Advances in Experimental Medicine and Biology 1131

Md. Shahidul Islam *Editor*

Calcium Signaling

Second Edition

Springer

Advances in Experimental Medicine and Biology

Volume 1131

More information about this series at http://www.springer.com/series/5584

Md. Shahidul Islam
Editor

Calcium Signaling

Second Edition

Springer

Editor
Md. Shahidul Islam
Department of Clinical Science
and Education
Södersjukhuset, Karolinska Institutet
Stockholm, Sweden

Department of Emergency Care
and Internal Medicine
Uppsala University Hospital
Uppsala, Sweden

Calcium signaling contains a unique selection of chapters that cover a wide range of contemporary topics in this ubiquitous and diverse system of cell signaling.

ISSN 0065-2598 ISSN 2214-8019 (electronic)
Advances in Experimental Medicine and Biology
ISBN 978-3-030-12456-4 ISBN 978-3-030-12457-1 (eBook)
https://doi.org/10.1007/978-3-030-12457-1

1st edition: © Springer Science+Business Media Dordrecht 2012

This Springer imprint is published by the registered company Springer Nature Switzerland AG.
The registered company address is: Gewerbestrasse 11, 6330 Cham, Switzerland

Dedicated to the living memory of
Roger Yonchien Tsien
(1952–2016)

Contents of Volume 1

Contents of Volume 2

Chapter 1
Calcium Signaling: From Basic to Bedside

Md. Shahidul Islam

Abstract Calcium signaling and its interacting networks are involved in mediating numerous processes including gene expression, excitation-contraction coupling, stimulus-secretion coupling, synaptic transmission, induction of synaptic plasticity, and embryonic development. Many structures, organelles, receptors, channels, calcium-binding proteins, pumps, transporters, enzymes, and transcription factors are involved in the generation and decoding of the different calcium signals in different cells. Powerful methods for measuring calcium concentrations, advanced statistical methods, and biophysical simulations are being used for modelling calcium signals. Calcium signaling is being studied in many cells, and in many model organisms to understand the mechanisms of many physiological processes, and the pathogenesis of many diseases, including cancers, diabetes, and neurodegenerative disorders. Studies in calcium signaling are being used for understanding the mechanisms of actions of drugs, and for discovery of new drugs for the prevention and treatment of many diseases.

Keywords Calcium signaling · Excitation-contraction coupling · Stimulus-secretion coupling · Calcium and gene expression · Calcium and diabetes · Calcium and cancer · Calcium channels · Calcium binding proteins · Calcium oscillations · Calcium pumps · Calcium-sensing receptor

Concentration of Ca^{2+} in the cytoplasm ($[Ca^{2+}]_c$) is >20, 000 times lower than that outside the cell. This is achieved by the Ca^{2+}-transporting ATPases, Na^+/Ca^{2+} exchangers, and Ca^{2+}-binding proteins. When activated by a variety of external stimuli, cells respond by an increase in the $[Ca^{2+}]_c$, in the form or Ca^{2+}-spikes and

M. S. Islam (✉)
Department of Clinical Science and Education, Södersjukhuset, Karolinska Institutet, Stockholm, Sweden

Department of Emergency Care and Internal Medicine, Uppsala University Hospital, Uppsala, Sweden
e-mail: Shahidul.Islam@ki.se

M. S. Islam (ed.), *Calcium Signaling*, Advances in Experimental Medicine and Biology 1131, https://doi.org/10.1007/978-3-030-12457-1_1

oscillations, which allosterically regulate many proteins leading to alterations of numerous processes like gene expression, meiotic resumption, gastrulation, somitogenesis, early embryonic development of different organs, left-right asymmetry, muscle contraction, exocytosis, synaptic transmission, and induction of synaptic plasticity, to name just a few.

The discovery of the method for measuring $[Ca^{2+}]_c$ by fluorescent Ca^{2+}-indicators [1] that are made temporarily membrane permeable [2] started a revolution in biology, and today many laboratories are using fluorescent Ca^{2+}-indicators for measuring $[Ca^{2+}]_c$. Since these indicators bind Ca^{2+}, it is necessary to assess to what extent the indicators attenuate the Ca^{2+} signal. At low concentration of the indicators, it is more likely that an un-attenuated Ca^{2+} signal is being measured, whereas at high concentration of the indicators, it is more likely that Ca^{2+}-flux is being measured [3]. Many investigators are using a variety of genetically encoded Ca^{2+} indicators suitable for measuring Ca^{2+} in different organelles and subcellular compartments [4]. The technology has advanced to the point that we can measure highly localized Ca^{2+} changes in femtoliter volume by high resolution laser microscopy. We can also measure the physiological changes in the membrane potential, and consequent changes in physiological Ca^{2+} currents, in living cells, in their native environment, by using fluorescence-based optical techniques. Pharmaceutical companies are using high- throughput fluorescence-based assays using a variety of Ca^{2+}-indicators, for screening of ion-channels and G-protein coupled receptor as drug targets, and for identifying novel lead compounds.

Plasma membrane Ca^{2+} transport ATPase (PMCA), Na^+/Ca^{2+} exchanger, and sarco/endoplasmic reticulum (SR/ER) Ca^{2+}-ATPase (SERCA) maintain $[Ca^{2+}]_c$ at a normal low level. More than 20 variants of PMCA, with different regulatory properties, cell-type-specific expressions, different localizations, and interactions with different signaling molecules, not only maintain Ca^{2+} homeostasis, but also shape the Ca^{2+} signals. Mutations or genetic variations in the PMCA genes have been associated with diseases like hypertension, preeclampsia, and neural disorders. Twelve isoforms of SERCA proteins encoded by three genes, are expressed in different patterns in different tissues. Impaired Ca^{2+} homeostasis and Ca^{2+} signaling caused by impaired functions of SERCA pumps have been implicated in the pathogenesis of Darier disease, and some neuropsychiatric and neurodegenerative disorders.

Cells contain numerous Ca^{2+}-binding proteins, some of which act as Ca^{2+}-sensors, others as Ca^{2+}-buffers, and some as both. Ca^{2+} is buffered by rapid binding to Ca^{2+}-binding proteins that vary in their Ca^{2+}-binding and -dissociation kinetics, their concentrations in different locations inside the cell, and in their diffusional mobility. Ca^{2+}-buffers make the $[Ca^{2+}]_c$ changes transient, and, thus, finely tune the timing and spatial extension of Ca^{2+} signaling.

Receptor activation increases incorporation of P^{32} into the phospholipids [5], due to activation of phospholipase C. Thirteen family members of phospholipase C, and their isoforms are regulated by numerous agonists in isozyme-selective manner; they perform distinct functions in signal transduction, and mediate a variety of

cellular responses, in almost every cells of the body. Activation of phospholipase C leads to the formation of the second messengers inositol 1,4,5 trisphosphate, and diacylglycerol [6, 7], which activates protein kinase C [8]. Inositol 1,4,5 trisphosphate activates 1,4,5 trisphosphate receptor, and releases Ca^{2+} from the ER [9]. In addition to mediating Ca^{2+} release, the three 1,4,5 trisphosphate receptors that form homotetramers, and heterotetramers, interact with >100 proteins, and signaling molecules. The expression of different isoforms of 1,4,5 trisphosphate receptor in different tissues, and their interactions with other proteins add to the complexity and diversity of the regulation of Ca^{2+} signaling in mediating many processes including apoptosis, autophagy, and cancer development.

The critical components of excitation-contraction coupling are the ryanodine receptors, the L-type voltage-gated Ca^{2+} channels and the junctophilins. From evolutionary perspective, Ca^{2+}-induced-Ca^{2+} release (CICR) (as in the cardiomyocytes) is the earliest form of excitation-contraction coupling, whereas depolarization-induced Ca^{2+} release from SR (DICR) through the type 1 ryanodine receptor mediated by direct protein-protein interaction between the ryanodine receptor and the L-type voltage-gated Ca^{2+} channel, (as in skeletal muscle cells) is a later development in the vertebrates. Four types of junctophilins link the ER to the plasma membrane, and support both CICR and DICR. Ca^{2+} regulates the three ryanodine receptors both positively and negatively (depending on concentration), by binding to the receptors, directly or indirectly through the Ca^{2+}-binding proteins, both from the cytosolic side and the luminal side. Release of Ca^{2+} from the ER /SR where Ca^{2+} is present in the form or "Ca^{2+}-lattice" bound to proteins, is a highly regulated process that prevents depletion of Ca^{2+} stores and consequent activation of ER stress response.

The pyridine nucleotide metabolite cyclic ADP ribose (cADPR) releases Ca^{2+} from the intracellular stores by mechanisms that may involve activation of the ryanodine receptors, but it is not clear how this happens, and to which protein cADPR binds. In heart, cADPR increases the gain of CICR. Another pyridine nucleotide metabolite, NAADP also releases Ca^{2+} from some acidic lysosomal Ca^{2+} stores by mechanisms that involve activation of the two pore channels (TPC). It is not clear whether NAADP binds to proteins other than TPCs. Stimulation of β-adrenergic receptors increases formation of NAADP, which releases Ca^{2+} from the acidic stores by binding to TPCs, but numerous questions remain unanswered. Endosomes and lysosomes are acidic organelles that contain Ca^{2+} in high concentration in readily releasable form. Ca^{2+} is loaded into these stores by the actions of vacuolar H^+-ATPase, and Ca^{2+}/H^+ exchange. Ca^{2+} can be released from these stores through the TRPML channel or the TPCs.

Receptor activation not only releases Ca^{2+} from the ER, but also leads to Ca^{2+} entry through the plasma membrane channels [10]. The stromal interaction molecule 1 (STIM1) senses the Ca^{2+} concentration in the ER Ca^{2+} stores, and it regulates the CRAC (Ca^{2+} release-activated Ca^{2+} channel) formed by Orai1, a highly calcium-selective channel located in the plasma membrane. STIM1 also regulates store-operated Ca^{2+} channel formed by TRPC1. Mutations in the STIM1/Orai1 have been associated with diseases like severe combined immune deficiency, Stormorken

syndrome, and tubular aggregate myopathy. Disturbances in store-operated Ca^{2+} entry have been implicated in promoting angiogenesis, tumor growth, muscle differentiation, and progression from cardiac hypertrophy to heart failure.

Mitochondria plays important roles in Ca^{2+} signaling. Mitochondria-associated ER membrane (MAM) provides a mechanism for communication between the ER and the mitochondria. The Sigma-1 receptor, a chaperone protein located in the MAM, is involved in Ca^{2+} exchange between the ER and the mitochondria. Ca^{2+} enters into the mitochondria through the mitochondrial Ca^{2+}-uniporter. Efflux of Ca^{2+} from the mitochondria is mediated by the Na^{+}/Ca^{2+} exchanger. Ca^{2+} regulates mitochondrial respiration, and ATP synthesis, but mitochondrial Ca^{2+} overload triggers the apoptosis pathways. The Sigma-1 receptor is also located near the plasma membrane, and it interacts with many other proteins. Mutations of the Sigma-1 receptor may lead to diseases like amyotrophic lateral sclerosis, and distal hereditary neuropathy.

The discovery of the transient receptor potential channels was helped by the clues obtained from the photoreceptor cells of drosophila mutants [11, 12]. These channels act as molecular sensors, and they participate in numerous cellular processes. Many cells express many of the TRP channels, and these channels appear to be involved in the pathogenesis of many diseases. In lungs, TRPC3 appears to be involved in mediating airway hyper-responsiveness seen in asthma. Dysregulation of several TRP channels has been implicated in promoting cancer growth, metastasis, and in determining sensitivity or resistance to chemotherapy. Some TRP channels that regulate tumorogenesis or tumor progression, are themselves targets of specific microRNAs, which are expressed in many cancer cells, and which function in RNA silencing. Manipulation of the TRP/miRNA interactive network is a potential way to treat cancer.

Ca^{2+} signals are decoded by numerous proteins, including, many ion channels, enzymes, transcription factors, and exocytotic proteins, which can be activated or inactivated by Ca^{2+}. Activation of protein kinase C [8] and multifunctional calcium/calmodulin stimulated protein kinases (CaMK) by Ca^{2+}, mediates a variety of cellular processes. The CaMKs, which are expressed in numerous cells, are activated following a variety of stimuli. Specificity of the functions of these kinases is determined by "molecular targeting" mechanisms mediated by some specific binding proteins. CaMK-II remains active in proportion to the frequency and amplitude of the Ca^{2+} signals, and the activation persists for some time even after $[Ca^{2+}]_c$ returns to the normal basal level. CaMK-II plays important roles in decoding Ca^{2+} signals to activate specific events during the embryonic development. Ca^{2+} singling regulates expression of many genes by acting at the level of gene transcription, gene translation, regulation of alternative splicing, and by regulating the epi-genetic mechanisms. Alteration in the expression of many genes can alter the so called "Ca^{2+} homeostasome" [13].

The Ca^{2+}-microdomains comprised of Ca^{2+} channels, Ca^{2+}-activated Ca^{2+} channels, Ca^{2+}-buffers, and other molecules, are fundamental elements of Ca^{2+} signaling. Different simulation strategies including stochastic method, deterministic method, Gillespie's method, and hybrid methods in multi-scale simulations, have been used for modeling of the Ca^{2+} signaling systems. Ca^{2+} signals occur in the

form of Ca^{2+} spikes, and Ca^{2+} oscillations, which are stochastic events. Advanced statistical approaches, and biophysical simulations are being used to obtain insight into the dynamics of Ca^{2+} oscillation, including the processes underlying the generation and decoding of the oscillations.

In biology, Ca^{2+} signaling is almost universal. Even bacteria use Ca^{2+} as a signal; they sense Ca^{2+} by using the so called two component regulatory systems consisting of a sensor kinase and a response element. To understand different biological phenomena, and many human diseases, Ca^{2+} signaling is being studied in many model organisms including *Drosophila melanogaster* [14], *Saccharomyces cerevisiae* [15], *Caenorhabditis elegans* [16], and zebrafish, and such researches have led to important discoveries. Study of Ca^{2+} imaging in the zebrafish has helped our understanding of the development processes, many other physiological processes, and the roles of disease-related genes in a vertebrate system.

Extracellular Ca^{2+} functions as charge carrier, and regulates neuromuscular excitability. Extracellular Ca^{2+} is sensed by a G-protein coupled receptor (calcium-sensing receptor), which regulates secretion of parathyroid hormone, and can be inhibited by the calcimimetic drug cinacalcet used in the treatment of hyperparathyroidism. In the bone marrow high extracellular Ca^{2+} leads to predominant osteoblast formation by acting through calcium-sensing receptor. High Ca^{2+} in the bone marrow also inhibits the differentiation and the bone-resorbing function of the osteoclasts. Extracellular matrix is the largest Ca^{2+} store in animals. The macromolecules of extracellular matrix interact with the receptor on the plasma membrane, and by that way regulate the $[Ca^{2+}]_c$ through complex mechanisms. Ca^{2+} also controls cell-extracellular matrix interaction through focal adhesions.

Study of Ca^{2+} signaling is helpful in understanding the pathogenesis of many diseases including that of diabetes, and the neurodegenerative diseases, and in understanding the mechanisms of action of drugs used in the treatment of these diseases. Many calcium channel blockers are being extensively used in the treatment of hypertension and atrial fibrillation. Over 400 million people in the world have diabetes. Studies of Ca^{2+} signaling have increased our understanding of the mechanisms underlying stimulus-secretion coupling in the β-cells, which is impaired in type 2 diabetes. Some of the commonly used antidiabetic drugs act by altering Ca^{2+} signaling in the β-cells [17]. It is likely that studies of Ca^{2+}-signaling and its interacting networks, will lead to new breakthroughs that will increase our understanding of the molecular mechanisms of many cellular processes that we do not fully understand today.

References

1. Tsien RY, Pozzan T, Rink TJ (1982) Calcium homeostasis in intact lymphocytes: cytoplasmic free calcium monitored with a new, intracellularly trapped fluorescent indicator. J Cell Biol 94(2):325–334
2. Tsien RY (1981) A non-disruptive technique for loading calcium buffers and indicators into cells. Nature 290(5806):527–528

3. Neher E (1995) The use of fura-2 for estimating Ca buffers and Ca fluxes. Neuropharmacology 34(11):1423–1442
4. Miyawaki A, Llopis J, Heim R, McCaffery JM, Adams JA, Ikura M et al (1997) Fluorescent indicators for Ca^{2+} based on green fluorescent proteins and calmodulin. Nature 388(6645):882–887
5. Hokin MR, Hokin LE (1953) Enzyme secretion and the incorporation of P32 into phospholipides of pancreas slices. J Biol Chem 203(2):967–977
6. Berridge MJ (1984) Inositol trisphosphate and diacylglycerol as second messengers. Biochem J 220(2):345–360
7. Michell RH (1975) Inositol phospholipids and cell surface receptor function. Biochim Biophys Acta 415(1):81–47
8. Nishizuka Y (1992) Intracellular signaling by hydrolysis of phospholipids and activation of protein kinase C. Science 258(5082):607–614
9. Maeda N, Niinobe M, Mikoshiba K (1990) A cerebellar Purkinje cell marker P400 protein is an inositol 1,4,5-trisphosphate (InsP3) receptor protein. Purification and characterization of InsP3 receptor complex. EMBO J 9(1):61–67
10. Putney JW Jr (1986) A model for receptor-regulated calcium entry. Cell Calcium 7(1):1–12
11. Cosens DJ, Manning A (1969) Abnormal electroretinogram from a Drosophila mutant. Nature 224(5216):285–287
12. Montell C, Rubin GM (1989) Molecular characterization of the Drosophila trp locus: a putative integral membrane protein required for phototransduction. Neuron 2(4):1313–1323
13. Schwaller B (2012) The regulation of a cell's Ca^{2+} signaling toolkit: the Ca^{2+} homeostasome. Adv Exp Med Biol 740:1–25
14. Hardie RC, Raghu P (2001) Visual transduction in Drosophila. Nature 413(6852):186–193
15. Cui J, Kaandorp JA, Sloot PM, Lloyd CM, Filatov MV (2009) Calcium homeostasis and signaling in yeast cells and cardiac myocytes. FEMS Yeast Res 9(8):1137–1147
16. Orrenius S, Zhivotovsky B, Nicotera P (2003) Regulation of cell death: the calcium-apoptosis link. Nat Rev Mol Cell Biol 4(7):552–565
17. Islam MS (2014) Calcium signaling in the islets. In: Islam MS (ed) Islets of langerhans, 2nd edn. Springer, Dordrecht, pp 605–632

Chapter 2
Measuring Ca^{2+} in Living Cells

Joseph Bruton, Arthur J. Cheng, and Håkan Westerblad

Abstract Measuring free Ca^{2+} concentration ($[Ca^{2+}]$) in the cytosol or organelles is routine in many fields of research. The availability of membrane permeant forms of indicators coupled with the relative ease of transfecting cell lines with biological Ca^{2+} sensors have led to the situation where cellular and subcellular $[Ca^{2+}]$ is examined by many non-specialists. In this chapter, we evaluate the most used Ca^{2+} indicators and highlight what their major advantages and disadvantages are. We stress the potential pitfalls of non-ratiometric techniques for measuring Ca^{2+} and the clear advantages of ratiometric methods. Likely improvements and new directions for Ca^{2+} measurement are discussed.

Keywords Ca^{2+} · Laser confocal microscopy · Fluorescence · Ratiometric · Non-ratiometric

Changes in the free Ca^{2+} concentration ($[Ca^{2+}]$) inside a cell can fulfil many different roles. Local changes in near membrane $[Ca^{2+}]$ can modify channels in the plasma membrane while changes in mitochondrial $[Ca^{2+}]$ can help to promote ATP production. Changes in nuclear $[Ca^{2+}]$ are critical for modulating gene replication and temporal aspects of these changes may provide valuable clues. One of the challenges in the field of Ca^{2+} signaling is to monitor the sites, amplitude and duration of free Ca^{2+} changes in response to physiological stimuli. Earlier researchers relied on a variety of methods, including atomic absorption and radioactive $^{45}Ca^{2+}$ to monitor Ca^{2+} in samples and Ca^{2+} movements across membranes and the likely underlying uptake and release mechanisms. Typically cell fragments were isolated by centrifugation and then Ca^{2+} uptake and storage capacity of isolated cellular organelles were examined. These methods were useful in the detection of relatively slow Ca^{2+} changes (seconds to minutes) but were unable to follow the short-term, transient Ca^{2+} movements induced by neural or

J. Bruton (✉) · A. J. Cheng · H. Westerblad
Department of Physiology & Pharmacology, Karolinska Institutet, Stockholm, Sweden
e-mail: Joseph.Bruton@ki.se

M. S. Islam (ed.), *Calcium Signaling*, Advances in Experimental Medicine and Biology 1131, https://doi.org/10.1007/978-3-030-12457-1_2

hormonal stimuli. Nonetheless, they provided valuable information about Ca^{2+} in cells e.g. the majority of tissue Ca^{2+} exists as bound to the glycocalyx (extracellular cell coat, Borle [4]) and is essential for maintaining excitability of neurons and muscle cells. X-ray microanalysis or electron probe analysis was the most ambitious of these attempts looking at both cellular and subcellular changes in Ca^{2+} but even at its best, this technique reported only the result of a physiological stimulus and not what happened during the period of stimulation itself.

All of these earlier techniques looked at changes in total Ca^{2+} and could not distinguish between bound and free Ca^{2+}, but what is most relevant to physiologists is the free Ca^{2+} concentration. Free Ca^{2+} concentration in the cytosol is often written as $[Ca^{2+}]_i$, which can be confusing since the 'i' can be interpreted as meaning free or bound or both. In this review, $[Ca^{2+}]_i$ will be used to refer to the free cytosolic Ca^{2+} concentration. When muscle cells are electrically stimulated, free cytosolic $[Ca^{2+}]$ (i.e. $[Ca^{2+}]_i$) can increase more than tenfold in a few ms, whereas the intracellular $[Ca^{2+}]$ remains essentially constant. The transient increase in $[Ca^{2+}]_i$ is due to Ca^{2+} release from the sarcoplasmic reticulum (SR) into the cytosol and subsequent active removal from the cytosol. Thus, Ca^{2+} moves from one cellular compartment to another and back again and overall total intracellular $[Ca^{2+}]$ does not change.

Multiple bioluminescent and fluorescent Ca^{2+} indicators are now available to measure $[Ca^{2+}]$ in cells and subcellular regions. Published results focus often on amplitude and time course of the signal and gloss over the possible pitfalls of interpretation. Since many users are not experts and try to follow or modify methods described earlier, the likelihood of errors and misinterpretation of data has increased. Our focus in this chapter is to highlight what can and cannot be done with available Ca^{2+} indicators.

2.1 Earlier Attempts to Measure $[Ca^{2+}]$ Inside Cells

Measurements of $[Ca^{2+}]_i$ were rather complicated before the invention of the various fluorescent Ca^{2+} indicators that are commonplace today. An invaluable source of information about these methods is to be found here [3].

1. *Ca^{2+}-activated photoproteins*. In 1961, Osamu Shimomura spent a stressful summer mashing up the light organs distributed along the edge of the bell of many thousands of *Aequorea* jellyfishes trying to isolate and characterize what was responsible for the blue-green glow. These jellyfishes are pretty colorless in real life and do not spontaneously glow. However if they are poked or disturbed in the water, then a greenish bioluminescence is seen, localised only around the margins of the bell but not found anywhere else on the jellyfish's body. After many trials two proteins were isolated, the bioluminescent protein aequorin that glowed blue upon the addition of Ca^{2+} and the green fluorescent protein which in the living jellyfish produces green light because of resonant energy transfer

from aequorin. Shimomura was awarded the Nobel prize in Chemistry in 2008 for the green fluorescent protein discovery. Other bioluminescent proteins were subsequently isolated from other organisms (e.g. obelin, berovin) but none of them approached the versatility of aequorin either in their native form or with targeted mutations and thus they are hardly used today.

An advantage of aequorin is that as a bioluminescent molecule it does not require any external stimulating light and thus the background signal or noise is extremely low. On the other hand, the bioluminescence signal is quite small and measurement of the light emitted is not as easy as it is for other currently used fluorescent indicators. In practice, it is barely sensitive enough to following changes in resting $[Ca^{2+}]_i$. Even when aequorin is used to monitor changes in the high physiological range of $[Ca^{2+}]_i$ (0.5–10 μM) that are induced by electrical or chemical stimulation, there are difficulties in interpreting the light emission which increases as approximately the third power of $[Ca^{2+}]$. Translating aequorin light signal into actual values of $[Ca^{2+}]_i$ is complicated further by its consumption (i.e. the signal decreases over time) and since $[Ca^{2+}]_i$ differs within different regions of the cell (highest at release sites), the signal will be heavily dominated by the regions with the highest $[Ca^{2+}]_i$. The light emitted by aequorin in the presence of $[Ca^{2+}]_i$, will be influenced by Mg^{2+} and the ionic strength which can change markedly during intense stimulation. Moreover, it is sensitive to changes in pH especially below pH 7. It is useful to imagine the Ca^{2+}-activated photoproteins as being "precharged" and Ca^{2+} binding to an photoprotein molecule causes an energy-consuming reaction with emission of light that discharges the molecule. Each molecule emits light only once, which means that the light-emitting capacity declines over time but with experience and modelling, one can minimise this potentially confounding factor. In earlier days, the major problem with native photoproteins was getting them into a cell. In large cells this was achieved by microinjection which was not practical for smaller (< 20 μm) cells. Other loading techniques have been tried and of these, incubation combined with mild centrifugation seems to be the best. Once the sequence of aequorin was known, it became feasible to transfect cells and induce expression of recombinant aequorin. This works well with many cultured cells and in embryos but is problematic when one tries to induce expression in adult cells in culture or in a living animal. An advantage with this technique is that the aequorin gene can be modified and targeted to different cellular compartments (e.g. mitochondria or endoplasmic reticulum) and the Ca^{2+} binding properties of the proteins can be modified appropriately. Photoprotein-based methods to measure $[Ca^{2+}]$ in organelles are useful because in some situations it is not possible to introduce other fluorescent probes into a subcellular compartment [1].

2. *Metallochromic Ca^{2+} dyes*. Murexide was the first of these and arsenazo III and antipylazo III followed soon afterwards. With these indicators, the light absorbance of the molecule is monitored by a photomultiplier and when $[Ca^{2+}]$ increases, the light measured will decrease. The advantage of these dyes is that they are fast and therefore can detect rapid $[Ca^{2+}]_i$ transients. This is because

they display a relatively low Ca^{2+} affinity, which means that they readily can detect high $[Ca^{2+}]_i$ levels and show little Ca^{2+} buffering. However, there have some unwanted characteristics which include complex Ca^{2+}-binding properties, marked Mg^{2+} and pH sensitivity, and a tendency to bind to intracellular proteins. The metallochromic Ca^{2+} dyes do not easily enter intact cells, and therefore these dyes were usually microinjected. Today, with one exception, these dyes are seldom used by anyone except specialists looking at the kinetics and other properties of Ca^{2+} release in muscle cells. The exception is calcein a metallochromic indicator used since 1956 to look at calcium in minerals and salts. It is not sensitive to monitor resting $[Ca^{2+}]$ in unstimulated cells but has found a niche as a live live/dead cell indicator and looking at opening of the mitochondrial permeability transition pore.

3. *Ca^{2+}-selective microelectrodes*. Electrophysiological techniques were already used to probe channels in the plasma membrane and thus they could be readily adapted when suitable Ca^{2+} resin and ligands were produced by chemists. Double barrelled electrodes were adapted quite early on so that only one microelectrode impalement of the cell was necessary to measure both membrane potential and Ca^{2+} (the signal detected by the Ca^{2+} sensor includes both the membrane potential and the Ca^{2+} potential and thus, the membrane potential has to be subtracted). Ca^{2+}-selective electrodes are rather difficult to make since a special silane coat has to be applied to the glass first before the Ca^{2+}-selective ligand is loaded in the electrode [8]. Microelectrodes with tips less than 1 μm are used to minimise cell damage when the electrodes are inserted into cells. Ca^{2+}-selective microelectrodes have good selectivity for Ca^{2+} over other cations in the physiological range. They suffer from two drawbacks that have limited their use in Ca^{2+}-signalling. First they report the free $[Ca^{2+}]_i$ only in the vicinity of the microelectrode tip and second even under the best possible recording conditions, their response time is slow, on the order of seconds when changing between solutions containing different free $[Ca^{2+}]$. Thus, they are not able to follow the rapid $[Ca^{2+}]_i$ transients that occur in excitable cells such as muscle or neurons. Nonetheless, various groups have used them to report resting free $[Ca^{2+}]$ in both animal and plant cells as being 50 nM to 150 nM, slightly higher than was measured later with diffusible Ca^{2+} indicators and reflecting the fact that underneath and close to the plasma membrane, free $[Ca^{2+}]$ is higher than in the bulk of the cytosol.

2.2 Fluorescent Ca^{2+} Indicators

Many of the common Ca^{2+} indicators used today were derived from the Ca^{2+} chelator BAPTA developed by Roger Tsien and his co-workers [14]. The Ca^{2+} indicator molecule consists of two parts: the Ca^{2+}-binding cavity that changes its shape when Ca^{2+} binds to it and the scaffold part of the molecule giving

the fluorescence changes in response to Ca^{2+} binding to or being released from the cavity. These indicators have high selectivity for Ca^{2+} over Mg^{2+} and other common monovalent cations and are relatively unaffected by modest changes in H^+. When Ca^{2+} binds into the Ca^{2+}-binding cavity, there are large absorbance and fluorescence changes. It should be remembered that even with a low affinity for Mg^{2+} and H^+, Ca^{2+} indicators can be affected by these ions in experiments that are designed to induce metabolic exhaustion and thus a rise in free Mg^{2+} or large changes in pH. Much work has gone into developing different Ca^{2+}-binding properties and fluorescent tails that are optimised to work in defined ranges of $[Ca^{2+}]$ and with different types of detection systems.

Ca^{2+} indicators can be conveniently divided into two groups: single-wavelength non-ratiometric indicators and dual-wavelength ratiometric indicators. Indicators have absorption and emission spectra that have been well characterised in vitro and which apply in general to the behaviour of the molecules inside cells. Optimal excitation and emission wavelengths for individual indicators can generally be found in the papers where they were originally described and have been gathered here with additional details (https://www.thermofisher.com/se/en/home/life-science/cell-analysis/cell-viability-and-regulation/ion-indicators/calcium-indicators.html#crs).

Non-ratiometric indicators generally show very little fluorescence at low (<100 nM) $[Ca^{2+}]$ but show up to a hundred-fold increase in fluorescence when $[Ca^{2+}]$ increases maximally inside a cell so that the indicator becomes saturated with Ca^{2+}. The expectation that the light signal faithfully reflects $[Ca^{2+}]_i$, is probably true under ideal conditions. However, to be able to directly compare signals from different experiments the following requirements have to be fulfilled: (1) cells exposed to similar loading conditions will have similar concentrations of indicator; (2) indicators remain in the cytosol and do not leak or get pumped out of the cytosol; (3) cell volume remains constant and there is no change in cell thickness; (4) the cell does not move; (5) the indicator is not affected by repeated exposure to excitation light. Unfortunately all these requirements are almost never fulfilled and so data obtained with non-ratiometric indicators should be carefully assessed to avoid errors (see Fig. 2.1 and discussion below).

Ratiometric indicators have the advantage that the Ca^{2+}-free and Ca^{2+}-bound forms of the indicator have distinct peaks at different wavelengths. Thus, measurements can be made at the two separate peaks and combined into a ratio. The ratio is usually constructed so that the signal recorded at the wavelength where the fluorescence shows a maximum at high $[Ca^{2+}]$ is divided by the signal recorded at the wavelength showing its maximum at low $[Ca^{2+}]$. Between the two wavelength peaks, there is an isosbestic point where the fluorescence does not depend on $Ca^{2+}]$. In some cases (e.g. measuring quenching of a dye by Mn^{2+}) measurements are best made at this isosbestic wavelength. The classical ratiometric indicator fura-2 requires excitation at two wavelengths while the emitted fluorescent light is measured at one wavelength (~510 nm). The isosbestic point for fura-2 excitation is ~360 nm and with increasing $[Ca^{2+}]$, the emitted light increases at shorter wavelengths and decreases at longer wavelengths. The ratio with maximal dynamic

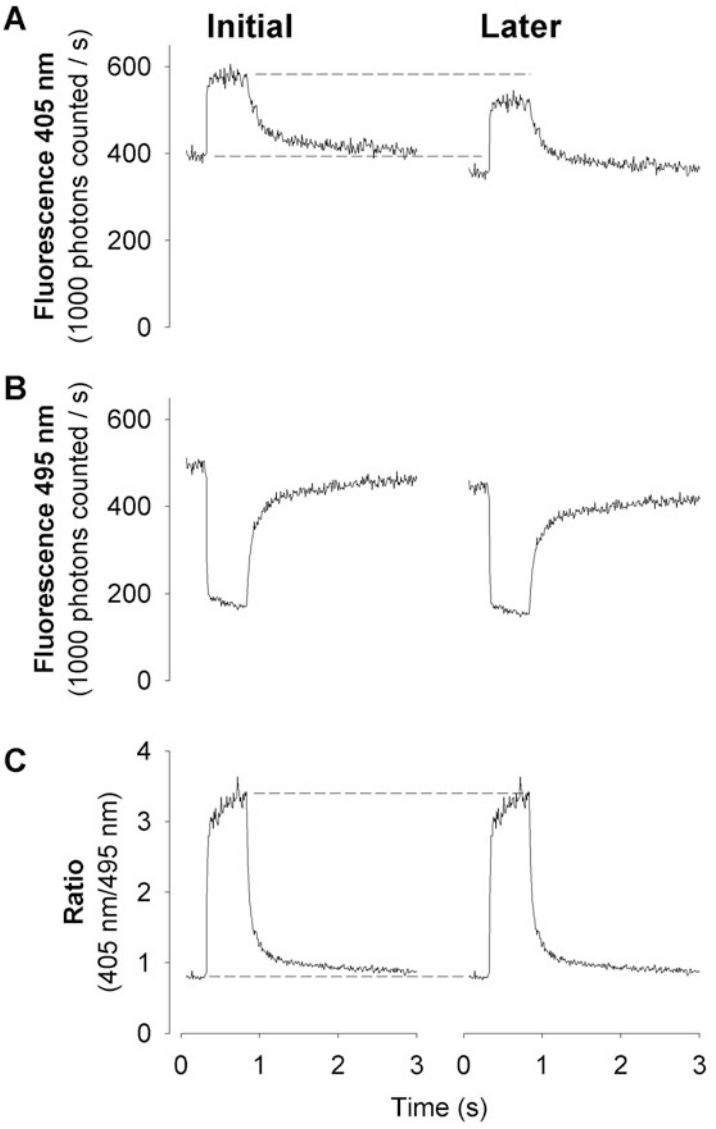

Fig. 2.1 Ratiometric indicators are best for experiments lasting hours. Indo-1 records obtained in a skeletal muscle cell stimulated to perform a tetanic contraction (70 Hz stimulation for 350 ms). Indo-1 was excited at 360 nm and the emitted light was measured simultaneously at 405 nm (**a**) and 495 nm (**b**) and the 405 nm/495 nm ratio was constructed (**c**). Over time, the ratio signal remained constant (dashed line in **c**) while the fluorescence intensity decreased for both the 405 nm (dashed line in **a**) and 495 nm signal. Note that the decline in the 405 nm trace seen in the right trace of the two shown in **a** is qualitatively similar to what would be seen if fluo-3 or another non-ratiometric indicator was used

range is then obtained by excitation below (~340 nm) divided by above (~380 nm) the isosbestic point. However, this requires continuous alteration between 340 nm and 380 nm excitation, which is technically troublesome, especially if rapid $[Ca^{2+}]_i$ transient are being measured. A simpler procedure is to measure the signal at the isosbestic point (360 nm) at regular intervals when constructing the ratio because the signal does not depend on $[Ca^{2+}]$. The preferred ratios will then be 340 nm/360 nm or 360 nm/380 nm, both of which will show an increase when $[Ca^{2+}]$ increases, albeit the ratio increase will not be as large as for the 340 nm/380 nm ratio. In our laboratory, we use the ratiometric dye indo-1 which requires excitation at only one wavelength and the emitted light be split into the $[Ca^{2+}]$-bound component (peaks about 400 nm) and the $[Ca^{2+}]$-free component (peaks about 475 nm).

The fundamental advantage of ratiometric over non-ratiometric indicators is exemplified in Fig. 2.1, which shows fluorescence records from a single skeletal muscle fiber at rest and during stimulation to produce a maximum contraction. Figure 2.1a shows the results as they would appear with a single wavelength indicator. As the experiments progressed, the fluorescent signal showed a general decline (probably representing pumping of the dye molecule out of the cell or transport by a non-specific anion transporter which can be blocked by probenecid or sulfinpyrazone), which might then be interpreted as a decrease in $[Ca^{2+}]_i$ both in the basal state and during contraction. However, the ratiometric indicator indo-1 was used in the experiment. In contrast to fura-2, this indicator is excited at one wavelength (~360 nm) and the emitted light is measured at two wavelengths (405 nm (increased signal with increasing $[Ca^{2+}]_i$) and 495 nm (decreased signal with increasing $[Ca^{2+}]_i$) in the depicted experiment). Figure 2.1b shows that there was a general decrease also in 495 nm signal as the experiment progressed. This means that there was no change in the 405 nm/495 nm ratio with time (Fig. 2.1c), which correctly reflects that there was no change in $[Ca^{2+}]_i$. The experimental traces in Fig. 2.1a show clearly that the signals from non-ratiometric indicators can result in completely erroneous conclusions if used without thinking. It should be noted that ratiometric indicators are not a cure for all problems. For instance, excessive UV light exposure can lead to qualitatively altered properties of the indicator (bleaching or inactivation), which cannot be corrected by ratioing [13].

2.3 Which Indicator Should One Use?

As outlined above, ratiometric indicators have clear advantages over non-ratiometric indicators and should be used whenever possible. Nowadays, visible-light laser scanning confocal microscopes are more common than any other Ca^{2+}-dedicated imaging systems meaning that a non-ratiometric indicator such as fluo-3/fluo-4 is often the first choice. Adding on a UV source to a microscope is reasonably straightforward and with suitable lens and filters, ratiometric indicators (i.e. fura-2 and indo-1 and their close relatives mag-fura-2 and mag-indo-1) could be used but this type of modification is rarely done.

In an ideal experiment, one would use an indicator which gives a fluorescence signal that shows large changes when $[Ca^{2+}]_i$ is changing and which is fast enough to follow the changes in $[Ca^{2+}]_i$ under study. However, the perfect indicator does not exist because some properties are difficult, or even impossible, to change. For instance, a Ca^{2+} indicator showing large changes in fluorescence with $[Ca^{2+}]_i$ changes in the low physiological range (~100 nM) is relatively slow and the opposite is also true. The relation between the intensity of the fluorescent signal (F) and $[Ca^{2+}]_i$ for a non-ratiometric indicator is given by the following equation (Eq. 2.1):

$$\left[Ca^{2+}\right]_i = K_d^* \ (F - F_{min}) / (F_{max} - F) , \tag{2.1}$$

where F_{min} and F_{max} mean the fluorescence intensity at virtually zero and saturating $[Ca^{2+}]_i$, respectively. K_d is the dissociation constant which in a plot of F against $[Ca^{2+}]_i$, will be the $[Ca^{2+}]$ where F is half-way between F_{min} and F_{max} and this is where the indicator displays its largest sensitivity. K_d is decided by an indicator's rates of Ca^{2+} binding (K_{on}) and dissociation (K_{off}), i.e. $K_d = K_{off}/K_{on}$. The on-rate constants of Ca^{2+}-binding are very fast and not that dissimilar whereas the rate that differs markedly between indicators is K_{off}. Accordingly, a slow indicator (low K_{off}) has a low K_d, which means that it is most sensitive at relatively low $[Ca^{2+}]_i$ and such indicators are therefore called high-affinity indicators. Conversely, a fast indicator has a high K_d and is referred to as a low-affinity indicator.

For ratiometric indicators, a slightly more complex equation describes the relation between fluorescence ratio (R) and $[Ca^{2+}]_i$ (Eq. 2.2):

$$\left[Ca^{2+}\right]_i = K_d^* \beta^* \ (R - R_{min}) / (R_{max} - R) , \tag{2.2}$$

where R_{min} and R_{max} is the fluorescence ratio at virtually zero and saturating $[Ca^{2+}]_i$, respectively. β is obtained by dividing the fluorescence intensity of the ratio's 2nd wavelength (denominator) acquired at virtually zero and saturating $[Ca^{2+}]_i$, respectively. Thus, the mid-point between R_{min} and R_{max} occurs at a $[Ca^{2+}]_i$ that equals $K_d * \beta$.

Figure 2.2 illustrates how the properties of two different Ca^{2+} indicators affect the change in fluorescence signal observed when $[Ca^{2+}]_i$ is changed in different concentration intervals. The comparison is between one high-affinity indicator, fura-2, and a low-affinity indicator, mag-fura-2. The name mag-fura-2 comes from the fact that it was designed to measure $[Mg^{2+}]$, but it has found its niche as a low-affinity Ca^{2+} indicator since $[Mg^{2+}]$ shows significant changes in the cytosol only when a cell is metabolically stressed by repetitive stimulation or exposed to poisons such as cyanide and its derivatives. $[Ca^{2+}]_i$ may vary dramatically between different physiological states. For instance, $[Ca^{2+}]_i$ peaks during contraction in a skeletal muscle cell may be up to 100-fold higher than resting $[Ca^{2+}]_i$. $[Ca^{2+}]_i$ is therefore often expressed as pCa or the negative $\log[Ca^{2+}]_i$ (analogous to the concept of pH). In Fig. 2.2, the 340 nm/380 nm ratio is shown for both indicators and β is set to

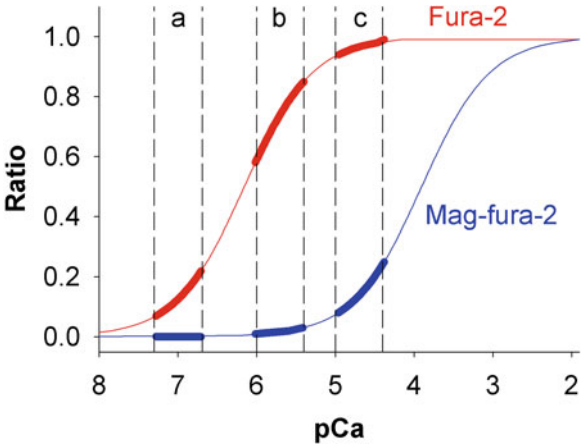

Fig. 2.2 High-affinity Ca^{2+}indicators are more sensitive to stable changes in $[Ca^{2+}]_i$in the normal physiological range. The relationships between $[Ca^{2+}]_i$ and fluorescence ratio (340 nm/380 nm excitation) are shown for the high-affinity indicator fura-2 and the low-affinity indicator mag-fura-2. $[Ca^{2+}]_i$ expressed as pCa ($-\log[Ca^{2+}]_i$) in order to cover a larger range of concentrations. The thick lines are used to emphasise the differences between the two indicators at different $[Ca^{2+}]$ (**a**) 50–200 nM; (**b**) 1–4 μM; (**c**) 10–40 μM

4. This means that the mid-point between R_{min} and R_{max} occurs at a $[Ca^{2+}]_i$ of 0.56 μM for fura-2 (K_d assumed to be 0.14 μM) and 100 μM for mag-fura-2 (K_d assumed to be 25 μM). The interval (a) in Fig. 2.2 shows the change in ratio signal obtained when $[Ca^{2+}]_i$ is changed in the range of normal resting values, 50–200 nM. Here the fura-2 ratio signal shows a substantial increase, whereas mag-fura-2 ratio signal changes hardly at all. Thus, fura-2 can readily detect changes in basal $[Ca^{2+}]_i$, whereas mag-fura-2 is useless. The interval (b) in Fig. 2.2 (1–4 μM) would reflect $[Ca^{2+}]_i$ in cells that are activated. Again fura-2 is a rather sensitive indicator in this interval, whereas mag-fura-2 shows little change in the ratio signal. Finally the area marked (c) reflects $[Ca^{2+}]_i$ (10–40 μM) in a cell stimulated to maximal activation. In this case, fura-2 is saturated and changes little in the face of large concentration changes, whereas mag-fura-2 is clearly able to report changes in $[Ca^{2+}]_i$.

As a rule of thumb, all buffers are useful for detecting changes in an interval between about tenfold below and tenfold above the mid-point. Thus inside a cell where free $[Ca^{2+}]$ varies between 50 nM and 2–3 μM a suitable Ca^{2+} indicator which readily detects $[Ca^{2+}]_i$, at rest and during activation will have a K_d of 200–300 nM. This is also the $[Ca^{2+}]_i$ interval where Ca^{2+} most easily binds to the indicator, which has the potential to cause buffering problems. The noise in the detected fluorescent light signal decreases with increasing emitted light intensity. From this perspective it would be advantageous to have a large concentration of fluorescent indicator in a cell. However, a high concentration of indicator with a K_d in the physiological $[Ca^{2+}]_i$ range will buffer $[Ca^{2+}]_i$ markedly as illustrated in Fig. 2.3. When a relatively low concentration of indicator is present in the cell

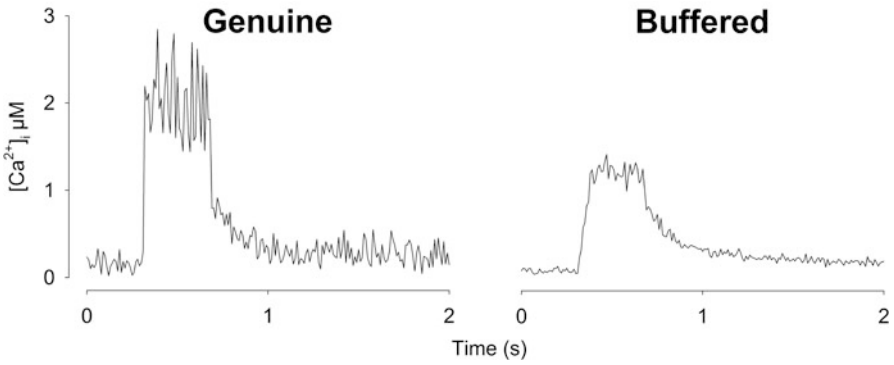

Fig. 2.3 Excessive cytosolic loading of Ca^{2+} indicator distorts $[Ca^{2+}]_i$ transients. Typical records from the same skeletal muscle cell illustrate the real $[Ca^{2+}]_i$ response to 70 Hz tetanic stimulation (left trace) and the response as it looked after further injections of the Ca^{2+} indicator, indo-1, that caused buffering of the $[Ca^{2+}]_i$ transient (right trace). Note the reduced noise, the reduced amplitude and the slower rate of rise and decay in the buffered Ca^{2+} transient compared to the original record

("Genuine") a rapid and relatively large change in $[Ca^{2+}]_i$ is recorded but the signal contains some irregular fluctuations (noise). A markedly higher concentration of indicator ("Buffered") gives a far less noisy signal but the time course of the rise and fall of $[Ca^{2+}]_i$ is slowed and the amplitude of the change is less. Thus, with high-affinity Ca^{2+} indicators there is a delicate balance between introducing a sufficiently high indicator concentration to obtain records with an acceptable noise level and having so much indicator that cytosolic Ca^{2+} is markedly buffered, which leads to distorted $[Ca^{2+}]_i$ signals as well as altered cell signalling or function.

Figure 2.2 shows that a high-affinity Ca^{2+} indicator is better than a low-affinity indicator at monitoring changes in $[Ca^{2+}]_i$ in the normal physiological range. However, the diagram in Fig. 2.2 refers to stable or slowly changing $[Ca^{2+}]_i$. As discussed above, a trade-off of high Ca^{2+} sensitivity is that the indicator may be too slow to follow rapid changes in $[Ca^{2+}]_i$. In Fig. 2.4 this is illustrated for $[Ca^{2+}]_i$ transients in a skeletal muscle cell, the same would be true for any other excitable cell. The $[Ca^{2+}]_i$ transient resulting from a single stimulation pulse lasts for ~10 ms. Figure 2.4a shows such a $[Ca^{2+}]_i$ transient as recorded with the high-affinity indicator indo-1. However, the indicator is not fast enough to accurately follow the rapid changes in $[Ca^{2+}]_i$ and the recorded transient is too slow and the amplitude too low. In Fig. 2.4b the signal has been kinetically corrected [15] to take account of the properties of indo-1 and the $[Ca^{2+}]_i$ transient now better represents the true situation. While a low-affinity Ca^{2+} indicator could follow $[Ca^{2+}]_i$ transients more accurately and would therefore be preferable in experiments where rapid $[Ca^{2+}]_i$ changes are being studied, there is the drawback that the change in fluorescent signal is going to be small and hence difficult to measure. Figure 2.4c shows $[Ca^{2+}]_i$ as recorded by indo-1 during tetanic stimulation (70 Hz, 350 ms duration) of the

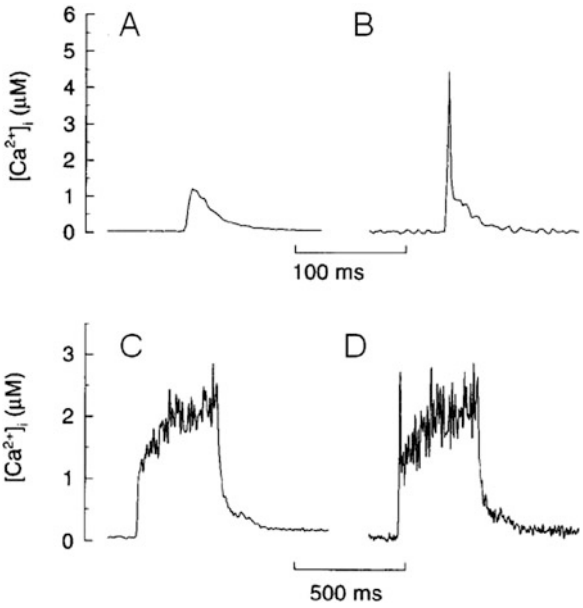

Fig. 2.4 Fast low-affinity Ca^{2+}indicators or kinetic correction of high-affinity Ca^{2+}indicator records are required to accurately portray rapid $[Ca^{2+}]_i$transients. $[Ca^{2+}]_i$ records measured with indo-1 in a skeletal muscle cell in response to a single stimulation pulse (**a**) and a tetanus (**c**). This high-affinity indicator is too slow to accurately follow the most rapid changes in $[Ca^{2+}]_i$. Kinetic correction reveals a faster and larger $[Ca^{2+}]_i$ transient with the single stimulation pulse (**b**) and a $[Ca^{2+}]_i$ spike at start of the tetanus (**d**). (Figure adapted from Westerblad and Allen [15])

muscle cell; in Fig. 2.4d the record is corrected for the slow response of indo-1. It can be seen that the initial "spike" of $[Ca^{2+}]_i$ is missed without correction, but otherwise the records are rather similar. To sum up, Fig. 2.4 thus illustrates that problems with slow, high-affinity Ca^{2+} indicators are substantial when recording rapid $[Ca^{2+}]_i$ transients but much less so during more prolonged $[Ca^{2+}]_i$ changes. Thus, again there is a delicate balance between being able to measure large and rapid $[Ca^{2+}]_i$ changes (low-affinity indicators are preferable) and measure small prolonged changes (high-affinity indicators are better).

The signals recorded by the PMT or CCD are always transferred and stored on a computer and this means that the sampling rate can be high as one wishes. Sampling theorems are available which can be used empirically to decide what the optimal sampling rate is. As a general rule, we use a sampling rate at least tenfold faster (100 Hz to 1 kHz) than the expected fastest speed of $[Ca^{2+}]_i$ transients under study. It is worth remembering that using a high sampling rate means that less light signal is integrated for each time point and hence the noise level is higher with fast than with slow sampling. On the other hand, rapid or small $[Ca^{2+}]_i$ transients might be missed or distorted with a low sampling rate.

2.3.1 How Easy Is It to Get Indicators into Cells?

Indicators are charged molecules and do not easily pass lipid membranes. While many cells display endocytotic behaviour, we consider that the amount of indicator that can enter the cell by endocytosis during a couple of hours will be small and unlikely to be enough to make reproducible and meaningful measurements. Ca^{2+}-indicator can be introduced into cells by pressure injection or by electrophoreses. Electroporation of the cell membrane using very brief, high voltage pulses opens transient small pores in the cell membrane through which indicator molecules pass. All of these techniques require specialised equipment and some skill, but they maximise the likelihood that the indicator will be found only in the cytosol and not move into sub-cellular compartments, such as the mitochondria or sarco-endoplasmic reticulum.

Fortunately, there is a much easier method for introducing fluorescent indicators into the interior of single cells or tissue. The principle behind the method is that lipophilic groups (acetoxymethyl or acetate ester (AM) groups) are added to the charged indicator molecule. In this way the charges are hidden and the indicator complex becomes lipophilic and hence membrane-permeant. Once the complex has entered into the cytosol, cytoplasmic esterases gradually cut off the lipophilic groups and the free indicator molecule is then trapped in the cytosol and ready to detect $[Ca^{2+}]_i$. This simple method of loading fluorescent indicators into cells gives many a chance to investigate the regulation of $[Ca^{2+}]$ in their favourite cell. The lipophilic AM-indicator complex is typically dissolved in a mixture of dimethylsulfoxide (usually written as DMSO) and the detergent Pluronic to disperse the indicator molecules and aid cell loading. Typically, cells are exposed to the indicator (1–10 μM) for 10–30 min. After the loading period is finished, the cells are washed to remove residual extracellular AM-indicator and left for a further 30 minutes to ensure that all lipophilic groups have been cleaved off by cytoplasmic esterases allowing the indicator molecule to interact with Ca^{2+}. We have successfully used this basic loading protocol to detect electrically- or chemical-induced transient changes in $[Ca^{2+}]_i$ in myoblasts, myotubes and muscle fibres [12], pancreatic beta-cells [5], hippocampal neurons [10] and cardiomyocytes [11].

Loading of the lipophilic AM-indicator complex is not without problems. The quantity loaded into cells cannot be directly controlled. This leads to the risk of excessive loading and resultant buffering of $[Ca^{2+}]_i$, which affects Ca^{2+} homeostasis inside the cell and gives erroneous estimates of changes in $[Ca^{2+}]_i$ amplitude and time course as well as affecting Ca^{2+}-dependent cellular signalling. An additional problem with AM-indicators is that they may pass across intracellular membranes into organelles and report changes in $[Ca^{2+}]$ in this compartment in addition to changes in the cytosol. Our experience is that these problems seem to be minimised if cells are loaded at room temperature rather than at the higher physiological temperature of mammals. Unfortunately there is no single set of conditions that produces optimal loading of all cells and procedures needs to be optimised for each new cell type. For example, in our hands, indo-1 AM does not

load into mouse cardiac myocytes but does load into rat cardiac myocytes. It should be noted that in tissues or densely coated cultured cells, indicator molecules can be trapped and cleaved by extracellular esterases to produce an indicator that reports extracellular [Ca^{2+}] and confounds the intracellular measurements [9].

For quantitative measurement within the cytosol of rapid or repeated transient [Ca^{2+}] in any intact neural or muscle cell, indo-1 is our first choice of fluorescent indicator. For slower changes lasting seconds or minutes, either indo-1 or fura-2 would be adequate. If one is interested only in the effect of a drug or other intervention and not the absolute numbers, then one could easily turn to fluo-3/fluo-4 as first choice indicators. For looking at intracellular organelles, the fluorescent indicator rhod-2 has been widely used to monitor changes in mitochondrial [Ca^{2+}] in neurones and muscles during and after stimulation by us and others. The low-affinity calcium indicator (K_{Ca} 90 μM) fluo-5 N has been used to monitor SR [Ca^{2+}] during repeated tetanic contractions. [Ca^{2+}] measurements can also be attempted using compartment-specific aequorin chimeras and other genetically engineered proteins [1, 7].

2.4 Equipment Overview

Typically, one uses the instruments that are available rather than those that are optimal for the task of measuring changes in [Ca^{2+}] inside a cell. The minimum needed to detect the fluorescence emitted from cells loaded with an indicator are a microscope with a light source to locate the cells and to excite the indicator, a detection device that is typically one or more photomultiplier tubes or a CCD camera and some recording or storage device. A simpler fluorometer-based system can be used if one is working with cell suspensions and is not interested in the response of individual cells. Filters are inserted into the light path to limit the wavelength and intensity of the light that excites the indicator and also to limit the wavelengths of the emitted light measured by the light detectors. The signals from the light detectors are generally digitised and stored on a computer. Newly purchased equipment dedicated to Ca^{2+} measurements is supplied with software controlling the various parameters related both to excitation wavelength and to detection of the emitted light that is more than capable of recording and performing a fast on-line analysis of signals.

The most important but often neglected part of the whole acquisition system is the light path and especially the objective lens. The lens is what allows one to magnify and focus on the cell or tissues. While magnification is important to see the sample, what is equally or more important is the ability of the lens to pass light of the appropriate wavelength and resolve fine specimen detail. The light collection effectiveness is described by the numerical aperture (N.A.) written on the lens casing. In general, one should have the lens with the highest N.A. possible (a more detailed description can be found here: http://micro.magnet.fsu.edu/primer/anatomy/numaperture.html). Lenses that are optimised to work with ultraviolet (UV) light are not optimal for visible light and vice versa. Lenses are

exposed to the dust and moisture in the working environment unlike most of the other elements of the system, which are encased in protective housing. Even if an acquisition system is handled carefully, the lens is liable to become dirty from the particles floating in the air. If the lens requires oil or water for its proper operation, the combination of liquid and dust can lead rather quickly to the formation of a film coating the lens surface and the light path deteriorates. We use a superfusion system routinely in our experiments and over the years we have had a variety of problems ranging from leaks in aged tubing, overflow of liquid out of the recording chamber resulting in fluid on and inside the lens leading to a rapid deterioration of the signal. If not spotted quickly, this can lead to salt deposits on the lens or, in the worst case scenario, fluid entering the lens casing with a salt coating both outside and inside the lens. Problems of this kind are easily recognised as increased noise in the fluorescence signal and in the worse cases inability to focus on the cells or tissue. It should be routine to check the lens before and at the end of an experiment and to clean the lens with lens paper and an air spray before and after experiments or immediately one sees that solution has dripped on to the lens. If solution has dried and formed salt crystals on the lens, we use distilled water to rinse the salts away and ethanol is used finally to clear off residual water.

Nowadays, the most common types of detection set-ups are epifluorescence microscopy and scanning confocal microscopy. In epifluorescence microscopy, the whole sample consisting of a single cell or group of cells loaded with an indicator is excited by light of the appropriate wavelength and the photons emitted from the indicator are collected both from the sample section in focus (typically 0.3 μm with an objective lens with a high numerical aperture of 1.3) and also from above and below this plane of focus. Emitted light travels to one or more photomultiplier tubes or a CCD camera. Epifluorescent microscopy is used most commonly with ratiometric dyes such as indo-1 or fura-2 that are excited with light in the UV region. This type of set-up is ideal for measuring changes in $[Ca^{2+}]_i$ in virtually any cell type over extended periods of time while using mechanical, electrical or chemical stimulation. The area of interest can be limited to a single cell or data can be collected from a larger number of cells. While this method allows one to measure from the total volume of the cell, it is difficult (or with photomultiplier tubes basically impossible) to focus in on discrete areas of the cell and visualise events such as the entry of extracellular Ca^{2+} through surface membrane Ca^{2+} channels. However, when combined with special indicators, one can measure $[Ca^{2+}]$ changes in discrete organelles. For example, rhod-2 is a Ca^{2+}-indicator that loads preferentially into the mitochondria and indo-5 N has been used for measurements of $[Ca^{2+}]$ in the sarcoplasmic reticulum. Several groups including us have measured changes in $[Ca^{2+}]$ in the vicinity of the plasma membrane rather than in the bulk of the cytoplasm using an indicator moiety conjugated to fatty acid chains called FIP-18 which preferentially anchors into the surface membrane and measures $[Ca^{2+}]$ nearby (e.g. https://www.scbt.com/scbt/sv/product/ffp-18-am).

Confocal microscopy uses much the same hardware and software as that used in epifluorescence microscopy with two important additions: a laser acting as a point light source that excites the indicator and an adjustable diaphragm or pinhole in the

emission pathway that when opened to its optimal size lets through light only from the focal plane, i.e. reducing light collection from cell regions outside the plane of focus. The fundamental advantage of the confocal microscope is that one can limit the focus to a very narrow section and thus measure discrete and rapid events such as localised release/entry of Ca^{2+} into the cytoplasm. While most confocal microscopes use lasers as light sources, this is not essential and the type of light source was not specified in the original patent (http://web.media.mit.edu/~minsky/papers/ConfocalMemoir.html).

Laser confocal microscopes come in three basic designs. These are (i) single photon laser scanning, (ii) the Nipkow or spinning disk, and (iii) two-photon versions.

(i) The single photon laser scanning confocal microscope is found in almost every biological/physiological institution. Most popular are those supplied by the major microscope manufacturers but nowadays for those who are technically proficient, it is possible to buy a confocal kit from the big optical suppliers (e.g. Thorlabs) and retrofit it to an existing microscope setup. In most systems, solid state lasers which have very precise and stable light emission and will work for many years have replaced Kr/Ar gas lasers. Physicists explain excitation of an indicator molecule as occurring when a single photon of the appropriate wavelength hits an indicator molecule and transiently lifts it from its ground state to a higher energy state. It remains in this higher energy state briefly (picoseconds) and then decays back to its original ground state by emitting a new photon with a longer wavelength than the original incident photon. An image of the sample is built up by moving a laser beam rapidly from one point to an adjacent point (pixel to pixel, typically dwelling a few to tens of μs on each pixel) along a horizontal line by means of a pair of mirrors (galvanometer-controlled or resonant-oscillating). A two dimensional image is built up by moving the laser beam vertically to a new line with a second pair of mirrors. The scanning and vertical movements are repeated until a full frame is obtained. This obviously takes a finite period of time and does not give an instantaneous view of what is happening in the cell. One can increase the scanning speed and obtain a full frame two to three times faster by reducing the "dwell time", i.e. the time for which the laser illuminates each pixel. The disadvantage of doing this is that the signal to noise ratio is reduced, which limits the ability to monitor small, spatially restricted changes in the fluorescence signal. If temporal resolution of a Ca^{2+} event in the cell is critical, the best approach is to abandon the two dimensional image acquisition approach and use the line scan mode instead. In this configuration, the laser beam scans the same line sequentially for a period of time. Line scans can be performed at over 1 kHz which is sufficiently fast to resolve even the most rapid change in local Ca^{2+} in a cell. The trade-off for the increased speed of data acquisition with line scanning is that only a single plane in a portion of the cell or tissue can be monitored. The line scan mode is extremely useful if one is trying to identify and characterise localised transient releases of Ca^{2+} from the

sarcoplasmic reticulum in muscle or trying to localise the sites of Ca^{2+} entry in a neuron. Conversely, the full frame ("x-y mode") is best if one is trying to see what happens in the whole cell in response to a stimulus.

(ii) Spinning disk laser confocal microscopes use a spinning disk (rotating at several thousand revolutions per minute) with multiple pinholes (> 1000) through which parallel light beams pass. These beams excite the fluorescent indicator in the cell and the emitted light returns through a second collector disk with a matching pattern of microlenses to the detection device, which is normally a very sensitive CCD camera operated at low temperatures to minimise noise. The current generation of spinning disk confocals can easily acquire images at rates of up to 50 frames per second, which makes them suitable for visualizing temporal and spatial [Ca^{2+}] changes in in a whole cell or cells rather than just a restricted line or set of lines using the line scan mode of a scanning confocal microscope. High frame rates generate large volumes of data but supplied software or ImageJ (download free from NIH) are sophisticated enough to select and analyze regions of interest only while masking data from uninteresting areas. The limited lack of popularity of these confocal microscopes may in part be due to the trade-off between spatial resolution and speed, i.e. greater spatial resolution generally requires a slower frame rate of acquisition and in part to the amount of incident light required that at best causes bleaching of the Ca^{2+} indicator only and at worst results cell damage and death.

(iii) The two- or multi-photon confocal microscopes overcome problems occurring when deeper parts of cells or tissues are being studied. Every microscope can be fitted with a motorised drive that accurately moves the plane of focus up or down in steps smaller than 1 μm. Thus, one can theoretically build up a three dimensional confocal image of a cell or tissue and check for possible hotspots or non-homogeneous change in [Ca^{2+}] throughout a cell, tissue slice or cell culture in response to a stimulus. However, with a simple laser confocal scanning microscope, image quality deteriorates as one penetrates deeper into a cell or tissue. This impaired performance is due to the fact that a laser beam is a stream of photons that will excite any indicator molecule it meets as it travels to the plane of focus. Thus, a lens will receive photons not just from the plane of focus but also some photons that have been deflected into the light collection path following collision with proteins. As the distance from the region of interest to the lens increases, some photons from the focal plane of interest will be lost and photons from uninteresting regions will be collected.

Two-photon confocal microscopes minimises this problem by delivering the longer wavelength pulses required to excite indicator molecules only to a very confined region. The longer wavelength improves penetration depth into tissue which is especially important when looking at the behaviour of nerves in the brain or secretory cells in isolated parotid or pancreatic ducts. The beauty of the two photon technique is that excitation of an indicator molecule can only occur if two photons each with twice the wavelength and half of the energy of a single photon

hit an indicator molecule. Indicator molecules hit by only one photon will not be excited. Longer wavelength light is less likely to cause damage to the cells. In a two-photon laser, the photons are sent out in femtosecond bursts. At the focal point, there is a high density of photons and the probability of two photons colliding with an indicator molecule is high. The major factor limiting more widespread usage of two-photon microscopy is the cost of the pulsed lasers themselves.

A final caution about experiments with lasers and intense light should be made. Children are routinely reminded to sunbathe in moderation and minimise prolonged exposure to ultraviolet light and avoid skin damage. The experience of seeing a cell start to bleb and die as one struggles to obtain the best record of $[Ca^{2+}]$ transients highlights the fact that light energy is dangerous to cells. One should be aware that the energy that each photon of light contains may impact on the measurements being made and should try to limit the intensity of the light to the minimum possible. An additional problem is that intense light may produce photodegradation or photobleaching of Ca^{2+} indicators whereby the indicator is converted into a fluorescent but Ca^{2+} insensitive form that results in false measurements of resting and transient changes in $[Ca^{2+}]_i$ [13]. Again, the problem can be avoided by minimising the intensity and duration of light exposure.

2.5 Calibration of the Fluorescent Signal

Some kind of calibration is usually attempted in order to translate fluorescence signals into $[Ca^{2+}]_i$. Before any calibration is attempted, it is important to recognise that there is always some background signal in fluorescence systems, arising from the detectors themselves and because of imperfect filters and leakage of the excitation light to the detectors. Moreover, each tissue or cell will have an intrinsic or auto-fluorescence. The autofluorescence arises predominantly from proteins containing the amino acids tyrosine, tryptophan, and phenylalanine. The amount of background and intrinsic fluorescence depends on the excitation and emission wavelengths being used. It is necessary to measure the background and intrinsic fluorescence in a sample before loading the Ca^{2+} indicator and to subtract this value from all subsequent measurements. Failure to do this can have dramatic effects on the translation of the indicator signals into $[Ca^{2+}]_i$. Complete and accurate calibrations are generally tiresome or even impossible to perform on a single cell and some simplifications are usually made. This has led to an increased tendency to completely ignore calibrations and take the viewpoint that the fluorescence light intensity (F, non-ratiometric indicators) or ratio (R, ratiometric indicators) of Ca^{2+} indicators is linearly related to $[Ca^{2+}]_i$, which clearly is a severe oversimplification (e.g. see Fig. 2.2). Numerous papers erroneously state that $[Ca^{2+}]_i$ increased/decreased by x%, whereas what actually occurred was an increase/decrease in fluorescence intensity or ratio of x%, which can represent

markedly different changes in $[Ca^{2+}]_i$. For instance, a minimal (<1%) change in fluorescence signal measured in a resting cell with a low-affinity indicator may represent a several-fold change in $[Ca^{2+}]_i$ (see Fig. 2.2). Similarly, a major increase in $[Ca^{2+}]_i$ may result in only a small increase in the fluorescence signal of a high-affinity indicator because the indicator was almost saturated with Ca^{2+} already before the increase.

Ca^{2+} indicators are affected by the surrounding protein and ionic environment and hence their properties inside a cell and in a test-tube will be markedly different. The relationship between fluorescence signals and $[Ca^{2+}]_i$ will also depend on the experimental setup. This means that all parameters in Eqs. 2.1 and 2.2 required to translate fluorescence signals into $[Ca^{2+}]_i$ should be established in the cell(s) using the same conditions and equipment as for the real experiments. This is of course easier said than done and some shortcuts are usually taken. In principle, the intracellular calibration is based on clamping $[Ca^{2+}]_i$ to a known value, without severe alterations of the cytosolic milieu, and then measure the fluorescence signal. The most important points to measure are at low/minimum $[Ca^{2+}]_i$, using EGTA or BAPTA to chelate Ca^{2+} to obtain F_{min} or R_{min}, and at saturating $[Ca^{2+}]_i$, to establish F_{max} or R_{max}. For ratiometric indicators, β is also obtained if R_{min} and R_{max} can be established without any major general decrease in fluorescence intensity. In addition, establishing K_d requires some intermediate $[Ca^{2+}]_i$. The reason why F_{min} or R_{min} and F_{max} or R_{max} are most important is because they set the limits between which the fluorescence signal can vary. Errors in measuring these parameters result in nonlinear errors when fluorescence signals are translated into $[Ca^{2+}]_i$. Erroneous estimates of F_{min} or R_{min} has the largest impact on the assessment of resting $[Ca^{2+}]_i$, whereas errors in F_{max} or R_{max} have the largest effects at high $[Ca^{2+}]_i$. On the other hand, K_d and β act as scaling factors and errors in these simply make the absolute changes in $[Ca^{2+}]_i$ smaller or larger, whereas relative changes during the course of an experiments are not affected.

Numerous methods have been used to perform a cytosolic calibration of $[Ca^{2+}]_i$. Most of these are based on introducing a strongly buffered solution with a set $[Ca^{2+}]$ to the cytosol. The solution can be introduced with methods similar to those described above for the introduction of the fluorescent indicator. An easy way of getting Ca^{2+} into cells is to add ionophores such as ionomycin or A23187 or even beta-escin to make the cell membrane leaky.

2.6 What Can We Hope for Now?

There have been marked improvements in the level of resolution. It was known and accepted for more than a century that separation of two objects closer than 250 nm in the horizontal plane was not possible with a standard single lens and

light source. However, the use of two opposing and matched objective lenses and a complementary approach that relies on the photochemical properties of the indicators have led to at least a threefold improvement in both axial and horizontal resolution. While these technical improvements are still expensive to implement and are not yet generally available as ready to use equipment packages, it is likely that super-resolution fluorescence microscopy techniques will be used to image Ca^{2+} fluxes through groups of ion channels in the future (the clearest non-technical introduction is given in Hell [6]).

In recent years, different groups have further developed genetically encoded Ca^{2+} indicators (GECI's) and focussed on improving different aspects of their performance. The key to these developments was the recognition that the green fluorescent protein (GFP) found in jellyfish could be modified relatively easily to produce variants in various colours.

Green fluorescent protein GECI can be split into two broad groups. The first group are proteins that consist of a fusion of circularly permutated green fluorescent protein (GFP) or red fluorescent protein, a Ca^{2+}-binding protein (usually calmodulin or troponin C) and M13 (a short Ca^{2+}-CaM-binding peptide derived from from myosin light chain kinase that acts as a spacer). This shows weak fluorescence in the absence of Ca^{2+}. When Ca^{2+} binds there is change in its conformation and the protein construct now fluoresces brightly. The second group consists of the cameleons that rely on resonance energy transfer (FRET) to signal changes in $[Ca^{2+}]$. FRET works only if the two molecules making up the FRET pair are very close together (< 10 nm). Cameleons are a fusion of calmodulin binding Ca^{2+} to M13 and flanked on one side by a blue-shifted GFP and on the other side by a longer wavelength shifted GFP. When Ca^{2+} binds to calmodulin, the distance between the GFP molecules is altered and FRET efficiency increases. The cameleons are inherently ratiometric allowing one in theory at least to translate the FRET pair ratio into real $[Ca^{2+}]$. Since these complex proteins are genetically encoded, they have been targeted successfully to subcellular compartments. Interference from native forms of the Ca^{2+}-binding protein has been reduced through selective mutations. Their dynamic range has improved markedly but the maximum change of about 50% on average is markedly less than the classical fluorescent indicators such as indo-1 and fluo-3.

The 22 kDa bioluminescent protein aequorin and its prosthetic protein (coelenterazine) that is oxidised and released when Ca^{2+} binds have been massively re-engineered to optimise the properties of the photoprotein for monitoring of Ca^{2+} at different sites inside a cell [2]. Despite all the improvements, the inherent limitations of low light emission (one photon per aequorin versus hundreds of photons for other indicator molecules) and its consumption continue to make recording and interpretation of experiments difficult. It is difficult to see further improvements in this area.

Acknowledgment Research reported from our laboratory was supported by the Swedish Research Council.

References

1. Agetsuma M, Matsuda T, Nagai T (2017) Methods for monitoring signaling molecules in cellular compartments. Cell Calcium 64:12–19
2. Alonso MT, Rodríguez-Prados M, Navas-Navarro P, Rojo-Ruiz J, García-Sancho J (2017) Using aequorin probes to measure Ca^{2+} in intracellular organelles. Cell Calcium 64:3–11
3. Blinks JR, Wier WG, Hess P, Prendergast FG (1982) Measurement of intracellular Ca^{2+} in living cells. Prog Biophys Mol Biol 40:1–114
4. Borle AB (1981) Control, modulation, and regulation of cell calcium. Rev Physiol Biochem Pharmacol 90:13–153
5. Bruton JD, Lemmens R, Shi CL, Persson-Sjögren S, Westerblad H, Ahmed M, Pyne NJ, Frame M, Furman BL, Islam MS (2003) Ryanodine receptors of pancreatic beta-cells mediate a distinct context-dependent signal for insulin secretion. FASEB J 17:301–303
6. Hell SW (2009) Microscopy and its focal switch. Nat Methods 6:24–32
7. Hossain MN, Suzuki K, Iwano M, Matsuda T, Nagai T (2018) Bioluminescent low-affinity Ca^{2+} indicator for ER with multicolor calcium imaging in single living cells. ACS Chem Biol 13:1862–1871
8. Hove-Madsen L, Baudet S, Bers DM (2010) Making and using calcium-selective mini- and microelectrodes. Methods Cell Biol 99:67–89
9. Jobsis PD, Rothstein EC, Balaban RS (2007) Limited utility of acetoxymethyl (AM) based intracellular delivery systems, in vivo: interference by extracellular esterases. J Microsc 226:74–81
10. Kloskowska E, Malkiewicz K, Winblad B, Benedikz E, Bruton JD (2008) APPswe mutation increases the frequency of spontaneous Ca^{2+}-oscillations in rat hippocampal neurons. Neurosci Lett 436:250–254
11. Llano-Diez M, Sinclair J, Yamada T, Zong M, Fauconnier J, Zhang SJ, Katz A, Jardemark K, Westerblad H, Andersson DC, Lanner JT (2016) The role of reactive oxygen species in β-adrenergic signaling in cardiomyocytes from mice with the metabolic syndrome. PLoS One 11(12):e0167090. https://doi.org/10.1371/journal.pone.0167090
12. Olsson K, Cheng AJ, Alam S, Al-Ameri M, Rullman E, Westerblad H, Lanner JT, Bruton JD, Gustafsson T (2015) Intracellular Ca^{2+}-handling differs markedly between intact human muscle fibers and myotubes. Skelet Muscle 162(3):285–293. https://doi.org/10.1186/s13395-015-0050-x
13. Scheenen WJ, Makings LR, Gross LR, Pozzan T, Tsien RY (1996) Photodegradation of indo-1 and its effect on apparent Ca^{2+} concentrations. Chem Biol 3:765–774
14. Tsien RY (1980) New calcium indicators and buffers with high selectivity against magnesium and protons: design, synthesis, and properties of prototype structures. Biochemistry 19: 2396–2404
15. Westerblad H, Allen DG (1996) Intracellular calibration of the calcium indicator indo-1 in isolated fibers of *Xenopus* muscle. Biophys J 71:908–917

Chapter 3
High-Throughput Fluorescence Assays for Ion Channels and GPCRs

Irina Vetter, David Carter, John Bassett, Jennifer R. Deuis, Bryan Tay, Sina Jami, and Samuel D. Robinson

Abstract Ca^{2+}, Na^{+} and K^{+}- permeable ion channels as well as GPCRs linked to Ca^{2+} release are important drug targets. Accordingly, high-throughput fluorescence plate reader assays have contributed substantially to drug discovery efforts and pharmacological characterization of these receptors and ion channels. This chapter describes some of the basic properties of the fluorescent dyes facilitating these assay approaches as well as general methods for establishment and optimisation of fluorescence assays for ion channels and G_q-coupled GPCRs.

Keywords High-throughput · High-content · Fluorescence imaging · G protein-coupled receptor · Voltage-gated ion channel · Ligand-gated ion channel · Assay development · Optimization · FLIPR

Abbreviations

ATP	adenosine triphosphate
Ca^{2+}	calcium ion
Ca_V and VGCC	Voltage-gated Ca^{2+} channels
DAG	diacylglycerol
FLIPR	Fluorescent Imaging Plate Reader
GPCR	G-protein coupled receptor
HTS	high throughput screening

I. Vetter (✉)
Institute for Molecular Bioscience, The University of Queensland, St. Lucia, QLD, Australia

School of Pharmacy, The University of Queensland, St. Lucia, QLD, Australia
e-mail: i.vetter@uq.edu.au

D. Carter · J. R. Deuis · B. Tay · S. Jami · S. D. Robinson
Institute for Molecular Bioscience, The University of Queensland, St. Lucia, QLD, Australia

J. Bassett
School of Pharmacy, The University of Queensland, St. Lucia, QLD, Australia

M. S. Islam (ed.), *Calcium Signaling*, Advances in Experimental Medicine and Biology 1131, https://doi.org/10.1007/978-3-030-12457-1_3

IP3	inositol-1,4,5,-triphosphate
LGCC	Ligand-gated Ca^{2+} channels
NCX	Na^{+}/Ca^{2+} exchanger
PIP_2	phosphatidylinositol 4, 5 bisphosphate
PMCA	Plasma Membrane Ca^{2+} ATPase
RyR	ryanodine receptors
SERCA	sarco/endoplasmic reticulum Ca^{2+} ATPase
EGTA	ethylene glycol-bis(2-aminoethylether)-*N*,*N*,*N*′,*N*′-tetraacetic acid.
APTRA	2-aminophenol-N,N,O-triacetic acid
BAPTA	1,2-bis(o-aminophenoxy)ethane-N,N,N′,N′-tetraacetic acid
K_d	dissociation constant
AM	acetoxymethyl
ER	endoplasmic reticulum
LED	light-emitting diode
CCD	charge-coupled device
EMCCD	Electron Multiplying Charge Coupled Device
ICDD	Intensified CCD
PDL	poly-D-lysine
PLL	poly-L-lysine
PLO	poly-L-ornithine
nAChR	nicotinic acetylcholine receptors
HEPES	4-(2-hydroxyethyl)-1-piperazineethanesulfonic acid
PAR2	protease-activated receptor 2
RFU	relative fluorescence unit
SBFI	Sodium-binding benzofuran isophthalate
PBFI	Potassium-binding benzofuran isophthalate
DRG	Dorsal Root Ganglion
RGS4	Regulator of G protein signalling 4
Na_V	voltage-gated sodium channel
MCU	mitochondrial Ca^{2+} uniporter
cAMP	cyclic adenosine monophosphate
CANDLES	Cyclic AMP iNdirect Detection by Light Emission from Sensor cells
GTP	guanosine triphosphate
TRP	Transient Receptor Potential
SK_{Ca}	small-conductance calcium-activated K^{+} channel
IK_{Ca}	intermediate-conductance calcium-activated K^{+} channel
BK_{Ca}	big-conductance calcium-activated K^{+} channel
IRK	Inwardly-rectifying K^{+} channel
TWIK	Tandem of pore domains in a Weakly Inward rectifying K^{+} channel
TREK	TWIK-related K^{+} channel

TASK	TWIK-related acid-sensitive K^+ channel
TALK	TWIK-related alkaline pH-activated K^+ channel
THIK	TWIK-related halothane-inhibited K^+ channel
TRESK	TWIK-related spinal cord K^+ channel
K_V or VGKC	voltage-gated K^+ channel
ANG-1 and ANG-2	Asante NaTRIUM Green-1 and -2
Di-4-ANEPPS	Pyridinium, 4-(2-(6(dibutylamino)-2-naphthalenyl)-1-(3-sulfopropyl)-hydroxide
$DiBAC_4(3)$	bis-(1,3-dibutylbarbituric acid) trimethine oxonol
FMP	FLIPR Membrane Potential
FRET	fluorescence resonance energy transfer
PeT	photoinduced electron transfer
CC2-DMPE	N-[6-chloro-7-hydroxycourmarin-3-carbonyl] dimyristroyl phosphatidyl ethanolamine
GEVI	genetically encoded voltage indicators
DPA	dipicrylamine
DiO	oxocyanine
LED	light-emitting diode
sCMOS	scientific complementary metal-oxide-semiconductor

3.1 Introduction

G-protein-coupled receptors and ion channels are, alongside kinases, the main protein families targeted by currently approved drugs [1]. Despite the considerable structural and functional diversity of these proteins, a common signalling mechanism involved in mediating some of their cellular effects is the directed flux of ions such as calcium (Ca^{2+}), sodium (Na^+) and potassium (K^+). Accordingly, over the past decades significant advances have been made towards the development of assays permitting high-throughput profiling of GPCRs or ion channels that are functionally coupled to ion flux. A particular focus of these efforts has been the development of high-throughput kinetic fluorescence plate reader assays for drug discovery and pharmacological characterisation of these targets, facilitated predominantly by fluorescent ion and membrane potential indicators (Fig. 3.1). Indeed, recent years have seen the development not only of fluorescent molecules and proteins capable of detecting physiologically relevant concentrations of Ca^{2+}, Na^+ and K^+, but also protons (H^+), chloride (Cl^-) and other halides which can detect the movement of these ions between subcellular compartments [2]. In combination with the development of sophisticated high-throughput and high-content plate readers incorporating fluid addition robots and kinetic read capabilities, these probes have significantly advanced our understanding of basic pharmacology of these important drug targets, not least by facilitating drug discovery programs that are accessible not only to pharmaceutical industry but also smaller academic groups.

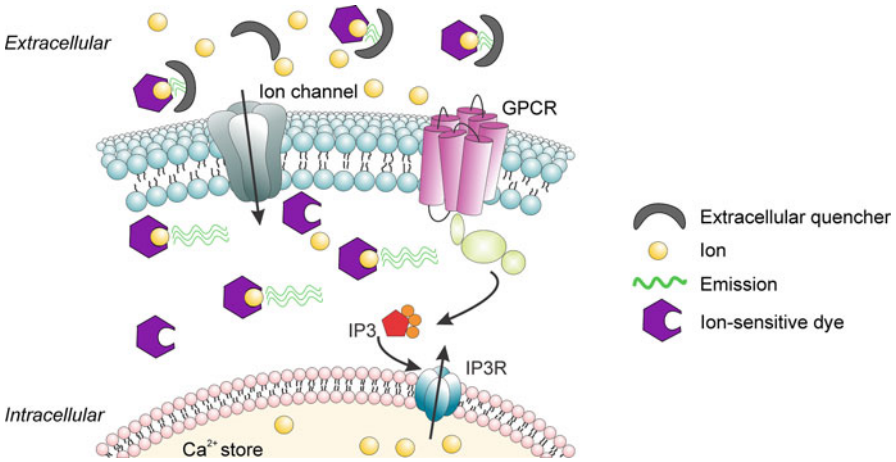

Fig. 3.1 Basic principle of fluorescent ion flux assays
Activation of ion channels and GPCRs leads to altered intracellular concentration of ions such as Ca^{2+}, Na^{+} or K^{+}. The emission of fluorescent ion-sensitive dyes (e.g. Fluo-4, Sodium Green) increases in response to binding of their cognate ions (e.g. Ca^{2+}, Na^{+}). In no-wash format, extracellular signal is eliminated through incorporation of fluorescence quenchers in extracellular assay buffer, permitting quantification of intracellular ion accumulation in high-throughput format

While fluorescence approaches cannot recapitulate mechanistic insight into the activation and gating mechanics leading to ionic flux *via* voltage-gated ion channels, fluorescence-based screening approaches have nonetheless found application in bioactive discovery programs. For example, novel modulators of voltage-gated sodium (Na_V) channels have been isolated from venoms using high-throughput fluorescent plate reader assays [3–9], and fluorescence assays have also been used for identification and pharmacological characterisation of small molecule modulators of voltage-gated ion channels [10–13]. In addition, these techniques – which can be complementary to more traditional assays such as electrophysiological recordings – have provided novel insight into ligand-gated ion channel pharmacology as well as the physiological or pathological roles of these channels.

This review will discuss the properties of the most important Ca^{2+}, Na^{+}, K^{+} and membrane potential dyes and fluorescent probes, as well as some of their applications in high-throughput and high-content kinetic fluorescence assays.

3.2 Ca^{2+} Signalling by Ion Channels and GPCRs

3.2.1 Calcium – A Universal Signalling Molecule

The calcium ion Ca^{2+} is often referred to as a ‘universal” signalling molecule; indeed, most biological processes involve Ca^{2+} signalling in one form or another

(for review, see [14, 15]). It is thus not surprising that Ca^{2+} is involved in diverse physiological functions ranging from differentiation, excitability and motility to apoptosis.

Because Ca^{2+} acts as a ubiquitous messenger molecule, a myriad of proteins are dedicated to its extrusion, chelation, sequestration and release, resulting in astonishingly precise temporal and spatial control of Ca^{2+} [14, 15]. At the cellular level, Ca^{2+} concentrations are extremely tightly controlled in the cytoplasm, where resting [Ca^{2+}] is approximately 100 nM. It is maintained at this level by extrusion to the extracellular space through pumps such as Plasma Membrane Ca^{2+} ATPase (PMCA) and the Na^{+}/Ca^{2+} exchanger (NCX) [16]. Ca^{2+} is also sequestered into intracellular stores such as the endoplasmic or sarcoplasmic reticulum by the sarco/endoplasmic reticulum Ca^{2+} ATPase (SERCA) and the mitochondria by the mitochondrial Ca^{2+} uniporter (MCU) [17]. As a result, extracellular Ca^{2+} concentrations are significantly higher at approximately 1.8–2 mM, and a large Ca^{2+} reserve also is found in intracellular compartments, where Ca^{2+} is stored in protein-bound form and also occurs at relatively high concentrations as free Ca^{2+} [18].

To initiate signalling events, Ca^{2+} can be derived from the extracellular space, where voltage- or ligand-gated ion channels permit flow of this ion down its approximately 20,000-fold concentration gradient. Ca^{2+} can also be released from intracellular stores such as the endoplasmic reticulum through activation of inositol-1,4,5,-triphosphate (IP3) receptors and ryanodine receptors (RyR), resulting in a net increase in cytoplasmic Ca^{2+}. Accordingly, intracellular Ca^{2+} concentrations can rise several fold relatively to baseline during Ca^{2+} signalling events, a phenomenon that can be conveniently exploited for the development of fluorescence Ca^{2+} signalling assays.

3.2.2 GPCRs

Activation of some G-protein coupled receptors (GPCR), in particular those coupled to $G_{q/11}$, results in activation of phospholipase C which in turn facilitates cleavage of phosphatidylinositol 4, 5 bisphosphate (PIP_2) into 1,4,5-inositol trisphosphate (IP3) and diacylglycerol (DAG). IP3 then activates IP3 receptors located on the endoplasmic reticulum, causing release of Ca^{2+} into the cytoplasm [19]. While $G_{\alpha s}$ and $G_{\alpha i}$-coupled GPCR do not signal through Ca^{2+} physiologically, co-expression of chimeric or promiscuous G-proteins, such as $G_{\alpha 15/16}$ [20–22], can couple activation of these receptors to increases in intracellular Ca^{2+} and thus allows development of functional high throughput (HTS) assays based on Ca^{2+} imaging. In addition, fluorescence assays have also been developed for detection of second messengers that are modulated downstream of $G\alpha_s$ and $G\alpha_{i/o}$ activation, such as cAMP (for review, see [23]). While most of the techniques adapted for this purpose, such as time-resolved fluorescence resonance transfer, gene reporter assays, and fluorescence polarisation, are end-point assays, this limitation has been overcome by the development of genetically-encoded cAMP sensors that enable monitoring

of real-time changes in intracellular cAMP concentrations (e.g. GloSensor™ cAMP (Promega); CANDLES (Cyclic AMP iNdirect Detection by Light Emission from Sensor cells); cADDis cAMP sensor (Montana Molecular) and CAMYEL, a cAMP sensor based on the BRET pair citrine-cp229 and *Renilla* luciferase which flank a human Epac1 (a cAMP-activated GTP exchange factor) protein) [24–26].

3.2.3 Ca^{2+}-Permeable Ion Channels

Voltage-gated Ca^{2+} channels (Ca_V), expressed in excitable cells, are large transmembrane proteins that undergo conformational changes in response to altered membrane potential [27]. As a result, activation of voltage-gated Ca^{2+} channels causes rapid influx of Ca^{2+} from the extracellular space, which controls processes such as muscle contractions or synaptic exocytosis. The properties of these channels can be exploited in the design of high throughput Ca^{2+} assays, where addition of extracellular KCl leads to membrane depolarization and thus channel opening [28, 29]. In addition, a plethora of Ca^{2+}-permeable transmembrane ion channels facilitate influx of extracellular Ca^{2+} along its concentration gradient in response to extra- or intracellular binding of ligands. These ligand-gated Ca^{2+} channels include, to name a few, ionotropic purinergic and glutamate receptors, nicotinic receptors and Transient Receptor Potential (TRP) channels and are indispensable to many physiological processes.

Accordingly, Ca^{2+} permeable ion channels and GPCRs linked to Ca^{2+} release are important drug targets, with modulation of Ca^{2+} signalling increasingly recognized as a valid therapeutic strategy in a range of diseases, including cardiac disease, neurological disorders such as Alzheimer's disease, and cancer [30–32].

3.3 Na^+-Permeable Ion Channels and Na^+ Signalling

3.3.1 Sodium – An Abundant Signalling Molecule

The sodium ion (Na^+) is the most abundant cation in the extracellular fluid, and as such, is essential for regulation of blood volume, osmotic equilibrium and cell membrane potential. At the cellular level, the concentration of Na^+ is predominantly maintained by the Na^+/K^+-ATPase, a membrane-bound protein that actively pumps Na^+ out of the cell in exchange for K^+, resulting in higher levels of extracellular Na^+ (145 mM) compared to intracellular Na^+ (10 mM) [33]. This maintains a negative membrane potential (−50 to −70 mV in neurons) that promotes an electrochemical gradient that drives Na^+ into the cell upon opening of Na^+-permeable channels [34]. Na^+-permeable channels are classified as either voltage-gated, which open in response to a change in membrane potential, or ligand-gated, which open upon binding of a ligand.

3.3.2 Voltage-Gated Na^+ Channels

Voltage-gated Na^+ channels (Na_Vs) are pore-forming membrane proteins that open in response to a positive change in membrane potential to allow Na^+ influx into the cell, resulting in the generation and propagation of action potentials in electrically excitable cells. In mammals, nine different Na_V subtypes have been described ($Na_V1.1$–1.9), each having distinct tissue expression profiles and biophysical properties. $Na_V1.1$, $Na_V1.2$, $Na_V1.3$ and $Na_V1.6$ are expressed in the central nervous system, $Na_V1.4$ is expressed in skeletal muscle, $Na_V1.5$ is expressed in cardiac tissue, and $Na_V1.1$, $Na_V1.6$, $Na_V1.7$, $Na_V1.8$, $Na_V1.9$ are expressed in the peripheral nervous system [35].

Despite the immense interest in Na_V modulators as therapeutic targets, high-throughput fluorescence assays of these channels have been comparatively limited, in part because of inherent difficulties in replicating the endogenous activation "signal" – a change in membrane voltage – in commonly available plate readers. Although allosteric modulators such as veratridine (activates $Na_V1.1$–1.7) and deltamethrin (activates $Na_V1.8$ & 1.9) can be used to elicit Na_V-mediated responses, they also alter channel kinetics such as reducing peak current and increasing sustained currents [4, 36]. This altered activity may interfere with screening assays and has the potential to generate false positive or negative results.

3.3.3 Ligand-Gated Na^+ Channels

Ligand-gated Na^+ channels are pore-forming membrane proteins that open in response to binding of a ligand to allow Na^+ influx into the cell. They can either be selective for Na^+, such as acid-sensing ion channels (ASICs) and epithelial sodium channels (eNaCs); or non-selective for Na^+, such as nicotinic acetylcholine receptors (nAChRs) or TRP channels, which can also conduct Ca^{2+} [37–39]. Indeed, the ionic selectivity of nAChR in particular is subtype-dependent, with the neuronal α7 nAChR being highly permeable to and selective for Ca^{2+}, while muscle nAChR subtypes are selective for Na^+ ions [37].

3.3.4 K^+-Permeable Ion Channels and K^+ Signalling

3.3.5 Potassium – A Comprehensive and Copious Counter to Calcium

K^+ flux generally opposes the function of Na^+ and Ca^{2+} signalling, with many (though not all) biological processes involving Ca^{2+} or Na^+ utilising K^+ as a physiological 'hand brake' to control and regulate signalling mechanisms. The intracellular K^+ concentration is typically high (140 mM) compared to the extracellular

environment (4 mM), thus creating a pronounced outward gradient. K^+-permeable ion channels are the most numerous and functionally diverse ion channels in nature [40, 41]. In mammals, they can be divided into four major functional groups: calcium-activated K^+ channels, inwardly rectifying K^+ channels, two pore K^+ channels and voltage-gated K^+ channels, each of which can be further classified into sub-families with unique functional roles.

The calcium-activated K^+ channels consist of three families: small-conductance ($SK_{Ca}1, 2, 3$), intermediate conductance ($IK_{Ca}1$) and large/big-conductance (BK_{Ca}), all of which are widely expressed in many different tissues such as smooth muscle, epithelia, endothelium and neurons. In these tissues, K_{Ca} channels generally regulate excitability by restoring resting membrane potential, thus forming a negative feedback loop for Ca^{2+}-mediated signalling since these channels are activated by Ca^{2+}. For example, in cerebellar Purkinje neurons normal activity is reliant on both Ca^{2+} channels to initiate firing and the calcium-activated K^+ channels to regulate the firing [42].

Inwardly-rectifying K^+ (IRK) channels are the 'wild-card' in the K^+-permeable ion channel superfamily, as they allow the passage of external K^+ into the cell instead of moving K^+ ions out of the cell [43]. IRK channels can be classified into four functional groups: transporters, classical, G-protein gated (GIRK) and ATP-sensitive. As a result, the functional consequences of IRK channel activation, in particular for GIRK channels which functionally couple to GPCRs, are very diverse [43]. Overall, the function of these channels is highly dependent on the tissue in which they are expressed. For example, ATP-sensitive IRK channels aid in glucose homeostasis by regulating insulin release, whilst classical IRK channels facilitate passive movement of K^+ ions in order to orchestrate the electrical excitability of membranes needed for neuronal signalling [43].

Compared with other K^+-permeable ion channels, the two-pore K^+ channels (K_{2P}) remain open at a range of physiological voltages, although their activity is largely unaffected by voltage [44]. They are considered to contribute to leak and background K^+ currents and restore resting membrane potential [44]. K_{2P} channels include a wide array of functionally distinct families, such as the TWIK (Tandem of pore domains in a Weakly Inward rectifying K^+ channel), TREK (TWIK-related K^+ channel), TASK (TWIK-related acid-sensitive K^+ channel), TALK (TWIK-related alkaline pH-activated K^+ channel), THIK (TWIK-related halothan-inhibited K^+ channel), and TRESK (TWIK-related spinal cord K^+ channel) channels [44].

By far the largest of the four families, the voltage-gated K^+ channels (K_Vs or VGKCs) are comprised of 40 known individual subunits which can form functional homomeric or heteromeric tetramers, leading to incredible physiological variety [41]. As the name suggests, VGKCs activate and inactivate in response to changes in the membrane potential [41]. As such, they have a significant role in excitable cells where they contribute to the downstroke of an action potential. However, VGKCs are widely expressed in many tissues and have many physiological functions. For example, $K_V1.3$, a VGKC expressed in immune cells, is a key regulator of chronically activated effector T memory cells [45].

3.4 High-Throughput Plate Reader Assays: Fluorescent Sensors

3.4.1 Chemical Ca^{2+} Indicator Dyes

Assessment of calcium signalling has been greatly aided by the development of Ca^{2+} dyes which exhibit changes in their fluorescence spectra and/or intensity upon binding of free Ca^{2+} ions, enabling assessment of Ca^{2+} signals at the single cell level or in high-throughput format. Most of these dyes were developed from the Ca^{2+} chelators EGTA, APTRA or BAPTA, and incorporate a fluorophore with the characteristic ion binding groups of these molecules [46–50]. Continuous improvement of these compounds has resulted in a diverse array of dyes with unique properties (Table 3.1). Differences in their Ca^{2+} dissociation constant (K_d) and thus dynamic range, binding kinetics, photostability, sequestration into intracellular compartments, fluorescence quenching characteristics as well as excitation and emission wavelengths govern the usefulness of these compounds in a variety of applications [79]. In particular, the K_d of chemical Ca^{2+} indicator dyes should be carefully matched to the expected Ca^{2+} concentration in the cellular environment, with the useful range over which changes in Ca^{2+} are most reliably detected approximating 0.1–10 x K_d [80]. Thus, measurement of cytoplasmic Ca^{2+} events require high affinity Ca^{2+} dyes, while low affinity dyes will be useful in high Ca^{2+} cellular compartments such as the mitochondria or endoplasmic reticulum [81]. It is, however, important to take into consideration that the K_d of these compounds is affected by pH, temperature, viscosity, ionic strength, protein binding and the presence of other ions such as Mg^{2+} [48, 58, 82–84]. Accordingly, the actual intracellular K_d of these dyes is frequently several orders of magnitude higher than the K_d determined in vitro, and can be expected to vary depending on the cell type and even the cellular compartment assessed [79, 83].

In addition, the binding kinetics of fluorescent Ca^{2+} indicators can affect temporal resolution of Ca^{2+} signals [52, 53, 80]. Ca^{2+} signals are generally transient, so that the binding kinetics of the dye need to be significantly faster than the change in Ca^{2+} concentration if Ca^{2+} signals are to be resolved with sufficient temporal precision [52]. Dyes with slow binding kinetics thus lead to substantial inaccuracies, particularly with respect to the temporal resolution of Ca^{2+} signals. This problem is further compounded by the Ca^{2+} buffering properties displayed by these compounds, especially if present at sufficiently high concentrations [52, 53]. Thus, bright fluorescent dyes which enable reduction in concentration are often preferable to dyes that require higher concentrations in order to achieve sufficient signal strength and similarly, dyes with fast dissociation kinetics are preferable for transient Ca^{2+} signals and high throughput applications.

In addition to these key characteristics, the spectrometric properties of these compounds determine selection of fluorescent Ca^{2+} indicators for specific applications. Principally, chemical Ca^{2+} indicators can be divided into ratiometric and single wavelength dyes.

Table 3.1 Properties of fluorescent indicators

Dye	Excitation wavelength (nm)		Emission wavelength (nm)		K_d (nM)	F_{Max}/F_{min}	K_{on} 1/(M^as)	K_{off} 1/s	References
	unbound	*ion-bound*	*unbound*	*ion-bound*					
Ca^{2+}dyes									
Quin-2	353	333	495	495	60	5–8			[49, 51]
Fura-2	363	335	512	505	135–258	13–25	4.0×10^8	103	[50–53]
Bis-Fura-2	366	338	511	504	370		5.5×10^8	257	[51, 53]
Fura-4F	366	336	511	505	770				[51, 54]
Fura-5F					400				[51]
Fura-6F	364	336	512	505	5300				[51, 54]
Fura-FF	364	335	510	506	5500				[51, 54]
Fura-PE3	364	335	508	500	250	18			[51, 55]
FFP18	364	335	475	408	331	7			[55, 56]
Fura-Red	472	436	657	637	140	5–12			[51, 57]
Mag-Fura-2	369	329	511	508	50,000	6–30	7.5×10^8	26,760	[53, 54]
Indo-1	346	330	485	410	250	20–80	9.4×10^8	180	[50, 58, 59]
Indo 1-PE3	346	330	475	408	260				[51]
Mag-Indo-1	349	328	480	390	35,000	12	2.3×10^5	> 1000	[58, 60]
Fluo-3	503	506	526	526	400	40–100	9.2×10^8	587/186	[47, 58, 61]
Fluo-4	491	494	–	516	345	100		350	[48, 62]
Mag-Fluo-4	490	493	–	516	22,000				[48, 51, 63]
Fluo-5F	491	494	–	518	2300			300	[53, 62, 64, 65]
Fluo-5 N	491	494	–	516	90,000				[51, 53, 62, 64, 65]
Fluo-4FF	491	494	–	516	9700				[51, 53, 62, 64, 65]
Fluo-8	490			514	389	> 200			[66]
Fluo-8H	490			514	232	> 200			[66]

Fluo-8 L	490			514	1860	> 200			[66]
Rhod-2,	556	553	576	576	1000	14–100			[51]
X-Rhod-1	576	580	–	602	700	4–100			[51]
Rhod-FF	551		556		19,000				[51]
X-Rhod-5F	576	580	–	602	1600				[51]
X-Rhod-FF	568		605		17,000				[51]
Rhod-5 N	547	549	–	576	320,000				[51]
Calcium-Green-1	506	506	532	532	190	38	0.79×10^9	178	[53, 67]
Calcium-Green-2	506	503	536	536	550	60–100			[51]
Calcium-Green-5 N	506	506	532	532	4000–19,000				[68–70]
Oregon Green 488 BAPTA-1	494	494	523	523	170	14			[51, 71]
Oregon Green 488 BAPTA-2	494	494	523	523	580	100			[51, 71]
Oregon Green 488 BAPTA-6F	494	494	523	523	3000				[51, 71]
Oregon Green 488 BAPTA-5 N	494	494	521	521	20,000	44			[51]
Calcium crimson	590	589	615	615	185	2.5	0.86×10^9	232	[51, 67]
Calcium Ruby	579		598		30,000	32			[72]
Calcium Orange	549	549	575	576	185	3	0.51×10^9	233	[51, 67]
Na^+dyes									
Asante Natrium Green-1	488–517		540		92,000,000	29			[73]
Asante Natrium Green-2	488–517		540		20,000 000	29			[73]
SBFI	379	340	505	505	4000 000	0.08[a]			[73]

(continued)

Table 3.1 (continued)

Dye	Excitation wavelength (nm)		Emission wavelength (nm)		K_d (nM)	F_{Max}/F_{min}	K_{on} 1/(M^as)	K_{off} 1/s	References
	unbound	*ion-bound*	*unbound*	*ion-bound*					
CoroNa Green	492	492	516	516	80,000,000	0.2[a]			[73]
CoroNa Red	547	547	576	576	200,000,000				[73]
Sodium Green	506		532		6,000,000				[73]
Membrane potential/voltage-sensitive dyes									
$DiBAC_2(3)$	535		560		n/a				[74]
$DiBAC_4(3)$	492		516		n/a				[75]
FMP dye	530		565		n/a				[76]
CC2-DMPE	425		435		n/a				[77]
K^+ dyes									
PBFI	390	340	500	500	8,000,000		2.7×10^8	1.4×10^9	[73, 78]
Asante Potassium Green-1	517	517	540	540	54,000,000				[73]
Asante Potassium Green-2	517	517	540	540	18,000,000				[73]

Fluorescence assays have been greatly aided by development of dyes that exhibit changes in fluorescence spectra and/or intensity upon binding of free Ca^{2+}, Na^+ or K^+ ions, or changes in membrane voltage. Ratiometric dyes exhibit a spectral shift, either in excitation or emission wavelength, upon ion binding, often in conjunction with altered fluorescence intensity, while binding of ions to single wavelength dyes elicits an increase in quantum efficiency, resulting in brighter fluorescence in the absence of spectral excitation or emission shifts. Differences in their dissociation constant (K_d) and thus dynamic range, binding kinetics (K_{on} and K_{off}), and fluorescence characteristics (emission and excitation maxima, F_{Max}/F_{Min}) govern the usefulness of these compounds in a variety of applications

[a]quantum yield; *n/a* not applicable

3.4.2 Ratiometric Dyes

Ratiometric dyes exhibit a spectral shift, either in excitation or emission wavelength, upon Ca^{2+} binding, often in conjunction with altered fluorescence intensity. This effectively results in increased and decreased fluorescence intensity, respectively, at wavelengths on either side of the isosbestic point. Ratiometric dyes are advantageous for measurement of Ca^{2+} in application where uneven dye loading, dye leakage, photobleaching, compartmentalization, or cell thickness occur, as the fluorescence ratio is independent of the absolute signal strength, thus compensating for these variables [85]. However, these advantages come at the cost of increased photodamage to cells by excitation wavelengths in the ultraviolet range, increased cellular autofluorescence as well as decreased compatibility with caged compounds. Ratiometric dyes are generally poorly suited for high-throughput applications due to the need for equipment capable of dual excitation or emission monitoring. However, as more recent high-throughput plate readers incorporate optics that are, at least in principle, suitable for these ratiometric dyes, these will be discussed here for completeness.

3.4.2.1 Quin-2

Quin-2 is a first generation Ca^{2+} dye developed by the research group of Roger Tsien [49]. It exhibits low quantum yield and absorptivity, necessitating high dye concentrations to achieve adequate signal strength. This is turn leads to problems with Ca^{2+} buffering [86] and has resulted in this dye being largely superseded by newer derivatives.

3.4.2.2 Fura-2

Fura-2 is a dual excitation, single emission ratiometric dye and has become the Ca^{2+} indicator of choice for fluorescence microscopy, where it is more practical to use dual excitation wavelengths and maintain a single emission wavelength [87]. Upon binding of Ca^{2+}, the maximum fluorescence excitation wavelength of Fura-2 shifts from 362 nm to 335 nm, with an accompanying two-fold increase in fluorescence quantum efficiency [50]. In contrast, the fluorescence emission maxima of the free Fura-2 anion and Ca^{2+}-bound Fura-2 are, at 512 and 505 nm, virtually unaltered [50]. Thus, excitation of Fura-2 at 340 and 380 nm results in increased and decreased fluorescence, respectively, at an emission wavelength of ~510 nm. The fluorescence ratio of 340/380 nm therefore increases with increasing concentrations of Ca^{2+}. With a K_d of approximately 135–258 nM, a K_{on} (1/(M.s)) of 4.0×10^8 and a K_{off} (1/s) of 103, Fura-2 and its derivatives are suitable for rapid, time-resolved measurement of cytoplasmic Ca^{2+} signals [50, 53]. In addition, Fura-2 has been

reported to be more resistant to photobleaching than Indo-1 [88, 89], although it tends to be more susceptible to intracellular departmentalization [90].

3.4.2.3 Bis-Fura-2

Bis-Fura-2 consists of two fluorophores incorporated with one BAPTA molecule, resulting in brighter signal strength with a slightly reduced K_d (370 nM). With excitation and emission spectra identical to Fura-2, Bis-Fura-2 is particularly suitable for applications which require better signal or tolerate Ca^{2+} buffering poorly and thus require reduced dye concentrations. While on-rates are similar to Fura-2 with a K_{on} (1/(M.s)) of 5.5×10^8, off-rates are slightly higher for Bis-Fura-2 with a K_{off} of 257 (1/s) [53].

3.4.2.4 Fura-4F, Fura-5F, Fura-6F and Fura-FF

These analogues of Fura-2 exhibit similar excitation and emission spectra upon binding of Ca^{2+}, however, the K_d of these compounds has been significantly shifted by addition of one (Fura-4F, Fura-5F, Fura-6F) or two (Fura-FF) fluorine substitutes at varying positions. With K_d values of 400 nM (Fura-5F), 770 nM (Fura-4F), 5300 nM (Fura-6F) and 5500 nM (Fura-FF) [51, 54], these fluorescent Ca^{2+} indicators exhibit intermediate Ca^{2+} affinities and are useful for applications where Ca^{2+} concentrations >1 μM occur.

3.4.2.5 Fura-PE3 (Fura-2 LeakRes)

Fura-PE3 was developed from an analogue of BAPTA, Fura-FF6, by addition of a positive charge in order to improve cytosolic retention of the dye and minimize compartmental sequestration [55]. The spectral properties of Fura-PE3 are identical to Fura-2, but this dye avoids problems associated with uneven loading and dye leakage.

3.4.2.6 FFP18

FFP18 is similar to Fura-PE3 but incorporates a hydrophobic tail that targets this dye to lipids such as cell membranes [55]. The spectral properties of FFP18 are similar to Fura-2, with a slightly decreased K_d of 331 nM [55] and improved hydrophilicity compared to other membrane-associating Ca^{2+} indicators. Thus, FFP18 appears suitable for measurement of membrane-associated Ca^{2+} events [56].

3.4.2.7 Fura-Red

Fura-Red is a Fura-2 analogue excited by visible light, with excitation maxima at approximately 450–500 nm, depending on the presence of Ca^{2+}, and a very long-wave emission maximum at approximately 660 nm. Fura-Red fluorescence decreases upon binding of Ca^{2+}, and in addition, the relatively low quantum efficiency of Fura-Red necessitates use of higher concentrations to achieve an adequate fluorescence signal. The in vitro K_d of Fura-Red is similar to Fura-2 at approximately 140 nM, although the K_d of Fura-Red has been reported to be significantly higher (~1100–1600 nM) in myoplasm [57]. The large Stokes shift of Fura-Red permits simultaneous measurement of Ca^{2+} as well as other fluorophores excited at ~488 nm. Accordingly, Fura-Red has been used for ratiometric Ca^{2+} measurement in conjunction with the single wavelength Ca^{2+} indicator Fluo-3 [91–93], although ratiometric imaging is also possible with Fura-Red alone using excitation wavelengths of 420/480 nm or 457/488 nm [57, 94].

3.4.2.8 Mag-Fura-2

Mag-Fura-2 (Furaptra) was, as the name suggests, originally developed to measure changes in Mg^{2+} concentration, and exhibits spectral properties similar to Fura-2.

Its propensity for intracellular departmentalization, in combination with its low affinity for Ca^{2+} with a K_d of approximately 50 μM [53, 95, 96], have seen application of this fluorescent indicator to measurement of Ca^{2+} in intracellular IP3-sensitive Ca^{2+} stores [97]. In addition, Mag-Fura-2 retains fast binding kinetics with a K_{on} (1/(M.s)) of 7.5 x 10^8 and particularly fast off-rates [53], enabling measurement of Ca^{2+} responses with little or no kinetic delay [98–100].

3.4.2.9 Indo-1

Like Fura-2, Indo-1 was developed as a BAPTA analogue by the research group of Roger Tsien [50]. However, in contrast to Fura-2, Indo-1 displays shifts in emission wavelength upon Ca^{2+} binding, with emission maxima of 485 nm and 410 nm in the absence and presence of Ca^{2+}, respectively [50]. Thus, this probe is generally more practical in flow cytometry applications, where it is easier to use a single excitation wavelength and monitor two emissions [101]. Indo-1 is also useful as it displays less compartmentalization than Fura-2, although it tends to photobleach more rapidly [90]. With a K_d of 250 nM, it displays slightly lower affinity for Ca^{2+} than Fura-2 and is useful for measurement of Ca^{2+} concentrations in the cytoplasmic range.

3.4.2.10 Indo-1-PE3 (Indo-1 LeakRes)

Like Fura-PE3, Indo-1-PE3 was developed as an Indo-1 analogue less prone to sequestration into intracellular compartments and dye extrusion [51]. Compared to the parent compound, Indo-1-PE3 displays the same spectral properties, but avoids problems with uneven loading, differences in cell thickness and uncontrolled loss of dye fluorescence due to extrusion or photobleaching [102, 103].

3.4.2.11 Mag-Indo-1

Mag-Indo-1 is a low affinity fluorescent Ca^{2+} indicator derived from Indo-1. Its spectral properties are virtually identical to its parent compound, except that they occur at significantly higher Ca^{2+} concentrations (K_d ~35 μM) [58, 60, 80]. In combination with extremely fast kinetics [58], this compound is useful for measurement of Ca^{2+} kinetics in environments with high Ca^{2+} concentration.

3.4.3 Single Wavelength Ca^{2+} Dyes

In contrast to ratiometric fluorescent probes, binding of Ca^{2+} to single wavelength dyes elicits an increase in quantum efficiency, resulting in brighter fluorescence in the absence of spectral excitation or emission shifts. This eliminates the need for sophisticated equipment capable of dual excitation or dual emission monitoring and greatly simplifies experimental protocols. However, while single wavelength dyes generally exhibit large increases in fluorescence intensity upon binding of Ca^{2+}, brightness is also dependant on dye concentration. Thus, in addition to Ca^{2+} binding, fluorescence intensity of single wavelength Ca^{2+} probes is also affected by variables relating to the amount of dye present in cells. Most notably, differences in dye loading, extrusion, compartmentalization and photobleaching, as well as cell thickness and cellular environment can lead to apparent changes in dye concentration or fluorescence. Thus, because fluorescence intensity is the only measure for single wavelength dyes, quantitation of Ca^{2+}, particularly at the single cell level, tends to be less accurate than for ratiometric dyes. As an alternative to wavelength ratioing, time-based ratioing has been suggested as a viable strategy for single wavelength dyes, where the change in fluorescence intensity is expressed relative to a baseline fluorescence value [47, 104]. In circumstances where cell volume and shape changes as well as photobleaching have not been significant, this ratiometric Δ F/F value will approximate changes in Ca^{2+} [47]. Thus, single wavelength dyes have significantly advanced fluorescent Ca^{2+} imaging and are invaluable particularly for high-throughput assessment of Ca^{2+} responses.

3.4.3.1 Fluo-3

Fluo-3 was developed by Roger Tsien and his research group from the calcium chelator BAPTA conjugated with a xanthene chromophore [47]. Fluo-3 is excited by visible light, with absorption and emission maxima at 506 and 526 nm, respectively [47]. While the AM ester of Fluo-3 is virtually non-fluorescent, emission intensity of Fluo-3 increases approximately 40-fold in the presence of Ca^{2+} [47]. With a K_d of 400 nM, this makes Fluo-3 well suited for high resolution of cytosolic Ca^{2+} signals while at the same time being less prone to saturation and Ca^{2+} buffering at resting cytosolic Ca^{2+} than ratiometric dyes such as Fura-2 [61]. Fluo-3 – like all Ca^{2+}-dyes – is pH-sensitive, with an apparent pKa of 6.2, necessitating careful consideration of intracellular pH when measuring Ca^{2+} [47, 61]. In addition, Fluo-3 exhibits biphasic Ca^{2+} dissociation constants which, while also pH-dependent, are faster than Quin-2 and thus allow high time resolution of Ca^{2+} responses at neutral or physiological pH [61].

3.4.3.2 Fluo-4

Fluo-4 is a di-fluoro analogue of Fluo-3, and accordingly exhibits very similar spectral properties with absorption and emission maxima of 494 and 516 nm, respectively [48]. However, Fluo-4 is considerably brighter and more photostable than Fluo-3, and with a K_d of 345 nM [48], has become the dye of choice for measurement of cytosolic Ca^{2+} particularly in high throughput applications. Fluo-4 fluorescence, when excited at 488 nm, increases more than 100-fold upon binding of Ca^{2+}, permitting both use of lower dye concentrations and shorter loading times.

3.4.3.3 Mag-Fluo-4

Mag-Fluo-4 is a low affinity analogue of Fluo-4, and with a K_d of 22 μM, is particularly suitable for measurement of Ca^{2+} in the low μM – mM range. Accordingly, Mag-Fluo-4 has been used for measurement of Ca^{2+} responses in sarcoplasmic reticulum, and due to its affinity for Mg^{2+}, has also found applications in the measurement of intracellular Mg^{2+} [105, 106]. The spectral properties of Mag-Fluo-4, with an excitation maximum of 493 nm and an emission maximum of 516 nm, are very similar to Fluo-4 [48]. In addition, similar to Mag-Fura-2, Mag-Fluo-4 has fast dissociation kinetics which make this dye suitable for measurement of high resolution Ca^{2+} kinetics [63].

3.4.3.4 Fluo-5F, Fluo-5Cl, Fluo-5 N and Fluo-4FF

These mono-or di-substituted Fluo-4 analogues exhibit similar spectral properties to Fluo-4 upon binding of Ca^{2+}, however, the addition of one or two fluorine, chlorine or NO_2 substitutes results in significantly decreased Ca^{2+} affinity. The relatively high K_d values of Fluo-5F (2.3 μM), Fluo-5Cl (6.2 μM), Fluo-4FF (9.7 μM) and Fluo-5 N (90 μM) make these dyes suitable for measurement of Ca^{2+} under conditions which would result in saturation of higher affinity dyes [48]. The dissociation rate constant for Fluo-4 and Fluo-5F were determined as approximately 200–300 s^{-1} in vitro, making these dyes kinetically similar to Fura-2 [53, 62, 64, 65].

3.4.3.5 Fluo-8, Fluo-8H and Fluo-8 L

Fluo-8 and its analogues (AAT Bioquest) are a novel green-emitting Ca^{2+} probe (excitation/emission maxima ~490 nm/514 nm) that have been reported to be considerably brighter than Fluo-3 and even Fluo-4, resulting in improved signal-to-noise [107]. With K_d values of 389 nM (Fluo-8), 232 nM (Fluo-8H) and 1.86 μM (Fluo-8 L), these dyes may prove to be viable alternatives to Fluo-3, Fluo-4 and their analogues [66].

3.4.3.6 Rhod-2, X-Rhod-1and Low Affinity Derivatives

Rhod-2 was developed by the research group of Roger Tsien as a BAPTA analogue incorporating a rhodamine-like fluorophore [47]. This dye exhibits an excitation maximum of 553 nm and an emission maximum of 576 nm, with a K_d in the low μM range (~ 1.0 μM) [47]; while the analogue X-Rhod-1 has slightly shifted absorption and emission maxima (~580/602 nm, respectively) and a K_d of approximately 800 nM [108]. The cationic AM-esters of Rhod-2 and X-Rhod-1 can accumulate, using optimized loading protocols, in negatively charged mitochondria [109, 110], making Rhod-2, X-Rhod-1, and their derivatives useful for measurement of mitochondrial Ca^{2+} [108, 111, 112]. However, due to their relatively higher K_d values and thus lower potential for saturation in high Ca^{2+} environments, the low affinity Rhod-2 derivatives Rhod-FF (K_d 19 μM), X-Rhod-5F (K_d 1.9 μM), X-Rhod-FF (K_d 17 μM) and Rhod-5 N (K_d 320 μM) are preferred for this application [81, 113–115].

3.4.3.7 Calcium-Green-1 and Calcium-Green-2 Indicators

The Calcium-Green indicators display increased fluorescence emission intensity with little spectral shift upon binding of Ca^{2+} [67]. With peak excitation at ~507 nm, peak emission at ~530 nm and K_d values of approximately 200 nM

and 550 nM for Calcium-Green-1 and Calcium-Green-2, respectively, these dyes are well suited to measurement of fast cytosolic Ca^{2+} responses [67].

In addition, Calcium-Green dyes have a higher quantum yield than Fluo-3, particularly at saturating Ca^{2+} concentrations, which improves brightness of these dyes at high Ca^{2+} concentrations and provides an excellent dynamic range [67]. In contrast to Fluo-3, Ca^{2+} dissociation from Calcium-Green dyes is mono- rather than bi-exponential with a K_{off} of approximately 180 s^{-1} [67]. Substitution of a NO_2 group in Calcium-Green-1 produced the low affinity analogue Calcium-Green-5 N, which has similar spectral properties but considerably lower Ca^{2+} affinity with a K_d of approximately 4–19 μM, making this dye less prone to saturation [68–70].

3.4.3.8 Oregon Green 488 BAPTA Indicators

Oregon Green 488 BAPTA-1, Oregon Green 488 BAPTA-2 and their derivatives are fluorinated analogues of Calcium-Green indicators that were developed to achieve increased excitation efficiencies by the 488 nm spectral line of an argon laser. Accordingly, peak excitation and emission wavelengths of these Oregon Ca^{2+} indicators are 494 nm/523 nm. Like the Calcium-green dyes, Oregon Green 488 BAPTA indicators are bright dyes with higher quantum efficiencies than Fluo-3. Oregon Green 488 BATPA-1 in particular, with a K_d of 170 nM, may thus be particularly well suited for measuring small changes in Ca^{2+} near resting cytosolic Ca^{2+}, while the K_d of Oregon Green 488 BAPTA-2, at ~ 580 nM, more closely resembles the Ca^{2+} affinity of Fluo-4 [71]. Oregon Green 488 BAPTA-6F and Oregon Green 488 BAPTA-5 N are the 6′-fluorine and 5′-nitro analogues of Oregon Green 488 BAPTA-1 with reduced Ca^{2+} affinities (Oregon Green 488 BAPTA-6F K_d for Ca^{2+} ~3 μM and Oregon Green 488 BAPTA-5 N K_d for Ca^{2+} ~20 μM) and thus more suitable for measurement of larger Ca^{2+} responses.

3.4.3.9 Calcium Crimson, Calcium Ruby and Calcium Orange

Like other single wavelength dyes, Calcium Crimson, Ruby and Orange exhibit increased fluorescence emission intensity with little or no spectral shift in the presence of Ca^{2+}. As their names suggest, the excitation and emission spectra of these indicators are red-shifted with peak excitation/emission at 549/576 nm (Calcium Orange), 590/615 nm (Calcium Crimson) and 579/598 nm (Calcium Ruby) [72]. Calcium Ruby in particular displays large increases in fluorescence intensity upon Ca^{2+} binding, while all of these indicators are particularly useful where cellular autofluorescence is problematic [72]. The K_ds of these red-emitting Ca^{2+} indicators vary from ~ 300 nM (Calcium Crimson) and ~ 400 nM (Calcium Orange) to 30 μM (Calcium Ruby), allowing selection of Ca^{2+} dyes suitable for most imaging applications [67, 72].

3.4.4 Genetically Encoded Ca^{2+} Indicators

Genetically encoded Ca^{2+} indicators are protein-based sensors whose fluorescence changes in a concentration-dependent manner with alterations in intracellular Ca^{2+}. These indicators may be transiently or stably expressed and have been applied in a range of in vitro and in vivo models [116–120]. Modern genetically encoded Ca^{2+} indicators have improved properties compared to predecessors, which were limited by factors including pH sensitivity and low brightness [51]. One example is the GCaMP6 family of genetically encoded Ca^{2+} indicators, which have favourable characteristics such as a large signal to noise ratio, increased brightness and improved sensitivity comparable to leading small molecule fluorescent dyes [121]. This series has gained widespread use, particularly for the assessment of Ca^{2+} changes associated with neuronal activity using in vivo models [122–126]. Genetically encoded Ca^{2+} indicators are advantageous for certain applications compared to small molecule fluorescent dyes. This includes the repeated measurement of Ca^{2+} alterations occurring over a long time course (e.g. hours, days or weeks) [127], where small molecule Ca^{2+} indicators are not well suited due to sequestration and dye leakage that occurs over time. An example of the utility of genetically encoded over small molecule Ca^{2+} sensors is the use of GCaMP6f to monitor cortical neuron activity in marmosets over several months using a cranial window [128]. An additional advantage of genetically encoded Ca^{2+} indicators is their ability to be targeted to specific subcellular locations, which can enable investigations into Ca^{2+} dynamics in organelles such as the endoplasmic reticulum or mitochondria [129]. Additionally, the relationship between organellar and global cytosolic Ca^{2+} changes can be investigated using co-expression of an organelle-targeted and cytosolic genetically encoded Ca^{2+} indicator with distinct fluorescence spectra. For example, co-expression of GCaMP6s (cytosolic) with R-CEPIA*er* (targeted to endoplasmic reticulum) in MA104 cells following rotavirus infection identified cytosolic Ca^{2+} increases and corresponding endoplasmic reticulum Ca^{2+} depletion occurring over several hours [119]. Following the introduction of a genetically encoded Ca^{2+} indicator transgene into a model organism or stable cell line, further validation should be undertaken to ensure appropriate expression levels of the sensor and preservation of the parental phenotype [130]. Use of genetically encoded Ca^{2+} indicators will likely continue to increase with the continued development of spectrally distinct sensors enabling simultaneous assessment of Ca^{2+} changes with other cell features and further improvements in the properties of those Ca^{2+} sensors targeted to organelles.

3.4.5 Na^+ Dyes

Compared to the number of available fluorescent calcium indicators (~40), there are currently only a limited number of useful fluorescent sodium indicators: SBFI

(sodium-binding benzofuran isophthalate), Sodium Green, CoroNa Green and Red, as well as Asante NaTRIUM Green-1 and -2 (ANG-1 and ANG-2) [2, 73, 131]. These have been used widely as probes in fluorescence imaging with conventional and confocal microscopes and have only relatively recently been adapted for high-throughput format [132, 133]. With the exception of CoroNa Red – which is lipophilic and thus readily crosses the plasma membrane – Na^+ indicators are also available in their acetomethyl (AM) ester-conjugated forms which cross the plasma membrane and become trapped in the cytosol after cleavage by endogenous esterases (see below). In addition, the net positive charge of CoroNa Red leads to accumulation of the dye in mitochondria [2, 73, 131].

Like Fura-2, SBFI is a ratiometric dye that exhibits changes in fluorescence quantum yield as well as excitation characteristics upon binding of Na^+ ions. Generally, the selectivity of SBFI for Na^+ is reduced compared to the selectivity of Fura-2 for Ca^{2+}, although the spectral properties of the dyes are similar and the same optical filters and equipment can be used for both. A disadvantage of SBFI, as well as the related K^+ dye PBFI (Potassium-binding Benzofuran Isophthalate), is their sensitivity to ionic strength, pH and temperature, which necessitates calibration using gramicidin or palytoxin [2].

In contrast, Sodium Green, CoroNa Green and Red as well as Asante NaTRIUM Green-1 and 2 are single wavelength dyes with excitation peaks in the visible spectrum, making them particularly useful for high-throughput systems. However, although the quantum yield of these dyes (e.g. 0.2 for CoroNa Green; 0.64 for ANG-2) is considerably greater than that of SBFI (0.08 for SBFI), the dynamic range of fluorescent Na^+ dyes remains considerably lower than that of many Ca^{2+} dyes [2, 73]. These issues are compound by the relatively small Na^+ gradient across the membrane (~10-fold compared to the ~10,000-fold difference in Ca^{2+} concentrations) which leads to a relatively small increase in intracellular Na^+ concentration in comparison with Ca^{2+} concentrations, which can increase several fold during signalling events. Accordingly, the signal-to-noise ratio for Na^+ detection is correspondingly – and inherently – low in comparison to other ions. Therefore, Na^+ channel activity is more commonly observed by electrophysiological means, or with surrogate measures such as membrane potential or voltage-sensitive dyes, as discussed below. In combination with difficulties relating to physiologically meaningful activation of Na_V channels – albeit these are also concerns with other voltage-gated channels such as K_V channels – these limitations have greatly hampered the use of Na^+ indicators for pharmacological characterisation of Na^+-selective channels, particularly those activated by changes in membrane voltage.

In practice, we have found only ANG-2 to have fluorescence characteristics compatible with high-throughput assay approaches of Na_V channels (unpublished data) and although TRPV1-expressing HEK293 cells loaded with CoroNa Green respond to capsaicin with an increase in fluorescence, these responses are considerably smaller than the corresponding changes in fluorescence in Fluo-4 loaded cells (Fig. 3.2).

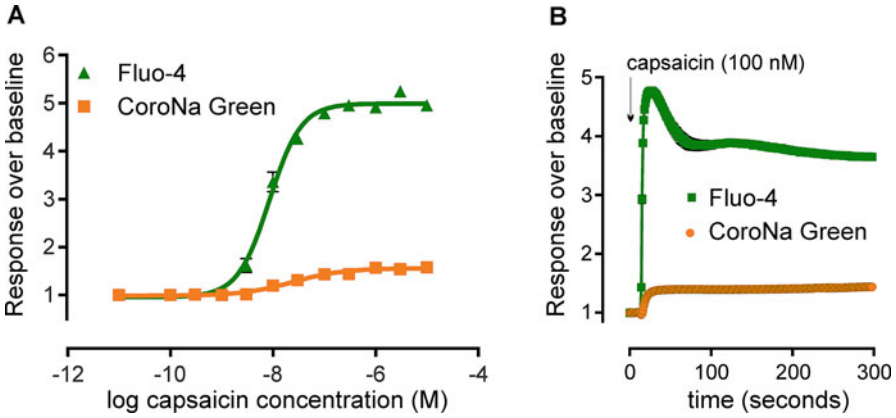

Fig. 3.2 Ca^{2+} and Na^{+} responses elicited by capsaicin in cells stably expressing TRPV1
Methods: HEK293 cells stably expressing TRPV1 were generated as previously described [209, 210], plated at a density of 50,000 cells/well on PDL-coated, black-walled 96-well imaging plates and incubated in a 37 deg./5% CO_2 incubator for 24 h
Fluo-4-AM (Invitrogen) or CoroNa Green-AM (Invitrogen) were prepared as 5 mM stock solutions in DMSO and diluted to final concentration of 5 μM in physiological salt solution (PSS; composition see [195]). Cells were incubated with 50 μl of the loading solution in a 37 deg./5% CO2 incubator for 45 minutes. After removal of dye solution, cells were washed twice with PSS prior to addition of 100 μl PSS/well and transfer to the FLIPR^{TETRAPlus}
TRPV1-HEK293 cells were stimulated by addition of 50 μl capsaicin (final concentration: 10 μM – 0.1 nM) prepared as a 3 x concentrated stock solution in PSS and imaged at 1 Hz for 300 reads (excitation/emission: 470–495/515–575 nm) using a FLIPR^{TetraPlus} Fluorescent Plate reader
Raw fluorescence values were converted to response over baseline values using the analysis tool of ScreenWorks 3.1 by subtracting baseline reads (read 1–10) from subsequent fluorescent reads
*Results:***(A)** Capsaicin-induced fluorescence responses were of significantly smaller magnitude in CoroNa Green-loaded cells (max. response over baseline 1.58 ± 0.02) compared with Fluo-4-loaded cells (max. response over baseline 4.96 ± 0.1); leading to an apparent decrease in the capsaicin EC_{50} in CoroNa Green-loaded cells (pEC_{50} 7.61 ± 0.07) compared with Fluo-4-loaded cells (pEC_{50} 8.07 ± 0.03). **(B)** Fluorescence responses to capsaicin (100 nM) differ in both magnitude and kinetics in Fluo-4- and CoroNa Green-loaded cells. Data presented as mean ± S.E.M. from n = 6 wells of the same plate. Error bars may be obscured by the data symbols

3.4.6 Membrane Potential and Voltage-Sensitive Dyes

Activity of Na^{+}-, K^{+}- and Ca^{2+}-permeable ion channels often leads to a change in membrane potential, or transmembrane charge distribution, which is most accurately measured using electrophysiological techniques. However, despite advances in high-throughput electrophysiology approaches (reviewed in [134]), these techniques remain technically challenging and relatively expensive. As the intracellular ion concentration may not be an accurate reflection of membrane potential or cell excitability, alternative imaging approaches are needed to measure membrane depolarisation. With the exception of Ca^{2+}, the flux of ions required to depolarise

a cell of 50 μm diameter by 60 mV (∼ 30 million ions) may not appreciably change the intracellular or extracellular ion concentration. Thus, the development of membrane potential dyes has greatly aided high-throughput assessment of cell excitability. These dyes generally incorporate into the lipid membrane of cells and exhibit a change in fluorescence spectra and/or intensity upon depolarisation. Examples include the fast responding styryl dyes, which have high temporal resolution (3 ms) but limited sensitivity; oxonol and carbocyanine dyes and their derivatives, including bis-(1,3-dibutylbarbituric acid) trimethine oxonol ($DiBAC_4(3)$); and FLIPR Membrane Potential (FMP) Dye which displays slower kinetics and moderate sensitivity. The use of two probes allows more sensitive detection of membrane potential changes via the measurement of fluorescence resonance energy transfer (FRET). More recently, the use of photoinduced electron transfer (PeT) has driven the development of dyes such as FluoVolt, which is both fast, sensitive and displays a higher fluorescent yield. Finally, there have been considerable advances in the effective use of genetically encoded membrane potential indicators. Membrane potential is an attractive output for high-throughput screening as it is sensitive, generic, and applicable to living cells.

Although membrane potential dyes act via different mechanisms, sensitivity to depolarisation is dependent on having a dynamic interaction with phospholipid bilayers. Generally, styryl, oxonol, and carbocyanine dyes move across lipid bilayers dependent on the Nernstian distribution during depolarisation [135, 136]. The direction depends on their charge, but results in a change in the concentration of intracellular and extracellular dye. The interactions of dye, membrane or cytosolic molecules results in changes to the emission spectra and/or quantum yield underpinning their usefulness as voltage-sensitive dyes. As the membrane potential of mitochondria can be as high as −180 mV, cationic dyes are less suitable for measuring depolarisation in the plasma membrane. However, they have been employed in limited circumstances to discriminate mitochondrial membrane potential [137, 138]. FMP Dye and $DiBAC_4(3)$ possess lipophilic tails, and negatively charged head groups, allowing these dyes to embed in cell membranes and act as voltage sensors. The negatively charged dyes preferentially sequester to the extracellular leaflet of a hyperpolarised cell membrane (inside the cell is negatively charged) and the presence of an extracellular quencher limits emissions in this state. Upon depolarisation, dye molecules are recruited to the cytosolic side of the plasma membrane, escaping the quencher, and increasing emissions. Despite sharing a mechanism of action, FLIPR Membrane Potential Dye display superior temporal and membrane potential sensitivity to $DiBAC_4(3)$ [76, 139].

In contrast, FRET relies on the dynamic interactions of the emission donor and/or acceptor within the membrane. The most commonly used system utilises a membrane bound coumarin derivative, N-[6-chloro-7-hydroxycourmarin-3-carbonyl] dimyristroyl phosphatidyl ethanolamine, CC2-DMPE) that acts as a FRET donor, co-loaded with a mobile voltage-sensitive oxonol acceptor, such as $DiBAC_4(3)$ [77, 140] . Other FRET systems co-load two oxonol derivatives (*e.g.* $DiBAC_1(3)$ and $DiBAC_1(5)$) into the plasma membrane as a donor/acceptor pair, respectively. Recording concurrent emission wavelength maxima from both molecules after exci-

tation of the donor results in transfer of emissions to the acceptor, proportional to the proximity of the two molecules. As the position of at least one of the donor/acceptor pair in the membrane is dependent on cell polarity, this allows the ratiometric measurement of membrane potential [141]. The catalogue of voltage-dependent dyes is ever expanding, with new "VoltageFluors" being developed to overcome the shortcomings of previously designed dyes. More recently, experimenters have utilised photoinduced electron transfer (PeT), by tethering a dichlorosulfoflorescein reporter to a dimethylaniline electron donor via a phenylenevinylene molecular "wire" [142]. The fluorescent reporter, embedded in the extracellular membrane leaflet is quenched by the electron donor when the cell is hyperpolarised. Depolarisation of the membrane decreases the dipole moment of the dye, allowing increased emissions from the fluorescein, proportional to the voltage difference across the membrane. Due to these slight differences in mechanism of action, voltage-sensitive dyes may require elaborate, highly sensitive detection equipment and/or labour intensive tissue preparation, while others are more useful for high-throughput screening applications.

In addition to dyes, there are many genetically encoded voltage indicators (GEVI) that have been developed over the past 20 years. There are two main structurally distinct GEVI. The first to be developed exploited the voltage-dependent structural rearrangement of voltage-sensing domains from potassium channels [143], sodium channels [144], phosphatases [145, 146], and proton channels [147]. These are generally tethered to one or more fluorescent molecules and the structural shift during depolarisation changes some spectral property of the fluorophore/s. In addition to those based on voltage-sensing domains are a contingent of GEVI engineered from microbial opsins [148]. These rely on membrane depolarisation changing the protonation of the opsin's retinal cofactor, resulting in changes to absorption or emission intensity from a conjugated fluorophore [149]. All GEVI offer similar advantages to calcium indicators, and can be selectively and stably expressed in cells and animal models, making this approach advantageous for in vivo imaging as well as imaging over multiple days. Some benefit has also been derived from combining GEVI and traditional voltage-sensitive dyes to assess membrane potential [150]. As GEVI have extensively reviewed in recent years, this chapter will not discuss them in detail, however comprehensive comparison can be found elsewhere [151–153].

When designing experiments for membrane potential assays, it is important to consider limitations in temporal resolution. Depending on the cell type, the duration of an action potential ranges from 1–2 ms in neurons, 2–5 ms in skeletal muscle cells, and 200–400 ms in cardiac muscle cells. With the exception of styryl dyes, PeT dyes, and some GEVIs, all membrane potentials dyes $t_{1/2}$ fall in the range between 1 s and >60 s, and are thus not capable of resolving the membrane potential changes characteristic of an action potential [139]. However, paramount to these considerations is the system in which compounds are being screened – many in vitro cell systems are not capable of firing action potentials and so the inability to resolve single action potentials is not necessarily a limitation.

Membrane potential dyes impart several advantages over ion-sensing dyes. One benefit of membrane potential dyes is the high stability, with stable signals being reported 4–15 h after loading [139, 154]. Unfortunately, due to their relatively insolubility in water, dye loading may require the addition of a pluronic surfactant, which may interfere with interactions between test compounds and molecular targets. Each cell system requires dye concentration titration with the aim of optimal loading to increase signal-to-noise ratio. This can be particularly laborious when using FRET-based assays, as multiple compounds require loading [140]. In addition, membrane potential dyes can be particularly prone to artefacts, with alterations in pH, quantity of cytosolic proteins and/or RNA, and membrane integrity leading to changes in fluorescence that can be misinterpreted as changes in membrane potential. Likewise, molecules – particularly charged compounds – can directly interact with dye molecules, and positive hits should be screened at least once in a cell free system or better yet, in the absence of the suspected molecular target.

3.4.6.1 Styryl Dyes

Styryl dyes offer the temporal resolution to accurately measure the onset of a single action potential and low background fluorescence [155]. One example is pyridinium, 4-(2-(6(dibutylamino)-2-naphthalenyl)-1-(3-sulfopropyl)-hydroxide (di-4 ANEPPS), which has been used in a number of different in vitro membrane potential measurements including red blood cells, squid giant axon, cardiomyocytes, and isolated membrane vesicles [156]. The excitation and emission wavelengths are dependent on the cell system, but ranges between 520 ± 20 nm (Ex) and >640 nm (Em). However, the relative fluorescence change upon depolarisation is limited (<10% with depolarisations of more than 100 mV) and the dye has proven incompatible with some cultured cell lines [157, 158]. Other styryl dyes, such as Di-2-ANEPEQ must be microinjected into cells, making them capable of distinguishing sub-cellular depolarisation [159]. Thus, stryryl dyes are well suited for use with highly optimized, low noise equipment, but ill-suited for high-throughput screening.

3.4.6.2 Carbocyanine Derivatives

Indo-, thia-, and oxo-cyanine dyes were some of the first potentiometric dyes used. Oxocyanine (DiO) $C_6(3)$, the most commonly used for this application, has excitation/emission maxima of 484/501 nm [160]. However, due to its high affinity for mitochondria and other intracellular organelles, its application for measurement of plasma membrane potential is limited. Another cyanine derivative, mercocyanine 540, was also initially used as a membrane potential probe, but its high phototoxicity limits its application in living cells [161].

3.4.6.3 Oxonol Derivatives

A diverse family of oxonol derivatives with a variety of fluorescent properties have been produced. Two examples of oxonol derivatives with potentiometric sensitivity are $DiBAC_2(3)$ and $DiBAC_4(3)$ with excitation/emission maxima of 537/554 nm and 492/516 nm, respectively. Due to their overall negative charge, these dye molecules are excluded from mitochondrial membranes, thus reducing noise. $DiBAC_4(3)$ is often used with an extracellular quencher (*e.g.* bromophenol blue) allowing a substantial improvement in signal to noise ratio when compared to other oxonol and carbocyanine derivatives. $DiBAC_4(3)$ also shows other advantages over $DiBAC_2(3)$ with more than 2 × fluorescence yield upon depolarisation and faster kinetics ($t_{½}$ = 30 s) [139]. However, the slow kinetics of activation leaves the dye susceptible to interference from temperature and pH changes as longer read times may be required to capture differences in membrane depolarisation [162]. Additionally, loading cells with $DiBAC_4(3)$ requires surfactant, and additional dye must be washed off before reading, making the application of these dyes difficult for poorly adherent cells.

3.4.6.4 FLIPR Membrane Potential Dye

The FMP dye is excited at 530 nm with emissions measured at 565 nm. There is the option of FMP dye being bundled with two proprietary quenchers, "red" and "blue", which must be optimised to individual assay conditions. FMP displays a relative fluorescence change of more than four times that of $DiBAC_4(3)$ during depolarisation [139]. This is accompanied by enhanced kinetics over oxonol and carbocyanine derivatives ($t_{½}$ = 8 s). The inclusion of a proprietary quencher offers more stability to changing temperatures, making them useful during short or long time-course experiments. The loading of cells is streamlined, with fast loading times (< 30 min) and the absences of wash steps making these dyes useful for poorly adherent cells while enhancing the reproducibility of assays [163, 164].

3.4.6.5 Fret-Based Membrane Potential Dyes

The most commonly used commercially available FRET system for measurement of membrane potential is based on the CC2-DMPE/$DiBAC_2(3)$ donor/acceptor pair. The donor is excited at 405 ± 15 nm with emission monitored at both 460 nm and 580 nm, leading to a ratiometric readout that is relatively resistant to changes in pH, temperature and bleaching [165]. While ratiometric systems offer the most sensitive measurement of membrane potential available, more complex loading procedures are required [139]. These include optimisation of the FRET donor concentration for each cell system assayed, and multiple wash steps which may limit application when cells are poorly adherent. Another fluorescent molecule, dipicrylamine (DPA, Abs 406 nM) has been paired with DiO for the measurement of membrane voltage

potential by FRET [166]. This system is applicable to two-photon imaging, allowing voltage measurement from deep within tissue slices [167].

3.4.6.6 FluoVolt™

Described as "molecular wires", these fluorophores display the favourable properties of both fast and slow membrane potential dyes [168]. The fast temporal dynamics allow the dye to change fluorescence and resolve single action potentials while displaying a greater relative fluorescence yield upon depolarisation (approx. 25% per 100 mV). As the conjugated fluorescein shares an excitation/emission maxima with GFP, standard filter sets can be used for imaging. Furthermore, the molecule can be applied for high throughput screening, and is easily loaded into cells with the use of a proprietary surfactant [169]. Due to emission overlap with other biologically useful molecules, a far-red fluorescent equivalent has also been developed [170]. Thus, one can record the membrane potential change of a cell, while simultaneously using GCAMP6 to record the resulting calcium spike, for example.

3.4.7 K^+ Dyes

Similar to Na^+-sensitive dyes, the repertoire of K^+ dyes is relatively limited. PBFI comprises a benzofuranyl fluorophore that is linked to a crown ether chelator [2] which confers some modest selectivity for K^+ ions, although the K_d is also affected by pH, temperature, ionic strength and the presence of Na^+ ions. Like SBFI and Fura-2, PBFI is a ratiometric dye with excitation/emission peaks of 336/557 and 338/507 nm in the K^+-free and K^+-bound state, respectively. Although the selectivity of PBFI for K^+ is sufficient for the quantification of intracellular K^+ concentrations in vitro – owing to the relatively higher concentration compared to Na^+ – the dye properties of PBFI make it poorly suited to high-throughput applications. In addition, dyes such as PBFI are less useful for high-throughput screening because of their broad excitation spectra, which can overlap with many optically active compounds in drug screening libraries [171].

More recently, single wavelength K^+ dyes – including Asante Potassium Green-1 and -2 – have been reported [73]. Although these have not been widely used as yet, at least in principle they could be useful for high-throughput and/or high-content applications in light of their more favourable properties, such as excitation/emission peaks of ~515/540 nm and more favourable loading [172].

Historically, rubidium ion (Rb^+) efflux was used to determine K^+ channel activity by incubating cells expressing the K^+ channel of interest in a Rb^+ rich buffer and examining the movement of Rb^+ using radioactive Rb^+ isotopes or Rb^+ ions in conjunction with atomic absorption spectroscopy (AAS) or as its commonly known, "flame photometry", to quantify the amount of Rb^+ [171, 173]. In addition to Rb^+, many K^+-permeable channels are also thallium (Tl^+) permeable. Although

permeability of K^+-permeable ion channels families and subtypes to Tl^+ has not been assessed systematically, the pore structure is relatively conserved and it is reasonable to assume that these channels are likely Tl^+ permeable [171]. Accordingly, a change in fluorescence occurs when Tl^+ enters a cell loaded with a Tl^+-sensitive dye via K^+ channels, thus providing a surrogate measure of K^+ channel activity [171].

3.4.8 Dye Loading

Several methods for introduction of Ca^{2+}, Na^+ and K^+ dyes into the cell cytoplasm have been developed; these include ATP-induced permeabilization, electroporation, hypo-osmotic shock, cationic liposomes, chelators mediating dye uptake through pinocytosis, microinjection as well as loading of dyes coupled to acetoxymethyl (AM) ester [58, 82, 83, 97, 174–177]. Of these, the acetoxymethyl (AM) ester loading technique has become popular due to its simplicity, ease of use and low toxicity and is particularly well suited to high-throughput applications.

3.4.9 AM Ester Loading Technique

As free poly-anionic, large fluorescent probes are unable to passively cross the cell membrane, fluorescent dyes can be conjugated to lipophilic acetoxymethyl (AM) groups to render them membrane-permeable. Once in the cytoplasm, ubiquitous esterases hydrolyse these derivatized indicators, which again become unable to passively cross the plasma membrane, thus effectively trapping the free fluorescent probe. As an additional advantage, these AM derivatives are often non-fluorescent, thus reducing or eliminating fluorescence from non-hydrolysed extracellular dye.

3.4.10 No-Wash Extracellular Quenchers

Because physiologically, extracellular Ca^{2+} and Na^+ concentrations are high, fluorescence signals from the extracellular compartment generally need to be excluded to enable measurement of the often relatively small changes in cytosolic ion concentration. This can be achieved either by physically removing extracellular dyes by media or buffer exchange (“washing”), or alternatively by incorporation of fluorescence quenchers in the extracellular media. Quenchers that have been used successfully include Trypan Blue, haemoglobin and Brilliant Black [178, 179]. In addition, several of these quenchers or “no-wash” kits are now commercially available, and they can provide significant improvements in assay performance particularly for cells that are only weakly adherent, or for cells that are prone

to dye extrusion. However, as the composition and nature of these quenchers is largely proprietary information, it can be difficult to assess potential interference of quenchers with assays or to design protocols for assay optimization [179].

3.4.11 Problems with AM Ester Loading

While the AM ester loading technique is undoubtedly one of the most widely used and easiest approaches to introducing fluorescent dyes into cells, a number of issues – including limited dye solubility, sequestration, incomplete hydrolysis and dye extrusion – can limit the applications of this approach. These issues are typically dye- and also cell-specific, and perhaps best understood (or appreciated) for fluorescent Ca^{2+} dyes. Specific considerations relating to each of these issues are thus described below in the context of Ca^{2+} dyes, although similar problems may also arise for other indicators.

Solubility By virtue of increased lipophilicity, many AM esters are poorly soluble in aqueous solutions, thus necessitating inclusion of dispersants such as pluronic acid in the loading media. However, satisfactory dye loading can be achieved in the absence of pluronic acid for several dyes (including e.g. Fluo-4, Fura-2 and ANG-2) provided they are prepared as 100x to 1000x stock solutions in dimethylsulfoxide and carefully stored frozen as aliquots to avoid water absorption and thus precipitation. Individual optimisation of loading conditions is thus advisable.

Sequestration Once introduced into the cell cytoplasm, fluorescent Ca^{2+} dyes start to accumulate into intracellular membrane-bound vacuoles and organelles such as the endoplasmic reticulum (ER) and mitochondria in a process commonly referred to as sequestration or compartmentalization [180]. This process is, however, not restricted to the AM ester loading technique and may result in increasing baseline fluorescence readings as the free dye accumulates in high Ca^{2+} intracellular compartments, as well as accompanying decreases in cytosolic Ca^{2+} responses due to dye loss. To minimize dye sequestration, loading with the lowest AM ester concentration that produces reliable Ca^{2+} signals, as well as loading for the shortest possible time is beneficial. Loading and imaging cells at room temperature rather than 37 °C can also help reduce dye sequestration, although restricting recordings to approximately 30 minutes largely avoids this problem. In addition, while for most applications, retention of the dye in the cell cytoplasm is desirable, dye sequestration can be exploited to assess calcium levels in organelles [181–184].

Incomplete AM Ester Hydrolysis Residual cytosolic non-hydrolysed dyes, due to insufficient intracellular esterase activity or failure to completely remove AM ester dyes, can lead to signal artefacts, most notably an apparent decrease in fluorescence response, as AM esters tend to be non-fluorescent [185, 186]. In addition, efficiency of ester hydrolysis can be highly variable and often depends on the cell type; incubation at 37 °C generally improves ester hydrolysis but optimal conditions

usually have to be determined empirically. In contrast, excessive extracellular ester hydrolysis leads to poor dye loading and as a result poor fluorescence signals, while extracellular hydrolysed probes tend to provide high fluorescence background [187].

Dye Extrusion Extrusion of hydrolysed intracellular Ca^{2+} probes by cellular anion transporters results in decreased available dye concentrations and thus, decreased signal strength. This problem is not restricted to the AM-loading technique, and can be a particular problem in certain cell types. Dye extrusion or leakage can be minimized by incorporation of anion transport inhibitors such as probenecid or sulphinpyrazone [180]. However, these compounds can alter cellular function and should thus be used with caution. Loading cells and measuring fluorescence a quickly as possible, as well as performing experiments at room temperature rather than 37 °C generally also aid in minimising dye extrusion [80].

3.5 Assay Platforms

3.5.1 High-Throughput Fluorescence Plate Readers

A number of plate reader platforms suitable for fluorescence assays in high-throughput format are available commercially. The industry-leading instruments are set apart from lower throughput instruments by the capacity to dispense liquids and measure fluorescence emission from 96,384 or 1536 wells simultaneously with high temporal resolution. This in turn negates some of the problems associated with conventional fluorescence imaging that arise from uneven dye loading, extrusion, intracellular compartmentalization or photobleaching, as loading and imaging conditions are constant across all wells. Thus, high-throughput imaging plate readers such as the FLIPR^{TetraPlus} (Molecular Devices), Hamamatsu FDSS7000EX (Hamamatsu), WaveFront Biosciences PanOptic (WaveFront Biosciences) and CellLux (Perkin Elmer) are well-suited for the primary identification of drug leads as well as detailed pharmacological characterization of compounds. Because functional responses are measured, pharmacological characterization of full or partial agonists as well as competitive and non-competitive antagonists at a range of targets can be accomplished.

While the precise specifications differ between these instruments, all combine sophisticated liquid handling systems with optics that permit real-time fluorescence readings before, during, and after compound addition to enable characterisation of kinetic responses. Desirable attributes of these high-throughput platforms include high-precision robotics in 96-, 384- or 1534-well format that permit custom configuration of aspiration and dispense height and speed to minimize disruption of cell monolayers and addition artefacts. The ability to program multiple additions is crucial for testing antagonists as well as agonists in the same experiment, with additional reagents plates permitting assessment of more complex responses such as Ca^{2+} influx through Orai-1 channels following store depletion [188].

The incorporation of state-of-the-art excitation and detection systems – such as two sets of customisable LED banks and an EMCCD cooled charge-coupled device (CCD) camera for fluorescence detection, or optionally an ICCD intensified CCD camera for the FLIPR^{TetraPlus}, or a variable-wattage white light xenon lamp with Hamamatsu fluorescence/luminescence camera for the FDSS7000EX – permit the versatile design of experiments. Measurements from an entire plate can be taken in as little as sub-second intervals, with up to 800 (FLIPR^{TetraPlus}) or 4000 (Hamamatsu FDSS7000EX) reads enabling prolonged real-time pre-incubation with antagonists as well as kinetics recordings for even the slowest fluorescent responses.

In addition, an increasing number of available emission filters, with wavelengths ranging from 340 nm to > 650 nm, permit selection of fluorescent dyes that are most suitable for individual applications. An important consideration is the number of excitation/emission filter sets that each instrument can be configured to, which in case of the FLIPR^{TetraPlus} is currently limited to 2 and 3, respectively.

While most high-throughput instruments include optional temperature-control, typically permitting heating from ambient to ∼ 40 °C, most assays perform well at ambient temperature and both the speed and precision of plate heating are insufficient for modulation of most temperature-sensitive pharmacological targets, although this feature could be useful if assaying poorly soluble compounds.

3.5.2 Single-Cell Imaging

In high-throughput plate reader assays, it is the sum of individual cellular responses in each well that is recorded and analysed. It is this relatively simple experimental output that has made this technology particularly amenable to high-throughput applications. However, for some studies, multiple readouts may be desirable. Such assays, where multiple cellular or subcellular responses or components are recorded individually and in parallel, have been described as "high-content" [189]. For example, changes in intracellular Ca^{2+} can be quantified simultaneously – in individual cells – with other cellular and subcellular features or events such as cell morphology, cell death or nuclear translocation [127].

High-content imaging assays are often considered as target-agnostic and provide information on cellular phenotypes – associated with one, or many, targets and signalling pathways – through the analysis of fluorescence microscopy images in high-throughput format. However, in the context of this review, the term "high-content imaging" will be used for single-cell, live imaging approaches that permit analysis of individual cellular responses rather than population responses that are assessed in high-throughput plate reader assays.

For high-content imaging assays, cells can be prepared and loaded in the same manner as for high-throughput imaging assays, but the imaging instrumentation and software used is necessarily different. At its most basic, cells are imaged by videomicroscopy using an inverted fluorescent microscope equipped with an appropriate light source, excitation and emission filters and a camera. However,

while this approach may be "high-content" in the sense that many single cells can be captured simultaneously, it is limited in its throughput as typically a single experiment (often from individual coverslips or wells on which cells were plated) is conducted. Nevertheless, because this type of single cell imaging provides information that is complementary to high-throughput approaches, it has found use in multiple applications. One of these is the systematic characterisation of distinct functional populations in heterogeneous cell populations such as primary cell cultures [190, 191]. In this application, researchers exploit a suite of well-defined pharmacological tools to functionally profile cell populations — an application that is complementary to immunocytochemistry or RNAseq-based techniques. In cases where a cell population is already well-defined, a second application becomes possible: defining the cellular mechanism of action of a compound of interest [192–194]. An example of this application is shown in Fig. 3.3, where high-content imaging of cultured DRG neurons was used to define the cellular mechanism of action of two algogenic toxins. Using a similar high-content imaging approach, the Na_V activator Pacific Ciguatoxin-1 was shown to selectively activate TRPA1-expressing sensory neurons in cultured DRG neurons [195]. While these example compounds act as agonists, it is worth mentioning that this type of experiment is equally relevant for the investigation of antagonists: a cellular response can be elicited by the application of a well-defined agonist in the presence/absence of the compound of interest and cellular responses recorded in the same manner. The information acquired through this type of high-content imaging assays, particularly when coupled with complementary immunocytochemistry, RNAseq or gene-knockout data, can be valuable in determining the molecular mechanism of action of a compound of interest.

In more recent years, single cell imaging has been adapted to automated platforms that permit imaging from cells plated in multi-well plates – so-called high-content plate readers, examples of which will be discussed in the following paragraphs – and have opened the door to other applications such as the parallel recording and quantitation of spatial redistribution of cellular or subcellular targets and/or individual cell and organelle morphology [189].

Temperature control and CO_2 regulation is available in some systems (e.g. ImageXpress Micro (Molecular Devices), Operetta CLS LIVE (PerkinElmer)) which permits live cell imaging over extended durations, such as time-lapse measurement of Ca^{2+} changes in cells undergoing cellular events. For example, using an ImageXpress Micro, global $[Ca^{2+}]_{CYT}$ increases were identified in the subset of MDA-MB-231 breast cancer cells undergoing cell death within 6 h of ceramide treatment [196]. The Kinetic Image Cytometer (Vala) can also be used for timelapse high content imaging and is capable of rapid image capture particularly suited to transient cellular events occurring over milliseconds. This instrument also has the option for electrical stimulation of cells, useful for applications such as neuronal screening. Wide-field imaging is commonly used for high-content systems, although confocal imaging is also available. The Opera Phenix (PerkinElmer) is an example of a confocal high content imaging system, which can also be configured with four sCMOS cameras to enable increased frame rates, low signal to noise ratio

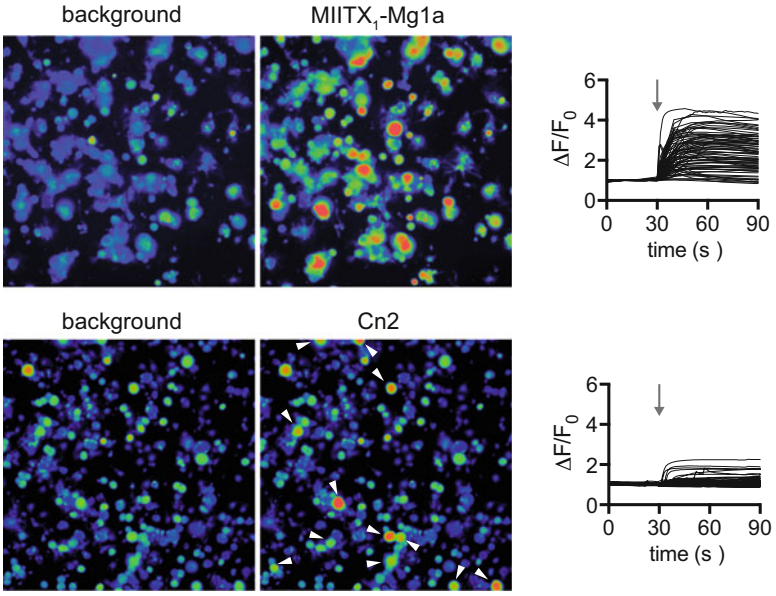

Fig. 3.3 High-content calcium imaging of the effects of algogenic toxins on DRG cells
Methods: Experiments involving animals were approved by the University of Queensland Animal ethics committee. DRGs from 6–8 week male C57BL/6 mice were dissociated as described [211], plated on a poly-D-lysine-coated 96-well culture plate and maintained in a 37 deg./5% CO_2 incubator overnight
Fluo-4-AM (Invitrogen) was prepared according to the manufacturer's instructions. Cells were loaded for 30 min in a 37 deg./5% CO_2 incubator, followed by 30 min equilibration at room temperature. After loading, the dye-containing solution was replaced with assay solution (1x Hanks' balanced salt solution, 20 mM HEPES), and the plate transferred to the inverted microscope setup
Fluorescence corresponding to $[Ca^{2+}]_i$ of 100–150 DRG cells per experiment was monitored in parallel using a Nikon Ti-E Deconvolution inverted microscope, equipped with a Lumencor Spectra LED Lightsource. Baseline fluorescence was monitored for 30 s, after which assay solution was replaced with $MIITX_1$-Mg1a (10 μM in assay solution; panel A) or Cn2 (500 nM in assay solution; panel B).
Raw fluorescence values were converted to $\Delta F/F_0$ (fluorescence minus baseline fluorescence, divided by baseline fluorescence)
Results: $MIITX_1$-Mg1a is the major peptide component of the venom of the giant red bull ant, *Myrmecia gulosa*. The toxin exerts algogenic activity in vivo, and causes a sustained increase in intracellular Ca^{2+} concentration in neuronal as well as non-neuronal cells obtained from a culture of dissociated dorsal root ganglia. This activity is suggestive of a widespread cellular target, and indeed, $MIITX_1$-Mg1a acts on cellular lipid bilayers where it causes a leak in membrane ion conductance, which, in neurons, triggers depolarization [211]. In contrast, the algogenic $Na_V1.6$-selective Cn2 – a major peptide component of the venom from the scorpion *Centruroides noxious* – caused a sustained increase in intracellular calcium concentration only in a subset of large diameter neurons (labelled with an arrowhead), indicative of a molecular target expressed only in this neuronal population. Snapshots shown are before and after addition of each compound. Each trace corresponds a single cell in each field of view. Arrows indicate toxin addition

and parallel measurement in four colour channels simultaneously. The ImageXpress Micro has the option for automated liquid addition, a feature that can be used for the assessment of transient Ca^{2+} changes following compound addition. However, as for automated high-throughput imaging systems – and in contrast to traditional setups that permit perfusion imaging – high-content imaging in microwell plates typically does not permit removal of compounds and is limited to cumulative additions. High-content imaging systems can also vary in number of objectives, filter configurations and ability to measure bright-field in addition to fluorescence (e.g. IN Cell Analyzer 6000 (GE Healthcare), CellInsight CX7 (Thermo Fisher Scientific)). A key challenge of high-content imaging approaches is the inherent generation of large datasets, which typically requires advanced computing solutions for analysis including large data storage capacity. Most instruments are packaged with analysis software, with open-source applications such as ImageJ and CellProfiler also used widely. For comprehensive reviews on high-content imaging in drug discovery, including live-cell and fluorescent Ca^{2+} imaging, see e.g. [197–200].

3.5.3 High-Throughput Electrophysiology Platforms

For assessment of ion channel function, in particular voltage-gated channels, electrophysiological assays remain the technique of choice as they assess the flux of ions across cell membranes in real time. However, these approaches are not only very low-throughput, but also require highly technically skilled operators and are thus generally limited to detailed characterisation of few compounds. A number of automated high-throughput electrophysiology platforms have been developed in recent years to overcome some of these limitations. These include the IonFlux 16, HT and Mercury (FluxIon Biosciences), IonWorks.

Barracuda Plus (Molecular Devices), IonWorks Quattro (Molecular Devices), PatchXpress 7000A (Molecular Devices), SyncroPatch (96 and 384/768 PE) (Nanion), Patchliner (Nanion), Port-a-Patch (Nanion), QPatch 8, 16 and HT (Sophion), QPatch II (Sophion), Qube (Sophion), Patch-Server (Multichannel Systems GmbH) as well as Robocyte2 for automated recording from oocytes (Multichannel Systems GmbH).

Most of these systems operate on the principle of planar patch-clamping, where cell membranes are patched though a small opening on a plate or chip which can be configured to achieve recordings from 4 to 384 cells in parallel. While the specific advantages and disadvantages of these systems are discussed in detail elsewhere [134, 201, 202], the arguably more physiologically relevant read-out of high-throughput electrophysiological assays is offset by the relatively greater purchasing and operating cost of these systems.

3.6 Technical Considerations

3.6.1 Design and Optimization of Fluorescence Assays

High-content and high-throughput fluorescence assays can be performed on cells either heterologously or endogenously expressing ion channels and GPCRs of interest [203]. While endogenously expressed targets may provide more physiologically relevant data owing to co-expression appropriate auxiliary subunits, there is usually little control over subtypes present or expression levels [203]. In contrast, heterologously expressed ion channels and GPCRs allow control of both subtype expression as well as selection of cells with appropriate target expression levels, and are thus often the favoured approach particularly for primary identification of novel lead compounds.

High-throughput fluorescence assays are generally possible with both adherent and suspension cell lines, though adherent cell lines tend to produce less addition artefacts. Suspension cell lines often require use of no-wash kits using extracellular quenchers, while this is optional for adherent cell lines. While commercial no-wash kits are considerably more expensive, they also require less time due to omission of washing steps and can improve assay performance particularly for poorly adherent cell lines. In addition, it is possible to use readily available dyes for in-house optimisation of no-wash protocols, which may be considerably cheaper than commercial kits which typically include quenchers of undisclosed composition.

The most important aspect of a successful high-content or high-throughput assays is the quality of cells. For adherent cell lines used in high-throughput applications, this optimally requires a 90–95% confluent monolayer of cells. As a rule of thumb, over-confluent cells tend to produce better assays than sub-confluent or patchy cells, although changes in cell morphology that occur as a result of confluency need to be considered. For example, some cancer cell lines differentiate when over-confluent, and receptor expression can also vary with cell confluency. In contrast, high-content assays ideally require well-defined "single" cells that grow evenly, do not clump and are not overly confluent. For both approaches, firmly adherent cells are desirable so no disruption of the cell layer occurs even with multiple washing or liquid addition steps. If cells can be even partially dislodged from their tissue culture flask by mechanical means, cell adhesion probably needs to be optimized for successful imaging assays.

Cell adherence can be improved by coating plates with poly-D-lysine (PDL), poly-L-lysine (PLL), collagen, Matrigel, laminin, poly-L-ornithine (PLO) or similar substances. Adhesion-promoting plates such as Cell^{BIND} (Corning) plates can also help, though improvement appears generally less dramatic than with coating. Typically, ideal plating conditions as well as coating substances and procedures need to be optimised according to specific cell, assay and research requirements. Generally, cells should be plated at least overnight, although cell viability and morphology is often improved with plating several days prior to the assay.

3.6.2 Agonists

In order to design successful fluorescence assays, cellular responses need to be elicited by addition of suitable agonists; the choice of agonist is often crucial to the success of the assay and will need to be determined carefully.

In the case of ligand-gated ion channels or GPCRs, these will generally consist of endogenous or exogenous ligands. For example, addition of nicotine or acetylcholine could be utilized to elicit Ca^{2+} responses mediated through nicotinic acetylcholine receptors (nAChR) [203]. Similarly, membrane depolarization can be induced through addition of KCl in order to activate voltage-gated Ca^{2+} channels, though in the case of N-type Ca_V ($Ca_v2.2$), addition of extracellular Ca^{2+} is required to elicit sufficiently robust responses [28]. It may also be necessary to co-express inward rectifier K^+ channels to adequately control membrane potential [204], or to include allosteric modulators to delay inactivation or enhance signalling, as is the case for α7 nAChR [203]. A more difficult application is high-throughput assays for voltage-gated Na^+ or K^+ channels; the former typically require use of allosteric modulators such as veratridine or deltamethrin which may skew the pharmacology of these channels in undesirable, or unexpected, ways.

3.6.3 Limitations

Fluorescence assays can be used for drug screening or the primary identification of novel drug leads, as well as for detailed pharmacological characterization of known or novel agonists and antagonists. However, while the most commonly used protocol involves addition of antagonists first, followed by addition of agonists, this setup can lead to ambiguous pharmacological profiles due to the kinetics of receptor/channel binding and the elicited fluorescence response. For example, the kinetics of Ca^{2+} responses measured using fluorescent approaches result from a combination of the binding rate constants of the Ca^{2+} dye, the binding kinetics of agonists and antagonists used, the rate of inactivation or desensitization of receptors and ion channels as well as extrusion and sequestration of Ca^{2+} by pumps such as PMCA or SERCA [205, 206]. This complex interplay may lead to functional profiles resembling irreversible rather than reversible agonism [207]. In addition, physical factors such as mixing of test compounds in the well – which in turn can be affected by fluid volume, addition speed, and the physicochemical properties of the compounds – may not only affect the kinetics but also the magnitude of the observed responses. While some of these difficulties are decreased by addition to, and measurement from, an entire multi-well plate simultaneously, it nonetheless is important to remember that fluorescent responses remain a surrogate measure of ion accumulation rather than ionic currents or receptor activation. In the case of membrane potential, Na^+ or K^+ responses, some of these issues are compounded by the unfavourable dye kinetics and, as discussed earlier, the need for non-physiological or allosteric agonists.

Nonetheless, response kinetics obtained using fluorescence imaging approaches can provide valuable information. For example, activation of IP3 receptors result in Ca^{2+} kinetics that are often quite distinct from those of voltage- or ligand ion channels. GPCR activation leads to relatively slow, concentration-dependent increases in intracellular Ca^{2+}, which peak approximately 5–20 s after ligand addition and return to baseline within ~ 100–180 s. In contrast, ion channels often display extremely rapid increases in Ca^{2+}, which, depending on the desensitization kinetics of the channel as well as the Ca^{2+} load, may or may not return to baseline (see e.g. Fig. 3.2). Thus, when using fluorescence imaging for pharmacological characterization of compounds, careful design and validation of individual assays is essential.

3.7 Future Directions

Development of the first fluorescence plate readers incorporating liquid handling robotics for the real-time measurement of intracellular Ca^{2+} concentrations began more than 20 years ago and has revolutionised screening of ion channel and GPCR drug targets. The long-standing industry-leader of these instruments – the FLIPR – was undoubtedly developed due to the availability of ever-improving fluorescent Ca^{2+} sensors, an area pioneered by the Nobel prize-winning Roger Tsien and colleagues [47]. While the miniaturisation and development of true high-throughput capacities of these platforms were driven predominantly by industry needs relating to high-throughput screening campaigns, these advances have also led to several advantages for mechanistic and pharmacological studies. These include for example the ability to obtain fluorescence reads from all wells in parallel, thus eliminating or at least considerably reducing assay errors arising from inconsistent dye loading or sequestration effects; as well as the ease with which large datasets can be collected. Thus, in conjunction with an ever-increasing repertoire of fluorescent indicators, optical capabilities and access to high-throughput platforms outside of large pharmaceutical companies, fluorescence assays are evolving to become invaluable tools addressing basic biological research questions. For example, using FLIPR-based fluorescence Ca^{2+} imaging, Regulator of G protein signalling 4 (RGS4) was found to negatively regulate muscarinic receptor 3 (M3R)-mediated Ca^{2+} signalling in pancreatic β-cells, leading to reduced glucose-stimulated insulin secretion, thus identifying novel mechanisms and drug targets for treatment of diabetes [208].

However, while high-throughput fluorescence assays are increasingly used as tools across many areas of research, these applications also highlight some of the limitations of these assays. Currently, most kinetic fluorescence plate reader assays are poorly suited to drug discovery or mechanistic studies of targets that are activated, or regulated, by temperature (in particular cool temperatures), mechanical stimuli, or membrane voltage. Nonetheless, high-throughput fluorescence assays remain an important and easily accessible methodology that is particularly powerful

when combined with complementary approaches such as single cell imaging, patch-clamp electrophysiology or multi-electrode arrays, as these techniques can inform on signalling events at the subcellular, channel and network excitability level, which cannot (yet) be captured by existing high-throughput fluorescence platforms. The utility and versatility of high-throughput fluorescence assays will undoubtedly continue to improve, particularly if instrumentation with routine capabilities for control of membrane voltage and temperature become available.

References

1. Santos R et al (2017) A comprehensive map of molecular drug targets. Nat Rev Drug Discov 16(1):19–34
2. Johnson I, Spence MTZ (eds) (2010) *Molecular probes handbook, a guide to fluorescent probes and labeling technologies*, 11th edn. Invitrogen, Carlsbad
3. Cardoso FC et al (2017) Modulatory features of the novel spider toxin mu-TRTX-Df1a isolated from the venom of the spider Davus fasciatus. Br J Pharmacol 174(15):2528–2544
4. Deuis JR et al (2016) Development of a muO-Conotoxin analogue with improved lipid membrane interactions and potency for the analgesic Sodium Channel NaV1.8. J Biol Chem 291(22):11829–11842
5. Deuis JR et al (2017) Pharmacological characterisation of the highly NaV1.7 selective spider venom peptide Pn3a. Sci Rep 7:40883
6. Jin AH et al (2015) delta-Conotoxin SuVIA suggests an evolutionary link between ancestral predator defence and the origin of fish-hunting behaviour in carnivorous cone snails. Proc Biol Sci 282(1811):pii: 20150817
7. Klint JK et al (2015) Seven novel modulators of the analgesic target NaV 1.7 uncovered using a high-throughput venom-based discovery approach. Br J Pharmacol 172(10):2445–2458
8. Vetter I et al (2012) Isolation, characterization and total regioselective synthesis of the novel muO-conotoxin MfVIA from Conus magnificus that targets voltage-gated sodium channels. Biochem Pharmacol 84(4):540–548
9. Vetter I et al (2012) Characterisation of Na(v) types endogenously expressed in human SH-SY5Y neuroblastoma cells. Biochem Pharmacol 83(11):1562–1571
10. Benjamin ER et al (2006) State-dependent compound inhibition of Nav1.2 sodium channels using the FLIPR Vm dye: on-target and off-target effects of diverse pharmacological agents. J Biomol Screen 11(1):29–39
11. Liu K et al (2010) High-throughput screening for Kv1.3 channel blockers using an improved FLIPR-based membrane-potential assay. J Biomol Screen 15(2):185–195
12. Trivedi S et al (2008) Cellular HTS assays for pharmacological characterization of Na(V)1.7 modulators. Assay Drug Dev Technol 6(2):167–179
13. Zhao F et al (2016) Development of a rapid throughput assay for identification of hNav1.7 antagonist using unique efficacious sodium channel agonist, antillatoxin. Mar Drugs 14(2):pii: E36
14. Clapham DE (2007) Calcium signaling. Cell 131(6):1047–1058
15. Berridge MJ, Lipp P, Bootman MD (2000) The versatility and universality of calcium signalling. Nat Rev Mol Cell Biol 1(1):11–21
16. Brini M, Carafoli E (2011) The plasma membrane Ca^{2+} ATPase and the plasma membrane sodium calcium exchanger cooperate in the regulation of cell calcium. Cold Spring Harb Perspect Biol 3(2):pii: a004168
17. Pathak T, Trebak M (2018) Mitochondrial Ca^{2+} signaling. Pharmacol Ther 192:112–123

18. Bygrave FL, Benedetti A (1996) What is the concentration of calcium ions in the endoplasmic reticulum? Cell Calcium 19(6):547–551
19. Berridge MJ (1993) Inositol trisphosphate and calcium signalling. Nature 361(6410):315–325
20. Liu AM et al (2003) Galpha(16/z) chimeras efficiently link a wide range of G protein-coupled receptors to calcium mobilization. J Biomol Screen 8(1):39–49
21. Zhu T, Fang LY, Xie X (2008) Development of a universal high-throughput calcium assay for G-protein- coupled receptors with promiscuous G-protein Galpha15/16. Acta Pharmacol Sin 29(4):507–516
22. Kostenis E, Waelbroeck M, Milligan G (2005) Techniques: promiscuous Galpha proteins in basic research and drug discovery. Trends Pharmacol Sci 26(11):595–602
23. Vasudevan NT (2017) cAMP assays in GPCR drug discovery. Methods Cell Biol 142:51–57
24. Jiang LI et al (2007) Use of a cAMP BRET sensor to characterize a novel regulation of cAMP by the sphingosine 1-phosphate/G13 pathway. J Biol Chem 282(14):10576–10584
25. Trehan A et al (2014) CANDLES, an assay for monitoring GPCR induced cAMP generation in cell cultures. Cell Commun Signal 12:70
26. Matthiesen K, Nielsen J (2011) Cyclic AMP control measured in two compartments in HEK293 cells: phosphodiesterase K(M) is more important than phosphodiesterase localization. PLoS One 6(9):e24392
27. Catterall WA (2000) Structure and regulation of voltage-gated Ca^{2+} channels. Annu Rev Cell Dev Biol 16:521–555
28. Benjamin ER et al (2006) Pharmacological characterization of recombinant N-type calcium channel (Cav2.2) mediated calcium mobilization using FLIPR. Biochem Pharmacol 72(6):770–782
29. Belardetti F et al (2009) A fluorescence-based high-throughput screening assay for the identification of T-type calcium channel blockers. Assay Drug Dev Technol 7(3):266–280
30. Monteith GR et al (2007) Calcium and cancer: targeting Ca^{2+} transport. Nat Rev Cancer 7(7):519–530
31. Duncan RS et al (2010) Control of intracellular calcium signaling as a neuroprotective strategy. Molecules 15(3):1168–1195
32. Talukder MA, Zweier JL, Periasamy M (2009) Targeting calcium transport in ischaemic heart disease. Cardiovasc Res 84(3):345–352
33. Suhail M (2010) Na, K-ATPase: Ubiquitous multifunctional transmembrane protein and its relevance to various pathophysiological conditions. J Clin Med Res 2(1):1–17
34. Davidson S et al (2014) Human sensory neurons: membrane properties and sensitization by inflammatory mediators. Pain 155(9):1861–1870
35. Catterall WA, Goldin AL, Waxman SG (2005) International Union of Pharmacology. XLVII. Nomenclature and structure-function relationships of voltage-gated sodium channels. Pharmacol Rev 57(4):397–409
36. Zhang XY et al (2018) Veratridine modifies the gating of human voltage-gated sodium channel Nav1.7. Acta Pharmacol Sin 39(11):1716–1724
37. Albuquerque EX et al (2009) Mammalian nicotinic acetylcholine receptors: from structure to function. Physiol Rev 89(1):73–120
38. Hanukoglu I, Hanukoglu A (2016) Epithelial sodium channel (ENaC) family: phylogeny, structure-function, tissue distribution, and associated inherited diseases. Gene 579(2):95–132
39. Kweon HJ, Suh BC (2013) Acid-sensing ion channels (ASICs): therapeutic targets for neurological diseases and their regulation. BMB Rep 46(6):295–304
40. Kuang Q, Purhonen P, Hebert H (2015) Structure of potassium channels. Cell Mol Life Sci 72(19):3677–3693
41. Grizel AV, Glukhov GS, Sokolova OS (2014) Mechanisms of activation of voltage-gated potassium channels. Acta Nat 6(4):10–26
42. Womack MD, Chevez C, Khodakhah K (2004) Calcium-activated potassium channels are selectively coupled to P/Q-type calcium channels in cerebellar Purkinje neurons. J Neurosci 24(40):8818–8822

43. Hibino H et al (2010) Inwardly rectifying potassium channels: their structure, function, and physiological roles. Physiol Rev 90(1):291–366
44. Feliciangeli S et al (2015) The family of K2P channels: salient structural and functional properties. J Physiol 593(12):2587–2603
45. Chiang EY et al (2017) Potassium channels Kv1.3 and KCa3.1 cooperatively and compensatorily regulate antigen-specific memory T cell functions. Nat Commun 8:14644
46. Otten PA, London RE, Levy LA (2001) A new approach to the synthesis of APTRA indicators. Bioconjug Chem 12(1):76–83
47. Minta A, Kao JP, Tsien RY (1989) Fluorescent indicators for cytosolic calcium based on rhodamine and fluorescein chromophores. J Biol Chem 264(14):8171–8178
48. Gee KR et al (2000) Chemical and physiological characterization of fluo-4 Ca^{2+}-indicator dyes. Cell Calcium 27(2):97–106
49. Tsien RY (1980) New calcium indicators and buffers with high selectivity against magnesium and protons: design, synthesis, and properties of prototype structures. Biochemistry 19(11):2396–2404
50. Grynkiewicz G, Poenie M, Tsien RY (1985) A new generation of Ca^{2+} indicators with greatly improved fluorescence properties. J Biol Chem 260(6):3440–3450
51. Whitaker M (2010) Genetically encoded probes for measurement of intracellular calcium. Methods Cell Biol 99:153–182
52. Kao JP, Tsien RY (1988) Ca^{2+} binding kinetics of fura-2 and azo-1 from temperature-jump relaxation measurements. Biophys J 53(4):635–639
53. Naraghi M (1997) T-jump study of calcium binding kinetics of calcium chelators. Cell Calcium 22(4):255–268
54. Wokosin DL, Loughrey CM, Smith GL (2004) Characterization of a range of fura dyes with two-photon excitation. Biophys J 86(3):1726–1738
55. Vorndran C, Minta A, Poenie M (1995) New fluorescent calcium indicators designed for cytosolic retention or measuring calcium near membranes. Biophys J 69(5):2112–2124
56. Etter EF et al (1996) Near-membrane [Ca^{2+}] transients resolved using the Ca^{2+} indicator FFP18. Proc Natl Acad Sci U S A 93(11):5368–5373
57. Kurebayashi N, Harkins AB, Baylor SM (1993) Use of fura red as an intracellular calcium indicator in frog skeletal muscle fibers. Biophys J 64(6):1934–1960
58. Lattanzio FA Jr (1990) The effects of pH and temperature on fluorescent calcium indicators as determined with Chelex-100 and EDTA buffer systems. Biochem Biophys Res Commun 171(1):102–108
59. Westerblad H, Allen DG (1996) Intracellular calibration of the calcium indicator indo-1 in isolated fibers of Xenopus muscle. Biophys J 71(2):908–917
60. Launikonis BS et al (2005) Confocal imaging of [Ca^{2+}] in cellular organelles by SEER, shifted excitation and emission ratioing of fluorescence. J Physiol 567(Pt 2):523–543
61. Eberhard M, Erne P (1989) Kinetics of calcium binding to fluo-3 determined by stopped-flow fluorescence. Biochem Biophys Res Commun 163(1):309–314
62. Goldberg JH et al (2003) Calcium microdomains in aspiny dendrites. Neuron 40(4):807–821
63. Hollingworth S, Gee KR, Baylor SM (2009) Low-affinity Ca^{2+} indicators compared in measurements of skeletal muscle Ca^{2+} transients. Biophys J 97(7):1864–1872
64. Scott R, Rusakov DA (2006) Main determinants of presynaptic Ca^{2+} dynamics at individual mossy fiber-CA3 pyramidal cell synapses. J Neurosci 26(26):7071–7081
65. Woodruff ML et al (2002) Measurement of cytoplasmic calcium concentration in the rods of wild-type and transducin knock-out mice. J Physiol 542(Pt 3):843–854
66. Falk S, Rekling JC (2009) Neurons in the preBotzinger complex and VRG are located in proximity to arterioles in newborn mice. Neurosci Lett 450(3):229–234
67. Eberhard M, Erne P (1991) Calcium binding to fluorescent calcium indicators: calcium green, calcium orange and calcium crimson. Biochem Biophys Res Commun 180(1):209–215
68. Stout AK, Reynolds IJ (1999) High-affinity calcium indicators underestimate increases in intracellular calcium concentrations associated with excitotoxic glutamate stimulations. Neuroscience 89(1):91–100

69. Rajdev S, Reynolds IJ (1993) Calcium green-5N, a novel fluorescent probe for monitoring high intracellular free Ca^{2+} concentrations associated with glutamate excitotoxicity in cultured rat brain neurons. Neurosci Lett 162(1–2):149–152
70. Eilers J et al (1995) Calcium signaling in a narrow somatic submembrane shell during synaptic activity in cerebellar Purkinje neurons. Proc Natl Acad Sci U S A 92(22):10272–10276
71. Agronskaia AV, Tertoolen L, Gerritsen HC (2004) Fast fluorescence lifetime imaging of calcium in living cells. J Biomed Opt 9(6):1230–1237
72. Gaillard S et al (2007) Synthesis and characterization of a new red-emitting Ca^{2+} indicator, calcium ruby. Org Lett 9(14):2629–2632
73. Teflabs (2011) Fluorescent ion indicator handbook, vol 1–44. Texas Teflabs, Austin
74. Sguilla FS, Tedesco AC, Bendhack LM (2003) A membrane potential-sensitive dye for vascular smooth muscle cells assays. Biochem Biophys Res Commun 301(1):113–118
75. Brauner T, Hulser DF, Strasser RJ (1984) Comparative measurements of membrane potentials with microelectrodes and voltage-sensitive dyes. Biochim Biophys Acta 771(2):208–216
76. Baxter DF et al (2002) A novel membrane potential-sensitive fluorescent dye improves cell-based assays for ion channels. J Biomol Screen 7(1):79–85
77. Adams DS, Levin M (2012) Measuring resting membrane potential using the fluorescent voltage reporters DiBAC4(3) and CC2-DMPE. Cold Spring Harb Protoc 2012(4):459–464
78. Meuwis K et al (1995) Photophysics of the fluorescent K^+ indicator PBFI. Biophys J 68(6):2469–2473
79. Thomas D et al (2000) A comparison of fluorescent Ca^{2+} indicator properties and their use in measuring elementary and global Ca^{2+} signals. Cell Calcium 28(4):213–223
80. Paredes RM et al (2008) Chemical calcium indicators. Methods 46(3):143–151
81. Yasuda R et al (2004) *Imaging calcium concentration dynamics in small neuronal compartments*. Sci STKE 2004(219):pl5
82. Oliver AE et al (2000) Effects of temperature on calcium-sensitive fluorescent probes. Biophys J 78(4):2116–2126
83. O'Malley DM, Burbach BJ, Adams PR (1999) Fluorescent calcium indicators: subcellular behavior and use in confocal imaging. Methods Mol Biol 122:261–303
84. Poenie M (1990) Alteration of intracellular Fura-2 fluorescence by viscosity: a simple correction. Cell Calcium 11(2–3):85–91
85. Dustin LB (2000) Ratiometric analysis of calcium mobilization. Clin Appl Immunol Rev 1(1):5–15
86. Hesketh TR et al (1983) Duration of the calcium signal in the mitogenic stimulation of thymocytes. Biochem J 214(2):575–579
87. O'Connor N, Silver RB (2007) Ratio imaging: practical considerations for measuring intracellular Ca^{2+} and pH in living cells. Methods Cell Biol 81:415–433
88. Becker PL, Fay FS (1987) Photobleaching of fura-2 and its effect on determination of calcium concentrations. Am J Phys 253(4 Pt 1):C613–C618
89. Scheenen WJ et al (1996) Photodegradation of indo-1 and its effect on apparent Ca^{2+} concentrations. Chem Biol 3(9):765–774
90. Wahl M, Lucherini MJ, Gruenstein E (1990) Intracellular Ca^{2+} measurement with Indo-1 in substrate-attached cells: advantages and special considerations. Cell Calcium 11(7):487–500
91. Floto RA et al (1995) IgG-induced Ca^{2+} oscillations in differentiated U937 cells; a study using laser scanning confocal microscopy and co-loaded fluo-3 and fura-red fluorescent probes. Cell Calcium 18(5):377–389
92. Lipp P, Niggli E (1993) Ratiometric confocal Ca^{2+}-measurements with visible wavelength indicators in isolated cardiac myocytes. Cell Calcium 14(5):359–372
93. Schild D, Jung A, Schultens HA (1994) Localization of calcium entry through calcium channels in olfactory receptor neurones using a laser scanning microscope and the calcium indicator dyes Fluo-3 and Fura-red. Cell Calcium 15(5):341–348
94. Lohr C (2003) Monitoring neuronal calcium signalling using a new method for ratiometric confocal calcium imaging. Cell Calcium 34(3):295–303

95. Martinez-Zaguilan R, Parnami J, Martinez GM (1998) Mag-Fura-2 (Furaptra) exhibits both low (microM) and high (nM) affinity for Ca^{2+}. Cell Physiol Biochem 8(3):158–174
96. Zhao M, Hollingworth S, Baylor SM (1996) Properties of tri- and tetracarboxylate Ca^{2+} indicators in frog skeletal muscle fibers. Biophys J 70(2):896–916
97. Hofer AM (2005) Measurement of free [Ca^{2+}] changes in agonist-sensitive internal stores using compartmentalized fluorescent indicators. Methods Mol Biol 312:229–247
98. Claflin DR et al (1994) The intracellular Ca^{2+} transient and tension in frog skeletal muscle fibres measured with high temporal resolution. J Physiol 475(2):319–325
99. Konishi M et al (1991) Myoplasmic calcium transients in intact frog skeletal muscle fibers monitored with the fluorescent indicator furaptra. J Gen Physiol 97(2):271–301
100. Berlin JR, Konishi M (1993) Ca^{2+} transients in cardiac myocytes measured with high and low affinity Ca^{2+} indicators. Biophys J 65(4):1632–1647
101. MacFarlane AWt, Oesterling JF, Campbell KS (2010) Measuring intracellular calcium signaling in murine NK cells by flow cytometry. Methods Mol Biol 612:149–157
102. Takahashi A et al (1999) Measurement of intracellular calcium. Physiol Rev 79(4):1089–1125
103. Overholt JL et al (2000) HERG-like potassium current regulates the resting membrane potential in glomus cells of the rabbit carotid body. J Neurophysiol 83(3):1150–1157
104. Smith SJ, Augustine GJ (1988) Calcium ions, active zones and synaptic transmitter release. Trends Neurosci 11(10):458–464
105. Lee S, Lee HG, Kang SH (2009) Real-time observations of intracellular Mg2+ signaling and waves in a single living ventricular myocyte cell. Anal Chem 81(2):538–542
106. Shmigol AV, Eisner DA, Wray S (2001) Simultaneous measurements of changes in sarcoplasmic reticulum and cytosolic. J Physiol 531(Pt 3):707–713
107. Bioquest A (2011) Quest fluo-8™ calcium reagents and screen quest™ Fluo-8 NW calcium assay kits. [cited 2011]
108. Gerencser AA, Adam-Vizi V (2005) Mitochondrial Ca^{2+} dynamics reveals limited intramitochondrial Ca^{2+} diffusion. Biophys J 88(1):698–714
109. Tao J, Haynes DH (1992) Actions of thapsigargin on the Ca^{2+}-handling systems of the human platelet. Incomplete inhibition of the dense tubular Ca^{2+} uptake, partial inhibition of the Ca^{2+} extrusion pump, increase in plasma membrane Ca^{2+} permeability, and consequent elevation of resting cytoplasmic Ca^{2+}. J Biol Chem 267(35):24972–24982
110. Trollinger DR, Cascio WE, Lemasters JJ (1997) Selective loading of Rhod 2 into mitochondria shows mitochondrial Ca^{2+} transients during the contractile cycle in adult rabbit cardiac myocytes. Biochem Biophys Res Commun 236(3):738–742
111. Davidson SM, Yellon D, Duchen MR (2007) Assessing mitochondrial potential, calcium, and redox state in isolated mammalian cells using confocal microscopy. Methods Mol Biol 372:421–430
112. Gerencser AA, Adam-Vizi V (2001) Selective, high-resolution fluorescence imaging of mitochondrial Ca^{2+} concentration. Cell Calcium 30(5):311–321
113. Pologruto TA, Yasuda R, Svoboda K (2004) Monitoring neural activity and [Ca^{2+}] with genetically encoded Ca^{2+} indicators. J Neurosci 24(43):9572–9579
114. David G, Talbot J, Barrett EF (2003) Quantitative estimate of mitochondrial [Ca^{2+}] in stimulated motor nerve terminals. Cell Calcium 33(3):197–206
115. Simpson AW (2006) Fluorescent measurement of [Ca^{2+}]c: basic practical considerations. Methods Mol Biol 312:3–36
116. Palmer AE et al (2004) Bcl-2-mediated alterations in endoplasmic reticulum Ca^{2+} analyzed with an improved genetically encoded fluorescent sensor. Proc Natl Acad Sci U S A 101(50):17404–17409
117. McCombs JE, Gibson EA, Palmer AE (2010) Using a genetically targeted sensor to investigate the role of presenilin-1 in ER Ca^{2+} levels and dynamics. Mol BioSyst 6(9): 1640–1649

118. Kuchibhotla KV et al (2008) Abeta plaques lead to aberrant regulation of calcium homeostasis in vivo resulting in structural and functional disruption of neuronal networks. Neuron 59(2):214–225
119. Perry JL et al (2015) Use of genetically-encoded calcium indicators for live cell calcium imaging and localization in virus-infected cells. Methods 90:28–38
120. Ouzounov DG et al (2017) In vivo three-photon imaging of activity of GCaMP6-labeled neurons deep in intact mouse brain. Nat Methods 14(4):388–390
121. Chen TW et al (2013) Ultrasensitive fluorescent proteins for imaging neuronal activity. Nature 499(7458):295–300
122. Cichon J, Gan WB (2015) Branch-specific dendritic Ca^{2+} spikes cause persistent synaptic plasticity. Nature 520(7546):180–185
123. Sheffield ME, Dombeck DA (2015) Calcium transient prevalence across the dendritic arbour predicts place field properties. Nature 517(7533):200–204
124. Sun W et al (2016) Thalamus provides layer 4 of primary visual cortex with orientation- and direction-tuned inputs. Nat Neurosci 19(2):308–315
125. Falkner S et al (2016) Transplanted embryonic neurons integrate into adult neocortical circuits. Nature 539(7628):248–253
126. Lee KS, Huang X, Fitzpatrick D (2016) Topology of ON and OFF inputs in visual cortex enables an invariant columnar architecture. Nature 533(7601):90–94
127. Bassett JJ, Monteith GR (2017) Genetically encoded calcium indicators as probes to assess the role of calcium channels in disease and for high-throughput drug discovery. Adv Pharmacol 79:141–171
128. Sadakane O et al (2015) Long-term two-photon calcium imaging of neuronal populations with subcellular resolution in adult non-human primates. Cell Rep 13(9):1989–1999
129. Suzuki J, Kanemaru K, Iino M (2016) Genetically encoded fluorescent indicators for Organellar calcium imaging. Biophys J 111(6):1119–1131
130. Tian L, Hires SA, Looger LL (2012) Imaging neuronal activity with genetically encoded calcium indicators. Cold Spring Harb Protoc 2012(6):647–656
131. Schreiner AE, Rose CR (2012) Quantitative imaging of intracellular sodium. In: Mendez-Vilas A (ed) Current microscopy contributions to advances in science and technology. Formatex Research Center, Badajoz, pp 119–129
132. O'Donnell GT et al (2011) *Evaluation of the sodium sensing dye asante natrium green 2 in a voltage-gated sodium channel assay in 1536-well format*. Merck & Co., Inc., Whitehouse Station
133. Antonia B et al (2016) *Overcoming historical challenges of Nav1.9 voltage gated sodium channel as a drug discovery target for treatment of pain*. Icagen, Durham
134. Priest BT et al (2004) Automated electrophysiology assays. In: Sittampalam GS et al (eds) Assay guidance manual. Eli Lilly & Company and the National Center for Advancing Translational Sciences, Bethesda
135. Sims PJ et al (1974) Studies on the mechanism by which cyanine dyes measure membrane potential in red blood cells and phosphatidylcholine vesicles. Biochemistry 13(16):3315–3330
136. Bashford CL, Chance B, Prince RC (1979) Oxonol dyes as monitors of membrane potential. Their behavior in photosynthetic bacteria. Biochim Biophys Acta 545(1):46–57
137. Rottenberg H, Wu S (1998) Quantitative assay by flow cytometry of the mitochondrial membrane potential in intact cells. Biochim Biophys Acta 1404(3):393–404
138. Huang SG (2002) Development of a high throughput screening assay for mitochondrial membrane potential in living cells. J Biomol Screen 7(4):383–389
139. Wolff C, Fuks B, Chatelain P (2003) Comparative study of membrane potential-sensitive fluorescent probes and their use in ion channel screening assays. J Biomol Screen 8(5):533–543
140. Gonzalez JE, Maher MP (2002) Cellular fluorescent indicators and voltage/ion probe reader (VIPR) tools for ion channel and receptor drug discovery. Receptors Channels 8(5–6):283–295

141. Dunlop J et al (2008) Ion channel screening. Comb Chem High Throughput Screen 11(7):514–522
142. Woodford CR et al (2015) Improved PeT molecules for optically sensing voltage in neurons. J Am Chem Soc 137(5):1817–1824
143. Siegel MS, Isacoff EY (1997) A genetically encoded optical probe of membrane voltage. Neuron 19(4):735–741
144. Ataka K, Pieribone VA (2002) A genetically targetable fluorescent probe of channel gating with rapid kinetics. Biophys J 82(1 Pt 1):509–516
145. Dimitrov D et al (2007) Engineering and characterization of an enhanced fluorescent protein voltage sensor. PLoS One 2(5):e440
146. Murata Y et al (2005) Phosphoinositide phosphatase activity coupled to an intrinsic voltage sensor. Nature 435(7046):1239–1243
147. Kang BE, Baker BJ (2016) Pado, a fluorescent protein with proton channel activity can optically monitor membrane potential, intracellular pH, and map gap junctions. Sci Rep 6:23865
148. Kralj JM et al (2011) Optical recording of action potentials in mammalian neurons using a microbial rhodopsin. Nat Methods 9(1):90–95
149. Maclaurin D et al (2013) Mechanism of voltage-sensitive fluorescence in a microbial rhodopsin. Proc Natl Acad Sci U S A 110(15):5939–5944
150. Mutoh H, Akemann W, Knopfel T (2012) Genetically engineered fluorescent voltage reporters. ACS Chem Neurosci 3(8):585–592
151. St-Pierre F, Chavarha M, Lin MZ (2015) Designs and sensing mechanisms of genetically encoded fluorescent voltage indicators. Curr Opin Chem Biol 27:31–38
152. Xu Y, Zou P, Cohen AE (2017) Voltage imaging with genetically encoded indicators. Curr Opin Chem Biol 39:1–10
153. Yang HH, St-Pierre F (2016) Genetically encoded voltage indicators: opportunities and challenges. J Neurosci 36(39):9977–9989
154. Whiteaker KL et al (2001) Validation of FLIPR membrane potential dye for high throughput screening of potassium channel modulators. J Biomol Screen 6(5):305–312
155. Muller W, Windisch H, Tritthart HA (1986) Fluorescent styryl dyes applied as fast optical probes of cardiac action potential. Eur Biophys J 14(2):103–111
156. Loew LM et al (1992) A naphthyl analog of the aminostyryl pyridinium class of potentiometric membrane dyes shows consistent sensitivity in a variety of tissue, cell, and model membrane preparations. J Membr Biol 130(1):1–10
157. Fluhler E, Burnham VG, Loew LM (1985) Spectra, membrane binding, and potentiometric responses of new charge shift probes. Biochemistry 24(21):5749–5755
158. Gross D, Loew LM (1989) Fluorescent indicators of membrane potential: microspectrofluorometry and imaging. Methods Cell Biol 30:193–218
159. Canepari M et al (2010) Imaging inhibitory synaptic potentials using voltage sensitive dyes. Biophys J 98(9):2032–2040
160. Waggoner AS (1979) Dye indicators of membrane potential. Annu Rev Biophys Bioeng 8:47–68
161. Picaud S, Wunderer HJ, Franceschini N (1988) 'Photo-degeneration' of neurones after extracellular dye application. Neurosci Lett 95(1–3):24–30
162. Yamada A et al (2001) Usefulness and limitation of DiBAC4(3), a voltage-sensitive fluorescent dye, for the measurement of membrane potentials regulated by recombinant large conductance Ca^{2+}−activated K^+ channels in HEK293 cells. Jpn J Pharmacol 86(3):342–350
163. Joesch C et al (2008) Use of FLIPR membrane potential dyes for validation of high-throughput screening with the FLIPR and microARCS technologies: identification of ion channel modulators acting on the GABA(A) receptor. J Biomol Screen 13(3):218–228
164. Molinski SV et al (2015) Facilitating structure-function studies of CFTR modulator sites with efficiencies in mutagenesis and functional screening. J Biomol Screen 20(10):1204–1217
165. Maher MP, Wu NT, Ao H (2007) pH-Insensitive FRET voltage dyes. J Biomol Screen 12(5):656–667

166. Bradley J et al (2009) Submillisecond optical reporting of membrane potential in situ using a neuronal tracer dye. J Neurosci 29(29):9197–9209
167. Fink AE et al (2012) Two-photon compatibility and single-voxel, single-trial detection of subthreshold neuronal activity by a two-component optical voltage sensor. PLoS One 7(8):e41434
168. Miller EW et al (2012) Optically monitoring voltage in neurons by photo-induced electron transfer through molecular wires. Proc Natl Acad Sci U S A 109(6):2114–2119
169. Bedut S et al (2016) High-throughput drug profiling with voltage- and calcium-sensitive fluorescent probes in human iPSC-derived cardiomyocytes. Am J Physiol Heart Circ Physiol 311(1):H44–H53
170. Huang YL, Walker AS, Miller EW (2015) A Photostable silicon rhodamine platform for optical voltage sensing. J Am Chem Soc 137(33):10767–10776
171. Weaver CD et al (2004) A thallium-sensitive, fluorescence-based assay for detecting and characterizing potassium channel modulators in mammalian cells. J Biomol Screen 9(8):671–677
172. Rimmele TS, Chatton JY (2014) A novel optical intracellular imaging approach for potassium dynamics in astrocytes. PLoS One 9(10):e109243
173. Terstappen GC (2004) Nonradioactive rubidium ion efflux assay and its applications in drug discovery and development. Assay Drug Dev Technol 2(5):553–559
174. Roe MW, Lemasters JJ, Herman B (1990) Assessment of Fura-2 for measurements of cytosolic free calcium. Cell Calcium 11(2–3):63–73
175. Tsien RY (1981) A non-disruptive technique for loading calcium buffers and indicators into cells. Nature 290(5806):527–528
176. Williams DA, Bowser DN, Petrou S (1999) Confocal Ca^{2+} imaging of organelles, cells, tissues, and organs. Methods Enzymol 307:441–469
177. Johnson I (1998) Fluorescent probes for living cells. Histochem J 30(3):123–140
178. Cronshaw DG et al (2006) Evidence that phospholipase-C-dependent, calcium-independent mechanisms are required for directional migration of T-lymphocytes in response to the CCR4 ligands CCL17 and CCL22. J Leukoc Biol 79(6):1369–1380
179. Mehlin C, Crittenden C, Andreyka J (2003) No-wash dyes for calcium flux measurement. BioTechniques 34(1):164–166
180. Di Virgilio F, Steinberg TH, Silverstein SC (1990) Inhibition of Fura-2 sequestration and secretion with organic anion transport blockers. Cell Calcium 11(2–3):57–62
181. Vetter I et al (2008) Rapid, opioid-sensitive mechanisms involved in transient receptor potential vanilloid 1 sensitization. J Biol Chem 283(28):19540–19550
182. Kabbara AA, Allen DG (2001) The use of the indicator fluo-5N to measure sarcoplasmic reticulum calcium in single muscle fibres of the cane toad. J Physiol 534(Pt 1):87–97
183. Rehberg M et al (2008) A new non-disruptive strategy to target calcium indicator dyes to the endoplasmic reticulum. Cell Calcium 44(4):386–399
184. Solovyova N, Verkhratsky A (2002) Monitoring of free calcium in the neuronal endoplasmic reticulum: an overview of modern approaches. J Neurosci Methods 122(1):1–12
185. Oakes SG et al (1988) Incomplete hydrolysis of the calcium indicator precursor fura-2 pentaacetoxymethyl ester (fura-2 AM) by cells. Anal Biochem 169(1):159–166
186. Gillis JM, Gailly P (1994) Measurements of $[Ca^{2+}]$i with the diffusible Fura-2 AM: can some potential pitfalls be evaluated? Biophys J 67(1):476–477
187. Jobsis PD, Rothstein EC, Balaban RS (2007) Limited utility of acetoxymethyl (AM)-based intracellular delivery systems, in vivo: interference by extracellular esterases. J Microsc 226(Pt 1):74–81
188. Azimi I et al (2017) Evaluation of known and novel inhibitors of Orai1-mediated store operated Ca^{2+} entry in MDA-MB-231 breast cancer cells using a fluorescence imaging plate reader assay. Bioorg Med Chem 25(1):440–449
189. Buchser W et al (2004) *Assay development guidelines for image-based high content screening, high content analysis and high content imaging*. In: Sittampalam GS et al (eds) Assay guidance manual. Eli Lilly & Company and the National Center for Advancing Translational Sciences, Bethesda

190. Teichert RW et al (2012) Characterization of two neuronal subclasses through constellation pharmacology. Proc Natl Acad Sci U S A 109(31):12758–12763
191. Teichert RW et al (2012) Functional profiling of neurons through cellular neuropharmacology. Proc Natl Acad Sci U S A 109(5):1388–1395
192. Siemens J et al (2006) Spider toxins activate the capsaicin receptor to produce inflammatory pain. Nature 444(7116):208–212
193. Imperial JS et al (2014) A family of excitatory peptide toxins from venomous crassispirine snails: using Constellation Pharmacology to assess bioactivity. Toxicon 89:45–54
194. Robinson SD et al (2015) Discovery by proteogenomics and characterization of an RF-amide neuropeptide from cone snail venom. J Proteome 114:38–47
195. Vetter I et al (2012) Ciguatoxins activate specific cold pain pathways to elicit burning pain from cooling. EMBO J 31(19):3795–3808
196. Bassett JJ et al (2018) Assessment of cytosolic free calcium changes during ceramide-induced cell death in MDA-MB-231 breast cancer cells expressing the calcium sensor GCaMP6m. Cell Calcium 72:39–50
197. Harrill JA (2018) Human-derived neurons and neural progenitor cells in high content imaging applications. Methods Mol Biol 1683:305–338
198. Esner M, Meyenhofer F, Bickle M (2018) Live-cell high content screening in drug development. Methods Mol Biol 1683:149–164
199. Adams CL, Sjaastad MD (2009) Design and implementation of high-content imaging platforms: lessons learned from end user-developer collaboration. Comb Chem High Throughput Screen 12(9):877–887
200. Shumate C, Hoffman AF (2009) Instrumental considerations in high content screening. Comb Chem High Throughput Screen 12(9):888–898
201. McManus OB (2014) HTS assays for developing the molecular pharmacology of ion channels. Curr Opin Pharmacol 15:91–96
202. Picones A et al (2016) Contribution of automated technologies to ion channel drug discovery. Adv Protein Chem Struct Biol 104:357–378
203. Gleeson EC et al (2015) Inhibition of N-type calcium channels by fluorophenoxyanilide derivatives. Mar Drugs 13(4):2030–2045
204. Dai G et al (2008) A high-throughput assay for evaluating state dependence and subtype selectivity of Cav2 calcium channel inhibitors. Assay Drug Dev Technol 6(2):195–212
205. Redondo PC et al (2005) Collaborative effect of SERCA and PMCA in cytosolic calcium homeostasis in human platelets. J Physiol Biochem 61(4):507–516
206. Brini M et al (2000) Effects of PMCA and SERCA pump overexpression on the kinetics of cell Ca^{2+} signalling. EMBO J 19(18):4926–4935
207. Vetter I (2012) Development and optimization of FLIPR high throughput calcium assays for ion channels and GPCRs. Adv Exp Med Biol 740:45–82
208. Ruiz de Azua I et al (2010) RGS4 is a negative regulator of insulin release from pancreatic beta-cells in vitro and in vivo. Proc Natl Acad Sci U S A 107(17):7999–8004
209. Vetter I et al (2006) The mu opioid agonist morphine modulates potentiation of capsaicin-evoked TRPV1 responses through a cyclic AMP-dependent protein kinase A pathway. Mol Pain 2:22
210. Vetter I et al (2008) Mechanisms involved in potentiation of transient receptor potential vanilloid 1 responses by ethanol. Eur J Pain 12(4):441–454
211. Samuel D, Robinson SD et al (2018) A comprehensive portrait of the venom of the giant red bull ant Myrmecia gulosa reveals a hyperdiverse hymenopteran toxin gene family. Sci Adv 4:eaau4640

Chapter 4
Imaging Native Calcium Currents in Brain Slices

Karima Ait Ouares, Nadia Jaafari, Nicola Kuczewski, and Marco Canepari

Abstract Imaging techniques may overcome the limitations of electrode techniques to measure locally not only membrane potential changes, but also ionic currents. Here, we review a recently developed approach to image native neuronal Ca^{2+} currents from brain slices. The technique is based on combined fluorescence recordings using low-affinity Ca^{2+} indicators possibly in combination with voltage sensitive dyes. We illustrate how the kinetics of a Ca^{2+} current can be estimated from the Ca^{2+} fluorescence change and locally correlated with the change of membrane potential, calibrated on an absolute scale, from the voltage fluorescence change. We show some representative measurements from the dendrites of CA1 hippocampal pyramidal neurons, from olfactory bulb mitral cells and from cerebellar Purkinje neurons. We discuss the striking difference in data analysis and interpretation between Ca^{2+} current measurements obtained using classical electrode techniques and the physiological currents obtained using this novel approach. Finally, we show how important is the kinetic information on the native Ca^{2+} current to explore the potential molecular targets of the Ca^{2+} flux from each individual Ca^{2+} channel.

K. Ait Ouares · N. Jaafari
Univ. Grenoble Alpes, CNRS, LIPhy, Grenoble, France

Laboratories of Excellence, Ion Channel Science and Therapeutics, France

N. Kuczewski
Centre de Recherche en Neurosciences de Lyon, INSERM U1028/CNRS UMR5292, Université Lyon1, Lyon, France

M. Canepari (✉)
Univ. Grenoble Alpes, CNRS, LIPhy, Grenoble, France

Laboratories of Excellence, Ion Channel Science and Therapeutics, France

Institut National de la Santé et Recherche Médicale (INSERM), Paris, France

Laboratoire Interdisciplinaire de Physique (UMR 5588), St Martin d'Hères cedex, France
e-mail: marco.canepari@univ-grenoble-alpes.fr

M. S. Islam (ed.), *Calcium Signaling*, Advances in Experimental Medicine and Biology 1131, https://doi.org/10.1007/978-3-030-12457-1_4

Keywords Calcium currents · Calcium imaging · Voltage sensitive dyes imaging · CA1 hippocampal pyramidal neuron · Olfactory bulb mitral cell · Purkinje neuron · Brain slices · Action potential · Synaptic potential · Biophysical modeling

4.1 Introduction

Optical measurements have been historically designed to monitor the electrical activity of the nervous system, a task where the use of electrode techniques has clear limitations [1]. In the last two decades, the development of new organic voltage sensitive dyes (VSD), in parallel with the progress of devices to excite and detect fluorescence [2], allowed optical recordings of sub-cellular membrane potential (V_m) changes <1 mV with a signal-to-noise ratio (S/N) comparable to that of patch clamp recordings [3]. This achievement suggested that voltage imaging can be used to investigate voltage-dependent proteins, in particular voltage-gated ion channels, in their physiological environment. The principal function of an ion channel is to allow an ion flux through a membrane, i.e. to produce an ionic current. Thus, the study of the biophysics of ion channels is routinely performed by measurements of ionic currents in single-electrode or two-electrode voltage clamp [4]. A way to investigate the biophysics of isolated native ion channels is to perform excised patches from ex-vivo membranes [5]. Alternatively, ion channels can be expressed in foreign cells such as oocytes or mammalian cell lines [6] and studied by using patch clamp techniques [7]. Yet, the physiological role and function of voltage-gated ion channels must be investigated in their natural environment, i.e. in their native cellular compartment and during physiological changes of V_m. To this purpose, the voltage clamp electrode approach has serious limitations for several reasons. First, the ionic current is measured by maintaining the cell at a given artificial V_m and even if the cell is dynamically clamped the V_m change is never a physiological signal [8]. Second, the current measured with the electrode is the summation of the filtered currents from all different cellular regions, including remote regions where V_m is unclamped, and no information is available on the site of origin of the current [9]. Third, different ionic currents contribute to the physiological change of V_m producing a functional coupling among the different ion channels [10]. Thus, a single native ionic current must be pharmacologically isolated from the total current mediated by the other channels, but the block of these channels will make the V_m change non-physiological.

In the last few years, we designed a novel approach to measure physiological Ca^{2+} currents from neurons in brain slices [11]. The method is based on fast Ca^{2+} optical measurements using low-affinity indicators that can be combined with sequential [12] or simultaneous [13] V_m optical recordings. The latter measurements can be calibrated in mV [14] using cell-specific protocols. Individual cells are loaded with Ca^{2+} and V_m indicators using a patch clamp recording. In contrast to voltage-clamp current measurements, the current approach permits independent

recordings of the V_m change and of the Ca^{2+} influx, i.e. the study of voltage gating during physiological V_m changes. Since the Ca^{2+} current is reconstructed by the measurement of Ca^{2+} locally binding to an indicator, this approach provides information on channels in different areas of the cell with a spatial resolution as good as the optical recording allows. Finally, the Ca^{2+} current is recorded without blocking all Na^+ and K^+ channels that are necessary to produce the physiological V_m change. The principle of obtaining an optical measurement of a fast Ca^{2+} current is based on the analysis of the dye-Ca^{2+} binding reaction in a cell, a scenario initially studied by Kao and Tsien [15]. According to their theoretical estimates and to our recent empirical measurements [16], the relaxation time of the dye-Ca^{2+} binding reaction is less than 200 μs for low-affinity indicators with equilibrium constant (K_D) ≥ 10 μM such as Oregon Green BAPTA-5N (OG5N, K_D = 35 μM, [17]) or Fura-FF (K_D = 10 μM, [18]). Therefore, a fast Ca^{2+} current with duration of a few milliseconds can be reliably tracked by low-affinity indicators if fluorescence is acquired at sufficiently high speed. The goal of this methodological article is to provide an exhaustive tool for those scientists aiming at performing this type of measurement. The next section addresses in detail the problem of extracting the Ca^{2+} current kinetics from Ca^{2+} fluorescence measurements under different cellular buffering conditions. The following section is devoted to the technical aspects of how to set up combined V_m and Ca^{2+} optical measurements and to calibrate V_m signals on an absolute scale. We then illustrate some examples of combined V_m and Ca^{2+} current measurements and we finally discuss how to correctly interpret the results and how to use this information to significantly advance our knowledge on Ca^{2+} channels function. All data shown here were from experiments performed at the Laboratoire Interdisciplinaire de Physique and approved by the Isere prefecture (Authorisation n. 38 12 01). These experiments were performed at 32–34 °C using brain slices from 21 to 40 postnatal days old C57Bl6 mice of both genders.

4.2 Extracting Ca^{2+} Current Kinetics from Ca^{2+} Fluorescence Measurements

4.2.1 Biophysical Foundations of Ca^{2+} Currents Imaging

An optical measurement of a Ca^{2+} signal is ultimately a measurement of the Ca^{2+} indicator bound to Ca^{2+} ions, which is proportional to the Ca^{2+} fractional change of fluorescence ($\Delta F/F_0$) if the indicator is not saturated. If the kinetics of the Ca^{2+}-binding reaction of the indicator is slower than the kinetics of the Ca^{2+} source, and imaging is performed at higher rate, the time-course of Ca^{2+} $\Delta F/F_0$ essentially tracks the kinetics of the chemical reaction. Alternatively, if the kinetics of the Ca^{2+}-

binding reaction is faster than the kinetics of the Ca^{2+} source, the Ca^{2+} $\Delta F/F_0$ signal tracks the kinetics of the Ca^{2+} source. It follows that the equilibration (or relaxation) time of the Ca^{2+}-indicator binding reaction is a crucial variable to use the technique to investigate the biophysics and the physiology of the Ca^{2+} source. The relaxation of the Ca^{2+}- binding reactions for early indicators was studied by Kao and Tsien [15] who established that the rate of association for all these molecules is limited by diffusion leading to an association constant of $\sim 6 \cdot 10^8$ M^{-1} s^{-1}. Thus, both the equilibrium constant (K_D) and the equilibrium time are determined by the dissociation constant, i.e. the lower is the affinity of the indicator the shorter is its equilibrium time. We have empirically demonstrated that indicators with $K_D \geq 10$ μM such as OG5N or FuraFF have relaxation time < 200 μs [16]. Since the kinetics of activation and deactivation of voltage-gated Ca^{2+} channels (VGCCs) during physiological changes of V_m (for instance action potentials), is governed by the kinetics of the V_m transient, it follows that the relaxation time for those indicators is shorter than the duration of the Ca^{2+} influx. Hence, since Ca^{2+} binds to the indicator linearly in time, the Ca^{2+} $\Delta F/F_0$ is proportional to the integral of the Ca^{2+} influx, i.e. to the integral of the Ca^{2+} current. In the cell, however, Ca^{2+} simultaneously binds to proteins that form the endogenous buffer and this binding is competing with the binding to the indicator. An endogenous buffer can be, in principle, at least as fast as the indicator in equilibrating. In this case, only a fraction of Ca^{2+} is bound to the indicator, but this fraction is proportional to the total Ca^{2+} entering the cell and therefore to the integral of the Ca^{2+} current. Alternatively, an endogenous buffer can equilibrate over a time scale that is longer than the duration of the Ca^{2+} current. In this case, Ca^{2+} first binds to the dye and later to the endogenous buffer, implying that part of Ca^{2+} moves from the indicator to the endogenous buffer during its relaxation time. Under this condition, the Ca^{2+} $\Delta F/F_0$ is not linear with the integral of the Ca^{2+} current over this time scale. To clarify this important concept we make use of two simple computer simulations shown in Fig. 4.1, produced by a model that takes into account the chemical reactions as well as an extrusion mechanism re-establishing the initial Ca^{2+} conditions over a time scale >100 ms. We analyse what hypothetically can happen if a Ca^{2+} current with Gaussian shape occurs in a cell filled with 2 mM OG5N. In the first simulation (Fig. 4.1a), the cell has only 1 mM of a fast endogenous buffer behaving with the same association constant of the indicator and $K_D = 10$ μM. In the second simulation (Fig. 4.1b), the cell has additional 400 μM of a slower endogenous buffer with association rate ~3 times slower than that of the indicator and $K_D = 0.2$ μM. In the first case, the time derivative of the Ca^{2+} $\Delta F/F_0$ signal matches the kinetics of the Ca^{2+} current (Fig. 4.1a). In contrast, in the presence of the slower buffer, the time derivative of the Ca^{2+} $\Delta F/F_0$ signal has a negative component and does not match the kinetics of the Ca^{2+} current (Fig. 4.1b). In the next two paragraphs, we present the analysis strategies that can be applied to extract the kinetics of Ca^{2+} currents from Ca^{2+} imaging recordings.

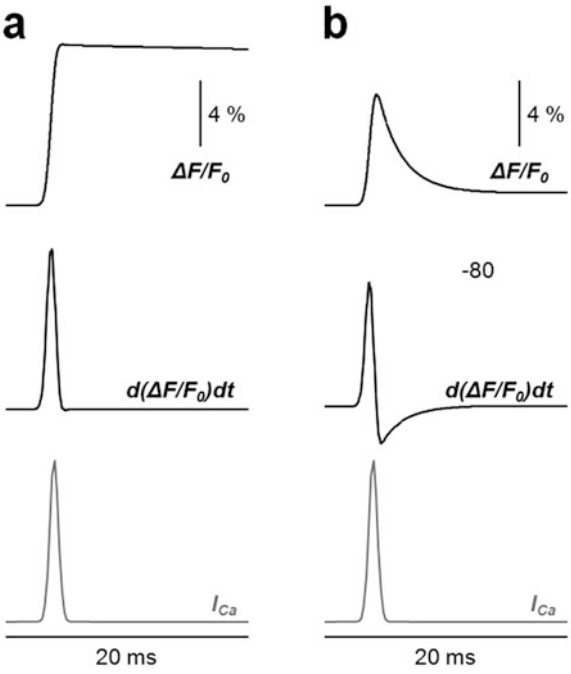

Fig. 4.1 Simulation of hypothetical Ca^{2+} $\Delta F/F_0$ signals from 2 mM OG5N in the presence of endogenous Ca^{2+} buffers. (**a**) Simulation of $\Delta F/F_0$ signal (top trace) following a Ca^{2+} current with simple Gaussian kinetics (I_{Ca}, gray trace on the bottom) in the presence of 1 mM of a fast endogenous Ca^{2+} buffer with same association constant of the Ca^{2+} indicator ($5.7 \cdot 10^8$ M^{-1} s^{-1}) and $K_D = 10$ μM. The kinetics of the $\Delta F/F_0$ time derivative (middle trace) matches the kinetics of the Ca^{2+} current. (**b**) Same as in the previous panel but in this case in the presence of additional 400 μM of a slower buffer with association constant equal to $2 \cdot 10^8$ M^{-1} s^{-1} and $K_D = 0.2$ μM. The kinetics of the $\Delta F/F_0$ time derivative (middle trace) does not matches the kinetics of the Ca^{2+} current

4.2.2 *The Case of Linearity Between Ca^{2+} Influx and Ca^{2+} Fluorescence Changes*

The proteins expressed in a cell determine whether or not the time course of the Ca^{2+} $\Delta F/F_0$ signal is linear with the kinetics of the Ca^{2+} current. As previously demonstrated [11], in the case of linear behaviour, the Ca^{2+} $\Delta F/F_0$ signal must reach its peak and remain constant for a few milliseconds afterwards, i.e. for the entire duration of the current. As shown in the simulation of Fig. 4.1a, the kinetics of Ca^{2+} extrusion producing a slow decrease of the Ca^{2+} $\Delta F/F_0$ signal has negligible effect on the time derivative. Thus, the estimate of the Ca^{2+} current kinetics is reliably obtained by the calculation of the time derivative of the Ca^{2+} $\Delta F/F_0$ signal. This calculation, however, requires the signal noise to be smaller than the signal change between two consecutive samples. The classical way to

achieve this necessary condition is to apply to the Ca^{2+} $\Delta F/F_0$ signal a "smoothing algorithm", i.e. a temporal filter that reduces the noise of the signal with minimal distortion of its kinetics. At 20 kHz acquisition rate, we have found that the Savitky-Golay algorithm [19] is an optimal filtering tool permitting noise reduction of the signal without significant temporal distortion using time-windows of up to 20–30 samples [11]. The applicability of this strategy has however limitations, i.e. if the signal or the region of measurement are too small, or if the light is too dim, the smoothing of the signal might not be sufficient to reduce the noise down to the level permitting calculation of the time derivative. In this case, the alternative strategy to apply consists in fitting the raw or the filtered Ca^{2+} $\Delta F/F_0$ signal with a model function obtaining a noiseless curve that mimics the time course of the Ca^{2+} $\Delta F/F_0$ signal. A simple choice of function that resembles the time course of the Ca^{2+} $\Delta F/F_0$ transient is the sigmoid. In particular, we found that the product of three sigmoid functions always provides an excellent fit of the Ca^{2+} $\Delta F/F_0$ signal associated with a backpropagating action potential in CA1 hippocampal pyramidal neurons [16]. As shown in the example of Fig. 4.2a both strategies are faithful in correctly calculating the time derivative of the $\Delta F/F_0$ signal. In this example, a CA1 hippocampal pyramidal neuron was filled with 2 mM OG5N and the dendritic Ca^{2+} $\Delta F/F_0$ signal associated with a backpropagating action potential was recorded at 20 kHz and averaged over 16 trials. This high sampling frequency was necessary to avoid signal aliasing and therefore distortion of the kinetics of the current. The filtering strategy is the straightforward approach that enables the calculation of the time derivative, but it produces a curve with noise. The noise can be reduced (if possible) by increasing the number of trials to average or by enlarging the dendritic area from where fluorescence is averaged. The fitting strategy is less direct but it produces a noiseless curve and it is therefore the only possible approach when the noise of the Ca^{2+} $\Delta F/F_0$ signal is above a certain level, as quantitatively estimated in an original report [16]. In particular, this is the case when the current must be extracted from single trials or when the recording is obtained from small or relatively dim regions.

4.2.3 The Case of Nonlinearity Between Ca^{2+} Influx and Ca^{2+} Fluorescence Changes

The method of estimating the kinetics of a Ca^{2+} current by calculating the Ca^{2+} $\Delta F/F_0$ time derivative fails when Ca^{2+} unbinds from the indicator over a time scale that is longer than the current duration, but sufficiently short to distort the estimate of Ca^{2+} influx dynamics by fluorescence measurement. In other words, this method fails when the Ca^{2+} $\Delta F/F_0$ signal decays rapidly, after correction for bleaching, generating a negative component in its time derivative. Such a situation occurs, for example, where slow buffering is produced by Calbindin-D28k [20, 21] and Parvalbumin [22, 23]. As shown in the example of Fig. 4.2b, the Ca^{2+}

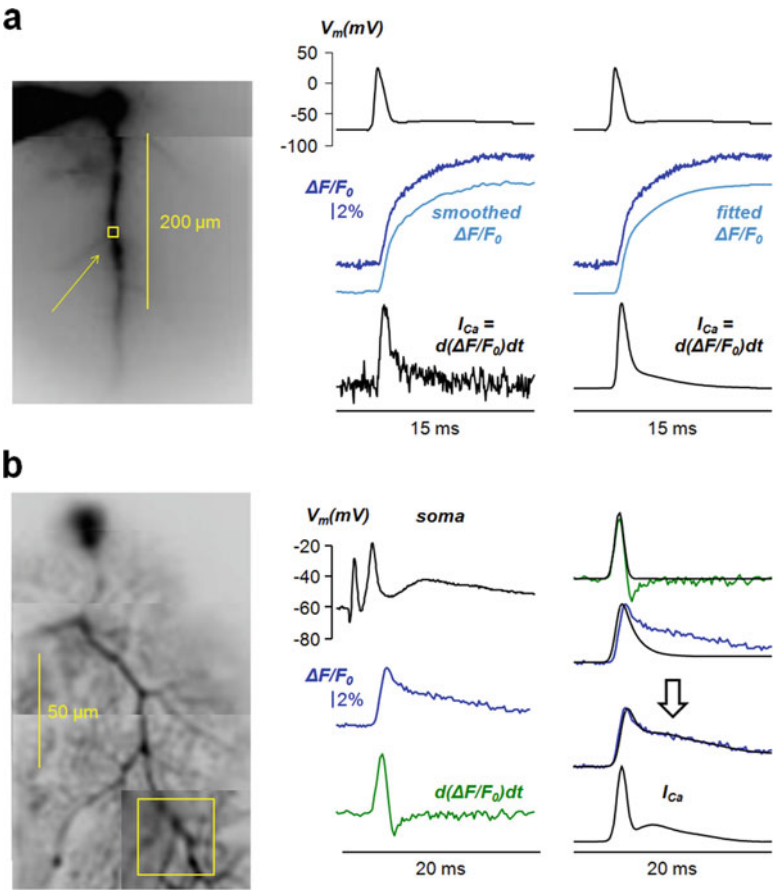

Fig. 4.2 Different strategies to estimate the kinetics of a Ca^{2+} current (**a**) On the left, fluorescence image of CA1 hippocampal pyramidal neuron filled with 2 mM OG5N with a small region of the apical dendrite outlined and indicated by the arrow. On the right, somatic V_m change associated with an action potential (top black traces) and Ca^{2+} $\Delta F/F_0$ signal in the indicated region (blue trace). The $\Delta F/F_0$ signal is either smoothed with a Savitky-Golay algorithm (left) or fitted with a 3-sigmoid function (right). The Ca^{2+} current kinetics (I_{Ca}) is then estimated by calculating the time derivative of the processed $\Delta F/F_0$ signal. The kinetics of the current is the same using the two strategies, but the curve obtained with the strategy of data fitting is noiseless. Data, recorded at 20 kHz, were from averages of 16 trials. (**b**) On the left, fluorescence image of PN filled with 2 mM OG5N with square region of interest outlined. On the right, somatic V_m change associated with a climbing fibre EPSP (top-left black trace) and Ca^{2+} $\Delta F/F_0$ signal in the indicated region (blue traces). The time derivative of the Ca^{2+} $\Delta F/F_0$ signal (green traces) does not match the kinetics of the current. To estimate the kinetics of the current we use a strategy that consists in matching the result of a computer simulation to the Ca^{2+} $\Delta F/F_0$ signal using an optimised two-buffer model [24]. We start from the Gaussian function fitting the rising phase of the $\Delta F/F_0$ time derivative (top-right black trace). We then correct the current with three additional Gaussian components until a match of the computer simulation with the Ca^{2+} $\Delta F/F_0$ signal is obtained (process indicated by the arrow. The curve producing this match (I_{Ca}, bottom-right black trace) is the estimate of the Ca^{2+} current kinetics. Data, recorded at 5 kHz, were from averages of 4 trials

$\Delta F/F_0$ signal associated with a climbing fibre excitatory postsynaptic potential (EPSP), recorded at 5 kHz from a dendritic region and averaged over four trials, decays rapidly after its maximum resulting in a negative component of its time derivative. The distortion from the linear behaviour produced by the slow buffers can be compensated by taking into account the kinetics of Ca^{2+} unbinding from the indicator. We have recently developed a successful method to achieve this goal [24]. The strategy is based on fitting the decay time of the Ca^{2+} $\Delta F/F_0$ signal with the result of a computer simulation of a model with a slow buffer. Initially the input current is the Gaussian function fitting the rising phase of the time derivative (that is still a good approximation of the initial part of the current). The kinetic parameters and the concentration of the slow buffer are set to obtain the best fit of the decay phase of the Ca^{2+} $\Delta F/F_0$ signal. Then, the kinetics of the Ca^{2+} current is obtained as summation of four Gaussian functions that maximise the match between the result of the computer simulation and the experimental Ca^{2+} $\Delta F/F_0$ signal. Although this new method provides only an indirect approximation of the kinetics of the Ca^{2+} current, this information is crucial at understanding the activation and deactivation of different types of VGCCs. In the dendrites of PNs, for instance, different Ca^{2+} current kinetics components are associated with the activation of P/Q-type VGCCs [25] and T-type Ca^{2+} channels [26] that can be in principle separated by pharmacological block of one component. Thus, the extrapolation of a curve that approaches the kinetics of the Ca^{2+} current can be used to quantitatively investigate the variability of channels activation at different dendritic sites, the modulation of channel activation due to physiological activity or to pharmacological action. Finally, it is important to say that such a strategy can be extended to estimate slower Ca^{2+} currents where the fitting procedure can be applied to the slower decay time due to Ca^{2+} extrusion [27].

4.3 Combining Membrane Potential and Ca^{2+} Imaging

4.3.1 Setting up Combined Voltage and Ca^{2+} Fluorescence Measurements

To combine V_m and Ca^{2+} optical measurements, the VSD and the Ca^{2+} indicator must have minimal overlap in the emission spectra. Water soluble voltage indicators with different excitation and emission spectra have been recently developed [28]. In particular, the red-excitable and IR emitting VSD ANBDQPTEA (or PY3283) is suitable for coupling with other optical techniques [29]. Nevertheless, the most used VSDs for single cell applications are still JPW3028 [30] and the commercially available JPW1114 [18]. These indicators have wide excitation spectrum in the blue/green region and they emit mainly in the red region. We have previously demonstrated that both indicators can be optimally combined with Fura indicators that are excited in the UV region and emit in the short green region [12]. In

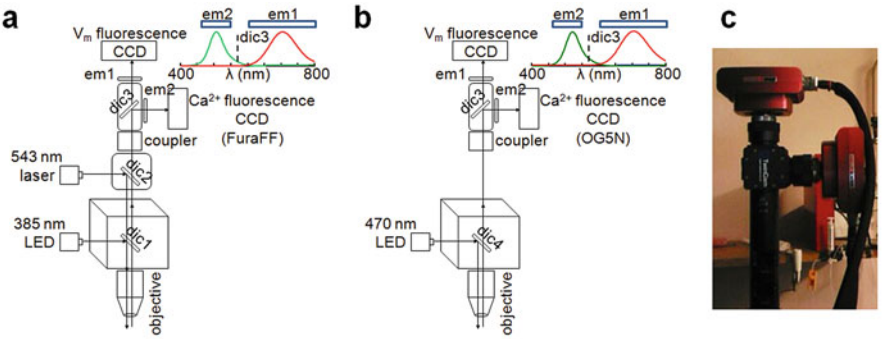

Fig. 4.3 Configurations and camera for combined voltage and Ca^{2+} fluorescence measurements. (**a**) Schematic drawing of the apparatus for simultaneous voltage and Ca^{2+} imaging using the VSD JPW1114 and the Ca^{2+} indicator FuraFF [13]; 385 nm LED light via the epifluorescence port of a commercial microscope is reflected by a 506 nm long-pass dichroic mirror (dic1); 543 nm laser light via the top of the microscope is reflected by a dual-band dichroic mirror transmitting wavelengths between 493 nm and 530 nm and wavelengths longer than 574 nm (dic2); the fluorescence images of the two dyes are demagnified and separated by a 565 nm long-pass dichroic mirror (dic3); The V_m image and the Ca^{2+} images are filtered by a 610 nm long-pass (em1) and by a 510 ± 42 nm band-pass filter (em2) respectively, then acquired by two CCD cameras; the emission spectra of FuraFF (green) and JPW1114 (red) are shown on the top-right. (**b**) Schematic drawing of the apparatus for simultaneous voltage and Ca^{2+} imaging using the VSD JPW1114 and the Ca^{2+} indicator OG5N [11]; 470 nm LED light via the epifluorescence port of a commercial microscope is reflected by a 495 nm long-pass dichroic mirror (dic4); the fluorescence images of the two dyes are demagnified and processed as in the previous configuration; the emission spectra of OG5N (green) and JPW1114 (red) are shown on the top-right. (**c**) "The dual NeuroCCD camera designed by RedshirtImaging for this type of measurement

this case, VSDs were excited at 543 nm using a laser and Fura indicators were excited at 385 nm using a light emitting diode (LED) as shown in the scheme of Fig. 4.3a. Alternatively, simultaneous voltage and Ca^{2+} imaging can be achieved using Oregon Green, Calcium Green or Fluo Ca^{2+} indicators using blue light (470–490 nm) to excite both VSDs and Ca^{2+} indicators [31]. Simultaneous imaging of JPW1114 and OG5N was adopted to obtain the first combined measurement of V_m and Ca^{2+} currents using the configuration of Fig. 4.3b. This type of measurement, however, has several disadvantages. First, OG5N fluorescence has a small tail component in the red region [31] which can be negligible or not depending on the ratio of the two dyes at each site as well as on the ratio between the two signals. Thus, for example, it works in proximal dendrites of CA1 pyramidal neurons for signals associated with action potentials [11], where V_m fluorescence is stronger than Ca^{2+} fluorescence, but it does not in distal dendrites of cerebellar Purkinje neurons (PNs, data not shown), where V_m fluorescence is weaker than Ca^{2+} fluorescence. A second disadvantage is that the JPW1114 signal at 470 nm excitation is ∼4 times smaller than that at 532 nm excitation. If simultaneous recordings are not critical, one can replace them with sequential recordings obtained by alternating 470 nm and 532 nm excitation as used in a recent study [32]. Finally,

a third disadvantage is that JPW1114 absorbs more in the blue range than in the green range, i.e. it exhibits toxic effects after fewer exposures. A crucial technical aspect to take into consideration while setting up combined voltage and Ca^{2+} fluorescence measurements is the ability to record the two signals simultaneously at high speed. To this purpose, the company RedShirtImaging (Decantur, GA) has developed a dual-head version of the SMQ NeuroCCD (Fig. 4.3c). This camera permits simultaneous image acquisitions from both heads at 5–20 kHz, i.e. at the required speed. A demagnifier developed by Cairn Research Ltd. (Faversham, UK) allows adjusting the size of the image before it is split in two images at the emission wavelengths of the two dyes. Thus, the alignment of the two heads of the camera allows obtaining, at each precise region of interest, the V_m and the Ca^{2+} signal.

4.3.2 Calibrating Membrane Potential Fluorescence Transients

The calibration of V_m optical signals on an absolute scale (in mV) is crucial to analyse the gating of Ca^{2+} channels at the same locations where Ca^{2+} recordings are performed. This is not, however, straightforward. Indeed, the fractional change of VSD fluorescence is proportional to V_m [33], but the linear coefficient between these two quantities depends on the ratio between the inactive dye and the active dye that varies from site to site. The inactive dye is bound to membranes that do not change potential and contributes only to the resting fluorescence, while the active dye is bound to the plasma membrane and contributes to the resting fluorescence, but also carries the signal. In particular, in experiments utilising intracellular application of the dye, inactive dye is the dye that binds to intracellular membranes and organelles. Since the sensitivity of recording varies from site to site, a calibration can be achieved only if a calibrating electrical signal that has known amplitude at all locations is available. Such a signal is different in different systems. In mitral cells of the olfactory bulb, the amplitude of an action potential is the same in the whole apical dendrite and it can be used to create a sensitivity profile of the measuring system [34]. Another type of calibrating electrical signal can be a slow electrical change spreading with minimal attenuation over relatively long distances. Such a signal can be used to reliably calibrate VSD signals in PNs [18]. An example of this type of calibration is reported in Fig. 4.4a. Starting from the resting V_m, that we assume nearly uniform over the entire cell, long current hyperpolarising or depolarising current pulses are injected to the soma *via* the patch pipette and the change in V_m is recorded. As shown by direct dendritic patch recording, the dendrite is hyperpolarised by the same amount of the soma [35]. Thus, the measurement of somatic hyperpolarisation can be used as voltage reference to calibrate the dendritic VSD fractional change of fluorescence (VSD $\Delta F/F_0$) optical signal, as shown in Fig. 4.4a. In contrast, a depolarisation step attenuates along the dendrite. A third type of calibrating signal is a uniform depolarisation over the entire dendritic tree

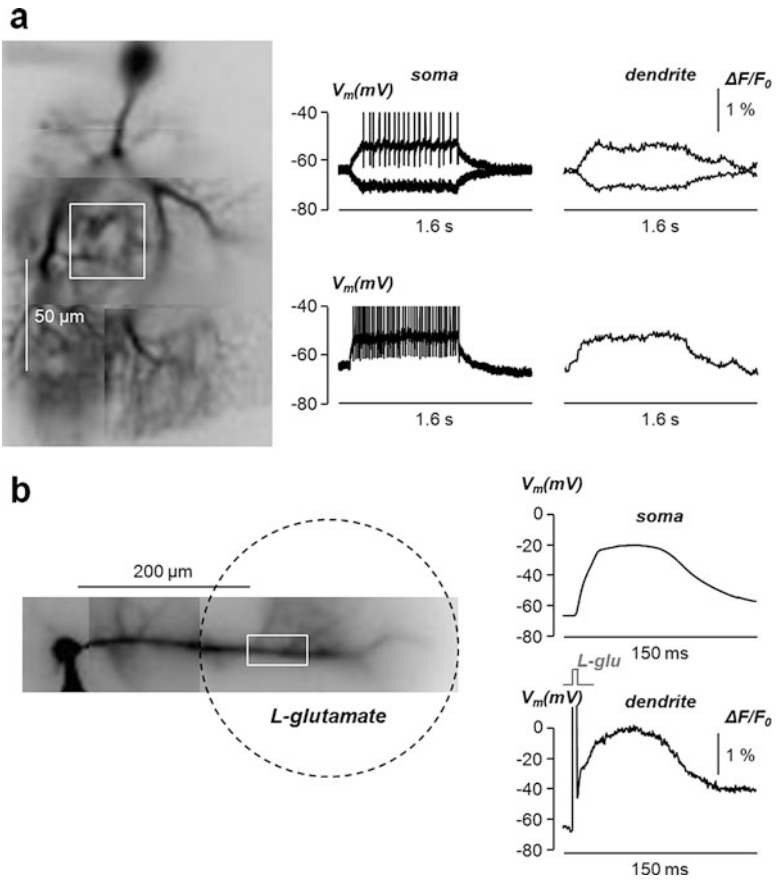

Fig. 4.4 Calibration methods for dendritic V_m optical signals. (**a**) On the left, fluorescence image of PN with square region of interest outlined. On the right, somatic V_m change associated with long hyperpolarising or depolarising steps and associated dendritic VSD $\Delta F/F_0$ signals in the region of interest; the hyperpolarising step spreads to the dendrites with negligible attenuation [35] and is used to calibrate the VSD $\Delta F/F_0$ signals; the weak depolarising step on the top also spreads with minimal attenuation, but the associated somatic action potentials do not propagate into the dendrites; in contrast, the strong depolarising step on the bottom attenuates. (**b**) On the left, fluorescence image of CA1 hippocampal pyramidal neuron with rectangular region, 200–250 µm from the soma, outlined. On the right, somatic V_m change associated with L-glutamate photorelease from MNI-glutamate [14] in the area limited by the dotted line and in the presence of 1 µM tetrodotoxin blocking action potentials; the dendritic VSD $\Delta F/F_0$ signal is reported on the bottom; the saturating L-glutamate concentration depolarises the illuminated area from the resting V_m (~ -70 mV) to the reversal potential of AMPA receptors (0 mV). All calibrations were from single trials

using L-glutamate photolysis from 4-Methoxy-7-nitroindolinyl-caged-L-glutamate (MNI-glutamate) [14]. This calibration procedure is applicable to all membrane expressing a relatively large number of glutamate receptors, i.e. to dendrites with

high densities of excitatory synapses. The calibration is based on the principle that if the ionotropic glutamate receptor becomes the dominant conductance in a particular neuronal compartment, its reversal potential will determine the membrane potential of the compartment. Thus, in the area where dominance of glutamate receptor conductance is obtained, the resulting V_m change will be the same and can be used to calibrate VSD signals. An example of this protocol to calibrate backpropagating action potentials in CA1 hippocampal pyramidal neurons is shown in Fig. 4.4b. The VSD $\Delta F/F_0$ signal associated with the backpropagating AP at different sites of the apical dendrites is variable and cannot be directly correlated with the absolute change of V_m. In the presence of 1 μM TTX, to block action potentials, L-glutamate is photoreleased to saturate glutamate receptors over the whole field of view. Since the recording is performed starting from the resting V_m, the size of the VSD $\Delta F/F_0$ corresponds to this potential in the whole illuminated area where V_m reaches the reversal potential of 0 mV. Thus, this information is used to extrapolate the V_m at each dendritic site.

4.4 Examples of Combined Voltage and Ca^{2+} Current Imaging

4.4.1 Ca^{2+} Currents Associated with Backpropagating Action Potentials in CA1 Hippocampal Pyramidal Neurons and in Olfactory Bulb Mitral Cells

In many neurons, action potentials generated in the axon hillock adjacent to the soma do not only propagate along the axon to reach neurotransmitter release terminals, but also backpropagate throughout dendrites to signal cell activation at the sites where the neuron receives the synaptic inputs. At least part of this information is given by the fast Ca^{2+} transients produced by activation of VGCCs caused by the dendritic depolarisation associated with the action potential. The analysis that can be performed using the present imaging method is therefore crucial at understanding signal processing in individual neurons, as well as the specific role and function of the diverse VGCCs activated in dendrites. The propagation of the action potential and the consequent activation of VGCCs may be very different in different neuronal systems. In CA1 hippocampal pyramidal neurons, action potentials attenuate along the dendrite and activate both high-voltage activated (HVA) and low-voltage activated (LVA) VGCCs [36, 37]. We have very recently demonstrated that HVA-VGCCs and LVA-VGCCs operate synergistically to stabilise Ca^{2+} signals during burst firing [32]. Somatic and dendritic action potentials, at nearly physiological temperature, have 1–4 ms duration as in the example shown in Fig. 4.5a. In agreement with this evidence, the kinetics of the Ca^{2+} current is similar to that of the action potential, with a peak delayed by a few hundred milliseconds from the peak of the action potential. In total contrast to the CA1 hippocampal pyramidal neuron, in

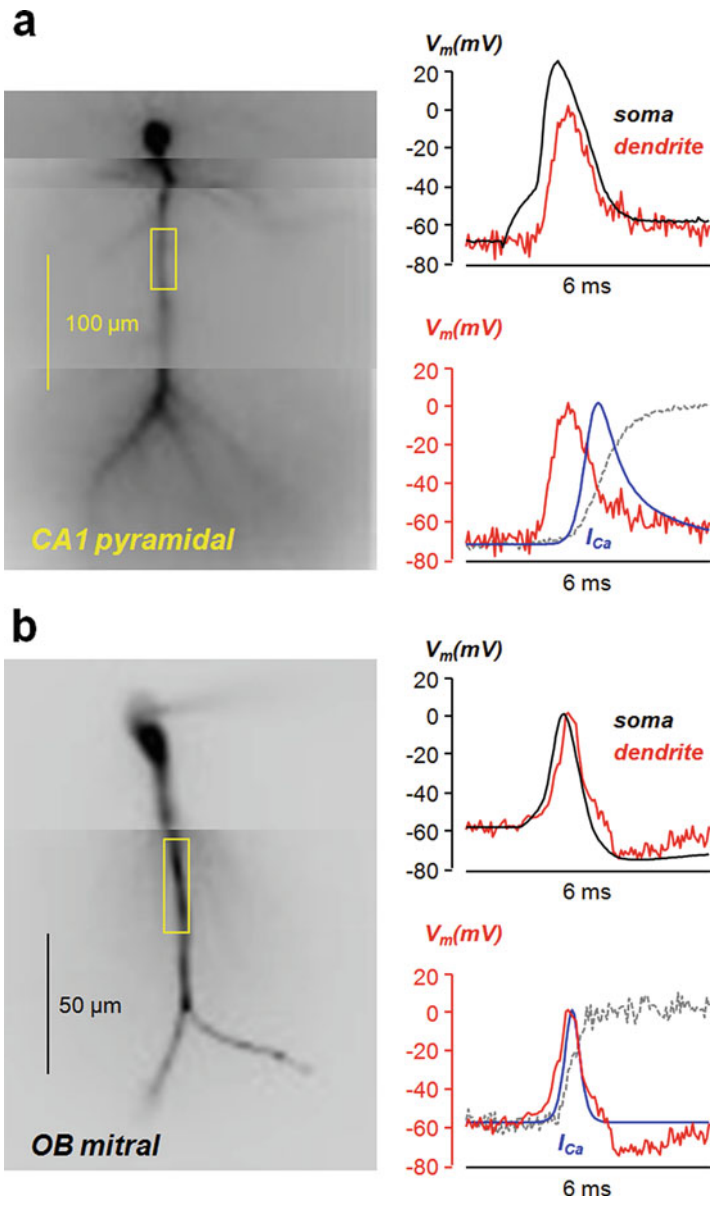

Fig. 4.5 Ca^{2+} currents associated with backpropagating action potentials in CA1 hippocampal pyramidal neurons and in olfactory bulb (OB) mitral cells (**a**) On the left, fluorescence image of CA1 hippocampal pyramidal neuron filled with JPW1114 and 2 mM OG5N with a region of the apical dendrite outlined. On the right, somatic V_m change associated with an action potential (black trace) in the soma and in the dendritic region. The associated Ca^{2+} current kinetics, obtained with the fitting strategy from the raw Ca^{2+} signal (dashed gray trace), is shown in the bottom. (**b**) On the left, fluorescence image of OB cell filled with JPW1114 and 2 mM OG5N with a region of the principal dendrite outlined. On the right, somatic V_m change associated with an action potential in the soma (black trace) and in the dendritic region (red trace). The associated Ca^{2+} current kinetics, obtained with the fitting strategy from the raw Ca^{2+} signal (dashed gray trace), is shown in the bottom (blue trace) superimposed to the dendritic action potential (red trace). Data, recorded at 20 kHz, were from averages of 4 trials. All experiments were performed at 32–34 °C

olfactory bulb mitral cells the action potential does not attenuate along the dendrites [38]. In addition, as shown in the representative example of Fig. 4.5b, the somatic and dendritic action potential at near physiological temperature (32–34 °C) has duration <1 ms. Thus, in this system, the activation and deactivation of VGCCs is also faster leading to a Ca^{2+} current with shorter duration and shorter delay from the V_m waveform peak. This preliminary comparison between the two cases indicates that the role of VGCCs, activated by the action potential, is different in different systems. For example, Ca^{2+} currents are delayed by ~100 μs in presynaptic terminals where the function of this signal is to trigger neurotransmitter release [39]. Here, the kinetics of the Ca^{2+} current was obtained by calculating the time derivative of the Ca^{2+} $\Delta F/F_0$ signal fit [16]. VGCCs contribute to the shape of the action potential directly and indirectly by activating K^+ channels, but also provide a precise time-locked Ca^{2+} transient capable to select fast-activated Ca^{2+} binding proteins. The possibility to locally investigate, using combined V_m and Ca^{2+} current optical measurements, the physiological occurrence of Ca^{2+} signals mediated by VGCCs will contribute enormously, in the near future, to the understanding of complex signal processing in neurons.

4.4.2 *Ca^{2+} Currents Associated with Climbing Fibre EPSPs in Cerebellar Purkinje Neurons*

In contrast to pyramidal neurons of the cortex and hippocampus, and to olfactory bulb mitral cells, somatic/axonal action potentials in PNs do not actively propagate in the dendrites [40]. The dendrites of PNs, however, express P/Q-type HVA-VGCCs [25] and T-type LVA-VGCCs [26] that are activated by the dendritic depolarisation produced by climbing fibre EPSPs. As shown in the example of Fig. 4.6, the shape of the dendritic V_m calibrated in Fig. 4.4a is quite different in the soma and in the dendrite, mainly reflecting the absence of Na^+ action potentials in the dendrite. In this system, the low-affinity Ca^{2+} indicator used to estimate the Ca^{2+} current was Fura-FF, since the larger Ca^{2+} signal produced by OG5N contaminated the optical V_m measurement. The prominent dendritic depolarisation produces a biphasic Ca^{2+} current, which is in this case obtained by applying our recent generalised method [24]. The fast and sharp component is nearly concomitant to the short period in which $V_m > -40$ mV and it is therefore likely mediated by HVA-VGCCs. The slower and more persistent component is instead mostly concomitant to the whole depolarisation transient and is therefore likely mediated by LVA-VGCCs, as demonstrated by selectively blocking T-type VGCCs (unpublished data not shown). The analysis of Ca^{2+} signalling associated with the climbing fibre EPSP is crucial for the understanding of synaptic plasticity in PNs [41]. Yet, while the role of the Ca^{2+} transient associated with the climbing fibre EPSP has been postulated to be auxiliary to the principal Ca^{2+} signal mediated by parallel fibre EPSPs, these first measurements of the Ca^{2+} current

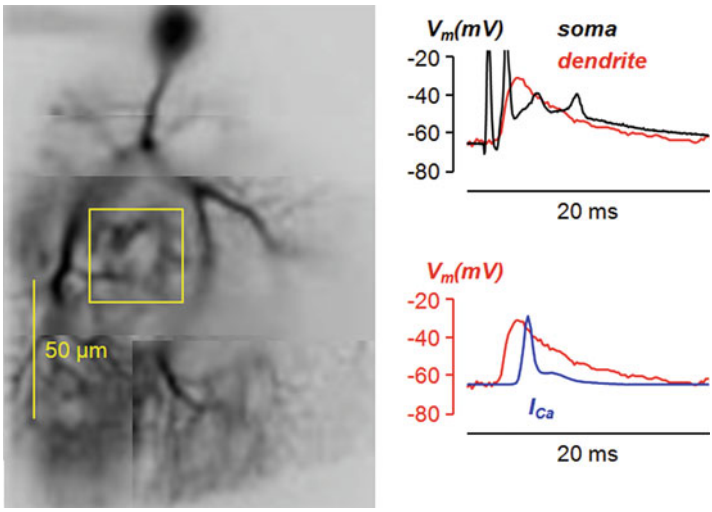

Fig. 4.6 Ca^{2+} currents associated with climbing fibre EPSPs in cerebellar Purkinje neurons. On the left, fluorescence image of the same PN of Fig. 4.4a filled with JPW1114 and 2 mM Fura-FF with a region of the dendrite outlined. On the right, somatic V_m change associated with climbing fibre EPSP (black trace) in the soma and in the dendritic region. The associated Ca^{2+} current kinetics, obtained with the generalised method [24], is shown in the bottom. Data, recorded at 5 kHz, were from averages of 4 trials. Experiments were performed at 32–34 °C

kinetics elucidate a quite precise timing of occurrence of the Ca^{2+} source that may eventually provide a less ambiguous explanation of the precise function of this spread dendritic depolarisation. In summary, the examples illustrated in this section show the potentials of this novel optical method in providing physiological information not available by using electrode techniques.

4.5 Data Interpretation and Future Prospective

The method described here has been developed to overcome the limitations of single-electrode or two-electrode voltage clamp techniques permitting the analysis of physiological Ca^{2+} currents of native Ca^{2+} channels. Indeed, in contrast to patch-clamp recordings, these Ca^{2+} optical currents can be measured in conditions of a physiological change of V_m and the measured currents are confined to the sites where they are recorded, as shown in apical dendrites of hippocampal pyramidal neurons [32]. The additional information on local V_m change, necessary to correlate the behaviour of the conductance with its biophysical properties, is obtained by combining VSD imaging. In cases of linear behaviour between Ca^{2+} influx and Ca^{2+} fluorescence changes the kinetics of the Ca^{2+} current can be extracted by calculating the time derivative of the Ca^{2+} $\Delta F/F_0$ signal using low-affinity Ca^{2+} indicators [11,

16]. In the case of nonlinear behaviour between Ca^{2+} influx and Ca^{2+} fluorescence, produced by Ca^{2+}-binding proteins with slower kinetics with respect to the Ca^{2+} current, the kinetics of the Ca^{2+} current can be still correctly estimated by taking into account the faster unbinding of Ca^{2+} from the low-affinity indicator [24]. In this last section we address the question of how data, obtained using this technique, should be interpreted. In Ca^{2+} current recordings from channels expressed in heterologous systems using voltage clamp, V_m is controlled artificially and its change is therefore independent of the channel deactivation. Under physiological conditions, Ca^{2+} channels contribute to the V_m change directly, through the ion flux, and indirectly by regulating other conductances. It follows that the channel deactivation changes the V_m waveform. We have shown that in CA1 hippocampal pyramidal neurons this phenomenon produces a modulation of LVA-VGCCs by HVA-VGCCs [32]. More in general, a Ca^{2+} current mediated by diverse VGCCs is always the result of a synergy among all different ion channels contributing to the V_m waveform. It follows that in a Ca^{2+} current optical measurement, a single component of the current cannot be extracted simply by blocking the underlying channel, since this block may affect the residual current as well. This evidence has important implications in the study of transgenic animals carrying Ca^{2+} channel mutations. In this case, a certain phenotype is likely to result from the combined modification of function of many different channels, rather than from the specific Ca^{2+} influx component, making the study of these animals as models for disease challenging. In summary, the investigation of the role and function of individual Ca^{2+} channels must be performed in the global context of activation of all channels participating to the local V_m waveform.

Another important aspect of data interpretation is the relation of the kinetics of Ca^{2+} current with the putative molecular targets of Ca^{2+} ions entering the cell. While importance is normally given to possible molecular coupling between the Ca^{2+} channel and the Ca^{2+} binding protein, the kinetics of the Ca^{2+} current can be a potent selector of the molecular pathway which is activated. To illustrate this important concept we make use of computer simulations using the same theoretical framework for simple Ca^{2+}-binding dynamics that we already used in the past [42]. We imagine the possible activation of two proteins: a "fast" protein with $K_{ON} = 5.7 \cdot 10^8\ M^{-1}\ s^{-1}$ and $K_D = 10\ \mu M$, expressed at the concentration of 500 μM; and a "slow" protein with $K_{ON} = 4 \cdot 10^8\ M^{-1}\ s^{-1}$ and $K_D = 0.4\ \mu M$, expressed at the concentration of 100 μM. In the first case, shown in Fig. 4.7a, the cell is receiving a fast Ca^{2+} current with $\sim$ 2 ms total duration which binds first to the fast protein and later to the slow protein. In the second case, shown in Fig. 4.7b, the cell is receiving a slower Ca^{2+} current that is smaller in amplitude but that carries approximately the same amount of Ca^{2+}. In this case the slow protein binds to Ca^{2+} with a slower kinetics but the amount of the fast protein binding to Ca^{2+} is less than half with respect to the first case. These simulations indicate that the ability to activate for a molecular pathway triggered by the fast protein strongly depends on the kinetics of the Ca^{2+} current. Thus, the approach described here should drastically improve our understanding of the physiological function of Ca^{2+} channels by providing the possibility to explore the biophysics of

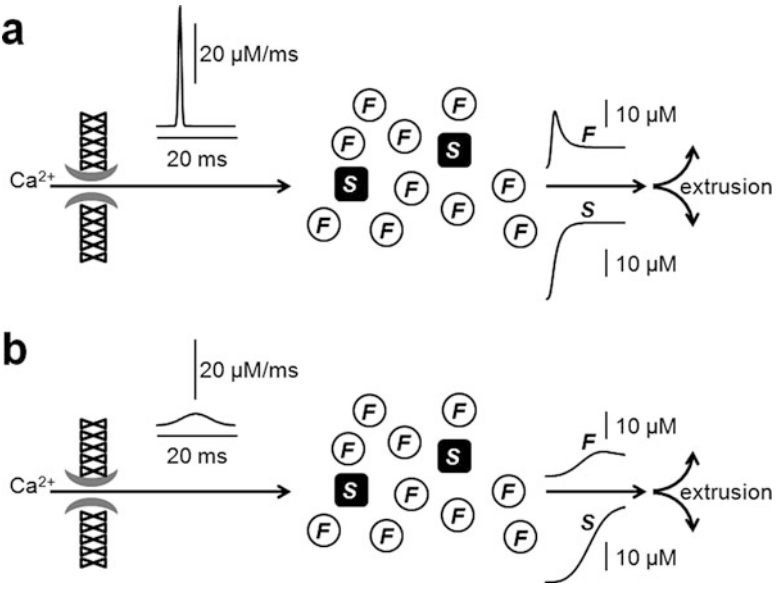

Fig. 4.7 Simulated activation of two different Ca^{2+}-binding proteins by Ca^{2+} currents. (**a**) In a cell containing 500 µM of a fast (*F*) buffer with $K_{ON} = 5.7 \cdot 10^8$ M^{-1} s^{-1} and $K_D = 10$ µM, and 100 µM of a slow (*S*) buffer with $K_{ON} = 4 \cdot 10^8$ M^{-1} s^{-1} and $K_D = 0.4$ µM, the curves on the right report the binding to Ca^{2+} of the *F* and *S* proteins following the fast Ca^{2+} current reported on the left. (**b**) Same as in the previous panel but following the slow Ca^{2+} current reported on the left

native channels during physiological activity locally within the complex neuronal architecture. The examples of combined V_m and Ca^{2+} current optical measurements from CA1 hippocampal pyramidal neurons, olfactory bulb mitral cells and PNs reported here are representative of the types of exploration that can be performed using this novel approach.

Acknowledgment This work was supported by the *Agence Nationale de la Recherche* through three grants: (1) Grant *WaveFrontImag*, program number ANR-14-CE17–0006-01; (2) Labex *Ion Channels Science and Therapeutics*, program number ANR-11-LABX-0015; (3) National Infrastructure France Life Imaging "Noeud Grenoblois"; and by the *Federation pour la recherché sur le Cerveau* (FRC) through the grant *Espoir en tête* (in partnership with Rotary France).

References

1. Braubach O, Cohen LB, Choi Y (2015) Historical overview and general methods of membrane potential imaging. Adv Exp Med Biol 859:3–26
2. Davies R, Graham J, Canepari M (2013) Light sources and cameras for standard in vitro membrane potential and high-speed ion imaging. J Microsc 251:5–13

3. Canepari M, Willadt S, Zecevic D, Vogt KE (2010) Imaging inhibitory synaptic potentials using voltage sensitive dyes. Biophys J 98:2032–2040
4. Sakmann B, Neher E (1986) Patch clamp techniques for studying ionic channels in excitable membranes. Annu Rev Physiol 46:455–472
5. Gray R, Johnston D (1985) Rectification of single GABA-gated chloride channels in adult hippocampal neurons. J Neurophysiol 54:134–142
6. Lester HA (1988) Heterologous expression of excitability proteins: route to more specific drugs? Science 241:1057–1063
7. Guy HR, Conti F (1990) Pursuing the structure and function of voltage-gated channels. Trends Neurosci 13:201–206
8. Antic SD (2016) Simultaneous recordings of voltage and current waveforms from dendrites. J Physiol 594:2557–2558
9. Williams SR, Mitchell SJ (2008) Direct measurement of somatic voltage clamp errors in central neurons. Nat Neurosci 11:790–798
10. Hodgkin AL, Huxley AF (1952) Currents carried by sodium and potassium ions through the membrane of the giant axon of Loligo. J Physiol 116:449–472
11. Jaafari N, De Waard M, Canepari M (2014) Imaging fast calcium currents beyond the limitations of electrode techniques. Biophys J 107:1280–1288
12. Canepari M, Vogt K, Zecevic D (2008) Combining voltage and calcium imaging from neuronal dendrites. Cell Mol Neurobiol 58:1079–1093
13. Vogt KE, Gerharz S, Graham J, Canepari M (2011a) High-resolution simultaneous voltage and Ca^{2+} imaging. J Physiol 589:489–494
14. Vogt KE, Gerharz S, Graham J, Canepari M (2011) Combining membrane potential imaging with L-glutamate or GABA photorelease. PLoS One 6:e24911
15. Kao JP, Tsien RY (1988) Ca^{2+} binding kinetics of fura-2 and azo-1 from temperature-jump relaxation measurements. Biophys J 53:635–639
16. Jaafari N, Marret E, Canepari M (2015) Using simultaneous voltage and calcium imaging to study fast Ca^{2+} channels. Neurophotonics 2:021010
17. Canepari M, Odgen D (2006) Kinetic, pharmacological and activity-dependent separation of two Ca^{2+} signalling pathways mediated by type 1 metabotropic glutamate receptors in rat Purkinje neurons. J Physiol 573:65–82
18. Canepari M, Vogt KE (2008) Dendritic spike saturation of endogenous calcium buffer and induction of postsynaptic cerebellar LTP. PLoS One 3:e4011
19. Savitzky A, Golay MJE (1964) Smoothing and differentiation of data by simplified least squares procedures. Anal Chem 36:1627–1639
20. Nägerl UV, Novo D, Mody I, Vergara JL (2000) Binding kinetics of calbindin-D(28k) determined by flash photolysis of caged Ca^{2+}. Biophys J 79:3009–3018
21. Airaksinen MS, Eilers J, Garaschuk O, Thoenen H, Konnerth A, Meyer M (1997) Ataxia and altered dendritic calcium signalling in mice carrying a targeted nullmutation of the calbindin D28k gene. Proc Natl Acad Sci U S A 94:1488–1493
22. Lee SH, Schwaller B, Neher E (2000) Kinetics of Ca^{2+} binding to parvalbumin in bovine chromaffin cells: implications for $[Ca^{2+}]$ transients of neuronal dendrites. J Physiol 525:419–432
23. Schmidt H, Stiefel KM, Racay P, Schwaller B, Eilers J (2003) Mutational analysis of dendritic Ca^{2+} kinetics in rodent Purkinje cells: role of parvalbumin and calbindin D28k. J Physiol 551:13–32
24. Ait Ouares K, Jaafari N, Canepari M (2016) A generalised method to estimate the kinetics of fast Ca^{2+} currents from Ca^{2+} imaging experiments. J Neurosci Methods 268:66–77
25. Usowicz MM, Sugimori M, Cherksey B, Llinás R (1992) P-type calcium channels in the somata and dendrites of adult cerebellar Purkinje cells. Neuron 9:1185–1199
26. Isope P, Hildebrand ME, Snutch TP (2012) Contributions of T-type voltage-gated calcium channels to postsynaptic calcium signaling within Purkinje neurons. Cerebellum 11:651–665

27. Miyakawa H, Lev-Ram V, Lasser-Ross N, Ross WN (1992) Calcium transients evoked by climbing fiber and parallel fiber synaptic inputs in guinea pig cerebellar Purkinje neurons. J Neurophysiol 68:1178–1189
28. Yan P, Acker CD, Zhou WL, Lee P, Bollensdorff C, Negrean A, Lotti J, Sacconi L, Antic SD, Kohl P, Mansvelder HD, Pavone FS, Loew LM (2012) Palette of fluorinated voltage-sensitive hemicyanine dyes. Proc Natl Acad Sci U S A 109:20443–20448
29. Willadt S, Canepari M, Yan P, Loew LM, Vogt KE (2014) Combined optogenetics and voltage sensitive dye imaging at single cell resolution. Front Cell Neurosci 8:311
30. Antic SD (2003) Action potentials in basal and oblique dendrites of rat neocortical pyramidal neurons. J Physiol 550:35–50
31. Bullen A, Saggau P (1998) Indicators and optical configuration for simultaneous high-resolution recording of membrane potential and intracellular calcium using laser scanning microscopy. Pflügers Arch 436:788–796
32. Jaafari N, Canepari M (2016) Functional coupling of diverse voltage-gated Ca^{2+} channels underlies high fidelity of fast dendritic Ca^{2+} signals during burst firing. J Physiol 594:967–983
33. Loew LM, Simpson LL (1981) Charge-shift probes of membrane potential: a probable electrochromic mechanism for p-aminostyrylpyridinium probes on a hemispherical lipid bilayer. Biophys J 34:353–365
34. Djurisic M, Antic S, Chen WR, Zecevic D (2004) Voltage imaging from dendrites of mitral cells: EPSP attenuation and spike trigger zones. J Neurosci 24:6703–6714
35. Roth A, Häusser M (2001) Compartmental models of rat cerebellar Purkinje cells based on simultaneous somatic and dendritic patch-clamp recordings. J Physiol 535:445–472
36. Spruston N, Schiller Y, Stuart G, Sakmann B (1995) Activity-dependent action potential invasion and calcium influx into hippocampal CA1 dendrites. Science 268:297–300
37. Canepari M, Djurisic M, Zecevic D (2007) Dendritic signals from rat hippocampal CA1 pyramidal neurons during coincident pre- and post-synaptic activity: a combined voltage- and calcium-imaging study. J Physiol 580:463–484
38. Bischofberger J, Jonas P (1997) Action potential propagation into the presynaptic dendrites of rat mitral cells. J Physiol 504:359–365
39. Sabatini BL, Regerh WG (1996) Timing of neurotransmission at fast synapses in the mammalian brain. Nature 384:170–172
40. Stuart G, Häusser M (1994) Initiation and spread of sodium action potentials in cerebellar Purkinje cells. Neuron 13:703–712
41. Vogt KE, Canepari M (2010) On the induction of postsynaptic granule cell-Purkinje neuron LTP and LTD. Cerebellum 9:284–290
42. Canepari M, Mammano F (1999) Imaging neuronal calcium fluorescence at high spatio-temporal resolution. J Neurosci Methods 87:1–11

Chapter 5
Molecular Diversity of Plasma Membrane Ca^{2+} Transporting ATPases: Their Function Under Normal and Pathological Conditions

Luca Hegedűs, Boglárka Zámbó, Katalin Pászty, Rita Padányi, Karolina Varga, John T. Penniston, and Ágnes Enyedi

Abstract Plasma membrane Ca^{2+} transport ATPases (PMCA1-4, *ATP2B1-4*) are responsible for removing excess Ca^{2+} from the cell in order to keep the cytosolic Ca^{2+} ion concentration at the low level essential for normal cell function. While these pumps take care of cellular Ca^{2+} homeostasis they also change the duration and amplitude of the Ca^{2+} signal and can create Ca^{2+} gradients across the cell. This is accomplished by generating more than twenty PMCA variants each having the character – fast or slow response, long or short memory, distinct interaction partners and localization signals – that meets the specific needs of the particular cell-type in which they are expressed. It has become apparent that these pumps are essential to normal tissue development and their malfunctioning can be linked to different pathological conditions such as certain types of neurodegenerative and heart diseases, hearing loss and cancer. In this chapter we summarize the complexity of PMCA regulation and function under normal and pathological conditions with particular attention to recent developments of the field.

L. Hegedűs
Department of Thoracic Surgery, Ruhrlandklinik, University Clinic Essen, Essen, Germany

B. Zámbó
Research Centre for Natural Sciences, Institute of Enzymology, Hungarian Academy of Sciences, Budapest, Hungary

K. Pászty
Department of Biophysics, Semmelweis University, Budapest, Hungary

R. Padányi · K. Varga · Á. Enyedi (✉)
2nd Department of Pathology, Semmelweis University, Budapest, Hungary
e-mail: enyedi.agnes@med.semmelweis-univ.hu

J. T. Penniston
Department of Neurosurgery, Massachusetts General Hospital, Boston, MA, USA

M. S. Islam (ed.), *Calcium Signaling*, Advances in Experimental Medicine and Biology 1131, https://doi.org/10.1007/978-3-030-12457-1_5

Keywords Plasma membrane Ca^{2+} ATPase (PMCA) · *ATP2B1-4* · Alternative splice · Calmodulin · Phosphatidylinositol-4, 5-bisphosphate · Actin cytoskeleton · Ca^{2+} signal · Genetic variation · Altered expression · Pathological condition

Abbreviations

AD	Alzheimer's disease
ATP	adenosine triphosphate
CaM	calmodulin
CaMKII	calcium/calmodulin-dependent protein kinase II
CASK	calcium/calmodulin-dependent serine protein kinase
CBS	calmodulin binding sequence
ER	endoplasmic reticulum
ERK	extracellular-signal regulated kinase
HDAC	histone deacetylase
HER2	human epidermal growth factor receptor 2
HUVEC	human umbilical vein endothelial cell
IP3	inositol 1,4,5-trisphosphate
IP_3R	inositol 1,4,5-trisphosphate receptor
IS	immunological synapse
MAGUK	membrane-associated guanylate kinase
MLEC	mouse lung endothelial cells
NFAT	nuclear factor of activated T-cell
NHERF2	Na^+/H^+ exchanger regulatory factor 2
nNOS	neural nitric oxide synthase
PIP2	phosphatidylinositol-4,5- bisphosphate
PKC	protein kinase C
PKA	protein kinase A
PMCA	plasma membrane Ca^{2+} ATPases
POST	partner of STIM
PSD-95	post synaptic density protein 95
RANKL	nuclear factor κB ligand
RASSF1	Ras association domain-containing protein 1
RBC	red blood cell
SCD	sickle cell disease
SERCA	sarco/endoplasmic reticulum Ca^{2+} ATPases
SNP	small nucleotide polymorphisms
SOCE	store operated Ca^{2+} entry
SPCA	secretory-pathway Ca^{2+} ATPase
STIM	stromal interacting molecule
TGF	transforming growth factor
TM domain	transmembrane domain

TSA	trichostatin A
VEGF	vascular endothelial growth factor
VSMC	vascular smooth muscle cell

5.1 Introduction

The plasma membrane Ca^{2+} transport ATPase (PMCA protein, *ATP2B gene*) was first described as a Ca^{2+} extrusion pump in red blood cells by Hans J. Schatzmann in 1966 [1]. It became evident that this pump is an essential element of the Ca^{2+} signaling toolkit, and that it plays a vital role in maintaining Ca^{2+} homeostasis in all mammalian cells [2]. After the first discovery of the PMCA many years were spent on identifying its regulators (for example calmodulin and acidic phospholipids) before it was cloned and sequenced at around the time when sequences for many of the other P-type ATPase family members also became available [3, 4]. Further structure-function studies concentrated on the PMCAs unique C-terminal regulatory region (often called the C-tail) and identified there calmodulin and PDZ-domain binding sequence motifs, a built-in inhibitor sequence, phosphorylation sites for protein kinases and a localization signal [5]. It became apparent that PMCAs comprise a P-type ATPase sub-family, encoded by four separate genes *ATP2B1-4* [6, 7] from which alternative splicing generates more than 20 variants with distinct biochemical characteristics that make them suitable to perform specific cellular functions [8, 9]. By now it is well documented that PMCAs are not simply Ca^{2+} extrusion pumps but by changing their abundance and variant composition, having different activation kinetics, locale and partners, they can actively modulate the Ca^{2+} signal in space and time, and hence affect Ca^{2+} mediated signaling events downstream. The PMCA variants are expressed in a tissue and cell type specific manner and many of them have specific function. Although, in the past decades these pumps have been extensively characterized their importance is rather underestimated. This is because only recently we gathered more information on their involvement in diseases such as cancer, neurological disorders, hearing loss and others. In this book chapter, therefore, we will summarize briefly the long known basic characteristics of these pumps paying more attention to the most recent findings on their roles under normal and pathophysiological conditions.

5.2 Structural Features of the PMCA

PMCAs (*ATP2B1-4 gene*) belong to the P-type ATPase family and share basic structural and catalytic features with them. The closest relatives of the PMCAs are the sarco/endoplasmic reticulum type Ca^{2+} pumps (SERCAs, *ATP2A1-3*) with an overall 30 % sequence homology between PMCA4 and SERCA1 [10]. Homology modeling using the SERCA1 structure as a template [11–13] has revealed four major domains shared with SERCA1, and a relatively large unstructured C-terminal region (30–130 residues depending on the isoforms and their variants), which is unique

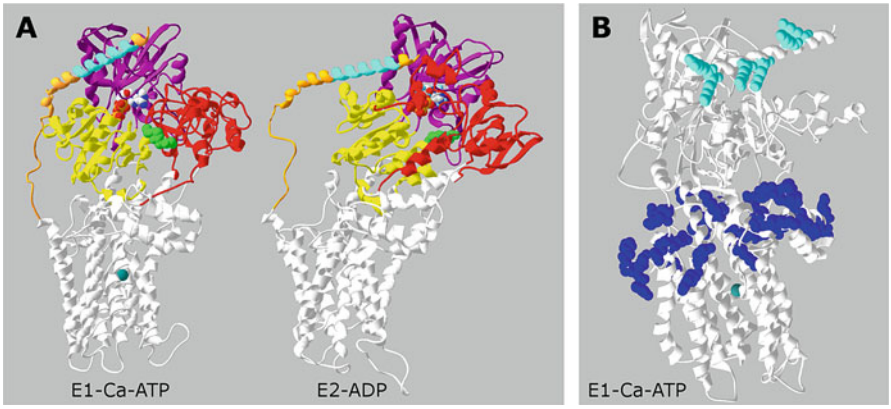

Fig. 5.1 Structural model of the PMCA in the E1-Ca-ATP and E2-ADP conformations. Structures of several intermediates in the enzyme cycle have been determined for SERCA [11–13]. Based on those, models of the intermediates have been constructed for PMCA4b (lacking 90 residues from the C-tail). (**a**): The models show 2 of the intermediates, E1 with Ca and ATP (SERCA PDB 1VFP and 1T5S) and E2 with ADP (SERCA PDB 2C88). In the latter, the Ca has been ejected into the extracellular space. They are colored as follows: A domain *red*; P domain *yellow*; N domain *purple*; stalk; insert and transmembrane domains *white*; C-tail *straw*; Calmodulin-binding domain *cyan*; Ca^{2+}*metallic blue-green*. (**b**): The positively charged residues of the PIP_2 binding regions are colored. The blue collar and the insert *blue*, the calmodulin-binding domain (CBD) *cyan*. The CBD would have the potential of releasing from the conformation shown and lying on the surface of the membrane in a PIP_2-rich region

to the PMCAs (Fig. 5.1a) (for a review see also [14]). The M-domain consists of 10 trans-membrane spanning helices that provide the coordinating ligands for the binding of one cytosolic Ca^{2+} ion to be transported. The N-domain binds an ATP molecule of which the terminal phosphate is transferred to a highly conserved aspartate in the P-domain forming a high-energy acyl-phosphate intermediate. As a result of these events hydrolysis of one ATP molecule provides sufficient energy to translocate one Ca^{2+} ion through the membrane [15] that is coupled to H^+ transport in return with a Ca^{2+}:H^+ ratio of 1:2 [16]. The A-domain coordinates the movements of the other three domains during the E1-E2 transition to complete a full reaction cycle [17]. While the catalytic domains N, P and the M-domain are largely conserved between the PMCAs the C-tail and the A-domain – where alternative splicing generates substantial sequence divergence – vary substantially. These variations in the C-tail and A-domain can generate PMCA proteins with distinct characteristics [18, 19].

The Blue Collar In contrast to the endoplasmic reticulum-resident SERCA pump a cluster of positively charged residues were found at the intracellular near-membrane region of the PMCA forming four binding pockets for the phosphorylated inositol ring of PIP2 (phosphatidylinositol-4,5-bisphosphate) [20], in addition to the previously determined linear PIP2 binding sequences near the A splice-site region at the A-domain [21, 22] and the calmodulin binding sequence at the C-tail [23]. Figure 5.1b shows a blue collar formed from the four PIP2 binding pockets and the

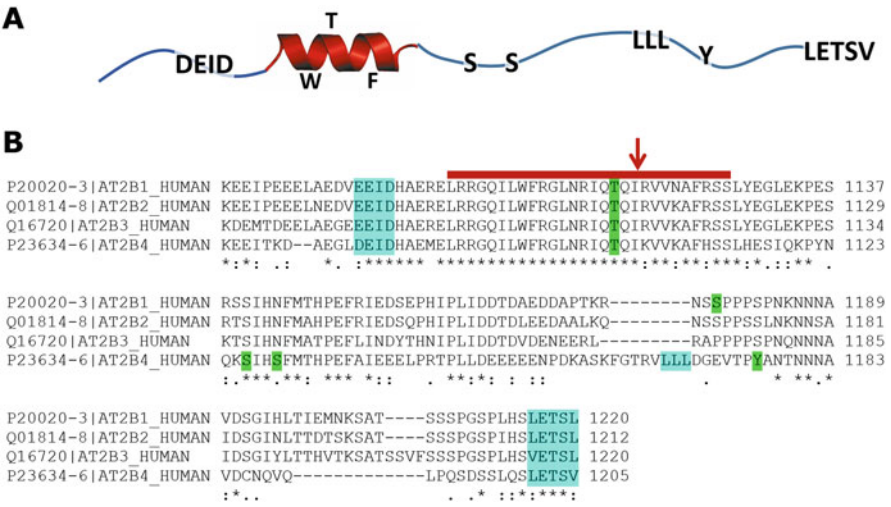

Fig. 5.2 C-tail of the "b" splice variants of PMCA1-4. (**a**) Schematic representation of the C-tail of PMCA4b emphasizing important sequence motifs highlighted below. Calmodulin-binding domain is colored *burgundy*. (**b**) An alignment of C-terminal sequences of "b" splice forms of PMCA1-4 demonstrates that the variants may have distinct regulatory features (i.e. the di-leucine motif in PMCA4b) however; some sequence motifs (caspase 3 sites and the PDZ-binding tails) are relatively conserved. These motifs are colored *cyan*. The PKA, PKC and tyrosine kinase phosphorylation sites are highlighted in *green* and the calmodulin-binding sequence is marked *burgundy*. The arrow indicates where alternative splice changes the sequence in the other splice variants of PMCA1-4

linear lipid binding region of the A domain around the stalk region of the PMCA. This arrangement of positively charged residues follows the positive inside role, which is quite common in plasma membrane proteins and often involved in PIP2 binding [24, 25].

The C-Tail The C-tail, which is also known as the main regulatory unit of these pumps, is the most characterized although the least conserved region of the PMCAs (Fig. 5.2). A major portion of this region is structurally disordered [5], containing multiple recognition sites: a DxxD caspase cleavage site [26, 27], a calmodulin-binding domain (CBD) with an overlapping auto-inhibitory region and acidic lipid binding side chains [3], several protein kinase phosphorylation sites [28, 29], a di-leucine-like localization signal [30] and a PDZ-domain-binding sequence motif at the C-terminus [31]. Some of these motifs are present in nearly all PMCAs (caspase 3 cleavage sites, CBD) while others are specific to certain variants; for instance the di-leucine-like motif is specific to PMCA4b whereas the PDZ-binding motif is present in all "b" splice variants. However, specificity of the PDZ binding may vary because the terminal amino acid is Val in PMCA4b but Leu in PMCA1-3. As an example the sodium-hydrogen exchange regulatory cofactor NHERF2 interacts with PMCA2b but not with PMCA4b [32].

Ca^{2+}-Calmodulin Binding is critical for PMCA function. Early studies identified a 28 residue long sequence at the C-tail of PMCA4b that could bind Ca^{2+}-calmodulin with high affinity. Extensive kinetic [33, 34] and NMR [35] studies with a peptide (c28) representing the complete 28-residue sequence region have revealed two anchor sites Phe-1110 and Trp-1093 in a relative position of 18 and 1, and two steps of Ca^{2+}-calmodulin binding in an anti-parallel manner (Fig. 5.3). In the first step the C-terminal lobe of calmodulin binds the N-terminal Trp-1093, followed by the second step, which is binding of the C-terminal Phe-1110 to the N-terminal lobe of calmodulin. As a result, calmodulin wraps around the c28 peptide that adopts an α-helix with its anchors buried in the hydrophobic pockets of the two distinct CaM lobes. This model correlates well with an earlier NMR structure of Ca^{2+}-calmodulin with a shorter c20 peptide lacking the second anchor Phe-1110 [36]. In that case the peptide could bind only to the C-terminal lobe of calmodulin, which retained its extended structure, as is expected (Fig. 5.3).

The w Insert Another structurally less defined region of the molecule is the sequence that couples the A domain to the third membrane spanning helix. An

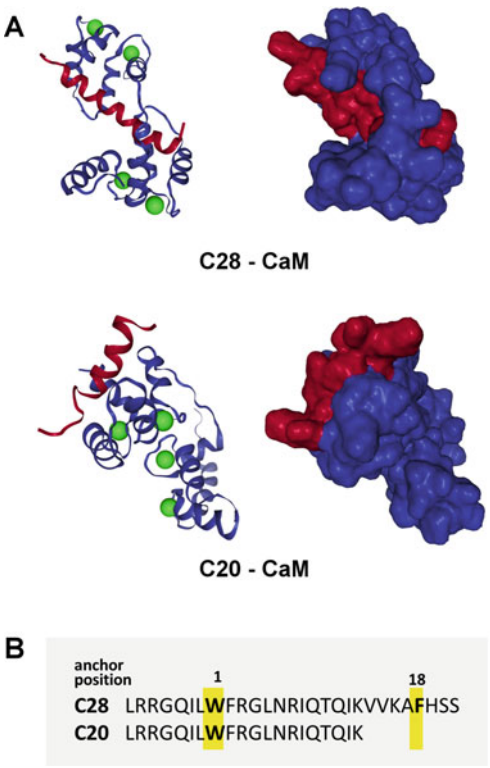

Fig. 5.3 NMR structure of calmodulin in complex with calmodulin binding peptides. (**a**)**:** Structures of C28-calmodulin (https://www.rcsb.org/structure/2KNE) and C20-calmodulin complexes (https://www.rcsb.org/structure/1CFF). C20 and C28 correspond to the appropriate calmodulin binding sequence of PMCA4b. Colors: calmodulin *blue*; peptide *burgundy*; green spheres correspond to the 4 Ca^{2+} bound to CaM. (**b**): Sequences of the peptides C20 and C28 with the anchors 18-1

alternative splice at splice site A changes the structure of this region by including or excluding a single exon, producing the x and z variants of the isoforms [37], however, no functional significance has been linked to these changes. In PMCA2, however, additional variations exist in which two more exons can be inserted generating the PMCA2 y and w forms. Importantly, the w insert – which is a 44-residue long sequence – is essential for targeting PMCA2 to the apical compartment of polarized cells.

5.3 Regulation of PMCA Expression and Function

PMCAs are encoded by four separate genes (*ATP2B1-4*) located at distinct chromosomes: 12q21–23, 3p25.3, Xq28 and 1q25–q32, respectively [8]. Two major alternative splice options at splice sites A and C of the primary transcripts of each *ATP2B* gene have the potential of generating >30 PMCA protein variants, however, only 20 of them have been identified in different tissues [38, 39]. In addition, mutations, single nucleotide polymorphisms and posttranslational modifications further increase PMCA variations. It is not surprising that to keep the level of calcium within a suitable range in the cytoplasm of different cell types with very different function tight regulation of PMCAs is required at the transcriptional, splicing, translational and protein levels.

5.3.1 Regulation at the Transcription Level

Transcriptional regulation of *ATP2B* genes is complex and still not well understood. The intricate regulatory structure of the promoter and enhancer regions of the genes allows the fine-tuning of each PMCA's transcription during embryonic development, in various tissues, as well as upon various stimuli. It has been shown that in mouse smooth muscle cells Atp2b1 expression during G1/S phase is reduced via c-myb binding to the promoter region of the gene [40]. This transcription factor is also involved in the down-regulation of Atp2b1 in differentiating B-lymphocytes [41]. The active form of vitamin D induces the transcription of *ATP2B1* in various tissues and cell types [42–45]. *ATP2B2* gene has four alternative promoters and alternatively spliced 5' exons, which showed higher expression and different promoter usage in mammary gland compared to neuronal cells [46]. EGR1 can bind to a specific region in the CpG island of the *ATP2B2* gene and controls the α-type promoter activity, which is specific to brain and auditory cells [47]. The *ATP2B4* gene contains an enhancer in the intron 1, which has an essential role in the erythroid differentiation, but has no effect in other cell types [48]. From these studies it appears that PMCAs possess general and specific transcription factor binding sites and regions, which only play role under certain conditions, under proper stimulus or differentiation state of the given cell type.

5.3.2 Regulation at the Protein Level

Auto-Inhibition PMCA activity is determined by the presence of an auto-inhibitory unit at the C-tail, which largely overlaps with the calmodulin-binding sequence [49]. This inhibitory unit binds to the N- and A-domains interfering with Ca^{2+} binding to the catalytic sites, and slowing down the reaction cycle by inhibiting the movements of the cytosolic domains [23]. The extent of the auto-inhibition differs from one isoform to the other and is affected by the alternative splice at splice site C [50–52]. As a result, PMCA4b is the only truly inactive pump at resting cytosolic Ca^{2+} ion concentration while all the other pumps are partially active, as determined in cell free systems.

Activation by Caspase 3 The auto-inhibitory C-tail is removed by the executor protease caspase 3 during apoptosis. Caspase 3 cleaves PMCA4b at a canonic caspase 3 cleavage site (DEID) just upstream of the CBD-auto-inhibitory sequence removing the complete auto-inhibitory region [26, 27]. While there has been a long debate on whether caspase 3 activates or inhibits PMCA4b during apoptosis [53] it is conceivable that deleting the auto-inhibitor should result in a gain-of- function pump [54], however, the overall outcome could depend on the given cell type, stimulus and conditions that need further studies.

Activation with Ca^{2+}-Calmodulin A functionally important feature of the PMCA variants is the difference in their activation with Ca^{2+}-calmodulin that determines the rate by which they can respond to the incoming Ca^{2+} signal, and equally important is the length of time during which they remain active after the stimulus [55]. Since pump and calmodulin compete for CBD-autoinhibitor it is expected that a strong pump-CBD-auto-inhibitor interaction will result not only in a low basal activity but also in a slow activation rate. Indeed, PMCA4b has both the lowest basal activity and the slowest activation with calmodulin among the isoforms (slow pump, $T_{1/2}$ is about 1 min) [56]. Although, PMCA4b is activated slowly its inactivation rate is even slower (long memory, remains active for about 20 min) because calmodulin remains bound to the pump for a long period of time [57]. An alternative splice that creates a shorter version of PMCA4 changes the response of the pump to Ca^{2+} completely so that PMCA4a binds Ca^{2+}-calmodulin quickly (fast pump, T1/2 is about 20 s) but then calmodulin dissociates also quickly, resulting in a fast responding pump that remains active for a relatively short period of time (short memory, active for less than a minute) [34]. It is important to note, that PMCA4a also has a relatively high basal activity suggesting weak interaction between pump and auto-inhibitor. All other forms – variants of PMCA2 and PMCA3 – that have been characterized are fast responding pumps having slow inactivation rates (long memory), and as mentioned above they also have relatively high activity even without activators [50, 57].

Activation with Acidic Phospholipids Acidic lipids like PS and the PIPs – PI, PIP and PIP2 – can activate the pump and the amount of activation is augmented as the negative charge of the phospholipid head group increases [58]. It has been

demonstrated that both the CBD and the linear basic sequence in the A-domain are involved in this type of activation [21–23]. It has been suggested that changes in the lipid composition may affect PMCA activity and that PMCAs might be more active in PIP2-rich lipid rafts [59]. Recently, it was demonstrated that the activity of the PMCA is also modulated by neutral phospholipids. The activity of PMCA4b was optimal when it was reconstituted in a 1,2-dimyristoyl-*sn*-glycero-3-phosphocholine (DMPC) bilayer of approximately 24 Å thickness [60]. Molecular simulation studies have revealed that in DMPC several lysine and arginine residues at the extracellular surface are exposed to the medium while in a thicker layer of 1,2-dioleoyl-sn-glycero-3-phosphocholine (DOPC) these residues are embedded in the hydrophobic core that could explain the reduced activity observed in DOPC.

Regulation by the Actin Cytoskeleton First it was shown that PMCAs interact with F-actin in activated platelets and they are associated with the F-actin rich cytoskeleton at or near the filopodia [61, 62]. Later it was documented that the purified PMCA4b can bind both monomeric and filamentous actin and while actin monomers activate the pump, F-actin may inhibit its function [63, 64]. These results were confirmed by using live HEK cells expressing isoforms PMCA2 and PMCA4 [65]. Based on these findings it has been suggested that PMCA can regulate actin dynamics through a series of feed-back regulations by lowering Ca^{2+} concentration in its vicinity and promoting actin polymerization, which in turn switches off the PMCA function allowing increase in Ca^{2+} levels and hence actin de-polymerization [66].

5.4 Function of the PMCAs in the Living Cell

It is quite remarkable how the above described diverse structural and biochemical characteristics of the PMCA proteins are translated into specific physiological functions in the different cell types. Distinct kinetics of the PMCAs are transcribed into distinct Ca^{2+} signaling properties while additional structural diversity between the PMCAs determines their localization and interaction patterns with different scaffolding and signaling molecules resulting in unique PMCA variant-specific cellular function (Table 5.2).

5.4.1 PMCAs Shape the Ca^{2+} Signal

It has been widely accepted that PMCAs play a role in the decay phase of the store-operated Ca^{2+} entry (SOCE). However, expression of PMCAs with distinct kinetic properties (see also Table 5.1 and Fig. 5.4) – fast or slow, with or without memories – resulted not only in a faster decay of the signal but also in very different Ca^{2+} signaling patterns in HEK and HeLa cells [67]. While the “slow with

Table 5.1 Distinct kinetic properties and distribution of the PMCAs

Basal activity	Activation with CaM	Memory	Pump variant	Cells, tissues
High	Fast	Short	PMCA4a	Smooth muscle, heart, sperm
High	Fast	Long	PMCA2b	Neuron, mammary gland
			PMCA2a	Neuron, cochlear hair cells
Low	Slow	Long	PMCA4b	Erythrocyte, breast, colon heart, kidney, HUVEC, melanoma

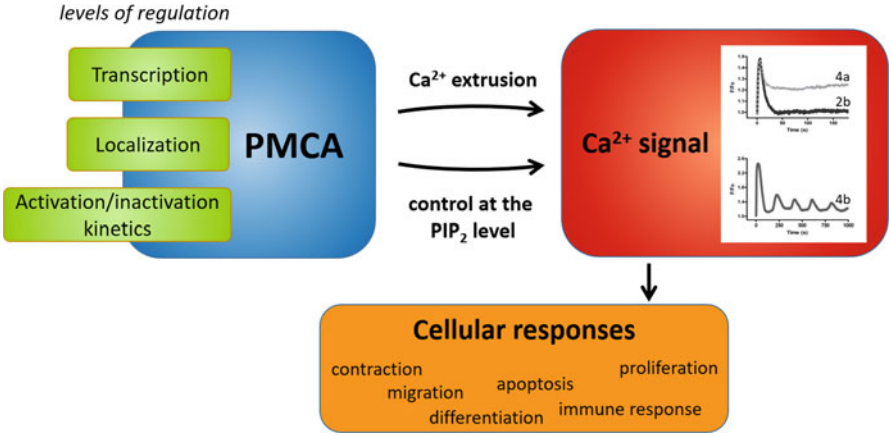

Fig. 5.4 Schematic representation of the role of PMCAs in Ca^{2+}signaling. The abundance of PMCA is regulated at the transcriptional and protein levels. Localization is affected by specific sequence motifs and interaction with other proteins. The activity is regulated by proteins (such as calmodulin) and acidic lipids. This can result in the modulation of the Ca^{2+} signal at two levels: (i) Ca^{2+} extrusion; (ii) IP_3-induced Ca^{2+} release. The resultant Ca^{2+} signal then might be translated to distinct cell responses

memory" PMCA4b induced Ca^{2+} oscillation after the first spike, the C-terminal splice variant of the PMCA4 isoform – the "fast without memory" PMCA4a – responds quickly to the incoming Ca^{2+} but then since it becomes inactivated also quickly the signal returns to an elevated level without oscillation. PMCA2b – a fast pump with memory – allows only short Ca^{2+} spikes and Ca^{2+} concentration always returns to the basal level quickly. It was also demonstrated that in addition to shaping the SOCE mediated Ca^{2+} signal PMCAs also control the formation of IP3 by controlling the availability of the signaling PIP2 molecules, and hence regulate the release of Ca^{2+} from the stores [20] (Fig. 5.4). It is important to note that the Ca^{2+} signal can also be altered through additional cell type-specific regulatory mechanisms of the PMCA. During T-cell activation, for example, it was shown that the activity of PMCA4b is inhibited by the interaction with the ER Ca^{2+} sensor protein STIM1 [68] and its partner scaffold protein POST [69] resulting in a more sustained elevation in intracellular Ca^{2+} concentration.

5.4.2 Cell Type Specific Expression of the PMCAs

Homozygous deletion of the *ATP2B1* gene in mice is lethal suggesting that PMCA1 is the housekeeping isoform [70]. The other isoforms PMCA2-4 are expressed at different stages of development [8]. The slow PMCA4b variant is present in erythrocytes, T lymphocytes and in epithelial cells but also abundantly expressed in the heart and smooth muscle cells [39]. PMCA4a is expressed in the brain and it is the only PMCA isoform present in the sperm tail [71]. Altered expression of *ATP2B4* in mice was associated with arrhythmias, cardiac hypertrophy and heart failure. Deletion of both copies of *ATP2B4* in mice caused male infertility [70, 72]. Interestingly, in activated sperm cells the pattern of the Ca^{2+} signal is similar to that seen in the PMCA4a expressing Hela cells [73]. Ca^{2+} pumps (PMCA1 and PMCA4) were shown to contribute to sustained Ca^{2+} oscillations in human mesenchymal stem cells [74] and airway smooth muscle cells [75].

The fast pumps PMCA2 and PMCA3 are abundantly expressed in excitable tissues such as the brain and skeletal muscle [76, 77]. The PMCA2w/a and PMCA2w/b forms are found in vestibular hair cells and in Purkinje neurons of the cerebellum where they can react quickly to the fast signals induced by the voltage-gated Ca^{2+} channels. A specific form PMCA2w/b is also expressed in the lactating mammary gland. Knock down of the *ATP2B2* gene induced ataxia, deafness [78] and reduced Ca^{2+} concentration in the milk [79]. These are just a few examples demonstrating how variations in PMCA expression contribute to cell-type specific functions (see more details in refs (39, 55, 76, 77) and in Table 5.1.

5.4.3 Polarized Expression of the PMCA

To perform their cellular function it is also important to target PMCA proteins to the appropriate membrane compartment. This is accomplished by intrinsic localization signals and/or by interaction with other proteins in a cell-type specific manner. In many cases these characteristics of the PMCAs are sensitive to alternative splicing. For example, the di-leucine-like localization motif is unique to the “b” splice variant of PMCA4 that was shown to direct this pump to endocytic vesicles in non-confluent epithelial cells [30]. Hence, PMCA4b localizes to the plasma membrane only in fully confluent differentiated cells where it can be stabilized and/or modulated by other interacting molecules [80]. Most recently, basigin/CD147 was identified as a novel interacting protein that may serve as a subunit of the PMCA [81]. It was demonstrated in a variety of cell types that PMCA1-4 interacts with basigin in the ER, which is essentially involved in functional targeting PMCAs to the plasma membrane.

PMCA proteins are localized to specific membrane compartments in polarized cells where they contribute to trans-cellular Ca^{2+} fluxes. While the lateral compartment seems to be the default place, in some cell types PMCAs localize apically.

PMCA2 for example can be directed to the apical compartment by an alternative splice option at site A that introduces a 44-residue long "w" sequence at the region that connects the A and TM domains [37]. The resultant PMCA2w/b and PMCA2w/a variants have very specific functions in the lactating mammary gland [79] and the stereocilia of hair cells [78, 82, 83] where PMCA2w/b is responsible for milk Ca^{2+} while PMCA2w/a contributes to hearing, respectively. The "b" splice variant of PMCA2w might be connected through PDZ-interactions with the scaffold protein NHERF2 to the actin cytoskeleton by which it is immobilized in the apical membrane [84]. In contrast, PMCA2w/a, which is lacking the PDZ-interacting tail, is very mobile, trafficking in and out of the stereocilia of hair cells [85]. In parotid gland acinar cells PMCA4b was found in the apical membrane compartment and its localization was modulated by PDZ-interaction with Homer2 [86]. In the same cells PMCA1 was also found in the apical membrane but only when it was phosphorylated by PKA [87]. PMCA4b plays an important role in the immune synapse where it is targeted to specific signaling micro domains beneath the mitochondria where it is actively involved in Ca^{2+} handling during T-cell activation controlling Ca^{2+} influx through the CRAC channels [88].

Polarized distribution of PMCA was also found in migrating cells. In collectively migrating human umbilical vein endothelial cells (HUVEC) PMCA located to the front of the cells by which it contributed to the front-to-rear Ca^{2+} gradient essential for directed cell migration [89]. In addition, downregulation of PMCA4 increased while its overexpression decreased cell migration in a wound-healing assay of HUVECs [90]. These data are in line with the latest finding demonstrating that PMCA4b interferes with cell migration of a highly motile BRAF mutant melanoma cell line [91]. These examples highlight the importance of PMCA targeting and demonstrate that different interacting partners may change the location of PMCAs resulting in distinct cellular functions (see Table 5.2).

5.4.4 Interaction of PMCAs with Signaling Molecules

Through interactions with other proteins PMCAs can influence downstream signaling events (Table 5.2). In many cases they influence the activity of the interacting signaling molecule by reducing the Ca^{2+} concentration in its vicinity. One example is the interaction of PMCA2 and PMCA4 with the Ca^{2+}-CaM dependent phosphatase calcineurin through their catalytic domain that was found to reduce the activity of the nuclear factor activated T-cell (NFAT) pathway [92, 93]. Inhibition of this interaction increased Fas-ligand expression and apoptosis in breast cancer cells [94], while PMCA4b overexpression in endothelial cells reduced VEGF initiated cell migration and angiogenesis [95]. Another example for this type of interaction was described between PMCA4b and calcium/calmodulin-dependent serine protein kinase (CASK) in rat brain and kidney where PMCA4b binds CASK through its C-terminal PDZ binding motif [96]. CASK together with Tbr-1 induces T-element dependent transcription; however, this is strongly decreased upon interaction with

Table 5.2 PMCA interactions

Interacting partner	Isoform preference	Type/place of interaction	Cell type	Effect	References
Effect of interacting on PMCA					
14-3-3ε	PMCA1, PMCA3, PMCA4	N-terminal	HeLa, CHO	Inhibition of PMCA activity	[233, 234]
G-actin (short oligomers)	PMCA4	Putative actin-binding site	Erythrocyte	Increasing PMCA activity	[63, 64, 235]
F-actin	PMCA4	Putative actin-binding site	Erythrocyte	Inhibition of PMCA activity	[64]
G/F-actin	PMCA4b	Through CLP36 and α-actinin	Platelet		[62, 236]
Calmodulin	All PMCA forms	Calmodulin-binding domain CaMBS1, CaMBS2	All kinds of cells	RELIEVING autoinhibition of the pump, increasing both Ca2+ affinity and pump rate	[237, 238]
CASK	PMCA4b	Via PDZ interaction	Mouse sperm	Reduced PMCA activity	[97]
Homer1	PMCA1-4 b-splice forms	Via PDZ interaction	Hippocampal neurons, MDCK, COS-7	Increasing PMCA activity	[239, 240]
Homer2	PMCA1b	Homer-binding	Mouse parotid gland acinar cells, HEK293	Inhibition of PMCA activity	[86]
	PMCA4b				

(continued)

Table 5.2 (continued)

Interacting partner	Isoform preference	Type/place of interaction	Cell type	Effect	References
Effect of PMCA on the interacting partner					
Calcineurin	PMCA4b	Main intracellular loop (amino acids 501–575)	HEK293, MCF-7, HUVEC, endothelial cells, cardiomyocytes	Inhibition of the calcineurin/NFAT signal transduction pathway	[92, 93, 95, 204]
	PMCA2(b)	Amino acids 462–684	Breast cancer cells, MCF-7, ZR-75-1, MDA-MB-231, T47D,HEK293	Inhibition of the calcineurin/NFAT signal transduction pathway	[93, 94]
CASK	PMCA4b	Via PDZ interaction	Rat brain and kidney, HEK293	Inhibition of CASK function	[96]
CD147 (basigin)	PMCA4		Jurkat E6.1	Negatively regulates IL-2 expression	[231]
nNOS	PMCA4b	Via PDZ interaction	HEK293, neuro-2a, cardiomyocytes, sperm	Decrease nNOS activity, decrease NO production	[197, 241, 242]
eNOS	PMCA4	Catalytic intracellular loop	Endothelial cells, sperm	Decrease eNOS activity, decrease NO production	[243]
Ras-associated factor-1	PMCA4b	Main intracellular loop (region 652–748)	HEK293, cardiomyocytes	Modulating the EGF-mediated Ras signaling pathways	[244]
α1-syntrophin	PMCA1b, PMCA4b	Main intracellular loop (region 652–748)	HEK293, heart	Inhibit NOS-I-mediated NO production	[200]

Changing localization of PMCA					
CLP36	PMCA4b	Via PDZ interaction	Platelet	Connect PMCA to the cytoskeleton	[62]
mGluR1–Homer3–IP3R1	PMCA2	via PDZ interaction	Purkinje neurons	Component of the mGluR1–Homer3–IP3R1 signaling complex	[245]
MAGUK family members: PSD95, PSD93, SAP97 and SAP102	PMCA2b, PMCA4b	Via PDZ interaction	MDCK, hippocampal neurons	Recruit PMCA to specific membrane domains	[31, 80, 246]
	Only PMCA4b	Via PDZ interaction			
neuroplastin or basigin	PMCA1-4	Heteromeric complexes of PMCAs1–4 and either neuroplastin or basigin	Brain, kidney	Stability and effective surface trafficking of PMCA	[81]
NHERF2	PMCA2(w)b	Via PDZ interaction	MDCK	NHERF2 anchors PMCA2w/b to the apical actin filaments via ezrin	[32, 84]
	PMCA1b	Via PDZ interaction	HT-29	Scaffolding and maintaining PMCA at the cell membrane	[247]
PISP	All PMCA b-splice forms	Via PDZ interaction	MDCK	Sorting of PMCAs to and from the plasma membrane	[248]

PMCA4b in HEK cells. Interestingly, CASK and PMCA4b interaction was also found in mouse sperm where CASK inhibited the activity of the pump resulting in an increased Ca^{2+} level and ultimately decreased motility of the sperm [97]. Several other interactions between PMCA proteins and their partners were described that influence downstream signaling events such as interactions with nNOS in the heart, CD147 in T-cells, STIM and POST in the immune synapse or with F- and G-actin. These results demonstrate that besides maintaining the low intracellular calcium level PMCAs are also important signaling molecules modulating the outcome of a variety of cell-type specific functions.

5.5 PMCAs in Disease Pathogenesis

PMCA proteins have been associated with several diseases in humans. Since many isoforms have highly specialized, cell type specific function alterations in their expression, localization, regulation or activity may contribute to the development of distinct pathological conditions (Table 5.3) [98]. Alterations of the PMCAs have been described in cardiovascular diseases, neurodegenerative disorders and cancer [99, 100]. More recently genetic variations in the *ATP2B* genes were also linked to certain pathological conditions.

5.5.1 Diseases Related to Genetic Variations in ATP2B1-4

ATP2B1 Small nucleotide polymorphisms (SNPs) found in the *ATP2B1* gene were associated with hypertension [101, 102], coronary artery disease [103–105] and early onset preeclampsia [106]. Preeclampsia is a disorder during pregnancy and it is characterized by high blood pressure and proteinuria. Reduced Ca^{2+}-ATPase activity of myometrium and the placental trophoblast was described in preeclamptic women [107], and a decreased expression of PMCA1 and PMCA4 in preeclamptic placental tissue was also found [108] suggesting a pivotal role of PMCAs in calcium homeostasis and transport through the placenta. The susceptibility to hypertension resulting in elevated blood pressure was linked to SNP rs11105378 in *ATP2B1* that was suggested to decrease PMCA1 expression in human umbilical artery smooth muscle cells [109]. In patients with chronic kidney disease, SNPs in ATB2B1 were associated with coronary atherosclerosis and myocardial infarction [105].

ATP2B2 SNPs in the *ATP2B2* gene were associated with autism in both European and Chinese population [110, 111]. Also, a missense mutation of PMCA2 (V586M) was shown to exacerbate the effect of the mutation in cadherin-23 leading to hearing loss [112, 113] in good accordance with the finding that ablation or missense mutations in PMCA2 cause deafness in mice [83, 114].

Table 5.3 PMCA related diseases

PMCA/*ATP2B*	Diseases associated with genetic variation in the *ATP2B1-4* genes	Diseases associated with altered expression, localization or activity of the PMCA proteins
PMCA1 (*ATP2B1*)	Hypertension	Multiple sclerosis
	Coronary artery disease	Reduced bone mineral density
	Myocardial infarction	Oral cancer
	Early onset preeclampsia	Ovarian cancer
PMCA2 (*ATP2B2*)	Hereditary deafness	Parkinson's disease
	Autism	Type 1 and type 2 diabetes
		Breast cancer
PMCA3 (*ATP2B3*)	X-linked cerebellar ataxia	Multiple sclerosis
	Aldosterone producing adenomas	
PMCA4 (*ATP2B4*)	Familial spastic paraplegia	Cardiac hypertrophy
	Developmental dysplasia of the hip	Hypertension
	Malaria resistance	Sickle cell disease
		Alzheimer's disease
		Chronic kidney disease
		Diabetes
		Adult idiopathic scoliosis
		Colon cancer
		Breast cancer
		Melanoma

ATP2B3 Missense mutation in the *ATP2B3* gene was found in patients with X-linked congenital cerebellar ataxia in two separate cases, in which the ability of the pump to decrease intracellular Ca^{2+} concentration after stimulation was compromised [115, 116]. Later it was demonstrated that the G1107D replacement altered both activation and auto-inhibition of this pump at low Ca^{2+} levels [117]. Mutations in the *ATP2B3* gene were also identified in some aldosterone producing adenomas (APA), and were linked to elevated aldosterone production compared with wild type APAs [118, 119]. In cellular models it was demonstrated that impaired PMCA3 function resulted in elevated intracellular Ca^{2+} levels and consequently increased aldosterone synthase production in the cells [120].

ATP2B4 Missense mutation in the *ATP2B4* gene was found in one family with familial spastic paraplegia that causes lower limb spasticity and weakness in patients [121]. Later it was shown that overexpression of the mutant PMCA4 protein in human neuroblastoma cells increased the resting cytosolic Ca^{2+} concentration and elevated the maximal Ca^{2+} surge after stimulation relative to the wild type pump [122]. Rear heterozygous variants in the *ATP2B4* and the *HSPG2* genes were described in a family with developmental dysplasia of the hip and based on *in silico* analysis an epistatic interaction was suggested between the genes [123]. SNPs in the *ATP2B4* gene were related to resistance against severe malaria that will be discussed in detail in the next chapter.

5.5.2 PMCAs in Red Blood Cell Related Diseases

PMCAs were among the first proteins described – and later characterized – in the membrane of red blood cells [124–126]. Since mature red cells (RBCs) are easily accessible, and have no internal membrane organelles involved in Ca^{2+} homeostasis, they have become important model cells for the examination of the enzymatic activity and kinetic parameters of the plasma membrane-bound PMCA protein [22, 127, 128]. Two isoforms have been identified in the RBC surface, PMCA1b and PMCA4b, of which PMCA4b appeared to be the most abundant [129–132]. These high affinity calcium pumps are responsible for maintaining the exceptionally low total Ca^{2+} content of red cells [133–135]. They have a crucial role in balancing cell calcium during shear stress in the microcirculation [136], volume control [137, 138] and in senescence and programmed cell death [131, 139, 140] of RBCs. Under certain pathological conditions – such as hereditary hemolytic anemia, malaria and diabetes mellitus – the intracellular Ca^{2+} levels in RBCs are altered [135, 141], therefore, the role of PMCAs in these cases emerges.

In Hereditary Hemolytic Anemia Ca^{2+} transport has a particular importance. In case of sickle cell anemia (SCD) and thalassemia, atypical hemoglobin (such as HbS) polymerization and deoxygenating processes lead to membrane deformation and activation of the mechanosensitive stretch-activated cation channel PIEZO1 [142]. As a result, Ca^{2+} permeability of these atypical RBCs increases. Subsequent stochastic activation of the Gardos or Ca^{2+}-sensitive potassium channel can lead to sickling and dehydration of red cells in SCD patients [131, 138, 143, 144]. It was found that PMCA inhibition is also involved in the maintenance of the high Ca^{2+} concentration needed for sickle cell dehydration [145, 146].

Severe Malaria is one of the most studied infectious diseases worldwide [147, 148]; however, the molecular mechanisms underlying the survival and growth of the parasite in the human body are still not fully understood. As a result of co-evolution of human and *Plasmodium* species, many alleles preserved in our genome, which provide some degree of protection against malaria infection [149, 150]. Majority of these alleles are important in the erythroid stage of the parasite [150] when it binds to the uninfected RBC, invades it and grows inside the red cells. The firstly described genetic factors linked to malaria protection were the hemoglobin genes [151, 152], but there are several other red cell related genetic variants involved in the susceptibility to malaria [148] including ABO blood group [153, 154], G6PD [151, 155], glycophorin genes [156, 157], CR1 [158], band 3 protein (*SLC4A1*) [157], pyruvate kinase (Pklv) [159], basigin [160] and ABCB6 [161]. It was recently discovered that PMCAs present in RBCs are involved in the survival and growth of the parasite and some variations in the *ATP2B4* (encoding PMCA4) gene may lead to malaria resistance [162–165].

The latest genome wide association (GWA) [163, 164] and multicenter [165] studies have shown that the *ATP2B4* gene also carries a haplotype that is involved in malaria protection and this haplotype showed association with red blood cell traits

such as mean corpuscular hemoglobin concentration (MCHC) [166]. According to Lessard et al. [167], this haplotype is located in the enhancer region of the protein, and the complete deletion of this region lead to complete loss of PMCA expression in some erythroid related cell lines, while in case of some other cell lines the deletion does not cause any change in its expression. It is also described [168] that this haplotype leads to reduced expression of PMCA4b in RBCs, but this change is not associated with any additional physiological conditions, probably because this genome region is only essential in erythrocyte development. It is also notable, that this haplotype is much more frequent in malaria-endemic than in malaria-free countries (NCBI and CDC databases). While the relationship between these variations in the *ATP2B4* gene and malaria susceptibility is apparent, the exact function of the PMCA in the parasite's lifecycle within RBCs is still not known [169]. There are controversial data [170] whether the parasitophorous vacuolar membrane (PVM), surrounding the parasite inside the RBCs, contains host membrane proteins [171] or they are excluded from it [172]. Although, the locale of the PMCA during RBC phase of the parasite lifecycle has not been determined, it has been suggested that PMCA remains in the vacuolar membrane, and the parasite may use this protein to maintain a sufficiently high concentration of Ca^{2+} within the vacuolar membrane to proliferate [162]. Thus, selective inhibition of the PMCA may offer a potential new treatment option for malaria in the future.

Diabetes In poorly controlled diabetic patients increased glycosylation and decreased Ca^{2+}-ATPase activity were detected [173]. In another study, oral glucose administration to healthy subjects also decreased the activity of the RBC Ca^{2+}-ATPase [174] Similar results were obtained when protein glycosylation and Ca^{2+}-ATPase activity were measured in membranes from normal erythrocytes pre-incubated with glucose [175]. It has also been shown that the activity of the pump decreases with cell age, however, this effect was independent of the patients' glucose level indicating that glycation could not be responsible for the age dependent decline in pump's activity [176].

5.5.3 PMCAs Linked to Neuronal Disorders and Other Diseases

Although, in several diseases no genetic alterations in the *ATP2B* genes have been identified, modified expression, altered activity or de-regulation of one or more PMCA isoforms could be associated with the disorder. For example, PMCAs have an important role in the brain where they have been linked to certain neurodegen-

erative disorders [100]. In Alzheimer's disease (AD) deposits of amyloid β-peptide are extensively formed and it was suggested that activation of the amyloidogenic pathway was associated with the remodeling of neuronal Ca^{2+} signaling [177]. First it was found that Ca^{2+} dependence of PMCAs was different in membrane vesicles prepared from human AD brains as compared to non-AD brains [178]. Later amyloid β-peptide aggregates were shown to bind to PMCA and inhibit its activity in the absence of calmodulin [179]. Furthermore, microtubule-associated regulatory protein tau, that is hyperphosphorylated and forms neurofibrillary tangles in AD, has been shown to interact with PMCA, as well, and inhibited its activity [180].

Altered activity of PMCA proteins in human brain tissue was also proposed in Parkinson's disease (PD) [181]. In an in vitro model of PD in neuroblastoma cells it was found that the resting cytosolic Ca^{2+} concentration was elevated while PMCA2 expression was decreased leading to decreased cell survival [182]. Alterations in the expression of PMCAs were also found in multiple sclerosis (MS), an inflammatory, demyelinating and neurodegenerative disorder of the central nervous system. In gene microarray analysis of brain lesions from MS patients both PMCA1 and PMCA3 expression was found to be downregulated compared to control [183]. Down-regulation of PMCA2 expression was also described in rats with experimental autoimmune encephalomyelitis (EAE), an animal model of MS. Interestingly, after disease recovery PMCA2 expression was restored in the animals, while in mouse models with chronic EAE PMCA2 level remained low throughout the disease course [184, 185].

Expression of PMCA4b has been shown to be increased in platelets from patient with both type I and type II diabetes compared to control; this might contribute to increased thrombus formation in diabetic patients [186]. In cellular models it was found that PMCA2 plays an important role in the regulation of pancreatic β-cell proliferation, survival and insulin secretion [187–189]. An analysis of PMCA expression in rat pancreatic islets showed that PMCA1 and PMCA4 are expressed in all islet cells while PMCA3 is present only in the β-cells [190]. In fructose rich diet induced insulin resistant rats PMCA expression was altered in the islet cells resulting in reduced total activity. This caused an elevation in the intracellular calcium level that contributes to the compensatory elevated insulin secretion in response to glucose [191]. Alterations in PMCA activity were related to kidney diseases, as well. Decreased PMCA activity and concomitantly increased cytosolic Ca^{2+} concentration was described in red blood cells of children with chronic kidney disease [192]. Furthermore, in patients with idiopathic hypercalciuria PMCA activity of the erythrocytes was increased compared to controls [193].

5.5.4 PMCA4 in Heart Diseases

During cardiac relaxation SERCA and NCX proteins are mainly responsible for Ca^{2+} removal and PMCA4 acts primarily as a signaling molecule in the heart. It plays a role in the regulation of cardiac β-adrenergic response, hypertrophy

and heart failure [194]. β-adrenergic stimulation can initiate neural nitric oxide synthase (nNOS) activity and NO production in cardiac myocytes [195] while nNOS regulates contractility and oxygen radical production [196]. It was demonstrated that PMCA4b can directly interact with the Ca^{2+} sensitive nNOS molecule through its C-terminal PDZ binding motif and it decreases nNOS activity by reducing the Ca^{2+} concentration in its vicinity [197]. In cardiac specific PMCA4b transgenic mice nNOS activity was reduced compared to WT animals and that caused a decreased responsiveness to β-adrenergic stimulation [198]. This interaction might play an important role in remodeling after myocardial infarction (MI). In mice, after induction of MI, nNOS and its adaptor protein CAPON (carboxy-terminal PDZ ligand of NOS1) relocate to caveolae where they make a complex also with PMCA and this way possibly protect the cardiomyocytes from calcium overload. In mice lacking nNOS the redistribution does not happen [199].

PMCA4 also forms a ternary complex in cardiac cells with α-1 syntrophin and nNOS [200]. A mutation in α-1 syntrophin (A390V-SNTA1) was found in patients with long QT syndrome and it was demonstrated that the mutation resulted in the disruption of the interaction with PMCA4. This led to increased nNOS activation and late sodium current causing arrhythmias [201]. Interestingly, in a GWAS study a mutation in CAPON was found to be associated with QT interval variations [202] and variants of the *ATP2B4* gene were associated with congenital ventricular arrhythmia [203].

PMCA4 can also influence cardiac hypertrophy. It is well established that the calcineurin-NFAT pathway is activated during cardiac hypertrophy and it was found that PMCA4 is able to inhibit this pathway through direct binding of calcineurin [92]. In mice overexpressing PMCA4 in the heart both the NFAT-calcineurin signaling and hypertrophy were reduced, while the mice lacking PMCA4 were more susceptible to hypertrophy [204]. Furthermore, after induction of experimental myocardial infarction in mice overexpression of PMCA4 in cardiomyocytes reduced infarct expansion, cardiac hypertrophy and heart failure [205]. However, deletion of PMCA4 in cardiac fibroblasts also prevented cardiac hypertrophy in mice. In the absence of PMCA4, intracellular Ca^{2+} level was elevated in the fibroblasts enhancing secreted frizzled related protein 2 (sFRP2) production and secretion which reduced Wnt signaling in the neighboring cardiomyocytes [206]. Interestingly, overexpression of PMCA4 in arterial smooth muscle cells in mice caused an increase in blood pressure through the inhibition of nNOS [207].

5.5.5 *The Role of PMCAs in the Intestine and Bone Mineralization*

PMCA1 plays a crucial role in the transcellular Ca^{2+} absorption both in the duodenum and in the large bowel. Its expression is induced by vitamin D metabolite 1,25-(OH)2D3 and by estrogens, as well [208]. In mice it was demonstrated that

high bone density correlated with PMCA expression and mucosal to serosal Ca^{2+} transport in the duodenum [209]. Treatment of mice with 1,25-(OH)2D3 strongly increased PMCA1 mRNA level in the duodenum [210] while selective deletion of PMCA1 in the intestinal absorptive cells caused reduced whole body bone mineral density and lower serum Ca^{2+} level [211]. Furthermore, in ovariectomized rats a negative Ca^{2+} balance was induced and this was associated with decreased PMCA1 mRNA expression in an estrogen dependent manner [212], a model for postmenopausal osteoporosis. Interestingly, in biopsies of ulcerative colitis patients reduced PMCA1 expression was also found [213].

PMCAs play an important role in the regulation of bone mineral density already during development. The expression level of PMCA3 in the placenta correlates with neonatal bone mineral content [214] while during lactation PMCA2 expression is strongly induced in the mammary epithelium and it provides Ca^{2+} into the breast milk that is required for the normal bone development of the offspring. In PMCA2-null mice the Ca^{2+} content of the milk was 60% less than in the wild type mice [79]. PMCA isoforms 1, 2 and 4 were described in human osteoblasts, and PMCA1 and PMCA4 in osteoclasts. In osteoblasts of patient with adolescent idiopathic scoliosis expression of PMCA4 was found to be downregulated [215]. During osteoclast differentiation PMCA4 was shown to have an anti-osteoclastogenic effect on one hand by reducing NF-κB ligand–induced Ca^{2+} oscillations, on the other hand by decreasing NO synthesis in the cells [216]. However in mature osteoclast PMCA had an anti-apoptotic effect on the cells. Furthermore, in premenopausal women PMCA4b level showed correlation with high peak bone mass.

5.5.6 Altered PMCA Expression Linked to Tumorigenesis

Ca^{2+} plays an important role in the regulation of many cellular processes such as proliferation, migration or cell death. In tumorous cells these processes are strongly altered and changes in the expression or activity of Ca^{2+} handling molecules in several cancer types have been described. These modifications can result in altered resting Ca^{2+} level in the cellular compartments and can change the spatial and temporal characteristics of the intracellular calcium transients [217].

Alterations in the expression of PMCA proteins have been described in several cancer types. In colorectal cancer a decrease in PMCA4 expression was found during the multistep carcinogenesis of the human colon [218]. In normal human colon mucosa samples PMCA4 was present both at the mRNA and protein levels, however, in high grade adenomas, adenocarcinomas and lymph node metastases the protein expression strongly decreased. Interestingly, the PMCA4 mRNA level was not altered in the samples. Furthermore, after spontaneous differentiation of the colorectal cancer cell line Caco-2 the expression of PMCA4 strongly increased, and treatment with the histone deacetylase (HDAC) inhibitor Trichostatin A induced differentiation and PMCA4 expression in several gastric and colon cancer cell

lines [219, 220]. PMCA1 was also found in colon cancer cells and its expression increased after 1,25-(OH)2D3 treatments, however, this was not accompanied by a change in cellular differentiation [221].

Expression of PMCA proteins was also analyzed in breast cancer. In normal breast epithelium PMCA4 is abundantly present [222], while PMCA2 expression is induced only in the lactating mammary glands. In breast cancer cell lines it was found that the mRNA level of PMCA1 and PMCA2 is increased compared to non-tumorigenic human breast epithelial cell lines [223, 224], while PMCA4 expression is downregulated [222]. In human breast cancer samples PMCA2 mRNA level showed association with higher tumor grade and docetaxel resistance in patients. In a tissue microarray analysis of 652 primary breast tumors PMCA2 expression showed positive correlation with lymph node metastasis and human epidermal growth factor receptor 2 (HER2) positivity. Furthermore, overexpression of PMCA2 in breast cancer cells reduced their sensitivity to apoptosis [225]. It was suggested that PMCA2 regulates HER2 signaling in breast cancer cells and knocking down PMCA2 inhibits HER2 mediated cell growth [226]. In another study PMCA2 expression was found in 9% of 96 breast tumors with various histological subtypes and there was no association with grade or hormone receptor status. However, higher PMCA2 expression was described in samples with basal histological subtype. It was also demonstrated that downregulation of PMCA2 level decreased breast cancer cell proliferation and increased the sensitivity to doxorubicin treatment [227]. While PMCA2 expression is upregulated in certain breast cancer cells, PMCA4 level seems to be downregulated. In MCF-7 breast cancer cells treatment with HDAC inhibitors or with phorbol 12-myristate 13-acetate (PMA) strongly induced PMCA4b expression and this effect was coupled with increased Ca^{2+} clearance from the cells [222].

Altered PMCA protein levels were described in melanomas. In melanoma cell lines with different BRAF and NRAS mutational status PMCA4 and PMCA1 isoforms were detected. Mutant BRAF specific inhibitor treatment selectively increased PMCA4b expression in BRAF mutant melanoma cells and this was coupled with faster Ca^{2+} clearance and strong inhibition of migration [91]. When PMCA4b was overexpressed in a BRAF mutant melanoma cell line A375, it strongly reduced the migratory and metastatic capacity of the cells both in vitro and in vivo, while it did not influence their proliferation rate. Furthermore, HDAC inhibitor treatment increased the expression of both PMCA4b and PMCA1 in melanoma cell lines independently from their BRAF mutational status [228]. Similarly to BRAF inhibitor treatment, HDAC inhibition also increased Ca^{2+} clearance and reduced the migratory activity of the highly motile A375 melanoma cells. These results suggested that PMCA4b plays an important role in the regulation of melanoma cell motility, and its expression is under epigenetic control.

PMCA1 was also found to be epigenetically downregulated in human oral cancer. PMCA1 expression was reduced both in primary oral squamous cell carcinomas (OSCCs) and in oral premalignant lesions (OPLs) compared to normal tissue. In OSCC derived cell lines it was demonstrated that decreased PMCA1 level was caused by the increased DNA methylation in the promoter region of PMCA1 [229].

The emerging role of PMCAs in the regulation of the immune response might also be considered in the treatment of malignant diseases**.** Immune checkpoint inhibitors are relatively new but promising treatment options in cancer therapy that are able to enhance cytotoxic T-cell activation by blocking the negative regulatory signals coming from tumor cells [230]. Recently, it was found that PMCA4 interacts with Ig-like glycoprotein CD147 upon T-cell activation and this interaction is necessary for the immunosuppressive effect of CD147 through the decrease of IL-2 production [231]. CD147 was shown to participate in the development and progression of several cancer types including malignant melanomas, and antibodies targeting CD147 are under development [232]. All these results show that remodeling of the activity and expression of PMCA proteins play an important role in altered cancer cell growth, motility, and in T-cell activation during the immune response to cancer cells that might influence therapy response, as well.

5.6 Conclusion

PMCAs comprise a big family of Ca^{2+} transport ATPases including four separate genes *(ATP2B1-4)* from which more than twenty different protein variants are transcribed. The variants have different regulatory properties, and hence they respond differently to the incoming Ca^{2+} signal, differ in their sub-plasma membrane localization and interact with different signaling molecules. The expression, and thus the abundance of the variants are also tightly regulated in a development and cell-type specific manner, by processes not yet very well understood. In the past we studied many aspects of the biochemical characteristics of these pumps, but we still know very little on how their transcription and translation are regulated and how stable the proteins are in the plasma membrane. Our main goal, therefore, should be to study further these mechanisms particularly because alterations in the PMCA expression and genetic variations in the *ATP2B* genes have been linked to several diseases such as cardiovascular and neurodegenerative disorders, and cancer. Understanding PMCA pathophysiology and learning more about the consequences of PMCA dysfunction may help finding ways to predict, prevent and/or cure such diseases.

Acknowledgement The authors are supported by grants from the Hungarian Scientific Research Funds NKFIH K119223 and FIKP-EMMI (AE).

References

1. Schatzmann HJ (1966) ATP-dependent Ca++-extrusion from human red cells. Experientia 22(6):364–365
2. Berridge MJ, Bootman MD, Roderick HL (2003) Calcium signalling: dynamics, homeostasis and remodelling. Nat Rev Mol Cell Biol 4(7):517–529

3. Penniston JT, Enyedi A (1998) Modulation of the plasma membrane Ca^{2+} pump. J Membr Biol 165(2):101–109
4. Strehler EE (1990) Plasma membrane Ca^{2+} pumps and Na^{+}/Ca^{2+} exchangers. Semin Cell Biol 1(4):283–295
5. Padanyi R, Paszty K, Hegedus L, Varga K, Papp B, Penniston JT et al (2016) Multifaceted plasma membrane Ca^{2+} pumps: from structure to intracellular Ca^{2+} handling and cancer. Biochim Biophys Acta 1863(6 Pt B):1351–1363
6. Axelsen KB, Palmgren MG (1998) Evolution of substrate specificities in the P-type ATPase superfamily. J Mol Evol 46(1):84–101
7. Thever MD, Saier MH Jr (2009) Bioinformatic characterization of p-type ATPases encoded within the fully sequenced genomes of 26 eukaryotes. J Membr Biol 229(3):115–130
8. Strehler EE, Zacharias DA (2001) Role of alternative splicing in generating isoform diversity among plasma membrane calcium pumps. Physiol Rev 81(1):21–50
9. Krebs J (2015) The plethora of PMCA isoforms: alternative splicing and differential expression. Biochim Biophys Acta 1853(9):2018–2024
10. Green NM (1989) ATP-driven cation pumps: alignment of sequences. Biochem Soc Trans 17(6):972
11. Toyoshima C, Mizutani T (2004) Crystal structure of the calcium pump with a bound ATP analogue. Nature 430(6999):529–535
12. Sorensen TL, Moller JV, Nissen P (2004) Phosphoryl transfer and calcium ion occlusion in the calcium pump. Science 304(5677):1672–1675
13. Jensen AM, Sorensen TL, Olesen C, Moller JV, Nissen P (2006) Modulatory and catalytic modes of ATP binding by the calcium pump. EMBO J 25(11):2305–2314
14. Sweadner KJ, Donnet C (2001) Structural similarities of Na,K-ATPase and SERCA, the Ca^{2+}-ATPase of the sarcoplasmic reticulum. Biochem J 356(Pt 3):685–704
15. Toyoshima C (2009) How Ca^{2+}-ATPase pumps ions across the sarcoplasmic reticulum membrane. Biochim Biophys Acta 1793(6):941–946
16. Thomas RC (2009) The plasma membrane calcium ATPase (PMCA) of neurones is electroneutral and exchanges 2 H^{+} for each Ca^{2+} or Ba^{2+} ion extruded. J Physiol 587(2):315–327
17. Carafoli E, Brini M (2000) Calcium pumps: structural basis for and mechanism of calcium transmembrane transport. Curr Opin Chem Biol 4(2):152–161
18. Strehler EE, Treiman M (2004) Calcium pumps of plasma membrane and cell interior. Curr Mol Med 4(3):323–335
19. Di Leva F, Domi T, Fedrizzi L, Lim D, Carafoli E (2008) The plasma membrane Ca^{2+} ATPase of animal cells: structure, function and regulation. Arch Biochem Biophys 476(1):65–74
20. Penniston JT, Padanyi R, Paszty K, Varga K, Hegedus L, Enyedi A (2014) Apart from its known function, the plasma membrane Ca^{2+}ATPase can regulate Ca^{2+} signaling by controlling phosphatidylinositol 4,5-bisphosphate levels. J Cell Sci 127(Pt 1):72–84
21. Filoteo AG, Enyedi A, Penniston JT (1992) The lipid-binding peptide from the plasma membrane Ca^{2+} pump binds calmodulin, and the primary calmodulin-binding domain interacts with lipid. J Biol Chem 267(17):11800–11805
22. Enyedi A, Flura M, Sarkadi B, Gardos G, Carafoli E (1987) The maximal velocity and the calcium affinity of the red cell calcium pump may be regulated independently. J Biol Chem 262(13):6425–6430
23. Brodin P, Falchetto R, Vorherr T, Carafoli E (1992) Identification of two domains which mediate the binding of activating phospholipids to the plasma-membrane Ca^{2+} pump. Eur J Biochem 204(2):939–946
24. Wang K, Sitsel O, Meloni G, Autzen HE, Andersson M, Klymchuk T et al (2014) Structure and mechanism of Zn2+-transporting P-type ATPases. Nature 514(7523):518–522
25. Hansen SB (2015) Lipid agonism: the PIP2 paradigm of ligand-gated ion channels. Biochim Biophys Acta 1851(5):620–628
26. Paszty K, Verma AK, Padanyi R, Filoteo AG, Penniston JT, Enyedi A (2002) Plasma membrane Ca^{2+}ATPase isoform 4b is cleaved and activated by caspase-3 during the early

phase of apoptosis. J Biol Chem 277(9):6822–6829
27. Schwab BL, Guerini D, Didszun C, Bano D, Ferrando-May E, Fava E et al (2002) Cleavage of plasma membrane calcium pumps by caspases: a link between apoptosis and necrosis. Cell Death Differ 9(8):818–831
28. Enyedi A, Elwess NL, Filoteo AG, Verma AK, Paszty K, Penniston JT (1997) Protein kinase C phosphorylates the "a" forms of plasma membrane Ca^{2+} pump isoforms 2 and 3 and prevents binding of calmodulin. J Biol Chem 272(44):27525–27528
29. Enyedi A, Verma AK, Filoteo AG, Penniston JT (1996) Protein kinase C activates the plasma membrane Ca^{2+} pump isoform 4b by phosphorylation of an inhibitory region downstream of the calmodulin-binding domain. J Biol Chem 271(50):32461–32467
30. Antalffy G, Paszty K, Varga K, Hegedus L, Enyedi A, Padanyi R (2013) A C-terminal di-leucine motif controls plasma membrane expression of PMCA4b. Biochim Biophys Acta 1833(12):2561–2572
31. DeMarco SJ, Strehler EE (2001) Plasma membrane Ca^{2+}-atpase isoforms 2b and 4b interact promiscuously and selectively with members of the membrane-associated guanylate kinase family of PDZ (PSD95/Dlg/ZO-1) domain-containing proteins. J Biol Chem 276(24):21594–21600
32. DeMarco SJ, Chicka MC, Strehler EE (2002) Plasma membrane Ca^{2+} ATPase isoform 2b interacts preferentially with Na^+/H^+ exchanger regulatory factor 2 in apical plasma membranes. J Biol Chem 277(12):10506–10511
33. Penniston JT, Caride AJ, Strehler EE (2012) Alternative pathways for association and dissociation of the calmodulin-binding domain of plasma membrane Ca^{2+}-ATPase isoform 4b (PMCA4b). J Biol Chem 287(35):29664–29671
34. Caride AJ, Filoteo AG, Penniston JT, Strehler EE (2007) The plasma membrane Ca^{2+} pump isoform 4a differs from isoform 4b in the mechanism of calmodulin binding and activation kinetics: implications for Ca^{2+} signaling. J Biol Chem 282(35):25640–25648
35. Juranic N, Atanasova E, Filoteo AG, Macura S, Prendergast FG, Penniston JT et al (2010) Calmodulin wraps around its binding domain in the plasma membrane Ca^{2+} pump anchored by a novel 18-1 motif. J Biol Chem 285(6):4015–4024
36. Elshorst B, Hennig M, Forsterling H, Diener A, Maurer M, Schulte P et al (1999) NMR solution structure of a complex of calmodulin with a binding peptide of the Ca^{2+} pump. Biochemistry 38(38):12320–12332
37. Chicka MC, Strehler EE (2003) Alternative splicing of the first intracellular loop of plasma membrane Ca^{2+}-ATPase isoform 2 alters its membrane targeting. J Biol Chem 278(20):18464–18470
38. Strehler EE (2013) Plasma membrane calcium ATPases as novel candidates for therapeutic agent development. J Pharm Pharm Sci 16(2):190–206
39. Strehler EE (2015) Plasma membrane calcium ATPases: from generic Ca^{2+} sump pumps to versatile systems for fine-tuning cellular Ca(2.). Biochem Biophys Res Commun 460(1):26–33
40. Afroze T, Husain M (2000) c-Myb-binding sites mediate G(1)/S-associated repression of the plasma membrane Ca^{2+}-ATPase-1 promoter. J Biol Chem 275(12):9062–9069
41. Habib T, Park H, Tsang M, de Alboran IM, Nicks A, Wilson L et al (2007) Myc stimulates B lymphocyte differentiation and amplifies calcium signaling. J Cell Biol 179(4):717–731
42. Zelinski JM, Sykes DE, Weiser MM (1991) The effect of vitamin D on rat intestinal plasma membrane CA-pump mRNA. Biochem Biophys Res Commun 179(2):749–755
43. Cai Q, Chandler JS, Wasserman RH, Kumar R, Penniston JT (1993) Vitamin D and adaptation to dietary calcium and phosphate deficiencies increase intestinal plasma membrane calcium pump gene expression. Proc Natl Acad Sci U S A 90(4):1345–1349
44. Glendenning P, Ratajczak T, Dick IM, Prince RL (2000) Calcitriol upregulates expression and activity of the 1b isoform of the plasma membrane calcium pump in immortalized distal kidney tubular cells. Arch Biochem Biophys 380(1):126–132
45. Glendenning P, Ratajczak T, Dick IM, Prince RL (2001) Regulation of the 1b isoform of the plasma membrane calcium pump by 1,25-dihydroxyvitamin D3 in rat osteoblast-like cells. J

Bone Miner Res 16(3):525–534
46. Silverstein RS, Tempel BL (2006) Atp2b2, encoding plasma membrane Ca^{2+}-ATPase type 2, (PMCA2) exhibits tissue-specific first exon usage in hair cells, neurons, and mammary glands of mice. Neuroscience 141(1):245–257
47. Minich RR, Li J, Tempel BL (2017) Early growth response protein 1 regulates promoter activity of alpha-plasma membrane calcium ATPase 2, a major calcium pump in the brain and auditory system. BMC Mol Biol 18(1):14
48. Lessard S, Gatof ES, Beaudoin M, Schupp PG, Sher F, Ali A et al (2017) An erythroid-specific ATP2B4 enhancer mediates red blood cell hydration and malaria susceptibility. J Clin Invest 127(8):3065–3074
49. Verma AK, Enyedi A, Filoteo AG, Penniston JT (1994) Regulatory region of plasma membrane Ca^{2+} pump. 28 residues suffice to bind calmodulin but more are needed for full auto-inhibition of the activity. J Biol Chem 269(3):1687–1691
50. Caride AJ, Filoteo AG, Penheiter AR, Paszty K, Enyedi A, Penniston JT (2001) Delayed activation of the plasma membrane calcium pump by a sudden increase in Ca^{2+}: fast pumps reside in fast cells. Cell Calcium 30(1):49–57
51. Enyedi A, Vorherr T, James P, McCormick DJ, Filoteo AG, Carafoli E et al (1989) The calmodulin binding domain of the plasma membrane Ca^{2+} pump interacts both with calmodulin and with another part of the pump. J Biol Chem 264(21):12313–12321
52. Ba-Thein W, Caride AJ, Enyedi A, Paszty K, Croy CL, Filoteo AG et al (2001) Chimaeras reveal the role of the catalytic core in the activation of the plasma membrane Ca^{2+} pump. Biochem J 356(Pt 1):241–245
53. Bruce JIE (2018) Metabolic regulation of the PMCA: role in cell death and survival. Cell Calcium 69:28–36
54. Paszty K, Antalffy G, Penheiter AR, Homolya L, Padanyi R, Ilias A et al (2005) The caspase-3 cleavage product of the plasma membrane Ca^{2+}-ATPase 4b is activated and appropriately targeted. Biochem J 391(Pt 3):687–692
55. Strehler EE, Caride AJ, Filoteo AG, Xiong Y, Penniston JT, Enyedi A (2007) Plasma membrane Ca^{2+} ATPases as dynamic regulators of cellular calcium handling. Ann N Y Acad Sci 1099:226–236
56. Caride AJ, Elwess NL, Verma AK, Filoteo AG, Enyedi A, Bajzer Z et al (1999) The rate of activation by calmodulin of isoform 4 of the plasma membrane Ca^{2+} pump is slow and is changed by alternative splicing. J Biol Chem 274(49):35227–35232
57. Caride AJ, Penheiter AR, Filoteo AG, Bajzer Z, Enyedi A, Penniston JT (2001) The plasma membrane calcium pump displays memory of past calcium spikes. Differences between isoforms 2b and 4b. J Biol Chem 276(43):39797–39804
58. Missiaen L, Raeymaekers L, Wuytack F, Vrolix M, de Smedt H, Casteels R (1989) Phospholipid-protein interactions of the plasma-membrane Ca^{2+}-transporting ATPase. Evidence for a tissue-dependent functional difference. Biochem J 263(3):687–694
59. Zaidi A, Adewale M, McLean L, Ramlow P (2018) The plasma membrane calcium pumps-The old and the new. Neurosci Lett 663:12–17
60. Pignataro MF, Dodes-Traian MM, Gonzalez-Flecha FL, Sica M, Mangialavori IC, Rossi JP (2015) Modulation of plasma membrane Ca^{2+}-ATPase by neutral phospholipids: effect of the micelle-vesicle transition and the bilayer thickness. J Biol Chem 290(10):6179–6190
61. Dean WL, Whiteheart SW (2004) Plasma membrane Ca^{2+}-ATPase (PMCA) translocates to filopodia during platelet activation. Thromb Haemost 91(2):325–333
62. Bozulic LD, Malik MT, Powell DW, Nanez A, Link AJ, Ramos KS et al (2007) Plasma membrane Ca^{2+} -ATPase associates with CLP36, alpha-actinin and actin in human platelets. Thromb Haemost 97(4):587–597
63. Dalghi MG, Fernandez MM, Ferreira-Gomes M, Mangialavori IC, Malchiodi EL, Strehler EE et al (2013) Plasma membrane calcium ATPase activity is regulated by actin oligomers through direct interaction. J Biol Chem 288(32):23380–23393
64. Vanagas L, de La Fuente MC, Dalghi M, Ferreira-Gomes M, Rossi RC, Strehler EE et al (2013) Differential effects of G- and F-actin on the plasma membrane calcium pump activity.

Cell Biochem Biophys 66(1):187–198
65. Dalghi MG, Ferreira-Gomes M, Montalbetti N, Simonin A, Strehler EE, Hediger MA et al (2017) Cortical cytoskeleton dynamics regulates plasma membrane calcium ATPase isoform-2 (PMCA2) activity. Biochim Biophys Acta 1864(8):1413–1424
66. Dalghi MG, Ferreira-Gomes M, Rossi JP (2017) Regulation of the plasma membrane calcium ATPases by the actin cytoskeleton. Biochem Biophys Res Commun
67. Paszty K, Caride AJ, Bajzer Z, Offord CP, Padanyi R, Hegedus L et al (2015) Plasma membrane Ca^{2+}-ATPases can shape the pattern of Ca^{2+} transients induced by store-operated Ca^{2+} entry. Sci Signal 8(364):ra19
68. Ritchie MF, Samakai E, Soboloff J (2012) STIM1 is required for attenuation of PMCA-mediated Ca^{2+} clearance during T-cell activation. EMBO J 31(5):1123–1133
69. Krapivinsky G, Krapivinsky L, Stotz SC, Manasian Y, Clapham DE (2011) POST, partner of stromal interaction molecule 1 (STIM1), targets STIM1 to multiple transporters. Proc Natl Acad Sci U S A 108(48):19234–19239
70. Okunade GW, Miller ML, Pyne GJ, Sutliff RL, O'Connor KT, Neumann JC et al (2004) Targeted ablation of plasma membrane Ca^{2+}-ATPase (PMCA) 1 and 4 indicates a major housekeeping function for PMCA1 and a critical role in hyperactivated sperm motility and male fertility for PMCA4. J Biol Chem 279(32):33742–33750
71. Schuh K, Cartwright EJ, Jankevics E, Bundschu K, Liebermann J, Williams JC et al (2004) Plasma membrane Ca^{2+} ATPase 4 is required for sperm motility and male fertility. J Biol Chem 279(27):28220–28226
72. Prasad V, Okunade GW, Miller ML, Shull GE (2004) Phenotypes of SERCA and PMCA knockout mice. Biochem Biophys Res Commun 322(4):1192–1203
73. Lefievre L, Nash K, Mansell S, Costello S, Punt E, Correia J et al (2012) 2-APB-potentiated channels amplify CatSper-induced Ca^{2+} signals in human sperm. Biochem J 448(2):189–200
74. Kawano S, Otsu K, Shoji S, Yamagata K, Hiraoka M (2003) Ca^{2+} oscillations regulated by $Na(+)$-Ca^{2+} exchanger and plasma membrane Ca^{2+} pump induce fluctuations of membrane currents and potentials in human mesenchymal stem cells. Cell Calcium 34(2):145–156
75. Chen YF, Cao J, Zhong JN, Chen X, Cheng M, Yang J et al (2014) Plasma membrane Ca^{2+}-ATPase regulates Ca^{2+} signaling and the proliferation of airway smooth muscle cells. Eur J Pharmacol 740:733–741
76. Prasad V, Okunade G, Liu L, Paul RJ, Shull GE (2007) Distinct phenotypes among plasma membrane Ca^{2+}-ATPase knockout mice. Ann N Y Acad Sci 1099:276–286
77. Cali T, Brini M, Carafoli E (2018) The PMCA pumps in genetically determined neuronal pathologies. Neurosci Lett 663:2–11
78. Ficarella R, Di Leva F, Bortolozzi M, Ortolano S, Donaudy F, Petrillo M et al (2007) A functional study of plasma-membrane calcium-pump isoform 2 mutants causing digenic deafness. Proc Natl Acad Sci U S A 104(5):1516–1521
79. Reinhardt TA, Lippolis JD, Shull GE, Horst RL (2004) Null mutation in the gene encoding plasma membrane Ca^{2+}-ATPase isoform 2 impairs calcium transport into milk. J Biol Chem 279(41):42369–42373
80. Padanyi R, Paszty K, Strehler EE, Enyedi A (2009) PSD-95 mediates membrane clustering of the human plasma membrane Ca^{2+} pump isoform 4b. Biochimica et Biophysica Acta 1793(6):1023–1032
81. Schmidt N, Kollewe A, Constantin CE, Henrich S, Ritzau-Jost A, Bildl W et al (2017) Neuroplastin and basigin are essential auxiliary subunits of plasma membrane Ca^{2+}-ATPases and key regulators of Ca^{2+} clearance. Neuron 96(4):827–38 e9
82. Grati M, Aggarwal N, Strehler EE, Wenthold RJ (2006) Molecular determinants for differential membrane trafficking of PMCA1 and PMCA2 in mammalian hair cells. J Cell Sci 119(Pt 14):2995–3007
83. Spiden SL, Bortolozzi M, Di Leva F, de Angelis MH, Fuchs H, Lim D et al (2008) The novel mouse mutation Oblivion inactivates the PMCA2 pump and causes progressive hearing loss. PLoS Genet 4(10):e1000238

84. Padanyi R, Xiong Y, Antalffy G, Lor K, Paszty K, Strehler EE et al (2010) Apical scaffolding protein NHERF2 modulates the localization of alternatively spliced plasma membrane Ca^{2+} pump 2B variants in polarized epithelial cells. J Biol Chem 285(41):31704–31712
85. Grati M, Schneider ME, Lipkow K, Strehler EE, Wenthold RJ, Kachar B (2006) Rapid turnover of stereocilia membrane proteins: evidence from the trafficking and mobility of plasma membrane Ca^{2+}-ATPase 2. J Neurosci 26(23):6386–6395
86. Yang YM, Lee J, Jo H, Park S, Chang I, Muallem S et al (2014) Homer2 protein regulates plasma membrane Ca^{2+}-ATPase-mediated Ca^{2+} signaling in mouse parotid gland acinar cells. J Biol Chem 289(36):24971–24979
87. Baggaley E, McLarnon S, Demeter I, Varga G, Bruce JI (2007) Differential regulation of the apical plasma membrane Ca^{2+} -ATPase by protein kinase A in parotid acinar cells. J Biol Chem 282(52):37678–37693
88. Quintana A, Pasche M, Junker C, Al-Ansary D, Rieger H, Kummerow C et al (2011) Calcium microdomains at the immunological synapse: how ORAI channels, mitochondria and calcium pumps generate local calcium signals for efficient T-cell activation. EMBO J 30(19):3895–3912
89. Tsai FC, Seki A, Yang HW, Hayer A, Carrasco S, Malmersjo S et al (2014) A polarized Ca^{2+}, diacylglycerol and STIM1 signalling system regulates directed cell migration. Nat Cell Biol 16(2):133–144
90. Kurusamy S, Lopez-Maderuelo D, Little R, Cadagan D, Savage AM, Ihugba JC et al (2017) Selective inhibition of plasma membrane calcium ATPase 4 improves angiogenesis and vascular reperfusion. J Mol Cell Cardiol 109:38–47
91. Hegedus L, Garay T, Molnar E, Varga K, Bilecz A, Torok S et al (2017) The plasma membrane Ca^{2+} pump PMCA4b inhibits the migratory and metastatic activity of BRAF mutant melanoma cells. Int J Cancer 140(12):2758–2770
92. Buch MH, Pickard A, Rodriguez A, Gillies S, Maass AH, Emerson M et al (2005) The sarcolemmal calcium pump inhibits the calcineurin/nuclear factor of activated T-cell pathway via interaction with the calcineurin A catalytic subunit. J Biol Chem 280(33):29479–29487
93. Holton M, Yang D, Wang W, Mohamed TM, Neyses L, Armesilla AL (2007) The interaction between endogenous calcineurin and the plasma membrane calcium-dependent ATPase is isoform specific in breast cancer cells. FEBS Lett 581(21):4115–4119
94. Baggott RR, Mohamed TM, Oceandy D, Holton M, Blanc MC, Roux-Soro SC et al (2012) Disruption of the interaction between PMCA2 and calcineurin triggers apoptosis and enhances paclitaxel-induced cytotoxicity in breast cancer cells. Carcinogenesis 33(12):2362–2368
95. Baggott RR, Alfranca A, Lopez-Maderuelo D, Mohamed TM, Escolano A, Oller J et al (2014) Plasma membrane calcium ATPase isoform 4 inhibits vascular endothelial growth factor-mediated angiogenesis through interaction with calcineurin. Arterioscler Thromb Vasc Biol 34(10):2310–2320
96. Schuh K, Uldrijan S, Gambaryan S, Roethlein N, Neyses L (2003) Interaction of the plasma membrane Ca^{2+} pump 4b/CI with the Ca^{2+}/calmodulin-dependent membrane-associated kinase CASK. J Biol Chem 278(11):9778–9783
97. Aravindan RG, Fomin VP, Naik UP, Modelski MJ, Naik MU, Galileo DS et al (2012) CASK interacts with PMCA4b and JAM-A on the mouse sperm flagellum to regulate Ca^{2+} homeostasis and motility. J Cell Physiol 227(8):3138–3150
98. Stafford N, Wilson C, Oceandy D, Neyses L, Cartwright EJ (2017) The plasma membrane calcium ATPases and their role as major new players in human disease. Physiol Rev 97(3):1089–1125
99. Giacomello M, De Mario A, Scarlatti C, Primerano S, Carafoli E (2013) Plasma membrane calcium ATPases and related disorders. Int J Biochem Cell Biol 45(3):753–762
100. Hajieva P, Baeken MW, Moosmann B (2018) The role of Plasma Membrane Calcium ATPases (PMCAs) in neurodegenerative disorders. Neurosci Lett 663:29–38
101. Johnson T, Gaunt TR, Newhouse SJ, Padmanabhan S, Tomaszewski M, Kumari M et al (2011) Blood pressure loci identified with a gene-centric array. Am J Hum Genet 89(6):688–700

102. Kato N, Takeuchi F, Tabara Y, Kelly TN, Go MJ, Sim X et al (2011) Meta-analysis of genome-wide association studies identifies common variants associated with blood pressure variation in east Asians. Nat Genet 43(6):531–538
103. Weng L, Taylor KD, Chen YD, Sopko G, Kelsey SF, Bairey Merz CN et al (2016) Genetic loci associated with nonobstructive coronary artery disease in Caucasian women. Physiol Genomics 48(1):12–20
104. Lu X, Wang L, Chen S, He L, Yang X, Shi Y et al (2012) Genome-wide association study in Han Chinese identifies four new susceptibility loci for coronary artery disease. Nat Genet 44(8):890–894
105. Ferguson JF, Matthews GJ, Townsend RR, Raj DS, Kanetsky PA, Budoff M et al (2013) Candidate gene association study of coronary artery calcification in chronic kidney disease: findings from the CRIC study (Chronic Renal Insufficiency Cohort). J Am Coll Cardiol 62(9):789–798
106. Wan JP, Wang H, Li CZ, Zhao H, You L, Shi DH et al (2014) The common single-nucleotide polymorphism rs2681472 is associated with early-onset preeclampsia in Northern Han Chinese women. Reprod Sci 21(11):1423–1427
107. Carrera F, Casart YC, Proverbio T, Proverbio F, Marin R (2003) Preeclampsia and calcium-ATPase activity of plasma membranes from human myometrium and placental trophoblast. Hypertens Pregnancy 22(3):295–304
108. Hache S, Takser L, LeBellego F, Weiler H, Leduc L, Forest JC et al (2011) Alteration of calcium homeostasis in primary preeclamptic syncytiotrophoblasts: effect on calcium exchange in placenta. J Cell Mol Med 15(3):654–667
109. Tabara Y, Kohara K, Kita Y, Hirawa N, Katsuya T, Ohkubo T et al (2010) Common variants in the ATP2B1 gene are associated with susceptibility to hypertension: the Japanese Millennium Genome Project. Hypertension 56(5):973–980
110. Yang W, Liu J, Zheng F, Jia M, Zhao L, Lu T et al (2013) The evidence for association of ATP2B2 polymorphisms with autism in Chinese Han population. PLoS One 8(4):e61021
111. Prandini P, Pasquali A, Malerba G, Marostica A, Zusi C, Xumerle L et al (2012) The association of rs4307059 and rs35678 markers with autism spectrum disorders is replicated in Italian families. Psychiatr Genet 22(4):177–181
112. Schultz JM, Yang Y, Caride AJ, Filoteo AG, Penheiter AR, Lagziel A et al (2005) Modification of human hearing loss by plasma-membrane calcium pump PMCA2. N Engl J Med 352(15):1557–1564
113. Bortolozzi M, Mammano F (2018) PMCA2 pump mutations and hereditary deafness. Neurosci Lett 663:18–24
114. Street VA, McKee-Johnson JW, Fonseca RC, Tempel BL, Noben-Trauth K (1998) Mutations in a plasma membrane Ca^{2+}-ATPase gene cause deafness in deafwaddler mice. Nat Genet 19(4):390–394
115. Zanni G, Cali T, Kalscheuer VM, Ottolini D, Barresi S, Lebrun N et al (2012) Mutation of plasma membrane Ca^{2+} ATPase isoform 3 in a family with X-linked congenital cerebellar ataxia impairs Ca^{2+} homeostasis. Proc Natl Acad Sci U S A 109(36):14514–14519
116. Cali T, Lopreiato R, Shimony J, Vineyard M, Frizzarin M, Zanni G et al (2015) A novel mutation in isoform 3 of the plasma membrane Ca^{2+} pump impairs cellular Ca^{2+} homeostasis in a patient with cerebellar ataxia and laminin subunit 1alpha mutations. J Biol Chem 290(26):16132–16141
117. Cali T, Frizzarin M, Luoni L, Zonta F, Pantano S, Cruz C et al (2017) The ataxia related G1107D mutation of the plasma membrane Ca^{2+} ATPase isoform 3 affects its interplay with calmodulin and the autoinhibition process. Biochim Biophys Acta 1863(1):165–173

118. Williams TA, Monticone S, Schack VR, Stindl J, Burrello J, Buffolo F et al (2014) Somatic ATP1A1, ATP2B3, and KCNJ5 mutations in aldosterone-producing adenomas. Hypertension 63(1):188–195
119. Kitamoto T, Suematsu S, Yamazaki Y, Nakamura Y, Sasano H, Matsuzawa Y et al (2016) Clinical and steroidogenic characteristics of aldosterone-producing adenomas with ATPase or CACNA1D gene mutations. J Clin Endocrinol Metab 101(2):494–503
120. Tauber P, Aichinger B, Christ C, Stindl J, Rhayem Y, Beuschlein F et al (2016) Cellular pathophysiology of an adrenal adenoma-associated mutant of the plasma membrane Ca^{2+}-ATPase ATP2B3. Endocrinology. 157(6):2489–2499
121. Li M, Ho PW, Pang SY, Tse ZH, Kung MH, Sham PC et al (2014) PMCA4 (ATP2B4) mutation in familial spastic paraplegia. PLoS One 9(8):e104790
122. Ho PW, Pang SY, Li M, Tse ZH, Kung MH, Sham PC et al (2015) PMCA4 (ATP2B4) mutation in familial spastic paraplegia causes delay in intracellular calcium extrusion. Brain Behav 5(4):e00321
123. Basit S, Albalawi AM, Alharby E, Khoshhal KI (2017) Exome sequencing identified rare variants in genes HSPG2 and ATP2B4 in a family segregating developmental dysplasia of the hip. BMC Med Genet 18(1):34
124. Schatzmann HJ, Rossi JL (1971) (Ca^{2+} + Mg2+)-activated membrane ATPases in human red cells and their possible relations to cation transport. Biochimica et 75659:379–392
125. Wolf HU (1972) Studies on a Ca^{2+}-dependent ATPase of human erythrocyte membranes – effects of Ca^{2+} and H^{+}. Biochimica et Biophysica Acta 66:361–375
126. Sarkadi B (1980) Active calcium transport in human red cells. Biochimica et Biophysica Acta 4:159–190
127. Schatzmann HJ (1975) Active calcium transport and Ca^{2+}-Activated ATPase in human red cells. Curr Topics Membr Transport 6:125–168
128. Strehler EE (1991) Recent advances in the molecular characterization of plasma membrane Ca^{2+} pumps. J Membr Biol 120:1–15
129. Borke JL, Minami J, Verma A, Penniston JT, Kumar R (1987) Monoclonal antibodies to human erythrocyte membrane Ca++-Mg++ adenosine triphosphatase pump recognize an epitope in the basolateral membrane of human kidney distal tubule cells. J Clin Invest 80:1225–1231
130. Caride AJ, Filoteo AG, Enyedi A, Verma AK, Penniston JT (1996) Detection of isoform 4 of the plasma membrane calcium pump in human tissues by using isoform-specific monoclonal antibodies. Biochem J 316:353–359
131. Bogdanova A, Makhro A, Wang J, Lipp P, Kaestner L (2013) Calcium in red blood cells – a perilous balance. Int J Mol Sci 14:9848–9872
132. Pasini EME, Kirkegaard M, Mortensen P, Lutz HU, Thomas AW, Mann M (2006) In-depth analysis of the membrane and cytosolic proteome of red blood cells. Blood 108:791–801
133. Harrison D, Long C (1968) The calcium content of human erythrocytes. J Physiol 199:367–381
134. Schatzmann HJ (1973) Dependence on calcium concentration and stoichiometry of the calcium pump in human red cells. J Physiol 235:551–569
135. Tiffert T, Bookchin RM, Lew VL (2003) Calcium homeostasis in normal and abnormal human red cells. In: Red cell membrane transport in health and disease. Springer, Berlin/Heidelberg, pp 373–405
136. Larsen FL, Katz S, Roufogalis BD, Brooks DE (1981) Physiological shear stresses enhance the Ca^{2+} permeability of human erythrocytes. Nature 294:667–668
137. Lew VL, Daw N, Perdomo D, Etzion Z, Bookchin RM, Tiffert T (2003) Distribution of plasma membrane Ca^{2+} pump activity in normal human red blood cells. Distribution 102:4206–4213
138. Lew VL, Tiffert T, Etzion Z, Perdomo D, Daw N, Macdonald L et al (2005) Distribution of dehydration rates generated by maximal Gardos-channel activation in normal and sickle red blood cells. Blood 105:361–367
139. Lew VL, Daw N, Etzion Z, Tiffert T, Muoma A, Vanagas L et al (2007) Effects of age-dependent membrane transport changes on the homeostasis of senescent human red blood

cells. Blood 110:1334–1342
140. Lew VL, Tiffert T (2017) On the mechanism of human red blood cell longevity: roles of calcium, the sodium pump, PIEZO1, and gardos channels. Front Physiol 8:977
141. Hertz L, Huisjes R, Llaudet-Planas E, Petkova-Kirova P, Makhro A, Danielczok JG, et al (2017) Is increased intracellular calcium in red blood cells a common component in the molecular mechanism causing anemia? Front Physiol 8
142. Vandorpe DH, Xu C, Shmukler BE, Otterbein LE, Trudel M, Sachs F et al (2010) Hypoxia activates a Ca^{2+}-permeable cation conductance sensitive to carbon monoxide and to GsMTx-4 in human and mouse sickle erythrocytes. PLoS One. 5(1):e8732
143. Gibson JS, Ellory JC (2002) Membrane transport in sickle cell disease. Blood Cells Mol Dis 28:303–314
144. Lew VL, Ortiz OE, Bookchin RM (1997) Stochastic nature and red cell population distribution of the sickling-induced Ca^{2+} permeability. J Clin Invest 99(11):2727–2735
145. Etzion Z, Tiffert T, Bookchin RM, Lew VL (1993) Effects of deoxygenation on active and passive Ca^{2+} transport and on the cytoplasmic Ca^{2+} levels of sickle cell anemia red cells. J Clin Investig 92:2489–2498
146. Lew VL, Bookchin RM (2005) Ion transport pathology in the mechanism of sickle cell dehydration. Physiol Rev 85(1):179–200
147. Wassmer SC, Taylor TE, Rathod PK, Mishra SK, Mohanty S, Arevalo-Herrera M et al (2015) Investigating the pathogenesis of severe malaria: a multidisciplinary and cross-geographical approach. Am J Trop Med Hyg 93:42–56
148. Marquet S (2018) Overview of human genetic susceptibility to malaria: from parasitemia control to severe disease. Infect Genet Evol 66:399–409
149. Min-Oo G, Gros P (2005) Erythrocyte variants and the nature of their malaria protective effect. Cell Microbiol 7:753–763
150. Williams TN (2006) Human red blood cell polymorphisms and malaria. Curr Opin Microbiol 9:388–394
151. Gilles HM, Fletcher KA, Hendrickse RG, Linder R, Reddy S, Allan N (1967) Glucose-6-phosphate-dehydrogenase deficiency, sickling, and malaria in African children in South Western Nigeria. Lancet 289(7482):138–140
152. Hill AVS, Allsopp CEM, Kwiatkowski D, Anstey NM, Twumasi P, Rowe PA et al (1991) Common West African HLA antigens are associated with protection from severe malaria. Nature 352:595–600
153. Lell B, May J, Schmidt-Ott RJ, Lehman LG, Luckner D, Greve B et al (1999) The role of red blood cell polymorphisms in resistance and susceptibility to malaria. Clin Infect Dis 28:794–799
154. Fischer PR, Boone P (1998) Short report: severe malaria associated with blood group. Am J Trop Med Hyg 58:122–123
155. Shah SS, Rockett KA, Jallow M, Sisay-Joof F, Bojang KA, Pinder M et al (2016) Heterogeneous alleles comprising G6PD deficiency trait in West Africa exert contrasting effects on two major clinical presentations of severe malaria. Malar J 15:1–8
156. Pasvol G, Wainscoat JS, Weatherall DJ (1982) Erythrocytes deficient in glycophorin resist invasion by the malarial parasite Plasmodium falciparum. Nature 297:64–66
157. Patel SS, King CL, Mgone CS, Kazura JW, Zimmerman PA (2004) Glycophorin C (Gerbich Antigen Blood Group) and Band 3 Polymorphisms in Two Malaria Holoendemic Regions of Papua New Guinea. Am J Hematol 75:1–5
158. Teeranaipong P, Ohashi J, Patarapotikul J, Kimura R, Nuchnoi P, Hananantachai H et al (2008) A functional single-nucleotide polymorphism in the CR1 promoter region contributes to protection against cerebral malaria. J Infect Dis 198:1880–1891
159. Durand PM, Coetzer TL (2008) Pyruvate kinase deficiency protects against malaria in humans. Haematologica 93:939–940
160. Crosnier C, Bustamante LY, Bartholdson SJ, Bei AK, Theron M, Uchikawa M et al (2011) Basigin is a receptor essential for erythrocyte invasion by Plasmodium falciparum. Nature 480(7378):534–537

161. Egan ES, Weekes MP, Kanjee U, Manzo J, Srinivasan A, Lomas-Francis C et al (2018) Erythrocytes lacking the Langereis blood group protein ABCB6 are resistant to the malaria parasite Plasmodium falciparum. Commun Biol 1(1):45
162. Gazarini ML, Thomas AP, Pozzan T, Garcia CRS (2003) Calcium signaling in a low calcium environment: how the intracellular malaria parasite solves the problem. J Cell Biol 161:103–110
163. Timmann C, Thye T, Vens M, Evans J, May J, Ehmen C et al (2012) Genome-wide association study indicates two novel resistance loci for severe malaria. Nature 489:443–446
164. Bedu-Addo G, Meese S, Mockenhaupt FP (2013) An ATP2B4 polymorphism protects against malaria in pregnancy. J Infect Dis 207:1600–1603
165. Rockett KA, Clarke GM, Fitzpatrick K, Hubbart C, Jeffreys AE, Rowlands K et al (2014) Reappraisal of known malaria resistance loci in a large multicenter study. Nat Genet 46:1197–1204
166. Li J, Glessner JT, Zhang H, Hou C, Wei Z, Bradfield JP et al (2013) GWAS of blood cell traits identifies novel associated loci and epistatic interactions in Caucasian and African-American children. Hum Mol Genet 22:1457–1464
167. Lessard S, Stern EN, Beaudoin M, Schupp PG, Sher F, Ali A et al (2017) An erythroid – specific enhancer of ATP2B4 mediates red blood cell hydration and malaria susceptibility. J Clin Investig 1:1–10
168. Zambo B, Varady G, Padanyi R, Szabo E, Nemeth A, Lango T et al (2017) Decreased calcium pump expression in human erythrocytes is connected to a minor haplotype in the ATP2B4 gene. Cell Calcium 65:73–79
169. Tiffert T, Staines HM, Ellory JC, Lew VL (2000) Functional state of the plasma membrane Ca^{2+} pump in Plasmodium falciparum-infected human red blood cells. J Physiol 525(Pt 1):125–134
170. Spielmann T, Montagna GN, Hecht L, Matuschewski K (2012) Molecular make-up of the Plasmodium parasitophorous vacuolar membrane. Int J Med Microbiol 302:179–186
171. Lauer S, VanWye J, Harrison T, McManus H, Samuel BU, Hiller NL et al (2000) Vacuolar uptake of host components, and a role for cholesterol and sphingomyelin in malarial infection. EMBO J 19:3556–3564
172. Dluzewski AR, Fryer PR, Griffiths S, Wilson RJ, Gratzer WB (1989) Red cell membrane protein distribution during malarial invasion. J cell Sci 92:691–699
173. Gonzalez Flecha FL, Castello PR, Caride AJ, Gagliardino JJ, Rossi JP (1993) The erythrocyte calcium pump is inhibited by non-enzymic glycation: studies in situ and with the purified enzyme. Biochem J 293(Pt 2):369–375
174. Davis FB, Davis PJ, Nat G, Blas SD, MacGillivray M, Gutman S et al (1985) The effect of in vivo glucose administration on human erythrocyte Ca^{2+}-ATPase activity and on enzyme responsiveness in vitro to thyroid hormone and calmodulin. Diabetes 34(7):639–646
175. Gonzalez Flecha FL, Bermudez MC, Cedola NV, Gagliardino JJ, Rossi JP (1990) Decreased Ca2(+)-ATPase activity after glycosylation of erythrocyte membranes in vivo and in vitro. Diabetes 39(6):707–711
176. Bookchin RM, Etzion Z, Lew VL, Tiffert T (2009) Preserved function of the plasma membrane calcium pump of red blood cells from diabetic subjects with high levels of glycated haemoglobin. Cell Calcium 45(3):260–263
177. Berridge MJ (2010) Calcium hypothesis of Alzheimer's disease. Pflugers Arch 459(3):441–449
178. Berrocal M, Marcos D, Sepulveda MR, Perez M, Avila J, Mata AM (2009) Altered Ca^{2+} dependence of synaptosomal plasma membrane Ca^{2+}-ATPase in human brain affected by Alzheimer's disease. FASEB J 23(6):1826–1834
179. Berrocal M, Sepulveda MR, Vazquez-Hernandez M, Mata AM (2012) Calmodulin antagonizes amyloid-beta peptides-mediated inhibition of brain plasma membrane Ca^{2+}-ATPase. Biochim Biophys Acta 1822(6):961–969
180. Berrocal M, Corbacho I, Vazquez-Hernandez M, Avila J, Sepulveda MR, Mata AM (2015) Inhibition of PMCA activity by tau as a function of aging and Alzheimer's neuropathology. Biochim Biophys Acta 1852(7):1465–1476

181. Zaidi A (2010) Plasma membrane Ca-ATPases: targets of oxidative stress in brain aging and neurodegeneration. World J Biol Chem 1(9):271–280
182. Brendel A, Renziehausen J, Behl C, Hajieva P (2014) Downregulation of PMCA2 increases the vulnerability of midbrain neurons to mitochondrial complex I inhibition. Neurotoxicology 40:43–51
183. Lock C, Hermans G, Pedotti R, Brendolan A, Schadt E, Garren H et al (2002) Gene-microarray analysis of multiple sclerosis lesions yields new targets validated in autoimmune encephalomyelitis. Nat Med 8(5):500–508
184. Nicot A, Kurnellas M, Elkabes S (2005) Temporal pattern of plasma membrane calcium ATPase 2 expression in the spinal cord correlates with the course of clinical symptoms in two rodent models of autoimmune encephalomyelitis. Eur J Neurosci 21(10):2660–2670
185. Kurnellas MP, Donahue KC, Elkabes S (2007) Mechanisms of neuronal damage in multiple sclerosis and its animal models: role of calcium pumps and exchangers. Biochem Soc Trans 35(Pt 5):923–926
186. Chaabane C, Dally S, Corvazier E, Bredoux R, Bobe R, Ftouhi B et al (2007) Platelet PMCA- and SERCA-type Ca^{2+} -ATPase expression in diabetes: a novel signature of abnormal megakaryocytopoiesis. J Thromb Haemost 5(10):2127–2135
187. Souza KLA, Elsner M, Mathias PCF, Lenzen S, Tiedge M (2004) Cytokines activate genes of the endocytotic pathway in insulin-producing RINm5F cells. Diabetologia 47(7):1292–1302
188. Jiang L, Allagnat F, Nguidjoe E, Kamagate A, Pachera N, Vanderwinden JM et al (2010) Plasma membrane Ca^{2+}-ATPase overexpression depletes both mitochondrial and endoplasmic reticulum Ca^{2+} stores and triggers apoptosis in insulin-secreting BRIN-BD11 cells. J Biol Chem 285(40):30634–30643
189. Pachera N, Papin J, Zummo FP, Rahier J, Mast J, Meyerovich K et al (2015) Heterozygous inactivation of plasma membrane Ca^{2+}-ATPase in mice increases glucose-induced insulin release and beta cell proliferation, mass and viability. Diabetologia 58(12):2843–2850
190. Garcia ME, Del Zotto H, Caride AJ, Filoteo AG, Penniston JT, Rossi JP et al (2002) Expression and cellular distribution pattern of plasma membrane calcium pump isoforms in rat pancreatic islets. J Membr Biol 185(1):17–23
191. Alzugaray ME, Garcia ME, Del Zotto HH, Raschia MA, Palomeque J, Rossi JP et al (2009) Changes in islet plasma membrane calcium-ATPase activity and isoform expression induced by insulin resistance. Arch Biochem Biophys 490(1):17–23
192. Polak-Jonkisz D, Purzyc L, Laszki-Szczachor K, Musial K, Zwolinska D (2010) The endogenous modulators of Ca^{2+}-Mg2+-dependent ATPase in children with chronic kidney disease (CKD). Nephrol Dial Transplant 25(2):438–444
193. Bianchi G, Vezzoli G, Cusi D, Cova T, Elli A, Soldati L et al (1988) Abnormal red-cell calcium pump in patients with idiopathic hypercalciuria. N Engl J Med 319(14):897–901
194. Cartwright EJ, Oceandy D, Austin C, Neyses L (2011) Ca^{2+} signalling in cardiovascular disease: the role of the plasma membrane calcium pumps. Sci China Life Sci 54(8):691–698
195. Queen LR, Ferro A (2006) Beta-adrenergic receptors and nitric oxide generation in the cardiovascular system. Cell Mol Life Sci 63(9):1070–1083
196. Cartwright EJ, Oceandy D, Neyses L (2009) Physiological implications of the interaction between the plasma membrane calcium pump and nNOS. Pflugers Arch 457(3):665–671
197. Schuh K, Uldrijan S, Telkamp M, Rothlein N, Neyses L (2001) The plasmamembrane calmodulin-dependent calcium pump: a major regulator of nitric oxide synthase I. J Cell Biol 155(2):201–205

198. Mohamed TM, Oceandy D, Prehar S, Alatwi N, Hegab Z, Baudoin FM et al (2009) Specific role of neuronal nitric-oxide synthase when tethered to the plasma membrane calcium pump in regulating the beta-adrenergic signal in the myocardium. J Biol Chem 284(18):12091–12098
199. Beigi F, Oskouei BN, Zheng M, Cooke CA, Lamirault G, Hare JM (2009) Cardiac nitric oxide synthase-1 localization within the cardiomyocyte is accompanied by the adaptor protein, CAPON. Nitric Oxide 21(3-4):226–233
200. Williams JC, Armesilla AL, Mohamed TM, Hagarty CL, McIntyre FH, Schomburg S et al (2006) The sarcolemmal calcium pump, alpha-1 syntrophin, and neuronal nitric-oxide synthase are parts of a macromolecular protein complex. J Biol Chem 281(33):23341–23348
201. Ueda K, Valdivia C, Medeiros-Domingo A, Tester DJ, Vatta M, Farrugia G et al (2008) Syntrophin mutation associated with long QT syndrome through activation of the nNOS-SCN5A macromolecular complex. Proc Natl Acad Sci U S A. 105(27):9355–9360
202. Arking DE, Pfeufer A, Post W, Kao WH, Newton-Cheh C, Ikeda M et al (2006) A common genetic variant in the NOS1 regulator NOS1AP modulates cardiac repolarization. Nat Genet. 38(6):644–651
203. Dewey FE, Grove ME, Priest JR, Waggott D, Batra P, Miller CL et al (2015) Sequence to medical phenotypes: a framework for interpretation of human whole genome DNA sequence data. PLoS Genet. 11(10):e1005496
204. Wu X, Chang B, Blair NS, Sargent M, York AJ, Robbins J et al (2009) Plasma membrane Ca^{2+}-ATPase isoform 4 antagonizes cardiac hypertrophy in association with calcineurin inhibition in rodents. J Clin Invest. 119(4):976–985
205. Sadi AM, Afroze T, Siraj MA, Momen A, White-Dzuro C, Zarrin-Khat D et al (2018) Cardiac-specific inducible overexpression of human plasma membrane Ca^{2+} ATPase 4b is cardioprotective and improves survival in mice following ischemic injury. Clin Sci (Lond). 132(6):641–654
206. Mohamed TM, Abou-Leisa R, Stafford N, Maqsood A, Zi M, Prehar S et al (2016) The plasma membrane calcium ATPase 4 signalling in cardiac fibroblasts mediates cardiomyocyte hypertrophy. Nat Commun. 7:11074
207. Gros R, Afroze T, You XM, Kabir G, Van Wert R, Kalair W et al (2003) Plasma membrane calcium ATPase overexpression in arterial smooth muscle increases vasomotor responsiveness and blood pressure. Circ Res. 93(7):614–621
208. Perez AV, Picotto G, Carpentieri AR, Rivoira MA, Peralta Lopez ME, Tolosa de Talamoni NG (2008) Minireview on regulation of intestinal calcium absorption. Emphasis on molecular mechanisms of transcellular pathway. Digestion. 77(1):22–34
209. Armbrecht HJ, Boltz MA, Hodam TL (2002) Differences in intestinal calcium and phosphate transport between low and high bone density mice. Am J Physiol Gastrointest Liver Physiol. 282(1):G130–G136
210. Lee SM, Riley EM, Meyer MB, Benkusky NA, Plum LA, DeLuca HF et al (2015) 1,25-Dihydroxyvitamin D3 Controls a Cohort of Vitamin D Receptor Target Genes in the Proximal Intestine That Is Enriched for Calcium-regulating Components. J Biol Chem. 290(29):18199–18215
211. Ryan ZC, Craig TA, Filoteo AG, Westendorf JJ, Cartwright EJ, Neyses L et al (2015) Deletion of the intestinal plasma membrane calcium pump, isoform 1, Atp2b1, in mice is associated with decreased bone mineral density and impaired responsiveness to 1, 25-dihydroxyvitamin D3. Biochem Biophys Res Commun 467(1):152–156
212. Dong XL, Zhang Y, Wong MS (2014) Estrogen deficiency-induced Ca balance impairment is associated with decrease in expression of epithelial Ca transport proteins in aged female rats. Life Sci. 96(1-2):26–32
213. Wu F, Dassopoulos T, Cope L, Maitra A, Brant SR, Harris ML et al (2007) Genome-wide gene expression differences in Crohn's disease and ulcerative colitis from endoscopic pinch biopsies: insights into distinctive pathogenesis. Inflamm Bowel Dis. 13(7):807–821

214. Martin R, Harvey NC, Crozier SR, Poole JR, Javaid MK, Dennison EM et al (2007) Placental calcium transporter (PMCA3) gene expression predicts intrauterine bone mineral accrual. Bone. 40(5):1203–1208
215. Bredoux R, Corvazier E, Dally S, Chaabane C, Bobe R, Raies A et al (2006) Human platelet Ca^{2+}-ATPases: new markers of cell differentiation as illustrated in idiopathic scoliosis. Platelets. 17(6):421–433
216. Kim HJ, Prasad V, Hyung SW, Lee ZH, Lee SW, Bhargava A et al (2012) Plasma membrane calcium ATPase regulates bone mass by fine-tuning osteoclast differentiation and survival. J Cell Biol. 199(7):1145–1158
217. Prevarskaya N, Ouadid-Ahidouch H, Skryma R, Shuba Y (2014) Remodelling of Ca^{2+} transport in cancer: how it contributes to cancer hallmarks? Philos Trans R Soc Lond B Biol Sci. 369(1638):20130097
218. Ruschoff JH, Brandenburger T, Strehler EE, Filoteo AG, Heinmoller E, Aumuller G et al (2012) Plasma membrane calcium ATPase expression in human colon multistep carcinogenesis. Cancer Invest. 30(4):251–257
219. Ribiczey P, Tordai A, Andrikovics H, Filoteo AG, Penniston JT, Enouf J et al (2007) Isoform-specific up-regulation of plasma membrane Ca^{2+}ATPase expression during colon and gastric cancer cell differentiation. Cell Calcium. 42(6):590–605
220. Aung CS, Kruger WA, Poronnik P, Roberts-Thomson SJ, Monteith GR (2007) Plasma membrane Ca^{2+}-ATPase expression during colon cancer cell line differentiation. Biochem Biophys Res Commun. 355(4):932–936
221. Ribiczey P, Papp B, Homolya L, Enyedi A, Kovacs T (2015) Selective upregulation of the expression of plasma membrane calcium ATPase isoforms upon differentiation and 1,25(OH)2D3-vitamin treatment of colon cancer cells. Biochem Biophys Res Commun. 464(1):189–194
222. Varga K, Paszty K, Padanyi R, Hegedus L, Brouland JP, Papp B et al (2014) Histone deacetylase inhibitor- and PMA-induced upregulation of PMCA4b enhances Ca^{2+} clearance from MCF-7 breast cancer cells. Cell calcium. 55(2):78–92
223. Lee WJ, Roberts-Thomson SJ, Holman NA, May FJ, Lehrbach GM, Monteith GR (2002) Expression of plasma membrane calcium pump isoform mRNAs in breast cancer cell lines. Cell Signal 14(12):1015–1022
224. Lee WJ, Roberts-Thomson SJ, Monteith GR (2005) Plasma membrane calcium-ATPase 2 and 4 in human breast cancer cell lines. Biochem Biophys Res Commun 337(3):779–783
225. VanHouten J, Sullivan C, Bazinet C, Ryoo T, Camp R, Rimm DL et al (2010) PMCA2 regulates apoptosis during mammary gland involution and predicts outcome in breast cancer. Proc Natl Acad Sci U S A. 107(25):11405–11410
226. Jeong J, VanHouten JN, Dann P, Kim W, Sullivan C, Yu H et al (2016) PMCA2 regulates HER2 protein kinase localization and signaling and promotes HER2-mediated breast cancer. Proc Natl Acad Sci U S A. 113(3):E282–E290
227. Peters AA, Milevskiy MJ, Lee WC, Curry MC, Smart CE, Saunus JM et al (2016) The calcium pump plasma membrane Ca^{2+}-ATPase 2 (PMCA2) regulates breast cancer cell proliferation and sensitivity to doxorubicin. Sci Rep. 6:25505
228. Hegedus L, Padanyi R, Molnar J, Paszty K, Varga K, Kenessey I et al (2017) Histone deacetylase inhibitor treatment increases the expression of the plasma membrane Ca^{2+} pump PMCA4b and inhibits the migration of melanoma cells independent of ERK. Front Oncol. 7:95
229. Saito K, Uzawa K, Endo Y, Kato Y, Nakashima D, Ogawara K et al (2006) Plasma membrane Ca^{2+} ATPase isoform 1 down-regulated in human oral cancer. Oncol Rep. 15(1):49–55
230. Farkona S, Diamandis EP, Blasutig IM (2016) Cancer immunotherapy: the beginning of the end of cancer? BMC Med. 14:73
231. Supper V, Schiller HB, Paster W, Forster F, Boulegue C, Mitulovic G et al (2016) Association of CD147 and calcium exporter PMCA4 uncouples IL-2 expression from early TCR signaling. J Immunol. 196(3):1387–1399

232. Hu X, Su J, Zhou Y, Xie X, Peng C, Yuan Z et al (2017) Repressing CD147 is a novel therapeutic strategy for malignant melanoma. Oncotarget. 8(15):25806–25813
233. Rimessi A, Coletto L, Pinton P, Rizzuto R, Brini M, Carafoli E (2005) Inhibitory interaction of the 14-3-3{epsilon} protein with isoform 4 of the plasma membrane Ca^{2+}-ATPase pump. J Biol Chem. 280(44):37195–37203
234. Linde CI, Di Leva F, Domi T, Tosatto SC, Brini M, Carafoli E (2008) Inhibitory interaction of the 14-3-3 proteins with ubiquitous (PMCA1) and tissue-specific (PMCA3) isoforms of the plasma membrane Ca^{2+} pump. Cell Calcium. 43(6):550–561
235. Vanagas L, Rossi RC, Caride AJ, Filoteo AG, Strehler EE, Rossi JP (2007) Plasma membrane calcium pump activity is affected by the membrane protein concentration: evidence for the involvement of the actin cytoskeleton. Biochim Biophys Acta. 1768(6):1641–1649
236. Zabe M, Dean WL (2001) Plasma membrane Ca^{2+}-ATPase associates with the cytoskeleton in activated platelets through a PDZ-binding domain. J Biol Chem. 276(18):14704–14709
237. James P, Maeda M, Fischer R, Verma AK, Krebs J, Penniston JT et al (1988) Identification and primary structure of a calmodulin binding domain of the Ca^{2+} pump of human erythrocytes. J Biol Chem. 263(6):2905–2910
238. Cali T, Brini M, Carafoli E (2017) Regulation of cell calcium and role of plasma membrane calcium ATPases. Int Rev Cell Mol Biol. 332:259–296
239. Sgambato-Faure V, Xiong Y, Berke JD, Hyman SE, Strehler EE (2006) The Homer-1 protein Ania-3 interacts with the plasma membrane calcium pump. Biochem Biophys Res Commun. 343(2):630–637
240. Salm EJ, Thayer SA (2012) Homer proteins accelerate Ca^{2+} clearance mediated by the plasma membrane Ca^{2+} pump in hippocampal neurons. Biochem Biophys Res Commun. 424(1):76–81
241. Oceandy D, Cartwright EJ, Emerson M, Prehar S, Baudoin FM, Zi M et al (2007) Neuronal nitric oxide synthase signaling in the heart is regulated by the sarcolemmal calcium pump 4b. Circulation. 115(4):483–492
242. Olli KE, Li K, Galileo DS, Martin-DeLeon PA (2018) Plasma membrane calcium ATPase 4 (PMCA4) co-ordinates calcium and nitric oxide signaling in regulating murine sperm functional activity. J Cell Physiol. 233(1):11–22
243. Holton M, Mohamed TM, Oceandy D, Wang W, Lamas S, Emerson M et al (2010) Endothelial nitric oxide synthase activity is inhibited by the plasma membrane calcium ATPase in human endothelial cells. Cardiovasc Res. 87(3):440–448
244. Armesilla AL, Williams JC, Buch MH, Pickard A, Emerson M, Cartwright EJ et al (2004) Novel functional interaction between the plasma membrane Ca^{2+} pump 4b and the proapoptotic tumor suppressor Ras-associated factor 1 (RASSF1). J Biol Chem. 279(30):31318–31328
245. Kurnellas MP, Lee AK, Li H, Deng L, Ehrlich DJ, Elkabes S (2007) Molecular alterations in the cerebellum of the plasma membrane calcium ATPase 2 (PMCA2)-null mouse indicate abnormalities in Purkinje neurons. Mol Cell Neurosci. 34(2):178–188
246. Kim E, DeMarco SJ, Marfatia SM, Chishti AH, Sheng M, Strehler EE (1998) Plasma membrane Ca^{2+} ATPase isoform 4b binds to membrane-associated guanylate kinase (MAGUK) proteins via their PDZ (PSD-95/Dlg/ZO-1) domains. J Biol Chem. 273(3):1591–1595
247. Kruger WA, Yun CC, Monteith GR, Poronnik P (2009) Muscarinic-induced recruitment of plasma membrane Ca^{2+}-ATPase involves PSD-95/Dlg/Zo-1-mediated interactions. J Biol Chem 284(3):1820–1830
248. Goellner GM, DeMarco SJ, Strehler EE (2003) Characterization of PISP, a novel single-PDZ protein that binds to all plasma membrane Ca^{2+}-ATPase b-splice variants. Ann N Y Acad Sci 986:461–471

Chapter 6
A Role for SERCA Pumps in the Neurobiology of Neuropsychiatric and Neurodegenerative Disorders

Aikaterini Britzolaki, Joseph Saurine, Benjamin Klocke, and Pothitos M. Pitychoutis

Abstract Calcium (Ca^{2+}) is a fundamental regulator of cell fate and intracellular Ca^{2+} homeostasis is crucial for proper function of the nerve cells. Given the complexity of neurons, a constellation of mechanisms finely tunes the intracellular Ca^{2+} signaling. We are focusing on the sarco/endoplasmic reticulum (SR/ER) calcium (Ca^{2+})-ATPase (SERCA) pump, an integral ER protein. SERCA's well established role is to preserve low cytosolic Ca^{2+} levels ($[Ca^{2+}]_{cyt}$), by pumping free Ca^{2+} ions into the ER lumen, utilizing ATP hydrolysis. The SERCA pumps are encoded by three distinct genes, *SERCA1-3*, resulting in 12 known protein isoforms, with tissue-dependent expression patterns. Despite the well-established structure and function of the SERCA pumps, their role in the central nervous system is not clear yet. Interestingly, SERCA-mediated Ca^{2+} dyshomeostasis has been associated with neuropathological conditions, such as bipolar disorder, schizophrenia, Parkinson's disease and Alzheimer's disease. We summarize here current evidence suggesting a role for SERCA in the neurobiology of neuropsychiatric and neurodegenerative disorders, thus highlighting the importance of this pump in brain physiology and pathophysiology.

Keywords SERCA · Calcium · Central nervous system · Bipolar disorder · Schizophrenia · Alzheimer's disease · Parkinson's disease

6.1 Introduction

Calcium (Ca^{2+}) is a critical and universal regulator of cell fate [1–3]. While Ca^{2+} is crucial for the electrophysiological properties of all cells, it also serves as a prominent second messenger triggering a cascade of intracellular molecular

A. Britzolaki · J. Saurine · B. Klocke · P. M. Pitychoutis (✉)
Department of Biology & Center for Tissue Regeneration and Engineering at Dayton (TREND), University of Dayton, Dayton, OH, USA
e-mail: ppitychoutis1@udayton.edu

M. S. Islam (ed.), *Calcium Signaling*, Advances in Experimental Medicine and Biology 1131, https://doi.org/10.1007/978-3-030-12457-1_6

processes [1, 4–8]. Neurons are no exception to this; Ca^{2+} is pivotal for their survival and function, and disruptions of intracellular Ca^{2+} homeostasis may elicit neuropathology [9–14]. Given the innate complexity of neurons and the importance of Ca^{2+} in maintaining proper neuronal function, nerve cells have developed an intricate Ca^{2+} signaling network. A variety of channels, pumps, exchangers and proteins ensure a finely-tuned handling of the intraneuronal Ca^{2+} distribution [1, 4, 15–18]. In this review, we are focusing on the sarco/endoplasmic reticulum (SR/ER) calcium (Ca^{2+})-ATPase (SERCA) pump, an integral ER protein. The SERCA pumps are major regulators of intracellular Ca^{2+} homeostasis, facilitating the influx of Ca^{2+} in the ER lumen, thus regulating the levels of free Ca^{2+} in the cytosol [2, 19]. SERCAs belong to the family of P-type ATPases which includes a variety of membrane pumps that utilize ATP hydrolysis and a phosphorylated enzyme intermediate to transport ions across cellular membranes [20–22]. Found in all eukaryotic cells, three distinct genes, *SERCA1-3* (or *ATPA1-3* in humans), encode SERCA, producing 12 known protein isoforms, mainly *via* alternate splicing [23]. Interestingly, although all SERCA isoforms have a highly conserved structure, their expression patterns, affinity for Ca^{2+} and turnover rates may differ [23–30].

The SERCA structure and function have been recently reviewed [26]. It is well-established that SERCA is composed of a 1000-amino-acid-long single 100 kDa polypeptide chain [29, 31–33]. Much of the current knowledge on the structure of the SERCA pumps was based on SERCA1a isoform crystallography studies [34]. In fact, the folded SERCA protein resides on the ER membrane, and it is comprised of three cytosolic domains (A, N and P), one short luminal loop, and ten transmembrane α-helices (M1-M10). The extension of four transmembrane α-helices (M2-M5) results in the formation of the three cytosolic domains; Ca^{2+} binding and release are mediated by the actuator (A) domain, the ATP-binding cavity is formed by the nucleotide-binding (N) domain, whereas the high-energy phosphorylation intermediate product is formed in the phosphorylation (P) domain [34–39]. Moreover, the transmembrane α-helices are crucial for the formation of the Ca^{2+} channel (M2, M5, M5 and M8), and facilitate the Ca^{2+} transportation across the ER membrane (M4-M6) [34, 36, 40, 41]. This organization is highly conserved amongst all SERCA isoforms with differences mainly detected in the C-terminus [26, 31, 42–47] (Fig. 6.1). Despite the plethora of the SERCA splice variants, the universal role of SERCA entails the pumping of Ca^{2+} into the ER, resulting in decreased free cytosolic Ca^{2+} levels ($[Ca^{2+}]_{cyt}$) and maintained internal Ca^{2+} storages. Specifically, SERCA couples the active transport of two Ca^{2+} ions at the expense of one ATP molecule throughout a cycle of conformational alterations between two biochemical states (E1/E2) [19, 24, 48–55] (Fig. 6.2). At the E1 state, once Ca^{2+} and ATP bind to the high-affinity cytosolic sites, ATP hydrolysis is triggered, and the high energy intermediate state is formed. Subsequently, ADP is released and SERCA is phosphorylated, leading to the conformational change of the transmembrane domain (E2 state). During this transition, Ca^{2+} is shortly occluded from both the cytosol and the ER lumen. At the E2 state, Ca^{2+} is exposed to the ER lumen and its binding affinity to SERCA is very low, resulting in its release into

SERCA isoform	Protein size	Carboxyl terminus sequence
SERCA1a	994aa; 109.3kDa	LDEILKFVARNYLEG
SERCA1b	1001aa; 110.5kDa	LDEILKFVARNYLEDPEDERRK
SERCA2a	997aa; 109.7kDa	LYVEPLP/LIFQITPLLNVTQWLMVLKISLPVILMDETLKFVARNYLEP/AILE
SERCA2b	1042aa; 114.8kDa	LYVEPLP/LIFQITPLLNVTQWLMVLKISLPVILMDETLKFVARNYLEP/GKECVQPATKS CSFSACTDGISWPFVLLIMPLVIYVYSTDTNFSDMFWS
SERCA2c	999aa; 109.9kDa	LYVEPLP/LIFQITPLLNVTQWLMVLKISLPVILMDETLKFVARNYLEP/VLSSEL
SERCA2d	1007aa; 110.6kDa	LYVEPLP/VSGWVGLGTSHLLPGEAGGVTRLPCVS/AHLPDHTAERDPVADGAENLLA RDSHG
SERCA3a	999aa; 109.2kDa	SRNHMH/EEMSQK
SERCA3b	1043aa; 113.9kDa	SRNHMH/ACLYPGLLRTVSQAWSRQPLTTSWTPDHTGRNEPEVSAGNRVESPVCTS D
SERCA3c	1029aa; 112.4kDa	SRNHMH/ACLYPGLLRTVSQAWSRQPLTTSWTPDHTGLASLKK
SERCA3d	1044aa; 114.1kDa	SRNHMH/ACLYPGLLRTVSQAWSRQPLTTSWTPDHTGARDTASSRCQSCSEREEAGK K
SERCA3e	1052aa; 114.9kDa	SRNHMH/ACLYPGLLRTVSQAWSRQPLTTSWTPDHTGLASLGQGHSIVSLSELLREG GSREEMSQK
SERCA3f	1033aa; 112.6kDa	SRNHMH/GPGTQHRLAVRAAQRGRKQGRNEPEVSAGNRVESPVCTSD

Fig. 6.1 The primary sequence of the carboxyl termini of all known human SERCA protein isoforms. SERCA pumps have a highly conserved structure, but differences are detected in the carboxyl termini amongst protein isoforms. Variants that are encoded by the same gene tend to be less different. The splice sites are marked with slashes

the ER lumen. Simultaneously, 2-3 H^+ ions bind to the pump. Afterwards, SERCA gets dephosphorylated and returns to its E1 state, while releasing H^+ into the cytosol [19, 36, 37, 39, 48, 56, 57]. Of note, ATP-binding is independent of whether Ca^{2+} is bound to SERCA, but Ca^{2+} is essential for the enzymatic cycle to proceed [36, 37, 58]. Taken together, these conformational changes mediate the SERCA-dependent Ca^{2+} shuttling from the cytosol into the ER.

Interestingly, certain SERCA functions are isoform-dependent, with different splice-variants presenting slight differences in the affinity for Ca^{2+} and turnover rate [26, 28, 31, 59–61]. Several studies have revealed that the different SERCA isoforms present distinct expression profiles, suggesting tissue-specific functions. Two SERCA1 isoforms have been identified so far; SERCA1a and SERCA1b. The gene encoding these protein isoforms, *SERCA1*, is expressed in both the neonatal and the adult period [46, 62], but alternative splicing determines which isoform will be expressed in each developmental period [46, 62, 63]. Hence, SERCA1a is considered the adult isoform, and SERCA1b the neonatal isoform [46, 62–64]. In addition to temporal expression, SERCA1 expression is also tissue-dependent. To date, functional SERCA1 protein expression has been found primarily in the fast-twitch skeletal muscle fibers [46, 62], while studies have also shown low expression of SERCA1 in the Purkinje neurons of the cerebellum [65].

Similarly, SERCA2 expression is spatially regulated in the different tissues of the body [27, 29, 43, 44, 66, 67]. To date, four SERCA2 splice variants (SERCA2a-

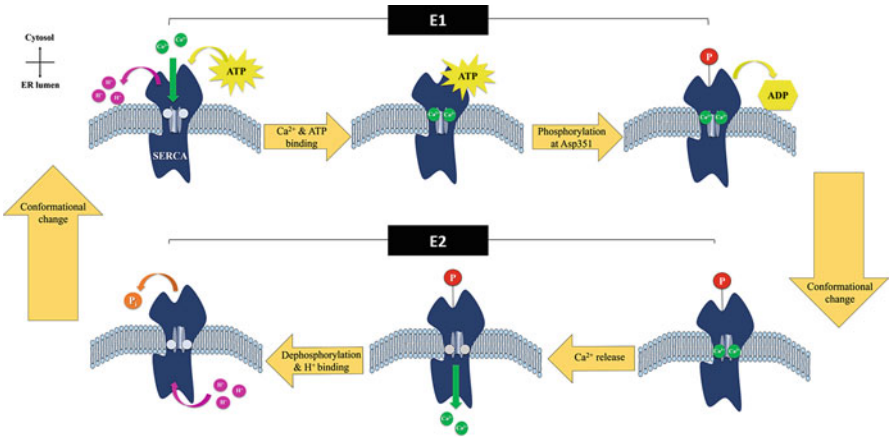

Fig. 6.2 SERCA-mediated Ca^{2+} transport across the ER membrane. SERCA facilitates the transport of two Ca^{2+} ions across the ER membrane in the expense of one ATP molecule, through a cycle of conformational changes (E1/E2 states). Upon Ca^{2+} and ATP binding (E1 state), SERCA gets phosphorylated due to ATP hydrolysis and changes conformation (E2 state). This conformational change allows Ca^{2+} release in the ER lumen. Afterwards, phosphate cleavage leads to dephosphorylation of SERCA, while two to three H^+ are coupled. SERCA dephosphorylation will reinforce a second conformational change to the initial E1 state. H^+ are released and SERCA is ready to bind new Ca^{2+} ions

d) have been identified with tissue-specific expression [26, 27, 42–44, 68–70]. Specifically, SERCA2a mRNA and protein have been detected in slow-twitch skeletal muscle, as well as in cardiac muscle fibers [44, 66, 67]. Furthermore, SERCA2a expression has been identified in the brain, albeit at low levels, and it is confined in the granular cells of cerebellar Purkinje neurons, as well as in the giant cells of the brainstem reticular formation [71–73]. In contrast, SERCA2b is constitutively expressed in all tissues including slow skeletal muscle fibers, smooth muscle cells, cardiac muscle fibers, neurons and astrocytes [27, 43, 44, 74]. SERCA2b has also been found to be the only isoform expressed in neuronal microsomes, synaptic plasma membrane vesicles, and synaptosomes [75]. The extensive expression pattern of SERCA2b in the CNS has been recently reviewed [26]. Given its constitutive expression, SERCA2b is considered an ER housekeeping enzyme, crucial for maintaining intracellular Ca^{2+} homeostasis [27, 44, 64]. About 15 years after the discovery of the SERCA2a and SERCA2b isoforms, a third splice variant, SERCA2c, was identified in hematopoietic, mesenchymal and epithelial cells, as well as in the brain at low levels [30, 31, 42]. Moreover, the mRNA expression of a fourth splice variant, SERCA2d, has been detected in skeletal muscle fibers [68].

The expression pattern of the third SERCA-encoding gene, *SERCA3*, was first discovered using northern blot analysis in rat tissues [64]. To date, at least six different SERCA3 isoforms (SERCA3a-f) have been identified with a complex expression pattern in many tissue types and in a wide variety of species [60, 61,

64, 76–79]. The SERCA3a, SERCA3b, and SERCA3c protein isoforms have been detected in human platelets and human immortalized T-lymphocytes, known as T-lymphoid Jurkat cells [78]. The most distributed SERCA3 isoforms are SERCA3a, SERCA3b and SERCA3d; their expression has been found in a wide variety of tissue types, including the brain [60]. Specifically, SERCA3a and SERCA3b mRNA expression has been identified in the brain, heart, lung, pancreas, liver and placenta [60]. SERCA3d mRNA has also been found in the same tissue types as well as in skeletal muscle fibers [60]. The expression of SERCA3e is rather confined to human lung and pancreatic tissues [60]. Further studies have revealed the expression of a sixth SERCA3 variant, SERCA3f, in hematopoietic and non-muscle cell lines, as well as in all human cell and tissue types [61]. Importantly, immunoblotting and immunohistochemical experiments have indicated the expression of SERCA3 protein in the rat cerebral cortex and cerebellar Purkinje neurons, as well as in the human choroid plexus [79–81].

6.2 The SERCA Pumps: Potential Indicators of Brain Pathophysiology?

Taking into consideration that SERCA plays a pivotal role in preserving intracellular Ca^{2+} homeostasis, and that specific SERCA isoforms are expressed in the brain, several studies have explored the role of this important Ca^{2+} regulator in brain pathophysiology. In this context we conduct a comprehensive review of contemporary experimental evidence suggesting a central role for SERCA in the pathophysiology of neuropsychiatric and neurodegenerative disorders. Moreover, we discuss the potential of SERCA pumps as molecular targets for the development of novel pharmacotherapies to combat such debilitating disorders.

6.3 A Role for SERCA in the Pathophysiology of Neuropsychiatric Disorders

Neuropsychiatric disorders such as schizophrenia (SZ) and bipolar disorder (BD) are characterized by high lifetime prevalence and early onset, with deleterious long-time effects on public health [82–85]. Of note, neuropsychiatric disorders account for approximately 70% of disabilities worldwide, with SZ and BD contributing approximately 7% each [86]. SZ is a clinically and genetically heterogenous neuropsychiatric disorder, that affects approximately 1% of the general population, and is associated with hallucinations, delusions and profound cognitive impairment [87, 88]. BD is a debilitating chronic mood disorder with a complex clinical and genetic background. About 1% of the general population is affected by BD, with episodes of depression, mania and hypomania being the characteristic symptoms of

the disease [89, 90]. Despite the devastating effects of these disorders and the rapid increase in incidence worldwide, their underlying pathophysiology is yet elusive. Interestingly, although SZ and BD are classified as distinct diagnostic categories, the two disorders greatly overlap in clinical presentation and genetic liability, as extensively discussed in recent association studies [91], highlighting the importance of understanding the common mechanisms underlying both disorders.

Intracellular Ca^{2+} signaling is believed to play a vital role in SZ etiology. In fact Ca^{2+} has been proposed as the common mechanism underlying SZ pathology [92, 93]. According to this theory, SZ symptomatology rises due to the disruption of the intracellular Ca^{2+} homeostasis, and the subsequent dysfunction of Ca^{2+}-mediated signal transduction processes [93]. The role of Ca^{2+} in SZ was first proposed by Jimerson et al., as a positive correlation was evidenced between psychotic episodes and increased cerebrospinal fluid (CSF) Ca^{2+} levels in SZ patients [92]. Since then, growing evidence has further supported the central role of Ca^{2+}-signaling in the pathogenesis of SZ, as discussed in several reviews [26, 93–96].

In addition to SZ, altered intracellular Ca^{2+} signaling has also been proposed as a potential mechanism underlying BD pathophysiology. In fact, ex vivo platelet studies have indicated that intracellular Ca^{2+} mobilization is dysregulated in BD. More specifically, an increase in serotonin- or thrombin-induced Ca^{2+} mobilization, as well as elevation of intracellular Ca^{2+} levels, have been observed in platelets harvested from BD patients [97–102]. Importantly, common pharmacological therapies for BD (i.e., lithium and valproate) have been reported to enhance the expression of proteins essential for Ca^{2+} sequestration, further supporting a possible role for Ca^{2+} in BD pathogenesis [103–109].

Disruption of intracellular Ca^{2+} homeostasis is crucial in the emergence of neuropsychiatric pathology. Indeed, recent Genome Wide Association Studies (GWAS) and meta-analyses have indicated the association of altered Ca^{2+} channel activity with SZ and BD [110–112]. More specifically, the expression of genes encoding several types of voltage-gated Ca^{2+} (Ca_v) channels have been linked to both SZ and BD [113–117]. Of note, Ca_v channels are central in regulating Ca^{2+} influx into neurons, and Ca_v channel blockers have been examined in clinical trials as potential therapeutic approach for SZ, highlighting the importance of altered Ca^{2+}-signaling mechanisms in the pathogenesis of this disorder [118]. Thus, efforts have focused on deciphering the possible role of Ca^{2+}-regulating mechanisms in SZ and BD.

6.3.1 Early Association Between SERCA2 Mutations and Psychosis in Darier's Disease Patients

The implication of SERCA in BD and SZ was first introduced almost two decades ago and since then, growing evidence has continued to support the importance of SERCA in the pathogenesis of these disorders. An early association between

SERCA and neuropsychiatric pathophysiology was made in patients with Darier's Disease (DD) [14, 119]. DD or Darier-White disease, also known as *keratosis follicularis*, is a rare autosomal dominant skin disorder with the presence of characteristic warty papules and keratotic plaques in seborrheic areas [120]. It is a highly penetrating disorder, with variable expressivity and early onset, affecting 1 in 100,000 individuals in the general population [120–123]. Mutations in the *ATP2A2* (i.e. SERCA2) gene on chromosome 12q23-24.1 have been identified as the underlying mechanism of DD pathogenesis, with at least 253 unique *ATP2A2* variants being reported in 353 familiar or sporadic DD cases throughout the years [124]. At least 75% of the reported mutations are unique to the affected family, many are *de novo* mutations and only a few are common between families [125]. Evidence indicates that the majority of *ATP2A2* mutations are missense (51%), while all mutations are dispersed throughout the gene without hotspots [121, 124–126]. It is also believed that the *ATP2A2* mutations lead to DD phenotype through haploinsufficiency, and that DD symptomatology occurs independently of the SERCA2 mutation type [124, 126]. Several studies have indicated that *ATP2A2* mutations might affect SERCA2 protein expression and function, as well as proteasomal degradation [24, 127–129]. Specifically, some *ATP2A2* mutants have shown reduced SERCA2 expression, subsequent decreased Ca^{2+} ATPase activity, Ca^{2+} turnover and phosphorylation rates [24, 127–129]. Other *ATP2A2* mutants only reduce Ca^{2+} affinity and sensitivity to feedback inhibition by ER Ca^{2+} [129]. Moreover, frameshift deletions and nonsense mutations have been reported to promote apoptosis by increasing proteasomal degradation [127]. Further in vitro experiments using missense, nonsense and deletion *ATPA2* variants have indicated that ER luminal Ca^{2+} is depleted in keratinocytes, leading to abnormal $[Ca^{2+}]_{cyt}$ [130, 131]. Additional experiments with cultured cells from DD patients have revealed abrogated post-translational protein trafficking to plasma membrane and induced ER stress, caused by diminished ER Ca^{2+} [132, 133]. More importantly, ER stress induced by SERCA-blockade in primary human keratinocytes has been associated with increased keratinocyte differentiation, further confirming the fundamental role of SERCA2 in DD [134].

Interestingly, as extensively discussed in recent reviews [26, 124, 135, 136], DD patients present with increased life-time prevalence of several neuropsychiatric disorders, including: major depression disorder (MDD-30%), BD (4%), epilepsy (3%), SZ (1%) and cognitive disabilities (4%) [137–143]. These early observations along with the fact that the ubiquitous expression of SERCA2b had been identified in the brain [144], raised the question whether skin and brain disorders occur independently, or due to a SERCA2 pleiotropic effect. Early studies in DD patients have associated mutations in the SERCA2 ATP-binding domain with dysthymia, hinge domain mutations with MDD and BD, and transmembrane domain mutations with epilepsy, MDD and cognitive disability [14]. Other studies have supported the implication of SERCA2 mutations in the neuropsychopathology of DD patients. Identified SERCA2 mutations affecting the phosphorylation, stalk, hinge or transduction domains, and the transmembrane M6/M7 loop, have been reported in clinical DD cases with concurrent mental disease and vegetative growth

[121]. More recent clinical reports have further supported the association between SERCA2 dysfunction and schizophrenic or bipolar symptomatology in DD patients by identifying novel or recurrent *ATP2A2* mutations [145–147]. Specifically, the same missense mutation in the stalk domain of the SERCA2 pump has been identified in two different clinical DD cases with concurrent SZ [145, 147], while an altered-splicing mutation in the acceptor site has been characterized in another DD patient with concurrent BD [146].

6.3.2 Altered SERCA Activity Associated with the Pathogenesis of Schizophrenia and Bipolar Disorder

The role of SERCA in SZ and BD pathophysiology has been further discussed in a variety of preclinical and clinical studies. Early studies have investigated the role of SERCA in the pathophysiology of BD; platelets derived from BD patients presented a higher increase in $[Ca^{2+}]_{cyt}$ upon SERCA blockade by thapsigargin when compared to healthy controls, indicating altered SERCA activity in BD [148]. Other studies have attempted to explore the role of SERCA in SZ using a common animal model for SZ, the *Df(16)1/+* mouse, carrying SZ-related 22q11 microdeletions. These *de novo* deletions are variable in size and occur on the 22q11.21 to 22q11.23 chromosomal region in humans [149–153], leading to haploinsufficiency of several genes [149, 154–160]. The syndrome associated with these microdeletions is known as the 22q11 deletion syndrome (22q11DS) or DiGeorge syndrome, and it affects 1in 4000 to 1 in 6000 individuals worldwide [161–165]. DiGeorge symptomatology includes mild to moderate cognitive deficits, intellectual and learning disabilities, with a progressive worsening of cognitive function [166–170]. Interestingly, DiGeorge patients present high life-time prevalence to SZ or psychotic spectrum disorders (25%) [171–176]. Moreover, DiGeorge-related and idiopathic psychosis are not distinguished from each other, presenting similar demographics, age-onset and symptomatology [177, 178]. Therefore, *Df(16)1/+* mice are widely used to study the mechanisms underlying SZ pathophysiology in vivo. In vivo and in vitro experiments have suggested profound neuromolecular and behavioral alterations in *Df(16)1/+* mice, such as hippocampus-dependent spatial memory deficits and enhanced long-term potentiation (LTP) at the Schaffer collateral synapses [13]. More specifically, presynaptic SERCA2 expression has been found to be enhanced in the hippocampus, subsequently increasing presynaptic glutamate release and altering Ca^{2+} dynamics in the axon terminal [13]. Additional studies in *Df(16)1/+* mice have indicated that SERCA2 expression is altered in a brain-specific manner, and that these alterations extend to other brain regions beyond the hippocampus, such as the cortex and cerebellum [179]. Interestingly, later studies have proposed that the microRNA-processing gene *Dgcr8* regulates SZ-related SERCA2 expression [179, 180]. Earls et al. identified the loss of two miRNAs, miR-25 and miR-185, in the brain of *Df(16)1/+* mice, leading to abnormal

LTP increase [179]. According to the study, miR-25 and miR-185 affect Ca^{2+} influx into the ER by targeting SERCA2. Hence, loss of these two miRNAs has been linked to significantly elevated presynaptic SERCA2 levels of the hippocampus. Strikingly, presynaptic injection of either miR-25 and miR-185, restored SERCA2 activity and rescued the LTP abnormalities, introducing novel targets for the development of pharmacotherapies for the treatment of SZ [179]. More importantly, the same study demonstrated that SERCA2 was upregulated in the prefrontal cortex and the hippocampus of SZ patients post-mortem, further supporting the mechanistic link between SZ, DiGeorge syndrome and SERCA2. These data collectively led the investigators to hypothesize that SERCA2 upregulation results in perturbation of presynaptic Ca^{2+} signaling that may ultimately lead to the cognitive deficits observed in SZ [179].

In agreement with previous studies, a recent GWAS assay identified *ATP2A2* as a risk gene for SZ [181]. In addition, a meta-analysis classified *ATP2A2* as a SZ risk gene that could synergistically contribute to the enhanced generation of thalamic delta oscillations, associated with both negative and positive symptoms of SZ [182]. Furthermore, recent studies using another SZ-relevant animal model, the Neonatal Lesion in Ventral Hippocampus (NLVH) rat, have identified decreased SERCA2 expression in the prefrontal cortex of NLVH rats [183]. Genis-Mendoza et al. used microarrays to assess the global transcriptomic profiles of the prefrontal cortex, hippocampus and nucleus accumbens in juvenile and adult NVLH rats. The investigators reported a marked decline in *ATP2A2* expression only in the prefrontal cortex of adult NVLH rats, but not in their juvenile counterparts. These data led to the hypothesis that decreased *ATP2A2* expression could result in elevated $[Ca^{2+}]_{cyt}$, thus activating Ca^{2+}-dependent transcription factors and kinases that could potentially exert genomic effects contributing to the cognitive defects observed in SZ [183, 184].

Adding to the proposed role of SERCA in the neurobiology of SZ, a very interesting study used a ketamine-induced pharmacological model of experimental psychosis to demonstrate brain region-specific alterations in SERCA3 expression [185]. Specifically, Lisek et al. treated rats repeatedly (5 consecutive days) with the non-competitive N-methyl-D-aspartate receptor (NMDAR) antagonist, ketamine (30 mg/kg); this protocol has been found to induce profound psychosis-like neurochemical, behavioral and neuroanatomical alterations in the rat brain [94, 186, 187]. The authors first observed that ketamine-treated rats presented severe stereotypic behavior (i.e., increased cumulative turning, weaving and bobbing), as assessed by open field (OF) tests. Interestingly, a marked increase of $[Ca^{2+}]_{cyt}$ in the striatum, cerebellum, cortex and hippocampus of ketamine-treated rats was reported. However, a positive correlation between hyperlocomotion and elevated $[Ca^{2+}]_{cyt}$ was only established in cortical and striatal neurons [185]. Moreover, SERCA3 expression was found decreased in the cortex, but increased in the cerebellum, hippocampus and striatum of ketamine-treated rats. Correlation studies linked the abnormal elevation of $[Ca^{2+}]_{cyt}$ to increased SERCA3 expression,

suggesting that overexpression of SERCA acted as a compensatory mechanism for the increased $[Ca^{2+}]_{cyt}$ [185].

Taken together, clinical and preclinical evidence point to altered SERCA activity in SZ and BD. SERCA dysregulation most likely affects downstream events, such as synaptic glutamate release and LTP in excitatory neurons, likely leading to characteristic neuropsychiatric symptomatology [13, 179, 180]. Evidently, SERCA pumps synergistically drive neuropsychiatric pathology, reinforcing the notion that this protein family might be an important target for the development of future pharmacological approaches in treating schizophrenia and bipolar disorder.

6.4 A Proposed Implication of SERCA Pump Dysregulation in Neurodegenerative Disorders

6.4.1 Ca^{2+} Aberrations in Alzheimer's Disease and Parkinson's Disease

Alzheimer's disease (AD) and Parkinson's disease (PD) are the two most common progressive neurodegenerative disorders amongst aging populations with high morbidity and mortality [188–190]. The majority of AD and PD cases are sporadic, but a few early-onset cases have been attributed to familial mutations [188, 190–193]. Interestingly, neuronal loss and malformed protein aggregations are characteristic features in both AD and PD. The pathophysiological hallmarks of PD include the loss of dopamine (DA) neurons in the substantia nigra *pars compacta* (SNc) as well as the presence of intraneuronal Lewy bodies, resulting in motor deficits manifested as bradykinesia, resting tremor and rigidity [194–196]. Likewise, AD is characterized by progressive cognitive loss and dementia due to the onset of extracellular senile amyloid (Aβ) plaques, intraneuronal neurofibrillary tangles (NFT), as well as the detrimental loss of neurons and synapses predominately in the hippocampus and the cerebral cortex [197–199].

Despite the distinct clinical presentation, recent studies have revealed a crosstalk in the molecular mechanisms underlying AD and PD pathophysiology, suggesting that common molecular mechanisms drive aging brain pathology [200–203]. As extensively reviewed recently [200], oxidative stress and the generation of free radicals could be caused by abnormal accumulation of proteins with altered conformation (i.e., proteinopathy). Subsequently, proteinopathy results in impaired proteasomal degradation of toxic proteins and subsequent proteotoxicity observed in AD and PD [200, 204–208]. Additionally, proteotoxicity has been associated with mitochondrial dysfunction in both disorders. Evidence has indicated that abnormal protein aggregation could result in disruption of bioenergetics and important mitochondrial functions, such as mitophagy and fusion/fission, and to a subsequent increase of free radicals that may trigger cell apoptosis [200, 209–215].

Taking into consideration that the molecular pathogenetic mechanisms underlying AD and PD appear to be highly similar, great effort has focused on revealing whether these two disorders share common mechanisms that reinforce a cross-talk. Interestingly, decreased ER Ca^{2+} levels and subsequent increased $[Ca^{2+}]_{cyt}$ have been associated with ER-stress induced apoptosis and neurodegeneration [198, 216–220]. As discussed in several reviews [26, 217, 221–225], evidence indicates an intricate interplay between intracellular Ca^{2+} homeostasis, amyloid metabolism, neurotransmission and plasticity in the pathophysiology of AD. Increase in intracellular Ca^{2+} concentrations is considered to be secondary to the characteristic AD lesions, including the accumulation Aβ and the hyperphosphorylation of TAU protein [11, 226–230]. The aftermath of such complex interactions is believed to be rendering the neurons more vulnerable to Ca^{2+} overload, causing a major remodeling of the neural Ca^{2+} circuits, that leads to apoptosis and progressive cognitive deterioration [11, 225, 231–233]. Many in vitro and in vivo studies have supported an association between dysfunctional amyloid precursor protein (APP), Aβ plaque deposition and Ca^{2+} overload with dendritic degeneration, leading to impaired spino-dendritic Ca^{2+} signaling and disrupted plasticity [234–237].

Similarly, intracellular Ca^{2+} dyshomeostasis is believed to be critical for the elicitation of PD-related histopathological features [238–241]. The possible implication of intraneuronal Ca^{2+} signaling in PD originated by the association between increased PD-related neuronal vulnerability and decreased levels of the Ca^{2+}-buffering protein, CB-D_{28k}, as well as between high $[Ca^{2+}]_{cyt}$ and a two- to threefold increase in DA levels in the cytosol of SNc DAergic neurons [242, 243]. Subsequent studies supported the involvement of Ca^{2+} in PD, as overexpression of familial PD-related proteins, such as DJ-1, Parkin and α-synuclein (αSYN) enhanced the ER-mitochondrial Ca^{2+} sequestration [244, 245]. More importantly, ER stress caused by the disruption of Ca^{2+} signaling and buffering in the SNc DAergic neurons has been linked to abnormal levels of αSYN and Parkin [239, 242, 246–249]. Thus, it seems that an intricate interplay exists between elevated $[Ca^{2+}]_{cyt}$ and DA levels, as well as αSYN overexpression in triggering the selective apoptosis of SNc DAergic neurons. Aggregation of αSYN has been shown to increase $[Ca^{2+}]_{cyt}$ and caspase-3-mediated cell death in cultured neurons and human neuroblastoma cell lines [250, 251]. Interestingly, it seems that αSYN aggregates regulate $[Ca^{2+}]_{cyt}$ in a biphasic fashion [252–257]; in vitro experiments in primary hippocampal neurons from αSYN-transgenic mice overexpressing αSYN, showed that the initial decline in $[Ca^{2+}]_{cyt}$ was followed by an increase 10 days later, suggesting a sophisticated a-SYN-dependent regulation of intracellular Ca^{2+} signaling in PD [257]. In addition, Ca^{2+} binding to the αSYN carboxyl terminus has been shown to accelerate the accumulation of the annular toxic form of αSYN in vitro [247, 258]. It has been also demonstrated that elevated intracellular Ca^{2+} and oxidative stress cooperatively stimulate αSYN accumulation. Goodwin et al. reported that when oxidative stress is induced in 1321N1 cells in vitro by treatment with the SERCA inhibitor thapsigargin, accumulation of αSYN aggregates increases dramatically [259]. In addition, αSYN aggregates might associate with ER in vivo, as demonstrated by experiments using transgenic mice

overexpressing WT or mutant αSYN and human brain tissue from PD patients [260]. According to Colla et al. a small subset of αSYN resides in the ER lumen leading to protein aggregation. Additionally, the initial appearance of aggregated αSYN precedes onset and increases with the progression of the disease, while ER-stress attenuation reduces αSYN aggregation and rescues disease phenotype [260]. Such observations, directly associated αSYN aggregation with ER stress and α-synucleinopathy, highlighting the importance of further investigation of ER-stress-associated mechanisms underlying PD pathology. Most importantly, clinical studies with hypertensive patients have suggested that Ca^{2+} channel blockers could decrease the risk for PD, thus suggesting intracellular Ca^{2+} regulation as a novel pharmacological approach for PD [261–265].

In the context of unraveling the molecular mechanisms underlying Ca^{2+} dysregulation in AD and PD pathogenesis, the role of SERCA in neurodegeneration has also been investigated. It is well established that SERCA pumps play an important role in oxidative stress, the generation of free radicals, and mitochondrial dysfunction, as aberrations in SERCA function lead to ER stress. Compelling studies have suggested that pharmacological activation and/or overexpression of SERCA may alleviate ER stress [266–268]. For instance, Park et al. infected mouse embryonic fibroblasts with an adenovirus encoding SERCA2b and challenged the cells with thapsigargin to induce ER stress, by blocking SERCA. Interestingly, the overexpression of SERCA2b resulted in the alleviation of ER stress and the increase of ER folding capacity [267]. ER stress-induced apoptosis may also be reduced by pharmacological activation of SERCA, as indicated by recent in vitro experiments in human embryonic cells [268]. In this study, ER stress was induced by H_2O_2 exposure in SERCA2b-expressing HEK293 cells, and viability assays were conducted in the presence and absence of a small allosteric specific SERCA activator (i.e., CDN1163). CDN1163-induced SERCA activation dramatically decreased H_2O_2-induced apoptosis, suggesting CDN1163 as a potential pharmacological treatment for ER stress-mediated cell death. SERCA activity maintains ER function and intracellular Ca^{2+} balance, ultimately preventing the activation of apoptotic pathways. Thus, it is very likely that SERCA is associated with proteotoxicity present in AD and PD.

6.4.2 Evidence for Altered SERCA Function in Alzheimer's Disease

In the quest of deciphering the role of SERCA in AD, several studies have sought for a possible correlation between fundamental disease features and SERCA activity. Indeed, studies have proposed an association between SERCA and proteins that are central in AD pathogenesis, namely presenilins (PS). Over 200 reported mutations on the genes encoding for PS1, PS2 and APP have been suggested as causatives of 30–50% of all familial AD (FAD) cases [269–273]. Of note, PS resides on

the ER membrane until it is cleaved to its N- and C-terminal fragments. These fragments then travel to the plasma membrane where they act as γ-secretase units, subsequently cleaving APP to form Aβ peptides [274–276]. Given the important role of γ-secretase in cleaving APP, PS mutations disturbing APP processing, result in the formation of cytotoxic Aβ peptides. In vitro studies utilizing mouse embryonic fibroblasts and *Xenopus laevis* oocytes introduced the concept of SERCA physically associating with PS [9]. Green et al. proposed that SERCA2 function was directly relying on the presence of PS, as shown by the elevated levels of SERCA2b in double-PS null-mutant (PSDKO) neuronal cells. Surprisingly, the levels of resting $[Ca^{2+}]_{cyt}$ was elevated while the ER Ca^{2+} load was diminished in the absence of PS, indicating impaired SERCA activity that led to a compensatory increase in SERCA expression. Their hypothesis was confirmed as SERCA2b levels were rescued in PS mutant cells in the presence of either PS1 or PS2. In addition, siRNA knockdown of SERCA2b in CHO cells mimicked the Ca^{2+} phenotype of PSDKO cells, further supporting their initial observations. The study also highlighted the importance of PS in Ca^{2+} sequestration by overexpressing PS1, PS2 and SERCA2b in *X. laevis* oocytes; cytosolic Ca^{2+} sequestration was accelerated in all cells, with PS2 overxpression showing the most robust effect. Interestingly, pharmacological blockade of SERCA2 by thapsigargin prevented the PS-mediated accelerated ER filling. Further immunohistochemical and immunoprecipitation experiments on WT mouse fibroblasts showed that SERCA2b and PS1/PS2 colocalize on the ER membrane and that PS1/PS2 specifically bind to SERCA2b. Moreover, the implication of SERCA2b in Aβ production was suggested in the same study; overexpression of SERCA2b in APP-expressing CHO cells resulted in elevated Aβ production, while siRNA knockdown of SERCA2b caused a drastic decline in Aβ40 and Aβ42 production [9].

Adding to the notion that SERCA and PS physically associate, in vitro experiments in human epithelial, glioma and neuroblastoma cell lines (HEK293, KNS-42 and GOTO) indicated the formation of a complex between SERCA2 and the PS1 holoprotein [277]. Jin et al. proposed that the PS1 holoprotein may act as an anti-apoptotic agent under stress by upregulating SERCA2, and thus preventing the disruption of intracellular Ca^{2+} homeostasis [277]. Further co-immunoprecipitation data, derived from untransfected and stably PS1-expressing cells, demonstrated the interaction between SERCA2b and the PS1 holoprotein. In addition, immunohistochemical analysis revealed that SERCA2b and PS1-holoprotein co-localize [277]. The importance of the interaction between PS and SERCA in AD pathogenesis was further supported by in vitro studies using HeLa cells, embryonic cells (HEK293), human neuroblastoma cells (SH-SY5Y) and fibroblasts expressing PS2 [278]. Brunello et al. showed that both WT PS2 and the FAD-related PS2-T122R mutation could reduce ER Ca^{2+} uptake by affecting SERCA2 activity. Indeed, overexpression of SERCA2b in PS2-T122R-expressing SH-SY5Y cells resulted in full restoration of ER Ca^{2+} uptake rate and steady-state levels, highlighting the inhibitory activity of PS2 on SERCA activity [278].

Apart from the PS-SERCA interaction, recent studies have also indicated another possible interaction between SERCA and a novel sporadic AD-associated protein,

known as the Ca^{2+} homeostasis modulator 1 (CALHM1) [218]. CALHM1 is preferentially expressed in the nervous system and is located on the neuronal plasma and ER membranes, while it is proposed to increase Aβ production by disrupting intracellular Ca^{2+} homeostasis [279]. Intriguingly, earlier in vitro experiments in CALHM1-transfected HEK-293 cells, showed that CALHM1 provokes ER stress by affecting the influx and efflux of Ca^{2+} into ER [218]; The CALHM1-transfected cells presented a drastic increase in the plasma membrane permeability to Ca^{2+}, whereas ER Ca^{2+} accumulation at the steady-state was significantly decreased. Such a reduction in ER Ca^{2+} uptake was initially hypothesized to be attributed to either enhanced ER Ca^{2+} leak by IP_3R and RyR, or diminished ER Ca^{2+} pumping by SERCA2. Further measurements of Ca^{2+} levels revealed that CALHM1 promoted ER Ca^{2+} leak, as indicated by the increased efflux of Ca^{2+} from the ER. Despite the increase in both plasma membrane-mediated Ca^{2+} influx and ER Ca^{2+} leak, the diminished intraluminal ER Ca^{2+} suggested that Ca^{2+} pumping into the ER might also be impaired. Further experiments using plasma membrane-permeabilized cells indicated that ER uptake was altered, as both Ca^{2+} transport capacity and Ca^{2+} affinity had been significantly reduced. Interestingly, the combined decline in ER pumping and increase in ER leak resulted to a 6-7-fold decrease in steady-state ER Ca^{2+} levels at physiological $[Ca^{2+}]_{cyt}$. Subsequently, Gallego-Sandin et al. proposed that the aftermath of such alterations in the ER Ca^{2+} levels could be the activation of store-operated Ca^{2+} entry, justifying the enhanced plasma membrane- mediated Ca^{2+} influx and the $[Ca^{2+}]_{cyt}$. In agreement with the notion that diminished ER Ca^{2+} promotes ER stress, the same study demonstrated the activation of ER stress-related genes in CALHM1-transfected cells. The derived data further supported the importance of maintaining SERCA activity and the detrimental consequences of dysfunctional SERCA in intracellular Ca^{2+} homeostasis, leading to AD-associated neuronal cell death [218].

Another intriguing pull-down assay employing human post-mortem brains identified that SERCA2 interacts with FE65, a cytosolic adapter protein as well as an APP-binding partner [280]. Of note, the FE65-APP interaction is believed to be critical for APP processing, apoptosis and neurite outgrowth [281–285]. Among other identified candidate proteins, SERCA2 was confirmed to interact with FE65, as supported by further co-immunoprecipitation assays from HEK293 cells overexpressing both SERCA2 and FE65. Notably, SERCA2 was found to be upregulated in primary hippocampal neurons derived from FE65/FE65L1 DKO mice, whereas HEK293 cells were more prone to thapsigargin-induced ER stress when FE65 was knocked down. According to Nensa et al. FE65 is possibly involved in the regulation of intracellular Ca^{2+} homeostasis, through its interaction with key components on the ER membrane. Taken together, it was suggested that the regulation of SERCA activity by PS may be attributed to the increased availability of APP intracellular domains (AICD) upon γ-secretase-mediated APP cleavage. Subsequently, the free AICDs bind to FE65 (or FE65 changes conformation), leading to further interaction with binding partners, such as SERCA2 [280].

As demonstrated by in vitro data, SERCA possibly holds an important role in AD pathology. Recently, promising in vivo experiments proposed that SERCA activation could alleviate AD-like pathology in mice [286]. Krajnak et al. employed the allosteric SERCA activator, CDN1163, which had been previously shown to increase ER Ca^{2+} uptake and SERCA activity in vivo [268]. To test whether CDN1163 had a therapeutic effect, double-transgenic APPSwe/PSEN1dE9 mice (i.e., transgenic mice carrying both mutant APP and PS1) were administered CDN1163 (10 mg/kg) for 4 weeks and were then subjected to a series of behavioral tests to assess learning and memory (i.e., Morris Water Maze; MWM), depressive-like behavior (i.e., tail suspension test; TST) and motor coordination (i.e., Rotarod). Strikingly, CDN1163-treated mice presented enhanced memory retention, better motor coordination and an antidepressant-like phenotype, as compared to vehicle-treated controls. These data collectively suggested SERCA as a therapeutic target in AD pathogenesis and CDN1163 as a promising drug candidate [286].

6.4.3 SERCA Dysregulation as a Proposed Mechanism Underlying Parkinson's Disease Pathophysiology

Similar to AD, SERCA activity has recently been linked to PD pathophysiology, further supporting the pivotal role of the pump in neurodegeneration. Growing evidence suggests that the intricate interplay between SERCA activity, αSYN aggregation and ER stress in neurons could be the main driving force of PD pathogenesis. Of note, several reviews have discussed the multifunctional properties of αSYN, including the regulation of synaptic transmission, synaptic function and plasticity, as well as the organization of membrane activity through interaction with intracellular membranes and lipid surfaces [287, 288]. Furthermore, synucleinopathies have been established as the genetic component of PD, as extensively discussed in a recent excellent review by Nussbaum; autosomal-dominant familial PD cases have been attributed to mutations on the αSYN-encoding *SNCA* gene, while *SNCA* gene variations have been linked with sporadic PD cases [287]. Previous studies have associated abnormal αSYN aggregation with ER stress, intracellular Ca^{2+} signaling alterations and subsequent neuronal cell death (reviewed in [289]). However, the association of SERCA with αSYN, and its subsequent implication in PD pathophysiology, has been only recently investigated. An interesting study showed that 6-hydroxy-DA (6-OHDA)-mediated oxidative stress affects SERCA2 activity in rats, and that physical exercise may rescue the PD phenotype, supporting the idea that SERCA dysregulation might be implicated in PD pathogenesis [290]. Prior to striatal stereotaxic injections of 6-OHDA, rats were challenged with an incremental running program on a treadmill for a total period of 8 weeks. One-week post-surgery, all animals were subjected to the Rotational test to assess ipsiversive and contraversive movement, and to detect any rotational asymmetry. Even though both untrained and trained 6-OHDA-lesioned rats presented high asymmetry, the trained

6-OHDA-lesioned group presented a marked decline in number of rotations when compared to their untrained counterparts, indicating that physical exercise could have a protective effect against PD-mediated motor deficits. Interestingly, a significant increase in αSYN levels accompanied by a decline in SERCA2 was observed in untrained 6-OHDA-lesioned rats as opposed to the non-lesioned group, suggesting a correlation between αSYN accumulation and SERCA2 downregulation. However, trained 6-OHDA-lesioned rats presented full restoration of αSYN and SERCA2 protein levels, further highlighting the potential neuroprotective effect of physical exercise. Taken together, the investigators proposed that abnormal accumulation of αSYN could lead to intracellular Ca^{2+} dyshomeostasis possibly *via* downregulation of SERCA2 activity, and that physical exercise could indirectly prevent these events most likely by reducing ER stress through restoring SERCA activity [290].

It has been previously shown that αSYN aggregation leads to biphasic alterations in $[Ca^{2+}]_{cyt}$ [252–256]. The hypothesized SERCA/αSYN interaction has been recently confirmed in vitro; aggregated, but not monomeric, αSYN specifically binds to SERCA, stimulating the activity of the pump and affecting downstream processes that drive intracellular Ca^{2+} dysregulation [257]. Betzer et al. investigated whether αSYN physically associates with SERCA using SH-SY5Y cells and primary hippocampal neurons from αSYN-overexpressing transgenic mice, human brain tissue and *C. elegans*. Interestingly, co-immunoprecipitation experiments showed that oligomeric αSYN preferentially binds to the E1 conformation of SERCA, indicating a high degree of structural specificity for the SERCA/αSYN interaction. Further, Proximity Ligation Assay (PLA) experiments in SH-SY5Y cells showed that the two proteins are in close proximity, confirming the proposed interaction, while inhibiting the abnormal aggregation of αSYN abolished the SERCA/αSYN interaction. Taken together, these data confirmed that SERCA specifically binds to oligomeric αSYN. In vitro biochemical experiments also revealed that aggregated αSYN increase SERCA-dependent ATP hydrolysis, thus accelerating Ca^{2+} transfer across the ER membrane [257]. Of note, β-synuclein (βSYN) and Tau proteins did not influence SERCA activity, highlighting the high specificity of this interaction. Further in vitro experiments using SERCA1a-containing microsomes showed that only αSYN aggregates (and not monomeric αSYN species) increased SERCA-dependent Ca^{2+} uptake and SERCA's dephosphorylation rate, suggesting that the aggregated protein form regulates the function of SERCA. Interestingly, cyclopiazonic acid (CPA)-mediated SERCA inhibition in SH-SY5Y cells resulted to the normalization of the elevated $[Ca^{2+}]_{cyt}$, reducing αSYN-mediated apoptosis via the reduction of total αSYN levels by 10% and αSYN/SERCA interaction by 50%. In the same study, it was revealed that αSYN aggregation may enhance dendritic loss in dopaminergic neurons by 40% in *C. elegans*, and that this could be rescued by CPA-induced SERCA inhibition [257]. Betzer et al. also reported that SERCA and αSYN oligomers interact in the brain of patients affected by PD, Lewy body dementia and multiple system atrophy (MSA). Taken together, the investigators proposed that at the early stages of disease αSYN accumulation most likely stimulates SERCA activity *via* direct interaction, affecting three key SERCA functions; Ca^{2+} pumping, ATP hydrolysis

and dephosphorylation. Subsequently Ca^{2+} uptake into the ER is increased and $[Ca^{2+}]_{cyt}$ is diminished, ultimately altering Ca^{2+} homeostasis and promoting cell death [257].

Strikingly, in vivo experiments have further supported the crucial role of SERCA activity in PD pathology [10]. Dahl demonstrated that the SERCA activator CDN1163 could alleviate dyskinesia in the 6-OHDA-lesioned rat model of PD. Adult male Wistar rats were unilaterally injected with 6-OHDA in the left SNc, and on day 11 post-surgery they were administered either L-DOPA (i.e., a current PD drug treatment)- or the SERCA activator CDN1163. Once the animals were pharmacologically challenged, they were subjected to three standardized akinesia tests; the Initiation Time (IT) test, the stepping test, and the cylinder test. Of note, the same tests were also conducted prior to surgery to establish a baseline response. As expected 6-OHDA-treated rats showed a delay in stepping initiation in the IT test that was reversed by L-DOPA treatment. Importantly, CDN1163 treatment also reversed 6-OH-DA-induced delay in stepping initiation. The stepping test was then employed to evaluate the degree of contralateral limb akinesia by measuring the number of adjusting steps the animal performed while moving sideways [291]. As expected, the lesioned animals presented a significantly reduced number of adjusting steps, while treatment with either L-DOPA or CDN1163 completely rescued this phenotype. Finally, the cylinder test aimed to assess spontaneous forelimb laterization by scoring for akinesia of the contralateral forelimb *via* measuring the number of contacts made with the cylinder wall [291, 292]. The 6-OHDA lesioned group showed a drastically decreased number of contacts. Treatment with L-DOPA restored forelimb laterization to almost baseline levels, while CDN1163-treated rats presented with a significantly increased number of contacts, restoring forelimb laterization to approximately 50% of baseline. Observing that administration of CDN1163 exerted similar therapeutic effects to L-DOPA treatment, the study proposed SERCA activation as a potential therapeutic target for PD.

6.5 Conclusions

It is well established that Ca^{2+} is a fundamental signaling molecule for cell survival and function, and that SERCA is a gatekeeper of intracellular Ca^{2+} homeostasis. Aberrations in the finely-tuned intraneuronal Ca^{2+} homeostasis may impose detrimental effects, leading to the emergence of brain pathology. Despite the extensive knowledge on SERCA distribution and function, the exact regulatory networks and mechanisms that operate in the brain are still elusive. In this context, we have presented current evidence regarding SERCA's involvement in the pathophysiology of neuropsychiatric and neurodegenerative disorders (for summary, see Fig. 6.3). Although only DD has been directly linked to SERCA2 mutations, compelling data supports that brain pathology is caused by alterations in SERCA activity, and that SERCA synergistically contributes to neuronal pathogenesis. It is yet unclear to what extent SERCA is involved and what upstream or downstream events participate in determining the fate of nerve cells. However, targeting SERCA activity could

SERCA isoform	SERCA modification	Study model	Associated disease
SERCA2	Missense mutation in stalk domain	Human tissue	DD with concurrent SZ (Takeichi, Sugiura et al. 2016, Noda, Takeichi et al. 2016)
SERCA2	Altered-splicing mutation in acceptor site	Human tissue	DD with concurrent BD (Nakamura et al., 2016)
SERCA2	Downregulation	Human platelets	BD (Hough, Lu et al. 1999)
SERCA2	Upregulation in hippocampus, cortex and cerebellum	Df(16)1/+ mice Human brain tissue	DiGeorge-related SZ (Earls, Bayazitov et al. 2010, Earls, Fricke et al. 2012)
SERCA2	Downregulation in prefrontal cortex	NLVH rats	SZ (Genis-Mendoza, Gallegos-Silva et al. 2018)
SERCA3	Downregulation in cortex/ Upregulation in hippocampus, striatum and cerebellum	Ketamine-induced psychotic rats	SZ (Lisek, Boczek et al. 2016)
SERCA2	Upregulation	PSDKO mouse neuronal cells	AD (Green, Demuro et al. 2008)
		APP-expressing CHO cells	
SERCA2	Downregulation	PS2-expressing SH-SY5Y cells CALHM1-transfected cells APPSwe/PSEN1dE9 mice	AD (Brunello, Zampese et al. 2009, Gallego-Sandin, Alonso et al. 2011, Krajnak and Dahl, 2018)
SERCA2	Upregulation	Primary hippocampal neurons of FE65/FE65L1 DKO mice	AD (Nensa, Neumann et al. 2014)
SERCA2	Downregulation	6-OHDA lesioned rats	PD (Tuon et al., 2012, Dahl, 2017)
SERCA2	Upregulation	αSYN-overexpressing cell lines	PD (Betzer et al., 2018)

Fig. 6.3 Clinical and preclinical experimental evidence of altered SERCA expression and/or activity in neuropsychiatric and neurodegenerative disor**ders.** SERCA2 mutations have been reported in Darier's disease (DD) patients with concurrent schizophrenia (SZ) or bipolar disease (BD). SERCA2 and SERCA3 alterations have been associated with SZ, BD, Alzheimer's disease (AD) and Parkinson's disease (PD)

reveal more protein interactions, shedding light on the neuromolecular circuitry involved in brain pathophysiology. Most importantly, advancing knowledge on the neuronal function of SERCA may contribute to the future development of safer and more effective therapeutic strategies to combat such incapacitating disorders.

Acknowledgements A.B. was supported by the *University of Dayton (UD) Graduate School* and by the *UD Office for Graduate Affairs* through the *Graduate Student Summer Fellowship* (GSSF) Program. J.S. was supported by a *Barry Goldwater Scholarship in Excellence and Education Award*, a *Biology Department Lancaster-McDougall Award, a CAS Dean Fellowship*, the *Berry Summer Thesis Institute*, and the *UD Honors Program*. P.M.P. was supported by an *inaugural STEM Catalyst grant and Start-up funding from UD*, as well as by *Research Council Seed Grants (RCSG) from the University of Dayton Research Institute (UDRI)*; this work was supported by the National Institute Of Neurological Disorders and Stroke of the National Institutes of Health under award number R03NS109836 (to P.M.P.). Funding sponsors had no further role in study design; in the collection, analysis and interpretation of data; in the writing of the report; and in the decision to submit the article for publication.

Conflict of Interest None.

References

1. Brini M et al (2014) Neuronal calcium signaling: function and dysfunction. Cell Mol Life Sci 71(15):2787–2814
2. Berridge MJ, Lipp P, Bootman MD (2000) The versatility and universality of calcium signalling. Nat Rev Mol Cell Biol 1(1):11–21
3. Orrenius S, Zhivotovsky B, Nicotera P (2003) Regulation of cell death: the calcium–apoptosis link. Nat Rev Mol Cell Biol 4(7):552–565
4. Berridge MJ, Bootman MD, Roderick HL (2003) Calcium signalling: dynamics, homeostasis and remodelling. Nat Rev Mol Cell Biol 4(7):517–529
5. Zucker RS (1999) Calcium-and activity-dependent synaptic plasticity. Curr Opin Neurobiol 9(3):305–313
6. Lyons MR, West AE (2011) Mechanisms of specificity in neuronal activity-regulated gene transcription. Prog Neurobiol 94(3):259–295
7. Neher E, Sakaba T (2008) Multiple roles of calcium ions in the regulation of neurotransmitter release. Neuron 59(6):861–872
8. Carafoli E (2003) The calcium-signalling saga: tap water and protein crystals. Nat Rev Mol Cell Biol 4(4):326–332
9. Green KN et al (2008) SERCA pump activity is physiologically regulated by presenilin and regulates amyloid beta production. J Gen Physiol 132(2):i1
10. Dahl R (2017) A new target for Parkinson's disease: small molecule SERCA activator CDN1163 ameliorates dyskinesia in 6-OHDA-lesioned rats. Bioorg Med Chem 25(1):53–57
11. LaFerla FM (2002) Calcium dyshomeostasis and intracellular signalling in Alzheimer's disease. Nat Rev Neurosci 3(11):862–872
12. Bezprozvanny I, Mattson MP (2008) Neuronal calcium mishandling and the pathogenesis of Alzheimer's disease. Trends Neurosci 31(9):454–463
13. Earls LR et al (2010) Dysregulation of presynaptic calcium and synaptic plasticity in a mouse model of 22q11 deletion syndrome. J Neurosci 30(47):15843–15855
14. Jacobsen NJ et al (1999) ATP2A2 mutations in Darier's disease and their relationship to neuropsychiatric phenotypes. Hum Mol Genet 8(9):1631–1636
15. Grienberger C, Konnerth A (2012) Imaging calcium in neurons. Neuron 73(5):862–885
16. Fucile S (2004) Ca^{2+} permeability of nicotinic acetylcholine receptors. Cell Calcium 35(1):1–8
17. Berridge MJ, Bootman MD, Lipp P (1998) Calcium – a life and death signal. Nature 395(6703):645–648
18. Schwaller B (2010) Cytosolic Ca^{2+} buffers. Cold Spring Harb Perspect Biol 2(11):a004051
19. Vandecaetsbeek I et al (2009) Structural basis for the high Ca^{2+} affinity of the ubiquitous SERCA2b Ca^{2+} pump. Proc Natl Acad Sci 106(44):18533–18538
20. Morth JP et al (2010) A structural overview of the plasma membrane Na^{+},K^{+}-ATPase and H^{+}-ATPase ion pumps. Nat Rev Mol Cell Biol 12:60
21. Toyoshima C (2008) Structural aspects of ion pumping by Ca^{2+}-ATPase of sarcoplasmic reticulum. Arch Biochem Biophys 476(1):3–11
22. Bublitz M et al (2010) In and out of the cation pumps: P-type ATPase structure revisited. Curr Opin Struct Biol 20(4):431–439
23. Bobe R et al (2005) How many Ca^{2+} ATPase isoforms are expressed in a cell type? A growing family of membrane proteins illustrated by studies in platelets. Platelets 16(3–4):133–150
24. Dode L et al (2003) Dissection of the functional differences between sarco (endo) plasmic reticulum Ca^{2+}-ATPase (SERCA) 1 and 2 isoforms and characterization of Darier disease (SERCA2) mutants by steady-state and transient kinetic analyses. J Biol Chem 278: 47877–47889
25. Dode L et al (2002) Dissection of the functional differences between sarco (endo) plasmic reticulum Ca^{2+}-ATPase (SERCA) 1 and 3 isoforms by steady-state and transient kinetic analyses. J Biol Chem 277(47):45579–45591

26. Britzolaki A et al (2018) The SERCA2: a gatekeeper of neuronal calcium homeostasis in the brain. Cell Mol Neurobiol 38:981–994
27. Lytton J, MacLennan DH (1988) Molecular cloning of cDNAs from human kidney coding for two alternatively spliced products of the cardiac Ca^{2+}-ATPase gene. J Biol Chem 263(29):15024–15031
28. Lytton J et al (1992) Functional comparisons between isoforms of the sarcoplasmic or endoplasmic reticulum family of calcium pumps. J Biol Chem 267(20):14483–14489
29. MacLennan DH et al (1985) Amino-acid sequence of a Ca^{2+} + Mg2+−dependent ATPase from rabbit muscle sarcoplasmic reticulum, deduced from its complementary DNA sequence. Nature 316(6030):696–700
30. Dally S et al (2010) Multiple and diverse coexpression, location, and regulation of additional SERCA2 and SERCA3 isoforms in nonfailing and failing human heart. J Mol Cell Cardiol 48(4):633–644
31. Dally S et al (2006) Ca^{2+}-ATPases in non-failing and failing heart: evidence for a novel cardiac sarco/endoplasmic reticulum Ca^{2+}-ATPase 2 isoform (SERCA2c). Biochem J 395(2):249–258
32. MacLennan DH (1970) Purification and properties of an adenosine triphosphatase from sarcoplasmic reticulum. J Biol Chem 245(17):4508–4518
33. Toyoshima C, Inesi G (2004) Structural basis of ion pumping by Ca^{2+}-ATPase of the sarcoplasmic reticulum. Annu Rev Biochem 73:269–292
34. Toyoshima C et al (2000) Crystal structure of the calcium pump of sarcoplasmic reticulum at 2.6 Å resolution. Nature 405(6787):647–655
35. Abu-Abed M et al (2002) Characterization of the ATP-binding domain of the sarco (endo) plasmic reticulum Ca^{2+}-ATPase: probing nucleotide binding by multidimensional NMR. Biochemistry 41(4):1156–1164
36. Toyoshima C, Nomura H (2002) Structural changes in the calcium pump accompanying the dissociation of calcium. Nature 418(6898):605–611
37. Smolin N, Robia SL (2015) A structural mechanism for calcium transporter headpiece closure. J Phys Chem B 119(4):1407–1415
38. Brini M, Carafoli E, Cali T (2017) The plasma membrane calcium pumps: focus on the role in (neuro)pathology. Biochem Biophys Res Commun 483(4):1116–1124
39. Møller JV et al (2005) The structural basis for coupling of Ca^{2+} transport to ATP hydrolysis by the sarcoplasmic reticulum Ca^{2+}-ATPase. J Bioenerg Biomembr 37(6):359–364
40. Guerini D (1998) The Ca^{2+} pumps and the Na^{+}/Ca^{2+} exchangers. Biometals 11(4):319–330
41. Zhang P et al (1998) Structure of the calcium pump from sarcoplasmic reticulum at 8-A resolution. Nature 392(6678):835–839
42. Gelebart P et al (2003) Identification of a new SERCA2 splice variant regulated during monocytic differentiation. Biochem Biophys Res Commun 303(2):676–684
43. Gunteski-Hamblin AM, Greeb J, Shull GE (1988) A novel Ca^{2+} pump expressed in brain, kidney, and stomach is encoded by an alternative transcript of the slow-twitch muscle sarcoplasmic reticulum Ca-ATPase gene. Identification of cDNAs encoding Ca^{2+} and other cation-transporting ATPases using an oligonucleotide probe derived from the ATP-binding site. J Biol Chem 263(29):15032–15040
44. Lytton J et al (1989) Molecular cloning of the mammalian smooth muscle sarco(endo)plasmic reticulum Ca^{2+}-ATPase. J Biol Chem 264(12):7059–7065
45. Zarain-Herzberg A, MacLennan D, Periasamy M (1990) Characterization of rabbit cardiac sarco (endo) plasmic reticulum Ca2 (+)-ATPase gene. J Biol Chem 265(8):4670–4677
46. Brandl CJ et al (1986) Two Ca^{2+} ATPase genes: homologies and mechanistic implications of deduced amino acid sequences. Cell 44(4):597–607
47. Dally S et al (2009) Multiple and diverse coexpression, location, and regulation of additional SERCA2 and SERCA3 isoforms in nonfailing and failing human heart. J Mol Cell Cardiol 48:633–644
48. Periasamy M, Kalyanasundaram A (2007) SERCA pump isoforms: their role in calcium transport and disease. Muscle Nerve 35(4):430–442

49. Hao L, Rigaud J-L, Inesi G (1994) Ca^{2+}/H^{+} countertransport and electrogenicity in proteoliposomes containing erythrocyte plasma membrane Ca-ATPase and exogenous lipids. J Biol Chem 269(19):14268–14275
50. Yu X et al (1993) H^{+} countertransport and electrogenicity of the sarcoplasmic reticulum Ca^{2+} pump in reconstituted proteoliposomes. Biophys J 64(4):1232–1242
51. Salvador JM et al (1998) Ca^{2+} transport by reconstituted synaptosomal ATPase is associated with H^{+} countertransport and net charge displacement. J Biol Chem 273(29):18230–18234
52. Brini M, Carafoli E (2009) Calcium pumps in health and disease. Physiol Rev 89(4):1341–1378
53. Hasselbach W, Makinose M (1961) The calcium pump of the "relaxing granules" of muscle and its dependence on ATP-splitting. Biochem Z 333:518–528
54. Lee C-H et al (2002) Ca^{2+} oscillations, gradients, and homeostasis in vascular smooth muscle. Am J Phys Heart Circ Phys 282(5):H1571–H1583
55. Dyla M et al (2018) Dynamics of P-type ATPase transport cycle revealed by single-molecule FRET. Biophys J 114(3):559a
56. Carafoli E, Brini M (2000) Calcium pumps: structural basis for and mechanism of calcium transmembrane transport. Curr Opin Chem Biol 4(2):152–161
57. Olesen C et al (2004) Dephosphorylation of the calcium pump coupled to counterion occlusion. Science 306(5705):2251–2255
58. Mueller B et al (2004) SERCA structural dynamics induced by ATP and calcium. Biochemistry 43(40):12846–12854
59. Verboomen H et al (1994) The functional importance of the extreme C-terminal tail in the gene 2 organellar Ca^{2+}-transport ATPase (SERCA2a/b). Biochem J 303(Pt 3):979–984
60. Martin V et al (2002) Three novel Sarco/endoplasmic reticulum Ca^{2+}-ATPase (SERCA) 3 isoforms expression, regulation, and function of the members of the SERCA3 family. J Biol Chem 277(27):24442–24452
61. Bobe R et al (2004) Identification, expression, function, and localization of a novel (sixth) isoform of the human sarco/endoplasmic reticulum Ca^{2+} ATPase 3 gene. J Biol Chem 279(23):24297–24306
62. Brandl CJ et al (1987) Adult forms of the Ca^{2+}ATPase of sarcoplasmic reticulum. Expression in developing skeletal muscle. J Biol Chem 262(8):3768–3774
63. Korczak B et al (1988) Structure of the rabbit fast-twitch skeletal muscle Ca^{2+}-ATPase gene. J Biol Chem 263(10):4813–4819
64. Burk SE et al (1989) cDNA cloning, functional expression, and mRNA tissue distribution of a third organellar Ca^{2+} pump. J Biol Chem 264(31):18561–18568
65. Wu KD et al (1995) Localization and quantification of endoplasmic reticulum ca(2+)-ATPase isoform transcripts. Am J Phys 269(3 Pt 1):C775–C784
66. Wuytack F et al (1989) Smooth muscle expresses a cardiac/slow muscle isoform of the $Ca^{2+}-$transport ATPase in its endoplasmic reticulum. Biochem J 257(1):117–123
67. Lompre A-M et al (1989) Characterization and expression of the rat heart sarcoplasmic reticulum Ca^{2+}-ATPase mRNA. FEBS Lett 249(1):35–41
68. Kimura T et al (2005) Altered mRNA splicing of the skeletal muscle ryanodine receptor and sarcoplasmic/endoplasmic reticulum Ca^{2+}-ATPase in myotonic dystrophy type 1. Hum Mol Genet 14(15):2189–2200
69. Miller KK et al (1991) Localization of an endoplasmic reticulum calcium ATPase mRNA in rat brain by in situ hybridization. Neuroscience 43(1):1–9
70. Sepulveda MR, Hidalgo-Sanchez M, Mata AM (2004) Localization of endoplasmic reticulum and plasma membrane Ca^{2+}-ATPases in subcellular fractions and sections of pig cerebellum. Eur J Neurosci 19(3):542–551
71. Baba-Aissa F et al (1996) Distribution of the organellar Ca^{2+} transport ATPase SERCA2 isoforms in the cat brain. Brain Res 743(1–2):141–153
72. Campbell AM, Wuytack F, Fambrough DM (1993) Differential distribution of the alternative forms of the sarcoplasmic/endoplasmic reticulum Ca^{2+}-ATPase, SERCA2b and SERCA2a, in the avian brain. Brain Res 605(1):67–76

73. Plessers L et al (1991) A study of the organellar Ca2(+)-transport ATPase isozymes in pig cerebellar Purkinje neurons. J Neurosci 11(3):650–656
74. Morita M, Kudo Y (2010) Growth factors upregulate astrocyte [Ca^{2+}]i oscillation by increasing SERCA2b expression. Glia 58(16):1988–1995
75. Salvador JM et al (2001) Distribution of the intracellular Ca^{2+}-ATPase isoform 2b in pig brain subcellular fractions and cross-reaction with a monoclonal antibody raised against the enzyme isoform. J Biochem 129(4):621–626
76. Dode L et al (1996) cDNA cloning, expression and chromosomal localization of the human sarco/endoplasmic reticulum Ca (2)-ATPase 3 gene. Biochem J 318(2):689–699
77. Wuytack F et al (1994) A sarco/endoplasmic reticulum Ca^{2+}-ATPase 3-type Ca^{2+} pump is expressed in platelets, in lymphoid cells, and in mast cells. J Biol Chem 269(2):1410–1416
78. KOVÁCS T et al (2001) All three splice variants of the human sarco/endoplasmic reticulum Ca^{2+}-ATPase 3 gene are translated to proteins: a study of their co-expression in platelets and lymphoid cells. Biochem J 358(3):559–568
79. Ait-Ghezali L et al (2014) Loss of endoplasmic reticulum calcium pump expression in choroid plexus tumours. Neuropathol Appl Neurobiol 40(6):726–735
80. Pottorf W et al (2001) Function of SERCA mediated calcium uptake and expression of SERCA3 in cerebral cortex from young and old rats. Brain Res 914(1–2):57–65
81. Baba-Aïssa F et al (1996) Purkinje neurons express the SERCA3 isoform of the organellar type Ca^{2+}−transport ATPase. Mol Brain Res 41(1–2):169–174
82. Kessler RC et al (2007) Age of onset of mental disorders: a review of recent literature. Curr Opin Psychiatry 20(4):359–364
83. Kessler RC et al (2005) Lifetime prevalence and age-of-onset distributions of DSM-IV disorders in the National Comorbidity Survey Replication. Arch Gen Psychiatry 62(6):593–602
84. Murray CJ, Lopez AD (1997) Global mortality, disability, and the contribution of risk factors: global burden of disease study. Lancet 349(9063):1436–1442
85. Murray CJ, Lopez AD (1997) Alternative projections of mortality and disability by cause 1990–2020: global burden of disease study. Lancet 349(9064):1498–1504
86. Whiteford HA et al (2013) Global burden of disease attributable to mental and substance use disorders: findings from the global burden of disease study 2010. Lancet 382(9904):1575–1586
87. Ohi K et al (2017) Cognitive clustering in schizophrenia patients, their first-degree relatives and healthy subjects is associated with anterior cingulate cortex volume. NeuroImage Clin 16:248–256
88. Purcell S, International Schizophrenia Consortium, Wray NR, Stone JL, Visscher PM, O'Donovan MC, Sullivan PF, Sklar P (2009) Common polygenic variation contributes to risk of schizophrenia and bipolar disorder. Nature 460:748–752
89. Grunze H (2015) Bipolar disorder. In: Neurobiology of brain disorders. Elsevier, pp 655–673
90. Miller S et al (2016) Mixed depression in bipolar disorder: prevalence rate and clinical correlates during naturalistic follow-up in the Stanley bipolar network. Am J Psychiatr 173(10):1015–1023
91. Allardyce J et al (2018) Association between schizophrenia-related polygenic liability and the occurrence and level of mood-incongruent psychotic symptoms in bipolar disorder. JAMA Psychiat 75(1):28–35
92. Jimerson DC et al (1979) CSF calcium: clinical correlates in affective illness and schizophrenia. Biol Psychiatry 14:37–51
93. Lidow MS (2003) Calcium signaling dysfunction in schizophrenia: a unifying approach. Brain Res Rev 43(1):70–84
94. Lajtha A, Tettamanti G, Goracci G (2009) Handbook of neurochemistry and molecular neurobiology. Springer, New York
95. Hertzberg L, Domany E (2018) *Commentary:* Integration of gene expression and GWAS results supports involvement of calcium signaling in Schizophrenia. J Ment Health Clin Psychol 2(3):5–7

96. Woon PS et al (2017) CACNA1C genomewide supported psychosis genetic variation affects cortical brain white matter integrity in Chinese patients with schizophrenia. J Clin Psychiatry 75(11):e1284–e1290
97. Dubovsky SL et al (1991) Elevated platelet intracellular calcium concentration in bipolar depression. Biol Psychiatry 29(5):441–450
98. Kusumi I, Koyama T, Yamashita I (1992) Thrombin-induced platelet calcium mobilization is enhanced in bipolar disorders. Biol Psychiatry 32(8):731–734
99. Kusumi I, Koyama T, Yamashita I (1994) Serotonin-induced platelet intracellular calcium mobilization in depressed patients. Psychopharmacology 113(3–4):322–327
100. Suzuki K et al (2003) Altered 5-HT-induced calcium response in the presence of staurosporine in blood platelets from bipolar disorder patients. Neuropsychopharmacology 28(6):1210–1214
101. Suzuki K et al (2004) Effects of lithium and valproate on agonist-induced platelet intracellular calcium mobilization: relevance to myosin light chain kinase. Prog Neuro-Psychopharmacol Biol Psychiatry 28(1):67–72
102. Suzuki K et al (2001) Serotonin-induced platelet intracellular calcium mobilization in various psychiatric disorders: is it specific to bipolar disorder? J Affect Disord 64(2–3):291–296
103. Manji HK, Moore GJ, Chen G (2000) Clinical and preclinical evidence for the neurotrophic effects of mood stabilizers: implications for the pathophysiology and treatment of manic–depressive illness. Biol Psychiatry 48(8):740–754
104. Chen G et al (1999) The mood-stabilizing agents Lithium and valproate RobustlIncrease the levels of the neuroprotective protein bcl-2 in the CNS. J Neurochem 72(2):879–882
105. Chen R-W, Chuang D-M (1999) Long term lithium treatment suppresses p53 and Bax expression but increases Bcl-2 expression A prominent role in neuroprotection against excitotoxicity. J Biol Chem 274(10):6039–6042
106. Manji HK et al (1996) Regulation of signal transduction pathways by mood-stabilizing agents: implications for the delayed onset of therapeutic efficacy. J Clin Psychiatry 57:34–46. discussion 47-8
107. Manji HK, Moore GJ, Chen G (1999) Lithium at 50: have the neuroprotective effects of this unique cation been overlooked? Biol Psychiatry 46(7):929–940
108. Manji HK, Moore GJ, Chen G (2000) Lithium up-regulates the cytoprotective protein Bcl-2 in the CNS in vivo: a role for neurotrophic and neuroprotective effects in manic depressive illness. J Clin Psychiatry 61:82–96
109. Wang J-F, Bown C, Young LT (1999) Differential display PCR reveals novel targets for the mood-stabilizing drug valproate including the molecular chaperone GRP78. Mol Pharmacol 55(3):521–527
110. Bhat S et al (2012) CACNA1C (Cav1.2) in the pathophysiology of psychiatric disease. Prog Neurobiol 99(1):1–14
111. Gonzalez S et al (2013) Suggestive evidence for association between L-type voltage-gated calcium channel (CACNA1C) gene haplotypes and bipolar disorder in Latinos: a family-based association study. Bipolar Disord 15(2):206–214
112. Isaac C, Januel D (2016) Neural correlates of cognitive improvements following cognitive remediation in schizophrenia: a systematic review of randomized trials. Socioaffect Neurosci Psychol 6(1):30054
113. Li W et al (2018) A molecule-based genetic association approach implicates a range of voltage-gated calcium channels associated with schizophrenia. Am J Med Genet B Neuropsychiatr Genet 177(4):454–467
114. Schizophrenia Working Group of the Psychiatric Genomics, C et al (2014) Biological insights from 108 schizophrenia-associated genetic loci. Nature 511:421–427
115. Li Z et al (2017) Genome-wide association analysis identifies 30 new susceptibility loci for schizophrenia. Nat Genet 49(11):1576–1583
116. Ferreira MAR et al (2008) Collaborative genome-wide association analysis supports a role for ANK3 and CACNA1C in bipolar disorder. Nat Genet 40(9):1056–1058

117. Sklar P et al (2011) Large-scale genome-wide association analysis of bipolar disorder identifies a new susceptibility locus near ODZ4. Nat Genet 43(10):977–983
118. Lencz T, Malhotra A (2015) Targeting the schizophrenia genome: a fast track strategy from GWAS to clinic. Mol Psychiatry 20(7):820–826
119. Craddock N et al (1994) Familial cosegregation of major affective disorder and Darier's disease (keratosis follicularis). Br J Psychiatry 164(3):355–358
120. Burge SM, Wilkinson JD (1992) Darier-white disease: a review of the clinical features in 163 patients. J Am Acad Dermatol 27(1):40–50
121. Ringpfeil F et al (2001) Darier disease–novel mutations in ATP2A2 and genotype-phenotype correlation. Exp Dermatol 10(1):19–27
122. Judge M, McLean W, Munro C (2010) Disorders of keratinization. In: Rook's textbook of dermatology, vol 1, pp 1–122
123. Munro C (1992) The phenotype of Darier's disease: penetrance and expressivity in adults and children. Br J Dermatol 127(2):126–130
124. Nellen RGL et al (2017) Mendelian disorders of cornification caused by defects in intracellular calcium pumps: mutation update and database for variants in ATP2A2 and ATP2C1 associated with Darier disease and Hailey–Hailey disease. Hum Mutat 38(4):343–356
125. Green EK et al (2013) Novel ATP2A2 mutations in a large sample of individuals with D arier disease. J Dermatol 40(4):259–266
126. Sakuntabhai A et al (1999) Mutations in ATP2A2, encoding a Ca^{2+} pump, cause Darier disease. Nat Genet 21(3):271–277
127. Ahn W et al (2003) Multiple effects of SERCA2b mutations associated with Darier's disease. J Biol Chem 278(23):20795–20801
128. Sato K et al (2004) Distinct types of abnormality in kinetic properties of three Darier disease-causing sarco (endo) plasmic reticulum Ca^{2+}-ATPase mutants that exhibit normal expression and high Ca^{2+} transport activity. J Biol Chem 279(34):35595–35603
129. Miyauchi Y et al (2006) Comprehensive analysis of expression and function of 51 sarco (endo) plasmic reticulum Ca^{2+}-ATPase mutants associated with Darier disease. J Biol Chem 281(32):22882–22895
130. Foggia L et al (2006) Activity of the hSPCA1 Golgi Ca^{2+} pump is essential for Ca^{2+}−mediated Ca^{2+} response and cell viability in Darier disease. J Cell Sci 119(4):671–679
131. Leinonen P et al (2005) Keratinocytes cultured from patients with Hailey–Hailey disease and Darier disease display distinct patterns of calcium regulation. Br J Dermatol 153(1):113–117
132. Hetz C (2012) The unfolded protein response: controlling cell fate decisions under ER stress and beyond. Nat Rev Mol Cell Biol 13(2):89–102
133. Savignac M et al (2014) SERCA2 dysfunction in Darier disease causes endoplasmic reticulum stress and impaired cell-to-cell adhesion strength: rescue by Miglustat. J Investig Dermatol 134(7):1961–1970
134. Celli A et al (2011) Endoplasmic reticulum Ca^{2+} depletion activates XBP1 and controls terminal differentiation in keratinocytes and epidermis. Br J Dermatol 164(1):16–25
135. Engin B et al (2015) Darier disease: a fold (intertriginous) dermatosis. Clin Dermatol 33(4):448–451
136. Suryawanshi H et al (2017) Darier disease: a rare genodermatosis. J Oral Maxillofac Pathol 21(2):321–321
137. Cheour M et al (2009) Darier's disease: an evaluation of its neuropsychiatric component. Encéphale 35(1):32–35
138. Wang SL et al (2002) Darier's disease associated with bipolar affective disorder: a case report. Kaohsiung J Med Sci 18(12):622–626
139. Gordon-Smith K et al (2010) The neuropsychiatric phenotype in Darier disease. Br J Dermatol 163(3):515–522
140. Jones I et al (2002) Evidence for familial cosegregation of major affective disorder and genetic markers flanking the gene for Darier's disease. Mol Psychiatry 7(4):424–427

141. Cederlöf M et al (2015) The association between Darier disease, bipolar disorder, and schizophrenia revisited: a population-based family study. Bipolar Disord 17(3):340–344
142. Cederlöf M et al (2015) Intellectual disability and cognitive ability in Darier disease: Swedish nation-wide study. Br J Dermatol 173(1):155–158
143. Dodiuk-Gad R et al (2016) Darier disease in Israel: combined evaluation of genetic and neuropsychiatric aspects. Br J Dermatol 174(3):562–568
144. Baba-Aissa F et al (1998) Distribution and isoform diversity of the organellar Ca^{2+} pumps in the brain. Mol Chem Neuropathol 33(3):199–208
145. Takeichi T et al (2016) Darier's disease complicated by schizophrenia caused by a novel ATP2A2 mutation. Acta Derm Venereol 96(7):993–994
146. Nakamura T et al (2016) Loss of function mutations in ATP2A2 and psychoses: a case report and literature survey. Psychiatry Clin Neurosci 70(8):342–350
147. Noda K et al (2016) Novel and recurrent ATP2A2 mutations in Japanese patients with Darier's disease. Nagoya J Med Sci 78(4):485–492
148. Hough C et al (1999) Elevated basal and thapsigargin-stimulated intracellular calcium of platelets and lymphocytes from bipolar affective disorder patients measured by a fluorometric microassay. Biol Psychiatry 46(2):247–255
149. Scambler PJ (2000) The 22q11 deletion syndromes. Hum Mol Genet 9(16):2421–2426
150. McDonald-McGinn DM et al (2001) Phenotype of the 22q11.2 deletion in individuals identified through an affected relative: cast a wide FISHing net! Genet Med 3(1):23–29
151. Schreiner MJ et al (2013) Converging levels of analysis on a genomic hotspot for psychosis: insights from 22q11. 2 deletion syndrome. Neuropharmacology 68:157–173
152. Chun S et al (2014) Specific disruption of thalamic inputs to the auditory cortex in schizophrenia models. Science 344(6188):1178–1182
153. Kobrynski LJ, Sullivan KE (2007) Velocardiofacial syndrome, DiGeorge syndrome: the chromosome 22q11.2 deletion syndromes. Lancet 370(9596):1443–1452
154. Yagi H et al (2003) Role of TBX1 in human del22q11.2 syndrome. Lancet 362(9393):1366–1373
155. Papangeli I, Scambler P (2013) The 22q11 deletion: DiGeorge and velocardiofacial syndromes and the role of TBX1. Wiley Interdiscip Rev Dev Biol 2(3):393–403
156. Devaraju P et al (2017) Haploinsufficiency of the 22q11. 2 microdeletion gene Mrpl40 disrupts short-term synaptic plasticity and working memory through dysregulation of mitochondrial calcium. Mol Psychiatry 22(9):1313–1326
157. Shi H, Wang Z (2018) Atypical microdeletion in 22q11 deletion syndrome reveals new candidate causative genes: a case report and literature review. Medicine 97(8):e9936
158. Ellegood J et al (2014) Neuroanatomical phenotypes in a mouse model of the 22q11.2 microdeletion. Mol Psychiatry 19(1):99–107
159. Mukai J et al (2015) Molecular substrates of altered axonal growth and brain connectivity in a mouse model of schizophrenia. Neuron 86(3):680–695
160. Karpinski BA et al (2014) Dysphagia and disrupted cranial nerve development in a mouse model of DiGeorge (22q11) deletion syndrome. Dis Model Mech 7(2):245–257
161. Oskarsdottir S, Vujic M, Fasth A (2004) Incidence and prevalence of the 22q11 deletion syndrome: a population-based study in Western Sweden. Arch Dis Child 89(2):148–151
162. Chow EW et al (2006) Neurocognitive profile in 22q11 deletion syndrome and schizophrenia. Schizophr Res 87(1):270–278
163. Pulver AE et al (1994) Psychotic illness in patients diagnosed with velo-cardio-facial syndrome and their relatives. J Nerv Ment Dis 182(8):476–477
164. Botto LD et al (2003) A population-based study of the 22q11.2 deletion: phenotype, incidence, and contribution to major birth defects in the population. Pediatrics 112(1 Pt 1):101–107
165. Bassett AS et al (2011) Practical guidelines for managing patients with 22q11.2 deletion syndrome. J Pediatr 159(2):332–339.e1
166. Bearden CE et al (2001) The neurocognitive phenotype of the 22q11. 2 deletion syndrome: selective deficit in visual-spatial memory. J Clin Exp Neuropsychol 23(4):447–464

167. Eliez S et al (2000) Young children with Velo-cardio-facial syndrome (CATCH-22). Psychological and language phenotypes. Eur Child Adolesc Psychiatry 9(2):109–114
168. Swillen A et al (2000) Chromosome 22q11 deletion syndrome: update and review of the clinical features, cognitive-behavioral spectrum, and psychiatric complications. Am J Med Genet A 97(2):128–135
169. Gothelf D et al (2007) Developmental trajectories of brain structure in adolescents with 22q11. 2 deletion syndrome: a longitudinal study. Schizophr Res 96(1):72–81
170. Rauch A et al (2006) Diagnostic yield of various genetic approaches in patients with unexplained developmental delay or mental retardation. Am J Med Genet A 140(19):2063–2074
171. Bassett AS, Chow EW (2008) Schizophrenia and 22q11.2 deletion syndrome. Curr Psychiatry Rep 10(2):148–157
172. Fung WL et al (2010) Elevated prevalence of generalized anxiety disorder in adults with 22q11.2 deletion syndrome. Am J Psychiatry 167(8):998
173. Karayiorgou M, Simon TJ, Gogos JA (2010) 22q11.2 microdeletions: linking DNA structural variation to brain dysfunction and schizophrenia. Nat Rev Neurosci 11:402–416
174. Schneider M et al (2014) Psychiatric disorders from childhood to adulthood in 22q11. 2 deletion syndrome: results from the international consortium on brain and behavior in 22q11. 2 deletion syndrome. Am J Psychiatr 171(6):627–639
175. Jonas RK, Montojo CA, Bearden CE (2014) The 22q11.2 deletion syndrome as a window into complex neuropsychiatric disorders over the lifespan. Biol Psychiatry 75(5):351–360
176. Green T et al (2009) Psychiatric disorders and intellectual functioning throughout development in velocardiofacial (22q11. 2 deletion) syndrome. J Am Acad Child Adolesc Psychiatry 48(11):1060–1068
177. Bassett AS et al (2003) The schizophrenia phenotype in 22q11 deletion syndrome. Am J Psychiatr 160(9):1580–1586
178. Tang SX et al (2017) The psychosis Spectrum in 22q11.2 deletion syndrome is comparable to that of nondeleted youth. Biol Psychiatry 82(1):17–25
179. Earls LR et al (2012) Age-dependent microRNA control of synaptic plasticity in 22q11 deletion syndrome and schizophrenia. J Neurosci 32(41):14132–14144
180. Earls LR, Zakharenko SS (2014) A synaptic function approach to investigating complex psychiatric diseases. Neuroscientist 20(3):257–271
181. Schizophrenia_Working_Group_of_the_Psychiatric_Genomics-Consortium (2014) Biological insights from 108 schizophrenia-associated genetic loci. Nature 511(7510):421–427
182. Richard EA et al (2017) Potential synergistic action of 19 schizophrenia risk genes in. Schizophr Res 180:64–69
183. Genis-Mendoza A et al (2018) Comparative analysis of gene expression profiles involved in calcium signaling pathways using the NLVH animal model of schizophrenia. J Mol Neurosci 64(1):111–116
184. Hagenston AM, Bading H (2011) Calcium signaling in synapse-to-nucleus communication. Cold Spring Harb Perspect Biol:a004564
185. Lisek M et al (2016) Regional brain dysregulation of Ca^{2+}−handling systems in ketamine-induced rat model of experimental psychosis. Cell Tissue Res 363(3):609–620
186. Stefani MR, Moghaddam B (2005) Transient N-methyl-D-aspartate receptor blockade in early development causes lasting cognitive deficits relevant to schizophrenia. Biol Psychiatry 57(4):433–436
187. Neill JC et al (2010) Animal models of cognitive dysfunction and negative symptoms of schizophrenia: focus on NMDA receptor antagonism. Pharmacol Ther 128(3):419–432
188. Chakrabarti S et al (2015) Metabolic risk factors of sporadic Alzheimer's disease: implications in the pathology, pathogenesis and treatment. Aging Dis 6(4):282–299
189. Davie CA (2008) A review of Parkinson's disease. Br Med Bull 86:109–127
190. Nussbaum RL, Ellis CE (2003) Alzheimer's disease and Parkinson's disease. N Engl J Med 348(14):1356–1364

191. Warner TT, Schapira AH (2003) Genetic and environmental factors in the cause of Parkinson's disease. Ann Neurol 53(S3):S16–S25
192. Cookson MR, Xiromerisiou G, Singleton A (2005) How genetics research in Parkinson's disease is enhancing understanding of the common idiopathic forms of the disease. Curr Opin Neurol 18(6):706–711
193. Gilks WP et al (2005) A common LRRK2 mutation in idiopathic Parkinson's disease. Lancet 365(9457):415–416
194. Forno LS (1996) Neuropathology of Parkinson's disease. J Neuropathol Exp Neurol 55(3):259–272
195. Braak H et al (2003) Staging of brain pathology related to sporadic Parkinson's disease. Neurobiol Aging 24(2):197–211
196. Gandhi S, Wood NW (2005) Molecular pathogenesis of Parkinson's disease. Hum Mol Genet 14(18):2749–2755
197. Sudo H et al (2001) Secreted Abeta does not mediate neurotoxicity by antibody-stimulated amyloid precursor protein. Biochem Biophys Res Commun 282(2):548–556
198. Mattson MP (2007) Calcium and neurodegeneration. Aging Cell 6(3):337–350
199. Mattson MP (2004) Pathways towards and away from Alzheimer's disease. Nature 430(7000):631–639
200. Ganguly G et al (2017) Proteinopathy, oxidative stress and mitochondrial dysfunction: cross talk in Alzheimer's disease and Parkinson's disease. Drug Des Devel Ther 11:797–810
201. Xie A et al (2014) Shared mechanisms of neurodegeneration in Alzheimer's disease and Parkinson's disease. Biomed Res Int 2014:648740
202. Bonda DJ et al (2011) The mitochondrial dynamics of Alzheimer's disease and Parkinson's disease offer important opportunities for therapeutic intervention. Curr Pharm Des 17(31):3374–3380
203. Perier C, Vila M (2012) Mitochondrial biology and Parkinson's disease. Cold Spring Harb Perspect Med 2(2):a009332
204. Sen CK, Packer L (1996) Antioxidant and redox regulation of gene transcription. FASEB J 10(7):709–720
205. Aiken CT et al (2011) Oxidative stress-mediated regulation of proteasome complexes. Mol Cell Proteomics 10(5):R110.006924
206. Pajares M et al (2015) Redox control of protein degradation. Redox Biol 6:409–420
207. Baillet A et al (2010) The role of oxidative stress in amyotrophic lateral sclerosis and Parkinson's disease. Neurochem Res 35(10):1530–1537
208. Zhou C, Huang Y, Przedborski S (2008) Oxidative stress in Parkinson's disease: a mechanism of pathogenic and therapeutic significance. Ann NY Acad Sci 1147(1):93–104
209. Protter D, Lang C, Cooper AA (2012) alphaSynuclein and mitochondrial dysfunction: a pathogenic partnership in parkinson's disease? Parkinsons Dis 2012:829207
210. Banerjee K et al (2010) Alpha-synuclein induced membrane depolarization and loss of phosphorylation capacity of isolated rat brain mitochondria: implications in Parkinson's disease. FEBS Lett 584(8):1571–1576
211. Wang X et al (2009) Impaired balance of mitochondrial fission and fusion in Alzheimer's disease. J Neurosci 29(28):9090–9103
212. Devi L et al (2006) Accumulation of amyloid precursor protein in the mitochondrial import channels of human Alzheimer's disease brain is associated with mitochondrial dysfunction. J Neurosci 26(35):9057–9068
213. Mounsey RB, Teismann P (2011) Mitochondrial dysfunction in Parkinson's disease: pathogenesis and neuroprotection. Parkinson's Dis 2011
214. Pacelli C et al (2011) Mitochondrial defect and PGC-1α dysfunction in parkin-associated familial Parkinson's disease. Biochim Biophys Acta (BBA) - Mol Basis Dis 1812(8):1041–1053
215. Wen Y et al (2011) Alternative mitochondrial electron transfer as a novel strategy for neuroprotection. J Biol Chem, 2011:jbc. M110. 208447

216. Stutzmann GE, Mattson MP (2011) Endoplasmic reticulum Ca^{2+} handling in excitable cells in health and disease. Pharmacol Rev:pr. 110.003814
217. Woods NK, Padmanabhan J (2012) Neuronal calcium signaling and Alzheimer's disease. In: Islam MS (ed) Calcium signaling. Springer Netherlands, Dordrecht, pp 1193–1217
218. Gallego-Sandin S, Alonso MT, Garcia-Sancho J (2011) Calcium homoeostasis modulator 1 (CALHM1) reduces the calcium content of the endoplasmic reticulum (ER) and triggers ER stress. Biochem J 437(3):469–475
219. Verkhratsky A (2005) Physiology and pathophysiology of the calcium store in the endoplasmic reticulum of neurons. Physiol Rev 85(1):201–279
220. Verkhratsky A (2002) The endoplasmic reticulum and neuronal calcium signalling. Cell Calcium 32(5–6):393–404
221. Corona C et al (2011) New therapeutic targets in Alzheimer's disease: brain deregulation of calcium and zinc. Cell Death Dis 2(6):e176
222. Mattson MP (2010) ER calcium and Alzheimer's disease: in a state of flux. Sci Signal 3(114):pe10–pe10
223. Magi S et al (2016) Intracellular calcium dysregulation: implications for Alzheimer's disease. Biomed Res Int 2016:1–14
224. Egorova P, Popugaeva E, Bezprozvanny I (2015) Disturbed calcium signaling in spinocerebellar ataxias and Alzheimer's disease. Semin Cell Dev Biol 40:127–133
225. Berridge MJ (2013) Dysregulation of neural calcium signaling in Alzheimer disease, bipolar disorder and schizophrenia. Prion 7(1):2–13
226. Mattson MP (1990) Antigenic changes similar to those seen in neurofibrillary tangles are elicited by glutamate and Ca^{2+} influx in cultured hippocampal neurons. Neuron 4(1):105–117
227. Mattson MP et al (1993) Comparison of the effects of elevated intracellular aluminum and calcium levels on neuronal survival and tau immunoreactivity. Brain Res 602(1):21–31
228. Kurbatskaya K et al (2016) Upregulation of calpain activity precedes tau phosphorylation and loss of synaptic proteins in Alzheimer's disease brain. Acta Neuropathol Commun 4(1):34
229. Mattson MP et al (1992) Beta-amyloid peptides destabilize calcium homeostasis and render human cortical neurons vulnerable to excitotoxicity. J Neurosci 12(2):376–389
230. Mattson MP, Tomaselli KJ, Rydel RE (1993) Calcium-destabilizing and neurodegenerative effects of aggregated β-amyloid peptide are attenuated by basic FGF. Brain Res 621(1):35–49
231. Khachaturian ZS (1989) Calcium, membranes, aging and Alzheimer's disease: introduction and overview. Ann NY Acad Sci 568(1):1–4
232. Shankar GM et al (2007) Natural oligomers of the Alzheimer amyloid-β protein induce reversible synapse loss by modulating an NMDA-type glutamate receptor-dependent signaling pathway. J Neurosci 27(11):2866–2875
233. Thibault O, Gant JC, Landfield PW (2007) Expansion of the calcium hypothesis of brain aging and Alzheimer's disease: minding the store. Aging Cell 6(3):307–317
234. Kamenetz F et al (2003) APP processing and synaptic function. Neuron 37(6):925–937
235. Cirrito JR et al (2003) In vivo assessment of brain interstitial fluid with microdialysis reveals plaque-associated changes in amyloid-β metabolism and half-life. J Neurosci 23(26):8844–8853
236. Kuchibhotla KV et al (2008) Aβ plaques lead to aberrant regulation of calcium homeostasis in vivo resulting in structural and functional disruption of neuronal networks. Neuron 59(2):214–225
237. Abramov E et al (2009) Amyloid-β as a positive endogenous regulator of release probability at hippocampal synapses. Nat Neurosci 12(12):1567–1576
238. Surmeier DJ et al (2017) Calcium and Parkinson's disease. Biochem Biophys Res Commun 483(4):1013–1019
239. Calì T, Ottolini D, Brini M (2011) Mitochondria, calcium, and endoplasmic reticulum stress in Parkinson's disease. Biofactors 37(3):228–240

240. Chan CS, Gertler TS, Surmeier DJ (2009) Calcium homeostasis, selective vulnerability and Parkinson's disease. Trends Neurosci 32(5):249–256
241. Surmeier DJ, Guzman JN, Sanchez-Padilla J (2010) Calcium, cellular aging, and selective neuronal vulnerability in Parkinson's disease. Cell Calcium 47(2):175–182
242. Mosharov EV et al (2009) Interplay between cytosolic dopamine, calcium, and α-synuclein causes selective death of substantia nigra neurons. Neuron 62(2):218–229
243. Nedergaard S, Flatman J, Engberg I (1993) Nifedipine-and omega-conotoxin-sensitive Ca^{2+} conductances in guinea-pig substantia nigra pars compacta neurones. J Physiol 466(1):727–747
244. Calì T et al (2013) Enhanced parkin levels favor ER-mitochondria crosstalk and guarantee Ca^{2+} transfer to sustain cell bioenergetics. Biochim Biophys Acta (BBA) - Mol Basis Dis 1832(4):495–508
245. Calì T et al (2012) α-Synuclein controls mitochondrial calcium homeostasis by enhancing endoplasmic reticulum-mitochondria interactions. J Biol Chem 287(22):17914–17929
246. Sandebring A et al (2009) Parkin deficiency disrupts calcium homeostasis by modulating phospholipase C signalling. FEBS J 276(18):5041–5052
247. Nath S et al (2011) Raised calcium promotes α-synuclein aggregate formation. Mol Cell Neurosci 46(2):516–526
248. Rcom H et al (2014) Interactions between calcium and alpha-Synuclein in neurodegeneration. Biomol Ther 4(3)
249. Surmeier DJ (2007) Calcium, ageing, and neuronal vulnerability in Parkinson's disease. Lancet Neurol 6(10):933–938
250. Danzer KM et al (2007) Different species of α-synuclein oligomers induce calcium influx and seeding. J Neurosci 27(34):9220–9232
251. Hettiarachchi NT et al (2009) α-Synuclein modulation of Ca^{2+} signaling in human neuroblastoma (SH-SY5Y) cells. J Neurochem 111(5):1192–1201
252. El-Agnaf OM et al (2004) A strategy for designing inhibitors of α-synuclein aggregation and toxicity as a novel treatment for Parkinson's disease and related disorders. FASEB J 18(11):1315–1317
253. Rockenstein E et al (2002) Differential neuropathological alterations in transgenic mice expressing α-synuclein from the platelet-derived growth factor and Thy-1 promoters. J Neurosci Res 68(5):568–578
254. Vekrellis K et al (2011) Pathological roles of α-synuclein in neurological disorders. Lancet Neurol 10(11):1015–1025
255. Vekrellis K et al (2009) Inducible over-expression of wild type α-synuclein in human neuronal cells leads to caspase-dependent non-apoptotic death. J Neurochem 109(5):1348–1362
256. Kragh CL et al (2009) α-Synuclein aggregation and Ser-129 phosphorylation-dependent cell death in oligodendroglial cells. J Biol Chem 284(15):10211–10222
257. Betzer C et al (2018) Alpha-synuclein aggregates activate calcium pump SERCA leading to calcium dysregulation. EMBO Rep 19:e44617
258. Lowe R et al (2004) Calcium (II) selectively induces α-synuclein annular oligomers via interaction with the C-terminal domain. Protein Sci 13(12):3245–3252
259. Goodwin J et al (2013) Raised calcium and oxidative stress cooperatively promote alpha-synuclein aggregate formation. Neurochem Int 62(5):703–711
260. Colla E et al (2012) Accumulation of toxic α-synuclein oligomer within endoplasmic reticulum occurs in α-synucleinopathy in vivo. J Neurosci 32(10):3301–3305
261. Hurley MJ et al (2013) Parkinson's disease is associated with altered expression of CaV1 channels and calcium-binding proteins. Brain 136(7):2077–2097
262. Pasternak B et al (2012) Use of calcium channel blockers and Parkinson's disease. Am J Epidemiol 175(7):627–635
263. Ritz B et al (2010) L-type calcium channel blockers and Parkinson disease in Denmark. Ann Neurol 67(5):600–606
264. Becker C, Jick SS, Meier CR (2008) Use of antihypertensives and the risk of Parkinson disease. Neurology 70(16 Part 2):1438–1444

265. Marras C et al (2012) Dihydropyridine calcium channel blockers and the progression of parkinsonism. Ann Neurol 71(3):362–369
266. Lytton J, Westlin M, Hanley MR (1991) Thapsigargin inhibits the sarcoplasmic or endoplasmic reticulum Ca-ATPase family of calcium pumps. J Biol Chem 266(26):17067–17071
267. Park SW et al (2010) Sarco (endo) plasmic reticulum Ca^{2+}-ATPase 2b is a major regulator of endoplasmic reticulum stress and glucose homeostasis in obesity. Proc Natl Acad Sci 2010:12044
268. Kang S et al (2015) Small molecular allosteric activator of the sarco/endoplasmic reticulum Ca^{2+}-ATPase (SERCA) attenuates diabetes and metabolic disorders. J Biol Chem, 2015:p. jbc. M115. 705012
269. Tanzi RE et al (1987) Amyloid beta protein gene: cDNA, mRNA distribution, and genetic linkage near the Alzheimer locus. Science 235(4791):880–884
270. Sherrington R et al (1995) Cloning of a gene bearing missense mutations in early-onset familial Alzheimer's disease. Nature 375(6534):754–760
271. Levy-Lahad E et al (1995) Candidate gene for the chromosome 1 familial Alzheimer's disease locus. Science 269(5226):973–977
272. Rogaev EI et al (1995) Familial Alzheimer's disease in kindreds with missense mutations in a gene on chromosome 1 related to the Alzheimer's disease type 3 gene. Nature 376:775
273. Cruts M, Theuns J, Van Broeckhoven C (2012) Locus-specific mutation databases for neurodegenerative brain diseases. Hum Mutat 33(9):1340–1344
274. Wolfe MS et al (1999) Two transmembrane aspartates in presenilin-1 required for presenilin endoproteolysis and γ-secretase activity. Nature 398(6727):513–517
275. Annaert WG et al (1999) Presenilin 1 controls γ-secretase processing of amyloid precursor protein in pre-Golgi compartments of hippocampal neurons. J Cell Biol 147(2):277–294
276. De Strooper B et al (1998) Deficiency of presenilin-1 inhibits the normal cleavage of amyloid precursor protein. Nature 391(6665):387–390
277. Jin H et al (2010) Presenilin-1 holoprotein is an interacting partner of sarco endoplasmic reticulum calcium-ATPase and confers resistance to endoplasmic reticulum stress. J Alzheimers Dis 20(1):261–273
278. Brunello L et al (2009) Presenilin-2 dampens intracellular ca(2+) stores by increasing ca(2+) leakage and reducing ca(2+) uptake. J Cell Mol Med 13(9b):3358–3369
279. Dreses-Werringloer U et al (2008) A polymorphism in CALHM1 influences Ca^{2+} homeostasis, Abeta levels, and Alzheimer's disease risk. Cell 133(7):1149–1161
280. Nensa FM et al (2014) Amyloid beta a4 precursor protein-binding family B member 1 (FE65) interactomics revealed synaptic vesicle glycoprotein 2A (SV2A) and sarcoplasmic/endoplasmic reticulum calcium ATPase 2 (SERCA2) as new binding proteins in the human brain. Mol Cell Proteomics 13(2):475–488
281. Ikin AF et al (2007) A macromolecular complex involving the amyloid precursor protein (APP) and the cytosolic adapter FE65 is a negative regulator of axon branching. Mol Cell Neurosci 35(1):57–63
282. Cao X, Südhof TC (2001) A transcriptively active complex of APP with Fe65 and histone acetyltransferase Tip60. Science 293(5527):115–120
283. Pietrzik CU et al (2004) FE65 constitutes the functional link between the low-density lipoprotein receptor-related protein and the amyloid precursor protein. J Neurosci 24(17):4259–4265
284. Kinoshita A et al (2002) The γ secretase-generated carboxyl-terminal domain of the amyloid precursor protein induces apoptosis via Tip60 in H4 cells. J Biol Chem 277(32):28530–28536
285. Santiard-Baron D et al (2005) Expression of human FE65 in amyloid precursor protein transgenic mice is associated with a reduction in β-amyloid load. J Neurochem 93(2):330–338
286. Krajnak K, Dahl R (2018) A new target for Alzheimer's disease: a small molecule SERCA activator is neuroprotective in vitro and improves memory and cognition in APP/PS1 mice. Bioorg Med Chem Lett 28(9):1591–1594
287. Nussbaum RL (2018) Genetics of synucleinopathies. Cold Spring Harb Perspect Med 8(6):a024109

288. Lashuel HA et al (2013) The many faces of α-synuclein: from structure and toxicity to therapeutic target. Nat Rev Neurosci 14(1):38–48
289. Ghiglieri V, Calabrese V, Calabresi P (2018) Alpha-Synuclein: from early synaptic dysfunction to neurodegeneration. Front Neurol 9:295
290. Tuon T et al (2012) Physical training exerts neuroprotective effects in the regulation of neurochemical factors in an animal model of. Neuroscience 227:305–312
291. Lundblad M et al (2002) Pharmacological validation of behavioural measures of akinesia and dyskinesia in a rat model of Parkinson's disease. Eur J Neurosci 15(1):120–132
292. Jouve L et al (2010) Deep brain stimulation of the center median–parafascicular complex of the thalamus has efficient anti-parkinsonian action associated with widespread cellular responses in the basal ganglia network in a rat model of Parkinson's disease. J Neurosci 30(29):9919–9928

Chapter 7
Cytoplasmic Calcium Buffering: An Integrative Crosstalk

Juan A. Gilabert

Abstract Calcium (Ca^{2+}) buffering is part of an integrative crosstalk between different mechanisms and elements involved in the control of free Ca^{2+} ions persistence in the cytoplasm and hence, in the Ca^{2+}-dependence of many intracellular processes. Alterations of Ca^{2+} homeostasis and signaling from systemic to subcellular levels also play a pivotal role in the pathogenesis of many diseases.

Compared with Ca^{2+} sequestration towards intracellular Ca^{2+} stores, Ca^{2+} buffering is a rapid process occurring in a subsecond scale. Any molecule (or binding site) with the ability to bind Ca^{2+} ions could be considered, at least in principle, as a buffer. However, the term Ca^{2+} buffer is applied only to a small subset of Ca^{2+} binding proteins containing acidic side-chain residues.

Ca^{2+} buffering in the cytoplasm mainly relies on mobile and immobile or fixed buffers controlling the diffusion of free Ca^{2+} ions inside the cytosol both temporally and spatially. Mobility of buffers depends on their molecular weight, but other parameters as their concentration, affinity for Ca^{2+} or Ca^{2+} binding and dissociation kinetics next to their diffusional mobility also contribute to make Ca^{2+} signaling one of the most complex signaling activities of the cell.

The crosstalk between all the elements involved in the intracellular Ca^{2+} dynamics is a process of extreme complexity due to the diversity of structural and molecular elements involved but permit a highly regulated spatiotemporal control of the signal mediated by Ca^{2+} ions. The basis of modeling tools to study Ca^{2+} dynamics are also presented.

Keywords Ca^{2+} buffering · Mobile buffers · Immobile buffers · Modeling Ca^{2+} signaling

J. A. Gilabert (✉)
Department of Pharmacology and Toxicology, Faculty of Veterinary Medicine, Complutense University of Madrid, Madrid, Spain
e-mail: jagilabe@ucm.es

M. S. Islam (ed.), *Calcium Signaling*, Advances in Experimental Medicine and Biology 1131, https://doi.org/10.1007/978-3-030-12457-1_7

7.1 Introduction

In the previous chapters the reader has had the opportunity to explore the properties and characteristics making of calcium ions (Ca^{2+}) the essential and more versatile messenger in the cells. But, how its concentration is so tightly regulated within the cells and for what reason?

Ca^{2+} ions are involved in many processes along the vital cycle of the cells. Notwithstanding, they also can be cytotoxic for living organisms across the entire phylogenetic tree (from bacteria to eukaryotic cells) making necessary an universal Ca^{2+} homeostasis system [1].

Ancestral cells probably faced to low Ca^{2+} levels in the prehistoric alkaline ocean, which millennia later became acidified and Ca^{2+} in the seawater started gradually to increase [2]. Thus, primitive cells had to face a massive, constant and toxic Ca^{2+} gradient. The appearance of a plasma membrane in the primitive cell was the border between extra- and intracellular spaces providing permeability features to enable a tight control of this cation concentration in the cytoplasm, with low concentrations inside against high concentrations in the extracellular milieu. This generates a huge gradient both in terms of concentration and of net charge considering the negative net charge of the intracellular milieu.

Moreover, since primitive cells successful mechanisms were developed very early in the evolution process to precisely regulate the cellular concentrations of free and bound/sequestered Ca^{2+} both in time and spatial dimensions. These mechanisms are essentially the same in prokaryote and eukaryote organisms: a low permeability of the cell membrane depending on influx mechanisms, a high intracellular buffering capacity, and an effective removal system [3, 4]. A significant difference in the mechanisms of buffering in eukaryotic cells is the presence of a nucleus and several sets of intracellular organelles, which can divide the cytoplasm into specialized compartments, with distinct mechanisms and capacities of Ca^{2+} handling [3].

At the cell level, Ca^{2+} homeostasis determines that basal cytosolic Ca^{2+} concentration ($[Ca^{2+}]_c$) is set at around 100 nM (10^{-7} M). This is crucial for a proper signaling process mediated by Ca^{2+} which as other effective signals, must be fast, with an adequate magnitude or dynamic range (to exceed a threshold) and finite in spatial and/or temporal terms.

This resting $[Ca^{2+}]_c$ works as a threshold to switch on any signaling processes mediated by Ca^{2+} against an electrochemical gradient due to a 10,000–20,000 times higher concentration in the extracellular milieu (around 1–2 mM). This threshold is kept by different mechanisms in a continuous and well-orchestrated crosstalk involving active transport expending energy (i.e. ATP-dependent) of Ca^{2+} out of the cell or into the organelles, antiport systems, Ca^{2+} buffering (mobile and immobile buffers) and ion condensation [5].

Ca^{2+} buffering in the cytoplasm relies on mobile or immobile buffers controlling the diffusion of free Ca^{2+} ions inside the cytosol both temporally and spatially. In other words, Ca^{2+} changes can occur in the whole cell space or be restricted to smaller areas around those elements involved in Ca^{2+} fluxes.

The importance of Ca^{2+} control mechanisms can be also seen at intercellular and multicellular levels in higher organisms. Thus, Ca^{2+} homeostasis also operates in the extracellular fluid where is influenced by dietary intake, Ca^{2+} absorption in the small intestine, exchange to and from the bones, and by excretion of Ca^{2+} in the urine. So, control of Ca^{2+} homeostasis in the cell and between cells underlies different physiological processes at the whole organism level [6].

Next, we will review these mechanisms with special attention to the role of cytoplasmic Ca^{2+} buffering in the generation of different spatiotemporal Ca^{2+} signals and its physiological relevance at the single cell (eukaryote) level.

7.2 Ca^{2+} Buffering: An Overview

The control of $[Ca^{2+}]_c$ at the resting level ($\sim 10^{-7}$ M range) involves several mechanisms, including Ca^{2+} influx (from the extracellular space), Ca^{2+} release (from internal Ca^{2+} stores), Ca^{2+} sequestration (towards internal Ca^{2+} stores), Ca^{2+} efflux (to the extracellular space) or Ca^{2+} buffering. Hence, Ca^{2+} persistence in the cytosol and derived Ca^{2+}-mediated actions are determined by two main processes: Ca^{2+} removal and Ca^{2+} diffusion (Fig. 7.1). Note that occasionally some of the efflux mechanisms can increase cytosolic Ca^{2+} as "slippage" of Ca^{2+} through Ca^{2+}-ATPases and the reverse-mode action of Na^+/Ca^{2+} exchanger) [7].

Ca^{2+} removal from the cytosol results from the combined action of Ca^{2+} sequestration and Ca^{2+} efflux, while Ca^{2+} diffusion is mainly determined by Ca^{2+} buffering. Ca^{2+} buffering is the rapid binding of Ca^{2+} entering cytosolic space to different cellular binding sites. Ca^{2+} buffering is an important process in Ca^{2+} signaling because it has been estimated that only about 1–5% of Ca^{2+} entering the cell remains as free Ca^{2+}, its physiologically active form [8–12].

In 1992, Neher and Augustine showed that Ca^{2+} buffering was a rapid process (time scale in subsecond range) kinetically distinct of Ca^{2+} sequestration, which is slower occurring in a tens of seconds scale. They also were able to determine using a combination of fura-2 microfluorimetry and Ca^{2+} current measurements in single adrenal chromaffin cells, the Ca^{2+} binding capacity of cytoplasm (κ_s) (bound Ca^{2+} over free Ca^{2+}) [13]. The κ_s value was approximately 75, which did not change during prolonged whole-cell recording (in a dialyzed cell with a disrupted membrane). Thus, they concluded that the majority of cellular Ca^{2+} binding sites were immobile [14].

Immobile buffers are represented by molecules of high molecular weight or Ca^{2+} binding sites anchored to intracellular structures. On the contrary, mobile buffers are molecules of low molecular size, typically less than 20–25 kDa, comprising soluble proteins or small organic anions and metabolites, like ATP. Their contribution can be difficult to estimate in some experiments involving whole-cell recordings where washout phenomena lead to the loss of some of these small molecules. In the presence of mobile buffers, immobile buffers increase the complexity of the spatiotemporal signaling repertoires, depending on the relative affinities, kinetics, and concentrations of the different buffers [15].

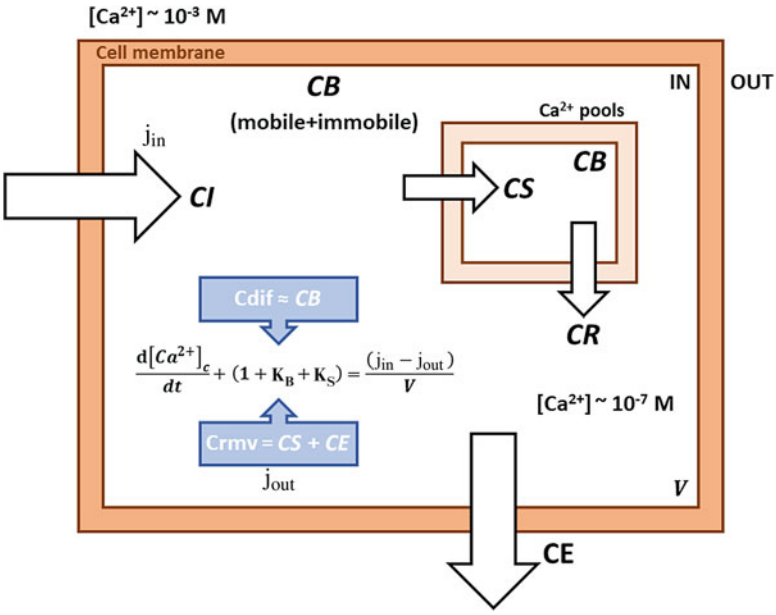

Fig. 7.1 Schematic representation of the main processes involved in the control of calcium concentration in the cytosol ($[Ca^{2+}]_c$) of a eukaryotic cell. *CI* calcium influx, *CR* calcium release, *CS* calcium sequestration, *CE* calcium efflux, and *CB* calcium buffering (mobile and immobile buffers). Ca^{2+} diffusion (Cdif) is mainly determined by cytoplasmic *CB*. *Ca^{2+}pools*, mainly represent the endoplasmic or sarcoplasmic reticulum and mitochondria. The combined action of these fluxes determines how $[Ca^{2+}]_c$ changes with time to generate different spatiotemporal signaling patterns. A basic transient in a cell of volume V and a Ca^{2+} influx (j_{in}) as consequence of a stimulus will produce an increase of $[Ca^{2+}]_c$ (see text for details). These Ca^{2+} ions will be partitioned into the cytoplasm between the endogenous Ca^{2+} buffer component and, in common experimental conditions, the exogenous Ca^{2+} indicator/buffer with constant Ca^{2+}-binding ratios κ_S and κ_B, respectively. Ca^{2+} removal from the cytoplasm (Crmv) (j_{out}) mainly reflects a combined action of *CS* and *CE*

Mobile buffers are estimated to have a Ca^{2+} binding capacity about one tenth of the cytoplasm Ca^{2+} binding capacity. One important mobile Ca^{2+} buffer is ATP, a highly mobile and effective Ca^{2+} chelator. ATP concentration in the cytosol is estimated to be around 2–3 mM, of which 0.4 mM is in a free form [16, 17].

But, which is the mobility of buffers in the cell? When a signal opens a Ca^{2+} route (i.e., a channel or a receptor) a fast Ca^{2+} flux reach the cytoplasm from extracellular space (or from organelles) driven by a large electrochemical gradient. More than 95% of Ca^{2+} are immediately bound to buffers within a distance of 10–50 nm from the focal point of Ca^{2+} entry [18, 19]. A mobile Ca^{2+} buffer will act to disperse such local domains of elevated $[Ca^{2+}]_c$ whereas fixed Ca^{2+} buffers will tend to prolong them.

Therefore, commonly used exogenous buffers/chelators for experimental purposes (EGTA, BAPTA or fluorescent Ca^{2+} indicators like fura-2) must be also considered since they compete with endogenous buffers increasing the transport of Ca^{2+} across the cell [20].

The presence of mobile and immobile buffers greatly reduces the diffusion spread of Ca^{2+}. The effective diffusion constant of free Ca^{2+} is between 200–300 $\mu m^2/s$, this being reduced more than 20 times (<16 $\mu m^2/s$) by cytoplasmic buffering [21, 22]. This fact was already described by Hodgkin and Keynes in 1957 in squid giant axon, where the retardation factor of radioactivity-labeled Ca^{2+} was about 40 [8]. However, the timescale of those experiments was of minutes so that Ca^{2+} buffering and Ca^{2+} sequestration could be equilibrated and hence the effects of buffers overestimated.

One parameter that offers an intuitive idea of Ca^{2+} diffusion is the mean distance covered by Ca^{2+} ions in one dimension. This distance can be calculated as $(2D_{eff}t)^{1/2}$, where D_{eff} is the effective diffusion coefficient for Ca^{2+} and t is the uptake time constant.

A stationary state situation (determining the basal level, usually around 100 nM) will be reached when Ca^{2+} influx or Ca^{2+} release to the cytoplasm space equals Ca^{2+} efflux plus Ca^{2+} buffering and sequestration into organelles [23, 24].

The results of simulations of the spatial and temporal pattern of Ca^{2+} changes following stimulation depend very much on assumptions regarding mobility of buffers [25, 26]. Thus, it is important to have experimental data on the mobility of cellular Ca^{2+} buffers. The result, showed by Neher and Augustine [13], that there is very little mobile buffer, would mean that the addition of even minute amounts of an exogenous mobile Ca^{2+} buffer, such as fura-2 (as in Ca^{2+} imaging experiments), should alter the temporal pattern of Ca^{2+} redistribution.

7.2.1 Ca^{2+} Buffers

Any molecule (or process) with the ability to bind Ca^{2+} ions could be considered, at least in principle, as a buffer. Thus, many molecules with several negatively charged groups can act as Ca^{2+} chelators. However, the term Ca^{2+} buffer is applied only to a small subset of Ca^{2+} binding proteins containing acidic side-chain residues [27, 28].

Ca^{2+} binding proteins can be found in the cytosol (as soluble proteins); but also, inside organelles (intraluminal proteins) [29] like the endoplasmic reticulum (ER) or as intrinsic proteins in membranes (plasma or organelle membranes) (see *Calcium Binding Proteins* chapter on this volume). The first of these proteins to be described was troponin C [30].

Different protein families bind Ca^{2+} through different structural motifs as EF-hands [31] or other well conserved Ca^{2+} binding domains founded in several proteins families (C2 domain proteins, annexins) [27, 32]. However, the term Ca^{2+}

buffer is applied only to a small subset of proteins of the EF-hand family, including parvalbumins (α and β isoforms), calbindin-D9k (CB-D9k), calbindin D-28k and calretinin in the cytosol [28].

In the ER, main intraluminal Ca^{2+} buffers are calsequestrin and calreticulin (which can also operate in the cytosol). These organellar Ca^{2+} buffers play a significant role as modulators in a dynamic network of organellar Ca^{2+} signaling [29].

Other Ca^{2+} binding proteins play a role as Ca^{2+} sensors more than as Ca^{2+} buffers due to its low concentration in the cell. Ca^{2+} ions bind to Ca^{2+} sensors inducing a conformational change, which permits them to interact with specific targets in a Ca^{2+}-regulated manner. A prototype of Ca^{2+} sensor is calmodulin [33].

On the other hand, depending on their diffusion characteristics, buffers can be considered as mobile or immobile. In addition, their Ca^{2+} binding and dissociation rate constants cover a wide range from slow buffers (with constant values about 1 s^{-1}) to fast buffers (constant values about 100 s^{-1}) [34].

The obvious consequence of the presence of Ca^{2+} buffers is the Ca^{2+} buffering capacity of the cytoplasm, which will be directly related to the concentration and spatial location of the Ca^{2+} buffers. However, other parameters as affinity for Ca^{2+}, Ca^{2+} binding and dissociation kinetics, and diffusional mobility also contribute to make Ca^{2+} signaling one of the most complex signaling activities of the cell.

7.2.2 Intracellular Concentration of Ca^{2+} Buffers

Intracellular or endogenous Ca^{2+} buffering capacity is directly related to the concentration of Ca^{2+} buffers located in the cytosol [19]. However, this unitless parameter is quite variable amongst different cells or even in the same type of cell depending of host tissue, species or clonality (e.g., PC12 *vs* adrenal chromaffin cells in Table 7.1) [19, 27, 35]. However, a minimal value could be 15 [15].

A useful approximation to endogenous Ca^{2+} buffering properties is to estimate the ratio of changes of buffer-bound Ca^{2+} over changes of free Ca^{2+}

Table 7.1 Values of Ca2+ binding ratio (κ) in different cell types

Cell type	κ	References
Motor neurons	40–50	[37, 41]
Adrenal chromaffin cells (PC12 cells)	40–75 (268)	[13, 14, 35]
Hippocampal neurons (excitatory/inhibitory)	60/150	[42]
Dopaminergic neurons	110–179	[40]
Smooth muscle (coronary artery)	150	[43]
Cerebellar Purkinje cells	900–2000	[38]
Pancreatic acinar cells	1500–2000	[39]

More details (as experimental conditions of measurements) can be founded in the respective original references. More values of Ca2+ binding ratios and their quantification for different types of neurons can be founded in Matthews and Dietrich [15]

($\kappa = d[BCa^{2+}]/d[Ca^{2+}] \approx [B]/K_d$) [15, 19, 36]. We can use this Ca^{2+} binding ratio to compare the values of κ of different cells ranging from low (below 50) for motor neurons [37] to very high (around 1000–2000) as that found in cerebellar Purkinje neurons [38] or pancreatic acinar cells [39] (Table 7.1). It indicates that lower values are probably needed in cells with a rapid Ca^{2+} signaling, as occurs in many neurons types [40]. In other words, a high buffering capacity means that very few Ca^{2+} will remain free following an action potential or other Ca^{2+}-generating event.

7.2.3 *Ca^{2+} Binding and Kinetics by Ca^{2+} Buffers*

EF-hands motifs are Ca^{2+}-binding sites with different selectivity and affinity for Ca^{2+} and Mg^{2+} [31, 44]. The Ca^{2+}-specific sites display affinities for Ca^{2+} from 10^{-3} to 10^{-7} M and significant lower ones for Mg^{2+} (10^{-1} to 10^{-2} M). The Ca^{2+} and Mg^{2+} sites bind Ca^{2+} with high (10^{-7} to 10^{-9} M) and Mg^{2+} with moderate (10^{-3} to 10^{-5} M) affinities (see [28]).

The majority of Ca^{2+} buffers have values of dissociation constants in the low micromolar range, such that, in a resting cell, Ca^{2+} buffers are mostly in a Ca^{2+}-free form. Another parameter to be considered is the kinetics of this binding. Ca^{2+} buffers considered as fast have rates $>10^8$ M^{-1} s^{-1} (as CB-D9k and troponin C and the synthetic buffers BAPTA or Fura-2), while those considered as slow have rates around 10^6 M^{-1} s^{-1} (as parvalbumins and the synthetic buffer EGTA). It is the presence of Mg^{2+} (0.5–1.0 mM in physiological conditions) that determines the Ca^{2+}-binding due to the slow Mg^{2+} off rate. Thus, in an experimental setting in the absence of Mg^{2+}, the on-rate of Ca^{2+} binding to parvalbumins is very rapid (around 10^8 M^{-1} s^{-1}) [45]. Usually, endogenous Ca^{2+} buffers possess several Ca^{2+} binding sites with different affinities and kinetics. The ratio between high:intermediate affinity sites can be 3:1 or 2:2 [46]. Likewise, Ca^{2+} binding sites (EF-hands) show allosterism in function of the occupied sites resulting in a non-linear Ca^{2+} buffering [47, 48], therefore increasing the complexity and versatility of the signaling mediated by Ca^{2+}.

7.2.4 *Intracellular Mobility of Ca^{2+} Buffers*

Ca^{2+} buffering is, at least in mechanistic terms a different process that Ca^{2+} sequestration. The majority of Ca^{2+} entering into the cell will be rapidly bound by Ca^{2+} buffers and later sequestered into Ca^{2+} storing organelles by slower processes [13]. Mobility of Ca^{2+} buffers is an important determinant of Ca^{2+} signaling since a mobile buffer will disperse a local increment of Ca^{2+} [15]. However, not only mobile buffers can alter the time course and spatial distribution of the Ca^{2+} signal. Immobile or fixed buffers (which also include some mobile Ca^{2+} binding

proteins that may change their mobility upon binding Ca^{2+}) have been proposed to participate in the generation of the repertoire of intracellular Ca^{2+} signaling [15, 49].

The mobility of a Ca^{2+} buffer is expressed by its diffusion coefficient, which is proportional to the molecular weight but also influenced by other factors. Molecular diffusion is a complex process determined by a dynamic and out of equilibrium environment as the cytoplasm. The rate of the diffusion of a molecule or particle is also a function of temperature (thermal Brownian movement), viscosity and its mass (i.e. radius) (see [50]). Therefore, the same molecule can have different diffusion coefficient values in different cellular compartments as occurs with parvalbumin that exhibits around 12 $\mu m^2/s$ in axons, somata and nuclei [51] versus 43 $\mu m^2/s$ in dendrites [52].

7.3 Physiological Relevance of Cytosolic Ca^{2+} Buffering

Ca^{2+} signaling can be observed and described at different levels of life organization ranging from the whole organism to the subcellular level, but they are closely related [53, 54]. Most of Ca^{2+} in higher organisms is bound to bones and teeth forming hydroxyapatite. In humans, from a total amount of Ca^{2+} of approximately 1250 g, only a few grams are in the extracellular and intracellular fluids, this level is controlled by the slow Ca^{2+} movements in and out of the bone deposits [55] under the influence of vitamin D and parathyroid hormone regulatory actions. Serum concentration of Ca^{2+} is quite variable in animals ranging from 1 to 15 mM. In man, normal range is 2.1–2.6 mM, but levels out of this range can produce uncontrollable muscle spasms and cardiac alterations [56].

As discussed above, extracellular (plasma) levels will determine the electrochemical gradient with respect to intracellular space and Ca^{2+} fluxes from the extracellular fluid to inside the cells are both signals and sources of Ca^{2+} for subcellular organelles as the ER, mitochondrion or nucleus. Thus, the extracellular pool acts as a large reservoir of free Ca^{2+}.

Intracellular Ca^{2+} homeostasis is finely tuned by different regulatory systems making of Ca^{2+} a crucial cation in the cellular physiopathology and cell fate. An increase of $[Ca^{2+}]_c$ is the key signal to initiate many physiological actions as synaptic transmission, muscle contraction, hormone secretion or gene expression [57, 58]. Moreover, Ca^{2+} signaling is also present throughout the life history of the cell from its birth (mitosis) to death (apoptosis) [23, 59]. Alterations of Ca^{2+} homeostasis and signaling from systemic to subcellular levels also play a pivotal role in the pathogenesis of many diseases [60–67].

Ca^{2+} signaling does not act solely by "on-off" changes in their concentration at the entire cytoplasm. Cells have developed a complex code of signals based on the modulation of Ca^{2+} concentration on different spatial and temporal basis [66]. Thus, Ca^{2+} signals can be graded from unitary and spatially located signals, with a very limited spread through the cell, to whole cell signals as Ca^{2+} waves or Ca^{2+}

oscillations with repetitive Ca^{2+} changes travelling across the cell over longer time periods. These global signals are possible due to a coordinated activity of Ca^{2+} entry, Ca^{2+} release and Ca^{2+} sequestration and finely tuned by Ca^{2+} buffering.

However, a signal to be effective as messenger must be finite. Ca^{2+} buffering and Ca^{2+} sequestration are mechanisms to make intracellular Ca^{2+} changes transient, permitting the cell to recover the basal values so that get ready again for a new signaling round.

In general, fast responses are mediated by rapid and highly localized Ca^{2+} spikes as in neurons during synaptic transmission. By contrast, repetitive Ca^{2+} transients or waves are involved in slower intracellular processes, like in astrocytes. Moreover, neuronal excitability can be modulated by Ca^{2+} buffering changing from a spike-based pattern to a bursting signaling [67].

7.3.1 Spatiotemporal Signaling

Intracellular Ca^{2+}signaling, as occurs with other second messengers-mediated signaling is coded by changes in amplitude and frequency. Likewise, the quality and quantity of an extracellular incoming signal are reflected in different domains in the cell [68]. Amplitude may be proportional to the strength of the stimulus while the frequency to its strength and quality. Localized increases of Ca^{2+} in restricted domains represents an additional way of coding the signal. The combination of all these three characteristics makes possible a wide variety of Ca^{2+} signals and slight modifications of the amplitude or the temporal and spatial features of Ca^{2+} signals can trigger deleterious processes involved in multiple pathogenic states, such as cancer, inflammation, heart failure, and neurodegeneration [58].

The elementary phenomena involved in Ca^{2+} dynamics at a cytosolic level can be the opening of a single channel in the plasma membrane or in an intracellular Ca^{2+}-store organelle leading to Ca^{2+} entry or Ca^{2+} release. Such events can act as starters of whole cell events (i.e. Ca^{2+} sparks and Ca^{2+} induced Ca^{2+} release from the sarcoplasmic reticulum). Many other different elementary Ca^{2+} signaling events have been described from many cell and tissue types [69].

In an elementary event, the opening is usually brief and leads to a small and local increase of Ca^{2+} concentration. This local increase results in the formation of submicron sharp Ca^{2+} concentration profile in the vicinity of the channel [70]. The temporal collapse of these Ca^{2+} domains after channel closing is believed to be achieved in the microsecond time scale.

Ca^{2+} microdomains are restrained by strong buffering and slow diffusion. The microdomain's size is a function of several parameters as the conductance and the opening duration of the channel (how many ions can pass through the channel pore by time unit) and the electrochemical driving force for Ca^{2+} (potential difference and free Ca^{2+} concentration on both sides of the channel) but it is strongly influenced by the properties of Ca^{2+} buffers.

7.3.2 Ca^{2+} Buffering and Organelles

In addition to Ca^{2+} buffering, Ca^{2+} pumping significantly influences cellular Ca^{2+} signaling, albeit in a slower time scale. Ca^{2+} diffusion throughout the cell is not only restrained by Ca^{2+} buffering, Ca^{2+} pumping (Ca^{2+} fluxes against the electrochemical gradients) removes Ca^{2+} from the cytosol towards the extracellular space (by plasma membrane Ca^{2+}-ATPases and Na^{+}/Ca^{2+} exchanger) or into the ER (by sarco/endoplasmic reticulum Ca^{2+}-ATPases or SERCA pumps). Therefore, Ca^{2+} can be sequestered into the mitochondria (by action of the mitochondrial Ca^{2+} uniporter). In the resting state or for small $[Ca^{2+}]_c$ changes the dominant pumping fluxes are into the ER and to the extracellular space, whereas larger Ca^{2+} signals (micromolar range) involves mitochondrial participation [71].

SERCA pumps are in charge of Ca^{2+} sequestration from the cytosol to inside of the ER, where Ca^{2+} binds to intraluminal Ca^{2+} binding proteins with high capacity (10 mol per mol of protein) but low affinity ($K_D \approx 1$ mM) which permit ER to store vast amounts of Ca^{2+} which can rapidly be exchanged with the cytosol. Many ER proteins bind Ca^{2+}, including calreticulin, protein disulfide isomerase (PDI), glucose regulated protein 94 (Grp94), immunoglobulin binding protein (BiP), and ERp57. In the sarcoplasmic reticulum the most abundant Ca^{2+} binding protein is calsequestrin. Sarcolumenin, a histidine-rich protein, junctin, junctate, and triadin are unique to their membrane providing buffering and structural support [72].

ER contribution to Ca^{2+} signaling is also mediated by inositol 1,4,5-trisphosphate (InsP3) and ryanodine receptors as well as by passive leak channels. An example of this coordinated exchange between ER Ca^{2+} pools and $[Ca^{2+}]_c$ is the propagation of Ca^{2+} waves observed in mature oocytes during activation [73].

Organellar buffers also play a multifunctional role in a variety of processes, including protein folding, regulation of apoptosis, and regulating Ca^{2+} release pathways [29]. Thus, organellar Ca^{2+} dynamics is also dependent both structural and functional relationships between different organelles and their respective buffers.

The total Ca^{2+} concentration in the ER has been estimated between 5 and 50 mM [74]. The majority of this Ca^{2+} is bound to proteins with a low affinity ($K_d = 1$–4 mM) like calreticulin/calsequestrin and other intraluminal proteins with additional function as chaperones. The high intraluminal content of Ca^{2+} and the low affinity of ER Ca^{2+} buffers suggest that free Ca^{2+} concentration inside the ER could be in the micromolar range (300–800 mM, depending on cell type) [75].

Mitochondria is another crucial organelle in Ca^{2+} homeostasis in the cell, being capable of store substantial amounts of Ca^{2+}. Moreover, Ca^{2+} play an important role linking Ca^{2+} signaling with mitochondrial energetic status (through the production of ATP necessary, among other functions, for active Ca^{2+} transport) and cell death by apoptosis [76].

The Ca^{2+} entry way to the mitochondria is the uniporter located in the organelle's inner membrane. This mitochondrial Ca^{2+} uniporter is a selective Ca^{2+} channel with low affinity (K_d estimated at ~10–50 μM) and high conductance [77].

Mitochondria becomes the predominant system of Ca^{2+} sequestration when the level of $[Ca^{2+}]_c$ is well above that reached during normal cell activation (around 1 μM) when work at saturation [78].

An additional mechanism of Ca^{2+} entry into the mitochondria known as rapid uptake mode or RaM was described in hepatocytes [79]. RaM functions could be to create a brief but high free Ca^{2+} elevation inside mitochondria, which may be enough to activate metabolic reactions with small amounts of Ca^{2+} uptake that are not capable to open mitochondrial membrane permeability transition pore [80]. Thus, mitochondria are the decoder between intensity of signaling and metabolic activity till apoptosis is induced when Ca^{2+} homeostasis is lost.

A final interesting point to understand Ca^{2+} dynamics in the cytoplasm is the crosstalk between organelles and plasma membrane. A good example of it is the mechanism, described by Putney in 1986 [81], known as capacitative calcium entry in which plasma membrane Ca^{2+} channels (like Ca^{2+} release activated Ca^{2+} or CRAC channels) open after depletion of ER Ca^{2+} stores to slowly replenish their resting Ca^{2+} levels [82].

This communication involves different signaling molecules and/or close interactions between subcellular structures. Ca^{2+} entry through store-operated Ca^{2+} channels involve two main proteins. The stromal interaction molecule 1 (STIM1), an ER-located Ca^{2+}-sensing protein and, Orai1, a pore-forming subunit located at the plasma membrane. After depletion of Ca^{2+} stores, STIM1 multimerizes and redistributes into discrete sites close to the plasma membrane and, STIM1 couples to and stimulates Orai, initiating the Ca^{2+} entry to replenish the empty stores [83].

The high-resolution imaging techniques have permitted to confirm that the mitochondrial network inside the cells can be very close or even in contact with the ER membrane and/or plasma membrane channels. Also mitochondria could be able to sense large, but spatially limited Ca^{2+} increments derived from $InsP_3$ receptor activation or other Ca^{2+} fluxes from plasma membrane channels as voltage-dependent calcium channels or store-operated calcium entry [84–86]. But, mitochondria can also increase Ca^{2+} buffering capacity by a local release of ATP which acts as an endogenous highly mobile and effective Ca^{2+} chelator. Thus, mitochondria located close to CRAC channels in T lymphocytes can regulate slow Ca^{2+}-dependent inactivation of the Ca^{2+} current through these channels by increasing the Ca^{2+} buffering capacity beneath the plasma membrane, mainly through the release of ATP [17].

7.4 Elements for Modeling Ca^{2+} Buffering and Signaling

Ca^{2+} dynamics can be seen as a process of extreme complexity due to the diversity of molecular and structural elements (i.e., pumps, channels, Ca^{2+} buffers, organelles, . . .) involved [23] which can be analyzed at several levels from unitary or elementary events (restricted to subcellular spaces) to global events (as waves or oscillations) occurring at the whole cell level.

First attempts to model intracellular Ca^{2+} dynamics focused in extracellular Ca^{2+} entry pathways (i.e. channels) considering the cytoplasm as a uniform medium. Later, more descriptive models were proposed to explain the activation kinetics of a single channel or the spatial arrangements of a group of channels, the role of mobile and immobile buffers or the alterations produced by experimentally-added exogenous buffers.

In general, the inositol 1,4,5-trisphosphate receptor (InsP3R), the ryanodine receptor, and the SERCA pumps govern most Ca^{2+} exchanges between the cytosol and the ER. When combined in a cellular model, they can explain many observations regarding signal-induced Ca^{2+} oscillations and waves. On the other hand, modeling also permits a predictive analysis of experimental results and to study the role of different elements in a complex system (see an excellent review by Dupont [87] about the relative contribution of the different elements in Ca^{2+} dynamics).

Mathematics behinds Ca^{2+} modeling can be hard for some of us (a comprehensive review about this issue have been written by Martin Falcke [88]). For it, only the main elements (variables) and their role in the control of cytoplasmic Ca^{2+} will be shortly described below.

A valuable approach to study the properties and contribution of buffers to Ca^{2+} signaling has been the microfluorimetry combined with single-cell electrophysiological techniques using Ca^{2+} indicators (as fura-2) [89]. They have also permitted to study the contribution of exogenous Ca^{2+} buffers (i.e. fluorescent Ca^{2+} probes) competing with endogenous Ca^{2+} buffers [19]. The method known as "added-buffer method" (see next section) allows to study endogenous buffer capacity by adding a competing exogenous buffer. Recently, new experimental approaches using minimal Ca^{2+} buffer (the low affinity Ca^{2+} indicator Fura-6F) concentrations, in order not to overwhelm endogenous Ca^{2+} buffers, have permitted more realistic intracellular conditions and to obtain more accurate values of parameters for modelling Ca^{2+} dynamics in neurons [90].

The basis to understand complex signals as Ca^{2+} waves or oscillations is the measurement of Ca^{2+} fluxes through a single channel and the subsequent estimation of its contribution to the global Ca^{2+} signal. The free Ca^{2+} increase due to a single channel opening (elementary events as blips or quarks) will depend mainly on the magnitude of the Ca^{2+} current and the buffering characteristics of the cytoplasm.

In early works, the aim was to estimate the cytosolic Ca^{2+} rise near the inner side of a single Ca^{2+} channel [91, 92] or a cluster of single channels [93]. These studies also allowed to make inferences about processes controlled by local Ca^{2+} signals like Ca^{2+}-dependent inactivation of Ca^{2+} channels [17], activation of Ca^{2+}-dependent potassium channels [94] or neurosecretion mediated by Ca^{2+} regulated exocytosis [95, 96].

The Ca^{2+} signal generated by a single channel is known as a nanodomain, which produces a Ca^{2+} elevation until 50 nm away from the channel pore in neurons [97]. Thus, any potential Ca^{2+}-dependent process controlled by a nanodomain should have a Ca^{2+} sensor in such distance range as occurs in rapid neurotransmitter release or the Ca^{2+} dependent modulation of ionic channels commented above.

Interestingly, small groups or clusters of channels can lead to the summation of nanodomains producing stronger signals called microdomains. These microdomains imply Ca^{2+} sensors that are placed within a fraction of a micrometer from the Ca^{2+} channel cluster center, to allow detection of summed signals.

The spread of Ca^{2+} during elemental events is the process most directly affected by buffer properties [26]. Thus, many efforts have been done to understand the cytosolic buffer dynamics and their influence in Ca^{2+} signaling from elementary events. However, Ca^{2+} nano or microdomains occurs in spatial and temporal scales that requires highly sensitive optical imaging techniques [98]. An alternative is the theoretical approach to study the influence of buffering on Ca^{2+} microdomains formation and diffusion [13, 16, 20, 99, 100]. At this level some other phenomena can be considered, as the stochastic behavior or the spatial grouping of Ca^{2+} permeating channels forming clusters [34], much more complex and demanding in order to design a reliable mathematical approach.

Despite several technological and methodological improvements in microfluorometry, such as the development of two-photon and super-resolution microscopy, we remain unable to trace Ca^{2+} dynamics over longer periods of time limiting our knowledge to their relevance in different physiological (or pathological) conditions [58].

An increased level of complexity of Ca^{2+} signaling is represented by global phenomena as waves or oscillations. They reflect the coordinated activity of release and diffusion processes involving several fluxes among different cellular compartments and organelles. These fluxes are usually visualized as a periodic behavior of $[Ca^{2+}]_c$ which spread across the cell and between cells. Ca^{2+} waves were first observed in fertilized fish oocytes [101], now we know different patterns from one-way linear displacement to spiral waves with a synchronous or asynchronous behavior depending of cell types [102, 103]. Ca^{2+} wave propagation can be modified by changing InsP3, buffer concentration, mitochondrial Ca^{2+} uptake or overexpressing SERCA pumps (see [88]). Repetitive Ca^{2+} spikes were instead first time observed in agonist-stimulated hepatocytes [104].

Ca^{2+} oscillations reflect an exchange of Ca^{2+} between the buffers and the ER mediated by InsP3R and the SERCA [25] with a dependence on external Ca^{2+} in most cells. Ca^{2+} oscillations and waves can be found in many cells from intra- to an intercellular (coordinated and cooperative responses in multicellular systems) level of signaling [105]. These transient events permit signaling based on frequency instead of amplitude; hence avoiding prolonged exposures to high Ca^{2+} concentrations potentially toxic for cells.

An additional challenge in the development of models is represented by the stochastic or deterministic nature of the signals involved in Ca^{2+} dynamics [87]. Some groups have concluded that Ca^{2+} dynamics remains as stochastic process even at the cellular level, mainly because of the poor communication between Ca^{2+}-releasing channels due to the low diffusivity of Ca^{2+} inside the cytoplasm [106–108].

The mathematical description of global phenomena can be very complex (in function of the number of variables considered, see [109]). However, Ca^{2+} signaling

involves a complex system with many elements and multiple interactions where modeling is a useful tool to understand the spatiotemporal behavior of Ca^{2+} signaling in a particular system.

There are three basic types of models: qualitative, phenomenological and quantitative or mechanistic. Qualitative models are presented in a diagrammatic rather than in mathematical form; they are easy to do and can serve to support an initial hypothesis. Phenomenological models are based and expressed in a mathematical form to explain the experimental observations. A main disadvantage of this sort of models is that widely differing mathematical expressions can behave in a comparable way. Finally, the quantitative or mechanistic models are based as far as possible on known mechanisms and experimentally validated parameters [110].

7.4.1 Ca^{2+}-Binding Ratio

Several experimental approaches have been employed to estimate Ca^{2+} fluxes and free Ca^{2+} concentration in cells being the most popular a combination of fluorescent imaging using Ca^{2+} indicator dyes with the electrophysiological measurements [42]. But, these Ca^{2+} indicators are exogenous Ca^{2+} buffers that contribute to cytoplasmic Ca^{2+} binding capacity.

In 1995, E. Neher developed the "added buffer method" to estimate the endogenous Ca^{2+} buffer [19]. It consists to measure the Ca^{2+} transients elicited by voltage or drug stimulation in the presence of different concentrations of an exogenous Ca^{2+} indicator. By extrapolating to zero concentration of added exogenous indicator it is possible to estimate the endogenous Ca^{2+} buffer.

In practice, to calculate κ_S we need to measure changes in both the fluorescent signal and in the total calcium entering the cytosol (valid for brief time intervals and small incremental elevations in $[Ca^{2+}]_c$). As explained before, κ_S can be estimated by different approaches like the analysis of Ca^{2+} signal or the amount of Ca^{2+} bound to buffer (see [18, 19] for alternative methods and problems measuring Ca^{2+}-binding ratio). Some limitations of the "added buffer method" regarding to the relative contributions of mobile and immobile buffers to the total buffering capacity are widely described in Matthews and Dietrich [15].

7.4.2 Calculating Changes in Free Ca^{2+} Concentration

The most basic scenario to model Ca^{2+} transients is to consider that they occur in a single compartment [13]. Consider a cell (or subcellular location, e.g. a dendritic segment) with a volume V and a Ca^{2+} influx (j_{in}) induced by a stimulus that produces an increase in the total Ca^{2+} concentration. Ca^{2+} will be partitioned between the endogenous Ca^{2+} buffer component (S) in the cytoplasm and the exogenous Ca^{2+} indicator/buffer (B) with constant Ca^{2+}-binding ratios κ_S and κ_B,

respectively. Ca^{2+} removal (j_{out}) is modeled as a linear extrusion mechanism with rate constant γ. The next equation describes the kinetics of Ca^{2+} changes (with conservation of total Ca^{2+}) [36]:

$$\frac{d\left[Ca^{2+}\right]_i}{dt} + \frac{d\,[BCa]}{dt} + \frac{d\,[SCa]}{dt} = \frac{(j_{in} - j_{out})}{V} \tag{7.1}$$

where [BCa] is the concentration of a mobile buffer (such as fura-2 or some other exogenous buffer) in its Ca^{2+}-bound form, [SCa] is the concentration of fixed (endogenous) Ca^{2+} buffer in the Ca^{2+}-bound form, and V is the accessible volume of the cell (or compartment).

The Eq. 7.1 can be expressed as a function of calcium binding capacities of κ_B and κ_S as

$$\frac{d\left[Ca^{2+}\right]_i}{dt}(1 + \kappa_B + \kappa_S) = \frac{(j_{in} - j_{out})}{V}$$

where

$$\kappa_B = \frac{d\,[BCa]}{d\left[Ca^{2+}\right]_i}$$

and

$$\kappa_S = \frac{d\,[SCa]}{d\left[Ca^{2+}\right]_i}$$

Thus, in a typical patch-clamp experiment we need to know the proportion of total current carried by Ca^{2+} ions, the accessible cell volume, and the cellular Ca^{2+} binding ratio to calculate the free Ca^{2+} concentration.

CalC ("Calcium Calculator") is a free modeling tool for simulating intracellular Ca^{2+} diffusion and buffering developed by Prof. Victor Matveev and available for download at https://web.njit.edu/matveev/calc.html [111]. CalC solves continuous reaction-diffusion partial differential equations describing the entry of Ca^{2+} into a volume through point-like channels, and its diffusion, buffering and binding to calcium "receptors".

The diffusion of calcium within a three-dimensional space in the presence of multiple buffers of mixed mobility is a more complex phenomenon, which it is described by a set of partial differential equations, which can be linearized to isolate individual interactions of Ca^{2+} with buffers at the nano and microdomain levels [16, 112].

An additional simplification assumes that interactions between Ca^{2+} and buffers are instantaneous ('Rapid Buffer Approximation') and that the spatiotemporal localization of Ca^{2+} depends only on the diffusion coefficients and affinities of the various buffers [20, 99, 100]. This yields a very useful analytical expression

describing Ca^{2+} diffusion in the presence of multiple buffers using a new, smaller diffusion coefficient of calcium (*Dapp*), depending on the number, amount and mobility of the calcium buffers present (see [15] for details):

$$Dapp = D_{Ca} \frac{\left(1 + \frac{D_{mobile}}{D_{Ca}} \kappa_{mobile}\right)}{(1 + \kappa_{mobile} + \kappa_{immobile})}$$

where, D_{Ca} is the diffusion coefficient of free Ca^{2+} in the cytosol, D_{mobile} is the diffusion coefficient of mobile buffers, and κ_{mobile} and $\kappa_{immobile}$ are the Ca^{2+} buffering capacities of mobile and immobile buffers, respectively. This equation dictates that adding a mobile buffer can accelerate Ca^{2+} diffusion (increasing *Dapp*), but only if the mobile buffer's diffusion coefficient is larger than the *Dapp* of the system in the absence of the mobile buffer.

References

1. Dominguez DC (2004) Calcium signalling in bacteria. Mol Microbiol 54:291–297
2. Kazmierczak J, Kempe S, Kremer B (2013) Calcium in the early evolution of living systems: a biohistorical approach. Curr Org Chem 17:1738–1750
3. Case RM, Eisner D, Gurney A, Jones O, Muallem S, Verkhratsky A (2007) Evolution of calcium homeostasis: from birth of the first cell to an omnipresent signalling system. Cell Calcium 42:345–350
4. Domínguez DC, Guragain M, Patrauchan M (2015) Calcium binding proteins and calcium signaling in prokaryotes. Cell Calcium 57:151–165
5. Ripoll C, Norris V, Thellier M (2004) Ion condensation and signal transduction. BioEssays 26:549–557
6. Bronner F (2001) Extracellular and intracellular regulation of calcium homeostasis. Sci World J. https://doi.org/10.1100/tsw.2001.489
7. Harzheim D, Roderick HL, Bootman MD (2010) Chapter 117 – Intracellular calcium signaling. In: Bradshaw RA, Dennis EA (eds) Handbook of cell signal, 2nd edn. Academic, San Diego, pp 937–942
8. Hodgkin AL, Keynes RD (1957) Movements of labelled calcium in squid giant axons. J Physiol 138:253–281
9. Smith SJ, Zucker RS (1980) Aequorin response facilitation and intracellular calcium accumulation in molluscan neurones. J Physiol 300:167–196
10. Gorman AL, Thomas MV (1980) Intracellular calcium accumulation during depolarization in a molluscan neurone. J Physiol 308:259–285
11. McBurney RN, Neering IR (1985) The measurement of changes in intracellular free calcium during action potentials in mammalian neurones. J Neurosci Methods 13:65–76
12. Ahmed Z, Connor JA (1988) Calcium regulation by and buffer capacity of molluscan neurons during calcium transients. Cell Calcium 9:57–69
13. Neher E, Augustine GJ (1992) Calcium gradients and buffers in bovine chromaffin cells. J Physiol 450:273–301
14. Zhou Z, Neher E (1993) Mobile and immobile calcium buffers in bovine adrenal chromaffin cells. J Physiol 469:245–273
15. Matthews EA, Dietrich D (2015) Buffer mobility and the regulation of neuronal calcium domains. Front Cell Neurosci 9:1–11

16. Naraghi M, Neher E (1997) Linearized buffered Ca^{2+} diffusion in microdomains and its implications for calculation of $[Ca^{2+}]$ at the mouth of a calcium channel. J Neurosci 17:6961–6973
17. Montalvo GB, Artalejo AR, Gilabert JA (2006) ATP from subplasmalemmal mitochondria controls Ca^{2+}-dependent inactivation of CRAC channels. J Biol Chem 281:35616–35623
18. Augustine GJ, Neher E (1992) Calcium requirements for secretion in bovine chromaffin cells. J Physiol 450:247–271
19. Neher E (1995) The use of fura-2 for estimating Ca buffers and Ca fluxes. Neuropharmacology 34:1423–1442
20. Wagner J, Keizer J (1994) Effects of rapid buffers on Ca^{2+} diffusion and Ca^{2+} oscillations. Biophys J 67:447–456
21. Gabso M, Neher E, Spira ME (1997) Low mobility of the Ca^{2+} buffers in axons of cultured Aplysia neurons. Neuron 18:473–481
22. Allbritton NL, Meyer T, Stryer L (1992) Range of messenger action of calcium ion and inositol 1,4,5-trisphosphate. Science 258:1812–1815
23. Berridge MJ, Lipp P, Bootman MD (2000) The versatility and universality of calcium signalling. Nat Rev Mol Cell Biol 1:11–21
24. Berridge MJ, Bootman MD, Roderick HL (2003) Calcium: calcium signalling: dynamics, homeostasis and remodelling. Nat Rev Mol Cell Biol 4:517–529
25. Sala F, Hernández-Cruz A (1990) Calcium diffusion modeling in a spherical neuron. Relevance of buffering properties. Biophys J 57:313–324
26. Nowycky MC, Pinter MJ (1993) Time courses of calcium and calcium-bound buffers following calcium influx in a model cell. Biophys J 64:77–91
27. Schwaller B (2010) Chapter 120 – Ca^{2+} buffers. In: Bradshaw RA, Dennis EA (eds) Handbook of cell signal, 2nd edn. Academic, San Diego, pp 955–962
28. Schwaller B (2010) Cytosolic Ca^{2+} buffers. Cold Spring Harb Perspect Biol 2:a004051
29. Prins D, Michalak M (2011) Organellar calcium buffers. Cold Spring Harb Perspect Biol 3:a004069
30. Ebashi S (1963) Third component participating in the superprecipitation of "natural actomyosin". Nature 200:1010
31. Gifford JL, Walsh MP, Vogel HJ (2007) Structures and metal-ion-binding properties of the Ca^{2+}-binding helix–loop–helix EF-hand motifs. Biochem J 405:199–221
32. Bindreither D, Lackner P (2009) Structural diversity of calcium binding sites. Gen Physiol Biophys 28 Spec No Focus:F82–F88
33. Chin D, Means AR (2000) Calmodulin: a prototypical calcium sensor. Trends Cell Biol 10:322–328
34. Falcke M (2003) Buffers and oscillations in intracellular Ca^{2+} dynamics. Biophys J 84: 28–41
35. Duman JG, Chen L, Hille B (2008) Calcium transport mechanisms of PC12 cells. J Gen Physiol 131:307–323
36. Mathias RT, Cohen IS, Oliva C (1990) Limitations of the whole cell patch clamp technique in the control of intracellular concentrations. Biophys J 58:759–770
37. Lips MB, Keller BU (1998) Endogenous calcium buffering in motoneurones of the nucleus hypoglossus from mouse. J Physiol 511:105–117
38. Fierro L, Llano I (1996) High endogenous calcium buffering in Purkinje cells from rat cerebellar slices. J Physiol 496:617–625
39. Mogami H, Gardner J, Gerasimenko OV, Camello P, Petersen OH, Tepikin AV (1999) Calcium binding capacity of the cytosol and endoplasmic reticulum of mouse pancreatic acinar cells. J Physiol 518:463–467
40. Foehring RC, Zhang XF, Lee JCF, Callaway JC (2009) Endogenous calcium buffering capacity of substantia nigral dopamine neurons. J Neurophysiol 102:2326–2333
41. Palecek J, Lips MB, Keller BU (1999) Calcium dynamics and buffering in motoneurones of the mouse spinal cord. J Physiol 520:485–502

42. Lee S-H, Rosenmund C, Schwaller B, Neher E (2000) Differences in Ca^{2+} buffering properties between excitatory and inhibitory hippocampal neurons from the rat. J Physiol 525:405–418
43. Ganitkevich VYa, Isenberg G (1995) Efficacy of peak Ca^{2+} currents (ICa) as trigger of sarcoplasmic reticulum Ca^{2+} release in myocytes from the guinea-pig coronary artery. J Physiol 484: 287–306
44. Kawasaki H, Kretsinger RH (2017) Structural and functional diversity of EF-hand proteins: evolutionary perspectives. Protein Sci 26:1898–1920
45. Lee S-H, Schwaller B, Neher E (2000) Kinetics of Ca^{2+} binding to parvalbumin in bovine chromaffin cells: implications for [Ca^{2+}] transients of neuronal dendrites. J Physiol 525: 419–432
46. Nägerl UV, Novo D, Mody I, Vergara JL (2000) Binding kinetics of calbindin-D(28k) determined by flash photolysis of caged Ca^{2+}. Biophys J 79:3009–3018
47. Schwaller B (2009) The continuing disappearance of "pure" Ca^{2+} buffers. Cell Mol Life Sci 66:275–300
48. Faas GC, Schwaller B, Vergara JL, Mody I (2007) Resolving the fast kinetics of cooperative binding: Ca^{2+} buffering by calretinin. PLoS Biol. https://doi.org/10.1371/journal.pbio.0050311
49. Matthews EA, Schoch S, Dietrich D (2013) Tuning local calcium availability: cell-type-specific immobile calcium buffer capacity in hippocampal neurons. J Neurosci 33:14431–14445
50. Brangwynne CP, Koenderink GH, MacKintosh FC, Weitz DA (2008) Cytoplasmic diffusion: molecular motors mix it up. J Cell Biol 183:583–587
51. Schmidt H, Arendt O, Brown EB, Schwaller B, Eilers J (2007) Parvalbumin is freely mobile in axons, somata and nuclei of cerebellar Purkinje neurones. J Neurochem 100:727–735
52. Schmidt H, Brown EB, Schwaller B, Eilers J (2003) Diffusional mobility of parvalbumin in spiny dendrites of cerebellar Purkinje neurons quantified by fluorescence recovery after photobleaching. Biophys J 84:2599–2608
53. Williams RJP (1998) Calcium: outside/inside homeostasis and signalling. Biochim Biophys Acta Mol Cell Res 1448:153–165
54. Williams RJP (2006) The evolution of calcium biochemistry. Biochim Biophys Acta Mol Cell Res 1763:1139–1146
55. Carafoli E (1987) Intracellular calcium homeostasis. Annu Rev Biochem 56:395–433
56. Soar J, Perkins GD, Abbas G et al (2010) European Resuscitation Council guidelines for resuscitation 2010 Section 8. Cardiac arrest in special circumstances: electrolyte abnormalities, poisoning, drowning, accidental hypothermia, hyperthermia, asthma, anaphylaxis, cardiac surgery, trauma, pregnancy, electrocution. Resuscitation 81:1400–1433
57. Carafoli E (2002) Calcium signaling: a tale for all seasons. Proc Natl Acad Sci 99:1115–1122
58. Giorgi C, Danese A, Missiroli S, Patergnani S, Pinton P (2018) Calcium dynamics as a machine for decoding signals. Trends Cell Biol 28:258–273
59. Krebs J, Michalak M (eds) (2007) Calcium: a matter of life or death, vol 41, 1st edn. Elsevier Science, Amsterdam
60. Peacock M (2010) Calcium metabolism in health and disease. Clin J Am Soc Nephrol 5: S23–S30
61. Chan CS, Gertler TS, Surmeier DJ (2009) Calcium homeostasis, selective vulnerability and Parkinson's disease. Trends Neurosci 32:249–256
62. Blair HC, Schlesinger PH, Huang CL-H, Zaidi M (2007) Calcium signalling and calcium transport in bone disease. Subcell Biochem 45:539–562
63. Feske S (2007) Calcium signalling in lymphocyte activation and disease. Nat Rev Immunol 7:690–702
64. Duchen MR, Verkhratsky A, Muallem S (2008) Mitochondria and calcium in health and disease. Cell Calcium 44:1–5
65. Lloyd-Evans E, Waller-Evans H, Peterneva K, Platt FM (2010) Endolysosomal calcium regulation and disease. Biochem Soc Trans 38:1458–1464

66. Bootman MD, Collins TJ, Peppiatt CM et al (2001) Calcium signalling—an overview. Semin Cell Dev Biol 12:3–10
67. Roussel C, Erneux T, Schiffmann SN, Gall D (2006) Modulation of neuronal excitability by intracellular calcium buffering: from spiking to bursting. Cell Calcium 39:455–466
68. Lipp P, Niggli E (1996) A hierarchical concept of cellular and subcellular Ca^{2+}-signalling. Prog Biophys Mol Biol 65:265–296
69. Niggli E, Shirokova N (2007) A guide to sparkology: the taxonomy of elementary cellular Ca^{2+} signaling events. Cell Calcium 42:379–387
70. Stern MD (1992) Buffering of calcium in the vicinity of a channel pore. Cell Calcium 13: 183–192
71. Saris NE, Carafoli E (2005) A historical review of cellular calcium handling, with emphasis on mitochondria. Biochemistry (Mosc) 70:187–194
72. Lee D, Michalak M (2010) Membrane associated Ca^{2+} buffers in the heart. BMB Rep 43:151–157
73. Kaneuchi T, Sartain CV, Takeo S, Horner VL, Buehner NA, Aigaki T, Wolfner MF (2015) Calcium waves occur as Drosophila oocytes activate. Proc Natl Acad Sci 112:791–796
74. Meldolesi J, Pozzan T (1998) The endoplasmic reticulum Ca^{2+} store: a view from the lumen. Trends Biochem Sci 23:10–14
75. Alvarez J, Montero M, García-Sancho J (1999) Subcellular Ca^{2+} dynamics. Physiology 14:161–168
76. Gunter TE, Gunter KK, Sheu SS, Gavin CE (1994) Mitochondrial calcium transport: physiological and pathological relevance. Am J Physiol Cell Physiol 267:C313–C339
77. Mishra J, Jhun BS, Hurst S, O-Uchi J, Csordás G, Sheu S-S (2017) The mitochondrial Ca^{2+} Uniporter: structure, function and pharmacology. Handb Exp Pharmacol 240:129–156
78. Alonso MT, Villalobos C, Chamero P, Alvarez J, García-Sancho J (2006) Calcium microdomains in mitochondria and nucleus. Cell Calcium 40:513–525
79. Sparagna GC, Gunter KK, Sheu S-S, Gunter TE (1995) Mitochondrial calcium uptake from physiological-type pulses of calcium. A description of the rapid uptake mode. J Biol Chem 270:27510–27515
80. Buntinas L, Gunter KK, Sparagna GC, Gunter TE (2001) The rapid mode of calcium uptake into heart mitochondria (RaM): comparison to RaM in liver mitochondria. Biochim Biophys Acta Bioenerg 1504:248–261
81. Putney JW (1986) A model for receptor-regulated calcium entry. Cell Calcium 7:1–12
82. Stathopulos PB, Ikura M (2017) Store operated calcium entry: from concept to structural mechanisms. Cell Calcium 63:3–7
83. Zhou Y, Meraner P, Kwon HT, Machnes D, Oh-hora M, Zimmer J, Huang Y, Stura A, Rao A, Hogan PG (2010) STIM1 gates the store-operated calcium channel ORAI1 in vitro. Nat Struct Mol Biol 17:112–116
84. Rizzuto R, Brini M, Murgia M, Pozzan T (1993) Microdomains with high Ca^{2+} close to IP3-sensitive channels that are sensed by neighboring mitochondria. Science 262:744–747
85. Rizzuto R, Pinton P, Carrington W, Fay FS, Fogarty KE, Lifshitz LM, Tuft RA, Pozzan T (1998) Close contacts with the endoplasmic reticulum as determinants of mitochondrial Ca^{2+} responses. Science 280:1763–1766
86. Gilabert JA, Bakowski D, Parekh AB (2001) Energized mitochondria increase the dynamic range over which inositol 1,4,5-trisphosphate activates store-operated calcium influx. EMBO J 20:2672–2679
87. Dupont G (2014) Modeling the intracellular organization of calcium signaling. Wiley Interdiscip Rev Syst Biol Med 6:227–237
88. Falcke M (2004) Reading the patterns in living cells—the physics of Ca^{2+} signaling. Adv Phys 53:255–440
89. Daub B, Ganitkevich VY (2000) An estimate of rapid cytoplasmic calcium buffering in a single smooth muscle cell. Cell Calcium 27:3–13

90. Lin K-H, Taschenberger H, Neher E (2017) Dynamics of volume-averaged intracellular Ca^{2+} in a rat CNS nerve terminal during single and repetitive voltage-clamp depolarizations. J Physiol 595:3219–3236
91. Chad JE, Eckert R (1984) Calcium domains associated with individual channels can account for anomalous voltage relations of CA-dependent responses. Biophys J 45:993–999
92. Neher E (1986) Concentration profiles of intracellular calcium in the presence of a diffusible chelator. In: Klee M, Neher E, Singer W, Heinemann U (eds) Calcium electrogenesis neuronal functioning. Springer, Berlin, pp 80–96
93. Fogelson AL, Zucker RS (1985) Presynaptic calcium diffusion from various arrays of single channels. Implications for transmitter release and synaptic facilitation. Biophys J 48:1003–1017
94. Fakler B, Adelman JP (2008) Control of KCa channels by calcium nano/microdomains. Neuron 59:873–881
95. Klingauf J, Neher E (1997) Modeling buffered Ca^{2+} diffusion near the membrane: implications for secretion in neuroendocrine cells. Biophys J 72:674–690
96. Pedersen MG, Tagliavini A, Cortese G, Riz M, Montefusco F (2017) Recent advances in mathematical modeling and statistical analysis of exocytosis in endocrine cells. Math Biosci 283:60–70
97. Augustine GJ, Santamaria F, Tanaka K (2003) Local calcium signaling in neurons. Neuron 40:331–346
98. Demuro A, Parker I (2006) Imaging single-channel calcium microdomains. Cell Calcium 40:413–422
99. Smith GD, Wagner J, Keizer J (1996) Validity of the rapid buffering approximation near a point source of calcium ions. Biophys J 70:2527–2539
100. Neher E (1998) Usefulness and limitations of linear approximations to the understanding of Ca++ signals. Cell Calcium 24:345–357
101. Gilkey JC, Jaffe LF, Ridgway EB, Reynolds GT (1978) A free calcium wave traverses the activating egg of the medaka, Oryzias latipes. J Cell Biol 76:448–466
102. Jaffe LF (2008) Calcium waves. Philos Trans R Soc Lond Ser B Biol Sci 363:1311–1317
103. Jaffe LF (1993) Classes and mechanisms of calcium waves. Cell Calcium 14:736–745
104. Woods NM, Cuthbertson KSR, Cobbold PH (1987) Agonist-induced oscillations in cytoplasmic free calcium concentration in single rat hepatocytes. Cell Calcium 8:79–100
105. MacQuaide N, Dempster J, Smith GL (2007) Measurement and modeling of Ca^{2+} waves in isolated rabbit ventricular cardiomyocytes. Biophys J 93:2581–2595
106. Thul R, Bellamy TC, Roderick HL, Bootman MD, Coombes S (2008) Calcium oscillations. Adv Exp Med Biol 641:1–27
107. Williams GSB, Molinelli EJ, Smith GD (2008) Modeling local and global intracellular calcium responses mediated by diffusely distributed inositol 1,4,5-trisphosphate receptors. J Theor Biol 253:170–188
108. Skupin A, Kettenmann H, Falcke M (2010) Calcium signals driven by single channel noise. PLoS Comput Biol. https://doi.org/10.1371/journal.pcbi.1000870
109. Schuster S, Marhl M, Höfer T (2002) Modelling of simple and complex calcium oscillations. Eur J Biochem 269:1333–1355
110. Sneyd J, Keizer J, Sanderson MJ (1995) Mechanisms of calcium oscillations and waves: a quantitative analysis. FASEB J 9:1463–1472
111. Matveev V, Sherman A, Zucker RS (2002) New and corrected simulations of synaptic facilitation. Biophys J 83:1368–1373
112. Zador A, Koch C (1994) Linearized models of calcium dynamics: formal equivalence to the cable equation. J Neurosci 14:4705–4715

Chapter 8
An Update to Calcium Binding Proteins

Jacobo Elíes, Matilde Yáñez, Thiago M. C. Pereira, José Gil-Longo, David A. MacDougall, and Manuel Campos-Toimil

Abstract Ca^{2+} binding proteins (CBP) are of key importance for calcium to play its role as a pivotal second messenger. CBP bind Ca^{2+} in specific domains, contributing to the regulation of its concentration at the cytosol and intracellular stores. They also participate in numerous cellular functions by acting as Ca^{2+} transporters across cell membranes or as Ca^{2+}-modulated sensors, i.e. decoding Ca^{2+} signals. Since CBP are integral to normal physiological processes, possible roles for them in a variety of diseases has attracted growing interest in recent years. In addition, research on CBP has been reinforced with advances in the structural characterization of new CBP family members. In this chapter we have updated a previous review on CBP, covering in more depth potential participation in physiopathological processes and candidacy for pharmacological targets in many diseases. We review intracellular CBP that contain the structural EF-hand domain: parvalbumin, calmodulin, S100 proteins, calcineurin and neuronal Ca^{2+} sensor proteins (NCS). We also address intracellular CBP lacking the EF-hand domain: annexins, CBP within intracellular Ca^{2+} stores (paying special attention to calreticulin and calsequestrin), proteins that

Authors Jacobo Elíes and Matilde Yáñez have contributed equally for this chapter

J. Elíes
Pharmacology and Experimental Therapeutics, Faculty of Life Sciences, University of Bradford, Bradford, UK

M. Yáñez · J. Gil-Longo · M. Campos-Toimil (✉)
Pharmacology of Chronic Diseases (CD Pharma), Centro de Investigación en Medicina Molecular y Enfermedades Crónicas (CIMUS), Universidad de Santiago de Compostela, Santiago de Compostela, Spain
e-mail: manuel.campos@usc.es

T. M. C. Pereira
Pharmaceutical Sciences Graduate Program, Vila Velha University (UVV), Vila Velha, ES, Brazil

Federal Institute of Education, Science and Technology (IFES), Vila Velha, ES, Brazil

D. A. MacDougall
Research and Enterprise, University of Huddersfield, Huddersfield, UK

M. S. Islam (ed.), *Calcium Signaling*, Advances in Experimental Medicine and Biology 1131, https://doi.org/10.1007/978-3-030-12457-1_8

contain a C2 domain (such as protein kinase C (PKC) or synaptotagmin) and other proteins of interest, such as regucalcin or proprotein convertase subtisilin kexins (PCSK). Finally, we summarise the latest findings on extracellular CBP, classified according to their Ca^{2+} binding structures: (i) EF-hand domains; (ii) EGF-like domains; (iii) ɣ-carboxyl glutamic acid (GLA)-rich domains; (iv) cadherin domains; (v) Ca^{2+}-dependent (C)-type lectin-like domains; (vi) Ca^{2+}-binding pockets of family C G-protein-coupled receptors.

Keywords Annexins · Ca^{2+} sensors · Calcineurin · Calmodulin · Calreticulin · EF-hand domain · Parvalbumin · Protein kinase C · S100 proteins · Synaptotagmin

8.1 Introduction

Calcium (Ca^{2+}) is a ubiquitous and highly versatile intracellular signal that operates over a wide spatial and temporal range to regulate many different cellular processes [1]. However, cellular Ca^{2+} overload can be cytotoxic and therefore a homeostatic system is necessary to regulate ionic balance. Calcium binding proteins (CBP), grouped together into a very large and heterogeneous family, not only regulate Ca^{2+} homeostasis but also control numerous Ca^{2+} signalling pathways [2]. Those that regulate Ca^{2+} levels are mainly membrane proteins (Ca^{2+} pumps) which maintain low cytosolic free Ca^{2+} concentrations under resting conditions (∼100 nM) to avoid calcium precipitation or excess of Ca^{2+} signal activity. Other CBP regulate a plethora of cellular functions by interacting with and modulating a wide range of proteins.

This review presents an update on discoveries pertaining to intracellular CBP with or without EF-hand domains, as well as extracellular CBP, in health and disease, based on our previous review [3]. Here we focus on CBP cellular functions and diseases associated with mutations and dysregulation of CPB, but not on the structural and Ca^{2+}-binding affinities of the CPB previously discussed [3].

We have also gathered evidence of how recently-developed experimental tools such as genetically encoded Ca^{2+} indicators (GECI), mutagenesis studies combined with in vivo calcium imaging, optogenetics and chemogenetics, have contributed to a better understanding of cellular Ca^{2+} signalling.

8.2 Intracellular Ca^{2+} Binding Proteins with EF-Hand Domains

The superfamily of EF-hand proteins includes a large number of members which share a common structural motif consisting of two alpha helices oriented perpendicular to each other (Fig. 8.1). The loop integrated in this sequence can

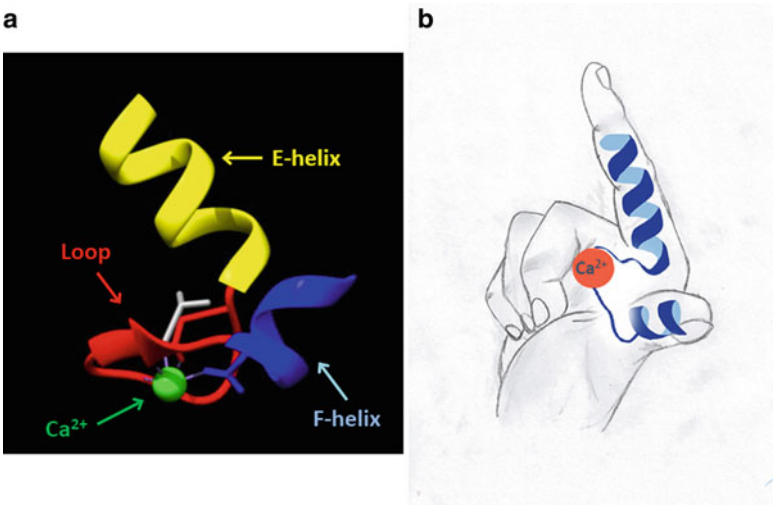

Fig. 8.1 (**a**) Representation of a EF-hand motif constituted by two alpha helices (E and F) perpendicularly placed and linked by a short loop region that facilitates Ca^{2+}binding. (**b**) The spatial arrangement of the EF-hand motif mimicks the spread thumb and the index finger of a human right hand

accommodate Ca^{2+} or Mg^{2+} with distinct geometries and the affinity for these ions is a determining factor for the function of the protein [4].

Commonly, EF-hand motifs occur in adjacent pairs giving rise to different structural and functional proteins. Conformational changes induced in EF-hand regulatory proteins usually lead to an increase in enzymatic activity or in signal transduction between cellular compartments [5]. Meanwhile, structural EF-hand domains play an important role in calcium buffering in the cytosol [3].

8.2.1 Parvalbumin Family Proteins

Traditionally, parvalbumin (PV) was considered a cytosolic Ca^{2+}-binding protein acting as a slow-onset Ca^{2+} buffer that modulates the shape of Ca^{2+} transients in fast-twitch muscles and a subpopulation of neurons. However, PV is also widely expressed in non-excitable cells like distal convoluted tubule (DCT) cells of the kidney, where it might act as an intracellular Ca^{2+} shuttle facilitating transcellular Ca^{2+} resorption by influencing mitochondrial Ca^{2+} buffering [6]. Two isoforms, alpha and beta parvalbumin, exist in vertebrates and are associated with several calcium-mediated cellular activities and physiological processes.

Parvalbumin-expressing GABAergic interneurons (PVIs), present in different brain regions, play a role in short-term synaptic plasticity [7], high frequency neuronal synchronization, maintaining a proper excitatory/inhibitory balance, and

voluntary movement tasks [8]. Their activity supports critical developmental trajectories, sensory and cognitive processing, and social behaviour [9–13]. Alterations in PVIs are commonly observed in post mortem brains of schizophrenia patients and are reported in bipolar and autism spectrum disorders [14]. Furthermore, dysregulation of PV (and calretinin) is associated with the development of affective disorders [15], anxiety, and fear extinction [16].

The use of designer receptors exclusively activated by designer drugs (DREADD) technology, a selective noninvasive chemogenetic approach, allowed the characterization of specific and reversible activation of PVIs in subregions of the hippocampus associated with social behaviour such as the dentate gyrus (DG) [17].

PVIs can generate feedforward inhibition that opposes seizure spread in both experimental models [18] and patients [19]. Moreover, in vivo optogenetic studies revealed that PVI activation interrupts spontaneous ongoing seizures [20–22].

Importantly, distribution of CBP (regulators of intracellular Ca^{2+} levels) is associated with functionally distinct neuronal subpopulations (with different neurotransmitter profiles), suggesting that CBP can serve as anatomical (and potentially functional) markers of locomotor network as recently demonstrated by Ca^{2+} imaging studies in zebra fish [23].

8.2.2 Calmodulin Family Proteins

The calmodulin family, represented by calmodulin, troponin C and essential and regulatory myosin light chains (ELC and RLC of myosin), is one of the most extensively characterized sets of the EF-hand Ca^{2+} sensor proteins. Calmodulin is a ubiquitous Ca^{2+} sensor molecule encoded by 3 distinct genes, CALM1-3. CALM modulates the activity of various proteins including ion channels [24–26] which play important roles in the generation and profile of cardiomyocyte action potentials. Mutagenesis studies in cardiac cells have identified that mutations in CALM genes are associated with severe early-onset of congenital long-QT syndrome (LQTS) [27–29], and idiopathic ventricular fibrillation [30]. A recent study of the calmodulin interactome characterised a pivotal role for this CBP in invadopodia formation associated with the invasive nature of glioblastoma multiforme (GBM) cells [31].

Troponin C, as a part of the troponin complex, is present in all striated muscle, being the protein trigger that initiates myocyte contraction [32]. Two isoforms of this protein have been described: fast skeletal muscle troponin C, which is activated by Ca^{2+} binding to two low-affinity sites on the N-terminal domain, and slow skeletal (and cardiac) muscle troponin C, which is activated by Ca^{2+} binding to a single affinity site [33].

ELC and RLC of myosin bind to the neck region (approximately 70 amino acids) of myosin heavy chain; the neighbouring head region contains the globular catalytic domain, responsible for binding to actin and hydrolysing of ATP [34].

Phosphorylation of RLC generates a structural signal transmitted between myosin molecules in the thick filament and finally to the thin filaments (actin), which forms the basis of contractile regulation in cardiac muscle [35].

8.2.3 S100 Family Proteins

The S100 proteins, a family of Ca^{2+}-binding cytosolic proteins expressed exclusively in vertebrates, constitute the major family of EF-hand calcium sensor proteins. S100 proteins are characterised by the presence of a unique S100-specific Ca^{2+}-binding loop named "pseudo EF-hand" [36], often involved in the formation of homo- or heterodimers, and the ability to bind other divalent metals such as Zn^{2+} and Cu^{2+} [37, 38].

S100 proteins have a wide range of intracellular and extracellular functions through regulating calcium balance, cell apoptosis, migration, differentiation, energy metabolism and inflammation [39–41].

Initial research showed that S100 proteins are involved in cell growth, division and differentiation [38, 42–46]. Nonetheless, more recent contributions have demonstrated the role of S100 proteins in cell migration and invasion [39, 40, 47, 48], neuronal plasticity [49, 50], cartilage repair [51], inflammation [41], and several types of cancer including lung [52], ovarian [53], pancreatic [54], and melanoma [55, 56].

The S100 family of calcium-binding proteins are gaining importance as both potential molecular key players and biomarkers in the aetiology, progression, manifestation, and therapy of neoplastic disorders, including lymphoma, pancreatic cancer and malignant melanoma [57]. For example, S100A2 is downregulated in melanoma, whilst S100A1, S100A4, S100A6, S100A13, S100B, and S100P are upregulated [56].

8.2.4 Calcineurin

Calcineurin is classified as a calmodulin-dependent serine/threonine phosphatase and is ubiquitously expressed in lower and higher eukaryotes [58]. Calcineurin plays a pivotal role in the information flow from local or global Ca^{2+} signals to effectors that control immediate cellular responses and alter gene transcription. It is a heterodimeric protein consisting of a catalytic A subunit (CNA), which is highly homologous to protein phosphatases 1 and 2, and a regulatory B subunit (CNB), that contains four EF-hand motifs and binds to CNA to regulate its phosphatase activity even in the absence of Ca^{2+} [59]. A malfunction in calcineurin-NFAT signalling can engender several pathologies, such as cardiac hypertrophy, autoimmune diseases, osteoporosis, and neurodegenerative diseases [60–62].

8.2.5 *Neuronal Ca^{2+} Sensor (NCS) Proteins*

Frequenin was the first NCS protein to be discovered and was originally designated NCS-1, due to its distribution in neuronal cell types [63]. Fourteen NCS proteins have since been identified, and classified into A-E subgroups on the basis of their amino acid sequences, including NCS-1, hippocalcin, neurocalcin-δ, VILIP1-3, recoverin, GCAP1-3 and KChIP1-4 [64]. Most are expressed only in neurons, where they have different roles in the regulation of neuronal function [65]. For instance, direct interaction of NCS1 and calneuron-1 with the GPCR cannabinoid CB1 Receptor (CB1R) determines cAMP/Ca^{2+} crosstalk which regulates the action of endocannabinoids [66]. Dysregulation of NCS proteins have been observed in several CNS disorders, such as Alzheimer's disease, schizophrenia, and cancer [67–69].

8.3 Intracellular Ca^{2+} Binding Proteins Without EF-Hand Domains

An important and heterogeneous group of proteins capable of binding Ca^{2+} but lacking the EF-hand domain are also found within eukaryotic cells. Important functional roles have been described for most of them, which has led to many being considered new potential therapeutic targets in various pathologies (see below). This is the case for annexins, whose role in different types of cancer, among other pathologies, is currently under investigation. Other CBP, such as calreticulin and calsequestrin, perform a fundamental role in Ca^{2+} homeostasis, since they fix the ion within the endoplasmic/sarcoplasmic reticulum (ER/SR), facilitating the role of these organelles as intracellular Ca^{2+} reservoirs. In addition, there are other proteins, such as regucalcin, calcium-and integrin-binding protein 1 (CIB1), proprotein convertases, or those that share a Ca^{2+}-binding domain named C2, whose Ca^{2+} binding ability serves as a regulatory mechanism for several cellular functions.

8.3.1 *Annexins*

Annexins, also known as lipocortins, are a multigene superfamily of Ca^{2+}-dependent phospholipid- and membrane-binding proteins. We have previously reviewed their classification and structure [3]. Briefly, annexins are classified into 5 families (A–E) [70–72]. The annexin A family, which is common to humans and other vertebrates, contains 12 members (annexin A1–11 and A13). Their structure consists of a highly conserved COOH-terminal core domain and a NH_2-terminal region that shows marked diversity and regulates membrane association and interaction with protein ligands [72, 73] (Fig. 8.2).

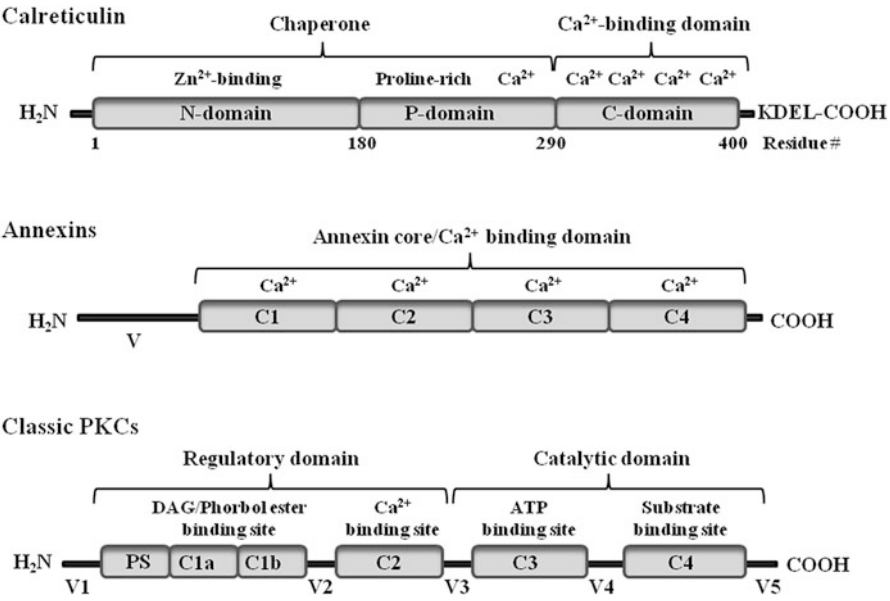

Fig. 8.2 Domain structures of calreticulin, annexins and classic PKCs. Calreticulin contains a KDEL signal that is responsible for the retrieval of ER proteins from the Golgi complex; *C* conserved regions, *V* variable regions, *PS* pseudosubstrate binding site. For more details, see main text

Upon binding and activation by Ca^{2+}, annexins undergo a conformational change which allows them to bind negatively charged membrane phospholipids and form a ternary complex bridging adjacent membranes [74].

Annexins can participate in a large number of cellular processes including anti-coagulation, anti-inflammation, endocytosis and exocytosis, membrane aggregation and fusion, regulation of membrane dynamics and organization, signal transduction, cell division, cell proliferation, differentiation, growth regulation and apoptosis (for detailed review see e.g. [75, 76]). Accordingly, their involvement in different disease states, including cancer, diabetes and inflammatory pathologies, has been extensively studied, and they have consequently become promising pharmacological targets [75–77].

Annexin A1 in particular has received much interest from multiple perspectives in the search for novel therapies. It participates in many important biological processes that encompass cell migration, recruitment, permeability, apoptosis, phagocytosis and proliferation [78, 79]. It makes up 2–4% of the total cytosolic protein in some cell types and can also be found in the nucleus [80]. The expression level of annexin A1 is modified in various tumours, suggesting a potential influence on tumorigenic and metastatic processes [81, 82] and has been found in breast cancer and squamous cancer cells [83, 84]. Annexin A1 may act as a modulator of inflammation and inflammatory pain [85, 86]. In fact, annexin 1 replicates anti-

inflammatory effects due to its potential for glucocorticoid sparing in rheumatoid arthritis [87]. As a result of these properties, annexin A1-based therapies could be used in myocardial ischaemia-reperfusion injury, limiting neutrophil infiltration and preserving both cardiomyocyte viability and left ventricular contractile function, thereby offering a novel route for treating myocardial inflammatory disorders [88].

Annexin A2 also fulfils a wide range of biological functions both at the plasma membrane and within multiple intracellular compartments [89]. It regulates tumour cell adhesion, proliferation, invasion, metastasis and tumour neovasculogenesis, thus playing a crucial role in tumour development, which in turn means it is a potential therapeutic target for efficient molecular-based strategies in tumour treatment [90] as well as a putative cancer biomarker [91, 92]. Other pathologies in which annexin A2 is identified as a potential target are ulcerative colitis [93], thrombosis and lupus [94].

Concerning annexin A3, its function either as a tumour suppressor or as a tumour promoter candidate for different cancers depending on the types of tumour cells and tissues has been investigated [95].

Annexin A4 is considered a promising therapeutic target for the treatment of platinum-resistant cancers [96]. Furthermore, studies on the function of this protein on tumour tissues have great potential importance not only for understanding cancer progression but also for developing diagnostic and therapeutic approaches [97].

Similarly, annexin A5 contributes to several aspects of tumour progression and drug resistance in certain types of cancer, so it can be used as a therapeutic target for broad applications in the diagnosis, treatment, and prognosis of tumours [98]. Other important functions that have been described for annexin A5 are its role in cell membrane repair [99, 100] and in the maintenance of pregnancy since it acts as an immunomodulator and anticoagulant at the level of the placenta [101].

Finally, other annexins with the potential to be pharmacological targets are: annexin A6 (which regulates converging steps of autophagy and endocytic trafficking in hepatocytes [102]; annexin A7 (abnormal expression of the Anxa7 gene is associated with several pathologies, including glioblastoma, melanoma, urinary bladder transitional cell carcinoma and Hodgkin lymphoma ovarian carcinoma [103]; and annexin A11 (dysregulation and mutation of this protein are involved in systemic autoimmune diseases and sarcoidosis, and are associated with the development, chemoresistance and recurrence of cancers [104].

8.3.2 Ca^{2+} Binding Proteins at Intracellular Ca^{2+} Stores

The SR and ER of eukaryotic cells act as intracellular reservoirs of readily-releasable Ca^{2+} ions. Several CBP within these organelles are essential for this function. Calreticulin, BiP/Grp78, glucose-regulated protein 94 (Grp 94) and protein disulfide isomerase (PDI) are CBP that participate in smooth muscle SR/ER-dependent Ca^{2+} homeostasis and act as protein chaperones [105, 106].

Amongst these CBP, calreticulin is arguably the most important. This protein consists of three distinct structural and functional domains (Fig. 8.2) [3, 107]. In addition to SR/ER, it is also present on the membrane of other subcellular organelles, cell surface and in the extracellular environment where it contributes to different physiological and pathological processes [108]. Calreticulin regulates Ca^{2+} uptake and release within the ER and mitochondria [109, 110], and it is a central component of the folding quality control system of glycoproteins [111, 112].

Outside of the ER, calreticulin also regulates critical biological functions including cell adhesion, gene expression, and RNA stability [107]. New roles of calreticulin in the extracellular space such as an involvement in cutaneous wound healing and possible diagnostic applications of calreticulin in blood or urine have also emerged [108].

A possible role for calreticulin in the development of several human pathologies, including congenital arrhythmias and some cancers (including oral, esophagus, breast, pancreas, gastric, colon, bladder, prostate, vagina, ovarian and neuroblastoma) has been described [107, 109, 112, 113]. Mutations in the calreticulin gene, for example, are present in myeloproliferative neoplasms [114]. Thus, the multifaceted properties of calreticulin may in the future provide a means to treat a number of diseases [115].

BiP/Grp78 is an immunoglobulin binding protein that can bind Ca^{2+} at relatively low stoichiometry [116]. As a consequence, its over-expression increases the Ca^{2+} pool available for transfer to mitochondria. Grp94 protein is a high affinity CBP whose inhibition induces Ca^{2+}-mediated apoptosis [117]. PDI is a major CBP of the ER that is also involved in protein folding and isomerization [118]. Increasing evidence suggests that PDI supports the survival and progression of several cancers. However, no PDI inhibitor has been approved for clinical use [119].

The storage and rapid release of Ca^{2+} from the skeletal and cardiac SR reservoirs has been associated with calsequestrin [120, 121], as previously reviewed [3]. Both calsequestrin 1 and calsequestrin 2 subtypes act as SR luminal sensors for skeletal or cardiac ryanodine receptors together with the proteins triadin and junctin [122, 123] (Fig. 8.3). Calsequestrin communicates changes in the luminal Ca^{2+} concentration to the cardiac ryanodine receptor channel [124] and it has been demonstrated that a lack of this protein causes important structural changes in the SR and alters the storage and release of appropriate levels of SR Ca^{2+} [125]. Alterations in calsequestrin expression are an underlying cause of cardiac complications. For example, loss of calsequestrin 2 causes abnormal SR Ca^{2+} release and selective interstitial fibrosis in the atrial pacemaker complex (which disrupts sinoatrial node pacemaking but enhances latent pacemaker activity) and creates conduction abnormalities and increased susceptibility to atrial fibrillation [126]. Also, a change in calsequestrin expression is involved in the pathogenesis of Duchenne progressive muscular dystrophy [127]. In addition, calsequestrin-1 knockout mice suffer episodes of exertional/environmental heatstroke when exposed to strenuous exercise and environmental heat, and aerobic training significantly reduces mortality rate by lowering oxidative stress [128].

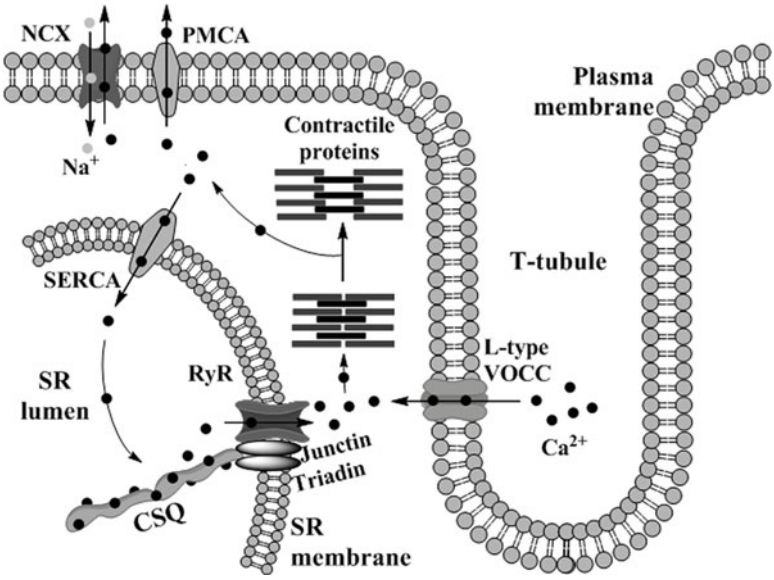

Fig. 8.3 Calsequestrin (CSQ) binds Ca^{2+} within the SR of cardiac myocytes. It is attached to the ryanonide receptor through the junctin-triadin protein complex. *NCX* Na^{2+}/Ca^{2+} exchanger, *PMCA* plasma membrane Ca^{2+} ATPase, *VOCC* voltage-operated Ca^{2+} channel, *SERCA* sarcoplasmic/endoplasmic reticulum Ca^{2+} ATPase, *RyR* ryanodine receptor

8.3.3 Ca^{2+} Binding Proteins with C2 Domains

The C2 domain is a Ca^{2+}-binding motif which also has the ability to bind phospholipids, inositol polyphosphates and some other intracellular proteins. It was first identified as Conserved Domain 2 of the PKC kinase family, hence its name [129, 130]. It has been found in well over two hundred different proteins, making it the second most common lipid binding domain [3, 131] and it mediates a wide range of intracellular processes, such as membrane trafficking, generation of lipid-second messengers, activation of GTPases, and control of protein phosphorylation [132]. Some of the best-known proteins that contain a C2 domain are PKC, synaptotagmins, phospholipase C (PLC) and phospholipase A (PLA).

PKC is composed of a large family of lipid-activated enzymes that regulate the function of other proteins via phosphorylation of serine and threonine residues (Fig. 8.2). Multiple isoforms of PKC, ten of them found in mammals, can exist in the cytosol in a soluble form or bind to the plasma membrane, participating in many functions, such as intracellular signalling, secretion, cell growth and differentiation [133, 134].

PKC activity depends on the presence of several lipid cofactors and Ca^{2+}, although these requirements vary for different isozymes. Three categories have been

established for mammalian PKCs: classical, novel and atypical isoforms, the last lacking the C2 domain [134, 135]. Classical isozymes contain a C2 type I Ca^{2+}- and phospholipid-binding domain and require Ca^{2+} in order to stabilize interaction with the plasma membrane [133]. On the other hand, novel isozymes contain a variant of the C2 domain (type 2) that lacks key Ca^{2+}-coordinating residues; as a result, novel isozymes are not sensitive to Ca^{2+} [135]. Therefore, classical PKC isoforms are activated by Ca^{2+} and diacylglycerol (DAG), whereas novel PKC isoforms are activated by DAG, but not Ca^{2+}. Atypical PKC isoforms require neither Ca^{2+} nor DAG for activation [136].

A role for different PKC isozymes has been described in a large number of diseases, including cardiac pathologies, cancer, dermatological diseases, lung and kidney diseases, autoimmune diseases, neurological diseases and some others (for detailed review see e.g. [137]).

Synaptotagmins are a family of transmembrane Ca^{2+} sensors found in synaptic vesicles and in secretory granules of endocrine cells that have a main role in exocytosis [2, 138, 139]. They bind Ca^{2+} with low affinity by means of two C2 domains: C2A and C2B [140]. The most studied protein in this family is synaptotagmin I, which functions as a sensor for evoked, synchronous neurotransmitter release in neurons [141].

Otoferlin is another transmembrane protein with a C2 domain that binds Ca^2 and membranes and triggers the fusion of neurotransmitter-filled vesicles with the plasma membrane, in conjunction with a specific ensemble of molecular machinery proteins [142]. Its significance in priming and fusion of synaptic vesicles during sound encoding is clear, and mutations in otoferlin cause human deafness [143].

Other proteins involved in the modification of lipids that also contain functional Ca^{2+}-binding C2 domains are phosphoinositide-specific PLC, which liberates IP_3 and DAG in response to mitogenic signals that raise intracellular Ca^{2+} levels [144] and PLA2, which liberates arachidonic acid from glycerophospholipids to initiate production of leukotrienes and prostaglandins, potent mediators of inflammation [145].

8.3.4 Other Intracellular CBP Without EF-Hand Domains

Regucalcin is a CBP with multiple physiological functions that has been localised to the cell nucleus and cytoplasm, as well as in the mitochondrial fraction [146]. It is involved in aging, participating in brain calcium signalling [147]. Also, it may be a key molecule in lipid metabolic disorder and diabetes [148]. In addition, regucalcin is implicated in carcinogenesis and the enhancement of regucalcin gene expression may reveal preventive and therapeutic effects in the progression of cancer cells. Thus, it has been suggested that targeting the regucalcin gene could be a useful tool in cancer therapy [149, 150].

Proprotein convertase subtilisin kexins (PCSK) are a family of CBP that activate other proteins. Nine subtypes of PCSKs with varying functions and tissue distri-

butions have been described [151]. Some of these proteins have been studied as possible therapeutic targets. For example, inhibition of PCSK9 holds considerable promise as a therapeutic option for decreasing cardiovascular disease risk, since it plays an important role in the regulation of cholesterol homeostasis [152]. Also, furin has been the most intensively researched member of the family with regard to tumur regulation, promotion, and progression [153] and there are numerous patents related to the uses of this protein and its inhibitors as therapeutics [154].

8.4 Extracellular Ca^{2+} Binding Proteins

The extracellular Ca^{2+} ($Ca^{2+}{}_o$) concentration in mammals is maintained at about 1.2 mM [155]. Deviations in this concentration lead to severe pathological malfunctions. Different organs and hormones must cooperate to regulate the uptake, excretion and recycling of calcium in the body and, as a consequence, serum Ca^{2+} concentration. To regulate $Ca^{2+}{}_o$ homeostasis in the body, cells must be equipped with the ability to monitor its level. In this regard, several extracellular Ca^{2+} binding proteins (ECBP) have been discovered and their roles investigated. The study of extracellular Ca^{2+} as a messenger has probably been hampered by the generally accepted (although erroneous) view that the Ca^{2+} concentration in the extracellular space does not fluctuate, as well as by the technical difficulties inherent in measuring spatial and temporal changes in extracellular Ca^{2+} concentration [156].

If the Ca^{2+} concentration in the extracellular space did not differ from that measured in serum, Ca^{2+} would not play an extracellular messenger role. ECBP would only use Ca^{2+} for static roles (e.g. formation of active sites in enzymes or active conformations in receptors, structure protein stabilization and formation of supramolecular structures with other proteins or carbohydrates) or to maintain extracellular Ca^{2+} homeostasis.

Despite the constant concentration of serum Ca^{2+}, there are clear demonstrations that Ca^{2+} levels of interstitial fluids in many tissues differ from those usually measured in serum and, do indeed fluctuate (e.g. fluctuations are very likely to occur during intracellular Ca^{2+} signalling events) [156, 157]. Therefore, extracellular Ca^{2+} could fulfil a more dynamic function as a 'first messenger' in extracellular signal transduction pathways and contributor to autocrine/paracrine cell-to-cell communication. This role for $Ca^{2+}{}_o$ is possible only if ECBP undergo a conformational change in response to physiological fluctuations in extracellular Ca^{2+} concentrations; this would allow interactions with, and modulation of, specific target proteins.

ECBP are modulators of numerous cellular functions (e.g. neuronal signalling, blood-clotting, complement activation, cell-cell interactions, cell-matrix interactions, receptor-ligand interactions, Ca^{2+} transport and Ca^{2+} homeostasis, cardiovascular remodelling, tumour cell migration and cancer metastasis regulation, gene expression, apoptosis, and more) and may serve as important therapeutic targets (see the following sections). In this section we review the main ECBP, focussing on some

proteins that could be $Ca^{2+}{}_o$ sensors and mediators of $Ca^{2+}{}_o$ signalling. We have grouped ECBP by shared Ca^{2+}-binding domain structures (also see Table 8.1).

8.4.1 Extracellular Ca^{2+} Binding Proteins with EF-Hand Domains

Ca^{2+}-binding proteins containing a pair of EF-hand motifs are present within cells as described in Sect. 8.2, and in the extracellular environment (or matrix). EF-hand proteins are widely found in animal genomes and distributed throughout the cell [158, 159]. These proteins are fundamental for many cellular functions and at the same time are associated with neuronal diseases, cardiac arrhythmias, cancer and autism [160]. Physiologically, all EF-hand proteins can be divided into two groups: (1) calcium buffers, controlling the level of free cytosolic Ca^{2+} or (2) calcium sensors, acting to translate the signal to various responses [160, 161]. In this context, some examples of these proteins will be explained below.

Osteonectin, also known as BM-40 or SPARC (secreted protein acidic and rich in cysteine), is a 32-kDa calcium-binding glycoprotein matrix protein that serves as the prototype of the osteonectin family [162]. Other members of this family are hevin, QR1, testicans 1-3, tsc 36, SMOC-1 and SMOC-2. The osteonectin family is characterized by a follistatin-like, cysteine rich domain and a C-terminal module with two EF-hand Ca^{2+}-binding domains; each EF-hand domain is predicted to bind one Ca^{2+} ion [163]. The EF-hand pair is very similar to those of intracellular EF-hand proteins such as calmodulin. The affinity of the Ca^{2+}-binding domain for Ca^{2+} is high; for example, osteonectin binds 2 Ca^{2+} with a K_{d1} of 490 nM and K_{d2} of 26 nM [164]. The osteonectin-like proteins modulate cell function by interacting with cell-surface receptors, metalloproteinases, growth factors and other bioeffector molecules and proteins of the matrix such as collagens, secreted by many types of cells, e.g. endothelial cells, fibroblasts, and fragments of megakaryocyte-platelets [162, 165]. Different lines of evidence link osteonectin-like proteins with human cancer progression [166, 167].

Another example is the FKBP65 (or FKBP10) protein. Its molecular structure includes four PPIase–FKBP type domains that are involved in activation of the release of ER Ca^{2+} stores. Moreover, its expression coincides with increased expression of tropoelastin and type I collagen expression [168, 169]. Although not all of its biological roles are known, emerging genetic studies have shown that, in humans, mutation of this protein might cause a form of osteogenesis imperfecta, a brittle bone disease resulting from deficient secretion of mature type I collagen [168, 169].

Table 8.1 Main extracellular Ca^{2+}- binding domain structures

Group and calcium-binding domain structure	Main proteins	Possible role of Ca^{2+}- binding to proteins
EF-hand domains	Osteonectin family: osteonectin, hevin, QR1, testicans 1–3, tsc 36, SMOC-1 and SMOC-2, FKBP65 (or FKBP10)	Formation of binding sites for extracellular ligands
		Ca^{2+} signal transmission?
EGF-like domains	EGF protein, Neuregulin, Transforming growth factor α, Coagulation factors VII, IX and X, protein C and protein S	Induction of protein conformation required for biological activity
	Fibrillin	Stabilization of proteins
	Notch and delta receptors	Ca^{2+} signal transmission?
	LDL receptors	
ɣ-Carboxyl glutamic acid-rich domains	Coagulation factors II, VII, IX and X, protein C and protein Z	Anchoring of proteins to membrane
	Osteocalcin, matrix GLA protein and periostin, telopeptide of type I collagen, bone alkaline phosphatase	Activation of proteins
	Growth arrest-specific protein 6, matrix Gla protein-MGP	
Cadherin domains	Cadherin family: classical cadherins, protocadherins, and atypical cadherins (Fat, Dachsous, and Flamingo)	Modulation of mechanical integrity and mechanotransduction capability of proteins (using an adaptor complex, cadherins connect to the cytoskeleton)
		Ca^{2+} signal transmission
(C)-type lectin-like domains	Selectins	Modulation of ligand binding
	Mannose receptor family	Stabilization of proteins
	Dendritic cell-specific ICAM-3 grabbing non-integrin molecule	Cell-cell adhesion
	Several collectins (e.g. mannose-binding protein)	Apoptotic process
Ca^{2+}-binding pockets of family C GPCRs	Ca^{2+} -sensing receptor	Change of receptor conformation
	Metabotropic glutamate receptors	Ca^{2+} signal transmission through G-proteins
	$GABA_B$ receptors	

All Ca^{2+}-binding domain structures have in common a highly negative surface potential usually associated with Asp or Glu residues

8.4.2 *Extracellular Ca^{2+} Binding Proteins with EGF-Like Domains*

The epidermal growth factor (EGF)-like domain is one of the most widely distributed disulfide-containing domains in nature and is involved in multiple cellular regulations [170]. Its name derives from the epidermal growth factor where it was first described [171]. Normally, EGF domains contain six cysteine residues that form disulphide bridges. Although many EGF-like domains participate in Ca^{2+}-dependent processes by responding to local Ca^{2+} concentrations, very little detail has been resolved concerning how this regulation is programmed at the molecular level [170]. What is known is that a subset of EGF-like domains also contains a Ca^{2+}-binding domain with a wide range of high Ca^{2+} affinities (K_d from 0.1 mM to nM values) and these represent prevalent extracellular Ca^{2+}-binding sites [172–179].

Among the proteins containing Ca^{2+}-binding EGF-like domains are those involved in cell growth (e.g. EGF, neuregulin and transforming growth factor α), blood coagulation, fibrinolysis and the complement system (e.g. factors VII, IX and X, protein C and protein S), matrix proteins (e.g. laminin, fibrillin and nidogen) and cell surface receptors (e.g. selectins, low density lipoprotein receptor and Notch receptor and their homologues) [3, 176, 177]. The coagulation enzymes, factors VII, IX and X and protein C, all have two EGF-like domains, whereas the cofactor of activated protein C, protein S, has four EGF-like domains in tandem [178]. On the other hand, fibrillin, low density lipoprotein receptor and the developmentally important receptor Notch have numerous EGF-like domains in tandem that might mediate heterophilic interactions with other family members based on binding between the EGF-like repeats of adjacent receptors [176, 179–181].

Additionally, recent studies have demonstrated that Ca^{2+} binding to an EGF-like domain is important to orient neighbouring domains and to induce the protein conformation required for biological activity [170, 178, 182]. For example, Ca^{2+} binding to an EGF-like domain contributes to protein stability [181, 182]. Moreover, the EGF-like domains seem to be involved in protein-protein interactions, receptor-ligand interactions and blood coagulation [175, 181]. Interestingly, some studies have demonstrated that mutations in EGF-like domains might be involved in hemophilia B, Marfan syndrome or hypercholesterolemia (due to mutation of factor IX, fibrillin and low-density lipoprotein receptor, respectively) [172, 183, 184].

8.4.3 *Extracellular Ca^{2+} Binding Proteins with ɣ-Carboxyl Glutamic Acid-Rich Domains*

Several human proteins have a ɣ-carboxyl glutamic acid (GLA)-rich domain that binds Ca^{2+}. These proteins play key roles in the regulation of blood coagulation

(factors II-prothrombin- VII, IX, X, protein C, protein S, and protein Z), bone metabolism (osteocalcin, matrix GLA protein, periostin, telopeptide of type I collagen and bone alkaline phosphatase) and vascular biology (growth arrest-specific protein 6, matrix Gla protein-MGP) [185–188]. It is important to emphasize that in addition to the GLA-rich domain, several blood-clotting proteins also have EGF-like domains as described above. The GLA-rich domain consists of approximately 45 amino acids, of which the 10–12 glutamic acids are carboxylated to GLA by a vitamin K dependent carboxylase [189–191]. In coagulation factors VII, IX and X and protein C, the GLA-rich domain occupies the N-terminal half of the molecule and is followed by two EGF-like domains. Regarding protein S, the GLA-rich domain also occupies the N-terminal half of the molecule and is followed by a thrombin-sensitive domain and four EGF-like domains [172, 192]. According to different structural studies, it is known that the number of Ca^{2+} ions associated with the GLA domains seems to be variable. For example, in the GLA domain of human FVIIa, nine of the ten GLA residues bind seven Ca^{2+} [193, 194].

More specifically, Ca^{2+} binding to blood-clotting proteins is required for initiation of the coagulation cascade at sites of injury. The GLA domains of most coagulation factors have similar Ca^{2+} affinities, the average K_d being ~0.5 mM [195, 196]. Thus, coagulation factors should generally be in the Ca^{2+}-saturated form in the extracellular space and Ca^{2+} should play a structural role rather a regulatory role. However, local fluctuations of Ca^{2+} levels have been described and a regulatory role of Ca^{2+} may occur in some circumstances [156]. For example, 4-hydroxycoumarin anticoagulants are currently used in clinical practice because they indirectly inhibit the vitamin K dependent carboxylation of several blood-clotting proteins; as a consequence, clotting proteins cannot bind Ca^{2+} and they cannot participate in the coagulation cascade [155, 197]. However, this intervention may not be free of risks. Since γ-carboxylated coagulation proteins are potent inhibitors of vascular calcification, some recent studies have suggested that anticoagulants such as warfarin may accelerate vascular calcification in addition to frequent or irregular heavy bleeding [198–200]. Although there are already studies demonstrating this effect, clinical data need to be supplemented with controlled studies to confirm this plausible hypothesis [200].

Another protein involved in arterial calcification is MGP, a 10-kDa vitamin K-dependent extracellular matrix protein. Although the normal physiological process by which MGP inhibits vascular calcification is still unknown, recent evidence demonstrates that MGP regulates vascular calcification by binding to and inhibiting bone morphogenic protein 2 and preventing the deposition of calcium phosphate in vascular matrix [201–203]. The association with vascular calcification and atherosclerotic disease may be justified by several single nucleotide polymorphisms (SNPs) of the MGP gene, compromising its function [203, 204].

8.4.4 *Extracellular Ca^{2+} Binding Proteins with Cadherin Domains*

As their name implies, cadherins are Ca^{2+}-dependent adherent receptors that mediate adhesion between cells (extracellular domains of cadherins from adjacent cells form trans bonds). Moreover, they sense and transmit several extracellular signals to the inside of the cell [205]. The cadherin family includes classical cadherins, desmosomal cadherins, protocadherins and atypical cadherins. All are single membrane-spanning proteins with the exception of flamingo, an atypical cadherin that is a seven-pass membrane protein. As we have previously reviewed [3], the different types of cadherins have diverse structures, but all possess Ca^{2+}-binding extracellular repeats of the same protein chain and may act as Ca^{2+} sensors that respond to external Ca^{2+} fluctuations [206, 207].

Once a cadherin has been activated by an appropriate signal, the cytoplasmic tails connect to the cytoskeleton using an adaptor complex formed by three proteins (p120 catenin, β-catenin and α-catenin) and, as a consequence, several important intracellular signalling pathways are modulated [205]. Cadherins are involved in development, morphogenesis, synaptogenesis, differentiation and carcinogenesis (for detailed review see e.g. [206]).

Because of their essential biological functions, cadherins are being investigated as drug targets, especially in oncology. For example, neural (N)-cadherin is involved in angiogenesis and the maintenance of blood vessel stability [208]. Since tumour growth depends on an adequate blood supply, it could be affected by N-cadherin antagonists [209]. Also, E-cadherin plays an important role in epithelial cell adhesion and the loss of its function is a major contributor to cancer progression because most solid tumours arise from epithelial tissue [210, 211].

8.4.5 *Extracellular Ca^{2+} Binding Proteins with Ca^{2+}-Dependent (C)-Type Lectin-Like Domains*

The superfamily of proteins containing C-type lectin-like domains (CTLDs) is a large group of extracellular proteins with diverse functions of biomedical interest. Curiously, the term ‘C-type lectin’ was introduced to distinguish a group of Ca^{2+}-dependent (C-type) carbohydrate-binding (lectin) animal lectins from the other (Ca^{2+}-independent) type [212].

CTLD are present not only in C-type lectins, but also in other extracellular proteins. They are found in more than 1000 proteins and represent a ligand-binding motif that is not necessarily restricted to binding sugars [213]. C-type lectins are found either as transmembrane proteins (e.g. selectins, the mannose receptor family and the dendritic cell-specific ICAM-3 grabbing non-integrin molecule) or as secreted soluble proteins (e.g. mannose-binding protein and other collectins) [3, 212]. The C-type lectin fold is rare and complex. It presents a compact

domain of approximately 120 amino acid residues with a double-looped ('loop-in-a-loop'), two-stranded antiparallel β-sheet formed by the amino-and carboxy-terminal residues connected by two α-helices and a three-stranded antiparallel β-sheet [213]. This secondary loop is involved in Ca^{2+}-dependent carbohydrate binding, the main CTLD function, and in interactions with other ligands [214]. Four Ca^{2+}-binding sites are consistently detected in the CTLD domain, but depending on the particular CTLD sequence and on experimental conditions, zero, one, two or three sites are occupied [212, 214]. Ca^{2+} is involved in ligand binding to C-type lectins and also serves to stabilize their molecular structure [215, 216]. Since changes in Ca^{2+} concentration dramatically enhance carbohydrate binding by C-type lectins, it has been suggested that physiological fluctuations of extracellular Ca^{2+} have a regulatory effect on ligand binding by C-type lectins [216, 217]. Additionally, C-type lectins are involved in many cell surface carbohydrate recognition events, e.g. cell-to-cell contact and recognition of pathogens, cell-to-cell adhesion and apoptosis [215, 218, 219].

8.4.6 Ca^{2+}-Binding Pockets of Family C G-Protein-Coupled Receptors

Family C of the superfamily of G protein-coupled receptors (GPCRs) includes the Ca^{2+}-sensing receptor (CaR), eight metabotropic glutamate receptors (mGluRs), two $GABA_B$ receptors, three taste (T1R) receptors, one L-amino acid receptor (GPRC6A), and five orphan receptors [220]. The function of some of these receptors is altered in response to small fluctuations in $Ca^{2+}{}_o$ concentrations, suggesting Ca^{2+} sensing and Ca^{2+} signalling regulator capabilities.

8.4.6.1 Ca^{2+}-Sensing Receptor (CaR; Also Named CaSR or CaS)

CaR was initially identified in bovine parathyroid glands as a plasma membrane-located GPCR and was the first GPCR recognised to have Ca^{2+} as its major physiological agonist. The main function originally ascribed to CaR was the control of $Ca^{2+}{}_o$ concentrations by modulating parathyroid hormone (PTH) secretion. Later, CaR was also identified on the surface of cells from multiple tissues, e.g. bone, thyroid, kidney, nervous system, gastrointestinal system, ovary, mamma, prostate, blood vessels and heart cells, pancreas as well as monocytes, macrophages, dendritic and intestine and haematopoietic stem cells [173, 221]. Furthermore, it was found that other agonists and allosteric modulators interact with CaR and influence its response to Ca^{2+}, and that CaR has several non-calciotropic roles.

CaR has a long extracellular amino-terminal domain of 612 amino acids called a Venus flytrap module, containing a ligand binding pocket that gives the receptor the necessary sensitivity to detect small fluctuations in external Ca^{2+} concentration.

According to Silve et al. [222], the Ca^{2+}-binding site in CaR hosts a set of polar residues directly involved in Ca^{2+} coordination (Ser-170, Asp-190, Gln-193, Ser-296, and Glu-297), and an additional set of residues that completes the coordination sphere of the cation (Phe-270, Tyr-218, and Ser-147). The Venus flytrap module is followed by a seven transmembrane helix cassette (250 amino acids) and a C-terminal domain (216 amino acids) [223]. CaR activity is modulated by changes in $Ca^{2+}{}_o$ concentrations occurring in the mM range. CaR is coupled through G-proteins, preferentially Gαq/11, Gαi/o, Gαs and Gα12/13 subunits, to intracellular signal transduction pathways involving phospholipase C, cytosolic phospholipase A_2 and various MAP kinase proteins [155, 156, 224].

An increase in serum Ca^{2+} concentration negatively regulates PTH secretion via CaR. The vital role of CaR in maintaining normal systemic Ca^{2+} homeostasis is illustrated by more than 230 different germline mutations in CaR that cause hypocalcemic and hypercalcemic disorders [225] and by mouse knockout models. Complete ablation of functional CaR is lethal, resulting in severe skeletal demineralization, extremely high Ca^{2+} serum concentration, growth defects and ultrastructural changes in the epidermis [157].

In vitro experiments have revealed that CaR on the cell surface responds to Ca^{2+} exported from the same or a neighbouring cell during Ca^{2+} signalling events; $Ca^{2+}{}_o$ might thus act as an autocrine/paracrine messenger via CaR [157]. CaR not only responds to Ca^{2+}, but also to other agonists (inorganic divalent and trivalent cations, polyamines, aminoglycoside antibiotics, basic polypeptides) and to allosteric modulators (L-amino acids, glutathione analogs, small molecule calcimimetics, small molecule calcilytics) that influence the effect of Ca^{2+} [156, 224]. CaR can discriminate between different ligands and selectively activate one signalling transduction pathway in response to a particular ligand (a phenomenon known as biased agonism) [224].

It is therefore not surprising that CaR is important for processes other than maintenance of systemic Ca^{2+} homeostasis, e.g. regulation of hormone and fluid secretion, activities of various ion channels, synaptic transmission and neuronal activity via multiple signaling pathways, gene expression, programmed cell death (apoptosis), cellular proliferation, development and more [155, 226, 227].

Activators of the Ca^{2+} binding site in CaR (orthosteric agonists and also termed type I calcimimetics), synthetic allosteric activators of CaR (termed type II calcimimetics) and inhibitors of CaR (termed calcilytics) have been developed for clinical use. Strontium, which can be considered a type I calcimimetic, is currently used in osteoporosis in the form of strontium ranelate. Cinnacalcet, a type II calcimimetic, is currently used in primary and secondary hyperparathyroidism and parathyroid carcinoma. Calcilytics failed in previous clinical trials as anabolic therapies for the treatment of osteoporosis but are now being evaluated for the treatment of some cases of hypocalcemic and hypercalciuric disorders [228]. Sustained elevations of PTH, as occurs in hyperparathyroid states, have a net catabolic effect on bone, favouring resorption, whereas short bursts are anabolic,

favouring formation [229]. Therefore, continuous administration of a calcimimetic or intermittent administration of a calcilytic could promote anabolic over catabolic actions.

Because Ca^{2+} and CaR are implicated in many physiopathological conditions, the use of calcilytics or CaR allosteric activators have been proposed for the treatment of a range of disorders [223]. For instance, the former could be beneficial for the treatment of Alzheimer's disease, osteolytic breast cancer, pulmonary hypertension, asthma and other inflammatory lung disorders, whilst the latter could be useful in inflammatory bowel disease, secretory diarrhoea, hypertension, and colon cancer.

8.4.6.2 Metabotropic Glutamate Receptors (mGluRs) and $GABA_B$ Receptors

Metabotropic glutamate receptors are family C GPCRs and structurally similar to CaR. On the basis of sequence homology to CaR and several experimental results, it was postulated that some mGluRs can respond to external Ca^{2+} fluctuations [157, 220]. mGluRs are expressed principally in the brain, where the levels of external Ca^{2+} are highly dynamic. A Ca^{2+}-binding site in the mGluR1α extracellular domain was recently identified: it comprises Asp-318, Glu-325 and Asp-322 and the carboxylate side chain of Glu-701 [230]. External Ca^{2+} has been proposed: (i) to directly activate mGluRs; (ii) to increase sensitivity of mGluRs to L-glutamate; (iii) to modulate mGluRs synergistically with L-glutamate; and (iv) to modulate actions of allosteric drugs targeting mGluRs [220, 230]. External Ca^{2+} also modulates other type C GPCRs, namely $GABA_B$ receptors, although it is not thought that this occurs directly [155]. The numerous clinical effects in which these receptors are involved have been the subject of a large number of studies and reviews (see e.g. [231–234]).

8.5 Concluding Remarks

Over the few last decades, research on CBP has resulted in a profusion of important advances. Crystallography, molecular biology, microscopy and other techniques have widened our knowledge on the sequence, structure, and functionality of CBP. Many new proteins equipped with the ability to bind Ca^{2+} have been discovered and there has been a great effort to rationally classify them. Currently, much of the research in this field is oriented towards understanding the physiological roles of these proteins. This is why ever more CBP are emerging as potential targets in therapeutic approaches for a staggering array of diseases. Nonetheless, differentiating between structural and regulatory roles for Ca^{2+} binding (especially in the case of extracellular CBP) remains a significant challenge. Also, although progress has been made, determining which proteins act exclusively as Ca^{2+} sensors and which act uniquely as Ca^{2+} buffers is still not straightforward and, indeed, for

some CBP, both functions are observed. A deeper understanding of the structure and function of CBP, together with a better definition of their physiological role, will allow us to further investigate targeting of these proteins in novel therapeutic strategies.

Author Contribution JE was responsible for the writing of Sect. 8.2; he also participated in the drafting of the Introduction and Concluding Remarks sections. MY was responsible for the writing of Sect. 8.2. TMCP and JGL were responsible for the writing of Sect. 8.4. DAM contributed throughout, provided focus and flow to the various sections of the review, and oversaw/edited written English. MCT was responsible for the writing of Sect. 8.3; he also participated in the writing of the Introduction and Concluding Remarks sections and in the coordination of all authors.

References

1. Berridge MJ, Bootman MD, Roderick HL (2003) Calcium signalling: dynamics, homeostasis and remodelling. Nat Rev Mol Cell Biol 4:517–529
2. Carafoli E, Santella L, Branca D, Brini M (2001) Generation, control, and processing of cellular calcium signals. Crit Rev Biochem Mol Biol 36:107–260
3. Yáñez M, Gil-Longo J, Campos-Toimil M (2012) Calcium binding proteins. Adv Exp Med Biol 740:461–482
4. Lewit-Bentley A, Réty S (2000) EF-hand calcium-binding proteins. Curr Opin Struct Biol 10:637–643
5. Skelton NJ, Kordel J, Akke M, Forsen S, Chazin WJ (1994) Signal transduction versus buffering activity in Ca^{2+}-binding proteins. Nat Struct Biol 1:239–245
6. Henzi T, Schwaller B (2015) Antagonistic regulation of parvalbumin expression and mitochondrial calcium handling capacity in renal epithelial cells. PLoS One 10:e0142005
7. Caillard O, Moreno H, Schwaller B, Celio MR, Marty A (2000) Role of the calcium-binding protein parvalbumin in short-term synaptic plasticity. Proc Natl Acad Sci 97:13372–13377
8. Estebanez L, Hoffmann D, Voigt BC, Poulet JFA (2017) Parvalbumin-expressing GABAergic neurons in primary motor cortex signal reaching. Cell Rep 20:308–318
9. Yizhar O, Fenno LE, Prigge M, Schneider F, Davidson TJ, O'Shea DJ et al (2011) Neocortical excitation/inhibition balance in information processing and social dysfunction. Nature 477:171–178
10. Inan M, Petros TJ, Anderson SA (2013) Losing your inhibition: linking cortical GABAergic interneurons to schizophrenia. Neurobiol Dis 53:36–48
11. Zikopoulos B, Barbas H (2013) Altered neural connectivity in excitatory and inhibitory cortical circuits in autism. Front Hum Neurosci 7:609
12. Hu H, Gan J, Interneurons JP (2014) Fast-spiking, parvalbumin(+) GABAergic interneurons: from cellular design to microcircuit function. Science 345:1255263
13. Hashemi E, Ariza J, Rogers H, Noctor SC, Martínez-Cerdeño V (2017) The number of parvalbumin-expressing interneurons is decreased in the medial prefrontal cortex in autism. Cereb Cortex 27:1931–1943
14. Steullet P, Cabungcal JH, Coyle J, Didriksen M, Gill K, Grace AA et al (2017) Oxidative stress-driven parvalbumin interneuron impairment as a common mechanism in models of schizophrenia. Mol Psychiatry 22:936–943
15. Brisch R, Bielau H, Saniotis A, Wolf R, Bogerts B, Krell D et al (2015) Calretinin and parvalbumin in schizophrenia and affective disorders: a mini-review, a perspective on the evolutionary role of calretinin in schizophrenia, and a preliminary post-mortem study of calretinin in the septal nuclei. Front Cell Neurosci 9:393

16. Soghomonian JJ, Zhang K, Reprakash S, Blatt GJ (2017) Decreased parvalbumin mRNA levels in cerebellar purkinje cells in autism. Autism Res 10:1787–1796
17. Zou D, Chen L, Deng D, Jiang D, Dong F, McSweeney C et al (2016) DREADD in parvalbumin interneurons of the dentate gyrus modulates anxiety, social interaction and memory extinction. Curr Mol Med 16:91–102
18. Cammarota M, Losi G, Chiavegato A, Zonta M, Carmignoto G (2013) Fast spiking interneuron control of seizure propagation in a cortical slice model of focal epilepsy. J Physiol 591:807–822
19. Schevon CA, Weiss SA, McKhann G Jr, Goodman RR, Yuste R, Emerson RG et al (2012) Evidence of an inhibitory restraint of seizure activity in humans. Nat Commun 3:1060
20. Krook-Magnuson E, Armstrong C, Oijala M, Soltesz I (2013) On-demand optogenetic control of spontaneous seizures in temporal lobe epilepsy. Nat Commun 4:1376
21. Paz JT, Davidson TJ, Frechette ES, Delord B, Parada I, Peng K et al (2013) Closed-loop optogenetic control of thalamus as a tool for interrupting seizures after cortical injury. Nat Neurosci 16:64–70
22. Sessolo M, Marcon I, Bovetti S, Losi G, Cammarota M, Ratto GM et al (2015) Parvalbumin-positive inhibitory interneurons oppose propagation but favor generation of focal epileptiform activity. J Neurosci 35:9544–9557
23. Berg EM, Bertuzzi M, Ampatzis K (2018) Complementary expression of calcium binding proteins delineates the functional organization of the locomotor network. Brain Struct Funct 223:2181–2196
24. Shamgar L, Ma L, Schmitt N, Haitin Y, Peretz A, Wiener R et al (2006) Calmodulin is essential for cardiac IKS channel gating and assembly: impaired function in long-QT mutations. Circ Res 98:1055–1063
25. Ciampa EJ, Welch RC, Vanoye CG, George AL Jr (2011) KCNE4 juxtamembrane region is required for interaction with calmodulin and for functional suppression of KCNQ1. J Biol Chem 286:4141–4149
26. Chang A, Abderemane-Ali F, Hura GL, Rossen ND, Gate RE, Minor DL Jr (2018) A calmodulin c-lobe Ca^{2+}-dependent switch governs Kv7 channel function. Neuron 97:836–852
27. Crotti L, Johnson CN, Graf E, De Ferrari GM, Cuneo BF, Ovadia M et al (2013) Calmodulin mutations associated with recurrent cardiac arrest in infants. Circulation 127:1009–1017
28. Makita N, Yagihara N, Crotti L, Johnson CN, Beckmann BM, Roh MS et al (2014) Novel calmodulin mutations associated with congenital arrhythmia susceptibility. Circ Cardiovasc Genet 7:466–474
29. Yamamoto Y, Makiyama T, Harita T, Sasaki K, Wuriyanghai Y, Hayano M et al (2017) Allele-specific ablation rescues electrophysiological abnormalities in a human iPS cell model of long-QT syndrome with a CALM2 mutation. Hum Mol Genet 26:1670–1677
30. Marsman RF, Barc J, Beekman L, Alders M, Dooijes D, van den Wijngaard A et al (2014) A mutation in CALM1 encoding calmodulin in familial idiopathic ventricular fibrillation in childhood and adolescence. J Am Coll Cardiol 63:259–266
31. Li T, Yi L, Hai L, Ma H, Tao Z, Zhang C et al (2018) The interactome and spatial redistribution feature of Ca^{2+} receptor protein calmodulin reveals a novel role in invadopodia-mediated invasion. Cell Death Dis 9:292
32. McDonald KS (2018) Jack-of-many-trades: discovering new roles for troponin C. J Physiol 596(19):4553–4554. https://doi.org/10.1113/JP276790
33. Gillis TE, Marshall CR, Tibbits GF (2007) Functional and evolutionary relationships of troponin C. Physiol Genomics 32:16–27
34. Trybus KM (1994) Role of myosin light chains. J Muscle Res Cell Motil 15:587–594
35. Kampourakis T, Sun YB, Irving M (2016) Myosin light chain phosphorylation enhances contraction of heart muscle via structural changes in both thick and thin filaments. Proc Natl Acad Sci U S A 113:E3039–E3047
36. Pechere JF (1968) Muscular parvalbumins as homologous proteins. Comp Biochem Physiol 24:289–295

37. Nishikawa T, Lee IS, Shiraishi N, Ishikawa T, Ohta Y, Nishikimi M (1997) Identification of S100b protein as copper-binding protein and its suppression of copper-induced cell damage. J Biol Chem 272:23037–23041
38. Fritz G, Botelho HM, Morozova-Roche LA, Gomes CM (2010) Natural and amyloid self-assembly of S100 proteins: structural basis of functional diversity. FEBS J 277:4578–4590
39. Gross SR, Sin CG, Barraclough R, Rudland PS (2014) Joining S100 proteins and migration: for better or for worse, in sickness and in health. Cell Mol Life Sci 71:1551–1579
40. Donato R, Sorci G, Giambanco I (2017) S100A6 protein: functional roles. Cell Mol Life Sci 74:2749–2760
41. Xia C, Braunstein Z, Toomey AC, Zhong J, Rao X (2018) S100 proteins as an important regulator of macrophage inflammation. Front Immunol 8:1908
42. Zimmer DB, Wright Sadosky P, Weber DJ (2003) Molecular mechanisms of S100-target protein interactions. Microsc Res Tech 60:552–559
43. Eckert RL, Broome AM, Ruse M, Robinson N, Ryan D, Lee K (2004) S100 proteins in the epidermis. J Invest Dermatol 123:23–33
44. Donato R, Sorci G, Riuzzi F, Arcuri C, Bianchi R, Brozzi F et al (2009) S100B's double life: intracellular regulator and extracellular signal. Biochim Biophys Acta 1793:1008–1022
45. He H, Li J, Weng S, Li M, Yu Y (2009) S100A11: diverse function and pathology corresponding to different target proteins. Cell Biochem Biophys 55:117–126
46. Sherbet GV (2009) Metastasis promoter S100A4 is a potentially valuable molecular target for cancer therapy. Cancer Lett 280:15–30
47. Naz S, Ranganathan P, Bodapati P, Shastry AH, Mishra LN, Kondaiah P (2012) Regulation of S100A2 expression by TGF-beta-induced MEK/ERK signalling and its role in cell migration/invasion. Biochem J 447:81–91
48. Donato R, Cannon BR, Sorci G, Riuzzi F, Hsu K, Weber DJ et al (2013) Functions of S100 proteins. Curr Mol Med 13:24–57
49. Brockett AT, Kane GA, Monari PK, Briones BA, Vigneron PA, Barber GA et al (2018) Evidence supporting a role for astrocytes in the regulation of cognitive flexibility and neuronal oscillations through the Ca^{2+} binding protein S100β. PLoS One 13:e0195726
50. Sakatani S, Seto-Ohshima A, Shinohara Y, Yamamoto Y, Yamamoto H, Itohara S et al (2008) Neuralactivity-dependent release of S100β from astrocytes enhances kainate-induced gamma oscillations in vivo. J Neurosci 28:10928–10936
51. Diaz-Romero J, Nesic D (2017) S100A1 and S100B: calcium sensors at the cross-roads of multiple chondrogenic pathways. J Cell Physiol 232:1979–1987
52. Wang T, Huo X, Chong Z, Khan H, Liu R, Wang T (2018) A review of S100 protein family in lung cancer. Clin Chim Acta 476:54–59
53. Tian T, Li X, Hua Z, Ma J, Liu Z, Chen H et al (2017) S100A1 promotes cell proliferation and migration and is associated with lymph node metastasis in ovarian cancer. Discov Med 23:235–245
54. Chen X, Liu X, Lang H, Zhang S, Luo Y, Zhang J (2015) S100 calcium-binding protein A6 promotes epithelial-mesenchymal transition through b-catenin in pancreatic cancer cell line. PLoS One 10:e0121319
55. Belter B, Haase-Kohn C, Pietzsch J (2017) Biomarkers in malignant melanoma: recent trends and critical perspective. In: Ward WH, Farma JM (eds) Cutaneous melanoma: etiology and therapy. Codon Publications, Brisbane
56. Bresnick AR, Weber DJ, Zimmer DB (2015) S100 proteins in cancer. Nat Rev Cancer 15:96–109
57. Tesarova P, Kalousova M, Zima T, Tesar V (2016) HMGB1, S100 proteins and other RAGE ligands in cancer-markers, mediators and putative therapeutic targets. Biomed Pap Med Fac Univ Palacky Olomouc Czech Repub 160:1–10
58. Rusnak F, Mertz P (2000) Calcineurin: form and function. Physiol Rev 80:1483–1521
59. Li J, Jia Z, Zhou W, Wei Q (2009) Calcineurin regulatory subunit B is a unique calcium sensor that regulates calcineurin in both calcium-dependent and calcium-independent manner. Proteins 77:612–623

60. Li H, Rao A, Hogan PG (2011) Interaction of calcineurin with substrates and targeting proteins. Trends Cell Biol 21:91–103
61. Parra V, Rothermel BA (2017) Calcineurin signaling in the heart: the importance of time and place. J Mol Cell Cardiol 103:121–136
62. Shah SZ, Hussain T, Zhao D, Yang L (2012) A central role for calcineurin in protein misfolding neurodegenerative diseases. Cell Mol Life Sci 74:1061–1074
63. Pongs O, Lindemeier J, Zhu XR, Theil T, Engelkamp D, Krah-Jentgens I et al (1993) Frequenin – a novel calcium-binding protein that modulates synaptic efficacy in the Drosophila nervous system. Neuron 11:15–28
64. Burgoyne RD, Haynes LP (2015) Sense and specificity in neuronal calcium signalling. Biochim Biophys Acta 1853:1921–1932
65. Burgoyne RD (2007) Neuronal calcium sensor proteins: generating diversity in neuronal Ca^{2+} signalling. Nat Rev Neurosci 8:182–193
66. Angelats E, Requesens M, Aguinaga D, Kreutz MR, Franco R, Navarro G (2018) Neuronal calcium and cAMP cross-talk mediated by cannabinoid CB1 receptor and EF-hand calcium sensor interactions. Front Cell Dev Biol 6:67
67. Braunewell KH (2005) The darker side of Ca^{2+} signaling by neuronal Ca^{2+}-sensor proteins: from Alzheimer's disease to cancer. Trends Pharmacol Sci 26:345–351
68. Kaeser PS, Regehr WG (2014) Molecular mechanisms for synchronous, asynchronous, and spontaneous neurotransmitter release. Annu Rev Physiol 76:333–363
69. Romanov RA, Alpár A, Hökfelt T, Harkany T (2017) Molecular diversity of corticotropin-releasing hormone mRNA-containing neurons in the hypothalamus. J Endocrinol 232:R161–R172
70. Gerke V, Moss SE (2002) Annexins: from structure to function. Physiol Rev 82:331–371
71. Moss SE, Morgan RO (2004) The annexins. Genome Biol 5:219
72. Rescher U, Gerke V (2004) Annexins -unique membrane binding proteins with diverse functions. J Cell Sci 117:2631–2639
73. Mishra S, Chander V, Banerjee P, Oh JG, Lifirsu E, Park WJ et al (2011) Interaction of annexin A6 with alpha actinin in cardiomyocytes. BMC Cell Biol 12:7
74. Santamaria-Kisiel L, Rintala-Dempsey AC, Shaw GS (2006) Calcium-dependent and-independent interactions of the S100 protein family. Biochem J 396:201–214
75. Raynal P, Pollard HB (1994) Annexins: the problem of assessing the biological role for a gene family of multifunctional calcium- and phospholipid-binding proteins. Biochim Biophys Acta 1197:63–93
76. Gerke V, Creutz CE, Moss SE (2005) Annexins: linking Ca2þ signalling to membrane dynamics. Nat Rev Mol Cell Biol 6:449–461
77. Fatimathas L, Moss SE (2010) Annexins as disease modifiers. Histol Histopathol 25:527–532
78. D'Acunto CW, Gbelcova H, Festa M, Ruml T (2014) The complex understanding of annexin A1 phosphorylation. Cell Signal 26:173–178
79. Leoni G, Nusrat A (2016) Annexin A1: shifting the balance towards resolution and repair. Biol Chem 397:971–979
80. Christmas P, Callaway J, Fallon J, Jones J, Haigler HT (1991) Selective secretion of annexin-1, a protein without a signal sequence, by the human prostate-gland. J Biol Chem 266:2499–2507
81. Guo C, Liu S, Sun M (2013b) Potential role of Anxa1 in cáncer. Future Oncol 9:1773–1793
82. Tu Y, Johnstone CN, Stewart AG (2017) Annexin A1 influences in breast cancer: controversies on contributions to tumour, host and immunoediting processes. Pharmacol Res 119:278–288
83. Boudhraa Z, Bouchon B, Viallard C, D'Incan M, Degoul F (2016) Annexin A1 localization and its relevance to cancer. Clin Sci 130:205–220
84. Yan Tu Y, Johnstone CN, Stewart AG (2017) Annexin A1 influences in breast cancer: Controversies on contributions to tumour, host and immunoediting processes. Pharmacol Res 119:278–288

85. Chen L, Lv F, Pei L (2014) Annexin 1: a glucocorticoid-inducible protein that modulates inflammatory pain. Eur J Pain 18:338–347
86. Sugimoto MA, Vago JP, Teixeira MM, Sousa LP (2016) Annexin A1 and the resolution of inflammation: modulation of neutrophil recruitment, apoptosis, and clearance. J Immunol Res 2016:8239258
87. Yang YH, Morand E, Leech M (2013) Annexin A1: potential for glucocorticoid sparing in RA. Nat Rev Rheumatol 9:595–603
88. Qin C, Yang YH, May L, Gao X, Stewart AG, Tu Y et al (2015) Cardioprotective potential of annexin-A1 mimetics in myocardial infarction. Pharmacol Ther 148:47–65
89. Luo M, Hajjar KA (2013) Annexin A2 system in human biology: cell surface and beyond. Semin Thromb Hemost 39:338–346
90. Xu XH, Pan W, Kang LH, Feng H, Song YQ (2015) Association of annexin A2 with cancer development. Oncol Rep 33:2121–2128
91. Wang C, Lin C (2014a) Annexin A2: its molecular regulation and cellular expression in cancer development. Dis Markers 2014:308976
92. Liu X, Ma D, Jing X, Wang B, Yang W, Qiu W (2015) Overexpression of ANXA2 predicts adverse outcomes of patients with malignant tumors: a systematic review and meta-analysis. Med Oncol 32:392
93. Tanida S, Mizoshita T, Ozeki K, Katano T, Kataoka H, Kamiya T et al (2015) Advances in refractory ulcerative colitis treatment: a new therapeutic target, Annexin A2. World J Gastroenterol 21:8776–8786
94. Cañas F, Simonin L, Couturaud F, Renaudineau Y (2015) Annexin A2 autoantibodies in thrombosis and autoimmune diseases. Thromb Res 135:226–230
95. Wu N, Liu S, Guo C, Hou Z, Sun MZ (2013) The role of annexin A3 playing in cancers. Clin Transl Oncol 15:106–110
96. Matsuzaki S, Serada S, Morimoto A, Ueda Y, Yoshino K, Kimura T et al (2014) Annexin A4 is a promising therapeutic target for the treatment of platinum-resistant cancers. Expert Opin Ther Targets 18:403–414
97. Wei B, Guo C, Liu S, Sun MZ (2015) Annexin A4 and cancer. Clin Chim Acta 447:72–78
98. Peng B, Guo C, Guan H, Liu S, Sun MZ (2014) Annexin A5 as a potential marker in tumors. Clin Chim Acta 427:42–48
99. Bouter A, Carmeille R, Gounou C, Bouvet F, Degrelle SA, Evain-Brion D et al (2015) Review: Annexin-A5 and cell membrane repair. Placenta 36:S43–S49
100. Carmeille R, Degrelle SA, Plawinski L, Bouvet F, Gounou C, Evain-Brion D, Brisson AR, Bouter A (2015) Annexin-A5 promotes membrane resealing in human trophoblasts. Biochim Biophys Acta 1853:2033–2044
101. Udry S, Aranda F, Latino O, de Larrañaga G (2013) Annexins and recurrent pregnancy loss. Medicina (B Aires) 73:495–500
102. Enrich C, Rentero C, Grewal T (2017) Annexin A6 in the liver: from the endocytic compartment to cellular physiology. Biochim Biophys Acta 1864:933–946
103. Guo C, Liu S, Greenaway F, Sun MZ (2013a) Potential role of annexin A7 in cancers. Clin Chim Acta 423:83–89
104. Wang J, Guo C, Liu S, Qi H, Yin Y, Liang R et al (2014b) Annexin A11 in disease. Clin Chim Acta 431:164–168
105. Coe H, Michalak M (2009) Calcium binding chaperones of the endoplasmic reticulum. Gen Physiol Biophys 28:F96–F103
106. Gutierrez T, Simmen T (2018) Endoplasmic reticulum chaperones tweak the mitochondrial calcium rheostat to control metabolism and cell death. Cell Calcium 70:64–75
107. Lu YC, Weng WC, Lee H (2015) Functional roles of calreticulin in cancer biology. Biomed Res Int 2015:526524
108. Zamanian M, Veerakumarasivam A, Abdullah S, Rosli R (2013) Calreticulin and cancer. Pathol Oncol Res 19:149–154
109. Nakamura K, Zuppini A, Arnaudeau S, Lynch J, Ahsan I, Krause R et al (2001) Functional specialization of calreticulin domains. J Cell Biol 154:961–972

110. Arnaudeau S, Frieden M, Nakamura K, Castelbou C, Michalak M, Demaurex N (2002) Calreticulin differentially modulates calcium uptake and release in the endoplasmic reticulum and mitochondria. J Biol Chem 277:46696–46705
111. Trombetta ES (2003) The contribution of N-glycans and their processing in the endoplasmic reticulum to glycoprotein biosynthesis. Glycobiology 13:77R–91R
112. Gelebart P, Opas M, Michalak M (2005) Calreticulin, a Ca^{2+}-binding chaperone of the endoplasmic reticulum. Int J Biochem Cell Biol 37:260–266
113. Zhu N, Wang Z (1999) Calreticulin expression is associated with androgen regulation of the sensitivity to calcium ionophore-induced apoptosis in LNCaP prostate cancer cells. Cancer Res 59:1896–1902
114. Clinton A, McMullin MF (2016) The Calreticulin gene and myeloproliferative neoplasms. J Clin Pathol 69:841–845
115. Eggleton P, Bremer E, Dudek E, Michalak M (2016) Calreticulin, a therapeutic target? Expert Opin Ther Targets 20:1137–1147
116. Lievremont JP, Rizzuto R, Hendershot L, Meldolesi J (1997) BiP: a major chaperone protein of the endoplasmic reticulum lumen, plays a direct and important role in the storage of the rapidly exchanging pool of Ca^{2+}. J Biol Chem 272:30873–30879
117. Taiyab A, Sreedhar AS, Rao CM (2009) Hsp90 inhibitors: GA and 17AAG, lead to ER stress-induced apoptosis in rat histiocytoma. Biochem Pharmacol 78:142–152
118. Narindrasorasak S, Yao P, Sarkar B (2003) Protein disulfide isomerase, a multifunctional protein chaperone, shows copper-binding activity. Biochem Biophys Res Commun 311:405–414
119. Xu S, Sankar S, Neamati N (2014) Protein disulfide isomerase: a promising target for cancer therapy. Drug Discov Today 19:222–240
120. MacLennan DH, Wong PT (1971) Isolation of a calcium-sequestering protein from sarcoplasmic reticulum. Proc Natl Acad Sci U S A 68:1231–1235
121. Novák P, Soukup T (2011) Calsequestrin distribution, structure and function, its role in normal and pathological situations and the effect of thyroid hormones. A review. Physiol Res 60:439–452
122. Gyorke I, Hester N, Jones LR, Gyorke S (2004) The role of calsequestrin, triadin, and junctin in conferring cardiac ryanodine receptor responsiveness to luminal calcium. Biophys J 86:2121–2128
123. Qin J, Valle G, Nani A, Nori A, Rizzi N, Priori SG et al (2008) Luminal Ca^{2+} regulation of single cardiac ryanodine receptors: insights provided by calsequestrin and its mutants. J Gen Physiol 131:325–334
124. Gaburjakova M, Bal NC, Gaburjakova J, Periasamy M (2013) Functional interaction between calsequestrin and ryanodine receptor in the heart. Cell Mol Life Sci 70:2935–2945
125. Paolini C, Quarta M, Nori A, Boncompagni S, Canato M, Volpe P et al (2007) Reorganized stores and impaired calcium handling in skeletal muscle of mice lacking calsequestrin-1. J Physiol 583:767–784
126. Glukhov AV, Kalyanasundaram A, Lou Q, Hage LT, Hansen BJ, Belevych AE et al (2015) Calsequestrin 2 deletion causes sinoatrial node dysfunction and atrial arrhythmias associated with altered sarcoplasmic reticulum calcium cycling and degenerative fibrosis within the mouse atrial pacemaker complex1. Eur Heart J 36:686–697
127. Pertille A, de Carvalho CL, Matsumura CY, Neto HS, Marques MJ (2010) Calcium-binding proteins in skeletal muscles of the mdx mice: potential role in the pathogenesis of Duchenne muscular dystrophy. Int J Exp Pathol 91:63–71
128. Guarnier FA, Michelucci A, Serano M, Pietrangelo L, Pecorai C, Boncompagni S et al (2018) Aerobic training prevents heatstrokes in calsequestrin-1 knockout mice by reducing oxidative stress. Oxidative Med Cell Longev 2018:4652480
129. Nishizuka Y (1998) The molecular heterogeneity of protein kinase C and its implications for cellular regulation. Nature 334:661–665
130. Kikkawa U, Kishimoto A, Nishizuka Y (1989) The protein kinase C family: heterogeneity and its implications. Annu Rev Biochem 58:31–44

131. Stahelin RV (2009) Lipid binding domains: more than simple lipid effectors. J Lipid Res 50:S299–S304
132. Nalefski EA, Falke JJ (1996) The C2 domain calcium-binding motif: structural and functional diversity. Protein Sci 5:2375–2390
133. Steinberg SF (2008) Structural basis of protein kinase C isoform function. Physiol Rev 88:1341–1378
134. Newton AC (2010) Protein kinase C: poised to signal. Am J Physiol Endocrinol Metab 298:E395–E402
135. Newton AC, Johnson JE (1998) Protein kinase C: a paradigm for regulation of protein function by two membrane-targeting modules. Biochim Biophys Acta 1376:155–172
136. Breitkreutz D, Braiman-Wiksman L, Daum N, Denning MF, Tennenbaum T (2007) Protein kinase C family: on the crossroads of cell signaling in skin and tumor epithelium. J Cancer Res Clin Oncol 133:793–808
137. Mochly-Rosen D, Das K, Grimes KV (2012) Protein kinase C, an elusive therapeutic target? Nat Rev Drug Discov 11:937–957
138. Perin MS, Fried VA, Mignery GA, Jahn R, Sudhof TC (1990) Phospholipid binding by a synaptic vesicle protein homologous to the regulatory region of protein kinase C. Nature 345:260–263
139. Jackman SL, Turecek J, Belinsky JE, Regehr WG (2016) The calcium sensor synaptotagmin 7 is required for synaptic facilitation. Nature 529:88–91
140. Fernandez I, Araç D, Ubach J, Gerber SH, Shin O, Gao Y et al (2001) Three-dimensional structure of the synaptotagmin 1 C2B-domain: synaptotagmin 1 as a phospholipid binding machine. Neuron 32:1057–1069
141. Fernández-Chacón R, Königstorfer A, Gerber SH, García J, Matos MF, Stevens CF et al (2001) Synaptotagmin I functions as a calcium regulator of release probability. Nature 410:41–49
142. Johnson CP, Chapman ER (2010) Otoferlin is a calcium sensor that directly regulates SNARE-mediated membrane fusion. J Cell Biol 191:187–197
143. Pangrsic T, Reisinger E, Moser T (2012) Otoferlin: a multi-C2 domain protein essential for hearing. Trends Neurosci 35:671–680
144. Bunney TD, Katan M (2011) PLC regulation: emerging pictures for molecular mechanisms. Trends Biochem Sci 36:88–96
145. Lee JC, Simonyi A, Sun AY, Sun GY (2011) Phospholipases A2 and neural membrane dynamics: implications for Alzheimer's disease. J Neurochem 116:813–819
146. Marques R, Maia CJ, Vaz C, Correia S, Socorro S (2014) The diverse roles of calcium-binding protein regucalcin in cell biology: from tissue expression and signalling to disease. Cell Mol Life Sci 71:93–111
147. Yamaguchi M (2012) Role of regucalcin in brain calcium signaling: involvement in aging. Integr Biol (Camb) 4:825–837
148. Yamaguchi M, Murata T (2013) Involvement of regucalcin in lipid metabolism and diabetes. Metab Clin Exp 62:1045–1051
149. Yamaguchi M (2013) Suppressive role of regucalcin in liver cell proliferation: involvement in carcinogenesis. Cell Prolif 46:243–253
150. Yamaguchi M (2015) Involvement of regucalcin as a suppressor protein in human carcinogenesis: insight into the gene therapy. J Cancer Res Clin Oncol 141:1333–1341
151. Seidah NG, Chrétien M (1999) Proprotein and prohormone convertases: a family of subtilases generating diverse bioactive polypeptides. Brain Res 848:45–62
152. Bergeron N, Phan BA, Ding Y, Fong A, Kraussn RM (2015) Proprotein convertase subtilisin/kexin type 9 inhibition: a new therapeutic mechanism for reducing cardiovascular disease risk. Circulation 132:1648–1666
153. Kadio B, Yaya S, Basak A, Djè K, Gomes J, Mesenge C (2016) Calcium role in human carcinogenesis: a comprehensive analysis and critical review of literature. Cancer Metastasis Rev 35:391–411

154. Couture F, Kwiatkowska A, Dory YL, Day R (2015) Therapeutic uses of furin and its inhibitors: a patent review. Expert Opin Ther Pat 25:379–396
155. Brown EM, MacLeod RJ (2001) Extracellular calcium sensing and extracellular calcium signaling. Physiol Rev 81:239–297
156. Colella M, Gerbino A, Hofer AM, Curci S (2016) Recent advances in understanding the extracellular calcium-sensing receptor. F1000Res 5:2535
157. Hofer AM (2005) Another dimension to calcium signaling: a look at extracellular calcium. J Cell Sci 118:855–862
158. Chazin WJ (2011) Relating form and function of EF-hand calcium binding proteins. Acc Chem Res 44:171–179
159. Martínez J, Cristóvão JS, Sánchez R, Gasset M, Gomes CM (2018) Preparation of amyloidogenic aggregates from EF-hand β-parvalbumin and S100 proteins. Methods Mol Biol 1779:167–179
160. Denessiouk K, Permyakov S, Denesyuk A, Permyakov E, Johnson MS (2014) Two structural motifs within canonical EF-hand calcium-binding domains identify five different classes of calcium buffers and sensors. PLoS One 9:e109287
161. Murphy-Ullrich JE, Sage EH (2014) Revisiting the matricellular concept. Matrix Biol 37:1–14
162. Wang H, Workman G, Chen S, Barker TH, Ratner BD, Sage EH et al (2006) Secreted protein acidic and rich in cysteine (SPARC/osteonectin/BM-40) binds to fibrinogen fragments D and E, but not to native fibrinogen. Matrix Biol 25:20–26
163. Bradshaw AD (2012) Diverse biological functions of the SPARC family of proteins. Int J Biochem Cell Biol 44:480–448
164. Busch E, Hohenester E, Timpl R, Paulsson M, Maurer P (2000) Calcium affinity, cooperativity, and domain interactions of extracellular EF-hands present in BM-40. J Biol Chem 275:25508–25515
165. Papapanagiotou A, Sgourakis G, Karkoulias K, Raptis D, Parkin E, Brotzakis P et al (2018) Osteonectin as a screening marker for pancreatic cancer: a prospective study. J Int Med Res 46:2769–2779
166. Podhajcer OL, Benedetti L, Girotti MR, Prada F, Salvatierra E, Llera AS (2008) The role of the matricellular protein SPARC in the dynamic interaction between the tumor and the host. Cancer Metastasis Rev 27:523–537
167. Vaz J, Ansari D, Sasor A, Andersson R (2015) SPARC: a potential prognostic and therapeutic target in pancreatic cancer. Pancreas 44:1024–1035
168. Murphy LA, Ramirez EA, Trinh VT, Herman AM, Anderson VC, Brewster JL (2011) Endoplasmic reticulum stress or mutation of an EF-hand Ca^{2+}-binding domain directs the FKBP65 rotamase to an ERAD-based proteolysis. Cell Stress Chaperones 16:607–619
169. Ishikawa Y, Holden P, Bächinger HP (2017) Heat shock protein 47 and 65-kDa FK506-binding protein weakly but synergistically interact during collagen folding in the endoplasmic reticulum. J Biol Chem 292:17216–17224
170. Wang CK, Ghani HA, Bundock A, Weidmann J, Harvey PJ, Edwards IA et al (2018) Calcium-mediated allostery of the EGF fold. ACS Chem Biol 13:1659–1667
171. Engel J (1989) EGF-like domains in extracellular matrix proteins: localized signals for growth and differentiation? FEBS Lett 251:1–7
172. Stenflo J, Stenberg Y, Muranyi A (2000) Calcium-binding EGF-like modules in coagulation proteinases: function of the calcium ion in module interactions. Biochim Biophys Acta 1477:51–63
173. Krebs J, Heizmann CW (2007) Calcium-binding proteins and the EF-hand principle. In: Krebs J, Michalak M (eds) Calcium: a matter of life or death. Elsevier, Amsterdam, pp 51–93
174. Rose-Martel M, Smiley S, Hincke MT (2015) Novel identification of matrix proteins involved in calcitic biomineralization. J Proteome 116:81–96
175. Hu P, Luo BH (2018) The interface between the EGF1 and EGF2 domains is critical in integrin affinity regulation. J Cell Biochem 119(9):7264–7273. https://doi.org/10.1002/jcb.26921

176. Balzar M, Briaire-de Bruijn IH, Rees-Bakker HA, Prins FA, Helfrich W, de Leij L et al (2001) Epidermal growth factor-like repeats mediate lateral and reciprocal interactions of Ep-CAM molecules in homophilic adhesions. Mol Cell Biol 21:2570–2580
177. Saha S, Boyd J, Werner JM, Knott V, Handford PA, Campbell ID et al (2001) Solution structure of the LDL receptor EGF-AB pair: a paradigm for the assembly of tandem calcium binding EGF domains. Structure 9:451–456
178. Wildhagen KC, Lutgens E, Loubele ST, ten Cate H, Nicolaes GA (2011) The structure-function relationship of activated protein C. Lessons from natural and engineered mutations. Thromb Haemost 106:1034–1045
179. Robertson I, Jensen S, Handford P (2011) TB domain proteins: evolutionary insights into the multifaceted roles of fibrillins and LTBPs. Biochem J 433:263–276
180. Andersen OM, Dagil R, Kragelund BB (2013) New horizons for lipoprotein receptors: communication by β-propellers. J Lipid Res 54:2763–2774
181. Jensen SA, Handford PA (2016) New insights into the structure, assembly and biological roles of 10-12 nm connective tissue microfibrils from fibrillin-1 studies. Biochem J 473:827–838
182. Pena F, Jansens A, van Zadelhoff G, Braakman I (2010) Calcium as a crucial cofactor for low density lipoprotein receptor folding in the endoplasmic reticulum. J Biol Chem 285:8656–8664
183. Wang F, Li B, Lan L, Li L (2015) C596G mutation in FBN1 causes Marfan syndrome with exotropia in a Chinese family. Mol Vis 21:194–200
184. Garvie CW, Fraley CV, Elowe NH, Culyba EK, Lemke CT, Hubbard BK et al (2016) Point mutations at the catalytic site of PCSK9 inhibit folding, autoprocessing, and interaction with the LDL receptor. Protein Sci 25:2018–2027
185. Cranenburg EC, Schurgers LJ, Vermeer C (2007) Vitamin K: the coagulation vitamin that became omnipotent. Thromb Haemost 98:120–125
186. Cristiani A, Maset F, De Toni L, Guidolin D, Sabbadin D, Strapazzon G, Moro S, De Filippis V, Foresta C (2014) Carboxylation-dependent conformational changes of human osteocalcin. Front Biosci 19:1105–1116
187. Palta S, Saroa R, Palta A (2014) Overview of the coagulation system. Indian J Anaesth 58:515–523
188. Zhao D, Wang J, Liu Y, Liu X (2015) Expressions and clinical significance of serum bone Gla-protein, bone alkaline phosphatase and C-terminal telopeptide of type I collagen in bone metabolism of patients with osteoporosis. Pak J Med Sci 31:91–94
189. Maurer P, Hohenester E, Engel J (1996) Extracellular calcium-binding proteins. Curr Opin Cell Biol 8:609–617
190. Viegas CS, Simes DC, Laizé V, Williamson MK, Price PA, Cancela ML (2008) Gla-rich protein (GRP), a new vitamin K-dependent protein identified from sturgeon cartilage and highly conserved in vertebrates. J Biol Chem 283:36655–36664
191. Tie JK, Carneiro JD, Jin DY, Martinhago CD, Vermeer C, Stafford DW (2016) Characterization of vitamin K-dependent carboxylase mutations that cause bleeding and nonbleeding disorders. Blood 127:1847–1855
192. Persson E, Madsen JJ, Olsen OH (2014) The length of the linker between the epidermal growth factor-like domains in factor VIIa is critical for a productive interaction with tissue factor. Protein Sci 23:1717–1727
193. Ohkubo YZ, Tajkhorshid E (2008) Distinct structural and adhesive roles of Ca^{2+} in membrane binding of blood coagulation factors. Structure 16:72–81
194. Sumarheni S, Hong SS, Josserand V, Coll JL, Boulanger P, Schoehn G et al (2014) Human full-length coagulation factor X and a GLA domain-derived 40-merpolypeptide bind to different regions of the adenovirus serotype 5 hexoncapsomer. Hum Gene Ther 25:339–349
195. Hansson K, Stenflo J (2005) Post-translational modifications in proteins involved in blood coagulation. J Thromb Haemost 3:2633–2648
196. Egorina EM, Sovershaev MA, Osterud B (2008) Regulation of tissue factor procoagulant activity by post-translational modifications. Thromb Res 122:831–837

197. Czogalla KJ, Watzka M, Oldenburg J (2015) Structural modeling insights into human VKORC1 phenotypes. Nutrients 7:6837–6851
198. Zhang YT, Tang ZY (2014) Research progress of warfarin-associated vascular calcification and its possible therapy. J Cardiovasc Pharmacol 63:76–82
199. Kapustin AN, Schoppet M, Schurgers LJ, Reynolds JL, McNair R, Heiss A et al (2017) Prothrombin loading of vascular smooth muscle cell-derived exosomes regulates coagulation and calcification. Arterioscler Thromb Vasc Biol 37:e22–e32
200. Siltari A, Vapaatalo H (2018) Vascular calcification, vitamin K and warfarin therapy – possible or plausible connection? Basic Clin Pharmacol Toxicol 122:19–24
201. Wallin R, Cain D, Hutson SM, Sane DC, Loeser R (2000) Modulation of the binding of matrix Gla protein (MGP) to bone morphogenetic protein-2 (BMP-2). Thromb Haemost 84:1039–1044
202. Lomashvili KA, Wang X, Wallin R, O'Neill WC (2011) Matrix Gla protein metabolism in vascular smooth muscle and role in uremic vascular calcification. J Biol Chem 286:28715–28722
203. Sheng K, Zhang P, Lin W, Cheng J, Li J, Chen J (2017) Association of Matrix Gla protein gene (rs1800801, rs1800802, rs4236) polymorphism with vascular calcification and atherosclerotic disease: a meta-analysis. Sci Rep 7:8713
204. Luo G, Ducy P, McKee MD, Pinero GJ, Loyer E, Behringer RR et al (1997) Spontaneous calcification of arteries and cartilage in mice lacking matrix GLA protein. Nature 386:78–81
205. Klezovitch O, Vasioukhin V (2015) Cadherin signaling: keeping cells in touch. F1000Res 4(F1000 Faculty Rev):550
206. Halbleib JM, Nelson WJ (2006) Cadherins in development: cell adhesion, sorting, and tissue morphogenesis. Genes Dev 20:3199–3214
207. Oroz J, Valbuena A, Vera AM, Mendieta J, Gomez-Puertas P, Carrion-Vazquez M (2011) Nanomechanics of the cadherin ectodomain: "canalization" by Ca^{2+} binding results in a new mechanical element. J Biol Chem 286:9405–9418
208. Gaengel K, Genové G, Armulik A, Betsholtz C (2009) Endothelial-mural cell signalling in vascular development and angiogenesis. Arterioscler Thromb Vasc Biol 29:630–638
209. Blaschuk OW (2015) N-cadherin antagonists as oncology therapeutics. Philos Trans R Soc B 370:20140039
210. Jeanes A, Gottardi CJ, Yap AS (2008) Cadherins and cancer: how does cadherin dysfunction promote tumor progression? Oncogene 27:6920–6929
211. Wong SHM, Fang CM, Chuah LH, Leong CO, Ngai SC (2018) E-cadherin: Its dysregulation in carcinogenesis and clinical implications. Crit Rev Oncol Hematol 121:11–22
212. Zelensky AN, Gready JE (2005) The C-type lectin-like domain superfamily. FEBS J 272:6179–6217
213. Varki A, Cummings RD, Esko JD, Stanley P, Hart GW, Aebi M et al (2017) Essentials of glycobiology, 3rd edn. Cold Spring Harbor Laboratory Press, New York
214. Aretz J, Wamhoff EC, Hanske J, Heymann D, Rademacher C (2014) Computational and experimental prediction of human C-type lectin receptor druggability. Front Immunol 5:323
215. Cambi A, Koopman M, Figdor CG (2005) How C-type lectins detect pathogens. Cell Microbiol 7:481–488
216. Abdian PL, Caramelo JJ, Ausmees N, Zorreguieta A (2013) RapA2 is a calcium-binding lectin composed of two highly conserved cadherin-like domains that specifically recognize *Rhizobium leguminosarum* acidic exopolysaccharides. J Biol Chem 288:2893–2904
217. Bravo R, Parra V, Gatica D, Rodriguez AE, Torrealba N, Paredes F et al (2013) Endoplasmic reticulum and the unfolded protein response: dynamics and metabolic integration. Int Rev Cell Mol Biol 301:215–290
218. Cambi A, Figdor C (2009) Necrosis: C-type lectins sense cell death. Curr Biol 19:R375–R378
219. Bellande K, Bono JJ, Savelli B, Jamet E, Canut H (2017) Plant lectins and lectin receptor-like kinases: how do they sense the outside? Int J Mol Sci 18:E1164
220. Zou J, Jiang JY, Yang JJ (2017) Molecular basis for modulation of metabotropic glutamate receptors and their drug actions by extracellular Ca^{2+}. Int J Mol Sci 18:672

221. Peterlik M, Kállay E, Cross HS (2013) Calcium nutrition and extracellular calcium sensing: relevance for the pathogenesis of osteoporosis, cancer and cardiovascular diseases. Nutrients 5:302–327
222. Silve C, Petrel C, Leroy C, Bruel H, Mallet E, Rognan D et al (2005) Delineating a Ca^{2+} binding pocket within the venus flytrap module of the human calcium-sensing receptor. J Biol Chem 280:37917–37923
223. Lopez-Fernandez I, Schepelmann M, Brennan SC, Yarova PL, Riccardi D (2015) The calcium-sensing receptor: one of a kind. Exp Physiol 100:1392–1399
224. Conigrave AD, Ward DT (2013) Calcium-sensing receptor (CaSR): pharmacological properties and signaling pathways. Best Pract Res Clin Endocrinol Metab 27:315–331
225. Hannan FM, Babinsky VN, Thakker RV (2016) Disorders of the calcium-sensing receptor and partner proteins: insights into the molecular basis of calcium homeostasis. J Mol Endocrinol 57:R127–R142
226. Riccardi D, Kemp PJ (2012) The calcium-sensing receptor beyond extracellular calcium homeostasis: conception, development, adult physiology, and disease. Rev Physiol 74:271–297
227. Jones BL, Smith SM (2016) Calcium-sensing receptor: a key target for extracellular calcium signaling in neurons. Front Physiol 7:116
228. Nemeth EF, Shoback D (2013) Calcimimetic and calcilytic drugs for treating bone and mineral-related disorders. Best Pract Res Clin Endocrinol Metab 27:373–384
229. Steddon SJ, Cunningham J (2005) Calcimimetics and calcilytics -fooling the calcium receptor. Lancet 365:2237–2239
230. Jiang Y, Huang Y, Wong HC, Zhou Y, Wang X, Yang J et al (2010) Elucidation of a novel extracellular calcium-binding site on metabotropic glutamate receptor 1{alpha} (mGluR1{alpha}) that controls receptor activation. J Biol Chem 285:33463–33474
231. Samardzic J (ed) (2018) GABA and glutamate. New developments in neurotransmission research. Intech Open, London
232. Willard SS, Koochekpour S (2013) Glutamate, glutamate receptors, and downstream signaling pathways. Int J Biol Sci 9:948–959
233. Jacobson LH, Vlachou S, Slattery DA, Li X, Cryan JF (2018) The gamma-aminobutyric acid B receptor in depression and reward. Biol Psychiatry 83:963–976
234. Benarroch EE (2012) GABAB receptors: structure, functions, and clinical implications. Neurology 78:578–584

Chapter 9
Phospholipase C

Colin A. Bill and Charlotte M. Vines

Abstract Phospholipase C (PLC) family members constitute a family of diverse enzymes. Thirteen different family members have been cloned. These family members have unique structures that mediate various functions. Although PLC family members all appear to signal through the bi-products of cleaving phospholipids, it is clear that each family member, and at times each isoform, contributes to unique cellular functions. This chapter provides a review of the current literature on PLC. In addition, references have been provided for more in-depth information regarding areas that are not discussed including tyrosine kinase activation of PLC. Understanding the roles of the individual PLC enzymes, and their distinct cellular functions, will lead to a better understanding of the physiological roles of these enzymes in the development of diseases and the maintenance of homeostasis.

Keywords Phospholipase C family · G protein-coupled receptors · Phosphatidylinositol 4 · 5 – bisphosphate · Diacylglycerol · Inositol 1 · 4 · 5 – triphosphate · Calcium · Isoform · Structure · Ubiquitous expression · Multiple functions

9.1 Discovery

In 1953, it was reported that the addition of acetylcholine or carbamylcholine to pancreatic cells led to the production of phospholipids [1]. In these studies, ^{32}P was used to detect a sevenfold increase in the levels of phospholipids in the samples treated with the drugs, when compared with control slices, which had remained un-stimulated. Although unrecognized at that time, this was the first evidence of

C. A. Bill · C. M. Vines (✉)
Department of Biological Sciences, Border Biomedical Research Center, The University of Texas at El Paso, El Paso, TX, USA
e-mail: cvines@utep.edu

M. S. Islam (ed.), *Calcium Signaling*, Advances in Experimental Medicine and Biology 1131, https://doi.org/10.1007/978-3-030-12457-1_9

the presence of phospholipase C (PLC) function in cells. More than 20 years later, in 1975, it was shown that impure preparations of PLC could be used to cleave phosphatidylinositol [2]. In 1981, the first purified preparation of PLC was isolated [3]. A couple of years later it was found that the inositol 1,4,5 trisphosphate (IP_3) generated from the cleavage of phosphatidyl inositol 4,5 bisphosphate (also known as PI (4,5)P_2 or PIP_2) could induce the release of Ca^{2+} from intracellular stores [4] (Figs. 9.1 and 9.2). This important observation provided new insight into the function of PLC in living organisms. Eventually, the PLCβ, PLCγ, PLCδ, PLCε, PLCη and PLCζ cDNAs were cloned [5–10]. Although PIP_2 is a minor phospholipid in the plasma membrane, it plays a central role in regulating a host of cellular processes. PLC is activated following stimulation of cells by either tyrosine kinase receptors, T-cell receptors, B-cell receptors, Fc receptors, integrin adhesion proteins or G protein-coupled receptors via cognate ligands including neurotransmitters, histamine, hormones and growth factors [11–15]. Signaling through PLC family members regulates diverse functions, which will be outlined within this chapter. In addition, we will discuss PLC mediated signaling, common structural domains found in this family of enzymes, current knowledge about the isoforms and areas that have yet to be explored.

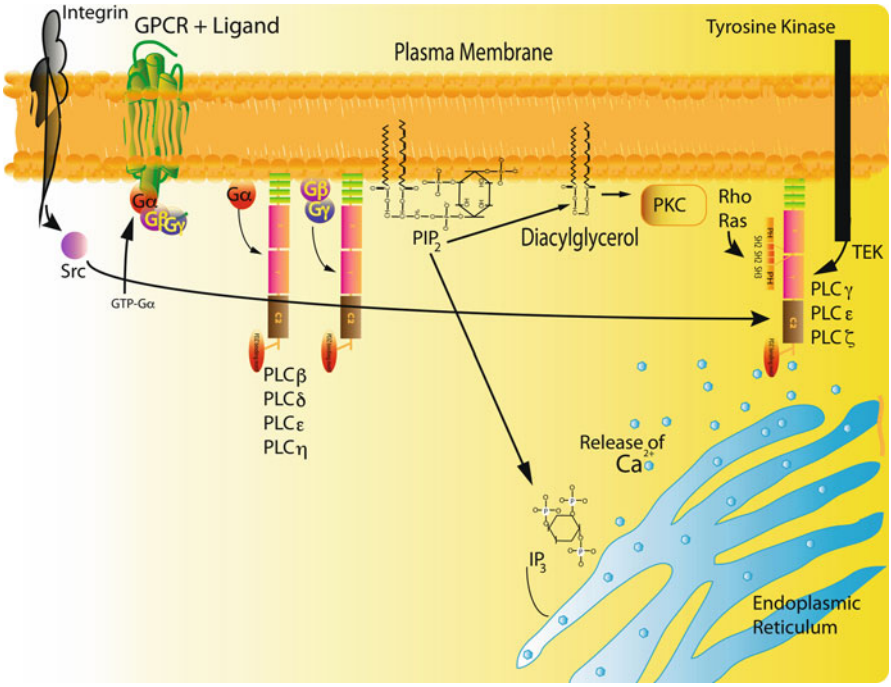

Fig. 9.1 Different effectors activate signaling through PLC to induce cleavage of PIP_2 to yield diacylglycerol and inositol triphosphate

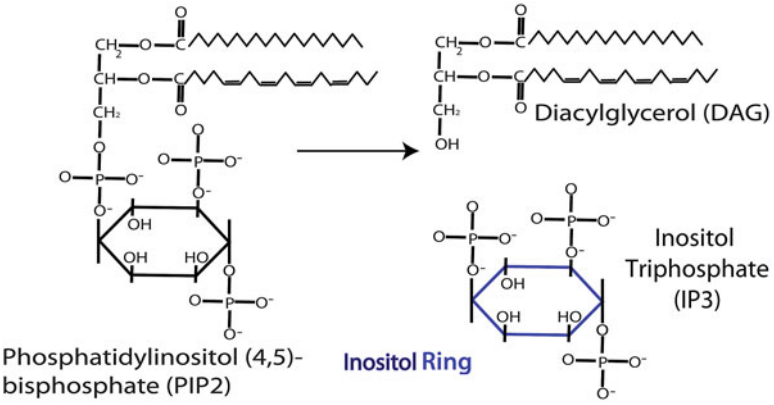

Fig. 9.2 PLC family members cleave PIP_2 to produce diacylglycerol and inositol triphosphate

9.2 Cleavage of PIP_2 and Signaling

PLC is a cytoplasmic protein that controls the levels of PIP_2 in cells by localizing within or outside of lipid rafts in the plasma membrane and catalyzing the hydrolysis of phosphorylated forms of phosphatidyl inositol in response to cellular stimuli (Figs. 9.1 and 9.2). These enzymes have been reported to increase the rate of lysis of phosphatidyl inositol >1000 s^{-1} at 30 °C at low concentrations of substrate, but is likely to reach rates of >5000 s^{-1} (as reviewed by [16]). Therefore, targeting of PLC to the plasma membrane plays a critical role in the functioning of this enzyme. The preferred substrate of PLC is PIP_2, a relatively uncommon phospholipid in the plasma membrane, followed by phosphatidyl inositol phosphate (PIP), and then phosphatidyl inositol (PI). Cleavage of PIP_2 leads to the generation of two products. One product, diacylglycerol (DAG), activates the calcium dependent protein kinase C (PKC), which then phosphorylates downstream effectors such as AKT to activate an array of cellular functions including regulating cell proliferation, cell polarity, learning, memory and spatial distribution of signals [17, 18]. DAG, which remains membrane bound, can then be cleaved to produce another signaling molecule, arachidonic acid. The second product of PLC action on PIP_2, IP_3 is a small water-soluble molecule, which diffuses away from the membrane, and through the cytosol to bind to IP_3 receptors on the endoplasmic reticulum inducing the release of Ca^{2+} from intracellular stores found within the organelle [4]. In turn, the cytoplasmic calcium levels are quickly elevated and cause the characteristic calcium spike that signals cell activation. Once the endoplasmic reticulum stores have been used up, they are replenished through the store-operated calcium channels. Ca^{2+} activates downstream transcription factors resulting in a plethora of gene activation pathways. In this way, signaling through PLC regulates proliferation, differentiation, fertilization, cell division, growth, sensory transduction, modification of gene expression, degranulation, secretion and motility [15, 19–26].

9.3 Structure of PLC

There are thirteen different PLC family members that can be subdivided into six classes, β, γ, δ, ε, η and ζ (Fig. 9.3). Different isoforms have been discovered in a wide range of species including mouse, rat and cattle. PLC-like isozymes have been found in *Drosophila melanogaster*, *Glycine max* (soybean), *Arabidopsis thaliana*, *Saccharomyces cerevisiae* and *Schizosaccharomyces pombe* [27, 28]. Overall, there is a low level of amino acid conservation between the family members; however, the similarity of the pleckstrin homology domains, the EF hand motifs, the X and Y domains and the C2 domains is greater than 40–50% [15]. Since these domains are common to all organisms they might represent a minimum requirement for a functioning PLC [29]. With the exception of the PH domain, which is not expressed on PLCζ, each family member shares all of the core domains. A description of each domain follows:

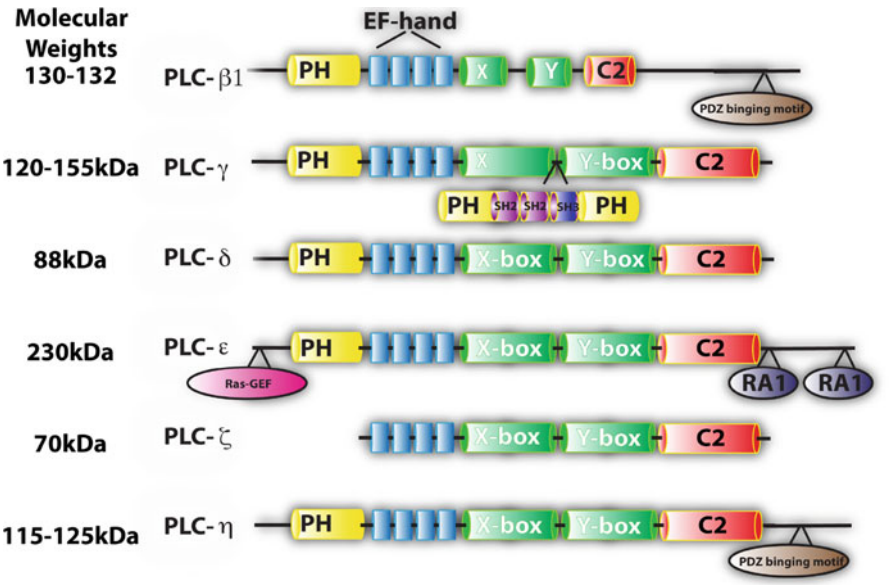

Fig. 9.3 Unique domains found in individual family members include the following: Post Synaptic density (PSD-95), Drosophila disc large tumor suppressor (DLgA) and Zonula Occludens-1 (ZO-1) (PDZ), src homology 2 (SH2)

9.3.1 Pleckstrin Homology (PH) Domains

As mentioned, with the exception of PLCζ, all PLC family members have N-terminal pleckstrin homology (PH) domains which consists of approximately 120 amino acids, and is the eleventh most common domain in the human genome. PH domains are found in a large number of distinct protein families involved in signal transduction [30]. PH domains can mediate recruitment of the PLC family members to the plasma membrane via phosphoinositides. Computer simulations and crystal structures of the PH domain found in kindlins, proteins which co-activate integrin adhesion proteins, have revealed that PH domains consist of 7 beta sheets and an alpha helix, and that the beta sheets form the PIP_2 binding site [31]. Surface plasmon resonance studies have revealed a 1mM affinity for PIP_2 within lipid bilayers.

Notably, membrane binding of PLCδ to PIP_2 is blocked by high levels of intracellular Ca^{2+} in hepatocytes due to generation of phosphoinositides [32]. This may also be due to the ability of Ca^{2+} to regulate the conformation of the headgroup of PIP_2 [33]. Unlike the PH domain of PLCδ1, which uses the PH domain to bind to the PIP_2 in the membrane, the PH domain of PLCβ2, cannot bind to phosphoinositides [34].

PLCγ contains 2 PH domains, one in the N-terminus and a C-terminal split PH domain. This PH domain of PLCγ is unique, since it is split between two tandem Src homology domains [35]. Early on, it was found that the carboxy-terminal region of the PH domains of PLCγ, PLCβ2 and PLCβ3 control the binding of heterotrimeric G protein βγ subunits to PLC following activation of G protein-coupled receptors [36, 37]. Interestingly, the binding of $G_{\beta\gamma}$ to the PH domain, and the binding of $G_{\beta\gamma}$ to Gα are mutually exclusive [36]. Therefore, this competition for binding to $G_{\beta\gamma}$ implicates PLC activation in preventing the regeneration of the $G\alpha/G_{\beta\gamma}$ heterotrimeric G proteins. In this way [34], PLC activation may regulate the signaling of proteins that are turned on in response to stimulation of G protein-coupled receptors. Additionally, downstream of SDF1α (CXCL12) binding to the G protein-coupled receptor CXC chemokine receptor 4 (CXCR4), the PH domains of PLCε1 promote lipase independent activation of Rap1, which leads to β2-integrin-mediated recruitment and adhesion of T-cells to sites of inflammation [38]. Overall, from these observations it can be inferred that PH domains have multiple roles in regulating the signaling via PLC.

In contrast to PLC signaling through heterotrimeric G-protein, it should be noted that Rap1 which belongs to the Rap-family of small GTPases and Ras-family small GTPases are also involved in PLC signaling. Rap and Ras are small, closely related GTP binding proteins. While Rap is an important factor in cell junctions and cell adhesion, Ras is linked to cell proliferation and survival [39]. Both of these small, monomeric G proteins also play critical roles in signaling through PLC as will be discussed below:

9.3.1.1 EF-Hand Motifs

The EF-hand motifs are helix-loop-helix motifs present in a number of calcium-binding proteins, such as myosin, calmodulin, calreticulin and troponin [40]. EF-hand motifs were first described for PLC when the crystal structure analysis of PLCδ1 revealed the characteristic helix-loop-helix motifs [41]. Within PLC, the EF-hand is part of the catalytic core that consists of an EF-hand, the X and Y and the C2 domains ([41] and see below). Upon binding to Ca^{2+}, the structure of PLC is stabilized as the EF-hand motifs undergo a conformational change to activate calcium-regulated functions, by exposing sites that become ligands for other proteins [42]. For example, in PLCβ, the EF-hands contain sites that mediate association with subunits of heterotrimeric G proteins, while in PLCγ, the EF-hands contain regions that lead to binding of tyrosine kinases [43]. Independent of the Ca^{2+} concentration, deletion of the EF-hands in the enzyme reduces PLC function, [44]; however, binding of Ca^{2+} to the EF-hand motifs can promote binding of PLC to PIP_2 via the PH domain. Lacking a PH domain, PLCζ may bind to membrane PIP_2 via cationic residues in the EF-hand [45] as well as the X-Y linker (as reviewed [46]).

9.3.1.2 X and Y Domains

So far, only PLCδ1 and PLCβ2 have been crystallized and their structures analyzed [34, 41]. The X and Y domains consist of approximately 300 amino acids and lie at the C-terminus of the EF-hand motifs. These domains consist of alternating α-helices and β-sheets that form aβaβaβaβ motif with a triosephosphate isomerase (TIM) barrel-like structure [41]. The X-region, containing all of the catalytic residues, is somewhat conserved across the PLC family members [27, 41]. The X-region forms one half of the TIM-barrel like structure. Within the X-region lies histidine residues that support the generation of the 1,2 cyclic inositol 4,5-bisphosphate [47]. The catalytic activity of this domain increases as the concentration of Ca^{2+} rises from 0.01μM to 10μM. Mutational analysis of rat PLCδ1 revealed that histidine^{311} and histidine^{356}, which are crucial for catalyzing the hydrolysis of PIP_2, have an important role within the X domain [47]. These residues are well conserved in PLC family members [47].

Structurally, the Y-domain (residues 489–606) forms the other half of the TIM-barrel-like architecture. This eightfold barrel structure is almost always found within an enzyme that regulates metabolism [48], although the functions of the enzymes are quite diverse. With the exception of an extended loop connection between the β5 and β6 strand, instead of a helix, this domain forms the second half of the TIM-barrel-like structure. This Y-domain is important for substrate recognition and regulates the preference of PLC for PIP_2, PIP and PI [49, 50].

PLCγ contains a unique region that splits the X and Y domains. This region contains the split PH domains at the ends and the middle consists of two N-terminal src homology (SH2) domains followed by an SH3 domain. The SH2

domains provide docking sites for tyrosine kinase growth factor receptors such as the platelet derived growth factor receptors (PDGFRs) and the epidermal growth factor receptors (EGFRs) to promote activation of this PLC family member [51–53]. The binding of tyrosine kinase receptors to PLCγ results in phosphorylation and activation of the enzymes [54, 55]. The SH3 domain directs the cellular localization of signaling proteins such as dynamin and the actin cytoskeleton. In addition, the SH3 domains have been found to mediate nerve growth factor-induced cell proliferation through activation of a guanine nucleotide exchange factor for phosphoinositide 3 kinase (PI3K) [56, 57].

9.3.1.3 C2 Domains

C2 domains are formed from about 120 amino acids [58] and can be found in more than 40 different proteins [41]. These motifs have several binding targets and have been implicated in signal transduction and membrane interactions. The C2 domains found within PLC family members are formed by an eight-stranded anti-parallel β-sandwich [41]. There are between three and four C2 domains found within PLCδ family members. In combination with Ca^{2+}, the C2 domain mediates the binding of PLCδ1 to anionic phospholipids to mediate signal transduction and membrane trafficking [43]. C2 domains have common structural motifs, which are found in PKCβ, rabphilin 3A [59, 60], and synaptotagmin I [61]. High cooperativity of calcium-dependent phospholipid binding sites implies that there are multiple sites that bind Ca^{2+}, which function synergistically [43].

C2 domains belong to the non-continuous Ca^{2+}-binding sites in which the Ca^{2+}-binding pockets are found far from each other in the amino acid sequence. In contrast EF-hands have binding pockets for Ca^{2+}produced by a stretch of continuous amino acids in the primary sequence [62, 63]. Functionally, the EF-hand motif, the most common Ca^{2+} binding motif in proteins, may compete for binding to Ca^{2+} with the C2 domains. The affinity of the EF-hand for Ca^{2+} is within the nanomolar to millimolar range, which overlaps the micromolar to millimolar binding constants of C2 domains [64, 65]. This broad affinity of C2 domains for [Ca^{2+}] reflects the diversity of the functions of proteins containing the C2 domains over a wide range of calcium concentrations [66–68].

9.3.1.4 PDZ Domains

PDZ (Post synaptic density (PSD)-95, Drosophila disc large tumor suppressor (DlgA), and Zonula occludens-1 protein (zo-1)) regions are separate from C2 domains, and are found in the C-terminal tails of PLCβ and PLCη lipases (Fig. 9.1) [58]. The PDZ domains are formed by 5 of 6 β-strands and 2 or 3 α-helices [69]. This common structural motif is found in many signaling proteins, where it functions as a scaffold for large molecular complexes [70]. In this way, the motif links many proteins to signaling from the cytoskeletal membranes. It has been postulated that

each PLCβ form may be used by different G protein-coupled receptors in regulating signaling events [71]. The sequences within the last five amino acids of the C-terminus are thought to regulate the specificity of the interaction of PLC with the Gα or Gβγ subunits [72].

9.4 Roles of Each PLC

As mentioned, there are six PLC family members (β, γ, δ, ε, η and ζ) consisting of thirteen different PLCs identified based on structure (Fig. 9.3) and activation mechanism. There is no alpha form of PLC, since the protein that was originally described as the α form turned out to be a protein disulfide isomerase without phospholipase activity [73]. Under most conditions, PLC is a cytoplasmic protein that moves to the plasma membrane. Its role within the membrane lipid rafts is somewhat controversial. For instance, PLC has been shown to accumulate within lipid rafts that consist of cholesterol, sphingomyelin and ceramide, *Xenopus* egg activation, catalyzing the hydrolysis of PIP_2 within these frog eggs [16, 74]. In contrast, PLC associates with the tyrosine kinase HER2 within non-raft domains in ovarian cancer cells [72]. In eggs and in ovarian cancer cells, PLC catalyzes hydrolysis of PIP_2 to promote classic functions (Fig. 9.2 and 9.3). With the exception of PLCγ2, there have been splice variants reported for each PLC isoform (as reviewed by [28, 44]). For PLC a different gene encodes each isoform. The diversity of the PLC isoforms is created with splice variants. PLC isoforms are quite distinct in regard to tissue distribution, cell localization, expression and regulation. PLCβ and PLCγ are typically activated by extracellular stimuli and are termed first line PLC's, whereas PLCδ, ε, η and ζ are activated by intracellular stimuli and known as secondary PLC's [75]. For the purposes of this chapter, we will focus on the general properties described for each isoform.

9.4.1 PLCβ1,2,3,4

There are four isoforms of PLCβ that range in size from 130 kDa for PLCβ4, 140 kDa for PLCβ2, 150 kDa for PLCβ1 and 152 kDa for PLCβ3. In addition, splice variants have been reported for each of these isoforms [76–78]. The PLCβ subfamily consists of a well-conserved core structure with an N-terminal PH domain, four EF-hands, a split X + Y catalytic domain, C2 domain and an extended C-terminal domain (Fig. 9.3). The catalytic domain being the most conserved domain of all PLC's isozymes with a substrate preference for PIP2 over PIP and PI [79]. PLCβ family members show distinct tissue expression and G protein regulation. PLCβ1 and PLCβ3 are ubiquitously expressed, whereas PLCβ2 and PLCβ4 are found only in hematopoietic and neuronal tissues, respectively [80]. These well-characterized isoforms of PLC are classically activated by G protein-coupled receptors and their

catalytic activity is entirely dependent upon Ca^{2+}. All four PLCβ isoforms are activated by $G\alpha_q$ subunit. PLCβ2 and PLCβ3 can also be activated by βγ subunits of the $G\alpha_{i/o}$ family of G proteins and by small GTPases such as Rac and Cdc42 (Figs. 9.1 and 9.3). In addition, PLCβ's are GTPase-activating proteins (GAPs) for the $G\alpha_q$ proteins that activate them [80, 81]. While $G\alpha_q$, $G\alpha_{11}$, and $G\alpha_{16}$ can activate PLCβ1, PCLβ2 and PLCβ3 family members [82]. In this case, the G protein-coupled receptor is stimulated by binding to its ligand, undergoing a conformational change to release $G\alpha_q$ or $G\alpha_{i/o}$ and Gβ/γ [81, 83, 84]. PLCβ is recruited to the membranes through interactions with Gβγ, but not Gαq [85]. In addition, PLCβ is recruited only through specific Gα subunits and the Gβγ subunits. These studies demonstrate that the PLC family members respond not only to Gα, but to Gβγ as well [37, 86]. Phosphoinositide-specific-phospholipase C β (PLCβ) is the main effector of $G\alpha_q$ stimulation that is coupled to receptors binding acetylcholine, dopamine, bradykinin, angiotensin II, other hormones and neurotransmitters [87].

The PLCβ family members have an additional 450 amino acid residues in the C-terminus (Fig. 9.3). While all PLCβ family members have been found in the nucleus, PLCβ1 is the major nuclear PLC [88–90]. Within this C-terminal 450 amino acid region, lies the greatest dissimilarity between PLC family members. In this region of the PLCβ1a and 1b splice variants is a nuclear localization signal, which directs localization of PLCβ1 isoforms, mostly to the nucleus while a nuclear export signal allows PLCβ1a to remain in the cytosol [77]. The likely consequence of DAG generation inside the nucleus is activation of nuclear PKC [91, 92]. Nuclear PLCβ1 regulates the cell cycle by modulating cyclin levels with cells overexpressing PLCβ1 producing increased levels of Cyclin D3 and a higher percentage of cells in S phase, in an erythroleukemia cell line [92, 93]. The binding site for Gαq is found within a region that mediates activation of Gαq by regulator of G protein signaling 4 (RGS4) and G alpha interacting protein (GAIP), which are GTPase-activating proteins (GAPs) [94]. This binding site blocks activation of PLCβ [95]. PLCβ1 is expressed at high levels in the cerebral cortex, retina, hippocampus and cardiomyocytes [96–98].

As mentioned, the expression of PLCβ2, which shares 48% identity with PLCβ1, appears to be restricted to cells of the hematopoietic lineages [99]. PLCβ2 can be activated by Rac, a member of the Rho-family of kinases [100]. The PH domain of PLCβ2 mediates binding of active forms of Rac (Rac1, Rac2 and Rac3), which leads to activation [101]. In contrast to PLCβ1 and PLCβ2, PLCβ3 lacks 10–20 amino acids within its C-terminus [102], although the significance of this difference is unknown. This PLC isoform is expressed by liver, brain and parotid gland [102].

PLCβ1 and PLCβ4 are expressed within the brain including the cerebral cortex, amygdala, hippocampus, and olfactory bulb and are thought to be involved in brain development and synaptic plasticity [91, 103–105]. Mis-regulation of PLCβ1 and/or PLCβ4 have been linked to several brain conditions such as schizophrenia, epilepsy, depression, Alzheimer's disease, bipolar disease and Huntington's disease [105–107]. In addition, studies of $PLC\beta1^{-/-}$ mice revealed roles for PLCβ1 in regulating

vision and central nervous system homeostasis and loss of PLCβ1 can lead to seizures and sudden death [108].

PLCβ1 plays important roles in cell differentiation, particularly in osteogenesis, hematopoiesis and myogenesis [79, 80, 109]. At least for myogenic differentiation, PLCβ1 signaling involves inositol polyphosphate multikinase and β -catenin as downstream effectors. By means of c-jun binding to cyclin D3 promoter, the activation of PLC β 1 pathway determines cyclin D3 accumulation and muscle cell differentiation [110]. Also, PLCβ participates in the differentiation and activation of immune cells involved in both the innate and adaptive immune systems including, macrophages, neutrophils, mast cells, T cells and B cells [79]. Consistent with a role of PLCβ3 in neutrophil development, it was reported that PLCβ3$^{-/-}$ mice develop myeloproliferative neoplasm with increased mature neutrophils [80].

A role for PLCβ in several cancers has been proposed. Recently, it has been reported that PLCβ2 acts as a negative regulator of triple negative breast cancer since up-regulation in invasive triple negative breast cancer cells was sufficient to lower the expression of surface antigens required for malignancy and to reduce the number of cells with a stem-like phenotype suggesting that enhancing PLCβ2 expression is a potential therapy for triple negative breast cancer [111]. Similarly, a high expression of PLCβ1 was associated with an enhanced long-term survival of patients with a proneural subtype high grade gliomas [112] and patients affected by myelodysplastic syndromes showed a reduced propensity to develop acute myeloid leukemia when the expression of nuclear PLCβ1 was reduced [91].

9.4.2 PLCγ$_{1,2}$

There are two isoforms of PLCγ, PLCγ1 and PLCγ2. PLCγ1 is ubiquitously expressed, and operates downstream of tyrosine kinase growth factor receptors such as vascular endothelial growth factor (VEGF), fibroblast growth factor (FGF), PDGF and EGF, whereas PLCγ2 is primarily expressed in hematopoietic cell lineages, often functioning downstream of immune cell receptors (Fig. 9.1 and [113, 114]). PLCγ subtypes are primarily activated by receptor tyrosine kinases (RTKs). Both PLCγ1 [115] and PLCγ2 can be activated by adhesion receptors, such as integrins [116]. PLCγ1 signaling acts via direct interactions with other signaling molecules via SH domains, as well as its lipase activity [117]. Some PLCγ signaling via nonreceptor tyrosine kinases has been reported [118, 119], including the B-cell receptor and via the Spleen tyrosine kinase (Syk)-activated PLCγ2 signaling in T cells [120] or osteogenic differentiation of bone marrow stromal cells [121]. PLCγ has important roles in differentiation, proliferation, transformation, calcium flux and tumorigenesis [22, 25, 122, 123]. In addition, it has been shown that PLC γ1 is activated by Src tyrosine kinase in Xenopus [124].

PLCγ can regulate proliferation by functions that are independent of its lipase activity. One example is that DNA synthesis does not require phospholipase function, but instead is regulated through the SH3 recruitment of a Ras exchange

factor, SOS1 [125]. In addition to the PH domain found in the N-terminus, these PLCγ family members have a second PH domain, which is split into an N-terminal domain of the PH domain that flanks two SH2 domains, followed by an SH3 domain and a C-terminal PH domain (Fig. 9.3). This C-terminal is thought to bind directly to the TRPC3 calcium channel, which then leads to agonist-induced calcium entry into the cell [35]. In addition, Vav1, c-Cbl and Slp76, via interactions with either the SH3 domain or the C-terminal SH2 domain are also required to help stabilize the recruitment of PLCγ1to the plasma membrane [126]. PLCγ2 and PKC are important upstream signals of macrophage-colony stimulating factor (M-CSF) and granulocyte-colony stimulating factor (G-CSF) that regulate myelopoiesis through cytokine production. These pathways activate ERK1/2, NFAT and JAK1/STAT-3 pathways [127]. PLCγ isoforms have been reported to be expressed in several innate immune cell types, including natural killer cells, macrophages, neutrophils and mast cells [128–131]. PLCγ activates the innate immune system by regulating respiratory bursts, phagocytosis, cell adhesion, and cell migration. PLCγ also modulates the inflammatory response by controlling Toll-like receptor-mediated signaling [132]. T cells express more PLCγ1 than PLCγ2 and PLCγ1 is activated by ligation of the T cell antigen receptor [126] and recruitment of PLCγ1 by Linker of Activated T cells (LAT) to the plasma membrane [133]. Phosphorylated LAT, in turn, serves as the primary docking site for the amino terminal SH2 domain of PLCγ1 to the membrane [134, 135]. All three SH domains of PLCγ1, however, are required to stabilize association of PLCγ1 with LAT, which is required to activate T cells [126]. Following engagement of the TCR, PLCγ1 production of DAG leads to activation of not only PKC, but also Ras guanyl releasing protein (GRP)-dependent signaling events [136, 137].

PLCγ1 is also activated by certain G protein-coupled receptors. We have shown that PLCγ1 can be activated following stimulation by the G protein-coupled receptor, C–C chemokine Receptor 7, a $G\alpha_{i/o}$ receptor, to mediate activation of β1 integrin, heterodimeric adhesion receptors [138]. In addition, PLCγ1 and PLCγ2 are both activated by the angiotensin and bradykinin G protein coupled receptors.

Homozygous disruption of PLCγ1 in a mouse model revealed that this PLC plays an essential role in growth and development [139]. In the absence of PLCγ1, the mice die at day E9.0, although until that stage of development the embryos appear normal. This mouse model revealed that although other PLCγ family members might be available, the role of PLCγ1 is essential and is not compensated by another PLC. In contrast, homozygous deletion of PLCγ2 leads to defects in platelet functions that are stimulated through β1 and β3 integrin adhesion proteins [140, 141]. PLCγ2 plays an essential role in B cell development, and function [20, 26]. Similar to PLCβ2, Rac, a member of the Rho-family of GTPases, can bind to and activate PLCγ2 [100]. This PLC family member can be activated through interactions with growth factor receptors, via phosphorylated tyrosines within their cytoplasmic tails via their intracellular tyrosine activation motifs (ITAMs). PLCγ2 also regulates calcium oscillations induced by the transcription factor, Nuclear Factor of Activated T cells (NFAT). Additionally, the SH2 domains can mediate activation of this receptor.

A role for PLCγ in neural development and certain neurological condition has become increasingly evident. PLCγ1 is highly expressed in the brain and is required for normal neuronal development and activation [114]. Since deregulation of PLCγ1 activation in response to brain derived neuronal factor can alter calcium influx and actin rearrangements that control neuronal migration, this PLC has been linked to diverse neurological disorders, including epilepsy, Huntington's disease and depression [114]. In this case mis-regulation of PLCγ1 function has been observed in animal models of Huntington's disease [142]. Moreover, genomic analysis has revealed a PLCγ2 variant that appears to be protective against Alzheimer's disease, possibly acting via microglia-modulated immune responses [143]. Other physiological roles for PLCγ are provided by recent evidence suggesting that PLCγ1 activates Akt-mediated Notch1 signaling, which is required for intima formation of blood vessels, and also plays a role in influenza viral entry into human epithelial cells [144, 145].

PLCγ1 is often mutated and highly expressed in several cancers being involved in tumorigenic processes including migration, invasion and in some cases, proliferation (as reviewed by [146]). Moderately to poorly differentiated breast tumors showed significantly higher levels of PLCγ1, compared with well differentiated tumors [147, 148]. Also, three distinct mutations in PLCγ2 were described in patients with chronic lymphocytic leukemia that were resistant to Ibrutinib treatment [148]. Indeed, studies have shown that mutated DNA sequences associated with human cancers and autoimmune diseases are well conserved between PLCγ1 und PLCγ2 and these mutations are gain-of-function effectors that destabilize normal regulatory signaling [149].

9.4.3 PLCδ$_{1, 3, 4}$

There are three identified isoforms of PLCδ with similar amino acid sequences that are highly evolutionary conserved from lower to higher eukaryotes [150]. PLCδ family members are activated by levels of calcium that are normally found in the cytoplasm (10^{-7}M to 10^{-5}M), making them one of the most calcium sensitive PLC isoforms [151, 152]. While PLCδ1 is localized to the cytoplasm in quiescent cells, this PLC isoform shuttles between the nucleus and the cytoplasm in active cells [153]. Human PLCδ4 was found to be primarily nuclear in human adipose derived mesenchymal stem cells [154]. Depletion of PLCδ1 leads to a block in the cell cycle [155]. PLCδ family members are thought to have a role in potentiating calcium signaling [151]. This form of PLC is similar to non-mammalian forms of PLC [15, 156] PLCδ1 can be activated by $G_{i/o}$ and Ga_q following stimulation of G protein-coupled receptors [157]. PLCδ is involved in regulating the activation of the actin cytoskeleton. Studies using PLCδ knockout mice have shown that PLCδ1 is required for maintenance of skin homeostasis; a recent study suggested that PLCδ1 is required for epidermal barrier integrity [158], whereas PLCδ3 regulates microvilli genesis within the intestine and the directed migration of neurons in

the cerebral cortex of developing brains [159, 160]. Knockout of both PLCδ1 and PLCδ3 resulted in embryonic lethality [161].

Similar to PLCγ1, mis-regulation of PLCδ1 has been linked to Alzheimer's disease [162]. Interestingly, this enzyme function is inhibited by sphingomyelin, a membrane lipid that is found in high concentrations in neurons. PLCδ1 is also mis-regulated in rat models of hypertension [163]. In addition, a decrease in PLCδ1 downregulation in cystic fibrosis cells resulted in dysregulation of Transient Receptor Potential Vanilloid 6 channel activity leading to an increase in the constitutive calcium influx, exacerbating cystic fibrosis effects [164].

PLCδ1 is expressed at high levels in hair follicles. Homozygous deletion of PLCδ1 leads to hair loss [165, 166]. The hair loss was due to an increase in leukocytes, specifically macrophages, neutrophils and T cells within the hair follicle [166]. Homozygous deletion of *Plcδ3* or *Plcδ4* had no apparent affect and the mice appeared normal.

During fertilization, a transient increase in Ca^{2+} precedes egg activation. Like other forms of PLC, this isoform appears to play a role in fertilization. Notably, PLCδ4$^{-/-}$ male mice are sterile [167, 168]. Even when PLCδ4$^{-/-}$ sperm were injected into eggs, few viable embryos developed. These studies implicate this family member in the regulation of fertilization [167]. In the same study, sperm isolated from PLCδ4 knockout mice were found to be inferior to sperm isolated from wild type mice in that the Ca^{2+} oscillations in these mice were delayed or did not occur at all [167].

Similar to several other PLC's, PLCδ's role in carcinogenesis is controversial. In one study, high expression levels of PLCδ significantly correlated with a shorter disease-free survival of patients with poorly-differentiated breast tumors suggesting a possible role as a tumor promoter [147]. In contrast, an unrelated study found that downregulation of PLCδ1 in breast cancers induced cell migration and invasion in an in vitro assay by inhibiting the phosphorylation of ERK1/2, suggesting a role as a tumor suppressor [169]. In support of the tumor suppressor effects, another study in colorectal cancer revealed that expression of PLCδ1, as shown by immunohistochemistry, was down-regulated in colorectal cancer samples, which was also linked to suppression of ERK1/2 phosphorylation [170] and increased autophagy of the colorectal cancer cells [171]. These results are in line with the concept that PLCδ1 may function as a tumor promoter or as tumor suppressor [147], and it is clear that further studies are needed to clarify the role of PLCδ in carcinogenesis.

9.4.4 PLCε

PLCε is the largest of the PLC family members with an apparent molecular weight of ~230 kDa and was originally described in 1998 as a Let-60 Ras binding protein [172]. Two splice variants of PLCε have been reported, termed PLCε1a and PLCε1b that are widely expressed, but distinct roles for these variants have

not been described [173]. PLCε is expressed at the highest levels in the heart, liver and lung, but can also be found in the skeletal muscle, spleen brain, lungs, kidneys, pancreas, testis, uterus, thymus and intestine [7, 174, 175]. This class of PLC, which was originally identified in *Caenorhabditis elegans*, and was later cloned in humans [7, 172, 174, 175]. The Ras-associated (RA) domains consist of approximately 100 amino acids that interact directly with the Ras-family GTPases, Ras [7, 175] and Rho [176]. A point mutation at a lysine residue in the RA2 domain of PLCε is sufficient to prevent Ras binding of the enzyme in a GTP-dependent manner [7]. Subsequently, it was found that PLCε could also be activated by the $G\alpha_{12}$ and Gβ/γ released by activated G protein-coupled receptors [175, 177]. Later, it was shown that hydrolysis of Golgi-associated phosphatidylinositol 4- phosphate (PI4P) in cardiac myocytes is mediated by Gβγ via the RA2 and N-terminal CDC25 and cysteine-rich domains [178, 179]. G protein-coupled receptors that activate PLCε include the adrenergic and PGE receptors. At the same time Gαs has been shown to stimulate activation of PLCε [180] while $G\alpha_{12}$ and $G\alpha_{13}$ can activate RhoA which can stimulate PLCε [180, 181]. Not only is this PLC family member activated by Ras and RhoA, it can also function as a guanine nucleotide exchange factor (GEF) for the Ras superfamily of GTPases [175]. In a contrasting study, the CDC25 domain of PLCε was found to serve as a GEF for Rap1 but not for other Ras family members [182]. These characteristics of PLCε reveal that this enzyme can be activated not only by subunits of heterotrimeric G proteins, but also by small GTPases.

This ability of PLCε to be regulated by both Ras and Rho suggest that it can contribute to both proliferation and to migration. More interestingly, since PLCβ can be activated by Rho, both PLC family members may work together to regulate signal transduction pathways that are activated following stimulation of cells by Rho to control cell migration. Similarly, since PLCε can be regulated by Ras, a downstream effector of PLCγ signaling following activation of growth factor receptors such as the EGF receptor, the signaling pathways may work together to promote proliferation. The ability of PLCε to coordinate signaling through these pathways points to regulatory mechanisms that may be more complex than originally thought.

Since PLCε can regulate inflammatory ligands for G protein-coupled receptors, it was suggested that PLCε may protect against ischemia/reperfusion injuries [183]. In contrast, in a separate study it was shown that PLCε is often upregulated in patients with heart failure [184] and recently it was shown that chronic activation of this isoform leads to cardiac hypertrophy [178]. Additionally, PLCε-null mice have abnormal development of aortic and pulmonary valves [185]. The role of PLCε in carcinogenesis is controversial, although the enzyme is thought to play important roles in the regulation of cancer development and progression, possibly acting as either an oncogene or tumor suppressor depending upon the type of tumor [186, 187]. Inflammatory processes induced by PLCε are thought to be involved in the progression towards cancer [188]. Mutation analysis of the PLCE1 gene landscape via The Cancer Genome Atlas (TCGA) database showed that PLCE1 is an often-

mutated gene in several types of cancer, in particular digestive tract cancer such as gastric cancer and esophageal squamous carcinoma, but also including skin cancer, lung cancer and head and neck cancers [187].

9.4.5 *PLCη$_{1,2}$*

PLCη consists of two members that are the most recently discovered PLC's and are most closely related to PLCδ subtype [189]. The sequence homology between PLCη$_1$ and PLCη$_2$ are ~50% similar. PLCη1 has an apparent molecular weight of 115 kDa in mouse and humans, while PLCη2 is larger at 125 kDa. PLCη can be activated by G protein-coupled receptors and RTK's [190] with PLC activity amplified by both intracellular Ca^{2+} mobilization and extracellular Ca^{2+} entry [191]. PLCη sequence analysis showed a novel EF-hand domain including a non-canonical EF-loop 2 sequence that is responsible for the enhanced binding of Ca^{2+} and enhanced hydrolysis of PIP_2 [189]. The PLCη$_1$ and PLCη$_{2,}$ isoforms are localized to the brain and neurons and are extremely sensitive to changes in calcium levels within the physiological range [8, 9, 192, 193]. Like PLCδ, this form of PLC responds to the 100 nM calcium concentrations found inside the cell [194]. However, PLCη is more sensitive than PLCδ [8] and PLCη can modulate a sustained Ca^{2+} release via production of IP_3 [189].

PLCη2 is expressed in the infant brain, specifically in the hippocampus, cerebral cortex and olfactory bulb [9], where it may play an important role in calcium mobilization required for axon growth and retraction, growth cone guidance, the generation of synapses and neurological responses [9]. In humans, loss of the human chromosomal region, which encodes PLCη2 has been linked to mental retardation [195] and role for PLCη2 in neurite growth has been postulated [196]. Alzheimer's disease has been linked to altered calcium homeostasis within neurons of the central nervous system with calcium accumulation occurring in disease affected neuronal cells [197]. Since PLCη is expressed in these same regions of the brain, a potential role for PLCη in Alzheimer's disease pathogenesis has been postulated [197].

9.4.6 *PLCζ*

PLCζ is the smallest of the mammalian PLC family members with a molecular mass of ~70 kDa in humans and ~74 kDa in mice [10, 198]. Interestingly, studies have shown PLC-like activities in plants with non-specific PLC hydrolyzing membrane phospholipids like phosphatidylcholine (PC) and phosphatidylethanolamine and another PLC with structural similarities to PLCζ [29]. In mammals, PLCζ expression has been confined to sperm heads [10, 198, 199] where it serves to activate eggs during fertilization [10, 200]. Subsequent studies have also identified further mammalian orthologues of PLCζ in human, hamster, monkey, and horse

sperm [201, 202]. Although some studies suggested the possibility that a post-acrosomal sheath WW domain-binding protein, termed PAWP, could be responsible for eliciting Ca^{2+} oscillations at egg activation [203–205], more recent studies now convincingly suggest that PAWP is not required to stimulate Ca^{2+} oscillations during egg activation, while strong evidence supports PLCζ as a soluble sperm factor responsible for the Ca^{2+} oscillations [206–210].

In line with its key role as a sperm factor, PLCζ generally localizes to distinct regions of the sperm head in mammals [211–213]. In humans, three distinct populations of PLCζ within the sperm head have been determined in the acrosomal, equatorial and post-acrosomal regions [211, 214–216]. Although this is the only isoform of PLC identified, which lacks the N-terminal PH domain, it shares the closest homology with PLCδ1 [217]. The absence of the PH domain demonstrates that presence is not required for membrane localization of PLCζ. It is unclear, however, how PLCζ targets the plasma membrane in the absence of the PH domain. There is some indication that the C2 domain may contribute to targeting PLCζ to membrane-bound PIP_2. Following fusion of sperm with the egg, PLCζ is released into an egg, which until that point, is arrested at the second meiotic division. Ca^{2+} oscillations that mediate activation of an egg are due to IP_3 mediated Ca^{2+} release. The presence of PLCζ within the cytoplasm leads to Ca^{2+} oscillations, which are classically observed during activation of the egg and release from the meiotic arrest [218]. In addition, immuno-depletion of PLCζ suppresses Ca^{2+} release. After the egg is fertilized the Ca^{2+} oscillations end when the pronuclei merge [219, 220]. Sperm from infertile men who are unable to activate eggs have been reported to exhibit reduced or abolished types of PLCζ [214, 216, 221]. Also, the proportion of sperm expressing PLCζ correlates with fertilization rates following intracytoplasmic sperm injection making PLCζ a diagnostic marker of fertilization [75].

9.5 Methods to Inhibit PLC

There are several chemical inhibitors that can be used to block PLC function. A commonly used pan inhibitor, 1-[6-((17β-3-methoxyestra-1,3,5(10)trien-17-yl)amino)hexyl)-1H-pyrrole-2,5-dione, (U73122), of phospholipase C, is thought to function by blocking translocation of the enzyme to the membrane [222]. For example, using 2 μM U73122 in contrast to the control U73343, we found that stimulation of CCR7 through one of its ligands, CCL21 [138], but not CCL19 promoted PLC dependent migration of T cells via β1 integrin adhesion proteins. In the same study, we were able to determine that the PLCγ1 isoform regulated migration by preventing CCL21 directed migration with targeted siRNA. This data suggests that one G protein-coupled receptor can activate PLCγ1 through two different ligands to control migration in T cells. In this case we speculate that PLCγ1

mediates integrin activation through inside-out signaling leading to activation of β1-integrins.

Recently, it has been shown that U73122 forms covalent associations with human PLCβ3, when the phospholipase is associated with mixed micelles [223]. While U73122 has been used as a pan inhibitor of PLC in numerous studies [21, 138, 224–228], in the study by Klein et al., instead of inhibiting PLC, U73122 activated human PLCγ1, human PLCβ2 and human PLCβ3, which had been incorporated into micelles to differing magnitudes. Since the PLC used in these studies was in a purified form, it is unclear, how U73122 functions to regulate the extent of PLC activation. In a second study, 1 μM U73122 was found to directly inhibit G protein activated inwardly rectifying potassium channels. This was in contrast to a second PLC inhibitor, 2-Nitro-4-carboxyphenylN,N -diphenylcarbamate (NCDC), which did not have that effect [229]. NCDC, however, is also thought to have non-specific effects that are not related to PLC functions [230].

It should also be noted that in rabbit parietal cells, use of the U73122 led to a number of unexpected effects including mis-regulation of Ca^{2+} mobilization, and acid secretion induced by an agonist. Of equal concern, the negative control U73343 blocked acid secretion [231]. Therefore, this PLC inhibitor when used, should be used with caution.

Similarly, there are at least three other known inhibitors and two activators of PLC, yet they are not specific. These inhibitors include O-(Octahydro-4,7-mthano-1H-iden-5-yl)carbonopotassium dithioate, [232], Edelfosine [233] and RHC 80267 (O,O′[1,6-Hexanediyl*bis*(iminocarbonyl)]dioxime cyclohexanone) [234]. The two activators are *m*-3M3FBS (2,4,6-Trimethyl-*N*-[3-(trifluoromethyl)phenyl]benzenesulfonamide), and the ortho version *o*-3M3FBS [235].

Heterozygous deletion of a specific PLC family member via siRNA, however, can yield targeted results [138]. As mentioned, in these studies, PLCγ1 specific siRNA was used to confirm the role of this PLC isoform in the regulation of β1 integrins during the adhesion of primary T cells. In the future it may be advisable to determine the specific PLC family member involved in a cellular response, by using siRNAs. More recently the discovery of Clustered Regularly Spaced Short Palindromic Repeats-Cas9 (CRISPR Cas9) technology, which was originally described in bacterial systems, allows for long-term targeted disruption or in some cases activation of specific genes [236, 237]. This technology, will likely be used to target specific PLC isoforms in the future.

The highly specific 3-phosphoinositide-dependent protein kinase 1(PDK1) inhibitor 2-O-benzyl-myo-inositol 1,3,4,5,6-pentakisphosphate (2-O-Bn-InsP5) can also block PLCγ1 dependent cell functions such as EGFR-induced phosphorylation of PLCγ1. This interaction takes place through the PH domain of PDK1. The loss of phosphorylation blocks PLCγ1 activity and downstream the cell migration and invasion [238], and has been considered as a lead compound for an anti-metastatic drug.

9.6 Future Directions

9.6.1 Hierarchy of Isozymes

It is unclear how the different isoforms of PLC are activated in cells receiving multiple stimuli from different receptors. With thirteen identified isoforms, expressed in multiple cell types, it will be important to define how the different signaling events that are linked to each isoform are controlled. Since PLC activation leads to release of IP_3 and DAG in response to activation, it will be important to determine how cells discriminates between multiple PLC signals to determine the hierarchy, intensity and duration of signaling events. As mentioned, PLCβ2 and PLCγ2 are activated by Rac while PLCε is activated by RhoA. These observations suggest that key regulators of cell motility function through different PLC family members, and may have pivotal roles in defining where and when a cell migrates.

PLC enzymes are found in every cell in the body, where they play critical roles in regulating diverse cellular responses (as reviewed in [28]). As mentioned, some family members serve as scaffolds for other signaling proteins, while others can serve as GAPs or GEFs, for secondary signaling proteins. Other PLCs function to amplify the Ca^{2+}oscillations in the cell. Certain PLC family members can travel to the nucleus to control signaling there. With PLC family members playing key roles in numerous cell functions, it will be important to define how each PLC is regulated and how the cellular environment affects the duration and intensity of the response.

References

1. Hokin MR, Hokin LE (1953) Enzyme secretion and the incorporation of P32 into phospholipides of pancreas slices. J Biol Chem 203(2):967–977
2. Michell RH, Allan D (1975) Inositol cyclis phosphate as a product of phosphatidylinositol breakdown by phospholipase C (Bacillus cereus). FEBS Lett 53(3):302–304
3. Takenawa T, Nagai Y (1982) Effect of unsaturated fatty acids and Ca^{2+} on phosphatidylinositol synthesis and breakdown. J Biochem 91(3):793–799
4. Streb H et al (1983) Release of Ca^{2+} from a nonmitochondrial intracellular store in pancreatic acinar cells by inositol-1,4,5-trisphosphate. Nature 306(5938):67–69
5. Suh PG et al (1988) Inositol phospholipid-specific phospholipase C: complete cDNA and protein sequences and sequence homology to tyrosine kinase-related oncogene products. Proc Natl Acad Sci U S A 85(15):5419–5423
6. Suh PG et al (1988) Cloning and sequence of multiple forms of phospholipase C. Cell 54(2):161–169
7. Kelley GG et al (2001) Phospholipase C(epsilon): a novel Ras effector. EMBO J 20(4):743–754
8. Hwang JI et al (2005) Molecular cloning and characterization of a novel phospholipase C, PLC-eta. Biochem J 389(Pt 1):181–186
9. Nakahara M et al (2005) A novel phospholipase C, PLC(eta)2, is a neuron-specific isozyme. J Biol Chem 280(32):29128–29134
10. Saunders CM et al (2002) PLC zeta: a sperm-specific trigger of Ca^{2+} oscillations in eggs and embryo development. Development 129(15):3533–3544

11. Albuquerque EX, Thesleff S (1967) Influence of phospholipase C on some electrical properties of the skeletal muscle membrane. J Physiol 190(1):123–137
12. Macchia V, Pastan I (1967) Action of phospholipase C on the thyroid. Abolition of the response to thyroid-stimulating hormone. J Biol Chem 242(8):1864–1869
13. Portela A et al (1966) Membrane response to phospholipase C and acetylcholine in cesium and potassium Ringer. Acta Physiol Lat Am 16(4):380–386
14. Trifaro JM et al (2002) Pathways that control cortical F-actin dynamics during secretion. Neurochem Res 27(11):1371–1385
15. Fukami K et al (2010) Phospholipase C is a key enzyme regulating intracellular calcium and modulating the phosphoinositide balance. Prog Lipid Res 49(4):429–437
16. Kadamur G, Ross EM (2013) Mammalian phospholipase C. Annu Rev Physiol 75:127–154
17. Sun MK, Alkon DL (2010) Pharmacology of protein kinase C activators: cognition-enhancing and antidementic therapeutics. Pharmacol Ther 127(1):66–77
18. Rosse C et al (2010) PKC and the control of localized signal dynamics. Nat Rev Mol Cell Biol 11(2):103–112
19. Akutagawa A et al (2006) Disruption of phospholipase Cdelta4 gene modulates the liver regeneration in cooperation with nuclear protein kinase C. J Biochem 140(5):619–625
20. Hashimoto A et al (2000) Cutting edge: essential role of phospholipase C-gamma 2 in B cell development and function. J Immunol 165(4):1738–1742
21. Hong J et al (2010) Bile acid reflux contributes to development of esophageal adenocarcinoma via activation of phosphatidylinositol-specific phospholipase Cgamma2 and NADPH oxidase NOX5-S. Cancer Res 70(3):1247–1255
22. Li M et al (2009) Phospholipase Cepsilon promotes intestinal tumorigenesis of Apc(Min/+) mice through augmentation of inflammation and angiogenesis. Carcinogenesis 30(8):1424–1432
23. Sun C et al (2009) Inhibition of phosphatidylcholine-specific phospholipase C prevents bone marrow stromal cell senescence in vitro. J Cell Biochem 108(2):519–528
24. Varela D et al (2007) Activation of H2O2-induced VSOR Cl^- currents in HTC cells require phospholipase Cgamma1 phosphorylation and Ca^{2+} mobilisation. Cell Physiol Biochem 20(6):773–780
25. Wahl MI et al (1989) Platelet-derived growth factor induces rapid and sustained tyrosine phosphorylation of phospholipase C-gamma in quiescent BALB/c 3T3 cells. Mol Cell Biol 9(7):2934–2943
26. Wang D et al (2000) Phospholipase Cgamma2 is essential in the functions of B cell and several Fc receptors. Immunity 13(1):25–35
27. Bunney TD, Katan M (2011) PLC regulation: emerging pictures for molecular mechanisms. Trends Biochem Sci 36(2):88–96
28. Suh PG et al (2008) Multiple roles of phosphoinositide-specific phospholipase C isozymes. BMB Rep 41(6):415–434
29. Rupwate SD, Rajasekharan R (2012) Plant phosphoinositide-specific phospholipase C: an insight. Plant Signal Behav 7(10):1281–1283
30. Harlan JE et al (1994) Pleckstrin homology domains bind to phosphatidylinositol-4,5-bisphosphate. Nature 371(6493):168–170
31. Ni T et al (2017) Structure and lipid-binding properties of the kindlin-3 pleckstrin homology domain. Biochem J 474(4):539–556
32. Kang JK et al (2017) Increased intracellular Ca^{2+} concentrations prevent membrane localization of PH domains through the formation of Ca^{2+}-phosphoinositides. Proc Natl Acad Sci U S A 114(45):11926–11931
33. Bilkova E et al (2017) Calcium directly regulates phosphatidylinositol 4,5-bisphosphate headgroup conformation and recognition. J Am Chem Soc 139(11):4019–4024
34. Jezyk MR et al (2006) Crystal structure of Rac1 bound to its effector phospholipase C-beta2. Nat Struct Mol Biol 13(12):1135–1140

35. Wen W, Yan J, Zhang M (2006) Structural characterization of the split pleckstrin homology domain in phospholipase C-gamma1 and its interaction with TRPC3. J Biol Chem 281(17):12060–12068
36. Touhara K et al (1994) Binding of G protein beta gamma-subunits to pleckstrin homology domains. J Biol Chem 269(14):10217–10220
37. Wang T et al (1999) Differential association of the pleckstrin homology domains of phospholipases C-beta 1, C-beta 2, and C-delta 1 with lipid bilayers and the beta gamma subunits of heterotrimeric G proteins. Biochemistry 38(5):1517–1524
38. Strazza M et al (2017) PLCepsilon1 regulates SDF-1alpha-induced lymphocyte adhesion and migration to sites of inflammation. Proc Natl Acad Sci U S A 114(10):2693–2698
39. Raaijmakers JH, Bos JL (2009) Specificity in Ras and Rap signaling. J Biol Chem 284(17):10995–10999
40. Kawasaki H, Kretsinger RH (1994) Calcium-binding proteins. 1: EF-hands. Protein Profile 1(4):343–517
41. Essen LO et al (1996) Crystal structure of a mammalian phosphoinositide-specific phospholipase C delta. Nature 380(6575):595–602
42. Rhee SG, Choi KD (1992) Regulation of inositol phospholipid-specific phospholipase C isozymes. J Biol Chem 267(18):12393–12396
43. Essen LO et al (1997) A ternary metal binding site in the C2 domain of phosphoinositide-specific phospholipase C-delta1. Biochemistry 36(10):2753–2762
44. Otterhag L, Sommarin M, Pical C (2001) N-terminal EF-hand-like domain is required for phosphoinositide-specific phospholipase C activity in Arabidopsis thaliana. FEBS Lett 497(2-3):165–170
45. Nomikos M et al (2015) Essential role of the EF-hand domain in targeting sperm phospholipase Czeta to membrane phosphatidylinositol 4,5-bisphosphate (PIP2). J Biol Chem 290(49):29519–29530
46. Theodoridou M et al (2013) Chimeras of sperm PLCzeta reveal disparate protein domain functions in the generation of intracellular Ca^{2+} oscillations in mammalian eggs at fertilization. Mol Hum Reprod 19(12):852–864
47. Ellis MV, S. U, Katan M (1995) Mutations within a highly conserved sequence present in the X region of phosphoinositide-specific phospholipase C-delta 1. Biochem J 307(Pt 1):69–75
48. Nagano N, Orengo CA, Thornton JM (2002) One fold with many functions: the evolutionary relationships between TIM barrel families based on their sequences, structures and functions. J Mol Biol 321(5):741–765
49. Williams RL (1999) Mammalian phosphoinositide-specific phospholipase C. Biochim Biophys Acta 1441(2-3):255–267
50. Ryu SH et al (1987) Bovine brain cytosol contains three immunologically distinct forms of inositolphospholipid-specific phospholipase C. Proc Natl Acad Sci U S A 84(19):6649–6653
51. Margolis B et al (1990) Effect of phospholipase C-gamma overexpression on PDGF-induced second messengers and mitogenesis. Science 248(4955):607–610
52. Meisenhelder J et al (1989) Phospholipase C-gamma is a substrate for the PDGF and EGF receptor protein-tyrosine kinases in vivo and in vitro. Cell 57(7):1109–1122
53. Wahl MI, Daniel TO, Carpenter G (1988) Antiphosphotyrosine recovery of phospholipase C activity after EGF treatment of A-431 cells. Science 241(4868):968–970
54. Ronnstrand L et al (1992) Identification of two C-terminal autophosphorylation sites in the PDGF beta-receptor: involvement in the interaction with phospholipase C-gamma. EMBO J 11(11):3911–3919
55. Kim HK et al (1991) PDGF stimulation of inositol phospholipid hydrolysis requires PLC-gamma 1 phosphorylation on tyrosine residues 783 and 1254. Cell 65(3):435–441
56. Gout I et al (1993) The GTPase dynamin binds to and is activated by a subset of SH3 domains. Cell 75(1):25–36
57. Bar-Sagi D et al (1993) SH3 domains direct cellular localization of signaling molecules. Cell 74(1):83–91

58. van Huizen R et al (1998) Two distantly positioned PDZ domains mediate multivalent INAD-phospholipase C interactions essential for G protein-coupled signaling. EMBO J 17(8):2285–2297
59. Yamaguchi T et al (1993) Two functionally different domains of rabphilin-3A, Rab3A p25/smg p25A-binding and phospholipid- and Ca^{2+}-binding domains. J Biol Chem 268(36):27164–27170
60. Luo JH, Weinstein IB (1993) Calcium-dependent activation of protein kinase C. The role of the C2 domain in divalent cation selectivity. J Biol Chem 268(31):23580–23584
61. Davletov BA, Sudhof TC (1993) A single C2 domain from synaptotagmin I is sufficient for high affinity Ca^{2+}/phospholipid binding. J Biol Chem 268(35):26386–26390
62. Kawasaki H, Nakayama S, Kretsinger RH (1998) Classification and evolution of EF-hand proteins. Biometals 11(4):277–295
63. Kim Y et al (2001) Chimeric HTH motifs based on EF-hands. J Biol Inorg Chem 6(2):173–181
64. Lomasney JW et al (1999) Activation of phospholipase C delta1 through C2 domain by a Ca^{2+}-enzyme-phosphatidylserine ternary complex. J Biol Chem 274(31):21995–22001
65. Montaville P et al (2007) The C2A-C2B linker defines the high affinity Ca^{2+} binding mode of rabphilin-3A. J Biol Chem 282(7):5015–5025
66. Busch E et al (2000) Calcium affinity, cooperativity, and domain interactions of extracellular EF-hands present in BM-40. J Biol Chem 275(33):25508–25515
67. Gifford JL, Walsh MP, Vogel HJ (2007) Structures and metal-ion-binding properties of the Ca^{2+}-binding helix-loop-helix EF-hand motifs. Biochem J 405(2):199–221
68. Linse S et al (1988) The role of protein surface charges in ion binding. Nature 335(6191):651–652
69. Fanning AS, Anderson JM (1996) Protein-protein interactions: PDZ domain networks. Curr Biol 6(11):1385–1388
70. Wang CK et al (2010) Extensions of PDZ domains as important structural and functional elements. Protein Cell 1(8):737–751
71. Kim JK et al (2011) Subtype-specific roles of phospholipase C-beta via differential interactions with PDZ domain proteins. Adv Enzym Regul 51(1):138–151
72. Paris L et al (2017) Phosphatidylcholine-specific phospholipase C inhibition reduces HER2-overexpression, cell proliferation and in vivo tumor growth in a highly tumorigenic ovarian cancer model. Oncotarget 8(33):55022–55038
73. Charnock-Jones DS, Day K, Smith SK (1996) Cloning, expression and genomic organization of human placental protein disulfide isomerase (previously identified as phospholipase C alpha). Int J Biochem Cell Biol 28(1):81–89
74. Bates RC et al (2014) Activation of Src and release of intracellular calcium by phosphatidic acid during Xenopus laevis fertilization. Dev Biol 386(1):165–180
75. Yelumalai S et al (2015) Total levels, localization patterns, and proportions of sperm exhibiting phospholipase C zeta are significantly correlated with fertilization rates after intracytoplasmic sperm injection. Fertil Steril 104(3):561–8.e4
76. Lagercrantz J et al (1995) Genomic organization and complete cDNA sequence of the human phosphoinositide-specific phospholipase C beta 3 gene (PLCB3). Genomics 26(3):467–472
77. Mao GF, Kunapuli SP, Koneti Rao A (2000) Evidence for two alternatively spliced forms of phospholipase C-beta2 in haematopoietic cells. Br J Haematol 110(2):402–408
78. Kim MJ et al (1998) A cytosolic, galphaq- and betagamma-insensitive splice variant of phospholipase C-beta4. J Biol Chem 273(6):3618–3624
79. Xiao W, Kawakami Y, Kawakami T (2013) Immune regulation by phospholipase C-beta isoforms. Immunol Res 56(1):9–19
80. Kawakami T, Xiao W (2013) Phospholipase C-beta in immune cells. Adv Biol Regul 53(3):249–257
81. Berstein G et al (1992) Phospholipase C-beta 1 is a GTPase-activating protein for Gq/11, its physiologic regulator. Cell 70(3):411–418

82. Runnels LW, Scarlata SF (1999) Determination of the affinities between heterotrimeric G protein subunits and their phospholipase C-beta effectors. Biochemistry 38(5):1488–1496
83. Hwang JI et al (2000) Regulation of phospholipase C-beta 3 activity by Na^+/H^+ exchanger regulatory factor 2. J Biol Chem 275(22):16632–16637
84. Camps M et al (1992) Isozyme-selective stimulation of phospholipase C-beta 2 by G protein beta gamma-subunits. Nature 360(6405):684–686
85. Lee SB et al (1993) Activation of phospholipase C-beta 2 mutants by G protein alpha q and beta gamma subunits. J Biol Chem 268(34):25952–25957
86. Wang T et al (1999) Selective interaction of the C2 domains of phospholipase C-beta1 and -beta2 with activated Galphaq subunits: an alternative function for C2-signaling modules. Proc Natl Acad Sci U S A 96(14):7843–7846
87. Scarlata S et al (2016) Phospholipase Cbeta connects G protein signaling with RNA interference. Adv Biol Regul 61:51–57
88. Martelli AM et al (1992) Nuclear localization and signalling activity of phosphoinositidase C beta in Swiss 3T3 cells. Nature 358(6383):242–245
89. Kim CG, Park D, Rhee SG (1996) The role of carboxyl-terminal basic amino acids in Gqalpha-dependent activation, particulate association, and nuclear localization of phospholipase C-beta1. J Biol Chem 271(35):21187–21192
90. Payrastre B et al (1992) A differential location of phosphoinositide kinases, diacylglycerol kinase, and phospholipase C in the nuclear matrix. J Biol Chem 267(8):5078–5084
91. Ratti S et al (2017) Nuclear inositide signaling via phospholipase C. J Cell Biochem 118(8):1969–1978
92. Poli A et al (2016) Nuclear phosphatidylinositol signaling: focus on phosphatidylinositol phosphate kinases and phospholipases C. J Cell Physiol 231(8):1645–1655
93. Piazzi M et al (2015) PI-PLCbeta1b affects Akt activation, cyclin E expression, and caspase cleavage, promoting cell survival in pro-B-lymphoblastic cells exposed to oxidative stress. FASEB J 29(4):1383–1394
94. Navaratnarajah P, Gershenson A, Ross EM (2017) The binding of activated Galphaq to phospholipase C-beta exhibits anomalous affinity. J Biol Chem 292(40):16787–16801
95. Wang HL (1997) Basic amino acids at the C-terminus of the third intracellular loop are required for the activation of phospholipase C by cholecystokinin-B receptors. J Neurochem 68(4):1728–1735
96. Adamski FM, Timms KM, Shieh BH (1999) A unique isoform of phospholipase Cbeta4 highly expressed in the cerebellum and eye. Biochim Biophys Acta 1444(1):55–60
97. Min DS et al (1993) Purification of a novel phospholipase C isozyme from bovine cerebellum. J Biol Chem 268(16):12207–12212
98. Alvarez RA et al (1995) cDNA sequence and gene locus of the human retinal phosphoinositide-specific phospholipase-C beta 4 (PLCB4). Genomics 29(1):53–61
99. Park D et al (1992) Cloning, sequencing, expression, and Gq-independent activation of phospholipase C-beta 2. J Biol Chem 267(23):16048–16055
100. Harden TK, Hicks SN, Sondek J (2009) Phospholipase C isozymes as effectors of Ras superfamily GTPases. J Lipid Res 50(Suppl):S243–S248
101. Snyder JT et al (2003) The pleckstrin homology domain of phospholipase C-beta2 as an effector site for Rac. J Biol Chem 278(23):21099–21104
102. Jhon DY et al (1993) Cloning, sequencing, purification, and Gq-dependent activation of phospholipase C-beta 3. J Biol Chem 268(9):6654–6661
103. Fukaya M et al (2008) Predominant expression of phospholipase Cbeta1 in telencephalic principal neurons and cerebellar interneurons, and its close association with related signaling molecules in somatodendritic neuronal elements. Eur J Neurosci 28(9):1744–1759
104. Watanabe M et al (1998) Patterns of expression for the mRNA corresponding to the four isoforms of phospholipase Cbeta in mouse brain. Eur J Neurosci 10(6):2016–2025
105. Yang YR et al (2016) Primary phospholipase C and brain disorders. Adv Biol Regul 61:80–85
106. Koh HY (2013) Phospholipase C-beta1 and schizophrenia-related behaviors. Adv Biol Regul 53(3):242–248

107. Schoonjans AS et al (2016) PLCB1 epileptic encephalopathies; Review and expansion of the phenotypic spectrum. Eur J Paediatr Neurol 20(3):474–479
108. Kim D et al (1997) Phospholipase C isozymes selectively couple to specific neurotransmitter receptors. Nature 389(6648):290–293
109. Cocco L et al (2016) Modulation of nuclear PI-PLCbeta1 during cell differentiation. Adv Biol Regul 60:1–5
110. Ramazzotti G et al (2017) PLC-beta1 and cell differentiation: An insight into myogenesis and osteogenesis. Adv Biol Regul 63:1–5
111. Brugnoli F et al (2017) Up-modulation of PLC-beta2 reduces the number and malignancy of triple-negative breast tumor cells with a CD133(+)/EpCAM(+) phenotype: a promising target for preventing progression of TNBC. BMC Cancer 17(1):617
112. Lu G et al (2016) Phospholipase C Beta 1: a candidate signature gene for proneural subtype high-grade glioma. Mol Neurobiol 53(9):6511–6525
113. Driscoll PC (2015) Exposed: the many and varied roles of phospholipase C gamma SH2 domains. J Mol Biol 427(17):2731–2733
114. Jang HJ et al (2013) Phospholipase C-gamma1 involved in brain disorders. Adv Biol Regul 53(1):51–62
115. Epple H et al (2008) Phospholipase Cgamma2 modulates integrin signaling in the osteoclast by affecting the localization and activation of Src kinase. Mol Cell Biol 28(11):3610–3622
116. Choi JH et al (2007) Phospholipase C-gamma1 potentiates integrin-dependent cell spreading and migration through Pyk2/paxillin activation. Cell Signal 19(8):1784–1796
117. Bunney TD et al (2012) Structural and functional integration of the PLCgamma interaction domains critical for regulatory mechanisms and signaling deregulation. Structure 20(12):2062–2075
118. Arkinstall S, Payton M, Maundrell K (1995) Activation of phospholipase C gamma in Schizosaccharomyces pombe by coexpression of receptor or nonreceptor tyrosine kinases. Mol Cell Biol 15(3):1431–1438
119. Phillippe M et al (2009) Role of nonreceptor protein tyrosine kinases during phospholipase C-gamma 1-related uterine contractions in the rat. Reprod Sci 16(3):265–273
120. Buitrago C, Gonzalez Pardo V, de Boland AR (2002) Nongenomic action of 1 alpha,25(OH)(2)-vitamin D3. Activation of muscle cell PLC gamma through the tyrosine kinase c-Src and PtdIns 3-kinase. Eur J Biochem 269(10):2506–2515
121. Kusuyama J et al (2018) Spleen tyrosine kinase influences the early stages of multilineage differentiation of bone marrow stromal cell lines by regulating phospholipase C gamma activities. J Cell Physiol 233(3):2549–2559
122. Rivas M, Santisteban P (2003) TSH-activated signaling pathways in thyroid tumorigenesis. Mol Cell Endocrinol 213(1):31–45
123. Kroczek C et al (2010) Swiprosin-1/EFhd2 controls B cell receptor signaling through the assembly of the B cell receptor, Syk, and phospholipase C gamma2 in membrane rafts. J Immunol 184(7):3665–3676
124. Sato K et al (2003) Reconstitution of Src-dependent phospholipase Cgamma phosphorylation and transient calcium release by using membrane rafts and cell-free extracts from Xenopus eggs. J Biol Chem 278(40):38413–38420
125. Kim MJ et al (2000) Direct interaction of SOS1 Ras exchange protein with the SH3 domain of phospholipase C-gamma1. Biochemistry 39(29):8674–8682
126. Braiman A et al (2006) Recruitment and activation of PLCgamma1 in T cells: a new insight into old domains. EMBO J 25(4):774–784
127. Barbosa CM et al (2014) PLCgamma2 and PKC are important to myeloid lineage commitment triggered by M-SCF and G-CSF. J Cell Biochem 115(1):42–51
128. Wen R et al (2002) Phospholipase C gamma 2 is essential for specific functions of Fc epsilon R and Fc gamma R. J Immunol 169(12):6743–6752
129. Todt JC, Hu B, Curtis JL (2004) The receptor tyrosine kinase MerTK activates phospholipase C gamma2 during recognition of apoptotic thymocytes by murine macrophages. J Leukoc Biol 75(4):705–713

130. Ting AT et al (1992) Fc gamma receptor activation induces the tyrosine phosphorylation of both phospholipase C (PLC)-gamma 1 and PLC-gamma 2 in natural killer cells. J Exp Med 176(6):1751–1755
131. Hiller G, Sundler R (2002) Regulation of phospholipase C-gamma 2 via phosphatidylinositol 3-kinase in macrophages. Cell Signal 14(2):169–173
132. Kagan JC, Medzhitov R (2006) Phosphoinositide-mediated adaptor recruitment controls Toll-like receptor signaling. Cell 125(5):943–955
133. Finco TS et al (1998) LAT is required for TCR-mediated activation of PLCgamma1 and the Ras pathway. Immunity 9(5):617–626
134. Stoica B et al (1998) The amino-terminal Src homology 2 domain of phospholipase C gamma 1 is essential for TCR-induced tyrosine phosphorylation of phospholipase C gamma 1. J Immunol 160(3):1059–1066
135. Zhang W et al (2000) Association of Grb2, Gads, and phospholipase C-gamma 1 with phosphorylated LAT tyrosine residues. Effect of LAT tyrosine mutations on T cell angigen receptor-mediated signaling. J Biol Chem 275(30):23355–23361
136. Dower NA et al (2000) RasGRP is essential for mouse thymocyte differentiation and TCR signaling. Nat Immunol 1(4):317–321
137. Ebinu JO et al (2000) RasGRP links T-cell receptor signaling to Ras. Blood 95(10):3199–3203
138. Shannon LA et al (2010) CCR7/CCL21 migration on fibronectin is mediated by phospholipase Cgamma1 and ERK1/2 in primary T lymphocytes. J Biol Chem 285(50):38781–38787
139. Ji QS et al (1997) Essential role of the tyrosine kinase substrate phospholipase C-gamma1 in mammalian growth and development. Proc Natl Acad Sci U S A 94(7):2999–3003
140. Wonerow P et al (2003) A critical role for phospholipase Cgamma2 in alphaIIbbeta3-mediated platelet spreading. J Biol Chem 278(39):37520–37529
141. Inoue O et al (2003) Integrin alpha2beta1 mediates outside-in regulation of platelet spreading on collagen through activation of Src kinases and PLCgamma2. J Cell Biol 160(5):769–780
142. Garcia-Diaz Barriga G et al (2017) 7,8-dihydroxyflavone ameliorates cognitive and motor deficits in a Huntington's disease mouse model through specific activation of the PLCgamma1 pathway. Hum Mol Genet 26(16):3144–3160
143. Sims R et al (2017) Rare coding variants in PLCG2, ABI3, and TREM2 implicate microglial-mediated innate immunity in Alzheimer's disease. Nat Genet 49(9):1373–1384
144. Jiang D et al (2017) Phospholipase Cgamma1 mediates intima formation through Akt-Notch1 signaling independent of the phospholipase activity. J Am Heart Assoc 6(7)
145. Zhu L et al (2016) PLC-gamma1 is involved in the inflammatory response induced by influenza A virus H1N1 infection. Virology 496:131–137
146. Jang HJ et al (2018) PLCgamma1: potential arbitrator of cancer progression. Adv Biol Regul 67:179–189
147. Cai S et al (2017) Expression of phospholipase C isozymes in human breast cancer and their clinical significance. Oncol Rep 37(3):1707–1715
148. Woyach JA et al (2014) Resistance mechanisms for the Bruton's tyrosine kinase inhibitor ibrutinib. N Engl J Med 370(24):2286–2294
149. Koss H et al (2014) Dysfunction of phospholipase Cgamma in immune disorders and cancer. Trends Biochem Sci 39(12):603–611
150. Meldrum E et al (1991) A second gene product of the inositol-phospholipid-specific phospholipase C delta subclass. Eur J Biochem 196(1):159–165
151. Allen V et al (1997) Regulation of inositol lipid-specific phospholipase cdelta by changes in Ca^{2+} ion concentrations. Biochem J 327(Pt 2):545–552
152. Kim YH et al (1999) Phospholipase C-delta1 is activated by capacitative calcium entry that follows phospholipase C-beta activation upon bradykinin stimulation. J Biol Chem 274(37):26127–26134
153. Yamaga M et al (1999) Phospholipase C-delta1 contains a functional nuclear export signal sequence. J Biol Chem 274(40):28537–28541

154. Kunrath-Lima M et al (2018) Phospholipase C delta 4 (PLCdelta4) is a nuclear protein involved in cell proliferation and senescence in mesenchymal stromal stem cells. Cell Signal 49:59–67
155. Stallings JD et al (2005) Nuclear translocation of phospholipase C-delta1 is linked to the cell cycle and nuclear phosphatidylinositol 4,5-bisphosphate. J Biol Chem 280(23):22060–22069
156. Yoko-o T et al (1993) The putative phosphoinositide-specific phospholipase C gene, PLC1, of the yeast Saccharomyces cerevisiae is important for cell growth. Proc Natl Acad Sci U S A 90(5):1804–1808
157. Murthy KS et al (2004) Activation of PLC-delta1 by Gi/o-coupled receptor agonists. Am J Phys Cell Phys 287(6):C1679–C1687
158. Kanemaru K et al (2017) Phospholipase Cdelta1 regulates p38 MAPK activity and skin barrier integrity. Cell Death Differ 24(6):1079–1090
159. Sakurai K et al (2011) Phospholipase Cdelta3 is a novel binding partner of myosin VI and functions as anchoring of myosin VI on plasma membrane. Adv Enzym Regul 51(1):171–181
160. Kouchi Z et al (2011) Phospholipase Cdelta3 regulates RhoA/Rho kinase signaling and neurite outgrowth. J Biol Chem 286(10):8459–8471
161. Nakamura Y et al (2005) Phospholipase C-delta1 and -delta3 are essential in the trophoblast for placental development. Mol Cell Biol 25(24):10979–10988
162. Shimohama S et al (1991) Aberrant accumulation of phospholipase C-delta in Alzheimer brains. Am J Pathol 139(4):737–742
163. Yagisawa H, Tanase H, Nojima H (1991) Phospholipase C-delta gene of the spontaneously hypertensive rat harbors point mutations causing amino acid substitutions in a catalytic domain. J Hypertens 9(11):997–1004
164. Vachel L et al (2015) The low PLC-delta1 expression in cystic fibrosis bronchial epithelial cells induces upregulation of TRPV6 channel activity. Cell Calcium 57(1):38–48
165. Nakamura Y et al (2008) Phospholipase C-delta1 is an essential molecule downstream of Foxn1, the gene responsible for the nude mutation, in normal hair development. FASEB J 22(3):841–849
166. Ichinohe M et al (2007) Lack of phospholipase C-delta1 induces skin inflammation. Biochem Biophys Res Commun 356(4):912–918
167. Fukami K et al (2003) Phospholipase Cdelta4 is required for Ca^{2+} mobilization essential for acrosome reaction in sperm. J Cell Biol 161(1):79–88
168. Fukami K et al (2001) Requirement of phospholipase Cdelta4 for the zona pellucida-induced acrosome reaction. Science 292(5518):920–923
169. Shao Q et al (2017) Phospholipase Cdelta1 suppresses cell migration and invasion of breast cancer cells by modulating KIF3A-mediated ERK1/2/beta- catenin/MMP7 signalling. Oncotarget 8(17):29056–29066
170. Satow R et al (2014) Phospholipase Cdelta1 induces E-cadherin expression and suppresses malignancy in colorectal cancer cells. Proc Natl Acad Sci U S A 111(37):13505–13510
171. Shimozawa M et al (2017) Phospholipase C delta1 negatively regulates autophagy in colorectal cancer cells. Biochem Biophys Res Commun 488(4):578–583
172. Shibatohge M et al (1998) Identification of PLC210, a Caenorhabditis elegans phospholipase C, as a putative effector of Ras. J Biol Chem 273(11):6218–6222
173. Sorli SC et al (2005) Signaling properties and expression in normal and tumor tissues of two phospholipase C epsilon splice variants. Oncogene 24(1):90–100
174. Lopez I et al (2001) A novel bifunctional phospholipase c that is regulated by Galpha 12 and stimulates the Ras/mitogen-activated protein kinase pathway. J Biol Chem 276(4):2758–2765
175. Song C et al (2001) Regulation of a novel human phospholipase C, PLCepsilon, through membrane targeting by Ras. J Biol Chem 276(4):2752–2757
176. Wing MR et al (2003) Direct activation of phospholipase C-epsilon by Rho. J Biol Chem 278(42):41253–41258
177. Wing MR, Bourdon DM, Harden TK (2003) PLC-epsilon: a shared effector protein in Ras-, Rho-, and G alpha beta gamma-mediated signaling. Mol Interv 3(5):273–280

178. Malik S et al (2015) G protein betagamma subunits regulate cardiomyocyte hypertrophy through a perinuclear Golgi phosphatidylinositol 4-phosphate hydrolysis pathway. Mol Biol Cell 26(6):1188–1198
179. Madukwe JC et al (2018) G protein betagamma subunits directly interact with and activate phospholipase C. J Biol Chem 293(17):6387–6397
180. Schmidt M et al (2001) A new phospholipase-C calcium signaling pathway mediated by cyclic AMP and a Rap GTPase. Nat Cell Biol 3(11):1020–1024
181. Evellin S et al (2002) Stimulation of phospholipase C-epsilon by the M3 muscarinic acetylcholine receptor mediated by cyclic AMP and the GTPase Rap2B. J Biol Chem 277(19):16805–16813
182. Jin TG et al (2001) Role of the CDC25 homology domain of phospholipase Cepsilon in amplification of Rap1-dependent signaling. J Biol Chem 276(32):30301–30307
183. Xiang SY et al (2013) PLCepsilon, PKD1, and SSH1L transduce RhoA signaling to protect mitochondria from oxidative stress in the heart. Sci Signal 6(306):ra108
184. Wang H et al (2005) Phospholipase C epsilon modulates beta-adrenergic receptor-dependent cardiac contraction and inhibits cardiac hypertrophy. Circ Res 97(12):1305–1313
185. Tadano M et al (2005) Congenital semilunar valvulogenesis defect in mice deficient in phospholipase C epsilon. Mol Cell Biol 25(6):2191–2199
186. Chan JJ, Katan M (2013) PLCvarepsilon and the RASSF family in tumour suppression and other functions. Adv Biol Regul 53(3):258–279
187. Tyutyunnykova A, Telegeev G, Dubrovska A (2017) The controversial role of phospholipase C epsilon (PLCepsilon) in cancer development and progression. J Cancer 8(5):716–729
188. Zhang RY et al (2016) PLCepsilon signaling in cancer. J Cancer Res Clin Oncol 142(4):715–722
189. Popovics P et al (2014) A canonical EF-loop directs Ca^{2+} -sensitivity in phospholipase C-eta2. J Cell Biochem 115(3):557–565
190. Smrcka AV, Brown JH, Holz GG (2012) Role of phospholipase Cepsilon in physiological phosphoinositide signaling networks. Cell Signal 24(6):1333–1343
191. Yang YR et al (2013) The physiological roles of primary phospholipase C. Adv Biol Regul 53(3):232–241
192. Stewart AJ et al (2005) Identification of a novel class of mammalian phosphoinositol-specific phospholipase C enzymes. Int J Mol Med 15(1):117–121
193. Zhou Y et al (2005) Molecular cloning and characterization of PLC-eta2. Biochem J 391(Pt 3):667–676
194. Kouchi Z et al (2005) The role of EF-hand domains and C2 domain in regulation of enzymatic activity of phospholipase Czeta. J Biol Chem 280(22):21015–21021
195. Lo Vasco VR (2011) Role of Phosphoinositide-Specific Phospholipase C eta2 in Isolated and Syndromic Mental Retardation. Eur Neurol 65(5):264–269
196. Popovics P et al (2013) Phospholipase C-eta2 is required for retinoic acid-stimulated neurite growth. J Neurochem 124(5):632–644
197. Popovics P, Stewart AJ (2012) Phospholipase C-eta activity may contribute to Alzheimer's disease-associated calciumopathy. J Alzheimers Dis 30(4):737–744
198. Cox LJ et al (2002) Sperm phospholipase Czeta from humans and cynomolgus monkeys triggers Ca^{2+} oscillations, activation and development of mouse oocytes. Reproduction 124(5):611–623
199. Fujimoto S et al (2004) Mammalian phospholipase Czeta induces oocyte activation from the sperm perinuclear matrix. Dev Biol 274(2):370–383
200. Jones KT et al (2000) Different Ca^{2+}-releasing abilities of sperm extracts compared with tissue extracts and phospholipase C isoforms in sea urchin egg homogenate and mouse eggs. Biochem J 346(Pt 3):743–749
201. Kashir J et al (2017) Antigen unmasking enhances visualization efficacy of the oocyte activation factor, phospholipase C zeta, in mammalian sperm. Mol Hum Reprod 23(1):54–67

202. Kashir J, Nomikos M, Lai FA (2018) Phospholipase C zeta and calcium oscillations at fertilisation: the evidence, applications, and further questions. Adv Biol Regul 67:148–162
203. Aarabi M et al (2014) Sperm-derived WW domain-binding protein, PAWP, elicits calcium oscillations and oocyte activation in humans and mice. FASEB J 28(10):4434–4440
204. Aarabi M et al (2010) Sperm-borne protein, PAWP, initiates zygotic development in Xenopus laevis by eliciting intracellular calcium release. Mol Reprod Dev 77(3):249–256
205. Wu AT et al (2007) PAWP, a sperm-specific WW domain-binding protein, promotes meiotic resumption and pronuclear development during fertilization. J Biol Chem 282(16):12164–12175
206. Escoffier J et al (2016) Homozygous mutation of PLCZ1 leads to defective human oocyte activation and infertility that is not rescued by the WW-binding protein PAWP. Hum Mol Genet 25(5):878–891
207. Kashir J et al (2015) PLCzeta or PAWP: revisiting the putative mammalian sperm factor that triggers egg activation and embryogenesis. Mol Hum Reprod 21(5):383–388
208. Nomikos M et al (2015) Functional disparity between human PAWP and PLCzeta in the generation of Ca^{2+} oscillations for oocyte activation. Mol Hum Reprod 21(9):702–710
209. Nomikos M et al (2014) Sperm-specific post-acrosomal WW-domain binding protein (PAWP) does not cause Ca^{2+} release in mouse oocytes. Mol Hum Reprod 20(10):938–947
210. Satouh Y, Nozawa K, Ikawa M (2015) Sperm postacrosomal WW domain-binding protein is not required for mouse egg activation. Biol Reprod 93(4):94
211. Grasa P et al (2008) The pattern of localization of the putative oocyte activation factor, phospholipase Czeta, in uncapacitated, capacitated, and ionophore-treated human spermatozoa. Hum Reprod 23(11):2513–2522
212. Kashir J et al (2014) Sperm-induced Ca^{2+} release during egg activation in mammals. Biochem Biophys Res Commun 450(3):1204–1211
213. Young C et al (2009) Phospholipase C zeta undergoes dynamic changes in its pattern of localization in sperm during capacitation and the acrosome reaction. Fertil Steril 91(5 Suppl):2230–2242
214. Heytens E et al (2009) Reduced amounts and abnormal forms of phospholipase C zeta (PLCzeta) in spermatozoa from infertile men. Hum Reprod 24(10):2417–2428
215. Kashir J et al (2013) Variance in total levels of phospholipase C zeta (PLC-zeta) in human sperm may limit the applicability of quantitative immunofluorescent analysis as a diagnostic indicator of oocyte activation capability. Fertil Steril 99(1):107–117
216. Yoon SY et al (2008) Human sperm devoid of PLC, zeta 1 fail to induce Ca^{2+} release and are unable to initiate the first step of embryo development. J Clin Invest 118(11):3671–3681
217. Swann K et al (2006) PLCzeta(zeta): a sperm protein that triggers Ca^{2+} oscillations and egg activation in mammals. Semin Cell Dev Biol 17(2):264–273
218. Nomikos M et al (2005) Role of phospholipase C-zeta domains in Ca^{2+}-dependent phosphatidylinositol 4,5-bisphosphate hydrolysis and cytoplasmic Ca^{2+} oscillations. J Biol Chem 280(35):31011–31018
219. Halet G et al (2003) Ca^{2+} oscillations at fertilization in mammals. Biochem Soc Trans 31(Pt 5):907–911
220. Marangos P, FitzHarris G, Carroll J (2003) Ca^{2+} oscillations at fertilization in mammals are regulated by the formation of pronuclei. Development 130(7):1461–1472
221. Amdani SN et al (2016) Phospholipase C zeta (PLCzeta) and male infertility: Clinical update and topical developments. Adv Biol Regul 61:58–67
222. Wang C et al (2005) Binding of PLCdelta1PH-GFP to PtdIns(4,5)P2 prevents inhibition of phospholipase C-mediated hydrolysis of PtdIns(4,5)P2 by neomycin. Acta Pharmacol Sin 26(12):1485–1491
223. Klein RR et al (2011) Direct activation of human phospholipase C by its well known inhibitor u73122. J Biol Chem 286(14):12407–12416
224. Dwyer L et al (2010) Phospholipase C-independent effects of 3M3FBS in murine colon. Eur J Pharmacol 628(1-3):187–194

225. Frei E, Hofmann F, Wegener JW (2009) Phospholipase C mediated Ca^{2+} signals in murine urinary bladder smooth muscle. Eur J Pharmacol 610(1-3):106–109
226. Xu S et al (2009) Phospholipase Cgamma2 is critical for Dectin-1-mediated Ca^{2+} flux and cytokine production in dendritic cells. J Biol Chem 284(11):7038–7046
227. Shi TJ et al (2008) Phospholipase C{beta}3 in mouse and human dorsal root ganglia and spinal cord is a possible target for treatment of neuropathic pain. Proc Natl Acad Sci U S A 105(50):20004–20008
228. Ibrahim S et al (2007) The transfer of VLDL-associated phospholipids to activated platelets depends upon cytosolic phospholipase A2 activity. J Lipid Res 48(7):1533–1538
229. Sickmann T et al (2008) Unexpected suppression of neuronal G protein-activated, inwardly rectifying K^+ current by common phospholipase C inhibitor. Neurosci Lett 436(2):102–106
230. Kim DD, Ramirez MM, Duran WN (2000) Platelet-activating factor modulates microvascular dynamics through phospholipase C in the hamster cheek pouch. Microvasc Res 59(1):7–13
231. Muto Y, Nagao T, Urushidani T (1997) The putative phospholipase C inhibitor U73122 and its negative control, U73343, elicit unexpected effects on the rabbit parietal cell. J Pharmacol Exp Ther 282(3):1379–1388
232. Amtmann E (1996) The antiviral, antitumoural xanthate D609 is a competitive inhibitor of phosphatidylcholine-specific phospholipase C. Drugs Exp Clin Res 22(6):287–294
233. Powis G et al (1992) Selective inhibition of phosphatidylinositol phospholipase C by cytotoxic ether lipid analogues. Cancer Res 52(10):2835–2840
234. Suzuki H et al (2002) Effects of RHC-80267, an inhibitor of diacylglycerol lipase, on excitation of circular smooth muscle of the guinea-pig gastric antrum. J Smooth Muscle Res 38(6):153–164
235. Bae YS et al (2003) Identification of a compound that directly stimulates phospholipase C activity. Mol Pharmacol 63(5):1043–1050
236. Bassett AR et al (2013) Highly efficient targeted mutagenesis of Drosophila with the CRISPR/Cas9 system. Cell Rep 4(1):220–228
237. Friedland AE et al (2013) Heritable genome editing in C. elegans via a CRISPR-Cas9 system. Nat Methods 10(8):741–743
238. Raimondi C et al (2016) A Small Molecule Inhibitor of PDK1/PLCgamma1 Interaction Blocks Breast and Melanoma Cancer Cell Invasion. Sci Rep 6:26142

Chapter 10
New Insights in the IP_3 Receptor and Its Regulation

Jan B. Parys and Tim Vervliet

Abstract The inositol 1,4,5-trisphosphate (IP_3) receptor (IP_3R) is a Ca^{2+}-release channel mainly located in the endoplasmic reticulum (ER). Three IP_3R isoforms are responsible for the generation of intracellular Ca^{2+} signals that may spread across the entire cell or occur locally in so-called microdomains. Because of their ubiquitous expression, these channels are involved in the regulation of a plethora of cellular processes, including cell survival and cell death. To exert their proper function a fine regulation of their activity is of paramount importance. In this review, we will highlight the recent advances in the structural analysis of the IP_3R and try to link these data with the newest information concerning IP_3R activation and regulation. A special focus of this review will be directed towards the regulation of the IP_3R by protein-protein interaction. Especially the protein family formed by calmodulin and related Ca^{2+}-binding proteins and the pro- and anti-apoptotic/autophagic Bcl-2-family members will be highlighted. Finally, recently identified and novel IP_3R regulatory proteins will be discussed. A number of these interactions are involved in cancer development, illustrating the potential importance of modulating IP_3R-mediated Ca^{2+} signaling in cancer treatment.

Keywords IP_3R · Ca^{2+} signaling · IP_3-induced Ca^{2+} release · Calmodulin · Bcl-2 · IRBIT · TESPA1 · PKM2 · BAP1 · Cancer

Abbreviations

a.a.	amino acids
BAP1	BRCA-associated protein 1
Bcl	B-cell lymphoma
BH	Bcl-2 homology

J. B. Parys (✉) · T. Vervliet
KU Leuven, Laboratory for Molecular and Cellular Signaling, Department of Cellular and Molecular Medicine & Leuven Kanker Instituut, Leuven, Belgium
e-mail: jan.parys@kuleuven.be

M. S. Islam (ed.), *Calcium Signaling*, Advances in Experimental Medicine and Biology 1131, https://doi.org/10.1007/978-3-030-12457-1_10

CaBP	neuronal Ca^{2+}-binding protein
CaM	calmodulin
CaM1234	calmodulin fully deficient in Ca^{2+} binding
cryo-EM	cryo-electron microscopy
DARPP-32	dopamine- and cAMP-regulated phosphoprotein of 32 kDa
ER	endoplasmic reticulum
IBC	IP_3-binding core
IICR	IP_3-induced Ca^{2+} release
IP_3	inositol 1,4,5-trisphosphate
IP_3R	IP_3 receptor
IRBIT	IP_3R-binding protein released by IP_3
MLCK	myosin light chain kinase
NCS-1	neuronal Ca^{2+} sensor-1
PK	pyruvate kinase
PKA	cAMP-dependent protein kinase
PKB	protein kinase B/Akt
PLC	phospholipase C
PTEN	phosphatase and tensin homolog
RyR	ryanodine receptor
TCR	T-cell receptor
TESPA1	thymocyte-expressed, positive selection-associated 1
TIRF	total internal reflection fluorescence
TKO	triple-knockout

10.1 Introduction

The inositol 1,4,5-trisphosphate (IP_3) receptor (IP_3R) is a ubiquitously expressed Ca^{2+}-release channel mainly located in the endoplasmic reticulum (ER) [1]. The IP_3R is activated by IP_3, produced by phospholipase C (PLC), following cell stimulation by for instance extracellular agonists, hormones, growth factors or neurotransmitters. The IP_3R is responsible for the initiation and propagation of complex spatio-temporal Ca^{2+} signals that control a multitude of cellular processes [2, 3]. Moreover, dysfunction of the IP_3R and deregulation of the subsequent Ca^{2+} signals is involved in many pathological situations [4–10].

There are at least three main reasons for the central role of the IP_3R in cellular signaling. First, IP_3R signaling is not only dependent on the production of IP_3, but is also heavily modulated by its local cellular environment, integrating multiple signaling pathways. Indeed, IP_3R activity is controlled by the cytosolic and the intraluminal Ca^{2+} concentrations, pH, ATP, Mg^{2+} and redox state, as well as by its phosphorylation state at multiple sites. Furthermore, a plethora of associated proteins can modulate localization and activity of the IP_3R [11–15]. Second, in higher organisms, three genes (ITPR1, ITPR2 and ITPR3) encode three isoforms (IP_3R1, IP_3R2, and IP_3R3). These isoforms have a homology of

about 75% at the a.a. level, allowing for differences in sensitivity towards IP_3 ($IP_3R2 > IP_3R1 > IP_3R3$) as well as towards the various regulatory factors and proteins [12, 16–19]. Splice isoforms and the possibility to form both homo- and heterotetramers further increase IP_3R diversity. Third, the intracellular localization of the IP_3Rs determines their local effect [1]. Recently, an increased appreciation for the existence and functional importance of intracellular Ca^{2+} microdomains was obtained, e.g. between ER and mitochondria, lysosomes or plasma membrane where IP_3-induced Ca^{2+} release (IICR) occurs, allowing Ca^{2+} to control very local processes [20–24].

As a number of excellent reviews on various aspects of IP_3R structure and function have recently appeared [25–32], we will in present review highlight the most recent advances concerning the understanding of IP_3R structure and regulation, with special focus on recent insights obtained in relation to IP_3R modulation by associated proteins.

10.2 New Structural Information on the IP_3R

The IP_3Rs form large Ca^{2+}-release channels consisting of 4 subunits, each about 2700 a.a. long, that assemble to functional tetramers with a molecular mass of about 1.2 MDa. Each subunit consists of five distinct domains (Fig. 10.1a): the N-terminal coupling domain or suppressor domain (for IP_3R1: a.a. 1–225), the IP_3-binding core (IBC, a.a. 226–578), the central coupling domain or modulatory and transducing domain (a.a. 579–2275), the channel domain with 6 trans-membrane helices (a.a. 2276–2589) and the C-terminal tail or gatekeeper domain (a.a. 2590–2749) [33].

The crystal structure of the two N-terminal domains of the IP_3R1 were first resolved separately at a resolution of 2.2 Å (IBC with bound IP_3, [34]) and 1.8 Å (suppressor domain, [35]). Subsequent studies analyzed the crystal structure of the full ligand-binding domain, i.e. the suppressor domain and the IBC together, resolved in the presence and absence of bound IP_3 at a resolution between 3.0 and 3.8 Å [36, 37]. These studies indicated that the N-terminus of IP_3R1 consisted of two successive β-trefoil domains (β-TF) followed by an α-helical armadillo repeat domain. IP_3 binds in a cleft between the second β-trefoil domain and the α-helical armadillo repeat, leading to a closure of the IP_3-binding pocket and a conformational change of the domains involved [36–38]. Recently, Mikoshiba and co-workers succeeded to perform X-ray crystallography on the complete cytosolic part of the IP_3R [39]. This study was performed using truncated IP_3R1 proteins (IP_3R^{2217} and IP_3R^{1585}) in which additional point mutations (resp. $R^{937}G$ and $R^{922}G$) were incorporated in order to increase the quality of the obtained crystals. In addition to the three domains mentioned above (the two β-trefoil domains and the α-helical armadillo repeat domain), three large α-helical domains were described, i.e. HD1 (a.a. 605–1009), HD2 (a.a. 1026–1493) and HD3 (1593–2217) (Fig. 10.1b). Binding of IP_3 induces a conformation change that is transmitted from the IBC through HD1 and HD3, whereby a short, 21 a.a.-long domain (a.a. 2195–2215) called the leaflet domain is essential for IP_3R function.

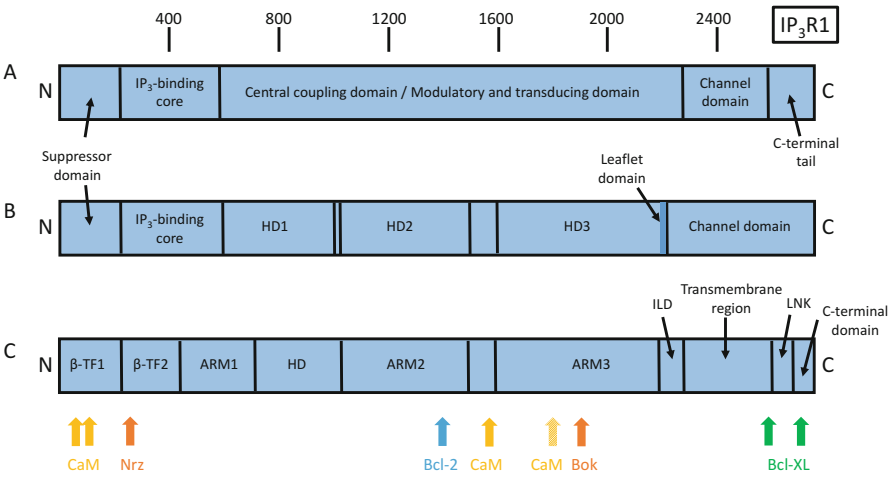

Fig. 10.1 Alignment of proposed IP_3R1 structures. (**a**) Linear representation of IP_3R1 [33]. (**b**) Linear representation of the IP_3R1 domains identified by X-ray crystallography [39]. (**c**) Linear representation of the IP_3R1 domains identified by cryo-EM [41]. For the various domains, the original nomenclature was used. Additionally, the interaction sites for calmodulin (CaM) and for the various Bcl-2 family members (Bcl-2, Bcl-XL, Nrz and Bok) are indicated with colored arrows at the bottom of the figure. Please note that the name of the interacting protein indicated at each arrow represents the protein for which binding was initially described. As discussed in the text, related proteins share in some cases common binding sites. The striped arrow indicates that this binding site is only present in a specific IP_3R1splice isoform. For further explanations, please see text

In parallel with the analysis of the IP_3R by X-ray crystallography, the structure of full-size IP_3R1 was investigated by several groups by cryo-electron microscopy (cryo-EM), obtaining increasingly better resolution [40]. The structure of the IP_3R1 at the highest resolution obtained by this method until now (4.7 Å) was published by Serysheva and co-workers and allowed modelling of the backbone topology of 2327 of the 2750 a.a [41]. As IP_3R1 was purified in the absence of IP_3 and as Ca^{2+} was depleted before vitrification, the obtained structure corresponds to the closed state of the channel (Fig. 10.2). In total, ten domains were identified: two contiguous β-trefoil domains (a.a. 1–436), followed by three armadillo solenoid folds (ARM1–ARM3, a.a. 437–2192) with an α-helical domain between ARM1 and 2, an intervening lateral domain (ILD, a.a. 2193–2272), the transmembrane region with six trans-membrane α-helices (TM1–6) (a.a. 2273–2600), a linker domain (LNK, a.a. 2601–2680) and the C-terminal domain containing an 80 Å α-helix (a.a. 2681–2731) (Fig. 10.1c). The latter domains of the four subunits form together with the four TM6 helices (~55 Å) a central core structure that is not found in other types of Ca^{2+} channels. The four transmembrane TM6 helices thereby line the Ca^{2+} conduction pathway and connect via their respective LNK domains with the cytosolic helices.

How binding of IP_3 is coupled to channel opening is still under investigation. An interesting aspect of the IP_3R structure thereby is the fact that either after

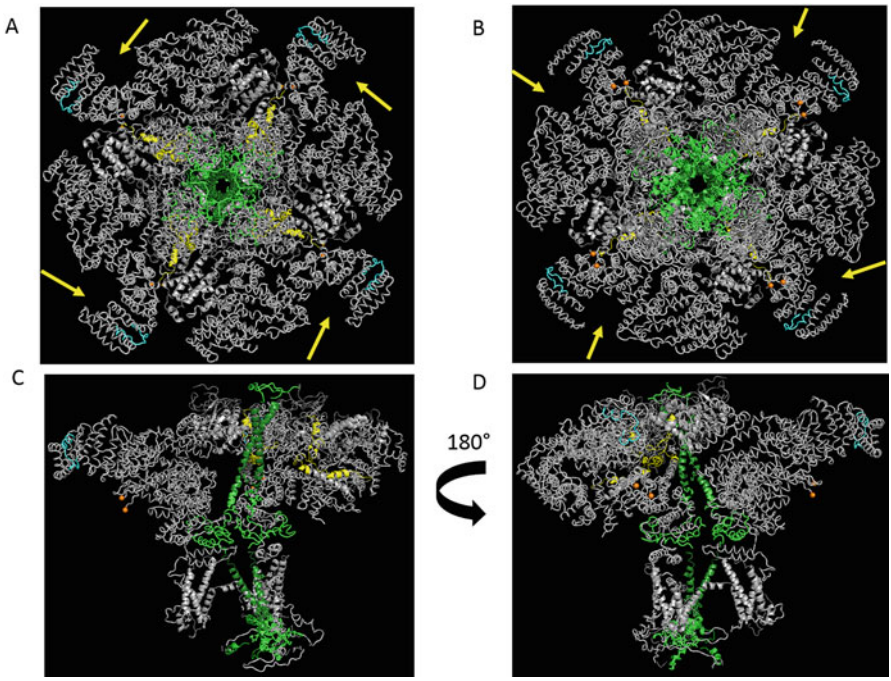

Fig. 10.2 Cryo-EM structure of IP_3R1. Structure of IP_3R1 fitted to the cryo-EM map (PDB 3JAV, [41]) showing (**a**) a cytosolic and (**b**) a luminal view of an IP_3R1 tetramer. (**c**, **d**) Side views of two neighboring IP_3R1 subunits as seen from the (**c**) inside or the (**d**) outside of the tetramer. The discontinuous CaM-binding site in the suppressor domain is indicated in yellow (a.a. 49–81 and a.a. 106–128). The yellow arrows in panels A and B indicate where the CaM-binding site in the central coupling domain should be located (a.a. 1564–1585). This could not be indicated on the structure itself because the part between a.a. 1488 and 1588 of the IP_3R is not resolved. The binding site for Bcl-2 and, to a lesser extent, Bcl-XL located in the central coupling domain is indicated in blue (a.a. 1389–1408). The C-terminal binding site for Bcl-2, Bcl-XL and Mcl-1 is shown in green (a.a. 2512–2749). The domains indicated in dark green (a.a. 2571–2606 and a.a. 2690–2732) thereby represent the BH3-like structures that were identified to bind to Bcl-XL. The region where Bok interacts with IP_3R1 (a.a. 1895–1903) was not resolved in this cryo-EM structure. The two orange spheres (a.a. 1883 and 1945) however show the boundaries of this non-characterized IP_3R1 region to which Bok binds. These images were obtained using PyMOL. For further explanations, please see text

mild trypsinisation of IP_3R1 [42] or after heterologous expression of the various IP_3R1 fragments corresponding to the domains obtained by trypsinisation [43], the resulting structure appeared both tetrameric and functional. This indicates that continuity of the polypeptide chain is not per se needed for signal transmission to the channel domain, although the resulting Ca^{2+} signals can differ, depending on the exact cleavage site and the IP_3R isoform under consideration [44, 45].

Meanwhile, various models for the transmission of the IP_3 signal to the channel region were proposed for IP_3R1, including a direct coupling between the N-terminus and the C-terminus [41, 46–48] and a long-range coupling mediated by the central

coupling domain [48], via intra- and/or inter-subunit interactions [41]. Mechanisms for the latter can involve β-TF1 ➔ ARM3 ➔ ILD [41] or IBC ➔ HD1 ➔ HD3 ➔ leaflet [39].

In addition to the structural studies on IP_3R1 described above, the structure of human IP_3R3 was recently analyzed at high resolution (between 3.3 and 4.3 Å) under various conditions. Its apo state was compared to the structures obtained at saturating IP_3 and/or Ca^{2+} concentrations [49]. In the presence of IP_3, five different conformational states were resolved, suggesting a dynamic transition between intermediate states eventually leading to channel opening. Ca^{2+} binding appeared to eliminate the inter-subunit interactions present in the apo and the IP_3-bound states and provoke channel inhibition. Two Ca^{2+}-binding sites were identified, one just upstream of ARM2 and one just upstream of ARM3, though their relative function cannot be inferred from structural data alone.

Although IP_3R1 and IP_3R3 are structurally quite similar, they are differentially activated and regulated (see Sect. 10.1). Additional work, including performing a high-resolution cryo-EM analysis of IP_3-bound IP_3R1 and the further investigation of the effect of Ca^{2+} and other IP_3R modulators, including associated proteins, on IP_3R structure will therefore be needed to fully unravel the underlying mechanism of activation and to understand the functional differences between the various IP_3R isoforms.

10.3 Complexity of IP_3R Activation and Regulation

Concerning the mechanisms of activation and regulation of the IP_3R, progress has been made on several points recently.

10.3.1 IP_3 Binding Stoichiometry

First, a long-standing question in the field concerned the number of IP_3 molecules needed to evoke the opening of the IP_3R/Ca^{2+}-release channel. Some studies demonstrated a high cooperativity of IP_3 binding to its receptor, and suggested that minimally 3 IP_3 molecules should be bound to the IP_3R to evoke Ca^{2+} release [50, 51]. In contrast herewith, co-expression of an IP_3R apparently defective in IP_3 binding ($R^{265}Q$) and of a channel-dead IP_3R mutant ($D^{2550}A$) resulted in a partial IP_3-induced Ca^{2+} release, suggesting that one IP_3R subunit can gate another and that therefore not all subunits need to bind IP_3 to form an active channel [52]. Moreover, these results fit with the most recent cryo-EM data discussed above (see Sect. 10.2.; [41]).

Recently, a comprehensive study by Yule and co-workers demonstrated in triple-knockout (TKO) cells, devoid of endogenous IP_3R expression (DT-40 TKO and HEK TKO), that the activity of recomplemented IP_3Rs depends on the occupation of the 4 IP_3-binding sites by their ligand [53]. The strongest evidence for this was obtained by the expression of a concatenated IP_3R1 containing 3 wild-type

subunits and 1 mutant subunit. The mutant subunit contained a triple mutation ($R^{265}Q/K^{508}Q/R^{511}Q$) in the ligand-binding domain precluding any IP_3 binding, as previously demonstrated [54], while the $R^{265}Q$ single mutant still retained 10% binding activity. Interestingly, the tetrameric IP_3R containing only 1 defective IP_3-binding site and expressed in cells fully devoid of endogenous IP_3Rs was completely inactive in Ca^{2+} imaging experiments, unidirectional Ca^{2+} flux experiments and in patch-clamp electrophysiological experiments [53]. Similar experiments were performed for IP_3R2, making use of its existing short splice isoform that lacks 33 a.a. in the suppressor domain rendering it non-functional [55]. These data strongly suggest that no opening of the IP_3R can occur, unless each subunit has bound IP_3. This characteristic would strongly limit the number of active IP_3Rs and protect the cell against unwanted Ca^{2+} release in conditions in which the IP_3 concentration is only slightly increased [50, 53]. However, in the case of IP_3R mutations affecting IP_3 binding / IP_3R activity it may explain why they are detrimental, even in heterozygous conditions [10].

10.3.2 Physiological Relevance of IP_3R Heterotetramer Formation

As already indicated above (see Sect. 10.1.), the high level of homology between the various IP_3R isoforms allows not only for the formation of homotetramers but also for that of heterotetramers [57–59]. The frequency of heterotetramer occurrence is however not completely clear. A study in COS-7 cells indicated that kinetic constrains affect the formation of heterotetramers and that therefore the level of heterotetramers composed of overexpressed IP_3R1 and of either endogenously expressed or overexpressed IP_3R3 was lower than what could be expected from a purely binomial distribution [60]. In contrast herewith, by using isoform-specific IP_3R antibodies for sequential depletion of the IP_3Rs, it was shown that in pancreas, over 90% of IP_3R3 is present in heterotetrameric complexes, generally with IP_3R2 [61]. This is significant as pancreas is a tissue in which IP_3R2 and IP_3R3 together constitute over 80% of the total amount of IP_3R [62, 63]. It is therefore meaningful to investigate whether the presence of IP_3R heterotetramers will contribute in increasing the diversity of the IP_3R Ca^{2+}-release channels, as is generally assumed. However, due to the fact that most cells express or can express various types of homo- and heterotetrameric IP_3Rs in unknown proportions, addressing this question is in most cell types not straightforward.

Overexpressing mutated IP_3R1 and IP_3R3 in COS-7 cells at least indicated that heterotetramers are functional [52]. The expression of concatenated dimeric IP_3R1-IP_3R2 (and IP_3R2-IP_3R1) in DT-40 TKO cells led to the formation of IP_3R heterotetramers with a defined composition (2:2) that could be compared with homotetrameric IP_3R1 or homotetrameric IP_3R2 that were similarly expressed [61]. Investigation of their electrophysiological properties via nuclear patch-clamp recordings indicated that in the IP_3R1-IP_3R2 2:2 heterotetramers the properties

of the IP_3R2 dominated with respect to the induction of Ca^{2+} oscillations and their regulation by ATP [61]. A more recent study based on the same approach but now including combinations of all three IP_3R isoforms, demonstrated that 2:2 heterotetrameric IP_3Rs display an IP_3 sensitivity that is intermediate to that of their respective homotetramers [64] indicating that heterotetramerization successfully increases IP_3R diversity. In addition, the obtained results also demonstrate that IP_3R2 properties with respect to both the induction of Ca^{2+} oscillations and the regulation by ATP also dominated in IP_3R2-IP_3R3 2:2 heterotetramers. In contrast, when a tetrameric IP_3R containing 3 IP_3R1 and 1 IP_3R2 subunit was expressed, its properties were similar to that of a homotetrameric IP_3R1 [64]. Taken together, these experiments indicate that IP_3R heterotetramers increase the diversity of the IP_3Rs with respect to Ca^{2+} release and that further studies are needed to fully understand how IP_3R heterotetramers are regulated by other factors, including associated proteins.

10.3.3 Novel Crosstalk Mechanism Between cAMP and IICR

cAMP and Ca^{2+}, the two most important intracellular messengers, have numerous crosstalks between them [65]. At the level of the IP_3R, the most evident crosstalk is the sensitization of IP_3R1 by cAMP-dependent protein kinase (PKA) [66], while a similar regulatory role is highly probable for IP_3R2 but less likely for IP_3R3 [15, 65].

A novel line of regulation was discovered some time ago when it was shown that cAMP can, independently from PKA or cAMP-activated exchange proteins, potentiate the IP_3R [67–69]. In particular, it was shown in HEK cells that adenylate cyclase 6, which in those cells accounts for only a minor portion of the adenylate cyclase isoforms, is responsible for providing cAMP to a microdomain surrounding IP_3R2, increasing its activity [69]. Such mechanism would form a specific signaling complex in which locally a very high concentration of cAMP could be reached, without affecting its global concentration [65]. Recent work provided further evidence concerning the importance of cAMP for IP_3R functioning, showing that the presence of cAMP can uncover IP_3Rs that were insensitive to IP_3 alone [56]. Indeed, in HEK cells heterologously expressing the parathyroid hormone (PTH) receptor, it appears that PTH, via production of cAMP, evokes Ca^{2+} release after full depletion of the carbachol-sensitive Ca^{2+} stores. Although the identity of the Ca^{2+} stores could not yet be established, the obtained results are indicative that cAMP unmasks IP_3Rs with a high affinity for IP_3. This fits with the previous observation that IP_3R2, the IP_3R with the highest affinity for IP_3 (reviewed in [19]), is regulated by cAMP [69]. The molecular mechanism on how cAMP interacts with the IP_3R remains to be determined. At this moment no discrimination can be made between a low-affinity cAMP-binding site on the IP_3R itself or a similar binding site on an associated protein [65]. The possibility that the IP_3R-binding protein

released by IP_3 (IRBIT), related to protein S-adenosylhomocysteine-hydrolase, known to bind cAMP, is involved was however already excluded by knockdown and overexpression experiments [56].

10.4 Complexity of Protein-Protein Interactions Affecting the IP_3R

In a comprehensive review published a few years ago, over 100 proteins that interact with the IP_3R have been listed [14]. For that reason, we will limit ourselves in the present review to either newly discovered interacting proteins or proteins for which new information about their interaction recently became available.

10.4.1 Calmodulin (CaM) and Related Ca^{2+}-Binding Proteins

CaM is the most ubiquitously expressed intracellular Ca^{2+} sensor. It is a relatively small protein (148 a.a.) with a typical dumbbell structure. A central, flexible linker region connects the globular N-terminal and C-terminal domains, each containing two Ca^{2+}-binding EF-hand motifs with a classical helix-loop-helix structure. The K_d of CaM for Ca^{2+} ranges between 5×10^{-7} and 5×10^{-6} M, with the C-terminal Ca^{2+}-binding sites having a three to five-fold higher affinity than the N-terminal ones [70]. CaM therefore displays the correct Ca^{2+} affinity to sense changes in intracellular Ca^{2+} concentrations and serve as Ca^{2+} sensor. While apo-CaM has a rather compact structure, Ca^{2+}-CaM exposes in each domain a hydrophobic groove with acidic residues at its extremities that will allow interaction with their target [71]. A plethora of target proteins that are modulated by CaM exists, including various Ca^{2+}-transporting proteins [72]. These various proteins contain CaM-binding sites that can be categorized into various types of motifs [73].

Although the interaction of CaM with the IP_3R was already observed soon after the identification of the IP_3R as IP_3-sensitive Ca^{2+}-release channel [74] its exact mechanism of action is still not completely elucidated. Moreover, there are a number of interesting features related to the binding of CaM to the IP_3R: (i) the existence of multiple binding sites, (ii) the possibility for both Ca^{2+}-CaM and apo-CaM to affect IP_3R function and (iii) the use of some of the CaM-binding sites by other Ca^{2+}-binding proteins. The aim of this paragraph therefore is to present a comprehensive view on the relation between CaM (and some related Ca^{2+}-binding proteins) and the IP_3R.

On IP_3R1, three CaM-binding sites were described (Fig. 10.1). A high-affinity CaM-binding site (a.a. 1564–1585; Fig. 10.2a–b, indicated by the yellow arrows) was described in the central coupling domain [75], while a low-affinity one was found in the suppressor domain [76]. The latter site is discontinuous (a.a. 49–81

and a.a. 106–128; Fig. 10.2**,** indicated in yellow) and can bind to both apo-CaM and Ca^{2+}-CaM [77]. Finally, a third site was described on the S2(−) IP_3R1 splice isoform in which a.a. 1693–1732 are removed [78, 79]. CaM binding to this newly formed site is inhibited by PKA-mediated phosphorylation, probably on Ser^{1589} [79].

CaM interaction with the two other IP_3R isoforms was studied in less detail, but an IP_3R2 construct overlapping with the CaM-binding site in the central coupling domain interacted with CaM, supporting the conservation of this site [75]. However, no direct interaction between CaM and IP_3R3 could be measured [75, 80] though CaM can bind to IP_3R1-IP_3R3 heterotetramers [79].

Functional effects on the IP_3R have been described for both apo-CaM and Ca^{2+}-CaM. In fact, apo-CaM is equally potent in inhibiting IP_3 binding to full-length IP_3R1 as Ca^{2+}-CaM [81]. In agreement with the absence of CaM binding to IP_3R3, full-length IP_3R3 remained insensitive to regulation by CaM [80]. In contrast, a Ca^{2+}-independent inhibition of IP_3 binding was observed for the isolated ligand-binding domain of IP_3R1 [82] as well as for that of IP_3R2 and IP_3R3 [83].

Concerning IP_3-induced Ca^{2+} release, the situation is somewhat more complex. Ca^{2+} release by IP_3R1 is inhibited by CaM in a Ca^{2+}-dependent way [84, 85] while similar results were subsequently found for IP_3R2 and IP_3R3 [76, 86]. However, linking these functional effects molecularly to a CaM-binding site appeared more difficult, not only because of the apparent absence of a Ca^{2+}-dependent CaM-binding site on IP_3R3 but also because the mutation $W^{1577}A$ that abolishes CaM binding to IP_3R1 [75], does not abolish the CaM-mediated inhibition of IICR [87].

Furthermore, other results suggested that the relation between CaM and the IP_3R was more complex than originally thought. A detailed analysis of the CaM-binding site located in the central coupling domain of IP_3R1 provided evidence that it consisted of a high-affinity Ca^{2+}-CaM and a lower affinity apo-CaM site [88]. Moreover, in the same study it was demonstrated that a CaM mutant deficient in Ca^{2+} binding (CaM1234) could inhibit IICR in a Ca^{2+}-dependent way with the same potency as CaM. In a separate study, it was demonstrated that a myosin light chain kinase (MLCK)-derived peptide, which binds to CaM with high affinity, fully inhibited the IP_3R [89]. This inhibition could be reversed by the addition of CaM but not of CaM1234 and the results were interpreted as evidence that endogenously bound CaM is needed for IP_3R activity. A follow-up study by another group [90] however proposed that the MLCK peptide is not removing endogenous CaM but is interacting with an endogenous CaM-like domain on IP_3R, thereby disrupting its interaction with a so-called 1–8-14 CaM-binding motif (a.a. 51–66) essential for IP_3R activity [91].

Meanwhile, the interaction of apo-CaM with the suppressor domain was studied via NMR analysis [92]. This study brought forward two main pieces of evidence. First, it was shown that the binding of apo-CaM to the suppressor domain induced an important, general conformational change to the latter. These changes further increased in the presence of Ca^{2+}. Secondly, analysis of the conformational change of CaM indicated that apo-CaM already binds with its C-lobe to the IP_3R1 suppressor domain, and that only after addition of Ca^{2+} also the N-lobe interacts

with the suppressor domain. These results can therefore explain the importance of the CaM-binding sites in the suppressor domain in spite of their difficult accessibility ([92]; Fig. 10.2).

Finally, some Ca^{2+}-binding proteins related to CaM (e.g. neuronal Ca^{2+}-binding protein (CaBP) 1, calmyrin, also known as CIB1, and neuronal Ca^{2+} sensor-1 (NCS-1)) also regulate the IP_3R. Similarly to CaM, these proteins contain 4 EF-hand motifs but in contrast with CaM, not all of them bind Ca^{2+}. In CaBP1 and NCS-1 only 3 EF hands are functional (EF1, EF3, EF4 and EF2, EF3, EF4 resp.) and in calmyrin only 2 (EF3 and EF4). Moreover, some of the EF hands bind Mg^{2+} rather than Ca^{2+}. Furthermore, those proteins are myristoylated. Although early results suggested that CaBP1 and calmyrin could, in the absence of IP_3, activate the IP_3R under some circumstances [93, 94], there is presently a large consensus that they, similarly to CaM, generally inhibit the IP_3R [93, 95, 96].

CaBP1 was proposed to interact with the IP_3R1 with a higher affinity than CaM itself [94, 96], while in contrast to CaM it does not affect the ryanodine receptor (RyR), another family of intracellular Ca^{2+}-release channels. Additionally, the interaction with the IP_3R would be subject to regulation by caseine kinase 2, an enzyme that can phosphorylate CaBP1 on S^{120} [96]. Similarly to CaM, CaBP1 binds in a Ca^{2+}-independent way to the IP_3R1 suppressor domain, but in contrast to CaM, only to the first of the two non-contiguous binding sites described for CaM (Fig. 10.1). However, CaM and CaBP1 similarly antagonized the thimerosal-stimulated interaction between the suppressor domain and the IBC of IP_3R1, suggesting a common mechanism of action whereby they disrupt intramolecular interactions needed for channel activation [97]. More recent work confirmed the inhibitory effect of CaBP1 on IP_3R1, while expanding the knowledge concerning the CaBP1 binding site. In particular, NMR analysis indicated that CaBP1 interacts with its C lobe with the suppressor domain of the IP_3R and that even at saturating Ca^{2+} concentrations EF1 is bound to Mg^{2+}, precluding a conformational change of the N lobe [98]. The same study demonstrated that Ca^{2+}-bound CaBP1 bound with an 10-fold higher affinity than Mg^{2+}-bound CaBP1 and an at least 100-fold higher affinity than CaM itself. Functional analysis performed in DT-40 cells solely expressing IP_3R1 demonstrated that CaBP1 stabilized the closed conformation of the channel, probably by clamping inter-subunit interactions [99]. The interaction of specific hydrophobic a.a. in the C lobe of CaBP1 (V^{101}, L^{104}, V^{162}) that become more exposed in the presence of Ca^{2+} with hydrophobic a.a. in the IBC (L^{302}, I^{364}, L^{393}) appeared hereby essential.

The action of NCS-1 on the IP_3R forms a slightly different story. It co-immunoprecipitates with IP_3R1 and IP_3R2 in neuronal cells and in heart thereby stimulating IICR in a Ca^{2+}-dependent way [100, 101]. Interestingly, paclitaxel by binding to NCS-1 increases its interaction with IP_3R1 and so induces Ca^{2+} oscillations in various cell types [102, 103]. This Ca^{2+}-signaling pathway was proposed to lead to calpain activation and to underlie the origin of paclitaxel-induced peripheral neuropathy [104]. However, the interaction site of NCS-1 on the IP_3R, either direct or indirect, has not yet been identified.

Taken together these results confirm that Ca^{2+}-binding proteins interact in a complex way with the IP_3R and that the various Ca^{2+}-binding proteins have distinct, though sometimes overlapping, roles. The functional effect of CaM has been studied in detail and it appears to inhibit the IP_3R. The results described above support a view that the main action of CaM on the IP_3R is at the level of the suppressor domain. Indeed, apo-CaM can via its C lobe bind to the suppressor domain of all three IP_3R isoforms while a subsequent binding of the N lobe will depend on the Ca^{2+} concentration. The binding of CaM in that domain can disturb an intra-IP_3R interaction needed for IP_3R function and therefore inhibits IICR. This behavior can be particularly important in cells having high CaM expression levels, as for example Purkinje neurons that also demonstrate high levels of IP_3R1. In that case, CaM was proposed to be responsible for suppressing basal IP_3R activity [81]. Moreover, as the intracellular distribution of CaM can depend on intracellular Ca^{2+} dynamics, it was also hypothesized that it allows IP_3R regulation is a non-uniform way [84]. Additionally, it should be emphasized that CaM can act on other Ca^{2+}-transporting proteins in the cell, like the RyR [105], the plasma membrane Ca^{2+} ATPase [106] and various plasma membrane Ca^{2+} channels including voltage-operated Ca^{2+} channels and transient receptor potential channels [107, 108]. In all these cases CaM tends to inhibit Ca^{2+} influx into the cytosol (inhibition of IP_3Rs, RyRs and plasma membrane Ca^{2+} channels) while promoting Ca^{2+} efflux out of the cell (stimulation of plasma membrane Ca^{2+} ATPase).

An IP_3R-inhibiting behavior can similarly be expected for CaM-related Ca^{2+}-binding proteins, though their interaction sites are not strictly identical to that of CaM. The binding site for NCS-1, which rather stimulates the IP_3R, is even still unknown. In comparison to CaM, CaBP1 demonstrates a much higher affinity for the IP_3R [99] and a higher specificity, as it does not affect the RyR [96]. In cells expressing CaBP1, the major control of IICR will therefore depend on the interaction of the IP_3R with CaBP1, while RyR activity will depend on the presence and activation of CaM. Further work will be needed to completely unravel the exact role of these various proteins in the control of intracellular Ca^{2+} signaling. From the present results, it can already be expected that the relative role of the various Ca^{2+}-binding proteins in the control of IICR will strongly depend on the exact cell type in consideration.

10.4.2 The Bcl-2-Protein Family

The B-cell lymphoma (Bcl)-2 protein family has been extensively studied as critical regulator of apoptosis [109]. This family consists of both anti- and pro-apoptotic members. The anti-apoptotic family members inhibit apoptosis in at least two different manners. First, at the mitochondria anti-apoptotic Bcl-2 proteins such as Bcl-2, Bcl-XL and Mcl-1, bind to the pro-apoptotic Bcl-2-family members thereby inhibiting the permeabilization of the outer mitochondrial membrane by Bax and

Bak and subsequent release of cytochrome C [110, 111]. Second, the anti-apoptotic Bcl-2-family members also affect intracellular Ca^{2+} signaling. On the one hand they promote pro-survival Ca^{2+} oscillations while on the other hand they inhibit pro-apoptotic Ca^{2+} release from the ER that otherwise could lead to mitochondrial Ca^{2+} overload [112]. These combined actions mean that anti-apoptotic Bcl-2 proteins can, by modulating several protein families involved in intracellular Ca^{2+} signaling, both fine tune mitochondrial bio-energetics and inhibit Ca^{2+}-mediated mitochondrial outer membrane permeabilization [113–116]. Both the interaction between Bcl-2-family members and their ability to regulate intracellular Ca^{2+} signaling is critically dependent on the presence of so-called Bcl-2 homology (BH) domains. Anti-apoptotic Bcl-2 proteins contain four of these domains (BH1, 2, 3 and 4) [111]. The BH1 to 3 domains together form a hydrophobic cleft that inactivates the pro-apoptotic Bcl-2-family members via interaction with their BH3 domain. For regulating intracellular Ca^{2+} signaling events, anti-apoptotic Bcl-2 proteins rely to a great extent, however not exclusively, on their BH4 domain. In this review we will focus on how IP_3Rs are regulated by Bcl-2 proteins. For a more extensive revision of how Bcl-2-family members regulate the various members of the intracellular Ca^{2+} signaling machinery we would like to refer to our recent review on the subject [112].

The various IP_3R isoforms are important targets for several anti-apoptotic Bcl-2-family members [112]. To complicate matters, multiple binding sites on the IP_3R have been described for anti-apoptotic Bcl-2 proteins [117]. First, Bcl-2, Bcl-XL and Mcl-1 were shown to target the C-terminal part (a.a. 2512–2749) of IP_3R1 (Fig. 10.2, indicated in green) thereby stimulating pro-survival Ca^{2+} oscillations [114, 115, 118]. Additionally, Bcl-2, and Bcl-XL with lesser affinity, also target the central coupling domain (a.a. 1389–1408 of IP_3R1; Figs. 10.1 and 10.2, indicated in blue) of the IP_3R where binding of these proteins inhibits pro-apoptotic Ca^{2+}-release events [116, 118–120]. Finally, the zebrafish protein Nrz [121] and its mammalian homolog Bcl-2-like 10 [122] were shown to interact with the IBC and inhibit IICR.

The group of Kevin Foskett performed a more in-depth study into how the IP_3R is regulated by Bcl-XL and proposed a mechanism unifying the regulation at the C-terminal and at the central coupling domain of the IP_3R [123]. Two domains containing BH3-like structures (a.a. 2571–2606 and a.a. 2690–2732; Figs. 10.1 and 10.2**,** indicated in dark green) were identified in the C-terminal part of the IP_3R. When Bcl-XL is, via its hydrophobic cleft, bound to both BH3-like domains it sensitizes the IP_3R to low concentrations of IP_3, thereby stimulating Ca^{2+} oscillations. If Bcl-XL binds to only one of these BH3 like domains while also binding to the central coupling domain, it will inhibit IICR. Whether Bcl-XL occupies one or the two BH3-like domains at the C-terminus of the IP_3R was proposed to be dependent on Bcl-XL levels and on the intensity of IP_3R stimulation. Whether Bcl-2 operates in a similar manner is still unclear. As there is evidence that Bcl-2 shows a greater affinity than Bcl-XL for the inhibitory binding site in the central coupling domain it is likely that this site is the preferential target for Bcl-2 [118]. In addition, for Bcl-2 not its hydrophobic cleft but rather its transmembrane domain seems to play an important role for targeting and regulating the IP_3R via both its C-terminus and the site located in the central coupling domain [124].

Based on the recent cryo-EM structure of IP_3R1 [29, 41], this central site in the coupling domain resides in a relatively easily accessible area of IP_3R1 (Fig. 10.2, indicated in blue). The C-terminal transmembrane domain of Bcl-2 may thus serve to concentrate the protein at the ER near the IP_3R from where its N-terminal BH4 domain can more easily bind to the central coupling domain. In addition, sequestering Bcl-2 proteins at the ER membrane via their transmembrane domain may increase their ability to interact with the C-terminus of the IP_3R (Fig. 10.2, indicated in green). As this C-terminal binding site seems to be located more at the inside of the IP_3R1 tetramer one can expect a local high concentration of Bcl-2 proteins to be necessary for this interaction. Besides directly modulating IICR, Bcl-2 can serve as an anchor for targeting additional regulatory proteins to the IP_3R. It was shown that Bcl-2 attracts dopamine- and cAMP-regulated phosphoprotein of 32 kDa (DARPP-32) and calcineurin to the IP_3R thereby regulating the phosphorylation state of the latter and consequently its Ca^{2+}-release properties [125]. Finally, recent data indicate also for Bcl-2 an additional interaction site in the ligand-binding domain [126] highlighting the complexity of the interaction of the anti-apoptotic Bcl-2-family members with the IP_3R. Further research will be needed to unravel the precise function of each of these sites.

Another Bcl-2-family member that regulates the IP_3R is the zebrafish protein Nrz. The latter was shown to bind via its BH4 domain to the IBC of zebrafish IP_3R1, whereby E^{255} appeared essential for interaction (Fig. 10.1). Nrz prevents IP_3 binding to the IP_3R thereby inhibiting IICR [121]. Interestingly, although the Nrz BH4 domain is sufficient for interaction with the IP_3R, inhibition of IICR required the BH4-BH3-BH1 domains. Furthermore, phosphorylation of Nrz abolished its interaction with the IP_3R. Recently, Bcl-2-like 10, the human orthologue of Nrz, was shown, just like Nrz in zebrafish, to interact with the IBC, indicating a conserved function for this protein [122].

Besides anti-apoptotic Bcl-2-family members, also pro-apoptotic Bcl-2 proteins and other BH3 domain-containing proteins are known to target and regulate IP_3Rs. For instance, Bok, a pro-apoptotic Bcl-2-family member, interacts with the IP_3R (a.a. 1895–1903 of IP_3R1; Figs. 10.1 and 10.2) [127]. This interaction protects IP_3R1 and IP_3R2 from proteolytic cleavage by caspase 3 that results in a Ca^{2+} leak that may contribute to mitochondrial Ca^{2+} overload and thus apoptosis [128, 129]. Subsequent work demonstrated that the majority of all cellular Bok is bound to the IP_3R thereby stabilizing the Bok protein [130]. Unbound, newly synthesized Bok is rapidly turned over by the proteasome pathway. Both the association of mature Bok with the IP_3R and the rapid degradation of newly synthesized Bok by the proteasome restrict the pro-apoptotic functions of Bok thus preventing cell death induction.

From the above it is clear that the IP_3R is heavily regulated by both pro- and anti-apoptotic Bcl-2-family members. The occurrence of multiple binding sites for the same Bcl-2-family member further increases the complexity [112]. Furthermore, it should be stressed that the regulation of the IP_3R by Bcl-2 proteins is conserved during evolution. This is illustrated by the ability of the zebrafish Nrz protein to regulate IICR via its BH4 domain [121] and is further validated by the observation

that the BH4 domains of Bcl-2 derived from different vertebrates are able to inhibit IICR with similar efficiency [131]. The large number of both pro-and anti-apoptotic Bcl-2 proteins that regulate the IP_3R, targeting it at multiple sites, suggests that throughout evolution regulating IICR became an important functional aspect of the Bcl-2-protein family.

Mcl-1, Bcl-2 and Bcl-XL all target the C-terminal region of the IP_3R stimulating the occurrence of pro-survival Ca^{2+} oscillations and thus Ca^{2+} transfer to the mitochondria [114, 115, 118]. These Ca^{2+} transfers into the mitochondria are important for normal cell functioning [113] but are also involved in cancer development and could potentially form a novel therapeutic target [132]. Mitochondrial Ca^{2+} contributes to maintaining proper ATP production. When Ca^{2+} transfer into the mitochondria is inhibited, ATP levels decrease, activating autophagy. At the same time the cell cycle progression is halted [113, 133]. In cancer cells, decreased Ca^{2+} transfer into the mitochondria, consecutive loss of ATP and the start of autophagy is not accompanied by a stop in the cell cycle. Continuing the cell cycle without sufficient building blocks and ATP results in necrotic cell death [132]. Cancer cells are therefore reliant on proper Ca^{2+} transfer to the mitochondria to maintain mitochondrial function, including the production of ATP and metabolites necessary for completing the cell cycle. It is therefore common for cancer cells to upregulate one or several anti-apoptotic Bcl-2 proteins. By interacting with the C-terminus of the IP_3R the Bcl-2 proteins may stimulate Ca^{2+} oscillations assuring proper mitochondrial Ca^{2+} uptake and an adequate mitochondrial metabolism. On the other hand, upregulation of Bcl-2 and/or Bcl-XL also protects the cells from excessive IP_3R-mediated Ca^{2+} release by binding to the central regulatory site [116, 118–120] and prevents apoptosis, even in the presence of cell death inducers [109, 134]. In healthy cells a similar regulation of IICR by Bcl-2 proteins occurs. However, when cell death is induced in the latter, the amount of anti-apoptotic Bcl-2 proteins declines [134] potentially decreasing the level of their association with the IP_3R. This alleviates the inhibitory actions on IICR allowing pro-death Ca^{2+} signals while also reducing the opportunities for the occurrence of pro-survival Ca^{2+} oscillations.

10.4.3 Beclin 1

Beclin 1 is a pro-autophagic BH3 domain-containing protein [135]. It interacts with various proteins involved in the regulation of autophagy, including Bcl-2 [136, 137]. The latter protein, by sequestering Beclin 1, prevents its pro-autophagic action. A first study presenting evidence that Beclin 1 also interacts with the IP_3R showed an interaction between Beclin 1 and the IP_3R that depended on Bcl-2 and which was disrupted by the IP_3R inhibitor xestospongin B [138]. The release of Beclin 1 from the Bcl-2/IP_3R complex resulted in the stimulation of autophagy which could be counteracted by overexpressing the IBC. This suggested that the IBC was able to sequester the xestospongin B-released Beclin 1 thus halting its pro-autophagic function. From subsequent work, it appeared that the role of Beclin 1 with respect

to the IP_3R was more complex [139]. Indeed, the binding of Beclin 1 to the ligand-binding domain was confirmed, though it appeared that in IP_3R1 and to a lesser degree in IP_3R3 the suppressor domain (a.a. 1–225) played a more prominent role in the interaction than the IBC. Interestingly, during starvation-induced autophagy Beclin 1 binding to the IP_3R sensitized IICR that was shown to be essential for the autophagy process [139]. Using the $F^{123}A$ Beclin 1 mutant that does not interact with Bcl-2, it was shown that the sensitization of the IP_3R by Beclin 1 was not due to counteracting the inhibitory effect of Bcl-2, although, in agreement with the previous study [138] it appeared that Beclin 1 binding to Bcl-2 may be needed to target the protein in proximity of the IP_3R.

10.4.4 IRBIT

IRBIT regulates IICR by targeting the IP_3R ligand-binding domain thereby competing with IP_3. Moreover, this interaction is promoted by IRBIT phosphorylation [140]. Besides the IP_3R, IRBIT binds to several other targets regulating a wide range of cellular processes [141]. How IRBIT determines which target to interact with and modulate was recently described [142]. First, various forms of IRBIT exist: IRBIT, the long-IRBIT homologue and its splice variants, which were shown to have distinct expression patterns. Besides this, the N-terminal region of the various members of the IRBIT-protein family showed distinct differences. These differences, obtained by N-terminal splicing, are important in maintaining protein stability and in determining which target to interact with.

Recently, it was shown that Bcl-2-like 10, which binds to a distinct site in the ligand-binding domain (see Sect. 10.4.2), functionally and structurally interferes with the action of IRBIT on the IP_3R [122]. When both proteins are present, Bcl-2-like 10, via its BH4 domain, interacts with IRBIT, thereby mutually strengthening their interaction with the IP_3R and decreasing IICR in an additive way. Upon dephosphorylation of IRBIT, both IRBIT and Bcl-2-like 10 are released from the IP_3R, increasing pro-apoptotic Ca^{2+} transfer from the ER to the mitochondria. Interestingly, this study also showed that IRBIT is involved in regulating ER-mitochondrial contact sites as IRBIT knockout reduced the number of these contact sites [122].

10.4.5 Thymocyte-Expressed, Positive Selection-Associated 1 (TESPA1)

T-cell receptor (TCR) stimulation triggers a signaling cascade ultimately leading to the activation of PLC, production of IP_3 and IICR important for T-cell maturation [143]. TESPA1, a protein involved in the development/selection of T cells [144], has

been shown to regulate these Ca^{2+} signals. TESPA1 has a significant homology with KRAS-induced actin-interacting protein [147], a protein that was already shown to interact with and control the IP_3R [145, 146]. TESPA1 similarly interacts with the various IP_3R isoforms and it appeared that the full ligand-binding domain was needed for this interaction. However, at first no functional effect was described for this interaction [147]. Recently this topic was revisited and it was shown that TESPA1 recruits IP_3R1 to the TCR where PLC signaling is initiated and IP_3 produced [143]. In this way, TESPA1 promotes IP_3R1 phosphorylation on Y^{353} by the tyrosine kinase Fyn, increasing the affinity of the IP_3R for IP_3. The combination of both these effects increases the efficiency by which Ca^{2+} signaling occurs after TCR stimulation, which is beneficial for T-cell selection and maturation [148]. Furthermore, in Jurkat cells TESPA1 interacts at the ER-mitochondria contact sites with GRP75 [149], a linker protein coupling IP_3R with the mitochondrial VDAC1 channel favoring Ca^{2+} transfer from ER to mitochondria [150]. Consequently, TESPA1 knockout diminished the TCR-evoked Ca^{2+} transfers to both mitochondria and cytosol and confirm the important role for TESPA1 in these processes.

10.4.6 Pyruvate Kinase (PK) M2

PKs catalyze the last step of glycolysis and convert phosphoenolpyruvate to pyruvate resulting in the production of ATP. Many cancer cells preferentially upregulate glycolysis over oxidative phosphorylation suggesting a potential role for the PK family in cancer development. Four distinct PK isoforms exists, having each a distinct tissue expression pattern but PKM2 has the peculiarity to be expressed at an elevated level in most tumoral cells where it has a growth-promoting function. Moreover, although PKM1 and PKM2 are nearly identical, differing in only 22 a.a., they are regulated differently and have non-redundant functions [151]. Besides its metabolic functions, PKM2 is also involved in several non-metabolic functions. The latter encompass a nuclear role in transcriptional regulation, protein kinase activity towards various proteins in different cellular organelles, and even an extracellular function as PKM2 is also present in exosomes [152, 153]. It is therefore interesting that also a role for PKM2 at the ER was described since a direct interaction was found between PKM2 and the central coupling domain of the IP_3R, inhibiting IICR in various cell types [154, 155]. Moreover, a recent study links the switch from oxidative phosphorylation to glycolysis in breast cancer cells with PKM2 methylation [156]. Methylated PKM2 promoted proliferation, migration and growth of various breast cancer cell lines. Strikingly, PKM2 methylation did not seem to alter its enzymatic activity but did however alter mitochondrial Ca^{2+} homeostasis by decreasing IP_3R levels. Finally, co-immunoprecipitation experiments showed an interaction between methylated PKM2 and IP_3R1 and IP_3R3, though in this study it was not investigated whether the interaction was direct or indirect [156]. As PKM2 is in a variety of cancers considered as a good prognostic marker with

a strong potential as therapeutic target [152] these new data, linking directly a metabolic enzyme with an intracellular Ca^{2+}-release channel and ER-mitochondria Ca^{2+} transfer, provide new possibilities for therapeutic intervention.

10.4.7 BRCA-Associated Protein 1 (BAP1) and the F-Box Protein FBXL2

Prolonged stimulation of IP_3Rs leads to a downregulation of the IP_3R levels [157–159]. This downregulation is mainly due to IP_3R ubiquitination followed by their degradation via the proteasomal pathway [31, 160]. Ubiquitination is therefore an important IP_3R modification that may severely impact IICR signaling to for instance the mitochondria, thereby greatly affecting cell death and cell survival decisions. Recently a number of proto-oncogenes and tumor suppressors have been identified that critically control IP_3R3 ubiquitination.

BAP1 is a tumor suppressor with deubiquitinase activity that is known to have important roles in regulating gene expression, DNA stability, replication, and repair and in maintaining chromosome stability [161–164]. Besides this, BAP1 was also shown to influence cellular metabolism, suggesting potential roles for BAP1 outside the nucleus [165, 166]. Heterozygous loss of BAP1 results in decreased mitochondrial respiration while increasing glycolysis [167, 168]. These cells produced a distinct metabolite signature, indicative for the occurrence of the Warburg effect that is supporting cells towards malignant transformation. Heterozygous loss of BAP1 leads to a decreased ER-mitochondria Ca^{2+} transfer and altered mitochondrial metabolism [167]. BAP1 regulates this Ca^{2+} transfer by interacting with the N-terminal part (a.a. 1–800) of IP_3R3, a region which contains the complete ligand-binding domain and a small part of the central coupling domain. The deubiquitinase activity of BAP1 prevents degradation of IP_3R3 by the proteasome. Loss of BAP1 consequently results in excessive reduction of IP_3R3 levels thereby lowering mitochondrial Ca^{2+} uptake. This not only reduces the cell its responsiveness to Ca^{2+}-induced cell death but also promotes glycolysis over oxidative phosphorylation, both important aspects of malignant cell transformation. The nuclear function of BAP1 with respect to maintaining DNA integrity [161–164] together with its extra-nuclear role in regulating cell metabolism and sensitivity to Ca^{2+}-induced cell death [165–168] suggests that this protein may be an excellent target for cancer drug development.

F-box protein FBXL2 that forms a subunit of a ubiquitin ligase complex has the opposite effect of BAP1 on IP_3R3. FBXL2 interacts with a.a. 545–566 of IP_3R3, promoting its ubiquitination and its subsequent degradation. Reduced IP_3R3 leads to a decreased transfer of Ca^{2+} to the mitochondria and a reduced sensitivity towards apoptosis, thus promoting tumor growth [169]. The phosphatase and tensin homolog (PTEN) tumor suppressor could inhibit this pro-tumorigenic effect of FBXL2. PTEN not only promotes apoptosis by inhibiting protein kinase B/Akt (PKB) [170–

172] thereby counteracting PKB-mediated IP_3R3 phosphorylation [173, 174] but also by directly binding to IP_3R3 [169]. Binding of PTEN to IP_3R3 displaces FBXL2 from its binding site, reducing IP_3R3 ubiquitination, stabilizing IP_3R3 levels, and thus increasing pro-apoptotic Ca^{2+} signaling to the mitochondria [169]. In accordance with the fact that the FBXL2-binding site is only partially conserved in IP_3R1 and IP_3R2, the stability of the two latter isoforms appeared to be affected neither by FBXL2 nor by PTEN.

In several tumors, PTEN function is impaired which results in accelerated IP_3R3 degradation and impaired apoptosis induction. Treatment with drugs that stabilize IP_3R levels may therefore also be of interest for cancer therapy in cases where PTEN is affected.

10.5 Conclusions

Intracellular Ca^{2+} signaling is involved in a plethora of cellular processes. The ubiquitously expressed IP_3R Ca^{2+}-release channels play an important role in the generation of these signals and serve as signaling hubs for several regulatory factors and proteins/protein complexes. Since the first identification of the IP_3R [175], IP_3R-interacting proteins and their modulating roles on Ca^{2+} signaling and (patho)physiological processes have been the subject of many studies and well over 100 interaction partners were reported [14], though for many of them it is unclear how they exactly interact with the IP_3R and how they affect IP_3R function. Moreover, for many regulatory proteins, multiple binding sites were described of which the relative importance is not directly apparent. The recent (and future) advances in the elucidation of the IP_3R structure will pave the way for a better understanding how IP_3R gating exactly occurs and how different cellular factors and regulatory proteins influence IICR. As several of these proteins affect life and death decisions and/or play important roles in tumor development, the exact knowledge of their interaction site and their action of the IP_3R may lead to the development of new therapies for e.g. cancer treatment.

Acknowledgements TV is recipient of a postdoctoral fellowship of the Research Foundation—Flanders (FWO). Work performed in the laboratory of the authors was supported by research grants of the FWO, the Research Council of the KU Leuven and the Interuniversity Attraction Poles Programme (Belgian Science Policy). JBP is member of the Transautophagy COST action CA15138.

References

1. Vermassen E, Parys JB, Mauger JP (2004) Subcellular distribution of the inositol 1,4,5-trisphosphate receptors: functional relevance and molecular determinants. Biol Cell 96:3–17
2. Berridge MJ, Bootman MD, Roderick HL (2003) Calcium signalling: dynamics, homeostasis and remodelling. Nat Rev Mol Cell Biol 4:517–529

3. Berridge MJ, Lipp P, Bootman MD (2000) The versatility and universality of calcium signalling. Nat Rev Mol Cell Biol 1:11–21
4. Berridge MJ (2016) The inositol trisphosphate/calcium signaling pathway in health and disease. Physiol Rev 96:1261–1296
5. Tada M, Nishizawa M, Onodera O (2016) Roles of inositol 1,4,5-trisphosphate receptors in spinocerebellar ataxias. Neurochem Int 94:1–8
6. Egorova PA, Bezprozvanny IB (2018) Inositol 1,4,5-trisphosphate receptors and neurodegenerative disorders. FEBS J 285:3547–3565
7. Hisatsune C, Mikoshiba K (2017) IP_3 receptor mutations and brain diseases in human and rodents. J Neurochem 141:790–807
8. Hisatsune C, Hamada K, Mikoshiba K (2018) Ca^{2+} signaling and spinocerebellar ataxia. Biochim Biophys Acta 1865:1733–1744
9. Kerkhofs M, Seitaj B, Ivanova H, Monaco G, Bultynck G, Parys JB (2018) Pathophysiological consequences of isoform-specific IP_3 receptor mutations. Biochim Biophys Acta 1865: 1707–1717
10. Terry LE, Alzayady KJ, Furati E, Yule DI (2018) Inositol 1,4,5-trisphosphate receptor mutations associated with human disease. Messenger 6:29–44
11. Fedorenko OA, Popugaeva E, Enomoto M, Stathopulos PB, Ikura M, Bezprozvanny I (2014) Intracellular calcium channels: Inositol-1,4,5-trisphosphate receptors. Eur J Pharmacol 739:39–48
12. Foskett JK, White C, Cheung KH, Mak DO (2007) Inositol trisphosphate receptor Ca^{2+} release channels. Physiol Rev 87:593–658
13. Parys JB, De Smedt H (2012) Inositol 1,4,5-trisphosphate and its receptors. Adv Exp Med Biol 740:255–279
14. Prole DL, Taylor CW (2016) Inositol 1,4,5-trisphosphate receptors and their protein partners as signalling hubs. J Physiol 594:2849–2866
15. Vanderheyden V, Devogelaere B, Missiaen L, De Smedt H, Bultynck G, Parys JB (2009) Regulation of inositol 1,4,5-trisphosphate-induced Ca^{2+} release by reversible phosphorylation and dephosphorylation. Biochim Biophys Acta 1793:959–970
16. Ivanova H, Vervliet T, Missiaen L, Parys JB, De Smedt H, Bultynck G (2014) Inositol 1,4,5-trisphosphate receptor-isoform diversity in cell death and survival. Biochim Biophys Acta 1843:2164–2183
17. Patel S, Joseph SK, Thomas AP (1999) Molecular properties of inositol 1,4,5-trisphosphate receptors. Cell Calcium 25:247–264
18. Taylor CW, Genazzani AA, Morris SA (1999) Expression of inositol trisphosphate receptors. Cell Calcium 26:237–251
19. Vervloessem T, Yule DI, Bultynck G, Parys JB (2015) The type 2 inositol 1,4,5-trisphosphate receptor, emerging functions for an intriguing Ca^{2+}-release channel. Biochim Biophys Acta 1853:1992–2005
20. Gutierrez T, Simmen T (2018) Endoplasmic reticulum chaperones tweak the mitochondrial calcium rheostat to control metabolism and cell death. Cell Calcium 70:64–75
21. La Rovere RM, Roest G, Bultynck G, Parys JB (2016) Intracellular Ca^{2+} signaling and Ca^{2+} microdomains in the control of cell survival, apoptosis and autophagy. Cell Calcium 60: 74–87
22. Marchi S, Bittremieux M, Missiroli S, Morganti C, Patergnani S, Sbano L et al (2017) Endoplasmic reticulum-mitochondria communication through Ca^{2+} signaling: the importance of mitochondria-associated membranes (MAMs). Adv Exp Med Biol 997:49–67
23. Marchi S, Patergnani S, Missiroli S, Morciano G, Rimessi A, Wieckowski MR et al (2018) Mitochondrial and endoplasmic reticulum calcium homeostasis and cell death. Cell Calcium 69:62–72
24. Raffaello A, Mammucari C, Gherardi G, Rizzuto R (2016) Calcium at the center of cell signaling: interplay between endoplasmic reticulum, mitochondria, and lysosomes. Trends Biochem Sci 41:1035–1049

25. Ando H, Kawaai K, Bonneau B, Mikoshiba K (2018) Remodeling of Ca^{2+} signaling in cancer: regulation of inositol 1,4,5-trisphosphate receptors through oncogenes and tumor suppressors. Adv Biol Regul 68:64–76
26. Garcia MI, Boehning D (2017) Cardiac inositol 1,4,5-trisphosphate receptors. Biochim Biophys Acta 1864:907–914
27. Kania E, Roest G, Vervliet T, Parys JB, Bultynck G (2017) IP_3 receptor-mediated calcium signaling and its role in autophagy in cancer. Front Oncol 7:140
28. Roest G, La Rovere RM, Bultynck G, Parys JB (2017) IP_3 receptor properties and function at membrane contact sites. Adv Exp Med Biol 981:149–178
29. Serysheva II, Baker MR, Fan G (2017) Structural insights into IP_3R function. Adv Exp Med Biol 981:121–147
30. Wang L, Alzayady KJ, Yule DI (2016) Proteolytic fragmentation of inositol 1,4,5-trisphosphate receptors: a novel mechanism regulating channel activity? J Physiol 594: 2867–2876
31. Wright FA, Wojcikiewicz RJ (2016) Chapter 4 – inositol 1,4,5-trisphosphate receptor ubiquitination. Prog Mol Biol Transl Sci 141:141–159
32. Eid AH, El-Yazbi AF, Zouein F, Arredouani A, Ouhtit A, Rahman MM et al (2018) Inositol 1,4,5-trisphosphate receptors in hypertension. Front Physiol 9:1018
33. Uchida K, Miyauchi H, Furuichi T, Michikawa T, Mikoshiba K (2003) Critical regions for activation gating of the inositol 1,4,5-trisphosphate receptor. J Biol Chem 278:16551–16560
34. Bosanac I, Alattia JR, Mal TK, Chan J, Talarico S, Tong FK et al (2002) Structure of the inositol 1,4,5-trisphosphate receptor binding core in complex with its ligand. Nature 420: 696–700
35. Bosanac I, Yamazaki H, Matsu-Ura T, Michikawa T, Mikoshiba K, Ikura M (2005) Crystal structure of the ligand binding suppressor domain of type 1 inositol 1,4,5-trisphosphate receptor. Mol Cell 17:193–203
36. Lin CC, Baek K, Lu Z (2011) Apo and $InsP_3$-bound crystal structures of the ligand-binding domain of an $InsP_3$ receptor. Nat Struct Mol Biol 18:1172–1174
37. Seo MD, Velamakanni S, Ishiyama N, Stathopulos PB, Rossi AM, Khan SA et al (2012) Structural and functional conservation of key domains in $InsP_3$ and ryanodine receptors. Nature 483:108–112
38. Bosanac I, Michikawa T, Mikoshiba K, Ikura M (2004) Structural insights into the regulatory mechanism of IP_3 receptor. Biochim Biophys Acta 1742:89–102
39. Hamada K, Miyatake H, Terauchi A, Mikoshiba K (2017) IP_3-mediated gating mechanism of the IP_3 receptor revealed by mutagenesis and X-ray crystallography. Proc Natl Acad Sci USA 114:4661–4666
40. Taylor CW, da Fonseca PC, Morris EP (2004) IP_3 receptors: the search for structure. Trends Biochem Sci 29:210–219
41. Fan G, Baker ML, Wang Z, Baker MR, Sinyagovskiy PA, Chiu W et al (2015) Gating machinery of $InsP_3R$ channels revealed by electron cryomicroscopy. Nature 527:336–341
42. Yoshikawa F, Iwasaki H, Michikawa T, Furuichi T, Mikoshiba K (1999) Trypsinized cerebellar inositol 1,4,5-trisphosphate receptor. Structural and functional coupling of cleaved ligand binding and channel domains. J Biol Chem 274:316–327
43. Wang L, Wagner LE 2nd, Alzayady KJ, Yule DI (2017) Region-specific proteolysis differentially regulates type 1 inositol 1,4,5-trisphosphate receptor activity. J Biol Chem 292:11714–11726
44. Wang L, Yule DI (2018) Differential regulation of ion channels function by proteolysis. Biochim Biophys Acta 1865:1698–1706
45. Wang L, Wagner LE 2nd, Alzayady KJ, Yule DI (2018) Region-specific proteolysis differentially modulates type 2 and type 3 inositol 1,4,5-trisphosphate receptor activity in models of acute pancreatitis. J Biol Chem 293:13112–13124
46. Chan J, Yamazaki H, Ishiyama N, Seo MD, Mal TK, Michikawa T et al (2010) Structural studies of inositol 1,4,5-trisphosphate receptor: coupling ligand binding to channel gating. J Biol Chem 285:36092–36099

47. Schug ZT, Joseph SK (2006) The role of the S4-S5 linker and C-terminal tail in inositol 1,4,5-trisphosphate receptor function. J Biol Chem 281:24431–24440
48. Yamazaki H, Chan J, Ikura M, Michikawa T, Mikoshiba K (2010) Tyr-167/Trp-168 in type 1/3 inositol 1,4,5-trisphosphate receptor mediates functional coupling between ligand binding and channel opening. J Biol Chem 285:36081–36091
49. Paknejad N, Hite RK (2018) Structural basis for the regulation of inositol trisphosphate receptors by Ca^{2+} and IP_3. Nat Struct Mol Biol 25:660–668
50. Marchant JS, Taylor CW (1997) Cooperative activation of IP_3 receptors by sequential binding of IP_3 and Ca^{2+} safeguards against spontaneous activity. Curr Biol 7:510–518
51. Meyer T, Holowka D, Stryer L (1988) Highly cooperative opening of calcium channels by inositol 1,4,5-trisphosphate. Science 240:653–656
52. Boehning D, Joseph SK (2000) Direct association of ligand-binding and pore domains in homo- and heterotetrameric inositol 1,4,5-trisphosphate receptors. EMBO J 19:5450–5459
53. Alzayady KJ, Wang L, Chandrasekhar R, Wagner LE 2nd, Van Petegem F, Yule DI (2016) Defining the stoichiometry of inositol 1,4,5-trisphosphate binding required to initiate Ca^{2+} release. Sci Signal 9:ra35
54. Yoshikawa F, Morita M, Monkawa T, Michikawa T, Furuichi T, Mikoshiba K (1996) Mutational analysis of the ligand binding site of the inositol 1,4,5-trisphosphate receptor. J Biol Chem 271:18277–18284
55. Iwai M, Tateishi Y, Hattori M, Mizutani A, Nakamura T, Futatsugi A et al (2005) Molecular cloning of mouse type 2 and type 3 inositol 1,4,5-trisphosphate receptors and identification of a novel type 2 receptor splice variant. J Biol Chem 280:10305–10317
56. Konieczny V, Tovey SC, Mataragka S, Prole DL, Taylor CW (2017) Cyclic AMP recruits a discrete intracellular Ca^{2+} store by unmasking hypersensitive IP_3 receptors. Cell Rep 18: 711–722
57. Joseph SK, Lin C, Pierson S, Thomas AP, Maranto AR (1995) Heteroligomers of type-I and type-III inositol trisphosphate receptors in WB rat liver epithelial cells. J Biol Chem 270:23310–23316
58. Monkawa T, Miyawaki A, Sugiyama T, Yoneshima H, Yamamoto-Hino M, Furuichi T et al (1995) Heterotetrameric complex formation of inositol 1,4,5-trisphosphate receptor subunits. J Biol Chem 270:14700–14704
59. Wojcikiewicz RJ, He Y (1995) Type I, II and III inositol 1,4,5-trisphosphate receptor co-immunoprecipitation as evidence for the existence of heterotetrameric receptor complexes. Biochem Biophys Res Commun 213:334–341
60. Joseph SK, Bokkala S, Boehning D, Zeigler S (2000) Factors determining the composition of inositol trisphosphate receptor hetero-oligomers expressed in COS cells. J Biol Chem 275:16084–16090
61. Alzayady KJ, Wagner LE 2nd, Chandrasekhar R, Monteagudo A, Godiska R, Tall GG et al (2013) Functional inositol 1,4,5-trisphosphate receptors assembled from concatenated homo- and heteromeric subunits. J Biol Chem 288:29772–29784
62. De Smedt H, Missiaen L, Parys JB, Henning RH, Sienaert I, Vanlingen S et al (1997) Isoform diversity of the inositol trisphosphate receptor in cell types of mouse origin. Biochem J 322:575–583
63. Wojcikiewicz RJ (1995) Type I, II, and III inositol 1,4,5-trisphosphate receptors are unequally susceptible to down-regulation and are expressed in markedly different proportions in different cell types. J Biol Chem 270:11678–11683
64. Chandrasekhar R, Alzayady KJ, Wagner LE 2nd, Yule DI (2016) Unique regulatory properties of heterotetrameric inositol 1,4,5-trisphosphate receptors revealed by studying concatenated receptor constructs. J Biol Chem 291:4846–4860
65. Taylor CW (2017) Regulation of IP_3 receptors by cyclic AMP. Cell Calcium 63:48–52
66. Wagner LE 2nd, Joseph SK, Yule DI (2008) Regulation of single inositol 1,4,5-trisphosphate receptor channel activity by protein kinase A phosphorylation. J Physiol 586:3577–3596
67. Meena A, Tovey SC, Taylor CW (2015) Sustained signalling by PTH modulates IP_3 accumulation and IP_3 receptors through cyclic AMP junctions. J Cell Sci 128:408–420

68. Tovey SC, Dedos SG, Rahman T, Taylor EJ, Pantazaka E, Taylor CW (2010) Regulation of inositol 1,4,5-trisphosphate receptors by cAMP independent of cAMP-dependent protein kinase. J Biol Chem 285:12979–12989
69. Tovey SC, Dedos SG, Taylor EJ, Church JE, Taylor CW (2008) Selective coupling of type 6 adenylyl cyclase with type 2 IP_3 receptors mediates direct sensitization of IP_3 receptors by cAMP. J Cell Biol 183:297–311
70. Chin D, Means AR (2000) Calmodulin: a prototypical calcium sensor. Trends Cell Biol 10:322–328
71. Villarroel A, Taglialatela M, Bernardo-Seisdedos G, Alaimo A, Agirre J, Alberdi A et al (2014) The ever changing moods of calmodulin: how structural plasticity entails transductional adaptability. J Mol Biol 426:2717–2735
72. Tidow H, Nissen P (2013) Structural diversity of calmodulin binding to its target sites. FEBS J 280:5551–5565
73. Yap KL, Kim J, Truong K, Sherman M, Yuan T, Ikura M (2000) Calmodulin target database. J Struct Funct Genom 1:8–14
74. Maeda N, Kawasaki T, Nakade S, Yokota N, Taguchi T, Kasai M et al (1991) Structural and functional characterization of inositol 1,4,5-trisphosphate receptor channel from mouse cerebellum. J Biol Chem 266:1109–1116
75. Yamada M, Miyawaki A, Saito K, Nakajima T, Yamamoto-Hino M, Ryo Y et al (1995) The calmodulin-binding domain in the mouse type 1 inositol 1,4,5-trisphosphate receptor. Biochem J 308:83–88
76. Adkins CE, Morris SA, De Smedt H, Sienaert I, Török K, Taylor CW (2000) Ca^{2+}-calmodulin inhibits Ca^{2+} release mediated by type-1, −2 and −3 inositol trisphosphate receptors. Biochem J 345:357–363
77. Sienaert I, Nadif Kasri N, Vanlingen S, Parys JB, Callewaert G, Missiaen L et al (2002) Localization and function of a calmodulin-apocalmodulin-binding domain in the N-terminal part of the type 1 inositol 1,4,5-trisphosphate receptor. Biochem J 365:269–277
78. Islam MO, Yoshida Y, Koga T, Kojima M, Kangawa K, Imai S (1996) Isolation and characterization of vascular smooth muscle inositol 1,4,5-trisphosphate receptor. Biochem J 316:295–302
79. Lin C, Widjaja J, Joseph SK (2000) The interaction of calmodulin with alternatively spliced isoforms of the type-I inositol trisphosphate receptor. J Biol Chem 275:2305–2311
80. Cardy TJ, Taylor CW (1998) A novel role for calmodulin: Ca^{2+}-independent inhibition of type-1 inositol trisphosphate receptors. Biochem J 334:447–455
81. Patel S, Morris SA, Adkins CE, O'Beirne G, Taylor CW (1997) Ca^{2+}-independent inhibition of inositol trisphosphate receptors by calmodulin: redistribution of calmodulin as a possible means of regulating Ca^{2+} mobilization. Proc Natl Acad Sci U S A 94:11627–11632
82. Sipma H, De Smet P, Sienaert I, Vanlingen S, Missiaen L, Parys JB et al (1999) Modulation of inositol 1,4,5-trisphosphate binding to the recombinant ligand-binding site of the type-1 inositol 1,4, 5-trisphosphate receptor by Ca^{2+} and calmodulin. J Biol Chem 274: 12157–12162
83. Vanlingen S, Sipma H, De Smet P, Callewaert G, Missiaen L, De Smedt H et al (2000) Ca^{2+} and calmodulin differentially modulate myo-inositol 1,4, 5-trisphosphate (IP_3)-binding to the recombinant ligand-binding domains of the various IP_3 receptor isoforms. Biochem J 346:275–280
84. Michikawa T, Hirota J, Kawano S, Hiraoka M, Yamada M, Furuichi T et al (1999) Calmodulin mediates calcium-dependent inactivation of the cerebellar type 1 inositol 1,4,5-trisphosphate receptor. Neuron 23:799–808
85. Missiaen L, Parys JB, Weidema AF, Sipma H, Vanlingen S, De Smet P et al (1999) The bell-shaped Ca^{2+} dependence of the inositol 1,4, 5-trisphosphate-induced Ca^{2+} release is modulated by Ca^{2+}/calmodulin. J Biol Chem 274:13748–13751
86. Missiaen L, DeSmedt H, Bultynck G, Vanlingen S, Desmet P, Callewaert G et al (2000) Calmodulin increases the sensitivity of type 3 inositol-1,4, 5-trisphosphate receptors to Ca^{2+} inhibition in human bronchial mucosal cells. Mol Pharmacol 57:564–567

87. Nosyreva E, Miyakawa T, Wang Z, Glouchankova L, Mizushima A, Iino M et al (2002) The high-affinity calcium-calmodulin-binding site does not play a role in the modulation of type 1 inositol 1,4,5-trisphosphate receptor function by calcium and calmodulin. Biochem J 365:659–367
88. Kasri NN, Bultynck G, Smyth J, Szlufcik K, Parys JB, Callewaert G et al (2004) The N-terminal Ca^{2+}-independent calmodulin-binding site on the inositol 1,4,5-trisphosphate receptor is responsible for calmodulin inhibition, even though this inhibition requires Ca^{2+}. Mol Pharmacol 66:276–284
89. Kasri NN, Török K, Galione A, Garnham C, Callewaert G, Missiaen L et al (2006) Endogenously bound calmodulin is essential for the function of the inositol 1,4,5-trisphosphate receptor. J Biol Chem 281:8332–8338
90. Sun Y, Taylor CW (2008) A calmodulin antagonist reveals a calmodulin-independent interdomain interaction essential for activation of inositol 1,4,5-trisphosphate receptors. Biochem J 416:243–253
91. Sun Y, Rossi AM, Rahman T, Taylor CW (2013) Activation of IP_3 receptors requires an endogenous 1-8-14 calmodulin-binding motif. Biochem J 449:39–49
92. Kang S, Kwon H, Wen H, Song Y, Frueh D, Ahn HC et al (2011) Global dynamic conformational changes in the suppressor domain of IP_3 receptor by stepwise binding of the two lobes of calmodulin. FASEB J 25:840–850
93. White C, Yang J, Monteiro MJ, Foskett JK (2006) CIB1, a ubiquitously expressed Ca^{2+}-binding protein ligand of the $InsP_3$ receptor Ca^{2+} release channel. J Biol Chem 281: 20825–20833
94. Yang J, McBride S, Mak DO, Vardi N, Palczewski K, Haeseleer F et al (2002) Identification of a family of calcium sensors as protein ligands of inositol trisphosphate receptor Ca^{2+} release channels. Proc Natl Acad Sci U S A 99:7711–7716
95. Haynes LP, Tepikin AV, Burgoyne RD (2004) Calcium-binding protein 1 is an inhibitor of agonist-evoked, inositol 1,4,5-trisphosphate-mediated calcium signaling. J Biol Chem 279:547–555
96. Kasri NN, Holmes AM, Bultynck G, Parys JB, Bootman MD, Rietdorf K et al (2004) Regulation of $InsP_3$ receptor activity by neuronal Ca^{2+}-binding proteins. EMBO J 23: 312–321
97. Bultynck G, Szlufcik K, Kasri NN, Assefa Z, Callewaert G, Missiaen L et al (2004) Thimerosal stimulates Ca^{2+} flux through inositol 1,4,5-trisphosphate receptor type 1, but not type 3, via modulation of an isoform-specific Ca^{2+}-dependent intramolecular interaction. Biochem J 381:87–96
98. Li C, Chan J, Haeseleer F, Mikoshiba K, Palczewski K, Ikura M et al (2009) Structural insights into Ca^{2+}-dependent regulation of inositol 1,4,5-trisphosphate receptors by CaBP1. J Biol Chem 284:2472–2481
99. Li C, Enomoto M, Rossi AM, Seo MD, Rahman T, Stathopulos PB et al (2013) CaBP1, a neuronal Ca^{2+} sensor protein, inhibits inositol trisphosphate receptors by clamping intersubunit interactions. Proc Natl Acad Sci U S A 110:8507–8512
100. Nakamura TY, Jeromin A, Mikoshiba K, Wakabayashi S (2011) Neuronal calcium sensor-1 promotes immature heart function and hypertrophy by enhancing Ca^{2+} signals. Circ Res 109:512–523
101. Schlecker C, Boehmerle W, Jeromin A, DeGray B, Varshney A, Sharma Y et al (2006) Neuronal calcium sensor-1 enhancement of $InsP_3$ receptor activity is inhibited by therapeutic levels of lithium. J Clin Invest 116:1668–1674
102. Zhang K, Heidrich FM, DeGray B, Boehmerle W, Ehrlich BE (2010) Paclitaxel accelerates spontaneous calcium oscillations in cardiomyocytes by interacting with NCS-1 and the $InsP_3R$. J Mol Cell Cardiol 49:829–835
103. Boehmerle W, Splittgerber U, Lazarus MB, McKenzie KM, Johnston DG, Austin DJ et al (2006) Paclitaxel induces calcium oscillations via an inositol 1,4,5-trisphosphate receptor and neuronal calcium sensor 1-dependent mechanism. Proc Natl Acad Sci USA 103: 18356–18361

104. Boeckel GR, Ehrlich BE (2018) NCS-1 is a regulator of calcium signaling in health and disease. Biochim Biophys Acta 1865:1660–1667
105. Meissner G (2017) The structural basis of ryanodine receptor ion channel function. J Gen Physiol 149:1065–1089
106. Brini M, Cali T, Ottolini D, Carafoli E (2013) The plasma membrane calcium pump in health and disease. FEBS J 280:5385–5397
107. Hasan R, Zhang X (2018) Ca^{2+} regulation of TRP ion channels. Int J Mol Sci 19:1256
108. Saimi Y, Kung C (2002) Calmodulin as an ion channel subunit. Annu Rev Physiol 64: 289–311
109. Letai AG (2008) Diagnosing and exploiting cancer's addiction to blocks in apoptosis. Nat Rev Cancer 8:121–132
110. Brunelle JK, Letai A (2009) Control of mitochondrial apoptosis by the Bcl-2 family. J Cell Sci 122:437–441
111. Davids MS, Letai A (2012) Targeting the B-cell lymphoma/leukemia 2 family in cancer. J Clin Oncol 30:3127–3135
112. Vervliet T, Parys JB, Bultynck G (2016) Bcl-2 proteins and calcium signaling: complexity beneath the surface. Oncogene 35:5079–5092
113. Cárdenas C, Miller RA, Smith I, Bui T, Molgó J, Müller M et al (2010) Essential regulation of cell bioenergetics by constitutive $InsP_3$ receptor Ca^{2+} transfer to mitochondria. Cell 142: 270–283
114. Eckenrode EF, Yang J, Velmurugan GV, Foskett JK, White C (2010) Apoptosis protection by Mcl-1 and Bcl-2 modulation of inositol 1,4,5-trisphosphate receptor-dependent Ca^{2+} signaling. J Biol Chem 285:13678–13684
115. White C, Li C, Yang J, Petrenko NB, Madesh M, Thompson CB et al (2005) The endoplasmic reticulum gateway to apoptosis by Bcl-X_L modulation of the $InsP_3R$. Nat Cell Biol 7: 1021–1028
116. Rong YP, Bultynck G, Aromolaran AS, Zhong F, Parys JB, De Smedt H et al (2009) The BH4 domain of Bcl-2 inhibits ER calcium release and apoptosis by binding the regulatory and coupling domain of the IP_3 receptor. Proc Natl Acad Sci USA 106:14397–14402
117. Parys JB (2014) The IP_3 receptor as a hub for Bcl-2 family proteins in cell death control and beyond. Sci Signal 7:pe4
118. Monaco G, Beckers M, Ivanova H, Missiaen L, Parys JB, De Smedt H et al (2012) Profiling of the Bcl-2/Bcl-X_L-binding sites on type 1 IP_3 receptor. Biochem Biophys Res Commun 428:31–35
119. Monaco G, Decrock E, Akl H, Ponsaerts R, Vervliet T, Luyten T et al (2012) Selective regulation of IP_3-receptor-mediated Ca^{2+} signaling and apoptosis by the BH4 domain of Bcl-2 versus Bcl-xl. Cell Death Differ 19:295–309
120. Rong YP, Aromolaran AS, Bultynck G, Zhong F, Li X, McColl K et al (2008) Targeting Bcl-2-IP_3 receptor interaction to reverse Bcl-2's inhibition of apoptotic calcium signals. Mol Cell 31:255–265
121. Bonneau B, Nougarede A, Prudent J, Popgeorgiev N, Peyrieras N, Rimokh R et al (2014) The Bcl-2 homolog Nrz inhibits binding of IP_3 to its receptor to control calcium signaling during zebrafish epiboly. Sci Signal 7:ra14
122. Bonneau B, Ando H, Kawaai K, Hirose M, Takahashi-Iwanaga H, Mikoshiba K (2016) IRBIT controls apoptosis by interacting with the Bcl-2 homolog, Bcl2l10, and by promoting ER-mitochondria contact. elife 5:e19896
123. Yang J, Vais H, Gu W, Foskett JK (2016) Biphasic regulation of $InsP_3$ receptor gating by dual Ca^{2+} release channel BH3-like domains mediates Bcl-xL control of cell viability. Proc Natl Acad Sci USA 113:E1953–E1962
124. Ivanova H, Ritaine A, Wagner L, Luyten T, Shapovalov G, Welkenhuyzen K et al (2016) The trans-membrane domain of Bcl-2α, but not its hydrophobic cleft, is a critical determinant for efficient IP_3 receptor inhibition. Oncotarget 7:55704–55720

125. Chang MJ, Zhong F, Lavik AR, Parys JB, Berridge MJ, Distelhorst CW (2014) Feedback regulation mediated by Bcl-2 and DARPP-32 regulates inositol 1,4,5-trisphosphate receptor phosphorylation and promotes cell survival. Proc Natl Acad Sci U S A 111:1186–1191
126. Ivanova H, Wagner LE, 2nd, Tanimura A, Vandermarliere E, Luyten T, Welkenhuyzen K et al (2019) Bcl-2 and IP_3 compete for the ligand-binding domain of IP_3Rs modulating Ca^{2+} signaling output. Cell Mol Life Sci. In press
127. Schulman JJ, Wright FA, Kaufmann T, Wojcikiewicz RJ (2013) The Bcl-2 protein family member Bok binds to the coupling domain of inositol 1,4,5-trisphosphate receptors and protects them from proteolytic cleavage. J Biol Chem 288:25340–25349
128. Assefa Z, Bultynck G, Szlufcik K, Nadif Kasri N, Vermassen E, Goris J et al (2004) Caspase-3-induced truncation of type 1 inositol trisphosphate receptor accelerates apoptotic cell death and induces inositol trisphosphate-independent calcium release during apoptosis. J Biol Chem 279:43227–43236
129. Hirota J, Furuichi T, Mikoshiba K (1999) Inositol 1,4,5-trisphosphate receptor type 1 is a substrate for caspase-3 and is cleaved during apoptosis in a caspase-3-dependent manner. J Biol Chem 274:34433–34437
130. Schulman JJ, Wright FA, Han X, Zluhan EJ, Szczesniak LM, Wojcikiewicz RJ (2016) The stability and expression level of Bok are governed by binding to inositol 1,4,5-trisphosphate receptors. J Biol Chem 291:11820–11828
131. Ivanova H, Luyten T, Decrock E, Vervliet T, Leybaert L, Parys JB et al (2017) The BH4 domain of Bcl-2 orthologues from different classes of vertebrates can act as an evolutionary conserved inhibitor of IP_3 receptor channels. Cell Calcium 62:41–66
132. Cárdenas C, Müller M, McNeal A, Lovy A, Jana F, Bustos G et al (2016) Selective vulnerability of cancer cells by inhibition of Ca^{2+} transfer from endoplasmic reticulum to mitochondria. Cell Rep 14:2313–2324
133. Finkel T, Hwang PM (2009) The Krebs cycle meets the cell cycle: mitochondria and the G_1-S transition. Proc Natl Acad Sci USA 106:11825–11826
134. Distelhorst CW (2018) Targeting Bcl-2-IP_3 receptor interaction to treat cancer: a novel approach inspired by nearly a century treating cancer with adrenal corticosteroid hormones. Biochim Biophys Acta 1865:1795–1804
135. He C, Levine B (2010) The Beclin 1 interactome. Curr Opin Cell Biol 22:140–149
136. Decuypere JP, Parys JB, Bultynck G (2012) Regulation of the autophagic Bcl-2/Beclin 1 interaction. Cell 1:284–312
137. Erlich S, Mizrachy L, Segev O, Lindenboim L, Zmira O, Adi-Harel S et al (2007) Differential interactions between Beclin 1 and Bcl-2 family members. Autophagy 3:561–568
138. Vicencio JM, Ortiz C, Criollo A, Jones AW, Kepp O, Galluzzi L et al (2009) The inositol 1,4,5-trisphosphate receptor regulates autophagy through its interaction with Beclin 1. Cell Death Differ 16:1006–1017
139. Decuypere JP, Welkenhuyzen K, Luyten T, Ponsaerts R, Dewaele M, Molgo J et al (2011) Ins(1,4,5)P_3 receptor-mediated Ca^{2+} signaling and autophagy induction are interrelated. Autophagy 7:1472–1489
140. Ando H, Mizutani A, Matsu-ura T, Mikoshiba K (2003) IRBIT, a novel inositol 1,4,5-trisphosphate (IP_3) receptor-binding protein, is released from the IP_3 receptor upon IP_3 binding to the receptor. J Biol Chem 278:10602–10612
141. Ando H, Kawaai K, Mikoshiba K (2014) IRBIT: a regulator of ion channels and ion transporters. Biochim Biophys Acta 1843:2195–2204
142. Kawaai K, Ando H, Satoh N, Yamada H, Ogawa N, Hirose M et al (2017) Splicing variation of long-IRBIT determines the target selectivity of IRBIT family proteins. Proc Natl Acad Sci USA 114:3921–3926
143. Liang J, Lyu J, Zhao M, Li D, Zheng M, Fang Y et al (2017) Tespa1 regulates T cell receptor-induced calcium signals by recruiting inositol 1,4,5-trisphosphate receptors. Nat Commun 8:15732

144. Wang D, Zheng M, Lei L, Ji J, Yao Y, Qiu Y et al (2012) Tespa1 is involved in late thymocyte development through the regulation of TCR-mediated signaling. Nat Immunol 13:560–568
145. Dingli F, Parys JB, Loew D, Saule S, Mery L (2012) Vimentin and the K-Ras-induced actin-binding protein control inositol-(1,4,5)-trisphosphate receptor redistribution during MDCK cell differentiation. J Cell Sci 125:5428–5440
146. Fujimoto T, Machida T, Tanaka Y, Tsunoda T, Doi K, Ota T et al (2011) KRAS-induced actin-interacting protein is required for the proper localization of inositol 1,4,5-trisphosphate receptor in the epithelial cells. Biochem Biophys Res Commun 407:438–443
147. Matsuzaki H, Fujimoto T, Ota T, Ogawa M, Tsunoda T, Doi K et al (2012) Tespa1 is a novel inositol 1,4,5-trisphosphate receptor binding protein in T and B lymphocytes. FEBS Open Bio 2:255–259
148. Malissen B, Gregoire C, Malissen M, Roncagalli R (2014) Integrative biology of T cell activation. Nat Immunol 15:790–797
149. Matsuzaki H, Fujimoto T, Tanaka M, Shirasawa S (2013) Tespa1 is a novel component of mitochondria-associated endoplasmic reticulum membranes and affects mitochondrial calcium flux. Biochem Biophys Res Commun 433:322–326
150. Szabadkai G, Bianchi K, Varnai P, De Stefani D, Wieckowski MR, Cavagna D et al (2006) Chaperone-mediated coupling of endoplasmic reticulum and mitochondrial Ca^{2+} channels. J Cell Biol 175:901–911
151. Dayton TL, Jacks T, Vander Heiden MG (2016) PKM2, cancer metabolism, and the road ahead. EMBO Rep 17:1721–1730
152. Hsu MC, Hung WC (2018) Pyruvate kinase M2 fuels multiple aspects of cancer cells: from cellular metabolism, transcriptional regulation to extracellular signaling. Mol Cancer 17:35
153. Dong G, Mao Q, Xia W, Xu Y, Wang J, Xu L et al (2016) PKM2 and cancer: the function of PKM2 beyond glycolysis. Oncol Lett 11:1980–1986
154. Lavik AR (2016) The role of inositol 1,4,5-trisphosphate receptor-interacting proteins in regulating inositol 1,4,5-trisphosphate receptor-dependent calcium signals and cell survival. PhD thesis, Case Western Reserve University, USA. https://etd.ohiolink.edu/!etd.send_file?accession=case1448532307&disposition=inline
155. Lavik A, Harr M, Kerkhofs M, Parys JB, Bultynck G, Bird G et al (2018) IP_3Rs recruit the glycolytic enzyme PKM2 to the ER, promoting Ca^{2+} homeostasis and survival in hematologic malignancies. In: Abstract 66, 15th International meeting of the European Calcium Society. Hamburg, Germany
156. Liu F, Ma F, Wang Y, Hao L, Zeng H, Jia C et al (2017) PKM2 methylation by CARM1 activates aerobic glycolysis to promote tumorigenesis. Nat Cell Biol 19:1358–1370
157. Sipma H, Deelman L, Smedt HD, Missiaen L, Parys JB, Vanlingen S et al (1998) Agonist-induced down-regulation of type 1 and type 3 inositol 1,4,5-trisphosphate receptors in A7r5 and DDT1 MF-2 smooth muscle cells. Cell Calcium 23:11–21
158. Wojcikiewicz RJ, Furuichi T, Nakade S, Mikoshiba K, Nahorski SR (1994) Muscarinic receptor activation down-regulates the type I inositol 1,4,5-trisphosphate receptor by accelerating its degradation. J Biol Chem 269:7963–7969
159. Wojcikiewicz RJ, Nakade S, Mikoshiba K, Nahorski SR (1992) Inositol 1,4,5-trisphosphate receptor immunoreactivity in SH-SY5Y human neuroblastoma cells is reduced by chronic muscarinic receptor activation. J Neurochem 59:383–386
160. Oberdorf J, Webster JM, Zhu CC, Luo SG, Wojcikiewicz RJ (1999) Down-regulation of types I, II and III inositol 1,4,5-trisphosphate receptors is mediated by the ubiquitin/proteasome pathway. Biochem J 339:453–461
161. Lee HS, Lee SA, Hur SK, Seo JW, Kwon J (2014) Stabilization and targeting of INO80 to replication forks by BAP1 during normal DNA synthesis. Nat Commun 5:5128
162. Zarrizi R, Menard JA, Belting M, Massoumi R (2014) Deubiquitination of γ-tubulin by BAP1 prevents chromosome instability in breast cancer cells. Cancer Res 74:6499–6508
163. Yu H, Pak H, Hammond-Martel I, Ghram M, Rodrigue A, Daou S et al (2014) Tumor suppressor and deubiquitinase BAP1 promotes DNA double-strand break repair. Proc Natl Acad Sci U S A 111:285–290

164. Yu H, Mashtalir N, Daou S, Hammond-Martel I, Ross J, Sui G et al (2010) The ubiquitin carboxyl hydrolase BAP1 forms a ternary complex with YY1 and HCF-1 and is a critical regulator of gene expression. Mol Cell Biol 30:5071–5085
165. Baughman JM, Rose CM, Kolumam G, Webster JD, Wilkerson EM, Merrill AE et al (2016) NeuCode proteomics reveals Bap1 regulation of metabolism. Cell Rep 16:583–595
166. Ruan HB, Han X, Li MD, Singh JP, Qian K, Azarhoush S et al (2012) O-GlcNAc transferase/host cell factor C1 complex regulates gluconeogenesis by modulating PGC-1α stability. Cell Metab 16:226–237
167. Bononi A, Giorgi C, Patergnani S, Larson D, Verbruggen K, Tanji M et al (2017) BAP1 regulates IP_3R3-mediated Ca^{2+} flux to mitochondria suppressing cell transformation. Nature 546:549–553
168. Bononi A, Yang H, Giorgi C, Patergnani S, Pellegrini L, Su M et al (2017) Germline BAP1 mutations induce a Warburg effect. Cell Death Differ 24:1694–1704
169. Kuchay S, Giorgi C, Simoneschi D, Pagan J, Missiroli S, Saraf A et al (2017) PTEN counteracts FBXL2 to promote IP_3R3- and Ca^{2+}-mediated apoptosis limiting tumour growth. Nature 546:554–558
170. Worby CA, Dixon JE (2014) PTEN. Annu Rev Biochem 83:641–669
171. Carnero A, Paramio JM (2014) The PTEN/PI3K/AKT pathway in vivo, cancer mouse models. Front Oncol 4:252
172. Milella M, Falcone I, Conciatori F, Cesta Incani U, Del Curatolo A, Inzerilli N et al (2015) PTEN: multiple functions in human malignant tumors. Front Oncol 5:24
173. Bittremieux M, Parys JB, Pinton P, Bultynck G (2016) ER functions of oncogenes and tumor suppressors: modulators of intracellular Ca^{2+} signaling. Biochim Biophys Acta 1863: 1364–1378
174. Bononi A, Bonora M, Marchi S, Missiroli S, Poletti F, Giorgi C et al (2013) Identification of PTEN at the ER and MAMs and its regulation of Ca^{2+} signaling and apoptosis in a protein phosphatase-dependent manner. Cell Death Differ 20:1631–1643
175. Furuichi T, Yoshikawa S, Miyawaki A, Wada K, Maeda N, Mikoshiba K (1989) Primary structure and functional expression of the inositol 1,4,5-trisphosphate-binding protein P_{400}. Nature 342:32–38

Chapter 11
Expression of the Inositol 1,4,5-Trisphosphate Receptor and the Ryanodine Receptor Ca^{2+}-Release Channels in the Beta-Cells and Alpha-Cells of the Human Islets of Langerhans

Fabian Nordenskjöld, Björn Andersson, and Md. Shahidul Islam

Abstract Calcium signaling regulates secretion of hormones and many other cellular processes in the islets of Langerhans. The three subtypes of the inositol 1,4,5-trisphosphate receptors (IP3Rs), inositol 1,4,5-trisphosphate receptor type 1 (IP3R1), 1,4,5-trisphosphate receptor type 2 (IP3R2), 1,4,5-trisphosphate receptor type 3 (IP3R3), and the three subtypes of the ryanodine receptors (RyRs), ryanodine receptor 1 (RyR1), ryanodine receptor 2 (RyR2) and ryanodine receptor 3 (RyR3) are the main intracellular Ca^{2+}-release channels. The identity and the relative levels of expression of these channels in the alpha-cells, and the beta-cells of the human islets of Langerhans are unknown. We have analyzed the RNA sequencing data obtained from highly purified human alpha-cells and beta-cells for quantitatively identifying the mRNA of the intracellular Ca^{2+}-release channels in these cells. We found that among the three IP3Rs the IP3R3 is the most abundantly expressed one in the beta-cells, whereas IP3R1 is the most abundantly expressed one in the alpha-cells. In addition to the IP3R3, beta-cells also expressed the IP3R2, at a lower level. Among the RyRs, the RyR2 was the most abundantly expressed one in the beta-cells, whereas the RyR1 was the most abundantly expressed one in the alpha-cells. Information on the relative abundance of the different intracellular Ca^{2+}-release channels in the human alpha-cells and the beta-cells may help the understanding

F. Nordenskjöld · B. Andersson
Department of Cell and Molecular Biology, Karolinska Institutet, Stockholm, Sweden

M. S. Islam (✉)
Department of Clinical Science and Education, Södersjukhuset, Karolinska Institutet, Stockholm, Sweden

Department of Emergency Care and Internal Medicine, Uppsala University Hospital, Uppsala, Sweden
e-mail: Shahidul.Islam@ki.se

M. S. Islam (ed.), *Calcium Signaling*, Advances in Experimental Medicine and Biology 1131, https://doi.org/10.1007/978-3-030-12457-1_11

of their roles in the generation of Ca^{2+} signals and many other related cellular processes in these cells.

Keywords Human islets of Langerhans · Inositol 1,4,5-trisphosphate receptors in the beta-cells · Inositol 1,4,5-trisphosphate receptors in the alpha-cells · Ryanodine receptors in the alpha cells · Ryanodine receptors in the beta-cells · Ca^{2+} signaling in the islets · Human alpha-cells · Human beta-cells · RNA-sequencing

11.1 Introduction

Human islets of Langerhans are microorgans that contain the glucagon-secreting α-cells, the insulin-secreting β-cells, and the somatostatin-secreting δ-cells, dispersed throughout the islets [1, 2]. Islet research is important because of the roles of these microorgans in the secretion of insulin and glucagon, and the impairment of such secretions in diabetes mellitus, which is a global public health problem. The human islets contain 28–75% β-cell, 10–65% α-cells, and 1.2–22% δ-cells [1]. It is important to understand the molecular mechanisms of hormone secretion from the islet cells to understand their roles in the pathogenesis of different diseases including diabetes mellitus and pancreatogenous hyperinsulinemic hypoglycemia. A major obstacle in islet research is the difficulty in obtaining pure preparations of individual islet cells in sufficient numbers for experiments.

Insulin secretion from the β-cells is triggered by an increase in the cytoplasmic free Ca^{2+} concentration ($[Ca^{2+}]_c$) [3, 4]. The mechanism of increase in the $[Ca^{2+}]_c$ include Ca^{2+} entry through the plasma membrane Ca^{2+} channels, and Ca^{2+} release from the intracellular Ca^{2+} stores [3]. The intracellular Ca^{2+}-release channels are activated by inositol 1,4,5-trisphosphate and/or by Ca^{2+}, the latter process being called calcium-induced calcium release (CICR) [3, 5].

The two main families of the intracellular Ca^{2+}-release channels are the inositol 1,4,5-trisphosphate (IP3) receptor (IP3R) and the ryanodine receptors (RyR). They form tetrameric ion channels. In mammals and other higher organisms, three genes *ITPR1*, *ITPR2* and *ITPR3* encode the IP3R1, IP3R2, and IP3R3 respectively. The homology between the three isoforms is about 75% at amino acid level. They usually form homotetramers, but can also form heterotetramers, thereby altering the regulatory properties of the IP3Rs, and increasing the diversity of the spatial and temporal aspects of Ca^{2+} signaling mediated by the IP3Rs [6]. Ca^{2+}, at modest concentrations, acts as a co-activator of the IP3Rs, since in the absence of Ca^{2+}, IP3 alone cannot activate the channel [7]. At higher concentrations Ca^{2+} inhibits IP3-induced Ca^{2+} release [7].

Three genes *RYR1*, *RYR2*, and *RYR3* encode the ryanodine receptor 1 (RyR1), the ryanodine receptor 2 (RyR2), and the ryanodine receptor 3 (RyR3) respectively [8]. Previous studies have shown that ryanodine receptors participate in the generation of Ca^{2+} signals through CICR in the human β-cells [3, 5, 9, 10].

From numerous studies we know that the β-cells and the α-cells have both the IP3Rs and the RyRs [3, 11]. The functional properties and molecular regulation of the different types of the IP3Rs and the RyRs are different. In spite of over three decades of research, it is not known which types of the IP3Rs and the RyRs are present in the human islet cells. It is difficult to identify different types of IP3Rs and RyRs by immunohistochemistry because of lack of antibodies that selectively discriminate between the receptor subtypes. Difficulties in preparing highly purified α-cells and β-cells in sufficient amounts have further hampered the identification of the intracellular Ca^{2+}-release channels by conventional molecular techniques.

RNA sequencing or whole transcriptome shotgun sequencing of cDNA by using "next generation sequencing" is a powerful method for identifying the presence of, and measuring the quantity of different species of mRNA in the cells [12]. RNA sequencing is more reliable than hybridization-based microarrays for gene expression studies. We have used this approach for quantitatively identifying the transient receptor potential channels in the human β-cells [13]. By analyzing the RNA sequencing data obtained from highly purified α-cells and β-cells, we have now identified the level of expression of the different subtypes of the IP3Rs and RyRs in the human α-cells and the β-cells.

11.2 Methods and Materials

For identifying the intracellular Ca^{2+}-release channels, we used the transcriptomes of the purified human α-cells and β-cells reported by Blodgett et al. [14]. These investigators isolated islets from deceased human donors, dissociated those into single cell suspensions, fixed and permeabilized the cells to stain for the intracellular hormones, and sorted the cells by using fluorescence activated cell sorter (FACS). They sorted highly purified (> 97% pure) human α-cells and β-cells identified by anti-glucagon and anti-insulin antibodies respectively, under experimental conditions that minimized RNA degradation [14]. The δ-cells were stained by anti-somatostatin, and were gated out to obtain homogenous preparations of highly purified α-cells and β-cells [14]. The methods have been described in details by Blodgett et al. [14]. In short, they extracted RNA from the purified α-cells and β-cells, purified, quantified, and analyzed RNA for integrity. They constructed libraries by RNA fragmentation, first- and second-strand cDNA synthesis, ligation of adaptors, amplification, library validation, and ribosomal RNA removal [14]. They performed 91 base pair, paired-end sequencing on Illumina HiSeq 2000 [14].

The RNA sequencing data were made available for the public on the GEO database (https://www.ncbi.nlm.nih.gov/geo). We analyzed the data obtained from the α-cell and the β-cell samples from the adult donors of both sexes (5 males, 1 female, 1 undefined) of variable ages (4–60 years), and BMI (21.5–37 kg/m^2) [14]. Of the seven α-cell samples, RNA-sequencing data were produced from six samples. All of the seven β-cell samples yielded β- cell RNA-sequencing data.

We analyzed the RNA-sequencing data that consisted of 13 samples (6 α-cell and 7 β-cell) from 7 adult donors. We first filtered the data for the mitochondrial reads.

The data were mas mapped against the human mitochondrial genome (http://www.ncbi.nlm.nih.gov/nuccore/NC_012920.1) by using bowtie 2, and any mapped reads were removed from the data (option–un-conc-gz). On average 18% of the reads of each sample mapped to the mitochondrial genome. We analyzed gene expression by using RSEM software package [15], with bowtie 2 as mapping software (RSEM v1.2.25, bowtie 2 v2.2.6, standard RSEM in-parameters for bowtie 2). The filtered reads were mapped to the annotated human genome (version GRCh37.2). The resulting expression counts were normalized by RSEM to TPM-values (transcripts per million). We preferred TPM instead of FPKM (fragments per kilobase million) because TPM makes it convenient to compare the proportion of reads that maps to a gene in each sample. Gene level differential expression analysis was done by using the EBSeq R-package, >99% confidence [16].

11.3 Results

Of the six genes analyzed, four (*RYR2*, *ITPR1*, *ITPR2*, *ITPR3*) appeared to be differentially expressed in the two cell types. According to our differential expression analysis, *ITPR1* had a higher expression in the α-cells than in the β-cells, while *RYR2*, *ITPR2* and *ITPR3* had a higher expression in the β-cells than in the α-cells.

Figure 11.1 shows a heat map of the gene expression values of the IP3Rs and RyRs in the FACS purified human α-cell and β-cell preparations. IP3R1 was expressed more abundantly in the α-cells than in the β-cells, where it was almost absent. IP3R3 was more abundantly expressed in the β-cells than in the α-cells, where it was almost absent. In the β-cells the expression of the IP3R2 was lower than that of the IP3R3, but was higher than the expression of the IP3R2 in the α-cells, where it was almost absent. Highest expression of IP3R2 was observed in one of the β-cell preparations (β-4, white).

The expression of the RYR1 was higher in the α-cells than in the β-cells, where it was almost absent (Fig. 11.1). On the other hand, the expression of the RYR2 was higher in the β-cells than in the α-cells, where it was almost absent. The expression of the RYR3 was highly variable both in the α-cells and in the β-cells. There was very low expression of RYR3 in two preparations of the α-cells (α-5, α-7), and four preparations of β-cells (β-1, β5–7).

Figure 11.2 shows the level of expression of the three IP3Rs in six purified α-cell and seven purified β-cell preparations. In all α-cell preparations, the expressions of the IP3R1 were higher than those in any of the β-cell preparations. In six β-cell preparations (β-1, β-2, β-4 to 7), the expressions of the IP3R3 were higher than those in the α-cells. In one β-cell preparation (β-3) the expression of the IP3R3 was lower, similar to that in the α-cells.

The level of expressions of the three RyRs in the α-cells and the β-cells are shown in Fig. 11.3. In general, both the α-cells and the β-cells expressed RyRs at a much lower level than the IP3Rs. We found that *RYR1* was expressed, at low level, in five α-cell preparations (a1, a3, a4-a6), whereas it was almost absent in one α-cell

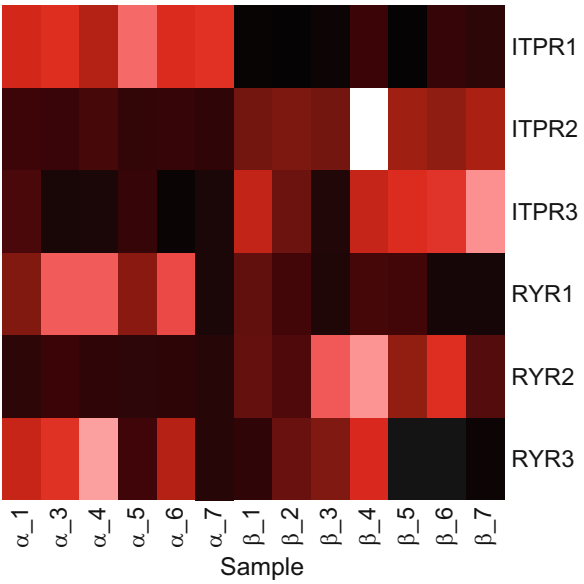

Fig. 11.1 Expression pattern of IP3Rs and the RyRs in the purified β-cells and α-cells of human islets of Langerhans. A heat map of the gene expression values is shown. The color indicates the relative expression of each gene (black, low; red, high; white, highest). For example, the expression of IP3R1 (*ITPR1*) is higher in the α-cells than in the β-cells (β-cells black); *RYR2* is more in the β-cells than in the α-cells (α-cells black)

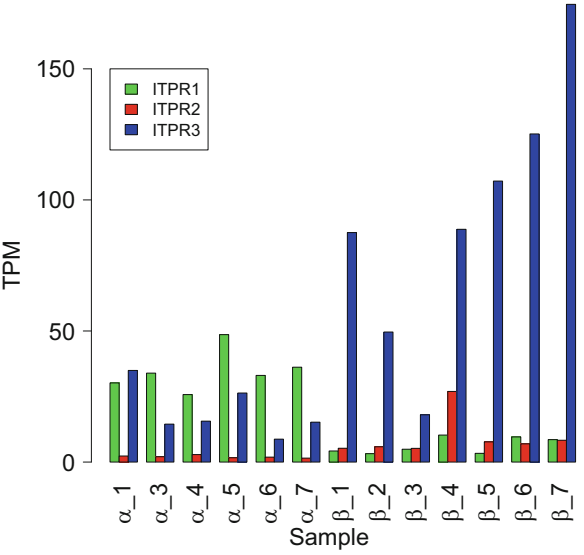

Fig. 11.2 Expression of the IP3Rs in the purified human β-cells and the α-cells of the islets of Langerhans. The scale is linear with all counts normalized to TPM. The figure shows the relative expression levels as bar plots. Green, IP3R1 (*ITPR1*); red, IP3R2 (*ITPR2*), blue, IP3R3 (*ITPR3*). TPM = transcripts per million. Results obtained from six α-cell preparations and seven β-cell preparations are shown

preparation (α-7). All of the seven samples of the β-cells expressed *RYR1* at very low level. On the other hand all of the samples of the β-cells expressed the *RYR2* at a level much higher than any of the α-cell preparations. The α-cells expressed *RYR2* only at very low level. We observed that both the α-cells and the β-cells expressed *RYR3* at low levels. Three of the β-cell preparations (β-2, β-3, β-4) expressed *RYR3* at low levels, whereas it was almost absent in the remaining four preparations (β-1, β-5, β-6, β-7). *RYR3* was expressed at a higher level in the α-cells than in the β-cells.

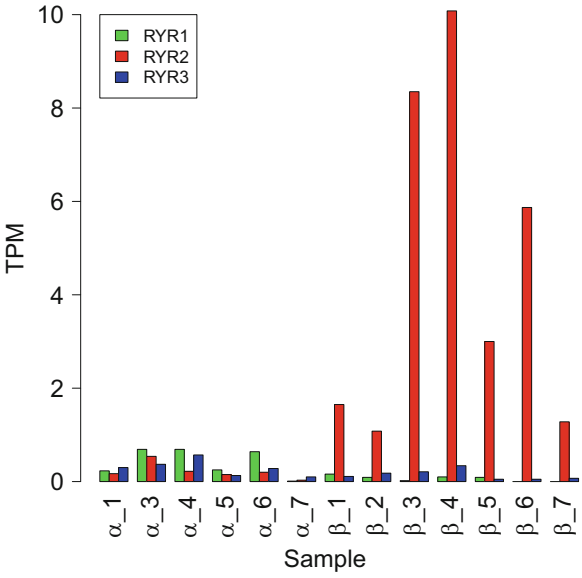

Fig. 11.3 Expression of the RyRs in the purified human β-cells and the α-cells of the islets of Langerhans. The figure shows the relative expression levels as bar plots. Green, RyR1 (*RYR1*); red, RyR2 (*RYR2*); blue, RyR3 (*RYR3*). The scale is linear with all counts normalized to TPM. TPM = transcripts per million. Note that the Y axis of this figure is different from that of Fig. 11.2. Results obtained from six α-cell preparations and seven β-cell preparations are shown

Four of the α-cell preparations expressed RYR3 at low level, whereas it was almost absent in the remaining two (α-5 and α-7).

11.4 Discussion

By analyzing the next generation RNA-sequencing data, we have identified the subtypes of the two major intracellular Ca^{2+}-release channels that are expressed in the two major types of cells in the human islets of Langerhans. The transcriptome data we used are reliable because these were obtained from α-cells and β-cells that were highly purified by FACS after staining the cells for insulin, glucagon and somatostatin, and after excluding the contaminating somatostatin-positive cells [14].

Our results showed that the most abundantly expressed IP3R in the β-cells was the IP3R3, and the most abundantly expressed IP3R in the α-cells was the IP3R1. The most abundantly expressed RyR in the β-cells was the RyR2 and the most abundantly expressed RyR in the α-cells was the RyR1. In both of the cell types the expression of IP3Rs was many fold higher than that of the RyRs.

A previous study reported that IP3R3 is readily detectable by immonoblotting in the rat insulinoma RINm5F cells, and a hamster-derived insulinoma cell line HIT-T15 cells [17, 18]. Wojcikiewicj et al. demonstrated that at protein level, 96% of the IP3Rs in the RINm5F cells are IP3R3 and 4% IP3R1 [19]. It was unclear whether the abundant expression of IP3R3 was a peculiarity limited to he transformed rodent β-cells. Our study showed that IP3R3 was expressed abundantly even in the primary human β-cells. Using RT-PCR, Blondel et al. could detect only IP3R3, but not IP3R2

and IP3R1 in the rat whole pancreatic islets [17]. Lee et al. showed that in the whole mouse islets, and rat islets the IP3R1 and the IP3R3 are the most abundant IP3Rs, respectively [20, 21]. In our study the primary human β-cells expressed the IP3R3 abundantly, and to a lesser extent also the IP3R2. This raises the possibility that in the β-cells IP3Rs may exist not only as homo-tetramers, but also as hetero-tetramers of IP3R3 and IP3R2. It may be noted that in pancreatic acinar cells, which express both IP3R3 and IP3R2, the majority of the IP3R3 form hetero-tetramer with IP3R2 [22]. IP3R hetero-tetramers composed of different IP3R subtypes show unique affinities for IP3 [6]. Chandrasekhar et al. have also shown that in IP3R hetero-tetramers, the properties of the IP3R2 dictates the regulatory properties and ATP sensitivity of the hetero-tetramer irrespective of the other subtypes present in the tetramer [6].

Even though the IP3Rs are primarily activated by inositol, 1,4,5-trisphosphate, and biphasically regulated by Ca^{2+}, there are many differences in the electrophysiological properties and molecular mechanisms that regulate the three subtypes of IP3Rs [6, 23, 24]. For instance, the three IP3Rs have different affinities for inositol, 1,4,5-trisphosphate (IP3R2 > IP3R1 > IP3R3).

The most abundant RyR in the β-cells was the RyR2. This is consistent with our previous report where we demonstrated by RNAse protection assay that mouse islets and βTC3 mouse insulinoma cells express RyR2 [25]. Mitchell et al. detected mRNA of both RyR1 and RyR2 but not of RyR3 in rat islets, mouse insulinoma MIN6 cells, and rat insulinoma INS-1 cells. Our results showed that primary human β-cells express RyR1 mRNA only at very low level. On the other hand, the most abundant RyR in the primary human α-cells was the RyR1, which was however expressed at a lower level compared to the RyR2 in the β-cells.

While all three RyRs can be activated by micromolar concentrations of Ca^{2+}, RyR2 is the one that is best known for physiological activation by Ca^{2+} entering through the voltage gated Ca^{2+} channels in the plasma membrane. Abundant expression of RyR2 in the β-cells as opposed to the α-cells, is consistent with the current views that CICR plays an important role in Ca^{2+} signaling in the β-cells [3, 5, 26]. Furthermore, in the β-cells, the RyR2-mediated CICR is facilitated by cAMP, and agonists like glucagon-like peptide 1, which increase cAMP [3, 25]. Glucagon-like peptide 1 and its analogues are frequently used in the treatment of type 2 diabetes.

We found that the expression of both the IP3Rs and the RyRs were highly variable in both the α-cell and the β-cell samples obtained from different donors. We speculate that the variability may partly be related to the procedures rather than the biology [14]. It should be noted that the human islets were collected after cold ischemia, and they were cultured prior to transport. These factors may reduce the yield of α-cells and β-cells after dissociation and FACS sorting, and may contribute to the variability of the RNA sequencing data from donor to donor.

It should be noted that we have estimated the relative abundance of the IP3R subtypes and the RyR subtypes in the human α-cells and β-cells only at the RNA level, and it remains a possibility that the expression of these channel subtypes at protein level may be different. At present, it is difficult to quantitatively estimate

the relative abundance of these channel proteins because of difficulty in obtaining highly purified human α-cells and β-cells in sufficient amounts, and lack of subtype specific antibodies against some of these channel proteins. Nevertheless, the comparison between the mRNA levels in the different cell types is still relevant and a strong indication of biological differences.

In summary, we have quantitatively identified the three subtypes of the IP3Rs and the RyRs in the human α-cells and β-cells, by analyzing the RNA sequencing data obtained from highly purified human α-cells and β-cells. Our results showed that the most abundant IP3R in the α-cells and the β-cells were the IP3R1 and the IP3R3 respectively; the most abundant RyRs in the α-cells and β-cells were the RyR1 and RyR2 respectively. Our results will be helpful in understanding the molecular mechanisms of generation of different types of Ca^{2+} signals and in regulating the Ca^{2+}-dependent processes in these two cell types of the human islets of Langerhans.

Acknowledgements Financial support was obtained from the Karolinska Institutet and the Uppsala County Council.

References

1. Brissova M, Fowler MJ, Nicholson WE, Chu A, Hirshberg B, Harlan DM et al (2005) Assessment of human pancreatic islet architecture and composition by laser scanning confocal microscopy. J Histochem Cytochem 53(9):1087–1097
2. Islam MS, Gustafsson AJ (2007) Islets of Langerhans: cellular structure and physiology. In: Ahsan N (ed) Chronic allograft failure: natural history, pathogenesis, diagnosis and management. Landes Bioscience, Austin, pp 229–232
3. Islam MS (2014) Calcium signaling in the islets. In: Islam MS (ed) Islets of Langerhans, 2nd edn. Springer, Dordrecht, pp 1–26
4. Islam MS (2010) Calcium signaling in the islets. Adv Exp Med Biol 654:235–259
5. Islam MS (2002) The ryanodine receptor calcium channel of beta-cells: molecular regulation and physiological significance. Diabetes 51(5):1299–1309
6. Chandrasekhar R, Alzayady KJ, Wagner LE 2nd, Yule DI (2016) Unique regulatory properties of heterotetrameric inositol 1,4,5-trisphosphate receptors revealed by studying concatenated receptor constructs. J Biol Chem 291(10):4846–4860
7. Taylor CW, Tovey SC (2010) IP(3) receptors: toward understanding their activation. Cold Spring Harb Perspect Biol 2(12):a004010
8. Santulli G, Lewis D, des Georges A, Marks AR, Frank J (2018) Ryanodine receptor structure and function in health and disease. Subcell Biochem 87:329–352
9. Holz GG, Leech CA, Heller RS, Castonguay M, Habener JF (1999) cAMP-dependent mobilization of intracellular Ca^{2+} stores by activation of ryanodine receptors in pancreatic beta-cells. A Ca^{2+} signaling system stimulated by the insulinotropic hormone glucagon-like peptide-1-(7-37). J Biol Chem 274(20):14147–14156
10. Gustafsson AJ, Islam MS (2005) Cellular calcium ion signalling–from basic research to benefits for patients. Lakartidningen 102(44):3214–3219
11. Hamilton A, Zhang Q, Salehi A, Willems M, Knudsen JG, Ringgaard AK et al (2018) Adrenaline stimulates glucagon secretion by Tpc2-dependent Ca^{2+} mobilization from acidic stores in pancreatic alpha-cells. Diabetes 67(6):1128–1139
12. Wang Z, Gerstein M, Snyder M (2009) RNA-Seq: a revolutionary tool for transcriptomics. Nat Rev Genet 10(1):57–63

13. Marabita F, Islam MS (2017) Expression of transient receptor potential channels in the purified human pancreatic beta-cells. Pancreas 46(1):97–101
14. Blodgett DM, Nowosielska A, Afik S, Pechhold S, Cura AJ, Kennedy NJ et al (2015) Novel observations from next-generation RNA sequencing of highly purified human adult and fetal islet cell subsets. Diabetes 64(9):3172–3181
15. Li B, Dewey CN (2011) RSEM: accurate transcript quantification from RNA-Seq data with or without a reference genome. BMC Bioinforma 12:323
16. Leng N, Dawson JA, Thomson JA, Ruotti V, Rissman AI, Smits BM et al (2013) EBSeq: an empirical Bayes hierarchical model for inference in RNA-seq experiments. Bioinformatics 29(8):1035–1043
17. Blondel O, Takeda J, Janssen H, Seino S, Bell GI (1993) Sequence and functional characterization of a third inositol trisphosphate receptor subtype, IP3R-3, expressed in pancreatic islets, kidney, gastrointestinal tract, and other tissues. J Biol Chem 268(15):11356–11363
18. De Smedt H, Missiaen L, Parys JB, Bootman MD, Mertens L, Van Den Bosch L et al (1994) Determination of relative amounts of inositol trisphosphate receptor mRNA isoforms by ratio polymerase chain reaction. J Biol Chem 269(34):21691–21698
19. Wojcikiewicz RJ (1995) Type I, II, and III inositol 1,4,5-trisphosphate receptors are unequally susceptible to down-regulation and are expressed in markedly different proportions in different cell types. J Biol Chem 270(19):11678–11683
20. Lee B, Bradford PG, Laychock SG (1998) Characterization of inositol 1,4,5-trisphosphate receptor isoform mRNA expression and regulation in rat pancreatic islets, RINm5F cells and betaHC9 cells. J Mol Endocrinol 21(1):31–39
21. Lee B, Laychock SG (2001) Inositol 1,4,5-trisphosphate receptor isoform expression in mouse pancreatic islets: effects of carbachol. Biochem Pharmacol 61(3):327–336
22. Alzayady KJ, Wagner LE 2nd, Chandrasekhar R, Monteagudo A, Godiska R, Tall GG et al (2013) Functional inositol 1,4,5-trisphosphate receptors assembled from concatenated homo- and heteromeric subunits. J Biol Chem 288(41):29772–29784
23. Vais H, Foskett JK, Mak DO (2010) Unitary Ca^{2+} current through recombinant type 3 InsP(3) receptor channels under physiological ionic conditions. J Gen Physiol 136(6):687–700
24. De Smet P, Parys JB, Vanlingen S, Bultynck G, Callewaert G, Galione A et al (1999) The relative order of IP3 sensitivity of types 1 and 3 IP3 receptors is pH dependent. Pflugers Arch 438(2):154–158
25. Islam MS, Leibiger I, Leibiger B, Rossi D, Sorrentino V, Ekstrom TJ et al (1998) In situ activation of the type 2 ryanodine receptor in pancreatic beta cells requires cAMP-dependent phosphorylation. Proc Natl Acad Sci U S A 95(11):6145–6150
26. Bruton JD, Lemmens R, Shi CL, Persson-Sjogren S, Westerblad H, Ahmed M et al (2003) Ryanodine receptors of pancreatic beta-cells mediate a distinct context-dependent signal for insulin secretion. FASEB J 17(2):301–303

Chapter 12
Evolution of Excitation-Contraction Coupling

John James Mackrill and Holly Alice Shiels

Abstract In mammalian cardiomyocytes, Ca^{2+} influx through L-type voltage-gated Ca^{2+} channels (VGCCs) is amplified by release of Ca^{2+} via type 2 ryanodine receptors (RyR2) in the sarcoplasmic reticulum (SR): a process termed Ca^{2+}-induced Ca^{2+}-release (CICR). In mammalian skeletal muscles, VGCCs play a distinct role as voltage-sensors, physically interacting with RyR1 channels to initiate Ca^{2+} release in a mechanism termed depolarisation-induced Ca^{2+}-release (DICR). In the current study, we surveyed the genomes of animals and their close relatives, to explore the evolutionary history of genes encoding three proteins pivotal for ECC: L-type VGCCs; RyRs; and a protein family that anchors intracellular organelles to plasma membranes, namely junctophilins (JPHs). In agreement with earlier studies, we find that non-vertebrate eukaryotes either lack VGCCs, RyRs and JPHs; or contain a single homologue of each protein. Furthermore, the molecular features of these proteins thought to be essential for DICR are only detectable within vertebrates and not in any other taxonomic group. Consistent with earlier physiological and ultrastructural observations, this suggests that CICR is the most basal form of ECC and that DICR is a vertebrate innovation. This development was accompanied by the appearance of multiple homologues of RyRs, VGCCs and junctophilins in vertebrates, thought to have arisen by 'whole genome replication' mechanisms. Subsequent gene duplications and losses have resulted in distinct assemblies of ECC components in different vertebrate clades, with striking examples being the apparent absence of RyR2 from amphibians, and additional duplication events for all three ECC proteins in teleost fish. This is consistent with teleosts possessing the most derived mode of DICR, with their $Ca_v1.1$ VGCCs completely lacking in Ca^{2+} channel activity.

J. J. Mackrill (✉)
Department of Physiology, School of Medicine, University College Cork, Cork, Ireland
e-mail: J.Mackrill@ucc.ie

H. A. Shiels
Division of Cardiovascular Sciences, Faculty of Biology, Medicine and Health, University of Manchester, Manchester, UK
e-mail: Holly.Shiels@manchester.ac.uk

M. S. Islam (ed.), *Calcium Signaling*, Advances in Experimental Medicine and Biology 1131, https://doi.org/10.1007/978-3-030-12457-1_12

Keywords Excitation-contraction coupling · Ryanodine receptor · Voltage-gated Ca^{2+} channel · Junctophilin · Evolution · Whole-genome duplication

12.1 Introduction

It is estimated that animals (Metazoa) evolved and diversified into major extant groups before the end of the Ediacaran Period, approximately 542 million years ago (Ma) [1]. Metazoa are taxonomically organised based on their degree of symmetry, Fig. 12.1. The body plan of radially symmetrical animals (Radiata) is circular and includes animals in the phyla Cnidaria and Ctenophora. Bilaterally symmetrical

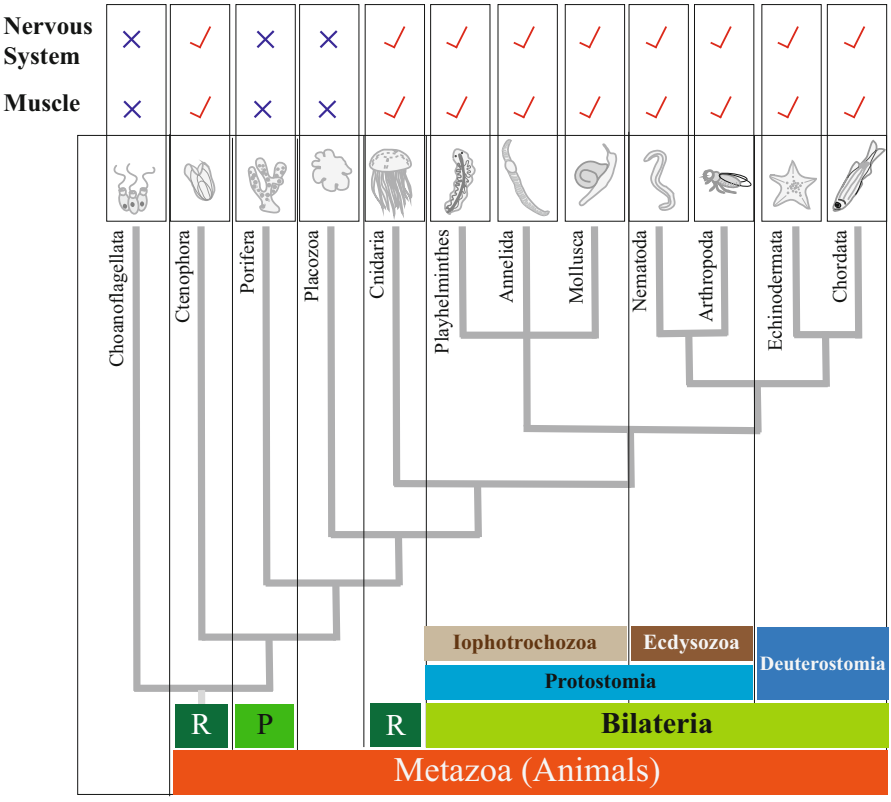

Fig. 12.1 Relationships between metazoan taxa in the context of excitation-contraction coupling (ECC). Diagrammatic representation of the relationships between major metazoan taxa and their sister group, Choanoflagellata. Also indicated is the presence of absence of nervous systems and muscles in these organisms: key players in ECC. Choanoflagellates are eukaryotes that are closely related to animals and can form colonies of cells. The relationships between basal metazoans, the Radiata ('R', ctenophores and cnidarians) and Parazoa ('P', poriferans) are unclear: shown is one consensus based on phylogenetic analysis of genomic data from these groups [36]

animals (Bilateria) have two symmetrical halves and are divided into three main groups that are differentiated by molecular and morphological characteristics: (1) the Ecdysozoa, which includes Arthropoda and Nematoda and have a three-layered cuticle that moults; (2) the Iophotrochozoa, a diverse group that includes the phyla Brachiopoda, Phoronida, Ectoprocta, Platyhelmintes, Nemertea, Mollusca and Annelida, who are characterised by the presence of either a lophophore, a crown of ciliated tentacles, or a distinct trocohophore larval stage (hence the name of this group: lopho + trocho); (3) the Deuterostoma, that include the phyla Echinodermata and Chordata who are distinguished by their embryonic development, during which the blastopore (the first opening) becomes the anus (as opposed to the mouth forming from the blastopore in the ecdysozoans and lophotrochozoans).

Molecular phylogenetic analyses indicate that certain metazoan lineages, the Poriferans (sponges) and Cnidarians (jellyfish, anemones and corals), emerged 750–800 Ma, during the Cryogenian Period [2]. Living cnidarians possess the characteristics that define animal life: multicellularity and the specialisation of particular tissue types. One innovation resulting from these developments was the evolution of specialised contractile myoepithelial and muscle cells, which generate force by interactions between ATP-dependent motors (myosins) and cytoskeletal components (actin) [2]. The concurrent development of the nervous system permitted the rapid regulation of force production by contractile tissues in response to intrinsic and extrinsic stimuli, such as neuronal inputs [3]. Regulation of force production in contractile cells initiated by such cues is termed excitation-contraction coupling (ECC). Prior to the development of actin-myosin dependent contractile machinery, eukaryotic cells moved exclusively using slower and weaker systems dependent on ciliary or flagellar beating. For example choanoflagellates, a closely related outgroup to metazoa, use the beating of their single flagellum to move and to ingest water and food. The development of ECC produced several selective advantages for metazoans, both in terms of capturing prey and of eluding predators [4].

12.1.1 Excitation-Contraction Coupling (ECC) in Various Muscle Types

Some features of ECC are conserved throughout animal evolution and in distinct types of muscle. In vertebrates, there are two main types of muscle: smooth and striated. Smooth muscle cells line the walls of hollow organs and are characterised by relatively slow contractions. They are defined by the net-like organisation of the contractile apparatus, which is anchored to structures called dense bodies. In contrast, cardiac and skeletal muscles are striated, due to an arrangement of the actin-myosin complexes within repeated units called sarcomeres, delimited by transverse structures called z-discs (also called z-lines).

As a second messenger, Ca^{2+} plays a key role in ECC in all muscle types. The rise of intracellular Ca^{2+} serves to activate the contractile apparatus in smooth muscle and in the cardiac and skeletal forms of striated muscle. The pathways subsequently diverge, with Ca^{2+} binding to the actin filament-associated troponin complex in striated muscles; but in smooth muscle, to calmodulin (CaM) forming an active complex which activates the myosin filament via myosin light chain kinase (MLCK). Ca^{2+} interactions with troponin, or activation of MLCK following binding of Ca^{2+}-CaM, initiates the cross-bridge cycling machinery and causes cell shortening, in line with the sliding filament theory of muscle contraction.

The excitatory mechanisms that raise intracellular Ca^{2+} and the effectors that transmit the chemical signal to mechanical force differ between muscle types. Cardiac- and skeletal muscle-type myosin heavy chain genes are thought to have arisen early during vertebrate evolution, prior to the divergence of Actinopterygian (ray-finned) and Sarcopterygian (lobe-finned) fish [5]. Furthermore, phylogenomic analyses indicate that the contractile machinery of striated muscles evolved independently in bilaterian and non-bilaterian animals. Radiata (cnidarians and ctenophores) lack key proteins of bilaterian striated muscle contractile machinery, such as components of the troponin complex. However, poriferans and non-metazoan eukaryotes possess homologues of other sarcomeric contractile proteins, such as muscle-type actins and myosins, even though they do not have muscle cells. Indeed, Ca^{2+}-stimulated, actin-myosin dependent contraction occurs in several single-celled eukaryote taxa, including amoebozoans (eg. *Amoeba, Dictyostelium*) and basal plants (eg. *Volvox*) [6]. This suggests that the metazoan contractile apparatus was derived by addition of new proteins to pre-existing actin-myosin force-producing machinery and that this occurred independently, in at least two animal lineages [7].

A key step in ECC is the delivery of sufficient quantities of Ca^{2+} to the vicinity of the contractile apparatus, to initiate and maintain cross-bridge cycling. Regardless of whether this Ca^{2+} is extracellular in origin or is released from intracellular stores, a major consideration is that Ca^{2+} is heavily buffered within the myoplasm. Buffering occurs through interactions of Ca^{2+} with anionic proteins and other large, negatively charged biomolecules. As a result, Ca^{2+} diffuses through cytoplasm about ten times more slowly than it does through water [8]. This places constraints on the distances within cells over which Ca^{2+} is able to operate effectively as a second messenger. This limitation has been circumvented in several ways during the evolution of metazoans, including the employment of muscles of small diameter (limiting distances over which Ca^{2+} has to diffuse), or of invaginations of the surface membrane called T-tubules. Slow movement of Ca^{2+} within the myoplasm is also a strength of this second messenger system, as it lends itself toward compartmentalisation, thus providing the scope for one signal to initiate multiple and distinct reactions separated in space and time [9].

12.1.2 Two Modes of Excitation-Contraction Coupling in Mammalian Striated Muscles

Mammalian cardiomyocytes use a mechanism of ECC considered to have developed early during animal evolution [10, 11]. Propagating action potentials, initiated in nodal cells, are detected by a constituent of L-type voltage-gated Ca^{2+} channel complexes (VGCCs) known as $Ca_v1.2$, or the α1C subunit of the cardiac dihydropyridine receptor [12]. This sarcolemmal protein acts as both a voltage-sensor and a Ca^{2+} channel, allowing this second messenger to enter the myoplasm [13]. Other components of L-type VGCC complexes are involved in modifying the electrophysiological properties and trafficking of these channels; and include the β, α2δ and γ subunits [14], see Sect. 12.2.

In mammalian cardiomyocytes, the quantity of Ca^{2+} influx via Ca_v1x channels (where 'x' means an undefined member of the Ca_v1 family) is insufficient to initiate contraction, and so it must be amplified by additional Ca^{2+} release from the sarcoplasmic reticulum (SR). This release occurs via an SR cation channel called the type 2 ryanodine receptor (RyR2), that is activated by Ca_v1x-dependent entry of this ion in a process termed Ca^{2+}-induced Ca^{2+}-release (CICR) [15]. Communication between $Ca_v1.2$ (plus $Ca_v1.3$) and RyR2 occurs at junctions between SR and sarcolemmal membranes, forming Ca^{2+} Release Units (CRUs) [16]. CRUs are found at the cell surface where the sarcolemmal and SR membrane systems interact in regions known as peripheral couplings. CRUs also exist at "dyadic" junctions between the SR and infoldings of the sarcolemma membrane called transverse- (T-) tubules. These invaginations allow membrane depolarisation to propagate deep into the myoplasm, circumventing the limitations on signalling imposed by Ca^{2+} buffering and permitting the development of cardiomyocytes of high cross-sectional area, capable of generating large forces [17]. However, not all cardiomyocytes possess well-developed T-tubular systems. For example, in mammals T-tubules can be completely absent or variable in density in adult atrial myocytes [18], and are lacking in all cardiomyocyte types of embryonic and newborn animals [19]. Moreover, T-tubules are absent in both the atria and the ventricle of non-mammalian vertebrates, namely aves, non-avian reptiles, the amphibians and fish [20, 21]. In these cases, ECC occurs at the peripheral couplings where VGCC and RyR2 channels form CRUs at the surface membrane. Here, and in mammalian myocytes without T-tubules, CICR-dependent propagation of Ca^{2+} waves travelling through the myoplasm are amplified by RyRs located within non-junctional, or "corbular" SR. These extra-junctional RyRs effectively act as "relay stations", propagating Ca^{2+} waves deeper into the myoplasm than would be practical by diffusion alone [20, 166].

In mammalian skeletal muscle fibres, ECC is initiated by nerve impulses at the end-plates of motor neurons. These action potentials propagate into myofibres via T-tubules, where a distinct member of the L-type VGCC family, based on the $Ca_v1.1$ protein, is enriched [21]. Instead of acting as Ca^{2+}-influx channels, myoplasmic regions of $Ca_v1.1$ communicate directly with RyR1 channels located in the terminal

cisternae of the SR. This allosteric, voltage-induced, or depolarisation-induced Ca^{2+}release (DICR) mechanism involves long-range protein-protein interactions, spanning the 10–12 nm gap between the T-tubule and apposed terminal cisternae SR [22]. Within myofibres, T-tubules are usually associated with paired termini of the SR, forming CRUs at "triad" junctions, see Fig. 12.2. Based on ultrastructural observations, DICR in skeletal muscle is an innovation that occurred either in pre-vertebrates or early during vertebrate evolution [10]. This mechanism displays a number of distinctions from the CICR-based ECC employed in cardiomyocytes: (1) no direct requirement for extracellular Ca^{2+} and influx of this ion (a voltage-dependent conformational change in the VGCC is communicated to the SR Ca^{2+} release channels); (2) faster kinetics, due to the lack of a requirement of triggering Ca^{2+} to diffuse through the junctional myoplasm; and (3) use of different members of the VGCC ($Ca_v1.1$ versus $Ca_v1.2$) and Ca^{2+} release channel (RyR1 versus RyR2) families.

In vertebrate skeletal muscle, not all RyR1 channels are directly coupled to $Ca_v1.1$ voltage-sensors. Ultrastructural data from toadfish skeletal myocytes indicate that alternate RyRs (which appear as "feet structures" by transmission electron microscopy) are directly coupled to "tetrads", likely to represent groups of four VGCC complexes [22]. Consequently, non-coupled RyR channels would have to be activated by an additional mechanism, with CICR triggered by Ca^{2+} release from neighbouring coupled RyR channels being the strongest candidate. Although present at low abundance in most mammalian muscle tissues, a third RyR type (RyR3) is thought to play a role in amplifying RyR1-mediated Ca^{2+} signals in some skeletal muscle types, via CICR at extra-junctional sites. This amplification of DICR occurs in neonatal skeletal myocytes [23] and in a subset of muscles of cephalic or somitomeric origin in adult mice [24]. RyR3 amplification of the Ca^{2+} signal is also present the heart; not in the working atrial and ventricular myocytes, but in cells of the conduction system [25].

In addition to the molecular communication between RyR and Ca_v1x channels, multiple other protein-protein interactions modulate the process of ECC in the striated muscles of mammals and other vertebrates [11]. These accessory proteins are associated with the sarcolemma (β-subunits of VGCCs), the myoplasm (calmodulin, FK506-binding proteins, protein kinases and phosphatases), the SR membrane (triadins, junctophilins, kinase anchor proteins, selenoprotein N) or the SR lumen (calsequestrin, histidine rich Ca^{2+} binding protein) [26]. Recently, it has been demonstrated that five proteins are essential for *de novo* reconstitution of the DICR-mode of ECC in a non-muscle mammalian cell-line: $Ca_v1.1$, RyR1, the β_{1a}-subunit of the VGCC, SH3 and cysteine rich domain 3 (STAC3) protein and junctophilin 2 (JPH2) [27]. Junctophilins are SR/ER integral membrane proteins that are essential for the formation of the junctions (peripheral, dyadic or triadic) between the SR and sarcolemmal membranes [28]. They hold the CRUs in register and thus together with the Ca^{2+} cycling proteins, are important for CICR and DICR, in facilitating ECC.

12.1.3 Aim of This Study

In order to simplify reconstruction of the evolutionary history of ECC, we have focused on three proteins that are essential for the formation of CRUs in striated muscles: the Ca_v1x subunit of L-type VGCCs; the RyR Ca^{2+} release channels; and the junctophilins, Fig. 12.2. Many of the observations in this study come from reviewing the literature. However, we also include significant novel *in silico* findings (Figs. 12.3, 12.4, 12.5, 12.6, and 12.7), where we test the hypotheses on the evolution of ECC gleaned from published work. The mode of ECC in vertebrate and invertebrate smooth muscle differs significantly from that in striated muscle and

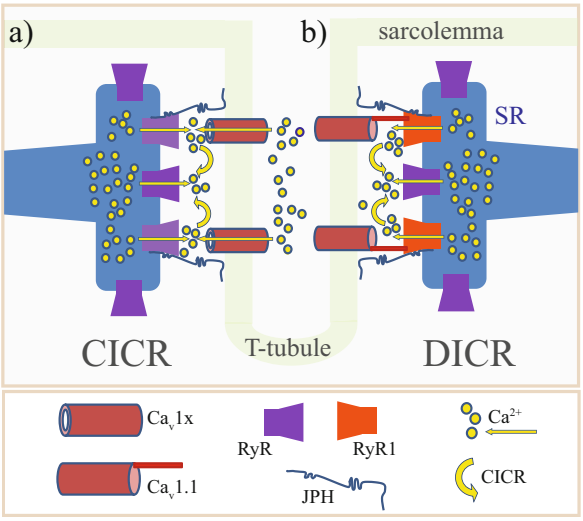

Fig. 12.2 Distinct modes of excitation-contraction coupling in mammalian striated muscles. Cartoon depicting the two modes of ECC employed within mammalian striated muscles: (**a**) Ca^{2+}-induced Ca^{2+} release (CICR) involves amplification of a small influx of Ca^{2+} via Ca_v1x VGCCs by calcium release via RyR channels in the SR [13, 15]. In mammals, this archetypally occurs at the dyad junctions of cardiomyocytes, but operates in other membranes and cell types, including the subplasmalemmal junctions of neurons [161] and of smooth muscle cells [29]. In the mammalian heart, junctophilin-2 (JPH2) plays critical roles in forming membrane junctions and in regulating communication between $Ca_v1.2$ and RyR2 [140, 141, 147]. This mode of ECC is evolutionarily most basal, with all of the necessary signalling protein components being present in choanoflagellates, a sister group to animals; (**b**) Depolarisation-induced Ca^{2+} release (DICR) in mammalian skeletal muscle involves direct, physical communication between $Ca_v1.1$ voltage-sensors in the T-tubule and RyR1 in the junctional SR. These interactions take place at triad junctions, whose formation is facilitated by both JPH1 and JPH2. This mode of signalling might operate in other mammalian cell types, including neurons [161]. In some cases, Ca^{2+} signals produced by DICR are amplified by CICR from RyRs that are not physically coupled to VGCCs [20, 22–24]. In terms of evolution, DICR appears to have arisen most recently and is probably a vertebrate innovation [10]

thus is not included in the subsequent analysis. For a detailed review of the smooth muscle literature *please see* [29].

12.2 The Evolutionary History of L-Type Voltage-Gated Ca^{2+} Channels (VGCC)

VGCC α subunits are part of a four-domain voltage-gated cation channel (FVCC) superfamily: proteins that share a common topology of four repeats, each containing six transmembrane helices, connected by extracellular and cytoplasmic loops [30]. The FVCC superfamily is comprised of five families: voltage-gated sodium channels (Na_v); Ca^{2+} channels that are activated by large changes in membrane potential ("high voltage activated" (HVA)); "low-voltage activated" (LVA) Ca^{2+} channels; sodium leak channels; and fungal Ca^{2+} channels [31]. Mammalian VGCCs consist of ten members grouped into three families, with Ca_v3x being LVA; and Ca_v1x and Ca_v2x being HVA. Of these, Ca_v1x forms L-type Ca^{2+} channels, characterised by their long open durations ("L-type") and sensitivity to dihydropyridine drugs [32]. There are four members of the Ca_v1x family in mammals, with $Ca_v1.1$ underlying ECC in skeletal muscle and $Ca_v1.2$ playing the predominant role in this process in cardiomyocytes. In addition to their channel-forming and voltage-sensing α1 subunit, L-type VGCCs complexes also contain β and α2δ subunits, along with a γ subunit in the case of $Ca_v1.1$ assemblies. These accessory proteins serve roles in channel complex trafficking and/or can modify VGCC electrophysiological properties [32]. The evolutionary histories of these accessory proteins have been described in detail elsewhere and will not be addressed further in the current work [33–35].

Published phylogenetic surveys have indicated that members of the FVCC superfamily were present in the common ancestor of all extant eukaryotes and subsequently diversified into five families, including the HVA (Ca_v1x and Ca_v2x) Ca^{2+} channels [31, 36]. Reconstruction of the evolution of the Ca_v1x family has been problematic, particularly because of controversies surrounding the relationships between early emerging animal groups [34, 36, 37]. Choanoflagellates are a sister group of metazoans, that morphologically resemble the choanocytes (flagellated "collar cells") of sponges. The genome of one member of this group, *Salpingoeca rossetta*, encodes one HVA and one LVA Ca_v homologue [33].

12.2.1 VGCC in Metazoan Invertebrates

Trichoplax adhaerens is the sole known living representative of the phylum Placozoa. Anatomically, these animals are the simplest that have been studied, comprising of only six cell types; lacking in muscle cells and in electrical or

chemical synapses [38]. Despite this apparent minimalism, the *T.adhaerens* genome encodes one member of each VGCC subfamily (Ca_v1x, Ca_v2x, Ca_v3x) and multiple homologues of proteins involved in neurotransmission [39]. Possession of Ca_v1x channels without the necessary cell-types to perform ECC might be resolved using similar rationales employed to explain paradoxes in the evolution of the actin-myosin contractile apparatus: such proteins were present prior to the development of these processes, but served distinct roles [7]. Recent investigation of *T.adhaerans* behaviours lends support to this hypothesis: this placozoan can alter its ciliary-based motility in response to gravity, or to neuropeptides, despite having no nervous system. These sensory responses utilise specialised crystal cells [40], or neurosecretory cells [41], respectively. In the latter case, the Ca_v3x homologue localises to secretory cells, suggesting that it plays a positive feedback role in secretion of neuropeptides: these neurotransmitter-like molecules could activate VGCCs, stimulating Ca^{2+} influx, which would elicit further exocytosis [42]. Elucidation of the roles of Ca_v1x channels in this organism could bring new insights into the evolution of ECC.

The sponge *Amphimedon queenslandica* possesses one gene encoding a HVA VGCC, which is intermediate between Ca_v1x and Ca_v2x in terms of its primary structure [33]. The ctenphore *Mnemiopsis leidyi* (the warty comb jelly) also has one HVA homologue, which is most closely related to vertebrate Ca_v2x proteins [33]. Some cnidarians, such as the starlet anemone *Nematostella vectensis* and the coral *Acropora millepora*, possess one Ca_v1x homologue, three members of the Ca_v2x family and two genes encoding Ca_v3x channels. In contrast, the hydra *Hydra magnipapillata*, another cnidarian, has only a single member of each family. This indicates expansion of Ca_v families in some cnidarian groups but not in others, presumably by lineage-specific gene duplication. Using *in situ* hybridisation microscopy, the mRNA encoding the Ca_v1x homologue was detected at greatest abundance in the muscle and/or motor neurons of *N.vectensis*, in keeping with a candidate role in ECC [33].

12.2.1.1 Protostomes

Among bilaterians (animals with bilateral symmetry), all protostomes (including arthropods, molluscs and worms) investigated have one representative of each of the three Ca_v subfamilies (Ca_v1x, Ca_v2x and Ca_v3x) [33, 35]. Nematode worms lack a heart and cardiomyocytes. They use either obliquely striated muscles in their body walls, or smooth muscles in other contractile organs. The contractile apparatus of obliquely striated muscles is anchored to staggered dense bodies, rather than to transverse z-discs such as those used by vertebrates [43]. The surface membrane of myofibres from these worms lacks T-tubules, but interacts with subsarcolemmal junctional SR to form candidate CRUs [44]. The model nematode *Caenorhabditis elegans* has a single Ca_v1x protein, encoded by the *egl-19* gene. Complete loss-of-function mutations in this gene cause embryonic lethality; partial loss-of-function mutants display hypotonia (flaccidity); and gain-of-function mutant worms are

myotonic, with impaired relaxation of the body [45, 46]. These observations strongly support an essential role for Ca_v1x VGCCs in nematode ECC.

All arthropod muscles are striated, with the contractile apparatus anchored to transverse z-discs [43]. Observations using transmission and freeze-fracture electron microscopy indicate that flight muscles from dragonflies, pedipalp muscles from a scorpion, or leg muscle from a fly, contain T-tubules. The SR-facing regions of these membranes bear large proteinaceous particles, resembling those which are accepted to be L-type VGCCs in vertebrate T-tubules [47]. In the fruit fly *Drosophila melanogaster*, a Ca_v1x protein is encoded by the *Dmca1D* gene and forms dihydropyridine-sensitive Ca^{2+} channel, required for contraction of the body wall muscles [48]. The *D.melanogaster* circulatory system is powered by a heart tube, which has both anterior and posterior pacemaker regions. Action potentials propagate from these sites in a manner that is dependent on Ca^{2+} influx through dihydropyridine-sensitive channels [49]. Biochemical, pharmacological and electrophysiological investigations indicate that crayfish striated muscle [50], isopod abdominal extensor muscles [51], and locust leg muscle [52] all possess dihydropyridine-sensitive Ca^{2+}-conducting L-type VGCCs. This suggests that ECC dependent on Ca^{2+}-influx through Ca_v1x channels, augmented to varying degrees by CICR from the SR, is a common feature of arthropod muscles. This is analogous to the type of ECC that occurs in vertebrate cardiomyocytes.

In contrast, the superficial abdominal flexor muscles of the shrimp *Atya lanipes* are electrically inexcitable and during contraction, Ca^{2+} influx is too small to be measured electrophysiologically. However, this contraction is strictly dependent on extracellular Ca^{2+} and could be modulated by agonistic (BayK 8644) or antagonistic (nifedipine) dihydropyridines [53, 54]. The proposed solution to these paradoxical observations is that "silent" L-type VGCCs allow an undetectable influx of Ca^{2+} into myocytes, which is amplified by CICR from the SR by a mechanism with extremely high gain. Consistent with this proposal, *A.lanipes* skeletal muscle has T-tubules, abundant SR and contracts in response to the RyR agonist caffeine [54]. Alternatively, this might represent development of the DICR mode of ECC in a relatively early branching group of bilaterians, with its dependency on extracellular Ca^{2+} being due to a requirement to replenish depleted intracellular Ca^{2+} stores, rather than due to a direct dependence on Ca^{2+} influx.

Annelids and molluscs use transversely striated, obliquely striated or smooth myocytes in different organ systems [43]. L-type Ca^{2+} channels have been reported in atrial cells from the Pacific oyster, *Crassostrea gigas* [55]. Ventricular myocytes of the pond snail *Lymnaea stagnalis* are myogenic, displaying rhythmic depolarization and contractions independently of neural inputs. These mollusc cardiomyocytes contain HVA and LVA VGCCs, which contribute to both pace-making and to ECC [56]. Heterologous expression and electrophysiological analysis of the Ca_v1x protein from *L.stagnalis* indicate that it has very similar electrophysiological properties to mammalian $Ca_v1.2$, with the most notable difference being a reduced sensitivity to dihydropyridine drugs [57]. Contraction of smooth muscle cells from the sea-slug *Aplysia kurodai* can be activated by acetylcholine or high extracellular K^+, via a mechanism that could be inhibited by nifedipine [58]. Similarly, contraction

of the obliquely striated muscle of *Octopus vulgaris* arms is dependent on rapidly activating and slowly inactivating currents carried by L-type VGCCs [59]. These findings demonstrate that Ca_v1x-dependent ECC, resembling that in vertebrate cardiomyocytes, is a common feature of molluscan muscles.

12.2.1.2 Deuterstomes

Deuterstomes are a major group of bilaterian animals that includes echinoderms (sea urchins, starfish, sea cucumbers and their relatives), hemichordates (such as acorn worms) and chordates (cephalochordates, tunicates and craniates). Of these, echinoderms use a distinctive mode of locomotion: walking on "tube-feet" (podia) dependent on hydrostatic forces powered by the contraction of smooth muscle-like cells of myoepithelial origin [60]. Although Ca^{2+} plays a key role in the contraction of these myocytes, there are no available data on the presence and function of L-type VGCCs in echinoderm contractile tissues [61]. However, Ca_v1x and Ca_v2x have been detected in sea urchin sperm, at the level of both mRNA and protein [62]. We were unable to find any published data on the role of L-type VGCC in the ECC of hemichordate muscles.

Chordates are bilaterian animals that possess a notochord: a flexible rod that runs along the long-axis of the body. Cephalochordates are a free-living, aquatic subphylum of chordates that superficially resemble fish or worms. They are exemplified by *Branchiostoma sp*., also known as lancelets or amphioxus. Like vertebrates, the body wall muscles of lancelets are striated and arranged in repeated segments called somites [63]. In the current study, we identified a single Ca_v1x homologue in the genome of *B. blecheri*. Lancelet somites are thin fibres, meaning that Ca^{2+} influx through VGCCs might be adequate for ECC [64]. However, electrophysiological and biochemical investigations indicate that *B. lanceolatum* trunk muscles possess dyad junctions and under certain conditions, can contract in the absence of extracellular Ca^{2+} [65, 66]. This suggests that the DICR mode of ECC could have evolved early in the chordate lineage [10].

Tunicates, or sea quirts, are a sister group to vertebrates and to cephalochordates, with a free-swimming larval stage and a sessile adult form. They possess skeletal, cardiac and smooth muscle types. Tunicate genomes encode a single Ca_v1x homologue, which displays low sensitivity to dihydropyridines [67]. There appears to be considerable diversity in the modes of ECC employed by tunicates. For example, muscle fibres from the body wall of adult *Doliolum denticulatum* lack T-tubules and an SR system, with their contraction being ablated by the dihydropyridine, nifedipine [68]. In contrast, caudal muscles from *Botryllus schlosseri* (the golden star tunicate) larvae possess a highly developed T-tubule system that forms dyad junctions with the SR [69].

12.2.2 VGCC in Metazoan Vertebrates

The two-rounds of whole genome duplication (2R-WGD) process, originally postulated by Susumu Ohno, describes a mechanism that facilitated the rapid evolution and expansion of vertebrates [70]. Gene duplication by polyploidy, and the resulting potential for functional diversification of duplicated genes, permitted rapid increases in the complexity and adaptability of this group. Phylogenetic and cytogenetic data support the concept of these rounds of genomic duplication occurring prior to the divergence of agnathan (jawless fish, including the cyclostomes) and gnathostome (jawed) vertebrates [71]. The 2R-WGD mechanism probably permitted the innovation of the DICR-mode of ECC in skeletal muscle, either prior to, or early during, the evolution of vertebrates. Cyclostomes are the most basal of extant vertebrates, comprising of hagfish and lampreys. Depolarisation-evoked contraction of caudal hearts (i.e. accessory hearts, analogous to those of the lymphatic system), slow-twitch and fast-twitch skeletal muscle from the inshore hagfish, *Eptatretus burgeri*, persists in nominally Ca^{2+}-free seawater, indicating a DICR mode of ECC [72]. Electrically-stimulated twitches in skeletal muscle fibres from the river lamprey, *Lampetra planeri*, were maintained in the presence of levels of colbalt ions that blocked Ca^{2+} influx via dihydropyridine-sensitive channels, again providing evidence for a DICR mechanism [73]. Freeze-fracture electron microscopy of skeletal muscle from the Pacific hagfish *E. stoutii* and the river lamprey, *L. planeri*, indicates that membrane particles corresponding to L-type VGCC complexes are arranged in tetrads [10], a feature thought to depend on physical interactions with underlying RyRs at CRUs [74]. Despite such physiological evidence of a DICR mode of ECC in cyclostome skeletal myocytes, we were only able to detect partial homologues of a Ca_v1 VGCC encoded in the genome of the sea lamprey *Petromyzon marinus*. Furthermore, this homologue displays greatest identity with $Ca_v1.2$, rather than $Ca_v1.1$. However, failure to detect homologues of skeletal muscle-type $Ca_v1.1$ in *P.marinus* might be a consequence of incomplete sequencing or poor annotation of its genome.

Amphibians, non-avian reptiles, birds and mammals generally have four Ca_v1x homologues ($Ca_v1.1$ to $Ca_v1.4$), probably generated by the 2R-WGD mechanism. This could have permitted functional specialisation of the $Ca_v1.1$ type in skeletal muscles, allowing it to mechanically couple to RyR1 in the SR. In mammalian skeletal muscle, Ca^{2+} influx via VGCCs is not required for ECC, since mice engineered with a non-conducting mutant of $Ca_v1.1$ (N617D) do not show any overt changes in skeletal myocyte function [75]. Teleosts are the largest group within the class Actinopterygii (ray-finned fish), that underwent an additional third round of WGD between 320 and 350 Ma [76]. This facilitated the development of new innovations, such as two non-conducting homologues of $Ca_v1.1$ in the skeletal muscles of teleost fish, including the zebrafish (*Danio rerio*), pike characin (*Ctenolucius hujeta*), and rice medaka (*Oryzias latipes*) [77]. Salmonids may be of particular interest in relation to functional specialisation of VGCCs, because of

an additional and relatively recent WGD event (the salmonid-specific 4R-WGD or Ss4R) that has been dated 25–100 Ma [78].

The sterlet *Acipenser ruthenus* is a basal ray-finned sturgeon, whose $Ca_v1.1$ homologue displays a Ca^{2+} conductance intermediate between that of mammals and teleosts. Together with phylogenetic evidence, this suggests that teleost non-conducting $Ca_v1.1$ voltage-sensors are the most derived forms, with Ca^{2+}-conducting $Ca_v1.1$ channels of mammals and other sarcopterygian (lobe-finned fish) descendants being the most basal [79].

12.3 Evolution of Ryanodine Receptor (RyR) Ca^{2+} Release Channels

Along with inositol 1,4,5-trisphosphate receptors (ITPRs), the ryanodine receptors (RyRs) form a superfamily of tetrameric, ligand-gated cation channels that release Ca^{2+} from intracellular storage organelles including the ER and SR [26]. ITPR homologues are encoded in the genomes of most eukaryotes, but have apparently been lost by some groups, such as late branching fungi and green plants [80]. The Ca^{2+} release channel superfamily is subdivided between the ITPR-A and ITPR-B families, the latter of which is probably ancestral to the RyRs [81]. Proteins related to RyRs, both in terms of sequence identity and protein domain architecture, first appeared over 950 Ma, prior to the divergence of metazoa and their sister groups choanoflagellata and filasterea [80].

12.3.1 RyRs of Invertebrates

Among animals, RyR homologues have been detected in the genomes of sponges such as *Amphimedon queenslandica*, *Oscarella carmela* and *Sycon ciliatum* [81], though not in ctenophores or cnidaria, Fig. 12.3. If sponges are basal metazoans [33, 82], this implies that RyRs were subsequently lost from ctenophore and cnidarian lineages. However, the striated swimming muscles of the hydrozoan jellyfish *Aglantha digitale* [83] and of the giant smooth muscles of the ctenophore *Beroe ovata* [84] are reported to contain an SR system. This indicates that either RyRs have not been detected in cnidarian and ctenophore genomes because of poor sequence quality or incomplete annotation; or that Ca^{2+} might be released from the SR of these organisms by a distinct mechanism, such as CICR via ITPRs. Of these possibilities, we consider the latter to be more likely, given the increasing numbers of cnidarian and ctenophore species whose genomes have been deduced. Furthermore, contraction of radial muscles from the jellyfish *Polyorchis penicillatus* is abolished by low extracellular Ca^{2+} or the Ca_v1x antagonist nitrendipine, but is also reduced by 25% in the presence of 10 mM caffeine [85]. In addition to its use as

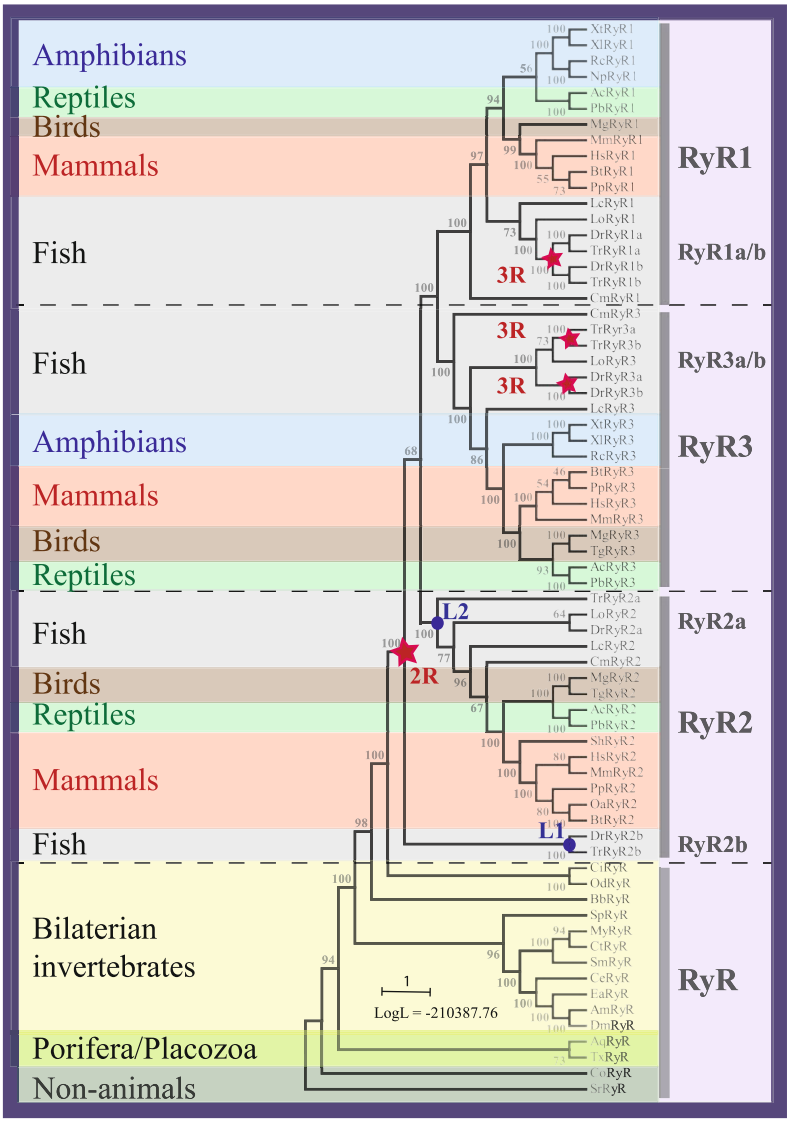

Fig. 12.3 Evolutionary history of RyR calcium release channels. The evolutionary history of proteins related to RyR2 from *Homo sapiens* (Accession Number Q92736.3) was inferred using the Maximum Parsimony method, conducted using MEGA5 [162]. The percentage of trees (from 500 replicates) in which taxa are clustered was determined by using the bootstrap method, with 50% being taken as significant [163]. Bootstrap values are indicated next to branches. Also shown is a scale-bar of the number of amino acid substitutions per position and the logarithmic likelihood value for this consensus tree. Red stars ('2R' and '3R') indicate potential whole genome duplications; blue circles ('L1' and 'L2') candidate gene losses. This analysis involved 68 proteins (full details available from the corresponding author, upon request). Species analysed were mammals: *Homo sapiens* ('Hs', human) *Mus musculus* ('Mm', house-mouse), *Bos taurus* ('Bt', cattle) and *Panthera pardus* ('Pp', leopard); birds: *Meleagris gallopavo* ('Mg', turkey) and

an RyR agonist, caffeine is also an antagonist of ITPRs [86]. Since this drug did not stimulate contraction of *P.penicillatus* striated muscles in its own right, its effects were probably mediated by ITPR antagonism, rather than depletion of intracellular stores by sustained activation of RyR channels.

12.3.1.1 Protostomes

Most bilaterian animal groups possess a single RyR homologue, most likely operating via CICR [80]. The extent of the contribution of Ca^{2+} released in this manner to contraction varies between organisms, tissues and muscle types. Platyhelminthes, or flatworms, are considered to be basal bilaterians: they lack a body cavity, do not possess a specialised cardiovascular system and contain two layers of smooth muscle-like contractile tissue in their body walls. The plant alkaloid ryanodine is specific, high-affinity and irreversible ligand for RyRs [87], that can only bind to these channels when they are in an open state. Consequently, [^{3}H]ryanodine binding has been employed to gauge the open state of RyR channels in response to physiological and pharmacological stimuli [26, 88]. Membrane vesicles prepared from the trematode flatworm *Schistosoma mansoni* contain binding sites for ryanodine, whose abundance could be increased by the RyR agonist caffeine and decreased by the antagonist dantrolene [88]. Both release of $^{45}Ca^{2+}$ from microsomal membranes and contraction of the body wall muscle of *S.mansoni* were enhanced by ryanodine [89]. Caffeine could stimulate body wall contraction in *S.mansoni* and in the turbellarian flatworms *Dugesia tigrina* and *Procerodes littoralis*, in a manner that was inhibited by high concentrations of ryanodine, although not by other characteristic antagonists of mammalian RyRs, neomycin and ruthenium red [90]. Along with phylogenomic data (Fig. 12.3), these observations suggest that a single RyR homologue contributes to muscle contraction in flatworms, and that their Ca^{2+} release channels are pharmacologically distinct from their vertebrate counterparts.

Fig. 12.3 (continued) *Taeniopygia guttata* ('Tg', zebrafinch); reptiles: *Anolis carolinensis* ('Ac', anole) and *Python bivittatus* ('Pb', python); amphibians: *Xenopus tropicalis* ('Xt', Western clawed frog), *Xenopus laevis* ('Xl', African clawed frog), *Rana catesbeiana* ('Rc', American bullfrog) and *Nanorana parkeri* ('Np', High Himalayan frog); fish: *Latimeria chalumnae* ('Lc', coelacanth), *Lepisosteus oculatus* ('Lc', spotted gar), *Danio rerio* ('Dr', zebrafish), *Takifugu rubripes* ('Tr', Japanese pufferfish) and *Callorhinchus milii* ('Cm', elephant shark); tunicates: *Ciona intestinalis* ('Ci', a sea squirt) and *Oikopleura dioica* ('Od'); cephalochordate: *Branchiostoma belcheri* ('Bb', Belcher's lancelet); echinoderm: *Strongylocentrotus purpuratus* ('Sp', Atlantic purple sea urchin); mollusc: *Mizuhopecten yessoensis* ('My', Yesso scallop); annelid: *Capitella teleta* ('Ct'); arthropods: *Eurytemora affinis* ('Ea', marine copepod), *Apis mellifera* ('Am', European honeybee) and *Drosophila melanogaster* ('Dm', fruit-fly); nematode: *Caenorhabditis elegans* ('Ce'); platyhelminth: *Schistosoma mansoni* ('Sm'); porifera: *Amphimedon queenslandica* ('Aq', sponge); placozoa: *Trichoplax adhaerens* ('Tr'); choanoflagellata: *Salpingoeca rosetta* ('Sr'); and filasterea *Capsaspora owczarzaki* ('Co')

Nematode worms are coelomate (possess a body cavity), but lack a specialised circulatory system. Deletion of the single RyR homologue (*unc-68*) in the model nematode worm *C.elegans* results in incomplete flaccid paralysis, indicating that this channel is not essential for, but is supportive of, body muscle ECC [91]. Contraction of body wall muscle from *Ascaris suum* (large roundworm of the pig), stimulated by the cholinergic ant-helminthic drug levamisole, was abolished in Ca^{2+}-free extracellular medium and inhibited by 44% by 100 nM ryanodine [92]. This might suggest that RyRs are non-essential for nematode ECC, but might augment this process under some circumstances. Alternatively, the *A.suum* RyRs might display a very low open probability under these experimental conditions, such that only a small proportion of them would be open and available to bind to ryanodine.

RyR-mediated Ca^{2+} release appears to play a critical role in arthropod ECC. One of the earliest reports of a physiological effect of ryanodine was an increase in oxygen consumption in the cockroach *Periplaneta americana*, probably due to enhanced muscle contraction and ATP utilisation [93]. An insertional mutagenesis strategy was used to demonstrate that a single RyR homologue is essential for ECC in the body wall, visceral and circulatory muscles of *D.melanogaster* [94]. In this fruit fly, high concentrations of ryanodine exerted a negative chronotropic effect on the cardiovascular system, slowing heart rate by about 60% [95]. Tritiated ryanodine binding to membranes prepared from thoracic tissues of the moth *Heliothis virescens* is biphasically dependent on Ca^{2+}, stimulated by ATP, but unaffected by caffeine. Single channel electrophysiology of RyR complexes isolated from the same tissue demonstrated a cation channel that was activated by Ca^{2+} and ATP; inhibited by ruthenium red; and modified by ryanodine [96]. In the honeybee, *Apis melifera*, both caffeine and 4-chloro-*meta*-cresol (another RyR agonist) could stimulate skeletal muscle contraction [97]. Overall, these studies support the presence of a single RyR homologue in insect muscles, which displays some characteristics that are similar to their vertebrate relatives, as well as some that are distinct. Such pharmacological differences have prompted the commercial development of insecticides selectively targeting insect RyRs, as a novel strategy for pest control [98].

Photolysis of a caged Ca^{2+} molecule, nitr-5, was used to directly demonstrate CICR in muscle fibres of the giant barnacle *Balanus nubilus* [99]. In skeletal muscle fibres from the crayfish *Procambarus clarkia*, the RyR antagonists procaine and tetracaine inhibit Ca^{2+} transients triggered by depolarisation, without decreasing Ca^{2+} currents across the sarcolemma [100]. Unlike in vertebrates, muscle from the intestine of this crustacean is striated and also uses a CICR-mode of ECC, as indicated by its dependence on extracellular Ca^{2+} and inhibition by ryanodine [101]. A RyR protein isolated from abdominal muscles the lobster *Homarus americanus*, displays single-channel properties that are similar to their vertebrate counterparts, with the exception of relative insensitivity to activating Ca^{2+}, or to the agonist caffeine [102, 103]. These studies demonstrate that arthropod muscles use Ca^{2+} influx to activate contraction, augmented to varying degrees by the release of Ca^{2+} from the SR via RyRs. This is further supported by ultrastructural observations of

insect and arachnid muscles, which display organised "feet structures" (presumed to be RyRs) at junctions with the sarcolemma, which lack overt tetrad organisation of the overlying membrane particles (thought to be Ca_v1 channel complexes) [47].

The obliquely striated abductor muscle from the Noble scallop, *Chlamys nobilis*, does not contain T-tubules, but bears feet structures at presumptive subsarcolemmal CRUs. A protein of similar biochemical properties to vertebrate RyRs was isolated from these muscles [104]. Ryanodine, caffeine and the second messenger cyclic ADP ribose all stimulated Ca^{2+} release from SR vesicles prepared from the abductor muscle of *Pecten jacobaeus*, the Mediterranean scallop [105]. In smooth muscle from the body wall of the wedge sea-hare *Dolabella auricularia*, extracellular K^+-induced depolarisation triggered contraction that persisted in the presence of the Ca^{2+} chelator ethylene glycol-bis(β-aminoethyl ether)-N,N,N′,N′-tetraacetic acid, but which was inhibited by the RyR antagonist procaine. Ultrastructural examination of these muscles indicated the presence of T-tubules coupled to SR, spanned by bridging feet structures [106]. This suggests that a DICR-like form of ECC operates in the muscles of at least some molluscs. The longitudinal muscle of the body wall (LMBW) of several echinoderms possesses subsarcolemmal SR, which can release Ca^{2+} in response to the RyR agonist caffeine, *for review see* [61].

12.3.1.2 Deuterstomes

Ryanodine increases the amplitude and decreases the frequency of spontaneous contractions of the LMBW of the sea-cucumber *Sclerodactyla briareus* [107]. This suggests that RyRs play a role in ECC in echinoderms. Indeed, there is strong similarity between the RyR from sea urchin eggs (suRyR) and mammalian RyRs in crucial regions such as the selectivity filter, the pore helix and helix bundle crossing region [108]. Interestingly, the activation of suRyR differs substantially from the mammalian RyR isoforms [109]; cyclic adenosine diphosphoribose can trigger release but 'crude sea urchin egg homogenate' was required to substantially activate the channels, suggesting the requirement of an unknown cellular activator and/or binding protein.

Among the chordates, the genome of the cephalochordate *B.belcheri* contains a single RyR gene, Fig. 12.3. This contrasts with an earlier suggestion that *B.floridae* contains three RyR orthologues [80]. The most likely cause of this discrepancy is that the original observation was based on conceptual translations of partial DNA sequences, the products of which were not definitively grouped with one RyR type or another. As discussed in Sect. 12.2.1, the trunk muscles of *B.lanceolatum* can contract in the absence of extracellular Ca^{2+} under some circumstances, including the presence of caffeine [64, 66]. This suggests that cephalochordates can use the DICR-mode of ECC under some conditions, but this conclusion conflicts with ultrastructural studies, which show that lancelet muscles lack a tetradic organisation of dihydropyridine receptor/VGCC complexes [10]. Sarcolemmal tetrads are thought to a hallmark of the molecular interaction between Ca_v1x and RyR proteins [74]. However, it is possible that several different mechanisms of DICR have evolved in

distinct metazoan lineages, not all of which are dependent on the arrangement of Ca_v1x in tetrads.

The muscles of some, though not all, tunicates contain RyR-dependent SR Ca^{2+} stores. For example, myocytes generated by differentiation of growth-arrested blastocysts from the ascidian *Halocynthia roretzi* (the sea pineapple) display functional coupling between VGCCs and caffeine-/ryanodine-sensitive intracellular Ca^{2+} stores [110]. BLAST searches of two tunicate genomes suggest that both *Oikopleura dioica* and *Ciona intestinalis* encode a single RyR homologue, Fig. 12.3.

12.3.2 RyRs of Vertebrates

Most vertebrates possess three RyR paralogues, indicative of two rounds of duplication during the 2R-WGD process, followed by loss of one member. These paralogues are employed for different physiological roles (DICR versus CICR) and display distinct but partially overlapping tissue distributions [111, 112]. For example, in mammals RyR1 is most abundant in skeletal muscle, whereas RyR2 is prevalent in cardiomyocytes. In addition, the teleost specific third round of WGD [76] has generated a greater number of these paralogues, with six (RyR1a, RyR1b, RyR2a, RyR3a and RyR3b) being reported in the genomes of *D.rerio* (zebrafish), *Fundulus heteroclitus* (Atlantic killifish), *Gasterosteus aculeatus* (three-spined stickleback) and *Takifugu rubripes* (Japanese pufferfish) [113]. The basal ray-finned fish *Polypterus ornatipinnis* (the ornate bichir) possesses duplicated RyR1 genes, but single copies of the two other vertebrate RyR types. The authors of this work proposed that this resulted from generation of multiple RyR paralogues during 3R-WGD, followed by losses of some of the duplicated genes [114]. However, other workers have suggested that the bichir RyR1a and RyR1b proteins are generated by alternate splicing of transcripts from a single gene, rather than being the products of separate genes. The current and earlier studies have demonstrated that another basal actinopterygian, *Lepisosteus oculatus* (the spotted gar), encodes just three RyR paralogues in its genome, Fig. 12.3 [113].

A novel observation in the current work is that in all four of the amphibian genomes investigated, the only RyR homologues that could be detected correspond to RyR1 and RyR3, i.e. this class of vertebrate apparently lacks RyR2. This is unexpected, because previous studies, based on use of anti-RyR2 antibodies of incompletely defined subtype selectivity, demonstrated that this channel protein is present in SR-enriched microsomal membranes prepared from the hearts of *Rana pipiens* (the Northern leopard frog) [115] and of *Xenopus laevis* (African clawed frog) [116]. It is unlikely that this disparity is due to poor quality or curation of genomes, since those of *X.laevis* and *X.tropicalis* (Western clawed frog) are particularly well annotated. Contraction of amphibian cardiomyocytes is largely dependent on extracellular Ca^{2+} influx, with release of this ion from the SR playing little part in ventricular myocyte ECC under normal conditions [117]. A lack of involvement of Ca^{2+} release in heart contraction has been reported in other ectothermic vertebrates,

such as fish, in which RyRs play an incompletely defined auxiliary role [11, 118], only contributing to this process under situations demanding increased cardiac output [119]. An investigation using immunofluorescent microscopy with a non-subtype selective antibody, indicate that RyRs are present in junctional SR of the atria of *Rana temporaria* (the European Common frog) [120]. Furthermore, mRNAs encoding RyR1 and RyR3 have been detected in the heart of *R.esculenta* (the Edible frog) [121].

It is hypothesised that a WGD event in a sterile, diploid, hybrid ancestor of *Xenopus sp.* generated a fertile, tetraploid species. As a consequence, *X.laevis* possesses two non-identical copies of each chromosome, termed the long ("L") and short ("S") forms. In cases where losses had not occurred (>56% of genes), this also resulted in the availability of four copies of each gene (two from each ancestor). Often, these genes evolved asymmetrically, with one ancestral pair being relatively preserved and the other being subject to deletion, divergence, loss or reduced transcription [122]. In the current study, searching of a boutique *Xenopus* genomic and transcriptomic database (Xenbase: http://www.xenbase.org/ [123]) revealed that the two copies of RyR1, termed RyR1L and RyR1S, are encoded by chromosomes 8L and 8S. In terms of transcription in adult animals, *X.laevis* RyR1L is expressed at highest levels in skeletal muscle and is also present in the eye; whereas RyR1S mRNA is not detected at high abundance in any tissue examined. Like RyR1, *X.laevis* RyR3 genes are located in chromosomes 8L and 8S. In adult African clawed frogs, the mRNA encoding RyR3L is most abundant in the heart, followed by skeletal muscle, brain and then the eye. RyR3S transcripts are also abundant in skeletal muscle, but were only present at low levels in the heart and in other tissues. These findings suggest a potential role for RyR3L in *Xenopus* cardiomyocyte ECC. This also implies redundancy among RyRs in this process, in that RyR3 might be able to substitute for RyR2 under some circumstances.

12.4 Evolution of Depolarisation-Induced Ca^{2+} Release

Although related processes might exist in some arthropods, molluscs, echinoderms and cephalochordates, the DICR mode of ECC, dependent on the organisation of VGCC into tetrads, is probably a vertebrate innovation [10, 74]. DICR is characteristic of skeletal muscle, but also plays roles in other tissues, such as the brain [124]. This form of ECC is dependent on physical interactions between $Ca_v1.1$-containing VGCCs in the sarcolemma and RyR1 Ca^{2+} release channels in the terminal cisternae of the SR. Additional accessory proteins, such as the β_{1a}-subunits of L-type VGCCs [27, 125], modulate DICR but are not critical for it. The three-dimensional architecture of interactions between RyR1 and L-type VGCCs are currently being unveiled using cryo-electron microscopy approaches [26, 126]. Although these models are currently of low resolution, it is likely that future advances in such techniques will reveal greater molecular detail of the RyR1-$Ca_v1.1$ interaction.

An investigation comparing rates of evolution between different RyRs and $Ca_v1.1$, as an indicator of co-evolution, generated some unexpected findings: that the only pairs of genes displaying significantly positive correlations were RyR3-RyR2 and RyR3-$Ca_v1.1$. It was anticipated that the evolution rates of RyR1 and $Ca_v1.1$ genes would be correlated, given that they encode a pair of interacting proteins. The authors explained the unexpected association between the evolutionary rates of RyR3 and $Ca_v1.1$ by suggesting an indirect effect: that DICR via RyR1 could trigger further release of Ca^{2+} via RyR3, which not directly coupled to VGCCs [127]. However, in this scenario, it would be predicted that RyR1 and RyR3 should also display significant co-evolution, which was not observed. An alternative explanation offered was that there could be a yet undiscovered direct interaction between RyR3 and $Ca_v1.1$ [127].

Clearer insights into the molecular mechanisms of DICR have been obtained by the generation of mutated and chimeric forms of the interacting partners involved. The spontaneously arising mouse mutant *dysgenic* lacks functional $Ca_v1.1$ gene and in its homozygous state, dies perinatally due to asphyxia. Myotubes cultured from the skeletal muscles of these mice provided an excellent system for testing which components of VGCC α1-subunits (Ca_v1) are critical for skeletal muscle-type DICR [128]. In a ground-breaking study, a panel of chimeras between cDNAs encoding $Ca_v1.1$ and $Ca_v1.2$ was generated and expressed in dysgenic myotubes, in order to determine which region(s) are required to restore DICR. This work established a key role for the cytoplasmic loop between transmembrane repeats II and III of $Ca_v1.1$ [129]. This "skeletal" II-III loop contains the information required not only for activation of RyR1 (orthograde signalling), but also for receiving a signal from the Ca^{2+} release channel that enhances VGCC currents. Chimeras containing $Ca_v1.1$ loops that could restore DICR to dysgenic myotubes also resulted in the formation of VGCC tetrads, as analysed by freeze-fracture electron microscopy. Constructs containing the mouse $Ca_v1.2$ ("cardiac") II-III loop did not form tetrads, whereas those bearing the II-III loop from the Ca_v1 homologue of *Musca domestica* (the housefly) did, despite being unable to support the DICR mode of ECC [130]. These observations suggest that the formation of VGCC tetrads is necessary, though not sufficient for DICR.

To further map the molecular features of the $Ca_v1.1$ II-III loop that are critical for DICR, constructs containing large deletions of this region were expressed in dyspedic myotubes. Using this strategy, it was found that deletion of residues 720–765 or 724–743 abolished depolarisation induced Ca^{2+} transients [131]. Such experiments have also revealed that additional regions of $Ca_v1.1$ such as the III-IV loop [132], or other components of the L-type VGCC such as the β_{1a}-subunit, contribute to DICR [125]. Introduction of a series of single amino acid substitutions into the II-III loop of *M.domestica*, revealed which features are critical for bidirectional communication between mammalian $Ca_v1.1$ and RyR1. These are: i) four conserved amino acid residues within a DICR motif; ii) a cluster of acid amino acid residues at the centre of this loop; and iii) the secondary structure of this negatively charged region [133]. Identification of these critical features has enabled us to search for them within all of the available Ca_v1 channel sequences from

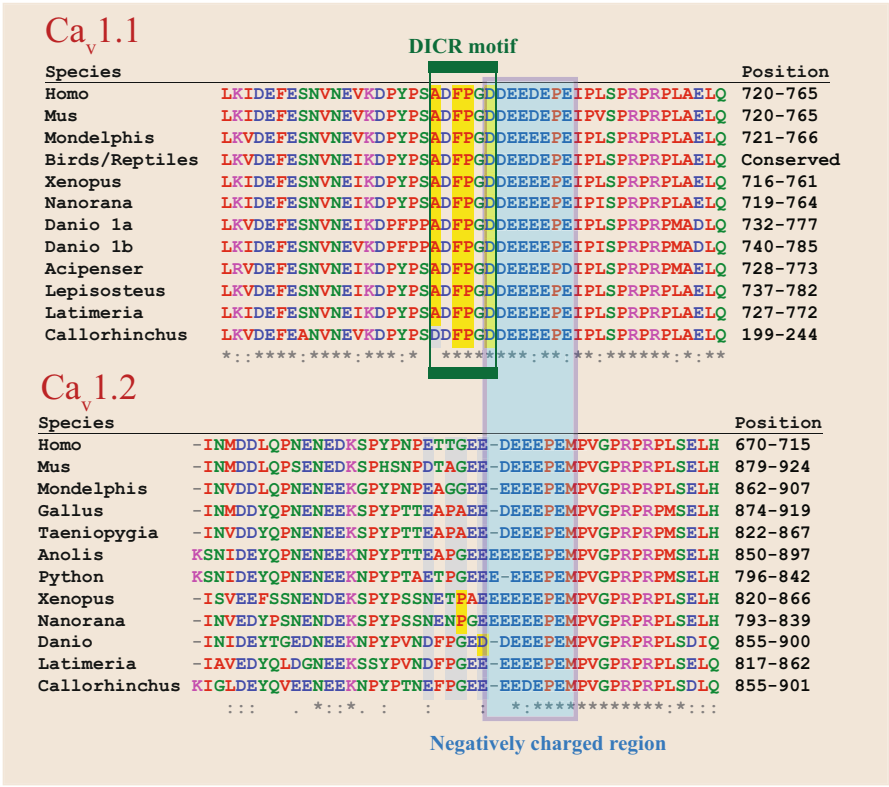

Fig. 12.4 Features of $Ca_v1.1$ required for depolarisation-induced calcium release (DICR). Multiple Sequence Alignment (MSA) of the region of the II-III loop of $Ca_v1.1$ that is critical for the DICR-mode of ECC. This region from *Homo sapiens* $Ca_v1.1$ (L720-Q765) was aligned to corresponding homologues from the following species, using Clustal Omega software (https://www.ebi.ac.uk/Tools/msa/clustalo/, [164]): *Mus musculus* (mouse), *Monodelphis domestica* (grey short-tailed opossum), *Gallus gallus* (chicken), *Taeniopygia guttata* (zebra-finch) *Python bivittatus* (Burmese python), *Anolis carolinensis* (anole, a lizard), *Xenopus laevis* (African clawed frog), *Nanorana parkeri* (High Himayalan frog), *Danio rerio* (zebrafish), *Acipenser ruthenus* (sterlet), *Lepisosteus oculatus* (spotted gar), *Latimeria chalumnae* (the coelacanth, a lobe-finned fish) and *Callorhinchus milii* (Elephant shark). Positions of these sequences are shown to the right; for $Ca_v1.1$ those from bird and reptile species listed are pooled, since they are 100% identical. The corresponding region from *C.milii* is derived from a partial sequence, explaining its distinct position in this protein. Also shown is an MSA from the corresponding region of $Ca_v1.2$ homologues. Below each alignment, asterisks (*) indicate amino acid identity, colons (:) homology and full-stops (.) similarity. Although these $Ca_v1.2$ II-III loops contain a negatively charged central region, they lack the DICR motif that is highly conserved among $Ca_v1.1$ homologues

metazoans, Fig. 12.4. Although limited by the availability or curation of genomes from basal vertebrates and non-vertebrate chordates, these searches support the notion that DICR, or skeletal muscle-type ECC, is a vertebrate innovation [10]. All vertebrate $Ca_v1.1$ proteins share the consensus four residue DICR motif followed

by a negatively charged region. The only exception to this is an alanine to aspartic acid substitution in the first residue of the motif, in the $Ca_v1.1$ II-III loop of *Callorhinchus milii* (the Elephant shark), a basal vertebrate. In contrast, the motif absent from the II-III loops of all vertebrate $Ca_v1.2$ proteins and from Ca_v1 proteins from non-vertebrates.

Mapping of the regions of RyR1 that are crucial for bidirectional communication with $Ca_v1.1$ has progressed using a similar combination of biochemical, molecular, electrophysiological and Ca^{2+}-imaging approaches. The availability of skeletal muscle myotubes from a transgenic RyR1 knockout mouse, termed *dyspedic* (lacking in feet structures), has facilitated determination of the functional effects of expressing RyR chimeras, deletions and point mutations. By monitoring in vitro interactions between fusion proteins, it has been demonstrated that a 37 amino acid region of RyR1, Arg1076-Asp1112, interacts with both the II-III and III-IV cytoplasmic loops of $Ca_v1.1$ [132, 134]. Analyses of RyR/RyR2 chimeras revealed that residues 1837–2168 of RyR1 contribute to DICR, but are not essential for it [135]. Assessment of additional RyR1/RyR2 chimeras for their ability to restore DICR and to promote assembly of L-type VGCC complexes into tetrads in dyspedic myotubes, revealed that multiple regions of RyR1 were important for these processes. In particular, chimeras containing residues 1635–3720 or 1635–2559 of RyR1 effectively restored DICR, whereas residues 1635–3720 or 2659–3720 strongly promoted tetrad formation [74].

Three regions within vertebrate RyRs, termed the divergent regions (DR1, DR2, DR3), display the lowest sequence identity between paralogues [136]. Deletion of DR2 (residues 1303-1406) of RyR1 abolishes DICR, without altering caffeine-mediated Ca^{2+} release in dyspedic myotubes. Additional regions of RyR1 must contribute to skeletal muscle-type ECC, since replacement of its DR2 with that from RyR2 did not alter reciprocal communication with $Ca_v1.1$ [137]. Similarly, replacement of residues 1-1680 in RyR3 with the corresponding region of RyR1 could restore DICR. Deletion of residues 1272-1455, containing DR2, from RyR1 abolished DICR. However, this region proved to be necessary but not sufficient for this mode of ECC, since it did not restore DICR to chimeras with an RyR3 backbone [138]. An *N*-ethyl-*N*-nitrosourea mutagenesis approach revealed that an E4242G mutation of RyR1 inhibited retrograde (RyR1 to $Ca_v1.1$), though not orthograde ($Ca_v1.1$ to RyR1) communication with VGCCs [139].

Overall, these investigations indicate that multiple regions of RyR1 participate in communication with $Ca_v1.1$. In the current work, we performed BLAST searches for the 37 residue RyR1 (R1076-N1112) sequence reported to interact with the II-III and III-V loops of $Ca_v1.1$ [132, 134]. As was the case for $Ca_v1.1$, this analysis of RyR1 lends support to the earlier preposition that DICR arose in vertebrates [10]. In addition, a partial RyR1 sequence from the lamprey *P.marinus* contains a sequence that is closely related to the 37 residue $Ca_v1.1$ binding region, Fig. 12.5. Multiple sequence alignments of this $Ca_v1.1$-interacting region of RyR1 homologues, and comparison with the corresponding region of RyR2 proteins, has uncovered novel detail of this molecular interaction. The alanine residue at position 1105 and the arginine at residue 1110 are found in all vertebrate RyR1 homologues examined,

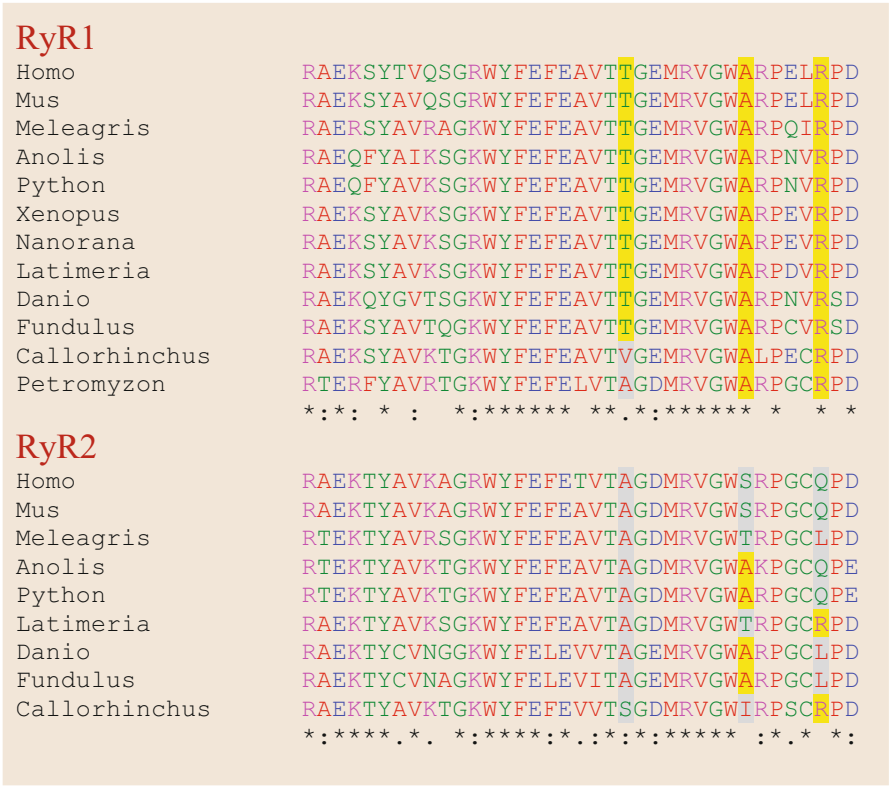

Fig. 12.5 Conservation of $Ca_v1.1$-interacting region from RyR1. Multiple Sequence Alignment (MSA) of the 37 amino acid $Ca_v1.1$-interacting region of RyR1. This region from *Homo sapiens* RyR1 (R1075-N1111) was aligned to corresponding homologues from the species listed in Fig. 12.4 and the following additional species, using Clustal Omega software [164]: *Meleagris gallopavo* (turkey), *Fundulus heteroclitus* (Atlantic killifish) and *Petromyzon marinus* (the sea lamprey). An MSA for the corresponding regions of RyR2 is also shown. Below each alignment, asterisks (*) indicate amino acid identity, colons (:) homology and full-stops (.) similarity. Yellow-shaded residues indicate those which are conserved in RyR1, though not in RyR2, suggesting that they could have a specific role in determining DICR

but are not conserved in RyR2. The threonine at position 1097 is not found in any RyR2 homologue, but is conserved in all RyR1 proteins, with the exception of those from the basal vertebrates *C.milii* and *P.marinus*, Fig. 12.5. The candidate role of these conserved residues in DICR is a compelling target for future mutagenesis, expression and functional reconstitution studies.

12.5 Junctophilins and ECC: Proteins that Bring It All Together

Junctophilins (JPHs) are a family of proteins that link intracellular membranes (ER and SR) to the plasma membrane, thereby promoting formation of junctions [28], Fig. 12.2. As such, they are critical for formation of CRUs and for supporting both CICR- and DICR-modes of ECC. This anchoring role is facilitated by a single ER/SR transmembrane region close to the C-terminus, an intervening helical domain and eight repeats of a lipid binding "membrane occupation and recognition nexus" (MORN) repeat motif, distributed between the middle and the N-terminus of these proteins [140, 141]. JPHs were discovered using an antibody-based biochemical approach to identify proteins that were highly enriched in rabbit skeletal muscle triads. Initially, three genes encoding JPHs were identified in mice: JPH1 is predominantly expressed in skeletal muscle; JPH2 in both skeletal and cardiac muscle; and JPH3 in the nervous system [28]. A fourth JPH paralogue, JPH4, was subsequently identified and found to be predominantly expressed in brain [142], but is also present in T-lymphocytes [143].

Genetic ablation of JPH2 in transgenic mice is lethal prior to mid-gestation, with the SR of heart tissues becoming enlarged, vacuolated and distributed at a greater distance from the sarcolemma than in wild-type animals [28]. Cardiomyocytes from the JPH2 knockout mice display abnormal spontaneous Ca^{2+}-transients, which are resistant to inhibition by removal of extracellular Ca^{2+}. Overexpression of JPH2, by means of adenovirus-delivered gene therapy, rescued deficits in ventricular contractility and T-tubule architecture in a mouse aortic constriction model of heart failure [144]. Conditional knockdown of JPH2 in mice, using RNA interference, decreased contractility; increased heart failure and death; and reduced gain during ECC. This impaired gain is due to enhanced spontaneous activity of RyR2 in JPH2 knockdown mice, leading to chronic depletion of SR Ca^{2+} stores. This indicates that there is an inhibitory interaction between the two proteins, supported by the observation that JPH2 co-immunoprecipitates with RyR2 [145]. In the dog left ventricular cardiomyocytes, JPH2 forms complexes with a range of Ca^{2+}-handling proteins, including RyR2, SERCA2a, calsequestrin and $Ca_v1.2$, increasing the amplitude of Ca^{2+} currents via L-type VGCCs [146]. Imaging of Ca^{2+} and single protein molecules in cardiomyocytes from transgenic mice overexpressing JPH2 showed an enlargement of the physical size of dyadic CRUs, without an anticipated increase in spontaneous Ca^{2+} release events. This was accompanied by an increase in the ratio between JPH2 and RyR2 at these CRUs, suggesting that these anchoring proteins inhibit gating of the Ca^{2+} release channels [147].

JPH1 knockout mice are deficient in milk suckling behaviour and die within a day of birth. Skeletal muscle from JPH1 deficient mice produces less force in response to low-frequency electrical stimulation than controls and displays reduced abundance

of triadic junctions [148]. Both JPH1 and JPH2 can interact with a 12-residue motif, close to the C-terminus of $Ca_v1.1$ (residues 1595-1606, EGIFRRTGGLFG). This motif is highly conserved amongst vertebrate $Ca_v1.1$ and $Ca_v1.2$ proteins, but is not found in mammalian $Ca_v2.1$, nor within invertebrate Ca_v1 homologues. When expressed in mouse C2C12 myotubes, a dominant negative form of JPH1, lacking the SR-anchoring transmembrane domain, inhibits DICR without modifying Ca^{2+} store loading [149]. Again, this implies that JPHs not only act as anchors in the formation of CRUs, but also regulate the Ca^{2+} signalling that occurs at these junctions.

Although the evolutionary history of JPH family has been investigated previously [150], its deeper relationships with other protein families have not been reported. In the current study, we have examined the phylogeny of JPHs and related families, throughout the tree of life. We have found that JPHs form part of a MORN repeat-containing superfamily of proteins, which contains members in bacteria, archaea and eukaryotes, suggesting that they arose early during the evolution of cellular life, Fig. 12.6. In addition to the MORN domain proteins previously reported to be related to JPHs, namely phosphatidylinositol-4-phosphate 5-kinases (PIP5Ks) and histone-lysine N-methyltransferases [150], we have found four families of MORN-repeat proteins (MORN1-4), 2-isopropylmalate synthases, ankyrin repeat and MYND domain-containing (ANKMY) proteins, radial spoke-head (RSPH) proteins and alsin-like (ALS) proteins. We have also identified candidate MORN superfamily members in the genomes of the viruses *Pandoravirus dulcis* and of *Bodo saltans* virus.

It is expected that all of these protein families are able to interact with lipids, in particular phospholipids, via their MORN repeats. As is the case for JPHs, certain MORN domain proteins play additional roles in determining the subcellular distribution and stability of protein complexes. For example, MORN4 family members act as adaptors, tethering class III myosin motor proteins to membranes [151]. In eukaryotes, RSPH proteins are located in the central pair of microtubules of cilia/flagellae and regulate force production by them, via interactions with the motor protein dynein [152]. Of all members of the MORN repeat superfamily, ALS proteins are most closely related to JPHs, Fig. 12.6. In humans, alsin is mutated in amyotrophic lateral sclerosis-2 [153], a disease characterised by progressive loss of motor neurons, leading to paralysis. ALS regulates endocytosis by activation of the small G-protein Rab5, again implying that the MORN family has conserved roles in cellular motility and trafficking [154].

A key difference between JPHs and all other MORN repeat proteins examined is that the former possesses a transmembrane segment, crucial for localising it to intracellular organelles. In the current analysis, the most basal organism possessing a JPH homologue was *Salpingoeca rossetta*, belonging to the phylum choanoflagellata, a sister group to metazoans, Fig. 12.6. This suggests that the *S.rossetta*

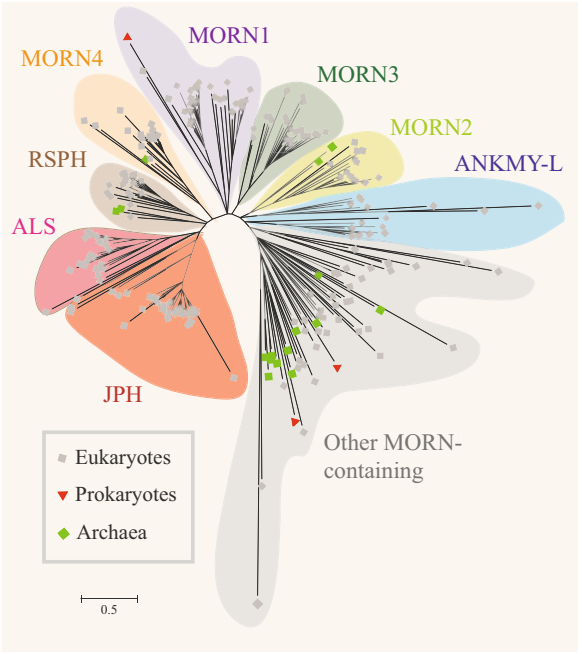

Fig. 12.6 Phylogenetic tree of the MORN repeat containing protein superfamily. An extensive evolutionary history of proteins related to JPH1 from *Homo sapiens* (Accession Number NP_065698.1), inferred using the Maximum Parsimony method, conducted using MEGA5 [162]. The tree is to scale, with branch lengths corresponding to amino acid substitutions per site, calculated using the average pathway method [165]. This analysis involved 238 amino acid sequences, from a range of eukaryotes, archaea and bacteria, the details of which are available upon request. The clustering of this tree has enabled us to envisage eight distinct families of protein containing membrane occupation and recognition nexus (MORN) repeat-containing proteins: the junctophilins (JPH), alsins (ALS), radial spokehead homology (RSPH) proteins, four MORN-containing families (MORN1 to MORN4) and an ankyrin repeat and MYND domain-containing protein 1-like (ANKMY-L) family; along with another less clearly defined group of proteins

genome encodes at least three of the proteins required for DICR (RyR, a HVA Ca_v1, JPH), but at present there is no experimental evidence to either reject or to support the hypothesis that this form of Ca^{2+}-signalling operates in a choanoflagellate. Furthermore, both RyR [80, 81, 155] and JPH homologues were undetectable in another choanoflagellates species, *Monsiga brevicolis*, suggesting that *S.rossetta* might represent a transitional stage in the evolution of Ca^{2+} signalling. JPH homologues were not found in filasterea, another sister group to animals represented by the organism *Capsaspora owczarzaki* [88].

In agreement with an earlier study, single JPH homologues were detected in placozoans (*T.adhaerens*), poriferans (*A.queenslandica*) and in cnidarians (*N.vectensis* and *H.vulgaris*) [150]. However, in the previous publication, the cnidarian JPH

homologues clustered with bilaterian animals such as echinoderms and vertebrates, whereas in the current work, they formed a separate group clustered with poriferans. This is likely to reflect the use of a distinct subset of proteins, with a greater range of JPH homologues from non-bilaterians; and the use of a more robust algorithm for reconstruction of phylogenetic trees (Maximum-Parsimony instead of Neighbour-Joining) [156]. Prediction of the transmembrane topology of these JPH homolgues, using both Phobius (http://phobius.sbc.su.se/ [157]) and THHM (http://www.cbs.dtu.dk/services/TMHMM-2.0/ [158]) points toward a lack of a transmembrane spanning segment in these proteins from *T.adhaerens*, *N.vectensis* and *H.vulgaris*. One explanation for this observation could be poor sequence quality or annotation, leading to artefactually truncated hypothetical proteins. Alternatively, these basal metazoan JPH homologues could play roles in the regulation of VGCC channels, as described for the engineered C-terminally truncated form of mammalian JPH1, that inhibits gating of $Ca_v1.1$ [149].

All other invertebrate genomes analysed are predicted to encode a single JPH homologue. For only a few organisms, the presence of a JPH homologue has been verified experimentally. In the nematode worm *C.elegans*, JPH is transcribed in muscle cells and knockdown of its mRNA leads to hypolocomotion, supporting a role in ECC [44]. Tissue-specific knockdown or overexpression of JPH in the insect *D.melanogaster* generates similar phenotypes to those that that arise through genetic modification of its mouse paralogues: skeletal myopathies for JPH1; alterations in T-tubule formation for JPH2; and neuronal defects in the case of JPH3 and/or JPH4 [159]. This implies that the single JPH protein in an arthropod can be functionally equivalent to its four mammalian paralogues.

Amongst vertebrates, amphibians, non-avian reptiles and mammals contain four JPH paralogues (JPH1, JPH2, JPH3 and JPH4), consistent with a 2R-WGD mechanism of evolution [70]. In contrast, elasmobranch (shark, ray and skate) and sarcopterygian (lobe-finned fish) genomes encode three JPH paralogues and lack JPH4, Figs. 12.7 and 12.8. This implies that an early vertebrate ancestor possessed four JPH genes and that one of these was lost in certain lineages, although not in others. Our preliminary analyses of teleost fish genomes show that they encode four JPH homologues, but in contrast to tetrapods (amphibians, reptiles, birds and mammals), these represent JPH2, JPH3 and a duplicated pair of JPH1 genes. A mechanism for the evolution of these genes could be duplication of the three ancestral JPH paralogues during the teleost-specific third round of WGD [76], followed by losses of one of the copies of JPH2 and of JPH3. In the tetrapod lineage, birds alone appear to have lost the JPH4 gene. Similar avian-specific gene losses have been reported for other protein families, such as components of the endocrine system that are highly conserved among other vertebrates [160].

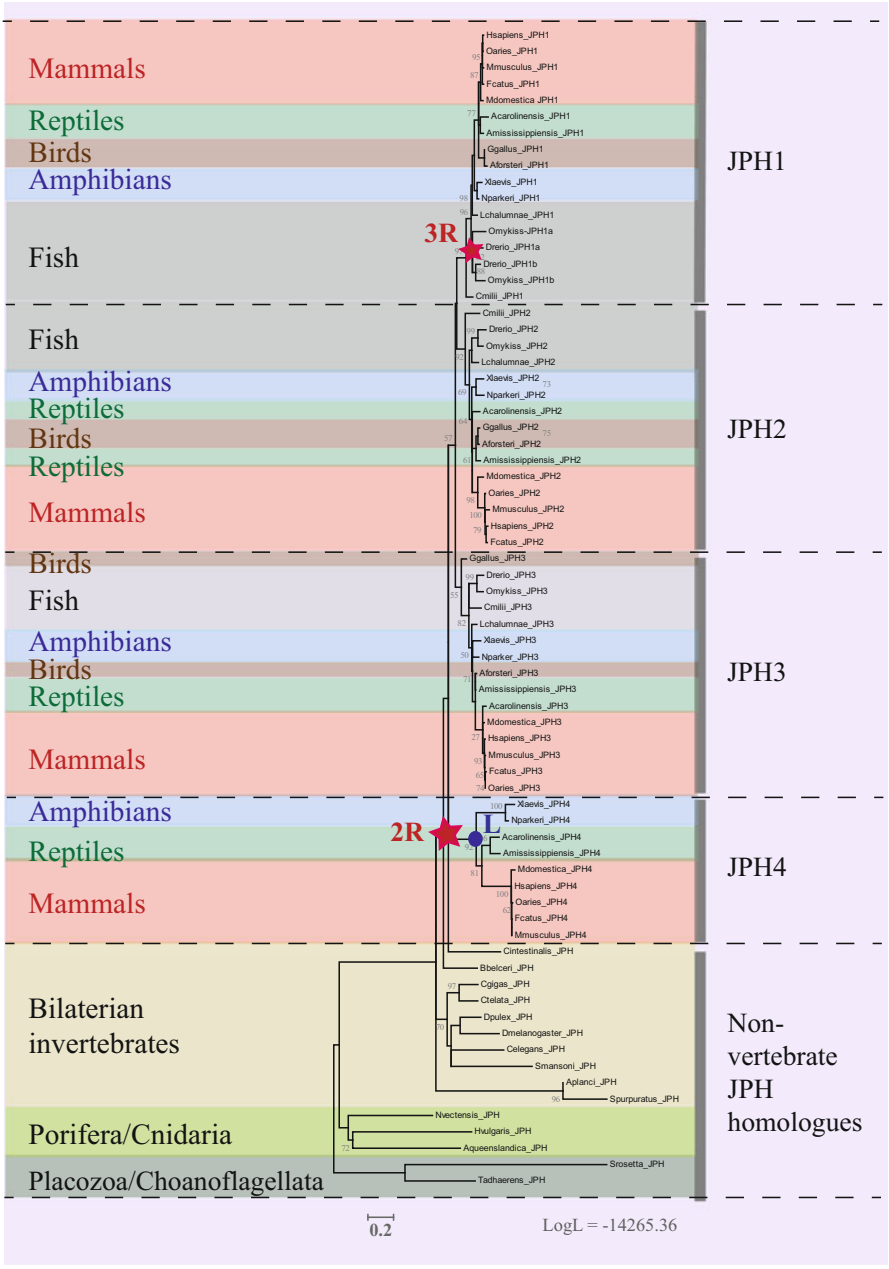

Fig. 12.7 Phylogenetic tree of the junctophilins. The evolutionary history of the junctophilin (JPH) family of MORN-repeat containing proteins was inferred using the methodology described in Fig. 12.5. This analysis involved 71 amino acid sequences, with full details being available upon request. Red stars ('2R' and '3R') indicate putative gene duplications; the blue circle ('L') candidate gene losses. This phylogenetic tree indicates that invertebrates possess a single JPH homologue and that this was duplicated twice early during vertebrate evolution to generate four paralogues. JPH4 was subsequently lost from fish and birds. In contrast, JPH1 was duplicated again in the teleost-specific 3R-WGD. Presumably, other JPH types were either not replicated in this event, or were duplicated and then one of the copies was subsequently lost

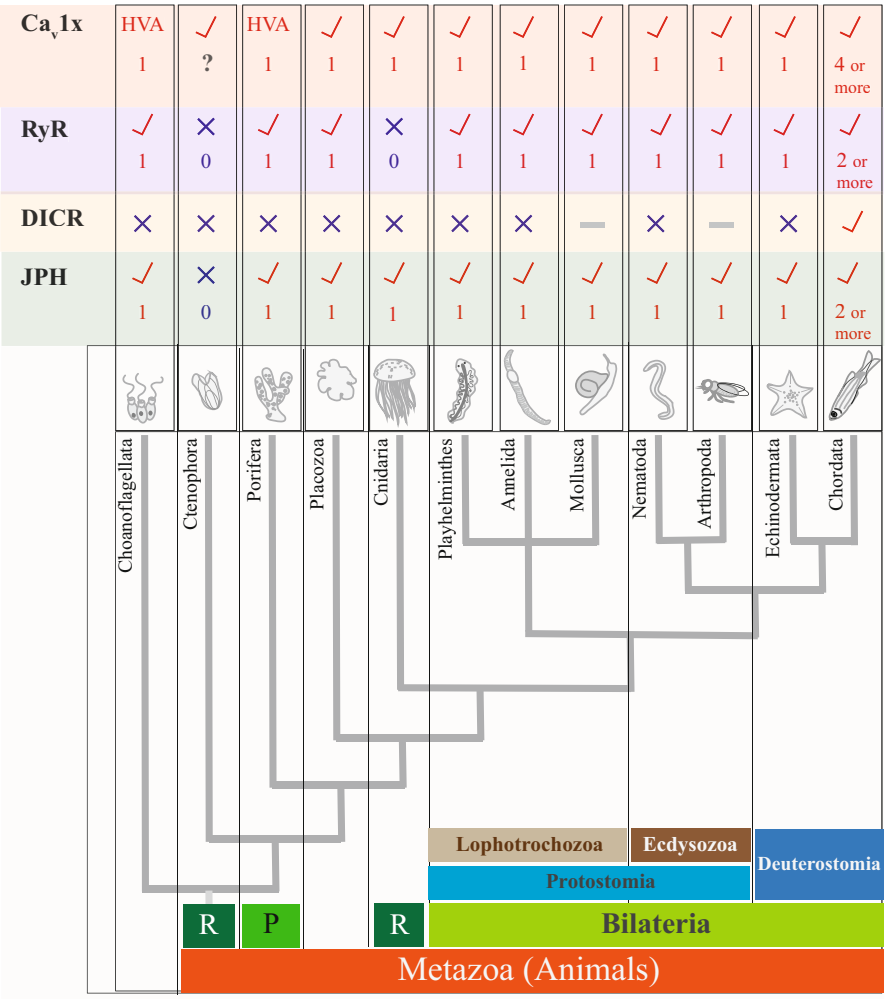

Fig. 12.8 Summary of the Presence of ECC components in metazoa and choanoflagellates. The presence of Ca_v1x (or HVA, high voltage-activated) voltage-gated calcium channels, ryanodine receptor (RyR) Ca^{2+} release channels, depolarisation-induced Ca^{2+}-release (DICR) and junctophilin (JPH) homologues in metazoa and choanoflagellata is indicated. The '?' indicates that Ca_v1x member used is unknown; the '-'indicates uncertainty of the mode of ECC employed. Where homologues of these ECC proteins have been found, the number detected is shown. Further details are given in Fig. 12.1

12.6 Conclusions and Future Directions

Our phylogenetic analyses and literature review of the evolution of ECC has generated several new insights into this group of signal transduction mecha-

nisms. Concordant with the physiological and ultrastructural investigations of other researchers, we have found that the DICR mode of ECC is likely to be a vertebrate innovation [10]. The CICR form of ECC is employed in the vertebrate heart and in different muscle types from the majority of invertebrates. The time at which this Ca^{2+} signalling process first appeared is less certain. Choanoflagellates, a sister group to animals, possess proteins related to those required for CICR and possibly, even for DICR [27]: RyRs, HVA Cav1 channels, a JPH homologue, VGCC β-subunits [33] and STAC3 paralogues (*JJM, preliminary analyses*). This could represent operation of ECC-like mechanisms in choanoflagellates, or by analogy to the development of the actin-myosin contractile apparatus [7], the possession of all components required for this process, prior to its development in the metazoan lineage.

Distinct modes of ECC are employed by different metazoan groups. RyR homologues could not be detected in cnidarians or ctenophores, hinting that ECC is largely dependent on Ca^{2+}-influx via VGCC in these animals. However, experimental evidence suggests that CICR occurs in some cnidarians, with a likely scenario being amplification of Ca^{2+}-influx by Ca^{2+} release via ITPRs. However, ctenophores also lack detectable ITPR homologues [80].

Some invertebrates, including arthropods, molluscs and lancelets, display forms of ECC that resemble DICR. This manifests mainly in the apparent lack of dependency on Ca^{2+}-influx. However, where data are available, RyR and Ca_v1 proteins of these organisms lack the molecular features that are required for DICR in vertebrates. Furthermore, their VGCCs are not ordered into tetrads in junctional membranes, another feature thought to be essential for DICR. Possible reasons for this discrepancy are either operation of CICR with very high gain, as proposed for ECC in the abdominal flexor muscles of the shrimp *A.lanipes*, or a yet uncharacterised mode of DICR that is distinct from that in vertebrate skeletal muscle.

The genes encoding proteins involved in ECC have been subject to expansions and losses in different vertebrate classes. Such events have underpinned the evolution of vertebrate innovations, such as the DICR-mode of ECC. This is exemplified in teleost fish, whereby the 3R-WGD process has allowed the development of duplicated non-conducting VGCCs ($Ca_v1.1a$ and $Ca_v1.1b$) and RyRs (RyR1a and RyR1b), which operate within distinct skeletal muscle fibre types. A remarkable example of gene loss appears to have occurred in amphibians, which apparently lack the gene encoding RyR2. This loss appears to have been compensated for by the expression of RyR3 and RyR1 in the heart, implying that there might be some redundancy between these Ca^{2+} release channels, at least within the CICR-mode of ECC.

Many of the observations in the current work are based on limited genomic and experimental data, making some of them tenuous. For improved understanding of the evolution of ECC, more information needs to be gathered. For example, the number of genomes sequenced and the quality of the annotation of these data needs to increase, in particular for some vertebrate species in which key events may have occurred, such as agnathans and amphibians. Although Ca^{2+} signalling has been

explored experimentally in some unicellular eukaryotes, such *C.owczarzaki* and *Paramecium tetraurelia* [155, 81], the roles of ECC proteins in choanoflagellates, a sister group of animals which lacks muscles, could be particularly informative. Contemporary technologies, such as genome-editing and determination of three-dimensional protein structures by cryo-electron microscopy, are likely to reveal the exquisite interactions that underlie ECC in greater detail, in a wider range of animal species and their relatives.

References

1. Cunningham JA, Liu AG, Bengtson S, Donoghue PC (2017) The origin of animals: can molecular clocks and the fossil record be reconciled? BioEssays 39(1):1–12. https://doi.org/10.1002/bies.201600120
2. Erwin DH (2015) Early metazoan life: divergence, environment and ecology. Philos Trans R Soc Lond Ser B Biol Sci 370(1684):20150036. https://doi.org/10.1098/rstb.2015.0036
3. Bosch TCG, Klimovich A, Domazet-Loso T, Grunder S, Holstein TW, Jekely G, Miller DJ, Murillo-Rincon AP, Rentzsch F, Richards GS, Schroder K, Technau U, Yuste R (2017) Back to the basics: cnidarians start to fire. Trends Neurosci 40(2):92–105. https://doi.org/10.1016/j.tins.2016.11.005
4. Seipel K, Schmid V (2005) Evolution of striated muscle: jellyfish and the origin of triploblasty. Dev Biol 282(1):14–26. https://doi.org/10.1016/j.ydbio.2005.03.032
5. McGuigan K, Phillips PC, Postlethwait JH (2004) Evolution of sarcomeric myosin heavy chain genes: evidence from fish. Mol Biol Evol 21(6):1042–1056. https://doi.org/10.1093/molbev/msh103
6. Brunet T, Arendt D (2016) From damage response to action potentials: early evolution of neural and contractile modules in stem eukaryotes. Philos Trans R Soc Lond Ser B Biol Sci 371(1685):20150043. https://doi.org/10.1098/rstb.2015.0043
7. Steinmetz PR, Kraus JE, Larroux C, Hammel JU, Amon-Hassenzahl A, Houliston E, Worheide G, Nickel M, Degnan BM, Technau U (2012) Independent evolution of striated muscles in cnidarians and bilaterians. Nature 487(7406):231–234. https://doi.org/10.1038/nature11180
8. Allbritton NL, Meyer T, Stryer L (1992) Range of messenger action of calcium ion and inositol 1,4,5-trisphosphate. Science 258(5089):1812–1815
9. Parekh AB (2011) Decoding cytosolic Ca^{2+} oscillations. Trends Biochem Sci 36(2):78–87. https://doi.org/10.1016/j.tibs.2010.07.013
10. Di Biase V, Franzini-Armstrong C (2005) Evolution of skeletal type e-c coupling: a novel means of controlling calcium delivery. J Cell Biol 171(4):695–704. https://doi.org/10.1083/jcb.200503077
11. Shiels HA, Galli GL (2014) The sarcoplasmic reticulum and the evolution of the vertebrate heart. Physiology 29(6):456–469. https://doi.org/10.1152/physiol.00015.2014
12. Catterall WA, Striessnig J, Snutch TP, Perez-Reyes E, International Union of P (2003) International Union of Pharmacology. XL. Compendium of voltage-gated ion channels: calcium channels. Pharmacol Rev 55(4):579–581. https://doi.org/10.1124/pr.55.4.8
13. Bers DM, Perez-Reyes E (1999) Ca channels in cardiac myocytes: structure and function in Ca influx and intracellular Ca release. Cardiovasc Res 42(2):339–360
14. Campiglio M, Flucher BE (2015) The role of auxiliary subunits for the functional diversity of voltage-gated calcium channels. J Cell Physiol 230(9):2019–2031. https://doi.org/10.1002/jcp.24998
15. Endo M (1977) Calcium release from the sarcoplasmic reticulum. Physiol Rev 57(1):71–108. https://doi.org/10.1152/physrev.1977.57.1.71

16. Franzini-Armstrong C, Protasi F, Ramesh V (1999) Shape, size, and distribution of Ca^{2+} release units and couplons in skeletal and cardiac muscles. Biophys J 77(3):1528–1539. https://doi.org/10.1016/S0006-3495(99)77000-1
17. Hong T, Shaw RM (2017) Cardiac T-tubule microanatomy and function. Physiol Rev 97(1):227–252. https://doi.org/10.1152/physrev.00037.2015
18. Dibb KM, Clarke JD, Eisner DA, Richards MA, Trafford AW (2013) A functional role for transverse (t-) tubules in the atria. J Mol Cell Cardiol 58:84–91. https://doi.org/10.1016/j.yjmcc.2012.11.001
19. Orchard C, Brette F (2008) t-Tubules and sarcoplasmic reticulum function in cardiac ventricular myocytes. Cardiovasc Res 77(2):237–244. https://doi.org/10.1093/cvr/cvm002
20. Perni S, Iyer VR, Franzini-Armstrong C (2012) Ultrastructure of cardiac muscle in reptiles and birds: optimizing and/or reducing the probability of transmission between calcium release units. J Muscle Res Cell Motil 33(2):145–152. https://doi.org/10.1007/s10974-012-9297-6
21. Brandt NR, Kawamoto RM, Caswell AH (1985) Dihydropyridine binding sites on transverse tubules isolated from triads of rabbit skeletal muscle. J Recept Res 5(2–3):155–170
22. Block BA, Imagawa T, Campbell KP, Franzini-Armstrong C (1988) Structural evidence for direct interaction between the molecular components of the transverse tubule/sarcoplasmic reticulum junction in skeletal muscle. J Cell Biol 107(6 Pt 2):2587–2600
23. Bertocchini F, Ovitt CE, Conti A, Barone V, Scholer HR, Bottinelli R, Reggiani C, Sorrentino V (1997) Requirement for the ryanodine receptor type 3 for efficient contraction in neonatal skeletal muscles. EMBO J 16(23):6956–6963. https://doi.org/10.1093/emboj/16.23.6956
24. Conti A, Reggiani C, Sorrentino V (2005) Selective expression of the type 3 isoform of ryanodine receptor Ca^{2+} release channel (RyR3) in a subset of slow fibers in diaphragm and cephalic muscles of adult rabbits. Biochem Biophys Res Commun 337(1):195–200. https://doi.org/10.1016/j.bbrc.2005.09.027
25. Daniels RE, Haq KT, Miller LS, Chia EW, Miura M, Sorrentino V, McGuire JJ, Stuyvers BD (2017) Cardiac expression of ryanodine receptor subtype 3; a strategic component in the intracellular Ca^{2+} release system of Purkinje fibers in large mammalian heart. J Mol Cell Cardiol 104:31–42. https://doi.org/10.1016/j.yjmcc.2017.01.011
26. Meissner G (2017) The structural basis of ryanodine receptor ion channel function. J Gen Physiol 149(12):1065–1089. https://doi.org/10.1085/jgp.201711878
27. Perni S, Lavorato M, Beam KG (2017) De novo reconstitution reveals the proteins required for skeletal muscle voltage-induced Ca^{2+} release. Proc Natl Acad Sci U S A 114(52):13822–13827. https://doi.org/10.1073/pnas.1716461115
28. Takeshima H, Komazaki S, Nishi M, Iino M, Kangawa K (2000) Junctophilins: a novel family of junctional membrane complex proteins. Mol Cell 6(1):11–22
29. Somlyo AV, Siegman MJ (2012) Smooth muscle myocyte ultrastructure and contractility. In: Hill JA, Olson EN (eds) Muscle. Boston/Waltham, Academic, pp 1117–1132. https://doi.org/10.1016/B978-0-12-381510-1.00083-1
30. Catterall WA (2010) Signaling complexes of voltage-gated sodium and calcium channels. Neurosci Lett 486(2):107–116. https://doi.org/10.1016/j.neulet.2010.08.085
31. Pozdnyakov I, Matantseva O, Skarlato S (2018) Diversity and evolution of four-domain voltage-gated cation channels of eukaryotes and their ancestral functional determinants. Sci Rep 8(1):3539. https://doi.org/10.1038/s41598-018-21897-7
32. Dolphin AC (2016) Voltage-gated calcium channels and their auxiliary subunits: physiology and pathophysiology and pharmacology. J Physiol 594(19):5369–5390. https://doi.org/10.1113/JP272262
33. Moran Y, Zakon HH (2014) The evolution of the four subunits of voltage-gated calcium channels: ancient roots, increasing complexity, and multiple losses. Genome Biol Evol 6(9):2210–2217. https://doi.org/10.1093/gbe/evu177
34. Moran Y, Barzilai MG, Liebeskind BJ, Zakon HH (2015) Evolution of voltage-gated ion channels at the emergence of Metazoa. J Exp Biol 218(Pt 4):515–525. https://doi.org/10.1242/jeb.110270

35. Jeziorski MC, Greenberg RM, Anderson PA (2000) The molecular biology of invertebrate voltage-gated Ca^{2+} channels. J Exp Biol 203(Pt 5):841–856
36. Senatore A, Raiss H, Le P (2016) Physiology and evolution of voltage-gated calcium channels in early diverging animal phyla: cnidaria, placozoa, porifera and ctenophora. Front Physiol 7:481. https://doi.org/10.3389/fphys.2016.00481
37. Whelan NV, Kocot KM, Moroz LL, Halanych KM (2015) Error, signal, and the placement of Ctenophora sister to all other animals. Proc Natl Acad Sci U S A 112(18):5773–5778. https://doi.org/10.1073/pnas.1503453112
38. Schierwater B, de Jong D, Desalle R (2009) Placozoa and the evolution of Metazoa and intrasomatic cell differentiation. Int J Biochem Cell Biol 41(2):370–379. https://doi.org/10.1016/j.biocel.2008.09.023
39. Smith CL, Varoqueaux F, Kittelmann M, Azzam RN, Cooper B, Winters CA, Eitel M, Fasshauer D, Reese TS (2014) Novel cell types, neurosecretory cells, and body plan of the early-diverging metazoan Trichoplax adhaerens. Curr Biol 24(14):1565–1572. https://doi.org/10.1016/j.cub.2014.05.046
40. Mayorova TD, Smith CL, Hammar K, Winters CA, Pivovarova NB, Aronova MA, Leapman RD, Reese TS (2018) Cells containing aragonite crystals mediate responses to gravity in Trichoplax adhaerens (Placozoa), an animal lacking neurons and synapses. PLoS One 13(1):e0190905. https://doi.org/10.1371/journal.pone.0190905
41. Senatore A, Reese TS, Smith CL (2017) Neuropeptidergic integration of behavior in Trichoplax adhaerens, an animal without synapses. J Exp Biol 220(Pt 18):3381–3390. https://doi.org/10.1242/jeb.162396
42. Smith CL, Abdallah S, Wong YY, Le P, Harracksingh AN, Artinian L, Tamvacakis AN, Rehder V, Reese TS, Senatore A (2017) Evolutionary insights into T-type Ca^{2+} channel structure, function, and ion selectivity from the Trichoplax adhaerens homologue. J Gen Physiol 149(4):483–510. https://doi.org/10.1085/jgp.201611683
43. Paniagua R, Royuela M, Garcia-Anchuelo RM, Fraile B (1996) Ultrastructure of invertebrate muscle cell types. Histol Histopathol 11(1):181–201
44. Yoshida M, Sugimoto A, Ohshima Y, Takeshima H (2001) Important role of junctophilin in nematode motor function. Biochem Biophys Res Commun 289(1):234–239. https://doi.org/10.1006/bbrc.2001.5951
45. Jospin M, Jacquemond V, Mariol MC, Segalat L, Allard B (2002) The L-type voltage-dependent Ca^{2+} channel EGL-19 controls body wall muscle function in Caenorhabditis elegans. J Cell Biol 159(2):337–348. https://doi.org/10.1083/jcb.200203055
46. Lee RY, Lobel L, Hengartner M, Horvitz HR, Avery L (1997) Mutations in the alpha1 subunit of an L-type voltage-activated Ca^{2+} channel cause myotonia in Caenorhabditis elegans. EMBO J 16(20):6066–6076. https://doi.org/10.1093/emboj/16.20.6066
47. Takekura H, Franzini-Armstrong C (2002) The structure of Ca^{2+} release units in arthropod body muscle indicates an indirect mechanism for excitation-contraction coupling. Biophys J 83(5):2742–2753. https://doi.org/10.1016/S0006-3495(02)75284-3
48. Hara Y, Koganezawa M, Yamamoto D (2015) The Dmca1D channel mediates Ca^{2+} inward currents in Drosophila embryonic muscles. J Neurogenet 29(2–3):117–123. https://doi.org/10.3109/01677063.2015.1054991
49. Lin N, Badie N, Yu L, Abraham D, Cheng H, Bursac N, Rockman HA, Wolf MJ (2011) A method to measure myocardial calcium handling in adult Drosophila. Circ Res 108(11):1306–1315. https://doi.org/10.1161/CIRCRESAHA.110.238105
50. Krizanova O, Novotova M, Zachar J (1990) Characterization of DHP binding protein in crayfish striated muscle. FEBS Lett 267(2):311–315
51. Erxleben C, Rathmayer W (1997) A dihydropyridine-sensitive voltage-dependent calcium channel in the sarcolemmal membrane of crustacean muscle. J Gen Physiol 109(3):313–326
52. Findsen A, Overgaard J, Pedersen TH (2016) Reduced L-type Ca^{2+} current and compromised excitability induce loss of skeletal muscle function during acute cooling in locust. J Exp Biol 219(Pt 15):2340–2348. https://doi.org/10.1242/jeb.137604

53. Monterrubio J, Lizardi L, Zuazaga C (2000) Silent calcium channels in skeletal muscle fibers of the crustacean Atya lanipes. J Membr Biol 173(1):9–17
54. Bonilla M, Garcia MC, Orkand PM, Zuazaga C (1992) Ultrastructural and mechanical properties of electrically inexcitable skeletal muscle fibers of the crustacean Atya lanipes. Tissue Cell 24(4):525–535
55. Pennec JP, Talarmin H, Droguet M, Giroux-Metges MA, Gioux M, Dorange G (2004) Characterization of the voltage-activated currents in cultured atrial myocytes isolated from the heart of the common oyster Crassostrea gigas. J Exp Biol 207(Pt 22):3935–3944. https://doi.org/10.1242/jeb.01221
56. Yeoman MS, Brezden BL, Benjamin PR (1999) LVA and HVA Ca^{2+} currents in ventricular muscle cells of the Lymnaea heart. J Neurophysiol 82(5):2428–2440. https://doi.org/10.1152/jn.1999.82.5.2428
57. Senatore A, Boone A, Lam S, Dawson TF, Zhorov B, Spafford JD (2011) Mapping of dihydropyridine binding residues in a less sensitive invertebrate L-type calcium channel (LCa v 1). Channels (Austin) 5(2):173–187. https://doi.org/10.4161/chan.5.2.15141
58. Huang Z, Ishii Y, Watari T, Liu H, Miyake S, Suzaki T, Tsuchiya T (2005) Sources of activator calcium ions in the contraction of smooth muscles in Aplysia kurodai. Zool Sci 22(8):923–932. https://doi.org/10.2108/zsj.22.923
59. Rokni D, Hochner B (2002) Ionic currents underlying fast action potentials in the obliquely striated muscle cells of the octopus arm. J Neurophysiol 88(6):3386–3397. https://doi.org/10.1152/jn.00383.2002
60. Cavey MJ, Wood RL (1981) Specializations for excitation-contraction coupling in the podial retractor cells of the starfish Stylasterias forreri. Cell Tissue Res 218(3):475–485
61. Hill RB (2001) Role of Ca^{2+} in excitation-contraction coupling in echinoderm muscle: comparison with role in other tissues. J Exp Biol 204(Pt 5):897–908
62. Granados-Gonzalez G, Mendoza-Lujambio I, Rodriguez E, Galindo BE, Beltran C, Darszon A (2005) Identification of voltage-dependent Ca^{2+} channels in sea urchin sperm. FEBS Lett 579(29):6667–6672. https://doi.org/10.1016/j.febslet.2005.10.035
63. Peachey LD (1961) Structure of the longitudinal body muscles of amphioxus. J Biophys Biochem Cytol 10(4 Suppl):159–176
64. Hagiwara S, Henkart MP, Kidokoro Y (1971) Excitation-contraction coupling in amphioxus muscle cells. J Physiol 219(1):233–251
65. Benterbusch R, Herberg FW, Melzer W, Thieleczek R (1992) Excitation-contraction coupling in a pre-vertebrate twitch muscle: the myotomes of Branchiostoma lanceolatum. J Membr Biol 129(3):237–252
66. Melzer W (1982) Twitch activation in Ca^{2+} -free solutions in the myotomes of the lancelet (Branchiostoma lanceolatum). Eur J Cell Biol 28(2):219–225
67. Okamura Y, Izumi-Nakaseko H, Nakajo K, Ohtsuka Y, Ebihara T (2003) The ascidian dihydropyridine-resistant calcium channel as the prototype of chordate L-type calcium channel. Neurosignals 12(3):142–158. https://doi.org/10.1159/000072161
68. Inoue I, Tsutsui I, Bone Q (2002) Excitation-contraction coupling in isolated locomotor muscle fibres from the pelagic tunicate Doliolum which lack both sarcoplasmic reticulum and transverse tubular system. J Comp Physiol B 172(6):541–546. https://doi.org/10.1007/s00360-002-0280-1
69. Schiaffino S, Nunzi MG, Burighel P (1976) T system in ascidian muscle: organization of the sarcotubular system in the caudal muscle cells of Botryllus schlosseri tadpole larvae. Tissue Cell 8(1):101–110
70. Ohno S (1993) Patterns in genome evolution. Curr Opin Genet Dev 3(6):911–914
71. Caputo Barucchi V, Giovannotti M, Nisi Cerioni P, Splendiani A (2013) Genome duplication in early vertebrates: insights from agnathan cytogenetics. Cytogenet Genome Res 141(2–3):80–89. https://doi.org/10.1159/000354098
72. Inoue I, Tsutsui I, Bone Q (2002) Excitation-contraction coupling in skeletal and caudal heart muscle of the hagfish Eptatretus burgeri Girard. J Exp Biol 205(Pt 22):3535–3541

73. Inoue I, Tsutsui I, Bone Q, Brown ER (1994) Evolution of skeletal muscle excitation-contraction coupling and the appearance of dihydropyridine-sensitive intramembrane charge movement. Proc R Soc London Ser B Biol Sci 255(1343):181–187
74. Protasi F, Paolini C, Nakai J, Beam KG, Franzini-Armstrong C, Allen PD (2002) Multiple regions of RyR1 mediate functional and structural interactions with alpha(1S)-dihydropyridine receptors in skeletal muscle. Biophys J 83(6):3230–3244. https://doi.org/10.1016/S0006-3495(02)75325-3
75. Dayal A, Schrotter K, Pan Y, Fohr K, Melzer W, Grabner M (2017) The Ca^{2+} influx through the mammalian skeletal muscle dihydropyridine receptor is irrelevant for muscle performance. Nat Commun 8(1):475. https://doi.org/10.1038/s41467-017-00629-x
76. Glasauer SM, Neuhauss SC (2014) Whole-genome duplication in teleost fishes and its evolutionary consequences. Mol Gen Genomics 289(6):1045–1060. https://doi.org/10.1007/s00438-014-0889-2
77. Schredelseker J, Shrivastav M, Dayal A, Grabner M (2010) Non-Ca^{2+}-conducting Ca^{2+} channels in fish skeletal muscle excitation-contraction coupling. Proc Natl Acad Sci U S A 107(12):5658–5663. https://doi.org/10.1073/pnas.0912153107
78. Lien S, Koop BF, Sandve SR, Miller JR, Kent MP, Nome T, Hvidsten TR, Leong JS, Minkley DR, Zimin A, Grammes F, Grove H, Gjuvsland A, Walenz B, Hermansen RA, von Schalburg K, Rondeau EB, Di Genova A, Samy JK, Olav Vik J, Vigeland MD, Caler L, Grimholt U, Jentoft S, Vage DI, de Jong P, Moen T, Baranski M, Palti Y, Smith DR, Yorke JA, Nederbragt AJ, Tooming-Klunderud A, Jakobsen KS, Jiang X, Fan D, Hu Y, Liberles DA, Vidal R, Iturra P, Jones SJ, Jonassen I, Maass A, Omholt SW, Davidson WS (2016) The Atlantic salmon genome provides insights into rediploidization. Nature 533(7602):200–205. https://doi.org/10.1038/nature17164
79. Schrotter K, Dayal A, Grabner M (2017) The mammalian skeletal muscle DHPR has larger Ca^{2+} conductance and is phylogenetically ancient to the early ray-finned fish sterlet (Acipenser ruthenus). Cell Calcium 61:22–31. https://doi.org/10.1016/j.ceca.2016.10.002
80. Mackrill JJ (2012) Ryanodine receptor calcium release channels: an evolutionary perspective. Adv Exp Med Biol 740:159–182. https://doi.org/10.1007/978-94-007-2888-2_7
81. Alzayady KJ, Sebe-Pedros A, Chandrasekhar R, Wang L, Ruiz-Trillo I, Yule DI (2015) Tracing the evolutionary history of inositol, 1, 4, 5-trisphosphate receptor: insights from analyses of Capsaspora owczarzaki Ca^{2+} Release Channel Orthologs. Mol Biol Evol 32(9):2236–2253. https://doi.org/10.1093/molbev/msv098
82. Simion P, Philippe H, Baurain D, Jager M, Richter DJ, Di Franco A, Roure B, Satoh N, Queinnec E, Ereskovsky A, Lapebie P, Corre E, Delsuc F, King N, Worheide G, Manuel M (2017) A large and consistent Phylogenomic dataset supports sponges as the sister group to all other animals. Curr Biol 27(7):958–967. https://doi.org/10.1016/j.cub.2017.02.031
83. Singla CL (1978) Locomotion and neuromuscular system of Aglantha digitale. Cell Tissue Res 188(2):317–327
84. Cario C, Malaval L, Hernandez-Nicaise ML (1995) Two distinct distribution patterns of sarcoplasmic reticulum in two functionally different giant smooth muscle cells of Beroe ovata. Cell Tissue Res 282(3):435–443
85. Lin YC, Grigoriev NG, Spencer AN (2000) Wound healing in jellyfish striated muscle involves rapid switching between two modes of cell motility and a change in the source of regulatory calcium. Dev Biol 225(1):87–100. https://doi.org/10.1006/dbio.2000.9807
86. Missiaen L, Parys JB, De Smedt H, Himpens B, Casteels R (1994) Inhibition of inositol trisphosphate-induced calcium release by caffeine is prevented by ATP. Biochem J 300(Pt 1):81–84
87. Sutko JL, Ito K, Kenyon JL (1985) Ryanodine: a modifier of sarcoplasmic reticulum calcium release in striated muscle. Fed Proc 44(15):2984–2988
88. Mackrill JJ (2010) Ryanodine receptor calcium channels and their partners as drug targets. Biochem Pharmacol 79(11):1535–1543. https://doi.org/10.1016/j.bcp.2010.01.014
89. Silva CL, Cunha VM, Mendonca-Silva DL, Noel F (1998) Evidence for ryanodine receptors in Schistosoma mansoni. Biochem Pharmacol 56(8):997–1003

90. Day TA, Haithcock J, Kimber M, Maule AG (2000) Functional ryanodine receptor channels in flatworm muscle fibres. Parasitology 120(Pt 4):417–422
91. Maryon EB, Coronado R, Anderson P (1996) unc-68 encodes a ryanodine receptor involved in regulating C. elegans body-wall muscle contraction. J Cell Biol 134(4):885–893
92. Robertson AP, Clark CL, Martin RJ (2010) Levamisole and ryanodine receptors. I: a contraction study in Ascaris suum. Mol Biochem Parasitol 171(1):1–7. https://doi.org/10.1016/j.molbiopara.2009.12.007
93. Hassett CC (1948) Effect of ryanodine on the oxygen consumption of Periplaneta americana. Science 108(2797):138–139. https://doi.org/10.1126/science.108.2797.138
94. Sullivan KM, Scott K, Zuker CS, Rubin GM (2000) The ryanodine receptor is essential for larval development in Drosophila melanogaster. Proc Natl Acad Sci U S A 97(11):5942–5947. https://doi.org/10.1073/pnas.110145997
95. Frolov RV, Singh S (2012) Inhibition of ion channels and heart beat in Drosophila by selective COX-2 inhibitor SC-791. PLoS One 7(6):e38759. https://doi.org/10.1371/journal.pone.0038759
96. Scott-Ward TS, Dunbar SJ, Windass JD, Williams AJ (2001) Characterization of the ryanodine receptor-Ca^{2+} release channel from the thoracic tissues of the lepidopteran insect Heliothis virescens. J Membr Biol 179(2):127–141
97. Collet C (2009) Excitation-contraction coupling in skeletal muscle fibers from adult domestic honeybee. Pflugers Arch 458(3):601–612. https://doi.org/10.1007/s00424-009-0642-6
98. Lahm GP, Cordova D, Barry JD (2009) New and selective ryanodine receptor activators for insect control. Bioorg Med Chem 17(12):4127–4133. https://doi.org/10.1016/j.bmc.2009.01.018
99. Lea TJ, Ashley CC (1990) Ca^{2+} release from the sarcoplasmic reticulum of barnacle myofibrillar bundles initiated by photolysis of caged Ca^{2+}. J Physiol 427:435–453
100. Gyorke S, Palade P (1992) Calcium-induced calcium release in crayfish skeletal muscle. J Physiol 457:195–210
101. Brenner TL, Wilkens JL (2001) Physiology and excitation-contraction coupling in the intestinal muscle of the crayfish Procambarus clarkii. J Comp Physiol B 171(7):613–621
102. Xiong H, Feng X, Gao L, Xu L, Pasek DA, Seok JH, Meissner G (1998) Identification of a two EF-hand Ca^{2+} binding domain in lobster skeletal muscle ryanodine receptor/Ca^{2+} release channel. Biochemistry 37(14):4804–4814. https://doi.org/10.1021/bi971198b
103. Zhang JJ, Williams AJ, Sitsapesan R (1999) Evidence for novel caffeine and Ca^{2+} binding sites on the lobster skeletal ryanodine receptor. Br J Pharmacol 126(4):1066–1074. https://doi.org/10.1038/sj.bjp.0702400
104. Abe T, Ishida H, Matsuno A (1997) Foot structure and foot protein in the cross striated muscle of a pecten. Cell Struct Funct 22(1):21–26
105. Panfoli I, Burlando B, Viarengo A (1999) Cyclic ADP-ribose-dependent Ca^{2+} release is modulated by free [Ca^{2+}] in the scallop sarcoplasmic reticulum. Biochem Biophys Res Commun 257(1):57–62. https://doi.org/10.1006/bbrc.1999.0405
106. Sugi H, Suzuki S (1978) Ultrastructural and physiological studies on the longitudinal body wall muscle of Dolabella auricularia. I. Mechanical response and ultrastructure. J Cell Biol 79(2 Pt 1):454–466
107. Devlin CL, Amole W, Anderson S, Shea K (2003) Muscarinic acetylcholine receptor compounds alter net Ca^{2+} flux and contractility in an invertebrate smooth muscle. Invertebr Neurosci 5(1):9–17. https://doi.org/10.1007/s10158-003-0023-3
108. Shiwa M, Murayama T, Ogawa Y (2002) Molecular cloning and characterization of ryanodine receptor from unfertilized sea urchin eggs. Am J Physiol Regul Integr Comp Physiol 282(3):R727–R737. https://doi.org/10.1152/ajpregu.00519.2001
109. Lokuta AJ, Darszon A, Beltran C, Valdivia HH (1998) Detection and functional characterization of ryanodine receptors from sea urchin eggs. J Physiol 510(Pt 1):155–164
110. Nakajo K, Chen L, Okamura Y (1999) Cross-coupling between voltage-dependent Ca^{2+} channels and ryanodine receptors in developing ascidian muscle blastomeres. J Physiol 515(Pt 3):695–710

111. Giannini G, Conti A, Mammarella S, Scrobogna M, Sorrentino V (1995) The ryanodine receptor/calcium channel genes are widely and differentially expressed in murine brain and peripheral tissues. J Cell Biol 128(5):893–904
112. Mackrill JJ, Challiss RA, O'Connell DA, Lai FA, Nahorski SR (1997) Differential expression and regulation of ryanodine receptor and myo-inositol 1,4,5-trisphosphate receptor Ca^{2+} release channels in mammalian tissues and cell lines. Biochem J 327(Pt 1):251–258
113. Holland EB, Goldstone JV, Pessah IN, Whitehead A, Reid NM, Karchner SI, Hahn ME, Nacci DE, Clark BW, Stegeman JJ (2017) Ryanodine receptor and FK506 binding protein 1 in the Atlantic killifish (Fundulus heteroclitus): a phylogenetic and population-based comparison. Aquat Toxicol 192:105–115. https://doi.org/10.1016/j.aquatox.2017.09.002
114. Darbandi S, Franck JP (2009) A comparative study of ryanodine receptor (RyR) gene expression levels in a basal ray-finned fish, bichir (Polypterus ornatipinnis) and the derived euteleost zebrafish (Danio rerio). Comp Biochem Physiol B Biochem Mol Biol 154(4):443–448. https://doi.org/10.1016/j.cbpb.2009.09.003
115. Lai FA, Liu QY, Xu L, el-Hashem A, Kramarcy NR, Sealock R, Meissner G (1992) Amphibian ryanodine receptor isoforms are related to those of mammalian skeletal or cardiac muscle. Am J Phys 263(2 Pt 1):C365–C372. https://doi.org/10.1152/ajpcell.1992.263.2.C365
116. Jeyakumar LH, Ballester L, Cheng DS, McIntyre JO, Chang P, Olivey HE, Rollins-Smith L, Barnett JV, Murray K, Xin HB, Fleischer S (2001) FKBP binding characteristics of cardiac microsomes from diverse vertebrates. Biochem Biophys Res Commun 281(4):979–986. https://doi.org/10.1006/bbrc.2001.4444
117. Klitzner T, Morad M (1983) Excitation-contraction coupling in frog ventricle. Possible Ca^{2+} transport mechanisms. Pflugers Arch 398(4):274–283
118. Shiels HA, Sitsapesan R (2015) Is there something fishy about the regulation of the ryanodine receptor in the fish heart? Exp Physiol 100(12):1412–1420. https://doi.org/10.1113/EP085136
119. Cros C, Salle L, Warren DE, Shiels HA, Brette F (2014) The calcium stored in the sarcoplasmic reticulum acts as a safety mechanism in rainbow trout heart. Am J Physiol Regul Integr Comp Physiol 307(12):R1493–R1501. https://doi.org/10.1152/ajpregu.00127.2014
120. Tijskens P, Meissner G, Franzini-Armstrong C (2003) Location of ryanodine and dihydropyridine receptors in frog myocardium. Biophys J 84(2 Pt 1):1079–1092. https://doi.org/10.1016/S0006-3495(03)74924-8
121. Perin P, Botta L, Tritto S, Laforenza U (2012) Expression and localization of ryanodine receptors in the frog semicircular canal. J Biomed Biotechnol 2012:398398. https://doi.org/10.1155/2012/398398
122. Session AM, Uno Y, Kwon T, Chapman JA, Toyoda A, Takahashi S, Fukui A, Hikosaka A, Suzuki A, Kondo M, van Heeringen SJ, Quigley I, Heinz S, Ogino H, Ochi H, Hellsten U, Lyons JB, Simakov O, Putnam N, Stites J, Kuroki Y, Tanaka T, Michiue T, Watanabe M, Bogdanovic O, Lister R, Georgiou G, Paranjpe SS, van Kruijsbergen I, Shu S, Carlson J, Kinoshita T, Ohta Y, Mawaribuchi S, Jenkins J, Grimwood J, Schmutz J, Mitros T, Mozaffari SV, Suzuki Y, Haramoto Y, Yamamoto TS, Takagi C, Heald R, Miller K, Haudenschild C, Kitzman J, Nakayama T, Izutsu Y, Robert J, Fortriede J, Burns K, Lotay V, Karimi K, Yasuoka Y, Dichmann DS, Flajnik MF, Houston DW, Shendure J, DuPasquier L, Vize PD, Zorn AM, Ito M, Marcotte EM, Wallingford JB, Ito Y, Asashima M, Ueno N, Matsuda Y, Veenstra GJ, Fujiyama A, Harland RM, Taira M, Rokhsar DS (2016) Genome evolution in the allotetraploid frog Xenopus laevis. Nature 538(7625):336–343. https://doi.org/10.1038/nature19840
123. Bowes JB, Snyder KA, Segerdell E, Gibb R, Jarabek C, Noumen E, Pollet N, Vize PD (2008) Xenbase: a Xenopus biology and genomics resource. Nucleic Acids Res 36(Database issue):D761–D767. https://doi.org/10.1093/nar/gkm826
124. Mouton J, Marty I, Villaz M, Feltz A, Maulet Y (2001) Molecular interaction of dihydropyridine receptors with type-1 ryanodine receptors in rat brain. Biochem J 354(Pt 3):597–603
125. Cheng W, Altafaj X, Ronjat M, Coronado R (2005) Interaction between the dihydropyridine receptor Ca^{2+} channel beta-subunit and ryanodine receptor type 1 strength-

ens excitation-contraction coupling. Proc Natl Acad Sci U S A 102(52):19225–19230. https://doi.org/10.1073/pnas.0504334102
126. Samso M (2015) 3D structure of the Dihydropyridine receptor of skeletal muscle. Eur J Transl Myol 25(1):4840. https://doi.org/10.4081/ejtm.2015.4840
127. McKay PB, Griswold CK (2014) A comparative study indicates both positive and purifying selection within ryanodine receptor (RyR) genes, as well as correlated evolution. J Exp Zool A Ecol Genet Physiol 321(3):151–163. https://doi.org/10.1002/jez.1845
128. Tanabe T, Beam KG, Powell JA, Numa S (1988) Restoration of excitation-contraction coupling and slow calcium current in dysgenic muscle by dihydropyridine receptor complementary DNA. Nature 336(6195):134–139. https://doi.org/10.1038/336134a0
129. Tanabe T, Beam KG, Adams BA, Niidome T, Numa S (1990) Regions of the skeletal muscle dihydropyridine receptor critical for excitation-contraction coupling. Nature 346(6284):567–569. https://doi.org/10.1038/346567a0
130. Takekura H, Paolini C, Franzini-Armstrong C, Kugler G, Grabner M, Flucher BE (2004) Differential contribution of skeletal and cardiac II-III loop sequences to the assembly of dihydropyridine-receptor arrays in skeletal muscle. Mol Biol Cell 15(12):5408–5419. https://doi.org/10.1091/mbc.E04-05-0414
131. Ahern CA, Bhattacharya D, Mortenson L, Coronado R (2001) A component of excitation-contraction coupling triggered in the absence of the T671-L690 and L720-Q765 regions of the II-III loop of the dihydropyridine receptor alpha(1s) pore subunit. Biophys J 81(6):3294–3307. https://doi.org/10.1016/S0006-3495(01)75963-2
132. Leong P, MacLennan DH (1998) The cytoplasmic loops between domains II and III and domains III and IV in the skeletal muscle dihydropyridine receptor bind to a contiguous site in the skeletal muscle ryanodine receptor. J Biol Chem 273(45):29958–29964
133. Kugler G, Weiss RG, Flucher BE, Grabner M (2004) Structural requirements of the dihydropyridine receptor alpha1S II-III loop for skeletal-type excitation-contraction coupling. J Biol Chem 279(6):4721–4728. https://doi.org/10.1074/jbc.M307538200
134. Leong P, MacLennan DH (1998) A 37-amino acid sequence in the skeletal muscle ryanodine receptor interacts with the cytoplasmic loop between domains II and III in the skeletal muscle dihydropyridine receptor. J Biol Chem 273(14):7791–7794
135. Proenza C, O'Brien J, Nakai J, Mukherjee S, Allen PD, Beam KG (2002) Identification of a region of RyR1 that participates in allosteric coupling with the alpha(1S) (Ca(V)1.1) II-III loop. J Biol Chem 277(8):6530–6535. https://doi.org/10.1074/jbc.M106471200
136. Sorrentino V, Volpe P (1993) Ryanodine receptors: how many, where and why? Trends Pharmacol Sci 14(3):98–103
137. Yamazawa T, Takeshima H, Shimuta M, Iino M (1997) A region of the ryanodine receptor critical for excitation-contraction coupling in skeletal muscle. J Biol Chem 272(13):8161–8164
138. Perez CF, Mukherjee S, Allen PD (2003) Amino acids 1-1,680 of ryanodine receptor type 1 hold critical determinants of skeletal type for excitation-contraction coupling. Role of divergence domain D2. J Biol Chem 278(41):39644–39652. https://doi.org/10.1074/jbc.M305160200
139. Bannister RA, Sheridan DC, Beam KG (2016) Distinct components of retrograde Ca(V)1.1-RyR1 coupling revealed by a lethal mutation in RyR1. Biophys J 110(4):912–921. https://doi.org/10.1016/j.bpj.2015.12.031
140. Takeshima H, Hoshijima M, Song LS (2015) Ca(2)(+) microdomains organized by junctophilins. Cell Calcium 58(4):349–356. https://doi.org/10.1016/j.ceca.2015.01.007
141. Landstrom AP, Beavers DL, Wehrens XH (2014) The junctophilin family of proteins: from bench to bedside. Trends Mol Med 20(6):353–362. https://doi.org/10.1016/j.molmed.2014.02.004
142. Nishi M, Sakagami H, Komazaki S, Kondo H, Takeshima H (2003) Coexpression of junctophilin type 3 and type 4 in brain. Brain Res Mol Brain Res 118(1–2):102–110
143. Woo JS, Srikanth S, Nishi M, Ping P, Takeshima H, Gwack Y (2016) Junctophilin-4, a component of the endoplasmic reticulum-plasma membrane junctions, regu-

lates Ca^{2+} dynamics in T cells. Proc Natl Acad Sci U S A 113(10):2762–2767. https://doi.org/10.1073/pnas.1524229113
144. Reynolds JO, Quick AP, Wang Q, Beavers DL, Philippen LE, Showell J, Barreto-Torres G, Thuerauf DJ, Doroudgar S, Glembotski CC, Wehrens XH (2016) Junctophilin-2 gene therapy rescues heart failure by normalizing RyR2-mediated Ca^{2+} release. Int J Cardiol 225:371–380. https://doi.org/10.1016/j.ijcard.2016.10.021
145. van Oort RJ, Garbino A, Wang W, Dixit SS, Landstrom AP, Gaur N, De Almeida AC, Skapura DG, Rudy Y, Burns AR, Ackerman MJ, Wehrens XH (2011) Disrupted junctional membrane complexes and hyperactive ryanodine receptors after acute junctophilin knockdown in mice. Circulation 123(9):979–988. https://doi.org/10.1161/CIRCULATIONAHA.110.006437
146. Jiang M, Zhang M, Howren M, Wang Y, Tan A, Balijepalli RC, Huizar JF, Tseng GN (2016) JPH-2 interacts with Cai-handling proteins and ion channels in dyads: contribution to premature ventricular contraction-induced cardiomyopathy. Heart Rhythm 13(3):743–752. https://doi.org/10.1016/j.hrthm.2015.10.037
147. Munro ML, Jayasinghe ID, Wang Q, Quick A, Wang W, Baddeley D, Wehrens XH, Soeller C (2016) Junctophilin-2 in the nanoscale organisation and functional signalling of ryanodine receptor clusters in cardiomyocytes. J Cell Sci 129(23):4388–4398. https://doi.org/10.1242/jcs.196873
148. Ito K, Komazaki S, Sasamoto K, Yoshida M, Nishi M, Kitamura K, Takeshima H (2001) Deficiency of triad junction and contraction in mutant skeletal muscle lacking junctophilin type 1. J Cell Biol 154(5):1059–1067. https://doi.org/10.1083/jcb.200105040
149. Nakada T, Kashihara T, Komatsu M, Kojima K, Takeshita T, Yamada M (2018) Physical interaction of junctophilin and the CaV1.1 C terminus is crucial for skeletal muscle contraction. Proc Natl Acad Sci U S A 115(17):4507–4512. https://doi.org/10.1073/pnas.1716649115
150. Garbino A, van Oort RJ, Dixit SS, Landstrom AP, Ackerman MJ, Wehrens XH (2009) Molecular evolution of the junctophilin gene family. Physiol Genomics 37(3):175–186. https://doi.org/10.1152/physiolgenomics.00017.2009
151. Mecklenburg KL, Freed SA, Raval M, Quintero OA, Yengo CM, O'Tousa JE (2015) Invertebrate and vertebrate class III myosins interact with MORN repeat-containing adaptor proteins. PLoS One 10(3):e0122502. https://doi.org/10.1371/journal.pone.0122502
152. Kohno T, Wakabayashi K, Diener DR, Rosenbaum JL, Kamiya R (2011) Subunit interactions within the Chlamydomonas flagellar spokehead. Cytoskeleton (Hoboken) 68(4):237–246. https://doi.org/10.1002/cm.20507
153. Sheerin UM, Schneider SA, Carr L, Deuschl G, Hopfner F, Stamelou M, Wood NW, Bhatia KP (2014) ALS2 mutations: juvenile amyotrophic lateral sclerosis and generalized dystonia. Neurology 82(12):1065–1067. https://doi.org/10.1212/WNL.0000000000000254
154. Topp JD, Gray NW, Gerard RD, Horazdovsky BF (2004) Alsin is a Rab5 and Rac1 guanine nucleotide exchange factor. J Biol Chem 279(23):24612–24623. https://doi.org/10.1074/jbc.M313504200
155. Plattner H (2015) Molecular aspects of calcium signalling at the crossroads of unikont and bikont eukaryote evolution – the ciliated protozoan Paramecium in focus. Cell Calcium 57(3):174–185. https://doi.org/10.1016/j.ceca.2014.12.002
156. Hasegawa M, Fujiwara M (1993) Relative efficiencies of the maximum likelihood, maximum parsimony, and neighbor-joining methods for estimating protein phylogeny. Mol Phylogenet Evol 2(1):1–5. https://doi.org/10.1006/mpev.1993.1001
157. Kall L, Krogh A, Sonnhammer EL (2004) A combined transmembrane topology and signal peptide prediction method. J Mol Biol 338(5):1027–1036. https://doi.org/10.1016/j.jmb.2004.03.016
158. Sonnhammer EL, von Heijne G, Krogh A (1998) A hidden Markov model for predicting transmembrane helices in protein sequences. Proc Int Conf Intell Syst Mol Biol 6:175–182
159. Calpena E, Lopez Del Amo V, Chakraborty M, Llamusi B, Artero R, Espinos C, Galindo MI (2018) The Drosophila junctophilin gene is functionally equivalent to its four mammalian counterparts and is a modifier of a Huntingtin poly-Q expansion and the Notch pathway. Dis Model Mech 11(1):dmm029082. https://doi.org/10.1242/dmm.029082

160. Mello CV, Lovell PV (2018) Avian genomics lends insights into endocrine function in birds. Gen Comp Endocrinol 256:123–129. https://doi.org/10.1016/j.ygcen.2017.05.023
161. Berridge MJ (1998) Neuronal calcium signaling. Neuron 21(1):13–26
162. Tamura K, Peterson D, Peterson N, Stecher G, Nei M, Kumar S (2011) MEGA5: molecular evolutionary genetics analysis using maximum likelihood, evolutionary distance, and maximum parsimony methods. Mol Biol Evol 28(10):2731–2739. https://doi.org/10.1093/molbev/msr121
163. Felsenstein J (1985) Confidence-limits on phylogenies – an approach using the bootstrap. Evolution 39(4):783–791
164. Sievers F, Wilm A, Dineen D, Gibson TJ, Karplus K, Li W, Lopez R, McWilliam H, Remmert M, Soding J, Thompson JD, Higgins DG (2011) Fast, scalable generation of high-quality protein multiple sequence alignments using Clustal omega. Mol Syst Biol 7:539. https://doi.org/10.1038/msb.2011.75
165. Nei M, Kumar S (2000) Molecular evolution and phylogenetics. Oxford University Press, New York
166. Sheard TM, Kharche SR, Pinali C, Shiels HA. 3D ultrastructural organisation of calcium release units in the avian sarcoplasmic reticulum. Journal of Experimental Biology. 2019 Jan 1:jeb-197640.

Chapter 13
Molecular Insights into Calcium Dependent Regulation of Ryanodine Receptor Calcium Release Channels

Naohiro Yamaguchi

Abstract Ryanodine receptor calcium release channels (RyRs) play central roles in controlling intracellular calcium concentrations in excitable and non-excitable cells. RyRs are located in the sarcoplasmic or endoplasmic reticulum, intracellular Ca^{2+} storage compartment, and release Ca^{2+} during cellular action potentials or in response to other cellular stimuli. Mammalian cells express three structurally related isoforms of RyR. RyR1 and RyR2 are the major RyR isoforms in skeletal and cardiac muscle, respectively, and RyR3 is expressed in various tissues along with the other two isoforms. A prominent feature of RyRs is that the Ca^{2+} release channel activities of RyRs are regulated by calcium ions; therefore, intracellular Ca^{2+} release controls positive- and negative-feedback phenomena through the RyRs. RyR channel activities are also regulated by Ca^{2+} indirectly, i.e. through Ca^{2+} binding proteins at both cytosolic and sarco/endoplasmic reticulum luminal sides. Here, I summarize Ca^{2+}-dependent feedback regulation of RyRs including recent progress in the structure/function aspects.

Keywords Ryanodine receptor · Excitation-contraction coupling · Calcium release channel · Intracellular calcium · Calmodulin

Transient increase of intracellular Ca^{2+} concentration plays a pivotal role in numerous cell functions, including muscle contraction, neuronal plasticity, and immune responses. Multiple sources of Ca^{2+} are involved in this signaling, including Ca^{2+} influx from the extracellular spaces and Ca^{2+} release from intracellular Ca^{2+} stores: the endo/sarcoplasmic reticulum (ER/SR), nuclear envelope, and mitochondria [1–3]. Ryanodine receptors (RyRs) are Ca^{2+} release channels located in the ER/SR

N. Yamaguchi (✉)
Cardiac Signaling Center, University of South Carolina, Medical University of South Carolina and Clemson University, Charleston, SC, USA

Department of Regenerative Medicine and Cell Biology, Medical University of South Carolina, Charleston, SC, USA
e-mail: yamaguch@musc.edu

M. S. Islam (ed.), *Calcium Signaling*, Advances in Experimental Medicine and Biology 1131, https://doi.org/10.1007/978-3-030-12457-1_13

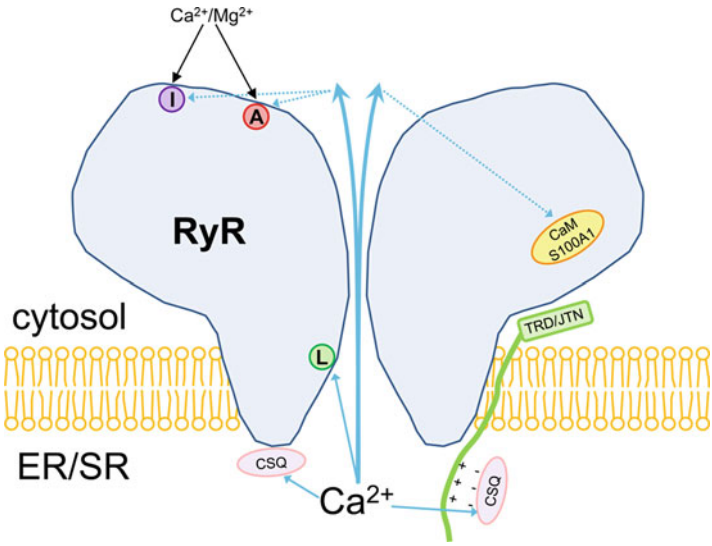

Fig. 13.1 A schematic of the RyR Ca^{2+} release channel regulation by Ca^{2+}. RyRs have been suggested to possess at least three Ca^{2+} regulatory sites; cytoplasmic high affinity activation (A) and low affinity inhibition (I) sites, and luminal regulatory (L) site. Mg^{2+} inhibits RyRs by binding to A or I sites. Calcium ions passing through the RyR from ER/SR lumen to the cytoplasm are considered to bind to RyR-A and I sites and cytoplasmic accessory proteins, CaM and S100A1. The low affinity luminal Ca^{2+} binding protein, CSQ, forms a macromolecular complex via its interaction with RyR accessory proteins, triadin (TRD) and junctin (JTN). CSQ may also bind to RyR directly

and play a primary role in Ca^{2+} release from SR during skeletal and cardiac muscle contraction [4–6]. Additionally, RyRs play an important role in smooth muscle, neurons, and other cell types by co-existing with another family of Ca^{2+} release channels called inositol-trisphosphate receptors [3]. RyRs release Ca^{2+} from the ER/SR and are regulated by Ca^{2+} [4–6], suggesting that RyRs have a self-regulatory mechanism controlled by Ca^{2+}, i.e. RyR-released Ca^{2+} regulates the same or neighboring RyRs. This chapter focuses on the structure-function aspect of RyR regulation by Ca^{2+} and Ca^{2+} binding proteins such as calmodulin and calsequestrin (Fig. 13.1).

13.1 Molecular Structure of RyRs

In striated muscle, RyRs are localized in the junctional SR membrane in close proximity to transverse (T)-tubule membranes, invaginations of the plasma membrane into the myofibrils. In skeletal muscle the SR is typically on both sides of the T-tubule (triad), while in cardiomyocytes, the SR is only on one side of the

T-tubule (dyad). In both triadic and dyadic junctions, electron microscopy shows foot structures spanning between the SR and T-tubule [4]. Molecular identification of RyRs was first performed with rabbit fast twitch skeletal muscle using ryanodine, a specific ligand of RyRs. Isolated RyRs are homotetramers of a ∼500 kDa polypeptide. Morphological analysis of the reconstituted purified proteins identified RyRs as the foot structures [7–10]. Molecular cloning of RyRs showed that mammals express three different RyR isoforms [11–16]. Skeletal muscle expresses primarily RyR1. The dominant RyR isoform in cardiac muscle is RyR2. RyR3 was initially identified in the brain; however, the brain expresses all three RyR isoforms. Although expression patterns depend on the locations in the brain, in general, RyR2 is widely dispersed over the whole brain [17]. RyR3 is also expressed together with RyR1 in the diaphragm and slow twitch muscle [18, 19], thus functional characterization of RyR1 is mainly performed with fast twitch muscle. In amphibians and avian skeletal muscle, two RyR isoforms, αRyR and βRyR, are recognized and correspond to the mammalian RyR1 and RyR3, respectively [20–22].

All three isoforms of RyR have a large cytoplasmic domain, which possesses multiple regulatory sites for channel activity. The carboxyl-terminal end of the RyR spans the SR membrane six times, in which a pore helix and the transmembrane segment form the channel pore [23–27]. RyRs are activated by micromolar Ca^{2+} and adenine nucleotide, and are inhibited by millimolar Ca^{2+} and Mg^{2+} [4–6]. A number of proteins have been found to interact with RyRs and regulate their channel activity. These include triadin, junctin, FK506-binding proteins, protein kinases and phosphatases, and Ca^{2+} binding proteins such as calmodulin and S100A1. Recently, cryo-electron microscopy and 3D image reconstruction of the purified full-length RyRs and crystal structural analysis of truncated recombinant RyRs have detailed the structures of RyR1 and RyR2 at near atomic resolution [24–30].

13.2 Activation by Cytoplasmic Ca^{2+}

Skeletal and cardiac muscle contractions are triggered by SR Ca^{2+} release mediated by RyR1 and RyR2. Two different mechanisms are now recognized to open RyRs. In skeletal muscle, direct interaction between RyR1 and the T-tubule voltage sensor, also recognized as the DHP receptor L-type Ca^{2+} channel (Cav1.1), opens RyR1 during skeletal action potential (voltage-induced Ca^{2+} release) [31]. Alternatively, in cardiac muscle, small Ca^{2+} influx through the cardiac L-type Ca^{2+} channel (Cav1.2) increases intracellular Ca^{2+}, and at ∼micromolar concentrations opens RyR2 by means of Ca^{2+}-induced Ca^{2+} release (CICR) [32]. The CICR mechanism was initially recognized in skeletal muscle contraction [33, 34]; however, elimination of Ca^{2+} from the extracellular space or blocking Ca^{2+} influx through Cav1.1 did not abolish voltage-dependent intracellular Ca^{2+} transients [35, 36]. Thus, CICR in skeletal muscle (RyR1) is not considered a trigger for muscle contraction.

Furthermore, slower kinetics of CICR in contrast to the rapid Ca^{2+} release in skeletal muscle also supported the idea that CICR is not a physiological trigger for skeletal muscle contraction [37]. However, CICR may play a role in amplifying Ca^{2+} signaling by activating RyR1s which do not couple with DHP receptors or the small population of RyR3s [38]. Calcium-dependent activation of RyR1 can be altered by RyR1 missense mutations associated with skeletal myopathies such as malignant hyperthermia, thus, CICR may impact these pathologies [37, 39]. Ca^{2+}-dependent activation of RyRs has been well characterized using isolated membrane fractions, intact cells and muscle fibers, purified RyR proteins, and recombinant RyRs by several different methods including muscle tension measurements, Ca^{2+} flux measurements using Ca^{2+} indicator dyes or radioactive $^{45}Ca^{2+}$, single channel recordings, and specific ligand ([^{3}H]ryanodine) binding assays [37, 40, 41]. All three mammalian RyR isoforms are activated by ~0.5–5 μM Ca^{2+} depending on assay conditions. Several potential Ca^{2+} binding sites were initially identified using truncated RyR1 proteins and $^{45}Ca^{2+}$ overlays [42–44]. Subsequently, site-directed mutagenesis showed that E3987 in RyR2 (E4032 in RyR1) was critical for Ca^{2+}-dependent activation of RyRs [45, 46]. The mutant RyRs showed impaired Ca^{2+} dependent activation in single channel recordings and [^{3}H]ryanodine binding assay. E4032A-RyR1 expressing myotubes were impaired in caffeine-induced Ca^{2+} release, but the aberrant function was restored in the presence of ryanodine [47]. Recently, near-atomic level cryo-electron microscopy analysis of RyR1 (~4 Å resolution) determined the open and closed state conformations of RyR1 [30]. The structure of RyR1 with 30 μM Ca^{2+}, which is optimal for RyR activation, identified a new Ca^{2+} binding site in RyR1. The Ca^{2+} binding site is formed by 3 essential amino acids, E3893, E3967, and T5001, together with two auxiliary amino acids, H3895 and Q3970, for secondary coordination of the Ca^{2+} sphere [30]. In this structural model, E4032 is distal from the bound calcium ion, but forms an interface with carboxyl terminal tail where T5001 locates. This suggests that E4032 contribute to stabilize the conformation of Ca^{2+} bound RyR1 [30]. Murayama and colleagues introduced point mutations on RyR2 amino acids corresponding to the RyR1 E3893, E3967, and Q3970, and found that the mutations altered Ca^{2+}-dependent activation of RyR2 [48]. These functional results support the idea that the identified Ca^{2+} binding site serves as a functional Ca^{2+} regulatory site. Further detail analysis including assessments of other amino acids combined in the presence of other channel agonists and antagonists will further advance structure and function relationship of Ca^{2+}-dependent activation of RyRs. Another ~6 Å resolution cryo-electron micrograph of RyR1 suggested that 10 mM Ca^{2+} changed the conformation of the EF hand-type Ca^{2+} binding domain of RyR1; therefore, it was proposed as a Ca^{2+} activation site [24]. However, studies with recombinant proteins including the EF hand domain showed Ca^{2+} affinity was >60 μM [49, 50], which is much higher than the RyR-activating Ca^{2+} concentration. Also, functional study scrambling of the EF hand sequence in RyR1 and deletion of the entire EF hand in RyR2 did not affect the Ca^{2+} activation of RyRs [51, 52]. Considering that the structural analysis was determined with 10 mM Ca^{2+}, the EF hand site is likely to be a Ca^{2+}

inactivation site [53]. We also found that the EF hand domain contributes to the isoform-specific regulation of RyRs by calmodulin (see below) [54].

Ca^{2+}-dependent activation of RyR1 and RyR2 are similar in single channel recordings and flux measurements in the SR vesicles; however, Ogawa and colleagues pointed out that RyR2 in rat ventricular SR or as a recombinant form exhibited a suppressed activity at 10–100 μM Ca^{2+} using [^{3}H]ryanodine equilibrium binding assay [55]. Similar suppressed RyR2 activities were observed in our own study with rabbit recombinant RyR2 using the same technique [56]. Surprisingly, this suppressed activity was restored by ~1 mM Mg^{2+} [55], which is usually considered to be an inhibitor of RyR channel activity by competing off Ca^{2+} at the Ca^{2+} activation site or binding to the Ca^{2+} inhibitory site [40, 57]. RyR2 in the rabbit ventricular SR showed this suppression only when AMP or caffeine, RyR activators, were added, suggesting that the suppressed effects depend on the type of RyR2 sample. One possibility for this mechanism is therefore that regulatory factors were removed during the sample preparations. Another possible explanation is that the RyR2 conformation is not very stable under long time (>8 h) equilibrium conditions in the [^{3}H]ryanodine binding assays. We found that replacement of the RyR1-EF hand domain with corresponding RyR2 sequence or the introduction of point mutations in the cytoplasmic loop between the second and the third transmembrane segments (S2-S3 loop) of RyR1 resulted in suppressed activity at 10–100 μM Ca^{2+} [53, 58]. The results suggested that the EF hand and S2-S3 cytoplasmic loop of RyRs are involved in the conformational stability and Ca^{2+}-dependent regulation (activation/inhibition) of RyR channels.

13.3 Inhibition by Cytoplasmic Ca^{2+}

While RyRs are activated by micromolar cytosolic Ca^{2+}, higher concentrations of Ca^{2+} (>1 mM) inhibit RyR channel activities. Thus, RyRs have a high affinity Ca^{2+} activation site and a low affinity Ca^{2+} inactivation site (A and I sites, respectively in Fig. 13.1). These sites are also implicated in Mg^{2+} inhibition, namely submillimolar Mg^{2+} competes with activating Ca^{2+} at A site and millimolar Mg^{2+} binds to the I site for inhibitory effect [57, 59]. Although the physiological significance of RyR inactivation by millimolar levels of Ca^{2+} has been questioned, local rise of cytosolic Ca^{2+} around the RyRs may be sufficient to inhibit RyR channel activity. Single channel recording showed that Ca^{2+} flux from the lumen to the cytosolic side resulted in a decrease of open probability of both the RyR1 and RyR2 channel, supporting Ca^{2+}-dependent inactivation of RyRs by the released Ca^{2+} in intact tissues [60, 61]. All three mammalian isoforms of RyR are inhibited by high concentrations of Ca^{2+}; however, affinity for inhibitory Ca^{2+} in RyR1 is 5–10 times higher than those in RyR2 and RyR3 [6, 53, 62]. Deletion of 52 amino acids including a large cluster (42 amino acids) of negatively charged amino acids in RyR1 resulted in a threefold decrease in Ca^{2+} inactivation affinity [63]; yet, this change in the local electrostatics property may have caused a large

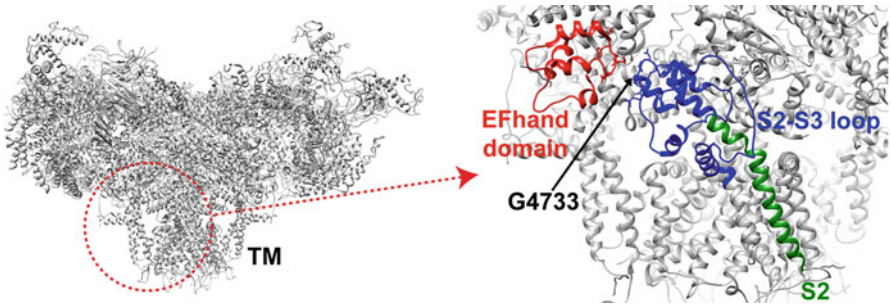

Fig. 13.2 High resolution cryo-electron microscopy structure of RyR1. The closed state of RyR1 (Protein Data Bank Accession 5TB0 [30]) is presented by UCSF Chimera program (https://www.cgl.ucsf.edu/chimera/) [121]. (*Left panel*) Structure of tetrameric RyR1. TM denotes transmembrane region. (*Right panel*) Enlargement of region marked with red circle in *left panel*. The EF hand domain (*red*) is shown to be adjacent to the S2-S3 loop (*blue*) in the neighboring subunit [25]. In this structure, Gly4733 and neighboring amino acids are located in close proximity to the EF hand domain, and point mutations on these amino acid residues altered Ca^{2+}-dependent inactivation of RyR1 [58]. Thus, the S2-S3 loop of RyR may transduce its Ca^{2+}-dependent inhibitory signal through the EF hand domain. Note that the S2 transmembrane (*green*) has also been shown to be involved in Ca^{2+}-dependent inactivation of RyRs [53]

conformational change. Construction and characterization of RyR1/RyR2 chimeras highlighted differences of Ca^{2+}-inactivation affinity between the two RyR isoforms. Chimeric RyRs showed that RyR isoform specific Ca^{2+} inactivation depends on the sequence of the carboxyl-terminal quarter (~1000 amino acids) [62, 64, 65]. Further characterization suggested that the second transmembrane segment (S2) and EF hand type Ca^{2+} binding motifs are involved in the isoform-specific Ca^{2+}-dependent inactivation of RyRs [53]. In agreement with these observations, scrambling one EF hand sequence (EF1) in RyR1 resulted in a twofold reduction in the affinity of Ca^{2+}-dependent inhibition [51]. In near-atomic level cryo-electron microscopy, the EF hand domain and S2-S3 cytoplasmic loop are in close proximity [25]. In another structural model, 10 mM Ca^{2+} changed the conformation of the EF hand domain [24]. Site-directed mutagenesis of the S2-S3 loop of RyR1 impaired the affinity for Ca^{2+}-dependent inactivation, and resulted in RyR2-type Ca^{2+}-dependent activity profiles [58]. Considering the Ca^{2+} affinity of the recombinant EF hand domain (60 μM-4 mM) [49, 50], the Ca^{2+} inactivation site of the RyR is the EF hand motif. One possible mechanism is that the S2-S3 loop transduces the signal of Ca^{2+} binding to the EF hand domain to the channel pore region including S2 [58]. It should be noted that a point mutation in G4733 of RyR1, which is in close proximity to the EF hand domain (Fig. 13.2), significantly suppressed Ca^{2+}-dependent inactivation [58].

13.4 Regulation by Luminal Ca^{2+}

RyRs could also be regulated by SR luminal Ca^{2+}, as during Ca^{2+} release the junctional SR Ca^{2+} concentration drastically drops. This suggests that RyR channel gating can be regulated directly by luminal Ca^{2+}; e.g. SR Ca^{2+} filling status regulates RyR channel opening and closing. It is known that the SR Ca^{2+} store with a certain level of Ca^{2+} exhibits spontaneous Ca^{2+} release in mammalian cardiac muscle cells [66, 67]. Chen and colleagues found that the store overload-induced Ca^{2+} release (SOICR) was observed in heterologous cells expressing recombinant RyR channels; therefore, it is likely an intrinsic property of RyRs. [68]. SOICR mechanisms were implicated in the aberrant Ca^{2+} signaling found in RyR mutation-related skeletal and cardiac muscle diseases [68–70]. The muscular disease-associated RyR mutations reduce the threshold for SOICR; therefore, spontaneous Ca^{2+} release (Ca^{2+} spills) occurs when the SR Ca^{2+} store loading is increased by the triggers of pathologies such as catecholamine release. The luminal Ca^{2+}-sensing gate of RyRs was investigated by site-directed mutagenesis, revealing that E4872 on the inner pore helix (S6 transmembrane segment) of RyR2 is essential for luminal Ca^{2+} activation of RyR2 and SOICR [71]. Knock-in mice harboring the E4872Q-RyR2 mutation were resistant to Ca^{2+}-dependent ventricular tachycardia, suggesting that SOICR is a critical mechanism for arrhythmogenesis [71].

It also should be noted that luminal Ca^{2+} can also access cytosolic Ca^{2+} activation and inactivation sites [60, 61] (Fig. 13.1). In single channel measurements of RyR1 and RyR2, luminal Ca^{2+} passed through RyRs to the cytosolic side in conjunction with potassium ions under a voltage gradient, and activated and inhibited the same RyR channels depending on luminal Ca^{2+} concentration [60, 61], which suggests that during excitation-contraction coupling, local cytoplasmic Ca^{2+} concentrations can reach millimolar levels and are sufficient for Ca^{2+}-dependent inactivation of RyRs.

13.5 Regulation by Calmodulin and S100A1

Calmodulin (CaM) is a 16.7-kDa protein that possesses 2 EF hand-type Ca^{2+} binding sites on both the amino and carboxyl-terminal. Thus, CaM works as a Ca^{2+} sensing subunit of multiple ion channels [72]. CaM modifies RyR channel function independently from regulation by Ca^{2+}; therefore, RyRs have "dual" cytosolic Ca^{2+} dependent regulatory mechanisms (direct and indirect). RyRs are regulated by not only the Ca^{2+} bound form of CaM, but also by CaM at cellular resting Ca^{2+} concentrations ($\sim$0.1 μM). Ca^{2+} bound CaM inhibits all three mammalian isoforms of RyR, while CaM activates RyR1 and RyR3 and inhibits RyR2 at submicromolar Ca^{2+} concentrations [73–77], suggesting that CaM constitutively binds to RyRs to regulate their channel activities by sensing cytoplasmic Ca^{2+} concentrations. In vitro experiments also showed that CaM regulation of the RyR depends on redox

state. Affinities for CaM regulation of RyR channel activity at the oxidized condition are 2–20 fold lower than at the reduced condition [77, 78]. The results are consistent with observations that CaM is dissociated from RyR2, resulting in a Ca^{2+} leak from SR in failing hearts [79], in which the redox balance possibly shifts to the more oxidized condition [80, 81].

Purified RyR1 and RyR2 as well as the recombinant RyR3 bind 4 CaM per tetrameric RyR, i.e. one RyR subunit binds one CaM [56, 77, 78, 82]. The CaM binding and regulatory domain was identified by trypsin digestion, binding of synthetic RyR1 peptides, and site directed mutagenesis of RyR1 amino acids 3614–3643 [82–84]. This domain was confirmed to be conserved in RyR2 and RyR3 by site-directed mutagenesis [56, 78]. Crystal structure analysis of a synthetic RyR1 peptide (amino acids 3614–3643) and CaM complex revealed that the carboxyl-terminal lobe of CaM binds to the peptide, while the amino-terminal lobe binds with low affinity or is free [85], which may explain that multiple RyR domain peptides or fusion proteins can bind to CaM [44, 86–88]. Point mutations in RyR1 3614–3643 or the corresponding RyR2 and RyR3 domains eliminated CaM binding and regulation of channel activities [56, 78, 82, 89]; thus, this conserved domain likely plays a primary role for CaM-dependent regulation. Although the primary CaM regulatory domain is well conserved, RyR isoform-specific CaM regulation at submicromolar (cellular resting level) Ca^{2+} concentrations, namely activation of RyR1 and RyR3 versus inhibition of RyR2, was investigated using RyR1/RyR2 chimera channels. Replacing the flanking regions of the RyR2 CaM binding domain with the RyR1 sequence abolished CaM regulation of RyR2 at submicromolar Ca^{2+} concentrations [90]. More recently, the EF hand domain and large N-terminal region were shown to be important for isoform-specific CaM regulation of RyRs [54]. These domains possibly mediate long-range interaction between the CaM binding domain and the functional effects on the channel, as the CaM binding domain is ~10 nm apart from the RyR channel pore region in cryo-electron micrographs [91].

In vivo significance of CaM regulation of RyR1 and RyR2 was studied with genetically modified mice. Knock-in mice carrying point mutations in the RyR2 CaM regulatory domain (W3587A/L3591D/F3603A: ADA mutations) were impaired in CaM binding and regulation of cardiac RyR2 [89]. The mice showed rapidly developing cardiac hypertrophy and died 2–3 weeks after birth. Cardiomyocytes isolated from the mutant mouse hearts exhibited long durations of the spontaneous Ca^{2+} transients or Ca^{2+} sparks, indicating that CaM inhibition of RyR2 contributes to the termination of SR Ca^{2+} release, which is important for heart physiology and growth [89, 92]. The knock-in ADA mice were impaired in CaM regulation of RyR2 at both diastolic (submicromolar) and systolic (micromolar) Ca^{2+} concentrations, while knock-in mice with a single mutation (L3591D), were only impaired in CaM regulation of RyR2 during diastole and showed more modest levels of cardiac hypertrophy, suggesting that CaM regulation of RyR2 at systolic Ca^{2+} levels plays a major role in vivo [93]. The corresponding RyR1 mutation (RyR1-L3624D) attenuated both CaM activation and inhibition at submicromolar and micromolar Ca^{2+} concentrations [82]. However, knock-in mice carrying RyR1-L3624D showed only modest effects on skeletal muscle excitation-contraction

coupling without lethality, suggesting that CaM regulation of RyR1 plays a minor role in skeletal physiology [94]. More recently, missense mutations in calmodulin genes were identified in patients with catecholaminergic polymorphic ventricular tachycardia (CPVT) [95], in which CaM mutations likely alter RyR2 regulation [96–98]. Thus, the CaM-RyR2 interaction can be a good therapeutic target for the cardiac pathologies [99].

S100A1, another EF hand type Ca^{2+} binding protein, is also expressed in skeletal and cardiac muscle and regulates intracellular Ca^{2+} signaling by interacting with multiple Ca^{2+} handling proteins including RyRs [100–103]. Competitive binding experiments showed that S100A1 shares a common binding site on RyR1 with CaM [104, 105]. Consistently, the L3624D-RyR1 mutation impaired both CaM and S100A1 activation of RyR1 at submicromolar Ca^{2+} concentrations in single channel recordings [94]. On the other hand, the corresponding L3591D-RyR2 mutation abolished CaM regulation only at submicromolar Ca^{2+} level, while S100A1 regulation of the mutant RyR2 was impaired at both submicromolar and micromollar Ca^{2+} concentrations [93]. The mutations and functional experiments suggested that S100A1 and CaM do not share exactly the same binding site in RyR2. Recent FRET experiments also showed that S100A1 interacts allosterically with the CaM binding site in RyR1 and RyR2 rather than through direct binding [106].

13.6 Regulation by Calsequestrin

On the SR luminal side, the low affinity but high capacity Ca^{2+} binding protein, calsequestrin (CSQ), localizes to the junctional SR [107, 108]. RyR-associated proteins, triadin and junctin appear to anchor CSQ to the junctional SR through charge interactions [109–111] (Fig. 13.1). In addition, it was recently shown that cardiac CSQ could also directly bind to the luminal side of RyR2 [112]. Two isoforms, CSQ1 and CSQ2, are dominantly expressed in skeletal and cardiac muscle, respectively. Direct regulation of RyR channel activities by CSQ have been investigated by planar bilayer single channel recordings, where luminal conditions can be controlled. CSQ regulates the RyR channel in a luminal Ca^{2+} concentration dependent manner. With high luminal Ca^{2+} concentrations, CSQ was dissociated from the RyR accessory proteins, triadin and junctin, while CSQ inhibited the RyR channel through the accessory proteins at the intermediate Ca^{2+} concentration [113–115].

Gene knockout of the CSQ in mice demonstrated both its physiological and pathological significance. CSQ1 (*Casq1*) knockout mice were viable and fertile; however, modest structural and functional changes were observed in the fast twitch skeletal muscle. Ablation of CSQ1 resulted in slightly slower force development and relaxation of the fast twitch muscle. Structural analysis showed that CSQ1 knockout muscle exhibited low SR volume and high mitochondria density, suggesting that CSQ1 is important for muscle development [116]. CSQ2 has been implicated in cardiac pathology. Missense mutations in human *CASQ2* gene, resulting in gene

knockout or single amino acid substitutions, were found in patients afflicted with catecholaminergic polymorphic ventricular tachycardia [117, 118]. Both mouse models exhibited arrhythmogenesis under the stress conditions of exercise or catecholamine infusion [119, 120]. Consistently, intracellular Ca^{2+} handling was altered by catecholamine in mutant cardiomyocytes isolated from mouse hearts. These results indicate that CSQ2 regulation of SR Ca^{2+} and RyR2 channels is pathologically important.

13.7 Closing Remarks

Almost 50 years have passed since Ca^{2+}-induced Ca^{2+} release, that we now know is associated with Ca^{2+}-dependent activation of RyR, was first reported [33, 34]. In the last 20 years molecular biology and genetic techniques greatly advanced our understanding of the structure/function relationship of RyR channel regulation by small molecules and proteins. More recently, high resolution three dimensional structural analyses have revealed the detailed protein conformations of the RyR channel complexes under different conditions corresponding to the open/closed channels [24–27, 30]. Combining these approaches and using computational modeling will provide more detailed molecular insights into RyR regulation by Ca^{2+} and Ca^{2+} binding proteins at near atomic levels.

Acknowledgements I would like to appreciate Dr. Gerhard Meissner for his mentorship on RyR structure/function analysis when I was working in his laboratory and for his continuous advices and encouragements on my current studies. I am very thankful to Dr. Martin Morad, the director of Cardiac Signaling Center, for providing me with wonderful environment to study Ca^{2+} signaling, and valuable suggestions and discussions on my studies. I am also grateful to Angela C. Gomez and Jordan S. Carter for their contributions to the RyR mutagenesis studies in my laboratory and for the comments on this manuscript. This study was supported by National Institutes of Health Grants R03AR061030, P20GM103499, and UL1TR001450.

References

1. Clapham DE (2007) Calcium signaling. Cell 131(6):1047–1058
2. Bootman MD (2012) Calcium signaling. Cold Spring Harb Perspect Biol 4(7):a011171
3. Berridge MJ (2016) The inositol trisphosphate/calcium signaling pathway in health and disease. Physiol Rev 96(4):1261–1296
4. Franzini-Armstrong C, Protasi F (1997) Ryanodine receptors of striated muscles: a complex channel capable of multiple interactions. Physiol Rev 77(3):699–729
5. Lanner JT, Georgiou DK, Joshi AD, Hamilton SL (2010) Ryanodine receptors: structure, expression, molecular details, and function in calcium release. Cold Spring Harb Perspect Biol 2(11):a003996
6. Meissner G (2017) The structural basis of ryanodine receptor ion channel function. J Gen Physiol 149(12):1065–1089
7. Inui M, Saito A, Fleischer S (1987) Purification of the ryanodine receptor and identity with feet structures of junctional terminal cisternae of sarcoplasmic reticulum from fast skeletal muscle. J Biol Chem 262(4):1740–1747

8. Imagawa T, Smith JS, Coronado R, Campbell KP (1987) Purified ryanodine receptor from skeletal muscle sarcoplasmic reticulum is the Ca^{2+}−permeable pore of the calcium release channel. J Biol Chem 262(34):16636–16643
9. Lai FA, Erickson HP, Rousseau E, Liu QY, Meissner G (1988) Purification and reconstitution of the calcium release channel from skeletal muscle. Nature 331(6154):315–319
10. Anderson K, Lai FA, Liu QY, Rousseau E, Erickson HP, Meissner G (1989) Structural and functional characterization of the purified cardiac ryanodine receptor-Ca^{2+} release channel complex. J Biol Chem 264(2):1329–1335
11. Takeshima H, Nishimura S, Matsumoto T, Ishida H, Kangawa K, Minamino N et al (1989) Primary structure and expression from complementary DNA of skeletal muscle ryanodine receptor. Nature 339(6224):439–445
12. Zorzato F, Fujii J, Otsu K, Phillips M, Green NM, Lai FA et al (1990) Molecular cloning of cDNA encoding human and rabbit forms of the Ca^{2+} release channel (ryanodine receptor) of skeletal muscle sarcoplasmic reticulum. J Biol Chem 265(4):2244–2256
13. Otsu K, Willard HF, Khanna VK, Zorzato F, Green NM, MacLennan DH (1990) Molecular cloning of cDNA encoding the Ca^{2+} release channel (ryanodine receptor) of rabbit cardiac muscle sarcoplasmic reticulum. J Biol Chem 265(23):13472–13483
14. Nakai J, Imagawa T, Hakamata Y, Shigekawa M, Takeshima H, Numa S (1990) Primary structure and functional expression from cDNA of the cardiac ryanodine receptor/calcium release channel. FEBS Lett 271(1–2):169–177
15. Hakamata Y, Nakai J, Takeshima H, Imoto K (1992) Primary structure and distribution of a novel ryanodine receptor/calcium release channel from rabbit brain. FEBS Lett 312(2–3):229–235
16. Takeshima H (1993) Primary structure and expression from cDNAs of the ryanodine receptor. Ann N Y Acad Sci 707:165–177
17. Furuichi T, Furutama D, Hakamata Y, Nakai J, Takeshima H, Mikoshiba K (1994) Multiple types of ryanodine receptor/Ca^{2+} release channels are differentially expressed in rabbit brain. J Neurosci 14(8):4794–4805
18. Conti A, Gorza L, Sorrentino V (1996) Differential distribution of ryanodine receptor type 3 (RyR3) gene product in mammalian skeletal muscles. Biochem J 316(Pt 1):19–23
19. Murayama T, Ogawa Y (1997) Characterization of type 3 ryanodine receptor (RyR3) of sarcoplasmic reticulum from rabbit skeletal muscles. J Biol Chem 272(38):24030–24037
20. Oyamada H, Murayama T, Takagi T, Iino M, Iwabe N, Miyata T et al (1994) Primary structure and distribution of ryanodine-binding protein isoforms of the bullfrog skeletal muscle. J Biol Chem 269(25):17206–17214
21. Percival AL, Williams AJ, Kenyon JL, Grinsell MM, Airey JA, Sutko JL (1994) Chicken skeletal muscle ryanodine receptor isoforms: ion channel properties. Biophys J 67(5):1834–1850
22. Ottini L, Marziali G, Conti A, Charlesworth A, Sorrentino V (1996) Alpha and beta isoforms of ryanodine receptor from chicken skeletal muscle are the homologues of mammalian RyR1 and RyR3. Biochem J 315(Pt 1):207–216
23. Du GG, Sandhu B, Khanna VK, Guo XH, MacLennan DH (2002) Topology of the Ca^{2+} release channel of skeletal muscle sarcoplasmic reticulum (RyR1). Proc Natl Acad Sci U S A 99(26):16725–16730
24. Efremov RG, Leitner A, Aebersold R, Raunser S (2015) Architecture and conformational switch mechanism of the ryanodine receptor. Nature 517(7532):39–43
25. Zalk R, Clarke OB, des Georges A, Grassucci RA, Reiken S, Mancia F et al (2015) Structure of a mammalian ryanodine receptor. Nature 517(7532):44–49
26. Yan Z, Bai X, Yan C, Wu J, Li Z, Xie T et al (2015) Structure of the rabbit ryanodine receptor RyR1 at near-atomic resolution. Nature 517(7532):50–55
27. Peng W, Shen H, Wu J, Guo W, Pan X, Wang R et al (2016) Structural basis for the gating mechanism of the type 2 ryanodine receptor RyR2. Science 354(6310):aah5324
28. Zhong X, Liu Y, Zhu L, Meng X, Wang R, Van Petegem F et al (2013) Conformational dynamics inside amino-terminal disease hotspot of ryanodine receptor. Structure 21(11):2051–2060

29. Yuchi Z, Yuen SM, Lau K, Underhill AQ, Cornea RL, Fessenden JD et al (2015) Crystal structures of ryanodine receptor SPRY1 and tandem-repeat domains reveal a critical FKBP12 binding determinant. Nat Commun 6:7947
30. des Georges A, Clarke OB, Zalk R, Yuan Q, Condon KJ, Grassucci RA et al (2016) Structural basis for gating and activation of RyR1. Cell 167(1):145–157. e17
31. Schneider MF, Chandler WK (1973) Voltage dependent charge movement of skeletal muscle: a possible step in excitation-contraction coupling. Nature 242(5395):244–246
32. Nabauer M, Callewaert G, Cleemann L, Morad M (1989) Regulation of calcium release is gated by calcium current, not gating charge, in cardiac myocytes. Science 244(4906):800–803
33. Ford LE, Podolsky RJ (1970) Regenerative calcium release within muscle cells. Science 167(3914):58–59
34. Endo M, Tanaka M, Ogawa Y (1970) Calcium induced release of calcium from the sarcoplasmic reticulum of skinned skeletal muscle fibres. Nature 228(5266):34–36
35. Brum G, Rios E, Stefani E (1988) Effects of extracellular calcium on calcium movements of excitation-contraction coupling in frog skeletal muscle fibres. J Physiol 398:441–473
36. Nakai J, Dirksen RT, Nguyen HT, Pessah IN, Beam KG, Allen PD (1996) Enhanced dihydropyridine receptor channel activity in the presence of ryanodine receptor. Nature 380(6569):72–75
37. Endo M (2009) Calcium-induced calcium release in skeletal muscle. Physiol Rev 89(4):1153–1176
38. Rios E (2018) Calcium-induced release of calcium in muscle: 50 years of work and the emerging consensus. J Gen Physiol 150(4):521–537
39. Murayama T, Kurebayashi N, Ogawa H, Yamazawa T, Oyamada H, Suzuki J et al (2016) Genotype-phenotype correlations of malignant hyperthermia and central Core disease mutations in the central region of the RYR1 channel. Hum Mutat 37(11):1231–1241
40. Meissner G (1994) Ryanodine receptor/Ca^{2+} release channels and their regulation by endogenous effectors. Annu Rev Physiol 56:485–508
41. Coronado R, Morrissette J, Sukhareva M, Vaughan DM (1994) Structure and function of ryanodine receptors. Am J Physiol 266(6 Pt 1):C1485–C1504
42. Chen SR, Zhang L, MacLennan DH (1992) Characterization of a Ca^{2+} binding and regulatory site in the Ca^{2+} release channel (ryanodine receptor) of rabbit skeletal muscle sarcoplasmic reticulum. J Biol Chem 267(32):23318–23326
43. Chen SR, Zhang L, MacLennan DH (1993) Antibodies as probes for Ca^{2+} activation sites in the Ca^{2+} release channel (ryanodine receptor) of rabbit skeletal muscle sarcoplasmic reticulum. J Biol Chem 268(18):13414–13421
44. Chen SR, MacLennan DH (1994) Identification of calmodulin-, Ca^{2+}-, and ruthenium red-binding domains in the Ca^{2+} release channel (ryanodine receptor) of rabbit skeletal muscle sarcoplasmic reticulum. J Biol Chem 269(36):22698–22704
45. Chen SR, Ebisawa K, Li X, Zhang L (1998) Molecular identification of the ryanodine receptor Ca^{2+} sensor. J Biol Chem 273(24):14675–14678
46. Li P, Chen SR (2001) Molecular basis of Ca^{2+} activation of the mouse cardiac Ca^{2+} release channel (ryanodine receptor). J Gen Physiol 118(1):33–44
47. Fessenden JD, Chen L, Wang Y, Paolini C, Franzini-Armstrong C, Allen PD et al (2001) Ryanodine receptor point mutant E4032A reveals an allosteric interaction with ryanodine. Proc Natl Acad Sci U S A 98(5):2865–2870
48. Murayama T, Ogawa H, Kurebayashi N, Ohno S, Horie M, Sakurai T (2018) A tryptophan residue in the caffeine-binding site of the ryanodine receptor regulates Ca^{2+} sensitivity. Commun Biol 1:98
49. Xiong H, Feng X, Gao L, Xu L, Pasek DA, Seok JH et al (1998) Identification of a two EF-hand Ca^{2+} binding domain in lobster skeletal muscle ryanodine receptor/Ca^{2+} release channel. Biochemistry 37(14):4804–4814
50. Xiong L, Zhang JZ, He R, Hamilton SL (2006) A Ca^{2+}-binding domain in RyR1 that interacts with the calmodulin binding site and modulates channel activity. Biophys J 90(1):173–182

51. Fessenden JD, Feng W, Pessah IN, Allen PD (2004) Mutational analysis of putative calcium binding motifs within the skeletal ryanodine receptor isoform, RyR1. J Biol Chem 279(51):53028–53035
52. Guo W, Sun B, Xiao Z, Liu Y, Wang Y, Zhang L et al (2016) The EF-hand Ca^{2+} binding domain is not required for cytosolic Ca^{2+} activation of the cardiac ryanodine receptor. J Biol Chem 291(5):2150–2160
53. Gomez AC, Yamaguchi N (2014) Two regions of the ryanodine receptor calcium channel are involved in Ca^{2+}-dependent inactivation. Biochemistry 53(8):1373–1379
54. Xu L, Gomez AC, Pasek DA, Meissner G, Yamaguchi N (2017) Two EF-hand motifs in ryanodine receptor calcium release channels contribute to isoform-specific regulation by calmodulin. Cell Calcium 66:62–70
55. Chugun A, Sato O, Takeshima H, Ogawa Y (2007) Mg^{2+} activates the ryanodine receptor type 2 (RyR2) at intermediate Ca^{2+} concentrations. Am J Physiol Cell Physiol 292(1):C535–C544
56. Yamaguchi N, Xu L, Pasek DA, Evans KE, Meissner G (2003) Molecular basis of calmodulin binding to cardiac muscle Ca^{2+} release channel (ryanodine receptor). J Biol Chem 278(26):23480–23486
57. Laver DR, Baynes TM, Dulhunty AF (1997) Magnesium inhibition of ryanodine-receptor calcium channels: evidence for two independent mechanisms. J Membr Biol 156(3):213–229
58. Gomez AC, Holford TW, Yamaguchi N (2016) Malignant hyperthermia-associated mutations in the S2-S3 cytoplasmic loop of type 1 ryanodine receptor calcium channel impair calcium-dependent inactivation. Am J Physiol Cell Physiol 311(5):C749–C757
59. Murayama T, Kurebayashi N, Ogawa Y (2000) Role of Mg^{2+} in Ca^{2+}-induced Ca^{2+} release through ryanodine receptors of frog skeletal muscle: modulations by adenine nucleotides and caffeine. Biophys J 78(4):1810–1824
60. Tripathy A, Meissner G (1996) Sarcoplasmic reticulum lumenal Ca^{2+} has access to cytosolic activation and inactivation sites of skeletal muscle Ca^{2+} release channel. Biophys J 70(6):2600–2615
61. Xu L, Meissner G (1998) Regulation of cardiac muscle Ca^{2+} release channel by sarcoplasmic reticulum lumenal Ca^{2+}. Biophys J 75(5):2302–2312
62. Du GG, MacLennan DH (1999) Ca^{2+} inactivation sites are located in the COOH-terminal quarter of recombinant rabbit skeletal muscle Ca^{2+} release channels (ryanodine receptors). J Biol Chem 274(37):26120–26126
63. Hayek SM, Zhu X, Bhat MB, Zhao J, Takeshima H, Valdivia HH et al (2000) Characterization of a calcium-regulation domain of the skeletal-muscle ryanodine receptor. Biochem J 351(Pt 1):57–65
64. Nakai J, Gao L, Xu L, Xin C, Pasek DA, Meissner G (1999) Evidence for a role of C-terminus in Ca^{2+} inactivation of skeletal muscle Ca^{2+} release channel (ryanodine receptor). FEBS Lett 459(2):154–158
65. Du GG, Khanna VK, MacLennan DH (2000) Mutation of divergent region 1 alters caffeine and Ca^{2+} sensitivity of the skeletal muscle Ca^{2+} release channel (ryanodine receptor). J Biol Chem 275(16):11778–11783
66. Fabiato A, Fabiato F (1979) Calcium and cardiac excitation-contraction coupling. Annu Rev Physiol 41:473–484
67. Orchard CH, Eisner DA, Allen DG (1983) Oscillations of intracellular Ca^{2+} in mammalian cardiac muscle. Nature 304(5928):735–738
68. Jiang D, Xiao B, Yang D, Wang R, Choi P, Zhang L et al (2004) RyR2 mutations linked to ventricular tachycardia and sudden death reduce the threshold for store-overload-induced Ca^{2+} release (SOICR). Proc Natl Acad Sci U S A 101(35):13062–13067
69. Jiang D, Wang R, Xiao B, Kong H, Hunt DJ, Choi P et al (2005) Enhanced store overload-induced Ca^{2+} release and channel sensitivity to luminal Ca^{2+} activation are common defects of RyR2 mutations linked to ventricular tachycardia and sudden death. Circ Res 97(11):1173–1181

70. Jiang D, Chen W, Xiao J, Wang R, Kong H, Jones PP et al (2008) Reduced threshold for luminal Ca^{2+} activation of RyR1 underlies a causal mechanism of porcine malignant hyperthermia. J Biol Chem 283(30):20813–20820
71. Chen W, Wang R, Chen B, Zhong X, Kong H, Bai Y et al (2014) The ryanodine receptor store-sensing gate controls Ca^{2+} waves and Ca^{2+}-triggered arrhythmias. Nat Med 20(2):184–192
72. Saimi Y, Kung C (2002) Calmodulin as an ion channel subunit. Annu Rev Physiol 64:289–311
73. Tripathy A, Xu L, Mann G, Meissner G (1995) Calmodulin activation and inhibition of skeletal muscle Ca^{2+} release channel (ryanodine receptor). Biophys J 69(1):106–119
74. Buratti R, Prestipino G, Menegazzi P, Treves S, Zorzato F (1995) Calcium dependent activation of skeletal muscle Ca^{2+} release channel (ryanodine receptor) by calmodulin. Biochem Biophys Res Commun 213(3):1082–1090
75. Chen SR, Li X, Ebisawa K, Zhang L (1997) Functional characterization of the recombinant type 3 Ca^{2+} release channel (ryanodine receptor) expressed in HEK293 cells. J Biol Chem 272(39):24234–24246
76. Fruen BR, Bardy JM, Byrem TM, Strasburg GM, Louis CF (2000) Differential Ca^{2+} sensitivity of skeletal and cardiac muscle ryanodine receptors in the presence of calmodulin. Am J Physiol Cell Physiol 279(3):C724–C733
77. Balshaw DM, Xu L, Yamaguchi N, Pasek DA, Meissner G (2001) Calmodulin binding and inhibition of cardiac muscle calcium release channel (ryanodine receptor). J Biol Chem 276(23):20144–20153
78. Yamaguchi N, Xu L, Pasek DA, Evans KE, Chen SR, Meissner G (2005) Calmodulin regulation and identification of calmodulin binding region of type-3 ryanodine receptor calcium release channel. Biochemistry 44(45):15074–15081
79. Ono M, Yano M, Hino A, Suetomi T, Xu X, Susa T et al (2010) Dissociation of calmodulin from cardiac ryanodine receptor causes aberrant Ca^{2+} release in heart failure. Cardiovasc Res 87(4):609–617
80. Terentyev D, Gyorke I, Belevych AE, Terentyeva R, Sridhar A, Nishijima Y et al (2008) Redox modification of ryanodine receptors contributes to sarcoplasmic reticulum Ca^{2+} leak in chronic heart failure. Circ Res 103(12):1466–1472
81. Oda T, Yang Y, Uchinoumi H, Thomas DD, Chen-Izu Y, Kato T et al (2015) Oxidation of ryanodine receptor (RyR) and calmodulin enhance Ca release and pathologically alter, RyR structure and calmodulin affinity. J Mol Cell Cardiol 85:240–248
82. Yamaguchi N, Xin C, Meissner G (2001) Identification of apocalmodulin and Ca^{2+}-calmodulin regulatory domain in skeletal muscle Ca^{2+} release channel, ryanodine receptor. J Biol Chem 276(25):22579–22585
83. Moore CP, Rodney G, Zhang JZ, Santacruz-Toloza L, Strasburg G, Hamilton SL (1999) Apocalmodulin and Ca^{2+} calmodulin bind to the same region on the skeletal muscle Ca^{2+} release channel. Biochemistry 38(26):8532–8537
84. Rodney GG, Moore CP, Williams BY, Zhang JZ, Krol J, Pedersen SE et al (2001) Calcium binding to calmodulin leads to an N-terminal shift in its binding site on the ryanodine receptor. J Biol Chem 276(3):2069–2074
85. Maximciuc AA, Putkey JA, Shamoo Y, Mackenzie KR (2006) Complex of calmodulin with a ryanodine receptor target reveals a novel, flexible binding mode. Structure 14(10):1547–1556
86. Menegazzi P, Larini F, Treves S, Guerrini R, Quadroni M, Zorzato F (1994) Identification and characterization of three calmodulin binding sites of the skeletal muscle ryanodine receptor. Biochemistry 33(31):9078–9084
87. Guerrini R, Menegazzi P, Anacardio R, Marastoni M, Tomatis R, Zorzato F et al (1995) Calmodulin binding sites of the skeletal, cardiac, and brain ryanodine receptor Ca^{2+} channels: modulation by the catalytic subunit of cAMP-dependent protein kinase? Biochemistry 34(15):5120–5129
88. Lau K, Chan MM, Van Petegem F (2014) Lobe-specific calmodulin binding to different ryanodine receptor isoforms. Biochemistry 53(5):932–946

89. Yamaguchi N, Takahashi N, Xu L, Smithies O, Meissner G (2007) Early cardiac hypertrophy in mice with impaired calmodulin regulation of cardiac muscle Ca^{2+} release channel. J Clin Invest 117(5):1344–1353
90. Yamaguchi N, Xu L, Evans KE, Pasek DA, Meissner G (2004) Different regions in skeletal and cardiac muscle ryanodine receptors are involved in transducing the functional effects of calmodulin. J Biol Chem 279(35):36433–36439
91. Samso M, Wagenknecht T (2002) Apocalmodulin and Ca^{2+}-calmodulin bind to neighboring locations on the ryanodine receptor. J Biol Chem 277(2):1349–1353
92. Arnaiz-Cot JJ, Damon BJ, Zhang XH, Cleemann L, Yamaguchi N, Meissner G et al (2013) Cardiac calcium signalling pathologies associated with defective calmodulin regulation of type 2 ryanodine receptor. J Physiol 591(17):4287–4299
93. Yamaguchi N, Chakraborty A, Huang TQ, Xu L, Gomez AC, Pasek DA et al (2013) Cardiac hypertrophy associated with impaired regulation of cardiac ryanodine receptor by calmodulin and S100A1. Am J Physiol Heart Circ Physiol 305(1):H86–H94
94. Yamaguchi N, Prosser BL, Ghassemi F, Xu L, Pasek DA, Eu JP et al (2011) Modulation of sarcoplasmic reticulum Ca^{2+} release in skeletal muscle expressing ryanodine receptor impaired in regulation by calmodulin and S100A1. Am J Physiol Cell Physiol 300(5):C998–C1012
95. Nyegaard M, Overgaard MT, Sondergaard MT, Vranas M, Behr ER, Hildebrandt LL et al (2012) Mutations in calmodulin cause ventricular tachycardia and sudden cardiac death. Am J Hum Genet 91(4):703–712
96. Hwang HS, Nitu FR, Yang Y, Walweel K, Pereira L, Johnson CN et al (2014) Divergent regulation of ryanodine receptor 2 calcium release channels by arrhythmogenic human calmodulin missense mutants. Circ Res 114(7):1114–1124
97. Sondergaard MT, Tian X, Liu Y, Wang R, Chazin WJ, Chen SR et al (2015) Arrhythmogenic calmodulin mutations affect the activation and termination of cardiac ryanodine receptor-mediated Ca^{2+} release. J Biol Chem 290(43):26151–26162
98. Vassilakopoulou V, Calver BL, Thanassoulas A, Beck K, Hu H, Buntwal L et al (2015) Distinctive malfunctions of calmodulin mutations associated with heart RyR2-mediated arrhythmic disease. Biochim Biophys Acta 1850(11):2168–2176
99. Liu B, Walton SD, Ho HT, Belevych AE, Tikunova SB, Bonilla I et al (2018) Gene transfer of engineered calmodulin alleviates ventricular arrhythmias in a calsequestrin-associated mouse model of catecholaminergic polymorphic ventricular tachycardia. J Am Heart Assoc 7(10):e008155
100. Treves S, Scutari E, Robert M, Groh S, Ottolia M, Prestipino G et al (1997) Interaction of S100A1 with the Ca^{2+} release channel (ryanodine receptor) of skeletal muscle. Biochemistry 36(38):11496–11503
101. Most P, Remppis A, Pleger ST, Loffler E, Ehlermann P, Bernotat J et al (2003) Transgenic overexpression of the Ca^{2+}-binding protein S100A1 in the heart leads to increased in vivo myocardial contractile performance. J Biol Chem 278(36):33809–33817
102. Volkers M, Rohde D, Goodman C, Most P (2010) S100A1: a regulator of striated muscle sarcoplasmic reticulum Ca^{2+} handling, sarcomeric, and mitochondrial function. J Biomed Biotechnol 2010:178614
103. Prosser BL, Hernandez-Ochoa EO, Schneider MF (2011) S100A1 and calmodulin regulation of ryanodine receptor in striated muscle. Cell Calcium 50(4):323–331
104. Prosser BL, Wright NT, Hernandez-Ochoa EO, Varney KM, Liu Y, Olojo RO et al (2008) S100A1 binds to the calmodulin-binding site of ryanodine receptor and modulates skeletal muscle excitation-contraction coupling. J Biol Chem 283(8):5046–5057
105. Wright NT, Prosser BL, Varney KM, Zimmer DB, Schneider MF, Weber DJ (2008) S100A1 and calmodulin compete for the same binding site on ryanodine receptor. J Biol Chem 283(39):26676–26683
106. Rebbeck RT, Nitu FR, Rohde D, Most P, Bers DM, Thomas DD et al (2016) S100A1 protein does not compete with calmodulin for ryanodine receptor binding but structurally alters the ryanodine receptor.Calmodulin complex. J Biol Chem 291(30):15896–15907

107. Saito A, Seiler S, Chu A, Fleischer S (1984) Preparation and morphology of sarcoplasmic reticulum terminal cisternae from rabbit skeletal muscle. J Cell Biol 99(3):875–885
108. Franzini-Armstrong C, Kenney LJ, Varriano-Marston E (1987) The structure of calsequestrin in triads of vertebrate skeletal muscle: a deep-etch study. J Cell Biol 105(1):49–56
109. Guo W, Campbell KP (1995) Association of triadin with the ryanodine receptor and calsequestrin in the lumen of the sarcoplasmic reticulum. J Biol Chem 270(16):9027–9030
110. Zhang L, Kelley J, Schmeisser G, Kobayashi YM, Jones LR (1997) Complex formation between junctin, triadin, calsequestrin, and the ryanodine receptor. Proteins of the cardiac junctional sarcoplasmic reticulum membrane. J Biol Chem 272(37):23389–23397
111. Kobayashi YM, Alseikhan BA, Jones LR (2000) Localization and characterization of the calsequestrin-binding domain of triadin 1. Evidence for a charged beta-strand in mediating the protein-protein interaction. J Biol Chem 275(23):17639–17646
112. Handhle A, Ormonde CE, Thomas NL, Bralesford C, Williams AJ, Lai FA et al (2016) Calsequestrin interacts directly with the cardiac ryanodine receptor luminal domain. J Cell Sci 129(21):3983–3988
113. Beard NA, Sakowska MM, Dulhunty AF, Laver DR (2002) Calsequestrin is an inhibitor of skeletal muscle ryanodine receptor calcium release channels. Biophys J 82(1 Pt 1):310–320
114. Gyorke I, Hester N, Jones LR, Gyorke S (2004) The role of calsequestrin, triadin, and junctin in conferring cardiac ryanodine receptor responsiveness to luminal calcium. Biophys J 86(4):2121–2128
115. Beard NA, Casarotto MG, Wei L, Varsanyi M, Laver DR, Dulhunty AF (2005) Regulation of ryanodine receptors by calsequestrin: effect of high luminal Ca^{2+} and phosphorylation. Biophys J 88(5):3444–3454
116. Paolini C, Quarta M, Nori A, Boncompagni S, Canato M, Volpe P et al (2007) Reorganized stores and impaired calcium handling in skeletal muscle of mice lacking calsequestrin-1. J Physiol 583(Pt 2):767–784
117. Lahat H, Pras E, Olender T, Avidan N, Ben-Asher E, Man O et al (2001) A missense mutation in a highly conserved region of CASQ2 is associated with autosomal recessive catecholamine-induced polymorphic ventricular tachycardia in bedouin families from Israel. Am J Hum Genet 69(6):1378–1384
118. Postma AV, Denjoy I, Hoorntje TM, Lupoglazoff JM, Da Costa A, Sebillon P et al (2002) Absence of calsequestrin 2 causes severe forms of catecholaminergic polymorphic ventricular tachycardia. Circ Res 91(8):e21–e26
119. Knollmann BC, Chopra N, Hlaing T, Akin B, Yang T, Ettensohn K et al (2006) Casq2 deletion causes sarcoplasmic reticulum volume increase, premature Ca^{2+} release, and catecholaminergic polymorphic ventricular tachycardia. J Clin Invest 116(9):2510–2520
120. Song L, Alcalai R, Arad M, Wolf CM, Toka O, Conner DA et al (2007) Calsequestrin 2 (CASQ2) mutations increase expression of calreticulin and ryanodine receptors, causing catecholaminergic polymorphic ventricular tachycardia. J Clin Invest 117(7):1814–1823
121. Pettersen EF, Goddard TD, Huang CC, Couch GS, Greenblatt DM, Meng EC et al (2004) UCSF chimera–a visualization system for exploratory research and analysis. J Comput Chem 25(13):1605–1612

Chapter 14
Sarco-Endoplasmic Reticulum Calcium Release Model Based on Changes in the Luminal Calcium Content

Agustín Guerrero-Hernández, Víctor Hugo Sánchez-Vázquez, Ericka Martínez-Martínez, Lizeth Sandoval-Vázquez, Norma C. Perez-Rosas, Rodrigo Lopez-Farias, and Adan Dagnino-Acosta

Abstract The sarcoplasmic/endoplasmic reticulum (SR/ER) is the main intracellular calcium (Ca^{2+}) pool in muscle and non-muscle eukaryotic cells, respectively. The reticulum accumulates Ca^{2+} against its electrochemical gradient by the action of sarco/endoplasmic reticulum calcium ATPases (SERCA pumps), and the capacity of this Ca^{2+} store is increased by the presence of Ca^{2+} binding proteins in the lumen of the reticulum. A diversity of physical and chemical signals, activate the main Ca^{2+} release channels, i.e. ryanodine receptors (RyRs) and inositol (1, 4, 5) trisphosphate receptors (IP_3Rs), to produce transient elevations of the cytoplasmic calcium concentration ($[Ca^{2+}]_i$) while the reticulum is being depleted of Ca^{2+}. This picture is incomplete because it implies that the elements involved in the Ca^{2+} release process are acting alone and independently of each other. However, it appears that the Ca^{2+} released by RyRs and IP_3Rs is trapped in luminal Ca^{2+} binding proteins (Ca^{2+} lattice), which are associated with these release channels, and the activation of these channels appears to facilitate that the trapped Ca^{2+} ions become available for release. This situation makes the initial stage of the Ca^{2+} release process a highly efficient one; accordingly, there is a large increase in the $[Ca^{2+}]_i$ with minimal reductions in the bulk of the free luminal SR/ER $[Ca^{2+}]$ ($[Ca^{2+}]_{SR/ER}$). Additionally, it has been shown that active SERCA pumps

A. Guerrero-Hernández (✉) · V. H. Sánchez-Vázquez · E. Martínez-Martínez
L. Sandoval-Vázquez
Department of Biochemistry, Cinvestav, Mexico city, Mexico
e-mail: aguerrero@cinvestav.mx

N. C. Perez-Rosas
Bioquant, University of Heidelberg, Heidelberg, Germany

R. Lopez-Farias
CONACYT-Consorcio CENTROMET, Querétaro, Mexico

A. Dagnino-Acosta
CONACYT-Universidad de Colima (Centro Universitario de Investigaciones Biomédicas), Colima, Mexico

M. S. Islam (ed.), *Calcium Signaling*, Advances in Experimental Medicine and Biology 1131, https://doi.org/10.1007/978-3-030-12457-1_14

are required for attaining this highly efficient Ca^{2+} release process. All these data indicate that Ca^{2+} release by the SR/ER is a highly regulated event and not just Ca^{2+} coming down its electrochemical gradient via the open release channels. One obvious advantage of this sophisticated Ca^{2+} release process is to avoid depletion of the ER Ca^{2+} store and accordingly, to prevent the activation of ER stress during each Ca^{2+} release event.

Keywords Endoplasmic reticulum (ER) · Sarcoplasmic reticulum (SR) · Ryanodine receptors (RyRs) · IP_3 receptors (IP_3Rs) · Sarco-endoplasmic reticulum calcium ATPase (SERCA pump) · Free luminal ER [Ca^{2+}] ($[Ca^{2+}]_{ER}$) · Cytoplasmic [Ca^{2+}] ($[Ca^{2+}]_i$) · Calcium buffer capacity · Kinetics on demand (KonD)

14.1 Elements of the SR/ER Involved in Ca^{2+} Release

14.1.1 Calcium Ion as Second Messenger

A transient elevation of the cytoplasmic calcium concentration ($[Ca^{2+}]_i$) leads to changes in a large array of cellular functions [1]. These are muscle contraction, gland secretion, neurotransmission, respiration, cell movement, cell proliferation, gene transcription, cell death, among others. There are two main sources of calcium ions, the external milieu and the intracellular calcium stores [2]. The latter, in turn, are formed by two main Ca^{2+} pools, the sarco-endoplasmic reticulum and the acidic Ca^{2+} stores. This review will focus on the former rather on the latter. However, before reviewing what we know on how the sarco-endoplasmic reticulum provides Ca^{2+} for different cellular events, we will discuss some principles associated with Ca^{2+} ion as one of the many different second messengers that cells use to respond to changes in the environment.

Calcium ions are toxic in principle [3], since a sustained elevation of the $[Ca^{2+}]_i$ leads to cell death. For this reason cells invest a considerable amount of energy, coming directly or indirectly from ATP hydrolysis, to keep cytoplasmic [Ca^{2+}] in the 100 nM range by actively transporting this ion to either outside the cell or inside intracellular compartments [2]. The latter are known as intracellular Ca^{2+} stores. Generally, second messengers are molecules synthesized and degraded by enzymes, which are essential in the initiation and termination of second messenger activities. However, the situation of Ca^{2+} being a second messenger is different, in this case Ca^{2+} is moved from one cell compartment to another and those concentration changes are recognized by proteins that lead to changes in cell behavior [2]. Therefore, the plasma membrane and the different intracellular membranes are endowed with a large variety of Ca^{2+} permeable ion channels that respond to different stimuli. Accordingly, the diffusion of Ca^{2+} through the open pore of these proteins occurs in response to different signals that are physical (voltage, heat, pressure) or chemical (hormones, neurotransmitters, etc.) in nature. Once the

$[Ca^{2+}]_i$ has been elevated by the increased activity of Ca^{2+} permeable ion channels, this divalent cation is bound by two different types of proteins, buffers and effectors, the former limit the increase of the $[Ca^{2+}]_i$ and this gives time to Ca^{2+} pumps to expel this ion out of the cytoplasm, while the latter are characterized by the ability of forming a Ca^{2+}-protein complex that modifies the activity of different enzymes (kinases, phosphatases, proteases, etc.) that change the cell behavior allowing cells to adapt and respond to different stimuli [2, 4].

14.1.2 Intracellular Calcium Stores

It has become evident then that intracellular Ca^{2+} pools are, at the same time, sources of Ca^{2+} in response to certain stimuli [1, 5] and also Ca^{2+} buffering compartments that help cells survive the cytotoxic effect of increased $[Ca^{2+}]_i$ [6–8]. This paradoxical situation has been the motor behind the evolution of very interesting solutions that will be reviewed below. There are basically two different types of internal Ca^{2+} stores, one represented by the sarcoplasmic/endoplasmic reticulum (SR/ER) and the other referred to as acidic Ca^{2+} store. The former is a single organelle while the latter encompasses a variety of organelles that have a luminal pH below 7.0, these are the Golgi apparatus [9, 10], lysosomes [11] and secretory granules [12], among other organelles. These two different types of stores can be observed using electron microscopy to detect intracellular sites with elevated $[Ca^{2+}]$ [13, 14]. Alternatively, these two stores can be observed by depleting the SR/ER followed by maneuvers to alkalinize and open Ca^{2+} permeable channels in the acidic organelles [10, 15].

The SR/ER is a membrane organelle that traverses all the cytoplasm. Actually, it forms the nuclear envelope and for this reason this organelle goes from the nucleus all the way to the plasma membrane at the periphery of the cell [16–18]. The reticulum is formed by tubules and saccules that are interconnected and it appears that their lumen do not have any diffusion barriers [7, 19–21]. At the same time these reticular structures are dynamic because they can move, to a certain degree, within the cytoplasm; using the microtubules as their rail-roads [17, 22, 23]. Reticular membranes also have the characteristic of being highly fusogenic, resulting in a constant reshaping of the reticulum [22–24].

The endoplasmic reticulum of muscle cells is the sarcoplasmic reticulum and, particularly in striated muscle cells, it has specialized in moving large quantities of Ca^{2+} for both muscle contraction and relaxation [25, 26]. In non-muscle cells, the endoplasmic reticulum is the main intracellular Ca^{2+} store, although this organelle also carries out many more functions such as protein and phospholipid synthesis, drug detoxification, synthesis of cholesterol, etc. [17]. The function of the sarcoplasmic/endoplasmic reticulum as Ca^{2+} store involves the following essential elements: (a) Ca^{2+} pumps to accumulate this ion in the store, against its electrochemical gradient, (b) release Ca^{2+} permeable channels and (c) luminal Ca^{2+} binding proteins that increase the capacity of the lumen to accumulate Ca^{2+} in the store. The characteristics of each one of these elements will be reviewed briefly.

14.1.3 SERCA Pumps

SERCA stands for Sarco-Endoplasmic Reticulum Calcium ATPase, is an SR/ER integral membrane protein codified by three different genes, ATP2A1, ATP2A2 and ATP2A3. All three messenger RNAs from these genes show alternative splicing in the 3′ end region, generating a large assortment of SERCA pumps. SERCA1a is the fastest pump and it is expressed in fast-twitch skeletal muscle, SERCA2a is expressed mainly in heart cells and SERCA2b is called house-keeping pump because it is present in smooth muscle cells and non-muscle cells having an ER [27].

Catalytic cycle of SERCA pumps consists of binding two Ca^{2+} ions from the cytoplasm, this in turn promotes ATP binding followed by SERCA own phosphorylation in a highly conserved aspartic residue, which results in conformational changes that close the access of cytoplasmic Ca^{2+} to the protein, and these would allow access to the lumen of the endoplasmic reticulum with a reduced affinity for Ca^{2+}. In the end, cytoplasmic Ca^{2+} is delivered into the lumen of the SR/ER in exchange for protons. This final event promotes dephosphorylation of the enzyme to reinitiate another catalytic cycle [28]. All these steps in the catalytic cycle involve large conformational changes whose structures have been determined by X-ray diffraction studies [29]. This series of conformational changes has very interesting implications for cell physiology. The slow rate of 100–1000 ions/second showed by SERCA pump [30] does not counteract the much higher Ca^{2+} rate of one million ions/sec in the RyR [31]. The leak activity of release channels then could be critical because it would impose an energy burden on the cell that could easily drain all its energy resources [32]. Accordingly, SERCA pump is one of the thermogenic sources in the body [33], to the extent that increased Ca^{2+} leakage from the SR, that in turn accelerates SERCA pump activity, can lead to malignant hyperthermia, a fatal side effect of anesthetics, like halothane, this complication can be overcome by using dantrolene, an inhibitor of Ca^{2+} release channel, by reducing the SR Ca^{2+} leak [34]. Furthermore, deletion of sarcolipin (a protein proposed to switch SERCA pump from Ca^{2+} translocation to thermogenesis) generates obese mice with the development of insulin resistance [35]. Thus, this catalytic cycle is essential for SERCA pump to produce heat and to accumulate Ca^{2+} in the lumen of the SR/ER.

It is easy to see then that any interference with the SERCA pump catalytic cycle will result in inhibition of its activity. It has been described a large variety of SERCA pump inhibitors that are either codified by the same cell or are chemicals from other sources. The former involve a series of peptides that are small, single span integral membrane proteins, that by binding to SERCA they inhibit its pump activity; these are phospholamban and sarcolipin [36], myoregulin, endorgulin, and another-regulin [37]. The second group of SERCA pump inhibitors comprises chemicals that bind to SERCA pump and inhibit the catalytic cycle, these are thapsigargin, cyclopiazonic acid and *tert*-butyl hydroquinone [38, 39]. Additionally, high levels of cholesterol and saturated fatty acids can also inhibit the activity of SERCA pump, allegedly by increasing the rigidity of the ER membrane [40]. Interestingly, it has

been found a peptide, codified by a long-noncoding RNA, named DWORF, which is able to increase the activity of SERCA pump by displacing the inhibitory peptides from the SERCA pump [41]. It is becoming clear that the activity of SERCA pump not only respond to an increase in the $[Ca^{2+}]_i$ but also to the presence of these regulatory peptides.

14.1.4 Calcium Release Channels

There are two main Ca^{2+} release channels in the SR/ER. The SR expresses the Ryanodine Receptor (RyR) while the ER is endowed with the IP_3R [42, 43]. These release channels are tetramers that form Ca^{2+} permeable, non-selective cation channels [44]. Both types of channels are activated by low cytoplasmic $[Ca^{2+}]$ and inhibited by higher concentrations of this divalent cation [45, 46]. The majority of the protein is facing in the cytoplasm and only a small fraction, in the carboxy terminal region of this protein, is inserted in the sarco-endoplasmic reticulum membrane to form the ion channel pore. Release channels are tetrameric, Ca^{2+} permeable non selective cation channels and each subunit of the RYR is more than 5000 amino acids long (the whole channel weighs around 2.2 MDa) while each subunit of the IP_3R is around 2500 amino acids long (the whole channel weight close to 1 MDa). There are three different genes for each one of these release channels and each gene produces alternative splicing isoforms. RyR1 is expressed mainly in fast-twitch skeletal muscle and is activated by what is known as mechanical coupling [47]. The membrane depolarization of the T tubules generates conformational changes in the voltage-gated calcium channels (VGCC, specifically the dihydropiridine receptor) that are directly transmitted to the RyR1 resulting in one of the fastest Ca^{2+} release events (1–2 msec time to peak). The key issue here is that RyRs in the SR require making contact with VGCC in the T tubules of the plasma membrane. Typically, each one of the subunits of RyRs connects with one VGCC, so one RyRs is connected with four VGCC. The RyRs alternate between those connected to the VGCC and those that are not connected, and the idea is that calcium-induced calcium release (CICR) would be activating those RyRs that are not connected [42]. The isoform 2 of RyR is expressed in heart cells and in this case the association with VGCCs is not that clear, RyR2s are not connected physically to VGCC, but these two proteins are located very close to each other [48]. The Ca^{2+} entering via VGCCs triggers the activation of RyR2s to produce Ca^{2+} release that results in heart cell contraction. It has been calculated that for all the Ca^{2+} involved in contraction, as much as 90% can be provided by RyR2s and only a small fraction by VGCCs, although these figures vary according to the species studied [49]. Finally, RyR3 was the last one to be cloned and is present in different type of cells, for instance in the diaphragm, brain cells and smooth muscle cells [47]. Actually, it is very interesting that smooth muscle cells express all three RyRs with different localization within the SR [50]. RyRs in smooth muscle cells appear to be involved more in relaxation than contraction [51], the idea here is that

localized Ca^{2+} release events involving the activation of RyRs, which are known as Ca^{2+} sparks, would activate Ca^{2+}-dependent, high conductance potassium channels that are heavily expressed in smooth muscle cells, this would result in membrane hyperpolarization and concomitant deactivation of VGCC, which provide most of the Ca^{2+} involved in smooth muscle contraction. This is the case because CICR is rather inefficient in smooth muscle cells [52, 53].

The IP_3R is activated by the combination of Ca^{2+} and IP_3 in a very complex manner, to the extent that IP_3Rs are activated in a very small window of IP_3 concentration [46]. This is very important because there is no correlation between the amount of IP_3 produced and the amplitude of the $[Ca^{2+}]_i$ response, actually, the main difference is time, because if an agonist produces a large amount of IP_3, this will reach the threshold for Ca^{2+} release, before the other agonist that has a much lower rate of IP_3 production [54, 55]. The IP_3 binding site is located in the amino terminus of the protein, while the ion channel is formed by the carboxy end of the IP_3R. The structure of this channel revealed by cryo-electron microscopy has shown that the very end of this protein, the carboxy terminal domain (CTD), is an alpha helix that goes all the way from the channel domain to contact the IP_3 binding region of the next subunit. This peculiar conformation of CTD might explain the allosterism displayed by IP_3 and Ca^{2+} to activate this release channel [56]. In addition to IP_3 and Ca^{2+} there are a number of proteins that can modulate the activity of IP_3Rs, examples are RACK, IRBIT, Homer, BCL2, Presenilin, Huntingtin, among others [57]. Thus, the activity of release channels is under the control of a large series of chemicals and protein interactions.

14.1.5 Luminal Calcium Binding Proteins

The $[Ca^{2+}]$ in the cytoplasm is in the submicromolar range and accordingly, the Ca^{2+} binding proteins that are present in the cytoplasm have high affinity and selectivity over Mg^{2+} to be able to bind Ca^{2+} and carry out their functions. This situation implies that the cytoplasmic Ca^{2+} binding proteins, participating in signal transduction, have evolved to display high affinity, but low capacity for Ca^{2+} ions [4].

This picture is completely different inside the lumen of the SR/ER where the free luminal $[Ca^{2+}]$ is in the submillimolar range and total $[Ca^{2+}]$ could be in the tens of millimolar range. There are two main luminal calcium binding proteins in the lumen of the reticulum, these are calsequestrin [58–60] and calreticulin [61]; the former appears to be the main Ca^{2+} binding protein in the lumen of the sarcoplasmic reticulum of striated muscles [62], while the latter is the main one in some smooth muscle cells and non-muscle cells [63]. These proteins are characterized by having low affinity but high capacity. This means that these proteins have several Ca^{2+} binding sites but their affinity for Ca^{2+} is low when compared with those proteins in the cytoplasm. The underlying idea is that these proteins are responsible for increasing the Ca^{2+} buffering power of the sarco-endoplasmic reticulum. That is, they increase the capacity of internal stores to accumulate Ca^{2+}, which allow

internal Ca^{2+} stores to be able to provide Ca^{2+} to the cytoplasm and to trigger cellular events that are driven by an increase of the $[Ca^{2+}]_i$.

Additionally, if the stores have a role in buffering the elevation of the $[Ca^{2+}]_i$, then these proteins increase the capacity of internal stores to accumulate Ca^{2+}, which in turn, avoid the cytotoxic effects of high levels of the $[Ca^{2+}]_i$. This situation has been clearly shown in neurons, where membrane depolarization activates VGCC that allow Ca^{2+} entry to the cytoplasm, and then SERCA pumps direct cytoplasmic Ca^{2+} to the lumen of the ER. Once Ca^{2+} is inside the ER, there are specific regions that accumulate this ion to concentrations as high as 40 mM [64]. These regions are adjacent to other regions of the ER that do not accumulate Ca^{2+} at all; this is not easy to explain since both regions are located within the same lumen of the ER [65]. The idea here is that the distribution of the Ca^{2+} binding proteins is not homogeneous [66], and that these proteins are trapping Ca^{2+} to reduce the activity of this ion (i.e. Ca^{2+} ions are no longer free). In the same neurons, it was observed that the inhibition of SERCA pumps with thapsigargin, leads to mitochondria Ca^{2+} accumulation due to the inability of the ER to buffer the incoming Ca^{2+} [64, 65]. Although it was not shown in this study, the increased mitochondrial matrix $[Ca^{2+}]$ would trigger mitochondria dysfunction and quite possible apoptosis [8].

Calsequestrin does not appear to be freely distributed inside the SR but it is associated with RyRs either directly [67] or indirectly via the association with triadin and junctin [47, 68]. However, it has been shown that the role of calsequestrin is more complex than the mere increase of the SR Ca^{2+} buffering capacity since it also regulates RyRs-mediated Ca^{2+} release events [58]. A very interesting example has been observed studying a single point mutation of $CASQ2^{R33Q}$, which was discovered in a patient afflicted with CPVT (catecholaminergic polymorphic ventricular tachycardia), an inherited arrhythmogenic condition that is life threatening [60]. Interestingly, the presence of CASQ2 confers RyR2s sensitivity to luminal $[Ca^{2+}]$ to the extent that there is a peak ion channel activity at 1 mM luminal $[Ca^{2+}]$ [69]. Remarkably, the mutant $CASQ2^{R33Q}$ increases the RyR2 ion channel activity by luminal Ca^{2+} at concentrations as low as 10 μM [69]. Then the presence of $CASQ2^{R33Q}$ makes RyR2 a leaky channel to the point that this results in a very low free luminal SR $[Ca^{2+}]$ in heart cells, even lower than the levels attained during normal Ca^{2+} release process [60]. Unexpectedly, this extremely low free luminal SR $[Ca^{2+}]$ with $CASQ2^{R33Q}$ results in Ca^{2+} waves and Ca^{2+} sparks of larger amplitude than those recorded in normal heart cells that have a much higher free luminal SR $[Ca^{2+}]$ [60]. Moreover, the Ca^{2+} systolic-induced contraction was only slightly smaller in myocytes expressing the mutant $CASQ^{R33Q}$ than in those expressing wild type CASQ [70]. Deletion of CASQ2 greatly decreased the amplitude of Ca^{2+} sparks despite having a normal reduction in the luminal SR $[Ca^{2+}]$ suggesting that CASQ2 is indeed the Ca^{2+} buffering protein in the SR of heart cells [60]. However, it is also clear that CASQ2 beyond being a Ca^{2+} buffering protein also has other roles in the Ca^{2+} release event since it shows a complex control of the activity of RyR2s. Assuming that the Kd for Ca^{2+} binding of $CASQ^{R33Q}$ is the same as the one for CASQ wild type, and because the free luminal SR $[Ca^{2+}]$ is

much smaller than normal, then the saturation of $CASQ^{R33Q}$ should also be much smaller, these two conditions (low free luminal SR $[Ca^{2+}]$ and smaller saturation of CASQ2) should result in a $[Ca^{2+}]_i$ response of smaller amplitude in the presence of $CASQ2^{R33Q}$. Since this is not the case [60], then it appears that $CSQ2^{R33Q}$ mutant clearly exemplifies the idea that the amount of Ca^{2+} that is released by activation of RyR2 cannot be predicted from the observed changes in the free luminal SR $[Ca^{2+}]$.

14.1.6 The Biophysical Vision of the SR/ER Ca^{2+} Stores

It is clear then that an intracellular Ca^{2+} store is a membrane compartment that forms a closed entity and involves the participation of several components, which are Ca^{2+} pumps, luminal Ca^{2+} binding proteins and Ca^{2+} release channels. The prevailing vision, particularly for mathematical models (Fig. 14.1), is that all these

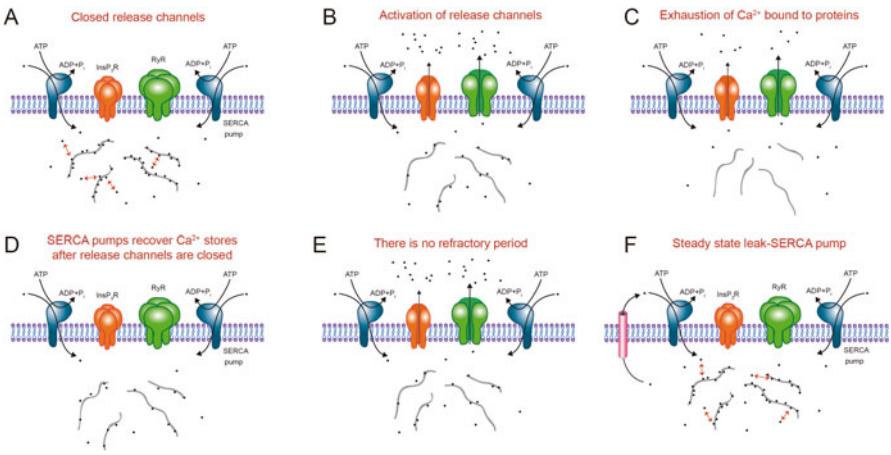

Fig. 14.1 Graphical model of Ca^{2+} release event where the free luminal SR/ER $[Ca^{2+}]$ is in equilibrium with the Ca^{2+} bound to the luminal proteins. This cartoon depicts the critical elements involved in a Ca^{2+} release event. (**a**) The Ca^{2+} bound to luminal proteins is in equilibrium with the free luminal SR/ER $[Ca^{2+}]$ (as represented by the double-headed arrows). (**b**) The activation of release channels would decrease the free luminal SR/ER $[Ca^{2+}]$ and this results in Ca^{2+} unbinding from luminal proteins, as long as the release channels stay open. This scenario cannot produce an increase of the free luminal SR/ER $[Ca^{2+}]$ in response to the activation of the release channels. (**c**) The Ca^{2+} release process terminates when all the Ca^{2+} bound to luminal proteins has been released. (**d**) SERCA pump needs that release channels to be close in order to recover the free luminal SR/ER $[Ca^{2+}]$. (**e**) This scenario cannot produce a refractory period for RyRs because the recovery of the free luminal SR/ER $[Ca^{2+}]$ implies also complete restauration of the Ca^{2+} bound to proteins. (**f**) The steady state implies that Ca^{2+} leak activity is counterbalanced by SERCA pump activity to keep constant the free luminal SR/ER $[Ca^{2+}]$ and also the total amount of Ca^{2+}. Any reduction in the free luminal SR/ER $[Ca^{2+}]$ implies a corresponding reduction in the total amount of Ca^{2+} stored in the SR/ER

three components work independently of each other and that it is only via changes in the free luminal [Ca^{2+}] that these three components communicate among each other [71, 72]. Accordingly, these models have explored the role played by free luminal [Ca^{2+}] in modulating the activity of both release channels and Ca^{2+} pumps. However, there are several experimental studies indicating that these three components are not working independently of each other. This situation was clearly unexpected particularly for SERCA pump and release channels, because they are supposed to be antagonistic elements of the Ca^{2+} pools since one increases while the other reduces the Ca^{2+} content of the intracellular store. Nevertheless, there is evidence, which will be discussed in the rest of the review, for a communication between Ca^{2+} release channels and SERCA pump to achieve an efficient Ca^{2+} release event (i.e. an increase in the $[Ca^{2+}]_i$ with minimal or no reduction in the free luminal SR/ER [Ca^{2+}]).

Mathematical models reflect our incomplete knowledge of the Ca^{2+} release event. One example can be found in a study investigating the role played by Ca^{2+} diffusion inside the SR in the termination of Ca^{2+} sparks [73, 74]. Interestingly, this model uses a previously reported Ca^{2+} diffusion coefficient in the non-junctional SR of 0.6×10^{-10} m^2/s [75], but to have an efficient Ca^{2+} release process, this coefficient has to be five-fold larger of 3.5×10^{-10} m^2/s in junctional SR [73, 74]. The problem with this difference is that the model uses a previously estimated concentration of calsequestrin of 6 mM [76], while the model needed to increase the concentration by five-fold (30 mM) in the junctional SR [73, 74]. These conditions generate a paradox because the idea is that calsequestrin is the main Ca^{2+} buffering protein in this compartment and since calsequestrin behaves as a non-mobile protein within the SR, because it is associated with the RyRs, therefore increasing the concentration of calsequestrin in the SR should lower the diffusion of Ca^{2+} ions. However, this is the opposite of what the model predicts to be happening in the junctional SR because it was increased five-fold. Thus, it appears then that our current picture of how calsequestrin is working would lead to a strong competition for the free luminal Ca^{2+} between RyRs and calsequestrin and since this does not seem to be happening in the Ca^{2+} release event, then there is still missing information on how these proteins produce an efficient Ca^{2+} release process.

14.2 Contributions of Noriaki Ikemoto to the SR Ca^{2+} Release Model

14.2.1 The Activation of RyR1 Produces an Initial Increase in the Free Luminal SR [Ca^{2+}] Before the Opening of this Release Channel

A very interesting observation made by Ikemoto's group consists in finding that stimulation of RyRs in skeletal muscle terminal cisterna SR vesicles produces an

elevation of the free luminal [Ca^{2+}] that occurs before any Ca^{2+} has come out from the store to the cytoplasm, in other words, the free luminal [Ca^{2+}] is increased in response to the activation of RyRs but before the opening of these channels [77]. The implications of this observation are so profound and paradigm changing that we are still in the process of incorporating them in our current models on how Ca^{2+} pools are working. The importance of this observation resides in the fact that current mathematical models of Ca^{2+} release cannot generate an increase in the free luminal [Ca^{2+}] in response to the activation of RyRs. The current idea on how Ca^{2+} release occurs requires the opening of RyRs to decrease the free luminal [Ca^{2+}], as an initial event, and this in turn would drive the dissociation of Ca^{2+} from calsequestrin to further amplify the amount of Ca^{2+} that is released from the SR. This model means that Ca^{2+} dissociation from calsequestrin is driven by a reduction of the free luminal [Ca^{2+}], which is the result of the opening of RyRs. This picture seems to coincide with the results obtained by Ikemoto using high concentrations of polylysine to activate RyRs [77]. However, using lower concentrations of polylysine resulted in a clear increase of the free luminal [Ca^{2+}], as measured with tetramethylmurexide, before any reduction in the total amount of Ca^{2+} (as measured with $^{45}Ca^{2+}$) stored in the SR vesicles [77]. This work suggests that activation of RyRs, before the opening of RyRs, results in the increase of the free luminal SR [Ca^{2+}] as an initial step followed then by the actual opening of these release channels.

14.2.2 Role of Calsequestrin in Producing a Transient Increase of the Luminal SR [Ca^{2+}]

Another crucial observation done by Ikemoto's laboratory concerns the role played by calsequestrin in generating an efficient Ca^{2+} release process [77]. They found that activation of RyRs with polylysine did not produce any increase in the free luminal [Ca^{2+}] when the SR vesicles were devoid of calsequestrin. This indicates that the Ca^{2+} bound to this protein is the one that is released by RyRs. However, the rather radical observation is that calsequestrin inside the SR vesicles is not enough to reconstitute the Ca^{2+} release event, but that calsequestrin needs to be associated with the RyRs of the SR vesicle to recover the increase in the free luminal [Ca^{2+}] response [77]. This signifies that the Ca^{2+} buffering power provided by calsequestrin is not enough to have a correct Ca^{2+} release event, but that RyRs and calsequestrin have to interact, either directly or indirectly, in order to reconstitute an efficient Ca^{2+} release event. Again the implications of this observation are so ample that it has been difficult to incorporate in our current thinking. The same conclusion was reached by a different group and their data was summarized in a model where there were two different RyRs, whose main difference was to have or not attached calsequestrin [78]. Those RyRs having attached calsequestrin respond very fast and produced more than 50% of the Ca^{2+} release event, while those without calsequestrin have a slower activation and provide less Ca^{2+} to the response [78]. It

is important to bear in mind that the rate of Ca^{2+} release is a critical characteristic to produce an increase in the $[Ca^{2+}]_i$ because, there are Ca^{2+} buffering proteins in the cytoplasm and Ca^{2+} pumps at the plasma membrane, that would reduce the effect of release channels on the $[Ca^{2+}]_i$. Accordingly, this means that those RyRs with calsequestrin bound would have a much higher effect on the $[Ca^{2+}]_i$ than those RyRs without calsequestrin, despite releasing similar amounts of Ca^{2+} from the SR but, the main difference is that one is faster than the other. These data are also suggesting that calsequestrin appears to be trapping Ca^{2+} next to the RyRs, meaning that this entrapped Ca^{2+} is not in equilibrium with the free luminal SR $[Ca^{2+}]$; if this is the case, then it is easy to explain why the activation of RyRs, before the opening of RyRs, produces an initial increase of the free luminal SR $[Ca^{2+}]$. Additionally, this situation also implies that the free luminal $[Ca^{2+}]$ is not a good predictor of the amount of Ca^{2+} released by activation of RyRs because the Ca^{2+} trapped by calsequestrin does not appear to be in equilibrium with the free luminal SR $[Ca^{2+}]$, which is the one reported by the fluorescent Ca^{2+} indicators. Yet another important consequence that can be derived from these works is that there will be a refractory period in the Ca^{2+} release event that would depend on the time taken by RyRs and calsequestrin to reconstitute the trapped Ca^{2+} complex. It appears that only closed conformation of RyRs allows the reconstitution of this complex, a conclusion that was derived from experiments using ryanodine in smooth muscle cells [79]. High concentrations of ryanodine lock RyRs in the open conformation but the Ca^{2+} flow is blocked because ryanodine binds to the open pore [45, 47]. In the cell, this effect of ryanodine allows SERCA pump to recover the luminal SR $[Ca^{2+}]$ because ryanodine has blocked the RyRs [79]. The most interesting observation is that in the presence of ryanodine and with normal SR luminal $[Ca^{2+}]$, the application of IP_3-producing agonists results in a much smaller increase of the $[Ca^{2+}]_i$ [79, 80]. Collectively, these data suggest that the SR Ca^{2+} store is still empty despite the presence of a high luminal SR $[Ca^{2+}]$. The interpretation for these data could be that the complex (release channel-Ca^{2+} binding protein) cannot be reassembled when the RyRs have been locked, by ryanodine, in the open conformation and this condition reduces the ability of nearby IP_3Rs to produce an efficient $[Ca^{2+}]_i$ response.

14.2.3 Evidence that There Is a Communication Between SERCA Pump and RyR1

At the end of the Ca^{2+} release event, the combined reduction in the free luminal SR/ER $[Ca^{2+}]$ and the associated increase of the $[Ca^{2+}]_i$ should lead to SERCA pump activation. At least that is the idea because high luminal $[Ca^{2+}]$ would make harder for SERCA pump the exchange of H^+ for Ca^{2+} in the lumen of the SR [81]. However, work done by Ikemoto's group has demonstrated that activation of RyR1s affects the activity of SERCA pump suggesting some kind

of communication between these two proteins [82–86]. The most interesting part is that this communication occurs right after the activation of RyRs and before any reduction in the free luminal SR [Ca^{2+}]. Even more difficult to explain is the observation that this activation of the SERCA pump occurs during the RyR-triggered increase of the free luminal [Ca^{2+}] [87]. This is quite paradoxical since it is expected that the increase in the free luminal [Ca^{2+}] should lead to further inhibition of the SERCA pump activity [81]. It is still unknown how the activation of RyRs, before their opening, results in SERCA pump activation; particularly because SERCA pump and RyRs are not necessarily localized next to each other in the SR; however, this communication could indirectly occur via luminal Ca^{2+} binding proteins [83]. Regardless how these two proteins communicate, it is easy to argue that this communication between release channels and SERCA pump is an important mechanism to avoid life-threatening situations such as ER-stress due to depletion of the ER Ca^{2+} store.

14.3 Simultaneous Recording of the Redution in the Free Luminal SR/ER [Ca^{2+}] and the Associated Changes in the [Ca^{2+}]$_i$

Since the 80's, when the organic fluorescent Ca^{2+} indicators were synthesized, it became customary to place cells in the absence of external [Ca^{2+}] to look at the [Ca^{2+}]$_i$ response induced by different stimuli, and to take amplitude of this response as an indirect measure of the amount of Ca^{2+} present in the SR/ER Ca^{2+} pools. However, this type of approach can be deceiving because there are different factors that shape the [Ca^{2+}]$_i$ response. One example of this problem was the observation in smooth muscle cells that two applications of saturating concentrations of caffeine, which are separated by only 30 s, results in a second [Ca^{2+}]$_i$ response that is 80% smaller than the first response [88]. The initial and incorrect interpretation of these data was that 30 s was not enough time to refill the SR Ca^{2+} pool, yet when using Mag-fura-2 to see the free luminal SR [Ca^{2+}], it became evident that the SR [Ca^{2+}] is fully recovered from caffeine-induced depletion after a time of only 30 s [89]. Therefore it is clear the importance of recording simultaneously the changes in the [Ca^{2+}]$_i$ and the luminal SR/ER [Ca^{2+}] with sufficiently high time resolution to be able to define an efficient Ca^{2+} release event. It is this approach what has made evident that the changes in the luminal SR/ER [Ca^{2+}] does not present a simple correlation with the corresponding changes in the [Ca^{2+}]$_i$.

Initial attempts to look at the luminal ER [Ca^{2+}] were carried out using Mag-fura-2, a low affinity Ca^{2+} indicator that does not go easily into the ER, and for this reason much of the work done with this indicator was carried out in permeabilized cells [90]. It turned out that Mag-fluo-4, a tricarboxylic low affinity Ca^{2+} indicator, goes into the ER more easily [91]. However, since Mag-fluo-4 lacks ER retention mechanism, not all dye stays in the ER, some of it goes into the Golgi

apparatus and from there goes into the vesicles of the secretory pathway [10]. The advantage of organic dyes is that they are easy to be loaded and to calibrate, their stoichiometry with Ca^{2+} is 1:1 and they are relatively insensitive to pH changes. Nevertheless, the main limitation is that they lack a targeting mechanism and this issue has been solved developing Genetically Encoded Ca Indicators (GECIs) that are targeted to different organelles, the ER/SR among others [10, 92]. These GECIs use EF-hand proteins as Ca^{2+} sensor moiety and the signal could be chemoluminescent or fluorescent in nature. The disadvantage of GECIs is that they are not homogeneously expressed in cells, their stoichiometry is not 1:1, and aequorin is irreversibly oxidized on Ca^{2+} binding, so it is a single shot Ca^{2+} indicator while GFP fluorescence is sensitive to changes in the pH [10].

Initial studies on the luminal ER $[Ca^{2+}]$ using aequorin in HeLa cells, found that the agonist-induced reduction in the free luminal ER $[Ca^{2+}]$ and the associated $[Ca^{2+}]_i$ response, were both of the same amplitude, whether the ER Ca^{2+} pool was fully loaded or practically depleted [93]. These data suggest that the Ca^{2+} released by the agonist is not in equilibrium with the free luminal ER $[Ca^{2+}]$. In pancreatic acinar cells it has been shown that a small concentration of acetylcholine (200 nM) increased the activity of Ca^{2+}-dependent Cl^- channels in the absence of any reduction in the luminal ER $[Ca^{2+}]$, despite the activation of IP_3R by acetylcholine [19]. These data indicate that activation of a small number of IP_3Rs produces no reduction in the free luminal ER $[Ca^{2+}]$ despite Ca^{2+} has been released. Again, these data suggest that the free luminal ER $[Ca^{2+}]$ is not in equilibrium with the Ca^{2+} that is released to the cytoplasm by IP_3Rs. A new cameleon targeted to the ER known as D1ER, showed that agonist-induced elevation of the $[Ca^{2+}]_i$ precedes any significant reduction in the free luminal $[Ca^{2+}]$. Actually, the majority of the reduction in the free luminal ER $[Ca^{2+}]$ occurs during the reduction of the agonist-induced $[Ca^{2+}]_i$ response [94]. These data suggest that the Ca^{2+} buffering capacity of the ER is extremely high, during the initial stages of Ca^{2+} release; later on, it switches to a form of low capacity [95–97]. This lack of correlation between the reduction in the free luminal ER $[Ca^{2+}]$ and the increase in the $[Ca^{2+}]_i$ cannot be explained by saturation of the luminal Ca^{2+} indicator. This is the case because in single uterine smooth muscle cells that were loaded with both fura-2 and Mag-fluo-4, the activation of SERCA pump increased the Mag-fluo-4 fluorescence implying that Mag-fluo-4 cannot be saturated inside the SR [91, 98]. This lack of correlation can be seen in different cell types and with activation of either RyRs or IP_3Rs. For instance, the addition of 1 mM ATP, to activate purinergic receptors in HeLa cells, results in the activation of IP_3Rs which produced a delayed reduction in the free luminal ER $[Ca^{2+}]$ with respect to the time course of the $[Ca^{2+}]_i$ response [99]. Another group studying HeLa cells that had been loaded with Indo-1 and an ER-targeted cameleon, observed that the histamine-induced increase of the $[Ca^{2+}]_i$ was associated with a rather small reduction of the free luminal ER $[Ca^{2+}]$ [100]. This was the case either in the presence or in the absence of external $[Ca^{2+}]$; indicating that the explanation for this lack of correlation is not due to the presence of Ca^{2+} entry at the plasma membrane. In heart cells, localized, fast, transient increases of the $[Ca^{2+}]_i$ known as Ca^{2+} sparks, which are due to the activation of a cluster

of RyR2s, are associated with a transient decreased of the free luminal SR [Ca^{2+}], known as blinks [101]. Remarkably, the large majority of these blinks show a slower Ca^{2+} decrease rate than the rate of Ca^{2+} increase seen with the corresponding spark [101, 102]. In skeletal muscle, the reduction in the free luminal SR [Ca^{2+}] that are associated with a Ca^{2+} spark are known as skraps [97], which also have a much slower time course when compared with their corresponding sparks [96, 97]. These data indicate that even at the subcellular level the time course of the reduction in the luminal SR [Ca^{2+}] does not coincide with the corresponding increase in the $[Ca^{2+}]_i$ [96]. To complicate matters even further, it has been shown in heart cells that activation of SERCA pump with isoproterenol produces an increase of the luminal SR [Ca^{2+}] while Ca^{2+} is simultaneously released to the cytoplasm [103, 104]. Moreover, an efficient Ca^{2+} wave propagation requires active SERCA pumps [105]. All these data indicate that there is no correlation between the changes in the free luminal SR/ER [Ca^{2+}] and the increase in the $[Ca^{2+}]_i$ despite the fact that the SR/ER is the source for the Ca^{2+} that appears in the cytoplasm.

A more detailed analysis of the Ca^{2+} release process carried out by either RyRs or IP_3Rs, in smooth muscle cells from the urinary bladder, reveals the existence of four different phases for a Ca^{2+} release event [95]. The first one involves the largest increase in the $[Ca^{2+}]_i$ with just a small reduction in the luminal SR [Ca^{2+}] (we call this an efficient Ca^{2+} release event); phase 2 is characterized by the largest reduction in the luminal SR [Ca^{2+}], without any effect on the $[Ca^{2+}]_i$; while phase three is defined by the reduction in the $[Ca^{2+}]_i$ but the luminal SR is still depleted because the release channels stay open and the fourth phase, is when release channels have been closed and the free luminal SR [Ca^{2+}] recovers to their normally high levels by the action of SERCA pumps [95]. Additionally, in the same work, it was used a low concentration of heparin, to partially inhibit IP_3Rs, and the application of carbachol, to activate IP_3Rs, results in both a transient elevation of the free luminal SR [Ca^{2+}] and a transient increase of the $[Ca^{2+}]_i$ [95]. The elevation in the $[Ca^{2+}]_{SR}$ occurred at the same time that the increase in the $[Ca^{2+}]_i$. The implication of these data is that activation of IP_3Rs unleashes Ca^{2+} trapped in luminal proteins that under normal conditions (fully activated IP_3Rs) will gain immediate access to the cytoplasm. However, with the use of heparin, to partially reduce the activity of IP_3Rs, the just liberated Ca^{2+} from luminal Ca^{2+} binding proteins, diffuses back to the bulk of the SR and it is seen as an increase of the $[Ca^{2+}]_{SR}$. This lack of correlation between the changes in the $[Ca^{2+}]_i$ and the SR/ER [Ca^{2+}] can also be detected using GECIs in cells, that are either isolated or in the tissue [92]. A newly developed GECI that uses apoaequorin to sense Ca^{2+} and GFP to have a fluorescence signal has been used together with Fura-2. Simultaneous recording of the luminal ER [Ca^{2+}] and the $[Ca^{2+}]_i$ show that the $[Ca^{2+}]_i$ response precedes the agonist-induced reduction in the luminal ER [Ca^{2+}] both in HeLa cells and neurons in hippocampal slices [92, 106]. Using a different set of GECIs, it was found that the application of both bradykinin and CPA results in a nuclear [Ca^{2+}] elevation, detected with H2B-D3cpv probe, that peaks well before the nadir of the free luminal ER [Ca^{2+}] reduction [107]. All these data undermine the idea that SR/ER is a Ca^{2+}

pool where the physical state of Ca^{2+} ions is switching from free to protein bound, but that this ion appears to be also trapped in protein complexes that release Ca^{2+} ions in response to the activation of RyRs or IP_3Rs, a picture that was portrayed by Ikemoto [77] and others [78].

The idea that Ca^{2+} does not seem to be in equilibrium inside the SR/ER has been shown using microanalysis with electron microscopes. The activation of VGCC in neurons, loads the ER with Ca^{2+} due to the activity of SERCA pump. However, the increase in Ca^{2+} was not homogenous inside the ER. The same cisterna, can have regions with high Ca^{2+} next to regions where the total amount of Ca^{2+} was not changed at all by the activity of SERCA pumps [64, 65]. Again, these data indicate that there are regions of the SR/ER where Ca^{2+} activity is reduced (meaning that Ca^{2+} has been trapped) without changing the Ca^{2+} activity of contiguous regions despite the absence of evident diffusion barriers. The easiest way to explain these observations is that Ca^{2+} is trapped by proteins and that these ions are not in equilibrium with the free luminal ER $[Ca^{2+}]$. If this is the case on how the SR/ER accumulates Ca^{2+} it might explain why there is a lack of correlation between the Ca^{2+} supplied to the cytoplasm by the SR/ER and the associated changes in the free luminal SR/ER $[Ca^{2+}]$.

A question that is still open is how luminal Ca^{2+} binding proteins are able to trap Ca^{2+} inside the SR/ER. Nevertheless, there are some hints on how this might be happening. It has been shown that calsequestrin is able to increase the number of Ca^{2+} binding sites as the Ca^{2+} concentration is increased. The underlying mechanism for the increase in Ca^{2+} binding sites depends on the ability of calsequestrin to polymerize [62]. However, since calsequestrin is not expressed by all cells and since an efficient Ca^{2+} release is a generalized cellular event, then there should be other proteins doing the same function as calsequestrin. Actually, knockout studies of both CSQ1 and CSQ2 have suggested that there must be other proteins in the lumen of the SR/ER because RyRs were still able to release Ca^{2+} [58]. Thus either calreticulin, or maybe other Ca^{2+} binding proteins in the lumen of the SR/ER, have also the property of increasing the number of Ca^{2+} binding sites in response to an increase of the luminal $[Ca^{2+}]$.

Another very interesting situation to study involves the phenomenon known as the refractory period of Ca^{2+} release that might reflect how the SR/ER is trapping releasable Ca^{2+} [88, 89, 101, 102]. If it is true that the free SR $[Ca^{2+}]$ is in equilibrium with the Ca^{2+} released by RyRs, then this time should be more than enough to fully recover the caffeine-induced $[Ca^{2+}]_i$ response. So the question remains on how to explain the presence of a refractory period for caffeine even when the free luminal SR $[Ca^{2+}]$ has reached normal levels. The same situation is observed in heart cells, where the refractory period between Ca^{2+} sparks from the same site is significantly longer than the time required for recovery of the free luminal SR $[Ca^{2+}]$ [101, 102]. Moreover, keep in mind that the inactivation of the RyRs cannot be the explanation for the presence of a refractory period because; it has been shown that the reduction in the free luminal SR $[Ca^{2+}]$ is basically the same for both Ca^{2+} release events. This observation implies that the same number

of RyRs was activated during the two Ca^{2+} release events although the second application of caffeine produced a five times smaller $[Ca^{2+}]_i$ response. Thus, all these data imply that the changes in the free luminal SR $[Ca^{2+}]$ does not reflect the total amount of Ca^{2+} that is released from the SR to the cytoplasm. If this is the case, then we think that the most likely explanation for the presence of a refractory period is that an efficient Ca^{2+} release event involves the liberation by RyRs of Ca^{2+} trapped by proteins, which are localized contiguous to the release channel [108]; however, it appears that this complex (RyRs-Ca^{2+} trapping proteins) takes a longer time to assemble than the time taken to recover the free luminal SR $[Ca^{2+}]$ (see Sect. 14.4.2).

14.4 Current View on How the SR/ER Ca^{2+} Store Is Working to Produce an Efficient Ca^{2+} Release Event

14.4.1 The Luminal Ca^{2+} Binding Proteins Compete for Ca^{2+} with the Open Release Channel

The picture depicted by Ikemoto in the '90s, on how the SR releases Ca^{2+}, appears to be a generalized situation not only for the SR but also for the ER, that is, for the IP_3Rs. However, this picture is still sketchy because we do not have enough spatial and temporal resolution to have all the elements involved in an efficient Ca^{2+} release event. For this reason, we have resorted on the use of mathematical models to find the conditions necessary to generate phase one during Ca^{2+} release from the ER/SR, as a reminder, phase one is characterized by an increase of the $[Ca^{2+}]_i$ without any reduction in the free luminal ER/SR $[Ca^{2+}]$ [95, 96]. The simplest solution we were able to figure out was reducing the number of luminal Ca^{2+} binding sites in response to a reduction of the luminal SR $[Ca^{2+}]$ [109]. We called this situation Kinetics on Demand (KonD) because the number of Ca^{2+} binding sites increases as the result of an elevation of the $[Ca^{2+}]$ while they are diminished by a reduction in the $[Ca^{2+}]$. This type of kinetics is completely different to the traditional one, where the number of Ca^{2+} binding sites is fixed and the reduction in the free $[Ca^{2+}]$ increases the number of Ca^{2+} binding sites that are unoccupied by Ca^{2+}. The mathematical model reveals that these unoccupied Ca^{2+}-binding sites, which are increasing in number during the Ca^{2+} release process, become a strong competitor for Ca^{2+} with the open release channels and naturally, this competition would slow the Ca^{2+} release process. This kind of problem would not be presented by KonD model because the number of Ca^{2+} binding sties is being reduced during the Ca^{2+} release event. We want to stress that KonD model was proposed based on the observation that the number of Ca^{2+} binding sites in calsequestrin increases as a function of its polymerization [62]. Therefore, the changes in the paradigm were based on understanding how calsequestrin is working and the main difference

consisted on assuming that the total number of Ca^{2+} binding sites are not fixed but varies depending on the presence of Ca^{2+} [62].

Phase one reflects a mechanism for an efficient Ca^{2+} release process and we think that involves Ca^{2+} trapped in luminal Ca^{2+}-binding proteins, next to release channels. This situation implies that the Ca^{2+} that is released by RyRs or IP_3Rs is not in equilibrium with the free luminal SR/ER [Ca^{2+}]. However, there could be alternative explanations for phase one, the idea that phase one is due to saturation of the luminal Ca^{2+} indicator has been discarded because there are different experimental conditions that produce an increase of the free luminal [Ca^{2+}], which argue against the idea that the Ca^{2+} indicator inside the SR/ER is saturated [91, 95, 97, 110]. In skeletal muscle it has been suggested that high cooperativity of Ca^{2+} binding to calsequestrin might explain phase one [58, 97, 111]. The main limitation with this explanation is that the high cooperativity means a smaller range of [Ca^{2+}] before reaching saturation and the ability of SR/ER to buffer Ca^{2+} is quite the opposite since it covers several orders of magnitude [64]. Mathematical models have suggested that luminal Ca^{2+} binding proteins diffuse away from the RyRs while Ca^{2+} would be diffusing towards the open release channels during the release process [73, 74]. We think this seems to be unlikely because we do not see what could be the driving force for Ca^{2+}-binding proteins to diffuse away from the RyRs. Another scenario might be a restricted diffusion of Mag-Fluo-4, which is kept in the bulk of the SR away from the RyRs, so this dye will not be in rapid equilibrium with calsequestrin, which is known to be associated with RyRs [112] and if Ca^{2+} slowly diffuses between these two compartments, then it is expected to see recovery of the free luminal SR Ca^{2+} level (provided that SERCA pumps are located where Mag-Fluo-4 is) even when the RyRs are still open. However, this scenario has not been observed. Release channels need to be in the closed conformation for SERCA pump being able to recover the free luminal SR/ER [Ca^{2+}]. This observation implies that there is no diffusion barrier for the Ca^{2+} indicator. The absence of diffusion barriers for Ca^{2+} and Ca^{2+} indicators within the lumen of the SR/ER should make it difficult to see the transition between phase one and phase two. Indeed, the fusion of these two phases in a single phase has been observed but only in particular conditions; for instance when SERCA pumps had been inhibited with thapsigargin [95] or when it has not given enough time for stores to recover from a previous release event [88, 109, 113]. These data add a new element of complexity since it argues for the importance of having an active SERCA pump to be able to see phase one separated from phase two. Additionally, our mathematical model has stressed the importance that Ca^{2+} binding proteins rapidly switch from high to low Ca^{2+} buffering capacity during the Ca^{2+} release process, a scenario that we have called Kinetics on Demand [109]. The importance of this switch is that the empty Ca^{2+}-binding sites of the luminal Ca^{2+}-binding proteins will not compete with release channels for free luminal Ca^{2+}. The absence of this competition is reflected in release channels having enough free luminal Ca^{2+} for an efficient release event even when the free luminal SR/ER [Ca^{2+}] is not decreasing. Obviously, it is important to know the molecular nature of the proteins responsible for sequestering Ca^{2+} next to

release channels and the molecular mechanism involved to switch from sequestered Ca^{2+} to free Ca^{2+} inside the SR/ER and how the activation of release channels gain access to this trapped Ca^{2+}. Based mainly, but not exclusively, on our own work and the work done by Ikemoto's group, we have developed a graphical model that might explain the differences observed for the time courses of the $[Ca^{2+}]_i$ and the $[Ca^{2+}]_{SR/ER}$ during a Ca^{2+} release event (Fig. 14.2).

14.4.2 Proposed Graphical Model on How Release Channels in the SR/ER Produce an Efficient $[Ca^{2+}]_i$ Response

The graphical model shown in Fig. 14.2 is a cartoon on how the activation of Ca^{2+} release channels leads to an efficient increase of the $[Ca^{2+}]_i$. Initially (Fig. 14.2a), release channels are closed and the Ca^{2+} lattice represents the luminal Ca^{2+} binding proteins that are present in the form of polymers attached to the RyRs [114]. These have trapped Ca^{2+} inside the lattice and accordingly, this Ca^{2+} will not be

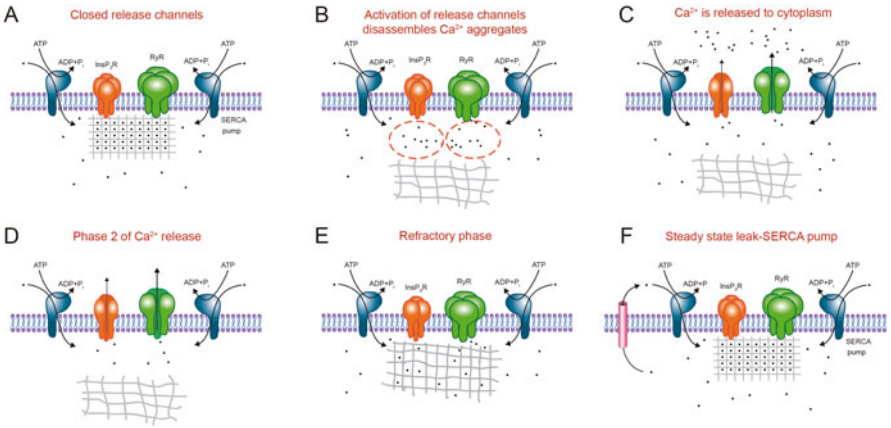

Fig. 14.2 Graphical model of an efficient Ca^{2+} release event by either RyRs or IP_3Rs in the SR/ER Ca^{2+} stores. This cartoon depicts those steps that are considered to be critical for generating an efficient Ca^{2+} release event that is reflected in a transient increase of the $[Ca^{2+}]_i$. (**a**) Ca^{2+} source is in the form of a lattice that is attached to the release channels but disconnected from the bulk of the free luminal SR/ER $[Ca^{2+}]$. (**b**) The activation of the release channels would liberate the Ca^{2+} trapped in the lattice. (**c**) The open conformation of release channels allow the movement of Ca^{2+}, down its electrochemical gradient, to the cytoplasm, without the need to reduce the bulk luminal SR/ER $[Ca^{2+}]$ (phase one). (**d**) Phase two of Ca^{2+} release, which is the inefficient part of the Ca^{2+} release event, mainly because the Ca^{2+} flux from the bulk of the SR/ER is rather slow when compared with the cytoplasmic Ca^{2+} removal mechanisms. (**e**) Once the release channels have been closed there will be a refractory period, because although the bulk of the free luminal SR/ER $[Ca^{2+}]$ has returned to normal levels, probably the Ca^{2+} lattice has not recovered just yet. (**f**) Once the Ca^{2+} lattice has reformed and reattached to the release channels, they are ready for another efficient Ca^{2+} release event

in equilibrium with the free luminal Ca^{2+} that is in the bulk of the SR/ER. This scenario might explain why there is an elevation in the free luminal SR/ER $[Ca^{2+}]$ in response to the activation of release channels; if this is the case then it is easy to see why the free luminal SR/ER $[Ca^{2+}]$ is an inadequate predictor of the amount of Ca^{2+} that the internal stores deliver to the cytoplasm. The activation of release channels (Fig. 14.2b) leads to conformational changes that disassemble the Ca^{2+} lattice producing a local elevation of the free luminal $[Ca^{2+}]$ next to the release channels. This elevation in the free luminal $[Ca^{2+}]$ might help release channels to reach the open conformation. If the release channel is not open or is blocked then this Ca^{2+} would start to diffuse to the bulk of the SR/ER, and this can be observed as a transient elevation of the free luminal SR/ER $[Ca^{2+}]$. This scenario might be the explanation behind the ability of polylysine, a substance that is both an activator and partial blocker of RyRs [115, 116], to reveal a transient elevation of the free luminal $[Ca^{2+}]$ during the activation of RyRs. Following this reasoning, we have used a low concentration of heparin to partially block IP_3Rs that had been previously activated in response to the application of carbachol in smooth muscle cells [117]. Actually, the rate of rising of the $[Ca^{2+}]_i$ when IP_3Rs had been inhibited by heparin, was strongly augmented [95]. The idea here is that Ca^{2+} would accumulate next to those partially blocked release channels and this will increase the driving force resulting in a higher Ca^{2+} exit via those few channels that were not blocked by heparin. Under normal circumstances, the release channels will be fully open (Fig. 14.2c) and this will allow free diffusion of Ca^{2+} from the SR/ER to the cytoplasm producing a significant, transient $[Ca^{2+}]_i$ response but with one very important characteristic, there will be basically no reduction of the bulk free luminal SR/ER $[Ca^{2+}]$. Since most of the Ca^{2+} indicator is in the bulk of the SR/ER, this dye will not see any reduction in the surrounding $[Ca^{2+}]$ because the Ca^{2+} next to the release channel is in a higher concentration than in the bulk of the SR/ER, at least initially in the release event. This is what we have called phase one of the Ca^{2+} release event [95], which is an efficient Ca^{2+} release process because there is an increase in the $[Ca^{2+}]_i$ with minimal or no reduction in the free luminal SR/ER $[Ca^{2+}]$. Phase one of the Ca^{2+} release process has been seen in all kind of cells, during slow or fast Ca^{2+} release events, for RyRs or IP_3Rs and using synthetic or genetically encoded Ca^{2+} indicators [96]. Phase two is observed when the Ca^{2+} supply that comes from the Ca^{2+} lattice has been exhausted and the free luminal Ca^{2+} in the bulk of the SR/ER starts to be drained via the still open release channels (Fig. 14.2d); however, in this case the Ca^{2+} movement is so slow that there is a clear reduction in the bulk of the SR/ER $[Ca^{2+}]$ but without any effect on the $[Ca^{2+}]_i$ (this is the unproductive part of the Ca^{2+} release event). Once the release channels are either closed or inactivated (Fig. 14.2e), then SERCA pump can start accumulating Ca^{2+} by hydrolyzing ATP until the high resting luminal SR/ER $[Ca^{2+}]$ has been reached, at least in the bulk of the SR/ER. However, there would be a time period larger than the time it will take to reach the normal free luminal $[Ca^{2+}]$, where it can be considered that the Ca^{2+} store has been refilled (high free luminal $[Ca^{2+}]$) but if the release channels were to be exposed to an activator in this time, the result would be an unproductive

Ca^{2+} release event [88, 95, 101, 102, 109]. We do not know the reason for this situation, but it is feasible that even when the free luminal SR/ER [Ca^{2+}] is high, close to the normal levels, the Ca^{2+} lattice appears that it has neither reassembled nor connected to the release channels yet. Thus, the characteristic of this stage is a small time window where the free luminal [Ca^{2+}] is basically normal but the activation of the release channels produces a much smaller $[Ca^{2+}]_i$ response [95, 101]. The implication of this situation is that Ca^{2+} buffering in the lumen of the SR/ER does not appear to be a reversible process. Actually, this process shows hysteresis [95, 96, 109], a situation that is not expected for proteins with a low affinity Ca^{2+} binding sites.

Activation of all RyRs, for instance with high concentrations of caffeine, displays this refractory phase in the order of tens of seconds [88, 95]. This implies that this is the time taken by RyRs to recover an efficient Ca^{2+} release event. Nevertheless, the frequency of Ca^{2+} release events in heart and skeletal muscle is much higher than the time taken by RyRs to recover an efficient Ca^{2+} release event. Then we think that muscles cope with this limitation by using only a fraction of all the RyRs present in the SR. In summary, a picture is emerging where the Ca^{2+} released by RyRs or IP_3Rs is trapped in a lattice that is not in equilibrium with the bulk of the SR/ER and it is essential for having an efficient $[Ca^{2+}]_i$ response. Additionally, we propose that the time it takes for this Ca^{2+} lattice to reconstitute itself and to attach to release channels determines the refractory period. We think that a reduction in the SERCA pump activity or the number of functional RyRs with an assembled Ca^{2+} lattice, or even worse, the presence of both conditions, lead to heart failure [118]. Under this condition, Ca^{2+} release via RyRs cannot be efficient since the Ca^{2+} flux is not fast enough to produce a large increase of the $[Ca^{2+}]_i$. One important issue here is that the formation of the Ca^{2+} lattice (Fig. 14.2f) requires both active SERCA pumps and release channels being in the close conformation. These two conditions are not met during heart failure and this might explain why the Ca^{2+} lattice would not be formed equally well and the Ca^{2+} release process is not efficient enough in this pathological condition. It is known that high concentrations of ryanodine lock RyRs in the open conformation, but at the same time, their ion pore is blocked by ryanodine [47]. This situation facilitates recovery of the high luminal $[Ca^{2+}]_{SR/ER}$ by the activity of SERCA pump after the application of caffeine, but it results in the lack of IP_3R-mediated $[Ca^{2+}]_i$ response despite the normal free luminal SR [Ca^{2+}] [79, 89, 117]. Thus, the idea is that the Ca^{2+} lattice to be reformed and attach to the release channels requires these channels to be in the closed conformation.

14.4.3 The Relevance of the Model Where Release Channels Used Ca^{2+} Trapped in the Ca^{2+} Lattice

The importance of this proposed mechanism used by the SR/ER to release Ca^{2+} is that these organelles can function as Ca^{2+} pools for cytoplasmic Ca^{2+} transients

without running the risk of triggering ER stress response due to depletion of the ER luminal [Ca^{2+}] [40, 119–121]. There would be no Ca^{2+} depletion of the SR/ER store when release channels stay open only for the period of time that encompasses phase one of the Ca^{2+} release process. The reason would be that release channels would not reach phase two of the release process and no depletion of the SR/ER would occur. The time required to reach phase two of Ca^{2+} release is much longer than the time involved in a Ca^{2+} spark or a Ca^{2+} puff. Therefore, this model of Ca^{2+} release has the compelling advantage that it can release large amounts of Ca^{2+} to the cytoplasm without eliciting depletion of the SR/ER and accordingly, without triggering the ER stress response that might limit the role of the SR/ER as Ca^{2+} pool. The price to pay for this type of Ca^{2+} release process is the presence of a refractory period because of the time needed for reassembling the Ca^{2+} lattice. However, this limitation can be overcome relatively easy by having a reserve of release channels with a Ca^{2+} lattice. The dynamic of this reserve might be compromised during the fatigue process [122].

This model of SR/ER Ca^{2+} release mechanism combines data obtained with different cell types, different Ca^{2+} indicators and with activation of either RyRs or IP_3Rs, and the observation by Ikemoto's group that activation of RyRs results in an elevation of the free luminal $[Ca^{2+}]_{SR}$ and that this effect requires calsequestrin attached to RyRs. Additionally, this model also considers that calsequestrin increases its Ca^{2+}-binding capacity as a function of its Ca^{2+}-induced polymerization [62, 109]. Despite all these data that support this model; it is still incomplete because the lack of information with sufficiently high temporal and spatial resolution to see the disassembling of the Ca^{2+} lattice induced by the activation of the release channels. To achieve these resolutions is not trivial since the distance is too short, a few nanometers, and the rate of this process is in the order of milliseconds. Additionally, it is quite feasible that calsequestrin might be one of many different proteins that can generate a Ca^{2+} lattice in association with RyRs and IP_3Rs because the double knockout of this protein was not lethal [58] and even worse, it resulted in a much smaller reduction than expected of skeletal muscle luminal Ca^{2+} buffer capacity [58]. The few attempts that have been done to see the disassembling of the Ca^{2+} lattice in real time have failed because it was tried by reducing the free luminal SR [Ca^{2+}] with ionomycin, instead of directly activating RyRs with caffeine [60]. Interestingly, the time constant for calsequestrin depolymerization was extremely slow when driven by a reduction in the luminal SR [Ca^{2+}], which made authors think that this mechanism cannot be operating in cardiac cells because systole has a much higher frequency. However, our own interpretation is that the reduction in the free luminal [Ca^{2+}] is not the signal that drives the fast disassemble of the Ca^{2+} lattice, it is the opening of the RyRs. This scenario might explain why in the absence of external Ca^{2+}, that reduces the free luminal ER [Ca^{2+}], IP_3-inducing agonists produce an $[Ca^{2+}]_i$ response that was barely decreased in amplitude by the absence of external Ca^{2+} [93]. In another study, it became clear that the spatial resolution was not good enough to see the subtle changes associated with modifications in the degree of calsequestrin polymerization during the reduction of the free luminal [Ca^{2+}] [123]. So these few attempts suggest that it will be more difficult than

previously thought to show the dynamics of the Ca^{2+} lattice associated with release channels during the Ca^{2+} release process.

14.5 Other Factors Involved in Having an Efficient Ca^{2+} Release Event

All these studies reviewed here clearly show that Ca^{2+} release from intracellular Ca^{2+} pools, particularly the SR/ER driven by release channels, is more complex than a simple analogy with a water tank (Fig. 14.1). The main difference appears to be that Ca^{2+} is trapped by luminal proteins and accordingly, it is not in equilibrium with the bulk of the SR/ER [Ca^{2+}]. It is only the activation of release channels (RyRs or IPRs) that liberates this Ca^{2+} from the lattice (Fig. 14.2). This situation implies that the change in the free luminal [Ca^{2+}] is not a good indicator of how much Ca^{2+} has been released to the cytoplasm. Additionally, the activity of release channels is under the control of both the luminal [Ca^{2+}] and the interaction with luminal proteins, as it is the case for RyRs and calsequestrin. Moreover, the distribution of release channels and Ca^{2+} binding proteins is not homogenous in the SR/ER and even when their lumen lack diffusion barriers, the tortuosity of these internal Ca^{2+} stores contribute with geometrical issues that also need to be considered. If all these factors are not adding enough complexity, there is still another layer of complexity due to the fact that all the elements involved in the Ca^{2+} release process work interconnected. In this regard, there is data showing that an efficient Ca^{2+} release process requires an active SERCA pump [89]. This was unexpected because these two activities, SERCA pump and release channels, should be antagonistic between each other and instead it turns out that an active SERCA pump is a critical element to achieve an efficient Ca^{2+} release event.

One example of this communication between SERCA pump and Ca^{2+} release channels is observed in the effect of activation of β adrenergic receptor in heart cells. In this case the phosphorylation of phospholamban by PKA dissociates this protein from SERCA pump resulting in a higher pump activity. However, this effect is reflected in a larger $[Ca^{2+}]_i$ response that paradoxically, cannot be explained by a higher free luminal SR [Ca^{2+}] [20]. Moreover, the high speed of Ca^{2+} wave propagation requires active SERCA pumps in heart cells [105], a condition that is unexpected. It has been shown that induction of Ca^{2+} release due to activation of RyR1 activates SERCA pump even during the initial phase of Ca^{2+} release when the free luminal SR [Ca^{2+}] is the highest [87], arguing against the idea that changes in the free luminal SR [Ca^{2+}] is the way that RyRs control the activity of SERCA pump [81]. Additionally, rapid inhibition of SERCA pump with thapsigargin decreases both the amplitude and the rate of rising of the cytoplasmic Ca^{2+} response to caffeine or to acetylcholine in smooth muscle cells. This is happening even when thapsigargin does not reduce immediately the free luminal [Ca^{2+}] [89]. All these data argue again for the need for active SERCA pumps to have

an efficient Ca^{2+} release event. Efficient histamine-induced Ca^{2+} release in HeLa cells also requires that SERCA pump is active [124]. Pancreatic acinar cells from RGS2 knockout mice express a compensatory twofold-increase in the expression of SERCA pump and this is associated with a larger and more sensitive $[Ca^{2+}]_i$ response to acetylcholine that cannot be explained by a larger production of IP_3 [125]. Although this type of experiment does not explain why the elimination of RGS2 has resulted in a compensatory two-fold increase in the expression of SERCA pump, these results are in line with the idea that higher activity of SERCA pump produces larger agonist-induced Ca^{2+} release events.

14.6 Ca^{2+} Signaling Between the SR/ER and Other Organelles

14.6.1 The Connection Between the ER and Mitochondria

It has been shown that close association between the ER and mitochondria plays an important role in ATP production, lipids synthesis, mitochondria dynamics and Ca^{2+} signaling [126, 127]. One of the first studies about this association showed that the majority of mitochondria, around 80%, was forming contacts sites with the ER [128]. However, using a high resolution microscope in the 90s, it was found that the mitochondrial surface in contact with the ER was estimated to be around 10% of the total mitochondrial network [129]. Subsequent works have found that the percentage of mitochondria in contact with the ER was close to 20%, and that these values can vary when cells are challenged with different experimental conditions, although this interaction has never reached 80% [130–133]. Interestingly, Scorrano's group has observed that the fraction of mitochondria interacting with the ER is near 80% [134], as it was initially described by Montisano et al. [128]. Recently, using super-resolution microscopes, it has been shown that mitochondria are the main organelle in association with the ER, although these studies did not quantify the degree of this interaction [23, 24, 135]. Collectively, these data show an uncertain scenario regarding the fraction of the mitochondrial network that is associated with the ER, since these numbers vary so widely. At the present time it is not clear the reason behind this variability among the different studies.

14.6.2 The Association Between Mitochondria and the ER Is Stabilized by a Large Assortment of Protein Tethers

At the biochemical level, it has been shown that the ER-mitochondria interaction is involved in phospholipids synthesis, this process involves the bidirectional exchange of phospholipids between the ER and mitochondria [136]. It has been shown that

this exchange occurs in specific contact sites called Mitochondria-associated ER membranes (MAMs). These structures facilitate different signaling transduction processes [137] and probably, Ca^{2+} transfer from the ER to mitochondria. Actually, it has been described several different protein tethers that modulate Ca^{2+} transfer from the ER to mitochondria [138].

It has been reported that the Voltage Dependent Anion Channel (VDAC), a resident protein in the outer mitochondrial membrane (OMM) connects with the IP_3R in the ER by interacting with the cytosolic chaperone glucose-regulated protein 75 (Grp75). This tether enhances the Ca^{2+} uptake by mitochondria [139]. Additionally, Cyclophilin D, a mitochondrial protein that modulates the opening of the permeability transition pore, interacts with the VDAC-Grp75-IP_3R complex; the loss of this protein decreases both ER-mitochondria interactions and Ca^{2+} transfer to mitochondria. This situation leads to insulin resistance in hepatic cells, suggesting that this tether might be controlling glucose homeostasis [140]. Moreover, the overexpression of α-synuclein (a central protein in Parkinson disease) in HeLa cells has promoted an increase in mitochondrial Ca^{2+} uptake by enhancing ER-mitochondria interactions. These data suggest that α-synuclein has an important role in mitochondrial Ca^{2+} homeostasis [141]. It is clear then, from these examples, that protein tethers are involved in Ca^{2+} signaling. Indeed, mitofusin 2 (Mfn-2) a GTPase that is located both in the OMM and the ER membrane, is involved in the formation of ER-mitochondria tethers. Mfn-2 ablation increases the distance between the ER and mitochondria, and this results in a reduced Ca^{2+} influx into mitochondria in response to IP_3 in both HeLa cells and mouse embryonic fibroblasts [134, 142]. Moreover, ablation of Mfn-2 leads to metabolic disorders such as glucose intolerance and impaired insulin signaling in both liver and muscle [143]. Conversely, Pozzan's group has demonstrated that silencing of Mfn-2 increases contact sites between the ER and mitochondria and augments mitochondria Ca^{2+} uptake. These data suggest that Mfn-2 appears to have a protective role because it forms a tether that prevents Ca^{2+} overload into the mitochondria [130]. Although both groups have shown that Mfn-2 is a molecular tether in the ER-mitochondria contact site, silencing this protein produces the opposite effects on Ca^{2+} signaling. Interestingly, a picture is emerging where Mfn-2 is able to increase the number of contact sites between the ER and mitochondria when they are low and it does the opposite when these sites are high. Further work is needed to understand the role played by Mfn-2 in Ca^{2+} transfer from the ER to mitochondria.

14.6.3 Mitocondrial Calcium Uniporter (MCU) Is a Finely Regulated Inner Mitochondrial Membrane Ion Channel

Ca^{2+} transfer from the ER to mitochondria is an essential event that regulates cell bioenergetics by increasing the activity of different Krebs cycle dehydrogenase; such as pyruvate dehydrogenase, isocitrate dehydrogenase and α-ketoglutarate

dehydrogenase [144]. This Ca^{2+} entry in the mitochondria matrix involves the activation of Ca^{2+} release channels from the ER, mainly the IP_3R [129]. Although the closeness between the ER and mitochondria should lead to mitochondria Ca^{2+} transient before that in the cytoplasm, it turns out that this is not the case. Indeed, GECIs targeted to mitochondria and the ER in combination with fura-2 to detect changes in cytoplasmic $[Ca^{2+}]$ have shown that despite mitochondria being close to the ER, the cytosolic Ca^{2+} increases well before it does in mitochondria [110], suggesting that closeness between these two organelles is not enough to elevate Ca^{2+} in mitochondria. Alternatively, mitochondria might have mechanisms that prevent an immediate Ca^{2+} entry in the mitochondrial matrix. The molecular identification of the Mitochondrial Ca^{2+} Uniporter or MCU [145, 146] as the mitochondria Ca^{2+} permeable channel for Ca^{2+} entry to the mitochondria matrix, has demonstrated that this channel is indeed a protein complex formed by different types of proteins, such as EMRE, MCUb and members of the MICU family [147]. MICU1, MICU2 and MICU3 are EF-hand proteins that inhibit MCU activity at low $[Ca^{2+}]_i$ (around 500 nM), thus acting as a channel gatekeeper that prevents mitochondria Ca^{2+} overload. Remarkably, MICU1 silencing leads to neurologic and muscular problems during development [148]. That is, these proteins act as natural inhibitors of MCU that block Ca^{2+} entry into the mitochondria. This might explain the mitochondria delayed Ca^{2+} increase after activation of IP_3R and increase of cytoplasm $[Ca^{2+}]$. In this regard, it has been shown that histamine, which produces a sustained Ca^{2+} release event, leads to a robust Ca^{2+} entry in mitochondria; however, glutamate, which produces a transient Ca^{2+} release event due to deactivation of IP_3Rs, produces a much smaller Ca^{2+} increase in mitochondria matrix [149]. These data suggest that Ca^{2+} entry in mitochondria requires more a sustained Ca^{2+} release from the ER than a localized elevation of cytoplasmic $[Ca^{2+}]$. Collectively, a picture is emerging showing that closeness between the ER and mitochondria is necessary but not sufficient for an elevation of the mitochondria $[Ca^{2+}]$. Moreover, an elevation of the mitochondrial $[Ca^{2+}]$ can trigger apoptosis [150]. In conclusion, the Ca^{2+} transfer from the ER to the mitochondria is important for cell respiration and for tuning ATP production while at the same time could lead to an apoptotic event. It is extremely complex how the same signal, i.e. Ca^{2+} ions, results in so divergent cell responses. Thus, essential pieces of the puzzle are still missing to fully unravel the role of Ca^{2+} in the interaction between the ER and mitochondria.

14.6.4 The Connection Between the ER and Lysosomes

The lysosome is another organelle that associates with the ER [23]. This organelle is vesicular in nature, it is filled with hydrolytic enzymes and characterized by having an extremely acidic luminal pH, around 5.0 [151]. This acidic pH is generated by the activity of a V-type proton ATPase [152, 153] and it has been considered that the activity of this pump is essential for the Ca^{2+} accumulating activity of

lysosomes [154, 155]. However, studies using Ca^{2+} indicators targeted directly to lysosomes and agonists for TRPML1 channel in lysosomes, have found that the acidic luminal pH is not essential for lysosomes to accumulate Ca^{2+} but that a still undefined mechanism allows lysosomes to accumulate Ca^{2+} that has been released by IP_3Rs from the ER [11, 156]. The dynamics of the ER and lysosomes has been recently observed with high spatial and temporal resolutions and it appears that lysosomes are able to reshape the ER [23]. However, it is still a long way to understand the regulation of Ca^{2+} transfer from the ER to lysosomes in the autophagic process [157]; although the presence of high spatial and temporal super-resolution microscopes, as GI-SIM [23], would make easier to unravel the role played by Ca^{2+} both in the lysosomes and in the ER in the activity of these acidic organelles.

14.7 Concluding Remarks

All these studies reviewed here allow us to depict a picture where an efficient Ca^{2+} release event from the SR/ER requires the activity not only of release channels, but also of SERCA pumps and the luminal Ca^{2+} binding proteins. Additionally, it is clear that the free luminal SR/ER $[Ca^{2+}]$ cannot predict the amount of Ca^{2+} that will be released to the cytoplasm, the most likely explanation is that the Ca^{2+} released during the activation of release channels involve the participation of luminal Ca^{2+} binding proteins that trap Ca^{2+} next to the release channels and that the formation of this complex requires active SERCA pumps. This scenario could explain several situations of the Ca^{2+} release event; for instance, why the amplitude of the Ca^{2+} release event in the cytoplasm does not show any correlation with the reduction in the free luminal SR/ER $[Ca^{2+}]$? Why the increase in the $[Ca^{2+}]_i$ during Ca^{2+} release is associated with a minimal reduction in the bulk free luminal SR/ER $[Ca^{2+}]$? Why is the refractory period for Ca^{2+} release longer than the recovery of the free luminal SR/ER $[Ca^{2+}]$? It is clear that we are still far from understanding how release channels produce an efficient Ca^{2+} release event but the development of the GI-SIM superresolution microscope should help [23]. This microscope has both enhanced spatial and temporal resolutions and can be used with the current Ca^{2+} indicators, so it should be easier to follow changes in the $[Ca^{2+}]$ of both the lumen of the ER and the cytoplasm to gather a better picture on how the Ca^{2+} lattice produces an efficient Ca^{2+} release event. Additionally, it is clear that the SR/ER is the main Ca^{2+} source, not only for the cytoplasm, but also for other organelles as mitochondria and lysosomes. In conclusion, it appears that an efficient Ca^{2+} release event occurs only during the initial Ca^{2+} release process and that this requires the participation of release channels, luminal Ca^{2+} binding proteins and the SERCA pump. This means that the communication among all these elements makes the Ca^{2+} release event more complex than previously envisioned but very

robust because it can successfully fulfill the role of SR/ER as Ca^{2+} source without interfering with the need of having a high luminal SR/ER [Ca^{2+}].

References

1. Berridge MJ, Bootman MD, Roderick HL (2003) Calcium signalling: dynamics, homeostasis and remodelling. Nat Rev Mol Cell Biol 4(7):517–529
2. Clapham DE (2007) Calcium signaling. Cell 131(6):1047–1058
3. Zhivotovsky B, Orrenius S (2011) Calcium and cell death mechanisms: a perspective from the cell death community. Cell Calcium 50(3):211–221
4. Yanez M, Gil-Longo J, Campos-Toimil M (2012) Calcium binding proteins. In: Calcium signaling. Springer, Dordrecht, pp 461–482
5. Berridge MJ, Lipp P, Bootman MD (2000) The versatility and universality of calcium signalling. Nat Rev Mol Cell Biol 1(1):11–21
6. Tombal B, Denmeade SR, Gillis JM, Isaacs JT (2002) A supramicromolar elevation of intracellular free calcium ([Ca^{2+}]i) is consistently required to induce the execution phase of apoptosis. Cell Death Differ 9(5):561–573
7. Verkhratsky A (2005) Physiology and pathophysiology of the calcium store in the endoplasmic reticulum of neurons. Physiol Rev 85(1):201–279
8. Rizzuto R, Marchi S, Bonora M, Aguiari P, Bononi A, De Stefani D et al (2009) Ca^{2+} transfer from the ER to mitochondria: when, how and why. Biochim Biophys Acta Bioenerg 1787(11):1342–1351
9. Llopis J, McCaffery JM, Miyawaki A, Farquhar MG, Tsien RY (1998) Measurement of cytosolic, mitochondrial, and Golgi pH in single living cells with green fluorescent proteins. Proc Natl Acad Sci U S A 95(12):6803–6808
10. Gallegos-Gómez M-L, Greotti E, López-Méndez M-C, Sánchez-Vázquez V-H, Arias J-M, Guerrero-Hernández A (2018) The trans golgi region is a labile intracellular Ca^{2+} store sensitive to emetine. Sci Rep 8(1):17143
11. Garrity AG, Wang W, Collier CMD, Levey SA, Gao Q, Xu H (2016) The endoplasmic reticulum, not the pH gradient, drives calcium refilling of lysosomes. elife 5:e15887
12. Dickson EJ, Duman JG, Moody MW, Chen L, Hille B (2012) Orai-STIM-mediated Ca^{2+} release from secretory granules revealed by a targeted Ca^{2+} and pH probe. Proc Natl Acad Sci U S A 109(51):E3539–E3548
13. Pezzati R, Bossi M, Podini P, Meldolesi J, Grohovaz F (1997) High-resolution calcium mapping of the endoplasmic reticulum-Golgi-exocytic membrane system. Electron energy loss imaging analysis of quick frozen-freeze dried PC12 cells. Mol Biol Cell 8(8):1501–1512
14. Yagodin S, Pivovarova NB, Andrews SB, Sattelle DB (1999) Functional characterization of thapsigargin and agonist-insensitive acidic Ca^{2+} stores in Drosophila melanogaster S2 cell lines. Cell Calcium 25(6):429–438
15. Fasolato C, Zottinis M, Clementis E, Zacchettis D, Meldolesi J, Pozzan T (1991) Intracellular Ca^{2+} pools in PC12 cells. J Biol Chem 266(30):20159–20167
16. Phillips MJ, Voeltz GK (2016) Structure and function of ER membrane contact sites with other organelles. Nat Rev Mol Cell Biol 17(2):69–82
17. Voeltz GK, Rolls MM, Rapoport TA (2002) Structural organization of the endoplasmic reticulum. EMBO Rep 3(10):944–950
18. Shibata Y, Voeltz GK, Rapoport TA (2006) Rough sheets and smooth tubules. Cell 126(3):435–439
19. Park MK, Petersen OH, Tepikin AV (2000) The endoplasmic reticulum as one continuous Ca^{2+} pool: visualization of rapid Ca^{2+} movements and equilibration. EMBO J 19(21):5729–5739

20. Bers DM, Shannon TR (2013) Calcium movements inside the sarcoplasmic reticulum of cardiac myocytes. J Mol Cell Cardiol 58(1):59–66
21. Jones VC, Rodríguez JJ, Verkhratsky A, Jones OT (2009) A lentivirally delivered photoactivatable GFP to assess continuity in the endoplasmic reticulum of neurones and glia. Pflugers Arch Eur J Physiol 458(4):809–818
22. Friedman JR, Webster BM, Mastronarde DN, Verhey KJ, Voeltz GK (2010) ER sliding dynamics and ER-mitochondrial contacts occur on acetylated microtubules. J Cell Biol 190(3):363–375
23. Guo Y, Li D, Zhang S, Lippincott-schwartz J, Betzig E, Guo Y et al (2018) Visualizing intracellular organelle and cytoskeletal interactions at nanoscale resolution on millisecond resource visualizing intracellular organelle and cytoskeletal interactions at nanoscale resolution on millisecond timescales. Cell 175:1430–1442
24. Shim S-H, Xia C, Zhong G, Babcock HP, Vaughan JC, Huang B et al (2012) Super-resolution fluorescence imaging of organelles in live cells with photoswitchable membrane probes. Proc Natl Acad Sci 109(35):13978–13983
25. Hernández-Ochoa EO, Schneider MF (2018) Voltage sensing mechanism in skeletal muscle excitation-contraction coupling: coming of age or midlife crisis? Skelet Muscle 8(1):22
26. Sweeney HL, Hammers DW (2018) Muscle contraction. Cold Spring Harb Perspect Biol 10(2):a023200
27. Zarain-Herzberg A, García-Rivas G, Estrada-Avilés R (2014) Regulation of SERCA pumps expression in diabetes. Cell Calcium 56(5):302–310
28. Toyoshima C, Inesi G (2004) Structural basis of ion pumping by Ca^{2+}-ATPase of the sarcoplasmic reticulum. Annu Rev Biochem 73:269–292
29. Toyoshima C, Nomura H, Tsuda T (2004) Lumenal gating mechanism revealed in calcium pump crystal structures with phosphate analogues. Nature 432(7015):361–368
30. Dyla M, Terry DS, Kjaergaard M, Sørensen TLM, Andersen JL, Andersen JP et al (2017) Dynamics of P-type ATPase transport revealed by single-molecule FRET. Nature 551(7680):346–351
31. Mejía-Alvarez R, Kettlun C, Ríos E, Stern M, Fill M (1999) Unitary Ca^{2+} current through cardiac ryanodine receptor channels under quasi-physiological ionic conditions. J Gen Physiol 113(2):177–186
32. Ikeda K, Kang Q, Yoneshiro T, Camporez JP, Maki H, Homma M et al (2017) UCP1-independent signaling involving SERCA2b mediated calcium cycling regulates beige fat thermogenesis and systemic glucose homeostasis. Nat Med 23(12):1454–1465
33. De Meis L, Arruda AP, Carvalho DP (2005) Role of sarco/endoplasmic reticulum Ca^{2+}-ATPase in thermogenesis. Biosci Rep 25(3–4):181–190
34. Fruen BR, Mickelson JR, Louis CF (1997) Dantrolene inhibition of sarcoplasmic reticulum Ca^{2+} release by direct and specific action at skeletal muscle ryanodine receptors. J Biol Chem 272(43):26965–26971
35. Bal NC, Maurya SK, Sopariwala DH, Sahoo SK, Gupta SC, Shaikh SA et al (2012) Sarcolipin is a newly identified regulator of muscle-based thermogenesis in mammals. Nat Med 18(10):1575–1579
36. Bhupathy P, Babu GJ, Periasamy M (2007) Sarcolipin and phospholamban as regulatos of cardiac sarcoplasmic reticulum Ca^{2+} ATPase. J Mol Cell Cardiol 42(5):903–911
37. Anderson DM, Makarewich CA, Anderson KM, Shelton JM, Bezprozvannaya S, Bassel-Duby R et al (2016) Widespread control of calcium signaling by a family of SERCA-inhibiting micropeptides. Sci Signal 9(457):ra119
38. Dettbarn C, Palade P (1998) Effects of three sarcoplasmic/endoplasmic reticulum Ca++ pump inhibitors on release channels of intracellular stores. J Pharmacol Exp Ther 285(2):739–745
39. Chen J, De Raeymaecker J, Hovgaard JB, Smaardijk S, Vandecaetsbeek I, Wuytack F et al (2017) Structure/activity relationship of thapsigargin inhibition on the purified golgi/secretory pathway Ca^{2+}/Mn2+−transport ATPase (SPCA1a). J Biol Chem 292(17):6938–6951

40. Gustavo Vazquez-Jimenez J, Chavez-Reyes J, Romero-Garcia T, Zarain-Herzberg A, Valdes-Flores J, Manuel Galindo-Rosales J et al (2016) Palmitic acid but not palmitoleic acid induces insulin resistance in a human endothelial cell line by decreasing SERCA pump expression. Cell Signal 28(1):53–59
41. Nelson BR, Makarewich CA, Anderson DM, Winders BR, Troupes CD, Wu F et al (2016) Muscle physiology: a peptide encoded by a transcript annotated as long noncoding RNA enhances SERCA activity in muscle. Science 351(6270):271–275
42. Fill M, Copello JA (2002) Ryanodine receptor calcium release channels. Physiol Rev 82(4):893–922
43. Mikoshiba K (2015) Role of IP_3 receptor signaling in cell functions and diseases. Adv Biol Regul 57:217–227
44. Seo M-D, Velamakanni S, Ishiyama N, Stathopulos PB, Rossi AM, Khan SA et al (2012) Structural and functional conservation of key domains in $InsP_3$ and ryanodine receptors. Nature 483(7387):108–112
45. Meissner G (2004) Molecular regulation of cardiac ryanodine receptor ion channel. Cell Calcium 35(6):621–628
46. Foskett JK, White C, Cheung K, Mak DD (2007) Inositol trisphosphate receptor Ca^{2+} release channels. Am Physiol Soc 87:593–658
47. Meissner G (2017) The structural basis of ryanodine receptor ion channel function. J Gen Physiol 149(12):1065–1089
48. Scriven DRL, Dan P, Moore EDW (2000) Distribution of proteins implicated in excitation-contraction coupling in rat ventricular myocytes. Biophys J 79(5):2682–2691
49. Bers DM (2002) Cardiac excitation–contraction coupling. Nature 415(6868):198–205
50. Clark JH, Kinnear NP, Kalujnaia S, Cramb G, Fleischer S, Jeyakumar LH et al (2010) Identification of functionally segregated sarcoplasmic reticulum calcium stores in pulmonary arterial smooth muscle. J Biol Chem 285(18):13542–13549
51. Nelson MT, Cheng H, Rubart M, Santana LF, Bonev AD, Knot HJ et al (1995) Relaxation of arterial smooth muscle by calcium sparks. Science 270(5236):633–637
52. Kirber MT, Guerrero-Hernández A, Bowman DS, Fogarty KE, Tuft RA, Singer JJ et al (2000) Multiple pathways responsible for the stretch-induced increase in Ca^{2+} concentration in toad stomach smooth muscle cells. J Physiol 524(1):3–17
53. Kotlikoff MI (2003) Calcium-induced calcium release in smooth muscle: the case for loose coupling. Prog Biophys Mol Biol 83(3):171–191
54. van der Wal J, Habets R, Várnai P, Balla T, Jalink K, Varnai P et al (2001) Monitoring agonist-induced phospholipase C activation in live cells by fluorescence resonance energy transfer. J Biol Chem 276(18):15337–15344
55. Dickson EJ, Falkenburger BH, Hille B (2013) Quantitative properties and receptor reserve of the IP3 and calcium branch of G(q)-coupled receptor signaling. J Gen Physiol 141(5):521–535
56. Baker MR, Fan G, Serysheva II (2017) Structure of IP_3R channel: high-resolution insights from cryo-EM. Curr Opin Struct Biol 46:38–47
57. Choe CU, Ehrlich BE (2006) The inositol 1,4,5-trisphosphate receptor (IP3R) and its regulators: sometimes good and sometimes bad teamwork. Sci STKE 2006(363):re15
58. Royer L, Ríos E (2009) Deconstructing calsequestrin. Complex buffering in the calcium store of skeletal muscle. J Physiol 587(13):3101–3111
59. Ikemoto N, Ronjat M, Meszaros LG, Koshita M (1989) Postulated role of calsequestrin in the regulation of calcium release from sarcoplasmic reticulum. Biochemistry 28(16):6764–6771
60. Terentyev D, Kubalova Z, Valle G, Nori A, Vedamoorthyrao S, Terentyeva R et al (2008) Modulation of SR Ca release by luminal Ca and calsequestrin in cardiac myocytes: effects of CASQ2 mutations linked to sudden cardiac death. Biophys J 95(4):2037–2048
61. Michalak M, Groenendyk J, Szabo E, Gold LI, Opas M (2009) Calreticulin, a multi-process calcium-buffering chaperone of the endoplasmic reticulum. Biochem J 417(3):651–666
62. Park H, Park IY, Kim E, Youn B, Fields K, Dunker AK et al (2004) Comparing skeletal and cardiac calsequestrin structures and their calcium binding: a proposed mechanism for coupled calcium binding and protein polymerization. J Biol Chem 279(17):18026–18033

63. Arnaudeau S, Frieden M, Nakamura K, Castelbou C, Michalak M, Demaurex N (2002) Calreticulin differentially modulates calcium uptake and release in the endoplasmic reticulum and mitochondria. J Biol Chem 277(48):46696–46705
64. Pozzo-Miller LD, Connor JA, Andrews B (2000) Microheterogeneity of calcium signalling in dendrites. J Physiol 525(1):53–61
65. Pozzo-Miller LD, Pivovarova NB, Connor JA, Reese TS, Andrews SB (1999) Correlated measurements of free and total intracellular calcium concentration in central nervous system neurons. Microsc Res Tech 46(6):370–379
66. Papp S, Dziak E, Michalak M, Opas M (2003) Is all of the endoplasmic reticulum created equal? The effects of the heterogeneous distribution of endoplasmic reticulum Ca^{2+}-handling proteins. J Cell Biol 160(4):475–479
67. Handhle A, Ormonde CE, Thomas NL, Bralesford C, Williams AJ, Lai FA et al (2016) Calsequestrin interacts directly with the cardiac ryanodine receptor luminal domain. J Cell Sci 129:3983–3988
68. Wang Y, Li X, Duan H, Fulton TR, Eu JP, Meissner G (2009) Altered stored calcium release in skeletal myotubes deficient of triadin and junctin. Cell Calcium 45(1):29–37
69. Qin J, Valle G, Nani A, Nori A, Rizzi N, Priori SG et al (2008) Luminal Ca^{2+} regulation of single cardiac ryanodine receptors: insights provided by Calsequestrin and its mutants. J Gen Physiol 131(4):325–334
70. Terentyev D, Viatchenko-Karpinski S, Gyorke I, Volpe P, Williams SC, Gyorke S (2003) Calsequestrin determines the functional size and stability of cardiac intracellular calcium stores: mechanism for hereditary arrhythmia. Proc Natl Acad Sci 100(20):11759–11764
71. Wray S, Burdyga T (2010) Sarcoplasmic reticulum function in smooth muscle. Physiol Rev 90(1):113–178
72. Laver DR (2007) Ca^{2+} stores regulate ryanodine receptor Ca^{2+} release channels via luminal and cytosolic Ca^{2+} sites. Biophys J 92(10):3541–3555
73. Laver DR, Kong CHT, Imtiaz MS, Cannell MB (2013) Termination of calcium-induced calcium release by induction decay: an emergent property of stochastic channel gating and molecular scale architecture. J Mol Cell Cardiol 54(1):98–100
74. Cannell MB, Kong CHT, Imtiaz MS, Laver DR (2013) Control of sarcoplasmic reticulum Ca^{2+} release by stochastic RyR gating within a 3D model of the cardiac dyad and importance of induction decay for CICR termination. Biophys J 104(10):2149–2159
75. Wu X, Bers DM (2006) Sarcoplasmic reticulum and nuclear envelope are one highly interconnected Ca^{2+} store throughout cardiac myocyte. Circ Res 99(3):283–291
76. Murphy RM, Mollica JP, Beard NA, Knollmann BC, Lamb GD (2011) Quantification of calsequestrin 2 (CSQ2) in sheep cardiac muscle and Ca^{2+}-binding protein changes in CSQ2 knockout mice. Am J Physiol Heart Circ Physiol 300(2):H595–H604
77. Ikemoto N, Antoniu B, Kang JJ, Mészáros LG, Ronjat M (1991) Intravesicular calcium transient during calcium release from sarcoplasmic reticulum. Biochemistry 30(21):5230–5237
78. Yamaguchi N, Igami K, Kasai M (1997) Kinetics of depolarization-induced calcium release from skeletal muscle triads in vitro. J Biochem 121(3):432–439
79. Gomez-Viquez L, Rueda A, Garcia U, Guerrero-Hernandez A (2005) Complex effects of ryanodine on the sarcoplasmic reticulum Ca^{2+} levels in smooth muscle cells. Cell Calcium 38:121–130
80. Rueda A, García L, Guerrero-Hernández A (2002) Luminal Ca^{2+} and the activity of sarcoplasmic reticulum Ca^{2+} pumps modulate histamine-induced all-or-none Ca^{2+} release in smooth muscle cells. Cell Signal 14(6):517–527
81. Inesi G, Tadini-Buoninsegni F (2014) Ca^{2+}/H^{+} exchange, lumenal Ca^{2+} release and Ca^{2+}/ATP coupling ratios in the sarcoplasmic reticulum ATPase. J Cell Commun Signal 8(1):5–11
82. Saiki Y, Ikemoto N (1999) Coordination between Ca^{2+} release and subsequent re-uptake in the sarcoplasmic reticulum. Biochemistry 38(10):3112–3119

83. Saiki Y, Ikemoto N (1997) Fluorescence probe study of the lumenal $Ca^{2+}$of the sarcoplasmic reticulum vesicles during Ca^{2+} uptake and Ca^{2+} release. Biochem Biophys Res Commun 241(1):181–186
84. Mészáros LG, Ikemoto N (1989) Non-identical behavior of the Ca^{2+}-ATPase in the terminal cisternae and the longitudinal tubules fractions of sarcoplasmic reticulum. Eur J Biochem 186(3):677–681
85. Yano M, Yamamoto T, Ikemoto N, Matsuzaki M (2005) Abnormal ryanodine receptor function in heart failure. Pharmacol Ther 107(3):377–391
86. Mészáros LG, Ikemoto N (1985) Conformational changes of the Ca^{2+}-ATPase as early events of Ca^{2+} release from sarcoplasmic reticulum. J Biol Chem 260(30):16076–16079
87. Ikemoto N, Yamamoto T (2000) The luminal Ca^{2+} transient controls Ca^{2+} release/re-uptake of sarcoplasmic reticulum. Biochem Biophys Res Commun 279(3):858–863
88. Guerrero A, Singer JJ, Fay FS (1994) Simultaneous measurement of Ca^{2+} release and influx into smooth muscle cells in response to caffeine. A novel approach for calculating the fraction of current carried by calcium. J Gen Physiol 104(2):395–422
89. Gómez-Viquez L, Guerrero-Serna G, García U, Guerrero-Hernández A (2003) SERCA pump optimizes Ca^{2+} release by a mechanism independent of store filling in smooth muscle cells. Biophys J 85(1):370–380
90. Hofer AM, Machen TE (1993) Technique for in situ measurement of calcium in intracellular inositol 1,4,5-trisphosphate-sensitive stores using the fluorescent indicator mag-fura-2 (gastric glands/thapsigargin/heparin). Proc Natl Acad Sci 90(April):2598–2602
91. Shmigol AV, Eisner DA, Wray S (2001) Simultaneous measurements of changes in sarcoplasmic reticulum and cytosolic [Ca^{2+}] in rat uterine smooth muscle cells. J Physiol 531(1):707–713
92. Navas-Navarro P, Rojo-Ruiz J, Rodriguez-Prados M, Ganfornina MD, Looger LL, Alonso MT et al (2016) GFP-aequorin protein sensor for ex vivo and in vivo imaging of Ca^{2+} dynamics in high-Ca^{2+} organelles. Cell Chem Biol 23(6):738–745
93. Barrero MJ, Montero M, Alvarez J (1997) Dynamics of [Ca^{2+}] in the endoplasmic reticulum and cytoplasm of intact HeLa cells: a comparative study. J Biol Chem 272(44):27694–27699
94. Palmer AE, Jin C, Reed JC, Tsien RY (2004) Bcl-2-mediated alterations in endoplasmic reticulum Ca^{2+} analyzed with an improved genetically encoded fluorescent sensor. Proc Natl Acad Sci 101(50):17404–17409
95. Dagnino-Acosta A, Guerrero-Hernández A (2009) Variable luminal sarcoplasmic reticulum Ca^{2+} buffer capacity in smooth muscle cells. Cell Calcium 46(3):188–196
96. Guerrero-Hernandez A, Dagnino-Acosta A, Verkhratsky A (2010) An intelligent sarcoendoplasmic reticulum Ca^{2+} store: release and leak channels have differential access to a concealed Ca^{2+} pool. Cell Calcium 48(2–3):143–149
97. Launikonis BS, Zhou J, Royer L, Shannon TR, Brum G, Ríos E (2006) Depletion "skraps" and dynamic buffering inside the cellular calcium store. Proc Natl Acad Sci U S A 103(8):2982–2987
98. Shmygol A, Wray S (2005) Modulation of agonist-induced Ca^{2+} release by SR Ca^{2+} load: direct SR and cytosolic Ca^{2+} measurements in rat uterine myocytes. Cell Calcium 37(3):215–223
99. Missiaen L, Van Acker K, Van Baelen K, Raeymaekers L, Wuytack F, Parys JB et al (2004) Calcium release from the Golgi apparatus and the endoplasmic reticulum in HeLa cells stably expressing targeted aequorin to these compartments. Cell Calcium 36(6):479–487
100. Ishii K, Hirose K, Iino M (2006) Ca^{2+} shuttling between endoplasmic reticulum and mitochondria underlying Ca^{2+} oscillations. EMBO Rep 7(4):390–396
101. Brochet DXP, Yang D, Di Maio A, Lederer WJ, Franzini-Armstrong C, Cheng H (2005) Ca^{2+} blinks: rapid nanoscopic store calcium signaling. Proc Natl Acad Sci U S A 102(8):3099–3104
102. Zima AV, Picht E, Bers DM, Blatter LA (2008) Termination of cardiac Ca^{2+} sparks: role of intra-SR [Ca^{2+}], release flux, and intra-SR Ca^{2+} diffusion. Circ Res 103(8):e105–e115

103. Maxwell JT, Blatter LA (2012) Facilitation of cytosolic calcium wave propagation by local calcium uptake into the sarcoplasmic reticulum in cardiac myocytes. J Physiol 590:6037–6045
104. Maxwell JT, Blatter LA (2017) A novel mechanism of tandem activation of ryanodine receptors by cytosolic and SR luminal Ca^{2+} during excitation–contraction coupling in atrial myocytes. J Physiol 595(12):3835–3845
105. Keller M, Kao JPY, Egger M, Niggli E (2007) Calcium waves driven by "sensitization" wavefronts. Cardiovasc Res 74(1):39–45
106. Rodriguez-Garcia A, Rojo-Ruiz J, Navas-Navarro P, Aulestia FJ, Gallego-Sandin S, Garcia-Sancho J et al (2014) GAP, an aequorin-based fluorescent indicator for imaging Ca^{2+} in organelles. Proc Natl Acad Sci U S A 111(7):2584–2589
107. Greotti E, Wong A, Pozzan T, Pendin D, Pizzo P (2016) Characterization of the ER-targeted low affinity Ca^{2+} probe D4ER. Sensors 16(9):1–13
108. Baddeley D, Crossman D, Rossberger S, Cheyne JE, Montgomery JM, Jayasinghe ID et al (2011) 4D super-resolution microscopy with conventional fluorophores and single wavelength excitation in optically thick cells and tissues. PLoS One 6(5):e20645
109. Perez-Rosas NC, Gomez-Viquez NL, Dagnino-Acosta A, Santillan M, Guerrero-Hernandez A (2015) Kinetics on demand is a simple mathematical solution that fits recorded caffeine-induced luminal SR Ca^{2+} changes in smooth muscle cells. PLoS One 10(9):e0138195
110. Suzuki J, Kanemaru K, Ishii K, Ohkura M, Okubo Y, Iino M (2014) Imaging intraorganellar Ca^{2+} at subcellular resolution using CEPIA. Nat Commun 5:4153
111. Manno C, Ríos E (2015) A better method to measure total calcium in biological samples yields immediate payoffs. J Gen Physiol 145(3):167–171
112. Györke I, Hester N, Jones LR, Györke S (2004) The role of calsequestrin, triadin, and junctin conferring cardiac ryanodine receptor responsiveness to luminal calcium. Biophys J 86(4):2121–2128
113. Gómez-Viquez NL, Guerrero-Serna G, Arvizu F, García U, Guerrero-Hernández A (2010) Inhibition of SERCA pumps induces desynchronized RyR activation in overloaded internal Ca^{2+} stores in smooth muscle cells. Am J Physiol Cell Physiol 298(5):C1038–C1046
114. Song XW, Tang Y, Lei CH, Cao M, Shen YF, Yang YJ (2016) In situ visualizing T-tubule/SR junction reveals the ultra-structures of calcium storage and release machinery. Int J Biol Macromol 82:7–12
115. Cifuentes ME, Ronjat M, Ikemoto N (1989) Polylysine induces a rapid Ca^{2+} release from sarcoplasmic reticulum vesicles by mediation of its binding to the foot protein. Arch Biochem Biophys 273(2):554–561
116. El-Hayekt R, Yano M, Ikemoto N (1995) A conformational change in the junctional foot protein is involved in the regulation of Ca^{2+} release from sarcoplasmic reticulum: studies on polylysine-induced Ca^{2+} release. J Biol Chem 270(26):15634–15638
117. Rueda A, García L, Soria-Jasso LE, Arias-Montaño JA, Guerrero-Hernández A (2002) The initial inositol 1,4,5-trisphosphate response induced by histamine is strongly amplified by Ca^{2+} release from internal stores in smooth muscle. Cell Calcium 31(4):161–173
118. Bers DM, Eisner DA, Valdivia HH (2003) Sarcoplasmic reticulum Ca^{2+} and heart failure. Circ Res 93(6):487–490
119. Park SW, Zhou Y, Lee J, Lee J, Ozcan U (2010) Sarco(endo)plasmic reticulum Ca^{2+}-ATPase 2b is a major regulator of endoplasmic reticulum stress and glucose homeostasis in obesity. Proc Natl Acad Sci U S A 107(45):19320–19325
120. Sammels E, Parys JB, Missiaen L, De Smedt H, Bultynck G (2010) Intracellular Ca^{2+} storage in health and disease: a dynamic equilibrium. Cell Calcium 47(4):297–314
121. Fu S, Watkins SM, Hotamisligil GS (2012) The role of endoplasmic reticulum in hepatic lipid homeostasis and stress signaling. Cell Metab 15(5):623–634
122. Allen DG, Lamb GD, Westerblad H (2007) Impaired calcium release during fatigue. J Appl Physiol 104(1):296–305

123. Manno C, Figueroa LC, Gillespie D, Fitts R, Kang C, Franzini-Armstrong C et al (2017) Calsequestrin depolymerizes when calcium is depleted in the sarcoplasmic reticulum of working muscle. Proc Natl Acad Sci 114(4):E638–E647
124. Aguilar-Maldonado B, Gómez-Viquez L, García L, Del Angel RM, Arias-Montaño JA, Guerrero-Hernández A (2003) Histamine potentiates IP3-mediated Ca^{2+} release via thapsigargin-sensitive Ca^{2+} pumps. Cell Signal 15(7):689–697
125. Wang X, Huang G, Luo X, Penninger JM, Muallem S (2004) Role of regulator of G protein signaling 2 (RGS2) in Ca^{2+} oscillations and adaptation of Ca^{2+} signaling to reduce excitability of $RGS2^{-/-}$ cells. J Biol Chem 279(40):41642–41649
126. Rowland AA, Voeltz GK (2012) Endoplasmic reticulum–mitochondria contacts: function of the junction. Nat Rev Mol Cell Biol 13(10):607–615
127. Csordás G, Renken C, Várnai P, Walter L, Weaver D, Buttle KF et al (2006) Structural and functional features and significance of the physical linkage between ER and mitochondria. J Cell Biol 174(7):915–921
128. Montisano D, Cascarano J, Pickett C, James T (1982) Association between mitochondria and rough endoplasmic reticulum in rat liver. Anat Rec 203:441–450
129. Rizzuto R (1998) Close contacts with the endoplasmic reticulum as determinants of mitochondrial Ca^{2+} responses. Science 280(5370):1763–1766
130. Filadi R, Greotti E, Turacchio G, Luini A, Pozzan T, Pizzo P (2015) Mitofusin 2 ablation increases endoplasmic reticulum–mitochondria coupling. Proc Natl Acad Sci 112(17):E2174–E2181
131. Bravo R, Vicencio JM, Parra V, Troncoso R, Munoz JP, Bui M et al (2011) Increased ER-mitochondrial coupling promotes mitochondrial respiration and bioenergetics during early phases of ER stress. J Cell Sci 124(14):2511–2511
132. Bravo-sagua R, López-crisosto C, Parra V, Rodriguez M, Rothermel BA, Quest AFG et al (2016) mTORC1 inhibitor rapamycin and ER stressor tunicamycin induce differential patterns of ER- mitochondria coupling. Sci Rep 6:36394
133. Harmon M, Larkman P, Hardingham G, Jackson M, Skehel P (2017) A Bi-fluorescence complementation system to detect associations between the endoplasmic reticulum and mitochondria. Sci Rep 7:1–12
134. de Brito OM, Scorrano L (2008) Mitofusin 2 tethers endoplasmic reticulum to mitochondria. Nature 456(7222):605–610
135. Valm AM, Cohen S, Legant WR, Melunis J, Hershberg U, Wait E et al (2017) Applying systems-level spectral imaging and analysis to reveal the organelle interactome. Nature 546(7656):162–167
136. Vance E (1990) Phospholipid synthesis in a membrane fraction associated with mitochondria. J Biol Chem 265(13):7248–7256
137. Filadi R, Theurey P, Pizzo P (2017) The endoplasmic reticulum-mitochondria coupling in health and disease: molecules, functions and significance. Cell Calcium 62:1–15
138. Marchi S, Patergnani S, Missiroli S, Morciano G, Rimessi A, Wieckowski MR et al (2018) Mitochondrial and endoplasmic reticulum calcium homeostasis and cell death. Cell Calcium 69:62–72
139. Szabadkai G, Bianchi K, Várnai P, De Stefani D, Wieckowski MR, Cavagna D et al (2006) Chaperone-mediated coupling of endoplasmic reticulum and mitochondrial Ca^{2+} channels. J Cell Biol 175(6):901–911
140. Rieusset J, Fauconnier J, Paillard M, Belaidi E, Tubbs E, Chauvin M et al (2016) Disruption of calcium transfer from ER to mitochondria links alterations of mitochondria-associated ER membrane integrity to hepatic insulin resistance. Diabetologia 59:614–623
141. Cali T, Ottolini D, Negro A, Brini M (2012) α-Synuclein controls mitochondrial calcium homeostasis by enhancing endoplasmic reticulum-mitochondria interactions. J Biol Chem 287(22):17914–17929
142. Naon D, Zaninello M, Giacomello M, Varanita T, Grespi F, Lakshminaranayan S et al (2016) Critical reappraisal confirms that Mitofusin 2 is an endoplasmic reticulum–mitochondria tether. Proc Natl Acad Sci 113(40):11249–11254

143. Sebastián D, Hernández-alvarez MI, Segalés J, Sorianello E (2012) Mitofusin 2 (Mfn2) links mitochondrial and endoplasmic reticulum function with insulin signaling and is essential for normal glucose homeostasis. Proc Natl Acad Sci 109(14):5523–5528
144. Rossi A, Pizzo P, Filadi R (2018) Calcium, mitochondria and cell metabolism: a functional triangle in bioenergetics. BBA Mol Cell Res 1865(11):1–33
145. De Stefani D, Raffaello A, Teardo E, Szabò I, Rizzuto R (2011) A forty-kilodalton protein of the inner membrane is the mitochondrial calcium uniporter. Nature 476(7360):336–340
146. Baughman JM, Perocchi F, Girgis HS, Plovanich M, Belcher-Timme CA, Sancak Y et al (2011) Integrative genomics identifies MCU as an essential component of the mitochondrial calcium uniporter. Nature 476(7360):341–345
147. Mammucari C, Gherardi G, Rizzuto R (2017) Structure, activity regulation, and role of the mitochondrial calcium uniporter in health and disease. Front Oncol 7:139
148. Liu JC, Liu J, Holmstrom KM, Menazza S, Parks RJ, Fergusson MM et al (2016) MICU1 serves as a molecular gatekeeper to prevent in vivo mitochondrial calcium overload. Cell Rep 16(6):1561–1573
149. Szabadkai G, Simoni AM, Rizzuto R (2003) Mitochondrial Ca^{2+} uptake requires sustained Ca^{2+} release from the endoplasmic reticulum. J Biol Chem 278(17):15153–15161
150. Pinton P, Giorgi C, Siviero R, Zecchini E, Rizzuto R (2008) Calcium and apoptosis: ER-mitochondria Ca^{2+} transfer in the control of apoptosis. Oncogene 27:6407–6418
151. Christensen KA, Myers JT, Swanson JA (2002) pH-dependent regulation of lysosomal calcium in macrophages. J Cell Sci 115(3):599–607
152. Bowman EJ, Siebers A, Altendorf K (1988) Bafilomycins: a class of inhibitors of membrane ATPases from microorganisms, animal cells, and plant cells. Proc Natl Acad Sci U S A 85(21):7972–7976
153. Yoshimori T, Yamamoto A, Moriyama Y, Futai M, Tashiro Y (1991) Bafilomycin A1, a specific inhibitor of vacuolar-type H^+-ATPase, inhibits acidification and protein degradation in lysosomes of cultured cells. J Biol Chem 266(26):17707–17712
154. Sanjurjo CIL, Tovey SC, Prole DL, Taylor CW (2012 Jan) Lysosomes shape IP_3-evoked Ca^{2+} signals by selectively sequestering Ca^{2+} released from the endoplasmic reticulum. J Cell Sci 126(Pt 1):289–300
155. Sanjurjo CIL, Tovey SC, Taylor CW (2014) Rapid recycling of Ca^{2+}between IP_3-sensitive stores and lysosomes. PLoS One 9(10):e111275
156. Ronco V, Potenza DM, Denti F, Vullo S, Gagliano G, Tognolina M et al (2015) A novel Ca^{2+}-mediated cross-talk between endoplasmic reticulum and acidic organelles: implications for NAADP-dependent Ca^{2+}signalling. Cell Calcium 57(2):89–100
157. Augustine MK, Choi MD, Ryter SW, Beth Levine MD (2014) Autophagy in human health and disease. N Engl J Med 368:651–662

Chapter 15
Pyridine Nucleotide Metabolites and Calcium Release from Intracellular Stores

Antony Galione and Kai-Ting Chuang

Abstract Ca^{2+} signals are probably the most common intracellular signaling cellular events, controlling an extensive range of responses in virtually all cells. Many cellular stimuli, often acting at cell surface receptors, evoke Ca^{2+} signals by mobilizing Ca^{2+} from intracellular stores. Inositol trisphosphate (IP_3) was the first messenger shown to link events at the plasma membrane to release Ca^{2+} from the endoplasmic reticulum (ER), through the activation of IP_3-gated Ca^{2+} release channels (IP_3 receptors). Subsequently, two additional Ca^{2+} mobilizing messengers were discovered, cADPR and NAADP. Both are metabolites of pyridine nucleotides, and may be produced by the same class of enzymes, ADP-ribosyl cyclases, such as CD38. Whilst cADPR mobilizes Ca^{2+} from the ER by activation of ryanodine receptors (RyRs), NAADP releases Ca^{2+} from acidic stores by a mechanism involving the activation of two pore channels (TPCs). In addition, other pyridine nucleotides have emerged as intracellular messengers. ADP-ribose and 2′-deoxy-ADPR both activate TRPM2 channels which are expressed at the plasma membrane and in lysosomes.

Keywords Calcium · Cyclic ADP-ribose · NAADP · CD38 · Ryanodine · Two-pore channels · Inositol trisphosphate · ADP-ribose · TRPM2 channel · Lysosome · Endoplasmic reticulum · Calcium microdomain

15.1 Introduction

Studies of cardiac contractility at the close of the nineteenth century by Sidney Ringer showed a requirement for Ca^{2+} ions in perfusion solutions [1]. Use of jellyfish photoproteins, such as aequorin, provided the first measurements of

A. Galione (✉) · K.-T. Chuang
Department of Pharmacology, University of Oxford, Oxford, UK
e-mail: antony.galione@pharm.ox.ac.uk; kai-ting_chuang@hms.harvard.edu

M. S. Islam (ed.), *Calcium Signaling*, Advances in Experimental Medicine and Biology 1131, https://doi.org/10.1007/978-3-030-12457-1_15

cytosolic Ca^{2+} in muscle cells. Importantly, Ca^{2+} transients were found to precede contractions and this realization was important in generating the concept of a messenger role for Ca^{2+} ions in cell contractility [2].

Work studying transmitter release from neurons and hormone secretion [3], also led to a growing appreciation of the role of Ca^{2+} ions in stimulus-response coupling. An important source of Ca^{2+} was that which could be mobilized from internal stores in response to hormones and neurotransmitters acting at cell surface receptors [4]. In the mid-1970s it was hypothesized that receptors could stimulate cellular Ca^{2+} signals by stimulating the hydrolysis of inositol lipids [5]. Importantly, the initial inositol lipid hydrolysed was found to be phosphatidylinositol 4,5 bisphosphate [6]. The enzyme involved, phospholipase C thus generated diacylglycerol which activates protein kinase C, and inositol 1,4,5 trisphosphate (IP_3). A pivotal finding was that IP_3 added to permeabilized pancreatic acinar cells released Ca^{2+} from a non-mitochondrial store in a way that was mimicked by activating plasma membrane muscarinic acetylcholine receptors [7]. Thus IP_3 was proposed as a Ca^{2+} mobilizing messenger linking the activation of cell surface receptors to mobilization of Ca^{2+} from intracellular stores. Biochemical purification studies [8, 9] and molecular cloning experiments [10, 11] defined the principal targets for IP_3 on intracellular stores as homo/heterotetrameric Ca^{2+} release channels termed IP_3 receptors (IP_3Rs). An understanding of how IP_3 regulates IP_3Rs has emerged from recent IP_3R structural studies [12]. The IP_3 signaling pathway is now well established, ubiquitous, and plays key roles in mediating many of the actions of a variety of cellular stimuli [13]. The first intact cell in which IP_3 was shown to evoke a cellular response was the sea urchin egg [14]. IP_3 microinjection induced exocytosis of cortical granules resulting in the raising of the fertilization envelope which acts as a barrier to polyspermy. At around the same time, sea urchin egg homogenates containing Ca^{2+} sequestering vesicles were found to be sensitive to IP_3 which discharged Ca^{2+} from non-mitochondrial stores [15] . Following the establishment of egg homogenates to study Ca^{2+} release mechanisms, Lee and colleagues found that in addition to IP_3, the pyridine nucleotides, NAD^+ and NADP, at micromolar concentrations, were also found to release Ca^{2+} by mechanisms independent from those regulated by IP_3 [16]. NAD^+ released Ca^{2+} from a subcellular fraction which was also sensitive to IP_3, but after a delay of several seconds. In contrast, NADP rapidly released Ca^{2+} from a denser fraction of vesicles. Subsequent analysis revealed that the Ca^{2+} mobilizing properties of NAD^+ was due to an enzyme-produced metabolite identified as cyclic ADP-ribose (cADPR) [17], and Ca^{2+} release evoked by NADP was due to a contaminant, nicotinic acid adenine dinucleotide phosphate (NAADP) [18]. An abbreviated summary of our current understanding of Ca^{2+} homeostasis in animal cells is shown in Fig. 15.1.

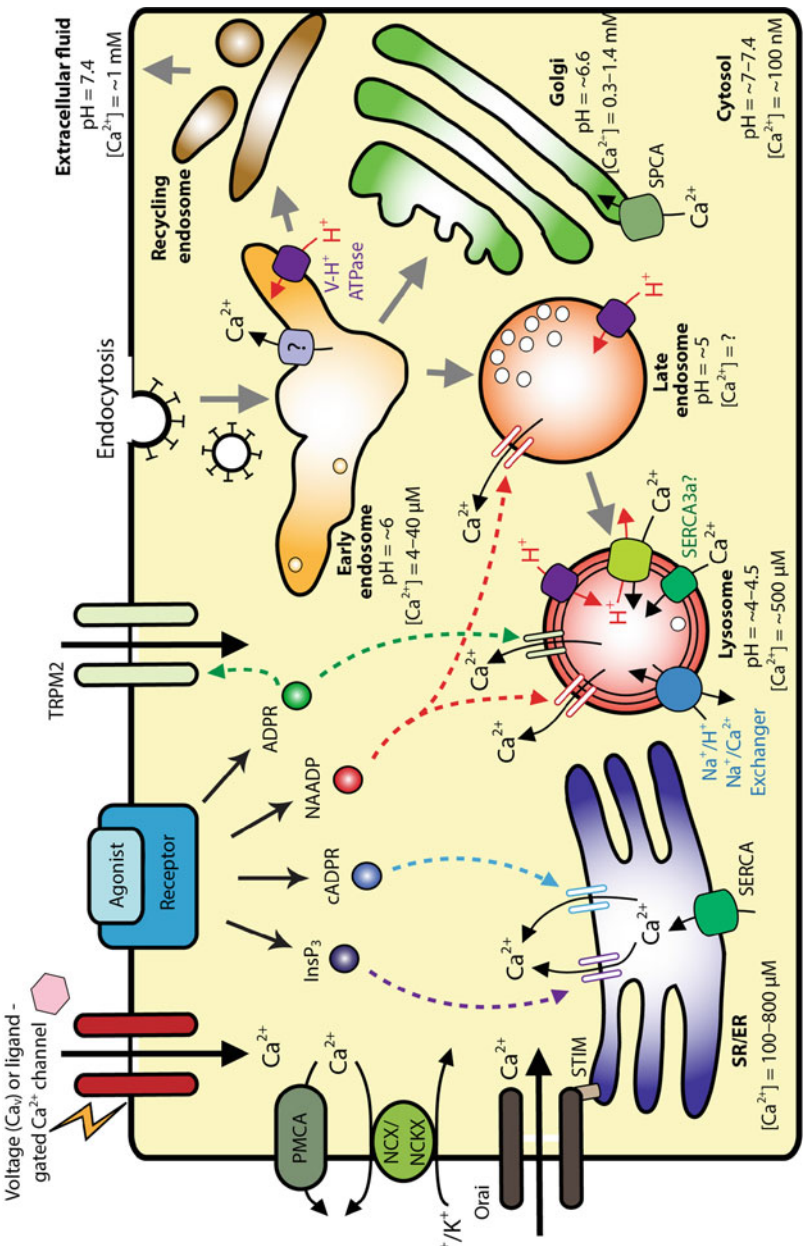

Fig. 15.1 Schematic representation of non-mitochondrial Ca^{2+} pools in animal cells. Ca^{2+} can enter the cytosol from the extracellular space via plasma membrane ion channels, or from intracellular Ca^{2+} sequestering stores such as the ER or the acidic Ca^{2+} stores in response to second messengers: IP_3, cADPR and NAADP. Ca^{2+} released to the cytosol is then exchanged or actively transported back to the Ca^{2+} stores or the extracellular space to restore a low cytosolic concentration of Ca^{2+}

15.2 Enzymology of cADPR and NAADP Synthesis and Metabolism

A family of multifunctional enzymes, termed ADP-ribosyl cyclases, has been characterized that are capable of both the synthesis and metabolism of both cADPR and NAADP. An enzyme activity responsible for the synthesis of cADPR was first indicated by the finding that NAD^+ mobilized Ca^{2+} with a delay from sea urchin egg homogenates but not from purified microsomes, indicating that egg homogenate supernatant contained an activity responsible for the conversion of NAD^+ to an active metabolite [16], later identified as cADPR [17]. This enzyme activity was also widespread in rat tissues and shown to be an enzyme showing stereo-specificity for substrate, pH and temperature-dependence, as well as protease-sensitivity [19]. The first ADP-ribosyl cyclase that was purified and characterized at the molecular level was that from *Aplysia* ovotestis [20–22]. The rationale for this was that during the study of ADP-ribosylation of G proteins by endotoxins in this tissue, a protein factor from ovotestis was uncovered that inhibited this reaction by competing for NAD^+ as a substrate. This protein factor, which was localized to ovotestis granules, was subsequently purified and cloned and found to catalyse the cyclization of NAD^+ to cADPR (Fig. 15.2). *Aplysia* ADP-ribosyl cyclase was the founding member of a class of enzymes that by sequence homology was found to include the mammalian proteins CD38 and CD157 [23]. In contrast to *Aplysia* ADP-ribosyl cyclase, CD38 is a multi- functional enzyme. It is an NAD glycohydrolase (NADase), producing ADP-ribose from NAD^+ [24]. But in addition, not only does it cyclize NAD to

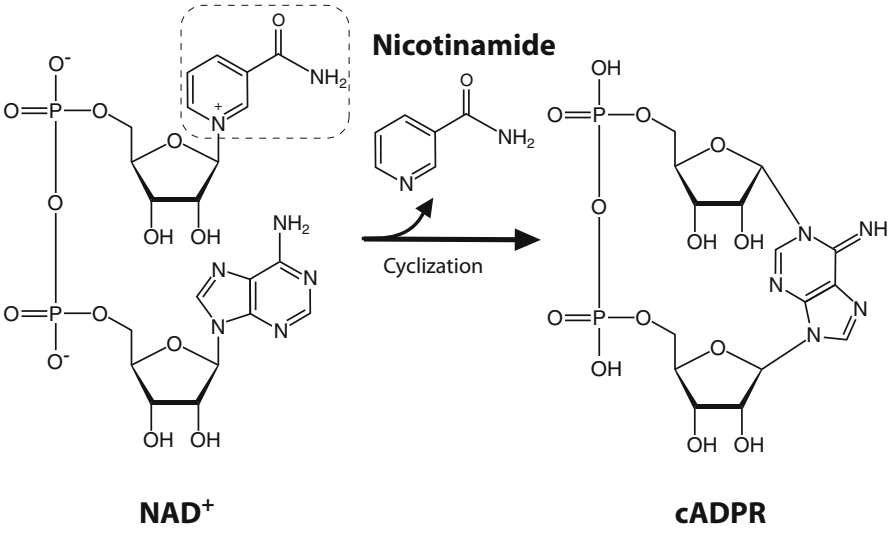

Fig. 15.2 cADPR synthesis. Synthesis of cADPR by cyclization of NAD^+ catalyzed by ADP-ribosyl cyclases

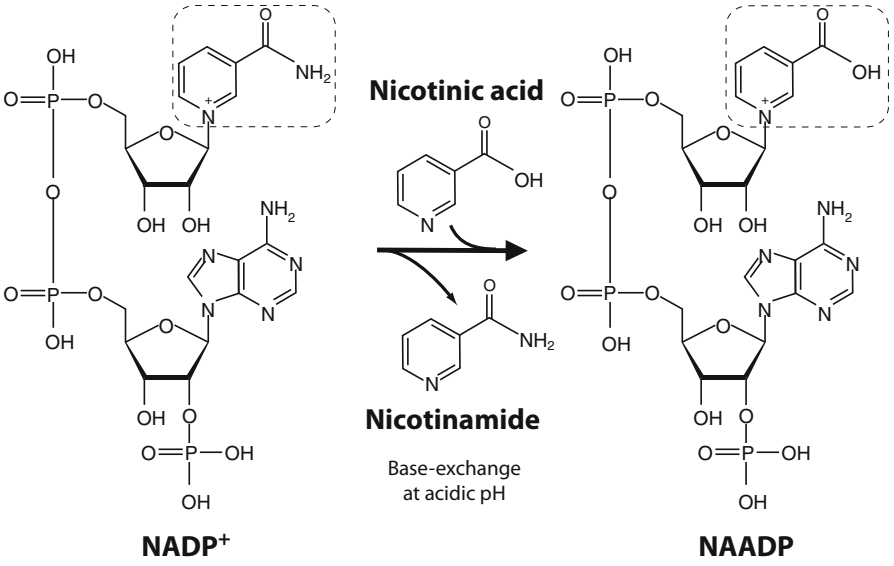

Fig. 15.3 NAADP synthesis. Synthesis of NAADP from NADP by base-exchange of the nicotinamide moiety for nicotinic acid at acidic pH catalyzed by ADP-ribosyl cyclases

cADPR, it also has an appreciable hydrolase activity that converts cADPR to ADP-ribose [25]. Furthermore, CD38 may also use the alternate substrate NADP, and in the presence of nicotinic acid may catalyse a base- exchange reaction generating NAADP too (Fig. 15.3) [26]. Evidence has also emerged that CD38 may also hydrolyse NAADP to ADP-ribose 2-phosphate [27], although cellular phosphatases may also convert NAADP to inactive NAAD [28]. Thus CD38 is responsible for both the synthesis of a number of Ca^{2+} signaling regulators, and may also catalyse their metabolism.

Detailed mechanistic studies following the crystallization of both *Aplysia* ADP-ribosyl cyclase and CD38 have emerged in recent years to explain the various activities of these proteins (reviewed in [29]). As also mentioned below, an expanded family of ADP-ribosyl cyclases have been cloned from sea urchins, and various forms are localized inside intracellular vesicles or expressed as ecto-enzymes at the cell surface [30–33].

15.3 cADPR-Mediated Ca^{2+} Release

Initial studies showed that IP_3, cADPR and NAADP likely released Ca^{2+} by activating distinct mechanisms in sea urchin eggs, since all three compounds independently self-desensitized their respective Ca^{2+} release mechanisms to a second challenge [18]. Pharmacological analysis of cADPR-evoked Ca^{2+} release in

sea urchin egg homogenates and intact eggs showed that the pathway for cADPR-evoked Ca^{2+} release was likely ryanodine receptors (RyRs) [34]. This is also the case in mammalian cells, where cADPR is now recognized as a widespread Ca^{2+} mobilizing messenger [35]. RyRs along with IP_3Rs, with which they share degrees of homology in both primary sequence and structure, were discovered as the principal Ca^{2+} release channels of the sarcoplasmic reticulum of striated muscle [36]. However, in common with IP_3Rs, they are also widely expressed in most cell types, including sea urchin eggs [37–39], where they are often both present together in the membranes of the endoplasmic reticulum (ER).

A key property of RyRs and indeed IP_3Rs are that they are also regulated by Ca^{2+} itself in a complex manner [40]. This may lead to Ca^{2+}-induced Ca^{2+} release (CICR), a phenomenon responsible for the globalization of local Ca^{2+} signals as propagating Ca^{2+} waves or repetitive Ca^{2+} spikes, hallmarks of Ca^{2+} signaling in all cells [41]. Increases in cytoplasmic Ca^{2+} were found to potentiate cADPR-evoked Ca^{2+} release both in cell free systems, and also in intact cells [42]. Thus it has been proposed that cADPR sensitizes RyRs to activation by Ca^{2+}. This hypothesis has a pleasing symmetry with the way in which IP_3 is thought to regulate IP_3R gating by also by modulating Ca^{2+} sensitivity of a Ca^{2+} release channel [43].

The exact mechanism by which cADPR regulates RyRs is currently unclear. However, pivotal roles for additional accessory proteins which interact with the large cytoplasmic domains of RyR subunits have been suggested. The radiolabelled photoaffinity cADPR derivative, [^{32}P]8-azido-cADPR, labels a 100 kDa and a140 kDa protein in sea urchin egg extracts, too small for RyRs, but these have not been identified. A key finding was that in the sea urchin egg microsomal system a soluble protein factor was required to confer cADPR-sensitivity of RyRs [44]. This was found to be calmodulin, a well-known component of RyR macromolecular complexes [45]. Furthermore, it was found that cycles of dissociation and re-association of calmodulin could account for the desensitization and resensitization of cADPR- evoked Ca^{2+} release from sea urchin egg homogenates [46]. In mammalian systems a role for FKBP12.6, an immunophilin with prolyl isomerase activity, has been proposed as important for RyR cADPR sensitivity [47–52]. cADPR has been suggested to induce the dissociation of FKBP12.6 from RyRs which destabilizes the channel causing an increased probability in their openings. The dependence of accessory proteins on the cADPR-sensitivity of RyRs may explain in part the variations in cADPR sensitivity of purified RyRs reconstituted in planar lipid bilayers [53]. More recently GADPH has been proposed to be a cADPR binding protein with a micromolar affinity for cADPR, and apparently required for cADPR-evoked Ca^{2+} release [54]. The development of 8-substituted analogues of cADPR as highly selective cADPR antagonists have been invaluable in dissecting cADPR-dependent signaling pathways [55, 56]. There is also some evidence that cADPR may activate SERCA pumps in some cells and thus increasing the Ca^{2+} loading of stores which could lead to increased Ca^{2+} release by a Ca^{2+} overload mechanism [57, 58].

15.4 NAADP-Mediated Ca^{2+} Release

Of the three major Ca^{2+} releasing messengers, NAADP is the most potent, often effective in cells at concentrations as low as 1–10 nM [59, 60]. Its mode of action intrigued researchers from its very discovery, since it appeared not to target the two principal Ca^{2+} release channels, IP_3Rs/RyRs, but rather a novel Ca^{2+} release channel. In sea urchin eggs and homogenates, NAADP-evoked Ca^{2+} release, which is rapid and likely mediated by a channel [61], is not affected by IP_3Rs/RyRs or cADPR inhibitors such as heparin, ryanodine or 8-amino-cADPR [18], but is selectively antagonized by voltage-gated cation channel blockers such as certain dihydropyridines [62]. In addition, in contrast to IP_3Rs or RyRs, the NAADP-sensitive Ca^{2+} release mechanism is not potentiated by divalent cations leading to the proposal that it does not function as a CICR channel [63, 64]. Furthermore, the NAADP- sensitive channel appeared not to reside on the ER [64, 65]. Fractionation of sea urchin egg homogenates showed that the NAADP-sensitive store was generally denser than IP_3 or cADPR-sensitive microsomes [16]. Treatment of homogenates with the SERCA pump inhibitor, thapsigargin, whilst completely abolishing Ca^{2+} release to either IP_3 or cADPR, did not prevent NAADP-evoked Ca^{2+} release. In studies in stratified eggs where ER accumulates near the nucleus, IP_3 and cADPR were found to mobilize Ca^{2+} from this region, whilst NAADP released Ca^{2+} from structures at the opposite pole. In detailed studies of NAADP-evoked Ca^{2+} release from sea urchin eggs, NAADP was found to induce an initial Ca^{2+} release which was followed by a series of further Ca^{2+} spikes [66, 67]. The initial Ca^{2+} release was insensitive to thapsigargin, whereas subsequent Ca^{2+} spikes were abolished by thapsigargin or IP_3 and RyR inhibitors [67]. It was therefore proposed that NAADP was initially releasing Ca^{2+} from a distinct organelle which then triggered further rounds of Ca^{2+} signals by stimulating Ca^{2+} release from the ER [67]. Further purification of the sea urchin egg NAADP- sensitive stores revealed them as rich in lysosomal markers and acidic in nature, since they stained with lysotracker red [68]. Furthermore, Ca^{2+} uptake whilst insensitive to thapsigargin, was dependent on proton gradients created by the action of bafilomycin-sensitive vacuolar proton pumps. In intact eggs, the lysomolytic agent, glycyl-L- phenylalanine 2-naphthylamide (GPN) was found to lyse lysotracker stained vesicles, which also caused bursts of localized Ca^{2+} release. Treatment with GPN also selectively abolished NAADP-evoked Ca^{2+} release whilst having no effect on either IP_3 or cADPR-induced Ca^{2+} signals. From this study it was proposed that NAADP selectively targets lysosome-like organelles in the sea urchin egg [68–70].

Building on these results from sea urchin eggs, the action of NAADP as a Ca^{2+} mobilizing molecule was investigated in a variety of mammalian cells. In the first study, pancreatic acinar cells were found to be exquisitely sensitive to NAADP which produced effects at considerably lower concentrations than either

IP_3 or cADPR [71]. Several important principles for mammalian NAADP signaling were proposed from this study. First the concentration-response curve for NAADP-evoked Ca^{2+} release (assessed by activation of Ca^{2+}-activated currents) is bell-shaped, with high concentrations of NAADP causing no effect on account of induction of rapid desensitization of NAADP receptors. Secondly, the response to NAADP required functional IP_3 Rs/RyRs, and thirdly, Ca^{2+} release by the secretagogue, cholecystokinin (CCK) required functional NAADP receptors. Until the development of selective NAADP antagonists such as Ned-19 [72], use of high, desensitizing, NAADP concentrations was the major way in which to implicate NAADP in Ca^{2+} signaling processes such as CCK signal transduction here [71]. The finding that NAADP required functional IP_3Rs/RyRs indicated that as in the sea urchin egg, one major action of NAADP-evoked Ca^{2+} release in mammalian cells is to trigger further Ca^{2+} release by recruiting ER-based CICR channels [73]. Similarly, activation of the lysosomal channel, TRPML1 causes similar recruitment of ER Ca^{2+} stores [74].

NAADP has now been shown to have a widespread if not universal action in cells as a mobilizer of Ca^{2+} from acidic stores such as lysosomes [60, 75] and endosomes [76]. Although these organelles contain considerably smaller amounts of Ca^{2+} than the ER, they nevertheless may play an important role in Ca^{2+} signaling by locally targeting Ca^{2+} to specific effectors. Questions still remain about the precise way in which Ca^{2+} is sequestered into lysosomes and related organelles. The proton gradient across organellar membranes is required and direct or indirect Ca^{2+}/H^{+} exchange has been proposed [68]. However, such exchangers are only expressed in lower vertebrates and invertebrates so additional mechanisms may operate [77]. In addition, SERCA3 has been proposed to mediate Ca^{2+} uptake in part, in NAADP-sensitive acidic Ca^{2+} stores of platelets [78]. Others have suggested that filling of Ca^{2+} occurs by privileged communication with the ER by a pH-independent mechanism [79]. Interestingly, in cells from patients with the lysosomal storage disease, Niemann Pick C, lysosomes have defects in Ca^{2+} sequestration, have a low intralysosomal Ca^{2+} concentration, and show a much reduced response to NAADP [80]. Whilst reduced calcium uptake was suggested to account for reduced lysosomal calcium and NAADP action, subsequent studies suggested that this may due to enhanced calcium release [81]

In sea urchin egg membranes, [^{32}P]NAADP binds with very high affinity [66, 82, 83]. Intriguingly, NAADP binding becomes essentially irreversible and it has been proposed that it becomes occluded due to a conformational change of the receptor, a phenomenon that requires the presence of K^{+} ions [84] and phospholipid [85]. Binding may stabilize protein complexes of solubilized proteins [86, 87]. These unusual binding phenomena have been linked with the equally unusual desensitization properties of the NAADP-sensitive Ca^{2+} release mechanism. Prior exposure with concentrations of NAADP which are subthreshold for evoking Ca^{2+} release can desensitize the mechanism to subsequent suprathreshold NAADP concentrations in a concentration and time-dependent manner [66, 88, 89].

15.5 Two Pore Channels as NAADP Targets

Two principles for NAADP-mediated Ca^{2+} release have emerged in recent years. The first was that NAADP-gated channels have distinct properties from known Ca^{2+} release channels such as IP_3Rs and RyRs, and their pharmacology more closely resembled that of voltage-gated cation and TRP channels [62]. Secondly, the NAADP-sensitive release mechanism principally resides on acidic stores such as lysosomes and lysosome-related organelles [68].

Inspection of genomic sequences emerging from a variety of organisms including that of sea urchins, pointed to two families of channels as possible targets. The first was mucolipin-1, a lysosomal TRP channel whose mutations may lead to the lysosomal storage disease, mucolipidosis IV [90–92], and second, a poorly characterized family of channels termed Two-pore channels (TPCs) [93]. TPCs are members of the superfamily of voltage-gated channels which comprise of around 150 members with predicted molecular weights ranging between 80 and 100 kDa. TPCs are predicted to have two domains each containing six transmembrane segments and a single pore loop for each domain. As such they represent a proposed evolutionary intermediate between single domain a subunits which tetramerise to form shaker-like K^+ channels, and the single pore-forming four homologous domain a subunits of voltage-gated Ca^{2+} and Na^+ channels. These channels are thought to have evolved by successive rounds of gene duplication [94–96].

A two pore channel (TPC1) had first been identified from sequences homologous to voltage-gated ion Ca^{2+} channels from rat kidney cDNA [97]. This was followed by the identification of a TPC1 from the genome of the plant *Arabidopsis* [98]. Thus it was the plant channel that was most intensively investigated initially. Importantly, it was shown to be localized to the plant vacuole, the principal acidic organelle in plants, and to act as a Ca^{2+} release channel [99]. On account of a pair of EF hands in the region between the two 6 transmembrane domain (TMD) repeats, not seen in mammalian TPCs, it was also proposed to function as a CICR channel. Electrophysiological analysis of AtTPC1 showed that it likely accounts for the slow vacuolar current and likely to play a key role in plant physiology [100].

At this time Michael Zhu cloned a novel mammalian TPC sequence termed TPC2, and heterologous expression showed that it largely localized to lysosomes, and thus TPCs emerged as plausible candidates as NAADP-gated channels. These data were finally reported in 2009 [101], as described below. Both mucoplin-1 and TPCs have now been proposed as NAADP-gated channels. Although there has been some evidence presented for mucoplin-1 as an NAADP-gated channel [102], this has not been seen by others [103, 104]. In contrast, a number of papers have emerged over the last few years firmly implicating TPCs as central components of NAADP-sensitive Ca^{2+} release channels [105, 106]. Heterologous expression of HsTPC2 in HEK293 cells greatly increased the responsiveness of these cells to NAADP so that now NAADP evoked biphasic Ca^{2+} signals [101]. Pharmacological analysis revealed that the initial Ca^{2+} release is due to Ca^{2+} release from acidic stores whilst the second larger release is mediated by activation

of IP3Rs. This coupling between lysosomes and ER nicely mirrors previous studies of NAADP mediated Ca^{2+} release through organellar cross-talk with NAADP acting in a triggering role [67, 71]. Indeed in pulmonary arteriolar smooth muscle cells, both endothelin-1 and NAADP mediated Ca^{2+} signals initiate in a subcellular region where lysosomes and ER are closely apposed [107, 108]. In contrast, expression of TPC1, which localizes to endosomal vesicles, when activated by NAADP, mediates localized Ca^{2+} signals apparently uncoupled from ER-based Ca^{2+} release mechanisms [101, 109]}. Importantly, sea urchins also express TPC isoforms, and expression of both TPC1 and TPC2 also enhance the responsiveness of cells to NAADP generating characteristic biphasic Ca^{2+} signals [110, 111]. Sea urchins, in common with many animals, express three isoforms, although TPC3 is not expressed in man, mouse or rats. In one report, TPC3 appeared to act as a dominant negative suppressing the effects of NAADP on both small endogenous Ca^{2+} release or enhanced release due to TPC2 overexpression [110]. Another important finding is that immunopurified endogenous TPCs bind [^{32}P]NAADP with nanomolar affinity and recapitulates key properties of NAADP binding to native egg membrane fractions [110]. Electrophysiological studies either from isolated lysosomes [112, 113], immunopurified TPC2 reconstituted into lipid bilayers [114] or channels redirected to the plasma membrane by mutating lysosomal targeting sequences [115] have shown that TPCs are indeed NAADP-gated cation channels which can pass Ca^{2+} ions.

Interestingly, TPC2 channel activity is modulated by luminal pH, and increased luminal Ca^{2+} greatly increases their sensitivity to activation by NAADP [114].

Evidence from cells derived from TPC2 knockout mice also supports a key role for TPC2 in mediating NAADP-evoked Ca^{2+} release. In pancreatic beta cells, NAADP evokes Ca^{2+} activated plasma membrane currents which are absent in those from *Tpcn2−/−* mice [101] and may be important in regulating insulin secretion [116]. Furthermore, application of exogenous NAADP to diabetic mice restores insulin secretion [117]. In bladder smooth muscle, whilst NAADP contracts permeabilised myocytes, it fails to do so in cells from *Tpcn2*$^{-/-}$ mice, and now agonist- mediated contractions are due entirely to SR-mediated Ca^{2+} release since agonist-coupling to Ca^{2+} release from acidic stores is now abolished [118]. RNA interference approaches are now emerging. For example, knockdown of TPC2 with siRNA has revealed important specific roles for the NAADP/TPC signaling pathway in striated muscle differentiation [119] Importantly, this effect is phenocopied by use of the membrane-permeant NAADP antagonist, Ned-19 or disruption of Ca^{2+} storage by lysosomes/acidic stores by bafilomycin [119]. Importantly, cells from *Tpcn1*$^{-/-}$*/Tpcn2*$^{-/-}$ mice do not mobilize Ca^{2+} in response to NAADP, but do so on expression of either TPC1 or TPC2 proteins, but not TRPML1 [120].

Taken together, there is now compelling evidence that TPCs are key components of the NAADP-sensitive Ca^{2+} release mechanism. A study comparing cADPR and NAADP actions shows clearly that in HEK293 cells, that expression of RyRs confers cADPR-sensitivity, but TPC expression is needed for NAADP-evoked Ca^{2+} release [109] crystallizing the hypotheses that cADPR targets RyRs whilst NAADP targets TPCs. Direct patch-clamping of lysosomes has given further insight into the biophysical properties of TPCs. TPCs are likely non-selective

cation channels with substantial Na^+ conductances [121]. However, even a minimal Ca^{2+} conductance may be sufficient to generate physiologically important Ca^{2+} microdomains particularly at lysosomal-ER contact sites [120].

Molecular structures of TPCs have recently been reported by X-ray crystallography or cryo-EM [122–126]. The role of TPCs is disease is a new and growing field [127, 128].

RyRs themselves have been proposed as direct targets for NAADP in some cell types [129, 130] although indirect activation of RyRs by local Ca^{2+} release from acidic stores is not trivial to discount. However, since it is likely that NAADP may bind to a channel accessory protein rather than a channel itself [131, 132], it is possible that NAADP may regulate multiple Ca^{2+} release channels under certain conditions [133, 134]. The requirement for an elusive NAADP-binding protein may explain why there is variability in responsiveness of TPC channel currents recorded under conditions of whole-lysosome patch clamp [112, 113, 121]. A similar case may operate for cADPR modulation of RyRs [54].

NAADP-evoked Ca^{2+} release from acidic stores has been proposed to work in three major ways to regulate cellular processes (Fig. 15.4) [135]. The first is to

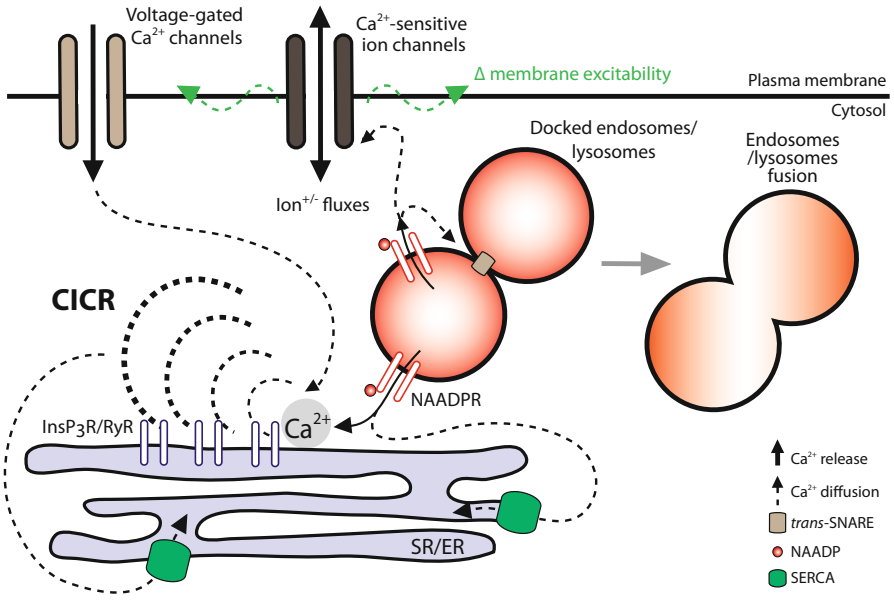

Fig. 15.4 Local to global Ca^{2+} responses mediated by NAADP. Locally, the Ca^{2+} release from acidic stores is likely to be important for normal functions of the endo-lysosomal system such as vesicle fusion or fission in lysosomal biogenesis. Small local Ca^{2+} release evoked by NAADP from lysosomes may also act as a trigger to initiate CICR from the SR/ER and generate global signals. NAADP-mediated Ca^{2+} release near the plasma membrane modulates membrane excitability (excitable cells), or ion fluxes (non-excitable cells) by opening Ca^{2+} activated channels. Changes in the membrane potential could further activate, for example, voltage-gated Ca^{2+} channels, to allow Ca^{2+} influx and initiate a global response via CICR

coordinate Ca^{2+} release by organelle cross-talk at junctions between lysosomes and the ER [136–138]. The second is to produce local Ca^{2+} signals in the sub-plasma membrane space to control Ca^{2+}-activated plasma membrane channels and thus regulate processes such as fluid secretion in non-excitable cells such as exocrine gland cells [71], or membrane excitability in excitable cells. Examples of the latter are the polyspermy blocking cortical flash in sea urchin eggs [139] or activation of membrane currents in starfish oocytes [140], and depolarization of pancreatic beta cells [101] or neurones [141]. Thirdly, local Ca^{2+} release via TPCs may regulate endolysosomal trafficking and organelle biogenesis by regulating membrane fission and fusion processes. Overexpression of TPCs or their block by the NAADP antagonist Ned-19 induces deregulation of endocytosis, lysosome biogenesis and trafficking mimicking features of lysosomal storage diseases [110, 142, 143] which may be relevant to disease [60, 128].

15.6 ADP-Ribose and Other Metabolites

As mentioned above, cADPR is metabolized to ADPR by CD38's intrinsic hydrolase activity. Other NADases may directly catalyse the formation of ADPR. ADPR although inactive at releasing Ca^{2+} from the ER, was found to stimulate Ca^{2+} influx. This was first observed in ascidian oocytes where low ADPR concentrations may activate plasma membrane currents [144]. An important target for ADPR is TRPM2. TRPM2 channels are polymodal-gated channels responding to not only pyridine nucleotides but also to calcium, oxidants and raised temperature [145]. They have been proposed as chanzymes in that they express an intrinsic enzyme activity, ADPR pyrophosphate conferred by a nudix box containing domain at their C-terminus [146], although this has been challenged [147]. Both cADPR and NAADP have also been reported to activate TRPM2, but at high micromolar concentrations, substantially higher than reported concentrations of these molecules in cells and tissues [148], although this has also been questioned [149]. In a T cell line, a second messenger role for ADP-ribose in mediating concanavalin A-activated Ca^{2+} influx via TRPM2 channels has been proposed [150]. Interestingly, although TRPM2 channels are mainly found in the plasma membrane, they have also been reported in lysosomes [151]. In addition to ADPR, ADP-ribosyl cyclases may also generate additional nucleotides including cADPR-phosphate, and adenine dinucleotides [152] which may also be active in some cells at generating Ca^{2+} signals. A recent report has suggested that 2′-deoxyadenosine 5′-diphosphoribose is an endogenous TRPM2 superagonist [153]. The recent description of the molecular structure of TRPM2 from cryo-EM studies will shed more light on the molecular architecture of the pyridine nucleotide binding site [154].

15.7 Receptor-Mediated NAADP and cADPR-Mediated Ca^{2+} Signaling

Both cADPR and NAADP have satisfied all the criteria originally mandated by Sutherland, to be unambiguously assigned as second or intracellular messengers [155].

Endogenous levels of both cADPR and NAADP are found in a wide range of tissues and cells from across the phyla. Similarly, increases in levels of cADPR [35] and NAADP [75] have been reported in response to cell activation by a variety of stimuli and cell surface receptor families. There have been two principal ways in which cADPR and NAADP levels have been measured [156]. The first are radioreceptor assays based on the high affinity binding sites for these molecules on sea urchin egg membranes [157, 158], and the second is a cycling assay using ADP-ribosyl cyclase in reverse to generate NAD which is then coupled to the generation of a fluorescent product [159, 160]. The latter requires initial treatment with enzymes to completely remove endogenous NAD before proceeding. An additional important development was the use of NGD as an alternative substrate to NAD. True ADP- ribosyl cyclase as opposed to most ADP glycohydrolases tend to cyclise NGD to cGDPR which is fluorescent [161]], and this assay has been extensively used to demonstrate ADP-ribosyl cylase activities in many preparations, and in some cases regulation of activities by various stimuli.

The first indication that cADPR levels could be regulated by phosphorylation processes was the finding that cGMP via G kinase stimulates Ca^{2+} release via cADPR synthesis in sea urchin eggs [162, 163]. cAMP on the other hand may selectively enhance NAADP forming base-exchange activity by PKA or EPAC [164], thus differential phosphorylation or regulation by cGMP or cAMP may dictate which messenger is generated on enzyme stimulation [165].

As a general principle, NAADP increases rapidly and transiently on cell stimulation, whilst cADPR remains elevated for many minutes [166, 167]. From this it has been proposed that NAADP plays a major role in triggering Ca^{2+} signals, whilst cADPR may have a longer term role in producing a long lasting increase in sensitivity of RyRs to CICR. Indeed prolonged elevations of cADPR have been associated with the circadian clock in plants as well as increased proliferative state of cells in culture [168].

CD38 knockout mice are providing important insights into the role of CD38 in agonist-mediated Ca^{2+} signaling mediated by both cADPR and NAADP. Several studies have indicated that various tissues from *Cd38*$^{-/-}$ mice have substantially reduced endogenous cADPR levels. In addition, the ability of a number of stimuli to elevate cADPR levels is impaired. Concomitantly, a number of important physiological processes are abrogated [23]. Defects include reduced insulin secretion from pancreatic beta cells [169], abolition of Ca^{2+} mobilization in pancreatic acinar cells [170, 171], cardiac hypertrophy [172], changes in airway [173] and vascular smooth muscle pharmaco-mechanical coupling [174], defects in neutrophil chemotaxis with increased susceptibility to bacterial infection [175], impaired oxytocin signaling with associated behavioral correlates [176].

A recent report has suggested a novel way in which cADPR signaling is regulated in sperm. These cells with minimal signaling machineries apparently acquire CD38 and RyRs from secreted prostasomes from prostate gland cells and competence in cADPR signaling is required for sperm motility and thus ability to fertilize ova [177].

The finding that, at least in vitro, CD38 can synthesise NAADP [27], has also led to the investigation of this enzyme in receptor-mediated NAADP production. Using cells from *Cd38−/−* mice it was found that in pancreatic acinar cells, NAADP production stimulated by physiological concentrations of CCK was abolished [171], as was that produced by angiotensin II in hepatic stellate cells [178], and by IL8 in lymphokine-activated killer cells [179]. Recent evidence has been presented to show that NAADP synthesis is also linked to beta- adrenergic signalling mechanisms in cardiac myocytes [180]. However, agonist-induced NAADP production has been reported in tissues from *Cd38−/−* mouse tissues, raising the possibility of alternate synthetic pathways [181]. CD157, also known as BST1, shows ADP-ribosyl cyclase activity, but apparently is poor at catalysing NAADP synthesis by base exchange [182].

The great plasticity of Ca^{2+} signaling pathways is exemplified by the ability of high affinity CCK receptors in Cd38−/− pancreatic acinar cells now to switch from NAADP production to IP -mediated Ca^{2+} signaling [171]. Conversely, CCK evoked Ca^{2+} signals in the ADP-ribosyl cyclase-deficient AR42J rat pancreatic cell line switch from IP -mediated Ca^{2+} signaling to NAADP signaling and Ca^{2+} release from acidic stores on transfection with CD38 cDNA [171].

A major question concerning the notion that CD38 is the major synthetic enzyme for cADPR and NAADP synthesis is the membrane topology of this protein [183]. It was originally noted as a plasma membrane ectoenzyme with its active site facing the extracellular space. De Flora and colleagues presented evidence that NAD may leak from the cell via connexins which is acted upon by extracellular CD38 to yield extracellular cADPR. cADPR may be transported back into the cell via nucleoside transporters [183]. However, an appreciable amount of CD38 is intracellular and associated with organelles such as secretory granules or endosomes, and this may increase on cell stimulation. This appears to be the case in sea urchin eggs, and evidence has been provided that NAD may be transported into organelles, converted to cADPR, which is transported into the cytoplasm to its site of action [30, 31]. This also raises the possibility that cADPR and NAADP may also be stored in intracellular compartments, and cell stimuli may act to regulate the egress of these molecules into the cytoplasm as for Ca^{2+} mobilization from intracellular stores. Another possibility, recently proposed, is that CD38 may exist in two topologies with the active site of one form, termed type III, actually facing the cytoplasm, [184, 185, 186]. The cytosolic facing form has been shown to interact with the Ca^{2+} binding CIB1 protein which may enhance its activity [186]. Whatever the situation, more clarification is needed to understand how cellular stimuli are coupled to increases in ADP-ribosyl cyclase activities.

15.8 Conclusions

The emergence of cADPR and NAADP as Ca^{2+} mobilizing messengers and the elucidation of their place in signaling pathways and the identification of their molecular targets over the last two decades has provided many surprises and advances in our understanding of cellular regulatory processes. The field has moved on from the role of these molecules at fertilization of invertebrate eggs to central players in mammalian Ca^{2+} homeostasis and signaling. We can expect more surprises and answers in the years to come, but the next key development will be to identify cADPR and NAADP binding proteins and ascertain how they modulate their respective targets.

References

1. Ringer S (1882) Concerning the influence exerted by each of the constituents of the blood on the contraction of the ventricle. J Physiol 3:380–393
2. Ashley CC, Ridgway EB (1968) Simultaneous recording of membrane potential, calcium transient and tension in single muscle fibers. Nature 219:1168–1169
3. Douglas WW, Poisner AM (1964) Stimulus-secretion coupling in a neurosecretory organ: the role of calcium in the release of vasopressin from the neurohypophysis. J Physiol 172:1–18
4. Nielsen SP, Petersen OH (1972) Transport of calcium in the perfused submandibular gland of the cat. J Physiol 223:685–697
5. Michell RH (1975) Inositol phospholipids and cell surface receptor function. Biochim Biophys Acta 415:81–47
6. Berridge MJ (1983) Rapid accumulation of inositol trisphosphate reveals that agonists hydrolyse polyphosphoinositides instead of phosphatidylinositol. Biochem J 212:849–858
7. Streb H, Irvine RF, Berridge MJ, Schulz I (1983) Release of Ca^{2+} from a nonmitochondrial intracellular store in pancreatic acinar cells by inositol-1,4,5-trisphosphate. Nature 306:67–69
8. Supattapone S, Worley PF, Baraban JM, Snyder SH (1988) Solubilization, purification, and characterization of an inositol trisphosphate receptor. J Biol Chem 263:1530–1534
9. Maeda N, Niinobe M, Mikoshiba K (1990) A cerebellar Purkinje cell marker P400 protein is an inositol 1,4,5-trisphosphate ($InsP_3$) receptor protein. Purification and characterization of InsP3 receptor complex. Embo J 9:61–67
10. Furuichi T, Yoshikawa S, Miyawaki A, Wada K, Maeda N, Mikoshiba K (1989) Primary structure and functional expression of the inositol 1,4,5-trisphosphate-binding protein P400. Nature 342:32–38
11. Mignery GA, Sudhof TC, Takei K, De Camilli P (1989) Putative receptor for inositol 1,4,5-trisphosphate similar to ryanodine receptor. Nature 342:192–195
12. Serysheva II, Baker MR, Fan G (2017) Structural Insights into IP^3R Function. Adv Exp Med Biol 981:121–147
13. Berridge MJ (1993) Inositol trisphosphate and calcium signalling. Nature 361: 315–325
14. Whitaker M, Irvine RF (1984) Inositol 1,4,5 trisphosphate microinjection activates sea urchin eggs. Nature 312:636–639
15. Clapper DL, Lee HC (1985) Inositol trisphosphate induces calcium release from nonmitochondrial stores i sea urchin egg homogenates. J Biol Chem 260:13947–13954

16. Clapper DL, Walseth TF, Dargie PJ, Lee HC (1987) Pyridine nucleotide metabolites stimulate calcium release from sea urchin egg microsomes desensitized to inositol trisphosphate. J Biol Chem 262:9561–9568
17. Lee HC, Walseth TF, Bratt GT, Hayes RN, Clapper DL (1989) Structural determination of a cyclic metabolite of NAD^+ with intracellular Ca^{2+}-mobilizing activity. J Biol Chem 264:1608–1615
18. Lee HC, Aarhus R (1995) A derivative of NADP mobilizes calcium stores insensitive to inositol trisphosphate and cyclic ADP-ribose. J Biol Chem 270:2152–2157
19. Rusinko N, Lee HC (1989) Widespread occurrence in animal tissues of an enzyme catalyzing the conversion of NAD^+ into a cyclic metabolite with intracellular Ca^{2+}-mobilizing activity. J Biol Chem 264:11725–11731
20. Hellmich MR, Strumwasser F (1991) Purification and characterization of a molluscan egg-specific NADase, a second-messenger enzyme. Cell Regul 2:193–202
21. Glick DL, Hellmich MR, Beushausen S, Tempst P, Bayley H, Strumwasser F (1991) Primary structure of a molluscan egg-specific NADase, a second-messenger enzyme. Cell Regul 2:211–218
22. Lee HC, Aarhus R (1991) ADP-ribosyl cyclase: an enzyme that cyclizes NAD^+ into a calcium-mobilizing metabolite. Cell Regul 2:203–209
23. Malavasi F, Deaglio S, Funaro A, Ferrero E, Horenstein AL, Ortolan E et al (2008) Evolution and function of the ADP ribosyl cyclase/CD38 gene family in physiology and pathology. Physiol Rev 88:841–886
24. Chini EN, Chini CCS, Espindola Netto JM, de Oliveira GC, van Schooten W (2018) The pharmacology of CD38/NADase: an emerging target in cancer and diseases of aging. Trends Pharmacol Sci 39:424–436
25. Howard M, Grimaldi JC, Bazan JF, Lund FE, Santos-Argumedo L, Parkhouse RM et al (1993) Formation and hydrolysis of cyclic ADP-ribose catalyzed by lymphocyte antigen CD38. Science 262:1056–1059
26. Aarhus R, Graeff RM, Dickey DM, Walseth TF, Lee HC (1995) ADP-ribosyl cyclase and CD38 catalyze the synthesis of a calcium-mobilizing metabolite from NADP. J Biol Chem 270:30327–30333
27. Graeff R, Liu Q, Kriksunov IA, Hao Q, Lee HC (2006) Acidic residues at the active sites of CD38 and ADP-ribosyl cyclase determine nicotinic acid adenine dinucleotide phosphate (NAADP) synthesis and hydrolysis activities. J Biol Chem 281:28951–28957
28. Berridge G, Cramer R, Galione A, Patel S (2002) Metabolism of the novel Ca^{2+}-mobilizing messenger nicotinic acid-adenine dinucleotide phosphate via a 2′-specific $Ca2^{2+}$-dependent phosphatase. Biochem J 365:295–301
29. Lee HC (2000) Enzymatic functions and structures of CD38 and homologs. Chem Immunol 75:39–59
30. Churamani D, Boulware MJ, Geach TJ, Martin AC, Moy GW, Su YH et al (2007) Molecular characterization of a novel intracellular ADP-ribosyl cyclase. PLoS One 2:e797
31. Davis LC, Morgan AJ, Ruas M, Wong JL, Graeff RM, Poustka AJ et al (2008) Ca^{2+} signaling occurs via second messenger release from intraorganelle synthesis sites. Curr Biol 18:1612–1618
32. Churamani D, Boulware MJ, Ramakrishnan L, Geach TJ, Martin AC, Vacquier VD et al (2008) Molecular characterization of a novel cell surface ADP-ribosyl cyclase from the sea urchin. Cell Signal 20:2347–2355
33. Ramakrishnan L, Muller-Steffner H, Bosc C, Vacquier VD, Schuber F, Moutin MJ et al (2010) A single residue in a novel ADP-ribosyl cyclase controls production of the calcium-mobilizing messengers cyclic ADP-ribose and nicotinic acid adenine dinucleotide phosphate. J Biol Chem 285:19900–19909
34. Galione A, Lee HC, Busa WB (1991) Ca^{2+}-induced Ca^{2+} release in sea urchin egg homogenates: modulation by cyclic ADP-ribose. Science 253:1143–1146
35. Galione A, Churchill GC (2000) Cyclic ADP ribose as a calcium-mobilizing messenger. Sci STKE 2000:pe1

36. Fill M, Copello JA (2002) Ryanodine receptor calcium release channels. Physiol Rev 82:893–922
37. McPherson SM, McPherson PS, Mathews L, Campbell KP, Longo FJ (1992) Cortical localization of a calcium release channel in sea urchin eggs. J Cell Biol 116:1111–1121
38. Lokuta AJ, Darszon A, Beltran C, Valdivia HH (1998) Detection and functional characterization of ryanodine receptors from sea urchin eggs. J Physiol 510:155–164
39. Shiwa M, Murayama T, Ogawa Y (2002) Molecular cloning and characterization of ryanodine receptor from unfertilized sea urchin eggs. Am J Physiol Regul Integr Comp Physiol 282:R727–R737
40. Taylor CW (1998) Inositol trisphosphate receptors: Ca^{2+}-modulated intracellular Ca^{2+} channels. Biochim Biophys Acta 1436:19–33
41. Roderick HL, Berridge MJ, Bootman MD (2003) Calcium-induced calcium release. Curr Biol 13:R425
42. Lee HC (1993) Potentiation of calcium- and caffeine-induced calcium release by cyclic ADP-ribose. J Biol Chem 268:293–299
43. Parys JB, De Smedt H (2012) Inositol 1,4,5-trisphosphate and its receptors. Adv Exp Med Biol 740:255–279
44. Lee HC, Aarhus R, Graeff RM (1995) Sensitization of calcium-induced calcium release by cyclic ADP-ribose and calmodulin. J Biol Chem 270:9060–9066
45. Zhu X, Ghanta J, Walker JW, Allen PD, Valdivia HH (2004) The calmodulin binding region of the skeletal ryanodine receptor acts as a self-modulatory domain. Cell Calcium 35: 165–177
46. Thomas JM, Summerhill RJ, Fruen BR, Churchill GC, Galione A (2002) Calmodulin dissociation mediates desensitization of the cADPR-induced Ca^{2+} release mechanism. Curr Biol 12:2018–2022
47. Morita K, Kitayama T, Kitayama S, Dohi T (2006) Cyclic ADP-ribose requires FK506-binding protein to regulate intracellular Ca^{2+} dynamics and catecholamine release in acetylcholine-stimulated bovine adrenal chromaffin cells. J Pharmacol Sci 101:40–51
48. Noguchi N, Takasawa S, Nata K, Tohgo A, Kato I, Ikehata F et al (1997) Cyclic ADP-ribose binds to FK506-binding protein 12.6 to release Ca^{2+} from islet microsomes. J Biol Chem 272:3133–3136
49. Tang WX, Chen YF, Zou AP, Campbell WB, Li PL (2002) Role of FKBP12.6 in cADPR-induced activation of reconstituted ryanodine receptors from arterial smooth muscle. Am J Physiol Heart Circ Physiol 282:H1304–H1310
50. Wang YX, Zheng YM, Mei QB, Wang QS, Collier ML, Fleischer S et al (2004) FKBP12.6 and cADPR regulation of Ca^{2+} release in smooth muscle cells. Am J Physiol Cell Physiol 286:C538–C546
51. Zhang X, Tallini YN, Chen Z, Gan L, Wei B, Doran R et al (2009) Dissociation of FKBP12.6 from ryanodine receptor type 2 is regulated by cyclic ADP-ribose but not beta-adrenergic stimulation in mouse cardiomyocytes. Cardiovasc Res 84:253–262
52. Zheng J, Wenzhi B, Miao L, Hao Y, Zhang X, Yin W et al (2010) Ca^{2+} release induced by cADP-ribose is mediated by FKBP12.6 proteins in mouse bladder smooth muscle. Cell Calcium 47:449–457
53. Copello JA, Qi Y, Jeyakumar LH, Ogunbunmi E, Fleischer S (2001) Lack of effect of cADP-ribose and NAADP on the activity of skeletal muscle and heart ryanodine receptors. Cell Calcium 30:269–284
54. Zhang K, Sun W, Huang L, Zhu K, Pei F, Zhu L et al (2017) Identifying glyceraldehyde 3-phosphate dehydrogenase as a cyclic adenosine diphosphoribose binding protein by photoaffinity protein-ligand labeling approach. J Am Chem Soc 139:156–170
55. Walseth TF, Lee HC (1993) Synthesis and characterization of antagonists of cyclic-ADP-ribose-induced Ca^{2+} release. Biochim Biophys Acta 1178:235–242
56. Sethi JK, Empson RM, Bailey VC, Potter BV, Galione A (1997) 7-Deaza-8-bromo-cyclic ADP-ribose, the first membrane-permeant, hydrolysis-resistant cyclic ADP-ribose antagonist. J Biol Chem 272:16358–16363

57. Lukyanenko V, Gyorke I, Wiesner TF, Gyorke S (2001) Potentiation of Ca^{2+} release by cADP-ribose in the heart is mediated by enhanced SR Ca^{2+} uptake into the sarcoplasmic reticulum. Circ Res 89:614–622
58. Yamasaki-Mann M, Demuro A, Parker I (2009) cADPR stimulates SERCA activity in Xenopus oocytes. Cell Calcium 45:293–299
59. Guse AH, Lee HC (2008) NAADP: a universal Ca^{2+} trigger. Sci Signal 1:re10
60. Galione A (2015) A primer of NAADP-mediated Ca^{2+} signalling: from sea urchin eggs to mammalian cells. Cell Calcium 58:27–47
61. Genazzani AA, Mezna M, Summerhill RJ, Galione A, Michelangeli F (1997) Kinetic properties of nicotinic acid adenine dinucleotide phosphate-induced Ca^{2+} release. J Biol Chem 272:7669–7675
62. Genazzani AA, Mezna M, Dickey DM, Michelangeli F, Walseth TF, Galione A (1997) Pharmacological properties of the Ca^{2+}-release mechanism sensitive to NAADP in the sea urchin egg. Br J Pharmacol 121:1489–1495
63. Chini EN, Dousa TP (1996) Nicotinate-adenine dinucleotide phosphate-induced Ca^{2+}-release does not behave as a Ca^{2+}-induced Ca^{2+}-release system. Biochem J 316:709–711
64. Genazzani AA, Galione A (1996) Nicotinic acid-adenine dinucleotide phosphate mobilizes Ca^{2+} from a thapsigargin-insensitive pool. Biochem J 315:721–725
65. Lee HC, Aarhus R (2000) Functional visualization of the separate but interacting calcium stores sensitive to NAADP and cyclic ADP-ribose. J Cell Sci 113:4413–4420
66. Aarhus R, Dickey DM, Graeff RM, Gee KR, Walseth TF, Lee HC (1996) Activation and inactivation of Ca^{2+} release by NAADP+. J Biol Chem 271:8513–8516
67. Churchill GC, Galione A (2001) NAADP induces Ca^{2+} oscillations via a two-pool mechanism by priming IP3- and cADPR-sensitive Ca^{2+} stores. EMBO J 20:2666–2671
68. Churchill GC, Okada Y, Thomas JM, Genazzani AA, Patel S, Galione A (2002) NAADP mobilizes Ca^{2+} from reserve granules, lysosome-related organelles, in sea urchin eggs. Cell 111:703–708
69. Morgan AJ, Platt FM, Lloyd-Evans E, Galione A (2011) Molecular mechanisms of endolysosomal Ca^{2+} signalling in health and disease. Biochem J 439:349–374
70. Lee HC (2012) Cyclic ADP-ribose and nicotinic acid adenine dinucleotide phosphate (NAADP) as messengers for calcium mobilization. J Biol Chem 287:31633–31640
71. Cancela JM, Churchill GC, Galione A (1999) Coordination of agonist-induced Ca^{2+}-signalling patterns by NAADP in pancreatic acinar cells. Nature 398:74–76
72. Naylor E, Arredouani A, Vasudevan SR, Lewis AM, Parkesh R, Mizote A et al (2009) Identification of a chemical probe for NAADP by virtual screening. Nat Chem Biol 5:220–226
73. Patel S, Churchill GC, Galione A (2001) Coordination of Ca^{2+} signalling by NAADP. Trends Biochem Sci 26:482–489
74. Kilpatrick BS, Yates E, Grimm C, Schapira AH, Patel S (2016) Endo-lysosomal TRP mucolipin-1 channels trigger global ER Ca^{2+} release and Ca^{2+} influx. J Cell Sci 129:3859–3867
75. Galione A, Morgan AJ, Arredouani A, Davis LC, Rietdorf K, Ruas M et al (2010) NAADP as an intracellular messenger regulating lysosomal calcium-release channels. Biochem Soc Trans 38:1424–1431
76. Menteyne A, Burdakov A, Charpentier G, Petersen OH, Cancela JM (2006) Generation of specific Ca^{2+} signals from Ca^{2+} stores and endocytosis by differential coupling to messengers. Curr Biol 16:1931–1937
77. Melchionda M, Pittman JK, Mayor R, Patel S (2016) Ca^{2+}/H^{+} exchange by acidic organelles regulates cell migration in vivo. J Cell Biol 212:803–813
78. Jardin I, Lopez JJ, Pariente JA, Salido GM, Rosado JA (2008) Intracellular calcium release from human platelets: different messengers for multiple stores. Trends Cardiovasc Med 18:57–61
79. Garrity AG, Wang W, Collier CM, Levey SA, Gao Q, Xu H (2016) The endoplasmic reticulum, not the pH gradient, drives calcium refilling of lysosomes. Elife 5

80. Lloyd-Evans E, Morgan AJ, He X, Smith DA, Elliot-Smith E, Sillence DJ et al (2008) Niemann-Pick disease type C1 is a sphingosine storage disease that causes deregulation of lysosomal calcium. Nat Med 14:1247–1255
81. Hoglinger D, Haberkant P, Aguilera-Romero A, Riezman H, Porter FD, Platt FM et al (2015) Intracellular sphingosine releases calcium from lysosomes. Elife 4
82. Billington RA, Genazzani AA (2000) Characterization of $NAADP^+$ binding in sea urchin eggs. Biochem Biophys Res Commun 276:112–116
83. Patel S, Churchill GC, Galione A (2000) Unique kinetics of nicotinic acid-adenine dinucleotide phosphate (NAADP) binding enhance the sensitivity of NAADP receptors for their ligand. Biochem J 352:725–729
84. Dickinson GD, Patel S (2003) Modulation of NAADP (nicotinic acid-adenine dinucleotide phosphate) receptors by K^{2+} ions: evidence for multiple NAADP receptor conformations. Biochem J 375:805–812
85. Churamani D, Dickinson GD, Patel S (2005) NAADP binding to its target protein in sea urchin eggs requires phospholipids. Biochem J 386:497–504
86. Berridge G, Dickinson G, Parrington J, Galione A, Patel S (2002) Solubilization of receptors for the novel Ca^{2+}-mobilizing messenger, nicotinic acid adenine dinucleotide phosphate. J Biol Chem 277:43717–43723
87. Churamani D, Dickinson GD, Ziegler M, Patel S (2006) Time sensing by NAADP receptors. Biochem J 397:313–320
88. Genazzani AA, Empson RM, Galione A (1996) Unique inactivation properties of NAADP-sensitive Ca^{2+} release. J Biol Chem 271:11599–11602
89. Churchill GC, Galione A (2001) Prolonged inactivation of nicotinic acid adenine dinucleotide phosphate-induced Ca^{2+} release mediates a spatiotemporal Ca^{2+} memory. J Biol Chem 276:11223–11225
90. Bargal R, Avidan N, Ben-Asher E, Olender Z, Zeigler M, Frumkin A et al (2000) Identification of the gene causing mucolipidosis type IV. Nat Genet 26:118–123
91. Sun M, Goldin E, Stahl S, Falardeau JL, Kennedy JC, Acierno JS Jr et al (2000) Mucolipidosis type IV is caused by mutations in a gene encoding a novel transient receptor potential channel. Hum Mol Genet 9:2471–2478
92. Bach G (2001) Mucolipidosis type IV. Mol Genet Metab 73:197–203
93. Galione A, Evans AM, Ma J, Parrington J, Arredouani A, Cheng X et al (2009) The acid test: the discovery of two-pore channels (TPCs) as NAADP-gated endolysosomal Ca^{2+} release channels. Pflugers Arch 458:869–876
94. Zhu MX, Ma J, Parrington J, Calcraft PJ, Galione A, Evans AM (2010) Calcium signaling via two-pore channels: local or global, that is the question. Am J Physiol Cell Physiol 298:C430–C441
95. Cai X, Patel S (2010) Degeneration of an intracellular ion channel in the primate lineage by relaxation of selective constraints. Mol Biol Evol 27:2352–2359
96. Rahman T, Cai X, Brailoiu GC, Abood ME, Brailoiu E, Patel S (2014) Two-pore channels provide insight into the evolution of voltage-gated Ca^{2+} and Na^+ channels. Sci Signal 7:ra109
97. Ishibashi K, Suzuki M, Imai M (2000) Molecular cloning of a novel form (two-repeat) protein related to voltage-gated sodium and calcium channels. Biochem Biophys Res Commun 270:370–376
98. Furuichi T, Cunningham KW, Muto S (2001) A putative two pore channel AtTPC1 mediates Ca^{2+} flux in Arabidopsis leaf cells. Plant Cell Physiol 42:900–905
99. Peiter E, Maathuis FJ, Mills LN, Knight H, Pelloux J, Hetherington AM et al (2005) The vacuolar Ca^{2+}-activated channel TPC1 regulates germination and stomatal movement. Nature 434:404–408
100. Hedrich R, Marten I (2011) TPC1-SV channels gain shape. Mol Plant 4:428–441
101. Calcraft PJ, Ruas M, Pan Z, Cheng X, Arredouani A, Hao X et al (2009) NAADP mobilizes calcium from acidic organelles through two-pore channels. Nature 459:596–600

102. Zhang F, Li PL (2007) Reconstitution and characterization of a nicotinic acid adenine dinucleotide phosphate (NAADP)-sensitive Ca^{2+} release channel from liver lysosomes of rats. J Biol Chem 282:25259–25269
103. Pryor PR, Reimann F, Gribble FM, Luzio JP (2006) Mucolipin-1 is a lysosomal membrane protein required for intracellular lactosylceramide traffic. Traffic 7:1388–1398
104. Yamaguchi S, Jha A, Li Q, Soyombo AA, Dickinson GD, Churamani D et al (2011) Transient receptor potential mucolipin 1 (TRPML1) and two-pore channels are functionally independent organellar ion channels. J Biol Chem 286:22934–22942
105. Zong X, Schieder M, Cuny H, Fenske S, Gruner C, Rotzer K et al (2009) The two-pore channel TPCN2 mediates NAADP-dependent Ca^{2+}-release from lysosomal stores. Pflugers Arch 458:891–899
106. Brailoiu E, Churamani D, Cai X, Schrlau MG, Brailoiu GC, Gao X et al (2009) Essential requirement for two-pore channel 1 in NAADP-mediated calcium signaling. J Cell Biol 186:201–209
107. Kinnear NP, Boittin FX, Thomas JM, Galione A, Evans AM (2004) Lysosome-sarcoplasmic reticulum junctions. A trigger zone for calcium signaling by nicotinic acid adenine dinucleotide phosphate and endothelin-1. J Biol Chem 279:54319–54326
108. Kinnear NP, Wyatt CN, Clark JH, Calcraft PJ, Fleischer S, Jeyakumar LH et al (2008) Lysosomes co-localize with ryanodine receptor subtype 3 to form a trigger zone for calcium signalling by NAADP in rat pulmonary arterial smooth muscle. Cell Calcium 44:190–201
109. Ogunbayo OA, Zhu Y, Rossi D, Sorrentino V, Ma J, Zhu MX et al (2011) Cyclic adenosine diphosphate ribose activates ryanodine receptors, whereas NAADP activates two-pore domain channels. J Biol Chem 286:9136–9140
110. Ruas M, Rietdorf K, Arredouani A, Davis LC, Lloyd-Evans E, Koegel H et al (2010) Purified TPC isoforms form NAADP receptors with distinct roles for Ca^{2+} signaling and endolysosomal trafficking. Curr Biol 20:703–709
111. Brailoiu E, Hooper R, Cai X, Brailoiu GC, Keebler MV, Dun NJ et al (2010) An ancestral deuterostome family of two-pore channels mediates nicotinic acid adenine dinucleotide phosphate-dependent calcium release from acidic organelles. J Biol Chem 285:2897–2901
112. Schieder M, Rotzer K, Bruggemann A, Biel M, Wahl-Schott CA (2010) Characterization of two-pore channel 2 (TPCN2)-mediated Ca^{2+} currents in isolated lysosomes. J Biol Chem 285:21219–21222
113. Jha A, Ahuja M, Patel S, Brailoiu E, Muallem S (2014) Convergent regulation of the lysosomal two-pore channel-2 by Mg^{2+}, NAADP, $PI(3,5)P_2$ and multiple protein kinases. Embo J 33:501–511
114. Pitt SJ, Funnell TM, Sitsapesan M, Venturi E, Rietdorf K, Ruas M et al (2010) TPC2 is a novel NAADP-sensitive Ca^{2+} release channel, operating as a dual sensor of luminal pH and Ca^{2+}. J Biol Chem 285:35039–35046
115. Brailoiu E, Rahman T, Churamani D, Prole DL, Brailoiu GC, Hooper R et al (2010) An NAADP-gated two-pore channel targeted to the plasma membrane uncouples triggering from amplifying Ca^{2+} signals. J Biol Chem 285:38511–38516
116. Arredouani A, Ruas M, Collins SC, Parkesh R, Clough F, Pillinger T et al (2015) Nicotinic Acid Adenine Dinucleotide Phosphate (NAADP) and endolysosomal two-pore channels modulate membrane excitability and stimulus-secretion coupling in mouse pancreatic beta cells. J Biol Chem 290:21376–21392
117. Park KH, Kim BJ, Shawl AI, Han MK, Lee HC, Kim UH (2013) Autocrine/paracrine function of nicotinic acid adenine dinucleotide phosphate (NAADP) for glucose homeostasis in pancreatic beta-cells and adipocytes. J Biol Chem 288:35548–35558
118. Tugba Durlu-Kandilci N, Ruas M, Chuang KT, Brading A, Parrington J, Galione A (2010) TPC2 proteins mediate nicotinic acid adenine dinucleotide phosphate (NAADP)- and agonist-evoked contractions of smooth muscle. J Biol Chem 285:24925–24932
119. Aley PK, Mikolajczyk AM, Munz B, Churchill GC, Galione A, Berger F (2010) Nicotinic acid adenine dinucleotide phosphate regulates skeletal muscle differentiation via action at two-pore channels. Proc Natl Acad Sci USA 107:19927–19932

120. Ruas M, Davis LC, Chen CC, Morgan AJ, Chuang KT, Walseth TF et al (2015) Expression of Ca^{2+}-permeable two-pore channels rescues NAADP signalling in TPC-deficient cells. Embo J 34:1743–1758
121. Wang X, Zhang X, Dong XP, Samie M, Li X, Cheng X et al (2012) TPC proteins are phosphoinositide- activated sodium-selective ion channels in endosomes and lysosomes. Cell 151:372–383
122. Guo J, Zeng W, Chen Q, Lee C, Chen L, Yang Y et al (2016) Structure of the voltage-gated two-pore channel TPC1 from Arabidopsis thaliana. Nature 531:196–201
123. Hedrich R, Mueller TD, Becker D, Marten I (2018) Structure and function of TPC1 vacuole SV channel gains shape. Mol Plant 11:764–775
124. Kintzer AF, Stroud RM (2016) Structure, inhibition and regulation of two-pore channel TPC1 from Arabidopsis thaliana. Nature 531:258–262
125. Kintzer AF, Stroud RM (2018) On the structure and mechanism of two-pore channels. Febs J 285:233–243
126. Patel S, Penny CJ, Rahman T (2016) Two-pore channels enter the atomic era: structure of plant TPC revealed. Trends Biochem Sci 41:475–477
127. Grimm C, Butz E, Chen CC, Wahl-Schott C, Biel M (2017) From mucolipidosis type IV to Ebola: TRPML and two-pore channels at the crossroads of endo-lysosomal trafficking and disease. Cell Calcium 67:148–155
128. Patel S, Kilpatrick BS (2018) Two-pore channels and disease. Biochim Biophys Acta Mol Cell Res 1865:1678–1686
129. Gerasimenko JV, Maruyama Y, Yano K, Dolman NJ, Tepikin AV, Petersen OH et al (2003) NAADP mobilizes Ca^{2+} from a thapsigargin-sensitive store in the nuclear envelope by activating ryanodine receptors. J Cell Biol 163:271–282
130. Dammermann W, Guse AH (2005) Functional ryanodine receptor expression is required for NAADP-mediated local Ca^{2+} signaling in T-lymphocytes. J Biol Chem 280:21394–21399
131. Lin-Moshier Y, Walseth TF, Churamani D, Davidson SM, Slama JT, Hooper R et al (2012) Photoaffinity labeling of nicotinic acid adenine dinucleotide phosphate (NAADP) targets in mammalian cells. J Biol Chem 287:2296–2307
132. Walseth TF, Lin-Moshier Y, Jain P, Ruas M, Parrington J, Galione A et al (2012) Photoaffinity labeling of high affinity nicotinic acid adenine dinucleotide phosphate (NAADP)-binding proteins in sea urchin egg. J Biol Chem 287:2308–2315
133. Galione A, Petersen OH (2005) The NAADP receptor: new receptors or new regulation? Mol Interv 5:73–79
134. Guse AH, Diercks BP (2018) Integration of nicotinic acid adenine dinucleotide phosphate (NAADP)-dependent calcium signalling. J Physiol 596:2735–2743
135. Galione A (2011) NAADP receptors. Cold Spring Harb Perspect Biol 3:a004036
136. Morgan AJ, Davis LC, Wagner SK, Lewis AM, Parrington J, Churchill GC et al (2013) Bidirectional Ca^{2+} signaling occurs between the endoplasmic reticulum and acidic organelles. J Cell Biol 200:789–805
137. Kilpatrick BS, Eden ER, Schapira AH, Futter CE, Patel S (2013) Direct mobilisation of lysosomal Ca^{2+} triggers complex Ca^{2+} signals. J Cell Sci 126:60–66
138. Kilpatrick BS, Eden ER, Hockey LN, Yates E, Futter CE, Patel S (2017) An endosomal NAADP-sensitive two-pore Ca^{2+} channel regulates ER-endosome membrane contact sites to control growth factor signaling. Cell Rep 18:1636–1645
139. Churchill GC, O'Neill JS, Masgrau R, Patel S, Thomas JM, Genazzani AA et al (2003) Sperm deliver a new second messenger: NAADP. Curr Biol 13:125–128
140. Moccia F, Lim D, Kyozuka K, Santella L (2004) NAADP triggers the fertilization potential in starfish oocytes. Cell Calcium 36:515–524
141. Brailoiu GC, Brailoiu E, Parkesh R, Galione A, Churchill GC, Patel S et al (2009) NAADP-mediated channel 'chatter' in neurons of the rat medulla oblongata. Biochem J 419:91–97.
142. Hockey LN, Kilpatrick BS, Eden ER, Lin-Moshier Y, Brailoiu GC, Brailoiu E et al (2015) Dysregulation of lysosomal morphology by pathogenic LRRK2 is corrected by TPC2 inhibition. J Cell Sci 128:232–238

143. Lin-Moshier Y, Keebler MV, Hooper R, Boulware MJ, Liu X, Churamani D et al (2014) The Two-Pore Channel (TPC) interactome unmasks isoform-specific roles for TPCs in endolysosomal morphology and cell pigmentation. Proc Natl Acad Sci USA 111:13087–13092
144. Wilding M, Russo GL, Galione A, Marino M, Dale B (1998) ADP-ribose gates the fertilization channel in ascidian oocytes. Am J Physiol 275:C1277–C1283
145. Sumoza-Toledo A, Penner R (2011) TRPM2: a multifunctional ion channel for calcium signalling. J Physiol 589:1515–1525
146. Perraud AL, Fleig A, Dunn CA, Bagley LA, Launay P, Schmitz C et al (2001) ADP-ribose gating of the calcium-permeable LTRPC2 channel revealed by Nudix motif homology. Nature 411:595–599
147. Iordanov I, Mihalyi C, Toth B, Csanady L (2016) The proposed channel-enzyme transient receptor potential melastatin 2 does not possess ADP ribose hydrolase activity. Elife 5: e17600
148. Beck A, Kolisek M, Bagley LA, Fleig A, Penner R (2006) Nicotinic acid adenine dinucleotide phosphate and cyclic ADP-ribose regulate TRPM2 channels in T lymphocytes. FASEB J 20:962–964
149. Toth B, Iordanov I, Csanady L (2015) Ruling out pyridine dinucleotides as true TRPM2 channel activators reveals novel direct agonist ADP-ribose-2′-phosphate. J Gen Physiol 145:419–430
150. Gasser A, Glassmeier G, Fliegert R, Langhorst MF, Meinke S, Hein D et al (2006) Activation of T cell calcium influx by the second messenger ADP-ribose. J Biol Chem 281:2489–2496
151. Lange I, Yamamoto S, Partida-Sanchez S, Mori Y, Fleig A, Penner R (2009) TRPM2 functions as a lysosomal Ca^{2+}-release channel in beta cells. Sci Signal 2:ra23
152. Basile G, Taglialatela-Scafati O, Damonte G, Armirotti A, Bruzzone S, Guida L et al (2005) ADP-ribosyl cyclases generate two unusual adenine homodinucleotides with cytotoxic activity on mammalian cells. Proc Natl Acad Sci USA 102:14509–14514
153. Fliegert R, Bauche A, Wolf Perez AM, Watt JM, Rozewitz MD, Winzer R et al (2017) 2′-Deoxyadenosine 5′-diphosphoribose is an endogenous TRPM2 superagonist. Nat Chem Biol 13:1036–1044
154. Huang Y, Winkler PA, Sun W, Lu W, Du J (2018) Architecture of the TRPM2 channel and its activation mechanism by ADP-ribose and calcium. Nature 562:145–149
155. Sutherland EW (1972) Studies on the mechanism of hormone action. Science 177:401–408
156. Morgan AJ, Galione A (2008) Investigating cADPR and NAADP in intact and broken cell preparations. Methods 46:194–203
157. Churamani D, Carrey EA, Dickinson GD, Patel S (2004) Determination of cellular nicotinic acid-adenine dinucleotide phosphate (NAADP) levels. Biochem J 380:449–454
158. Lewis AM, Masgrau R, Vasudevan SR, Yamasaki M, O'Neill JS, Garnham C et al (2007) Refinement of a radioreceptor binding assay for nicotinic acid adenine dinucleotide phosphate. Anal Biochem 371:26–36
159. Graeff R, Lee HC (2002) A novel cycling assay for cellular cADP-ribose with nanomolar sensitivity. Biochem J 361:379–384
160. Graeff R, Lee HC (2002) A novel cycling assay for nicotinic acid-adenine dinucleotide phosphate with nanomolar sensitivity. Biochem J 367:163–168
161. Graeff RM, Walseth TF, Fryxell K, Branton WD, Lee HC (1994) Enzymatic synthesis and characterizations of cyclic GDP-ribose. A procedure for distinguishing enzymes with ADP-ribosyl cyclase activity. J Biol Chem 269:30260–30267
162. Galione A, White A, Willmott N, Turner M, Potter BV, Watson SP (1993) cGMP mobilizes intracellular Ca^{2+} in sea urchin eggs by stimulating cyclic ADP-ribose synthesis. Nature 365:456–459
163. Graeff RM, Franco L, De Flora A, Lee HC (1998) Cyclic GMP-dependent and -independent effects on the synthesis of the calcium messengers cyclic ADP-ribose and nicotinic acid adenine dinucleotide phosphate. J Biol Chem 273:118–125

164. Kim BJ, Park KH, Yim CY, Takasawa S, Okamoto H, Im MJ et al (2008) Generation of nicotinic acid adenine dinucleotide phosphate and cyclic ADP-ribose by glucagon-like peptide-1 evokes Ca^{2+} signal that is essential for insulin secretion in mouse pancreatic islets. Diabetes 57:868–878
165. Wilson HL, Galione A (1998) Differential regulation of nicotinic acid-adenine dinucleotide phosphate and cADP-ribose production by cAMP and cGMP. Biochem J 331(Pt 3):837–843
166. Yamasaki M, Thomas JM, Churchill GC, Garnham C, Lewis AM, Cancela JM et al (2005) Role of NAADP and cADPR in the induction and maintenance of agonist-evoked Ca^{2+} spiking in mouse pancreatic acinar cells. Curr Biol 15:874–878
167. Gasser A, Bruhn S, Guse AH (2006) Second messenger function of nicotinic acid adenine dinucleotide phosphate revealed by an improved enzymatic cycling assay. J Biol Chem 281:16906–16913
168. Dodd AN, Gardner MJ, Hotta CT, Hubbard KE, Dalchau N, Love J et al (2007) The Arabidopsis circadian clock incorporates a cADPR-based feedback loop. Science 318:1789–1792
169. Kato I, Yamamoto Y, Fujimura M, Noguchi N, Takasawa S, Okamoto H (1999) CD38 disruption impairs glucose-induced increases in cyclic ADP-ribose, $[Ca^{2+}]i$, and insulin secretion. J Biol Chem 274:1869–1872
170. Fukushi Y, Kato I, Takasawa S, Sasaki T, Ong BH, Sato M et al (2001) Identification of cyclic ADP-ribose-dependent mechanisms in pancreatic muscarinic Ca^{2+} signaling using CD38 knockout mice. J Biol Chem 276:649–655
171. Cosker F, Cheviron N, Yamasaki M, Menteyne A, Lund FE, Moutin MJ et al (2010) The ecto-enzyme CD38 is a nicotinic acid adenine dinucleotide phosphate (NAADP) synthase that couples receptor activation to Ca^{2+} mobilization from lysosomes in pancreatic acinar cells. J Biol Chem 285:38251–38259
172. Takahashi J, Kagaya Y, Kato I, Ohta J, Isoyama S, Miura M et al (2003) Deficit of CD38/cyclic ADP-ribose is differentially compensated in hearts by gender. Biochem Biophys Res Commun 312:434–440
173. Deshpande DA, White TA, Guedes AG, Milla C, Walseth TF, Lund FE et al (2005) Altered airway responsiveness in CD38-deficient mice. Am J Respir Cell Mol Biol 32:149–156
174. Mitsui-Saito M, Kato I, Takasawa S, Okamoto H, Yanagisawa T (2003) CD38 gene disruption inhibits the contraction induced by alpha-adrenoceptor stimulation in mouse aorta. J Vet Med Sci 65:1325–1330
175. Partida-Sanchez S, Cockayne DA, Monard S, Jacobson EL, Oppenheimer N, Garvy B et al (2001) Cyclic ADP-ribose production by CD38 regulates intracellular calcium release, extracellular calcium influx and chemotaxis in neutrophils and is required for bacterial clearance in vivo. Nat Med 7:1209–1216
176. Jin D, Liu HX, Hirai H, Torashima T, Nagai T, Lopatina O et al (2007) CD38 is critical for social behaviour by regulating oxytocin secretion. Nature 446:41–45
177. Park KH, Kim BJ, Kang J, Nam TS, Lim JM, Kim HT et al (2011) Ca^{2+} signaling tools acquired from prostasomes are required for progesterone-induced sperm motility. Sci Signal 4:ra31
178. Kim SY, Cho BH, Kim UH (2010) CD38-mediated Ca^{2+} signaling contributes to angiotensin II-induced activation of hepatic stellate cells: attenuation of hepatic fibrosis by CD38 ablation. J Biol Chem 285:576–582
179. Rah SY, Mushtaq M, Nam TS, Kim SH, Kim UH (2010) Generation of cyclic ADP-ribose and nicotinic acid adenine dinucleotide phosphate by CD38 for Ca^{2+} signaling in interleukin-8-treated lymphokine-activated killer cells. J Biol Chem 285:21877–21887
180. Lin WK, Bolton EL, Cortopassi WA, Wang Y, O'Brien F, Maciejewska M et al (2017) Synthesis of the Ca^{2+}-mobilizing messengers NAADP and cADPR by intracellular CD38 enzyme in the mouse heart: role in beta-adrenoceptor signaling. J Biol Chem 292: 13243–13257

181. Soares S, Thompson M, White T, Isbell A, Yamasaki M, Prakash Y et al (2007) NAADP as a second messenger: neither CD38 nor base-exchange reaction are necessary for in vivo generation of NAADP in myometrial cells. Am J Physiol Cell Physiol 292:C227–C239
182. Higashida H, Liang M, Yoshihara T, Akther S, Fakhrul A, Stanislav C et al (2017) An immunohistochemical, enzymatic, and behavioral study of CD157/BST-1 as a neuroregulator. BMC Neurosci 18:35
183. De Flora A, Guida L, Franco L, Zocchi E (1997) The CD38/cyclic ADP-ribose system: a topological paradox. Int J Biochem Cell Biol 29:1149–1166
184. Lee HC (2011) Cyclic ADP-ribose and NAADP: fraternal twin messengers for calcium signaling. Sci China Life Sci 54(8):699–711
185. Zhao YJ, Lam CM, Lee HC (2012) The membrane-bound enzyme CD38 exists in two opposing orientations. Sci Signal 5:ra67
186. Liu J, Zhao YJ, Li WH, Hou YN, Li T, Zhao ZY et al (2017) Cytosolic interaction of type III human CD38 with CIB1 modulates cellular cyclic ADP-ribose levels. Proc Natl Acad Sci USA

Chapter 16
Calcium Signaling in the Heart

Derek A. Terrar

Abstract The aim of this chapter is to discuss evidence concerning the many roles of calcium ions, Ca^{2+}, in cell signaling pathways that control heart function. Before considering details of these signaling pathways, the control of contraction in ventricular muscle by Ca^{2+} transients accompanying cardiac action potentials is first summarized, together with a discussion of how myocytes from the atrial and pacemaker regions of the heart diverge from this basic scheme. Cell signaling pathways regulate the size and timing of the Ca^{2+} transients in the different heart regions to influence function. The simplest Ca^{2+} signaling elements involve enzymes that are regulated by cytosolic Ca^{2+}. Particularly important examples to be discussed are those that are stimulated by Ca^{2+}, including Ca^{2+}-calmodulin-dependent kinase (CaMKII), Ca^{2+} stimulated adenylyl cyclases, Ca^{2+} stimulated phosphatase and NO synthases. Another major aspect of Ca^{2+} signaling in the heart concerns actions of the Ca^{2+} mobilizing agents, inositol trisphosphate (IP_3), cADP-ribose (cADPR) and nicotinic acid adenine dinucleotide phosphate, (NAADP). Evidence concerning roles of these Ca^{2+} mobilizing agents in different regions of the heart is discussed in detail. The focus of the review will be on short term regulation of Ca^{2+} transients and contractile function, although it is recognized that Ca^{2+} regulation of gene expression has important long term functional consequences which will also be briefly discussed.

Keywords Heart · Cardiac · Calcium · Signaling · Calcium-stimulated enzymes · CaMKII · AC1 · AC8 · IP_3 · cADPR · NAADP

D. A. Terrar (✉)
Department of Pharmacology, University of Oxford, Oxford, UK
e-mail: derek.terrar@pharm.ox.ac.uk

M. S. Islam (ed.), *Calcium Signaling*, Advances in Experimental Medicine and Biology 1131, https://doi.org/10.1007/978-3-030-12457-1_16

16.1 Introduction

Readers of this volume will be well aware of the importance of calcium in all plant and animal species arising from the many roles of calcium ions in all biological processes. The statement that calcium is everything (generally attributed to Loewi) might be regarded as inspiring awe or exasperation in relation to the design of experiments to explore the functions of calcium. The focus of this chapter concerns the many roles of calcium ions, Ca^{2+}, in the heart.

The primary function of the heart is to provide a co-ordinated muscle contraction system to pump blood to the lungs and body, enabling the body tissues to receive oxygen and nutrients. The elements of the process that couples electrical activity to contraction of cardiac muscle will be outlined briefly to set the scene for how this relatively simple process might be regulated by many calcium-dependent systems. These calcium-dependent regulatory pathways will make up the bulk of the chapter. They include calcium-dependent enzymes (including the Ca^{2+}-calmodulin-dependent protein kinase, CaMKII, and other enzymes influenced by Ca^{2+}, particularly those that regulate cAMP and cGMP signaling systems), as well as the pathways involving the Ca^{2+} mobilizing agents inositol trisphosphate (IP_3), cADP-ribose (cADPR) and nicotinic acid adenine-dinucleotide phosphate (NAADP). In the case of cADPR and NAADP, evidence concerning the actions of these substances will be reviewed separately, but a brief summary will discuss the possibility of synergistic actions of these two substance in the heart, since their actions appear to be complementary and it has recently been suggested that the synthesis of both is catalyzed by the same enzyme, CD38, in the heart [1].

Although the headlines of the process coupling the electric signal of the action potential to contraction (EC coupling) are simple and generally agreed (see reviews [2]; [3]), there are details of the underlying mechanisms that remain open to debate. The outstanding questions are difficult to address experimentally precisely because of the many overlapping roles of calcium. These experimental problems are further compounded by the nature of different compartments inside cardiac cells, not just different membrane delimited compartments (such as the sarcoplasmic reticulum, mitochondria and lysosomes) but also the presence of microdomains in the cytosol where the concentration of Ca^{2+} might differ for functionally important periods of time from that in the bulk cytosol, for example in the subsarcolemmal space beneath the plasma membrane, or spaces between intracellular organelles. Although the poorly understood aspects of EC coupling are functionally important, most of the discussion of the calcium-dependent signaling pathways that form the bulk of this chapter can be followed with just a knowledge of the agreed simple framework.

In addition to the rapid processes controlling contraction, many of the roles of Ca^{2+} in the heart concern long term processes involving turning genes on or off to change protein expression, and are important not only in development but in adaptive processes such as hypertrophy that might be either beneficial or harmful. These roles of Ca^{2+} over periods of days or longer will be covered here only in

summary, and such long-term calcium signaling mechanisms are described in detail in: [4]; [5].

Before addressing our knowledge of calcium signaling in the heart, it should be emphasized that although all of the points raised above relate to cardiac muscle in general, there are important differences between cell types in different regions of the heart with particular functions. Much of the discussion will concern ventricular muscle that has generally received most extensive experimental study, but it is clear that cells from the upper atrial chambers of the heart show important variations in the control of their Ca^{2+} signals that are related to their different functions, and an even greater divergence from the ventricular pattern is shown in the pacemaker cells from the SA node. These differences are addressed in particular sections below, after first outlining a basic scheme for ventricular myocytes. The atrioventricular node and conduction systems also show particular specialisations but will not be discussed in detail here (see [6]).

16.2 Simple Scheme of EC Coupling in Ventricular Myocytes

Excitation-contraction (EC) coupling in the heart has been extensively reviewed, for example in [2], [7], as well as in an excellent recent paper from [3], from which Fig. 16.1a is taken. EC coupling links electrical activity in the form of a cardiac action potential, generally lasting hundreds of ms, to a rise in free Ca^{2+} in the cytosol, which in turn activates the contractile machinery of the actin and myosin filaments. Ventricular myocytes show a striated appearance arising from overlap of the thick myosin and thin actin filaments, but also reflecting the division of the length of the myocyte into sarcomeres, which are slightly less than 2 μm long and act as functional units. Each end of a sarcomere in ventricular muscle is bounded by a transverse tubule, which is an invagination of the surface membrane running deep into the myocyte, as shown schematically in Fig. 16.1a (from [3]), together with a confocal image in Fig. 16.1b illustrating an example of this arrangement in a rabbit ventricular myocyte (from [8]). An important membrane system within the myocyte is the endoplasmic reticulum (termed sarcoplasmic reticulum, SR, in myocytes), and this functions as a Ca^{2+} store in which the luminal Ca^{2+} concentration far exceeds that in the cytoplasm. The regions where the SR approaches the transverse tubules are referred to as terminal cisternae, and these two membrane components, together with the restricted space between them, form an important unit for EC coupling, as shown in Figs. 16.1a and 16.1b. This unit of transverse tubule and SR in cardiac muscle is generally referred to as a dyad. The headline of EC coupling is that Ca^{2+} enters the cytosol from the extracellular space to trigger further release of Ca^{2+} ions from the SR by a process termed Ca^{2+}-induced-Ca^{2+}-release (CICR). The Ca^{2+} enters via voltage-gated L-type Ca^{2+} channels located predominantly in the transverse tubules, and the release of Ca^{2+} is via ryanodine receptors (RyR2) in the terminal cisternae of the SR. At body temperature the L-type Ca^{2+} channels are rapidly activated by the depolarization of the action potential, reaching a peak

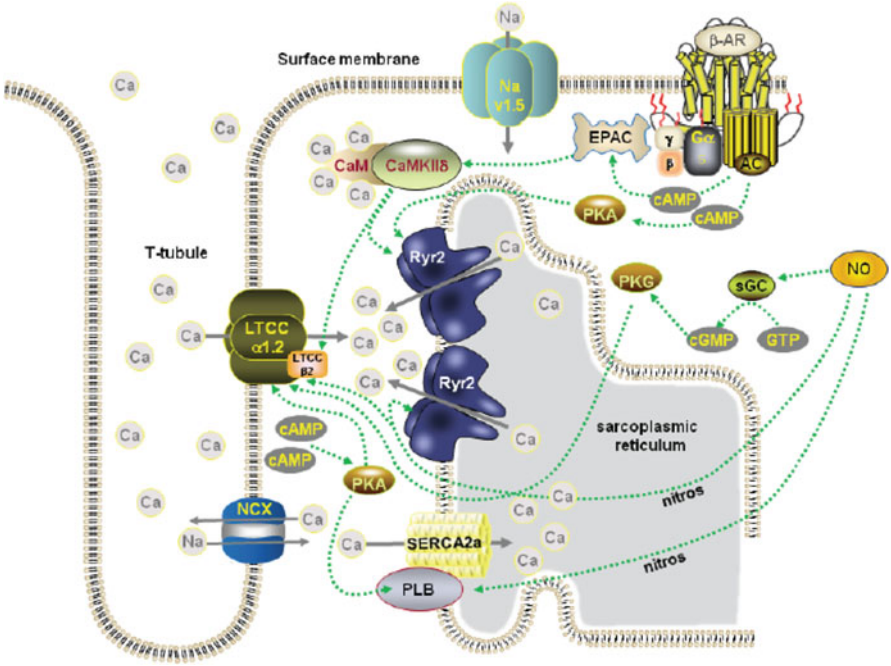

Fig. 16.1a Schematic diagram of the main proteins involved in EC coupling in a ventricular myocyte and the main mechanisms for their phosphorylation or nitrosylation. LTCC = L-type Ca channel, Cav1.2; Nav1.5 = cardiac isoform of the Na channel; NCX = Na/Ca exchange; RyR2 = ryanodine receptor; PLB = phospholamban; AC = adenylyl cyclase; sGC = soluble guanylyl cyclase; EPAC = exchange protein activated by cAMP; PKA = protein kinase A; PKG = protein kinase G. The transverse tubule (T tubule) is shown as an invagination of the surface membrane forming a dyad with the adjacent terminal cisterna of the SR. CICR occurs in the microdomain of the dyad between these two structures. (Reproduced from [3])

of activation in about 3 ms, and this leads to CICR via RyR2 within the dyad followed by a rise in bulk cytosolic Ca^{2+} concentration to activate the myofilaments. The RyR2 is key to this process and is a large protein with multiple regulatory sites (see: [9–12]). The brief rise in Ca^{2+} in the bulk cytosol associated with this process of CICR is termed the Ca^{2+} transient, CaT. Restoration of cytosolic Ca^{2+} concentration back to the resting level (resulting in the decline of the CaT) is largely achieved by pumping of Ca^{2+} back into the SR by a sarcoplasmic-endoplasmic reticulum Ca^{2+} ATP-ase, SERCA, and by extrusion of Ca^{2+} back into the extracellular space, predominantly by the secondarily active and electrogenic Na^{+}/Ca^{2+} exchange, NCX. There is a minor role in most circumstances of a Ca^{2+} ATP-ase in the surface membrane.

It is worth briefly mentioning mitochondria which occupy about a third of the cellular volume of ventricular myocytes and are essential for supplying ATP to meet the energy demands associated with ion transport and contraction. In the context of

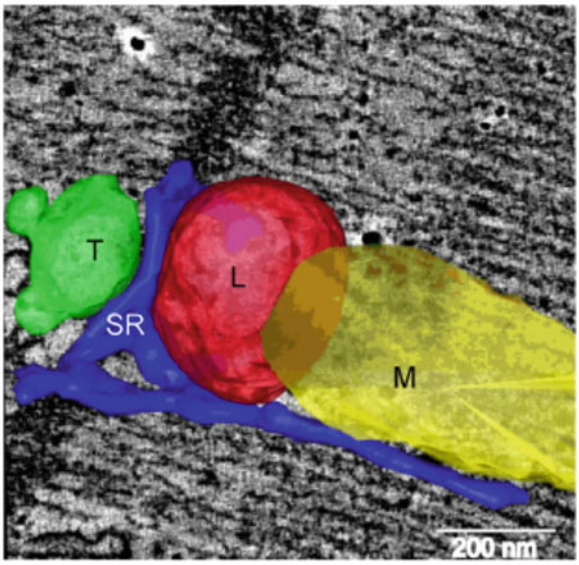

Fig. 16.1b 3D Electron Tomography reconstruction of lysosomes, SR, t-tubules and mitochondria. Representative electron tomography (ET) image of lysosomes near calcium signalling organelles, showing reconstructed organelles in 3D of sarcoplasmic reticulum, mitochondria and t-tubule in rabbit left ventricular tissue. Dual-axis ET and IMOD software were used to image, reconstruct and model lysosomes (L, red), sarcoplasmic reticulum (SR, blue), mitochondria (M, yellow), and t-tubules (T, green) in 3D. Isovolumetric voxel size = 1.206 nm, Z-depth = 275 nm. Scale bar = 200 nm. See original paper for Supplementary Video 1 for 3D animation of tomographic reconstruction of cell. The structural element formed by the t-tubule and SR is important for CICR, while the microdomains between the lysosome and the SR, and between the lysosome and the mitochondria, will be discussed in the section concerning cardiac actions of the Ca^{2+} mobilising agent, NAADP. (Reproduced from [8])

Ca^{2+} signaling, mitochondria may influence changes in cytosolic Ca^{2+} during EC coupling [13], and in turn Ca^{2+} within the mitochondria regulates ATP production [14]. Mitochondria may play a particular role in shaping cytosolic Ca^{2+} signals in atrial myocytes [15].

The potentially explosive process of CICR is subject to local control, and clusters of RyR2 act as release units, giving rise to Ca^{2+} 'sparks' [16]. These are transient localized increases in cytosolic Ca^{2+} arising from Ca^{2+} release from the SR, and it is generally believed the CaT is made of many Ca^{2+} spark-like events; see: [17–19]. These Ca^{2+} sparks are approximately elliptical when viewed in 2D and cover a distance comparable to the sarcomere spacing. The occurrence of sparks is influenced by Ca^{2+} close to RyR2 both in the cytosol and in the lumen of the SR. Recent discussions of the influences of cytosolic and luminal SR Ca^{2+} on RyR2 function can be found in: [20]; [21]; and [19] (and see [22]).

A key aspect of the EC coupling process described above concerns the timing of the CaT relative to the time course of the action potential. It is important to

note that all the processes of CICR are very temperature dependent. Temperature is particularly influential for Ca^{2+} entry via L-type Ca^{2+} channels [23] and for Ca^{2+} release from the SR via RyR2 [24]. The transport processes that are responsible for Ca^{2+} extrusion from the cell (principally Na^{+}/Ca^{2+} exchange) and for Ca^{2+} uptake into the SR (by the sarcoplasmic/endoplasmic reticulum ATP-ase, SERCA) are also very temperature dependent. In the ventricular muscle of most mammalian species, including human (although not adult rat or mouse), the action potential that controls contraction has a prolonged plateau at a potential that is much more depolarized than the resting level of approximately −85 mV. This plateau lasts hundreds of ms and is often close to 0 mV. At body temperature the peak and a substantial part of the decline of the CaT occurs while the plateau is still elevated. This is illustrated in Fig. 16.2 (from [25]; see also [26]).

One aspect of the importance of temperature and the timing of CaT relative to the AP plateau concerns the balance between Ca^{2+} extrusion from the cytosol to the extracellular space (predominantly by NCX) and uptake of Ca^{2+} from the cytosol into the SR. These two Ca^{2+} removal processes are essentially in competition. Extrusion of Ca^{2+} via NCX depends on the cytosolic concentration of Ca^{2+} ions (which changes rapidly in the subsarcolemmal space from the resting level of 100 nM to a peak concentration at least 100 times greater, though still much smaller than the free extracellular Ca^{2+} concentration of 1–2 mM), and on the concentrations of sodium ions on either side of the membrane (which are likely to be relatively stable during a single action potential at over 100 mM on the extracellular side and approximately 5 mM in the cytosol, since the influx of Na^{+} is too small on this time scale to have any substantial effect on these relatively large Na^{+} concentrations). The other determinant of NCX is the membrane potential since Ca^{2+} extrusion normally depends primarily on the driving force for Na^{+} entry (though the Ca^{2+} gradient is also important). The precise reversal potential

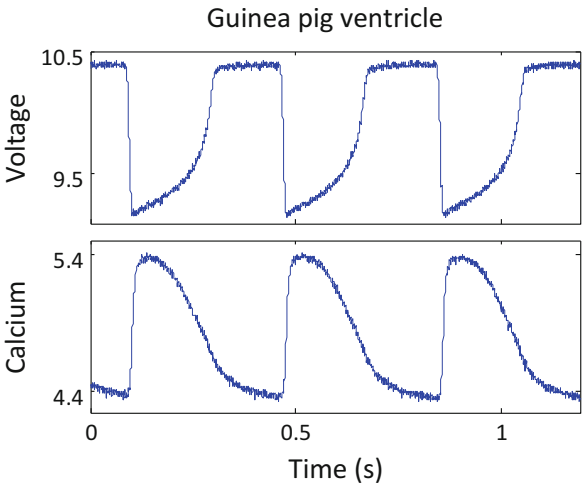

Fig. 16.2 Simultaneous recording of AP and CaT measured using optical methods in whole guinea-pig heart at body temperature. The AP waveform is shown as optical signal in which depolarization is represented as a downward deflection, inverting the normal AP appearance. The CaT is shown below the AP. It is clear that the peak and a major component of the decay of CaT occurred during the AP plateau (see text). (Reproduced from [25])

(in other words the potential for zero net current) for NCX is controversial, and will change as the subsarcolemmal Ca^{2+} changes, but it is clear that the extrusion of Ca^{2+} at a plateau potential close to 0 mV will be much less than that at the resting potential of approximately −85 mV because the driving force for Na^{+} entry will be much greater at the resting potential. It could be argued that one factor underlying the evolution of action potentials with a prolonged plateau results from the above arguments concerning Ca^{2+} balance: while the action potential remains at the plateau potential the balance between Ca^{2+} extrusion via NCX and Ca^{2+} uptake into the SR by SERCA greatly favours Ca^{2+} uptake. This might be seen as an efficient mechanism so that the large fraction of Ca^{2+} release from the SR (contributing perhaps 75% of the amplitude of the CaT, depending on species) can be taken back into the SR with minimal opposition from NCX at plateau potentials.

Note that at room temperature (which is often used even for experiments on mammalian ventricular myocytes) the time course of the CaT is greatly prolonged relative to the timing of the action potential so that even the peak but also generally all of the decay of the CaT occur at or close to the resting potential, which favours Ca^{2+} extrusion from the cytosol via NCX over uptake of Ca^{2+} back into the SR by SERCA. This situation departs from the physiological and can give rise to difficulties in the interpretation of some experimental observations.

One area where these difficulties are particularly important in the context of Ca^{2+} signaling in the heart concerns the effect of an agent that increases the Ca^{2+} sensitivity of RyR2 to cytosolic Ca^{2+}, as appears to be the case for caffeine. Some have argued that both on theoretical and experimental grounds such an agent will have only a transient effect since although there is an initial increase in CaT amplitude, the increase is not sustained because the amount of Ca^{2+} loaded in the SR declines until there is an exact compensation of SR Ca^{2+} load to restore the original CaT amplitude. When caffeine or similar agent is removed there is an initial decline in CaT amplitude followed by restoration of CaT amplitude as the SR Ca^{2+} load re-adjusts [27]. It is stressed that in the steady state Ca^{2+} influx equals Ca^{2+} efflux during every beat. The experiments to investigate this compensation have generally been done under conditions in which the peak of the CaT occurs after repolarization of the initiating AP or voltage-clamp pulse (mostly at room temperature). We have found that in guinea-pig ventricular myocytes maintained close to body temperature (36 °C), a low concentration of caffeine (250 μM) caused an increase in CaT amplitude, and although there was some decline after the initial effect presumably reflecting partial compensation, the CaT remained elevated for the 30 s of caffeine exposure (unpublished observations of Rakovic & Terrar, presented to the 2006 meeting of Biophysical Society). However, at room temperature (after the heater for the cell superfusion system was turned off) the full compensation described by Eisner et al. was observed. One interpretation of these apparently conflicting observations is that full compensation occurs when there is a clear separation between the timing of the initiating Ca^{2+} influx via L-type Ca^{2+} channels and Ca^{2+} removal from the cytosol by SERCA and NCX (particularly when NCX dominates over SERCA at potentials close to the resting level), as is the case when the timing of the CaT is clearly slower than the action potential at room temperature.

However, at body temperature when the bulk of the CaT occurs at plateau potentials, additional Ca^{2+} released from the SR can be taken back up by SERCA with little or no opposition from NCX, and therefore without contravening the need to maintain equal Ca^{2+} influx and efflux during every beat at the steady state.

Measuring the amount and timing of Ca^{2+} entry via voltage-activated L-type Ca^{2+} channels during an action potential with a long positive plateau is also difficult, if not impossible, to measure with currently available methods. It might be thought that the availability of very selective blockers for L-type Ca^{2+} channels, such as nisoldipine, would allow estimation of this current by difference methods. However, if the action potential waveform is applied under voltage clamp conditions, and nisoldipine is added this will block not only the current through L-type Ca^{2+} channels but also any effects of the Ca^{2+} entering the cell on other processes that could affect other currents (such as Ca^{2+}-dependent changes in K^+, or Ca^{2+}-activated Cl^- currents), but in particular the current associated with extrusion of Ca^{2+} by electrogenic NCX. The best experiments (e.g [28]) have tried to take account of NCX with the use of cytosolic Ca^{2+} buffers such as BAPTA, but the difficulty here is that such buffers may also have effects in addition to suppressing NCX (such as a reduced inactivation of L-type Ca^{2+} channels). Often modeling of ventricular APs includes a significant amount of L-type Ca^{2+} current towards the end of the plateau (e.g [29]), although this does not seem to fit with the substantial inactivation of L-type Ca^{2+} channels towards the end of the plateau, as reported by [30] and [31].

It should be also noted that many aspects of the structure and function of ventricular myocytes are altered in the failing heart, as summarized in [3].

16.3 Atria

The purpose of this section is to outline major differences between atrial and ventricular myocytes that are relevant for understanding of calcium-signaling pathways described below. Recent reviews of the mechanism of EC coupling in atrial myocytes can be found in [32].

The most important feature of atrial myocytes is that transverse tubules are either absent, or present at a much lower density, than is the case in ventricular cells, with the consequence that CICR operates with major differences from the scheme outlined above. Fig. 16.3a-e shows a confocal image of an atrial myocyte stained with an antibody recognizing RyR2. It can be seen that there is a line of RyR2 at the periphery, consistent with a location just beneath the sarcolemma. This is referred to as the junctional SR. There are additional bands of SR with a separation consistent with sarcomere spacing of slightly less than 2 μm and this is referred to as non-junctional SR. In terms of EC coupling, the simplest scheme is that Ca^{2+} enters through L-type Ca^{2+} channels in the surface membrane and activates Ca^{2+} release via RyR in the junctional SR.

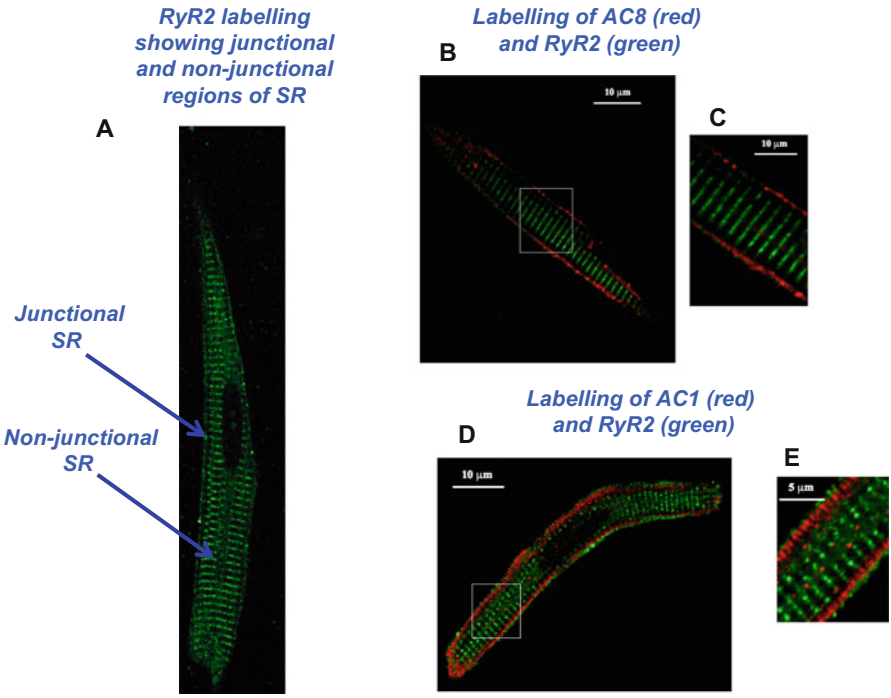

Fig. 16.3(a-e) Organisation of RyR2 and related elements in atrial myocytes. (**a**). Labelling of RyR2 (green) to show junctional and non-junctional SR (observation by T.P. Collins in the Terrar lab). (**b–e**) (Reproduced from [33]). Immunolocalisation of RyRs and Ca^{2+}-stimulated adenylyl cyclases B, RyR2 (green) and AC1 (red). C, enlarged section of panel A identified by white box. D, RyR2 (green) and AC8 (red). (**e**), enlarged section of panel C identified by white box

The way in which the rise in Ca^{2+} at the surface propagates to regions deeper within the atrial myocyte is the subject of intense recent research. It is clear that the spread of Ca^{2+} from periphery to centre is normally slow relative to that in a ventricular myocytes (in which transverse tubules greatly speed the spread of Ca^{2+} release). To gain insight into the underlying mechanisms in atrial myocytes, confocal microscopy has been used to make simultaneous measurements of Ca^{2+} in the cytosol (using rhod-2) and SR (using fluo-5N) [34]. The magnitude of the cytosolic CaT close to junctional SR was higher than that in the vicinity of non-junctional SR. As might be expected the fall in junctional SR Ca^{2+} was well synchronised with the local rise in cytosolic Ca^{2+}, but in the non-junctional SR there was a small rise in SR Ca^{2+} as the Ca^{2+} wavefront progressed deeper into the cell, presumably resulting from Ca^{2+} uptake by SERCA, with the additional luminal Ca^{2+} leading to sensitization of RyR2 to the Ca^{2+} signal in the cytosol. The rise of cytosolic Ca^{2+} at individual release sites of the non-junctional SR thus preceded the depletion of SR Ca^{2+} accompanying Ca^{2+} release in this region. It was proposed that Ca^{2+} release from non-junctional SR is activated by both cytosolic and luminal

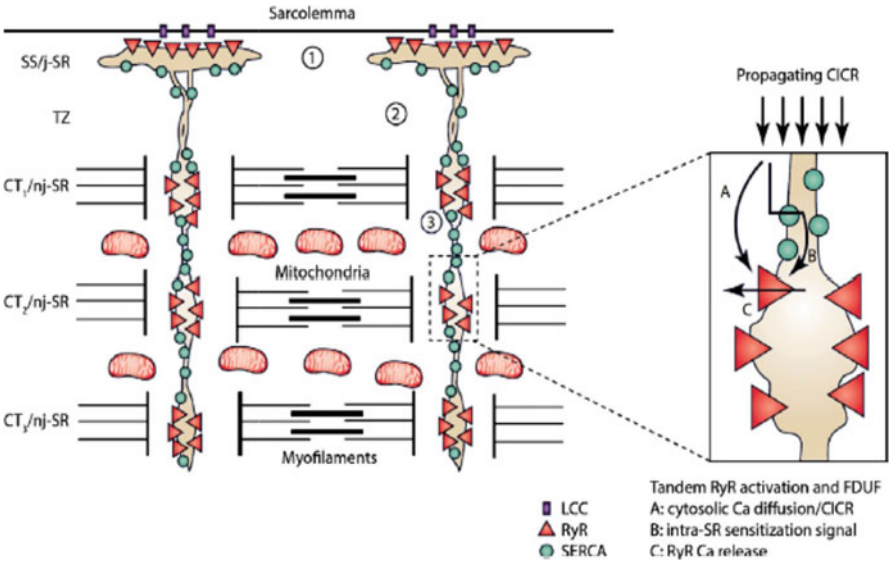

Fig. 16.3f Atrial ECC: tandem RyR activation and FDUF mechanism. AP-induced Ca^{2+} release from junctional-SR (jSR) by L-type Ca^{2+} channel activation [1], followed by propagation through mitochondria-free transition zone (TZ; 2) and activation of centripetal propagating CICR [3] from central (CT) non-junctional (nj-SR) CRUs (CT1 → CT2 → CT3 → . . .). Inset: FDUF mechanism. Tandem RyR activation by cytosolic CICR (**a**) and luminal RyR sensitization (**b**) by elevated [Ca]SR (SR Ca^{2+} sensitization signal) resulting in Ca^{2+} release (**c**). SR Ca^{2+} sensitization signal is generated by Ca uptake at the activation front by SERCA. (Reproduced from [32])

Ca^{2+}. This was described as tandem RyR activation and was thought to occur via a novel 'fire-diffuse-uptake-fire' or FDUF mechanism, in which Ca^{2+} uptake by SERCA at the propagation front elevates local SR Ca^{2+}, which in turn causes RyR sensitization, lowering the threshold for activation of CICR by cytosolic Ca^{2+} [34]. This is shown schematically in Fig. 16.3f. Recent discussion of these mechanisms can be found in: [20] and [19].

The above evidence is both intriguing and convincing, but there may also be some functions of sparse transverse tubules in atrial myocytes, as described in an interesting rapid signaling mechanism involving axial tubule junctions [35].

Particular roles of Ca^{2+} stimulated adenylyl cyclases and of CaMKII in atrial myocytes are discussed below.

16.4 SA Node

The mechanisms underlying pacemaker activity in the SA node remain poorly understood and are the subject of extensive discussion. It could be argued that since pacemaker activity initiates the heartbeat that is essential for life, evolution has led

to the development of a system of several potentially redundant mechanisms that combine to create a secure system in which if one component should fail another can step forward to ensure that the heart never stops beating. Two major lines of argument in this field in recent years concern whether the primary mechanism for controlling the timing of pacemaker activity in the SA node is a 'membrane' clock or a 'calcium' clock, but it seems most likely that under normal physiological conditions both these timing mechanisms play important roles in an integrated system, as reviewed in [36] and [37]. It will be argued that both membrane and calcium clock components are subject to modification by Ca^{2+} signaling processes.

For the membrane clock the timing is controlled by the ebb and flow of ionic currents, determined predominantly by the sequential opening and closing of different ion channels (see [38] and [39] for recent work in this area).

For the calcium clock the cyclic nature of uptake and release of Ca^{2+} by the SR provides another timing mechanism. Some proponents of the calcium clock give prominence to 'local Ca^{2+} release events' which are similar to Ca^{2+} sparks in SA node cells [36], although others argue that these events are not essential for pacemaker activity [37]. Although there is an excellent correlation between the timing of local release events and the rate of firing of spontaneous action potentials in the SA node, this relationship need not be causal. The timing of the repetitive cyclic activity of uptake and release of Ca^{2+} from the SR might perhaps depend on a mechanism to sense the level of Ca^{2+} in the SR (as appears to be the case in ventricular myocytes under 'overload' conditions [40]).

Some proponents of a membrane clock give prominence to the 'funny' current (I_f, or in neurons I_h) which is activated by hyperpolarization, or repolarization of the action potential under physiological conditions. This current usually exerts a depolarizing influence, and is sometimes referred to as 'the' pacemaker current, but while it often exerts a modulatory influence on heart rate, some authors argue that it is not essential for pacemaker activity. The cardiac channels supporting this current are located primarily in the SA node, and are referred to as HCN since they are activated by hyperpolarization and regulated by cyclic nucleotides. Another very important specific characteristic of the SA node concerns the lack of I_{K1} channels that set the 'resting' potential in atria and ventricular muscle. In the absence of I_{K1} channels, de-activation of voltage-activated K channels (such as I_{Kr} and I_{Ks}) can make an important contribution to pacemaker depolarization. Two other channel types contributing to this slow depolarization provide 'background' current and sustained inward current, both carried at least in part by Na^+. Recent evidence shows that the sustained inward current channels are related to Ca_V 1.3, a voltage-gated Ca^{2+} channel [41]. Ca_V 1.3 channels can in their own right also exert a slow depolarizing influence, in addition to supplementing opening of Ca_V 1.2 channels during the upstroke of the action potential [38]. Other ion channels must also be taken into account, including the I_{KACh} channel that is activated by ACh, but can be open to conduct ions even in the absence of this neurotransmitter. (See [37] for detailed discussion).

In addition to currents through ion channels, ionic currents through the Na^+/Ca^{2+} exchange mechanism (NCX) contribute to both membrane and Ca^{2+}

clock mechanisms (and may provide a link between the two). Some argue that NCX plays a role throughout the cardiac cycle [42]. Interesting new insights concerning the role of NCX during pacemaker activity can be found in [43].

It is interesting to consider whether the wave like spread of Ca^{2+} described in atrial myocytes based on the work of [34] might have a parallel in SA node cells. Labelling of RyR2 in SA node cells shows what appear to be junctional and non-junctional components (see Fig. 1 in [44]), though these possible compartments were not described in this way at the time of publication. This topic deserves further experimental investigation.

Clinical observations and results of genetic manipulation show that heart rate is disturbed when there are abnormalities in components of either the membrane or Ca^{2+} clock mechanisms. It seems likely that pacemaker activity is a complex summation of a variety of the above mechanisms, although it seems clear that Ca^{2+} ions play essential and diverse roles in the initiation and regulation of the pacemaker activity controlling the heartbeat.

16.5 CaMKII

Perhaps the most important Ca^{2+}-stimulated enzyme in cardiac myocytes is the Ca^{2+} and calmodulin dependent protein kinase, CaMKII, which is central to Ca^{2+}-dependent regulation of cardiac function and has been the subject of many reviews (e.g [45–54]. Since this enzyme has been so extensively discussed, only a summary of its contributions will be presented here.

Two targets of CaMKII, L-type Ca^{2+} channels and RyR2 are shown in Fig. 16.1. One function of CaMKII concerns facilitation of I_{CaL} during repetitive stimulation. This arises because during repetitive electrical stimulation, extra Ca^{2+} enters through L-type Ca^{2+} channel as the heart rate increases, and this additional Ca^{2+} stimulates CaMKII leading to phosphorylation of the same channels to enhance their activity [55]; [56]. A second function of CaMKII concerns phosphorylation of RyR2 to modulate its sensitivity to Ca^{2+}, particularly following β-adrenoceptor stimulation [57]. There is also a frequency-dependent acceleration of relaxation, which is thought to arise from an effect of CaMKII to increase SERCA activity, although this was not thought to require phosphorylation of phospholamban [58]. In addition to the link between PKA and CaMKII, a parallel activation pathway involving EPAC. exchange protein activated by cAMP, needs to be taken into account [59].

In addition to effects of CaMKII on L-type Ca^{2+} channels and RyR2, there are also regulatory effects on voltage-gated K^+ and Na^+ channels (e.g [60–63]).

CaMKII makes particularly important contributions to the pacemaker function of the SA node [49]. Additional discussion of CaMKII in atria is included below.

16.6 AC1 and AC8

Work in neurons first established a role for Ca^{2+}-stimulated adenylyl cyclases to control neural activity, predominantly via HCN ion channels that are activated by hyperpolarization and directly regulated by cAMP (e.g [64]; and see [65]; [66]. The first work in heart on this topic showed the presence of AC1 and AC8 in SA node and atrial myocytes but not ventricular myocytes [67]. One function of these Ca^{2+}-stimulated adenylyl cyclases appeared to be regulation of HCN in guinea pig SA node cells. Activation of HCN currents by hyperpolarization was reduced (shifted in the hyperpolarizing direction) following application of membrane permeant BAPTA-AM to load the cells with Ca^{2+} chelator or by the adenylyl cyclase inhibitor, MDL12330A, but the effects of MDL12330 were reduced or abolished in cells pre-treated with BAPTA-AM. Immunohistochemistry showed an intracellular location of AC1 and AC8 in atrial and SA node cells primarily close to the cell surface [67]. Additional work on spontaneous CaT accompanying action potentials in SA node also supports the functional importance of AC1 and AC8 in pacemaker cells, as well as a location of these enzymes at or close to the surface membrane [68]. Interestingly in dogs that have had pacemaker function suppressed by blockade of the atrio-ventricular node, introduction of AC1/HCN2 constructs into left bundle branches provided a highly efficient biological pacing mechanism [69], demonstrating the ability of this Ca^{2+} stimulated enzyme pathway to determine pacemaker function under these conditions.

The functional importance of Ca^{2+}-stimulated adenylyl cyclases has also been demonstrated in atrial myocytes. The presence and activity of these enzymes in the absence of hormonal or neurotransmitter stimulation, probably accounts for the ability of muscarinic acetylcholine antagonists or NO to reduce CaT and L-type Ca^{2+} currents in atrial myocytes, in contrast to ventricular myocytes which lack resting adenylyl cyclase activity, with the major adenylyl cyclases being AC5 and AC6 [70]. Ventricular myocytes do, however, respond to agents that inhibit adenylyl cyclase once this has been activated for example by isoproterenol. In guinea pig atrial myocytes, MDL12,330A reduced the amplitudes of CaT and L-type Ca^{2+} currents, as did application of BAPTA-AM. However, BAPTA-AM was without effect on the amplitude of L-type Ca^{2+} currents in cells loaded with a high concentration of cAMP (100 micro M) from a patch pipette. Immunohistochemistry showed that AC8 appeared to be localized together with RyR2 in the junctional SR just beneath the membrane (although it is difficult to exclude some location in nearby caveolae of the plasmalemma), while AC1 appeared to be in the space between junctional and non-junctional SR [33], and see Fig. 16.3b–e.

An interesting additional conclusion from the above experiments was that the location and function of CaMKII appeared to differ in atrial and ventricular myocytes. In guinea-pig atrial myocytes, the CaMKII appeared to be present with RyR2 in the non-junctional SR, but the junctional SR showed RyR with little or no CaMKII. In other words the CaMKII seemed to be quite distant from L-type Ca^{2+} channels, though close to non-junctional RyR in atrial myocytes. In contrast,

ventricular cells showed the usual striated pattern of RyR2 presumably close to L-type Ca^{2+} channels in dyads formed by SR and transverse tubules (which are rare or absent in guinea-pig atrial myocytes), and there was a reasonable amount of colocalization with CaMKII. It therefore appears that in ventricular myocytes, CaMKII is located close to L-type Ca^{2+} channels in transverse tubules as expected from its important role in determining the rate-dependence of this current.

L-type Ca^{2+} currents in guinea pig ventricular myocytes were reduced by the CaMKII kinase inhibitor, KN93, with little effect of the inactive analogue KN92, while BAPTA-AM was without effect in the presence of KN93. In other words all of the effects of BAPTA-AM in ventricular myocytes can be attributed to inhibition of CaMKII rather than adenylyl cyclase. In the case of guinea pig atrial myocytes, KN93 again reduced L-type Ca^{2+} currents, and there was no effect of KN92, but addition of BAPTA-AM in the presence of KN93 caused a further reduction of L-type Ca^{2+} current amplitude. Nevertheless, as mentioned above, BAPTA-AM was without effect in atrial myocytes under conditions in which the cytosolic cAMP concentrations were maintained at a high level from a patch pipette. If the actions of BAPTA-AM in atrial myocytes result entirely from inhibition of Ca^{2+}-stimulated adenylyl cyclase, how might the effects of KN-93 on L-type Ca^{2+} current arise? It was suggested that in atrial myocytes, the primary effect of inhibition of CaMKII is on SR proteins leading to a reduction in the Ca^{2+} released from the SR, as a consequence of effects on uptake and or release, leading to partial inhibition of adenylyl cyclase activity. In support of this view, inhibition of SR function with a combination of ryanodine and thapsigargin reduced L-type Ca^{2+} current, but under these conditions inhibition of CaMKII with KN-93 had no further effect. In summary, CaMKII influences SR proteins and L-type Ca^{2+} channels in ventricular myocytes, while in atrial myocytes CaMKII only affects SR proteins. The effects of Ca^{2+} chelation in atrial myocytes can be entirely accounted for by suppression of Ca^{2+}-stimulated adenylyl cyclase activity, but some activation of these adenylyl cyclases results from Ca^{2+} release from the SR [33].

Possible activation of AC8 or AC1 by Ca^{2+} release from the SR via the action of the IP_3-dependent Ca^{2+} signaling system in atrial myocytes will be considered later.

16.7 Other Calcium-Sensitive Enzymes

An interesting early discussion of Ca^{2+} regulation of enzymes can be found in [71]. This includes an account of how Ca^{2+} stimulation of phosphodiesterase was discovered by Cheung in 1970. In more recent experiments on cardiac muscle, expression of the Ca^{2+} stimulated phosphodiesterase, PDE1A, was found to be fivefold greater in SA node tissues than ventricle. Interestingly nimodipine was thought to act as a selective PDE1 inhibitor, and this compound suppressed total PDE activity by approximately 40% in SA node cell lysates but by only 4% in ventricular cell lysates. In SA node cells that had been permeabilised to avoid effects

of nimodipine on L-type Ca^{2+} channels, the PDE1 inhibitor increased the activity of local Ca^{2+} release events. In spontaneously beating HL-1 cells, suppression of PDE1 protein with a selective siRNA increased spontaneous beating frequency. Immunohistochemistry in rabbit SA node cells showed that PDE1A was located on the cytosolic side of the HCN protein in the surface membrane, and separated by approximately 150 nm [72].

It is interesting to note here that Ca^{2+} signaling pathways have been implicated in the cardiac hypertrophy that arises as a maladaptive response to increased workload and excessive cardiac stimulation by hormones including Angiotensin II and β-adrenoceptor agonists; calcineurin and CaMKII are among calcium signaling molecules that have been proposed to play key roles in the development of cardiac hypertrophy [73]. This is a topic that will be revisited in discussion below of the actions of IP_3, cADPR and NAADP. In the case of PDE1C, this enzyme has also been proposed to be involved in cardiac hypertrophy [74]. When hypertrophy was induced by aortic constriction, PDE1C expression was increased. In addition mice that were deficient in PDE1C showed reduced hypertrophy compared to WT in response to aortic constriction. Ventricular myocytes grown in culture for 72 h after isolation from mice that were deficient in PDE1C showed a reduced hypertrophic response to Angiotensin II compared with myocytes from WT mice [74].

NO synthase enzymes have calmodulin containing domains allowing regulation by cytosolic Ca^{2+} [75]. The roles of endothelial NO synthase (eNOS) and neuronal NO synthase (nNOS) have been reviewed by [76] [10] and [77]. Despite the names of these enzymes, which are based on tissues in which they were first discovered, eNOS and nNOS are present in cardiac muscle and eNOS is located predominantly in caveolae, which are invaginations of the surface membrane, while nNOS is associated with SR, at least under normal physiological conditions in healthy heart. Regulation of eNOS by Ca^{2+} released from the SR by IP_3 will be discussed later.

The above summary of Ca^{2+}-regulated enzymes is not an exhaustive list, and it seems likely that there will be many additions to this family.

16.8 IP_3 Signaling

Effects of inositol-(1,4,5)- trisphosphate (IP_3) on CICR in the heart can be traced back at least to observations from Fabiato [78]. However, interest in IP_3-dependent Ca^{2+} signaling as a physiological mechanism for short term effects on CaT associated with action potentials was established by the work of Lipp et al. [79]. These observations showed that the relative importance of IP_3 dependent signaling for short term effects on CaT was much greater in atrial than ventricular muscle, and atrial actions of IP_3 will be discussed first, though in ventricular myocytes there are functionally import long term changes resulting from modification of gene expression following activation of IP_3 receptors in perinuclear membranes [4], and perhaps other effects of IP_3 receptors in the cardiac cell periphery. The functional

importance of junctional SR beneath the plasmalemma in atrial myocytes was discussed above, and it was noted that Ca^{2+} entry through L-type Ca^{2+} channels triggers CICR directly in these membranes. Type II IP_3 receptors (IP_3R) are present in atrial myocytes, and interestingly show a precise location in the juntional SR, but not the non-junctional SR that runs deep within the cell with the usual sarcomere spacing. The location of IP_3R in junctional but not non-junctional SR (in contrast to RyR2 which were present in all SR membranes) was shown in both 2D and 3D images from the immunohistochemical observations. To test for functional effects of IP_3, Lipp et al. [79] applied a membrane permeant ester, IP_3-BM, to atrial myocytes leading to cytosolic release of IP_3 following the action of intracellular esterases. Using these methods, cytosolic IP_3 was shown to increase the amplitude of CaT accompanying action potentials in electrically stimulated cells. Application of IP_3-BM also increased Ca^{2+} spark frequency in atrial myocytes. Long exposures to IP_3-BM, presumably achieving higher concentrations of cytosolic IP_3 led to the development of arrhythmogenic Ca^{2+} waves [79].

One cell surface receptor in cat atrial myocytes that appears to be linked to the IP_3-dependent Ca^{2+} signaling pathway is that activated by endothelin-1, which caused an increase in the amplitude of CaT accompanying action potentials initiated by electrical stimulation. Endothelin-1 also caused the appearance of spontaneous arrhythmogenic Ca^{2+} events. In atrial cells that were not electrically stimulated, endothelin-1 increased the frequency and amplitude of Ca^{2+} sparks. All these effects of endothelin-1 were blocked by 2-aminoethoxydiphenylborane, 2-APB, at 2 μM, a concentration which appears to be reasonably selective for IP_3R. In permeabilised atrial myocytes, direct application of IP_3 increased Ca^{2+} spark frequency, as did the IP_3R activator, adenophostin. The effects of IP_3 in permeabilized cells were blocked by the IP_3 antagonists, heparin and 2-APB. These effects are all consistent with the importance of the IP_3 signaling pathway and atrial myocytes and the effectiveness of endothelin-1 in activating this pathway [80].

Ca^{2+} release events via RyRs are generally referred to as Ca^{2+} sparks, while those through IP_3Rs are referred to as Ca^{2+} 'puffs' [81]. These Ca^{2+} puffs are smaller in amplitude and slower to rise and decay than Ca^{2+} sparks, and in the presence of tetracaine to block Ca^{2+} sparks via RyR, both IP_3 and adenophostin were observed to cause the appearance of Ca^{2+} puffs with appropriate amplitude and time characteristics [80].

Further evidence in support of the importance of an IP_3-dependent signaling pathway for effects of endothelin-1 in atria was provided in experiments using transgenic mice, in which atrial myocytes from mice lacking Type II IP_3R failed to show an increase in CaT amplitude following endothelin-1 application, while myocytes from WT mice showed the usual enhancement, and this was blocked by 2-APB [82].

Another surface receptor pathway that appears to be linked to IP_3-dependent Ca^{2+} signaling is the α_1-adrenoceptor. Phenylephrine caused an approximate doubling of L-type Ca^{2+} current in cat atrial myocytes, and these effects were blocked by the α_1-adrenoceptor antagonist, prazosin. The effects of phenylephrine on Ca^{2+} currents were blocked by cytosolic heparin, 2-APB and the IP_3 inhibitor

xestospongin, all of which would be expected to reduce IP_3 cellular actions. Interestingly, the effects were also suppressed by L-N^5–1-iminoethylornithine, an inhibitor of NO synthase, by oxadiazolo [4,3-alpha] quinoxaline-1-one (ODQ), an inhibitor of guanylate cyclase, and by H89, a PKA inhibitor. Taken together these observations are consistent with an α-adrenoceptor mediated increase in IP_3 causing Ca^{2+} release from junctional SR where the IP_3 receptors are located which activates NO synthase (eNOS) in nearby caveolae in the plasmalemma, and the resultant NO activates guanylyl cyclase leading in turn to cGMP-dependent inhibition of phosphodiesterase thus causing an increase in cAMP and PKA dependent enhancement of L-type Ca^{2+} channel activity [83]. Further evidence in support of this mechanism was provided by direct measurements of NO production in atrial myocytes in response to phenylephrine, and the observations that NO production was suppressed by 2-APB and by ryanodine [83].

The evidence for the dominance of the NO mediated pathway involving IP_3-dependent Ca^{2+} release is convincing for cat atrial myocytes, although another simpler pathway deserves consideration, perhaps more important in other species. In guinea pig atrial myocytes, the Type II IP_3R again seem to be preferentially located in junctional SR, and phenylephrine caused an increase in the amplitude of CaT accompanying action potential. These effects were suppressed by prazosin and by 2-APB, consistent with α-adrenoceptor activation of the IP_3-dependent pathway to bring about the increase in CaT [84]. The importance of Ca^{2+}-stimulated adenylyl cyclases, AC8 and AC1, in atrial myocytes was reported above, and these enzymes were thought to be located either in junctional SR (for AC8) or in the space between junctional and non-junctional SR (for AC1). IP_3-mediated Ca^{2+} release could therefore directly activate nearby AC8, and perhaps even AC1, without the intervention of the NO-dependent pathway. Recent observations show that photoreleased IP_3 increased CaT and that these effects were reduced by the adenylyl cyclase inhibitor, MDL-12,330, and by 2-APB [85], but the possible involvement of eNOS and cGMP-dependent pathways in these effects has yet to be tested.

Additional detailed reviews of IP_3-dependent Ca^{2+} signaling in atrial myocytes can be found in [86–89]; [32].

It was mentioned above that in ventricular myocytes IP_3 receptors in the perinuclear membrane may be important for local Ca^{2+} signals that may function to regulate gene expression [4].

Although IP_3 receptors are thought to play less of a role in controlling CaT in ventricular myocytes, effects of stimulation of enothelin-1 receptors have been shown to increase the amplitude of CaT accompanying action potentials in rabbit ventricular myocytes, and the effects were suppressed by low concentrations of 2-APB, supporting a role for the IP_3-dependent signaling mechanism [90]. Recent evidence also supports a role for IP_3 and stimulation of CaMKII in the hypertrophic effects of both endothelin and the α-adrenoceptor agonist phenylephrine in rat ventricular myocytes [91].

Effects of phenylephrine on Ca^{2+} spark-like events with increased width, perhaps involving IP_3 actions at Type I IP_3R in the perinuclear region have been described by [92]. Evidence concerning IP_3-dependent nuclear Ca^{2+} signaling in the mammalian heart has been presented by [93]

In view of the major effects of IP_3 in atrial myocyes described above, it is perhaps unsurprising that IP_3 also appears to play a prominent role in SA node. Application of the membrane permeant form of IP_3 (IP_3-BM) was shown to exert a positive chronotropic effect [94] in mouse SA node cells. In these experiments, Type II IP_3R appeared to be located close to the surface membrane, but also deeper in the cells perhaps associated with both junctional and non-junctional SR, although IP_3R were said to be predominantly close to the plasmalemma. In these cells, application of IP_3-BM increased the frequency of Ca^{2+} sparks particularly close to the cell surface. IP_3-BM also increased both the spontaneous frequency and the amplitude of CaT accompanying action potentials in mouse SA node cells. In mice lacking Type II IP_3R, the effect of endothelin-1 on the amplitude and frequency of CaT was prevented as expected, while the effects of isoproterenol acting through β-adrenoceptor pathways appeared to be unchanged [94]. A summary of these effects, with new observations, was presented in a review again showing that IP_3-BM increased Ca^{2+} spark activity, particularly at the periphery of SA node cells, and that endothelin-1 increased the frequency and amplitude of whole cell CaT [95].

Interesting new observations, broadly supporting the above hypotheses have recently been presented comparing effects of 2-APB (a membrane permeant IP_3 receptor antagonist) in SA node myocytes from WT mice and KO mice lacking NCX. SA node myocytes from WT mice showed spontaneous whole cell CaT that were synchronized across the cell by the accompanying action potentials, while those from mice lacking NCX showed spontaneous Ca^{2+} transients that were 'uncoupled' from the surface membrane in that these events were not able to initiate action potentials to accompany the Ca^{2+} transients [43]. These spontaneous Ca^{2+} transients in cells lacking NCX were nevertheless surprisingly regular in their frequency, but very irregular in their spatial characteristics, presumably because of the lack of synchronizing influence of the action potential. 2-APB at a concentration of 2 μM had a surprisingly large effect to reduce the frequency of CaT in SA node from WT mice, and it was argued that the effects might result from blockade of IP_3R, but perhaps also from non-specific effects, for example on L-type Ca^{2+} currents. In the case of the spontaneous activity of SA node cells from mice lacking NCX, 2-APB also greatly reduced the frequency of spontaneous activity, which could not be attributed to effects of 2-APB on surface membrane channels, but was interpreted again to reflect the importance of IP_3-signaling to influence spontaneous rate [43]. In addition, blockade of phospholipase C (which is essential for IP_3 production from PIP2) abolished spontaneous activity in both WT SA node cells and those lacking NCX, while an inactive structural analogue was without effect. Phenylephrine increased the spontaneous frequency of whole cell Ca^{2+} transients in both WT and pacemaker cells lacking NCX, and in both types of cell the effects were greatly suppressed by 2-APB. Interestingly, a high concentration of ryanodine (100 μM) completely suppressed spontaneous CaT activity in WT SA node cells, and under these conditions phenylephrine was unable to restore activity, while there still seemed to be Ca^{2+} in the SR that could be released with a high concentration of caffeine [43].

Overall the observations provide a convincing case for a contribution of IP_3-dependent Ca^{2+} signaling both at rest and after stimulation by endothelin-1 or the alpha-adrenoceptor agonist, phenylephrine.

Before moving on to other Ca^{2+} mobilization agents, two other points should be mentioned. First, IP_3-dependent Ca^{2+} signaling may make an increased contribution under conditions of heart failure, and this has been shown to be functionally important in atrial myocytes [96]. In addition to activation of IP_3-dependent mechanisms by coupling to hormones and neurotransmitter receptors, the possible influence of mechanical stimuli must also be considered, since another interesting activator of IP_3-dependent mechanisms in atrial myocytes is shear stress [97], [98].

16.9 cADPR/NAADP Signaling

The Ca^{2+} mobilizing agents cADP-ribose and NAADP are now widely recognized as playing major roles in a wide variety of plant and animal cells, and influence the function in processes as diverse as egg fertilization, neuronal processing and the closing of stomata on leaves. General reviews of the actions of these substances can be found in [99–103].

These two signaling molecules are included under a single heading here since it is becoming clearer that in the heart they play a co-operative and perhaps synergistic role. Cardiac actions of cADP-ribose (reviewed in [104] and [9]) will be discussed first, before going on to NAADP actions, which have been reviewed more recently [105], and finally the possible parallel combined actions of these two signaling molecules will be considered. The general view presented here is that cADPR actions primarily increase Ca^{2+} release from the SR, while NAADP actions primarily increase Ca^{2+} uptake into the SR, though qualifications of this broad statement will be necessary. An important recent observation is that the CD38 enzyme (an ADP-ribosyl cyclase) in the heart appears to be located at the SR and can catalyse the synthesis of both cADPR and NAADP [1], as discussed in more detail below. A scheme to represent current hypotheses is shown in Fig. 16.6.

16.10 cADP-Ribose

The first observations concerning cADPR in cardiac tissue showed increased Ca^{2+} release from cardiac microsomes, and enhanced opening of Ca^{2+} release channels (RyR2) incorporated into artificial membranes [106]. Some of the these early observed effects on RyR2 channel opening were difficult to reconcile with observations that cADPR competed with ATP for sites on RyR2 [107]. More recently, evidence concerning how cADP might increase Ca^{2+} release from SR via RyR2 in cardiac myocytes has been reviewed in [9], and this question will be considered in more detail below.

16.10.1 Detection of cADPR in Cardiac Muscle and Possible Synthetic Mechanisms

Synthesis of cADPR by cardiac tissue was first shown by [108]. A variety of tissue extracts, including heart, were shown to support cADPR synthesis when incubated with NAD. Endogenous cADPR was detected by Walseth et al. [109], at approximately 1 pmol/mg protein, and the cytosolic concentration was estimated to be about 200 nM. The kinetics of cADPR synthesis from NAD by heart muscle were investigated by [110].

An important observation concerning the regulation of cADPR synthesis showed that this was enhanced by exposure of rat cardiac myocytes to a beta-agonist [111]. This was studied either as [^{3}H]cADPR from [^{3}HJ]NAD, or in a fluorescent assay in which the βNGD, a fluorescent analogue of NAD, was converted to cGDPR. Isoproterenol increased the synthesis in a concentration dependent manner, and the effects were inhibited by the β-adrenoceptor antagonist, propranolol. The ability of isoproterenol to stimulate cADPR synthesis was blocked by cholera toxin, supporting a role for the stimulatory G protein, Gs, in the pathway coupling the β-adrenoceptor to enhancement of the activity of the synthetic enzyme [111].

Using the NGD assay, synthesis of cADPR by guinea-pig cardiac ventricular membranes was shown to be enhanced following application of the catalytic subunit of PKA. In whole guinea pig hearts, exposure to isoprenaline increased cADPR levels, and these effects were blocked by both propranolol and H89, consistent with involvement of PKA in these effects [104]. More recent observations supporting an increase in cADPR levels following exposure to isoproterenol is provided by [113].

Another signalling pathway that leads to increased cADPR synthesis is that linked to Angiotensin II receptors [114].

16.10.2 Role of CD38 in Cardiac cADPR Synthesis

Several ADP-ribosyl cyclase enzymes have been identified that can synthesise cADPR from betaNAD [115].

Gul et al. [116], [117] have presented evidence for such a synthetic enzyme in the heart with activity increased by Angiotensin II, but this enzyme was not thought to be CD38 since synthetic activity was still observed in cardiac muscle from *CD38*$^{-/-}$ mice lacking the ability to express CD38.

However, CD38 in endosomes was thought to be responsible for an increase in cADPR synthesis following beta-adrenoceptor stimulation by isoproterenol, since this increase was no longer observed in cardiac tissue from *CD38*$^{-/-}$ mice [118]. As expected from information above concerning PKA, the effects of isoproterenol on cADPR synthesis were blocked by H89 [118].

In our experiments on mixed membrane preparations from mouse heart, a resting synthesis of cADPR was present in WT but not *CD38*$^{-/-}$ mice [1], consistent with

CD38 as the major synthesizing enzyme under these conditions. A sheep heart SR preparation that is commonly used for the study of cardiac SR proteins also supported cADPR synthesis [1].

SAN4825 is a drug developed to inhibit cardiac ADP-ribosyl cyclases, and was shown to suppress the ability of a rat SR membrane preparation to synthesize fluorescent cGDPR from NGD [119]. SAN4825 also inhibited cGDPR synthesis in the mixed membrane preparation from mouse heart in which CD38 was thought to be the major synthetic enzyme [1].

16.10.3 cADPR Actions on Ca^{2+} Transients Associated with Contraction

The first evidence that cADPR exerts a functional effect in intact cardiac myocytes came from the use of the 8-amino-cADPR, which had been shown to suppress cADPR-induced Ca^{2+} release through RyR in sea urchin egg preparations [120]. Ca^{2+} transients (CaT) accompanying action potentials were recorded in guinea pig ventricular myocytes. These were investigated both using the fluorescent probe, fura-2 and by a less direct method involving measurement of 'Ca^{2+}-activated' currents predominantly carried by NCX. Both methods of measurement showed a reduction in the amplitude of CaT following cytosolic application of 8-amino-cADPR. The less direct method based on measurements 'Ca^{2+}-activated' currents was thought to provide a more accurate indication of the timing of the CaT since it avoids the inevitable buffering caused by fluorescent probes (which increases as the affinity of the probe for Ca^{2+} increases). Myocyte contractions accompanying action potentials were recorded in the same myocytes. All experiments were carried out close to body temperature (36 °C). In these experiments, 8-amino-cADPR caused an approximately 40% reduction of the amplitude of both CaT and contraction [121]. Under voltage-clamp conditions, 8-amino-cADPR did not cause any reduction of L-type Ca^{2+} currents. In additional experiments using fura-2, 8-amino-cADPR was again found to reduce the amplitude of CaT. When SR function was inhibited with ryanodine, the CaT constructed from 'Ca^{2+}-activated' currents was greatly reduced (particularly the early peak that occurred approximately 50 ms after the upstroke of the action potential that appears to be associated with CICR), as was the accompanying contraction, and under these conditions 8-amino-cADPR did not cause any further reductions in CaT or contraction [121]. The observations were thought to be consistent with a role for cADPR to promote Ca^{2+} release from the SR, as proposed for sea urchin egg and many other tissues, in response to Ca^{2+} entry via L-type Ca^{2+} currents during the action potential.

In the above experiments, the amount of Ca^{2+} stored in the SR under these conditions was estimated from the size of the contraction associated with a rapid application of a high concentration of caffeine. Under the conditions in which 8-amino-cADPR reduced the amplitudes of CaT and contractions, in the same cells

8-amino-cADPR did not reduce the amount of Ca^{2+} stored in the SR, and indeed there appeared to be a small but significant increase in SR Ca^{2+} load under these conditions [121].

The first experiments to detect an effect cADPR applied from a patch pipette in intact myocytes showed an increase in the amplitude of contractions associated with action potentials (1 Hz), and the increase in contraction showed a concentration-dependence with an EC_{50} of 2–3 μM. CaT amplitude measured with fura-2 was also increased by patch-applied cADPR. These enhancing effects of exogenous cADPR were blocked by 8-amino-cADPR. Pretreatment of these guinea pig ventricular myocytes with ryanodine and thapsigargin to suppress SR function also prevented the effects of exogenous cADPR [122].

Another convincing demonstration of cADPR actions to increase the amplitude of CaT in intact guinea-pig ventricular myocytes was provided by experiments in which cADPR was photoreleased from a caged compound. In these experiments CaT was measured with fluo-3 (a probe with lower Ca^{2+} affinity than fura-2). The cells were stimulated to fire action potentials once every 2 s, and following a single photorelease of cADPR there was a progressive increase in the amplitudes of CaT over a period of about 15 s. Accompanying the change in amplitude of CaT, there was a change in its time course, so that the peak appeared slightly earlier in the action potential [123]. Further observations supported an increase in the amplitude of CaT and contractions accompanying action potentials following cADPR applied either by photorelease or directly from a patch pipette, and in both cases there was no change in SR Ca^{2+} load [124]. As above SR load was judged from the response to rapid application of a high concentration of caffeine, but in these experiments two different methods were used to assess SR Ca^{2+}. In one SR Ca^{2+} was estimated from the amplitude of the cytosolic Ca^{2+} change measured using fluo4 following rapid caffeine exposure, and in the other the amount of SR Ca^{2+} was assessed from the time integral of caffeine-induced current under voltage-clamp conditions (predominantly NCX while extruding the Ca^{2+} released from the SR). With both assessment methods, SR Ca^{2+} appeared unchanged while the CaT or contraction accompanying action potentials was clearly enhanced by the cADPR application [124]. In another series of experiments, CaT were evoked by repeating voltage-clamp pulses (from −40 to 0 mV for 200 ms; 0.33 Hz) rather than action potentials, and photoreleased cADPR increased the amplitude of CaT without changing the decay time, and without changing the amplitude of the L-type Ca^{2+} current that evoked the CaT, again consistent with an increase in the gain of CICR [124].

16.10.4 cADPR Actions on the Frequency and Amplitude of Ca^{2+} Sparks

Guinea pig ventricular myocytes are unusual in showing few if any Ca^{2+} sparks, while rat ventricular myocytes regularly show Ca^{2+} spark activity. Before measur-

ing this Ca^{2+} spark activity, photorelease of cADPR in rat myocytes was again shown to increase the amplitude of CaT measured with fluo-3. In rat myocytes at rest (not stimulated to fire action potentials) photorelease of cADPR caused an increase in Ca^{2+} spark frequency by approximately two to threefold. Prior application of 8-amino-cADPR prevented the effect of photoreleased cADPR on Ca^{2+} spark frequency. It is important to note that spark characteristics, in particular spark amplitude were not changed, as would have been the case if SR Ca^{2+} load had been increased [123]. Further observations in support of this hypothesis, with effects of cADPR to increase CaT amplitude, and at high doses to provoke Ca^{2+} waves have been made in rat ventricular myocytes [125].

Taken together the observations so far described above are consistent with the hypothesis that cytosolic cADPR in some way increases the gain of CICR via RyR2, though this should not be taken to imply that a direct effect of cADPR on RyR2 is necessarily involved.

It is important to recognize that not all reports show observations consistent with the above hypothesis, and some have failed to detect effects of cADPR and 8-amino-cADPR on CaT in rat ventricular myocytes [126]. However, these negative observations were made at room temperature, and it was later shown that the effects of cADPR, and of the antagonists, 8-amino-cADPR and 8-Br-cADPR, were all temperature dependent, showing clear agonist or antagonist effects at 36 °C, but not having detectable effects on CaT when the cell superfusion heater was switched off [122].

The above observations on Ca^{2+} sparks in rat ventricular myocytes were from intact cells. Different conclusions were made on the basis of later observations on saponin permeabilised rat ventricular myocytes, and on rat heart microsomes, all at room temperature, and it has been claimed that the primary target for cADPR in the heart is SERCA-dependent Ca^{2+} uptake into the SR [127]. Under the conditions of these experiments in permeabilised myocytes, unlike all the observations reported above, there was a change in the amount of Ca^{2+} loaded into the SR following exposure to cADPR, tested by rapid application of caffeine. The measurements of SR content were made 5 min after application of cADPR in permeabilized myocytes. The observations also showed that when rat heart microsomes had been exposed to cADPR (in the presence of ruthenium red to block Ca^{2+} release via RyR2), the Ca^{2+} uptake by the microsomes was faster in the presence than in the absence of cADPR, consistent with an enhanced activity of SERCA [127]. These observations provoked a re-investigation of cADPR actions, and it was found that in rat saponin permeabilised ventricular myocytes at 36 °C application of 10 μM cADPR caused an approximate doubling in Ca^{2+} spark frequency after 30 s, while the SR Ca^{2+} load tested with rapid caffeine application was not increased at this time [124]. The increase in spark frequency caused by cADPR after 30 s was prevented by prior exposure to the antagonist, 8-amino-cADPR. However, if the exposure to cADPR was prolonged to 10 min, the increase in Ca^{2+} spark frequency was maintained but under these conditions there was indeed an increase in SR Ca^{2+} load as assessed from the response to rapid caffeine application [124].

Furthermore, while the increase in Ca^{2+} spark frequency at 30s occurred without a change in spark amplitude or decay time (consistent with no change in SR load or uptake by SERCA), in contrast after 10 min exposure to cADPR under these conditions Ca^{2+} spark amplitude was increased and Ca^{2+} spark decay time was quickened [124]. These changes in spark characteristics after 10 min exposure to cADPR are consistent with an increase in SERCA activity, since it has been shown that even at room temperature SERCA contributes significantly to spark decay, and isoproterenol was observed to shorten Ca^{2+} spark decay time [128]. In these experiments the protocol was designed to maintain a comparable SR Ca^{2+} load in the presence and absence of isoproterenol, and therefore to avoid an increase in Ca^{2+} spark amplitude that might otherwise have occurred.

The main conclusion from the above experiments is that there is a clear effect of cADPR on Ca^{2+} release from the SR at short exposure times that does not depend on an increased loading of the SR with Ca^{2+}. The effect of cADPR on Ca^{2+} uptake by SERCA at very long exposure times has been observed in particular conditions (permeabilization of the cell membrane with saponin, or isolated microsomal preparations). It is not yet clear how the slow increase in SERCA activity arises, and whether it might be a secondary consequence of the cytosolic Ca^{2+} changes associated with the rapid effects of cADPR. The mechanism involving an increase in SERCA activity may represent an additional slow pathway for effects of cADPR on CaT (perhaps involving activation of CaMKII by the additional Ca^{2+} associated with a prolonged increase in Ca^{2+} spark frequency), and it remains for future study whether this pathway also operates under physiological conditions in intact myocytes. However, it is clear that cADPR has important effects apparently to increase the gain of CICR under conditions in which there is little or no change in SR Ca^{2+} load, and that these effects are associated with an increase in the CaT accompanying action potentials.

16.10.5 Possible Mechanisms for the Increase in Release of Ca^{2+} from the SR Mediated by cADPR

Although the observations summarized above provide strong support for an effect of an increase in cytosolic cADPR (whether from patch applied or photoreleased cADPR) to increase CICR without a change in SR Ca^{2+} load, the underlying mechanism of action of cADPR remains unclear. It should first be acknowledged that these methods of application of cADPR to the bulk cytosol are unlikely to simulate the precise consequences of synthesis of cADPR, perhaps by CD38 in a signaling microdomain close to ryanodine receptors. It has already been mentioned that a direct effect of cADPR on RyR seems difficult to reconcile with observations on RyR2 activity under well controlled conditions [9]. It remains possible that a binding protein for cADPR (or another intermediary step) may be interposed between synthesis of cADPR and the consequential change in CICR in intact

myocytes. It was mentioned in the EC coupling section that some have argued that an agent acting to increase the amount of Ca^{2+} released via RyRs cannot have a lasting effect, since the SR Ca^{2+} load will adjust to compensate [27]. It was, however, argued above that at body temperature when a substantial fraction of the CaT occurs while the AP is at elevated plateau potentials, additional Ca^{2+} can be released from the SR and taken back up with little or no opposition from NCX and therefore without contravening the need for balance between Ca^{2+} influx and efflux for a single beat. Whatever the merits of the theoretical arguments, repeated observations described in this section show increases in CaT amplitude which follow cADPR application to the cytosol by different methods in both atrial and ventricular myocytes without a change in the measured SR Ca^{2+} load. Additional information relating to possible mechanisms is listed below.

16.10.6 Possible Influence of Calmodulin (and CaMKII)

In sea urchin egg homogenates, it has been shown that calmodulin is a necessary requirement for cADPR mediated Ca^{2+} release [129–131], and it appears that CaMKII is required for cADPR effects in pancreatic islets [132]. More recently calmodulin dissociation from RyR has been shown to underlie the specific 'densensitization' of the cADPR-induced Ca^{2+} release mechanism in sea urchin homogenates, so that binding of calmodulin to RyR appears to be essential for the cADPR mediated Ca^{2+} release [133]. In guinea pig ventricular myocytes, effects of patch applied cADPR on the amplitude of CaT accompanying action potentials were prevented by the calmodulin antagonists, calmidazolium and W7, while calmidazolium also prevented the effect of photoreleased cADPR on the amplitude of CaT. Effects of photoreleased cADPR on CaT were also prevented by the CaMKII antagonist KN93 [104]. The underlying mechanisms deserve further study.

16.10.7 Possible Influence of FKBP

FKB12.6 is a protein that associates with RyR2, although its functions are controversial [9]. Evidence for an involvement of this protein in the actions of cADPR has been provided by experiments in which cADPR increased Ca^{2+} spark frequency in permeabilized myocytes from WT mice, but not those lacking FKB12.6 [134]. The possible significance of these observations is discussed in more detail in [9].

16.10.8 Contributions of cADPR Signaling to Cardiac Arrhythmia and Hypertrophy

The ability of beta-adrenoceptor agonists to increase cADPR synthesis in heart muscle has been described in detail above. High concentrations of beta-adrenoceptor agonist are known to provoke arrhythmias, and it is interesting to investigate whether cADPR-dependent mechanisms might contribute to the arrhythmogenic effects in addition to the well known involvement of other proteins including L-type Ca^{2+} channels, phospholamban in conjunction with SERCA, and perhaps RyR2 (as reviewed in [7]). High concentrations of isoproterenol (50 nM) gave rise to spontaneous action potentials and Ca^{2+} waves associated with SR Ca^{2+} overload in guinea pig ventricular myocytes, and these spontaneous events were suppressed by application of the cADPR antagonist, 8-amino-cADPR [135].

Gul et al. have shown that the hypertrophy that is normally seen following chronic exposure to isoproterenol is reduced in mice lacking CD38 as compared to WT, and propose that this results at least in part from reduction in cADPR synthesis [118]. It has been shown that the acute arrhythmogenic response of isolated hearts to high concentrations of isoproterenol is reduced in hearts from *CD38*$^{-/-}$ mice as compared to WT, and that the ADP-ribosyl cyclase inhibitor, SAN4825 also reduced isoproterenol-induced arrhythmias in WT hearts, consistent with a contribution of the cADPR signaling pathway to arrhythmogenic mechanisms [1], although the possible combined actions of cADPR and NAADP acting in concert on different aspects of the control of CaT amplitude in heart will be discussed later.

It was mentioned above that Angiotensin II can increase cADPR formation in neonatal rat cardiac myocytes [114], and chronic stimulation of this pathway is thought to lead to cardiac hypertrophy since the cADPR antagonist, 8-Br-cADPR, suppressed cardiac hypertrophy caused by AngII [117]. More recently it has been shown that ROS and AngII mechanisms co-operate to bring about cardiac hypertrophy [136].

16.11 NAADP

The first observations of actions of NAADP in heart showed the presence of binding sites for NAADP and the ability of NAADP to release Ca^{2+} from rabbit heart microsomes [137].

16.11.1 Detection of NAADP in Cardiac Muscle and Possible Synthetic Mechanisms

The ability of rat heart tissue to synthesise NAADP was shown by [138], and endogenous levels of NAADP in mammalian hearts were reported by [139]. It is important to note that the levels of NAADP that are necessary for activation of this signaling system in a variety of cell types seem to be in the submicromolar range (generally less than 100 nM), and indeed higher levels of NAADP can cause a self-inactivation or desensitization of the pathway [103]. The physiological levels are therefore likely to be very low and consequently difficult to measure. Synthetic mechanisms for NAADP remain controversial. Evidence was presented in the preceding section that ADP-ribosyl cyclases can catalyse cADPR formation, and that CD38 is the most likely candidate enzyme in the heart [1]. At least under in vitro conditions, CD38 can also catalyse the formation of NAADP from NADP and nicotinic acid by a base exchange mechanism in a variety of cell systems [103]. Support for the action of CD38 to underlie NAADP synthesis in mouse heart is provided by the observation that a cardiac membrane fraction from WT mice was able to catalyse the formation of NAADP from NADP and nicotinic acid, but this synthesis was not observed with cardiac membrane from *CD38*$^{-/-}$ mice. The base exchange reaction for formation of NAADP occurs most readily at acidic pH [140] [103], but NAADP synthesis from NADP and nicotinic acid was observed at a cytosolic pH of 7.2 in both in mouse cardiac mixed membranes and in a sheep cardiac SR preparation [1] that has been used to study SR proteins including RyR2 [141]. When mouse cardiac myocytes were permeabilised with saponin to allow access of NADP and nicotinic acid to the cytoplasm, NAADP synthesis was detected, but little or no synthesis was detected in the absence of saponin. This substance primarily permeabilises the cholesterol-containing membranes such as the plasmalemma, while Triton-X-100 permeabilises all cell membranes including the SR, and might potentially expose additional enzymes (including those with lumen-facing active sites in various organelles). However, there was little or no difference between saponin and Triton-X-100, applied alone or in combination, to permit NAADP synthesis, consistent with NAADP synthesis by an enzyme with an active site facing the cytosol [1].

It should be noted that another paper takes a different view, agreeing that CD38 promotes cADPR synthesis in the heart, but proposing that an additional enzyme is responsible for NAADP synthesis [118]. In these experiments CaTs accompanying action potentials were not recorded (see [1] for more detailed discussion).

An enzyme inhibitor, SAN4825, was developed to suppress cADPR synthesis [119], and in our experiments mentioned above, SAN4825 was found to inhibit cADPR production by cardiac membrane preparations. In addition, NAADP production by cardiac membrane preparations was also inhibited by SAN4825, and in silico modeling studies supported binding of SAN4825 at a single site on CD38 to inhibit both cADPR and NAADP synthesis [1].

Evidence was presented above that the amounts of cADPR synthesised in cardiac preparations, and the functional effects of cADPR in intact myocytes and whole hearts were increased following beta-adrenoceptor stimulation. Exposure of guinea-pig hearts to beta-adrenoceptor stimulation also increased NAADP synthesis, as detected by two different methods [142], [113]. This seems unsurprising if the same enzyme, CD38, is responsible for synthesis of cADPR and NAADP, although more work is needed to show how modification of CD38, perhaps by PKA dependent mechanisms, increases synthesis of cADPR and NAADP by two very different chemical reactions.

16.11.2 Location of CD38 in Cardiac Myocytes

The location of CD38 in heart is of particular interest in view of its possible functions supporting synthesis of both cADPR and NAADP. Observations in mouse WT cardiac myocytes showed that an antibody against CD38 appeared to be predominantly localized at the SR (although there was also a small subfraction associated with the plasmalemma). Labelling showed a banded appearance corresponding to the striations of the SR (separation slightly less than 2 μm). However, cardiac myocytes lacking CD38 showed minimal labeling without striations, supporting the selectivity of the antibody for CD38 in the mouse WT myocytes. Experiments were also performed on rabbit ventricular and atrial myocytes, and again the pattern and spacing of immunolabeling of CD38 was consistent with a location of this enzyme at or close to the SR. When antibodies to RyR2 and CD38 were applied to the same rabbit ventricular myocytes, there was a close correspondence between the two labeling patterns, again supporting an SR location for CD38 [1]. The location of CD38 in cardiac myocytes is illustrated in Fig. 16.4.

16.11.3 Orientation of CD38

CD38 is generally thought of as a type II transmembrane protein with its catalytic domain located on the outside of the cell, or pointing away from the cytosol in intracellular organelles, but recent evidence shows that this is not always the case [143–145] and the possible cytosolic synthesis of cADPR and NAADP by CD38 associated with SR in cardiac myocytes is discussed in detail in [1]. Future research will be necessary to provide clear information on the orientation of CD38 in cardiac membranes, but the suggestion that NAADP production can occur in the cytosol is consistent with the observations mentioned above that NAADP production occurs in media at pH7.2 after permeabilisation of cardiac myocytes with saponin, and is similar when Triton X100 is used as the permeabilisation agent.

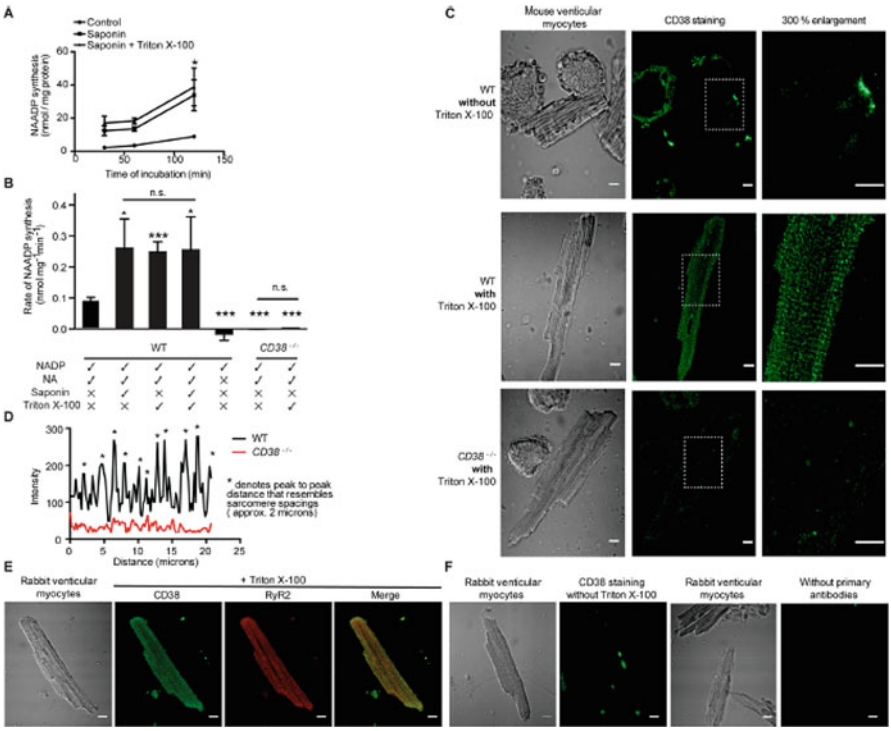

Fig. 16.4 Permeabilization of cardiac myocytes with Triton X-100 and/or saponin enhanced NAADP production and permitted immunolabeling of CD38. (**a**), the rate of NAADP synthesis was higher after permeabilization of the cell membranes with saponin alone, and permeabilization with Triton X-100 in addition to saponin did not further increase the rate of NAADP synthesis (n = 3 in each group). (**b**), this point is further illustrated in the bar graph, which also shows that the ability to synthesize NAADP was lost in myocytes from $CD38^{-}/^{-}$ mice (n = 4). Omission of NA also abolished synthesis of NAADP in intact cells (n = 5). (**c**), immunolabeling of CD38 using rabbit anti-human CD38 antibody without Triton X-100 showed little staining, although there were surface patches with higher fluorescence intensity (top panels). Following membrane permeabilization with Triton X-100 to allow access of the antibody to the cell interior, there was clear staining with a striated pattern in WT (center panels) but not in permeabilized $CD38^{-}/^{-}$ cardiac myocytes (bottom panels). (**d**), the representative intensity-distance plot (bottom panel) shows that, in permeabilized cells, the staining observed in the WT myocyte had a much higher intensity than in the $CD38^{-}/^{-}$ myocyte and showed multiple peaks with a repeating distance interval that resembled the sarcomere spacing. (**e**), similar observations in rabbit ventricular myocytes. The fluorescent images of myocytes permeabilized with Triton X-100 showed clear labeling with CD38 antibody. There was a striated pattern with a similar spacing as that shown by immunolabeling of RyR2. (**f**), no labeling with a striated pattern was observed when Triton X-100 or primary antibodies were omitted. The images show representative staining of the major observation (> 75%) in each group (n > 20). Scale bars 10 mm, n = number of cells. Data are expressed as mean % S.E. *, $p < 0.05$; ***, $p < 0.001$; n.s., not significant. (Reproduced from [1])

16.11.4 Importance of Lysosomes for Cardiac Actions of NAADP

In a variety of cell types the actions of NAADP appear to depend on the presence and function of acidic organelles, such as lysosomes or similar structures [146], [103]. An important experimental tool to investigate these pathways is bafilomycin A which blocks a V-type H^+ ATP-ase that sets up the proton gradient that is necessary for the functions of acidic organelles, including uptake of Ca^{2+} by a Ca^{2+}/H^+ exchange mechanism. Ca^{2+} release from acidic organelles has been shown to be a key component of the actions of NAADP in many cell types, and bafilomycin A is well established as useful experimental tool to suppress these NAADP effects [103]. The term lysosome will be used here to describe the acidic organelle involved in NAADP actions in the heart, although it is recognized that it is difficult to distinguish between lysosomes and other related organelles such as endosomes [147]. In our experiments described below on the functional effects of NAADP on Ca^{2+} transients and contraction of cardiac myocytes, bafilomycin A consistently suppressed NAADP actions, supporting the key role of acidic lysosomes for NAADP actions in the heart.

Given the proposed location of CD38 at or close to SR membranes and the proposed role of CD38 for NAADP synthesis, it is of special interest that lysosomes in the heart are localized close to the SR. This was shown by immunohistochemistry with conventional microscopy, labeling microsomes with lysotracker, and with EM methods [8]; see Figs. 16.1b and 16.5. Conventional 2D EM studies showed a close association of approximately 20 nm between lysosomes and SR. In the case of studies using 3D electron tomography the separation between SR and lysosomes appeared to be 3.3 nm. These separations are clearly consistent with microdomains between lysosomes and SR that may be important for proposed actions of NAADP to release Ca^{2+} from lysosomes, with actions of the released Ca^{2+} in the interposed microdomains to influence SR function. It is interesting to note that in addition to the positioning of lysosomes close to the SR it was found that lysosomes also form close associations with mitochondria. In this case 3D electron tomography showed a median separation of 6.2 nm [8]. This additional possible signaling microdomain will be important for some of the functional effects of NAADP that involve mitochondria and these are described in more detail below.

16.11.5 Importance of TPC2 and TPC1 Proteins for Cardiac Actions of NAADP

Generally actions of NAADP in heart are consistent with reported actions of this Ca^{2+} signaling molecule in many other tissues. The target of NAADP action, whether directly or after the intervention of an associated binding protein, is thought to be two-pore cation channels (TPCs) in a variety of tissues [148], [149]. There are

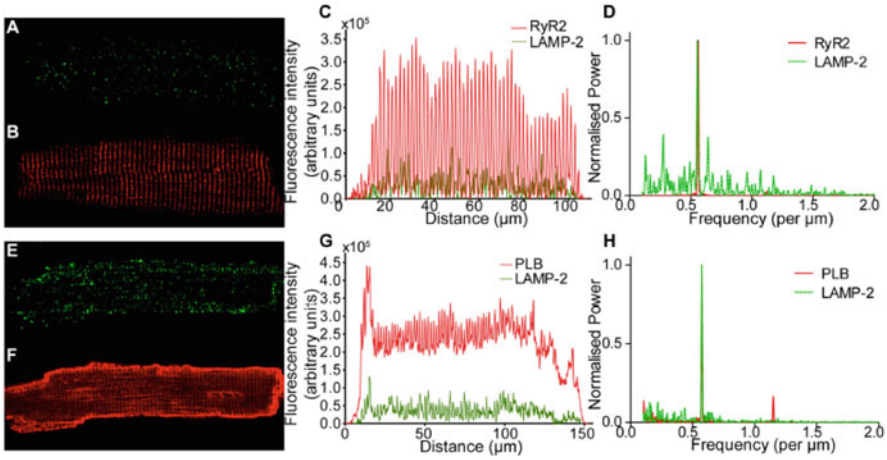

Fig. 16.5 Lysosomes are localised in a periodic pattern with sarcomeric distribution, similar to RyR and PLB, in fixed, isolated rabbit ventricular myocytes. (Top line) Representative example of LAMP-2 and RyR2 co-labelling experiment. Immunolabelling of LAMP-2 (**a**) and RyR2 (**b**) co-stained in the same, fixed, myocyte. (**c**) Intensity plot illustrating total pixel intensity for each column of pixels, for the two stains. Results of Fourier analyses (**d**) indicate a dominant frequency of 0.56 striations μm^{-1}, or a signal peak every 1.79 μm, for RyR2 and LAMP-2. (Middle line) Representative example of LAMP-2 and PLB co-labelling experiment. Confocal images of LAMP-2 (**e**) and PLB (**f**) with merged column intensity plot of both stains (**g**). Fourier analysis (**h**) of each signal indicate a dominant frequency of 0.57 signal peaks μm^{-1} for both PLB and LAMP-2, equivalent to a peak every 1.74 μm. A correlation plot of dominant frequencies for LAMP-2 against either RyR2 or PLB in co-labelling experiments (not shown; see original paper) revealed strong correlation (Pearson product-moment correlation co-efficient (r) = 0.72, n = 22 cells (n = 18 for RyR2 vs LAMP-2 and n = 4 for PLB vs LAMP-2). (Reproduced from [8])

at least three types of these channels, although TPC1 and TPC2 are thought to be most important in mammalian tissues. There is some controversy over the major cations that flow to support the functional effects of NAADP, and some propose that TPCs are channels activated by PI(3,5)P2 and that the primary cation flowing through the channels is Na^+ [150], although at least under some conditions NAADP activates Ca^{2+} flux through lysosomal TPC2 [149], [151]. Our evidence in the heart also supports the hypothesis of NAADP activated Ca^{2+} flux, and experiments comparing NAADP actions in cardiac muscle from WT mice or those lacking TPC2 proteins show that NAADP effects require TPC2. This was true both for isolated ventricular myocytes and for intact hearts [152], and the involvement of TPC2 proteins in the effects of NAADP on calcium transients, contraction and related processes are discussed in more detail below.

A useful chemical tool for the study of NAADP mechanisms is Ned-19, which acts as an antagonist of NAADP [153]. When used in conjunction with genetic methods to suppress the expression of TPC2, Ned-19 would be predicted to have effects in WT mice but to have little or no effect KO mice lacking TPC2, as was

found to be the case in [152], for NAADP actions concerning effects on Ca^{2+} transients, hypertrophy and arrhythmias that are described in detail below.

It appears that TPC1 proteins may be involved in a quite separate set of actions of NAADP in heart. When the heart is subject to a restricted blood flow, and then reperfused with oxygenated solution, the cardiac myocytes show substantial damage and sometimes cell death. The damage caused by such exposures to ischaemia and reperfusion is associated with Ca^{2+} oscillations. Cell death associated with ischaemia and subsequent perfusion was reduced by an antagonist of NAADP termed Ned-K (a structural analogue of the Ned-19 described above), supporting a role for NAADP in the underlying mechanisms of these effects [154]. It seems likely that mitochondria are involved in these actions of NAADP, and the observation described above that lysosomes are located close to mitochondria [8] is consistent with a signaling microdomain between these two organelles for actions of Ca^{2+} released from the lysosomes. Interestingly, transgenic mice lacking TPC1 proteins showed reduced injury following ischaemia and reperfusion, consistent with the importance of TPC1 proteins in this particular aspect of NAADP dependent Ca^{2+} signaling [154].

Most of the actions of NAADP described in this chapter concern involvement of cytosolic NAADP on intracellular signaling pathways, but there are some additional reported extracellular effects that appear to be related to the observations concerning ischaemia and reperfusion. Extracellular NAADP can increase intracellular levels of cADPR and NAADP by activating a signaling pathway that is thought to be mediated by a P2Y11 GPCR receptor on the surface membrane that is antagonised by NF157 [155]. Production of cADPR and NAADP in neonatal rat cardiomyocyte cultures was also enhanced by the selective P2Y11 agonist, NF456 [155]. The possible link with the observations above on TPC1 proteins involved in ischaemia-reperfusion injury is that 1 μM extracellular NAADP was observed to have a significant protective effect, and P2Y11 antagonist, NF157 suppressed this protection [156].

16.11.6 NAADP Actions on Ca^{2+} Transients Associated with Contraction

The discussion above alludes to a key signaling role of NAADP in cardiac muscle involving modulation of the Ca^{2+} transients, CaT, and contractions associated with action potentials that are essential for the normal physiology of the heart. Effects of cytosolic NAADP on CaT associated with action potentials were first shown in experiments in which NAADP was photoreleased from a caged compound that was applied to the cytosol of guinea-pig ventricular myocytes via a patch pipette [142]. CaTs were measured in cells in which action potentials were stimulated every 2 s, and a single pulse of UV light to photorelease NAADP caused a progressive increase in CaT amplitude accompanying successive action potentials. The effects on CaT

amplitude continued to develop for at least a minute after a single photorelease, and were dependent on concentration of caged compound over the range 0.5–5 μM. It is difficult to be sure of the cytosolic concentration of free NAADP corresponding to these concentrations of caged compound, but this is likely to have been less than 100 nM, perhaps between 10 and 100 nM if the efficiency of release from the caged compound at the above concentrations were approximately 2%.

It is difficult to record similar effects of NAADP applied directly to the cytosol from a patch pipette because it seems likely that there will be overlap between the possibly enhancing effects of low concentrations NAADP and the self-inactivating or desensitizing effects of higher concentrations of this messenger [157], as mentioned at the start of this section on NAADP. However, high concentrations of 0.1 or 1 mM NAADP predominantly cause self-inactivation of the NAADP signaling mechanism, and as expected prior application of NAADP from a patch pipette reduced (0.1 mM) or abolished (1 mM) the effects of photoreleased NAADP on the amplitude of CaT [142].

The effects of photoreleased NAADP on CaT amplitude were also suppressed by prior application of bafilomycin A, consistent with the involvement of lysosomes [142].

There were no detectable effects of photoreleased NAADP on the amplitude of L-type Ca^{2+} currents and it therefore seems likely that the actions of NAADP on CaT amplitude involve the SR, and perhaps the signaling microdomain proposed above between lysosomes and SR. As expected pretreatment of myocytes with thapsigargin and ryanodine (to inhibit both uptake and release of Ca^{2+} by the SR) prevented the effects of photoreleased NAADP on CaT. The effects of photoreleased NAADP were accompanied by an increased amount of Ca^{2+} loaded into the SR (as tested by a rapid caffeine application to release SR Ca^{2+}), and taken together the observations are consistent with an effect of NAADP to release Ca^{2+} from the lysosome leading to an increase in SR Ca^{2+} and therefore the amplitude of the CaT [142]. The possibility of an amplification mechanism so that the amount of extra Ca^{2+} loaded into the SR may be greater than that released from the lysosome will be described later.

Another method for application of NAADP is to apply a membrane permeant ester (NAADP-AM) to the extracellular solution, allowing intracellular accumulation of NAADP-AM followed by release of free NAADP resulting from the action of cytosolic esterases [158]. Applying this approach to guinea pig cardiac ventricular cells, rapid application of 60 nM NAADP-AM (to favour the enhancing effects of low concentrations of NAADP before the development of high self-inactivating cytosolic concentrations of NAADP) increased the amplitude of contractions in cells stimulated to fire action potentials. In rat ventricular cells, which show Ca^{2+} sparks, application of 60 nM NAADP increased both the frequency and amplitude of Ca^{2+} sparks (effects which are both consistent with the proposed increase in amount of Ca^{2+} loaded into the SR). The effects NAADP-AM on contractions in guinea pig ventricular myocytes and on Ca^{2+} spark characteristics in rat myocytes were suppressed by bafilomycin A, again consistent with the involvement of the proposed lysosomal pathway in these effects [142].

Some have argued that the predominant effect of NAADP is to have a direct influence on sensitivity of RyR2 to increase Ca^{2+} release (e.g [159], [160]). This would be consistent with the increase in Ca^{2+} spark frequency mentioned above, but not the increase in amplitude. Interesting effects of patch applied NAADP have been observed in mouse ventricular myocyte, which unlike those from guinea pig, retain Ca^{2+} in the SR even when the myocytes are not electrically stimulated to fire action potentials. Under these conditions, NAADP applied from a patch pipette cause a slow wave of Ca^{2+} release from the SR. The concentration dependence of this effect showed a bell shaped curve, in which the response to 375 nM NAADP was substantially smaller than that to 37.5 nM, consistent with the desensitizing or self-inactivating effects of NAADP described above. The response to 37.5 nM NAADP was suppressed by a selective NAADP antagonist (BZ194, 10 microM), as well as by ruthenium red (which prevents Ca^{2+} release from SR) and bafilomycin A (consistent with the involvement of lysosomes as described above).

Observations described above in this section have all been made in ventricular myocytes, though it seems likely that the NAADP signaling system may be present throughout the heart. In atrial myocytes, effects of NAADP on CaT accompanying action potentials have been found to be broadly similar to those in ventricular cells. This was shown again using photorelease of NAADP from a caged compound, with a single release of cytosolic NAADP causing a progressive increase in the amplitude of successive CaT over a 2 min period [161]. As with the observations in ventricular cells there was no effect of NAADP on L-type Ca^{2+} currents, but the actions of NAADP were prevented when SR release of Ca^{2+} was suppressed with a combination of thapsigargin and ryanodine. Once again, the effects appeared to be dependent on lysosomes since the effects of photoreleased NAADP were prevented by prior exposure to bafilomycin A [161].

Guinea pig atrial myocytes (surprisingly unlike ventricular myocytes from the same species) show Ca^{2+} sparks in perhaps 30–50% of cells, and it is interesting that, as had been observed in rat ventricular myocytes, membrane-permeant NAADP-AM caused an increase in Ca^{2+} spark amplitude. This was consistent with an increase in the amount of Ca^{2+} loaded into the SR following the intracellular actions of NAADP, and this interpretation was further reinforced by the observation that Ca^{2+} release from the SR caused by rapid application of a high concentration of caffeine was also increased following NAADP-AM application. Broadly the increase in SR Ca^{2+} in atrial myocytes following the increased levels of cytosolic NAADP under these conditions appeared to be approximately 30% [161].

16.11.7 An Amplification Mechanism Linking Lysosomal Ca^{2+} Release and Increased Ca^{2+} Uptake by the SR in the Heart

Given the relatively small size of lysosomes compared with the extensive SR system, it seems unlikely that lysosomes could release sufficient Ca^{2+} to account directly for the substantial observed increase in SR Ca^{2+} content. One obvious potential

amplification mechanism is CaMKII, particularly taking into account the evidence for a signaling microdomain between lysosomes and SR [8] that was described above.

This was tested in a series of experiments using two inhibitors of CaMKII, KN93 and the peptide AIP (autocamtide inhibitor peptide). The observations were made in guinea pig ventricular myocytes, mouse ventricular myocytes and guinea pig atrial myocytes. In all cases inhibition of CaMKII suppressed the ability of photoreleased NAADP to increase the amplitude of CaT accompanying action potentials. The interpretation that the observed effects of KN93 arose from inhibition of CaMKII was further supported by the failure of KN92, a structural analogue of KN93 without effects on CaMKII, to prevent actions of NAADP on CaT [152].

16.11.8 Extent of Ongoing Activity in NAADP Signaling Pathway Under Resting Conditions in Cardiac Muscle

The evidence presented above using photorelease of NAADP from a caged compound or application of the membrane permeant NAADP-AM make a convincing case for cytosolic actions of NAADP, predominantly to increase Ca^{2+} content of the SR and therefore the amplitude of CaT. It seems reasonable to ask whether there might be ongoing activity of this signaling system at rest and whether resting activity might be enhanced, for example following actions of hormones or neurotransmitters. Early evidence for a resting role for NAADP in guinea-pig ventricular cells came from the observation that the amplitude of CaT accompanying action potentials was reduced both by a high concentration of NAADP (presumably by the desensitizing or self inactivation mechanism) and by bafilomycin A (to suppress lysosomal function), and this reduction was approximately 20–25% [142].

An ongoing activity of the NAADP signaling system also seemed to operate in atrial myocytes, since bafilomycin A again caused a reduction in the amplitude of CaT accompanying action potentials. Interestingly the resting activity of the NAADP system seemed to be greater in atrial than in ventricular myocytes, since the reduction in CaT amplitude following bafilomycin was approximately 50% [161]. Whether this apparent difference between ventricular and atrial myocytes is real deserves further study in other species, but it is interesting to note in this context that atrial cells show an ongoing activity of adenyl cyclases (thought to be AC1 and AC8) as described above in the section on Ca^{2+} stimulated adenylyl cyclases, and ongoing activity of adenylyl cyclases is not observed in resting ventricular myocytes. One possibility is that the ongoing activity of adenylyl cyclases in atrial myocytes acts via a cAMP dependent pathway to increase NAADP synthesis by CD38, which in turn increases the contribution of the NAADP signaling pathway to the control of the amplitude of the CaT. The ability of beta-adrenoceptor stimulation to increase levels of NAADP in myocytes and whole hearts was described above, and the importance of cAMP dependent mechanisms to regulate functionally important aspects of NAADP signaling will be discussed in more detail in the next section.

16.11.9 Enhanced NAADP Effects Following Beta-Adrenoceptor Stimulation in Heart

Early evidence showing the influence of β-adrenoceptor stimulation on the function of NAADP signaling pathway in controlling CaT amplitude was provided in experiments taking advantage of the desensitizing or self inactivating effect of high concentrations of NAADP. It was found that high concentrations (1 mM) of NAADP applied via a patch pipette in guinea pig ventricular myocytes caused a larger reduction in CaT amplitude in the presence than in the absence of β-adrenoceptor stimulation, consistent with a greater role of this pathway when cAMP levels are elevated. If NAADP concentrations are substantially increased following beta-adrenoceptor signalling, it might be expected that further addition of NAADP would have less effect than would be the case when NAADP levels are at their resting level, and consistent with this line of argument photoreleased NAADP had a smaller effect on CaT amplitude after beta-adrenoceptor stimulation than under resting conditions [142].

In guinea pig atrial myocytes, the effects of beta-adrenoceptor stimulation to increase the amplitude of CaT were less when lysosomal function was inhibited by bafilomycin A. Another experimental procedure to suppress lysosomal function is to apply GPN to disrupt these organelles. As expected, pretreatment with GPN also reduced the increase in CaT caused by beta-adrenoceptor stimulation [161]. It should be noted even if there were a functionally important contribution of the NAADP signaling pathway to the effects of beta-adrenoceptor stimulation, this would be expected to be additional to the well known effects of β-adrenoceptor stimulation to increase the amplitude of Ca^{2+} currents (e.g [23]. and review by [7]) and to increase Ca^{2+} uptake by SERCA into the SR following phosphorylation of phospholamban [7]. Based on the observations with bafilomycin and GPN it appears that in guinea-pig atrial myocytes the NAADP Ca^{2+} signaling mechanism involving lysosomes contributes over 30% to the total increase in CaT caused by beta-adrenoceptor stimulation.

A separate piece of evidence supporting an involvement of lysosomes in the effects of β-adrenoceptor stimulation comes from observations in which the pH of the normally acidic lysosomes was measured. Isoproterenol caused an alkalinisation of lysosomes in atrial myocytes similar to that caused by NAADP-AM [161]. The maintenance of a relatively high concentration of Ca^{2+} within the lysosome is thought to depend on Ca^{2+}/H^{+} exchange, and alkalinisation may occur following Ca^{2+} release from the lysosome, potentially by a change in the lysosomal buffering capacity or in the direction of Ca^{2+}/H^{+} exchange.

Two further tests of the ability of β-adrenoceptor stimulation to increase the functional effects of NAADP signaling are to use the NAADP-antagonist, Ned-19 or to use myocytes lacking TPC2 receptors. In guinea pig ventricular myocytes Ned-19 pretreatment reduced the effects of β-adrenoceptor stimulation to a similar extent as that observed in separate experiments in which lysosomal function was suppressed by bafilomycin A. As expected, the effects of beta-adrenoceptor stimulation on the

amplitude of L-type Ca^{2+} currents was unaffected by Ned-19. Mouse ventricular myocytes from WT and those lacking TPC2 proteins were compared, and the effects of β-adrenoceptor stimulation on CaT and contraction were less in myocytes lacking TPC2 proteins. However, the effects of β-adrenoceptor stimulation on the amplitude of L-type Ca^{2+} currents were similar in WT myocytes and those lacking TPC2 proteins [152].

Another important piece of evidence concerns the synthetic pathway for NAADP, and observations described above support the key role of CD38. While bafilomycin A reduced the increase in CaT in response to β-adrenoceptor stimulation in WT mice, there was no such effect of bafilomycin A in mice lacking CD38 [1].

Taken together, the observations above are consistent with the hypothesis that β-adrenoceptor stimulation increases NAADP synthesis, and that NAADP causes Ca^{2+} release from lysosomes via TPC2 proteins into a signaling domain between lysosomes and SR, and this leads to increased Ca^{2+} uptake by the SR by a CaMKII dependent mechanism. The contribution of the NAADP signaling pathway to the effects of β-adrenoceptor stimulation in atrial and ventricular myocytes appeared to be about 30%.

16.11.10 Involvement of NAADP Signaling in Cardiac Arrhythmia and Hypertrophy

Cardiac arrhythmias associated with NAADP actions following high concentrations of beta-adrenoceptor agonist have been described by Guse and colleagues. In these experiments on mouse ventricular myocytes, high concentrations of beta adrenoceptor agonist increased the amplitude of CaT associated action potentials, but also led to additional spontaneous Ca^{2+} transients that were taken to indicate arrhythmias. The spontaneous events were suppressed by bafilomycin A and by an NAADP antagonist, BZ194 [159]. In a subsequent paper, measurements of cytosolic Ca^{2+} were supplemented by additional detection of changes in SR luminal Ca^{2+} using the low affinity Ca^{2+} probe, mag-fura-2. High concentrations of beta-adrenoceptor agonist again caused spontaneous arrhythmogenic activity, and in the spontaneous activity was suppressed by SAN4825, which as described above inhibits synthesis of both cADPR and NAADP [160].

Cardiac arrhythmias measured in an in vivo mouse model when exposed to high concentrations of β-adrenoceptor agonist were suppressed by the NAADP antagonist, BZ194, supporting a role for the NAADP pathway in arrhythmias at the whole animal level [159].

Another approach supporting a role for NAADP in arrhythmogenic properties is to compare the effects of a high concentration of beta-adrenoceptor agonist in WT mice and those lacking TPC2 proteins that were shown to be essential for the arrhythmogenic response, as described above. Isolated whole hearts from

Tpcn2$^{-/-}$ mice were resistant to arrhythmias caused by high concentrations of beta-adrenoceptor agonist as compared to hearts from WT animals [152].

Hearts from *CD38*$^{-/-}$ mice lacking CD38, the key enzyme for synthesis of NAADP, were also resistant to arrhythmias caused by high concentrations of beta adrenoceptor agonist as compared to WT hearts. A similar suppression of the arrhythmogenic effects of beta-adrenoceptor stimulation was seen following exposure of WT hearts to SAN4825, the inhibitor of cADPR and NAADP synthesis [1].

Prolonged exposure of animals to beta-agonist also causes cardiac hypertrophy. The involvement of the NAADP signaling mechanism in the stress pathway linking β-adrenoceptor stimulation to cardiac hypertrophy was demonstrated by the observation that following chronic exposure to β-adrenoceptor agonist hearts from *Tpcn2*$^{-/-}$ mice showed less cardiac hypertrophy and an increased threshold for arrhythmogenesis compared to WT controls [152]. In addition, hearts from *CD38*$^{-/-}$ mice were also resistant to cardiac hypertrophy and associated arrhythmias following chronic β-adrenoceptor stimulation compared to WT [118].

16.11.11 Trigger Hypothesis

The trigger hypothesis in which a transient change in NAADP concentration leads to important functional effects is well supported by very convincing evidence in a wide variety of cell types [162], [163], but this may not necessarily be the case in heart. As discussed above the evidence in heart seems to support an ongoing activity of the NAADP pathway under resting conditions (in the sense that cells were not exposed to hormones or neurotransmitters), so that suppression of the pathway, for example by bafilomycin A, reduces CaT accompanying action potentials by 20–25% in ventricular myocytes, and by approximately 50% in atrial myocytes. Although in whole hearts following beta-adrenoceptor stimulation with isoproterenol the rise in NAADP levels appeared to be transient in comparison with the changes in cADPR concentrations, the effects of isoproterenol on contraction were also transient [113]. The reason for the transience of the effect of isoproterenol on contraction are unknown, but might perhaps result from the difficulty of maintaining oxygen supply and cytosolic pH when contraction is substantially increased in hearts perfused with physiological solution rather than blood. Oxygen supply and pH can be more easily maintained in isolated myocytes, but changes in NAADP levels have not yet been measured in myocytes exposed to isoproterenol in the superfusing solution. However, the component of the effects of isoproterenol on CaT and contraction that involves NAADP (blocked by bafilomycin A and absent in myocytes lacking TPC2) appears to be well maintained at least over the several minutes that effects were measured [152]. Further experiments are required to shed more light on the question of whether NAADP acts as a trigger or an ongoing influence in cardiac muscle, both at rest and following β-adrenoceptor stimulation.

16.12 Combined Actions of cADPR and NAADP

It is argued above that there are maintained concentrations of both cADPR and NAADP for their effects in heart muscle on CaT and associated contractions accompanying action potentials under physiological conditions. Both agents are produced by CD38, which in mouse heart appeared to be the major synthetic enzyme for these two Ca^{2+} mobilizing messengers. Evidence was presented that CD38 in heart is predominantly associated with SR, and there appears to be an important Ca^{2+} signaling domain between lysosomes and the SR. TPC2 proteins appear to be essential for NAADP actions on CaT and contractions (while TPC1 proteins are important for ischaemia-reperfusion effects, perhaps involving a separate signaling microdomain between lysosomes and mitochondria). β-adrenoceptor stimulation increased the levels of both substances, and in ventricular myocytes both cADPR and NAADP pathways seemed to contribute to the β-adrenoceptor mediated effects on the amplitudes of CaT and contractions accompanying action potentials.

The evidence also supports the contention that at least for short periods (perhaps less than 3 min) the predominant effect of cADPR alone is on Ca^{2+} release from the SR (though this should not be taken to indicate that this necessarily results from a direct effect on RyR2) without a change in the amount of Ca^{2+} loaded into the SR, while NAADP actions primarily result from increased Ca^{2+} loading into the SR. It is the author's belief that any additional effects of cADPR alone on Ca^{2+} uptake into the SR after prolonged exposure to cADPR in permeabilised myocytes are less important than those on the Ca^{2+} release process (and have yet to be established under more physiological conditions), but this seems a fruitless argument if cADPR and NAADP normally act in concert as a result of their synthesis by the same enzyme, CD38, associated with the SR, and their complementary actions on CICR. In a similar way, the argument discussed above about whether cADPR could have a sustained effect on the amplitude of CaT and contractions if its only action were to influence Ca^{2+} release via RyR seems unlikely to be productive for a physiological situation in which cADPR and NAADP act together. The dual effects of NAADP on Ca^{2+} load and cADPR on Ca^{2+} release are expected to combine to create a powerful effect on CaT and contractions accompanying action potentials. One reservation arises from the presumed location of SERCA and RyR2 in various schemes of EC coupling in which these two proteins are normally shown far apart with the RyR2 at the terminal cisternae, and the SERCA closer to the middle of the sarcomere, as might be expected if Ca^{2+} is taken up after contraction in one part of the SR before transport of Ca^{2+} to the terminal cisternae for release via RyR2. However, recent evidence supports the presence of both SERCA and RyR2 in the terminal cisternae [112] (See also [19] for discussion of JSR and NSR)

A scheme summarizing the actions of cADPR and NAADP is shown in Fig. 16.6.

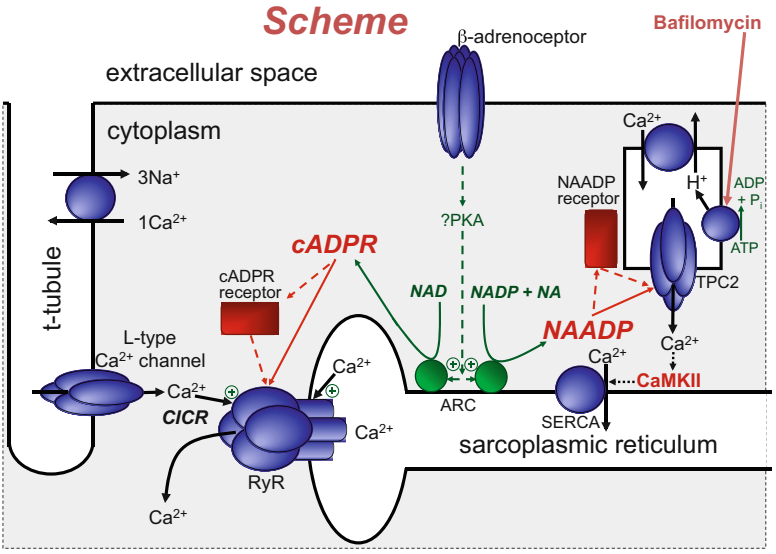

Fig. 16.6 ADP-ribosyl cyclase (ARC) is thought to be equivalent to CD38 and appears to be located on (or close to) the SR (see text). Cardiac ARC catalyses formation of both cADPR (with NAD as substrate) and NAADP (from NADP and nicotinic acid (NA)). cADPR appears to act primarily on RyRs, although there may be an intermediary step possibly involving a binding protein, and additional slow effects of cADPR on Ca^{2+} uptake by the SR cannot be excluded. NAADP causes Ca^{2+} to be released from endolysosomes via TPC2 proteins (perhaps with mediation of an additional NAADP receptor protein). The Ca^{2+} released from the endolysosome leads to additional Ca^{2+} uptake by the SR (an effect that appears to involve CaMKII, perhaps by phosphorylation of phospholamban to increase SERCA activity). Additional Ca^{2+} loaded into the SR will increase CICR both by providing a greater gradient for Ca^{2+} release and by increasing opening probability of RyRs. Additional effects of NAADP on RyRs cannot be excluded. cADPR and NAADP may function together in a cooperative or synergistic way in ventricular myocytes (perhaps also interacting with IP3-dependent Ca^{2+} signaling in atrial myocytes). Stimulation of beta-adrenoceptors increases synthesis of both cADPR and NAADP, by mechanism that remains to be fully determined, but may involve an action of PKA on ARC

16.13 Summary

It was recognized at the outset of this article that Ca^{2+} is involved in all aspects of biology, and evidence presented here shows that Ca^{2+} in the heart not only controls its primary function to provide rhythmic contractions to pump blood to the lungs and tissues, but also that diverse Ca^{2+} signaling pathways regulate this basic function. The simplest regulatory elements are Ca^{2+} stimulated enzymes. In addition Ca^{2+} mobilizing agents play important roles in stimulating Ca^{2+} release from the intracellular organelles of the SR and lysosomes. These Ca^{2+} regulated processes form an interconnecting network that determines function, and not surprisingly there are variations in the contributions and relative importance of components of this network in different regions of the heart with different functions.

IP_3 is particularly important for the short term control of Ca^{2+} transients in atria and pacemaker tissue of the SA node, although long term effects on gene expression occur throughout the heart. It is suggested that cADPR and NAADP are synthesized in heart by the same enzyme, CD38, located at or close to the SR, where these two substances act in a complementary way to regulate Ca^{2+} release by increasing the gain of CICR and increasing the amount of Ca^{2+} stored in the SR. Although the relationship between cADPR and NAADP actions is argued to be particularly close, it is recognized that overall function is determined by complex interactions with IP_3 and Ca^{2+} stimulated enzymes. Actions of hormones and neurotransmitters provide a regulatory influence on these complex pathways. The contributions of Ca^{2+} signaling pathways to the overall effect of receptor stimulation on Ca^{2+} transients are often surprisingly large. Although disentangling the complex interacting Ca^{2+}-dependent processes provides a challenge for the design of experiments, it is clear that Ca^{2+} signaling in the heart is a major determinant of function.

References

1. Lin WK, Bolton EL, Cortopassi WA, Wang Y, O'Brien F, Maciejewska M et al (2017) Synthesis of the Ca^{2+}-mobilizing messengers NAADP and cADPR by intracellular CD38 enzyme in the mouse heart: role in beta-adrenoceptor signaling. J Biol Chem 292(32):13243–13257
2. Bers DM (2002) Cardiac excitation-contraction coupling. Nature 415(6868):198–205
3. MacLeod KT (2016) Recent advances in understanding cardiac contractility in health and disease. F1000 Res 5:1770
4. Dewenter M, von der Lieth A, Katus HA, Backs J (2017) Calcium signaling and transcriptional regulation in cardiomyocytes. Circ Res 121(8):1000–1020
5. Harada M, Luo X, Murohara T, Yang B, Dobrev D, Nattel S (2014) MicroRNA regulation and cardiac calcium signaling: role in cardiac disease and therapeutic potential. Circ Res 114(4):689–705
6. Li J, Greener ID, Inada S, Nikolski VP, Yamamoto M, Hancox JC et al (2008) Computer three-dimensional reconstruction of the atrioventricular node. Circ Res 102(8):975–985
7. Bers DM (2008) Calcium cycling and signaling in cardiac myocytes. Annu Rev Physiol 70:23–49
8. Aston D, Capel RA, Ford KL, Christian HC, Mirams GR, Rog-Zielinska EA et al (2017) High resolution structural evidence suggests the sarcoplasmic reticulum forms microdomains with acidic stores (lysosomes) in the heart. Sci Rep 7:40620
9. Venturi E, Pitt S, Galfre E, Sitsapesan R (2012) From eggs to hearts: what is the link between cyclic ADP-ribose and ryanodine receptors? Cardiovasc Ther 30(2):109–116
10. Lim G, Venetucci L, Eisner DA, Casadei B (2008) Does nitric oxide modulate cardiac ryanodine receptor function? Implications for excitation-contraction coupling. Cardiovasc Res 77(2):256–264
11. O'Brien F, Venturi E, Sitsapesan R (2015) The ryanodine receptor provides high throughput Ca^{2+}−release but is precisely regulated by networks of associated proteins: a focus on proteins relevant to phosphorylation. Biochem Soc Trans 43(3):426–433
12. Camors E, Valdivia HH (2014) CaMKII regulation of cardiac ryanodine receptors and inositol triphosphate receptors. Front Pharmacol 5:101
13. Lukyanenko V, Chikando A, Lederer WJ (2009) Mitochondria in cardiomyocyte Ca^{2+} signaling. Int J Biochem Cell Biol 41(10):1957–1971

14. Williams GS, Boyman L, Lederer WJ (2015) Mitochondrial calcium and the regulation of metabolism in the heart. J Mol Cell Cardiol 78:35–45
15. Hohendanner F, Maxwell JT, Blatter LA (2015) Cytosolic and nuclear calcium signaling in atrial myocytes: IP3-mediated calcium release and the role of mitochondria. Channels 9(3):129–138
16. Cheng H, Lederer WJ, Cannell MB (1993) Calcium sparks: elementary events underlying excitation-contraction coupling in heart muscle. Science 262(5134):740–744
17. Cannell MB, Kong CH, Imtiaz MS, Laver DR (2013) Control of sarcoplasmic reticulum Ca^{2+} release by stochastic RyR gating within a 3D model of the cardiac dyad and importance of induction decay for CICR termination. Biophys J 104(10):2149–2159
18. Wescott AP, Jafri MS, Lederer WJ, Williams GS (2016) Ryanodine receptor sensitivity governs the stability and synchrony of local calcium release during cardiac excitation-contraction coupling. J Mol Cell Cardiol 92:82–92
19. Sobie EA, Williams GSB, Lederer WJ (2017) Ambiguous interactions between diastolic and SR Ca^{2+} in the regulation of cardiac Ca^{2+} release. J Gen Physiol 149(9):847–855
20. Rios E (2017) Perspectives on "control of Ca release from within the cardiac sarcoplasmic reticulum". J Gen Physiol 149(9):833–836
21. Jones PP, Guo W, Chen SRW (2017) Control of cardiac ryanodine receptor by sarcoplasmic reticulum luminal Ca(2). J Gen Physiol 149(9):867–875
22. Ching LL, Williams AJ, Sitsapesan R (2000) Evidence for Ca^{2+} activation and inactivation sites on the luminal side of the cardiac ryanodine receptor complex. Circ Res 87(3):201–206
23. Mitchell MR, Powell T, Terrar DA, Twist VW (1983) Characteristics of the second inward current in cells isolated from rat ventricular muscle. Proc R Soc Lond Ser B Biol Sci 219(1217):447–469
24. Sitsapesan R, Montgomery RA, MacLeod KT, Williams AJ (1991) Sheep cardiac sarcoplasmic reticulum calcium-release channels: modification of conductance and gating by temperature. J Physiol 434:469–488
25. Lee P, Wang K, Woods CE, Yan P, Kohl P, Ewart P et al (2012) Cardiac electrophysiological imaging systems scalable for high-throughput drug testing. Pflugers Arch: Eur J Physiol 464(6):645–656
26. Winter J, Bishop MJ, Wilder CDE, O'Shea C, Pavlovic D, Shattock MJ (2018) Sympathetic nervous regulation of calcium and action potential alternans in the intact heart. Front Physiol 9:16
27. Eisner DA, Caldwell JL, Kistamas K, Trafford AW (2017) Calcium and excitation-contraction coupling in the heart. Circ Res 121(2):181–195
28. Janvier NC, Harrison SM, Boyett MR (1997) The role of inward $Na(+)$-Ca^{2+} exchange current in the ferret ventricular action potential. J Physiol 498(Pt 3):611–625
29. O'Hara T, Virag L, Varro A, Rudy Y (2011) Simulation of the undiseased human cardiac ventricular action potential: model formulation and experimental validation. PLoS Comput Biol 7(5):e1002061
30. White E, Terrar DA (1992) Inactivation of Ca current during the action potential in guinea-pig ventricular myocytes. Exp Physiol 77(1):153–164
31. Linz KW, Meyer R (1998) Control of L-type calcium current during the action potential of guinea-pig ventricular myocytes. J Physiol 513(Pt 2):425–442
32. Blatter LA (2017) The intricacies of atrial calcium cycling during excitation-contraction coupling. J Gen Physiol 149(9):857–865
33. Collins TP, Terrar DA (2012) Ca^{2+}-stimulated adenylyl cyclases regulate the L-type Ca^{2+} current in guinea-pig atrial myocytes. J Physiol 590(8):1881–1893
34. Maxwell JT, Blatter LA (2017) A novel mechanism of tandem activation of ryanodine receptors by cytosolic and SR luminal Ca^{2+} during excitation-contraction coupling in atrial myocytes. J Physiol 595(12):3835–3845
35. Brandenburg S, Kohl T, Williams GS, Gusev K, Wagner E, Rog-Zielinska EA et al (2016) Axial tubule junctions control rapid calcium signaling in atria. J Clin Invest 126(10):3999–4015

36. Lakatta EG, Maltsev VA, Vinogradova TM (2010) A coupled system of intracellular Ca^{2+} clocks and surface membrane voltage clocks controls the timekeeping mechanism of the heart's pacemaker. Circ Res 106(4):659–673
37. Capel RA, Terrar DA (2015) The importance of Ca^{2+}-dependent mechanisms for the initiation of the heartbeat. Front Physiol 6:80
38. Mesirca P, Torrente AG, Mangoni ME (2015) Functional role of voltage gated Ca^{2+} channels in heart automaticity. Front Physiol 6:19
39. DiFrancesco D (2015) HCN4, sinus bradycardia and atrial fibrillation. Arrhythmia Electrophysiol Rev 4(1):9–13
40. Chen W, Wang R, Chen B, Zhong X, Kong H, Bai Y et al (2014) The ryanodine receptor store-sensing gate controls Ca^{2+} waves and Ca^{2+}−triggered arrhythmias. Nat Med 20(2):184–192
41. Toyoda F, Mesirca P, Dubel S, Ding WG, Striessnig J, Mangoni ME et al (2017) CaV1.3 L-type Ca^{2+} channel contributes to the heartbeat by generating a dihydropyridine-sensitive persistent Na(+) current. Sci Rep 7(1):7869
42. Sanders L, Rakovic S, Lowe M, Mattick PA, Terrar DA (2006) Fundamental importance of Na^{+}-Ca^{2+} exchange for the pacemaking mechanism in guinea-pig sino-atrial node. J Physiol 571(Pt 3):639–649
43. Kapoor N, Tran A, Kang J, Zhang R, Philipson KD, Goldhaber JI (2015) Regulation of calcium clock-mediated pacemaking by inositol-1,4,5-trisphosphate receptors in mouse sinoatrial nodal cells. J Physiol 593(12):2649–2663
44. Rigg L, Heath BM, Cui Y, Terrar DA (2000) Localisation and functional significance of ryanodine receptors during beta-adrenoceptor stimulation in the guinea-pig sino-atrial node. Cardiovasc Res 48(2):254–264
45. Maier LS (2012) Ca^{2+}/calmodulin-dependent protein kinase II (CaMKII) in the heart. Adv Exp Med Biol 740:685–702
46. Swaminathan PD, Purohit A, Hund TJ, Anderson ME (2012) Calmodulin-dependent protein kinase II: linking heart failure and arrhythmias. Circ Res 110(12):1661–1677
47. Gray CB, Heller BJ (2014) CaMKIIdelta subtypes: localization and function. Front Pharmacol 5:15
48. Mustroph J, Maier LS, Wagner S (2014) CaMKII regulation of cardiac K channels. Front Pharmacol 5:20
49. Wu Y, Anderson ME (2014) CaMKII in sinoatrial node physiology and dysfunction. Front Pharmacol 5:48
50. Hund TJ, Mohler PJ (2015) Role of CaMKII in cardiac arrhythmias. Trends Cardiovasc Med 25(5):392–397
51. Mattiazzi A, Bassani RA, Escobar AL, Palomeque J, Valverde CA, Vila Petroff M et al (2015) Chasing cardiac physiology and pathology down the CaMKII cascade. Am J Physiol Heart Circ Physiol 308(10):H1177–H1191
52. Johnston AS, Lehnart SE, Burgoyne JR (2015) Ca^{2+} signaling in the myocardium by (redox) regulation of PKA/CaMKII. Front Pharmacol 6:166
53. Anderson ME (2015) Oxidant stress promotes disease by activating CaMKII. J Mol Cell Cardiol 89(Pt B):160–167
54. Feng N, Anderson ME (2017) CaMKII is a nodal signal for multiple programmed cell death pathways in heart. J Mol Cell Cardiol 103:102–109
55. Richard S, Perrier E, Fauconnier J, Perrier R, Pereira L, Gomez AM et al (2006) 'Ca^{2+}-induced Ca^{2+} entry' or how the L-type Ca^{2+} channel remodels its own signalling pathway in cardiac cells. Prog Biophys Mol Biol 90(1–3):118–135
56. Xu L, Lai D, Cheng J, Lim HJ, Keskanokwong T, Backs J et al (2010) Alterations of L-type calcium current and cardiac function in CaMKII{delta} knockout mice. Circ Res 107(3):398–407
57. Ferrero P, Said M, Sanchez G, Vittone L, Valverde C, Donoso P et al (2007) Ca^{2+}/calmodulin kinase II increases ryanodine binding and Ca^{2+}−induced sarcoplasmic reticulum Ca^{2+} release kinetics during beta-adrenergic stimulation. J Mol Cell Cardiol 43(3):281–291

58. DeSantiago J, Maier LS, Bers DM (2002) Frequency-dependent acceleration of relaxation in the heart depends on CaMKII, but not phospholamban. J Mol Cell Cardiol 34(8):975–984
59. Pereira L, Metrich M, Fernandez-Velasco M, Lucas A, Leroy J, Perrier R et al (2007) The cAMP binding protein Epac modulates Ca^{2+} sparks by a Ca^{2+}/calmodulin kinase signalling pathway in rat cardiac myocytes. J Physiol 583(Pt 2):685–694
60. Bers DM, Grandi E (2009) Calcium/calmodulin-dependent kinase II regulation of cardiac ion channels. J Cardiovasc Pharmacol 54(3):180–187
61. Nerbonne JM (2011) Repolarizing cardiac potassium channels: multiple sites and mechanisms for CaMKII-mediated regulation. Heart Rhythm 8(6):938–941
62. Grandi E, Herren AW (2014) CaMKII-dependent regulation of cardiac Na(+) homeostasis. Front Pharmacol 5:41
63. Belardinelli L, Giles WR, Rajamani S, Karagueuzian HS, Shryock JC (2015) Cardiac late Na(+) current: proarrhythmic effects, roles in long QT syndromes, and pathological relationship to CaMKII and oxidative stress. Heart Rhythm 12(2):440–448
64. Luthi A, McCormick DA (1999) Modulation of a pacemaker current through Ca^{2+}-induced stimulation of cAMP production. Nat Neurosci 2(7):634–641
65. Halls ML, Cooper DM (2011) Regulation by Ca^{2+}−signaling pathways of adenylyl cyclases. Cold Spring Harb Perspect Biol 3(1):a004143
66. Wang H, Zhang M (2012) The role of Ca(2)(+)-stimulated adenylyl cyclases in bidirectional synaptic plasticity and brain function. Rev Neurosci 23(1):67–78
67. Mattick P, Parrington J, Odia E, Simpson A, Collins T, Terrar D (2007) Ca^{2+}−stimulated adenylyl cyclase isoform AC1 is preferentially expressed in guinea-pig sino-atrial node cells and modulates the I(f) pacemaker current. J Physiol 582(Pt 3):1195–1203
68. Younes A, Lyashkov AE, Graham D, Sheydina A, Volkova MV, Mitsak M et al (2008) Ca^{2+}-stimulated basal adenylyl cyclase activity localization in membrane lipid microdomains of cardiac sinoatrial nodal pacemaker cells. J Biol Chem 283(21):14461–14468
69. Boink GJ, Nearing BD, Shlapakova IN, Duan L, Kryukova Y, Bobkov Y et al (2012) Ca^{2+}-stimulated adenylyl cyclase AC1 generates efficient biological pacing as single gene therapy and in combination with HCN2. Circulation 126(5):528–536
70. Timofeyev V, Myers RE, Kim HJ, Woltz RL, Sirish P, Heiserman JP et al (2013) Adenylyl cyclase subtype-specific compartmentalization: differential regulation of L-type Ca^{2+} current in ventricular myocytes. Circ Res 112(12):1567–1576
71. Cheung WY (1980) Calmodulin plays a pivotal role in cellular regulation. Science 207(4426):19–27
72. Lukyanenko YO, Younes A, Lyashkov AE, Tarasov KV, Riordon DR, Lee J et al (2016) Ca^{2+}/calmodulin-activated phosphodiesterase 1A is highly expressed in rabbit cardiac sinoatrial nodal cells and regulates pacemaker function. J Mol Cell Cardiol 98:73–82
73. Tham YK, Bernardo BC, Ooi JY, Weeks KL, McMullen JR (2015) Pathophysiology of cardiac hypertrophy and heart failure: signaling pathways and novel therapeutic targets. Arch Toxicol 89(9):1401–1438
74. Knight WE, Chen S, Zhang Y, Oikawa M, Wu M, Zhou Q et al (2016) PDE1C deficiency antagonizes pathological cardiac remodeling and dysfunction. Proc Natl Acad Sci U S A 113(45):E7116–E7E25
75. Forstermann U, Sessa WC (2012) Nitric oxide synthases: regulation and function. Eur Heart J 33(7):829–837, 37a–37d
76. Casadei B (2006) The emerging role of neuronal nitric oxide synthase in the regulation of myocardial function. Exp Physiol 91(6):943–955
77. Zhang YH (2017) Nitric oxide signalling and neuronal nitric oxide synthase in the heart under stress. F1000 Res 6:742
78. Fabiato A (1992) Two kinds of calcium-induced release of calcium from the sarcoplasmic reticulum of skinned cardiac cells. Adv Exp Med Biol 311:245–262
79. Lipp P, Laine M, Tovey SC, Burrell KM, Berridge MJ, Li W et al (2000) Functional InsP3 receptors that may modulate excitation-contraction coupling in the heart. Curr Biol: CB 10(15):939–942

80. Zima AV, Blatter LA (2004) Inositol-1,4,5-trisphosphate-dependent Ca^{2+} signalling in cat atrial excitation-contraction coupling and arrhythmias. J Physiol 555(Pt 3):607–615
81. Yao Y, Choi J, Parker I (1995) Quantal puffs of intracellular Ca^{2+} evoked by inositol trisphosphate in xenopus oocytes. J Physiol 482(Pt 3):533–553
82. Li X, Zima AV, Sheikh F, Blatter LA, Chen J (2005) Endothelin-1-induced arrhythmogenic Ca^{2+} signaling is abolished in atrial myocytes of inositol-1,4,5-trisphosphate(IP3)-receptor type 2-deficient mice. Circ Res 96(12):1274–1281
83. Wang YG, Dedkova EN, Ji X, Blatter LA, Lipsius SL (2005) Phenylephrine acts via IP3-dependent intracellular NO release to stimulate L-type Ca^{2+} current in cat atrial myocytes. J Physiol 567(Pt 1):143–157
84. Collins TP, Mikoshiba K, Terrar DA (2007) Possible novel mechanism for the positive inotropic action of alpha-1 adrenoceptor agonists in guinea-pig isolated atrial myocytes. Biophys J:433A–433A
85. Terrar DA, Capel RA, Collins TP, Rajasumdaram S, Ayagamar T, Burton RAB (2018) Cross talk between IP3 and adenylyl cyclase signaling pathways in cardiac atrial Myocytes. Biophys J 114(3):466A–466A
86. Kockskamper J, Zima AV, Roderick HL, Pieske B, Blatter LA, Bootman MD (2008) Emerging roles of inositol 1,4,5-trisphosphate signaling in cardiac myocytes. J Mol Cell Cardiol 45(2):128–147
87. Berridge MJ (2009) Inositol trisphosphate and calcium signalling mechanisms. Biochim Biophys Acta 1793(6):933–940
88. Hohendanner F, McCulloch AD, Blatter LA, Michailova AP (2014) Calcium and IP3 dynamics in cardiac myocytes: experimental and computational perspectives and approaches. Front Pharmacol 5:35
89. Garcia MI, Boehning D (2017) Cardiac inositol 1,4,5-trisphosphate receptors. Biochim Biophys Acta 1864(6):907–914
90. Domeier TL, Zima AV, Maxwell JT, Huke S, Mignery GA, Blatter LA (2008) IP3 receptor-dependent Ca^{2+} release modulates excitation-contraction coupling in rabbit ventricular myocytes. Am J Physiol Heart Circ Physiol 294(2):H596–H604
91. Subedi KP, Son MJ, Chidipi B, Kim SW, Wang J, Kim KH et al (2017) Signaling pathway for endothelin-1- and phenylephrine-induced cAMP response element binding protein activation in rat ventricular Myocytes: role of inositol 1,4,5-Trisphosphate receptors and CaMKII. Cell Physiol Biochem 41(1):399–412
92. Hirose M, Stuyvers B, Dun W, Ter Keurs H, Boyden PA (2008) Wide long lasting perinuclear Ca^{2+} release events generated by an interaction between ryanodine and IP3 receptors in canine Purkinje cells. J Mol Cell Cardiol 45(2):176–184
93. Zima AV, Bare DJ, Mignery GA, Blatter LA (2007) IP3-dependent nuclear Ca^{2+} signalling in the mammalian heart. J Physiol 584(Pt 2):601–611
94. Ju YK, Liu J, Lee BH, Lai D, Woodcock EA, Lei M et al (2011) Distribution and functional role of inositol 1,4,5-trisphosphate receptors in mouse sinoatrial node. Circ Res 109(8):848–857
95. Ju YK, Woodcock EA, Allen DG, Cannell MB (2012) Inositol 1,4,5-trisphosphate receptors and pacemaker rhythms. J Mol Cell Cardiol 53(3):375–381
96. Hohendanner F, Walther S, Maxwell JT, Kettlewell S, Awad S, Smith GL et al (2015) Inositol-1,4,5-trisphosphate induced Ca^{2+} release and excitation-contraction coupling in atrial myocytes from normal and failing hearts. J Physiol 593(6):1459–1477
97. Kim JC, Woo SH (2015) Shear stress induces a longitudinal Ca^{2+} wave via autocrine activation of P2Y1 purinergic signalling in rat atrial myocytes. J Physiol 593(23):5091–5109
98. Son MJ, Kim JC, Kim SW, Chidipi B, Muniyandi J, Singh TD et al (2016) Shear stress activates monovalent cation channel transient receptor potential melastatin subfamily 4 in rat atrial myocytes via type 2 inositol 1,4,5-trisphosphate receptors and Ca^{2+} release. J Physiol 594(11):2985–3004
99. Lee HC (2001) Physiological functions of cyclic ADP-ribose and NAADP as calcium messengers. Annu Rev Pharmacol Toxicol 41:317–345

100. Higashida H, Salmina AB, Olovyannikova RY, Hashii M, Yokoyama S, Koizumi K et al (2007) Cyclic ADP-ribose as a universal calcium signal molecule in the nervous system. Neurochem Int 51(2–4):192–199
101. Lee HC (2012) Cyclic ADP-ribose and nicotinic acid adenine dinucleotide phosphate (NAADP) as messengers for calcium mobilization. J Biol Chem 287(38):31633–31640
102. Wei W, Graeff R, Yue J (2014) Roles and mechanisms of the CD38/cyclic adenosine diphosphate ribose/Ca^{2+} signaling pathway. World J Biol Chem 5(1):58–67
103. Galione A (2015) A primer of NAADP-mediated Ca^{2+} signalling: from sea urchin eggs to mammalian cells. Cell Calcium 58(1):27–47
104. Rakovic S, Terrar DA (2002) Calcium signaling by cADPR in cardiac myocytes. In: Lee HC (ed) Cyclic ADP-ribose and NAADP. Structures, metabolism and functions. Kluwer, Dordecht, pp 319–341
105. Terrar DA (2015) The roles of NAADP, two-pore channels and lysosomes in Ca^{2+} signaling in cardiac muscle. Messenger 4:23–33
106. Meszaros LG, Bak J, Chu A (1993) Cyclic ADP-ribose as an endogenous regulator of the non-skeletal type ryanodine receptor Ca^{2+} channel. Nature 364(6432):76–79
107. Sitsapesan R, McGarry SJ, Williams AJ (1994) Cyclic ADP-ribose competes with ATP for the adenine nucleotide binding site on the cardiac ryanodine receptor Ca^{2+}-release channel. Circ Res 75(3):596–600
108. Rusinko N, Lee HC (1989) Widespread occurrence in animal tissues of an enzyme catalyzing the conversion of NAD+ into a cyclic metabolite with intracellular Ca^{2+}−mobilizing activity. J Biol Chem 264(20):11725–11731
109. Walseth TF, Aarhus R, Zeleznikar RJ Jr, Lee HC (1991) Determination of endogenous levels of cyclic ADP-ribose in rat tissues. Biochim Biophys Acta 1094(1):113–120
110. Meszaros V, Socci R, Meszaros LG (1995) The kinetics of cyclic ADP-ribose formation in heart muscle. Biochem Biophys Res Commun 210(2):452–456
111. Higashida H, Egorova A, Higashida C, Zhong ZG, Yokoyama S, Noda M et al (1999) Sympathetic potentiation of cyclic ADP-ribose formation in rat cardiac myocytes. J Biol Chem 274(47):33348–33354
112. Kolstad TR, Stokke MK, Stang E, Brorson SH, William LE, Sejersted OM (2015) Serca located in the junctional SR shapes calcium release in cardiac myocytes. Biophys J 108(2):503A–503A
113. Lewis AM, Aley PK, Roomi A, Thomas JM, Masgrau R, Garnham C et al (2012) Beta-adrenergic receptor signaling increases NAADP and cADPR levels in the heart. Biochem Biophys Res Commun 427(2):326–329
114. Higashida H, Zhang J, Hashii M, Shintaku M, Higashida C, Takeda Y (2000) Angiotensin II stimulates cyclic ADP-ribose formation in neonatal rat cardiac myocytes. Biochem J 352(Pt 1):197–202
115. Ferrero E, Lo Buono N, Horenstein AL, Funaro A, Malavasi F (2014) The ADP-ribosyl cyclases–the current evolutionary state of the ARCs. Front Biosci 19:986–1002
116. Gul R, Kim SY, Park KH, Kim BJ, Kim SJ, Im MJ et al (2008) A novel signaling pathway of ADP-ribosyl cyclase activation by angiotensin II in adult rat cardiomyocytes. Am J Physiol Heart Circ Physiol 295(1):H77–H88
117. Gul R, Park JH, Kim SY, Jang KY, Chae JK, Ko JK et al (2009) Inhibition of ADP-ribosyl cyclase attenuates angiotensin II-induced cardiac hypertrophy. Cardiovasc Res 81(3):582–591
118. Gul R, Park DR, Shawl AI, Im SY, Nam TS, Lee SH et al (2016) Nicotinic Acid Adenine Dinucleotide Phosphate (NAADP) and Cyclic ADP-Ribose (cADPR) mediate Ca^{2+} signaling in cardiac hypertrophy induced by beta-adrenergic stimulation. PLoS One 11(3):e0149125
119. Kannt A, Sicka K, Kroll K, Kadereit D, Gogelein H (2012) Selective inhibitors of cardiac ADPR cyclase as novel anti-arrhythmic compounds. Naunyn Schmiedeberg's Arch Pharmacol 385(7):717–727
120. Walseth TF, Lee HC (1993) Synthesis and characterization of antagonists of cyclic-ADP-ribose-induced Ca^{2+} release. Biochim Biophys Acta 1178(3):235–242

121. Rakovic S, Galione A, Ashamu GA, Potter BV, Terrar DA (1996) A specific cyclic ADP-ribose antagonist inhibits cardiac excitation-contraction coupling. Curr Biol: CB 6(8):989–996
122. Iino S, Cui Y, Galione A, Terrar DA (1997) Actions of cADP-ribose and its antagonists on contraction in guinea pig isolated ventricular myocytes. Influence Temp Circ Res 81(5):879–884
123. Cui Y, Galione A, Terrar DA (1999) Effects of photoreleased cADP-ribose on calcium transients and calcium sparks in myocytes isolated from guinea-pig and rat ventricle. Biochem J 342(Pt 2):269–273
124. Macgregor AT, Rakovic S, Galione A, Terrar DA (2007) Dual effects of cyclic ADP-ribose on sarcoplasmic reticulum Ca^{2+} release and storage in cardiac myocytes isolated from guinea-pig and rat ventricle. Cell Calcium 41(6):537–546
125. Prakash YS, Kannan MS, Walseth TF, Sieck GC (2000) cADP ribose and $[Ca^{2+}](i)$ regulation in rat cardiac myocytes. Am J Physiol Heart Circ Physiol 279(4):H1482–H1489
126. Guo X, Laflamme MA, Becker PL (1996) Cyclic ADP-ribose does not regulate sarcoplasmic reticulum Ca^{2+} release in intact cardiac myocytes. Circ Res 79(1):147–151
127. Lukyanenko V, Gyorke I, Wiesner TF, Gyorke S (2001) Potentiation of Ca^{2+} release by cADP-ribose in the heart is mediated by enhanced SR Ca^{2+} uptake into the sarcoplasmic reticulum. Circ Res 89(7):614–622
128. Gomez AM, Cheng H, Lederer WJ, Bers DM (1996) Ca^{2+} diffusion and sarcoplasmic reticulum transport both contribute to $[Ca^{2+}]$i decline during Ca^{2+} sparks in rat ventricular myocytes. J Physiol 496(Pt 2):575–581
129. Lee HC, Aarhus R, Graeff R, Gurnack ME, Walseth TF (1994) Cyclic ADP ribose activation of the ryanodine receptor is mediated by calmodulin. Nature 370(6487):307–309
130. Lee HC, Aarhus R, Graeff RM (1995) Sensitization of calcium-induced calcium release by cyclic ADP-ribose and calmodulin. J Biol Chem 270(16):9060–9066
131. Tanaka Y, Tashjian AH Jr (1995) Calmodulin is a selective mediator of Ca^{2+}-induced Ca^{2+} release via the ryanodine receptor-like Ca^{2+} channel triggered by cyclic ADP-ribose. Proc Natl Acad Sci U S A 92(8):3244–3248
132. Takasawa S, Ishida A, Nata K, Nakagawa K, Noguchi N, Tohgo A et al (1995) Requirement of calmodulin-dependent protein kinase II in cyclic ADP-ribose-mediated intracellular Ca^{2+} mobilization. J Biol Chem 270(51):30257–30259
133. Thomas JM, Summerhill RJ, Fruen BR, Churchill GC, Galione A (2002) Calmodulin dissociation mediates desensitization of the cADPR-induced Ca^{2+} release mechanism. Curr Biol: CB 12(23):2018–2022
134. Zhang X, Tallini YN, Chen Z, Gan L, Wei B, Doran R et al (2009) Dissociation of FKBP12.6 from ryanodine receptor type 2 is regulated by cyclic ADP-ribose but not beta-adrenergic stimulation in mouse cardiomyocytes. Cardiovasc Res 84(2):253–262
135. Rakovic S, Cui Y, Iino S, Galione A, Ashamu GA, Potter BV et al (1999) An antagonist of cADP-ribose inhibits arrhythmogenic oscillations of intracellular Ca^{2+} in heart cells. J Biol Chem 274(25):17820–17827
136. Gul R, Shawl AI, Kim SH, Kim UH (2012) Cooperative interaction between reactive oxygen species and Ca^{2+} signals contributes to angiotensin II-induced hypertrophy in adult rat cardiomyocytes. Am J Physiol Heart Circ Physiol 302(4):H901–H909
137. Bak J, Billington RA, Timar G, Dutton AC, Genazzani AA (2001) NAADP receptors are present and functional in the heart. Curr Biol: CB 11(12):987–990
138. Chini EN, Dousa TP (1995) Enzymatic synthesis and degradation of nicotinate adenine dinucleotide phosphate (NAADP), a Ca^{2+}-releasing agonist, in rat tissues. Biochem Biophys Res Commun 209(1):167–174
139. Chini EN, Chini CC, Kato I, Takasawa S, Okamoto H (2002) CD38 is the major enzyme responsible for synthesis of nicotinic acid-adenine dinucleotide phosphate in mammalian tissues. Biochem J 362(Pt 1):125–130
140. Vasudevan SR, Galione A, Churchill GC (2008) Sperm express a Ca^{2+}−regulated NAADP synthase. Biochem J 411(1):63–70

141. Galfre E, Pitt SJ, Venturi E, Sitsapesan M, Zaccai NR, Tsaneva-Atanasova K et al (2012) FKBP12 activates the cardiac ryanodine receptor Ca^{2+}−release channel and is antagonised by FKBP12.6. PLoS One 7(2):e31956
142. Macgregor A, Yamasaki M, Rakovic S, Sanders L, Parkesh R, Churchill GC et al (2007) NAADP controls cross-talk between distinct Ca^{2+} stores in the heart. J Biol Chem 282(20):15302–15311
143. Zhao YJ, Zhang HM, Lam CM, Hao Q, Lee HC (2011) Cytosolic CD38 protein forms intact disulfides and is active in elevating intracellular cyclic ADP-ribose. J Biol Chem 286(25):22170–22177
144. Zhao YJ, Lam CM, Lee HC (2012) The membrane-bound enzyme CD38 exists in two opposing orientations. Sci Signal 5(241):ra67
145. Zhao YJ, Zhu WJ, Wang XW, Zhang LH, Lee HC (2015) Determinants of the membrane orientation of a calcium signaling enzyme CD38. Biochim Biophys Acta 1853(9):2095–2103
146. Churchill GC, Okada Y, Thomas JM, Genazzani AA, Patel S, Galione A (2002) NAADP mobilizes Ca^{2+} from reserve granules, lysosome-related organelles, in sea urchin eggs. Cell 111(5):703–708
147. Repnik U, Cesen MH, Turk B (2013) The endolysosomal system in cell death and survival. Cold Spring Harb Perspect Biol 5(1):a008755
148. Ruas M, Rietdorf K, Arredouani A, Davis LC, Lloyd-Evans E, Koegel H et al (2010) Purified TPC isoforms form NAADP receptors with distinct roles for Ca^{2+} signaling and endolysosomal trafficking. Curr Biol: CB 20(8):703–709
149. Ruas M, Davis LC, Chen CC, Morgan AJ, Chuang KT, Walseth TF et al (2015) Expression of Ca(2)(+)-permeable two-pore channels rescues NAADP signalling in TPC-deficient cells. EMBO J 34(13):1743–1758
150. Wang X, Zhang X, Dong XP, Samie M, Li X, Cheng X et al (2012) TPC proteins are phosphoinositide- activated sodium-selective ion channels in endosomes and lysosomes. Cell 151(2):372–383
151. Jentsch TJ, Hoegg-Beiler MB, Vogt J (2015) Departure gate of acidic Ca(2)(+) confirmed. EMBO J 34(13):1737–1739
152. Capel RA, Bolton EL, Lin WK, Aston D, Wang Y, Liu W et al (2015) Two-pore channels (TPC2s) and nicotinic acid adenine dinucleotide phosphate (NAADP) at Lysosomal-sarcoplasmic reticular junctions contribute to acute and chronic beta-adrenoceptor signaling in the heart. J Biol Chem 290(50):30087–30098
153. Naylor E, Arredouani A, Vasudevan SR, Lewis AM, Parkesh R, Mizote A et al (2009) Identification of a chemical probe for NAADP by virtual screening. Nat Chem Biol 5(4):220–226
154. Davidson SM, Foote K, Kunuthur S, Gosain R, Tan N, Tyser R et al (2015) Inhibition of NAADP signalling on reperfusion protects the heart by preventing lethal calcium oscillations via two-pore channel 1 and opening of the mitochondrial permeability transition pore. Cardiovasc Res 108(3):357–366
155. Djerada Z, Millart H (2013) Intracellular NAADP increase induced by extracellular NAADP via the P2Y11-like receptor. Biochem Biophys Res Commun 436(2):199–203
156. Djerada Z, Peyret H, Dukic S, Millart H (2013) Extracellular NAADP affords cardioprotection against ischemia and reperfusion injury and involves the P2Y11-like receptor. Biochem Biophys Res Commun 434(3):428–433
157. Cancela JM, Churchill GC, Galione A (1999) Coordination of agonist-induced Ca^{2+}−signalling patterns by NAADP in pancreatic acinar cells. Nature 398(6722):74–76
158. Parkesh R, Lewis AM, Aley PK, Arredouani A, Rossi S, Tavares R et al (2008) Cell-permeant NAADP: a novel chemical tool enabling the study of Ca^{2+} signalling in intact cells. Cell Calcium 43(6):531–538
159. Nebel M, Schwoerer AP, Warszta D, Siebrands CC, Limbrock AC, Swarbrick JM et al (2013) Nicotinic acid adenine dinucleotide phosphate (NAADP)-mediated calcium signaling and arrhythmias in the heart evoked by beta-adrenergic stimulation. J Biol Chem 288(22):16017–16030

160. Warszta D, Nebel M, Fliegert R, Guse AH (2014) NAD derived second messengers: role in spontaneous diastolic Ca^{2+} transients in murine cardiac myocytes. DNA Repair 23:69–78
161. Collins TP, Bayliss R, Churchill GC, Galione A, Terrar DA (2011) NAADP influences excitation-contraction coupling by releasing calcium from lysosomes in atrial myocytes. Cell Calcium 50(5):449–458
162. Zhu MX, Ma J, Parrington J, Calcraft PJ, Galione A, Evans AM (2010) Calcium signaling via two-pore channels: local or global, that is the question. Am J Physiol Cell Physiol 298(3):C430–C441
163. Kinnear NP, Boittin FX, Thomas JM, Galione A, Evans AM (2004) Lysosome-sarcoplasmic reticulum junctions. A trigger zone for calcium signaling by nicotinic acid adenine dinucleotide phosphate and endothelin-1. J Biol Chem 279(52):54319–54326

Chapter 17
Molecular Basis and Regulation of Store-Operated Calcium Entry

Jose J. Lopez, Isaac Jardin, Letizia Albarrán, Jose Sanchez-Collado, Carlos Cantonero, Gines M. Salido, Tarik Smani, and Juan A. Rosado

Abstract Store-operated Ca^{2+} entry (SOCE) is a ubiquitous mechanism for Ca^{2+} influx in mammalian cells with important physiological implications. Since the discovery of SOCE more than three decades ago, the mechanism that communicates the information about the amount of Ca^{2+} accumulated in the intracellular Ca^{2+} stores to the plasma membrane channels and the nature of these channels have been matters of intense investigation and debate. The stromal interaction molecule-1 (STIM1) has been identified as the Ca^{2+} sensor of the intracellular Ca^{2+} compartments that activates the store-operated channels. STIM1 regulates two types of store-dependent channels: the Ca^{2+} release-activated Ca^{2+} (CRAC) channels, formed by Orai1 subunits, that conduct the highly Ca^{2+} selective current I_{CRAC} and the cation permeable store-operated Ca^{2+} (SOC) channels, which consist of Orai1 and TRPC1 proteins and conduct the non-selective current I_{SOC}. While the crystal structure of *Drosophila* CRAC channel has already been solved, the architecture of the SOC channels still remains unclear. The dynamic interaction of STIM1 with the store-operated channels is modulated by a number of proteins that either support the formation of the functional STIM1-channel complex or protect the cell against Ca^{2+} overload.

Keywords SOCE · Orai · STIM · CRAC · Transient receptor potential (TRP) channels

J. J. Lopez · I. Jardin (✉) · L. Albarrán · J. Sanchez-Collado · C. Cantonero · G. M. Salido · J. A. Rosado
Department of Physiology, Cell Physiology Research Group and Institute of Molecular Pathology Biomarkers, University of Extremadura, Cáceres, Spain
e-mail: ijp@unex.es

T. Smani
Department of Medical Physiology and Biophysics and Group of Cardiovascular Pathophysiology, Institute of Biomedicine of Sevilla (IBiS), Hospital Universitario Virgen del Rocío/CSIC/University of Sevilla, Sevilla, Spain

M. S. Islam (ed.), *Calcium Signaling*, Advances in Experimental Medicine and Biology 1131, https://doi.org/10.1007/978-3-030-12457-1_17

Abbreviations

$[Ca^{2+}]_c$	cytosolic free Ca^{2+} concentration
AMPA	alpha-amino-3-hydroxy-5-methylisoxazole-4-propionate
CRAC channels	Ca^{2+}-release activated Ca^{2+} channels
CTID	C-terminal inhibitory domain
ER	endoplasmic reticulum
IP_3	inositol 1,4,5-trisphosphate
NAADP	nicotinic acid adenine dinucleotide phosphate
NMDA	N-methyl-D-aspartate
OAG	1-oleoyl-2-acetyl-sn-glycerol
PM	plasma membrane
ROC	receptor-operated channels
ROS	reactive oxygen species
SERCA	sarco/endoplasmic reticulum Ca^{2+} ATPase
SMOC	second messenger-operated channels
SOAP	STIM1-Orai1 Association Pocket
SOC channels	store-operated Ca^{2+} channels
SOCE	store-operated Ca^{2+} entry

17.1 Receptor-Operated Calcium Entry

Among the second messengers that mediate the function of cellular agonists, cytosolic free-Ca^{2+} stands out both for its versatility and ubiquity. In contrast to other intracellular messengers, Ca^{2+} signals do not depend on the reversible generation or covalent modification of signalling molecules but on the transport of Ca^{2+} across membranes. Cellular agonists increase cytosolic free-Ca^{2+} concentration ($[Ca^{2+}]_c$) either by releasing compartmentalized Ca^{2+} and/or by promoting Ca^{2+} influx from the extracellular medium through plasma membrane (PM) channels [1]. Both mechanisms occur in favour of an electrochemical gradient and, therefore, do not consume energy. Once cellular stimulation is terminated a number of mechanisms, involved in the recovery and maintenance of low resting $[Ca^{2+}]_c$, activate in order to allow further Ca^{2+} signals and to prevent cytosolic Ca^{2+} overload. Ca^{2+} removal from the cytosol is mediated by different mechanisms that includes Ca^{2+} reuptake by the sarco/endoplasmic reticulum Ca^{2+}-ATPase (SERCA) into intracellular organelles, especially the sarcoplasmic/endoplasmic reticulum [2, 3] and a variety of acidic, lysosome-related, organelles [4, 5]. SERCA pumps are also responsible to maintain a low resting $[Ca^{2+}]_c$ by opposing Ca^{2+} leak into the cytosol from the intracellular stores [6]. Further mechanisms for cytosolic Ca^{2+} clearance includes Ca^{2+} extrusion across the PM through the collaborative actions of the plasma membrane Ca^{2+}-ATPase and the Na^+/Ca^{2+} exchangers [7] (Fig. 17.1), as well as mitochondrial Ca^{2+} uptake, which also shapes the responses to agonists.

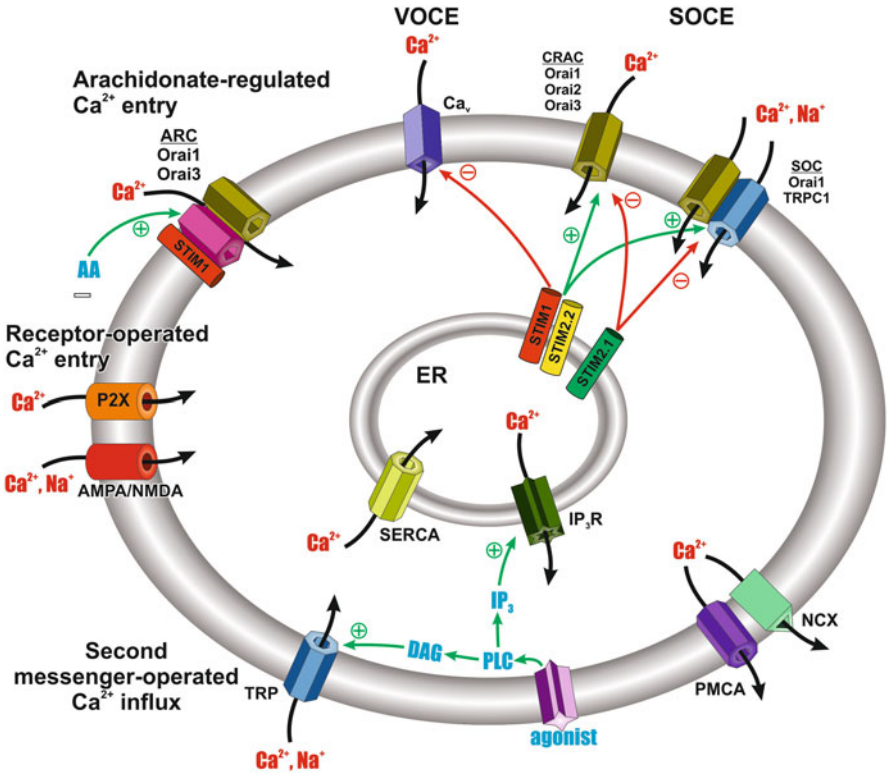

Fig. 17.1 Schematic representation of the main cellular Ca^{2+} entry mechanims. Cell stimulation with physiological agonists results in the activation of phospholipase C (PLC), which, in turn, leads to the generation of inositol 1,4,5 trisphosphate (IP_3) and diacylglycerol (DAG). IP_3 releases Ca^{2+} from intracellular stores, which results in the activation of store-operated Ca^{2+} entry (SOCE)via CRAC and SOC channels through the participation of STIM1 and STIM2.2 isoforms and the modulator STIM2.1. On the other hand, DAG is the endogenous activator of certain TRP channels that participate in second messenger-operated Ca^{2+} influx. PLA_2-generated arachidonate activates a Ca^{2+} selective channel formed by Orai1 and Orai3 subunits named arachidonate-regulated channels (ARC). Agonists might also induce direct receptor-operated Ca^{2+} entry gating ionotropic receptors such as purinergic P2X and AMPA o NMDA glutamate receptors. Finally, voltage-operated Ca^{2+} channels play a major role in Ca^{2+} entry in electrically excitable cells. Calcium removal from the cytosol is mediated by ATPases and transporters, such as the sarco/endoplasmic reticulum Ca^{2+} ATPase (SERCA), the plasma membrane Ca^{2+} ATPase (PMCA) and the Na^+/Ca^{2+} exchangers

Physiological agonists induce Ca^{2+} release from intracellular compartments through the generation of a variety of signalling molecules that gate Ca^{2+} channels located in the membrane of the internal Ca^{2+} stores, i.e. the ER, secretory granules and lysosome-related organelles. Ca^{2+}-releasing molecules include the inositol 1,4,5-trisphosphate (IP_3), nicotinic acid adenine dinucleotide phosphate (NAADP), cyclic ADP ribose or sphingosine 1-phosphate [8, 9]. Given the negligible electrical

potential across the ER membrane [10], Ca^{2+} efflux from this organelles is only driven by a chemical gradient generated by SERCA pumps. This is most likely the mechanism involved in Ca^{2+} efflux from secretory vesicles and lysosome-related organelles, where a slightly positive membrane potential (lumen positive) has been reported [11, 12].

Ca^{2+} efflux from finite intracellular compartments is transient and sometimes insufficient for the activation of certain cellular processes that require higher or more sustained rises in $[Ca^{2+}]_c$. In this context Ca^{2+} entry through PM Ca^{2+}-permeable channels plays an essential functional role. Ca^{2+} influx leads to more sustained and/or greater increase in $[Ca^{2+}]_c$, which is required for intracellular Ca^{2+} store refilling and full activation of certain cellular processes. Extracellular Ca^{2+} might enter the cell by different mechanisms including voltage-operated Ca^{2+} entry and receptor-operated Ca^{2+} entry.

Voltage-operated Ca^{2+} entry takes place in electrically excitable cells where membrane depolarization leads to the opening of Ca^{2+} channels, which, in turn, results in Ca^{2+} transients that initiate different physiological events (Fig.17.1). Voltage-operated Ca^{2+} channels are heteromeric complexes where the pore-forming $\alpha 1$ subunits consists of four repeated domains, each containing six transmembrane domains (S1–S6) and a loop between transmembrane segments S5 and S6. The channel also contains an intracellular β subunit, a disulphide-linked $\alpha 2\delta$ dimer and a transmembrane γ subunit [13]. Voltage-operated Ca^{2+} channels are named according to the principal permeation ion (Ca) followed by the principal physiological modulator, i.e. voltage (v) as a subscript (Ca_v), then the numerical order corresponds to the nomenclature of the $\alpha 1$ subunit [14]. According to this nomenclature, three subfamilies have been described: Ca_v1, which mediate L-type Ca^{2+} currents, Ca_v2, responsible of the P/Q-type, N-type and R-type currents, and Ca_v3, which mediate T-type Ca^{2+} currents [15].

Despite a functional expression of voltage-gated Ca^{2+} channels has been reported in a variety of electrically nonexcitable cells, such as T and B lymphocytes and mast cells [16–19], their role in cell biology is not as relevant as in excitable cells. In non-excitable cells, Ca^{2+} influx is mostly mediated by receptor-operated pathways. Heterologous regulation of voltage-operated channels upon activation of certain receptor-operated pathways has been described, where STIM1, the ER Ca^{2+} sensor for the activation of SOCE, induces inactivation of voltage-gated Ca^{2+} channels [20, 21] (Fig. 17.1). Receptor-operated Ca^{2+} entry groups the pathways for Ca^{2+} influx activated by membrane receptor occupation. This includes the Ca^{2+} currents that occurs by gating the receptor-channel itself, the properly named receptor-operated Ca^{2+} channels (ROC) and the currents via second messenger-operated channels (SMOC) or store-operated channels [22].

Receptor-operated Ca^{2+} entry occurs through a number of Ca^{2+} permeable ionotropic receptors activated by different ligands, such as the purinergic P2X receptors [23] or the N-methyl-D-aspartate (NMDA) and alpha-amino-3-hydroxy-5-methylisoxazole-4-propionate (AMPA) receptors activated by glutamate [24–26] (Fig. 17.1). On the other hand, second messenger-operated Ca^{2+} entry is medi-

ated by Ca^{2+}-permeable SMOCs activated by diffusible messengers, which are generated by receptor occupation. Among the second messengers that have been reported to gate SMOCs are the phospholipase C product diacylglycerol, or its membrane permeant analogue 1-oleoyl-2-acetyl-sn-glycerol (OAG) [27–30], cyclic ADP ribose [31] or arachidonate [32–35]. The function of different SMOCs is modulated by phosphoinositides, such as phosphatidylinositol 4,5-bisphosphate [36, 37]. The third major pathway for Ca^{2+} influx activated by receptor occupation is store-operated Ca^{2+} entry (SOCE), a route regulated by the Ca^{2+} concentration into the agonist-sensitive stores [38].

17.2 Store-Operated Ca^{2+} Entry

Probably the most ubiquitous mechanism for receptor-operated Ca^{2+} influx is store-operated Ca^{2+} entry (SOCE), a mechanism for the entry of Ca^{2+} across PM-resident channels that is activated when the Ca^{2+} concentration decreases in the intracellular Ca^{2+} stores [39]. SOCE has been demonstrated upon discharge of different agonist-sensitive intracellular Ca^{2+} pools, including the ER [40] and bafilomycin A1-sensitive acidic compartments [41]. Store-operated or "capacitative" Ca^{2+} entry was initially proposed by Putney in 1986 [40] as a mechanism for Ca^{2+} influx regulated by the filling state of the intracellular Ca^{2+} stores. A previous study by Casteels and Droogmans reported similar observations in vascular smooth muscle cells, suggesting two pathways for the transport of Ca^{2+} from the extracellular medium to the noradrenalin-sensitive intracellular store including a direct route into the store [42]. This hypothesis, which limited the role of SOCE to the refilling of the intracellular Ca^{2+} compartments during or after agonist stimulation, was later on demonstrated to be imprecise as reported by Kwan and co-workers in 1990 [43]. In this study the authors used lanthanum to prevent Ca^{2+} entry and extrusion and demonstrated that Ca^{2+} released into the cytoplasm could replenish the stores. These findings provide initial evidence that the refilling process does not involve a direct route into the intracellular stores but rather is the result of a sequential Ca^{2+} transport into the cytoplasm and subsequent uptake from the stores by SERCA pumps [43, 44]. Therefore, SOCE is a relevant mechanism for Ca^{2+} store refilling and is also essential to sustain a number of cellular functions, including cell proliferation, differentiation, platelet aggregation and secretion, contraction or migration [45–52]. The study by Kwan and co-workers also provided a key conceptual characteristic of SOCE, by demonstrating that SOCE does not require the synthesis of IP_3 since Ca^{2+} influx mediated by methacholine and thapsigargin, an inhibitor of SERCA that is unable to increase the cellular level of IP_3, was mediated by the same mechanism activated by the discharge of the intracellular Ca^{2+} stores [43].

Since the identification of SOCE both the nature of the channels in the PM and the mechanism of activation of Ca^{2+} influx have been widely investigated. Early studies on the activation mechanism led to a variety of mutually exclusive

hypotheses that can be grouped into (1) those suggesting a constitutive conformational coupling between elements in the ER and the PM, (2) the indirect coupling between the ER and the PM via diffusible messengers, (3) the insertion in the PM of preformed channels located in internal vesicles and (4) a reversible *de novo* conformational coupling between a Ca^{2+} sensor in the ER and the Ca^{2+} channels in the PM [53]. In 2005, the *ST*romal *I*nteraction *M*olecule-1 (STIM1) was identified as the ER Ca^{2+} sensor, using an RNA interference-based screen to identify genes involved in thapsigargin-evoked Ca^{2+} entry [54]. Furthermore, it was found that STIM1 communicates the information about the filling state of the ER to the SOC channels, as demonstrated by immunofluorescence, electron microscopy and EF-hand mutants of STIM1 that result in store-independent SOCE activation [55] (Fig. 17.1).

17.3 STIM1

Human STIM1 is a type-1 transmembrane protein of 685 amino acids that was initially reported to be involved in cell-to-cell interaction [56] and cell growth suppression with a relevant role in tumoral progression [57, 58]. STIM1 has been presented as a 90-kDa phosphoprotein ubiquitously expressed in the PM as well as in intracellular membranes of a number of human primary and tumoral cells [59]. The C-terminal region of STIM1 is cytosolic whatever its location (ER or PM), while the N-terminal region is located either in the ER lumen (for STIM1 located in the ER membrane) or the extracellular medium (for PM-resident STIM1) [60–62]. Structural studies revealed several functional domains in the STIM1 N-terminal region, including an ER signal peptide (aa 1–22), a canonical EF-hand Ca^{2+}-binding motif (aa 63–96) as well as a hidden EF-hand (aa 97–128), and a sterile alpha motif (SAM; aa 132–200) that plays an important role in protein-protein interaction [63–65]. STIM1 transmembrane domain (aa 214–234) is followed by the cytosolic region, which contains an ezrin/radixin/moesin domain, highly conserved among the STIM proteins. This region includes three coiled-coil domains, named CC1 (aa 238–342), CC2 (aa 364–389) and CC3 (aa 399–423), a CRAC-modulatory domain (aa 470–491), a proline/serine-rich region (aa 600–629), and a polybasic lysine-rich region (aa 671–685) [66–70].

The key region of STIM1 for the interaction with the store-operated channels was identified almost at the same time by four research groups. This region overlaps with the coiled-coil domains present in the cytosolic region of STIM1 and received different names: SOAR (STIM1 Orai-activating region, aa 344–442) [68], OASF (Orai-activating small fragment, 233–450; an extended version of OASF encompasses aa 234–491) [71, 72], CAD (CRAC-activating domain, aa 342–448) [73] and CCb9 (for coiled-coil domain containing region b9 encompassing aa 339–444) [74]. The crystal structure of the SOAR domain has revealed that SOAR appears as a dimer. Each subunit comprises four α-helical regions (α1, α2, α3, α4) [75], where the proposed strong Orai1 activation site is located between helixes α1

and α3, with the F^{394} residue playing a predominant role, and the α4 helix plays a relevant role in the maintenance of the SOAR dimer [76].

Overlapping with the CRAC-modulatory domain, a C-terminal inhibitory domain (CTID) has been described to modulate STIM1 function through the interaction with the modulator SARAF (see below). Deletion of the CTID region has been reported to induce spontaneous clustering of STIM1 and activation of Orai1 independently of the filling state of the Ca^{2+} stores [77]. STIM1 is subjected to a variety of post-translational modifications, including phosphorylation on serine [78] and tyrosine residues [79], and N-linked glycosylation at N^{131} and N^{171} located within in the SAM domain [80].

An alternative spliced long variant, STIM1L, has been found to be expressed in human skeletal muscle [81, 82], neonatal rat cardiomyocytes [83] and differentiated myotubes [82]. STIM1L is generated by alternative splicing and extension of exon 11 leading to a variant that contains an extra 106 amino acids (aa 515-620) insert in the cytosolic region. This region has been reported to provide STIM1 the ability to interact with Orai1 channels leading to the formation of permanent STIM1-Orai1 clusters that is associated with the rapid (< 1 s) activation of SOCE in skeletal muscle cells in comparison with other cells [84].

17.4 STIM2

The STIM1 homologue, STIM2, was identified in 2001 as a ubiquitously expressed protein that in vivo forms oligomers with STIM1 indicating a possible functional interaction between both proteins [78]. STIM2 is a type-1 transmembrane protein with similar structure to STIM1. The N-terminal region contains the functional Ca2+-binding EF-hand motif (aa 67–100) and SAM domain (aa 136–204). The cytosolic C-terminal region contains the ezrin/radixin/moesin domain with three coiled-coil domains [85]. The SOAR overlaps with this domain [86], and, as for STIM1, is involved in the activation of Orai [87]. Adjacent to the SOAR domain there is a proline- and histidine-rich region whose function is still unclear [78, 88]. Close to the end of the C-terminal region there is a calmodulin-binding region and a polybasic lysine-rich region [88, 89].

STIM2 is expressed in human and mouse tissues [78, 90], and it is the dominant STIM isoform in mouse brain, pancreas, placenta and heart; however, STIM2 is almost absent in skeletal muscle, kidney, liver and lung. It has been found co-expressed together with STIM1 in many human cell lines [78] and cell types [91–93], which indicates that both STIM isoforms co-exist and suggesting that they might interact functionally. STIM2 has been observed located in the ER membrane and in acidic intracellular stores [41, 85, 94], but, at present, no description of its location in the plasma membrane has been reported, in contrast to STIM1 [61, 67, 95, 96].

Three STIM2 splice variants have been described to date STIM2.1 (STIM2β), STIM2.2 (STIM2α) and STIM2.3. The best known and characterized variant is

STIM2.2 [97] and most of the previously published studies on STIM2 refer to STIM2.2 [98]. The *STIM2* gene comprises 13 exons, but the STIM2.2 mRNA is encoded by 12 exons (excluding exon 9) leading to a protein of 833 amino acids [87]. The STIM2.1 variant contains an eight-residue insert (383-VAASYLIQ-392) within the SOAR domain encoded by exon 9 that was initially found to impair the interaction with Orai1 and its activation [87]. However, more recent studies have revealed that the heterodimer consisting of the SOAR regions of STIM1 and STIM2.1 is able to induce full activation of Orai1 while preventing cross-linking and clustering of this channel [99]. STIM2.1 is ubiquitously expressed and might heterodimerize with STIM1 and STIM2.2 leading to the attenuation of Ca^{2+} influx through SOCE [87]. The third STIM2 variant, STIM2.3, expresses an alternative exon 13 that results in an upstream end of translation leading to a protein approximately 17 kDa smaller [97]. The expression of STIM2.3 is limited and its function is still uncertain [97].

The EF-hand motif of STIM1 and STIM2 binds Ca^{2+} and provide STIM proteins the ability to sense the ER Ca^{2+} concentration ($[Ca^{2+}]_{ER}$). STIM2 EF-hand exhibits a greater affinity for Ca^{2+} than that of STIM1 (STIM2 EF-hand motif Kd∼0.5 mM, STIM1 EF-hand motif Kd∼0.6 mM) [64, 100]. As a result, STIM2 is expected to show a greater sensitivity to minor changes in $[Ca^{2+}]_{ER}$ than STIM1. Consequently, STIM2 has been reported to be partially active at resting $[Ca^{2+}]_{ER}$ and is further activated by small reductions in $[Ca^{2+}]_{ER}$; on the other hand, STIM1 requires larger reductions in $[Ca^{2+}]_{ER}$ to become active [101]. The greater sensitivity for free-Ca^{2+} confers STIM2 the ability to sense $[Ca^{2+}]_{ER}$ fluctuations, stabilizing both basal cytosolic and endoplasmic reticulum Ca^{2+} levels, as well as to activate earlier than STIM1 upon agonist stimulation [101]. Furthermore, STIM2 has been reported to trigger a conformational remodeling of STIM1 C-terminus, leading to STIM1-Orai1 interaction at relatively high $[Ca^{2+}]_{ER}$ [102].

The characterization of STIM1 as the Ca^{2+} sensor facilitated the identification of the channels involved in SOCE. After intense research and debate two types of STIM1-modulated SOC channels have been described so far: the Ca^{2+}-release activated Ca^{2+} (CRAC) channels, which involves Orai1 subunits, and store-operated Ca^{2+} (SOC) channels, involving subunits of Orai1 and the canonical transient receptor potential (TRPC) family member TRPC1 [103–106].

17.5 STIM and Orai: CRAC Channels

Soon after the identification of SOCE, a highly Ca^{2+}-selective current activated by discharge of the intracellular Ca^{2+} stores was identified in mast cells and named Calcium-Release Activated Current (I_{CRAC}). This current was described as a voltage-insensitive current with a characteristic inward rectification [107]. More than a decade after the identification of I_{CRAC}, in 2006, the channel conducting this current was identified, through whole-genome screening of *Drosophila* S2 cells and gene mapping in patients with the hereditary severe combined immune deficiency

(SCID) syndrome induced by I_{CRAC} deficiency, as the protein Orai1 [108–110]. In Greek mythology the Orai is the keeper of the heaven´s gate [111]. Orai1 is a protein that shares no homology with other known ion channels. It is a protein of 301 amino acids that shows four transmembrane domains (TM1-TM4) and cytosolic N- and C-terminal tails [112–115], which are both required for STIM1 interaction and regulation [68, 71, 73, 116–118].

Despite the initial studies pointed out to a tetramer as the most likely Orai1 subunit stoichiometry of the mammalian CRAC channels [119–121], crystallization of *Drosophila* Orai has revealed that the channel consists of an hexameric assembly of Orai subunits [122]. Although the crystal structure of mammalian Orai1 is not available the analysis of the biophysical properties of concatenated hexameric and tetrameric human Orai1 channels has shown that a tetrameric architecture displays the highly Ca^{2+}-selective conductance characteristic of I_{CRAC} and endogenous CRAC channels, while the hexameric structure forms a non-selective cation channel [123].

Concerning the hexameric CRAC channel, the pore is located amid the hexamer formed by the six TM1 domains and also including the residues 74–90 (named ETON region) within the N-terminus, which is essential for the interaction with STIM1 [116]. The channel pore has been reported to acts as a funnel formed by an external vestibule, which consist of negatively charged residues (D110, D112 and D114) that attract Ca^{2+} to the immediacies to the pore, followed by the selectivity filter (aa E106), which is required for the CRAC channel high Ca^{2+} selectivity [124, 125], a hydrophobic region (aa V102, F99 and L95) and a basic region (aa R91, K87 and R83). The channel pore is surrounded by three rings comprised by TM2, TM3 and TM4 [122]. A number of residues within TM2-TM4 have been reported to be key regulators of CRAC channel function. The Orai1 mutations L138F and P245L, located in TM2 and TM4, have been shown to trigger constitutive currents that underlie the pathogenesis of different disorders, such as tubular aggregate myopathy (TAM) [126] and Stormorken disease [127], respectively.

The Orai family includes three human homologs, Orai1, Orai2 and Orai3. All three Orai isoforms are activated by Ca^{2+} store depletion when co-expressed with STIM1 [128, 129]; however, the Orai isoforms show different sensitivity to 2-aminoethoxydiphenyl borate (2-APB), an IP_3 receptor antagonist and Ca^{2+} channel blocker [130, 131]. While 2-APB has been reported to act as a direct Orai3 activator, its effect on Orai1 and Orai2 function is concentration-dependent. Low 2-APB concentrations (5–10 μM) activate Orai1 and Orai2 currents when co-expressed with STIM1; by contrast, at high concentrations (50 μM), 2-APB is a potent inhibitor of Orai1 currents [124, 132, 133]. In addition to the inhibitory role on Orai1 channels, 2-APB can also directly inhibit STIM1 function by promoting intramolecular interaction between the CC1 and SOAR regions of STIM1 [134]. Orai3 expression has recently been reported to be regulated by the protein stanniocalcin-2 in mouse platelets, so that platelets from mice lacking stanniocalcin-2 exhibit a significantly greater Orai3 expression, leading to enhanced agonist-induced Ca^{2+} mobilization and platelet aggregation [135].

The mechanism of activation of CRAC channels by STIM1 has long been investigated. In its resting state the canonical EF-hand domain is occupied by Ca^{2+}, STIM1 appears as a dimer and the SOAR region is hidden from the channel due to an autoinhibitory electrostatic interaction between an acidic segment within the CC1 and a polybasic region (aa 382–386) within the SOAR domain [136, 137]. Discharge of the ER upon agonist stimulation leads to Ca^{2+} dissociation from the EF-hand, which, in turn, changes the EF-hand-SAM conformation facilitating the formation of STIM1 oligomers [100, 138]. This conformational change lessens the angle of interaction of the TM region within the ER membrane bringing the C-termini together [139] and inducing the release of the SOAR domain from the autoinhibitory interaction with the CC1 region [116, 140–142]. STIM1 interacts with the N- and C-termini of Orai1. The interaction between STIM1 and Orai1 C-terminus was solved by NMR and involves the positively charged residues that interact with the CC1 autoinhibitory domain (K382, K384, K385 and K386), two aromatic residues Y361 and Y362 and four hydrophobic amino acids (L347, L351, L373 and A376) within STIM1 as well as Orai1 residues L273, L276, R281, L286 and R289 from its C-terminus, forming altogether the so called STIM1-Orai1 Association Pocket (SOAP) [141]. It has been reported that STIM binding to the Orai C-terminus orients STIM for effective interaction with the N-terminus [143]. The interaction between STIM1 and Orai1 N-terminus is essential for channel gating [144]; however, the sequence in STIM1 and in Orai1 N-terminus is not completely solved yet, although it has been proposed that Orai1 N-terminus might interact with a sequence adjacent to the SOAP previously described [145]. Furthermore, the STIM1-Orai1 stoichiometry in an efficient interaction has not been determined yet and further studies are still required to define these aspects.

17.6 STIM1, Orai1 and TRPC1: SOC Channels

In addition to I_{CRAC}, a number of store-operated currents with different biophysical properties have been described in a variety of cell types, including A431 epidermal cells, messangial cells, endothelial cells as well as aortic, portal vein and pulmonary artery myocytes, which have been named I_{SOC}. I_{SOC} currents are not selective for Ca^{2+} and exhibit a greater conductance than I_{CRAC} [146]. The activation of I_{SOC} involves the interaction among STIM1, Orai1 and TRPC1 [103, 104, 106, 147–150].

The TRP proteins form non-selective cation channels identified in the trp mutant of *Drosophila*. In 1969, Cosens and Manning reported a *Drosophila* mutant with altered electroretinogram [151]. In *Drosophila* photoreceptors, the sustained light-sensitive ionic current due to Na^{+} and Ca^{2+} influx is conducted by two Ca^{2+}-permeable channels encoded by the *trp* and *trpl* genes [152, 153]. By contrast, the trp mutant exhibited transient, rather than sustained, light-sensitive receptor potential, which gave the name to transient receptor potential (TRP) channels [154]. Soon after the identification of *Drosophila* TRP proteins, the first mammalian TRP was identified, TRPC1, both in human [155, 156] and in mouse [157]. Since the

identification of TRPC1 several TRP proteins have been identified in vertebrates, which have been grouped into seven subfamilies: four are closely related to *Drosophila* TRP (TRPC, TRPV, TRPA and TRPM), two are more distantly related subfamilies (TRPP and TRPML), and, finally, the TRPN group, which is expressed in fish, flies and worms [158]. Each subfamily includes different members, i.e. the TRPC subfamily comprises seven members (TRPC1-TRPC7), the vanilloid TRP subfamily (TRPV) includes six members (TRPV1–TRPV6), the TRPA (ankyrin) subfamily includes only one protein, TRPA1, the melastatin TRP subfamily (TRPM) comprises eight members (TRPM1-TRPM8) and both the TRPP (polycystin) and the TRPML (mucolipin) subfamilies include three members each [159, 160].

TRP channels are permeable to monovalent and divalent cations and exhibit a Ca^{2+}/Na^{+} permeability ratio <10 [156], with some exceptions such as TRPM4 and TRPM5, which are selective for monovalent cations, and the highly Ca^{2+} selective TRPV5 and TRPV6 [161, 162]. The lack of Ca^{2+} selectivity for TRP channels raises the possibility that these channels are involved in the SOC channels [104]. TRP proteins share a common architecture, which resembles other ionic channels, including six transmembrane domains (TM1-TM6), with cytosolic N- and C-termini and a pore loop region between TM5 and TM6 [156, 163]. The C-terminal region includes a characteristic TRP signature motif (EWKFAR), involved in allosteric channel activation [164] and a CIRB (calmodulin/IP_3 receptor-binding) region, involved in the regulation of TRP channel gating [165, 166]. The N- and C-termini of TRP channels included coiled-coil domains that play a relevant role in the interaction with STIM1 [167].

Despite *Drosophila* TRP channels were described as receptor-operated channels activated by second messengers [168], the involvement of TRP channels in SOCE has been widely investigated and debated. Particular attention has been focused on the TRPC subfamily members, which have been found to be gated by Ca^{2+} store depletion in a number of cell types by using different approaches, from overexpression of specific TRPC proteins to knockdown of endogenous TRPs and knockout models [169–172]. There is now a consensus that TRPC1 forms a complex with STIM1 and Orai1, which is responsible of the less selective I_{SOC} current. There are two hypotheses concerning the molecular basis of I_{SOC}. One such hypothesis supports that the I_{SOC} current represents the sum of I_{CRAC} and a less selective current through TRPC channels [173], whereas another model suggests that I_{SOC} involves channels, of still unknown composition, but including both TRPC1 and Orai1 subunits [174].

STIM1 has been reported to interact with TRPC channels by direct association of the STIM1 SOAR domain with the N- and C-terminal coiled-coil domains of TRPC, as single mutations in these domains has been shown to reduce the interaction and activation of TRPC1 by STIM1 [167]. Apparently, STIM1 directly associates with certain TRPC proteins, such as TRPC1, TRPC4 and TRPC5, but the regulation of other TRPC channels, such as TRPC3 or TRPC6, is indirect and depends on TRPC1 and TRPC4, respectively. According to this model, at the resting state, TRPC3 N- and C-terminal coiled-coil domains interact with each other to prevent the interaction of the C-terminal coiled-coil domain with STIM1. Upon store depletion,

the TRPC1 C-terminal coiled-coil domain dissociates this interaction to allow the association between the SOAR region within STIM1 and the TRPC3 C-terminal coiled-coil domain, and, thus, the regulation of TRPC3 channel by STIM1 [167]. In addition to the interaction between STIM1 and TRPCs described above, the activation of these channels by STIM1 require the electrostatic interaction between two positively charged residues located in the polybasic lysine-rich domain of STIM1 (K^{684} and K^{685}) and two negatively charged aspartates in TRPC1 (D^{639} and D^{640}), with a similar sequence described in TRPC3 [175].

17.7 Regulation of SOCE

Given the functional relevance of SOCE in cell biology, this mechanism is finely regulated by a number of biochemical interactions involving signalling molecules, physico-chemical conditions or Ca^{2+} itself. Soon after the identification of I_{CRAC} it was reported that an elevated $[Ca^{2+}]_c$ was able to inactivate the channel function in two different ways termed fast Ca^{2+}-dependent inactivation (FCDI), which occurs within milliseconds, and slow Ca^{2+}-dependent inactivation (SCDI) that initiates tens of seconds after CRAC channel activation [176–179].The rapid activation of FCDI, together with the fact that it does not depend on the I_{CRAC} amplitude led to the proposal that the inactivation is driven by Ca^{2+} binding to nearby cytosolic inactivating sites in close proximity to the channel pore [176, 180]. Different regions of Orai1 have been analysed and the two most prominent residues were identified as W76 and Y80 [181], located in the proposed Orai1 calmodulin-binding domain. However, the more recent publication of the crystal architecture of the pore-forming region of Orai1 revealed that residues W76 and Y80 face the pore lumen and, therefore, they are not freely accessible to calmodulin, as predicted [122]. Further studies using calmodulin dominant negative mutants have confirmed that FCDI might occur independently of calmodulin and suggest that W76 and Y80 might participate in a conformational change within the pore region leading to FCDI [182].

In contrast to FCDI, SCDI depends on global rises in $[Ca^{2+}]_c$ [177, 179]. Mitochondria have been reported to play a role in the modulation of SCDI. Ca^{2+} uptake by mitochondria upon rises in $[Ca^{2+}]_c$ due to the opening of CRAC channels slows down store refilling and attenuates the rate and extent of SCDI [183]. Current evidence supports a role of the protein SARAF (store-operated Ca^{2+} entry associated regulatory factor) in the activation of SCDI. SARAF is a 339-amino acid type I transmembrane protein that has been found to be located in the ER [184], as well as in the PM [35], location where its expression is regulated by STIM1 [185]. SARAF has been reported to interact with STIM1 modulating the Ca^{2+} fluxes and protecting the cell against Ca^{2+} overload [184]. Despite no functional domains have been identified yet, studies using SARAF constructs have revealed that the N-terminal region is essential for SARAF activity, while the C-terminal region is responsible for the interaction with STIM1 and the migration to ER-PM junctions in a STIM1-dependent manner [184]. SARAF interacts with the STIM1 SOAR

region at rest to prevent spontaneous activation of STIM1 [184]. The interaction of SARAF with the SOAR region is modulated by an adjacent region termed CTID (aa 448–530), so that, in the resting state, the STIM1 SOAR-CTID region facilitates access of SARAF to SOAR to prevent spontaneous activation of SOCE, while store depletion, leading to a conformational change in STIM1, induces the dissociation of SARAF from the SOAR domain that facilitates the activation of SOCE. This process is followed by a more sustained reinteraction of SARAF with STIM1 (Fig. 17.2), which has been proposed as the mechanism underlying SCDI [77]. Analysis of the SARAF-STIM1 interaction has revealed that this association reaches a minimum 30s after store depletion by thapsigargin and then rises [186], a time-course that is compatible with the activation of SCDI [177, 179]. In addition to STIM1, we have recently reported that SARAF interacts with and modulates the function of Orai1 and TRPC1 channels. Studies in cells with low STIM1 expression have revealed that SARAF enhances Orai1-mediated Ca^{2+} entry and, conversely, attenuates Ca^{2+} influx mediated by TRPC1 channels [186, 187]. Altogether, the role of SARAF in the regulation of Orai1 and TRPC1 function strongly depends on STIM1 expression. In STIM1-expressing cells, SARAF negatively regulates Ca^{2+} influx through the

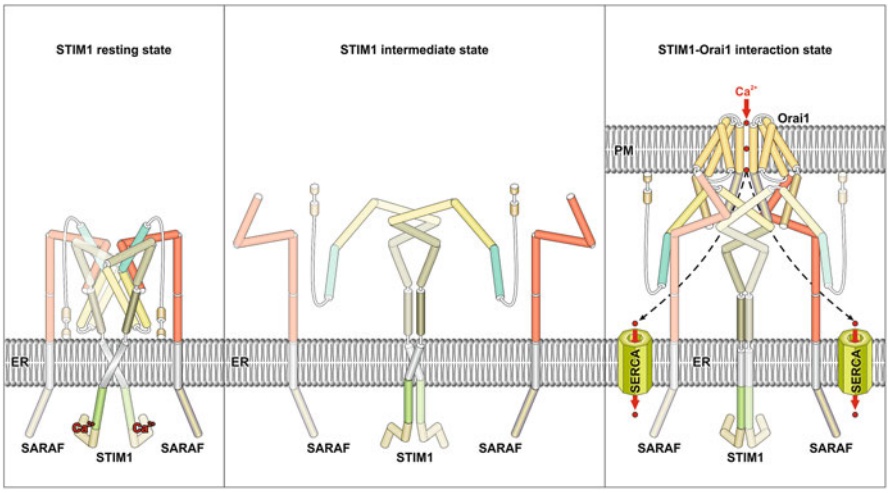

Fig. 17.2 Interaction of SARAF with STIM1. In the resting state, the canonical EF-hand motif is occupied by Ca^{2+} and STIM1 appears as a dimer in a autoinhibited configuration mediated by electrostatic interaction between an acidic segment within the CC1 and a polybasic region within the SOAR domain [136, 137]. In this configuration, SARAF is associated with the SOAR region. Discharge of the intracellular Ca^{2+} stores is followed by Ca^{2+} dissociation from the EF-hand motif, which leads to the beginning of the conformational change of STIM1 towards an extended state and the dissociation of SARAF. STIM1, in the extended state, interacts with Orai1 channels in the plasma membrane and a few seconds after the discharge of the Ca^{2+} stores SARAF re-associates with STIM1, which might lead to SCDI [77]. The Ca^{2+} that enters the cytoplasm through the Orai1 channels is pumped into the ER by the sarco/endoplasmic reticulum Ca^{2+} ATPase (SERCA)

channels modulated by STIM1, including the store-operated CRAC and SOC channels [77, 184, 186], and the store-independent arachidonate-regulated Ca^{2+} (ARC) channel [35], probably as a mechanism to prevent Ca^{2+} overload. On the other hand, in the absence of STIM1, SARAF enhances Orai1 function while attenuating TRPC1 activation [186, 187], probably as a mechanism to prevent cation influx through a channel with greater conductance and facilitate Ca^{2+} entry through a more selective low-conductance channel. The role of SARAF in SCDI is observed only when the STIM1-Orai1 complex is located within $PI(4,5)P_2$-rich microdomain [188], which indicates that plasma membrane nanodomains play an important role in STIM1-Orai1 function [145].

In addition to SARAF, other molecular modulators have been proposed to regulate SOCE to prevent excessive Ca^{2+} influx. Among them, Golli, a member of the family of myelin basic proteins, has been reported to attenuate SOCE in Jurkat T cells, while T cells from Golli-deficient mice exhibits enhanced Ca^{2+} influx evoked by T cell receptor activation [189]. Although the mechanism of regulation is still uncertain, Golli has been found to interact with the C-terminal domain of STIM1 following store depletion and modulated by $[Ca^{2+}]_c$ [190]. Furthermore, the protein orosomucoid-like 3 (ORMDL3) has also been reported to act as a negative modulator of I_{CRAC} and SOCE in T cells. ORMDL3 attenuates Ca^{2+} uptake by mitochondria, thus resulting in inhibition of I_{CRAC} and SOCE by SCDI [191]. More recently, filamin A has been shown as a modulator of the interaction of STIM1 with the actin cytoskeleton and Orai1. Thus, in cells lacking filamin A, as well as in cells where filamin A expression had been attenuated using siRNA, it has been reported enhancement of the STIM1-Orai1 interaction and SOCE [192]. Other SOCE modulators includes CRACR2A, a cytosolic Ca^{2+}-binding protein that modulates STIM1–Orai1 complexes [193], and STIMATE, an ER-resident protein and facilitates STIM1 puncta formation and the activation of CRAC channels [194] (Table 17.1).

SOCE is further subjected to a variety of physico-chemical conditions. For instance, Ca^{2+} influx through SOCE is subjected to the electrochemical gradient across the cell membrane, which, at physiological conditions, favours Ca^{2+} entry into the cytoplasm. However, the opening of non-selective cation channels or closure of K^+ channels might significantly alter the membrane potential and, thus, the driving force for Ca^{2+} influx. Similarly, Orai1 has been found to be sensitive to pH,

Table 17.1 Biochemical components of the STIM1-regulated Ca^{2+} channels

Channel	Components	Regulators	Refs.
CRAC	Orai1α/Orai1β, Orai2, Orai3	STIM1, STIM2.1, STIM2.2, SARAF, CRACR2A, Golli, ORMDL3, STIMATE, filamin A.	[87, 97, 103, 128, 129, 189, 191–194]
SOC	Orai1α/Orai1β, TRPC1	STIM1, STIM2.1, STIM2.2, CRACR2A, Golli, ORMDL3, SARAF, filamin A.	[87, 97, 103, 190, 191, 193]
ARC	Orai1α, Orai3	STIM1, SARAF	[32, 33, 103]

with a decrease in Orai1 function at mildly acidic pH and opposite effects observed upon mild alkalinisation [145, 195]. The expression of STIM and Orai proteins has also been found to be sensitive to hypoxia, which has been reported to upregulate the expression of STIM1, STIM2, Orai1, Orai2 and TRPC6 at the protein level [196]. Finally, reactive oxygen species (ROS) have also been reported to alter STIM1-Orai1 function. For instance, ROS have been reported to activate SOCE in human platelets [197]. Furthermore, oxidative stress in DT40 cells has been found to induce STIM1 S-glutathionylation at C^{56}, an event that has been associated to a decrease in the affinity of STIM1 for $[Ca^{2+}]_{ER}$, thus mimicking the effect of store depletion and enhancing SOCE [198]. In sum, these mechanisms, together with different covalent modifications of the key players, such as phosphorylation of STIM1 [79, 199, 200] and Orai1 [201], fine tune SOCE in order to provide functional Ca^{2+} signals.

Acknowledgements This work was supported by MINECO (Grant BFU2016-74932-C2-1-P/2-P) and Junta de Extremadura-FEDER (IB16046 and GR18061). IJ and JJL were supported by Juan de la Cierva Program (IJCI_2015-25665) and Junta de Extremadura-FEDER (IB16046), respectively.

References

1. Berridge MJ, Bootman MD, Roderick HL (2003) Calcium signalling: dynamics, homeostasis and remodelling. Nat Rev Mol Cell Biol 4(7):517–529
2. Bobe R, Bredoux R, Wuytack F, Quarck R, Kovacs T, Papp B, Corvazier E, Magnier C, Enouf J (1994) The rat platelet 97-kDa Ca^{2+}ATPase isoform is the sarcoendoplasmic reticulum Ca^{2+}ATPase 3 protein. J Biol Chem 269(2):1417–1424
3. Wuytack F, Papp B, Verboomen H, Raeymaekers L, Dode L, Bobe R, Enouf J, Bokkala S, Authi KS, Casteels R (1994) A sarco/endoplasmic reticulum Ca^{2+}-ATPase 3-type Ca^{2+} pump is expressed in platelets, in lymphoid cells, and in mast cells. J Biol Chem 269(2):1410–1416
4. Cavallini L, Coassin M, Alexandre A (1995) Two classes of agonist-sensitive Ca^{2+} stores in platelets, as identified by their differential sensitivity to 2,5-di-(tert-butyl)-1,4-benzohydroquinone and thapsigargin. Biochem J 310(Pt 2):449–452
5. Lopez JJ, Camello-Almaraz C, Pariente JA, Salido GM, Rosado JA (2005) Ca^{2+} accumulation into acidic organelles mediated by Ca^{2+}- and vacuolar H^+-ATPases in human platelets. Biochem J 390(Pt 1):243–252
6. Juska A, Redondo PC, Rosado JA, Salido GM (2005) Dynamics of calcium fluxes in human platelets assessed in calcium-free medium. Biochem Biophys Res Commun 334(3):779–786
7. Brini M, Carafoli E (2011) The plasma membrane Ca(2)+ ATPase and the plasma membrane sodium calcium exchanger cooperate in the regulation of cell calcium. Cold Spring Harb Perspect Biol 3(2)
8. Cancela JM (2001) Specific Ca^{2+} signaling evoked by cholecystokinin and acetylcholine: the roles of NAADP, cADPR, and IP_3. Annu Rev Physiol 63:99–117
9. Choe CU, Ehrlich BE (2006) The inositol 1,4,5-trisphosphate receptor (IP3R) and its regulators: sometimes good and sometimes bad teamwork. Sci STKE 2006(363):re15
10. Lam AK, Galione A (2013) The endoplasmic reticulum and junctional membrane communication during calcium signaling. Biochim Biophys Acta 1833(11):2542–2559
11. Loh YP, Tam WW, Russell JT (1984) Measurement of delta pH and membrane potential in secretory vesicles isolated from bovine pituitary intermediate lobe. J Biol Chem 259(13):8238–8245

12. Koivusalo M, Steinberg BE, Mason D, Grinstein S (2011) In situ measurement of the electrical potential across the lysosomal membrane using FRET. Traffic 12(8):972–982
13. Catterall WA (2011) Voltage-gated calcium channels. Cold Spring Harb Perspect Biol 3(8):a003947
14. Ertel EA, Campbell KP, Harpold MM, Hofmann F, Mori Y, Perez-Reyes E, Schwartz A, Snutch TP, Tanabe T, Birnbaumer L, Tsien RW, Catterall WA (2000) Nomenclature of voltage-gated calcium channels. Neuron 25(3):533–535
15. Catterall WA, Perez-Reyes E, Snutch TP, Striessnig J (2005) International Union of Pharmacology. XLVIII. Nomenclature and structure-function relationships of voltage-gated calcium channels. Pharmacol Rev 57(4):411–425
16. Suzuki Y, Inoue T, Ra C (2010) L-type Ca^{2+} channels: a new player in the regulation of Ca^{2+} signaling, cell activation and cell survival in immune cells. Mol Immunol 47(4):640–648
17. Suzuki Y, Yoshimaru T, Inoue T, Ra C (2009) Ca v 1.2 L-type Ca^{2+} channel protects mast cells against activation-induced cell death by preventing mitochondrial integrity disruption. Mol Immunol 46(11–12):2370–2380
18. Yoshimaru T, Suzuki Y, Inoue T, Ra C (2009) L-type Ca^{2+} channels in mast cells: activation by membrane depolarization and distinct roles in regulating mediator release from store-operated Ca^{2+} channels. Mol Immunol 46(7):1267–1277
19. Matza D, Flavell RA (2009) Roles of Ca(v) channels and AHNAK1 in T cells: the beauty and the beast. Immunol Rev 231(1):257–264
20. Dionisio N, Smani T, Woodard GE, Castellano A, Salido GM, Rosado JA (2015) Homer proteins mediate the interaction between STIM1 and Cav1.2 channels. Biochim Biophys Acta 1853(5):1145–1153
21. Wang Y, Deng X, Mancarella S, Hendron E, Eguchi S, Soboloff J, Tang XD, Gill DL (2010) The calcium store sensor, STIM1, reciprocally controls Orai and CaV1.2 channels. Science 330(6000):105–109
22. Sage SO (1992) Three routes for receptor-mediated Ca^{2+} entry. Curr Biol 2(6):312–314
23. North RA (2002) Molecular physiology of P2X receptors. Physiol Rev 82(4):1013–1067
24. Kyrozis A, Goldstein PA, Heath MJ, MacDermott AB (1995) Calcium entry through a subpopulation of AMPA receptors desensitized neighbouring NMDA receptors in rat dorsal horn neurons. J Physiol 485(Pt 2):373–381
25. Salazar H, Eibl C, Chebli M, Plested A (2017) Mechanism of partial agonism in AMPA-type glutamate receptors. Nat Commun 8:14327
26. Twomey EC, Yelshanskaya MV, Grassucci RA, Frank J, Sobolevsky AI (2017) Channel opening and gating mechanism in AMPA-subtype glutamate receptors. Nature 549(7670):60–65
27. Hofmann T, Obukhov AG, Schaefer M, Harteneck C, Gudermann T, Schultz G (1999) Direct activation of human TRPC6 and TRPC3 channels by diacylglycerol. Nature 397(6716):259–263
28. Venkatachalam K, Zheng F, Gill DL (2003) Regulation of canonical transient receptor potential (TRPC) channel function by diacylglycerol and protein kinase C. J Biol Chem 278(31):29031–29040
29. Berna-Erro A, Galan C, Dionisio N, Gomez LJ, Salido GM, Rosado JA (2012) Capacitative and non-capacitative signaling complexes in human platelets. Biochim Biophys Acta 1823(8):1242–1251
30. Jardin I, Gomez LJ, Salido GM, Rosado JA (2009) Dynamic interaction of hTRPC6 with the Orai1/STIM1 complex or hTRPC3 mediates its role in capacitative or non-capacitative Ca^{2+} entry pathways. Biochem J 420:267–276
31. Togashi K, Hara Y, Tominaga T, Higashi T, Konishi Y, Mori Y, Tominaga M (2006) TRPM2 activation by cyclic ADP-ribose at body temperature is involved in insulin secretion. EMBO J 25(9):1804–1815
32. Shuttleworth TJ (2009) Arachidonic acid, ARC channels, and Orai proteins. Cell Calcium 45(6):602–610

33. Shuttleworth TJ, Thompson JL, Mignen O (2007) STIM1 and the noncapacitative ARC channels. Cell Calcium 42(2):183–191
34. Shuttleworth TJ, Thompson JL, Mignen O (2004) ARC channels: a novel pathway for receptor-activated calcium entry. Physiology (Bethesda) 19:355–361
35. Albarran L, Lopez JJ, Woodard GE, Salido GM, Rosado JA (2016) Store-operated Ca^{2+} entry-associated regulatory factor (SARAF) plays an important role in the regulation of arachidonate-regulated Ca^{2+} (ARC) channels. J Biol Chem 291(13):6982–6988
36. Rohacs T, Nilius B (2007) Regulation of transient receptor potential (TRP) channels by phosphoinositides. Pflugers Arch 455(1):157–168
37. Jardin I, Redondo PC, Salido GM, Rosado JA (2008) Phosphatidylinositol 4,5-bisphosphate enhances store-operated calcium entry through hTRPC6 channel in human platelets. Biochim Biophys Acta 1783(1):84–97
38. Putney JW (2011) The physiological function of store-operated calcium entry. Neurochem Res 36(7):1157–1165
39. Putney JW Jr (2005) Capacitative calcium entry: sensing the calcium stores. J Cell Biol 169(3):381–382
40. Putney JW Jr (1986) A model for receptor-regulated calcium entry. Cell Calcium 7(1):1–12
41. Zbidi H, Jardin I, Woodard GE, Lopez JJ, Berna-Erro A, Salido GM, Rosado JA (2011) STIM1 and STIM2 are located in the acidic Ca^{2+} stores and associates with Orai1 upon depletion of the acidic stores in human platelets. J Biol Chem 286(14):12257–12270
42. Casteels R, Droogmans G (1981) Exchange characteristics of the noradrenaline-sensitive calcium store in vascular smooth muscle cells or rabbit ear artery. J Physiol 317:263–279
43. Kwan CY, Takemura H, Obie JF, Thastrup O, Putney JW Jr (1990) Effects of MeCh, thapsigargin, and La3+ on plasmalemmal and intracellular Ca^{2+} transport in lacrimal acinar cells. Am J Physiol 258(6 Pt 1):C1006–C1015
44. Rosado JA (2006) Discovering the mechanism of capacitative calcium entry. Am J Physiol Cell Physiol 291(6):C1104–C1106
45. Abdullaev IF, Bisaillon JM, Potier M, Gonzalez JC, Motiani RK, Trebak M (2008) Stim1 and Orai1 mediate CRAC currents and store-operated calcium entry important for endothelial cell proliferation. Circ Res 103(11):1289–1299
46. Darbellay B, Arnaudeau S, Konig S, Jousset H, Bader C, Demaurex N, Bernheim L (2009) STIM1- and Orai1-dependent store-operated calcium entry regulates human myoblast differentiation. J Biol Chem 284(8):5370–5380
47. Feske S (2011) Immunodeficiency due to defects in store-operated calcium entry. Ann NY Acad Sci 1238:74–90
48. Stiber J, Hawkins A, Zhang ZS, Wang S, Burch J, Graham V, Ward CC, Seth M, Finch E, Malouf N, Williams RS, Eu JP, Rosenberg P (2008) STIM1 signalling controls store-operated calcium entry required for development and contractile function in skeletal muscle. Nat Cell Biol 10(6):688–697
49. Yoshida J, Iwabuchi K, Matsui T, Ishibashi T, Masuoka T, Nishio M (2012) Knockdown of stromal interaction molecule 1 (STIM1) suppresses store-operated calcium entry, cell proliferation and tumorigenicity in human epidermoid carcinoma A431 cells. Biochem Pharmacol 84(12):1592–1603
50. Avila-Medina J, Calderon-Sanchez E, Gonzalez-Rodriguez P, Monje-Quiroga F, Rosado JA, Castellano A, Ordonez A, Smani T (2016) Orai1 and TRPC1 proteins Co-localize with CaV1.2 channels to form a signal complex in vascular smooth muscle cells. J Biol Chem 291(40):21148–21159
51. Diez-Bello R, Jardin I, Salido GM, Rosado JA (2017) Orai1 and Orai2 mediate store-operated calcium entry that regulates HL60 cell migration and FAK phosphorylation. Biochim Biophys Acta 1864(6):1064–1070
52. Galan C, Zbidi H, Bartegi A, Salido GM, Rosado JA (2009) STIM1, Orai1 and hTRPC1 are important for thrombin- and ADP-induced aggregation in human platelets. Arch Biochem Biophys 490(2):137–144

53. Albarran L, Lopez JJ, Salido GM, Rosado JA (2016) Historical overview of store-operated Ca^{2+} entry. Adv Exp Med Biol 898:3–24
54. Roos J, DiGregorio PJ, Yeromin AV, Ohlsen K, Lioudyno M, Zhang S, Safrina O, Kozak JA, Wagner SL, Cahalan MD, Velicelebi G, Stauderman KA (2005) STIM1, an essential and conserved component of store-operated Ca^{2+} channel function. J Cell Biol 169(3):435–445
55. Zhang SL, Yu Y, Roos J, Kozak JA, Deerinck TJ, Ellisman MH, Stauderman KA, Cahalan MD (2005) STIM1 is a Ca^{2+} sensor that activates CRAC channels and migrates from the Ca^{2+} store to the plasma membrane. Nature 437(7060):902–905
56. Oritani K, Kincade PW (1996) Identification of stromal cell products that interact with pre-B cells. J Cell Biol 134(3):771–782
57. Parker NJ, Begley CG, Smith PJ, Fox RM (1996) Molecular cloning of a novel human gene (D11S4896E) at chromosomal region 11p15.5. Genomics 37(2):253–256
58. Sabbioni S, Barbanti-Brodano G, Croce CM, Negrini M (1997) GOK: a gene at 11p15 involved in rhabdomyosarcoma and rhabdoid tumor development. Cancer Res 57(20):4493–4497
59. Manji SS, Parker NJ, Williams RT, van Stekelenburg L, Pearson RB, Dziadek M, Smith PJ (2000) STIM1: a novel phosphoprotein located at the cell surface. Biochim Biophys Acta 1481(1):147–155
60. Lopez JJ, Salido GM, Pariente JA, Rosado JA (2006) Interaction of STIM1 with endogenously expressed human canonical TRP1 upon depletion of intracellular Ca^{2+} stores. J Biol Chem 281(38):28254–28264
61. Spassova MA, Soboloff J, He LP, Xu W, Dziadek MA, Gill DL (2006) STIM1 has a plasma membrane role in the activation of store-operated Ca^{2+} channels. Proc Natl Acad Sci USA 103(11):4040–4045
62. Jardin I, Lopez JJ, Redondo PC, Salido GM, Rosado JA (2009) Store-operated Ca^{2+} entry is sensitive to the extracellular Ca^{2+} concentration through plasma membrane STIM1. Biochim Biophys Acta 1793(10):1614–1622
63. Stathopulos PB, Zheng L, Li GY, Plevin MJ, Ikura M (2008) Structural and mechanistic insights into STIM1-mediated initiation of store-operated calcium entry. Cell 135(1):110–122
64. Zheng L, Stathopulos PB, Li GY, Ikura M (2008) Biophysical characterization of the EF-hand and SAM domain containing Ca^{2+} sensory region of STIM1 and STIM2. Biochem Biophys Res Commun 369(1):240–246
65. Baba Y, Hayashi K, Fujii Y, Mizushima A, Watarai H, Wakamori M, Numaga T, Mori Y, Iino M, Hikida M, Kurosaki T (2006) Coupling of STIM1 to store-operated Ca^{2+} entry through its constitutive and inducible movement in the endoplasmic reticulum. Proc Natl Acad Sci USA 103(45):16704–16709
66. Derler I, Fahrner M, Muik M, Lackner B, Schindl R, Groschner K, Romanin C (2009) A Ca^{2+} release-activated Ca^{2+} (CRAC) Modulatory Domain (CMD) within STIM1 mediates fast Ca^{2+}-dependent Inactivation of ORAI1 channels. J Biol Chem 284(37):24933–24938
67. Jardin I, Dionisio N, Frischauf I, Berna-Erro A, Woodard GE, Lopez JJ, Salido GM, Rosado JA (2013) The polybasic lysine-rich domain of plasma membrane-resident STIM1 is essential for the modulation of store-operated divalent cation entry by extracellular calcium. Cell Signal 25(5):1328–1337
68. Yuan JP, Zeng W, Dorwart MR, Choi YJ, Worley PF, Muallem S (2009) SOAR and the polybasic STIM1 domains gate and regulate Orai channels. Nat Cell Biol 11(3):337–343
69. Li Z, Lu J, Xu P, Xie X, Chen L, Xu T (2007) Mapping the interacting domains of STIM1 and Orai1 in Ca^{2+} release-activated Ca^{2+} channel activation. J Biol Chem 282(40):29448–29456
70. Muik M, Frischauf I, Derler I, Fahrner M, Bergsmann J, Eder P, Schindl R, Hesch C, Polzinger B, Fritsch R, Kahr H, Madl J, Gruber H, Groschner K, Romanin C (2008) Dynamic coupling of the putative coiled-coil domain of ORAI1 with STIM1 mediates ORAI1 channel activation. J Biol Chem 283(12):8014–8022
71. Muik M, Fahrner M, Derler I, Schindl R, Bergsmann J, Frischauf I, Groschner K, Romanin C (2009) A cytosolic homomerization and a modulatory domain within STIM1 C terminus

determine coupling to ORAI1 channels. J Biol Chem 284(13):8421–8426
72. Muik M, Fahrner M, Schindl R, Stathopulos P, Frischauf I, Derler I, Plenk P, Lackner B, Groschner K, Ikura M, Romanin C (2011) STIM1 couples to ORAI1 via an intramolecular transition into an extended conformation. EMBO J 30(9):1678–1689
73. Park CY, Hoover PJ, Mullins FM, Bachhawat P, Covington ED, Raunser S, Walz T, Garcia KC, Dolmetsch RE, Lewis RS (2009) STIM1 clusters and activates CRAC channels via direct binding of a cytosolic domain to Orai1. Cell 136(5):876–890
74. Kawasaki T, Lange I, Feske S (2009) A minimal regulatory domain in the C terminus of STIM1 binds to and activates ORAI1 CRAC channels. Biochem Biophys Res Commun 385(1):49–54
75. Yang X, Jin H, Cai X, Li S, Shen Y (2012) Structural and mechanistic insights into the activation of Stromal interaction molecule 1 (STIM1). Proc Natl Acad Sci USA 109(15):5657–5662
76. Nwokonko RM, Cai X, Loktionova NA, Wang Y, Zhou Y, Gill DL (2017) The STIM-Orai pathway: conformational coupling between STIM and Orai in the activation of store-operated Ca^{2+} entry. Adv Exp Med Biol 993:83–98
77. Jha A, Ahuja M, Maleth J, Moreno CM, Yuan JP, Kim MS, Muallem S (2013) The STIM1 CTID domain determines access of SARAF to SOAR to regulate Orai1 channel function. J Cell Biol 202(1):71–79
78. Williams RT, Manji SS, Parker NJ, Hancock MS, Van Stekelenburg L, Eid JP, Senior PV, Kazenwadel JS, Shandala T, Saint R, Smith PJ, Dziadek MA (2001) Identification and characterization of the STIM (stromal interaction molecule) gene family: coding for a novel class of transmembrane proteins. Biochem J 357(Pt 3):673–685
79. Lopez E, Jardin I, Berna-Erro A, Bermejo N, Salido GM, Sage SO, Rosado JA, Redondo PC (2012) STIM1 tyrosine-phosphorylation is required for STIM1-Orai1 association in human platelets. Cell Signal 24(6):1315–1322
80. Williams RT, Senior PV, Van Stekelenburg L, Layton JE, Smith PJ, Dziadek MA (2002) Stromal interaction molecule 1 (STIM1), a transmembrane protein with growth suppressor activity, contains an extracellular SAM domain modified by N-linked glycosylation. Biochim Biophys Acta 1596(1):131–137
81. Horinouchi T, Higashi T, Higa T, Terada K, Mai Y, Aoyagi H, Hatate C, Nepal P, Horiguchi M, Harada T, Miwa S (2012) Different binding property of STIM1 and its novel splice variant STIM1L to Orai1, TRPC3, and TRPC6 channels. Biochem Biophys Res Commun 428(2):252–258
82. Darbellay B, Arnaudeau S, Bader CR, Konig S, Bernheim L (2011) STIM1L is a new actin-binding splice variant involved in fast repetitive Ca^{2+} release. J Cell Biol 194(2):335–346
83. Luo X, Hojayev B, Jiang N, Wang ZV, Tandan S, Rakalin A, Rothermel BA, Gillette TG, Hill JA (2012) STIM1-dependent store-operated Ca(2)(+) entry is required for pathological cardiac hypertrophy. J Mol Cell Cardiol 52(1):136–147
84. Rosado JA, Diez R, Smani T, Jardin I (2015) STIM and Orai1 variants in store-operated calcium entry. Front Pharmacol 6:325
85. Soboloff J, Spassova MA, Hewavitharana T, He LP, Xu W, Johnstone LS, Dziadek MA, Gill DL (2006) STIM2 is an inhibitor of STIM1-mediated store-operated Ca^{2+} Entry. Curr Biol 16(14):1465–1470
86. Wang JY, Sun J, Huang MY, Wang YS, Hou MF, Sun Y, He H, Krishna N, Chiu SJ, Lin S, Yang S, Chang WC (2014) STIM1 overexpression promotes colorectal cancer progression, cell motility and COX-2 expression. Oncogene 34:4358–4367
87. Rana A, Yen M, Sadaghiani AM, Malmersjo S, Park CY, Dolmetsch RE, Lewis RS (2015) Alternative splicing converts STIM2 from an activator to an inhibitor of store-operated calcium channels. J Cell Biol 209(5):653–669

88. Ercan E, Chung SH, Bhardwaj R, Seedorf M (2012) Di-arginine signals and the K-rich domain retain the Ca(2)(+) sensor STIM1 in the endoplasmic reticulum. Traffic 13(7):992–1003
89. Bauer MC, O'Connell D, Cahill DJ, Linse S (2008) Calmodulin binding to the polybasic C-termini of STIM proteins involved in store-operated calcium entry. Biochemistry 47(23):6089–6091
90. Berna-Erro A, Braun A, Kraft R, Kleinschnitz C, Schuhmann MK, Stegner D, Wultsch T, Eilers J, Meuth SG, Stoll G, Nieswandt B (2009) STIM2 regulates capacitive Ca^{2+} entry in neurons and plays a key role in hypoxic neuronal cell death. Sci Signal 2(93):ra67
91. Schuhmann MK, Stegner D, Berna-Erro A, Bittner S, Braun A, Kleinschnitz C, Stoll G, Wiendl H, Meuth SG, Nieswandt B (2010) Stromal interaction molecules 1 and 2 are key regulators of autoreactive T cell activation in murine autoimmune central nervous system inflammation. J Immunol 184(3):1536–1542
92. Oh-Hora M, Yamashita M, Hogan PG, Sharma S, Lamperti E, Chung W, Prakriya M, Feske S, Rao A (2008) Dual functions for the endoplasmic reticulum calcium sensors STIM1 and STIM2 in T cell activation and tolerance. Nat Immunol 9(4):432–443
93. Darbellay B, Arnaudeau S, Ceroni D, Bader CR, Konig S, Bernheim L (2010) Human muscle economy myoblast differentiation and excitation-contraction coupling use the same molecular partners, STIM1 and STIM2. J Biol Chem 285(29):22437–22447
94. Liou J, Kim ML, Heo WD, Jones JT, Myers JW, Ferrell JE Jr, Meyer T (2005) STIM is a Ca^{2+} sensor essential for Ca^{2+}-store-depletion-triggered Ca^{2+} influx. Curr Biol 15(13):1235–1241
95. Dionisio N, Galan C, Jardin I, Salido GM, Rosado JA (2011) Lipid rafts are essential for the regulation of SOCE by plasma membrane resident STIM1 in human platelets. Biochim Biophys Acta 1813(3):431–437
96. Mignen O, Thompson JL, Shuttleworth TJ (2007) STIM1 regulates Ca^{2+} entry via arachidonate-regulated Ca^{2+}-selective (ARC) channels without store depletion or translocation to the plasma membrane. J Physiol 579(Pt 3):703–715
97. Miederer AM, Alansary D, Schwar G, Lee PH, Jung M, Helms V, Niemeyer BA (2015) A STIM2 splice variant negatively regulates store-operated calcium entry. Nat Commun 6:6899
98. Berna-Erro A, Jardin I, Salido GM, Rosado JA (2017) Role of STIM2 in cell function and physiopathology. J Physiol 595(10):3111–3128
99. Zhou Y, Nwokonko RM, Cai X, Loktionova NA, Abdulqadir R, Xin P, Niemeyer BA, Wang Y, Trebak M, Gill DL (2018) Cross-linking of Orai1 channels by STIM proteins. Proc Natl Acad Sci USA 115(15):E3398–E3407
100. Stathopulos PB, Li GY, Plevin MJ, Ames JB, Ikura M (2006) Stored Ca^{2+} depletion-induced oligomerization of stromal interaction molecule 1 (STIM1) via the EF-SAM region: An initiation mechanism for capacitive Ca^{2+} entry. J Biol Chem 281(47):35855–35862
101. Brandman O, Liou J, Park WS, Meyer T (2007) STIM2 is a feedback regulator that stabilizes basal cytosolic and endoplasmic reticulum Ca^{2+} levels. Cell 131(7):1327–1339
102. Subedi KP, Ong HL, Son GY, Liu X, Ambudkar IS (2018) STIM2 induces activated conformation of STIM1 to control Orai1 function in ER-PM junctions. Cell Rep 23(2): 522–534
103. Desai PN, Zhang X, Wu S, Janoshazi A, Bolimuntha S, Putney JW, Trebak M (2015) Multiple types of calcium channels arising from alternative translation initiation of the Orai1 message. Sci Signal 8(387):ra74
104. Ambudkar IS, de Souza LB, Ong HL (2017) TRPC1, Orai1, and STIM1 in SOCE: friends in tight spaces. Cell Calcium 63:33–39
105. Chung WY, Jha A, Ahuja M, Muallem S (2017) Ca^{2+} influx at the ER/PM junctions. Cell Calcium 63:29–32
106. Jardin I, Lopez JJ, Salido GM, Rosado JA (2008) Orai1 mediates the interaction between STIM1 and hTRPC1 and regulates the mode of activation of hTRPC1-forming Ca^{2+} channels. J Biol Chem 283(37):25296–25304
107. Hoth M, Penner R (1992) Depletion of intracellular calcium stores activates a calcium current in mast cells. Nature 355(6358):353–356

108. Feske S, Gwack Y, Prakriya M, Srikanth S, Puppel SH, Tanasa B, Hogan PG, Lewis RS, Daly M, Rao A (2006) A mutation in Orai1 causes immune deficiency by abrogating CRAC channel function. Nature 441(7090):179–185
109. Vig M, Peinelt C, Beck A, Koomoa DL, Rabah D, Koblan-Huberson M, Kraft S, Turner H, Fleig A, Penner R, Kinet JP (2006) CRACM1 is a plasma membrane protein essential for store-operated Ca^{2+} entry. Science 312(5777):1220–1223
110. Zhang SL, Yeromin AV, Zhang XH, Yu Y, Safrina O, Penna A, Roos J, Stauderman KA, Cahalan MD (2006) Genome-wide RNAi screen of Ca^{2+} influx identifies genes that regulate Ca^{2+} release-activated Ca^{2+} channel activity. Proc Natl Acad Sci USA 103(24):9357–9362
111. Guo RW, Huang L (2008) New insights into the activation mechanism of store-operated calcium channels: roles of STIM and Orai. J Zhejiang Univ Sci B 9(8):591–601
112. Mercer JC, Dehaven WI, Smyth JT, Wedel B, Boyles RR, Bird GS, Putney JW Jr (2006) Large store-operated calcium selective currents due to co-expression of Orai1 or Orai2 with the intracellular calcium sensor, Stim1. J Biol Chem 281(34):24979–24990
113. Peinelt C, Vig M, Koomoa DL, Beck A, Nadler MJ, Koblan-Huberson M, Lis A, Fleig A, Penner R, Kinet JP (2006) Amplification of CRAC current by STIM1 and CRACM1 (Orai1). Nat Cell Biol 8(7):771–773
114. Prakriya M, Feske S, Gwack Y, Srikanth S, Rao A, Hogan PG (2006) Orai1 is an essential pore subunit of the CRAC channel. Nature 443(7108):230–233
115. Soboloff J, Spassova MA, Tang XD, Hewavitharana T, Xu W, Gill DL (2006) Orai1 and STIM reconstitute store-operated calcium channel function. J Biol Chem 281(30):20661–20665
116. Derler I, Plenk P, Fahrner M, Muik M, Jardin I, Schindl R, Gruber HJ, Groschner K, Romanin C (2013) The extended transmembrane Orai1 N-terminal (ETON) region combines binding interface and gate for Orai1 activation by STIM1. J Biol Chem 288(40):29025–29034
117. Palty R, Isacoff EY (2015) Cooperative binding of Stromal Interaction Molecule 1 (STIM1) to the N and C termini of calcium release-activated calcium modulator 1 (Orai1). J Biol Chem 291:334–341
118. Palty R, Stanley C, Isacoff EY (2015) Critical role for Orai1 C-terminal domain and TM4 in CRAC channel gating. Cell Res 25(8):963–980
119. Penna A, Demuro A, Yeromin AV, Zhang SL, Safrina O, Parker I, Cahalan MD (2008) The CRAC channel consists of a tetramer formed by Stim-induced dimerization of Orai dimers. Nature 456(7218):116–120
120. Maruyama Y, Ogura T, Mio K, Kato K, Kaneko T, Kiyonaka S, Mori Y, Sato C (2009) Tetrameric Orai1 is a teardrop-shaped molecule with a long, tapered cytoplasmic domain. J Biol Chem 284(20):13676–13685
121. Mignen O, Thompson JL, Shuttleworth TJ (2008) Orai1 subunit stoichiometry of the mammalian CRAC channel pore. J Physiol 586(2):419–425
122. Hou X, Pedi L, Diver MM, Long SB (2012) Crystal structure of the calcium release-activated calcium channel Orai. Science 338(6112):1308–1313
123. Thompson JL, Shuttleworth TJ (2013) How many Orai's does it take to make a CRAC channel? Sci Rep 3:1961
124. Peinelt C, Lis A, Beck A, Fleig A, Penner R (2008) 2-Aminoethoxydiphenyl borate directly facilitates and indirectly inhibits STIM1-dependent gating of CRAC channels. J Physiol 586(13):3061–3073
125. Yamashita M, Navarro-Borelly L, McNally BA, Prakriya M (2007) Orai1 mutations alter ion permeation and Ca^{2+}-dependent fast inactivation of CRAC channels: evidence for coupling of permeation and gating. J Gen Physiol 130(5):525–540
126. Endo Y, Noguchi S, Hara Y, Hayashi YK, Motomura K, Miyatake S, Murakami N, Tanaka S, Yamashita S, Kizu R, Bamba M, Goto Y, Matsumoto N, Nonaka I, Nishino I (2015) Dominant mutations in ORAI1 cause tubular aggregate myopathy with hypocalcemia via constitutive activation of store-operated Ca(2)(+) channels. Hum Mol Genet 24(3):637–648
127. Nesin V, Wiley G, Kousi M, Ong EC, Lehmann T, Nicholl DJ, Suri M, Shahrizaila N, Katsanis N, Gaffney PM, Wierenga KJ, Tsiokas L (2014) Activating mutations in STIM1 and ORAI1 cause overlapping syndromes of tubular myopathy and congenital miosis. Proc Natl Acad Sci USA 111(11):4197–4202

128. Frischauf I, Muik M, Derler I, Bergsmann J, Fahrner M, Schindl R, Groschner K, Romanin C (2009) Molecular determinants of the coupling between STIM1 and Orai channels: differential activation of Orai1-3 channels by a STIM1 coiled-coil mutant. J Biol Chem 284(32):21696–21706
129. Lis A, Peinelt C, Beck A, Parvez S, Monteilh-Zoller M, Fleig A, Penner R (2007) CRACM1, CRACM2, and CRACM3 are store-operated Ca^{2+} channels with distinct functional properties. Curr Biol 17(9):794–800
130. Ma HT, Patterson RL, van Rossum DB, Birnbaumer L, Mikoshiba K, Gill DL (2000) Requirement of the inositol trisphosphate receptor for activation of store-operated Ca^{2+} channels. Science 287(5458):1647–1651
131. Diver JM, Sage SO, Rosado JA (2001) The inositol trisphosphate receptor antagonist 2-aminoethoxydiphenylborate (2-APB) blocks Ca^{2+} entry channels in human platelets: cautions for its use in studying Ca^{2+} influx. Cell Calcium 30(5):323–329
132. Wang Y, Deng X, Zhou Y, Hendron E, Mancarella S, Ritchie MF, Tang XD, Baba Y, Kurosaki T, Mori Y, Soboloff J, Gill DL (2009) STIM protein coupling in the activation of Orai channels. Proc Natl Acad Sci USA 106(18):7391–7396
133. Prakriya M, Lewis RS (2001) Potentiation and inhibition of Ca^{2+} release-activated Ca^{2+} channels by 2-aminoethyldiphenyl borate (2-APB) occurs independently of IP(3) receptors. J Physiol 536(Pt 1):3–19
134. Wei M, Zhou Y, Sun A, Ma G, He L, Zhou L, Zhang S, Liu J, Zhang SL, Gill DL, Wang Y (2016) Molecular mechanisms underlying inhibition of STIM1-Orai1-mediated Ca^{2+} entry induced by 2-aminoethoxydiphenyl borate. Pflugers Arch 468(11–12):2061–2074
135. Lopez JJ, Jardin I, Cantonero Chamorro C, Duran ML, Tarancon Rubio MJ, Reyes Panadero M, Jimenez F, Montero R, Gonzalez MJ, Martinez M, Hernandez MJ, Brull JM, Corbacho AJ, Delgado E, Granados MP, Gomez-Gordo L, Rosado JA, Redondo PC (2018) Involvement of stanniocalcins in the deregulation of glycaemia in obese mice and type 2 diabetic patients. J Cell Mol Med 22(1):684–694
136. Fahrner M, Derler I, Jardin I, Romanin C (2013) The STIM1/Orai signaling machinery. Channels (Austin) 7(5):330–343
137. Korzeniowski MK, Manjarres IM, Varnai P, Balla T (2010) Activation of STIM1-Orai1 involves an intramolecular switching mechanism. Sci Signal 3(148):ra82
138. Stathopulos PB, Zheng L, Ikura M (2009) Stromal interaction molecule (STIM) 1 and STIM2 calcium sensing regions exhibit distinct unfolding and oligomerization kinetics. J Biol Chem 284(2):728–732
139. Ma G, Wei M, He L, Liu C, Wu B, Zhang SL, Jing J, Liang X, Senes A, Tan P, Li S, Sun A, Bi Y, Zhong L, Si H, Shen Y, Li M, Lee MS, Zhou W, Wang J, Wang Y, Zhou Y (2015) Inside-out Ca^{2+} signalling prompted by STIM1 conformational switch. Nat Commun 6:7826
140. Fahrner M, Muik M, Schindl R, Butorac C, Stathopulos P, Zheng L, Jardin I, Ikura M, Romanin C (2014) A coiled-coil clamp controls both conformation and clustering of Stromal Interaction Molecule 1 (STIM1). J Biol Chem 289(48):33231–33244
141. Stathopulos PB, Schindl R, Fahrner M, Zheng L, Gasmi-Seabrook GM, Muik M, Romanin C, Ikura M (2013) STIM1/Orai1 coiled-coil interplay in the regulation of store-operated calcium entry. Nat Commun 4:2963
142. Hirve N, Rajanikanth V, Hogan PG, Gudlur A (2018) Coiled-coil formation conveys a STIM1 signal from ER Lumen to cytoplasm. Cell Rep 22(1):72–83
143. McNally BA, Somasundaram A, Jairaman A, Yamashita M, Prakriya M (2013) The C- and N-terminal STIM1 binding sites on Orai1 are required for both trapping and gating CRAC channels. J Physiol 591(11):2833–2850
144. Gudlur A, Quintana A, Zhou Y, Hirve N, Mahapatra S, Hogan PG (2014) STIM1 triggers a gating rearrangement at the extracellular mouth of the ORAI1 channel. Nat Commun 5:5164
145. Hogan PG, Rao A (2015) Store-operated calcium entry: mechanisms and modulation. Biochem Biophys Res Commun 460(1):40–49
146. Parekh AB, Putney JW Jr (2005) Store-operated calcium channels. Physiol Rev 85(2): 757–810

147. Brechard S, Melchior C, Plancon S, Schenten V, Tschirhart EJ (2008) Store-operated Ca^{2+} channels formed by TRPC1, TRPC6 and Orai1 and non-store-operated channels formed by TRPC3 are involved in the regulation of NADPH oxidase in HL-60 granulocytes. Cell Calcium 44(5):492–506
148. Galan C, Dionisio N, Smani T, Salido GM, Rosado JA (2011) The cytoskeleton plays a modulatory role in the association between STIM1 and the Ca^{2+} channel subunits Orai1 and TRPC1. Biochem Pharmacol 82(4):400–410
149. Sabourin J, Le Gal L, Saurwein L, Haefliger JA, Raddatz E, Allagnat F (2015) Store-operated Ca^{2+} entry mediated by Orai1 and TRPC1 participates to insulin secretion in Rat beta-Cells. J Biol Chem 290(51):30530–30539
150. Sampieri A, Zepeda A, Saldaña C, Salgado A, Vaca L (2008) STIM1 converts TRPC1 from a receptor-operated to a store-operated channel: moving TRPC1 in and out of lipid rafts. Cell Calcium 44(5):479–491
151. Cosens DJ, Manning A (1969) Abnormal electroretinogram from a Drosophila mutant. Nature 224(5216):285–287
152. Hardie RC, Minke B (1992) The trp gene is essential for a light-activated Ca^{2+} channel in Drosophila photoreceptors. Neuron 8(4):643–651
153. Phillips AM, Bull A, Kelly LE (1992) Identification of a Drosophila gene encoding a calmodulin-binding protein with homology to the trp phototransduction gene. Neuron 8(4):631–642
154. Minke B (1977) Drosophila mutant with a transducer defect. Biophys Struct Mech 3(1): 59–64
155. Wes PD, Chevesich J, Jeromin A, Rosenberg C, Stetten G, Montell C (1995) TRPC1, a human homolog of a Drosophila store-operated channel. Proc Natl Acad Sci USA 92(21):9652–9656
156. Zhu X, Chu PB, Peyton M, Birnbaumer L (1995) Molecular cloning of a widely expressed human homologue for the Drosophila trp gene. FEBS Lett 373(3):193–198
157. Petersen CC, Berridge MJ, Borgese MF, Bennett DL (1995) Putative capacitative calcium entry channels: expression of Drosophila trp and evidence for the existence of vertebrate homologues. Biochem J 311(Pt 1):41–44
158. Montell C, Birnbaumer L, Flockerzi V, Bindels RJ, Bruford EA, Caterina MJ, Clapham DE, Harteneck C, Heller S, Julius D, Kojima I, Mori Y, Penner R, Prawitt D, Scharenberg AM, Schultz G, Shimizu N, Zhu MX (2002) A unified nomenclature for the superfamily of TRP cation channels. Mol Cell 9(2):229–231
159. Flockerzi V, Nilius B (2014) TRPs: truly remarkable proteins. Handb Exp Pharmacol 222: 1–12
160. Salido GM, Jardin I, Rosado JA (2011) The TRPC Ion channels: association with Orai1 and STIM1 proteins and participation in capacitative and non-capacitative calcium entry. Adv Exp Med Biol 704:413–433
161. Montell C (2003) The venerable inveterate invertebrate TRP channels. Cell Calcium 33(5–6):409–417
162. Montell C, Birnbaumer L, Flockerzi V (2002) The TRP channels, a remarkably functional family. Cell 108(5):595–598
163. Rosado JA, Brownlow SL, Sage SO (2002) Endogenously expressed Trp1 is involved in store-mediated Ca^{2+} entry by conformational coupling in human platelets. J Biol Chem 277(44):42157–42163
164. Gregorio-Teruel L, Valente P, Gonzalez-Ros JM, Fernandez-Ballester G, Ferrer-Montiel A (2014) Mutation of I696 and W697 in the TRP box of vanilloid receptor subtype I modulates allosteric channel activation. J Gen Physiol 143(3):361–375
165. Wedel BJ, Vazquez G, McKay RR, St JBG, Putney JW Jr (2003) A calmodulin/inositol 1,4,5-trisphosphate (IP3) receptor-binding region targets TRPC3 to the plasma membrane in a calmodulin/IP3 receptor-independent process. J Biol Chem 278(28):25758–25765
166. Dionisio N, Albarran L, Berna-Erro A, Hernandez-Cruz JM, Salido GM, Rosado JA (2011) Functional role of the calmodulin- and inositol 1,4,5-trisphosphate receptor-binding (CIRB) site of TRPC6 in human platelet activation. Cell Signal 23(11):1850–1856

167. Lee KP, Choi S, Hong JH, Ahuja M, Graham S, Ma R, So I, Shin DM, Muallem S, Yuan JP (2014) Molecular determinants mediating gating of Transient Receptor Potential Canonical (TRPC) channels by stromal interaction molecule 1 (STIM1). J Biol Chem 289(10):6372–6382
168. Hardie RC (2003) Regulation of TRP channels via lipid second messengers. Annu Rev Physiol 65:735–759
169. Huang GN, Zeng W, Kim JY, Yuan JP, Han L, Muallem S, Worley PF (2006) STIM1 carboxyl-terminus activates native SOC, I(crac) and TRPC1 channels. Nat Cell Biol 8(9):1003–1010
170. Pani B, Liu X, Bollimuntha S, Cheng KT, Niesman IR, Zheng C, Achen VR, Patel HH, Ambudkar IS, Singh BB (2013) Impairment of TRPC1-STIM1 channel assembly and AQP5 translocation compromise agonist-stimulated fluid secretion in mice lacking caveolin1. J Cell Sci 126(Pt 2):667–675
171. Lopez E, Berna-Erro A, Salido GM, Rosado JA, Redondo PC (2013) FKBP52 is involved in the regulation of SOCE channels in the human platelets and MEG 01 cells. Biochim Biophys Acta 1833(3):652–662
172. Jardin I, Lopez JJ, Salido GM, Rosado JA (2008) Functional relevance of the de novo coupling between hTRPC1 and type II IP_3 receptor in store-operated Ca^{2+} entry in human platelets. Cell Signal 20(4):737–747
173. Cheng KT, Liu X, Ong HL, Swaim W, Ambudkar IS (2011) Local Ca^{2+} entry via Orai1 regulates plasma membrane recruitment of TRPC1 and controls cytosolic Ca^{2+} signals required for specific cell functions. PLoS Biol 9(3):e1001025
174. Ong EC, Nesin V, Long CL, Bai CX, Guz JL, Ivanov IP, Abramowitz J, Birnbaumer L, Humphrey MB, Tsiokas L (2013) A TRPC1 protein-dependent pathway regulates osteoclast formation and function. J Biol Chem 288(31):22219–22232
175. Zeng W, Yuan JP, Kim MS, Choi YJ, Huang GN, Worley PF, Muallem S (2008) STIM1 gates TRPC channels, but not Orai1, by electrostatic interaction. Mol Cell 32(3):439–448
176. Zweifach A, Lewis RS (1995) Rapid inactivation of depletion-activated calcium current (ICRAC) due to local calcium feedback. J Gen Physiol 105(2):209–226
177. Zweifach A, Lewis RS (1995) Slow calcium-dependent inactivation of depletion-activated calcium current. Store-dependent and -independent mechanisms. J Biol Chem 270(24):14445–14451
178. Parekh AB (2017) Regulation of CRAC channels by Ca^{2+}-dependent inactivation. Cell Calcium 63:20–23
179. Parekh AB (1998) Slow feedback inhibition of calcium release-activated calcium current by calcium entry. J Biol Chem 273(24):14925–14932
180. Fierro L, Parekh AB (1999) Fast calcium-dependent inactivation of calcium release-activated calcium current (CRAC) in RBL-1 cells. J Membr Biol 168(1):9–17
181. Liu Y, Zheng X, Mueller GA, Sobhany M, DeRose EF, Zhang Y, London RE, Birnbaumer L (2012) Crystal structure of calmodulin binding domain of orai1 in complex with Ca^{2+} calmodulin displays a unique binding mode. J Biol Chem 287(51):43030–43041
182. Mullins FM, Yen M, Lewis RS (2016) Orai1 pore residues control CRAC channel inactivation independently of calmodulin. J Gen Physiol 147(2):137–152
183. Gilabert JA, Parekh AB (2000) Respiring mitochondria determine the pattern of activation and inactivation of the store-operated Ca^{2+} current I(CRAC). EMBO J 19(23):6401–6407
184. Palty R, Raveh A, Kaminsky I, Meller R, Reuveny E (2012) SARAF inactivates the store operated calcium entry machinery to prevent excess calcium refilling. Cell 149(2):425–438
185. Albarran L, Regodon S, Salido GM, Lopez JJ, Rosado JA (2017) Role of STIM1 in the surface expression of SARAF. Channels (Austin) 11(1):84–88
186. Albarran L, Lopez JJ, Ben Amor N, Martín-Cano FE, Berna-Erro A, Smani T, Salido GM, Rosado JA (2016) Dynamic interaction of SARAF with STIM1 and Orai1 to modulate store-operated calcium entry. Scientific Reports 6:24452
187. Albarran L, Lopez JJ, Gomez LJ, Salido GM, Rosado JA (2016) SARAF modulates TRPC1, but not TRPC6, channel function in a STIM1-independent manner. Biochem J 473(20):3581–3595

188. Maleth J, Choi S, Muallem S, Ahuja M (2014) Translocation between PI(4,5)P2-poor and PI(4,5)P2-rich microdomains during store depletion determines STIM1 conformation and Orai1 gating. Nat Commun 5:5843
189. Feng JM, Hu YK, Xie LH, Colwell CS, Shao XM, Sun XP, Chen B, Tang H, Campagnoni AT (2006) Golli protein negatively regulates store depletion-induced calcium influx in T cells. Immunity 24(6):717–727
190. Walsh CM, Doherty MK, Tepikin AV, Burgoyne RD (2010) Evidence for an interaction between Golli and STIM1 in store-operated calcium entry. Biochem J 430(3):453–460
191. Carreras-Sureda A, Cantero-Recasens G, Rubio-Moscardo F, Kiefer K, Peinelt C, Niemeyer BA, Valverde MA, Vicente R (2013) ORMDL3 modulates store-operated calcium entry and lymphocyte activation. Hum Mol Genet 22(3):519–530
192. Lopez JJ, Albarran L, Jardin I, Sanchez-Collado J, Redondo PC, Bermejo N, Bobe R, Smani T, Rosado JA (2018) Filamin A modulates store-operated Ca^{2+} entry by regulating STIM1 (Stromal Interaction Molecule 1)-Orai1 association in human platelets. Arterioscler Thromb Vasc Biol 38:386–397
193. Srikanth S, Jung HJ, Kim KD, Souda P, Whitelegge J, Gwack Y (2010) A novel EF-hand protein, CRACR2A, is a cytosolic Ca^{2+} sensor that stabilizes CRAC channels in T cells. Nat Cell Biol 12(5):436–446
194. Jing J, He L, Sun A, Quintana A, Ding Y, Ma G, Tan P, Liang X, Zheng X, Chen L, Shi X, Zhang SL, Zhong L, Huang Y, Dong MQ, Walker CL, Hogan PG, Wang Y, Zhou Y (2015) Proteomic mapping of ER-PM junctions identifies STIMATE as a regulator of Ca(2)(+) influx. Nat Cell Biol 17(10):1339–1347
195. Beck A, Fleig A, Penner R, Peinelt C (2014) Regulation of endogenous and heterologous Ca(2)(+) release-activated Ca(2)(+) currents by pH. Cell Calcium 56(3):235–243
196. He X, Song S, Ayon RJ, Balisterieri A, Black SM, Makino A, Wier WG, Zang WJ, Yuan JX (2018) Hypoxia selectively upregulates cation channels and increases cytosolic [Ca^{2+}] in pulmonary, but not coronary, arterial smooth muscle cells. Am J Physiol Cell Physiol 314(4):C504–C517
197. Rosado JA, Redondo PC, Salido GM, Gomez-Arteta E, Sage SO, Pariente JA (2004) Hydrogen peroxide generation induces pp60src activation in human platelets: evidence for the involvement of this pathway in store-mediated calcium entry. J Biol Chem 279(3):1665–1675
198. Hawkins BJ, Irrinki KM, Mallilankaraman K, Lien YC, Wang Y, Bhanumathy CD, Subbiah R, Ritchie MF, Soboloff J, Baba Y, Kurosaki T, Joseph SK, Gill DL, Madesh M (2010) S-glutathionylation activates STIM1 and alters mitochondrial homeostasis. J Cell Biol 190(3):391–405
199. Smyth JT, Petranka JG, Boyles RR, DeHaven WI, Fukushima M, Johnson KL, Williams JG, Putney JW Jr (2009) Phosphorylation of STIM1 underlies suppression of store-operated calcium entry during mitosis. Nat Cell Biol 11(12):1465–1472
200. Sundivakkam PC, Natarajan V, Malik AB, Tiruppathi C (2013) Store-operated Ca^{2+} entry (SOCE) induced by protease-activated receptor-1 mediates STIM1 protein phosphorylation to inhibit SOCE in endothelial cells through AMP-activated protein kinase and p38beta mitogen-activated protein kinase. J Biol Chem 288(23):17030–17041
201. Kawasaki T, Ueyama T, Lange I, Feske S, Saito N (2010) Protein kinase C-induced phosphorylation of Orai1 regulates the intracellular Ca^{2+} level via the store-operated Ca^{2+} channel. J Biol Chem 285(33):25720–25730

Chapter 18
Canonical Transient Potential Receptor-3 Channels in Normal and Diseased Airway Smooth Muscle Cells

Yong-Xiao Wang, Lan Wang, and Yun-Min Zheng

Abstract All seven canonical transient potential receptor (TRPC1–7) channel members are expressed in mammalian airway smooth muscle cells (ASMCs). Among this family, TRPC3 channel plays an important role in the control of the resting $[Ca^{2+}]_i$ and agonist-induced increase in $[Ca^{2+}]_i$. This channel is significantly upregulated in molecular expression and functional activity in airway diseases. The upregulated channel significantly augments the resting $[Ca^{2+}]_i$ and agonist-induced increase in $[Ca^{2+}]_i$, thereby exerting a direct and essential effect in airway hyperresponsiveness. The increased TRPC3 channel-mediated Ca^{2+} signaling also results in the transcription factor nuclear factor-κB (NF-κB) activation via protein kinase C-α (PKCα)-dependent inhibitor of NFκB-α (IκBα) and calcineurin-dependent IκBβ signaling pathways, which upregulates cyclin-D1 expression and causes cell proliferation, leading to airway remodeling. TRPC3 channel may further interact with intracellular release Ca^{2+} channels, Orai channels and Ca^{2+}-sensing stromal interaction molecules, mediating important cellular responses in ASMCs and the development of airway diseases.

Keywords Canonical transient potential receptor channel · Inositol 1 · 4 · 5-trisphosphate receptor · Ryanodine receptor · Orai channel · Stromal interaction molecule · Nuclear factor κB · Protein kinase C · Calcineurin · Airway hyperresponsiveness · Airway remodeling · Airway diseases

Authors "Yong-Xiao Wang and Lan Wang" have contributed equally for this chapter

Y.-X. Wang · Y.-M. Zheng (✉)
Department of Molecular and Cellular Physiology, Albany Medical College, Albany, NY, USA

L. Wang
Department of Molecular and Cellular Physiology, Albany Medical College, Albany, NY, USA

Department of Cardiopulmonary Circulation, Shanghai Pulmonary Hospital, Tongji University School of Medicine, Shanghai, China
e-mail: zhengy@amc.edu

M. S. Islam (ed.), *Calcium Signaling*, Advances in Experimental Medicine and Biology 1131, https://doi.org/10.1007/978-3-030-12457-1_18

Abbreviations

$[Ca^{2+}]i$	Intracellular Ca^{2+} concentration
ASMCs	Airway smooth muscle cells
COPD	chronic obstructive pulmonary disease
DAG	Diacylglycerol
GPCR	G protein-coupled receptor
IP_3	Inositol 1,4,5-trisphosphate
IP_3R	IP_3 receptor
IκB	Nuclear factor κB inhibitor
JNK	Jun amino-terminal kinase
mAch	Methacholine
NF-κB	Nuclear factor κB
NPo	Open probability
NSCC	Non-selective cation channel
OAG	1-oleoyl-2-acetyl-sn-glycerol
PIP_2	Phosphatidylinositol 4,5-bisphosphate
PKCα	Protein kinase C-α
PLC	Phospholipase C
RyR	Ryanodine receptor
SOCE	Store-operated Ca^{2+} entry
SR	Sarcoplasmic reticulum
STIM	Stromal interaction molecule
TNFα	Tumor necrosis factor-α
TRPC	Canonical transient potential receptor
Vm	Membrane potential

18.1 Introduction

The canonical transient potential receptor (TRP) channels are encoded by genes that most closely related resemble the *trp* gene, which was originally identified in *Drosophila* [1]. Photoreceptor cells in *Drosophila* produce a transient receptor potential in response to light. This potential is comprised of an initial rapid spike followed by a sustained phase. Both phases are mediated by TRP encoded and TRP-like channels. The first mammalian TRP gene was cloned from the human brain using an expressed sequence tag, categorized into the TRPC channel family based on its primary amino acid sequence, and thus termed TRPC1 channel [2]. The TRPC channel family is known to consist of seven members designated TRPC1–7 channels.

TRPC channels have been well investigated in a number of cell types; however, their functional roles and underlying signaling mechanisms are not well known in airway smooth muscle cells (ASMCs). A series of our recent studies using the patch clamp technique, genetically-manipulated approach and other methods have started

to meticulously address whether, which and how TRPC channels play an important role in physiological and pathological cellular responses in ASMCs. In this article, we intend to provide a comprehensive overview of the major exciting findings from our research works and others, with particularly focus on the molecular expression, functional roles and underlying signaling mechanisms of TRPC3 channels in physiological cellular responses in ASMCs and airway diseases.

18.2 Multiple TRPC Channel Members Are Expressed, but TRPC3 Channel Is the Predominant Member in ASMCs

Ong HL et al. reported that TRPC1, TRPC2, TRPC3, TRPC4, TRPC5 and TRPC6 channel mRNAs are detected in primary isolated guinea-pig airway SMCs [3]. It has also been reported that TRPC1, TRPC3, TRPC4 and TRPC6, but not TRPC2 and TRPC5 channel mRNAs are present in cultured human ASMCs [4]. In cultured human ASMCs, TRPC1, TRPC3, TRPC4, TRPC5 and TRPC6, but not TRPC2 channel mRNAs have been found [5]. Prior studies detected expression of TRPC1,TRPC3 and TRPC6 channel proteins in primary isolated guinea pig airway SM cells and tissues [3, 6], TRPC1, TRPC3/6/7 and TRPC4 channel proteins in freshly isolated porcine airway SM tissues [7], TRPC6 channel protein in primary isolated guinea pig and cultured human airway SMCs [4, 8], and TRPC1, TRPC3, TRPC4, TRPC5 and TRPC6 channel proteins in cultured human ASMCs [5]. Our studies reveal that TRPC1 and TRPC3 channel mRNAs and proteins are expressed in freshly isolated mouse ASMCs [9].

Researchers have found that non-selective cation channels (NSCCs), which are permeable to both Na^+ and Ca^{2+}, with higher permeability to Na^+, are present in freshly isolated bovine and human ASMCs [10–13]. We have further characterized NSCCs in freshly isolated mouse ASMCs using the excised inside-out single channel recording [9]. The channel open probability in freshly isolated mouse ASMCs is significantly higher at positive than negative potentials, suggesting that the native NSCCs exhibit outward rectification in ASMCs. A diacylglycerol analogue, 1-oleoyl-2-acetyl-sn-glycerol (OAG), significantly increases the channel activity. The channel activity is augmented by elevating extracellular Ca^{2+} concentration and inhibited by reducing extracellular Ca^{2+} concentration. Thus, constitutively-active NSCCs in ASMCs possess diacylglycerol- and Ca^{2+}-gated properties, which are very similar to native constitutively-active NSCCs in vascular SMCs [14].

Our study also reveals that application of specific TRPC3 channel antibodies blocks the activity of native single NSCCs by ~80% in freshly isolated ASMCs [9]. TRPC3 channel gene silencing by specific siRNAs inhibits the single channel activity to a very similar extent in primary isolated cells. These patch clamp and genetic studies for the first time provide compelling evidence that native constitutively-active NSCCs are mainly encoded by TRPC3 channel in ASMCs

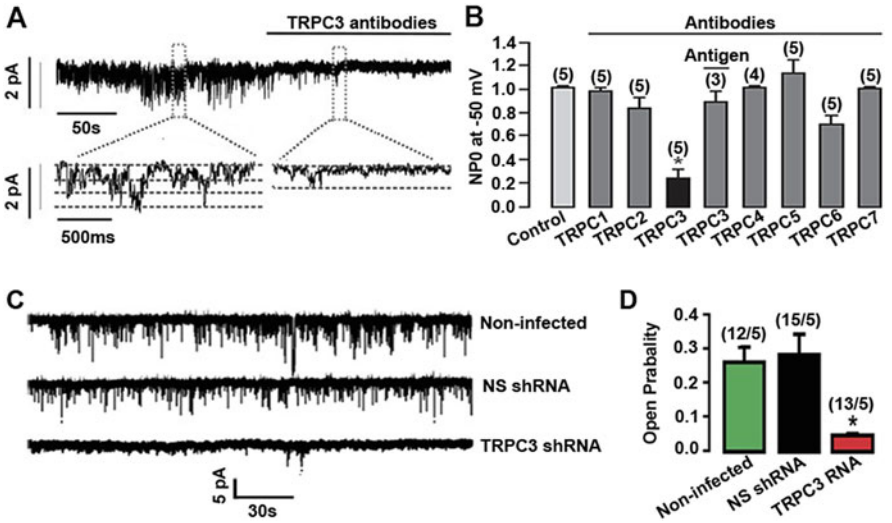

Fig. 18.1 TRPC3 channel is a predominant member of the TRPC channel family showing functional activity in ASMCs. (**a**) Specific TRPC3 channel antibodies inhibit the activity of single native constitutively active NSCCs in freshly isolated ASMCs (adopted from Xiao et al, *Am J Respir Cell Mol Biol*, 43: 17–25, 2010). An original recording of single NSCCs in an inside-out patch at −50 mV before and after bath application of specific TRPC3 channel antibodies (1:200 dilution). The *inserts* exhibit the channel recording at an extended time scale. (**b**) Summary of the effect of TRPC1 – TRPC6 antibodies on the activity of single NSCCs (unpublished data). The relative open probability (NPo) is presented as the difference in the channel activity recorded before and after application of individual TRPC antibodies (Ab). Numbers in parentheses indicate the numbers of cells from different mice examined. $^*P < 0.05$ compared with control cells (without application of TRPC antibodies). (**c**) TRPC3 channel activity in ASMCs isolated from noninfected mice and mice receiving intravenous injection of NS and TRPC3 shRNAs (adopted from Song et al, *FASEB J*, 30: 214–29, 2016). TRPC3 channel activity in ASMCs isolated from noninfected mice (not receiving lentiviral SM22-driven shRANs) and mice receiving intravenous injection of lentiviral SM22-driven non-silencing (NS) and TRPC3 channel shRNAs. The channel activity was recorded in excised membrane patches from ASMCs using the inside-out single-channel recording. $^*P < 0.05$ compared with cells from control (noninfected) mice

(Fig. 18.1), These findings also suggest that TRPC3 channel may form homomeric and/or heteromeric NSCCs with different conductance states.

18.3 TRPC3 Channel Is Important for Controlling Resting Membrane Potential and $[Ca^{2+}]_i$ in ASMCs

The resting membrane potential (Vm) in ASMCs is between −40 and − 50 mV, similar to other types of SMCs, and significantly less negative than a K^+ equilibrium potential of ∼ − 85 mV [15, 16]. Consistent with these prior reports, we have also found that the resting Vm is −44 mV in freshly isolated ASMCs [9]. More importantly, our data reveal that specific TRPC3 channel antibodies and gene

silencing both result in a pronounced hyperpolarization of the resting membrane potential by approximately 14 mV. Conversely, TRPC1 channel antibodies and gene silencing have no obvious effect on the resting Vm. Thus, TRPC3 channel predominates the control of resting Vm in ASMCs, consistent with the vital role of TRPC3 channel in mediating the activity of constitutively-active NSCCs.

Comparable to the effect on the resting membrane potential, we have found that siRNA-mediated TRPC3 channel gene silencing significantly lowers the resting $[Ca^{2+}]_i$ in primary isolated ASMCs [9]. However, TRPC1 channel gene silencing does not alter the resting $[Ca^{2+}]$i. These findings provide evidence that TRPC3, but not TRPC1 channel, play an important role in the control of the resting $[Ca^{2+}]_i$ in ASMCs. We have also shown that IP_3, an important intracellular second messenger, can activate TRPC3 channel to cause extracellular Ca^{2+} influx [17]. This novel extracellular Ca^{2+} entry route may play a significant role in mediating IP_3-mediated numerous cellular response in ASMCs.

18.4 TRPC3 Channel Is Involved in Agonist-Induced Increase in $[Ca^{2+}]_i$ in ASMCs

Using the patch clamp recording technique, we and other investigators have shown that muscarinic agonists acetylcholine and methacholine (mAch) activate NSCCs in freshly isolated canine, equine, guinea-pig and swine ASMCs [18–22]. Simultaneous measurements of membrane currents and $[Ca^{2+}]_i$ reveal that activation of NSCCs during muscarinic stimulation is always accompanied by a sustained increase in $[Ca^{2+}]_i$ due to extracellular Ca^{2+} influx [19–22]. The sustained increase in $[Ca^{2+}]_i$ induced by mACH and other agonists are largely inhibited or abolished by the general NSCC blockers $Ni2^+$, Cd^{2+}, La^{3+}, Gd^{3+} and SKF-96365 [12, 15, 20, 22–28]. Thus, functional NSCCs mediate agonist-induced Ca^{2+} influx and associated increase in $[Ca^{2+}]_i$ in ASMCs.

We have started to identify which of the TRPC channels are responsible for agonist-induced increase in $[Ca^{2+}]_i$. Our recent study reveals that TRPC3 channel gene silencing inhibits mACH-evoked increase in $[Ca^{2+}]_i$ in primary isolated ASMCs. Similarly, a previous report has shown that TRPC3 channel gene silencing blocks acetylcholine- and tumor necrosis factor-α (TNFα)-induced increase in $[Ca^{2+}]_i$ and cultured human ASMCs [5]. Moreover, OAG, a putative activator for TRPC channels [29, 30], causes a significant increase in $[Ca^{2+}]_i$ in primary isolated guinea pig ASMCs. Collectively, TRPC3 channel is vital for agonist-induced Ca^{2+} responses in airway myocytes. Relative to Ca^{2+} release from the sarcoplasmic reticulum (SR), extracellular Ca^{2+} influx through TRPC3 channel makes a smaller contribution to agonist-induced initial increase in $[Ca^{2+}]_i$, whereas TRPC3 channel-mediated Ca^{2+} signaling is persistent during agonist stimulation. This persistent Ca^{2+} signaling may be essential for maintaining cell contraction and other cellular responses, as well as refilling intracellular Ca^{2+} stores to start a new response.

Activation of muscarinic receptors or other G protein-coupled receptors can result in production of IP_3, which causes the opening of TRPC3 channel, serving

as a novel mechanism for Ca^{2+} signaling to mediate cellular responses in ASMCs. In support, we have found that TRPC3 channel knockdown significantly decreases mACH-induced Ca^{2+} influx in ASMCs. The mACH-evoked contraction (cell shortening) is also inhibited by TRPC3 channel knockdown.

18.5 TRPC3 Channel Is Increased in Expression and Activity in ASMCs from Airway Diseases

TRPC3 channel in ASMCs has been shown to make an important contribution to the pathogenesis of asthma. TRPC3 channel is up-regulated in ASMCs isolated from asthma model mice [9, 31, 32] and human ASM [33], and has the ability to regulate cell proliferation of asthmatic mouse and human ASMCs in vivo and in vitro [32, 33]. In cultured human ASMCs, TRPC3 channel mRNA and protein expression is significantly increased following treatment with TNFα. Furthermore, TRPC3 channel gene silencing inhibits TNFα-induced Ca^{2+} influx, the associated increase in $[Ca^{2+}]_i$, and TNFα-mediated augmentation of acetylcholine-evoked increase in $[Ca^{2+}]_i$ [5]. In ovalbumin-sensitized/challenged asthmatic mice, TRPC1 channel protein expression level is not changed in freshly isolated asthmatic ASM tissue, but TRPC3 channel protein expression level is increased significantly [5, 9]. The asthmatic membrane depolarization is blocked by specific TRPC3 channel antibodies. We have also revealed that the asthmatic ASMCs increase in the activity of constitutively active NSCCs and depolarization in the membrane potential are both blocked by TRPC3 channel antibodies. Thus, TRPC3 channel is upregulated in its molecular expression and functional activity, which contributes to membrane depolarization and increased $[Ca^{2+}]_i$ in ASMCs, leading to airway hyperresponsiveness, remodeling and asthma [32, 34].

In a recent study, we have demonstrated that intravenous injection of lentiviral SM-specific promoter-driven TRPC3 channel shRNAs can sufficiently knockdown TRPC3 channel expression and activity in ASMC of mice in vivo and can block allergen-induced airway hyperresponsiveness and remodeling [32] (Fig. 18.2). It is interesting to point out that in-vivo administration of specific pharmacological

Fig. 18.2 (continued) normal and asthmatic mice following intranasal inhalation of vehicle (control) or the specific pharmacological inhibitor of TRPC3 channel Pyr3. (**c**) In-vitro airway muscle contractile responses to mAch were recorded in freshly sliced lung tissues from normal, AIAD (asthmatic), and asthmatic mice treated with NS or TRPC3 shRNAs. Scale bars represent 25 μm in length. Graph shows the quantification of airway lumen changes. (**d**) Immunohistochemistrical co-stains of α-smooth muscle actin (pink) and Ki67 (brown) in airways in normal, AIAD (asthmatic), asthmatic mice treated with lentiviral SM22-driven NS or TRPC3 shRNAs in vivo. Scale bars indicate 20 μm in length. Green arrows indicate colocalization of α-SM actin and Ki67. The insert shows an enlarged part of ASM layers, illustrating the colocalization of Ki67 and α-SM actin. Bar graph displays the quantification of ASM areas and summary of Ki67-positive cells in ASM layers in each group. Numbers in parentheses indicate the numbers of airways/mice examined. $^{*}P < 0.05$ compared with noninfected ASMCs or normal mice. $^{\#}P < 0.05$ compared with asthmatic mice treated with NS. The figure is adopted from Song et al, *FASEB J*, 30: 214–29, 2016

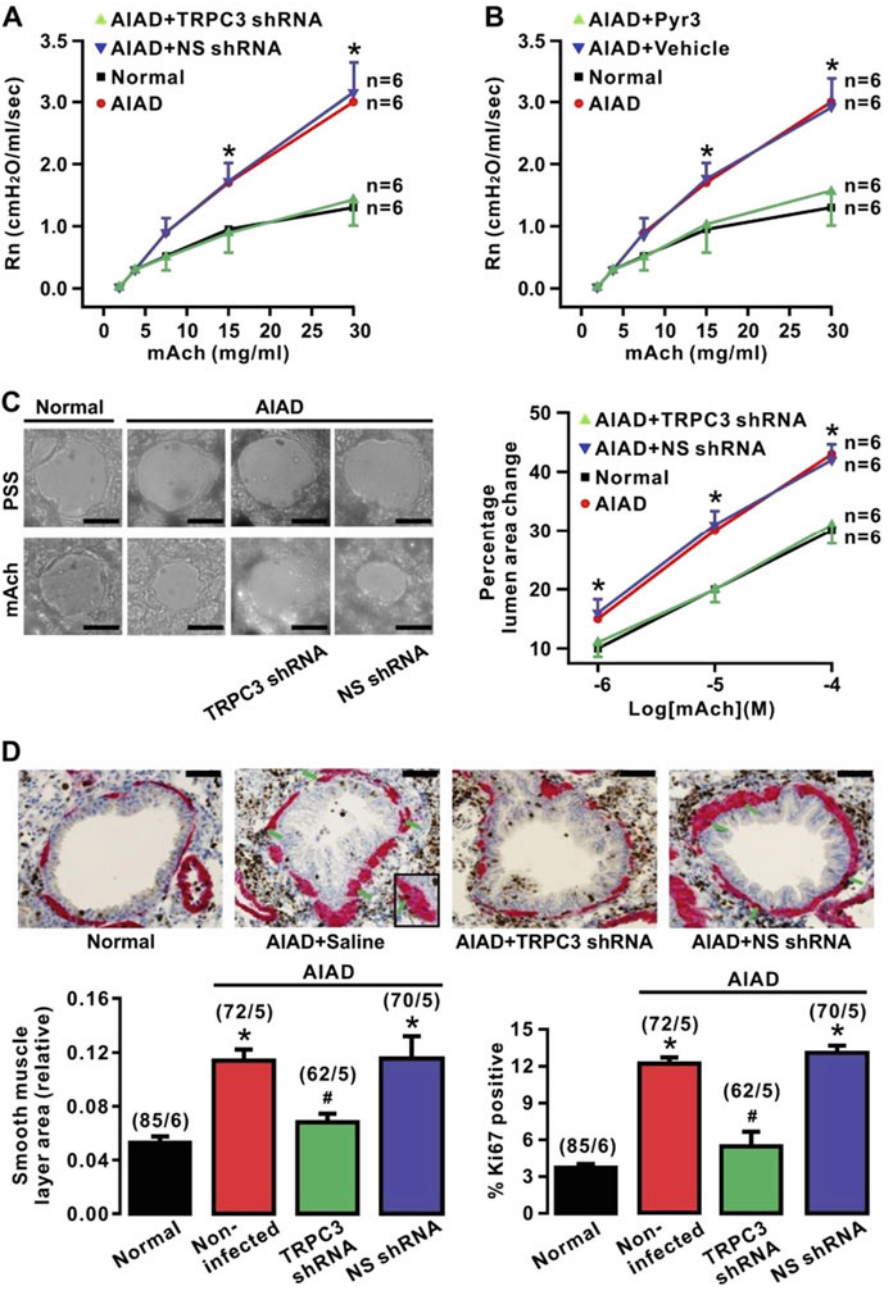

Fig. 18.2 Role of TRPC3 channel in airway smooth muscle hyperresponsiveness and remodeling in mice with allergen (ovalbumin)-induced airway disease (AIAD, asthma). (**a**) Inhibitory effect of SMC-specific TRPC3 channel knockdown on in-vivo airway muscle contractile responses to the muscarinic agonist methacholine (mAch) in mice with asthma (AIAD). The in-vivo airway muscle contractile responses in non-asthmatic (normal) mice, asthmatic mice, and asthmatic mice following intravenous injection of lentiviral SM22 (SMC promoter)-driven non-silencing (NS) or TRPC3 channel shRNAs were determined by assessing conducting airway (Newtonian) resistance (Rn) using an invasive FlexiVent device. (**b**) In-vivo airway muscle contractile responses (Rn) in

inhibitors of TRPC3 channel produce similar effects. These results are consistent with reports from our group and others, in which among all 7 members, only TRPC3 channel exhibits a predominant functional activity in normal ASMCs and an increase in the activity and expression in asthmatic ASMCs [5, 9, 31].

18.6 Upregulated TRPC3 Channel Can Activate NF-κB to Mediate Asthma and Other Airway Diseases Via PKCα–Dependent IκBα and Calcineurin-Reliant IκBβ Signaling Pathways in ASMCs

The recent studies have revealed that expression of protein kinase C-α (PKCα), a Ca^{2+}-sensitive PKC isoform that may activate nuclear factor-κB (NF-κB) by decreasing its inhibitor-α (IκBα) activity in cancer cells and ASMCs [32, 35] and induce cyclin D1 expression to promote proliferation in ASMCs, is increased in ASMCs from asthmatic subjects [32]. More importantly, TRPC3 channel-over expression increases PKCα expression in asthmatic and normal ASMCs, whereas TRPC3 channel knockdown blocks the increased PKC-α expression in asthmatic ASMCs with no effect in normal cells [32]. NF-κB activity in asthmatic ASMCs can also be inhibited by a PKCα antagonist. This information supports that up-regulated TRPC3 channel induces an increased Ca^{2+} influx, which stimulates PKCα, inactivates IκBα, and increase NF-κB activity, leading to cyclin expression, cell proliferation, airway hyperresponsiveness and remodeling, and ultimately asthma. However, this PKCα–dependent signaling pathway may not be functional in normal ASMCs.

We and others have found that calcineurin expression is increased in asthmatic ASMCs [32, 36–38]. The increased calcineurin expression is inhibited by TRPC3 channel knockdown, but augmented by TRPC3 channel overexpression. Similarly, specific calcineurin inhibition blocks, while its activation enhances, NF-κB activity. These findings unveil that in addition to PKCα/IκBα signaling pathway, TRPC3 channel can also stimulate calcineurin and inhibit IκBβ, leading to the activation of NF-κB and induction of cyclin D1 in asthmatic ASMCs [32]. It has been proven that calcineurin plays an important role in TRPC3 channel-mediated activation of NF-κB in neurons and myocardiocytes [39–41]. Perceptibly, PKCα–dependent IκBα and calcineurin-reliant IκBβ inhibition, the two distinct signaling pathways, are critical for TRPC3 channel-mediated increased activity of NF-κB (Fig. 18.3), which plays a vital role in the development of airway hyperresponsiveness and remodeling, eventually leading to asthma and possibly other airway diseases [32].

The upregulated TRPC3 channel has also been found to induce p-p38, p-Jun amino-terminal kinase (JNK), cleaved caspase-3, and Bcl-2 expression, as well as promote cell cycle in asthmatic mouse ASMCs. Moreover, the Ca^{2+} chelator EGTA

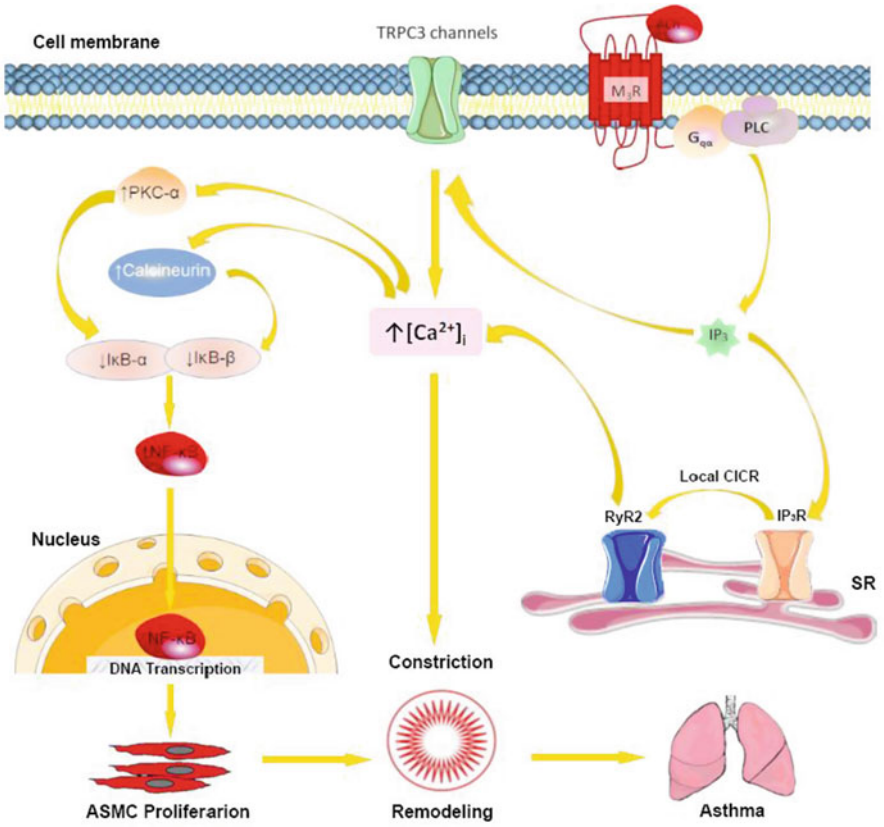

Fig. 18.3 A schematic diagram for signaling mechanisms underlying the role of TRPC3 channel in asthma. The asthmatic stimuli increase TRPC3 channel expression and activity leading to an increase in $[Ca^{2+}]_i$ in ASMCs. In addition to the direct role in mediating airway hyperresponsiveness, the increased $[Ca^{2+}]_i$ not only stimulates PKCα and then inhibits IκBα, but also stimulates calcineurin and inhibits IκBβ. The inhibited IκBα and IκBβ together result in NF-κB activation, cyclin induction, and cell proliferation, ultimately airway hyperresponsiveness, airway remodeling, and asthma. Stimulation of muscarinic receptors or other GPCRs activates PLC to produce DAG and IP_3. DAG causes a direct opening of TRPC3 channel. In a traditional view, IP_3 opens its receptors and induces Ca^{2+} release from the SR to mediate cellular responses. Notably, there is a new paradigm for the molecular functions of IP_3 at least in ASMCs, in which IP_3-induced Ca^{2+} release through IP_3R is significantly amplified by RyR2 due to their local interaction. In addition to Ca^{2+} release, IP may activate TRPC3 channel and cause extracellular Ca^{2+} influx to mediate cell contraction and proliferation, playing an important role in airway hyperresponsiveness, remodeling and diseases

or BAPTA significantly diminishes the effects of TRPC3 channel knockdown on the cell viability, cell cycle and the increased protein expression levels of p-p38, p-JNK, cleaved caspase-3 and Bcl-2 in asthmatic mouse ASMCs [42], which is consistent with the functional role of Ca^{2+} influx through TRPC3 channel.

18.7 TRPC3 Channel Is Regulated by Orai Channel and Ca^{2+}-Sensing Stromal Interaction Molecule

Store-operated Ca^{2+} entry (SOCE) is a vital route in controlling $[Ca^{2+}]_i$ in various types of cells including ASMCs [43, 44]. Ca^{2+} store depletion may result in activation of stromal interaction molecule 1 (STIM1) that is located on the sarco/endoplasmic reticulum [45]. The activated STIM1 is translocated from the ER to the ER-PM junctions, where it interacts with Orai1 channel that permits Ca^{2+} from the extracellular space to the cytosol [46–50]. STIM1 and Orai1 work together as mediators of SOCE in ASMCs, and SOCE has been shown to be increased in proliferative ASMCs accompanied by a modest increase in STIM1 mRNA expression and significant increase in Orai1 channel mRNA expression [47]. Gene knockdown of STIM1 or Orai1 channel by shRNAs significantly attenuates proliferation of ASMCs [47]. Moreover, STIM1 and Orai1 are involved in PDGF-mediated SOCE [51]. Overall, STIM1 and Orai1 are important contributors to SOCE in ASMCs that exhibit hyperplasia [52, 53].

It has been shown that Orail1 channel physically interacts with the N and C terminus of TRPC3 channel, and overexpressing TRPC3 channel only becomes sensitive to the store depletion in cells that also express exogenous Orai channel; thus, Orai channel interacts with TRPC3 channel to form a functional integrative unit that confers STIM1-mediated store depletion sensitivity to these two channels [54].

Interestingly, an elegant study has found that under the resting state, the N and C terminus coiled-coil domains of both TRPC3 and TRPC1 channel interact with each other to shield the STIM1 binding site, thereby preventing the role of STIM1 in regulating the activity of TRPC3 and TRPC1 channel [55]. However, cell stimulation can facilitate the formation of TRPC3/TRPC1 channel heteromultimers, enhance both interaction, and also dissociate between the TRPC1 channel N and C terminus coiled-coil domains. As such, the free TRPC1 channel C terminus coiled-coil domain interacts with the TRPC3 channel coiled-coil domains to dissociate them, making the TRPC3 channel C terminus coiled-coil domain available for interaction with STIM1, thereby allowing STIM1 to activate TRPC3 channel [55]. These novel results provide an important molecular mechanism for the regulatory interaction of STIM1 with TRPC3 channel and also potentially other TRPC channel members.

18.8 TRPC3 Channel May Interact with Ca^{2+} Release Channels

TRPC3 channel can be regulated by muscarinic receptors and other G protein-coupled receptors (GPCRs) in ASMCs [43, 56]. Stimulation of GPCRs causes activation of phospholipase C (PLC), which hydrolyzes phosphatidylinositol

4,5-bisphosphate (PIP_2) to produce diacylglycerol (DAG) and inositol 1,4,5-trisphosphate (IP_3). These two-important intracellular second messengers will possibly mediate the role of GPCRs in controlling the activity of TRPC3 channel. Indeed, we have demonstrated that the DAG analog 1-oleyl-2-acetyl-sn-glycerol (OAG) activates TRPC3 channel in ASMCs [9]. A similar effect of OAG on TRPC3 channel has also been observed in ear artery SMCs [57, 58].

IP_3 is generally considered to elevate $[Ca^{2+}]_i$ by activating IP_3 receptor/Ca^{2+} release channel (IP_3R) to induce intracellular Ca^{2+} release from the SR [59]. Interestingly, we have discovered that Ca^{2+} release through IP_3R can activate adjacent ryanodine receptor-2/Ca^{2+} reelase channel (RyR2) to induce further Ca^{2+} release from the SR, termed a local IP_3R/RyR2 interaction-meidated Ca^{2+}-induced Ca^{2+} release process [59–61]. Equally importantly, our more recent investigations have found that IP_3, can notably increase the activity of single NSCCs [17]. The effects of IP_3 can be fully blocked by shRNA-mediated TRPC3 channel knockdown. The stimulatory effect of IP_3 is also abolished by heparin, an IP_3R antagonist that blocks the IP_3-binding site, but not by xestospongin C, an IP_3R antagonist that has no effect on the IP_3-binding site. In contrast, shRNA-mediated knockdown of IP_3R1, IP_3R2, or IP_3R3 does not change the excitatory effect of IP_3 on the activity of TRPC channel. Furthermore, TRPC3 channel knockdown significantly diminishes IP_3-induced increase in $[Ca^{2+}]_i$. IP_3R1 knockdown produces a similar inhibitory effect. TRPC3 channel and IP_3R1 knockdown both diminish the muscarinic receptor agonist methacholine-evoked Ca^{2+} responses. IP_3 may also produce a stimulatory effect on the activity of TRPC3 channel in the absence of OAG in vascular SMCs [62, 63]. Taken together, IP_3 can not only open IP_3Rs to induce intracellular Ca^{2+} release, but also activate TRPC3 channel to cause extracellular Ca^{2+} influx.

It should be noted there are limited studies on the interaction of TRPC3 channel with Ca^{2+} release channels in ASMC. Further studies to determine how TRPC3 channels are regulated in normal and diseased (e.g., asthmatic) ASMCs are necessary.

18.9 TRPC3 Channel May Become a Novel and Effective Drug Target in Lung Diseases

It is well established that airway hyperresponsiveness and remodeling are the two major cellular responses in asthma [43, 45, 64–67]. We have recently demonstrated that lentivirus-based, shRNA-mediated, SMC-specific TRPC3 channel gene knockdown in vivo blocks the development of hyperresponsiveness and remodeling in mice with allergic asthma [32]. As lentivirus- and/or shRNA-mediated loss and gain of gene function embody a promising human gene therapy [68], our findings may provide a new, specific and effective therapeutic avenue in the treatment of asthma. Consistent with this view, we have further revealed that intranasal administration of the TRPC3 channel blocker Pyr3 also abolishes allergen-induced asthma in animals

[32]. It is interesting to point out that a number of TRP channels have been identified as the novel 'druggable' targets in numerous diseases; some of pharmacological blockers of these channels, although not the TRPC3 channel, have been in clinical trials [68–70]. Convincingly, the TRPC3 channel is an advantageous drug target in the therapy of asthma.

Similar to asthma, chronic obstructive pulmonary disease (COPD) is a common devastating airway disease. Indeed, this disease is the fifth leading cause of death worldwide and expected to be the third cause of mortality by 2020 [71]. Airway hyperresponsiveness develops in COPD, and thus is the rationale for using bronchodilators as the first-line therapy for COPD [72–77]. Airway remodeling has been increasingly recognized in COPD [45, 64, 67, 78–83]. Cigarette smoke is a primary factor in 80% to 90% of COPD [84–86]. Interestingly, cigarette smoking increases TRPC3 channel expression and associated Ca^{2+} influx, altering airway structure and function [87]. Presumably, lentivirus-based shRNA-mediated genetic inhibition and pharmacological inhibitors of TRPC3 channel may also become valuable therapeutics for COPD.

It has been reported that TRPC3 channel expression levels are correlated with differentiation of non-small cell lung cancer, regulate cancer cell differentiation and proliferation, and mediate the inhibitory effect of all-trans-retinoic acid [88]. In support, a recent study has found that TRPC3 methylation variation is prominent in lung cancer tissues [89]. These data suggest that in addition to asthma and COPD, TRPC3 channel may also serve as a valuable drug target in lung cancer.

18.10 Conclusion

Multiple TRPC channels are expressed in animal and human ASMCs; however, TRPC3 channel is a major functional member of the TRPC family. This channel plays an important role in controlling the resting $[Ca^{2+}]_i$ and mediating agonist-evoked increase in $[Ca^{2+}]_i$ in ASMCs. TRPC3 channel is significantly increased in expression and activity in ASMCs from subjects with asthma or other airway diseases. The increased TRPC3 channel causes excessive extracellular Ca^{2+} influx, which serves as a very important player in mediating airway hyperresponsiveness in asthma and other relevant airway disorders. In addition to this direct imperative role, the excessive extracellular Ca^{2+} influx through the upregulated TRPC3 channel can also cause the suppression of PKCα–dependent IκBα and calcineurin-reliant IκBβ signaling pathways, activation of NF-κB, induction of cyclin expression, and cell proliferation in ASMCs, which may not only lead to airway remodeling, but can also contribute to airway hyperresponsiveness, thereby mediating the development of asthma and other airway diseases.

In-vivo administration of lentiviral SMC-specific TRPC3 channel shRNAs or specific TRPC3 channel blockers blocks airway hyperresponsiveness and remodeling, thus preventing the development of asthma. These findings promote the

potential use of gene therapies or pharmacological interventions specifically targeting at TRPC3 channel in the clinical treatment of asthma and other airway diseases.

Studies suggest that the plasmalemmal TRPC3 channel well interacts with the plasmalemmal Orai channel, cytosolic STIM, and sarcolemmal Ca^{2+} release channels in ASMCs. This coordinative network may provide a unique system in precisely controlling and regulating $[Ca^{2+}]_i$ to meet adequate physiological cellular responses, further indicating the functional significance of TRPC3 channel in ASMCs. Clearly, further investigations to determine whether, which, and how TRPC3 channel is involved in cellular responses in normal and diseased (e.g., asthmatic) ASMCs are needed, with hopes of yielding novel and important findings to enhance our understanding of the functional roles, regulatory mechanisms and signaling processes of TRPC3, as well as aid in the creation of effective therapeutic targets for the treatment of asthma and other respiratory diseases.

References

1. Montell C, Jones K, Hafen E, Rubin G (1985) Rescue of the drosophila phototransduction mutation trp by germline transformation. Science (New York, NY) 230(4729):1040–1043
2. Wes PD, Chevesich J, Jeromin A, Rosenberg C, Stetten G, Montell C (1995) TRPC1, a human homolog of a drosophila store-operated channel. Proc Natl Acad Sci U S A 92(21):9652–9656
3. Ong HL, Brereton HM, Harland ML, Barritt GJ (2003) Evidence for the expression of transient receptor potential proteins in Guinea pig airway smooth muscle cells. Respirology 8(1):23–32
4. Corteling RL, Li S, Giddings J, Westwick J, Poll C, Hall IP (2004) Expression of transient receptor potential C6 and related transient receptor potential family members in human airway smooth muscle and lung tissue. Am J Respir Cell Mol Biol 30(2):145–154
5. White TA, Xue A, Chini EN, Thompson M, Sieck GC, Wylam ME (2006) Role of transient receptor potential C3 in TNF-alpha-enhanced calcium influx in human airway myocytes. Am J Respir Cell Mol Biol 35(2):243–251
6. Ong HL, Chen J, Chataway T, Brereton H, Zhang L, Downs T et al (2002) Specific detection of the endogenous transient receptor potential (TRP)-1 protein in liver and airway smooth muscle cells using immunoprecipitation and Western-blot analysis. Biochem J 364(Pt 3):641–648
7. Ay B, Prakash YS, Pabelick CM, Sieck GC (2004) Store-operated Ca^{2+} entry in porcine airway smooth muscle. Am J Physiol Lung Cell Mol Physiol 286(5):L909–L917
8. Godin N, Rousseau E (2007) TRPC6 silencing in primary airway smooth muscle cells inhibits protein expression without affecting OAG-induced calcium entry. Mol Cell Biochem 296(1–2):193–201
9. Xiao JH, Zheng YM, Liao B, Wang YX (2010) Functional role of canonical transient receptor potential 1 and canonical transient receptor potential 3 in normal and asthmatic airway smooth muscle cells. Am J Respir Cell Mol Biol 43(1):17–25
10. Snetkov VA, Pandya H, Hirst SJ, Ward JP (1998) Potassium channels in human fetal airway smooth muscle cells. Pediatr Res 43(4 Pt 1):548–554
11. Snetkov VA, Ward JP (1999) Ion currents in smooth muscle cells from human small bronchioles: presence of an inward rectifier K^+ current and three types of large conductance K^+ channel. Exp Physiol 84(5):835–846
12. Snetkov VA, Hapgood KJ, McVicker CG, Lee TH, Ward JP (2001) Mechanisms of leukotriene D4-induced constriction in human small bronchioles. Br J Pharmacol 133(2):243–252
13. Helli PB, Janssen LJ (2008) Properties of a store-operated nonselective cation channel in airway smooth muscle. Eur Respir J 32(6):1529–1539

14. Albert AP, Large WA (2001) Comparison of spontaneous and noradrenaline-evoked non-selective cation channels in rabbit portal vein myocytes. J Physiol 530(Pt 3):457–468
15. Hirota S, Helli P, Janssen LJ (2007) Ionic mechanisms and Ca^{2+} handling in airway smooth muscle. Eur Respir J 30(1):114–133
16. Liu XS, Xu YJ (2005) Potassium channels in airway smooth muscle and airway hyperreactivity in asthma. Chin Med J 118(7):574–580
17. Song T, Hao Q, Zheng YM, Liu QH, Wang YX (2015) Inositol 1,4,5-trisphosphate activates TRPC3 channels to cause extracellular Ca^{2+} influx in airway smooth muscle cells. Am J Physiol Lung Cell Mol Physiol 309(12):L1455–L1466
18. Janssen LJ, Sims SM (1992) Acetylcholine activates non-selective cation and chloride conductances in canine and Guinea-pig tracheal myocytes. J Physiol 453:197–218
19. Wang YX, Fleischmann BK, Kotlikoff MI (1997) M2 receptor activation of nonselective cation channels in smooth muscle cells: calcium and Gi/G(o) requirements. Am J Phys 273(2 Pt 1):C500–C508
20. Fleischmann BK, Wang YX, Kotlikoff MI (1997) Muscarinic activation and calcium permeation of nonselective cation currents in airway myocytes. Am J Phys 272(1 Pt 1):C341–C349
21. Wang YX, Kotlikoff MI (2000) Signalling pathway for histamine activation of non-selective cation channels in equine tracheal myocytes. J Physiol 523(Pt 1):131–138
22. Yamashita T, Kokubun S (1999) Nonselective cationic currents activated by acetylcholine in swine tracheal smooth muscle cells. Can J Physiol Pharmacol 77(10):796–805
23. Murray RK, Kotlikoff MI (1991) Receptor-activated calcium influx in human airway smooth muscle cells. J Physiol 435:123–144
24. Parvez O, Voss AM, de Kok M, Roth-Kleiner M, Belik J (2006) Bronchial muscle peristaltic activity in the fetal rat. Pediatr Res 59(6):756–761
25. Dai JM, Kuo KH, Leo JM, Pare PD, van Breemen C, Lee CH (2007) Acetylcholine-induced asynchronous calcium waves in intact human bronchial muscle bundle. Am J Respir Cell Mol Biol 36(5):600–608
26. Dai JM, Kuo KH, Leo JM, van Breemen C, Lee CH (2006) Mechanism of ACh-induced asynchronous calcium waves and tonic contraction in porcine tracheal muscle bundle. Am J Physiol Lung Cell Mol Physiol 290(3):L459–L469
27. Gorenne I, Labat C, Gascard JP, Norel X, Nashashibi N, Brink C (1998) Leukotriene D4 contractions in human airways are blocked by SK&F 96365, an inhibitor of receptor-mediated calcium entry. J Pharmacol Exp Ther 284(2):549–552
28. Hirota S, Janssen LJ (2007) Store-refilling involves both L-type calcium channels and reverse-mode sodium-calcium exchange in airway smooth muscle. Eur Respir J 30(2):269–278
29. Nilius B, Owsianik G, Voets T, Peters JA (2007) Transient receptor potential cation channels in disease. Physiol Rev 87(1):165–217
30. Abramowitz J, Birnbaumer L (2009) Physiology and pathophysiology of canonical transient receptor potential channels. FASEB J 23(2):297–328
31. Wang L, Li J, Zhang J, He Q, Weng X, Huang Y et al (2017) Inhibition of TRPC3 downregulates airway hyperresponsiveness, remodeling of OVA-sensitized mouse. Biochem Biophys Res Commun 484(1):209–217
32. Song T, Zheng YM, Vincent PA, Cai D, Rosenberg P, Wang YX (2016) Canonical transient receptor potential 3 channels activate NF-kappaB to mediate allergic airway disease via PKC-alpha/IkappaB-alpha and calcineurin/IkappaB-beta pathways. FASEB J 30(1):214–229
33. Wylam ME, Sathish V, VanOosten SK, Freeman M, Burkholder D, Thompson MA et al (2015) Mechanisms of cigarette smoke effects on human airway smooth muscle. PLoS One 10(6):e0128778
34. Wang YX, Zheng YM (2011) Molecular expression and functional role of canonical transient receptor potential channels in airway smooth muscle cells. Adv Exp Med Biol 704:731–747
35. Vertegaal AC, Kuiperij HB, Yamaoka S, Courtois G, van der Eb AJ, Zantema A (2000) Protein kinase C-alpha is an upstream activator of the IkappaB kinase complex in the TPA signal transduction pathway to NF-kappaB in U2OS cells. Cell Signal 12(11–12):759–768

36. Hai CM (2007) Airway smooth muscle cell as therapeutic target of inflammation. Curr Med Chem 14(1):67–76
37. Walczak-Drzewiecka A, Ratajewski M, Wagner W, Dastych J (2008) HIF-1alpha is up-regulated in activated mast cells by a process that involves calcineurin and NFAT. J Immunol 181(3):1665–1672
38. Said SI, Hamidi SA, Gonzalez Bosc L (2010) Asthma and pulmonary arterial hypertension: do they share a key mechanism of pathogenesis? Eur Respir J 35(4):730–734
39. Rosenberg P, Hawkins A, Stiber J, Shelton JM, Hutcheson K, Bassel-Duby R et al (2004) TRPC3 channels confer cellular memory of recent neuromuscular activity. Proc Natl Acad Sci U S A 101(25):9387–9392
40. Nakayama H, Wilkin BJ, Bodi I, Molkentin JD (2006) Calcineurin-dependent cardiomyopathy is activated by TRPC in the adult mouse heart. FASEB J 20(10):1660–1670
41. Poteser M, Schleifer H, Lichtenegger M, Schernthaner M, Stockner T, Kappe CO et al (2011) PKC-dependent coupling of calcium permeation through transient receptor potential canonical 3 (TRPC3) to calcineurin signaling in HL-1 myocytes. Proc Natl Acad Sci U S A 108(26):10556–10561
42. Zhang X, Zhao Z, Ma L, Guo Y, Li X, Zhao L et al (2018) The effects of transient receptor potential channel (TRPC) on airway smooth muscle cell isolated from asthma model mice. J Cell Biochem 119(7):6033–6044
43. Xiao JH, Wang YX, Zheng YM (2014) Transient receptor potential and Orai channels in airway smooth muscle cells. In: Wang YX (ed) Calcium signaling in airway smooth muscle cells. Springer, Cham, pp 35–45
44. Ong HL, Ambudkar IS (2017) STIM-TRP pathways and microdomain organization: contribution of TRPC1 in store-operated Ca^{2+} entry: impact on Ca^{2+} signaling and cell function. Adv Exp Med Biol 993:159–188
45. Song T, Zheng Y-M, Wang YX (2014) Calcium signaling in airway smooth muscle Remodeling. In: YX W (ed) Calcium signaling in airway smooth muscle cells. Springer, Cham, pp 393–407
46. Dolmetsch RE, Xu K, Lewis RS (1998) Calcium oscillations increase the efficiency and specificity of gene expression. Nature 392(6679):933–936
47. Zou JJ, Gao YD, Geng S, Yang J (2011) Role of STIM1/Orai1-mediated store-operated Ca(2)(+) entry in airway smooth muscle cell proliferation. J Appl Physiol (1985) 110(5):1256–1263
48. Spinelli AM, Gonzalez-Cobos JC, Zhang X, Motiani RK, Rowan S, Zhang W et al (2012) Airway smooth muscle STIM1 and Orai1 are upregulated in asthmatic mice and mediate PDGF-activated SOCE, CRAC currents, proliferation, and migration. Pflugers Archiv Eur J Physiol 464(5):481–492
49. Chin D, Means AR (2000) Calmodulin: a prototypical calcium sensor. Trends Cell Biol 10(8):322–328
50. Feske S, Prakriya M (2013) Conformational dynamics of STIM1 activation. Nat Struct Mol Biol 20(8):918–919
51. Ogawa A, Firth AL, Smith KA, Maliakal MV, Yuan JX (2012) PDGF enhances store-operated Ca^{2+} entry by upregulating STIM1/Orai1 via activation of Akt/mTOR in human pulmonary arterial smooth muscle cells. Am J Physiol Cell Physiol 302(2):C405–C411
52. Peel SE, Liu B, Hall IP (2008) ORAI and store-operated calcium influx in human airway smooth muscle cells. Am J Respir Cell Mol Biol 38(6):744–749
53. Peel SE, Liu B, Hall IP (2006) A key role for STIM1 in store operated calcium channel activation in airway smooth muscle. Respir Res 7:119
54. Liao Y, Erxleben C, Yildirim E, Abramowitz J, Armstrong DL, Birnbaumer L (2007) Orai proteins interact with TRPC channels and confer responsiveness to store depletion. Proc Natl Acad Sci U S A 104(11):4682–4687
55. Lee KP, Choi S, Hong JH, Ahuja M, Graham S, Ma R et al (2014) Molecular determinants mediating gating of Transient Receptor Potential Canonical (TRPC) channels by stromal interaction molecule 1 (STIM1). J Biol Chem 289(10):6372–6382

56. Brightbill HD, Jeet S, Lin Z, Yan D, Zhou M, Tan M et al (2010) Antibodies specific for a segment of human membrane IgE deplete IgE-producing B cells in humanized mice. J Clin Invest 120(6):2218–2229
57. Albert AP, Piper AS, Large WA (2005) Role of phospholipase D and diacylglycerol in activating constitutive TRPC-like cation channels in rabbit ear artery myocytes. J Physiol 566(Pt 3):769–780
58. Albert AP, Pucovsky V, Prestwich SA, Large WA (2006) TRPC3 properties of a native constitutively active Ca^{2+}−permeable cation channel in rabbit ear artery myocytes. J Physiol 571(Pt 2):361–369
59. Mei L, Zheng YM, Wang YX (2014) Ryanodine and inositol trisphosphate receptors/Ca^{2+} release channels in airway smooth muscle cells. In: Wang YX (ed) Calcium signaling in airway smooth muscle cells. Springer, Cham, pp 1–20
60. Liu QH, Zheng YM, Korde AS, Yadav VR, Rathore R, Wess J et al (2009) Membrane depolarization causes a direct activation of G protein-coupled receptors leading to local Ca^{2+} release in smooth muscle. Proc Natl Acad Sci U S A 106(27):11418–11423
61. Liu QH, Savoia C, Wang YX, Zheng YM (2014) Local calcium signaling in airway smooth muscle cells. In: YX W (ed) Calcium signaling in airway smooth muscle cells. Springer, Cham, pp 107–120
62. Adebiyi A, Thomas-Gatewood CM, Leo MD, Kidd MW, Neeb ZP, Jaggar JH (2012) An elevation in physical coupling of type 1 inositol 1,4,5-trisphosphate (IP3) receptors to transient receptor potential 3 (TRPC3) channels constricts mesenteric arteries in genetic hypertension. Hypertension 60(5):1213–1219
63. Xi Q, Adebiyi A, Zhao G, Chapman KE, Waters CM, Hassid A et al (2008) IP3 constricts cerebral arteries via IP3 receptor-mediated TRPC3 channel activation and independently of sarcoplasmic reticulum Ca^{2+} release. Circ Res 102(9):1118–1126
64. Prakash YS (2016) Emerging concepts in smooth muscle contributions to airway structure and function: implications for health and disease. Am J Physiol Lung Cell Mol Physiol 311(6):L1113–L1l40
65. Panettieri RA, Pera T, Liggett SB, Benovic JL, Penn RB (2018) Pepducins as a potential treatment strategy for asthma and COPD. Curr Opin Pharmacol 40:120–125
66. Alves MF, da Fonseca DV, de Melo SAL, Scotti MT, Scotti L, Dos Santos SG et al (2018) New therapeutic targets and drugs for the treatment of asthma. Mini Rev Med Chem 18(8):684–696
67. Prakash YS, Halayko AJ, Gosens R, Panettieri RA Jr, Camoretti-Mercado B, Penn RB (2017) An official American Thoracic Society research statement: current challenges facing research and therapeutic advances in airway remodeling. Am J Respir Crit Care Med 195(2):e4–e19
68. Tiapko O, Groschner K (2018) TRPC3 as a target of novel therapeutic interventions. Cell 7(7):83
69. Nilius B, Szallasi A (2014) Transient receptor potential channels as drug targets: from the science of basic research to the art of medicine. Pharmacol Rev 66(3):676–814
70. Cui C, Merritt R, Fu L, Pan Z (2017) Targeting calcium signaling in cancer therapy. Acta Pharm Sin B 7(1):3–17
71. Vestbo J, Hurd SS, Agusti AG, Jones PW, Vogelmeier C, Anzueto A et al (2013) Global strategy for the diagnosis, management, and prevention of chronic obstructive pulmonary disease: GOLD executive summary. Am J Respir Crit Care Med 187(4):347–365
72. Vestbo J, Hansen EF (2001) Airway hyperresponsiveness and COPD mortality. Thorax 56(Suppl 2):ii11–ii14
73. Scichilone N, Battaglia S, La Sala A, Bellia V (2006) Clinical implications of airway hyperresponsiveness in COPD. Int J Chron Obstruct Pulmon Dis 1(1):49–60
74. van den Berge M, Vonk JM, Gosman M, Lapperre TS, Snoeck-Stroband JB, Sterk PJ et al (2012) Clinical and inflammatory determinants of bronchial hyperresponsiveness in COPD. Eur Respir J 40(5):1098–1105
75. Prakash YS (2013) Airway smooth muscle in airway reactivity and remodeling: what have we learned? Am J Physiol Lung Cell Mol Physiol 305(12):L912–L933

76. Fricker M, Deane A, Hansbro PM (2014) Animal models of chronic obstructive pulmonary disease. Expert Opin Drug Discovery 9(6):629–645
77. Tkacova R, Dai DLY, Vonk JM, Leung JM, Hiemstra PS, van den Berge M et al (2016) Airway hyperresponsiveness in chronic obstructive pulmonary disease: a marker of asthma-chronic obstructive pulmonary disease overlap syndrome? J Allergy Clin Immunol 138(6):1571–1579. e10
78. Hogg JC (2004) Pathophysiology of airflow limitation in chronic obstructive pulmonary disease. Lancet (London, UK) 364(9435):709–721
79. Chung KF (2005) The role of airway smooth muscle in the pathogenesis of airway wall remodeling in chronic obstructive pulmonary disease. Proc Am Thorac Soc 2(4):347–354; discussion 71–2
80. Kim V, Rogers TJ, Criner GJ (2008) New concepts in the pathobiology of chronic obstructive pulmonary disease. Proc Am Thorac Soc 5(4):478–485
81. Jones RL, Noble PB, Elliot JG, James AL (2016) Airway remodelling in COPD: it's not asthma! Respirology 21(8):1347–1356
82. Kistemaker LE, Oenema TA, Meurs H, Gosens R (2012) Regulation of airway inflammation and remodeling by muscarinic receptors: perspectives on anticholinergic therapy in asthma and COPD. Life Sci 91(21–22):1126–1133
83. Nayak AP, Deshpande DA, Penn RB (2018) New targets for resolution of airway remodeling in obstructive lung diseases. F1000 Res 7:680
84. Dewar M, Curry RW Jr (2006) Chronic obstructive pulmonary disease: diagnostic considerations. Am Fam Physician 73(4):669–676
85. Zeller M (2016) The deeming rule: keeping pace with the modern tobacco marketplace. Am J Respir Crit Care Med 194(5):538–540
86. Temitayo Orisasami I, Ojo O (2016) Evaluating the effectiveness of smoking cessation in the management of COPD. Br J Nurs (Mark Allen Publishing) 25(14):786–791
87. Vogel ER, VanOosten SK, Holman MA, Hohbein DD, Thompson MA, Vassallo R et al (2014) Cigarette smoke enhances proliferation and extracellular matrix deposition by human fetal airway smooth muscle. Am J Physiol Lung Cell Mol Physiol 307(12):L978–L986
88. Jiang HN, Zeng B, Zhang Y, Daskoulidou N, Fan H, Qu JM et al (2013) Involvement of TRPC channels in lung cancer cell differentiation and the correlation analysis in human non-small cell lung cancer. PLoS One 8(6):e67637
89. Kettunen E, Hernandez-Vargas H, Cros MP, Durand G, Le Calvez-Kelm F, Stuopelyte K et al (2017) Asbestos-associated genome-wide DNA methylation changes in lung cancer. Int J Cancer 141(10):2014–2029

Chapter 19
Pathophysiological Significance of Store-Operated Calcium Entry in Cardiovascular and Skeletal Muscle Disorders and Angiogenesis

Javier Avila-Medina, Isabel Mayoral-González, Isabel Galeano-Otero, Pedro C. Redondo, Juan A. Rosado, and Tarik Smani

Abstract Store-Operated Ca^{2+} Entry (SOCE) is an important Ca^{2+} influx pathway expressed by several excitable and non-excitable cell types. SOCE is recognized as relevant signaling pathway not only for physiological process, but also for its involvement in different pathologies. In fact, independent studies demonstrated the implication of essential protein regulating SOCE, such as STIM, Orai and TRPCs, in different pathogenesis and cell disorders, including cardiovascular disease, muscular dystrophies and angiogenesis. Compelling evidence showed that dysregulation in the function and/or expression of isoforms of STIM, Orai or TRPC play pivotal roles in cardiac hypertrophy and heart failure, vascular remodeling and hypertension, skeletal myopathies, and angiogenesis. In this chapter, we summarized the current

J. Avila-Medina · I. Galeano-Otero
Department of Medical Physiology and Biophysics, University of Seville, Sevilla, Spain

Institute of Biomedicine of Seville (IBiS), University Hospital of Virgen del Rocío/CSIC/University of Seville, Sevilla, Spain

I. Mayoral-Gonzàlez
Department of Medical Physiology and Biophysics, University of Seville, Sevilla, Spain

Institute of Biomedicine of Seville (IBiS), University Hospital of Virgen del Rocío/CSIC/University of Seville, Sevilla, Spain

Department of Surgery, University of Seville, Sevilla, Spain

P. C. Redondo · J. A. Rosado
Department of Physiology, Cell Physiology Research Group and Institute of Molecular Pathology Biomarkers, University of Extremadura, Cáceres, Spain

T. Smani (✉)
Department of Medical Physiology and Biophysics, University of Seville, Sevilla, Spain

Institute of Biomedicine of Seville (IBiS), University Hospital of Virgen del Rocío/CSIC/University of Seville, Sevilla, Spain

CIBERCV, Madrid, Spain
e-mail: tasmani@us.es

M. S. Islam (ed.), *Calcium Signaling*, Advances in Experimental Medicine and Biology 1131, https://doi.org/10.1007/978-3-030-12457-1_19

knowledge concerning the mechanisms underlying abnormal SOCE and its involvement in some diseases, as well as, we discussed the significance of STIM, Orai and TRPC isoforms as possible therapeutic targets for the treatment of angiogenesis, cardiovascular and skeletal muscle diseases.

Keywords Cardiac disease · Vascular disorders · Skeletal muscle · Angiogenesis

Abbreviations

CRAC	Ca^{2+}-Release Activated Ca^{2+} Channels
CREB	cAMP Response Element-Binding
DMD	Duchenne Muscular Dystrophy
EC	Endothelial Cell
EPC	Endothelial Progenitor Cell
ER/SR	Endoplasmic/Sarcoplasmic Reticulum
HF	Heart Failure
MD	Muscular Dystrophy
NFAT	Nuclear Factor of Activated T-cell
PAH	Pulmonary Arterial Hypertension
PASMC	Pulmonary Artery Smooth Muscle Cell
PDGF	Platelet-Derived Growth Factor
SERCA	Sarco/Endoplasmic Reticulum Ca^{2+} ATPase
siRNA	small interfering RNA
SOCC	Store-Operated Ca^{2+} Channel
SOCE	Store-Operated Ca^{2+} Entry
STIM1/2/1L	Stromal Interaction Molecule 1/2/1Large
TAC	Transverse Aortic Constriction
TRPC	Transient Receptor Potential-Canonical
VEGF	Vascular Endothelial Growth Factor
VSMC	Vascular Smooth Muscle Cell

19.1 General Overview of Store-Operated Ca^{2+} Entry

Store-Operated Ca^{2+} Entry (SOCE) is a ubiquitous mechanism for the entry of Ca^{2+} across ion channels located in the plasma membrane as illustrated in Fig. 19.1. SOCE is activated when the luminal Ca^{2+} concentration decreases in the intracellular Endoplasmic Reticulum (ER) Ca^{2+} stores [1]. More than a decade ago, Stromal Interacting Molecules 1 (STIM1) and Orai1 proteins were identified as the most relevant molecular components of SOCE [2, 3]. STIM1 was characterized as the ER luminal Ca^{2+} sensor that can interact and activates Orai channels upon ER

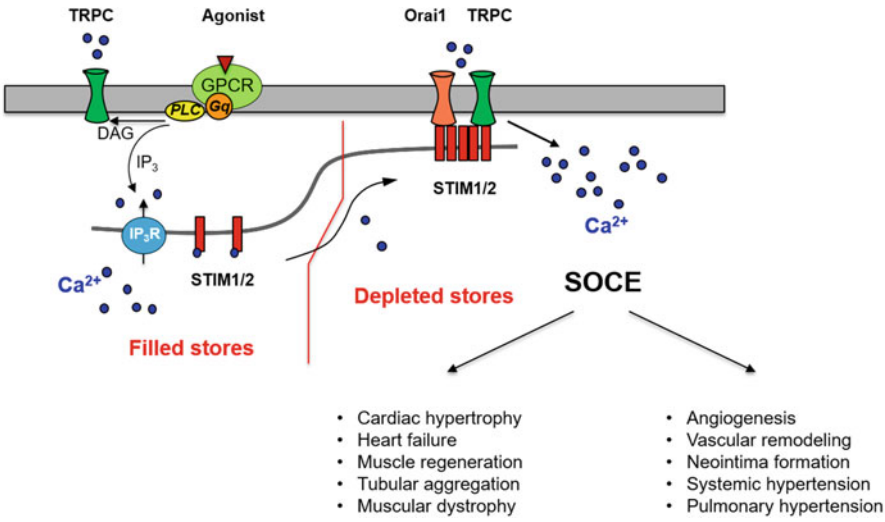

Fig. 19.1 Consensus model and standard molecular components of SOCE. Agonist binding to G-protein coupled receptor (GPCR), induces Ca^{2+} release from intracellular stores, STIM1/2 oligomerization in puncta and translocation to the plasma membrane, activation of Ca^{2+} entry through Orai1 and/or TRPCs. Agonists might also stimulate store-independent Ca^{2+} entry through others TRPCs activated by diacylglycerol (DAG). Several reports demonstrated that dysregulation in the expression and/or activation of STIM, Orai or TRPCs is associated with pathogenesis of different diseases such as cardiac hypertrophy and heart failure, muscle generation, tubular aggregation and dystrophies, angiogenesis, vascular remodeling, systemic and pulmonary hypertension

depletion [2]. Another isoform of STIM, STIM2, also senses the Ca^{2+} concentration in ER. This isoform apparently has a greater sensitivity for free intraluminal Ca^{2+} than STIM1 [4]. STIM2 can be partially active by resting ER Ca^{2+} concentration and it is further activated by small Ca^{2+} concentrations reductions in ER [4]. Along with STIM1, an alternative spliced long variant, STIM1L, has been related to SOCE especially in skeletal and cardiac muscle [5]. STIM1L is colocalized with Orai1 as well as others channels, such as Transient Receptor Potential-Canonical (TRPC) channels: TRPC1, TRPC3, TRPC4 and TRPC6 [6–8]. STIM1L is thought to form permanent clusters with Orai1 that are responsible for the rapid (<1 s) activation of SOCE in skeletal muscle cells in comparison to other cells [5].

Soon after the identification of STIM1, Orai1 was identified as the pore-forming subunit of Store-Operated Ca^{2+} Channels (SOCCs) [9, 10]. SOCE is generally mediated by the highly Ca^{2+}-selective channel, known as Ca^{2+} Release-Activated Ca^{2+} channel (CRAC) formed by homo- or hetero-multimeric Orai subunits (Orai1/2) [11, 12]. Along with Orai1, Ca^{2+} store depletion also activates other isoforms of Orai, Orai2 and Orai3 [13]. Although, Orai3 also contributes to store-independent Ca^{2+} channels, such as the Arachidonate Regulated Ca^{2+} (ARC) channels [14] and Leukotriene C4-Regulated Ca^{2+} (LRC) channels [15].

In addition to the highly selective CRAC channel, independent studies showed that SOCE can be also mediated by a non-selective SOCCs, involving Orai subunits interacting with members of TRPC channels, which are permeable to monovalent and divalent cations [16, 17]. This non-selective SOCCs has been largely described in excitable cells such as cardiac myocytes [18], Vascular Smooth Muscle Cells (VSMCs) [19] and skeletal muscle cells [20, 21]. Like Orai proteins, different members of the TRPC family can be activated by store depletion or by a variety of extracellular signals leading to changes in the Ca^{2+} concentration in spatially restricted microdomains underneath the plasma membrane, which support various Ca^{2+} dependent intracellular pathways [22].

Ca^{2+} influx via SOCE has been reported to be necessary for numerous cellular functions as VSMCs contraction and proliferation [19, 23, 24]; the contractile function in the skeletal and cardiac muscle [25, 26]; the insulin secretion [27, 28], etc. Given the physiological importance of SOCE, compelling evidences confirmed that alterations in the mechanism of activation, maintenance or inactivation of SOCE might lead to a pathophysiological phenotype. Loss- or gain-of-function gene mutations in the key components of SOCE have been reported to underlie a number of human diseases [29]. Actually, as resumed in Fig. 19.1 activation of SOCE as well as the level of expression of its molecular determinant, STIM1, Orai1 and TRPCs, have been implicated in the development of angiogenesis and several types of cancer [22], in the alteration of cardiac conduction and ventricle adverse remodeling [30], in skeletal muscle myopathy and tubular aggregation [31], and in vascular disorders [32].

In this chapter we will describe direct or indirect observations supporting the critical role of SOCE in cardiovascular and skeletal muscle disorders and angiogenesis.

19.2 SOCE in Cardiac Hypertrophy and Heart Failure

Most of the described molecular determinants of SOCE are also expressed in both excitable and non-excitable cardiac cells, such as fibroblasts, although the contribution of SOCE to normal cardiac physiology is still under debate [17, 26]. Growing set of experiments showed that stimulation of cardiomyocytes with agonists that activated G-protein coupled receptors or treatment with inhibitors of SERCA evokes persistent Ca^{2+} influx sensitive to classical blockers of SOCE. Whereas, they are insensitive to the inhibition of L-type Ca^{2+} channel [18, 33–35]. Interestingly, SOCE emerged as potential key player in Ca^{2+} dysregulation in cardiomyocytes. Therefore, most reports focused on its role in cardiac disease such as cardiac adverse remodeling, hypertrophy and consequent heart failure (HF), arrhythmia or cardiac conduction disorders [36–38]. In this chapter we will focus on the role of SOCE in cardiac hypertrophy and consequent HF. Cardiac hypertrophy can be reversible, nevertheless prolonged stress on the heart promotes deleterious

remodeling of cardiomyocytes, leading to a weaker dilated heart and potentially HF [36, 39].

Cardiac hypertrophy occurs to preserve the pump function in response to a greater hemodynamic demand or to different stress such as myocardial infarction or hypertension-induced pressure overload [40, 41]. It is well known that the calcineurin-Nuclear Factor of Activated T-cells (NFAT) complex, which requires cytosolic Ca^{2+} increase, is one of the key mechanisms that switches on the fetal genes causing cardiac hypertrophy [36]. Growing evidences suggest that STIM1/Orai1-mediated SOCE provide Ca^{2+} signals necessary to initiate cardiac hypertrophy, mainly through the calcineurin/NFAT signaling [42]. Actually, the overexpression of STIM1 is associated with an increase in neonatal cardiomyocytes size and an enhanced NFAT activity, which are abolished in the presence of SOCC inhibitors [43]. Furthermore, silencing of STIM1 and Orai1 prevents phenylephrine-mediated hypertrophic neonatal cardiomyocyte growth [44]. Likewise, a more recent report found that STIM1 deletion protects the heart from pressure overload induced cardiac hypertrophy [45]. Previously, Luo et al. [46] demonstrated that STIM1L is barely expressed in adult cardiomyocytes but it reemerges with hypertrophic agonists or in mice subjected to transverse aortic constriction during 3 weeks to trigger cardiac hypertrophy. Conversely, STIM1L levels correlate with exacerbated SOCE, and the expression of STIM1L is induced in isolated adult cardiomyocytes stimulated with phenylephrine [46].

On the other hand, independent studies demonstrated significant upregulation of TRPCs in several animal models of cardiac hypertrophy and heart failure [22, 37, 38]. In fact, experiments using pharmacological and molecular silencing or overexpression demonstrated that essential proteins of SOCE (STIM1, Orai1 and TRPC1/3/4 and 6) are involved in hypertrophy mainly through calcineurin/NFAT signaling [22, 38, 47]. Seth et al. [48] demonstrated in TRPC1 knockout mice that the calcineurin/NFAT pathway is inhibited, which reduces the hypertrophic response related to a better survival after Transverse Aortic Constriction (TAC) treatment. In this way, another study further confirmed that TRPC1/4 double knockout prevents cardiac hypertrophy and fibrotic infiltration after TAC and chronic neurohumoral stimulation [47].

Recent studies tried to demonstrate the involvement of SOCE in the transition from cardiac hypertrophy to HF. An early study demonstrated that TRPC3 protein levels are elevated in failing hearts of 20-months-old rats. This study also determined, specific increase in the expression of mRNA and protein levels of TRPC5 in heart failure patients comparing to non-failing heart [49]. Whereas, other research showed that TRPC6 is also significantly upregulated in human failing heart and HF was observed in transgenic mice overexpressing TRPC6 [50]. Horton et al. [51] showed that Orai1-knock out mice submitted to TAC develop earlier loss of cardiac function and greater dilatation of the left ventricle comparing to WT mice. However, Orai1 role in HF is still unclear. Recently, Correll et al. [52] showed that STIM1 overexpression increases SOCE in heart and enhances sudden death in transgenic mice at 6 weeks of age. Authors observed that when these mice reached 12 weeks, they develop HF with prominent hypertrophy, loss of ventricular

function, and pulmonary edema. Moreover, when submitted to pressure overload or neurohormonal stimulation these transgenic mice display accelerated hypertrophic [52]. In contrast, other study showed that specific STIM1 silencing in heart promotes the rapid transition from cardiac hypertrophy to HF [53]. Therefore, the presence of STIM1 is likely required for the persistence of adaptive cardiac hypertrophy.

Altogether, these studies suggest that different SOCE components play pivotal roles in the pathogenesis of heart disease, although many questions remain unanswered and require more detailed investigations.

19.3 SOCE in Vascular Disorder

Considerable interest has been focused towards the influence of ion channels plasticity and gene expression in VSMCs, which are normally quiescent and contractile. However, they can change to a proliferative and migratory state in certain conditions as arterial injury or inflammation [54]. This change is considered a characteristic step in the pathogenesis of multiple vascular diseases. Compelling evidence indicate that changes in the handling of SOCE originated by an alteration of STIM and Orai proteins is a significant contributor to the development of numerous vascular diseases [32], such as occlusive diseases, atherosclerosis or restenosis following angioplasty or those involving arterial remodeling like hypertension [15, 55–57].

Earlier studies demonstrated that vasoactive agonists and growth factors stimulate VSMCs growth, proliferation or migration through SOCE activation. In fact, angiotensin-II activates STIM1 and Orai1- dependent SOCE to stimulate aortic VSMCs growth and proliferation [58, 59]. Also, the addition of urotensin-II to aortic VSMCs activates I_{CRAC} and SOCE, stimulates Ca^{2+}/cAMP Response Element-Binding (CREB) transcription factor and promotes cells proliferation [24]. Urotensin-II mechanism requires a complex signaling pathway that involves STIM1, Orai1, and TRPC1 activation. On the other hand, Platelet-Derived Growth Factor (PDGF) activates Ca^{2+} entry and VSMCs migration involving STIM1 and Orai1 pathway, but not TRPC1/4/6 and Orai2/3 proteins [55]. Conversely, another study demonstrated that PDGF-induced proliferation VSMCs is strongly reduced in smooth muscle-specific STIM1 Knockout (sm-STIM1KO) mice, due to the diminution of NFAT activation dependent of Ca^{2+} entry through SOCE [60].

Interestingly, the use of in vivo animal model of angioplasty, performed generally by mechanical injury procedure of rat carotid arteries, helped to confirm that SOCE play a critical role in migration and proliferation of VSMCs on luminal side of injured vessels to form neointima [61]. Actually, inhibition of STIM1 and Orai1 with lentivirus attenuates neointima formation and prevents the increase of both proteins 14 days post-injury in the medial and neointimal layer. Moreover, STIM1 and Orai1 knockdown inhibits NFAT activation, which correlates with decreasing VSMCs proliferation compared to control [62]. In the same way, Guo et al. [59, 63] showed that angiotensin-II increases significantly the expression of STIM1 and Orai1 in the neointima layer. They also demonstrated that silencing

of Orai1 and STIM1 reduces VSMCs proliferation and inhibits the accelerated neointimal growth induced by angiotensin-II in balloon-injured rat carotid arteries. Consistent with these data, Mancarella et al. described a significantly attenuation of neointima formation after carotid artery ligation in sm-STIM1KO mice compared to control mice [60]. Recently, a role of Homer1, a scaffolding protein that bind to several Ca^{2+}-signaling proteins [64], was characterized in VSMCs proliferation and neointima formation [65]. This study showed that Homer1 is upregulated in neointimal VSMCs after balloon-injured rat carotid arteries, interacting with TRPC1/3/4/6 channels and Orai1. Furthermore, knockdown of Homer 1 in vivo by AAV virus expressing a short hairpin RNA against Homer1, and in vitro by transfection with siRNAs, evokes a significant reduction of neointimal area and SOCE, which attenuate VSMCs proliferation and migration [65].

SOCE has also been implicated in the pathogenesis of systemic and pulmonary hypertension in different animal models. SOCE activation, associated with augmented levels of Orai1 and STIM1, is increased in aorta from spontaneously hypertensive rats compared to wild-type rats [56]. In mesenteric artery from ouabain-induced hypertensive rats compared to normotensive rats, SOCE is also increased and correlates with an enhanced expression of TRPC1, but not of TRPC4/5 [66]. Meanwhile, STIM1 upregulation was observed after hypertension development by ethanol consumption in rats [67]. Similarly, an augmented SOCE associated with an increase in TRPC channels expression was observed in Pulmonary Artery Smooth Muscle Cells (PASMCs) isolated from patients with idiopathic or hypoxic Pulmonary Arterial Hypertension (PAH) patients compared to normotensive patients [68, 69]. Likewise, others reported the participation of Orai1, STIM1 and/or STIM2 in SOCE and PASMCs proliferation in patients with idiopathic PAH [70–72]. Recently, it has been described that hypoxic conditions in PASMCs upregulated expression of STIM1/2 and Orai1/2/3 disturbing resting Ca^{2+} and SOCE, which could explain why hypoxic PAH causes pulmonary arterial vasoconstriction [73, 74].

Therefore, several players of SOCE play critical roles in VSMCs proliferation and migration making them fair therapeutic targets to mitigate vascular remodeling.

19.4 SOCE in Skeletal Muscle: Differentiation and Myopathies

The role of SOCE in the skeletal muscle contraction was neglected for a long time, however it is now commonly accepted that Ca^{2+} entry via SOCE is essential to sustain muscle contraction [25, 75, 76]. In the skeletal muscle, SOCE machinery involves a signaling complex located at the triad, the structure formed by a T-tubule with a sarcoplasmic reticulum (SR) known as the terminal cisterna, containing STIM1, STIM1L, Orai1, TRPCs and ryanodine receptors [17, 31]. These proteins control Ca^{2+} influx to refill sarcoplasmic reticulum Ca^{2+} store. This occurs not

only in repetitive tetanic stimulation, but also in an immediate basis [77]. SOCE has a specific feature in the skeletal muscle related to its very fast kinetics of activation. In fact, the process leading to SOCE involving STIM1 aggregation and ER translocation to the plasma membrane and Orai1 opening takes place in less than a second [78, 79]. This feature is apparently due to the architecture of the sarcoplasmic reticulum. It is located permanently close to T-tubules at the triad allowing the proximity of STIM1 and Orai1 even before store depletion. SOCE seems also involved in the muscle contractions during tetanic stimulations in vigorous exercise and fatigue [80]. Actually, the absence of SOCE in the skeletal muscle results in mice more prone to fatigue, displaying a reduced muscle mass and force [25, 81].

SOCE also plays a role for muscle regeneration process to repair everyday life injuries or in case of myopathies partially the damage [8]. In fact, in human skeletal muscle the first event described during the differentiation process is an influx of Ca^{2+} caused by the activation of SOCE where STIM1, STIM2 and Orai1 proteins seem strongly involved [82]. Moreover, silencing of STIM1, Orai1 and Orai3 reduces the amplitude of SOCE and affects to myoblast differentiation. In contrast, the overexpression of STIM1 together with Orai1 increases SOCE and accelerates muscle differentiation [82].

An early study by Olah et al. [83] suggested that the overexpression of TRPC1 enhances SOCE in myotubes but it delays muscle differentiation leading to the formation of small myotubes. In contrast, TRPC1 overexpression enhances SOCE and accelerates the process of myogenesis in human muscle [84]. This finding was supported by recent data by Xia et al. [85] where they determined that TRPC1 downregulation by siRNA delays significantly the muscle regeneration. Similarly, a recent study demonstrated that TRPC1/4 and STIM1L are necessary for SOCE and are required for a proper skeletal muscle differentiation [6]. So far TRPC1, which is likely accepted as a channel necessary for the proper muscle differentiation both in human and murine models, can be activated by store depletion as well as stretch.

In addition to its role in muscle differentiation the alteration of the Ca^{2+} influx through SOCCs is related to different myopathies. Patients with the hereditary Severe Combined Immunodeficiency (SCID) syndrome have depressed SOCE because of loss-of-function associated to mutations of STIM1 and Orai1 genes. They manifest atrophy in skeletal-muscle fibers, hypotonia and a severe chronic pulmonary problem due to respiratory muscle weakness [29]. Interestingly, gain-of-function mutations in STIM1 or Orai1 genes results as well in muscular weakness, mainly associated with tubular aggregate myopathy syndrome [86]. Moreover, several reports suggested an important role of SOCE in Muscular Dystrophies (MD), which developed progressively accompanied with an increase of muscular weakness, atrophy and fatigue. SOCE is proposed to be a cause of Ca^{2+} overload which could initiate the characteristic cell necrosis in MD [78, 87]. Duchenne Muscular Dystrophy (DMD) is the most common form of MD in children and it is characterized by a progressive muscle degeneration and weakness [88]. DMD is caused by the absence of dystrophin, a cohesive protein located between the sarcolemma and the myofilaments in skeletal muscle cells. When the myofilaments

lack of dystrophin occurs a pathological Ca^{2+} dynamic where SOCE is exacerbated [89]. Significant increase in the expression of STIM1, Orai1 and TRPC1 is associated with Ca^{2+} overload in fiber of a mouse model of DMD (*mdx*) [78, 89, 90]. Moreover, STIM1L isoform is upregulated in *mdx* fiber, meanwhile STIM2 does not participate [91, 92]. Furthermore, the inhibition of TRPC1 and TRPC4 in *mdx* recovered Ca^{2+} homeostasis suggesting a role of these TRPCs [8, 90]. On the other hand, TRPC3 is also overexpressed in MD although its function seems independent of SOCE [93, 94].

Taking everything into account, it is confirmed that STIM1/1L, Orai1 and different isoforms of TRPCs are relevant for Ca^{2+} influx and for the progression of skeletal muscle disease such as DMD. Hence, molecular determinants of SOCE could be potential therapeutic targets to attenuate the impact of different myopathies.

19.5 SOCE and Angiogenesis

Angiogenesis is understood as the growth of new blood vessels from existing vasculature [95, 96]. This process is tightly regulated and may occur in a number of situations including prolonged exercise [97], reproduction [98], physiological repair (e.g. regeneration of heart after a myocardial infarction [99–101], and different pathologies such as diabetes, endometriosis [102] and cancer [103]). Basically, angiogenesis is initiated in hypoxic environment because a variety of growth factors, including vascular endothelial growth factor (VEGF), fibroblast growth factor (FGF), and epidermal growth factor (EGF). The last one stimulates proliferation, migration and tube formation of endothelial cells (ECs), resulting in the generation of new capillary tubes [104]. Increasing evidences confirmed an expression of different SOCE proteins in ECs, which are intimately related to tumor progression and angiogenesis [105–108]. Chen et al. [106] demonstrated that STIM1 overexpression remarkably enhances tumor growth, local spread and angiogenesis; whereas, knockdown of STIM1 significantly decreases tumor growth and tumor vessels number. Independent studies showed that VEGF increases cytosolic Ca^{2+} due to SOCE in ECs [102, 105, 109]. Li et al. [102] demonstrated that specific inhibition of CRAC channels prevented VEGF-induced Ca^{2+} influx and tube formation. Using siRNAs, a dominant negative or neutralizing antibodies, they also demonstrated that Orai1 instead of TRPC1 is involved in VEGF-induced Ca^{2+} increase and angiogenesis [102]. Moreover, beside the implication of Orai1/STIM1, a recent study suggested a role for Orai3 in VEGF-induced ECs tube formation both in vitro and in vivo [110].

Although there is a consensus in the role of STIM1 and Orai1 in angiogenesis, TRPCs involvement is still under debate [111]. Indeed, knockdown of TRPC1 did not have a significant effect on the in vitro formation of human umbilical vein-derived endothelial tubes [112]. Besides, TRPC1 knockout mice developed the

vasculature normally [113]. Furthermore, Antigny et al. [112] reported that silencing of TRPC3, TRPC4, or TRPC5 expression inhibited endothelial tube formation in vitro, suggesting a possible role of these TRPC channels in angiogenesis. Therefore, additional studies about the role of TRPCs in angiogenesis will be welcomed.

SOCE proteins are also expressed in Endothelial Progenitor Cells (EPCs) [114], and they are significantly enhanced in EPCs isolated from patients with renal cellular carcinoma [115]. The exacerbated SOCE correlates with an upregulation of STIM1, Orai1 and TRPC1, which controls proliferation and in vitro tubulogenesis both in normal EPCs and in their malignant counterparts [116].

Taken together, these studies suggest that STIM1, Orai1 and some TRPCs stand out as promising molecular target of anti-angiogenic therapies to prevent tumor neovascularization. Therefore, SOCE signaling pathway is worth to take in consideration as alternative strategy to hit highly vasculogenic tumors.

19.6 Conclusion and Perspectives

Over the last decades, the rapid progress in SOCE research has revealed that different proteins of the SOCE mechanism play pivotal roles not only in the regulation of basal Ca^{2+} homeostasis but also in several pathogenesis related to heart and vascular diseases, skeletal myopathies and angiogenesis. Nevertheless, many questions remain unanswered and require future investigations to decipher the physiological and pathological roles of SOCE in different systems. Given that STIM, Orai and TRPC isoforms are widely expressed in different cell types, using transgenic mouse models or tissue specific knockout of these genes will undoubtedly provide more precise information about the causative role of these proteins in the development of each disease. For this reason, many studies are now focusing on such proteins as therapeutic targets to consider for pharmacological intervention in the treatment of these pathologies.

Acknowledgements This work was supported by FEDER funds and by Spanish Ministry of Economy and Competitiveness [BFU2016-74932-C2]; Institute of Carlos III [PI15/00203; CB16/11/00431]; and by the Andalusia Government [P12-CTS-1965; PI-0313-2016].

References

1. Putney JW (1986) A model for receptor-regulated calcium entry. Cell Calcium 7:1–12
2. Roos J, DiGregorio PJ, Yeromin AV et al (2005) STIM1, an essential and conserved component of store-operated Ca^{2+} channel function. J Cell Biol 169:435–445
3. Hogan PG, Rao A (2015) Store-operated calcium entry: mechanisms and modulation. Biochem Biophys Res Commun 460:40–49
4. Brandman O, Liou J, Park WS, Meyer T (2007) STIM2 is a feedback regulator that stabilizes basal cytosolic and endoplasmic reticulum Ca^{2+} levels. Cell 131:1327–1339

5. Rosado JA, Diez R, Smani T, Jardín I (2015) STIM and Orai1 variants in store-operated calcium entry. Front Pharmacol 6:325
6. Antigny F, Sabourin J, Saüc S, Bernheim L, Koenig S, Frieden M (2017) TRPC1 and TRPC4 channels functionally interact with STIM1L to promote myogenesis and maintain fast repetitive Ca^{2+} release in human myotubes. Biochim Biophys Acta 1864:806–813
7. Horinouchi T, Higashi T, Higa T et al (2012) Different binding property of STIM1 and its novel splice variant STIM1L to Orai1, TRPC3, and TRPC6 channels. Biochem Biophys Res Commun 428:252–258
8. Saüc S, Frieden M (2017) Neurological and motor disorders: TRPC in the skeletal muscle. Adv Exp Med Biol 993:557–575
9. Feske S, Gwack Y, Prakriya M, Srikanth S, Puppel SH, Tanasa B, Hogan PG, Lewis RS, Daly M, Rao A (2006) A mutation in Orai1 causes immune deficiency by abrogating CRAC channel function. Nature 441:179–185
10. Vig M, Beck A, Billingsley JM et al (2006) CRACM1 multimers form the ion-selective pore of the CRAC channel. Curr Biol 16:2073–2079
11. Desai PN, Zhang X, Wu S, Janoshazi A, Bolimuntha S, Putney JW, Trebak M (2015) Multiple types of calcium channels arising from alternative translation initiation of the Orai1 message. Sci Signal 8:ra74
12. Vaeth M, Yang J, Yamashita M et al (2017) ORAI2 modulates store-operated calcium entry and T cell-mediated immunity. Nat Commun 8:14714
13. Lis A, Peinelt C, Beck A, Parvez S, Monteilh-Zoller M, Fleig A, Penner R (2007) CRACM1, CRACM2, and CRACM3 are store-operated Ca^{2+} channels with distinct functional properties. Curr Biol CB 17:794–800
14. Mignen O, Thompson JL, Shuttleworth TJ (2008) Both Orai1 and Orai3 are essential components of the arachidonate-regulated Ca^{2+}−selective (ARC) channels. J Physiol 586:185–195
15. Gonzalez-Cobos JC, Zhang X, Zhang W et al (2013) Store-independent Orai1/3 channels activated by intracrine leukotriene C4: role in neointimal hyperplasia. Circ Res 112:1013–1025
16. Ambudkar IS, de Souza LB, Ong HL (2017) TRPC1, Orai1, and STIM1 in SOCE: friends in tight spaces. Cell Calcium 63:33–39
17. Avila-Medina J, Mayoral-Gonzalez I, Dominguez-Rodriguez A, Gallardo-Castillo I, Ribas J, Ordoñez A, Rosado JA, Smani T (2018) The complex role of store operated calcium entry pathways and related proteins in the function of cardiac, skeletal and vascular smooth muscle cells. Front Physiol 9:257
18. Domínguez-Rodríguez A, Ruiz-Hurtado G, Sabourin J, Gómez AM, Alvarez JL, Benitah J-P (2015) Proarrhythmic effect of sustained EPAC activation on TRPC3/4 in rat ventricular cardiomyocytes. J Mol Cell Cardiol 87:74–78
19. Avila-Medina J, Calderon-Sanchez E, Gonzalez-Rodriguez P, Monje-Quiroga F, Rosado JA, Castellano A, Ordonez A, Smani T (2016) Orai1 and TRPC1 proteins co-localize with CaV1.2 channels to form a signal complex in vascular smooth muscle cells. J Biol Chem 291:21148–21159
20. Lyfenko AD, Dirksen RT (2008) Differential dependence of store-operated and excitation-coupled Ca^{2+} entry in skeletal muscle on STIM1 and Orai1. J Physiol 586:4815–4824
21. Stiber J, Hawkins A, Zhang Z-S et al (2008) STIM1 signalling controls store-operated calcium entry required for development and contractile function in skeletal muscle. Nat Cell Biol 10:688–697
22. Smani T, Shapovalov G, Skryma R, Prevarskaya N, Rosado JA (2015) Functional and physiopathological implications of TRP channels. Biochim Biophys Acta 1853:1772–1782
23. Dominguez-Rodriguez A, Diaz I, Rodriguez-Moyano M, Calderon-Sanchez E, Rosado JA, Ordonez A, Smani T (2012) Urotensin-II signaling mechanism in rat coronary artery: role of STIM1 and Orai1-dependent store operated calcium influx in vasoconstriction. Arter Thromb Vasc Biol 32:1325–1332

24. Rodriguez-Moyano M, Diaz I, Dionisio N, Zhang X, Avila-Medina J, Calderon-Sanchez E, Trebak M, Rosado JA, Ordonez A, Smani T (2013) Urotensin-II promotes vascular smooth muscle cell proliferation through store-operated calcium entry and EGFR transactivation. Cardiovasc Res 100:297–306
25. Wei-Lapierre L, Carrell EM, Boncompagni S, Protasi F, Dirksen RT (2013) Orai1-dependent calcium entry promotes skeletal muscle growth and limits fatigue. Nat Commun 4:2805
26. Bootman MD, Rietdorf K (2017) Tissue specificity: store-operated Ca^{2+} entry in cardiac myocytes. Adv Exp Med Biol 993:363–387
27. Chang H-Y, Chen S-L, Shen M-R, Kung M-L, Chuang L-M, Chen Y-W (2017) Selective serotonin reuptake inhibitor, fluoxetine, impairs E-cadherin-mediated cell adhesion and alters calcium homeostasis in pancreatic beta cells. Sci Rep 7:3515
28. Sabourin J, Le Gal L, Saurwein L, Haefliger J-A, Raddatz E, Allagnat F (2015) Store-operated Ca^{2+} entry mediated by Orai1 and TRPC1 participates to insulin secretion in rat β-cells. J Biol Chem 290:30530–30539
29. Lacruz RS, Feske S (2015) Diseases caused by mutations in ORAI1 and STIM1. Ann N Y Acad Sci 1356:45–79
30. Eder P (2017) Cardiac remodeling and disease: SOCE and TRPC signaling in cardiac pathology. Adv Exp Med Biol 993:505–521
31. Pan Z, Brotto M, Ma J (2014) Store-operated Ca^{2+} entry in muscle physiology and diseases. BMB Rep 47:69–79
32. Tanwar J, Trebak M, Motiani RK (2017) Cardiovascular and hemostatic disorders: role of STIM and Orai proteins in vascular disorders. Adv Exp Med Biol 993:425–452
33. Hunton DL, Zou L, Pang Y, Marchase RB (2004) Adult rat cardiomyocytes exhibit capacitative calcium entry. Am J Physiol Heart Circ Physiol 286:H1124–H1132
34. Kojima A, Kitagawa H, Omatsu-Kanbe M, Matsuura H, Nosaka S (2012) Presence of store-operated Ca^{2+} entry in C57BL/6J mouse ventricular myocytes and its suppression by sevoflurane. Br J Anaesth 109:352–360
35. Uehara A, Yasukochi M, Imanaga I, Nishi M, Takeshima H (2002) Store-operated Ca^{2+} entry uncoupled with ryanodine receptor and junctional membrane complex in heart muscle cells. Cell Calcium 31:89–96
36. Eder P, Molkentin JD (2011) TRPC channels as effectors of cardiac hypertrophy. Circ Res 108:265–272
37. Bartoli F, Sabourin J (2017) Cardiac remodeling and disease: current understanding of STIM1/Orai1-mediated store-operated Ca^{2+} entry in cardiac function and pathology. Adv Exp Med Biol 993:523–534
38. Yue Z, Xie J, Yu AS, Stock J, Du J, Yue L (2015) Role of TRP channels in the cardiovascular system. Am J Physiol Heart Circ Physiol 308:H157–H182
39. Ljubojevic S, Radulovic S, Leitinger G et al (2014) Early remodeling of perinuclear Ca^{2+} stores and nucleoplasmic Ca^{2+} signaling during the development of hypertrophy and heart failure. Circulation 130:244–255
40. Samak M, Fatullayev J, Sabashnikov A et al (2016) Cardiac hypertrophy: an introduction to molecular and cellular basis. Med Sci Monit Basic Res 22:75–79
41. McMullen JR, Jennings GL (2007) Differences between pathological and physiological cardiac hypertrophy: novel therapeutic strategies to treat heart failure. Clin Exp Pharmacol Physiol 34:255–262
42. Collins HE, Zhu-Mauldin X, Marchase RB, Chatham JC (2013) STIM1/Orai1-mediated SOCE: current perspectives and potential roles in cardiac function and pathology. Am J Physiol Heart Circ Physiol 305:H446–H458
43. Hulot J-S, Fauconnier J, Ramanujam D et al (2011) Critical role for stromal interaction molecule 1 in cardiac hypertrophy. Circulation 124:796–805
44. Voelkers M, Salz M, Herzog N et al (2010) Orai1 and Stim1 regulate normal and hypertrophic growth in cardiomyocytes. J Mol Cell Cardiol 48:1329–1334
45. Parks C, Alam MA, Sullivan R, Mancarella S (2016) STIM1-dependent Ca^{2+} microdomains are required for myofilament remodeling and signaling in the heart. Sci Rep 6:25372

46. Luo X, Hojayev B, Jiang N, Wang ZV, Tandan S, Rakalin A, Rothermel BA, Gillette TG, Hill JA (2012) STIM1-dependent store-operated Ca^{2+} entry is required for pathological cardiac hypertrophy. J Mol Cell Cardiol 52:136–147
47. Camacho Londoño JE, Tian Q, Hammer K et al (2015) A background Ca^{2+} entry pathway mediated by TRPC1/TRPC4 is critical for development of pathological cardiac remodelling. Eur Heart J 36:2257–2266
48. Seth M, Zhang Z-S, Mao L et al (2009) TRPC1 channels are critical for hypertrophic signaling in the heart. Circ Res 105:1023–1030
49. Bush EW, Hood DB, Papst PJ, Chapo JA, Minobe W, Bristow MR, Olson EN, McKinsey TA (2006) Canonical transient receptor potential channels promote cardiomyocyte hypertrophy through activation of calcineurin signaling. J Biol Chem 281:33487–33496
50. Kuwahara K, Wang Y, McAnally J, Richardson JA, Bassel-Duby R, Hill JA, Olson EN (2006) TRPC6 fulfills a calcineurin signaling circuit during pathologic cardiac remodeling. J Clin Invest 116:3114–3126
51. Horton JS, Buckley CL, Alvarez EM, Schorlemmer A, Stokes AJ (2014) The calcium release-activated calcium channel Orai1 represents a crucial component in hypertrophic compensation and the development of dilated cardiomyopathy. Channels Austin Tex 8:35–48
52. Correll RN, Goonasekera SA, van Berlo JH et al (2015) STIM1 elevation in the heart results in aberrant Ca^{2+} handling and cardiomyopathy. J Mol Cell Cardiol 87:38–47
53. Bénard L, Oh JG, Cacheux M et al (2016) Cardiac Stim1 silencing impairs adaptive hypertrophy and promotes heart failure through inactivation of mTORC2/Akt signaling. Circulation 133:1458–1471; discussion 1471
54. House SJ, Potier M, Bisaillon J, Singer HA, Trebak M (2008) The non-excitable smooth muscle: calcium signaling and phenotypic switching during vascular disease. Pflugers Arch 456:769–785
55. Bisaillon JM, Motiani RK, Gonzalez-Cobos JC, Potier M, Halligan KE, Alzawahra WF, Barroso M, Singer HA, Jourd'heuil D, Trebak M (2010) Essential role for STIM1/Orai1-mediated calcium influx in PDGF-induced smooth muscle migration. Am J Physiol Cell Physiol 298:C993–C1005
56. Giachini FR, Chiao CW, Carneiro FS, Lima VV, Carneiro ZN, Dorrance AM, Tostes RC, Webb RC (2009) Increased activation of stromal interaction molecule-1/Orai-1 in aorta from hypertensive rats: a novel insight into vascular dysfunction. Hypertension 53:409–416
57. Kassan M, Ait-Aissa K, Radwan E et al (2016) Essential role of smooth muscle STIM1 in hypertension and cardiovascular dysfunction. Arter Thromb Vasc Biol 36:1900–1909
58. Simo-Cheyou ER, Tan JJ, Grygorczyk R, Srivastava AK (2017) STIM-1 and ORAI-1 channel mediate angiotensin-II-induced expression of Egr-1 in vascular smooth muscle cells. J Cell Physiol 232:3496–3509
59. Guo RW, Yang LX, Li MQ, Pan XH, Liu B, Deng YL (2012) Stim1- and Orai1-mediated store-operated calcium entry is critical for angiotensin II-induced vascular smooth muscle cell proliferation. Cardiovasc Res 93:360–370
60. Mancarella S, Potireddy S, Wang Y et al (2013) Targeted STIM deletion impairs calcium homeostasis, NFAT activation, and growth of smooth muscle. FASEB J 27:893–906
61. Zhang W, Trebak M (2014) Vascular balloon injury and intraluminal administration in rat carotid artery. J Vis Exp. https://doi.org/10.3791/52045
62. Zhang W, Halligan KE, Zhang X et al (2011) Orai1-mediated I (CRAC) is essential for neointima formation after vascular injury. Circ Res 109:534–542
63. Guo RW, Wang H, Gao P, Li MQ, Zeng CY, Yu Y, Chen JF, Song MB, Shi YK, Huang L (2009) An essential role for stromal interaction molecule 1 in neointima formation following arterial injury. Cardiovasc Res 81:660–668
64. Jardin I, Albarrán L, Bermejo N, Salido GM, Rosado JA (2012) Homers regulate calcium entry and aggregation in human platelets: a role for Homers in the association between STIM1 and Orai1. Biochem J 445:29–38
65. Jia S, Rodriguez M, Williams AG, Yuan JP (2017) Homer binds to Orai1 and TRPC channels in the neointima and regulates vascular smooth muscle cell migration and proliferation. Sci Rep 7:5075

66. Pulina MV, Zulian A, Berra-Romani R, Beskina O, Mazzocco-Spezzia A, Baryshnikov SG, Papparella I, Hamlyn JM, Blaustein MP, Golovina VA (2010) Upregulation of Na^+ and Ca^{2+} transporters in arterial smooth muscle from ouabain-induced hypertensive rats. Am J Physiol Heart Circ Physiol 298:H263–H274
67. Souza Bomfim GH, Mendez-Lopez I, Arranz-Tagarro JA, Ferraz Carbonel AA, Roman-Campos D, Padin JF, Garcia AG, Jurkiewicz A, Jurkiewicz NH (2017) Functional upregulation of STIM-1/Orai-1-mediated store-operated Ca^{2+} contributing to the hypertension development elicited by chronic EtOH consumption. Curr Vasc Pharmacol 15:265–281
68. Lin MJ, Leung GP, Zhang WM, Yang XR, Yip KP, Tse CM, Sham JS (2004) Chronic hypoxia-induced upregulation of store-operated and receptor-operated Ca^{2+} channels in pulmonary arterial smooth muscle cells: a novel mechanism of hypoxic pulmonary hypertension. Circ Res 95:496–505
69. Zhang S, Patel HH, Murray F, Remillard CV, Schach C, Thistlethwaite PA, Insel PA, Yuan JX (2007) Pulmonary artery smooth muscle cells from normal subjects and IPAH patients show divergent cAMP-mediated effects on TRPC expression and capacitative Ca^{2+} entry. Am J Physiol Lung Cell Mol Physiol 292:L1202–L1210
70. Ogawa A, Firth AL, Smith KA, Maliakal MV, Yuan JX (2012) PDGF enhances store-operated Ca^{2+} entry by upregulating STIM1/Orai1 via activation of Akt/mTOR in human pulmonary arterial smooth muscle cells. Am J Physiol Cell Physiol 302:C405–C411
71. Hou X, Chen J, Luo Y, Liu F, Xu G, Gao Y (2013) Silencing of STIM1 attenuates hypoxia-induced PASMCs proliferation via inhibition of the SOC/Ca^{2+}/NFAT pathway. Respir Res 14:2
72. Fernandez RA, Wan J, Song S, Smith KA, Gu Y, Tauseef M, Tang H, Makino A, Mehta D, Yuan JX (2015) Upregulated expression of STIM2, TRPC6, and Orai2 contributes to the transition of pulmonary arterial smooth muscle cells from a contractile to proliferative phenotype. Am J Physiol Cell Physiol 308:C581–C593
73. Wang J, Xu C, Zheng Q, Yang K, Lai N, Wang T, Tang H, Lu W (2017) Orai1, 2, 3 and STIM1 promote store-operated calcium entry in pulmonary arterial smooth muscle cells. Cell Death Discov 3:17074
74. He X, Song S, Ayon RJ, Balisterieri A, Black SM, Makino A, Wier WG, Zang WJ, Yuan JX (2018) Hypoxia selectively upregulates cation channels and increases cytosolic [Ca^{2+}] in pulmonary, but not coronary, arterial smooth muscle cells. Am J Physiol Cell Physiol. https://doi.org/10.1152/ajpcell.00272.2017
75. Dirksen RT (2009) Checking your SOCCs and feet: the molecular mechanisms of Ca^{2+} entry in skeletal muscle. J Physiol 587:3139–3147
76. Stiber JA, Rosenberg PB (2011) The role of store-operated calcium influx in skeletal muscle signaling. Cell Calcium 49:341–349
77. Sztretye M, Geyer N, Vincze J et al (2017) SOCE is important for maintaining sarcoplasmic calcium content and release in skeletal muscle fibers. Biophys J 113:2496–2507
78. Edwards JN, Friedrich O, Cully TR, von Wegner F, Murphy RM, Launikonis BS (2010) Upregulation of store-operated Ca^{2+} entry in dystrophic mdx mouse muscle. Am J Physiol Cell Physiol 299:C42–C50
79. Launikonis BS, Stephenson DG, Friedrich O (2009) Rapid Ca^{2+} flux through the transverse tubular membrane, activated by individual action potentials in mammalian skeletal muscle. J Physiol 587:2299–2312
80. Allen DG, Lamb GD, Westerblad H (2008) Skeletal muscle fatigue: cellular mechanisms. Physiol Rev 88:287–332
81. Li T, Finch EA, Graham V, Zhang Z-S, Ding J-D, Burch J, Oh-hora M, Rosenberg P (2012) STIM1-Ca^{2+} signaling is required for the hypertrophic growth of skeletal muscle in mice. Mol Cell Biol 32:3009–3017
82. Darbellay B, Arnaudeau S, König S, Jousset H, Bader C, Demaurex N, Bernheim L (2009) STIM1- and Orai1-dependent store-operated calcium entry regulates human myoblast differentiation. J Biol Chem 284:5370–5380

83. Oláh T, Fodor J, Ruzsnavszky O, Vincze J, Berbey C, Allard B, Csernoch L (2011) Overexpression of transient receptor potential canonical type 1 (TRPC1) alters both store operated calcium entry and depolarization-evoked calcium signals in C2C12 cells. Cell Calcium 49:415–425
84. Antigny F, Koenig S, Bernheim L, Frieden M (2013) During post-natal human myogenesis, normal myotube size requires TRPC1- and TRPC4-mediated Ca^{2+} entry. J Cell Sci 126:2525–2533
85. Xia L, Cheung K-K, Yeung SS, Yeung EW (2016) The involvement of transient receptor potential canonical type 1 in skeletal muscle regrowth after unloading-induced atrophy. J Physiol 594:3111–3126
86. Böhm J, Chevessier F, Koch C et al (2014) Clinical, histological and genetic characterisation of patients with tubular aggregate myopathy caused by mutations in STIM1. J Med Genet 51:824–833
87. Goonasekera SA, Davis J, Kwong JQ, Accornero F, Wei-LaPierre L, Sargent MA, Dirksen RT, Molkentin JD (2014) Enhanced Ca^{2+} influx from STIM1-Orai1 induces muscle pathology in mouse models of muscular dystrophy. Hum Mol Genet 23:3706–3715
88. Brandsema JF, Darras BT (2015) Dystrophinopathies. Semin Neurol 35:369–384
89. Kiviluoto S, Decuypere J-P, De Smedt H, Missiaen L, Parys JB, Bultynck G (2011) STIM1 as a key regulator for Ca^{2+} homeostasis in skeletal-muscle development and function. Skelet Muscle 1:16
90. Vandebrouck C, Martin D, Schoor MC-V, Debaix H, Gailly P (2002) Involvement of TRPC in the abnormal calcium influx observed in dystrophic (mdx) mouse skeletal muscle fibers. J Cell Biol 158:1089–1096
91. Cully TR, Edwards JN, Friedrich O, Stephenson DG, Murphy RM, Launikonis BS (2012) Changes in plasma membrane Ca-ATPase and stromal interacting molecule 1 expression levels for Ca^{2+} signaling in dystrophic mdx mouse muscle. Am J Physiol Cell Physiol 303:C567–C576
92. Cully TR, Launikonis BS (2013) Store-operated Ca^{2+} entry is not required for store refilling in skeletal muscle. Clin Exp Pharmacol Physiol 40:338–344
93. Shirokova N, Niggli E (2013) Cardiac phenotype of duchenne muscular dystrophy: insights from cellular studies. J Mol Cell Cardiol 58:217–224
94. Millay DP, Goonasekera SA, Sargent MA, Maillet M, Aronow BJ, Molkentin JD (2009) Calcium influx is sufficient to induce muscular dystrophy through a TRPC-dependent mechanism. Proc Natl Acad Sci U S A 106:19023–19028
95. Fraisl P, Mazzone M, Schmidt T, Carmeliet P (2009) Regulation of angiogenesis by oxygen and metabolism. Dev Cell 16:167–179
96. Stapor P, Wang X, Goveia J, Moens S, Carmeliet P (2014) Angiogenesis revisited – role and therapeutic potential of targeting endothelial metabolism. J Cell Sci 127:4331–4341
97. Egginton S (2009) Invited review: activity-induced angiogenesis. Pflugers Arch 457:963–977
98. Logsdon EA, Finley SD, Popel AS, Mac Gabhann F (2014) A systems biology view of blood vessel growth and remodelling. J Cell Mol Med 18:1491–1508
99. Ingason AB, Goldstone AB, Paulsen MJ, Thakore AD, Truong VN, Edwards BB, Eskandari A, Bollig T, Steele AN, Woo YJ (2018) Angiogenesis precedes cardiomyocyte migration in regenerating mammalian hearts. J Thorac Cardiovasc Surg 155:1118–1127.e1
100. Reddy K, Khaliq A, Henning RJ (2015) Recent advances in the diagnosis and treatment of acute myocardial infarction. World J Cardiol 7:243–276
101. Melly L, Cerino G, Frobert A et al (2018) Myocardial infarction stabilization by cell-based expression of controlled vascular endothelial growth factor levels. J Cell Mol Med. https://doi.org/10.1111/jcmm.13511
102. Li J, Cubbon RM, Wilson LA et al (2011) Orai1 and CRAC channel dependence of VEGF-activated Ca^{2+} entry and endothelial tube formation. Circ Res 108:1190–1198
103. Folkman J (1971) Tumor angiogenesis: therapeutic implications. N Engl J Med 285:1182–1186

104. Kohn EC, Alessandro R, Spoonster J, Wersto RP, Liotta LA (1995) Angiogenesis: role of calcium-mediated signal transduction. Proc Natl Acad Sci U S A 92:1307–1311
105. Chen Y-F, Hsu K-F, Shen M-R (2016) The store-operated Ca^{2+} entry-mediated signaling is important for cancer spread. Biochim Biophys Acta 1863:1427–1435
106. Chen Y-F, Chiu W-T, Chen Y-T, Lin P-Y, Huang H-J, Chou C-Y, Chang H-C, Tang M-J, Shen M-R (2011) Calcium store sensor stromal-interaction molecule 1-dependent signaling plays an important role in cervical cancer growth, migration, and angiogenesis. Proc Natl Acad Sci U S A 108:15225–15230
107. Fiorio Pla A, Gkika D (2013) Emerging role of TRP channels in cell migration: from tumor vascularization to metastasis. Front Physiol 4:311
108. Martial S (2016) Involvement of ion channels and transporters in carcinoma angiogenesis and metastasis. Am J Physiol Cell Physiol 310:C710–C727
109. Dragoni S, Laforenza U, Bonetti E et al (2011) Vascular endothelial growth factor stimulates endothelial colony forming cells proliferation and tubulogenesis by inducing oscillations in intracellular Ca^{2+} concentration. Stem Cells Dayt Ohio 29:1898–1907
110. Li J, Bruns A-F, Hou B et al (2015) Orai3 surface accumulation and calcium entry evoked by vascular endothelial growth factor. Arterioscler Thromb Vasc Biol 35:1987–1994
111. Earley S, Brayden JE (2015) Transient receptor potential channels in the vasculature. Physiol Rev 95:645–690
112. Antigny F, Girardin N, Frieden M (2012) Transient receptor potential canonical channels are required for in vitro endothelial tube formation. J Biol Chem 287:5917–5927
113. Schmidt K, Dubrovska G, Nielsen G et al (2010) Amplification of EDHF-type vasodilatations in TRPC1-deficient mice. Br J Pharmacol 161:1722–1733
114. Sánchez-Hernández Y, Laforenza U, Bonetti E et al (2010) Store-operated Ca^{2+} entry is expressed in human endothelial progenitor cells. Stem Cells Dev 19:1967–1981
115. Lodola F, Laforenza U, Bonetti E et al (2012) Store-operated Ca^{2+} entry is remodelled and controls in vitro angiogenesis in endothelial progenitor cells isolated from tumoral patients. PLoS One 7:e42541
116. Moccia F, Poletto V (2015) May the remodeling of the Ca^{2+} toolkit in endothelial progenitor cells derived from cancer patients suggest alternative targets for anti-angiogenic treatment? Biochim Biophys Acta 1853:1958–1973

Chapter 20
Calcium Signaling and the Regulation of Chemosensitivity in Cancer Cells: Role of the Transient Receptor Potential Channels

Giorgio Santoni, Maria Beatrice Morelli, Oliviero Marinelli, Massimo Nabissi, Matteo Santoni, and Consuelo Amantini

Abstract Cancer cells acquire the ability to modify the calcium signaling network by altering the expression and functions of cation channels, pumps or transporters. Calcium signaling pathways are involved in proliferation, angiogenesis, invasion, immune evasion, disruption of cell death pathways, ECM remodelling, epithelial-mesenchymal transition (EMT) and drug resistance. Among cation channels, a pivotal role is played by the Transient Receptor Potential non-selective cation-permeable receptors localized in plasma membrane, endoplasmic reticulum, mitochondria and lysosomes. Several findings indicate that the dysregulation in calcium signaling induced by TRP channels is responsible for cancer growth, metastasis and chemoresistance. Drug resistance represents a major limitation in the application of current therapeutic regimens and several efforts are spent to overcome it. Here we describe the ability of Transient Receptor Potential Channels to modify, by altering the intracellular calcium influx, the cancer cell sensitivity to chemotherapeutic drugs.

G. Santoni · M. Nabissi
School of Pharmacy, Immunopathology and Molecular Medicine Laboratory, University of Camerino, Camerino, Italy

M. B. Morelli · O. Marinelli
School of Pharmacy, Immunopathology and Molecular Medicine Laboratory, University of Camerino, Camerino, Italy

School of Biosciences and Veterinary Medicine, University of Camerino, Camerino, Italy

M. Santoni
Clinic and Oncology Unit, Macerata Hospital, Macerata, Italy

C. Amantini (✉)
School of Biosciences and Veterinary Medicine, University of Camerino, Camerino, Italy
e-mail: consuelo.amantini@unicam.it

M. S. Islam (ed.), *Calcium Signaling*, Advances in Experimental Medicine and Biology 1131, https://doi.org/10.1007/978-3-030-12457-1_20

Keywords Ca^{2+} dysregulation · TRPC5 · TRPC6 · TRPM7 · TRPM8 · TRPV1 · TRPV2 · TRPV6 · Chemoresistance · Cancer

20.1 Calcium Signaling in Cancer

Intracellular calcium ions (Ca^{2+}), the most abundant and important second messenger, play a pivotal role in controlling cell proliferation, differentiation, migration and death [1–4]. Thus, it is essential to keep under tight control the Ca^{2+} signals in the form of oscillations, wave or spikes [2]. The disruption of normal Ca^{2+} signaling contributes to the development of the malignant phenotypes; in fact, cancer cells are able to modify the Ca^{2+} signaling network in order to increase proliferation, immortalization, angiogenesis, invasion, immune evasion, disruption of cell death pathways, ECM remodelling, epithelial-mesenchymal transition (EMT) and drug resistance [5, 6]. Several Ca^{2+} channels, transporters and Ca^{2+}-ATPases, as voltage-gated Ca^{2+} channel (VGCC), Transient Receptor Potential (TRP), Ca^{2+} release activated Ca^{2+} channel (CRAC), inositol 1,4,5-triphosphate receptor (IP3R) and mitochondrial Ca^{2+} uniporter (MCU) are altered in cancer. Moreover, their impairment has been found to be involved in the tumorigenesis [2] (Fig. 20.1). The aim of this chapter is to address the role of TRP channels in modulating sensitivity to chemotherapeutic drugs in different cancer types.

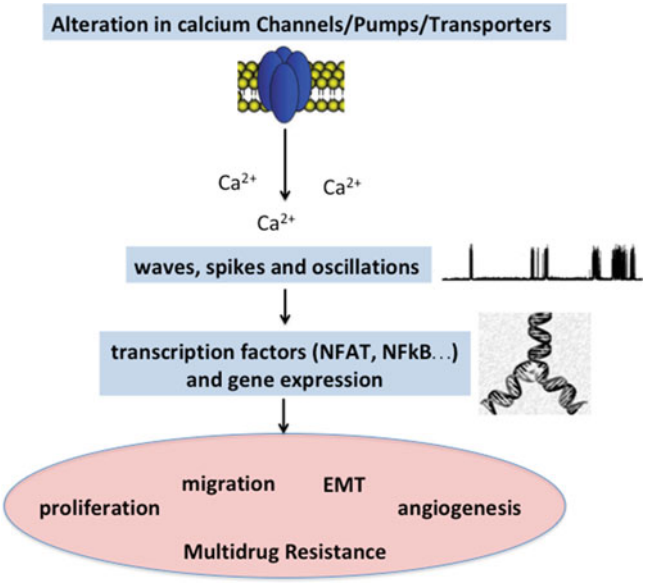

Fig. 20.1 Alterations in expression and functions of Ca^{2+} channels/pumps/transporters lead to dysregulation in calcium signaling promoting malignant phenotype and chemoresistance

20.1.1 Cation Disruption in Cancer: The Transient Receptor Potential Family

The TRP channels are non-selective cation permeable receptors localized in plasma membrane, endoplasmic reticulum, mitochondria and lysosomes [7]. They play a key role in regulating cellular Ca^{2+} concentration and membrane voltage. To date, about 30 TRPs have been identified and, on the basis of their structural homology, they are classified in: TRPC1-7, TRPV1-6, TRPM1-8, TRPP2,3,5, TRPML1-3 and TRPA1 [8]. Several findings indicate that alterations in expression and functions of TRP channels are responsible for cancer growth, metastasis and chemoresistance [9]. In particular, dysregulation of TRPC, TRPM or TRPV members has been mainly correlated with malignant growth and progression [10], so that cancer can now be considered like a "channellopathy" [11]. The central role of TRPs in cancer is to impair the Ca^{2+} homeostasis by stimulating Ca^{2+} entry or altering membrane potential. For this reason, in the recent years an increased interest in discovering agents targeting TRP channels in cancer, has been emerged and several pharmacological modulators are now used to characterize the implications of TRP channels in whole-cell membrane currents, resting membrane potential regulation or intracellular Ca^{2+} signaling [12, 13].

20.2 Drug Resistance in Cancer

Initially, cancers are susceptible to chemotherapy but over time they develop resistance by activating different strategies to limit drug efficacy eluding cell death. Thus, cancer cells become tolerant to pharmacological treatments [14]. Drug resistance can be achieved through several mechanisms involving Ca^{2+} signaling as drug inactivation, drug efflux, drug target alterations, acquisition of EMT, evasion from cell death pathways, increased DNA damage tolerance and dysregulation of critical genes (Fig. 20.2). Many chemotherapeutic agents require metabolic

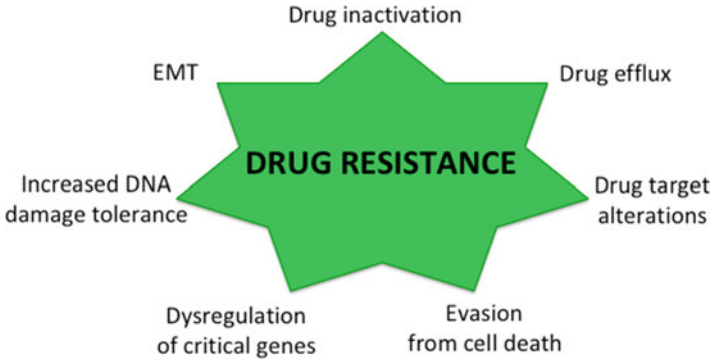

Fig. 20.2 Mechanisms promoting the acquisition of chemoresistance in cancer

conversion to be active; mutations or down-regulation of the enzymes responsible for the drug activation, as cytochrome P 450 system, glutathione-S-transferase (GST) and uridine diphospho-glucuronosyltransferase (UGT) super-families, are often present in cancer cells [15]. In addition, changes in the expression or functions of drug targets such as topoisomerase II, epidermal growth factor receptor family, Ras, Src, Raf, MEK, AKT and PTEN, lead to resistance. One of the most studied mechanisms of cancer drug resistance involves the increasing drug efflux with subsequent reduction in cellular drug concentration. ATP-binding cassette (ABC) members, multidrug resistance protein 1 (MDR1), known as P glycoprotein (P-gp), multidrug resistance-associated protein 1 (MRP1), and breast cancer resistance protein (BCRP), represent the main transporters involved in the efflux mechanism causing the non-accumulation of anti-tumoral agents in cancer cells [16].

20.2.1 TRPC5 and TRPC6 in Multidrug Resistance

TRPC5 forms homo and hetero-oligomeric complex with other TRPs and it stimulates Ca^{2+} flux in response to different stimuli as stress, growth factors, lysophospholipids, nitric oxide or thioredoxin [17]. Abnormal expression of this channel has been found to be associated with several diseases. In addition, it is well known that TRPC5 alterations, interfering with the normal Ca^{2+} homeostasis, are involved in the development of cancer progression and acquisition of chemoresistance. During therapy, the majority of cancer cell types starts to over-express P-gp, a well-known membrane efflux pump [18]. Recently [19], TRPC5 channel has been found to be overexpressed together with P-gp in adriamycin-resistant breast cancer cell line (MCF-7/ADM). As demonstrated by patch clamp, the TRPC5-dependent calcium current was higher in MCF-7/ADM cells compared to wild type indicating that the over-expressed TRPC5 is functional.

By using the TRPC5-specific blocking antibody T5E3, authors showed that the TRPC5 inhibition is associated with both marked down-regulation of P-gp expression and increase of adriamycin accumulation, demonstrating that TRPC5 is crucial for P-gp expression and chemoresistance in MCF-7/ADM cells. Moreover, the high Ca^{2+} current generated by TRPC5 activation was able to activate the nuclear factor of activated T cells cytoplasmic 3 ($NFAT_C3$) that, stimulating the transcription, promotes P-gp over-expression. In vivo studies using athymic nude mouse model of ADM-human breast tumor, showed an evident decrease of cancer growth induced by the suppression of TRPC5 channel. Thus, the TRPC5-NFATc3-P-gp signaling cascade plays an important role in promoting drug-resistance in breast cancer cells [19].

Micro RNAs (miRNAs) are single-stranded 19–25 nucleotide short RNAs that modulate gene expression at post-transcriptional stage by targeting mRNAs. It is now well accepted that they can regulate several processes closely associated with tumor progression as chemoresistance, apoptosis, cell cycle or stemness transition. In the recent years, the attention was mainly focused on miR-230a

since its expression has been found to be strongly down-regulated in MCF-7/ADM cells compared to MCF-7 cells, suggesting that it is involved in the development of chemoresistance [20]. Moreover, low miR-320a expression is associated with clinical chemoresistance and poor patient outcome. As showed by Targescan and miRDB software analysis, this miRNA specifically targets TRPC5 and NFATC3 mRNAs. Therefore, its down-regulation has been found to be responsible for TRPC5 over-expression and related drug resistance in breast cancer [20].

For cancer progression, cell-cell communication in the tumor microenvironment is fundamental [21]. To this aim, cancer cells produce soluble factors and secrete membrane-encapsulated vesicles containing regulatory signals. These membrane-limited vesicles are known as Extracellular Vesicles (EVs) and they include exosomes, microvesicles and apoptotic bodies [21]. It has been recently demonstrated [22] that TRPC5, involved in growth factor-regulated local vesicular trafficking, by mediating Ca^{2+} flux, plays a role in the EVs formation and secretion in MCF-7/ADM. Since EVs membrane phospholipid bilayer is composed by the plasma membrane of the donor cells, TRPC5 channel is packaged in the developing vesicles and, in this way, transported into recipient cells where it promotes P-gp expression by increasing Ca^{2+} flux. Thus, the TRPC5-containing EVs represent a mechanism used by cancer cells to disseminate the acquisition of chemoresistance. Furthermore, immunohistochemistry analysis performed on breast cancer tissues, collected before and after the chemotherapy, showed a marked increase in the TRPC5 expression mainly in samples from not responsive patients indicating the close association between TRPC5 and chemoresistance [22]. Since TRPC5-containing EV levels correlate with acquired chemoresistance and EVs can be easily monitored in the blood of breast cancer patients [23], TRPC5-containing EVs represent a new potential diagnostic biomarker for real time measurement of chemoresistance in breast cancer.

In addition, it has been demonstrated that endothelial cells of the tumor microenvironment acquire resistance thanks to TRPC5-containing EVs released by ADM/MCF-7 [24]. As already described, the transmitted TRPC5, by activating NFATC3 in a Ca^{2+} dependent manner, stimulates the expression of P-gp.

Autophagy, an evolutionarily conserved lysosomal pathway, has been reported to show paradoxical roles in cancer: it can inhibit or promote tumorigenesis by inducing cell death or survival, respectively [25]. Since intracellular Ca^{2+} plays an important role in both basal and induced autophagy, TRP channels are now recognized as autophagy regulators [26].

Zhang and co-workers demonstrated that TRPC5 regulates the chemotherapy-induced autophagy in breast cancer cells. In fact, TRPC5, by inducing Ca^{2+} flux, initiates the autophagy via CaMKKβ/AMPKα/mTOR pathway in response to chemotherapy. Authors also showed that the TRPC5-induced autophagy functions as pro-survival mechanism promoting chemoresistance, as demonstrated by the reduction in autophagy and enhancement in ADM sensitivity in TRPC5 silenced MCF-7 cells [27].

Over-expression of TRPC5 was also found to be involved in the development of 5-Fluorouracil (5-Fu) resistance in colon rectal cancer [28]. TRPC5 is up-regulated

together with the efflux pump ABC subfamily B, both at mRNA and protein levels, in resistant human HCT-8 and LoVo colon rectal cancer cells. TRPC5, by inducing intracellular Ca^{2+} flux, promotes β-catenin translocation in the nucleus, increases glycolysis and provides ATP production to avoid Ca^{2+} influx overload. Moreover it stimulates ACB and cyclin D1 expression contributing to the development of 5-Fu resistance. In fact, its suppression markedly inhibits the canonical Wnt/β-catenin signal pathway and reduces efflux pump activity reverting the chemoresistance. By contrast, the forced expression of TRPC5 results in an activated Wnt/β-catenin signal pathway and up-regulation of ABC. High expression of TRPC5 has also been found to be associated with glucose transporter 1 (GLUT1) up-regulation in colon rectal cancer cells and increased glycolysis often occurs in chemoresistance cells [29]. Taken together, these findings demonstrate in human colon rectal cancer cells an important role of TRPC5 in drug resistance via stimulating nuclear β-catenin, ABC and GLUT1 over-expression [28–30].

Cancer cells become more resistant to drugs also thanks to the EMT, a process involved in the acquisition of invasive and migratory phenotype [31]. In hepatocellular carcinoma (HCC), it has been recently demonstrated that chemoresistance to doxorubicin occurs through up-regulation of Vimentin and down-regulation of E-cadherin and Claudin1, typical EMT markers. In fact, prolonged treatment with doxorubicin, by enhancing Ca^{2+} influx, induces EMT promoting chemoresistance. The channel involved in this process is TRPC6 that, via calcium signaling, stimulates STAT3 activation inducing the EMT [32]. The role of TRPC6 in chemoresistance was also explored in xenograft models of HCC using TRPC6-silenced and wild type Huh-7 HCC cells. Results showed that tumors, derived from the injection of TRPC6-silenced cells, grow slower than normal cells and they are more sensitive to doxorubicin [32].

20.2.2 TRPM Channels in Chemoresistance

TRPM7 is a highly Ca^{2+} and Mg^{2+} permeable member of the TRPM family activated by ATP and characterized in the C-terminal region by the presence of a kinase domain. Recent findings showed that Vacquinol-1 (Vac) promotes in glioma cells the methuosis cell death based on cell blebbing followed by rupture of the plasma membrane. This new type of cell death, caused by inefficient vacuole-lysosome fusion, is caspase-dependent and it is reverted by exogenous ATP [33]. The ATP-mediated inhibitory effect on Vac-induced cell death is due to TRPM7 activation that, by a marked Ca^{2+} influx, stimulates the phosphoinositide 3-kinase (PI3K) restoring the vacuole-lysosome fusion. Thus, the Ca^{2+} current induced by TRPM7, often found to be overexpressed in cancer cells, is responsible for the development of Vac-resistance in glioma cell lines (Fig. 20.3). It has also been demonstrated that the expression of TRPM7 is required to prevent apoptotic cell death in pancreatic adenocarcinoma [34]. The targeted silencing of TRPM7

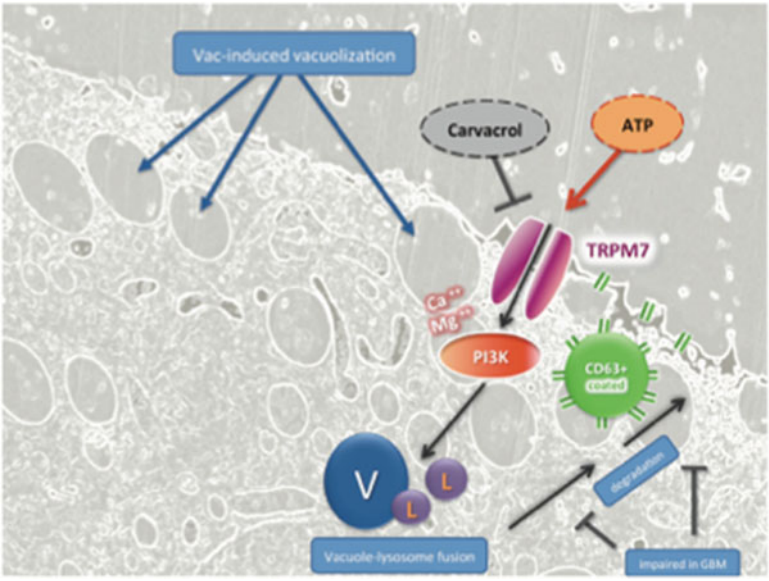

Fig. 20.3 TRPM7 activation induced by exogenous ATP stimulates Ca^{2+} influx that promotes PI3K activation increasing vesicle fusion (V) with lysosomes (L). [From reference 33]

increases the expression of senescence-associated genes inducing the replicative senescence in pancreatic cancer cells. The down-regulation of TRPM7 expression also enhances the cytotoxicity mediated by gemcitabine treatment in pancreatic cancer suggesting that its expression is strongly associated with resistance to apoptosis induction [34].

Moreover, in Lewis lung cancer cells (LLC-2), TRPM8, showing a plasma membrane and a membrane rafts localisation, is involved in the induction of proliferation, invasion and migration [35]. In addition, TRPM8, by activating Uncoupling Protein 2, contributes to the acquisition of resistance against both activated spleen CD8 T lymphocytes and doxorubicin contributing to the development of the malignant phenotype. The ability of TRPM8 to promote the acquisition of chemoresistance is also supported by data obtained in in vitro studies on prostate cancer cells [36]. By enhancing the HIF-1α protein levels, the cold-sensitive Ca^{2+} channel protein TRPM8 promotes hypoxic growth capacities and drug resistance. In particular, the TRPM8 activation induces the suppression of HIF-1α ubiquitination and enhances HIF-1 transactivation both in hypoxia- and normoxia-exposed prostate cancer cells. The potential involvement of TRPM8 channel in chemosensitivity has been also shown in osteosarcoma cells [37]. Knockdown of TRPM8 by siRNA in osteosarcoma cells leads to alterations in intracellular Ca^{2+} concentration. This Ca^{2+} imbalance induces the inhibition of several pathways as Akt-GSK-3β, ERK1/2 and FAK, promoting strong decrease in proliferation, invasion and migration.

Moreover, although TRPM8 silencing alone does not increase apoptotic cell death, it enhances the epirubicin-induced apoptosis indicating that the over expression of TRPM8 in osteosarcoma cells is associated with impaired Ca^{2+} signaling and induction of drug resistance [37].

20.2.3 Chemosensitivity and TRPV-Mediated Calcium Signaling

Calcium signaling is also required for the development of the neoplastic features in Retinoblastoma, a common intraocular pediatric cancer arising from immature cells of the retina [38]. TRPs and cannabinoid receptors are expressed in retinoblastoma cells. Their expression levels are considered useful as prognostic factors, since they correlate with tumor progression and are associated with the acquisition of etoposide-resistance. Interestingly, capsaicin, the specific agonist of TRPV1 receptor, is able to evoke Ca^{2+} influx in etoposide-resistant but not in etoposide-sensitive WERI-Rb1 retinoblastoma cells, suggesting the key role played by TRPV1-mediated calcium signaling in the acquisition of drug chemoresistance [38].

TRPV1 is also involved in the enhancement of chemosentitivity to cisplatin induced by Alpha-lipoic acid (ALA) in breast cancer cells. ALA administration, through TRPV1 activation, increases the apoptosis induced by cisplatin stimulating mitochondrial membrane depolarization, reactive oxygen species (ROS) production, lipid peroxidation, PARP1, caspase 3 and 9 expression. The ALA-dependent stimulation of TRPV1, via calcium signaling, enhances the oxidative stress making breast cancer cells more sensitive to the action of the chemotherapeutic drug [39].

Among TRPV family members, the role of TRPV2, with Ca^{2+} permeation properties, in the regulation of glioblastoma cell growth and progression, has been addressed. The aggressive behaviour of glioblastoma is mainly due to high resistance to the standard chemotherapy as Temozolomide (TMZ), Carmustine (BCNU) or Doxorubicin characterized by limited efficacy. The over-expression of TRPV2 by gene transfection in glioma cells increases the sensitivity to FAS- and BCNU-induced cytotoxicity [40, 41]. Moreover, the activation of the TRPV2 channel, induced by treatment with cannabidiol (CBD), strongly reduced the BCNU resistance in glioma cells. In fact, CBD, by generating a TRPV2-dependent Ca^{2+} influx, inhibits the Ras/Raf/MEK/ERK pathway and promotes the drug retention in glioma cells, reverting the chemoresistant phenotype and improving the apoptosis induced by TMZ, BCNU and doxorubicin [40, 41]. Mutations of the TRPV2 pore completely cancel the CBD-induced Ca^{2+} signaling demonstrating the essential role of the TRPV2 permeant cation region in chemoresistance. In addition, glioma stem-like cells represent a major problem in the treatment of glioblastoma because they maintain stem cell properties and show marked resistance to radiation and conven-

tional drugs. Reduce their drug resistance is fundamental to increase the patient survival. At this regard, CBD, through TRPV2 activation, stimulates autophagy in glioma stem-like cells promoting cell differentiation and increasing the sensitivity to the apoptosis induced by BCNU and TMZ [42].

Furthermore, TRPV2 is expressed in multiple myeloma cells, a malignancy characterised by clonal proliferation of plasma cells and subsequent accumulation in the bone marrow [43]. Recent data demonstrated that CBD treatment induces in myeloma cells up-regulation of TRPV2 expression enhancing the sensitivity to Bortezomib, a specific proteosome inhibitor. The specific TRPV2 activation, induced by CBD, strongly reduces proliferation and improves cytotoxic effects of bortezomib by enhancing cell growth inhibition, cell cycle arrest at the G1 phase, mitochondrial and ROS-dependent necrosis mainly in TRPV2-transfected RPMI8226 and U266 multiple myeloma cells. The cell death induced by the co-administration of CBD and Bortezomib is also characterized by down-regulation of the ERK, AKT and NF-κB pathways. These findings provide a rationale for the use of TRPV2 activators (e.g., CBD) to increase the activity of proteasome inhibitors in myeloma multiple patients [43].

The TRPV6 channel, which is highly selective for Ca^{2+}, is upregulated, by a gene amplification mechanism, in breast cancer cell lines and in breast carcinoma samples compared with normal mammary gland tissue. By microarray analysis, it has been shown that the TRPV6 over-expression, associated with reduced patient overall survival, is a feature of estrogen receptor-negative breast tumors as well as HER2-positive tumors. Down-regulation of TRPV6 expression reduces the basal Ca^{2+} influx leading to decrease in cellular proliferation and DNA synthesis [44]. It has been showed, using TRPV6-transfected *Xenopus* oocytes, that tamoxifen, the most common therapy used in breast cancer treatment, inhibits the Ca^{2+} uptake regulated by this channel. In addition, tamoxifen treatment markedly reduces the expression of TRPC6 at mRNA levels in breast cancer cell lines [45]. Silencing of TRPV6 enhances the pro-apoptotic activity of tamoxifen suggesting that the increase of Ca^{2+} influx, mediated by TRPV6 over-expression in breast cancer cells, is responsible for the reduced sensitivity to tamoxifen treatment. These findings support the hypothesis that a combination therapy using tamoxifen and TRPV6 inhibitor could represent a promising strategy to improve the treatment of breast cancer [44, 46].

20.3 Conclusion

It is becoming evident that dysregulation in Ca^{2+} homeostasis plays a pivotal role in tumor progression, functioning as a driving signal in the acquisition of the aggressive phenotype. In fact, cancer cells, by changing the expression of ion channels/transporters/pumps acquire the ability to modulate Ca^{2+} intracellular concentration creating pro-survival conditions. Several evidences support the idea that Ca^{2+} signaling pathways are also involved in regulating sensitiv-

Table 20.1 Chemosensitivity and TRP roles in cancer cells

TRPs activation	Pathway mediated by Ca^{2+} dysregulation	Drug	Cancer cell line	References
TRPCS	NFATc3 activation promoting P-gp over-expression	↑Adryamycin	MCF-7	[19]
	Prosurvival autophagy via CaMKKβ/AMPKα/mTOR	↑Adryamycin	MCF-7	[27]
	ACB and cyclin D1 over-expression via β-catenin	↑5-Fluorouracil	HCT8 and LoVo	[28–30]
TRPC6	STAT3 activation inducing EMT	↑Doxorubicin	Huh-7	[32]
TRPM7	PI3K activation restoring vacuole/lysosome fusion	↑Vaquinol-1	U-87 and #12537-GB	[33]
	Prevention of non apoptotic cell death	↑Gemcitabine	BxPC3 and PANIC-1	[34]
TRPM8	Uncoupling Protein 2 activation	↑Doxorubicin	LLC-2	[35]
	Akt-GSK-3β, ERK1/2 and FAK activation	↑Epirubicin	MG-63, U2OS, SaOS2 and HOS	[37]
TRPV1	Oxidative stress	↓Cisplatin	MCF-7	[39]
TRPV2		↓Temozolomide		
	Ras/Raf/MEK/ERK activation	↓Carmustine	U-37, MZC, GSC,	[40–42]
		↓Doxorubicine		
	Inhibition of NF-kB	↓Bortezomib	RPMI3226 and U266	[43]
TRPV6	Promotes cell proliferation	↑Tamoxifen	T47D	[46]

ity to chemotherapeutic drugs. Drug resistance represents a major limitation in the application of current therapeutic regimens and several efforts are spent to overcome it. The targeting of the Ca^{2+} channels, by altering their expression and functions, has been demonstrated be effective in improving of cytotoxicity induced by the most common chemotherapeutic agents. Among Ca^{2+} channels, TRPs influence the expression and function of many drug resistance-related proteins and pathways contributing to the development of pharmacological tolerance in cancer (Table 20.1). Therefore, targeting the TRP expression and activity, can be now considered a promising and fascinating strategy to inhibit cancer growth and progression and restore/improve the sensitivity of cancer cells to chemotherapeutic drugs [10].

References

1. Giorgi C, Danese A, Missiroli S, Patergnani S, Pinton P (2018) Calcium dynamics as a machine for decoding signals. Trends Cell Biol 28(4):258–273
2. Cui C, Merritt R, Fu L, Pan Z (2017) Targeting calcium signaling in cancer therapy. Acta Pharm Sin B 7(1):3–17
3. Zhang X, Yuan D, Sun Q, Xu L, Lee E, Lewis AJ, Zuckerbraun BS, Rosengart MR (2017) Calcium/calmodulin-dependent protein kinase regulates the PINK1/Parkin and DJ-1 pathways of mitophagy during sepsis. FASEB J 31(10):4382–4395
4. Bootman MD, Chehab T, Bultynck G, Parys JB, Rietdorf K (2018) The regulation of autophagy by calcium signals: do we have a consensus? Cell Calcium 70:32–46
5. Busselberg D, Florea AM (2017) Targeting intracellular calcium signaling ($[Ca^{2+}]_i$) to overcome multiddrug resistance of cancer cells: a mini-overview. Cancers 9:48
6. Xu MM, Seas A, Kijan M, Ji KSY, Bell HN (2018) A temporal examination of calcium signaling in cancer-from tumorigenesis, to immune evasion, and metastasis. Cell Biosci 8:25
7. La Rovere RM, Roest G, Bultynck G, Parys JB (2016) Intracellular Ca^{2+} signaling and Ca^{2+} microdomains in the control of cell survival, apoptosis and autophagy. Cell Calcium 60(2):74–87
8. Nilius B, Owsianik G (2011) The transient receptor potential family of ion channels. Genome Biol 12(3):218
9. Shapovalov G, Ritaine A, Skryma R, Prevarskaya N (2016) Role of TRP ion channels in cancer and tumorigenesis. Semin Immunopathol 38(3):357–369
10. Gautier M, Dhennin-Duthille I, Ay AS, Rybarczyk P, Korichneva I, Ouadid-Ahidouch H (2014) New insights into pharmacological tools to TR(i)P cancer up. Br J Pharmacol 171:2582–2592
11. Litan A, Langhans SA (2015) Cancer as a channelopathy: ion channels and pumps in tumor development and progression. Front Cell Neurosci 9:86
12. Santoni G, Farfariello V, Amantini C (2011) TRPV channels in tumor growth and progression. Adv Exp Med Biol 704:947–967
13. Santoni G, Farfariello V (2011) TRP channels and cancer: new targets for diagnosis and chemotherapy. Endocr Metab Immune Disord Drug Targets 11:54–67
14. Housman G, Byler S, Heerboth S, Lapinska K, Longacre M, Snyder N, Sarkar S (2014) Drug resistance in cancer: an overview. Cancers (Basel) 6:1769–1792
15. Michael M, Doherty MM (2005) Tumoral drug metabolism: overview and its implications for cancer therapy. J Clin Oncol 23:205–229
16. Stavrovskaya AA (2000) Cellular mechanisms of multidrug resistance of tumor cells. Biochemistry (Mosc) 65:95–106
17. He DX, Ma X (2016) Transient receptor potential channel C5 in cancer chemoresistance. Acta Pharmacol Sin 37:19–24
18. Binkhathlan Z, Lavasanifar A (2013) P-glycoprotein inhibition as a therapeutic approach for overcoming multidrug resistance in cancer: current status and future perspectives. Curr Cancer Drug Targets 13:326–346
19. Ma X, Cai Y, He D, Zou C, Zhang P, Lo CY, Xu Z, Chan FL, Yu S, Chen Y, Zhu R, Lei J, Jin J, Yao X (2012) Transient receptor potential channel TRPC5 is essential for P-glycoprotein induction in drug-resistant cancer cells. Proc Natl Acad Sci U S A 109:16282–16287
20. He DX, Gu XT, Jiang L, Jin J, Ma X (2014) A methylation-based regulatory network for microRNA 320a in chemoresistant breast cancer. Mol Pharmacol 86:536–547
21. Xu R, Rai A, Chen M, Suwakulsiri W, Greening DW, Simpson RJ (2018) Extracellular vesicles in cancer – implications for future improvements in cancer care. Nat Rev Clin Oncol 15(10):617–638. https://doi.org/10.1038/s41571-018-0036-9
22. Ma X, Chen Z, Hua D, He D, Wang L, Zhang P, Wang J, Cai Y, Gao C, Zhang X, Zhang F, Wang T, Hong T, Jin L, Qi X, Chen S, Gu X, Yang D, Pan Q, Zhu Y, Chen Y, Chen D, Jiang L, Han X, Zhang Y, Jin J, Yao X (2014) Essential role for TrpC5-containing extracellular vesicles in breast cancer with chemotherapeutic resistance. Proc Natl Acad Sci U S A 111:6389–6394

23. Wang T, Ning K, Lu TX, Sun X, Jin L, Qi X, Jin J, Hua D (2017) Increasing circulating exosomes-carrying TRPC5 predicts chemoresistance in metastatic breast cancer patients. Cancer Sci 108:448–454
24. Dong Y, Pan Q, Jiang L, Chen Z, Zhang F, Liu Y, Xing H, Shi M, Li J, Li X, Zhu Y, Chen Y, Bruce IC, Jin J, Ma X (2014) Tumor endothelial expression of P-glycoprotein upon microvesicular transfer of TrpC5 derived from adriamycin-resistant breast cancer cells. Biochem Biophys Res Commun 446:85–90
25. Singh SS, Vats S, Chia AY, Tan TZ, Deng S, Ong MS, Arfuso F, Yap CT, Goh BC, Sethi G, Huang RY, Shen HM, Manjithaya R, Kumar AP (2018) Dual role of autophagy in hallmarks of cancer. Oncogene 37:1142–1158
26. Sukumaran P, Schaar A, Sun Y, Singh BB (2016) Functional role of TRP channels in modulating ER stress and autophagy. Cell Calcium 60:123–132
27. Zhang P, Liu X, Li H, Chen Z, Yao X, Jin J, Ma X (2017) TRPC5-induced autophagy promotes drug resistance in breast carcinoma via CaMKKβ/AMPKα/mTOR pathway. Sci Rep 7(1):3158
28. Wang T, Chen Z, Zhu Y, Pan Q, Liu Y, Qi X, Jin L, Jin J, Ma X, Hua D (2015) Inhibition of transient receptor potential channel 5 reverses 5-fluorouracil resistance in human colorectal Cancer cells. J Biol Chem 290:448–456
29. Wang T, Ning K, Lu TX, Hua D (2017) Elevated expression of TrpC5 and GLUT1 is associated with chemoresistance in colorectal cancer. Oncol Rep 37:1059–1065
30. Wang T, Ning K, Sun X, Zhang C, Jin L-f, Hua D (2018) Glycolysis is essential for chemoresistance induced by transient receptor potential channel C5 in colorectal cancer. BMC Cancer 18:207
31. Bhatia S, Monkman J, Toh AKL, Nagaraj SH, Thompson EW (2017) Targeting epithelial-mesenchymal plasticity in cancer: clinical and preclinical advances in therapy and monitoring. Biochem J 474:3269–3306
32. Wen L, Liang C, Chen E, Chen W, Liang F, Zhi X, Wei T, Xue F, Li G, Yang Q, Gong W, Feng X, Bai X, Liang T (2016) Regulation of multi-drug resistance in hepatocellular carcinoma cells is TRPC6/calcium dependent. Sci Rep 6:23269
33. Sander P, Mostafa H, Soboh A, Schneider JM, Pala A, Baron AK, Moepps B, Wirtz CR, Georgieff M, Schneider M (2017) Vacquinol-1 inducible cell death in glioblastoma multiforme is counter regulated by TRPM7 activity induced by exogenous ATP. Oncotarget 8:35124–35137
34. Yee NS, Zhou W, Lee M, Yee RK (2012) Targeted silencing of TRPM7 ion channel induces replicative senescence and produces enhanced cytotoxicity with gemcitabine in pancreatic adenocarcinoma. Cancer Lett 318:99–105
35. Du GJ, Li JH, Liu WJ, Liu YH, Zhao B, Li HR, Hou XD, Li H, Qi XX, Duan YJ (2014) The combination of TRPM8 and TRPA1 expression causes an invasive phenotype in lung cancer. Tumour Biol 35:1251–1261
36. Yu S, Xu Z, Zou C, Wu D, Wang Y, Yao X, Ng CF, Chan FL (2014) Ion channel TRPM8 promotes hypoxic growth of prostate cancer cells via an O2 -independent and RACK1-mediated mechanism of HIF-1α stabilization. J Pathol 234:514–525
37. Wang Y, Yang Z, Meng Z, Cao H, Zhu G, Liu T, Wang X (2013) Knockdown of TRPM8 suppresses cancer malignancy and enhances epirubicin-induced apoptosis in human osteosarcoma cells. Int J Biol Sci 10:90–102
38. Mergler S, Cheng Y, Skosyrski S, Garreis F, Pietrzak P, Kociok N, Dwarakanath A, Reinach PS, Kakkassery V (2012) Altered calcium regulation by thermosensitive transient receptor potential channels in etoposide-resistant WERI-Rb1 retinoblastoma cells. Exp Eye Res 94:157–173
39. Nur G, Nazıroğlu M, Deveci HA (2017) Synergic prooxidant, apoptotic and TRPV1 channel activator effects of alpha-lipoic acid and cisplatin in MCF-7 breast cancer cells. J Recept Signal Transduct Res 37:569–577
40. Nabissi M, Morelli MB, Amantini C, Farfariello V, Ricci-Vitiani L, Caprodossi S, Arcella A, Santoni M, Giangaspero F, De Maria R, Santoni G (2010) TRPV2 channel negatively controls glioma cell proliferation and resistance to Fas-induced apoptosis in ERK-dependent manner. Carcinogenesis 31(5):794–803

41. Nabissi M, Morelli MB, Santoni M, Santoni G (2013) Triggering of the TRPV2 channel by cannabidiol sensitizes glioblastoma cells to cytotoxic chemotherapeutic agents. Carcinogenesis 34:48–57
42. Nabissi M, Morelli MB, Amantini C, Liberati S, Santoni M, Ricci-Vitiani L, Pallini R, Santoni G (2015) Cannabidiol stimulates Aml-1a-dependent glial differentiation and inhibits glioma stem-like cells proliferation by inducing autophagy in a TRPV2-dependent manner. Int J Cancer 137:1855–1869
43. Morelli MB, Nabissi M, Amantini C, Farfariello V, Ricci-Vitiani L, di Martino S, Pallini R, Larocca LM, Caprodossi S, Santoni M, De Maria R, Santoni G (2012) The transient receptor potential vanilloid-2 cation channel impairs glioblastoma stem-like cell proliferation and promotes differentiation. Int J Cancer 131:E1067–E1077
44. Peters AA, Simpson PT, Bassett JJ, Lee JM, Da Silva L, Reid LE, Song S, Parat MO, Lakhani SR, Kenny PA, Roberts-Thomson SJ, Monteith GR (2012) Calcium channel TRPV6 as a potential therapeutic target in estrogen receptor-negative breast cancer. Mol Cancer Ther 11:2158–2168
45. Bolanz KA, Kovacs GG, Landowski CP, Hediger MA (2009) Tamoxifen inhibits TRPV6 activity via estrogen receptor-independent pathways in TRPV6-expressing MCF-7 breast cancer cells. Mol Cancer Res 7:2000–2010
46. Bolanz KA, Hediger MA, Landowski CP (2008) The role of TRPV6 in breast carcinogenesis. Mol Cancer Ther 7:271–279

Chapter 21
Widespread Roles of CaMK-II in Developmental Pathways

Sarah C. Rothschild and Robert M. Tombes

Abstract The multifunctional Ca^{2+}/calmodulin-dependent protein kinase type 2 (CaMK-II) was first discovered in brain tissue and shown to have a central role in long term potentiation, responding to Ca^{2+} elevations through voltage dependent channels. CaMK-II has a unique molecular mechanism that enables it to remain active in proportion to the degree (frequency and amplitude) of Ca^{2+} elevations, long after such elevations have subsided. Ca^{2+} is also a rapid activator of early development and CaMK-II is expressed and activated in early development. Using biochemical, pharmacological and genetic approaches, the functions of CaMK-II overlap remarkably well with those for Ca^{2+} elevations, post-fertilization. **Conclusion.** Activated CaMK-II plays a central role in decoding Ca^{2+} signals to activate specific events during early development; a majority of the known functions of elevated Ca^{2+} act though CaMK-II.

Keywords CaMK-II · Calcium · Calmodulin · Development · Gastrulation · Kidney · Cilia · Cardiac · Laterality · Ear · Phosphorylation

21.1 Introduction

21.1.1 Calcium Signaling During Early Development

Ca^{2+} at Fertilization Ca^{2+} elevations in living cells were first visualized in fertilized eggs from vertebrate and invertebrate species. These studies used luminescent (aequorin) or fluorescent (fura-2) indicators on species as varied as sea urchin, medaka and mice [1–4]. Multiple studies demonstrated a role for Ca^{2+} in promoting the exocytosis of cortical granules, leading to fertilization envelope elevation and the

S. C. Rothschild (✉) · R. M. Tombes
Life Sciences, Virginia Commonwealth University, Richmond, VA, USA
e-mail: chasese@vcu.edu

M. S. Islam (ed.), *Calcium Signaling*, Advances in Experimental Medicine and Biology 1131, https://doi.org/10.1007/978-3-030-12457-1_21

activation of early development. These studies have been summarized in excellent and comprehensive reviews [5, 6].

Ca^{2+} During Early Development Ca^{2+} signaling also influences oocyte maturation and other early developmental events [7]. The multi-functionality of Ca^{2+} in post-fertilization events may be reflected by the frequency, amplitude and location of its modulation [8] and supports its importance as a developmental controller, but also makes it challenging to identify specific roles. For instance, injection of the Ca^{2+} chelator, BAPTA, just after fertilization in mouse and zebrafish embryos, blocks all subsequent cleavages and development [9, 10], even though Ca^{2+} signals continue throughout early zebrafish development. Zebrafish Ca^{2+} elevations were observed during three stages: (1) the early rapid cleavages, (2) gastrulation and dorsal-ventral specification and (3) segmentation [10]. With enhanced spatial and temporal sensitivity, transient elevations of Ca^{2+} have been more specifically attributed to cells of the outer enveloping layer of zebrafish embryos at the blastoderm margin [11, 12], primarily on the dorsal [10] or ventral aspect [5]. In zebrafish, it was concluded [10] that Ca^{2+} signals during the discrete developmental window (6-8hpf) that corresponds to gastrulation are not necessary for specification but are important for convergent extension, through cell motility and migration [5].

Ca^{2+} at Gastrulation Coordinated inductive and morphogenetic processes generate the three germ layers and shape the embryonic body during vertebrate gastrulation. Three modes of cell migration enable these rearrangements and include (a) epiboly, (b) internalization of the presumptive mesendoderm and (c) convergent extension (CE). CE movements narrow the germ layers mediolaterally (convergence) and elongate them anteroposteriorly (extension) to define the embryonic axis. The non-canonical Wnt (ncWnt) pathway has been identified as an evolutionarily conserved signaling pathway that regulates CE cell movements during vertebrate gastrulation [13]. During development, suppression of the ncWnts, Wnt5 [14–17] and Wnt11 [18–21], leads to a shortened anterior-posterior body axis, wider dorsal structures and defects in segmentation, which are stereotypical of CE defects [22, 23]. Wnt5 and Wnt11 have been identified as essential modulators of these cellular movements and are known to cause intracellular Ca^{2+} release [24–26], whereas mutations in Wnt5 and Wnt11, reduce Ca^{2+} levels [26]. Wnt5a is known to induce prolonged Ca^{2+} elevations when injected into zebrafish embryos [24]. The zebrafish *wnt5* mutant is known as *pipetail* (*ppt*). Ppt mutant (−/−) embryos exhibit altered Ca^{2+} modulation, widened somites and in some cases, split axes, indicative of defects in convergent extension [27]. Wnt11 appears responsible for the Ca^{2+} elevation that leads to directed rapid cell migration [28], whereas Wnt5/ppt acts later to influence cell intercalation. Wnt11 appears to be more important for the morphological changes associated with CE and not specification [16]. This is consistent with a cytosolic, not a nuclear role for Wnt11 in CE. CE movements in mouse embryos are also dependent on Wnt5 and Wnt11 [23].

Ca^{2+} in LR Asymmetry Laterality disorders are characterized by the misplacement of one or more organs across the left-right (LR) axis and occur as often as once in every 6000 newborn humans [29]. The positioning of internal organs in diverse

vertebrate organisms is initiated by signals originating from a transient posterior structure, known as the mouse embryonic node or zebrafish Kupffer's vesicle (KV) [30]. The KV is a fluid-filled organ that forms at the posterior end of the notochord at the early somite stages of teleosts [31]. The KV, like the mouse ventral node, is lined by epithelial cells that contain motile cilia whose resultant fluid flow is necessary to establish left-right asymmetry [32, 33].

Fluid flow is believed to yield asymmetric Ca^{2+} elevations through the TRP channel, PKD2 (polycystin-2) [34, 35] and may be the earliest asymmetric event [36] responsible for developing normal laterality. Ca^{2+} elevations on the left side of the embryonic node have been detected in mice [37, 38], chick [39, 40] and zebrafish [41, 42]. Disruption of Ca^{2+} signaling causes randomization of heart and visceral organs [41].

In addition to PKD2, Ca^{2+} release has also been linked to ryanodine receptors [40, 42] and inositol phosphate dependent signals [41]. Gap junctions may enable Ca^{2+} to spread through target cells on the left side of the embryonic node [43, 44] and the H^+K^+ATPase may help maintain the driving force for Ca^{2+} elevations [40]. PKD2 targeted to endomembranes in KV cells may be more important than plasma membrane PKD2 for left-right asymmetry in zebrafish [45]. The importance of PKD2 is further supported by observations that *pkd2* morphants and mutants randomize organ placement and mis-express *spaw* (Southpaw) [34, 35]. PKD2-deficient mouse embryos also lack the normal Ca^{2+} elevation on the left side of the ventral node, fail to express *nodal* and have randomized organs [37, 46].

Ca^{2+} in Somitogenesis Zebrafish somitogenesis is accompanied by transient elevations in Ca^{2+} at the posterior end of forming somites [10, 47]. Ca^{2+} signals have also been observed in developing *Xenopus* myotome [48]. Pharmacological studies support a role for GPCR coupled PL-C activation leading to the Ca^{2+} release necessary for the formation of somites and notochord [26]. L690330, an inhibitor of Inositol monophosphatase, causes widening of somites [26] which is also observed in Wnt5 and Wnt 11 morphants [21]. These effects on somitogenesis could be due to effects on convergence and extension, as described above.

Ca^{2+} in Heart Development Ca^{2+} signals have also been implicated in the morphogenic process by which the heart tube transforms into a chambered heart. In zebrafish and mouse embryos, Ca^{2+} channel blockers, Ca^{2+} chelators, disruption of either the Na^+/Ca^{2+} exchanger, NCX, or SERCA2, the sarcoplasmic reticulum (SR) Ca^{2+} ATPase, all interfere with cardiac looping [10, 49, 50].

Ca^{2+} in Kidney Development Kidney tubules form in *Xenopus* animal caps treated with activin and retinoic acid and this is accompanied by an elevation in Ca^{2+} [51]. Activin/retinoic acid-treated animal caps do not form tubules when treated with the Ca^{2+} chelator BAPTA; the Ca^{2+} ionophore A23187 and ammonium chloride, two agents that elevate Ca^{2+} in activin-treated caps, can substitute for retinoic acid in stimulating the appearance of kidney tubules. Ca^{2+} released from IP_3 receptors during a specific time is important for the cell movements necessary to properly position zebrafish pronephric tissue [52].

Ca^{2+} in Ear Development Embryonic tissues that require motile cilia for development [32] are also sites of Ca^{2+} signaling. In addition to the KV and the kidney, the embryonic ear is also a member of this tissue category. The zebrafish inner ear contains both motile and immotile cilia; the immotile cilia, also known as kinocilia, emanate from "hair cells" and are hypothesized to contain an otolith precursor-binding factor [53]. Beating cilia appear transiently, adjacent to the kinocilia, in order to create a steady fluid flow that ensures the uniform formation of otoliths [54]. Ca^{2+} channels, such as TRP family members, have been implicated as the sensory transduction channel in hair cells [55–58]. However, well before the ear becomes a sensory organ, free Ca^{2+} is elevated in otic placode cells [10], suggesting its role in the differentiation of the ear.

21.1.2 CaMK-II Activation During Early Development

CaMK-II as a Ca^{2+} Sensor The "multifunctional" Ca^{2+}/calmodulin-dependent protein kinase, type 2 (CaMK-II) is often linked to central nervous system function, where it functions in long term potentiation (LTP) and comprises as much as 1% of the total protein in the hippocampus [59]. However, CaMK-II is evolutionarily conserved, has been found during development and in every adult mammalian tissue [60] and is expressed across all metazoan species [61]. CaMK-II is activated by Ca^{2+}-calmodulin that forms upon intracellular release of Ca^{2+} to phosphorylate protein substrates involved in functions that include transcription, secretion, cytoskeletal re-organization and ion channel regulation [59].

CaMK-II has a unique ability to oligomerize and autophosphorylate (at T^{287}) upon Ca^{2+}/CaM stimulation, distinguishing it from other CaM-dependent kinases and leading to its depiction as a "memory molecule" [62]. T^{287} autophosphorylation converts the enzyme into an "autonomous" or Ca^{2+}-independent active state where it "remembers" its activation by Ca^{2+}. Activated (P-T^{287}) CaMK-II can be localized in fixed tissue as described [63] and its level has been shown to be proportional to autonomous CaMK-II enzymatic activity, including in zebrafish embryonic extracts [64]. This method can be used to provide a snapshot of Ca^{2+} signaling in zebrafish embryos as early as the 10 somite stage [64] and in locations that include the olfactory placode, apical pronephric duct and cloaca, and at the base of inner ear hair cell kinocilia [65]. These locations represent a subset of the locations where total CaMK-II is expressed such as the embryonic forebrain, olfactory placode, spinal cord, somites, ear and pronephric kidney, which are consistent with the locations of CaMK-II mRNA expression [66]. By 60hpf, CaMK-II becomes activated and located (P-T^{287}) in retina, fins, anterior pituitary, neuromasts of the lateral line, with continued activation in the ear, somites, and kidney [65]. There is significant potential for using this method to define subcellular locations of Ca^{2+} signaling that act via CaMK-II in a wide variety of tissues, species and even disease states.

Two other potentially relevant and regulatory CaMK-II phosphorylation sites exist at T^{253} and T^{307}. Both of these sites are conserved across all metazoans [61]. T^{307} is an autophosphorylation site [67] that fine-tunes synaptic signaling, while T^{253} phosphorylation has been linked to G2-M progression [68]. The prevalence, overlap with P-T^{287} location and the function of these phosphorylation sites during embryogenesis has not yet been evaluated.

CaMK-II activity can be reversibly inhibited with the CaM-binding antagonist, KN-93, in mammalian cells [69, 70] and in zebrafish embryos [71]. Dominant negative CaMK-II constructs have also been used to interfere with the normal activation of CaMK-II [65].

Importance of CaMK-II at Fertilization and Resumption of Meiosis CaMK-II does not play a central role in cortical granule exocytosis or the activation of protein synthesis at fertilization, but may participate in the block to polyspermy [72]. However, in species, like humans and mice, where fertilization causes the resumption of meiosis II, CaMK-II has been strongly implicated in the release from metaphase II arrest. Such a role for CaMK-II was first proposed over 20 years ago using *Xenopus* oocyte extracts [73] and was supported by mathematical models [74]. Empirical support was also obtained in intact mouse oocytes that were pre-treated with KN-93 and then activated in vitro by ethanol [75], a treatment known to release Ca^{2+} from internal stores. Knockout or knockdown of γ CaMK-II [76, 77], but not other CaMK-IIs [78–81], interferes with mouse meiotic resumption at egg activation. Subsequent dissection of this pathway revealed a collaboration with a polo-like kinase [82, 83] in releasing spindles from metaphase II arrest. In embryos where fertilization occurs after the completion of meiosis at the pronuclear stage (sea urchins), a role for CaMK-II at fertilization has not been reported. This further supports the concept that CaMK-II is involved in meiotic resumption, not the specific Ca^{2+}-dependent activation events that accompany fertilization.

Role of CaMK-II in Cell Migration During Early Development CaMK-II is detected early in development at the time [66, 84] when important Ca^{2+} transients occur [5, 12, 85]. CaMK-II is activated by ncWnt family members [25] and can rescue mutant phenotypes of certain non-canonical Wnts (ncWnts), whose roles are to promote morphogenic cell movements [86]. CaMK-II is known to mediate cell migration [87–91] by enabling focal adhesion turnover. A reported role for CaMK-II on the ventral side of the embryo [25] is consistent with the ventral expression of zebrafish CaMK-IIs during early development [66, 92].

In zebrafish, CaMK-II is encoded by seven genes that give rise to at least two dozen splice variants in early embryos [66, 92]. CaMK-II morphants exhibit a similar phenotype to morphants and mutants of the non-canonical Wnts, Wnt11 and Wnt5. In fact, at first glance, the *camk2b1* morphant has an undulated notochord [92], exactly like the Wnt5/*ppt* morphant/mutant [21], while the *camk2g1* morphant [65] has segmentation defects similar to the Wnt11/*slb* mutant [21]. The expression patterns of *camk2b1* and *camk2g1* are consistent with tissues that exhibit CE cell movements. Previous studies have shown that *camk2b1* and *camk2g1* are expressed

during gastrulation in both the mesendoderm and neuroectoderm layers where CE cell movements occur [66]. The non-variable regions encoded by *camk2b1* and *camk2g1* are 92% identical at the amino acid level, with their splice variants exhibiting different exon utilization and thus potential subcellular targeting [66]. Of the two dozen splice variants expressed from zebrafish CaMK-II genes during early development [65, 66, 92], all four that are expressed from *camk2g1* encode putative cytosolic targeting domains while two of the three that are expressed from *camk2b1* encode nuclear targeting domains. It is known that CaMK-IIs freely hetero-oligomerize [93] to form their stereotypical dodecameric structures yielding even further potential variations. Consequently, it is possible that *camk2b1* or *camk2g1* could hetero-oligomerize and target the entire complex to a location that might not be predicted based on the variants encoded by each gene.

During gastrulation, it is likely that CaMK-IIs encoded by *camk2b1* and *camk2g1* are activated by ncWnt-mediated Ca^{2+} elevations to directly enable cell migration. Oscillations of Ca^{2+} are known to occur during gastrulation [7, 94], which would activate CaMK-II to enable cell migration [91]. Interestingly, the migration of cells in culture and in embryos is compromised when CaMK-II is either hyperactivated, inhibited or eliminated [91]. A model in which ncWnts cause Ca^{2+} oscillations to transiently activate CaMK-II and enable focal adhesion turnover and thus cell migration is also consistent with findings that were described as apparently contradictory in which both Wnt5/Wnt11 gain of function and loss of function mutants inhibit convergent extension [95]. No specific focal adhesion protein has yet been identified as the target of CaMK-II phosphorylation that would enable focal adhesion turnover.

Role of CaMK-II in Cell Proliferation During Early Development CaMK-II has previously been strongly implicated in the early cell cycles of frog, sea urchin and mouse cell divisions [84, 96–100] and in cell cycle progression through cyclin D1 and cyclin dependent kinase inhibitors like $p27^{kip1}$ in cells in culture [69, 70, 84, 101]. In early sea urchin embryos, CaMK-II activity cycles with the cell cycle, like CDK1, and may actually interact with CDK1 [84]. An additional role for P-T^{253} CaMK-II has also been implicated at the G2-M boundary [68].

Importance of CaMK-II in Cardiac Development CaMK-II has been extensively implicated in cardiovascular disease [102–104] and has been proposed as a therapeutic target to minimize remodeling, arrhythmias and hypertrophy [105–107]. Substrates or binding partners of CaMK-II known to influence cardiac function include phospholamban [108], L-type Ca^{2+} channels [109–111], ryanodine receptors [112] and histone deacetylases [113, 114]. Even in embryos, KN-93 reversibly slows heart rates, supporting a role for CaMK-II phosphorylation in excitation-contraction coupling [115].

During morphogenesis, the ncWnts, Wnt11 and Wnt11-R, have been implicated in cardiac specification and/or morphogenesis [116–118]. In addition, the T-box protein, Tbx5, promotes CaMK-II expression (*camk2b2*) during zebrafish cardiac development [92]. CaMK-II binding proteins or substrates, which may influence

cardiac morphogenesis through cell polarity, cell migration or cell cycle control, have been identified and include Tiam1 and Flightless-I [91, 119, 120].

Importance of CaMK-II in Somitogenesis Somite broadening, notochord thickening and axis duplication were observed in Wnt5 and Wnt11 mutant embryos [21, 27] and in embryos expressing dominant negative CaMK-II [25]. While total CaMK-II is found throughout somites, activated CaMK-II is found in sarcomeres and somite boundaries [65].

Role of CaMK-II in Laterality and Kidney Development CaMK-II is a known target of polycystin2 (PKD2)-dependent Ca^{2+} signals necessary for left-right patterning but also kidney development [64, 65]. PKD2, also known as TRPP2, is a member of the TRP family of Ca^{2+} conducting channels and is mutated in patients with autosomal dominant polycystic kidney disease (ADPKD) [121]. Suppression of zebrafish PKD2 or CaMK-II causes pronephric kidney cysts and the loss of normal organ asymmetry [64, 65, 122].

A potential target of CaMK-II in this role is the histone deacetylase, HDAC4 [115]. In muscle tissue, CaMK-II directly phosphorylates HDAC4, retaining it in the cytosol to upregulate MEF2C target genes [114, 123, 124]. HDAC4 is the only class II HDAC that bears a specific CaMK-II docking site [125]. However, HDAC4 and HDAC5 can form hetero-dimers, rendering HDAC5 responsive to CaMK-II and enabling export and retention of HDAC5 in the cytosol [123].

HDAC4 and HDAC5 are known to influence MEF2C-dependent gene transcription [114, 123, 126]. MEF2C is a Ca^{2+}-dependent mediator of differentiation and development that is known to couple signaling to transcription [127]. When HDACs are exported from the nucleus, p300/CBP can then transcriptionally activate MEF2C-dependent genes through histone acetylation [127]. MEF2C target genes are not just involved in myogenesis and include *MTSS1 (MIM)*, which is necessary for ciliogenesis and actin cytoskeletal organization [128, 129]. MEF2C, and MIM are also important signaling molecules in kidney disease; loss of MEF2C or MIM leads to polycystic kidneys [130]. In addition, HDAC5 suppression or treatment with the pan-specific HDAC inhibitor, TSA, partially reverses cystogenesis in PKD2 mutants [130].

It stands to reason that CaMK-II provides a previously unknown linkage between Ca^{2+} signals and HDAC family members in ciliated embryonic tissues such as the kidney. CaMK-II may serve to refine the action of HDACs in cells where Ca^{2+} is elevated. Activated CaMK-II sequesters HDAC4 in the cytosol, presumably enabling transcription of target genes that are necessary for kidney morphogenesis and cilia stability.

Role for CaMK-II in Ear Development While the location of activated CaMK-II (P-T^{287} CaMK-II) provided insight into many of the potential roles of CaMK-II during early development, the intensity and location of P-T^{287} CaMK-II in the inner ear [65] suggested that CaMK-II could be essential for translating external stimuli into an intracellular response.

The organization of sensory epithelial cells must occur at the appropriate time and place during development to ensure normal otolith biomineralization. Alterations in this process lead to malformed otoliths and therefore impaired hearing. Signaling molecules necessary for inner ear sensory epithelial cell patterning include Delta-Notch family members, as demonstrated by the *mindbomb* (*mib*) mutant, which leads to supernumerary hair cells [131]. The *mib* locus encodes an E3 ubiquitin ligase, which ubiquitylates and then internalizes Delta ligands [132, 133]. CaMK-II (*camk2g1*) is responsible for the patterning of inner ear sensory cells through the Delta-Notch pathway. Like *mib* mutants, suppression of *camk2g1* also leads to supernumerary hair cells, which may contribute directly or indirectly to ectopic or malformed otoliths.

The enrichment of CaMK-II in the hair cells, but not in the surrounding support cells is consistent with CaMK-II influencing the Delta ligand and not the Notch receptor. Upon Delta binding to Notch, the Delta-Notch extracellular domain undergoes transendocytosis causing the Notch receptor to be proteolytically cleaved and the Notch intracellular domain (NICD) to enter the nucleus and activate gene expression [134]. Delta ligands are ubiquitylated, internalized, and degraded, but in the *mib* mutant, DeltaD is not endocytosed and degraded, causing an upregulation of DeltaD mRNA expression and increased DeltaD protein localization to the membrane with retention in endocytic vesicles [133, 135]. Suppression of *camk2g1* also causes an increase of DeltaD in particles that appeared to represent intracellular vesicles, but do not accumulate at the cell surface. These results suggest that the DeltaD protein is being synthesized in *camk2g1* morphants, but is not being transported to the membrane, therefore accumulating in secretory vesicles in the cytosol.

CaMK-II is known to phosphorylate proteins important in trafficking, docking and fusion of secretory vesicles. Substrates include synapsin I [136], synaptotagmin [137] and synaptobrevin, a vesicle associated membrane protein [138]. Although these proteins are essential in the secretion of neurotransmitters, they also function in non-neuronal tissues [139]. In the zebrafish KV, CaMK-II may be necessary for the secretion of Southpaw (Spaw) to the left lateral plate mesoderm, enabling the expression of left sided genes and therefore left-right organ asymmetry [64]. Likewise, a role for CaMK-II in promoting recycling and trafficking of the Delta ligand would explain its role in enabling Delta signaling to Notch expressing cells. In the absence or reduction of Delta ligands at the plasma membrane, expression of key genes would be inhibited, causing alterations in sensory epithelial cell patterning. Delta-Notch signaling has been linked to the differentiation of ciliated embryonic cells in other organisms as well [140]. While CaMK-II has previously been shown to activate Notch signaling in Notch expressing cells [141, 142], this role for CaMK-II in Delta ligand processing is distinct and acts through an undetermined protein target.

Protein Targets of CaMK-II During Development For a multifunctional protein kinase like CaMK-II, it stands to reason that there are many different potential substrates of phosphorylation during early development. However, histone deacetylase,

HDAC4, is a known substrate of CaMK-II and may be responsible for many of these developmental processes through epigenetics [115]. Nonetheless, there are other potential substrates that have also been identified. For Wnt signaling, Flightless-I may be a protein that is not itself phosphorylated, but binds to autophosphorylated CaMK-II and thus impacts downstream pathways, such as cell migration and gene expression [120]. While phospholamban has not been explicitly evaluated in the embryonic heart, its role as a target of cyclical phosphorylation by CaMK-II during excitation-contraction coupling [108] makes it an ideal candidate to explain the effect of reversible CaMK-II inhibition on heart rates. As described above, there are multiple CaMK-II substrates, including synapsin, that could mediate the effect of CaMK-II on secretion and thereby explain both its role in Delta-Notch signaling in the ear and in Southpaw secretion in the embryonic node. A characterization of these substrates in early development would be justified.

Other Protein Targets of Calcium During Development Among alternative Ca^{2+} targets including PK-C, calcineurin and CaM kinases, only CaMK-II has the molecular capability of decoding Ca^{2+} of different amplitude, duration and frequency [74, 143, 144]. In addition, it is represented by a family of genes whose alternatively spliced products are differentially targeted to membranes and subcellular compartments [61]. While PKC-delta has been implicated in convergent extension in Xenopus [145] and PK-C lambda in cell polarity [146], neither PK-C or calcineurin have been implicated as targets of the asymmetric Ca^{2+} signal [5].

21.2 Conclusion

Ca^{2+} signals have long been known to play an important role during early development. CaMK-II is a multifunctional, ubiquitously expressed protein kinase that built its reputation as regulating long-term potentiation (LTP) in the central nervous system. The features of CaMK-II that make it structurally and enzymatically attractive in the CNS are also advantageous for frequency decoding and sustained activation in a variety of cellular and tissue settings during early development.

So far, evidence is strong for a role for *camk2b1* in gastrulation and the nervous system [66], while *camk2g1* is pleiotropic and has been linked to functions found primarily in ciliated cells, such as the development and function of the ear, kidney and KV, all of which rely on cilia [64, 65, 71]. Interestingly, investigators have been stymied in their quest to prepare a knockout *camk2g1* CRISPR mutant to this clearly important early developmental gene due to a poorly understood, but gene-specific repair mechanism, which appears to act on a limited number of critical genes, including *camk2g1* [147]. While this suggests an important role for *camk2g1* in early zebrafish development, it has made it difficult to prepare *camk2g1* mutants. Activated CaMK-II plays a central role in decoding Ca^{2+} signals to activate specific events during early development. A majority of the known Ca^{2+} elevations act though CaMK-II and not other known Ca^{2+} targets (Table 21.1). Not

Table 21.1 Roles for calcium and calcium targets during development

Event	Calcium	PK-C	Calcineurin	CaMK-II
Meiotic resumption	Essential	NO	NO	YES via PLK
Gastrulation	Elevates ventrally	YES, PK-C delta	YES	Wnt/Ca pathway
Somitogenesis	Preceding somites	NO	NO	YES, compression
Heart Development	Elevates at looping	YES, "Heart and Soul" zebrafish mutant	NO	YES, by Tbx5
Kidney Development	Ventrally high	NO	NO	YES, with PKD2
LR Asymmetry	Transient on left side	NO	NO	YES, on left
Ears	TRP channel dependent	NO	NO	YES, Delta-Notch

only do Ca^{2+} signals and CaMK-II functionally overlap during meiotic resumption, gastrulation, somitogenesis, heart morphogenesis and function, kidney development and laterality and ear development, but the localization of Ca^{2+} signals, whether they be transient or sustained coincides with the location and sometimes intensity of activated CaMK-II. Linkages of CaMK-II with upstream (Tbx5, PKD2) and downstream (HDAC4) partners that are associated with human disease further supports these relationships.

References

1. Steinhardt R, Zucker R, Schatten G (1977) Intracellular calcium release at fertilization in the sea urchin egg. Dev Biol 58:185–196
2. Gilkey JC, Jaffe LF, Ridgway EB, Reynolds GT (1978) A free calcium wave traverses the activating egg of the medaka, Oryzias Latipes. J Cell Biol 76:448–466
3. Ridgway EB, Gilkey JC, Jaffe LF (1977) Free calcium increases explosively in activating medaka eggs. Proc Natl Acad Sci U S A 74:623–627
4. Cuthbertson KSR, Whittingham DG, Cobbold PH (1981) Free Ca^{2+} increases in exponential phases during mouse oocyte activation. Nature 294:754–757
5. Whitaker M (2006) Calcium at fertilization and in early development. Physiol Rev 86(1): 25–88
6. Stricker SA (1999) Comparative biology of calcium signaling during fertilization and egg activation in animals. Dev Biol 211(2):157–176
7. Webb SE, Miller AL (2003) Calcium signalling during embryonic development. Nat Rev Mol Cell Biol 4(7):539–551
8. Berridge MJ, Lipp P, Bootman MD (2000) The versatility and universality of calcium signalling. Nat Rev Mol Cell Biol 1(1):11–21
9. Tombes RM, Simerly C, Borisy GG, Schatten G (1992) Meiosis, egg activation and nuclear envelope breakdown are differentially reliant on Ca^{2+}, whereas germinal vesicle breakdown is Ca^{2+}-independent in the mouse oocyte. J Cell Biol 117:799–812
10. Creton R, Speksnijder JE, Jaffe LF (1998) Patterns of free calcium in zebrafish embryos. J Cell Sci 111(Pt 12):1613–1622
11. Reinhard E, Yokoe H, Niebling KR, Allbritton NL, Kuhn MA, Meyer T (1995) Localized calcium signals in early zebrafish development. Dev Biol 170(1):50–61

12. Gilland E, Miller AL, Karplus E, Baker R, Webb SE (1999) Imaging of multicellular large-scale rhythmic calcium waves during zebrafish gastrulation. Proc Natl Acad Sci U S A 96(1):157–161
13. Kühl M, Sheldahl LC, Park M, Miller JR, Moon RT (2000) The Wnt/Ca^{2+} pathway: a new vertebrate Wnt signaling pathway takes shape. Trends Genetics 16(7):279–283
14. Lin S, Baye LM, Westfall TA, Slusarski DC (2010) Wnt5b-Ryk pathway provides directional signals to regulate gastrulation movement. J Cell Biol 190(2):263–278
15. Zhu S, Liu L, Korzh V, Gong Z, Low BC (2006) RhoA acts downstream of Wnt5 and Wnt11 to regulate convergence and extension movements by involving effectors Rho kinase and Diaphanous: use of zebrafish as an in vivo model for GTPase signaling. Cell Signal 18(3):359–372
16. Kilian B, Mansukoski H, Barbosa FC, Ulrich F, Tada M, Heisenberg CP (2003) The role of Ppt/Wnt5 in regulating cell shape and movement during zebrafish gastrulation. Mech Dev 120(4):467–476
17. Moon RT, Campbell RM, Christian JL, McGrew LL, Shih J, Fraser S (1993) Xwnt-5A: a maternal Wnt that affects morphogenetic movements after overexpression in embryos of Xenopus laevis. Development 119(1):97–111
18. Matsui T, Raya A, Kawakami Y, Callol-Massot C, Capdevila J, Rodriguez-Esteban C et al (2005) Noncanonical Wnt signaling regulates midline convergence of organ primordia during zebrafish development. Genes Dev 19(1):164–175
19. Marlow F, Topczewski J, Sepich D, Solnica-Krezel L (2002) Zebrafish Rho kinase 2 acts downstream of Wnt11 to mediate cell polarity and effective convergence and extension movements. Curr Biol 12(11):876–884
20. Heisenberg CP, Tada M, Rauch GJ, Saude L, Concha ML, Geisler R et al (2000) Silberblick/Wnt11 mediates convergent extension movements during zebrafish gastrulation. Nature 405(6782):76–81
21. Lele Z, Bakkers J, Hammerschmidt M (2001) Morpholino phenocopies of the swirl, snailhouse, somitabun, minifin, silberblick, and pipetail mutations. Genesis 30(3):190–194
22. Wallingford JB, Fraser SE, Harland RM (2002) Convergent extension: the molecular control of polarized cell movement during embryonic development. Dev Cell 2(6):695–706
23. Andre P, Song H, Kim W, Kispert A, Yang Y (2015) Wnt5a and Wnt11 regulate mammalian anterior-posterior axis elongation. Development 142(8):1516–1527
24. Slusarski DC, Corces VG, Moon RT (1997) Interaction of Wnt and a Frizzled homologue triggers G-protein-linked phosphatidylinositol signalling. Nature 390(6658):410–413
25. Kühl M, Sheldahl L, Malbon CC, Moon RT (2000) Ca^{2+}/calmodulin-dependent protein kinase II is stimulated by Wnt and Frizzled homologs and promotes ventral Cell fates in xenopus. J Biol Chem 275:12701–12711
26. Westfall TA, Hjertos B, Slusarski DC (2003) Requirement for intracellular calcium modulation in zebrafish dorsal-ventral patterning. Dev Biol 259(2):380–391
27. Westfall TA, Brimeyer R, Twedt J, Gladon J, Olberding A, Furutani-Seiki M et al (2003) Wnt-5/pipetail functions in vertebrate axis formation as a negative regulator of Wnt/beta-catenin activity. J Cell Biol 162(5):889–898
28. Ulrich F, Concha ML, Heid PJ, Voss E, Witzel S, Roehl H et al (2003) Slb/Wnt11 controls hypoblast cell migration and morphogenesis at the onset of zebrafish gastrulation. Development 130(22):5375–5384
29. Peeters H, Devriendt K (2006) Human laterality disorders. Eur J Med Genet 49(5):349–362
30. Hirokawa N, Tanaka Y, Okada Y, Takeda S (2006) Nodal flow and the generation of left-right asymmetry. Cell 125(1):33–45
31. Essner JJ, Amack JD, Nyholm MK, Harris EB, Yost HJ (2005) Kupffer's vesicle is a ciliated organ of asymmetry in the zebrafish embryo that initiates left-right development of the brain, heart and gut. Development 132(6):1247–1260
32. Kramer-Zucker AG, Olale F, Haycraft CJ, Yoder BK, Schier AF, Drummond IA (2005) Cilia-driven fluid flow in the zebrafish pronephros, brain and Kupffer's vesicle is required for normal organogenesis. Development 132(8):1907–1921

33. Lee JD, Anderson KV (2008) Morphogenesis of the node and notochord: the cellular basis for the establishment and maintenance of left-right asymmetry in the mouse. Dev Dyn 237(12):3464–3476
34. Bisgrove BW, Snarr BS, Emrazian A, Yost HJ (2005) Polaris and Polycystin-2 in dorsal forerunner cells and Kupffer's vesicle are required for specification of the zebrafish left-right axis. Dev Biol 287(2):274–288
35. Schottenfeld J, Sullivan-Brown J, Burdine RD (2007) Zebrafish curly up encodes a Pkd2 ortholog that restricts left-side-specific expression of southpaw. Development 134(8): 1605–1615
36. Tabin CJ, Vogan KJ (2003) A two-cilia model for vertebrate left-right axis specification. Genes Dev 17(1):1–6
37. McGrath J, Somlo S, Makova S, Tian X, Brueckner M (2003) Two populations of node monocilia initiate left-right asymmetry in the mouse. Cell 114(1):61–73
38. Tanaka Y, Okada Y, Hirokawa N (2005) FGF-induced vesicular release of Sonic hedgehog and retinoic acid in leftward nodal flow is critical for left-right determination. Nature 435(7039):172–177
39. Raya A, Kawakami Y, Rodriguez-Esteban C, Ibanes M, Rasskin-Gutman D, Rodriguez-Leon J et al (2004) Notch activity acts as a sensor for extracellular calcium during vertebrate left-right determination. Nature 427(6970):121–128
40. Garic-Stankovic A, Hernandez M, Flentke GR, Zile MH, Smith SM (2008) A ryanodine receptor-dependent Ca(i)(2+) asymmetry at Hensen's node mediates avian lateral identity. Development 135(19):3271–3280
41. Sarmah B, Latimer AJ, Appel B, Wente SR (2005) Inositol polyphosphates regulate zebrafish left-right asymmetry. Dev Cell 9(1):133–145
42. Jurynec MJ, Xia R, Mackrill JJ, Gunther D, Crawford T, Flanigan KM et al (2008) Selenoprotein N is required for ryanodine receptor calcium release channel activity in human and zebrafish muscle. Proc Natl Acad Sci U S A 105(34):12485–12490
43. Levin M, Mercola M (1999) Gap junction-mediated transfer of left-right patterning signals in the early chick blastoderm is upstream of Shh asymmetry in the node. Development 126(21):4703–4714
44. Hatler JM, Essner JJ, Johnson RG (2009) A gap junction connexin is required in the vertebrate left-right organizer. Dev Biol 336(2):183–191
45. Fu X, Wang Y, Schetle N, Gao H, Putz M, von Gersdorff G et al (2008) The subcellular localization of TRPP2 modulates its function. J Am Soc Nephrol 19(7):1342–1351
46. Pennekamp P, Karcher C, Fischer A, Schweickert A, Skryabin B, Horst J et al (2002) The ion channel polycystin-2 is required for left-right axis determination in mice. Curr Biol 12(11):938–943
47. Webb SE, Miller AL (2000) Calcium signalling during zebrafish embryonic development. BioEssays 22(2):113–123
48. Ferrari MB, Spitzer NC (1999) Calcium signaling in the developing Xenopus myotome. Dev Biol 213(2):269–282
49. Porter GA Jr, Makuck RF, Rivkees SA (2003) Intracellular calcium plays an essential role in cardiac development. Dev Dyn 227(2):280–290
50. Ebert AM, Hume GL, Warren KS, Cook NP, Burns CG, Mohideen MA et al (2005) Calcium extrusion is critical for cardiac morphogenesis and rhythm in embryonic zebrafish hearts. Proc Natl Acad Sci U S A 102(49):17705–17710
51. Leclerc C, Webb SE, Miller AL, Moreau M (2008) An increase in intracellular Ca^{2+} is involved in pronephric tubule differentiation in the amphibian Xenopus laevis. Dev Biol 321(2):357–367
52. Lam PY, Webb SE, Leclerc C, Moreau M, Miller AL (2009) Inhibition of stored Ca^{2+} release disrupts convergence-related cell movements in the lateral intermediate mesoderm resulting in abnormal positioning and morphology of the pronephric anlagen in intact zebrafish embryos. Develop Growth Differ 51(4):429–442

53. Stooke-Vaughan GA, Huang P, Hammond KL, Schier AF, Whitfield TT (2012) The role of hair cells, cilia and ciliary motility in otolith formation in the zebrafish otic vesicle. Development 139(10):1777–1787
54. Colantonio JR, Vermot J, Wu D, Langenbacher AD, Fraser S, Chen JN et al (2009) The dynein regulatory complex is required for ciliary motility and otolith biogenesis in the inner ear. Nature 457(7226):205–209
55. Amato V, Vina E, Calavia MG, Guerrera MC, Laura R, Navarro M et al (2012) TRPV4 in the sensory organs of adult zebrafish. Microsc Res Tech 75(1):89–96
56. Corey DP (2006) What is the hair cell transduction channel? J Physiol 576(Pt 1):23–28
57. Shin JB, Adams D, Paukert M, Siba M, Sidi S, Levin M et al (2005) Xenopus TRPN1 (NOMPC) localizes to microtubule-based cilia in epithelial cells, including inner-ear hair cells. Proc Natl Acad Sci U S A 102(35):12572–12577
58. Sidi S, Friedrich RW, Nicolson T (2003) NompC TRP channel required for vertebrate sensory hair cell mechanotransduction. Science 301(5629):96–99
59. Hudmon A, Schulman H (2002) Neuronal Ca^{2+}/calmodulin-dependent protein kinase II: the role of structure and autoregulation in cellular function. Annu Rev Biochem 71:473–510
60. Tobimatsu T, Fujisawa H (1989) Tissue-specific expression of four types of rat calmodulin-dependent protein kinase II mRNAs. J Biol Chem 264:17907–17912
61. Tombes RM, Faison MO, Turbeville C (2003) Organization and evolution of multifunctional Ca^{2+}/CaM-dependent protein kinase (CaMK-II) genes. Gene 322:17–31
62. Swulius MT, Waxham MN (2008) Ca($^{2+}$)/calmodulin-dependent protein kinases. Cell Mol Life Sci 65(17):2637–2657
63. Rothschild SC, Francescatto L, Tombes RM (2016) Immunostaining phospho-epitopes in ciliated organs of whole mount zebrafish embryos. J Visual Exp JoVE 108:53747
64. Francescatto L, Rothschild SC, Myers AL, Tombes RM (2010) The activation of membrane targeted CaMK-II in the zebrafish Kupffer's vesicle is required for left-right asymmetry. Development 137(16):2753–2762
65. Rothschild SC, Francescatto L, Drummond IA, Tombes RM (2011) CaMK-II is a PKD2 target that promotes pronephric kidney development and stabilizes cilia. Development 138(16):3387–3397
66. Rothschild SC, Lister JA, Tombes RM (2007) Differential expression of CaMK-II genes during early zebrafish embryogenesis. Dev Dyn 236(1):295–305
67. Lou L, Schulman H (1989) Distinct autophosphorylation sites sequantially produce autonomy and inhibition of the multifunctional Ca^{2+}/calmodulin-dependent protein kinase. J Neurosci 9(6):2020–2032
68. Hoffman A, Carpenter H, Kahl R, Watt LF, Dickson PW, Rostas JA et al (2014) Dephosphorylation of CaMKII at T253 controls the metaphase-anaphase transition. Cell Signal 26(4):748–756
69. Tombes RM, Grant S, Westin EH, Krystal G (1995) G1 cell cycle arrest and apoptosis are induced in NIH 3T3 cells by KN-93, an inhibitor of CaMK-II (the multifunctional Ca^{2+}/CaM kinase). Cell Growth Differ 6(9):1063–1070
70. Rasmussen G, Rasmussen C (1995) Calmodulin-dependent protein kinase II is required for G1/S progression in HeLa cells. Biochem Cell Biol 73:201–207
71. Rothschild SC, Lahvic J, Francescatto L, McLeod JJ, Burgess SM, Tombes RM (2013) CaMK-II activation is essential for zebrafish inner ear development and acts through Delta-Notch signaling. Dev Biol 381(1):179–188
72. Gardner AJ, Knott JG, Jones KT, Evans JP (2007) CaMKII can participate in but is not sufficient for the establishment of the membrane block to polyspermy in mouse eggs. J Cell Physiol 212(2):275–280
73. Morin N, Abrieu A, Lorca T, Martin F, Dorée M (1994) The proteolysis-dependent metaphase to anaphase transition: calcium/calmodulin-dependent protein kinase II mediates onset of anaphase in extracts prepared from unfertilized Xenopus eggs. EMBO J 13(18):4343–4352
74. Dupont G (1998) Link between fertilization-induced Ca^{2+} oscillations and relief from metaphase II arrest in mammalian eggs: a model based on calmodulin-dependent kinase II activation. Biophys Chem 72(1–2):153–167

75. Tatone C, Iorio R, Francione A, Gioia L, Colonna R (1999) Biochemical and biological effects of KN-93, an inhibitor of calmodulin-dependent protein kinase II, on the initial events of mouse egg activation induced by ethanol. J Reprod Fertil 115(1):151–157
76. Backs J, Stein P, Backs T, Duncan FE, Grueter CE, McAnally J et al (2010) The gamma isoform of CaM kinase II controls mouse egg activation by regulating cell cycle resumption. Proc Natl Acad Sci U S A 107(1):81–86
77. Chang HY, Minahan K, Merriman JA, Jones KT (2009) Calmodulin-dependent protein kinase gamma 3 (CamKIIgamma3) mediates the cell cycle resumption of metaphase II eggs in mouse. Development 136(24):4077–4081
78. Silva A, Stevens C, Tonegawa S, Wang Y (1992) Deficient hippocampal long term-potentiation in a-calcium-calmodulin kinase II mutant mice. Science 257:201–206
79. Silva AJ, Paylor R, Wehner JM, Tonegawa S (1992) Impaired spatial learning in alpha-calcium-calmodulin kinase II mutant mice. Science 257(5067):206–211
80. van Woerden GM, Hoebeek FE, Gao Z, Nagaraja RY, Hoogenraad CC, Kushner SA et al (2009) betaCaMKII controls the direction of plasticity at parallel fiber-Purkinje cell synapses. Nat Neurosci 12:823–825
81. Backs J, Backs T, Neef S, Kreusser MM, Lehmann LH, Patrick DM et al (2009) The delta isoform of CaM kinase II is required for pathological cardiac hypertrophy and remodeling after pressure overload. Proc Natl Acad Sci U S A 106(7):2342–2347
82. Liu J, Maller JL (2005) Calcium elevation at fertilization coordinates phosphorylation of XErp1/Emi2 by Plx1 and CaMK II to release metaphase arrest by cytostatic factor. Curr Biol 15(16):1458–1468
83. Hansen DV, Tung JJ, Jackson PK (2006) CaMKII and polo-like kinase 1 sequentially phosphorylate the cytostatic factor Emi2/XErp1 to trigger its destruction and meiotic exit. Proc Natl Acad Sci U S A 103(3):608–613
84. Tombes RM, Peppers LS (1995) Sea urchin fertilization stimulates CaM kinase-II (multifunctional (type II) Ca^{2+}/CaM Kinase) activity and association with $p34^{cdc2}$. Dev Growth Differ 37(5):589–596
85. Creton R (2004) The calcium pump of the endoplasmic reticulum plays a role in midline signaling during early zebrafish development. Brain Res Dev Brain Res 151(1–2):33–41
86. Kohn AD, Moon RT (2005) Wnt and calcium signaling: beta-catenin-independent pathways. Cell Calcium 38(3–4):439–446
87. Pfleiderer PJ, Lu KK, Crow MT, Keller RS, Singer HA (2004) Modulation of vascular smooth muscle cell migration by calcium/calmodulin-dependent protein kinase II-delta 2. Am J Physiol Cell Physiol 286(6):C1238–C1245
88. Bilato C, Curto KA, Monticone RE, Pauly RR, White AJ, Crow MT (1997) The inhibition of vascular smooth muscle cell migration by peptide and antibody antagonists of the alphavbeta3 integrin complex is reversed by activated calcium/calmodulin- dependent protein kinase II. J Clin Invest 100(3):693–704
89. Bouvard D, Block MR (1998) Calcium/calmodulin-dependent protein kinase II controls integrin alpha5beta1-mediated cell adhesion through the integrin cytoplasmic domain associated protein-1alpha. Biochem Biophys Res Commun 252(1):46–50
90. Lundberg MS, Curto KA, Bilato C, Monticone RE, Crow MT (1998) Regulation of vascular smooth muscle migration by mitogen-activated protein kinase and calcium/calmodulin-dependent protein kinase II signaling pathways. J Mol Cell Cardiol 30(11):2377–2389
91. Easley CA, Brown CM, Horwitz AF, Tombes RM (2008) CaMK-II promotes focal adhesion turnover and cell motility by inducing tyrosine dephosphorylation of FAK and paxillin. Cell Motil Cytoskeleton 65(8):662–674
92. Rothschild SC, Easley CA, Francescatto L, Lister JA, Garrity DM, Tombes RM (2009) Tbx5-mediated expression of Ca^{2+}/calmodulin-dependent protein kinase II is necessary for zebrafish cardiac and pectoral fin morphogenesis. Dev Biol 330(1):175–184
93. Lantsman K, Tombes RM (2005) CaMK-II oligomerization potential determined using CFP/YFP FRET. Biochim Biophys Acta 1746(1):45–54

94. Webb SE, Miller AL (2006) Ca^{2+} signaling and early embryonic patterning during the Blastula and Gastrula Periods of Zebrafish and Xenopus development. Biochim Biophys Acta 1763:1192–1208
95. Kuhl M, Geis K, Sheldahl LC, Pukrop T, Moon RT, Wedlich D (2001) Antagonistic regulation of convergent extension movements in Xenopus by Wnt/beta-catenin and Wnt/Ca^{2+} signaling. Mech Dev 106(1–2):61–76
96. Baitinger C, Alderton J, Poenie M, Schulman H, Steinhardt RA (1990) Multifunctional Ca^{2+}/calmodulin-dependent protein kinase is necessary for nuclear envelope breakdown. J Cell Biol 111:1763–1773
97. Knott JG, Gardner AJ, Madgwick S, Jones KT, Williams CJ, Schultz RM (2006) Calmodulin-dependent protein kinase II triggers mouse egg activation and embryo development in the absence of Ca^{2+} oscillations. Dev Biol 296(2):388–395
98. Markoulaki S, Matson S, Ducibella T (2004) Fertilization stimulates long-lasting oscillations of CaMKII activity in mouse eggs. Dev Biol 272(1):15–25
99. Markoulaki S, Matson S, Abbott AL, Ducibella T (2003) Oscillatory CaMKII activity in mouse egg activation. Dev Biol 258(2):464–474
100. Johnson J, Bierle BM, Gallicano GI, Capco DG (1998) Calcium/calmodulin-dependent protein kinase II and calmodulin: regulators of the meiotic spindle in mouse eggs. Dev Biol 204(2):464–477
101. Morris TA, DeLorenzo RJ, Tombes RM (1998) CaMK-II inhibition reduces cyclin D1 levels and enhances the association of $p27^{kip1}$ with cdk2 to cause G1 arrest in NIH 3T3 cells. Exp Cell Res 240:218–227
102. Zhu W, Woo AY, Yang D, Cheng H, Crow MT, Xiao RP (2007) Activation of CaMKIIdeltaC is a common intermediate of diverse death stimuli-induced heart muscle cell apoptosis. J Biol Chem 282(14):10833–10839
103. Hagemann D, Bohlender J, Hoch B, Krause EG, Karczewski P (2001) Expression of Ca^{2+}/calmodulin-dependent protein kinase II delta-subunit isoforms in rats with hypertensive cardiac hypertrophy. Mol Cell Biochem 220(1–2):69–76
104. Zhang T, Maier LS, Dalton ND, Miyamoto S, Ross J Jr, Bers DM et al (2003) The deltaC isoform of CaMKII is activated in cardiac hypertrophy and induces dilated cardiomyopathy and heart failure. Circ Res 92(8):912–919
105. Zhang R, Khoo MS, Wu Y, Yang Y, Grueter CE, Ni G et al (2005) Calmodulin kinase II inhibition protects against structural heart disease. Nat Med 11(4):409–417
106. Grueter CE, Colbran RJ, Anderson ME (2007) CaMKII, an emerging molecular driver for calcium homeostasis, arrhythmias, and cardiac dysfunction. J Mol Med (Berlin, Germany) 85(1):5–14
107. Yang Y, Zhu WZ, Joiner ML, Zhang R, Oddis CV, Hou Y et al (2006) Calmodulin kinase II inhibition protects against myocardial cell apoptosis in vivo. Am J Physiol 291(6):H3065–H3075
108. Baltas LG, Karczewski P, Krause EG (1995) The cardiac sarcoplasmic reticulum phospholamban kinase is a distinct delta-CaM kinase isozyme. FEBS Lett 373(1):71–75
109. Grueter CE, Abiria SA, Dzhura I, Wu Y, Ham AJ, Mohler PJ et al (2006) L-type Ca^{2+} channel facilitation mediated by phosphorylation of the beta subunit by CaMKII. Mol Cell 23(5):641–650
110. Hudmon A, Schulman H, Kim J, Maltez JM, Tsien RW, Pitt GS (2005) CaMKII tethers to L-type Ca^{2+} channels, establishing a local and dedicated integrator of Ca^{2+} signals for facilitation. J Cell Biol 171(3):537–547
111. Lee TS, Karl R, Moosmang S, Lenhardt P, Klugbauer N, Hofmann F et al (2006) Calmodulin kinase II is involved in voltage-dependent facilitation of the L-type Cav1.2 calcium channel: identification of the phosphorylation sites. J Biol Chem 281(35):25560–25567
112. Zalk R, Lehnart SE, Marks AR (2007) Modulation of the ryanodine receptor and intracellular calcium. Annu Rev Biochem 76:367–385
113. Backs J, Song K, Bezprozvannaya S, Chang S, Olson EN (2006) CaM kinase II selectively signals to histone deacetylase 4 during cardiomyocyte hypertrophy. J Clin Invest 116(7):1853–1864

114. Little GH, Bai Y, Williams T, Poizat C (2007) Nuclear calcium/calmodulin-dependent protein kinase IIdelta preferentially transmits signals to histone deacetylase 4 in cardiac cells. J Biol Chem 282(10):7219–7231
115. Rothschild SC, Lee HJ, Ingram SR, Mohammadi DK, Walsh GS, Tombes RM (2018) Calcium signals act through histone deacetylase to mediate pronephric kidney morphogenesis. Dev Dyn 247(6):807–817
116. Garriock RJ, D'Agostino SL, Pilcher KC, Krieg PA (2005) Wnt11-R, a protein closely related to mammalian Wnt11, is required for heart morphogenesis in Xenopus. Dev Biol 279(1):179–192
117. Eisenberg CA, Eisenberg LM (1999) WNT11 promotes cardiac tissue formation of early mesoderm. Dev Dyn 216(1):45–58
118. Pandur P, Lasche M, Eisenberg LM, Kuhl M (2002) Wnt-11 activation of a non-canonical Wnt signaling pathway is required for cardiogenesis. Nature 418(6898):636–641
119. Fleming IN, Elliott CM, Buchanan FG, Downes CP, Exton JH (1999) Ca^{2+}/calmodulin-dependent protein kinase II regulates Tiam1 by reversible protein phosphorylation. J Biol Chem 274(18):12753–12758
120. Seward ME, Easley CA, McLeod JJ, Myers AL, Tombes RM (2008) Flightless-I, a gelsolin family member and transcriptional regulator, preferentially binds directly to activated cytosolic CaMK-II. FEBS Lett 582(17):2489–2495
121. Tsiokas L (2009) Function and regulation of TRPP2 at the plasma membrane. Am J Physiol Renal Physiol 297(1):F1–F9
122. Obara T, Mangos S, Liu Y, Zhao J, Wiessner S, Kramer-Zucker AG et al (2006) Polycystin-2 immunolocalization and function in zebrafish. J Am Soc Nephrol 17(10):2706–2718
123. Backs J, Backs T, Bezprozvannaya S, McKinsey TA, Olson EN (2008) Histone deacetylase 4 confers CaM kinase II responsiveness to histone deacetylase 5 by oligomerization. Mol Cell Biol 28(10):3437–3445
124. Zhang T, Kohlhaas M, Backs J, Mishra S, Phillips W, Dybkova N et al (2007) CaMKIIdelta isoforms differentially affect calcium handling but similarly regulate HDAC/MEF2 transcriptional responses. J Biol Chem 282(48):35078–35087
125. Di Giorgio E, Brancolini C (2016) Regulation of class IIa HDAC activities: it is not only matter of subcellular localization. Epigenomics 8(2):251–269
126. Di Giorgio E, Clocchiatti A, Piccinin S, Sgorbissa A, Viviani G, Peruzzo P et al (2013) MEF2 is a converging hub for histone deacetylase 4 and phosphatidylinositol 3-kinase/Akt-induced transformation. Mol Cell Biol 33(22):4473–4491
127. McKinsey TA, Zhang CL, Olson EN (2002) MEF2: a calcium-dependent regulator of cell division, differentiation and death. Trends Biochem Sci 27(1):40–47
128. Bershteyn M, Atwood SX, Woo WM, Li M, Oro AE (2010) MIM and cortactin antagonism regulates ciliogenesis and hedgehog signaling. Dev Cell 19(2):270–283
129. Saarikangas J, Mattila PK, Varjosalo M, Bovellan M, Hakanen J, Calzada-Wack J et al (2011) Missing-in-metastasis MIM/MTSS1 promotes actin assembly at intercellular junctions and is required for integrity of kidney epithelia. J Cell Sci 124(Pt 8):1245–1255
130. Xia S, Li X, Johnson T, Seidel C, Wallace DP, Li R (2010) Polycystin-dependent fluid flow sensing targets histone deacetylase 5 to prevent the development of renal cysts. Development 137(7):1075–1084
131. Haddon C, Jiang YJ, Smithers L, Lewis J (1998) Delta-Notch signalling and the patterning of sensory cell differentiation in the zebrafish ear: evidence from the mind bomb mutant. Development 125(23):4637–4644
132. Haddon C, Mowbray C, Whitfield T, Jones D, Gschmeissner S, Lewis J (1999) Hair cells without supporting cells: further studies in the ear of the zebrafish mind bomb mutant. J Neurocytol 28(10–11):837–850
133. Itoh M, Kim CH, Palardy G, Oda T, Jiang YJ, Maust D et al (2003) Mind bomb is a ubiquitin ligase that is essential for efficient activation of Notch signaling by Delta. Dev Cell 4(1):67–82

134. Kandachar V, Roegiers F (2012) Endocytosis and control of Notch signaling. Curr Opin Cell Biol 24(4):534–540
135. Matsuda M, Chitnis AB (2009) Interaction with Notch determines endocytosis of specific Delta ligands in zebrafish neural tissue. Development 136(2):197–206
136. Matsumoto K, Fukunaga K, Miyazaki J, Shichiri M, Miyamoto E (1995) Ca^{2+}/calmodulin-dependent protein kinase II and synapsin I-like protein in mouse insulinoma MIN6 cells. Endocrinology 136(9):3784–3793
137. Nielander HB, Onofri F, Valtorta F, Schiavo G, Montecucco C, Greengard P et al (1995) Phosphorylation of VAMP/synaptobrevin in synaptic vesicles by endogenous protein kinases. J Neurochem 65(4):1712–1720
138. Popoli M (1993) Synaptotagmin is endogenously phosphorylated by Ca^{2+}/calmodulin protein kinase II in synaptic vesicles. FEBS Lett 317(1–2):85–88
139. Bustos R, Kolen ER, Braiterman L, Baines AJ, Gorelick FS, Hubbard AL (2001) Synapsin I is expressed in epithelial cells: localization to a unique trans-Golgi compartment. J Cell Sci 114(Pt 20):3695–3704
140. Marcet B, Chevalier B, Luxardi G, Coraux C, Zaragosi LE, Cibois M et al (2011) Control of vertebrate multiciliogenesis by miR-449 through direct repression of the Delta/Notch pathway. Nat Cell Biol 13(6):693–699
141. Ann EJ, Kim HY, Seo MS, Mo JS, Kim MY, Yoon JH et al (2012) Wnt5a controls Notch1 signaling through CaMKII-mediated degradation of the SMRT corepressor protein. J Biol Chem 287(44):36814–36829
142. Mamaeva OA, Kim J, Feng G, McDonald JM (2009) Calcium/calmodulin-dependent kinase II regulates notch-1 signaling in prostate cancer cells. J Cell Biochem 106(1):25–32
143. Bayer KU, De Koninck P, Schulman H (2002) Alternative splicing modulates the frequency-dependent response of CaMKII to Ca^{2+} oscillations. EMBO J 21(14):3590–3597
144. De Koninck P, Schulman H (1998) Sensitivity of CaM kinase II to the frequency of Ca^{2+} oscillations. Science 279(5348):227–230
145. Kinoshita N, Iioka H, Miyakoshi A, Ueno N (2003) PKC delta is essential for Dishevelled function in a noncanonical Wnt pathway that regulates Xenopus convergent extension movements. Genes Dev 17(13):1663–1676
146. Horne-Badovinac S, Lin D, Waldron S, Schwarz M, Mbamalu G, Pawson T et al (2001) Positional cloning of heart and soul reveals multiple roles for PKC lambda in zebrafish organogenesis. Curr Biol 11(19):1492–1502
147. Gagnon JA, Valen E, Thyme SB, Huang P, Ahkmetova L, Pauli A et al (2014) Efficient mutagenesis by Cas9 protein-mediated oligonucleotide insertion and large-scale assessment of single-guide RNAs. PLoS One 9(5):e98186

Chapter 22
Calcium Signaling and Gene Expression

Basant K. Puri

Abstract Calcium signaling plays an important role in gene expression. At the transcriptional level, this may underpin mammalian neuronal synaptic plasticity. Calcium influx into the postsynaptic neuron via: *N*-methyl-D-aspartate (NMDA) receptors activates small GTPase Rac1 and other Rac guanine nucleotide exchange factors, and stimulates calmodulin-dependent kinase kinase (CaMKK) and CaMKI; α-amino-3-hydroxy-5-methyl-4-isoxazolepropionic acid receptors that are not impermeable to calcium ions, that is, those lacking the glutamate receptor-2 subunits, leads to activation of Ras guanine nucleotide-releasing factor proteins, which is coupled with activation of the mitogen-activated protein kinases/extracellular signal-regulated kinases signaling cascade; L-type voltage-gated calcium channels activates signaling pathways involving CaMKII, downstream responsive element antagonist modulator and distinct microdomains. Key members of these signaling cascades then translocate into the nucleus, where they alter the expression of genes involved in neuronal synaptic plasticity. At the post-transcriptional level, intracellular calcium level changes can change alternative splicing patterns; in the mammalian brain, alterations in calcium signaling via NMDA receptors is associated with exon silencing of the CI cassette of the NMDA R1 receptor (*GRIN1*) transcript by UAGG motifs in response to neuronal excitation. Regulation also occurs at the translational level; transglutaminase-2 (TG2) mediates calcium ion-regulated crosslinking of Y-box binding protein-1 (YB-1) translation-regulatory protein in TGFβ1-activated myofibroblasts; YB-1 binds smooth muscle α-actin mRNA and regulates its translational activity. Calcium signaling is also important in epigenetic regulation, for example in respect of changes in cytosine bases. Targeting calcium signaling may provide therapeutically useful options, for example to induce epigenetic reactivation of tumor suppressor genes in cancer patients.

B. K. Puri (✉)
CAR, Cambridge, UK
e-mail: bpuri@cantab.net

M. S. Islam (ed.), *Calcium Signaling*, Advances in Experimental Medicine and Biology 1131, https://doi.org/10.1007/978-3-030-12457-1_22

Keywords Alternative splicing patterns · AMPA receptors · Calcium signaling · Epigenetic regulation · Gene expression · Gene reactivation · L-type voltage-gated calcium channels · NMDA receptors · Transcription · Translation

22.1 Introduction

Gene expression is the process by which the information in a DNA sequence in a gene is used to biosynthesize an RNA or polypeptide [1]. In turn, this involves transcription, that is, the synthesis of an RNA copy from a DNA template, and, in the case of polypeptides, translation, that is, protein synthesis on a messenger RNA (mRNA) template [1]. It has recently become increasingly apparent that calcium signaling is relevant to the regulation of eukaryotic transcription, alternative splicing patterns, and translation. In this chapter, the roles of calcium ion signaling in these processes and in the regulation of epigenetic mechanisms will be discussed.

Calcium ion binding, and associated phosphorylation, are associated with changes in protein electrical charge, conformation and interactions; phosphate moieties can be removed by protein kinases from adenosine-5′-triphosphate (ATP) and attached covalently to the three common amino acid residues which have free hydroxyl groups, namely the polar amino acids serine, threonine and tyrosine [2, 3]. Thus, calcium ions and phosphate ions can effect signal transduction [2, 3]. Aside from its role in gene expression, calcium ion signaling, both intercellular and intracellular, has numerous other important functions, ranging from mitochondrial functioning and innate immunity to apoptosis and cell death pathways [2, 4, 5]. Other chapters of this work deal with many of these. An excellent review from the year 2000 which considers the versatility and universality of calcium signaling is that of Berridge, Lipp and Bootman [6], while Putney and Tomita review the role of phospholipase C signaling and calcium influx [7]; in this chapter, the focus is on the role of calcium ion signaling in respect of gene expression.

22.2 Pre-translation

22.2.1 Eukaryotic Transcription

Eukaryotic transcription occurs on a chromatin template (unlike the case for prokaryotes, in which a DNA template is used for transcription); the following three classes of RNA polymerase are involved: RNA polymerase I, which transcribes 18S/28S ribosomal RNA (rRNA); RNA polymerase II, which transcribes mRNA and certain small RNAs; and RNA polymerase III, which transcribes transfer RNA (tRNA), 5S rRNA and certain small RNAs [1].

22.2.2 Calcium-Related Transcriptional Regulation

Calcium-dependent gene expression regulation at the transcriptional level is thought to underlie animal neuronal synaptic plasticity and thereby mediate learning and adaptation to the environment [8]. In mammalian neurons, such regulation involves a complex cascade of signaling molecules, beginning with influx of calcium ions into the postsynaptic neuron via *N*-methyl-D-aspartate (NMDA) receptors (for glutamate), α-amino-3-hydroxy-5-methyl-4-isoxazolepropionic acid (AMPA) receptors (also for glutamate), or L-type voltage-gated calcium channels (VGCCs) [9–11]. Each of these three possibilities will be briefly considered in turn.

Calcium ion influx through NMDA receptors activates small GTPase Rac1 (also known as Ras-related C3 botulinum toxin substrate 1), which acts as a pleiotropic activator of actin, and also activates other Rac guanine nucleotide exchange factors (GEFs) such as kalirin-7 and betaPIX (βPIX) [12, 13]. It also stimulates calmodulin-dependent kinase kinase (CaMKK) and CaMKI, which in turn phosphorylates βPIX [13]. Kalirin-7 interacts with AMPA receptors, controlling their synaptic expression [12]. While most AMPA receptors are calcium impermeable, those lacking the glutamate receptor-2 (GluR2) subunits do allow calcium ion flow. Calcium ion influx through such calcium-permeable AMPA receptors leads to activation of Ras guanine nucleotide-releasing factor (RasGRF) proteins, which in turn is coupled with activation of the mitogen-activated protein kinases/extracellular signal-regulated kinases (MAPK/ERK; also known as the Ras-ERK or Ras-Raf-MEK-ERK) signaling cascade [14]. Finally, calcium ion influx through L-type VGCCs appears to activate signaling pathways involving CaMKII, downstream responsive element antagonist modulator (DREAM), distinct microdomains (MD-I and MD-II), and possibly the distal C-terminal (dCT) fragment of the L-type receptor and beta subunits [15]. These consequences of calcium ion influx through NMDA, AMPA receptors and VGCCs are summarized in Table 22.1.

In turn, key members of the above signaling cascades, such as CAMKII, nuclear factor kappa-light-chain-enhancer of activated B cells (NF-κB), MAPK/ERK, GTP-Rac, DREAM, MD-I, MD-II, and possibly dCT and β4c, cross from the cytoplasm into the nucleus [8, 15]. Here, they alter the expression of, amongst others, the non-

Table 22.1 Primary activated molecules following calcium ion influx through NMDA and AMPA receptors and VGCCs

Type of calcium ion receptor or channel	NMDA receptors	AMPA receptors	VGCCs
Primary activated molecules	Small GTPase Rac1	RasGRF	CaMKII
	Kalirin-7		DREAM
	βPIX		MD-I
	CaMKK		MD-II
	CaMKI		dCT
			β subunits

coding RNA (ncRNA) miR-132 (which is a microRNA), *CREM* (which encodes the protein cyclic adenosine monophosphate (cAMP) responsive element modulator), *BDNF* (which encodes brain-derived neurotrophic factor), the proto-oncogene *c-Fos*, *PDYN* (which encodes a preproprotein which, following proteolysis, gives rise to several opioid peptides), *WNT2* (wingless-type MMTV integration site family, member 2; encoding signaling proteins relating to the Wnt signal transduction pathways), *BCL2* (encoding B-cell lymphoma 2 or Bcl-2), *SOD2* or *MnSOD* (encoding superoxide dismutase 2, mitochondrial), *XIAP* (X-linked inhibitor of apoptosis family of proteins), *NR4A1* or *Nur77* (nuclear receptor subfamily 4 group A member 1 or nerve growth factor IB), *ARC* (which encodes activity-regulated cytoskeleton-associated protein), HOMER1 (Homer scaffold protein 1 or Homer1a), *SLC8A1* or *NCX1* (solute carrier family 8 member A1 or sodium/calcium exchanger), and *SLC8A3* or *NCX3*. These are involved in synaptic development, dendritic growth, and neuronal plasticity; changes in their expression, as well as mutations in some of these loci, may be associated with neurocognitive disorders [8, 15]. Furthermore, EphB receptor tyrosine kinases, localized at excitatory synapses, cluster with NMDA receptors and modulate the function of the latter during early synaptogenesis [16].

A similar picture exists in respect of the mammalian heart, from which efflux of calcium ions normally takes place via plasma membrane calcium ATPases (PMCAs). Sustained increase in intracellular calcium ion concentration in cardiac cells activates the calcineurin moiety of PMCA4, which in turn dephosphorylates nuclear factor of activated T-cells (NFAT), which then translocates to the nucleus where it activates genes involved in cardiac hypertrophy [17].

The above examples have been drawn from animal cells. Calcium-related transcriptional regulation has also been shown to be important in plants. This has been studied in the unicellular green alga *Chlamydomonas reinhardtii*, which has a relatively short life-cycle and a fully sequenced genome [18–20]. In chloroplasts of this alga, calcium ion signaling and the calcium ion-binding protein CAS, acting in response to cues such as biotic and abiotic stress and carbon dioxide concentrating mechanisms, ultimately act upon a number of nuclear targets, including: *APX* (encoding ascorbate peroxidase); flg22 (flagellin 22); *HSF*s (heat shock transcription factors); *HSP*s (heat shock proteins); and *LHCRS3* (light-harvesting complex stress-related protein 3) [21]. These result in changes in basal defense responses and carbon dioxide concentration mechanisms [21].

22.2.3 Changes in Alternative Splicing Patterns

At the post-transcriptional, but pre-translational, level, intracellular calcium ion level changes can also alter gene expression by causing changes in alternative splicing patterns, whereby the same pre-mRNA generates mRNAs (post-splicing) which have different exon combinations [1].

In the mammalian brain, it has been shown that alterations in calcium ion signaling via NMDA receptors is associated with exon silencing of the CI cassette (exon 19) of the NMDA R1 receptor (*GRIN1*) transcript by UAGG motifs in response to neuronal excitation [22]. CI mediates targeting of NMDA R1 to the plasma membrane, has an endoplasmic reticulum retention signal, and contains a binding site for calcium/calmodulin [23, 24]. This may offer a powerful strategy for neuronal adaptation to hyperstimulation and may explain the diverse properties of NMDA receptors in different groups of neurons [22, 24].

Mechanical stimulation of hair cells of the basilar papilla of the avian inner ear, which is homologous to the organ of Corti, or spiral organ, of mammals, is associated with changes in intracellular calcium ion concentration via changes in the kinetic properties of calcium-ion-activated potassium ion channels; in turn, changes in calcium concentration have been found to be associated with alternative mRNA splicing patterns which tune individual hair cells to specific auditory frequencies [25–27].

In a similar vein, it is also noteworthy that GH3 pituitary cell depolarization has been shown to repress *KCNMA1* or *STREX* (potassium calcium-activated channel subfamily M alpha 1, previously stress-axis regulated exon) exon splicing in BK (big potassium, also known as Maxi-K, Kcal.1 or slo1) potassium ion channel transcripts via CaMKs [28].

Mammalian VGCCs are able to be activated over a relatively wide range of electrical potential differences, whereas the activation voltage dependence of calcium channel isoforms found in different tissues are tuned to their specific corresponding physiological functions. For example, the type known as 1.1 is the VGCC least responsive to depolarization and it has been found to achieve this electrical property through alternative splicing [29]. It acts both as a calcium ion channel in embryonic muscle and as a sensor of electrical potential difference in mature skeletal muscle for excitation-contraction coupling, and its relative lack of responsiveness to depolarization serves these functions well [29, 30]. On the other hand, the type of VGCC known as 1.2, which is the main type found in the brain and the cardiovascular system, is more responsive to depolarization; interestingly, the adjustment of its optimum activation voltage-dependency has recently been shown not to result from alternative splicing, showing that more than one mechanism is involved in fine tuning VGCCs [30].

22.3 Translation

Calcium regulation of gene expression at the translational level has been demonstrated in human cultured cells. The peptide transforming growth factor beta (TGFβ) controls cell proliferation in many tissues, including connective tissue [31]. In particular, repair of mammalian tissue injury can be initiated by TGFβ1 receptor signaling [32–35]. Indeed, poor regulation of this process may lead to dysfunctional cardiopulmonary fibrosis and chronic myofibroblast differentiation [36–38]. In

2013, it was shown, by Willis and colleagues, that the protein cross-linking enzyme transglutaminase-2 (TG2) mediates calcium ion-regulated crosslinking of Y-box binding protein-1 (YB-1) translation-regulatory protein in TGFβ1-activated myofibroblasts; YB-1 binds smooth muscle α-actin (*SMαA*) mRNA and regulates its translational activity [39].

22.4 Epigenetics

22.4.1 Epigenetic Mechanisms

Tollefsbol has defined epigenetic processes as 'changes of a biochemical nature to the DNA or its associated proteins or RNA that do not change the DNA sequence itself but do impact the level of gene expression' [40]. These biochemical changes are reversible and include DNA methylation, modifications in chromatin, nucleosome positioning, and ncRNA profile alterations [41]. The study of epigenetics is a rapidly developing field of research, which is of relevance to the study of diseases and, at a fundamental level, to a deeper understanding of intracellular communication [40–42]. It has recently become increasingly clear that calcium ion signaling plays an important role in epigenetic regulation.

22.4.2 Calcium-Related Epigenetic Regulation

A few recent examples are given to illustrate the important role of calcium signaling in epigenetic regulation.

Regarding DNA methylation, it has been shown that changes in the calcium content of murine diets can induce methylation changes in DNA cytosine bases. For example, a calcium-deficient diet in pregnant and nursing rats is associated with hypomethylation of the pup hepatic *HSD11B2* promoter region; this gene encodes the NAD^+-dependent enzyme corticosteroid 11-β-dehydrogenase isozyme 2 (also known as 11-β-hydroxysteroid dehydrogenase 2), and such pups have higher serum corticosterone levels than matched control pups from mothers fed a normal diet [43].

Raynal and colleagues tested a number of drugs which re-activate silenced gene expression in human cancer cells [44]. They found 11 newly identified pharmacological agents, such as cardiac glycosides, which induce methylated and silenced CpG island promoters which drive *GFP*, the gene for green fluorescent protein, and endogenous tumor suppressor genes in cancer cell lines. Surprisingly, rather than causing local DNA methylation changes or global histone changes, all 11 agents were found to alter calcium ion signaling and trigger CaMK activity; in turn, this released methyl CpG binding protein 2 (MeCP2), a methyl-binding protein, from silenced promoters, thus causing gene activation [44–46]. Given

that epigenetic changes are, in principle, reversible, this suggests that a potential therapeutic approach to the treatment of cancer might involve targeting calcium signaling in order to induce epigenetic reactivation of tumor suppressor genes [44].

It has been pointed out that the calcium ion influx through postsynaptic NMDA receptors and VGCCs mentioned above, which can lead to changes in *BDNF* expression, for example, also cause epigenetic changes such DNA hypomethylation (unmethylated cytosines) and histone acetylation; indeed, histone modification and changes in DNA methylation appear to be important features of the mediation of the risk of the development of major depressive disorder [47].

It should also be noted that epigenetic changes can also regulate calcium ion homeostasis. For example, epigenetic modification of the promoter region of *SERCA2a*, which encodes sarcoplasmic reticulum Ca^{2+}-ATPase and which is rich in CpG islands, changes the expression of this gene and is associated with alterations in calcium ion homeostasis; indeed, it has been suggested that demethylation in this promoter region, induced by the hydrazinophthalazine antihypertensive pharmacological agent hydralazine, may lead to modulated cardiomyocytic calcium homeostasis and consequent improved cardiac functioning [48].

22.5 Discussion

The examples given above have shown that calcium signaling has an important role in gene expression. This may involve regulation at the level of gene transcription; it may involve the regulation of alternative splicing; it may occur at the level of gene translation; and it may entail epigenetic mechanisms. Furthermore, these regulatory processes are bidirectional, in that changes in gene expression can themselves affect calcium ion homeostasis and calcium ion signaling. These findings offer important potential therapeutic avenues for the treatment of numerous diseases.

References

1. Krebs JE, Goldstein ES, Kilpatrick ST (2018) Lewin's genes XII. Jones & Bartlett Learning, Burlington
2. Clapham DE (2007) Calcium signaling. Cell 131(6):1047–1058
3. Westheimer FH (1987) Why nature chose phosphates. Science 235(4793):1173–1178
4. Morris G, Puri BK, Walder K, Berk M, Stubbs B, Maes M et al (2018) The endoplasmic reticulum stress response in neuroprogressive diseases: emerging pathophysiological role and translational implications. Mol Neurobiol 55(12):8765–8787
5. Puri BK, Morris G (2018) Potential therapeutic interventions based on the role of the endoplasmic reticulum stress response in progressive neurodegenerative diseases. Neural Regen Res 13(11):1887–1889
6. Berridge MJ, Lipp P, Bootman MD (2000) The versatility and universality of calcium signalling. Nat Rev Mol Cell Biol 1:11

7. Putney JW, Tomita T (2012) Phospholipase C signaling and calcium influx. Adv Biol Regul 52(1):152–164
8. Greer PL, Greenberg ME (2008) From synapse to nucleus: calcium-dependent gene transcription in the control of synapse development and function. Neuron 59(6):846–860
9. Berridge MJ (1998) Neuronal calcium signaling. Neuron 21(1):13–26
10. Berridge MJ, Bootman MD, Lipp P (1998) Calcium–a life and death signal. Nature 395(6703):645–648
11. Jonas P, Burnashev N (1995) Molecular mechanisms controlling calcium entry through AMPA-type glutamate receptor channels. Neuron 15(5):987–990
12. Xie Z, Srivastava DP, Photowala H, Kai L, Cahill ME, Woolfrey KM et al (2007) Kalirin-7 controls activity-dependent structural and functional plasticity of dendritic spines. Neuron 56(4):640–656
13. Saneyoshi T, Wayman G, Fortin D, Davare M, Hoshi N, Nozaki N et al (2008) Activity-dependent synaptogenesis: regulation by a CaM-kinase kinase/CaM-kinase I/betaPIX signaling complex. Neuron 57(1):94–107
14. Tian X, Feig LA (2006) Age-dependent participation of Ras-GRF proteins in coupling calcium-permeable AMPA glutamate receptors to Ras/Erk signaling in cortical neurons. J Biol Chem 281(11):7578–7582
15. Naranjo JR, Mellström B (2012) Ca^{2+}-dependent transcriptional control of Ca^{2+} homeostasis. J Biol Chem 287(38):31674–31680
16. Takasu MA, Dalva MB, Zigmond RE, Greenberg ME (2002) Modulation of NMDA receptor-dependent calcium influx and gene expression through EphB receptors. Science 295(5554):491–495
17. Cartwright EJ, Oceandy D, Austin C, Neyses L (2011) Ca^{2+} signalling in cardiovascular disease: the role of the plasma membrane calcium pumps. Sci China Life Sci 54(8):691–698
18. Jain M, Shrager J, Harris EH, Halbrook R, Grossman AR, Hauser C et al (2007) EST assembly supported by a draft genome sequence: an analysis of the Chlamydomonas reinhardtii transcriptome. Nucleic Acids Res 35(6):2074–2083
19. Merchant SS, Prochnik SE, Vallon O, Harris EH, Karpowicz SJ, Witman GB et al (2007) The Chlamydomonas genome reveals the evolution of key animal and plant functions. Science 318(5848):245–250
20. Misumi O, Yoshida Y, Nishida K, Fujiwara T, Sakajiri T, Hirooka S et al (2008) Genome analysis and its significance in four unicellular algae, Cyanidioschyzon [corrected] merolae, Ostreococcus tauri, Chlamydomonas reinhardtii, and Thalassiosira pseudonana. J Plant Res 121(1):3–17
21. Rea G, Antonacci A, Lambreva MD, Mattoo AK (2018) Features of cues and processes during chloroplast-mediated retrograde signaling in the alga Chlamydomonas. Plant Sci 272:193–206
22. An P, Grabowski PJ (2007) Exon silencing by UAGG motifs in response to neuronal excitation. PLoS Biol 5(2):e36
23. Black DL, Grabowski PJ (2003) Alternative pre-mRNA splicing and neuronal function. Prog Mol Subcell Biol 31:187–216
24. Zukin RS, Bennett MV (1995) Alternatively spliced isoforms of the NMDARI receptor subunit. Trends Neurosci 18(7):306–313
25. Black DL (1998) Splicing in the inner ear: a familiar tune, but what are the instruments? Neuron 20(2):165–168
26. Navaratnam DS, Bell TJ, Tu TD, Cohen EL, Oberholtzer JC (1997) Differential distribution of $Ca^{2+}-$activated K^+ channel splice variants among hair cells along the tonotopic axis of the chick cochlea. Neuron 19(5):1077–1085
27. Rosenblatt KP, Sun ZP, Heller S, Hudspeth AJ (1997) Distribution of $Ca^{2+}-$activated K^+ channel isoforms along the tonotopic gradient of the chicken's cochlea. Neuron 19(5):1061–1075
28. Xie J, Black DL (2001) A CaMK IV responsive RNA element mediates depolarization-induced alternative splicing of ion channels. Nature 410(6831):936–939

29. Tuluc P, Yarov-Yarovoy V, Benedetti B, Flucher BE (2016) Molecular interactions in the voltage sensor controlling gating properties of CaV calcium channels. Structure 24(2):261–271
30. Coste de Bagneaux P, Campiglio M, Benedetti B, Tuluc P, Flucher BE (2018) Role of putative voltage-sensor countercharge D4 in regulating gating properties of CaV1.2 and CaV1.3 calcium channels. Channels (Austin) 12(1):249–261
31. Canney PA, Dean S (1990) Transforming growth factor beta: a promotor of late connective tissue injury following radiotherapy? Br J Radiol 63(752):620–623
32. Sun X, Liu W, Cheng G, Qu X, Bi H, Cao Z et al (2017) The influence of connective tissue growth factor on rabbit ligament injury repair. Bone Joint Res 6(7):399–404
33. Toomey D, Condron C, Wu QD, Kay E, Harmey J, Broe P et al (2001) TGF-beta1 is elevated in breast cancer tissue and regulates nitric oxide production from a number of cellular sources during hypoxia re-oxygenation injury. Br J Biomed Sci 58(3):177–183
34. Wang S, Denichilo M, Brubaker C, Hirschberg R (2001) Connective tissue growth factor in tubulointerstitial injury of diabetic nephropathy. Kidney Int 60(1):96–105
35. Desmouliere A, Geinoz A, Gabbiani F, Gabbiani G (1993) Transforming growth factor-beta 1 induces alpha-smooth muscle actin expression in granulation tissue myofibroblasts and in quiescent and growing cultured fibroblasts. J Cell Biol 122(1):103–111
36. Gabbiani G (2003) The myofibroblast in wound healing and fibrocontractive diseases. J Pathol 200(4):500–503
37. Grotendorst GR, Rahmanie H, Duncan MR (2004) Combinatorial signaling pathways determine fibroblast proliferation and myofibroblast differentiation. FASEB J 18(3):469–479
38. Chen G, Grotendorst G, Eichholtz T, Khalil N (2003) GM-CSF increases airway smooth muscle cell connective tissue expression by inducing TGF-beta receptors. Am J Phys Lung Cell Mol Phys 284(3):L548–L556
39. Willis WL, Hariharan S, David JJ, Strauch AR (2013) Transglutaminase-2 mediates calcium-regulated crosslinking of the Y-Box 1 (YB-1) translation-regulatory protein in TGFβ1-activated myofibroblasts. J Cell Biochem 114(12):2753–2769
40. Tollefsbol TO (2016) An overview of medical epigenetics. In: Tollefsbol TO (ed) Medical epigenetics. Elsevier, Amsterdam, pp 3–7
41. Kanwal R, Gupta K, Gupta S (2015) Cancer epigenetics: an introduction. Methods Mol Biol 1238:3–25
42. Huang B, Jiang C, Zhang R (2014) Epigenetics: the language of the cell? Epigenomics 6(1):73–88
43. Takaya J, Iharada A, Okihana H, Kaneko K (2013) A calcium-deficient diet in pregnant, nursing rats induces hypomethylation of specific cytosines in the 11beta-hydroxysteroid dehydrogenase-1 promoter in pup liver. Nutr Res 33(11):961–970
44. Raynal NJ, Lee JT, Wang Y, Beaudry A, Madireddi P, Garriga J et al (2016) Targeting calcium signaling induces epigenetic reactivation of tumor suppressor genes in cancer. Cancer Res 76(6):1494–1505
45. Martinowich K, Hattori D, Wu H, Fouse S, He F, Hu Y et al (2003) DNA methylation-related chromatin remodeling in activity-dependent BDNF gene regulation. Science 302(5646):890–893
46. Chen WG, Chang Q, Lin Y, Meissner A, West AE, Griffith EC et al (2003) Derepression of BDNF transcription involves calcium-dependent phosphorylation of MeCP2. Science 302(5646):885–889
47. Nagy C, Vaillancourt K, Turecki G (2018) A role for activity-dependent epigenetics in the development and treatment of major depressive disorder. Genes Brain Behav 17(3):e12446
48. Kao YH, Cheng CC, Chen YC, Chung CC, Lee TI, Chen SA et al (2011) Hydralazine-induced promoter demethylation enhances sarcoplasmic reticulum Ca^{2+} -ATPase and calcium homeostasis in cardiac myocytes. Lab Investig 91(9):1291–1297

Chapter 23
Review: Structure and Activation Mechanisms of CRAC Channels

Carmen Butorac, Adéla Krizova, and Isabella Derler

Abstract Ca^{2+} release activated Ca^{2+} (CRAC) channels represent a primary pathway for Ca^{2+} to enter non-excitable cells. The two key players in this process are the stromal interaction molecule (STIM), a Ca^{2+} sensor embedded in the membrane of the endoplasmic reticulum, and Orai, a highly Ca^{2+} selective ion channel located in the plasma membrane. Upon depletion of the internal Ca^{2+} stores, STIM is activated, oligomerizes, couples to and activates Orai. This review provides an overview of novel findings about the CRAC channel activation mechanisms, structure and gating. In addition, it highlights, among diverse STIM and Orai mutants, also the disease-related mutants and their implications.

Keywords Calcium · CRAC channel · STIM1 · Orai1 · STIM-Orai interaction · Orai gating · Gain-of-function mutants · Electrophysiology · FRET · Structural resolution

Abbreviations

2-APB	2-aminoethoxydiphenyl borate
aa	amino acid
ADP	adenosine diphosphate
ATP	adenosine triphosphate
ANSGA	4-point mutation in hinge region aa position 261-265
ATPase	adenosine triphosphatase
BK	large conductance, Ca^{2+}-activated potassium channels
cCAD	*C. elegans* CAD
cOrai	*C. elegans* Orai
cSTIM	*C. elegans* STIM

C. Butorac · A. Krizova · I. Derler (✉)
Institute of Biophysics, Johannes Kepler University of Linz, Linz, Austria
e-mail: isabella.derler@jku.at

M. S. Islam (ed.), *Calcium Signaling*, Advances in Experimental Medicine and Biology 1131, https://doi.org/10.1007/978-3-030-12457-1_23

Ca^{2+}	calcium ion
CAD	Ca^{2+} Release-Activated Ca^{2+} activating domain
CaM	calmodulin
CAR	Ca^{2+} accumulating region
CC	coiled-coil
Ccb9	coiled-coil domain containing region b9
cEF	canonical EF hand
CFP	cyan fluorescent protein
CRAC	Ca^{2+} release-activated Ca^{2+}
CRACR2A	calcium release activated channel regulator 2A
Cs^{+}	cesium ion
Δ	represents deletion mutants
dOrai	*Drosophila melanogaster* Orai
DVF	divalent-free
EGTA	ethylene glycol tetraacetic acid
ER	endoplasmic reticulum
ERK1/2	extracellular-signal-regulated kinases 1 and 2
ETON	extended transmembrane Orai1 N-terminal
FCDI	fast calcium dependent inactivation
FIRE	FRET-derived interaction in a restricted environment
FRAP	fluorescence recovery after photobleaching
FRET	fluorescence resonance energy transfer
GoF	gain of function
HEK	Human Embryonic Kidney
I/V	current voltage relationship
I_{Ca2+}	CRAC current
I_{Na+}	sodium current in sodium divalent free solution
ID	inhibitory domain
IH	inhibitory helix
IP3	inositol-triphosphate
K^{+}	potassium ion
Kir	inward-rectifier potassium channels
L1-L3	Loop 1-3 (of Orai channels)
L-type	long-lasting Calcium channel
LRET	luminescence resonance energy transfer
MD simulations	molecular dynamics simulations
Na^{+}-DVF	sodium divalent free
nEF	non-canonical EF hand
nAChR	nicotinic acetylcholine receptors
NMR	nuclear magnetic resonance
OASF	Orai – activating small fragment
Orai 1-3	Orai proteins (also as O1-3)
P/S	proline/serine
PIP_2	phosphatidylinositol 4,5-bisphosphate

PM	plasma membrane
RASSF4	Ras association domain family member 4
RNAi	RNA interference
SAM	sterile α-motif
S	signal peptide
SCDI	slow calcium dependent inactivation
SCID	Severe Combined Immune Deficiency
SOAP	STIM – Orai association pocket
SOAR	STIM – Orai activating region
SOC	store operated channel
SOCE	store-operated calcium entry
SPCA2	Secretory Pathway Ca^{2+}-ATPase
STIM	stromal interaction molecule
TM	transmembrane helices
TRP	transient receptor potential ion channel (C-canonical, M-melastatin, V-vallinoid)
WT	wild-type

23.1 Introduction

Ca^{2+} is a very important second messenger in eukaryotic cells. Sustaining Ca^{2+}-homeostasis within the cell is indispensable for immune cell function and activity of neurons. Perturbations in Ca^{2+} levels can lead to severe diseases such as cancer or immune deficiencies [1, 2]. In many cell types, one well-known Ca^{2+} entry pathway is the Ca^{2+} release activated Ca^{2+} (CRAC) channel [3]. This pathway is composed of two molecular key players STIM1, which belongs to the stromal interaction molecule (STIM) family (STIM1 and STIM2) and Orai1, which belongs to the Orai family (Orai1, Orai2, Orai3). Both of these have been identified via a systematic RNA interference (RNAi) screen [4]. Intact communication of STIM and Orai proteins maintains proper cell function, especially of immune cells and neurons, while abnormal up- or downregulation of these proteins can lead to defects in signaling pathways [5]. Additionally, several mutations in STIM1 and Orai1 are currently known to lead to either gain- [6] or loss-of-function [7] and have been associated with diseases like Severe Combined Immune Deficiency (SCID), Stormorken Syndrome and tubular aggregate myopathy, highlighting their clinical relevance [2, 8]. A list of most currently known STIM and Orai mutants and their functional effects are summarized in Tables 23.1 and 23.2, which also states whether they are disease-related.

Upon binding of IP_3 to receptors in the membrane of the endoplasmic reticulum (ER), Ca^{2+} is released from the ER, which initiates the activation of STIM1 [3]. STIM1 is a single transmembrane spanning protein within the ER membrane that senses the ER-lumenal Ca^{2+} concentration via its N-terminal EF-hand motif. It is uniformly distributed within the ER membrane in the resting state [9]. Once

Table 23.1 Mutations in STIM1

Mutation	Domain	Orai coupling	Current	Related disease	References
H72Q	EF-hand	Yes	CONSTITUTIVE	Tubular aggregate myopathy	[218]
D76A	EF-hand	Yes	Constitutive		[11]
N80T	EF-hand	Yes	Constitutive	Tubular aggregate myopathy	[219]
G81D	EF-hand	Yes	Constitutive	Tubular aggregate myopathy	[220]
D84G	EF-hand	Yes	Constitutive	Tubular aggregate myopathy	[218]
E87A	EF-hand	Yes	Constitutive		[23]
L96V	EF-hand	Yes	Constitutive	Tubular aggregate myopathy	[219]
F108I/L	EF-hand	Yes	Constitutive	Tubular aggregate myopathy	[219]
H109R/N	EF-hand	Yes	Constitutive	Tubular aggregate myopathy	[218]
I115F	EF-hand	Yes	Constitutive	Tubular aggregate myopathy; York platelet syndrome	[221, 222]
E136X	SAM	No	Inactive	Combined immune deficiency	[223]
P165Q	SAM	Yes	Store-operated	Late-onset immunodeficiency	[224]
I220W	TM	Yes	Constitutive		[40]
C227W	TM	Yes	Constitutive		[40]
L248S	CC1	Yes	Constitutive		[86]
L251S	CC1	Yes	Constitutive		[86]
R304W	CC1	Yes	Constitutive	Stormorken Syndrome	[8]
Y316A	CC1	Yes	Constitutive		[87]
E318/319/320/322A	CC1	Yes	Constitutive		[225]
I364A	CC2	Yes	Store-operated (enhanced)		[114]
A369K	CC2	Yes	Constitutive		[74]
A376K	CC2	Yes	Constitutive		[74]
A380R	CC2	Yes	Constitutive		[16]
K382/384/385/386E	CC2	No	Inactive		[16]
F394H	CC2	Reduced	Inactive		[52]
R426L	CC3	No	Inactive		[86]
R429C	CC3	No	Inactive	Combined immune deficiency	[97]

STIM1 has been activated, it homomerizes and oligomerizes into ER-PM-junctions, where it can bind to and activate Orai1 via the cytosolic C-terminus [2, 10–12]. Orai1 represents a highly Ca^{2+} selective pore in the plasma membrane [12, 13]. A milestone was reached in 2012, when Hou et al. [14] managed to crystallize the Orai channel of *Drosophila melanogaster* (dOrai), revealing the hexameric stoichiometry of this channel complex. Recently, the structure of a dOrai mutant representing a potential open Orai state was also resolved [15]. Furthermore, structural resolutions

Table 23.2 Mutations in Orai1

Mutation	Domain	Pm-localization	STIM1 coupling	Current	Related disease	References
L74I	N-term.	Yes	Yes	Store-operated (enhanced)		[113]
Y80S	N-term.	Yes	Yes	Store-operated (enhanced)		[113]
L74/W76E/ R/S	N-term.	Yes	Yes	Store-operated (reduced)		[64]
K85E	N-term.	Yes	Reduced	Inactive		[109]
R91W	TM1	Yes		Inactive	SCID	[2]
S97C	TM1	Yes		Constitutive	Tubular aggregate myopathy	[226]
G98C/D/P	TM1	Yes	Yes	Constitutive		[69, 156]
G98R	TM1	No	No	Inactive	CID; autoimmunity; EDA	[227]
G98S	TM1	Yes		Constitutive	Tubular aggregate myopathy	[71]
F99C/G/M/ S/T/Y/W	TM1	Yes	Yes	Constitutive		[69]
V102A/C/ G/S/T	TM1	Yes	Yes	Constitutive		[67]
V102I/L/M/V	TM1	Yes	Yes	Store-operated		[67]
A103E	TM1	No	No	Inactive	Immunodeficiency	[228]
E106Q	TM1	Yes	Yes	Inactive		[154]
V107M	TM1	Yes		Constitutive	Tubular aggregate myopathy	[71]
H134S/A/C/ T/V/Q/E/M	TM2	Yes	Yes	Constitutive		[68, 73]
H134K/W	TM2	Yes	Yes	Inactive		[73]
A137V	TM2	Yes		Constitutive	Colorectal tumor	[68, 229]
L138F	TM2	Yes		Constitutive	Tubular aggregate myopathy	[72]
M139V	TM2	Yes		Constitutive	Stomach carcinoma	[68, 229]
S141C	TM2	Yes		Constitutive		[73]
S159L	Loop2	Yes		Constitutive	Uterine carcinoma	[68, 229]
L174D	TM3	Yes	Reduced	Inactive		[65]

(continued)

Table 23.2 (continued)

Mutation	Domain	Pm-localization	STIM1 coupling	Current	Related disease	References
W176C	TM3	Yes	Yes	Constitutive		[162]
A177D	TM3	Yes		Constitutive		[68, 229]
V181SfsX8	TM3	No	No	Inactive	CID; autoimmunity; EDA	[227]
G183A	TM3	Yes		Inactive		[162]
G183D	TM3	No	No	Inactive	Glioblastoma	[68, 229]
T184M	TM3	Yes	Yes	Store-operated	Tubular aggregate myopathy	[71]
F187C	TM3	Yes		Constitutive		[73]
E190C	TM3	Yes	Yes	Constitutive		[73]
E190Q	TM3	Yes		Reduced		[13]
L194P	TM3	No	No	Inactive	CID; autoimmunity; EDA; immunodeficiency	[227, 228]
A235C	TM4	Yes	Yes	Constitutive		[73]
S239C	TM4	Yes		Constitutive		[73]
G247S	TM4	Yes		Constitutive	Neck carcinoma	[68, 229]
F250C	TM4	Yes		Constitutive		[73]
P245L	TM4	Yes	Yes	Constitutive	Stormorken-like syndrome	[8]
L273S	C-term.	Yes	No	Inactive		[89]
L273D	C-term.	Yes	No	Inactive		[127]
L276D	C-term.	Yes	No	Inactive		[230]

of STIM1 N- and C-terminal fragments as well as an interacting complex formed by C-terminal fragments of STIM1 and Orai1 are currently available [16, 17]. This structural data together with functional and simulation studies improve our understanding of the STIM/Orai coupling and activation mechanism.

23.2 Composition and Structure of the Molecular Key Players of CRAC Channels

23.2.1 Structure of STIM

The STIM protein family, includes STIM1 and STIM2, two isoforms which share ~61% sequence identity [18, 19]. They are expressed in the endoplasmic reticulum [9, 11, 20, 21] and, at lower levels, in the plasma membrane [19, 20, 22]. STIM1 located in the plasma membrane has been suggested to control the extent of store-operated Ca^{2+} entry [23]. The activity of arachidonic acid regulated channels (ARC) has been proposed to solely depend on plasma membrane resident STIM1 [24–26]. According to recent reports, STIM proteins are also expressed in the acidic stores of lysosome-related organelles and the dense granules of the human platelets [27–29]. However, their roles there have so far remained elusive. In this review, we focus particularly on the role, function and structure of STIM proteins expressed in the ER, which are essential for the activation of CRAC channels [30].

The family of STIM proteins is further enriched in splice variants of STIM1 (STIM1L) and STIM2 (STIM 2.1 or STIM2β, STIM 2.2 or STIM2α, STIM2.3) [31–33] (see sequence alignment – Fig. 23.1).

Briefly, key domains in the STIM proteins (Fig. 23.2a) are the N-terminus embedded in the ER lumen, containing the Ca^{2+} – sensing region, a single TM spanning region of ~20-amino acids and the long cytosolic C-terminus, which binds to Orai channels in the plasma membrane [34]. Whereas the N-terminus of STIM is well conserved, the C- terminus is relatively varied among diverse species [35]. So far, only one luminal and two different C-terminal portions of STIM1 have been crystallized [16, 17, 36, 37], while a structural resolution of full-length STIM1 is still lacking.

23.2.2 STIM1

The Ca^{2+}-sensor protein STIM1 is composed of 685 amino acids (Fig. 23.2a) including the ER signal peptide (aa 1-22), a luminal EF hand (a canonical aa 63-96 and a non-canonical aa 97-128 EF hand), a sterile α-motif (SAM aa 132-200) followed by an α-helical TM domain (aa 212-234) and the C-terminus (aa 238-685). The first third of the cytosolic segment includes the three highly conserved

Fig. 23.1 Sequence alignment of STIM isoforms

Fig. 23.1 (continued)

coiled-coil (CC1-CC3) helices (aa 238-437), CC1 aa: 238-343, CC2 aa: 345-391, CC3 aa: 393-437. Afterwards, the inhibitory domain (aa 470-491), containing the CRAC modulatory domain (aa 475-483), a proline/serine-rich (aa 600-629) and a positively charged lysine-rich region (aa 672-685) follow (Fig. 23.2a).

The structure of the N-terminal Ca^{2+} sensor, the STIM1 EF-SAM complex has been resolved via NMR in the Ca^{2+}-bound state [37]. The EF hand domain consists of two EF hand motifs, a canonical and a non-canonical one. They both possess typical helix-loop-helix structures, α1-loop1-α2 for the canonical and α3-loop2-α4 for the non-canonical (Fig. 23.2b, left) motif, respectively. While the canonical EF hand motif coordinates a single Ca^{2+} ion, the non-canonical one lacks this ability and contributes to structural stabilization of the canonical EF hand [26, 37]. The canonical EF hand includes several negatively charged residues that have been proposed to contribute to Ca^{2+} binding [36] (Fig. 23.2b, left).

The EF hand domain is linked to the SAM domain via a short helical structure. The SAM region forms a five α-helix bundle structure (Fig. 23.2b, left) and represents another essential region of the STIM1 protein, which is vital for the regulation of store-operated Ca^{2+} entry [16, 26]. Deletion of the SAM domain has been shown to alter inducible punctae formation [38].

The EF-hand and SAM domains form a complex via hydrophobic interactions, under resting conditions. Here, two hydrophobic amino acids L195 and L199, positioned within the last α-helical segment of the SAM domain, couple to the hydrophobic cleft of the EF-hand domain [26, 37].

The TM domain of STIM1 links the EF-SAM domain to STIM1 C-terminus, in order to enable signal transmission from the N- to the C-terminus [39]. This helical portion includes three glycines (G223, G225, G226) which provide it with

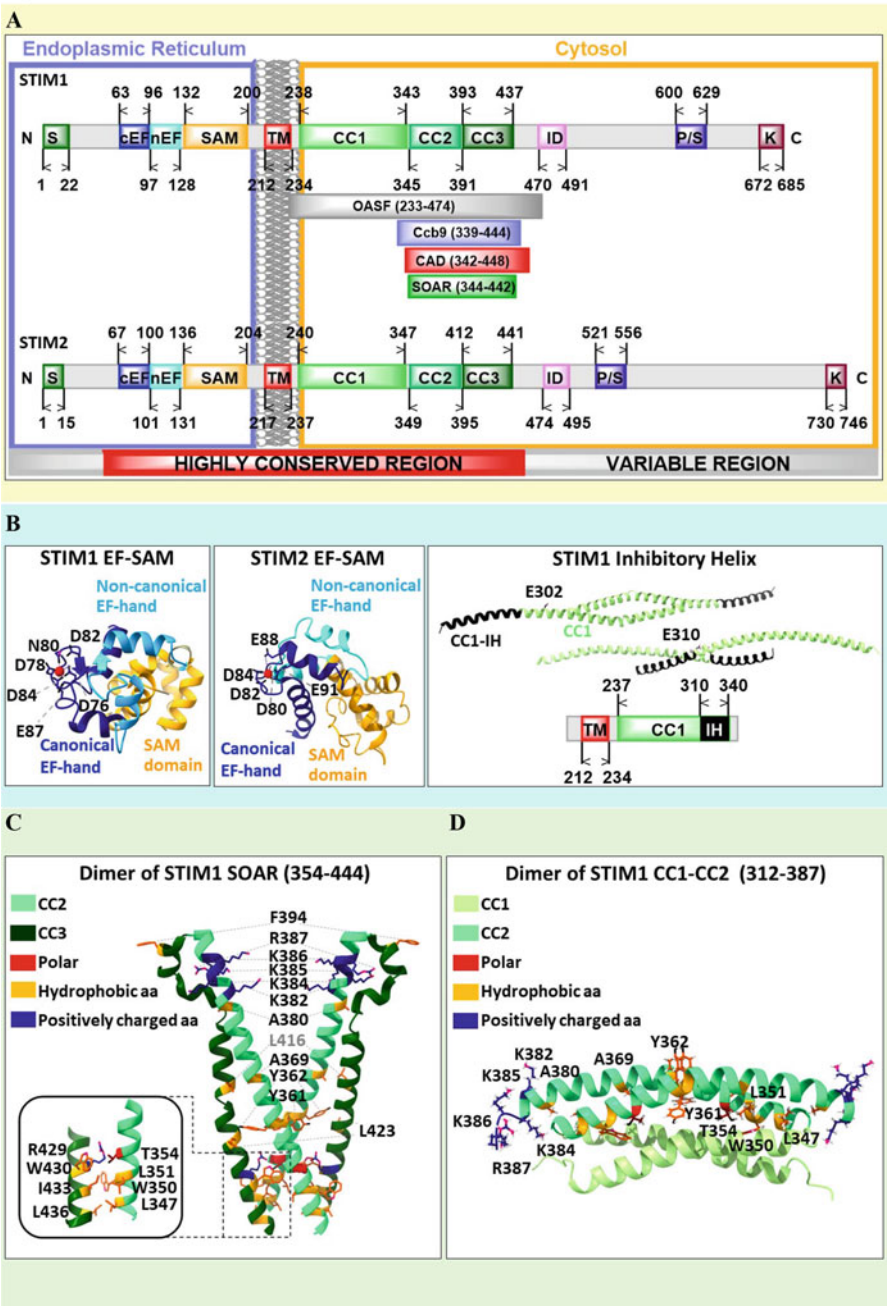

Fig. 23.2 Stromal interaction molecule 1 and 2 (STIM1, STIM2) (**a**) Scheme showing a comparison of a full-length human STIM1 (top) and STIM2 (bottom) with respect to regions critical for the regulation of the STIM1/Orai1 signaling cascade (upper part). Important fragments, such as

the flexibility required for conformational changes upon STIM1 activation [40]. Structural alterations will be addressed in more detail in the following sections.

STIM1 C-terminus has been shown to include minimal fragments such as the Orai1 activating small fragment: OASF (aa 233-474) [41], Ccb9 (aa 339-444) [42], the CRAC-activating domain: CAD (aa 342-448) [43] and the STIM Orai activating region: SOAR (aa 344-442) [44], which is sufficient to activate Orai channels. Structural predictions have revealed that the long putative CC1 domain contains three α-helical regions $CC1_{\alpha1}$ (aa 238-271), $CC1_{\alpha2}$ (aa 278-304), $CC1_{\alpha3}$ (aa 308-337), respectively [45]. Currently structural resolutions of two distinct portions of STIM1 C-terminus are available: a STIM1-C-terminal, SOAR-like fragment aa 354-444 [17] (Fig. 23.2c) and a SOAR overlapping fragment aa 312-387 (Fig. 23.2d) [16]. Both fragments incorporate parts of STIM1 CC2 (aa: 345-391) and CC3 (aa: 393-437) that are supposed to be critical for oligomerization of STIM1 proteins, coupling to and activation of CRAC channels [41]. It is noteworthy that both structures of STIM1 C-terminal fragments reveal a dimeric assembly, while the two monomers assemble in an antiparallel manner with a cross point at residue Y361 (Fig. 23.2c, d). Within the crystal structure of the SOAR-like fragments arranged as dimers, the two monomers together exhibit an overall V-shaped conformation (Fig. 23.2c). The structure of each monomer resembles the capital letter "R", that is constituted by four α-helices $S_{\alpha1}$-$S_{\alpha4}$ ($S_{\alpha1}$ (aa 345-391), $S_{\alpha2}$ (aa 393-398), $S_{\alpha3}$ (aa 400-403) and $S_{\alpha4}$ (aa 408-437)). Within the NMR structure of the SOAR dimer, each monomer forms a bend between the two helical portions $CC1_{\alpha3}$ and CC2 [16, 17] (Fig. 23.2d).

The inhibitory (aa 470-491) [46] or CRAC modulatory domain (aa 474-485) [47] contains seven negatively charged residues which are critical for the maintenance of typical biophysical characteristics of CRAC channels, as explained later in this review.

Downstream of the C-terminal coiled-coil regions STIM1 possesses a Ser/Pro-rich region (aa 600-629) which is important for proper targeting of STIM1 into clusters close to the cell membrane upon Ca^{2+} store depletion [48].

Fig. 23.2 (continued) OASF, Ccb9, CAD and SOAR are further represented as insets. (**b**) The left and middle panels show high resolution EF-SAM domains structures of human STIM1 and STIM2, each loaded with a Ca^{2+} ion (red spheres), respectively. The residues with proposed Ca^{2+} binding ability are highlighted. The right panel displays the portion of the STIM1 CC1- inhibitory helix with the critical residues highlighted. (**c**) The crystallographic structure of the STIM1 SOAR dimer, forming a V-shape, consists of CC2 and CC3 domains. Each monomer resembles the capital letter ‚R". Residues that represent potential interaction sites within the dimer and those mediating coupling to Orai1 are highlighted. Left inset: Magnified view of amino acids involved in dimer interactions between the N-terminal portion of the first SOAR monomer and the C-terminal portion of the second SOAR monomer. (**d**) The NMR structure consists of a dimer of STIM1 $CC1_{\alpha3}$-CC2 monomers that couple in an antiparallel manner. Each monomer bends with a sharp kink between the two coiled-coil domains

Furthermore, a lysine-rich region at the end of STIM1 C-terminus [34, 49] also participates in correct STIM1 targeting. However, it is dispensable for CRAC channel activation [50]. It resembles a phosphatidyl inositol-4,5-bisphosphat (PIP_2) binding domain [50, 51]. The role of PIP_2 in STIM1 regulation will be explained in the section entitled "Lipid mediated regulation of the STIM1/Orai1 complex.".

23.2.3 STIM2

The STIM2 protein contains 746 amino acids (Fig. 23.2a) and critical domains are analogous to those for STIM1 as described above. Briefly, this protein includes the ER signal peptide (aa 1-15), a luminal EF hand (a canonical aa 67-100 and a non-canonical aa 101-131 EF hand) (Fig. 23.2b, middle), a sterile α-motif (SAM aa 136-204) followed by an α helical TM domain (aa 217-237) and the large cytosolic part, which includes the three coiled-coil (CC1-CC3) helices (aa 240-441; CC1 aa: 240-347, CC2 aa: 349-395, CC3 aa: 412-441), a proline/serine-rich (aa 521-556) and a positively charged lysine-rich region (aa 730-746).

Despite the many similarities and ∼61% sequence identity of STIM1 and STIM2 isoforms, STIM2 possesses several notable differences compared to STIM1, providing evidence for distinctions in its structure and function.

STIM1 and STIM2 EF-SAM domains possess significant differences, despite having a sequence similarity of ∼85%. Specifically, the SAM domain of STIM2 (Fig. 23.2b middle), in contrast to that of STIM1, consists of an additional third non-polar residue V201 that packs into its hydrophobic cleft. Thus, the hydrophobic core of STIM2 – unlike STIM1 – shows not only an enhancement in size but also in stability in the presence of bound Ca^{2+}. Additional support for the stability of STIM2 is provided by the existence of a possible ionic bond between D200 in the SAM domain and K103 in the EF hand domain. Thus, due to the presence of more stable hydrophobic and electrostatic interactions, the STIM2 SAM domain oligomerizes more efficiently than that in STIM1 [26, 37].

A comparison of STIM1 and STIM2 C-termini exhibits considerable differences within the last third, termed as variable region. Homology modelling of the STIM1 C-terminal SOAR region predicts an almost identical structure. Nevertheless, one main difference represents the non-conserved residue F394 in SOAR of STIM1 [52], corresponding to L398 in STIM2. Chimera and single point mutation studies by Wang et al. [52] revealed clear functional differences in the dependence of the introduced residue at this position, which will be outlined in detail in the section entitled "Activation mechanisms of the STIM1/Orai signaling machinery".

The lysine-rich region at the very end of STIM2 is notably larger than that of STIM1 and possesses an enhanced affinity for PIP_2, as explained in more detail in the section entitled "Lipid-mediated regulation of the STIM1/Orai1 complex" [51].

23.2.4 Orai Proteins

The Orai protein family includes three highly conserved isoforms, Orai1-3, expressed in the plasma membrane. Orai, as the pore-forming subunit of CRAC channels, is unique among the huge diversity of Ca^{2+} ion channels due to its high degree of Ca^{2+} selectivity as well as its hexameric structure. [2, 12, 14, 53] In native cells, Orai proteins are assumed to form homo- as well as heteromeric assemblies [54, 55]. Each Orai subunit is composed of four transmembrane (TM) domains that are connected via one intracellular and two extracellular loops and flanked by a cytosolic N- and C-terminal strand (Fig. 23.3a, b) [56–58]. The TM1 segment (aa 92-106) is fully conserved among the protein family, while TM2 (aa 118-140), TM3 (aa 174-197) and TM4 (aa 236-258) share ~81-87% sequence identity. Flanking strands and connecting loops possess major isoform specific structural differences (Fig. 23.2) [59]. Specifically, the cytosolic N- (aa 1-90) and C-terminal (aa 265-301) strands show only 34% and 46% sequence identity, respectively [60]. Furthermore, especially the cytosolic extension of TM2 has been suggested as longer in Orai3 than in Orai1. Thus, Orai3 in contrast to Orai1, contains a shorter flexible loop2 portion connecting TM2 and TM3 [61].

In 2012, Hou et al. [14] published the crystal structure of *Drosophila melanogaster* dOrai, that exhibits a hexameric stoichiometry (Fig. 23.3c). In accord with the dOrai crystal structure, the results of concatemeric studies confirmed that the functional state of human Orai1 represents a hexameric assembly [62, 63]. The Orai pore is formed by the six TM1 domains arranged as a ring in the center of the channel complex. Its detailed composition (Fig. 23.3d) is explained in the section entitled "Ca^{2+} ion conduction pathway". The other TM regions, TM2 – TM4 are arranged around the pore in two rings, whereas TM2 and TM3 form the second and TM4 the third ring. The TM1 domains extend further into the cytosol [14] culminating into a conserved, helical region, that has been termed the so-called ETON (Extended TM Orai1 NH_2-terminal; aa 73-90 in hOrai1) region [64] (Fig. 23.3d, e) for hOrai homologues. It is approximately 20 Å long and includes the last 20 amino acids of the Orai N-terminus. Both, TM2 and TM3 have been shown to expand into the cytosol by a couple of helical turns [14]. TM4 is divided by a kink at P245 in hOrai (corresponding to P288 in dOrai) into two regions. Helical extensions of TM4 exposed to the cytosol, represent the Orai C-termini and are connected to TM4 via a highly conserved hinge region (aa 261-265). Within a hexamer, three dimers of Orai subunits exhibit antiparallel oriented C-termini, which respectively form an angle of 152° [14, 65]. Thereby, they capture a belt-like assembly surrounding the intracellular side of the channel [15]. The structural properties of the Orai C-termini provide in addition to the sixfold, a threefold symmetry to the Orai channel. (Fig. 23.3c). Unfortunately, structural resolution of the more flexible Orai segments including the intracellular, both extracellular loops and approximately the first ~70 residues of the N- terminal strands are still missing. Nevertheless, flexible loop portions have been integrated into a hOrai1 model that is based on the dOrai X-ray structure [66].

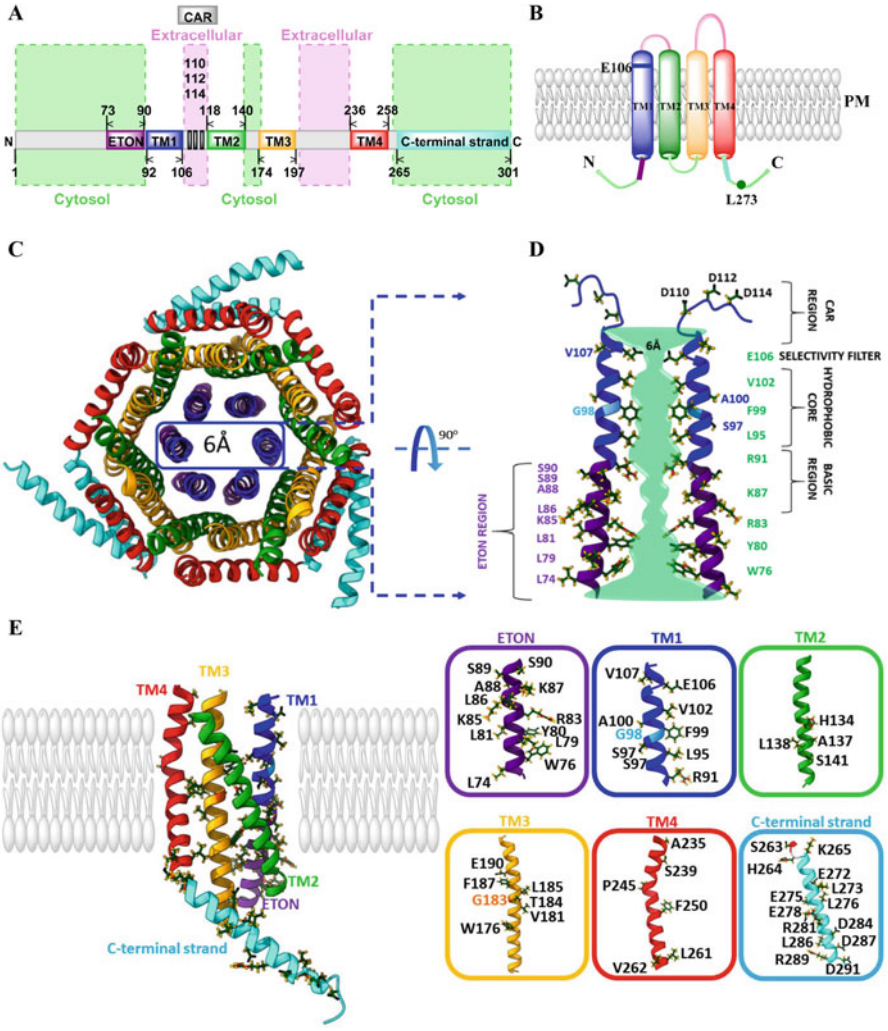

Fig. 23.3 Orai1 channel (**a**) Scheme depicting the full-length human Orai1 channel with highlighted regions and residues that are essential for Orai1 function. (**b**) Scheme of overall full-length human Orai1 subunit structure representing distinct extracellular, cytosolic and transmembrane-spanning regions. The selectivity filter of the channel, E106, is depicted as a blue line; the residue L273 that causes impaired STIM1 binding upon single point mutation is shown as a green circle. (**c**) The cartoon shows the Orai1 channel possessing a hexameric assembly based on the *Drosophila* dOrai X-ray structure. While the inner ring surrounding the pore is formed by TM1, other TM domains within the six subunits are constituted into concentric rings around the pore. (**d**) The cartoon displays two opposite TM1 domains with the cytosolic and extracellular helical extension and highlights the essential residues lining the pore of the channel depicted in teal. Residues of the N-terminal region, ETON, are depicted in purple. On the C-terminal side is the CAR region with its residues depicted in black. The selectivity filter, hydrophobic core and basic region of the pore are highlighted. (**e**) The cartoon of one Orai1 subunit with four TM segments along with N- and C- terminal helices depicted in distinct colors (same as applied within **a**–**d**) displays the residues in more detail that are known to manifest proper Orai1 channel function and maintain the closed state of the Orai1 channel

Fig. 23.4 Sequence alignment of Orai isoforms

It is noteworthy that several residues (Fig. 23.4e) within Orai TM domains have recently been reported as important for maintaining the entire channel complex in the closed state, since their single or multiple point mutations have resulted in constitutively active channels. These are known as gain-of-function mutations [65, 67–73]. One recently described gain-of-function point mutant Orai1 H134A (dOrai H206A) [68] has been utilized for further crystallographic studies representing one open conformation of the channel [15], in contrast to the potential quiescent state of the dOrai structure published in 2012 [14].

In accordance with the dOrai crystal structure, the novel dOrai H206A (corresponds to H134A in hOrai1) mutant structure exhibits also a hexameric assembly [15]. Main conformational alterations have been observed in the basic region of the pore as well as the TM4 regions. Unlike to the dOrai closed pore, the open state of the dOrai mutant displays an extension of approximately 10Å at dOrai K159 (corresponding to K87 in hOrai1) within the basic pore region. While in the quiescent state TM4 is separated into two regions by a kink at P288 (corresponds to P245) and connected to the C-terminus via another kink, the so-called nexus (in hOrai1 aa 261-265) [65], the open state of the Orai mutant exhibits a straight helix formed by the two TM4 segments and the C-terminus thus, expanding approximately 45Å into the cytosol [15].

It is important to note that the Orai crystal structures available so far display the channel's potential open and closed conformations only in the absence of STIM1. However, physiologically, Orai channels are activated via their coupling to STIM1, which potentially leads to a distinct conformation that differ from the structure of specific gain-of-function point mutants. Thus, the structural resolution of a STIM1-Orai1 complex would represent the ultimate goal to provide insights in Orai conformational changes from the closed to the open state at a more physiological level.

23.3 Activation Mechanisms of the STIM1/Orai Signaling Machinery

23.3.1 STIM1 in the Resting State

The STIM1 conformation in the resting state is controlled by STIM1 N-terminal, transmembrane and C-terminal domains, which is explained in detail in the following. Inactive STIM1 proteins exist as dimers [41, 74] that are uniformly distributed throughout the ER membrane. They are stably connected to microtubules [75, 76] and their average diffusion velocity is 0.22 ±0.07 μm/s [75].

In the quiescent state, the EF-hand domain at the luminal N-terminus of STIM1 binds Ca^{2+} via negatively charged residues (aspartates and glutamates) [77]. Mutations of some of these residues (D76A, D76/78N, E87Q) lead to the loss of Ca^{2+} binding ability and, hence, to constitutive STIM1 activity [9, 11, 78]. The resting conformation of the EF-SAM domain represents a compact structure consisting of mainly α-helices (Fig. 23.2b). They are stabilized by hydrophobic interactions between the EF-hand and the SAM domain (see previous section) [36]. Several studies have revealed that the EF-SAM domain exists as a stable monomer in the quiescent state, while it forms dimers upon dissociation of Ca^{2+}, findings that are in line with STIM1 oligomerization upon store-depletion [36, 37]. In contrast, Huang et al. [77] have shown that the EF-hand domains isolated from STIM1 tend to form dimers already in the presence of Ca^{2+}, in accord with the STIM1 dimeric state under resting conditions.

STIM2 already leaves the quiescent state upon smaller changes in the luminal Ca^{2+} concentration than STIM1, although Orai channel activation by STIM2 is slower compared to STIM1 [37]. This underlies differences in sequence and structure of the EF-SAM domain of STIM1 and STIM2 that lead to distinct affinities for Ca^{2+} with a K_d of 200 μM and 500 μM for STIM1 and STIM2, respectively [36, 37, 79]. While the canonical EF-hand of STIM2 possesses a lower Ca^{2+} affinity than that of STIM1, hydrophobic and electrostatic interactions between the EF-hands and the SAM domains are more stable in STIM2 than in STIM1. Thus, the STIM1 EF-SAM domain undergoes faster unfolding and aggregation upon dissociation of Ca^{2+} than that of STIM2 [26, 37]. Furthermore Subedi et al. [80] recently revealed that STIM2 is already located in ER-PM junctions in the resting state and assists STIM1 in unfolding and coupling to Orai1 upon minimal store-depletion. In addition, a splice variant STIM1L has been shown to be located in the ER-PM junctions in the resting state, which has been found to underlie a 106 aa long extension in its C-terminus. The latter enables the anchoring of STIM1L to the cytoskeleton [81].

In addition to the EF-SAM domain, the conformation of the TM domains also controls the resting state of STIM proteins. Chemical crosslinking and computational modeling have revealed that the TM domains of two STIM1 proteins mainly interact at their C-terminal portions (aa 221-232) whereas their N-terminal parts (aa 212-220) are kept apart via a crossing angle of approximately 45° in the resting state [40] (Fig. 23.5a). A tryptophan-scanning approach was used by Zhou et al. [40]

to identify two residues (I220, C227) within the transmembrane domain that keep STIM1 in the closed state, as their mutation (I220W, C227W) leads to constitutive STIM1 activity.

The dimeric state of STIM1 C-termini under resting conditions [38, 41, 82–85] is mediated by CAD/SOAR and further supported by CC1 [74]. Based on the crystal structure of human SOAR, STIM1 dimer formation is maintained via hydrophobic, hydrogen bond and stacking interactions between C-terminal residues of one SOAR (R429, W430, I433, L436 in α4) and N-terminal residues of another one (L347, W350, L351, T354, Y361 in α1). Their importance is evident from the results of mutagenesis studies, as interference with the dimer formation at those positions impairs the SOAR binding to Orai. [17] Moreover, the NMR structure of the overlapping SOAR domain resolves the interactions of $CC1_{\alpha 3}$ (aa 320-331) and CC2 (aa 355-369) within the monomers, respectively [16] (Figs. 23.2c, d and 23.5a). These NMR data provide valuable information on the SOAR structure. Nevertheless, one still has to keep in mind that the STIM1 fragment (aa 312-387), which has been structurally resolved, is unable to bind to and activate Orai1 [41].

The cytosolic part of STIM1 is also involved in controlling the inactive state via an intramolecular clamp between CC1 and SOAR (Fig. 23.5a), particularly between $CC1_{\alpha 1}$ and CC3 [45, 86]. Single point mutations within $CC1_{\alpha 1}$ (L248S, L251S, L258S) and CC3 (L416S, L423S) engineered in a double labeled OASF fragment resulted in decreased FRET values, indicating that these residues are involved in maintaining the tight conformation of STIM1 [83, 86]. Additionally, Y316 in CC3 has been shown to contribute to the inactive state of STIM1, as a mutation to an alanine (Y316A) leads to STIM1 cluster formation without store-depletion [87]. In contrast, mutating the arginine at position 426 in CC3 to a leucine (R426L) strengthened the CC1-CC3 clamp, thereby stabilizing the quiescent state of STIM1 [86]. Moreover, four other residues, L258 and L261 in $CC1_{\alpha 1}$ and V419 and L416 in CC3 have been proposed to support this intramolecular clamp, keeping STIM1 in the closed state [40].

The gain-of-function point mutant STIM1 R304W, which has been associated with Stormorken Syndrome, suggests that residue R304 in CC1 supports the maintenance of STIM1 in the closed state [8]. A recent study on this mutant revealed that this specific point mutation induces an extension of the $CC1_{\alpha 2}$ helix and lead to increased CC1 homomerization [88], which is in line with the observed destabilizing effect of $CC1_{\alpha 2}$ leading to an open state as mentioned in the next section.

In contrast to STIM1, the CC1-CC3 interaction within STIM2 has been found to be much weaker, thus providing one potential explanation for the observed clustering of STIM2 within the ER-PM junction in unstimulated cells [80].

In summary, several parts of STIM1 are involved in keeping the protein in the resting state, including the EF-hand domain as long as Ca^{2+} is bound, specific residues within the crossing TM domains of a STIM1 dimer as well as the C-terminus via the intramolecular clamp between CC1 and SOAR.

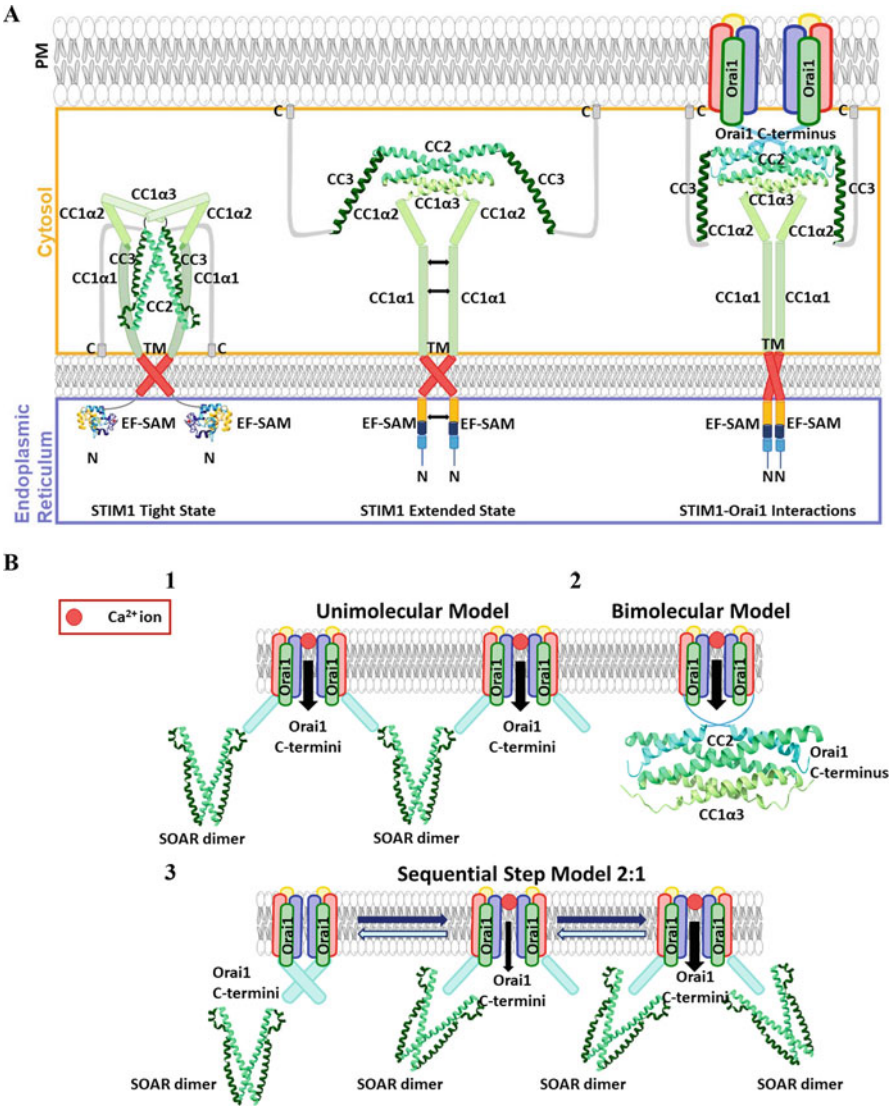

Fig. 23.5 Hypothetical model of the binding of STIM1 to Orai1 (**a**) As long as Ca^{2+} ions are bound to the EF-hand of STIM1, the latter stays in an inactive, tight state (left part). However, upon store depletion, when the EF-hand domain of STIM1 loses the Ca^{2+} ion, conformational changes are induced, and STIM1 proteins reassemble into the active, extended state (middle part). Subsequently, the crossing angle of the STIM1 TM helices is altered and the inhibitory, intramolecular clamp between CC1α1 and CC3 is released, which finally results in a STIM1 interaction with the Orai channel in the plasma membrane (right). (**b**) Three different stoichiometries of the functional STIM1-Orai1 complex have been proposed (according to

23.3.2 STIM1 Oligomerization and Conformational Changes Upon Activation

STIM1 activation is initiated upon store-depletion and induces conformational changes in STIM1 that propagate from the N-terminus via the TM domain to the C-terminus. This leads to STIM1 oligomerization, punctae formation and finally coupling to and activation of Orai. Initial studies employing FRET microscopy have revealed an increase in the STIM1 homomeric interaction following store-depletion which decreases upon store-refilling [50, 89]. It is worth mentioning, that STIM1 oligomerization occurs prior to STIM1-Orai1 coupling [50].

The first step in the STIM1 activation cascade is the dissociation of the EF-hand bound Ca^{2+} ion upon store-depletion, which leads to the structural destabilization of the EF-SAM motif [79, 90]. Hydrophobic regions become exposed, leading to the dimerization of neighboring STIM1 N-termini. In accordance with this observation, STIM1 mutants lacking the entire C-terminus have been reported to form multimers upon the loss of Ca^{2+} binding [74]. Oligomerization upon Ca^{2+} store-depletion is in line with the constitutive punctae formation seen in the STIM1 EF-hand mutants (D76A, E87A), that are defect in Ca^{2+} binding [9, 23]. In addition, oxidative stress has been hypothesized to reduce the Ca^{2+}-binding affinity of STIM1, as native CRAC currents have been shown to activate in the presence of micromolar concentrations of H_2O_2 [91–94].

Structural rearrangements within the STIM1 N-terminus lead to conformational changes in the TM domains, allowing the transmission of the activation signal to the C-terminus. STIM1-TM domains have been found to possess distinct conformations in the closed versus the open state. NMR and LRET experiments have revealed that store-depletion decreases the crossing angle of interacting TM regions thereby bringing the N-terminal parts (aa 214-220) closer together [40]. In line with this observation, cysteine crosslinking experiments have shown that the TM helices

Fig. 23.5 (continued) [16, 217]). (1) In the unimolecular SOAR-Orai coupling model (STIM1-Orai1 1:1 ratio) one of the SOAR monomers of a SOAR dimer interacts with a single Orai1 channel subunit and induces gating (upper part left). The second monomer of the dimer binds to another Orai channel, thus enabling clustering of Orai channels. (2) Bimolecular coupling model shows (STIM1-Orai1 1:1 ratio), based on the NMR [16] structure using isolated partial SOAR fragments and SOAR-coupling C-terminal strand of Orai, a dimer of STIM1 which binds to the crossing C-termini of two adjacent Orai1 subunits in the hexameric Orai1 channel, thus inducing gating (left). (3) The sequential step model shows, first, the resting state of the Orai channel which possesses the assembly with an antiparallel configuration of neighboring Orai1 C-terminal strands providing the binding site for a SOAR dimer (lower part, left). In the next step, Orai1 C-terminal strands extend towards the cytosol leading to only a partial pore opening (middle). Finally, the dissociated Orai1 C terminal strands of the partially active channel represent a new binding site for the SOAR dimer with a final 2:1 stoichiometry (right)

of two STIM1 proteins move closer together after store-depletion and undergo a change in the orientation towards each other, as the crosslinking of residues L216, S219, G223, G226, A230 and Q233, when mutated to a cysteine, has only been visible in the active state [40, 95]. Due to their high flexibility, three glycines (G223, G225, G226) within the transmembrane domain likely facilitate the conformational changes necessary to transmit the activation signal from the luminal side to STIM1 C-terminus [40, 96]. It is worth mentioning that STIM1 TM rearrangements are not only triggered by luminal Ca^{2+} but can also be governed by alterations in the C-terminus, as has been shown via the L251S mutation. The latter induces constitutive activity of STIM1 and already allows in the presence of Ca^{2+}a TM cysteine crosslinking pattern [95], as observed under wild-type conditions in the absence of Ca^{2+}. Thus, while the activation signal within STIM1 is transmitted from the N- to the C-terminus, conformational changes within STIM1 have been assumed to occur in a bidirectional manner.

The final step in the activation cascade of STIM1 represents the signal transmission from the TM domain to the C-terminus inducing conformational changes together with oligomerization. Here, one main step represents the release of the intramolecular clamp between CC1 and CC3, thereby exposing SOAR [40, 45, 83]. By labeling STIM1 fragments on both sides a reduction in intramolecular FRET/LRET has been observed upon the release of the intramolecular clamp either upon coupling to Orai1, single point mutations such as L248S, L251S, L258S or the deletion of CC1 domain [83, 86]. Along the same lines, ER-targeted CC1 domains are unable to couple to SOAR/CAD fragments when mutated (e.g. at L251S) [40, 45]. Moreover, while CC1 occurs as a monomer in solution and binds to CAD, artificially crosslinked CC1 fragments form dimers that exhibit impaired interaction with cytosolic CAD/SOAR [83] that is compatible with a di-/homomerization of the CC1 region and contributes to the switch into an extended conformation [83]. Additionally, FIRE (FRET-derived Interaction in a Restricted Environment) experiments have shown that $CC1_{\alpha 2}$ plays a destabilizing role, as the deletion of this region significantly delays the activation of Orai1 by STIM1 $\Delta CC1_{\alpha 2}$. Breakup of the CC1-CC3 clamp leads to enhanced CC1 homomerization and SOAR exposure, while CC3 is involved in formation of higher order STIM1 oligomers [16, 40, 41, 45, 83, 86]. Mutation of residue R429 in CC3 to a cysteine (R429C), associated with combined immune deficiency [97], does not affect the STIM1 transition to the active state, but reduces STIM1 oligomerization and its coupling to Orai1 [98]. A C-terminal region overlapping with CC3 (aa 421-450) forms the STIM1 homomerization domain (SHD), the deletion of which leads to drastically reduced STIM1 oligomerization and loss of Orai1 activation [41].

In contrast to STIM1, clustering of STIM2 is more pronounced, probably due to the more relaxed and open conformation of OASF in STIM2 than in STIM1. Herewith, STIM2 helps STIM1 to transit into the active state, thus enabling STIM1/Orai1 activation [80]. Furthermore, the accessory protein STIMATE, a

STIM-activating enhancer located in the ER membrane, has been found to interact with STIM1 CC1 in order to support the release of SOAR upon store-depletion [99].

A STIM2 splice variant, STIM2.1 has been found to couple to, but not gate Orai1, and it functions as a negative regulator for STIM1 and STIM2 wild-type. This inhibitory function arises due to an insertion of 8 aa in the CAD region of STIM2, which potentially interferes with stable CAD formation. [33]

In addition to Ca^{2+} dependent regulation of STIM1 function, STIM1 glycosylation sites within the SAM domain have been found to control its function depending on the properties of the inserted amino acids. Specifically, a STIM1 N131D N171Q mutation has been found to create gain-of-function, thus enabling not constitutive but faster Orai channel activation, suggesting that these mutations facilitate STIM1's transition from the closed to the open state. Intriguingly, this STIM1 DQ mutant reduced the amount of Orai protein in the cell. This suggests that an alternative mechanism leads to enhanced Orai activation, likely due to enhanced oligomerization rates or potentially increased STIM1 dimer fusion. [100]

Further phosphorylation sites in Orai1 possess regulatory roles. Specifically, the N-terminus includes two serines, S27 and S30, which, when mutated, enhance CRAC channel activation upon mutation. This suggests that protein kinase C (PKC) inhibits CRAC channel activation upon phosphorylation of these sites [101]. The residue Y361 in STIM1 CC2 has been found to be phosphorylated by the proline-rich kinase 2 upon store-depletion. Knocking out this phosphorylation site (Y361F) still leads to STIM1 punctae formation, but coupling to Orai is completely abolished [102]. Additional phosphorylation sites within the STIM1 C-terminus (S468, S668) regulate store-operated Ca^{2+} currents during meiosis and mitosis [20, 103, 104]. Furthermore, STIM1 has been reported to be regulated by the extracellular-signal-regulated kinases 1 and 2 (ERK1/2) [105], involving the phosphorylation of specific sites within the STIM1 C-terminal serine/proline-rich region.

In summary, upon store-depletion and dissociation of the Ca^{2+} ion from the STIM1 EF-hand domain, the activation signal is transmitted via the TM domain to the C-terminus. Subsequently, the intramolecular clamp between CC1 and CC3 in the C-terminus is released, thereby exposing SOAR, the binding domain for Orai. In addition, STIMATE, glycosylation sites and several phosphorylation sites are involved in the regulation of the STIM's active state.

23.4 STIM/Orai Coupling

Upon store-triggered conformational changes of STIM1, this Ca^{2+} sensor protein interacts with the pore forming CRAC channel component, Orai. In the following section, the main coupling domains within STIM1 and Orai that establish their assembly and activation will be explained in detail.

23.4.1 Main Coupling Domains Within STIM1

The STIM1 C-terminus located in the cytoplasm contains sites that are essential for direct coupling to Orai1. In the STIM1 C-terminus, OASF, SOAR, CAD or Ccb9 (Fig. 23.2a) are sufficient for Orai activation [41–44]. All of these fragments comprise the CC2 (aa 345-391) as well as parts of the extended CC3 (aa 393-450) domain, the latter including the STIM1 homomerization domain (SHD, aa 421-450) [41]. Park et al. [43] showed a direct interaction between CAD and Orai1. Additional studies with STIM1 C-terminal and Orai1 cytosolic fragments have revealed a strong interaction between CAD and Orai1 C-terminus and, a weak one with the N-terminus, and no interaction with the loop2 [43, 61, 64]. By employing a slightly longer Orai1 loop2 fragment, our recent study revealed interactions with a STIM1-C-terminal fragment [61].

The NMR structure of the so-called SOAP (STIM-Orai association pocket) clearly shows that two STIM1 C-terminal fragments (aa312-387) bind to two Orai C-termini in an antiparallel manner [16]. The residues involved in this association are L347, L351 of one CC2, Y362, L373 and A376 of the second CC2, but also a positively charged cluster (K382, K384, K385 and K386) [16]. This findings are in line with those reported in previous publications which have shown that mutations within this region (L347R, L351R, L373S, A376K) disrupt STIM1 binding to Orai1 [16, 106].

A more recent discovery shows that the α2 domain of SOAR (aa 393-398), located between CC2 and CC3, plays a role in the coupling as well as activation process of SOCE, as the non-conserved residue F394 therein seems to represent an important interaction site within STIM1 [52]. It is worth mentioning that residue F394 is the only non-conserved residue between STIM1 and STIM2 (L398) within α2 of SOAR, which may also contribute to the distinct behavior of the two homologues. F394 in STIM1 has been hypothesized to interact either with the Orai1 N-terminus or the Orai1 hinge plate [65], a region between TM3 and TM4 that forms hydrophobic interactions (L174, L261) at the more cytosolic side of Orai1 [52, 107].

In summary, SOAR, located within the STIM1 C-terminus, represents an essential binding site for Orai channels. While the binding of STIM1 C-terminal residues to the Orai1 C-terminus has been clearly defined, residues mediating potential interactions with other Orai cytosolic sites are currently elusive.

23.4.2 Main Coupling Domains Within Orai1

STIM1 coupling to and activation of Orai1 involves cytosolic domains of the Orai protein for either direct or indirect interaction. The main STIM1 binding site within Orai1 represents the C-terminus. The Orai1 C-terminus contains two hydrophobic residues (L273, L276) which have been identified as important for STIM1 coupling, as their mutation to more hydrophilic amino acids (S/D) completely abolished

STIM1 binding to Orai1 [48, 89]. Interestingly, only double, but not single point mutations in the C-termini of Orai2 and Orai3 are sufficient to abolish STIM1 binding [106]. Besides L273 and L276, the resolution of the SOAP structure uncovered additional residues within Orai1 C-terminus that are involved in STIM1 binding: R281, L286 and R289 [16]. The crystal structure of dOrai reveals that the C-termini of two adjacent subunits are crossing each other in an antiparallel manner at a crossing angle of 152° [14]. Crosslinking of cysteines at positions L273 and L276 impaired STIM1 mediated Orai1 channel activation, thus locking it into the inactive state [108]. The Orai1 C-terminus is connected to TM4 by a bent region [14], the so-called nexus (aa261-265). It is assumed to alter its configuration upon STIM1 coupling and initiates signal transmission to the pore [15, 65]. Indeed, point mutations within the nexus (L261A V262N H264G K265A; Orai1 ANSGA) can lead to a constitutively active channel that is accompanied by a reduction in STIM1 binding. This suggests that an altered Orai1 C-terminus conformation affects both STIM1 coupling and the channel's active state [65]. Thus, there is evidence that the orientation of the C-termini for proper STIM1 binding is the key to preserving store-operated Orai1 channel activation.

The Orai1 C-terminus representing the main and indispensable binding site for STIM1 [43, 48, 89], but there is also evidence for the involvement of the N-terminus in coupling, although to a weaker extent [43, 64]. These findings are based on in vitro interaction studies with N-terminal fragments. Overexpression studies of Orai1 N- and C-terminal truncation or single point mutants have allowed researchers to clearly distinguish between STIM1 binding either to the N- or C-terminus, as a deletion of or single point mutation within the C-terminus has led to total loss of STIM1 binding. This suggests that if there is STIM1 binding to other cytosolic domains of Orai1, STIM1 coupling to the Orai C-terminus is an inalienable prerequisite for this. Nevertheless, both N-terminal truncation ($\Delta N_{1\text{-}76/78}$) and point mutations (L74/W76EE/RR/SS, R83/K87A and K85E) within the extended transmembrane Orai1 N-terminal (ETON) region (aa 73-90), lead to reduced STIM1 binding, pointing to a potential direct or indirect involvement of the Orai N-terminus in STIM1 coupling. [64, 109]. It is worth mentioning that although the entire ETON region is conserved among the Orai homologues, Orai1 activation is lost upon N-terminal truncation up to residue 76 (Orai1 $\Delta N_{1\text{-}76}$), whereas Orai3 activation is only lost upon deletion of the first 57 residues (Orai3 $\Delta N_{1\text{-}57}$), corresponding to residue 82 in Orai1 [110]. These observations suggest an inhibitory role for Orai1 loop2 [61].

Thus, the loop2 of Orai1 has also been assumed to play a role in the gating process. Exchanging the loop2 in Orai1 with that of Orai3 allows the recovery of activation for some inactive Orai1 N-terminal mutants (e.g. Orai1 $\Delta N_{1\text{-}78}$, Orai1 L74E W76E) [61] (Fig. 23.6a), indicating that loop2 has distinct properties in the two homologues. The observed effects are accompanied by enhanced STIM1 coupling to the N-truncated Orai1-Orai3-loop2 chimera. Indeed, experiments employing the FIRE system have revealed an interaction between a STIM1 C-terminal and the Orai1 loop2 fragment; this interaction, however, has the same extent as with the analogous Orai3-loop2 segment [61]. Further investigation of the

role of loop2 revealed that it already impacts CRAC channels at the level of Orai independent of STIM1. Specifically, diverse gain-of-function Orai mutants, that lose their function upon N-terminal truncation, recover their activity upon swapping Orai3-loop2, even without co-expression of STIM1, except for Orai1 ANSGA (Fig. 23.6m). MD simulations revealed that the helical extension of TM2 into the cytosol is shorter in Orai1 than in Orai3, resulting in a longer and more flexible loop2 segment in Orai1 as compared to that in Orai3 [61]. This higher flexibility may facilitate interactions between loop2 and the truncated N-terminus in Orai1, causing this inhibitory effect within Orai1 $\Delta N_{1\text{-}78}$, but not within Orai1 $\Delta_{1\text{-}78}$ Orai3-L2. This altered Orai conformation at the cytosolic side is thought to affect STIM1 binding either in a direct or indirect manner. It is probable that the loop2 and the N-terminus function as individual binding sites or form a new binding site, but this requires further proof. Cysteine crosslinking experiments have shown that STIM1 induced Orai1 currents are drastically diminished upon the crosslinking of K78 in the N-terminus and E166 in loop2 [61]. Thus, in wild-type Orai1 a permissive communication between the N-terminus and loop2 is required to maintain STIM1 mediated Orai activation. In contrast, a non-functional Orai1 ANSGA N-truncation mutant does not regain function (Fig. 23.6m) upon swapping Orai3-loop2. This suggests that this mutant employs a distinct signal propagation pathway compared to wild-type Orai1 and other constitutive Orai1 mutants, which probably bypasses the loop2. A recent study on STIM and Orai in C. *elegans* revealed a distinct gating mechanism compared to that in mammals, where the binding of cSTIM or cCAD to the loop2 of cOrai is sufficient to gate the channel [111], indicating that the gating mechanism of SOCE has evolved over time.

In addition, although STIM1 and Orai1 are sufficient for CRAC channel activation [84], accessory proteins further adjust their interplay. Certain regulatory molecules have been reported to modulate CRAC channel function via coupling to Orai N-terminus, and especially to the ETON region [43, 112–115], as it has been shown for calmodulin (CaM). It adjusts CRAC channel inactivation, as outlined in detail in "Ca^{2+} dependent inactivation of Orai channels" [116]. CRACR2A has been reported to regulate the clustering of STIM1 and Orai1 upon store-depletion via positively charged residues in the N-terminus [115]. Furthermore, SPCA2, a Golgi secretory pathway Ca^{2+}-ATPase, has been found to bind directly to Orai1, whereas the region of interaction has been narrowed down to Orai1 N-terminus (aa 48-91) [117]. It mediates Ca^{2+} entry across Orai1 channels independent of STIM1 or ER-Ca^{2+}-store-depletion. Moreover, the lipid cholesterol has been shown to regulate CRAC channel function [113]. Detailed mechanisms for all these regulatory proteins are summarized in the following studies and reviews [59, 118–120], while more detailed insights on lipid mediated CRAC channel regulation are provided at the end of this review.

In summary, Orai1 C-terminus represents the main and best-characterized binding site for STIM1. Other Orai cytosolic fragments are essential for CRAC channel activation and maintenance of authentic CRAC channel hallmarks (as outlined in "Maintenance of CRAC channel hallmarks") but it remains unclear whether they directly interact with the STIM1 C-terminus.

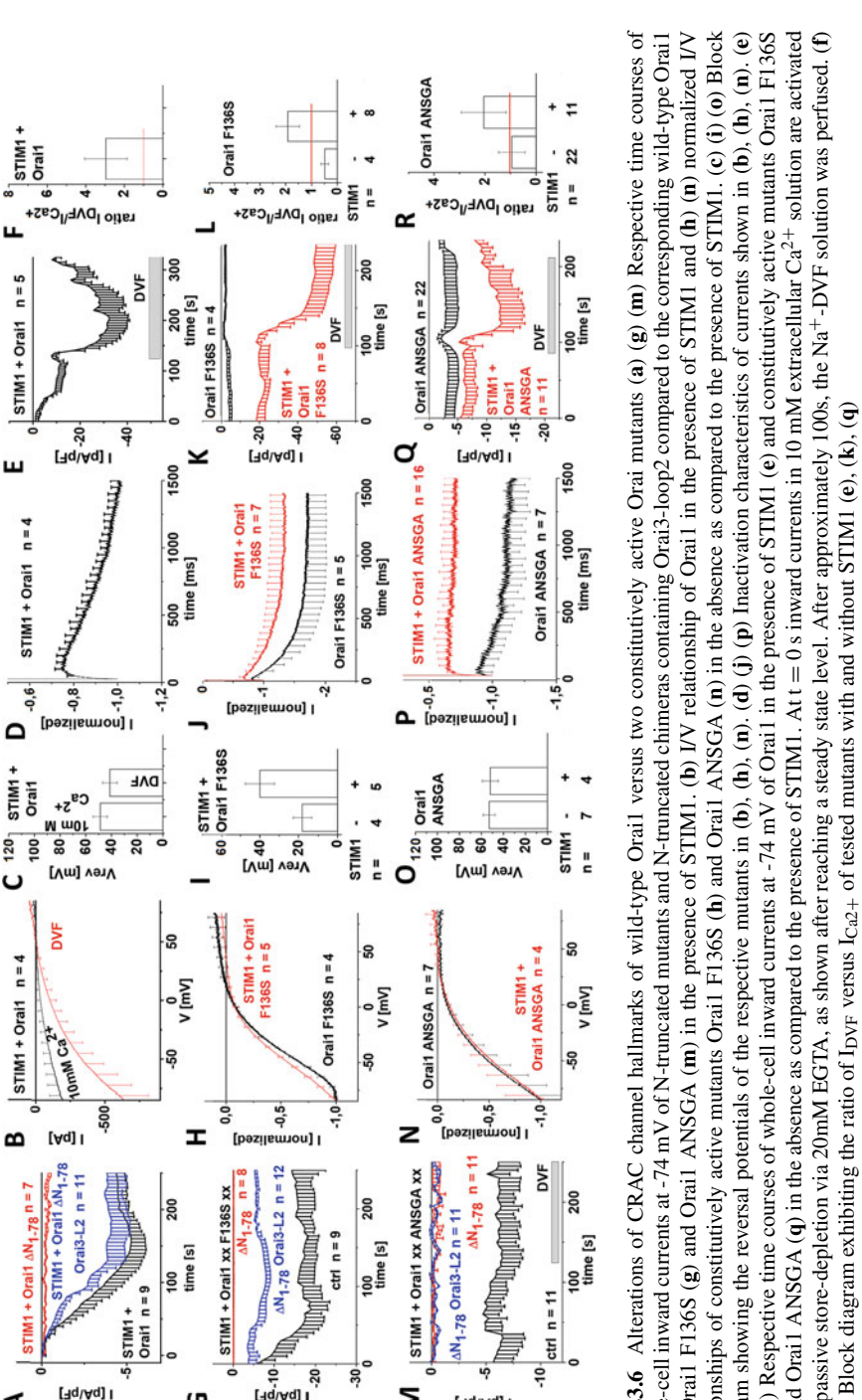

Fig. 23.6 Alterations of CRAC channel hallmarks of wild-type Orai1 versus two constitutively active Orai mutants (**a**) (**g**) (**m**) Respective time courses of whole-cell inward currents at -74 mV of N-truncated mutants and N-truncated chimeras containing Orai3-loop2 compared to the corresponding wild-type Orai1 (**a**), Orai1 F136S (**g**) and Orai1 ANSGA (**m**) in the presence of STIM1. (**b**) I/V relationship of Orai1 in the presence of STIM1 and (**h**) (**n**) normalized I/V relationships of constitutively active mutants Orai1 F136S (**h**) and Orai1 ANSGA (**n**) in the absence as compared to the presence of STIM1. (**c**) (**i**) (**o**) Block diagram showing the reversal potentials of the respective mutants in (**b**), (**h**), (**n**). (**d**) (**j**) (**p**) Inactivation characteristics of currents shown in (**b**), (**h**), (**n**). (**e**) (**k**) (**q**) Respective time courses of whole-cell inward currents at -74 mV of Orai1 in the presence of STIM1 (**e**) and constitutively active mutants Orai1 F136S (**k**) and Orai1 ANSGA (**q**) in the absence as compared to the presence of STIM1. At t = 0 s inward currents in 10 mM extracellular Ca^{2+} solution are activated upon passive store-depletion via 20mM EGTA, as shown after reaching a steady state level. After approximately 100s, the Na^{+}-DVF solution was perfused. (**f**) (**l**) (**r**) Block diagram exhibiting the ratio of I_{DVF} versus I_{Ca2+} of tested mutants with and without STIM1 (**e**), (**k**), (**q**)

23.5 Potential CRAC Channel Activation Mechanism via STIM1-Orai1 Coupling

The Orai channel activation cascade is initiated via the coupling of STIM1-SOAR to Orai1 C-terminus, which has been assumed to induce a conformational change in the C-terminus and the connected TM4 as outlined in the previous chapter. In line, comparison of the crystallographic resolution of a closed and an open conformation of dOrai suggests a straightening of TM4-C-terminus together with a widening of the pore in the basic region upon Orai pore opening [15]. However, a straightened TM4-C-terminus has also been observed for an Orai1 R91S mutant, which remains inactive in the absence of STIM1, in line with a lack of pore widening in the basic region. Thus, a straightening of TM4-C-terminus is not sufficient for pore opening. Additional conformational changes within the Orai channel complex are required to enable pore widening of the basic region. [15] Further investigations are required to determine how the signal of STIM1 binding to Orai1 C-terminus is transmitted to the pore helices located toward the N-terminal side of each subunit.

On the one hand, it is probable that Orai1 channel activation requires, both STIM1 coupling to Orai1 C-terminus and coupling to the cytosolic loop2 and/or the N-terminus, as are required for STIM1 mediated activation [61, 64, 110, 121]. Palty et al. [122] clearly demonstrated via local enrichment of STIM1 SOAR, that both the Orai1 N- and C-terminus contribute synergistically to STIM1 mediated Orai1 activation. Specifically, they have shown that Orai1 tethered to CAD remains active upon partial deletion (Δ1-76 or Δ276-301) of both the N- and the C-terminal strand. In contrast, while single point mutations (K85E or L273S) in either the N- or the C-terminus leave the fusion construct active, mutations within both cytosolic strands lead to total loss of function [122]. Apparently, the local attachment of CAD/SOAR is able to circumvent the need for two intact cytosolic strands as is usually seen with full-length STIM1 or cytosolic STIM1 fragments. Thus, Palty et al. [122] even hypothesized, as an alternative to a potential stepwise STIM1 coupling, which initially starts with STIM1 binding to the Orai1 C-terminus and continues to the N-terminus, that the N- and C-terminal binding sites assemble into a distinct binding pocket for STIM1 that controls the gating and selectivity of Orai1 channels. It is still unclear whether and how STIM1 bridges the potential signal transmission from the Orai1 C-terminus via the loop2 to the N-terminus.

On the other hand, it is possible that STIM1 coupling to Orai1 C-terminus solely initiates signal transmission emanating from the nexus via all the Orai1 TM domains, thus enabling Orai1 pore opening. Indeed, mutations within the nexus can lead to a channel that is constitutively active, but has reduced STIM1 affinity [65]. The nexus comprises the flexible hinge region (SHK, aa 263-265) and the hinge plate (LV, aa 261-262). Here, two residues L261 (TM4) and L174 (TM3) form potential hydrophobic interactions to mediated close proximity of TM3 and TM4 [65]. They may contribute to the transmission of the gating signal from the C-terminus towards the pore, as mutation of one of these residues to an aspartate (L261D, L174D) drastically decreased or completely abolished channel activation,

respectively [65]. Additionally, cysteine crosslinking experiments with L174C and L261C revealed enhanced activation, suggesting that these two residues change their orientation towards each other upon Orai1 activation [65]. Whether the hinge plate represents another target for STIM1 coupling as has been suggested by Zhou et al. [107] still requires further investigations. Conformational changes within the C-terminus and the nexus region might be potentially transferred to loop2 and the N-terminus [61], in line with the observations that their permissive communication is essential for Orai channel activation.

In summary, STIM1 SOAR binding to Orai1 C-terminus represents the trigger for pore opening. However, how the signal is further propagated to the pore and whether STIM1 requires further cytosolic coupling sites still needs to be clarified. Potential rearrangements within the Orai1 TM domains upon pore opening will be highlighted in the following sections, based on several gain-of-function point mutants.

23.6 Structure and Stoichiometry of the STIM/Orai Complex

Upon Ca^{2+} store-depletion, the direct interaction between STIM1 and Orai1 is initiated and results in the formation of an oligomeric, heteromeric complex (Fig. 23.5a). However, the exact stoichiometry of these coupling subunits is still unclear. According to the published X-ray dOrai structures and Orai concatemeric studies [62, 63], Orai is known to form a hexamer. Therefore, one might assume that, within a STIM1-Orai complex, six STIM1 molecules bind to the hexameric complex. Along those lines, NMR studies by Stathopulos et al. [16] indicate that the antiparallel oriented Orai1 C-terminal strands are attached to a dimer of STIM1 C-terminal fragments which would fits with the 1:1 STIM1:Orai1 stoichiometry, termed as the bimolecular binding model (Fig. 23.5b2). In contrast to this bimolecular model, a recent study by Zhou et al. [107] revealed a completely distinct STIM1-Orai1 interaction model. Through super-resolution microscopy and FRAP studies, the authors have discovered that SOAR dimers induced substantial clustering of Orai channels. A single point mutant, STIM1 F394H [52], impaired coupling to and activation of Orai1. Introduction of this single point mutation within one subunit of a SOAR dimer still enables the full activation of Orai1 channels, however, but lacked the ability to crosslink Orai1 channels [123]. This outcome suggests, in contrast to the bimolecular model, a unimolecular interaction, with an overall 1:1 stoichiometry (Fig. 23.5b1). However, in the latter model two monomers of one STIM1 dimer each interact with one Orai subunit of two distinct Orai channels, enabling local clustering of Orai channels.

Alternatively, several studies have demonstrated that maximal Orai1 activation requires a ratio of 2:1 of STIM1:Orai1 subunits [124–127]. Here, twelve STIM1 proteins would be required to activate one Orai hexamer. A recent study by Palty et al. [128] which employ a constitutively active Orai1 mutant (Orai1 P245L) proposes a sequential activation mechanism of Orai1 via STIM1, whereby the authors assumed a final 2:1 STIM1:Orai1 stoichiometry (Fig. 23.5b3). They sup-

posed that, in a first step, one C-terminal strand of a STIM1 dimer is coupled to an Orai1 C-terminus, thereby inducing partial activation and leading to conformational rearrangements within the Orai channel. The latter enables binding of the second C-terminus of the STIM1 dimer to the same Orai subunit to trigger full Orai1 activation [128]. At this point, however, it remains unclear whether the second STIM1 monomer of the dimer also binds to the C-terminus or some other cytosolic site in the Orai protein.

The amount of bound STIM1 has been reported to alter the Orai channels' biophysical characteristics. Scrimgeour et al. [125, 126] reported that a lower number of STIM1 proteins bound to the Orai1 channel corresponds to a reduced extent of typical fast Ca^{2+} dependent inactivation of CRAC channels. The decreased STIM1:Orai1 ratio has been shown to lead to a slower increment in divalent cation selectivity together with reduced 2-aminoethoxydiphenyl borate (2-APB) current potentiation. [125, 126] The amount of bound STIM1 also determines Orai1 channel Ca^{2+} selectivity, as it has been shown for Orai1 and Orai1 V102A proteins tethered to a single CAD/SOAR domain, as opposed to a tandem one [67].

Overall, the stoichiometry of an active STIM1-Orai1 channel complex is currently still controversial. Thus far, three distinct scenarios have been proposed including a uni- and a bimolecular model as well as a sequential activation model (Fig. 23.5b). Functional studies have suggested that Orai1 channel activation can occur at distinct STIM1:Orai1 ratios, while the biophysical characteristics might be distinct depending on the respective ratios. Full clarification of the stoichiometry of a functional CRAC channel would require additional functional studies together with the structural resolution of the STIM1-Orai1 channel complex (Figs. 23.5a and 23.7).

23.7 Orai Channel Activation

23.7.1 CRAC/Orai Channel Permeability

CRAC channels are characterized by two main properties: high Ca^{2+} selectivity and low single channel conductance [13, 129, 130]. Among a myriad of Ca^{2+} ion channels, this type of store-operated Ca^{2+} channel is one of the most selective ones. Its high Ca^{2+} selectivity is characterized by a 1000 times higher permeation for Ca^{2+} than for the more prevalent Na^{+} ion [131]. This appears in the strong inward rectification of the CRAC channel's whole cell currents, which exhibit a reversal potential higher than +50 mV [129, 130]. At the structural level, high Ca^{2+} selectivity is determined by a ring of glutamates (E106) at the external pore mouth, forming the selectivity filter together with three negatively charged residues (D110/112/114) in the first extracellular loop, the so-called CAR region [66]. Despite the fact that CRAC channels exhibit a 20-fold lower binding affinity for Ca^{2+} than for, for example, Ca_V channels [132], their high level of Ca^{2+} selectivity is justified by a slow rate of ion flux [133]. Additionally, the Ca^{2+} selectivity of

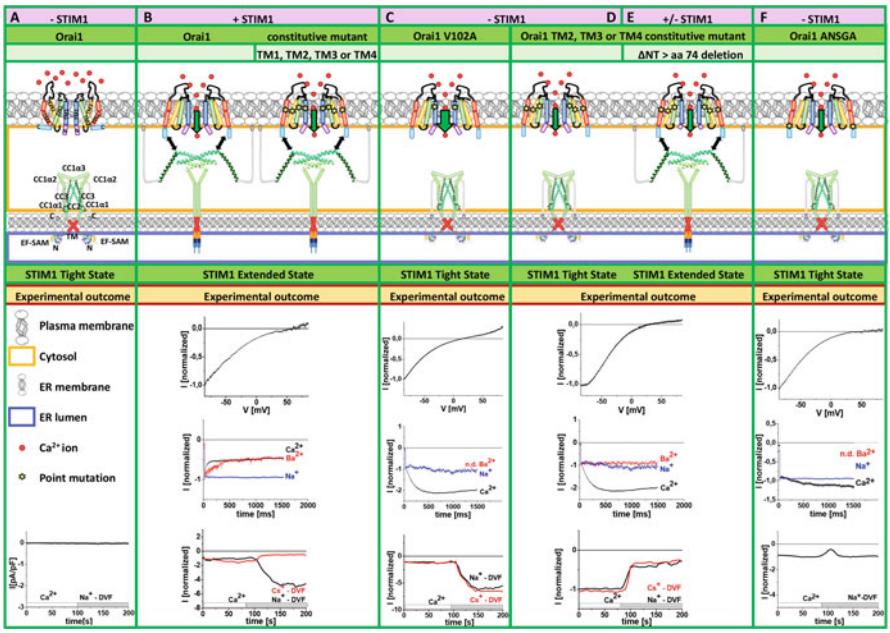

Fig. 23.7 Hypothetical models for gating of Orai1 channel The cartoon depicts how Orai channel activation via STIM1 or point mutation inducing constitutive activity or both is related to CRAC channel hallmarks. (**a**) Orai1 wild-type in the absence of STIM1 shows no activation. (**b**) STIM1 mediated activation of Orai1 wild-type or most constitutive Orai1 mutants leads to maintenance of CRAC channel hallmarks, with $V_{rev} > 50$mV, strong inactivation in a Ca^{2+} containing solution and a ratio of $I_{DVF}/I_{Ca2+} > 1$. Inactivation is preserved in a Ba^{2+} containing solution, while it is lost in a Na^{+} containing divalent free solution. Furthermore, the STIM1 activated Orai proteins are impermeable to Cs^{+}. (**c**–**f**) In the absence of STIM1 or the deletion of at least the first 74 N-terminal amino acids of Orai1, constitutively active mutants loose the typical CRAC channel characteristics shown in (**b**). The mutants show differences and can be categorized in three groups (**c**, **d**, **f**). Orai1 V102A/C (**c**) show a V_{rev} of +20 mV, reactivation, but maintain a ratio of $I_{DVF}/I_{Ca2+} > 1$. Orai1 TM2/TM3/TM4 point mutants (**d**) show constitutive activity, a V_{rev} of 30–40mV, reactivation and a ratio of $I_{DVF}/I_{Ca2+} < 1$. (**e**) Deletion of the N-terminus of the constitutively active mutants in (**d**) leads to mutants with comparable properties as described in (**d**). Orai1 ANSGA (**f**) exhibits a V_{rev} of +50mV and loss of inactivation, but no reactivations and a ratio of $I_{DVF}/I_{Ca2+} = 1$

Orai is maintained via the conserved glutamate E190 in TM3. Its substitution to an alanine or glutamine (E190A/Q) results in increased permeation of Cs^{+}, an increased pore diameter to 7Å and decreased activation via the compound 2-APB [134]. It has been suggested that E190 allosterically affects the pore, probably through alterations in the intramolecular TM interactions. Novel MD simulations of dOrai revealed that the mutation E262Q (corresponding to E190Q in hOrai1) severely impacts the hydration pattern of the pore and the dynamics of a positively charged residue K270 (corresponds to K198 in hOrai1) in TM3. It has been suggested that high Ca^{2+} selectivity relies on a counterbalancing effect of E262 and K270 which is lost for the E262Q mutant [135].

Furthermore, the Ca^{2+} selectivity of CRAC channels is not only determined by the Orai pore, but also by STIM1 binding, making it a dynamic rather than a fixed property of the channel [64, 67].

The low unitary conductance represents the second, more poorly understood property of CRAC channels and thus far precludes these Ca^{2+} channels from direct single channel current recordings [136]. Only non-stationary noise analysis has enabled researchers to determine CRAC channel open probabilities and unitary conductance [137]. To date, promising studies at the single molecule level have only been obtained via optical recordings on Orai proteins fused to a genetically encoded Ca^{2+} indicator, which allowed to monitor single channel opening events [138]. Upon co-expression of CAD/SOAR, the Orai activity was resolved as periodic fluctuations with multiple conductance states [138].

Besides Ca^{2+}, CRAC channels also conduct small monovalent ions such as Na^+, Li^+ or K^+, however, only as long as divalent ions are lacking in the monovalent solution. One typical CRAC channel hallmark represents the 5–6 fold enhancement of currents in a divalent free Na^+- versus a Ca^{2+}-containing solution. The anomalous mole fraction behaviour for Ca^{2+} versus Na^+ currents has revealed that Na^+ currents are blocked by the addition of Ca^{2+} in the μM range. [46, 131, 137, 139–145] Unlike other Ca^{2+} ion channels such as L-type and TRPV6, Cs^+ ions are impermeable across CRAC channels. This is thought to be due to the very narrow pore diameters of CRAC channels, which are in the range of 3.8–3.9 Å and are significantly narrower than for Ca_V channels. [134, 137, 146] Intriguingly, the dOrai crystal structure displays a diameter of 6 Å at the narrowest part of the pore [14] (Fig. 23.3c, d), which seems to vary little compared to the novel structure of the gain-of-function mutant dOrai H206A [15]. The variance in pore diameter between structural and experimental [134] data can probably be explained by distinct pore diameters in the absence or the presence of STIM1. In order to clarify this, the structural resolution of an Orai complex bound to STIM1 proteins is required.

STIM1 possesses the ability to narrow the pore diameter of Orai channels, as it has been shown for a constitutive Orai1 mutant, Orai1 V102A/C. This mutant exhibits non-selective currents together with an enhanced pore diameter of around 6.9 Å in the absence of STIM1, while Orai1 V102A/C currents become selective and exhibit a pore diameter of 4.9 Å in the presence of STIM1, which is comparable to that observed for the STIM1-bound Orai1 pore. [67]

23.7.2 Ca^{2+} Ion Conduction Pathway

The Ca^{2+} permeation pathway of Orai channels is formed by TM1 together with the N-terminal helical extension, the so-called ETON region (aa 73-90) (see Fig. 23.3c, d). An initial idea of the pore conformation has been obtained by conclusive electrophysiological studies, cysteine scanning mutagenesis experiments and the characterization of the inhibition of Orai currents by oxidative crosslinking of either cysteines or block via cadmium [134, 147, 148]. The crystal structure of dOrai,

elucidated in 2012, finally confirmed the concept of the Orai pore [14] and showed that the conduction pathway is formed by an association of six TM1 helices in the center of the Orai channel. The Orai pore (see Fig. 23.3d) is composed of a Ca^{2+} accumulating region (CAR) at the external side [66], the selectivity filter, followed by a hydrophobic cavity and finally a basic region at the cytosolic side [14, 149, 150]. Their detailed roles will be explained in the following section.

The external CAR region (see Fig. 23.3d) is constituted by the loops connecting TM1 and TM2 (TM1-TM2 loops). Substituted cysteine accessibility method (SCAM), disulphide crosslinking and Cd^{+} block experiments have shown that the 1st loops are highly flexible portions within the Orai channel complex [148, 151]. Each first loop segment contains three negatively charged amino acids (D110, D112, D114) that attract Ca^{2+} ions [66] thereby reducing the energetic barrier for Ca^{2+} ions to enter the pore. While the mutation of all three residues to alanines changes the ion selectivity and widens the pore diameter [134], single cysteine or alanine point mutations do not affect Ca^{2+} selectivity [66, 148]. Molecular dynamics simulations have revealed that in particular, D110 and D112 act as transient Ca^{2+} binding sites before the Ca^{2+} ions bind to E106, the selectivity filter, which is 1.2 nm away from the CAR region. Indeed, Ca^{2+} permeation is reduced upon substitution of D110 to an alanine (D110A), especially at lower extracellular Ca^{2+} concentrations. The reason for this might be that Ca^{2+} binding shifts to D112 and D114, leading to an increased energy barrier between CAR and the selectivity filter. Ca^{2+} accumulation at the pore is fine-tuned still further by electrostatic interactions between TM1-TM2 loop1 and the TM3-TM4 connecting loop3 [66].

In contrast to the three glutamines found in the first loop of Orai1, Orai2 and Orai3 contain a mixture of glutamates, glutamines and aspartates. This difference leaves homomeric Orai assemblies unaffected, but heteromeric Orai1/Orai3 channels exhibit reduced Ca^{2+} selectivity and higher Cs^{+} permeation [152]. These findings suggest that the acidic Ca^{2+} coordination site in the first loop regulates not only the Ca^{2+} permeation, but also the Ca^{2+} selectivity of Orai channels. Interestingly, co-expression of Orai1 and Orai2 maintained the Ca^{2+} selectivity of store-operated currents at a level comparable to that seen in wild-type conditions [153].

Originating from the CAR region, Ca^{2+} ions are guided toward to the selectivity filter, which is exclusively formed by E106 at the more extracellular side of TM1 [13, 14, 154, 155]. While single point mutants Orai1 E106A/Q lose function, Orai1 E106D exhibits reduced Ca^{2+} selectivity and a widened pore diameter of about 5.4 Å [134]. The coordination of the Ca^{2+} ions is established by the close proximity of the residues E106 and a high rigidity of the residues aa 99-104 in the TM1 helix [147]. MD simulations showed that a single Ca^{2+} ion is bound to E106 under equilibrium conditions [66]. The novel crystal structure of the constitutively open dOrai H206A (equal to Orai1 H134A) mutant, representing an open channel state, revealed that either one or two ions directly coordinate the side chains of the glutamate ring (E178 in dOrai, corresponds to E106 in hOrai1) [15]. This ring of E106 residues forming the selectivity filter establishes a negative electrostatic potential and has been suggested to act as a potential gate for Ca^{2+} ions to enter the channel [67].

After passing the selectivity filter, Ca^{2+} ions enter a wide, hydrophobic cavity, that is composed of V102, F99 and L95 [14] (see Fig. 23.3d). Furthermore, this area includes a glycine G98 that has been suggested to function as a flexible gating hinge [156], as is known for many other ion channels [157–159]. Cysteine crosslinking studies suggest that V102 and L95 point directly into the ion conduction pathway [147]. In support of this observation, Cd^{+} blockage experiments showed the significant inhibition of V102C, G98C, L95C mutant currents [151]. Single point mutations of Orai1 V102 (V102C/A/G) and Orai1 F99 (F99Y/M/S/T/W/C/G) lead to constitutively active function, thus somehow locking Orai1 in an open state [69]. In line with these findings, molecular dynamics simulations for the dOrai channel showed that a F171Y and V174A mutation (corresponding to F99Y and V102A in human Orai1, respectively) provided a more favourable permeation pathway than the WT channel, based on potentials of mean force for the translocation of a single Na^{+} ion [160] and enhanced hydration of the hydrophobic zone within the pore [67, 69].

The flexible glycine G98 within this hydrophobic cavity [156] is assumed to provide flexibility for the upstream pore-lining region, enabling Ca^{2+} ions to easily pass through the pore after passing the selectivity filter. Single point mutations of G98 (G98 S/T/Q/H/N/K/E/D) induce constitutive activity [69]. Recent studies suggest that, while F99 points into the pore in the closed state, it moves out and G98 moves into the pore upon STIM1 coupling, thus decreasing the hydrophobic barrier for Ca^{2+} permeation [69]. Diverse constitutive Orai1 mutants that contain substitutions at the positions G98, F99 or V102 exhibited non-selective currents in the absence of STIM1, but became selective in the presence of STIM1. Thus, the potential rotation within the hydrophobic portion in TM1 is assumed to govern the Ca^{2+} selectivity of the Orai channel. [69]

The attachment of Tb^{3+} to the pore close to the selectivity filter has revealed alterations in the luminescence upon STIM1 coupling [67, 161]. In line with these findings, a comparison of the dOrai crystal structure in a closed versus an open conformation showed an altered positioning of Ba^{2+} around the selectivity filter, indicating that the latter undergoes subtle changes upon Orai pore opening [15]. Altogether, these studies suggest that the hydrophobic cavity together with E106 contribute as one gate of the CRAC channel and that ion selectivity and gating of Orai channels are closely coupled [67, 161].

The hydrophobic cavity is followed by a basic region that is already located in the elongated Orai1 helix in the cytosol connecting TM1 to the Orai1 N-terminus, the so-called ETON region [64]. The ETON region potentially forms an electrostatic barrier via the three positively charged amino acids R91, K87 and R83 (see Fig. 23.3d). The crystal structure suggests that all three residues point into the pore, in line with the results of crosslinking experiments with Orai1 R91C [147, 151]. These residues are suggested to inhibit Ca^{2+} entry in the closed channel state probably either simply via electrostatic repulsion in this region or due to bound anions [14]. MD simulations on wild-type Orai1 versus a constitutively open Orai1 mutant, where a Ca^{2+} ion has been pulled through the pore, suggested that the side chains

of R91 are moved more out of the pore in the Ca^{2+} permeable state [68]. Severe Combined Immune Deficiency (SCID) is associated with a substitution of R91 by a hydrophobic amino acid which assumedly generates a robust hydrophobic barrier [14], hindering Ca^{2+} flow through the elongated pore. Currently, it is being debated whether the ETON region, with the positively charged residues pointing into the pore, functions as a potential second gate or merely a barrier. Furthermore, it still remains to be determined whether it contributes to STIM1 coupling [64].

In summary, Ca^{2+} permeation through the Orai1 pore starts upon the attraction of Ca^{2+} ions by the external CAR region. Ca^{2+} ions are then moved toward the selectivity filter that is formed by the single glutamate E106. This functions together with the hydrophobic region as one gate of the Orai channel. Subsequently, Ca^{2+} ions pass through an electrostatic barrier and finally, they are guided into the cytosol potentially via the repulsion of positively charged residues at the end of the pore [136].

23.7.3 Gating of Orai Channels

Gating of Orai channels implicitly requires the coupling of STIM1 to the Orai C-terminus. However, how this activation is finally transmitted to the pore helix at the N-terminal side of each Orai subunit is currently unclear. As described above it has been hypothesized that other cytosolic Orai domains are also involved in channel activation by STIM1 either via direct binding or indirectly. Recent studies additionally suggest that Orai TM domains are involved in signal propagation to the pore. Within this section, we aim to provide a picture of how the activation signal of STIM1 binding propagates across Orai TM helices to the pore.

Site-directed mutagenesis studies have revealed that the closed state of the Orai channel is not only maintained by the pore-lining helix TM1, but also by the other three TM helices and the hinge region that connects TM4 and the C-terminus of the Orai subunit, even if these do not line the pore [39, 70, 73]. A series of point mutations at positions throughout all TM domains, identified individually [68–71] as well as by a systematic screen [73], have been shown to lead to constitutive Orai activation. Some of those gain-of-function mutants have also been associated with diseases such as cancer, Stormorken syndrome, tubular aggregate myopathy (TAM) and hypocalcemia [68, 72] (see Table 23.2). Additionally, mutagenesis studies have revealed that a cluster of hydrophobic contacts between TM1-TM3 contribute to proper pore opening [73]. Below, we provide an overview of the diversity of mutants that are currently known.

Along the pore-lining helix TM1, S97, G98, F99, A100, V102 and V107 (Fig. 23.3d) have been discovered to contribute to the establishment of the closed state [67, 73, 156] as their mutation to small and/or polar residues leads to constitutive activity. Furthermore, the V107M mutation, which is associated with tubular aggregate myopathy (TAM) or Stormorken syndrome, results in constitutively active Orai1 mutant channels [71]. As mentioned in the previous section, studies on diverse

other constitutive Orai1 TM1 mutants (e.g. Orai1 V102A/C) together with Cd^{+} block experiments [67, 69] have suggested that Orai1 pore opening is accompanied by a rotation of the pore helix TM1 [69, 70, 122, 136] at least at position G98 and F99.

In TM2, H134, F136 (Fig. 23.6g) A137 [68], L138 [72], M139 [68] and S141 [73] are suggested to keep the Orai1 channel in the closed state, as single point mutation of these residues (H134A/C, A137V, L138F, S141C) lead to constitutively active currents [68, 73]. In addition, Orai1 M139V enhances Ca^{2+} levels independent of STIM1 [68]. MD simulations together with Cd^{+} block experiments provide a potential explanation for facilitated Ca^{2+} transport across the constitutive Orai1 mutants, containing substitutions at H134. In two independent studies enhanced water permeation was observed through the pore of constitutive Orai1 H134A/S mutants in MD simulations [68, 73]. Furthermore, pulling a Ca^{2+} ion through the pore of hOrai1 H134A revealed an unaffected movement of the R91 side chain, in contrast to Orai1 wild-type [68]. In addition, Cd^{+} crosslinking experiments showed that Orai1 H134S exhibits no rotation of TM1 around G98/F99, as G98 points already into the pore region in the absence of STIM1 [68, 73]. The crystal structure of the dOrai H206A analogue of the Orai1 H134A mutant displays a strongly dilated pore together with a fully extended TM4-C-terminus region [15].

In TM3, W176, V181, G183, T184, L185, F187, E190 have been demonstrated to keep the Orai1 channel in the closed state, as their substitution to a cysteine or several other small, polar residues can lead to constitutive activity and/or altered selectivity [61, 73, 110, 162]. A mutation of W176 to a cysteine (W176C) induces constitutive, but fewer Ca^{2+} selective currents, in the absence or presence of STIM1 [162]. While a single substitution of V181 or L185 to an alanine results in small, constitutively active Orai currents [61], a double point mutation L185A F250A of two opposing residues in TM3 and TM4 lead to strongly enhanced constitutive activity that was not further enhanced upon STIM1 coupling [110]. Interestingly, Orai3 F160A, unlike the analogue Orai1 L185A, has revealed much higher constitutive currents, indicating isoform specific signal propagation [61, 110]. These critical residues of the two Orai isoforms in TM3 are located opposite to TM4. At this point, further examination is required to determine whether mutations in TM3 that lead to constitutive activity, induce conformational changes such as the movement of TM3 closer to or farther apart from the adjacent TM4. Moreover, the single point mutant T184M, associated with TAM and Stormorken syndrome, exhibits constitutive activity.

A235, S239, P245 and F250 in TM4 have also been discovered to contribute to the maintenance of the closed state [70, 73]. P245 is located at the kink of TM4 (Fig. 23.3e). A GoF point mutation P245L, associated with the Stormorken-like syndrome [8], and the analogue Orai3 P254L mutant [110] have been shown to cause constitutive activation. Interestingly, substitution of this proline by any other amino acids leads to constitutive activation suggesting that only the proline keeps Orai1 in the closed state [122]. Since this proline is located at and responsible for the kink in TM4, it might be assumed that this kink contributes to keeping Orai1 in the closed state.

The nexus region connecting TM4 and the C-terminus also contributes to the maintenance of the closed state of the Orai channel. A double (L261A V262N) and a fourfold point mutation (L261A V262N H264G K265A corresponds to Orai1 ANSGA) in this kink region, which is 80% conserved among all Orai homologues, resulted in constitutively active Orai1 channels with high selectivity and a V_{rev} of +60 mV (Fig. 23.6n, o, 5) [65].

The gain-of-function point mutants mentioned above exhibit a partially open state, that probably represents one step in the structural change that occurs upon STIM1 binding [122]. At this point, it is worth noting that these diverse GoF mutants exhibit distinct biophysical characteristics in the absence of STIM1, potentially in line with slightly distinct partially active states, as outlined in the section entitled "Authentic CRAC channel hallmarks are tuned by STIM1 and Orai1 N-terminus".

In addition, atomic packing analysis revealed a close density of residues around TM1-TM2/3 situated within the same membrane plane as E106 and V102. Mutational analysis of hydrophobic residues in this area, such as L96, M101, M104, F187, yielded a finding that they contribute to proper communication with the pore helix, because their substitution by an alanine impairs Orai activation [73].

In summary, several residues throughout all Orai TM helices contribute to the maintenance of the closed state of Orai channels and are likely displaced upon STIM1 binding. Thus, Orai pore opening is governed by a concerted, overall conformational change in the Orai channel complex rather than the sole rearrangement of TM1 helices [73]. Furthermore, the establishment of the open state requires an intact communication of the residues in a TM1-TM2/3 hydrophobic clamp [73]. It is noticeable that several residues, not lining the pore, are all located within the same membrane plane of the Orai1 channel complex and affect gating and/or permeation of Orai channels indirectly.

A long the same line, a comparison of the crystal structures of dOrai and a mutant (H206) form, exhibiting either a potentially closed or open form, indicated that conformational rearrangements take place throughout all TM domains. Hence, STIM1 coupling probably initially releases the belt formed by the crossing Orai C-termini, which likely provides to all TM helices more freedom to move. Subsequently, a signal is propagated to the pore, sequentially altering the conformations of TM4, TM3 and TM2, which finally leads to a pore dilation in the basic region to around 10 Å. However, as these assumptions are only based on the comparison of two dOrai states, more structural resolutions – especially of a human Orai channel complexed together with STIM1 – are needed to draw firm conclusions. This would provide information on how STIM1 binds to the channel and rearranges the orientation of the TM helices to finally stabilize the open state [65, 136].

23.7.4 Regulatory Residues in Orai TM Domains

In addition to the huge variety of sites within the Orai TM domains that are known to control Orai channel gating, a few other positions have been found to possess distinct functional roles in Orai1.

Unlike the constitutive Orai1 G183C mutant, the G183A mutation leads to fully abolished store-operated activation and an altered sensitivity to 2-APB [162]. Furthermore, this glycine in TM3 ensures proper plasma membrane insertion, as several amino acid substitutions at this position have resulted in loss of plasma membrane expression [68]. The analogue Orai3 G158C exhibits altered kinetics in response to 2-APB and an impaired closing of the channel upon 2-APB washout [163]. These effects of G158C in Orai3 have been attributed to a potential TM2-TM3 interaction with an endogenous cysteine C101, which probably controls the activation state of Orai3 channels [163].

Oxidative stress has also been reported to control Orai channel function via TM3. While H_2O_2 blocks the activation of Orai1 channels, it leaves Orai3 channels unaffected. This isoform specific sensitivity to H_2O_2 underlies a cysteine C195, which is located at the extracellular side of TM3 in Orai1 and is lacking in Orai3. [164]. This inhibitory mechanism underlies a reduction in subunit interactions within the oxidized Orai1 channel. Specifically, the oxidized C195 has been proposed to form inhibitory interactions with S239 in TM4, which locks Orai1 into the closed state [165].

23.7.5 Ca^{2+} Dependent Inactivation of Orai Channels

Ca^{2+} dependent inactivation (CDI) governs the inhibition of Orai/CRAC channel activity. It represents an important feedback mechanism to regulate cytosolic Ca^{2+} levels and can be separated into fast (FCDI) and slow Ca^{2+}-dependent inactivation (SCDI) [166]. FCDI can typically be monitored as a decrease in CRAC currents during a hyperpolarizing voltage step that takes place over tens of milliseconds [3, 131, 167, 168]. In contrast, SCDI requires several minutes for full completion [3, 168].

The CDI of CRAC channels is regulated by several components: STIM1 and Orai as well as the accessory proteins, CaM and SARAF [118]. Here, the cytosolic regions of STIM1 and Orai1 especially contribute to the inactivation of Orai channels.

The extent of inactivation has been suggested to depend on the STIM1-Orai ratio [125, 126]. Moreover, the CRAC Modulatory Domain (CMD), an acidic cluster (aa 475-483) in the STIM1 C-terminus is required for the FCDI of Orai/CRAC channels [47, 116, 169]. Mutation of these negatively charged amino acids in the CMD to alanines has led to a reduction in inactivation of all Orai isoforms as well as native CRAC currents in RBL-2H3 cells [47, 169]. Moreover, studies of several

gain-of-function Orai mutants have shown that FCDI, which is typical for STIM1 mediated Orai currents, can only be established in the presence of STIM1 and an intact N-terminus, which includes the whole ETON region [73, 110].

Fast and slow CDI of STIM1-Orai mediated currents have also been shown to be regulated by SARAF, another protein localized in the ER [166, 170, 171]. So far, only its role in SCDI is understood, while the mechanisms underlying the regulation of FCDI via SARAF are still elusive [166, 170, 172]. SARAF only binds to the CAD/SOAR domain of STIM1 in the presence of Orai1 [170]. STIM1-mediated regulation by SARAF occurs via a domain downstream from SOAR, the so-called C-terminal inhibitory domain (CTID). Here, SARAF interacts with different portions of CTID to accomplish SCDI of Orai channels [170]. Briefly, in the presence of SARAF, STIM1-induced Orai1 currents exhibit SCDI that is reduced when PIP_2 is depleted, the polybasic cluster is lacking, or STIM1 proteins are targeted to PIP_2-poor regions [172]. The interplay between STIM1 and SARAF is further supported by septin 4 and ESyt1, which helps to keep STIM1/Orai1 complexes in PIP_2-rich regions [166, 172].

All three isoforms (Orai1, Orai2 and Orai3) display fast CDI that occurs within the first 100 ms of a voltage step. However, it is three times weaker for Orai1 and Orai2 compared to Orai3 [129, 152, 169]. Orai1 currents exhibit a late reactivation phase after FCDI, while Orai2 and Orai3 channels subsequently show a slow inactivation phase over a 2s voltage step [129, 152]. Unlike overexpressed Orai subunits, the native CRAC currents in RBL-2H3 mast cells [47, 167] display FCDI without the subsequent, typical reactivation phase known for Orai1 currents. This suggests that other cellular components may contribute to the inactivation of native CRAC channels.

Several cytosolic domains in the Orai channel have been reported to maintain its FCDI.

Within the Orai1 N-terminus, a proline/arginine-rich region aa 1 – 47 was found to induce reactivation [173]. Furthermore, CaM has been suggested to regulate inactivation of Orai channels via its binding to the N-terminus [116, 173, 174]. However, recent studies have found no alteration in Orai channel's inactivation via overexpression of CaM or CaM_{MUT} [175]. Specific residues (W76, Y80, R83) that line the pore have been proposed to adjust inactivation via the side chain properties of the respective amino acids [145].

Chimeric and mutagenesis studies have shown that the intracellular loop2 of Orai1 connecting TM2 and TM3 is also involved in the modulation of fast and slow inactivation [173, 176]. Specifically, the mutation of the amino acid stretch 151-VSNV-154 to a sequence of four alanines compromises fast inactivation. A short peptide (aa 153-157) including this region has been shown to reduce CRAC currents, suggesting that loop2 probably functions either as a blocking particle or affects inactivation in an allosteric manner.

The Orai C-terminus also modulates Orai channel's fast inactivation. Orai2 and Orai3 chimeras, in which the C-terminus was exchanged with that of Orai1, exhibited diminished fast inactivation [169], potentially due to three glutamates that are only present in the C-termini of Orai2 and Orai3 [169].

Thus, Orai channels utilize diverse regions to regulate CDI. The cytosolic N- and C-termini and loop2 seem to regulate Orai inactivation/gating in a cooperative manner [173]. Moreover, the FCDI is adjusted by negatively charged residues within the outer pore vestibule of Orai channels [134]. The interpretation of potential inactivation sites may require a strict control of STIM/Orai stoichiometry [124, 126].

In summary, the FCDI of Orai channels is controlled by negatively charged residues in STIM1 as well as all three cytosolic portions of Orai channels, the two cytosolic strands as well as the loop2 region. Orai channel current's SCDI underlies the regulation via STIM1 and SARAF. However, whether Orai domains are also involved in SCDI is still unclear.

23.7.6 Authentic CRAC Channel Hallmarks are Tuned by STIM1 and Orai1 N-terminus

STIM1 plays several roles in CRAC channel activation. It triggers not only CRAC channel gating but also adjusts authentic CRAC channel hallmarks [110]. The latter include high Ca^{2+} selectivity ($V_{rev} \sim +50mV$) (Fig. 23.6b, c), fast Ca^{2+} dependent inactivation (FCDI) (Fig. 23.6d) and enhancement of currents upon the switch from a Ca^{2+} containing to a Na^{+} containing divalent free solution (Fig. 23.6e, f).

The high Ca^{2+} selectivity of CRAC channels is triggered upon functional coupling of STIM1 to the Orai channel. This finding has been proven by studies with a series of constitutively active mutants throughout all TM helices [67, 70, 73, 110] (see section "Gating of Orai channels"). In the absence of STIM1, these mutants exhibit constitutive, non-selective currents, whereas constitutive Orai1 TM mutants (e.g., Orai1 V102A/C) show a lower V_{rev} and are less Ca^{2+} selective than most other mutants that contain substitutions in the outer TM regions TM2/TM3/TM4 [110] (Fig. 23.7d). Contrary to the absence of STIM1, in its presence the Ca^{2+} selectivity of all constitutive mutants is enhanced to levels comparable to wild-type STIM1-Orai-mediated currents [73, 110] (Fig. 23.7b). As a representative for most constitutive TM2/TM3/TM4 mutants, the typical CRAC channel hallmarks of the constitutively active Orai1 TM2 mutants (Orai1 F136S) are shown in Fig. 23.6g–l. The ability of STIM1 to fine-tune Ca^{2+} selectivity is not unique to constitutive mutant channels. Wild-type Orai1 currents have also been shown to display increased ion selectivity with a progressive amount of bound STIM1 proteins [67]. Exceptions to this are some other non-selective constitutive TM1 mutants (e.g. S97C/M/V/L/I) that cannot regain Ca^{2+} selectivity in the presence of STIM1, potentially due to constrained motions of TM helices that trap the channel in a non-selective state [73, 156]. In addition, constitutive Orai1 H134A/S/C (mutations in TM2) [68, 73] and the TM4-C-terminus hinge mutant (Orai1 ANSGA) [65] (Fig. 23.6n, o) have revealed comparable V_{rev} in both the absence and presence of STIM1, suggesting that these mutants possess similar conformational alterations and properties as those observed for activated endogenous CRAC and STIM1-induced Orai1 currents.

Both the Orai channels' Ca^{2+} selectivity and their fast Ca^{2+}-dependent inactivation (FCDI) is maintained only in the presence of STIM1 (Fig. 23.6d, 23.7b), which has been visualized with constitutively active mutants. Constitutive Orai1 TM mutants display strong reactivation in the absence of STIM1 upon the application of a hyperpolarizing voltage step [67, 70, 73, 110] as shown for Orai1 F136S exemplarily (Fig. 23.6j). It is worth mentioning, that the extent of reactivation in the absence of STIM1 is less pronounced for Orai1 ANSGA (Fig. 23.6p) compared to all other Orai1 TM mutants [73, 110]. The FCDI of all constitutive Orai mutant currents is maintained only in the presence of STIM1, but, it lacks the typical reactivation phase after FCDI within the first 100ms [110] (Fig. 23.6d, j, p), potentially due to altered STIM1 coupling (see "Main coupling domains within Orai1").

Another common CRAC channel characteristic represents the increase in I_{DVF} compared to I_{Ca2+} (Fig. 23.6e, f). For CRAC channels, it has been hypothesized that this prominent enhancement in current densities correlates with the extent of inactivation [137]. In a Ca^{2+}-containing solution, CRAC channels display FCDI, but in a divalent free Na^{+}-containing solution, CRAC channel currents exhibit no inactivation, similar to constitutively active mutants in the presence of STIM1 [110]. This possibly explains the increased current levels observed in a solution containing Na^{+}-compared to Ca^{2+}- as a charge carrier [13]. This correlation has been suggested to potentially underlie an altered open probability in a Ca^{2+}- versus Na^{+}- containing solution [137]. Indeed, diverse studies [46, 137, 144, 167] have suggested that Ca^{2+} dependent inactivation is likely to reduce the open probability when Ca^{2+} rather than Na^{+} is the charge carrier. In accordance with these findings, the extent of the FCDI of Orai1 and Orai3, which is much more pronounced for Orai3, also correlates with larger current enhancements for Orai3 in a Na^{+} versus Ca^{2+} containing solution compared to Orai1 [129].

Interestingly, in the absence of STIM1 the currents of several constitutively active mutants, especially those in the outer TM regions, TM2-TM4, exhibit decreased I_{DVF} versus I_{Ca2+} in a reversible manner, a feature that was reported for the first time by Derler et al. [110] and is here exemplarily shown for Orai1 F136S (Fig. 23.6k, l; 5D). A potential explanation might be a distinct inactivation behaviour found in Ca^{2+}- versus Na^{+}-containing solutions. While hyperpolarizing voltage steps have shown loss of inactivation, but strong reactivation in the presence of Ca^{2+}, in a Na^{+}-containing divalent-free solution, these mutants yielded only loss of inactivation, and lack reactivation. Thus, this difference in the "inactivation behavior" in a Ca^{2+}-versus Na^{+}-containing solution might account for reduced I_{DVF} versus I_{Ca2+}. One exception represents Orai1 H134A, as it shows enhancements in I_{DVF} versus I_{Ca2+} [68], thus, probably matches the STIM1 bound Orai1 open state even more than other Orai1 TM2-TM4 constitutively active mutants.

Intriguingly, in contrast to the TM2/3/4 mutants, the poorly Ca^{2+}-selective Orai1 V102A/C mutants displayed strongly increased Na^{+} divalent-free versus Ca^{2+} currents, both, in the absence and presence of STIM1 [67]. Other investigations of various constitutively active TM mutants have revealed differences in Cs^{+} per-

meation. As mentioned in the section entitled "CRAC/Orai channel permeability", Cs^+ is known to be impermeable for CRAC or STIM1/Orai1 channels [67]. The non-selective Orai1 V102A/C allow permeation of Cs^+ [110], due to an enhanced pore diameter. In the presence of STIM1, Cs^+ permeation across Orai1 V102A/C is abolished, as STIM1 coupling narrows the pore, thus restoring the pore dimensions of the wild-type Orai1 channel. In contrast to Orai1 V102A/C, other constitutively active TM3/TM4 mutants are impermeable to Cs^+ in the absence of STIM1, suggesting that their pore diameters are comparable in the absence or presence of STIM1 [110]. Thus, differences in current size in a Ca^{2+} containing versus Na^+ containing divalent free solution of different constitutively active mutants are probably determined by the differences in pore diameter, which still requires further clarification.

However, at this point, it is unclear why Orai1 V102A/C and other Orai TM mutants exhibit an identical inactivation behaviour, despite so far discussed differences in V_{rev} and I_{DVF}/I_{Ca2+}, [110, 148] (Fig. 23.7c, d). All constitutive Orai mutants exhibit reactivation in the absence of STIM1 and inactivation in the presence of STIM1. It is probable that an enhanced pore diameter, as is the case for Orai1 V102A, does not additionally enhance the extent of reactivation, but this supposition requires further evaluation and direct comparisons.

The Orai1 ANSGA mutant represents another exception, with respect to the enhancements in currents in a Na^+ divalent free solution, in the absence of STIM1. The current ratio I_{DVF}/I_{Ca2+} amounts to 1 (Fig. 23.6q, r; 5F), showing that currents in a Ca^{2+}-containing solution exhibit levels comparable to those in divalent free Na^+-containing solution only for this mutant.

Maintenance of authentic CRAC channel hallmarks not only requires STIM1, but also an intact Orai N-terminus. Using Orai1 V102A it has been impressively shown that an N-terminal deletion up to aa 78 still preserves constitutive activity, while the Ca^{2+} selectivity in the presence of STIM1 is lost. Only a deletion up to aa 74 fully maintains Ca^{2+} selectivity in line with the preserved store-operated activation of wild-type Orai1 upon deletion up to aa 74/75 in the presence of STIM1 [64, 67, 110, 121]. Other constitutive Orai1 mutants lead to loss of function upon deletion up to aa 78, while the function can be restored via the swap of Orai3 loop2 (Fig. 23.6g) as in the wild-type Orai1 (Fig. 23.6a) and in line with preserved function of analogue Orai3 N-terminal deletion mutants [61, 110]. N-truncation Orai1-Orai3-loop2 chimeras and analogue Orai3 N-truncation mutants have revealed that the reversal potential is not altered in the presence of STIM1 to more positive values, underlining the fact that residues upstream of aa 78, including the entire ETON region, are required to maintain the Ca^{2+} selectivity of Orai channels [110].

Furthermore, N-truncated constitutive mutants in the outer TM regions, TM2-TM4, have been employed to clarify the role of the N-terminus in maintaining the other CRAC channel hallmarks (FCDI and the ratio of I_{DVF}/I_{Ca2+}). We have discovered that a deletion of the first 74 residues already leads to abolished FCDI and enhancement of I_{DVF} versus I_{Ca2+} also in the presence of STIM1, suggesting that residues upstream of position 74 are required for full maintenance of authentic CRAC channel characteristics [110]. Moreover, this holds not only for the

constitutively active mutants, but also for wild-type Orai proteins. Thus, in contrast to store-operated activation which requires only the last half of the ETON region (aa 80-90), for maintenance of CRAC channel hallmarks the whole ETON region is indispensable. Furthermore, we have shown that the interplay of the N-terminus with loop2 governs the maintenance of authentic CRAC channel characteristics, as a swap of loop2 between Orai1 and Orai3 N-truncation mutants alters CRAC channel properties in various ways. It is noteworthy that the Orai1 ANSGA mutant loses function upon N-terminal deletion up to aa 78. However, the function cannot be recovered via the switch of the Orai3 loop2 for this mutant function (Fig. 23.6m). This suggests that conformational alterations within the hinge region disrupt the communication with the loop2 region pointing to distinct conformational alterations via ANSGA compared to the diversity of other constitutively active mutants [61].

In summary, authentic CRAC channel hallmarks are only maintained in the presence of STIM1 and an intact Orai N-terminus. Otherwise, typical CRAC channel characteristics are fully abolished, as shown with diverse constitutively active Orai mutants. The latter, however, exhibit differences in their biophysical properties and thus can be categorized into three groups: Orai1 V102A, most TM2/TM3/TM4 constitutively active mutants and the Orai1 ANSGA mutant (Fig. 23.7). Obviously, these different constitutively active mutants adjust distinct partially open states. At this point, however, it remains unclear if STIM1 mediated Orai activation induces comparable structural alterations at some point as observed for the constitutively active mutants before reaching the final open state. Moreover, it is elusive, whether STIM1 binding and the Orai N-terminus establish these authentic CRAC channel properties via direct or indirect communication which should be ultimately addressed at a structural level.

23.8 Lipid Mediated Regulation of the STIM1/Orai Channel Complex

STIM1 and Orai1 proteins can fully reconstitute CRAC channel currents [84]. However, several components [115, 117, 171, 177–190] in the cell have been found to modulate the interplay, interaction and activation of the STIM1-Orai channel complex. Some regulatory proteins, such as SARAF, STIMATE or CRACR2A have already been briefly mentioned in this review, while a detailed presentation of these can be found in the following reviews [59, 118–120]. Here, we provide an overview of lipid mediated regulation of the STIM1/Orai channel complex. Among the lipids, PIP_2 and cholesterol have been found to predominantly regulate CRAC channels.

PIP_2 represents a minor phospholipid that is found in the inner leaflet of the plasma membrane and plays an essential role in the modulation of several ion channels [191–193]. Furthermore, it reportedly regulates STIM proteins. Both, STIM1 and STIM2 contain a lysine-rich domain at the very end of their C-termini, which resembles a PIP_2 binding site [50]. This domain is larger in STIM2 [51].

The STIM1-Orai1 clustering, STIM1 targeting to ER-PM junctions and stable interaction between STIM1 and the plasma membrane have been shown to be affected upon reduction of PIP_2 or PIP_3 levels [50, 183–185]. Nevertheless, store-operated currents are maintained upon PIP_2 depletion [183, 185]. Enhanced PIP_2 levels in liposomes enabled preferential binding of STIM2 [51], suggesting that PIP_2 contributes to STIM2 recruitment to the plasma membrane. In contrast, the reduction in PIP_2 levels affects STIM1 translocation only mildly, although CRAC currents are strongly impaired [183]. Recently, a novel regulatory protein RASSF4 was found to control SOCE and ER-PM junctions by affecting steady state PIP_2 levels in the plasma membrane. Knock-down of RASSF4 leads to reduced PIP_2 levels and in consequence to decreased STIM1-Orai1 mediated currents [194, 195].

Cholesterol represents a class that is distinct from other membrane lipids, as it cannot form membranes on its own and it penetrates less deeply into the hydrophobic layer of membrane leaflets [196]. Moreover, cholesterol is a highly mobile lipid, and drug-induced modulation of the cholesterol levels in the membrane can have a large impact on virus replication and trafficking pathways [196]. Membrane rafts have been suggested to contain high concentrations of cholesterol as well as sphingolipids [196].

Among the diversity of ion channels (nAChR, Kir, BK, TRPV [197]), the CRAC channel components, STIM1 and Orai1 have also been recently found to be regulated by cholesterol [112–114]. Enzymatically or chemically induced cholesterol depletion enhances SOCE or Ca^{2+} currents from STIM1/Orai1 expressing HEK cells and increases endogenous CRAC currents in mast cells [113]. The latter also leads to enhanced mast cell degranulation as pathophysiologically observed in hypocholesterolemia patients associated with the Smith-Lemli-Opitz syndrome [198]. In support of these observations, both, STIM1 and Orai1 have been shown to bind cholesterol which affects STIM1 mediated Orai1 currents in an inhibitory manner [113, 114].

Cholesterol can interact with membrane proteins via specific cholesterol binding motifs, such as the cholesterol recognition amino acid consensus motif (CRAC) [197, 199, 200]. The CRAC motif, with the consensus sequence -L/V-$(X)_{(1-5)}$-Y-$(X)_{(1-5)}$-R/K-, is located at the protein-lipid interface of a transmembrane domain [200]. Cholesterol as part of the membrane is located either in the outer or inner leaflet of the membrane, and its head groups (-OH group in cholesterol) are aligned in a row with the head groups of the other lipids located in the upper or lower leaflet. Due to considerable variability of the consensus sequence for cholesterol binding motifs, other criteria such as its close proximity to a TM region, formation of an α-helical structure and/or its incorporation in a protein located within lipid rafts is required [196, 201, 202]. The STIM1 C-terminus and Orai1 N-terminus have been shown to contain a putative cholesterol binding motif. The cholesterol binding motif within Orai1 N-terminus is located in the conserved ETON region that extends from aa 74-83 [113]. In STIM1 C-terminus it is located within the SOAR domain, specifically at aa 357 – 366 in CC2 [114]. Mutations of those cholesterol binding motifs (L74I, Y80S in Orai1, I364A in STIM1), that lead to abolished cholesterol binding, have been shown to strongly enhance Orai1 currents mediated

by STIM1 or STIM1-C-terminal fragments, and these findings are in line with the enhancements observed upon chemically induced cholesterol depletion. A lack of cholesterol binding does not affect the selectivity of CRAC currents and retains the association of STIM1 to Orai1. Overall, these findings clearly indicate that the CRAC channel function can be modulated by lipids such as PIP_2 and cholesterol.

23.9 Perspectives

Over the past decade, considerable progress has been made in understanding the key molecular components of CRAC channels. Currently, two 3D atomic structures of the Orai protein are available; one showing the closed and one the open state. Nevertheless, several questions remain to be answered in the CRAC channel field.

With regard to STIM1, structural resolutions are currently only available for cytosolic C-terminal fragments. Furthermore, the two different, available structures of STIM1 C-terminal portions have revealed significant differences. Hence, further structural studies are needed, particularly on longer STIM1 C-terminal fragments in order to clarify the intra- and intermolecular interactions that govern the activation of STIM1. Mutations within STIM1 proteins locking them in the active, extended conformation e.g. L251S probably helps to obtain structures that mimic the active state of cytosolic STIM1.

Unlike STIM1, the dOrai structure has already been resolved in two conformations, which are assumed to represent the closed and the open state, respectively. Nevertheless, the structure of the gain-of-function mutant represents an open state in the absence of STIM1. Thus, it is unclear whether this structure mimics the STIM1-bound Orai open conformation. The novel structure indicates a huge structural rearrangement within TM4-C-terminus, but a great deal of energy would be required to stabilize this conformation. Thus, the provision of additional structures for other gain-of-function mutants (e.g. Orai1 P245X) or the STIM1-Orai complex as well as a structure for a human Orai would further clarify the pore opening mechanisms of CRAC channels.

The detailed molecular mechanism of how STIM1 gates Orai channels into the open state is still only partially understood. Thus far, only the NMR structure of a complex of C-terminal fragments of STIM1 and Orai1 is available and this has been a key to characterizing the main STIM1-Orai1 interaction sites. There is clear evidence that other cytosolic strands within Orai are involved in the STIM1 mediated gating process. However, whether this occurs via direct or indirect interaction still remains to be resolved. In addition, structural resolutions of a STIM1-Orai1 complex might also provide further insight into essential binding sites of STIM1 within Orai. These studies may reveal the structural alterations that take place upon activation of the Orai channel including re-arrangements of the cytosolic strands that are linked with those in the TM regions. Here, single particle cryo-EM [203, 204] represents another valuable approach, that can be used, as this has been successfully used with ion channels such as TRPV1 [205], TRPML3 [206] and the IP_3-receptor [207] to obtain resolutions that are similar to those obtained using crystallography.

As a complement to structural resolutions, the precise and dynamic resolution of the CRAC channel function was obtained using light [40, 208–210]. This sophisticated optogenetics approach can be capitalized upon to control and understand the STIM1-Orai communication more effectively and elucidate the structure-function relationship in more detail.

The current achievements hat have been made in the understanding of the communication between STIM and Orai proteins have allowed to enhance our knowledge of physiological down-stream signaling for the CRAC channels [211, 212]. The native CRAC channel system becomes even more complex when considering the accessory cellular components that regulate the STIM/Orai communication, such as SARAF [171], STIMATE [213] and cholesterol [112–114] and potentially enables fine-tuned interference with drugs. Even though several CRAC channel blockers are currently available [214–216], their precise sites of action have remained elusive. In addition to the classical pore blockers, the complexity of the CRAC channel machinery allows a variety of interventions to be made, which can interfere with the coupling of CRAC channel components or their conformational changes from the closed to the open state in order. Hence, novel CRAC channel modulators with significant therapeutic potential in immune deficiency, autoimmune or allergic disorders can potentially be uncovered.

Acknowledgements This work was supported by the Austrian Science Fund (FWF projects P27641 and P30567 to I.D.).

References

1. Misceo D, Holmgren A, Louch WE, Holme PA, Mizobuchi M, Morales RJ, De Paula AM, Stray-Pedersen A, Lyle R, Dalhus B, Christensen G, Stormorken H, Tjonnfjord GE, Frengen E (2014) A dominant STIM1 mutation causes Stormorken syndrome. Hum Mutat 35(5):556–564. https://doi.org/10.1002/humu.22544
2. Feske S, Gwack Y, Prakriya M, Srikanth S, Puppel SH, Tanasa B, Hogan PG, Lewis RS, Daly M, Rao A (2006) A mutation in Orai1 causes immune deficiency by abrogating CRAC channel function. Nature 441(7090):179–185
3. Parekh AB, Putney JW Jr (2005) Store-operated calcium channels. Physiol Rev 85(2):757–810. https://doi.org/10.1152/physrev.00057.2003
4. Zhang SL, Yeromin AV, Zhang XH, Yu Y, Safrina O, Penna A, Roos J, Stauderman KA, Cahalan MD (2006) Genome-wide RNAi screen of Ca^{2+} influx identifies genes that regulate Ca^{2+} release-activated Ca^{2+} channel activity. Proc Natl Acad Sci U S A 103(24):9357–9362. https://doi.org/10.1073/pnas.0603161103
5. Berna-Erro A, Woodard GE, Rosado JA (2012) Orais and STIMs: physiological mechanisms and disease. J Cell Mol Med 16(3):407–424. https://doi.org/10.1111/j.1582-4934.2011.01395.x
6. Morin G, Bruechle NO, Singh AR, Knopp C, Jedraszak G, Elbracht M, Bremond-Gignac D, Hartmann K, Sevestre H, Deutz P, Herent D, Nurnberg P, Romeo B, Konrad K, Mathieu-Dramard M, Oldenburg J, Bourges-Petit E, Shen Y, Zerres K, Ouadid-Ahidouch H, Rochette J (2014) Gain-of-function mutation in STIM1 (P.R304W) is associated with stormorken syndrome. Hum Mutat 35(10):1221–1232. https://doi.org/10.1002/humu.22621

7. Thompson JL, Mignen O, Shuttleworth TJ (2009) The Orai1 severe combined immune deficiency mutation and calcium release-activated Ca^{2+} channel function in the heterozygous condition. J Biol Chem 284(11):6620–6626. https://doi.org/10.1074/jbc.M808346200
8. Nesin V, Wiley G, Kousi M, Ong EC, Lehmann T, Nicholl DJ, Suri M, Shahrizaila N, Katsanis N, Gaffney PM, Wierenga KJ, Tsiokas L (2014) Activating mutations in STIM1 and ORAI1 cause overlapping syndromes of tubular myopathy and congenital miosis. Proc Natl Acad Sci U S A 111(11):4197–4202. https://doi.org/10.1073/pnas.1312520111 1312520111 [pii]
9. Zhang SL, Yu Y, Roos J, Kozak JA, Deerinck TJ, Ellisman MH, Stauderman KA, Cahalan MD (2005) STIM1 is a Ca^{2+} sensor that activates CRAC channels and migrates from the Ca^{2+} store to the plasma membrane. Nature 437(7060):902–905. doi:nature04147 [pii] https://doi.org/10.1038/nature04147
10. Roos J, DiGregorio PJ, Yeromin AV, Ohlsen K, Lioudyno M, Zhang S, Safrina O, Kozak JA, Wagner SL, Cahalan MD, Velicelebi G, Stauderman KA (2005) STIM1, an essential and conserved component of store-operated Ca^{2+} channel function. J Cell Biol 169(3):435–445. https://doi.org/10.1083/jcb.200502019
11. Liou J, Kim ML, Heo WD, Jones JT, Myers JW, Ferrell JE Jr, Meyer T (2005) STIM is a Ca^{2+} sensor essential for Ca^{2+}-store-depletion-triggered Ca^{2+} influx. Curr Biol 15(13):1235–1241
12. Vig M, Peinelt C, Beck A, Koomoa DL, Rabah D, Koblan-Huberson M, Kraft S, Turner H, Fleig A, Penner R, Kinet JP (2006) CRACM1 is a plasma membrane protein essential for store-operated Ca^{2+} entry. Science 312(5777):1220–1223
13. Prakriya M, Feske S, Gwack Y, Srikanth S, Rao A, Hogan PG (2006) Orai1 is an essential pore subunit of the CRAC channel. Nature 443(7108):230–233. https://doi.org/10.1038/nature05122
14. Hou X, Pedi L, Diver MM, Long SB (2012) Crystal structure of the calcium release-activated calcium channel Orai. Science 338(6112):1308–1313. https://doi.org/10.1126/science.1228757
15. Hou X, Burstein SR, Long S (2018) Structures reveal opening of the store-operated calcium channel Orai. bioRxiv. https://doi.org/10.1101/284034
16. Stathopulos PB, Schindl R, Fahrner M, Zheng L, Gasmi-Seabrook GM, Muik M, Romanin C, Ikura M (2013) STIM1/Orai1 coiled-coil interplay in the regulation of store-operated calcium entry. Nat Commun 4:2963. https://doi.org/10.1038/ncomms3963
17. Yang X, Jin H, Cai X, Li S, Shen Y (2012) Structural and mechanistic insights into the activation of Stromal interaction molecule 1 (STIM1). Proc Natl Acad Sci U S A 109(15):5657–5662. https://doi.org/10.1073/pnas.1118947109
18. Soboloff J, Rothberg BS, Madesh M, Gill DL (2012) STIM proteins: dynamic calcium signal transducers. Nat Rev Mol Cell Biol 13(9):549–565. https://doi.org/10.1038/nrm3414
19. Cahalan MD (2009) STIMulating store-operated Ca^{2+} entry. Nat Cell Biol 11(6):669–677. https://doi.org/10.1038/ncb0609-669
20. Manji SS, Parker NJ, Williams RT, van Stekelenburg L, Pearson RB, Dziadek M, Smith PJ (2000) STIM1: a novel phosphoprotein located at the cell surface. Biochim Biophys Acta 1481(1):147–155
21. Soboloff J, Spassova MA, Tang XD, Hewavitharana T, Xu W, Gill DL (2006) Orai1 and STIM reconstitute store-operated calcium channel function. J Biol Chem 281(30):20661–20665. https://doi.org/10.1074/jbc.C600126200
22. Ambily A, Kaiser WJ, Pierro C, Chamberlain EV, Li Z, Jones CI, Kassouf N, Gibbins JM, Authi KS (2014) The role of plasma membrane STIM1 and Ca^{2+}entry in platelet aggregation. STIM1 binds to novel proteins in human platelets. Cell Signal 26(3):502–511. https://doi.org/10.1016/j.cellsig.2013.11.025
23. Spassova MA, Soboloff J, He LP, Xu W, Dziadek MA, Gill DL (2006) STIM1 has a plasma membrane role in the activation of store-operated Ca^{2+} channels. Proc Natl Acad Sci U S A 103(11):4040–4045. https://doi.org/10.1073/pnas.0510050103
24. Shuttleworth TJ (2009) Arachidonic acid, ARC channels, and Orai proteins. Cell Calcium 45(6):602–610. https://doi.org/10.1016/j.ceca.2009.02.001

25. Thompson JL, Shuttleworth TJ (2012) A plasma membrane-targeted cytosolic domain of STIM1 selectively activates ARC channels, an arachidonate-regulated store-independent Orai channel. Channels (Austin) 6(5):370–378. https://doi.org/10.4161/chan.21947
26. Novello MJ, Zhu J, Feng Q, Ikura M, Stathopulos PB (2018) Structural elements of stromal interaction molecule function. Cell Calcium 73:88–94. https://doi.org/10.1016/j.ceca.2018.04.006
27. Varga-Szabo D, Braun A, Nieswandt B (2011) STIM and Orai in platelet function. Cell Calcium 50(3):270–278. https://doi.org/10.1016/j.ceca.2011.04.002
28. Braun A, Vogtle T, Varga-Szabo D, Nieswandt B (2011) STIM and Orai in hemostasis and thrombosis. Front Biosci (Landmark Ed) 16:2144–2160
29. Zbidi H, Jardin I, Woodard GE, Lopez JJ, Berna-Erro A, Salido GM, Rosado JA (2011) STIM1 and STIM2 are located in the acidic Ca^{2+} stores and associates with Orai1 upon depletion of the acidic stores in human platelets. J Biol Chem 286(14):12257–12270. https://doi.org/10.1074/jbc.M110.190694
30. Soboloff J, Spassova MA, Dziadek MA, Gill DL (2006) Calcium signals mediated by STIM and Orai proteins – a new paradigm in inter-organelle communication. Biochim Biophys Acta 1763(11):1161–1168. https://doi.org/10.1016/j.bbamcr.2006.09.023
31. Rosado JA, Diez R, Smani T, Jardin I (2015) STIM and Orai1 variants in store-operated calcium entry. Front Pharmacol 6:325. https://doi.org/10.3389/fphar.2015.00325
32. Rana A, Yen M, Sadaghiani AM, Malmersjo S, Park CY, Dolmetsch RE, Lewis RS (2015) Alternative splicing converts STIM2 from an activator to an inhibitor of store-operated calcium channels. J Cell Biol 209(5):653–669. https://doi.org/10.1083/jcb.201412060
33. Miederer AM, Alansary D, Schwar G, Lee PH, Jung M, Helms V, Niemeyer BA (2015) A STIM2 splice variant negatively regulates store-operated calcium entry. Nat Commun 6:6899. https://doi.org/10.1038/ncomms7899
34. Hewavitharana T, Deng X, Soboloff J, Gill DL (2007) Role of STIM and Orai proteins in the store-operated calcium signaling pathway. Cell Calcium 42(2):173–182. https://doi.org/10.1016/j.ceca.2007.03.009
35. Cai X (2007) Molecular evolution and functional divergence of the Ca^{2+} sensor protein in store-operated Ca^{2+} entry: stromal interaction molecule. PLoS One 2(7):e609. https://doi.org/10.1371/journal.pone.0000609
36. Stathopulos PB, Zheng L, Li GY, Plevin MJ, Ikura M (2008) Structural and mechanistic insights into STIM1-mediated initiation of store-operated calcium entry. Cell 135(1):110–122. https://doi.org/10.1016/j.cell.2008.08.006
37. Zheng L, Stathopulos PB, Schindl R, Li GY, Romanin C, Ikura M (2011) Auto-inhibitory role of the EF-SAM domain of STIM proteins in store-operated calcium entry. Proc Natl Acad Sci U S A 108(4):1337–1342. https://doi.org/10.1073/pnas.1015125108
38. Baba Y, Hayashi K, Fujii Y, Mizushima A, Watarai H, Wakamori M, Numaga T, Mori Y, Iino M, Hikida M, Kurosaki T (2006) Coupling of STIM1 to store-operated Ca^{2+} entry through its constitutive and inducible movement in the endoplasmic reticulum. Proc Natl Acad Sci U S A 103(45):16704–16709. https://doi.org/10.1073/pnas.0608358103
39. Derler I, Jardin I, Romanin C (2016) Molecular mechanisms of STIM/Orai communication. Am J Physiol Cell Physiol 310(8):C643–C662. https://doi.org/10.1152/ajpcell.00007.2016
40. Ma G, Wei M, He L, Liu C, Wu B, Zhang SL, Jing J, Liang X, Senes A, Tan P, Li S, Sun A, Bi Y, Zhong L, Si H, Shen Y, Li M, Lee MS, Zhou W, Wang J, Wang Y, Zhou Y (2015) Inside-out Ca^{2+} signalling prompted by STIM1 conformational switch. Nat Commun 6:7826. https://doi.org/10.1038/ncomms8826
41. Muik M, Fahrner M, Derler I, Schindl R, Bergsmann J, Frischauf I, Groschner K, Romanin C (2009) A cytosolic homomerization and a modulatory domain within STIM1 C terminus determine coupling to ORAI1 channels. J Biol Chem 284(13):8421–8426. https://doi.org/10.1074/jbc.C800229200
42. Kawasaki T, Lange I, Feske S (2009) A minimal regulatory domain in the C terminus of STIM1 binds to and activates ORAI1 CRAC channels. Biochem Biophys Res Commun 385(1):49–54. https://doi.org/10.1016/j.bbrc.2009.05.020

43. Park CY, Hoover PJ, Mullins FM, Bachhawat P, Covington ED, Raunser S, Walz T, Garcia KC, Dolmetsch RE, Lewis RS (2009) STIM1 clusters and activates CRAC channels via direct binding of a cytosolic domain to Orai1. Cell 136(5):876–890. https://doi.org/10.1016/j.cell.2009.02.014
44. Yuan JP, Zeng W, Dorwart MR, Choi YJ, Worley PF, Muallem S (2009) SOAR and the polybasic STIM1 domains gate and regulate Orai channels. Nat Cell Biol 11(3):337–343. https://doi.org/10.1038/ncb1842
45. Fahrner M, Muik M, Schindl R, Butorac C, Stathopulos P, Zheng L, Jardin I, Ikura M, Romanin C (2014) A coiled-coil clamp controls both conformation and clustering of stromal interaction molecule 1 (STIM1). J Biol Chem 289(48):33231–33244. https://doi.org/10.1074/jbc.M114.610022
46. Mullins FM, Lewis RS (2016) The inactivation domain of STIM1 is functionally coupled with the Orai1 pore to enable Ca^{2+}-dependent inactivation. J Gen Physiol 147(2):153–164. https://doi.org/10.1085/jgp.201511438
47. Derler I, Fahrner M, Muik M, Lackner B, Schindl R, Groschner K, Romanin C (2009) A Ca2(+)release-activated Ca2(+) (CRAC) modulatory domain (CMD) within STIM1 mediates fast Ca2(+)-dependent inactivation of ORAI1 channels. J Biol Chem 284(37):24933–24938. doi:C109.024083 [pii] https://doi.org/10.1074/jbc.C109.024083
48. Li Z, Lu J, Xu P, Xie X, Chen L, Xu T (2007) Mapping the interacting domains of STIM1 and Orai1 in Ca^{2+} release-activated Ca^{2+} channel activation. J Biol Chem 282(40):29448–29456. https://doi.org/10.1074/jbc.M703573200
49. Hogan PG, Lewis RS, Rao A (2010) Molecular basis of calcium signaling in lymphocytes: STIM and ORAI. Annu Rev Immunol 28:491–533. https://doi.org/10.1146/annurev.immunol.021908.132550
50. Liou J, Fivaz M, Inoue T, Meyer T (2007) Live-cell imaging reveals sequential oligomerization and local plasma membrane targeting of stromal interaction molecule 1 after Ca^{2+} store depletion. Proc Natl Acad Sci U S A 104(22):9301–9306. https://doi.org/10.1073/pnas.0702866104
51. Ercan E, Momburg F, Engel U, Temmerman K, Nickel W, Seedorf M (2009) A conserved, lipid-mediated sorting mechanism of yeast Ist2 and mammalian STIM proteins to the peripheral ER. Traffic 10(12):1802–1818. doi:TRA995 [pii] https://doi.org/10.1111/j.1600-0854.2009.00995.x
52. Wang X, Wang Y, Zhou Y, Hendron E, Mancarella S, Andrake MD, Rothberg BS, Soboloff J, Gill DL (2014) Distinct Orai-coupling domains in STIM1 and STIM2 define the Orai-activating site. Nat Commun 5:3183. https://doi.org/10.1038/ncomms4183
53. Bogeski I, Al-Ansary D, Qu B, Niemeyer BA, Hoth M, Peinelt C (2010) Pharmacology of ORAI channels as a tool to understand their physiological functions. Expert Rev Clin Pharmacol 3(3):291–303. https://doi.org/10.1586/ecp.10.23
54. Vanden Abeele F, Dubois C, Shuba Y, Prevarskaya N (2015) Disrupting the dynamic equilibrium of ORAI channels determines the phenotype of malignant cells. Mol Cell Oncol 2(2):e975631. https://doi.org/10.4161/23723556.2014.975631
55. Dubois C, Vanden Abeele F, Lehen'kyi V, Gkika D, Guarmit B, Lepage G, Slomianny C, Borowiec AS, Bidaux G, Benahmed M, Shuba Y, Prevarskaya N (2014) Remodeling of channel-forming ORAI proteins determines an oncogenic switch in prostate cancer. Cancer Cell 26(1):19–32. https://doi.org/10.1016/j.ccr.2014.04.025
56. Ji W, Xu P, Li Z, Lu J, Liu L, Zhan Y, Chen Y, Hille B, Xu T, Chen L (2008) Functional stoichiometry of the unitary calcium-release-activated calcium channel. Proc Natl Acad Sci U S A 105(36):13668–13673. doi:0806499105 [pii] https://doi.org/10.1073/pnas.0806499105
57. Mignen O, Thompson JL, Shuttleworth TJ (2008) Orai1 subunit stoichiometry of the mammalian CRAC channel pore. J Physiol 586(2):419–425. doi:jphysiol.2007.147249 [pii] https://doi.org/10.1113/jphysiol.2007.147249
58. Penna A, Demuro A, Yeromin AV, Zhang SL, Safrina O, Parker I, Cahalan MD (2008) The CRAC channel consists of a tetramer formed by Stim-induced dimerization of Orai dimers. Nature 456(7218):116–120. https://doi.org/10.1038/nature07338

59. Hogan PG, Rao A (2015) Store-operated calcium entry: mechanisms and modulation. Biochem Biophys Res Commun 460(1):40–49. https://doi.org/10.1016/j.bbrc.2015.02.110
60. Shuttleworth TJ (2012) Orai3 – the 'exceptional' Orai? J Physiol 590(Pt 2):241–257. https://doi.org/10.1113/jphysiol.2011.220574
61. Fahrner M, Pandey SK, Muik M, Traxler L, Butorac C, Stadlbauer M, Zayats V, Krizova A, Plenk P, Frischauf I, Schindl R, Gruber HJ, Hinterdorfer P, Ettrich R, Romanin C, Derler I (2018) Communication between N terminus and loop2 tunes Orai activation. J Biol Chem 293(4):1271–1285. https://doi.org/10.1074/jbc.M117.812693
62. Yen M, Lokteva LA, Lewis RS (2016) Functional analysis of Orai1 concatemers supports a hexameric stoichiometry for the CRAC channel. Biophys J 111(9):1897–1907. https://doi.org/10.1016/j.bpj.2016.09.020
63. Cai X, Zhou Y, Nwokonko RM, Loktionova NA, Wang X, Xin P, Trebak M, Wang Y, Gill DL (2016) The Orai1 store-operated calcium channel functions as a hexamer. J Biol Chem 291(50):25764–25775. https://doi.org/10.1074/jbc.M116.758813
64. Derler I, Plenk P, Fahrner M, Muik M, Jardin I, Schindl R, Gruber HJ, Groschner K, Romanin C (2013) The extended transmembrane Orai1 N-terminal (ETON) region combines binding interface and gate for Orai1 activation by STIM1. J Biol Chem 288(40):29025–29034. https://doi.org/10.1074/jbc.M113.501510
65. Zhou Y, Cai X, Loktionova NA, Wang X, Nwokonko RM, Wang X, Wang Y, Rothberg BS, Trebak M, Gill DL (2016) The STIM1-binding site nexus remotely controls Orai1 channel gating. Nat Commun 7:13725. https://doi.org/10.1038/ncomms13725
66. Frischauf I, Zayats V, Deix M, Hochreiter A, Jardin I, Muik M, Lackner B, Svobodova B, Pammer T, Litvinukova M, Sridhar AA, Derler I, Bogeski I, Romanin C, Ettrich RH, Schindl R (2015) A calcium-accumulating region, CAR, in the channel Orai1 enhances Ca^{2+} permeation and SOCE-induced gene transcription. Sci Signal 8(408):ra131. https://doi.org/10.1126/scisignal.aab1901
67. McNally BA, Somasundaram A, Yamashita M, Prakriya M (2012) Gated regulation of CRAC channel ion selectivity by STIM1. Nature 482(7384):241–245. https://doi.org/10.1038/nature10752
68. Frischauf I, Litvinukova M, Schober R, Zayats V, Svobodova B, Bonhenry D, Lunz V, Cappello S, Tociu L, Reha D, Stallinger A, Hochreiter A, Pammer T, Butorac C, Muik M, Groschner K, Bogeski I, Ettrich RH, Romanin C, Schindl R (2017) Transmembrane helix connectivity in Orai1 controls two gates for calcium-dependent transcription. Sci Signal 10(507). https://doi.org/10.1126/scisignal.aao0358
69. Yamashita M, Yeung PS, Ing CE, McNally BA, Pomes R, Prakriya M (2017) STIM1 activates CRAC channels through rotation of the pore helix to open a hydrophobic gate. Nat Commun 8:14512. https://doi.org/10.1038/ncomms14512
70. Palty R, Stanley C, Isacoff EY (2015) Critical role for Orai1 C-terminal domain and TM4 in CRAC channel gating. Cell Res 25(8):963–980. https://doi.org/10.1038/cr.2015.80
71. Bohm J, Bulla M, Urquhart JE, Malfatti E, Williams SG, O'Sullivan J, Szlauer A, Koch C, Baranello G, Mora M, Ripolone M, Violano R, Moggio M, Kingston H, Dawson T, DeGoede CG, Nixon J, Boland A, Deleuze JF, Romero N, Newman WG, Demaurex N, Laporte J (2017) ORAI1 mutations with distinct channel gating defects in tubular aggregate myopathy. Hum Mutat 38(4):426–438. https://doi.org/10.1002/humu.23172
72. Endo Y, Noguchi S, Hara Y, Hayashi YK, Motomura K, Miyatake S, Murakami N, Tanaka S, Yamashita S, Kizu R, Bamba M, Goto Y, Matsumoto N, Nonaka I, Nishino I (2015) Dominant mutations in ORAI1 cause tubular aggregate myopathy with hypocalcemia via constitutive activation of store-operated Ca(2)(+) channels. Hum Mol Genet 24(3):637–648. https://doi.org/10.1093/hmg/ddu477
73. Yeung PS, Yamashita M, Ing CE, Pomes R, Freymann DM, Prakriya M (2018) Mapping the functional anatomy of Orai1 transmembrane domains for CRAC channel gating. Proc Natl Acad Sci U S A 115(22):E5193–E5202. https://doi.org/10.1073/pnas.1718373115
74. Covington ED, Wu MM, Lewis RS (2010) Essential role for the CRAC activation domain in store-dependent oligomerization of STIM1. Mol Biol Cell 21(11):1897–1907. https://doi.org/10.1091/mbc.E10-02-0145

75. Grigoriev I, Gouveia SM, van der Vaart B, Demmers J, Smyth JT, Honnappa S, Splinter D, Steinmetz MO, Putney JW Jr, Hoogenraad CC, Akhmanova A (2008) STIM1 is a MT-plus-end-tracking protein involved in remodeling of the ER. Curr Biol 18(3):177–182. https://doi.org/10.1016/j.cub.2007.12.050
76. Honnappa S, Gouveia SM, Weisbrich A, Damberger FF, Bhavesh NS, Jawhari H, Grigoriev I, van Rijssel FJ, Buey RM, Lawera A, Jelesarov I, Winkler FK, Wuthrich K, Akhmanova A, Steinmetz MO (2009) An EB1-binding motif acts as a microtubule tip localization signal. Cell 138(2):366–376. https://doi.org/10.1016/j.cell.2009.04.065
77. Huang Y, Zhou Y, Wong HC, Chen Y, Wang S, Castiblanco A, Liu A, Yang JJ (2009) A single EF-hand isolated from STIM1 forms dimer in the absence and presence of Ca^{2+}. FEBS J 276(19):5589–5597. https://doi.org/10.1111/j.1742-4658.2009.07240.x
78. Mercer JC, Dehaven WI, Smyth JT, Wedel B, Boyles RR, Bird GS, Putney JW Jr (2006) Large store-operated calcium selective currents due to co-expression of Orai1 or Orai2 with the intracellular calcium sensor, Stim1. J Biol Chem 281(34):24979–24990. https://doi.org/10.1074/jbc.M604589200
79. Brandman O, Liou J, Park WS, Meyer T (2007) STIM2 is a feedback regulator that stabilizes basal cytosolic and endoplasmic reticulum Ca^{2+} levels. Cell 131(7):1327–1339. https://doi.org/10.1016/j.cell.2007.11.039
80. Subedi KP, Ong HL, Son GY, Liu X, Ambudkar IS (2018) STIM2 induces activated conformation of STIM1 to control Orai1 function in ER-PM junctions. Cell Rep 23(2):522–534. https://doi.org/10.1016/j.celrep.2018.03.065
81. Darbellay B, Arnaudeau S, Bader CR, Konig S, Bernheim L (2011) STIM1L is a new actin-binding splice variant involved in fast repetitive Ca^{2+} release. J Cell Biol 194(2):335–346. https://doi.org/10.1083/jcb.201012157
82. Huang GN, Zeng W, Kim JY, Yuan JP, Han L, Muallem S, Worley PF (2006) STIM1 carboxyl-terminus activates native SOC, I(crac) and TRPC1 channels. Nat Cell Biol 8(9):1003–1010. https://doi.org/10.1038/ncb1454
83. Zhou Y, Srinivasan P, Razavi S, Seymour S, Meraner P, Gudlur A, Stathopulos PB, Ikura M, Rao A, Hogan PG (2013) Initial activation of STIM1, the regulator of store-operated calcium entry. Nat Struct Mol Biol 20(8):973–981. https://doi.org/10.1038/nsmb.2625
84. Zhou Y, Meraner P, Kwon HT, Machnes D, Oh-hora M, Zimmer J, Huang Y, Stura A, Rao A, Hogan PG (2010) STIM1 gates the store-operated calcium channel ORAI1 in vitro. Nat Struct Mol Biol 17(1):112–116. https://doi.org/10.1038/nsmb.1724
85. Williams RT, Senior PV, Van Stekelenburg L, Layton JE, Smith PJ, Dziadek MA (2002) Stromal interaction molecule 1 (STIM1), a transmembrane protein with growth suppressor activity, contains an extracellular SAM domain modified by N-linked glycosylation. Biochim Biophys Acta 1596(1):131–137
86. Muik M, Fahrner M, Schindl R, Stathopulos P, Frischauf I, Derler I, Plenk P, Lackner B, Groschner K, Ikura M, Romanin C (2011) STIM1 couples to ORAI1 via an intramolecular transition into an extended conformation. EMBO J 30(9):1678–1689. https://doi.org/10.1038/emboj.2011.79
87. Yu J, Zhang H, Zhang M, Deng Y, Wang H, Lu J, Xu T, Xu P (2013) An aromatic amino acid in the coiled-coil 1 domain plays a crucial role in the auto-inhibitory mechanism of STIM1. Biochem J 454(3):401–409. https://doi.org/10.1042/BJ20130292
88. Fahrner M, Stadlbauer M, Muik M, Rathner P, Stathopulos P, Ikura M, Muller N, Romanin C (2018) A dual mechanism promotes switching of the Stormorken STIM1 R304W mutant into the activated state. Nat Commun 9(1):825. https://doi.org/10.1038/s41467-018-03062-w
89. Muik M, Frischauf I, Derler I, Fahrner M, Bergsmann J, Eder P, Schindl R, Hesch C, Polzinger B, Fritsch R, Kahr H, Madl J, Gruber H, Groschner K, Romanin C (2008) Dynamic coupling of the putative coiled-coil domain of ORAI1 with STIM1 mediates ORAI1 channel activation. J Biol Chem 283(12):8014–8022. doi:M708898200 [pii] https://doi.org/10.1074/jbc.M708898200

90. Stathopulos PB, Li GY, Plevin MJ, Ames JB, Ikura M (2006) Stored Ca^{2+} depletion-induced oligomerization of stromal interaction molecule 1 (STIM1) via the EF-SAM region: an initiation mechanism for capacitive Ca^{2+} entry. J Biol Chem 281(47):35855–35862. https://doi.org/10.1074/jbc.M608247200
91. Grupe M, Myers G, Penner R, Fleig A (2010) Activation of store-operated I(CRAC) by hydrogen peroxide. Cell Calcium 48(1):1–9. doi: S0143-4160(10)00085-0 [pii] https://doi.org/10.1016/j.ceca.2010.05.005
92. Hawkins BJ, Irrinki KM, Mallilankaraman K, Lien YC, Wang Y, Bhanumathy CD, Subbiah R, Ritchie MF, Soboloff J, Baba Y, Kurosaki T, Joseph SK, Gill DL, Madesh M (2010) S-glutathionylation activates STIM1 and alters mitochondrial homeostasis. J Cell Biol 190(3):391–405. doi:jcb.201004152 [pii] https://doi.org/10.1083/jcb.201004152
93. Droge W (2002) Free radicals in the physiological control of cell function. Physiol Rev 82(1):47–95. https://doi.org/10.1152/physrev.00018.2001
94. Rhee SG (2006) Cell signaling. H2O2, a necessary evil for cell signaling. Science 312(5782):1882–1883. doi: 312/5782/1882 [pii] https://doi.org/10.1126/science.1130481
95. Hirve N, Rajanikanth V, Hogan PG, Gudlur A (2018) Coiled-coil formation conveys a STIM1 signal from ER lumen to cytoplasm. Cell Rep 22(1):72–83. https://doi.org/10.1016/j.celrep.2017.12.030
96. Dong H, Sharma M, Zhou HX, Cross TA (2012) Glycines: role in alpha-helical membrane protein structures and a potential indicator of native conformation. Biochemistry 51(24):4779–4789. https://doi.org/10.1021/bi300090x
97. Fuchs S, Rensing-Ehl A, Speckmann C, Bengsch B, Schmitt-Graeff A, Bondzio I, Maul-Pavicic A, Bass T, Vraetz T, Strahm B, Ankermann T, Benson M, Caliebe A, Folster-Holst R, Kaiser P, Thimme R, Schamel WW, Schwarz K, Feske S, Ehl S (2012) Antiviral and regulatory T cell immunity in a patient with stromal interaction molecule 1 deficiency. J Immunol 188(3):1523–1533. https://doi.org/10.4049/jimmunol.1102507
98. Maus M, Jairaman A, Stathopulos PB, Muik M, Fahrner M, Weidinger C, Benson M, Fuchs S, Ehl S, Romanin C, Ikura M, Prakriya M, Feske S (2015) Missense mutation in immunodeficient patients shows the multifunctional roles of coiled-coil domain 3 (CC3) in STIM1 activation. Proc Natl Acad Sci U S A 112(19):6206–6211. https://doi.org/10.1073/pnas.1418852112
99. Hooper R, Soboloff J (2015) STIMATE reveals a STIM1 Transitional State. Nat Cell Biol 17(10):1232–1234. https://doi.org/10.1038/ncb3245
100. Kilch T, Alansary D, Peglow M, Dorr K, Rychkov G, Rieger H, Peinelt C, Niemeyer BA (2013) Mutations of the Ca^{2+}-sensing stromal interaction molecule STIM1 regulate Ca^{2+} influx by altered oligomerization of STIM1 and by destabilization of the Ca^{2+} channel Orai1. J Biol Chem 288(3):1653–1664. https://doi.org/10.1074/jbc.M112.417246
101. Kawasaki T, Ueyama T, Lange I, Feske S, Saito N (2010) Protein kinase C-induced phosphorylation of Orai1 regulates the intracellular Ca^{2+} level via the store-operated Ca^{2+} channel. J Biol Chem 285(33):25720–25730. doi:M109.022996 [pii] https://doi.org/10.1074/jbc.M109.022996
102. Yazbeck P, Tauseef M, Kruse K, Amin MR, Sheikh R, Feske S, Komarova Y, Mehta D (2017) STIM1 phosphorylation at Y361 recruits Orai1 to STIM1 puncta and induces Ca^{2+} entry. Sci Rep 7:42758. https://doi.org/10.1038/srep42758
103. Yu F, Sun L, Machaca K (2009) Orai1 internalization and STIM1 clustering inhibition modulate SOCE inactivation during meiosis. Proc Natl Acad Sci U S A 106(41):17401–17406. doi:0904651106 [pii] https://doi.org/10.1073/pnas.0904651106
104. Smyth JT, Petranka JG, Boyles RR, DeHaven WI, Fukushima M, Johnson KL, Williams JG, Putney JW Jr (2009) Phosphorylation of STIM1 underlies suppression of store-operated calcium entry during mitosis. Nat Cell Biol 11(12):1465–1472. doi:ncb1995 [pii] https://doi.org/10.1038/ncb1995
105. Pozo-Guisado E, Campbell DG, Deak M, Alvarez-Barrientos A, Morrice NA, Alvarez IS, Alessi DR, Martin-Romero FJ (2010) Phosphorylation of STIM1 at ERK1/2 target sites modulates store-operated calcium entry. J Cell Sci 123(Pt 18):3084–3093. doi:jcs.067215 [pii] https://doi.org/10.1242/jcs.067215

106. Frischauf I, Muik M, Derler I, Bergsmann J, Fahrner M, Schindl R, Groschner K, Romanin C (2009) Molecular determinants of the coupling between STIM1 and Orai channels: differential activation of Orai1-3 channels by a STIM1 coiled-coil mutant. J Biol Chem 284(32):21696–21706. https://doi.org/10.1074/jbc.M109.018408
107. Zhou Y, Cai X, Nwokonko RM, Loktionova NA, Wang Y, Gill DL (2017) The STIM-Orai coupling interface and gating of the Orai1 channel. Cell Calcium 63:8–13. https://doi.org/10.1016/j.ceca.2017.01.001
108. Tirado-Lee L, Yamashita M, Prakriya M (2015) Conformational changes in the Orai1 C-terminus evoked by STIM1 binding. PLoS One 10(6):e0128622. https://doi.org/10.1371/journal.pone.0128622
109. Lis A, Zierler S, Peinelt C, Fleig A, Penner R (2010) A single lysine in the N-terminal region of store-operated channels is critical for STIM1-mediated gating. J Gen Physiol 136(6):673–686. https://doi.org/10.1085/jgp.201010484
110. Derler I, Butorac C, Krizova A, Stadlbauer M, Muik M, Fahrner M, Frischauf I, Romanin C (2018) Authentic CRAC channel activity requires STIM1 and the conserved portion of the Orai N terminus. J Biol Chem 293(4):1259–1270. https://doi.org/10.1074/jbc.M117.812206
111. Kim KM, Wijerathne T, Hur JH, Kang UJ, Kim IH, Kweon YC, Lee AR, Jeong SJ, Lee SK, Lee YY, Sim BW, Lee JH, Baig C, Kim SU, Chang KT, Lee KP, Park CY (2018) Distinct gating mechanism of SOC channel involving STIM-Orai coupling and an intramolecular interaction of Orai in Caenorhabditis elegans. Proc Natl Acad Sci U S A 115(20):E4623–e4632. https://doi.org/10.1073/pnas.1714986115
112. Bohorquez-Hernandez A, Gratton E, Pacheco J, Asanov A, Vaca L (2017) Cholesterol modulates the cellular localization of Orai1 channels and its disposition among membrane domains. Biochim Biophys Acta 1862(12):1481–1490. https://doi.org/10.1016/j.bbalip.2017.09.005
113. Derler I, Jardin I, Stathopulos PB, Muik M, Fahrner M, Zayats V, Pandey SK, Poteser M, Lackner B, Absolonova M, Schindl R, Groschner K, Ettrich R, Ikura M, Romanin C (2016) Cholesterol modulates Orai1 channel function. Sci Signal 9(412):ra10. https://doi.org/10.1126/scisignal.aad7808
114. Pacheco J, Dominguez L, Bohorquez-Hernandez A, Asanov A, Vaca L (2016) A cholesterol-binding domain in STIM1 modulates STIM1-Orai1 physical and functional interactions. Sci Rep 6:29634. https://doi.org/10.1038/srep29634
115. Srikanth S, Jung HJ, Kim KD, Souda P, Whitelegge J, Gwack Y (2010) A novel EF-hand protein, CRACR2A, is a cytosolic Ca^{2+} sensor that stabilizes CRAC channels in T cells. Nat Cell Biol 12(5):436–446. https://doi.org/10.1038/ncb2045
116. Mullins FM, Park CY, Dolmetsch RE, Lewis RS (2009) STIM1 and calmodulin interact with Orai1 to induce Ca^{2+}-dependent inactivation of CRAC channels. Proc Natl Acad Sci U S A 106(36):15495–15500. https://doi.org/10.1073/pnas.0906781106
117. Feng M, Grice DM, Faddy HM, Nguyen N, Leitch S, Wang Y, Muend S, Kenny PA, Sukumar S, Roberts-Thomson SJ, Monteith GR, Rao R (2010) Store-independent activation of Orai1 by SPCA2 in mammary tumors. Cell 143(1):84–98. https://doi.org/10.1016/j.cell.2010.08.040
118. Lopez JJ, Albarran L, Gomez LJ, Smani T, Salido GM, Rosado JA (2016) Molecular modulators of store-operated calcium entry. Biochim Biophys Acta 1863(8):2037–2043. https://doi.org/10.1016/j.bbamcr.2016.04.024
119. Shaw PJ, Qu B, Hoth M, Feske S (2013) Molecular regulation of CRAC channels and their role in lymphocyte function. Cell Mol Life Sci 70(15):2637–2656. https://doi.org/10.1007/s00018-012-1175-2
120. Srikanth S, Gwack Y (2013) Molecular regulation of the pore component of CRAC channels, Orai1. Curr Top Membr 71:181–207. https://doi.org/10.1016/B978-0-12-407870-3.00008-1
121. McNally BA, Somasundaram A, Jairaman A, Yamashita M, Prakriya M (2013) The C- and N-terminal STIM1 binding sites on Orai1 are required for both trapping and gating CRAC channels. J Physiol 591(Pt 11):2833–2850. https://doi.org/10.1113/jphysiol.2012.250456
122. Palty R, Isacoff EY (2016) Cooperative binding of stromal interaction molecule 1 (STIM1) to the N and C termini of calcium release-activated calcium modulator 1 (Orai1). J Biol Chem 291(1):334–341. https://doi.org/10.1074/jbc.M115.685289

123. Zhou Y, Nwokonko RM, Cai X, Loktionova NA, Abdulqadir R, Xin P, Niemeyer BA, Wang Y, Trebak M, Gill DL (2018) Cross-linking of Orai1 channels by STIM proteins. Proc Natl Acad Sci U S A 115(15):E3398–E3407. https://doi.org/10.1073/pnas.1720810115
124. Hoover PJ, Lewis RS (2011) Stoichiometric requirements for trapping and gating of Ca^{2+} release-activated Ca^{2+} (CRAC) channels by stromal interaction molecule 1 (STIM1). Proc Natl Acad Sci U S A 108(32):13299–13304. https://doi.org/10.1073/pnas.1101664108
125. Scrimgeour NR, Wilson DP, Barritt GJ, Rychkov GY (2014) Structural and stoichiometric determinants of Ca^{2+} release-activated Ca^{2+} (CRAC) channel Ca^{2+}-dependent inactivation. Biochim Biophys Acta 1838(5):1281–1287. https://doi.org/10.1016/j.bbamem.2014.01.019
126. Scrimgeour N, Litjens T, Ma L, Barritt GJ, Rychkov GY (2009) Properties of Orai1 mediated store-operated current depend on the expression levels of STIM1 and Orai1 proteins. J Physiol 587(Pt 12):2903–2918. https://doi.org/10.1113/jphysiol.2009.170662
127. Li Z, Liu L, Deng Y, Ji W, Du W, Xu P, Chen L, Xu T (2011) Graded activation of CRAC channel by binding of different numbers of STIM1 to Orai1 subunits. Cell Res 21(2):305–315. https://doi.org/10.1038/cr.2010.131
128. Palty R, Fu Z, Isacoff EY (2017) Sequential steps of CRAC channel activation. Cell Rep 19(9):1929–1939. https://doi.org/10.1016/j.celrep.2017.05.025
129. Lis A, Peinelt C, Beck A, Parvez S, Monteilh-Zoller M, Fleig A, Penner R (2007) CRACM1, CRACM2, and CRACM3 are store-operated Ca^{2+} channels with distinct functional properties. Curr Biol 17(9):794–800. https://doi.org/10.1016/j.cub.2007.03.065
130. Hoth M, Penner R (1992) Depletion of intracellular calcium stores activates a calcium current in mast cells. Nature 355(6358):353–356
131. Hoth M, Penner R (1993) Calcium release-activated calcium current in rat mast cells. J Physiol 465:359–386
132. Sather WA, McCleskey EW (2003) Permeation and selectivity in calcium channels. Annu Rev Physiol 65:133–159. https://doi.org/10.1146/annurev.physiol.65.092101.142345
133. Yamashita M, Prakriya M (2014) Divergence of Ca^{2+} selectivity and equilibrium Ca^{2+} blockade in a Ca^{2+} release-activated Ca^{2+} channel. J Gen Physiol 143(3):325–343. https://doi.org/10.1085/jgp.201311108
134. Yamashita M, Navarro-Borelly L, McNally BA, Prakriya M (2007) Orai1 mutations alter ion permeation and Ca^{2+}-dependent fast inactivation of CRAC channels: evidence for coupling of permeation and gating. J Gen Physiol 130(5):525–540. https://doi.org/10.1085/jgp.200709872
135. Alavizargar A, Berti C, Ejtehadi MR, Furini S (2018) Molecular dynamics simulations of Orai reveal how the third transmembrane segment contributes to hydration and Ca^{2+} selectivity in calcium release-activated calcium channels. J Phys Chem B 122(16):4407–4417. https://doi.org/10.1021/acs.jpcb.7b12453
136. Yeung PS, Yamashita M, Prakriya M (2016) Pore opening mechanism of CRAC channels. Cell Calcium. https://doi.org/10.1016/j.ceca.2016.12.006
137. Prakriya M, Lewis RS (2006) Regulation of CRAC channel activity by recruitment of silent channels to a high open-probability gating mode. J Gen Physiol 128(3):373–386. https://doi.org/10.1085/jgp.200609588
138. Dynes JL, Amcheslavsky A, Cahalan MD (2015) Genetically targeted single-channel optical recording reveals multiple Orai1 gating states and oscillations in calcium influx. Proc Natl Acad Sci U S A. https://doi.org/10.1073/pnas.1523410113
139. Lepple-Wienhues A, Cahalan MD (1996) Conductance and permeation of monovalent cations through depletion-activated Ca^{2+} channels (ICRAC) in Jurkat T cells. Biophys J 71(2):787–794. https://doi.org/10.1016/S0006-3495(96)79278-0
140. Bakowski D, Parekh AB (2002) Permeation through store-operated CRAC channels in divalent-free solution: potential problems and implications for putative CRAC channel genes. Cell Calcium 32(5-6):379–391
141. Prakriya M, Lewis RS (2002) Separation and characterization of currents through store-operated CRAC channels and Mg2+-inhibited cation (MIC) channels. J Gen Physiol 119(5):487–507

142. Su Z, Shoemaker RL, Marchase RB, Blalock JE (2004) Ca^{2+} modulation of Ca^{2+} release-activated Ca^{2+} channels is responsible for the inactivation of its monovalent cation current. Biophys J 86(2):805–814. https://doi.org/10.1016/S0006-3495(04)74156-9
143. Mullins FM, Yen M, Lewis RS (2016) Correction: Orai1 pore residues control CRAC channel inactivation independently of calmodulin. J Gen Physiol 147(3):289. https://doi.org/10.1085/jgp.20151143701262016c
144. Mullins FM, Yen M, Lewis RS (2016) Orai1 pore residues control CRAC channel inactivation independently of calmodulin. J Gen Physiol 147(2):137–152. https://doi.org/10.1085/jgp.201511437
145. Prakriya M, Lewis RS (2015) Store-operated calcium channels. Physiol Rev 95(4):1383–1436. https://doi.org/10.1152/physrev.00020.2014
146. McCleskey EW, Almers W (1985) The Ca channel in skeletal muscle is a large pore. Proc Natl Acad Sci U S A 82(20):7149–7153
147. Zhou Y, Ramachandran S, Oh-Hora M, Rao A, Hogan PG (2010) Pore architecture of the ORAI1 store-operated calcium channel. Proc Natl Acad Sci U S A 107(11):4896–4901. https://doi.org/10.1073/pnas.1001169107
148. McNally BA, Prakriya M (2012) Permeation, selectivity and gating in store-operated CRAC channels. J Physiol 590(Pt 17):4179–4191. https://doi.org/10.1113/jphysiol.2012.233098
149. Rothberg BS, Wang Y, Gill DL (2013) Orai channel pore properties and gating by STIM: implications from the Orai crystal structure. Sci Signal 6(267):pe9. https://doi.org/10.1126/scisignal.2003971
150. Derler I, Fahrner M, Carugo O, Muik M, Bergsmann J, Schindl R, Frischauf I, Eshaghi S, Romanin C (2009) Increased hydrophobicity at the N terminus/membrane interface impairs gating of the severe combined immunodeficiency-related ORAI1 mutant. J Biol Chem 284(23):15903–15915. https://doi.org/10.1074/jbc.M808312200
151. McNally BA, Yamashita M, Engh A, Prakriya M (2009) Structural determinants of ion permeation in CRAC channels. Proc Natl Acad Sci U S A 106(52):22516–22521. https://doi.org/10.1073/pnas.0909574106
152. Schindl R, Frischauf I, Bergsmann J, Muik M, Derler I, Lackner B, Groschner K, Romanin C (2009) Plasticity in Ca^{2+} selectivity of Orai1/Orai3 heteromeric channel. Proc Natl Acad Sci U S A 106(46):19623–19628. doi:0907714106 [pii] https://doi.org/10.1073/pnas.0907714106
153. Vaeth M, Yang J, Yamashita M, Zee I, Eckstein M, Knosp C, Kaufmann U, Karoly Jani P, Lacruz RS, Flockerzi V, Kacskovics I, Prakriya M, Feske S (2017) ORAI2 modulates store-operated calcium entry and T cell-mediated immunity. Nat Commun 8:14714. https://doi.org/10.1038/ncomms14714
154. Vig M, Beck A, Billingsley JM, Lis A, Parvez S, Peinelt C, Koomoa DL, Soboloff J, Gill DL, Fleig A, Kinet JP, Penner R (2006) CRACM1 multimers form the ion-selective pore of the CRAC channel. Curr Biol 16(20):2073–2079. https://doi.org/10.1016/j.cub.2006.08.085
155. Yeromin AV, Zhang SL, Jiang W, Yu Y, Safrina O, Cahalan MD (2006) Molecular identification of the CRAC channel by altered ion selectivity in a mutant of Orai. Nature 443(7108):226–229. https://doi.org/10.1038/nature05108
156. Zhang SL, Yeromin AV, Hu J, Amcheslavsky A, Zheng H, Cahalan MD (2011) Mutations in Orai1 transmembrane segment 1 cause STIM1-independent activation of Orai1 channels at glycine 98 and channel closure at arginine 91. Proc Natl Acad Sci U S A 108(43):17838–17843. https://doi.org/10.1073/pnas.1114821108
157. Webster SM, Del Camino D, Dekker JP, Yellen G (2004) Intracellular gate opening in Shaker K^+ channels defined by high-affinity metal bridges. Nature 428(6985):864–868. https://doi.org/10.1038/nature02468
158. Payandeh J, Scheuer T, Zheng N, Catterall WA (2011) The crystal structure of a voltage-gated sodium channel. Nature 475(7356):353–358. https://doi.org/10.1038/nature10238
159. Zhao Y, Yarov-Yarovoy V, Scheuer T, Catterall WA (2004) A gating hinge in Na^+ channels; a molecular switch for electrical signaling. Neuron 41(6):859–865

160. Dong H, Fiorin G, Carnevale V, Treptow W, Klein ML (2013) Pore waters regulate ion permeation in a calcium release-activated calcium channel. Proc Natl Acad Sci U S A 110(43):17332–17337. https://doi.org/10.1073/pnas.1316969110
161. Gudlur A, Quintana A, Zhou Y, Hirve N, Mahapatra S, Hogan PG (2014) STIM1 triggers a gating rearrangement at the extracellular mouth of the ORAI1 channel. Nat Commun 5:5164. https://doi.org/10.1038/ncomms6164
162. Srikanth S, Yee MK, Gwack Y, Ribalet B (2011) The third transmembrane segment of orai1 protein modulates Ca^{2+} release-activated Ca^{2+} (CRAC) channel gating and permeation properties. J Biol Chem 286(40):35318–35328. https://doi.org/10.1074/jbc.M111.265884
163. Amcheslavsky A, Safrina O, Cahalan MD (2013) Orai3 TM3 point mutation G158C alters kinetics of 2-APB-induced gating by disulfide bridge formation with TM2 C101. J Gen Physiol 142(4):405–412. https://doi.org/10.1085/jgp.201311030
164. Bogeski I, Kummerow C, Al-Ansary D, Schwarz EC, Koehler R, Kozai D, Takahashi N, Peinelt C, Griesemer D, Bozem M, Mori Y, Hoth M, Niemeyer BA (2010) Differential redox regulation of ORAI ion channels: a mechanism to tune cellular calcium signaling. Sci Signal 3(115):ra24. doi:3/115/ra24 [pii] https://doi.org/10.1126/scisignal.2000672
165. Alansary D, Schmidt B, Dorr K, Bogeski I, Rieger H, Kless A, Niemeyer BA (2016) Thiol dependent intramolecular locking of Orai1 channels. Sci Rep 6:33347. https://doi.org/10.1038/srep33347
166. Cao X, Choi S, Maleth JJ, Park S, Ahuja M, Muallem S (2015) The ER/PM microdomain, PI(4,5)P(2) and the regulation of STIM1-Orai1 channel function. Cell Calcium 58(4):342–348. https://doi.org/10.1016/j.ceca.2015.03.003
167. Zweifach A, Lewis RS (1995) Rapid inactivation of depletion-activated calcium current (ICRAC) due to local calcium feedback. J Gen Physiol 105(2):209–226
168. Prakriya M, Lewis RS (2003) CRAC channels: activation, permeation, and the search for a molecular identity. Cell Calcium 33(5-6):311–321
169. Lee KP, Yuan JP, Zeng W, So I, Worley PF, Muallem S (2009) Molecular determinants of fast Ca^{2+}-dependent inactivation and gating of the Orai channels. Proc Natl Acad Sci U S A 106(34):14687–14692. doi:0904664106 [pii] https://doi.org/10.1073/pnas.0904664106
170. Jha A, Ahuja M, Maleth J, Moreno CM, Yuan JP, Kim MS, Muallem S (2013) The STIM1 CTID domain determines access of SARAF to SOAR to regulate Orai1 channel function. J Cell Biol 202(1):71–79. https://doi.org/10.1083/jcb.201301148
171. Palty R, Raveh A, Kaminsky I, Meller R, Reuveny E (2012) SARAF inactivates the store operated calcium entry machinery to prevent excess calcium refilling. Cell 149(2):425–438. https://doi.org/10.1016/j.cell.2012.01.055
172. Maleth J, Choi S, Muallem S, Ahuja M (2014) Translocation between PI(4,5)P2-poor and PI(4,5)P2-rich microdomains during store depletion determines STIM1 conformation and Orai1 gating. Nat Commun 5:5843. https://doi.org/10.1038/ncomms6843
173. Frischauf I, Schindl R, Bergsmann J, Derler I, Fahrner M, Muik M, Fritsch R, Lackner B, Groschner K, Romanin C (2011) Cooperativeness of Orai cytosolic domains tunes subtype-specific gating. J Biol Chem 286(10):8577–8584. doi:M110.187179 [pii] https://doi.org/10.1074/jbc.M110.187179
174. Bergsmann J, Derler I, Muik M, Frischauf I, Fahrner M, Pollheimer P, Schwarzinger C, Gruber HJ, Groschner K, Romanin C (2011) Molecular determinants within N terminus of Orai3 protein that control channel activation and gating. J Biol Chem 286(36):31565–31575. https://doi.org/10.1074/jbc.M111.227546
175. Litjens T, Harland ML, Roberts ML, Barritt GJ, Rychkov GY (2004) Fast Ca^{2+}-dependent inactivation of the store-operated Ca^{2+} current (ISOC) in liver cells: a role for calmodulin. J Physiol 558(Pt 1):85–97. https://doi.org/10.1113/jphysiol.2004.065870
176. Srikanth S, Jung HJ, Ribalet B, Gwack Y (2010) The intracellular loop of Orai1 plays a central role in fast inactivation of Ca^{2+} release-activated Ca^{2+} channels. J Biol Chem 285(7):5066–5075. doi:M109.072736 [pii] https://doi.org/10.1074/jbc.M109.072736
177. Howie D, Nolan KF, Daley S, Butterfield E, Adams E, Garcia-Rueda H, Thompson C, Saunders NJ, Cobbold SP, Tone Y, Tone M, Waldmann H (2009) MS4A4B

is a GITR-associated membrane adapter, expressed by regulatory T cells, which modulates T cell activation. J Immunol 183(7):4197–4204. doi:jimmunol.0901070 [pii] https://doi.org/10.4049/jimmunol.0901070
178. Walsh CM, Doherty MK, Tepikin AV, Burgoyne RD (2010) Evidence for an interaction between Golli and STIM1 in store-operated calcium entry. Biochem J 430(3):453–460. doi:BJ20100650 [pii] https://doi.org/10.1042/BJ20100650
179. Krapivinsky G, Krapivinsky L, Stotz SC, Manasian Y, Clapham DE 2011 POST, partner of stromal interaction molecule 1 (STIM1), targets STIM1 to multiple transporters. Proc Natl Acad Sci U S A 108 (48):19234-19239. doi:1117231108 [pii] https://doi.org/10.1073/pnas.1117231108
180. Deb BK, Pathak T, Hasan G (2016) Store-independent modulation of Ca^{2+} entry through Orai by Septin 7. Nat Commun 7. https://doi.org/10.1038/ncomms11751
181. Sharma S, Quintana A, Findlay GM, Mettlen M, Baust B, Jain M, Nilsson R, Rao A, Hogan PG (2013) An siRNA screen for NFAT activation identifies septins as coordinators of store-operated Ca^{2+} entry. Nature 499(7457):238–242. https://doi.org/10.1038/nature12229
182. Srivats S, Balasuriya D, Pasche M, Vistal G, Edwardson JM, Taylor CW, Murrell-Lagnado RD (2016) Sigma1 receptors inhibit store-operated Ca^{2+} entry by attenuating coupling of STIM1 to Orai1. J Cell Biol 213(1):65–79. https://doi.org/10.1083/jcb.201506022
183. Korzeniowski MK, Popovic MA, Szentpetery Z, Varnai P, Stojilkovic SS, Balla T (2009) Dependence of STIM1/Orai1-mediated calcium entry on plasma membrane phosphoinositides. J Biol Chem 284(31):21027–21035. doi:M109.012252 [pii] https://doi.org/10.1074/jbc.M109.012252
184. Chvanov M, Walsh CM, Haynes LP, Voronina SG, Lur G, Gerasimenko OV, Barraclough R, Rudland PS, Petersen OH, Burgoyne RD, Tepikin AV (2008) ATP depletion induces translocation of STIM1 to puncta and formation of STIM1-ORAI1 clusters: translocation and re-translocation of STIM1 does not require ATP. Pflugers Arch 457(2):505–517. https://doi.org/10.1007/s00424-008-0529-y
185. Walsh CM, Chvanov M, Haynes LP, Petersen OH, Tepikin AV, Burgoyne RD (2010) Role of phosphoinositides in STIM1 dynamics and store-operated calcium entry. Biochem J 425(1):159–168. doi:BJ20090884 [pii] https://doi.org/10.1042/BJ20090884
186. Galan C, Woodard GE, Dionisio N, Salido GM, Rosado JA Lipid rafts modulate the activation but not the maintenance of store-operated Ca^{2+} entry. Biochim Biophys Acta 1803(9):1083–1093. doi:S0167-4889(10)00176-X [pii] https://doi.org/10.1016/j.bbamcr.2010.06.006
187. Jardin I, Salido GM, Rosado JA (2008) Role of lipid rafts in the interaction between hTRPC1, Orai1 and STIM1. Channels (Austin) 2(6). doi:7055 [pii]
188. Liao Y, Plummer NW, George MD, Abramowitz J, Zhu MX, Birnbaumer L (2009) A role for Orai in TRPC-mediated Ca^{2+} entry suggests that a TRPC:Orai complex may mediate store and receptor operated Ca^{2+} entry. Proc Natl Acad Sci U S A 106(9):3202–3206. doi:0813346106 [pii] https://doi.org/10.1073/pnas.0813346106
189. Martin AC, Willoughby D, Ciruela A, Ayling LJ, Pagano M, Wachten S, Tengholm A, Cooper DM (2009) Capacitative Ca^{2+} entry via Orai1 and stromal interacting molecule 1 (STIM1) regulates adenylyl cyclase type 8. Mol Pharmacol 75(4):830–842. doi:mol.108.051748 [pii] https://doi.org/10.1124/mol.108.051748
190. Korade Z, Kenworthy AK (2008) Lipid rafts, cholesterol, and the brain. Neuropharmacology 55(8):1265–1273. doi:S0028-3908(08)00064-6 [pii] https://doi.org/10.1016/j.neuropharm.2008.02.019
191. Toth BI, Oberwinkler J, Voets T (2016) Phosphoinositide regulation of TRPM channels – TRPM3 joins the club! Channels (Austin) 10(2):83–85. https://doi.org/10.1080/19336950.2015.1113719
192. Hille B, Dickson EJ, Kruse M, Vivas O, Suh BC (2015) Phosphoinositides regulate ion channels. Biochim Biophys Acta 1851(6):844–856. https://doi.org/10.1016/j.bbalip.2014.09.010
193. Zaydman MA, Cui J (2014) PIP2 regulation of KCNQ channels: biophysical and molecular mechanisms for lipid modulation of voltage-dependent gating. Front Physiol 5:195. https://doi.org/10.3389/fphys.2014.00195

194. Dickson EJ (2017) RASSF4: Regulator of plasma membrane PI(4,5)P2. J Cell Biol 216(7):1879–1881. https://doi.org/10.1083/jcb.201706042
195. Chen YJ, Chang CL, Lee WR, Liou J (2017) RASSF4 controls SOCE and ER-PM junctions through regulation of PI(4,5)P2. J Cell Biol 216(7):2011–2025. https://doi.org/10.1083/jcb.201606047
196. Schroeder C (2010) Cholesterol-binding viral proteins in virus entry and morphogenesis. Subcell Biochem 51:77–108. https://doi.org/10.1007/978-90-481-8622-8_3
197. Levitan I, Singh DK, Rosenhouse-Dantsker A (2014) Cholesterol binding to ion channels. Front Physiol 5:65. https://doi.org/10.3389/fphys.2014.00065
198. Kovarova M, Wassif CA, Odom S, Liao K, Porter FD, Rivera J (2006) Cholesterol deficiency in a mouse model of Smith-Lemli-Opitz syndrome reveals increased mast cell responsiveness. J Exp Med 203(5):1161–1171. https://doi.org/10.1084/jem.20051701
199. Fantini J, Barrantes FJ (2013) How cholesterol interacts with membrane proteins: an exploration of cholesterol-binding sites including CRAC, CARC, and tilted domains. Front Physiol 4:31. https://doi.org/10.3389/fphys.2013.00031
200. Baier CJ, Fantini J, Barrantes FJ (2011) Disclosure of cholesterol recognition motifs in transmembrane domains of the human nicotinic acetylcholine receptor. Sci Rep 1:69. https://doi.org/10.1038/srep00069
201. Epand RM (2006) Cholesterol and the interaction of proteins with membrane domains. Prog Lipid Res 45(4):279–294. doi:S0163-7827(06)00015-4 [pii] https://doi.org/10.1016/j.plipres.2006.02.001
202. Epand RM (2008) Proteins and cholesterol-rich domains. Biochim Biophys Acta 1778(7-8):1576–1582
203. Cheng Y (2015) Single-particle Cryo-EM at crystallographic resolution. Cell 161(3):450–457. https://doi.org/10.1016/j.cell.2015.03.049
204. Bai XC, McMullan G, Scheres SH (2015) How cryo-EM is revolutionizing structural biology. Trends Biochem Sci 40(1):49–57. https://doi.org/10.1016/j.tibs.2014.10.005
205. Liao M, Cao E, Julius D, Cheng Y (2013) Structure of the TRPV1 ion channel determined by electron cryo-microscopy. Nature 504(7478):107–112. https://doi.org/10.1038/nature12822
206. Zhou X, Li M, Su D, Jia Q, Li H, Li X, Yang J (2017) Cryo-EM structures of the human endolysosomal TRPML3 channel in three distinct states. Nat Struct Mol Biol 24(12):1146–1154. https://doi.org/10.1038/nsmb.3502
207. Fan G, Baker ML, Wang Z, Baker MR, Sinyagovskiy PA, Chiu W, Ludtke SJ, Serysheva II (2015) Gating machinery of InsP3R channels revealed by electron cryomicroscopy. Nature 527(7578):336–341. https://doi.org/10.1038/nature15249
208. Ishii T, Sato K, Kakumoto T, Miura S, Touhara K, Takeuchi S, Nakata T (2015) Light generation of intracellular Ca^{2+} signals by a genetically encoded protein BACCS. Nat Commun 6:8021. https://doi.org/10.1038/ncomms9021
209. He L, Zhang Y, Ma G, Tan P, Li Z, Zang S, Wu X, Jing J, Fang S, Zhou L, Wang Y, Huang Y, Hogan PG, Han G, Zhou Y (2015) Near-infrared photoactivatable control of Ca^{2+} signaling and optogenetic immunomodulation. elife 4. https://doi.org/10.7554/eLife.10024
210. Ma G, Wen S, Huang Y, Zhou Y (2017) The STIM-Orai pathway: light-operated Ca^{2+} entry through engineered CRAC channels. Adv Exp Med Biol 993:117–138. https://doi.org/10.1007/978-3-319-57732-6_7
211. Parekh AB (2008) Store-operated channels: mechanisms and function. J Physiol 586(13):3033. https://doi.org/10.1113/jphysiol.2008.156885
212. Kar P, Parekh AB (2015) Distinct spatial Ca^{2+} signatures selectively activate different NFAT transcription factor isoforms. Mol Cell 58(2):232–243. https://doi.org/10.1016/j.molcel.2015.02.027
213. Jing J, He L, Sun A, Quintana A, Ding Y, Ma G, Tan P, Liang X, Zheng X, Chen L, Shi X, Zhang SL, Zhong L, Huang Y, Dong MQ, Walker CL, Hogan PG, Wang Y, Zhou Y (2015) Proteomic mapping of ER-PM junctions identifies STIMATE as a regulator of Ca influx. Nat Cell Biol. https://doi.org/10.1038/ncb3234

214. Parekh AB (2010) Store-operated CRAC channels: function in health and disease. Nat Rev Drug Discov 9(5):399–410. https://doi.org/10.1038/nrd3136
215. Putney JW (2010) Pharmacology of store-operated calcium channels. Mol Interv 10(4):209–218. https://doi.org/10.1124/mi.10.4.4
216. Jairaman A, Prakriya M (2013) Molecular pharmacology of store-operated CRAC channels. Channels (Austin) 7(5):402–414. https://doi.org/10.4161/chan.25292
217. Zhou Y, Wang X, Wang X, Loktionova NA, Cai X, Nwokonko RM, Vrana E, Wang Y, Rothberg BS, Gill DL (2015) STIM1 dimers undergo unimolecular coupling to activate Orai1 channels. Nat Commun 6:8395. https://doi.org/10.1038/ncomms9395
218. Bohm J, Chevessier F, Maues De Paula A, Koch C, Attarian S, Feger C, Hantai D, Laforet P, Ghorab K, Vallat JM, Fardeau M, Figarella-Branger D, Pouget J, Romero NB, Koch M, Ebel C, Levy N, Krahn M, Eymard B, Bartoli M, Laporte J (2013) Constitutive activation of the calcium sensor STIM1 causes tubular-aggregate myopathy. Am J Hum Genet 92(2):271–278. https://doi.org/10.1016/j.ajhg.2012.12.007
219. Bohm J, Chevessier F, Koch C, Peche GA, Mora M, Morandi L, Pasanisi B, Moroni I, Tasca G, Fattori F, Ricci E, Penisson-Besnier I, Nadaj-Pakleza A, Fardeau M, Joshi PR, Deschauer M, Romero NB, Eymard B, Laporte J (2014) Clinical, histological and genetic characterisation of patients with tubular aggregate myopathy caused by mutations in STIM1. J Med Genet 51(12):824–833. https://doi.org/10.1136/jmedgenet-2014-102623
220. Walter MC, Rossius M, Zitzelsberger M, Vorgerd M, Muller-Felber W, Ertl-Wagner B, Zhang Y, Brinkmeier H, Senderek J, Schoser B (2015) 50 years to diagnosis: autosomal dominant tubular aggregate myopathy caused by a novel STIM1 mutation. Neuromuscul Disord 25(7):577–584. https://doi.org/10.1016/j.nmd.2015.04.005
221. Hedberg C, Niceta M, Fattori F, Lindvall B, Ciolfi A, D'Amico A, Tasca G, Petrini S, Tulinius M, Tartaglia M, Oldfors A, Bertini E (2014) Childhood onset tubular aggregate myopathy associated with de novo STIM1 mutations. J Neurol 261(5):870–876. https://doi.org/10.1007/s00415-014-7287-x
222. Markello T, Chen D, Kwan JY, Horkayne-Szakaly I, Morrison A, Simakova O, Maric I, Lozier J, Cullinane AR, Kilo T, Meister L, Pakzad K, Bone W, Chainani S, Lee E, Links A, Boerkoel C, Fischer R, Toro C, White JG, Gahl WA, Gunay-Aygun M (2015) York platelet syndrome is a CRAC channelopathy due to gain-of-function mutations in STIM1. Mol Genet Metab 114(3):474–482. https://doi.org/10.1016/j.ymgme.2014.12.307
223. Picard C, McCarl CA, Papolos A, Khalil S, Luthy K, Hivroz C, LeDeist F, Rieux-Laucat F, Rechavi G, Rao A, Fischer A, Feske S (2009) STIM1 mutation associated with a syndrome of immunodeficiency and autoimmunity. N Engl J Med 360(19):1971–1980. https://doi.org/10.1056/NEJMoa0900082
224. Schaballie H, Rodriguez R, Martin E, Moens L, Frans G, Lenoir C, Dutre J, Canioni D, Bossuyt X, Fischer A, Latour S, Meyts I, Picard C (2015) A novel hypomorphic mutation in STIM1 results in a late-onset immunodeficiency. J Allergy Clin Immunol 136(3):816–819.e814. https://doi.org/10.1016/j.jaci.2015.03.009
225. Korzeniowski MK, Manjarres IM, Varnai P, Balla T (2010) Activation of STIM1-Orai1 involves an intramolecular switching mechanism. Sci Signal 3(148):ra82. https://doi.org/10.1126/scisignal.2001122
226. Garibaldi M, Fattori F, Riva B, Labasse C, Brochier G, Ottaviani P, Sacconi S, Vizzaccaro E, Laschena F, Romero NB, Genazzani A, Bertini E, Antonini G (2017) A novel gain-of-function mutation in ORAI1 causes late-onset tubular aggregate myopathy and congenital miosis. Clin Genet 91(5):780–786. https://doi.org/10.1111/cge.12888
227. Lian J, Cuk M, Kahlfuss S, Kozhaya L, Vaeth M, Rieux-Laucat F, Picard C, Benson MJ, Jakovcevic A, Bilic K, Martinac I, Stathopulos P, Kacskovics I, Vraetz T, Speckmann C, Ehl S, Issekutz T, Unutmaz D, Feske S (2017) ORAI1 mutations abolishing store-operated Ca^{2+} entry cause anhidrotic ectodermal dysplasia with immunodeficiency. J Allergy Clin Immunol. https://doi.org/10.1016/j.jaci.2017.10.031

228. McCarl CA, Picard C, Khalil S, Kawasaki T, Rother J, Papolos A, Kutok J, Hivroz C, Ledeist F, Plogmann K, Ehl S, Notheis G, Albert MH, Belohradsky BH, Kirschner J, Rao A, Fischer A, Feske S (2009) ORAI1 deficiency and lack of store-operated Ca^{2+} entry cause immunodeficiency, myopathy, and ectodermal dysplasia. J Allergy Clin Immunol 124(6):1311–1318.e1317. https://doi.org/10.1016/j.jaci.2009.10.007
229. Cancer Genome Atlas Network. https://cancergenome.nih.gov/
230. Navarro-Borelly L, Somasundaram A, Yamashita M, Ren D, Miller RJ, Prakriya M (2008) STIM1-Orai1 interactions and Orai1 conformational changes revealed by live-cell FRET microscopy. J Physiol 586(Pt 22):5383–5401. https://doi.org/10.1113/jphysiol.2008.162503

Chapter 24
Targeting Transient Receptor Potential Channels by MicroRNAs Drives Tumor Development and Progression

Giorgio Santoni, Maria Beatrice Morelli, Matteo Santoni, Massimo Nabissi, Oliviero Marinelli, and Consuelo Amantini

Abstract Transient receptor potential (TRP) cation channel superfamily plays important roles in a variety of cellular processes such polymodal cellular sensing, adhesion, polarity, proliferation, differentiation and apoptosis. The expression of TRP channels is strictly regulated and their de-regulation can stimulate cancer development and progression.

In human cancers, specific miRNAs are expressed in different tissues, and changes in the regulation of gene expression mediated by specific miRNAs have been associated with carcinogenesis. Several miRNAs/TRP channel pairs have been reported to play an important role in tumor biology. Thus, the TRPM1 gene regulates melanocyte/melanoma behaviour via TRPM1 and microRNA-211 transcripts. Both miR-211 and TRPM1 proteins are regulated through microphthalmia-associated transcription factor (MIFT) and the expression of miR-211 is decreased during melanoma progression. Melanocyte phenotype and melanoma behaviour strictly depend on dual TRPM1 activity, with loss of TRPM1 protein promoting melanoma aggressiveness and miR-211 expression supporting tumour suppressor. TRPM3 plays a major role in the development and progression of human clear cell renal cell carcinoma (ccRCC) with von Hippel-Lindau (VHL) loss. TRPM3, a direct target of miR-204, is enhanced in ccRCC with inactivated or deleted VHL. Loss of VHL inhibits miR-204 expression that lead to increased oncogenic autophagy. Therefore,

G. Santoni (✉) · M. B. Morelli · M. Nabissi
School of Pharmacy, Experimental Medicine Section, University of Camerino, Camerino, Italy
e-mail: giorgio.santoni@unicam.it

M. Santoni
Clinic and Oncology Unit, Macerata Hospital, Macerata, Italy

O. Marinelli
School of Pharmacy, Experimental Medicine Section, University of Camerino, Camerino, Italy

School of Biosciences and Veterinary Medicine, University of Camerino, Camerino, Italy

C. Amantini
School of Biosciences and Veterinary Medicine, University of Camerino, Camerino, Italy

M. S. Islam (ed.), *Calcium Signaling*, Advances in Experimental Medicine and Biology 1131, https://doi.org/10.1007/978-3-030-12457-1_24

the understanding of specific TRP channels/miRNAs molecular pathways in distinct tumors could provide a clinical rationale for target therapy in cancer.

Keywords TRP channels · miRNAs · Channelopathies · Tumor progression · Target therapy · Calcium/calcineurin signaling · TRPV · TRPA1 · TRPP · TRPM

Abbreviations

BRAF	proto-oncogene protein B-raf
$BRAF^{V600}$	BRAF harbouring somatic missense mutations at the amino acid residue V600
BRN2	POU-domain transcription factor (POU3F2)
ccRCC	human clear cell renal cell carcinoma
CRC	colorectal cancer
EC	endometrial cancer
EOC	epithelial ovarian cancer
ETS-1	erythroblastosis virus E26 oncogene homolog 1
FGR2	fibroblast growth factor receptor type 2
HCC	hepatocellular carcinoma cells
LUAD	lung adenocarcinoma
MIFT	microphthalmia-associated transcription factor
miR	MicroRNAs
mRNA	messenger RNA
MTSS1	metastasis suppressor gene 1
NCX1	Na^+/Ca^{2+} exchanger-1
NFAT5	nuclear factor of activated T-cells 5
NFATC3	nuclear factor of activated T-cells isoform c3
NSCLC	non-small cell lung carcinoma
OC	ovarian cancer
PCa	prostate cancer
PKD	Polycystic kidney disease
pri-miRs	primary miRNAs
TrkB	Tropomyosin receptor kinase B
TRPA	Transient receptor potential ankyrin
TRPC	Transient receptor potential canonical
TRPM	Transient receptor potential melastatin
TRPP	Transient receptor potential polycystic
TRPV	Transient receptor potential vanilloid
UTR	untranslated region
VHL	von Hippel-Lindau

24.1 Introduction

Ion channels belonging to the Transient Receptor Potential (TRP) family are expressed in every living cell, where they participate in controlling a lot of biological processes and physiological functions, such as cell excitation, electrical activity, cellular osmolarity, as well as growth and death. They show common features in the structure such us the presence of six transmembrane segments with intracellular N- and C-termini and varying degrees of sequence homology. They are grouped into seven subfamilies: TRPC ("C" for canonical), TRPV ("V" for vanilloid), TRPM ("M" for melastatin), TRPN ("N" for no mechanoreceptor potential C), TRPA ("A" for ankyrin), TRPP ("P" for polycystic) and TRPML ("ML" for mucolipin). The majority of TRPs is permeable to Ca^{2+} and these channels are considered as multiple signal integrators. In fact they play critical roles in chemosensation, mechanosensation, thermosensation and nociception sensing stimuli from both external and local environments [1]. Expression of TRP channels is tightly regulated and their expression deregulation can trigger abnormal processes, leading to pathologies, called channelopathies. Several transcription factors play a critical role in controlling the transcriptome of TRP channels by acting on the 5′-flanking gene region. Microribonucleic acids (miRNAs), a small non-coding ribonucleic acids (RNAs) of approximately 22 bp, induce RNA interference by base-pairing with the 3′ untranslated region (UTR) of mRNA, which triggers either mRNA translational repression or RNA degradation [2, 3]. In this manner, miRNAs function as sequence-specific inhibitors of gene expression. miRNAs are initially transcribed as precursor transcripts called primary miRNAs (pri-miRNAs). pri-miRNAs are at first processed in the nucleus to precursor miRNAs (pre-miRNAs) by the class 2 RNase III enzyme Drosha, then, after the transport into the cytoplasm, they become mature miRNAs by the action of Dicer, an RNase III type protein. Finally they are integrated into the Argonaute protein to produce the effector RNA-induced silencing complex (RISC). RISCs target mRNAs recognized through partial sequence complementarity promoting either translational repression or mRNA degradation [4]. Over 1000 different miRNAs are encoded by the human genome; approximately 20–30% of all genes are targeted by miRNAs, and a single miRNA may target up to 200 genes [5]. In human cancers, specific miRNAs are expressed in different tissues, and changes in the control of gene expression have been associated with carcinogenesis [6], including in endometrial, colorectal, prostate cancers and melanomas [7–11]. Furthermore, miRNAs cooperatively exert their function with certain transcription factors in the regulation of mutual sets of target genes, allowing coordinated modulation of gene expression both transcriptionally and post-transcriptionally [12]. In addition, these small noncoding RNAs regulate the expression of different genes involved also in cardiac excitability, pain, brain edema etc. [3]. Future studies might decode other miRNAs/TRP deregulation in human diseases (Table 24.1).

Table 24.1 Expression of miRs and TRP channels in cancers

Tumors	TRP gene	miR	Refs.
Breast cancer	TRPC5	miR-320a (−)	[28]
Renal cell cancer	TRPM3	miR-204 (−)	[54, 56]
Melanoma	TRPM1	miR-211 (−)	[7, 8, 17–20]
Endometrial cancer	TRPM3	miR-204 (−)	[9]
Prostate cancer	TRPM8	miR-26a (+)	[11]
Colon-rectal cancer	TRPV6	miR-122 (+)	[30]
	TRPC1 (?)	miR-135a (+)	[73]
Epithelial ovarian cancer	TRPM1	miR-211 (−)	[26]
	TRPM3	mir-204 (−)	[62]
	TRPC1	miR-135b (+)	[76]
Hepatocarcinoma	TRPC6 (?)	miR-30 (?)	[64]
Lung adenocarcinoma	TRPA1	miR-142 (?)	[31]
Non small cell lung carcinoma	TRPP2	miR-106b (−)[a]	[29]

TRP: Transient receptor potential channels; (?): correlation has been suggested; (−): down-regulated; (+): up-regulated
[a]Cisplatin cell resistant vs sensitive

24.1.1 miR-211 and Its Target Genes in Melanoma Progression

Malignant melanoma has increased the frequency of its occurrence in the last years [13]. Surgical removal of superficial primary tumors is satisfactory in term of survival. However, metastatic melanoma shows a poor survival rate [14]. Transient receptor potential melastatin channel 1 (TRPM1) transcripts are over-expressed in benign nevi, dysplastic nevi and melanomas *in situ*; it is variably expressed in invasive melanomas and is absent in most melanoma metastasis [15]. TRPM1 is regulated by a microphthalmia-associated transcription factor (MITF) [16]. The expression of miR-211, which decreases during melanoma progression [7], is driven by the TRPM1 promoter sequences in a MITF-dependent manner [17]. The gene encoding miR-211 is located within the sixth intron of the TRPM1 gene, and both miR-211 and TRPM1 channel protein are regulated by MITF. The miR-211 directly targets potassium calcium-activated channel subfamily M alpha 1 (KCNMA1) which is often associated with both cell proliferation and migration/invasion in various cancers [7]. Moreover, it has been demonstrated that miR-211 expression is greatly decreased in melanoma cells compared to normal melanocytes [18]. Levy and co-workers have demonstrated by over-expression and knockdown of either TRPM1 channel protein or miR-211, respectively, that miR-211, rather than TRPM1 channel protein, modified the melanoma invasiveness [17]. They also identified that miR-211 regulates insulin-like growth factor 2 (IGF2R), transforming growth factor beta receptor II (TGFBR2), and nuclear factor of activated T-cells 5 (NFAT5) signal transduction pathways to have a suppressive effect on a tumour. These data support the hypothesis that TRPM1 gene regulates melanocyte/melanoma behaviour via generation of two transcripts including TRPM1 protein, and miR-211: the loss of TRPM1 protein is an excellent marker of melanoma aggressiveness while

the miR-211 expression is linked to the tumour suppressor functions. Therefore, different RNA transcription program (i.e. TRPM1 mRNA and/or miR-211) decides on the melanocyte phenotype and melanoma behaviour. Clarifying this phenomenon requires future in vitro studies with targeted modulation of TRPM1 expression and clinic-pathologic correlation using large clinical cohorts of melanoma patients [8]. Furthermore, another miR-211 target, BRN2, also known as POU-domain transcription factor (POU3F2) has been identified. In melanocyte, miR-211 modulates BRN2 expression by repressing its translation [18]. In melanoma miR-211 is expressed at low levels and is related to an over-expression of BRN2, that mediates the de-differentiated and invasive phenotype [18]. The identification of miR-211 and its TRPM1 and BRN2 target genes, could suggest a new therapeutic strategy for the treatment of metastatic melanomas.

24.1.2 miR-211/TRPM1 in BRAF^{V600} Malignant Melanoma

About 50% of malignant melanomas showed proto-oncogene protein B-raf (BRAF) somatic missense mutations at the amino acid residue V600 (BRAF^{V600}) [19]. Inhibition of BRAF^{V600} with vemurafenib induces a rapid regression of metastatic BRAF^{V600} melanomas. Recently, by studying the secretome of melanoma-derived extracellular CD81^{+} and TSG-101^{+} vesicles in vemurafenib-treated cells, an increased expression of several miRNAs including miR-211-5p was evidenced (Table 24.2). In melanomas harboring Braf^{V600} mutation, the expression of miR-211-5p because of BRAF inhibition was induced by increased MIFT expression. The later transcriptional factor that up-regulates the TRPM1 gene expression induces miR-211-5p expression, resulting in activation of survival pathway through the Bcl-2 and Melan-A anti-apoptotic molecules [20]. Bcl-2 is a direct target of

Table 24.2 Vemurofenib treatment increases the microRNA levels in exosomes-derived and BRAF^{V600} melanoma cells, compared to not treated cells

	Melanoma cells		Exosomes	
Type	Fold changes	p-value	Fold changes	p-value
microRNA-211-5p	4.07	0.03		
microRNA-34a-5p	1.91	0.04		
microRNA-15b-5p	−2.11	0.01		
microRNA-1307-3p	−1.72	0.01		
microRNA-1301-3p	−2.22	0.02		
microRNA-1307-5p	−2,25	0.03		
microRNA-339-5p	−2.23	0.01		
microRNA-574-3p			−1.40	0.00
microRNA-9-5p			−1.40	0.04
microRNA-7-5p			−1.50	0.04

Table shows the microRNA changes (fold expression) from sequencing analysis in exosome-secreted from and melanoma cells. Fold change is utilized as microRNA up- or down-regulation. Data are presented as the ±SEM. $p < 0.05$

MIFT and modulation of Bcl-2 regulates Melan-A [21]. Inhibition of $BRAF^{V600}$ leads to down-regulation of pERK1/2 that increases MIFT expression [22].

MIFT transcriptionally activates TRPM1 and simultaneously up-regulates the intronic miR-211-5p. Recently has been reported that MIFT induces miR-211 target genes such as AP1S2, SOX11, IGFBP5 and SERINC3 that increase melanoma cell invasion. In addition, also a role for miR-211 as metabolic regulator in melanoma cells, by targeting the hypoxia inducible factor 1a (HIF-1α) has been reported [23].

24.1.3 miR-211 in Ovarian Cancer

The miR-211 is located on intron 6 of the TRPM1 gene at 15q13-q21, a locus frequently lost in neoplasms [24, 25]. It has been demonstrated that miR-211 expression is significantly down-regulated in ovarian cancer. The miR-211 negatively regulates the activity of CDK6 and Cyclin D1 by directly binding to 3'UTR sequences of the related mRNAs repressing their translation into proteins [26]. The cyclin D controls the CDK6 activity and has been reported to regulate angiogenesis, growth factor-stimulated proliferation and the promotion of G1 phase progression. Moreover, miR-211 suppresses the expression of PHF19, promoting apoptosis and inhibiting cell migration [27]. Overall, the cyclin D1/CDK6 and PHF19 are key players in epithelial ovarian cancer (EOC) tumorigenesis and TRPM1/miR-211 might provides new data in the diagnosis, prognosis and therapy for EOC [26, 27].

24.2 TRPC5/miR-320a and TRPP2/miR-106-5p in Breast and Lung Cancer Drug Sensitivity

Over-expression of the transient receptor potential canonical 5 (TRPC5) channel and the nuclear factor of activated T-cells isoform c3 (NFATC3) are essential for breast cancer chemoresistance. However, the mechanism by which TRPC5 and NFATC3 are regulated are unknown. The miR-320a was found to be downregulated in chemoresistant breast cancer cells. It directly targeted TRPC5 and NFATC3 and downregulation of miR-320a triggered TRPC5 and NFATC3 over-expression. In chemoresistant breast cancer cells, downregulation of miR-320a was associated with promoter methylation of the miR-320a coding sequence [28]. Furthermore, the transcription factor v-ets erythroblastosis virus E26 oncogene homolog 1 (ETS-1), which inhibits the miR-320a expression, was found to be activated in chemoresistant breast cancer cells and such activation was associated with hypomethylation of the ETS-1 promoter [28]. Finally, downregulation of miR-320a and enhanced expression of TRPC5, NFATC3, and ETS-1 were verified in clinically chemoresistant breast cancer samples. Low expression of miR-320a was also found to be a significant unfavourable predictor for clinic outcome.

In addition, a role for the miR-106b-5p and the transient receptor potential polycystic channel 2 (TRPP2) channel in the sensitivity of non-small cell lung

carcinoma (NSCLC) to cisplatin treatment has been reported [29]. Treatment of NSCL patients with cisplatin is hindered by cisplatin resistance. Yu e co-workers, have demonstrated in human lung adenocarcinoma MDRA549/cisplatin (A549/DDP) and its progenitor A549 cell line, that miR-106b-5p was decreased in A549/DDP cells. The miR-106b-5p affected the tolerance of cancer lung cells to cisplatin treatment, by negatively regulating the TRPP2 channel [29]. Up-regulation of the miR-106b-5p or down-regulation of the TRPP2 channel expression increased the sensitivity of A549/DDP cells to cisplatin treatment, suggesting that mR-106b-5p may represent a clinical strategy in the treatment of NSCLC [29].

24.3 TRPV6/miR-122 in Colorectal Liver Metastasis

Control of liver metastasis is an important goal in the treatment of colorectal cancer (CRC). In liver metastasis of primary CRCs, the most abundant miRNA, compared with primary tumors, is miR-122 [30].

The expression levels of transient receptor potential vanilloid channel 6 (TRPV6) channels, the cationic amino acid transporter 1 (CAT1), a negative target gene of miR-122, were found to be lower in liver metastases than in primary tumors. The expression levels of TRPV6 evaluated in 132 formalin-fixed paraffin-embedded primary tumors and their corresponding metastatic liver tumors isolated by using laser capture microdissection, were negatively correlated with synchronous liver metastasis and tumor stage. Results from the analysis on 121 CRC patients without synchronous liver metastasis, demonstrated that patients with low TRPV6 expression showed significantly shorter liver metastasis-free survival, but not disease-free survival. Over-expression of miR-122 and concomitant suppression of TRPV6 in the primary CRC appears to play important roles in the development of colorectal liver metastasis.

Thus, expression of TRPV6 in the primary CRC represents a novel biomarker to predict the risk of postoperative liver metastasis of CRC patients [30].

24.4 TRPA1 Channel-Targeting Exosomal miR-142-3p

The transient receptor potential ankyrin channel A1 (TRPA1) channel has been suggested to play an important role in lung cancers [31, 32]. Recent studies have demonstrated the capability of the TRPA1 to form a complex with the fibroblast growth factor receptor type 2 (FGR2) in lung adenocarcinoma (LUAD), a diffuse lung cancer that metastasizes in different organs and brain [33]. As in other lung tumors, in LUAD, FGFR2 is a major factor responsible of tumor progression [34, 35]. In this regard, the TRPA1 channel through the ankyrin repeats, has been demonstrated to bind the terminal prolin-rich region of FGR2. This binding that it is induced, independently by external stimulation, inhibits TRPA1 channel activity, resulting in FGFR2 signaling activation that leads to increased cell proliferation and metastatic spread invasion [33, 34]. In addition, Berrout and coworkers also

demonstrated that the dormant state of LUAD cells observed in the brain upon astrocytes encounter, may be related to a crosstalk between cancer cells and astrocytes. Previously, has been reported that the miR-142-3p targeting the TRPA1 channel can suppress NSC lung cancer progression [35, 36]. In regard to LUAD, astrocytes have been found to be able to transfer micro-vesicles called exosomes containing miRNA (e.g. miR-142-3p) specifically targeting the TRP channel. The binding of miRNA-142-3p to the 3'-UTR of TRPA1 triggers the depletion of TRPA1 expression in metastatic LUAD cells and subsequently abrogation of the FGFR2-driven cell proliferation and invasion of lung cancer cells in the brain.

24.5 TRPM8 and miRNAs in Prostate Cancer

Prostate cancer (PCa) is the second most frequent tumor and the 60 leading cause of cancer related death among males worldwide [37]. TRPM8 is an androgen-responsive gene and essential for the survival of PCa cells [38]. It is involved in the regulation of the intracellular Ca^{2+} concentration and exhibited an elevated expression in PCa cells. TRPM8 shows a significant association with age, serum prostate specific antigen concentration, tumor state, Gleason score or metastasis at prostatectomy. The analysis of a possible correlation between the expression of selected miRNAs and the TRPM8 gene, have evidenced a moderate inverse correlation between high TRPM8 expression and low miR-26a expression. It was found that miR-26a expression was decreased in PCa tissues and cell lines, with androgen-independent prostate cancer showing lower miR-26a expression compared to androgen-dependent prostate cancer [39]. Over-expression of miR-26a enhances apoptosis, and this upregulation is triggered by cytochrome *c* oxidase subunit II inhibition. In addition, a low miR-26a density resulted in an evidently poor prognosis. Further research is warranted to confirm a direct regulatory effect of miRNA on their potential target genes and to the development of miRNA-based therapy [11].

24.6 miR-17/TRPP Channels in Polycystic Kidney Disease and Cancers

The miR-17 and related miRNAs are derived from three miRNA clusters: miR-17 ~ 92, miR-106a-363 and miR-106b ~ 25 clusters. The genomic organization and coding sequences of these miRNA clusters are evolutionarily conserved in vertebrates. Based on their seed sequence, miRNAs derived from these three clusters can be classified into four families: the miR-17, miR-18, miR-19 and miR-25 families. Since members of each family have an identical seed sequence, they are predicted to target the same mRNAs. Interestingly, miR-17 ~ 92 and related clusters

are enriched in developing tissues and are essential for heart and lung development [40]. The miR-17 and related miRNAs are also implicated in the pathogenesis of Polycystic kidney disease (PKD) [41], a most common genetic cause of chronic kidney failure characterized by the presence of numerous, progressively enlarging fluid-filled cysts in the renal parenchyma [41]. By bioinformatics analysis has been reported that miR-17 directly targets the 3′UTR of TRPP2 (PKD2) and post-transcriptionally represses its expression [42]. Dysregulated miRNA expression is observed in PKD, with miR-17 ~ 92, that is upregulated in a mouse model of PKD. Kidney-specific transgenic over-expression of miR-17 ~ 92 produces kidney cysts in mice. Conversely, kidney-specific inactivation of miR-17 ~ 92 in a mouse model of PKD retards kidney cyst growth, improves renal function, and prolongs survival. miR-17 ~ 92 may mediate these effects by promoting proliferation and through post-transcriptional repression of the TRPP1 and TRPP2 genes (Pkd1 and Pkd2, respectively) and of the hepatocyte nuclear factor-1β [41]. The cysts arise from renal tubules and are lined by abnormally functioning and hyperproliferative epithelial cells.

In addition, two major lines of evidence also implicate miR-17 and related miRs in the pathogenesis of various cancers [43, 44]. First, these miRs are amplified in numerous human cancers, promote proliferation [45] and cause tumor growth in vivo [44]. Second, the oncogenic transcription factor c-Myc has been demonstrated to bind to the miR-17 ~ 92 promoter and to induce its transcription [46]. Further studies should be required to completely address the oncogenic role of miR-17 and TRPP channels.

24.6.1 miR-204/TRPM3 and Cancer Survival and Apoptosis

At present, several data on the role of miR-204 in cancers have been provided. Roldo and coworkers showed the upregulation of miR-204 in insulinoma [47]. Similar results were also reported by Zanette in the acute lymphoblastic leukemia [48]. By contrast, decreased miR-204 expression was reported in glioblastoma [49], gastric, bladder and lung cancers, suggesting that miR-204 may also be a tumor suppressor gene. In hepatocarcinoma, miR-204 has been found to inhibit the expression of long non-coding RNA (IncRNA) for homeobox A distal transcript antisense RNA (HOTTIP), through interference with the argonaute-2 pathway [50]. BCL-2 represents a target for miR-204, and apoptosis represents the suppressive mechanism regulated by miR-204 by binding to the 3′-UTR of BCL-2 [51]. The miR-204 suppression has been reported to inhibit the transition from epithelial to mesenchymal, IL-11, SOX4 and SIX1 target gene expression [52] and bone metastasis in breast cancer cells by reduction of the 68-kDa Src-associated protein in mitosis (SAM68) activity [53].

The miR-204-encoding gene is located in the sixth intron of TRPM3, and expression of mature miR-204 and pri-miR-204 strictly correlates in vitro and in vivo with that of TRPM3 gene [54].

24.6.2 Loss of miR-204 Triggers TRPM3-Mediated Oncogenic Autophagy in Clear Cell Renal Cell Carcinoma

Autophagy is an important homeostatic process for lysosome degradation of damaged organelles and proteins. Interestingly, alterations of the crosstalk between miRs and ion channels belonging to the TRP family, alter the homeostatic control and trigger oncogenic autophagy to survive to stressful stimuli [55]. Among TRP ion channels, TRPM3 plays a major role in the development and progression of clear cell renal cell carcinoma (ccRCC) with von Hippel-Lindau (VHL) loss mutation. TRPM3 expression is enhanced in human ccRCC with inactivated or deleted VHL. Loss of VHL inhibits the expression of miR-204 that in turn leads to increased oncogenic autophagy in ccRCC, resulting in an augmented expression of TRPM3, a direct target of miR-204 [54, 56, 57]. Binding of miR-204 to the 3′UTR of TRPM3 inhibits the TRPM3 translation. Similarly, binding of miR-204 to the 3′-UTR of caveolin 1 (CAV1) inhibits the CAV1 expression required for TRPM3 expression (Fig. 24.1). TRPM3 activation by stimulating of Ca^{2+} influx rise, triggers oncogenic autophagy through increased autophagosomes and CAMKK2

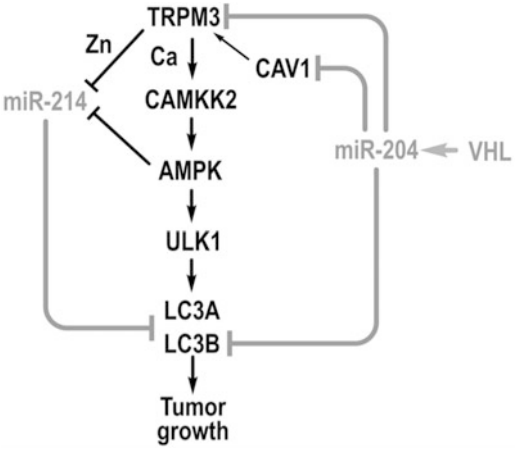

Fig. 24.1 Robust control of the autophagic network by microRNAs and calcium- and zinc-activated pathways. Calcium and zinc entering the cell through the TRPM3 channel stimulate oncogenic autophagy mediated by LC3A and LC3B through a dual mechanism. Calcium stimulates phagophore initiation through Ca^{2+}-dependent activation of CAMKK2 and AMPK, and the resulting phosphorylation of ULK1. Calcium and zinc also inhibit miR-214, which directly targets LC3A and LC3B. The VHL tumor suppressor inhibits expression of TRPM3 directly and indirectly through the effect of miR-204 on CAV1. In addition, miR-204 directly targets LC3B. AMPK, AMP-activated protein kinase; CAMKK2, calcium/calmodulin-dependent protein kinase kinase 2, β; CAV1, caveolin 1; LC3A, microtubule-associated protein 1 light chain 3 α; LC3B, microtubule-associated protein 1 light chain 3 β; TRPM3, transient receptor potential melastatin 3; ULK1, unc-51 like autophagy activating kinase 1; VHL, Von Hippel-Lindau [52]. (Courtesy Hall et al., Cancer Cell. 2014; 26(5): 738–753)

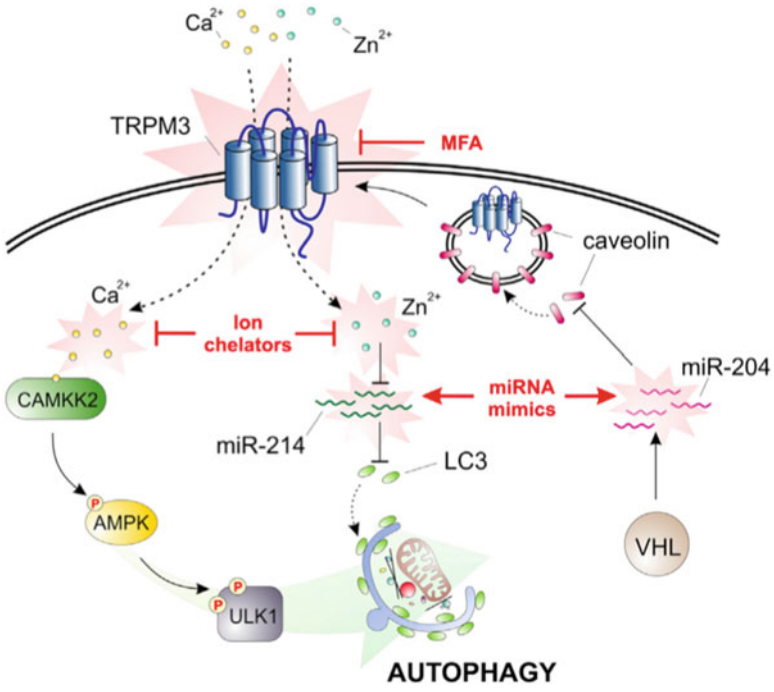

Fig. 24.2 Novel autophagy pathway important in ccRCC, centered on the ion channel TRPM3. The possible strategies to manipulate this pathway at several steps are indicated in red [53]. (Courtesy of Cecconi and Jaattela, Cancer Cell. 2014;26(5):599–600)

and AMPK activation, resulting in ULK1 phosphorylation; by contrast miR-204 inhibits oncogenic autophagy [56]. In addition, TRPM3-induced Ca^{2+} and Zn^{2+} influx and CAMKK2-AMPK pathway activation, inhibit the expression of miR-214 directly targeting the LC3A and LC3B proteins (Fig. 24.2) [58, 59]. Overall, the inhibition of TRPM3-induced oncogenic autophagy in VHL-mutated ccRCC may provide a clinical rationale therapy leading to ccRCC regression. On the other hand, the signal transducer and activator of transcription (STAT)-3 has been demonstrated to down-regulate the miR-204 expression in nasopharyngeal carcinoma [60] and endometrial carcinoma [9].

24.6.3 TRPM3/TrkB/miR-204 Interplay in the Endometrial Cancer

Endometrial carcinoma (EC) is the most common gynecological malignancy worldwide [61]. A recent study identifies a novel TrkB–STAT3–miR-204-5p signaling axis playing an important role in EC growth through the accumulation of the key

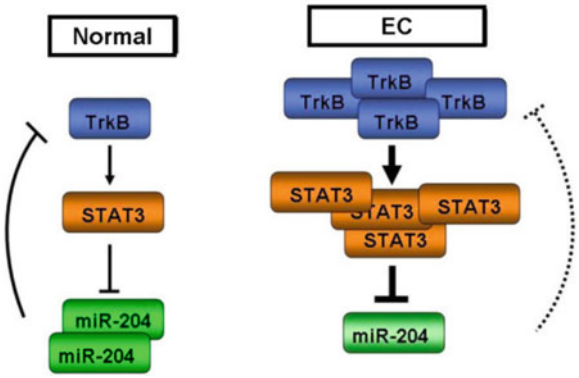

Fig. 24.3 Left: In normal cells, a recurrent auto-regulatory circuit involving the expression of TrkB induces phosphorylation of STAT3 to negatively regulate the expression of miR-204-5p. MiR-204-5p, in turn, represses TrkB expression. The expression of miR-204 within this circuit maintains endometrial cells in a normal differentiated state. Right: In endometrial cancer cells, this circuit becomes dysregulated due to increased activity of the TrkB–STAT3 component of the circuit, which constitutively represses miR-204-5p. In the absence of sufficient miR-204 tumor suppressor activity, TrkB is left uncontrolled, thereby leading to carcinogenesis [7]. (Courtesy of Bao et al. Mol Cancer. 2013; 12: 155)

tumor oncogene, TrkB [9]. The TrkB oncogene is a novel target of miR-204-5p. In normal cells, a recurrent auto-regulatory circuit involving the expression of TrkB induces phosphorylation of STAT3 that negatively regulates the miR-204-5p expression. The miR-204-5p in turn, represses the TrkB expression. The expression of miR-204 in this circuit maintains the endometrial cells in a normal differentiated state. On the other hand, in EC cells, this circuit becomes dysregulated due to increased activity of the TrkB–STAT3 component, which constitutively represses the miR-204-5p. In the absence of sufficient miR-204 tumor suppressor activity, the TrkB oncogene is left uncontrolled, thereby leading to carcinogenesis (Fig. 24.3).

Ectopic over-expression or knockdown of TrkB expression caused changes in miR expression in EC cells. qRT-PCR showed that elevated TrkB repressed miR-204-5p expression in EC cells. Furthermore, TrkB over-expression in Ishikawa^{TrkB} cells increased JAK2 and STAT3 phosphorylation, which was aborted by TrkB knockdown in HEC-1B^{shTrkB} cells. Moreover, by ChIP assays, phospho-STAT3 direct binding to STAT3-binding sites near the TRPM3 promoter region, upstream of miR-204-5p, has been reported [9]. The miR-204-5p suppresses the clonogenic growth, migration and invasion of EC cells and also inhibits the growth of tumor xenografts bearing human EC cells. Interestingly, lower miR-204-5p expression was associated with lymph node metastasis and lowered the survival in EC patients. Finally, it has been also recently reported in EOC [62] that IL-6 treated EOC via IL-6R, triggers STAT3 activation that in turn represses miR-204 near to the TRPM3 promoter. This effect is required for IL-6-induced cisplatin resistance [62]. Collectively, the reestablishment of miR-204-5p expression could be explored as a potential new therapeutic target for this disease.

24.6.4 TRPC6 and miR-30 in Hepatocellular Carcinoma Invasion

TRPC6 channel is a critical component of calcium/calcineurin signaling together with protein phosphatase 3 family member 3CA/B, R1 (PPP3CA/B, PPP3R1) and NFATC3. This channel is highly expressed in several types of cancer [63]. Recently, a role for TRPC6 in driven TGFβ-mediated migration and invasion of human hepatocellular carcinoma cells (HCC) by forming a complex with the Na^+/Ca^{2+} exchanger-1 (NCX1) has been reported [64]. This complex-mediating Ca^{2+} signaling regulates the effects of TGFβ on the migration, invasion in HepG2 and Huh7 cells, and intrahepatic metastasis of human HCC cells in nude mice. TGFβ upregulates TRPC6 and NCX1 expression and induces the formation and activation of the TRPC6/NCX1 molecular complex, generating a positive feedback between TRPC6/NCX1 and Smad signaling. The expression of both TRPC6 and NCX1 was markedly increased in native human HCC tissues, and their expression levels positively correlated with advancement of HCC in patients. These data reveal the relevance of TRPC6/NCX1 molecular complex in HCC suggesting it as potential targets for therapy [64]. TRPC6 is a target gene of miR-30 [65] found to inhibit cell proliferation and invasion in different tumors [66]. However, at present the mechanisms regulating the miR-30/TRPC6 molecular interaction in HCC are still unknown. In parallel to TRPC6 upregulation that increases cell proliferation, TRPC1 silencing suppressed proliferation. Thus, it may be suggested that miR-30 by targeting TRPC1 and TRPC6 channels may take a part in the mechanism regulating HCC cell proliferation [67].

24.6.5 MiR-135 by Targeting TRPC1 Promotes Cancer Invasion and Chemotherapy Resistance

The miR-135 family comprises two members, miR-135a and miR-135b. miR-135a functions as a tumor suppressor gene in gastric [68], prostate [69] and renal cancers [70], malignant glioma [71] and colon cancer [72]. An in vitro study has demonstrated that in SW480 and SW620 CRC cell lines miR-135a promotes mobility and invasion via the metastasis suppressor gene 1 (MTSS1) [73]. In contrast, inhibition of miR-135a reduced their invasive capability. The miR-135a-mediated cell mobility and invasion were reduced after MTSS1 knocked-down by small interfering RNA, indicating that miR-135a promotes the invasion of CRC cells, partially through targeting MTSS1 [73].

By luciferase reporter assay, TRPC1 was identified as other target gene of miR-135a [63]. In cultured podocytes, TGFβ stimulation and adriamycin treatment promote miR-135a expression and TRPC1 down-regulation. Ectopic expression of miR-135a led to severe podocyte injury and disarray of podocyte cytoskeleton, which was reversed by TRPC1 [63]. Thus, in the view of the important role of miR-

135a in cytoskeleton stability, a contribute of this miRNA in cancer migration and metastatic invasion could be suggested. A role of TRPC1 in cancer development and progression, such as a role in apoptosis of hepatocellular carcinoma [67], metastasis of nasopharyngeal carcinoma [74], proliferation of NSCL carcinoma [75] as well as proliferation and tumorigenesis in ovarian cancer (OC) has been reported. A marked decrease in TRPC1 mRNA levels in human OC and cisplatin-resistant OC cells was observed [76]. TRPC1 directly interacts with several proteins/genes (MORC4, EGFR, STAT3, PDCD4, MET, OGDHL, BCL2, PTEN, SPARCL1, PIK3C3) implicated in drug resistance of OC. In the same way 5 miRs (miR-135b, miR-186, miR-26a, miR-497 and miR-548b-3p) targeting TRPC1, controlling drug resistance in OC [76] have been identified, with increased miR-135b and miR-186 expression that significantly correlates with the reduction of TRPC1 expression. The miR-135a regulates HOXA10 expression in epithelial OC, which correlates with platinum resistance [77]; moreover, a role for the TRPC1/SPARCL1 in the regulation of the autophagy and drug resistance in OC has been suggested.

24.7 Conclusion

MicroRNA are single stranded 19–25 nucleotides short RNAs that modulate gene expression at posttranslational level by targeting mRNAs and through binding of the 3′-untranslated region (UTR) of mRNAs. In the last years, miRNAs have attracted great interest from the oncologists for their versatility to regulate every phase of the carcinogenesis processes. A growing body of evidence suggests that miRNAs are aberrantly expressed in many human cancers (Table 24.1). Some high expressed miRNAs may function as oncogenes by repressing tumor suppressors, whereas other miRNAs are down-regulated and negatively regulate oncogenes, thus functioning as tumor suppressor. miRNAs have a pivotal role in tumorigenesis and the understanding of their functions may help to provide new cancer therapies.

In the last years it was demonstrated that several members of TRP family are target of miRNAs. Considering that these not selective cation channels fulfill several roles in cell physiology and in pathology such as regulating tumorigenesis and tumor progression, they became promising therapeutic targets in cancer treatment. Indeed, the interruption of one or more of the above described signaling network could be more effective than a single target gene to overcome cancer.

Interestingly, RNA molecules are not only retained in the cytoplasm of the cells, but they can also be released into the extracellular milieu, often in extracellular vesicles. These extracellular vesicles can transfer functional RNA between cells. In addition, different types of vesicles such as apoptotic bodies, microvesicles and exosomes contain distinct RNA molecules, especially miRNAs.

MiRNAs dysregulation was also involved in cancer chemoresistance, by regulating specific TRP-mediated pathway developed as consequence of high selection pressure in response to a disadvantageous microenvironment.

Future studies should be required to identify the TRP channels and miRNAs expression and their role played in distinct phase of tumor development and progression. Much work still remains to do; we are only at the beginning to develop strategies to treat cancer manipulating the TRP/miRNA interactive network.

References

1. Zheng J (2013) Molecular mechanism of TRP channels. Compr Physiol 3:221–242
2. Bartel DP (2004) MicroRNAs: genomics, biogenesis, mechanism, and function. Cell 12:281–297
3. Wang Z (2013) miRNA in the regulation of ion channel/transporter expression. Compr Physiol 3:599–653
4. Hyun YJ, Changchun X (2015) MicroRNA mechanisms of action: what have we learned from mice? Front Genet 6:328
5. Krek A, Grun D, Poy MN, Wolf R, Rosenberg L, Epstein EJ, MacMenamin P, da Piedade I, Gunsalus KC, Stoffel M, Rajewsky N (2005) Combinatorial microRNA target predictions. Nat Genet 12:495–500
6. Lu J, Getz G, Miska EA, Alvarez-Saavedra E, Lamb J, Peck D, Sweet-Cordero A, Ebert BL, Mak RH, Ferrando AA (2005) MicroRNA expression profiles classify human cancers. Nature 12:834–838
7. Mazar J, DeYoung K, Khaitan D, Meister E, Almodovar A, Goydos J, Ray A, Perera RJ (2010) The regulation of miRNA-211 expression and its role in melanoma cell invasiveness. PLoS One 5:e13779
8. Guo H, Carlson JA, Slominski A (2012) Role of TRPM in melanocytes and melanoma. Exp Dermatol 21(9):650–654
9. Bao W, Wang HH, Tian FJ, He XY, Qiu MT, Wang JY (2013) A TrkB-STAT3-miR-204-5p regulatory circuitry controls proliferation and invasion of endometrial carcinoma cells. Mol Cancer 12:155
10. Banno K, Yanokura M, Kisu I, Yamagami W, Susumu N, Aoki D (2013) MicroRNAs in endometrial cancer. Int J Clin Oncol 12:186–192
11. Erdmann K, Kaulke K, Thomae C, Huebner D, Sergon M, Froehner M, Wirth MP, Fuessel S (2014) Elevated expression of prostate cancer-associated genes is linked to down-regulation of microRNAs. BMC Cancer 14:82
12. Shalgi R, Lieber D, Oren M, Pilpel Y (2007) Global and local architecture of the mammalian microRNA-transcription factor regulatory network. PLoS Comput Biol 3(7):e131
13. Australian Institute of Health and Welfare (AIHW) (2008) Australia Cancer Incidence and Mortality (ACIM) books: incidence numbers and rates from 1982 to 2005, and mortality numbers and rates from 1968 to 2006
14. Thompson JF, Scolyer RA, Kefford RF (2005) Cutaneous melanoma. Lancet 365(9460):687–701
15. Deeds J, Cronin F, Duncan LM (2000) Patterns of melastatin mRNA expression in melanocytic tumors. Hum Pathol 31(11):1346–1356
16. Miller AJ, Du J, Rowan S, Hershey CL, Widlund HR, Fisher DE (2004) Transcriptional regulation of the melanoma prognostic marker melastatin (TRPM1) by MITF in melanocytes and melanoma. Cancer Res 64(2):509–516
17. Levy C, Khaled M, Iliopoulos D, Janas MM, Schubert S, Pinner S, Chen PH, Li S, Fletcher AL, Yokoyama S, Scott KL, Garraway LA, Song JS, Granter SR, Turley SJ, Fisher DE, Novina CD (2010) Intronic miR-211 assumes the tumor suppressive function of its host gene in melanoma. Mol Cell 40:841–849

18. Boyle GM, Woods SL, Bonazzi VF, Stark MS, Hacker E, Aoude LG, Dutton-Regester K, Cook AL, Sturm RA, Hayward NK (2011) Melanoma cell invasiveness is regulated by miR-211 suppression of the BRN2 transcription factor. Pigment Cell Melanoma Res 24:525–537
19. Davies H, Bignell GR, Cox C, Stephens P, Edkins S, Clegg S, Teague J, Woffendin H, Garnett MJ, Bottomley W, Davis N, Dicks E, Ewing R, Floyd Y, Gray K, Hall S, Hawes R, Hughes J, Kosmidou V, Menzies A, Mould C, Parker A, Stevens C, Watt S, Hooper S, Wilson R, Jayatilake H, Gusterson BA, Cooper C, Shipley J, Hargrave D, Pritchard-Jones K, Maitland N, Chenevix-Trench G, Riggins GJ, Bigner DD, Palmieri G, Cossu A, Flanagan A, Nicholson A, Ho JW, Leung SY, Yuen ST, Weber BL, Seigler HF, Darrow TL, Paterson H, Marais R, Marshall CJ, Wooster R, Stratton MR, Futreal PA (2002) Mutation of the BRAF gene in human cancer. Nature 417:949–954
20. Lunavat TR, Cheng L, Einarsdottir BO, Olofsson Bagge R, Veppil Muralidharan S, Sharples RA, Lässer C, Gho YS, Hill AF, Nilsson JA, Lötvall J (2017) BRAF(V600) inhibition alters the microRNA cargo in the vesicular secretome of malignant melanoma cells. Proc Natl Acad Sci U S A 114(29):E5930–E5939
21. De Luca T, Pelosi A, Trisciuoglio D, D'Aguanno S, Desideri M, Farini V, Di Martile M, Bellei B, Tupone MG, Condiloro A, Regazzo G, Rizzo MG, Del Bufalo D (2016) miR-211 and MIFT modulation by Bcl-2 protein in melanoma cells. Mol Carcinog 55:2304–2312
22. Wellbrock C, Arozarena I (2015) Microphthalmia-associated transcription factor in melanoma development and MAP-kinase pathway targed therapy. Pigment Cell Melanoma Res 28:390–406
23. Margue C, Philippidou D, Reinsbach SE, Schmitt M, Behrmann I, Kreis S (2013) New target genes of MITF-induced microRNA-211 contribute to melanoma cell invasion. PLoS One 8(9):e73473
24. Natrajan R, Louhelainen J, Williams S, Laye J, Knowles MA (2003) High-resolution deletion mapping of 15q13.2-q21.1 in transitional cell carcinoma of the bladder. Cancer Res 63:7657–7662
25. Poetsch M, Kleist B (2006) Loss of heterozygosity at 15q21.3 correlates with occurrence of metastases in head and neck cancer. Mod Pathol 19:1462–1469
26. Xia B, Yang S, Liu T, Lou G (2015) miR-211 suppresses epithelial ovarian cancer proliferation and cell-cycle progression by targeting Cyclin D1 and CDK6. Mol Cancer 14:57
27. Tao F, Tian X, Ruan S, Shen M, Zhang Z (2018) miR-211 sponges lncRNA MALAT1 to suppress tumor growth and progression through inhibiting PHF19 in ovarian carcinoma. FASEB J 6:fj201800495RR
28. He DX, Gu XT, Jiang L, Jin J, Ma X (2014) A methylation-based regulatory network for microRNA 320a in chemoresistant breast cancer. Mol Pharmacol 86(5):536–547
29. Yu S, Qin X, Chen T, Zhou L, Xu X, Feng J (2017) MicroRNA-106b-5p regulates cisplatin chemosensitivity by targeting polycystic kidney disease-2 in non-small-cell lung cancer. Anti-Cancer Drugs 28(8):852–860
30. Iino I, Kikuchi H, Myyazaki S, Hiramatsu Y, Ohta M, Kamiya K, Kusama Y, Baba S, Setou M, Konno H (2013) Effect of mir-122 and its target gene cationic aminoacid transporter 1 on colorectal liver metastasis. Cancer Sci 104:624–630
31. Shapiro D, Deering-Rice CE, Romero EG, Hughen RW, Light AR, Veranth JM, Reilly CA (2013) Activation of transient receptor potential ankyrin-1 (TRPA1) in lung cells by wood smoke particulate material. Chem Res Toxicol 26(5):750–758
32. Zygmunt PM, Hogestatt ED (2014) Trpa1. Handb Exp Pharmacol 222:583–630
33. Berrout J, Kyriakopoulou E, Moparthi L, Hogea AS, Berrout L, Ivan C, Lorger M, Boyle J, Peers C, Muench S, Gomez JE, Hu X, Hurst C, Hall T, Umamaheswaran S, Wesley L, Gagea M, Shires M, Manfield I, Knowles MA, Davies S, Suhling K, Gonzalez YT, Carragher N, Macleod K, Abbott NJ, Calin GA, Gamper N, Zygmunt PM, Timsah Z (2017) TRPA1-FGFR2 binding event is a regulatory oncogenic driver modulated by miRNA-142-3p. Nat Commun 8(1):947
34. Turner N, Grose R (2010) Fibroblast growth factor signalling: from development to cancer. Nat Rev Cancer 10:116–129

35. Timsah Z, Berrout J, Suraokar M, Behrens C, Song J, Lee JJ, Ivan C, Gagea M, Shires M, Hu X, Vallien C, Kingsley CV, Wistuba I, Ladbury JE (2015) Expression pattern of FGFR2, Grb2 and Plcγ1 acts as a novel prognostic marker of recurrence recurrence-free survival in lung adenocarcinoma. Am J Cancer Res 5(10):3135–3148
36. Peng X, Liu WL (2015) MiR-142-3p functions as a potential tumour suppressor directly targeting HMGB1 in non-small-cell lung carcinoma. Int J Clin Exp Pathol 8(9):10800
37. Jemal A, Bray F, Center MM, Ferlay J, Ward E, Forman D (2011) Global cancer statistics. CA Cancer J Clin 61(2):69–90
38. Zhang L, Barritt GJ (2004) Evidence that TRPM8 is an androgen-dependent Ca^{2+} channel required for the survival of prostate cancer cells. Cancer Res 64(22):8365–8373
39. Zhang J, Liang J, Huang J (2016) Downregulated microRNA-26a modulates prostate cancer cell proliferation and apoptosis by targeting COX-2. Oncol Lett 12(5):3397–3402
40. Tong MH, Mitchell DA, McGowan SD, Evanoff R, Griswold MD (2012) Two miRNA clusters, Mir-17-92 (Mirc1) and Mir-106b-25 (Mirc3), are involved in the regulation of spermatogonial differentiation in mice. Biol Reprod 86(3):72
41. Patel V, Williams D, Hajarnis S, Hunter R, Pontoglio M, Somlo S, Igarashi P (2013) miR-17∼92 miRNA cluster promotes kidney cyst growth in polycystic kidney disease. Proc Natl Acad Sci U S A 110(26):10765–10770
42. Sun H, Li QW, Lv XY, Ai JZ, Yang QT, Duan JJ, Bian GH, Xiao Y, Wang YD, Zhang Z, Liu YH, Tan RZ, Yang Y, Wei YQ, Zhou Q (2010) MicroRNA-17 post-transcriptionally regulates polycystic kidney disease-2 gene and promotes cell proliferation. Mol Biol Rep 37:2951–2958
43. Mendell JT (2008) miRiad roles for the miR-17-92 cluster in development and disease. Cell 133(2):217–222
44. Conkrite K, Sundby M, Mukai S, Thomson JM, Mu D, Hammond SM, MacPherson D (2011) miR-17∼92 cooperates with RB pathway mutations to promote retinoblastoma. Genes Dev 25(16):1734–1745
45. Cloonan N, Brown MK, Steptoe AL, Wani S, Chan WL, Forrest AR, Kolle G, Gabrielli B, Grimmond SM (2008) The miR-17-5p microRNA is a key regulator of the G1/S phase cell cycle transition. Genome Biol 9(8):R127
46. O'Donnell KA, Wentzel EA, Zeller KI, Dang CV, Mendell JT (2005) c-Myc-regulated microRNAs modulate E2F1 expression. Nature 435(7043):839–843
47. Roldo C, Missiaglia E, Hagan JP, Falconi M, Capelli P, Bersani S, Calin GA, Volinia S, Liu CG, Scarpa A, Croce CM (2006) MicroRNA expression abnormalities in pancreatic endocrine and acinar tumors are associated with distinctive pathologic features and clinical behavior. J Clin Oncol 24(29):4677–4684
48. Zanette DL, Rivadavia F, Molfetta GA, Barbuzano FG, Proto-Siqueira R, Silva WA Jr, Falcão RP, Zago MA (2007) miRNA expression profiles in chronic lymphocytic and acute lymphocytic leukemia. Braz J Med Biol Res 40(11):1435–1440
49. Xin J, Zheng L-M, Sun D-K, Li X-F, Xu P, Tian L-Q (2018) miR-204 functions as a tumor suppressor gene, at least partly by suppressing CYP27A1 in glioblastoma. Oncol Lett 16:1439–1448
50. Ge Y, Yan X, Jin Y, Yang X, Yu X, Zhou L, Han S, Yuan Q, Yang M (2015) fMiRNA-192 and miRNA-204 directly suppress lncRNA HOTTIP and interrupt GLS1-mediated glutaminolysis in hepatocellular carcinoma. Terracciano L ed. PLoS Genet 11(12):e1005726
51. Kuwano Y, Nishida K, Kajita K, Satake Y, Akaike Y, Fujita K, Kano S, Masuda K, Rokutan K (2015) Transformer 2beta and miR-204 regulate apoptosis through competitive binding to 3′ UTR of BCL2 mRNA. Cell Death Differ 22(5):815–825
52. Imam JS, Plyler JR, Bansal H, Prajapati S, Bansal S, Rebeles J, Chen HI, Chang YF, Panneerdoss S, Zoghi B, Buddavarapu KC, Broaddus R, Hornsby P, Tomlinson G, Dome J, Vadlamudi RK, Pertsemlidis A, Chen Y, Rao MK (2012) Genomic loss of tumor suppressor miRNA-204 promotes cancer cell migration and invasion by activating AKT/mTOR/Rac1 signaling and actin reorganization. PLoS One 7(12):e52397
53. Wang L, Tian H, Yuan J, Wu H, Wu J, Zhu X (2015) CONSORT. Sam68 is directly regulated by MiR-204 and promotes the self-renewal potential of breast cancer cells by activating the Wnt/Beta-catenin signaling pathway. Medicine 94(49):e2228

54. Hall DP, Cost NG, Hegde S, Kellner E, Mikhaylova O, Stratton Y, Ehmer B, Abplanalp WA, Pandey R, Biesiada J, Harteneck C, Plas DR, Meller J, Czyzyk-Krzeska MF (2014) TRPM3 and miR-204 establish a regulatory circuit that controls oncogenic autophagy in clear cell renal cell carcinoma. Cancer Cell 26(5):738–753
55. Cecconi F, Jäättelä M (2014) Targeting ions-induced autophagy in cancer. Cancer Cell 26(5):599–600
56. Cost NG, Czyzyk-Krzeska MF (2015) Regulation of autophagy by two products of one gene: TRPM3 and miR-204. Mol Cell Oncol 2(4):e1002712
57. Harteneck C (2005) Function and pharmacology of TRPM cation channels. Naunyn Schmiedeberg's Arch Pharmacol 371:307–314
58. Chow TF, Youssef YM, Lianidou E, Romaschin AD, Honey RJ, Stewart R, Pace KT, Youssef GM (2010) Differential expression profiling of microRNAs and their potential involvement in renal cell carcinoma pathogenesis. Clin Biochem 43:150–158
59. Osanto S, Qin Y, Buermans HP, Berkers J, Lerut E, Goeman JJ, van Poppel H (2012) Genome-wide microRNA expression analysis of clear cell renal cell carcinoma by next generation deep sequencing. PLoS One 7:e38298
60. Ma L, Deng X, Wu M, Zhang G, Huang J (2014) Down-regulation of miRNA-204 by LMP-1 enhances CDC42 activity and facilitates invasion of EBV-associated nasopharyngeal carcinoma cells. FEBS Lett 588(9):1562–1570
61. Siegel R, Naishadham D, Jemal A (2013) Cancer statistics, 2013. CA Cancer J Clin 12:11–30
62. Zhu X, Shen H, Yin X, Long L, Chen X, Feng F, Liu Y, Zhao P, Xu Y, Li M, Xu W, Li Y (2017) IL-6R/STAT3/miR-204 feedback loop contributes to cisplatin resistance of epithelial ovarian cancer cells. Oncotarget 8(24):39154–39166
63. Shapovalov G, Ritaine A, Skryma R, Prevarskaya N (2016) Role of TRP ion channels in cancer and tumorigenesis. Semin Immunopathol 38(3):357–369
64. Xu J, Yang Y, Xie R, Liu J, Nie X, An J, Wen G, Liu X, Jin H, Tuo B (2018) The NCX1/TRPC6 complex mediates TGFβ-driven migration and invasion of human hepatocellular carcinoma cells. Cancer Res 78(10):2564–2576
65. Wu J, Zheng C, Wang X, Yun S, Zhao Y, Liu L, Lu Y, Ye Y, Zhu X, Zhang C, Shi S, Liu Z (2015) MicroRNA-30 family members regulate calcium/calcineurin signaling in podocytes. J Clin Invest 125(11):4091–4106
66. Liu Y, Zhou Y, Gong X, Zhang C (2017) MicroRNA-30a-5p inhibits the proliferation and invasion of gastric cells by targeting insulin-like growth factor 1 receptor. Exp Ther Med 14:173–180
67. Selli C, Erac Y, Tosun M (2015) Simultaneous measurement of cytosolic and mitochondrial calcium levels: observations in TRPC1-silenced hepatocellular carcinoma cells. J Pharmacol Toxicol Methods 72:29–34
68. Zhang C, Chen X, Chen X, Wang X, Ji A, Jiang L, Sang F, Li F (2016) miR-135a acts as a tumor suppressor in gastric cancer in part by targeting KIFC1. Onco Targets Ther 9:3555–3563
69. Wan X, Pu H, Huang W, Yang S, Zhang Y, Kong Z, Yang Z, Zhao P, Li A, Li T, Li Y (2016) Androgen-induced miR-135a acts as a tumor suppressor through downregulating RBAK and MMP11, and mediates resistance to androgen deprivation therapy. Oncotarget 7:51284–51300
70. Yamada Y, Hidaka H, Seki N, Yoshino H, Yamasaki T, Itesako T, Nakagawa M, Enokida H (2013) Tumor-suppressive microRNA-135a inhibits cancer cell proliferation by targeting the c-MYC oncogene in renal cell carcinoma. Cancer Sci 104:304–312
71. Wu S, Lin Y, Xu D, Chen J, Shu M, Zhou Y, Zhu W, Su X, Zhou Y, Qiu P, Yan G (2012) MiR-135a functions as a selective killer of malignant glioma. Oncogene 31:3866–3874
72. Nagel R, le Sage C, Diosdad B, van der Waal M, Oude Vrielink JA, Bolijn A, Meijer GA, Agami R (2008) Regulation of the adenomatous polyposis coli gene by the miR-135 family in colorectal cancer. Cancer Res 68:5795–5802
73. Zhou W, Li X, Liu F, Xiao Z, He M, Shen S, Liu S (2012) MiR-135a promotes growth and invasion of colorectal cancer via metastasis suppressor 1 in vitro. Acta Biochim Biophys Sin Shanghai 44:838–846

74. He B, Liu F, Ruan J, Li A, Chen J, Li R, Shen J, Zheng D, Luo R (2012) Silencing TRPC1 expression inhibits invasion of CNE2 nasopharyngeal tumor cells. Oncol Rep 27:1548–1554
75. Tajeddine N, Gailly P (2012) TRPC1 protein channel is major regulator of epidermal growth factor receptor signaling. J Biol Chem 287:16146–16157
76. Liu X, Zou J, Su J, Lu Y, Zhang J, Li L, Yin F (2016) Downregulation of transient receptor potential cation channel, subfamily C, member 1 contributes to drug resistance and high histological grade in ovarian cancer. Int J Oncol 48(1):243–252
77. Tang W, Jiang Y, Mu X, Xu L, Cheng W, Wang X (2014) MiR-135a functions as a tumor suppressor in epithelial ovarian cancer and regulates HOXA10 expression. Cell Signal 26:1420–1426

Chapter 25
Calcium Channels and Calcium-Regulated Channels in Human Red Blood Cells

Lars Kaestner, Anna Bogdanova, and Stephane Egee

Abstract Free Calcium (Ca^{2+}) is an important and universal signalling entity in all cells, red blood cells included. Although mature mammalian red blood cells are believed to not contain organelles as Ca^{2+} stores such as the endoplasmic reticulum or mitochondria, a 20,000-fold gradient based on a intracellular Ca^{2+} concentration of approximately 60 nM vs. an extracellular concentration of 1.2 mM makes Ca^{2+}-permeable channels a major signalling tool of red blood cells. However, the internal Ca^{2+} concentration is tightly controlled, regulated and maintained primarily by the Ca^{2+} pumps PMCA1 and PMCA4. Within the last two decades it became evident that an increased intracellular Ca^{2+} is associated with red blood cell clearance in the spleen and promotes red blood cell aggregability and clot formation. In contrast to this rather uncontrolled deadly Ca^{2+} signals only recently it became evident, that a temporal increase in intracellular Ca^{2+} can also have positive effects such as the modulation of the red blood cells O_2 binding properties or even be vital for brief transient cellular volume adaptation when passing constrictions like small capillaries or slits in the spleen. Here we give an overview of Ca^{2+} channels and Ca^{2+}-regulated channels in red blood cells, namely the Gárdos channel, the non-selective voltage dependent cation channel, Piezo1, the NMDA receptor, VDAC, TRPC channels, $Ca_V2.1$, a Ca^{2+}-inhibited channel novel to red blood cells and i.a. relate these channels to the molecular unknown sickle cell disease conductance P_{sickle}. Particular attention is given to correlation of functional measurements with

L. Kaestner (✉)
Theoretical Medicine and Biosciences, Saarland University, Homburg, Germany

Experimental Physics, Saarland University, Saarbrücken, Germany
e-mail: lars_kaestner@me.com

A. Bogdanova
Red Blood Cell Research Group, Institute of Veterinary Physiology, Vetsuisse Faculty and the Zürich Center for Integrative Human Physiology (ZIHP), University of Zürich, Zürich, Switzerland

S. Egee
CNRS, UMR8227 LBI2M, Sorbonne Université, Roscoff, France

Laboratoire d'Excellence GR-Ex, Paris, France

M. S. Islam (ed.), *Calcium Signaling*, Advances in Experimental Medicine and Biology 1131, https://doi.org/10.1007/978-3-030-12457-1_25

molecular entities as well as the physiological and pathophysiological function of these channels. This view is in constant progress and in particular the understanding of the interaction of several ion channels in a physiological context just started. This includes on the one hand channelopathies, where a mutation of the ion channel is the direct cause of the disease, like Hereditary Xerocytosis and the Gárdos Channelopathy. On the other hand it applies to red blood cell related diseases where an altered channel activity is a secondary effect like in sickle cell disease or thalassemia. Also these secondary effects should receive medical and pharmacologic attention because they can be crucial when it comes to the life-threatening symptoms of the disease.

Keywords Gárdos channel · Non-selective voltage dependent cation channel · Piezo1 · NMDA receptor · VDAC · TRPC channel · $Ca_V2.1$ · Calcium-inhibited channel · P_{sickle} · Anaemia

25.1 Introduction to Calcium in Red Blood Cells

Free Calcium (Ca^{2+}) is an important and universal second messenger in all cells [1, 2], red blood cells (RBCs) included [3–5]. This results in the abundance of Ca^{2+}-binding proteins in RBCs with differing Ca^{2+} sensitivities as outlined in Fig. 25.1. Mature mammalian RBCs are believed to not contain organelles as Ca^{2+} stores such as the endoplasmic reticulum or mitochondria [6]. Compared to other cell types, where the Ca^{2+} liberated from stores within intracellular organelles can be used in the regulation of free cytosolic Ca^{2+} concentration and thereby Ca^{2+} signalling, in mammalian erythrocytes the control of free intracellular Ca^{2+} concentration must be done by regulation of membrane transport. A 20,000-fold gradient based on an intracellular Ca^{2+} concentration of approximately 60 nM vs. an extracellular concentration of 1.2 mM makes Ca^{2+}-permeable channels a major signalling tool of RBCs. As historically RBCs served as the model cell to investigate membrane transport, it is well known that the internal Ca^{2+} concentration is tightly controlled, regulated and maintained primarily by the Ca^{2+} pumps PMCA1 and PMCA4 [4, 7]. The Ca^{2+} pumping in turn is regulated by multiple factors, such as the Ca^{2+} concentration itself [8], calmodulin [9], calpain [10], phospholipids and various kinases [11] or even self-association [12]. Within the last two decades it became evident that an increased intracellular Ca^{2+} is associated with RBC clearance in the spleen and promotes RBCs aggregability and clot formation [3, 13–16]. There was a long debate within the community whether this process should be called eryptosis [17], which is no longer recommended [18]. In contrast to this rather uncontrolled deadly Ca^{2+} signals (resulting in Ca^{2+} overload), within the recent years it became evident that a temporal increase in intracellular Ca^{2+} can also have positive effects such as the modulation of the RBCs O_2 binding properties [19] or even be vital for brief transient cellular volume adaptation when passing constrictions like small capillaries or slits in the spleen [5, 20, 21] as depicted in Fig. 25.2. The perilous balance of Ca^{2+} in RBCs was recently reviewed [3].

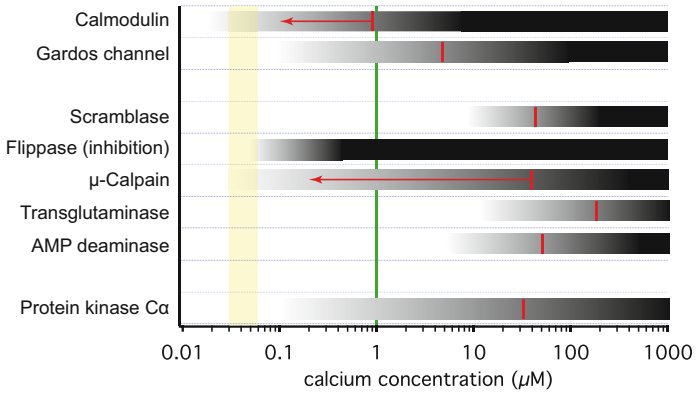

Fig. 25.1 Overview of concentration dependence of Ca^{2+}activated proteins in RBCs. The yellow column indicates the estimated range of RBCs'resting free Ca^{2+} [96]. The gray/black bars indicate the activation of the proteins with the intensity of darkness related to the activation level (details see below). The red lines depict the half activation concentration. For orientation the green line provides the in vivo k_D for Fluo-4 [101], probably the most appropriate Ca^{2+} fluorophore to be used in RBCs [102]. The universal intermediate messenger calmodulin has a dissociation constant for Ca^{2+} of 920 nM [103], which can be shifted down to 100 nM, indicated by the red arrow. The Gárdos channel has an open probability of EC_{50} of 4.7 μM with a Hill slope factor of approximately 1 [104]. Values were measured in excised patches at a membrane potential of 0 mV. The curve of the opening frequency is almost superimposable (EC_{50} of 4.3 μM) [104] keeping the values given in the figure valid also for whole cell and hence population based investigations. The values for half maximal activation of the scramblase was determined by different studies with varying methodologies and a slightly different result. Values varied between approximately 30 μM determined in liposomes [105] and 70 μM measured in RBC ghosts [106]. The flippase displays almost full inhibition already at a Ca^{2+} concentration of 400 nM [107]. μ-Calpain, a protein that cleaves cytoskeleton and membrane proteins depicts an half activation at 40 μM Ca^{2+} [108] but can be activated and then shifting half-maximal activation down to 200 nM [109]. Transglutaminase mediating polymerisation of RBC membrane proteins in its native form has a dissociation constant for Ca^{2+} of 190 μM [110]. Adenosine monophosphate (AMP) deaminase is an enzyme that converts AMP into inosin monophosphate and is directly stimulated by Ca^{2+} at a half maximal concentration of 50 μM free Ca^{2+} [111]. The binding of Ca^{2+} to the C2-domain of PKCα was determined in vitro to be 35 μM with a Hill coefficient of 0.9 [112]. Although the Ca^{2+} dependence of the membrane binding was measured to be one order of magnitude lower [112], the initial Ca^{2+} binding is the crucial step for PKCα activation and therefore the relevant number in this compilation. (This figure is reproduced from Bogdanova et al. 2013 [3])

25.2 The Gárdos Channel – A Calcium-Activated Potassium Channel

The Gárdos channel is one of the Ca^{2+} sensors in RBCs transferring Ca^{2+} uptake into K^+ and water loss and mediating thereby Ca^{2+}-dependent volume regulation and changes in RBC rheology. It is also annotated as KCNN4, $K_{Ca}3.1$, IK1 or SK4. It is the first channel we describe in this chapter because it was the first channel found in RBCs [22, 23], i.e. utilising the patch-clamp technique as a direct read-out of channel activity. However, its name goes back to the effect of Ca^{2+} dependent

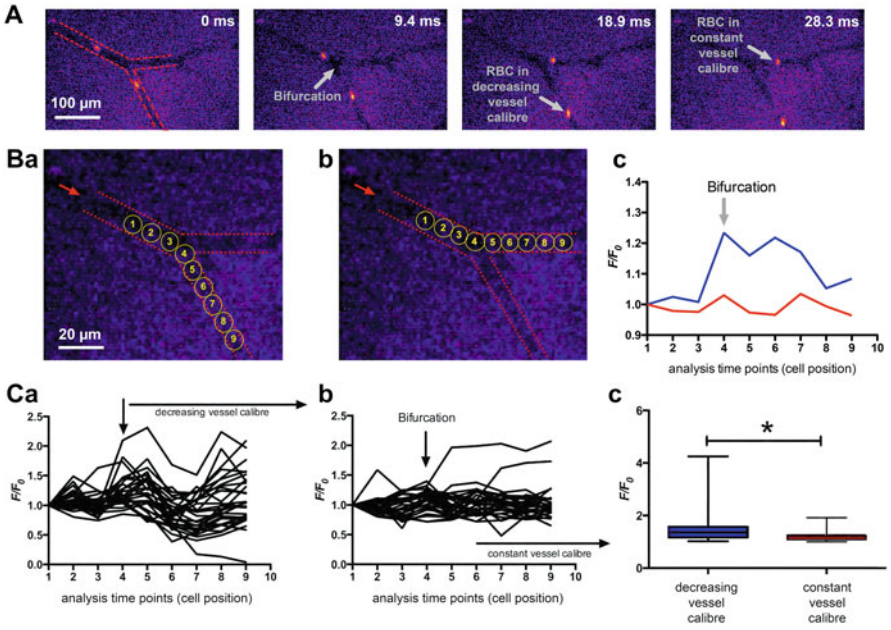

Fig. 25.2 In vivo Ca^{2+}-signalling of mouse RBCs when passing through capillaries. Mouse RBCs were ex vivo stained with Fluo-4 and then re-injected into the mouse circulation. Fluorescence imaging of capillaries was performed in the dorsal skinfold chamber. (A) shows representative snapshots of RBCs passing a bifurcation. For the 30 ms sequence only every second recorded image is presented. For a better orientation the vessel walls are indicated by red dashed lines in the leftmost image and further annotations (grey) are added in the other images. (B) depicts the positions where fluorescence intensity (F/F_0) was analysed for a decreasing vessel calibre (Ba) and for a constant vessel calibre (Bb) of the same example section as in (A). The dashed red lines mark the vessel walls, the red arrow indicates the blood flow direction and the yellow circles depict the analysis positions which are plotted in the following diagrams. Example fluorescence traces of the two cells analysed as pointed out in (Ba) and (Bb) are shown in (Bc). (C) depicts the analysis of 30 cells passing through a capillary with decreasing vessel calibre and 28 cells passing through a capillary with constant vessel calibre. Analysis was performed at 3 vessel-bifurcations in 2 mice. The fluorescence intensity (F/F_0) traces of all measured RBCs passing through a capillary with decreasing vessel calibre is plotted in (Ca), while the traces of all measured RBCs passing a capillary with constant vessel calibre is plotted in (Cb). The statistical analysis of the maximal fluorescence intensity (F/F_0) of RBCs from both groups is depicted in (Cc). The increase in Ca^{2+}, while passing through a vessel with decreasing calibre is significant ($p = 0.014$; *). (This figure is reproduced from Danielczok et al. 2017 [5])

K^+ efflux found in RBCs by G. Gárdos once metabolic pathways are poisoned [24, 25]. As the molecular identity of this transport in RBCs was not known, it was referred to as Gárdos effect and later, when it turned out to be ion channel mediated, the involved transport protein was called Gárdos channel. Even after its molecular identification in 2003 [26] in the RBC field it remained to be referred to as Gárdos channel. Figure 25.3 provides the milestones in the Gárdos channel research. A comprehensive review of the Gárdos channel structure and function was published

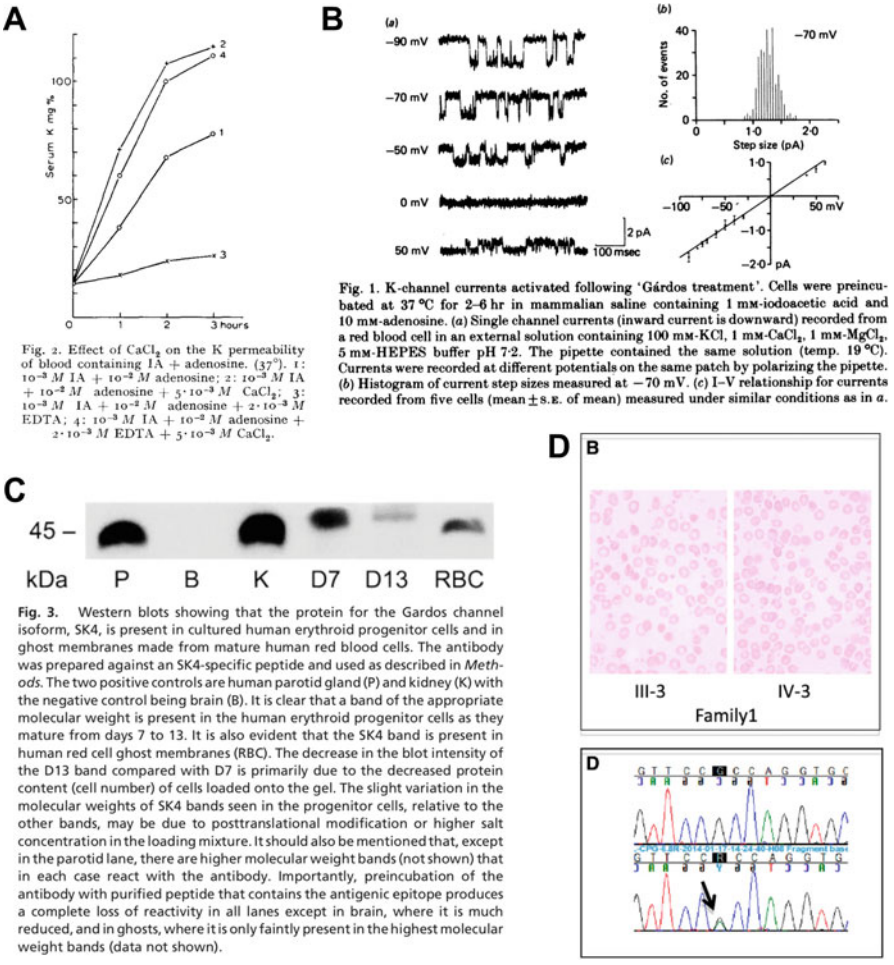

Fig. 2. Effect of $CaCl_2$ on the K permeability of blood containing IA + adenosine. (37°). 1: 10^{-3} *M* IA + 10^{-2} *M* adenosine; 2: 10^{-3} *M* IA + 10^{-2} *M* adenosine + $5 \cdot 10^{-3}$ *M* $CaCl_2$; 3: 10^{-3} *M* IA + 10^{-2} *M* adenosine + $2 \cdot 10^{-3}$ *M* EDTA; 4: 10^{-3} *M* IA + 10^{-2} *M* adenosine + $2 \cdot 10^{-3}$ *M* EDTA + $5 \cdot 10^{-3}$ *M* $CaCl_2$.

Fig. 1. K-channel currents activated following 'Gárdos treatment'. Cells were preincubated at 37 °C for 2–6 hr in mammalian saline containing 1 mM-iodoacetic acid and 10 mM-adenosine. (*a*) Single channel currents (inward current is downward) recorded from a red blood cell in an external solution containing 100 mM-KCl, 1 mM-$CaCl_2$, 1 mM-$MgCl_2$, 5 mM-HEPES buffer pH 7·2. The pipette contained the same solution (temp. 19 °C). Currents were recorded at different potentials on the same patch by polarizing the pipette. (*b*) Histogram of current step sizes measured at −70 mV. (*c*) I–V relationship for currents recorded from five cells (mean ± S.E. of mean) measured under similar conditions as in *a*.

Fig. 3. Western blots showing that the protein for the Gardos channel isoform, SK4, is present in cultured human erythroid progenitor cells and in ghost membranes made from mature human red blood cells. The antibody was prepared against an SK4-specific peptide and used as described in *Methods*. The two positive controls are human parotid gland (P) and kidney (K) with the negative control being brain (B). It is clear that a band of the appropriate molecular weight is present in the human erythroid progenitor cells as they mature from days 7 to 13. It is also evident that the SK4 band is present in human red cell ghost membranes (RBC). The decrease in the blot intensity of the D13 band compared with D7 is primarily due to the decreased protein content (cell number) of cells loaded onto the gel. The slight variation in the molecular weights of SK4 bands seen in the progenitor cells, relative to the other bands, may be due to posttranslational modification or higher salt concentration in the loading mixture. It should also be mentioned that, except in the parotid lane, there are higher molecular weight bands (not shown) that in each case react with the antibody. Importantly, preincubation of the antibody with purified peptide that contains the antigenic epitope produces a complete loss of reactivity in all lanes except in brain, where it is much reduced, and in ghosts, where it is only faintly present in the highest molecular weight bands (data not shown).

Fig. 25.3 Milestones in Gárdos channel research. (**a**) Reprint from Gárdos 1958 [25]; a one page article mentioning a dependence of K^+-efflux from Ca^{2+} in the category "preliminary notes" was retrospectively sufficient for the naming of an ion channel. IA stands for iodoacedic acid. (**b**) Reprint from Hamill 1981 [23]; the first published single channel current traces from the Gárdos channel appeared in a poster Abstract for the Physiological Society (London) meeting. Numerous patch-clamp based characterisations followed this initial recording [22, 28, 104, 103–107]. (**c**) Reprint from Hoffman et al. 2003 [26] providing the molecular identification of the Gárdos channel to be KCNN4 ($K_{Ca}3.1$, IK1, SK4). (**d**) Reprint from Rapetti-Maus et al. 2015 [29] providing the first report of a Gárdos channel mutation and its link to a pathophysiological setting. Upper panel: Blood film smears for two patients with the Gárdos channel mutation p.Arg352His (mother and son). Lower panel KCNN4 transcript sequencing; upper line presents the wild type sequence and the lower line the transcript with mutation c.1055G.A (p.Arg352His)

some 15 years ago [27]. An interesting property of the channel is its temperature dependence. With decreasing temperature, a continuous decrease of Gárdos channel conductance is observed. The Arrhenius plot of the unitary channel conductance between 0 °C and 47 °C is strictly linear and has a slope which corresponds to an activation energy of 29.6 ± 0.4 kJ/mol. Nevertheless, simultaneously, altered gating kinetics results in an increase of channel opening probability at reduced temperatures. At saturating concentration of intracellular Ca^{2+} (10 μM), reducing the temperature from 35 to 30 °C results in a change of the opening and closing kinetic of the Gárdos channel. Brief channel openings and closing are progressively replaced by longer openings and shorter closing states [28]. More importantly, reducing the Ca^{2+} concentration at the intracellular face of the channel at half the EC_{50} for Ca^{2+} and temperature close to 0 °C drastically increases open probability indicating that even at very low Ca^{2+} concentrations the Gárdos channel may be activated. Knowing that blood samples for analyses and RBC concentrates for blood transfusion are kept refrigerated, one has to keep in mind this peculiar property of the Gárdos channel that may have deleterious effects respective to the cell volume.

The physiological function of the Gárdos channel was a speculative topic for many decades although a link to RBC cell volume threatening was clear, since activation of the Gárdos channel results in cellular K^+ loss associated with Cl^- and osmotically obliged water loss may lead to rapid cell shrinkage. In this context the channel was believed to be a 'suicide mechanism' triggered by the intracellular increase in Ca^{2+}. This was proposed to happen in the process of clot formation, in thrombotic events as well as during RBC clearance. With the finding of the first mutations in the Gárdos channel [29, 30] (see also Fig. 25.3D) and the associated pathophysiology, a physiological function of the Gárdos channel was doubtless proven. Although the initial reports link the mutation of the Gárdos channel to Hereditary Xerocytosis [29, 30], further studies revealed that 'Gárdos channelopathy' is its own disease or at least an own variant of Hereditary Stomatocytosis [31]. Any prolonged Gárdos channel activation lead to changes in cell volume which eventually affect rheological, stiffness and rigidity properties that compromise their survival within the circulation especially during their passage within the slits of the spleen. The mutations reported so far resulted in a gain of function that could be treated with a Gárdos channel inhibitor. There are numerous Gárdos channel inhibitors available some of them already clinically tested for other diseases, like clotrimazole for topical applications or senicapoc [32]. The Gárdos channel also shows an increased activity in other haemolytic diseases, such as sickle cell disease. Therefore one has tried to use the Gárdos channel as a pharmacological target to treat sickle cell disease [33] overlooking the fact that upstream of the signalling cascade is an increase in intracellular Ca^{2+} through a pathway named P_{sickle} for which we are still seeking molecular identity (see below) and triggers numerous other pathophysiological processes in the RBCs (compare Fig. 25.1) leaving the Gárdos channel only a minor portion to account for the cellular symptoms of sickle cell disease [34]. However, what failed in sickle cell disease may still work out well in Gárdos Channelopathy [31, 35].

25.3 Non-selective Cation Channels Permeable for Calcium

25.3.1 Non-selective Voltage Dependent Cation Channel and Piezo1

RBCs contain a variety of non-selective ion channels that are permeable to Ca^{2+}. First there is a non-selective voltage dependent cation channel initially described by Christophersen and Bennekou [36, 37] and later to be reported to be Ca^{2+} permeable [38]. However, the molecular identity of this channel is still not quite clear [39, 40]. Although it was proposed to be a conductive state of the voltage-dependent anion channel (VDAC) [41], recent reports rather make a link to the Piezo1 [42, 43]. Figure 25.4 provides a comparison of the non-selective voltage dependent cation channel and Piezo1. The unique hysteresis-like open probability was also modelled successfully [44].

PIEZO1 and in particular mutations of the channel have been associated with the RBC-related disease Hereditary Xerocytosis [45, 46]. Therefore it seems obvious that this channel, originally described as a mechanosensitive channel, is present in the RBC membrane. Furthermore, knock-out approaches in zebrafish [21] and mice [20] gave further evidence for the conserved abundance of Piezo1 in RBCs as well as for its function (see below). Piezo1 and its mutations were mainly characterised in heterologous overexpressing cell lines and initial measurements of Piezo1 in RBC have been rather episodic [47]. However, the discovery of the pharmacological activation of Piezo1 by Yoda1 [48] lead to the development of high throughput patch-clamp assays as potential diagnostic tools that were recently implemented [49].

The interplay of Piezo1 (in particular its property to mediate Ca^{2+} entry) with the above mentioned Gardos channel [5, 20, 21] provides additional evidence for a functional Piezo1 in RBCs. Furthermore, the interplay between the channels was proposed to be vital for the RBCs to maintain their ion homeostasis [50]. In pathophysiology, Piezo1 seems to play a mayor role in an increased RBC Ca^{2+}-homeostasis. The reported mutations of Piezo1 [45, 46, 51–54] are mostly gain of function mutations suggesting an easier and more pronounced Ca^{2+} entry. The consequent increase in intracellular Ca^{2+} is most likely the trigger for the early removal of the RBC from the circulation and hence the reason for the anaemic symptoms [55]. One of the clinical treatments to handle severe anaemias is splenectomy. Interestingly splenectomy introduces comorbidity, namely thrombotic events, in a subpopulation of Hereditary Xerocytosis patients. This could be explained by an active participation of RBCs in the thrombus formation due to increased intracellular Ca^{2+} [13, 14, 56–58]. Surprisingly such thrombotic events were not reported for splenectomised Gárdos Channelopathy patients [31].

It is worthwhile to mention that in sickle cells an increased conductance carrying also Ca^{2+} was reported and named P_{sickle} [59, 60]. It is likely that P_{sickle} resembles the superposition of several ion channel entities. The sensitivity of P_{sickle} to GsMTx-4 [61], a toxin that inhibits Piezo1 [62] points to this mechanosensitive channel, while the increased abundance of *N*-methyl-D-aspartate (NMDA) receptors in sickle cells [63] is a very strong indicator for these ionotrope glutamate receptors (see below).

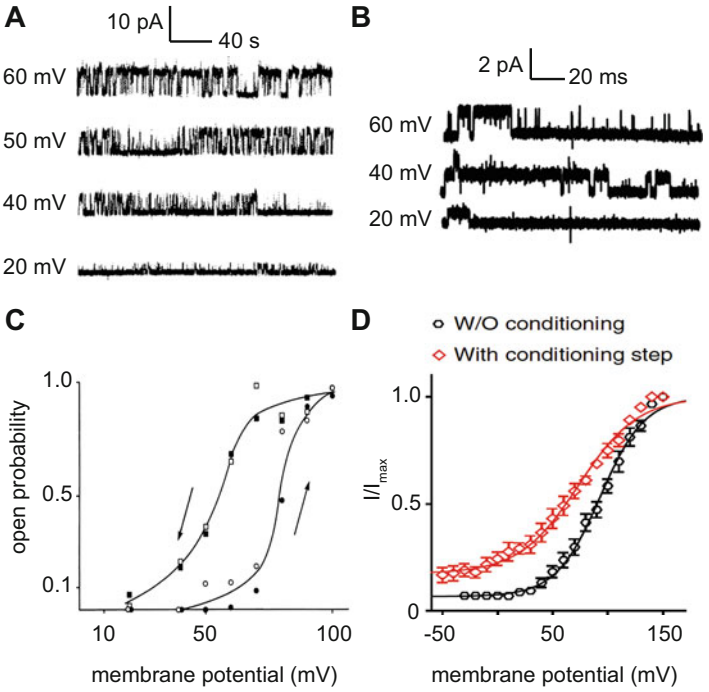

Fig. 25.4 Comparison of the non-selective voltage activated cation channel recorded in RBCs and Piezo1 recorded in overexpressing Neuro2A cells. (**a**) Current traces of the non-selective voltage activated cation channel in inside-out patches of RBCs in symmetrical KCl-solution in mM (500 KCl, 5 MOPS, 4 NMDG, 1 EGTA, 0.02 Ca^{2+}, pH = 7.4). (**b**) Current traces of Piezo1 in outside-out patches of overexpressing Neuro2A cells in symmetrical NaCl-solution in mM (140 NaCl, 10 HEPES, 5 EGTA, pH = 7.4). The difference in ion strength between panels **a** and **b** could explain the different current amplitudes shown in the single channel openings. (**c**) The open state probability as function of the membrane potential. Filled symbols represent data from the experiment shown panel **a**. Open symbols represent data from an identical experiment performed on the same patch after 15 min. In both series, the open probability was calculated from 3 min of continuous recording at each potential. The curves were drawn by eye. (**d**) Tail currents from individual cells were normalized to their maximum and fitted to a Boltzmann relationship. Pooled data are shown as mean ± SEM. (Panels **a** and **c** are reproduced from Kaestner et al. 2000 [38] and panels **b** and **d** from Moroni et al. 2018 [42])

25.3.2 N-Methyl D-Aspartate Receptor

There is clear evidence for the abundance of erythroid N-methyl D-aspartate (NMDA)-receptors in RBCs in particular in the young cell population [19, 64, 65] and its abnormally high prevalence and activity in sickle cell patients [34, 63]. Inhibition of these receptors by oral administration of memantine, the pore-targeting antagonist of NMDARs, results in a decrease of the intracellular Ca^{2+} (Fig. 25.5). In general, cells stemming from myeloid lineage are expressing

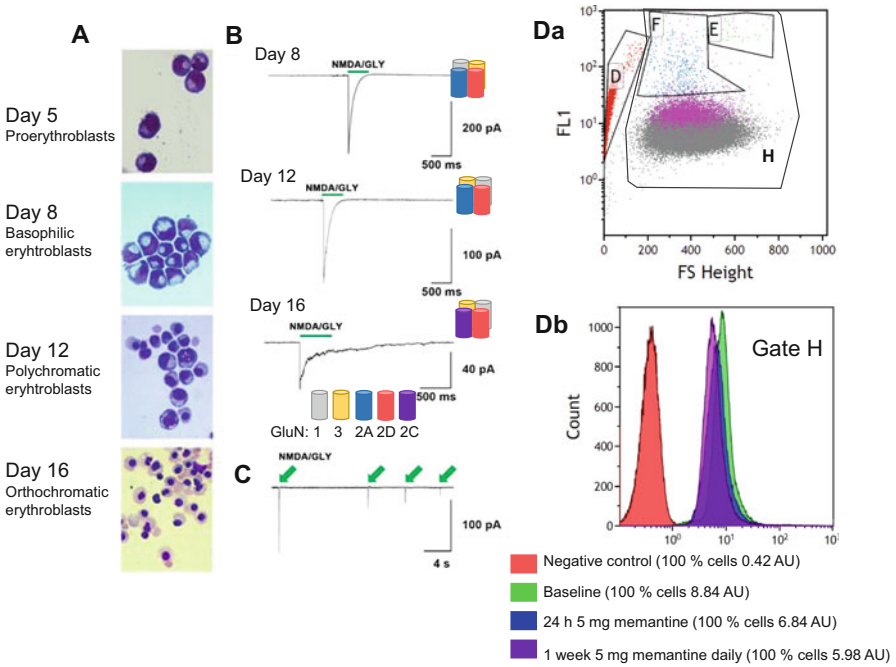

Fig. 25.5 NMDA receptors structure and function. (A) Erythroid NMDA receptors are expressed early on in differentiating erythroid progenitor cells starting from proerythroblasts (CD34 + -derived cells on day 5 in culture) to orthochromatic erythroblasts (day 16 in culture). (B) Electrophysiological recordings of currents mediated by treatment of these cells with agonists NMDA and glycine reveal the change in subunit composition of the receptor during differentiation. Whereas proerythroblasts and polychromatic erythroblasts are equipped with receptors built by glycine-binding GluN1 and 3A/B and glutamate/NMDA-binding Glun2A and 2D (see cartoons), late orthochromatic erythroblasts and reticulocytes contain receptors in which GluN2A is replaced by GluN2C. As a result channels with high current amplitudes and short times to inactivation in early progenitors turn into slowly inactivating channels with lower amplitude in late progenitors and circulating RBCs. For details see [67]. (C) Repeated activation of eNMDARs triggers inactivation of the channels. (D) Changes in the intracellular Ca^{2+} concentration in RBCs upon systemic administration of memantine in patients with sickle cell disease. (Da) Dot plot showing the heterogeneity of free Ca^{2+} levels in RBCs (gates F, E, and H) and RBC-derived vesicles (gate D). (Db) shows a histogram of Ca^{2+}-dependent fluorescence (all cells in population, gate H) in unstained cells (negative control, red), at baseline before the onset of treatment with 5 mg memantine a day (green) after 24 h (blue) and 1 week (pink) of therapy with 5 mg Memantin Mepha daily. The treatment was performed within the MemSID clinical trial (ClinicalTrials.gov Identifier: NCT02615847 approved by SWISSMEDIC (# 2015DR2096) and Cantonal ethic committee of canton Zurich (#2015–0297)). (Panels A–C are reproduced from Hänggi et al. 2015 [67] and panel D from Makhro et al. 2017 [66])

particular type of ionotropic glutamate receptors making immune responses, clotting and RBC function sensitive to the changes in ambient glutamate levels [66]. Subunit composition of erythroid NMDA receptors (eNMDARs) as well as the number of receptor copies changes in the course of differentiation (Fig. 25.5A–C).

Receptor abundance declines from thousand copies in proerythroblasts to about 30 in reticulocytes and about 5 (on average) in mature RBCs [19, 67]. At the same time high amplitude currents with short inactivation time carried by the GluN2A/2D-containing receptors in proerythroblasts are replaced by the currents mediated by the receptors built by the GluN2C/2D subunits with much smaller amplitude and prolonged inactivation time in ortho/polychromatic erythroblasts and reticulocytes [67], (Fig. 25.5A–C). eNMDARs are highly permeable for Ca^{2+} [19, 64] and are actively involved in Ca^{2+}-driven signaling during differentiation and maintenance of intracellular Ca^{2+} in mature RBCs [19, 67]. Clearance of eNMDARs in reticulocytes released into the circulation most likely occurs by way of 'shedding' when receptors are released together with other membrane proteins from the membrane in the form of vesicles. Whereas no direct measurements of eNMDARs in vesicles were performed so far, inability to clear eNMDARs from membranes of RBCs of patients with sickle cell disease is an indirect evidence for this hypothesis. In erythroid precursor cells obtained by differentiation of peripheral CD34+ cells of sickle cell disease patients the number of eNMDAR copies was like that in cells of healthy patients [67]. However, circulating RBCs of patients were presented with abnormally high abundance and activity levels of eNMDARs. As a result, basal Ca^{2+} levels in RBCs of sickle cell disease patients were exceeding that in cells of healthy subjects. Pharmacological inhibition of the receptors decreased Ca^{2+} levels and resulted in rehydration and reduction in oxidative load [67]. First pilot clinical trial MemSID in which patients with sickle cell disease were treated with the antagonist of NMDA receptors, memantine, revealed that these receptors may be an attractive pharmacological target for this group of patients [68, 69] (Fig. 25.5D). Among physiological factors that may control eNMDARs are endurance exercises that are associated with glutamate release into the circulation [70].

25.3.3 Voltage-Dependent Anion Channel

Another multifunctional channel with a clear molecular identity in RBCs that also conducts Ca^{2+} is the Voltage-Dependent Anion Channel (VDAC) [41, 71]. VDACs have originally been characterized as mitochondrial porins [72]. Three different isoforms of VDAC have been identified so far: VDAC1, VDAC2 and VDAC3. Showing the expression of 'Porin 31HL' in the plasmalemma of human B lymphocytes, gave first evidence on the multitopological localisation of VDAC [73]. The existence in the membrane of RBCs of a 32 kDa associated voltage dependent anion channel (VDAC) in a peripheral benzodiazepine receptor-like PBR protein complex to 18 kDa protein TSPO 'translocator proteins' and 30 kDa ANT 'adenine nucleotide transporter' proteins has been demonstrated [41, 74]. It has a nanomolar affinity for PK11195, Ro5–4864 and Diazepam ligands [75,

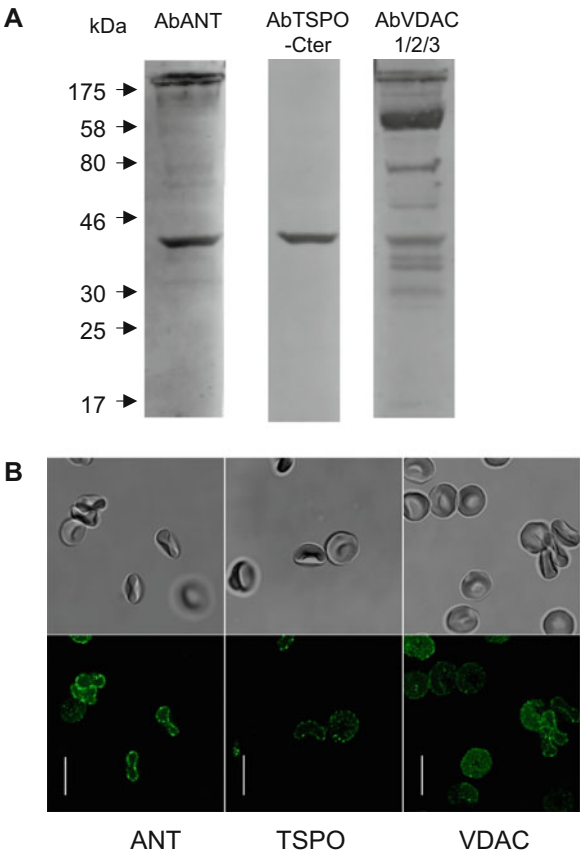

Fig. 25.6 VDAC, ANT and TSPO detection in human red blood cell ghosts. (**a**) Samples (15 μg of protein) of whole lysates were subjected to SDS-PAGE (10% acrylamide) and analysed by Western blotting using polyclonal anti-ANT (1:1000 dilution), polyclonal goat anti-TSPO raised against the C terminus of human TSPO (1:1000) or rabbit polyclonal anti VDAC 1–2-3 (1:100 dilution). Multiple bands at different molecular weights is consistent with the oligomerisation of VDAC proteins. ANT and TSPO proteins are also clearly visible. (**b**) Immunofluorescence experiments were performed on smears Dilution were 1/5 for primary and 1/20 for secondary antibodies. Scale bars represent 10 μm. (This figure is reproduced from Bouyer et al. 2011 [41])

76]. All blood cells have a population of receptors with micromolar affinity for PK11195 ranging from approximately 750,000 sites for lymphocytes to over one hundred sites for RBCs [77, 78]. These indications are corroborated by analysis of messenger RNA expression data provided by GeneAtlas U133A where 3 isoforms of VDAC, 2 isoforms of ANT and 2 isoforms of TSPO were found in erythroid progenitors from CD34+ to CD71+ (Fig. 25.6). VDAC is a protein that has remarkably well-preserved structural and functional characteristics, despite major variations in the sequence [79]. Although it is also present in the plasma membrane, most of the information we have on its structure function comes from studies on mitochondrial proteins [80, 81]. The maximum conductances reach 4–5 nS in the

presence of 1 M NaCl or KCl, 350–450 pS for more physiological concentrations (NaCl or 150 mM KCl). Conductance and selectivity are voltage dependent; at low voltages, close to −10 mV, the channel is stable and remains open, whereas at positive or negative potentials higher than 40 mV, VDAC has multiple sub states of different permeabilities and selectivities, as well as closing episodes of which frequency increases with voltage [82, 83]. The highest levels are permeable to small ions (Na^+, K^+, Cl^-, etc.) but also to large anions (glutamate, ATP) and large cations (acetylcholine, dopamine, Tris, etc.). They have a preference for anions (2:1) when saline solutions are composed of ions of equal mobility such as NaCl or KCl. More importantly, at low conductances, VDAC is more permeable to small ions with, apparently, a marked preference for cations and higher permeability to Ca^{2+} ions than in large conductances [82–84]. VDAC may have different oligomerization states: mono-, di-, tri, tetra-, hexamers or even more. Indeed, atomic force microscopy revealed the presence of VDAC1 monomers as well as dimers and larger oligomers showcasing the interaction of the pore with itself, however, dimers are more frequent. Very little is known about the activation and regulation mechanisms of the channel. Nevertheless, when the pores dimerize, the selectivity for Ca^{2+} increases. Various studies support the function of VDAC (more precisely VDAC1 the most studied yet) in the transport of Ca^{2+} and in cellular Ca^{2+} homeostasis. Lipids-reconstituted bilayer incorporating VDAC1 in the presence of different $CaCl_2$ concentration gradients showed well-defined voltage-dependent channel conductance, as observed with either NaCl or KCl solution, with higher permeability to Ca^{2+} once VDAC is in the low conductance state. It is obvious that the permeability ratios of VDAC1 for Ca^{2+} is very low compared to Cl^- (P_{Ca2+}/P_{Cl-} is 0.02–0.38) [83] but considering the tremendous electrochemical gradient for Ca^{2+} between intra- and extracellular face of RBCs (see Introduction) a short activation may represent a significant input of Ca^{2+} into the cell.

25.3.4 Transient Receptor Potential Channels of Canonical Type

Yet another type of non-selective cation channels that are believed to be abundant in RBCs are Transient Receptor Potential channels of Canonical type (TRPC channels). Indications point to a different expression pattern of isoforms in precursor cells compared to mature RBCs and also differences between mammalian species seem likely [85–88]. In humans it is believed that TRPC6 is abundant in RBCs [39, 89, 90]. So far a dedicated physiological function of TRPC6 in mature RBCs remains elusive.

25.4 Voltage-Activated Calcium Channels and Their Regulation

Evidence for the existence of a number of voltage-activated Ca^{2+} channels in RBCs has been reported [91, 92], and the most convincing evidence is for $Ca_V2.1$, based on molecular biology data (Western blot) [93] and, presumably, $Ca_V2.1$-specific pharmacological interactions (ω-agatoxinTK) [93, 94] – both are shown in Fig. 25.7A, B. Nevertheless, so far, we and others have failed to obtain direct functional evidence for the existence of $Ca_V2.1$ or other voltage-activated Ca^{2+} channels in RBCs by patch-clamp techniques [95]. However, also RBCs although non-excitable cells meet the condition of voltage jumps necessary to activate voltage-activated channels such as $Ca_V2.1$ [95]. In particular when the Gárdos channel (see Sect. 25.2) is activated, the resting membrane potential changes from approximately −10 mV to approximately −70 mV [96]. Not hyperpolarisation but depolarisation is required to activate $Ca_V2.1$ [97]. Nevertheless, hyperpolarisation is a requirement to switch $Ca_V2.1$ channels from the inactivated state to the closed state, which is a prerequisite to subsequently transition to the open state [98] (Fig. 25.7C). Closing of the Gárdos channels after their initial activation could well provide the necessary conditions for subsequent depolarisation to activate $Ca_V2.1$ [95]. Such a proposed mechanism is sensible also in the context of other voltage-activated channels in the RBC membrane (compare Sect. 25.3).

25.5 Evidence for a Calcium-Inhibited Channel

There is also evidence for a non-selective cation channel in RBCs that is activated when extracellular Ca^{2+} is removed [99]. Original recordings and an I–V curve are shown in Fig. 25.8A, B. There are two conceptual question related to this recent report (a) if the channel is abundant in almost all RBCs why it was not reported before (in four decades of patch-clamping RBCs) and (b) since divalent cations in general and Ca^{2+} in particular support seal formation, a removal of Ca^{2+} could impair the seal quality/tightness. Under these circumstances it is almost impossible to discriminate a leak in the seal from an ion channel. However, here are also two arguments in favour of the existence of this channel: (A) The suspicion of the phenomenon described in (b) could have prevented scientists to report about the channel (a). The non-ohmic behaviour of the I-V curve (Fig. 25.8B) is in favour of a channel rather than a leak. (B) A channel activated by the removal of Ca^{2+} is an ideal explanation of the dissipation of the monovalent cation gradients when

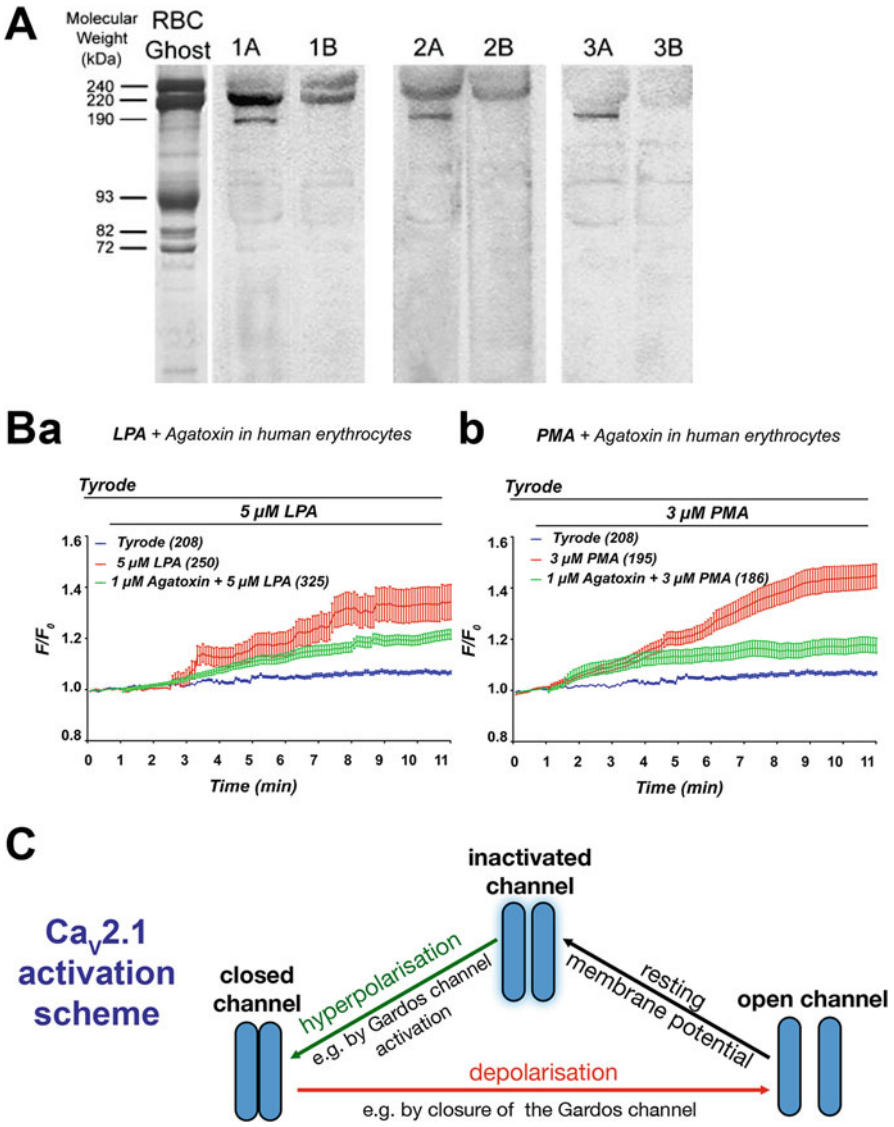

Fig. 25.7 $Ca_V2.1$ in human RBCs. (A) Western blot analysis of the 1A subunit of voltage-gated calcium channels in human erythrocyte ghosts from 3 different donors. RBC membrane proteins were separated electrophoretically at high protein loads (80 µg). After electrophoretic transfer to nitrocellulose paper, blots were stained with antibodies directed against residues 865 to 881 of the α_{1A} subunit of the rat brain voltage-gated calcium channel (lanes 1A, 2A, 3A). Because several nonspecific bands were also visualized, competition of $Ca_V2.1$ antibody staining using its specific peptide was also performed. For this purpose, 10 µg of the $Ca_V2.1$ antibody was preincubated with 10 µg of antibody-specific peptide for 1 h at 22 °C and then further incubated with the blot for 2 h at 22 °C (lanes 1B, 2B, 3B). Polypeptides with M_r of approximately 190,000 and 220,000 are characteristic of the major splicing variants of the α_{1A} subunit of $Ca_V2.1$ in the brain. An SDS-PAGE Coomassie blue–stained gel of RBC membranes (left lane; "RBC Ghost") serves as an

cells are placed in tubes containing Ca^{2+}-chelating anticoagulants as exemplified in Fig. 25.8C. This experimental result is a showcase of the cation gradient dissipation associated with RBC storage lesions [100].

Fig. 25.7 (continued) approximate molecular weight marker. (B) Kinetics of lysophosphatidic acid (LPA; phospholipid released by activated platelets)-induced (Ba) and Phorbol 12-myristate 13-acetate (PMA; protein kinase C activator)-induced (Bb) Ca^{2+} entry in the presence and absence of ω-agatoxin TK. Average traces of single cells derived from live cell imaging experiments are presented as self-ratio values. Labelled lines above the traces indicate the stimulation regime. The traces are the mean values of 3 independent experiments, and the numbers in brackets at the end of the colour legend refer to the number of cells measured. (C) Activation scheme for the $Ca_V2.1$ channel modulated by underlying Gardos channel activity. Closing of the Gardos channels after their initial activation could provide the necessary conditions for subsequent depolarisation to activate $Ca_V2.1$. Since the hypothetical switching behaviour of the Gardos channel would be crucial for the activation of $Ca_V2.1$, we propose three principle modes by which this switching could occur: (i) Because channel activity is a stochastic event and because the number of Gardos channels per RBC is rather low (in the single digit numbers [114, 118]), depolarisation could be the result of stochastic Gardos channel closures. This hypothesis is supported by the rather sparse whole cell patch-clamp recordings of Gardos channel activity in human RBCs [31, 119–121]. Whole cell current traces do not show a smooth appearance but rather a flickering pattern similar to that observed with single channel recordings, especially at higher (positive and negative) membrane potentials. (ii) When looking at Gardos channel-induced changes in the membrane potential of cell populations, a gradual Ca^{2+} concentration-dependent effect can be seen [122], i.e., the hyperpolarisation observed in RBC suspensions is a gradual Ca^{2+} concentration-dependent effect. However, the abovementioned study [122] as well as another report [123] showed that the activation of the Gardos channel at the cellular level is an all-or-none response. This means that the gradual change in membrane potential would be the result of the summation of cells with open or closed Gardos channels. Taking into consideration that the Ca^{2+} pump [124] continuously operates in response to any increase in intracellular Ca^{2+} levels, one would imagine that the state of the Gardos channels is exclusively modulated by variations in intracellular Ca^{2+} concentrations. Hence, the switching behaviour of the Gardos channel would be the direct consequence of continuous variations in RBC intracellular Ca^{2+} concentrations. (iii) Localized interactions between the Gárdos channel and $Ca_V2.1$ in RBCs could occur in lipid rafts or nanodomains, as is the case with closely related ion transporters in other cell types, for example, within the fuzzy space or dyadic cleft in myocytes [125]. Although RBCs do not possess membrane-constricted subspaces, there are indications for functional compartments in the immediate vicinity of the plasma membrane [126]. Colocalization of ion channels is common in excitable cells [127, 128]. For RBCs, it is still unknown if the different ion channels colocalize or cluster to allow their interaction in nanodomains. However, in support of this idea is the observation that local activation of mechanosensitive channels (most likely Piezo 1) by patch-clamp micropipettes resulted in local activation (single-channel recordings) of the Gardos channel [124]. (Panels A, B and C are reproduced from Andrews et al. 2000 [93], Wagner-Britz et al. 2013 [94] and Kaestner et al. 2018 [95], respectively)

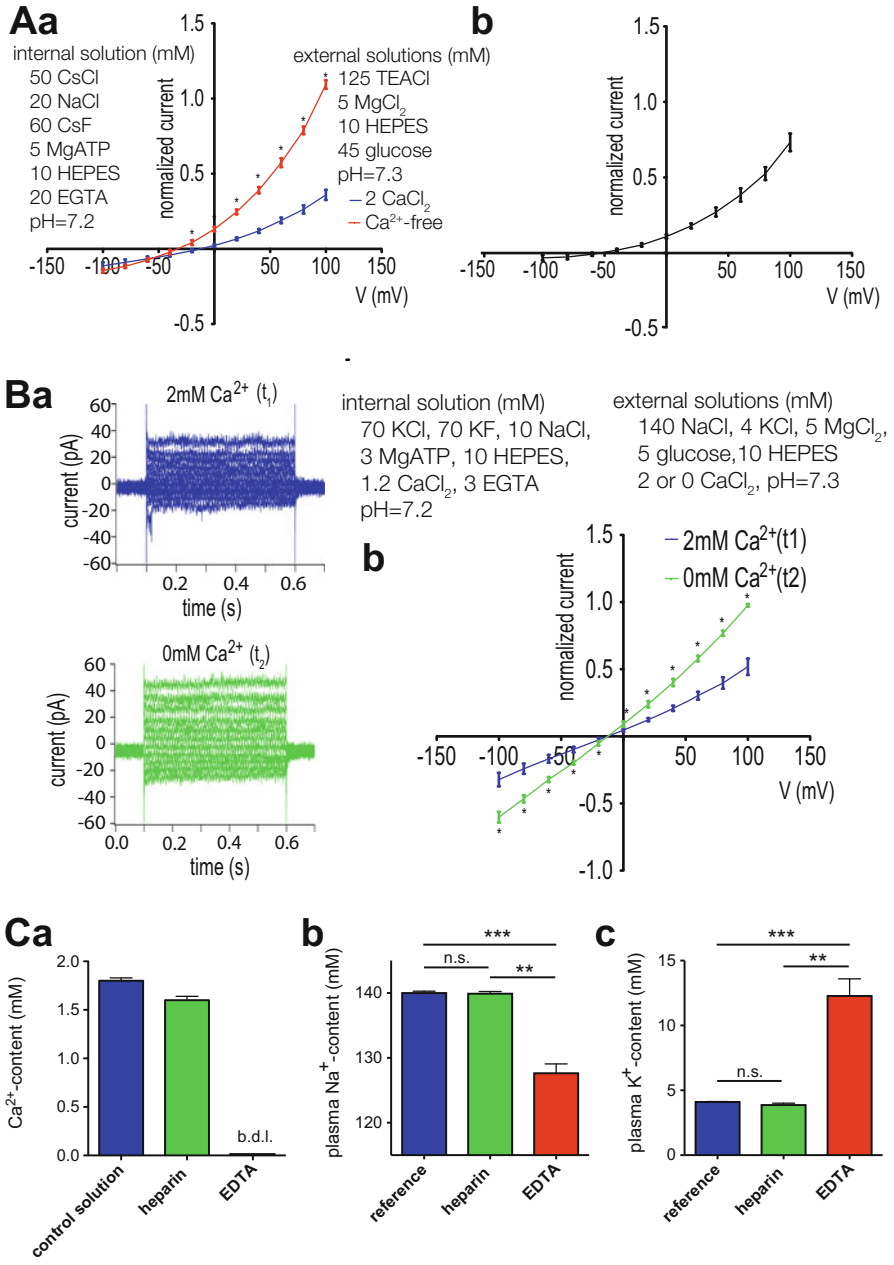

Fig. 25.8 Evidence for non-selective cation channel activated by the removal of Ca^{2+}. (A) Whole-cell patch clamp recordings in a Cs^{+}-based internal and a TEACl-based external solutions (Aa) I/V curves with 2 mM $CaCl_2$ (blue) and 0 mM $CaCl_2$ (red) in the external solution (n = 5). (Ab) I/V curve of the Ca^{2+} blocked current – the current recorded in 2 mM $CaCl_2$-external solution was subtracted from the current recorded in 0 mM $CaCl_2$ -external solution. Currents were elicited

25.6 Summary

The importance of Ca^{2+} in the membrane transport regulation and mediation of RBCs was early recognised. However, only in the recent years it became evident how this ion transport is related to ion channels and a correlation to molecular entities could be performed. This process is everything but finished and in particular the understanding of the interaction of several ion channels in a physiological context just started. This includes also pathophysiological conditions, on the one hand channelopathies, where a mutation of the ion channel is the direct cause of the disease, like the above described Hereditary Xerocytosis [45] and the Gárdos Channelopathy [31]. On the other hand it applies to RBC related diseases where an altered channel activity is a secondary effect like in sickle cell disease [34, 63] or thalassemia. Also these secondary effects should receive medical and pharmacologic attention because they can be crucial when it comes to the life-threatening symptoms of the disease [55]. An overview of the involvement of Ca^{2+} and Ca^{2+}-conducting channels as general components in anaemias is summarised in Fig. 25.9. However, this scheme can only be regarded as a current snapshot of our knowledge about Ca^{2+} and Ca^{2+}-conducting channels in RBCs. Further investigations on a better match between functional and molecular knowledge will arise as well as a better understanding of the activity of Ca^{2+} and Ca^{2+}-conducting channels within the signalling networks in RBCs.

Fig. 25.8 (continued) by voltage steps from −100 mV to 100 mV for 500 ms in 20 mV increments at $V_h = -30$ mV. Detailed solutions composition is given next to the graphs. Data are presented as mean ± SEM, with n being the number of cells. Significance is assessed with a paired Student's t test and set at $p < 0.05$. For better visualization, a significance anywhere below $p < 0.05$ is denoted with one star. (B) Whole-cell patch clamp recordings in physiological (a K^+-based internal and a Na^+-based external) solutions (Ba) Raw current traces from a representative RBC in an external solution containing 2 mM $CaCl_2$ at t_1 (dark blue) and 0 mM $CaCl_2$ at t_2 (green). Detailed solutions composition is given next to the current traces. (Bb) I/V curves in 2 mM $CaCl_2$ (t_1) (dark blue) and 0 mM $CaCl_2$ (t_2) (green) external solutions ($n = 7$). (C) Blood plasma ion content of healthy adults in heparin and EDTA. (Ca) Ca^{2+} content of a control aqueous non-buffered 1.8 mM $CaCl_2$ solution filled in heparin and EDTA vacutainers. The abbreviation b.d.l. denotes 'below detection limit'. (Cb) Na^+ plasma content, (Cc) K^+ plasma content of blood anticoagulated with heparin and EDTA. Measurements in heparin and EDTA were performed on blood of healthy adults ($n = 3$) collected in heparin and EDTA vacutainers, respectively and reference values were taken from Liappis, 1972 [130]. Error bars represent SEM and stars denote significances as follows: n.s for not significant, ** for $p < 0.01$ and *** for $p < 0.001$. (This figure is reproduced from Petkova-Kirowa et al. 2018 [99])

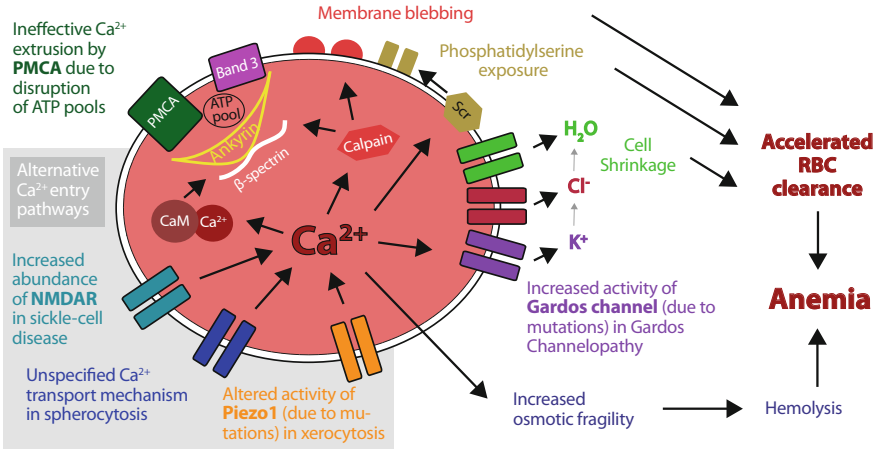

Fig. 25.9 Proposed mechanisms leading to increased intracellular Ca^{2+}levels in diseased RBCs and accordingly to accelerated clearance of cells from the blood stream. Alternative or cumulating Ca^{2+} entry pathways are highlighted with grey background: increased abundance of NMDA-receptors (NMDAR), e.g., in sickle cell disease, altered activity of Piezo1, e.g. in Hereditary Xerocytosis, increased activity of Gárdos Channel, e.g. in Gárdos Channelopathy, or unspecified Ca^{2+} transport mechanisms. Additionally, ineffective extrusion of Ca^{2+} due to disruption of ATP pools fueling the plasma membrane Ca^{2+} ATPase (PMCA) can contribute. Several downstream processes follow Ca^{2+} overload in RBCs, e.g.: activation of calmodulin by formation of the Ca^{2+}-calmodulin complex (Ca-CaM) and activation of calpain, thereby loosening the cytoskeletal structure; activation of the scramblase (Scr) leading to exposure of phosphatidylserine on the outer leaflet of the membrane; activation of the Gárdos channel followed by the efflux of K^+, Cl^- and H_2O and consecutive cell shrinkage. (This figure is reproduced from Hertz et al. 2017 [55])

References

1. Berridge MJ (1994) The biology and medicine of calcium signalling. Mol Cell Endocrinol 98:119–124
2. Berridge MJ (2006) Calcium microdomains: organization and function. Cell Calcium 40:405–412
3. Bogdanova A, Makhro A, Wang J et al (2013) Calcium in red blood cells-a perilous balance. Int J Mol Sci 14:9848–9872. https://doi.org/10.3390/ijms14059848
4. Lew VL, Tsien RY, Miner C, Bookchin RM (1982) Physiological [Ca^{2+}]i level and pump-leak turnover in intact red cells measured using an incorporated Ca chelator. Nature 298:478–481
5. Danielczok JG, Terriac E, Hertz L et al (2017) Red blood cell passage of small capillaries is associated with transient Ca^{2+}-mediated adaptations. Front Physiol 8:979. https://doi.org/10.3389/fphys.2017.00979
6. Hammer K, Ruppenthal S, Viero C et al (2010) Remodelling of Ca^{2+} handling organelles in adult rat ventricular myocytes during long term culture. J Mol Cell Cardiol 49:427–437. https://doi.org/10.1016/j.yjmcc.2010.05.010
7. Schatzmann HJ (1983) The red cell calcium pump. Annu Rev Physiol 45:303–312. https://doi.org/10.1146/annurev.ph.45.030183.001511
8. Scharff O, Foder B (1977) Low Ca^{2+} concentrations controlling two kinetic states of Ca^{2+}-ATPase from human erythrocytes. Biochim Biophys Acta 483:416–424

9. Kosk-Kosicka D, Bzdega T (1990) Effects of calmodulin on erythrocyte Ca2(+)-ATPase activation and oligomerization. Biochemistry 29:3772–3777
10. Wang KK, Roufogalis BD, Villalobo A (1990) Calpain I activates Ca^{2+} transport by the human erythrocyte plasma membrane calcium pump. Adv Exp Med Biol 269:175–180
11. Wang KK, Villalobo A, Roufogalis BD (1992) The plasma membrane calcium pump: a multiregulated transporter. Trends Cell Biol 2:46–52
12. Kosk-Kosicka D, Bzdega T (1988) Activation of the erythrocyte Ca^{2+}-ATPase by either self-association or interaction with calmodulin. J Biol Chem 263:18184–18189
13. Andrews DA, Low PS (1999) Role of red blood cells in thrombosis. Curr Opin Hematol 6:76–82
14. Kaestner L, Tabellion W, Lipp P, Bernhardt I (2004) Prostaglandin E2 activates channel-mediated calcium entry in human erythrocytes: an indication for a blood clot formation supporting process. Thromb Haemost 92:1269–1272. https://doi.org/10.1267/THRO04061269
15. Lang KS, Duranton C, Poehlmann H et al (2003) Cation channels trigger apoptotic death of erythrocytes. Cell Death Differ 10:249–256. https://doi.org/10.1038/sj.cdd.4401144
16. Kaestner L, Minetti G (2017) The potential of erythrocytes as cellular aging models. Cell Death Differ 24:1475–1477. https://doi.org/10.1038/cdd.2017.100
17. Lang KS, Lang PA, Bauer C et al (2005) Mechanisms of suicidal erythrocyte death. Cell Physiol Biochem 15:195–202
18. Galluzzi L, Vitale I, Aaronson SA et al (2018) Molecular mechanisms of cell death: recommendations of the Nomenclature Committee on Cell Death 2018. Cell Death Differ:1–56. https://doi.org/10.1038/s41418-017-0012-4
19. Makhro A, Hanggi P, Goede JS et al (2013) N-methyl D-aspartate (NMDA) receptors in human erythroid precursor cells and in circulating red blood cells contribute to the intracellular calcium regulation. Am J Physiol Cell Physiol. https://doi.org/10.1152/ajpcell.00031.2013
20. Cahalan SM, Lukacs V, Ranade SS et al (2015) Piezo1 links mechanical forces to red blood cell volume. Elife 4:e07370. https://doi.org/10.7554/eLife.07370
21. Faucherre A, Kissa K, Nargeot J et al (2014) Piezo1 plays a role in erythrocyte volume homeostasis. Haematologica 99:70–75. https://doi.org/10.3324/haematol.2013.086090
22. Hamill OP (1983) Potassium and chloride channels in red blood cells. In: Sakmann B, Neher E (eds) Single channel recording. Plenum Press, New York/London, pp 451–471
23. Hamill OP (1981) Potassium channel currents in human red blood cells. J Physiol Lond 319:97P–98P
24. Gardos G (1956) The permeability of human erythrocytes to potassium. Acta Physiol Hung 10:185–189
25. Gardos G (1958) The function of calcium in the potassium permeability of human erythrocytes. Biochim Biophys Acta 30:653–654
26. Hoffman JF, Joiner W, Nehrke K et al (2003) The hSK4 (KCNN4) isoform is the Ca^{2+}-activated K^+ channel (Gardos channel) in human red blood cells. Proc Natl Acad Sci U S A 100:7366–7371. https://doi.org/10.1073/pnas.1232342100
27. Maher AD, Kuchel PW (2003) The Gárdos channel: a review of the Ca^{2+}-activated K^+ channel in human erythrocytes. Int J Biochem Cell Biol 35:1182–1197
28. Grygorczyk R (1987) Temperature dependence of Ca^{2+}-activated K^+ currents in the membrane of human erythrocytes. Biochim Biophys Acta 902:159–168
29. Rapetti-Mauss R, Lacoste C, Picard V et al (2015) A mutation in the Gardos channel is associated with hereditary xerocytosis. Blood 126:1273–1280. https://doi.org/10.1182/blood-2015-04-642496
30. Glogowska E, Lezon-Geyda K, Maksimova Y et al (2015) Mutations in the Gardos channel (KCNN4) are associated with hereditary xerocytosis. Blood 126:1281–1284. https://doi.org/10.1182/blood-2015-07-657957
31. Fermo E, Bogdanova A, Petkova-Kirova P et al (2017) "Gardos Channelopathy": a variant of hereditary stomatocytosis with complex molecular regulation. Sci Rep 7:1744. https://doi.org/10.1038/s41598-017-01591-w
32. Mankad VN (2001) Exciting new treatment approaches for pathyphysiologic mechanisms of sickle cell disease. Pediatr Pathol Mol Med 20:1–13

33. Ataga KI, Reid M, Ballas SK et al (2011) Improvements in haemolysis and indicators of erythrocyte survival do not correlate with acute vaso-occlusive crises in patients with sickle cell disease: a phase III randomized, placebo-controlled, double-blind study of the Gardos channel blocker senicapoc (ICA-17043). Br J Haematol 153:92–104. https://doi.org/10.1111/j.1365-2141.2010.08520.x
34. Bogdanova A, Makhro A, Kaestner L (2015) Calcium handling in red blood cells of sicke cell disease patients. In: Lewis ME (ed) Sickle cell disease: *Genetics, Management and Prognosis*, Nova Publishing, pp 29–59
35. Rapetti-Mauss R, Soriani O, Vinti H et al (2016) Senicapoc: a potent candidate for the treatment of a subset of Hereditary Xerocytosis caused by mutations in the Gardos channel. Haematologica 2016:149104. https://doi.org/10.3324/haematol.2016.149104
36. Christophersen P, Bennekou P (1991) Evidence for a voltage-gated, non-selective cation channel in the human red cell membrane. Biochim Biophys Acta 1065:103–106
37. Bennekou P (1993) The voltage-gated non-selective cation channel from human red cells is sensitive to acetylcholine. Biochim Biophys Acta 1147:165–167
38. Kaestner L, Christophersen P, Bernhardt I, Bennekou P (2000) The non-selective voltage-activated cation channel in the human red blood cell membrane: reconciliation between two conflicting reports and further characterisation. Bioelectrochemistry 52:117–125
39. Kaestner L (2011) Cation channels in erythrocytes – historical and future perspective. Open Biol J 4:27–34
40. Bouyer G, Thomas S, Egée S (2012) Patch-clamp analysis of membrane transport in erythrocytes. In: Patch clamp technique. InTech, Rijeka, pp 171–202
41. Bouyer G, Cueff A, Egée S et al (2011) Erythrocyte peripheral type benzodiazepine receptor/voltage-dependent anion channels are upregulated by Plasmodium falciparum. Blood 118:2305–2312. https://doi.org/10.1182/blood-2011-01-329300
42. Moroni M, Servin-Vences MR, Fleischer R et al (2018) Voltage gating of mechanosensitive PIEZO channels. Nat Commun 9:1096. https://doi.org/10.1038/s41467-018-03502-7
43. Kaestner L, Egee S (2018) Commentary: voltage gating of mechanosensitive PIEZO channels. Front Physiol 9:1565
44. Andersson T (2010) Exploring voltage-dependent ion channels in silico by hysteretic conductance. Math Biosci 226:16–27. https://doi.org/10.1016/j.mbs.2010.03.004
45. Zarychanski R, Schulz VP, Houston BL et al (2012) Mutations in the mechanotransduction protein PIEZO1 are associated with hereditary xerocytosis. Blood 120:1908–1915. https://doi.org/10.1182/blood-2012-04-422253
46. Bae C, Gnanasambandam R, Nicolai C et al (2013) Xerocytosis is caused by mutations that alter the kinetics of the mechanosensitive channel PIEZO1. Proc Natl Acad Sci U S A 110:E1162–E1168. https://doi.org/10.1073/pnas.1219777110
47. Kaestner L (2015) Channelizing the red blood cell: molecular biology competes with patch-clamp. Front Mol Biosci 2:46. https://doi.org/10.3389/fmolb.2015.00046
48. Syeda R, Xu J, Dubin AE et al (2015) Chemical activation of the mechanotransduction channel Piezo1. Elife. https://doi.org/10.7554/eLife.07369
49. Rotordam GM, Fermo E, Becker N et al (2019) A novel gain-of-function mutation of Piezo1 is functionally affirmed in red blood cells by high-throughput patch clamp. Haematologica 104(5). https://doi.org/10.3324/haematol.2018.201160
50. Lew VL, Tiffert T (2017) On the mechanism of human red blood cell longevity: roles of calcium, the sodium pump, PIEZO1, and Gardos channels. Front Physiol 8:977. https://doi.org/10.3389/fphys.2017.00977
51. Albuisson J, Murthy SE, Bandell M et al (2013) Dehydrated hereditary stomatocytosis linked to gain-of-function mutations in mechanically activated PIEZO1 ion channels. Nat Commun 4:1884. https://doi.org/10.1038/ncomms2899
52. Andolfo I, Alper SL, De Franceschi L et al (2013) Multiple clinical forms of dehydrated hereditary stomatocytosis arise from mutations in PIEZO1. Blood 121:3925–3935. https://doi.org/10.1182/blood-2013-02-482489
53. Archer NM, Shmukler BE, Andolfo I et al (2014) Hereditary xerocytosis revisited. Am J Hematol 89:1142–1146. https://doi.org/10.1002/ajh.23799

54. Glogowska E, Schneider ER, Maksimova Y et al (2017) Novel mechanisms of PIEZO1 dysfunction in hereditary xerocytosis. Blood 130:1845–1856. https://doi.org/10.1182/blood-2017-05-786004
55. Hertz L, Huisjes R, Llaudet-Planas E et al (2017) Is increased intracellular calcium in red blood cells a common component in the molecular mechanism causing anemia? Front Physiol 8:673. https://doi.org/10.3389/fphys.2017.00673
56. Steffen P, Jung A, Nguyen DB et al (2011) Stimulation of human red blood cells leads to Ca^{2+}-mediated intercellular adhesion. Cell Calcium 50:54–61. https://doi.org/10.1016/j.ceca.2011.05.002
57. Kaestner L, Steffen P, Nguyen DB et al (2012) Lysophosphatidic acid induced red blood cell aggregation in vitro. Bioelectrochemistry 87:89–95. https://doi.org/10.1016/j.bioelechem.2011.08.004
58. Chung SM, Bae ON, Lim KM et al (2007) Lysophosphatidic acid induces thrombogenic activity through phosphatidylserine exposure and procoagulant microvesicle generation in human erythrocytes. Arterioscler Thromb Vasc Biol 27:414–421
59. Lew VL, Ortiz OE, Bookchin RM (1997) Stochastic nature and red cell population distribution of the sickling-induced Ca^{2+} permeability. J Clin Invest 99:2727–2735. https://doi.org/10.1172/JCI119462
60. Browning JA, Robinson HC, Ellory JC, Gibson JS (2007) Deoxygenation-induced non-electrolyte pathway in red cells from sickle cell patients. Cell Physiol Biochem 19:165–174. https://doi.org/10.1159/000099204
61. Ma Y-L, Rees DC, Gibson JS, Ellory JC (2012) The conductance of red blood cells from sickle cell patients: ion selectivity and inhibitors. J Physiol Lond 590:2095–2105. https://doi.org/10.1113/jphysiol.2012.229609
62. Bae C, Sachs F, Gottlieb PA (2011) The mechanosensitive ion channel Piezo1 is inhibited by the peptide GsMTx4. Biochemistry 50:6295–6300. https://doi.org/10.1021/bi200770q
63. Hanggi P, Makhro A, Gassmann M et al (2014) Red blood cells of sickle cell disease patients exhibit abnormally high abundance of N-methyl D-aspartate receptors mediating excessive calcium uptake. Br J Haematol 167:252–264. https://doi.org/10.1111/bjh.13028
64. Makhro A, Wang J, Vogel J et al (2010) Functional NMDA receptors in rat erythrocytes. Am J Physiol Cell Physiol 298:C1315–C1325. https://doi.org/10.1152/ajpcell.00407.2009
65. Bogdanova A, Makhro A, Goede J et al (2009) NMDA receptors in mammalien erythrocytes. Clin Biochem 42:1858–1859
66. Makhro A, Kaestner L, Bogdanova A (2017) NMDA receptor activity in circulating red blood cells: methods of detection. Methods Mol Biol 1677:265–282, 484. https://doi.org/10.1007/978-1-4939-7321-7_15
67. Hanggi P, Telezhkin V, Kemp PJ et al (2015) Functional plasticity of the N-methyl-d-aspartate receptor in differentiating human erythroid precursor cells. Am J Physiol Cell Physiol 308:C993–C1007. https://doi.org/10.1152/ajpcell.00395.2014
68. Hegemann I, Sasselli C, Valeri F, Makhro A, Müller R, Bogdanova A, Manz MG, Gassmann M, Goede JS. Memantine treatment is well tolerated by sickle cell patients and improves erythrocyte stability: phase II study MemSID (submitted)
69. Bogdanova A, Makhro A, Hegemann I, Seiler E, Bogdanov N, Simionato G, Kaestner L, Claveria V, Saselli C, Torgeson P, Manz M, Goede J, Gassmann M. Improved maturation and increased stability of red blood cells of sickle cell patients on memantine treatment (submitted)
70. Makhro A, Haider T, Wang J et al (2016) Comparing the impact of an acute exercise bout on plasma amino acid composition, intraerythrocytic Ca^{2+} handling, and red cell function in athletes and untrained subjects. Cell Calcium 60:235–244. https://doi.org/10.1016/j.ceca.2016.05.005
71. Thomas SLY, Bouyer G, Cueff A et al (2011) Ion channels in human red blood cell membrane: actors or relics? Blood Cells Mol Dis 46:261–265. https://doi.org/10.1016/j.bcmd.2011.02.007
72. Schein SJ, Colombini M, Finkelstein A (1976) Reconstitution in planar lipid bilayers of a voltage-dependent anion-selective channel obtained from paramecium mitochondria. J Membr Biol 30:99–120

73. Thinnes FP, Flörke H, Winkelbach H et al (1994) Channel active mammalian porin, purified from crude membrane fractions of human B lymphocytes or bovine skeletal muscle, reversibly binds the stilbene-disulfonate group of the chloride channel blocker DIDS. Biol Chem Hoppe Seyler 375:315–322
74. Marginedas-Freixa I, Hattab C, Bouyer G et al (2016) TSPO ligands stimulate ZnPPIX transport and ROS accumulation leading to the inhibition of P. falciparum growth in human blood. Sci Rep 6:33516. https://doi.org/10.1038/srep33516
75. McEnery MW, Snowman AM, Trifiletti RR, Snyder SH (1992) Isolation of the mitochondrial benzodiazepine receptor: association with the voltage-dependent anion channel and the adenine nucleotide carrier. Proc Natl Acad Sci U S A 89:3170–3174
76. Le Fur G, Vaucher N, Perrier ML et al (1983) Differentiation between two ligands for peripheral benzodiazepine binding sites, [3H]RO5-4864 and [3H]PK 11195, by thermodynamic studies. Life Sci 33:449–457
77. Olson JM, Ciliax BJ, Mancini WR, Young AB (1988) Presence of peripheral-type benzodiazepine binding sites on human erythrocyte membranes. Eur J Pharmacol 152:47–53
78. Canat X, Carayon P, Bouaboula M et al (1993) Distribution profile and properties of peripheral-type benzodiazepine receptors on human hemopoietic cells. Life Sci 52:107–118
79. Shoshan-Barmatz V, De Pinto V, Zweckstetter M et al (2010) VDAC, a multifunctional mitochondrial protein regulating cell life and death. Mol Asp Med 31:227–285. https://doi.org/10.1016/j.mam.2010.03.002
80. Moran O, Sorgato MC (1992) High-conductance pathways in mitochondrial membranes. J Bioenerg Biomembr 24:91–98
81. Benz R (1994) Permeation of hydrophilic solutes through mitochondrial outer membranes: review on mitochondrial porins. Biochim Biophys Acta 1197:167–196
82. Hodge T, Colombini M (1997) Regulation of metabolite flux through voltage-gating of VDAC channels. J Membr Biol 157:271–279
83. Gincel D, Silberberg SD, Shoshan-Barmatz V (2000) Modulation of the voltage-dependent anion channel (VDAC) by glutamate. J Bioenerg Biomembr 32:571–583
84. Báthori G, Csordás G, Garcia-Perez C et al (2006) Ca^{2+}-dependent control of the permeability properties of the mitochondrial outer membrane and voltage-dependent anion-selective channel (VDAC). J Biol Chem 281:17347–17358. https://doi.org/10.1074/jbc.M600906200
85. Tong Q, Hirschler-Laszkiewicz I, Zhang W et al (2008) TRPC3 is the erythropoietin-regulated calcium channel in human erythroid cells. J Biol Chem 283:10385–10395. https://doi.org/10.1074/jbc.M710231200
86. Hirschler-Laszkiewicz I, Tong Q, Conrad K et al (2009) TRPC3 activation by erythropoietin is modulated by TRPC6. J Biol Chem 284:4567–4581. https://doi.org/10.1074/jbc.M804734200
87. Kucherenko YV, Bhavsar SK, Grischenko VI et al (2010) Increased cation conductance in human erythrocytes artificially aged by glycation. J Membr Biol 235:177–189. https://doi.org/10.1007/s00232-010-9265-2
88. Danielczok J, Hertz L, Ruppenthal S et al (2017) Does erythropoietin regulate TRPC channels in red blood cells? Cell Physiol Biochem 41:1219–1228. https://doi.org/10.1159/000464384
89. Foller M, Kasinathan RS, Koka S et al (2008) TRPC6 contributes to the Ca^{2+} leak of human erythrocytes. Cell Physiol Biochem 21:183–192
90. Dietrich A, Gudermann T (2014) TRPC6: physiological function and pathophysiological relevance. Handb Exp Pharmacol 222:157–188. https://doi.org/10.1007/978-3-642-54215-2_7
91. Pinet C, Antoine S, Filoteo AG et al (2002) Reincorporated plasma membrane Ca^{2+}-ATPase can mediate B-type Ca^{2+} channels observed in native membrane of human red blood cells. J Membr Biol 187:185–201. https://doi.org/10.1007/s00232-001-0163-5
92. Romero PJ, Romero EA, Mateu D et al (2006) Voltage-dependent calcium channels in young and old human red cells. Cell Biochem Biophys 46:265–276. https://doi.org/10.1385/CBB:46:3:265
93. Andrews DA, Yang L, Low PS (2002) Phorbol ester stimulates a protein kinase C-mediated agatoxin-TK-sensitive calcium permeability pathway in human red blood cells. Blood 100:3392–3399

94. Wagner-Britz L, Wang J, Kaestner L, Bernhardt I (2013) Protein kinase Cα and P-type Ca channel CaV2.1 in red blood cell calcium signalling. Cell Physiol Biochem 31:883–891. https://doi.org/10.1159/000350106
95. Kaestner L, Wang X, Hertz L, Bernhardt I (2018) Voltage-activated ion channels in non-excitable cells – a viewpoint regarding their physiological justification. Front Physiol 9:450
96. Tiffert T, Bookchin RM, Lew VL (2003) Calcium homeostasis in normal and abnormal human red cells. In: Bernhardt I, Ellory C (eds) Red cell membrane transport in health and disease. Springer, Berlin, pp 373–405
97. Catterall WA (2011) Voltage-gated calcium channels. Cold Spring Harb Perspect Biol 3:a003947. https://doi.org/10.1101/cshperspect.a003947
98. Catterall WA (2000) Structure and regulation of voltage-gated Ca^{2+} channels. Annu Rev Cell Dev Biol 16:521–555. https://doi.org/10.1146/annurev.cellbio.16.1.521
99. Petkova-Kirova P, Hertz L, Makhro A et al (2018) A previously unrecognized Ca^{2+}-inhibited non-selective cation channel in red blood cells. HemaSphere, 2:e146
100. Flatt JF, Bawazir WM, Bruce LJ (2014) The involvement of cation leaks in the storage lesion of red blood cells. Front Physiol 5:214. https://doi.org/10.3389/fphys.2014.00214
101. Lipp P, Kaestner L (2014) Detecting calcium in cardiac muscle: fluorescence to dye for. Am J Physiol Heart Circ Physiol 307:H1687–H1690. https://doi.org/10.1152/ajpheart.00468.2014
102. Kaestner L, Tabellion W, Weiss E et al (2006) Calcium imaging of individual erythrocytes: problems and approaches. Cell Calcium 39:13–19. https://doi.org/10.1016/j.ceca.2005.09.004
103. Jarrett HW, Kyte J (1979) Human erythrocyte calmodulin. Further chemical characterization and the site of its interaction with the membrane. J Biol Chem 254:8237–8244
104. Leinders T, van Kleef RG, Vijverberg HP (1992) Single Ca^{2+}-activated K^+ channels in human erythrocytes: Ca^{2+} dependence of opening frequency but not of open lifetimes. Biochim Biophys Acta 1112:67–74
105. Stout JG, Zhou Q, Wiedmer T, Sims PJ (1998) Change in conformation of plasma membrane phospholipid scramblase induced by occupancy of its Ca^{2+} binding site. Biochemistry 37:14860–14866. https://doi.org/10.1021/bi9812930
106. Woon LA, Holland JW, Kable EP, Roufogalis BD (1999) Ca^2+ sensitivity of phospholipid scrambling in human red cell ghosts. Cell Calcium 25:313–320
107. Bitbol M, Fellmann P, Zachowski A, Devaux PF (1987) Ion regulation of phosphatidylserine and phosphatidylethanolamine outside-inside translocation in human erythrocytes. Biochim Biophys Acta 904:268–282
108. Murakami T, Hatanaka M, Murachi T (1981) The cytosol of human erythrocytes contains a highly Ca^{2+}-sensitive thiol protease (calpain I) and its specific inhibitor protein (calpastatin). J Biochem 90:1809–1816
109. Salamino F, De Tullio R, Mengotti P et al (1993) Site-directed activation of calpain is promoted by a membrane-associated natural activator protein. Biochem J 290(Pt 1):191–197
110. Bergamini CM, Signorini M (1993) Studies on tissue transglutaminases: interaction of erythrocyte type-2 transglutaminase with GTP. Biochem J 291(Pt 1):37–39
111. Almaraz L, García-Sancho J, Lew VL (1988) Calcium-induced conversion of adenine nucleotides to inosine monophosphate in human red cells. J Physiol Lond 407:557–567
112. Kohout SC, Corbalán-García S, Torrecillas A et al (2002) C2 domains of protein kinase C isoforms alpha, beta, and gamma: activation parameters and calcium stoichiometries of the membrane-bound state. Biochemistry 41:11411–11424. https://doi.org/10.1021/bi026401k
113. Schwarz W, Grygorczyk R, Hof D (1989) Recording single-channel currents from human red cells. Methods Enzymol 173:112–121
114. Grygorczyk R, Schwarz W, Passow H (1984) Ca^{2+}-activated K^+ channels in human red cells. Comparison of single-channel currents with ion fluxes. Biophys J 45:693–698. https://doi.org/10.1016/S0006-3495(84)84211-3
115. Grygorczyk R, Schwarz W (1985) Ca^{2+}-activated K^+ permeability in human erythrocytes: modulation of single-channel events. Eur Biophys J 12:57–65

116. Leinders T, van Kleef RG, Vijverberg HP (1992) Distinct metal ion binding sites on Ca^{2+}-activated K^+ channels in inside-out patches of human erythrocytes. Biochim Biophys Acta 1112:75–82
117. Dunn PM (1998) The action of blocking agents applied to the inner face of Ca^{2+}-activated K^+ channels from human erythrocytes. J Membr Biol 165:133–143
118. Wolff D, Cecchi X, Spalvins A, Canessa M (1988) Charybdotoxin blocks with high affinity the Ca-activated K^+ channel of Hb A and Hb S red cells: individual differences in the number of channels. J Membr Biol 106:243–252
119. Qadri SM, Kucherenko Y, Lang F (2011) Beauvericin induced erythrocyte cell membrane scrambling. Toxicology 283:24–31. https://doi.org/10.1016/j.tox.2011.01.023
120. Kucherenko Y, Zelenak C, Eberhard M et al (2012) Effect of casein kinase 1α activator pyrvinium pamoate on erythrocyte ion channels. Cell Physiol Biochem 30:407–417. https://doi.org/10.1159/000339034
121. Kucherenko YV, Wagner-Britz L, Bernhardt I, Lang F (2013) Effect of chloride channel inhibitors on cytosolic Ca^{2+} levels and Ca^{2+}-activated K^+ (Gardos) channel activity in human red blood cells. J Membr Biol 246:315–326. https://doi.org/10.1007/s00232-013-9532-0
122. Baunbaek M, Bennekou P (2008) Evidence for a random entry of Ca^{2+} into human red cells. Bioelectrochemistry 73:145–150. https://doi.org/10.1016/j.bioelechem.2008.04.006
123. Seear RV, Lew VL (2011) IKCa agonist (NS309)-elicited all-or-none dehydration response of human red blood cells is cell-age dependent. Cell Calcium 50:444–448. https://doi.org/10.1016/j.ceca.2011.07.005
124. Schatzmann HJ (1973) Dependence on calcium concentration and stoichiometry of the calcium pump in human red cells. J Physiol Lond 235:551–569
125. Lines GT, Sande JB, Louch WE et al (2006) Contribution of the Na^+/Ca^{2+} exchanger to rapid Ca^{2+} release in cardiomyocytes. Biophys J 91:779–792. https://doi.org/10.1529/biophysj.105.072447
126. Chu H, Puchulu-Campanella E, Galan JA et al (2012) Identification of cytoskeletal elements enclosing the ATP pools that fuel human red blood cell membrane cation pumps. Proc Natl Acad Sci U S A 109:12794–12799. https://doi.org/10.1073/pnas.1209014109
127. Bers DM (2002) Cardiac excitation-contraction coupling. Nature 415:198–205. https://doi.org/10.1038/415198a
128. Rasband MN, Shrager P (2000) Ion channel sequestration in central nervous system axons. J Physiol Lond 525(Pt 1):63–73. https://doi.org/10.1111/j.1469-7793.2000.00063.x
129. Dyrda A, Cytlak U, Ciuraszkiewicz A et al (2010) Local membrane deformations activate Ca^{2+}-dependent K^+ and anionic currents in intact human red blood cells. PLoS One 5:e9447. https://doi.org/10.1371/journal.pone.0009447
130. Liappis N (1972) Sodium-, potassium- and chloride-concentrations in the serum of infants, children and adults. Monatsschr Kinderheilkd 120:138–142

Chapter 26
Regulation of Multifunctional Calcium/Calmodulin Stimulated Protein Kinases by Molecular Targeting

Kathryn Anne Skelding and John A. P. Rostas

Abstract Multifunctional calcium/calmodulin-stimulated protein kinases control a broad range of cellular functions in a multitude of cell types. This family of kinases contain several structural similarities and all are regulated by phosphorylation, which either activates, inhibits or modulates their kinase activity. As these protein kinases are widely or ubiquitously expressed, and yet regulate a broad range of different cellular functions, additional levels of regulation exist that control these cell-specific functions. Of particular importance for this specificity of function for multifunctional kinases is the expression of specific binding proteins that mediate molecular targeting. These molecular targeting mechanisms allow pools of kinase in different cells, or parts of a cell, to respond differently to activation and produce different functional outcomes.

Keywords CaMKK · CaMKI · CaMKII · CaMKIV · Casein kinase I · Targeting

Abbreviations

α-KAP	αCaMKII anchoring protein
AMPK	AMP-activated protein kinase

K. A. Skelding
Priority Research Centre for Cancer Research, Innovation and Translation, School of Biomedical Sciences and Pharmacy, Faculty of Health and Medicine, The University of Newcastle, Callaghan, NSW, Australia

Hunter Medical Research Institute, New Lambton Heights, NSW, Australia

J. A. P. Rostas
Hunter Medical Research Institute, New Lambton Heights, NSW, Australia

Priority Research Centre for Brain and Mental Health, and Priority Research Centre for Stroke and Brain Injury, School of Biomedical Sciences and Pharmacy, Faculty of Health and Medicine, The University of Newcastle, Callaghan, NSW, Australia
e-mail: John.Rostas@newcastle.edu.au

M. S. Islam (ed.), *Calcium Signaling*, Advances in Experimental Medicine and Biology 1131, https://doi.org/10.1007/978-3-030-12457-1_26

ATP	Adenosine triphosphate
Ca^{2+}	Calcium ions
CaM	Calmodulin
CaMK	Calcium/calmodulin stimulated protein kinases
CaMKI	Calcium/calmodulin stimulated protein kinase I
CaMKII	Calcium/calmodulin stimulated protein kinase II
CaMKIV	Calcium/calmodulin stimulated protein kinase IV
CaMKK	Calcium/calmodulin stimulated protein kinase kinase
CK1	Casein kinase 1
CLK2	CDC-like kinase 2
GSK-3	Glycogen synthase kinase 3
PKA	cAMP-dependent protein kinase
PKB	Protein kinase B; Akt
PSD	Post-synaptic density
S	Serine
T	Threonine

26.1 Introduction

Calcium is a major second messenger in all cells, and is integral in many important signalling pathways. Changes in intracellular Ca^{2+} regulate many biological processes, including neurotransmitter release, gene expression, and the cell cycle. Though free Ca^{2+} can activate a number of proteins directly (for example myosin, phospholipase A_2, and protein kinase C), it regulates the activity of many enzymes indirectly via a number of low molecular weight Ca^{2+} binding proteins, the most abundant of which is calmodulin (CaM). CaM consists of two globular lobes, each of which contain two Ca^{2+}-binding sites. Binding of Ca^{2+} dramatically changes the conformation of CaM, allowing Ca^{2+}/CaM to interact with a variety of other proteins, including several classes of protein kinases.

Many proteins that bind Ca^{2+}/CaM do so via an α-helical region consisting of approximately 20 amino acids, which contain positively charged amino acids among hydrophobic residues. There are two classes of CaM binding motif [1]. The ***IQ motif*** (IQXXXRGXXXR) is present in proteins that bind CaM in the absence of Ca^{2+}. The majority, if not all, of the proteins that contain this motif are not enzymes, and appear to limit the concentration of diffusible CaM during periods of low intracellular Ca^{2+}. The second class of motifs are related to each other, and indicate CaM binding in the presence of Ca^{2+}. These motifs include ***1-12***, ***1-14***, ***1-5-10***, and ***1-8-14*** (named based on the conserved hydrophobic residues within these motifs). However, several identified/putative CaM binding sites have sequence motifs that are called ***unclassified*** because they do not conform to either of the preceding sequence motifs.

Ca^{2+}/CaM stimulated protein kinases are classified based on their substrate specificity, and there are two main types: ***restricted*** kinases, which only phosphory-

late one, or a small number, of substrates, and ***multifunctional*** kinases, which have broad substrate specificity and regulate multiple functions in the same and different cell types.

There are three main families of restricted Ca^{2+}/CaM stimulated protein kinases: phosphorylase kinase (PhK), elongation factor 2 kinase (eEF2K) and myosin light chain kinase (MLCK). These kinase families do not share a common protein domain structure and, though they are all regulated by multiple mechanisms, only MLCK appears to be controlled by molecular targeting. For a description of the molecular structures and control mechanisms of the restricted kinases, the reader is referred to our previous review [2]. This review will focus on the multifunctional kinases and the molecular regulatory mechanisms that allow these widely expressed kinases to produce functional responses that are both stimulus- and cell type-specific.

Multifunctional kinases control a plethora of functions within multiple cell types and, consequently, there are multiple levels of control that regulate the functions of these protein kinases. The most basic method of controlling kinase function is via the regulation of Ca^{2+} dynamics, specifically the frequency, amplitude and duration of oscillations in the intracellular concentration of Ca^{2+}. This is most commonly controlled by ion channels and many kinases can be directly regulated by intracellular Ca^{2+} fluxes. For example, the multifunctional Ca^{2+}/CaM-stimulated protein kinase II (CaMKII) can translate the frequency of Ca^{2+} spikes into corresponding amounts of kinase activity [3]. However, several additional mechanisms exist that produce extra forms of control of kinase activity. Modulation of the response to changes in Ca^{2+} can be controlled by expression of different splice forms of the kinase which are differentially sensitive to the various control mechanisms, phosphorylation, or by the kinase becoming autonomously active (i.e. no longer require Ca^{2+}/CaM for activity) [4–6]. Another level of control has also been identified that provides both temporal, tissue-specific and cellular site-specific control of kinase function. This mechanism is termed 'molecular targeting' and involves the interactions between kinases and specific binding proteins. This chapter will examine the role of molecular regulation and targeting in controlling the function of multifunctional Ca^{2+}/CaM stimulated protein kinases (Table 26.1). We will focus particularly on CaMKII because it has been most extensively studied with respect to molecular targeting.

26.2 Multifunctional Calcium/Calmodulin Stimulated Protein Kinases

26.2.1 Two Families of Kinases with Homologous Domain Structures

The multifunctional calcium/calmodulin stimulated protein kinases can be classified into two broad families based on the homology of their domain structures

Table 26.1 Structural and functional properties of multifunctional Ca^{2+}/CaM-stimulated kinases

	Multifunctional Ca^{2+}/CaM-stimulated kinases				
	CaMKK	CaMKI	CaMKIV	CaMKII	CK1
Genes	2 (*CAMKK1, CAMKK2*)	4 (*CAMK1A, CAMK1B, CAMK1G, CAMK1D*)	1 *(CAMK4)*	4 (*CAMK2A, CAMK2B, CAMK2G, CAMK2D*)	7 (*CSNK1A1, CSNK1B, CSNK1G1, CSNK1G2, CSNK1G3, CSNK1D, CSNK1E*)
Splice Variants	Multiple	Multiple	At least 1	Multiple	Multiple
Subunit (kDa)	54–68	38–53	65–67	50–60	37–51
Structure	Monomer	Monomer	Monomer	Multimer	Monomer
CaM Binding Motif	Unclassified	1-14 motif	1-8-14 motif	1-5-10 motif	Unclassified
Contains an Autoinhibitory Region?	Yes	Yes	Yes	Yes	Yes (proposed)
Expression	Neuronal, immune, testis	Ubiquitous	Neuronal, immune, testis	Ubiquitous	Ubiquitous
Regulated by Targeting?	Yes	Yes	Yes	Yes	Yes
Requirement for Activation	Ca^{2+}/CaM	Ca^{2+}/CaM	Ca^{2+}/CaM,and phosphorylation	Ca^{2+}/CaM	Constitutively active
Capable of Autonomous Activity?	Yes	No	Yes	Yes	Yes
Number of Phosphorylation Sites	Multiple	T174 to T180 (depending on isoform)	T196 and S332 (CaMKIVα)	Multiple	Multiple
Regulation by Phosphorylation	Phosphorylation by PKA (α) or CDK, GSK (β) inhibitors kinase activity. Autophosphorylation at S74 may regulate targeting	Phosphorylation by CaMKK activates kinase activity	Phosphorylation by CaMKK activates kinase activity	Autophosphorylation regulates both kinase activity (inhibitory and activating) and targeting	Autophosphorylation inhibits kinase activity

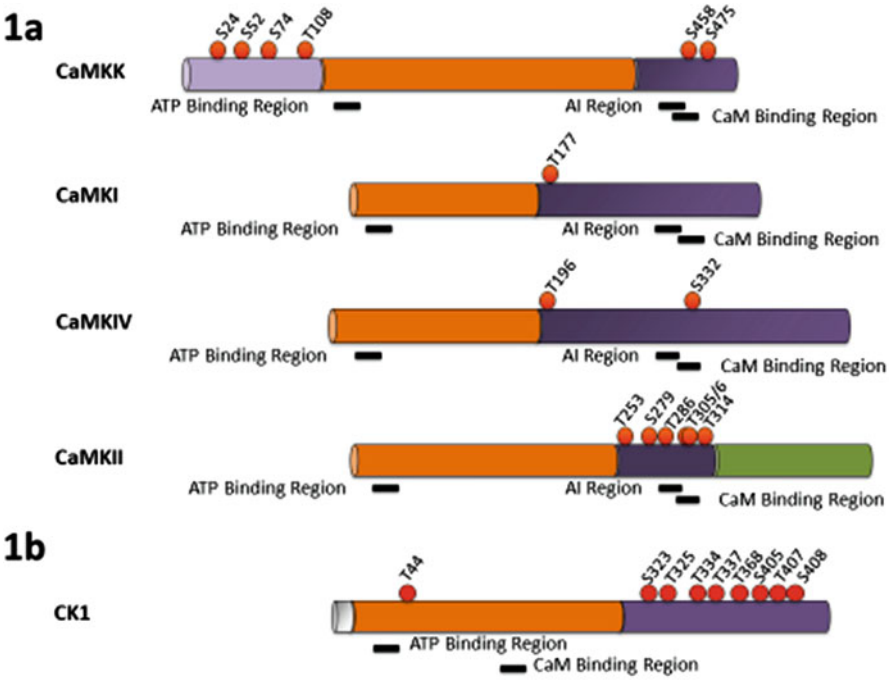

Fig. 26.1 Schematic representation, drawn to relative scale, of the domain structures of the multifunctional Ca^{2+}/CaM stimulated protein kinases. Domain structures of the α isoforms of the four homologous kinases: CaMKK, CaMKI, CaMKIV and CaMKII (**a**) and the ε isoform of casein kinase I (CK1) (**b**). Each kinase has a similar domain structure illustrated as catalytic (orange), regulatory (purple), and putative regulatory (lilac) domains. CaMKII also has an association domain (green). The major characterised phosphorylation sites (red balls) are also indicated. Black bars indicate the locations of ATP binding regions, autoinhibitory (AI) pseudosubstrate regions and calcium/calmodulin (CaM) binding regions

(Fig. 24.1a, b). Each of these kinases in both families has a regulatory domain (purple) and a catalytic domain (orange) linked to its N-terminus. Calcium/calmodulin stimulated protein kinase II (CaMKII) is the only member of these families that is multimeric (Table 26.1) and its multimeric structure is held together by interactions between the association domains (green) of the subunits which are attached to the C-terminus of their regulatory domains (Fig. 26.1).

The four kinases which form one family (Fig. 24.1a) – calcium/calmodulin stimulated protein kinase kinase (CaMKK) and calcium/calmodulin stimulated protein kinase I, IV and II (CaMKI, CaMKIV and CaMKII) – all have the following common features in their regulatory domains: (i) an autoinhibitory (AI) pseudosubstrate region which acts like a substrate and binds to the active site of the kinase, thereby inhibiting it until the binding of calcium/calmodulin causes the displacement of the autoinhibitory pseudosubstrate region and activates the kinase; (ii) a calcium/calmodulin binding region that partially overlaps with the

autoinhibitory region; and (iii) one or more phosphorylation sites (red balls) that modify the activity of the kinase but are not necessary for kinase activity. The autoinhibitory and calcium/calmodulin binding regions provide an obvious area of homology and point for alignment for the kinases in Fig. 24.1a. There is no consensus in the literature on the precise extents of the regulatory domains. We have chosen to define the extent of the regulatory domains in CaMKI and CaMKIV based on CaMKII whose regulatory mechanisms have been characterised most extensively. For the purposes of Fig. 24.1a, we have placed the N-terminal boundary of the regulatory domain of CaMKII to include T253, whose phosphorylation has been shown to regulate molecular targeting in vivo, and the C-terminal boundary to include the first of the four splice sites in the C terminal part of CaMKII because the functional differences between the alternative spice variants in this region are all related to regulatory properties. The N termini of the regulatory domains of CaMKI and CaMKIV have been chosen to include T196 in CaMKIV and T177 in CaMKI because phosphorylation of these sites has been shown to regulate kinase activity. As CaMKK, CaMKI and CaMKIV are monomeric we have assumed that the regulatory domains of these kinases extend to their C termini. As the N terminal domain of CaMKK contains three phosphorylation sites that regulate CaMKK activity, we have designated this domain as a putative second regulatory domain and coloured it lilac to differentiate it from the well-established C-terminal regulatory domain.

The multiple variants of casein kinase I form another family of homologous kinases with a variable C-terminal regulatory domain (purple) and a conserved catalytic domain (orange) attached to its N-terminus (Fig. 24.1b). There is also a short N-terminal extension (white) to the catalytic domain whose function is not known.

26.2.2 Calcium/Calmodulin Stimulated Protein Kinase Kinase (CaMKK)

Calcium/calmodulin stimulated protein kinase kinase (CaMKK) is a multifunctional protein kinase encoded by two genes (*CAMKK1* and *CAMKK2*) that produce CaMKKα and CaMKKβ, respectively. Several splice isoforms of the monomeric enzyme are generated [7], which are between 54 and 68 kDa in size. CaMKK is primarily expressed in the brain, but is also present in the thymus, spleen, and testis [5, 8]. The expression pattern of CaMKKβ appears to parallel that of CaMKIV [9]. CaMKK phosphorylates CaMKI and CaMKIV, but can also phosphorylate other proteins in their activation loop, such as AMP activated protein kinase (AMPK) [10] and protein kinase B (PKB/Akt) [11].

CaMKK, CaMKI and CaMKIV have been shown to form a signalling pathway termed the Ca^{2+}/CaM-dependent kinase cascade, which has been implicated in several cellular processes, including axonal and dendritic outgrowth and elongation, adiposity regulation, glucose homeostasis, hematopoietic stem cell maintenance,

cell proliferation, apoptosis, and normal immune cell function [5, 12–17]. An unusual aspect of this cascade is that binding of Ca^{2+}/CaM to both CaMKK and its substrates (CaMKI and CaMKIV) is required for phosphorylation of their activation loops [18]. Whilst unusual, this mechanism has been noted in other signalling pathways, including the AMP-kinase cascade [19].

CaMKK requires Ca^{2+}/CaM for maximal activity [18], however, CaMKKβ exhibits partially autonomous activity in the absence of Ca^{2+}/CaM, whereas CaMKKα is completely dependent on the binding of Ca^{2+}/CaM for activity [9, 20]. The major site of autosphorylation of CaMKKα is S24 [21], but CaMKK can also autophosphorylate at S74 in the presence of Ca^{2+}/CaM, however, it is very slow, substochiometric, and does not appear to affect catalytic activity [9, 22]. A possible role for this phosphorylation in regulating molecular targeting has not been investigated.

The activity of CaMKKα is regulated by phosphorylation at multiple sites. cAMP-dependent protein kinase (PKA) can phosphorylate S52, S74, T108, S458, and S475 on CaMKKα [21], and S100, S495 and S511 on CaMKKβ [5]. Binding of Ca^{2+}/CaM blocks phosphorylation at S52, S74, T108, and S458, but enhances phosphorylation at S475 [21]. CaMKKα activity is negatively regulated by phosphorylation on S74, T108 and S458 [23–25] and phosphorylation of S458 blocks Ca^{2+}/CaM binding. Cyclin dependent kinase 5 (CDK5) phosphorylates CaMKKβ at S137, thereby priming CaMKKβ for phosphorylation by glycogen synthase kinase 3β (GSK-3β) at S129 and S133 [26]. Phosphorylation at these sites decreases the autonomous activity and the half-life of CaMKKβ. In addition, phosphorylation of CaMKKβ by GSK-3β and CDK5 is critical for its role in neurite development [26]. Furthermore, CaMKK binding partners can alter CaMKK kinetics. Whilst 14-3-3 protein binding to CaMKKβ does not inhibit the catalytic activity of phosphorylated CaMKK, it slows down its dephosphorylation by affecting the structure of several regions of CaMKKβ outside of the 14-3-3- binding motifs [27].

Evidence indicates that molecular targeting plays a role in regulating CaMKK function, as CaMKKα is known to translocate to the nucleus [28]. Furthermore, inhibition of this translocation prevents type-II monocytic cells from being activated [28]. However, whether this targeting is regulated by phosphorylation has not been identified.

26.2.3 Calcium/Calmodulin Stimulated Protein Kinase I (CaMKI)

The CaMKI family is composed of four members, which are encoded by four different genes: CAMK1 (CaMKIα), PNCK (CaMKIβ/Pnck), CAMK1G (CaMKIγ/CLICK3) and CAMK1D (CaMKIδ/CKLiK). Each gene produces at least one splice variant and all members of this family are monomeric with sizes between 38 and 53 kDa. The various isoforms of CaMKI are widely expressed in rat brain

and other tissues, with CaMKIα being found in most mammalian cells [29]. CaMKI has been implicated in a variety of cellular functions, including the control of synapsin in nerve terminals, growth cone motility and axon outgrowth, aldosterone synthase expression, the visual signalling process, and the cell cycle [30–35].

In addition to activation by binding of Ca^{2+}/CaM, CaMKI is activated through phosphorylation by CaMKK, and phosphorylation of the conserved T (T174 to T180, depending on the isoform) in the activation loop by CaMKK is required for maximal CaMKI activity [36] in a substrate dependent manner [37], suggesting that targeting may also be involved in the regulation of CaMKI. Additionally, once CaMKIδ is phosphorylated by CaMKK, it becomes resistant to protein phosphatases, which induces a 'primed' state, where it can more readily be activated in response to Ca^{2+} signals than other CaMKI enzymes [38].

Subcellular localisation regulates CaMKI function, and several CaMKI isoforms can translocate to the nucleus. For example, the translocation of CaMKIα to the nucleus (mediated by interacting with a CRM1 complex) is enhanced by Ca^{2+}/CaM, suggesting that nuclear export may be enhanced by activation of the kinase [39]. Furthermore, nuclear translocation of CaMKIδ is triggered by stimuli that produce an influx of intracellular Ca^{2+} (potassium depolarisation or glutamate stimulation) [40]. The mechanisms and functions involved, however, remain to be determined.

26.2.4 Calcium/Calmodulin Stimulated Protein Kinase IV (CaMKIV)

CaMKIV is encoded by one gene (CAMK4) which encodes the α isoform and produces at least one splice variant (β); both are monomeric and are 65 and 67 kDa, respectively in size. The two isoforms, CaMKIVα and CaMKIVβ, are identical, except CaMKIVβ contains a 28 aa N-terminal extension, of unknown function. As mentioned previously, the CaMKIV expression pattern is similar to that of CaMKKβ, with CaMKIV primarily expressed in the brain, but also present in immune cells and in the testis and ovary [8, 14, 41, 42]. The *CAMK4* gene also encodes calspermin, a Ca^{2+}/CaM binding protein of unknown function that is expressed exclusively in spermatids in the testes [42]. CaMKIV has been implicated in the regulation of cyclic AMP element binding protein (CREB), homeostatic plasticity, neurite outgrowth, fear memory, immune and inflammatory responses, tau accumulation, neuropathic pain, and cell cycle control [31, 43–51].

CaMKIV requires Ca^{2+}/CaM to become active, as well as phosphorylation of the conserved T in the activation loop by CaMKK [6], which generates an autonomously active kinase. Phosphorylation of S332 within the CaM binding region prevents CaM binding [52]. Phosphorylation at T196 enhances glucokinase promoter activity [53], suggesting that CaMKIV phosphorylation can regulate insulin secretion and glucose homeostasis. Additionally, a subfraction of hyper-phosphorylated CaMKIV (identified by its shift in electrophoretic mobility) has

been identified specifically localised to the nuclear matrix in spermatids [42], however the precise molecular function regulated by this is yet to be elucidated. The subcellular distribution of CaMKIV is dynamic as CaMKIV can translocate between the cytoplasm and nucleus, however, catalytic activity is required for this translocation, as catalytically inactive CaMKIV remains in the cytoplasm [54]. CaMKIV translocates to the nucleus in neocortical neurons after disruption of sensory input [55], whereas CaMKIV translocates to the cytoplasm in luteinised ovarian granulosa cells [41]. This indicates that targeting plays a role in regulating CaMKIV function, but the mechanisms involved require further investigation.

26.2.5 Calcium/Calmodulin Stimulated Protein Kinase II (CaMKII)

Ca^{2+}/CaM stimulated protein kinase II (CaMKII) is encoded by four genes (α, β, γ, and δ) [56], which produce over 30 isoforms ranging in size from 50 to 60 kDa. There are four main variable regions (V1-4) in the regulatory and association domains at which the alternative splicing occurs [57]. The V1 region, which we have included at the C-terminal of the regulatory domain, is the primary site for divergence among the four CaMKII genes. The functional differences between the splice variants are all regulatory e.g. altered sensitivity to intracellular Ca^{2+} and altered molecular targeting by interaction with different CaMKII binding proteins (Table 26.2). One or more members of this family are found in virtually every tissue, and mediate diverse physiological functions. CaMKIIα is expressed most abundantly in neurons (where it can account for up to 1% of total protein [58]), and is involved in regulating many aspects of normal neuronal function, including neurotransmitter synthesis and release, cellular morphology and neurite extension, cortical neuron migration, long-term plasticity, learning, memory consolidation, and memory erasure following retrieval [59–68]. Non-neuronal CaMKII has been implicated in the regulation of other biological processes, such as fertilisation, cell proliferation, osteogenic differentiation, the maintenance of vascular tone, normal cardiac function and heart failure, and cancer cell invasion and migration [69–79].

The three-dimensional structure of CaMKII is in fact highly unusual [80], and in contrast to the other CaMKI family members, CaMKII associates into a multimeric form through interactions between the association domains of its subunits (Fig. 24.1a). The CaMKIIα crystal is an asymmetric unit that consists of two autoinhibited catalytic domains in a symmetric dimer held together by interactions between anti-parallel coiled-coil structures formed by the regulatory domains. The regulatory domains are joined by a hinge to the C-terminus of the catalytic domain [80]. The regulatory domain functions like a gate (with T286 as its hinge), so that it is positioned to block the protein substrate and adenosine triphosphate (ATP) binding sites when CaMKII is autoinhibited and is 'open' when Ca^{2+}/CaM is bound or CaMKII is autophosphorylated at T286. Therefore, CaMKII

Table 26.2 Identified CaMKII targeting proteins

Binding protein		CaMKII used in study		Refs.
Protein	Function	Phosphorylation state	Isoform	
α-actinin-1	Microfilament protein	Non-phosphorylated	α (β, γ, δ nt)	[161]
α-actinin-2	Microfilament protein	Autophosphorylated (radiolabelled CaMKII)[a]	α (β, γ, δ nt)	[162]
F-actin	Actin cytoskeleton	Asp286-CaMKII does not bind.	α, β (γ, δ nt)	[163]
BAALC 1-6-8	Marker of human hematopoietic progenitor cells; proposed lipid raft targeting protein in neurons	Non-phosphorylated and Asp286-CaMKII both bind, Asp253-CaMKII binds more strongly through a different binding site	α binds, β does not (γ, δ nt)	[70, 164]
Calcium channel α-subunit isoforms (L-type)	Calcium influx	Non-phosphorylated CaMKII binds α1, α2a, α3, and α4, while pThr286 only binds α1 and α2a	δ2 (α, β, γ nt)	[165]
Calcium channel, N-type	Pre-synaptic calcium influx	Non-phosphorylated	Not specified	[166]
Camguk/CASK	Synaptic protein targeting and synaptic plasticity	Non-phosphorylated CaMKII binds Camguk, pThr305/306 decreases binding	Not specified	[167]
CARMA1	Regulator of NFκB activation of lymphocytes	Autophosphorylated (radiolabelled CaMKII)[a]	γ (α, β, δ nt)	[168]
Cdk5 activators p35 and p39	Proline-directed serine/threonine kinase	Non-phosphorylated	α (β, γ, δ nt)	[161]
Cytoplasmic polyadenylation element binding protein (CPEB)	Regulates protein synthesis and initiates mRNA polyadenylation and translation	pThr286	Not specified	[169]

Densin-180	Dendritic scaffolding protein	pThr286 enhances binding compared to non-phosphorylated CaMKII	α (β, γ, δ nt)	[170, 171]
Desmin	Muscle intermediate filament	Non-phosphorylated CaMKII binds desmin, Asp286 and Asp253 increases binding	Purified from rat brain	[70, 172, 173]
MAP-2	Microtubule assembly	Non-phosphorylated binds MAP-2, Asp286 increases binding	Purified from rat brain	[70, 172, 173]
Myelin Basic Protein	Major myelin sheath protein	Autophosphorylated (radiolabelled CaMKII)[a]	γ (α, β, δ nt)	[174]
		Non-phosphorylated binds, Asp286 slightly decreases binding, Asp253 completely blocks binding	α (β, γ, δ nt)	[70]
NR2A/B	Voltage sensitive ionotropic glutamate receptor involved in synaptic plasticity	pThr286 enhances binding compared to non-phosphorylated CaMKII	α (β, γ, δ nt)	[84, 175–177]
PP2A	Serine/threonine protein phosphatase	Non-phosphorylated	α (β, γ, δ nt)	[178]
Projectin	Integral protein of insect flight muscle	pThr286 decreases binding compared to non-phosphorylated CaMKII	Purified from rat brain	[179]
Rad	GTP binding protein	Autophosphorylated (radiolabelled CaMKII)[a]	Not specified	[180]
SCP3	PP2C-type protein phosphatase	Non-phosphorylated	γ (G-2 variant) (α, β, δ nt)	[181]

(continued)

Table 26.2 (continued)

Binding protein		CaMKII used in study		Refs.
Protein	Function	Phosphorylation state	Isoform	
STOP	Microtubule associated protein	pThr286	Purified from rat brain	[182]
Synapsin 1	Synaptic vesicle binding protein	Autophosphorylated (radiolabelled CaMKII)[a]	α (β, γ, δ nt)	[183]
Syntaxin 1A	Component of exocytotic molecular machinery	Only pThr286 bound syntaxin 1A (non-phosphorylated CaMKII did not interact)	α (β, γ, δ nt)	[59]
Tau	Microtubule assembly	Non-phosphorylated and Asp253 CaMKII bind tau, Asp286 increases binding	Purified from rat brain	[70, 173, 184]
Tyrosine hydroxylase (rat)	Catecholamine biosynthesis	Non-phosphorylated	α (β, γ, δ nt)	[185]
Tyrosine hydroxylase isoform 2 (human)	Catecholamine biosynthesis	Non-phosphorylated and Asp286 CaMKII bind, Asp253 increases binding	α (β, γ, δ nt)	[70]
Tyrosine hydroxylase isoform 2 (human), phosphorylated at Ser19 and Ser40	Catecholamine biosynthesis	Binding is enhanced for non-phosphorylated, Asp286, and Asp253 CaMKII when compared to non-phosphorylated tyrosine hydroxylase	α (β, γ, δ nt)	[70]

nt not tested

[a]When autophosphorylated, CaMKII will be predominantly (though not always exclusively) phosphorylated at Thr286 Asp286-CaMKII and Asp253-CaMKII are phosphomimic mutants of CaMKII in which an aspartatic acid has been substituted for threonine at positions 286 and 253, respectively

is comprised of six mutually inhibited dimers. Homomers of α, β, γ, and δ all exhibit the same basic structure. Whilst heteromultimers are known to exist [81], their structures are unknown.

The biological properties of CaMKII are regulated by a variety of post-translational modifications (including phosphorylation and oxidation by reactive oxygen species in pathological conditions) and targeting to specific subcellular locations through interactions with other proteins. These two control mechanisms can also influence one another, as the interaction between CaMKII and some binding partners can be modified by the phosphorylation state of the kinase, as well as by phosphorylation of the binding partner [4, 70].

Purified CaMKII requires the presence of Ca^{2+}/CaM for enzyme activity. Binding of two CaM molecules to two adjacent subunits within a holoenzyme allows autophosphorylation of one or both of these subunits to occur at T286 [82]. Autophosphorylation of T286 in CaMKIIα (T287 in CaMKIIβ, γ, and δ) occurs quickly, greatly enhances the affinity of CaMKII for Ca^{2+}/CaM by more than 100 fold, changes enzyme activity, and alters targeting to specific subcellular sites. CaMKII phosphorylation at T286 allows the enzyme to remain active even after CaM has dissociated from it (autonomous activity), and can also regulate the function of the enzyme by increasing the binding of CaMKII to specific subcellular sites [83–85]. However, phosphorylation of T286 is not required for kinase activity.

Once the kinase activity of CaMKII is Ca^{2+}-independent (autonomous), and Ca^{2+}/CaM is no longer bound to the kinase, secondary sites that are within the CaM-binding site can be phosphorylated (T305/306 in CaMKIIα, and T306/307 in CaMKIIβ, γ, and δ) but these phosphorylation changes occur slowly because the rate of dissociation of Ca^{2+}/CaM is greatly decreased by phosphorylation at T286 [86, 87]. Once these sites are phosphorylated, CaM can no longer bind so CaMKII becomes insensitive to changes in Ca^{2+}/CaM but CaMKII remains active until T286/7 is dephosphorylated [88].

CaMKII can also be directly activated by Zn^{2+} independent of Ca^{2+}/CaM resulting in autophosphorylation of T306, T286 and S279. The level of phosphorylation of S279 in vitro increases with increasing Zn^{2+} concentration and inhibits CaMKII activity [89]. This may be particularly relevant in certain pathological conditions that involve elevated intracellular Zn^{2+} concentrations [90].

However, not all CaMKII phosphorylation sites modulate Ca^{2+}/CaM binding and kinase activity. A phosphorylation site on CaMKII at T253 was identified in vivo [91]. T253 has previously been overlooked as a phosphorylation site of interest because: (i) T253 phosphorylation has no direct effect on the kinase activity or Ca^{2+}/CaM binding of purified CaMKII in vitro [91]; (ii) T253 autophosphorylation of purified CaMKII in vitro occurs relatively slowly (at least 10 times slower than the phosphorylation of T286) under standard assay conditions [91]; and (iii) the overall stoichiometry of T253 phosphorylation in tissues and cells in vivo is relatively low [91] . However, subsequent studies have shown that the rate and extent of T253 phosphorylation is very sensitive to the molecular environment so that: (i) the rate of T253 phosphorylation in vivo can be very fast depending on the cell type and stimulus [70, 91–93]; (ii) by inducing interaction with specific binding

proteins, T253 phosphorylation can lead to allosteric activation of CaMKII [94]; and (iii) T253 phosphorylation only occurs in particular subpopulations of CaMKII at specific cellular locations and the stoichiometry of T253 phosphorylation at these locations can be high [91]. Therefore, T253 phosphorylation exerts its regulatory effects on CaMKII through modifying molecular targeting.

Other sites, such as S279 and S314, are phosphorylated both in vitro [89, 95, 96] and in vivo [97–99], but the stoichiometry of phosphorylation is relatively low and phosphorylation of S314 does not affect CaMKII activity in vitro. Although these sites have not been investigated for their effects on targeting, it is possible that, as with T253, their major functional role is to regulate molecular targeting rather than to directly modify enzyme activity.

Other forms of post-translational modification have also been demonstrated to alter CaMKII kinase activity. Specifically, a pair of methionine residues in CaMKII (M281/282), present in β, γ, and δ, but not α, isoforms, can become oxidised during periods of elevated reactive oxygen species and produce a conformational change in CaMKII similar to that produced following T286 phosphorylation leading to an autonomous activation of CaMKII [100]. Consequently, one might expect that M281/282 oxidation would also modify molecular targeting in a way that is similar to T286 phosphorylation, but this has not yet been investigated.

A detailed discussion of the mechanisms involved in molecular targeting is given in Section 2 with a specific focus on CaMKII.

26.2.6 Casein Kinase 1 (CK1)

The casein kinase 1 (CK1) family of multifunctional serine/threonine protein kinases are abundantly expressed in all eukaryotic organisms [101], and in a variety of tissues [102]. All organisms contain several isoforms [103], and 7 isoforms have been identified in vertebrates (α1, β, γ1, γ2, γ3, δ, ε), [104–106]. In addition, several splice variants exhibiting different biochemical and cellular properties also exist [107]. CK1 phosphorylates a variety of proteins that are involved in many cellular processes, including cell division, neurite outgrowth, differentiation, antiviral responses, circadian rhythms and metabolism [108–111].

CK1 phosphorylates a wide range of substrates [112–117] and shows a strong preference for 'primed' pre-phosphorylated substrates at N-3 (e.g. pS/T-X-X-S/T). However, CK1 can also phosphorylate unprimed substrates that contain a cluster of acidic amino acids in the N-3 position. Furthermore, CK1 purified from erythrocytes and Xenopus oocytes is able to phosphorylate tyrosine residues in vitro [118, 119], though it has not been determined whether this activity occurs in vivo.

The different isoforms/variants of CK1 are highly conserved within their catalytic domains but vary significantly in the length and structure of their regulatory domains, which contain multiple phosphorylation sites [120–122]. The catalytic domain of CK1 is similar to other kinases, with a smaller N-terminal lobe, a large C-terminal lobe, and an intermediate catalytic cleft where ATP and substrates bind.

CK1δ, ε, and γ3 have large C-terminal domains, which have been suggested to function as pseudosubstrates which, when phosphorylated, inhibit kinase activity [120, 123, 124]. The CK1 family of kinases have been described as monomeric, constitutively active enzymes. However, CK1δ has been suggested to form dimers [124], with this dimerisation potentially inhibiting its activity. This hypothesis has yet to be proven.

The precise mechanisms involved in regulating CK1 function have not been fully elucidated. CK1 was initially identified as being stimulated by Ca^{2+}/CaM [125, 126]. However, because CK1 is constitutively active, mechanisms controlled by second messengers can modify its activity but are not required for its initial activation, unlike many other kinases. The function of CK1 is regulated via a combination of phosphorylation and targeting to specific subcellular locations and via interactions with specific binding proteins. In addition, CK1ε can undergo limited proteolysis, which produces a protease-resistant core kinase with increased activity [121].

CK1 does not require phosphorylation on its activation loop for activity. CK1 can be autophosphorylated, or phosphorylated by PKA, PKB/Akt, CLK2 (CDC-like kinase 2) and PKC. Phosphorylation of CK1δ by these kinases at S370 decreases substrate phosphorylation efficiency [127]. Additionally, CK1ε can autophosphorylate at T44 in vivo, and phosphomimic mutation of this site activates TCF/LEF-driven transcription in breast cancer cell lines [128]. Several inhibitory autophosphorylation sites have been identified for CK1δ and ε (CK1δ at S331, S370, S382, D383, S384, S411 and CK1ε at S323, T325, T324, T337, S368, S405, T407, S408) [122, 123, 129–131]. Although CK1 can autophosphorylate in vivo, it is actively maintained in its dephosphorylated, active state by protein phosphatases [132, 133].

Similarly to CaMKII, there is a large body of evidence demonstrating that targeting is an important regulatory mechanism for controlling CK1 function in vivo. Studies in yeast [134–136], and more recently in higher organisms [137, 138], have demonstrated that the function of constitutively active CK1 is regulated by its subcellular localisation. For example, CK1α exhibits a cell cycle dependent subcellular distribution, interacting with cytosolic vesicles and nuclear structures during interphase, and the mitotic spindle during mitosis [139–142], with this localisation being controlled by the activity of CK1 [137]. In addition, domain swapping experiments performed with yeast CK1 demonstrate the interaction between CK1 and its substrates is controlled by subcellular distribution. Yeast encode four homologues of CK1, 3 of which localise to the plasma membrane, with the fourth being located at the nucleus [135, 143]. However, these homologues functionally complement each other when the localisation signals are switched [135], strongly supporting a role for subcellular targeting in regulating the function of CK1. Additionally, phosphorylation of CK1δ at T347 regulates CK1δ activity towards the PER protein, which regulates the circadian clock [144]. Furthermore, alternative splicing of isoforms influences substrate binding and subcellular location [107, 145–147] highlighting another layer of complexity in the regulation of CK1.

In addition, the function of CK1 varies depending on the proteins with which it is associated. For example, CK1ε only phosphorylates CRY when both proteins are

bound to PGR [148]. The phosphorylation state of CK1 can also affect its ability to interact with proteins. For example, the interaction between CK1α and 14-3-3 is dependent upon phosphorylation of CK1α [149]. By contrast, dephosphorylation of CK1ε increases activity towards the SV40 large T antigen, IκB and Ets-1 [121]. These examples highlight the importance of molecular targeting in mediating cell and tissue specific CK1 function in vivo.

26.3 Mechanisms of Molecular Targeting

Molecular targeting is an important regulatory mechanism for all the multifunctional calcium/calmodulin stimulated protein kinases but it has been most extensively studied in CaMKII. This is because the high level of expression of CaMKII in neurons, and the morphological complexity of neurons, made it easier to identify the heterogeneity of the responses of pools of CaMKII molecules in different cellular locations. Therefore, in this section, we will discuss the mechanisms involved in molecular targeting using CaMKII as the specific example, but the general principles outlined here apply to all the multifunctional kinases.

A wide range of proteins with varied functions have been shown to bind CaMKII (Table 26.2). The expression patterns of CaMKII binding proteins vary with cell type and also subcellular localisation. Additionally, phosphorylation of either the binding partner or CaMKII can alter their ability to bind CaMKII [4, 70]. As cells contain multiple pools of CaMKII (with different post-translational modifications and hence affinity for binding partners) these pools of CaMKII can respond differently to cellular stimulation, depending on the binding partner with which they are associated.

Fig. 26.2 shows a schematic diagram depicting how molecular targeting can generate different functional responses to cellular stimulation by multiple pools of CaMKII. Non-phosphorylated CaMKII, which has a protein binding site represented by a square on its surface, interacts with three different proteins in different cellular locations (A). When cellular stimulation produces a rise in intracellular Ca^{2+} and activation of CaMKII by Ca^{2+}/CaM, the different molecular environments provided by the three binding proteins cause the three pools of CaMKII to respond with a different pattern of autophosphorylation (A). This difference may be due to proximity to different ion channels or conformational changes induced in CaMKII by the interaction with the binding protein. The autophosphorylation induces a conformational change in the CaMKII that hides the binding site through which non-phosphorylated CaMKII interacted with its binding partners causing the phosphorylated CaMKII to dissociate from those binding proteins. Each pattern of autophosphorylation exposes a different binding site on the surface of CaMKII (pT286 – trapezium; pT253 – triangle; pT286+pT253 – circle) which allows that pool of CaMKII to interact with a different binding protein (purple) that has a matching complementary binding site (B and C). These events may involve translocation of CaMKII between protein complexes in the same region of the cell

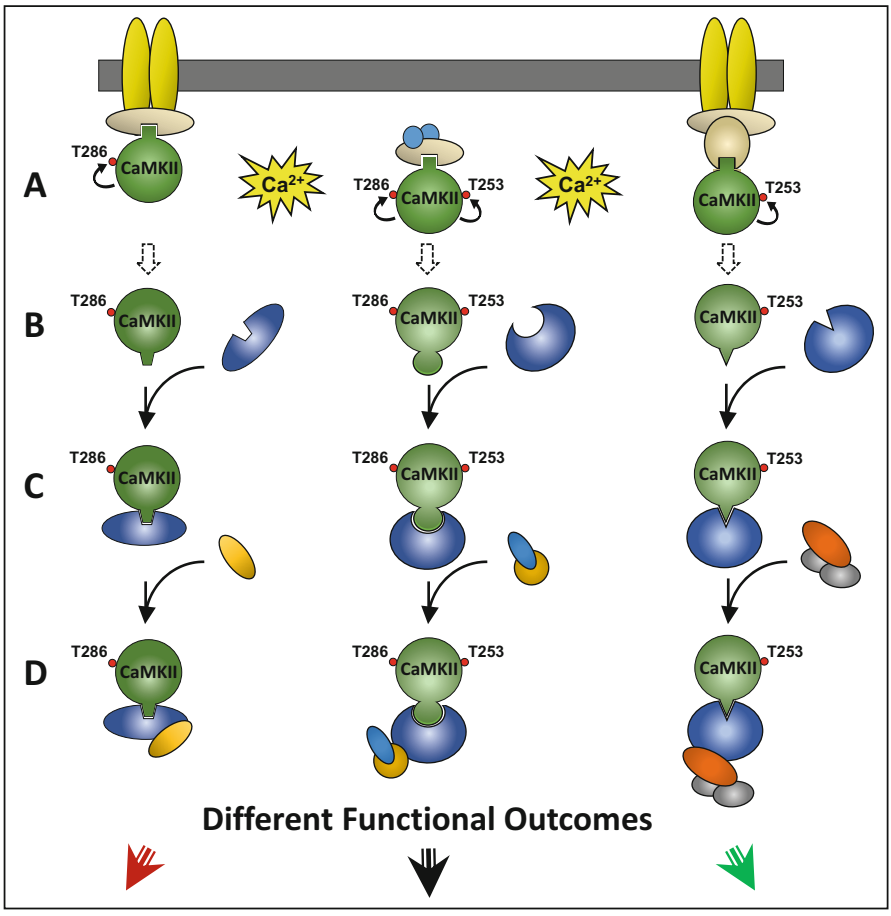

Fig. 26.2 Schematic diagram depicting how molecular targeting can create multiple pools of CaMKII that can generate different functional responses to cellular stimulation. (**a**) Non-phosphorylated CaMKII, which has a protein binding site represented by a square on its surface, interacts with three different proteins in different cellular locations. When cellular stimulation produces a rise in intracellular Ca^{2+} and activation of CaMKII by Ca^{2+}/CaM, the different molecular environments provided by the three binding proteins cause the three pools of CaMKII to respond with different patterns of autophosphorylation (curved arrows and red balls on CaMKII), namely phosphorylation at T286 (left) alone, T253 (right) alone or both T286 and T253 (middle). (**b**) This autophosphorylation induces a conformational change in CaMKII that hides the binding site through which non-phosphorylated CaMKII interacted with its binding partners causing the phosphorylated CaMKII to dissociate from those binding proteins. Each pattern of autophosphorylation exposes a different binding site on the surface of CaMKII (pT286 – trapezium; pT253 – triangle; pT286+pT253 – circle). (**c**) This allows that pool of CaMKII to interact with a different binding protein (dark blue) that has a matching complementary binding site. (**d**) Each CaMKII-binding protein complex then interacts with a different group of additional proteins targeting that pool of CaMKII to different substrates, possibly at different cellular locations, resulting in the activation of different downstream molecular events producing different functional outcomes

or in different subcellular compartments. Each CaMKII-binding protein complex then interacts with a different group of additional proteins targeting that pool of CaMKII to different substrates, possibly at different cellular locations (D), resulting in the activation of different downstream molecular events producing different functional outcomes. These targeted pools of CaMKII may be activated in their new location by Ca^{2+}/CaM following a subsequent rise in intracellular Ca^{2+}, or may be autonomously active due to phosphorylation at T286 or allosteric activation of pT253-CaMKII [150].

We have shown that phosphorylation of CaMKII at T253 is essential for CaMKII-mediated ischaemia-induced cell death [94]. Brain regions with enhanced sensitivity to ischaemic damage show enhanced ischaemia/excitotoxicty-induced phosphorylation of CaMKII at T253, but not T286 or T305/306, and this difference in response is intrinsic to the tissue and independent of blood perfusion, since excitotoxic stimulation of brain slices from different regions in vitro faithfully mimics the responses to cerebral ischaemia in vivo. [93]. Brain regions with enhanced sensitivity to ischaemia also express different patterns of CaMKII binding proteins compared to regions that are more resistant [70]. The interaction of pT253-CaMKII with one or more specific binding proteins activates the pT253-CaMKII by an induced conformational change that is independent of Ca^{2+}-calmodulin [150]. The binding protein targets the pT253-CaMKII to proteins associated with cell death pathway(s) allowing the sustained CaMKII activity to activate cell death responses. The specificity of these targeting mechanisms provides an opportunity for therapeutic intervention in conditions such as stroke through selectively disrupting the interaction between pT253-CaMKII and its specific binding protein. Using a peptide or other small molecule that mimics the pT253-induced binding site on CaMKII for the specific binding protein, the pT253-CaMKII could be displaced, thereby preventing the sustained CaMKII activity and its targeting to cell death pathways and consequently reducing the amount of cell death [150]. Importantly, such a small molecule inhibitor would specifically act on the key pool of pT253-CaMKII molecules without inhibiting the CaMKII molecules in other pools within the same cell or in other cells. Such an approach offers the potential of neuroprotective therapy with enhanced tissue specificity and reduced side effects. The fact that each CaMKII-mediated functional outcome depends on the interaction of a particular pool of CaMKII with a specific binding protein that targets it to molecular pathway involved, means that developing specific inhibitors of the interaction between CaMKII and particular targeting proteins has the potential of producing highly selective therapeutic agents in many clinical conditions.

In addition to differences in phosphorylation state, interaction with specific binding proteins can also be regulated by other factors. Several binding proteins interact with only particular isoforms or splice variants of CaMKII (Table 26.2). All four CaMKII genes undergo alternative splicing in their variable regions [151], which produces some variability in the kinase properties in vitro. However, the number of splice variants is much greater than the differences observed in enzyme activity and the splicing occurs in parts of the molecule well away from the catalytic domain and the autoinhibitory and Ca^{2+}/CaM binding regions suggesting that the

primary function of many of the splicing isoforms is not to alter enzyme activity. The αCaMKII-anchoring protein (αKAP), provides an unusual example of targeting. RNA splicing of CaMKIIα produces αKAP as a truncated, enzymatically inactive protein, which is mostly comprised of the association domain of CaMKIIα, and an N-terminal hydrophobic anchor sequence. αKAP is found in skeletal muscle and the heart, and is expressed at low levels in the lung, kidney, and testis [152]. αKAP can form heteromultimers with full length CaMKII, thereby targeting the active kinase subunits to the sarcoplasmic reticulum membrane in rat skeletal muscle [153].

A small number of splice variants of CaMKII contain a consensus nuclear localisation sequence and others contain specific binding sites for individual proteins (for example, the binding sequence for actin is specific to the CaMKIIβ isoform [154]). The fact that the association domain and the C-terminal part of the regulatory domain contain all the main sequence variations between isoforms of CaMKII suggests that these regions contains part or all of the binding sites for other proteins.

The change in interaction between CaMKII and its specific binding protein partners as a consequence of stimulus induced phosphorylation highlights the mobility of CaMKII involved in targeting. This was first identified in the brain where it was recognised that CaMKII is highly concentrated in certain cellular locations, such as the post synaptic density (PSD) and the cytoskeleton, and that the concentration at such sites can change by translocation from the cytoplasm. Translocation to the PSD can occur slowly during the normal maturation phase of brain development by a process that is sensitive to thyroid hormone [155]. Translocation can also occur rapidly to the cytoskeleton [156] and also to the PSD in response to excitotoxic stimulation, hypoxia or post-mortem delay [85, 157, 158]. Phosphorylation of CaMKII at T305/306 decreases the amount of CaMKII bound to the PSD and stimulates the translocation from the PSD to the cytosol [159]. By contrast, phosphorylation at either T286 or T253 stimulates translocation from the cytosol to the PSD and enhances binding to the PSD through different binding proteins [91]. Once located at the PSD CaMKII can bind to, and move between, a number of proteins and phosphorylate a variety of substrates [160].

Figure 26.3 shows a schematic representation of how stimulus-induced short distance translocation of CaMKII between different binding proteins in protein complexes (such as found in the PSD or the cytoskeleton) can modify CaMKII-mediated functional responses to stimulation. Panel A shows the effects of two sequential stimulus-induced rises in intracellular Ca^{2+} on CaMKII bound to a protein as part of a protein complex. Non-phosphorylated CaMKII is bound to one protein in the protein complex. The initial stimulus-induced rise in intracellular Ca^{2+} allows the non-phosphorylated CaMKII to be activated by Ca^{2+}/CaM and to phosphorylate itself and a nearby protein substrate in the protein complex (this functional response is denoted as response ①). The phospho-CaMKII dissociates from the protein to which the non-phosphorylated CaMKII was bound and binds to a neighbouring protein. When a subsequent stimulus-induced rise in intracellular Ca^{2+} activates the translocated phospho-CaMKII, it is able to phosphorylate two different sites on neighbouring proteins (this different functional response is denoted as response ②).

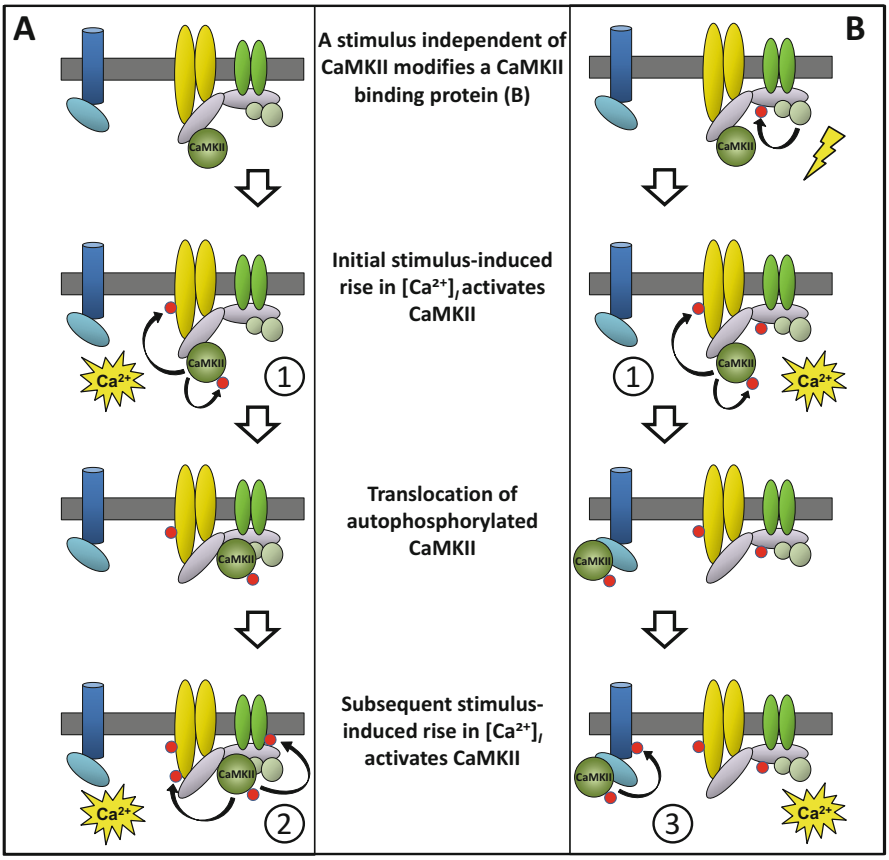

Fig. 26.3 A schematic representation of how stimulus-induced short distance translocation of CaMKII and cross talk between different signalling pathways can alter CaMKII-mediated responses. (**a**) The effects of two sequential stimulus-induced rises in intracellular Ca^{2+} on CaMKII bound to a protein as part of a protein complex. Non-phosphorylated CaMKII is bound to one protein in the protein complex. The initial stimulus-induced rise in intracellular Ca^{2+} allows the non-phosphorylated CaMKII to be activated by Ca^{2+}/CaM and to phosphorylate itself and a nearby protein substrate in the protein complex (curved arrows and red balls). This is functional response ①. The pCaMKII dissociates from the protein to which the non-phosphorylated CaMKII was bound and binds to a neighbouring protein. When a subsequent stimulus-induced rise in intracellular Ca^{2+} activates the translocated pCaMKII, it is able to phosphorylate two different sites on neighbouring proteins (functional response ②) (**b**) How cross talk between different signalling pathways can alter CaMKII-mediated responses. Non-phosphorylated CaMKII is bound to the same protein as in A when a different stimulus (yellow lightning bolt) activates a CaMKII-independent signalling pathway that phosphorylates the protein that binds pCaMKII following functional response ① in panel A. The initial stimulus-induced rise in intracellular Ca^{2+} produces the same functional response ① as in A. However, the pCaMKII now translocates to another pCaMKII binding protein in a nearby complex because the prior CaMKII-independent phosphorylation has prevented pCaMKII binding to the same protein as in A. When a subsequent stimulus-induced rise in intracellular Ca^{2+} activates the translocated pCaMKII, it is able to phosphorylate a different site on a neighbouring protein in the complex (functional response ③)

Therefore, the CaMKII-mediated functional outcome of the second stimulus can be altered by a previous stimulus of the same type. Panel B shows how cross talk between different signalling pathways can alter CaMKII-mediated responses. Non-phosphorylated CaMKII is bound to the same protein as in Panel A when a different stimulus (yellow lightning bolt) activates a CaMKII-independent signalling pathway that phosphorylates the protein which binds phospho-CaMKII following functional response ① in panel A′, inhibiting the ability of that protein to bind phospho-CaMKII. Following this change, the initial stimulus-induced rise in intracellular Ca^{2+} allows the non-phosphorylated CaMKII to be activated by Ca^{2+}/CaM and to produce the same functional response ① as in Panel A. However, when the phospho-CaMKII dissociates from the protein to which the non-phosphorylated CaMKII was bound, it can no longer bind to the same phospho-CaMKII binding protein as in Panel A because it has been phosphorylated in response to the earlier stimulus, so it binds to another phospho-CaMKII binding protein in a nearby complex. When a subsequent stimulus-induced rise in intracellular Ca^{2+} activates the translocated phospho-CaMKII, it is able to phosphorylate a different site on a neighbouring protein in the complex (this different functional response is denoted as response ③).

26.4 Conclusions

Multifunctional Ca^{2+}/CaM stimulated protein kinases are abundant, expressed in most tissues and are responsible for regulating a broad range of physiological functions. We have examined the multiple molecular control mechanisms that regulate the functional responses of these multifunctional kinases. We have focussed particularly on the mechanism of molecular targeting whereby the interaction of these kinases with specific binding proteins enables these enzymes to produce tissue-specific and stimulus-specific responses despite having broad substrate specificities.

As different cells express different complements of binding proteins, the microenvironment in which the kinase is located affects its response to different stimuli and the functional outcome from the stimulus. Understanding molecular targeting will allow us to have a better understanding of molecular mechanisms underlying normal and pathological cellular events. In addition, if cell specific mechanisms controlling kinase function can be identified, then drugs can be designed that will selectively disrupt interactions between widely expressed kinases and their substrates only in specific tissues or in response to specific stimuli. In the past, such widely expressed, multifunctional kinases have not been regarded as suitable drug targets for fear that lack of tissue- or stimulus-specificity would produce unwanted side-effects. But, with our developing understanding of how targeting can produce cell- and stimulus-specific responses in widely expressed kinases, the potential has arisen to achieve specific therapeutic outcomes for a variety of conditions and pathologies by developing drugs that disrupt specific

molecular targeting interactions, as proposed above in the case of pT253-CaMKII and ischaemia.

References

1. Rhoads AR, Friedberg F (1997) Sequence motifs for calmodulin recognition. FASEB J 11(5):331–340
2. Skelding KA, Rostas JA (2012) The role of molecular regulation and targeting in regulating calcium/calmodulin stimulated protein kinases. Adv Exp Med Biol 740:703–730
3. De Koninck P, Schulman H (1998) Sensitivity of CaM kinase II to the frequency of Ca^{2+} oscillations. Science 279(5348):227–230
4. Skelding KA, Rostas JA (2009) Regulation of CaMKII in vivo: the importance of targeting and the intracellular microenvironment. Neurochem Res 34(10):1792–1804
5. Racioppi L, Means AR (2012) Calcium/calmodulin-dependent protein kinase kinase 2: roles in signaling and pathophysiology. J Biol Chem 287(38):31658–31665
6. Selbert MA, Anderson KA, Huang QH, Goldstein EG, Means AR, Edelman AM (1995) Phosphorylation and activation of Ca^{2+}-calmodulin-dependent protein kinase IV by Ca^{2+}-calmodulin-dependent protein kinase Ia kinase. Phosphorylation of threonine 196 is essential for activation. J Biol Chem 270(29):17616–17621
7. Hsu LS, Chen GD, Lee LS, Chi CW, Cheng JF, Chen JY (2001) Human Ca^{2+}/calmodulin-dependent protein kinase kinase beta gene encodes multiple isoforms that display distinct kinase activity. J Biol Chem 276(33):31113–31123
8. Ohmstede CA, Jensen KF, Sahyoun NE (1989) Ca^{2+}/calmodulin-dependent protein kinase enriched in cerebellar granule cells. Identification of a novel neuronal calmodulin-dependent protein kinase. J Biol Chem 264(10):5866–5875
9. Anderson KA, Means RL, Huang QH, Kemp BE, Goldstein EG, Selbert MA et al (1998) Components of a calmodulin-dependent protein kinase cascade. Molecular cloning, functional characterization and cellular localization of Ca^{2+}/calmodulin-dependent protein kinase kinase beta. J Biol Chem 273(48):31880–31889
10. Hawley SA, Selbert MA, Goldstein EG, Edelman AM, Carling D, Hardie DG (1995) 5′-AMP activates the AMP-activated protein kinase cascade, and Ca^{2+}/calmodulin activates the calmodulin-dependent protein kinase I cascade, via three independent mechanisms. J Biol Chem 270(45):27186–27191
11. Yano S, Tokumitsu H, Soderling TR (1998) Calcium promotes cell survival through CaM-K kinase activation of the protein-kinase-B pathway. Nature 396(6711):584–587
12. Anderson KA, Means AR (2002) Defective signaling in a subpopulation of CD4(+) T cells in the absence of Ca^{2+}/calmodulin-dependent protein kinase IV. Mol Cell Biol 22(1):23–29
13. Neal AP, Molina-Campos E, Marrero-Rosado B, Bradford AB, Fox SM, Kovalova N et al (2010) CaMKK-CaMKI signaling pathways differentially control axon and dendrite elongation in cortical neurons. J Neurosci 30(8):2807–2809
14. Kitsos CM, Sankar U, Illario M, Colomer-Font JM, Duncan AW, Ribar TJ et al (2005) Calmodulin-dependent protein kinase IV regulates hematopoietic stem cell maintenance. J Biol Chem 280(39):33101–33108
15. Kahl CR, Means AR (2004) Regulation of cyclin D1/Cdk4 complexes by calcium/calmodulin-dependent protein kinase I. J Biol Chem 279(15):15411–15419
16. Anderson KA, Ribar TJ, Illario M, Means AR (1997) Defective survival and activation of thymocytes in transgenic mice expressing a catalytically inactive form of Ca^{2+}/calmodulin-dependent protein kinase IV. Mol Endocrinol 11(6):725–737
17. Wayman GA, Lee YS, Tokumitsu H, Silva AJ, Soderling TR (2008) Calmodulin-kinases: modulators of neuronal development and plasticity. Neuron 59(6):914–931

18. Tokumitsu H, Soderling TR (1996) Requirements for calcium and calmodulin in the calmodulin kinase activation cascade. J Biol Chem 271(10):5617–5622
19. Hawley SA, Davison M, Woods A, Davies SP, Beri RK, Carling D et al (1996) Characterization of the AMP-activated protein kinase kinase from rat liver and identification of threonine 172 as the major site at which it phosphorylates AMP-activated protein kinase. J Biol Chem 271(44):27879–27887
20. Edelman AM, Mitchelhill KI, Selbert MA, Anderson KA, Hook SS, Stapleton D et al (1996) Multiple Ca^{2+}-calmodulin-dependent protein kinase kinases from rat brain. Purification, regulation by Ca^{2+}-calmodulin, and partial amino acid sequence. J Biol Chem 271(18):10806–10810
21. Okuno S, Kitani T, Fujisawa H (2001) Regulation of Ca^{2+}/calmodulin-dependent protein kinase kinase alpha by cAMP-dependent protein kinase: I. Biochemical analysis. J Biochem 130(4):503–513
22. Tokumitsu H, Takahashi N, Eto K, Yano S, Soderling TR, Muramatsu M (1999) Substrate recognition by Ca^{2+}/Calmodulin-dependent protein kinase kinase. Role of the arg-pro-rich insert domain. J Biol Chem 274(22):15803–15810
23. Davare MA, Saneyoshi T, Guire ES, Nygaard SC, Soderling TR (2004) Inhibition of calcium/calmodulin-dependent protein kinase kinase by protein 14-3-3. J Biol Chem 279(50):52191–52199
24. Wayman GA, Tokumitsu H, Soderling TR (1997) Inhibitory cross-talk by cAMP kinase on the calmodulin-dependent protein kinase cascade. J Biol Chem 272(26):16073–16076
25. Matsushita M, Nairn AC (1999) Inhibition of the Ca^{2+}/calmodulin-dependent protein kinase I cascade by cAMP-dependent protein kinase. J Biol Chem 274(15):10086–10093
26. Green MF, Scott JW, Steel R, Oakhill JS, Kemp BE, Means AR (2011) Ca^{2+}/calmodulin-dependent protein kinase kinase beta is regulated by multisite phosphorylation. J Biol Chem 286(32):28066–28079
27. Psenakova K, Petrvalska O, Kylarova S, Lentini Santo D, Kalabova D, Herman P et al (2018) 14-3-3 protein directly interacts with the kinase domain of calcium/calmodulin-dependent protein kinase kinase (CaMKK2). Biochim Biophys Acta. ePub ahead of print
28. Guest CB, Deszo EL, Hartman ME, York JM, Kelley KW, Freund GG (2008) Ca^{2+}/calmodulin-dependent kinase kinase alpha is expressed by monocytic cells and regulates the activation profile. Plos One 3(2):e1606
29. Picciotto MR, Zoli M, Bertuzzi G, Nairn AC (1995) Immunochemical localization of calcium/calmodulin-dependent protein kinase I. Synapse 20(1):75–84
30. Rasmussen CD (2000) Cloning of a calmodulin kinase I homologue from Schizosaccharomyces pombe. J Biol Chem 275(1):685–690
31. Skelding KA, Rostas JA, Verrills NM (2011) Controlling the cell cycle: the role of calcium/calmodulin-stimulated protein kinases I and II. Cell Cycle 10(4):631–639
32. Nairn AC, Greengard P (1987) Purification and characterization of Ca^{2+}/calmodulin-dependent protein kinase I from bovine brain. J Biol Chem 262(15):7273–7281
33. Wayman GA, Kaech S, Grant WF, Davare M, Impey S, Tokumitsu H et al (2004) Regulation of axonal extension and growth cone motility by calmodulin-dependent protein kinase I. J Neurosci 24(15):3786–3794
34. Condon JC, Pezzi V, Drummond BM, Yin S, Rainey WE (2002) Calmodulin-dependent kinase I regulates adrenal cell expression of aldosterone synthase. Endocrinology 143(9):3651–3657
35. Jusuf AA, Sakagami H, Kikkawa S, Terashima T (2016) Expression of beta subunit 2 of Ca(2)+/calmodulin-dependent protein kinase I in the developing rat retina. Kobe J Med Sci 61(4):E115–E123
36. Haribabu B, Hook SS, Selbert MA, Goldstein EG, Tomhave ED, Edelman AM et al (1995) Human calcium-calmodulin dependent protein-kinase-I – CDNA cloning, domain-structure and activation by phosphorylation at threonine-177 by calcium-calmodulin dependent protein-kinase-I kinase. EMBO J 14(15):3679–3686

37. Hook SS, Kemp BE, Means AR (1999) Peptide specificity determinants at P-7 and P-6 enhance the catalytic efficiency of Ca^{2+}/calmodulin-dependent protein kinase I in the absence of activation loop phosphorylation. J Biol Chem 274(29):20215–20222
38. Senga Y, Ishida A, Shigeri Y, Kameshita I, Sueyoshi N (2015) The phosphatase-resistant isoform of CaMKI, Ca(2)(+)/calmodulin-dependent protein kinase Idelta (CaMKIdelta), remains in its "Primed" form without Ca(2)(+) stimulation. Biochemistry 54(23):3617–3630
39. Stedman DR, Uboha NV, Stedman TT, Nairn AC, Picciotto MR (2004) Cytoplasmic localization of calcium/calmodulin-dependent protein kinase I-alpha depends on a nuclear export signal in its regulatory domain. FEBS Lett 566(1-3):275–280
40. Sakagami H, Kamata A, Nishimura H, Kasahara J, Owada Y, Takeuchi Y et al (2005) Prominent expression and activity-dependent nuclear translocation of Ca^{2+}/calmodulin-dependent protein kinase I delta in hippocampal neurons. Eur J Neurosci 22(11):2697–2707
41. Wu JY, Gonzalez-Robayana IJ, Richards JS, Means AR (2000) Female fertility is reduced in mice lacking Ca^{2+}/calmodulin-dependent protein kinase IV. Endocrinology 141:4777–4783
42. Wu JY, Means AR (2000) Ca^{2+}/calmodulin-dependent protein kinase IV is expressed in spermatids and targeted to chromatin and the nuclear matrix. J Biol Chem 275(11):7994–7999
43. Kimura Y, Corcoran EE, Eto K, Gengyo-Ando K, Muramatsu MA, Kobayashi R et al (2002) A CaMK cascade activates CRE-mediated transcription in neurons of Caenorhabditis elegans. EMBO Rep 3(10):962–966
44. Bleier J, Toliver A (2017) Exploring the role of CaMKIV in homeostatic plasticity. J Neurosci 37(48):11520–11522
45. Takemura M, Mishima T, Wang Y, Kasahara J, Fukunaga K, Ohashi K et al (2009) Ca^{2+}/calmodulin-dependent protein kinase IV-mediated LIM kinase activation is critical for calcium signal-induced neurite outgrowth. J Biol Chem 284(42):28554–28562
46. Wei F, Qiu CS, Liauw J, Robinson DA, Ho N, Chatila T et al (2002) Calcium calmodulin-dependent protein kinase IV is required for fear memory. Nat Neurosci 5(6):573–579
47. Racioppi L, Means AR (2008) Calcium/calmodulin-dependent kinase IV in immune and inflammatory responses: novel routes for an ancient traveller. Trends Immunol 29(12):600–607
48. Gu R, Ding M, Shi D, Huang T, Guo M, Yu L et al (2018) Calcium/calmodulin-dependent protein kinase IV mediates IFN-gamma-induced immune behaviors in skeletal muscle cells. Cell Physiol Biochem 46(1):351–364
49. Shi D, Gu R, Song Y, Ding M, Huang T, Guo M et al (2018) Calcium/calmodulin-dependent protein kinase IV (CaMKIV) mediates acute skeletal muscle inflammatory response. Inflammation 41(1):199–212
50. Wei YP, Ye JW, Wang X, Zhu LP, Hu QH, Wang Q et al (2018) Tau-induced Ca^{2+}/calmodulin-dependent protein kinase-IV activation aggravates nuclear Tau hyperphosphorylation. Neurosci Bull 34(2):261–269
51. Zhao X, Shen L, Xu L, Wang Z, Ma C, Huang Y (2016) Inhibition of CaMKIV relieves streptozotocin-induced diabetic neuropathic pain through regulation of HMGB1. BMC Anesthesiol 16(1):27
52. Swulius MT, Waxham MN (2008) Ca^{2+}/calmodulin-dependent protein kinases. Cell Mol Life Sci 65(17):2637–2657
53. Murao K, Li J, Imachi H, Muraoka T, Masugata H, Zhang GX et al (2009) Exendin-4 regulates glucokinase expression by CaMKK/CaMKIV pathway in pancreatic beta-cell line. Diabetes Obes Metab 11(10):939–946
54. Lemrow SM, Anderson KA, Joseph JD, Ribar TJ, Noeldner PK, Means AR (2004) Catalytic activity is required for calcium/calmodulin-dependent protein kinase IV to enter the nucleus. J Biol Chem 279(12):11664–11671
55. Lalonde J, Lachance PE, Chaudhuri A (2004) Monocular enucleation induces nuclear localization of calcium/calmodulin-dependent protein kinase IV in cortical interneurons of adult monkey area V1. J Neurosci 24(2):554–564

56. Miller SG, Kennedy MB (1985) Distinct forebrain and cerebellar isozymes of type II Ca^{2+}/calmodulin-dependent protein kinase associate differently with the postsynaptic density fraction. J Biol Chem 260(15):9039–9046
57. Hudmon A, Schulman H (2002) Neuronal CA^{2+}/calmodulin-dependent protein kinase II: the role of structure and autoregulation in cellular function. Annu Rev Biochem 71:473–510
58. Lisman J, Schulman H, Cline H (2002) The molecular basis of CaMKII function in synaptic and behavioural memory. Nat Rev Neurosci 3(3):175–190
59. Ohyama A, Hosaka K, Komiya Y, Akagawa K, Yamauchi E, Taniguchi H et al (2002) Regulation of exocytosis through Ca^{2+}/ATP-dependent binding of autophosphorylated Ca^{2+}/calmodulin-activated protein kinase II to syntaxin 1A. J Neurosci 22(9):3342–3351
60. Giese KP, Fedorov NB, Filipkowski RK, Silva AJ (1998) Autophosphorylation at Thr286 of the alpha calcium-calmodulin kinase II in LTP and learning. Science 279(5352):870–873
61. Miller S, Yasuda M, Coats JK, Jones Y, Martone ME, Mayford M (2002) Disruption of dendritic translation of CaMKIIalpha impairs stabilization of synaptic plasticity and memory consolidation. Neuron 36(3):507–519
62. Soderling TR, Derkach VA (2000) Postsynaptic protein phosphorylation and LTP. Trends Neurosci 23(2):75–80
63. Taha S, Hanover JL, Silva AJ, Stryker MP (2002) Autophosphorylation of alphaCaMKII is required for ocular dominance plasticity. Neuron 36(3):483–491
64. Cao X, Wang H, Mei B, An S, Yin L, Wang LP et al (2008) Inducible and selective erasure of memories in the mouse brain via chemical-genetic manipulation. Neuron 60(2):353–366
65. von Hertzen LS, Giese KP (2005) Alpha-isoform of Ca^{2+}/calmodulin-dependent kinase II autophosphorylation is required for memory consolidation-specific transcription. Neuroreport 16(12):1411–1414
66. Vigil FA, Giese KP (2018) Calcium/calmodulin-dependent kinase II and memory destabilization: a new role in memorymaintenance. J Neurochem.. ePub ahead of print
67. Li X, Goel P, Wondolowski J, Paluch J, Dickman D (2018) A glutamate homeostat controls the presynaptic inhibition of neurotransmitter release. Cell Rep 23(6):1716–1727
68. Nicole O, Bell DM, Leste-Lasserre T, Doat H, Guillemot F, Pacary E (2018) A novel role for CAMKIIbeta in the regulation of cortical neuron migration: implications for neurodevelopmental disorders. Mol Psychiatry. ePub ahead of print.
69. Jones KT (2007) Intracellular calcium in the fertilization and development of mammalian eggs. Clin Exp Pharmacol Physiol 34(10):1084–1089
70. Skelding KA, Suzuki T, Gordon S, Xue J, Verrills NM, Dickson PW et al (2010) Regulation of CaMKII by phospho-Thr253 or phospho-Thr286 sensitive targeting alters cellular function. Cell Signal 22(5):759–769
71. Hoffman A, Carpenter H, Kahl R, Watt LF, Dickson PW, Rostas JAP et al (2014) Dephosphorylation of CaMKII at T253 controls the metaphase-anaphase transition. Cellular Signal 26(4):748–756
72. Shin MK, Kim MK, Bae YS, Jo I, Lee SJ, Chung CP et al (2008) A novel collagen-binding peptide promotes osteogenic differentiation via Ca^{2+}/calmodulin-dependent protein kinase II/ERK/AP-1 signaling pathway in human bone marrow-derived mesenchymal stem cells. Cell Signal 20(4):613–624
73. Munevar S, Gangopadhyay SS, Gallant C, Colombo B, Sellke FW, Morgan KG (2008) CaMKIIT287 and T305 regulate history-dependent increases in alpha agonist-induced vascular tone. J Cell Mol Med 12(1):219–226
74. Maier LS, Bers DM (2007) Role of Ca^{2+}/calmodulin-dependent protein kinase (CaMK) in excitation-contraction coupling in the heart. Cardiovasc Res 73(4):631–640
75. Chi M, Evans H, Gilchrist J, Mayhew J, Hoffman A, Pearsall EA et al (2016) Phosphorylation of calcium/calmodulin-stimulated protein kinase II at T286 enhances invasion and migration of human breast cancer cells. Sci Rep 6:33132
76. Liu Z, Han G, Cao Y, Wang Y, Gong H (2014) Calcium/calmodulindependent protein kinase II enhances metastasis of human gastric cancer by upregulating nuclear factorkappaB and Aktmediated matrix metalloproteinase9 production. Mol Med Rep 10(5):2459–2464

77. Abdul Majeed ABB, Pearsall E, Carpenter H, Brzozowski J, Dickson PW, Rostas JAP et al (2014) CaMKII kinase activity, targeting and control of cellular functions: effect of single and double phosphorylation of CaMKIIalpha. Calcium Signal 1:36–51
78. Sun X, Cao H, Zhan L, Yin C, Wang G, Liang P et al (2018) Mitochondrial fission promotes cell migration by Ca^{2+} /CaMKII/ERK/FAK pathway in hepatocellular carcinoma. Liver Int 38(7):1263–1272
79. Yu G, Cheng CJ, Lin SC, Lee YC, Frigo DE, Yu-Lee LY et al (2018) Organelle-derived acetyl-CoA promotes prostate cancer cell survival, migration, and metastasis via activation of calmodulin kinase II. Cancer Res 78(10):2490–2502
80. Rosenberg OS, Deindl S, Sung RJ, Nairn AC, Kuriyan J (2005) Structure of the autoinhibited kinase domain of CaMKII and SAXS analysis of the holoenzyme. Cell 123(5):849–860
81. Kolb SJ, Hudmon A, Ginsberg TR, Waxham MN (1998) Identification of domains essential for the assembly of calcium/calmodulin-dependent protein kinase II holoenzymes. J Biol Chem 273(47):31555–31564
82. Hanson PI, Meyer T, Stryer L, Schulman H (1994) Dual role of calmodulin in autophosphorylation of multifunctional cam kinase may underlie decoding of calcium signals. Neuron 12(5):943–956
83. Meyer T, Hanson PI, Stryer L, Schulman H (1992) Calmodulin trapping by calcium-calmodulin-dependent protein kinase. Science 256(5060):1199–1202
84. Strack S, Colbran RJ (1998) Autophosphorylation-dependent targeting of calcium/calmodulin-dependent protein kinase II by the NR2B subunit of the N-methyl- D-aspartate receptor. J Biol Chem 273(33):20689–20692
85. Strack S, Choi S, Lovinger DM, Colbran RJ (1997) Translocation of autophosphorylated calcium/calmodulin-dependent protein kinase II to the postsynaptic density. J Biol Chem 272(21):13467–13470
86. Hanson PI, Schulman H (1992) Inhibitory autophosphorylation of multifunctional Ca^{2+}/calmodulin-dependent protein kinase analyzed by site-directed mutagenesis. J Biol Chem 267(24):17216–17224
87. Patton BL, Miller SG, Kennedy MB (1990) Activation of type II calcium/calmodulin-dependent protein kinase by Ca^{2+}/calmodulin is inhibited by autophosphorylation of threonine within the calmodulin-binding domain. J Biol Chem 265:11204–11212
88. Kato K, Iwamoto T, Kida S (2013) Interactions between alphaCaMKII and calmodulin in living cells: conformational changes arising from CaM-dependent and -independent relationships. Mol Brain 6:37
89. Lengyel I, Fieuw-Makaroff S, Hall AL, Sim AT, Rostas JA, Dunkley PR (2000) Modulation of the phosphorylation and activity of calcium/calmodulin-dependent protein kinase II by zinc. J Neurochem 75(2):594–605
90. Mizuno D, Kawahara M (2013) The molecular mechanisms of zinc neurotoxicity and the pathogenesis of vascular type senile dementia. Int J Mol Sci 14(11):22067–22081
91. Migues PV, Lehmann IT, Fluechter L, Cammarota M, Gurd JW, Sim ATR et al (2006) Phosphorylation of CaMKII at Thr253 occurs in vivo and enhances binding to isolated postsynaptic densities. J Neurochem 98(1):289–299
92. Gurd JW, Rawof S, Zhen Huo J, Dykstra C, Bissoon N, Teves L et al (2008) Ischemia and status epilepitcus result in enhanced phosphorylation of calcium and calmodulin-stimulated protein kinase II on threonine 253. Brain Res 1218:158–165
93. Skelding KA, Spratt NJ, Fluechter L, Dickson PW, Rostas JAP (2012) alpha CaMKII is differentially regulated in brain regions that exhibit differing sensitivities to ischemia and excitotoxicity. J Cerebr Blood F Met 32(12):2181–2192
94. Rostas JA, Hoffman A, Murtha LA, Pepperall D, McLeod DD, Dickson PW et al (2017) Ischaemia- and excitotoxicity-induced CaMKII-Mediated neuronal cell death: the relative roles of CaMKII autophosphorylation at T286 and T253. Neurochem Int. 104:6–10
95. Hanson PI, Kapiloff MS, Lou LL, Rosenfeld MG, Schulman H (1989) Expression of a multifunctional Ca^{2+}/calmodulin-dependent protein kinase and mutational analysis of its autoregulation. Neuron. 3(1):59–70

96. Colbran RJ, Soderling TR (1990) Calcium calmodulin-independent autophosphorylation sites of calcium calmodulin-dependent protein kinase-II – studies on the effect of phosphorylation of threonine-305/306 and serine-314 on calmodulin binding using synthetic peptides. J Biol Chem 265(19):11213–11219
97. Jaffe H, Vinade L, Dosemeci A (2004) Identification of novel phosphorylation sites on postsynaptic density proteins. Biochem Biophys Res Commun 321(1):210–218
98. Molloy SS, Kennedy MB (1991) Autophosphorylation of type II Ca^{2+}/calmodulin-dependent protein kinase in cultures of postnatal rat hippocampal slices. Proc Natl Acad Sci U S A 88(11):4756–4760
99. Collins MO, Yu L, Coba MP, Husi H, Campuzano I, Blackstock WP et al (2005) Proteomic analysis of in vivo phosphorylated synaptic proteins. J Biol Chem 280(7):5972–5982
100. Erickson JR, Joiner ML, Guan X, Kutschke W, Yang J, Oddis CV et al (2008) A dynamic pathway for calcium-independent activation of CaMKII by methionine oxidation. Cell 133(3):462–474
101. Tuazon PT, Traugh JA (1991) Casein kinase I and II–multipotential serine protein kinases: structure, function, and regulation. Adv Second Messenger Phosphoprotein Res 23:123–164
102. Nakajo S, Hagiwara T, Nakaya K, Nakamura Y (1987) Tissue distribution of casein kinases. Biochem Int 14(1):701–707
103. Manning G, Whyte DB, Martinez R, Hunter T, Sudarsanam S (2002) The protein kinase complement of the human genome. Science 298(5600):1912–1934
104. Rowles J, Slaughter C, Moomaw C, Hsu J, Cobb MH (1991) Purification of casein kinase I and isolation of cDNAs encoding multiple casein kinase I-like enzymes. Proc Natl Acad Sci U S A 88(21):9548–9552
105. Tapia C, Featherstone T, Gomez C, Taillon-Miller P, Allende CC, Allende JE (1994) Cloning and chromosomal localization of the gene coding for human protein kinase CK1. FEBS Lett 349(2):307–312
106. Fish KJ, Cegielska A, Getman ME, Landes GM, Virshup DM (1995) Isolation and characterization of human casein kinase I epsilon (CKI), a novel member of the CKI gene family. J Biol Chem 270(25):14875–14883
107. Burzio V, Antonelli M, Allende CC, Allende JE (2002) Biochemical and cellular characteristics of the four splice variants of protein kinase CK1alpha from zebrafish (Danio rerio). J Cell Biochem 86(4):805–814
108. Vielhaber E, Virshup DM (2001) Casein kinase I: from obscurity to center stage. IUBMB Life 51(2):73–78
109. Zhang L, Li H, Chen Y, Gao X, Lu Z, Gao L et al (2017) The down-regulation of casein kinase 1 alpha as a host defense response against infectious bursal disease virus infection. Virology 512:211–221
110. Bischof J, Muller A, Fander M, Knippschild U, Fischer D (2011) Neurite outgrowth of mature retinal ganglion cells and PC12 cells requires activity of CK1delta and CK1epsilon. PLoS One. 6(6):e20857
111. Zhang B, Butler AM, Shi Q, Xing S, Herman PK (2018) P-body localization of the Hrr25/CK1 protein kinase is required for the completion of meiosis. Mol Cell Biol. ePub ahead of print.
112. Pulgar V, Marin O, Meggio F, Allende CC, Allende JE, Pinna LA (1999) Optimal sequences for non-phosphate-directed phosphorylation by protein kinase CK1 (casein kinase-1) – a re-evaluation. Eur J Biochem 260(2):520–526
113. Marin O, Bustos VH, Cesaro L, Meggio F, Pagano MA, Antonelli M et al (2003) A noncanonical sequence phosphorylated by casein kinase 1 in beta-catenin may play a role in casein kinase 1 targeting of important signaling proteins. P Natl Acad Sci USA 100(18):10193–10200
114. Flotow H, Graves PR, Wang AQ, Fiol CJ, Roeske RW, Roach PJ (1990) Phosphate groups as substrate determinants for casein kinase I action. J Biol Chem 265(24):14264–14269
115. Flotow H, Roach PJ (1991) Role of acidic residues as substrate determinants for casein kinase-I. J Biol Chem 266(6):3724–3727

116. Meggio F, Perich JW, Reynolds EC, Pinna LA (1991) A synthetic beta-casein phosphopeptide and analogs as model substrates for casein kinase-1, a ubiquitous, phosphate directed protein-kinase. Febs Letters 283(2):303–306
117. Bustos VH, Marin O, Meggio F, Cesaro L, Allende CC, Allende JE et al (2005) Generation of protein kinase Ck1alpha mutants which discriminate between canonical and non-canonical substrates. Biochem J 391(Pt 2):417–424
118. Pulgar V, Tapia C, Vignolo P, Santos J, Sunkel CE, Allende CC et al (1996) The recombinant alpha isoform of protein kinase CK1 from Xenopus laevis can phosphorylate tyrosine in synthetic substrates. Eur J Biochem 242(3):519–528
119. Braun S, Raymond WE, Racker E (1984) Synthetic tyrosine polymers as substrates and inhibitors of tyrosine-specific protein-kinases. J Biol Chem 259(4):2051–2054
120. Graves PR, Roach PJ (1995) Role of COOH-terminal phosphorylation in the regulation of casein kinase I delta. J Biol Chem 270(37):21689–21694
121. Cegielska A, Gietzen KF, Rivers A, Virshup DM (1998) Autoinhibition of casein kinase I epsilon (CKI epsilon) is relieved by protein phosphatases and limited proteolysis. J Biol Chem 273(3):1357–1364
122. Gietzen KF, Virshup DM (1999) Identification of inhibitory autophosphorylation sites in casein kinase I epsilon. J Biol Chem 274(45):32063–32070
123. Zhai L, Graves PR, Robinson LC, Italiano M, Culbertson MR, Rowles J et al (1995) Casein kinase I gamma subfamily. Molecular cloning, expression, and characterization of three mammalian isoforms and complementation of defects in the Saccharomyces cerevisiae YCK genes. J Biol Chem 270(21):12717–12724
124. Longenecker KL, Roach PJ, Hurley TD (1998) Crystallographic studies of casein kinase I delta toward a structural understanding of auto-inhibition. Acta Crystallogr D Biol Crystallogr 54(Pt 3):473–475
125. Kuret J, Schulman H (1984) Purification and characterization of a Ca^{2+}/calmodulin-dependent protein kinase from rat brain. Biochemistry 23(23):5495–5504
126. Brooks CL, Landt M (1984) Calcium-ion and calmodulin-dependent kappa-casein kinase in rat mammary acini. Biochem J 224(1):195–200
127. Giamas G, Hirner H, Shoshiashvili L, Grothey A, Gessert S, Kuhl M et al (2007) Phosphorylation of CK1delta: identification of Ser370 as the major phosphorylation site targeted by PKA in vitro and in vivo. Biochem J 406(3):389–398
128. Foldynova-Trantirkova S, Sekyrova P, Tmejova K, Brumovska E, Bernatik O, Blankenfeldt W et al (2010) Breast cancer-specific mutations in CK1epsilon inhibit Wnt/beta-catenin and activate the Wnt/Rac1/JNK and NFAT pathways to decrease cell adhesion and promote cell migration. Breast Cancer Res 12(3):R30
129. Graves PR, Haas DW, Hagedorn CH, DePaoli-Roach AA, Roach PJ (1993) Molecular cloning, expression, and characterization of a 49-kilodalton casein kinase I isoform from rat testis. J Biol Chem 268(9):6394–6401
130. Carmel G, Leichus B, Cheng X, Patterson SD, Mirza U, Chait BT et al (1994) Expression, purification, crystallization, and preliminary x-ray analysis of casein kinase-1 from Schizosaccharomyces pombe. J Biol Chem 269(10):7304–7309
131. Schittek B, Sinnberg T (2014) Biological functions of casein kinase 1 isoforms and putative roles in tumorigenesis. Mol Cancer 13:231
132. Rivers A, Gietzen KF, Vielhaber E, Virshup DM (1998) Regulation of casein kinase I epsilon and casein kinase I delta by an in vivo futile phosphorylation cycle. J Biol Chem 273(26):15980–15984
133. Swiatek W, Tsai IC, Klimowski L, Pepler A, Barnette J, Yost HJ et al (2004) Regulation of casein kinase I epsilon activity by Wnt signaling. J Biol Chem 279(13):13011–13017
134. Wang PC, Vancura A, Mitcheson TG, Kuret J (1992) Two genes in Saccharomyces cerevisiae encode a membrane-bound form of casein kinase-1. Mol Biol Cell 3(3):275–286
135. Vancura A, Sessler A, Leichus B, Kuret J (1994) A prenylation motif is required for plasma membrane localization and biochemical function of casein kinase I in budding yeast. J Biol Chem 269(30):19271–19278

136. Ho Y, Mason S, Kobayashi R, Hoekstra M, Andrews B (1997) Role of the casein kinase I isoform, Hrr25, and the cell cycle-regulatory transcription factor, SBF, in the transcriptional response to DNA damage in Saccharomyces cerevisiae. Proc Natl Acad Sci U S A 94(2):581–586
137. Milne DM, Looby P, Meek DW (2001) Catalytic activity of protein kinase CK1 delta (casein kinase 1delta) is essential for its normal subcellular localization. Exp Cell Res 263(1):43–54
138. Yin H, Laguna KA, Li G, Kuret J (2006) Dysbindin structural homologue CK1BP is an isoform-selective binding partner of human casein kinase-1. Biochemistry 45(16):5297–5308
139. Gross SD, Hoffman DP, Fisette PL, Baas P, Anderson RA (1995) A phosphatidylinositol 4,5-bisphosphate-sensitive casein kinase I alpha associates with synaptic vesicles and phosphorylates a subset of vesicle proteins. J Cell Biol 130(3):711–724
140. Gross SD, Simerly C, Schatten G, Anderson RA (1997) A casein kinase I isoform is required for proper cell cycle progression in the fertilized mouse oocyte. J Cell Sci 110:3083–3090
141. Brockman JL, Gross SD, Sussman MR, Anderson RA (1992) Cell cycle-dependent localization of casein kinase I to mitotic spindles. Proc Natl Acad Sci U S A 89(20):9454–9458
142. Elmore ZC, Guillen RX, Gould KL (2018) The kinase domain of CK1 enzymes contains the localization cue essential for compartmentalized signaling at the spindle pole. Mol Biol Cell. ePub ahead of print. mbcE18020129
143. Wang X, Hoekstra MF, DeMaggio AJ, Dhillon N, Vancura A, Kuret J et al (1996) Prenylated isoforms of yeast casein kinase I, including the novel Yck3p, suppress the gcs1 blockage of cell proliferation from stationary phase. Mol Cell Biol 16(10):5375–5385
144. GWL E, Edison, Virshup DM (2017) Site-specific phosphorylation of casein kinase 1 delta (CK1delta) regulates its activity towards the circadian regulator PER2. PLoS One 12(5):e0177834
145. Zhang J, Gross SD, Schroeder MD, Anderson RA (1996) Casein kinase I alpha and alpha L: alternative splicing-generated kinases exhibit different catalytic properties. Biochemistry 35(50):16319–16327
146. Takano A, Hoe HS, Isojima Y, Nagai K (2004) Analysis of the expression, localization and activity of rat casein kinase 1epsilon-3. Neuroreport 15(9):1461–1464
147. Kannanayakal TJ, Tao H, Vandre DD, Kuret J (2006) Casein kinase-1 isoforms differentially associate with neurofibrillary and granulovacuolar degeneration lesions. Acta Neuropathol 111(5):413–421
148. Eide EJ, Vielhaber EL, Hinz WA, Virshup DM (2002) The circadian regulatory proteins BMAL1 and cryptochromes are substrates of casein kinase Iepsilon. J Biol Chem 277(19):17248–17254
149. Clokie S, Falconer H, Mackie S, Dubois T, Aitken A (2009) The interaction between casein kinase Ialpha and 14-3-3 is phosphorylation dependent. FEBS J. 276(23):6971–6984
150. Rostas JAP, Spratt NJ, Dickson PW, Skelding KA (2017) The role of Ca^{2+}-calmodulin stimulated protein kinase II in ischaemic stroke – A potential target for neuroprotective therapies. Neurochem Int 107:33–42
151. Hudmon A, Schulman H (2002) Structure-function of the multifunctional Ca^{2+}/calmodulin-dependent protein kinase II. Biochem J 364(Pt 3):593–611
152. Sugai R, Takeuchi M, Okuno S, Fujisawa H (1996) Molecular cloning of a novel protein containing the association domain of calmodulin-dependent protein kinase II. J Biochem 120(4):773–779
153. Bayer KU, Harbers K, Schulman H (1998) alphaKAP is an anchoring protein for a novel CaM kinase II isoform in skeletal muscle. EMBO J 17(19):5598–5605
154. O'Leary H, Lasda E, Bayer KU (2006) CaMKIIbeta association with the actin cytoskeleton is regulated by alternative splicing. Mol Biol Cell 17(11):4656–4665
155. Wang X, Rostas JA (1996) Effect of hypothyroidism on the subcellular distribution of Ca^{2+}/calmodulin-stimulated protein kinase II in chicken brain during posthatch development. J Neurochem 66(4):1625–1632
156. Lin YC, Redmond L (2008) CaMKIIbeta binding to stable F-actin in vivo regulates F-actin filament stability. Proc Natl Acad Sci U S A 105(41):15791–15796

157. Kolb SJ, Hudmon A, Waxham MN (1995) Ca^{2+}/calmodulin kinase II translocates in a hippocampal slice model of ischemia. J Neurochem 64(5):2147–2156
158. Suzuki T, Okumuranoji K, Tanaka R, Tada T (1994) Rapid translocation of cytosolic Ca^{2+}/calmodulin-dependent protein-kinase-II into postsynaptic density after decapitation. J Neurochem 63(4):1529–1537
159. Elgersma Y, Fedorov NB, Ikonen S, Choi ES, Elgersma M, Carvalho OM et al (2002) Inhibitory autophosphorylation of CaMKII controls PSD association, plasticity, and learning. Neuron 36(3):493–505
160. Bayer KU, Schulman H (2001) Regulation of signal transduction by protein targeting: the case for CaMKII. Biochem Biophys Res Commun 289(5):917–923
161. Dhavan R, Greer PL, Morabito MA, Orlando LR, Tsai LH (2002) The cyclin-dependent kinase 5 activators p35 and p39 interact with the alpha-subunit of Ca^{2+}/calmodulin-dependent protein kinase II and alpha-actinin-1 in a calcium-dependent manner. J Neurosci 22(18):7879–7891
162. Robison AJ, Bartlett RK, Bass MA, Colbran RJ (2005) Differential modulation of Ca^{2+}/calmodulin-dependent protein kinase II activity by regulated interactions with N-methyl-D-aspartate receptor NR2B subunits and alpha-actinin. J Biol Chem 280(47):39316–39323
163. Khan S, Conte I, Carter T, Bayer KU, Molloy JE (2016) Multiple CaMKII binding modes to the actin cytoskeleton revealed by single-molecule imaging. Biophys J 111(2):395–408
164. Wang X, Tian QB, Okano A, Sakagami H, Moon IS, Kondon H et al (2005) BAALC 1-6-8 protein is targeted to postsynaptic lipid rafts by its N-terminal myristoylation and palmitoylation, and interacts with alpha, but not beta, subunit of Ca^{2+}/calmodulin-dependent protein kinase II. J Neurochem 92:647–659
165. Grueter CE, Abiria SA, Wu Y, Anderson ME, Colbran RJ (2008) Differential regulated interactions of calcium/calmodulin-dependent protein kinase II with isoforms of voltage-gated calcium channel beta subunits. Biochemistry 47(6):1760–1767
166. Hell JW, Appleyard SM, Yokoyama CT, Warner C, Catterall WA (1994) Differential phosphorylation of two size forms of the N-type calcium channel alpha 1 subunit which have different COOH termini. J Biol Chem 269(10):7390–7396
167. Lu CS, Hodge JJ, Mehren J, Sun XX, Griffith LC (2003) Regulation of the Ca^{2+}/CaM-responsive pool of CaMKII by scaffold-dependent autophosphorylation. Neuron 40(6):1185–1197
168. Ishiguro K, Green T, Rapley J, Wachtel H, Giallourakis C, Landry A et al (2006) Ca^{2+}/calmodulin-dependent protein kinase II is a modulator of CARMA1-mediated NF-kappaB activation. Mol Cell Biol 26(14):5497–5508
169. Atkins CM, Nozaki N, Shigeri Y, Soderling TR (2004) Cytoplasmic polyadenylation element binding protein-dependent protein synthesis is regulated by calcium/calmodulin-dependent protein kinase II. J Neurosci 24(22):5193–5201
170. McNeill RB, Colbran RJ (1995) Interaction of autophosphorylated Ca^{2+}/calmodulin-dependent protein kinase II with neuronal cytoskeletal proteins. Characterization of binding to a 190-kDa postsynaptic density protein. J Biol Chem 270(17):10043–10049
171. Robison AJ, Bass MA, Jiao Y, MacMillan LB, Carmody LC, Bartlett RK et al (2005) Multivalent interactions of calcium/calmodulin-dependent protein kinase II with the postsynaptic density proteins NR2B, densin-180, and alpha-actinin-2. J Biol Chem 280(42):35329–35336
172. Jefferson AB, Schulman H (1991) Phosphorylation of microtubule-associated protein-2 in GH3 cells. Regulation by cAMP and by calcium. J Biol Chem 266(1):346–354
173. Yamamoto H, Fukunaga K, Goto S, Tanaka E, Miyamoto E (1985) Ca^{2+}, calmodulin-dependent regulation of microtubule formation via phosphorylation of microtubule-associated protein 2, tau factor, and tubulin, and comparison with the cyclic AMP-dependent phosphorylation. J Neurochem 44(3):759–768
174. Shoju H, Sueyoshi N, Ishida A, Kameshita I (2005) High level expression and preparation of autonomous Ca^{2+}/calmodulin-dependent protein kinase II in Escherichia coli. J Biochem 138(5):605–611

175. Bayer KU, De Koninck P, Leonard AS, Hell JW, Schulman H (2001) Interaction with the NMDA receptor locks CaMKII in an active conformation. Nature 411(6839):801–805
176. Gardoni F, Caputi A, Cimino M, Pastorino L, Cattabeni F, Di Luca M (1998) Calcium/calmodulin-dependent protein kinase II is associated with NR2A/B subunits of NMDA receptor in postsynaptic densities. J Neurochem 71(4):1733–1741
177. Gardoni F, Schrama LH, van Dalen JJ, Gispen WH, Cattabeni F, Di Luca M (1999) AlphaCaMKII binding to the C-terminal tail of NMDA receptor subunit NR2A and its modulation by autophosphorylation. FEBS Lett 456(3):394–398
178. Yamashita T, Inui S, Maeda K, Hua DR, Takagi K, Fukunaga K et al (2006) Regulation of CaMKII by alpha4/PP2Ac contributes to learning and memory. Brain Res 1082(1):1–10
179. Fahrmann M, Erfmann M, Beinbrech G (2002) Binding of CaMKII to the giant muscle protein projectin: stimulation of CaMKII activity by projectin. Biochim Biophys Acta 1569(1–3):127–134
180. Moyers JS, Bilan PJ, Zhu J, Kahn CR (1997) Rad and Rad-related GTPases interact with calmodulin and calmodulin-dependent protein kinase II. J Biol Chem 272(18):11832–11839
181. Gangopadhyay SS, Gallant C, Sundberg EJ, Lane WS, Morgan KG (2008) Regulation of Ca^{2+}/calmodulin kinase II by a small C-terminal domain phosphatase. Biochem J 412(3):507–516
182. Baratier J, Peris L, Brocard J, Gory-Faure S, Dufour F, Bosc C et al (2006) Phosphorylation of microtubule-associated protein STOP by calmodulin kinase II. J Biol Chem 281(28):19561–19569
183. Benfenati F, Valtorta F, Rubenstein JL, Gorelick FS, Greengard P, Czernik AJ (1992) Synaptic vesicle-associated Ca^{2+}/calmodulin-dependent protein kinase II is a binding protein for synapsin I. Nature. 359(6394):417–420
184. Bennecib M, Gong CX, Grundke-Iqbal I, Iqbal K (2001) Inhibition of PP-2A upregulates CaMKII in rat forebrain and induces hyperphosphorylation of tau at Ser 262/356. Febs Letters 490(1–2):15–22
185. Lehmann IT, Bobrovskaya L, Gordon SL, Dunkley PR, Dickson PW (2006) Differential regulation of the human tyrosine hydroxylase isoforms via hierarchical phosphorylation. J Biol Chem 281(26):17644–17651

Chapter 27
Readily Releasable Stores of Calcium in Neuronal Endolysosomes: Physiological and Pathophysiological Relevance

Koffi L. Lakpa, Peter W. Halcrow, Xuesong Chen, and Jonathan D. Geiger

Abstract Neurons are long-lived post-mitotic cells that possess an elaborate system of endosomes and lysosomes (endolysosomes) for protein quality control. Relatively recently, endolysosomes were recognized to contain high concentrations (400–600 μM) of readily releasable calcium. The release of calcium from this acidic organelle store contributes to calcium-dependent processes of fundamental physiological importance to neurons including neurotransmitter release, membrane excitability, neurite outgrowth, synaptic remodeling, and cell viability. Pathologically, disturbances of endolysosome structure and/or function have been noted in a variety of neurodegenerative disorders including Alzheimer's disease (AD) and HIV-1 associated neurocognitive disorder (HAND). And, dysregulation of intracellular calcium has been implicated in the neuropathogenesis of these same neurological disorders. Thus, it is important to better understand mechanisms by which calcium is released from endolysosomes as well as the consequences of such release to inter-organellar signaling, physiological functions of neurons, and possible pathological consequences. In doing so, a path forward towards new therapeutic modalities might be facilitated.

Keywords Endosomes · Lysosomes · Endolysosomes · Calcium · Store-operated calcium entry · N-type calcium channels · Neurodegenerative diseases · HIV-1 associated neurocognitive disorder · Alzheimer's disease · Neurons

K. L. Lakpa · P. W. Halcrow · X. Chen · J. D. Geiger (✉)
Department of Biomedical Sciences, University of North Dakota School of Medicine and Health Sciences, Grand Forks, ND, USA
e-mail: Jonathan.geiger@und.edu

M. S. Islam (ed.), *Calcium Signaling*, Advances in Experimental Medicine and Biology 1131, https://doi.org/10.1007/978-3-030-12457-1_27

27.1 An Evolutionary Perspective on Calcium, Intracellular Organelles and Endolysosomes

Intracellular calcium regulates many essential functions of neurons including neurotransmitter release, excitability, synaptic plasticity, and cell viability [1]. Levels of intraneuronal calcium are very tightly regulated both temporally and spatially by various mechanisms including calcium release from intracellular stores, calcium influx across plasma membranes, and its association with a whole host of calcium binding proteins. Because of its importance both physiologically and pathologically, we start our story about the presence and functional significance of readily releasable stores of calcium in neuronal endolysosomes with a brief evolutionary perspective about calcium and intracellular organelles.

Calcium is well-known to be important for signal transduction in most cells including neurons. Indeed, calcium has been referred to as a universal second messenger in eukaryotic cells. The approximate 10,000-fold gradient of extracellular to intracellular calcium originated evolutionarily because of the gradual rise in calcium levels from about 100 nM during the period when the basic building blocks of life developed in thermal ducts under the ocean floor to about 1 mM during the Pre-Cambrian period when multicellular life evolved [2, 3]. Due to the toxic nature of millimolar levels of calcium, evolutionary pressure was applied such that cellular survival dictated that semipermeable membranes appeared and a variety of mechanisms were formed to maintain appropriate calcium gradients across plasma membranes [3]. Simultaneously, embedded in the plasma membranes were newly developed calcium pumps and calcium binding proteins which helped with calcium homeostasis [3]. Together, in neurons, these evolutionary changes provide unique and complex spatial and temporal handling of calcium that is essential for not only proper cellular signaling but also neuronal cell life and death.

It was also during this billion-year evolutionary period that intracellular organelles began appearing including mitochondria resulting from symbiotic relationships with bacteria and the development of functional endocytic machinery [4]. Mitochondria are integral to the maintenance of cellular energetics and they are important ‘sinks’ for intracellular calcium [5]. However, when too much calcium is up-taken into mitochondria cellular energetics are compromised and the resulting calcium overload can lead to a cascade of events including increased oxidative stress and cell death. It has also become increasingly appreciated that organelles including endoplasmic reticulum, endosomes and lysosomes (hereafter referred to as endolysosomes) have readily releasable and functionally important pools of intracellular calcium. Although less well known, the approximate 500 μM levels of calcium in endolysosomes are similar to the calcium concentrations present in endoplasmic reticulum [6]. This is a very important concept because endoplasmic reticulum is commonly referred to as the principal intracellular store of readily releasable calcium. Furthermore, as the field of inter-organellar signaling as well as physical and chemical crosstalk between organelles has grown over the past decade

it is prudent of us to now posit that this relatively new and highly complicated area of modern cell biology is key to our understanding of the regulation and dysregulation of calcium [7].

With this as a very quick trip across 1 billion years of evolutionary biology, here we embark on a brief but focused summary of findings that neuronal endolysosomes contain readily releasable stores of calcium and once released this calcium can lead to calcium influx into cells, calcium release from other organelles, and calcium dysregulation-induced neurotoxicity. The relevance of such an important upstream store of calcium to the regulation of physiological functions and pathophysiological events is obvious and will be discussed with particular relevance to the pathogenesis of two neurodegenerative disorders; Alzheimer's disease (AD) and HIV-1 associated neurocognitive disorder (HAND).

27.2 Endolysosomes Contain Readily Releasable Pools of Calcium

Neurons are long-lived post-mitotic cells that possess an elaborate endolysosome system for quality control especially for proteins. Endolysosomes are well known to be acidic organelles that contain high levels of cations including calcium, iron, zinc and copper. However, for the cation calcium it was not until fairly recently that these organelles were described as being 'acidic calcium stores' because the luminal pH of endolysosomes is acidic and endolysosomes contain high (400–600 μM) levels of readily releasable calcium [8, 9].

Neuronal calcium signals display spectacular spatiotemporal complexity and understanding how calcium signals are generated spatially and temporally is necessary to understand calcium-dependent cellular processes. Endolysosome calcium levels are maintained by a variety of uptake and efflux mechanisms. Essential for uptake of calcium into endolysosomes, proton gradients are established mainly by vacuolar H^+-ATPase (v-ATPase) that pumps H^+ into the lumen and this helps regulate Ca^{2+} levels [9–11]. Four main mechanisms for calcium release from endolysosomes have been described including: (1) Calcium release through two-pore channels (TPCs) triggered by nicotinic acid adenine dinucleotide phosphate (NAADP) [12–17]; (2) Elevation of endolysosome pH with, for example, the selective v-ATPase inhibitor bafilomycin (BAF) or the alkaline lysosomotropic agents NH_4Cl and chloroquine [8, 18, 19]; (3) Involvement of TRPML1 mucolipin-type channels and P2X4 receptors [20–22]; and (4) Selective disruption of endolysosome membranes with Gly-Phe-β-naphtylamide (GPN) [23, 24]. Of physiological significance, calcium released from endolysosomes has been shown to contribute to a variety of calcium-dependent neuronal processes including neurotransmitter release, neuronal excitability, neurite outgrowth, synaptic remodeling, and cell viability [25–27].

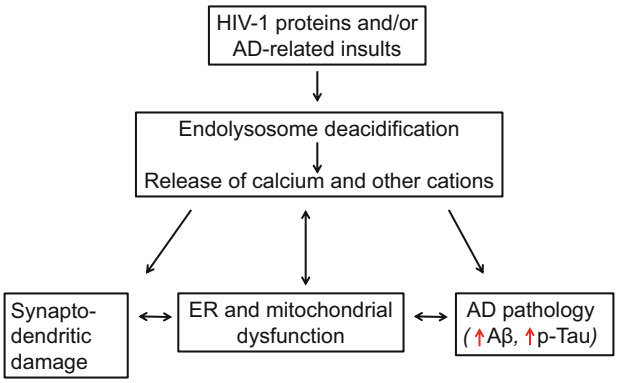

Fig. 27.1 HIV-1 proteins and other neurotoxic insults can cause deacidification of endolysosomes. Increasing endolysosome pH can release calcium and other cations from endolysosomes. Calcium released from readily releasable stores in endolysosomes can increase the release of calcium from other intracellular stores and can increase the influx of extracellular calcium. Such increases in pH and calcium levels can cause endoplasmic reticulum (ER) and mitochondrial dysfunction, Alzheimer's disease (AD)-like pathology, and synaptodendritic damage

Endolysosomes can release calcium transiently and in a highly localized and distinct fashion [17, 28, 29]. Endolysosome calcium can affect the release of calcium from organellar stores as well as through plasma membrane-based calcium influx mechanisms. The inter-organellar signaling and signaling with the plasma membrane is explained at least in part by findings that endolysosomes are highly mobile in cells, are highly dynamic metabolically, have high rates of biogenesis, and can interact physically and functionally with other intracellular organelles (Fig. 27.1).

At least three models of acidic store-induced calcium signaling mechanisms have been described [9]. (1) Acidic stores of calcium might communicate with endoplasmic reticulum calcium stores such that calcium released from endolysosomes can enhance endoplasmic reticulum calcium loading [30] and calcium-induced calcium release [13, 15]. (2) Changes in endolysosome pH may release calcium from a subgroup of acidic calcium stores and the released calcium may affect other subgroups of acidic stores through mechanisms such as vesicular fusion of late endosomes and lysosomes [9, 15, 31]. (3) Calcium released from acidic calcium stores might depolarize plasma membranes, evoke calcium-dependent currents, and stimulate calcium influx across plasma membranes [12].

27.3 Acidic Store-Operated Calcium Entry in Neurons

Acidic store-operated calcium entry (aSOCE) is a unique mechanism that links readily releasable calcium in endolysosomes with influx of extracellular calcium into neurons. This is a novel means by which intraneuronal stores of calcium can contribute to spatial and temporal integration of calcium signaling. In support of this novel mechanism, we found that calcium could be released from endolysosomes following stimulation of a number of different mechanisms, that the calcium release could be independent of other organellar stores of calcium, that release of calcium from endolysosomes triggered calcium influx, and that the calcium influx was regulated by N-type calcium channels and lysosome exocytosis (Fig. 27.2).

Capacitative influx of calcium into cells was described over 30 years ago [32]. Such calcium influx mechanisms, that are now commonly referred to as store-operated calcium entry (SOCE), are principally initiated by a reduction in

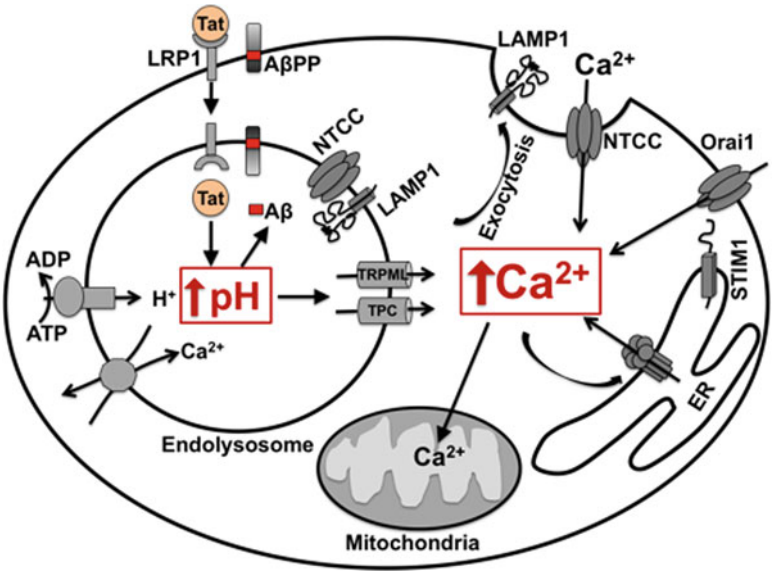

Fig. 27.2 HIV-1 Tat de-acidifies endolysosomes, increases amyloidogenesis, and releases calcium from readily releasable stores in endolysosomes. Calcium released from endolysosomes can affect mitochondrial and endoplasmic reticulum (ER) calcium stores, and increase store operated calcium (SOCE) mechanisms. Mechanistically, following de-acidification endolysosome calcium is released through TRPML1 and two pore channels (TPCs). The calcium signals can be amplified by releasing calcium from other organelles including mitochondria and ER, and by activating ER-based SOCE involving STIM1 and Orai channels as well as acidic store operated calcium entry involving N-type calcium channels (NTCCs)

endoplasmic reticulum calcium stores followed by influx of extracellular calcium in a variety of cells including neurons in order to refill the depleted stores of calcium. Mechanistically, depleting endoplasmic reticulum calcium stores drives the oligomerization and translocation of stromal interaction molecule 1 (STIM1) proteins to endoplasmic reticulum junctions close to the plasma membrane. Such STIM1 translocation induces the clustering of calcium release-activated calcium modulator 1 (Orai1) channels and/or transient receptor potential (TRP) cation channels into plasma membranes thereby enabling extracellular calcium entry [33].

Conceptually, but not mechanistically, we observed similar store-operated calcium entry involving endolysosomes in neurons. Using primary cultures of rat cortical neurons, we found that calcium was released from endolysosomes following treatment with the two-pore channel agonist NAADP-AM, the v-ATPase inhibitor BAF, and the lysosomotropic agent GPN; all of which de-acidify endolysosomes [34]. However, when these experiments were conducted in the absence of extracellular calcium, de-acidification of endolysosomes with NAADP-AM, BAF and GPN increased only slightly levels of free cytosolic calcium. When these same experiments were conducted in the presence of extracellular calcium, NAADP-AM, BAF and GPN all increased significantly the levels of free cytosolic calcium. Although it is not well understood currently, the relatively small release of calcium from endolysosomes causes a much larger influx of extracellular calcium and this might be due to plasma membrane depolarization as is accompanied by NAADP-induced endolysosome calcium release [34, 35]. Besides neurons, phenomena similar to aSOCE have been described in other cell types where NAADP has been found to induce endolysosome calcium release and large influxes of calcium across plasma membranes [12, 36–39]. These observations suggested to us that endolysosome de-acidification by three completely different mechanisms led directly or indirectly to an enhanced influx of calcium into neurons. Accordingly, we next tested more specifically the extent to which a store-operated mechanism might control the observed calcium influx across the plasma membrane.

Using approaches similar to those used by others and us, we began studying store-operated calcium mechanisms including the classical endoplasmic reticulum-based capacitative SOCE. Indeed, we confirmed that in the absence of extracellular calcium and following depletion of endoplasmic reticulum calcium with the SERCA pump inhibitor thapsigargin (TG) there was a significant increase in levels of free intracellular calcium only when calcium was re-introduced to the extracellular medium. With this positive control for the functional presence of endoplasmic reticulum-based SOCE in our cultured neurons, we conducted similar experiments with agents that de-acidify endolysosomes and release calcium from endolysosome stores. Even after depleting ER pools of calcium with TG, application of NAADP-AM, BAF and GPN still caused increased influx of extracellular calcium and still induced increased levels of intracellular calcium. Thus, in these neurons there appeared to be at least two separate and functional store-operated calcium mechanisms; one governed by endoplasmic reticulum and the other by endolysosomes.

In testing the distinctive nature of the two store-operated calcium mechanisms governed by endoplasmic reticulum or endolysosomes, we used pharmacological and molecular/genetic strategies. Using siRNA to knock-down protein expression levels of STIM1, a protein that is central to SOCE, and the SOCE blockers SKF-96365 and 2-APB we were able to block significantly TG-induced release of calcium from endoplasmic reticulum, but we were unable to block significantly NAADP-AM-, BAF- and GPN-induced calcium influx. However, we were able to block significantly NAADP-AM-, BAF- and GPN-induced calcium influx with the selective N-type calcium channel (NTCC) blocker (ω-conotoxin). The selective and specific nature of this inhibition by ω-conotoxin was confirmed further by showing that NAADP-AM-, BAF- and GPN-induced calcium influx was not blocked by inhibitors of L-type (nimodipine, verapamil) and P/Q-type (ω-agatoxin) calcium channels. Moreover, we confirmed these pharmacological findings by showing that siRNA knockdown of NTCCs attenuated significantly NAADP-AM-, BAF- and GPN-induced calcium influx, but did not affect TG-induced SOCE. Together, the above results demonstrated that calcium released from endolysosomes can be distinct from calcium released from endoplasmic reticulum through SOCE mechanisms and that the calcium released from endolysosomes is capable of activating cell surface calcium channels to stimulate calcium influx. These findings support and extend earlier findings that calcium released from endolysosomes did not stimulate endoplasmic reticulum-dependent SOCE in MDCK epithelial cells [23]. Accordingly, this new mechanism was termed by us as "acidic store-operated calcium entry" (aSOCE) [34].

27.4 Role of Lysosome Exocytosis in Acidic Store-Operated Calcium Entry (aSOCE)

Multiple mechanisms might control aSOCE involving NTCCs. One such mechanism might involve lysosome exocytosis because we have shown using a quantitative biotinylation of surface proteins assay that NAADP-AM, BAF and GPN all increased cell surface protein expression levels of NTCCs and lysosome-associated glycoprotein 1 (LAMP1). Next, we addressed the possibility that lysosome exocytosis and NTCCs were linked directly by conducting co-immunoprecipitation studies and found a physical interaction between NTCCs and LAMP1. Because LAMP1 is critical for lysosome exocytosis [40], those observations suggested to us that lysosome exocytosis might be a functional partner in aSOCE especially because aSOCE was inhibited following siRNA knockdown of protein expression levels of LAMP1. Thus, de-acidification of endolysosomes might be of central importance because NAADP-AM, BAF and GPN through very different initial mechanisms all appeared to enhance lysosome exocytosis and the recycling of NTCCs to the plasma membrane where they participated in calcium influx generally and aSOCE more specifically. Physically, this makes sense as well because of findings that

de-acidification of endolysosomes changes cellular distribution patterns of these organelles from a mostly peri-nuclear pattern to one where the endolysosomes migrate close to the plasma membrane [41]. Thus, functionally and physically there is evidence favoring endolysosomes and endolysosome exocytosis in calcium entry.

27.5 Physical Interactions and Functional Relevance of Inter-organellar Signaling

In addition to physical interactions between endolysosomes and plasma membranes, it is becoming increasingly clear that endolysosomes physically and functionally interact as well with other intracellular organelles including mitochondria and endoplasmic reticulum. Such recognition has led to an appreciation for dynamic physical and chemical communications between intracellular organelles including those regulated by pH and calcium.

Physical interactions between mitochondria and endoplasmic reticulum were first described about 60 years ago and the functional significance of mitochondria-associated membranes was first characterized about 30 years ago [42]. Even today, there continues to be work focused on the physical and functional interactions between organelles [43] as well as the role that organellar interactions plays in the pathogenesis of neurodegenerative diseases [44, 45]. As it relates to endolysosomes, it is now known that there are extensive physical interactions between endolysosomes and mitochondria and that these inter-organellar communications participate in lipid and metabolite exchange as well as mitochondrial quality control [46]. Conversely, mitochondrial dysfunction has been found to negatively affect lysosome structure and function through reactive oxygen species-dependent mechanisms [47]. Extensive membrane contact sites have been described between lysosomes and endoplasmic reticulum, that these contact sites were evolutionarily conserved, and that calcium released from lysosomes was sufficient to stimulate endoplasmic reticulum-dependent calcium-induced calcium release [48, 49, 50]. However, only recently was it shown that endolysosomes maintain their 1000-fold calcium concentration gradient in cells in part by refilling endolysosome stores of calcium from IP_3-regulated stores of calcium in endoplasmic reticulum [51]. Some of the differences in findings as to calcium movements between organelles might be because of cell-specific mechanisms. In addition, the difficult nature of understanding inter-organellar calcium dynamics is highlighted by work showing that STIM1 and STIM2 are expressed in endolysosomes, at least in platelets, and that depletion of acidic organellar stores of calcium can increase protein-protein interactions between STIM proteins with Orai1 and TRPC channels to induce SOCE [52]. It is further complicated by findings that calcium released through endolysosome-resident TRML1 channels can cause calcium release from endoplasmic reticulum and calcium influx [53] and that NAADP has been implicated in this “cross-talk” [54].

27.6 Possible Role of Endolysosomes and aSOCE in Pathogenesis of Alzheimer's Disease and HIV-1 Associated Neurocognitive Disorder (HAND)

Disturbances in endolysosome structure and/or function have been noted in a variety of neurodegenerative disorders including Alzheimer's disease (AD) and HIV-1 neurocognitive disorder (HAND) [55–59]. AD is a devastating age-related neurodegenerative disease that is the commonest cause of dementia in people over the age of 65. People with HAND, on the other hand, exhibit neurological complications ranging from mild (mild cognitive impairment) to severe (dementia). In the current era of anti-retroviral therapeutics HIV-1 infected individuals are living almost full life-spans, but are now experiencing a prevalence rate of over 50% for HAND [60, 61]. Clinically and pathologically people living with neuroHIV-1 are exhibiting AD-like symptoms including learning and memory deficits as well as increased amyloidogenesis. Although the pathogenesis of HAND is not fully understood, HIV-1 proteins including the HIV-1 transactivator of transcription protein Tat have been implicated by others and us to be causative virotoxins in HAND [62–69]. Among the HIV-1 viral proteins, HIV-1 Tat is present in brains of HIV-1 infected individuals and its levels stay elevated in CSF even when HIV-1 viral levels are immeasurable [70]. Others and we have shown that HIV-1 Tat directly excites neurons [65, 71, 72], disturbs neuronal calcium homeostasis [64, 73], disrupts synaptic integrity [74, 75], and induces neurotoxicity [68, 76].

Endolysosome dysfunction has been implicated in the development of at least two pathological hallmarks of AD and HAND; Aβ accumulation and neurofibrillary tangle formation. Endolysosomes are very important for amyloidogenic processing of AβPP to Aβ because amyloid β precursor protein (AβPP) is first endocytosed, the amyloidogenic enzymes BACE-1 and γ-secretase are almost exclusively located in endosomes and lysosomes, the acidic environment of endolysosomes is favorable for amyloidogenic metabolism of AβPP, and Aβ can be either accumulated in or released by exocytosis from endolysosomes [77–83]. Tau is a microtubule-associated protein, and when hyperphosphorylated it aggregates and contributes to the formation of neurofibrillary tangles. Tau aggregates can be degraded by cathepsin D in autophagosomes-lysosomes [84, 85], and endolysosome dysfunction contributes to tau aggregation and neurofibrillary tangle formation [86, 87]. On the other hand, transcriptional activation of lysosome biogenesis can clear aggregated tau [88]. Thus, endolysosomes are important sites for development of these neurological disorders.

Dysregulation of intracellular calcium has also been implicated in the neuropathogenesis of these same neurological disorders. And it is clear (see above) that de-acidification of endolysosomes releases calcium from these acidic stores [28, 89, 90]. We found that HIV-1 Tat protein elevated endolysosome pH and disturbed the structure and function of endolysosomes [74], a prominent and early pathological feature of HAND [57, 58]. Clearly, endolysosome calcium stores

contribute to neuronal calcium signaling and function [91–93] and calcium release from endolysosomes triggers calcium release from endoplasmic reticulum [11, 17] and through plasma membranes via aSOCE (see above).

HIV-1 proteins including HIV-1 Tat, and anti-retroviral therapeutic drugs contribute to the development of AD-like pathology including increases in Aβ levels [94–99]. HIV-1 Tat enters neurons via receptor-mediated endocytosis [100–102]. The Tat-induced de-acidification of endolysosomes and resulting effects on calcium dyshomeostasis likely results from the ability of HIV-1 Tat to decrease the levels and activity of vacuolar-ATPase as well as compensatory increases in cathepsin D and LAMP-1 [103]. The consequences of such alterations in calcium dynamics and homeostasis are synaptic disruption and neurotoxicity [104–106].

Endolysosomes contain physiologically important levels of calcium that is readily releasable by a number of stimuli and insults. The calcium can exit through a number of channels including TRPML and two pore channels. Once released the calcium can signal other organelles to release calcium and for greater influx of calcium through plasma membrane-resident calcium channels especially N-type calcium channels. These effects on endolysosome structure and function have clear implications to the pathogenesis of AD and HAND; neurological disorders that show overlap in terms of clinical and pathological features. We are excited to be part of this emerging area of cell biology focused on inter-organellar signaling and look forward to further studies elucidating physiological and pathological consequences of calcium release from endolysosome stores.

Acknowledgements The authors gratefully acknowledge the funding provided by the NIH for our work; P30GM103329, R01MH100972, R01MH105329, R01MH119000, R01NS065957, and R01DA032444.

References

1. Berridge MJ, Bootman MD, Roderick HL (2003) Calcium signalling: dynamics, homeostasis and remodelling. Nat Rev Mol Cell Biol 4:517–529
2. Jaiswal JK (2001) Calcium – how and why? J Biosci 26(3):357–363
3. Case RM, Eisner D, Gurney A, Jones O, Muallem S, Verkhratsky A (2007) Evolution of calcium homeostasis: from birth of the first cell to an omnipresent signalling system. Cell Calcium 42(4–5):345–350
4. Wideman JG, Leung KF, Field MC, Dacks JB (2014) The cell biology of the Endocytic system from an evolutionary perspective. Cold Spring Harb Perspect Biol [Internet] 6(4):a016998. Apr 1 [cited 2018 July 16]. Available from: http://www.ncbi.nlm.nih.gov/pubmed/24478384
5. Carafoli E (2010) The fateful encounter of mitochondria with calcium: how did it happen? Biochim Biophys Acta Bioenerg [Internet] 1797(6–7):595–606. June 1 [cited 2018 July 16]. Available from: https://www.sciencedirect.com/science/article/pii/S0005272810001301#fig1
6. Patel S, Cai X (2015) Evolution of acidic Ca^{2+}stores and their resident Ca^{2+}−permeable channels [internet]. Cell Calcium 57:222–230. [cited 2018 July 14]. Available from: https://www.sciencedirect.com/science/article/pii/S0143416014002012

7. Raffaello A, Mammucari C, Gherardi G, Rizzuto R (2016) Calcium at the Center of Cell Signaling: interplay between endoplasmic reticulum, mitochondria, and lysosomes. Trends Biochem Sci 41:1035–1049. [cited 2017 May 17]. Available from: http://www.cell.com/trends/biochemical-sciences/pdf/S0968-0004(16)30147-5.pdf
8. Christensen KA, Myers JT, JA S (2002) pH-dependent regulation of lysosomal calcium in macrophages. J Cell Sci 115(Pt 3):599–607
9. Morgan AJ, Platt FM, Lloyd-Evans E, Galione A (2011) Molecular mechanisms of endolysosomal Ca^{2+} signalling in health and disease. Biochem J [Internet] 439(3):349–374. Available from: http://www.biochemj.org/content/439/3/349.abstract
10. Moreno SNJ, Docampo R (2009) The role of acidocalcisomes in parasitic protists. J Eukaryot Microbiol 56:208–213
11. Patel S, Docampo R (2010) Acidic calcium stores open for business: expanding the potential for intracellular Ca^{2+} signaling. Trends Cell Biol 20:277–286
12. Brailoiu E, Churamani D, Cai X, Schrlau MG, Brailoiu GC, Gao X et al (2009) Essential requirement for two-pore channel 1 in NAADP-mediated calcium signaling (a). J Cell Biol 186(2):201–209
13. Calcraft PJ, Ruas M, Pan Z, Cheng X, Arredouani A, Hao X et al (2009) NAADP mobilizes calcium from acidic organelles through two-pore channels. Nature 459(7246):596–600
14. Zong X, Schieder M, Cuny H, Fenske S, Gruner C, Rötzer K et al (2009) The two-pore channel TPCN2 mediates NAADP-dependent Ca^{2+}−release from lysosomal stores. Pflugers Arch Eur J Physiol [Internet] 458(5):891–899. Sept 26 [cited 2018 July 14]. Available from: http://www.ncbi.nlm.nih.gov/pubmed/19557428
15. Ruas M, Rietdorf K, Arredouani A, Davis LC, Lloyd-Evans E, Koegel H et al (2010) Purified TPC isoforms form NAADP receptors with distinct roles for Ca^{2+} signaling and Endolysosomal trafficking. Curr Biol [Internet] 8(20):703–709. Apr 27 [cited 2018 July 27]. Available from: http://www.ncbi.nlm.nih.gov/pubmed/20346675
16. Schieder M, Rötzer K, Brüggemann A, Biel M, Wahl-Schott CA (2010) Characterization of two-pore channel 2 (TPCN2)-mediated Ca^{2+} currents in isolated lysosomes. J Biol Chem [Internet] 285(28):21219–21222. July 9 [cited 2018 July 14]. Available from: http://www.ncbi.nlm.nih.gov/pubmed/20495006
17. Zhu MX, Ma J, Parrington J, Calcraft PJ, Galione A, Evans AM (2010) Calcium signaling via two-pore channels: local or global, that is the question. AJP Cell Physiol [Internet] 298(3):C430–C441. Available from: http://ajpcell.physiology.org/cgi/doi/10.1152/ajpcell.00475.2009
18. Camacho M, Machado JD, Alvarez J, Borges R (2008) Intravesicular calcium release mediates the motion and exocytosis of secretory organelles: a study with adrenal chromaffin cells. J Biol Chem 283(33):22383–22389
19. Machado JD, Camacho M, Alvarez J, Borges R (2009) On the role of intravesicular calcium in the motion and exocytosis of secretory organelles. Commun Integr Biol 2(2):71–73
20. Starkus JG, Fleig A, Penner R (2010) The calcium-permeable non-selective cation channel TRPM2 is modulated by cellular acidification. J Physiol 588(8):1227–1240
21. Kiselyov K, Colletti GA, Terwilliger A, Ketchum K, CWP L, Quinn J et al (2011) TRPML: transporters of metals in lysosomes essential for cell survival? Cell Calcium 50:288–294
22. Cao Q, Zhong XZ, Zou Y, Murrell-Lagnado R, Zhu MX, Dong XP (2015) Calcium release through P2X4 activates calmodulin to promote endolysosomal membrane fusion. J Cell Biol 209(6):879–894
23. Haller T, Dietl P, Deetjen P, Völkl H (1996) The lysosomal compartment as intracellular calcium store in MDCK cells: a possible involvement in InsP3-mediated Ca^{2+} release. Cell Calcium 19(2):157–165
24. McGuinness L, Bardo SJ, Emptage NJ (2007) The lysosome or lysosome-related organelle may serve as a Ca^{2+} store in the boutons of hippocampal pyramidal cells. Neuropharmacology 52(1):126–135
25. Repnik U, Česen MH, Turk B (2013) The endolysosomal system in cell death and survival. Cold Spring Harb Perspect Biol [Internet] 5(1):a008755. Jan 1 [cited 2017 Oct 16]. Available from: http://www.ncbi.nlm.nih.gov/pubmed/23284043

26. Ferguson SM (2018) Neuronal lysosomes. Neurosci Lett [Internet]. Available from: http://linkinghub.elsevier.com/retrieve/pii/S030439401830260X
27. Goo MS, Sancho L, Slepak N, Boassa D, Deerinck TJ, Ellisman MH et al (2017) Activity-dependent trafficking of lysosomes in dendrites and dendritic spines. J Cell Biol 216(8):2499–2513
28. Galione A, Morgan AJ, Arredouani A, Davis LC, Rietdorf K, Ruas M et al (2010) NAADP as an intracellular messenger regulating lysosomal calcium-release channels. Biochem Soc Trans [Internet] 38(6):1424–1431. Available from: http://biochemsoctrans.org/lookup/doi/10.1042/BST0381424
29. Shen D, Wang X, Li X, Zhang X, Yao Z, Dibble S et al (2012) Lipid storage disorders block lysosomal trafficking by inhibiting a TRP channel and lysosomal calcium release. Nat Commun 3:731
30. Macgregor A, Yamasaki M, Rakovic S, Sanders L, Parkesh R, Churchill GC et al (2007) NAADP controls cross-talk between distinct Ca^{2+} Stores in the Heart. J Biol Chem [Internet] 282(20):15302–15311. May 18 [cited 2018 July 16]. Available from: http://www.ncbi.nlm.nih.gov/pubmed/17387177
31. Galione A, Parrington J, Funnell T (2011) Physiological roles of NAADP-mediated Ca^{2+} signaling. Sci China Life Sci [Internet] 54(8):725–732. Available from: http://link.springer.com/10.1007/s11427-011-4207-5
32. Putney JW (1986) A model for receptor-regulated calcium entry. Cell Calcium 7(1):1–12
33. Putney JW (2009) Capacitative calcium entry: from concept to molecules. Immunol Rev 231:10–22
34. Hui L, Geiger NH, Bloor-Young D, Churchill GC, Geiger JD, Chen X (2015) Release of calcium from endolysosomes increases calcium influx through N-type calcium channels: evidence for acidic store-operated calcium entry in neurons. Cell Calcium [Internet] 58:617–627. [cited 2017 May 31]. Available from: http://ac.els-cdn.com/S0143416015001529/1-s2.0-S0143416015001529-main.pdf?_tid=d155fae0-460a-11e7-a743-00000aab0f02&acdnat=1496239973_5d092efe55666657b3cd6c5dc4881cf0
35. Arredouani A, Ruas M, Collins SC, Parkesh R, Clough F, Pillinger T et al (2015) Nicotinic acid adenine dinucleotide phosphate (NAADP) and endolysosomal two-pore channels modulate membrane excitability and stimulus-secretion coupling in mouse pancreatic β cells. J Biol Chem [Internet] 290(35):21376–21392. Aug 28 [cited 2018 July 14]. Available from: http://www.ncbi.nlm.nih.gov/pubmed/26152717
36. Moccia F, Lim D, Nusco GA, Ercolano E, Santella L (2003) NAADP activates a Ca^{2+} current that is dependent on F-actin cytoskeleton. FASEB J 17(13):1907–1909
37. Moccia F, Billington RA, Santella L (2006) Pharmacological characterization of NAADP-induced Ca^{2+} signals in starfish oocytes. Biochem Biophys Res Commun 348(2):329–336
38. Naylor E, Arredouani A, Vasudevan SR, Lewis AM, Parkesh R, Mizote A et al (2009) Identification of a chemical probe for NAADP by virtual screening. Nat Chem Biol 5(4):220–226
39. Churchill GC, O'Neill JS, Masgrau R, Patel S, Thomas JM, Genazzani AA et al (2003) Sperm deliver a new second messenger: NAADP. Curr Biol 13(2):125–128
40. Yogalingam G, Bonten EJ, van de Vlekkert D, Hu H, Moshiach S, Connell SA et al (2008) Neuraminidase 1 is a negative regulator of Lysosomal exocytosis. Dev Cell 15(1):74–86
41. Li X, Rydzewski N, Hider A, Zhang X, Yang J, Wang W et al (2016) A molecular mechanism to regulate lysosome motility for lysosome positioning and tubulation. Nat Cell Biol 18(4):404–417
42. Herrera-Cruz MS, Simmen T (2017) Over six decades of discovery and characterization of the architecture at mitochondria-associated membranes (MAMs). Adv Exp Med Biol 997:13–31
43. Wu Y, Whiteus C, Xu CS, Hayworth KJ, Weinberg RJ, Hess HF et al (2017) Contacts between the endoplasmic reticulum and other membranes in neurons. Proc Natl Acad Sci [Internet] 114(24):E4859–E4867. Available from: http://www.pnas.org/lookup/doi/10.1073/pnas.1701078114

44. Schon EA, Area-Gomez E (2013) Mitochondria-associated ER membranes in Alzheimer disease. Mol Cell Neurosci [Internet] 55:26–36. July [cited 2018 July 27]. Available from: http://www.ncbi.nlm.nih.gov/pubmed/22922446
45. Joshi AU, Kornfeld OS, Mochly-Rosen D (2016) The entangled ER-mitochondrial axis as a potential therapeutic strategy in neurodegeneration: a tangled duo unchained. Cell Calcium 60:218–234
46. Soto-Heredero G, Baixauli F, Mittelbrunn M (2017) Interorganelle communication between mitochondria and the Endolysosomal system. Front Cell Dev Biol [Internet] 5:95. Available from: http://journal.frontiersin.org/article/10.3389/fcell.2017.00095/full
47. Demers-Lamarche J, Guillebaud G, Tlili M, Todkar K, Bélanger N, Grondin M et al (2016) Loss of mitochondrial function impairs lysosomes$_*$. J Biol Chem [Internet] 291(19):10263–10276. May 6 [cited 2017 Dec 8]. Available from: http://www.ncbi.nlm.nih.gov/pubmed/26987902
48. Kilpatrick BS, Eden ER, Schapira AH, Futter CE, Patel S (2013) Direct mobilisation of lysosomal Ca^{2+} triggers complex Ca^{2+} signals. J Cell Sci [Internet] 126(Pt 1):60–66. Available from: http://www.ncbi.nlm.nih.gov/pubmed/23108667%5Cnhttp://jcs.biologists.org/content/joces/126/1/60.full.pdf
49. Penny CJ, Kilpatrick BS, Eden ER, Patel S (2015) Coupling acidic organelles with the ER through Ca^{2+} microdomains at membrane contact sites. Cell Calcium 58:387–396
50. Hariri H, Ugrankar R, Liu Y, Henne WM (2016) Inter-organelle ER-endolysosomal contact sites in metabolism and disease across evolution. Communicative and Integrative Biology 9(3):e1156278
51. Garrity AG, Wang W, Collier CM, Levey SA, Gao Q, Xu H (2016) The endoplasmic reticulum, not the pH gradient, drives calcium refilling of lysosomes. Elife [Internet] 5:e15887. May 23 [cited 2017 May 11]. Available from: http://www.ncbi.nlm.nih.gov/pubmed/27213518
52. Zbidi H, Jardin I, Woodard GE, Lopez JJ, Berna-Erro A, Salido GM et al (2011) STIM1 and STIM2 are located in the acidic Ca^{2+} stores and associates with Orai1 upon depletion of the acidic stores in human platelets. J Biol Chem 286(14):12257–12270
53. Kilpatrick BS, Yates E, Grimm C, Schapira AH, Patel S (2016) Endo-lysosomal TRP mucolipin-1 channels trigger global ER Ca^{2+} release and Ca^{2+} influx. J Cell Sci [Internet]. 129(20):3859–3867. [cited 2018 July 27]. Available from: http://www.ncbi.nlm.nih.gov/pubmed/27577094
54. Ronco V, Potenza DM, Denti F, Vullo S, Gagliano G, Tognolina M et al (2015) A novel Ca^{2+}−mediated cross-talk between endoplasmic reticulum and acidic organelles: implications for NAADP-dependent Ca^{2+}signalling. Cell Calcium [Internet] 57(2):89–100. Feb 1 [cited 2018 July 14]. Available from: https://www.sciencedirect.com/science/article/pii/S0143416015000020
55. Tate BA, Mathews PM (2006) Targeting the role of the endosome in the pathophysiology of Alzheimer's disease: a strategy for treatment. Sci Aging Knowl Environ [Internet] 2006(10):re2–re2. June 28 [cited 2018 July 27]. Available from: http://www.ncbi.nlm.nih.gov/pubmed/16807486
56. Boland B, Kumar A, Lee S, Platt FM, Wegiel J, Yu WH et al (2008) Autophagy induction and Autophagosome clearance in neurons: relationship to Autophagic pathology in Alzheimer's disease. J Neurosci [Internet] 28(27):6926–6937. July 2 [cited 2018 July 27]. Available from: http://www.ncbi.nlm.nih.gov/pubmed/18596167
57. Gelman BB, Soukup VM, Holzer CE 3rd, Fabian RH, Schuenke KW, Keherly MJ et al (2005) Potential role for white matter lysosome expansion in HIV-associated dementia. J Acquir Immune Defic Syndr 39(4):422–425
58. Spector SA, Zhou D (2008) Autophagy: an overlooked mechanism of HIV-1 pathogenesis and neuroAIDS? Autophagy [Internet] 4(5):704–706. July [cited 2018 July 27]. Available from: http://www.ncbi.nlm.nih.gov/pubmed/18424919

59. Cysique LA, Hewitt T, Croitoru-Lamoury J, Taddei K, Martins RN, Chew CS et al (2015) APOE ε4 moderates abnormal CSF-abeta-42 levels, while neurocognitive impairment is associated with abnormal CSF tau levels in HIV+ individuals – a cross-sectional observational study. BMC Neurol [Internet] 15(1):51. Dec 1 [cited 2018 July 27]. Available from: http://www.ncbi.nlm.nih.gov/pubmed/25880550
60. Ellis RJ, Rosario D, Clifford DB, McArthur JC, Simpson D, Alexander T et al (2010) Continued high prevalence and adverse clinical impact of human immunodeficiency virus–associated sensory neuropathy in the era of combination antiretroviral therapy. Arch Neurol [Internet] 67(5):552. May 1 [cited 2018 July 27]. Available from: http://www.ncbi.nlm.nih.gov/pubmed/20457954
61. Heaton RK, Clifford DB, Franklin DR, Woods SP, Ake C, Vaida F et al (2010) HIV-associated neurocognitive disorders persist in the era of potent antiretroviral therapy: charter study. Neurol Int 75(23):2087–2096. Dec 7 [cited 2017 Sept 13]. Available from: http://www.ncbi.nlm.nih.gov/pubmed/21135382
62. Sabatier JM, Vives E, Mabrouk K, Benjouad A, Rochat H, Duval A et al (1991) Evidence for neurotoxic activity of tat from human immunodeficiency virus type 1. J Virol [Internet] 65(2):961–967. Feb [cited 2018 July 27]. Available from: http://www.ncbi.nlm.nih.gov/pubmed/1898974
63. Weeks BS, Lieberman DM, Johnson B, Roque E, Green M, Loewenstein P et al (1995) Neurotoxicity of the human immunodeficiency virus type 1 tat transactivator to PC12 cells requires the tat amino acid 49-58 basic domain. J Neurosci Res [Internet] 42(1):34–40. Sept 1 [cited 2018 July 27]. Available from: http://doi.wiley.com/10.1002/jnr.490420105
64. Haughey NJ, Holden CP, Nath A, Geiger JD (1999) Involvement of inositol 1,4,5-trisphosphate-regulated stores of intracellular calcium in calcium dysregulation and neuron cell death caused by HIV-1 protein tat. J Neurochem [Internet] 73(4):1363–1374. Oct [cited 2018 July 27]. Available from: http://www.ncbi.nlm.nih.gov/pubmed/10501179
65. Nath A, Haughey NJ, Jones M, Anderson C, Bell JE, Geiger JD (2000) Synergistic neurotoxicity by human immunodeficiency virus proteins tat and gp120: protection by memantine. Ann Neurol [Internet] 47(2):186–194. Feb [cited 2018 July 27]. Available from: http://www.ncbi.nlm.nih.gov/pubmed/10665489
66. Pérez A, Probert AW, Wang KK, Sharmeen L (2001) Evaluation of HIV-1 tat induced neurotoxicity in rat cortical cell culture. J Neurovirol [Internet] 7(1):1–10. Feb 1 [cited 2018 July 27]. Available from: http://www.ncbi.nlm.nih.gov/pubmed/11519477
67. King JE, Eugenin EA, Buckner CM, Berman JW (2006) HIV tat and neurotoxicity. Microbes Infect [Internet] 8(5):1347–1357. Apr [cited 2018 July 27]. Available from: http://www.ncbi.nlm.nih.gov/pubmed/16697675
68. Buscemi L, Ramonet D, Geiger JD (2007) Human immunodeficiency virus type-1 protein tat induces tumor necrosis factor-alpha-mediated neurotoxicity. Neurobiol Dis [Internet] 26(3):661–670. June [cited 2018 June 1]. Available from: http://www.ncbi.nlm.nih.gov/pubmed/17451964
69. Agrawal L, Louboutin J-P, Reyes BAS, Van Bockstaele EJ, Strayer DS (2012) HIV-1 tat neurotoxicity: a model of acute and chronic exposure, and neuroprotection by gene delivery of antioxidant enzymes. Neurobiol Dis [Internet] 45(2):657–670. Feb [cited 2018 July 27]. Available from: http://www.ncbi.nlm.nih.gov/pubmed/22036626
70. Johnson TP, Patel K, Johnson KR, Maric D, Calabresi PA, Hasbun R et al (2013) Induction of IL-17 and nonclassical T-cell activation by HIV-tat protein. Proc Natl Acad Sci U S A [Internet] 110(33):13588–13593. Aug 13 [cited 2017 July 20]. Available from: http://www.ncbi.nlm.nih.gov/pubmed/23898208
71. DSK M, Jsnudsen BE, Geiger JD, Brownstone RM, Nath A (1995) Human lmmunodehclency V m s lype 1 tat activates non-N-Methyla-aspartate excitatory ammo acid receptors and causes neurotoxicity. Ann Neurol [Internet] 37(3):373–380. [cited 2017 Nov 20]. Available from: https://med-und.illiad.oclc.org/illiad/illiad.dll?Action=10&Form=75&Value=116096

72. Nath A, Psooy K, Martin C, Knudsen B, Magnuson DS, Haughey N et al (1996) Identification of a human immunodeficiency virus type 1 tat epitope that is neuroexcitatory and neurotoxic. J Virol [Internet] 3(70):1475–1480. [cited 2018 June 13]. Available from: https://www.ncbi.nlm.nih.gov/pmc/articles/PMC189968/pdf/701475.pdf
73. Haughey NJ, Mattson MP (2002) Calcium dysregulation and neuronal apoptosis by the HIV-1 proteins tat and gp120. J Acquir Immune Defic Syndr [Internet] 31(Suppl 2):S55–S61. Oct 1 [cited 2018 July 27]. Available from: http://www.ncbi.nlm.nih.gov/pubmed/12394783
74. Kim HJ, Martemyanov KA, Thayer SA (2008) Human immunodeficiency virus protein tat induces synapse loss via a reversible process that is distinct from cell death. J Neurosci [Internet] 28(48):12604–12613. Nov 26 [cited 2018 July 27]. Available from: http://www.ncbi.nlm.nih.gov/pubmed/19036954
75. Fitting S, Xu R, Bull C, Buch SK, El-Hage N, Nath A et al (2010) Interactive comorbidity between opioid drug abuse and HIV-1 tat: chronic exposure augments spine loss and sublethal dendritic pathology in striatal neurons. Am J Pathol [Internet] 177(3):1397–1410. Sept [cited 2018 July 27]. Available from: http://www.ncbi.nlm.nih.gov/pubmed/20651230
76. Hui L, Chen X, Haughey NJ, Geiger JD (2012) Role of Endolysosomes in HIV-1 tat-induced neurotoxicity. ASN Neuro [Internet] 4(4):AN20120017. Apr 3 [cited 2018 July 27]. Available from: http://www.ncbi.nlm.nih.gov/pubmed/22591512
77. Rajendran L, Annaert W (2012) Membrane trafficking pathways in Alzheimer's disease. Traffic [Internet] 13(6):759–770. June [cited 2018 July 27]. Available from: http://www.ncbi.nlm.nih.gov/pubmed/22269004
78. Morel E, Chamoun Z, Lasiecka ZM, Chan RB, Williamson RL, Vetanovetz C et al (2013) Phosphatidylinositol-3-phosphate regulates sorting and processing of amyloid precursor protein through the endosomal system. Nat Commun [Internet] 4(1):2250. Dec 2 [cited 2018 July 27]. Available from: http://www.ncbi.nlm.nih.gov/pubmed/23907271
79. Jiang S, Li Y, Zhang X, Bu G, Xu H, Zhang Y (2014) Trafficking regulation of proteins in Alzheimer's disease. Mol Neurodegener [Internet] 9:6. Jan 11 [cited 2018 July 27]. Available from: http://www.ncbi.nlm.nih.gov/pubmed/24410826
80. Nixon RA (2005) Endosome function and dysfunction in Alzheimer's disease and other neurodegenerative diseases. Neurobiol Aging [Internet] 26(3):373–382. Mar [cited 2018 July 27]. Available from: http://www.ncbi.nlm.nih.gov/pubmed/15639316
81. Rajendran L, Schneider A, Schlechtingen G, Weidlich S, Ries J, Braxmeier T et al (2008) Efficient inhibition of the Alzheimer's disease -Secretase by membrane targeting. Science (80-) [Internet] 320(5875):520–523. Apr 25 [cited 2018 July 27]. Available from: http://www.ncbi.nlm.nih.gov/pubmed/18436784
82. Shimizu H, Tosaki A, Kaneko K, Hisano T, Sakurai T, Nukina N (2008) Crystal structure of an active form of BACE1, an enzyme responsible for amyloid protein production. Mol Cell Biol [Internet] 28(11):3663–3671. June 1 [cited 2018 July 27]. Available from: http://www.ncbi.nlm.nih.gov/pubmed/18378702
83. Sannerud R, Declerck I, Peric A, Raemaekers T, Menendez G, Zhou L et al (2011) ADP ribosylation factor 6 (ARF6) controls amyloid precursor protein (APP) processing by mediating the endosomal sorting of BACE1. Proc Natl Acad Sci [Internet] 108(34):E559–E568. Aug 23 [cited 2018 July 27]. Available from: http://www.ncbi.nlm.nih.gov/pubmed/21825135
84. Hamano T, Gendron TF, Causevic E, Yen S-H, Lin W-L, Isidoro C et al (2008) Autophagic-lysosomal perturbation enhances tau aggregation in transfectants with induced wild-type tau expression. Eur J Neurosci [Internet] 27(5):1119–1130. Mar [cited 2018 July 27]. Available from: http://www.ncbi.nlm.nih.gov/pubmed/18294209
85. Chesser AS, Pritchard SM, GVW J (2013) Tau clearance mechanisms and their possible role in the pathogenesis of Alzheimer disease. Front Neurol [Internet] 4:122. Sept 3 [cited 2018 July 27]. Available from: http://www.ncbi.nlm.nih.gov/pubmed/24027553

86. Jo C, Gundemir S, Pritchard S, Jin YN, Rahman I, GVW J (2014) Nrf2 reduces levels of phosphorylated tau protein by inducing autophagy adaptor protein NDP52. Nat Commun [Internet] 5(1):3496. Dec 25 [cited 2018 July 27]. Available from: http://www.nature.com/articles/ncomms4496
87. Bi X, Liao G (2007) Erratum: Autophagic-lysosomal dysfunction and neurodegeneration in Niemann-pick type C mice: lipid starvation or indigestion? (autophagy) [internet]. Autophagy 3:646–648. [cited 2018 July 27]. Available from: http://www.ncbi.nlm.nih.gov/pubmed/17921694
88. Polito VA, Li H, Martini-Stoica H, Wang B, Yang L, Xu Y et al (2014) Selective clearance of aberrant tau proteins and rescue of neurotoxicity by transcription factor EB. EMBO Mol Med [Internet] 6(9):1142–1160. Sept 1 [cited 2018 July 27]. Available from: http://www.ncbi.nlm.nih.gov/pubmed/25069841
89. Masgrau R, Churchill GC, Morgan AJ, Ashcroft SJH (2003) Galione a. NAADP: a new second messenger for glucose-induced Ca^{2+} responses in clonal pancreatic beta cells. Curr Biol [Internet] 13(3):247–251. Feb 4 [cited 2018 July 27]. Available from: http://www.ncbi.nlm.nih.gov/pubmed/12573222
90. Mitchell KJ, Lai FA, Rutter GA (2003) Ryanodine receptor type I and nicotinic acid adenine dinucleotide phosphate receptors mediate Ca^{2+} release from insulin-containing vesicles in living pancreatic β-cells (MIN6). J Biol Chem [Internet] 278(13):11057–11064. Mar 28 [cited 2018 July 27]. Available from: http://www.ncbi.nlm.nih.gov/pubmed/12538591
91. Haas E, Bhattacharya I, Brailoiu E, Damjanovic M, Brailoiu GC, Gao X et al (2009) Regulatory role of G protein-coupled estrogen receptor for vascular function and obesity. Circ Res [Internet] 104(3):288–291. Feb 13 [cited 2018 July 27]. Available from: http://www.ncbi.nlm.nih.gov/pubmed/19179659
92. Pandey V, Chuang C-C, Lewis AM, Aley PK, Brailoiu E, Dun NJ et al (2009) Recruitment of NAADP-sensitive acidic Ca^{2+} stores by glutamate. Biochem J [Internet] 422(3):503–512. Sept 15 [cited 2018 July 27]. Available from: http://www.ncbi.nlm.nih.gov/pubmed/19548879
93. Dickinson GD, Churchill GC, Brailoiu E, Patel S (2010) Deviant nicotinic acid adenine dinucleotide phosphate (NAADP)-mediated Ca^{2+} signaling upon lysosome proliferation. J Biol Chem [Internet] 285(18):13321–13325. Apr 30 [cited 2018 July 27]. Available from: http://www.ncbi.nlm.nih.gov/pubmed/20231291
94. Rempel HC, Pulliam L (2005) HIV-1 tat inhibits neprilysin and elevates amyloid β. AIDS [Internet] 19(2):127–135. Jan 28 [cited 2018 July 27]. Available from: http://www.ncbi.nlm.nih.gov/pubmed/15668537
95. Giunta B, Hou H, Zhu Y, Rrapo E, Tian J, Takashi M et al (2009) HIV-1 tat contributes to Alzheimer's disease-like pathology in PSAPP mice. Int J Clin Exp Pathol [Internet] 5(2):433–443. [cited 2018 July 27]. Available from: http://www.ncbi.nlm.nih.gov/pubmed/19294002
96. Aksenov MY, Aksenova MV, Mactutus CF, Booze RM (2010) HIV-1 protein-mediated amyloidogenesis in rat hippocampal cell cultures. Neurosci Lett [Internet] 475(3):174–178. May 21 [cited 2018 July 27]. Available from: http://www.ncbi.nlm.nih.gov/pubmed/20363291
97. Chen X, Hui L, Geiger NH, Haughey NJ, Geiger JD (2013) Endolysosome involvement in HIV-1 transactivator protein-induced neuronal amyloid beta production. Neurobiol Aging [Internet] 34(10):2370–2378. Oct [cited 2017 Aug 8]. Available from: http://www.ncbi.nlm.nih.gov/pubmed/23673310
98. Kim J, Yoon JH, Kim YS (2013) HIV-1 tat interacts with and regulates the localization and processing of amyloid precursor protein. Chauhan A, editor. PLoS One [Internet] 8(11):e77972. Nov 29 [cited 2018 July 27]. Available from: http://www.ncbi.nlm.nih.gov/pubmed/24312169
99. Fields JA, Dumaop W, Crews L, Adame A, Spencer B, Metcalf J et al (2015) Mechanisms of HIV-1 tat neurotoxicity via CDK5 translocation and hyper-activation: role in HIV-associated neurocognitive disorders. Curr HIV Res [Internet] 13(1):43–54. [cited 2018 July 27]. Available from: http://www.ncbi.nlm.nih.gov/pubmed/25760044

100. Liu Y, Jones M, Hingtgen CM, Bu G, Laribee N, Tanzi RE et al (2000) Uptake of HIV-1 tat protein mediated by low-density lipoprotein receptor-related protein disrupts the neuronal metabolic balance of the receptor ligands. Nat Med [Internet] 6(12):1380–1387. Dec 1 [cited 2018 July 27]. Available from: http://www.ncbi.nlm.nih.gov/pubmed/11100124
101. Deshmane SL, Mukerjee R, Fan S, Sawaya BE (2011) High-performance capillary electrophoresis for determining HIV-1 tat protein in neurons. Kashanchi F, editor. PLoS One [Internet] 6(1):e16148. Jan 7 [cited 2018 July 27]. Available from: http://dx.plos.org/10.1371/journal.pone.0016148
102. Vendeville A, Rayne F, Bonhoure A, Bettache N, Montcourrier P, Beaumelle B (2004) HIV-1 tat enters T cells using coated pits before translocating from acidified endosomes and eliciting biological responses. Mol Biol Cell [Internet] 15(5):2347–2360. May [cited 2018 July 27]. Available from: http://www.ncbi.nlm.nih.gov/pubmed/15020715
103. Mangieri LR, Mader BJ, Thomas CE, Taylor CA, Luker AM, Tse TE et al (2014) ATP6V0C knockdown in Neuroblastoma cells alters autophagy-lysosome pathway function and metabolism of proteins that accumulate in neurodegenerative disease. Srinivasula SM, editor. PLoS One [Internet] 9(4):e93257. Apr 2 [cited 2018 July 27]. Available from: http://dx.plos.org/10.1371/journal.pone.0093257
104. Bendiske J, Caba E, Brown QB, Bahr BA (2002) Intracellular deposition, microtubule destabilization, and transport failure: an "early" pathogenic Cascade leading to synaptic decline. J Neuropathol Exp Neurol [Internet] 61(7):640–650. July 1 [cited 2018 July 27]. Available from: https://academic.oup.com/jnen/article-lookup/doi/10.1093/jnen/61.7.640
105. Bendiske J, Bahr BA (2003) Lysosomal activation is a compensatory response against protein accumulation and associated synaptopathogenesis–an approach for slowing Alzheimer disease? J Neuropathol Exp Neurol [Internet] 62(5):451–463. May [cited 2018 July 27]. Available from: http://www.ncbi.nlm.nih.gov/pubmed/12769185
106. Kanju PM, Parameshwaran K, Vaithianathan T, Sims CM, Huggins K, Bendiske J et al (2007) Lysosomal dysfunction produces distinct alterations in synaptic alpha-amino-3-hydroxy-5-methylisoxazolepropionic acid and N-methyl-D-aspartate receptor currents in hippocampus. J Neuropathol Exp Neurol [Internet] 66(9):779–788. Sept [cited 2018 July 27]. Available from: http://www.ncbi.nlm.nih.gov/pubmed/17805008

Chapter 28
At the Crossing of ER Stress and MAMs: A Key Role of Sigma-1 Receptor?

Benjamin Delprat, Lucie Crouzier, Tsung-Ping Su, and Tangui Maurice

Abstract Calcium exchanges and homeostasis are finely regulated between cellular organelles and in response to physiological signals. Besides ionophores, including voltage-gated Ca^{2+} channels, ionotropic neurotransmitter receptors, or Store-operated Ca^{2+} entry, activity of regulatory intracellular proteins finely tune Calcium homeostasis. One of the most intriguing, by its unique nature but also most promising by the therapeutic opportunities it bears, is the sigma-1 receptor (Sig-1R). The Sig-1R is a chaperone protein residing at mitochondria-associated endoplasmic reticulum (ER) membranes (MAMs), where it interacts with several partners involved in ER stress response, or in Ca^{2+} exchange between the ER and mitochondria. Small molecules have been identified that specifically and selectively activate Sig-1R (Sig-1R agonists or positive modulators) at the cellular level and that also allow effective pharmacological actions in several pre-clinical models of pathologies. The present review will summarize the recent data on the mechanism of action of Sig-1R in regulating Ca^{2+} exchanges and protein interactions at MAMs and the ER. As MAMs alterations and ER stress now appear as a common track in most neurodegenerative diseases, the intracellular action of Sig-1R will be discussed in the context of the recently reported efficacy of Sig-1R drugs in pathologies like Alzheimer's disease, Parkinson's disease, Huntington's disease, or amyotrophic lateral sclerosis.

Keywords Sigma-1 receptor · Calcium · Mitochondria · ER stress · UPR · MAMs · Neurodegenerative disease · Alzheimer's disease · Amyotrophic lateral sclerosis · Addiction · Pain

B. Delprat (✉) · L. Crouzier · T. Maurice
MMDN, University of Montpellier, EPHE, INSERM, U1198, Montpellier, France
e-mail: benjamin.delprat@inserm.fr

T.-P. Su
Cellular Pathobiology Section, Integrative Neuroscience Branch, Intramural Research Program, National Institute on Drug Abuse, NIH, DHHS, IRP, NIDA/NIH, Baltimore, MD, USA

M. S. Islam (ed.), *Calcium Signaling*, Advances in Experimental Medicine and Biology 1131, https://doi.org/10.1007/978-3-030-12457-1_28

28.1 Introduction: Physiopathology of Sigma-1 Receptor (Sig-1R)

The Sigma-1 receptor (Sig-1R), discovered in the mid 1970s [1] was identified as a 223-amino acid protein only in the mid-1990s [2, 3]. Although its involvement in physiopathology started to be documented earlier, its cellular role was precised only 10 years ago [4] and cellular biology studies continue to precise its intracellular partners and functions. It shares no homology with any other known protein, except some steroid related/emopamyl-binding enzymes [2, 5, 6]. The protein was initially viewed as a receptor since, very early, specific and selective small molecules have been identified binding to Sig-1Rs and triggering (for so-called agonists) or preventing (for so-called antagonists) biological responses. However, its activation by physiological triggers, including ER stress or oxidative stress [4, 7, 8], and its mode of action, relying on modifications of protein-protein interactions rather than coupling to second messenger systems, suggested more a chaperone-like identity than a classical receptor nature [4]. Indeed, the present review will detail the effects of Sig-1R at intracellular organelles and show that it offers a unique opportunity to finely tune its activity, thereby impacting numerous physiopathological pathways, through a very classical pharmacological approach involving agonists, positive modulators or antagonists.

The Sig-1Rs are expressed in numerous organs, including liver, heart, lung, gonads and the nervous system, and numerous cell types, including, in the latter, neurons and glial cells (astrocytes, microglia, oligodendrocytes, Schwann cells) and vascular cells [9–11]. The particular density of Sig-1R in the nervous system is coherent with its importance in numerous psychiatric and neurological conditions. Sig1-Rs have indeed been involved in epilepsy [12, 13], stroke [14–16], drug abuse [17–19], pain [20, 21], and neurodegenerative pathologies. Interestingly, the last field of research is currently very active and recent evidence show both that Sig-1Rs play a role in the physiopathology of several neurodegenerative disease and that Sig-1R agonists have effective neuroprotective effects in preclinical models that deserve translation in clinical trials and better understanding of the mechanism of action of Sig-1R drugs against neurodegeneration. In parallel to the accumulating evidences that small molecules acting as Sig-1R agonist have pharmacological action in preclinical models of neurodegenerative diseases, and thus therapeutic potential, arguments are also brought confirming that Sig-1R exerts its cell homeostatic and cytoprotective activities mainly by directly targeting ER/mitochondria communication. We will here detail these arguments.

28.2 Sig-1R at the MAM

The ER of a cell spread almost all over a cell either in close proximity or in direct contacts with other subcellular components including the Golgi, mitochondria, nucleus, and plasma membrane. Through those close encounters, the ER plays

many critical functions in the cell. One such important contact site for the ER is the mitochondria-associated ER membrane, termed the MAM [22], which harbors not only the lipid exchange [22], mitochondrial DNA exchange, Ca^{2+} signaling between the ER and mitochondria [4, 23–27] but also plays a role in the ER-nucleus signaling for cellular survival [28]. Recent evidences also indicate that the MAM is the origin of the isolated membrane for autophagy [29]. In addition, the MAM is critical in the formation of inflammasome [30, 31].

The MAM contains a plethora of functional proteins [24, 32]. Among those is the Sig-1R which is an ER molecular chaperone with two transmembrane regions from cellular biology studies [4, 33] but only one from the X-ray crystallographic study [34]. At the MAM, the Sig-1R chaperones the inositol-1,4,5 trisphosphate receptor type 3 (IP_3R3) which would otherwise degrade after the stimulation of IP_3, ensuring thus proper Ca^{2+} signaling from the ER into mitochondria [4, 35]. At the MAM, the Sig-1R also chaperones inositol-requiring enzyme 1 (IRE-1), one of the ER stress sensors, to facilitate the signaling of the unfolded protein response from the ER into nucleus to call for the transcriptional activation of antioxidant proteins and chaperones [28]. The Sig-1R was also found to attenuate free radical formation around the MAM area to reduce the activation of caspase that would have degraded the guanine nucleotide exchange factor to inactivate Rac GTPase that is essential for dendritic spine formation [36]. The Sig-1R also plays a role, likely at the MAM, in binding and transferring myristic acid to p35 to facilitate the p35 degradation by proteasome at the plasma membrane, thereby diverting p35 from forming p25 that would otherwise stun the axon elongation [37]. However, it remains to be totally clarified how those molecular actions of the Sig-1R at the MAM may contribute to the overall cellular and physiological functions of the MAM in general in a cell.

Upon the stimulation of Sig-1R agonists, Sig-1Rs dissociate from innate co-chaperone binding immunoglobulin protein (BiP) and translocate to other parts of cell to interact with and regulate the function of receptors, ion channels, and other functional proteins at the plasma membrane, mitochondria, ER reticular network, and nucleus [38, 39]. Thus, due to the nature and dynamics of Sig-1Rs, the receptor plays multiple physiological roles in living systems.

One of the important physiological roles of the Sig-1R is to regulate Ca^{2+} signaling not only at the MAM but also at the ER reticular network and plasma membrane. Sig-1Rs at the MAM facilitate Ca^{2+} influx from the ER into mitochondria by chaperoning IP_3R3 at the MAM [4]. At the ER reticular network, the supranormal release of Ca^{2+} from the ER in medium spiny neurons of the YAC128 transgenic Huntington's disease mice was attenuated by a Sig-1R agonist [40]. The release of Ca^{2+} from the ER reticular network is mainly controlled by the IP_3R type 1 and the ryanodine receptor. Thus, this report suggests an inhibitory effect of Sig-1Rs on the IP_3R1 or the ryanodine receptor, which is in contrast to the facilitative effect of Sig-1Rs on IP_3R3. More experiments are needed as such.

The following three studies showed inconsistent effects of Sig-1Rs on the $[Ca^{2+}]_i$ in nevertheless different systems. Also, the site of action of Sig-1Rs were not identified. By using cultured cortical neurons, Sig-1R agonists were found to attenuate the ischemia-induced increase of $[Ca^{2+}]_i$ [41]. A recent study showed an

increased $[Ca^{2+}]_i$ when Sig-1Rs were activated by agonists in cultured embryonic mouse spinal neurons from ALS-causing mutants [42]. As well, methamphetamine-induced increase of $[Ca^{2+}]_i$ was shown to be attenuated by Sig-1R agonists in dopaminergic neurons [43]. Again, sites of action of Sig-1Rs in those three studies were not identified. It remains to be seen if those actions of Sig-1Rs were at the MAM, the ER reticular network, or the plasma membrane. Possibility exists that results were manifestation of concerted actions at all of those sites.

At the plasma membrane, Sig-1Rs showed a presynaptic action in inhibiting N-type Ca^{2+} channels in cholinergic interneurons in rat striatum, resulting in a decrease in presynaptic $[Ca^{2+}]_i$ [44]. The Sig-1R co-immunoprecipitated and co-localized with the N-type Ca^{2+} channel [24]. In rat brain microvascular endothelial cells, the store-operated calcium entry (SOCE) was attenuated by a Sig-1R agonist cocaine [45]. The mechanism of this interesting action of Sig-1R was reported in an elegant study in the same year. The Sig-1R was shown to bind stromal interaction molecule 1 (STIM1) at the ER when extracellular Ca^{2+} was depleted, and, as a result slowed down the recruitment of STIM1 to the ER-plasma membrane junction where STIM1 binds Orai1 [46]. The resultant inhibition of SOCE was seen when Sig-1Rs were overexpressed or when cells were treated with Sig-1R agonists. The Sig-1R antagonists or shSig-1R treatment enhanced the SOCE [46].

The calcium channels on the plasma membrane were examined in autonomous neurons taken from neonatal rat intracardiac and superior cervical ganglia (SCG). It was found that Sig-1Rs depressed high-voltage activated calcium currents from all calcium channel subtypes found on the cell body of these neurons, which includes N-, L-, P/Q-, and R-type calcium channels [47]. This study suggests that the activation of sigma receptors on sympathetic and parasympathetic neurons may modulate cell-to-cell signaling in autonomic ganglia and thus the regulation of cardiac function by the peripheral nervous system [47]. No direct interaction between Sig-1Rs and those calcium channels were demonstrated in this study however. The effect of Sig-1Rs on the potassium chloride-induced Ca^{2+} influx was examined by using retinal ganglion cell line (RGC)-5 and rat primary RGCs by the whole-cell patch clamp technique [48]. Sig-1R agonists inhibited the calcium influx and the Sig-1R antagonist reversed the inhibitory effect of Sig-1R agonist [48]. The Sig-1R was found to co-immunoprecipitate with the L-type calcium channels in this study.

Calcium homeostasis is critical to cellular physiology and plays an important role in many central nervous system (CNS) diseases, in particular the neurodegenerative diseases [49–54]. Since Sig-1Rs play critical role in calcium signaling at several loci of a cell, Sig-1Rs may be related to neurodegenerative diseases which show dysfunctional calcium homeostasis. However, a direct link between Sig-1R-regulated calcium signaling and a neurodegenerative disease has only been recently demonstrated in Huntington's disease as mentioned above [40].

Nevertheless, because Sig-1Rs reside mainly at the MAM which is increasingly recognized as an important loci related to many neurodegenerative diseases

[25, 49, 52, 53, 55, 56], it is possible that the Sig-1R at the MAM may participate in those diseases in a manner either directly related to calcium signaling or *via* other yet-to-be-revealed mechanisms at the MAM.

A study has specifically examined the role of Sig-1Rs at the MAM on ALS. Using primary motor neuron cultures, the study found that the pharmacological or genetic inactivation of Sig-1Rs led to motor neuron axonal degeneration [57]. They also found that the disruption of Sig-1R function in motor neurons disturbed ER-mitochondria contacts and affected intracellular calcium signaling, and was accompanied by activation of ER stress and defects in mitochondrial dynamics and transport (direct quotes) [57]. It is interesting to note that several other studies have implicated Sig-1Rs in ALS although they did not directly examine if the action of Sig-1Rs was at the MAM [58–61].

Sig-1Rs have been related to Alzheimer's disease (AD). Several Sig-1R agonists, including PRE-084, MR-22, afobasole, ANAVEX1-41, ANAVEX2-73 or dehydroepiandrosterone, prevented amyloid-$\beta_{25\text{-}35}$ ($A\beta_{25\text{-}35}$)-induced toxicity in rat neuronal cultures [62, 63] and/or $A\beta_{25\text{-}35}$-induced toxicity and learning impairments in mice in vivo [64–69]. Among the biochemical markers of toxicity in both in vitro and in vivo models, the Sig-1R drugs appear particularly effective in alleviating oxidative stress. Similar data were obtained in transgenic animal models of AD by Fisher et al. [70] who reported that AF710B, a mixed M1 mAChR/Sig-1R agonist, administered for 2 months in female 3xTg-AD mice, attenuated memory impairments and neurotoxicity. The drug also diminished soluble and insoluble Aβ species accumulation, the number of plaques and Tau hyperphosphorylation [70], thus confirming the neuroprotection and potentially disease-modifying effects of the drug. Moreover, invalidation of the Sig-1R expression, using Sig-1R knockout mice or a repeated treatment with the Sig-1R antagonist NE-100, increased learning deficits and neurotoxicity in $A\beta_{25\text{–}35}$-injected mice or after cross-breeding with $APP_{Swe,Ldn}$ mice [71]. Therefore, it appeared that the absence of Sig-1R could worsen Aβ toxicity and behavioral deficits while it activation by therapeutic drugs showed neuroprotection.

The role of the MAM in the pathogenesis of AD remains an important area of research. Interestingly, a study has related the toxicity of Aβ to the increase of $[Ca^{2+}]_i$ and the overload of mitochondrial calcium [72]. Nanomolar concentrations of Aβ was shown to increase MAM-associated proteins and caused an increase of the MAM [55]. Importantly, knockdown of Sig-1Rs resulted in neurodegeneration [55, 71]. Moreover, a direct examination of the effects of Sig-1R drugs in isolated mitochondria exposed to β-amyloid peptide showed that agonists decreased $A\beta_{1\text{–}42}$-induced increase in reactive oxygen species (ROS) and attenuated $A\beta_{1\text{–}42}$-induced alterations in mitochondrial respiration related to decreases in complex I and IV activity [73]. The Sig-1R agonists increased complex I activity, in a Ca^{2+}-dependent and Sig-1R antagonist-sensitive manner in physiological conditions. These observations identified direct consequences on mitochondria of Sig-1R activity. However, further research on the involvement of the MAM in Alzheimer's disease is certainly warranted.

Moreover, Sig-1R agonists, and particularly PRE-084, have been shown to be neuroprotective in mouse models of Parkinson's disease [74], Huntington's disease [75], amyotrophic lateral sclerosis (ALS) [76, 77], multiple sclerosis [78] or retinal neurodegeneration [79, 80], notably. Several recent reviews addressed the different progresses made so far [17, 51, 81–86]. For instance, a study examined the role of Sig-1Rs in Parkinsonism in a mouse model of intrastriatal lesion by 6-hydroxydopamine and found that the Sig-1R agonist significantly improved the fore-limb use [74]. At the molecular level, the study found that the agonist increased the density of dopaminergic fibers at the most denervated striatal regions and also caused an increase of neurotrophic factor brain-derived neurotrophic factor (BDNF) [74]. Interestingly, the agonist treatment induced a wider intracellular distribution of Sig-1Rs [74]. Because Sig-1Rs can translocate to other parts of neuron upon the stimulation by an agonist, it is tempting to speculate that the action of Sig-1Rs in the improvement of Parkinsonism may occur at the MAM as well other parts of neuron.

The Sig-1R has been shown to relate to Huntington's disease. Most of the evidence cam from studies using a drug called pridopidine which was effective against Huntington's disease in preclinical models and in phase two clinical trial at the secondary end-point level [87]. Originally thought to be a dopamine D2 ligand, pridopidine was nevertheless found to have a 100-fold higher affinity at the Sig-1R than at the dopamine D2 receptor [88]. In an in vivo radioligand binding assay, behaviorally relevant doses of pridopidine blocked about 57–85% of radiotracer binding to Sig-1Rs while blocked only negligible fraction of D2 receptor [89]. Recently, pridopidine was found to attenuate the phencyclidine-induced memory impairment through the Sig-1R-mediated mechanism as the effect of pridopidine was blocked by a Sig-1R antagonist NE-100 [90].

The exact mechanism and therefore the cellular site of action of Sig-1Rs underlying the action of pridopidine against Huntington's disease are however not fully clarified. However, couple of studies provide some interesting results. In Q175 knock-in (Q175 KI) *vs* Q25 WT mouse models, the effect of pridopidine versus sham treatment on genome-wide expression profiling in the rat striatum was analyzed and compared to the pathological expression profile. Then a broad, unbiased pathway analysis was conducted, followed by testing the enrichment of relevant pathways [87]. Results showed that pridopidine upregulated the BDNF pathway ($P = 1.73E\text{-}10$), and its effect on BDNF secretion was Sig-1R-dependent [87]. It remains to be investigated how Sig-1Rs may upregulate BDNF at the molecular level. As mentioned before, the action of pridopidine was examined in a mouse model of Huntington's disease with a specific focus on intracellular calcium signaling [40]. Results showed that pridopidine attenuates spine loss of medium spiny neurons and the effect was absent with the neuronal deletion of Sig-1Rs [40]. Pridopidine suppressed supranormal ER Ca^{2+} release, restored ER calcium levels and reduced excessive SOCE entry into spines. Interestingly, normalization of ER Ca^{2+} levels by pridopidine was prevented by Sig-1R deletion [40]. Whether those effects of Sig-1Rs originate at the MAM or beyond are not clear at present.

28.3 Sig-1R and ER Stress

The ER is an essential organelle of the cell that plays important role in protein folding and quality control [91, 92], lipid synthesis [93] and Ca^{2+} homeostasis [94]. During the life of the cell, different factors may perturb these functions, leading to a cellular state referred to as 'ER stress'. These stressors may be intrinsic, *i.e.*, cancer [95–98], neurodegenerative disease [99, 100], or diabetes [101, 102], or extrinsic, *i.e.*, micro-environmental stress [103], exposure to ER stressors [104], temperature [105] or reactive oxygen species production [106, 107]. Nevertheless, every time the ER is stressed, it triggers an adaptive response. This adaptive response is called the unfolded protein response (UPR). This UPR will help the cells to counter the stress by attenuating protein synthesis, clearing the unfolded proteins and enhancing the ability of the ER to fold proteins.

The UPR is an intracellular signal transduction mechanism that protects cells from ER stress. Three ER-resident transmembrane proteins function as stress sensors: RNA-activated protein kinase (PKR)-like endoplasmic reticular kinase (PERK); activating transcription factor 6 (ATF6); and IRE1. In basal state, these three transmembrane proteins are bound to BiP, an ER resident chaperone and are inactive [108, 109]. Upon a stress, the folding capacity of the ER is surpassed, leading to the dissociation of BiP from PERK, ATF6 and IRE1. This dissociation allows the activation of the three sensors [110]. Their activations transduce the unfolded protein stress signal across ER membrane and lead to UPR activation [111]. PERK is transmembrane ER resident protein of 1116 amino acids with two functional domains, a luminal and a cytosolic Ser/Thr kinase domain [112]. The dissociation of BiP from the luminal domain leads to oligomerization [108] and trans-autophosphorylation [113]. Activation of the PERK pathway leads to attenuation of general protein translation by phosphorylation of the α subunit of eukaryotic translation initiation factor 2 (eIF2α) [114]. Phosphorylated eIF2α inhibits eukaryotic translation initiation 2B activity, thus leading to a decrease of protein synthesis [115]. The blockage of the translation during ER stress diminishes the protein load on the ER folding machinery and is a prerequisite to a reestablishment of the ER homeostasis. In contrast to its attenuation of translation, eIF2α phosphorylation can selectively enhance the translation of mRNAs containing inhibitory upstream open reading frames in their 5′ untranslated region, such as activating transcription factor 4 (ATF4) [116]. The production of ATF4 induces the expression of a plethora of adaptive genes involved in amino acid transport, metabolism, protection from oxidative stress, protein homeostasis and autophagy [117]. Finally, ATF4 favors the expression of CAAT/enhancer-binding protein (C/EBP) homologous protein (CHOP), which will result in the expression of genes that are involved in protein synthesis and the UPR. If the expression of CHOP is sustained, the increased protein synthesis will lead to oxidative stress and cell death [118].

The second ER stress sensor is ATF6. ATF6 is also an ER resident transmembrane protein of 670 amino acids and two functional domains, an N-terminal

cytosolic containing basic leucine zipper and a C-terminal luminal domain. When BiP dissociates from ATF6, this one is exported to the Golgi where it will be cleaved by site-1 and site-2 proteases [119]. This cleavage releases a fragment of 400 amino acids corresponding to ATF6 cytosolic N-terminal domain. This released fragment of ATF6 will then translocate to the nucleus in order to act as a transcription factor. ATF6 will bind to the promoter of UPR-inducible genes, resulting in an upregulations of proteins, which role is to adjust ER protein folding, including ER chaperones and X-box-binding protein-1 (XBP-1) [120, 121].

The last ER stress sensor is IRE1. IRE1 is, like the two other sensors, an ER resident transmembrane proteins of 977 amino acids with three functional domains, an N-terminal luminal domain, a C-terminal Ser/Thr kinase domain and a C-terminal RNase L domain. The dissociation with BiP triggers oligomerization and activation of its cytosolic kinase domain. This activation facilitates the unconventional splicing of XBP-1 mRNA and subsequent translation of an active transcription factor, XBP1s [111, 121]. XBP1s is a basic leucine zipper transcription factor [122]. XBP1s controls the expression of several targets including chaperones, foldases and components of the ER-associated degradation (ERAD) pathway, in order to stop the ER stress and restore homeostasis [123]. The ERAD system destroys unfolded proteins through degradation in the cytosol [124]. Indeed, unfolded ER proteins are retro-translocated across the ER membrane into the cytosol in order to be degraded by the proteasome, following ubiquitination by ubiquitin-conjugating enzymes [125, 126]. Finally, the RNase activity of IRE1 may also target other genes *via* a mechanism named regulated IRE1-dependent decay (RIDD) [127]. RIDD is a conserved mechanism in eukaryotes by which IRE1 cleaves its target substrates [128]. The cleaved transcripts are degraded by exoribonucleases [129]. Therefore, RIDD seems to be required for the maintenance of ER homeostasis by diminishing ER protein load *via* mRNA degradation. Notably, it has been recently suggested that the physiological activity of RIDD may increase with the severity of the ER stress [130].

Interestingly, a substantial number of proteins involved in UPR are localized in MAMs [23]. Indeed, two of the three major proteins involved in UPR, PERK [131] and IRE1 [28], are enriched in MAMs. Intriguingly, some ER chaperones involved in UPR are also enriched in MAMs. For example, Calnexin, a type I integral membrane protein which helps in folding newly synthetize proteins which is essential in mitigating ER stress, is expressed in MAMs [132]. Another chaperone expressed in MAMs is the Sig-1R. The first evidence of the role of Sig-1R in ER stress came from the observation that under Ca^{2+} depletion or when stimulated by its ligand, Sig-1R dissociates from BiP, thus allowing a sustained Ca^{2+} efflux from the ER via IP_3R [4]. In addition, under ER stress following treatment with tunicamycin or thapsigargin, Sig-1R is upregulated, suggesting that it is protective against ER stress. Interestingly, overexpression on Sig-1R suppressed ER stress-induced activation of PERK and ATF6. IRE1 is expressed in MAMs and Sig-1R regulates the stability of IRE1 [28]. This enhanced stability favors the phosphorylation level of IRE1 under ER stress. Notably, the Sig-1R knock down potentiates the apoptosis of cells under ER stress. They showed that increased

apoptosis was due to a diminution of the Xbp1 splicing [28]. In addition, activation of Sig-1R increases Bcl-2 expression, allowing Bcl-2/IP3R interaction, leading to increased mitochondrial Ca^{2+} uptake and ATP production [133] (see Penke et al. for review [134]).

It is well known that Sig-1R plays an important protective role in retinal disease [85]. Using *in situ* hybridization, Ola et al. [135] detected the Sig-1R mRNA in retinal ganglion cells, cells of the inner nuclear layer, photoreceptor and retinal pigment epithelium. The mRNA expression was confirmed by immunohistochemistry. Ha et al. [136] described that in Müller cells of the retina from Sig-1R KO mice, the expression of PERK, IRE1 and ATF4 was decreased, whereas the expression of BiP, CHOP and ATF6 was increased. Intriguingly, no difference was detected in whole brain or whole retina. Similar to what was described by Yang et al. [133], Ha et al. saw a decrease expression of Bcl-2 associated with decrease in NFkB and pERK1/2 [136]. Moreover, Wang et al. [137] demonstrated that loss of Sig-1R in a model of retinitis pigmentosa (rd10), aggravates the degeneration of the photoreceptors. They revealed that at P28, the expression level of Xbp1 and CHOP is increased in the rd10 mice without Sig-1R expression.

Since Sig-1R is a receptor that can be activated or inhibited, different groups determined the effect of its activation or inhibition in following ER stress. Ha et al. [138] treated RGC-5 cells with (+)-pentazocine, a potent Sig-1R agonist. RGC-5 cells are a rat retinal ganglion cell line [139]. They showed that whereas the protein level of PERK, ATF4, ATF6 IRE1 and CHOP was upregulated during oxidative stress, in the presence of (+)-pentazocine, their expression level decreased, suggesting that Sig-1R plays a pivotal role in the UPR response. These results confirmed the initial observation of Wang et al. [140] that stimulation of Sig-1R protects against oxidative stress. Indeed, in human cell line FHL124, H_2O_2 treatment induces apoptosis, associated to an increase level of BiP, ATF6 and p-eIF2α. Application of (+)-pentazocine suppressed the induction of BiP and p-eIF2α. Another agonist, fluvoxamine, alleviates induction of CHOP, cleaved caspase 3 and 4 in cancer neuronal cell SK-N-SH [141]. In another experiment, Omi et al. [142] showed that treatment of neuronal cell line Neuro2a induces overexpression of Sig-1R. This expression is mediated by ATF4, a downstream element of PERK activation. Interestingly, this overexpression is achieved without activating UPR. Intriguingly, the increased translation of ATF4 is dependent of the presence/function of Sig-1R since if the concomitant treatment of Neuro2a cells with Fluvoxamine and NE-100, a Sig-1R antagonist, abolished the ATF4 translation. This result was confirmed by the use of mouse embryonic fibroblasts (MEF) from Sig-1R KO mice. Indeed, fluvoxamine treatment of these MEF did not increase ATF4 expression. Morihara et al. [143] treated mice with Sig-1R agonist aniline derivative compound (Comp-AD) following ischemic stroke, since it is well known that Sig-1R protects against ischemic stroke but the role of ER stress was unknown. So, treatment of mice after 90 min of transient middle cerebral artery, diminished the expression level of p-PERK and p-IRE1, suggesting that activation of Sig-1R protects against ischemic stroke *via* the attenuation of ER stress.

If Sig-1R activation suppresses effectively ER stress, it should be expected that inhibition of Sig-1R should do the contrary. This was demonstrated by Ono et al. [144] using Sig-1R antagonist, by Hong et al. [145] using Sig-1R KO, and Alam et al. [146] using siRNA to knock down Sig-1R. Ono et al. [144] showed that NE-100 protects ER stress induced cell death in hippocampal HT22 cells after tunicamycin treatment. Indeed, NE-100 application attenuated the upregulation of CHOP. Interestingly, NE-100 treatment alone was capable of upregulate the expression of both ATF6 and BiP. Total ablation of Sig-1R in dopaminergic neurons of substantia nigra in mice led to an elevation of the expression level of p-eIF2α and CHOP [145]. In cardiomyocytes treated with tunicamycin, the downregulation of Sig-1R by siRNA led to an increase of CHOP expression. They also showed that Sig-1R downregulation diminished IRE1 phosphorylation and Xbp1 splicing [146].

Mutations of Sig-1R in human may lead to Juvenile [58] and classic ALS [147] or distal hereditary neuropathy (dHMN) [148–151]. Interestingly, E102Q mutation, which induces juvenile ALS, leads to ER stress [59, 152]. Indeed, over-expression of Sig-1R mutant in MCF7 cells induced an aggregation of the mutant protein into the ER in contrast to the overexpression of the wild-type Sig-1R, which is localized in the ER, the nuclear envelope end ER-Golgi intermediate compartment. Using ER stress response element (ERSE) reporter assay, they detected an increase in ER stress in MCF7 cells. There was an increase expression level of p-eIF2α, BiP, HSP70, GADD. Moreover, they showed a co-localization of ubiquitin-positive Sig-1R mutant aggregates with 20S proteasome subunit, suggesting possible interference with the ubiquitin proteasome system machinery [59]. In parallel, they demonstrated that the proteasome activity was greatly reduced. In order to confirm the results observed in transfected cells, they generated immortalized primary lymphoblastoid cells (PLCs) from blood samples of ALS patients. In PLCs, they also showed an aggregation of mutant Sig-1R in the ER associated with an increase level of BiP and p-eIF2α together with an increase of HSP70, GADD and ubiquitin conjugates [59].

28.4 Sig-1R in the Nucleus

Although Sig-1R is known to be particularly enriched in MAMs, observation of Sig-1Rs at the nuclear envelope (NE) and within nucleoplasms have also been reported. First, after stimulation by agonists such as cocaine, Sig-1Rs were found to translocate from ER to the NE, where they bind NE protein emerin and recruit chromatin-remodeling molecules [37]. These partners include lamin A/C, barrier-to-autointegration factor, and histone deacetylase (HDAC), to form a complex with the gene repressor specific protein 3 (Sp3). The dynamics of the interaction was

confirmed when knockdown of Sig-1Rs attenuated the complex formation [37]. These observations were confirmed and developed by Mavlyutov et al. [153] who expressed APEX2 peroxidase fused to Sig1R-GFP in a Sig1R-null NSC34 neuronal cell line generated with CRISPR-Cas9. They observed that Sig1R actually resides in the nucleoplasmic reticulum, a specialized nuclear compartment formed via NE invagination into the nucleoplasm. A major consequence for this localization appears to be related to neurodegenerative pathologies since accumulation of Sig-1R may be common to neuronal nuclear inclusions in various proteinopathies [154]. Sig-1R immunoreactivity was shown to be co-localized with neuronal nuclear inclusions in TDP-43 proteinopathy, five polyglutamine diseases and intranuclear inclusion body disease, as well as in intranuclear Marinesco bodies in aged normal controls [154]. These authors interestingly proposed that Sig-1Rs might shuttle between the nucleus and the cytoplasm and likely play an important role in neurodegenerative diseases, characterized by neuronal nuclear inclusions, and known to particularly rely on ER-related degradation machinery as a common pathway for the degradation of aberrant proteins [154].

28.5 Conclusion

The Sig-1R protein is not specifically a MAM or ER protein, and direct interactions have been described at or close to the plasma membrane with potassium or sodium ion channels, ether-a-gogo-related gene (ERG) ionophores and metabotropic neurotransmitter receptors [39]. One of the complexity seen with Sig-1R is the multiplicity of its intracellular partners and consequent target pathways affected by its activation, as summarized in Fig. 28.1. This multiplicity of actions within different types of cells, in the brain as well as in other tissues, explain its involvement in numerous physiopathological processes and its value as a potential therapeutic target. Moreover, the well-known observation that bearing a relatively simple pharmacophore, Sig-1R binds small molecules, and even steroids or peptides, of diverse nature with high affinity, contributed to poorly considered it as a pertinent pharmacological target for therapeutic intervention. The data we discussed in this review allow to realize that we are now accumulating evidence on the mechanisms of action of Sig-1R, on its major role at MAMs and the ER, on its efficacy to maintain, and putatively restore cellular integrity and Ca^{2+} homeostasis (Fig. 28.1). The recent progression of several molecules in clinical phases in Alzheimer's disease or Huntington's disease strengthened the validity of Sig-1R as a pharmacological target. Moreover, their efficacies in preclinical models of different pathologies outlined the importance of MAM and ER alterations in neurodegenerative processes.

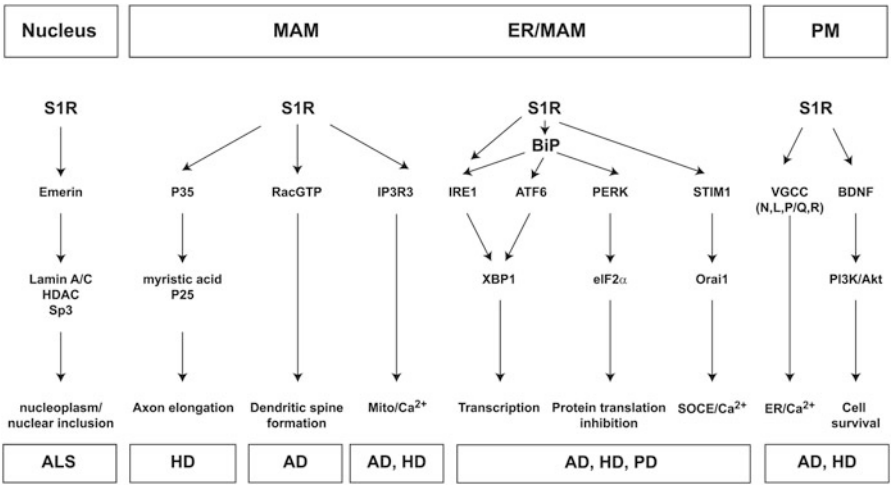

Fig. 28.1 Schematic diagram of the role of 1R in different compartment of the cell and putative major impacts in neurodegenerative diseases (AD, PD, HD, ALS)
In the nucleus, S1R interacts with Emerin [37]. This interaction leads to the recruitment of chromatin-remodeling molecules such as Lamin A/C and HDAC. This interaction is necessary for the creation of a supercomplex with Sp3. In the MAM, S1R interacts with P35 [37]. This will leads to the myristoylation of P25 and axon elongation. S1R interacts with RacGTP in order to foster dendritic spine formation [155]. S1R interacts with IP_3R3 in order to allow the proper Ca^{2+} efflux from the ER to the mitochondria [4]. In the ER, S1R interacts with BiP [4]. Upon stimulation, the dissociation of S1R with BiP induces activation of IRE1 [28] and ATF6 [136, 138, 144]. This will induce the splicing of XBP1 and the transcription of chaperones. The activation of PERK [144, 156] will induce the phosphorylation of eIF2α, to stop protein translation. Finally, S1R interacts with STIM1 and this interaction will regulate Ca^{2+} fluxes into the ER thought the STIM1/Orai1 axe [46]. In the plasma membrane, S1R interacts with voltage-gated calcium channels (for review, [157]) in order to modulate Ca^{2+} homeostasis. S1R favors BDNF secretion [74, 87]. BDNF will activate the PI3K/Akt pathway in order to improve cell survival

References

1. Martin WR, Eades CG, Thompson JA, Huppler RE, Gilbert PE (1976) The effects of morphine- and nalorphine- like drugs in the nondependent and morphine-dependent chronic spinal dog. J Pharmacol Exp Ther 197(3):517–532
2. Hanner M, Moebius FF, Flandorfer A, Knaus HG, Striessnig J, Kempner E et al (1996) Purification, molecular cloning, and expression of the mammalian $sigma_1$-binding site. Proc Natl Acad Sci U S A 93(15):8072–8077
3. Kekuda R, Prasad PD, Fei YJ, Leibach FH, Ganapathy V (1996) Cloning and functional expression of the human type 1 sigma receptor (hSigmaR1). Biochem Biophys Res Commun 229(2):553–558
4. Hayashi T, Su TP (2007) Sigma-1 receptor chaperones at the ER-mitochondrion interface regulate Ca^{2+} signaling and cell survival. Cell 131(3):596–610
5. Maurice T, Gregoire C, Espallergues J (2006) Neuro(active)steroids actions at the neuromodulatory $sigma_1$ (σ_1) receptor: biochemical and physiological evidences, consequences in neuroprotection. Pharmacol Biochem Behav 84(4):581–597

6. Moebius FF, Reiter RJ, Hanner M, Glossmann H (1997) High affinity of sigma 1-binding sites for sterol isomerization inhibitors: evidence for a pharmacological relationship with the yeast sterol C8-C7 isomerase. Br J Pharmacol 121(1):1–6
7. Meunier J, Hayashi T (2010) Sigma-1 receptors regulate Bcl-2 expression by reactive oxygen species-dependent transcriptional regulation of nuclear factor kappaB. J Pharmacol Exp Ther 332(2):388–397
8. Pal A, Fontanilla D, Gopalakrishnan A, Chae YK, Markley JL, Ruoho AE (2012) The sigma-1 receptor protects against cellular oxidative stress and activates antioxidant response elements. Eur J Pharmacol 682(1-3):12–20
9. Alonso G, Phan V, Guillemain I, Saunier M, Legrand A, Anoal M et al (2000) Immunocytochemical localization of the sigma$_1$ receptor in the adult rat central nervous system. Neuroscience 97(1):155–170
10. Palacios G, Muro A, Vela JM, Molina-Holgado E, Guitart X, Ovalle S et al (2003) Immunohistochemical localization of the sigma$_1$-receptor in oligodendrocytes in the rat central nervous system. Brain Res 961(1):92–99
11. Tagashira H, Bhuiyan S, Shioda N, Hasegawa H, Kanai H, Fukunaga K (2010) Sigma1-receptor stimulation with fluvoxamine ameliorates transverse aortic constriction-induced myocardial hypertrophy and dysfunction in mice. Am J Physiol Heart Circ Physiol 299(5):H1535–H1545
12. Meurs A, Clinckers R, Ebinger G, Michotte Y, Smolders I (2007) Sigma 1 receptor-mediated increase in hippocampal extracellular dopamine contributes to the mechanism of the anticonvulsant action of neuropeptide Y. Eur J Neurosci 26(11):3079–3092
13. Vavers E, Svalbe B, Lauberte L, Stonans I, Misane I, Dambrova M et al (2017) The activity of selective sigma-1 receptor ligands in seizure models in vivo. Behav Brain Res 328:13–18
14. Harukuni I, Bhardwaj A, Shaivitz AB, DeVries AC, London ED, Hurn PD et al (2000) sigma$_1$-receptor ligand 4-phenyl-1-(4-phenylbutyl)-piperidine affords neuroprotection from focal ischemia with prolonged reperfusion. Stroke 31(4):976–982
15. Lesage AS, De Loore KL, Peeters L, Leysen JE (1995) Neuroprotective sigma ligands interfere with the glutamate-activated NOS pathway in hippocampal cell culture. Synapse 20(2):156–164
16. Shen YC, Wang YH, Chou YC, Liou KT, Yen JC, Wang WY et al (2008) Dimemorfan protects rats against ischemic stroke through activation of sigma-1 receptor-mediated mechanisms by decreasing glutamate accumulation. J Neurochem 104(2):558–572
17. Cai Y, Yang L, Niu F, Liao K, Buch S (2017) Role of sigma-1 receptor in cocaine abuse and neurodegenerative disease. Adv Exp Med Biol 964:163–175
18. Maurice T, Martin-Fardon R, Romieu P, Matsumoto RR (2002) Sigma$_1$ (σ_1) receptor antagonists represent a new strategy against cocaine addiction and toxicity. Neurosci Biobehav Rev 26(4):499–527
19. Su TP, Hayashi T (2001) Cocaine affects the dynamics of cytoskeletal proteins via sigma$_1$ receptors. Trends Pharmacol Sci 22(9):456–458
20. Diaz JL, Zamanillo D, Corbera J, Baeyens JM, Maldonado R, Pericas MA et al (2009) Selective sigma-1 (σ_1) receptor antagonists: emerging target for the treatment of neuropathic pain. Cent Nerv Syst Agents Med Chem 9(3):172–183
21. Zamanillo D, Romero L, Merlos M, Vela JM (2013) Sigma 1 receptor: a new therapeutic target for pain. Eur J Pharmacol 716(1-3):78–93
22. Vance JE (1990) Phospholipid synthesis in a membrane fraction associated with mitochondria. J Biol Chem 265(13):7248–7256
23. Carreras-Sureda A, Pihan P, Hetz C (2017) The unfolded protein response: at the intersection between endoplasmic reticulum function and mitochondrial bioenergetics. Front Oncol 7:55
24. Hayashi T, Rizzuto R, Hajnoczky G, Su TP (2009) MAM: more than just a housekeeper. Trends Cell Biol 19(2):81–88
25. Raturi A, Simmen T (2013) Where the endoplasmic reticulum and the mitochondrion tie the knot: the mitochondria-associated membrane (MAM). Biochim Biophys Acta 1833(1): 213–224

26. Rizzuto R, Duchen MR, Pozzan T (2004) Flirting in little space: the ER/mitochondria Ca^{2+} liaison. Sci STKE 2004(215):re1
27. Walter L, Hajnoczky G (2005) Mitochondria and endoplasmic reticulum: the lethal interorganelle cross-talk. J Bioenerg Biomembr 37(3):191–206
28. Mori T, Hayashi T, Hayashi E, Su TP (2013) Sigma-1 receptor chaperone at the ER-mitochondrion interface mediates the mitochondrion-ER-nucleus signaling for cellular survival. PLoS One 8(10):e76941
29. Hamasaki M, Furuta N, Matsuda A, Nezu A, Yamamoto A, Fujita N et al (2013) Autophagosomes form at ER-mitochondria contact sites. Nature 495(7441):389–393
30. Sutterwala FS, Haasken S, Cassel SL (2014) Mechanism of NLRP3 inflammasome activation. Ann N Y Acad Sci 1319:82–95
31. Zhou R, Yazdi AS, Menu P, Tschopp J (2011) A role for mitochondria in NLRP3 inflammasome activation. Nature 469(7329):221–225
32. Poston CN, Krishnan SC, Bazemore-Walker CR (2013) In-depth proteomic analysis of mammalian mitochondria-associated membranes (MAM). J Proteome 79:219–230
33. Fontanilla D, Hajipour AR, Pal A, Chu UB, Arbabian M, Ruoho AE (2008) Probing the steroid binding domain-like I (SBDLI) of the sigma-1 receptor binding site using N-substituted photoaffinity labels. Biochemistry 47(27):7205–7217
34. Schmidt HR, Zheng S, Gurpinar E, Koehl A, Manglik A, Kruse AC (2016) Crystal structure of the human $sigma_1$ receptor. Nature 532(7600):527–530
35. Wu Z, Bowen WD (2008) Role of sigma-1 receptor C-terminal segment in inositol 1,4,5-trisphosphate receptor activation: constitutive enhancement of calcium signaling in MCF-7 tumor cells. J Biol Chem 283(42):28198–28215
36. Tsai SY, Hayashi T, Harvey BK, Wang Y, Wu WW, Shen RF et al (2009) Sigma-1 receptors regulate hippocampal dendritic spine formation via a free radical-sensitive mechanism involving Rac1xGTP pathway. Proc Natl Acad Sci U S A 106(52):22468–22473
37. Tsai SY, Pokrass MJ, Klauer NR, Nohara H, Su TP (2015) Sigma-1 receptor regulates Tau phosphorylation and axon extension by shaping p35 turnover via myristic acid. Proc Natl Acad Sci U S A 112(21):6742–6747
38. Maurice T, Su TP (2009) The pharmacology of sigma-1 receptors. Pharmacol Ther 124(2):195–206
39. Su TP, Su TC, Nakamura Y, Tsai SY (2016) The sigma-1 receptor as a pluripotent modulator in living systems. Trends Pharmacol Sci 37(4):262–278
40. Ryskamp D, Wu J, Geva M, Kusko R, Grossman I, Hayden M et al (2017) The sigma-1 receptor mediates the beneficial effects of pridopidine in a mouse model of Huntington disease. Neurobiol Dis 97(Pt A):46–59
41. Katnik C, Guerrero WR, Pennypacker KR, Herrera Y, Cuevas J (2006) Sigma-1 receptor activation prevents intracellular calcium dysregulation in cortical neurons during in vitro ischemia. J Pharmacol Exp Ther 319(3):1355–1365
42. Tadic V, Malci A, Goldhammer N, Stubendorff B, Sengupta S, Prell T et al (2017) Sigma 1 receptor activation modifies intracellular calcium exchange in the G93A(hSOD1) ALS model. Neuroscience 359:105–118
43. Sambo DO, Lin M, Owens A, Lebowitz JJ, Richardson B, Jagnarine DA et al (2017) The sigma-1 receptor modulates methamphetamine dysregulation of dopamine neurotransmission. Nat Commun 8(1):2228
44. Zhang K, Zhao Z, Lan L, Wei X, Wang L, Liu X et al (2017) Sigma-1 receptor plays a negative modulation on N-type calcium channel. Front Pharmacol 8:302
45. Brailoiu GC, Deliu E, Console-Bram LM, Soboloff J, Abood ME, Unterwald EM et al (2016) Cocaine inhibits store-operated Ca^{2+} entry in brain microvascular endothelial cells: critical role for sigma-1 receptors. Biochem J 473(1):1–5
46. Srivats S, Balasuriya D, Pasche M, Vistal G, Edwardson JM, Taylor CW et al (2016) Sigma1 receptors inhibit store-operated Ca^{2+} entry by attenuating coupling of STIM1 to Orai1. J Cell Biol 213(1):65–79

47. Zhang H, Cuevas J (2002) Sigma receptors inhibit high-voltage-activated calcium channels in rat sympathetic and parasympathetic neurons. J Neurophysiol 87(6):2867–2879
48. Tchedre KT, Huang RQ, Dibas A, Krishnamoorthy RR, Dillon GH, Yorio T (2008) Sigma-1 receptor regulation of voltage-gated calcium channels involves a direct interaction. Invest Ophthalmol Vis Sci 49(11):4993–5002
49. Erpapazoglou Z, Mouton-Liger F, Corti O (2017) From dysfunctional endoplasmic reticulum-mitochondria coupling to neurodegeneration. Neurochem Int 109:171–183
50. Joshi AU, Kornfeld OS, Mochly-Rosen D (2016) The entangled ER-mitochondrial axis as a potential therapeutic strategy in neurodegeneration: a tangled duo unchained. Cell Calcium 60(3):218–234
51. Nguyen L, Lucke-Wold BP, Mookerjee S, Kaushal N, Matsumoto RR (2017) Sigma-1 receptors and neurodegenerative diseases: towards a hypothesis of sigma-1 receptors as amplifiers of neurodegeneration and neuroprotection. Adv Exp Med Biol 964:133–152
52. Ottolini D, Cali T, Negro A, Brini M (2013) The Parkinson disease-related protein DJ-1 counteracts mitochondrial impairment induced by the tumour suppressor protein p53 by enhancing endoplasmic reticulum-mitochondria tethering. Hum Mol Genet 22(11):2152–2168
53. Ouyang YB, Giffard RG (2012) ER-mitochondria crosstalk during cerebral ischemia: molecular chaperones and ER-mitochondrial calcium transfer. Int J Cell Biol 2012:493934
54. Zundorf G, Reiser G (2011) Calcium dysregulation and homeostasis of neural calcium in the molecular mechanisms of neurodegenerative diseases provide multiple targets for neuroprotection. Antioxid Redox Signal 14(7):1275–1288
55. Hedskog L, Pinho CM, Filadi R, Ronnback A, Hertwig L, Wiehager B et al (2013) Modulation of the endoplasmic reticulum-mitochondria interface in Alzheimer's disease and related models. Proc Natl Acad Sci U S A 110(19):7916–7921
56. Prudent J, McBride HM (2017) The mitochondria-endoplasmic reticulum contact sites: a signalling platform for cell death. Curr Opin Cell Biol 47:52–63
57. Bernard-Marissal N, Medard JJ, Azzedine H, Chrast R (2015) Dysfunction in endoplasmic reticulum-mitochondria crosstalk underlies SIGMAR1 loss of function mediated motor neuron degeneration. Brain 138(Pt 4):875–890
58. Al-Saif A, Al-Mohanna F, Bohlega S (2011) A mutation in sigma-1 receptor causes juvenile amyotrophic lateral sclerosis. Ann Neurol 70(6):913–919
59. Dreser A, Vollrath JT, Sechi A, Johann S, Roos A, Yamoah A et al (2017) The ALS-linked E102Q mutation in sigma receptor-1 leads to ER stress-mediated defects in protein homeostasis and dysregulation of RNA-binding proteins. Cell Death Differ 24(10):1655–1671
60. Luty AA, Kwok JB, Dobson-Stone C, Loy CT, Coupland KG, Karlstrom H et al (2010) Sigma nonopioid intracellular receptor 1 mutations cause frontotemporal lobar degeneration-motor neuron disease. Ann Neurol 68(5):639–649
61. Prause J, Goswami A, Katona I, Roos A, Schnizler M, Bushuven E et al (2013) Altered localization, abnormal modification and loss of function of Sigma receptor-1 in amyotrophic lateral sclerosis. Hum Mol Genet 22(8):1581–1600
62. Behensky AA, Yasny IE, Shuster AM, Seredenin SB, Petrov AV, Cuevas J (2013) Afobazole activation of sigma-1 receptors modulates neuronal responses to amyloid-β_{25-35}. J Pharmacol Exp Ther 347(2):468–477
63. Marrazzo A, Caraci F, Salinaro ET, Su TP, Copani A, Ronsisvalle G (2005) Neuroprotective effects of sigma-1 receptor agonists against beta-amyloid-induced toxicity. Neuroreport 16(11):1223–1226
64. Antonini V, Marrazzo A, Kleiner G, Coradazzi M, Ronsisvalle S, Prezzavento O et al (2011) Anti-amnesic and neuroprotective actions of the sigma-1 receptor agonist (−)-MR22 in rats with selective cholinergic lesion and amyloid infusion. J Alzheimers Dis 24(3):569–586
65. Lahmy V, Meunier J, Malmstrom S, Naert G, Givalois L, Kim SH et al (2013) Blockade of Tau hyperphosphorylation and $A\beta_{1-42}$ generation by the aminotetrahydrofuran derivative ANAVEX2-73, a mixed muscarinic and $sigma_1$ receptor agonist, in a nontransgenic mouse model of Alzheimer's disease. Neuropsychopharmacology 38(9):1706–1723

66. Meunier J, Ieni J, Maurice T (2006) The anti-amnesic and neuroprotective effects of donepezil against amyloid β_{25-35} peptide-induced toxicity in mice involve an interaction with the σ_1 receptor. Br J Pharmacol 149(8):998–1012
67. Villard V, Espallergues J, Keller E, Alkam T, Nitta A, Yamada K et al (2009) Antiamnesic and neuroprotective effects of the aminotetrahydrofuran derivative ANAVEX1-41 against amyloid β_{25-35}-induced toxicity in mice. Neuropsychopharmacology 34(6):1552–1566
68. Villard V, Espallergues J, Keller E, Vamvakides A, Maurice T (2011) Anti-amnesic and neuroprotective potentials of the mixed muscarinic receptor/sigma$_1$ (σ_1) ligand ANAVEX2-73, a novel aminotetrahydrofuran derivative. J Psychopharmacol 25(8):1101–1117
69. Yang R, Chen L, Wang H, Xu B, Tomimoto H, Chen L (2012) Anti-amnesic effect of neurosteroid PREGS in Aβ_{25-35}-injected mice through σ_1 receptor- and α_7 nAChR-mediated neuroprotection. Neuropharmacology 63(6):1042–1050
70. Fisher A, Bezprozvanny I, Wu L, Ryskamp DA, Bar-Ner N, Natan N et al (2016) AF710B, a Novel M1/σ_1 agonist with therapeutic efficacy in animal models of Alzheimer's disease. Neurodegener Dis 16(1-2):95–110
71. Maurice T, Strehaiano M, Duhr F, Chevallier N (2018) Amyloid toxicity is enhanced after pharmacological or genetic invalidation of the sigma1 receptor. Behav Brain Res 339:1–10
72. Sanz-Blasco S, Valero RA, Rodriguez-Crespo I, Villalobos C, Nunez L (2008) Mitochondrial Ca^{2+} overload underlies Aβ oligomers neurotoxicity providing an unexpected mechanism of neuroprotection by NSAIDs. PLoS One 3(7):e2718
73. Goguadze N, Zhuravliova E, Morin D, Mikeladze D, Maurice T (2019) Sigma-1 receptor agonists induce oxidative stress in mitochondria and enhance complex I activity in physiological condition but protect against pathological oxidative stress. Neurotox Res 35(1):1–18
74. Francardo V, Bez F, Wieloch T, Nissbrandt H, Ruscher K, Cenci MA (2014) Pharmacological stimulation of sigma-1 receptors has neurorestorative effects in experimental parkinsonism. Brain 137(Pt 7):1998–2014
75. Hyrskyluoto A, Pulli I, Tornqvist K, Ho TH, Korhonen L, Lindholm D (2013) Sigma-1 receptor agonist PRE084 is protective against mutant huntingtin-induced cell degeneration: involvement of calpastatin and the NF-κB pathway. Cell Death Dis 4:e646
76. Mancuso R, Olivan S, Rando A, Casas C, Osta R, Navarro X (2012) Sigma-1R agonist improves motor function and motoneuron survival in ALS mice. Neurotherapeutics 9(4): 814–826
77. Peviani M, Salvaneschi E, Bontempi L, Petese A, Manzo A, Rossi D et al (2014) Neuroprotective effects of the Sigma-1 receptor (S1R) agonist PRE-084, in a mouse model of motor neuron disease not linked to SOD1 mutation. Neurobiol Dis 62:218–232
78. Oxombre B, Lee-Chang C, Duhamel A, Toussaint M, Giroux M, Donnier-Marechal M et al (2015) High-affinity sigma1 protein agonist reduces clinical and pathological signs of experimental autoimmune encephalomyelitis. Br J Pharmacol 172(7):1769–1782
79. Smith SB, Duplantier J, Dun Y, Mysona B, Roon P, Martin PM et al (2008) In vivo protection against retinal neurodegeneration by sigma receptor 1 ligand (+)-pentazocine. Invest Ophthalmol Vis Sci 49(9):4154–4161
80. Zhao L, Chen G, Li J, Fu Y, Mavlyutov TA, Yao A et al (2017) An intraocular drug delivery system using targeted nanocarriers attenuates retinal ganglion cell degeneration. J Control Release 247:153–166
81. Francardo V, Schmitz Y, Sulzer D, Cenci MA (2017) Neuroprotection and neurorestoration as experimental therapeutics for Parkinson's disease. Exp Neurol 298(Pt B):137–147
82. Mancuso R, Navarro X (2017) Sigma-1 receptor in motoneuron disease. Adv Exp Med Biol 964:235–254
83. Maurice T, Goguadze N (2017) Role of σ_1 receptors in learning and memory and Alzheimer's disease-type dementia. Adv Exp Med Biol 964:213–233
84. Maurice T, Goguadze N (2017) Sigma-1 (σ_1) receptor in memory and neurodegenerative diseases. Handb Exp Pharmacol 244:81–108
85. Smith SB, Wang J, Cui X, Mysona BA, Zhao J, Bollinger KE (2018) Sigma 1 receptor: a novel therapeutic target in retinal disease. Prog Retin Eye Res 67:130–149

86. Weng TY, Tsai SA, Su TP (2017) Roles of sigma-1 receptors on mitochondrial functions relevant to neurodegenerative diseases. J Biomed Sci 24(1):74
87. Geva M, Kusko R, Soares H, Fowler KD, Birnberg T, Barash S et al (2016) Pridopidine activates neuroprotective pathways impaired in Huntington disease. Hum Mol Genet 25(18):3975–3987
88. Sahlholm K, Arhem P, Fuxe K, Marcellino D (2013) The dopamine stabilizers ACR16 and (−)-OSU6162 display nanomolar affinities at the sigma-1 receptor. Mol Psychiatry 18(1): 12–14
89. Sahlholm K, Sijbesma JW, Maas B, Kwizera C, Marcellino D, Ramakrishnan NK et al (2015) Pridopidine selectively occupies sigma-1 rather than dopamine D2 receptors at behaviorally active doses. Psychopharmacology 232(18):3443–3453
90. Sahlholm K, Valle-Leon M, Fernandez-Duenas V, Ciruela F (2018) Pridopidine reverses phencyclidine-induced memory impairment. Front Pharmacol 9:338
91. Braakman I, Bulleid NJ (2011) Protein folding and modification in the mammalian endoplasmic reticulum. Annu Rev Biochem 80:71–99
92. Hebert DN, Molinari M (2007) In and out of the ER: protein folding, quality control, degradation, and related human diseases. Physiol Rev 87(4):1377–1408
93. Fagone P, Jackowski S (2009) Membrane phospholipid synthesis and endoplasmic reticulum function. J Lipid Res 50(Suppl):S311–S316
94. Meldolesi J, Pozzan T (1998) The endoplasmic reticulum Ca^{2+} store: a view from the lumen. Trends Biochem Sci 23(1):10–14
95. Corazzari M, Gagliardi M, Fimia GM, Piacentini M (2017) Endoplasmic reticulum stress, unfolded protein response, and cancer cell fate. Front Oncol 7:78
96. Hanahan D, Weinberg RA (2011) Hallmarks of cancer: the next generation. Cell 144(5): 646–674
97. Hetz C, Papa FR (2018) The unfolded protein response and cell fate control. Mol Cell 69(2):169–181
98. Jain BP (2017) An overview of unfolded protein response signaling and its role in cancer. Cancer Biother Radiopharm 32(8):275–281
99. Hetz C, Saxena S (2017) ER stress and the unfolded protein response in neurodegeneration. Nat Rev Neurol 13(8):477–491
100. Xiang C, Wang Y, Zhang H, Han F (2017) The role of endoplasmic reticulum stress in neurodegenerative disease. Apoptosis 22(1):1–26
101. Ariyasu D, Yoshida H, Hasegawa Y (2017) Endoplasmic reticulum (ER) stress and endocrine disorders. Int J Mol Sci 18(2):382
102. Harding HP, Ron D (2002) Endoplasmic reticulum stress and the development of diabetes: a review. Diabetes 51(Suppl 3):S455–S461
103. Giampietri C, Petrungaro S, Conti S, Facchiano A, Filippini A, Ziparo E (2015) Cancer microenvironment and endoplasmic reticulum stress response. Mediat Inflamm 2015:417281
104. Foufelle F, Fromenty B (2016) Role of endoplasmic reticulum stress in drug-induced toxicity. Pharmacol Res Perspect 4(1):e00211
105. Liu Y, Sakamoto H, Adachi M, Zhao S, Ukai W, Hashimoto E et al (2012) Heat stress activates ER stress signals which suppress the heat shock response, an effect occurring preferentially in the cortex in rats. Mol Biol Rep 39(4):3987–3993
106. Bhandary B, Marahatta A, Kim HR, Chae HJ (2012) An involvement of oxidative stress in endoplasmic reticulum stress and its associated diseases. Int J Mol Sci 14(1):434–456
107. Cao SS, Kaufman RJ (2014) Endoplasmic reticulum stress and oxidative stress in cell fate decision and human disease. Antioxid Redox Signal 21(3):396–413
108. Bertolotti A, Zhang Y, Hendershot LM, Harding HP, Ron D (2000) Dynamic interaction of BiP and ER stress transducers in the unfolded-protein response. Nat Cell Biol 2(6):326–332
109. Shen J, Chen X, Hendershot L, Prywes R (2002) ER stress regulation of ATF6 localization by dissociation of BiP/GRP78 binding and unmasking of Golgi localization signals. Dev Cell 3(1):99–111

110. Almanza A, Carlesso A, Chintha C, Creedican S, Doultsinos D, Leuzzi B et al (2018) Endoplasmic reticulum stress signalling – from basic mechanisms to clinical applications. FEBS J 286:241–278
111. Schroder M, Kaufman RJ (2005) The mammalian unfolded protein response. Annu Rev Biochem 74:739–789
112. Harding HP, Zhang Y, Ron D (1999) Protein translation and folding are coupled by an endoplasmic-reticulum-resident kinase. Nature 397(6716):271–274
113. McQuiston A, Diehl JA (2017) Recent insights into PERK-dependent signaling from the stressed endoplasmic reticulum. F1000Res 6:1897
114. Schroder M (2006) The unfolded protein response. Mol Biotechnol 34(2):279–290
115. Rowlands AG, Panniers R, Henshaw EC (1988) The catalytic mechanism of guanine nucleotide exchange factor action and competitive inhibition by phosphorylated eukaryotic initiation factor 2. J Biol Chem 263(12):5526–5533
116. Lu PD, Harding HP, Ron D (2004) Translation reinitiation at alternative open reading frames regulates gene expression in an integrated stress response. J Cell Biol 167(1):27–33
117. Quiros PM, Prado MA, Zamboni N, D'Amico D, Williams RW, Finley D et al (2017) Multi-omics analysis identifies ATF4 as a key regulator of the mitochondrial stress response in mammals. J Cell Biol 216(7):2027–2045
118. Han J, Back SH, Hur J, Lin YH, Gildersleeve R, Shan J et al (2013) ER-stress-induced transcriptional regulation increases protein synthesis leading to cell death. Nat Cell Biol 15(5):481–490
119. Ye J, Rawson RB, Komuro R, Chen X, Dave UP, Prywes R et al (2000) ER stress induces cleavage of membrane-bound ATF6 by the same proteases that process SREBPs. Mol Cell 6(6):1355–1364
120. Yamamoto K, Sato T, Matsui T, Sato M, Okada T, Yoshida H et al (2007) Transcriptional induction of mammalian ER quality control proteins is mediated by single or combined action of ATF6α and XBP1. Dev Cell 13(3):365–376
121. Yoshida H, Matsui T, Yamamoto A, Okada T, Mori K (2001) XBP1 mRNA is induced by ATF6 and spliced by IRE1 in response to ER stress to produce a highly active transcription factor. Cell 107(7):881–891
122. Liou HC, Boothby MR, Finn PW, Davidon R, Nabavi N, Zeleznik-Le NJ et al (1990) A new member of the leucine zipper class of proteins that binds to the HLA DR alpha promoter. Science 247(4950):1581–1584
123. Travers KJ, Patil CK, Wodicka L, Lockhart DJ, Weissman JS, Walter P (2000) Functional and genomic analyses reveal an essential coordination between the unfolded protein response and ER-associated degradation. Cell 101(3):249–258
124. Bonifacino JS, Weissman AM (1998) Ubiquitin and the control of protein fate in the secretory and endocytic pathways. Annu Rev Cell Dev Biol 14:19–57
125. Hwang J, Qi L (2018) Quality control in the endoplasmic reticulum: crosstalk between ERAD and UPR pathways. Trends Biochem Sci 43(8):593–605
126. Wu X, Rapoport TA (2018) Mechanistic insights into ER-associated protein degradation. Curr Opin Cell Biol 53:22–28
127. Hollien J, Lin JH, Li H, Stevens N, Walter P, Weissman JS (2009) Regulated Ire1-dependent decay of messenger RNAs in mammalian cells. J Cell Biol 186(3):323–331
128. Oikawa D, Tokuda M, Hosoda A, Iwawaki T (2010) Identification of a consensus element recognized and cleaved by IRE1α. Nucleic Acids Res 38(18):6265–6273
129. Hollien J, Weissman JS (2006) Decay of endoplasmic reticulum-localized mRNAs during the unfolded protein response. Science 313(5783):104–107
130. Maurel M, Chevet E, Tavernier J, Gerlo S (2014) Getting RIDD of RNA: IRE1 in cell fate regulation. Trends Biochem Sci 39(5):245–254
131. Verfaillie T, Rubio N, Garg AD, Bultynck G, Rizzuto R, Decuypere JP et al (2012) PERK is required at the ER-mitochondrial contact sites to convey apoptosis after ROS-based ER stress. Cell Death Differ 19(11):1880–1891

132. Lynes EM, Bui M, Yap MC, Benson MD, Schneider B, Ellgaard L et al (2012) Palmitoylated TMX and calnexin target to the mitochondria-associated membrane. EMBO J 31(2):457–470
133. Yang S, Bhardwaj A, Cheng J, Alkayed NJ, Hurn PD, Kirsch JR (2007) Sigma receptor agonists provide neuroprotection in vitro by preserving bcl-2. Anesth Analg 104(5):1179–1184
134. Penke B, Fulop L, Szucs M, Frecska E (2018) The role of sigma-1 receptor, an intracellular chaperone in neurodegenerative diseases. Curr Neuropharmacol 16(1):97–116
135. Ola MS, Moore P, El-Sherbeny A, Roon P, Agarwal N, Sarthy VP et al (2001) Expression pattern of sigma receptor 1 mRNA and protein in mammalian retina. Brain Res Mol Brain Res 95(1-2):86–95
136. Ha Y, Shanmugam AK, Markand S, Zorrilla E, Ganapathy V, Smith SB (2014) Sigma receptor 1 modulates ER stress and Bcl2 in murine retina. Cell Tissue Res 356(1):15–27
137. Wang J, Saul A, Cui X, Roon P, Smith SB (2017) Absence of sigma 1 receptor accelerates photoreceptor cell death in a Murine model of retinitis pigmentosa. Invest Ophthalmol Vis Sci 58(11):4545–4558
138. Ha Y, Dun Y, Thangaraju M, Duplantier J, Dong Z, Liu K et al (2011) Sigma receptor 1 modulates endoplasmic reticulum stress in retinal neurons. Invest Ophthalmol Vis Sci 52(1):527–540
139. Krishnamoorthy RR, Agarwal P, Prasanna G, Vopat K, Lambert W, Sheedlo HJ et al (2001) Characterization of a transformed rat retinal ganglion cell line. Brain Res Mol Brain Res 86(1-2):1–12
140. Wang L, Eldred JA, Sidaway P, Sanderson J, Smith AJ, Bowater RP et al (2012) Sigma 1 receptor stimulation protects against oxidative damage through suppression of the ER stress responses in the human lens. Mech Ageing Dev 133(11-12):665–674
141. Tanimukai H, Kudo T (2015) Fluvoxamine alleviates paclitaxel-induced neurotoxicity. Biochem Biophys Rep 4:202–206
142. Omi T, Tanimukai H, Kanayama D, Sakagami Y, Tagami S, Okochi M et al (2014) Fluvoxamine alleviates ER stress via induction of Sigma-1 receptor. Cell Death Dis 5:e1332
143. Morihara R, Yamashita T, Liu X, Nakano Y, Fukui Y, Sato K et al (2018) Protective effect of a novel sigma-1 receptor agonist is associated with reduced endoplasmic reticulum stress in stroke male mice. J Neurosci Res 96:1707–1716
144. Ono Y, Tanaka H, Tsuruma K, Shimazawa M, Hara H (2013) A sigma-1 receptor antagonist (NE-100) prevents tunicamycin-induced cell death via GRP78 induction in hippocampal cells. Biochem Biophys Res Commun 434(4):904–909
145. Hong J, Wang L, Zhang T, Zhang B, Chen L (2017) Sigma-1 receptor knockout increases alpha-synuclein aggregation and phosphorylation with loss of dopaminergic neurons in substantia nigra. Neurobiol Aging 59:171–183
146. Alam S, Abdullah CS, Aishwarya R, Orr AW, Traylor J, Miriyala S, et al. (2017) SigmaR1 regulates endoplasmic reticulum stress-induced C/EBP-homologous protein expression in cardiomyocytes. Biosci Rep 37(4)
147. Watanabe S, Ilieva H, Tamada H, Nomura H, Komine O, Endo F et al (2016) Mitochondria-associated membrane collapse is a common pathomechanism in SIGMAR1- and SOD1-linked ALS. EMBO Mol Med 8(12):1421–1437
148. Gregianin E, Pallafacchina G, Zanin S, Crippa V, Rusmini P, Poletti A et al (2016) Loss-of-function mutations in the SIGMAR1 gene cause distal hereditary motor neuropathy by impairing ER-mitochondria tethering and Ca^{2+} signalling. Hum Mol Genet 25(17):3741–3753
149. Horga A, Tomaselli PJ, Gonzalez MA, Laura M, Muntoni F, Manzur AY et al (2016) SIGMAR1 mutation associated with autosomal recessive Silver-like syndrome. Neurology 87(15):1607–1612
150. Li X, Hu Z, Liu L, Xie Y, Zhan Y, Zi X et al (2015) A SIGMAR1 splice-site mutation causes distal hereditary motor neuropathy. Neurology 84(24):2430–2437

151. Nandhagopal R, Meftah D, Al-Kalbani S, Scott P (2018) Recessive distal motor neuropathy with pyramidal signs in an Omani kindred: underlying novel mutation in the SIGMAR1 gene. Eur J Neurol 25(2):395–403
152. Fukunaga K, Shinoda Y, Tagashira H (2015) The role of SIGMAR1 gene mutation and mitochondrial dysfunction in amyotrophic lateral sclerosis. J Pharmacol Sci 127(1):36–41
153. Mavlyutov TA, Yang H, Epstein ML, Ruoho AE, Yang J, Guo LW (2017) APEX2-enhanced electron microscopy distinguishes sigma-1 receptor localization in the nucleoplasmic reticulum. Oncotarget 8(31):51317–51330
154. Miki Y, Mori F, Kon T, Tanji K, Toyoshima Y, Yoshida M et al (2014) Accumulation of the sigma-1 receptor is common to neuronal nuclear inclusions in various neurodegenerative diseases. Neuropathology 34(2):148–158
155. Natsvlishvili N, Goguadze N, Zhuravliova E, Mikeladze D (2015 Apr 30) Sigma-1 receptor directly interacts with Rac1-GTPase in the brain mitochondria. BMC Biochem 16:11
156. Mitsuda T, Omi T, Tanimukai H, Sakagami Y, Tagami S, Okochi M, Kudo T, Takeda M (2011 Nov 25) Sigma-1Rs are upregulated via PERK/eIF2α/ATF4 pathway and execute protective function in ER stress. Biochem Biophys Res Commun 415(3):519–525
157. Kourrich S (2017) Sigma-1 receptor and neuronal excitability. Handb Exp Pharmacol 244:109–130. https://doi.org/10.1007/164_2017_8

Chapter 29
ER-Mitochondria Calcium Transfer, Organelle Contacts and Neurodegenerative Diseases

Francesca Vallese, Lucia Barazzuol, Lorenzo Maso, Marisa Brini, and Tito Calì

Abstract It is generally accepted that interorganellar contacts are central to the control of cellular physiology. Virtually, any intracellular organelle can come into proximity with each other and, by establishing physical protein-mediated contacts within a selected fraction of the membrane surface, novel specific functions are acquired. Endoplasmic reticulum (ER) contacts with mitochondria are among the best studied and have a major role in Ca^{2+} and lipid transfer, signaling, and membrane dynamics.

Their functional (and structural) diversity, their dynamic nature as well as the growing number of new players involved in the tethering concurred to make their monitoring difficult especially in living cells. This review focuses on the most established examples of tethers/modulators of the ER-mitochondria interface and on the roles of these contacts in health and disease by specifically dissecting how Ca^{2+} transfer occurs and how mishandling eventually leads to disease. Additional functions of the ER-mitochondria interface and an overview of the currently available methods to measure/quantify the ER-mitochondria interface will also be discussed.

Keywords Calcium · Mitochondria · Endoplasmic reticulum · ER-mitochondria contact sites · Neurodegenerative diseases · Organelle communication · Signalling · MAM · Protein tethers · Bioenergetics

F. Vallese · L. Barazzuol
Department of Biomedical Sciences, University of Padua, Padua, Italy

L. Maso · M. Brini (✉)
Department of Biology, University of Padua, Padua, Italy
e-mail: marisa.brini@unipd.it

T. Calì (✉)
Department of Biomedical Sciences, University of Padua, Padua, Italy

Padua Neuroscience Center (PNC), Padua, Italy
e-mail: tito.cali@unipd.it

M. S. Islam (ed.), *Calcium Signaling*, Advances in Experimental Medicine and Biology 1131, https://doi.org/10.1007/978-3-030-12457-1_29

29.1 Introduction

Eukaryotic cells are characterized by the presence of defined intracellular membranous structures, the organelles that enable the compartmentalization of metabolites and the spatial separation of biological processes.

This chapter focuses on the most recent findings on the tethering complexes found between the endoplasmic reticulum (ER) and mitochondria, the so-called MAMs (mitochondria-associated ER membranes) region, the currently available methods for their monitoring, and their multiple physiological functions including Ca^{2+} signaling and lipid synthesis. How alterations in these connections are linked to the onset of neurodegenerative diseases such as Alzheimer's Disease (AD), Parkinson's Disease (PD) and Amyotrophic Lateral Sclerosis (ALS), will also be discussed.

29.2 Players at the ER-Mitochondria Interface

The maintenance of a correct tethering between the ER and mitochondria is guaranteed by several pairs of cytosolic proteins and integral membrane proteins, that keep the distance between the organelles in a proper range [1–4] (Fig. 29.1). The tethering complex composition and thickness, however, are not constant and

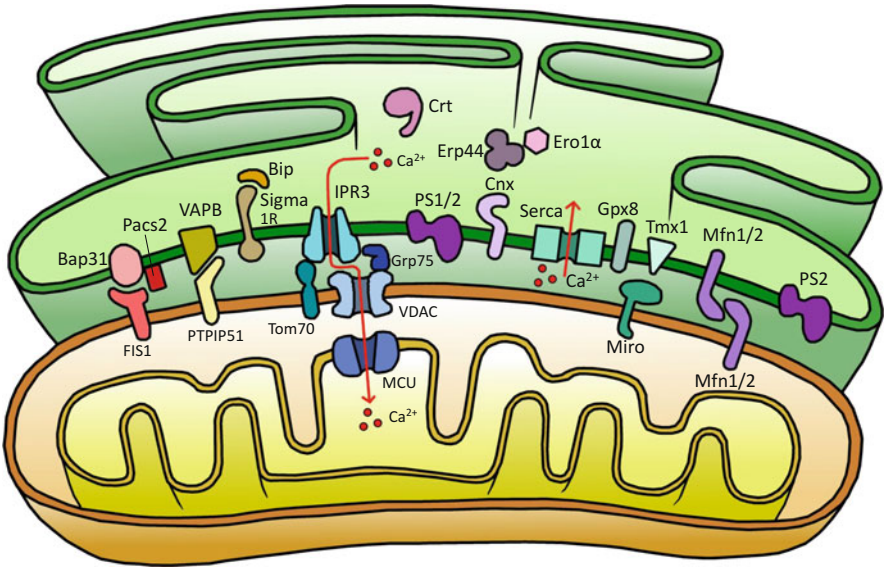

Fig. 29.1 ER-mitochondria contact sites and Ca^{2+} homeostasis. The figure depicts the main MAM proteins involved in Ca^{2+} exchange between ER and mitochondria

the distance between the ER and the outer mitochondrial membrane (OMM) can range from 10 nm up to 80–100 nm depending on the cell needs and response to different conditions [5]. In the following section the most established examples of tethers/modulators will be considered, for a general view of the growing number of proposed new players at this interface the reader is referred to [6–9].

29.2.1 MFN2

Mitofusin 2 (MFN2) is a large GTPase, it is involved in the fusion of mitochondrial outer membrane and it is enriched in MAMs. It is widely accepted that this protein is a major regulator of mitochondria-ER interface in different tissues [10, 11], however the exact role played at the mitochondria-ER contacts is still unclear. MFN2 located in the ER can form hetero- or homo-dimers in trans with mitochondrial mitofusins (i.e., MFN1 or MFN2) to fine tune the MAMs-dependent functions in a concerted manner. Although the precise mechanism by which the distance between the ER and mitochondria is adapted to cope with the cell needs must still be fully elucidated [12–15], the idea that the ER-mitochondria contacts can functionally and physically occur at different distances to perform specific functions is recently emerging [15, 16]. Accordingly, MFN2 has been shown to have opposite effects in the crosstalk between mitochondria and the rough or the smooth ER [15], a finding that was also confirmed by using a novel genetically encoded probe for the evaluation of narrow and wide organelle interactions [17].

29.2.2 VAPB-PTPIP51

Vesicle-associated membrane protein-associated protein B (VAPB) is an integral protein in the ER membrane that is involved in unfolded protein response (UPR) and in the regulation of cellular Ca^{2+} homeostasis [18]. VAPB interacts with a mitochondrial outer membrane protein, the tyrosine phosphatase-interacting protein-51 (PTPIP51) and its overexpression increases ER-mitochondria tethering, while knockdown of either protein decreases the tethering between the two organelles [19]. Multiple approaches demonstrated that VAPB and PTPIP51 are ER-mitochondria tethers: (i) VAPB is enriched in MAMs, and PTPIP51 is a known outer mitochondrial membrane protein [20, 21]. (ii) VAPB and PTPIP51 directly interact and their modulation affects Ca^{2+} exchange between ER and mitochondria [19, 20, 22, 23]. (iii) the manipulation of VAPB and/or PTPIP51 expression induces changes in ER-mitochondria contacts [19, 24].

29.2.3 Fis1-Bap31

Fis1-Bap31 interaction creates a preformed scaffold complex that is proven to tether ER and mitochondria together. B-cell receptor-associated protein 31 (Bap31) is an integral membrane chaperone protein of the ER that forms several protein complexes and controls the fate of newly synthesized integral membrane proteins. Recently, the mitochondrial fission protein 1 homologue (Fis1) has been shown to interact with Bap31 to form an ER-mitochondrial platform which is essential for either the recruitment and activation of procaspase 8 and for the conveyance of the apoptotic signal from mitochondria to the ER [25]. The tethering function of Bap31 may be modulated by phosphofurin acidic cluster sorting protein 2 (PACS-2), a multifunctional cytosolic protein. Downregulation of PACS-2 causes Bap31-dependent mitochondrial fragmentation and uncoupling from the ER along with inhibition of Ca^{2+} signal transmission [26, 27].

29.2.4 IP3R-Grp75-VDAC1

The ER Ca^{2+} channel inositol 1,4,5-trisphosphate receptor (IP3R) and the OMM protein VDAC1 (voltage-dependent anion channel 1) interact via the mitochondrial chaperone Grp75 (glucose-regulated protein 75) [28, 29]. This complex may not have a proper physical tethering role, but rather it is essential to functionally couple ER and mitochondria and favour Ca^{2+} exchanges. A role of TOM70 in the formation of this complex has also been recently demonstrated: it clusters at ER-mitochondria contacts, where it recruits IP3R and promotes inter-organelle Ca^{2+} transfer (likely through the IP3R-Grp75-VDAC1 complex), cell bioenergetics and proliferation [30].

29.3 Ca^{2+} Transfer at the ER-Mitochondria Interface

Ca^{2+} ion is one of the most important second messenger in eukaryotic cells, being a multitude of biological processes associated to the transient variation of its intracellular concentration. Basal levels of free cytoplasmic Ca^{2+} are maintained in the nM range by energy-dependent mechanisms regulated by proteins such as the plasma membrane Ca^{2+} ATPase (PMCA), the SR/ER Ca^{2+} ATPase (SERCA) and the secretory pathway Ca^{2+} ATPase (SPCA) of the Golgi apparatus. Ca^{2+} pumps, together with the plasma membrane Na^{+}/Ca^{2+} exchanger (NCX), promptly counteract cytosolic Ca^{2+} increases by extruding Ca^{2+} ions in the extracellular milieu or by pumping it in the intracellular stores, thus guaranteeing their refilling [31–33]. It is also well known that intracellular organelles, such as mitochondria, participate in the control of cytosolic Ca^{2+} signal. Evidence that Ca^{2+} is taken up

by mitochondria has been clear since the 60s, when it was found that the respiratory chain generates, across the inner mitochondrial membrane (IMM), an electrochemical gradient responsible for the import of the cation in the mitochondrial matrix [34, 35]. Only 50 years later, the molecular identity of the channel that mediates this ion transfer was discovered. The Mitochondrial Ca^{2+} uniporter (MCU) was identified in 2011 [36, 37]. Molecularly, the fungal and metazoan MCU is assembled in a tetrameric structure to form the active Ca^{2+} channel [38–41] while MCU from *C. elegans* is a homo-oligomer with pentameric symmetry [42]. The complex also includes a dominant negative isoform called MCUb [43]. Their expression level also differs among the tissues, possibly representing a way to regulate MCU activity according to the different cells type demands [43, 44]. A regulatory dimer formed by the two EF-hand containing proteins MICU1 and MICU2 [45, 46] gates the opening of MCU and depends on the extra-mitochondrial Ca^{2+} concentration. Additional components have also been identified, among them MICU3 [47, 48], highly expressed in neuronal tissue, EMRE [49], an essential protein for the correct assembly of the complex and MCUR1 [50], whose role and the inclusion in the MCU complex is still debated. As already documented by numerous studies before its molecular identification, MCU is characterized by a very low affinity for Ca^{2+} (K_d 15–20 μM), amply far away from the physiological Ca^{2+} concentration values reached in the cytosol of living cells, which are in the range of 50–100 nM in resting conditions and of 1–3 μM upon stimulation. This problem was solved by Rizzuto and co-workers, who showed for the first time that Ca^{2+} uptake by mitochondria occurs preferentially at the sites of contact between ER and mitochondria [1, 51]. Indeed, they observed that the two organelles are strategically located in close proximity, allowing the formation of Ca^{2+} hotspots that overcome the low affinity threshold of mitochondrial Ca^{2+} uptake mechanism. We now know that alterations of the interaction between ER and mitochondria lead to a disruption of Ca^{2+} transfer between the organelles and to ER stress [26]. Ca^{2+} accumulation into mitochondria is crucial not only for the maintenance of cellular Ca^{2+} homeostasis [52] but also for mitochondrial metabolism and adenosine triphosphate (ATP) production, especially for neuronal cells which are highly energy demanding. Ca^{2+} transport proteins, especially those located in MAMs, play a key role in buffering and shaping cytosolic Ca^{2+} transients [53–55] (Fig. 29.1).

The multiprotein complex involved in ER-mitochondria Ca^{2+} transfer is the IP3R-VDAC-Grp75 complex [28]. When MAMs are disrupted, the release of Ca^{2+} from the ER mediated by IP3R is suppressed and ATP production and cell survival are impaired [9, 56]. At the opposite, massive and/or a prolonged accumulation of Ca^{2+} into mitochondria can lead to the opening of the permeability transition pore (PTP) in the IMM, the swelling of the organelles and the induction of apoptosis [57].

SERCA pump, in addition to play a key role in maintaining bulk cytosolic Ca^{2+} at basal level and in replenishing intracellular stores, controls local Ca^{2+} transfer at ER-mitochondrial contacts level [3]. Several mechanisms regulate SERCA activity at MAMs level. Phosphorylation of the transmembrane chaperone calnexin (CNX) has been proposed to inhibit SERCA activity and, on the other

side, its dephosphorylation occurs upon IP3R-mediated Ca^{2+} release, suggesting a tight regulation via the phosphorylation status of the CNX cytosolic domain [58]. However CNX has also been suggested to act as a positive SERCA2b regulator [59, 60]. In conjunction with CNX, thioredoxin-related TMX1 has been shown to inhibit SERCA2b activity [8] and promote ER-mitochondria contact formation, thus suggesting that inhibition of SERCA2b might be a compensatory measure to reduce Ca^{2+} levels in the ER and to prevent possible mitochondrial Ca^{2+} overload [61]. Recently, the glutathione peroxidase (GPX8), another ER membrane and MAMs resident redox regulator, has been shown to decrease SERCA2b activity [62].

Ca^{2+} fluxes at the ER-mitochondria interface are thus tightly tuned, it is not surprising that many components acting at the MAM are indeed influenced by Ca^{2+} itself acting as a key regulator of many components required to sustain the plethora of physiologic processes occurring at this location [63]. On the mitochondrial side, there is the mitochondrial Rho GTPase (Miro), an essential protein for the regulation of mitochondrial movements. Interestingly, it responds to Ca^{2+} above a concentration range that is never attained in the bulk cytosol of living cells (10–100 μM) [64], but that might be easily reached at the ER-mitochondria contact sites. On the ER side, the above mentioned CNX, as well as calreticulin (CRT) and the Binding immunoglobulin protein BiP are MAMs-specific Ca^{2+} -binding and glucose regulated chaperones [65, 66] and serve as high-capacity Ca^{2+} pools in the ER [67, 68]. CRT has also a regulatory role on Ca^{2+} signaling since its overexpression has an inhibitory effect on the IP3R [69], while its downregulation impaired Ca^{2+} homeostasis [70]. The oxidoreductase Ero1a and its co-chaperone ERp44 [71] are enriched at the MAMs and regulate the activity of the IP3R via a direct interaction [72, 73]. Furthermore, Ero1a has been shown to directly regulate ER-mitochondria Ca^{2+} fluxes and to influence the activity of the mitochondrial transporters [74]. Analogously, the ER protein Sigma-1 receptor (Sig-1R), a Ca^{2+}-sensitive chaperone, operates at MAMs forming a complex with another chaperone, Bip. Upon ER Ca^{2+} depletion, Sig-1R dissociates from BiP, leading to a prolonged Ca^{2+} signaling into mitochondria via IP3Rs [65].

29.4 ER-Mitochondria Ca^{2+} Mishandling in Neurodegenerative Diseases

Neurodegenerative diseases, including PD, AD and ALS/FTD (fronto-temporal dementia), affect millions of people worldwide and are characterized by progressive nervous system dysfunction. Common pathogenic mechanisms have been described for these diseases, including abnormal proteostasis, often associated with the formation of intracellular and/or extracellular protein inclusions, ER and oxidative stress, mitochondrial dysfunction, and neuroinflammation [75, 76]. The existence of ER-mitochondria contacts also in neuronal cells, which are mainly dependent from Ca^{2+} influx from the extracellular ambient for the control of their function, suggests

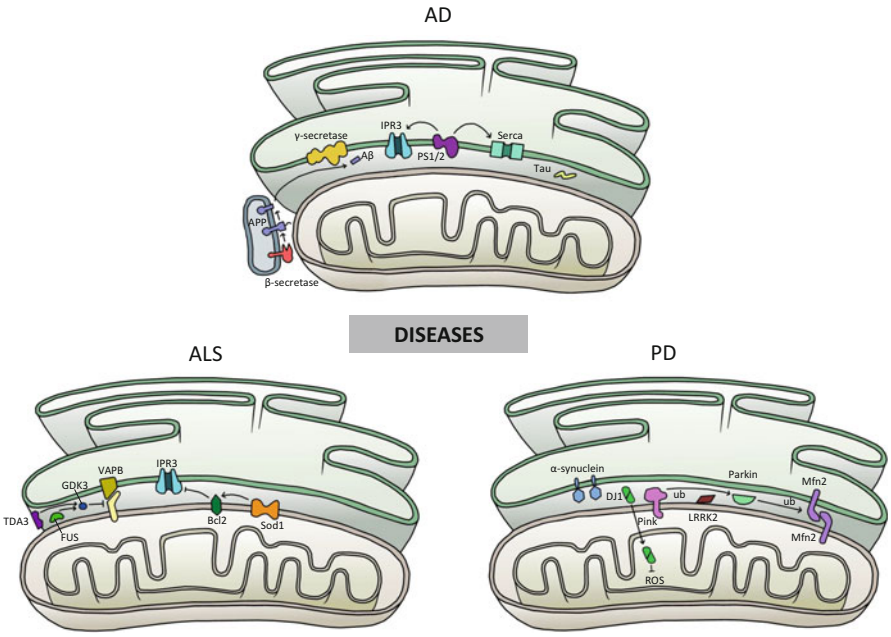

Fig. 29.2 ER-mitochondria contact sites in neurodegenerative diseases. The figure depicts the main players of MAMs involved in the pathogenesis of Alzheimer's disease (AD), Parkinson's disease (PD) and amyotrophic lateral sclerosis (ALS)

that MAMs may have a critical role also in regulating synaptic activity [77, 78]. Over the last decade, alterations in the contact sites between ER and mitochondria have been found as a common characteristic in many neurodegenerative diseases, consistently with the fact that several disease-related proteins are transiently or constitutively associated with the ER-mitochondria interface. The presence of mutations in these proteins has been shown to alter the structural and functional features of this subcellular compartment (Fig. 29.2). In the following sections, we will focus on representative examples of altered ER-mitochondria communication in the context of AD, PD and ALS.

29.4.1 Alzheimer's Disease (AD)

The first evidence on ER-mitochondria contacts involvement in neurodegeneration has been highlighted in the study of AD. AD is an irreversible neurodegenerative disorder characterized by progressive loss of episodic memory and by cognitive and behavioral impairment caused by degeneration of hippocampal and cortical neurons. All the familial forms of AD (FAD) so far identified are related to mutations in the genes coding for amyloid precursor protein (APP) or for presenilins (PS1 and

PS2), the major components of the γ-secretase complex that processes APP to release Amiloid β (Aβ) peptide. The generation or the accumulation of Aβ is tightly associated with the onset and progression of the disease, but this is not the unique phenotypic feature directly related to this pathology: alterations in Ca^{2+} and lipids homeostasis, ROS levels, autophagy, axonal transport and mitochondrial dynamics are commonly observed [79].

In the last years, a link between AD and MAMs dysfunction has become increasingly evident [21, 80] (Fig. 29.2). In particular, PSs, which play an important role in Ca^{2+} homeostasis [81, 82], have been found at the MAMs [6, 83] and proposed to form ER Ca^{2+} channels [84], as well as to act as modulators of the IP3R or ryanodine receptor (RyR) open probability [85, 86] or of the SERCA pump activity [87, 88]. Pizzo and coworkers have reported that PS2 action in Ca^{2+} signaling is dependent on the modulation of ER-mitochondria interactions and their Ca^{2+} cross talk [89, 90]. Pathogenic mutations of PS2 have been associated with increased ER-mitochondria juxtaposition and enhanced ER-mitochondria Ca^{2+} transfer in FAD-mutant PS1 and APP expressing cells. Increased ER-mitochondria connections (resembling those induced by mutated PS2) have also been reported in fibroblasts from patients with familial and sporadic forms of AD [83]. Intriguingly, the possibility that ER-mitochondria contact impairments might be the common feature in different neurodegenerative conditions becomes even more consistent considering that Parkin, a PD-related protein, has been recently shown to differently modulate PS1 and PS2 expression at the transcriptional level [91]. Interestingly, when primary hippocampal neurons are incubated with nM concentrations of oligomeric Aβ, ER-mitochondria proximity and Ca^{2+} exchanges between the two organelles increase [92].

Another typical feature of AD is the accumulation of intracellular neurofibrillary tangles (NFT) composed by tau and Aβ plaques. Both of them have also been shown to have a direct influence on several mitochondria-related activities: interestingly, a fraction of tau protein has been recently found at the OMM and within the inner mitochondrial space (IMS) [93], suggesting a potential tau-dependent regulation of mitochondrial functions and the possibility that alterations in its distribution may precede the appearance of the detrimental effects induced by its aggregation. Mis-handling and defects in the ER-mitochondria communications might be an important pathological event in tau-related dysfunction and thereby contributing to neurodegeneration [93, 94].

29.4.2 Parkinson's Disease (PD)

PD is the second most common neurodegenerative disease after AD. PD patients typically develop slowness of movements (bradykinesia), involuntary shaking (tremor), increased resistance to passive movement (rigidity) and postural instability [95, 96].

The phenotypes of both sporadic and familial forms of PD are essentially indistinguishable, implying that they might share common underlying etiological

mechanisms. Dominant forms of the disease are related to mutations in three proteins, α-synuclein, LRRK2 (Leucine-rich repeat kinase 2), and VPS35 (Vacuolar protein sorting-associated protein 35), whereas mutations in Parkin, PINK1 (PTEN-induced putative kinase 1), and DJ-1 cause autosomal recessive-inherited forms [97]. Recently, many studies have found dysfunctions in ER-mitochondria communication in different cellular models for PD (Fig. 29.2) and consequently alterations in many different pathways depending on it [21, 94, 98].

α-synuclein is a protein with a central role in the modulation of synaptic integrity and function, its disease-related mutations alter a plethora of physiological processes that are regulated by the signaling between ER and mitochondria, and, consistently, α-synuclein has been shown to play a key role at the ER–mitochondria contacts by favouring Ca^{2+} transfer between the organelles and sustaining mitochondrial metabolism [99–102]. PINK1 and Parkin are associated with mitochondria and in addition to play an important role in the process of mitochondrial quality control (mitophagy) [103–106], they may be involved in the modulation of the ER-mitochondria apposition, thus suggesting that mutations in the two proteins could be linked to MAMs anomalies. Furthermore, contact regions between ER and mitochondria have been shown to be prime locations for Parkin-mediated mitophagy and local recruitment of autophagosome precursors. Parkin was also shown to be present at the ER and the mitochondrial membranes under basal conditions [107–112] and to have a role in the modulation of the mitochondrial-ER interactions [111] and the proteosome activity. Cumulating evidence strongly supports a role for Parkin in general protein quality control and ER stress pathways [113–118]. The absence of Parkin in mice fibroblast or the presence of Parkin mutations in PD-patients fibroblasts have been shown to decrease the ER-mitochondrial tethering and, interestingly, mutant MFN2 that cannot be ubiquitinated, failed to restore ER-mitochondria contacts, suggesting that Parkin mediated ubiquitination of MFN2 may be required for inter-organelle association [119].

Mutations in DJ-1 protein have been linked to autosomal recessive early-onset parkinsonism [120]. DJ-1 protein plays a protective role against oxidative stress and it is essential to maintain proper mitochondria dynamics. It is mainly localized in the cytosol and in the nucleus, but it has also been found in mitochondria [121] and at MAMs level [122]. DJ-1 overexpression in cell models increased the ER–mitochondria association, whereas its downregulation caused mitochondria fragmentation and decreased mitochondrial Ca^{2+} uptake, suggesting a direct role of this protein in MAMs functions [122].

29.4.3 Amyotrophic Lateral Sclerosis (ALS)

ALS is the most common form of motor neuron disease that leads to a progressive muscle paralysis caused by a prominent degeneration of upper and lower motor neurons that communicate with muscle cells, leading to death within few years of

diagnosis [123]. Over 90% of ALS cases occur sporadically, while familial ALS (FALS) patients with known genetic mutations are relatively rare. Approximately 50% of the familial forms of the disease are associated with mutations in VAPB, TAR-DNA binding protein 43 (TDP43), fused in sarcoma (FUS) and superoxide dismutase 1 (SOD1). All the studies on these proteins strongly suggest that alterations of the ER-mitochondria platform could be an early event at the basis of ALS (Fig. 29.2). VAPB is an ER membrane anchored-protein enriched at the MAMs [20] and it is involved in the regulation of the ER stress response and consequent Ca^{2+}-mediated death in motor neurons [124]. VAPB interacts with PTPIP51 (a mitochondrial outer membrane protein) and this interaction is necessary to support ER-mitochondria Ca^{2+} transfer between the two organelles. Indeed, mutation of VAPB (P56S) induces impaired mitochondria Ca^{2+} uptake, increased cytosolic Ca^{2+} levels and mitochondria clustering [20, 125].

Concerning the involvement of TDP-43 in ALS, its overexpression in both wt and mutated form decreases ER-mitochondria physical and functional coupling by disrupting VAPB-PTPIP51 interaction through the activation of GSK-3 [19]. The disassembling of the VAPB-PTPIP51 tethering complex via GSK-3 is also induced upon FUS overexpression (both in the wt and ALS-linked mutant form) [23]. Impaired ER-mitochondria juxtaposition caused by the overexpression of these proteins results in all cases in defects in Ca^{2+} transfer and, consequently, in mitochondrial ATP production.

SOD1 is the most frequent mutated protein in ALS, accounting for the 20% of the familial cases [126]. SOD1 is a key enzyme in the defense against oxidative stress. At the moment, the best model for the study of ALS is represented by the transgenic mice expressing mutant SOD1. The overexpression of the ALS-related hSOD1 mutant G93A has been observed to alter ER and mitochondrial Ca^{2+} homeostasis in mouse embryonic motor neurons [127, 128]. The aberrant interactions of mutant SOD1 with Bcl-2 [129], a protein present both at mitochondrial and ER membranes, could in part define the mechanisms whereby mutant SOD1 affects Ca^{2+} regulation, as Bcl-2 has been proposed to modulate IP3R activity [130] and control ER Ca^{2+} levels [131].

29.5 Additional Cellular Functions Associated with the ER-Mitochondria Interface

Functional roles of ER-mitochondria contacts were first uncovered in phospholipid biosynthesis and transport [132, 133]. Subsequently, ER-mitochondria contacts were implicated in other different cellular processes (Ca^{2+} and ROS homeostasis, phosphoregulation, mitochondrial fission and fusion, autophagy), emerging as a complex hub fundamental for the correct integration of numerous signaling pathways [4, 134–136] (Fig. 29.3).

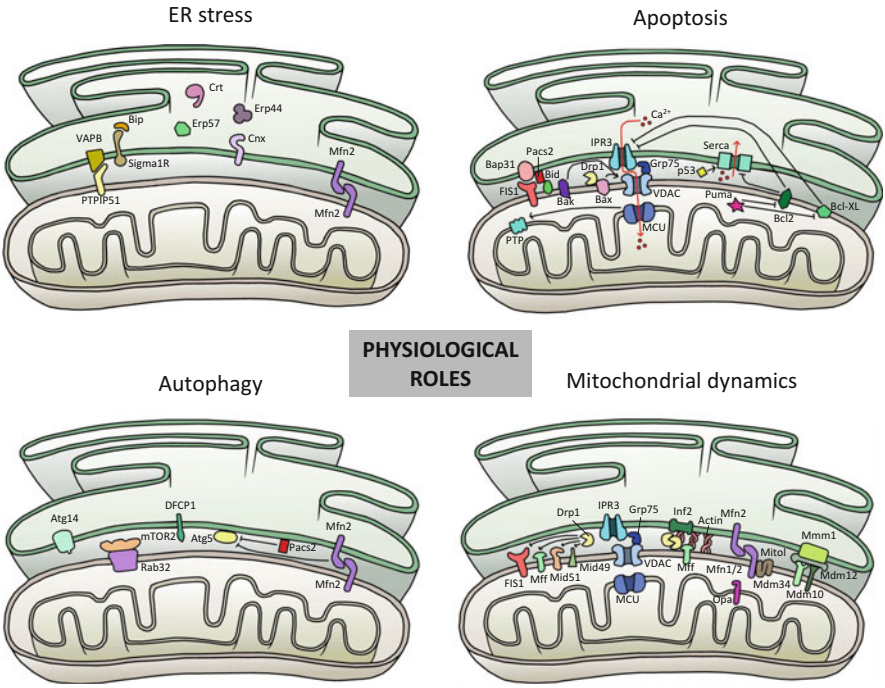

Fig. 29.3 Main physiological roles of MAM junctions. The figure summarizes the most important key components of MAMs involved in ER stress, apoptosis, autophagy and mitochondrial dynamics

29.5.1 Mithocondrial Dynamics

The best studied connection between ER-mitochondria contacts and mitochondrial dynamics involves mitochondrial fission and fusion machinery. Mitochondrial fission is mediated by human dynamin-related protein 1 (Drp1). It localizes primarily at the cytoplasm and is recruited to mitochondria by different proteins: Fis [137], the mitochondrial fission factor (Mff) [138] and the mitochondrial dynamics 51 and 49 kDa proteins (MiD51 and MiD49) [2] that regulate mitochondrial fission by anchoring Drp1 on the outer mitochondrial membrane [139]. Drp1 associates with the OMM, where, thanks to a conformational change due to its GTPase activity, forms oligomers that wrap around the constricted portions of the mitochondria membrane and lead to a fission event [140, 141]. However, it has been observed that mitochondrial fission may start even when Drp1 or Mff are down-regulated [2] since ER membranes were able to wrap around the mitochondrial tubules, indicating that ER-mitochondria contact represents a conserved platform for the regulation of mitochondrial division. Accordingly, recent findings from the Higgs group proposed a potential mechanism for ER association-induced mitochondrial fission involving actin polymerization and a ER-localized protein, i.e. the inverted

formin 2 (INF2) [142]. INF2 is activated to polymerize actin, which in turn might generate the driving force for the initial constriction of mitochondria [136, 142]. Once assembled, the ER-associated constricted mitochondria enable polymerized Drp1 to spiral around the mitochondria to mediate their fission [143].

Mitochondrial fusion is mainly orchestrated by MFN1 and MFN2, but while MFN1 plays a critical role in mitochondrial docking and fusion, MFN2 coordinates the interactions between mitochondria [144]. As mentioned above, MFN2 located in the ER membrane is crucial for tethering the ER to the mitochondria and stabilizing MAMs formation by forming both homo- and heterotypic interactions with mitochondrial MFN1 and 2 [12]. The mitochondrial ubiquitin ligase protein, MITOL, regulates MFN2 activity at the ER–mitochondria interface interacting with mitochondrial MFN2 and mediating its ubiquitination and its subsequent oligomerization, a fundamental step in MFN2-induced ER-mitochondria tethering [145]. The dual role of MFN2 in both mitochondrial fusion and ER-mitochondria tethering suggests that the establishment of ER–mitochondria contact might be a critical event in MFN2-dependent mitochondrial fusion.

29.5.2 Lipid Homeostasis at the ER-Mitochondria Interface

The maintenance of a defined lipid composition in mitochondrial membranes depends on bidirectional lipid trafficking between the ER and mitochondria. ER is the predominant production site for lipids and makes close contacts with other organelles to ensure lipid exchange [146]. Enzymes involved in phospholipid biosynthesis are enriched at MAMs [147, 148]. Despite of the important role of MAMs in phospholipid exchange between ER and mitochondria is well recognized, the precise role of the proteins involved in the ER-mitochondria tether in mammalian cells remain to be defined [149]. In yeast, the ER-mitochondrial encounter structure (ERMES) that mediates ER-mitochondria contacts has been well characterized: it is composed by Mdm34 (mitochondrial distribution and morphology 34) and Mdm10 that are integral OMM proteins, Mmm1 (maintenance of mitochondrial morphology 1) that resides in the ER membrane and Mdm12 that is associated with OMM peripherally [150–152]. It is believed that ERMES complex may act as a lipid transferase, since Mmm1, Mdm12, and Mdm34 contain a synaptotagmin-like mitochondrial-lipid-binding protein (SMP) domain, which forms a hydrophobic cavity and likely binds to hydrophobic molecules such as phospholipids [153, 154].

29.5.3 Apoptosis

The role of ER-mitochondria communication during apoptosis has been extensively documented, in particular in relation with Ca^{2+} transfer from ER to mitochondria,

that is essential to sustain mitochondrial function but can also be deleterious and promote cell death. This process is modulated by the presence of various Bcl-2 family proteins on the membranes of both organelles [155, 156], whose role has been discussed in several excellent reviews on the field [157–159]. In a simplified view, the anti-apoptotic members Bcl-2 and Bcl-XL inhibit ER Ca^{2+} release and apoptosis [160, 161], whereas the pro-apoptotic members Bax/Bak Puma and Bik acts as positive regulators [162–164].

Upon induction of apoptosis, mitochondrial permeability transition pore (MPTP) opening occurs, the mitochondrial network fragments and cytochrome c are released activating downstream caspases. Among the targets of caspases there is BAP31, an ER-membrane protein. Cleavage of BAP31 generates a pro-apoptotic p20 fragment that remains at the ER membrane and stimulates ER Ca^{2+} release that consequently induces mitochondrial uptake and the recruitment of the dynamin-related protein Drp1 that promotes mitochondrial fragmentation [165]. Exogenous inducers of apoptosis promote physical contacts between BAP31 and Fis1. This interaction is required for the activation of caspase-8 and the generation of the p20 fragment, demonstrating a bi-directional communication between the two organelles and a pattern of feedback amplification. Consistent with this, cell death caused by Fis1 over-expression is dependent on the ER-mitochondria Ca^{2+} transfer [166]. Mitochondrial dynamics are strictly related to apoptosis, indeed, during this process, Drp1 is massively recruited to the OMM, where it assembles into foci that mediate mitochondrial division, causing a dramatic fragmentation of the mitochondrial network. The pro-apoptotic protein Bax behaves similarly to Drp1 during apoptosis; it is recruited at the OMM, where it inserts and oligomerizes to form foci that are functionally associated with OMM permeabilization. Under apoptotic conditions, Drp1 and MFN2 were both found in foci with Bax [167] [168].

29.5.4 Autophagy

Autophagy is a regulated mechanism of the cell that controls both the specific disassembles of unnecessary or dysfunctional cellular components and the non-selective response to the deprivation of nutrients. Defects in autophagy may play a significant role in several human pathologies, including cancer and neurodegeneration [169]. The selective degradation of damaged mitochondria is called mitophagy. During this processes mitochondria are first excluded from the mitochondrial network, through fission events, and then delivered to the lysosomes by the autophagy machinery [170]. The recognition of mitochondria that need to be degraded takes place through specific molecular pathways which involve the OMM protein NIP3-like protein X (NIX; also known as BNIP3L) and PINK1/Parkin [106]. The generation of the autophagosome is central for the autophagic process and several observations suggest that phagophore membranes could be formed primarily from the ER. Moreover, the evidence for a connection between mitochondria and autophagosome is very strong: several autophagy-related proteins can localize to the mitochondria,

different mitochondrial proteins can modulate the autophagic process, and the OMM participates in autophagosome biogenesis under starvation conditions [171]. In recent studies, it has been shown that dynamic crosstalk between the ER and mitochondria is critical for autophagosome formation [172]. For example, when autophagy is induced upon starvation, the pre-autophagosome marker ATG14 (present at cytosolic and ER sites under resting conditions) and the omegasome marker DFCP1 (present in the MAMs fractions during starvation) are markedly concentrated at the MAMs and serves as a platform for autophagosome formation [172]. Additionally, ATG5, which is critical for autophagosome formation, translocate to the MAMs compartment during phagophore biogenesis and then dissociates from MAMs upon completion of the autophagosome formation, thus establishing a stable interaction with the ER and transient associations with the mitochondria. Autophagosome formations is prevented when there is an interference in the formation of ER-mitochondria contacts. The ER-mitochondria interface and autophagy are thus tightly linked and, interestingly, the diverse MAMs related functions are also coordinated and fine-tuned to keep cell homeostasis. One such example is represented by the mTOR complex 2 (mTORC2) [173], a MAMs resident complex that regulates autophagosome formation and mitochondrial dynamics in a Rab32 dependent manner [174], additionally, mTORC2 has been shown to control Ca^{2+} uptake, mitochondrial bioenergetics and apoptosis via Akt-mediated regulation of IP3R, hexokinase2 and PACS2 [175] suggesting that the ER-mitochondria interface is not only important for sensing cellular stress and coordinating Ca^{2+} transfer and the apoptotic response, but it also represents the primary platform for autophagosome formation and integration of many fundamental cell processes.

29.5.5 The ER Stress Response at the MAMs

ER stress consists in a perturbation of ER homeostasis that alters protein folding process and activates the unfolded protein response (UPR), an intracellular signaling pathway that is activated by the accumulation of unfolded proteins in the lumen of the ER and stimulates transcriptional responses of the genes that encode ER chaperones (such as BiP, CNX or CTR) or ER biosynthetic machinery components to increase the protein-folding/degradation capacity of the ER [176, 177]. ER-mitochondria contacts have been linked to ER stress and UPR, in particular, ER stress leads to a redistribution of mitochondrial and reticular networks at the perinuclear zone, with increased contact points and Ca^{2+} transfer. Chaperone complexes containing Grp75, and other proteins such as Rab32 [178] or PACS-2 [26], are involved in the adaptive response to ER stress. A variety of ER chaperones involved in protein folding, such as BiP, CNX, CRT, ERp44, ERp57, and the Sigma-1 receptor are enriched at MAMs [63], in addition, some players whose roles are apparently unrelated to the ER folding/degradation processes have also been shown to play a role in the UPR by influencing the ER-stress response, for example Mfn2 and VAPB can modulate the UPR and mitochondrial function via PERK and ATF6,

respectively [179, 180]. The observation that structural uncoupling of ER from mitochondria induces ER stress by impeding a correct unfolded protein response [26] suggests that the crosstalk between ER and mitochondria at MAMs level may have a role in facilitating UPR.

29.6 Methods to Measure ER-Mitochondria Contact Sites

Several approaches are currently available to study ER-mitochondria contact sites. The oldest and more consolidate approach to elucidate the structure of ER-mitochondria contacts and to calculate their distance is the electron microscopy (EM) [2, 12, 139, 181, 182].

Starting from 1958 EM studies produced a complete and detailed view of the ER-mitochondria contacts: different 3D reconstructions of these structures were generated by serial, tilt-angle tomography in yeast cells [139] as well as by focused ion beam scanning EM at 4-nm resolution in neurons from mice brain slices [78], and soft X-ray tomography with 50-nm resolution in mammalian lymphoblastoid cells [183]. However, the acquisition and reconstruction processes for these 3D approaches remain laborious and therefore they are not yet widely applicable. Furthermore, EM analysis is not able to generate sufficient data for statistical comparisons of organelle geometry. Historically, the existence of the MAMs fraction has been proven when it was found that, during cell-fractionation experiments, sub compartmentalized ER membranes co-sedimented with mitochondria [184]. To date, subcellular fractionation is still considered the standard method to prove presence/levels of specific players at the ER-mitochondria interface [185]. Other approaches, mainly based on the co-localization of ER and mitochondrial markers, are described in the literature and helped to describe ER-mitochondria contacts architecture [14, 51, 186, 187], but none of them has yet been applied to quantify the overall extent or geometry of the interface. The *in-situ* proximity ligation assay (PLA) also allows to visualize and quantify endogenous ER-mitochondria interactions in fixed cells by using pairs of primary antibodies against proteins on opposing membranes [188]. This technique is widely used [23, 189, 190] though it can only be applied to fixed cells and is limited by the availability as well as by the specificity of the antibodies. For the specific detection and quantification of the contact points it has been developed a tool based on the system of rapamycin-inducible linkers that were tagged with a pair of fluorophores capable of generating Förster resonance energy transfer (FRET) [191]. One half of the linker was targeted to the OMM and tagged with CFP, while the other half was targeted to the ER surface and tagged with YFP. A short treatment with rapamycin or its analogues causes the linkage of the two halves, whenever they are in sufficient close proximity. The linkage can be visualized as an increase in FRET signal. Major limitations in the use of this FRET-based probe are due to the fact that it requires equimolar expression of the two moieties [13] and that its in vivo applications are limited by the use of rapamycin, a potent inducer of autophagy [192]. Novel tools to measure

inter organelle proximity have been recently developed [17, 193–197]. The sensor developed by our group, called SPLICS (split-GFP-based Contact site Sensor), specifically allows to detect ER-mitochondria contact sites in living cells and in vivo [17]. Two non-fluorescent portions of the superfolder GFP, the $GFP_{1–10}$ moiety and the GFP β-strand 11 [198, 199], engineered to fluoresce when are in close proximity, were targeted to the ER and the OMM by the addition of targeting sequences. Two SPLICS versions were generated that efficiently measured narrow (8–10 nm) and wide (40–50 nm) juxtapositions between ER and mitochondria, and interestingly, they were able to document the existence of at least two types of contact sites in human cells that undergo to differential modulation upon different pharmacological treatments or conditions [17].

Acknowledgements This work was supported by grants from the Università degli Studi di Padova (Progetto di Ateneo 2015 n. CPDA 153402 to MB, Progetto Giovani 2012 n.GRIC128SP0 to TC and Progetto di Ateneo 2016 n. CALI_SID16_01 to TC) and from the Ministry of University and Research (Bando SIR 2014 n. RBSI14C65Z to TC).

References

1. Rizzuto R (1998) Close contacts with the endoplasmic reticulum as determinants of mitochondrial Ca^{2+} responses. Science 280(5370):1763–1766. https://doi.org/10.1126/science.280.5370.1763
2. Friedman JR, Lackner LL, West M, DiBenedetto JR, Nunnari J, Voeltz GK (2011) ER tubules mark sites of mitochondrial division. Science 334(6054):358–362. https://doi.org/10.1126/science.1207385
3. Csordas G, Hajnoczky G (2001) Sorting of calcium signals at the junctions of endoplasmic reticulum and mitochondria. Cell Calcium 29(4):249–262. https://doi.org/10.1054/ceca.2000.0191
4. Wu H, Carvalho P, Voeltz GK (2018) Here, there, and everywhere: the importance of ER membrane contact sites. Science 361(6401):eaan5835. https://doi.org/10.1126/ science.aan5835
5. Giacomello M, Pellegrini L (2016) The coming of age of the mitochondria-ER contact: a matter of thickness. Cell Death Differ 23(9):1417–1427. https://doi.org/10.1038/cdd.2016.52
6. Csordas G, Weaver D, Hajnoczky G (2018) Endoplasmic reticulum-mitochondrial contactology: structure and signaling functions. Trends Cell Biol 28(7):523–540. https://doi.org/10.1016/j.tcb.2018.02.009
7. Herrera-Cruz MS, Simmen T (2017) Over six decades of discovery and characterization of the architecture at Mitochondria-Associated Membranes (MAMs). Adv Exp Med Biol 997:13–31. https://doi.org/10.1007/978-981-10-4567-7_2
8. Raturi A, Gutierrez T, Ortiz-Sandoval C, Ruangkittisakul A, Herrera-Cruz MS, Rockley JP, Gesson K, Ourdev D, Lou PH, Lucchinetti E, Tahbaz N, Zaugg M, Baksh S, Ballanyi K, Simmen T (2016) TMX1 determines cancer cell metabolism as a thiol-based modulator of ER-mitochondria Ca^{2+} flux. J Cell Biol 214(4):433–444. https://doi.org/10.1083/jcb.201512077
9. Rowland AA, Voeltz GK (2012) Endoplasmic reticulum-mitochondria contacts: function of the junction. Nat Rev Mol Cell Biol 13(10):607–625. https://doi.org/10.1038/nrm3440
10. Naon D, Scorrano L (2014) At the right distance: ER-mitochondria juxtaposition in cell life and death. Biochim Biophys Acta 1843(10):2184–2194. https://doi.org/10.1016/j.bbamcr.2014.05.011

11. Filadi R, Pendin D, Pizzo P (2018) Mitofusin 2: from functions to disease. Cell Death Dis 9(3):330. https://doi.org/10.1038/s41419-017-0023-6
12. de Brito OM, Scorrano L (2008) Mitofusin 2 tethers endoplasmic reticulum to mitochondria. Nature 456(7222):605–610. https://doi.org/10.1038/nature07534
13. Naon D, Zaninello M, Giacomello M, Varanita T, Grespi F, Lakshminaranayan S, Serafini A, Semenzato M, Herkenne S, Hernandez-Alvarez MI, Zorzano A, De Stefani D, Dorn GW 2nd, Scorrano L (2016) Critical reappraisal confirms that Mitofusin 2 is an endoplasmic reticulum-mitochondria tether. Proc Natl Acad Sci U S A 113(40):11249–11254. https://doi.org/10.1073/pnas.1606786113
14. Filadi R, Greotti E, Turacchio G, Luini A, Pozzan T, Pizzo P (2015) Mitofusin 2 ablation increases endoplasmic reticulum-mitochondria coupling. Proc Natl Acad Sci U S A 112(17):E2174–E2181. https://doi.org/10.1073/pnas.1504880112
15. Wang PT, Garcin PO, Fu M, Masoudi M, St-Pierre P, Pante N, Nabi IR (2015) Distinct mechanisms controlling rough and smooth endoplasmic reticulum contacts with mitochondria. J Cell Sci 128(15):2759–2765. https://doi.org/10.1242/jcs.171132
16. Bravo-Sagua R, Lopez-Crisosto C, Parra V, Rodriguez-Pena M, Rothermel BA, Quest AF, Lavandero S (2016) mTORC1 inhibitor rapamycin and ER stressor tunicamycin induce differential patterns of ER-mitochondria coupling. Sci Rep 6:36394. https://doi.org/10.1038/srep36394
17. Cieri D, Vicario M, Giacomello M, Vallese F, Filadi R, Wagner T, Pozzan T, Pizzo P, Scorrano L, Brini M, Cali T (2017) SPLICS: a split green fluorescent protein-based contact site sensor for narrow and wide heterotypic organelle juxtaposition. Cell Death Differ 25(6):1131–1145. https://doi.org/10.1038/s41418-017-0033-z
18. Kanekura K, Nishimoto I, Aiso S, Matsuoka M (2006) Characterization of amyotrophic lateral sclerosis-linked P56S mutation of vesicle-associated membrane protein-associated protein B (VAPB/ALS8). J Biol Chem 281(40):30223–30233. https://doi.org/10.1074/jbc.M605049200
19. Stoica R, De Vos KJ, Paillusson S, Mueller S, Sancho RM, Lau KF, Vizcay-Barrena G, Lin WL, Xu YF, Lewis J, Dickson DW, Petrucelli L, Mitchell JC, Shaw CE, Miller CC (2014) ER-mitochondria associations are regulated by the VAPB-PTPIP51 interaction and are disrupted by ALS/FTD-associated TDP-43. Nat Commun 5:3996. https://doi.org/10.1038/ncomms4996
20. De Vos KJ, Morotz GM, Stoica R, Tudor EL, Lau KF, Ackerley S, Warley A, Shaw CE, Miller CC (2012) VAPB interacts with the mitochondrial protein PTPIP51 to regulate calcium homeostasis. Hum Mol Genet 21(6):1299–1311. https://doi.org/10.1093/hmg/ddr559
21. Paillusson S, Stoica R, Gomez-Suaga P, Lau DH, Mueller S, Miller T, Miller CC (2016) There's something wrong with my MAM; the ER-mitochondria axis and neurodegenerative diseases. Trends Neurosci 39(3):146–157. https://doi.org/10.1016/j.tins.2016.01.008
22. Huttlin EL, Ting L, Bruckner RJ, Gebreab F, Gygi MP, Szpyt J, Tam S, Zarraga G, Colby G, Baltier K, Dong R, Guarani V, Vaites LP, Ordureau A, Rad R, Erickson BK, Wuhr M, Chick J, Zhai B, Kolippakkam D, Mintseris J, Obar RA, Harris T, Artavanis-Tsakonas S, Sowa ME, De Camilli P, Paulo JA, Harper JW, Gygi SP (2015) The BioPlex network: a systematic exploration of the human interactome. Cell 162(2):425–440. https://doi.org/10.1016/j.cell.2015.06.043
23. Stoica R, Paillusson S, Gomez-Suaga P, Mitchell JC, Lau DH, Gray EH, Sancho RM, Vizcay-Barrena G, De Vos KJ, Shaw CE, Hanger DP, Noble W, Miller CC (2016) ALS/FTD-associated FUS activates GSK-3beta to disrupt the VAPB-PTPIP51 interaction and ER-mitochondria associations. EMBO Rep 17(9):1326–1342. https://doi.org/10.15252/embr.201541726
24. Galmes R, Houcine A, van Vliet AR, Agostinis P, Jackson CL, Giordano F (2016) ORP5/ORP8 localize to endoplasmic reticulum-mitochondria contacts and are involved in mitochondrial function. EMBO Rep 17(6):800–810. https://doi.org/10.15252/embr.201541108

25. Iwasawa R, Mahul-Mellier AL, Datler C, Pazarentzos E, Grimm S (2011) Fis1 and Bap31 bridge the mitochondria-ER interface to establish a platform for apoptosis induction. EMBO J 30(3):556–568. https://doi.org/10.1038/emboj.2010.346
26. Simmen T, Aslan JE, Blagoveshchenskaya AD, Thomas L, Wan L, Xiang Y, Feliciangeli SF, Hung CH, Crump CM, Thomas G (2005) PACS-2 controls endoplasmic reticulum-mitochondria communication and Bid-mediated apoptosis. EMBO J 24(4):717–729. https://doi.org/10.1038/sj.emboj.7600559
27. Betz C, Stracka D, Prescianotto-Baschong C, Frieden M, Demaurex N, Hall MN (2013) mTOR complex 2-Akt signaling at mitochondria-associated endoplasmic reticulum membranes (MAM) regulates mitochondrial physiology. Proc Natl Acad Sci U S A 110(31):12526–12534. https://doi.org/10.1073/pnas.1302455110
28. Szabadkai G, Bianchi K, Varnai P, De Stefani D, Wieckowski MR, Cavagna D, Nagy AI, Balla T, Rizzuto R (2006) Chaperone-mediated coupling of endoplasmic reticulum and mitochondrial Ca^{2+} channels. J Cell Biol 175(6):901–911. https://doi.org/10.1083/jcb.200608073
29. De Stefani D, Bononi A, Romagnoli A, Messina A, De Pinto V, Pinton P, Rizzuto R (2012) VDAC1 selectively transfers apoptotic Ca^{2+} signals to mitochondria. Cell Death Differ 19(2):267–273. https://doi.org/10.1038/cdd.2011.92
30. Filadi R, Leal NS, Schreiner B, Rossi A, Dentoni G, Pinho CM, Wiehager B, Cieri D, Calì T, Pizzo P, Ankarcrona M (2018) TOM70 sustains cell bioenergetics by promoting IP3R3-mediated ER to mitochondria Ca 2+ transfer. Curr Biol 28(3):369–382.e6. https://doi.org/10.1016/j.cub.2017.12.047
31. Berridge MJ, Bootman MD, Roderick HL (2003) Calcium signalling: dynamics, homeostasis and remodelling. Nat Rev Mol Cell Biol 4(7):517–529. https://doi.org/10.1038/nrm1155
32. Clapham DE (2007) Calcium signaling. Cell 131(6):1047–1058. https://doi.org/10.1016/j.cell.2007.11.028
33. Brini M, Carafoli E (2009) Calcium pumps in health and disease. Physiol Rev 89(4):1341–1378. https://doi.org/10.1152/physrev.00032.2008
34. Deluca HF, Engstrom GW (1961) Calcium uptake by rat kidney mitochondria. Proc Natl Acad Sci U S A 47:1744–1750
35. Mitchell P (1961) Coupling of phosphorilation to electron transfer by a chemi-osmotic type of mechanism. Nature 191(4784):144–148
36. De Stefani D, Raffaello A, Teardo E, Szabo I, Rizzuto R (2011) A forty-kilodalton protein of the inner membrane is the mitochondrial calcium uniporter. Nature 476(7360):336–340. https://doi.org/10.1038/nature10230
37. Baughman JM, Perocchi F, Girgis HS, Plovanich M, Belcher-Timme CA, Sancak Y, Bao XR, Strittmatter L, Goldberger O, Bogorad RL, Koteliansky V, Mootha VK (2011) Integrative genomics identifies MCU as an essential component of the mitochondrial calcium uniporter. Nature 476(7360):341–345. https://doi.org/10.1038/nature10234
38. Fan C, Fan M, Orlando BJ, Fastman NM, Zhang J, Xu Y, Chambers MG, Xu X, Perry K, Liao M, Feng L (2018) X-ray and cryo-EM structures of the mitochondrial calcium uniporter. Nature 559(7715):575–579. https://doi.org/10.1038/s41586-018-0330-9
39. Nguyen NX, Armache JP, Lee C, Yang Y, Zeng W, Mootha VK, Cheng Y, Bai XC, Jiang Y (2018) Cryo-EM structure of a fungal mitochondrial calcium uniporter. Nature 559(7715):570–574. https://doi.org/10.1038/s41586-018-0333-6
40. Yoo J, Wu M, Yin Y, Herzik MA Jr, Lander GC, Lee SY (2018) Cryo-EM structure of a mitochondrial calcium uniporter. Science 361(6401):506–511. https://doi.org/10.1126/science.aar4056
41. Baradaran R, Wang C, Siliciano AF, Long SB (2018) Cryo-EM structures of fungal and metazoan mitochondrial calcium uniporters. Nature 559(7715):580–584. https://doi.org/10.1038/s41586-018-0331-8
42. Oxenoid K, Dong Y, Cao C, Cui T, Sancak Y, Markhard AL, Grabarek Z, Kong L, Liu Z, Ouyang B, Cong Y, Mootha VK, Chou JJ (2016) Architecture of the mitochondrial calcium uniporter. Nature 533(7602):269–273. https://doi.org/10.1038/nature17656

43. Raffaello A, De Stefani D, Sabbadin D, Teardo E, Merli G, Picard A, Checchetto V, Moro S, Szabo I, Rizzuto R (2013) The mitochondrial calcium uniporter is a multimer that can include a dominant-negative pore-forming subunit. EMBO J 32(17):2362–2376. https://doi.org/10.1038/emboj.2013.157
44. De Stefani D, Rizzuto R, Pozzan T (2016) Enjoy the trip: calcium in mitochondria back and forth. Annu Rev Biochem 85:161–192. https://doi.org/10.1146/annurev-biochem-060614-034216
45. Patron M, Checchetto V, Raffaello A, Teardo E, Vecellio Reane D, Mantoan M, Granatiero V, Szabo I, De Stefani D, Rizzuto R (2014) MICU1 and MICU2 finely tune the mitochondrial Ca^{2+} uniporter by exerting opposite effects on MCU activity. Mol Cell 53(5):726–737. https://doi.org/10.1016/j.molcel.2014.01.013
46. Perocchi F, Gohil VM, Girgis HS, Bao XR, McCombs JE, Palmer AE, Mootha VK (2010) MICU1 encodes a mitochondrial EF hand protein required for Ca^{2+} uptake. Nature 467(7313):291–296. https://doi.org/10.1038/nature09358
47. Plovanich M, Bogorad RL, Sancak Y, Kamer KJ, Strittmatter L, Li AA, Girgis HS, Kuchimanchi S, De Groot J, Speciner L, Taneja N, Oshea J, Koteliansky V, Mootha VK (2013) MICU2, a paralog of MICU1, resides within the mitochondrial uniporter complex to regulate calcium handling. PLoS One 8(2):e55785. https://doi.org/10.1371/journal.pone.0055785
48. Patron M, Granatiero V, Espino J, Rizzuto R, De Stefani D (2018) MICU3 is a tissue-specific enhancer of mitochondrial calcium uptake. Cell Death Differ 26(1):179–195. https://doi.org/10.1038/s41418-018-0113-8
49. Sancak Y, Markhard AL, Kitami T, Kovacs-Bogdan E, Kamer KJ, Udeshi ND, Carr SA, Chaudhuri D, Clapham DE, Li AA, Calvo SE, Goldberger O, Mootha VK (2013) EMRE is an essential component of the mitochondrial calcium uniporter complex. Science 342(6164):1379–1382. https://doi.org/10.1126/science.1242993
50. Mallilankaraman K, Cardenas C, Doonan PJ, Chandramoorthy HC, Irrinki KM, Golenar T, Csordas G, Madireddi P, Yang J, Muller M, Miller R, Kolesar JE, Molgo J, Kaufman B, Hajnoczky G, Foskett JK, Madesh M (2012) MCUR1 is an essential component of mitochondrial Ca^{2+} uptake that regulates cellular metabolism. Nat Cell Biol 15(1):123. https://doi.org/10.1038/ncb2669
51. Rizzuto R, Brini M, Murgia M, Pozzan T (1993) Microdomains with high Ca^{2+} close to IP3-sensitive channels that are sensed by neighboring mitochondria. Science 262(5134):744–747
52. Pinton P, Giorgi C, Siviero R, Zecchini E, Rizzuto R (2008) Calcium and apoptosis: ER-mitochondria Ca^{2+} transfer in the control of apoptosis. Oncogene 27(50):6407–6418. https://doi.org/10.1038/onc.2008.308
53. Calì T, Ottolini D, Brini M (2012) Mitochondrial Ca^{2+} as a key regulator of mitochondrial activities. Adv Exp Med Biol 942:53–73. https://doi.org/10.1007/978-94-007-2869-1_3
54. Calì T, Ottolini D, Brini M (2012) Mitochondrial Ca^{2+} and neurodegeneration. Cell Calcium 52(1):73–85. https://doi.org/10.1016/j.ceca.2012.04.015
55. Rizzuto R, De Stefani D, Raffaello A, Mammucari C (2012) Mitochondria as sensors and regulators of calcium signalling. Nat Rev Mol Cell Biol 13(9):566–578. https://doi.org/10.1038/nrm3412
56. Cardenas C, Muller M, McNeal A, Lovy A, Jana F, Bustos G, Urra F, Smith N, Molgo J, Diehl JA, Ridky TW, Foskett JK (2016) Selective vulnerability of cancer cells by inhibition of Ca^{2+} transfer from endoplasmic reticulum to mitochondria. Cell Rep 14(10):2313–2324. https://doi.org/10.1016/j.celrep.2016.02.030
57. Bononi A, Bonora M, Marchi S, Missiroli S, Poletti F, Giorgi C, Pandolfi PP, Pinton P (2013) Identification of PTEN at the ER and MAMs and its regulation of Ca^{2+} signaling and apoptosis in a protein phosphatase-dependent manner. Cell Death Differ 20(12):1631–1643. https://doi.org/10.1038/cdd.2013.77
58. Roderick HL, Lechleiter JD, Camacho P (2000) Cytosolic phosphorylation of calnexin controls intracellular Ca^{2+} oscillations via an interaction with SERCA2b. J Cell Biol 149(6):1235–1248

59. Lynes EM, Raturi A, Shenkman M, Ortiz Sandoval C, Yap MC, Wu J, Janowicz A, Myhill N, Benson MD, Campbell RE, Berthiaume LG, Lederkremer GZ, Simmen T (2013) Palmitoylation is the switch that assigns calnexin to quality control or ER Ca^{2+} signaling. J Cell Sci 126(Pt 17):3893–3903. https://doi.org/10.1242/jcs.125856
60. Lynes EM, Bui M, Yap MC, Benson MD, Schneider B, Ellgaard L, Berthiaume LG, Simmen T (2012) Palmitoylated TMX and calnexin target to the mitochondria-associated membrane. EMBO J 31(2):457–470. https://doi.org/10.1038/emboj.2011.384
61. Krols M, Bultynck G, Janssens S (2016) ER-mitochondria contact sites: a new regulator of cellular calcium flux comes into play. J Cell Biol 214(4):367–370. https://doi.org/10.1083/jcb.201607124
62. Yoboue ED, Rimessi A, Anelli T, Pinton P, Sitia R (2017) Regulation of calcium fluxes by GPX8, a type-II transmembrane peroxidase enriched at the mitochondria-associated endoplasmic reticulum membrane. Antioxid Redox Signal 27(9):583–595. https://doi.org/10.1089/ars.2016.6866
63. Hayashi T, Rizzuto R, Hajnoczky G, Su TP (2009) MAM: more than just a housekeeper. Trends Cell Biol 19(2):81–88. https://doi.org/10.1016/j.tcb.2008.12.002
64. Wang X, Schwarz TL (2009) The mechanism of Ca^{2+} -dependent regulation of kinesin-mediated mitochondrial motility. Cell 136(1):163–174. https://doi.org/10.1016/j.cell.2008.11.046
65. Hayashi T, Su TP (2007) Sigma-1 receptor chaperones at the ER-mitochondrion interface regulate Ca^{2+} signaling and cell survival. Cell 131(3):596–610. https://doi.org/10.1016/j.cell.2007.08.036
66. Myhill N, Lynes EM, Nanji JA, Blagoveshchenskaya AD, Fei H, Carmine Simmen K, Cooper TJ, Thomas G, Simmen T (2008) The subcellular distribution of calnexin is mediated by PACS-2. Mol Biol Cell 19(7):2777–2788. https://doi.org/10.1091/mbc.E07-10-0995
67. Bastianutto C, Clementi E, Codazzi F, Podini P, De Giorgi F, Rizzuto R, Meldolesi J, Pozzan T (1995) Overexpression of calreticulin increases the Ca^{2+} capacity of rapidly exchanging Ca^{2+} stores and reveals aspects of their lumenal microenvironment and function. J Cell Biol 130(4):847–855
68. Hendershot LM (2004) The ER function BiP is a master regulator of ER function. Mt Sinai J Med 71(5):289–297
69. Camacho P, Lechleiter JD (1995) Calreticulin inhibits repetitive intracellular Ca^{2+} waves. Cell 82(5):765–771
70. Michalak M, Groenendyk J, Szabo E, Gold LI, Opas M (2009) Calreticulin, a multi-process calcium-buffering chaperone of the endoplasmic reticulum. Biochem J 417(3):651–666. https://doi.org/10.1042/BJ20081847
71. Anelli T, Alessio M, Mezghrani A, Simmen T, Talamo F, Bachi A, Sitia R (2002) ERp44, a novel endoplasmic reticulum folding assistant of the thioredoxin family. EMBO J 21(4):835–844
72. Higo T, Hattori M, Nakamura T, Natsume T, Michikawa T, Mikoshiba K (2005) Subtype-specific and ER lumenal environment-dependent regulation of inositol 1,4,5-trisphosphate receptor type 1 by ERp44. Cell 120(1):85–98. https://doi.org/10.1016/j.cell.2004.11.048
73. Li G, Mongillo M, Chin KT, Harding H, Ron D, Marks AR, Tabas I (2009) Role of ERO1-alpha-mediated stimulation of inositol 1,4,5-triphosphate receptor activity in endoplasmic reticulum stress-induced apoptosis. J Cell Biol 186(6):783–792. https://doi.org/10.1083/jcb.200904060
74. Anelli T, Bergamelli L, Margittai E, Rimessi A, Fagioli C, Malgaroli A, Pinton P, Ripamonti M, Rizzuto R, Sitia R (2012) Ero1alpha regulates Ca^{2+} fluxes at the endoplasmic reticulum-mitochondria interface (MAM). Antioxid Redox Signal 16(10):1077–1087. https://doi.org/10.1089/ars.2011.4004
75. Ghavami S, Shojaei S, Yeganeh B, Ande SR, Jangamreddy JR, Mehrpour M, Christoffersson J, Chaabane W, Moghadam AR, Kashani HH, Hashemi M, Owji AA, Los MJ (2014) Autophagy and apoptosis dysfunction in neurodegenerative disorders. Prog Neurobiol 112:24–49. https://doi.org/10.1016/j.pneurobio.2013.10.004

76. Millecamps S, Julien JP (2013) Axonal transport deficits and neurodegenerative diseases. Nat Rev Neurosci 14(3):161–176. https://doi.org/10.1038/nrn3380
77. Mironov SL, Symonchuk N (2006) ER vesicles and mitochondria move and communicate at synapses. J Cell Sci 119(Pt 23):4926–4934. https://doi.org/10.1242/jcs.03254
78. Wu Y, Whiteus C, Xu CS, Hayworth KJ, Weinberg RJ, Hess HF, De Camilli P (2017) Contacts between the endoplasmic reticulum and other membranes in neurons. Proc Natl Acad Sci U S A 114(24):E4859–E4867. https://doi.org/10.1073/pnas.1701078114
79. Goedert M (2015) NEURODEGENERATION. Alzheimer's and Parkinson's diseases: the prion concept in relation to assembled Abeta, tau, and alpha-synuclein. Science 349(6248):1255555. https://doi.org/10.1126/science.1255555
80. Area-Gomez E, de Groof A, Bonilla E, Montesinos J, Tanji K, Boldogh I, Pon L, Schon EA (2018) A key role for MAM in mediating mitochondrial dysfunction in Alzheimer disease. Cell Death Dis 9(3):335. https://doi.org/10.1038/s41419-017-0215-0
81. Bezprozvanny I (2013) Presenilins and calcium signaling-systems biology to the rescue. Sci Signal 6(283):pe24. https://doi.org/10.1126/scisignal.2004296
82. Popugaeva E, Pchitskaya E, Bezprozvanny I (2017) Dysregulation of neuronal calcium homeostasis in Alzheimer's disease – a therapeutic opportunity? Biochem Biophys Res Commun 483(4):998–1004. https://doi.org/10.1016/j.bbrc.2016.09.053
83. Area-Gomez E, de Groof AJ, Boldogh I, Bird TD, Gibson GE, Koehler CM, Yu WH, Duff KE, Yaffe MP, Pon LA, Schon EA (2009) Presenilins are enriched in endoplasmic reticulum membranes associated with mitochondria. Am J Pathol 175(5):1810–1816. https://doi.org/10.2353/ajpath.2009.090219
84. Tu H, Nelson O, Bezprozvanny A, Wang Z, Lee SF, Hao YH, Serneels L, De Strooper B, Yu G, Bezprozvanny I (2006) Presenilins form ER Ca^{2+} leak channels, a function disrupted by familial Alzheimer's disease-linked mutations. Cell 126(5):981–993. https://doi.org/10.1016/j.cell.2006.06.059
85. Cheung KH, Shineman D, Muller M, Cardenas C, Mei L, Yang J, Tomita T, Iwatsubo T, Lee VM, Foskett JK (2008) Mechanism of Ca^{2+} disruption in Alzheimer's disease by presenilin regulation of InsP3 receptor channel gating. Neuron 58(6):871–883. https://doi.org/10.1016/j.neuron.2008.04.015
86. D'Adamio L, Castillo PE (2013) Presenilin-ryanodine receptor connection. Proc Natl Acad Sci U S A 110(37):14825–14826. https://doi.org/10.1073/pnas.1313996110
87. Green KN, Demuro A, Akbari Y, Hitt BD, Smith IF, Parker I, LaFerla FM (2008) SERCA pump activity is physiologically regulated by presenilin and regulates amyloid beta production. J Cell Biol 181(7):1107–1116. https://doi.org/10.1083/jcb.200706171
88. Brunello L, Zampese E, Florean C, Pozzan T, Pizzo P, Fasolato C (2009) Presenilin-2 dampens intracellular Ca^{2+} stores by increasing Ca^{2+} leakage and reducing Ca^{2+} uptake. J Cell Mol Med 13(9B):3358–3369. https://doi.org/10.1111/j.1582-4934.2009.00755.x
89. Zampese E, Fasolato C, Kipanyula MJ, Bortolozzi M, Pozzan T, Pizzo P (2011) Presenilin 2 modulates endoplasmic reticulum (ER)-mitochondria interactions and Ca^{2+} cross-talk. Proc Natl Acad Sci U S A 108(7):2777–2782. https://doi.org/10.1073/pnas.1100735108
90. Kipanyula MJ, Contreras L, Zampese E, Lazzari C, Wong AK, Pizzo P, Fasolato C, Pozzan T (2012) Ca^{2+} dysregulation in neurons from transgenic mice expressing mutant presenilin 2. Aging Cell 11(5):885–893. https://doi.org/10.1111/j.1474-9726.2012.00858.x
91. Duplan E, Sevalle J, Viotti J, Goiran T, Druon C, Renbaum P, Levy-Lahad E, Gautier C, Corti O, Leroudier N, Checler F, da Costa CA (2013) Parkin differently regulates presenilin-1 and presenilin-2 function by direct control of their promoter transcription. J Mol Cell Biol 5(2):132–142. https://doi.org/10.1093/jmcb/mjt003
92. Hedskog L, Pinho CM, Filadi R, Ronnback A, Hertwig L, Wiehager B, Larssen P, Gellhaar S, Sandebring A, Westerlund M, Graff C, Winblad B, Galter D, Behbahani H, Pizzo P, Glaser E, Ankarcrona M (2013) Modulation of the endoplasmic reticulum-mitochondria interface in Alzheimer's disease and related models. Proc Natl Acad Sci U S A 110(19):7916–7921. https://doi.org/10.1073/pnas.1300677110

93. Cieri D, Vicario M, Vallese F, D'Orsi B, Berto P, Grinzato A, Catoni C, De Stefani D, Rizzuto R, Brini M, Cali T (2018) Tau localises within mitochondrial sub-compartments and its caspase cleavage affects ER-mitochondria interactions and cellular Ca^{2+} handling. Biochim Biophys Acta Mol basis Dis 1864(10):3247–3256. https://doi.org/10.1016/j.bbadis.2018.07.011
94. Cieri D, Brini M, Cali T (2016) Emerging (and converging) pathways in Parkinson's disease: keeping mitochondrial wellness. Biochem Biophys Res Commun 483(4):1020–1030. https://doi.org/10.1016/j.bbrc.2016.08.153
95. Poewe W, Seppi K, Tanner CM, Halliday GM, Brundin P, Volkmann J, Schrag AE, Lang AE (2017) Parkinson disease. Nat Rev Dis Primers 3:17013. https://doi.org/10.1038/nrdp.2017.13
96. Calì T, Ottolini D, Brini M (2014) Calcium signaling in Parkinson's disease. Cell Tissue Res 357:439–454. https://doi.org/10.1007/s00441-014-1866-0
97. Lin MK, Farrer MJ (2014) Genetics and genomics of Parkinson's disease. Genome Med 6(6):48. https://doi.org/10.1186/gm566
98. Rodriguez-Arribas M, SMS Y-D, JMB P, Gomez-Suaga P, Gomez-Sanchez R, Martinez-Chacon G, Fuentes JM, Gonzalez-Polo RA, Niso-Santano M (2017) Mitochondria-Associated Membranes (MAMs): overview and its role in Parkinson's disease. Mol Neurobiol 54(8):6287–6303. https://doi.org/10.1007/s12035-016-0140-8
99. Calì T, Ottolini D, Negro A, Brini M (2012) alpha-synuclein controls mitochondrial calcium homeostasis by enhancing endoplasmic reticulum-mitochondria interactions. J Biol Chem 287(22):17914–17929. https://doi.org/10.1074/jbc.M111.302794
100. Ottolini D, Cali T, Szabo I, Brini M (2017) Alpha-synuclein at the intracellular and the extracellular side: functional and dysfunctional implications. Biol Chem 398(1):77–100. https://doi.org/10.1515/hsz-2016-0201
101. Vicario M, Cieri D, Brini M, Calì T (2018) The close encounter between alpha-synuclein and mitochondria. Front Neurosci 12:388. https://doi.org/10.3389/fnins.2018.00388
102. Guardia-Laguarta C, Area-Gomez E, Schon EA, Przedborski S (2015) A new role for alpha-synuclein in Parkinson's disease: alteration of ER-mitochondrial communication. Mov Disord 30(8):1026–1033. https://doi.org/10.1002/mds.26239
103. Gan L, Cookson MR, Petrucelli L, La Spada AR (2018) Converging pathways in neurodegeneration, from genetics to mechanisms. Nat Neurosci 21(10):1300–1309. https://doi.org/10.1038/s41593-018-0237-7
104. Palikaras K, Lionaki E, Tavernarakis N (2018) Mechanisms of mitophagy in cellular homeostasis, physiology and pathology. Nat Cell Biol 20(9):1013–1022. https://doi.org/10.1038/s41556-018-0176-2
105. Pickles S, Vigie P, Youle RJ (2018) Mitophagy and quality control mechanisms in mitochondrial maintenance. Curr Biol 28(4):R170–R185. https://doi.org/10.1016/j.cub.2018.01.004
106. Youle RJ, Narendra DP (2011) Mechanisms of mitophagy. Nat Rev Mol Cell Biol 12(1):9–14. https://doi.org/10.1038/nrm3028
107. Van Laar VS, Roy N, Liu A, Rajprohat S, Arnold B, Dukes AA, Holbein CD, Berman SB (2014) Glutamate excitotoxicity in neurons triggers mitochondrial and endoplasmic reticulum accumulation of Parkin, and, in the presence of N-acetyl cysteine, mitophagy. Neurobiol Dis 74:180–193. https://doi.org/10.1016/j.nbd.2014.11.015
108. Darios F, Corti O, Lucking CB, Hampe C, Muriel MP, Abbas N, Gu WJ, Hirsch EC, Rooney T, Ruberg M, Brice A (2003) Parkin prevents mitochondrial swelling and cytochrome c release in mitochondria-dependent cell death. Hum Mol Genet 12(5):517–526
109. Shin JH, Ko HS, Kang H, Lee Y, Lee YI, Pletinkova O, Troconso JC, Dawson VL, Dawson TM (2011) PARIS (ZNF746) repression of PGC-1alpha contributes to neurodegeneration in Parkinson's disease. Cell 144(5):689–702. https://doi.org/10.1016/j.cell.2011.02.010
110. Bertolin G, Ferrando-Miguel R, Jacoupy M, Traver S, Grenier K, Greene AW, Dauphin A, Waharte F, Bayot A, Salamero J, Lombes A, Bulteau AL, Fon EA, Brice A, Corti O (2013) The TOMM machinery is a molecular switch in PINK1 and PARK2/PARKIN-dependent mitochondrial clearance. Autophagy 9(11):1801–1817. https://doi.org/10.4161/auto.25884

111. Calì T, Ottolini D, Negro A, Brini M (2013) Enhanced parkin levels favour ER-mitochondria crosstalk and guarantee Ca^{2+} transfer to sustain cell bioenergetics. BBA-Mol Basis Dis 1832(4):495–508. https://doi.org/10.1016/j.bbadis.2013.01.004
112. Imai Y, Soda M, Inoue H, Hattori N, Mizuno Y, Takahashi R (2001) An unfolded putative transmembrane polypeptide, which can lead to endoplasmic reticulum stress, is a substrate of Parkin. Cell 105(7):891–902
113. Wang HQ, Imai Y, Kataoka A, Takahashi R (2007) Cell type-specific upregulation of Parkin in response to ER stress. Antioxid Redox Signal 9(5):533–542. https://doi.org/10.1089/ars.2006.1522
114. Bouman L, Schlierf A, Lutz AK, Shan J, Deinlein A, Kast J, Galehdar Z, Palmisano V, Patenge N, Berg D, Gasser T, Augustin R, Trumbach D, Irrcher I, Park DS, Wurst W, Kilberg MS, Tatzelt J, Winklhofer KF (2011) Parkin is transcriptionally regulated by ATF4: evidence for an interconnection between mitochondrial stress and ER stress. Cell Death Differ 18(5):769–782. https://doi.org/10.1038/cdd.2010.142
115. Imai Y, Soda M, Hatakeyama S, Akagi T, Hashikawa T, Nakayama KI, Takahashi R (2002) CHIP is associated with Parkin, a gene responsible for familial Parkinson's disease, and enhances its ubiquitin ligase activity. Mol Cell 10(1):55–67
116. Avraham E, Rott R, Liani E, Szargel R, Engelender S (2007) Phosphorylation of Parkin by the cyclin-dependent kinase 5 at the linker region modulates its ubiquitin-ligase activity and aggregation. J Biol Chem 282(17):12842–12850. https://doi.org/10.1074/jbc.M608243200
117. Yao D, Gu Z, Nakamura T, Shi ZQ, Ma Y, Gaston B, Palmer LA, Rockenstein EM, Zhang Z, Masliah E, Uehara T, Lipton SA (2004) Nitrosative stress linked to sporadic Parkinson's disease: S-nitrosylation of parkin regulates its E3 ubiquitin ligase activity. Proc Natl Acad Sci U S A 101(29):10810–10814. https://doi.org/10.1073/pnas.0404161101
118. Han K, Hassanzadeh S, Singh K, Menazza S, Nguyen TT, Stevens MV, Nguyen A, San H, Anderson SA, Lin Y, Zou J, Murphy E, Sack MN (2017) Parkin regulation of CHOP modulates susceptibility to cardiac endoplasmic reticulum stress. Sci Rep 7(1):2093. https://doi.org/10.1038/s41598-017-02339-2
119. Basso V, Marchesan E, Peggion C, Chakraborty J, von Stockum S, Giacomello M, Ottolini D, Debattisti V, Caicci F, Tasca E, Pegoraro V, Angelini C, Antonini A, Bertoli A, Brini M, Ziviani E (2018) Regulation of endoplasmic reticulum-mitochondria contacts by Parkin via Mfn2. Pharmacol Res 138:43–56. https://doi.org/10.1016/j.phrs.2018.09.006
120. van der Merwe C, Jalali Sefid Dashti Z, Christoffels A, Loos B, Bardien S (2015) Evidence for a common biological pathway linking three Parkinson's disease-causing genes: parkin, PINK1 and DJ-1. Eur J Neurosci 41(9):1113–1125. https://doi.org/10.1111/ejn.12872
121. Cali T, Ottolini D, Soriano ME, Brini M (2014) A new split-GFP-based probe reveals DJ-1 translocation into the mitochondrial matrix to sustain ATP synthesis upon nutrient deprivation. Hum Mol Genet 24(4):1045–1160. https://doi.org/10.1093/hmg/ddu519
122. Ottolini D, Calì T, Negro A, Brini M (2013) The Parkinson disease-related protein DJ-1 counteracts mitochondrial impairment induced by the tumour suppressor protein p53 by enhancing endoplasmic reticulum-mitochondria tethering. Hum Mol Genet 22(11):2152–2168. https://doi.org/10.1093/hmg/ddt068
123. Hardiman O, Al-Chalabi A, Chio A, Corr EM, Logroscino G, Robberecht W, Shaw PJ, Simmons Z, van den Berg LH (2017) Amyotrophic lateral sclerosis. Nat Rev Dis Primers 3:17071. https://doi.org/10.1038/nrdp.2017.71
124. Langou K, Moumen A, Pellegrino C, Aebischer J, Medina I, Aebischer P, Raoul C (2010) AAV-mediated expression of wild-type and ALS-linked mutant VAPB selectively triggers death of motoneurons through a Ca^{2+}-dependent ER-associated pathway. J Neurochem 114(3):795–809. https://doi.org/10.1111/j.1471-4159.2010.06806.x
125. Morotz GM, De Vos KJ, Vagnoni A, Ackerley S, Shaw CE, Miller CC (2012) Amyotrophic lateral sclerosis-associated mutant VAPBP56S perturbs calcium homeostasis to disrupt axonal transport of mitochondria. Hum Mol Genet 21(9):1979–1988. https://doi.org/10.1093/hmg/dds011

126. Rosen DR (1993) Mutations in Cu/Zn superoxide dismutase gene are associated with familial amyotrophic lateral sclerosis. Nature 364(6435):362. https://doi.org/10.1038/364362c0
127. Damiano M, Starkov AA, Petri S, Kipiani K, Kiaei M, Mattiazzi M, Flint Beal M, Manfredi G (2006) Neural mitochondrial Ca^{2+} capacity impairment precedes the onset of motor symptoms in G93A Cu/Zn-superoxide dismutase mutant mice. J Neurochem 96(5):1349–1361. https://doi.org/10.1111/j.1471-4159.2006.03619.x
128. Parone PA, Da Cruz S, Han JS, McAlonis-Downes M, Vetto AP, Lee SK, Tseng E, Cleveland DW (2013) Enhancing mitochondrial calcium buffering capacity reduces aggregation of misfolded SOD1 and motor neuron cell death without extending survival in mouse models of inherited amyotrophic lateral sclerosis. J Neurosci 33(11):4657–4671. https://doi.org/10.1523/JNEUROSCI.1119-12.2013
129. Pedrini S, Sau D, Guareschi S, Bogush M, Brown RH Jr, Naniche N, Kia A, Trotti D, Pasinelli P (2010) ALS-linked mutant SOD1 damages mitochondria by promoting conformational changes in Bcl-2. Hum Mol Genet 19(15):2974–2986. https://doi.org/10.1093/hmg/ddq202
130. Eckenrode EF, Yang J, Velmurugan GV, Foskett JK, White C (2010) Apoptosis protection by Mcl-1 and Bcl-2 modulation of inositol 1,4,5-trisphosphate receptor-dependent Ca^{2+} signaling. J Biol Chem 285(18):13678–13684. https://doi.org/10.1074/jbc.M109.096040
131. Pinton P, Ferrari D, Magalhaes P, Schulze-Osthoff K, Di Virgilio F, Pozzan T, Rizzuto R (2000) Reduced loading of intracellular Ca^{2+} stores and downregulation of capacitative Ca^{2+} influx in Bcl-2-overexpressing cells. J Cell Biol 148(5):857–862
132. Dimmer KS, Rapaport D (2017) Mitochondrial contact sites as platforms for phospholipid exchange. Biochim Biophys Acta Mol Cell Biol Lipids 1862(1):69–80. https://doi.org/10.1016/j.bbalip.2016.07.010
133. Vance JE (2015) Phospholipid synthesis and transport in mammalian cells. Traffic 16(1):1–18. https://doi.org/10.1111/tra.12230
134. Csordas G, Hajnoczky G (2009) SR/ER-mitochondrial local communication: calcium and ROS. Biochim Biophys Acta 1787(11):1352–1362. https://doi.org/10.1016/j.bbabio.2009.06.004
135. Raffaello A, Mammucari C, Gherardi G, Rizzuto R (2016) Calcium at the center of cell signaling: interplay between endoplasmic reticulum, mitochondria, and lysosomes. Trends Biochem Sci 41(12):1035–1049. https://doi.org/10.1016/j.tibs.2016.09.001
136. Phillips MJ, Voeltz GK (2016) Structure and function of ER membrane contact sites with other organelles. Nat Rev Mol Cell Biol 17(2):69–82. https://doi.org/10.1038/nrm.2015.8
137. Yoon Y, Krueger EW, Oswald BJ, McNiven MA (2003) The mitochondrial protein hFis1 regulates mitochondrial fission in mammalian cells through an interaction with the dynamin-like protein DLP1. Mol Cell Biol 23(15):5409–5420
138. Otera H, Wang C, Cleland MM, Setoguchi K, Yokota S, Youle RJ, Mihara K (2010) Mff is an essential factor for mitochondrial recruitment of Drp1 during mitochondrial fission in mammalian cells. J Cell Biol 191(6):1141–1158. https://doi.org/10.1083/jcb.201007152
139. Murley A, Lackner LL, Osman C, West M, Voeltz GK, Walter P, Nunnari J (2013) ER-associated mitochondrial division links the distribution of mitochondria and mitochondrial DNA in yeast. elife 2:e00422. https://doi.org/10.7554/eLife.00422
140. Mears JA, Lackner LL, Fang S, Ingerman E, Nunnari J, Hinshaw JE (2011) Conformational changes in Dnm1 support a contractile mechanism for mitochondrial fission. Nat Struct Mol Biol 18(1):20–26. https://doi.org/10.1038/nsmb.1949
141. Zhao J, Liu T, Jin S, Wang X, Qu M, Uhlen P, Tomilin N, Shupliakov O, Lendahl U, Nister M (2011) Human MIEF1 recruits Drp1 to mitochondrial outer membranes and promotes mitochondrial fusion rather than fission. EMBO J 30(14):2762–2778. https://doi.org/10.1038/emboj.2011.198
142. Korobova F, Ramabhadran V, Higgs HN (2013) An actin-dependent step in mitochondrial fission mediated by the ER-associated formin INF2. Science 339(6118):464–467. https://doi.org/10.1126/science.1228360
143. Yoon Y, Pitts KR, McNiven MA (2001) Mammalian dynamin-like protein DLP1 tubulates membranes. Mol Biol Cell 12(9):2894–2905. https://doi.org/10.1091/mbc.12.9.2894

144. Koshiba T, Detmer SA, Kaiser JT, Chen H, McCaffery JM, Chan DC (2004) Structural basis of mitochondrial tethering by mitofusin complexes. Science 305(5685):858–862. https://doi.org/10.1126/science.1099793
145. Sugiura A, Nagashima S, Tokuyama T, Amo T, Matsuki Y, Ishido S, Kudo Y, McBride HM, Fukuda T, Matsushita N, Inatome R, Yanagi S (2013) MITOL regulates endoplasmic reticulum-mitochondria contacts via Mitofusin2. Mol Cell 51(1):20–34. https://doi.org/10.1016/j.molcel.2013.04.023
146. Lev S (2012) Nonvesicular lipid transfer from the endoplasmic reticulum. Cold Spring Harb Perspect Biol 4(10):a013300. https://doi.org/10.1101/cshperspect.a013300
147. Achleitner G, Zweytick D, Trotter PJ, Voelker DR, Daum G (1995) Synthesis and intracellular transport of aminoglycerophospholipids in permeabilized cells of the yeast, Saccharomyces cerevisiae. J Biol Chem 270(50):29836–29842
148. Vance JE (1990) Phospholipid synthesis in a membrane fraction associated with mitochondria. J Biol Chem 265(13):7248–7256
149. Kornmann B (2013) The molecular hug between the ER and the mitochondria. Curr Opin Cell Biol 25(4):443–448. https://doi.org/10.1016/j.ceb.2013.02.010
150. Kornmann B, Currie E, Collins SR, Schuldiner M, Nunnari J, Weissman JS, Walter P (2009) An ER-mitochondria tethering complex revealed by a synthetic biology screen. Science 325(5939):477–481. https://doi.org/10.1126/science.1175088
151. Kornmann B, Walter P (2010) ERMES-mediated ER-mitochondria contacts: molecular hubs for the regulation of mitochondrial biology. J Cell Sci 123(Pt 9):1389–1393. https://doi.org/10.1242/jcs.058636
152. Hirabayashi Y, Kwon SK, Paek H, Pernice WM, Paul MA, Lee J, Erfani P, Raczkowski A, Petrey DS, Pon LA, Polleux F (2017) ER-mitochondria tethering by PDZD8 regulates Ca^{2+} dynamics in mammalian neurons. Science 358(6363):623–630. https://doi.org/10.1126/science.aan6009
153. Kawano S, Tamura Y, Kojima R, Bala S, Asai E, Michel AH, Kornmann B, Riezman I, Riezman H, Sakae Y, Okamoto Y, Endo T (2018) Structure-function insights into direct lipid transfer between membranes by Mmm1-Mdm12 of ERMES. J Cell Biol 217(3):959–974. https://doi.org/10.1083/jcb.201704119
154. AhYoung AP, Jiang J, Zhang J, Khoi Dang X, Loo JA, Zhou ZH, Egea PF (2015) Conserved SMP domains of the ERMES complex bind phospholipids and mediate tether assembly. Proc Natl Acad Sci U S A 112(25):E3179–E3188. https://doi.org/10.1073/pnas.1422363112
155. Crompton M, Costi A, Hayat L (1987) Evidence for the presence of a reversible Ca^{2+}-dependent pore activated by oxidative stress in heart mitochondria. Biochem J 245(3):915–918
156. Deniaud A, Sharaf el dein O, Maillier E, Poncet D, Kroemer G, Lemaire C, Brenner C (2008) Endoplasmic reticulum stress induces calcium-dependent permeability transition, mitochondrial outer membrane permeabilization and apoptosis. Oncogene 27(3):285–299. https://doi.org/10.1038/sj.onc.1210638
157. Adams JM, Cory S (2018) The BCL-2 arbiters of apoptosis and their growing role as cancer targets. Cell Death Differ 25(1):27–36. https://doi.org/10.1038/cdd.2017.161
158. Strzyz P (2017) Cell death: BCL-2 proteins feed their own expression. Nat Rev Mol Cell Biol 18(11):652–653. https://doi.org/10.1038/nrm.2017.106
159. Giorgi C, Danese A, Missiroli S, Patergnani S, Pinton P (2018) Calcium dynamics as a machine for decoding signals. Trends Cell Biol 28(4):258–273. https://doi.org/10.1016/j.tcb.2018.01.002
160. Rong YP, Bultynck G, Aromolaran AS, Zhong F, Parys JB, De Smedt H, Mignery GA, Roderick HL, Bootman MD, Distelhorst CW (2009) The BH4 domain of Bcl-2 inhibits ER calcium release and apoptosis by binding the regulatory and coupling domain of the IP3 receptor. Proc Natl Acad Sci U S A 106(34):14397–14402. https://doi.org/10.1073/pnas.0907555106
161. White C, Li C, Yang J, Petrenko NB, Madesh M, Thompson CB, Foskett JK (2005) The endoplasmic reticulum gateway to apoptosis by Bcl-X(L) modulation of the InsP3R. Nat Cell Biol 7(10):1021–1028. https://doi.org/10.1038/ncb1302

162. Mathai JP, Germain M, Shore GC (2005) BH3-only BIK regulates BAX,BAK-dependent release of Ca^{2+} from endoplasmic reticulum stores and mitochondrial apoptosis during stress-induced cell death. J Biol Chem 280(25):23829–23836. https://doi.org/10.1074/jbc.M500800200
163. Nutt LK, Pataer A, Pahler J, Fang B, Roth J, McConkey DJ, Swisher SG (2002) Bax and Bak promote apoptosis by modulating endoplasmic reticular and mitochondrial Ca^{2+} stores. J Biol Chem 277(11):9219–9225. https://doi.org/10.1074/jbc.M106817200
164. Shibue T, Suzuki S, Okamoto H, Yoshida H, Ohba Y, Takaoka A, Taniguchi T (2006) Differential contribution of Puma and Noxa in dual regulation of p53-mediated apoptotic pathways. EMBO J 25(20):4952–4962. https://doi.org/10.1038/sj.emboj.7601359
165. Breckenridge DG, Stojanovic M, Marcellus RC, Shore GC (2003) Caspase cleavage product of BAP31 induces mitochondrial fission through endoplasmic reticulum calcium signals, enhancing cytochrome c release to the cytosol. J Cell Biol 160(7):1115–1127. https://doi.org/10.1083/jcb.200212059
166. Alirol E, James D, Huber D, Marchetto A, Vergani L, Martinou JC, Scorrano L (2006) The mitochondrial fission protein hFis1 requires the endoplasmic reticulum gateway to induce apoptosis. Mol Biol Cell 17(11):4593–4605. https://doi.org/10.1091/mbc.e06-05-0377
167. Karbowski M, Lee YJ, Gaume B, Jeong SY, Frank S, Nechushtan A, Santel A, Fuller M, Smith CL, Youle RJ (2002) Spatial and temporal association of Bax with mitochondrial fission sites, Drp1, and Mfn2 during apoptosis. J Cell Biol 159(6):931–938. https://doi.org/10.1083/jcb.200209124
168. Cleland MM, Norris KL, Karbowski M, Wang C, Suen DF, Jiao S, George NM, Luo X, Li Z, Youle RJ (2011) Bcl-2 family interaction with the mitochondrial morphogenesis machinery. Cell Death Differ 18(2):235–247. https://doi.org/10.1038/cdd.2010.89
169. He C, Klionsky DJ (2009) Regulation mechanisms and signaling pathways of autophagy. Annu Rev Genet 43:67–93. https://doi.org/10.1146/annurev-genet-102808-114910
170. MacVicar T (2013) Mitophagy. Essays Biochem 55:93–104. https://doi.org/10.1042/bse0550093
171. Hailey DW, Rambold AS, Satpute-Krishnan P, Mitra K, Sougrat R, Kim PK, Lippincott-Schwartz J (2010) Mitochondria supply membranes for autophagosome biogenesis during starvation. Cell 141(4):656–667. https://doi.org/10.1016/j.cell.2010.04.009
172. Hamasaki M, Furuta N, Matsuda A, Nezu A, Yamamoto A, Fujita N, Oomori H, Noda T, Haraguchi T, Hiraoka Y, Amano A, Yoshimori T (2013) Autophagosomes form at ER-mitochondria contact sites. Nature 495(7441):389–393. https://doi.org/10.1038/nature11910
173. Sarbassov DD, Guertin DA, Ali SM, Sabatini DM (2005) Phosphorylation and regulation of Akt/PKB by the rictor-mTOR complex. Science 307(5712):1098–1101. https://doi.org/10.1126/science.1106148
174. Hirota Y, Tanaka Y (2009) A small GTPase, human Rab32, is required for the formation of autophagic vacuoles under basal conditions. Cell Mol Life Sci 66(17):2913–2932. https://doi.org/10.1007/s00018-009-0080-9
175. Betz C, Stracka D, Prescianotto-Baschong C, Frieden M, Demaurex N, Hall MN (2013) Feature Article: mTOR complex 2-Akt signaling at mitochondria-associated endoplasmic reticulum membranes (MAM) regulates mitochondrial physiology. Proc Natl Acad Sci U S A 110(31):12526–12534. https://doi.org/10.1073/pnas.1302455110
176. Bernales S, Soto MM, McCullagh E (2012) Unfolded protein stress in the endoplasmic reticulum and mitochondria: a role in neurodegeneration. Front Aging Neurosci 4:5. https://doi.org/10.3389/fnagi.2012.00005
177. Wang M, Kaufman RJ (2016) Protein misfolding in the endoplasmic reticulum as a conduit to human disease. Nature 529(7586):326–335. https://doi.org/10.1038/nature17041
178. Bui M, Gilady SY, Fitzsimmons RE, Benson MD, Lynes EM, Gesson K, Alto NM, Strack S, Scott JD, Simmen T (2010) Rab32 modulates apoptosis onset and mitochondria-associated membrane (MAM) properties. J Biol Chem 285(41):31590–31602. https://doi.org/10.1074/jbc.M110.101584

179. Munoz JP, Ivanova S, Sanchez-Wandelmer J, Martinez-Cristobal P, Noguera E, Sancho A, Diaz-Ramos A, Hernandez-Alvarez MI, Sebastian D, Mauvezin C, Palacin M, Zorzano A (2013) Mfn2 modulates the UPR and mitochondrial function via repression of PERK. EMBO J 32(17):2348–2361. https://doi.org/10.1038/emboj.2013.168
180. Gkogkas C, Middleton S, Kremer AM, Wardrope C, Hannah M, Gillingwater TH, Skehel P (2008) VAPB interacts with and modulates the activity of ATF6. Hum Mol Genet 17(11):1517–1526. https://doi.org/10.1093/hmg/ddn040
181. Mannella CA, Buttle K, Rath BK, Marko M (1998) Electron microscopic tomography of rat-liver mitochondria and their interaction with the endoplasmic reticulum. Biofactors 8(3–4):225–228
182. Csordas G, Renken C, Varnai P, Walter L, Weaver D, Buttle KF, Balla T, Mannella CA, Hajnoczky G (2006) Structural and functional features and significance of the physical linkage between ER and mitochondria. J Cell Biol 174(7):915–921. https://doi.org/10.1083/jcb.200604016
183. Elgass KD, Smith EA, LeGros MA, Larabell CA, Ryan MT (2015) Analysis of ER-mitochondria contacts using correlative fluorescence microscopy and soft X-ray tomography of mammalian cells. J Cell Sci 128(15):2795–2804. https://doi.org/10.1242/jcs.169136
184. Rusinol AE, Cui Z, Chen MH, Vance JE (1994) A unique mitochondria-associated membrane fraction from rat liver has a high capacity for lipid synthesis and contains pre-Golgi secretory proteins including nascent lipoproteins. J Biol Chem 269(44):27494–27502
185. Wieckowski MR, Giorgi C, Lebiedzinska M, Duszynski J, Pinton P (2009) Isolation of mitochondria-associated membranes and mitochondria from animal tissues and cells. Nat Protoc 4(11):1582–1590. https://doi.org/10.1038/nprot.2009.151
186. Brunstein M, Wicker K, Herault K, Heintzmann R, Oheim M (2013) Full-field dual-color 100-nm super-resolution imaging reveals organization and dynamics of mitochondrial and ER networks. Opt Express 21(22):26162–26173. https://doi.org/10.1364/OE.21.026162
187. Bottanelli F, Kromann EB, Allgeyer ES, Erdmann RS, Wood Baguley S, Sirinakis G, Schepartz A, Baddeley D, Toomre DK, Rothman JE, Bewersdorf J (2016) Two-colour live-cell nanoscale imaging of intracellular targets. Nat Commun 7:10778. https://doi.org/10.1038/ncomms10778
188. Tubbs E, Rieusset J (2016) Study of endoplasmic reticulum and mitochondria interactions by in situ proximity ligation assay in fixed cells. J Vis Exp: JoVE (118). https://doi.org/10.3791/54899
189. Gomez-Suaga P, Paillusson S, Stoica R, Noble W, Hanger DP, Miller CC (2017) The ER-mitochondria tethering complex VAPB-PTPIP51 regulates autophagy. Curr Biol 27(3):371–385. https://doi.org/10.1016/j.cub.2016.12.038
190. Paillusson S, Gomez-Suaga P, Stoica R, Little D, Gissen P, Devine MJ, Noble W, Hanger DP, Miller CCJ (2017) alpha-Synuclein binds to the ER-mitochondria tethering protein VAPB to disrupt Ca^{2+} homeostasis and mitochondrial ATP production. Acta Neuropathol 134(1):129–149. https://doi.org/10.1007/s00401-017-1704-z
191. Csordas G, Varnai P, Golenar T, Roy S, Purkins G, Schneider TG, Balla T, Hajnoczky G (2010) Imaging interorganelle contacts and local calcium dynamics at the ER-mitochondrial interface. Mol Cell 39(1):121–132. https://doi.org/10.1016/j.molcel.2010.06.029
192. Ravikumar B, Duden R, Rubinsztein DC (2002) Aggregate-prone proteins with polyglutamine and polyalanine expansions are degraded by autophagy. Hum Mol Genet 11(9):1107–1117
193. Shi F, Kawano F, Park SE, Komazaki S, Hirabayashi Y, Polleux F, Yazawa M (2018) Optogenetic control of endoplasmic reticulum-mitochondria tethering. ACS Synth Biol 7(1):2–9. https://doi.org/10.1021/acssynbio.7b00248
194. Yang Z, Zhao X, Xu J, Shang W, Tong C (2018) A novel fluorescent reporter detects plastic remodeling of mitochondria-ER contact sites. J Cell Sci 131(1):jcs208686. https://doi.org/10.1242/jcs.208686

195. Harmon M, Larkman P, Hardingham G, Jackson M, Skehel P (2017) A Bi-fluorescence complementation system to detect associations between the endoplasmic reticulum and mitochondria. Sci Rep 7(1):17467. https://doi.org/10.1038/s41598-017-17278-1
196. Kakimoto Y, Tashiro S, Kojima R, Morozumi Y, Endo T, Tamura Y (2018) Visualizing multiple inter-organelle contact sites using the organelle-targeted split-GFP system. Sci Rep 8(1):6175. https://doi.org/10.1038/s41598-018-24466-0
197. Shai N, Yifrach E, van Roermund CWT, Cohen N, Bibi C, IJ L, Cavellini L, Meurisse J, Schuster R, Zada L, Mari MC, Reggiori FM, Hughes AL, Escobar-Henriques M, Cohen MM, Waterham HR, Wanders RJA, Schuldiner M, Zalckvar E (2018) Systematic mapping of contact sites reveals tethers and a function for the peroxisome-mitochondria contact. Nat Commun 9(1):1761. https://doi.org/10.1038/s41467-018-03957-8
198. Cabantous S, Terwilliger TC, Waldo GS (2005) Protein tagging and detection with engineered self-assembling fragments of green fluorescent protein. Nat Biotechnol 23(1):102–107. https://doi.org/10.1038/nbt1044
199. Pedelacq JD, Cabantous S, Tran T, Terwilliger TC, Waldo GS (2006) Engineering and characterization of a superfolder green fluorescent protein. Nat Biotechnol 24(1):79–88. https://doi.org/10.1038/nbt1172

Chapter 30
The Role of Mitochondrial Calcium Signaling in the Pathophysiology of Cancer Cells

Andra M. Sterea and Yassine El Hiani

Abstract The pioneering work of Richard Altman on the presence of mitochondria in cells set in motion a field of research dedicated to uncovering the secrets of the mitochondria. Despite limitations in studying the structure and function of the mitochondria, advances in our understanding of this organelle prompted the development of potential treatments for various diseases, from neurodegenerative conditions to muscular dystrophy and cancer. As the powerhouses of the cell, the mitochondria represent the essence of cellular life and as such, a selective advantage for cancer cells. Much of the function of the mitochondria relies on Ca^{2+} homeostasis and the presence of effective Ca^{2+} signaling to maintain the balance between mitochondrial function and dysfunction and subsequently, cell survival. Ca^{2+} regulates the mitochondrial respiration rate which in turn increases ATP synthesis, but too much Ca^{2+} can also trigger the mitochondrial apoptosis pathway; however, cancer cells have evolved mechanisms to modulate mitochondrial Ca^{2+} influx and efflux in order to sustain their metabolic demand and ensure their survival. Therefore, targeting the mitochondrial Ca^{2+} signaling involved in the bioenergetic and apoptotic pathways could serve as potential approaches to treat cancer patients. This chapter will review the role of Ca^{2+} signaling in mediating the function of the mitochondria and its involvement in health and disease with special focus on the pathophysiology of cancer.

Keywords Mitochondria · Calcium signaling · Cancer · Calcium uptake · ROS · Mitochondrial dysfunction · Cancer treatment

A. M. Sterea · Y. El Hiani (✉)
Departments of Physiology and Biophysics, Dalhousie University, Halifax, NS, Canada
e-mail: yassine.elhiani@dal.ca

M. S. Islam (ed.), *Calcium Signaling*, Advances in Experimental Medicine and Biology 1131, https://doi.org/10.1007/978-3-030-12457-1_30

30.1 An Introduction to Calcium Signaling

Calcium signaling is an important process in all aspects of cellular function and at its center lies the calcium atom, an element first isolated in 1808 [1, 2]. This method of communication within cells evolved as a means of adaptation to a changing environment, a survival strategy involving a multitude of complex and dynamic signaling cascades. Initially, low amounts of calcium where present on Earth and as a result, primitive cells contained very little calcium in their cytoplasm [3, 4]. Because of the low environmental calcium, the cell machinery evolved to tolerate nanomolar concentrations of this element. However, as the Earth's crust began to release more calcium, the accumulation of this element within cells became toxic; thus, initiating the evolution of calcium removal systems. Interestingly, unlike its ability to alter proteins and modulate cellular processes, calcium itself cannot be chemically modified [5, 6]. This property of the calcium atom along with the increasing calcium concentration in the atmosphere prompted the cell to establish methods of control over the levels of calcium in the cytosol through chelation, sequestration within organelles and extrusion [7, 8]. These processes require numerous calcium-binding proteins, sensors, pumps and ion channels. In its ionic form, Ca^{2+} concentrations vary depending on its location within the cell. For example, at rest, the cytoplasmic Ca^{2+} concentration is around 100 nM while the extracellular and endoplasmic reticulum Ca^{2+} reaches concentrations of approximately 1 mM and 0.5 mM, respectively [9]. These values are subject to change, in particular upon cell stimulation when calcium-selective ion channels open and allow for Ca^{2+} influx; thus, setting the basis for calcium signaling as an intricate signal transduction network. Furthermore, calcium signaling is involved in muscle contraction, cell growth, cellular motility, synaptic plasticity, but can also impact apoptosis, the permeability of ion channels and the cytoskeleton [10–18].

The concept of Ca^{2+} signaling and the importance of Ca^{2+} as a ubiquitous second messenger became apparent more than 100 years ago (circa 1883) when studies on heart cells demonstrated that the presence of Ca^{2+} was necessary for the contraction of cardiomyocytes [18]. These experiments set the stage for Ca^{2+} as an important intracellular regulator of muscle contraction. However, during the 1960s, studies moved beyond muscle research and established a pivotal role for Ca^{2+} as a modulator of cellular processes and identified the presence of buffering systems that can accommodate for the change in Ca^{2+} concentration. Ca^{2+} is naturally present in the extracellular environment and it enters cells via two types of proteins, channels and pumps which are gated by external messengers (receptor-operated receptors, ROCs) or voltage (voltage-gated receptors, VOCs) [19]. These proteins are present within the plasma membrane and upon stimulation (e.g. stretch, agonists, depletion of intracellular stores, etc.), they allow the inflow of Ca^{2+} and the initiation of Ca^{2+} signaling pathways [20]. Furthermore, the cell can also generate Ca^{2+} signals internally through the activation of Phospholipase C (PLC) found in the plasma membrane. Upon activation of PLC, phosphatidylinositol 4,5-biphosphate gets hydrolyzed to IP3 and DAG [21]. IP3 then binds to its receptors

on the surface of the endoplasmic reticulum (ER) and stimulates the release of Ca^{2+} from the ER [20]. The mitochondria and the ER have a web-like distribution throughout the cell which facilitates the uptake of Ca^{2+}, but also its distribution. Ca^{2+} is transported within the mitochondria via a uniporter (MCU) which allows for the rapid inflow of Ca^{2+} from the cytosol or the ER [22–25]. Once inside the matrix of the mitochondria, Ca^{2+} can alter the mitochondrial function, especially their ability to produce ATP [26]. Studies have shown that an elevation in the Ca^{2+} concentration inside the matrix can increase mitochondrial respiration and ATP synthesis [27–29]. This bioenergetic dependence of the mitochondria on the presence of Ca^{2+} allows these organelles to coordinate ATP synthesis with the needs of the cell while maintaining Ca^{2+} homeostasis. Nonetheless, excessive buildup of Ca^{2+} can lead to mitochondrial swelling and cell death, a feature that has been exploited in cancer in efforts to eliminate aberrant cells [30, 31]. In addition, while Ca^{2+} can modulate the function of the mitochondria, the organelle itself can in turn affect Ca^{2+} signaling. Numerous research groups have shifted their focus on the involvement of mitochondria Ca^{2+} signaling and its role in disease, especially in cancer cells which are metabolically distinct from normal cells as evidenced by their dependence on mitochondrial ATP to sustain cell proliferation. This chapter will focus on mitochondrial Ca^{2+} signaling, its impact on the pathophysiology of cancer and current mitochondria-based therapies for the treatment of cancer patients.

30.2 Mitochondria, a Historical Overview and Functional Analysis

Commonly referred to as the powerhouses of the cell, the mitochondria have been the subject of extensive scientific interest, from cytology and biochemistry to molecular biology. Early records of mitochondria-like features date back to the 1840s, a time when these structures were yet to be identified as the double membraned organelles we know today. However, in 1890, Richard Altmann, a German pathologist was the first to report the existence of mitochondria within cells, describing them as “living, elementary organisms” or “bioblasts” [32, 33]. Altmann believed that the presence of “bioblasts” was essential for cell metabolism and various genetic functions; thus, making them a vital component of the cell’s physiology, a belief that would soon dominate the research world, giving rise to theories on the origins of the mitochondria and their place as the driving force behind the evolution of eukaryotes [32]. Two main evolutionary scenarios stemming from the same endosymbiosis theory have attempted to explain the origin of the mitochondria and the basis behind the cell’s energetic dependence on these organelles [34, 35]. The symbiogenesis scenario provides evidence supporting the existence of mitochondria as free-living α-proteobacteria that were engulfed by a prokaryotic cell forming a symbiotic relationship between the mitochondria and the host cell [36–38]. With time, the symbiont reduced its genome size by transferring

its genetic material to the host cell and eventually becoming an organelle. This theory maintains the idea that the complexity of the modern eukaryotic cell evolved after this symbiotic event [39]. In contrast, in the archezoan scenario, the host cell was an early eukaryotic cell as opposed to a prokaryotic cell [39]. This model suggests that primitive eukaryotic cells became what we now refer to as eukaryotic cells before the mitochondria was integrated within the host cell. Nonetheless, despite the accumulating body of evidence supporting the symbiogenesis theory, the exact origin of the mitochondria and their place within the evolutionary timeframe has proven to be much more ambiguous and complicated to pinpoint. Elements from both scenarios can be used to explain the evolution of the mitochondria, but neither possibility can be rejected with unwavering certainty at this time.

The morphological heterogeneity of the mitochondria was confirmed by various studies demonstrating the existence of the mitochondria as small spheres, but also tubular structures as a consequence of the balance between fusion and fission, more commonly referred to as mitochondrial dynamics [40–42]. True to their name, the mitochondria have become the epitope of structural and functional complexity that extends far beyond their double membranes and serves as an example of the intimate relationship between morphology and functionality. The most distinct structural characteristic of the mitochondrion is the presence of a smooth outer membrane and a folded inner membrane surrounding the mitochondrial matrix [41, 43]. Each fold in the inner membrane creates cristae which act to increase the surface area of the mitochondria to allow for greater processing efficiency [44]. Interestingly, the outer and inner membranes are compositionally different and functionally independent from one another, with each membrane performing distinct roles necessary to maintain the viability of the mitochondrion and subsequently, the cell [45–47]. The outer mitochondrial membrane contains many porins or pore-forming membrane proteins which allow for the passage of ions and other uncharged molecules resulting in the lack of a membrane potential [48]. In contrast, molecules and ions can only cross the inner mitochondrial membrane when bound to specific transporter proteins or by passing through ion channels (e.g. MCU, discussed later); thus, creating an electrochemical gradient across the inner membrane which in turn, dictates its ion selectivity [48]. The presence of an electrochemical gradient is also indicative of the function of the inner mitochondrial membrane as the center for oxidative phosphorylation and the electron transport chain. Within the inner membrane there are four complexes (I: NADPH dehydrogenase, II: Succinate dehydrogenase, III: Cytochrome c reductase and IV: Cytochrome c oxidase) which facilitate the synthesis of ATP through ion trafficking across the membrane [49, 50]. However, despite the difference in the composition of their membranes, one of the most striking features of the mitochondrion is the presence of mitochondrial DNA (mtDNA) within the matrix compartment, a remnant of their bacterial ancestry [51]. Unlike other organelles, the mitochondrion harbors its own circular DNA which is transcribed and replicated in the matrix and can be inherited (in mammals it occurs only through maternal inheritance) [51]. This mitochondrial genome is packed into nucleoids which contain DNA binding proteins for DNA repair and signaling [52, 53]. These nucleoids also facilitate the development of a signaling network between

the mitochondria and the nucleus [54]. During nutrient starvations or mitochondrial damage, signals are sent from the mitochondria to the nucleus where they can induce mitochondrial gene transcription [54, 55]. While it is fascinating that a single organelle can influence nuclear gene expression, the nucleus is not the only organelle that shares a functional relationship with the mitochondria. The "social organelle network" of the mitochondria also includes the endoplasmic reticulum (ER) and lysosomes, two organelles essential for the maintenance of calcium homeostasis in the cell [9, 56, 57].

The mitochondria perform a myriad of functions, each orchestrated in a way as to accommodate the needs of the cell. Aside from generating energy for the cell through oxidative phosphorylation and the electron transport chain, the mitochondria are also responsible for Ca^{2+} signaling, apoptosis, fatty acid and amino acid metabolism [58–62]. Changes in mitochondrial metabolism often leads to the production of reactive oxygen species (ROS), hence the classification of the mitochondrion as a major site of ROS output [63, 64]. The presence of ROS is often regarded as Pandora's box where failure to maintain optimal levels of ROS can be detrimental to the cell and contribute to the development of diseases such as cancer [65–67]. However, although the accumulation of ROS can promote the onset of different pathologies, sustained ROS can damage the mitochondria and ultimately lead to cell death [68]. Normally, ROS act as signaling molecules that can modulate various intracellular pathways that influence cellular function. The levels of ROS are maintained by the cell's antioxidant system through the activity of catalases and peroxiredoxins [69]. As with many of the functions of the mitochondria, one of the factors that can affect the production of ROS is Ca^{2+} [70, 71]. Many studies have shown that the presence of Ca^{2+} promotes the production of ATP inside the mitochondria while excess Ca^{2+} increases ROS production [72, 73]. The interplay between Ca^{2+} and the mitochondria is well studied, but a few pieces of the puzzle are still missing. Research efforts are still focusing on mitochondrial Ca^{2+} signaling and how these Ca^{2+}-dependent pathways help shape the fate of the cell.

30.3 Mitochondria and Calcium Signaling

The mitochondria control many facets of the cell's normal physiology by acting as a Ca^{2+} buffer and sensor. In response to various stimuli, the mitochondria can modulate Ca^{2+} signaling directly by importing it via specific transporters or indirectly by releasing metabolites that can act on the Ca^{2+} signaling machinery and in turn, Ca^{2+} regulates mitochondrial function [74]. This dynamic relationship between the mitochondria and Ca^{2+} signaling affects cell metabolism and survival. However, it was only in the 1960s when scientists discovered that mitochondria can uptake and accumulate Ca^{2+}, but it took another 50 years to identify the mechanism behind this process [75–77]. Most discoveries regarding the mitochondrial Ca^{2+}

uptake mechanism and the proteins involved were made within the last 10 years due to advancements in molecular techniques to study the structure of the mitochondria. The paragraphs below will discuss the mitochondrial Ca^{2+} uptake and release system, modulation of mitochondrial functions by Ca^{2+} and the impact of mitochondrial Ca^{2+} signaling on cellular function (Fig. 30.1).

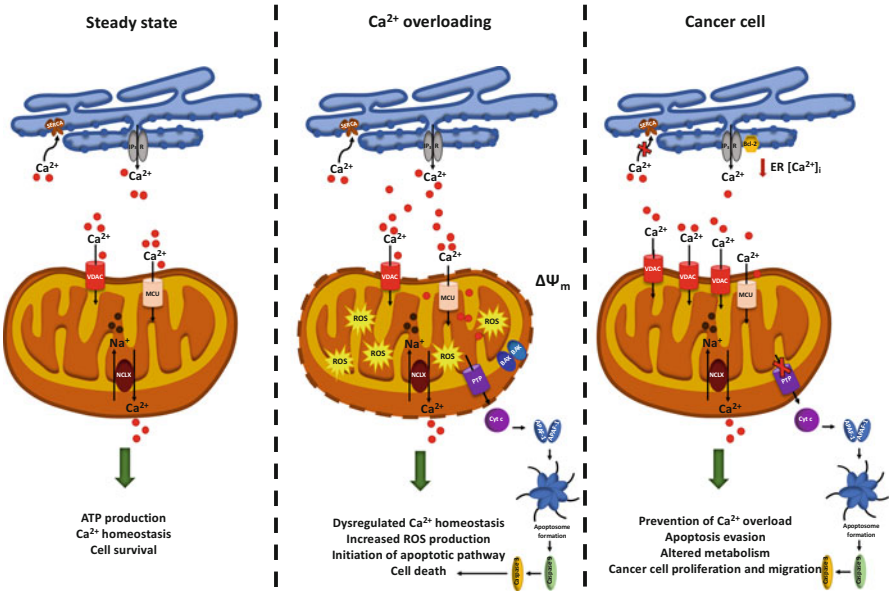

Fig. 30.1 The mitochondrion during steady state, Ca^{2+}overloading and cancer. As the powerhouses of the cell, the mitochondria utilize Ca^{2+} to make ATP in order to supply the cell's metabolic demands. The mitochondria uptake calcium mainly via two Ca^{2+} channels: VDAC (outer mitochondrial membrane) and MCU (inner mitochondrial membrane). In addition, to prevent overloading and to maintain cellular Ca^{2+} homeostasis, the Ca^{2+} must be removed from the mitochondria, a process mediated by the NCLX exchanger. However, if Ca^{2+} accumulates within the mitochondria, PTP opens, the outer membrane depolarizes and cytochrome c is release; thus, initiating the apoptosis pathway. Ca^{2+} overloading can also increase ROS production through the electron transport (located in the inner mitochondrial membrane) which ultimately leads to DNA damage and cell death. Given the importance of the mitochondria in normal cell physiology, these organelles represent a selective advantage for cancer cells. One of the many hallmarks of cancer is their ability to alter their metabolism to sustain proliferation. Unlike normal cells, cancer cells adopt a aerobic glycolysis phenotype whereas normal cells rely mainly on oxidative phosphorylation. Furthermore, cancer cells have evolved mechanisms to hijack the cell's machinery to prevent mitochondrial Ca^{2+} overloading and the activation of the apoptosis pathway. By depleted the ER stores and/or decreasing Ca^{2+} uptake into the ER., cancer cells are able to bypass the calcium induced mitochondrial apoptotic pathway. In addition, the presence of Ca^{2+} influences the expression of VDAC which in turn increases the uptake of Ca^{2+} and promotes cancer cell migration

30.3.1 Mitochondrial Calcium Uptake and Release

As mentioned in the introduction section, when the cytosolic Ca^{2+} concentration is high, Ca^{2+} is passively transported across the inner mitochondrial membrane via the Mitochondrial Calcium Uniporter (MCU), an inward rectifying Ca^{2+} tetrameric channel [25, 77, 78]. The movement of Ca^{2+} through MCU is driven by the negative mitochondrial membrane potential, unlike the outer membrane where the Ca^{2+} passes through porins [79]. MCU requires the binding of the Ca^{2+} to its cytosolic domain in order to be activated. However, MCU appears to work in a biphasic manner where extremely high cytosolic Ca^{2+} inhibit the channel; thus, preventing the accumulation of Ca^{2+} inside the mitochondria and potentially acting as a regulatory mechanism for the uptake of Ca^{2+}. Furthermore, due to its low affinity for Ca^{2+}, MCU allows for micromolar concentrations of Ca^{2+} ($\sim$10–20 μM) to pass through it [80]. With advances in molecular proteomic techniques, some of the architectural components of MCU were identified which enabled us to better understand the mechanism behind MCU-mediated Ca^{2+} uptake in the mitochondria. Studies have shown that the MCU channel pore is formed by three subunits: Mitochondrial Calcium Uniporter (MCU, found in plants and most vertebrates), Mitochondrial Ca^{2+} Uniporter b (MCUb, present in most vertebrates) and Essential MCU Regulator (EMRE, not found in plants, fungi and protozoa) [81]. While MCU and MUCb share 50% sequence similarity, MUCb is believed to function as a negative subunit that inhibits Ca^{2+} entry and reduces the activity of the MCU uniporter complex [82]. Furthermore, EMRE was found as necessary for the transport of Ca^{2+} into the mitochondria by maintaining MCU in an open confirmation while recruiting Mitochondrial Calcium Uptake 1 (MICU1) and 2 (MICU2), two of the three regulatory proteins forming the MCU complex [83, 84]. Experimental manipulation demonstrated that the knockdown of EMRE prevented the influx of Ca^{2+} into the mitochondria. Interestingly, the loss of EMRE leads to a decrease in the size of the MCU complex which suggests a possible role for EMRE as a regulator of MCU complex assembly. As mentioned in previous sentences, the MCU uniporter complex also consists of three regulatory proteins MICU1, 2 and 3. These proteins form a heterodimer and act as gatekeepers of the MCU channel. MCU2 was demonstrated as the inhibitory subunit whose inhibition is released upon MCU channel activation while MCU1 was found to control the activation of MCU and Ca^{2+} uptake [85–89]. Of note, because of the interaction of MCU1 with EMRE and their involvement in promoting the opening/activation of the MCU channel, the loss of either of these subunits leads to a decrease in Ca^{2+} influx into the mitochondria [83]. In addition, in 2018, MICU3 was described as an enhancer of Ca^{2+} uptake upon binding to MICU1, but not MICU2 [90]. Furthermore, the loss of MICU3 was shown to impair Ca^{2+} influx in cortical neurons; thus, suggesting an important role of MICU3 in neuronal function [90]. Moreover, recent studies have identified another protein responsible for calcium uptake through MCU and mitochondrial bioenergetics. Scientists have found that MCU regulator 1 (MCUR1) functions as a scaffold protein necessary for MCU

complex formation and subsequently, the loss of MCUR1 prevents the formation of the MCU complex leading to impaired mitochondrial metabolism [91, 92].

Aside from the Ca^{2+} influx through the MCU uniporter, mitochondria have developed contact sites with the ER, the cell's main Ca^{2+} stores [93, 94]. These contact sites are composed of several proteins (e.g. Mitofusin1 and 2) that form tethers between the mitochondria and the ER known as mitochondria-associated membranes (MAM) [95–97]. The MAMs express IP_3 receptors (IP_3Rs, responsible for the Ca^{2+} release from the ER) in close proximity to voltage-dependent anion channels type 1 (VDAC1, a ruthenium red- sensitive Ca^{2+} channel) present on the outer mitochondrial membrane [98]. These two channels form a stable physical connection via Grp75, a chaperon part of the heat shock protein family [99]. Other proteins have been proposed as potential mediators of Ca^{2+} influx including the leucine zipper-EF-hand-containing transmembrane protein 1 (Letm1) and ryanodine receptor (RyR); however, the experimental evidence supporting these suggestions is insufficient as proof of concept [100]. Nonetheless, to prevent Ca^{2+} overloading within the mitochondrial matrix and damage to the mitochondria, efflux mechanisms are set in place to release the excess Ca^{2+}. The efflux of Ca^{2+} is mediated by the presence of the Na^+/Ca^{2+} exchanger, NCLX within the inner mitochondrial membrane [101]. Numerous research groups have demonstrated that the loss of NCLX abolished Ca^{2+} efflux while overexpression of this exchanger enhanced the removal of Ca^{2+} from the mitochondria [101]. The mechanism behind the NCLX-mediated Ca^{2+} efflux is largely unknown, but studies suggest that the Na^+/Ca^{2+} is powered by an electrochemical gradient generated by the presence of high levels of Na^+ in the cytosol [102, 103]. Subsequently, the change in the mitochondrial inner membrane potential facilitates the exchange of three Na^+ for every one Ca^{2+} extruded from the mitochondrial matrix; however, the exchange stoichiometry of NCLX is controversial with some scientists supporting the 3:1 ion ratio while others suggesting a 2:1 ratio of Na^+ to Ca^{2+} [104, 105]. Interestingly, the NCLX exchanger is also involved in the transport of Li^+, a characteristic unique to NCLX [106]. Nonetheless, our knowledge regarding the exact structure and mode of action of NCLX is limited, partially due to the difficulty in isolating the inner mitochondrial membrane. Scientists speculate that the structure of NCLX is similar to that of NCX, a plasma membrane transporter [107]. Furthermore, in order to maintain a steady-state, the influx and efflux mechanisms of the mitochondria must perform in a synchronized manner as to allow the appropriate amount of Ca^{2+} in and out of the mitochondria. Once the Ca^{2+} is released from the mitochondria it is redistributed throughout the cell where it is likely taken up by various organelles including the ER and the lysosomes.

30.3.2 Calcium Modulation of Mitochondrial Function

The main function of the mitochondria is the maintenance of cell metabolism, mainly through oxidative phosphorylation, a characteristic that is heavily influenced

by the presence of Ca^{2+} [27]. The passage of calcium across the inner mitochondrial membrane is driven by a large, negative mitochondrial membrane potential which favors passive Ca^{2+} entry, but also the transport of Ca^{2+} down its electrochemical gradient [108]. Generated by mitochondrial respiration, the negative membrane potential (150–200 mV) coupled with the low Ca^{2+} concentration inside the matrix facilitates the transport of Ca^{2+} across the inner mitochondrial membrane [109, 110]. In turn, Ca^{2+} entry causes the depolarization of the mitochondrial membrane [78]. Upon entering the mitochondrial matrix, the Ca^{2+} concentration rises and activates various enzymes necessary for the initiation of the Krebs cycle, and the synthesis of ATP [111, 112]. In particular, the Ca^{2+}-binding α-ketoglutarate dehydrogenase and isocitrate dehydrogenase [113, 114]. Additionally, pyruvate dehydrogenase, an enzyme associated with the conversion of pyruvate to acetyl-CoA becomes activated by a Ca^{2+}-dependent phosphatase [114]. The activation of these rate-limiting enzymes increases the mitochondrial respiration rate and subsequently, enhancing the ATP production rate [115, 116]. The elegant orchestration of the Ca^{2+} signal and the output of energy further emphasizes the dynamic relationship between Ca^{2+} and the mitochondria.

30.3.3 Mitochondrial Calcium Overloading

While Ca^{2+} uptake is a normal, regulatory process for the mitochondria, excessive accumulation of this element can have detrimental consequences, not only for the organelle, but for the whole cell. The Permeability Transition Pore (PTP) is a large conductance channel found in the mitochondrial membrane and its activation represents the pathological effect of Ca^{2+} overloading (Fig. 30.1) [117, 118]. PTP is activated by elevated Ca^{2+} levels inside the mitochondria and results in the permeabilization of the outer mitochondrial membrane (MOMP, mitochondrial outer membrane permeabilization) [119, 120]. The PTP channel is believed to be regulated by several proteins including VDAC, cyclophilin D and Adenine nucleotide translocator (ANT); however, the exact structure of this channel remains unknown [121–123]. When the channel is activated, PTP opens and triggers the release of cytochrome c into the cytosol, an initiating event preceding the beginning of the apoptotic signaling cascade [124–126]. Normally, cytochrome c is involved in the electron transport chain and the generation of ATP, but once released from the confinements of the mitochondria, cytochrome c binds to apoptotic peptidase activating factor 1 (APAF-1) leading to the formation of the apoptosome [127, 128]. The apoptosome then activates procaspase-9 and subsequently caspase 3, ultimately resulting in the death of the cell [128, 129]. The opening of the PTP disrupts the mitochondrial membrane potential and Ca^{2+} leaks out, keeping the channel open. Due to the significance of MOMP in determining whether the cell lives or dies, the process of permeabilizing the outer mitochondrial membrane is tightly regulated by pro- and anti-apoptotic proteins. The anti-apoptotic proteins

are part of the Bcl-2 (Bcl-2, Bcl-xL, MCL-1, A1, Bcl-B and Bcl-w) family while the pro-apoptotic proteins are BAX and BAK along with other proteins belonging to the BH3 family (BID, BIM, BAD, PUMA, etc.) [130, 131]. The activation of BAX and BAK removes the apoptotic suppression set by the Bcl-2 proteins and initiates MOMP, and the release of cytochrome c [132–136]. Moreover, the initiation of the apoptotic pathway increases the production of reactive oxygen species (ROS) and decreases ATP synthesis; thus, altering the Ca^{2+} homeostasis within the mitochondria. Additionally, ROS generation maintains the PTP channel in its open conformation [137].

30.4 Defective Mitochondrial Calcium Signaling and Disease

Although the mitochondria play an integral role in normal cell physiology, these organelles proved to be of significance in the development and progression of various pathologies. The seemingly paradoxical relationship between the mitochondria and Ca^{2+} acts as a double edge sword where optimal Ca^{2+} levels benefit the cell while too much Ca^{2+} serves as the basis of many diseases including neurodegenerative and muscular diseases. For example, many research groups have identified that mitochondrial Ca^{2+} overloading contributes to the pathogenesis of Huntington's disease (HD), a neurodegenerative condition characterized by emotional instability and motor impairment [138]. In HD humans and mouse models, neuronal mitochondria are particularly susceptible to MOMP due to a decreased Ca^{2+} holding capacity [139–141]. Furthermore, Ca^{2+} overloading during diastole causes mitochondrial dysfunction and the overproduction of ROS [142]. The excessive ROS generation is thought to impair cardiac function after infarction and as such, contributing to heart failure [142]. Mitochondrial Ca^{2+} signaling has also been implicated in Alzheimer's disease (AD), Parkinson's disease (PD) and Amyotrophic lateral sclerosis (ALS); however, these topics are beyond the scope of this chapter and will not be discussed further [143–149].

30.5 Mitochondrial Calcium Handling in the Pathophysiology of Cancer

Cancer cells are characterized by uncontrolled proliferation and the ability to invade distant tissues; however, one of the emerging hallmarks of cancer cells comes in the form of metabolic reprogramming [150, 151]. Normally, cells generate energy through oxidative phosphorylation to meet their metabolic demand. But unlike normal cells, cancer cells undergo a metabolic shift that switches their cellular machinery from oxidative phosphorylation to aerobic glycolysis [152]. This peculiar event was first described by Otto Warburg who hypothesized that

the metabolic change is due defects in the mitochondria, a theory that was later challenged, but never completely disproved [153, 154]. Regardless of the state of the mitochondria, the driver behind ATP generation is Ca^{2+}; hence, for the cancer cell, Ca^{2+} represents the ability to produce enough energy to sustain their aberrant growth (Fig. 30.1). For the scientist, Ca^{2+}-driven metabolism represents a potential target for the development of new anti-cancer drugs.

30.5.1 IP_3R

As stated in previous paragraphs, Ca^{2+} overloading triggers the mitochondrial apoptotic pathway. Nonetheless, insufficient Ca^{2+} transfer from the ER to the mitochondria leads to decreased mitochondrial Ca^{2+} uptake and the activation of autophagy, a well-known degradation process. A paper published in 2010 demonstrated the role of Ca^{2+} transfer through ER IP_3Rs as a major determinant of normal cell bioenergetics [155]. In their paper, Cardenas et al. provided evidence that Ca^{2+} released specifically through IP_3Rs activates AMP-activated kinase (AMPK) which then activates the mechanistic target of Rapamycin (mTOR) and initiates the autophagy pathway [155]. AMPK becomes activated in the absence of adequate levels of ATP from the mitochondria and signals to the cell to start breaking down biomolecules to supply the cell with energy for survival. In terms of a cancer cell, this increase in autophagy is beneficial as it allows the cell to bypass the apoptotic pathway normally triggered by increased ER Ca^{2+} transfer to the mitochondria. This is of particular benefit to cancer cells when exposed to chemotherapeutics targeted at increasing ER Ca^{2+} release. This seemingly paradoxical alteration in function was shown in acute promyelocytic leukemia (APL) where the loss-of-function in the promyelocytic leukemia (PML) tumor suppressor prevented the release of Ca^{2+} from the ER and induced autophagy, promoting cancer cell survival as a result [156, 157]. To further support their work, the same research group conducted experiments on breast, prostate and cervix cancer cells where they found that inhibition of IP_3R induced a "bioenergetic crisis" and ultimately, cell death [158]. The underlying mechanism behind the diminished viability of IP_3R inhibited cancer cells was attributed to the attempt of cancer cells to proliferate while energetically-compromised [158]. Because cancer cells are able to bypass the intrinsic mitochondrial apoptotic pathway by reducing either Ca^{2+} uptake or release, they induce autophagy to supply their metabolic needs. However, in this case, when IP_3R was inhibited, autophagy activation was insufficient to support cell division resulting in cell cycle arrest and necrosis [158]. Another facet of the involvement of IP_3R in cancer was found in glioblastoma were the overexpression IP_3R subtype 3 (IP_3R3) promoted migration. Interestingly, caffeine inhibition of IP_3R3 prevented Ca^{2+} release and hampered the ability of glioblastoma cells to migrate and invade [159]. The caffeine-induced inhibition also decreased glioblastoma cell viability [159].

30.5.2 MCU

Studies performed in human colon cancer have identified a MCU-targeting microRNA (miR-25) able to downregulate the expression of MCU in the mitochondria [160, 161]. The research conducted by Marchi et al. found that miR-25 is overexpressed in colon cancer where it correlates with a decrease in Ca^{2+} uptake by the mitochondria and favors survival of cancer cells by enhancing proliferation [160]. In addition, re-expression of MCU sensitized colon cancer cells to apoptotic signals from the mitochondria [160]. However, in contrast to the results presented in the Marchi suty, a recent paper published in 2018 revealed that the interaction between the receptor-interacting protein kinase 1 (RIPK1) and MCU promotes colon cancer cell proliferation [162]. The study found that overexpression of RIPK1 in colon cancer cell lines increased mitochondrial Ca^{2+} uptake through MCU which resulted in an increase in cell proliferation [162]. In addition, upon analysis of the protein and mRNA expression level of RIPK1, the authors observed a significant increase in the expression of RIPK1 in colorectal cancer patient tissues as compared to normal tissues suggesting a potential for the RIPK1:MCU pathway as a target for colorectal cancer [162]. However, despite the evidence provided by the two studies described above, the role of MCU in colon cancer remains controversial.

The involvement of MCU in the carcinogenesis has also been described in breast cancer models where the expression of MCU increased the migration and invasion abilities of breast cancer cells under the regulation of the microRNA miR-340 [163]. This microRNA was found to be suppressed in breast cancer cells; thus, allowing for the expression of MCU. This concept was further confirmed by knocking down MCU and observing a decrease in migration [163]. Additional research on MCU and breast cancer uncovered the underlying mechanism behind its effect on migration. In 2016, work performed by Tosatto and colleagues found that MCU expression caused an increase in Ca^{2+} uptake by breast cancer cells leading to the production of ROS [164]. Moreover, the ROS released from the mitochondria induced the transcription of Hypoxia-inducible factor 1-alpha (*HIF1α*) [164]. The downstream pathways affected by *HIF1α* are responsible for migration, glycolytic protein expression and invasion. These effects were lost upon silencing of MCU expression. Aside from the mechanistic involvement of MCU in breast cancer, scientists have found a negative correlation between breast cancer patient survival and the expression of MCU [165].

The impact of mitochondrial Ca^{2+} signaling extends into hepatocellular carcinomas where the expression of mitochondrial MCUR1 was found to be enhanced [166]. In accordance with previous studies showing similar mechanisms, the overexpression of MCUR1 increased the uptake of Ca^{2+} into the mitochondria allowing the cancer cells to overcome any pro-apoptotic challenges. Subsequently, the loss of MCURI restored the mitochondrial Ca^{2+} signaling pathway. The authors concluded that the effects seen in hepatocellular carcinoma cells were in part due to the production of ROS and the activation of the AKT/MDM2 pathway [166]. Activation of this pathway triggers the ubiquitination and degradation of p53, a

major regulator of p53-dependent apoptosis [166]. The degradation of p53 then promotes the survival of cancer cells by preventing cell death.

30.5.3 VDAC

VDAC is an essential mediator in the cross talk between the mitochondria and the cell [167]. In addition to facilitating the flow of Ca^{2+} into and out of the mitochondria, VDAC also interacts with hexokinases (HK) to allow for the bridge between oxidative phosphorylation and glycolysis [168–170]. As mentioned in the paragraphs above, cancer cells undergo a metabolic switch to sustain cell division making VDAC an important determinant of the metabolic phenotype of a cancer cell. In addition, VDAC is upregulated in many cancer and its expression is influenced by the level of Ca^{2+} in the cell [171]. As such, it is unsurprising that the loss of VDAC1 (three VDAC isoforms exist) resulted in decreased cell growth and migration in lung, pancreatic and colon cancer cell lines in vitro, but also in vivo [172]. This decrease was concomitant with diminished ATP levels, suggesting that VDAC1 downregulation interferes with cancer cell metabolism; thus creating energetically unfavorable conditions for the cancer cell [172]. These studies were further confirmed in breast cancer where VDAC was demonstrated to interact with Bcl-xL to promote migration. The underlying mechanism behind the enhanced cancer cell migration was mediated by the interaction of Bcl-xL, CD95 and VDAC [173]. Together, these proteins facilitated the influx of Ca^{2+} from the ER to the mitochondria and the subsequent production of ATP which supplied the cancer cells with enough energy to migrate [173]. Similar studies were conducted in other cancers [174–176].

30.5.4 Bcl-2

Besides the involvement of MCU and IP_3R in cancer bioenergetics, the Bcl-2 protein family has also been demonstrated to affect Ca^{2+} flux into the mitochondria through an ER-mediated manner. In fact, one mechanism through which Bcl-2 proteins can affect cancer cell survival is by decreasing the Ca^{2+} concentration in the ER and preventing mitochondrial Ca^{2+} overloading [177]. Bcl-2 has been shown to inhibit the sarco/endoplasmic reticulum calcium ATPase (SERCA) to decrease Ca^{2+} levels within the ER and as such, protecting the mitochondria against Ca^{2+} overloading [178]. Several other modes of actions have been proposed to explain the impact of Bcl-2 on mitochondrial Ca^{2+} uptake such as the potential of Bcl-2 existing as an IP_3R sensitizer to reduce the level of Ca^{2+} in the ER. In addition, Bcl-2 is believed to be able to bind to IP_3R directly and inhibit its function, limiting Ca^{2+} release from the ER as a result. Furthermore, Bcl-2 was also found to be overexpressed in a number of cancers including non-small cell lung

carcinoma, breast, neuroblastoma, B-cell lymphoma, chronic lymphocytic leukemia and others [179–183]. Interestingly, experimental evidence has demonstrated that cells overexpressing Bcl-2 experience an increase in Ca^{2+} leakage from the ER which limits the level of Ca^{2+} available for release and mitochondrial uptake [184–186]. Although Bcl-2 is able to affect intracellular Ca^{2+} in various ways, the common goal is to protect the cancer cell against mitochondrial-induced cell death.

30.6 Closing Remarks

The availability of cancer treatments along with resistance against current therapeutics represent factors that limit a patient's chance at survival and their quality of life. Research efforts have been aimed at discovering novel targets to advance cancer therapy and improve patient outcome. These targets include mitochondrial Ca^{2+} signaling and metabolism. One of the major hallmarks of cancer is their ability to divide uncontrollability, a quality that requires a constant supply of energy. Therefore, as the main sources of ATP in the cell, the mitochondria hold tremendous potential as therapeutic targets for the treatment of cancer. In addition, the mitochondria are involved in mediating apoptosis making them an attractive option in the quest for an effective tool to eliminate cancer cells. However, although the role of the mitochondria in cancer is undeniable, our knowledge regarding the mechanisms behind the cancer cell's energetic dependence on this organelle are not well understood; a limitation which is currently putting a damper on the development of mitochondria-targeted therapies. Part of the reason behind our information gaps stems from the unavailability of proper tools to study the mitochondria, in particular the inner membrane of the mitochondria. But despite the difficulty in studying the mitochondrial structure and function, progress has been made in terms of identifying potential therapeutic targets [187, 188]. As of date, numerous compounds targeting the mitochondria are being tested and some even undergoing clinical trials. For example, paclitaxel, a Taxol-based drug used to treat breast and ovarian cancer, has been shown to modulate the cytosolic Ca^{2+} signal by acting on the mitochondria and inducing the opening of the permeability transition pore in pancreatic acinar cells [189]. The opening of this channel disturbs the mitochondrial membrane potential and leads to the loss of Ca^{2+} from the mitochondria [189]. Another example of drug-induced modulation of mitochondrial Ca^{2+} currently under testing is arsenic trioxide [190]. This drug was demonstrated to induce apoptosis in multiple myeloma cells by promoting the release of cytochrome c from the mitochondria through the upregulation of VDAC [190]. Furthermore, aspirin, a common drug for the treatment of fevers and pain, has also been shown to induce apoptosis in cervical cancer cells through the modulation of VDAC1 [191]. In addition, Ca^{2+} influx modulation through MCU has been shown to sensitize pancreatic cancer cells to gemcitabine-induced apoptosis [192]. Other methods of targeting the mitochondrial function in cancer cells include the synthesis of peptides designed to act on the Bcl-2 proteins to induce apoptosis

[193, 194]. Although targeting the mitochondria poses some challenges, advances in our knowledge of the mitochondrial structure and function are bringing researchers closer to developing effective cancer treatments.

Acknowledgements AS is supported through the cancer research training program (CRTP) administered by the Beatrice Hunter Cancer Research Institute (BHCRI) and funded by The Canadian Institute of Health Research (CIHR), Terry Fox Research Institute (TFRI), Cancer Care Nova Scotia, Dalhousie Medical Research Foundation (DMRF) and the Canadian Cancer Society Nova Scotia Division.

Conflict of Interest The authors declare no conflict of interest.

References

1. E.S.T. Sir Humphry Davy (1873) Notes queries s4-XI(276):304. https://doi.org/10.1093/nq/s4-XI.276.304-i
2. Brini M, Carafoli E (2000) Calcium signalling: a historical account, recent developments and future perspectives. Cell Mol Life Sci 57(3):354–370
3. Case RM, Eisner D, Gurney A, Jones O, Muallem S, Verkhratsky A (2007) Evolution of calcium homeostasis: from birth of the first cell to an omnipresent signalling system. Cell Calcium 42(4–5):345–350. https://doi.org/10.1016/j.ceca.2007.05.001
4. Verkhratsky A, Parpura V (2014) Calcium signalling and calcium channels: evolution and general principles. Eur J Pharmacol 739(C):1–3. https://doi.org/10.1016/j.ejphar.2013.11.013
5. Kazmierczak J, Kempe S, Kremer B (2013) Calcium in the early evolution of living systems: a biohistorical approach. Curr Org Chem 17(16):1738–1750. https://doi.org/10.2174/13852728113179990081
6. Cai X, Wang X, Patel S, Clapham DE (2015) Insights into the early evolution of animal calcium signaling machinery: a unicellular point of view. Cell Calcium 57(3):166–173. https://doi.org/10.1016/j.ceca.2014.11.007
7. Kass GEN, Orrenius S (1999) Calcium signaling and cytotoxicity. Environ Health Perspect 107(SUPPL. 1):25–35. https://doi.org/10.1289/ehp.99107s125
8. Montero M, Brini M, Marsault R et al (1995) Monitoring dynamic changes in free Ca^{2+} concentration in the endoplasmic reticulum of intact cells. EMBO J 14:5467
9. Raffaello A, Mammucari C, Gherardi G, Rizzuto R (2016) Calcium at the center of cell signaling: interplay between endoplasmic reticulum, mitochondria, and lysosomes. Trends Biochem Sci 41(12):1035–1049. https://doi.org/10.1016/j.tibs.2016.09.001
10. Hepler PK (1994) The role of calcium in cell division. Cell Calcium 16(4):322–330. https://doi.org/10.1016/0143-4160(94)90096-5
11. Mattson MP, Chan SL (2003) Calcium orchestrates apoptosis. Nat Cell Biol 5(12):1041–1043. https://doi.org/10.1038/ncb1203-1041
12. McConkey DJ, Orrenius S (1997) The role of calcium in the regulation of apoptosis. Biochem Biophys Res Commun 59(239):775–783. https://doi.org/10.1006/bbrc.1997.7409
13. Pinto MCX, Kihara AH, Goulart VAM et al (2015) Calcium signaling and cell proliferation. Cell Signal 27(11):2139–2149. https://doi.org/10.1016/j.cellsig.2015.08.006
14. Berridge MJ (1995) Calcium signalling and cell proliferation. BioEssays 17(6):491–500. https://doi.org/10.1002/bies.950170605
15. Hepler PK (2016) The cytoskeleton and its regulation by calcium and protons. Plant Physiol 170(1):3–22. https://doi.org/10.1104/pp.15.01506
16. Fitzjohn SM, Collingridge GL (2002) Calcium stores and synaptic plasticity. Cell Calcium 32(5–6):405–411. https://doi.org/10.1016/S0143-4160(02)00199-9

17. Lamont MG, Weber JT (2012) The role of calcium in synaptic plasticity and motor learning in the cerebellar cortex. Neurosci Biobehav Rev 36(4):1153–1162. https://doi.org/10.1016/j.neubiorev.2012.01.005
18. Ringer S (1883) A further contribution regarding the influence of the different constituents of the blood on the contraction of the heart. J Physiol 4(1):29–42. https://doi.org/10.1113/jphysiol.1883.sp000120
19. McFadzean I, Gibson A (2002) The developing relationship between receptor-operated and store-operated calcium channels in smooth muscle. Br J Pharmacol 135(1):1–13. https://doi.org/10.1038/sj.bjp.0704468
20. Berridge MJ, Bootman MD, Roderick HL (2003) Calcium signalling: dynamics, homeostasis and remodelling. Nat Rev Mol Cell Biol. https://doi.org/10.1038/nrm1155
21. Putney JW, Tomita T (2012) Phospholipase C signaling and calcium influx. Adv Biol Regul. https://doi.org/10.1016/j.advenzreg.2011.09.005
22. Carafoli E, Lehninger AL (1971) A survey of the interaction of calcium ions with mitochondria from different tissues and species. Biochem J. https://doi.org/10.1042/bj1220681
23. Gunter KK, Gunter TE (1994) Transport of calcium by mitochondria. J Bioenerg Biomembr. https://doi.org/10.1007/BF00762732
24. Rizzuto R, Simpson AWM, Brini M, Pozzan T (1992) Rapid changes of mitochondrial Ca^{2+} revealed by specifically targeted recombinant aequorin. Nature. https://doi.org/10.1038/358325a0
25. De Stefani D, Raffaello A, Teardo E, Szabó I, Rizzuto R (2011) A forty-kilodalton protein of the inner membrane is the mitochondrial calcium uniporter. Nature. https://doi.org/10.1038/nature10230
26. Denton RM, McCormack JG (1980) The role of calcium in the regulation of mitochondrial metabolism. Biochem Soc Trans. https://doi.org/10.1042/bst0080266
27. Denton RM, McCormack JG (1980) On the role of the calcium transport cycle in heart and other mammalian mitochondria. FEBS Lett. https://doi.org/10.1016/0014-5793(80)80986-0
28. Glancy B, Willis WT, Chess DJ, Balaban RS (2013) Effect of calcium on the oxidative phosphorylation cascade in skeletal muscle mitochondria. Biochemistry. https://doi.org/10.1021/bi3015983
29. Territo PR, Mootha VK, French SA, Balaban RS (2000) Ca^{2+} activation of heart mitochondrial oxidative phosphorylation: role of the F(0)/F(1)-ATPase. Am J Physiol Cell Physiol. https://doi.org/10.1152/ajpcell.2000.278.2.C423
30. Huang X, Zhai D, Huang Y (2000) Study on the relationship between calcium-induced calcium release from mitochondria and PTP opening. Mol Cell Biochem. https://doi.org/10.1023/A:1007138818124
31. Ichas F, Mazat JP (1998) From calcium signaling to cell death: two conformations for the mitochondrial permeability transition pore. Switching from low- to high-conductance state. Biochim Biophys Acta Bioenerg. https://doi.org/10.1016/S0005-2728(98)00119-4
32. O'Rourke B (2010) From bioblasts to mitochondria: ever expanding roles of mitochondria in cell physiology. Front Physiol. https://doi.org/10.3389/fphys.2010.00007
33. Ernster L, Schatz G (1981) Mitochondria: a historical review. J Cell Biol. https://doi.org/10.1083/jcb.91.3.227s
34. Check C (2012, Jan 1) Mitochondrial evolution 2–4
35. Gray MW, Burger G, Lang BF (1999) Mitochondrial evolution. Science (80-). https://doi.org/10.1126/science.283.5407.1476
36. Martin WF, Müller M (2007) Origin of mitochondria and hydrogenosomes. https://doi.org/10.1007/978-3-540-38502-8
37. Dyall SD, Brown MT, Johnson PJ (2004) Ancient invasions: from endosymbionts to organelles. Science (80-). https://doi.org/10.1126/science.1094884
38. Embley TM, Martin W (2006) Eukaryotic evolution, changes and challenges. Nature. https://doi.org/10.1038/nature04546
39. Gray MW (2014) The pre-endosymbiont hypothesis: a new perspective on the origin and evolution of mitochondria. Cold Spring Harb Perspect Biol. https://doi.org/10.1101/cshperspect.a016097

40. Westermann B (2012) Bioenergetic role of mitochondrial fusion and fission. Biochim Biophys Acta Bioenerg. https://doi.org/10.1016/j.bbabio.2012.02.033
41. McCarron JG, Wilson C, Sandison ME et al (2013) From structure to function: mitochondrial morphology, motion and shaping in vascular smooth muscle. J Vasc Res. https://doi.org/10.1159/000353883
42. Rafelski SM (2013) Mitochondrial network morphology: building an integrative, geometrical view. BMC Biol. https://doi.org/10.1186/1741-7007-11-71
43. Sjöstrand FS (1953) Electron microscopy of mitochondria and cytoplasmic double membranes: ultra-structure of rod-shaped mitochondria. Nature. https://doi.org/10.1038/171030a0
44. PALADE GE (1953) An electron microscope study of the mitochondrial structure. J Histochem Cytochem. https://doi.org/10.1177/1.4.188
45. Comte J, Maisterrena B, Gautheron DC, Mary SM (1976) Lipid composition and protein profiles of outer and inner membranes from pig heart mitochondria: comparison with microsomes. Biochim Biophys Acta. https://doi.org/10.1016/0005-2736(76)90353-9
46. Gohil VM, Greenberg ML (2009) Mitochondrial membrane biogenesis: phospholipids and proteins go hand in hand. J Cell Biol. https://doi.org/10.1083/jcb.200901127
47. Prasai K (2017) Regulation of mitochondrial structure and function by protein import: a current review. Pathophysiology. https://doi.org/10.1016/j.pathophys.2017.03.001
48. K?hlbrandt W (2015) Structure and function of mitochondrial membrane protein complexes. BMC Biol. https://doi.org/10.1186/s12915-015-0201-x
49. Davies KM, Strauss M, Daum B et al (2011) Macromolecular organization of ATP synthase and complex I in whole mitochondria. Proc Natl Acad Sci. https://doi.org/10.1073/pnas.1103621108
50. Lodish H, Berk A, Zipursky SL, Matsudaira P, Baltimore D, Darnell J (2000) Molecular cell biology. 4th ed. https://doi.org/10.1017/CBO9781107415324.004
51. Taanman J-W (1999) The mitochondrial genome: structure, transcription, translation and replication. Biochim Biophys Acta Bioenerg. https://doi.org/10.1016/S0005-2728(98)00161-3
52. Satoh M, Kuroiwa T (1991) Organization of multiple nucleoids and DNA molecules in mitochondria of a human cell. Exp Cell Res. https://doi.org/10.1016/0014-4827(91)90467-9
53. Bogenhagen DF (2012) Mitochondrial DNA nucleoid structure. Biochim Biophys Acta Gene Regul Mech. https://doi.org/10.1016/j.bbagrm.2011.11.005
54. Iborra FJ, Kimura H, Cook PR (2004) The functional organization of mitochondrial genomes in human cells. BMC Biol. https://doi.org/10.1186/1741-7007-2-9
55. Shaw AK, Kalem MC, Zimmer SL (2016) Mitochondrial gene expression is responsive to starvation stress and developmental transition in *Trypanosoma cruzi*. mSphere. https://doi.org/10.1128/mSphere.00051-16
56. Diogo CV, Yambire KF, Fernández Mosquera L, Branco FT, Raimundo N (2017) Mitochondrial adventures at the organelle society. Biochem Biophys Res Commun. https://doi.org/10.1016/j.bbrc.2017.04.124
57. Murley A, Nunnari J (2016) The emerging network of mitochondria-organelle contacts. Mol Cell. https://doi.org/10.1016/j.molcel.2016.01.031
58. Kunau WH, Dommes V, Schulz H (1995) β-oxidation of fatty acids in mitochondria, peroxisomes, and bacteria: a century of continued progress. Prog Lipid ResProg Lipid Res. https://doi.org/10.1016/0163-7827(95)00011-9
59. Bartlett K, Eaton S (2004) Mitochondrial beta-oxidation. Eur J Biochem. https://doi.org/10.1046/j.1432-1033.2003.03947.x
60. Guda P, Guda C, Subramaniam S (2007) Reconstruction of pathways associated with amino acid metabolism in human mitochondria. Genomics Proteomics Bioinformatics. https://doi.org/10.1016/S1672-0229(08)60004-2
61. Hutson SM, Fenstermacher D, Mahar C (1988) Role of mitochondrial transamination in branched chain amino acid metabolism. J Biol Chem
62. Liu X, Kim CN, Yang J, Jemmerson R, Wang X (1996) Induction of apoptotic program in cell-free extracts: requirement for dATP and cytochrome c. Cell. https://doi.org/10.1016/S0092-8674(00)80085-9

63. Chandel NS, Maltepe E, Goldwasser E, Mathieu CE, Simon MC, Schumacker PT (1998) Mitochondrial reactive oxygen species trigger hypoxia-induced transcription. Proc Natl Acad Sci U S A. https://doi.org/10.1073/pnas.95.20.11715
64. Finkel T (1998) Oxygen radicals and signaling. Curr Opin Cell Biol. https://doi.org/10.1016/S0955-0674(98)80147-6
65. Sena LA, Chandel NS (2012) Physiological roles of mitochondrial reactive oxygen species. Mol Cell. https://doi.org/10.1016/j.molcel.2012.09.025
66. De Sá Junior PL, Câmara DAD, Porcacchia AS et al (2017) The roles of ROS in cancer heterogeneity and therapy. Oxidative Med Cell Longev. https://doi.org/10.1155/2017/2467940
67. Liou M-Y, Storz P (2010) Reactive oxygen species in cancer. Free Radic Res 44:479–496. https://doi.org/10.3109/10715761003667554
68. Fleury C, Mignotte B, Vayssière J-L (2002) Mitochondrial reactive oxygen species in cell death signaling. Biochimie. https://doi.org/10.1016/S0300-9084(02)01369-X
69. Kotiadis VN, Duchen MR, Osellame LD (2014) Mitochondrial quality control and communications with the nucleus are important in maintaining mitochondrial function and cell health. Biochim Biophys Acta Gen Subj. https://doi.org/10.1016/j.bbagen.2013.10.041
70. Sohal RS, Allen RG (1985) Relationship between metabolic rate, free radicals, differentiation and aging: a unified theory. In: Molecular biology of aging. https://doi.org/10.1007/978-1-4899-2218-2_4
71. Görlach A, Bertram K, Hudecova S, Krizanova O (2015) Calcium and ROS: a mutual interplay. Redox Biol. https://doi.org/10.1016/j.redox.2015.08.010
72. Li X, Fang P, Mai J, Choi ET, Wang H, Yang X (2013) Targeting mitochondrial reactive oxygen species as novel therapy for inflammatory diseases and cancers. J Hematol Oncol. https://doi.org/10.1186/1756-8722-6-19
73. Brookes PS (2004) Calcium, ATP, and ROS: a mitochondrial love-hate triangle. AJP Cell Physiol. https://doi.org/10.1152/ajpcell.00139.2004
74. Walsh C, Barrow S, Voronina S, Chvanov M, Petersen OH, Tepikin A (2009) Modulation of calcium signalling by mitochondria. Biochim Biophys Acta Bioenerg. https://doi.org/10.1016/j.bbabio.2009.01.007
75. Deluca HF, Engstrom GW (1961) Calcium uptake by rat kidney mitochondria. Proc Natl Acad Sci U S A. https://doi.org/10.1073/pnas.47.11.1744
76. Vasington FD, Murphy J (1962) Ca++ ion uptake by rat kidney mitochondria and its dependence on respiration and phosphorylation. J Biol Chem. https://doi.org/10.1016/J.CELL.2008.08.006
77. Baughman JM, Perocchi F, Girgis HS et al (2011) Integrative genomics identifies MCU as an essential component of the mitochondrial calcium uniporter. Nature. https://doi.org/10.1038/nature10234
78. Kirichok Y, Krapivinsky G, Clapham DE (2004) The mitochondrial calcium uniporter is a highly selective ion channel. Nature. https://doi.org/10.1038/nature02246
79. Bernardi P (1999) Mitochondrial transport of cations: channels, exchangers, and permeability transition. Physiol Rev. https://doi.org/10.1152/physrev.1999.79.4.1127
80. Marchi S, Pinton P (2014) The mitochondrial calcium uniporter complex: molecular components, structure and physiopathological implications. J Physiol. https://doi.org/10.1113/jphysiol.2013.268235
81. De Stefani D, Rizzuto R, Pozzan T (2016) Enjoy the trip: calcium in mitochondria back and forth. Annu Rev Biochem. https://doi.org/10.1146/annurev-biochem-060614-034216
82. Raffaello A, De Stefani D, Sabbadin D et al (2013) The mitochondrial calcium uniporter is a multimer that can include a dominant-negative pore-forming subunit. EMBO J. https://doi.org/10.1038/emboj.2013.157
83. Sancak Y, Markhard AL, Kitami T, et al (2013) EMRE is an essential component of the mitochondrial calcium uniporter complex. Science (80-). https://doi.org/10.1126/science.1242993
84. Baradaran R, Wang C, Siliciano AF, Long SB (2018) Cryo-EM structures of fungal and metazoan mitochondrial calcium uniporters. Nature. https://doi.org/10.1038/s41586-018-0331-8

85. Csordás G, Golenár T, Seifert EL et al (2013) MICU1 controls both the threshold and cooperative activation of the mitochondrial Ca^{2+}uniporter. Cell Metab. https://doi.org/10.1016/j.cmet.2013.04.020
86. Hoffman NE, Chandramoorthy HC, Shamugapriya S et al (2013) MICU1 motifs define mitochondrial calcium uniporter binding and activity. Cell Rep. https://doi.org/10.1016/j.celrep.2013.11.026
87. Kamer KJ, Mootha VK (2014) MICU1 and MICU2 play nonredundant roles in the regulation of the mitochondrial calcium uniporter. EMBO Rep. https://doi.org/10.1002/embr.201337946
88. Perocchi F, Gohil VM, Girgis HS et al (2010) MICU1 encodes a mitochondrial EF hand protein required for Ca^{2+}uptake. Nature. https://doi.org/10.1038/nature09358
89. Mallilankaraman K, Doonan P, Cárdenas C et al (2012) MICU1 is an essential gatekeeper for mcu-mediated mitochondrial Ca 2+ uptake that regulates cell survival. Cell. https://doi.org/10.1016/j.cell.2012.10.011
90. Patron M, Granatiero V, Espino J (2018) MICU3 is a tissue-speci fi c enhancer of mitochondrial calcium uptake. Cell Death Differ. https://doi.org/10.1038/s41418-018-0113-8
91. Tomar D, Dong Z, Shanmughapriya S et al (2016) MCUR1 is a scaffold factor for the MCU complex function and promotes mitochondrial bioenergetics. Cell Rep. https://doi.org/10.1016/j.celrep.2016.04.050
92. Mallilankaraman K, Cardenas C, Doonan PJ et al (2012) MCUR1 is an essential component of mitochondrial Ca^{2+} uptake that regulates cellular metabolism. Nat Cell Biol. https://doi.org/10.1038/ncb2622
93. Rizzuto R, Pinton P, Carrington W, et al (1998) Close contacts with the endoplasmic reticulum as determinants of mitochondrial Ca^{2+} responses. Science (80-). https://doi.org/10.1126/science.280.5370.1763
94. Csordás G, Renken C, Várnai P et al (2006) Structural and functional features and significance of the physical linkage between ER and mitochondria. J Cell Biol. https://doi.org/10.1083/jcb.200604016
95. Wieckowski MRMR, Giorgi C, Lebiedzinska M, Duszynski J, Pinton P (2009) Isolation of mitochondria-associated membranes and mitochondria from animal tissues and cells. Nat Protoc. https://doi.org/10.1038/nprot.2009.151
96. Giorgi C, Missiroli S, Patergnani S, Duszynski J, Wieckowski MR, Pinton P (2015) Mitochondria-associated membranes: composition, molecular mechanisms, and physiopathological implications. Antioxid Redox Signal. https://doi.org/10.1089/ars.2014.6223
97. De Brito OM, Scorrano L (2008) Mitofusin 2 tethers endoplasmic reticulum to mitochondria. Nature. https://doi.org/10.1038/nature07534
98. Rowland AA, Voeltz GK (2012) Endoplasmic reticulum-mitochondria contacts: function of the junction. Nat Rev Mol Cell Biol. https://doi.org/10.1038/nrm3440
99. Szabadkai G, Bianchi K, Várnai P et al (2006) Chaperone-mediated coupling of endoplasmic reticulum and mitochondrial Ca^{2+} channels. J Cell Biol. https://doi.org/10.1083/jcb.200608073
100. Jiang D, Zhao L, Clapham DE (2009) Genome-wide RNAi screen identifies Letm1 as a mitochondrial Ca^{2+}/H^{+} antiporter. Science (80-). https://doi.org/10.1126/science.1175145
101. Palty R, Silverman WF, Hershfinkel M et al (2010) NCLX is an essential component of mitochondrial Na^{+}/Ca^{2+} exchange. Proc Natl Acad Sci. https://doi.org/10.1073/pnas.0908099107
102. CROMPTON M, KÜNZI M, CARAFOLI E (1977) The calcium-induced and sodium-induced effluxes of calcium from heart mitochondria: evidence for a sodium-calcium carrier. Eur J Biochem. https://doi.org/10.1111/j.1432-1033.1977.tb11839.x
103. Carafoli E, Tiozzo R, Lugli G, Crovetti F, Kratzing C (1974) The release of calcium from heart mitochondria by sodium. J Mol Cell Cardiol. https://doi.org/10.1016/0022-2828(74)90077-7
104. Brand MD (1985) The stoichiometry of the exchange catalysed by the mitochondrial calcium/sodium antiporter. Biochem J. https://doi.org/10.1042/bj2290161

105. Baysal K, Jung DW, Gunter KK, Gunter TE, Brierley GP (1994) Na(+)-dependent Ca^{2+} efflux mechanism of heart mitochondria is not a passive $Ca^{2+}/2Na^{+}$ exchanger. Am J Phys
106. Palty R, Ohana E, Hershfinkel M et al (2004) Lithium-calcium exchange is mediated by a distinct potassium-independent sodium-calcium exchanger. J Biol Chem. https://doi.org/10.1074/jbc.M401229200
107. Palty R, Hershfinkel M, Sekler I (2012) Molecular identity and functional properties of the mitochondrial Na +/Ca^{2+} exchanger. J Biol Chem. https://doi.org/10.1074/jbc.R112.355867
108. Duchen M (2000) Mitochondria and Ca^{2+} in cell physiology and pathophysiology. Cell Calcium
109. Brand MD, Chen CH, Lehninger AL (1976) Stoichiometry of H^{+} ejection during respiration dependent accumulation of Ca^{2+} by rat liver mitochoneria. J Biol Chem
110. Pozzan T, Magalhães P, Rizzuto R (2000) The comeback of mitochondria to calcium signalling. Cell Calcium. https://doi.org/10.1054/ceca.2000.0166
111. Hansford RG, Zorov D (1998) Role of mitochondrial calcium transport in the control of substrate oxidation. Mol Cell Biochem
112. McCormack JG, Halestrap AP, Denton RM (1990) Role of calcium ions in regulation of mammalian intramitochondrial metabolism. Physiol Rev. https://doi.org/10.1152/physrev.1990.70.2.391
113. Traaseth N, Elfering S, Solien J, Haynes V, Giulivi C (2004) Role of calcium signaling in the activation of mitochondrial nitric oxide synthase and citric acid cycle. Biochim Biophys Acta. https://doi.org/10.1016/j.bbabio.2004.04.015
114. Wan B, LaNoue KF, Cheung JY, Scaduto RC (1989) Regulation of citric acid cycle by calcium. J Biol Chem
115. Jouaville LS, Pinton P, Bastianutto C, G a R, Rizzuto R (1999) Regulation of mitochondrial ATP synthesis by calcium: evidence for a long-term metabolic priming. Proc Natl Acad Sci U S A. https://doi.org/10.1073/pnas.96.24.13807
116. Fink BD, Bai F, Yu L, Sivitz WI (2017) Regulation of ATP production: dependence on calcium concentration and respiratory state. Am J Phys Cell Phys. https://doi.org/10.1152/ajpcell.00086.2017
117. Giorgi C, Romagnoli A, Pinton P, Rizzuto R (2008) Ca^{2+} signaling, mitochondria and cell death. Curr Mol Med. https://doi.org/10.2174/156652408783769571
118. Hunter DR, Haworth RA, Southard JH (1976) Relationship between configuration, function, and permeability in calcium treated mitochondria. J Biol Chem. https://doi.org/10.1016/0304-4157(95)00003-A
119. Chalmers S, Nicholls DG (2003) The relationship between free and total calcium concentrations in the matrix of liver and brain mitochondria. J Biol Chem. https://doi.org/10.1074/jbc.M212661200
120. Basso E, Fante L, Fowlkes J, Petronilli V, Forte MA, Bernardi P (2005) Properties of the permeability transition pore in mitochondria devoid of cyclophilin D. J Biol Chem. https://doi.org/10.1074/jbc.C500089200
121. Crompton M, Ellinger H, Costi A (1988) Inhibition by cyclosporin A of a Ca^{2+}-dependent pore in heart mitochondria activated by inorganic phosphate and oxidative stress. Biochem J
122. Griffiths EJ, Halestrap AP (1991) Further evidence that cyclosporin A protects mitochondria from calcium overload by inhibiting a matrix peptidyl-prolyl cis-trans isomerase. Implications for the immunosuppressive and toxic effects of cyclosporin. Biochem J
123. Belzacq AS, Vieira HLA, Kroemer G, Brenner C (2002) The adenine nucleotide translocator in apoptosis. Biochimie. https://doi.org/10.1016/S0300-9084(02)01366-4
124. Green DR, Kroemer G (2004) The pathophysiology of mitochondrial cell death. Science (80-). https://doi.org/10.1126/science.1099320
125. Crompton M (1999) The mitochondrial permeability transition pore and its role in cell death. Biochem J. https://doi.org/10.1042/BJ3410233
126. Orrenius S, Zhivotovsky B, Nicotera P (2003) Regulation of cell death: the calcium-apoptosis link. Nat Rev Mol Cell Biol. https://doi.org/10.1038/nrm1150

127. Von Ahsen O, Waterhouse N, Kuwana T, Newmeyer D, Green D (2000) The "harmless" release of cytochrome C. Cell Death Differ. https://doi.org/10.1038/sj.cdd.4400782
128. Zou H, Li Y, Liu X, Wang X (1999) An APAf-1 · cytochrome C multimeric complex is a functional apoptosome that activates procaspase-9. J Biol Chem. https://doi.org/10.1074/jbc.274.17.11549
129. Thornberry NA (1998) Caspases: enemies within. Science (80-). https://doi.org/10.1126/science.281.5381.1312
130. Wei MC, Zong WX, Cheng EHY et al (2001) Proapoptotic BAX and BAK: a requisite gateway to mitochondrial dysfunction and death. Science (80-). https://doi.org/10.1126/science1059108
131. Kuwana T, Newmeyer DD (2003) Bcl-2-family proteins and the role of mitochondria in apoptosis. Curr Opin Cell Biol. https://doi.org/10.1016/j.ceb.2003.10.004
132. Jurgensmeier JM, Xie Z, Deveraux Q, Ellerby L, Bredesen D, Reed JC (1998) Bax directly induces release of cytochrome c from isolated mitochondria. Proc Natl Acad Sci. https://doi.org/10.1073/pnas.95.9.4997
133. Finucane DM, Bossy-Wetzel E, Waterhouse NJ, Cotter TG, Green DR (1999) Bax-induced caspase activation and apoptosis via cytochrome c release from mitochondria is inhibitable by Bcl-xL. J Biol Chem. https://doi.org/10.1074/jbc.274.4.2225
134. Luo X, Budihardjo I, Zou H, Slaughter C, Wang X (1998) Bid, a Bcl2 interacting protein, mediates cytochrome c release from mitochondria in response to activation of cell surface death receptors. Cell. https://doi.org/10.1016/S0092-8674(00)81589-5
135. Kluck RM (1997) The release of cytochrome c from mitochondria: a primary site for Bcl-2 regulation of apoptosis. Science (80-). https://doi.org/10.1126/science.275.5303.1132
136. Kuwana T, Bouchier-Hayes L, Chipuk JE et al (2005) BH3 domains of BH3-only proteins differentially regulate Bax-mediated mitochondrial membrane permeabilization both directly and indirectly. Mol Cell. https://doi.org/10.1016/j.molcel.2005.02.003
137. Vercesi AE, Kowaltowski AJ, Grijalba MT, Meinicke AR, Castilho RF (1997) The role of reactive oxygen species in mitochondrial permeability transition. Biosci Rep
138. Walker FO (2007) Huntington's disease. Semin Neurol. https://doi.org/10.1055/s-2007-971176
139. Choo YS, Johnson GVW, MacDonald M, Detloff PJ, Lesort M (2004) Mutant huntingtin directly increases susceptibility of mitochondria to the calcium-induced permeability transition and cytochrome c release. Hum Mol Genet. https://doi.org/10.1093/hmg/ddh162
140. Panov AV, Gutekunst CA, Leavitt BR et al (2002) Early mitochondrial calcium defects in Huntington's disease are a direct effect of polyglutamines. Nat Neurosci. https://doi.org/10.1038/nn884
141. Lim D, Fedrizzi L, Tartari M et al (2008) Calcium homeostasis and mitochondrial dysfunction in striatal neurons of Huntington disease. J Biol Chem. https://doi.org/10.1074/jbc.M704704200
142. Santulli G, Xie W, Reiken SR, Marks AR (2015) Mitochondrial calcium overload is a key determinant in heart failure. Proc Natl Acad Sci U S A. https://doi.org/10.1073/pnas.1513047112
143. Luth ES, Stavrovskaya IG, Bartels T, Kristal BS, Selkoe DJ (2014) Soluble, prefibrillar α-synuclein oligomers promote complex I-dependent, Ca^{2+}-induced mitochondrial dysfunction. J Biol Chem. https://doi.org/10.1074/jbc.M113.545749
144. Gómez-Suaga P, Bravo-San Pedro JM, González-Polo RA, Fuentes JM, Niso-Santano M (2018) ER-mitochondria signaling in Parkinson's disease review-article. Cell Death Dis. https://doi.org/10.1038/s41419-017-0079-3
145. Guardia-Laguarta C, Area-Gomez E, Rub C et al (2014) α-synuclein is localized to mitochondria-associated ER membranes. J Neurosci. https://doi.org/10.1523/JNEUROSCI.2507-13.2014
146. Paillusson S, Gomez-Suaga P, Stoica R et al (2017) α-synuclein binds to the ER–mitochondria tethering protein VAPB to disrupt Ca^{2+} homeostasis and mitochondrial ATP production. Acta Neuropathol. https://doi.org/10.1007/s00401-017-1704-z

147. Picone P, Nuzzo D, Caruana L, Scafidi V, Di Carlo MD (2014) Mitochondrial dysfunction: different routes to Alzheimer's disease therapy. Oxidative Med Cell Longev. https://doi.org/10.1155/2014/780179
148. Magi S, Castaldo P, MacRi ML et al (2016) Intracellular calcium dysregulation: implications for Alzheimer's disease. Biomed Res Int 2016. https://doi.org/10.1155/2016/6701324
149. Yi J, Ma C, Li Y et al (2011) Mitochondrial calcium uptake regulates rapid calcium transients in skeletal muscle during excitation-contraction (E-C) coupling. J Biol Chem. https://doi.org/10.1074/jbc.M110.217711
150. Oermann EK, Wu J, Guan KL, Xiong Y (2012) Alterations of metabolic genes and metabolites in cancer. Semin Cell Dev Biol. https://doi.org/10.1016/j.semcdb.2012.01.013
151. Hanahan D, Weinberg RA (2011) Hallmarks of cancer: the next generation. Cell. https://doi.org/10.1016/j.cell.2011.02.013
152. Vander Heiden MG, Cantley LC, Thompson CB (2009) Understanding the Warburg effect: cell proliferation. Science (80-). https://doi.org/10.1126/science.1160809
153. Warburg O (1956) On the origin of cancer cells on the origin of cance. Source Sci New Ser. https://doi.org/10.1126/science.123.3191.309
154. Koppenol WH, Bounds PL, Dang CV (2011) Otto Warburg's contributions to current concepts of cancer metabolism. Nat Rev Cancer. https://doi.org/10.1038/nrc3038
155. Cárdenas C, Miller RA, Smith I et al (2010) Essential regulation of cell bioenergetics by constitutive InsP3 receptor Ca^{2+} transfer to mitochondria. Cell. https://doi.org/10.1016/j.cell.2010.06.007
156. Giorgi C, Ito K, Lin HK, et al (2010) PML regulates apoptosis at endoplasmic reticulum by modulating calcium release. Science (80-). https://doi.org/10.1126/science.1189157
157. Missiroli S, Bonora M, Patergnani S et al (2016) PML at mitochondria-associated membranes is critical for the repression of autophagy and cancer development. Cell Rep. https://doi.org/10.1016/j.celrep.2016.07.082
158. Cárdenas C, Müller M, McNeal A et al (2016) Selective vulnerability of cancer cells by inhibition of Ca^{2+} transfer from endoplasmic reticulum to mitochondria. Cell Rep. https://doi.org/10.1016/j.celrep.2016.02.030
159. Kang SS, Han KS, Ku BM et al (2010) Caffeine-mediated inhibition of calcium release channel inositol 1,4,5-trisphosphate receptor subtype 3 blocks glioblastoma invasion and extends survival. Cancer Res. https://doi.org/10.1158/0008-5472.CAN-09-2886
160. Marchi S, Lupini L, Patergnani S et al (2013) Downregulation of the mitochondrial calcium uniporter by cancer-related miR-25. Curr Biol. https://doi.org/10.1016/j.cub.2012.11.026
161. Marchi S, Pinton P (2013) Mitochondrial calcium uniporter, MiRNA and cancer. Commun Integr Biol. https://doi.org/10.4161/cib.23818
162. Zeng F, Chen X, Cui W et al (2018) RIPK1 binds MCU to mediate induction of mitochondrial Ca2þuptake and promotes colorectal oncogenesis. Cancer Res. https://doi.org/10.1158/0008-5472.CAN-17-3082
163. Yu C, Wang Y, Peng J et al (2017) Mitochondrial calcium uniporter as a target of microRNA-340 and promoter of metastasis via enhancing the Warburg effect. Oncotarget. https://doi.org/10.18632/oncotarget.19747
164. Tosatto A, Sommaggio R, Kummerow C et al (2016) The mitochondrial calcium uniporter regulates breast cancer progression via HIF-1α. EMBO Mol Med. https://doi.org/10.15252/emmm.201606255
165. Mammucari C, Gherardi G, Rizzuto R (2017) Structure, activity regulation, and role of the mitochondrial calcium uniporter in health and disease. Front Oncol. https://doi.org/10.3389/fonc.2017.00139
166. Xing J, Ren T, Wang J et al (2017) MCUR1-mediated mitochondrial calcium signaling facilitates cell survival of hepatocellular carcinoma via ROS-dependent P53 degradation. Antioxid Redox Signal. https://doi.org/10.1089/ars.2017.6990
167. Shoshan-Barmatz V, De Pinto V, Zweckstetter M, Raviv Z, Keinan N, Arbel N (2010) VDAC, a multi-functional mitochondrial protein regulating cell life and death. Mol Asp Med. https://doi.org/10.1016/j.mam.2010.03.002

168. Wu W, Zhao S (2013) Metabolic changes in cancer: beyond the Warburg effect. Acta Biochim Biophys Sin Shanghai. https://doi.org/10.1093/abbs/gms104
169. Pastorino JG, Hoek JB (2008) Regulation of hexokinase binding to VDAC. J Bioenerg Biomembr. https://doi.org/10.1007/s10863-008-9148-8
170. Mathupala SP, Ko YH, Pedersen PL (2009) Hexokinase-2 bound to mitochondria: cancer's stygian link to the "Warburg effect" and a pivotal target for effective therapy. Semin Cancer Biol. https://doi.org/10.1016/j.semcancer.2008.11.006
171. Weisthal S, Keinan N, Ben-Hail D, Arif T, Shoshan-Barmatz V (2014) Ca^{2+}-mediated regulation of VDAC1 expression levels is associated with cell death induction. Biochim Biophys Acta Mol Cell Res. https://doi.org/10.1016/j.bbamcr.2014.03.021
172. Arif T, Vasilkovsky L, Refaely Y, Konson A, Shoshan-Barmatz V (2014) Silencing VDAC1 expression by siRNA inhibits cancer cell proliferation and tumor growth in vivo. Mol Ther Nucleic Acids. https://doi.org/10.1038/mtna.2014.9
173. Fouqué A, Lepvrier E, Debure L et al (2016) The apoptotic members CD95, BclxL, and Bcl-2 cooperate to promote cell migration by inducing Ca^{2+}flux from the endoplasmic reticulum to mitochondria. Cell Death Differ. https://doi.org/10.1038/cdd.2016.61
174. Arif T, Krelin Y, Nakdimon I et al (2017) VDAC1 is a molecular target in glioblastoma, with its depletion leading to reprogrammed metabolism and reversed oncogenic properties. Neuro-Oncology. https://doi.org/10.1093/neuonc/now297
175. Abu-Hamad S, Sivan S, Shoshan-Barmatz V (2006) The expression level of the voltage-dependent anion channel controls life and death of the cell. Proc Natl Acad Sci U S A. https://doi.org/10.1073/pnas.0600103103
176. Shoshan-Barmatz V, Ben-Hail D, Admoni L, Krelin Y, Tripathi SS (2014) The mitochondrial voltage-dependent anion channel 1 in tumor cells. Biochim Biophys Acta. https://doi.org/10.1016/j.bbamem.2014.10.040
177. Sammels E, Parys JB, Missiaen L, De Smedt H, Bultynck G (2010) Intracellular Ca^{2+} storage in health and disease: a dynamic equilibrium. Cell Calcium. https://doi.org/10.1016/j.ceca.2010.02.001
178. MacLennan DH, Rice WJ, Green NM (1997) The mechanism of Ca^{2+} transport by sarco(endo)plasmic reticulum Ca^{2+}-ATPases. J Biol Chem. https://doi.org/10.1074/jbc.272.46.28815
179. Coustan-Smith E, Kitanaka A, Pui CH et al (1996) Clinical relevance of BCL-2 overexpression in childhood acute lymphoblastic leukemia. Blood
180. Noujaim D, van Golen CM, van Golen KL, Grauman A, Feldman EL (2002) N-Myc and Bcl-2 coexpression induces MMP-2 secretion and activation in human neuroblastoma cells. Oncogene. https://doi.org/10.1038/sj.onc.1205552
181. Del Bufalo D, Biroccio a LC, Zupi G (1997) Bcl-2 overexpression enhances the metastatic potential of a human breast cancer line. FASEB J
182. Choi J, Choi K, Benveniste EN et al (2005) Bcl-2 promotes invasion and lung metastasis by inducing matrix metalloproteinase-2. Cancer Res. https://doi.org/10.1158/0008-5472.CAN-04-4570
183. Sánchez-Beato M, Sánchez-Aguilera A, Piris MA (2003) Cell cycle deregulation in B-cell lymphomas. Blood. https://doi.org/10.1182/blood-2002-07-2009
184. Foyouzi-Youssefi R, Arnaudeau S, Borner C et al (2000) Bcl-2 decreases the free Ca^{2+} concentration within the endoplasmic reticulum. Proc Natl Acad Sci. https://doi.org/10.1073/pnas.97.11.5723
185. Pinton P, Ferrari D, Magalhaes P et al (2000) Reduced loading of intracellular Ca^{2+} stores and downregulation of capacitative Ca^{2+} influx in Bcl-2-overexpressing cells. J Cell Biol. https://doi.org/10.1083/jcb.148.5.857
186. Chiu W-T, Chang H-A, Lin Y-H et al (2018) Bcl-2 regulates store-operated Ca^{2+} entry to modulate ER stress-induced apoptosis. Cell Death Dis. https://doi.org/10.1038/s41420-018-0039-4
187. Hockenbery DM (2010) Targeting mitochondria for cancer therapy. Environ Mol Mutagen. https://doi.org/10.1002/em.20552

188. Weinberg SE, Chandel NS (2015) Targeting mitochondria metabolism for cancer therapy. Nat Chem Biol. https://doi.org/10.1038/nchembio.1712
189. Kidd JF, Pilkington MF, Schell MJ et al (2002) Paclitaxel affects cytosolic calcium signals by opening the mitochondrial permeability transition pore. J Biol Chem. https://doi.org/10.1074/jbc.M106802200
190. Zheng Y, Shi Y, Tian C et al (2004) Essential role of the voltage-dependent anion channel (VDAC) in mitochondrial permeability transition pore opening and cytochrome c release induced by arsenic trioxide. Oncogene. https://doi.org/10.1038/sj.onc.1207205
191. Tewari D, Majumdar D, Vallabhaneni S, Bera AK (2017) Aspirin induces cell death by directly modulating mitochondrial voltage-dependent anion channel (VDAC). Sci Rep. https://doi.org/10.1038/srep45184
192. Chen L, Sun Q, Zhou D et al (2017) HINT2 triggers mitochondrial Ca^{2+}influx by regulating the mitochondrial Ca^{2+}uniporter (MCU) complex and enhances gemcitabine apoptotic effect in pancreatic cancer. Cancer Lett. https://doi.org/10.1016/j.canlet.2017.09.020
193. Wang J-L, Liu D, Zhang Z-J, et al (2000) Structure-based discovery of an organic compound that binds Bcl-2 protein and induces apoptosis of tumor cells. Proc Natl Acad Sci U S A. 97/13/7124 [pii]
194. Inoue-Yamauchi A, Jeng PS, Kim K et al (2017) Targeting the differential addiction to anti-apoptotic BCL-2 family for cancer therapy. Nat Commun. https://doi.org/10.1038/ncomms16078

Chapter 31
Simulation Strategies for Calcium Microdomains and Calcium Noise

Nicolas Wieder, Rainer H. A. Fink, and Frederic von Wegner

Abstract In this article, we present an overview of simulation strategies in the context of subcellular domains where calcium-dependent signaling plays an important role. The presentation follows the spatial and temporal scales involved and represented by each algorithm. As an exemplary cell type, we will mainly cite work done on striated muscle cells, i.e. skeletal and cardiac muscle. For these cells, a wealth of ultrastructural, biophysical and electrophysiological data is at hand. Moreover, these cells also express ubiquitous signaling pathways as they are found in many other cell types and thus, the generalization of the methods and results presented here is straightforward.

The models considered comprise the basic calcium signaling machinery as found in most excitable cell types including Ca^{2+} ions, diffusible and stationary buffer systems, and calcium regulated calcium release channels. Simulation strategies can be differentiated in stochastic and deterministic algorithms. Historically, deterministic approaches based on the macroscopic reaction rate equations were the first models considered. As experimental methods elucidated highly localized Ca^{2+} signaling events occurring in femtoliter volumes, stochastic methods were

N. Wieder
Broad Institute of MIT and Harvard, Cambridge, MA, USA

Department of Medicine, Brigham and Women's Hospital and Harvard Medical School, Boston, MA, USA

Medical Biophysics Group, Institute of Physiology and Pathophysiology, University of Heidelberg, Heidelberg, Germany

R. H. A. Fink
Medical Biophysics Group, Institute of Physiology and Pathophysiology, University of Heidelberg, Heidelberg, Germany

F. von Wegner (✉)
Department of Neurology and Brain Imaging Center, Goethe University Frankfurt, Frankfurt am Main, Germany

Medical Biophysics Group, Institute of Physiology and Pathophysiology, University of Heidelberg, Heidelberg, Germany
e-mail: vonWegner@med.uni-frankfurt.de

M. S. Islam (ed.), *Calcium Signaling*, Advances in Experimental Medicine and Biology 1131, https://doi.org/10.1007/978-3-030-12457-1_31

increasingly considered. However, detailed simulations of single molecule trajectories are rarely performed as the computational cost implied is too large. On the mesoscopic level, Gillespie's algorithm is extensively used in the systems biology community and with increasing frequency also in models of microdomain calcium signaling. To increase computational speed, fast approximations were derived from Gillespie's exact algorithm, most notably the chemical Langevin equation and the τ-leap algorithm. Finally, in order to integrate deterministic and stochastic effects in multiscale simulations, hybrid algorithms are increasingly used. These include stochastic models of ion channels combined with deterministic descriptions of the calcium buffering and diffusion system on the one hand, and algorithms that switch between deterministic and stochastic simulation steps in a context-dependent manner on the other. The basic assumptions of the listed methods as well as implementation schemes are given in the text. We conclude with a perspective on possible future developments of the field.

Keywords Calcium · Calcium signaling · Microdomains · Stochastic modeling · Calcium noise · Colored noise · Chemical master equation · Gillespie's algorithm · Langevin equation · IP3R

31.1 Biological Relevance of Calcium Microdomains

Ca^{2+} is an important second messenger in virtually every cell type. It acts as a signaling molecule in a variety of different cellular processes, ranging from synaptic neurotransmitter release and exocytosis in general to muscle contraction, the regulation of gene networks and many others [1]. Over the last decades, it became clear that the distribution of Ca^{2+} inside a cell cannot be considered to be homogenous. Quite the contrary, it emerged that Ca^{2+} signaling has a strong spatial component [2]. Ca^{2+} release sites were found to be highly organized entities that allow for cytosolic Ca^{2+} elevations in specific signaling relevant locations. The extent of these release events is controlled by a large cytosolic Ca^{2+} buffer capacity, Ca^{2+} pumps and transporters that transfer Ca^{2+} against a steep concentration gradient out of the cytosol and predefined morphological substructures such as neuronal synapses or the dyadic cleft in skeletal muscle cells. These transient, subcellular elevations of Ca^{2+} create temporary signaling entities that are termed Ca^{2+} microdomains [3].

From a systemic perspective, Ca^{2+} microdomains constitute the most fundamental building blocks of Ca^{2+} signaling networks and their biological relevance has been studied extensively. Ca^{2+} microdomains play an important role in the generation of complex spatio-temporal signaling patterns such as waves and oscillations. They are based on synchronized openings of endoplasmic reticulum (ER) Ca^{2+} release channels which are limited by negative feedback mechanisms such as membranous Ca^{2+} pumps. Well studied examples are insulin release from pancreatic beta cells [4], fertilization, muscle contraction and the regulation of gene networks [5]. Another prominent example where Ca^{2+} microdomains play

a crucial role in fundamental cellular processes are contact sites between the endoplasmic reticulum and mitochondria, known as mitochondria-associated membranes (MAMs). An interplay between clusters of endoplasmic Ca^{2+} release channels (e.g. IP_3R receptors) and the mitochondrial Ca^{2+} uniporter (MCU) allows to shuttle Ca^{2+} ions from the ER to the mitochondria via localized Ca^{2+} release events at MAMs. The impairment of this mechanism has been associated with different disease relevant cellular states such as inflammation [6], metabolism [7] and apoptosis [8]. A well understood example of structurally confined Ca^{2+} microdomains are neuronal synapses where highly spatially organized Ca^{2+} microdomains play an important role in synaptic plasticity and the generation of long term potentation (LTPs) that is involved in learning and memory [9]. The list of relevant examples goes on, but a comprehensive review of Ca^{2+} microdomains lies beyond the scope of this book chapter. For a more detailed discussion the reader is referred to [1–3, 10].

31.2 Canonical Models of Calcium Microdomains

Identical subcellular compartments and systems have been modeled using different strategies. Synaptic activation including vesicle release at the neuronal synapse, for instance, has been modeled with different approaches [11, 12] ranging from simulations at the scale of individual molecules to deterministic reaction rate equations. Similarly, different model classes of subcellular calcium dynamics in cardiomyocytes and skeletal muscle fibers are still being evaluated for their explanatory and predictive power. The simulated volume and average reactant concentrations can help to decide which simulation strategy is the most adequate for a given problem.

Virtually all cell types share a common family of molecules involved in the regulation of the local, subcellular calcium concentration and many cell lines even share common modules, i.e. small signaling networks that regulate key processes such as cell cycle regulation, adaptation of the metabolic rate, vesicle secretion, motility and excitability [13]. In order to keep the presentation of simulation strategies compact, we here focus on some key molecular species, in particular calcium buffers and calcium channels, from where the transfer to more specific problems should be easy. For a more general introduction to modeling and the simulation of chemical reactions, the reader is referred to [14–17].

The presentation and the implementation of the models used here is further facilitated by the fact that it is sufficient to take into account chemical reactions of second order, at most. In this context, zero-order reactions model the constant generation or degradation of a molecular species at a fixed rate, for instance, when a molecule is assumed to be unstable on time scales relevant for the simulation. Zero-order reactions also come into play when certain reaction networks are not simulated in detail but one of their products (resp. educts) appears as a reaction partner in the system that is simulated in detail. Also, ion channel currents can be modeled as zero-order reactions occurring in time intervals when the channel

is in an open state. Modeling ion channel currents as chemical reaction events has the advantage that the inclusion of channel currents does not require major modifications of the computational model but only the addition of another reaction type. First-order reactions are mainly concerned when a calcium-bound molecular complex dissociates and thereby liberates a calcium ion. Second-order reactions describe the corresponding association reaction of a calcium ion and a calcium-binding molecule such as buffer proteins, calcium-sensitive enzymes, membrane constituents, ion channels or fluorescent dye molecules. In principle, any of these calcium-binding molecules can be considered a calcium buffer.

The molecular species used in this presentation are calcium ions (Ca^{2+}), a set of calcium buffers (B_i, $I = 1, \ldots, N_B$) that can be either diffusible or immobile and calcium-regulated ion channels (Ch). In the case of ion channels, those regulated by calcium ions but conducting another ionic species (e.g. calcium regulated chloride or potassium channels) must be distinguished from calcium-regulated calcium channels. The latter, e.g. IP_3- and RyR-channels, provide a highly localized, nonlinear calcium-sensitive feedback system since these channels have activating as well as inhibitory calcium binding sites [18, 19].

31.3 Microscopic Simulation

To achieve a maximum of spatial detail, one has to simulate the Brownian motion of all molecules and introduce reaction events whenever a molecular collision of sufficiently high energy (the activation energy of the reaction) occurs [20]. The price of this level of detail is paid in computation time. Runtime scales unfavorably with increasing simulation volume and increasing number of reactants as diffusion events occur at much higher rates than chemical reactions and the number of trajectories grows linearly with the number of reactants. In the context of calcium dynamics, simulations of individual molecular trajectories are used less frequently than the approaches explained below. They can be found mainly in the context of calcium-regulated synaptic signaling [11, 21, 22] as well as Ca^{2+} dynamics in cardiac myocytes [23–26]. Practically, these systems can be implemented with the freely available software package MCell developed by the Salk Institute (www.mcell.cnl.salk.edu).

31.4 Mesoscopic Stochastic Simulation

Mesoscopic simulation approaches have been a growing area in computational cell biology in the past 15 years [15, 27]. Using the mesoscopic perspective, the fluctuating number of molecules of each type is tracked by one of several stochastic algorithms. To better understand different mesoscopic algorithms, it is necessary to introduce some notation and a few definitions. The state of a given model system

of N molecular species $S_1. \ldots, S_N$ will from here on be described by the time-dependent ***state vector*** $X_t = (x_t^{(1)}, \ldots, x_t^{(N)})$ that contains the ***copy number*** $x_t^{(i)}$ of each species (index i) at time t. By copy number, we understand the number of molecules of a certain molecular species in a defined volume at a given time, e.g. a Ca^{2+} concentration of 100 nM in a 1 fl volume yields a copy number of 60. The term copy number is mostly used in the context of small reaction volumes and low molar concentrations resulting in relatively few molecules of each type. The N chemical species in our model system interact through M types of chemical reactions R_j, $j = 1, \ldots, M$. Next, a ***state change vector*** V_j is introduced for each reaction R_j. The component v_{ji} describes the change in the copy number of molecular species S_i caused by a single occurrence of reaction type R_j. After a reaction R_j occurs, the state vector is updated according to $X_t \leftarrow X_t + V_j$. Furthermore, we assume that given a state X_t, there is a defined probability for each reaction R_j to occur within a small (infinitesimal) time interval $[t, t + dt]$. In the context of chemical reactions, this probability equals $a_j(X_t)dt$, and $a_j(X_t)$ is called the ***reaction propensity*** of reaction R_j. As the state vector X_t is time-dependent, the reaction propensity $a_j(X_t)$ is also time-dependent, however, this notation is often suppressed for the sake of simplicity. The following stochastic algorithms can all be derived from the chemical master equation (CME). The CME is a deterministic differential (or difference) equation that describes the temporal evolution of the probability density $p(X_t)$, i.e. the multivariate distribution of the state vector X_t. Using the notation introduced above, the CME reads:

$$\partial_t p\left(X_t\right) = \sum_{j=1}^{M} \left[a_j\left(X_t - V_j\right) p\left(X_t - V_j\right) - a_j\left(X_t\right) p\left(X_t\right)\right] \tag{31.1}$$

In words, the CME states that the change in $p(X_t)$ is calculated as the net probability flow conveyed by flows from state $X_t - V_j$ into state X_t (via reaction R_j) and the reverse flows out of state X_t. A closed-form, analytical solution for $p(X_t)$ is only accessible for very simple systems (8). As for many other stochastic systems, this is where Monte Carlo sampling schemes come into play. Numerical solutions are also difficult or impossible to obtain due to the large state space that arises when all possible combinations of molecule counts are considered. An approach to circumvent or approximate the CME problem is given by the Finite State projection algorithm [28].

31.5 Gillespie's Algorithm

Gillespie's algorithm or Stochastic Simulation Algorithm (SSA), provides a Monte Carlo simulation scheme that samples the time-dependent probability density $p(X_t)$ exactly [29]. The crucial point in Gillespie's algorithm is the insight that the

evolution of the state vector X_t follows a multivariate Markov process on the N-dimensional integer lattice Z_N. The transition rate between the lattice points X_t and $X_t + V_j$ is given by the reaction propensity $a_j(X_t)$. As Markov processes are characterized by exponential waiting time distributions, the waiting time until the next reaction event can be calculated in a single step. The waiting time distribution is parametrized by the cumulative reaction rate

$$a_0(X_t) = \sum_{j=1}^{M} a_j(X_t) \tag{31.2}$$

The rate $a_0(X_t)$ determines the probability $p(\tau, j|X_t)$ that, given state X_t at time t, the next reaction event will be of type R_j and will occur in the small time interval $[t + \tau, t + \tau + dt]$:

$$p(\tau, j \mid X_t) = a_j(X_t)\, e^{-a_0(X_t)\tau} \tag{31.3}$$

In the actual algorithm, the probability is factored in two parts. First, the waiting times τ for the next event are obtained as samples from an exponential distribution with parameter $a_0(X_t)$ according to

$$\tau = \frac{-\ln(r_1)}{a_0(X_t)} \tag{31.4}$$

where $r_1 \sim U_{[0,1]}$ is a uniformly distributed random variable. Here it is assumed that a_j remains constant during the next time step τ. Next, a second uniformly distributed random variable $r_2 \sim U_{[0,1]}$ is drawn which determines the next reaction type R_j according to the ratios of $\frac{a_j(X_t)}{a_0(X_t)}$.

Thus, the complete Gillespie algorithm reads:

1. ***Initialization***: initialize the state vector components $X_{t=0}$ with the copy number of chemical species S_i expected in equilibrium or any other desired initial condition. Calculate all individual reaction propensities $a_j(X_t)$ and the cumulative propensity $a_0(X_t)$.
2. ***Waiting time and reaction selection***: sample a waiting time τ and a reaction index j from the distribution (Eq. 31.3).
3. ***Update state and time***: $X_t \leftarrow X_t + V_j$ and $t \leftarrow t + \tau$.
4. ***Exit condition***: if $t \geq T_{max}$ where T_{max} is the desired length of the simulation.
5. ***Update propensities***: recalculate the propensities of all reactions affected by the last state change.
6. go to step 2.

An efficient implementation based on the dependency structure between reactions and the reuse of random numbers was developed later [30]. The result of Gillespie's algorithm is a set of N time series reflecting the fluctuating copy number of each molecular species S_i. The advantage of the algorithm becomes most clear

when compared to earlier approaches. An alternative approach to simulate the reaction process relies on the fact that the probability of reaction R_j to occur in a small interval $[t, t + dt]$ equals $a_j(X_t)dt$. If dt is chosen small enough to ensure that $a_j(X_t)dt \ll 1$, assuming that only one reaction occurs during dt, one can iteratively advance the simulation time by dt, accepting or rejecting reaction events by comparison with the value of a uniformly distributed random variable r. This strategy is not recommended however, as one will find that most time steps dt will pass without any reaction event happening. The problem becomes even worse when the desired precision demands a small time step dt. Gillespie's algorithm overcomes the problem by sampling the exponential waiting time distribution directly and by jumping to the next event time without further checks. Moreover, no fixed integration time step dt has to be chosen and therefore, the algorithm is stochastically 'exact'. Though widely used in systems biology, there are comparatively few examples for the use of Gillespie's algorithm in the modeling of intracellular calcium dynamics [31]. Gillespie's algorithm has been used to model stochastic resonance effects in whole cells [32, 33], calmodulin-dependent synaptic plasticity in dendritic spine microdomains [12] and to model calcium microdomains in the vicinity of individual L-type calcium channels [34]. Although the algorithm can be used for arbitrary simulation volumes, computation time quickly increases for larger volumes because the copy numbers enter the propensity terms in a combinatorial way. Therefore, several approximations of the exact simulation algorithm have been developed.

31.6 The Binomial and the τ-leap Methods

For small time steps dt, the probability for a reaction R_j to occur in the next time interval $[t, t + dt]$ is given by $a_j(X_t)dt$. Assuming that the propensity $a_j(X_t)$ remains approximately constant during the time span τ, the number of times the reaction R_j occurs during the span τ is a Poisson-distributed random variable with expected value $a_j(X_t)\tau$ [35]. Now, if τ is small enough to guarantee approximately constant reaction propensities $a_j(X_t)$ and at the same time large enough so that $a_j(X_t)\tau \gg 1$, i.e. a significant number of reactions will occur during the time interval of length τ, then Gillespie's algorithm can be accelerated by using the larger time step τ and by sampling the number of reactions from Poissonian distributions with parameters $a_j(X_t)\tau$ directly. This procedure is called the ***τ-leap method*** [15]. Obviously, the main task is to set the right time step τ adaptively throughout the simulation. Small time steps will produce low numbers of reactions (even zero), and in this situation the exact Gillespie algorithm could be used instead. Too large time steps however, lead to a larger error compared to the exact solution and furthermore, can lead to negative molecule numbers. A detailed discussion of τ-selection procedures can be found in the literature [36]. Using Poisson random numbers, there is always a risk of producing negative entries in the state vector as Poisson variables range from zero to infinity. As an alternative, the ***binomial leap method*** has been proposed.

Instead of Poisson variables, appropriately parametrized binomial random variables are used, the main advantage being that the range of the variable can be bounded by the current copy number of each molecule [37]. Irrespective of the method used, the update rule can be written as

$$x_{t+\tau}^{(i)} = x_t^{(i)} + \sum_{j=1}^{M} v_{ji} \xi_j \left(a_j \left(X_t \right) \right) \tag{31.5}$$

where ξ_j represents either a Poissonian or a binomial random variable. Applications and systematic evaluations of these methods for the simulation of calcium microdomains are still scarce, a comparative study can be found in [37].

31.7 The Chemical Langevin and Fokker-Planck Equations

The approximation of the number of reactions that occur in a given time interval by samples from a defined probability density can be taken a step further. In the case of the chemical Langevin equation (CLE), the number of reactions R_j occurring in a small time interval of length dt is sampled from a normal distribution with mean and variance equal to $a_j(X_t)dt$. From a statistical point of view, this approach is justified as the Poisson random variable introduced in the last paragraph converges to a normal distribution in the case of a large mean value. When the expected number of reactions is too small, the symmetric normal distribution does not yield a good approximation of the corresponding right-skewed Poisson distribution and negative molecule counts can be obtained. This becomes clear when considering models with a single ion channel [34, 38]. When each state of the ion channel is modeled as a distinct chemical species, e.g. open and closed states, the count of each state is either 0 or 1. Chemical reactions including the ion channel can therefore not be modeled adequately by the CLE approach. For these cases, alternative schemes have been proposed in the literature [39, 40]. In our code, we set $X_t = 0$ whenever the integration yields $X_t < 0$, as proposed for the Cox-Ingersoll-Ross process in [41]. The most important differences of the CLE approach are (i) that the time interval dt is fixed, and (ii) that, due to the normally distributed random variable, the copy numbers are real numbers rather than integers. The updating rule is given by

$$x_{t+dt}^{(i)} = x_t^{(i)} + \sum_{j=1}^{M} v_{ji} a_j \left(X_t \right) dt + \sum_{j=1}^{M} v_{ji} \sqrt{a_j \left(X_t \right)}\, dW_t \tag{31.6}$$

where dW_t are the increments of M mutually independent standard Wiener processes [14]. Using Eq. 31.6 in simulations directly corresponds to the Euler-Maruyama integration scheme for stochastic differential equations [17]. The first sum in Eq. (31.6) contains the deterministic dynamics that will be discussed in the following

paragraph while the second sum adds appropriately scaled stochastic fluctuations. Compared to the algorithms discussed so far, the CLE provides an extremely fast way to obtain an approximate solution of the CME. A basic result in the theory of stochastic processes allows a transformation of the Langevin equation to an associated Fokker-Planck equation (FPE) that describes the temporal evolution of the probability density $p(X_t)$ [14]. For discrete variables, the dynamics are captured completely by the CME, a family of first-order differential equations for the probabilities over all possible system states. For a Markov process, the CME is identical to the Chapman-Kolmogorov equation describing the dynamics of the transition probabilities $P(X_{t+n} = y|X_t = x)$. The CME's Taylor expansion in the spatial step size dx is called the Kramers-Moyal expansion. It generates a deterministic PDE from the integro-differential CME, both describing the dynamics of the system's underlying probability distributions. Using a second-order truncation of the infinite Kramers-Moyal expansion yields the Fokker-Planck equation [14]. Applications can focus on individual sample paths, in analogy to a single run of an experiment, or on distributions, summarizing the full stochastic structure of the system at hand. Ideally, all solutions would provide the complete distributions of all variables, but in practice, computation times often force the user to analyze a few representative sample paths, as produced by the CLE, for instance. Implementations of the CLE approach have been presented for calcium-dependent signaling pathways in neurons [42], IP_3-mediated calcium sensitive pathways in non-excitable cells [32, 43, 44] and Ca^{2+} release events in general [45]. An example of the FPE method to calcium dynamics in the dyadic cleft of cardiomyocytes is given in [46].

31.8 Deterministic Simulation

When stochastic effects in the dynamics of the modeled system are ignored, the classical deterministic reaction-rate equations are recovered. These correspond to the deterministic terms found in the chemical Langevin equation [35]. From a statistical physics point of view, the deterministic dynamics reflect the limit of an infinitely large simulation volume while keeping all reactant concentrations constant:

$$x_{t+dt}^{(i)} = x_t^{(i)} + \sum_{j=1}^{M} v_{ji} a_j (X_t)\, dt \tag{31.7}$$

Simulating the deterministic system using Eq. 31.7 directly represents a first-order Euler integration scheme. As stochastic effects are no longer present, a set of ordinary differential equations is obtained that can be conveniently integrated using standard schemes as implemented in most numerical software packages. If diffusion is included in the model, an additional diffusion term arises for each diffusible species. In deterministic simulations, diffusion would be modeled by a

discrete Laplace operator applied to the spatial concentration profile of the diffusing species. In the stochastic setting, diffusion is modeled as a pair of additional chemical reactions, as detailed further below. The model is now described by set of partial differential equations. Deterministic methods represent the major part of the literature on calcium dynamics in excitable and non-excitable cells. In the context of microdomain calcium dynamics in cardiac and skeletal muscle cells, we list only a small selection of representative and landmark studies [47–51].

31.9 Hybrid Simulation

Complex subcellular systems often generate patterns across several temporal scales, especially when the participating reactions have rate constants that span several orders of magnitude. In these cases, it may happen that Gillespie's exact algorithm performs quite slowly due to the exact tracking of effectively irrelevant fluctuations while the system's dynamics may perform in an almost deterministic way. Moreover, models of subcellular calcium dynamics often contain plasma membrane or endoplasmic reticulum ion channels that modulate the local calcium concentration or are modulated by Ca^{2+} ions. As ion channel gating is almost exclusively described with stochastic methods, mainly with Markov chain models, the introduction of ion channels in deterministic models is not obvious. For these cases, hybrid models combining several of the aforementioned techniques have been developed. For instance, hybrid models using deterministic reaction dynamics for the subset of calcium diffusion, permeation and buffering reactions and stochastic models of ion channel gating have successfully been used for the modeling of skeletal and cardiac muscle cells [46, 52, 53] as well as for generic cell types with an IP_3 regulated calcium signaling system [54]. Other approaches switch adaptively between deterministic dynamics and the CLE-approximation [55], or between the Gillespie algorithm, the CLE-approximation and the τ-leap method [56].

31.10 Reaction Propensities for Calcium Microdomains

In the preceding sections, reaction propensities were introduced in an abstract way to calculate certain probability densities. Now, we will give some explicit expressions for reaction types essential to microdomain calcium signaling.

1. ***Chemical reactions***. $a_j(X_t) = c_j h_j(X_t)$, where c_j is the stochastic reaction rate and $h_j(X_t)$ denotes the number of possible molecular combinations available for reaction R_j at time t. The stochastic rates are calculated from the macroscopic reaction rate constants k_j and the system volume V, for monomolecular reactions we get $c_j = k_j$, for bimolecular reactions $c_j = \frac{k_j}{V}$. Calcium buffering reactions

consist of a pair of reactions, a second-order association reaction and a first-order dissociation reaction. Calcium pumps can be modeled in the same way.

2. ***Ion channel gating***. Given a gating scheme and the associated transition rates, transitions between channel substates can be treated as first-order chemical reactions where the different channel states are seen as different chemical species that are transformed into each other as specified by the gating scheme. Calcium-sensitive gating steps are modeled as a second-order association reaction between a calcium ion and the unbound channel state. The propensity terms are identical to the preceding case.
3. ***Ion channel currents***. If the mean channel current amplitude is known, the process of ion conduction and release from the channel pore can be simplified as a zero-order reaction, i.e. a Poisson process with a fixed rate [34]. Even though a constant release rate may only be a rough approximation of the real permeation process [57], the model yields the correct mean current and furthermore takes into account the quantal nature (release of a single ion at a time) and stochasticity inherent to ion channel currents. Conversion of the current amplitude I_{ch} to a stochastic rate constant is achieved by

$$c_j = \left| \frac{I_{ch}}{e \times z_{ion}} \right|$$

where e is the elementary charge and z_{ion} is the charge of the permeating ion. A calcium current of 1 pA, for instance, has an 'event rate' of $c_j \approx 3000/ms$. The factor $h_j(X_t)$ is equal to the number of *open* channels at time t, which is easily implemented as each channel state is regarded as a separate chemical species.
4. ***Diffusion***. Assuming a multivoxel simulation geometry, diffusion at the mesoscopic level can be implemented using the concept of stochastic event rates [58]. In analogy to the previously introduced techniques, the diffusion event rate of species S_i is calculated from the macroscopic diffusion constant D_i in order to yield the correct behavior in the deterministic limit. At the microscopic level, the diffusion event constant controls the speed of the molecular random walk. Assuming a voxel side length δx, the rate is given by

$$a_j = \frac{D_i}{(\delta x)^2} x_t^{(i)}$$

where $x_t^{(i)}$ is the copy number of species S_i at time t. In practice, diffusion rates of small molecules often lie several orders of magnitude above the common reaction rates. This can lead to a significant increase in computation time. However, even in single voxel simulations the implementation of diffusion may be necessary to avoid accumulation of e.g. calcium ions released from calcium channels [34]. In the single voxel case, this reduces to a fixed efflux rate of the ion.

31.11 The Colored Noise Interpretation

The chemical Langevin equation transforms the discrete picture of individual molecules, diffusing and reacting within the reaction volume, into a continuous stochastic process. While the copy number of any molecular species can only change by an integer value in the discrete models, the mesoscopic description provided by the chemical Langevin equation allows arbitrarily small changes in all variables. The mesoscopic CLE model represents an intermediate scale between discrete molecule counts and continuous chemical concentrations.

Conceptually, the CLE describes chemical reaction dynamics within the mathematical framework of stochastic differential equations, for which a large body of theoretical and numerical results exist [14]. Though Eq. (31.6) is a generic way to describe chemical reactions stochastically, the application to microdomain calcium signaling may not be straightforward. Moreover, we are interested in approximations that simplify the expression in Eq. (31.6), while still representing physical reality to a reasonable extent. The theory for calcium ions binding to a single or multiple buffers, with and without diffusion, has been developed in Ref. [10, 59]. In order to illustrate the procedure, we here present the elemental case of calcium ions interacting with a single buffer species. We consider the reversible bimolecular reaction of Ca^{2+} with a single buffer species B:

$$Ca^{2+} + B \rightleftharpoons CaB$$

In terms of the macroscopic, deterministic reaction rates k^+ and k^-, the stochastic association and dissociation rates for the reaction volume V are $c^+ = \frac{k^+}{V}$ and $c^- = k^-$, respectively.

Next, let x_t denote the copy number of free calcium ions, Ca^{2+}, y_t the copy number of free buffer molecules B, and z_t the number of calcium bound buffer molecules CaB. The total amount of calcium in the system is $x_T = x_t + z_t$, and the total number of buffer molecules is $y_T = y_t + z_t$.

As we model two reactions, the full chemical Langevin equation of the system contains two independent Wiener processes $dW_t^{(1)}$ and $dW_t^{(2)}$, that can be combined into a single process dW_t, as detailed in [10]. In order to simplify the CLE, we will apply the excess buffer approximation [60], which assumes that the fluctuations in the number of free calcium ions is small compared to the number of free buffer molecules. Therefore, the number of free buffer molecules y_t can be approximated by its equilibrium concentration, denoted y_{eq} [10]. Though the assumption may fail in case of a massive intracellular calcium increase, it is appropriate for resting conditions. The simplified CLE then reads:

$$dx_t = -\left(c^+ y_{eq} + c^-\right) x_t dt + c^- x_T + \sqrt{c^+ x_t y_{eq} + c^- z_t}\, dW_t$$

Defining the constants $C_1 = c^+ y_{eq} + c^-$ and $C_2 = c^- x_T$, we obtain

$$dx_t = -C_1 \left(x_t - \frac{C_2}{C_1} \right) dt + \sqrt{c^+ x_t y_{eq} + c^- z_t} dW_t$$

The equilibrium calcium concentration is given by $[Ca^{2+}]_{\text{eq}} V = x_{eq} = \frac{C_2}{C_1}$, and defining the relaxation time $\tau = \frac{1}{C_1}$ and the time-dependent variance $\sigma_t = \sqrt{c^+ x_t y_{eq} + c^- z_t}$, the expression is

$$dx_t = -\frac{1}{\tau} \left(x_t - x_{eq} \right) dt + \sigma_t dW_t$$

A further approximation can be introduced by considering a stationary variance term.

$\sigma_t = \sqrt{c^+ x_{eq} y_{eq} + c^- z_{eq}}$, using the equilibrium calcium concentration x_{eq} rather than the time-dependent exact calcium concentration x_t. The resulting expression

$$dx_t = -\frac{1}{\tau} \left(x_t - x_{eq} \right) dt + \sigma dW_t$$

is the so-called Ornstein-Uhlenbeck process, a generic stochastic process with well known analytical properties [14]. The Ornstein-Uhlenbeck process is a Markovian process often used to represent and to generate so-called colored noise samples. To summarize linear noise properties, the time autocorrelation function, or equivalently, the power spectral density of a noisy time series can be used. Formally, the time series has to be time-stationary for these methods to work. For an oscillatory system, for instance, an oscillation frequency of $f = 1/T$ leads to a spectral peak at frequency f in the power spectrum, and to a dominant time lag of T in the autocorrelation function. Temporally uncorrelated noise yields a flat power spectrum, hence the name 'white' noise, in correspondence to the physical spectrum of white light. In contrast, a non-flat electromagnetic spectrum yields colored light, therefore the name colored noise for stochastic processes with non-flat spectrum. The Ornstein-Uhlenbeck process is the minimal representation of an exponentially autocorrelated, Gaussian distributed noise. Thus, realistic calcium noise samples with realistic first and second-order statistical properties, i.e. identical mean, variance and auto-correlation function, can be generated very quickly using a simple Ornstein-Uhlenbeck process. Moreover, the wealth of exact stochastic properties derived for the Ornstein-Uhlenbeck process can be transferred to the environment of microdomain calcium signaling. Using the calculations presented in this paragraph, direct algebraic relations between physico-chemical constants and stochastic properties like the relaxation time and the time-dependent variance can be derived in many cases, including multiple buffers and calcium diffusion [10, 59].

31.12 The Impact of Microdomain Calcium Noise on IP_3R Gating

The relevance of noise in non-linear systems in nature has received increasing attention over the last years [38, 61–63]. Considering the non-linear dynamics of many downstream Ca^{2+} effectors, one could hypothesize about a physiological relevant information content of Ca^{2+} fluctuations [64]. A suiting model system for the investigation of such an effect is the endoplasmic, homotetrameric inositol 1,4,5-trisphosphate receptor (IP_3R), a fundamental part of the intracellular Ca^{2+} signaling apparatus [65]. It is crucially involved in the generation and regulation of complex spatiotemporal Ca^{2+} signals [66], which have been observed in a variety of different cell types [67]. Each of the four channel subunits has a binding site for the second messenger IP_3 and two Ca^{2+} binding sites that give rise to the typical bell-shaped Ca^{2+} response curve of IP_3Rs [18]. For low Ca^{2+} concentrations a high-affinity Ca^{2+} binding site induces a positive feedback known as calcium-induced calcium release, while a low-affinity Ca^{2+} binding site is responsible for the negative feedback mechanism which eventually induces the inactivation of the IP_3 receptor at higher $[Ca^{2+}]$ [19]. The DeYoung-Keizer model is a well-established mathematical representation of the IP_3R gating dynamics [68] and was therefore used in the here presented study. The investigation of Ca^{2+} noise induced effects to more recent mathematical models of the IP_3R [69, 70] lies beyond the scope of the here presented example but will be subject of future studies. As discussed above, Ca^{2+} noise is shaped by diffusion and the presence of Ca^{2+} binding molecules, such as endogenous Ca^{2+} buffer proteins [59]. For a stochastically exact representation of those effects, one has to model the system at least at the mesoscopic level [31]. Considering the timescales of channel gating events (up to seconds), Gillespie's algorithm constitutes the only feasible approach to capture the exact noise phenomena of interest. A minimal system capable of exhibiting noise induced effects on the non-linear gating dynamics of the IP_3R should contain at least a single IP_3R in the DeYoung-Keizer representation, a constant IP_3 concentration and Ca^{2+} diffusion. The variation of Ca^{2+} diffusion coefficients allows us to tune the autocorrelation of Ca^{2+} noise in this model. The IP_3R can be functionally characterized by its open probability, its mean open time and its mean channel close time. A C++ implementation of Gillespie's algorithm, developed for the simulation of the here introduced model, is available on github (https://github.com/nwieder/SSTS).

In order to investigate the potential effects of Ca^{2+} noise on downstream signaling pathways, while maintaining computational feasibility, it is necessary to reduce a biological model system to its core elements. Hence, following an example detailed in [38], we assume an in-silico experiment where we first model a single non-conducting IP_3R in the absence of diffusion and buffer dynamics with a constant number of Ca^{2+} ions. In a second step, we introduce Ca^{2+} diffusion, hence Ca^{2+} fluctuations to the system. For each of these conditions we generate trajectories for different mean Ca^{2+} concentrations, essentially generating the characteristic bell-

shaped open probability curve of IP_3Rs for each of the different conditions as a read out. Interestingly, we find that the modulations of noise autocorrelation time by diffusion, indeed influences the shape of the IP_3R response curves in a $[Ca^{2+}]$ dependent manner. Figure 31.1 summarizes IP_3R gating properties for different theoretical Ca^{2+} diffusion constants. The dashed line (empty squares) represents a model in the absence of Ca^{2+} diffusion and thus the absence of Ca^{2+} fluctuations. This condition mimics a deterministic setting with a constant Ca^{2+} concentration. With the introduction of Ca^{2+} diffusion (solid lines), noise is added to the system. Considering a physiological Ca^{2+} diffusion coefficient $D_{Ca} = 200\ \mu m^2 s^{-1}$ (solid triangles), for $[Ca^{2+}] > 10\ \mu M$ the presence of Ca^{2+} fluctuations does induce a significant increase in open probability, mean open times and a decrease in mean closed times. For increasing diffusion constants, the noise autocorrelation time decreases and the IP_3R open probability for $[Ca^{2+}] > 1\ \mu M$ increases as a function of the diffusion constant and hence the autocorrelation time τ. In summary, this example demonstrates how the introduction of Ca^{2+} fluctuations alters IP_3R gating characteristics, which in turn has the potential to affect the properties of more complex spatiotemporal Ca^{2+} signals.

We are well aware of the fact that this example is based on an oversimplified model, accounting only for a fraction of known biologically relevant interactions between Ca^{2+} signaling molecules and endoplasmic Ca^{2+} release channels. Most importantly, the IP_3R was modeled as a non-conducting ion channel. This has two reasons: (a) Experimental quantification of Ca^{2+} dependent IP_3R gating dynamics has been conducted in a setting where Ca^{2+} was replaced by K^+ as primary charge carrier to extract information about the Ca^{2+} dependence of the IP_3R [19]. This experimental dataset was used to verify the here presented modeling approach. (b) The introduction of Ca^{2+} to the modeled system changes the mean number of Ca^{2+} ions in the system and hence alters the amplitude of Ca^{2+} fluctuations. Both these quantities need to be kept constant to isolate the effect of colored Ca^{2+} noise on the IP_3R. Hence the simplification is necessary to carefully extract a causal link between Ca^{2+} fluctuations (here induced by diffusion or Ca^{2+} buffers) and the non-linear dynamics of the down-stream effector (here the IP_3R). In [38], it has been shown that the presence of noise, as well its stochastic characteristics, has the potential to affect the dynamics of key components of biological signaling networks. Based on those observations, we argue that the relevance of stochastic fluctuations will most likely scale up to more complex systems found in living systems.

Over the last decades, Ca^{2+} microdomains emerged as the most fundamental entity of Ca^{2+} signaling [2]. In neurons and muscle cells, structurally distinct microdomains, such as dendritic spines or the dyadic cleft of cardiac myocytes, are recognized for their functional relevance in learning, memory, and heart- beat generation [71–73]. Even though the importance of stochastic Ca^{2+} fluctuations in such microdomains received increasing attention over the last years [66], the question to what extent such fluctuations influence global Ca^{2+} signals in general remains yet unanswered. The difficulties in painting a full picture is largely due to the immense complexity of Ca^{2+} signaling networks as well as the limited experimental approaches at hand to investigate noise induced effects. Nevertheless,

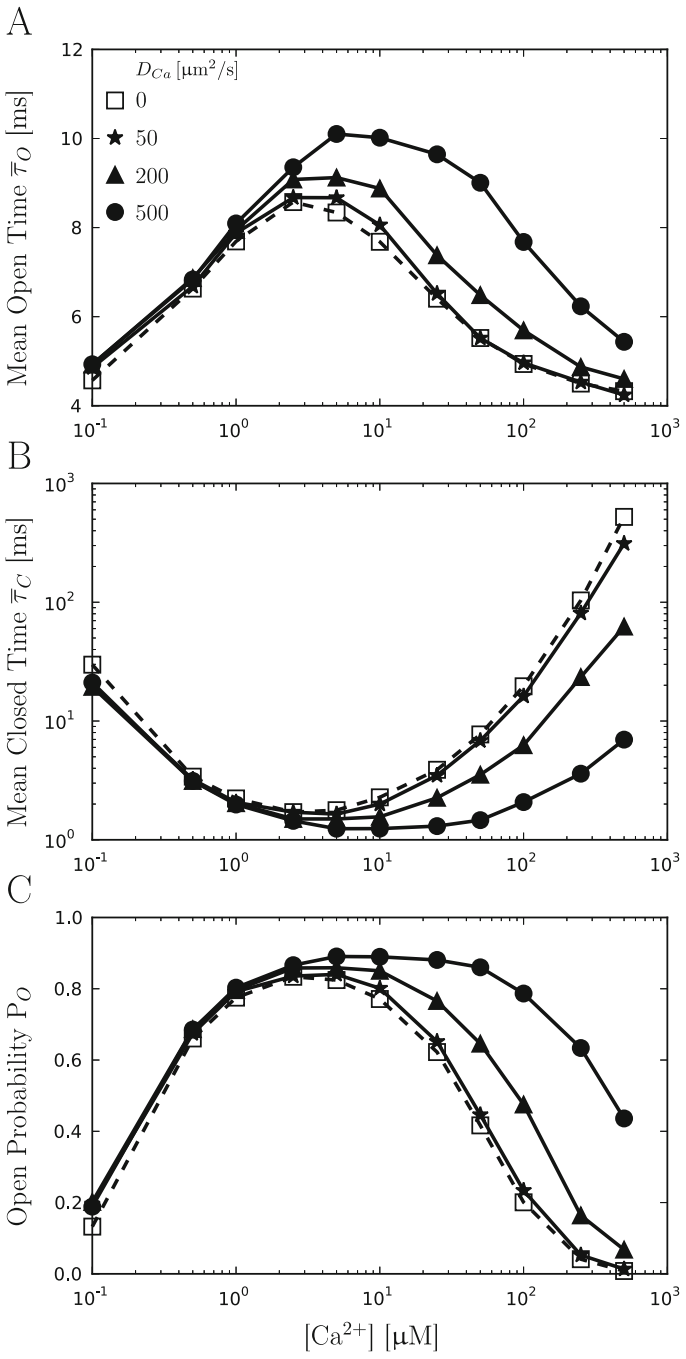

Fig. 31.1 Summary of the characteristic, bell shaped gating properties of the IP_3R for increasing diffusion coefficients D_{Ca}. Empty squares (dashed curve) show results for the zero noise model and represent expected results from deterministic algorithms. Solid curves show results for increasing diffusion coefficients $D_{Ca} = 50\,\mu m^2\,s^{-1}$ (stars), $200\mu m^2\,s^{-1}$ (triangles) and $500\mu m^2\,s^{-1}$ (circles). For low $[Ca^{2+}]$, Ca^{2+} noise has no obvious influence on the IP_3R. Starting at $[Ca^{2+}] = 1\,\mu M$, (**a**) mean open times τ_O increase with increasing D_{Ca}, whereas (**b**) mean close times τ_c decrease. (**c**) consequently, the channel open probability P_O increases with increasing D_{Ca}. (Reprint from [38])

this example emphasizes the importance of thermodynamic noise and its potential to scale up to the magnitude of intracellular signaling networks. We therefore have to keep in mind that, whenever low molecular copy numbers of key molecules meet nonlinear signaling effectors, deterministic assumptions might be limited and molecular noise has to be considered.

31.13 Working Examples

Example 1: We consider a simple system that contains Ca^{2+} ions and two buffers, called $B1$ and $B2$. The model geometry is given by a cube with a side length of 1 μm, i.e. the system volume is 1 *fl*. The copy numbers of the five molecular species, in the order $[Ca^{2+}, B_1, B_2, CaB_1, CaB_2]$ are stored in the state vector $X_t = [x_t^{(1)}, \ldots, x_t^{(5)}]$. We assume an equilibrium concentration of $[Ca^{2+}]_{eq} = 0.1\ \mu M$ (free Ca^{2+}), and total buffer concentrations of $[B_1]_T = [B_2]_T = 100\ \mu M$. To convert deterministic reaction rate constants into stochastic rate constants, we use the reaction propensities defined above (Sect. 31.10). Starting with the simulation box length l given in nm, we have $V = l^3 10^{-24}$ liters. Using Avogadro's number N_A, we get $c_{on} = k_{on}/(V{*}N_A{*}10^{-6})$ and $c_{off} = k_{off}$. The rate constants are set here to $k_1^+ = 0.1\ \mu M^{-1} ms^{-1}$, $k_1^- = 0.1 ms^{-1}$ for the reaction of Ca^{2+} and the first buffer B_1, and to $k_2^+ = 0.01\ \mu M^{-1} ms^{-1}$, $k_2^- = 0.01 ms^{-1}$ for the reaction of Ca^{2+} with the second buffer B_2. Thus, the four reactions read as follows.

Buffer 1:

$$Ca^{2+} + B_1 \rightarrow CaB_1$$

$$CaB_1 \rightarrow Ca^{2+} + B_1$$

Buffer 2:

$$Ca^{2+} + B_2 \rightarrow CaB_2$$

$$CaB_2 \rightarrow Ca^{2+} + B_2$$

The corresponding state change matrix $V = (v_{ji})$ contains the state change vector V_j at row index j, from which the stoichiometric coefficients can be read off directly:

$$V = \begin{pmatrix} -1 & -1 & 0 & 1 & 0 \\ 1 & 1 & 0 & -1 & 0 \\ -1 & 0 & -1 & 0 & 1 \\ 1 & 0 & 1 & 0 & -1 \end{pmatrix}$$

If we want to start the system in equilibrium, we obtain the initial state vector (after rounding) $X_0 = [60, 54755, 54755, 5476, 5476]$. The stochastic rate constants c_j are calculated as explained in the preceding paragraph and yield $c_1^+ = 1.66 * 10^{-4} ms^{-1}$, $c_1^- = 0.1 ms^{-1}$, $c_2^+ = 1.66 * 10^{-5} ms^{-1}$ and $c_2^- = 0.01 ms^{-1}$. For convenience, we adapted the notation using superscripts in order to better recognize the relation with macroscopic rate constants, i.e. c_1^+ is the stochastic rate constant associated with the macroscopic rate k_1^+. The time and state dependent propensities $a_j(X_t)$ are given by:

$$a_1(X_t) = c_1^+ x_t^{(1)} x_t^{(2)}$$

$$a_2(X_t) = c_1^- x_t^{(4)}$$

$$a_3(X_t) = c_2^+ x_t^{(1)} x_t^{(3)}$$

$$a_4(X_t) = c_2^- x_t^{(5)}$$

Finally, using the cumulative propensity $a_0(X_t) = a_1(X_t) + \cdots + a_4(X_t)$ and the initial state vector X_0, all parameters to run the Gillespie algorithm as defined above are given. Using the state change matrix and the propensities defined above, we obtain the corresponding chemical Langevin Eq. (31.6):

$$\begin{aligned} dx_t^{(1)} = &-a_1(X_t)\,dt - \sqrt{a_1(X_t)}\mathrm{d}W_t^{(1)} + a_2(X_t)\,dt + \sqrt{a_2(X_t)}dW_t^{(2)} \\ &-a_3(X_t)\,dt - \sqrt{a_3(X_t)}dW_t^{(3)} + a_4(X_t)\,dt + \sqrt{a_4(X_t)}dW_t^{(4)} \end{aligned}$$

$$dx_t^{(2)} = -a_1(X_t)\,dt - \sqrt{a_1(X_t)}dW_t^{(1)} + a_2(X_t)\,dt + \sqrt{a_2(X_t)}dW_t^{(2)}$$

$$dx_t^{(3)} = -a_3(X_t)\,dt - \sqrt{a_3(X_t)}dW_t^{(3)} + a_4(X_t)\,dt + \sqrt{a_4(X_t)}dW_t^{(4)}$$

$$dx_t^{(4)} = a_1(X_t)\,dt + \sqrt{a_1(X_t)}dW_t^{(1)} - a_2(X_t)\,dt - \sqrt{a_2(X_t)}dW_t^{(2)}$$

$$dx_t^{(5)} = a_3(X_t)\,dt + \sqrt{a_3(X_t)}dW_t^{(3)} - a_4(X_t)\,dt - \sqrt{a_4(X_t)}dW_t^{(4)}$$

Here, $dW_t^{(j)}$ represents the increments of four independent Brownian motions, i.e. each $dW_t^{(j)}$ is an independent and identically distributed Gaussian random process with mean zero and variance dt. A first-order, explicit Euler integration scheme is often satisfactory and allows a straightforward implementation of the above formulas in virtually any programming language. Sample code (Octave, Python) can be obtained from the authors.

Example 2: We consider a 1 fl single voxel system of diffusible Ca^{2+} ions and a single, immobile buffer B_1. The simulation volume is surrounded by a 'constant pool', i.e. an infinite volume with constant (equilibrium) calcium concentration. The state vector $X_t = [x_t^{(1)}, x_t^{(2)}, x_t^{(3)}]$ represents the copy numbers of $[Ca^{2+}, B_1, CaB_1]$. We again set $[Ca^{2+}]_{eq} = 0.1\ \mu M$, $[B_1]_T = 100\ \mu M$ and $k_1^+ = 0.1\mu M^{-1}ms^{-1}$, $k_1^- = 0.1ms^{-1}$ and set the diffusion coefficient of free calcium ions to $D_{Ca} = 200\ \mu m^2 s^{-1}$. Including the diffusion reactions of Ca^{2+} ions out of the simulation volume and influx of Ca^{2+} ions from the constant pool into the simulation volume, we get the following set of reactions.

Buffer 1:

$$Ca^{2+} + B_1 \rightarrow CaB_1$$

$$CaB_1 \rightarrow Ca^{2+} + B_1$$

Diffusion:

$$Ca^{2+} \rightarrow \varnothing$$

$$\varnothing \rightarrow Ca^{2+}$$

The state change matrix V now reads:

$$V = \begin{pmatrix} -1 & -1 & 1 \\ 1 & 1 & -1 \\ -1 & 0 & 0 \\ 1 & 0 & 0 \end{pmatrix}$$

Under equilibrium conditions, we obtain the initial state vector $X_0 = [60, 54755, 5476]$. The stochastic rate constants c_1^+ and c_1^- have the same magnitude as in the preceding example, and the stochastic diffusion rate c_D, calculated as explained in the preceding paragraph, evaluates to $c_D = 0.2\ ms^{-1}$. The diffusion propensities a_j are

$$a_3(X_t) = c_D x_t^{(1)}$$

$$a_4(X_t) = c_D x_0^{(1)}$$

Note that the rate $a_4(X_t)$ is constant as the surrounding calcium concentration is assumed to be fixed. The according chemical Langevin equation is

$$dx_t^{(1)} = -a_1(X_t)\,dt - \sqrt{a_1(X_t)}dW_t^{(1)} + a_2(X_t)\,dt + \sqrt{a_2(X_t)}dW_t^{(2)} - a_3(X_t)\,dt - \sqrt{a_3(X_t)}dW_t^{(3)} + a_4(X_t)\,dt + \sqrt{a_4(X_t)}dW_t^{(4)}$$

$$dx_t^{(2)} = -a_1(X_t)\,dt - \sqrt{a_1(X_t)}dW_t^{(1)} + a_2(X_t)\,dt + \sqrt{a_2(X_t)}dW_t^{(2)}$$

$$dx_t^{(3)} = a_1(X_t)\,dt + \sqrt{a_1(X_t)}dW_t^{(1)} - a_2(X_t)\,dt - \sqrt{a_2(X_t)}dW_t^{(2)}$$

Example 3: In the last example, we extend the system considered in Example 2 by a single ion channel that has a closed (C) and an open open substate (O) and conducts Ca^{2+} ions. It is convenient to model the two sub-states as different molecular species that can be transformed into each other. Obviously, the channel substate species are not diffusible. The state vector $X_t = [x_t^{(1)}, \ldots, x_t^{(5)}]$ represents the copy numbers of $[Ca^{2+}, B_1, CaB_1, C, O]$. As we consider a single ion channel, both $x_t^{(4)}$ and $x_t^{(5)}$ must be equal to either zero or one and $x_t^{(4)} + x_t^{(5)} = 1$ must be fulfilled at all times t. Introducing an extra reaction that models Ca^{2+} ion release from the O state (reaction 5), we extend the set of reactions introduced in the Example 2 by three ion channel related reactions.

Channel gating:

$$C \rightarrow O$$

$$O \rightarrow C$$

Calcium permeation:

$$O \rightarrow O + Ca^{2+}$$

The state change matrix V now reads:

$$\begin{pmatrix} -1 & -1 & 1 & 0 & 0 \\ 1 & 1 & -1 & 0 & 0 \\ -1 & 0 & 0 & 0 & 0 \\ 1 & 0 & 0 & 0 & 0 \\ 0 & 0 & 0 & -1 & 1 \\ 0 & 0 & 0 & 1 & -1 \\ 1 & 0 & 0 & 0 & 0 \end{pmatrix}$$

Reaction propensities for the new reactions are derived from the assumed channel kinetics and the channel permeability, respectively. As channel substate transitions are first-order reactions, we write $a_5(X_t) = c_{ch}^{+} x_t^{(4)}$ and $a_6(X_t) = c_{ch}^{-} x_t^{(5)}$ where $c_{ch}^{+} = k_{ch}^{+}$ and $c_{ch}^{-} = k_{ch}^{-}$ and k_{ch}^{+}, k_{ch}^{-} are the macroscopic rate constants for channel opening and closing as determined from electrophysiological measurements

for instance. Finally, Ca^{2+} ion release is modeled by $a_7(X_t) = c_P x_t^{(5)}$ with $c_P = I_{ch}/(2e)$.

In this case, it is important to note that a chemical Langevin equation approach cannot be applied because the system contains only a single ion channel and due to the use of normally distributed random numbers, negative values for $x_t^{(4)}$ or $x_t^{(5)}$ are highly probable. Negative copy numbers in turn lead to negative reaction propensities and render the square root terms in the CLE undefined.

31.14 Comparision of SSA and CLE Solutions

We ran $N = 20$ simulations of $T = 100\,ms$ length each, using an equilibrium calcium concentration of 0.1 $\mu mol/l$, a total buffer concentration of 10 $\mu mol/l$ and reaction rate constants of $k^+ = 0.5\ \mu mol/ms$ and $k^- = 0.25\ /ms$. To study the dependency of simulation accuracy and computation times on the simulation volume, we considered cubes of side length $L = 100$, 250, 500, 1000, 2500 and 5000 nm, corresponding to volumes of $V = 0.001$, 0.016, 0.125, 1.0, 15.625 and 125 fl, respectively. The CLE was numerically solved using a fixed integration time step of $dt = 0.01\ ms$ and an Euler-Maruyama integration scheme. As the basis of the SSA are randomly sampled time intervals between individual reactions, the generated time series of molecular counts are irregularly spaced. Before further processing, SSA-generated time series are linearly interpolated to the same sampling interval as the CLE solution, i.e. $dt = 0.01\ ms$.

Figure 31.2 shows four exemplary samples. The first two panels (A, B) show simulations of a small reaction volume ($L = 250\ nm$, $V = 1/64\ fl$). The upper panel

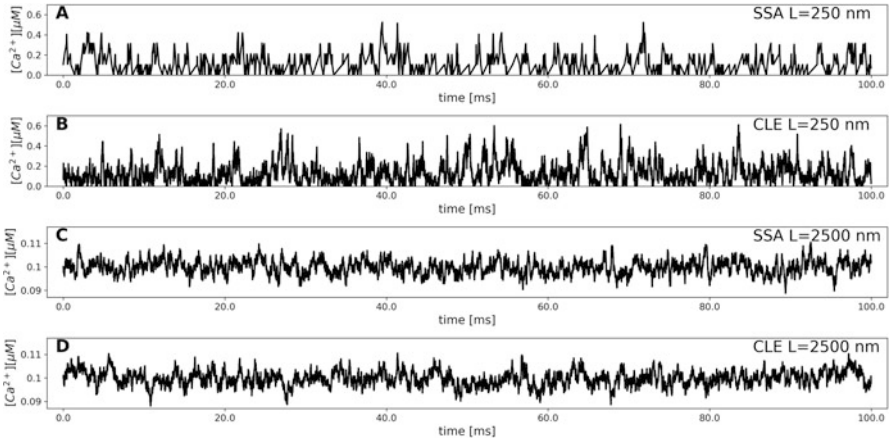

Fig. 31.2 Comparison between simulated 100 ms trajectories generated with either the SSA (A,C) or the CLE (B,D) approach for a small volume V = 1/64 fl and a large volume V = 15.625 fl

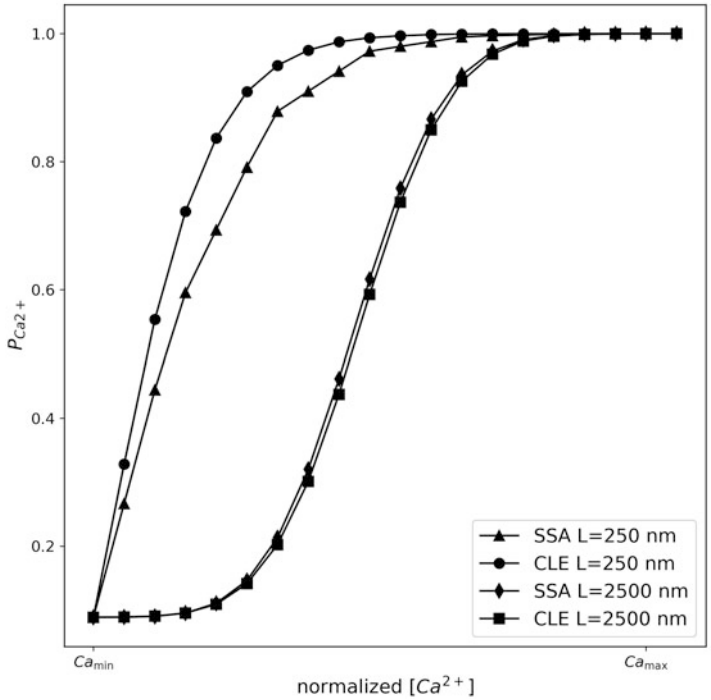

Fig. 31.3 Comparison of cumulative Ca^{2+} distributions from N = 20 simulation runs of the models presented in Fig. 31.2

shows the SSA solution, that is recognized by the discrete steps in the Ca^{2+} ion count. The corresponding CLE solution looks more continuous due to the small increments generated by the Brownian motion. We also observe that the Ca^{2+} concentration in both cases hits zero, indicating that the formal requirements of the CLE are not met for this small volume. Panels C (SSA) and D (CLE) show the case of a larger simulation volume ($L = 2500\ nm$, $V = 15.625\ fl$). Both solutions, SSA and CLE, are visually very similar and far from zero counts.

The accuracy of the two algorithms for the same volumes as shown in Fig. 31.2 is further analyzed in Fig. 31.3. To compare the algorithms, we plot the cumulative probability distribution of the calcium concentration (P_{Ca}), pooling the results of $N = 20$ simulations. To show the results of both simulation volumes in the same plot, we use a normalized calcium concentration on the abscissa. The values increase linearly from the minimum to the maximum calcium concentration obtained in each case. This visualization step is necessary as the width (or variance) of the calcium distribution for the larger volume is much smaller as that of the small reaction volume. We observe that the calcium distribution in the SSA and CLE solutions for the small volume (triangles and circles, respectively) differ to a larger degree than those in the large volume case (diamonds and squares, respectively).

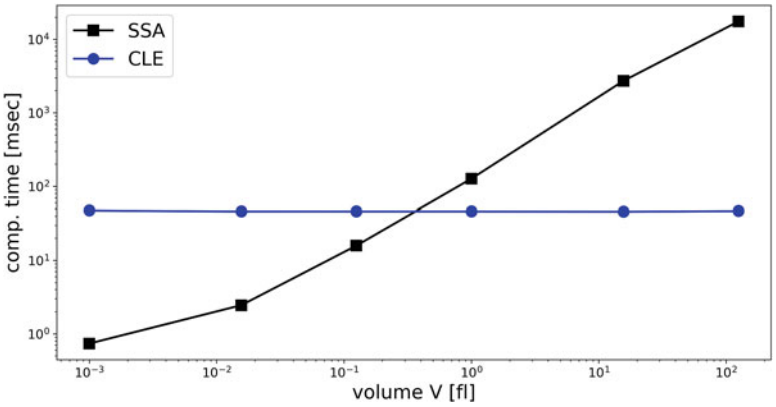

Fig. 31.4 Comparison of computation times between SSA (blue) and CLE (black) for increasing simulation volumes V

Taking the SSA solution as a reference, the difference of the CLE derived calcium distribution quantifies the accuracy of the CLE for a given volume. Even though a Kolmogorov-Smirnov test distinguishes the two solutions for both volumes, the better approximation for the larger simulation volume is clearly observed.

Finally, we address the computation times associated with both algorithms, SSA and CLE. Figure 31.4 shows the mean computation times of $N = 20$ simulations, as a function of the simulation volume, using the same parameters as given above. For the SSA algorithm, we expect the computation time to be approximately proportional to the number of molecules present in the simulation volume. For fixed concentrations, the computation time should therefore increase with the first power of the volume V, or with the third power of the simulation box length L, i.e. $T_c \sim L^3$. This increase is shown in log-log coordinates in Fig. 31.4 (black line and squares). A least-squares fit of L vs. T_c gives an empirical exponent of 2.7, comparable to the expected value of 3. The computation time of the CLE algorithm does not vary with the simulation volume, as expected for the Euler-Maruyama integration scheme with a fixed time interval dt (blue line and circles).

31.15 Outlook

Stochastic methods have received an increasing amount of attention in the modeling of subcellular signaling systems. Given the central role of calcium ions in the regulation of many cellular functions and the very low number of calcium ions present in the relevant volumes, e.g. a calcium concentration of 100 *nM* translates to some 60 calcium ions in a 1 μm^3 volume, surprisingly few studies model the stochastic effects of calcium diffusion and buffering in small volumes [34, 46]. Here, it is important to note that possibly important effects such as bistability of a signaling

pathway can even be missed completely when only deterministic dynamics are modeled [74]. The rising interest in simulating large systems with several interacting subsystems in some of which deterministic dynamics may dominate while in others stochastic effects may be important will lead to novel approaches combining deterministic and stochastic simulations. Most importantly, the validity of different approaches on a given scale will have to be evaluated for numerous experimental systems. At the same time, stochastic models of subcellular reactions will help to estimate the parameters of experimentally recorded signals, in which stochastic effects are uncovered thanks to technical advances such as high-resolution laser microscopy.

References

1. Clapham DE (2007) Calcium Signaling. Cell 131:1047–1058
2. Berridge MJ (2006) Calcium microdomains: organization and function. Cell Calcium 40:405–412. https://doi.org/10.1016/j.ceca.2006.09.002
3. Rizzuto R, Pozzan T (2006) Microdomains of intracellular ca 2+ : molecular determinants and functional consequences. Physiol Rev 86:369–408. https://doi.org/10.1152/physrev.00004.2005
4. Martín F, Soria B (1996) Glucose-induced [Ca^{2+}]i oscillations in single human pancreatic islets. Cell Calcium 20:409–414. https://doi.org/10.1016/S0143-4160(96)90003-2
5. Jaffe LF (1999) Organization of early development by calcium patterns. BioEssays 21:657–667
6. Giorgi C, Missiroli S, Patergnani S et al (2015) Mitochondria-associated membranes: composition, molecular mechanisms, and physiopathological implications. Antioxid Redox Signal 22(12):995–1019. https://doi.org/10.1089/ars.2014.6223
7. Rieusset J, Fauconnier J, Paillard M et al (2016) Disruption of calcium transfer from ER to mitochondria links alterations of mitochondria-associated ER membrane integrity to hepatic insulin resistance. Diabetologia 59:614–623. https://doi.org/10.1007/s00125-015-3829-8
8. Orrenius S, Zhivotovsky B, Nicotera P (2003) Regulation of cell death: the calcium-apoptosis link. Nat Rev Mol Cell Biol 4:552–565
9. Myoga MH, Regehr WG (2011) Calcium microdomains near R-type calcium channels control the induction of presynaptic long-term potentiation at parallel Fiber to Purkinje cell synapses. J Neurosci 31:5235–5243. https://doi.org/10.1523/JNEUROSCI.5252-10.2011
10. von Wegner F, Wieder N, Fink RHA (2014) Microdomain calcium fluctuations as a colored noise process. Front Genet 5:376. https://doi.org/10.3389/fgene.2014.00376
11. Keller DX, Franks KM, Bartol TM, Sejnowski TJ (2008) Calmodulin activation by calcium transients in the postsynaptic density of dendritic spines. PLoS One 3:e2045. https://doi.org/10.1371/journal.pone.0002045
12. Zeng S, Holmes WR (2010) The effect of noise on CaMKII activation in a dendritic spine during LTP induction. J Neurophysiol 103:1798–1808. https://doi.org/10.1152/jn.91235.2008
13. Berridge MJ (2009) Inositol trisphosphate and calcium signalling mechanisms. Biochim Biophys Acta, Mol Cell Res 1793:933–940
14. Gardiner CW (1996) Handbook of stochastic methods: for physics, chemistry and the natural sciences, Springer series in synergetics. Springer, Berlin
15. Gillespie DT (2007) Stochastic simulation of chemical kinetics. Annu Rev Phys Chem 58:35–55. https://doi.org/10.1146/annurev.physchem.58.032806.104637
16. Higham DJ (2008) Modeling and simulating chemical reactions. SIAM Rev 50:347–368. https://doi.org/10.1137/060666457

17. Higham DJ, Higham DJ (2001) An algorithmic introduction to numerical simulation of stochastic differential equations. SIAM Rev 43:525–546. https://doi.org/10.1137/S0036144500378302
18. Bezprozvanny I, Watras J, Ehrlich BE (1991) Bell-shaped calcium-response curves of lns(l,4,5)P3- and calcium-gated channels from endoplasmic reticulum of cerebellum. Nature 351:751–754. https://doi.org/10.1038/351751a0
19. Mak D-OD, McBride S, Foskett JK (1998) Inositol 1,4,5-tris-phosphate activation of inositol tris-phosphate receptor Ca^{2+} channel by ligand tuning of Ca^{2+} inhibition. Proc Natl Acad Sci 95:15821–15825. https://doi.org/10.1073/pnas.95.26.15821
20. Andrews SS, Bray D (2004) Stochastic simulation of chemical reactions with spatial resolution and single molecule detail. Phys Biol 1:137–151. https://doi.org/10.1088/1478-3967/1/3/001
21. Franks KM, Bartol TM, Sejnowski TJ (2002) A Monte Carlo model reveals independent signaling at central glutamatergic synapses. Biophys J 83:2333–2348. https://doi.org/10.1016/S0006-3495(02)75248-X
22. Shahrezaei V, Delaney KR (2004) Consequences of molecular-level Ca^{2+} channel and synaptic vesicle colocalization for the Ca^{2+} microdomain and neurotransmitter exocytosis: a Monte Carlo study. Biophys J 87:2352–2364. https://doi.org/10.1529/biophysj.104.043380
23. Tanskanen AJ, Greenstein JL, O'Rourke B, Winslow RL (2005) The role of stochastic and modal gating of cardiac L-type Ca^{2+} channels on early after-depolarizations. Biophys J 88:85–95. https://doi.org/10.1529/biophysj.104.051508
24. Hake J, Lines GT (2008) Stochastic binding of Ca^{2+} ions in the dyadic cleft; continuous versus random walk description of diffusion. Biophys J 94:4184–4201. https://doi.org/10.1529/biophysj.106.103523
25. Flegg MB, Rüdiger S, Erban R (2013) Diffusive spatio-temporal noise in a first-passage time model for intracellular calcium release. J Chem Phys 138:154103. https://doi.org/10.1063/1.4796417
26. Dobramysl U, Rüdiger S, Erban R (2016) Particle-based multiscale modeling of calcium puff dynamics. Multiscale Model Simul 14:997–1016. https://doi.org/10.1137/15M1015030
27. Nguyen V, Mathias R, Smith GD (2005) A stochastic automata network descriptor for Markov chain models of instantaneously coupled intracellular Ca^{2+}channels. Bull Math Biol 67:393–432. https://doi.org/10.1016/j.bulm.2004.08.010
28. Munsky B, Khammash M (2006) The finite state projection algorithm for the solution of the chemical master equation. J Chem Phys 124:044104. https://doi.org/10.1063/1.2145882
29. Gillespie DT (1977) Exact stochastic simulation of coupled chemical reactions. J Phys Chem 81:2340–2361. https://doi.org/10.1021/j100540a008
30. Gibson MA, Bruck J (2000) Efficient exact stochastic simulation of chemical systems with many species and many channels. J Phys Chem A 104:1876–1889. https://doi.org/10.1021/jp993732q
31. Weinberg SH (2016) Microdomain [ca 2+] fluctuations Alter temporal dynamics in models of ca 2+ −dependent signaling cascades and synaptic vesicle release. Neural Comput 28:493–524. https://doi.org/10.1162/NECO_a_00811
32. Li H, Hou Z, Xin H (2005) Internal noise stochastic resonance for intracellular calcium oscillations in a cell system. Phys Rev E Stat Nonlin Soft Matter Phys 71:061916. https://doi.org/10.1103/PhysRevE.71.061916
33. Kummer U, Krajnc B, Pahle J et al (2005) Transition from stochastic to deterministic behavior in calcium oscillations. Biophys J 89:1603–1611. https://doi.org/10.1529/biophysj.104.057216
34. Von Wegner F, Fink RHA (2010) Stochastic simulation of calcium microdomains in the vicinity of an L-type calcium channel. Eur Biophys J 39:1079–1088
35. Gillespie DT (2000) Chemical Langevin equation. J Chem Phys 113:297–306. https://doi.org/10.1063/1.481811
36. Cao Y, Gillespie DT, Petzold LR (2006) Efficient step size selection for the tau-leaping simulation method. J Chem Phys 124:044109. https://doi.org/10.1063/1.2159468

37. Tian T, Burrage K (2004) Binomial leap methods for simulating stochastic chemical kinetics. J Chem Phys 121:10356–10364. https://doi.org/10.1063/1.1810475
38. Wieder N, Fink R, Von Wegner F (2015) Exact stochastic simulation of a calcium microdomain reveals the impact of Ca^{2+} fluctuations on IP3R gating. Biophys J 108:557–567. https://doi.org/10.1016/j.bpj.2014.11.3458
39. Goldwyn JH, Imennov NS, Famulare M, Shea-Brown E (2011) Stochastic differential equation models for ion channel noise in Hodgkin-Huxley neurons. Phys Rev E Stat Nonlin Soft Matter Phys 83:041908. https://doi.org/10.1103/PhysRevE.83.041908
40. Dangerfield CE, Kay D, Burrage K (2012) Modeling ion channel dynamics through reflected stochastic differential equations. Phys Rev E Stat Nonlin Soft Matter Phys 85:051907. https://doi.org/10.1103/PhysRevE.85.051907
41. Alfonsi A (2005) On the discretization schemes for the CIR (and Bessel squared) processes. Monte Carlo Methods Appl 11:355–384. https://doi.org/10.1163/156939605777438569
42. Manninen T, Linne M-L, Ruohonen K (2006) Developing Itô stochastic differential equation models for neuronal signal transduction pathways. Comput Biol Chem 30:280–291. https://doi.org/10.1016/j.compbiolchem.2006.04.002
43. Zhang J, Hou Z, Xin H (2004) System-size biresonance for intracellular calcium signaling. ChemPhysChem 5:1041–1045. https://doi.org/10.1002/cphc.200400089
44. lian ZC, Jia Y, Liu Q et al (2007) A mesoscopic stochastic mechanism of cytosolic calcium oscillations. Biophys Chem 125:201–212. https://doi.org/10.1016/j.bpc.2006.08.001
45. Wang X, Hao Y, Weinberg SH, Smith GD (2015) $Ca^{2+}-$activation kinetics modulate successive puff/spark amplitude, duration and inter-event-interval correlations in a Langevin model of stochastic Ca^{2+}release. Math Biosci 264:101–107. https://doi.org/10.1016/j.mbs.2015.03.012
46. Winslow RL, Tanskanen A, Chen M, Greenstein JL (2006) Multiscale modeling of calcium signaling in the cardiac dyad. Ann NY Acad Sci 1080:362–375
47. Soeller C, Cannell MB (1997) Numerical simulation of local calcium movements during L-type calcium channel gating in the cardiac diad. Biophys J 73:97–111. https://doi.org/10.1016/S0006-3495(97)78051-2
48. Cannell MB, Soeller C (1997) Numerical analysis of ryanodine receptor activation by L-type channel activity in the cardiac muscle diad. Biophys J. doi: S0006-3495(97)78052-4 [pii]\r10.1016/S0006-3495(97)78052-4, vol 73, pp 112–122
49. Smith GD, Keizer JE, Stern MD et al (1998) A simple numerical model of calcium spark formation and detection in cardiac myocytes. Biophys J 75:15–32. https://doi.org/10.1016/S0006-3495(98)77491-0
50. Jiang YH, Klein MG, Schneider MF (1999) Numerical simulation of Ca^{2+} "sparks" in skeletal muscle. Biophys J 92:308–332. https://doi.org/10.1016/j.pbiomolbio.2005.05.016
51. Baylor SM, Hollingworth S (2007) Simulation of ca $^{2+}$ movements within the sarcomere of fast-twitch mouse fibers stimulated by action potentials. J Gen Physiol 130:283–302. https://doi.org/10.1085/jgp.200709827
52. Stern MD, Pizarro G, Ríos E (1997) Local control model of excitation-contraction coupling in skeletal muscle. J Gen Physiol 110:415–440. https://doi.org/10.1085/jgp.110.4.415
53. Greenstein JL, Winslow RL (2002) An integrative model of the cardiac ventricular myocyte incorporating local control of Ca^{2+} release. Biophys J 83:2918–2945. https://doi.org/10.1016/S0006-3495(02)75301-0
54. Rüdiger S, Shuai JW, Huisinga W et al (2007) Hybrid stochastic and deterministic simulations of calcium blips. Biophys J 93:1847–1857. https://doi.org/10.1529/biophysj.106.099879
55. Kalantzis G (2009) Hybrid stochastic simulations of intracellular reaction-diffusion systems. Comput Biol Chem 33:205–215. https://doi.org/10.1016/j.compbiolchem.2009.03.002
56. Choi T, Maurya MR, Tartakovsky DM, Subramaniam S (2010) Stochastic hybrid modeling of intracellular calcium dynamics. J Chem Phys 133:165101. https://doi.org/10.1063/1.3496996
57. Krishnamurthy V, Chung SH (2007) Large-scale dynamical models and estimation for permeation in biological membrane ion channels. Proc IEEE 95:853–880. https://doi.org/10.1109/JPROC.2007.893246

58. Elf J, Doncic A, Ehrenberg M (2003) Mesoscopic reaction-diffusion in intracellular signaling. In: Bezrukov S, Frauenfelder H, Moss F (eds) Fluctuations and noise in biological, biophysical, and biomedical systems. Proceedings of the SPIE, pp 114–124
59. Weinberg SH, Smith GD (2014) The influence of Ca^{2+} buffers on free $[Ca^{2+}]$ fluctuations and the effective volume of Ca^{2+} microdomains. Biophys J 106:2693–2709. https://doi.org/10.1016/j.bpj.2014.04.045
60. Sherman A, Smith GD, Dai L, Miura RM (2001) Asymptotic analysis of buffered calcium diffusion near a point source. SIAM J Appl Math 61:1816–1838. https://doi.org/10.1137/S0036139900368996
61. Li QS, Wang P (2004) Internal signal stochastic resonance induced by colored noise in an intracellular calcium oscillations model. Chem Phys Lett 387:383–387. https://doi.org/10.1016/j.cplett.2004.02.042
62. Blomberg C (2006) Fluctuations for good and bad: the role of noise in living systems. Phys Life Rev 3:133–161
63. Faisal AA, Selen LPJ, Wolpert DM (2008) Noise in the nervous system. Nat Rev Neurosci 9:292–303
64. Zhong S, Qi F, Xin H (2001) Internal stochastic resonance in a model system for intracellular calcium oscillations. Chem Phys Lett 342:583–586. https://doi.org/10.1016/S0009-2614(01)00625-X
65. Thul R, Falcke M (2004) Release currents of IP3 Receptor Channel clusters and concentration profiles. Biophys J 86:2660–2673. https://doi.org/10.1016/S0006-3495(04)74322-2
66. Skupin A, Falcke M (2009) From puffs to global Ca^{2+} signals: how molecular properties shape global signals. Chaos 19:037111. https://doi.org/10.1063/1.3184537
67. Marchant JS, Parker I (2001) Role of elementary Ca^{2+} puffs in generating repetitive Ca^{2+} oscillations. EMBO J 20:65–76. https://doi.org/10.1093/emboj/20.1.65
68. De Young GW, Keizer J (1992) A single-pool inositol 1,4,5-trisphosphate-receptor-based model for agonist-stimulated oscillations in Ca^{2+} concentration. Proc Natl Acad Sci 89:9895–9899. https://doi.org/10.1073/pnas.89.20.9895
69. Ullah G, Daniel Mak D-O, Pearson JE (2012) A data-driven model of a modal gated ion channel: the inositol 1,4,5-trisphosphate receptor in insect Sf9 cells. J Gen Physiol 140:159–173. https://doi.org/10.1085/jgp.201110753
70. Siekmann I, Wagner LE, Yule D et al (2012) A kinetic model for type i and II IP3R accounting for mode changes. Biophys J 103:658–668. https://doi.org/10.1016/j.bpj.2012.07.016
71. Xu T, Yu X, Perlik AJ et al (2009) Rapid formation and selective stabilization of synapses for enduring motor memories. Nature 462:915–919. https://doi.org/10.1038/nature08389
72. Bers DM (2002) Cardiac excitation contraction coupling. Nature 415:198–215. https://doi.org/10.1016/B978-0-12-378630-2.00221-8
73. Bers DM, Despa S (2013) Cardiac excitation-contraction coupling. In: Lennarz WJ, Lane MD (eds) The Encyclopedia of biological chemistry, 2nd edn. Academic Press, Waltham, MA, pp 379–383
74. Artyomov MN, Das J, Kardar M, Chakraborty AK (2007) Purely stochastic binary decisions in cell signaling models without underlying deterministic bistabilities. Proc Natl Acad Sci U S A 104:18958–18963. https://doi.org/10.1073/pnas.0706110104

Chapter 32
A Statistical View on Calcium Oscillations

Jake Powell, Martin Falcke, Alexander Skupin, Tomas C. Bellamy, Theodore Kypraios, and Rüdiger Thul

Abstract Transient rises and falls of the intracellular calcium concentration have been observed in numerous cell types and under a plethora of conditions. There is now a growing body of evidence that these whole-cell calcium oscillations are stochastic, which poses a significant challenge for modelling. In this review, we take a closer look at recently developed statistical approaches to calcium oscillations. These models describe the timing of whole-cell calcium spikes, yet their parametrisations reflect subcellular processes. We show how non-stationary calcium spike sequences, which e.g. occur during slow depletion of intracellular calcium stores or in the presence of time-dependent stimulation, can be analysed with the help of so-called intensity functions. By utilising Bayesian concepts, we demonstrate how values of key parameters of the statistical model can be inferred from single cell calcium spike sequences and illustrate what information whole-cell statistical models can provide about the subcellular mechanistic processes that drive calcium oscillations. In particular, we find that the interspike interval distribution of HEK293 cells under constant stimulation is captured by a Gamma distribution.

J. Powell · T. Kypraios · R. Thul (✉)
Centre for Mathematical Medicine and Biology, School of Mathematical Sciences, University of Nottingham, Nottingham, UK
e-mail: pmxjp8@exmail.nottingham.ac.uk; theodore.kypraios@nottingham.ac.uk; ruediger.thul@nottingham.ac.uk

M. Falcke
Max Delbrück Centre for Molecular Medicine, Berlin, Germany

Department of Physics, Humboldt University, Berlin, Germany
e-mail: martin.falcke@mdc-berlin.de

A. Skupin
Luxembourg Centre for Systems Biomedicine, University of Luxembourg, Belval, Luxembourg

National Biomedical Computation Resource, University California San Diego, La Jolla, CA, USA
e-mail: alexander.skupin@uni.lu

T. C. Bellamy
School of Life Sciences, University of Nottingham, Nottingham, UK
e-mail: tomas.bellamy@nottingham.ac.uk

M. S. Islam (ed.), *Calcium Signaling*, Advances in Experimental Medicine and Biology 1131, https://doi.org/10.1007/978-3-030-12457-1_32

Keywords Calcium spikes · Bayesian inference · Intensity functions · Heterogeneous cell populations

32.1 Introduction

Calcium (Ca^{2+}) oscillations have long been recognised as a centrepiece in the world of intracellular Ca^{2+} signals [1–9]. Acting as a ubiquitous and versatile signalling mechanism, Ca^{2+} oscillations are responsible for inducing gene expression [10–12], controlling hormone secretion [13–17], orchestrating fertilisation [18–20] and steering bacterial invasion [21], to name but a few cellular functions. The notion of Ca^{2+} oscillations usually refers to transient increases in the whole-cell Ca^{2+} concentration that present themselves as a series of Ca^{2+} spikes. Since whole-cell calcium recordings yield averaged concentration values, it has often been assumed that mathematical models of intracellular Ca^{2+} oscillations can be directly based on the averaged Ca^{2+} concentration. To illustrate this concept, consider Ca^{2+} oscillations driven by Ca^{2+} release from the endoplasmic reticulum (ER) through inositol-1,4,5-trisphosphate ($InsP_3$) receptors ($InsP_3Rs$). In its simplest incarnation, these mathematical models assume that Ca^{2+} transport through all open $InsP_3Rs$ and the activity of all sarco-endoplasmic Ca^{2+} ATP (SERCA) pumps can be averaged across the cell to yield averaged Ca^{2+} release and resequestration, respectively. Since the activity of both $InsP_3Rs$ and SERCA pumps depends on the cytosolic Ca^{2+} concentration, these models implicitly assume that the gating of $InsP_3Rs$ and SERCA pumps is controlled by averaged Ca^{2+} concentration values.

This assumption may serve as a starting point to explore Ca^{2+} dynamics in systems for which detailed Ca^{2+} measurements are missing, and models based on averaged Ca^{2+} concentrations have been instrumental in furthering our understanding of Ca^{2+} oscillations [13, 16, 22–48]. However, the notion of mean Ca^{2+} values generally falls short of capturing the biology that underlies Ca^{2+} oscillations. The main reason for this is that $InsP_3Rs$ form clusters that are distributed throughout the cell at distances of 2–7μm [49–53]. This entails that the dynamics of $InsP_3Rs$ is controlled by the *local* Ca^{2+} concentration, not a global average. In other words, measuring the Ca^{2+} concentration across a cell, taking the spatial average and determining the gating of all $InsP_3Rs$ subject to the averaged Ca^{2+} concentration misrepresents the actual $InsP_3R$ dynamics. In addition, there are only a few tens of $InsP_3Rs$ per cluster [54–56]. Since binding of Ca^{2+} and $InsP_3$ to $InsP_3Rs$ is random and hence transitions between different states of the $InsP_3R$ occur stochastically, the relative fluctuation in the number of open $InsP_3Rs$ is considerable. This stochasticity might even be enhanced by the fact that at basal Ca^{2+} concentration, the actual numbers of Ca^{2+} ions in the vicinity of an $InsP_3$ is small [57–60]. Taken together, these observations strongly suggest that intracellular Ca^{2+} is a spatially extended stochastic medium, which prompts the question on how to best describe $InsP_3$ mediated Ca^{2+} oscillations mathematically.

One approach starts with the dynamics of single $InsP_3Rs$, groups them into clusters and then places the clusters into a three-dimensional representation of the

cytosol—see [61] for a recent perspective. In these models, $InsP_3Rs$ are described by stochastic models known as Markov chains, which consist of different states of the $InsP_3R$ such as open, closed and inhibited and contain rules for stochastic transitions between different states. Clusters of $InsP_3Rs$ communicate with each other through Ca^{2+} diffusion. One advantage of such hierarchical modelling lies in its mechanistic interpretation. It allows questions to be answered about how Ca^{2+} oscillations are shaped by e.g. the distance between $InsP_3R$ clusters, single channel current and Ca^{2+} buffers. However, these models require as input a significant number of parameters, such as gating constants for the $InsP_3R$, and are computationally expensive. In order to reduce the computational load, Langevin-type models have been put forward. In essence, they approximate the exact stochastic dynamics of the Markov chains.

In terms of modelling philosophy, the above approaches fall into the category of bottom-up techniques. At the other end of the spectrum lie so-called top-down methods. Here, we construct models that directly describe key properties of Ca^{2+} spikes such as amplitude and frequency without explicitly incorporated mechanistic details as e.g. the possible states of an $InsP_3R$. At first sight, this might appear less advantageous as different model behaviours cannot immediately be linked to specific molecular processes. However, there are distinct advantages. Firstly, the computational demand is significantly lower than with bottom-up approaches. This puts us in an ideal position to generate large numbers of realistic Ca^{2+} spike sequences, which in turn can serve as input to signalling cascades that decode Ca^{2+} spikes. Secondly, top-down models provide a powerful framework for fitting data and testing hypotheses on Ca^{2+} spike generation. Consequentially, we can use the knowledge gained from top-down models to improve bottom-up approaches, which in turn will advance our mechanistic understanding of Ca^{2+} oscillations.

In this review, we present the current state of statistical modelling of Ca^{2+} oscillations. The techniques that we employ are well established amongst statisticians, but are less familiar to modellers and experimentalists in the field of Ca^{2+} signalling. We therefore mainly focus on describing the underlying concepts and how they are related to the physiology of Ca^{2+} signalling. We discuss practical approaches for how to ascertain whether our statistical assumptions are consistent with measured Ca^{2+} spike sequences and what we can learn from our statistical analysis regarding the mechanisms that underlie Ca^{2+} spike generation.

32.2 Interspike Interval Statistics

We outlined in the introduction the mechanistic reasons for why Ca^{2+} oscillations are stochastic. At this point, one might argue—as is often done—that the molecular fluctuations present at $InsP_3R$ clusters average out at the whole-cell level. In other words, since a cell can contain a large number of $InsP_3R$ clusters, the stochastic contributions cancel. To test this hypothesis, Skupin et al [62] measured spontaneous Ca^{2+} oscillations in microglia, astrocytes and PLA cells as well as carbachol-induced oscillations in HEK293 cells. They found that their data is

consistent with stochastic whole-cell Ca^{2+} oscillations, which was also confirmed in later experiments [63]. This conclusion rests on results as shown in Fig. 32.1. We plot representative fluorescence traces for carbachol stimulated HEK293 cells in Fig. 32.1a, b. Cells were initially stimulated with 20 μM carbachol before the solution was switched to 50 μM carbachol. Figure 32.1a illustrates the well-known phenomenon of frequency encoding, by which the frequency of Ca^{2+} oscillations increases with an increase in stimulation strength. In Fig. 32.1c we plot the Ca^{2+} spike times for a larger number of cells. If Ca^{2+} oscillations were deterministic and governed by averaged Ca^{2+} concentrations, we would expect an almost constant spread of Ca^{2+} spike times, i.e. an almost constant value for the interspike interval (ISI), not the observed large variability, which is present at both stimulation strengths. Our argument for stochastic Ca^{2+} oscillations is further strengthened by the results shown in Fig. 32.1d. Here, each triangle corresponds to a sequence of Ca^{2+} spikes from one cell and denotes its mean μ and its standard deviation σ. We observe that the standard deviation is of the same magnitude as the mean, which is another strong indicator of stochastic behaviour. Importantly, similar results have been obtained for a number of additional cell types and under different conditions [61, 62], which lends even more support for the stochasticity of Ca^{2+} oscillations. Given the insights that $\sigma - \mu$ plots can provide into the nature of Ca^{2+} oscillations, we have recently released CaSiAn [64], a user friendly tool that allows for automatic ISI detection from fluorescence time course data and interactive investigation of the relationship between μ and σ.

To appreciate the fact that μ and σ are of the same order of magnitude, we introduce a key concept for this review: the conditional Ca^{2+} spike intensity $q(t|s)$, $t > s$. Based on it, we obtain the conditional Ca^{2+} spike probability $q(t|s)\mathrm{d}t$, which represents the probability to observe a Ca^{2+} spike in the time interval $[t, t + \mathrm{d}t]$ given a Ca^{2+} spike at time s. In [62], the following ansatz was made:

$$q(t|s) = \begin{cases} 0\,, & s \le t \le T_r + s\,, \\ \lambda\left[1 - \mathrm{e}^{-\xi(t-s-T_r)}\right], & T_r + s \le t\,. \end{cases} \tag{32.1}$$

Here, T_r denotes the cellular refractory period. Numerous experiments have shown that there exists a minimal amount of time T_r after a Ca^{2+} spike before another Ca^{2+} spike can be triggered [62, 63, 66]. Therefore, the conditional intensity vanishes, i.e. $q = 0$, for a time T_r after the last Ca^{2+} spike. It is important to note that T_r is significantly longer than the recovery time of $InsP_3Rs$ [63]. Once the refractory period has passed, the conditional intensity for a Ca^{2+} spike starts to increase at a rate ξ and eventually approaches an equilibrium value λ. This reflects the notion that a cell has to recover from the last Ca^{2+} spike. While ξ is a single number, it subsumes numerous recovery processes such as refilling of the ER or replenishment of $InsP_3$ following degradation by $InsP_3$-3-kinase and $InsP_3$-5-phosphatase. The values of T_r, ξ and λ can be directly inferred from Fig. 32.1d as outlined below. Due to the strong linear relationship between the mean and the standard deviation, we posit that

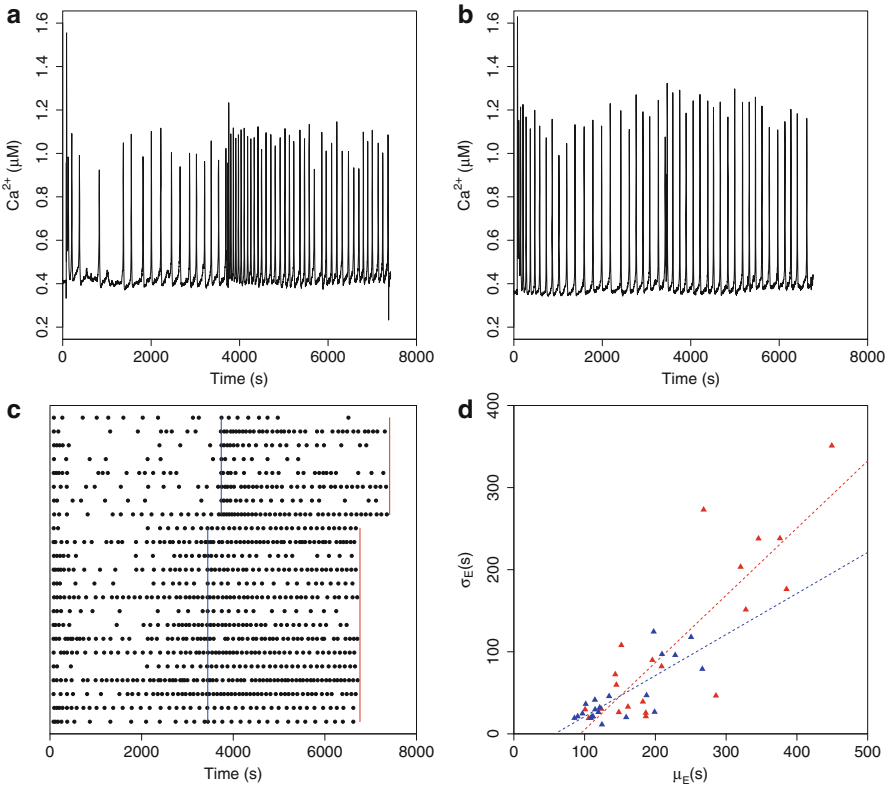

Fig. 32.1 (**a**, **b**) Fura-2 fluorescence intensity traces of two HEK293 cells stimulated first with 20 μM carbachol and then with 50 μM carbachol. The solution was exchanged at 3738s in (**a**) and at 3444s in (**b**). (**c**) Raster plot of Ca^{2+} spike times for the same stimulus protocol as in (**a**, **b**). The blue line indicates solution exchange and the red line denotes the end of the experiment. (**d**) Relationship between the standard deviation σ_E and the mean μ_E for the data shown in (**c**). Each triangle corresponds to data from one cell, and the line is the best linear fit. Red refers to 20 μM carbachol, and blue to 50 μM carbachol. (For details of the experiments see [65])

$$\sigma = \alpha(\mu - T_r)\,, \tag{32.2}$$

a relationship that has been shown to hold true for another 8 cell types and 10 conditions (see [61] for further discussion). When the standard deviation equals zero, successive Ca^{2+} spikes are separated by a constant period. Such Ca^{2+} spike sequences appear deterministic since there is no variation in the ISI, but the interpretation is different. The lack of ISI variability results from the fact that when the Ca^{2+} spike generation probability is high, i.e. λ is large, a Ca^{2+} spike is initiated as soon as the cell exits its refractory period. Therefore, the mean of the ISI distribution at a vanishing standard deviation equals T_r. This corresponds to the intersections of the red and blue lines with the x-axis in Fig. 32.1d, respectively. To

determine ξ and λ, we start from Eq. (32.1) and derive the ISI probability density $f(t, s)$, i.e. the probability density for Ca^{2+} spikes to occur at times t and s. This is equivalent to the probability of a Ca^{2+} spike at t given that the last spike occurred at s and no Ca^{2+} spike during the time $(s - t)$. Based on this interpretation of the ISI probability, we obtain

$$f(t, s) = q(t|s) \exp\left\{-\int_s^t q(u|s)\mathrm{d}u\right\}, \tag{32.3}$$

where the exponential term corresponds to the absence of Ca^{2+} spikes between s and t. The mean μ and the standard deviation σ of the ISI distribution then follow from Eq. (32.3) as

$$\mu = \int_0^\infty t f(t, 0)\mathrm{d}t\,, \qquad \sigma^2 = \int_0^\infty t^2 f(t, 0)\mathrm{d}t - \mu^2\,. \tag{32.4}$$

For practical purposes, we can set $T_r = 0$ in the computation of μ and σ, since a constant T_r only shifts the mean and does not affect the standard deviation. To put it another way, we evaluate Eq. (32.4) for $T_r = 0$ and then add T_r to obtain the mean ISI μ. Next, we fit the equations in (32.4) to data such as shown in Fig. 32.1d to obtain cell specific values for ξ and λ. This is achieved in a two-step process. Firstly, we determine the experimental mean μ_E and standard deviation σ_E from individual Ca^{2+} spike sequences as shown in Fig. 32.1c. This gives one data point in Fig. 32.1d. Since μ and σ^2 in Eq. (32.4) depend on ξ and λ through $f(t, 0)$ via $q(t|s)$, we can perform a least square fit of Eq. (32.4) to the experimental data μ_E and σ_E to obtain single cell estimates for ξ and λ. Figure 32.2a, b display results for HEK293 cells stimulated with 30 μM carbachol. While the distribution for ξ exhibits a localised peak, the distribution of λ is much broader. A similar behaviour is observed for spontaneously spiking astrocytes as seen in Fig. 32.2c, d. A comparison of the Ca^{2+} spike rate λ reveals that it is almost an order of magnitude larger for HEK293 cells than for astrocytes, which might be attributed to the fact that the former is stimulated, but the latter is not. Intriguingly, the time scale for recovery ξ is almost 10-fold larger for HEK293 cells than for astrocytes, indicating that HEK293 cells recover more slowly than astrocytes after a Ca^{2+} spike. The existence of wide distributions for ξ and λ also points towards significant cell-to-cell variability, which provides another argument in favour of a statistical description of Ca^{2+} spikes.

It is now instructive to evaluate Eq. (32.4) for a constant conditional intensity function $q = r > 0$, which corresponds to a homogenous Poisson process. It emerges from the general form of the conditional intensity function in Eq. (32.1) in the limit of fast recovery, i.e. a large value of ξ. In this case, the integrals can be computed analytically and we obtain $\mu = \sigma = r$, which is consistent with the scaling in Eq. (32.2). This provides further intuition for the statement made above that stochastic effects need to be taken into account when the mean and the standard deviation are of similar magnitude.

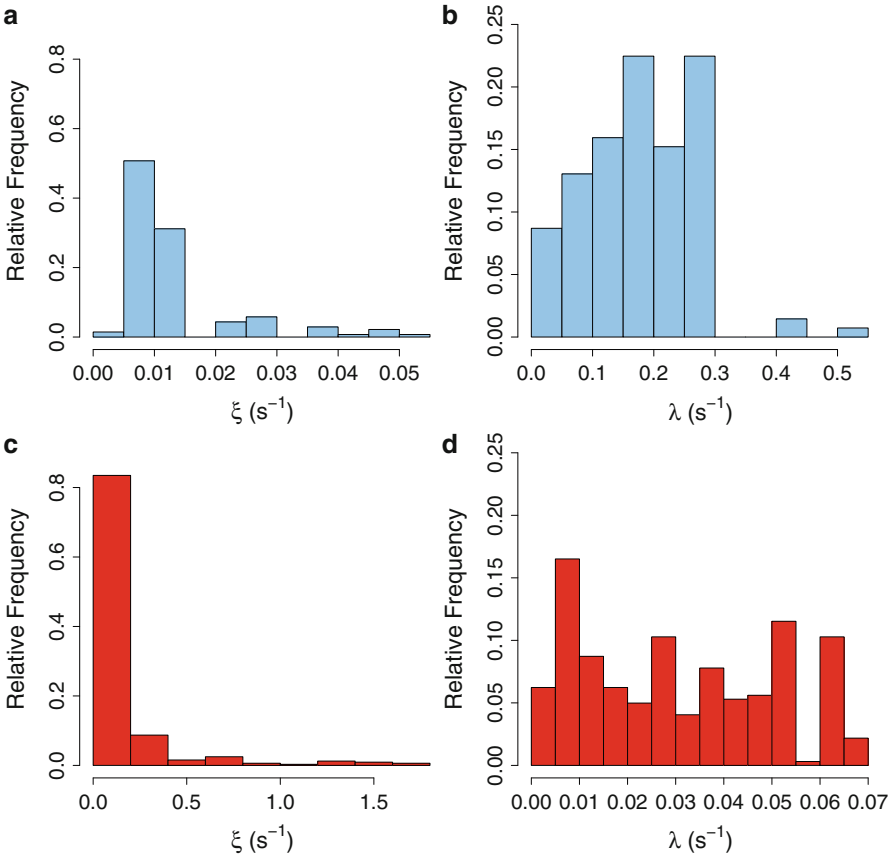

Fig. 32.2 Relative frequency for ξ (**a**, **c**) and λ (**b**, **d**) for HEK293 cells (top, blue) and astrocytes (bottom, red). HEK293 cells were stimulated with 30 μM carbachol, while Ca^{2+} spikes in astrocytes were spontaneous. $N = 138$ for HEK293 cells and $N = 321$ astrocytes. For experimental details, see [62]

Equation (32.3) expresses the ISI distribution in terms of the conditional intensity function. It is often convenient to reverse the approach and start from an ISI distribution. Firstly, we obtain ISIs directly from experimental recordings, which inform us about the possible shapes of ISI distributions. Secondly, some ISI distributions that have been shown to capture experimental data cannot be derived from closed form intensity functions as e.g. in Eq. (32.1). A point in case is the Gamma distribution, which is consistent with Ca^{2+} oscillations in HEK293 cells [67] and also with voltage spikes in neurons [68, 69]. One common representation for the density of the Gamma distribution reads as

$$f_{\mathrm{G}}(t,s) = \frac{\beta^{\alpha}}{\Gamma(\alpha)}(t-s)^{\alpha-1}\mathrm{e}^{-\beta(t-s)}\,, \tag{32.5}$$

where α and β are called the shape parameter and rate, respectively, and Γ denotes the standard Gamma function. Suppose for a moment that the time between successive Ca^{2+} puffs follows a Poisson distribution with rate β. In contrast to Ca^{2+} spikes, Ca^{2+} puffs correspond to localised Ca^{2+} liberation through a cluster of $InsP_3Rs$. In addition to Ca^{2+} release through single $InsP_3Rs$, Ca^{2+} puffs are considered the basic building blocks in the hierarchy of Ca^{2+} signals [2, 61, 70]. A Gamma distribution where α is a positive integer returns the probability that α Ca^{2+} puffs have occurred for the first time. In other words, the Gamma distribution is a probability distribution for a combination of events to happen for the first time. This interpretation makes it an appealing candidate for Ca^{2+} spikes. The reason is that Ca^{2+} spikes are thought to form when a small number of Ca^{2+} puffs generates a region of elevated Ca^{2+} in the cell, which then initiates Ca^{2+} release throughout the cell. Alternatively, recent experiments in astrocytes suggest that the co-occurrence of a certain number of Ca^{2+} puffs is sufficient to trigger a Ca^{2+} spike [71]. This also fits well with a body of research that shows that Ca^{2+} puffs and Ca^{2+} spikes can be described as first-passage time problems [63, 72–76]. As an interesting observation, note that the mean ISI for Eq. (32.5) is α/β, so that the mean interpuff interval for α puffs is $1/\beta$, which is consistent with the mean interpuff time when puffs are described by a Poisson process with rate β. To relate a given ISI distribution to the conditional intensity function, we find that

$$q(t|s) = \frac{f(t,s)}{1 - \int_s^t f(u,s)\mathrm{d}u}\,, \tag{32.6}$$

which is equivalent to Eq. (32.3) as shown in Appendix 1. Equations (32.3) and (32.6) allow us to switch between conditional intensity functions and ISI distributions depending on what our modelling question requires.

32.3 Beyond Stationary Ca^{2+} Spike Sequences

The discussion so far assumed that successive Ca^{2+} spikes are independent and are described by the same statistics. The conditional intensity function $q(t|s)$ only depends on the time since the last spike $(t - s)$, but not on the absolute Ca^{2+} spike times t and s. Hence, the probability for two spikes to be separated by say $80s$ is the same irrespective of whether the first spike occurs 10s into the experiment or 1000s. The same holds true for the ISI density in Eq. (32.5) which only depends on the time difference $(t - s)$ between successive Ca^{2+} spikes. A consequence of the independence of Ca^{2+} spikes is that we can immediately write down the probability density for n Ca^{2+} spikes occurring at times $y_1, y_2, \ldots, y_n$. If we collect the Ca^{2+} spike times in a set $\mathbf{y} = \{y_1, \ldots y_n\}$ the probability density for the entire Ca^{2+} spike sequence is given by

$$p(\mathbf{y}) = f_1(y_1, 0) f(y_2, y_1) \cdots f(y_n, y_{n-1}) f_n(T, y_n)\,, \tag{32.7}$$

where $f_1(y_1, 0)$ denotes the probability density for the first spike to occur at y_1 and $f_n(T, y_n)$ is the probability that no spike happens after y_n until the end of the experiment at time T. The probability for a Ca^{2+} spike sequence factorises in the probabilities of individual and identical ISIs, which are properties often referred to as independence and stationarity, respectively. We separate out the contributions from f_1 and f_n since they do not correspond to ISI probabilities and hence are often modelled by different probability distributions, e.g. a Poisson distribution.

However, there are numerous reasons for why ISI probabilities do not remain constant over time and hence ISIs at different times of the experiment follow different probability distributions. For example, while the ER refills between Ca^{2+} spikes, the level of refilling can decrease as Ca^{2+} leaves the cell across the plasma membrane. In most experiments, $InsP_3$ is formed in response to activation of cell surface receptors, but the efficiency of this pathway may decrease over time. Both factors lower the propensity for the generation of Ca^{2+} spikes as the experiment progresses and introduces trends when plotting ISIs. When analysing Ca^{2+} spikes, we can remove trends and only consider Ca^{2+} spikes after initial transients. This presents a sensible approach when cells experience constant stimulation such as in step change experiments. However, under physiological conditions, hormones arrive in a time-dependent manner, so do neurotransmitters and paracrine signals. To mimic such an in vivo environment, cells need to be challenged with time-varying stimuli. As soon as we introduce an explicit time-dependence, ISI distributions are no longer stationary, but depend on the absolute time of the experiment.

This raises the question on how to mathematically describe the non-stationarity of Ca^{2+} spike sequences. One approach is to introduce an explicit time-dependence into the ISI distribution by making the parameters change over time. While conceptually appealing, the practicalities of this approach are limited. For instance, if we believe that the parameters change continuously over time, it is not apparent how to constrain the model best given that we sample the values of the parameters at only a few discrete time points, viz. the times of Ca^{2+} spikes. Another issue arises from the fact that the probability of a Ca^{2+} spike sequence does not necessarily factorise any more as in Eq. (32.7), but we need to consider the full multivariate probability $p(\mathbf{y}) = p(y_1, \ldots, y_n)$, which can pose significant challenges.

A more practical approach was put forward in [68]. At the heart of it lies a time transformation that maps the time of the original experiment, denoted by t, to a new time u via

$$u(t) = \int_0^t x(v)\mathrm{d}v\,, \tag{32.8}$$

where x is called the intensity function and relates to the level of Ca^{2+} spiking as we will illustrate below. As such, x is always strictly positive and hence associates each value of t with a unique values of u through Eq. (32.8). A consequence of this

mapping is that in the new time u, ISIs become independent [68]. This means that the probability density for a Ca^{2+} spike sequence factorises again and we have

$$p(\mathbf{y}|x) = g_1(u_1, 0|x)g(u_2, u_1|x)\cdots g(u_n, u_{n-1}|x)g_n(U, u_n|x)\,, \tag{32.9}$$

where $u_i = u(y_i)$, $U = u(T)$ and the dependence of $\mathbf{y}$ on the left hand side enters on the right hand side through u being a function of t. We explicitly include x to emphasise that the transformation depends on the intensity function. What makes Eq. (32.9) particularly useful is that the probability density g is related to the original ISI probability density f via

$$g(u_i, u_{i-1}|x) = x(y_i)f(u_i, u_{i-1})\,, \tag{32.10}$$

which follows from the conservation of probability [67, 77]. We illustrate a practical calculation for Eq. (32.10) in Appendix 2.

At this point, it might appear that the intensity function is mathematically convenient, but detached from the actual biology. As it turns out, the contrary holds true. For the models of Ca^{2+} spiking considered here, $x(t)$ corresponds to the probability of Ca^{2+} spiking *independent* of the history of the Ca^{2+} spike sequence. Put differently, if there are N identical Ca^{2+} spiking cells, $Nx(t)$ is the expected number of Ca^{2+} spikes at time t. To illustrate this concept, we chose an intensity function (red line in Fig. 32.3), generated 10,000 Ca^{2+} spike sequences from it and binned them (light blue histogram). By using a large number of Ca^{2+} spike sequences, binning is equivalent to taking the average across all possible histories that led to a Ca^{2+} spike in the respective bin. The excellent agreement between the intensity function and the histogram confirms the above interpretation of $x(t)$. For the practicalities of generating the Ca^{2+} spike sequences, we refer the reader to Appendix 3.

32.4 Bayesian Computation

A main motivation for pursuing a statistical approach is to fit models of Ca^{2+} spike generation more easily to experimental data and hence learn more about the nature of Ca^{2+} oscillations. This requires us to infer the parameters of the ISI distribution, e.g. α and β for the Gamma distribution, and the time course of $x(t)$ from measured Ca^{2+} spike sequences. For ease of reference, we will call all unknowns of the model, i.e. the intensity function and the parameters of the ISI distribution, hyperparameters and denote them by θ.

There are a number of ways for achieving this goal. Here, we will make use of Bayesian inference, that addresses the following question: what does the data tell us about the parameters of the model? Expressed more formally, we are interested in $p(\theta|\mathbf{y})$, i.e. the probability distribution of the hyperparameters given a Ca^{2+} spike sequence. This probability is called the *posterior* distribution. The advantage of this

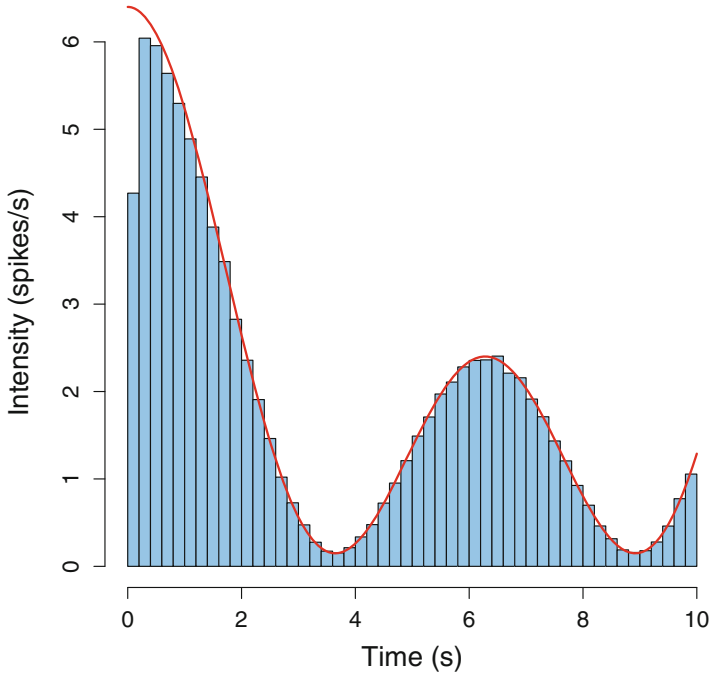

Fig. 32.3 Intensity function (red) and peristimulus-time histogram (blue) obtained from 10,000 Ca^{2+} spikes when the ISI distribution is given by a Gamma distribution. Parameter values are $x(t) = 2\cos(t) + 2\cos(0.5t) + 2.4$ and $\alpha = 6.2$ and $\beta = 6.2$s

approach is that we do not merely obtain a single value, but the full probability distribution for the parameters that are consistent with the data. This allows us to judge how well the model captures the data and what parameter values to use to describe the underlying biology. For instance, consider one of the hyperparameters, say θ_1. If the distribution for θ_1 is sharply peaked around a value θ_1^*, we can be confident that θ_1^* is a sensible estimate for θ_1. On the other hand, if the probability distribution is broad or exhibits multiple maxima, we are pressed much harder to interpret the results. It might also indicate that we based our original model on incorrect assumptions. In addition to these conceptual benefits, the posterior distribution is all we need to answer any question we have about the experiment. For instance, we can determine summary statistics such as mean and variance as well as the behaviour of functions that depend on hyperparameters.

To compute the posterior probability, we make use of Bayes' theorem, which states that

$$p(\theta|\mathbf{y}) = \frac{p(\mathbf{y}|\theta)p(\theta)}{p(\mathbf{y})}\,. \tag{32.11}$$

The right hand side contains the likelihood function $p(\mathbf{y}|\theta)$, the so-called prior $p(\theta)$ and the normalisation

$$p(\mathbf{y}) = \int p(\mathbf{y}|\theta)\, p(\theta) \mathrm{d}\theta \,. \tag{32.12}$$

The conceptual appeal of Eq. (32.11) stems from its numerator. We already encountered an example for a likelihood function in Eq. (32.9). It represents how likely it is to observe what we have measured for a given θ and hence reflects our believes about the potential mechanisms that drive Ca^{2+} spike generation. The prior distribution allows us to provide sensible input for the hyperparameter values before we see the data. For instance, if we believe that some hyperparameter, say θ_1 again, has a value close to some θ_1^0, we pick a probability distribution that is centred around θ_1^0. On the other hand, if we are uncertain about possible values of θ_1, we choose a wider prior. Thinking about priors for hyperparameters that are numbers immediately leads us to probability distributions in the classical sense such as Poisson distributions or Gamma distributions. But what about a prior for the intensity function $x(t)$? To answer this question, it is helpful to return to the biological interpretation of $x(t)$, viz. the probability density for a Ca^{2+} spike at time t irrespective of the history of the Ca^{2+} spike sequence. If we challenge cells with a constant stimulus as in e.g. a step-change experiment, a reasonable assumption is that $x(t)$ remains constant over longer periods of time, but not necessarily at the same value for the entire experiment. For instance, as the experiment continues, Ca^{2+} spikes may become less frequent compared to the beginning of the experiment due to receptor desensitisation or changes to ER Ca^{2+} load. We can mimic this biological response by assuming an $x(t)$ that has a large constant value when the experiment is started and smaller constant value towards the end. In this particular illustration, we assumed that there are two different levels. To allow more flexibility, suppose that there are k levels and that the probability for having k levels is Poissonian with rate γ. If we further assume that each level h_i is drawn from a Gamma distribution with parameters a and b, we find that the prior for the intensity function is

$$p(x) = \mathrm{e}^{-\gamma} \frac{\gamma^k}{k!} \prod_{i=1}^{k} \frac{a^b}{\Gamma(a)} h_i^{a-1} \mathrm{e}^{-b h_i} \,. \tag{32.13}$$

Because the number of changepoints is independent from the levels h_i, which again are independent from each other, $p(x)$ factorises into individual contributions [78]. In Fig. 32.4a we illustrate three candidates for such piecewise constant priors with different numbers of changepoints and different level values.

While piecewise linear intensity functions possess computational advantages—e.g. the integral in Eq. (32.22) in Appendix 2 can be computed analytically—one issue with them is that they are discontinuous, i.e. they have jumps. This might be undesirable in some situation, which leads us to priors for continuous functions. An example for this is when cells are challenged with a time-varying stimulus as e.g.

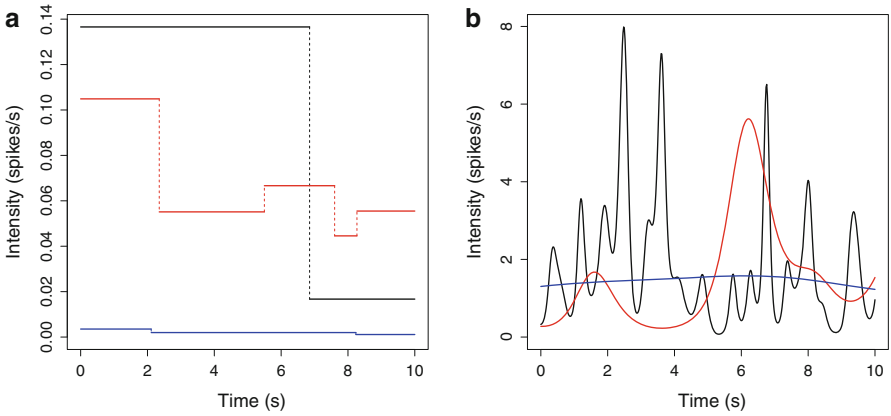

Fig. 32.4 Candidate intensity functions for (**a**) a piecewise linear prior and (**b**) a GP prior. The different colours indicate (**a**) different numbers of change points and different levels and (**b**) different values of κ. Here, blue corresponds to $\kappa = 5$s, red to $\kappa = 1$ s and black to $\kappa = 0.2$ s

in [67]. Since the stimulus changes smoothly over time, a reasonable assumption is that the intensity function inherits this smoothness. Among the different choices that can be made for continuous intensity functions, we here focus on so-called Gaussian processes (GPs). Consider the intensity function at some time point t. Instead of fixing a unique value $x = x(t)$, we prescribe a probability distribution $g(x)$. In other words, for a fixed time t there is a probability $g(x(t))\mathrm{d}x$ that the value of the intensity function lies in the interval $[x(t), x(t) + \mathrm{d}x]$. We here assume that the logarithm of the intensity function follows a Gaussian distribution of the form

$$f_{\mathrm{GP}}(x) = \frac{1}{\sqrt{2\pi\sigma^2}} \exp\left\{\frac{(\mu - x)^2}{2\sigma^2}\right\}, \tag{32.14}$$

where μ denotes the mean and σ the standard deviation, respectively. GPs derive their name from the fact that we employ a Gaussian distribution. The reason for assuming that $\log x(t)$ rather than $x(t)$ itself follows a Gaussian distribution is that $x(t)$ is always positive, but a Gaussian distribution can yield negative values. By using the logarithm, we enforce the positiveness of the intensity function. To ensure that the intensity function is continuous, we need to guarantee that the values of x at two close-by time points t and s are not too far apart. This is achieved by imposing a correlation function

$$\Sigma(s, t) = \sigma^2 \exp\left\{\frac{(s - t)^2}{\kappa^2}\right\}, \tag{32.15}$$

which we have chosen to be a squared exponential. Here, σ is the same as in Eq. (32.14) and κ measures how smooth the GP is. The larger κ the smoother

the intensity function. Figure 32.4b shows three different realisations of a GP for varying values of κ. Observe that all three functions are smooth, and that there are less wiggles for larger values of κ, which is consistent with the interpretation above. Since we have to discretise time for any practical computation, suppose that there are n time points, i.e. we represent the time of the experiments at n discrete time points ranging from $t_1 = 0$ to $t_n = T$, where T is the duration of the experiment. A practical representation for these time points are the values at which the Ca^{2+} concentration is measured and is determined by e.g. the frame rate of the microscope cameras. The prior for a GP is a multivariate Gaussian distribution and reads as

$$p(x) = \frac{1}{\sqrt{(2\pi)^n \det \Sigma}} \exp\left\{\frac{1}{2}(\mathbf{t}-\boldsymbol{\mu})\Sigma^{-1}(\mathbf{t}-\boldsymbol{\mu})\right\}, \tag{32.16}$$

where $\mathbf{t}$ is a vector of length n representing the discretised time of the experiment, $\boldsymbol{\mu}$ is a vector of length n denoting the mean of the GP at each time point t_n, and Σ is given by Eq. (32.15).

Having introduced different priors for the hyperparameters of the model including the intensity function x, we can return to Eq. (32.11). While it is conceptually appealing and offers us a full picture of the parameters of the model as constrained by the experiment, it is computationally challenging. The reason is the integral in the denominator, which runs over the entire hyperparameter space. Since this can be high-dimensional, we require computationally efficient methods as a direct integration is often prohibitively expensive if not impossible. There are various methods for tackling this problem. For instance, instead of computing $p(\theta|\mathbf{y})$ directly including the integration of the denominator, we can determine the maximum of the distribution and its variance [79, 80]. This will provide us e.g. with the most likely intensity function that is consistent with the data as well as confidence intervals, see [67]. A different approach is to try and sample from $p(\theta|\mathbf{y})$ without having to explicitly compute it. The main idea is that if we can sample from a probability distribution, we know the possible values and the associated probabilities (values that are more likely than others are sampled more frequently) without having to determine a closed form solution. This often suffices for practical purposes. A technique that does this is known as Markov chain Monte Carlo [81].

32.5 Analysing Ca^{2+} Spike Sequences

Having introduced key concepts for a statistical analysis of Ca^{2+} spike sequences in the previous sections, we now apply them to different experiments. A crucial input to our model is the ISI probability density, see Eq. (32.9). However, we do not know *a priori* which distribution is most consistent with the data. To establish this, we can make use of the following transformation. Let the measured Ca^{2+} spike times be given by $y_1, \ldots y_n$ again. We define transformed ISIs by

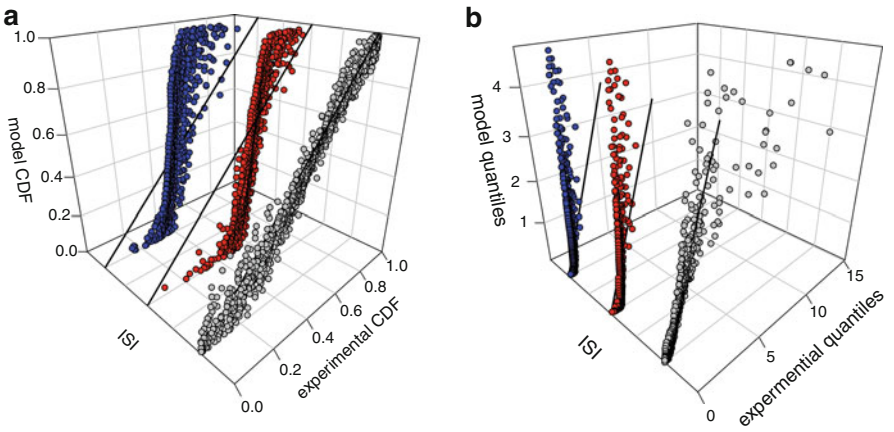

Fig. 32.5 K-S (**a**) and Q-Q (**b**) plots for data from 23 individual cells stimulated with carbachol cells. The initial concentration was 20 μM, which was increased to 50 μM. The ISI distributions are inverse Gaussian (blue), Poisson (red) and Gamma (grey). We used piecewise linear functions as prior for the intensity function

$$\tau_k = \int_{y_{k-1}}^{y_k} q(s|y_{k-1})\mathrm{d}s\,, \tag{32.17}$$

with q given by Eq. (32.6). It can now be shown that if the mechanisms that generate the observed Ca^{2+} spikes are consistent with the ISI distribution that we use in Eq. (32.6), the transformed ISIs τ_k are exponentially distributed with unit rate [82]. This leaves us with the task of comparing two probability distributions: the standard exponential distribution and the distribution of the transformed ISIs. The quantile-quantile (Q-Q) plot and the Kolmogorov Smirnov (K-S) plot are two powerful graphical approaches to examine differences between probability distributions. In Fig. 32.5 we show Q-Q and K-S plots for HEK293 cells in a multistep experiment. We tested three different ISI distributions: a Poisson, an inverse Gaussian and a Gamma distribution. Each cell was analysed individually and gave rise to a separate sequence of dots; no data assimilation was performed. For the Q-Q plot, we determine the quantiles of the transformed ISIs and plot them against the quantiles of the exponential distributions. For the K-S plot, we compute the cumulative distributions of the transformed ISIs and the exponential distribution, respectively, and plot them against each other. Identical probability distributions possess identical quantiles and identical cumulative distributions, respectively. Hence any deviation from a 45° straight line in the Q-Q and K-S plot points towards differences between the distributions and hence indicates that we need to improve our assumptions about the ISI distributions.

For both, the K-S and the Q-Q plot, the data points deviate significantly from a straight line with slope 1 for the Poisson and the inverse Gaussian distribution. On the other hand, we observe a strong correlation between the 45° line and the data points for the Gamma distribution. This visual inspection is corroborated by

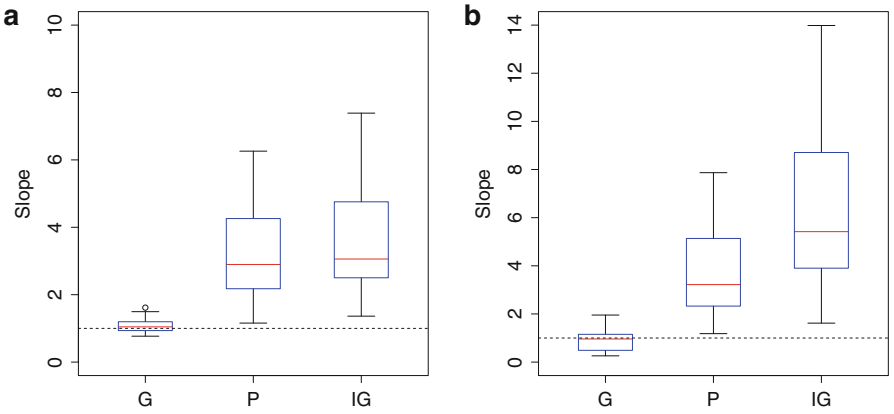

Fig. 32.6 Box and whisker plots for the data presented in Fig. 32.5 showing results for the (**a**) K-S plot and (**b**) Q-Q plot. The red line represents the median of the distribution, and the box delineates the range of data from the first to the third quartile. The whiskers indicate the spread of the data

the box-and-whisker plots in Fig. 32.6. Because we treated cells individually, we can determine the slope of a linear fit for each cell. The plots in Fig. 32.6 show the statistics for these slopes. The box represents the spread of data within the second and third quartile, and the red line indicates the median. The whiskers provide a measure for the overall spread of the data. Generally speaking, the smaller the box and the closer the whiskers to the box, the less spread is in the data. The Poisson and the inverse Gaussian distribution generally exhibit a larger spread than the Gamma distribution. Moreover, the median of the Gamma distribution is closer to one. In [67], we found that for HEK293 cells stimulated with 10 μM and 100 μM charbachol, respectively, the Gamma distribution worked best. These results and the new analysis presented here strongly suggest that the ISI statistics for Ca^{2+} spike sequences are captured by a Gamma distribution. A further argument to support this conclusion is that the data in [67] and [65] were acquired independently in different labs with different setups.

In order to obtain the results in Figs. 32.5 and 32.6 we had to estimate the intensity function $x(t)$ for each cell. Figure 32.7 displays $x(t)$ for two different cells. Since we analyse step change experiments, we first chose piecewise constant functions as a prior for x as discussed in Sect. 32.4. The mean intensity function is shown as a solid blue line, while the 95% confidence interval is represented by the shaded blue area. We clearly see an increase in the intensity function as the stimulus strength is stepped up. Moreover, during extended periods of time, the intensity function is almost constant, which has significant consequences for the interpretation of the mechanisms that drive Ca^{2+} spike generation as discussed below.

As pointed out in Sect. 32.4, piecewise constant functions are not the only possible prior. GPs constitute another possible class, and corresponding results are

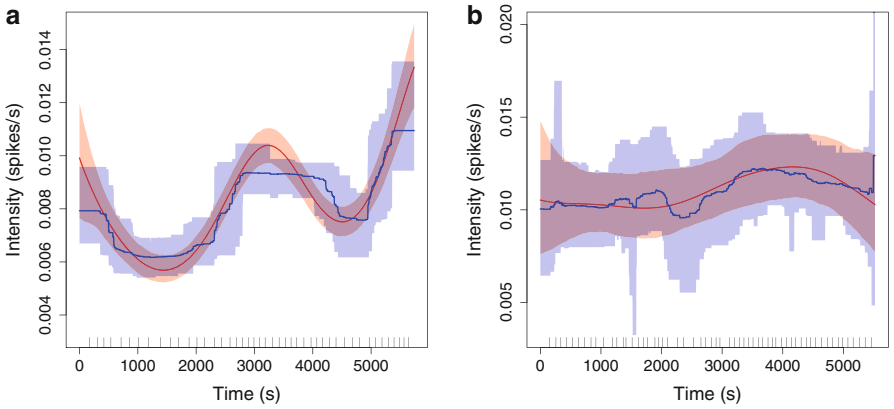

Fig. 32.7 Intensity functions (solid lines) and 95% confidence interval (shaded regions) for two cells in a multistep experiment. The initial stimulus was 20 μM carbachol and changed to 50 μM carbachol at $t = 2581$s (**a**) and $t = 2524$s (**b**). The prior for the intensity function is a GP (red) or piecewise constant (blue). The ticks along the x-axes indicate the Ca^{2+} spike times

shown in red in Fig. 32.7. Vitally, the intensity function obtained with a GP prior closely follows that derived from a piecewise constant prior. Given that the two priors represent significantly different functional forms of the intensity function, the consistency between the two approaches lends strong support for the validity of the derived intensity functions. Moreover, if we were to only use GPs as priors, a valid step is to interpolate the smooth prior with a piecewise linear function, which allows us to compute the mean ISI.

Having identified intensity functions that are consistent with measured Ca^{2+} spike sequences, we can now determine the conditional intensity functions $q(t|s) = q(y_i|y_{i-1})$. We start from Eq. (32.6), set $t = y_i$, $s = y_{i-1}$ and then replace $f(y_i, y_{i-1})$ with $g(u_i, u_{i-1}|x)$ from Eq. (32.10) by using Eq. (32.8) (see also Appendix 2). In other words, the conditional intensity function $q(t|s)$ is a highly nonlinear transformation of the estimated intensity function $x(t)$ given the Ca^{2+} spike times. In Fig. 32.8 we plot $q(t|s)$ for the data shown in Fig. 32.7. We notice that immediately after a Ca^{2+} spike $q(t|s)$ remains almost zero for some time before it increases. This indicates that during this period, Ca^{2+} spikes cannot occur, which is equivalent to saying that there is a refractory period. Importantly, we did not include an explicit refractory period in our model, i.e. we did not choose an ISI probability distribution that vanishes for a certain amount after the last Ca^{2+} spike. For instance, the Gamma distribution in Eq. (32.5) does not *per se* stay close to zero for small values of $(t - s)$. It only does so for certain values of α. Since the value of α is part of estimating $x(t)$, the vanishing of the conditional intensity function is an emergent result of the model. These findings are consistent with the presence of a refractory period T_r in the ansatz in Eq. (32.1). There, we chose the conditional intensity function and derived the ISI distribution, while for Fig. 32.8, we decided upon a certain ISI distribution and derived the conditional intensity function. The

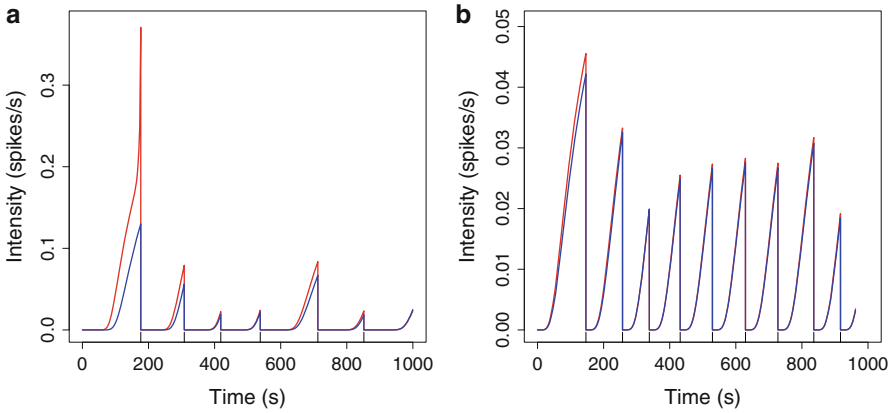

Fig. 32.8 Conditional intensity functions corresponding to the data in Fig. 32.7. The ticks along the x-axes indicate the Ca^{2+} spike times

agreement between the ansatz in Eq. (32.1) and the estimated conditional intensity function in Fig. 32.8 lends strong support to the former.

In addition to the conditional intensity function, we can also interrogate the ISI distribution. For a time-dependent intensity function $x(t)$, the corresponding ISI distribution is time-dependent as well, see Eqs. (32.21) and (32.22) in Appendix 2. However, when the intensity function is constant, this time-dependence is lost, and we can use the *same* ISI distribution for the entire period that x does not change. Inspecting Fig. 32.7a, we observe that the intensity function obtained with a PWL prior (blue line) is almost constant between 600s and 2000s, while a similar behaviour is seen in Fig. 32.7b during the first 2000s for the GP prior (red curve). Taking these values for x together with the inferred parameter values for the Gamma distribution, we now plot the corresponding ISI distributions in Fig. 32.9 based on Eq. (32.25). For the stronger stimulus (50 μM, blue line), the ISI distribution is shifted towards the left compared to the weaker stimulus (20 μM, red curve). In addition, the variance is more pronounced in the former than in the latter. To quantify this, we compute the mean μ and the standard deviation σ using the inferred intensity function x and the associated values of the Gamma distribution. We obtain $\mu = 159.07$s and $\sigma = 22.50$s for the small stimulus and $\mu = 96.73$s and $\sigma = 32.24$s for the stronger stimulus, respectively. We can compare this with the mean and standard deviation determined directly from the Ca^{2+} spike sequences shown in Fig. 32.7. We find $\mu_E = 166.57$s and $\sigma_E = 24.416$s at 20 μM and $\mu_E = 96.31$s and $\sigma_E = 27.03$s at 50 μM, respectively. The good agreement between the experimentally determined statistics (μ_E, σ_E) and the estimated quantities (μ, σ) demonstrates the usefulness of the Bayesian inference approach that we have employed here.

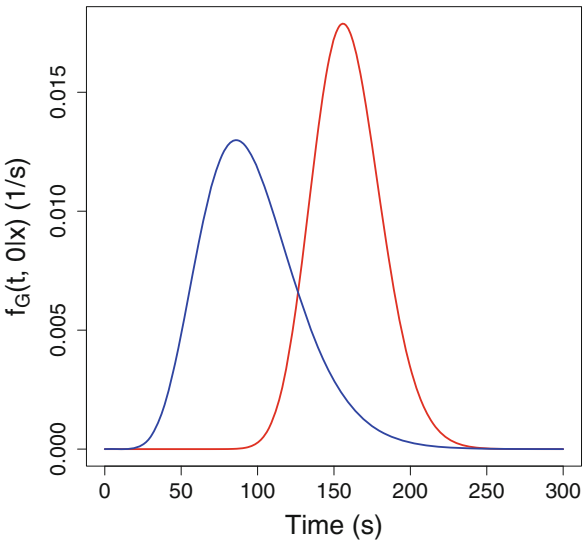

Fig. 32.9 ISI probability density $f_G(t, 0|x)$ for the data shown in Fig. 32.7a (red) and Fig. 32.7b (blue) for t between approximately 600s and 2000s (red) and t between 1s and 2000s (blue)

32.6 Concluding Discussion

Ca^{2+} spikes constitute a well-established mode of intracellular Ca^{2+} signalling across a large number of cell types. We can now draw on a substantial body of experimental measurements that have identified and characterised the cellular components that drive Ca^{2+} oscillations. Despite these successes, central questions remain open. Amongst them is a seemingly innocuous query: given a stimulus, can we predict the sequence of Ca^{2+} spikes? Since there is wide-ranging consensus that information about the stimulus is encoded in the properties of Ca^{2+} spike sequences, answering this question is critical for our understanding of intracellular Ca^{2+} signalling.

Addressing this issue from a modelling perspective is challenging for two reasons. The generation of Ca^{2+} spikes is firstly stochastic and secondly driven by the interaction of spatially distributed clusters of $InsP_3$ receptors. One avenue to make progress is to simulate partial differential equations for the intracellular calcium concentration (see [61] for a recent perspective). Here, we have reviewed a different framework that is a conceptual antipode to the first approach. While partial differential equations rely on mechanistic details and build oscillations from the bottom-up, the statistical ideas in this review aim at describing Ca^{2+} spikes directly at the cell level.

One advantage of a statistical model lies in its computational demands. It is considerably cheaper to generate Ca^{2+} spike sequences from a statistical model than to solve partial differential equations. This is particularly useful when studying cell populations, where intercellular heterogeneity calls for multiple Ca^{2+} spike sequences with different parameter values. But statistical models may also help

conceptually. Ultimately, Ca^{2+} dependent signalling is driven in many instances by the sequence of Ca^{2+} spikes. Hence, the properties of Ca^{2+} spikes such as their ISI distribution are of central interest. Since it is conceivable that different microscopic models based on detailed molecular processes all lead to the same cellular behaviour, statistical frameworks are ideally placed to capture this common identity of Ca^{2+} spiking.

The first step in our statistical analysis is to derive a model for whole-cell Ca^{2+} spiking. Since Ca^{2+} spikes are stochastic, we can express their occurrence most naturally in the language of probabilities. A core ingredient is the ISI distribution $f(t, s)$, or equivalently the conditional intensity function $q(t|s)$. It is worth noting that both depend on only two times, i.e. we assume that the generation of a Ca^{2+} spike only depends on the history since the last Ca^{2+} spike. This independence of successive Ca^{2+} spikes has been shown for astrocytes, PLA cells and HEK293 cells in [83] for constant stimulation. In general, however, this might be too strong an assumption. In particular, when cells are challenged with continuously changing stimuli—in order to mimic a more realistic cellular environment—correlations within the signal might be inherited by the Ca^{2+} spikes. One possibility is to generalise the conditional intensity function. Instead of depending only on the last time t, it now relies on the entire Ca^{2+} spike history H_t, i.e. $q = q(t|H_t)$. This, however, does not necessarily lead to a mathematically tractable problem. A more practical approach is the introduction of an intensity function. Essentially, it transforms the original Ca^{2+} spike times in such a way that they become independent. As a consequence, we can use the original ISI distributions $f(t, s)$ or conditional intensity functions $q(t|s)$, which entails that the parameters of the model are those of the ISI distribution and the intensity function, respectively.

This leaves us with the task of finding the parameter values given the Ca^{2+} spike sequences. The last condition is of particular relevance to the current approach. Our goal is to derive a model that is constrained by experimental data and whose parameter values can be sensibly estimated. We have achieved this by employing Bayesian ideas, which allow us to determine the probability distribution of the parameters given the Ca^{2+} spike sequences, i.e. $p(\theta|\mathbf{y})$. This is a distinct advantage of the Bayesian framework. Other methods, such as maximum likelihood estimators, also provide information about the parameters of the model. However, they only deliver *one* set of parameter values associated with a standard error, not entire probability distributions. Moreover, these approaches come with numerical challenges and are hard to pursue in higher dimensions.

Since the ISI distribution is a core component of the model, we first ascertained if our choices are consistent with the recorded Ca^{2+} spike sequences. As Figs. 32.5 and 32.6 illustrate, the Gamma distribution captures the data well, while the inverse Gaussian and the Poisson distribution fail to do so. It is worth noting that the data analysed here were obtained in different experiments than those used in [67], yet both data sets lead to the same conclusion: Ca^{2+} spikes are well described by a Gamma distribution. This might point to the mechanisms that generate Ca^{2+} spikes. Since the Gamma distribution returns the probability of the first time that

α events have occurred (see Eq. (32.5)), it is consistent with the interpretation that the formation of a critical nucleus of elevated Ca^{2+}, driven by the occurrence of a certain number of Ca^{2+} puffs, underlies the generation of a Ca^{2+} spike. At the moment, we cannot rule out that other probability distributions that we have not tested yet describe Ca^{2+} spikes equally well or even better. The advantage of our Bayesian modelling framework is that it works for *any* probability distribution, which allows us to test more candidate distributions in the future. Moreover, we have two complementary tests at our disposal, the Q-Q and the K-S plot. While both approaches check whether two probability distributions coincide, the K-S plot is more sensitive towards the centre of the distribution, while the Q-Q plot focusses on the tails.

When testing for the most likely ISI distribution, we had to estimate the intensity function $x(t)$ at the same time, since the ISI distribution explicitly depends on $x(t)$ (see Eqs. (32.21) and (32.22)). Following on from our results so far, we focussed on intensity functions obtained for the Gamma distribution. The intensity function is central to our understanding of Ca^{2+} spike generation. An almost constant intensity function indicates that Ca^{2+} spikes originate from *stationary* dynamics. This means that the ISI distribution is identical for each recorded Ca^{2+} spike time, which allows us to compute the mean and the variance of a Ca^{2+} spike sequence (see Fig. 32.9). From a biological perspective, this corresponds to a cell with no explicitly time-dependent processes such as a continuous depletion of the ER or an accumulating degree of receptor desensitisation. In the latter, this does not mean that receptor desensitisation does not occur, but that the fraction of desensitised receptors across the cell stays constant. A change of experimental conditions is directly translated into changes of the intensity functions. For instance, recent experiments with sinusoidal stimuli led to intensity functions that reflect the rises and falls of the applied agonist [67]. Moreover, since intensity functions are estimated from Ca^{2+} spike sequences of individual cells, they mirror the variability of observed responses. A key line of research is therefore to quantify and classify such diverse intensity functions.

Using both the ISI distribution and the intensity function we can compute the conditional intensity function $q(t|s)$, which corresponds to the probability of a Ca^{2+} spike at time t given that a Ca^{2+} spike occurred at time s. The shape of q allows us to discuss potential mechanisms that are involved in Ca^{2+} spike generation. For instance, as Fig. 32.8 illustrates, the conditional intensity function remains small after a Ca^{2+} spike before it increases. This period of low Ca^{2+} spiking probability is consistent with the observations of refractoriness. Plots like Fig. 32.8 also allow us to estimate the range of refractory periods, which we can then compare to the refractory period obtained from plots of the mean ISI against the ISI standard deviation as seen in Fig. 32.1d. In addition, we can compare the rise time of the conditional probability function with known timescales of e.g. ER refilling or $InsP_3$ receptor recovery to ascertain whether any of the molecular timescales match the cellular time scale, or whether we deal with an emergent timescale.

One motivation for pursuing a statistical approach is to obtain *distributions* for the parameter values that govern Ca^{2+} spike generation. The reason for why

distributions exist in the first place—and not a single parameter value only—lies in the inherent single-cell variability. Consider e.g. the variation of ξ and λ shown in Fig. 32.2. The recovery from global cellular inhibition is controlled by ξ. This involves inter alia resequestration of Ca^{2+} from the cytosol to the ER via SERCA pumps or recovery of $InsP_3$ levels. Since expression levels of SERCA pumps can vary amongst cells, recovery proceeds at different speed in different cells, which is captured by the variability of ξ. As for λ it controls the asymptotic Ca^{2+} spike rate. As Ca^{2+} spikes are believed to occur via the formation of a critical nucleus of elevated Ca^{2+} and subsequent propagation of a Ca^{2+} wave, the spatial distributions of $InsP_3Rs$ and SERCA pumps are crucial. These distributions vary significantly between cells, which directly impacts on the spread of λ.

As with all modelling approaches, the methodology presented here is not without its caveats. In its current form, we only consider Ca^{2+} spike times and leave aside other Ca^{2+} spike properties such as amplitude, duration, shape, or baseline Ca^{2+} concentration levels. However, these characteristics have been shown to impact on a number of Ca^{2+} dependent processes [4]. An interesting point in this respect is a potential interplay between release amplitude, release duration and the absolute refractory period. Our results in [65] suggest that the absolute refractory period is not controlled by cell variability and hence that there is only one value for all cells. We can further test this hypothesis by extending the model for a Ca^{2+} spike as in Eq. (32.25) in Appendix 3 to explicitly include a distributed refractory period. The advantage of the Bayesian approach is that the estimation process remains conceptually the same, but we need to estimate additional parameters. As stated above, one incentive for the current work is to relate the estimated parameter values to biophysical processes. Care needs to be taken here as different processes can potentially give rise to the same whole cell parameter values that we infer. Hence further tests are needed to discriminate between different alternatives. A consequence of this consideration is that cells might employ a number of different strategies to generate the same whole cell signal, and it will be fascinating to tease apart the advantages and disadvantages of specific routes to global Ca^{2+} signals.

The preceding discussion illustrates that advanced statistical modelling can provide valuable insights into the dynamics of Ca^{2+} spiking. Vitally, our approach works for cells that are dynamically stimulated with agonist time courses that mimic physiological conditions in vivo, which allows us to model cellular Ca^{2+} spiking in a realistic environment. By inferring parameter values from single cell measurements, we can determine their ISI distribution, which is a central ingredient to modelling Ca^{2+} spikes. Moreover, it allows us to compute statistical properties such as means and variances, which in turn quantify stochastic Ca^{2+} spikes. In addition, we showed how the statistical model allows us to infer potential mechanisms of Ca^{2+} spike generation. This connects the statistical approach with the mechanistic framework of simulating partial differential equations for Ca^{2+} signalling. In the future, it will be desirable to see these two complementary techniques working hand in hand, which has the potential to significantly enhance our understanding of the Ca^{2+} signalling toolkit.

Appendix 1

We here show the equivalence of Eqs. (32.3) and (32.6). For this, it is convenient to introduce

$$F(t,s) = 1 - \int_s^t f(u,s)\mathrm{d}u\,. \tag{32.18}$$

The right hand side of Eq. (32.6) can be written as a full derivative in the form

$$q(t|s) = -\frac{\mathrm{d}}{\mathrm{d}t}\ln F(t,s) \tag{32.19}$$

Multiplying through by (-1) and integrating both sides with respect to t yields

$$-\int_s^t q(u|s)\mathrm{d}u = \ln F(t,s)\,, \tag{32.20}$$

noting that $\ln F(s,s) = 0$. When we exponentiate both sides and use the fact that $F(t,s) = f(t,s)/q(t|s)$ as per Eq. (32.6) we arrive at Eq. (32.3).

Appendix 2

Here, we demonstrate how to practically apply Eq. (32.10) when f is given by the density for the Gamma distribution as in Eq. (32.5). We obtain

$$g_{\mathrm{G}}(u_i, u_{i-1}|x) = x(y_i)\frac{\beta^\alpha}{\Gamma(\alpha)}X_{i,i-1}^{\alpha-1}\mathrm{e}^{-\beta X_{i,i-1}}\,, \tag{32.21}$$

where

$$X_{i,i-1} = \int_{y_{i-1}}^{y_i} x(v)\mathrm{d}v\,, \tag{32.22}$$

since the difference $(t-s)$ in the transformed time u is given by

$$u(t) - u(s) = u(y_i) - u(y_{i-1}) = \int_0^{y_i} x(v)\mathrm{d}v - \int_0^{y_{i-1}} x(v)\mathrm{d}v = \int_{y_{i-1}}^{y_i} x(v)\mathrm{d}v\,. \tag{32.23}$$

A common choice for f_1 and f_n is a Poisson distribution, which leads to

$$g_1(u_1, 0|x) = x(y_1)\mathrm{e}^{-X_{1,0}}\,, \qquad g_n(U, u_n|x) = e^{-X_{n+1,n}}\,, \tag{32.24}$$

in the transformed time, where we have set $y_0 = 0$ and $y_{n+1} = T$.

Appendix 3

To generate the Ca^{2+} spikes that underlie the histogram in Fig. 32.3 we use inverse sampling [84]. Since $x(t)$ is non-constant, we need to use the time-dependent ISI density $g(u_i, u_{i-1}|x)$ from Eq. (32.10). For ease of presentation, we rewrite Eq. (32.10) in terms of the non-transformed Ca^{2+} spike times y_i using the results from Appendix 2 as

$$f_{\mathrm{G}}(y_i, y_{i-1}|x) = x(y_i)\frac{\beta^{\alpha}}{\Gamma(\alpha)}\left[\int_{y_{i-1}}^{y_i} x(v)\mathrm{d}v\right]^{\alpha-1} \exp\left\{-\beta\int_{y_{i-1}}^{y_i} x(v)\mathrm{d}v\right\}, \tag{32.25}$$

which we use in the definition of the cumulative probability function

$$F_{\mathrm{G}}(t, y_{i-1}|x) = \int_{y_{i-1}}^{t} f_{\mathrm{G}}(s, y_{i-1}|x)\mathrm{d}s\,. \tag{32.26}$$

Suppose now that the last Ca^{2+} spike occurred at time y_{i-1}. We find the next Ca^{2+} spike time as $y_i = y_{i-1} + \Delta$, where

$$\Delta = \inf\{t|F_{\mathrm{G}}(t, y_{i-1}|x) > \omega\}\,, \tag{32.27}$$

and ω is a random number that is uniformly distributed between 0 and 1. To put it another way, we need to integrate the ISI probability density f_G from y_{i-1} until we obtain a value of ω for the integral and then add the corresponding upper bound of the integral to the previous Ca^{2+} spike time y_{i-1}.

References

1. Berridge MJ, Galione A (1988) Cytosolic calcium oscillators. FASEB J 2:3074–3082
2. Berridge MJ, Lipp P, Bootman MD (2000) The versatility and universality of calcium signalling. Nat Rev Mol Cell Biol 1:11–21
3. Parekh AB (2011) Decoding cytosolic Ca^{2+} oscillations. Trends Biochem Sci 36:78–87
4. Dupont G, Combettes L (2016) Fine tuning of cytosolic Ca^{2+} oscillations. F1000Research 5. https://f1000research.com/articles/5-2036/v1
5. Thul R, Bellamy TC, Roderick HL, Bootman MD, Coombes S (2008) Calcium oscillations. Adv Exp Med Biol 641:1–27
6. Dupont G, Combettes L, Bird GS, Putney JW (2011) Calcium oscillations. Cold Spring Harb Perspect Biol 3:pii:a004226
7. Dupont G, Falcke M, Kirk V, Sneyd J (2016) Models of calcium signalling. Interdisciplinary Applied Mathematics, vol 43. Springer, Cham
8. Schuster S, Marhl M, Höfer T (2002) Modelling of simple and complex calcium oscillations. From single-cell responses to intercellular signalling. Eur J Biochem 269:1333–1355
9. Uhlén P, Fritz N (2010) Biochemistry of calcium oscillations. Biochem Biophys Res Commun 396:28–32

10. Dolmetsch RE, Xu K, Lewis RS (1998) Calcium oscillations increase the efficiency and specificity of gene expression. Nature 392:933–936
11. Noren DP, Chou WH, Lee SH, Qutub AA, Warmflash A, Wagner DS et al (2016) Endothelial cells decode VEGF-mediated Ca^{2+} signaling patterns to produce distinct functional responses. Sci Signal 9:ra20–ra20
12. Di Capite J, Ng SW, Parekh AB (2009) Decoding of cytoplasmic Ca^{2+} oscillations through the spatial signature drives gene expression. Curr Biol 19:853–858
13. Nunemaker CS, Bertram R, Sherman A, Tsaneva-Atanasova K, Daniel CR, Satin LS (2006) Glucose modulates $[Ca^{2+}]_i$ oscillations in pancreatic islets via ionic and glycolytic mechanisms. Biophys J 91:2082–2096
14. Tse A, Tse FW, Almers W, Hille B (1993) Rhythmic exocytosis stimulated by GnRH-induced calcium oscillations in rat gonadotropes. Science (New York, NY). 260:82–84
15. Colsoul B, Schraenen A, Lemaire K, Quintens R, Van Lommel L, Segal A et al (2010) Loss of high-frequency glucose-induced Ca^{2+} oscillations in pancreatic islets correlates with impaired glucose tolerance in $Trpm5^{-/-}$ mice. Proc Natl Acad Sci U S A 107:5208–5213
16. Tsaneva-Atanasova K, Yule DI, Sneyd J (2005) Calcium oscillations in a triplet of pancreatic acinar cells. Biophys J 88:1535–1551
17. Tse A, Lee AK, Tse FW (2012) Ca^{2+} signaling and exocytosis in pituitary corticotropes. Cell Calcium 51:253–259
18. Santella L, Lim D, Moccia F (2004) Calcium and fertilization: the beginning of life. Trends Biochem Sci 29:400–408
19. Whitaker M (2006) Calcium at fertilization and in early development. Physiol Rev 86:25–88
20. Denninger P, Bleckmann A, Lausser A, Vogler F, Ott T, Ehrhardt DW et al (2014) Male-female communication triggers calcium signatures during fertilization in arabidopsis. Nat Commun 5:4645
21. Van Nhieu GT, Clair C, Bruzzone R, Mesnil M, Sansonetti P, Combettes L (2003) Connexin-dependent inter-cellular communication increases invasion and dissemination of Shigella in epithelial cells. Nat Cell Biol 5:720–726
22. Ullah G, Jung P, Machaca K (2007) Modeling Ca^{2+} signaling differentiation during oocyte maturation. Cell Calcium 42:556–564
23. Ullah G, Jung P (2006) Modeling the statistics of elementary calcium release events. Biophys J 90:3485–3495
24. Shuai JW, Jung P (2003) Optimal ion channel clustering for intracellular calcium signaling. Proc Natl Acad Sci U S A 100:506–510
25. Shuai JW, Jung P (2002) Stochastic properties of Ca^{2+} release of inositol 1,4,5-trisphosphate receptor clusters. Biophys J 83:87–97
26. Shuai J, Jung P (2002) Optimal intracellular calcium signaling. Phys Rev Lett 88:068102
27. De Young GW, Keizer J (1992) A single-pool inositol 1,4,5-trisphosphate-receptor-based model for agonist-stimulated oscillations in Ca^{2+} concentration. Proc Natl Acad Sci U S A 89:9895–9899
28. Li Y, Rinzel J (1994) Equations for $InsP_3$ receptor-mediated $[Ca^{2+}]_i$ oscillations derived from a detailed kinetic model: a Hodgkin-Huxley like formalism. J Theor Biol 166:461–473
29. Tang Y, Stephenson J, Othmer H (1996) Simplification and analysis of models of calcium dynamics based on IP_3-sensitive calcium channel kinetics. Biophys J 70:246–263
30. Gaspers LD, Bartlett PJ, Politi A, Burnett P, Metzger W, Johnston J et al (2014) Hormone-induced calcium oscillations depend on cross-coupling with inositol 1,4,5-trisphosphate oscillations. Cell Rep 9:1209–1218
31. Politi A, Gaspers LD, Thomas J, Höfer T (2006) Models of IP_3 and Ca^{2+} oscillations: frequency encoding and identification of underlying feedbacks. Biophys J 90:3120–3133
32. Sun CH, Wacquier B, Aguilar DI, Carayol N, Denis K, Boucherie S et al (2017) The Shigella type III effector IpgD recodes Ca^{2+} signals during invasion of epithelial cells. EMBO J 36(17):2567–2580
33. Bessonnard S, De Mot L, Gonze D, Barriol M, Dennis C, Goldbeter A et al (2014) Gata6, Nanog and Erk signaling control cell fate in the inner cell mass through a tristable regulatory network. Development (Cambridge, England) 141:3637–3648

34. De Caluwé J, Dupont G (2013) The progression towards Alzheimer's disease described as a bistable switch arising from the positive loop between amyloids and Ca^{2+}. J Theor Biol 331:12–18
35. Dupont G, Lokenye EFL, Challiss RAJ (2011) A model for Ca^{2+} oscillations stimulated by the type 5 metabotropic glutamate receptor: an unusual mechanism based on repetitive, reversible phosphorylation of the receptor. Biochimie 93:2132–2138
36. Dupont G, Abou-Lovergne A, Combettes L (2008) Stochastic aspects of oscillatory Ca^{2+} dynamics in hepatocytes. Biophys J 95:2193–2202
37. Swillens S, Champeil P, Combettes L, Dupont G (1998) Stochastic simulation of a single inositol 1,4,5-trisphosphate-sensitive Ca^{2+} channel reveals repetitive openings during 'blip-like' Ca^{2+} transients. Cell Calcium. 23:291–302
38. Tran Van Nhieu G, Kai Liu B, Zhang J, Pierre F, Prigent S, Sansonetti P et al (2013) Actin-based confinement of calcium responses during Shigella invasion. Nat Commun 4:1567
39. Salazar C, Zaccaria Politi A, Höfer T (2008) Decoding of calcium oscillations by phosphorylation cycles: analytic results. Biophys J 94:1203–1215
40. Kummer U, Olsen LF, Dixon CJ, Green AK, Bornberg-Bauer E, Baier G (2000) Switching from simple to complex oscillations in calcium signaling. Biophys J 79:1188–1195
41. Kummer U, Krajnc B, Pahle J, Green AK, Dixon CJ, Marhl M (2005) Transition from stochastic to deterministic behavior in calcium oscillations. Biophys J 89:1603–1611
42. Sneyd J, Han JM, Wang L, Chen J, Yang X, Tanimura A et al (2017) On the dynamical structure of calcium oscillations. Proc Natl Acad Sci U S A 114:1456–1461
43. Cao P, Tan X, Donovan G, Sanderson MJ, Sneyd J (2014) A deterministic model predicts the properties of stochastic calcium oscillations in airway smooth muscle cells. PLoS Comput Biol 10:e1003783
44. Wang IY, Bai Y, Sanderson MJ, Sneyd J (2010) A mathematical analysis of agonist- and KCl-induced Ca^{2+} oscillations in mouse airway smooth muscle cells. Biophys J 98:1170–1181
45. Higgins ER, Cannell MB, Sneyd J (2006) A buffering SERCA pump in models of calcium dynamics. Biophys J 91:151–163
46. Sneyd J, Tsaneva-Atanasova K, Yule DI, Thompson JL, Shuttleworth TJ (2004) Control of calcium oscillations by membrane fluxes. Proc Natl Acad Sci U S A 101:1392–1396
47. Sneyd J, Tsaneva-Atanasova K, Reznikov V, Bai Y, Sanderson MJ, Yule DI (2006) A method for determining the dependence of calcium oscillations on inositol trisphosphate oscillations. Proc Natl Acad Sci USA 103:1675–1680
48. Nowacki J, Mazlan S, Osinga HM, Tsaneva-Atanasova K (2010) The role of large-conductance Calcium-activated K^+ (BK) channels in shaping bursting oscillations of a somatotroph cell model. Physica D Nonlinear Phenomena 239:485–493
49. Bootman M, Niggli E, Berridge M, Lipp P (1997) Imaging the hierarchical Ca^{2+} signalling system in HeLa cells. J Physiol 499 (Pt 2):307–314
50. Smith IF, Wiltgen SM, Parker I (2009) Localization of puff sites adjacent to the plasma membrane: functional and spatial characterization of Ca^{2+} signaling in SH-SY5Y cells utilizing membrane-permeant caged IP_3. Cell Calcium 45:65–76
51. Taufiq-Ur-Rahman, Skupin A, Falcke M, Taylor CW (2009) Clustering of $InsP_3$receptors by $InsP_3$retunes their regulation by $InsP_3$ and Ca^{2+}. Nature 458:655–659
52. Keebler MV, Taylor CW (2017) Endogenous signalling pathways and caged IP_3 evoke Ca^{2+} puffs at the same abundant immobile intracellular sites. J Cell Sci 130:3728–3739
53. Konieczny V, Keebler MV, Taylor CW (2012) Spatial organization of intracellular Ca^{2+} signals. Semin Cell Dev Biol 23:172–180
54. Bruno L, Solovey G, Ventura AC, Dargan S, Dawson SP (2010) Quantifying calcium fluxes underlying calcium puffs in Xenopus laevis oocytes. Cell Calcium 47:273–286
55. Shuai J, Pearson JE, Foskett JK, Mak DOD, Parker I (2007) A kinetic model of single and clustered IP_3 receptors in the absence of Ca^{2+} feedback. Biophys J 93:1151–1162
56. Smith IF, Parker I (2009) Imaging the quantal substructure of single IP_3R channel activity during Ca^{2+} puffs in intact mammalian cells. Proc Natl Acad Sci U S A 106:6404–6409

57. Flegg MB, Rüdiger S, Erban R (2013) Diffusive spatio-temporal noise in a first-passage time model for intracellular calcium release. J Chem Phys 138:154103
58. Dobramysl U, Rüdiger S, Erban R (2016) Particle-based multiscale modeling of calcium puff dynamics. Multiscale Model Simul 14:997–1016
59. Weinberg SH, Smith GD (2014) The influence of Ca^{2+} buffers on free [Ca^{2+}] fluctuations and the effective volume of Ca^{2+} microdomains. Biophys J 106:2693–2709
60. Wieder N, Fink R, von Wegner F (2015) Exact stochastic simulation of a calcium microdomain reveals the impact of Ca^{2+} fluctuations on IP_3R gating. Biophys J 108:557–567
61. Falcke M, Moein M, Tilunaite A, Thul R, Skupin A (2018) On the phase space structure of IP_3 induced Ca^{2+} signalling and concepts for predictive modeling. Chaos (Woodbury, NY) 28:045115
62. Skupin A, Kettenmann H, Winkler U, Wartenberg M, Sauer H, Tovey SC et al (2008) How does intracellular Ca^{2+} oscillate: by chance or by the clock? Biophys J 94:2404–2411
63. Thurley K, Smith IF, Tovey SC, Taylor CW, Parker I, Falcke M (2011) Timescales of IP_3-evoked Ca^{2+} spikes emerge from Ca^{2+} puffs only at the cellular level. Biophys J 101:2638–2644
64. Moein M, Grzyb K, Gonçalves Martins T, Komoto S, Peri F, Crawford A et al (2018) CaSiAn: a calcium signaling analyzer tool. Bioinformatics (Oxford, England) 1:11
65. Thurley K, Tovey SC, Moenke G, Prince VL, Meena A, Thomas J et al (2014) Reliable encoding of stimulus intensities within random sequences of intracellular Ca^{2+} spikes. Sci Signal 7:ra59
66. Rooney TA, Sass EJ, Thomas AP (1990) Agonist-induced cytosolic calcium oscillations originate from a specific locus in single hepatocytes. J Biol Chem 265:10792–10796
67. Tilunaite A, Croft W, Russell N, Bellamy TC, Thul R (2017) A Bayesian approach to modelling heterogeneous calcium responses in cell populations. PLoS Comput Biol 13:e1005794
68. Barbieri R, Quirk MC, Frank LM, Wilson MA, Brown EN (2001) Construction and analysis of non-Poisson stimulus-response models of neural spiking activity. J Neurosci Methods 105:25–37
69. Miura K, Tsubo Y, Okada M, Fukai T (2007) Balanced excitatory and inhibitory inputs to cortical neurons decouple firing irregularity from rate modulations. J Neurosci 27:13802–13812
70. Thurley K, Skupin A, Thul R, Falcke M (2012) Fundamental properties of Ca^{2+} signals. Biochim Biophys Acta 1820:1185–1194
71. Croft W, Reusch K, Tilunaite A, Russel N, Thul R, Bellamy TC (2016) Probabilistic encoding of stimulus strength in astrocyte global calcium signals. Glia 64:537–552
72. Thul R, Falcke M (2006) Frequency of elemental events of intracellular Ca^{2+} dynamics. Phys Rev E 73(6 Pt 1):061923
73. Thul R, Falcke M (2007) Waiting time distributions for clusters of complex molecules. Europhys Lett 79:38003
74. Thul R, Thurley K, Falcke M (2009) Toward a predictive model of Ca^{2+} puffs. Chaos (Woodbury, NY) 19:037108
75. Thurley K, Falcke M (2011) Derivation of Ca^{2+} signals from puff properties reveals that pathway function is robust against cell variability but sensitive for control. Proc Natl Acad Sci U S A 108:427–432
76. Moenke G, Falcke M, Thurley K (2012) Hierarchic stochastic modelling applied to intracellular Ca^{2+} signals. PLoS One 7:e51178
77. Papoulis A, Pillai SU (2002) Probability, random variables and stochastic processes, 4th edn. McGraw Hill, Boston
78. Ross SM (2003) Introduction to probability models, 8th edn. Academic, Amsterdam
79. Cunningham JP, Shenoy KV, Sahani M (2008) Fast gaussian process methods for point process intensity estimation. In: Proceedings of the 25th International Conference on Machine Learning, Stanford University, Palo Alto, pp 192–199

80. Cunningham JP, Yu B, Shenoy K, Sahani M (2008) Inferring neural firing rates from spike trains using gaussian processes. In: Platt JC, Koller D, Singer Y, Roweis S (eds) Advances in neural information processing systems, vol 20. MIT Press. Cambridge, MA, pp 329–336
81. Robert CP, Casella G (2005) Monte Carlo statistical methods. Springer Texts in Statistics. Springer, New York
82. Brown EN, Barbieri R, Ventura V, Kass RE, Frank LM (2002) The time-rescaling theorem and its application to neural spike train data analysis. Neural Comput 14:325–346
83. Skupin A, Falcke M (2010) Statistical analysis of calcium oscillations. Eu Phys J Spec Top 187:231–240
84. Devroye L (1986) Non-uniform random variate generation. Springer, New York

Chapter 33
Calcium Regulation of Bacterial Virulence

Michelle M. King, Biraj B. Kayastha, Michael J. Franklin, and Marianna A. Patrauchan

Abstract Calcium (Ca^{2+}) is a universal signaling ion, whose major informational role shaped the evolution of signaling pathways, enabling cellular communications and responsiveness to both the intracellular and extracellular environments. Elaborate Ca^{2+} regulatory networks have been well characterized in eukaryotic cells, where Ca^{2+} regulates a number of essential cellular processes, ranging from cell division, transport and motility, to apoptosis and pathogenesis. However, in bacteria, the knowledge on Ca^{2+} signaling is still fragmentary. This is complicated by the large variability of environments that bacteria inhabit with diverse levels of Ca^{2+}. Yet another complication arises when bacterial pathogens invade a host and become exposed to different levels of Ca^{2+} that (1) are tightly regulated by the host, (2) control host defenses including immune responses to bacterial infections, and (3) become impaired during diseases. The invading pathogens evolved to recognize and respond to the host Ca^{2+}, triggering the molecular mechanisms of adhesion, biofilm formation, host cellular damage, and host-defense resistance, processes enabling the development of persistent infections. In this review, we discuss: (1) Ca^{2+} as a determinant of a host environment for invading bacterial pathogens, (2) the role of Ca^{2+} in regulating main events of host colonization and bacterial virulence, and (3) the molecular mechanisms of Ca^{2+} signaling in bacterial pathogens.

Keywords Calcium signaling · Calcium channels · Calcium sensors · Toxins · Adhesins · Biofilm · Attachment · Two component regulatory systems · Secretion · Bacterial pathogens

M. M. King · B. B. Kayastha · M. A. Patrauchan (✉)
Department of Microbiology and Molecular Genetics, Oklahoma State University, Stillwater, OK, USA
e-mail: m.patrauchan@okstate.edu

M. J. Franklin
Department of Microbiology and Center for Biofilm Engineering, Montana State University, Bozeman, MT, USA

M. S. Islam (ed.), *Calcium Signaling*, Advances in Experimental Medicine and Biology 1131, https://doi.org/10.1007/978-3-030-12457-1_33

33.1 Elevated External Calcium (Ca^{2+}) Regulates Adaptation of Bacterial Pathogens to Their Host Environment

33.1.1 Host-Associated Ca^{2+}

In order to survive, bacteria must sense the chemical landscape of their environment and respond to it by adjusting their biological activities. Bacterial pathogens have an additional challenge of recognizing the transition between outside and inside the host and efficiently rearranging their gene expression to enable survival in the hostile host. The environment inside the host has a drastically different chemistry regulated by complex signaling systems, including one of the most versatile intracellular messengers, calcium (Ca^{2+}).

Ca^{2+} signaling has been widely studied in eukaryotes [1, 2]. Ca^{2+} signaling is based on tightly regulated fluctuations in the levels of the ion in different cellular compartments, that trigger multiple molecular pathways. Whereas the cytoplasmic concentration of free Ca^{2+} is maintained at high nanomolar level, the extracellular concentration of the ion reaches millimolar levels [3–5] differing between different body fluids, tissues, and organs. Several examples are summarized in Table 33.1.

Since Ca^{2+} signaling regulates most essential cellular processes, slight abnormalities in Ca^{2+} homeostasis cause diseases or are a result of certain pathologies. For example, in cystic fibrosis (CF) [6, 7], different types of cells, including skin fibroblasts and bronchial epithelium cells, show elevated intracellular Ca^{2+} pools [8, 9]. In addition, abnormally elevated levels of Ca^{2+} were registered in multiple body fluids of CF patients (Table 33.1). Further, the elevation of cytosolic Ca^{2+} concentration was shown to trigger host immune responses against invading pathogens. For example, intestinal epithelial cells infected with *Salmonella* serotype Typhimurium require an increased cytosolic Ca^{2+} to express pro-inflammatory chemokine IL-8 [10]. Elevated Ca^{2+} in CF sputum positively correlates with the release of IL-8 in the necrotic immune cells [11]. As a part of the innate immunity defense, production of antimicrobial peptides (AMPs) by epidermal keratinocytes in response to infection by *Pseudomonas aeruginosa, Staphylococcus aureus* and

Table 33.1 Examples of free Ca^{2+} levels in human body fluids

Body fluid	$[Ca^{2+}]$	References
Joint fluids	4 mM	[26]
Plasma	1.3–1.5 mM	[23, 27–29]
Serum	0.7 to 1.4 mM.	[23, 30–34]
Saliva (in CF patients)	0.3 mM (4.8 ± 0.7 mM)	[35–41]
Nasal secretions (in CF patients)	3.1 ± 1.6 mM (4.7 ± 2.2 mM)	[42–44]
Sputum (in CF patients)	1.1 mM (2.5 mM)	[11]
Urine	1.6–5 mM	[45]

other pathogens is induced by elevated levels of Ca^{2+} [12]. Some of the AMPs, including a family of Ca^{2+} binding EF-hand S100 family, require Ca^{2+} for their interactions with targets [13].

Some bacterial pathogens are able to alter the hosts $[Ca^{2+}]_{in}$ levels through activating Ca^{2+} flux across the plasma membrane and, releasing Ca^{2+} from the intracellular stores into the cytosol [10, 14–17]. These interactions can be mediated by bacterial surface associated proteins such as PilC of *Neisseria meningitidis* [17], FliC of *P. aeruginosa* and *Salmonella* [18], and FimH of *Escherichia coli* [19] or by secreted effectors, such as hemolysin A from *S. aureus* [20], pyocyanin and homoserine lactones from *P. aeruginosa* and *Serratia liquefaciens* [21–25]. Such alterations in the host Ca^{2+} have been shown to facilitate bacterial adherence and subsequent internalization into the host cells.

In plants, Ca^{2+} is one of the earliest signaling elements that coordinate adaptive immune responses to invading pathogenic bacteria. Cytoplasmic Ca^{2+} ($[Ca^{2+}]_{cyt}$) increases in response to infecting pathogens, such as *P. syringae* [46]. A sustained elevation of $[Ca^{2+}]_{cyt}$ serves as an important early signal, which links the recognition of infection to downstream defenses including generation of reactive oxygen species (ROS) and oxidative burst [47, 48]. The ROS burst may lead to cell death preventing the pathogen establishment inside the plant [49].

Overall, Ca^{2+} is an essential component of the host environment that both responds to the presence of bacterial pathogens, and regulates specific defense mechanisms. Ca^{2+} levels in a host may signal to the invading pathogens that they are entering a host and also indicate the status of immune protection in the host. Therefore, recognizing the host Ca^{2+} level can be beneficial to the invaders and trigger their adaptation to the host environment, and lead to their increased virulence and survival of the pathogen.

33.1.2 Ca^{2+} Triggers Life Style Switches in Bacterial Pathogens

Bacteria possess efficient regulatory systems that enable their adaptation to continuously changing environments. Regulation of gene expression is key for bacterial survival in a variety of environments. One particularly efficient and complex mechanism of surviving hostile environments is a switch between free-swimming or planktonic lifestyle to sessile life as surface-associated community, called biofilm. This transition is enabled by major molecular rearrangements ultimately enabling increased resistance, cell-cell communication and efficient metabolism [50, 51]. This mechanism is of particularly high importance to extracellular pathogenic bacteria colonizing host surfaces and surviving both host defenses and antimicrobial treatments.

There is a growing body of evidence that Ca^{2+} plays both a structural and a regulatory role in the transition to surface-associated biofilm lifestyle. Bacterial

adhesion is the first step in biofilm formation, and itself is a survival mechanism, as nutrients, for example, tend to accumulate at surfaces [52]. The effect of Ca^{2+} on adhesion is partially due to electrostatic interactions, but also due to strong interactions of the surfaces with the cell structures, such as pili and fimbriae [53–55], and other macromolecules including teichoic acids, adhesins, lipopolysaccharide (LPS), and extracellular polysaccharides (EPS). It was shown that cell surface properties and their electrostatic interactions with the substratum contribute to Ca^{2+}-enhanced adhesion of non-motile and motile *P. aeruginosa* [56]. Ca^{2+}-enhanced cell adhesion to diverse host molecules and in vitro substrates, as well as cell-cell aggregation, relies on the presence of type I and type IV pili in a number of pathogens, including *Xylella fastidiosa,* [53], *P. aeruginosa* [57], *Vibrio vulnificus* [58], and *N. gonorrhoeae* [59]. The Ca^{2+} regulation of the type IV pilus is determined by its binding to pilus-biogenesis factor, PilY1, enabling pilus extension and retraction [60]. This interaction is also required for the bacterium twitching motility. By interacting with type I pili and fimbriae, Ca^{2+} modulates invasion of bacterial pathogens, such as *E. coli,* into host cells [19, 61].

Ca^{2+} also enhances bacterial adhesion via large cell surface Ca^{2+}-binding adhesins, such as SdrC and SdrD in *S. aureus* [62, 63] and BapA in *Paracoccus denitrificans* [64]. The former contain EF hand-like motifs that bind Ca^{2+} required for protein folding. The latter belongs to repeats-in-toxin (RTX) family, containing multiple nonapeptide Ca^{2+}-binding domains, secreted via Type I Secretion System (TISS), and serving a variety of functions, including cell-cell or cell-surface interactions or contributing to protection against hostile environments by forming bacterial surface (S)-layers (reviewed in [65]). In *Listeria monocytogenes,* elevated Ca^{2+} has been reported to stabilize the complex between the adhesin InlA (Internalin A) and the human extracellular E-cadherin domain 1 (hEC1). Once inside the host cell, where Ca^{2+} concentrations are lower, the InlA-hEC1 complex dissociates, which facilitates the liberation of the bacteria from the host cell membrane into the cytosol [66]. Ca^{2+} is required for multimerization of large adhesin LapF involved in colonization, microcolony formation, and biofilm maturation of *P. putida* [67–69].

Due to its interactions with surface proteins and by forming ionic bridges between negatively charged macromolecules, Ca^{2+} enhances cell aggregation and strengthens biofilm matrixes, including cell aggregation in oral *Streptococci* [70] and alginate cross-linking of *P. aeruginosa* biofilm matrix [71]. Ca^{2+} was also shown to bind extracellular DNA (eDNA), another important component of biofilm matrix, and this thermodynamically favorable binding increases bacterial aggregation in several Gram-positive and Gram-negative species, including *S. aureus* and *P. aeruginosa*. The authors concluded that Ca^{2+} did not affect DNA release [72]. However, this observation is likely species- and strain-specific [73], as Ca^{2+} was shown to induce production of *P. aeruginosa* pyocyanin, which promotes DNA release [74]. Furthermore, the presence of Ca^{2+} increased eDNA release, contributing to biofilm formation in *Streptococcus mutans* [75]. Ca^{2+} was also shown to increase the adhesive nature of *P. fluorescence* biofilm, but reduced its elastic properties [76].

In different bacterial species, elevated Ca^{2+} either stimulates or reduces biofilm formation. Positive regulation was observed in response to 1–10 mM Ca^{2+} in *Pectobacterium carotovorum* [77], *Rhizobium leguminosarum* [78], *Pseudoalteromonas* sp. [79], *Shewanella oneidensis* [80], *P. aeruginosa* [73], *X. fastidiosa* [81], *V. cholerae* [82], and *V. fischeri* [83]. This regulation was shown to be mediated by diverse mechanisms. For example, elevated Ca^{2+} activates the transcription of genes responsible for production of surface adhesins and EPS: alginate in *P. aeruginosa* [73] and *P. syringae* [84]*;* symbiosis polysaccharide (*syp)* or cellulose in *V. fisheri*. Ca^{2+}-dependent hemophilic interactions of surface-associated adhesin SdrC promotes biofilm formation in *S. aureus* [62].

Negative regulation of biofilm by elevated Ca^{2+} was reported in *S. aureus* [85] and *V. cholerae* [86]. In *V. cholerae,* this regulation is mediated by negatively regulated two-component system CarSR and *vps* (Vibrio polysaccharide) genes. However, *V. cholerae* also produces Vps-independent biofilm, which is preferred under high Ca^{2+} sea water conditions, where Ca^{2+} interacts directly with the O-antigen polysaccharide [87]. *S. aureus* produces several surface adhesins, such as clumping factors A and B (ClfA and ClfB) [88, 89] and biofilm-associated protein (Bap) [85]. These proteins contain Ca^{2+}-binding EF-hand-like motifs, and binding the ion inhibits their role in cell adhesion and biofilm formation. A point mutation in protease aureolysin (*aur)* gene in one of *S. aureus* strains led to increased activity of ClfB, required for biofilm growth under Ca^{2+}-depleted conditions [90].

Some factors contributing to biofilm formation are known to be regulated by cyclic-di-GMP (c-di-GMP) (reviewed in [91]) and quorum sensing (QS) (reviewed in [92]). This raises the possibility of interconnections between c-di-GMP, QS and Ca^{2+} regulatory networks that warrant further studies.

33.1.3 Virulence Factors Regulated by Ca^{2+}

Factors that enable pathogenic bacteria to cause diseases can be broadly grouped into several categories, such as penetration, colonization, damage of host cells, evasion of host defenses, and proliferation, all ultimately contributing to the developing infections. Colonization requires pathogens to establish interactions with host tissues by producing extracellular or cell-associated molecules. It may also involve communication between invaders themselves or those with commensals. The relationship between some of these factors and Ca^{2+} is discussed above. Here we outline virulence factors attributed to more invasive host-pathogen interactions that are directly or indirectly regulated by Ca^{2+}.

Bacterial invasion is commonly facilitated by the production and secretion of molecules that cause enzymatic or non-enzymatic damage to the host cells [93, 94]. A number of secreted enzymes are known to be regulated by Ca^{2+} in bacterial pathogens. For example, in *P. aeruginosa,* Ca^{2+} promotes the production of extracellular proteases LasB, LasA, PrpL (protease IV), and AprA [73, 95–97].

In the case of elastase LasB, Ca^{2+} not only increases the production of the protein, but modulates its processing, export, stability and enzymatic activity [95, 98, 99]. The enzymatic activity covers a wide repertoire of substrates, including elastin, collagen, and human immunoglobulins, underlining the significance of the protein and its Ca^{2+} regulation in *P. aeruginosa* pathogenicity. The alkaline protease A (AprA) binds Ca^{2+} through its C-terminal RTX domain, enabling folding of both C- and N-terminal proteolytic domains, which is required for stable conformation and enzymatic activity of the protease [73, 80, 96]. Both AprA and LasB are capable of degrading exogenous flagellin monomers under Ca^{2+}-replete condition, which prevents flagellin-mediated immune recognition and killing of *P. aeruginosa via* complement-mediated phagocytosis [99, 100]. The Ca^{2+}-enhanced production of the two proteases with anti-flagellin activity provides a robust strategy for *P. aeruginosa* to escape the detection by the complement system.

Our earlier studies showed that production of pyocyanin, the extracellular redox cycling compound and a virulence factor of *P. aeruginosa* [101, 102] is up-regulated in response to elevated Ca^{2+} [73]. Pyocyanin is found in pulmonary fluids of CF patients and shown to disrupt Ca^{2+} homeostasis of the host epithelial cells [21, 103], potentially contributing to a further increase of extracellular host Ca^{2+} and therefore induction of Ca^{2+}-regulated virulence.

Toxins represent one of the most powerful strategies of bacterial pathogens to conquer a host. Ca^{2+} modulates the production, secretion, and function of several toxins in a number of pathogens. In *E. coli,* Ca^{2+} is required for Hemolysin A (HlyA) binding to erythrocytes [104]. Binding Ca^{2+} causes conformational change in the toxin increasing its surface hydrophobicity and promoting the irreversible binding to the lipid bilayer of erythrocytes. This interaction preludes and ensures the lytic effect [105]. In *V. cholerae*, Ca^{2+} enhances bile salt-dependent activation of virulence. The mechanism relies on Ca^{2+} promoting the bile salt-induced activation of transmembrane virulence regulator TcpP, which then induces the production of major virulence factors, including toxin-coregulated pilus (TCP) [106]. The presence of Ca^{2+} has been reported to be essential for the toxicity of anthrax-edema toxin (composed of protective antigen and edema factor) produced by *Bacillus anthracis* [107]. The edema factor has adenylate cyclase activity synthesizing cAMP. Once in the host cytosol, the edema factor produces cAMP, which causes a rapid influx of Ca^{2+}. The accumulation of cAMP in the cytosol requires the presence of extracellular Ca^{2+}. As a potent inhibitor of immune response, accumulated cAMP leads to suppression of proinflammatory cytokines, phagocytosis and bactericidal activity of leukocytes thereby facilitating the survival of bacteria in the host [107, 108].

On the other hand, elevated host Ca^{2+} may have a negative regulatory effect on virulence and thus contribute to host defenses. One example is a cell wall degrading enzyme endopolygalacturonase (PehA) that is down-regulated by high (10–30 mM) levels of Ca^{2+} in a plant pathogen *Pectobacterium carotovorum*. This prevents the pathogen from infecting the plant [109].

Overall, Ca^{2+} regulates many virulence factors of invading bacterial pathogens, which stresses the importance of a detailed understanding of Ca^{2+} regulatory pathways in these pathogens.

33.1.4 Ca^{2+}-Regulated Secretion Systems

Most bacteria can respond to and manipulate their environment through the secretion of extracellular proteins. Bacterial secreted proteins are often involved in breakdown of macromolecules, such as polysaccharides or polypeptides to simple sugars or amino acids that the bacteria can take up and utilize as carbon, nitrogen, and energy sources. Secreted proteins may also act as virulence factors, as in the case for the proteases described above, LasA, LasB, PrpL, and AprA, which modulate immune effectors and degrade elastic tissues [73, 95, 96, 99, 100]. Pathogenic bacteria also use protein secretion to kill other cells, including eukaryotic cells [110] and, in some cases, competing bacteria within biofilm communities [111]. Extracellular Ca^{2+} concentration plays a direct or indirect signaling role in many of the bacterial protein secretion systems.

Bacteria use at least six different strategies to secrete proteins (termed: T1SS to T6SS) reviewed in [112]. The T1SS transports specific proteins directly from the cytoplasm to the extracellular medium, with no apparent periplasmic intermediate. The Ca^{2+} requiring protease, AprA [113], is secreted by the T1SS, composed of three components, AprDEF, which include cytoplasmic ATPase, an inner membrane protein component, and an outer membrane protein [114]. These proteins form a molecular complex, dedicated to the export of AprA [113]. AprA accumulates in the biofilms of *P. aeruginosa* under Ca^{2+}-replete conditions, but not under Ca^{2+} – limiting conditions [73]. The other protease virulence factors described above that require Ca^{2+} for activity or structural integrity, LasA, LasB, and the PrpL [98], are secreted by the T2SS [115–117]. The T2SS is a general pathway for secretion of a variety of extracellular proteins. In the T2SS, proteins with N-terminal export signal peptides, are first exported to the periplasm by either the Sec export machinery or the twin-arginine translocation (TAT) system [118, 119]. Sec, exports proteins in an unfolded state, then folds the proteins into their three dimensional confirmation in the periplasm, with the help of proteins such as disulfide bond isomerase, DsbA. The TAT system exports folded proteins into the periplasm. Once in the periplasm, proteins are secreted across the outer member *via* the secretion apparatus. For example, in *P. aeruginosa* the secretion apparatus is composed of the Xcp proteins (XcpA and XcpP-Z) or the homologous system, Hxc (composed of HxcP-Z) [112]. In addition to secretion of enzymes into the extracellular medium, the T2SS also plays a role in generation of certain types of pili, the Type IV pilus, which plays role in bacterial attachment and movement along surface. In twitching motility, bacteria move along surfaces by extension and retraction of the pili, through polymerization and depolymerization of the pilin subunits. Some bacteria,

including *E. coli* and several *Vibrio* spps, requires Ca^{2+} for structural integrity of the major pseudopilin subunit, GspG [120].

The type III secretion system (T3SS), encoded on pathogenicity islands of many pathogenic bacteria, delivers effector protein toxins directly into the cytosol of eukaryotic cells during infection. The toxins, including enzymes such as ADP-ribosyltransferases, phospholipases, or adenylate cyclases, disrupt such host cell activities as actin remodeling, and gene regulation [112]. Perhaps the most interesting role of Ca^{2+} in secretion of bacterial virulence factors is its direct role in expression regulation (activation or repression) of the genes encoding the secretion apparatuses. It has been known for many years that expression of the T3SS genes is induced by either host-cell contact or by chelation of Ca^{2+} from the medium (low [Ca^{2+}]) [121, 122]. The T3SS forms a complex needle-like structure that is related to the bacterial flagella basal body [123]. The T3SS includes inner and outer membrane ring structures, and cytoplasmic protein components that dock to the inner membrane ring. The needle-like structure protrudes from the basal body, punctures the host cell membrane, and secretes toxins directly into the host cells. For this reason, the T3SS has also been termed the injectosome.

Regulation of expression of the T3SS gene clusters by host cell contact has been well characterized in *P. aeruginosa* [124, 125]. Transcription of the T3SS in *P. aeruginosa* is controlled by the transcriptional activator, ExsA, an AraC/XylS-type regulator. ExsA is inhibited by a cascade of protein-protein interactions that prevent ExsA binding to the DNA. The cascade involves interactions of ExsA, ExsD, ExsC, and ExsE. Expression of the T3SS genes is induced when ExsE is translocated from the cell through the T3SS, ultimately titrating the anti-activator, ExsD away from the ExsA and allowing transcription. If translocation of ExsE through the T3SS is functional (e.g. during host cell contact or at low Ca^{2+}), transcription of the TS33 genes is activated. If ExsE builds up in the cell due to lack of host cell contact, then further transcription of the TS33 genes is inhibited.

Another role of Ca^{2+} in regulation of T3SS was recently shown to involve the Ca^{2+}-sensor protein, LadS [126]. LadS is a hybrid membrane-bound sensor, containing both a histidine kinase domain and a periplasmic Ca^{2+}-binding DISMED2 domain. Broder et al. [126] mutated potential Ca^{2+}-binding residues in *P. aeruginosa* and found that the resulted T3SS gene expression became insensitive to Ca^{2+} conditions. Ca^{2+} binding to the LadS DISMED2 domain is the first step in a regulatory cascade that responds to external Ca^{2+}. The cascade involves two component system GacCS, two small regulatory RNAs, RsmY and RsmZ, and the RNA binding protein, RsmA. Ultimately, binding of RsmA to specific mRNA sequences results in gene regulation at the translational level [126].

Assembly of the T3SS is a dynamic process that responds to external Ca^{2+}. Using *Yersinia entercolitica*, Diepold et al. [127] tagged components of the T3SS with fluorescent reporter proteins, so that they could image the membrane and cytosolic components. Using Fluorescence correlation spectroscopy, they calculated the diffusion rates of the T3SS cytoplasmic components under inducing (low Ca^{2+}) and non-inducing (high Ca^{2+}) conditions, as they assembled. They found that the

rate of diffusion of the cytoplasmic components changed with the external Ca^{2+} concentration and proposed this as a novel mechanism for the role of Ca^{2+} in regulation of T3SS assembly.

The switch between expression of T3SS (low Ca^{2+}) to more recently discovered type T6SS [128] may correlate with the switch from acute to chronic infections of *P. aeruginosa* [126]. The T6SS also uses direct injection of effector proteins into other cells, which may be host cells, or other competing bacteria [111]. However, rather than being evolutionarily related to the flagella basal body, the T6SS appears related to bacteriophage tail-associated proteins [129]. The tail-spike is used to puncture the membranes of cells, and the effector molecules at the tip of the spike are injected directly into the cytosol. Regulation of expression of T6SS is not well characterized and the role of Ca^{2+} in regulation of T6SS is not well known. However, Allsopp et al. [130] using a transposon mutagenesis screening approach identified the RNA binding protein, RsmA as a primary component involved in the regulation of all the three T6SS gene operons of *P. aeruginosa*. Therefore, a common link in the inverse regulation of T3SS and T6SS involves the RNA binding protein RsmA.

33.2 Molecular Mechanisms of Ca^{2+} Responses in Pathogens

33.2.1 Two Component Systems

As discussed above, Ca^{2+} levels differ within a host, fluctuate during disease progression, and thus form a complex signaling landscape for invading pathogens. Therefore, sensing host Ca^{2+} is an important task enabling pathogens to efficiently adjust to the host environment by triggering the expression of genes responsible for virulence and resistance. Bacteria accomplish this in part by employing two-component regulatory systems (TCS). A traditional TCS consists of a sensor kinase and a response regulator. The sensor kinase is usually embedded into the inner membrane with the sensor region often facing the periplasm. Upon signal binding, the sensor kinase auto-phosphorylates followed by phosphorylating the response regulator, typically regulating transcription of a set of target genes [131–133].

Several Ca^{2+} sensing TCSs have been identified. Some of them are positively and some are negatively regulated by elevated Ca^{2+} (Table 33.2). To test whether the relationship with the ion is defined by the recognition sequence within the TCS sensor, we aligned the sensor sequences of the TCS experimentally shown to be regulated by Ca^{2+}. Based on the Clustal Omega alignment, a maximum likelihood tree was constructed using MEGA4 algorithm [134, 135] (Fig.33.1). The distinct grouping of positively and negatively regulated sensors supports the idea of sequence-dependent relationship with Ca^{2+}.

The TCSs that are negatively regulated by Ca^{2+} have been studied in more details. PhoPQ is a well-characterized TCS, found in a variety of Gram-negative pathogens, such as *P. aeruginosa*, *E. coli*, *Yersinia pestis, Shigella flexneri* and *S.*

Table 33.2 Sensors from two-component regulatory systems (TCS) regulated by Ca^{2+}

Name	GenBank ID	Stimuli	Ca^{2+}-dependent regulatory targets	Regulated Phenotype	Organism	References
Positively Regulated by Elevated Ca^{2+}						
CarS	AAG06044.1	Ca^{2+}	*carP, carO*	Virulence	*P. aeruginosa*	[153]
CvsS	AAO56858.1	Ca^{2+}	*hspR, algU*	Biofilm formation, cellulose production, virulence, T3SS	*P. syringae*	[84]
AtoS	AEH68827.1	Ca^{2+} SpermidineHistamineAcetoacetate	*Ato operon*	Synthesis of PHB-PP, motility	*E. coli*	[154–157]
VicK	PNM00564.1	Ca^{2+}, Mn^{2+}, sucrose	*atlA* operon	eDNA release, response to host immunity, attachment, and biofilm formation	*S. mutans*	[91, 158, 159]
Negatively Regulated by Elevated Ca^{2+}						
PhoQ	AIB53821.1	Mg^{2+}, Ca^{2+}, acetate		LPS modification	*E. coli*	[137, 147]
PhoQ	P0DM80.1	Mg^{2+}, Ca^{2+}		LPS modification, SOS response	*S. enterica*	[136, 145, 160]
PhoQ	AEU17992.1	Mg^{2+}, Ca^{2+}		LPS modification	*P. aeruginosa*	[137, 141, 143]
PehS	BAJ11971.1	Ca^{2+}	*pehA*	Virulence	*P. carotovorum*	[148]
CiaH	P0A4I6.1	Ca^{2+}	*ciaX*	Ca^{2+} mediated cell functions and biofilm production	*S. pneumoniae*	[161]
CarS	2,614,773	Ca^{2+}	*vps*	Vps-dependent biofilms, antibiotic resistance	*V. cholerae*	[86, 162]

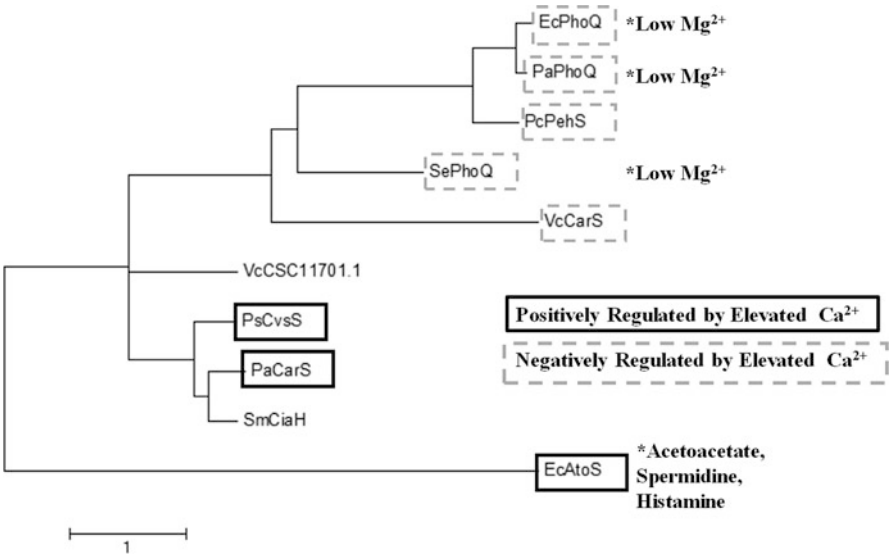

Fig. 33.1 Molecular Phylogenetic analysis of Ca^{2+}regulated TCS. To analyze the sequences of Ca^{2+} regulated TCS sensors, we first determined the sensor regions by selecting the periplasmic loop of the proteins based on TMHMM analyses. After the 11 sequences were aligned, all positions containing gaps and missing data were eliminated. The phylogenetic relationship of the sensor regions was inferred by using the Maximum Likelihood algorithm based on the JTT matrix-based model [1] in MEGA7 [2]. The tree with the highest log likelihood (−2667.30) is shown. The tree is drawn to scale, with branch lengths measured in the number of substitutions per site

enterica [82, 131, 136–138]. PhoPQ systems regulate multiple virulence factors, resistance and motility. The PhoPQ regulon includes the SOS response of *S. enterica* [139], and the *arn* operon of *P. aeruginosa*, which is responsible for lipid A modifications and increased resistance to antimicrobial peptides [138, 140–144]. Interestingly, PhoPQ systems are also repressed by elevated Mg^{2+}, and two-distinct Mg^{2+} and Ca^{2+} binding regions were identified in PhoQ sensor of *S. enterica* [136]. These regions are conserved in other PhoQ homologs [145, 146]. While the PhoPQ systems share overall sequence similarly, they differ in their responses. Thus, mutating Ca^{2+}-binding residues in PhoQ have less of an impact on transcriptional regulation in *E. coli* than in *S. enterica* [146]. PhoQ interactions with ligands also differ in different species: Mg^{2+} binds to PhoQ dimer causing destabilization and preventing signal transduction in *P. aeruginosa* PhoQ (*Pa*PhoQ), but not in *E. coli* PhoQ (*Ec*PhoQ) [137]. Finally, PhoQ may respond to additional ligands such as acetate in the *E. coli* PhoQ [147]. The TCS most closely grouped with PhoPQ is PehSR from a plant pathogen *Pectobacterium carotovorum* (Fig. 33.1). This system regulates the production of a secreted endopolygalacturonase, PehA which is required for initial invasion of the pathogen into a host [109, 148–150]. Homologs of PehA, although not yet characterized, have been identified in another plant pathogen *Erwinia chrysanthemi* [151, 152].

Another TCS negatively regulated by elevated Ca^{2+} is CarSR from *V. cholera* [86]. CarSR regulates *Vibrio* polysaccharide (*vps*), the main matrix component of *vps*-dependent biofilms. Although elevated Ca^{2+} decreases the formation of *vps*-dependent biofilms, it increases the formation of *vps*-independent biofilm in *V. cholerae,* as well as production of bile-salt-dependent virulence factors required for colonization of the gut [82, 163, 164]. The mechanisms for this positive Ca^{2+} regulation of *V. cholerae* virulence are not known and potentially involve an alternative TCS that is positively regulated by Ca^{2+}. To predict such a TCS, we performed BLASTP alignment of the sensor region from the positively regulated by Ca^{2+} *P. aeruginosa* CarS against the *V. cholerae* genome and identified a putative Ca^{2+} responsive sensor protein CSC11701.1. The close grouping of its sensor sequence with *P. aeruginosa* CarS and *P. syringae* CvsS supports its potentially positive regulation by Ca^{2+} (Fig. 33.1).

An atypical TCS, CiaHR, was identified in *Streptococcus mutans.* CiaHR contains a third component, CiaX, a small protein, which upon binding Ca^{2+}, interacts with the sensor portion of CiaH and prevents the phosphor-relay. The system was shown to regulate antibiotic resistance, biofilm formation, eDNA uptake, as well as stress response [161, 165–167]. Interestingly, CiaH grouped closely with the positively regulated sensors, indicating a possibility that CiaH itself may be regulated by Ca^{2+}. In addition, *S. mutans* biofilm formation and eDNA release can be positively regulated in response to Ca^{2+} *via* the TCS VicKR [91, 159, 168, 169]. However, VicK is more distantly related to the positively regulated Ca^{2+} sensors, which could be attributed to its potential to respond to other stimuli (Fig. 33.1).

The TCS that are positively regulated by elevated Ca^{2+} were shown to be involved in regulating virulence and resistance factors in response to Ca^{2+}. Earlier, our group identified a TCS that is positively regulated by Ca^{2+} in *P. aeruginosa.* It was named it Calcium Regulated Senor/ Regulator, CarSR [153]. This system regulates at least two identified targets, CarO and CarP, involved in Ca^{2+}–induced production of virulence factors pyocyanin and pyoverdine and contributes to the regulation of the intracellular Ca^{2+} homeostasis and tolerance to elevated Ca^{2+}. Recently, another Ca^{2+}-induced TCS was found in plant pathogen *P. syringae*, named Calcium, Virulence, and Swarming Sensor and Regulator, CvsSR. CvsSR is required for *P. syringae* pathogenicity in plants by enhancing transcription of genes for T3SS and small RNAs while repressing alginate and flagella biosynthesis [84]. In *E. coli*, synthesis of the polyhydoxybutyrate polyphosphate (PHB-PP) Ca^{2+} channels is positively regulated by the AtoSC TCS. These non-proteinaceous Ca^{2+} channels play a role in eDNA uptake and folding of the outer membrane protein OmpA [154, 170, 171]. In addition, AtoSC regulates other processes, such as motility in response to acetoacetate, histamine, and spermidine [155–157]. This may be reflected in its distant grouping from CarSR and CvsSR (Fig. 33.1).

In summary, bacterial pathogens utilize multiple TCS to recognize changes in the environmental Ca^{2+} and adjust their transcriptional activity. These systems are versatile as they evolved to enable bacterial adaptations to multi-variant environments. Understanding the regulation by TCS is challenged by several factors: the presence

of multiple systems in one organism, sensors responding to different stimuli, and additional components involved in signal recognition [172–175]. Different TCS may also cross-talk enabling multiple signals to control similar responses, as in the case of SypFG, proposed to mediate Ca^{2+} induction of biofilm formation in *V. fischeri* [83]. The sensing portion of SypF, however, was not required for Ca^{2+} induction, and involved an alternative sensor kinase RscS phosphorylating SypF in response to Ca^{2+} [83]. A much better understanding of the TCS signaling networks triggered by Ca^{2+} is needed to fully appreciate their role in Ca^{2+}-mediated communication between invading pathogens and their hosts.

33.2.2 Ca^{2+} Sensors

In eukaryotes, members of the calmodulin superfamily are the best studied Ca^{2+} sensors [176, 177]. Calmodulin (CaM) contains two canonical EF-hand motifs coordinating Ca^{2+} binding [178, 179]. Upon binding Ca^{2+}, CaM undergoes conformational changes enabling binding and activating diverse target proteins [180]. Therefore, searches for components of Ca^{2+} signaling networks in bacteria have focused on proteins with EF hands [181]. In addition, proteins that play roles in translocating or buffering Ca^{2+} have been studied [182–188]. A number of calmodulin-like proteins have been reported based on their sequence and structure similarity to CaM and binding to anti-calmodulin antibodies. Several of these Ca^{2+} sensors are summarized in Table 33.3. The first proposed bacterial Ca^{2+} sensor was CasA, from *Rhizobium etli.* CasA has three pairs of EF hand domains, similarly to eukaryotic calbindin and calretinin [189]. CasA mediates Ca^{2+}-dependent symbiotic relationship between *R. etli* and its plant host. Our group identified a homolog of CasA in *P. aeruginosa* and named it EfhP (EF-hand protein) [190]. EfhP is required for maintaining $Ca^{2+}{}_{in}$ homeostasis and involved in Ca^{2+} regulation of *P. aeruginosa* virulence. Our current studies verified the ability of this protein to selectively bind Ca^{2+} and undergo Ca^{2+}–dependent conformational changes supporting its role as a Ca^{2+} sensor (Kayastha et al. in preparation). Another EF hand protein, proposed to function as a Ca^{2+}-sensor, is CabD from *Streptomyces coelicolor*. CabD contributes to Ca^{2+} regulation of aerial mycelium formation. CabD has high- and low-affinity Ca^{2+}-binding sites, suggesting their distinct roles in mediating Ca^{2+}-regulatory and buffering roles, respectively [177].

CaM-like proteins have been reported in *Mycobacteria* and are suggested to play a role in sensing Ca^{2+} [199]. The CaM-like protein, Rv1211 of *M. tuberculosis* binds Ca^{2+} through its single EF hand domain and stimulates the activities of NAD kinase and phosphodiesterase (PDE), targets that are similar to those of eukaryotic CaM. Reduced expression of this protein has been shown to impair *M. tuberculosis* growth and survival in macrophages, suggesting its importance during infection [192, 193]. A homologous CaM-like protein from *M. smegmatis* has been shown to stimulate phosphodiesterase activity and regulate the metabolism of phospholipids [200] supporting the role of this protein as a Ca^{2+} sensor.

Table 33.3 Ca^{2+} Sensors

Protein name/GenBank ID	Organism	Function/Properties	Domain	References
EfhP AAG07494.1	*P. aeruginosa*	Regulates Ca^{2+} induced virulence and intracellular Ca^{2+} homeostasis	One pair of EF hands	Kayastha et al. (in preparation)
CasA AF288533	*R. etli*	Mediates Ca^{2+} dependent symbiosis with leguminous host	Three pairs of EF hands	[189]
CabD 3AKA_A	*S. coelicolor*	Affects formation of aerial mycelium	Two pairs of EF hands	[177]
Protein S WP_020477824	*M. xanthus*	Required for assembly of spore coat	Beta-gamma crystalline fold	[191]
CAMLP NP_215727	*M. tuberculosis*	Activates NAD kinase and phosphodiesterase upon Ca^{2+} binding	Single EF hand motif	[192, 193]
CAMLP AY319523.1	*M. smegmatis*	Activates phosphodiesterase	Single EF hand motif	[194]
CALP YP_004243569	*B. subtilis*	Activates phosphodiesterase in Ca^{2+} dependent manner		[195]
CLP	*B. pertussis*	Activates adenylate cyclase in Ca^{2+} dependent manner		[196]
LadS AAG07361	*P. aeruginosa*	Ca^{2+} dependent phosphor-relay to GacSA	Histidine kinase, 7 transmembrane, DISMED2	[197, 198]

Protein S from *Myxococcus xanthus* is a member of ßγ-crystalline family. This protein shares structural similarity to CaM and binds Ca^{2+}, which is required for the protein assembly on the surface of the spores [201]. A more recent report showed that the protein's Ca^{2+}-binding site forms a high charge density pocket similar to that in calsequestrin and human Hsp70. However it is still not clear whether the Ca^{2+}-induced conformational changes in protein S play roles in signaling events [191].

Recently, a hybrid histidine kinase LadS was shown to trigger a Ca^{2+}-induced switching between acute and chronic type of virulence in *P. aeruginosa* [198]. As discussed above, LadS belongs to a unique class of bacterial sensors that possess histidine kinase, seven transmembrane, and the periplasmic DISMED2 domain. The latter was shown to bind Ca^{2+} *via* Asp80 and Asp90 residues and activate the kinase activity leading to phosphorelay cascade [197, 198]. In contrast to typical sensors of TCS that phosphorylate partnered response regulators, LadS phosphorylates the TCS GacSA and thus activates GacS/Rsm pathway responsible for the global regulation of chronic infection-type virulence and tolerance [88]. *In silico* analysis of the sequence conservation of LadS showed that this protein is unique to *Pseudomonas*. Interestingly, during searches for homologous DISMED2

domains among selected bacterial pathogens, we identified several proteins including putative alkaline phosphatase synthesis sensors CJK91172.1 and CJK40304.1, and a membrane protein with GGDEF domain, CJK88170.1, in *S. pneumoniae*. The GGDEF domain is known to act as a diguanylate cyclase responsible for synthesis of cyclic-di-GMP, a second messenger mainly regulating biofilm formation [202]. In addition to DISMED2 domain, these proteins contain the two residues (Asp80 and Asp90) required for Ca^{2+} recognition, suggesting they may sense and respond to Ca^{2+}.

Pathogenic bacteria possess Ca^{2+}-sensing proteins that play an important role in modulating their pathogenicity. However, despite evidence of the significance of Ca^{2+} regulation in bacterial physiology and virulence, the knowledge on Ca^{2+} sensors and regulators in bacteria is still limited. Further studies are needed to determine whether these proteins sense the changes in the intracellular Ca^{2+} and thus enable Ca^{2+} to serve as second messenger.

33.3 Components of Intracellular Ca^{2+} Signaling in Pathogenic Bacteria Mediating Ca^{2+} Regulation of Virulence

A number of studies have shown that bacterial metabolic processes respond to elevated Ca^{2+} (reviewed in [203–205]). Some of these processes are regulated by extracellular Ca^{2+} levels and are mediated by TCS. However, other processes may respond to the transient changes in the intracellular Ca^{2+} ($Ca^{2+}{}_{in}$), thus implicating Ca^{2+} as a second messenger. Although the latter still requires experimental proof, here we discuss the components of $Ca^{2+}{}_{in}$ signaling network that have been shown to play a role in Ca^{2+} regulation, supporting the idea of a regulatory role of $Ca^{2+}{}_{in}$ in bacteria.

Similarly to eukaryotic cells, bacteria maintain their basal $[Ca^{2+}]_{in}$ at high nanomolar level and generate transient changes in $[Ca^{2+}]_{in}$ in response to diverse stimuli [206–210]. These stimuli include a variety of extracellular factors, such as $Ca^{2+}{}_{ex}$, pH, mechanical stimulation, intermediates of carbohydrate metabolism, and oxidative stress; all factors potentially to be encountered upon entering a host [206, 208, 210–213]. A number of proteins have been shown to contribute to the maintenance of $Ca^{2+}{}_{in}$ homeostasis and to the generation of $Ca^{2+}{}_{in}$ fluctuations [203, 206]. However, it is still not clear whether bacteria have an intracellular source of Ca^{2+} for these fluctuations (e.g. a compartment for storing and releasing Ca^{2+} into the cytoplasm) or if they rely on influx of extracellular Ca^{2+}. *E. coli* accumulates Ca^{2+} in the periplasm to millimolar levels when grown in the presence of millimolar extracellular Ca^{2+} [207]. It is possible that the periplasmic Ca^{2+} may be released into the cytoplasm and used for generating intracellular Ca^{2+} transients. However, further mechanistic studies are imperative.

33.3.1 Ca^{2+} Channels

Several types of Ca^{2+} transporters have been identified in bacteria. The transporters contribute to the regulation of virulence and host-pathogen interactions. First, the poly-β-hydroxybutyrate polyphosphate (PHB-PP) in *E. coli* forms non-proteinaceous Ca^{2+} channels and translocates Ca^{2+} into the cytoplasm [214]. In addition, PHB-PP channels are required for Ca^{2+}-dependent genetic competence, which plays a key role in uptake of foreign DNA, eventually enhancing bacterial adaptation to the host environment and resistance [215]. The production of the corresponding PHB-PP synthases was shown to be induced by elevated extracellular Ca^{2+} and several other stimuli *via* Ca^{2+}-dependent TCS AtoSC [154].

Another type of Ca^{2+} channels, a pH-dependent Ca^{2+} leak channel, YetJ was identified in *B. subtilis* [216]. This protein contains a BAX-1 inhibitor domain homologous to the one in a Ca^{2+} leak channel found in the endoplasmic reticulum (ER) membrane. Eukaryotic channels containing transmembrane BAX inhibitor-1 motif (TMBIM) mediate $Ca^{2+}{}_{in}$ homeostasis and apoptosis [217]. Interestingly, this highly conserved domain has been identified in a number of bacterial proteins. Initially, this domain was identified in *E. coli* protein YccA, and was shown to play a role in biofilm maturation [99]. While more research is needed to determine the roles of YetJ and YccA in *B. subtilis* and *E. coli* physiology, our group recently identified another homolog of the channel in *P. aeruginosa* [Guragain et al. in preparation]. We named it CalC for $\underline{Ca}^{2+}$ $\underline{L}$eak $\underline{C}$hannel and determined that the protein is responsible for generating transient changes in $[Ca^{2+}]$ in the *P. aeruginosa* cytoplasm in response to extracellular Ca^{2+}. Transcriptional profiling of the mutant strain with disrupted *calC* revealed that the responses to elevated Ca^{2+} were impaired, particularly for genes encoding virulence factors and biofilm determinants [Guragain et al. in preparation]. This work provides experimental proof of the regulatory role of $Ca^{2+}{}_{in}$ transients in bacterial responses to Ca^{2+}. Furthermore, homology searches identified a number of putative BAX-1 Ca^{2+} leak channels in bacterial pathogens including *S. pneumoniae*, *P. carotovorum*, *Coexiella burnetti*, *S. enterica*, and *H. pylori,* indicating the conserved nature of the Ca^{2+} leak channel in bacterial pathogens, and possibly suggesting a role in the pathogenic life style.

Mechanosensitive channels (MSC) are large, non-selective channels that usually allow the passage of ions in response to mechanical or osmotic stress (reviewed in [205, 218, 219]). MSC are found in a variety of different bacteria including human and plant pathogens [220–222]. In *B. subtilis,* MSC SpoVAC releases Ca-dipicolinic acid complex, which is required for spore formation [223]. Mechanical stress in *E. coli* was shown to cause an increase in $[Ca^{2+}]_{in}$ leading to altered gene expression [212]. However, the MSC, MscL in this organism did not impact $Ca^{2+}{}_{in}$ homeostasis [224], raising a possibility of an alternative Ca^{2+} channel responding to mechanical stress. Our studies with *P. aeruginosa* identified several Ca^{2+} transporters including a putative MSC encoded by PA4614, which contributed to the restoration of the $[Ca^{2+}]_{in}$ basal level and the regulation of Ca^{2+}-induced swarming motility [206].

33.3.2 Ca^{2+} Pumps

Elevated levels of free $Ca^{2+}{}_{in}$ can be toxic to bacterial cells, and the recovery to the basal $[Ca^{2+}]_{in}$ is critical for re-sensitizing cells for the next wave of $[Ca^{2+}]_{in}$ signaling. Therefore, the mechanisms of Ca^{2+} efflux are of high importance for cellular survival and for $Ca^{2+}{}_{in}$ regulation. Underlining their physiological significance, multiple families of efflux transporters have evolved and been shown to play a role in bacterial physiology and virulence (reviewed in [203]). The first group includes two types (P and F) of ATPases that couple Ca^{2+} export to ATP hydrolysis [60, 225, 226]. These proteins are highly conserved and were identified in diverse bacterial pathogens. In addition to translocating Ca^{2+}, or likely because of it, some of these proteins are important in diverse bacterial processes related to survival in a host. For example, CaxP plays a role in host colonization by *S. pneumoniae* [227], CtpE of *M. smegmatis* contributes to cell surface integrity [228], and PA3920 and PA2435 of *P. aeruginosa* mediate Ca^{2+} regulation of swarming motility [206]. The second group includes ion exchange transporters coupling Ca^{2+} export to co-transport of other ions. Although many of these transporters have been identified in bacterial pathogens (reviewed in [203]), there is little evidence yet about their role in virulence.

33.3.3 Predicting Novel Components of Ca^{2+} Signaling Network

To expand our knowledge on the components of $Ca^{2+}{}_{in}$ signaling network in pathogenic bacteria, we aimed to predict novel Ca^{2+}-recognizing or translocating proteins based on their homology to well-characterized components of eukaryotic Ca^{2+} network. For this, we selected well-characterized eukaryotic Ca^{2+}-binding proteins, whose homologs in bacteria have not been reported. All sequence alignments were carried out using NCBI BLASTP [76, 229]. CarR, a Ca^{2+} sensor that is a G protein-coupled receptor, plays an essential role in fluctuating intracellular Ca^{2+} homeostasis in response to minute changes in $[Ca^{2+}]_{ex}$ and other stimuli [230–234]. The protein contains three cooperative Ca^{2+} binding sites. To our surprise, four (underlined) out of five (in bold) residues required for Ca^{2+} binding (**R**XX**E**XX**EE**A**E**ERD) were found in a large number of bacterial proteins involved in a variety of life-sustaining functions, including recruitment of replisome in *S. aureus* [235], cell division protein FtsA in *E. persicina* [236], putative Rhs toxin and DNA recombination regulation system in *E. coli* [237–239], and putative pili assembly gene in *Enterobacter cloacae*. Another eukaryotic Ca^{2+} signaling protein is RyR1, which is a Ca^{2+} channel known to release Ca^{2+} stored in the sarcoplasmic reticulum into the cytoplasm [240]. Sequence homology searches against bacterial genomes identified only a small fragment of the protein as aligning with bacterial proteins. This region happened to be located within the lining of the

pore required for Ca^{2+} sensitivity [240–242]. Four (underlined) out of five residues E3893, H3895, E3967, Q3970, T5001 required for Ca^{2+} binding were found with similar spacing in several putative ABC transporters of pathogenic bacteria, including *S. aureus* and *S. pneumoniae*. We also detected these residues in putative bestrophin transporters of many bacterial species including *P. aeruginosa* and *E. coli*, in an orphan transcriptional regulator unique to a *P. aeruginosa* clinical isolate, and in several enzymes including a putative purine phosphatase of *P. aeruginosa.* The discovery of a putative Ca^{2+} binding site in bacterial bestrophin channels is particularly interesting, since human bestrophin is a Ca^{2+}-gated potassium channel [243]. However, the only characterized bacterial bestrophin channel (in *K. pneumoniae*) was shown to not require Ca^{2+} for its function [244] nor did it contain the Ca^{2+}-binding site found in the human bestrophin. This raises a possibility of two types of bestrophin channels in bacteria, Ca^{2+}-dependent and Ca^{2+}-independent. Interestingly, the eukaryotic bestrophin has been demonstrated to possess multiple splicing variants: with and without Ca^{2+} binding region [245]. Overall, these findings suggest that a significantly greater number of bacterial processes are likely regulated by Ca^{2+} than already known. The fact that most of these predicted Ca^{2+}-binding proteins were detected in bacterial pathogens suggests the importance of Ca^{2+} regulation in their physiology and, possibly, interactions with hosts, whose vital processes are regulated by Ca^{2+}.

33.4 Concluding Remarks

Bacteria have very dynamic and complex responses to Ca^{2+}. Over the past 10 years, the evidence that bacteria utilize Ca^{2+} for signaling has grown, yet important pieces are still missing. An area that needs study is on intracellular Ca^{2+} signaling. While a number of Ca^{2+} sensors and Ca^{2+}-dependent regulatory systems have been shown to regulate essential functions, most of the findings are of correlative nature with no direct experimental evidence linking the changes in the intracellular Ca^{2+} to the regulation of transcription or translation. Even less is known about how the amplitude and the frequency of intracellular Ca^{2+} signals modulate the response. An interesting aspect is the conservation of many Ca^{2+}-binding domains in eukaryotes and bacteria indicating an evolutionary lineage between Ca^{2+} signaling networks in these domains of life. One technical problem, that is worth mentioning, is the disregard for the presence of Ca^{2+} in commonly used rich bacteriological growth media, such as LB or BHI. Consequently, Ca^{2+} regulation of the resultant bacterial phenotypes may be underestimated. Overall, Ca^{2+} signaling in bacteria is an exciting and quickly developing field, which is providing not only the fundamental understanding of bacterial life and evolution but also generating insights into the regulation of bacterial pathogenicity.

References

1. Edel KH, Kudla J (2015) Increasing complexity and versatility: how the calcium signaling toolkit was shaped during plant land colonization. Cell Calcium 57(3):231–246
2. Permyakov EA, Kretsinger RH (2009) Cell signaling, beyond cytosolic calcium in eukaryotes. J Inorg Biochem 103(1):77–86
3. Clapham DE (1995) Calcium signaling. Cell 80(2):259–268
4. Bush DS, Jones RL (1990) Measuring intracellular Ca^{2+} levels in plant cells using the fluorescent probes, Indo-1 and Fura-2: progress and prospects. Plant Physiol 93(3):841–845
5. Bose J et al (2011) Calcium efflux systems in stress signaling and adaptation in plants. Front Plant Sci 2:85
6. Von Ruecker AA, Bertele R, Harms HK (1984) Calcium metabolism and cystic fibrosis: mitochondrial abnormalities suggest a modification of the mitochondrial membrane. Pediatr Res 18(7):594
7. Aris RM et al (1999) Altered calcium homeostasis in adults with cystic fibrosis. Osteoporos Int 10(2):102–108
8. Ceder O, Roomans G, Hösli P (1982) Increased calcium content in cultured fibroblasts from trisomy patients: comparison with cystic fibrosis fibroblasts. Scan Electron Microsc 1982(Pt 2):723–730
9. Roomans GM (1986) Calcium and cystic fibrosis. Scan Electron Microsc 1986(Pt 1):165–178
10. Gewirtz AT et al (2000) Salmonella typhimurium induces epithelial IL-8 expression via Ca^{2+}−mediated activation of the NF-κB pathway. J Clin Invest 105(1):79–92
11. Smith DJ et al (2014) Elevated metal concentrations in the CF airway correlate with cellular injury and disease severity. J Cyst Fibros 13(3):289–295
12. Büchau AS, Gallo RL (2007) Innate immunity and antimicrobial defense systems in psoriasis. Clin Dermatol 25(6):616–624
13. Donato R (2001) S100: a multigenic family of calcium-modulated proteins of the EF-hand type with intracellular and extracellular functional roles. Int J Biochem Cell Biol 33(7):637–668
14. Pace J, Hayman MJ, Galán JE (1993) Signal transduction and invasion of epithelial cells by S. Typhimurium. Cell 72(4):505–514
15. Gekara NO et al (2007) The multiple mechanisms of Ca^{2+} signalling by listeriolysin O, the cholesterol-dependent cytolysin of Listeria monocytogenes. Cell Microbiol 9(8):2008–2021
16. Hu Y et al (2011) Structures of Anabaena calcium-binding protein CcbP INSIGHTS INTO CA^{2+} SIGNALING DURING HETEROCYST DIFFERENTIATION. J Biol Chem 286(14):12381–12388
17. Asmat TM et al (2011) Streptococcus pneumoniae infection of host epithelial cells via polymeric immunoglobulin receptor transiently induces calcium release from intracellular stores. J Biol Chem 286(20):17861–17869
18. Nhieu GT et al (2004) Calcium signalling during cell interactions with bacterial pathogens. Biol Cell 96(1):93–101
19. Khan NA et al (2007) FimH-mediated Escherichia coli K1 invasion of human brain microvascular endothelial cells. Cell Microbiol 9(1):169–178
20. Eichstaedt S et al (2009) Effects of Staphylococcus aureus-hemolysin a on calcium signalling in immortalized human airway epithelial cells. Cell Calcium 45(2):165–176
21. Denning GM et al (1998) Pseudomonas pyocyanine alters calcium signaling in human airway epithelial cells. Am J Phys Lung Cell Mol Phys 274(6):L893–L900
22. Schwarzer C et al (2010) Pseudomonas aeruginosa homoserine lactone activates store-operated cAMP and cystic fibrosis transmembrane regulator-dependent cl− secretion by human airway epithelia. J Biol Chem 285(45):34850–34863
23. Forsen S, Kordel J (1994) Calcium in biological systems. University Science Books, Mill Valley, CA, p 107

24. Vikström E et al (2010) Role of calcium signalling and phosphorylations in disruption of the epithelial junctions by Pseudomonas aeruginosa quorum sensing molecule. Eur J Cell Biol 89(8):584–597
25. Werthén M, Lundgren T (2001) Intracellular Ca^{2+} mobilization and kinase activity during acylated homoserine lactone-dependent quorum sensing in Serratia liquefaciens. J Biol Chem 276(9):6468–6472
26. Maroudas A (1979) Physicochemical properties of articular cartilage. In: Freeman MAS (ed) Adult articular cartilage. Pitman Medical, Tunbridge Wells, pp 215–290
27. Prohaska C, Pomazal K, Steffan I (2000) Determination of ca, mg, Fe, cu, and Zn in blood fractions and whole blood of humans by ICP-OES. Fresenius J Anal Chem 367(5):479–484
28. Baker S, Worthley L (2002) *The essentials of calcium, magnesium and phosphate metabolism: part I. Physiology.* Critical care and. Resuscitation 4:301–306
29. Oreskes I et al (1968) Measurement of ionized calcium in human plasma with a calcium selective electrode. Clin Chim Acta 21(3):303–313
30. Sava L et al (2005) Serum calcium measurement: total versus free (ionized) calcium. Indian J Clin Biochem 20(2):158–161
31. Moore EW (1970) Ionized calcium in normal serum, ultrafiltrates, and whole blood determined by ion-exchange electrodes. J Clin Invest 49(2):318–334
32. Schwartz H, McConville B, Christopherson E (1971) Serum ionized calcium by specific ion electrode. Clin Chim Acta 31(1):97–107
33. Reinhart RA (1988) Magnesium metabolism: a review with special reference to the relationship between intracellular content and serum levels. Arch Intern Med 148(11):2415–2420
34. Fanconi A, Rose GA (1958) The ionized, complexed, and protein-bound fractions of calcium in plasma: an investigation of patients with various diseases which affect calcium metabolism, with an additional study of the role of calcium ions in the prevention of tetany. Q J Med 27:463–494
35. Fiyaz M et al (2013) Association of salivary calcium, phosphate, pH and flow rate on oral health: a study on 90 subjects. J Ind Soc Periodontol 17(4):454
36. Blomfield J, Warton KL, Brown J (1973) Flow rate and inorganic components of submandibular saliva in cystic fibrosis. Arch Dis Child 48(4):267–274
37. Chernick WS, Barbero GJ, Parkins FM (1961) Studies on submaxillary saliva in cystic fibrosis. J Pediatr 59(6):890–898
38. Marmar J, Barbero GJ, Sibinga MS (1966) The pattern of parotid gland secretion in cystic fibrosis of the pancreas. Gastroenterology 50(4):551–556
39. Blomfield J et al (1976) Parotid gland function in children with cystic fibrosis and child control subjects. Pediatr Res 10(6):574
40. Moreira A et al (2009) Flow rate, pH and calcium concentration of saliva of children and adolescents with type 1 diabetes mellitus. Braz J Med Biol Res 42(8):707–711
41. Agha-Hosseini F, Dizgah IM, Amirkhani S (2006) The composition of unstimulated whole saliva of healthy dental students. J Contemp Dent Pract 7(2):104–111
42. Halmerbauer G et al (2000) The relationship of eosinophil granule proteins to ions in the sputum of patients with cystic fibrosis. Clin Exp Allergy 30(12):1771–1776
43. Lorin MI, Gaerlan PF, Mandel ID (1972) Quantitative composition of nasal secretions in normal subjects. J Lab Clin Med 80(2):275–281
44. Lorin M et al (1976) Composition of nasal secretion in patients with cystic fibrosis. J Lab Clin Med 88(1):114–117
45. Taylor EN, Curhan GC (2007) Differences in 24-hour urine composition between black and white women. J Am Soc Nephrol 18(2):654–659
46. Nemchinov LG, Shabala L, Shabala S (2008) Calcium efflux as a component of the hypersensitive response of Nicotiana benthamiana to Pseudomonas syringae. Plant Cell Physiol 49(1):40–46
47. Grant M et al (2000) The RPM1 plant disease resistance gene facilitates a rapid and sustained increase in cytosolic calcium that is necessary for the oxidative burst and hypersensitive cell death. Plant J 23(4):441–450

48. Zhang L, Du L, Poovaiah B (2014) Calcium signaling and biotic defense responses in plants. Plant Signal Behav 9(11):e973818
49. Ma W, Berkowitz GA (2007) The grateful dead: calcium and cell death in plant innate immunity. Cell Microbiol 9(11):2571–2585
50. Hall-Stoodley L, Costerton JW, Stoodley P (2004) Bacterial biofilms: from the natural environment to infectious diseases. Nat Rev Microbiol 2(2):95–108
51. Sauer K (2003) The genomics and proteomics of biofilm formation. Genome Biol 4(6):219
52. van Loosdrecht MC et al (1990) Influence of interfaces on microbial activity. Microbiol Rev 54(1):75–87
53. Cruz LF, Cobine PA, De La Fuente L (2012) Calcium increases Xylella fastidiosa surface attachment, biofilm formation, and twitching motility. Appl Environ Microbiol 78(5):1321–1331
54. Romantschuk M (1992) Attachment of plant pathogenic bacteria to plant surfaces. Annu Rev Phytopathol 30(1):225–243
55. Yamaguchi T et al (2009) Gene cloning and characterization of Streptococcus intermedius fimbriae involved in saliva-mediated aggregation. Res Microbiol 160(10):809–816
56. Kerchove AJ, Elimelech M (2008) Calcium and magnesium cations enhance the adhesion of motile and nonmotile pseudomonas aeruginosa on alginate films. Langmuir 24(7):3392–3399
57. Johnson MD et al (2011) Pseudomonas aeruginosa PilY1 binds integrin in an RGD-and calcium-dependent manner. PLoS One 6(12):e29629
58. Williams TC, Ayrapetyan M, Oliver JD (2015) Molecular and physical factors that influence attachment of Vibrio vulnificus to chitin. Appl Environ Microbiol 81(18):6158–6165
59. Cheng Y et al (2013) Mutation of the conserved calcium-binding motif in Neisseria gonorrhoeae PilC1 impacts adhesion but not piliation. Infect Immun 81(11):4280–4289
60. Orans J et al (2010) Crystal structure analysis reveals Pseudomonas PilY1 as an essential calcium-dependent regulator of bacterial surface motility. Proc Natl Acad Sci U S A 107(3):1065–1070
61. Eto DS et al (2008) Clathrin, AP-2, and the NPXY-binding subset of alternate endocytic adaptors facilitate FimH-mediated bacterial invasion of host cells. Cell Microbiol 10(12):2553–2567
62. Barbu EM et al (2014) SdrC induces staphylococcal biofilm formation through a homophilic interaction. Mol Microbiol 94(1):172–185
63. Josefsson E et al (1998) The binding of calcium to the B-repeat segment of SdrD, a cell surface protein of Staphylococcus aureus. J Biol Chem 273(47):31145–31152
64. Kumar S, Spiro S (2017) Environmental and genetic determinants of biofilm formation in Paracoccus denitrificans. mSphere 2(5):e00350-17
65. Linhartova I et al (2010) RTX proteins: a highly diverse family secreted by a common mechanism. FEMS Microbiol Rev 34(6):1076–1112
66. Niemann HH, Schubert W-D, Heinz DW (2004) Adhesins and invasins of pathogenic bacteria: a structural view. Microbes Infect 6(1):101–112
67. Martínez-Gil M et al (2012) Calcium causes multimerization of the large adhesin LapF and modulates biofilm formation by Pseudomonas putida. J Bacteriol 194(24):6782–6789
68. Martínez-Gil M, Yousef-Coronado F, Espinosa-Urgel M (2010) LapF, the second largest Pseudomonas putida protein, contributes to plant root colonization and determines biofilm architecture. Mol Microbiol 77(3):549–561
69. Espinosa-Urgel M, Salido A, Ramos J-L (2000) Genetic analysis of functions involved in adhesion of Pseudomonas putida to seeds. J Bacteriol 182(9):2363–2369
70. Rose RK (2000) The role of calcium in oral streptococcal aggregation and the implications for biofilm formation and retention. BBA-Gen Subjects 1475(1):76–82
71. Korstgens V et al (2001) Influence of calcium ions on the mechanical properties of a model biofilm of mucoid Pseudomonas aeruginosa. Water Sci Technol 43(6):49–57
72. Das T et al (2014) Influence of calcium in extracellular DNA mediated bacterial aggregation and biofilm formation. PLoS One 9(3):e91935

73. Sarkisova S et al (2005) Calcium-induced virulence factors associated with the extracellular matrix of mucoid Pseudomonas aeruginosa biofilms. J Bacteriol 187(13):4327–4337
74. Das T, Manefield M (2012) Pyocyanin promotes extracellular DNA release in Pseudomonas aeruginosa. PLoS One 7(10):e46718
75. Jung CJ et al (2017) AtlA mediates extracellular DNA release, which contributes to Streptococcus mutans biofilm formation in an experimental rat model of infective endocarditis. Infect Immun 85(9):pii: e00252-17
76. Safari A et al (2014) The significance of calcium ions on Pseudomonas fluorescens biofilms - a structural and mechanical study. Biofouling 30(7):859–869
77. Haque MM et al (2017) CytR homolog of Pectobacterium carotovorum subsp. carotovorum controls air-liquid biofilm formation by regulating multiple genes involved in cellulose production, c-di-GMP signaling, motility, and type III secretion system in response to nutritional and environmental signals. Front Microbiol 8:972
78. Vozza NF et al (2016) A rhizobium leguminosarum CHDL- (cadherin-like-) Lectin participates in assembly and remodeling of the biofilm matrix. Front Microbiol 7:1608
79. Patrauchan MA et al (2005) Calcium influences cellular and extracellular product formation during biofilm-associated growth of a marine Pseudoalteromonas sp. Microbiology-Sgm 151:2885–2897
80. Theunissen S et al (2010) The 285 kDa bap/RTX hybrid cell surface protein (SO4317) of Shewanella oneidensis MR-1 is a key mediator of biofilm formation. Res Microbiol 161(2):144–152
81. Parker JK et al (2016) Calcium transcriptionally regulates the biofilm machinery of Xylella fastidiosa to promote continued biofilm development in batch cultures. Environ Microbiol 18(5):1620–1634
82. Hay AJ et al (2017) Calcium enhances bile salt-dependent virulence activation in Vibrio cholerae. Infect Immun 85(1):pii: e00707-16
83. Tischler AH et al (2018) Discovery of calcium as a biofilm-promoting signal for Vibrio fischeri reveals new phenotypes and underlying regulatory complexity. J Bacteriol 200(15):pii: e00016-18
84. Fishman MR et al (2018) Ca^{2+}-induced two-component system CvsSR regulates the type III secretion system and the Extracytoplasmic function sigma factor AlgU in Pseudomonas syringae pv. Tomato DC3000. J Bacteriol 200(5):e00538-17
85. Arrizubieta MJ et al (2004) Calcium inhibits bap-dependent multicellular behavior in Staphylococcus aureus. J Bacteriol 186(22):7490–7498
86. Bilecen K, Yildiz FH (2009) Identification of a calcium-controlled negative regulatory system affecting Vibrio cholerae biofilm formation. Environ Microbiol 11(8):2015–2029
87. Watnick PI et al (2001) The absence of a flagellum leads to altered colony morphology, biofilm development and virulence in Vibrio cholerae O139. Mol Microbiol 39(2):223–235
88. O'Connell DP et al (1998) The fibrinogen-binding MSCRAMM (clumping factor) of Staphylococcus aureus has a Ca^{2+}−dependent inhibitory site. J Biol Chem 273(12):6821–6829
89. Eidhin DN et al (1998) Clumping factor B (ClfB), a new surface-located fibrinogen-binding adhesin of Staphylococcus aureus. Mol Microbiol 30(2):245–257
90. Abraham NM, Jefferson KK (2012) Staphylococcus aureus clumping factor B mediates biofilm formation in the absence of calcium. Microbiology 158(Pt 6):1504–1512
91. Romling U, Galperin MY, Gomelsky M (2013) Cyclic di-GMP: the first 25 years of a universal bacterial second messenger. Microbiol Mol Biol Rev 77(1):1–52
92. Whiteley M, Diggle SP, Greenberg EP (2017) Progress in and promise of bacterial quorum sensing research. Nature 551(7680):313–320
93. Wilson J, Schurr M, LeBlanc C (2002) Mechanisms of bacterial pathogenicity. Postgrad Med J 78:216–224
94. Ribet D, Cossart P (2015) How bacterial pathogens colonize their hosts and invade deeper tissues. Microbes Infect 17(3):173–183

95. Olson JC, Ohman DE (1992) 1992, *Efficient production and processing of elastase and LasA by Pseudomonas aeruginosa require zinc and calcium ions*. J Bacteriol 174:4140–4147
96. Zhang L, Conway JF, Thibodeau PH (2012) Calcium-induced folding and stabilization of the Pseudomonas aeruginosa alkaline protease. J Biol Chem 287(6):4311–4322
97. Marquart ME et al (2005) Calcium and magnesium enhance the production of Pseudomonas aeruginosa protease IV, a corneal virulence factor. Med Microbiol Immunol 194(1-2):39–45
98. Thayer M, Flaherty KM, McKay DB (1991) Three-dimensional structure of the elastase of Pseudomonas aeruginosa at 1.5-a resolution. J Biol Chem 266(5):2864–2871
99. Casilag F et al (2016) The LasB elastase of Pseudomonas aeruginosa acts in concert with alkaline protease AprA to prevent flagellin-mediated immune recognition. Infect Immun 84(1):162–171
100. Laarman AJ et al (2012) Pseudomonas aeruginosa alkaline protease blocks complement activation via the classical and lectin pathways. J Immunol 188(1):386–393
101. Hall S et al (2016) Cellular effects of pyocyanin, a secreted virulence factor of Pseudomonas aeruginosa. Toxins 8(8):236
102. Rada B, Leto TL (2011) The redox-active Pseudomonas virulence factor pyocyanin induces formation of neutrophil extracellular traps. FASEB J 25(1 Supplement):360.1–360.1
103. Ran H, Hassett DJ, Lau GW (2003) Human targets of Pseudomonas aeruginosa pyocyanin. Proc Natl Acad Sci 100(24):14315–14320
104. Boehm DF (1990) R a Welch, and I S Snyder., *Calcium Is Required for Binding of Escherichia Coli Hemolysin (HlyA) to Erythrocyte Membranes*. Infect Immun 58(6):1951–1958
105. Bakas L et al (1998) Calcium-dependent conformation of E. coli α-haemolysin. Implications for the mechanism of membrane insertion and lysis. Biochim Biophys Acta 1368(2):225–234
106. Hay AJ et al (2017) Calcium enhances bile salt-dependent virulence activation in Vibrio cholerae. Infect Immun 85(1):e00707–e00716
107. Kumar P, Ahuja N, Bhatnagar R (2002) Anthrax edema toxin requires influx of calcium for inducing cyclic AMP toxicity in target cells. Infect Immun 70(9):4997–5007
108. Serezani CH et al (2008) Cyclic AMP: master regulator of innate immune cell function. Am J Respir Cell Mol Biol 39(2):127–132
109. Flego D et al (1997) Control of virulence gene expression by plant calcium in the phytopathogen Erwinia carotovora. Mol Microbiol 25(5):831–838
110. Deng W et al (2017) Assembly, structure, function and regulation of type III secretion systems. Nat Rev Microbiol 15(6):323–337
111. Ho BT, Dong TG, Mekalanos JJ (2014) A view to a kill: the bacterial type VI secretion system. Cell Host Microbe 15(1):9–21
112. Filloux A (2011) Protein secretion Systems in Pseudomonas aeruginosa: an essay on diversity, evolution, and function. Front Microbiol 2:155
113. Baumann U et al (1993) Three-dimensional structure of the alkaline protease of Pseudomonas aeruginosa: a two-domain protein with a calcium binding parallel beta roll motif. EMBO J 12(9):3357–3364
114. Duong F et al (1992) Sequence of a cluster of genes controlling synthesis and secretion of alkaline protease in Pseudomonas aeruginosa: relationships to other secretory pathways. Gene 121:47–54
115. Kessler E et al (1993) Secreted LasA of Pseudomonas aeruginosa is a staphylolytic protease. J Biol Chem 268(10):7503–7508
116. Thayer MM, Flaherty KM, McKay DB (1991) Three-dimensional structure of the elastase of Pseudomonas aeruginosa at 1.5-Å resolution. J Biol Chem 266(5):2864–2871
117. Wilderman PJ et al (2001) Characterization of an endoprotease (PrpL) encoded by a PvdS-regulated gene in Pseudomonas aeruginosa. Infect Immun 69(9):5385–5394
118. Palmer T, Berks BC (2012) The twin-arginine translocation (tat) protein export pathway. Nat Rev Microbiol 10(7):483–496
119. Papanikou E, Karamanou S, Economou A (2007) Bacterial protein secretion through the translocase nanomachine. Nat Rev Microbiol 5(11):839–851

120. Korotkov KV et al (2009) Calcium is essential for the major pseudopilin in the type 2 secretion system. J Biol Chem 284(38):25466–25470
121. Dasgupta N et al (2006) Transcriptional induction of the Pseudomonas aeruginosa type III secretion system by low Ca^{2+} and host cell contact proceeds through two distinct signaling pathways. Infect Immun 74(6):3334–3341
122. Vallis AJ et al (1999) Regulation of ExoS production and secretion by Pseudomonas aeruginosa in response to tissue culture conditions. Infect Immun 67(2):914–920
123. Schraidt O, Marlovits TC (2011) Three-dimensional model of Salmonella's needle complex at subnanometer resolution. Science 331(6021):1192–1195
124. Vakulskas CA, Brutinel ED, Yahr TL (2010) ExsA recruits RNA polymerase to an extended −10 promoter by contacting region 4.2 of sigma-70. J Bacteriol 192(14):3597–3607
125. Brutinel ED, Vakulskas CA, Yahr TL (2010) ExsD inhibits expression of the Pseudomonas aeruginosa type III secretion system by disrupting ExsA self-association and DNA binding activity. J Bacteriol 192(6):1479–1486
126. Broder UN, Jaeger T, Jenal U (2016) LadS is a calcium-responsive kinase that induces acute-to-chronic virulence switch in Pseudomonas aeruginosa. Nat Microbiol 2:16184
127. Diepold A et al (2017) A dynamic and adaptive network of cytosolic interactions governs protein export by the T3SS injectisome. Nat Commun 8:15940
128. Mougous JD et al (2006) A virulence locus of Pseudomonas aeruginosa encodes a protein secretion apparatus. Science 312(5779):1526–1530
129. Leiman PG et al (2009) Type VI secretion apparatus and phage tail-associated protein complexes share a common evolutionary origin. Proc Natl Acad Sci U S A 106(11):4154–4159
130. Allsopp LP et al (2017) RsmA and AmrZ orchestrate the assembly of all three type VI secretion systems in Pseudomonas aeruginosa. Proc Natl Acad Sci U S A 114(29):7707–7712
131. He X, Wang S (2014) DNA consensus sequence motif for binding response regulator PhoP, a virulence regulator of Mycobacterium tuberculosis. Biochemistry 53(51):8008–8020
132. Kreamer NN, Costa F, Newman DK (2015) The ferrous iron-responsive BqsRS two-component system activates genes that promote cationic stress tolerance. MBio 6(2):e02549
133. Schaaf S, Bott M (2007) Target genes and DNA-binding sites of the response regulator PhoR from Corynebacterium glutamicum. J Bacteriol 189(14):5002–5011
134. Sievers F et al (2011) Fast, scalable generation of high-quality protein multiple sequence alignments using Clustal omega. Mol Syst Biol 7:539–539
135. Tamura K et al (2007) MEGA4: molecular evolutionary genetics analysis (MEGA) software version 4.0. Mol Biol Evol 24(8):1596–1599
136. Vescovi EG et al (1997) Characterization of the bacterial sensor protein PhoQ. Evidence for distinct binding sites for Mg^{2+} and Ca^{2+}. J Biol Chem 272(3):1440–1443
137. Lesley JA, Waldburger CD (2001) Comparison of the Pseudomonas aeruginosa and Escherichia coli PhoQ sensor domains: evidence for distinct mechanisms of signal detection. J Biol Chem 276(33):30827–30833
138. Cai X et al (2011) The effect of the potential PhoQ histidine kinase inhibitors on Shigella flexneri virulence. PLoS One 6(8):e23100
139. Tu X et al (2006) The PhoP/PhoQ two-component system stabilizes the alternative sigma factor RpoS in Salmonella enterica. Proc Natl Acad Sci 103(36):13503–13508
140. Bishop RE et al (2004) Enzymology of lipid a palmitoylation in bacterial outer membranes. J Endotoxin Res 10(2):107–112
141. Macfarlane EL et al (1999) PhoP–PhoQ homologues in Pseudomonas aeruginosa regulate expression of the outer-membrane protein OprH and polymyxin B resistance. Mol Microbiol 34(2):305–316
142. Shin D et al (2006) A positive feedback loop promotes transcription surge that jump-starts Salmonella virulence circuit. Science 314(5805):1607–1609
143. Macfarlane EL, Kwasnicka A, Hancock RE (2000) Role of Pseudomonas aeruginosa PhoP-PhoQ in resistance to antimicrobial cationic peptides and aminoglycosides. Microbiology 146(10):2543–2554

144. Gooderham WJ et al (2009) The sensor kinase PhoQ mediates virulence in Pseudomonas aeruginosa. Microbiology 155(3):699–711
145. Chamnongpol S, Cromie M, Groisman EA (2003) Mg^{2+} sensing by the Mg^{2+} sensor PhoQ of Salmonella enterica. J Mol Biol 325(4):795–807
146. Regelmann AG et al (2002) Mutational analysis of the Escherichia coli PhoQ sensor kinase: differences with the Salmonella enterica serovar typhimurium PhoQ protein and in the mechanism of Mg^{2+} and Ca^{2+} sensing. J Bacteriol 184(19):5468–5478
147. Lesley JA, Waldburger CD (2003) Repression of Escherichia coli PhoP-PhoQ signaling by acetate reveals a regulatory role for acetyl coenzyme a. J Bacteriol 185(8):2563–2570
148. Flego D et al (2000) A two-component regulatory system, pehR-pehS, controls Endopolygalacturonase production and virulence in the plant pathogen Erwinia carotovora subsp. carotovora. Mol Plant-Microbe Interact 13(4):447–455
149. Kariola T et al (2003) Erwinia carotovora subsp carotovora and Erwinia-derived elicitors HrpN and PehA trigger distinct but interacting defense responses and cell death in Arabidopsis. Mol Plant-Microbe Interact 16(3):179–187
150. Palomaki T et al (2002) A putative three-dimensional targeting motif of polygalacturonase (PehA), a protein secreted through the type II (GSP) pathway in Erwinia carotovora. Mol Microbiol 43(3):585–596
151. Kaneshiro WS et al (2008) Characterization of Erwinia chrysanthemi from a bacterial heart rot of pineapple outbreak in Hawaii. Plant Dis 92(10):1444–1450
152. Hugouvieux-Cotte-Pattat N, Shevchik VE, Nasser W (2002) PehN, a Polygalacturonase homologue with a low hydrolase activity, is Coregulated with the other Erwinia chrysanthemi Polygalacturonases. J Bacteriol 184(10):2664–2673
153. Guragain M et al (2016) The Pseudomonas aeruginosa PAO1 two-component regulator CarSR regulates calcium homeostasis and calcium-induced virulence factor production through its regulatory targets CarO and CarP. J Bacteriol 198(6):951–963
154. Theodorou MC et al (2006) Involvement of the AtoS-AtoC signal transduction system in poly-(R)-3-hydroxybutyrate biosynthesis in Escherichia coli. Biochim Biophys Acta 1760(6):896–906
155. Theodorou MC, Theodorou EC, Kyriakidis DA (2012) Involvement of AtoSC two-component system in Escherichia coli flagellar regulon. Amino Acids 43(2):833–844
156. Theodorou MC et al (2007) Spermidine triggering effect to the signal transduction through the AtoS-AtoC/Az two-component system in Escherichia coli. Biochim Biophys Acta 1770(8):1104–1114
157. Theodorou EC, Theodorou MC, Kyriakidis DA (2013) Regulation of poly-(R)-(3-hydroxybutyrate-co-3-hydroxyvalerate) biosynthesis by the AtoSCDAEB regulon in phaCAB(+) Escherichia coli. Appl Microbiol Biotechnol 97(12):5259–5274
158. Jung C-J et al (2017) AtlA mediates extracellular DNA release, which contributes to Streptococcus mutans biofilm formation in an experimental rat model of infective endocarditis. Infect Immun 85(9):e00252–e00217
159. Downey JS et al (2014) In vitro manganese-dependent cross-talk between Streptococcus mutans VicK and GcrR: implications for overlapping stress response pathways. PLoS One 9(12):e115975
160. Kawasaki K (2012) Complexity of lipopolysaccharide modifications in Salmonella enterica: its effects on endotoxin activity, membrane permeability, and resistance to antimicrobial peptides. Food Res Int 45(2):493–501
161. He X et al (2008) The cia operon of Streptococcus mutans encodes a unique component required for calcium-mediated autoregulation. Mol Microbiol 70(1):112–126
162. Bilecen K et al (2015) Polymyxin B resistance and biofilm formation in Vibrio cholerae are controlled by the response regulator CarR. Infect Immun 83(3):1199–1209
163. Kierek K, Watnick PI (2003) The Vibrio cholerae O139 O-antigen polysaccharide is essential for ca²⁺−dependent biofilm development in sea water. Proc Natl Acad Sci 100(24):14357–14362

164. Kierek K, Watnick PI (2003) Environmental determinants of Vibrio cholerae biofilm development. Appl Environ Microbiol 69(9):5079–5088
165. Giammarinaro P, Sicard M, Gasc AM (1999) Genetic and physiological studies of the CiaH-CiaR two-component signal-transducing system involved in cefotaxime resistance and competence of Streptococcus pneumoniae. Microbiology 145(Pt 8):1859–1869
166. Ibrahim YM et al (2004) Control of virulence by the two-component system CiaR/H is mediated via HtrA, a major virulence factor of Streptococcus pneumoniae. J Bacteriol 186(16):5258–5266
167. Wu C et al (2010) Regulation of ciaXRH operon expression and identification of the CiaR regulon in Streptococcus mutans. J Bacteriol 192(18):4669–4679
168. Jung CJ et al (2017) AtlA mediates extracellular DNA release, which contributes to Streptococcus mutans biofilm formation in an experimental rat model of infective endocarditis. Infect Immun 85(9):10
169. Senadheera MD et al (2005) A VicRK signal transduction system in Streptococcus mutans affects gtfBCD, gbpB, and ftf expression, biofilm formation, and genetic competence development. J Bacteriol 187(12):4064–4076
170. Reusch R (2013) The role of short-chain conjugated poly-(R)-3-Hydroxybutyrate (cPHB) in protein folding. Int J Mol Sci 14(6):10727
171. Theodorou MC, Tiligada E, Kyriakidis DA (2009) Extracellular Ca^{2+} transients affect poly-(R)-3-hydroxybutyrate regulation by the AtoS-AtoC system in Escherichia coli. Biochem J 417(3):667–672
172. Yamamoto K et al (2005) Functional characterization in vitro of all two-component signal transduction systems from Escherichia coli. J Biol Chem 280(2):1448–1456
173. Rodrigue A et al (2000) Cell signalling by oligosaccharides. Two-component systems in Pseudomonas aeruginosa: why so many? Trends Microbiol 8(11):498–504
174. Siryaporn A, Goulian M (2008) Cross-talk suppression between the CpxA–CpxR and EnvZ–OmpR two-component systems in E. Coli. Mol Microbiol 70(2):494–506
175. Wanner BL (1992) Is cross regulation by phosphorylation of two-component response regulator proteins important in bacteria? J Bacteriol 174(7):2053
176. Chin D, Means AR (2000) Calmodulin: a prototypical calcium sensor. Trends Cell Biol 10(8):322–328
177. Zhao X et al (2010) Structural basis for prokaryotic calciummediated regulation by a Streptomyces coelicolor calcium binding protein. Protein Cell 1(8):771–779
178. Zhang M et al (2012) Structural basis for calmodulin as a dynamic calcium sensor. Structure 20(5):911–923
179. Ikura M (1996) Calcium binding and conformational response in EF-hand proteins. Trends Biochem Sci 21(1):14–17
180. Crivici A, Ikura M (1995) Molecular and structural basis of target recognition by calmodulin. Annu Rev Biophys Biomol Struct 24(1):85–116
181. Zhou Y et al (2006) Prediction of EF-hand calcium-binding proteins and analysis of bacterial EF-hand proteins. Proteins 65(3):643–655
182. Inouye S, Franceschini T, Inouye M (1983) Structural similarities between the development-specific protein S from a gram-negative bacterium, Myxococcus xanthus, and calmodulin. Proc Natl Acad Sci 80(22):6829–6833
183. Iwasa Y et al (1981) Calmodulin-like activity in the soluble fraction of Escherichia coli. Biochem Biophys Res Commun 98(3):656–660
184. Kerson GW, Miernyk JA, Budd K (1984) Evidence for the occurrence of, and possible physiological role for, cyanobacterial calmodulin. Plant Physiol 75(1):222–224
185. Leadlay PF, Roberts G, Walker JE (1984) Isolation of a novel calcium-binding protein from streptomyces erythreus. FEBS Lett 178(1):157–160
186. Swan D et al (1989) Cloning, characterization, and heterologous expression of the Saccharopolyspora erythraea (Streptomyces erythraeus) gene encoding an EF-hand calcium-binding protein. J Bacteriol 171(10):5614–5619

187. Swan DG et al (1987) A bacterial calcium-binding protein homologous to calmodulin. Nature 329(6134):84
188. Yonekawa T, Ohnishi Y, Horinouchi S (2005) A calmodulin-like protein in the bacterial genus Streptomyces. FEMS Microbiol Lett 244(2):315–321
189. Xi C et al (2000) Symbiosis-specific expression of rhizobium etli casA encoding a secreted calmodulin-related protein. Proc Natl Acad Sci 97(20):11114–11119
190. Sarkisova SA et al (2014) A Pseudomonas aeruginosa EF-hand protein, EfhP (PA4107), modulates stress responses and virulence at high calcium concentration. PLoS One 9(6):e98985
191. Scholl ZN et al (2016) Single-molecule force spectroscopy reveals the calcium dependence of the alternative conformations in the native state of a βγ-Crystallin protein. J Biol Chem 291(35):18263–18275
192. Koul, S., et al., A novel calcium binding protein in Mycobacterium tuberculosis—potential target for trifluoperazine. 2009
193. Advani MJ, Rajagopalan M, Reddy PH (2014) Calmodulin-like protein from M. Tuberculosis H37Rv is required during infection. Sci Rep 4:6861
194. Reddy PT et al (2003) Cloning and expression of the gene for a novel protein from Mycobacterium smegmatis with functional similarity to eukaryotic calmodulin. J Bacteriol 185(17):5263–5268
195. Fry I, Becker-Hapak M, Hageman J (1991) Purification and properties of an intracellular calmodulinlike protein from Bacillus subtilis cells. J Bacteriol 173(8):2506–2513
196. Nagai M et al (1994) Purification and characterization of Bordetella calmodulin-like protein. FEMS Microbiol Lett 116(2):169–174
197. Vincent F et al (2010) Distinct oligomeric forms of the Pseudomonas aeruginosa RetS sensor domain modulate accessibility to the ligand binding site. Environ Microbiol 12(6):1775–1786
198. Broder UN, Jaeger T, Jenal U (2017) LadS is a calcium-responsive kinase that induces acute-to-chronic virulence switch in Pseudomonas aeruginosa. Nat Microbiol 2(1):16184
199. Falah A et al (1988) On the presence of calmodulin-like protein in mycobacteria. FEMS Microbiol Lett 56(1):89–93
200. Burra SS et al (1991) Calmodulin-like protein and the phospholipids of Mycobacterium smegmatis. FEMS Microbiol Lett 80(2-3):189–194
201. Teintze M, Inouye M, Inouye S (1988) Characterization of calcium-binding sites in development-specific protein S of Myxococcus xanthus using site-specific mutagenesis. J Biol Chem 263(3):1199–1203
202. Ryjenkov DA et al (2005) Cyclic diguanylate is a ubiquitous signaling molecule in bacteria: insights into biochemistry of the GGDEF protein domain. J Bacteriol 187(5):1792–1798
203. Dominguez DC, Guragain M, Patrauchan M (2015) Calcium binding proteins and calcium signaling in prokaryotes. Cell Calcium 57(3):151–165
204. Dominguez DC (2004) Calcium signalling in bacteria. Mol Microbiol 54(2):291–297
205. Booth IR et al (2015) The evolution of bacterial mechanosensitive channels. Cell Calcium 57(3):140–150
206. Guragain M et al (2013) Calcium homeostasis in Pseudomonas aeruginosa requires multiple transporters and modulates swarming motility. Cell Calcium 54(5):350–361
207. Jones HE, Holland IB, Campbell AK (2002) Direct measurement of free Ca^{2+} shows different regulation of Ca^{2+} between the periplasm and the cytosol of Escherichia coli. Cell Calcium 32(4):183–192
208. Naseem R et al (2008) pH and monovalent cations regulate cytosolic free Ca^{2+} in E. Coli. Biochim Biophys Acta Biomembr 1778(6):1415–1422
209. Knight MR et al (1991) Recombinant aequorin as a probe for cytosolic free Ca^{2+} in Escherichia coli. FEBS Lett 282(2):405–408
210. Jones HE et al (1999) Slow changes in cytosolic free Ca^{2+} inEscherichia colihighlight two putative influx mechanisms in response to changes in extracellular calcium. Cell Calcium 25(3):265–274
211. Campbell AK et al (2007) Fermentation product butane 2, 3-diol induces Ca^{2+} transients in E. Coli through activation of lanthanum-sensitive Ca^{2+} channels. Cell Calcium 41(2):97–106

212. Bruni GN et al (2017) Voltage-gated calcium flux mediates Escherichia coli mechanosensation. Proc Natl Acad Sci 114(35):9445–9450
213. Herbaud M-L et al (1998) Calcium signalling in Bacillus subtilis. Biochim Biophys Acta 1448(2):212–226
214. Pavlov E et al (2005) A high-conductance mode of a poly-3-hydroxybutyrate/calcium/polyphosphate channel isolated from competent Escherichia coli cells. FEBS Lett 579(23):5187–5192
215. Huang R, Reusch RN (1995) Genetic competence in Escherichia coli requires poly-beta-hydroxybutyrate/calcium polyphosphate membrane complexes and certain divalent cations. J Bacteriol 177(2):486–490
216. Chang Y et al (2014) Structural basis for a pH-sensitive calcium leak across membranes. Science 344(6188):1131–1135
217. Liu Q (2017) TMBIM-mediated Ca^{2+} homeostasis and cell death. BBA-Mol Cell Res 1864(6):850–857
218. Haswell ES, Phillips R, Rees DC (2011) Mechanosensitive channels: what can they do and how do they do it? Structure 19(10):1356–1369
219. Martinac B (2004) Mechanosensitive ion channels: molecules of mechanotransduction. J Cell Sci 117(12):2449–2460
220. Moe PC, Blount P, Kung C (1998) Functional and structural conservation in the mechanosensitive channel MscL implicates elements crucial for mechanosensation. Mol Microbiol 28(3):583–592
221. Chang G et al (1998) Structure of the MscL homolog from Mycobacterium tuberculosis: a gated mechanosensitive ion channel. Science 282(5397):2220–2226
222. Blount P et al (1996) Membrane topology and multimeric structure of a mechanosensitive channel protein of Escherichia coli. EMBO J 15(18):4798–4805
223. Velasquez J et al (2014) Bacillus subtilis spore protein SpoVAC functions as a mechanosensitive channel. Mol Microbiol 92(4):813–823
224. Cox CD et al (2013) Selectivity mechanism of the mechanosensitive channel MscS revealed by probing channel subconducting states. Nat Commun 4:2137
225. Kühlbrandt W (2004) Biology, structure and mechanism of P-type ATPases. Nat Rev Mol Cell Biol 5:282
226. Rensing C et al (2000) CopA: an Escherichia coli cu(I)-translocating P-type ATPase. Proc Natl Acad Sci 97(2):652–656
227. Rosch JW et al (2008) Calcium efflux is essential for bacterial survival in the eukaryotic host. Mol Microbiol 70(2):435–444
228. Gupta HK, Shrivastava S, Sharma R (2017) A novel calcium uptake transporter of uncharacterized P-type ATPase family supplies calcium for cell surface integrity in Mycobacterium smegmatis. MBio 8(5):e01388-17
229. States DJ, Gish W (1994) Combined use of sequence similarity and codon bias for coding region identification. J Comput Biol 1(1):39–50
230. Huang Y et al (2009) Multiple Ca^{2+} binding sites in the extracellular domain of Ca^{2+}-sensing receptor corresponding to cooperative Ca^{2+} response. Biochemistry 48(2):388–398
231. Hendy GN et al (2000) Mutations of the calcium-sensing receptor (CASR) in familial hypocalciuric hypercalcemia, neonatal severe hyperparathyroidism, and autosomal dominant hypocalcemia. Hum Mutat 16(4):281–296
232. Holstein DM et al (2004) Calcium-sensing receptor-mediated ERK1/2 activation requires Gαi2 coupling and dynamin-independent receptor internalization. J Biol Chem 279(11):10060–10069
233. Di Mise A et al (2018) Activation of calcium-sensing receptor increases intracellular calcium and decreases cAMP and mTOR in PKD1 deficient cells. Sci Rep 8(1):5704
234. Smith KA et al (2016) Calcium-sensing receptor regulates cytosolic [Ca^{2+}] and plays a major role in the development of pulmonary hypertension. Front Physiol 7:517

235. Huang Y-H et al (2016) Characterization of Staphylococcus aureus Primosomal DnaD protein: highly conserved C-terminal region is crucial for ssDNA and PriA helicase binding but not for DnaA protein-binding and self-Tetramerization. PLoS One 11(6):e0157593
236. Mosyak L et al (2000) The bacterial cell-division protein ZipA and its interaction with an FtsZ fragment revealed by X-ray crystallography. EMBO J 19(13):3179–3191
237. Koskiniemi S et al (2013) Rhs proteins from diverse bacteria mediate intercellular competition. Proc Natl Acad Sci U S A 110(17):7032–7037
238. Drees JC et al (2006) Inhibition of RecA protein function by the RdgC protein from Escherichia coli. J Biol Chem 281(8):4708–4717
239. Briggs GS et al (2007) Ring structure of the Escherichia coli DNA-binding protein RdgC associated with recombination and replication fork repair. J Biol Chem 282(17):12353–12357
240. Hernández-Ochoa EO et al (2015) Critical role of intracellular RyR1 calcium release channels in skeletal muscle function and disease. Front Physiol 6:420
241. Xu L et al (2018) G4941K substitution in the pore-lining S6 helix of the skeletal muscle ryanodine receptor increases RyR1 sensitivity to cytosolic and luminal Ca^{2+}. J Biol Chem 293(6):2015–2028
242. Clarke OB, Hendrickson WA (2016) Structures of the colossal RyR1 calcium Release Channel. Curr Opin Struct Biol 39:144–152
243. Kane Dickson V, Pedi L, Long SB (2014) Structure and insights into the function of a Ca^{2+}-activated Cl(−) channel. Nature 516(7530):213–218
244. Yang T et al (2014) Structure and selectivity in bestrophin ion channels. Science 346(6207):355–359
245. Kuo YH et al (2014) Effects of alternative splicing on the function of bestrophin-1 calcium-activated chloride channels. Biochem J 458:575–583

Chapter 34
Ca^{2+} Signaling in *Drosophila* Photoreceptor Cells

Olaf Voolstra and Armin Huber

Abstract In *Drosophila* photoreceptor cells, Ca^{2+} exerts regulatory functions that control the shape, duration, and amplitude of the light response. Ca^{2+} also orchestrates light adaptation allowing *Drosophila* to see in light intensity regimes that span several orders of magnitude ranging from single photons to bright sunlight. The prime source for Ca^{2+} elevation in the cytosol is Ca^{2+} influx from the extracellular space through light-activated TRP channels. This Ca^{2+} influx is counterbalanced by constitutive Ca^{2+} extrusion via the Na^{+}/Ca^{2+} exchanger, CalX. The light-triggered rise in intracellular Ca^{2+} exerts its regulatory functions through interaction with about a dozen well-characterized Ca^{2+} and Ca^{2+}/CaM binding proteins. In this review we will discuss the dynamic changes in Ca^{2+} concentration upon illumination of photoreceptor cells. We will present the proteins that are known to interact with Ca^{2+} (/CaM) and elucidate the physiological functions of these interactions.

Keywords Arrestin · Calcium signaling · *Drosophila* · Light adaptation · Phospholipase C · Phototransduction · Protein kinase C · Rhodopsin · TRP channel · Vision

34.1 Introduction

The signaling cascade in photoreceptor cells of the *Drosophila* compound eye is among the best studied G protein-coupled, phosphoinositide-mediated signal transduction pathways. Identification of the components of this signaling cascade began in the 1970s when Bill Pak and others performed genetic screens directed to identify genes encoding proteins of the visual signaling pathway [1]. Now, a long list of proteins were found to be involved in fly vision and *Drosophila* mutants for

O. Voolstra · A. Huber (✉)
Department of Biochemistry, Institute of Physiology, University of Hohenheim, Stuttgart, Germany
e-mail: armin.huber@uni-hohenheim.de

M. S. Islam (ed.), *Calcium Signaling*, Advances in Experimental Medicine and Biology 1131, https://doi.org/10.1007/978-3-030-12457-1_34

each of these proteins are available (see e.g [2–6]). This list includes, for example, the first cloned invertebrate rhodopsin (RH1) and, importantly, the first ion channels of the TRP class of ion channels to be discovered. Because the light-activated TRP channels are Ca^{2+} permeable, activation of the visual cascade results in a profound increase in the intracellular Ca^{2+} concentration. Ca^{2+} in turn feeds back on several components of the signaling cascade, thereby ensuring fast photoresponses and adaptation to variable light intensities. Many of these Ca^{2+} feedback mechanisms have been clarified only recently and some are still elusive. The role of Ca^{2+} in fly photoreceptors has been dealt with in other reviews e.g [4, 7–9]. In this review, we focus mainly on more recent results elucidating new aspects of Ca^{2+} signaling in fly photoreceptor cells.

34.2 Regulation of Ca^{2+} Levels in *Drosophila* Photoreceptor Cells

34.2.1 Activation of the Phototransduction Cascade

The compound eye of *Drosophila* is composed of ~800 unit eyes, called ommatidia. Each ommatidium consists of a lens to gather the light, eight photoreceptor cells, and auxiliary cells. The elongated photoreceptor cells harbor a light-guiding structure, the rhabdomere that is built from its apical plasma membrane. ~40,000 finger-like evaginations of this membrane, called microvilli, form the rhabdomere. In the rhabdomere, the components of the phototransduction cascade, including the visual pigment rhodopsin, are located. Absorption of a photon triggers the phototransduction cascade by converting rhodopsin to its active state, metarhodopsin. Metarhodopsin activates a heterotrimeric G protein causing the exchange of GDP bound to the α subunit with cytosolic GTP and the release of the α subunit from the βγ subunits. The activated α subunit diffuses to its effector protein, phospholipase Cβ (PLCβ), and activates it (Fig. 34.1). PLCβ in turn cleaves the membrane component phosphatidylinositol-4,5-bisphosphate (PIP_2), to yield water-soluble inositol-1,4,5-trisphosphate ($InsP_3$), membrane-bound diacyl glycerol (DAG), and a proton leading to the opening of the ion channels TRP and TRPL. Currently, the exact activation mechanism of the plasma membrane channels is still a matter of debate. It has been shown that the decrease in PIP_2 together with the hitherto neglected generation of protons causes the opening of the channels [10]. Additionally, the removal of the bulky hydrophilic $InsP_3$ group from PIP_2, which leaves the much smaller lipid DAG in the microvillar membrane results in a change of lipid packing and generation of mechanical forces that might contribute to the gating of the TRP and TRPL ion channels [11]. The mechanical forces generated by PIP_2 cleavage are revealed by a contraction of the entire rhabdomere upon bright light illumination that was quantified by atomic force microscopy and shown to strictly depend on activation of the phototransduction cascade [11]. On the other

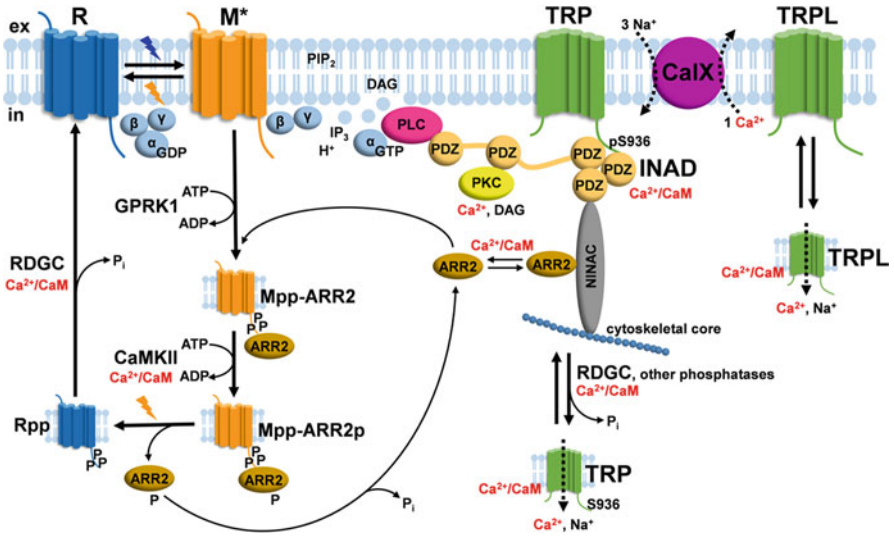

Fig. 34.1 The rhodopsin cycle and the phototransduction cascade. Absorption of a photon converts rhodopsin (R) to metarhodopsin (M*). M* can be directly converted back to R by absorption of another photon. If no photon is absorbed by M* within ~5 ms, the phototransduction cascade is activated [68]. The α subunit of the heterotrimeric G protein exchanges GDP for GTP and diffuses from the βγ subunits. Then it activates phospholipase Cβ that in turn cleaves phosphatidylinositol 4,5-bisphosphate (PIP_2) to yield diacylglycerol (DAG), inositol 1,4,5-trisphosphate (IP_3), and a proton (H^+). This reduction of PIP_2 levels and buildup of protons, together with mechanical forces that result from the removal of the bulky IP_3 head groups trigger the opening of the TRP channels [10, 11]. Ca^{2+} and Na^+ ions enter the photoreceptor cell generating the photoreceptor potential. Ca^{2+} then interacts with numerous targets. Activated metarhodopsin (M*) constitutes a substrate for the G protein-coupled receptor kinase 1 (GPRK1) that phosphorylates metarhodopsin at its C-terminus [54, 56]. Ca^{2+}/CaM releases ARR2 from NINAC and ARR2 binds to M* to inactivate it. CaMKII is activated by Ca^{2+}/CaM and phosphorylates ARR2 that is bound to Mpp. Phosphorylation of ARR2 facilitates its release from Mpp [71]. Absorption of another photon converts Mpp to Rpp and triggers the release of ARR2p [58]. RDGC that is activated by Ca^{2+}/CaM dephosphorylates Rpp or Mpp to yield R. Ca^{2+} together with DAG activate eye-specific protein kinase C (PKC) that in turn phosphorylates INAD and TRP [89, 93–97]. The TRP ion channel is phosphorylated in the dark at S936 by a yet unknown kinase and becomes RDGC-dependently dephosphorylated in the light. The phosphorylation state of S936 influences the kinetics of the channel opening [75, 102]. Ca^{2+} alone or together with CaM has strong regulatory effects on the TRP and TRPL ion channels. Low Ca^{2+} concentrations of ~300 nM facilitate channel opening whereas higher concentrations of ~1 μM promote closing of the channel. Concentrations of ~50 μM that are only reached transiently in vivo, inhibit PLC activity in a PKC-dependent manner. To reestablish resting Ca^{2+} concentrations, the Na^+/Ca^{2+} exchanger CalX extrudes 1 Ca^{2+} for every 3 Na^+ that are taken up. (Parts of the Figure were modified from [68])

hand, Delgado and co-workers reported on evidence that points to DAG as the endogenous TRP agonist [12]. It is also important to mention that TRP can be activated by polyunsaturated fatty acids (PUFAs) which could be generated by hydrolysis of PUFAs from DAG [13]. However, to date, only a DAG lipase, INAE,

that cleaves off the saturated but not the unsaturated fatty acid from DAG has been discovered [14]. Thus, the role of PUFAs in the activation of TRP ion channels in vivo remains questionable.

34.2.2 Generation of the Photoreceptor Potential by Na^+ and Ca^{2+} Influx

The light-triggered opening of the ion channels TRP and TRPL results in an influx of Ca^{2+} and Na^+ ions into the photoreceptor cell. The influx of cations depolarizes the photoreceptor cell and generates the photoreceptor potential. Thus, the light stimulus is converted into an electrical signal in the photoreceptor cell. The resting Ca^{2+} concentration in dark-adapted photoreceptors was measured using INDO-1 calcium indicator dye [15] and the genetically-encoded calcium indicator GCaMP6f [16]. Usage of INDO-1 resulted in an intracellular Ca^{2+} concentration of ~160 nM and usage of GCaMP6f in ~80 nM. These results are not too far from each other and provide a rough estimate of the intracellular resting Ca^{2+} concentration. Since these measurements were carried out on isolated ommatidia and depend on some calibration and assumptions, it is not clear if they reliably represent the in *vivo dark* level of photoreceptor Ca^{2+} concentration, which can be much lower. During a photoreceptor potential, the Ca^{2+} concentration can transiently reach almost millimolar concentrations within the small volume of the rhabdomeral microvilli where Ca^{2+} enters the cell mainly through TRP and to a smaller extent through TRPL channels [17–20]. Ca^{2+} diffuses from the rhabdomere into the cell body where it is diluted and buffered [17, 21] so that the cellular Ca^{2+} concentration reaches maximally 10 μM [8, 17, 18, 22]. Resting concentrations of Ca^{2+} are restored mainly by CalX, a Na^+/Ca^{2+} exchanger that extrudes one Ca^{2+} ion from the photoreceptor cell in exchange for the uptake of three Na^+ ions [23]. Loss of CalX function resulted in a transient light response to sustained light, a decrease in signal amplification, and abnormally rapid light adaptation [24]. Conversely, overexpression of CalX led to the opposite effects and rescued retinal degeneration caused by a constitutively active TRP variant [24]. Interestingly, the Na^+/Ca^{2+} exchange equilibrium can be manipulated to experimentally control intracellular Ca^{2+} concentrations [25] (see Chap. 3.3). Besides Ca^{2+} extrusion by CalX, uptake of Ca^{2+} into internal stores might constitute an additional mechanism to restore resting concentrations of Ca^{2+}. The sarcoendoplasmic reticulum Ca^{2+} ATPase (SERCA) mediates the uptake of Ca^{2+} into the endoplasmic reticulum (ER). SERCA is expressed in *Drosophila* photoreceptor cells [26] and pharmacological inhibition of SERCA resulted in elevated intracellular Ca^{2+} concentrations [20, 27]. However, the relative contribution of SERCA to the re-establishment of resting Ca^{2+} concentrations is elusive.

The source of the Ca^{2+} ions entering the cytosol of the photoreceptor cell upon light stimulation is somewhat controversial. It is general consensus that the

extracellular Ca^{2+} that enters the cell through TRP and TRPL channels is the major source for light-triggered Ca^{2+} elevation in the cytosol. However, $InsP_3$ that is generated by PLC action in *Drosophila* photoreceptor cells could activate an $InsP_3$ receptor in the endoplasmatic reticulum leading to Ca^{2+} release from intracellular stores. In photoreceptor cells of other invertebrates, for example in compound eyes of bees or in the ventral photoreceptor of *Limulus*, release of Ca^{2+} from internal stores is the major source of cellular Ca^{2+} elevation, which is well documented [28, 29]. In the *Drosophila* genome, a single *insP3* receptor gene exists. Two groups investigated *insP3* receptor mutant flies but did not find impairments in phototransduction [30, 31]. Thereafter, the idea of light-dependent Ca^{2+} release from intracellular stores in *Drosophila* photoreceptor cells was abandoned until Kohn and co-workers took up the topic again [32]. The authors used a *gmr-gal4* construct to drive $InsP_3$ receptor-RNAi transcription. Using RNAi to reduce $InsP_3$ receptor levels, they were able to circumvent structural eye damage that was found in $InsP_3$ receptor mutants. Additionally, Kohn and co-workers used a genetically-encoded calcium indicator, GCaMP6F, to monitor intracellular Ca^{2+} concentrations. They found that reduced $insP_3$ receptor levels or Ca^{2+} store depletion resulted in a reduction in light sensitivity and concluded that release of Ca^{2+} from intracellular stores plays an essential role in light excitation. The findings by Kohn and colleagues were challenged by Bollepalli and co-workers who found no effect of $insP_3$ receptor RNAi or $insP_3$ receptor mutation on photoresponses or Ca^{2+} influx, but observed that Gal4 expression under control of the *gmr* promotor resulted in altered photoreceptor physiology [33]. To avoid problems with *gmr*-driven GAL4 expression, Asteriti and colleagues used a fly expressing GCaMP6f under direct control of the *rh1* promoter [16]. Using dissociated photoreceptor cells from this fly, they were able to manipulate the ionic composition of the extracellular buffer. Under physiological conditions, rises in GCaMP6f fluorescence were observed 10–25 ms after a light stimulus and exhibited increases of up to 20fold. In contrast, in Ca^{2+}-free bath, latencies increased to 200 ms and fluorescence increases dropped to 4fold. Mutation of the $insP_3$ receptor had no effect showing that the residual signal was not generated by Ca^{2+} release from internal stores. Fluorescence increases were abolished in a *trpl*;*trp* double mutant, in a *calX* mutant, or when Na^+ was omitted from the bath, suggesting dependence on Na^+ and activity of the Na^+/Ca^{2+} exchanger. Thus, light-dependent rises in the fluorescence of calcium indicators under Ca^{2+}-free conditions can most probably be explained by the reversal of the Na^+/Ca^{2+} exchange [16]. It was proposed that extracellular Ca^{2+} that is resistant to buffering probably enters the photoreceptor cell through the reversed Na^+/Ca^{2+} exchange and leads to generation of the residual fluorescence. A question remains about the nature and location of this proposed pool of buffering-resistant extracellular Ca^{2+}. Alternatively, a fraction of CalX could be located in the membrane of intracellular Ca^{2+} stores and pump Ca^{2+} from these stores into the cytosol, when operating in reverse mode under high cytosolic Na^+ conditions [16].

34.2.3 Contribution of Ca^{2+} to the Photoreceptor Potential

Because Ca^{2+} is a charge carrier in the generation of the photoreceptor potential, but also serves a multitude of regulatory functions as we will discuss in Chap. 3, the determination of the fractional contribution of Ca^{2+} to the light-induced current (LIC) has been of general interest. The fractional current carried by Ca^{2+} influx can theoretically be estimated by the Goldman-Hodgkin-Katz (GHK) theory [34, 35]. However, Chu and colleagues doubted that the assumptions of this theory were met by the *Drosophila* photoreceptor cell. The authors therefore exploited the existence of a tail current that is caused by the CalX-dependent Ca^{2+}/Na^{+} exchange to experimentally determine the fractional current that is evoked by influx of Ca^{2+} into the photoreceptor cell [36]. While the GHK theory predicts the fractional Ca^{2+} current to be 42%, Chu and co-workers experimentally determined the fractional Ca^{2+} current to be 26%. The remaining fractional current can largely be attributed to Na^{+}. Collectively, Ca^{2+} significantly contributes to the LIC, but does not represent the largest fraction of the LIC. While the permeability of the TRP ion channel for Ca^{2+} is about 50 times higher than for Na^{+}, the permeability of the TRPL ion channel for Ca^{2+} is only about 4 times higher than for Na^{+} [37, 38]. The fact that Ca^{2+} does not generate the largest fractional current is due to the extracellular ion composition where the concentration of Na^{+} is 120 mM and that of Ca^{2+} is 1.5 mM [39].

34.3 Effects that Ca^{2+} Exerts in the Photoreceptor Cell

Through interaction with a variety of target proteins, Ca^{2+} exerts regulatory functions that control underlying processes to influence the shape, duration, and amplitude of the light response. Ca^{2+} mediates positive as well as negative feedback, resulting in a fast rising electrophysiological response to a light stimulus [40, 41]. Furthermore, Ca^{2+} orchestrates light adaptation allowing *Drosophila* to see in light intensity regimes that span several orders of magnitude ranging from single photons to bright sunlight ($\sim 10^6$ photons/photoreceptor/s). Proteins of fly photoreceptor cells that interact with Ca^{2+} are listed in Table 34.1.

34.3.1 General Ca^{2+} Binding Proteins

34.3.1.1 Ca^{2+} Buffering by Calphotin

Calphotin is a 85 kDa Ca^{2+} binding protein that is located in a defined cytoplasmic region in *Drosophila* photoreceptor cells adjacent to the base of the rhabbdomere [42, 43]. This cellular region is virtually free of electron dense structures and

Table 34.1 Ca^{2+}-interacting proteins in *Drosophila* photoreceptor cells

Protein	Function of this protein	Loss-of-function phenotype	Effect of Ca^{2+}
Calmodulin	Ca^{2+} sensor/adaptor to convey Ca^{2+} regulation	Prolonged deactivation of the phototransduction cascade [53]	Triggers binding of CaM to target proteins
Calphotin	Ca^{2+} buffer	Light-dependent retinal degeneration [21]	
CaMKII	Phosphorylation of ARR2 [48]	ARR2 hypophosphorylation and strong binding to rhodopsin [71]	Activation (together with CaM)
INAD	Scaffold for TRP, NINAC, PKC, and PLC	Mislocalization of signaling complex members, retinal degeneration	Ca^{2+}/CaM binding has unknown consequences
Myosin V	Translocation of pigment granula		Movement along RTW filament towards the rhabdomere base
Neurocalcin		Rhodopsin hyperphosphorylation? [116]	Inhibition of rhodopsin phosphorylation [116]
NINAC	Binding of ARR2	Light-dependent retinal degeneration, electrophysiological defect	Ca^{2+}/CaM triggers release of ARR2
PKC	Phosphorylation of INAD, TRP, and possibly other substrates	Prolonged deactivation of the photoresponse, transient receptor potential	Activation (together with DAG)
PKC53E	Phosphorylation of INAD, TRP, and possibly other substrates	No apparent phenotype	Activation (together with DAG)
PLC	Cleavage of PIP_2	No receptor potential	Activation at ≤ 1 μM
			Inhibition at 50 μM
RDGC	Dephosphorylation of rhodopsin and TRP	Light-dependent retinal degeneration, prolonged deactivation of the phototransduction cascade, premature entrance into PDA	Activation (together with CaM)
TRP	Na^+/Ca^{2+} channel	Transient receptor potential, light-dependent retinal degeneration	Activation at ~300 nM
			Inhibition at 0.1–10 μM
TRPL	Na^+/Ca^{2+} channel	Minor electrophysiological defects	Inhibition at 0.1–10 μM

separates the rhabdomeres from organelles in the cell body. Upon illumination, Ca^{2+} concentrations reach high values in the near millimolar range within the microvilli of the rhabdomere, but Ca^{2+} concentrations in the photoreceptor cell body do not rise above 10 μM [8, 17, 18, 22]. In part, this can simply be attributed to the higher volume of the cell body compared to the very small volume of the rhabdomeral microvilli. In addition, calphotin seems to act as a Ca^{2+} buffer that binds Ca^{2+} ions that diffuse out of the rhabdomeral compartment and thereby prevents high Ca^{2+} concentrations in the cell body [21]. Using calcium imaging, Weiss and colleagues observed an abnormally fast rise in intracellular Ca^{2+} levels upon illumination of photoreceptors that expressed reduced amounts of calphotin [21]. The attenuation of high Ca^{2+} concentrations in the cell body by calphotin may help to avoid toxic effects of high cellular calcium. Indeed, mutations in the calphotin gene result in retinal degeneration and in rough eyes [21, 44]. Interestingly, retinal degeneration in calphotin-defective flies was rescued by overexpression of CalX resulting in enhanced extrusion of Ca^{2+} ions [21]. These results indicate that calphotin acts as an immobile Ca^{2+} buffer that attenuates free Ca^{2+} concentrations that spread from the rhabdomeric compartment to the cell body of light-activated photoreceptor cells.

34.3.1.2 Calmodulin

Calmodulin is a ubiquitous, Ca^{2+}-binding, regulatory protein. Calmodulin can bind four Ca^{2+} ions and, upon binding, changes its conformation. Ca^{2+}/Calmodulin in turn exerts its regulatory roles upon binding to target proteins. Among the major signal transduction proteins in the *Drosophila* eye, calmodulin can bind to the cation channels TRP [45] and TRPL [46], NINAC [47], Ca^{2+}/calmodulin-dependent kinase II (CamKII) [48], RDGC [49], and INAD [50]. Additional calmodulin binding proteins comprise the ryanodine receptor [51] as well as additional Ca^{2+}/calmodulin-dependent protein kinases and phosphatases [52]. The physiological role of calmodulin binding to these target proteins will be discussed in detail below. Target proteins harbor calmodulin binding sites that are hard to predict from the amino acid sequence.

cam mutant flies exhibit a prolonged deactivation of the photoresponse that is also reflected in the elementary responses of the photoreceptor cells, called quantum bumps. In contrast to wild type photoreceptors, *cam* mutant photoreceptors produce a train of quantum bumps upon stimulation with a single photon [53]. These findings suggest an involvement of calmodulin in the termination of the photoresponse.

34.3.2 Ca^{2+}-Interacting Proteins and the Rhodopsin Cycle

When rhodopsin (R) absorbs a photon, the 11-*cis* 3-OH retinal chromophore is isomerized into its all-*trans* form and rhodopsin is converted to its active form,

metarhodopsin (M*) that triggers the phototransduction cascade (Fig. 34.1). M* can be reconverted to R by absorption of a second photon and thereby becomes inactivated. An alternative way for M* inactivation is binding to arrestin 2 that sterically hinders activation of the Gq protein. At least a fraction of arrestin 2 is bound to an unconventional myosin, NINAC, in the dark, from which it has to be released for binding to M*. M* becomes phosphorylated by a G protein-coupled receptor kinase, GPRK1 [54], although this phosphorylation is not required for arrestin 2 binding and M* inactivation [55–57]. Arrestin 2 becomes phosphorylated by CamKII [48]. After reconversion of M to R by absorption of a photon, arrestin 2 dissociates from the receptor and rhodopsin becomes dephosphorylated by RDGC and returns to its ground state [58, 59]. Three events in this circle involve Ca^{2+}: (1) The release of arrestin 2 from NINAC, (2) the phosphorylation of arrestin 2 by CamKII, and (3) the dephosphorylation of rhodopsin by RDGC.

34.3.2.1 NINAC

Like the other *nina* and *ina* mutants, *ninaC* was originally isolated in a mutagenesis screen in which mutations were identified by their electroretinogram phenotype [1]. The *ninaC* locus encodes a 132 kDa (p132) and a 174 kDa (p174) protein variant. The two variants share an N-terminal protein kinase domain, a domain that is homologous to the head region of the myosin heavy chain, and a calmodulin binding site. p174 harbors an additional calmodulin binding site and extends farther in the C-terminal direction [47, 60]. p132 is localized to the cytosol of the photoreceptor cell and p174 is localized to the rhabdomeres [61, 62]. Mutation of *ninaC* results in light- and age-dependent retinal degeneration and in an electrophysiological defect that is independent from this retinal degeneration [61]. While disruption of p132 alone had no effect, elimination of p174 alone resulted in a phenotype reminiscent of the *ninaC* null mutant [61]. To assign roles to the kinase and myosin domains, Porter and Montell mutated these domains in p174. Upon mutation of the kinase domain, they observed an ERG defect but no retinal degeneration. Deletion of the myosin domain resulted in an altered subcellular localization, an ERG defect, and retinal degeneration [63]. To investigate the roles of the CaM binding domains, Porter and colleagues deleted each of these or both in the p174 variant [47]. All these mutations resulted in a higher susceptibility to enter the prolonged depolarizing afterpotential (PDA) state. A PDA manifests in a persisting depolarization after cessation of the light stimulus [64]. The authors concluded that the CaM binding sites in NINAC function in termination of the light response. It has then been proposed that NINAC actively transports arrestin 2-loaded vesicles into the rhabdomeres, interacting with PIP_3 in the vesicle membrane [65, 66]. However, Satoh and Ready did not observe a requirement of NINAC for ARR2 translocation [67]. In an elegant set of experiments, Liu and co-workers used a fly expressing the UV-sensitive opsin, RH3, under control of the *ninaE* promoter in a *ninaE* null background [68]. The benefit of using RH3 was that absorption maxima of the inactivated (R) and the activated (M*) form are better separated than for RH1. This enabled the authors

to convert a large portion of R to M* and M* to R by using the respective light qualities. They observed a rapid, Ca^{2+}-dependent inactivation of M* in wild type flies. However, the Ca^{2+} dependence was abolished in *cam* and *ninaC* mutant flies. Therefore, the authors proposed that NINAC is an arrestin 2 binding protein that releases arrestin 2 upon Ca^{2+}/CaM binding so that arrestin 2 can inactivate M*. Further evidence for a diffusion-based translocation mechanism of arrestin 2 is the finding that arrestin 2 translocation to the rhabdomeres is stoichiometric to R to M* isomerization [69]. Light-dependent arrestin 2 translocation into the rhabdomere constitutes a light adaptation mechanism (see 3.4).

34.3.2.2 CamKII

Phosphorylation of arrestin 2 at serine 366 is the earliest light-induced phosphorylation step in *Drosophila* photoreceptors [70]. This phosphorylation is catalyzed by the Ca^{2+}/calmodulin-dependent kinase II (CaMKII) [48]. Alloway and Dolph showed that mutation of serine 366 to alanine had no effect on the binding of arrestin 2 to rhodopsin, but it hindered release of arrestin 2 from rhodopsin [71]. It was also known that hyperphosphorylation of rhodopsin results in a strong interaction of arrestin and rhodopsin and that the resulting complexes are internalized into the photoreceptor cell and trigger retinal degeneration (see RDGC). Therefore, Kristaponyte and colleagues tried to dissect the consequences of rhodopsin hyperphosphorylation and arrestin 2 hypophosphorylation [72]. They used phospholipase C null ($norpA^{P24}$) flies since in these flies, no Ca^{2+} enters the photoreceptor cells to activate RDGC and CaMKII. Thus, in $norpA^{P24}$ flies, arrestin 2 should remain dephosphorylated and rhodopsin should become hyperphosphorylated upon illumination. To test the consequences of permanent arrestin 2 dephosphorylation alone, the authors used a fly that expresses an inhibitory peptide of the CaMKII [73]. As a result, inhibition of CaMKII by inhibitory peptides did not result in photoreceptor degeneration while induction of rhodopsin hyperphosphorylation did. These results indicate that photoreceptor degeneration due to reduced Ca^{2+} influx after light activation, as in the $norpA^{P24}$ mutant, is a consequence of rhodopsin hyperphosphorylation rather than a lack of arrestin 2 phosphorylation.

34.3.2.3 RDGC

Drosophila retinal degeneration C (RDGC) is the founding member of the protein phosphatases with EF hands (PPEF) family. RDGC is expressed in the retina, in ocelli, in the mushroom bodies of the brain, and to a lower extend, in the lamina and medulla [74]. The *rdgC* locus encodes three different RDGC protein isoforms [49]. RDGC isoforms harbor an N-terminal IQ domain that interacts with Ca^{2+}/Calmodulin [49], a catalytic domain, and C-terminal EF hand domains that probably directly interact with Ca^{2+}. Upon Ca^{2+} activation, RDGC mediates dephosphorylation of rhodopsin [56] and the TRP ion channel at S936 [75]. *rdgC*

null mutant flies exhibit rhodopsin and TRP hyperphosphorylation [56, 75]. Hyperphosphorylation of rhodopsin results in an abnormally strong interaction between rhodopsin and arrestin. As an immediate consequence, arrestin 2 molecules are no longer available to deactivate metarhodopsin, resulting in prolonged deactivation of the phototransduction cascade upon orange light stimulation and higher susceptibility for persistent activation upon blue light stimulation (prolonged depolarizing afterpotential) [56]. Additionally, rhodopsin/arrestin complexes are internalized from the rhabdomeric membrane into the photoreceptor cell triggering apoptosis and ultimately resulting in photoreceptor degeneration. Collectively, Ca^{2+}-mediated regulation of RDGC ensures proper photoreceptor function and prevents retinal degeneration.

34.3.3 Ca^{2+}-Mediated Positive and Negative Feedback for Generating Highly Time-Resolved Photoreceptor Responses

Absorption of a single photon both in *Drosophila* and in vertebrate photoreceptors activates the phototransduction cascade and results in a distinct electrical response, termed quantum bump [76]. In *Drosophila* a quantum bump probably corresponds to the opening of TRP and TRPL channels within a single rhabdomeral microvillus [8]. The quantum bumps of *Drosophila* have an average amplitude of 12 pA at −70 mV membrane voltage and a duration of less than 50 ms. A macroscopic response to brighter illumination represents the summation of generated quantum bumps. The *Drosophila* quantum bump is much shorter than vertebrate quantum bumps resulting in better time resolved visual responses and a better time resolution of the fly visual system as compared to vertebrate eyes [76]. The sharpness of *Drosophila* quantum bumps is largely due to Ca^{2+}-mediated positive and negative feedback. In addition, it has been suggested that the assembly of main signaling components of the phototransduction cascade into a signaling complex by the scaffolding protein INAD may ensure specific and fast signal transduction [77, 78].

34.3.3.1 Positive and Negative Feedback on the TRP Channels

In 1991, Hardie as well as Ranganathan and co-workers observed that the time to peak of the photoresponse was shortened when the concentration of Ca^{2+} in the bath was elevated in dissociated ommatidia preparations [40, 79]. Release of caged Ca^{2+} during the rising phase of the photoresponse facilitated the LIC. This facilitation was mediated through the TRP but not the TRPL channel [80]. The EC_{50} of this facilitation was later measured to be ∼300 nM [81]. Besides positive feedback, Ca^{2+} apparently also promotes negative feedback on the TRP channels [79, 80]. Release of caged Ca^{2+} during the plateau phase of the light response resulted in

an accelerated inactivation of the photoresponse [80]. Through manipulation of the Na^+/Ca^{2+} exchange equilibrium, Gu and colleagues varied the intracellular Ca^{2+} concentration [25]. They observed inhibition of the LIC within a range of 0.1–10 μM Ca^{2+} (IC50 ~1 μM). At these concentrations, PLC activity was not affected, leading Gu and colleagues to the assumption that inhibition takes place at the level of the ion channels. In line with this suggestion is the presence of CaM binding sites within both the TRP and TRPL channels [45, 46]. TRP harbors CaM binding site within its C-terminus that bind CaM in a Ca^{2+}-independent manner [45, 82–84]. TRPL harbors two calmodulin binding sites in its C-terminus, one that exhibits Ca^{2+}-dependent CaM binding and one that shows Ca^{2+}-independent CaM binding [46]. Mutation of the Ca^{2+}-dependent CaM binding site resulted in prolonged inactivation of the light response [53]. Hypomorphic cam^{352}/cam^{339} mutants expressing less than 10% CaM of the wild type showed a similar phenotype [53].

It was proposed that the facilitation of rising and falling phase of the photoresponse that accompanies the rise of the intracellular Ca^{2+} concentration is caused by sensitization and desensitization of TRP channels and the following model was suggested [76]. Upon illumination, PLC action leads to accumulation of second messengers and an increase in membrane tension until a certain threshold is reached and the first TRP channel opens. Influx of Ca^{2+} ions through the first channel into the photoreceptor cell results in an almost instantaneous rise of the Ca^{2+} concentration in the respective microvillus because of its restricted volume. The other TRP channels present in the microvillus are rendered more sensitive towards second messengers and also open. When Ca^{2+} reaches a yet higher concentration, it inhibits the TRP and TRPL channels resulting in fast deactivation of the photoresponse.

34.3.3.2 Ca^{2+}-Mediated Feedback on PLC

In vitro studies showed that *Drosophila* PLC is stimulated at Ca^{2+} concentrations up to 1 μM while higher Ca^{2+} concentrations (5 μM) inhibited its activity [85]. A requirement of Ca^{2+} for PLC activity was also shown in intact photoreceptor cells [86, 87]. On the other hand and in line with positive as well as negative feedback of Ca^{2+} on PLC, Gu and colleagues observed inhibition of the PLC at Ca^{2+} concentrations of 50 μM or higher [25]. Such concentrations are only reached transiently in vivo [17, 18, 22]. The authors proposed that Ca^{2+}-mediated inhibition of PLC is a mechanism to avoid depletion of the PIP_2 pool in vivo. This observation might also provide an explanation for the *trp* phenotype. In a *trp* null mutant fly, due to the lack of the major Ca^{2+}-selective channel, Ca^{2+} influx into the photoreceptor cells is drastically reduced. Reduction of Ca^{2+} influx results in a transient receptor potential, meaning that the photoreceptor potential repolarizes back to resting voltages during a light stimulus. This transient receptor potential correlates with a depletion of the membrane component PIP_2. Due to the drastic reduction in Ca^{2+} influx, Ca^{2+}-dependent negative feedback mechanisms are not activated and PLC is not inhibited so that PLC cleaves all available PIP_2 molecules

to IP_3 and DAG. *trp* null mutant flies undergo light dependent retinal degeneration that has been shown to be caused by PIP_2 depletion [88]. Ca^{2+}-mediated inhibition of the PLC depended on eye-PKC [25]. Thus, a possible mechanism is that eye-PKC is activated by high Ca^{2+} concentrations and phosphorylates a target that inactivates PLC. This phosphorylation target does not seem to be PLC itself as phosphorylation of PLC so far has neither been observed in vitro [89] nor in vivo (Voolstra and Huber, unpublished results). In accordance with a role of ePKC in PLC inactivation, *inaC* null mutant flies exhibit quantum bumps that do not terminate properly. Additionally, these flies exhibit an ERG phenotype that can be described as a transient receptor potential combined with a prolonged deactivation. Like in the *trp* null mutant, the transient receptor potential phenotype of the *inaC* mutant might be attributed to PIP_2 depletion that results from the inability to phosphorylate target proteins to switch off phototransduction. In contrast to the *trp* null mutant, the $inaC^{P209}$ fly still expresses a functional TRP channel. It has been demonstrated that the TRP channel is less sensitive towards PIP_2 depletion than the TRPL channel [90]. This might explain why in the *inaC* mutant, transient receptor potential phenotype is less pronounced than in the *trp* mutant. Alternatively, a second protein kinase C, PKC53E, that probably resulted from a gene duplication event of the *inaC* gene and is also expressed in photoreceptor cells, may partially substitute for eye-PKC function in the *inaC* null mutant [91]. It has to be noted, however, that it is not understood how PIP_2 depletion is a prerequisite for TRP channel activation [10] but at the same time causes channel inhibition. Additionally, the transient receptor potential phenotype and early retinal degeneration is rescued in an *rdgA*;;*trp* double mutant [92]. This is astonishing since in this fly, due to the *trp* mutation, the Ca^{2+} influx is drastically lowered and solely the PIP_2 depletion-sensitive TRPL channel is expressed. It would thus be interesting to investigate PIP_2 levels in an *rdgA*;;*trp* double mutant. However, DAG-dependent activation of the TRP channels has been reported [12] and therefore, excessive DAG levels resulting from the *rdgA* mutation might mask effects of PIP_2 depletion. The TRP ion channel and the INAD scaffolding protein constitute targets of eye-PKC [89, 93–97]. However, mutation of putative eye-PKC phosphorylation sites in TRP or INAD did not evoke an electrophysiological phenotype that resembled the *inaC* mutant phenotype (Voolstra and Huber, unpublished results). It can therefore be concluded that either the relevant phosphorylation sites on TRP and INAD have not yet been identified or that other eye-PKC target proteins exist. In future work, the identification of these target proteins would contribute significantly to the understanding of the regulation of the visual response in *Drosophila*.

After PLC-mediated cleavage of PIP_2 to DAG and IP_3, PIP_2 is regenerated from DAG (for review, see [98]). Enzymes that are involved in the regeneration of PIP_2 represent potential targets for Ca^{2+} regulation. However, Ca^{2+}-mediated regulation of phospholipid cycle enzymes other than PLC is not likely. Using a fluorescently-tagged PIP_2 probe in intact flies, wild type and *trp* null mutant flies showed similar time courses of PIP_2 resynthesis and various background illumination intensities that were applied to trigger Ca^{2+} influx failed to accelerate PIP_2 synthesis in the wild type [90].

34.3.4 Ca^{2+}-Mediated Light Adaptation

34.3.4.1 General Aspects of Light Adaptation

Ambient light intensities span eleven orders of magnitude during a typical cycle of day and night [99]. Therefore, animals had to develop strategies to broaden the dynamic range of their visual systems in order to obtain information of relative brightness (contrast) of different objects in their environment at different levels of ambient light intensities. This is called light adaptation and it is achieved by shifting the relatively steep operational range (V-log I curve) along the 11 orders of magnitude of ambient light intensities. A second aspect of light adaptation affects the temporal resolution of a visual system, which preserves the contrast sensitivity when photoreceptors become light-adapted. Light adaptation in *Drosophila* is Ca^{2+}-dependent and takes place at different time scales by different mechanisms. First, *Drosophila* uses a pupil mechanism achieved by pigment granula migration [100, 101]. Second, during illumination, excitatory components of the phototransduction cascade are translocated out of the rhabdomere while inhibitory components are translocated into the rhabdomere [3]. Pigment granula migration and translocation of inhibitory and excitatory components constitute long-term light adaptation mechanisms. Third, short-term light adaptation is achieved by Ca^{2+} (/CaM) binding directly to the ion channels TRP and TRPL [25]. This mechanism has the strongest effect on light adaptation. Recently, an additional light adaptation mechanism was unraveled. The phosphorylation state of serine 936 of the TRP ion channel influences kinetic features of the photoresponse [75, 102]. We will discuss these aspects of Ca^{2+}-mediated light adaptation in detail below.

34.3.4.2 Short Term Light Adaptation

By manipulating cytosolic Ca^{2+} via the Na^{+}/Ca^{2+} exchange equilibrium, Gu and colleages found that Ca^{2+} inhibited the light-induced current (LIC) over a range corresponding to steady-state light-adapted Ca^{2+} levels (0.1–10 μM) and accurately mimicked light adaptation [25]. In contrast, PLC activity was unaffected by the steady-state Ca^{2+} concentrations reached during light adaptation, but it was inhibited over the range of concentrations experienced during the Ca^{2+} transients and this effect may be involved in contrast sensitivity.

28 phosphorylation sites have been identified within the TRP ion channel [97]. 15 of these sites are phosphorylated in the light and become dephosphorylated in the dark. The phosphorylation of most of these sites depends on the phototransduction cascade and on the activity of the TRP ion channel. Most probably, phosphorylation thus depends on Ca^{2+} ion influx into the photoreceptor cell. The physiological function of these phosphorylation sites is still elusive. Besides these sites that show increased phosphorylation in the light, a single site, S936, exhibits elevated phosphorylation in the dark and becomes dephosphorylated in the light. The

dephosphorylation of this site directly depends on Ca^{2+} and at least in part is mediated by the RDGC phosphatase [75]. The S936 phosphorylation site is involved in aspects of light adaptation related to temporal resolution of a visual system. In the light, when S936 is dephosphorylated, photoreceptors are able to immediately follow a light stimulus flickering at high frequency. In the dark, when S936 is phosphorylated, it takes several seconds for photoreceptors to follow the same light stimulus. Thus, phosphorylation at S936 is regulated by Ca^{2+} and is involved in one aspect of light adaptation.

34.3.4.3 Long Term Light Adaptation by Subcellular Translocation of Signaling Components

The properties of neurons depend on the abundance of signaling components in the plasma membrane. Hence, removal from or reinsertion into the plasma membrane of receptors, ion channels, or other signaling components can function as a mechanism for light adaptation. At least three *Drosophila* photoreceptor proteins undergo a light-triggered translocation between the rhabdomeral plasma membrane and the cell body: the TRPL ion channel, ARR2 and the Gαq subunit of the visual G-protein [66, 103, 104]. The TRPL ion channel is located to the rhabdomeres in the dark. Upon illumination, it translocates into the photoreceptor cell body [103]. Light-dependent TRPL translocation occurs in two stages which comprise transport of TRPL to the base of the rhabdomere and the adjacent stalk membrane in the first stage and a vesicle-mediated transport into the cell body within several hours [105, 106]. TRPL translocation depends on the phototransduction cascade and on Ca^{2+} influx [107].

The Gαq subunit is also partially removed from the rhabdomere upon illumination, thus reducing the amount of available G-protein for phototransduction [103]. This mechanism has been shown to significantly reduce the sensitivity of fly photoreceptors [107]. The association of Gαq to the membrane-attached Gβγ in the dark after illumination requires NINAC [108, 109]. Translocation of Gαq may be mediated by dynamic palmitoylation/depalmitoylation of the subunit but it is not known whether it depends on the light-induced Ca^{2+} influx [104].

Arrestin 2 is translocated in the opposite direction, i.e. it is highly abundant in the rhabdomere in the light but diffuses out of the rhabdomere in the dark [66]. As mentioned in Chap. 3.2, Ca^{2+} affects translocation of arrestin 2 into the rhabdomere as it is required to release arrestin 2 from NINAC [68].

34.3.4.4 Pupil Mechanism Mediated by Myosin V

Rhabdomeres act as optical light guides comparable to glass fibers. Therefore, photons that pass the dioptric apparatus enter the rhabdomere at its distal end and are guided through the rhabdomere towards the proximal end until they

are eventually absorbed by a rhodopsin molecule or leave the rhabdomere at its proximal end. Upon light-induced Ca^{2+} influx, pigment granules within the *Drosophila* photoreceptor cell migrate from the cytosol towards the base of the rhabdomere where they can absorb photons travelling through the rhabdomere [100, 101]. This mechanism in effect progressively reduces the light intensity in the rhabdomeres and has been compared to the effect of a closing pupil in vertebrate eyes. This "pupil mechanism" accounts for an attenuation of 0.8 log units and constitutes an important part of light adaptation [110, 111]. Satoh and coworkers showed that the migration of pigment molecules is mediated by myosin V. Upon illumination, myosin V that is loaded with a pigment granule migrates along a rhabdomere terminal web (RTW) filament towards the rhabdomere base in a Ca^{2+}- and calmodulin-dependent manner [112].

34.3.5 Ca^{2+} Interactions with a Still Elusive Physiological Role

34.3.5.1 INAD

INAD is a scaffolding protein that tethers some of the components of the phototransduction cascade resulting in short diffusion times and high fidelity of the system [113]. INAD binds CaM in a Ca^{2+}-dependent manner [45]. Using calmodulin overlay assays, Xu and colleagues showed direct interaction of calmodulin with an INAD protein fragment spanning amino acids 146 to 235 [50]. The exact consequences of calmodulin binding to INAD are elusive. However, recently, it has become increasingly clear that INAD has to be regarded as a dynamic machine rather than a rigid scaffold. This notion is corroborated by the finding that INAD undergoes a light-dependent conformational change to transiently release one of its binding partners, probably TRP, to ensure proper termination of visual response [95, 114].

34.3.5.2 Regulation of Neurocalcin

Drosophila neurocalcin was first identified in a polymerase chain reaction approach searching for recoverin-like proteins [115]. Neurocalcin is expressed in the central nervous system and in the eye [115] (flyatlas.org). The deduced amino acid sequence revealed three putative EF hands and an N-terminal myristoylation site. Indeed, recombinantly-expressed neurocalcin bound $^{45}Ca^{2+}$ and displayed a Ca^{2+}-dependent mobility shift in electrophoresis assays. Coexpression of neurocalcin with N-myristoyl transferase in bacteria in the presence of [^{3}H]myristic acid resulted in radioactive labeling of neurocalcin [115]. These results showed that *Drosophila* neurocalcin is myristoylated and can bind Ca^{2+}. Myristoylated neurocalcin exhibited a Ca^{2+}-dependent translocation to membranes [116]. Since it had been reported

that vertebrate recoverin inhibits phosphorylation of rhodopsin [117], Faurobert and colleagues tested this for *Drosophila* neurocalcin [116]. Indeed, the authors observed a Ca^{2+}- and myristoylation-dependent inhibition of phosphorylation of bovine rhodopsin by neurocalcin in vitro. However, the exact physiological role of neurocalcin in flies is elusive. It might be interesting to analyze neurocalcin-defective flies for rhodopsin hyperphosphorylation and concomitant.

34.4 Concluding Remarks

After ~50 years of *Drosophila* vision research, many interesting aspects of the *Drosophila* phototransduction cascade have been elucidated. We are now able to describe quantitatively how absorption of a photon ultimately leads to the generation of the photoreceptor potential [118]. As elaborated above, Ca^{2+} plays a major role in the regulation of the underlying processes. It controls positive and negative feedback mechanisms to increase the fidelity of the light response and regulates the sensitivity of the whole visual system to increase the dynamic range.

However, several questions have not been answered so far: How does the Ca^{2+}- and eye-PKC-dependent inactivation of the photoresponse operate? There is evidence that eye-PKC is mandatory for Ca^{2+}-dependent inhibition of PLCβ, but PLCβ does not seem to be a direct substrate of this protein kinase C. How does Ca^{2+} interact with the TRP and TRPL ion channels to provide positive and negative feedback? How can low Ca^{2+} concentrations promote channel opening while high Ca^{2+} concentrations inhibit channel opening? Finally, Ca^{2+}-mediated light adaptation is not well understood. Although it is likely that light adaptation occurs at the level of the TRP ion channels, it is not clear how this mechanism operates. Future studies will continue to increase our understanding of the role of Ca^{2+} in biological signaling pathways.

Acknowledgements Work in the laboratory of the authors has been supported by the German Research Foundation (DFG Hu839/7-1, Vo1741/1-1).

References

1. Pak WL, Grossfield J, Arnold KS (1970) Mutants of the visual pathway of *Drosophila melanogaster*. Nature 227(257):518–520
2. Smith DP, Stamnes MA, Zuker CS (1991) Signal transduction in the visual system of Drosophila. AnnuRevCell Biol 7:161–90: 161–190
3. Wang T, Montell C (2007) Phototransduction and retinal degeneration in *Drosophila*. Pflugers Arch 454(5):821–847
4. Minke B, Hardie RC (2000) Genetic dissection of Drosophila phototransduction. In: Stavenga D, DeGrip WJ, Pugh EN Jr (eds) Handbook of biological physics, Molecular mechanisms in visual transduction, vol 3. Elsevier, Amsterdam/London/New York/Oxford/Paris/Shannon/Tokyo, pp 449–525

5. Huber A (2004) Invertebrate phototransduction: multimolecular signaling complexes and the role of TRP and TRPL channels. In: Frings S, Bradley J (eds) Transduction channels in sensory cells. WILEY-VCH, Weinheim, pp 179–206
6. Tian Y, Hu W, Tong H et al (2012) Phototransduction in *Drosophila*. Sci China Life Sci 55(1):27–34. https://doi.org/10.1007/s11427-012-4272-4
7. O'Tousa JE (2002) $Ca2^{+}$ regulation of Drosophila phototransduction. Adv Exp Med Biol 514:493–505
8. Hardie RC, Juusola M (2015) Phototransduction in Drosophila. Curr Opin Neurobiol 34:37–45. https://doi.org/10.1016/j.conb.2015.01.008
9. Katz B, Minke B (2018) The *Drosophila* light-activated TRP and TRPL channels - targets of the phosphoinositide signaling cascade. Prog Retin Eye Res 66:200–219. https://doi.org/10.1016/j.preteyeres.2018.05.001
10. Huang J, Liu C-S, Hughes SA et al (2010) Activation of TRP channels by protons and Phosphoinositide depletion in *Drosophila* photoreceptors. Curr.Biol. 20:189–197
11. Hardie RC, Franze K (2012) Photomechanical responses in *Drosophila* photoreceptors. Science 338(6104):260–263
12. Delgado R, Muñoz Y, Peña-Cortés H et al (2014) Diacylglycerol activates the light-dependent channel TRP in the photosensitive microvilli of Drosophila melanogaster photoreceptors. J Neurosci 34(19):6679–6686. https://doi.org/10.1523/JNEUROSCI.0513-14.2014
13. Chyb S, Raghu P, Hardie RC (1999) Polyunsaturated fatty acids activate the Drosophila light-sensitive channels TRP and TRPL. Nature 397(6716):255–259
14. Leung HT, Tseng-Crank J, Kim M et al (2008) DAG lipase activity is necessary for TRP channel regulation in *Drosophila* photoreceptors. Neuron 58(6):825–827
15. Hardie RC (1996) INDO-1 measurements of absolute resting and light-induced $Ca2^{+}$ concentration in Drosophila photoreceptors. J.Neurosci. 16(9):2924–2933
16. Asteriti S, Liu C-H, Hardie RC (2017) Calcium signalling in Drosophila photoreceptors measured with GCaMP6f. Cell Calcium 65:40–51. https://doi.org/10.1016/j.ceca.2017.02.006
17. Oberwinkler J, Stavenga DG (2000) Calcium transients in the rhabdomeres of dark- and light-adapted fly photoreceptor cells. J.Neurosci. 20(5):1701–1709
18. Postma M, Oberwinkler J, Stavenga DG (1999) Does Ca^{2+} reach millimolar concentrations after single photon absorption in *Drosophila* photoreceptor microvilli? Biophys.J. 77(4):1811–1823
19. Peretz A, Suss-Toby E, Rom-Glas A et al (1994) The light response of *Drosophila* photoreceptors is accompanied by an increase in cellular calcium: effects of specific mutations. Neuron 12(6):1257–1267
20. Ranganathan R, Bacskai BJ, Tsien RY et al (1994) Cytosolic calcium transients: spatial localization and role in Drosophila photoreceptor cell function. Neuron 13(4):837–848
21. Weiss S, Kohn E, Dadon D et al (2012) Compartmentalization and $Ca2^{+}$ buffering are essential for prevention of light-induced retinal degeneration. J Neurosci 32(42):14696–14708. https://doi.org/10.1523/JNEUROSCI.2456-12.2012
22. Hardie RC (1996) A quantitative estimate of the maximum amount of light-induced Ca^{2+} release in *Drosophila* photoreceptors. JPhotochemPhotobiolB 35(1–2):83–89
23. Schwarz EM, Benzer S (1997) Calx, a Na-ca exchanger gene of *Drosophila melanogaster*. Proc Natl Acad Sci U S A 94(19):10249–10254
24. Wang T, Xu H, Oberwinkler J et al (2005) Light activation, adaptation, and cell survival functions of the Na^{+}/Ca^{2+} exchanger CalX. Neuron 45(3):367–378. https://doi.org/10.1016/j.neuron.2004.12.046
25. Gu Y, Oberwinkler J, Postma M et al (2005) Mechanisms of light adaptation in *Drosophila* photoreceptors. CurrBiol 15(13):1228–1234
26. Magyar A, Bakos E, Váradi A (1995) Structure and tissue-specific expression of the *Drosophila* melanogaster organellar-type Ca^{2+}-ATPase gene. Biochem J 310(Pt 3):757–763
27. Hardie RC (1996) Excitation of Drosophila photoreceptors by BAPTA and ionomycin: evidence for capacitative $Ca2^{+}$ entry? Cell Calcium 20(4):315–327

28. Walz B, Baumann O (1995) Structure and cellular physiology of Ca^{2+} Stores in Invertebrate Photoreceptors. Cell Calcium 18(4):342–351
29. Brown JE, Blinks JR (1974) Changes in intracellular free calcium concentration during illumination of invertebrate photoreceptors. Detection with aequorin. J Gen Physiol 64(6):643–665
30. Acharya JK, Jalink K, Hardy RW et al (1997) InsP3 receptor is essential for growth and differentiation but not for vision in *Drosophila*. Neuron 18(6):881–887
31. Raghu P, Colley NJ, Webel R et al (2000) Normal phototransduction in *Drosophila* photoreceptors lacking an InsP(3) receptor gene. MolCell Neurosci 15(5):429–445
32. Kohn E, Katz B, Yasin B et al (2015) Functional cooperation between the IP3 receptor and phospholipase C secures the high sensitivity to light of *Drosophila* photoreceptors in vivo. J Neurosci 35(6):2530–2546. https://doi.org/10.1523/JNEUROSCI.3933-14.2015
33. Bollepalli MK, Kuipers ME, Liu C-H et al (2017) Phototransduction in Drosophila is compromised by Gal4 expression but not by InsP3 receptor knockdown or mutation. eNeuro 4(3):ENEURO.0143–ENEU17.2017. https://doi.org/10.1523/ENEURO.0143-17.2017
34. Schneggenburger R, Zhou Z, Konnerth A et al (1993) Fractional contribution of calcium to the cation current through glutamate receptor channels. Neuron 11(1):133–143
35. Hille B (2001) Ionic channels of excitable membranes, 3rd edn. Sinauer Associates, Sunderland
36. Chu B, Postma M, Hardie RC (2013) Fractional $Ca(2^{+})$ currents through TRP and TRPL channels in Drosophila photoreceptors. BiophysJ 104(9):1905–1916
37. Reuss H, Mojet MH, Chyb S et al (1997) In vivo analysis of the drosophila light-sensitive channels, TRP and TRPL. Neuron 19(6):1249–1259
38. Liu CH, Wang T, Postma M et al (2007) *In vivo* identification and manipulation of the Ca^{2+} selectivity filter in the *Drosophila* transient receptor potential channel. J Neurosci 27(3):604–615. https://doi.org/10.1523/JNEUROSCI.4099-06.2007
39. Hofstee CA, Stavenga DG (1996) Calcium homeostasis in photoreceptor cells of Drosophila mutants inaC and trp studied with the pupil mechanism. VisNeurosci 13(2):257–263
40. Hardie RC (1991) Whole-cell recordings of the light induced current in dissociated *Drosophila* photoreceptors: evidence for feedback by calcium permeating the light-sensitive channels. Proc R Soc Lond Ser B Biol Sci 245(1314):203–210. https://doi.org/10.1098/rspb.1991.0110
41. Hardie RC, Minke B (1994) Calcium-dependent inactivation of light-sensitive channels in *Drosophila* photoreceptors. JGenPhysiol 103(3):409–427
42. Ballinger DG, Xue N, Harshman KD (1993) A Drosophila photoreceptor cell-specific protein, calphotin, binds calcium and contains a leucine zipper. Proc Natl Acad Sci U S A 90(4):1536–1540
43. Martin JH, Benzer S, Rudnicka M et al (1993) Calphotin: a Drosophila photoreceptor cell calcium-binding protein. Proc Natl Acad Sci U S A 90(4):1531–1535
44. Yang Y, Ballinger D (1994) Mutations in calphotin, the gene encoding a Drosophila photoreceptor cell-specific calcium-binding protein, reveal roles in cellular morphogenesis and survival. Genetics 138(2):413–421
45. Chevesich J, Kreuz AJ, Montell C (1997) Requirement for the PDZ domain protein, INAD, for localization of the TRP store-operated channel to a signaling complex. Neuron 18(1):95–105
46. Warr CG, Kelly LE (1996) Identification and characterization of two distinct calmodulin-binding sites in the Trpl ion-channel protein of *Drosophila* melanogaster. Biochem J 314(Pt 2):497–503
47. Porter JA, Minke B, Montell C (1995) Calmodulin binding to *Drosophila* NinaC required for termination of phototransduction. EMBO J 14(18):4450–4459
48. Kahn ES, Matsumoto H (1997) Calcium/calmodulin-dependent kinase II phosphorylates Drosophila visual arrestin. JNeurochem 68(1):169–175
49. Lee SJ, Montell C (2001) Regulation of the rhodopsin protein phosphatase, RDGC, through interaction with calmodulin. Neuron 32(6):1097–1106

50. Xu XZ, Choudhury A, Li X et al (1998) Coordination of an array of signaling proteins through homo- and heteromeric interactions between PDZ domains and target proteins. J.Cell Biol. 142(2):545–555
51. Hasan G, Rosbash M (1992) *Drosophila* homologs of two mammalian intracellular Ca(2$^+$)-release channels: identification and expression patterns of the inositol 1,4,5-triphosphate and the ryanodine receptor genes. Development 116(4):967–975
52. Xu XZS, Wes PD, Chen H et al (1998) Retinal targets for calmodulin include proteins implicated in synaptic transmission. In: The journal of biological chemistry (USA), vol 273, pp 31297–31307
53. Scott K, Sun Y, Beckingham K et al (1997) Calmodulin regulation of *Drosophila* light-activated channels and receptor function mediates termination of the light response in vivo. Cell 91(3):375–383
54. Lee SJ, Xu H, Montell C (2004) Rhodopsin kinase activity modulates the amplitude of the visual response in Drosophila. ProcNatlAcadSciUSA 101(32):11874–11879
55. Plangger A, Malicki D, Whitney M et al (1994) Mechanism of arrestin 2 function in rhabdomeric photoreceptors. J.Biol.Chem. 269(43):26969–26975
56. Vinos J, Jalink K, Hardy RW et al (1997) A G protein-coupled receptor phosphatase required for rhodopsin function. Science 277(5326):687–690
57. Kiselev A, Socolich M, Vinos J et al (2000) A molecular pathway for light-dependent photoreceptor apoptosis in *Drosophila*. Neuron 28(1):139–152
58. Byk T, Bar-Yaacov M, Doza YN et al (1993) Regulatory arrestin cycle secures the fidelity and maintenance of the fly photoreceptor cell. ProcNatlAcadSciUSA 90(5):1907–1911
59. Selinger Z, Doza YN, Minke B (1993) Mechanisms and genetics of photoreceptors desensitization in *Drosophila* flies. BiochimBiophysActa 1179(3):283–299
60. Montell C, Rubin GM (1988) The Drosophila ninaC locus encodes two photoreceptor cell specific proteins with domains homologous to protein kinases and the myosin heavy chain head. Cell 52(5):757–772
61. Porter JA, Hicks JL, Williams DS et al (1992) Differential localizations of and requirements for the two Drosophila ninaC kinase/myosins in photoreceptor cells. J.Cell Biol. 116(3):683–693
62. Hicks JL, Williams DS (1992) Distribution of the myosin I-like ninaC proteins in the *Drosophila* retina and ultrastructural analysis of mutant phenotypes. J Cell Sci 101(Pt 1):247–254
63. Porter JA, Montell C (1993) Distinct roles of the Drosophila ninaC kinase and myosin domains revealed by systematic mutagenesis. JCell Biol 122(3):601–612
64. Minke B (2012) The history of the prolonged depolarizing afterpotential (PDA) and its role in genetic dissection of Drosophila phototransduction. J Neurogenet 26(2):106–117. https://doi.org/10.3109/01677063.2012.666299
65. Lee S-J, Montell C (2004) Light-dependent translocation of visual arrestin regulated by the NINAC myosin III. Neuron 43(1):95–103. https://doi.org/10.1016/j.neuron.2004.06.014
66. Lee S-J, Xu H, Kang L-W et al (2003) Light adaptation through phosphoinositide-regulated translocation of Drosophila visual arrestin. Neuron 39(1):121–132
67. Satoh AK, Ready DF (2005) Arrestin1 mediates light-dependent rhodopsin endocytosis and cell survival. Curr.Biol. 15(19):1722–1733
68. Liu CH, Satoh AK, Postma M et al (2008) Ca2$^+$−dependent metarhodopsin inactivation mediated by calmodulin and NINAC myosin III. Neuron 59(5):778–789. https://doi.org/10.1016/j.neuron.2008.07.007
69. Satoh AK, Xia H, Yan L et al (2010) Arrestin translocation is stoichiometric to rhodopsin isomerization and accelerated by phototransduction in Drosophila photoreceptors. Neuron 67(6):997–1008. https://doi.org/10.1016/j.neuron.2010.08.024
70. Komori N, Usukura J, Kurien B et al (1994) Phosrestin I, an arrestin homolog that undergoes light-induced phosphorylation in dipteran photoreceptors. Insect Biochem Mol Biol 24(6):607–617

71. Alloway PG, Dolph PJ (1999) A role for the light-dependent phosphorylation of visual arrestin. Proc.Natl.Acad.Sci.U.S.A 96(11):6072–6077
72. Kristaponyte I, Hong Y, Lu H et al (2012) Role of rhodopsin and arrestin phosphorylation in retinal degeneration of Drosophila. J.Neurosci. 32(31):10758–10766
73. Griffith LC, Verselis LM, Aitken KM et al (1993) Inhibition of calcium/calmodulin-dependent protein kinase in Drosophila disrupts behavioral plasticity. Neuron 10(3):501–509
74. Steele FR, Washburn T, Rieger R et al (1992) *Drosophila* retinal-degeneration-C (Rdgc) encodes a novel serine threonine protein phosphatase. Cell 69(4):669–676
75. Voolstra O, Rhodes-Mordov E, Katz B et al (2017) The phosphorylation state of the *Drosophila* TRP channel modulates the frequency response to oscillating light in vivo. J Neurosci 37(15):4213–4224. https://doi.org/10.1523/JNEUROSCI.3670-16.2017
76. Hardie RC, Raghu P (2001) Visual transduction in *Drosophila*. Nature 413(6852):186–193
77. Huber A, Sander P, Gobert A et al (1996) The transient receptor potential protein (Trp), a putative store-operated Ca^{2+} channel essential for phosphoinositide-mediated photoreception, forms a signaling complex with NorpA, InaC and InaD. EMBO J 15(24):7036–7045
78. Scott K, Zuker CS (1998) Assembly of the Drosophila phototransduction cascade into a signalling complex shapes elementary responses. Nature 395(6704):805–808
79. Ranganathan R, Harris GL, Stevens CF et al (1991) A *Drosophila* mutant defective in extracellular calcium-dependent photoreceptor deactivation and rapid desensitization. Nature 354(6350):230–232
80. Hardie RC (1995) Photolysis of caged $Ca2^{+}$ facilitates and inactivates but does not directly excite light-sensitive channels in Drosophila photoreceptors. J Neurosci 15(1 Pt 2):889–902
81. Chu B, Liu C-H, Sengupta S et al (2013) Common mechanisms regulating dark noise and quantum bump amplification in Drosophila photoreceptors. J Neurophysiol 109(8):2044–2055. https://doi.org/10.1152/jn.00001.2013
82. Tang J, Lin Y, Zhang Z et al (2001) Identification of common binding sites for calmodulin and inositol 1,4,5-trisphosphate receptors on the carboxyl termini of trp channels. J Biol Chem 276(24):21303–21310. https://doi.org/10.1074/jbc.M102316200
83. Zheng Y-H, Liu W (2016) Identification and characterization of a new Calmodulin binding site at the C-terminus of Drosophila TRP Channel. Chinese J Biochem Mol Biol 32(7):790–797. https://doi.org/10.13865/j.cnki.cjbmb.2016.07.09
84. Sun Z, Zheng Y, Liu W (2018) Identification and characterization of a novel calmodulin binding site in Drosophila TRP C-terminus. Biochem Biophys Res Commun 501:434–439. https://doi.org/10.1016/j.bbrc.2018.05.007
85. Running Deer JL, Hurley JB, Yarfitz SL (1995) G protein control of *Drosophila* photoreceptor phospholipase C. J.Biol.Chem. 270(21):12623–12628
86. Katz B, Minke B (2012) Phospholipase C-mediated suppression of dark noise enables single-photon detection in Drosophila photoreceptors. J Neurosci 32(8):2722–2733. https://doi.org/10.1523/JNEUROSCI.5221-11.2012
87. Hardie RC (2005) Inhibition of phospholipase C activity in *Drosophila* photoreceptors by 1,2-bis(2-aminophenoxy)ethane N,N,N',N'-tetraacetic acid (BAPTA) and di-bromo BAPTA. Cell Calcium 38(6):547–556. https://doi.org/10.1016/j.ceca.2005.07.005
88. Sengupta S, Barber TR, Xia H et al (2013) Depletion of PtdIns(4,5)P(2) underlies retinal degeneration in Drosophila trp mutants. J Cell Sci 126(Pt 5):1247–1259. https://doi.org/10.1242/jcs.120592
89. Huber A, Sander P, Bahner M et al (1998) The TRP Ca^{2+} channel assembled in a signaling complex by the PDZ domain protein INAD is phosphorylated through the interaction with protein kinase C (ePKC). FEBS Lett 425(2):317–322
90. Hardie RC, Liu C-H, Randall AS et al (2015) In vivo tracking of phosphoinositides in Drosophila photoreceptors. J Cell Sci 128(23):4328–4340. https://doi.org/10.1242/jcs.180364
91. Schaeffer E, Smith D, Mardon G et al (1989) Isolation and characterization of two new Drosophila protein kinase C genes, including one specifically expressed in photoreceptor cells. Cell 57(3):403–412

92. Raghu P, Usher K, Jonas S et al (2000.Apr.;26.(1.):169.-79) Constitutive activity of the light-sensitive channels TRP and TRPL in the Drosophila diacylglycerol kinase mutant, rdgA. Neuron 26(1):169–179
93. Huber A, Sander P, Paulsen R (1996) Phosphorylation of the InaD gene product, a photoreceptor membrane protein required for recovery of visual excitation. JBiolChem 271(20):11710–11717
94. Liu M, Parker LL, Wadzinski BE et al (2000) Reversible phosphorylation of the signal transduction complex in *Drosophila* photoreceptors. J.Biol.Chem. 275(16):12194–12199
95. Mishra P, Socolich M, Wall MA et al (2007) Dynamic scaffolding in a G protein-coupled signaling system. Cell 131(1):80–92
96. Voolstra O, Spät P, Oberegelsbacher C et al (2015) Light-dependent phosphorylation of the Drosophila inactivation no afterpotential D (INAD) scaffolding protein at Thr170 and Ser174 by eye-specific protein kinase C. PLoS One 10(3):e0122039. https://doi.org/10.1371/journal.pone.0122039
97. Voolstra O, Bartels J-P, Oberegelsbacher C et al (2013) Phosphorylation of the *Drosophila* transient receptor potential ion channel is regulated by the phototransduction cascade and involves several protein kinases and phosphatases. PLoS One 8(9):e73787. https://doi.org/10.1371/journal.pone.0073787
98. Balakrishnan SS, Basu U, Raghu P (2015) Phosphoinositide signalling in *Drosophila*. Biochim Biophys Acta 1851(6):770–784. https://doi.org/10.1016/j.bbalip.2014.10.010
99. Rodieck RW (1998) The first steps in seeing. Sinauer Associates, Inc, Sunderland
100. Kirschfeld K, Franceschini N (1969) Ein Mechanismus zur Steuerung des Lichtflusses in den Rhabdomeren des Komplexauges von Musca (a mechanism for the control of the light flow in the rhabdomeres of the complex eye of Musca). Kybernetik 6(1):13–22
101. Kirschfeld K, Vogt K (1980) Calcium ions and pigment migration in fly photoreceptors. Naturwissenschaften 67(10):516–517. https://doi.org/10.1007/BF01047639
102. Katz B, Voolstra O, Tzadok H et al (2017) The latency of the light response is modulated by the phosphorylation state of Drosophila TRP at a specific site. Channels (Austin) 11(6):678–685. https://doi.org/10.1080/19336950.2017.1361073
103. Bähner M, Frechter S, Da Silva N et al (2002) Light-regulated subcellular translocation of *Drosophila* TRPL channels induces long-term adaptation and modifies the light-induced current. Neuron 34:83–93
104. Kosloff M, Elia N, Joel-Almagor T et al (2003) Regulation of light-dependent Gq alpha translocation and morphological changes in fly photoreceptors. EMBO J 22(3):459–468
105. Cronin MA, Lieu MH, Tsunoda S (2006) Two stages of light-dependent TRPL-channel translocation in Drosophila photoreceptors. JCell Sci 119:2935–2944
106. Oberegelsbacher C, Schneidler C, Voolstra O et al (2011) The Drosophila TRPL ion channel shares a Rab-dependent translocation pathway with rhodopsin. EurJCell Biol 90(8):620–630
107. Meyer NE, Joel-Almagor T, Frechter S et al (2006) Subcellular translocation of the eGFP-tagged TRPL channel in Drosophila photoreceptors requires activation of the phototransduction cascade. J.Cell Sci. 119:2592–2603
108. Frechter S, Elia N, Tzarfaty V et al (2007) Translocation of Gq alpha mediates long-term adaptation in *Drosophila* photoreceptors. J.Neurosci. 27(21):5571–5583
109. Cronin MA, Diao F, Tsunoda S (2004) Light-dependent subcellular translocation of Gqalpha in Drosophila photoreceptors is facilitated by the photoreceptor-specific myosin III NINAC. J.Cell Sci. 117(Pt 20):4797–4806
110. Stavenga DG (2004) Angular and spectral sensitivity of fly photoreceptors. III. Dependence on the pupil mechanism in the blowfly Calliphora. J Comp Physiol A Neuroethol Sens Neural Behav Physiol 190(2):115–129. https://doi.org/10.1007/s00359-003-0477-0
111. Franceschini N (1972) Pupil and Pseudopupil in the compound eye of Drosophila. In: Wehner R (ed) Information processing in the visual Systems of Anthropods: symposium held at the Department of Zoology, University of Zurich, March 6–9, 1972. Springer, Berlin/Heidelberg, pp 75–82

112. Satoh AK, Li BX, Xia H et al (2008) Calcium-activated myosin V closes the Drosophila pupil. Curr Biol 18(13):951–955. https://doi.org/10.1016/j.cub.2008.05.046
113. Tsunoda S, Zuker CS (1999) The organization of INAD-signaling complexes by a multivalent PDZ domain protein in Drosophila photoreceptor cells ensures sensitivity and speed of signaling. Cell Calcium 26(5):165–171
114. Liu W, Wen W, Wei Z et al (2011) The INAD scaffold is a dynamic, redox-regulated modulator of signaling in the *Drosophila* eye. Cell 145(7):1088–1101. https://doi.org/10.1016/j.cell.2011.05.015
115. Teng DH, Chen CK, Hurley JB (1994) A highly conserved homologue of bovine neurocalcin in Drosophila melanogaster is a $Ca(2^+)$-binding protein expressed in neuronal tissues. J Biol Chem 269(50):31900–31907
116. Faurobert E, Chen CK, Hurley JB et al (1996) Drosophila neurocalcin, a fatty acylated, $Ca2^+$−binding protein that associates with membranes and inhibits in vitro phosphorylation of bovine rhodopsin. J Biol Chem 271(17):10256–10262
117. Kawamura S, Hisatomi O, Kayada S et al (1993) Recoverin has S-modulin activity in frog rods. J Biol Chem 268(20):14579–14582
118. Song Z, Postma M, Billings SA et al (2012) Stochastic, adaptive sampling of information by microvilli in fly photoreceptors. Curr Biol 22(15):1371–1380. https://doi.org/10.1016/j.cub.2012.05.047

Chapter 35
Calcium Imaging in *Drosophila melanogaster*

Nicola Vajente, Rosa Norante, Paola Pizzo, and Diana Pendin

Abstract *Drosophila melanogaster*, colloquially known as the fruit fly, is one of the most commonly used model organisms in scientific research. Although the final architecture of a fly and a human differs greatly, most of the fundamental biological mechanisms and pathways controlling development and survival are conserved through evolution between the two species. For this reason, *Drosophila* has been productively used as a model organism for over a century, to study a diverse range of biological processes, including development, learning, behavior and aging. Ca^{2+} signaling comprises complex pathways that impact on virtually every aspect of cellular physiology. Within such a complex field of study, *Drosophila* offers the advantages of consolidated molecular and genetic techniques, lack of genetic redundancy and a completely annotated genome since 2000. These and other characteristics provided the basis for the identification of many genes encoding Ca^{2+} signaling molecules and the disclosure of conserved Ca^{2+} signaling pathways. In this review, we will analyze the applications of Ca^{2+} imaging in the fruit fly model, highlighting in particular their impact on the study of normal brain function and pathogenesis of neurodegenerative diseases.

Keywords Calcium imaging · *Drosophila* · Calcium indicators · GECI · Calcium signaling · Neurodegenerative diseases

Nicola Vajente and Rosa Norante have contributed equally.

N. Vajente · R. Norante
Department of Biomedical Sciences, University of Padova, Padova, Italy

P. Pizzo · D. Pendin (✉)
Department of Biomedical Sciences, University of Padova, Padova, Italy

Neuroscience Institute, National Research Council (CNR), Padova, Italy
e-mail: diana.pendin@unipd.it

M. S. Islam (ed.), *Calcium Signaling*, Advances in Experimental Medicine and Biology 1131, https://doi.org/10.1007/978-3-030-12457-1_35

35.1 A Brief History

The path of *Drosophila* as a research model is a history of groundbreaking achievements, underpinned by 6 Nobel Prizes since 1933. The first went to Thomas Hunt Morgan, who delineated the theory of inheritance by using *Drosophila* to define genes location on chromosomes [1]. Some years later, Hermann Muller defined the effects of X-rays on mutation rate in fruit flies [2], opening the field to modern genetics. These seminal discoveries allowed the generation of genetic tools that still prosper, *e.g.*, balancer chromosomes, special chromosomes that, preventing meiotic crossing-over, are used to maintain complex stocks with multiple mutations on single chromosomes over generations [3]. New genetic tools developed over the years allowed the fruit fly to move with times. As a significant example, CRISPR/Cas9 genome editing strategies allow simple and rapid engineering of the fly genome [4].

What makes *Drosophila* the model organism of choice of many researchers is the observation that relevant genes, cellular processes and basic building blocks in cellular and animal biology are conserved between flies and mammals [5]. Moreover, compared to vertebrate models, *Drosophila* has considerably less genetic redundancy, making the characterization of protein function less complicated. The function of a gene product can be inferred by generating fly lines for its up- or down-regulation and then analyzing the resulting phenotypes. The fruit fly represents also an ideal model organism to study human diseases. Remarkably, over 60% of known human disease-causing genes have a fly orthologue [6]. Most of the cellular processes known to be involved in human disorders pathogenesis, including apoptosis signaling cascades, intracellular calcium (Ca^{2+}) homeostasis, as well as oxidative stress, are conserved in flies. Of note, the high accessibility of the nervous system at different developmental stages, makes also neuroscience experiments feasible in the fly model. Moreover, flies exhibit complex behaviors and, like in humans, many of these behaviors, including learning, memory and motor ability, deteriorate with age [7, 8].

Box 35.1 Advantages of Using *Drosophila* as a Research Animal Model
Beside genetics, the strongest selling point of using *Drosophila* as an animal model are: (i) *Drosophila* are relatively inexpensive and easy to keep, as they are raised in bottles or vials containing cheap jelly-like food. (ii) Generally, there are very few restrictions, minimal ethical and safety issues on their laboratory use. (iii) Flies life cycle is very fast, lasting about 10–12 days at 25 °C. Newly laid eggs take 24 h to undergo embryogenesis before hatching into first instar larvae, which develop into second, and then third instar larvae. The duration of these stages varies with the temperature: at 20 °C, the average length of the egg-larval period is 8 days; at 25 °C it is reduced to 5 days. Larvae transform into immobile pupa, undergo metamorphosis and eclose in the adult form 5–7 days later. (iv) A single fly can produce hundreds

(continued)

Box 35.1 (continued)
of offspring within days, thus it is relatively easy to quickly generate large numbers of embryos, larvae or flies of a given genotype. Individual flies are easily manipulated when anaesthetized with carbon dioxide, allowing identification of selectable phenotypic features under a stereomicroscope [9].

35.2 *Drosophila* Ca^{2+} Toolkit

The Ca^{2+} ion is the major intracellular messenger, mediating a variety of physiological responses to chemical and electrical stimulations. Therefore, cell Ca^{2+} concentration [Ca^{2+}] must be tightly controlled in terms of both space and time, a task that is accomplished by several Ca^{2+} transporting and buffering systems. Easily accessible knock-down and knock-out strategies, applicable to cell lines, as well as to living animals, have helped discovering in flies a number of molecules involved in Ca^{2+} signaling. As in mammals, basal cytosolic Ca^{2+} levels are controlled in flies by the interplay of Ca^{2+} transport systems, localized in the plasma membrane (PM) and the membranes of intracellular organelles that function as internal Ca^{2+} stores (Fig. 35.1). This toolkit, together with a number of Ca^{2+}-binding proteins, concurs in creating and regulating the dynamics and spatial localization of Ca^{2+} signals. The major players in Ca^{2+} signaling in *Drosophila* are briefly described below; the interested reader is referred to a more extensive review on the topic [10].

Ca^{2+} enters the PM through Ca^{2+} channels, *e.g.*, voltage- and ligand- gated. As for voltage-gated Ca^{2+} channels, the fly genome encodes three α1 subunits (Ca-α1D, cacophony, Ca-α1T) forming Ca_v1, Ca_v2, and Ca_v3 type channels, respectively, mainly expressed in the nervous system and muscles [10]. Among ligand-gated channels, glutamate-gated ionotropic receptors (iGluRs) are represented in *Drosophila* by 15 genes encoding different subunits. As in other animal species, *Drosophila* uses glutamate as a fast neurotransmitter in neuromuscular junctions (NMJs), and highly Ca^{2+} permeable iGluRs are clustered in active zones in postsynaptic motor neuron terminals [11]. Cations enter sensory neurons through Transient Receptor Potential (TRP) channels. The gene encoding the first member of the trp superfamily was identified in *Drosophila* photoreceptors as a PM Ca^{2+} permeable channel, required for mediating the light response [12]. A vast number of trp homologs were found in vertebrates that have been classified in seven major subfamilies in metazoans.

Cytosolic Ca^{2+} increase can be also triggered by the activation of phospholipase C (PLC), which produces inositol 1,4,5-trisphosphate (IP_3) that interacts with Ca^{2+} channels located in the Endoplasmic Reticulum (ER) and Golgi apparatus (GA), causing their opening. Three IP_3 receptor (IP_3R) isoforms are expressed in mammals, while a single IP_3R is present in *Drosophila* (itpr) [13]. The channel shares the highest level of similarity as well as functional properties (channel conductance, gating properties, IP_3- and Ca^{2+}-dependence) with the mouse IP_3R1. The release of Ca^{2+} from intracellular stores occurs also through Ryanodine

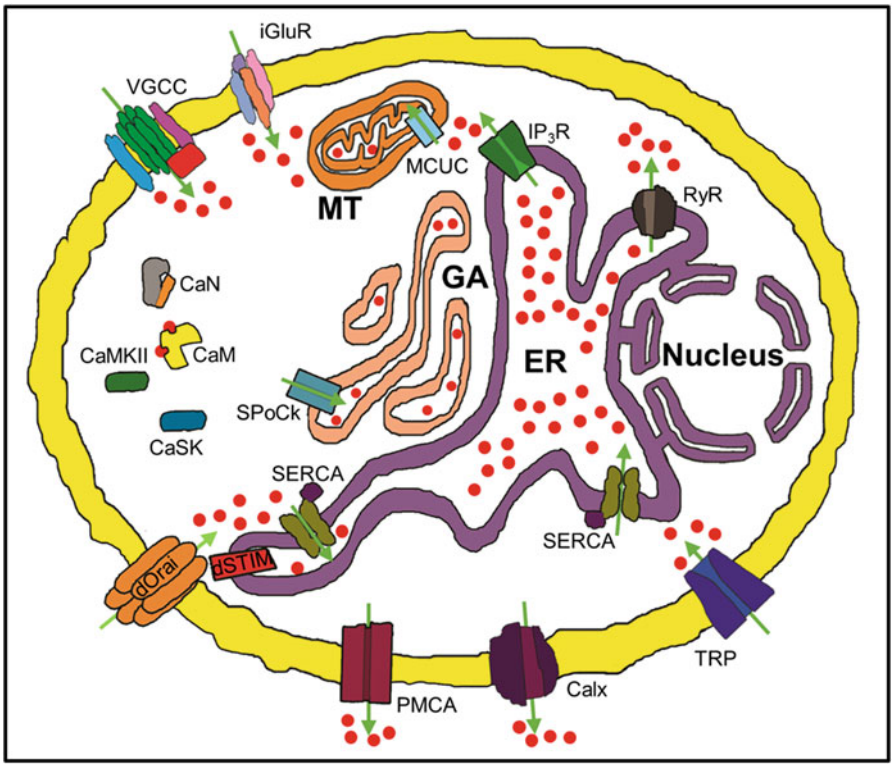

Fig. 35.1 A *Drosophila* cell with its Ca^{2+} toolkit. The movement of Ca^{2+} ions (red spots) are indicated as green arrows. The Ca^{2+} handling proteins inserted in the PM, from the upper left corner, are: Voltage-Gated Ca^{2+} channels (VGCC), glutamate-gated ionotropic receptors (iGluRs), Transient Receptor Potential (TRP) channels, Na^{+}/Ca^{2+} exchanger (Calx), PM Ca^{2+} ATPase (PMCA) and ORAI1 oligomers forming a channel. In the ER membrane from the upper left side are present: inositol 1,4,5-trisphosphate receptor (IP_3R), Ryanodine Receptor (RyR), Sarco-Endoplasmic Reticulum Ca^{2+} ATPase (SERCA) and STIM1. In the GA membrane is present the Secretory Pathway Ca^{2+} ATPase (SPoCk). The inner mitochondrial membrane hosts the mitochondrial calcium uniporter complex (MCUC). Different Ca^{2+} interacting proteins are resident in the cytosol: Calcineurin (CaN), Calmodulin (Cam), Ca^{2+}/Calmodulin-dependent protein kinase II (CaMKII), and Ca^{2+}/Calmodulin-dependent serine protein kinase (CaSK)

Receptor (RyR), located in the sarco/endoplasmic reticulum (SER) membrane. In vertebrates, three isoforms are described (RyR 1–3), while the *Drosophila* genome contains a single RyR gene that encodes a protein with approximately 45% identity with the vertebrate family members [14, 15].

Ca^{2+} release from intracellular stores is most often accompanied by Ca^{2+} influx through PM channels in the regulated process of Store-Operated Ca^{2+} Entry (SOCE). The molecular basis of SOCE, whereby Ca^{2+} influx across the PM is activated in response to depletion of ER Ca^{2+} stores, has been under investigation for more than 20 years and was finally revealed thanks to the identification of the two

molecular key players in RNAi screens performed in *Drosophila* S2 cells [16, 17]. The presence of a single fly homologue for stromal interacting molecule 1 (STIM1) and ORAI1, whereas mammals have two and three copies respectively, offered a flying start for the identification of the proteins.

The main route for Ca^{2+} uptake into mitochondria is through the mitochondrial calcium uniporter (MCU) complex, a Ca^{2+}-selective ion channel located at the inner mitochondrial membrane. The channel subunit MCU is regulated through other regulatory components, i.e. MICU1/2/3 and EMRE [18]. A MCU homologue has been identified and characterized in *Drosophila* [19, 20], along with its regulatory subunits MICU1 [19, 20] and EMRE [21].

Ca^{2+} signals are terminated by the combined activities of Ca^{2+} ATPases, located on PM, ER, GA membranes and the Na^{+}/Ca^{2+} exchanger, NCX. PM Ca^{2+} ATPase (PMCA) is a protein present in all animals, characterized by a high Ca^{2+} affinity and a low-transport capacity that extrudes Ca^{2+} from the cytosol to maintain $[Ca^{2+}]$ at the basal value of about 100 nM. In humans and other mammals, four major PMCA isoforms are encoded by separate genes, while the *Drosophila* genome encodes a single, ubiquitously expressed PMCA [22]. The ATPases located on ER and GA membranes acts to re-accumulate the cation in the organelles' lumen. The SER Ca^{2+} ATPase (SERCA), transports inside ER/SR two Ca^{2+} ions per ATP hydrolyzed. In vertebrates, three SERCA protein isoforms are encoded by three distinct genes, while in *Drosophila* a single gene was identified [23]. Fly SERCA has a higher identity with mammalian SERCA1 and SERCA2 (71–73%) and is expressed at a very high level in the central nervous system (CNS) and muscles. A single homolog of the Secretory Pathway Ca^{2+} ATPase (SPCA) is present in *Drosophila*, named SPoCk. The gene results in three isoforms, but only one (SPoCk-A) has been reported to localize in GA membranes, as its mammalian counterpart [24]. The other two variants have been reported to localize in the ER and peroxisomal membranes. The NCX is a non-ATP-dependent antiporter that mediates the efflux of Ca^{2+} ions in exchange for Na^{2+} import. The *Drosophila* NCX, named Calx, is highly expressed in brain and muscle and has 55% identity with the three mammalian isoforms NCX1, NCX2 and NCX3, which are differentially expressed mainly in the heart, brain and skeletal muscles, respectively [25].

35.3 Experimental Set Up for Ca^{2+} Imaging in *Drosophila*

The conserved Ca^{2+} molecular toolkit, together with the advantages of the model depicted above (Box 35.1), set the basis for the fruit fly to be a major model organism for Ca^{2+} signaling research. Thanks to the development of a broad range of Ca^{2+} indicators (Box 35.2), Ca^{2+} imaging procedures have been specifically designed for their application in flies.

Advancements in Ca^{2+} imaging techniques have proceeded through two distinct although interconnected avenues: the improvement of Ca^{2+} indicators and the development of appropriate instrumentations. In the field of Ca^{2+} imaging of live tissues/animals, the application of wide-field microscopy is limited by light scattering across the z-axis of extended pieces of tissue, thus the use of two-photon

(2P) microscopy is usually preferred. 2P microscopy have allowed measurements in the intact brain of an entire transgenic animal, improving spatial resolution by restricting the excitation of chromophores to defined focal planes.

In order to perform optical Ca^{2+} imaging experiments in *Drosophila*, the access of light for excitation to the structures of interest must be assured. The simplest possibility is to excite the genetically encoded Ca^{2+} indicator (GECI, see Box 35.2, Fig. 35.2) directly through the animal's cuticle without any surgical manipulation. When baseline fluorescence of the GECI used is strong enough, the partial transparency of third instar larvae allows for optical access of brain, dorsal sensory neurons and muscles. Since imaging is hurdled by continuous larval movements, a few experimental tips have been developed, *e.g.*, immobilization of the larva on the coverslip with a transparent sticky tape [26] or in microfluidic clamps [27]. Despite the immobilization, slight contractions and movements cannot be completely eliminated, possibly leading to shifts in the focal plane and thus alterations in the fluorescence intensity. The problem can be overcome by using ratiometric GECIs (Box 35.2).

Box 35.2 Ca^{2+} Indicators for Imaging in Flies

Approximately 30 years ago, scientists started to design and engineer organic fluorescent Ca^{2+} indicators, opening the door for cellular Ca^{2+} imaging. Since then, a variety of probes have been developed, which differ in their mode of action, Ca^{2+} affinities, intrinsic baseline fluorescence and kinetic properties. Two major classes of Ca^{2+} indicators have been developed, *i.e.*, chemical probes and genetically encoded Ca^{2+} indicators (GECIs).

Chemical indicators (*e.g.*, fura-2, indo-1, fluo-4) are small fluorescent molecules that are able to chelate Ca^{2+} ions. These molecules are based on BAPTA, an EGTA homologue with high selectivity for Ca^{2+}. The Ca^{2+} chelating carboxyl groups are usually masked as acetoxymethyl esters, making the molecule more lipophilic and allowing an easy entrance into cells. Once the molecule is inside the cell, the Ca^{2+} binding domains are freed by cellular esterases. Binding of a Ca^{2+} ion to the molecule leads to either an increase in quantum yield of fluorescence or an emission/excitation wavelength shift. Chemical indicators are mostly used to measure cytosolic $[Ca^{2+}]$. Early attempts to measure presynaptic $[Ca^{2+}]$ in *Drosophila* employed membrane permeant chemical Ca^{2+} indicators [30]. However, this technique is hardly reliable due to uneven dye loading, high background fluorescence and lack of cell type selectivity. To overcome current limitations, dextran-conjugated fluorescent Ca^{2+} indicators have been loaded in cut axons. The approach allowed to measure resting $[Ca^{2+}]$ and nerve-evoked Ca^{2+} signals during high-frequency activity [31].

GECIs include different types of engineered proteins, such as single fluorescent protein-based indicators (*e.g.*, GCaMP), bioluminescent probes (*e.g.*, aequorin) and fluorescence (or Förster) resonance energy transfer (FRET)-based indicators (*e.g.*, cameleons) [32].

(continued)

Box 35.2 (continued)

GCaMP is one of the most used GECIs, based on a circularly-permuted variant of Green Fluorescent Protein (cpGFP). The N-terminus of the cpGFP is connected to the M13 fragment of the myosin light chain kinase, while the C-terminus ends with the Ca^{2+}-binding region of calmodulin (CaM). In the presence of Ca^{2+}, M13 wraps around Ca^{2+}-bound CaM, leading to a conformational change that increases the fluorescence protein (FP) fluorescence intensity [33] (Fig. 35.2, panel a). During recent years, different variants of GCaMP indicators have been developed, with improved characteristics in terms of Ca^{2+} affinity, brightness, dynamic range. Other variants of FPs, *e.g.*, red-coloured, have been used to develop sensors allowing simultaneous measurement in different organelles, making GCaMPs a whole family of great tools to follow Ca^{2+} dynamics.

One limitation in the use of GCaMPs, and in general of single protein-based GECIs, is the sensitivity to movement artifacts as well as focal plane shifts, which can be mistaken for $[Ca^{2+}]$ changes. A method used to correct for this type of artifacts is to co-express a FP together with the GECI [34]. Alternatively, the limit can be overcome by using ratiometric indicators, such as cameleon. This molecule uses the same Ca^{2+} binding domains of the GCaMP (M13 and CaM), that are bound to two different variants of the GFP: a cyan (CFP) and a yellow (YFP) variant. In the absence of Ca^{2+}, the excited CFP emits at 480 nm, while in the presence of Ca^{2+} the interaction between Ca^{2+}, CaM and M13 brings the two FPs at a closer distance (2–6 nm), and the energy released from the CFP is absorbed by the YFP, that emits at a different wavelength (535 nm) (Fig. 35.2, panel b). By calculating the ratio of EYFP/ECFP emissions, one obtains a clear indication of intracellular $[Ca^{2+}]$ variations, excluding changes of fluorescence caused by artefactual movements of the sample.

GECIs allow the monitoring of Ca^{2+} not only in the cytosol, but also in organelles (*e.g.*, ER, mitochondria, GA, etc.) thanks to the addition of specific targeting sequences. GECIs have demonstrated valuable in the measurement of $[Ca^{2+}]$ in cells and within organelles in several in vivo models. Notably, in flies, the ease of transgenesis allowed the generation of several lines for the expression of GECIs, both cytosolic and organelle-targeted. Moreover, the Gal4-UAS expression system [35, 36] allows the targeting of the probes to specific tissues or even cell subtypes. In this two-part approach, one fly strain carries the Ca^{2+} sensor cDNA under the control of an upstream activator sequence (UAS), so that the gene is silent in the absence of the transcription factor Gal4. A second fly strain expressing Gal4 in a cell type-specific manner is mated to the UAS strain, resulting in progeny expressing the probe in a transcriptional pattern that reflects the expression pattern of the Gal4 line promoter.

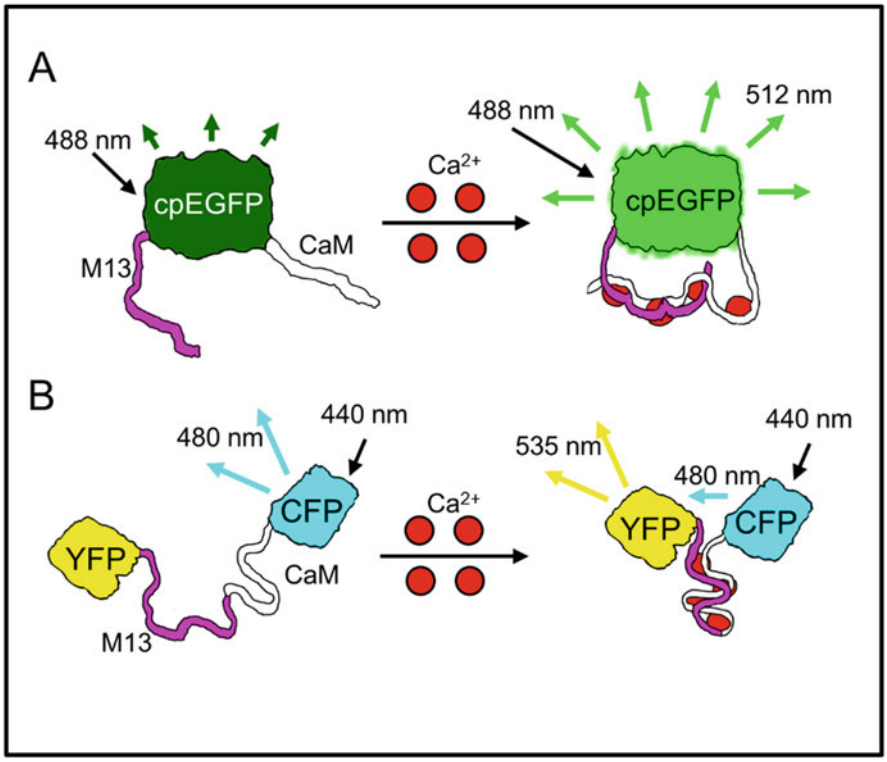

Fig. 35.2 Most used indicators for in vivo Ca^{2+} imaging in *Drosophila*. (**a**) The single-wavelength indicator GCaMP is composed by: the M13 fragment of the myosin light chain kinase domain (M13, pink), the circularly-permutated enhanced Green Fluorescent Protein (cpEGFP, green) and Ca^{2+}-binding region of calmodulin (CaM, white). The FP is excited at 488 nm and the emission is detected at 512 nm. Upon Ca^{2+} binding, a conformational change increases the emitted fluorescence intensity. (**b**) The FRET-based Cameleon probe, composed by: Yellow Fluorescent Protein (YFP, yellow), the M13 domain (pink), the CaM domain (white) and the Cyan Fluorescent Protein (CFP, cyan). The protein is excited at 440 nm and in absence of Ca^{2+} the emission is detected at 480 nm; upon Ca^{2+} binding, conformational changes provide the optimal distance to get Forster Resonance Energy Transfer (FRET), and the YFP emission is detected at 535 nm

Imaging Ca^{2+} activities in the CNS of adult flies usually requires a surgical intervention to achieve optical access to the brain. However, trans-cuticular imaging have also been applied to intact adult brains using 3P microscopy [28]. We report, as an example, a protocol applied to monitor odor-evoked Ca^{2+} dynamics. Anesthetized flies are restrained between a sticky tape and a fine-meshed metal grid which enables air exchange around the abdomen. A small hole cut through the sticky tape into the head capsule allows the exposure of the brain and the antennal lobes expressing the GECI. The odors are then applied to the fly's antennae and the temporal dynamics and spatial distribution of Ca^{2+} activities are monitored using an imaging microscope [26] (Fig. 35.3). Since movements are reduced in these

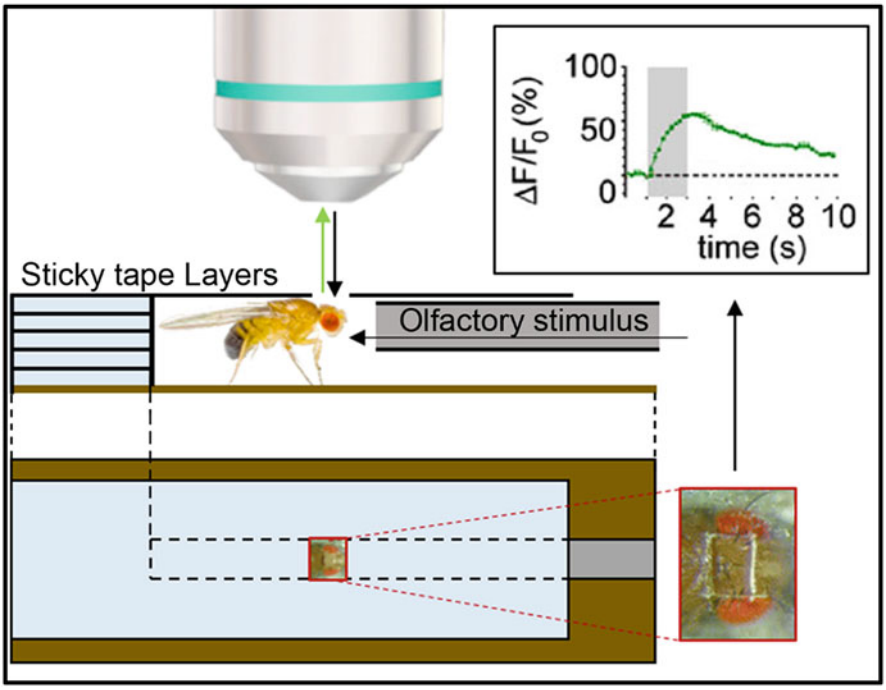

Fig. 35.3 Schematic illustration of a set up for in vivo odor-stimulated Ca^{2+}imaging in Drosophila. A grid is placed on the microscope slide and fixed with several layers of sticky tape. A small passage is cut into the layers of tape, fitting a single fly and a small tube for the delivery of the odor. The chamber is sealed with another layer of adhesive tape where a small window is cut, providing access to the fly's head. The dynamics of intracellular Ca^{2+} in the olfactory sensory neurons of the antennal lobe has been detected upon application of 3-octanol using the sensor G-CaMP 3.0. The duration of the odor stimulus is indicated as a grey bar. (Adapted from: Ref. [29])

preparations, single-wavelength GECIs, such as GCaMPs, are usually preferred, due to their higher dynamic range and because they permit the use of simpler imaging systems.

Thanks to the parallel development of indicators and imaging systems, Ca^{2+} imaging has matured over the years into a powerful tool for imaging of cellular activity in living animals. We propose now an overview of Ca^{2+} imaging experiments that can be performed in *Drosophila*, aware that by far this is not all encompassing, and the list of interesting investigations could certainly be extended.

35.4 Ca^{2+} Imaging: Sensory Neuroscience and Beyond

Drosophila melanogaster contributed to many aspects of neuroscience. In the past, the analysis of fly brain function has been challenging due to the small size of

neurons that initially restricted electrophysiological recordings to specific highly accessible regions, *e.g.*, larval preparations of NMJs [37]. Recently, whole-cell patch-clamp recordings have been performed on fly central neurons [38], providing insights into neuronal activity with an excellent temporal precision. However, as in the brains of vertebrates, *Drosophila* sensory stimuli, motor outputs as well as central processing events, are encoded as spatio-temporal activity patterns that require the concerted activity of many neurons. As a consequence, besides recordings from individual neurons, monitoring the activity across many cells is mandatory to explore complex circuits. In neurons, membrane depolarization is accompanied by fast Ca^{2+} influx via voltage-gated Ca^{2+} channels, as well as slower Ca^{2+} signals deriving from the ER and mitochondrial Ca^{2+} pools [39]. The easiest way to indirectly measure membrane depolarization is measuring the variations in $[Ca^{2+}]$ inside the cells. The development of GECIs allowed for these measurements in vivo in multi-cellular animals, by targeting the probes to specific cells and sub-cellular compartments.

Different types of scientific questions concerning the function of the *Drosophila* brain can be addressed using optical Ca^{2+} imaging. One of the most extensively explored fields regards the mechanisms of sensory processing, *i.e.*, how neural activity encodes sensory input in behavioral output. Sensory cells and directly coupled downstream neurons encode the sensory stimuli by membrane depolarization-induced action potential frequencies. High-intensity stimuli result in high-firing frequencies, leading to strong intracellular Ca^{2+} transients, allowing to fully exploit the potential of GECIs. A number of studies in this field have helped identify and measure the response of specific brain regions to various sensory stimuli including olfaction, taste, and thermosensation [26]. We present here some significant examples.

Optical Ca^{2+} imaging has been successfully applied to study neuronal activity in the olfactory system of the fly's brain. Flies display robust odor-evoked behaviors in response to cues from plants or other flies. More than 1000 olfactory sensory neurons located in the olfactory sensory organs of the head (*i.e.*, the third segment of the antenna and the maxillary palps) project with their axons to the antennal lobe, the primary olfactory center of the fly's brain. The neuronal terminal arborizations are organized into spherical structures called glomeruli that contact projection neurons and local interneurons. Projection neurons signal to higher brain centers, such as the mushroom body and the lateral horn. Since each sensory neuron expresses a limited number of olfactory receptors with a specific ligand-binding profile, each odor information is represented as a specific spatiotemporal code before it is sent to higher brain centers. Optical Ca^{2+} imaging has been performed in each order of olfactory neurons, including the antennal lobe (example in: [40]; protocol in [41]) and the neurons of the mushroom bodies (Kenyon cells) [42]. The mushroom body has been shown over many years to be a brain region necessary and sufficient for the association of odor stimuli through learning with rewarding or punishing cues [43, 44]. Electrophysiological studies on individual cells allowed to propose a model for odors encoding in the mushroom bodies. The model proposed that only very few out of a large array of Kenyon cells are selectively responding to any given odor

stimulus, due to the convergence of several projection neurons onto a given Kenyon cell, combined with the high firing thresholds of Kenyon cells. The use of GECIs recently allowed to confirm the proposed model: the activity of >100 mushroom body neurons was simultaneously monitored in vivo by two-photon imaging of the Ca^{2+} indicator GCaMP3, allowing the visualization of the distinct patterns of sparse mushroom body neurons activated upon different odors stimulation [45].

Ca^{2+} imaging has also proven to be of enormous value for the analysis of how auditory stimuli are encoded in flies. The structure that has been primarily associated with hearing is the Johnston's organ, located on the second antennal segment. Interestingly, Ca^{2+} imaging experiments performed in intact animals demonstrated that Johnston's organ contains also wind-sensitive neurons. GCaMP-1.3 was expressed under the control of different Gal4 enhancer trap lines in distinct groups of neurons in Johnston's organ. Live flies were mounted in an inverted orientation under a two-photon microscope, and an air flow or a near-field sound, were delivered while recording Ca^{2+} dynamics. Optical Ca^{2+} imaging represented here a powerful tool to dissect this novel circuit, providing evidence that a common sensory organ is used to encode sound-evoked stimuli and air movements [46].

Other relevant aspects for which optical Ca^{2+} imaging using GECIs has been successfully applied to sensory neuroscience comprise: propagation of fly taste perception [47], neuronal plasticity underlying associative learning and memory formation [42], visual circuits dissection [48], mapping of mechanosensory circuits [49].

An interesting recent work, exploiting whole-brain Ca^{2+} imaging in adult flies, aimed at assessing intrinsic functional connectivity. Ca^{2+} signals were acquired from the central brain and functional data were assigned to atlas regions. This allowed to correlate activity between distinct brain regions, providing a framework for using *Drosophila* to study functional large-scale brain networks [50]. Whole-brain imaging has also been attempted during open field behavior in adult flies [51], allowing functional imaging of brain activity of untethered, freely walking flies during sensorial and socially evoked behaviors. Of note, despite imaging over extended periods in live animals is critical to dissect the mechanisms of plasticity, neural development, degeneration and aging, chronic preparations for long-term (>24 h) microscopy have been difficult in *Drosophila*, due to the fly's fragility and opaque exoskeleton. Only recently, laser microsurgery has been employed to create a chronic fly preparation for repeated imaging of neural dynamics for up to 50 days. Ca^{2+} and voltage imaging was performed in fly mushroom body neurons, in particular odor-evoked Ca^{2+} transients were recorded over 7 weeks [52]. This chronic preparation is compatible with a broad range of optical techniques to address in live flies biological questions previously unanswerable.

An interesting approach developed to evaluate functional connections is the combination of Ca^{2+} imaging with genetically encoded optogenetic tools. Optogenetic activation in presynaptic neurons and Ca^{2+} imaging in postsynaptic neurons have been used to map circuits governing different aspects of fly behavior, *e.g.*, antennal grooming behavior [53], courtship [54] and aggression [55]. Some critical aspects need to be taken into account when setting up this kind of experiments, *i.e.*,

minimize spectral overlaps and use independent gene expression systems for the two transgenes [56].

Another example of the power of combined functional imaging in the fly takes advantage of both GECIs and Genetically Encoded Voltage Indicators (GEVIs) (reviewed in [57]). Yang and colleagues compared voltage and Ca^{2+} responses within compartments of the same neuron, using the ultrafast GCaMP6f sensor together with a newly developed GFP-based voltage sensor, named Asap2f. *In vivo* two-photon imaging of the two indicators was performed in the *Drosophila* visual system. Remarkably, intracellular [Ca^{2+}] do not simply follow the decay of voltage signals. Instead, Ca^{2+} responses appear compartmentalized, *i.e.*, they are different in their amplitude and kinetics among distinct regions of the same cell [58]. Voltage and Ca^{2+} signals appear distinct and neurons may convey varying information to their postsynaptic partners in different synaptic layers. The unprecedented resolution afforded by both indicators allowed to shed light on local neural computations during visual information processing.

In addition to adult flies, also other developmental stages can be subjected to Ca^{2+} imaging. In a recent paper, insight in the molecular pathway underlying network refinement was obtained by performing Ca^{2+} imaging at the embryonic NMJs. The authors demonstrated that oscillatory Ca^{2+} signals via voltage-gated Ca^{2+} channels orchestrate the activity of several kinases and phosphatases, key components in pruning aberrant synapses during embryonic synaptic refinement [59].

Another developmental stage much studied and appreciated for its accessibility and well-established organization is the larval stage. Ca^{2+} imaging has been performed in intact larvae, as well as in isolated larval CNS. An interesting recent example that underpins the power of the fly model is represented by a screen of unknown compounds for their potential to function as anticonvulsants [60]. In this work, GCaMP was expressed in motoneurons and the isolated CNS of third instar larvae was imaged to evaluate the effectiveness of novel anticonvulsive compounds to reduce seizure-like CNS activity.

Whole-brain imaging has also been performed in larvae (*e.g.*, imaging of ventral nerve cord during motor programs execution [61]; imaging of isolated CNS during coordinated motor pattern generation [62]).

Photoactivatable GECIs have been exploited for targeted neuronal imaging in cultured neurons and in fruit fly larvae [63]. Light-induced photoactivation allows single cells to be selected out of dense populations, for visualization of morphology and high signal-to-noise measurements of activity, synaptic transmission and connectivity. This tool combines the reporting Ca^{2+} activity with the selective highlighting of individual cells *in situ* in live tissues, facilitating tracking fine neuronal processes with a clarity that cannot be achieved with dense expression of standard FPs.

Besides the obvious importance in neurotransmission, Ca^{2+} signaling is fundamental for the survival and welfare of all cell types. Indeed, Ca^{2+} imaging experiments have been performed in other tissues, most relevantly in fly muscles. As an interesting recent example, an attempt to image all flight muscles together has

been tried in intact flying animals. In flies, wing motion is adjusted for both quick voluntary maneuvers and slow compensatory reflexes using only a dozen pairs of muscles. By applying visual motion stimuli while recording the pattern of activity across the complete set of steering muscles using GCaMP6f, the authors propose a model whereby the motor array regulates aerodynamically functional features of wing motion [64].

35.4.1 Ca^{2+} Imaging Inside Organelles

Organelle Ca^{2+} handling plays a fundamental role in cell Ca^{2+} homeostasis. At the cellular level, techniques to measure intra-organelle Ca^{2+} are nowadays available and routinely used. However, this type of measurements is still poorly exploited in living animals and few examples are available in *Drosophila*. Among them, the most commonly measured is mitochondrial Ca^{2+} [20, 65] although some attempts have also been done in other organelles.

As a recent example, Drago and Davis revealed a developmental role for the MCUC in memory formation in adult flies. The authors generated a transgenic line for a mitochondria-targeted GCaMP (named 4mtGCaMP3) that was expressed in MB neurons to measure mitochondria Ca^{2+} uptake upon downregulation of the MCUC components MCU or MICU1. Ca^{2+} imaging experiments have been associated to behavioral studies, demonstrating that the inhibition of mitochondrial Ca^{2+} entry in the developing fly MB neurons causes memory impairment [20].

A sensor of the GFP-aequorin protein (GAP) family, optimized for measurements in high-[Ca^{2+}] environments have been also developed and used in drosophila [66]. Among other applications, the authors propose the imaging of SR Ca^{2+} dynamics in the muscle of transgenic flies in vivo, providing evidence for a valuable tool to explore subcellular complex Ca^{2+} signaling in flies.

35.5 *Drosophila* Models of Neurodegenerative Diseases

Changes in intracellular [Ca^{2+}] mediate a wide range of cellular processes that are relevant to neurodegenerative disorder etiology, including learning and memory, as well as cell death. Indeed, a close link between the pathogenesis of different neurodegenerative disorders and Ca^{2+} regulating systems, the so called "Ca^{2+} hypothesis of neurodegenerative diseases", has been convincingly corroborated by several experimental findings [67, 68]. The potential of the approaches described above makes flies a powerful model system to elucidate pathogenic processes in neurobiology. Indeed, a wide collection of fly models of neurodegenerative disorders have been developed. Often, the model consists of targeted expression of human disease-associated protein. In the case of loss of function pathologic mutations, also knock out/knock down approaches have proved successful in

mimicking the pathology. In many cases, robust neurodegeneration is observed in these models.

Ca^{2+} imaging experiments performed in fly models of neurodegenerative disorders have helped unravel the pathogenesis of diseases, including Alzheimer's disease (AD), Parkinson's Disease (PD), Huntington Disease (HD). AD is a neurodegenerative disorder characterized by deposition of amyloid β (Aβ) in extracellular neuritic plaques, formation of intracellular neurofibrillary tangles and neuronal cell death. Among familial (FAD) cases, approximately 50% have been attributed to mutations in three genes: amyloid β precursor protein (*APP*) [69], presenilin 1 (*PSEN1*) [70] and presenilin 2 (*PSEN2*) [71]. The fly genome encodes a single Presenilin gene (*Psn*) [72] and a single APP orthologue (*Appl*) which encodes for β-amyloid precursor-like protein. *Drosophila* models of AD have been developed, mostly expressing wild type and FAD-mutant forms of human APP and presenilins, reproducing AD phenotypes, such as Aβ deposition, progressive learning defects, extensive neurodegeneration and ultimately a shortened lifespan [73]. It is now accepted that FAD-linked presenilins mutants are responsible for a dysregulation of cellular Ca^{2+} homeostasis. An imbalance of Ca^{2+} homeostasis is supposed to represent an early event in the pathogenesis of FAD, but the mechanisms through which FAD-linked mutants affect Ca^{2+} homeostasis are controversial [74]. Using a fly model of FAD, Michno et al. [75], showed that expression of wild type or FAD-mutant Psn in *Drosophila* cholinergic neurons results in cell-autonomous deficits in Ca^{2+} stores, highlighted using the chemical Ca^{2+} probe Fura-2. Importantly, these deficits occur independently of Aβ generation. They also describe a novel genetic, physiological and physical interaction between Psn and Calmodulin, a key regulator of intracellular Ca^{2+} homeostasis. More recently, a study conducted by Li et al. [76] exploited Ca^{2+} probes and confocal imaging to demonstrate that Imidazole, by decreasing the level of intracellular Ca^{2+}, can rescue the mental defect in Aβ42-expressing flies.

PD is the most common movement disorder, typically affecting people between 50 and 60 years of age. The disease is mostly sporadic, only a small fraction of PD cases have been linked to mutations in specific genes, including a-synuclein [77], parkin [78], PINK1 [79]. Cytoplasmic aggregates mainly formed by α-synuclein protein, called Lewy bodies [80], are usually found in the *substantia nigra* of brain tissue. Dopaminergic neurons are the most susceptible to degeneration in PD. Fruit flies are largely used as model for PD. Expression of human α-synuclein in flies leads to selective loss of dopaminergic neurons in the adult brain over time and accumulation of protein in cytoplasmic inclusions [81]. Pan-neural expression of α-synuclein either wild type or carrying PD-linked mutations results in premature loss of climbing ability. Noteworthy, the first animal models revealing an interaction between the two PD genes homologues Pink1 and parkin have been developed in *Drosophila* [82, 83]. Recently, Ca^{2+}-induced neurotoxicity have been explored in a *Drosophila* model of retinal degeneration. The authors found that increasing the autophagic flux prevented cell death in mutant flies, and this depended on the Pink1/parkin pathway [84]. The results indicated that maintaining mitochondrial homeostasis via Pink1/parkin-dependent mitochondrial quality control could potentially alleviate cell death in a wide range of neurodegenerative diseases.

HD is a progressive brain disorder characterized by uncontrolled movements, emotional problems, and loss of cognition. The disease is caused by autosomal dominant mutations in the gene encoding for huntingtin (*HTT*), resulting in an abnormal expansion of the number of CAG triplets, encoding for Glutamine. A *Drosophila* model of HD have helped investigating the mechanisms by which expanded full-length huntingtin (htt) impairs synaptic transmission [85]. The authors showed that expression of expanded full-length htt led to increased neurotransmitter release and increased resting intracellular Ca^{2+} levels, compared to controls. Moreover, mutations in voltage-gated Ca^{2+} channels restored the elevated [Ca^{2+}] and improved neurotransmitter release efficiency, as well as neurodegenerative phenotypes. This suggests that a defect in Ca^{2+} homeostasis contributes to the pathogenesis of the disease, which is in agreement with observations in mammalian systems [86–89].

Drosophila models have been created recapitulating many other diseases affecting the neuronal system, e.g. Hereditary Spastic Paraplegias (HSPs), are a group of inherited neurodegenerative disorders characterized by retrograde degeneration of corticospinal neurons, leading to muscle weakness and spasticity of the lower limbs. HSPs are highly genetically heterogeneous, with over 70 spastic paraplegia gene (SPG) loci associated [90]. Despite this diversity, it is now clear that one of the most common causes of HSPs are mutations in genes encoding proteins that, directly or indirectly, regulate ER morphology and/or distribution. Proper shape is necessary for the ER diverse functions, that are crucial for neuronal welfare [91]. Among these functions, Ca^{2+} sequestration and release play a fundamental role in shaping cytosolic signals [92]. *Drosophila* models have been generated for many HSP-related genes, among them the homologues of Atlastin-1 (SPG3A) [93], Spastin (SPG4) [94], Reticulon-2 (SPG12), ARL6IP1 (SPG61) [95]. Available tools for Ca^{2+} imaging applied to these models would provide valuable insights in the role of Ca^{2+} in the pathogenesis of HSPs.

35.6 Conclusions and Future Perspectives

Ca^{2+} signaling plays a critical role in cellular physiology and, in particular, in fundamental neuronal functions, such as synaptic transmission, synaptogenesis, neuronal plasticity, memory and cell survival. Understanding how the concerted action of neurons, synapses and circuits underlie brain function is a core challenge for neuroscience. The examples we described in this review underscore the contribution of *Drosophila* as a model system to explore cellular and circuits neurophysiology, highlighting potential future directions in the field. Given its genetic accessibility, complex behavioral repertoire and functional similarities with mammalian brain, the fruit fly represents an attractive model organism to approach relevant physiological and pathological questions. The combination of Ca^{2+} imaging with other tools, such as voltage indicators or optogenetics, provides a valuable developing strategy for investigating neural function and dysfunction. New variants of both green and red Ca^{2+} indicators are continually developed, offering improved sensitivity, brightness, photostability and kinetics and can be fruitfully applied to the *Drosophila* model.

Acknowledgments The authors thank the CARIPARO Foundation for Starting Grant 2015 to DP and University of Padova for a fellowship to RN.

References

1. Hunt TM, Bridges CB (1916) Sex linked inheritance in Drosophila, vol 352. Carnegie Institution of Washington, Washington, DC
2. Muller HJ (1928 Sep) The production of mutations by X-rays. Proc Natl Acad Sci U S A 14(9):714–726
3. Lindsley DL, Zimm GG (1992) The genome of Drosophila melanogaster. Annu Rev Genomics Hum Genet 4:89–117
4. Ewen-Campen B, Yang-Zhou D, Fernandes VR, González DP, Liu L-P, Tao R et al (2017) Optimized strategy for in vivo Cas9-activation in *Drosophila*. Proc Natl Acad Sci 114:9409–9414
5. Yoshihara M, Ensminger AW, Littleton JT (2001) Neurobiology and the Drosophila genome. Funct Integr Genomics 1:235–240
6. Wangler MF, Yamamoto S, Bellen HJ (2015) Fruit flies in biomedical research. Genetics 199(3):639–653
7. Mockett RJ, Bayne ACV, Kwong LK, Orr WC, Sohal RS (2003) Ectopic expression of catalase in Drosophila mitochondria increases stress resistance but not longevity. Free Radic Biol Med 34(2):207–217
8. Simon AF, Liang DT, Krantz DE (2006) Differential decline in behavioral performance of Drosophila melanogaster with age. Mech Ageing Dev 127(7):647–651
9. Stocker H, Gallant P (2008) Getting started : an overview on raising and handling Drosophila. Methods Mol Biol 420:27–44
10. Chorna T, Hasan G (2012) The genetics of calcium signaling in Drosophila melanogaster. Biochim Biophys Acta 1820(8):1269–1282
11. DiAntonio A (2006) Glutamate receptors at the Drosophila neuromuscular junction. Int Rev Neurobiol 75:165–179
12. Hardie RC, Minke B (1992) The trp gene is essential for a light-activated Ca^{2+} channel in Drosophila photoreceptors. Neuron 8(4):643–651
13. Yoshikawa S, Tanimura T, Miyawaki A, Nakamura M, Yuzaki M, Furuichi T et al (1992) Molecular cloning and characterization of the inositol 1,4,5-trisphosphate receptor in Drosophila melanogaster. J Biol Chem 267(23):16613–16619
14. Takeshima H, Nishi M, Iwabe N, Miyata T, Hosoya T, Masai I et al (1994) Isolation and characterization of a gene for a ryanodine receptor/calcium release channel in Drosophila melanogaster. FEBS Lett 337(1):81–87
15. Hasan G, Rosbash M (1992) Drosophila homologs of two mammalian intracellular ca(2+)-release channels: identification and expression patterns of the inositol 1,4,5-triphosphate and the ryanodine receptor genes. Development 116(4):967–975
16. Zhang SL, Yeromin AV, Zhang XH-F, Yu Y, Safrina O, Penna A et al (2006) Genome-wide RNAi screen of Ca^{2+} influx identifies genes that regulate Ca^{2+} release-activated Ca^{2+} channel activity. Proc Natl Acad Sci 103(24):9357–9362
17. Roos J, DiGregorio PJ, Yeromin AV, Ohlsen K, Lioudyno M, Zhang S et al (2005) STIM1, an essential and conserved component of store-operated Ca^{2+} channel function. J Cell Biol 169(3):435–445
18. Pendin D, Greotti E, Pozzan T (2014) The elusive importance of being a mitochondrial Ca^{2+} uniporter. Cell Calcium 55(3):139–145
19. Walkinshaw E, Gai Y, Farkas C, Richter D, Nicholas E, Keleman K et al (2015) Identification of genes that promote or inhibit olfactory memory formation in Drosophila. Genetics 199(4):1173–1182

20. Drago I, Davis RL (2016) Inhibiting the mitochondrial calcium uniporter during development impairs memory in adult Drosophila. Cell Rep 16(10):2763–2776
21. Choi S, Quan X, Bang S, Yoo H, Kim J, Park J et al (2017) Mitochondrial calcium uniporter in Drosophila transfers calcium between the endoplasmic reticulum and mitochondria in oxidative stress-induced cell death. J Biol Chem 292(35):14473–14485
22. Bai J, Binari R, Ni J-Q, Vijayakanthan M, Li H-S, Perrimon N (2008) RNA interference screening in Drosophila primary cells for genes involved in muscle assembly and maintenance. Development 135(8):1439–1449
23. Magyar A, Váradi A (1990) Molecular cloning and chromosomal localization of a sarco/endoplasmic reticulum-type Ca^{2+}-ATPase of drosophila melanogaster. Biochem Biophys Res Commun 173(3):872–877
24. Southall TD (2006) Novel subcellular locations and functions for secretory pathway Ca^{2+}/Mn^{2+}-ATPases. Physiol Genomics 26(1):35–45
25. Schwarz EM, Benzer S (1997) Calx, a Na-Ca exchanger gene of Drosophila melanogaster. Proc Natl Acad Sci U S A 94(19):10249–10254
26. Riemensperger T, Pech U, Dipt S, Fiala A (2012) Optical calcium imaging in the nervous system of Drosophila melanogaster. Biochim Biophys Acta Gen Subj 1820:1169–1178
27. Ghaemi R, Rezai P, Nejad FR, Selvaganapathy PR (2017) Characterization of microfluidic clamps for immobilizing and imaging of Drosophila melanogaster larva's central nervous system. Biomicrofluidics 11(3):034113
28. Tao X, Lin H-H, Lam T, Rodriguez R, Wang JW, Kubby J (2017) Transcutical imaging with cellular and subcellular resolution. Biomed Opt Express 8(3):1277–1289
29. Optical calcium imaging using DNA-encoded fluorescence sensors in transgenic fruit flies, Drosophila melanogaster. Dipt S, Riemensperger T, Fiala A. Methods Mol Biol. 2014;1071:195–206
30. Karunanithi S, Georgiou J, Charlton MP, Atwood HL (1997) Imaging of calcium in Drosophila larval motor nerve terminals. J Neurophysiol 78(6):3465–3467
31. Macleod GT (2002) Fast calcium signals in Drosophila motor neuron terminals. J Neurophysiol 88(5):2659–2663
32. Pendin D, Greotti E, Lefkimmiatis K, Pozzan T (2016) Exploring cells with targeted biosensors. J Gen Physiol 149(1):1–36
33. Nakai J, Ohkura M, Imoto K (2001) A high signal-to-noise Ca^{2+} probe composed of a single green fluorescent protein. Nat Biotechnol 19(2):137–141
34. Berry JA, Cervantes-Sandoval I, Chakraborty M, Davis RL (2015) Sleep facilitates memory by blocking dopamine neuron-mediated forgetting. Cell 161(7):1656–1667
35. Brand AH, Perrimon N (1993) Targeted gene expression as a means of altering cell fates and generating dominant phenotypes. Development 118(2):401–415
36. Klueg KM, Alvarado D, Muskavitch MAT, Duffy JB (2002) Creation of a GAL4/UAS-coupled inducible gene expression system for use in Drosophila cultured cell lines. Genesis 34(1–2):119–122
37. Broadie KS (1994) Synaptogenesis in Drosophila: coupling genetics and electrophysiology. J Physiol Paris 88(2):123–139
38. Wilson RI, Turner GC, Laurent G (2004) Transformation of olfactory representations in the Drosophila antennal lobe. Science 303(5656):366–370
39. Berridge MJ (1998) Neuronal calcium signaling. Neuron 21(1):13–26
40. Strube-Bloss MF, Grabe V, Hansson BS, Sachse S (2017) Calcium imaging revealed no modulatory effect on odor-evoked responses of the Drosophila antennal lobe by two populations of inhibitory local interneurons. Sci Rep 7(1):7854
41. Silbering AF, Bell R, Galizia CG, Benton R (2012) Calcium imaging of odor-evoked responses in the Drosophila antennal lobe. J Vis Exp 60:1–10
42. Barnstedt O, Owald D, Felsenberg J, Brain R, Moszynski JP, Talbot CB et al (2016) Memory-relevant mushroom body output synapses are cholinergic. Neuron 89(6):1237–1247
43. Heisenberg M (2003) Mushroom body memoir: from maps to models. Nat Rev Neurosci 4(4):266–275

44. Menzel R (2014) The insect mushroom body, an experience-dependent recoding device. J Physiol Paris 108(2–3):84–95
45. Honegger KS, Campbell RAA, Turner GC (2011) Cellular-resolution population imaging reveals robust sparse coding in the Drosophila mushroom body. J Neurosci 31(33):11772–11785
46. Yorozu S, Wong A, Fischer BJ, Dankert H, Kernan MJ, Kamikouchi A et al (2009) Distinct sensory representations of wind and near-field sound in the Drosophila brain. Nature 458(7235):201–205
47. Harris DT, Kallman BR, Mullaney BC, Scott K (2015) Representations of taste modality in the Drosophila Brain. Neuron 86(6):1449–1460
48. Schnaitmann C, Haikala V, Abraham E, Oberhauser V, Thestrup T, Griesbeck O et al (2018) Color processing in the early visual system of Drosophila. Cell 172(1–2):318–318.e18
49. Patella P, Wilson RI (2018) Functional maps of Mechanosensory features in the Drosophila Brain. Curr Biol 28:1189–1203.e5
50. Mann K, Gallen CL, Clandinin TR (2017) Whole-Brain calcium imaging reveals an intrinsic functional network in Drosophila. Curr Biol 27(15):2389–2396.e4
51. Grover D, Katsuki T, Greenspan RJ (2016) Flyception: imaging brain activity in freely walking fruit flies. Nat Methods 13(7):569–572
52. Huang C, Maxey JR, Sinha S, Savall J, Gong Y, Schnitzer MJ (2018) Long-term optical brain imaging in live adult fruit flies. Nat Commun 9(1):872
53. Hampel S, Franconville R, Simpson JH, Seeds AM (2015) A neural command circuit for grooming movement control. elife 4(9):e08758
54. Shirangi TR, Wong AM, Truman JW, Stern DL (2016) *Doublesex* regulates the connectivity of a neural circuit controlling *Drosophila* male courtship song. Dev Cell 37(6):533–544
55. Hoopfer ED, Jung Y, Inagaki HK, Rubin GM, Anderson DJ (2015) P1 interneurons promote a persistent internal state that enhances inter-male aggression in Drosophila. elife 4(12):pii: e11346
56. Simpson JH, Looger LL (2018) Functional imaging and optogenetics in drosophila. Genetics 208(4):1291–1309
57. Kaschula R, Salecker I (2016) Neuronal computations made visible with subcellular resolution. Cell 166:18–20
58. Yang HHH, St-Pierre F, Sun X, Ding X, Lin MZZ, Clandinin TRR (2016) Subcellular imaging of voltage and calcium signals reveals neural processing in vivo. Cell 166(1):245–257
59. Vonhoff F, Keshishian H (2017) In vivo calcium signaling during synaptic refinement at the Drosophila neuromuscular junction. J Neurosci 37(22):2922–2916
60. Streit AK, Fan YN, Masullo L, Baines RA (2016) Calcium imaging of neuronal activity in Drosophila can identify anticonvulsive compounds. PLoS One 11(2):e0148461
61. Lemon WC, Pulver SR, Höckendorf B, McDole K, Branson K, Freeman J et al (2015) Whole-central nervous system functional imaging in larval Drosophila. Nat Commun 6:7924
62. Pulver SR, Bayley TG, Taylor AL, Berni J, Bate M, Hedwig B (2015) Imaging fictive locomotor patterns in larval *Drosophila*. J Neurophysiol 114(5):2564–2577
63. Berlin S, Carroll EC, Newman ZL, Okada HO, Quinn CM, Kallman B et al (2015) Photoactivatable genetically encoded calcium indicators for targeted neuronal imaging. Nat Methods 12(9):852–858
64. Lindsay T, Sustar A, Dickinson M (2017) The function and organization of the motor system controlling flight maneuvers in flies. Curr Biol 27(3):345–358
65. Ivannikov MV, Macleod GT (2013) Mitochondrial free Ca^{2+} levels and their effects on energy metabolism in drosophila motor nerve terminals. Biophys J 104(11):2353–2361
66. Navas-Navarro P, Rojo-Ruiz J, Rodriguez-Prados M, Ganfornina MD, Looger LL, Alonso MT et al (2016) GFP-Aequorin protein sensor for Ex vivo and in vivo imaging of Ca 2+ dynamics in high-Ca 2+ organelles. Cell Chem Biol 23(6):738–745
67. Mattson MR (2007) Calcium and neurodegeneration. Aging Cell 6:337–350
68. Mattson MP (2004) Pathways towards and away from Alzheimer's disease. Nature 430:631–639

69. Goate A, Chartier-Harlin MC, Mullan M, Brown J, Crawford F, Fidani L et al (1991) Segregation of a missense mutation in the amyloid precursor protein gene with familial Alzheimer's disease. Nature 349(6311):704–706
70. Sherrington R, Rogaev EI, Liang Y, Rogaeva EA, Levesque G, Ikeda M et al (1995) Cloning of a gene bearing missense mutations in early-onset familial Alzheimer's disease. Nature 375(6534):754–760
71. Rogaev EI, Sherrington R, Rogaeva EA, Levesque G, Ikeda M, Liang Y et al (1995) Familial Alzheimer's disease in kindreds with missense mutations in a gene on chromosome 1 related to the Alzheimer's disease type 3 gene. Nature 376(6543):775–778
72. Boulianne GL, Livne-Bar I, Humphreys JM, Liang Y, Lin C, Rogaev E et al (1997) Cloning and characterization of the Drosophila presenilin homologue. Neuroreport 8(4):1025–1029
73. Iijima K, Liu H-P, Chiang A-S, S a H, Konsolaki M, Zhong Y (2004) Dissecting the pathological effects of human Abeta40 and Abeta42 in Drosophila: a potential model for Alzheimer's disease. Proc Natl Acad Sci U S A 101(17):6623–6628
74. Agostini M, Fasolato C (2016) When, where and how? Focus on neuronal calcium dysfunctions in Alzheimer's disease. Cell Calcium 60:289–298
75. Michno K, Knight D, Campussano JM, van de Hoef D, Boulianne GL (2009) Intracellular calcium deficits in Drosophila cholinergic neurons expressing wild type or FAD-mutant presenilin. PLoS One 4(9):e6904
76. Li M, Zhang W, Wang W, He Q, Yin M, Qin X et al (2018 Apr) Imidazole improves cognition and balances Alzheimer's-like intracellular calcium homeostasis in transgenic Drosophila model. Neurourol Urodyn 37(4):1250–1257
77. Polymeropoulos MH, Lavedan C, Leroy E, Ide SE, Dehejia A, Dutra A et al (1997) Mutation in the alpha-synuclein gene identified in families with Parkinson's disease. Science 276(5321):2045–2047
78. Kitada T, Asakawa S, Hattori N, Matsumine H, Yamamura Y, Minoshima S et al (1998) Mutations in the parkin gene cause autosomal recessive juvenile parkinsonism. Nature 392(6676):605–608
79. Valente EM, Abou-Sleiman PM, Caputo V, Muqit MMK, Harvey K, Gispert S et al (2004) Hereditary early-onset Parkinson's disease caused by mutations in PINK1. Science 304(5674):1158–1160
80. Spillantini MG, Schmidt ML, Lee VM-Y, Trojanowski JQ, Jakes R, Goedert M (1997) Alpha-synuclein in Lewy bodies. Nature 388(6645):839–840
81. Feany MB, Bender WW (2000) A Drosophila model of Parkinson's disease. Nature 404(6776):394–398
82. Park J, Lee SB, Lee S, Kim Y, Song S, Kim S et al (2006) Mitochondrial dysfunction in Drosophila PINK1 mutants is complemented by parkin. Nature 441(7097):1157–1161
83. Clark IE, Dodson MW, Jiang C, Cao JH, Huh JR, Seol JH et al (2006) Drosophila pink1 is required for mitochondrial function and interacts genetically with parkin. Nature 441(7097):1162–1166
84. Huang Z, Ren S, Jiang Y, Wang T (2016) PINK1 and Parkin cooperatively protect neurons against constitutively active TRP channel-induced retinal degeneration in Drosophila. Cell Death Dis 7:e2179
85. Romero E, Cha GH, Verstreken P, Ly CV, Hughes RE, Bellen HJ et al (2008) Suppression of neurodegeneration and increased neurotransmission caused by expanded full-length huntingtin accumulating in the cytoplasm. Neuron 57(1):27–40
86. Bezprozvanny I, Hayden MR (2004) Deranged neuronal calcium signaling and Huntington disease. Biochem Biophys Res Commun 322:1310–1317
87. Cepeda C, Ariano MA, Calvert CR, Flores-Hernández J, Chandler SH, Leavitt BR et al (2001) NMDA receptor function in mouse models of Huntington disease. J Neurosci Res 66(4):525–539
88. Hodgson JG, Agopyan N, Gutekunst CA, Leavitt BR, Lepiane F, Singaraja R et al (1999) A YAC mouse model for Huntington's disease with full-length mutant huntingtin, cytoplasmic toxicity, and selective striatal neurodegeneration. Neuron 23(1):181–192

89. Tang T-S, Slow E, Lupu V, Stavrovskaya IG, Sugimori M, Llinas R et al (2005) Disturbed Ca^{2+} signaling and apoptosis of medium spiny neurons in Huntington's disease. Proc Natl Acad Sci 102(7):2602–2607
90. Blackstone C (2012) Cellular pathways of hereditary spastic paraplegia. Annu Rev Neurosci 35(1):25–47
91. Renvoisé B, Blackstone C (2010) Emerging themes of ER organization in the development and maintenance of axons. Curr Opin Neurobiol 20:531–537
92. Verkhratsky A (2005) Physiology and pathophysiology of the calcium store in the endoplasmic reticulum of neurons. Physiol Rev 85(1):201–279
93. Orso G, Pendin D, Liu S, Tosetto J, Moss TJ, Faust JE et al (2009) Homotypic fusion of ER membranes requires the dynamin-like GTPase Atlastin. Nature 460(7258):978–983
94. Trotta N, Orso G, Rossetto MG, Daga A, Broadie K (2004) The hereditary spastic paraplegia gene, spastin, regulates microtubule stability to modulate synaptic structure and function. Curr Biol 14(13):1135–1147
95. Fowler PC, O'Sullivan NC (2016) ER-shaping proteins are required for ER and mitochondrial network organization in motor neurons. Hum Mol Genet 25(13):2827–2837

Chapter 36
Calcium Imaging in the Zebrafish

Petronella Kettunen

Abstract The zebrafish (*Danio rerio*) has emerged as a widely used model system during the last four decades. The fact that the zebrafish larva is transparent enables sophisticated in vivo imaging, including calcium imaging of intracellular transients in many different tissues. While being a vertebrate, the reduced complexity of its nervous system and small size make it possible to follow large-scale activity in the whole brain. Its genome is sequenced and many genetic and molecular tools have been developed that simplify the study of gene function in health and disease. Since the mid 90's, the development and neuronal function of the embryonic, larval, and later, adult zebrafish have been studied using calcium imaging methods. This updated chapter is reviewing the advances in methods and research findings of zebrafish calcium imaging during the last decade. The choice of calcium indicator depends on the desired number of cells to study and cell accessibility. Synthetic calcium indicators, conjugated to dextrans and acetoxymethyl (AM) esters, are still used to label specific neuronal cell types in the hindbrain and the olfactory system. However, genetically encoded calcium indicators, such as aequorin and the GCaMP family of indicators, expressed in various tissues by the use of cell-specific promoters, are now the choice for most applications, including brain-wide imaging. Calcium imaging in the zebrafish has contributed greatly to our understanding of basic biological principles during development and adulthood, and the function of disease-related genes in a vertebrate system.

Keywords Calcium · Development · Genetically encoded calcium indicator · Transgenic · Zebrafish · Embryo · Olfaction · Mauthner · Circuit · Tectum

P. Kettunen (✉)
Institute of Neuroscience and Physiology, Sahlgrenska Academy at the University of Gothenburg, Gothenburg, Sweden
e-mail: petronella.kettunen@neuro.gu.se

M. S. Islam (ed.), *Calcium Signaling*, Advances in Experimental Medicine and Biology 1131, https://doi.org/10.1007/978-3-030-12457-1_36

36.1 Introduction

The zebrafish (*Danio rerio*) (Fig. 36.1) has emerged as a widely used model system during the last four decades. Its attractiveness as an experimental system stems from a number of factors that are pushing the zebrafish to the forefront as a model system for biomedical research. The fact that the zebrafish embryo is transparent during its first days, and can stay transparent longer with chemical treatment or as non-pigmented strains (Fig. 36.1b) [1] enables sophisticated in vivo imaging. While being a vertebrate, the reduced complexity of its nervous system and small size make it possible to follow large-scale activity in the whole brain. Its genome is sequenced and many genetic and molecular tools have been developed that simplify the study of gene function. For example, a variety of mutants strains have been isolated in large mutagenesis screens and identification of cell-specific enhancers and promoters has been used for the development of transgenic animals. Moreover, proteins can be easily overexpressed transiently or as stable lines using RNA and DNA injections into the fertilized egg. Similarly, genes can be knocked out using the CRISPR/Cas9 technology, and proteins can be transiently down-regulated during the first 5 days by the use of morpholino oligonucleotides, resulting in so-called morphants [2].

Due to its external and fast embryonic development, the zebrafish initially attracted developmental scientists. With time, the zebrafish has showed usefulness in different areas, including cardiovascular research [3], neurodegenerative diseases [4], psychiatry [5] and cancer research [6]. One quickly growing field using the zebrafish is high-throughput chemical and toxicological screening benefitting from the small size and simplicity of drug delivery through the skin [7]. In addition, various techniques such as electrophysiological recordings, calcium imaging and behavioral tests have demonstrated the convenience of the zebrafish as a model system. Particularly, the combination of in vivo physiological and behavioral techniques in wild-type, mutant or transgenic zebrafish has made it possible to perform studies that would be hard or impossible in other preparations.

The aim of this updated chapter is to give a broad summary of the calcium indicators and labeling techniques used to record intracellular calcium in various zebrafish preparations and review new findings from projects using calcium imaging in the zebrafish since the last edition of this chapter [8].

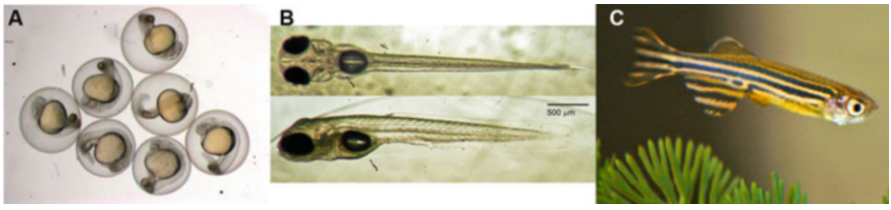

Fig. 36.1 The zebrafish can be studied at various ages. (**a**) Photo of wild-type zebrafish embryos, ~24 h post-fertilization. (Reprinted from Kaufman et al. [169] by permission from Springer Nature, Nature Protocols, Copyright 2009). (**b**) Zebrafish *nacre* mutant larva at ~72 h post-fertilization. (Photo: Todd O. Anderson. (**c**) Adult male zebrafish. Photo: Todd O. Anderson)

36.2 Calcium Indicators

The main advantages of using the zebrafish for calcium imaging are the variety of labeling methods and the small size, enabling in vivo imaging of many different structures in anesthetized or awake animals. Since the mid 90's, the embryonic development and neuronal function of the larval, and later, adult zebrafish have been studied using calcium imaging methods. Calcium indicators can be divided according to their chemical structure, optical properties and means of delivery [9]. Dextran-conjugated indicators, membrane-permeable acetoxymethyl (AM) ester dyes and genetically encoded calcium indicators (GECIs) have all been used in the zebrafish, studying phenomena ranging from the fertilization of the oocyte to neuronal activation in the adult animal. The choice of calcium indicator depends on the desired number of cells to study and cell accessibility. For example, dextran indicators can label a limited number of cells of a cell type that lacks appropriate cell specific promoters, or label cells in a cell lineage during development [10]. In contrast to dextrans, the perfusion of AM esters permits labeling of larger areas of tissue using multi-cell bolus loading [11] or can be used to label isolated organs or cells in culture [12]. During the last decade, expression of GECIs has been replacing the use of AM esters for general labeling of large volumes of cells, since general promoters, such as the neuronal promoter *HuC* (referred to as *elavl3* (ELAV like neuron-specific RNA binding protein 3) throughout the text) can label the whole nervous system [13, 14]. In contrast, the use of cell-specific gene enhancers or promoters can also give expression that is limited to a set of specific neurons at a specific time during development.

36.2.1 Synthetic Calcium Indicators

36.2.1.1 Dextrans

The water-soluble dextran-conjugated calcium indicators have a wide variety of applications, ranging from injection into developing eggs, dialysis into cells or injection into axonal pathways, which leads to local dye uptake with subsequent anterograde and retrograde transport over hours and days. Dextran dyes can fill structures far away, meaning that imaging can be done at a distance from the injection site where the tissue might be damaged and nonspecifically stained, increasing the background fluorescence. In comparison with the AM ester dyes, they show no compartmentalization and have low toxicity.

Calcium green-1 dextran is the first and most common visible light-excitable calcium imaging dye used in the embryonic and larval zebrafish [15]. When injected into the spinal cord it can backfill neurons in the spinal cord, hindbrain and midbrain by severing axonal tracts [16]. Injections of calcium green-1 dextran into eggs at the one-cell stage have helped showing calcium fluctuations during fertilization,

cleavage and blastula period [17–21]. If injected embryos are let to develop, the dye is retained in developing cells allowing imaging of those at later developmental stages.

The related dye Oregon green 488 BAPTA-1 has low calcium-binding affinity, high fluorescence yield and great resistance to photobleaching. It has been used similarly to retrograde label neurons and to stain cells following egg injections. It has been used together with Texas red dextran for ratiometric calcium measurements during gastrulation [22]. Both dextrans of calcium green-1 and Oregon green BAPTA-1 has been implemented in in vivo calcium imaging of the adult zebrafish tectum, via delivery to tectal cells via electroporation or tungsten pin injections of dye crystals [23].

36.2.1.2 AM Esters

Cell-permeable AM esters diffuse into cells where endogenous esterases will cleave the ester groups, trapping the indicators inside the cells. AM esters can simultaneously and nonselectively label numerous cells in a tissue. AM esters also serve as a faster means of labeling cells (30 min) than dextran dye backfilling (12–24 h) [24]. AM esters are often mixed with pluronic acid, increasing the solubilization of water-insoluble dyes.

The first attempt to label larger portions of the larval zebrafish spinal cord was done by Brustein and colleagues in 2003, using bolus injections of AM ester calcium dyes [24]. However, this method has since then not been generally used, perhaps due to the parallel development of GECIs at the same time. Oregon green 488 BAPTA-1 AM labeling has on the other hand been very useful when labeling large structures in the tectum [25]. In addition, embryonic hearts and isolated myocytes have been successfully labeled with fluo-4 AM before imaging [26–28]. Fluo-5N AM, an analog of fluo-4 with lower calcium-binding affinity which prevents saturation of signal in cells with high intracellular calcium levels, has been used to image calcium fluctuations in isolated muscle fibers [29]. In the red spectra, rhod-2 AM is often used to label the adult zebrafish olfactory bulb neurons in explant preparations [30].

36.2.2 Genetically Encoded Calcium Indicators

36.2.2.1 Bioluminescent Aequorins

Protein-based calcium indicators can be divided into being fluorescent or bioluminescent, i.e. either emitting light when excited by light, or emitting visible light following a chemical reaction in a living organism. The first bioluminescent calcium-sensitive photoprotein used in the zebrafish was aequorin, derived from the jellyfish *Aequorea victoria* [31, 32]. The binding of calcium ions to the photoprotein

starts an enzymatic reaction leading to an emission of blue light. In contrast to fluorescent reporters, aequorin has no background light emission at basal calcium levels and does not require excitation light. Since no input of radiation energy is required, problems with photobleaching, phototoxicity and autofluorescence are avoided.

Recombinant aequorin has been directly injected into the zebrafish egg before fertilization to study calcium patterns during the whole embryogenesis up to ~24 h post-fertilization (hpf), from fertilization to the formation of somites [19, 33]. To allow calcium imaging at later stages, mRNA coding for the native apoaequorin has been injected into the fertilized egg, expressing the fluorescent protein in somites and the trunk as late as 48 hpf [34].

Despite a good signal to noise ratio, the low quantum yield of aequorin has limited its use. However, aequorin naturally exists in complex with green fluorescent protein (GFP), and energy from the chemical reaction of aequorin is transferred to GFP, leading to an emission of green light. This association with GFP is increasing the efficiency of calcium-dependent photoemission from aequorin from 10% to 90%, which inspired the development of a GFP-aequorin fusion protein [35]. Injection of chimeric GFP-aequorin mRNA gives protein expression as early as blastula stage [36] until at least 48 hpf [34]. Zebrafish with GFP-apoaequorin expression driven by the *neuro-β-tubulin* promoter in hypocretin neurons as late as 7 days post-fertilization (dpf) have been used to study neuronal activity during natural behaviors [37]. More recently, a zebrafish line with selective expression of an optimized version of aequorin in motor neurons was combined with treatment of the GFP-aequorin substrate coelenterazine, allowing imaging of calcium transients in freely moving larvae [38]. Finally, injections of mRNA coding for a red form of aequorin, Redquorin, have been used to image calcium transients associated with twitching behavior in developing zebrafish embryos during segmentation [39].

36.2.2.2 GFP-Derived Fluorescent Indicators

Cameleon

A majority of the fluorescent GECIs are derivatives of GFP [40], emitting light in the green spectra. The first GEICs used in zebrafish, cameleon and pericams (a detailed review of the use of pericams in zebrafish is found here [8]), have now mostly been replaced with the GCaMP family of indicators. Cameleon is a hybrid protein in which cyan fluorescent protein (CFP) and yellow fluorescent protein (YFP) are linked by calmodulin and a calmodulin-binding peptide of myosin light-chain kinase (M13) [41]. When calcium levels are increasing, calcium binds to calmodulin, resulting in fluorescence resonance energy transfer (FRET) from CFP to YFP [42]. When excited by a wavelength appropriate for CFP excitation, an increase in calcium concentration causes an increase in the YFP/CFP fluorescence intensity ratio. Thus, cameleon serves as a ratiometric calcium indicator.

Yellow cameleon 2.1 (YC2.1), YC2.12 and YC2.6 have been generally expressed in the zebrafish brain using the *elavl3* promoter, in myocytes using heat shock protein 8A (*hsp8A*) [43] and in spinal neurons using the ISL LIM homeobox 1 (*isl1*) promoter [44]. Injection of YC2.12 mRNA into the fertilized egg gives YC expression between 3 and 33 hpf [42, 45] making it possible to follow calcium changes from gastrulation to the early pharyngula period.

GCaMP Family

In 2001, Nakai and coworkers developed a calcium probe based on a single GFP molecule with high calcium affinity named GCaMP [46]. GCaMP, 1.6, 2, 3, 4.1, 6, 6 s and 7 have all been expressed in zebrafish and the latest studies will be described further on.

GCaMP-HS (GCaMP-*h*yper *s*ensitive) [47] is brighter at the resting level and more sensitive to the change of intracellular calcium concentrations than the previous GCaMP indicators. It has been used in larval zebrafish to record spontaneous activity in motoneurons [47], retinal bipolar cells [48], Mauthner cells and spiral fiber neurons [49], and visual responses in tectum and dorsal telencephalon [50].

SyGCaMP2 is a fusion of GCaMP2 to the cytoplasmic side of synaptophysin, a transmembrane protein in synaptic vesicles [51]. By imaging zebrafish in vivo, it has been demonstrated that SyGCaMP2 can be used to monitor visual activity in synapses of spiking neurons in the optic tectum and neurons in the retina, sampling hundreds of terminals simultaneously [51, 52]. Imaging of SyGCaMP2 in bipolar cell terminals in the retina has also revealed modulation visual processing by olfactory signals [53] and crossover inhibition in the inner retina [54].

To this date, few red-emitting GECIs have been used in the zebrafish, although red indicators allow for deeper imaging into tissue, reduced cytotoxicity, and can be used in combination with the opsins that are activated by blue light. R-GECO-1 and the synaptic form SyRGECO, which is fused to the protein synaptophysin, were tested in the retinotectal system of zebrafish larvae [55]. A group of red GECIs, including RCaMP [56], jRCaMP1a, jRCaMP1b and jRGECO1a [57], has been evaluated after expression in trigeminal neurons. K-GECO1, which is based on a circularly permutated RFP derived from the sea anemone *Entacmaea quadricolor*, has been transiently expressed in spinal Rohon-Beard cells visualizing calcium fluctuations in response to skin stimulation [58].

An alternative way to monitor changes in intracellular calcium levels in freely moving animals has been to make use of the calcium indicator calcium-modulated photoactivatable ratiometric integrator (CaMPARI), which undergoes irreversible green-to-red conversion only when elevated intracellular calcium and UV illumination coincide. In this way, individual cells and brain areas, with elevated calcium during a specific time period, can be identified [59].

In conclusion, depending on the cell-specificity and temporal resolution required, calcium photoproteins can be delivered and used in different ways. Injecting a purified photoprotein, such as aequorin, enables detection of calcium signals already at fertilization, while injection of mRNA or use of some promoters delay the time when the photoprotein is available, but gives a prolonged window of protein expression. Transgenic animals expressing GECIs driven by cell-specific promoters can give precise spatiotemporal patterns. Due to the external development of the zebrafish embryo, the ease of genetic manipulations and the possibility of in vivo imaging, the zebrafish has been a valuable model system for the development of new calcium probes.

36.3 Calcium Imaging Studies in the Zebrafish

36.3.1 Development

The popularity of the zebrafish initially started among the developmental biologists, hence leading to the outcome that the first zebrafish calcium imaging experiments were to study calcium signaling in the zebrafish egg and early embryo [60]. Embryological studies of the zebrafish are particularly rewarding since the developmental process is done *ex utero*. Fertilized eggs are collected from breeding couples in the morning and can then be studied throughout the day, reaching the segmentation period within the first 24 h. The early development of the zebrafish embryo is comparably fast, and the speed of development can be manipulated by increasing or decreasing the temperature of the eggs/embryos. The precise developmental periods have been described by Kimmel and colleagues [61]. When incubated at 28.5 °C the times for the developmental stages are the following: zygote (0–0.75 hpf), cleavage period (0.75–2.25 hpf), blastula period (2.25–5.25 hpf), gastrula period (5.25–10.33 hpf), segmentation period (10.33–24 hpf), pharyngula period (24–48 hpf) and hatching period (48–72 hpf).

Calcium signaling has been studied throughout the whole development of the zebrafish embryo [19, 43, 62, 63]. The zygote and cleavage periods are dominated by intracellular calcium signals, but as the embryonic cell number increases, there is an appearance of localized intercellular signals along with the intracellular ones [18]. This transition proceeds through the blastula and early gastrula periods. Then, as global patterning processes start during the rest of the gastrula period, pan-embryonic intercellular signals associated with the dramatic morphological events of gastrulation can be observed [64]. Once the germ layers and major body axes are established, there is a return to localized intercellular signals associated with the generation of specific structures, for example somite formation, brain partitioning, eye development, and heart formation [33].

Fluctuations in intracellular calcium during **fertilization** and later developmental periods has been studied using injections of recombinant aequorin [19, 65], mRNA

of YC2.12 and dextran dyes [8, 17, 20, 66, 67], since imaging would require very early labeling of the egg and embryo. However, the identification of the constitutively active promoter *hsp8A* has made it possible to express YC2.60 and follow calcium signals from fertilization to segmentation [43]. Similarly, the early and ubiquitous activity of the *βactin2* promoter has allowed researchers to drive GCaMP6s expression as early as 30 min post-fertilization (mpf), throughout cleavage and the blastula stage [68].

When monitoring the calcium patterns during fertilization, the oocytes are held in place using an egg injection chamber when carefully injected with the calcium indicator without affecting the normal development of the oocyte [65]. In the zebrafish oocyte, the blastodisc (animal pole) is located on top of the yolk cell (vegetal pole). Activation and fertilization of the oocyte are then done under the confocal microscope to monitor the calcium changes during these processes. The unfertilized zebrafish oocyte exhibits little evidence of calcium signaling, however both activation with water and fertilization trigger rapid increases in intracellular calcium in the oocyte cortex. This fluorescence continues to increase during the first 12–15 min post-insemination (mpi), particularly at the animal pole [17]. The initial transient is followed by a more prolonged transient reaching a higher amplitude with a maximum at 8–10 mpi [17]. These two initial transients are followed by later calcium oscillations (30–60 mpi) associated with blastodisc expansion and cytokinesis [19, 65, 69].

Protein-tyrosine kinase 2-beta (PTK2B/PYK2), a calcium-sensitive protein tyrosine kinase was found to be activated in response to fertilization of the zebrafish oocyte [20]. Oocytes were injected with calcium green-1 dextran and then monitored by confocal microscopy. Fertilization-induced Ptk2b activation could be blocked by suppressing calcium transients via injection of BAPTA as a calcium chelator. Suppression of Ptk2b activity by chemical inhibition or by injection of a dominant-negative construct encoding the N-terminal ERM domain of Ptk2b inhibited formation of an organized fertilization cone and reduced the frequency of successful sperm incorporation.

The zebrafish **cleavage period** is represented by six rapid and synchronical cell cleavages, with one blastomere division approximately every 15 min (Fig. 36.2). The zebrafish embryo undergoes discoidal cleavage, meaning that the blastodisc is located at the animal pole and is divided with cleavage furrows that do not penetrate or divide the yolk. The cells remain interconnected by cytoplasmic bridges. Elevation of intracellular calcium can be seen at the cleavage furrow before the first cell cleavage, i.e. the furrow positioning signal, then during the furrow formation and deepening of the furrow [70]. Next, calcium elevations can be observed along the equators of the dividing cells, where the second cleavage furrow emerges (Fig. 36.2c, d). Thus, it appears that there is a close spatial correlation between elevated calcium and the formation of a cell cleavage furrow [68, 69, 71]. The calcium signals at cleavage furrows [72] and subsequent cell divisions [69] have indeed been prevented by injection of the calcium chelator BAPTA into the embryo, indicating the importance of calcium for cell division [73].

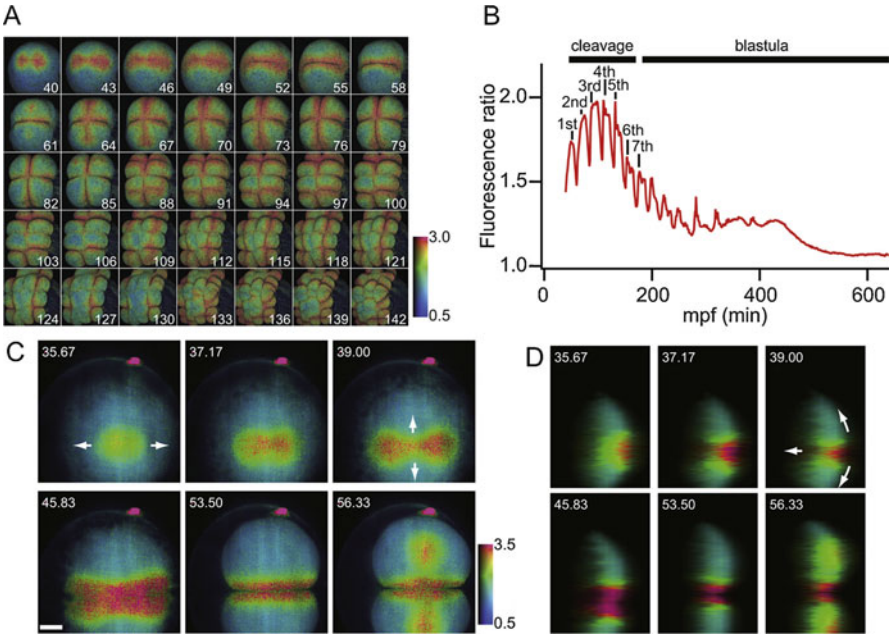

Fig. 36.2 Imaging of localized calcium propagations along the cleavage furrow. Zebrafish embryos are expressing yellow cameleon (YC) 2.60 driven by the promoter for shock protein 8A (*hsp8A*). The numbers on the images indicate minutes post fertilization (mpf). Images are pseudo-color ratiometric z-projections in intensity modulated display (IMD). (**a**) Montage of two-photon images of the calcium responses during the cleavage period. (**b**) Intensity trace of the fluorescence ratio from the whole embryo during two-photon imaging. The time for the 1st to 7th cleavage events are indicated. Bars on the top indicate the cleavage and blastula periods. (**c**) Images from line-scanning microscopy of calcium fluctuations during cleavage. (**d**) Cross sections performed using line-scanning microscopy showing calcium propagations along the cleavage furrow. Arrows in (**c**) and (**d**) indicate directions of calcium propagation. Scale bars are 100 μm. (Reprinted from Mizuno et al. [43])

Recently, Eno et al. showed that *nebel* mutants exhibit reduced furrow-associated slow calcium waves, caused by defective enrichment of calcium stores [66]. The imaging made use of labeling with the ratiometric indicator fura-2 dextran, Oregon green 488 BAPTA-1 dextran, and the transgenic line *Tg(βactin2:GCaMP6s)*.

At the 256-cell stage, the **blastula period** begins with the start of asynchronous cell divisions and zygotic gene transcription. During this period, the yolk syncytial layer (YSL) forms, and epiboly begins. This means spreading and flattening of the blastula to finally cover the whole yolk at the end of epiboly. During this period, there is a transition from intracellular signals to intercellular signals within the blastula. Fast, short-range, and slow, long-range calcium waves propagate exclusively through the external YSL (E-YSL), mainly initiated from the dorsal side (Figs. 36.3, 36.4) [74]. Bonneau and coauthors injected calcium green-1 dextran at the 128-cell stage to study the calcium waves in the YSL. They could conclude that

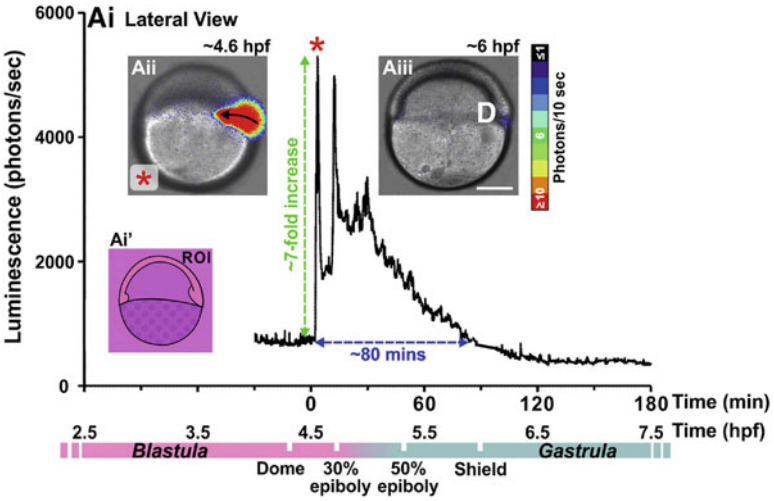

Fig. 36.3 Characterization of calcium signaling in the external yolk syncytial layer during the late blastula and early gastrula periods. (A) An embryo, injected with f-aequorin at the 128-cell stage, was imaged from a lateral view, where the location of the dorsal side remained constant throughout the experimental period. (Ai) Temporal profile of the aequorin-generated luminescence from ∼ 4 h post-fertilization (hpf) to 7.5 hpf, collected from the region of interest (ROI) in panel Ai′. The duration of and maximum increase in luminescence of the calcium signals are indicated by the blue and green dashed arrows, respectively. (Aii, Aiii) Luminescence images were superimposed on to the corresponding bright-field images to show the orientation, morphology and calcium signals generated at: (Aii) the beginning of the signaling period (the calcium signal corresponds to peak marked by a red asterisk in panel Ai), and (Aiii) at the shield stage (D is dorsal). Scale bar is 200 μm. (Reprinted from Yuen et al. [74], Copyright 2013, with permission from Elsevier)

phosphorylation of the protein Bcl-2–like 10 (Nrz) enables the generation of YSL calcium waves at the beginning of epiboly [21].

Moreover, localized elevations of calcium, so called calcium spikes, are generated in individual cells or small groups of cells in the blastoderm. These signals are restricted to the enveloping layer (EVL) cells and appear to propagate as calcium waves [18, 43, 68].

During the **gastrula period**, each germ layer (endoderm, mesoderm, and ectoderm) is spatially organized so that organs and tissues can form in the correct location. The morphogenetic movements of involution, convergence, and extension form the epiblast, hypoblast, and embryonic axis through the end of epiboly [22]. The level of intracellular calcium reaches a maximum during early gastrulation (6.5 hpf), when epiboly resumes and the embryonic shield starts to extend towards the animal pole [19]. Fast intracellular calcium waves have been observed around the blastoderm margin during late epiboly, moving up the trunk in an anterior direction [62, 64]. The function of these axial waves are unknown but are thought to contribute to the calcium waves that underlie the large-scale migrations of cells during this period.

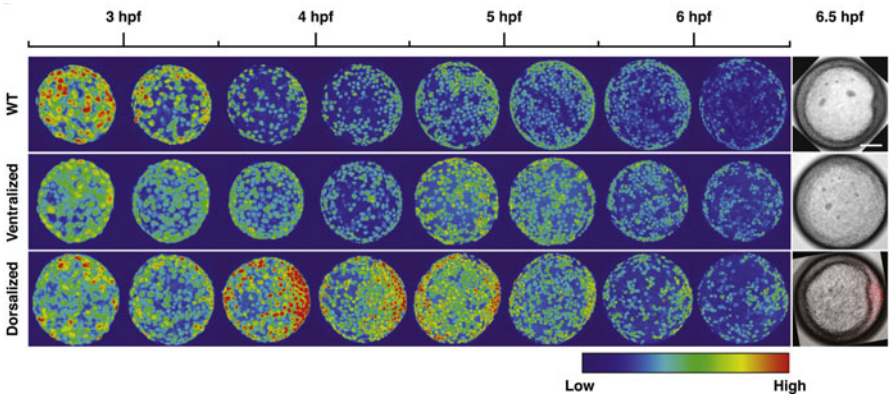

Fig. 36.4 External yolk syncytial layer calcium signaling pattern in ventralized and dorsalized embryos. Recordings of 30-min time-lapse overlay of calcium signals in wild-type, ventralized, and dorsalized *Tg(βactin2:GCaMP6s)* embryos from 2.5 h post-fertilization (hpf) to 6.5 hpf. Images were captured using a spinning-disk confocal microscope, showing that dorsal-biased calcium signaling was diminished in ventralized embryos and was ectopically induced in dorsalized ones. The ventralized phenotype was acquired using *ichabod/β-catenin2* mutant embryos and the dorsalized phenotype by injection of *β-catenin1* mRNA. Scale bar is 150 μm. (Reprinted from Chen et al. [68], Copyright 2017, with permission from Elsevier)

Other calcium release events that are seen during gastrulation are aperiodic transient fluxes found mainly in the EVL and dorsal forerunner cells becoming the Kupffer's vesicle, a structure implicated in laterality [75]. To answer whether an intraciliary calcium signal at the Kupffer's vesicle causes left-right development, Yuan et al. targeted GECIs into cilia via fusion to the ciliary protein Arl13b, a small GTPase [76]. *arl13b-GCaMP6* mRNA was injected into embryos at the one-cell stage and animals were imaged at the 1–4 somite stage. Confocal microscopy of the Kupffer's vesicle revealed the presence of highly dynamic intracellular calcium oscillations. The oscillations depended on polycystic kidney disease 2 (Pkd2) and were left-biased at the Kupffer's vesicle in response to ciliary motility. Suppression of oscillations using a cilia-targeted calcium sink revealed that they were essential for left-right development.

Following the dramatic global rearrangements during gastrulation, the embryo now undergoes a series of more localized morphogenetic movements that make up the **segmentation period**. Somites and the neural cord develop during this period, as well as the primary organs. The earliest body movements can be seen at this time. At 10–11 hpf, distinct calcium patterns can be recognized along the antero-posterior axis of the embryo [19]. High calcium levels can be observed in the presumptive mid- and forebrain in contrast to low calcium in the presumptive hindbrain (Fig. 36.5). This specific calcium pattern in the brain remains clearly visible for several hours and precedes morphological patterning of the brain [19]. Apart from the calcium patterns in the head, various calcium waves, gradients, and spikes can be observed in the trunk and tail region. The most pronounced is an ultraslow calcium

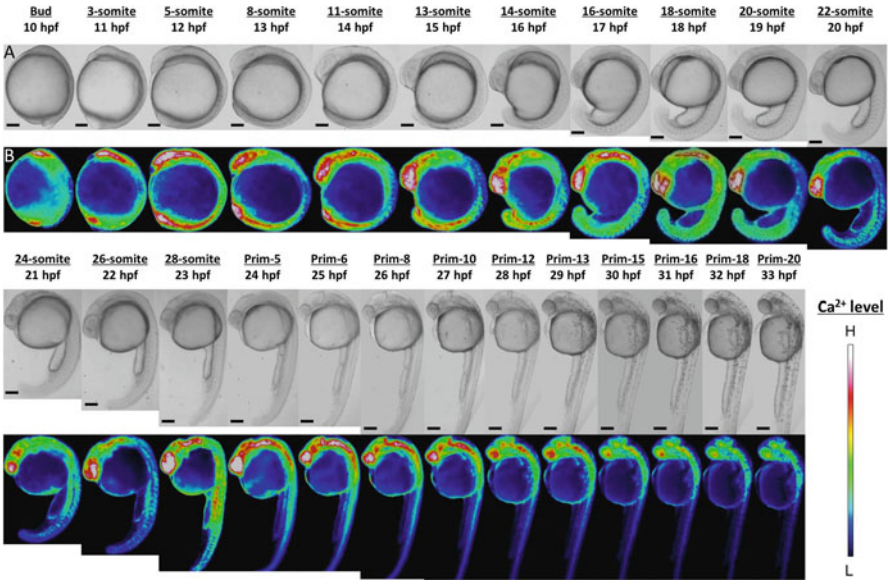

Fig. 36.5 Calcium dynamics in the late gastrula, segmentation, and early pharyngula periods. The genetically encoded calcium indicator yellow cameleon, YC2.12, was expressed in developing zebrafish embryos after mRNA injection at the one-cell stage. Imaging was performed on a fluorescent microscope. (**a**) Bright field image. (**b**) Color-coded image. Scale bar is 200 μm. The color-coded images show high calcium levels as white and low calcium levels as blue. High intracellular calcium levels could be observed in the anterior and posterior body regions from bud to 16-somite (10–17 h post-fertilization) stages. In the anterior trunk, the calcium levels reached a peak at 18-somite stage, whereas in the posterior trunk the calcium peak was present at 28-somite stage. (Reprinted from Tsuruwaka et al. [45])

wave moving posteriorly along with the formation of the somites and neural keel at 10–14 hpf [19].

In one experiment, YC2.12, injected as mRNA at the one-cell stage, was used to study calcium patterns up to the pharyngula period (Fig. 36.5). High levels of intracellular calcium were observed in the anterior and posterior body regions from bud to 16-somite (10–17 hpf) stages. In the anterior trunk, the calcium level reached a peak at 18-somite stage, whereas in the posterior trunk the calcium peak was shown at 28-somite stage [45].

The zebrafish embryo enters the **pharyngula period** at 24 hpf when the body axis begins to straighten. The circulation system develops and the heart starts to beat. The brain has now five distinct lobes and the pharyngula shows tactile sensitivity and uncoordinated movement. The **hatching** embryo (48–72 hpf) continues to form the primary organ systems and the sensory systems are complemented by hair cells and olfactory placodes [61]. The zebrafish is considered a **larva** from 72 hpf to 30 days (Fig. 36.1B) when it grows in size to become an adult animal (Fig. 36.1C). Pigmentation of the zebrafish skin starts around 24 hpf which requires 1-phenyl-2-thiourea treatment to keep embryos transparent, or the use of non-pigmented strains

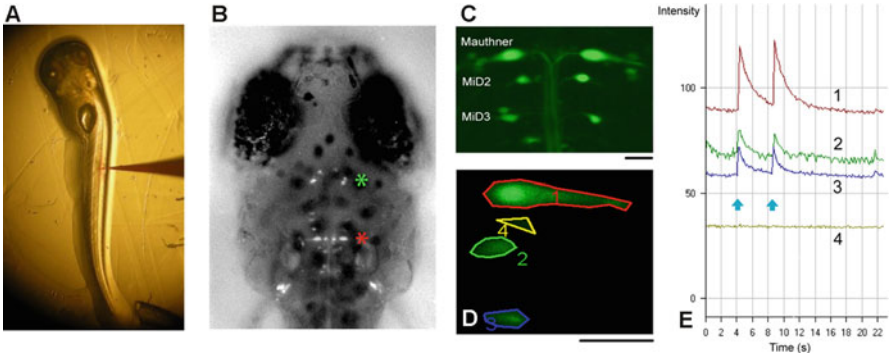

Fig. 36.6 Labeling of reticulospinal neurons in the larval zebrafish and recording of changes in intracellular calcium during the startle response. (**a**) Injection of a dextran dye (here calcium-insensitive rhodamine dextran) into the spinal cord of a larval zebrafish. (**b**) Descending projection neurons labeled with calcium green-1 dextran (10 kDa) in a wild-type larva with normal pigmentation 24 h after injection. The pair of Mauthner cells is marked with a red asterisk and the midbrain neurons with a green asterisk. (**c**) Confocal microscopy image showing Mauthner cells and their homologs labeled with calcium green-1 dextran in a 5-day-old larva. Scale bar is 25 μm. (**d**) The region of interest (ROI) 1 marks one Mauthner cell, ROI 2 marks the closest segmental homolog, MiD2cm, and ROI 3 marks the homolog MiD3cm. Background activity from non-labeled cells is recorded from ROI 4. Scale bar is 25 μm. (**e**) Intensity traces of the changes in intracellular calcium levels from ROIs 1–4 during weak electrical stimulation of the skin. The x-axis indicates time. Two skin shocks to the head are marked by the blue arrows. The y-axis indicates the fluorescence intensity in arbitrary units. The value 0 represents no fluorescence; the value of maximal fluorescence is 256. The numbering of traces corresponds to the ROIs in (**d**). The two skin shocks produced two fast peaks in intracellular calcium in the Mauthner cell and the segmental homologs. Each of the calcium transient lasted about 5 s. (Images: Petronella Kettunen)

like *nacre* [1], *casper* [77] or *crystal* [78]. Calcium imaging of different parts of the nervous system and muscle cells during these later stages will be described in the next sections of this chapter.

36.3.2 Locomotor Circuits

36.3.2.1 Reticulospinal Neurons

At the time when developmental biologists started to monitor calcium signaling events during development, physiologists started to inject dextran-conjugated calcium green-1 into the spinal cord to investigate firing properties of neurons in the spinal circuits and hindbrain [15, 79]. Since then, calcium imaging has been an important noninvasive tool in larval zebrafish to study neuronal activity and connectivity, simultaneously from a population of neurons.

The Mauthner cell network is one of the first circuits in the zebrafish brain that was studied using calcium imaging [15, 79]. The Mauthner cell is a large reticulospinal neuron located in the hindbrain (Fig. 36.6b, c) and responsible for the

startle response, elicited by various sensory stimuli such as touch, sound, and visual input. It has two prominent dendrites and its axon crosses over to the contralateral side where it activates motoneurons, contracting the muscles to propel the fish trough the water. Two homologous reticulospinal neurons, MiD2cm and MiD3cm, are located in adjacent segments (Fig. 36.6c) and can elicit a startle response if the Mauthner cell is deleted [80].

Our knowledge of the structure and function of reticulospinal neurons has grown during the last three decades. As these neurons are large and their morphology easily distinguishable, and the fact that their activation leads to a distinct response make this system very useful to functional investigations of genetic modifications. With the discovery of a variety of mutant strains, generated in large-scale genetic screens, the possibilities to learn about the formation and function of the nervous system are unlimited. For example, in the large-scale screen for behavioral locomotive defects performed in 1996, over 150 motility mutants were identified [81]. Interestingly, many of these mutants had defects in the Mauthner cell networks, and calcium imaging of these mutants has taught us much about this circuit [8].

Labeling of reticulospinal neurons via pressure injection of calcium sensitive dextran dyes is still a used method. However, with the discovery of new cell-specific promoters for cells in the Mauthner cell network, this technique will probably be less used with time. For example, the enhancer *Gal4FF-62a* that selectively labels Mauthner cells [82] has been used to drive expression of GCaMP6s in experiments investigating calcium signaling during startle habituation [83] and regulation of the innate startle threshold in 5 dpf zebrafish larvae [84].

Soon, the field of reticulospinal cell imaging expanded to involve networks feeding into the Mauthner cell, regulating its function. For example, investigations were made of the three different inhibitory connections of the Mauthner cell network; recurrent inhibition mediated by an ipsilateral collateral of the Mauthner cell axon, feed-forward inhibition driven by sensory afferents, and reciprocal inhibition between bilaterally opposed Mauthner cells [85]. This inhibition could be confirmed by confocal recordings of calcium signals in Mauthner cells when these inhibitory connections were stimulated.

Spiral fiber neurons are excitatory interneurons, which project to the Mauthner cell axon hillock. Researchers took advantage of the *Tg(–6.7FRhcrtR:gal4VP16; UAS:GCaMP5)* line that has labeled spiral fiber neurons [49]. In these fish, Mauthner cells could be laser-ablated after backfilling using dextran dyes, which revealed that spiral fiber neurons are active in response to aversive stimuli capable of eliciting escapes.

The nucleus of the medial longitudinal fasciculus (nMLF) consists of a small group of reticulospinal neurons in the zebrafish midbrain that is the most rostral of the descending projecting neurons. They have previously been implicated in escape, swimming and prey capture behaviors [16, 86]. One common way to label these cells has been to perform spinal injections of dextran dyes. Sankrithi and O'Malley performed calcium imaging in Oregon green 488 BAPTA-1-labeled 3–5 dpf animals [87]. Calcium responses were monitored simultaneously with recording swimming, turning and struggling movements, elicited by head taps and abrupt illumination.

This type of preparation shows the advantage of using the transparent zebrafish larvae to study which cells are active during certain behaviors, which would be more complicated in other vertebrate systems.

Dye injection was also used by Wang and McLean labeling motoneurons and descending neurons from the nMLF with calcium greeen-1 dextran [88]. Locomotor responses to light via an LED were monitored in both cell groups using calcium imaging and simultaneous motor nerve recordings. Both light onset and offset activated nMLF neurons while mainly ventral (rather than dorsal) motoneurons were consistently activated by this stimulus.

Thiele et al. identified a Gal4 driver fish line, *Tg(Gal4^{s1171t})*, allowing targeted expression of proteins in nMLF neurons [89]. By crossing this fish line with one carrying *UAS:GCaMP6*, it was possible to monitor calcium fluctuations in 6 dpf fish using two-photon imaging while simultaneously monitoring tail movements during spontaneous behaviors with a high-speed camera. The calcium signals in different nMLF neurons were correlated with swimming, flips and struggles, showing that most nMLF cells were active during swimming.

36.3.2.2 Spinal Cord

In parallel with the start of labeling and recording activity in reticulospinal neurons, imaging of the downstream spinal cord neurons started. Each hemisegment of the zebrafish spinal cord consists of three primary motoneurons (PMNs), the caudal primary (CaP), middle primary (MiP), and rostral primary (RoP), and around 30 secondary motoneurons (SMNs). The development of spinal cord networks is partly regulated by spontaneous activity (Fig. 36.7). The first motor behavior performed by zebrafish embryos is the gap junction-driven coiling behavior present at 17–25 hpf. Researchers expressed the constructs *UAS:GCaMP3* and *Gal4^{s1020t}* in the embryonic spinal cord to follow the development of this spontaneous activity using a spinning disc confocal microscope (Fig. 36.7) [90]. *Gal4^{s1020t}* drives expression of the target protein in PMNs and SMNs, as well as in both ascending and descending interneurons. Spinal cord activity imaged at 18 hpf was sporadic, while 2 h later, at 20 hpf, the activity was organized in bursts of alternation between the left and right sides. Optogenetic inhibition revealed changes in functional connectivity between ipsilateral neurons during development.

Using the same transgenic GECI line, Plazas and colleagues followed calcium activity in individual PMNs during axonal extension and pathfinding between 17 and 24 hpf [91]. By suppressing calcium spiking activity selectively in single PMNs, they could observe errors in axon pathfinding of MiP and RoP axons, but not of CaP axons. This activity-dependent competition was mediated by modulation of the chemotropic receptor PlexinA3.

An alternative way to specifically silence synaptic activity was developed by Sternberg and colleagues [92]. A zebrafish-optimized botulinum neurotoxin light chain fused to GFP (*BoTxBLC-GFP*) was expressed in zebrafish embryonic and lar-

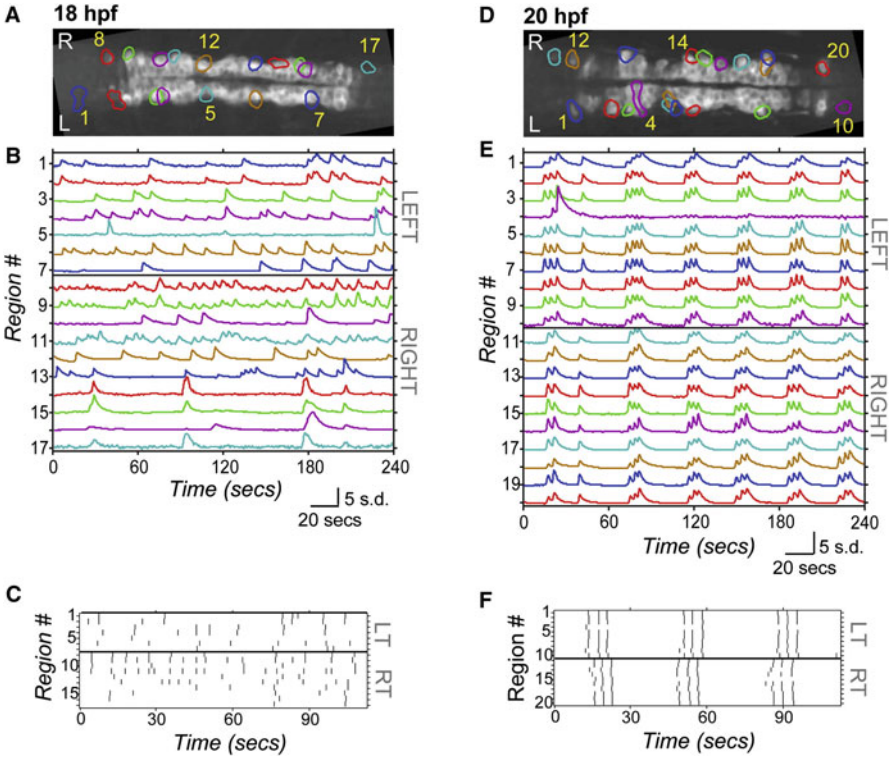

Fig. 36.7 Imaging of spontaneous calcium activity in spinal cord neurons during segmentation. Zebrafish *Tg(Gal4^{s1020t};UAS:GCaMP3)* embryos were imaged at 18 and 20 h post-fertilization (hpf) using a spinning disc confocal microscope. (**a** and **d**) Dorsal views of GCaMP3 baseline fluorescence with circled regions of interest (rostral to the left). (**b** and **e**) Normalized intensity traces for active regions (identified on y-axis) for the left and right sides of the spinal cord at 18 hpf and 20 hpf. (**c** and **f**) Raster plots of detected events for a subsection of the data in (**b**) and (**e**), showing how population activity went from uncoordinated (**b**) to synchronized (**e**) bursting. (Reprinted from Warp et al. [90], Copyright 2012, with permission from Elsevier)

val spinal cord using *Gal4^{s1020t}*. Fish expressing this construct failed at performing the coiling behavior. Interestingly, imaging revealed that calcium signals were still present, showing that the effects of BoTxBLC-GFP were limited to abolishment of synaptic release.

Gal4^{s1020t} was also used to drive expression of GCaMP5 in the spinal cord, in experiments investigating the effect of nonvisual light stimulation of the locomotor circuits via the vertebrate ancient long opsin A (VALopA) [93]. Using illumination at 488 nm, the coiling behavior as well as the calcium activity, monitored via two-photon imaging, could be reduced in 24 hpf embryos after knockdown of *valopa*.

Other promoters/enhancers have been used to drive expression of GECIs in specific subsets of neurons in the spinal cord of zebrafish. For example, the gene trap driver *SAIGFF213A* gives expression in a subset of spinal neurons including the

CaP motoneurons [47]. *Tg(SAIGFF213A;UAS:GCaMP7a)* embryos were used for tracking spontaneous calcium signals using a confocal microscope in CaP neurons at 18 or 24 hpf [94]. In this study, it was found that inhibition of two-pore channels (TPCs) that mediate calcium release from intracellular acidic compartments, prevent the high-frequency calcium transients in CaPs corresponding to network maturation.

It has also been possible to record calcium fluctuations in presynaptic boutons, by the use of the synaptophysin (*syp*) promoter as a driver for GECIs. In the spinal cord, V2a excitatory premotor interneurons are recruited during increase in swimming speed. In a study by Menelaou et al., spinning disc confocal imaging with parallel motor nerve recordings was used to track calcium transients in GCaMP3-labeled synaptic terminals of V2a neurons following electrical skin stimulation [95].

Cerebrospinal fluid-contacting neurons (CSF-cNs) are GABAergic ciliated cells surrounding the central canal in the ventral spinal cord, specifically expressing the polycystic kidney disease 2-like 1 (PKD2L1) channel. Böhm and coauthors investigated the role of CSF-cNs in locomotion by using the zebrafish lines *Tg(pkd2l1:GCaMP5G)icm07* and *Tg(UAS:GCaMP6f;cryaa:mCherry)icm06*, allowing expression of GECIs in this cell type [96]. Two-photon imaging of 5–6 dpf larvae revealed that the CSF-cNs were not activated during fictive escapes elicited by a water jet, which activated motoneurons (labeled with the *mnx1:Gal4, UAS:GCaMP6f;cryaa:mCherry* constructs). On the other hand, CSF-cNs showed a strong activation of in response to muscle contractions during tail bends, which could be abolished in mutants for *pkd2l1*. In the subsequent paper from the group, calcium imaging confirmed that ventral CSF-cNs are recruited during spontaneous longitudinal contractions, allowing the fish to maintain balance during locomotion [97].

Recently, the use of codon-optimized aequorin has simplified the monitoring of spinal calcium signaling [98]. Global bioluminescence from the motoneurons was recorded from *Tg(mnx1:gal4;UAS:GFP-aequorin-opt)* 4 dpf zebrafish larvae during escape behaviors and swimming. Calcium signals from individual neurons were monitored with the *Tg(mnx1:gal4;UAS:GCaMP6f,cryaa:mCherry)* line. The authors showed that mechanosensory feedback enhances the recruitment of motor pools during active locomotion.

36.3.3 Visual System

36.3.3.1 Retina

The zebrafish retina is organized into three nuclear layers: outer nuclear layer (ONL), inner nuclear layer (INL) and ganglion cell layer (GCL) that are separated by synaptic/plexiform layers. The ONL harbors rod and cone photoreceptors. The INL harbors horizontal, bipolar, amacrine and Müller glial cells. The GCL harbors retinal ganglion cells whose axons make up the optic nerve. After being fairly inaccessible to calcium indicator labeling in vivo, the zebrafish retina research has

benefitted highly from the development of constructs expressing GECIs in specific retinal cells.

One of the first zebrafish lines used to investigate retinal responses to light onset and offset expressed *SyGCaMP2* by the ribeye a (*ctbp2*) promoter, targeting the expression to ribbon synapses of bipolar cells within the inner plexiform layer. SyGCaMP2 is a fusion protein of synaptophysin and GCaMP2, allowing for calcium measurements at presynaptic synaptic boutons [51]. In a study by Odermatt and coauthors, SyGCaMP2 fluorescence was imaged in retinas in 9–12 dpf zebrafish larvae in response to on- and offset of a LED, investigating the luminance sensitivities of the bipolar cell synapses [99].

The same setup was used for investigation of crossover inhibition between bipolar cells and amacrine cells; the latter labeled by the *ptf1a:gal4;UAS:SyGCaMP3* constructs [54]. In OFF bipolar cells, sustained transmission was found to depend on crossover inhibition from the ON pathway through GABAergic amacrine cells. In ON bipolar cells, the amplitude of low-frequency signals was regulated by glycinergic amacrine cells, while GABAergic inhibition regulated the gain of band-pass signals.

The same group has also investigated the regulation of bipolar cell function by olfactory stimuli in 8–11 dpf larvae [53]. Zebrafish expressing SyGCaMP2 in bipolar cell terminals and GCaMP3.5 in ganglion cells, under the enolase 2 (*eno2*) promoter, were exposed to light flashes and oscillations during a bath application of the amino acid (AA) methionine. Two-photon calcium imaging revealed that olfactory stimulation reduced the gain and increased the sensitivity of responses to luminance and contrast transmitted through OFF bipolar cells. Activation of dopamine receptors increased the gain of synaptic transmission in vivo and potentiated synaptic calcium currents in isolated bipolar cells. These results indicate that olfactory stimuli alter the sensitivity of the retina through the dopaminergic regulation of presynaptic calcium channels that control the gain of synaptic transmission through OFF bipolar cells.

Tg(Isl2b:Gal4;UAS:SyGCaMP3) transgenic larvae were used to investigate the function of the cell-adhesive transmembrane protein Teneurin-3 (Tenm3) in structural and functional connectivity of retinal ganglion cells [100]. *tenm3* knockout animals showed mistargeting of dendritic processes and laminar arborization defects of these cells. Functional analysis of retinal ganglion cells targeting the tectum revealed a selective deficit in the development of orientation selectivity after *tenm3* knockdown.

The ribeye promoter was also used in an experiment, to express GCaMPHS in bipolar cell of zebrafish larvae (Fig. 36.8) [48]. Via optogenetic activation of the bipolar cell axon terminals, the authors could elicit calcium waves traveling over the retina.

Plasticity of the excitatory synapses formed by bipolar cells on retinal ganglion cells has been investigated by the combination of perforated whole-cell recordings and two-photon calcium imaging of 4 dpf transgenic *Tg(Gal4-VP16^{xfz43},UAS:GCaMP1.6)* larvae [101]. The driver *Gal4-VP16^{xfz43}* allows for labeling of a subset of bipolar cells in the retina [102]. Both repeated electrical

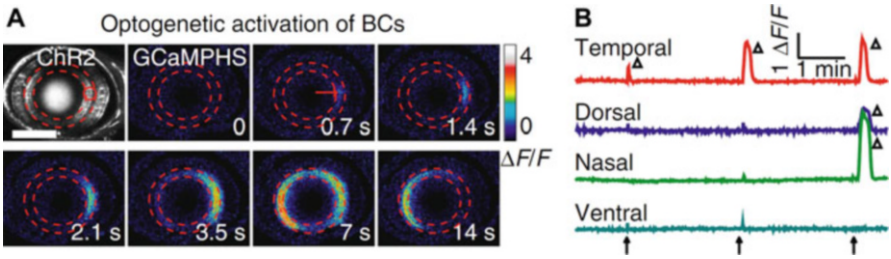

Fig. 36.8 Recording of retinal calcium waves induced by optogenetic activation of retinal bipolar cells. (**a**) Time-lapse images showing a retinal calcium wave evoked by optogenetic stimulation of a cluster of Channelrhodopsin-2 (ChR2) expressing bipolar cell terminals (red circle in first picture) in a transgenic *Tg(ctbp2:ChR2-CFP,Gal4-VP16xfz43,UAS:GCaMPHS)* larva. For optogenetic stimulation during calcium imaging, a 0.5 s pulse of 440 nm laser was activating the axon terminals, while calcium imaging data was simultaneously collected with a 900 nm or 488 nm laser using a two-photon microscope. Scale is 100 μm. (**b**) Calcium intensity traces during optogenetic stimulations of retinal bipolar cells in four different locations of the retina. Arrows mark repetitive optogenetic stimulations that induced calcium waves (triangles). (Reprinted from Zhang et al. [48])

and visual stimulations induced long-term potentiation (LTP) of bipolar cell synapses in larval but not juvenile zebrafish. LTP induction required the activation of postsynaptic N-methyl-D-aspartate (NMDA) receptors, and its expression involved arachidonic acid-dependent presynaptic changes in calcium dynamics and neurotransmitter release [101].

Finally, GCaMP3 has been selectively expressed in cone photoreceptors, by the use of the alpha subunit of cone transducin promoter (*TαCP*) [103]. Using this line, the authors analyzed whether photoreceptor degeneration induced by mutations in the phosphodiesterase-6 (*pde6*) gene was driven by excessive intracellular calcium levels. GCaMP3-expressing 5–6 dpf larvae were analyzed using multiphoton laser scanning. The time-lapse imaging monitored both changes in calcium transients and in cell shape every 20 min in a session that extended up to 9 h. In contrast to laser-killed cones, the ones in *pde6* mutants did not show elevated levels of intracellular calcium normally present at cell death [104].

36.3.3.2 Tectum

The zebrafish retinotectal system is responsible for converting moving visual inputs to the appropriate motor outputs, thus analogous to the mammalian superior colliculus [105]. The embryonic/larval tectum is located just beneath the skin and is therefore easily accessible to imaging and manipulations (Fig. 36.9a). The topographic map of the visual field present in the retina is conveyed into the tectum. Each retinal ganglion cell axon is targeted to a single lamina, and arborizes exclusively in this lamina. Information flows primarily from the superficial to the deeper layers in the tectum (Fig. 36.9b). In the deeper neuropil layers, information

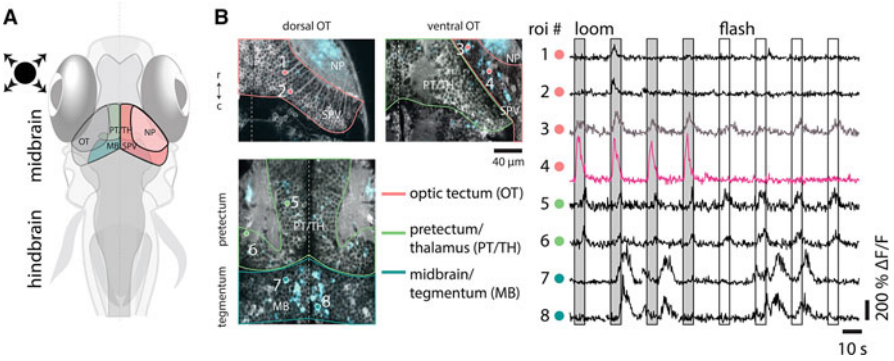

Fig. 36.9 Imaging calcium responses to visual stimuli from the tectum. (**a**) Schematic image of the brain regions processing visual information in larval zebrafish: the optic tectum (OT) with its neuropil (NP) and cell body layers (stratum periventriculare, SPV), the pretectum/thalamus (PT/TH), and the midbrain tegmental region (MB). (**b**) Neurons that responded to a looming visual stimuli, as well as to light flashes, were investigated in 5–6 days post-fertilization *Tg(elval3:GCaMP5G)* larvae using two-photon microscopy. Stimuli were presented onto a screen underneath the fish using a digital light processing (DLP) projector. The left picture shows the three brain regions imaged, i.e. the dorsal and ventral OT, the PT/TH, and the MB, where the recorded calcium activity is marked with blue. The regions of interest (ROIs) are marked as numbered circles, and they correspond to the time traces in the right diagram. Both neurons in the dorsal OT (1 and 2) and ventral OT (3 and 4) responded to looming stimuli. Neurons in the PT/TH (5 and 6) responded to both looming and flashed stimuli. Neurons in MB (7 and 8) acted spontaneously and not to the visual stimuli. (Reprinted from Dunn et al. [170], Copyright 2016, with permission from Elsevier)

is transmitted from the axons of interneurons to tectal projection neurons reaching premotor areas in the midbrain and hindbrain [106].

The first recordings of calcium activity in the larval zebrafish tectum were done after bolus labeling of Oregon green 488 BAPTA-1 AM into the tectal neuropil at 60 hpf to 9 dpf prior to visual stimulation using a miniature LCD screen [25]. Larvae were not anesthetized during imaging, as the agarose was sufficient to restrain them and prevent eye movements. A two-photon microscope collected images of visually evoked calcium fluctuation in tectal neurons, showing that zebrafish receptive field properties could be determined, such as visual topography, receptive field width, and direction and size selectivity [25].

Since then, this type of setup has been used in numerous studies investigating visual processing of diverse visual inputs, including moving dots, shadows, bars and the on- and offset of LEDs. However, today, the use of GECIs has almost entirely replaced the use of synthetic dyes for imaging of the tectum and therefore, the rest of this section will focus on research using GECIs. Due to the possibilities to combine calcium imaging of either individual cell types or entire brains in larval zebrafish in response to visual information, and to track the subsequent behavior, the studies of the visual system in zebrafish has grown exponentially during the last couple of years.

Researchers have investigated how visual information is encoded in the population activity of retinal ganglion cells. To address this, they used a genetically encoded reporter of presynaptic function (SyGCaMP3) to record visually evoked activity in the population of retinal ganglion cell axons innervating the zebrafish tectum [107]. Calcium imaging was performed using 7 dpf *Tg(isl2b:Gal4;UAS:SyGCaMP3)* zebrafish larvae with SyGCaMP3 expression in retinal ganglion cell axons within the tectal neuropil. Fish were presented light or dark drifting bars that were moving in 12 directions to one eye. Visually evoked SyGCaMP3 responses were recorded in the contralateral tectum. Analysis of SyGCaMP3 signals identified three subtypes of direction-selective and two subtypes of orientation-selective retinal input.

The same group then further studied the direction-selective and orientation-selective cells in the tectum in response to moving dark bars [108]. Imaging was performed using Oregon green 488 BAPTA-1 AM as well as the transgenic lines *Tg(Isl2b:Gal4; UAS:SyGCaMP3)* and *Tg(elavl3:GCaMP5)*, confirming that direction-selectivity is established in both the retina and tectum.

Gabriel et al. also used the *Tg(elavl3:Gal4;UAS:GFP)* line to better understand the direction-selective neurons in the tectum [109]. The team also developed new driver lines for tectal labeling with reduced labeling of retinal afferents. The two lines, *Tg(Oh:G-3)* and *Tg(Oh:G-4)*, are based on the gene orthopedia a (*otpa*) and a heat shock basal promoter fused to *Gal4VP16*. The driver lines were crossed with the *Tg(UAS:GCaMP3)* line to monitor calcium spikes in cell types of opposite directional tuning. A few years later, the group produced the *Tg(Oh:GCaMP6s)* transgene, used to map the activity of a group of superficial interneurons (SINs), showing exhibited distinct size-tuning properties [110].

Visual reflexes, such as the optomotor response, which is an orienting behavior evoked by visual motion, have been studied using calcium imaging in the zebrafish larva. In one study, the whole brains of 5–7 dpf *Tg(elavl3:GCaMP5G)* and *Tg(elavl3:GCaMP2)* zebrafish were scanned when the fish were exposed to moving gratings [111]. The fictive motor behavior was mapped simultaneously using motor nerve recordings. Interesting, the optomotor response was found to be processed by diverse neural response types distributed across multiple brain regions.

Prey capture behavior serves as a meaningful behavior to study in larval fish, as the visual stimulus and subsequent behavior are possible to induce in the lab by showing small moving objects to the test fish. A number of studies have investigated various aspects of prey capture behavior. In one of them, the *Tg(isl2b:Gal4, UAS:GCaMP6s)* line was used to label tectal cells in 8 dpf larvae [112]. The fish were restrained in agarose and were shown white dots on a black background. Two-photon calcium imaging revealed that a small visual area, AF7, was activated specifically by the optimal prey stimulus. This pretectal region was found to be innervated by two types of retinal ganglion cells, which also send collaterals to the optic tectum. The behavioral test was also performed with real paramecia, and laser ablations of AF7 neuropil confirmed the involvement of the brain region in prey capture behavior.

36.3.4 Olfaction

One of the few neural systems that has regularly involved calcium imaging of adult zebrafish is the olfactory system, due to the small size, transparent nature, and accessibility of the adult olfactory bulb for labeling, imaging and neuronal stimulation. In the nasal cavity, olfactory receptor neurons (ORNs) are stimulated by odors, and send a single unbranched axon to the first relay station in the central nervous system, the olfactory bulb (OB). ORN axons synapse onto mitral cells (MCs) and local interneurons in the olfactory glomeruli [113]. Each glomerulus receives convergent input from sensory neurons expressing the same odorant receptor [114]. MC axons exit the OB and project to several higher brain areas, such as the dorsal telencephalic area Dp, the homolog of olfactory cortex [115].

Initially, dextran and AM dyes were used to label neurons in the olfactory system, but with the development of transgenic lines expressing GECIs, these have been combined with synthetic dyes to allow for cell-specific labeling, activation and monitoring of cellular activity. Electrophysiology, as well as optogenetics [116] have successfully been used to map the functional connectivities in the networks processing olfactory information.

An explant preparation of the intact zebrafish brain and nose has been used extensively [117], allowing for two-photon imaging of different cell types in response to olfactory activation [118]. Olfactory stimuli such as AAs, bile acids or food extracts are applied to the naris of one olfactory epithelium. In this preparation, it is possible to monitor patterns of presynaptic activity in the OB and glomeruli induced by repeated applications in the same animal. In preparations where the telencephalon is spared [118], it is possible to record odor-generated activity in the telencephalic targets.

Calcium imaging from the zebrafish OB has shown that AAs and bile acids stimulate different parts of the OB [119]. AAs induce complex patterns of active glomerular modules that are unique for different stimuli and concentrations. Interestingly, the similarity of odorant-induced activity patterns is the highest for AAs that are chemically close.

Researchers used the explant preparation of the nose and brain from adult zebrafish to investigate the role of dopamine for olfactory signaling. The olfactory sensory neurons were loaded with Oregon green 488 BAPTA-1 dextran, and the preparation was exposed to amino acids. Here, dopamine had no effect on odorant-evoked calcium signals in sensory axon terminals. Next, neurons in the OB were loaded with rhod-2 AM by bolus injection in *Tg(elavl3:YC2.1)* zebrafish, a transgene where MCs are labeled with YC2.1. Electrophysiology showed that direct exposure by dopamine caused MCs cells to hyperpolarize. However, multiphoton calcium imaging of MCs showed that the mean response to odorants increased slightly, but not significantly, in the presence of DA [120]. In the following publication from the group, the role of dopaminergic modulation of the telencephalic area

Dp was investigated using bolus loading of rhod-2 AM into the tissue. Multiphoton calcium imaging showed that population responses of Dp neurons to olfactory tract stimulation or odor application were enhanced by dopamine [121].

Calcium activity patterns evoked by repeated odor stimulation were measured in the adult OB and Dp. Recordings of odor-evoked activity patterns of MCs in the OB were performed using the *Tg(elavl3:GCaMP5)* line while calcium responses in Dp was measured by bolus loading of rhod-2 AM. Whereas odor responses in the OB were highly reproducible, responses of Dp neurons were variable and reduced over trials. This data indicates that odor representations in higher brain areas are continuously modified by experience [122].

A group of GABAergic interneurons in the OB expresses the homeobox genes *dlx4* and *dlx6*. Zhu et al. combined electrophysiology with imaging of the dlx4/6 neurons by using the zebrafish line *Tg(dlx-itTA; Ptet-GCaMP2)*. In the ex vivo preparation, AA odorants or food extracts evoked widespread calcium changes throughout the glomerular layer. Individual dlx4/6 neurons responded to subsets of odorants and different odorants stimulated distributed, partially overlapping combinations of dlx4/6 neurons. Increasing odorant concentration enhanced responses and recruited additional dlx4/6 neurons. To examine how dlx4/6 neurons shape OB output during an odor response, the authors used optogenetics to silence dlx4/6 neurons while recording AA-stimulated MCs, labeled with rhod-2 AM. The inhibition of dlx4/6 cells suppressed the response of MCs to low odor concentrations, but enhanced their response to high concentrations [123].

Prostaglandin $F_{2\alpha}$ ($PGF_{2\alpha}$) is involved in reproductive behavior in fish, and it was found that it specifically activates two odorant receptors, or114-1 and or114-2 [124]. Imaging experiments were performed in the ex vivo preparation of the intact brain and nose from adult male zebrafish that were carrying the promoter for the olfactory marker protein (*omp*) which drove expression of *GCaMP7* or *GCaMP-HS* in ciliated olfactory sensory neurons. $PGF_{2\alpha}$ exposure gave rise to calcium signals in two ventromedular glomeruli in the OB. A low concentration of $PGF_{2\alpha}$ induced a calcium increase in one of the two glomeruli, while higher concentrations activated both glomeruli. Mutant male zebrafish, deficient in the high-affinity receptor or114-1, exhibited loss of attractive response to $PGF_{2\alpha}$ and impaired courtship behaviors toward female fish [124].

Labeling of ciliated olfactory sensory neurons by *Tg(omp:Gal4FF;UAS:GCaMP7)* has also been used in experiments aiming at understanding the signaling of the adenosine receptor A2c in the OB. Calcium imaging experiments of the nose-attached intact brain from adult male fish confirmed that adenine nucleotides (ATP, ADP and AMP) and adenosine, but not other nucleotides, nucleosides, AAs, or bile acids, specifically activated a single, large, identifiable glomerulus named lG2. The ATP- and alanine-induced neural activation in higher brain centers was investigated by c-Fos *in situ* hybridization. ATP and alanine applications resulted in significant increase in the number of c-Fos-positive neurons in multiple brain areas [125].

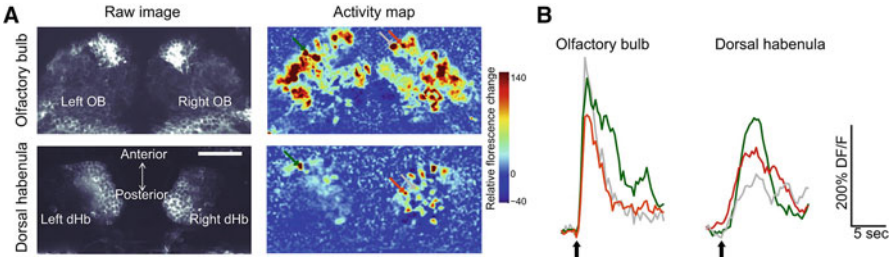

Fig. 36.10 Calcium signals in the olfactory bulb and dorsal habenula in response to odor stimulation. (**a**) Raw images and pseudo-colored food odor-evoked activity maps of the olfactory bulb and dorsal habenula recorded in 25-day-old *Tg(elavl3:GCaMP5)* zebrafish using two-photon microscopy. (**b**) Intensity traces of calcium signals in the two regions in response to food odor (black arrows). Colors of the traces correspond to the color of the arrows in (**a**). (Reprinted from Jetti et al. [126], Copyright 2014, with permission from Elsevier)

Due to its small size, the olfactory networks of larval and juvenile zebrafish can be imaged in the intact animal (Fig. 36.10). In most of these experiments, different versions of GCaMP have been expressed using the *elavl3* promoter, as it labels the MCs. In order to better understand the function of the habenular circuits and how habenulae process olfactory information, Jetti et al. measured and compared odor responses in the OB and the dorsal habenula (dHb) using two-photon calcium imaging, in 3- to 4-week-old *Tg(elavl3:GCaMP5)* zebrafish (Fig. 36.10) [126]. The fish were exposed to a large panel of odors, i.e. skin extract, urea, bile acid mixture, nucleotide mixture, chondroitin-6-sulfate, trimethylamine-n-oxide (TNO), putrescine, AA mixture, and food odor. Odor responses in the dHb were asymmetric and were primarily in the right dHb, unlike the symmetric odor responses in the OB. Interestingly, the odors evoked responses with different amplitudes in the OB, but amplitudes and distribution of dHb odor responses were indifferent to the stimulus strength as measured by OB activity.

Tree- to five-week-old larvae carrying the *Tα1:GCaMP2* construct were used to monitor odor-evoked neuronal activity in the OB related to fear responses. Exposure of odorants to the olfactory pits revealed that purified skin extracts and purified shark chondroitin sulfate activated one region of the OB, while bile acids and AA activated other regions [127].

To test the hypothesis that that zebrafish perceive MHC peptides as odorants, 6 dpf *Tg(elavl3:GCaMP2)* zebrafish larvae were exposed to a mixture of different MHC peptides. Multiphoton imaging was used to detect the odor-evoked calcium signals in the OB. Basal indicator fluorescence was higher in the mitral cell layer than in deeper, interneuron layers. Upon stimulation with the MHC peptides, fluorescence changes were observed in small, scattered populations of neurons and neuropil regions in the MC and interneuron layers [128].

OlfCc1 is a C family G-protein-coupled receptor that is expressed in a large population of microvillous sensory neurons in the zebrafish olfactory epithelium. It is a calcium-dependent, low-sensitivity receptor specific for the hydrophobic AAs isoleucine, leucine, and valine. DeMaria used three different promoters to drive expression of *GCaMP1.6* in the olfactory system of zebrafish larvae: *omp* for expression in ciliated olfactory sensory neurons, transient receptor potential cation channel C2 (*trpc2*) for expression in microvillous olfactory neurons, and *elavl3* for pan-neuronal expression in excitatory neurons throughout the CNS, including the OB. A confocal microscope was used to monitor activity to food extract, AA mix; bile acid mix and amine mix in 4.5 dpf animals. Morpholino knockdown of *olfcc1* demonstrated its importance in detecting various types of AAs [129].

Recently, researchers investigated the role of beating cilia in the nose of zebrafish in modulating the olfactory response. They made use of the *schmalhans* (*smh*) mutant line that displays ciliary motility defects. Fluorescently labeled food odor was delivered by a capillary, and odor flow dynamics and neural responses to odors were imaged using two-photon microscopy in 4 dpf wild-type and mutant *Tg(elavl3:GCaMP6s)* zebrafish. The experiments showed that beating cilia in the nose of zebrafish attract odors to the nose pit and facilitate detection of odors by the olfactory system. Flow fields from cilia facilitate odor detection and elicit odor responses at the ORNs and the OB. On the contrary, *smh*-/- zebrafish failed to attract odors to the nose and showed no detectable odor responses in ORNs or in the OB [130].

36.3.5 Brain-Wide Imaging

The small size and the transparency of the larval zebrafish allows for imaging experiments that are generally not feasible in many other vertebrates, i.e. the possibility to image activity of the entire nervous system in an awake animal while it is responding to sensory stimuli. The development of GECIs, in particular the GCaMP family of indicators, expressed by the generally expressed *elavl3* promoter has given rise to an exponentially increasing number of complex studies, often combined with new imaging techniques, such as light-sheet microscopy (Fig. 36.11) [131–136]. Just a few examples of studies performed using different forms of brain-wide imaging in transgenic zebrafish lines include monitoring of visually-induced brain activity during the optomotor [111] and optokinetic [137] responses, as well as brain activity during pharmacologically induced seizures [138, 139]. Selective plane illumination microscope (SPIM) imaging of *Tg(elavl3:H2B:GCaMP6f)* 6 dpf larvae has revealed brain regions and individual cells responsive for auditory processing [140]. Moreover, calcium imaging has successfully been performed in freely moving animals undergoing swimming [141] and prey capture behavior (Fig. 36.12) [142–144].

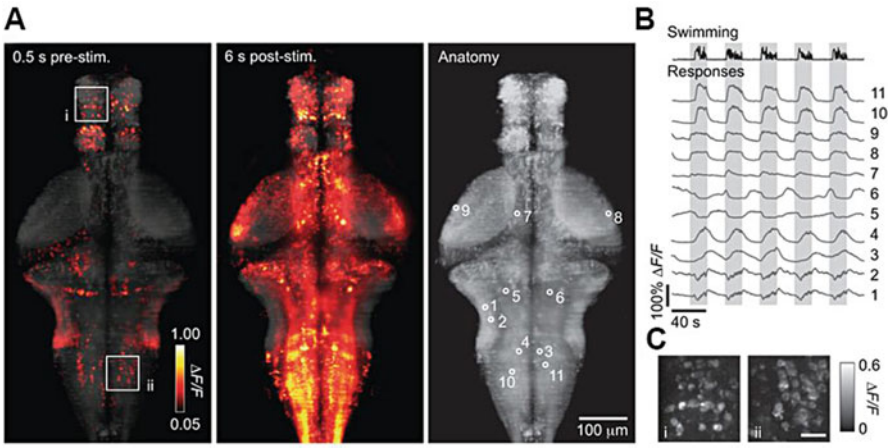

Fig. 36.11 Brain-wide calcium imaging of the optomotor response using light-sheet microscopy. A custom-built light-sheet microscope was used to image the full brains of 5–7 days post-fertilization *Tg(elavl3:GCaMP6s)* zebrafish larvae. The authors induced the optomotor response (OMR) in which swimming was elicited by visual gratings moving in the tail-to-head direction. Two extracellular suction electrodes recorded fictive swimming from the tail. (**a**) Maximum-intensity projections of ΔF/F over the entire volume before and after onset of grating movement averaged over 24 trials. The localizations of regions of interest (ROIs) are seen to the right. (**b**) Intensity traces of single neurons or patches of neuropil ROIs during fictive behavior. (**c**) Magnification of regions boxed in (**a**), showing single-neuron resolution. Scale bar is 20 μm. (Reprinted from Vladimirov et al. [136], Copyright 2014)

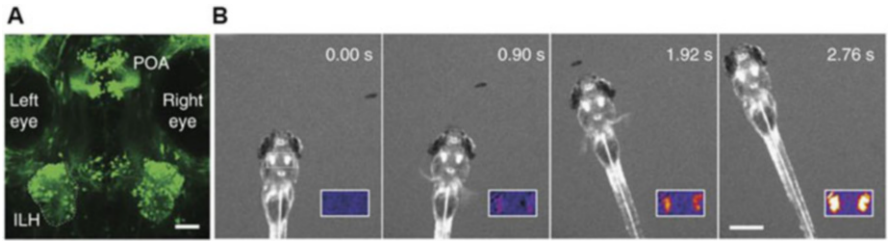

Fig. 36.12 Calcium imaging of freely swimming zebrafish larvae during prey capture behavior. (**a**) Labeling of the inferior lobe of the hypothalamus (ILH) of a 5 days post-fertilization (dpf) larva resulting from crossing the *Gal4* driver line *Tg(hspGFFDMC76A)* with *Tg(UAShspzGCaMP6s)* fish. POA: preoptic area. Scale bar is 50 μm. (**b**) ILH activation during prey capture behavior in a previously unfed 4 dpf larva. The imaging was performed using an epifluorescent microscope equipped with a complementary metal–oxide–semiconductor (CMOS) camera. Images show frames from a time-lapse recording during the behavior. Insets: Pseudo-color images of the frame divided by an averaged frame. Scale bar is 500 μm. (Reprinted from Muto et al. [144])

36.3.6 Muscle

Excitation–contraction coupling is the process that regulates contractions by skeletal muscle. A change in membrane voltage activates release of calcium from the sarcoplasmic reticulum (SR) via activation of ryanodine receptors (RyRs) type 1 or 3, leading to the initiation of muscle contraction via shortening of the myocyte myofilaments [145]. Although it has technically been possible to perform in vivo imaging of muscle fiber in the zebrafish to study this process, it has not commonly been done. One reason could be the ease of performing patch clamp recordings of muscle fibers in vivo [146]. In the cases when calcium signals have been recorded from myocytes, incubation with AM esters has been used, as well as injections of dextran dyes at the one-cell stage, or labeling using GECIs.

Lin et al. investigated the role of *microRNA 3906* (*miR-3906*) and *homer 1b* for muscle fiber differentiation (Fig. 36.13) [147]. They injected one-cell zebrafish embryos with a solution containing calcium green-1 and rhodamine dextran that was

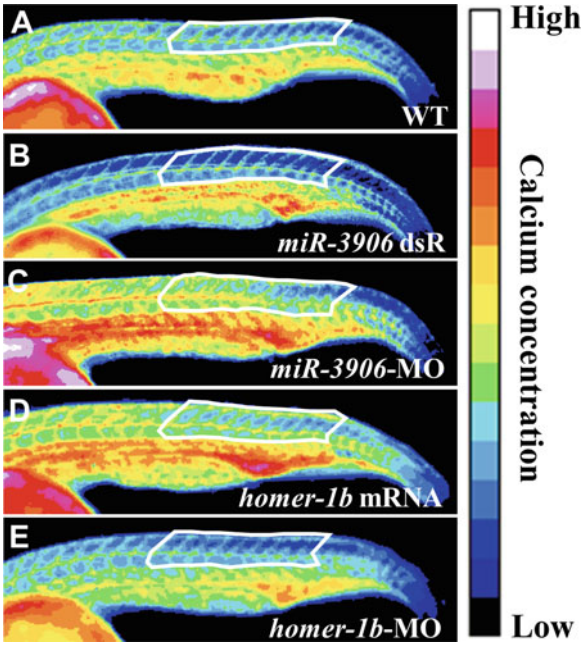

Fig. 36.13 Calcium imaging of myocytes in vivo. The contributions of the gene *homer1b* and microRNA *miR-3906* to development of calcium dynamics in zebrafish myocytes were investigated. A solution containing calcium green-1 and tetramethylrhodamine dextran was mixed with either: (**a**) buffer, (**b**) double-stranded *miR-3906* dsR, (**c**) *miR-3906* morpholino, (**d**) *homer1b* mRNA or (**e**) *homer1b* morpholino and was microinjected individually into one-cell zebrafish embryos. The fluorescent image of each embryo was captured by a fluorescent microscope at 24 h post-fertilization. The region of interest consisting of 11–20 trunk somites from where the calcium levels were recorded is marked with a white line. (Reprinted from Lin et al. [147])

mixed with morpholinos or RNA for either *miR-3906* or *homer 1b* to knock down or overexpress these in vivo. The fluorescent image of each embryo was captured at 24 hpf revealed that either *homer1b* overexpression or *miR-3906* knockdown increased the calcium concentration within muscle cells.

The role of RyRs has been investigated in zebrafish muscle. Klatt Shaw and coauthors made use of the RyR inhibitor azumolene and the RyR1 agonist 4-chloro-m-cresol (4-CmC) to manipulate RyR1 signaling [148]. Developing *Tg(act2b:GCaMP6f)* embryos were incubated in vehicle or drug from the gastrula stage (6 hpf) and onward. At 24 hpf, muscle contractions were electrically stimulated and calcium fluxes associated with muscle contraction were recorded. Under these conditions, azumolene acted in a dose-dependent manner to reduce calcium fluxes associated with muscle stimulation, whereas 4-CmC potentiated RyR activity, increasing both the duration and maximum levels of released calcium.

In another experiment, the role of RyR3 in calcium signaling and muscle function was investigated using morpholino knockdown [149]. Calcium sparks from the SR were monitored using confocal imaging of fluo-4 AM-loaded isolated tail myocytes from 72 hpf larvae. The bathing solution included caffeine to stimulate SR calcium release. It was found that the number of calcium sparks was reduced in the morphants, while the muscle function remained normal.

Two-pore channel type 2 (TPC2) is regulating differentiation of slow muscle fibers, and TPC2 has been implicated in intracellular calcium signaling as it has been suggested that the channel can mediate calcium release from internal stores. Researchers approached this theory by pharmacologically inhibiting, knocking down and overexpressing *tpc2* in zebrafish *Tg(α-actin-apoaequorin-IRES-EGFP)* [150]. Active aequorin was then reconstituted in vivo, by incubating transgenic embryos from the 4- to 64-cell stage to the ∼16-somite stage with f-coelenterazine. Embryos were then transferred to a photomultiplier tube (PMT)-based luminescence detection systems for luminescence detection [150]. The resulting data indicated that localized calcium release via Tpc2 might trigger the generation of more global calcium release from the SR via calcium-induced calcium release.

Xiyuan and coauthors investigated the role of the nitric oxide-soluble guanylyl cyclase (NO-sGC) pathway on calcium release and muscle contraction in zebrafish [151]. Isolated skeletal muscle cells from 5–7 dpf zebrafish larvae were incubated with fluo-4 AM and were then electrically activated using platinum electrodes. Myocytes were treated with S-Nitroso-N-acetyl-DL-penicillamin (SNAP), a NO-donor, or N(G)-Nitro-L-arginine methyl ester (L-NAME), an unspecific blocker of nitric oxide synthase. The authors concluded that endogenous NO reduced force production through negative modulation of calcium transients via the NO-sGC pathway.

The cytosolic protein SH3 and cysteine rich domain 3 (Stac3) has been identified as an essential component for skeletal muscle excitation–contraction coupling and a mutation in human *STAC3* causes the debilitating Native American myopathy, a severe disorder characterized by altered skeletal muscle structure and function. The group of John Kuwada has investigated the role of Stac3 in zebrafish by either loading dissociated muscle fibers with fluo-4 AM [152] or by injecting the

one-cell embryo with a plasmid carrying *α-actin:GCaMP3*, resulting in embryos that mosaically expressed GCaMP3 within skeletal muscle [153]. By performing calcium imaging of electrically stimulated isolated muscle fibers carrying the human *STAC3* mutation, it was found that Stac3 participates in excitation–contraction coupling in muscles [152]. Introduction of the mutated *stac3* in fish lacking the wild-type gene resulted in decreased calcium transients in fast-twitch muscles at 48 hpf and defective swimming [153].

Another myopathy, the autosomal recessive centronuclear myopathy, is caused by mutations in bridging integrator 1 (*BIN1*). To understand the role of Bin1 in muscle contraction, zebrafish embryos were injected at the one-cell stage with a plasmid encoding *GCaMP3–EGFP* under control of an *α-actin* promoter, alone or in combination with a *bin1* morpholino [154]. Calcium imaging of wild-type and *bin1* morphant embryos was done at 3 dpf using a spinning disk confocal microscope. KCl was used to initiate muscle contraction and relative fluorescence intensity changes of induced calcium transients in individual myofibers were recorded. Recordings confirmed that muscle calcium signaling was impaired in *bin1* morphants.

Another cause of centronuclear myopathy is mutations in the gene of dynamin 2 (*DNM2*), a ubiquitously expressed GTPase that regulates multiple subcellular processes. Expression of mutated human *DNM2-S619L* in zebrafish led to the accumulation of aberrant vesicular structures and to defective excitation-contraction coupling [155]. Embryos were co-injected with cDNA for *GCaMP3* and RNA for wildtype or mutant *DNM2* and calcium measurements of spontaneous muscle contractions were performed at 24 hpf. Although *DNM2-S619L* embryos displayed spontaneous muscle contractions with normal timing, there was no increase in intracellular calcium corresponding to calcium sparks.

The development of lines that selectively express GECIs in either fast or slow muscle fibers has big potential for the field. In a study by Jackson et al., the promoter for the slow myosin heavy chain 1 (*smyhc1*) was used to drive *GCaMP3* expression in slow-twitch muscle fibers [156]. Fast-twitch-specific transients could be monitored using the *Tg(mylz2:GCaMP3)* transgene, making use of the myosin light chain 2 promoter (*mylz2*).

Calcium imaging of 2 dpf *Tg(smyhc1:GCaMP3)* embryos was done with a confocal microscope, while muscle contractions were induced by pentylenetetrazol (PTZ) [156]. In wild-type embryos, the response time of slow-twitch fibers was shorter than in fast-twitch fibers, while the change in amplitude was smaller. The response time of *sox6* mutant fast-twitch fibers was significantly shorter than in wild types, resembling more that of wild-type slow-twitch fibers, whereas the amplitude change was unaffected. These findings indicate that the transcription factor Sox6 controls the calcium response of fast-twitch fibers.

Shahid et al. established an in vivo biosensor system to quantify potential toxicant effects on motor function, by generating a GFP line based on the regulatory element of the heat shock protein family B (small) member 11 (*hspb11*), i.e. *TgBAC(hspb11:GFP)* [157]. Exposure to substances that interfered with motor function induced a dose-dependent increase of GFP intensity, while also inducing

muscle hyperactivity with increased calcium spike height and frequency. This was monitored by developing the muscle specific calcium biosensor line Tg(*[-505/-310]unc45b:GCaMP5A*), where the promoter for unc-45 myosin chaperone B is driving the *GCaMP5A* expression.

Finally, spontaneous calcium activity in embryonic myocytes has been observed in a zebrafish line containing the constitutively active promoter *hspa8* and the gene for YC2.60 [43]. At 24 hpf, twitching behavior only caused calcium signals in slow muscles while the calcium concentration in the fast muscles stayed at basal level. During stronger contraction, when left and right side myocytes contracted alternately and repeatedly, rises in calcium were observed both in the slow and fast muscles. Alternating contractions of left- and right-side myocytes were also observed at 51 hpf.

36.3.7 Heart

The development of the heart and cardiovascular system has been extensively studied in the zebrafish [158, 159]. Still, there is information lacking regarding the intracellular calcium handling of the zebrafish heart. The zebrafish heart has a simple structure, composed of the sinus venosus, the atrium, the ventricle, and the bulbus arteriosus connected in series. The heart is the first organ to form and function during development, and the heart of the embryonic and larval zebrafish are particularly easily imaged during this time. The first calcium imaging studies of the zebrafish heart made use of labeling of embryonic and larval hearts with dextran and AM ester indicators [8], while later studies have benefitted from transgenic zebrafish lines expressing GECIs via the heart-specific cardiac myosin light chain 2 (*cmlc2*)/myosin light chain 7 (*myl7*) promoter (referred to as *myl7* here) [160]. By crossing this line with mutant lines displaying heart defects such as contraction problems, researchers have gained significant molecular knowledge underlying the development and function of the heart as well as dysfunction related to cardiomyopathies.

Isolated zebrafish myocytes or intact hearts can be loaded with AM esters. Bove et al. used confocal imaging to investigate the role of SR in calcium signaling of isolated cardiac myocytes loaded with fluo-4 AM [26]. They found that contrary to mammalian myocytes, only 20% of the action potential-induced calcium transients in zebrafish are mediated via calcium release from the SR, and the majority was originating from calcium influx via L-type calcium channels.

Embryonic zebrafish hearts can be isolated and incubated with calcium indicators despite their small size. Researchers were interested in understanding the function of *pkd2* mutations that are causing autosomal dominant polycystic kidney disease in humans, with comorbidity of cardiovascular disease [27]. Hearts from 3 dpf wild-type and *pkd2* mutant embryos were isolated and labeled with fluo-4 AM. Cardiac contractions were stopped with blebbistatin to eliminate motion artifacts. Isolated *pkd2* mutant hearts displayed impaired intracellular calcium cycling and calcium alternans.

Moreover, recordings from embryonic hearts were performed both after isolation and incubation with fluo-4 AM and in vivo in the *Tg(cmlc2:gCaMP)*^{s878} line [28]. The goal was to understand how 3-O-sulfotransferase (3-OST) 7 affects cardiac calcium processing since *3-ost-7* knockdown results in a noncontracting cardiac ventricle at 48 hpf. Interestingly, the noncontracting ventricle in *3-ost-7* morphants generated normal action potentials and calcium transients. In addition, calcium activation and conduction velocity proceeded normally in *3-ost-7* morphants in vivo. It was found that elevated bone morphogenetic protein (BMP) signaling in the morphants leads to disruption of sarcomere assembly, leading to the defect in myocyte contraction.

Light-sheet microscopy has been used for detailed in vivo cardiac imaging in zebrafish embryos. *Tg(myl7:GCaMP5G-Arch)D95N* embryos between 36 and 52 hpf were imaged with a custom-built light-sheet microscope [161]. Using this technique, the authors could map the three-dimensional calcium signals of all cells in the entire electro-mechanically uncoupled heart during the looping stage.

Fukuda et al. were interested in better understanding the formation of heart tissue during development [162]. They made use of a mutant fish line for ankyrin repeat and SOCS box containing 2 (*asb2b*), an E3 ubiquitin ligase that functions to specify target proteins for proteasome-dependent degradation. Although *asb2b* mutants displayed cardiac dysfunction, imaging with a spinning disc confocal microscope revealed no calcium signaling dysfunction in 50 hpf mutant *Tg(myl7:gCaMP)*^{s878} zebrafish, when compared to wild-type fish. It was found that *asb2b* is required for myocyte maturation, causing structural defects in the mutants.

Cardiac trabeculation is a crucial morphogenetic process by which clusters of ventricular cardiomyocytes extrude and expand to form sheet-like projections. Liu et al. found that in zebrafish Erb-B2 receptor tyrosine kinase 2 (*erbb2*) mutants lack cardiac trabeculae and display a dysfunctional cardiac function [163]. Optical mapping of 3 and 10 dpf wild-type and *erbb2* mutants crossed to *Tg(cmlc2:gCaMP)s878* were embedded and cardiac contraction was suppressed with 2,3-butanedione monoxime before imaging using a high-speed camera. At 3 dpf, when trabeculae start to form in wild type fish, optical mapping revealed that the activation patterns in wild-type and *erbb2* mutant ventricles were indistinguishable. By contrast, following the formation of trabeculae, the ventricular calcium wave in 10 dpf wild-type hearts was different from that of *erbb2* mutant hearts. These findings indicate an important role for cardiac trabeculae and ErbB2 signaling in the maturation of the ventricular conduction system.

The zebrafish mutant line *tremblor* (*tre*^{tc318}) lacks the gene for the Na^+/Ca^{2+} exchanger 1, *slc8a1a*, giving it an irregular heart rhythm since its myocytes are unable to efficiently remove calcium ions from the cytoplasm. Via drug screening, it was possible to identify a compound, efsevin, that could restore the heartbeat in the *tre*^{tc318} mutants [164]. The *Tg(myl7:GCaMP4.1)* zebrafish line was used to record calcium waves in vivo at 36 dpf, confirming that efsevin could normalize the calcium signals in the hearts of mutants.

BIN1 is not only involved in centronuclear myopathy, but is also involved in intracellular calcium processing in cardiomyocytes, as it allows the correct

processing of voltage-dependent calcium channels Cav1.2 to the cardiac T-tubules. *bin1* was knocked down in *Tg(cmlc2:gCaMP)*^{s878} zebrafish embryos where calcium transients and cardiac contractility were analyzed in vivo [165]. The analysis confirmed that calcium transients in 70 hpf *bin1* morphants was reduced, and the ventricular contractions were impaired.

The Popeye domain containing gene 2 (*popdc2*) encodes a transmembrane protein that expresses in the myocardium and transiently in the craniofacial and tail musculature. When *popdc2* was knocked down, the animals showed defects in skeletal muscle and the heart (Fig. 36.14) [166]. SPIM was used to image calcium oscillations in 5–6 dpf wild-type and *popdc2 Tg(cmlc2:gCaMP)*^{s878} embryos confirming the presence of a severe arrhythmia phenotype.

Desminopathies belong to a family of muscle disorders called myofibrillar myopathies that are caused by desmin mutations and lead to protein aggregates in muscle fibers. Desmin is involved in the formation of sarcomere architecture. The *desmin a* (*desma*) gene is homologous to human desmin and was further studied in the *desma*$^{sa5-/-}$ knock-out line and the *desma*^{Ct122aGt} gene trap mutant where citrine was inserted between AAs 460 and 461 in the C terminus of desmin a [167]. These lines were crossed with *Tg(myl7:galFF; UAS:GCaMP3)* animals to allow for confocal imaging of calcium transients in the heart. Calcium signals were measured from different regions of the heart, revealing reduced calcium signals at the tip of the ventricle in the mutant lines compared to controls.

Finally, calcium imaging has been performed in the endocardial cells that are sensing the flow forces of the heart at the time of the heart valve formation [168]. This was studied at the early stages of heart development, at 48 hpf, in the *Tg(fli1a:gal4ff; UAS:GCaMP3)* line that labels endothelial cells. It was observed that calcium levels were increased in the atrio-ventricular canal and was lower in the atrium and ventricle. The endocardial calcium response and the flow-responsive Kruppel-like factor 2a (*klf2a*) promoter were modulated by the oscillatory flow-through transient receptor potential cation channel subfamily V member 4 (Trpv4), a mechanosensitive ion channel specifically expressed in the endocardium during heart valve development.

36.4 Conclusion

The described preparations and experiments show the diversity of studies that have benefitted from calcium imaging in zebrafish cells, tissues and intact animals. These studies have contributed greatly to our understanding of basic biological principles during development and adulthood, as well as the function of disease-related genes in a vertebrate system. However, it is evident that we still lack knowledge in certain biomedical areas, where new preparations of the zebrafish would be valuable. Nevertheless, the technical advances in biomedical research promise exciting possibilities. For example, the discovery of new cell-specific promoters in combination with GECIs will undoubtedly continue to be of great importance for

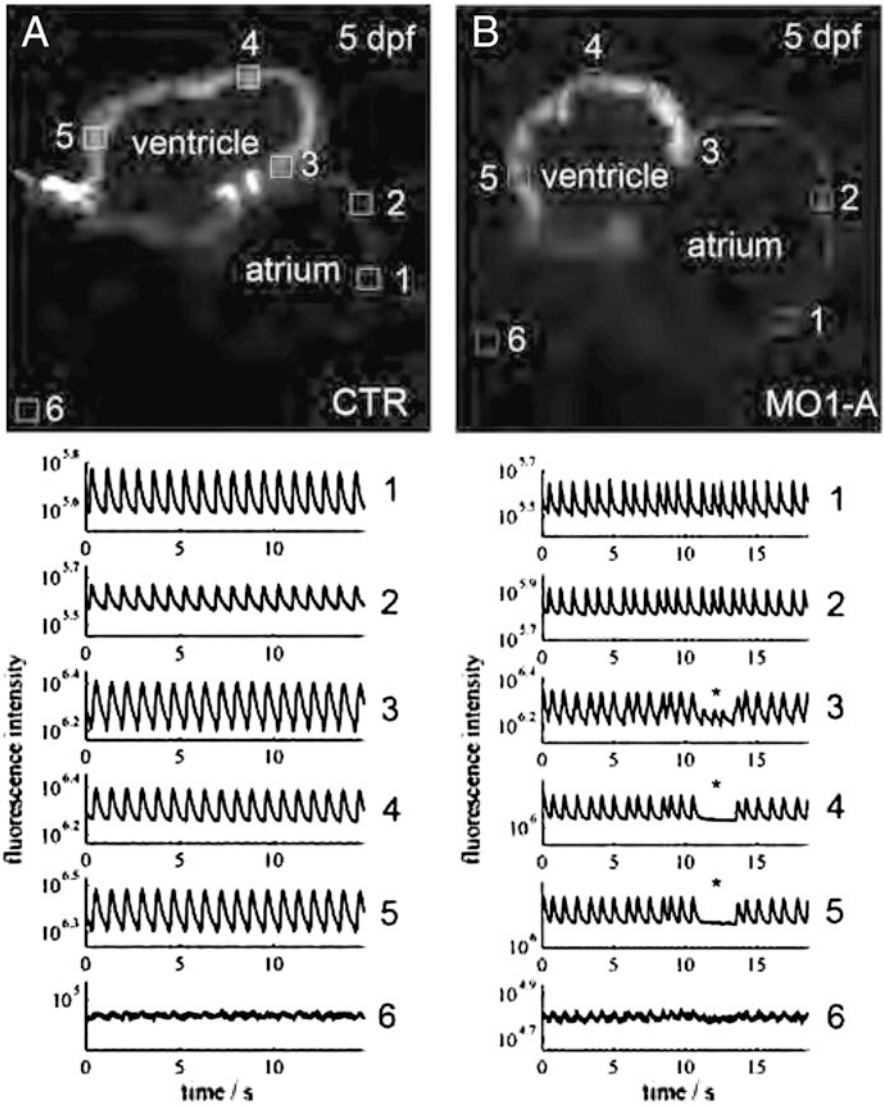

Fig. 36.14 Imaging of cardiomyocyte calcium signaling in vivo. The hearts of 5-day-old Popeye domain containing 2 (*popdc2*) morphants displayed cardiac conduction defects. A single plane illumination microscope (SPIM) was used to record videos of the heart of *Tg(cmlc2:gCaMP)s878* zebrafish embryos injected with (**a**) control (CTR) morpholino and (**b**) *MO1-popdc2* morpholino. The individual movies were processed to determine the fluorescence intensity of selected regions of the heart over time. Each selected region has a corresponding number plotted below. (**a**) In a control heart, fluorescence intensity varied with time in atrial and ventricular regions as the depolarization wave propagated through the heart. (**b**) The morphant heart displayed an atrioventricular (AV) block (asterisks). (Reprinted from Kirchmaier et al. [166], Copyright 2012, with permission from Elsevier)

future analyses of neuronal cell types and regions that so far have been unreachable by conventional labeling methods. Moreover, the combination of optogenetics with calcium imaging within the brain will mean valuable dissections of network function and connectivity. The development of new microscopy techniques with increased resolution, speed and imaging depth, such as light-sheet microscopy, will also be critical for the advancements of calcium imaging in the zebrafish, allowing the monitoring of processes in older animals and larger brain areas. New large-scale imaging methods and sophisticated analysis of activity from neuronal ensembles will bring our understanding of neuronal processing even further. The emerging use of the zebrafish as a model system for diseases, e.g. in the field of psychiatry, will mean exciting findings in the years to come. My hope is that this chapter will serve as an inspiration to continue the development of the zebrafish as a model organism to study the physiological processes and the complex biomedical mechanisms that are vital for biological beings.

References

1. Lister JA, Robertson CP, Lepage T, Johnson SL, Raible DW (1999) nacre encodes a zebrafish microphthalmia-related protein that regulates neural-crest-derived pigment cell fate. Development 126:3757–3767
2. Nasevicius A, Ekker SC (2000) Effective targeted gene 'knockdown' in zebrafish. Nat Genet 26:216–220
3. Asnani A, Peterson RT (2014) The zebrafish as a tool to identify novel therapies for human cardiovascular disease. Dis Model Mech 7:763–767
4. Xi Y, Noble S, Ekker M (2011) Modeling neurodegeneration in zebrafish. Curr Neurol Neurosci Rep 11:274–282
5. Norton WH (2013) Toward developmental models of psychiatric disorders in zebrafish. Front Neural Circuits 7:79
6. White R, Rose K, Zon L (2013) Zebrafish cancer: the state of the art and the path forward. Nat Rev Cancer 13:624–636
7. MacRae CA, Peterson RT (2015) Zebrafish as tools for drug discovery. Nat Rev Drug Discov 14:721–731
8. Kettunen P (2012) Calcium imaging in the zebrafish. Adv Exp Med Biol 740:1039–1071
9. Gobel W, Helmchen F (2007) In vivo calcium imaging of neural network function. Physiology (Bethesda) 22:358–365
10. O'Donovan MJ, Ho S, Sholomenko G, Yee W (1993) Real-time imaging of neurons retrogradely and anterogradely labelled with calcium-sensitive dyes. J Neurosci Methods 46:91–106
11. Stosiek C, Garaschuk O, Holthoff K, Konnerth A (2003) In vivo two-photon calcium imaging of neuronal networks. Proc Natl Acad Sci U S A 100:7319–7324
12. Tsien RY (1981) A non-disruptive technique for loading calcium buffers and indicators into cells. Nature 290:527–528
13. Park HC, Kim CH, Bae YK, Yeo SY, Kim SH, Hong SK, Shin J, Yoo KW, Hibi M, Hirano T, Miki N, Chitnis AB, Huh TL (2000) Analysis of upstream elements in the HuC promoter leads to the establishment of transgenic zebrafish with fluorescent neurons. Dev Biol 227:279–293
14. Ahrens MB, Li JM, Orger MB, Robson DN, Schier AF, Engert F, Portugues R (2012) Brain-wide neuronal dynamics during motor adaptation in zebrafish. Nature 485:471–477

15. Fetcho JR, O'Malley DM (1995) Visualization of active neural circuitry in the spinal cord of intact zebrafish. J Neurophysiol 73:399–406
16. Gahtan E, Sankrithi N, Campos JB, O'Malley DM (2002) Evidence for a widespread brain stem escape network in larval zebrafish. J Neurophysiol 87:608–614
17. Sharma D, Kinsey WH (2008) Regionalized calcium signaling in zebrafish fertilization. Int J Dev Biol 52:561–570
18. Reinhard E, Yokoe H, Niebling KR, Allbritton NL, Kuhn MA, Meyer T (1995) Localized calcium signals in early zebrafish development. Dev Biol 170:50–61
19. Creton R, Speksnijder JE, Jaffe LF (1998) Patterns of free calcium in zebrafish embryos. J Cell Sci 111(Pt 12):1613–1622
20. Sharma D, Kinsey WH (2013) PYK2: a calcium-sensitive protein tyrosine kinase activated in response to fertilization of the zebrafish oocyte. Dev Biol 373:130–140
21. Bonneau B, Nougarede A, Prudent J, Popgeorgiev N, Peyrieras N, Rimokh R, Gillet G (2014) The Bcl-2 homolog Nrz inhibits binding of IP3 to its receptor to control calcium signaling during zebrafish epiboly. Sci Signal 7:ra14
22. Kreiling JA, Balantac ZL, Crawford AR, Ren Y, Toure J, Zchut S, Kochilas L, Creton R (2008) Suppression of the endoplasmic reticulum calcium pump during zebrafish gastrulation affects left-right asymmetry of the heart and brain. Mech Dev 125:396–410
23. Hollmann V, Lucks V, Kurtz R, Engelmann J (2015) Adaptation-induced modification of motion selectivity tuning in visual tectal neurons of adult zebrafish. J Neurophysiol 114:2893–2902
24. Brustein E, Marandi N, Kovalchuk Y, Drapeau P, Konnerth A (2003) "In vivo" monitoring of neuronal network activity in zebrafish by two-photon Ca^{2+} imaging. Pflugers Arch 446:766–773
25. Niell CM, Smith SJ (2005) Functional imaging reveals rapid development of visual response properties in the zebrafish tectum. Neuron 45:941–951
26. Bovo E, Dvornikov AV, Mazurek SR, de Tombe PP, Zima AV (2013) Mechanisms of Ca(2)+ handling in zebrafish ventricular myocytes. Pflugers Arch 465:1775–1784
27. Paavola J, Schliffke S, Rossetti S, Kuo IY, Yuan S, Sun Z, Harris PC, Torres VE, Ehrlich BE (2013) Polycystin-2 mutations lead to impaired calcium cycling in the heart and predispose to dilated cardiomyopathy. J Mol Cell Cardiol 58:199–208
28. Samson SC, Ferrer T, Jou CJ, Sachse FB, Shankaran SS, Shaw RM, Chi NC, Tristani-Firouzi M, Yost HJ (2013) 3-OST-7 regulates BMP-dependent cardiac contraction. PLoS Biol 11:e1001727
29. Robin G, Allard B (2015) Voltage-gated Ca^{2+} influx through L-type channels contributes to sarcoplasmic reticulum Ca^{2+} loading in skeletal muscle. J Physiol 593:4781–4797
30. Yaksi E, Judkewitz B, Friedrich RW (2007) Topological reorganization of odor representations in the olfactory bulb. PLoS Biol 5:e178
31. Shimomura O, Johnson FH, Saiga Y (1962) Extraction, purification and properties of aequorin, a bioluminescent protein from the luminous hydromedusan, Aequorea. J Cell Comp Physiol 59:223–239
32. Chiesa A, Rapizzi E, Tosello V, Pinton P, de Virgilio M, Fogarty KE, Rizzuto R (2001) Recombinant aequorin and green fluorescent protein as valuable tools in the study of cell signalling. Biochem J 355:1–12
33. Webb SE, Miller AL (2000) Calcium signalling during zebrafish embryonic development. BioEssays 22:113–123
34. Cheung CY, Webb SE, Meng A, Miller AL (2006) Transient expression of apoaequorin in zebrafish embryos: extending the ability to image calcium transients during later stages of development. Int J Dev Biol 50:561–569
35. Baubet V, Le Mouellic H, Campbell AK, Lucas-Meunier E, Fossier P, Brulet P (2000) Chimeric green fluorescent protein-aequorin as bioluminescent Ca^{2+} reporters at the single-cell level. Proc Natl Acad Sci U S A 97:7260–7265
36. Ashworth R, Brennan C (2005) Use of transgenic zebrafish reporter lines to study calcium signalling in development. Brief Funct Genomic Proteomic 4:186–193

37. Naumann EA, Kampff AR, Prober DA, Schier AF, Engert F (2010) Monitoring neural activity with bioluminescence during natural behavior. Nat Neurosci 13:513–520
38. Knafo S, Prendergast A, Thouvenin O, Figueiredo SN, Wyart C (2017) Bioluminescence monitoring of neuronal activity in freely moving Zebrafish larvae. Bio Protoc 7:e2550
39. Bakayan A, Domingo B, Miyawaki A, Llopis J (2015) Imaging Ca^{2+} activity in mammalian cells and zebrafish with a novel red-emitting aequorin variant. Pflugers Arch 467:2031–2042
40. Pologruto TA, Yasuda R, Svoboda K (2004) Monitoring neural activity and [Ca^{2+}] with genetically encoded Ca^{2+} indicators. J Neurosci 24:9572–9579
41. Miyawaki A, Llopis J, Heim R, McCaffery JM, Adams JA, Ikura M, Tsien RY (1997) Fluorescent indicators for Ca^{2+} based on green fluorescent proteins and calmodulin. Nature 388:882–887
42. Tsuruwaka Y, Konishi T, Miyawaki A, Takagi M (2007) Real-time monitoring of dynamic intracellular Ca^{2+} movement during early embryogenesis through expression of yellow cameleon. Zebrafish 4:253–260
43. Mizuno H, Sassa T, Higashijima S, Okamoto H, Miyawaki A (2013) Transgenic zebrafish for ratiometric imaging of cytosolic and mitochondrial Ca^{2+} response in teleost embryo. Cell Calcium 54:236–245
44. Higashijima S, Masino MA, Mandel G, Fetcho JR (2003) Imaging neuronal activity during zebrafish behavior with a genetically encoded calcium indicator. J Neurophysiol 90:3986–3997
45. Tsuruwaka Y, Shimada E, Tsutsui K, Ogawa T (2017) Ca^{2+} dynamics in zebrafish morphogenesis. PeerJ 5:e2894
46. Nakai J, Ohkura M, Imoto K (2001) A high signal-to-noise Ca^{2+} probe composed of a single green fluorescent protein. Nat Biotechnol 19:137–141
47. Muto A, Ohkura M, Kotani T, Higashijima S, Nakai J, Kawakami K (2011) Genetic visualization with an improved GCaMP calcium indicator reveals spatiotemporal activation of the spinal motor neurons in zebrafish. Proc Natl Acad Sci U S A 108:5425–5430
48. Zhang RW, Li XQ, Kawakami K, Du JL (2016) Stereotyped initiation of retinal waves by bipolar cells via presynaptic NMDA autoreceptors. Nat Commun 7:12650
49. Lacoste AM, Schoppik D, Robson DN, Haesemeyer M, Portugues R, Li JM, Randlett O, Wee CL, Engert F, Schier AF (2015) A convergent and essential interneuron pathway for Mauthner-cell-mediated escapes. Curr Biol 25:1526–1534
50. Riley E, Kopotiyenko K, Zhdanova I (2015) Prenatal and acute cocaine exposure affects neural responses and habituation to visual stimuli. Front Neural Circuits 9:41
51. Dreosti E, Odermatt B, Dorostkar MM, Lagnado L (2009) A genetically encoded reporter of synaptic activity in vivo. Nat Methods 6:883–889
52. Dorostkar MM, Dreosti E, Odermatt B, Lagnado L (2010) Computational processing of optical measurements of neuronal and synaptic activity in networks. J Neurosci Methods 188:141–150
53. Esposti F, Johnston J, Rosa JM, Leung KM, Lagnado L (2013) Olfactory stimulation selectively modulates the OFF pathway in the retina of zebrafish. Neuron 79:97–110
54. Rosa JM, Ruehle S, Ding H, Lagnado L (2016) Crossover Inhibition Generates Sustained Visual Responses in the Inner Retina. Neuron 90:308–319
55. Walker AS, Burrone J, Meyer MP (2013) Functional imaging in the zebrafish retinotectal system using RGECO. Front Neural Circuits 7:34
56. Akerboom J, Carreras Calderon N, Tian L, Wabnig S, Prigge M, Tolo J, Gordus A, Orger MB, Severi KE, Macklin JJ, Patel R, Pulver SR, Wardill TJ, Fischer E, Schuler C, Chen TW, Sarkisyan KS, Marvin JS, Bargmann CI, Kim DS, Kugler S, Lagnado L, Hegemann P, Gottschalk A, Schreiter ER, Looger LL (2013) Genetically encoded calcium indicators for multi-color neural activity imaging and combination with optogenetics. Front Mol Neurosci 6:2
57. Dana H, Mohar B, Sun Y, Narayan S, Gordus A, Hasseman JP, Tsegaye G, Holt GT, Hu A, Walpita D, Patel R, Macklin JJ, Bargmann CI, Ahrens MB, Schreiter ER, Jayaraman V, Looger LL, Svoboda K, Kim DS (2016) Sensitive red protein calcium indicators for imaging neural activity. elife 5:pii: e12727

58. Shen Y, Dana H, Abdelfattah AS, Patel R, Shea J, Molina RS, Rawal B, Rancic V, Chang YF, Wu L, Chen Y, Qian Y, Wiens MD, Hambleton N, Ballanyi K, Hughes TE, Drobizhev M, Kim DS, Koyama M, Schreiter ER, Campbell RE (2018) A genetically encoded Ca^{2+} indicator based on circularly permutated sea anemone red fluorescent protein eqFP578. BMC Biol 16:9
59. Fosque BF, Sun Y, Dana H, Yang CT, Ohyama T, Tadross MR, Patel R, Zlatic M, Kim DS, Ahrens MB, Jayaraman V, Looger LL, Schreiter ER (2015) Neural circuits. Labeling of active neural circuits in vivo with designed calcium integrators. Science 347:755–760
60. Meng CL, Chang DC (1994) Study of calcium signaling in cell cleavage using confocal microscopy. Biol Bull 187:234–235
61. Kimmel CB, Ballard WW, Kimmel SR, Ullmann B, Schilling TF (1995) Stages of embryonic development of the zebrafish. Dev Dyn 203:253–310
62. Webb SE, Miller AL (2003) Imaging intercellular calcium waves during late epiboly in intact zebrafish embryos. Zygote 11:175–182
63. Webb SE, Fluck RA, Miller AL (2011) Calcium signaling during the early development of medaka and zebrafish. Biochimie 93:2112–2125
64. Gilland E, Miller AL, Karplus E, Baker R, Webb SE (1999) Imaging of multicellular large-scale rhythmic calcium waves during zebrafish gastrulation. Proc Natl Acad Sci U S A 96:157–161
65. Lee KW, Webb SE, Miller AL (1999) A wave of free cytosolic calcium traverses zebrafish eggs on activation. Dev Biol 214:168–180
66. Eno C, Gomez T, Slusarski DC, Pelegri F (2018) Slow calcium waves mediate furrow microtubule reorganization and germ plasm compaction in the early zebrafish embryo. Development 145:dev156604
67. Wu SY, Shin J, Sepich DS, Solnica-Krezel L (2012) Chemokine GPCR signaling inhibits beta-catenin during zebrafish axis formation. PLoS Biol 10:e1001403
68. Chen J, Xia L, Bruchas MR, Solnica-Krezel L (2017) Imaging early embryonic calcium activity with GCaMP6s transgenic zebrafish. Dev Biol 430:385–396
69. Chang DC, Meng C (1995) A localized elevation of cytosolic free calcium is associated with cytokinesis in the zebrafish embryo. J Cell Biol 131:1539–1545
70. Chang DC, Lu P (2000) Multiple types of calcium signals are associated with cell division in zebrafish embryo. Microsc Res Tech 49:111–122
71. Webb SE, Lee KW, Karplus E, Miller AL (1997) Localized calcium transients accompany furrow positioning, propagation, and deepening during the early cleavage period of zebrafish embryos. Dev Biol 192:78–92
72. Leung CF, Webb SE, Miller AL (1998) Calcium transients accompany ooplasmic segregation in zebrafish embryos. Develop Growth Differ 40:313–326
73. Webb SE, Li WM, Miller AL (2008) Calcium signalling during the cleavage period of zebrafish development. Philos Trans R Soc Lond Ser B Biol Sci 363:1363–1369
74. Yuen MY, Webb SE, Chan CM, Thisse B, Thisse C, Miller AL (2013) Characterization of Ca^{2+} signaling in the external yolk syncytial layer during the late blastula and early gastrula periods of zebrafish development. Biochim Biophys Acta 1833:1641–1656
75. Schneider I, Houston DW, Rebagliati MR, Slusarski DC (2008) Calcium fluxes in dorsal forerunner cells antagonize beta-catenin and alter left-right patterning. Development 135:75–84
76. Yuan S, Zhao L, Brueckner M, Sun Z (2015) Intraciliary calcium oscillations initiate vertebrate left-right asymmetry. Curr Biol 25:556–567
77. White RM, Sessa A, Burke C, Bowman T, LeBlanc J, Ceol C, Bourque C, Dovey M, Goessling W, Burns CE, Zon LI (2008) Transparent adult zebrafish as a tool for in vivo transplantation analysis. Cell Stem Cell 2:183–189
78. Antinucci P, Hindges R (2016) A crystal-clear zebrafish for in vivo imaging. Sci Rep 6:29490
79. O'Malley DM, Kao YH, Fetcho JR (1996) Imaging the functional organization of zebrafish hindbrain segments during escape behaviors. Neuron 17:1145–1155

80. Liu KS, Fetcho JR (1999) Laser ablations reveal functional relationships of segmental hindbrain neurons in zebrafish. Neuron 23:325–335
81. Granato M, van Eeden FJ, Schach U, Trowe T, Brand M, Furutani-Seiki M, Haffter P, Hammerschmidt M, Heisenberg CP, Jiang YJ, Kane DA, Kelsh RN, Mullins MC, Odenthal J, Nusslein-Volhard C (1996) Genes controlling and mediating locomotion behavior of the zebrafish embryo and larva. Development 123:399–413
82. Yamanaka I, Miki M, Asakawa K, Kawakami K, Oda Y, Hirata H (2013) Glycinergic transmission and postsynaptic activation of CaMKII are required for glycine receptor clustering in vivo. Genes Cells 18:211–224
83. Marsden KC, Granato M (2015) In vivo Ca^{2+} imaging reveals that decreased dendritic excitability drives startle habituation. Cell Rep 13:1733–1740
84. Marsden KC, Jain RA, Wolman MA, Echeverry FA, Nelson JC, Hayer KE, Miltenberg B, Pereda AE, Granato M (2018) A Cyfip2-dependent excitatory interneuron pathway establishes the innate startle threshold. Cell Rep 23:878–887
85. Takahashi M, Narushima M, Oda Y (2002) In vivo imaging of functional inhibitory networks on the mauthner cell of larval zebrafish. J Neurosci 22:3929–3938
86. O'Malley DM, Sankrithi NS, Borla MA, Parker S, Banden S, Gahtan E, Detrich HW 3rd (2004) Optical physiology and locomotor behaviors of wild-type and nacre zebrafish. Methods Cell Biol 76:261–284
87. Sankrithi NS, O'Malley DM (2010) Activation of a multisensory, multifunctional nucleus in the zebrafish midbrain during diverse locomotor behaviors. Neuroscience 166:970–993
88. Wang WC, McLean DL (2014) Selective responses to tonic descending commands by temporal summation in a spinal motor pool. Neuron 83:708–721
89. Thiele TR, Donovan JC, Baier H (2014) Descending control of swim posture by a midbrain nucleus in zebrafish. Neuron 83:679–691
90. Warp E, Agarwal G, Wyart C, Friedmann D, Oldfield CS, Conner A, Del Bene F, Arrenberg AB, Baier H, Isacoff EY (2012) Emergence of patterned activity in the developing zebrafish spinal cord. Curr Biol 22:93–102
91. Plazas PV, Nicol X, Spitzer NC (2013) Activity-dependent competition regulates motor neuron axon pathfinding via PlexinA3. Proc Natl Acad Sci U S A 110:1524–1529
92. Sternberg JR, Severi KE, Fidelin K, Gomez J, Ihara H, Alcheikh Y, Hubbard JM, Kawakami K, Suster M, Wyart C (2016) Optimization of a neurotoxin to investigate the contribution of excitatory interneurons to speed modulation in vivo. Curr Biol 26:2319–2328
93. Friedmann D, Hoagland A, Berlin S, Isacoff EY (2015) A spinal opsin controls early neural activity and drives a behavioral light response. Curr Biol 25:69–74
94. Kelu JJ, Webb SE, Galione A, Miller AL (2018) TPC2-mediated Ca^{2+} signaling is required for the establishment of synchronized activity in developing zebrafish primary motor neurons. Dev Biol 438:57–68
95. Menelaou E, VanDunk C, McLean DL (2014) Differences in the morphology of spinal V2a neurons reflect their recruitment order during swimming in larval zebrafish. J Comp Neurol 522:1232–1248
96. Bohm UL, Prendergast A, Djenoune L, Nunes Figueiredo S, Gomez J, Stokes C, Kaiser S, Suster M, Kawakami K, Charpentier M, Concordet JP, Rio JP, Del Bene F, Wyart C (2016) CSF-contacting neurons regulate locomotion by relaying mechanical stimuli to spinal circuits. Nat Commun 7:10866
97. Hubbard JM, Bohm UL, Prendergast A, Tseng PB, Newman M, Stokes C, Wyart C (2016) Intraspinal sensory neurons provide powerful inhibition to motor circuits ensuring postural control during locomotion. Curr Biol 26:2841–2853
98. Knafo S, Fidelin K, Prendergast A, Tseng PB, Parrin A, Dickey C, Bohm UL, Figueiredo SN, Thouvenin O, Pascal-Moussellard H, Wyart C (2017) Mechanosensory neurons control the timing of spinal microcircuit selection during locomotion. elife 6:pii: e25260
99. Odermatt B, Nikolaev A, Lagnado L (2012) Encoding of luminance and contrast by linear and nonlinear synapses in the retina. Neuron 73:758–773

100. Antinucci P, Nikolaou N, Meyer MP, Hindges R (2013) Teneurin-3 specifies morphological and functional connectivity of retinal ganglion cells in the vertebrate visual system. Cell Rep 5:582–592
101. Wei HP, Yao YY, Zhang RW, Zhao XF, Du JL (2012) Activity-induced long-term potentiation of excitatory synapses in developing zebrafish retina in vivo. Neuron 75:479–489
102. Zhao XF, Ellingsen S, Fjose A (2009) Labelling and targeted ablation of specific bipolar cell types in the zebrafish retina. BMC Neurosci 10:107
103. Smyth VA, Di Lorenzo D, Kennedy BN (2008) A novel, evolutionarily conserved enhancer of cone photoreceptor-specific expression. J Biol Chem 283:10881–10891
104. Ma EY, Lewis A, Barabas P, Stearns G, Suzuki S, Krizaj D, Brockerhoff SE (2013) Loss of Pde6 reduces cell body Ca^{2+} transients within photoreceptors. Cell Death Dis 4:e797
105. Fraser SE (1992) Patterning of retinotectal connections in the vertebrate visual system. Curr Opin Neurobiol 2:83–87
106. Nevin LM, Robles E, Baier H, Scott EK (2010) Focusing on optic tectum circuitry through the lens of genetics. BMC Biol 8:126
107. Nikolaou N, Lowe AS, Walker AS, Abbas F, Hunter PR, Thompson ID, Meyer MP (2012) Parametric functional maps of visual inputs to the tectum. Neuron 76:317–324
108. Hunter PR, Lowe AS, Thompson ID, Meyer MP (2013) Emergent properties of the optic tectum revealed by population analysis of direction and orientation selectivity. J Neurosci 33:13940–13945
109. Gabriel JP, Trivedi CA, Maurer CM, Ryu S, Bollmann JH (2012) Layer-specific targeting of direction-selective neurons in the zebrafish optic tectum. Neuron 76:1147–1160
110. Preuss SJ, Trivedi CA, vom Berg-Maurer CM, Ryu S, Bollmann JH (2014) Classification of object size in retinotectal microcircuits. Curr Biol 24:2376–2385
111. Naumann EA, Fitzgerald JE, Dunn TW, Rihel J, Sompolinsky H, Engert F (2016) From whole-brain data to functional circuit models: the zebrafish optomotor response. Cell 167:947–960.e920
112. Semmelhack JL, Donovan JC, Thiele TR, Kuehn E, Laurell E, Baier H (2014) A dedicated visual pathway for prey detection in larval zebrafish. elife 3:e04878
113. Shepherd GM (1993) Principles of specificity and redundancy underlying the organization of the olfactory system. Microsc Res Tech 24:106–112
114. Mombaerts P (2001) How smell develops. Nat Neurosci 4(Suppl):1192–1198
115. Shipley MT, Ennis M (1996) Functional organization of olfactory system. J Neurobiol 30:123–176
116. Blumhagen F, Zhu P, Shum J, Scharer YP, Yaksi E, Deisseroth K, Friedrich RW (2011) Neuronal filtering of multiplexed odour representations. Nature 479:493–498
117. Friedrich RW, Laurent G (2001) Dynamic optimization of odor representations by slow temporal patterning of mitral cell activity. Science 291:889–894
118. Yaksi E, von Saint Paul F, Niessing J, Bundschuh ST, Friedrich RW (2009) Transformation of odor representations in target areas of the olfactory bulb. Nat Neurosci 12:474–482
119. Friedrich RW, Korsching SI (1997) Combinatorial and chemotopic odorant coding in the zebrafish olfactory bulb visualized by optical imaging. Neuron 18:737–752
120. Bundschuh ST, Zhu P, Scharer YP, Friedrich RW (2012) Dopaminergic modulation of mitral cells and odor responses in the zebrafish olfactory bulb. J Neurosci 32:6830–6840
121. Scharer YP, Shum J, Moressis A, Friedrich RW (2012) Dopaminergic modulation of synaptic transmission and neuronal activity patterns in the zebrafish homolog of olfactory cortex. Front Neural Circuits 6:76
122. Jacobson GA, Rupprecht P, Friedrich RW (2018) Experience-dependent plasticity of odor representations in the telencephalon of zebrafish. Curr Biol 28:1–14.e13
123. Zhu P, Frank T, Friedrich RW (2013) Equalization of odor representations by a network of electrically coupled inhibitory interneurons. Nat Neurosci 16:1678–1686
124. Yabuki Y, Koide T, Miyasaka N, Wakisaka N, Masuda M, Ohkura M, Nakai J, Tsuge K, Tsuchiya S, Sugimoto Y, Yoshihara Y (2016) Olfactory receptor for prostaglandin F2alpha mediates male fish courtship behavior. Nat Neurosci 19:897–904

125. Wakisaka N, Miyasaka N, Koide T, Masuda M, Hiraki-Kajiyama T, Yoshihara Y (2017) An adenosine receptor for olfaction in fish. Curr Biol 27:1437–1447.e1434
126. Jetti SK, Vendrell-Llopis N, Yaksi E (2014) Spontaneous activity governs olfactory representations in spatially organized habenular microcircuits. Curr Biol 24:434–439
127. Mathuru AS, Kibat C, Cheong WF, Shui G, Wenk MR, Friedrich RW, Jesuthasan S (2012) Chondroitin fragments are odorants that trigger fear behavior in fish. Curr Biol 22:538–544
128. Hinz C, Namekawa I, Behrmann-Godel J, Oppelt C, Jaeschke A, Muller A, Friedrich RW, Gerlach G (2013) Olfactory imprinting is triggered by MHC peptide ligands. Sci Rep 3:2800
129. DeMaria S, Berke AP, Van Name E, Heravian A, Ferreira T, Ngai J (2013) Role of a ubiquitously expressed receptor in the vertebrate olfactory system. J Neurosci 33:15235–15247
130. Reiten I, Uslu FE, Fore S, Pelgrims R, Ringers C, Diaz Verdugo C, Hoffman M, Lal P, Kawakami K, Pekkan K, Yaksi E, Jurisch-Yaksi N (2017) Motile-cilia-mediated flow improves sensitivity and temporal resolution of olfactory computations. Curr Biol 27:166–174
131. Quirin S, Vladimirov N, Yang CT, Peterka DS, Yuste R, Ahrens MB (2016) Calcium imaging of neural circuits with extended depth-of-field light-sheet microscopy. Opt Lett 41:855–858
132. Ahrens MB, Orger MB, Robson DN, Li JM, Keller PJ (2013) Whole-brain functional imaging at cellular resolution using light-sheet microscopy. Nat Methods 10:413–420
133. Yang Z, Mei L, Xia F, Luo Q, Fu L, Gong H (2015) Dual-slit confocal light sheet microscopy for in vivo whole-brain imaging of zebrafish. Biomed Opt Express 6:1797–1811
134. Tomer R, Lovett-Barron M, Kauvar I, Andalman A, Burns VM, Sankaran S, Grosenick L, Broxton M, Yang S, Deisseroth K (2015) SPED light sheet microscopy: fast mapping of biological system structure and function. Cell 163:1796–1806
135. Dunn TW, Mu Y, Narayan S, Randlett O, Naumann EA, Yang CT, Schier AF, Freeman J, Engert F, Ahrens MB (2016) Brain-wide mapping of neural activity controlling zebrafish exploratory locomotion. elife 5:e12741
136. Vladimirov N, Mu Y, Kawashima T, Bennett DV, Yang CT, Looger LL, Keller PJ, Freeman J, Ahrens MB (2014) Light-sheet functional imaging in fictively behaving zebrafish. Nat Methods 11:883–884
137. Portugues R, Feierstein CE, Engert F, Orger MB (2014) Whole-brain activity maps reveal stereotyped, distributed networks for visuomotor behavior. Neuron 81:1328–1343
138. Winter MJ, Windell D, Metz J, Matthews P, Pinion J, Brown JT, Hetheridge MJ, Ball JS, Owen SF, Redfern WS, Moger J, Randall AD, Tyler CR (2017) 4-dimensional functional profiling in the convulsant-treated larval zebrafish brain. Sci Rep 7:6581
139. Turrini L, Fornetto C, Marchetto G, Mullenbroich MC, Tiso N, Vettori A, Resta F, Masi A, Mannaioni G, Pavone FS, Vanzi F (2017) Optical mapping of neuronal activity during seizures in zebrafish. Sci Rep 7:3025
140. Vanwalleghem G, Heap LA, Scott EK (2017) A profile of auditory-responsive neurons in the larval zebrafish brain. J Comp Neurol 525:3031–3043
141. Kim DH, Kim J, Marques JC, Grama A, Hildebrand DGC, Gu W, Li JM, Robson DN (2017) Pan-neuronal calcium imaging with cellular resolution in freely swimming zebrafish. Nat Methods 14:1107–1114
142. Cong L, Wang Z, Chai Y, Hang W, Shang C, Yang W, Bai L, Du J, Wang K, Wen Q (2017) Rapid whole brain imaging of neural activity in freely behaving larval zebrafish (Danio rerio). elife 6:pii: e28158
143. Muto A, Kawakami K (2016) Calcium imaging of neuronal activity in free-swimming larval zebrafish. Methods Mol Biol 1451:333–341
144. Muto A, Lal P, Ailani D, Abe G, Itoh M, Kawakami K (2017) Activation of the hypothalamic feeding centre upon visual prey detection. Nat Commun 8:15029
145. Stephenson DG, Lamb GD, Stephenson GM (1998) Events of the excitation-contraction-relaxation (E-C-R) cycle in fast- and slow-twitch mammalian muscle fibres relevant to muscle fatigue. Acta Physiol Scand 162:229–245
146. Wen H, Brehm P (2005) Paired motor neuron-muscle recordings in zebrafish test the receptor blockade model for shaping synaptic current. J Neurosci 25:8104–8111

147. Lin CY, Chen JS, Loo MR, Hsiao CC, Chang WY, Tsai HJ (2013) MicroRNA-3906 regulates fast muscle differentiation through modulating the target gene homer-1b in zebrafish embryos. PLoS One 8:e70187
148. Klatt Shaw D, Gunther D, Jurynec MJ, Chagovetz AA, Ritchie E, Grunwald DJ (2018) Intracellular calcium mobilization is required for sonic hedgehog signaling. Dev Cell 45:512–525.e515
149. Perni S, Marsden KC, Escobar M, Hollingworth S, Baylor SM, Franzini-Armstrong C (2015) Structural and functional properties of ryanodine receptor type 3 in zebrafish tail muscle. J Gen Physiol 145:173–184
150. Kelu JJ, Webb SE, Parrington J, Galione A, Miller AL (2017) Ca^{2+} release via two-pore channel type 2 (TPC2) is required for slow muscle cell myofibrillogenesis and myotomal patterning in intact zebrafish embryos. Dev Biol 425:109–129
151. Xiyuan Z, Fink RHA, Mosqueira M (2017) NO-sGC pathway modulates Ca^{2+} release and muscle contraction in zebrafish skeletal muscle. Front Physiol 8:607
152. Linsley JW, Hsu IU, Groom L, Yarotskyy V, Lavorato M, Horstick EJ, Linsley D, Wang W, Franzini-Armstrong C, Dirksen RT, Kuwada JY (2017) Congenital myopathy results from misregulation of a muscle Ca^{2+} channel by mutant Stac3. Proc Natl Acad Sci U S A 114:E228–E236
153. Horstick EJ, Linsley JW, Dowling JJ, Hauser MA, McDonald KK, Ashley-Koch A, Saint-Amant L, Satish A, Cui WW, Zhou W, Sprague SM, Stamm DS, Powell CM, Speer MC, Franzini-Armstrong C, Hirata H, Kuwada JY (2013) Stac3 is a component of the excitation-contraction coupling machinery and mutated in Native American myopathy. Nat Commun 4:1952
154. Smith LL, Gupta VA, Beggs AH (2014) Bridging integrator 1 (Bin1) deficiency in zebrafish results in centronuclear myopathy. Hum Mol Genet 23:3566–3578
155. Gibbs EM, Davidson AE, Telfer WR, Feldman EL, Dowling JJ (2014) The myopathy-causing mutation DNM2-S619L leads to defective tubulation in vitro and in developing zebrafish. Dis Model Mech 7:157–161
156. Jackson HE, Ono Y, Wang X, Elworthy S, Cunliffe VT, Ingham PW (2015) The role of Sox6 in zebrafish muscle fiber type specification. Skelet Muscle 5:2
157. Shahid M, Takamiya M, Stegmaier J, Middel V, Gradl M, Kluver N, Mikut R, Dickmeis T, Scholz S, Rastegar S, Yang L, Strahle U (2016) Zebrafish biosensor for toxicant induced muscle hyperactivity. Sci Rep 6:23768
158. Gore AV, Monzo K, Cha YR, Pan W, Weinstein BM (2012) Vascular development in the zebrafish. Cold Spring Harb Perspect Med 2:a006684
159. Bakkers J (2011) Zebrafish as a model to study cardiac development and human cardiac disease. Cardiovasc Res 91:279–288
160. Chi NC, Shaw RM, Jungblut B, Huisken J, Ferrer T, Arnaout R, Scott I, Beis D, Xiao T, Baier H, Jan LY, Tristani-Firouzi M, Stainier DY (2008) Genetic and physiologic dissection of the vertebrate cardiac conduction system. PLoS Biol 6:e109
161. Weber M, Scherf N, Meyer AM, Panakova D, Kohl P, Huisken J (2017) Cell-accurate optical mapping across the entire developing heart. elife 6:pii: e28307
162. Fukuda R, Gunawan F, Beisaw A, Jimenez-Amilburu V, Maischein HM, Kostin S, Kawakami K, Stainier DY (2017) Proteolysis regulates cardiomyocyte maturation and tissue integration. Nat Commun 8:14495
163. Liu J, Bressan M, Hassel D, Huisken J, Staudt D, Kikuchi K, Poss KD, Mikawa T, Stainier DY (2010) A dual role for ErbB2 signaling in cardiac trabeculation. Development 137:3867–3875
164. Shimizu H, Schredelseker J, Huang J, Lu K, Naghdi S, Lu F, Franklin S, Fiji HD, Wang K, Zhu H, Tian C, Lin B, Nakano H, Ehrlich A, Nakai J, Stieg AZ, Gimzewski JK, Nakano A, Goldhaber JI, Vondriska TM, Hajnoczky G, Kwon O, Chen JN (2015) Mitochondrial Ca^{2+} uptake by the voltage-dependent anion channel 2 regulates cardiac rhythmicity. elife 4:pii: e04801

165. Hong TT, Smyth JW, Chu KY, Vogan JM, Fong TS, Jensen BC, Fang K, Halushka MK, Russell SD, Colecraft H, Hoopes CW, Ocorr K, Chi NC, Shaw RM (2012) BIN1 is reduced and Cav1.2 trafficking is impaired in human failing cardiomyocytes. Heart Rhythm 9:812–820
166. Kirchmaier BC, Poon KL, Schwerte T, Huisken J, Winkler C, Jungblut B, Stainier DY, Brand T (2012) The Popeye domain containing 2 (popdc2) gene in zebrafish is required for heart and skeletal muscle development. Dev Biol 363:438–450
167. Ramspacher C, Steed E, Boselli F, Ferreira R, Faggianelli N, Roth S, Spiegelhalter C, Messaddeq N, Trinh L, Liebling M, Chacko N, Tessadori F, Bakkers J, Laporte J, Hnia K, Vermot J (2015) Developmental alterations in heart biomechanics and skeletal muscle function in desmin mutants suggest an early pathological root for desminopathies. Cell Rep 11:1564–1576
168. Heckel E, Boselli F, Roth S, Krudewig A, Belting HG, Charvin G, Vermot J (2015) Oscillatory flow modulates mechanosensitive klf2a expression through trpv4 and trpp2 during heart valve development. Curr Biol 25:1354–1361
169. Kaufman CK, White RM, Zon L (2009) Chemical genetic screening in the zebrafish embryo. Nat Protoc 4:1422–1432
170. Dunn TW, Gebhardt C, Naumann EA, Riegler C, Ahrens MB, Engert F, Del Bene F (2016) Neural circuits underlying visually evoked escapes in larval zebrafish. Neuron 89:613–628

Chapter 37
Stimulus-Secretion Coupling in Beta-Cells: From Basic to Bedside

Md. Shahidul Islam

Abstract Insulin secretion in humans is usually induced by mixed meals, which upon ingestion, increase the plasma concentration of glucose, fatty acids, amino acids, and incretins like glucagon-like peptide 1. Beta-cells can stay in the off-mode, ready-mode or on-mode; the mode-switching being determined by the open state probability of the ATP-sensitive potassium channels, and the activity of enzymes like glucokinase, and glutamate dehydrogenase. Mitochondrial metabolism is critical for insulin secretion. A sound understanding of the intermediary metabolism, electrophysiology, and cell signaling is essential for comprehension of the entire spectrum of the stimulus-secretion coupling. Depolarization brought about by inhibition of the ATP sensitive potassium channel, together with the inward depolarizing currents through the transient receptor potential (TRP) channels, leads to electrical activities, opening of the voltage-gated calcium channels, and exocytosis of insulin. Calcium- and cAMP-signaling elicited by depolarization, and activation of G-protein-coupled receptors, including the free fatty acid receptors, are intricately connected in the form of networks at different levels. Activation of the glucagon-like peptide 1 receptor augments insulin secretion by amplifying calcium signals by calcium induced calcium release (CICR). In the treatment of type 2 diabetes, use of the sulfonylureas that act on the ATP sensitive potassium channel, damages the beta cells, which eventually fail; these drugs do not improve the cardiovascular outcomes. In contrast, drugs acting through the glucagon-like peptide-1 receptor protect the beta-cells, and improve cardiovascular outcomes. The use of the glucagon-like peptide 1 receptor agonists is increasing and that of sulfonylurea is decreasing. A better understanding of the stimulus-secretion coupling may lead to the discovery of other molecular targets for development of drugs for the prevention and treatment of type 2 diabetes.

M. S. Islam (✉)
Department of Clinical Science and Education, Södersjukhuset, Karolinska Institutet, Stockholm, Sweden

Department of Emergency Care and Internal Medicine, Uppsala University Hospital, Uppsala, Sweden
e-mail: Shahidul.islam@ki.se

M. S. Islam (ed.), *Calcium Signaling*, Advances in Experimental Medicine and Biology 1131, https://doi.org/10.1007/978-3-030-12457-1_37

Keywords Insulin secretion · Beta-cells · Glucokinase · Glutamate dehydrogenase · Glucagon-like peptide-1 · Calcium induced calcium release · ATP-sensitive potassium channel · Stimulus-secretion coupling · Islets of Langerhans · Voltage-gated calcium channels and insulin secretion · Transient receptor potential channels and insulin secretion · Mitochondria and insulin secretion · Type 2 diabetes

Abbreviations

$[Ca^{2+}]_c$	Cytoplasmic free Ca^{2+} concentration
EPAC	Exchange protein directly activated by cAMP
K_{ATP}	ATP-sensitive potassium channel
NBD	Nucleotide binding domain
PKA	Protein kinase A
SCHAD	short chain 3-hydroxyacyl-CoA dehydrogenase
SUR1	Sulfonylurea receptor 1
VGCC	Voltage-gated Ca^{2+} channel

37.1 Introduction

The β-cells of the islets of Langerhans sense primarily the changes in the concentration of glucose in the plasma, and respond promptly and precisely by changing the rate of secretion of insulin to maintain the concentration of glucose within the physiologic range. They act as fuel sensors by virtue of possessing the glucose sensor glucokinase, and the ATP sensor, the ATP-sensitive potassium (K_{ATP}) channel. These cells are rendered "glucose-competent" by the incretin hormone glucagon-like peptide-1 (GLP-1) [1]. Strictly speaking, the physiological stimulus for insulin secretion is food, which is taken in the form of mixed meals, and which increases the concentration of not only glucose, but also of other nutrients, including the 20 amino acids, and many fatty acids, in the plasma. Foods increase not only the plasma concentrations of the nutrients, but also of several gut-derived peptides including GLP-1, and gastric inhibitory polypeptide (GIP). In their native environment in the normal human body, the β-cells do not have any resting state; they secrete insulin, albeit at low rates, even during the fasting state [2]. The concentration of glucose in the plasma must be maintained above a certain level to prevent hypoglycemia, which is life threatening. For this reason, insulin secretion is tightly coupled to the concentration of glucose. These cells switch between three overlapping modes of secretion: the "off-mode", the "ready-mode", and the "on-mode" [3]. At the molecular level, the open state probability of the ATP-sensitive potassium (K_{ATP}) channel partly determines the switching between the three modes.

In normal β-cells, when the concentration of glucose in the plasma plunges into the hypoglycemic range, the open state probability of the K_{ATP} channel increases, switching the cells rapidly to the off-mode, and shutting off the insulin secretion. Concentration of glucose in the hypoglycemic range minimizes metabolism of glucose because the enzyme glucokinase that phosphorylates glucose in the first step of the glycolytic pathway has high K_m for glucose. This reduces the concentration of ATP, and increases the concentration of MgADP in the cytoplasm, leading to an increase in the open state probability of K_{ATP} channel, hyperpolarization of membrane potential, closure of the voltage-gated Ca^{2+} channels (VGCC), reduction of the cytoplasmic free Ca^{2+} concentration ($[Ca^{2+}]_c$) to the resting level, and cessation of insulin secretion. In this scenario, the K_{ATP} channel acts as an emergency safety device for rapidly shutting off insulin secretion. If the K_{ATP} channel is absent, or if the channel do not open normally due to some mutations, then the channel does not open even when the glucose concentration reaches the hypoglycemic range. Inactivating mutations of K_{ATP} channel genes permanently switch the β-cells to the ready-mode or the on-mode. The *KCNJ11* gene encodes the pore forming $K_{ir}6.2$ subunit of the K_{ATP} channel. Activating mutations in the *KCNJ11* gene switches the β-cells to the off-mode [4]. When the β-cells are in the off-mode due to mutations in the K_{ATP} channel genes, glucose and GLP-1 cannot stimulate insulin secretion, and the result is permanent neonatal diabetes mellitus. In normal subjects, during the fasting condition, when the plasma glucose concentration is ∼5.5 mmol/L, the β-cells are in the ready-mode.

37.2 Calcium Signaling in the β-Cells

Glucose enters the β-cells through glucose transporter 2 following the concentration gradient, and it is phosphorylated by glucokinase. Further metabolism through the glycolytic pathway, and the mitochondrial metabolism increases the concentration of ATP, and reduces the concentration of ADP, both of which remain partly in the free forms, and partly in the magnesium bound forms. The binding of these different forms of the nucleotides to the sulfonylurea receptor 1 (SUR1) and $K_{ir}6.2$ subunits of the K_{ATP} channel determines the open state probability of the channel.

Critical events in the stimulus-secretion coupling in the β-cells are membrane depolarization, increase of $[Ca^{2+}]_c$, and increase of cAMP. Membrane depolarization occurs due to the reduction in the open state probability of the K_{ATP} channel, and activation of inward depolarizing currents mediated by several ion channels, including some transient receptor potential (TRP) channels [3, 5]. When the membrane potential reaches the respective thresholds for the activation of the VGCCs, the channels open, and Ca^{2+} enters into the cytoplasm. Ca^{2+} entering through the VGCCs triggers further Ca^{2+} release from the endoplasmic reticulum (ER) Ca^{2+} stores, a process called Ca^{2+}-induced Ca^{2+}-release (CICR) [6]. Stimulations of the β-cells by nutrients and agonists that induce insulin secretion increase the $[Ca^{2+}]_c$, often in the form of oscillations, and an increase in the $[Ca^{2+}]_c$ in the β-cells in

response to different stimuli is seen as a sign of β-cell activation [7–10]. Activation of the phospholipase-C-linked G-protein coupled receptors by agonists like the neurotransmitter acetylcholine increases $[Ca^{2+}]_c$ by releasing Ca^{2+} from the ER through activation of the inositol 1,4,5 trisphosphate receptors [11]. GLP-1 activates the GLP-1 receptor leading to the increases of cAMP, which has pleiotropic effects that enhance insulin secretion [12]. Cross talks between Ca^{2+}- and cAMP-signaling occurs at multiple levels, and it is nearly impossible to dissect between pure Ca^{2+} signaling, and pure cAMP signaling.

37.3 Hexokinases

Insulin secretion is "supply driven". Glucokinase (hexokinase 4), one of the four members of the hexokinase family of enzymes, is the primary glucose sensor. It phosphorylates glucose to glucose-6 phosphate. The affinity of glucokinase for glucose is low, compared to that of other hexokinases. The half saturation (the concentration of glucose at which the enzyme is half saturated, $S_{0.5}$) is about 8 mmol/L. The low affinity of glucokinase for glucose ensures that the concentration of glucose in the plasma is kept within the physiologic range.

Glucokinase is the only hexokinase expressed in the adult β-cells. In the neonatal period hexokinase 1 is also expressed in the β-cells, but its expression is down-regulated after birth. Some mutations in the non-coding region of HK1 can impair the process of normal suppression of HK1 expression [13]. Persistent expression of HK1 after birth leads to congenital hyperinsulinism in neonates and infants [14]. These subjects develop hypoglycemia during prolonged fasting. Some human insulinoma cells express hexokinase-1, which can explain excessive insulin secretion even during hypoglycemia [15]. Some of these patients can be treated by diazoxide for variable length of time, but those who have severe hypoglycemia, and those who do not respond to diazoxide, need near total pancreratectomy.

Activating mutations of glucokinase shifts the glucose-dependency curve to the left, reduces glucose $S_{0.5,}$ and increases the activity index of the enzyme. People who have activating mutations of glucokinase have hyperinsulinism, and variable degrees of hypoglycemia, ranging from severe hypoglycemia during neonatal period to milder hypoglycemia later in life. In vitro experiments with islets isolated from mice that express an activating mutation (A456V) of glucokinase show that the threshold for glucose stimulated insulin secretion is shifted to the left [16]. Hypoglycemia in some of these subjects can be treated by diazoxide that binds to the SUR1 subunit of the K_{ATP} channel, and increases the open state probability of the channel. Some subjects do not respond to diazoxide and may need the somatostatin analogs for reducing insulin secretion, and others may need near-total pancreatectomy.

Inactivating mutations of glucokinase increase the $S_{0.5}$ of the enzyme for glucose when the mutations are located in the glucose-binding site, and reduces the K_m for ATP when the mutations are located in the ATP-binding site. These mutations decrease the calculated activity index of glucokinase. Heterozygous inactivating

mutations of glucokinase usually cause "maturity onset diabetes of the young type 2" (MODY2). MODY2 subjects have only a mild form of diabetes with mild fasting hyperglycemia (5.5–8 mmol/L), and HbA1C 40–60 mmol/mol. MODY2 subjects do not suffer from the long term complications of diabetes, and treatment is not recommended outside pregnancy [17].

Completely inactive glucokinase due to homozygous or compound heterozygous mutations, which occur rarely, causes permanent neonatal diabetes mellitus (PNDM), requiring lifelong insulin therapy for severe hyperglycemia [18].

37.4 K_{ATP} Channel

The K_{ATP} channel of the β-cells is composed of two proteins, the regulatory sulfonylurea receptor 1 (SUR1) encoded by the *ABCC8* gene, and the pore-forming inwardly rectifying (ir) potassium channel $K_{ir}6.2$ (encoded by the *KCNJ11* gene). SUR1 binds the sulfonylurea class of antidiabetic drugs that promote insulin secretion. $K_{ir}6.2$ is an inward-rectifier K^+ channel, (which means that it has a greater tendency to allow K^+ to enter into a cell rather than flow out of a cell. Each K_{ATP} channel consists of eight subunits, four $K_{ir}6.2$ in the center surrounded by four SUR1 in the periphery. *ABCC8* and *KCNJ11* are two adjacent genes located on the short arm (p) of the chromosome 11 at position 15.1 (cytogenetic location 11p15.1). Opening of the K_{ATP} channel polarizes, and closure of the channel depolarizes the membrane potential of β-cells.

ATP potently inhibits the K_{ATP} channel activity by binding to the $K_{ir}6.2$ subunit. This binding and inhibitory action of ATP is independent of Mg^{2+}. On the other hand Mg-nucleotides, including both MgATP and MgADP activate the K_{ATP} channel by binding to the nucleotide binding domain (NBD) of SUR1 subunit. Binding of MgADP to the SUR1 is more efficacious than binding of MgATP to SUR1 in activating the K_{ATP} channel [19]. Sulfonylurea drugs inhibit K_{ATP} channel activity mostly by direct binding to the SUR1, but also by preventing the MgATP binding to the SUR1 and MgATP-mediated activation of the channel. Like MgADP and MgATP, diazoxide also activates K_{ATP} channel by binding to SUR1, although the exact site of diazoxide action is not known.

37.4.1 Inactivating Mutations of K_{ATP} Channel

Some mutations of the two K_{ATP} channel genes inhibit the ability of the channels to open, and other mutations impair the biogenesis or trafficking of the channels to the plasma membrane. These "inactivating" mutations cause persistent depolarization of the membrane, and persistent insulin secretion, despite hypoglycemia. Such β-cells are unable to switch to the off-mode, which normal β-cells would do when there is hypoglycemia. Inactivating mutations of the K_{ATP} channel genes

are the commonest causes of hypoglycemia due to congenital hyperinsulinism. Some mutations impair K_{ATP} channel activity, and the degree of the impairments determines the responsiveness of the mutant K_{ATP} channel to diazoxide [20].

Some of these mutations act in a recessive, and others act in a dominant fashion. Recessive mutations in the *ABCC8* and *KCNJ11* genes impair trafficking of the channels to the plasma membrane causing almost total loss of the channel in all of the β-cells. For this reason, the hyperinsulinism caused by the recessive mutations do not respond to the treatment by diazoxide. On the other hand the dominant mutations allow normal trafficking of the channels to the plasma membrane, but these mutations impair response to MgADP or diazoxide to variable degrees. Hyperinsulinism caused by some of these dominant mutations are diazoxide-responsive, and others are diazoxide-unresponsive [20]. Paradoxically, diazoxide can also stimulate insulin secretions in some of these cases, the mechanism of which remains unknown [14, 21].

There are two histological forms of K_{ATP} hyperinsulinism: the diffuse form, and the focal form. In the diffuse form, all the β-cells in the pancreas are affected. In the focal form, the β-cells of only parts of the pancreas are affected, but the β-cells located outside the affected area of the pancreas are normal. Diffuse form of K_{ATP} hyperinsulinism is due to recessive mutations in the K_{ATP} channel genes, *ABCC8 or KCNJ11*.

The focal form is caused by "two hits". The first is a mono-allelic recessive mutation in the *ABCC8* or *KCNJ11* gene that is paternally transmitted. The second "hit" is loss of heterozygosity due to a somatic loss of maternal 11p15.1 with paternal isodisomy at the same locus, inside the focal lesion in the pancreas [22, 23]. The 11p15.1 region contains not only the K_{ATP} channel genes, but also some imprinted genes including *H19*, *IGF2*, and *CDKN1C*, which are involved in the regulation of cell proliferation [24]. The *CDKN1C* gene encodes cyclin dependent kinase inhibitor 1C, which is a tumor suppressor. Absence of cyclin dependent kinase inhibitor 1C is one of the factors that probably contributes to the development of the β-cell hyperplasia in the focal form of the K_{ATP} hyperinsulinism [24]. In the focal form of K_{ATP}-hyperinsulinism, there is not only complete loss of K_{ATP}-channel function, but also formation of β-cell "tumors" [24]. The β-cells in the "unaffected" part of the pancreas, in the focal form of $_{KAP}$ hyperinsulinism have only mono-allelic recessive mutation of the K_{ATP} channel genes, but no loss of maternal 11p15.1. As expected, these β-cells function normally [25].

It is important to identify people who have the focal form of the disease, because this form can be completely cured by selective surgical resection of the pathologic area of the pancreas. The diffuse form, if they are not responsive to medical treatments, requires 95–98% pancreatectomy. Genetic analysis is useful in identifying the diffuse forms and the focal forms of K_{ATP} hyperinsulinism. If there are two recessive mutations in the K_{ATP} channel genes then the hyperinsulinism is more likely to be caused by the diffuse form. If there is only one heterozygous recessive mutation in either *ABCC8* or *KCNJ11* gene, then the hyperinsulinism is highly likely to be due to the focal form of the disease [26]. β-cells selectively incorporate 18-Fluorodihydroxy phenylalanine (18F-DOPA). 18F-DOPA PET scan

is currently the most accurate and specific method for identifying the focal lesions, but the facility is available only in a few advanced centers [27].

Inactivating mutations of the K_{ATP} channels cause inappropriately increased insulin secretion even during the fasting state leading to hypoglycemia. At first sight it may appear that absence of the K_{ATP} channel, or defective opening of these channels leads to persistent depolarization of the membrane-potential of the β-cells, opening of the VGCCs, increase of $[Ca^{2+}]_c$, leading to exocytosis of insulin, but the situation is more complicated than that. These cells secrete insulin even when the concentration of glucose is <5 mmol/L, when glucose metabolism through the high K_m glucokinase is dramatically reduced, suggesting that these cells metabolize glucose through other low K_m hexokinases. In fact, it turns out that in these cells there is a 16-fold increase in the expression of the hexokinase 1 (*HK1*) gene, and marked reduction in the expression of the glucokinase (*GCK*) gene. Expression of other important glycolytic enzymes is also increased in these cells. As a result, there is increased glycolysis, as measured by ^{13}C tracer studies, in these cells [28].

While these β-cells secrete insulin under fasting state, their response to glucose challenge is reduced or abolished [25, 28]. The insulin content of these islets is lower than that of the normal islets. Basal insulin secretion from these islets is higher, but there is little or no increase in insulin secretion upon glucose stimulation [25, 28]. In normal β-cells, glucose stimulates insulin secretion by depolarizing the membrane potential leading to the opening of the VGCCs, and elevating the $[Ca^{2+}]_c$, but in the β-cells where the K_{ATP} channel is absent or inactivated, the membrane potential and the $[Ca^{2+}]_c$ are already elevated under basal conditions leading to high basal insulin secretion [25, 28]. Sulfonylureas that close K_{ATP} channel, increase insulin secretion from normal islets, but fail to do so in the islets from patients with inactivating mutations of K_{ATP} channel [25]. Normal glucose sensing in these cells is impaired because of reduced expression of glucokinase, and increased expression of hexokinase 1, as mentioned before [28]. In these islets, metabolism of glucose is abnormal in many other ways too. For instance, glucose is used for synthesis of the amino acids glycine, serine and glutamine [28]. The expression of 3-phosphoglycerate dehydrogenase (PHGDH), the enzyme important for serine/glycine biosynthesis, is increased 38 fold [28]. Expression of another key enzyme for serine/glycine biosynthesis, phosphoserine aminotransferase is also increased tenfold [28].

While the insulin response of these cells to glucose challenge is reduced, their response to amino acid is increased [29]. These patients develop hypoglycemia after ingesting protein-rich meals. The absence or the closure of the K_{ATP} channel switches the β-cells from off-mode to the ready-mode. When in the ready mode, the cells can be easily switched to the on-mode by many stimuli, including many amino acids. In in vitro experiments, stimulation of islets isolated from patients who have inactivating mutations of the K_{ATP} channel, by a mixture of amino acids, increases insulin secretion, whereas stimulation of the normal islets fails to do so [28]. This may be due to increased amino acid metabolism as a consequence of activation of the enzyme glutamate dehydrogenase (GDH) in the β-ells that have K_{ATP}-channel with inactivating mutations [28, 30].

Inactivation of the K_{ATP} during the development of the β-cells, leads to persistent increase of $[Ca^{2+}]_c$. This induces homeostatic, adaptive or compensatory changes in the components of the Ca^{2+} signaling toolkit, by mechanisms that are not well understood. This phenomenon has been named "Ca^{2+} homeostasome" [31]. Thus, the phenotypes that we see in the inactivating mutations of the K_{ATP} channel, are not primarily the results of the alterations of the function of the $_{KATP}$ channel, rather the net results of global homeostatic reorganization of the cellular signaling network. As a consequence of the chronic inactivation of the K_{ATP} channel, numerous genes are upregulated, and numerous other genes are downregulated, leading to alterations in glucose and amino acid metabolism, to name a few [28].

37.4.2 Activating Mutations of the KATP Channel Genes

Activating mutations of the *KCNJ11* and the *ABCC8* genes increase the open state probability of the K_{ATP} channel. The ability of ATP to inhibit the channel is reduced to a variable extent depending on different mutations. These mutations switch the β-cells to the off-mode. The membrane potential of these β-cells remain hyperpolarized, the VGCCs cannot open, $[Ca^{2+}]_c$ remains low, and insulin secretion is reduced. These mutations account for ~ 50% of neonatal diabetes mellitus, which are commonly treated with insulin in the beginning. Once the genetic diagnosis is established, > 90% of these infants, children and young adults can be treated effectively, and safely by the sulfonylurea class of anti-diabetic drugs, for many years, perhaps for rest of their lives [32]. The doses of sulfonylurea drugs needed for the treatment of these patients are usually high, and vary depending on the severity of the mutations. The sulfonylurea drugs reduce the open state probability of the K_{ATP} channels in these subjects. In this scenario, the sulfonylureas switch the β-cells from the off-mode to the ready-mode, when the insulin secretion can be stimulated further by glucose, and other nutrients, and by glucagon-like peptide 1 (GLP-1) [4].

37.5 Voltage-Gated Potassium Channel

Voltage-gated K^+ (K_v) channels are activated by depolarization; they mediate the repolarizing phase of the action potential, and limit insulin secretion [33]. Activation of GLP-1 receptor can reduce K_v currents, and may thereby extend action potential, leading to increased Ca^{2+} entry through the VGCCs. This may be one of the many mechanisms that contribute to the GLP-1-induced augmentation of insulin secretion.

The pore forming α-subunit of one of the K_v channels, the $K_v7.1$ is encoded by the *KCNQ1* gene, which is expressed both in the human heart, and in the human β-cells [34]. Some mutations in the *KCNQ1* gene cause one particular type of long QT syndrome (LQTS). These subjects have lower plasma glucose concentration, and they have increased insulin response to oral glucose load. They get episodes of

hypoglycemia 3–5 h after meals [34]. As a sequelae of increased insulin secretion and hypoglycemia, these patients also tend to have hypokalemia, which further increases the risk of cardiac arrhythmia, and cardiac death. Variants in the *KCNQ1* gene are also associated with susceptibility to type 2 diabetes [35].

37.6 GLP-1

Oral glucose is more effective than intravenous glucose in stimulating insulin secretion, even when the plasma glucose concentration is maintained at the same level. This is called incretin effect. In healthy persons, 25–75% of insulin release after a glucose load is due to the incretin effect, which is mediated mostly by GLP-1, and gastric inhibitory polypeptide (GIP) [36]. In type 2 diabetes the incretin effect is almost abolished. Two active forms of endogenous GLP-1 are GLP1 (7-36)NH2, and GLP1 [7–37].

GLP-1 is secreted by the L-cells located in the small and large intestine, from duodenum to the colon. There are more L-cells particularly in the ileum. After ingestion of foods the concentration of GLP-1 in the plasma increases rapidly. If the β-cells are in the ready-mode, which is the case when the glucose concentration in the plasma is above the threshold for insulin secretion (∼5 mmol/L), then GLP-1 switches the β-cells to the on-mode. When the glucose concentration in the plasma is <5 mmol/L, the β-cells are not in the ready-mode, and GLP-1 cannot switch the β-cells to the on-mode despite increasing the cAMP concentration in the cell.

GLP-1 binds to the glucagon-like-peptide-1 receptor (GLP-1 receptor), which is expressed at variable levels, in numerous tissues, including the human β-cells, δ-cells and α-cells. Activation of the GLP-1 receptor of human β-cells leads to activation of adenylyl cyclase (not clear which isoform), and increase of cAMP in the cells. cAMP activates protein kinase A (PKA) and EPAC (exchange protein directly activated by cAMP), both of which act on many target proteins, including ion channels, enzymes, and the proteins that mediate exocytosis. Activation of the GLP-1 receptor facilitates inhibition of K_{ATP} channel [37], activation of the transient receptor potential channel subfamily M member 4 (TRPM4) [38, 39], and transient receptor potential channel subfamily M member 2 [40, 41], facilitating membrane depolarization. The effects of GLP-1 on the changes in the $[Ca^{2+}]_c$ is particularly dramatic [42–46]. GLP-1 augments Ca^{2+} signals qualitatively and quantitatively. It increases Ca^{2+} current through the L-type voltage-gated Ca^{2+} channel by a cAMP dependent manner [47–50]. GLP-1, through PKA and EPAC facilitates CICR that amplifies Ca^{2+} signals [43, 51–53] and amplifies insulin secretion.

PKA-mediated phosphorylation of serine-103 of the essential Ca^{2+}-sensor synaptotagmin 7 increases exocytosis of insulin [54]. The precise mechanism is unclear because PKA phosphorylation of the serine-103 does not increase the Ca^{2+}-sensitivity of exocytosis [see figure S3 of Wu et al. [54]].

Excess glucagon contributes to the pathogenesis of type 2 diabetes [55]. While GLP-1 increases insulin secretion, it inhibits glucagon secretion. The expression

of GLP-1 receptor in human α-cells is low, compared to that in the human β-cells and δ-cells [56]. GLP-1 inhibits glucagon secretion from the human α-cells through direct activation of the GLP-1 receptor, formation of cAMP, and activation of the protein kinase A, which leads to phosphorylation and inhibition of the P/Q type of VGCCs of the α-cells [57].

The half-life of GLP-1 in the plasma is only 1–2 min because of its rapid degradation by dipeptidyl peptidase 4 (DPP4), which is ubiquitously expressed. Inhibitors of DPP4 increase the concentration of GLP-1, and the inhibitors are used in the treatment of type 2 diabetes. GLP-1 analogs with long half-life have been developed by substitution of some of the amino acids, and by attaching fatty acids to the molecule. These changes promote self-aggregation, albumin-binding, slow absorption of the injected GLP-1 analog from the subcutaneous injection site, slow degradation, and slow renal elimination. The long half-life of semaglutide, a long-acting GLP-1 analog, means that it is enough to take one injection per week.

A large population-based study showed that GLP-1 secretion is reduced in prediabetes, and screen-detected diabetes, as well as in the obese and overweight individuals, suggesting that reduced secretion of GLP-1 leads to impaired regulation of glucose metabolism and appetite [58]. Other studies suggest that impaired insulin secretion in type 2 diabetes is not due to diminished secretion of GLP-1, but is due to diminished responsiveness of the β-cells to GLP-1 [42, 59, 60].

In addition to enhancing insulin secretion, GLP-1 inhibits, glucagon secretion, promotes satiety, delays gastric emptying, reduces weight, and promotes natriuresis. Antidiabetic drugs that act on the K_{ATP} channel do not reduce, rather they may increase the risk of cardiovascular events, and mortality [61]. On the other hand, some of the GLP-1 receptor agonists e.g. liraglutide, and semaglutide, reduce the risk of cardiovascular events and mortality [62, 63]. For this reason, the use of sulfonylureas in the treatment of type 2 diabetes is decreasing, and that of some GLP-1 analogs is increasing.

37.7 Somatostatin (Also Called Somatotropin Release-Inhibiting Factor, SRIF)

The δ-cells, which resemble small neurons with long slender processes and secretory granule-rich knob-like endings, secrete somatostatin. Somatostatin is also secreted from the pituitary gland, brain and gastrointestinal tract. Two forms of somatostatin, somatostatin 14 and somatostatin 28 are known; somatostatin-14 is the predominant form secreted from the δ-cells. Somatostatin inhibits secretion of many hormones, including insulin and specially glucagon. There are five somatostatin receptors (SST) 1–5 [64], all coupled to the G-proteins $G_{i/o}$. In rodent islets, somatostatin inhibits glucagon secretion by activating the SST2 receptor and inhibits insulin secretion by activating the SST5 receptor [65, 66]. In human islets SST2 is the dominant receptor in both the α-cells and the β-cells, but both cells express also other somatostatin receptors at low level [67, 68]. Selective inhibition of SST5

increases secretion of insulin, and also of GLP-1 [69]. Glucose stimulates secretion of insulin and inhibits secretion of glucagon in an oscillatory fashion, where the glucagon oscillations are anti-parallel to those of insulin and somatostatin [70]. Apparently, each pulse of somatostatin inhibits glucagon secretion by paracrine interactions.

Somatostatin inhibits insulin secretion by hyperpolarizing the membrane potential through activation of the G-protein coupled inwardly rectifying K (GIRK) channel, a process mediated by $G_{\beta\gamma}$. The GIRK channel of the islet cells consists of hetero-multimers of $K_{ir}3.1$, $K_{ir}3.2$, or $K_{ir}3.4$. Somatostatin inhibits the P/Q type VGCC of β-cells through G-protein mediated mechanisms. It activates $G_{i/o}$, which causes inhibition of adenylyl cyclase, and reduced formation of cAMP. In addition to these, somatostatin also inhibits exocytosis by mechanisms that are not fully clear [68].

Patients who have inoperable insulinoma, glucagonoma, or other carcinoid tumors, are often symptomatically treated, with variable degree of success, by one of the somastatin analogues e.g. octreotide, lanreotide and pasireotide that bind mostly to SST2 or SST5, [71].

37.8 Mitochondrial Uncoupling Protein 2 (UCP2)

UCP2 has only mild uncoupling activity, but it has other exchange/transport activities, which are more prominent. It exchanges four carbon (C4) intermediates e.g. malate, oxaloacetate, and aspartate, for cytoplasmic phosphate, and it exports C4 metabolites from mitochondria to the cytoplasm [72]. These processes are driven by electrical potential and pH gradient across the inner mitochondrial membrane. Glucose metabolism can be shifted towards aerobic glycolysis or mitochondrial oxidation, depending on the activity of UCP2. High activity of UCP2 reduces concentration of oxaloacetate in the mitochondria, and thereby reduces glucose oxidation through the citric acid cycle, lowers ATP:ADP ratio, production of reactive oxygen species (ROS), and increases glycolysis. Decreased activity of UCP2 increases mitochondrial glucose oxidation, and reduces glycolysis. Metformin, the most commonly used drug for the treatment of type 2 diabetes, induces UCP2 expression [73]. This reduces metabolically active citric acid cycle intermediates in the mitochondria, and cells utilize more glucose through aerobic glycolysis, which can partly explain how metformin increases glucose utilization in the peripheral tissues.

In the β-cells high activity of UCP2 reduces glucose oxidation in the mitochondria, lowers the ATP:ADP ratio, and ROS production. These effects reduce insulin secretion. On the other hand, inactivating mutations of the *UCP2* gene increase oxidation of glucose in the mitochondria, increase ATP:ADP ratio, increase insulin secretion, and cause congenital hyperinsulinism [72, 74]. Hypoglycemia in patients with inactivating mutations of UCP2 occurs usually after 24 h of fasting, and it can often be treated by diazoxide.

37.9 Glutamate Dehydrogenase

Glutamate dehydrogenase I (GDH-I) located in the mitochondrial matrix, catalyzes oxidative deamination of glutamate to α-ketoglutarate and ammonia, in a reversible manner. For insulin secretion, GDH is an important enzyme that is highly regulated. It is inhibited to near zero by GTP, and the inhibition can be relieved by ADP. [ADP] > 35 uM rapidly increases activity of GDH-1. The amino acid leucine allosterically activates GDH-I by promoting ADP binding. When glucose concentration falls below the threshold for insulin secretion, i.e. <4–5 mmol/L, the concentration of ADP increases, which increases GDH-I activity. Some mutations of the *GLUD1* gene that encodes GDH-I, activate the enzyme either by increasing the maximal rate or by reducing the sensitivity to inhibition by GTP. Subjects with such mutations suffer from episodes of hypoglycemia and hyperammonemia about 2–6 h after a protein-rich meal.

37.10 3-Hydroxyacyl CoA Dehydrogenase

3-Hydroxyacyl CoA dehydrogenase (also called short chain 3-hydroxyacyl-CoA dehydrogenase, SCHAD) is a mitochondrial enzyme that catalyzes the third step of β-oxidation of fatty acids, i.e. it catalyzes formation of 3-ketoacyl-CoA from 3-hydroxyacyl-CoA. Inactivating mutations in the *HADH* gene that encodes for SCHAD, cause deficiency of SCHAD. These subjects have increased insulin secretion and episodes of hypoglycemia in response to protein-rich meals. The increase in the insulin secretion is due to the increase in the activity of GDH. Normally SCHAD inhibits GDH; deficiency of SCHAD removes the inhibition, and GDH is activated by leucine present in the protein-rich meal, leading to increased insulin secretion [75]. The hypoglycemia caused by SCHAD can be prevented by diazoxide, which switches the β-cells to the off-mode by increasing the open state probability of the K_{ATP} channel.

37.11 Free Fatty Acid Receptors

The four free fatty acid receptors, FFA1, FFA2, FFA3 and FFA4 are encoded by *FFAR1*, *FFAR2*, *FFAR3*, and *FFAR4* genes respectively [76]. FFA1 and FFA4 are activated by long chain fatty acids; FFA2 and FFA3 are activated by short chain fatty acids.

FFA1 (GPR40, G-protein coupled receptor 40): FFA1 is activated by long chain fatty acids (myristic acid, palmitic acid, oleic acid, linoleic acid, alpha-linoleic acid, arachidonic acid, ecosapentanoic acid, and docosahexanoic acid). FFA1 is coupled to $G_{\alpha q}$, and activation of the receptor triggers Ca^{2+} signals through the

PLC-inositol 1,4,5 trisphosphate pathway [77, 78]. Activation of FFA1 enhances glucose-stimulated insulin secretion. FFA1 is also expressed in the intestinal L-cells, where its activation elicits Ca^{2+} signals leading to the secretion of GLP-1 [79]. FFA1 is a potential target for developing drugs that promote insulin secretion in a glucose-dependent manner [80].

FFA4 (GPR120, G-protein coupled receptor 120): FFA4 is activated by long chain fatty acids. It is coupled to $G_{q/11}$. Interestingly, activation of FFA4 increases secretion of GLP-1, which enhance insulin secretion in a glucose-dependent manner [81].

GPR119 (G-protein coupled receptor 119): GPR119 is not strictly a free fatty acid receptor, but it is activated by lipid compounds like N-oleoylethanolamide, and N-palmitoylethanolamide. This receptor is highly expressed in the β-cells and in the L-cells of small intestine that secrete GLP-1. Activation of GPR119 by orally active synthetic agonists increases GLP-1 level and enhances insulin secretion in a glucose-dependent manner [82].

37.12 Hepatocyte Nuclear Factor 4 Alpha

Loss of function mutations in the hepatocyte nuclear factor 4 alpha (*HNF4A*), (also called *MODY1*) gene reduces both glucose- and arginine-induced insulin secretion by mechanisms that are not fully clear [83]. It has been demonstrated that HNF4A directly induces expression of x-box protein 1 (XBP1). XBP1 protein is a transcription factor encoded by the *XBP1* gene. Loss of function mutations of *HNF4A* that cause "maturity onset diabetes of the young type 1" (MODY1), reduce expression of XBP1, which in turn reduces the area of the ER network, the concentration of Ca^{2+} in the ER, and the magnitude of the glucose-induced increase of $[Ca^{2+}]_c$ [84]. These patients present with diabetes during early childhood or adolescence, and are initially treated by insulin as in type 1 diabetes. Once the molecular diagnosis is established, many of these patients can be treated by sulfonylureas for variable period, but later on when sulfonylureas fail, they need insulin therapy.

37.13 Mitochondria

Mitochondrial ATP production is essential for stimulating normal insulin secretion. In β-cells, which lack lactate dehydrogenase, pyruvate, the end-product of glycolysis, is metabolized in the mitochondria, which is essential for robust insulin secretion in response to glucose [85].

Mitochondrial dysfunction caused by mutations in the mitochondrial DNA often cause impaired insulin secretion and diabetes. The A3243G mutation in the mitochondrially encoded tRNA leucine 1 (*MT-TL1*) gene causes maternally

inherited diabetes and deafness (MIDD). The mutation impairs the ability of the β-cells to secrete insulin probably due to impaired generation of ATP by the mutant mitochondria [86].

"Transcription factor B1, mitochondrial" (*TFB1M*) gene encodes for a dimethyltransferase that dimethylates mitochondrial 12S rRNA. It is also necessary for mitochondrial gene expression. A common variant (rs950994) in the *TFB1M* gene is associated with impaired insulin secretion and increased risk for developing type 2 diabetes [87]. Studies using knockout mice and clonal β-cells, show that the risk SNP leads to reduced level of TFB1M protein, reduced mitochondrial translation, reduced oxidative phosphorylation, reduced production of ATP, and consequent impairment of insulin secretion [87].

37.14 Insulin Secretion in Type 2 Diabetes

Insulin secretion in response to intake of mixed meals is not biphasic [88, 89]. The so called biphasic insulin secretion is an experimental artifact generated by rapid and sustained stimulation of the β-cells with glucose [90]. In type 2 diabetes, insulin secretion, especially the first phase of the insulin secretion, in response to rapid and sustained stimulation by glucose, is impaired. This impairment is seen even in the early stages of the natural history of diabetes [91], and even in the normoglycemic first-degree relatives of people who have diabetes [92, 93]. There is strong evidence that the impairment of insulin secretion is essential for the development of type 2 diabetes. In fact, most of the genes that are strongly associated with type 2 diabetes, appear to be important for the development, and the function of β-cells [94, 95]. One of the cornerstone of the treatment of diabetes is to improve insulin secretion either by drugs that act on the K_{ATP} channel or the GLP-1 receptor.

Sulfonylureas and glinides reduce the open state probability of the K_{ATP} channel and modestly improve food induced increase in insulin secretion in people with type 2 diabetes. Apparently, in type 2 diabetes, a proportion of β-cells remain in the off-mode, and by binding to the SUR1 subunit of the K_{ATP} channel, these drugs switch these β-cells to the ready-mode. In normal subjects, these drugs shift the dose-response curve of glucose-induced insulin secretion to the left. In diabetes, the dose-response curves of glucose-induced insulin secretion, are flatter and shifted to the right, compared to those in the normal subjects. Sulfonylureas almost normalize, and shift the curve to left in people with prediabetes, but their effects in people with diabetes are only modest [96]. The insulin response to the sulfonylureas remains lower in people with diabetes compared to that in the normal subjects. Prolonged treatment with sulfonylureas makes the β-cells unresponsive to the treatment, usually permanently [97]. Apparently, persistent depolarization, and consequent chronic elevation of the $[Ca^{2+}]_c$ in the β-cells, lead to adaptive, or compensatory changes that ultimately make the β-cells unresponsive to glucose [31]. We see a similar "glucose-blindness" in the SUR1 knockout mice [98], and in patients who have inactivating mutations of the K_{ATP} channel genes [25, 28].

Drugs that act on the K_{ATP} channel have been used in the treatment of diabetes for decades, but their use is declining since they often induce hypoglycemia, increase weight, and most importantly, they do not improve the cardiovascular outcomes [61].

Impaired insulin secretion in type 2 diabetes can be treated preferably by drugs that act, directly or indirectly, on the GLP-1 receptor. These drugs increase secretion of insulin in a glucose-dependent manner, and at the same time reduce secretion of glucagon [99].

In contrast to the drugs that act on the K_{ATP} channel or the GLP-1 receptor, metformin, the first line drug for the treatment of diabetes, impairs glucose-induced $[Ca^{2+}]_c$ response in the β-cells, and thereby reduce insulin secretion [100, 101]. It is possible that, in the β-cells, metformin, by inducing UCP2 expression [73] reduces mitochondrial oxidation, and promotes glucose utilization through aerobic glycolysis. This may be seen as a way to achieve "β-cell rest".

In type 2 diabetes impairment of β-cells function probably appears first, which then leads to a decrease of β-cell mass as the disease progresses [102, 103]. It appears that, one population of the β-cells remains in the off-mode, and they can be switched to the ready-mode by the anti-diabetic sulfonylurea drugs. A second population of β-cells remains in the ready-mode, and they can be switched to the on-mode by drugs that act on the GLP-1 receptor. A third population of β-cells remains in the on-mode, and these can be granted "rest" by metformin. A fourth population of β-cells are in the process of dying because of many factors including amyloid deposition, and apoptosis. Drugs that act on the GLP-1 receptor appear to protect all the three population of β-cells by preventing apoptosis, and possibly even by supporting proliferation of the cells [12].

Acknowledgements Financial support was obtained from the Karolinska Institutet and the Uppsala County Council.

References

1. Holz GG, Kuhtreiber WM, Habener JF (1993) Pancreatic beta-cells are rendered glucose-competent by the insulinotropic hormone glucagon-like peptide-1(7-37). Nature 361(6410):362–365
2. Song SH, McIntyre SS, Shah H, Veldhuis JD, Hayes PC, Butler PC (2000) Direct measurement of pulsatile insulin secretion from the portal vein in human subjects. J Clin Endocrinol Metab 85(12):4491–4499
3. Islam MS (2011) TRP channels of islets. Adv Exp Med Biol 704:811–830
4. Gloyn AL, Pearson ER, Antcliff JF, Proks P, Bruining GJ, Slingerland AS et al (2004) Activating mutations in the gene encoding the ATP-sensitive potassium-channel subunit Kir6.2 and permanent neonatal diabetes. N Engl J Med 350(18):1838–1849
5. Islam MS (2014) Calcium signaling in the islets. In: Islam MS (ed) Islets of Langerhans, 2nd edn. Springer, Dordrecht, pp 605–632
6. Islam MS (2002) The ryanodine receptor calcium channel of beta-cells: molecular regulation and physiological significance. Diabetes 51(5):1299–1309

7. Martin F, Soria B (1996) Glucose-induced [Ca^{2+}]i oscillations in single human pancreatic islets. Cell Calcium 20(5):409–414
8. Quesada I, Todorova MG, Alonso-Magdalena P, Beltra M, Carneiro EM, Martin F et al (2006) Glucose induces opposite intracellular Ca^{2+} concentration oscillatory patterns in identified alpha- and beta-cells within intact human islets of Langerhans. Diabetes 55(9):2463–2469
9. Kindmark H, Kohler M, Arkhammar P, Efendic S, Larsson O, Linder S et al (1994) Oscillations in cytoplasmic free calcium concentration in human pancreatic islets from subjects with normal and impaired glucose tolerance. Diabetologia 37(11):1121–1131
10. Hellman B, Gylfe E, Bergsten P, Grapengiesser E, Lund PE, Berts A et al (1994) Glucose induces oscillatory Ca^{2+} signalling and insulin release in human pancreatic beta cells. Diabetologia 37(Suppl 2):S11–S20
11. Nordenskjöld F, Andersson B, Islam MS (2019) Expression of the inositol 1,4,5-trisphosphate receptor and the ryanodine receptor Ca^{2+}-release channels in the beta-cells and alpha- cells of the human islets of Langerhans. Adv Exp Med Biol 1131:271–281
12. Rowlands J, Heng J, Newsholme P, Carlessi R (2018) Pleiotropic effects of GLP-1 and analogs on cell signaling, metabolism, and function. Front Endocrinol (Lausanne) 9:672
13. Pinney SE, Ganapathy K, Bradfield J, Stokes D, Sasson A, Mackiewicz K et al (2013) Dominant form of congenital hyperinsulinism maps to HK1 region on 10q. Horm Res Paediatr 80(1):18–27
14. Henquin JC, Sempoux C, Marchandise J, Godecharles S, Guiot Y, Nenquin M et al (2013) Congenital hyperinsulinism caused by hexokinase I expression or glucokinase-activating mutation in a subset of beta-cells. Diabetes 62(5):1689–1696
15. Henquin JC, Nenquin M, Guiot Y, Rahier J, Sempoux C (2015) Human Insulinomas show distinct patterns of insulin secretion in vitro. Diabetes 64(10):3543–3553
16. Pino MF, Kim KA, Shelton KD, Lindner J, Odili S, Li C et al (2007) Glucokinase thermolability and hepatic regulatory protein binding are essential factors for predicting the blood glucose phenotype of missense mutations. J Biol Chem 282(18):13906–13916
17. Chakera AJ, Steele AM, Gloyn AL, Shepherd MH, Shields B, Ellard S et al (2015) Recognition and Management of Individuals with Hyperglycemia because of a heterozygous Glucokinase mutation. Diabetes Care 38(7):1383–1392
18. Bennett K, James C, Mutair A, Al-Shaikh H, Sinani A, Hussain K (2011) Four novel cases of permanent neonatal diabetes mellitus caused by homozygous mutations in the glucokinase gene. Pediatr Diabetes 12(3 Pt 1):192–196
19. Gribble FM, Tucker SJ, Haug T, Ashcroft FM (1998) MgATP activates the beta cell KATP channel by interaction with its SUR1 subunit. Proc Natl Acad Sci U S A 95(12):7185–7190
20. Macmullen CM, Zhou Q, Snider KE, Tewson PH, Becker SA, Aziz AR et al (2011) Diazoxide-unresponsive congenital hyperinsulinism in children with dominant mutations of the beta-cell sulfonylurea receptor SUR1. Diabetes 60(6):1797–1804
21. Ponmani C, Gannon H, Hussain K, Senniappan S (2013) Paradoxical hypoglycaemia associated with diazoxide therapy for hyperinsulinaemic hypoglycaemia. Horm Res Paediatr 80(2):129–133
22. de Lonlay P, Fournet JC, Rahier J, Gross-Morand MS, Poggi-Travert F, Foussier V et al (1997) Somatic deletion of the imprinted 11p15 region in sporadic persistent hyperinsulinemic hypoglycemia of infancy is specific of focal adenomatous hyperplasia and endorses partial pancreatectomy. J Clin Invest 100(4):802–807
23. Kapoor RR, Flanagan SE, Arya VB, Shield JP, Ellard S, Hussain K (2013) Clinical and molecular characterisation of 300 patients with congenital hyperinsulinism. Eur J Endocrinol 168(4):557–564
24. Sempoux C, Guiot Y, Dahan K, Moulin P, Stevens M, Lambot V et al (2003) The focal form of persistent hyperinsulinemic hypoglycemia of infancy: morphological and molecular studies show structural and functional differences with insulinoma. Diabetes 52(3):784–794
25. Henquin JC, Nenquin M, Sempoux C, Guiot Y, Bellanne-Chantelot C, Otonkoski T et al (2011) In vitro insulin secretion by pancreatic tissue from infants with diazoxide-resistant congenital hyperinsulinism deviates from model predictions. J Clin Invest 121(10):3932–3942

26. Snider KE, Becker S, Boyajian L, Shyng SL, MacMullen C, Hughes N et al (2013) Genotype and phenotype correlations in 417 children with congenital hyperinsulinism. J Clin Endocrinol Metab 98(2):E355–E363
27. Yorifuji T, Horikawa R, Hasegawa T, Adachi M, Soneda S, Minagawa M et al (2017) Clinical practice guidelines for congenital hyperinsulinism. Clin Pediatr Endocrinol 26(3):127–152
28. Li C, Ackermann AM, Boodhansingh KE, Bhatti TR, Liu C, Schug J et al (2017) Functional and metabolomic consequences of KATP channel inactivation in human islets. Diabetes 66(7):1901–1913
29. Thornton PS, MacMullen C, Ganguly A, Ruchelli E, Steinkrauss L, Crane A et al (2003) Clinical and molecular characterization of a dominant form of congenital hyperinsulinism caused by a mutation in the high-affinity sulfonylurea receptor. Diabetes 52(9):2403–2410
30. Wilson DF, Cember ATJ, Matschinsky FM (2018) Glutamate dehydrogenase: role in regulating metabolism and insulin release in pancreatic beta-cells. J Appl Physiol (1985) 125(2):419–428
31. Schwaller B (2012) The regulation of a cell's Ca^{2+} signaling toolkit: the Ca^{2+} homeostasome. Adv Exp Med Biol 740:1–25
32. Bowman P, Sulen A, Barbetti F, Beltrand J, Svalastoga P, Codner E et al (2018) Effectiveness and safety of long-term treatment with sulfonylureas in patients with neonatal diabetes due to KCNJ11 mutations: an international cohort study. Lancet Diabetes Endocrinol 6(8):637–646
33. MacDonald PE, Salapatek AM, Wheeler MB (2002) Glucagon-like peptide-1 receptor activation antagonizes voltage-dependent repolarizing K(+) currents in beta-cells: a possible glucose-dependent insulinotropic mechanism. Diabetes 51(Suppl 3):S443–S447
34. Torekov SS, Iepsen E, Christiansen M, Linneberg A, Pedersen O, Holst JJ et al (2014) KCNQ1 long QT syndrome patients have hyperinsulinemia and symptomatic hypoglycemia. Diabetes 63(4):1315–1325
35. Yasuda K, Miyake K, Horikawa Y, Hara K, Osawa H, Furuta H et al (2008) Variants in KCNQ1 are associated with susceptibility to type 2 diabetes mellitus. Nat Genet 40(9):1092–1097
36. Nauck MA, Meier JJ (2018) Incretin hormones: their role in health and disease. Diabetes Obes Metab 20(Suppl 1):5–21
37. Light PE, Manning Fox JE, Riedel MJ, Wheeler MB (2002) Glucagon-like peptide-1 inhibits pancreatic ATP-sensitive potassium channels via a protein kinase A- and ADP-dependent mechanism. Mol Endocrinol 16(9):2135–2144
38. Ma Z, Bjorklund A, Islam MS (2017) A TRPM4 inhibitor 9-Phenanthrol inhibits glucose- and glucagon-like peptide 1-induced insulin secretion from rat islets of Langerhans. J Diabetes Res 2017:5131785
39. Marabita F, Islam MS (2017) Expression of transient receptor potential channels in the purified human pancreatic beta-cells. Pancreas 46(1):97–101
40. Pang B, Kim S, Li D, Ma Z, Sun B, Zhang X et al (2017) Glucagon-like peptide-1 potentiates glucose-stimulated insulin secretion via the transient receptor potential melastatin 2 channel. Exp Ther Med 14(5):5219–5227
41. Bari MR, Akbar S, Eweida M, Kuhn FJ, Gustafsson AJ, Luckhoff A et al (2009) H2O2-induced Ca^{2+} influx and its inhibition by N-(p-amylcinnamoyl) anthranilic acid in the beta-cells: involvement of TRPM2 channels. J Cell Mol Med 13(9B):3260–3267
42. Hodson DJ, Mitchell RK, Bellomo EA, Sun G, Vinet L, Meda P et al (2013) Lipotoxicity disrupts incretin-regulated human beta cell connectivity. J Clin Invest 123(10):4182–4194
43. Islam MS (2010) Calcium signaling in the islets. Adv Exp Med Biol 654:235–259
44. Krishnan K, Ma Z, Bjorklund A, Islam MS (2015) Calcium signaling in a genetically engineered human pancreatic beta-cell line. Pancreas 44(5):773–777
45. Holz GG, Leech CA, Heller RS, Castonguay M, Habener JF (1999) cAMP-dependent mobilization of intracellular Ca^{2+} stores by activation of ryanodine receptors in pancreatic beta-cells. A Ca^{2+} signaling system stimulated by the insulinotropic hormone glucagon-like peptide-1-(7-37). J Biol Chem 274(20):14147–14156

46. Kang G, Joseph JW, Chepurny OG, Monaco M, Wheeler MB, Bos JL et al (2003) Epac-selective cAMP analog 8-pCPT-2′-O-Me-cAMP as a stimulus for Ca^{2+}-induced Ca^{2+} release and exocytosis in pancreatic beta-cells. J Biol Chem 278(10):8279–8285
47. Suga S, Kanno T, Nakano K, Takeo T, Dobashi Y, Wakui M (1997) GLP-I(7-36) amide augments Ba^{2+} current through L-type Ca^{2+} channel of rat pancreatic beta-cell in a cAMP-dependent manner. Diabetes 46(11):1755–1760
48. Jacobo SM, Guerra ML, Hockerman GH (2009) Cav1.2 and Cav1.3 are differentially coupled to glucagon-like peptide-1 potentiation of glucose-stimulated insulin secretion in the pancreatic beta-cell line INS-1. J Pharmacol Exp Ther 331(2):724–732
49. Gromada J, Bokvist K, Ding WG, Holst JJ, Nielsen JH, Rorsman P (1998) Glucagon-like peptide 1 (7-36) amide stimulates exocytosis in human pancreatic beta-cells by both proximal and distal regulatory steps in stimulus-secretion coupling. Diabetes 47(1):57–65
50. Yada T, Itoh K, Nakata M (1993) Glucagon-like peptide-1-(7-36)amide and a rise in cyclic adenosine 3′,5′-monophosphate increase cytosolic free Ca^{2+} in rat pancreatic beta-cells by enhancing Ca^{2+} channel activity. Endocrinology 133(4):1685–1692
51. Kang G, Chepurny OG, Rindler MJ, Collis L, Chepurny Z, Li WH et al (2005) A cAMP and Ca^{2+} coincidence detector in support of Ca^{2+}-induced Ca^{2+} release in mouse pancreatic beta cells. J Physiol 566(Pt 1):173–188
52. Dyachok O, Gylfe E (2004) Ca^{2+}-induced Ca^{2+} release via inositol 1,4,5-trisphosphate receptors is amplified by protein kinase A and triggers exocytosis in pancreatic beta-cells. J Biol Chem 279(44):45455–45461
53. Bruton JD, Lemmens R, Shi CL, Persson-Sjogren S, Westerblad H, Ahmed M et al (2003) Ryanodine receptors of pancreatic beta-cells mediate a distinct context-dependent signal for insulin secretion. FASEB J 17(2):301–303
54. Wu B, Wei S, Petersen N, Ali Y, Wang X, Bacaj T et al (2015) Synaptotagmin-7 phosphorylation mediates GLP-1-dependent potentiation of insulin secretion from beta-cells. Proc Natl Acad Sci U S A 112(32):9996–10001
55. Unger RH, Cherrington AD (2012) Glucagonocentric restructuring of diabetes: a pathophysiologic and therapeutic makeover. J Clin Invest 122(1):4–12
56. Zhang Y, Parajuli KR, Fava GE, Gupta R, Xu W, Nguyen LU et al (2018) GLP-1 receptor in pancreatic alpha cells regulates glucagon secretion in a glucose-dependent bidirectional manner. Diabetes 68(1):34–44
57. Ramracheya R, Chapman C, Chibalina M, Dou H, Miranda C, Gonzalez A et al (2018) GLP-1 suppresses glucagon secretion in human pancreatic alpha-cells by inhibition of P/Q-type Ca^{2+} channels. Physiol Rep 6(17):e13852
58. Faerch K, Torekov SS, Vistisen D, Johansen NB, Witte DR, Jonsson A et al (2015) GLP-1 response to Oral glucose is reduced in prediabetes, screen-detected type 2 diabetes, and obesity and influenced by sex: the ADDITION-PRO Study. Diabetes 64(7):2513–2525
59. Calanna S, Christensen M, Holst JJ, Laferrere B, Gluud LL, Vilsboll T et al (2013) Secretion of glucagon-like peptide-1 in patients with type 2 diabetes mellitus: systematic review and meta-analyses of clinical studies. Diabetologia 56(5):965–972
60. Ruetten H, Gebauer M, Raymond RH, Calle RA, Cobelli C, Ghosh A et al (2018) Mixed meal and intravenous L-arginine tests both stimulate incretin release across glucose tolerance in man: lack of correlation with beta cell function. Metab Syndr Relat Disord 16(8):406–415
61. Azoulay L, Suissa S (2017) Sulfonylureas and the risks of cardiovascular events and death: a methodological meta-regression analysis of the observational studies. Diabetes Care 40(5):706–714
62. Marso SP, Bain SC, Consoli A, Eliaschewitz FG, Jodar E, Leiter LA et al (2016) Semaglutide and cardiovascular outcomes in patients with type 2 diabetes. N Engl J Med 375(19):1834–1844
63. Marso SP, Daniels GH, Brown-Frandsen K, Kristensen P, Mann JF, Nauck MA et al (2016) Liraglutide and cardiovascular outcomes in type 2 diabetes. N Engl J Med 375(4):311–322
64. Gunther T, Tulipano G, Dournaud P, Bousquet C, Csaba Z, Kreienkamp HJ et al (2018) International Union of Basic and Clinical Pharmacology. CV. Somatostatin receptors: structure,

function, ligands, and new nomenclature. Pharmacol Rev 70(4):763–835
65. Strowski MZ, Parmar RM, Blake AD, Schaeffer JM (2000) Somatostatin inhibits insulin and glucagon secretion via two receptors subtypes: an in vitro study of pancreatic islets from somatostatin receptor 2 knockout mice. Endocrinology 141(1):111–117
66. Strowski MZ, Kohler M, Chen HY, Trumbauer ME, Li Z, Szalkowski D et al (2003) Somatostatin receptor subtype 5 regulates insulin secretion and glucose homeostasis. Mol Endocrinol 17(1):93–106
67. Braun M (2014) The somatostatin receptor in human pancreatic beta-cells. Vitam Horm 95:165–193
68. Kailey B, van de Bunt M, Cheley S, Johnson PR, MacDonald PE, Gloyn AL et al (2012) SSTR2 is the functionally dominant somatostatin receptor in human pancreatic beta- and alpha-cells. Am J Physiol Endocrinol Metab 303(9):E1107–E1116
69. Liu W, Shao PP, Liang GB, Bawiec J, He J, Aster SD et al (2018) Discovery and pharmacology of a novel somatostatin subtype 5 (SSTR5) antagonist: synergy with DPP-4 inhibition. ACS Med Chem Lett 9(11):1082–1087
70. Salehi A, Qader SS, Grapengiesser E, Hellman B (2007) Pulses of somatostatin release are slightly delayed compared with insulin and antisynchronous to glucagon. Regul Pept 144(1–3):43–49
71. Oberg K (2018) Management of functional neuroendocrine tumors of the pancreas. Gland Surg 7(1):20–27
72. Vozza A, Parisi G, De Leonardis F, Lasorsa FM, Castegna A, Amorese D et al (2014) UCP2 transports C4 metabolites out of mitochondria, regulating glucose and glutamine oxidation. Proc Natl Acad Sci U S A 111(3):960–965
73. Anedda A, Rial E, Gonzalez-Barroso MM (2008) Metformin induces oxidative stress in white adipocytes and raises uncoupling protein 2 levels. J Endocrinol 199(1):33–40
74. Ferrara CT, Boodhansingh KE, Paradies E, Fiermonte G, Steinkrauss LJ, Topor LS et al (2017) Novel hypoglycemia phenotype in congenital hyperinsulinism due to dominant mutations of uncoupling protein 2. J Clin Endocrinol Metab 102(3):942–949
75. Li C, Chen P, Palladino A, Narayan S, Russell LK, Sayed S et al (2010) Mechanism of hyperinsulinism in short-chain 3-hydroxyacyl-CoA dehydrogenase deficiency involves activation of glutamate dehydrogenase. J Biol Chem 285(41):31806–31818
76. Davenport AP, Alexander SP, Sharman JL, Pawson AJ, Benson HE, Monaghan AE et al (2013) International union of basic and clinical pharmacology. LXXXVIII. G protein-coupled receptor list: recommendations for new pairings with cognate ligands. Pharmacol Rev 65(3):967–986
77. Zhao Y, Wang L, Qiu J, Zha D, Sun Q, Chen C (2013) Linoleic acid stimulates $[Ca^{2+}]$i increase in rat pancreatic beta-cells through both membrane receptor- and intracellular metabolite-mediated pathways. PLoS One 8(4):e60255
78. Fujiwara K, Maekawa F, Yada T (2005) Oleic acid interacts with GPR40 to induce Ca^{2+} signaling in rat islet beta-cells: mediation by PLC and L-type Ca^{2+} channel and link to insulin release. Am J Physiol Endocrinol Metab 289(4):E670–E677
79. Psichas A, Larraufie PF, Goldspink DA, Gribble FM, Reimann F (2017) Chylomicrons stimulate incretin secretion in mouse and human cells. Diabetologia 60(12):2475–2485
80. Guo B, Guo S, Huang J, Li J, Li J, Chen Q et al (2018) Design and optimization of 2,3-dihydrobenzo[b][1,4]dioxine propanoic acids as novel GPR40 agonists with improved pharmacokinetic and safety profiles. Bioorg Med Chem 26(22):5780–5791
81. Sundstrom L, Myhre S, Sundqvist M, Ahnmark A, McCoull W, Raubo P et al (2017) The acute glucose lowering effect of specific GPR120 activation in mice is mainly driven by glucagon-like peptide 1. PLoS One 12(12):e0189060
82. Matsumoto K, Yoshitomi T, Ishimoto Y, Tanaka N, Takahashi K, Watanabe A et al (2018) DS-8500a, an orally available G protein-coupled receptor 119 agonist, upregulates glucagon-like Peptide-1 and enhances glucose-dependent insulin secretion and improves glucose homeostasis in type 2 diabetic rats. J Pharmacol Exp Ther 367(3):509–517

83. Yamagata K, Senokuchi T, Lu M, Takemoto M, Fazlul Karim M, Go C et al (2011) Voltage-gated K^+ channel KCNQ1 regulates insulin secretion in MIN6 beta-cell line. Biochem Biophys Res Commun 407(3):620–625
84. Moore BD, Jin RU, Lo H, Jung M, Wang H, Battle MA et al (2016) Transcriptional regulation of X-box-binding protein one (XBP1) by hepatocyte nuclear factor 4alpha (HNF4Alpha) is vital to Beta-cell function. J Biol Chem 291(12):6146–6157
85. Malmgren S, Nicholls DG, Taneera J, Bacos K, Koeck T, Tamaddon A et al (2009) Tight coupling between glucose and mitochondrial metabolism in clonal beta-cells is required for robust insulin secretion. J Biol Chem 284(47):32395–32404
86. Fex M, Nicholas LM, Vishnu N, Medina A, Sharoyko VV, Nicholls DG et al (2018) The pathogenetic role of beta-cell mitochondria in type 2 diabetes. J Endocrinol 236(3):R145–RR59
87. Koeck T, Olsson AH, Nitert MD, Sharoyko VV, Ladenvall C, Kotova O et al (2011) A common variant in TFB1M is associated with reduced insulin secretion and increased future risk of type 2 diabetes. Cell Metab 13(1):80–91
88. Sorenson RL, Lindell DV, Elde RP (1980) Glucose stimulation of somatostatin and insulin release from the isolated, perfused rat pancreas. Diabetes 29(9):747–751
89. Grodsky GM (1972) A threshold distribution hypothesis for packet storage of insulin and its mathematical modeling. J Clin Invest 51(8):2047–2059
90. Henquin JC, Ishiyama N, Nenquin M, Ravier MA, Jonas JC (2002) Signals and pools underlying biphasic insulin secretion. Diabetes 51(Suppl 1):S60–S67
91. Davies MJ, Rayman G, Grenfell A, Gray IP, Day JL, Hales CN (1994) Loss of the first phase insulin response to intravenous glucose in subjects with persistent impaired glucose tolerance. Diabet Med 11(5):432–436
92. Nyholm B, Porksen N, Juhl CB, Gravholt CH, Butler PC, Weeke J et al (2000) Assessment of insulin secretion in relatives of patients with type 2 (non-insulin-dependent) diabetes mellitus: evidence of early beta-cell dysfunction. Metabolism 49(7):896–905
93. O'Rahilly S, Turner RC, Matthews DR (1988) Impaired pulsatile secretion of insulin in relatives of patients with non-insulin-dependent diabetes. N Engl J Med 318(19):1225–1230
94. Prasad RB, Groop L (2015) Genetics of type 2 diabetes-pitfalls and possibilities. Genes (Basel) 6(1):87–123
95. Wood AR, Jonsson A, Jackson AU, Wang N, van Leewen N, Palmer ND et al (2017) A genome-wide association study of IVGTT-based measures of first-phase insulin secretion refines the underlying physiology of type 2 diabetes variants. Diabetes 66(8):2296–2309
96. Cerasi E, Efendic S, Thornqvist C, Luft R (1979) Effect of two sulphonylureas on the dose kinetics of glucose-induced insulin release in normal and diabetic subjects. Acta Endocrinol 91(2):282–293
97. Delawter DE, Moss JM, Tyroler S, Canary JJ (1959) Secondary failure of response to tolbutamide treatment. J Am Med Assoc 171:1786–1792
98. Doliba NM, Qin W, Vatamaniuk MZ, Li C, Zelent D, Najafi H et al (2004) Restitution of defective glucose-stimulated insulin release of sulfonylurea type 1 receptor knockout mice by acetylcholine. Am J Physiol Endocrinol Metab 286(5):E834–E843
99. Gutniak M, Orskov C, Holst JJ, Ahren B, Efendic S (1992) Antidiabetogenic effect of glucagon-like peptide-1 (7-36)amide in normal subjects and patients with diabetes mellitus. N Engl J Med 326(20):1316–1322

100. Gelin L, Li J, Corbin KL, Jahan I, Nunemaker CS (2018) Metformin inhibits mouse islet insulin secretion and alters intracellular calcium in a concentration-dependent and duration-dependent manner near the circulating range. J Diabetes Res 2018:9163052
101. Leclerc I, Woltersdorf WW, da Silva XG, Rowe RL, Cross SE, Korbutt GS et al (2004) Metformin, but not leptin, regulates AMP-activated protein kinase in pancreatic islets: impact on glucose-stimulated insulin secretion. Am J Physiol Endocrinol Metab 286(6):E1023–E1031
102. Meier JJ, Bonadonna RC (2013) Role of reduced beta-cell mass versus impaired beta-cell function in the pathogenesis of type 2 diabetes. Diabetes Care 36(Suppl 2):S113–S119
103. Chen C, Cohrs CM, Stertmann J, Bozsak R, Speier S (2017) Human beta cell mass and function in diabetes: recent advances in knowledge and technologies to understand disease pathogenesis. Mol Metab 6(9):943–957

Chapter 38
Calcium Dynamics and Synaptic Plasticity

Pedro Mateos-Aparicio and Antonio Rodríguez-Moreno

Abstract Synaptic plasticity is a fundamental property of neurons referring to the activity-dependent changes in the strength and efficacy of synaptic transmission at preexisting synapses. Such changes can last from milliseconds to hours, days, or even longer and are involved in learning and memory as well as in development and response of the brain to injuries. Several types of synaptic plasticity have been described across neuronal types, brain regions, and species, but all of them share in one way or another capital importance of Ca^{2+}-mediated processes. In this chapter, we will focus on the Ca^{2+}-dependent events necessary for the induction and expression of multiple forms of synaptic plasticity.

Keywords Synaptic plasticity · NMDA · AMPA · calcium · LTP · LTD · Short-term plasticity · Second messengers · Transmitter release · Kinases

38.1 Introduction

Calcium (Ca^{2+}) is a divalent cation essential for all known forms of life. It is involved in the regulation of a myriad of cellular events such as metabolic control, mitochondrial function, apoptosis, intracellular signaling cascades, gene expression or cellular motility [1]. In neurons, Ca^{2+} acts as a second messenger controlling neuronal excitability, development of neuronal morphology, formation of synapses, synaptic release, gene expression, and synaptic plasticity [2]. While extracellular Ca^{2+} concentration ranges in the mM scale, intracellular free Ca^{2+} concentration is tightly maintained within the nM range (∼100 nM). In order to achieve and maintain such steep concentration gradient, neurons have developed multiple strategies over the course of evolution to keep cytosolic Ca^{2+} ions compartmentalized or

P. Mateos-Aparicio (✉) · A. Rodríguez-Moreno (✉)
Laboratorio de Neurociencia Celular y Plasticidad, Departamento de Fisiología, Anatomía y Biología Celular, Universidad Pablo de Olavide, Sevilla, Spain
e-mail: pmatmor@upo.es; arodmor@upo.es

M. S. Islam (ed.), *Calcium Signaling*, Advances in Experimental Medicine and Biology 1131, https://doi.org/10.1007/978-3-030-12457-1_38

sequestered as well as extruded outside the cell. Most of the processes involved in Ca^{2+} function and regulation are carried by a vast array of membrane proteins (i.e. ion channels and exchanger pumps) that permit Ca^{2+} influx through the plasma membrane or release Ca^{2+} from intracellular organelles or stores. In addition, the specific functions of Ca^{2+} depend upon numerous Ca^{2+}-binding proteins (i.e. Ca^{2+} buffers and Ca^{2+} sensors) that regulate numerous neuronal intracellular cascades. When a signal such as membrane depolarization or an action potential occurs in neurons, it can trigger the opening of plasma membrane and organelle Ca^{2+} channels, resulting in a sudden increase in intracellular Ca^{2+} concentration which modifies the conformation of signaling proteins which in turn translate the Ca^{2+} signal into downstream cellular effects.

Synaptic plasticity is a fundamental property of neurons referring to the activity-dependent changes in the strength and efficacy of synaptic transmission at preexisting synapses [3]. Such changes can last from milliseconds to hours, days, or even longer and are involved in the correct development of the brain, learning and memory processes, and recovery of the brain after injuries [4, 5]. Multiple types of synaptic plasticity have been described across neuronal types, brain regions, and species, but all of them share in one way or another capital importance of Ca^{2+}-mediated processes. Here, we review the Ca^{2+}-dependent events necessary for the induction and expression of different forms of synaptic plasticity.

38.2 The Structure of Ca^{2+} Signaling During Synaptic Plasticity

In the plasma membrane, Ca^{2+} ions can flow into the neuron through voltage-gated Ca^{2+} channels (VGCCs) and the Ca^{2+}-permeable type of glutamate receptor N-methyl-D-aspartate receptors (NMDARs). In some synapses, an unconventional type of α-amino-3-hydroxy-5-methyl-4-isoxazolepropionic acid receptors (AMPARs), so-called Ca^{2+}-permeable AMPARs (CP-AMPARs) has been reported in some types of plasticity [6] as has been some types of Kainate receptors (KAR) [7–13]. Neuronal VGCCs are heteromultimeric proteins composed by a pore-forming α1 subunit and auxiliary β, α2, δ, and γ subunits [14]. Ten different α1 subunits define three channel families that conduct Ca^{2+} currents with different physiological and pharmacological properties [14–16]. L-type Ca^{2+} currents, carried by Ca_v 1.1–1.4 channels, show high-voltage activation, large single channel conductance and slow voltage-dependent inactivation. In most cases, they are typically located in the postsynaptic membrane and provide the main Ca^{2+} signal that triggers postsynaptic forms of plasticity. N-, P/Q-, and R-type currents are carried by Ca_v 2.1, 2.2, and 2.3, respectively. In most cases, these channels are inserted in the presynaptic terminal, mediating fast synaptic transmission and providing the Ca^{2+} influx necessary for transmitter release. Finally, T-type currents

carried by Ca_v 3.1–3.3 channels show the lowest voltage dependence (also called low voltage-gated Ca^{2+} channels). Given their low voltage-dependent activation, they can facilitate synaptic plasticity by depolarizing the postsynaptic membrane potential and therefore allowing the activation of other Ca^{2+} channels types and/or NMDA receptors.

Inside the neuron, Ca^{2+} can be released from intracellular stores including the endoplasmic reticulum (ER), mitochondria, lysosomes, endosomes, Golgi vesicles, and secretory granules [1]. The most prominent contribution of intracellular stores during plasticity is that from the ER. The lumen contains Ca^{2+}-binding proteins in a concentration of 3–4 orders of magnitude higher than the cytosol (luminal total $Ca^{2+} > 1$ mM; free Ca^{2+} 100–700 μM) [17]. Release of Ca^{2+} from the ER is mediated by the inositol 1,4,5-triphosphate receptors ($InsP_3Rs$) and ryanodine receptors (RyRs). Both types of receptors are highly Ca^{2+} sensitive so they can mediate Ca^{2+}-induced Ca^{2+} release upon Ca^{2+} influx from membrane VGCCs or NMDA receptors [2]. $InsP_3Rs$ are Ca^{2+}-selective cation channels that open upon binding the second messenger $InsP_3$ and Ca^{2+} [18, 19]. Therefore, following rises in cytoplasmic Ca^{2+} and production of the second messenger $InsP_3$, $InsP_3Rs$ open and allow Ca^{2+} movement to the cytoplasm. RyRs are sensitive to Ca^{2+} entering either from outside or neighboring receptors [1]. They are also responsible for ER Ca^{2+} release. There are three isoforms of RyRs and although all of them have been reported in neurons, the RyR2 and 3 isoforms are the most commonly found in the brain [20]. Ca^{2+} binding increases the RyRs sensitivity to other ligands such as caffeine or adenosine diphosphate ribose (rADP). When active, they interact closely with multiple Ca^{2+}-binding proteins, Ca^{2+}-dependent enzymes (protein kinases and phosphatases) or even Ca_v 1 channels [20].

Synaptic terminals are tightly packed with numerous proteins that can bind Ca^{2+} and activate multiple downstream signaling cascades, modify gene expression, or interact with the release machinery. Ca^{2+} entry produces a local and transient increase in cytosolic Ca^{2+} concentration with temporal and spatial properties that differ between neurons, depending on the type and distribution of Ca^{2+}-binding proteins that transduce the rise of Ca^{2+} levels into biochemical responses. If a Ca^{2+} source is tightly coupled to the release machinery, it is known as Ca^{2+} nano-domain, however loose coupling defines local Ca^{2+} micro-domains where the source of Ca^{2+} and release machinery are separated by μm [21]. Neurons express a vast number of Ca^{2+} sensor proteins that are essential for the multiple effects of Ca^{2+} [22]. Among the most studied are the family of synaptotagmins (Syt1-7), important Ca^{2+} sensors of fast kinetics that mediate fast synaptic release in presynaptic terminals such as the calyx of Held or inhibitory synapses [23–26]. In addition, a wide variety of Ca^{2+} sensors contains EF-hand motifs, a highly conserved Ca^{2+}-binding motif [22, 27, 28] as for example is the ubiquitous Ca^{2+} sensor protein calmodulin (CaM) [29–31]. CaM binds Ca^{2+}, resulting in a conformational change and subsequent regulation of multiple target proteins, such as Ca^{2+}/CaM-dependent protein kinases or phosphatases of key importance in long-lasting plasticity.

Finally, another important group of cytosolic Ca^{2+}-binding proteins are the so-called "Ca^{2+}-buffers" [32]. Ca^{2+}-buffers are a subset of intracellular EF-hand containing proteins that do not belong to the Ca^{2+} sensor family, including parvalbumins, calbindin-D9k, calbindin-D28k, and calretinin [32–34]. Ca^{2+}-buffers chelate Ca^{2+} signals whenever there is a rise in cytosolic Ca^{2+} concentration and shape the properties, kinetics, and signaling properties of Ca^{2+} currents.

As seen, there are a vast number of elements affecting Ca^{2+} regulation during basal conditions and synaptic plasticity (Table 38.1). The precise contribution of each element to synaptic transmission and plasticity is probably synapse-specific and although in some synapses some elements are well known, many others still

Table 38.1 Historical overview of important events related with calcium dynamics during synaptic plasticity

Year	Milestones in calcium dynamics and synaptic plasticity
1954–65	Early discoveries on Ca^{2+} signaling in myofibrils
1964–73	Discovery of long-term potentiation in rabbit hippocampus by Bliss and Lømo
1965	Eric Kandel discovered Short-term facilitation in Aplysia
1967	Hagiwara and Nakajima describe the pharmacology of calcium spikes
	Harald Reuter provides the first voltage-clamp recordings of Ca^{2+} currents in neurons
1968	Katz and Miledi formulate the residual calcium hypothesis
	Discovery of calmodulin
	Discovery of cAMP
	Donald Walsh and Ed Krebs discover PKA
1977	Lynch and colleagues uncover LTD
1978	Bert Sakmann and Erwin Neher develop the patch-clamp technique
1981	Llinás and Yarom discover low-threshold Ca^{2+} spikes (T-type)
1983	Collingridge and colleagues demonstrated the involvement of NMDARs in LTP
1985	Discovery of N-type Ca^{2+} channels
	Llinás and colleagues discover P-type Ca^{2+} channels in Purkinje neurons
	Neuronal L-type channels
1986	Regulation of CaMKII
	Ca^{2+}-permeability of NMDARs
1991	Ca^{2+}-permeable AMPARs
	Participation of PKC in LTD
1992–97	Erwin Neher studies on Ca^{2+} buffering
1993	First evidence of a role of N-type Ca^{2+} channels in neurotransmission
1995	Q-type Ca^{2+} current terminology
1995–97	First evidence of STDP in neocortex
1998	Pharmacological separation of R-type currents
	Intracellular stores required for LTD
2003	Neocortical NMDA-dependent presynaptic LTD
2005	NMDAR-independent LTP in mossy fibers
2007	CP-AMPARs can induce LTP

remain unknown. In the next section, we review representative examples of several forms of synaptic plasticity and how the elements listed before interact to give rise a complex chain of events leading to short or long-lasting increases or decreases of synaptic strength.

38.3 Calcium Dynamics in Short-Term Plasticity

Short-term plasticity (STP) is a form of potentiation or depression of synaptic transmission present in probably all types of synapses [3, 35]. STP lasts from milliseconds to several minutes and is thought to be important in fast adaptations to sensory inputs, transient changes in behavioral states, and short-lasting forms of memory [3]. An action potential arriving to the presynaptic terminal can evoke influx of Ca^{2+} ions which bind to specialized Ca^{2+} sensor proteins that mediate fusion of synaptic vesicles and exocytosis [36]. Most forms of STP rely on transient accumulation of Ca^{2+} triggered by a short burst of action potentials. Presynaptic Ca^{2+} accumulation then modifies the probability of neurotransmitter release by modulating the biochemical events that produce the exocytosis of synaptic vesicles. STP can be induced following paired-pulse protocols and repetitive or tetanic stimulation at high frequencies [35]. It is important to note that multiple forms of STP coexist in the majority of synapses and the net synaptic strength is the result of an interaction between these forms, although the relative contribution of each one is controlled by the initial release probability and presynaptic activity pattern [37].

Short-term facilitation (STF) describes the increase in transmitter release lasting from milliseconds up to several seconds or minutes. Several forms of STF have been described including paired-pulse facilitation in response to paired-pulse protocols, augmentation (lasting seconds) and post-tetanic potentiation (PTP, lasting minutes) following high-frequency repetitive stimulation protocols. The main presynaptic Ca^{2+} current involved in STF is the P/Q-type current, carried by Ca_v 2.1 channels [38–43]. Ca_v 2.2 and 2.3 channels, carrying N- and R-type Ca^{2+} currents respectively, also contribute to synaptic transmission but lack the unique high-affinity Ca^{2+}-induced facilitation properties of Ca_v 2.1 channels [44].

Over the years, a mechanistic explanation of STF has remained elusive. However, substantial advances have been done in the past 20 years and several non-exclusive mechanisms have been proposed to explain STF [37]. The residual Ca^{2+} hypothesis, initially suggested in 1968 [45], proposes that an action potential evokes a local Ca^{2+} signal from tens to hundreds of millimolar that triggers release, but then lower levels of Ca^{2+} persist in the presynaptic terminal (residual Ca^{2+}) [37]. A second action potential would evoke another Ca^{2+} signal that would build-up over the residual Ca^{2+} thus causing facilitation. This would be the case if residual Ca^{2+} is a significant fraction of the local Ca^{2+} signal [37]. However, estimations of local and residual Ca^{2+} suggested that residual Ca^{2+} is about 1% of the local Ca^{2+} signal [46], so the enhancement of transmission after the second action potential would be very small, insufficient to account for paired-pulse facilitation.

Synapses can overcome this limitation by expressing two types of Ca^{2+} sensors, slow high-affinity (*e.g.* Syt7) and fast low-affinity proteins (*e.g.* Syt1, 2, 5/9) [24]. Thus, presynaptic residual Ca^{2+} can activate the high-affinity sensor to produce facilitation [37]. Third, the existence of Ca^{2+} buffers such as calbindin can reduce the initial probability of release by chelating local Ca^{2+}, however if Ca^{2+} levels are high enough to saturate local Ca^{2+} buffers, further incoming Ca^{2+} following subsequent action potentials would reach the release site, contributing to facilitation [37]. Finally, a fourth mechanism is the use-dependent facilitation of VGCCs mediated by the activation of CaM after Ca^{2+} entry [47, 48].

Short-term depression (STD) refers to the chain of events causing short-lasting decreases in transmitter release probability. As for STF, several mechanisms have been proposed over the years to account for the properties of STD observed following paired-pulse or tetanic stimulation. The simplest depletion model of STD proposes that the first stimulus triggers the release of a large fraction of the readily releasable pool (RRP) [37]. If the second action potential arrives and released vesicles are not replaced, the RRP is depleted and the response is depressed. The model implies that the initial fraction of RRP released must be large. This model accounts for the basic properties of paired-pulse depression observed in many synapses, however, in some hippocampal synapses the extent of depression does not correlate with the initial release [49]. Other models including inactivation of release sites or inactivation of VGCCs have been suggested to explain differences between synapses [37].

38.4 Calcium Dynamics in Long-Term Plasticity

Long-term potentiation (LTP) and long-term depression (LTD), lasting from minutes to hours or days, are thought to be a main neural substrate for learning and memory processes. Nowadays, multiple forms of LTP and LTD have been described, many of them depending upon Ca^{2+} dynamics at the presynaptic or postsynaptic sites. In the recent years, significant advances in the understanding of the molecular mechanisms involved in long-lasting decrease of synaptic strength, called long-term depression (LTD), have also been made [50]. LTD is important in hippocampus-dependent learning and memory processes, fear conditioning in amygdala, recognition memory in perirhinal cortex, development of visual and somatosensory cortices, impairments in learning and memory induced by acute stress, Fragile X syndrome, psychiatric disorders, or drug-addiction and cortico-limbic-striatal circuits [50]. LTD is typically induced using low-frequency stimulation, pairing stimulation with depolarization, and using spike-timing dependent (STDP) protocols (typically post-pre protocols, although some forms of LTD can be induced following pre-post protocols, depending on the developmental stage). In this section we outline the role of Ca^{2+} dynamics in the induction and expression of different known forms of LTP and LTD at different synapses.

38.4.1 Long-Term Potentiation

38.4.1.1 Postsynaptic NMDAR-Dependent LTP (Fig. 38.1a)

The best studied example of LTP is the NMDA-dependent LTP at CA3-CA1 synapses (Schaffer collateral-CA1) of the hippocampus [51, 52]. Most of the knowledge about this type of plasticity has been obtained using the brain slice preparation. The induction of this form of LTP requires activation of NMDA receptors during strong postsynaptic depolarization, which leads to an increase in postsynaptic Ca^{2+} concentration subsequently activating downstream biochemical processes [51, 53, 54]. Postsynaptic NMDA-dependent LTP can be experimentally induced following high-frequency tetanic stimulation, using a so-called "pairing-protocol" in which the postsynaptic cell is persistently depolarized while low-frequency stimulation is applied [55], or by using STDP protocols [56]. Upon repetitive stimulation, activation of postsynaptic NMDA receptors leads to Ca^{2+} influx restricted to the dendritic spine, increasing postsynaptic Ca^{2+} concentration and subsequent activation of the calcium/calmodulin-dependent protein kinase II, also known as CaMKII [30, 55, 57–59]. The increase in postsynaptic Ca^{2+} concentration leads to the activation of other protein kinases. For example, Ca^{2+} ions can bind calmodulin and activate the membrane enzyme adenylyl cyclase, resulting in increased cytosolic concentration of cyclic adenosine monophosphate (cAMP) which ultimately can activate the protein kinase A (PKA). PKA has been shown to indirectly boost the activity of CAMKII [60–62]. Recently, it was shown that an isoform of protein kinase C (PKC), which is also activated by raises in spine Ca^{2+} through NMDARs, termed PKCα, is directly involved in the induction and maintenance of LTP [63]. The activity of the above-mentioned kinases results in augmented single-channel conductance of dendritic AMPARs [64, 65] as well as in the incorporation of a higher number of AMPARs to the postsynaptic membrane during the expression and maintenance of LTP [66–69].

38.4.1.2 Postsynaptic NMDAR-Independent LTP (Fig. 38.1b)

Although the classical form of NMDA-dependent LTP has been object of intense research effort since its discovery, other forms of LTP independent of postsynaptic activation of NMDARs have been demonstrated [15]. VGCCs, in particular L-type currents conducted by $Ca_v1.2$ and $Ca_v1.3$ channels, are involved in several forms of NMDA-independent LTP. Inhibition of L-type current reduced LTP induced chemically by blockade of voltage-gated K^+ (K_v) channels with tetraethylammonium (TEA) [70, 71]. Also, LTP induced in vivo is partly blocked by $Ca_v1.2$ inhibition [72]. Moreover, LTP induced after NMDAR blockade or low-level theta stimulation has been shown to depend on $Ca_v1.2$ channels [73, 74]. Therefore, there is accumulating evidence for some forms of NMDA-independent LTP which depend on Ca^{2+} influx through Ca_v1 channels.

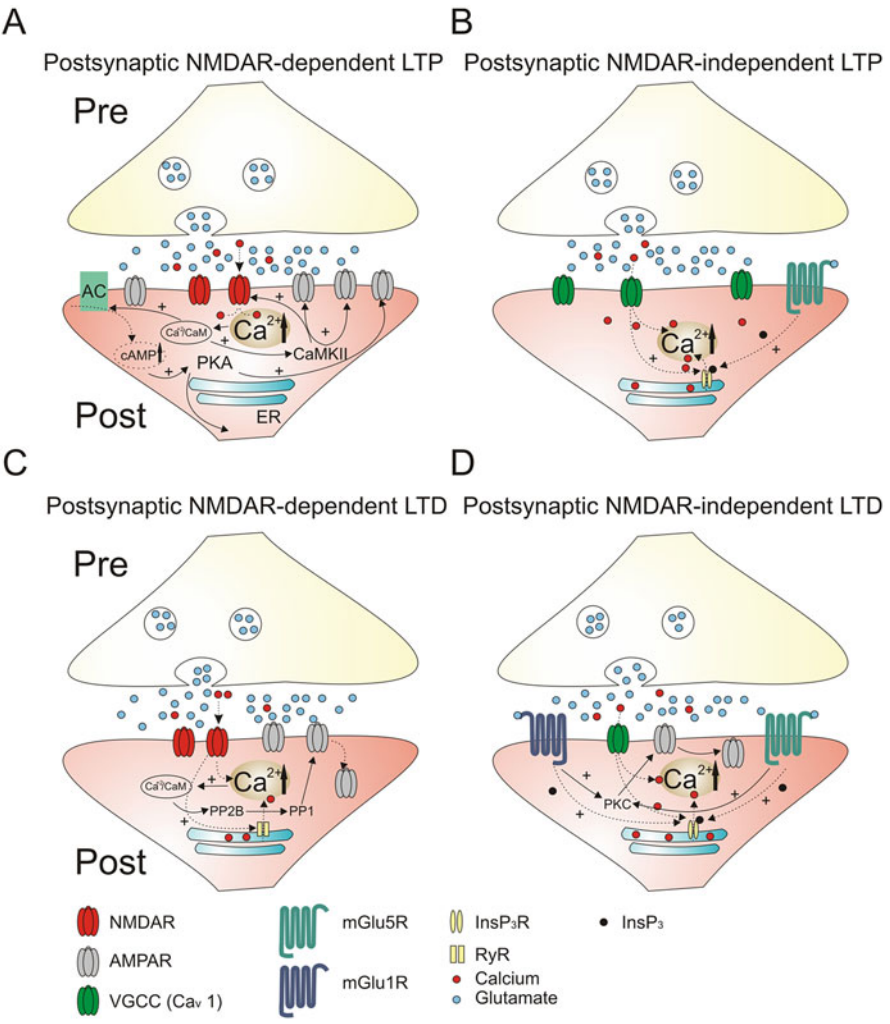

Fig. 38.1 Schematic examples of Ca^{2+}-related events during postsynaptic, NMDA-dependent and independent forms of LTP/LTD. (**a**) Ca^{2+} rise in the postsynaptic membrane through NMDA receptors activates the Ca^{2+}/CaM-activated AC and produces a subsequent increase in cAMP levels and PKA activation. Also, the Ca^{2+}/CaM complex can activate CaM-dependent kinases such as CaMKII. PKA and CaMKII activity lead to the insertion of additional AMPARs in the postsynaptic membrane, increasing synaptic strength. (**b**) Other forms of LTP include Ca^{2+} entry through postsynaptic VGCCs and activation of mGluRs, leading to the accumulation of second messenger and Ca^{2+}release from internal stores. (**c**) In prototypic cases of NMDA-dependent LTD, Ca^{2+} influx through postsynaptic NMDA receptors and ER-RyRs triggers the activation of a Ca^{2+}/CaM complex which in turn activates the phosphatase PP2B or calcineurin, leading to endocytosis of AMPAR. (**d**) In mGluR-dependent, NMDA-independent forms of LTD, activation of mGlu1R and mGlu5R and production of second messengers lead to activation of PKC-dependent pathways that will end in AMPAR endocytosis. In this form of LTD there is also Ca^{2+} influx from postsynaptic VGCCs. Solid arrow lines represent enzyme-dependent pathways whereas dashed arrow lines represent ion movement or production of second messengers

38.4.1.3 Presynaptic LTP (Fig. 38.2a)

Less studied than other forms of LTP, presynaptic LTP (preLTP) involves long-lasting modifications in the probability of neurotransmitter release [75–77]. This form of plasticity is ubiquitously expressed in the mammalian brain and may underlie behavioral responses occurring in vivo. In this section, we will review some of the best known examples of preLTP and their underlying Ca^{2+} dynamics.

In general, the mechanisms of induction of preLTP occur either in the presynaptic terminal or require the presence of a retrograde messenger produced by the postsynaptic neuron. The best characterized and prototypic form of preLTP can be found at the synapses established between the axons (mossy fibers, MF) of dentate gyrus granule cells and pyramidal CA3 neurons [78]. In this synapse, high-frequency stimulation or firing patterns occurring in vivo [79, 80] elicit an increase in Ca^{2+} concentration within the MF terminal [81–83] which results in a long-lasting increase of presynaptic release probability. Ca^{2+} influx mediated by Ca_v 2.3 channels (R-type currents) play a minor role in the overall Ca^{2+} influx during basal synaptic transmission (mostly mediated by N- and P/Q-type Ca^{2+} mediated by Ca_v 2.1 and 2.2 channels respectively) [84, 85], however Ca_v 2.3 channels contribute significantly to this type of preLTP. Presynaptic Ca^{2+} influx then activates a Ca^{2+}/CaM-dependent adenylyl cyclase, increasing presynaptic cAMP levels and subsequent activation of PKA, which ultimately phosphorylates other presynaptic substrates, resulting in a long-lasting increase of glutamate release probability [86–90].

Therefore, this type of preLTP is independent of NMDARs and cAMP/PKA-dependent. It has been found in other brain regions such as cerebellum [91], thalamus [92], subiculum [93], amygdala [94], and neocortex [95]. In MF-CA3 as well as MF-interneuron synapses [96–98], it has been proposed an additional mechanism for preLTP, consisting on the postsynaptic release of a retrograde messenger following postsynaptic Ca^{2+} increase mediated by Ca_v 1 channels and group I mGluR-dependent Ca^{2+} release from internal stores [99–101].

Although there is accumulating evidences pointing towards the presence of presynaptic NMDARs in some synapses, their roles in synaptic plasticity remain under debate [102]. NMDA-dependent preLTP has been described in some synapses of the amygdala and cerebellar cortex [75]. In this case, Ca^{2+} influx through NMDARs located in the presynaptic terminal is the main signal triggering downstream cascades that increase the presynaptic transmitter release probability during hours. The most common form of NMDA-dependent preLTP involves the increase of presynaptic levels of cAMP (presumably by activating the Ca^{2+}/CaM-dependent adenylyl cyclase) and subsequent PKA activation which phosphorylates target molecules of the presynaptic release machinery [103–106].

The expression mechanisms of preLTP also involve Ca^{2+} influx into presynaptic terminals. For example, at perforant path synapses contacting CA1 pyramidal neurons, a long-lasting increase of Ca_v 2.1 (N-type) channel activity has been demonstrated [107]. In addition, another study in the lateral amygdala showed a persistently increased Ca_v 1 (L-type) channel activity that mediates a long-lasting

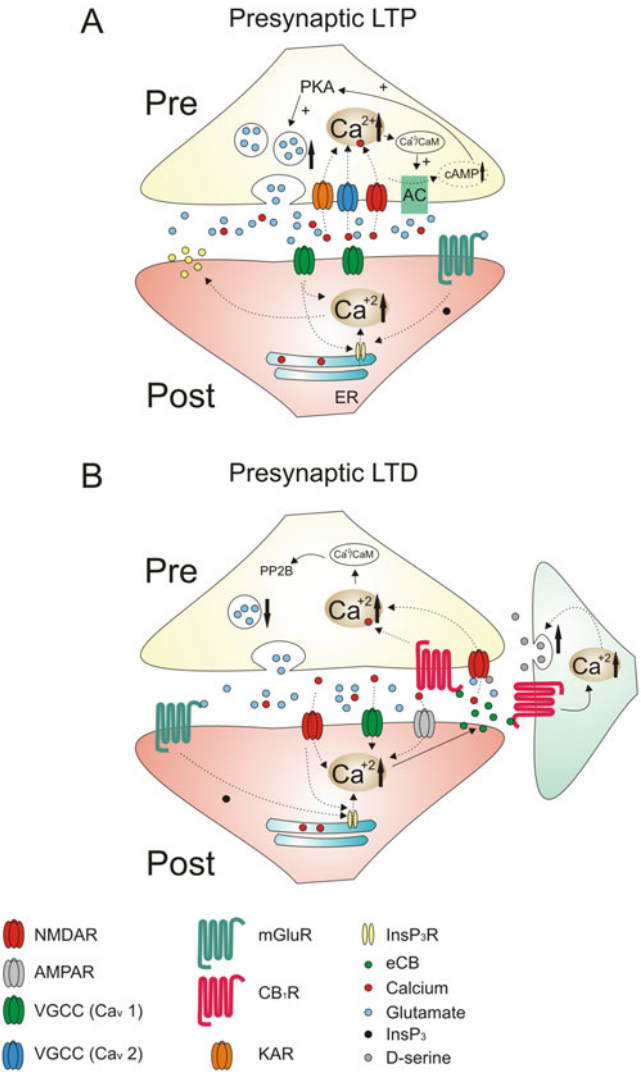

Fig. 38.2 Representation of Ca^{2+}-dependent events during presynaptic LTP/LTD. (**a**) In presynaptic forms of LTP, Ca^{2+} entry through NMDA (i.e. NMDA-dependent), VGCCs (Ca_v 2 channels), or KARs lead to presynaptic activation of Ca^{2+}/CaM complex, production of cAMP and activation of PKA, increasing the probability of transmitter release. In addition, coincident activation of postsynaptic mGluRs and Ca^{2+} influx through VGCCs and release from internal stores, and release of retrograde messengers (yellow) is required in some forms of preLTP. (**b**) During presynaptic LTD, presynaptic Ca^{2+} influx through NMDARs increase Ca^{2+} levels, activating Ca^{2+}/CaM-dependent phosphatases such as calcineurin, which in turn reduces the transmitter release probability. In addition, postsynaptic Ca^{2+} elevation through NMDARs, VGCCs, CP-AMPARs, or release from internal stores lead to eCB release, activating presynaptic eCB_1Rs (increasing presynaptic Ca^{2+} level) and astroglial eCB_1Rs. Glial CB_1R activation results in release of D-serine, boosting presynaptic NMDA activity. Solid arrow lines represent enzyme-dependent pathways whereas dashed arrow lines represent ion movement or production of second messengers

increase in glutamate release [108]. However, in the MF-CA3 of the hippocampus and the parallel fiber-Purkinje synapse in the cerebellum no changes in Ca^{2+} influx were observed following preLTP, suggesting that the expression mechanisms in these synapses occur downstream Ca^{2+} entry [75, 109–112]. Therefore, variability in the induction and expression of preLTP mechanisms indicate that further research is required to elucidate the molecular mechanisms more in detail. Given the increasing attention that presynaptic forms of LTP are receiving in the past few years, significant advances in this matter are expected to come in the upcoming future.

38.4.2 Long-Term Depression

38.4.2.1 Postsynaptic NMDAR-Dependent LTD (Fig. 38.1c)

As for LTP, NMDAR-dependency of LTD was first discovered at hippocampal CA3-CA1 synapses [113, 114]. One year later, in 1993, a similar form of LTD was also found in neocortical synapses [115]. In NMDAR-dependent LTD induced by low-frequency stimulation or STDP protocols, the main signal triggering downstream cascades that will end up in a sustained reduction in transmitter release is mainly postsynaptic Ca^{2+} influx through NMDA receptors [114]. The classical view is that LTD requires a modest increase in Ca^{2+} whereas LTP is elicited when Ca^{2+} levels increase beyond an induction threshold [51, 116]. However, further investigation has revealed that this is not always the case [117]. In this view, Ca^{2+} influx through NMDARs binds CaM, then activating a Ca^{2+} -dependent protein phosphatase cascade composed by Ca^{2+}/CaM-dependent phosphatase calcineurin which dephosphorylates inhibitor-1, leading to the activation of protein phosphatase 1 (PP1) [3, 50, 118–120], responsible for dephosphorilations either in AMPAR subunits or kinases that will end up in the endocytosis of postsynaptic AMPARs and LTD. The expression mechanisms of NMDAR-dependent LTD involve mainly endocytosis or removal of AMPARs from the postsynaptic membrane. This process involves different phosphatases that are directly or indirectly activated by Ca^{2+} influx. In addition, some studies suggest that protein kinases may be involved in the expression of this form of LTD [50]. Finally, the Ca^{2+} sensor hippocalcin has been suggested to mediate the coupling between Ca^{2+} signals and AMPAR endocytosis [121].

38.4.2.2 Postsynaptic NMDAR-Independent LTD (Fig. 38.1d)

As knowledge about LTD mechanisms in different synapses increased, new forms of LTD were uncovered across brain regions. NMDAR-independent LTD has been found in the hippocampus, cerebellum, ventral tegmental area, neostriatum, neocortex, or nucleus accumbens, for example.

The best studied form of NMDAR-independent LTD is that mediated by metabotropic glutamate receptors or mGluR-LTD. In the hippocampus [122], cerebellum [123], and perirhinal cortex [124], mGluR-LTD is dependent on Group I mGluRs (mGluR1 and 5) [125]. Since Group I mGluRs are located extrasynaptically, the induction of Group I mGluR-LTD is typically achieved by high-frequency trains (up to 300 Hz), burst or short trains at 66 Hz, paired-pulses of low frequency stimulation, or bath application of Group I mGluR agonists such as DHPG [126]. Afferent stimulation induces the opening of postsynaptic VGCCs and Group I mGluRs results in a postsynaptic elevation of second messengers such as $InsP_3$ pathway that will induce Ca^{2+} release from intracellular stores. Ca^{2+} influx activates the PKC pathway, eventually leading to removal of AMPARs in the postsynaptic membrane. In addition, DHPG-induced LTD can be observed in absence of Ca^{2+} and unaffected by PKC inhibition, suggesting that mGluR-LTD involves Ca^{2+}-dependent and -independent pathways [127, 128]. A role of Ca^{2+} entering into the cell trough calcium-permeable KARs has also been described.

Other forms of NMDAR-independent LTD involve postsynaptic release of endogenous endocannabinoids (eCBs) which act as retrograde messengers at the astrocyte or the presynaptic terminal (see below). In this form of LTD, neuronal activity triggers eCB release from the postsynaptic site, which binds to eCB_1Rs in the presynaptic site, suppressing neurotransmitter release at glutamatergic and GABAergic synapses [75]. Typically, presynaptic CB_1R activation is required during the induction of plasticity but not necessarily afterwards. In addition, postsynaptic Ca^{2+} rise through VGCCs is required for eCB release. At the presynaptic terminal, CB_1R activation inhibits presynaptic VGCCs, thereby reducing synaptic release.

38.4.2.3 Presynaptic LTD (Fig. 38.2b)

Conversely to preLTD, presynaptic LTD (preLTD) refers to long-lasting presynaptic changes that decrease synaptic strength [75]. As for preLTP, preLTD is widely expressed in many brain regions [75, 76]. There is evidence suggesting that preLTD may play important roles in certain behaviors, for example exploration of large spatial landmarks facilitates preLTD at MF-CA3 synapses [129]. In addition, fear extinction in the amygdala is linked to preLTD of prefrontal cortex-basolateral amygdala synapses [130]. At layer 4 to layer 2/3 synapses of developing barrel cortex, sensory evoked activity patterns induced preLTD potentially playing a role in synaptic pruning and refinement of cortical circuits during development [131].

NMDAR-Dependent PreLTD

Although currently subject of debate [102], accumulating evidence suggests that presynaptic NMDARs can mediate LTD in several synapses. A number of studies in visual and somatosensory cortices as well as in the hippocampus have provided

the strongest evidence for a role of presynaptic NMDARs in LTD [102, 131–142]**.** Here, the induction of NMDA-dependent preLTD requires presynaptic Ca^{2+} influx through NMDA receptors and, within a narrow time window, coincident activation of postsynaptic Group I mGluRs and Ca_v 1 channels and the release of endocannabinoids, acting as retrograde messengers at the presynaptic terminal or astrocytes [137, 139, 143] producing a long-lasting reduction of transmitter release by activating CB_1Rs and presynaptic NMDARs. Precise details at molecular level beyond presynaptic NMDARs activation remains to be determined.

Recently, a similar form of preLTD was found in developing CA3-CA1 synapses [139]. In this case, the induction of preLTD involves presynaptic Ca^{2+} influx and activation of the Ca^{2+}-dependent phosphatase calcineurin.

NMDAR-Independent PreLTD

The MF-CA3 synapse not only expresses preLTP as discussed before, a form of preLTD independent of NMDARs has also been reported [144, 145]. In this case, although the precise mechanism is not clear, it potentially involves mGluRs and metabotropic kainate receptors. There is presynaptic Ca^{2+} influx through VGCCs and subsequent activation of CaM and Ca^{2+}/CaM-dependent kinases [11, 146–148]. Another form of preLTD has been described in synapses established between mossy fibers and *stratum lucidum* interneurons [149]. In this case, the induction of preLTD is mediated by postsynaptic Ca^{2+} increase through CP-AMPARs and presynaptic Ca_v 2.1 channels presumably through postsynaptic release of unidentified retrograde messenger. The reduction of presynaptic Ca^{2+} influx leads to long-lasting reduction of neurotransmitter release probability.

38.5 Concluding Remarks

Ca^{2+} dynamics and signaling in mammalian cells and especially in neurons is an extremely complex phenomenon producing variable effects in different neurons. The huge variability of mechanisms found in relation to synaptic plasticity is a major challenge for the future. Traditionally, it has been proposed that high Ca^{2+} influx is required for LTP whereas moderate Ca^{2+} rises induced LTD under some conditions. More realistic protocols based on firing patterns found in vivo or STDP protocols have revealed that the traditional assumption does not hold in some synapses [117]. Future research will be required to investigate in detail the chain of events involved in Ca^{2+} signaling at different synapses. For example, a detailed knowledge of receptor subunits composition, Ca^{2+} sensors and buffers involved, and Ca^{2+}-dependent enzymatic processes will be of great help in the quest for a general mechanistic framework of synaptic plasticity. In addition, novel roles of NMDA receptors must be investigated in detail to clarify the relevance of presynaptic and/or putative metabotropic NMDA receptors and relevant signaling molecules. How the

complex machinery regulating Ca^{2+} dynamics controls the physiological aspects of neuronal communication in vivo and affects behavior in health and disease will be a major challenge for the future of the field.

Acknowlegments Work in the group is supported by the Ministerio de Economía y Competitividad (MINECO/FEDER) of Spain (Grant BFU2015-68655-P to A.R.-M.). P.M.-A. is supported by a postdoctoral "Juan de la Cierva-Formación" Fellowship from MINECO.

References

1. Clapham DE (2007) Calcium signaling. Cell 131(6):1047–1058
2. Berridge MJ (1998) Neuronal calcium signaling. Neuron 21(1):13–26
3. Citri A, Malenka RC (2008) Synaptic plasticity: multiple forms, functions, and mechanisms. Neuropsychopharmacology 33(1):18–41
4. Cramer SC, Sur M, Dobkin BH, O'Brien C, Sanger TD, Trojanowski JQ et al (2011) Harnessing neuroplasticity for clinical applications. Brain 134(6):1591–1609
5. Cooke SF, Bliss TVP (2006) Plasticity in the human central nervous system. Brain 129(7):1659–1673
6. Lalanne T, Oyrer J, Farrant M, Sjöström PJ (2018) Synapse type-dependent expression of calcium-permeable AMPA receptors. Front Synaptic Neurosci 10:34
7. Sihra TS, Flores G, Rodríguez-Moreno A (2014) Kainate receptors: multiple roles in neuronal plasticity. Neuroscientist 20(1):29–43
8. Negrete-Díaz JV, Duque-Feria P, Andrade-Talavera Y, Carrión M, Flores G, Rodríguez-Moreno A (2012) Kainate receptor-mediated depression of glutamatergic transmission involving protein kinase A in the lateral amygdala. J Neurochem 121(1):36–43
9. Rodríguez-Moreno A, Sihra TS (2011) Kainate receptors. Novel signaling insights. Adv Exp Med Biol 717:vii–xi, xiii
10. Rodríguez-Moreno A, Sihra TS (2007) Kainate receptors with a metabotropic modus operandi. Trends Neurosci 30(12):630–637
11. Negrete-Díaz JV, Sihra TS, Delgado-García JM, Rodríguez-Moreno A (2007) Kainate receptor-mediated presynaptic inhibition converges with presynaptic inhibition mediated by Group II mGluRs and long-term depression at the hippocampal mossy fiber-CA3 synapse. J Neural Transm (Vienna) 114(11):1425–1431
12. Negrete-Díaz JV, Sihra TS, Delgado-García JM, Rodríguez-Moreno A (2006) Kainate receptor-mediated inhibition of glutamate release involves protein kinase A in the mouse hippocampus. J Neurophysiol 96(4):1829–1837
13. Rodríguez-Moreno A, Lerma J (1998) Kainate receptor modulation of GABA release involves a metabotropic function. Neuron 20(6):1211–1218
14. Catterall WA (2011) Voltage-gated calcium channels. Cold Spring Harb Perspect Biol 3(8):a003947
15. Nanou E, Catterall WA (2018) Calcium Channels, Synaptic Plasticity, and Neuropsychiatric Disease. Neuron 98(3):466–481
16. Zamponi GW, Striessnig J, Koschak A, Dolphin AC (2015) The physiology, pathology, and pharmacology of voltage-gated calcium channels and their future therapeutic potential. Pharmacol Rev 67(4):821–870
17. Foskett JK, White C, Cheung K-H, Mak D-OD (2007) Inositol trisphosphate receptor Ca^{2+} release channels. Physiol Rev 87(2):593–658
18. Ferris CD, Huganir RL, Supattapone S, Snyder SH (1989) Purified inositol 1,4,5-trisphosphate receptor mediates calcium flux in reconstituted lipid vesicles. Nature 342(6245):87–89

19. Maeda N, Kawasaki T, Nakade S, Yokota N, Taguchi T, Kasai M et al (1991) Structural and functional characterization of inositol 1,4,5-trisphosphate receptor channel from mouse cerebellum. J Biol Chem 266(2):1109–1116
20. Lanner JT, Georgiou DK, Joshi AD, Hamilton SL (2010) Ryanodine receptors: structure, expression, molecular details, and function in calcium release. Cold Spring Harb Perspect Biol 2(11):a003996-a
21. Eggermann E, Bucurenciu I, Goswami SP, Jonas P (2011) Nanodomain coupling between Ca^{2+} channels and sensors of exocytosis at fast mammalian synapses. Nat Rev Neurosci 13(1):7–21
22. McCue HV, Haynes LP, Burgoyne RD (2010) The diversity of calcium sensor proteins in the regulation of neuronal function. Cold Spring Harb Perspect Biol 2(8):a004085
23. Chen C, Arai I, Satterfield R, Young SM Jr, Jonas P (2017) Synaptotagmin 2 Is the Fast Ca^{2+} Sensor at a Central Inhibitory Synapse. Cell Rep 18(3):723–736
24. Chen C, Jonas P (2017) Synaptotagmins: that's why so many. Neuron 94(4):694–696
25. Chen C, Satterfield R, Young SM Jr, Jonas P (2017) Triple function of synaptotagmin 7 ensures efficiency of high-frequency transmission at central GABAergic synapses. Cell Rep 21(8):2082–2089
26. Luo F, Südhof TC (2017) Synaptotagmin-7-mediated asynchronous release boosts high-fidelity synchronous transmission at a central synapse. Neuron 94(4):826–39 e3
27. Burgoyne RD (2007) Neuronal calcium sensor proteins: generating diversity in neuronal Ca^{2+} signalling. Nat Rev Neurosci 8(3):182–193
28. Burgoyne RD, Haynes LP (2012) Understanding the physiological roles of the neuronal calcium sensor proteins. Mol Brain 5(1):2
29. Malenka RC, Kauer JA, Perkel DJ, Mauk MD, Kelly PT, Nicoll RA et al (1989) An essential role for postsynaptic calmodulin and protein kinase activity in long-term potentiation. Nature 340(6234):554–557
30. Lledo PM, Hjelmstad GO, Mukherji S, Soderling TR, Malenka RC, Nicoll RA (1995) Calcium/calmodulin-dependent kinase II and long-term potentiation enhance synaptic transmission by the same mechanism. Proc Natl Acad Sci U S A 92(24):11175–11179
31. Lisman J, Malenka RC, Nicoll RA, Malinow R (1997) Learning mechanisms: the case for CaM-KII. Science 276(5321):2001–2002
32. Schwaller B (2010) Cytosolic Ca^{2+} buffers. Cold Spring Harb Perspect Biol 2(11):a004051
33. Blaustein MP (1988) Calcium transport and buffering in neurons. Trends Neurosci 11(10):438–443
34. Matthews EA, Dietrich D (2015) Buffer mobility and the regulation of neuronal calcium domains. Front Cell Neurosci 9:48
35. Zucker RS, Regehr WG (2002) Short-term synaptic plasticity. Annu Rev Physiol 64:355–405
36. Südhof TC (2013) Neurotransmitter release: the last millisecond in the life of a synaptic vesicle. Neuron 80(3):675–690
37. Regehr WG (2012) Short-term presynaptic plasticity. Cold Spring Harb Perspect Biol 4(7):a005702
38. Borst JG, Sakmann B (1998) Facilitation of presynaptic calcium currents in the rat brainstem. J Physiol 513(Pt 1):149–155
39. Cuttle MF, Tsujimoto T, Forsythe ID, Takahashi T (1998) Facilitation of the presynaptic calcium current at an auditory synapse in rat brainstem. J Physiol 512(Pt 3):723–729
40. Lee A, Scheuer T, Catterall WA (2000) Ca^{2+}/calmodulin-dependent facilitation and inactivation of P/Q-type Ca^{2+} channels. J Neurosci 20(18):6830–6838
41. Lee A, Westenbroek RE, Haeseleer F, Palczewski K, Scheuer T, Catterall WA (2002) Differential modulation of Ca(v)2.1 channels by calmodulin and Ca^{2+}-binding protein 1. Nat Neurosci 5(3):210–217
42. Lee A, Wong ST, Gallagher D, Li B, Storm DR, Scheuer T et al (1999) Ca^{2+}/calmodulin binds to and modulates P/Q-type calcium channels. Nature 399(6732):155–159
43. Lee A, Zhou H, Scheuer T, Catterall WA (2003) Molecular determinants of Ca^{2+}/calmodulin-dependent regulation of Ca(v)2.1 channels. Proc Natl Acad Sci U S A 100(26):16059–16064

44. Liang H, DeMaria CD, Erickson MG, Mori MX, Alseikhan BA, Yue DT (2003) Unified mechanisms of Ca^{2+} regulation across the Ca^{2+} channel family. Neuron 39(6):951–960
45. Katz B, Miledi R (1968) The role of calcium in neuromuscular facilitation. J Physiol 195(2):481–492
46. Schneggenburger R, Neher E (2005) Presynaptic calcium and control of vesicle fusion. Curr Opin Neurobiol 15(3):266–274
47. Catterall WA, Few AP (2008) Calcium channel regulation and presynaptic plasticity. Neuron 59(6):882–901
48. Mochida S, Few AP, Scheuer T, Catterall WA (2008) Regulation of presynaptic Ca(V)2.1 channels by Ca^{2+} sensor proteins mediates short-term synaptic plasticity. Neuron 57(2):210–216
49. Chen G, Harata NC, Tsien RW (2004) Paired-pulse depression of unitary quantal amplitude at single hippocampal synapses. Proc Natl Acad Sci U S A 101(4):1063–1068
50. Collingridge GL, Peineau S, Howland JG, Wang YT (2010) Long-term depression in the CNS. Nat Rev Neurosci 11:459–473
51. Malenka RC, Nicoll RA (1993) NMDA-receptor-dependent synaptic plasticity: multiple forms and mechanisms. Trends Neurosci 16(12):521–527
52. Nicoll RA (2017) A brief history of long-term potentiation. Neuron 93(2):281–290
53. Malenka RC (1991) Postsynaptic factors control the duration of synaptic enhancement in area CA1 of the hippocampus. Neuron 6(1):53–60
54. Malenka RC (1991) The role of postsynaptic calcium in the induction of long-term potentiation. Mol Neurobiol 5(2–4):289–295
55. Herring BE, Nicoll RA (2016) Long-term potentiation: from CaMKII to AMPA receptor trafficking. Annu Rev Physiol 78(1):351–365
56. Markram H, Lubke J, Frotscher M, Sakmann B (1997) Regulation of synaptic efficacy by coincidence of postsynaptic APs and EPSPs. Science 275(5297):213–215
57. Pettit DL, Perlman S, Malinow R (1994) Potentiated transmission and prevention of further LTP by increased CaMKII activity in postsynaptic hippocampal slice neurons. Science 266(5192):1881–1885
58. Silva AJ, Stevens CF, Tonegawa S, Wang Y (1992) Deficient hippocampal long-term potentiation in alpha-calcium-calmodulin kinase II mutant mice. Science 257(5067):201–206
59. Silva AJ, Wang Y, Paylor R, Wehner JM, Stevens CF, Tonegawa S (1992) Alpha calcium/calmodulin kinase II mutant mice: deficient long-term potentiation and impaired spatial learning. Cold Spring Harb Symp Quant Biol 57:527–539
60. Blitzer RD, Connor JH, Brown GP, Wong T, Shenolikar S, Iyengar R et al (1998) Gating of CaMKII by cAMP-regulated protein phosphatase activity during LTP. Science 280(5371):1940–1942
61. Lisman J (1989) A mechanism for the Hebb and the anti-Hebb processes underlying learning and memory. Proc Natl Acad Sci U S A 86(23):9574–9578
62. Makhinson M, Chotiner JK, Watson JB, O'Dell TJ (1999) Adenylyl cyclase activation modulates activity-dependent changes in synaptic strength and Ca^{2+}/calmodulin-dependent kinase II autophosphorylation. J Neurosci 19(7):2500–2510
63. Colgan LA, Hu M, Misler JA, Parra-Bueno P, Moran CM, Leitges M et al (2018) PKCα integrates spatiotemporally distinct Ca^{2+} and autocrine BDNF signaling to facilitate synaptic plasticity. Nat Neurosci 21:1027–1037
64. Benke TA, Luthi A, Isaac JT, Collingridge GL (1998) Modulation of AMPA receptor unitary conductance by synaptic activity. Nature 393(6687):793–797
65. Soderling TR, Derkach VA (2000) Postsynaptic protein phosphorylation and LTP. Trends Neurosci 23(2):75–80
66. Bredt DS, Nicoll RA (2003) AMPA receptor trafficking at excitatory synapses. Neuron 40(2):361–379
67. Collingridge GL, Isaac JT, Wang YT (2004) Receptor trafficking and synaptic plasticity. Nat Rev Neurosci 5(12):952–962

68. Sheng M, Kim MJ (2002) Postsynaptic signaling and plasticity mechanisms. Science 298(5594):776–780
69. Song I, Huganir RL (2002) Regulation of AMPA receptors during synaptic plasticity. Trends Neurosci 25(11):578–588
70. Huber KM, Mauk MD, Kelly PT (1995) LTP induced by activation of voltage-dependent Ca^{2+} channels requires protein kinase activity. Neuroreport 6(9):1281–1284
71. Huber KM, Mauk MD, Kelly PT (1995) Distinct LTP induction mechanisms: contribution of NMDA receptors and voltage-dependent calcium channels. J Neurophysiol 73(1):270–279
72. Freir DB, Herron CE (2003) Inhibition of L-type voltage dependent calcium channels causes impairment of long-term potentiation in the hippocampal CA1 region in vivo. Brain Res 967(1–2):27–36
73. Moosmang S, Haider N, Klugbauer N, Adelsberger H, Langwieser N, Muller J et al (2005) Role of hippocampal Cav1.2 Ca^{2+} channels in NMDA receptor-independent synaptic plasticity and spatial memory. J Neurosci 25(43):9883–9892
74. Staubli U, Lynch G (1987) Stable hippocampal long-term potentiation elicited by 'theta' pattern stimulation. Brain Res 435(1–2):227–234
75. Castillo PE (2012) Presynaptic LTP and LTD of excitatory and inhibitory synapses. Cold Spring Harb Perspect Biol 4(2):pii: a005728
76. Monday HR, Younts TJ, Castillo PE (2018) Long-term plasticity of neurotransmitter release: emerging mechanisms and contributions to brain function and disease. Annu Rev Neurosci 41(1):299–322
77. Yang Y, Calakos N (2013) Presynaptic long-term plasticity. Front Synaptic Neurosci 5:8
78. Nicoll RA, Schmitz D (2005) Synaptic plasticity at hippocampal mossy fibre synapses. Nat Rev Neurosci 6:863–876
79. Gundlfinger A, Breustedt J, Sullivan D, Schmitz D (2010) Natural spike trains trigger short- and long-lasting dynamics at hippocampal mossy fiber synapses in rodents. PLoS One 5(4):e9961
80. Mistry R, Dennis S, Frerking M, Mellor JR (2011) Dentate gyrus granule cell firing patterns can induce mossy fiber long-term potentiation in vitro. Hippocampus 21(11):1157–1168
81. Mellor J, Nicoll RA (2001) Hippocampal mossy fiber LTP is independent of postsynaptic calcium. Nat Neurosci 4(2):125–126
82. Zalutsky RA, Nicoll RA (1990) Comparison of two forms of long-term potentiation in single hippocampal neurons. Science 248(4963):1619–1624
83. Zalutsky RA, Nicoll RA (1991) Comparison of two forms of long-term potentiation in single hippocampus neurons. Correct Sci 251(4996):856
84. Breustedt J, Vogt KE, Miller RJ, Nicoll RA, Schmitz D (2003) Alpha1E-containing Ca^{2+} channels are involved in synaptic plasticity. Proc Natl Acad Sci U S A 100(21):12450–12455
85. Dietrich D, Kirschstein T, Kukley M, Pereverzev A, von der Brelie C, Schneider T et al (2003) Functional specialization of presynaptic Cav2.3 Ca^{2+} channels. Neuron 39(3):483–496
86. Huang YY, Li XC, Kandel ER (1994) cAMP contributes to mossy fiber LTP by initiating both a covalently mediated early phase and macromolecular synthesis-dependent late phase. Cell 79(1):69–79
87. Villacres EC, Wong ST, Chavkin C, Storm DR (1998) Type I adenylyl cyclase mutant mice have impaired mossy fiber long-term potentiation. J Neurosci 18(9):3186–3194
88. Wang H, Pineda VV, Chan GC, Wong ST, Muglia LJ, Storm DR (2003) Type 8 adenylyl cyclase is targeted to excitatory synapses and required for mossy fiber long-term potentiation. J Neurosci 23(30):9710–9718
89. Weisskopf MG, Castillo PE, Zalutsky RA, Nicoll RA (1994) Mediation of hippocampal mossy fiber long-term potentiation by cyclic AMP. Science 265(5180):1878–1882
90. Andrade-Talavera Y, Duque-Feria P, Negrete-Díaz JV, Sihra TS, Flores G, Rodríguez-Moreno A (2012) Presynaptic kainate receptor-mediated facilitation of glutamate release involves Ca^{2+} -calmodulin at mossy fiber-CA3 synapses. J Neurochem 122(5):891–899
91. Salin PA, Malenka RC, Nicoll RA (1996) Cyclic AMP mediates a presynaptic form of LTP at cerebellar parallel fiber synapses. Neuron 16(4):797–803

92. Castro-Alamancos MA, Calcagnotto ME (1999) Presynaptic long-term potentiation in corticothalamic synapses. J Neurosci 19(20):9090–9097
93. Behr J, Wozny C, Fidzinski P, Schmitz D (2009) Synaptic plasticity in the subiculum. Prog Neurobiol 89(4):334–342
94. López de Armentia M, Sah P (2007) Bidirectional synaptic plasticity at nociceptive afferents in the rat central amygdala. J Physiol 581(Pt 3):961–970
95. Chen HX, Jiang M, Akakin D, Roper SN (2009) Long-term potentiation of excitatory synapses on neocortical somatostatin-expressing interneurons. J Neurophysiol 102(6):3251–3259
96. Galván EJ, Calixto E, Barrionuevo G (2008) Bidirectional Hebbian plasticity at hippocampal mossy fiber synapses on CA3 interneurons. J Neurosci 28(52):14042–14055
97. Galván EJ, Cosgrove KE, Barrionuevo G (2011) Multiple forms of long-term synaptic plasticity at hippocampal mossy fiber synapses on interneurons. Neuropharmacology 60(5):740–747
98. Galván EJ, Cosgrove KE, Mauna JC, Card JP, Thiels E, Meriney SD et al (2010) Critical involvement of postsynaptic protein kinase activation in long-term potentiation at hippocampal mossy fiber synapses on CA3 interneurons. J Neurosci 30(8):2844–2855
99. Jaffe D, Johnston D (1990) Induction of long-term potentiation at hippocampal mossy-fiber synapses follows a Hebbian rule. J Neurophysiol 64(3):948–960
100. Kapur A, Yeckel MF, Gray R, Johnston D (1998) L-Type calcium channels are required for one form of hippocampal mossy fiber LTP. J Neurophysiol 79(4):2181–2190
101. Yeckel MF, Kapur A, Johnston D (1999) Multiple forms of LTP in hippocampal CA3 neurons use a common postsynaptic mechanism. Nat Neurosci 2(7):625–633
102. Bouvier G, Larsen RS, Rodríguez-Moreno A, Paulsen O, Sjöström PJ (2018) Towards resolving the presynaptic NMDA receptor debate. Curr Opin Neurobiol 51:1–7
103. Fourcaudot E, Gambino F, Humeau Y, Casassus G, Shaban H, Poulain B et al (2008) cAMP/PKA signaling and RIM1alpha mediate presynaptic LTP in the lateral amygdala. Proc Natl Acad Sci U S A 105(39):15130–15135
104. Lachamp PM, Liu Y, Liu SJ (2009) Glutamatergic modulation of cerebellar interneuron activity is mediated by an enhancement of GABA release and requires protein kinase A/RIM1alpha signaling. J Neurosci 29(2):381–392
105. Liu SJ, Lachamp P (2006) The activation of excitatory glutamate receptors evokes a long-lasting increase in the release of GABA from cerebellar stellate cells. J Neurosci 26(36):9332–9339
106. Samson RD, Pare D (2005) Activity-dependent synaptic plasticity in the central nucleus of the amygdala. J Neurosci 25(7):1847–1855
107. Ahmed MS, Siegelbaum SA (2009) Recruitment of N-Type Ca^{2+} channels during LTP enhances low release efficacy of hippocampal CA1 perforant path synapses. Neuron 63(3):372–385
108. Fourcaudot E, Gambino F, Casassus G, Poulain B, Humeau Y, Luthi A (2009) L-type voltage-dependent Ca^{2+} channels mediate expression of presynaptic LTP in amygdala. Nat Neurosci 12(9):1093–1095
109. Kamiya H, Umeda K, Ozawa S, Manabe T (2002) Presynaptic Ca^{2+} entry is unchanged during hippocampal mossy fiber long-term potentiation. J Neurosci 22(24):10524–10528
110. Regehr WG, Tank DW (1991) The maintenance of LTP at hippocampal mossy fiber synapses is independent of sustained presynaptic calcium. Neuron 7(3):451–459
111. Reid CA, Dixon DB, Takahashi M, Bliss TV, Fine A (2004) Optical quantal analysis indicates that long-term potentiation at single hippocampal mossy fiber synapses is expressed through increased release probability, recruitment of new release sites, and activation of silent synapses. J Neurosci 24(14):3618–3626
112. Chen C, Regehr WG (1997) The mechanism of cAMP-mediated enhancement at a cerebellar synapse. J Neurosci 17(22):8687–8694

113. Dudek SM, Bear MF (1992) Homosynaptic long-term depression in area CA1 of hippocampus and effects of N-methyl-D-aspartate receptor blockade. Proc Natl Acad Sci U S A 89(10):4363–4367
114. Mulkey RM, Malenka RC (1992) Mechanisms underlying induction of homosynaptic long-term depression in area CA1 of the hippocampus. Neuron 9(5):967–975
115. Kirkwood A, Dudek SM, Gold JT, Aizenman CD, Bear MF (1993) Common forms of synaptic plasticity in the hippocampus and neocortex in vitro. Science 260(5113):1518–1521
116. Cummings JA, Mulkey RM, Nicoll RA, Malenka RC (1996) Ca^{2+} signaling requirements for long-term depression in the hippocampus. Neuron 16(4):825–833
117. Evans RC, Blackwell KT (2015) Calcium: amplitude, duration, or location? Biol Bull 228(1):75–83
118. Isaac J (2001) Protein phosphatase 1 and LTD: synapses are the architects of depression. Neuron 32(6):963–966
119. Morishita W, Connor JH, Xia H, Quinlan EM, Shenolikar S, Malenka RC (2001) Regulation of synaptic strength by protein phosphatase 1. Neuron 32(6):1133–1148
120. Kirkwood A, Bear MF (1994) Homosynaptic long-term depression in the visual cortex. J Neurosci 14(5 Pt 2):3404–3412
121. Palmer CL, Lim W, Hastie PG, Toward M, Korolchuk VI, Burbidge SA et al (2005) Hippocalcin functions as a calcium sensor in hippocampal LTD. Neuron 47(4):487–494
122. Oliet SH, Malenka RC, Nicoll RA (1997) Two distinct forms of long-term depression coexist in CA1 hippocampal pyramidal cells. Neuron 18(6):969–982
123. Linden DJ, Connor JA (1991) Participation of postsynaptic PKC in cerebellar long-term depression in culture. Science 254(5038):1656–1659
124. Jo J, Heon S, Kim MJ, Son GH, Park Y, Henley JM et al (2008) Metabotropic glutamate receptor-mediated LTD involves two interacting Ca^{2+} sensors, NCS-1 and PICK1. Neuron 60(6):1095–1111
125. Lüscher C, Huber KM (2010) Group 1 mGluR-dependent synaptic long-term depression: mechanisms and implications for circuitry and disease. Neuron 65(4):445–459
126. Bellone C, Luscher C, Mameli M (2008) Mechanisms of synaptic depression triggered by metabotropic glutamate receptors. Cell Mol Life Sci 65(18):2913–2923
127. Fitzjohn SM, Palmer MJ, May JE, Neeson A, Morris SA, Collingridge GL (2001) A characterisation of long-term depression induced by metabotropic glutamate receptor activation in the rat hippocampus in vitro. J Physiol 537(Pt 2):421–430
128. Schnabel R, Kilpatrick IC, Collingridge GL (1999) An investigation into signal transduction mechanisms involved in DHPG-induced LTD in the CA1 region of the hippocampus. Neuropharmacology 38(10):1585–1596
129. Hagena H, Manahan-Vaughan D (2011) Learning-facilitated synaptic plasticity at CA3 mossy fiber and commissural-associational synapses reveals different roles in information processing. Cereb Cortex 21(11):2442–2449
130. Cho JH, Deisseroth K, Bolshakov VY (2013) Synaptic encoding of fear extinction in mPFC-amygdala circuits. Neuron 80(6):1491–1507
131. Rodríguez-Moreno A, Gonzalez-Rueda A, Banerjee A, Upton AL, Craig MT, Paulsen O (2013) Presynaptic self-depression at developing neocortical synapses. Neuron 77(1):35–42
132. Bender VA, Bender KJ, Brasier DJ, Feldman DE (2006) Two coincidence detectors for spike timing-dependent plasticity in somatosensory cortex. J Neurosci 26(16):4166–4177
133. Bender KJ, Allen CB, Bender VA, Feldman DE (2006) Synaptic basis for Whisker deprivation-induced synaptic depression in rat somatosensory cortex. J Neurosci 26(16):4155–4165
134. Larsen Rylan S, Smith Ikuko T, Miriyala J, Han Ji E, Corlew Rebekah J, Smith Spencer L et al (2014) Synapse-specific control of experience-dependent plasticity by presynaptic NMDA receptors. Neuron 83(4):879–893
135. Rodríguez-Moreno A, Paulsen O (2008) Spike timing-dependent long-term depression requires presynaptic NMDA receptors. Nat Neurosci 11(7):744–745

136. Nevian T, Sakmann B (2006) Spine Ca^{2+} signaling in spike-timing-dependent plasticity. J Neurosci 26(43):11001–11013
137. Sjöström PJ, Turrigiano GG, Nelson SB (2003) Neocortical LTD via coincident activation of presynaptic NMDA and cannabinoid receptors. Neuron 39(4):641–654
138. Rodríguez-Moreno A, Banerjee A, Paulsen O (2010) Presynaptic NMDA receptors and spike timing-dependent depression at cortical synapses. Front Synaptic Neurosci 2:18
139. Andrade-Talavera Y, Duque-Feria P, Paulsen O, Rodríguez-Moreno A (2016) Presynaptic spike timing-dependent long-term depression in the mouse hippocampus. Cereb Cortex 26(8):3637–3654
140. Banerjee A, Gonzalez-Rueda A, Sampaio-Baptista C, Paulsen O, Rodríguez-Moreno A (2014) Distinct mechanisms of spike timing-dependent LTD at vertical and horizontal inputs onto L2/3 pyramidal neurons in mouse barrel cortex. Phys Rep 2(3):e00271
141. Pérez-Rodríguez M, Arroyo-García LE, Prius-Mengual J, Andrade-Talavera Y, Armengol JA, Pérez-Villegas EM et al (2018) Adenosine receptor-mediated developmental loss of spike timing-dependent depression in the hippocampus. Cereb Cortex. https://doi.org/10.1093/cercor/bhy194
142. Rodríguez-Moreno A, Kohl MM, Reeve JE, Eaton TR, Collins HA, Anderson HL et al (2011) Presynaptic induction and expression of timing-dependent long-term depression demonstrated by compartment-specific photorelease of a use-dependent NMDA receptor antagonist. J Neurosci 31(23):8564–8569
143. Duguid I, Sjöström PJ (2006) Novel presynaptic mechanisms for coincidence detection in synaptic plasticity. Curr Opin Neurobiol 16(3):312–322
144. Yokoi M, Kobayashi K, Manabe T, Takahashi T, Sakaguchi I, Katsuura G et al (1996) Impairment of hippocampal mossy fiber LTD in mice lacking mGluR2. Science 273(5275):645–647
145. Kobayashi K, Manabe T, Takahashi T (1996) Presynaptic long-term depression at the hippocampal mossy fiber-CA3 synapse. Science 273(5275):648–650
146. Tzounopoulos T, Janz R, Südhof TC, Nicoll RA, Malenka RC (1998) A role for cAMP in long-term depression at hippocampal mossy fiber synapses. Neuron 21(4):837–845
147. Kobayashi K, Manabe T, Takahashi T (1999) Calcium-dependent mechanisms involved in presynaptic long-term depression at the hippocampal mossy fibre-CA3 synapse. Eur J Neurosci 11(5):1633–1638
148. Lyon L, Borel M, Carrion M, Kew JN, Corti C, Harrison PJ et al (2011) Hippocampal mossy fiber long-term depression in Grm2/3 double knockout mice. Synapse 65(9):945–954
149. Maccaferri G, Toth K, McBain CJ (1998) Target-specific expression of presynaptic mossy fiber plasticity. Science 279(5355):1368–1370

Chapter 39
Calcium Signaling During Brain Aging and Its Influence on the Hippocampal Synaptic Plasticity

Ashok Kumar

Abstract Calcium (Ca^{2+}) ions are highly versatile intracellular signaling molecules and are universal second messenger for regulating a variety of cellular and physiological functions including synaptic plasticity. Ca^{2+} homeostasis in the central nervous system endures subtle dysregulation with advancing age. Research has provided abundant evidence that brain aging is associated with altered neuronal Ca^{2+} regulation and synaptic plasticity mechanisms. Much of the work has focused on the hippocampus, a brain region critically involved in learning and memory, which is particularly susceptible to dysfunction during aging. The current chapter takes a specific perspective, assessing various Ca^{2+} sources and the influence of aging on Ca^{2+} sources and synaptic plasticity in the hippocampus. Integrating the knowledge of the complexity of age-related alterations in neuronal Ca^{2+} signaling and synaptic plasticity mechanisms will positively shape the development of highly effective therapeutics to treat brain disorders including cognitive impairment associated with aging and neurodegenerative disease.

Keywords Calcium homeostasis · Aging · Hippocampus · N-methyl-D-aspartate receptor · Voltage-dependent calcium channels · Intracellular calcium stores · Synaptic plasticity · LTP · LTD

39.1 Introduction

The Calcium (Ca^{2+}) ions are primary signaling molecules regulating a plethora of diverse and important cellular processes including apoptosis, energy production, gene regulation, cell proliferation, membrane excitability, and synaptic plasticity [1–5]. Due to the omnipresent environment of Ca^{2+} signaling, Ca^{2+} is one of the most highly regulated ions. The cytoplasmic concentration of Ca^{2+} is maintained

A. Kumar (✉)
Department of Neuroscience, McKnight Brain Institute, University of Florida, Gainesville, FL, USA
e-mail: kash@ufl.edu

M. S. Islam (ed.), *Calcium Signaling*, Advances in Experimental Medicine and Biology 1131, https://doi.org/10.1007/978-3-030-12457-1_39

considerably lower than the concentration in the extracellular space [6–8]. Therefore, any variation in Ca^{2+} signaling mechanisms, unless compensated by another mechanism, will result in a modification of cell function. Ca^{2+} signaling within a neuron is very complex, and an extremely precise and dynamic regulation of Ca^{2+} concentration is required for normal functioning. Ca^{2+} signaling depends primarily on a prompt and momentary increase in intracellular Ca^{2+} concentration through influx of Ca^{2+} from various sources including Ca^{2+} permeable plasma membrane receptors, ion channels, and internal Ca^{2+} sources. In most cells, multiple mechanisms exist whereby an augmentation in intracellular Ca^{2+} concentrations may ensue.

The major sources of intracellular Ca^{2+} include Ca^{2+} influx through various voltage-dependent Ca^{2+} channels (VDCCs), ligand-gated nonselective glutamate receptors, such as N-methyl-D-aspartate (NMDA) receptor, store-operated Ca^{2} channels (SOCs) as well as the release of Ca^{2+} from intracellular Ca^{2} stores (ICS) [9–13]. The transient receptor potential (TRP) channels, which are non-selective cation channels with high Ca^{2+} permeability, also contribute to influx of Ca^{2+} into the cell cytoplasm [14–19] (Fig. 39.1). The relative contribution of these sources will depend on the cell type: neuron, astrocyte, oligodendrocyte or microglia. In the case of neurons, Ca^{2+} sources will vary depending on their size, transmitter system, and location in excitatory or inhibitory neural circuits.

An elevation in intracellular concentration of free Ca^{2} plays an important role in the induction and maintenance of activity-dependent synaptic plasticity [20–22]. The level of Ca^{2} in response to synaptic activity determines the degree and direction of synaptic efficacy. Long-term potentiation (LTP) and long-term depression (LTD), the two major forms of activity-dependent synaptic plasticity, are the best cellular correlates of learning and memory, and are studied extensively across various brain regions [23–27]. LTP is a long lasting increase in synaptic strength in response to intense synaptic activity [20, 28, 29]. The induction of LTP requires activation of postsynaptic NMDA receptors resulting in a large, yet brief, influx of Ca^{2+} through the NMDA receptor channel. In turn, this large rise in intracellular Ca^{2+} activates Ca^{2+} sensitive kinases such Ca^{2+}/calmodulin-dependent kinase II (CaMKII). Kinase activity increases the strength of the synaptic response through phosphorylation of α-amino-3-hydroxy-5-methyl-4-isoxazolepropionic acid (AMPA) glutamate receptors, which leads to insertion of additional AMPA-glutamate receptors into the post-synaptic membrane [30–35]. In contrast to LTP, LTD is induced by low synaptic activity, which leads to a modest and prolonged rise in intracellular Ca^{2+} concentration [36–40]. The modest and sustained rise in intracellular Ca^{2+} concentration activates Ca^{2+}-sensitive phosphatases that decrease synaptic transmission through dephosphorylation of AMPA-glutamate receptors, resulting in their removal from the post-synaptic membrane [41] (Fig. 39.2). Due to the differential level of Ca^{2+} involved in the generation of the various forms of synaptic plasticity, any treatment that modifies Ca^{2+} influx into the cytoplasm can influence the direction and degree of synaptic plasticity. The dependence on differential intracellular Ca^{2+} levels in determining the form of synaptic plasticity underlies the observation that stimulation patterns for the induction of LTP and LTD tend toward high and low-

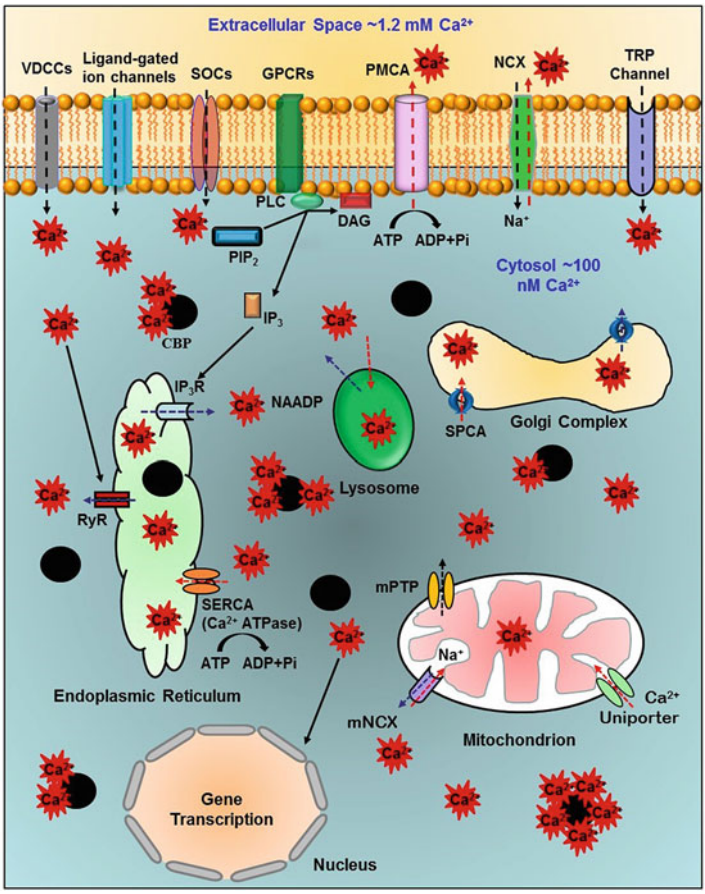

Fig. 39.1 The schematic illustration of various Ca^{2+} sources including ligand-gated ion channels (such as ionotropic glutamate NMDA receptor), voltage-dependent Ca^{2+} channels (*VDCC*), G protein-coupled receptors (*GPCRs*), store-operated Ca^{2} channels (SOCs), and transient receptor potential channels (TRP channels). Various channels permeable to Ca^{2+} exist and are expressed both on cell plasma membrane and on membrane of organelles. Alterations in cytosolic Ca^{2+} are dynamically regulated through interplay of various Ca^{2+}channels, exchange pumps, and transporters. Ca^{2+} (*red spark*) influxes into the cytosol (*black dashed arrows*) through various sources in a healthy cell. NMDA receptor and VDCCs are highly selective plasma proteins that mediate Ca^{2+} signals in response to membrane depolarization. The release of Ca^{2+} into the cytoplasm also occurs from the intracellular Ca^{2+} stores through ryanodine receptors (*RyR*), and inositol (1,4,5)-trisphosphate receptor (*IP3R*) involving phospholipase C (PLC), diacylglycerol (DAG), and inositol (1,4,5) trisphosphate (IP_3). Organelles, including endoplasmic reticulum, mitochondria, and lysosomes act as a Ca^{2+} buffering system, releasing, and sequestering Ca^{2+} in and out of the cytosol. Further, the model depicts Ca^{2+} buffering and extrusion pathways (*red dashed arrows*), involving plasma membrane Ca^{2+} ATPase (PMCA), sodium-calcium exchangers (NCX) located on plasma membrane and mitochondria (mNCX), sarcoplasmic reticulum Ca^{2+} ATPases (*SERCA*), various Ca^{2+} binding proteins (*CBP*), nicotinic acid adenine dinucleotide phosphate (NAADP), mitochondrial Ca^{2+} uniporter, mitochondrial permeability transition pore (*mPTP*), and secretory pathway Ca^{2+}-ATPases (*SPCA*)

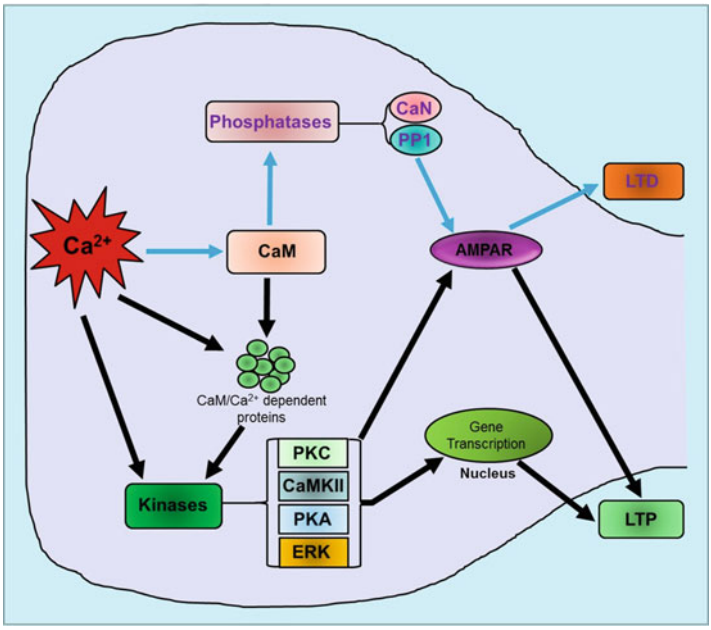

Fig. 39.2 Schematic representation of Ca^{2+} signaling in two major forms of synaptic plasticity, LTD and LTP. The homeostasis of intracellular Ca^{2+} is dynamically regulated. Ca^{2+} is required by a large number of proteins to mediate various cellular functions including synaptic plasticity. Activity-dependent changes in synaptic function results in elevation of intracellular Ca^{2+} levels through influx from various sources including VDCCs, NMDA receptor, and ICS. The large, but brief rise in intracellular Ca^{2+} following intense synaptic activity activates Ca^{2+} sensitive kinases and Ca^{2+} calmodulin (CaM)-dependent proteins. Activation of various kinase-dependent signaling cascades, including protein kinase C (PKC), CaM-dependent kinase II (CaMKII), protein kinase A (PKA), and extracellular regulated kinase (ERK), increases the strength of the synaptic response (LTP) through phosphorylation of AMPA type glutamate receptors (AMPAR), which leads to insertion of additional AMPA-glutamate receptors into the post-synaptic membrane (black arrows). LTD is induced by low synaptic activity, which leads to a modest and prolonged rise in intracellular Ca^{2+} concentration. The modest and sustained rise in intracellular Ca^{2+} activates Ca^{2+}-sensitive phosphatases including calcineurin (CaN) and protein phosphatase 1 (PP1) via CaM and induces a decrease in synaptic transmission (LTD) through dephosphorylation of AMPAR, resulting in their removal from the post-synaptic membrane (blue arrows)

frequency patterns, respectively. Theoretical models suggest that synaptic plasticity is a function of synaptic activity, such that low frequency stimulation induces LTD. As neural activity increases, there is a transition from net LTD to induction of LTP [40, 42]. The thresholds for induction of LTD and LTP, as defined by afferent activity, are thought to reflect activity-dependent changes in the level of intracellular Ca^{2+}, which in turn, activate Ca^{2+}-dependent enzymes. The current chapter centers on age-associated changes on various Ca^{2+} sources and how these alterations in Ca^{2+} signaling in the CA1 region of the hippocampus contributes to altered synaptic plasticity.

39.2 Ca^{2+} Hypothesis of Brain Aging and Influence of Aging on Various Ca^{2+} Sources

The Ca^{2+} 'dysregulation' hypothesis of brain aging and Alzheimer's disease formulated in the 1980s was based on discrete observations of alterations in processes that are regulated by Ca^{2+} [43–46]. Almost four decades of research, has accumulated substantial evidence for alterations in neuronal Ca^{2+} homeostasis in contributing to changes in various processes including cellular senescence and neurodegenerative diseases [47–60]. However, no single mechanism for Ca^{2+} dysregulation has been established. Rather, the causes and consequences of Ca^{2+} dysregulation vary across the central nervous system. As we increase our sophistication for identifying molecular and cellular processes, we are likely to find complex patterns of impaired/spared cellular function related to multiple Ca^{2+} regulating mechanisms. Normal aging is not associated with a loss of neurons [61, 62], so altered Ca^{2+} dependent physiology hypothesis including senescent synaptic plasticity is proposed. Age-associated changes in Ca^{2+} signaling mechanisms, including Ca^{2+} sources, contribute to alteration in synaptic function and presumably account for impaired cognitive function [21, 46, 55, 56, 60, 63–68].

39.3 Voltage-Dependent Ca^{2+} Channels

Voltage-dependent Ca^{2+} channels (VDCCs) are highly selective plasma membrane proteins, which open in response to membrane depolarization and allow Ca^{2+} influx into the cell from the extracellular space. These proteins, are heteromultimers composed of an α_1 subunit and three auxiliary subunits, $\alpha_2\delta$, $\beta_{1-4,}$ and γ [69–72], provide one of the most effective sources of Ca^{2+} influx into the neuron [73]. The pore forming α_1 subunit (190 kDa) of VDCCs is the primary subunit essential for channel functioning. Each α_1 subunit has four homologous domains (I-IV), which are composed of six transmembrane helices. The fourth transmembrane helix of each domain contains the voltage-sensing motif. Two classes of VDCCs have been described; high-voltage-gated and low-voltage-gated channels, which are activated by strong and weak depolarization, respectively. Based on differential biophysical properties and sensitivity to pharmacological agents, high-voltage-gated channels are further classified into the L ($Ca_v1.1$-3), P/Q ($Ca_v2.1$), and N ($Ca_v2.2$) type channels. The low-voltage-gated channels include the T ($Ca_v3.1$) type channels. In addition, an intermediate-voltage-gated channel, R ($Ca_v2.3$) type is expressed throughout the central nervous system [74–80].

In aged animals, the whole-cell L-type Ca^{2+} currents in CA1 pyramidal neurons are enhanced [81, 82], and there is an increase in the density of functional L-type VDCCs [65]. The idea that L-channels are augmented in the hippocampus during aging is also supported by mRNA and protein expression studies indicating an increase in $Ca_v1.3$ [83–86]. Furthermore, posttranslational changes including

the phosphorylation state of the $Ca_v1.2$ channel could contribute to age-associated increase in activity [87–89]. However, L-channel associated intracellular Ca^{2+} transients may demonstrate region specific variations within the hippocampus itself. For example, result indicates that CA3 interneurons in aged hippocampus exhibit no alterations in intracellular Ca^{2+} transients at resting state; however, larger Ca^{2+} transients are evident in the presence of external excitatory drive produced by kainate application [90].

It is not clearly elucidated why L-channels increase in the hippocampus during aging. The enhancement in L-channel function appears to be specific to hippocampal pyramidal cells. The expression of L-channels in the hippocampus is regulated by the sex steroid estrogen, such that an increased expression is associated with the decline of the hormone during aging [91]. Finally, it is possible that the increased L-channel function, enhanced the amplitude of afterhyperpolarization (AHP), and reduction in cell excitability represent compensatory mechanisms associated with Ca^{2+} dysregulation during senescence, which attempts to restrict depolarization and further influx of Ca^{2+} through NMDA receptors [21, 22, 63, 92]. Several cellular biomarkers of senescent physiology in the hippocampus are dependent on VDCC function, and L-type channel blockers can reverse age-related changes in the magnitude of the AHP and spike frequency adaptation [39, 44, 46, 65, 93, 94].

39.4 Ligand-Gated Ion Channels: N-Methyl-D-Aspartate (NMDA) Receptor

Various less-selective ligand-gated ion channels, including NMDA receptors, allow influx of Ca^{2+} into intracellular space. NMDA receptors are ionotropic non-selective cationic glutamate receptors, which play a critical role in the rapid regulation of synaptic plasticity. NMDA receptors are hetero-tetrameric protein complexes composed of two classes of subunits, the ubiquitously expressed and essential subunit (GluN1) and a modulatory subunit (GluN2A- GluN2D) [95–100]. The majority of NMDA receptors are assemblies of two GluN1 subunits, the ubiquitously expressed and obligatory subunit, and two GluN2A-D subunits, a modulatory subunit. In addition, GluN3 subunits (GluN3A and GluN3B), without involving GluN2 subunits, can assemble with GluN1 subunits to form functional receptors [101–105]. The activation of NMDA receptors requires binding of a ligand (glutamate), membrane depolarization (to remove the Mg^{2+} block of the channel), and binding of a co-agonist, glycine. Since NMDA receptor is a non-selective cation channel, its activation and opening leads to simultaneous influx of Na^+ and Ca^{2+} ions [106]. However, between the two predominant ionotropic glutamate receptors (AMPA and NMDA) subtypes, the NMDA receptors are the most permeable to Ca^{2+} ions [107].

There is considerable evidence to indicate that aging is associated with a decline in NMDA receptor function within brain regions involved in higher brain

function including learning and memory [108–115]. Perhaps the strongest evidence for a reduction in NMDA receptor function comes from electrophysiological studies, which indicate that the NMDA receptor mediated excitatory post synaptic potentials in the Schaeffer collateral pathway of the hippocampus are reduced by approximately 50% in aged animals [64, 110, 111, 116–120]. Several studies indicate a decrease in the level of NMDA receptor protein expression in the hippocampus during aging [114, 115, 121–129]; further, the decrease has primarily been localized to region CA1 [112, 130–132]. These studies report reduced binding of [^{3}H] glutamate (agonist site), [^{3}H] glycine (GluN1 site), [^{3}H] CPP (a competitive antagonist to the L-glutamate binding site), and [^{3}H] MK-801 (an open channel blocker) in the hippocampus of aged rats. However, others have reported no age-related change in antagonist binding [122, 125, 133, 134] or an increased MK-801 binding in animals with learning and retention deficits [135, 136]. It is interesting to note that MK-801 binds to the hydrophobic channel domain of NMDA receptor, exclusively labeling open channels. Thus, an apparent increase in NMDA receptor channel open time may act as a compensatory mechanism for the decrease in receptor number [137]. However, the majority of reports indicate that the net function of the NMDA receptors decreases at CA3-CA1 hippocampal synaptic contacts during senescence [116–120].

One of the potential mechanisms for the observed decrease in the NMDA receptor function is related to altered expression of specific NMDA receptor subunits [138]. Significant decreases have been observed in the expression of GluN1 protein [111, 139, 140] and GluN1 mRNA [141] levels in the aged hippocampus. In contrast, other studies report no age-related decrease in GluN1 protein expression in the whole hippocampus [115, 142]. Despite the lack of congruent changes in the expression levels in the hippocampus, other brain regions exhibit a decline in GluN1 mRNA expression during aging. Indeed, senescence-related decrease in the GluN1 mRNA expression has been observed in the medial basal hypothalamus-median eminence [113], in the medial and lateral prefrontal cortices [143], and in the insular, orbital, and somatosensory cortices [129]. Results indicate age-related changes in the modulatory GluN2 subunits. A decrease in the GluN2A protein expression has been observed in the hippocampus [114, 142]. Furthermore, GluN2A mRNA expression was reported to decline in the ventral hippocampus [141]. In contrast, results from other studies report no significant change in the GluN2A protein expression levels in the hippocampus [142, 144]. Age-related changes have also been reported for GluN2B subunit of the NMDA receptor; in particular the expression of GluN2B protein [115, 140] and GluN2B mRNA [141, 145] declines in the hippocampus.

From a physiological standpoint, the changes in the expression of specific GluN2 subunits could have dramatic influences on NMDA receptor function through the regulation of mean channel open time and conductance of the NMDA receptors. Studies on recombinant NMDA receptor expressed in *Xenopus* oocytes demonstrate that NMDA receptors containing the GluN2A subunit (GluN2A-NMDARs) have faster deactivation kinetics relative to GluN2B containing NMDARs (GluN2B-NMDARs) [95], such that smaller ion flux is observed for the GluN2A-NMDARs,

relative to the GluN2B-NMDA receptors. Thus, a shift in the level of GluN2 subunit expression could modify the time course and magnitude of the Ca^{2+} signal leading to reduced Ca^{2+} influx associated with loss of GluN2B. A shift in GluN2A and GluN2B expression is thought to contribute to developmental changes in cognition and synaptic function [146].

Alternatively, it is possible that alterations in the NMDA receptor localization through the insertion of receptors into the membrane or recruitment of extra-synaptic receptors into the synapse will have important effects on NMDA receptor function during aging. It has been suggested that GluN2B containing receptors may be more prevalent at extra-synaptic sites [147], which could temporarily house the NMDA receptors, before being internalized into the cytoplasm [148, 149]. Results indicate that extra-synaptic NMDA receptors couple to different signaling cascades, initiate mechanisms that oppose synaptic potentiation, by shutting off the activity of cAMP response element binding protein and decreasing expression of brain-derived neurotropic factor [150, 151]. However, it remains to be clearly investigated whether altered localization of the NMDA receptors (specifically extra-synaptic localization) is the mechanism by which the NMDA receptor function declines during senescence.

Another likely candidate mechanism for regulating NMDA receptor function during aging is posttranslational modification of the receptor. In particular, the function of the NMDA receptor is influenced by its phosphorylation state. Activation of the tyrosine kinase [152, 153], protein kinase C [154, 155] and protein kinase A [156] increases NMDA receptor mediated currents. In contrast, protein phosphatases, including calcineurin (CaN) and protein phosphatase 1, decrease NMDA receptor currents [153, 156, 157]. Phosphorylation state of GluN2A and GluN2B subunits can rapidly regulate surface expression and localization of these receptors [158–161]. For example, phosphorylation of serine residues within the alternatively spliced cassettes of the C-terminal tail of GluN1 promotes receptor trafficking from the endoplasmic reticulum and insertion into the postsynaptic membrane [162, 163]. Finally, increased phosphatase activity has been linked to the internalization of NMDA receptors [164]. Thus, the kinases and phosphatases act as molecular switches which increase or decrease NMDA receptor function, respectively. Interestingly, aging is associated with a shift in the balance of kinase/phosphatase activity, favoring an increase in the phosphatase activity [22, 88, 165]. Thus, alterations in the phosphorylation state of the NMDA receptor could underlie the decrease in the NMDA receptor function during aging [166].

NMDA receptor function can be altered by the oxidation and reduction of sulfhydryl moieties on their structure. Previous research demonstrates that oxidizing agents like 5,5′-dithiobis(2-nitrobenzoic acid) [167], hydroxyl radicals generated by xanthine/xanthine oxidase [168] and oxidized glutathione [169] decrease NMDA receptor function in the neuronal cell cultures. The decrease in NMDA receptor function under oxidizing conditions is thought to result from the formation of disulfide bonds on the sulfhydryl group containing amino acid residues in NMDA receptors [170–172]. The aging brain is associated with an increase in the levels of oxidative stress and/or a decrease in redox buffering capacity [173–175], conditions

that should promote a decrease in NMDA receptor function. Little or no effect of oxidizing agents was observed for older animals, suggesting that cells were already in an oxidized state. In contrast, reducing conditions enhanced NMDA receptor mediated synaptic responses in hippocampus of aged animals [64, 118–120, 176–179]. Results provide evidence for a link between the redox-mediated decrease in NMDA receptor function and the emergence of an age-related cognitive phenotype with impairment in the rapid acquisition and retention of novel spatial information [118, 119]. Further, results demonstrate that the age-related decrease in NMDA receptor-mediated synaptic responses at CA3-CA1 hippocampal synapses is related to redox state such that the reducing agent significantly enhanced the NMDA receptor component of the synaptic response to a greater extent in cognitively impaired animals relative to unimpaired animals [118, 180].

NMDA receptor function in neurons is regulated by local supporting cells, astrocytes and microglia, thus acting as an additional possible mechanism for the age-related changes to NMDA receptor function. Astrocytes are a major source of D-serine, an endogenous co-agonist for the NMDA receptor, which binds to the glycine site [181]. An age-related loss of D-serine is observed in the hippocampus of rats [182]. Furthermore, the age-related decline in the NMDA receptor function is rescued by D-cycloserine [128]. Microglia contribute to the brain's immune system and activated microglia can also release D-serine [183, 184]. In accordance with this idea, recent reports suggest that microglia can potentiate the NMDA receptor-mediated synaptic responses in cortical neurons [185, 186]. Finally, there is evidence for a feedback reduction in NMDA receptors due to excess synaptic glutamate activity during microglial activation [187, 188]. In light of the interactions of NMDA receptors and glial cells, it is important to consider the possibility that the decrease in NMDA receptor function might represent a compensatory neuroprotective mechanism associated with inappropriate receptor activity or increased Ca^{2+} due to other mechanisms. Thus, impaired NMDA receptor-dependent synaptic plasticity and memory decline may be epiphenomena due to processes for cell preservation [21, 22, 63, 92]. Indeed, upregulation of GluN2B subunits improves synaptic plasticity and memory in aged mice [117, 189] indicating that increased NMDA receptor function can ameliorate physiological aging.

39.5 Ca^{2+} Release from Intracellular Ca^{2+} Stores

Intracellular Ca^{2+} stores (ICS), in addition to Ca^{2+} influx from outside the cell, dynamically participate and play a significant role in regulating larger Ca^{2+} signals [190, 191]. Organelles, including the endoplasmic reticulum (ER), mitochondria, nuclear envelope, neurotransmitter vesicles, and lysosomes play a dual role by acting as a Ca^{2+} buffering-sequestering system for intracellular Ca^{2+} and releasing Ca^{2+} into the cytoplasm [58, 192–202]. Thus, there are at least two possible

mechanisms by which ICS regulate Ca^{2+} homeostasis: (1) release of stored Ca^{2+} to enhance Ca^{2+} signals and (2) removing cytosolic Ca^{2+} following a large influx.

Two independent pathways, Ca^{2+}-induced Ca^{2+} release (CICR) and inositol (1,4,5)-trisphosphate (IP_3)-induced Ca^{2+} release (IICR) control Ca^{2+} release from intracellular stores. The CICR is a Ca^{2+} augmentation process initiated by Ca^{2+} influx through the plasma membrane that activates ryanodine receptors (RyRs), while IICR is IP_3-acivated release of Ca^{2+} from intracellular sources [193]. The release of Ca^{2+} from the ER is initiated by the activation of G protein-coupled receptors (GPCRs). GPCRs activate phospholipase C (PLC) to form diacylglycerol (DAG) and IP_3 that act on IP_3 receptors (IP_3Rs) to release Ca^{2+} from ICS. Several studies indicate age-related changes in GPCRs or PLC [203–205]. Despite a general decrease in the receptor, the literature suggests that a decrease in IP_3 induced Ca^{2+} release is either limited to cortical cells [206] or no age-related change is observed [206–210]. The disconnect between a reduction in IP_3R expression and the apparent absence of an effect of age on IP_3-induced Ca^{2+} release may be due to increased oxidation of the IP_3Rs which has been demonstrated to increase IP_3R function in brain cells [211, 212]. As such, reduced expression may act as compensation for an altered redox state, in order to maintain proper IP_3 signaling.

CICR is a Ca^{2+} amplification process that is initiated by influx of Ca^{2+} through membrane channels or from ICS through the activation of IP_3Rs. The intracellular Ca^{2+} binds RyRs to release additional Ca^{2+} into the cytosol from the ER. Accumulating evidence supports a role of altered CICR in contributing to altered physiology of normal aging. Rather, an age-related increase in oxidative stress and a shift in the intracellular redox state may enhance the responsiveness of RyRs to intracellular Ca^{2+} [68, 213–215]. Ca^{2+} release from ICS contributes towards enhancing NMDA-receptor mediated Ca^{2+} influx for induction of LTP [216–219]. Recent results reveal that activation of Ca^{2+} release from RyRs receptor facilitated LTD while attenuation of RyR-mediated Ca^{2+} release significantly prevented the induction of LTD in young animals [220]. Aging is associated with an increase RyRs protein content in hippocampal tissue and enhanced oxidation of cysteine residues located on RyRs [221]. Increased CICR appears to contribute to altered physiology in hippocampal neurons [38, 177, 222–224]. As noted above, hippocampal cells exhibit increase Ca^{2+} from L-type Ca^{2+} channels, which could provide a source of Ca^{2+} to fill ICS and activate CICR from ICS. Thus, the contribution of CICR to aging physiology in hippocampal cells may be due to a summation of various mechanisms.

39.6 Influence of Aging-Associated Altered Ca^{2+} Regulation on Synaptic Plasticity: LTP and LTD

Complex and synergistic molecular and cellular processes probably contribute to memory formation and storage in the brain. Several evidence suggest that multiple

mechanisms including synaptic changes and intrinsic neuronal excitability are involved in information processing and storage [23–27, 225, 226]. Aging is a complex process; in general, aging is associated with a shift in synaptic plasticity favoring decreased synaptic transmission (i.e. LTD) and a reduced ability to enhance synaptic transmission through LTP. Indeed, the impairment in LTP may begin in middle age [227]. It has been suggested that the shift in synaptic plasticity, favoring LTD over LTP, contributes to the decrease in synaptic transmission observed in aged animals [21, 22, 63, 92]. In considering the mechanism for synaptic plasticity involvement in regulating synaptic transmission during aging, it is important to note that the shift in synaptic modifiability is not due to a change in the expression mechanisms. For example, there is no age-related difference in the maximal LTP magnitude observed under conditions in which strong burst of synaptic stimulation is delivered [228–231]. In addition, maximal LTP can be observed in aged animals when single pulses are combined with strong postsynaptic depolarization [232], or weak stimulation is combined with increased Ca^{2+} in the recording medium [233] suggesting that the NMDA receptor/Ca^{2+}-dependent signaling pathways for the induction of LTP are maintained.

Similarly, the increase in LTD in aged animals is not due to an enhancement in the expression mechanism or an increase in the maximum amplitude of LTD. Robust LTD can be observed in adults when Ca^{2+} levels are elevated in the recording media [228]. In addition, a substantial level of LTD can be observed by using more effective induction protocols involving paired-pulse low-frequency stimulation [234, 235]. In fact, administration of multiple episodes of the paired-pulse low-frequency stimulation produces similar levels of LTD in aged and adult animals [231]. Thus, it can be concluded that the age-related difference in synaptic modifiability is not due to a change in the expression mechanisms.

One possibility for a shift in the balance of LTP and LTD is an adjustment in the induction mechanisms, which are engaged to initiate synaptic modifications. The original reports of increased susceptibility to LTD in aged animals hypothesized that altered Ca^{2+} regulation resulted in a shift in the threshold for induction of synaptic plasticity over the life span [21, 60, 228]. Indeed, the ability to generate LTD using the weaker stimulation protocol decreases as animals mature from juvenile to adult [235, 236], and the propensity to induce LTD is once again augmented with advanced age [38, 228, 237, 238]. The dependence on Ca^{2+} regulation for LTD induction is readily demonstrated by altering the Ca^{2+}/Mg^{2+} ratio in the recording medium. While LTD is observed for aged animals and little or no LTD is observed for adult animals under Ca^{2+}/Mg^{2+} conditions that mimic cerebral spinal fluid, LTD can be readily observed in adults if the level of Ca^{2+} is increased relative to Mg^{2+}. Moreover, the elevation of Ca^{2+}/Mg^{2+} ratio may prevent LTD in the oldest animals due to a shift in intracellular Ca^{2+} levels beyond the range needed for LTD-induction or possibly due to increased susceptibility to toxic effects of higher Ca^{2+} in the oldest animals.

Interestingly, an age-related reduction in susceptibility to LTP is observed when stimulation parameters are set near the threshold for LTP-induction [223, 237, 239–241]. The induction mechanism for LTP involves the activation of NMDA

receptors through the coincident binding of glutamate to the receptor and sufficient postsynaptic depolarization to remove the Mg^{2+} block from the NMDA receptor channel. In turn, weaken synaptic depolarization or disruption of NMDA receptors could contribute to impairments in induction of LTP. Evidence has been provided that NMDA receptor function may be compromised due to altered Ca^{2+} regulation leading to increased activity of the Ca^{2+}-dependent phosphatase, CaN. The activity of CaN depends on a modest rise in intracellular Ca^{2+} and aged memory impaired animals exhibit an increase in CaN activity [165]. In turn, CaN can act on NMDA receptors to reduce Ca^{2+} influx [157, 242].

The idea that induction of LTP is subdued as a result of a reduction in NMDA receptor activation is supported by research showing that induction deficits can be overcome by strong postsynaptic depolarization [232]. Indeed, there are several reasons to believe that an inability to achieve sufficient postsynaptic depolarization, a prerequisite for NMDA receptor activation, may be more problematic for LTP induction during aging. The reduced synaptic strength of aged animals may result in a reduced afferent cooperativity in depolarizing the postsynaptic neuron and an inability to reach the level of depolarization needed for NMDA receptor activation. The AHP, a Ca^{2+}-dependent, K^{+} mediated process, contributes to hyperpolarization and controls the cell excitability. Importantly, generation of the AHP depends on Ca^{2+} and all three AHP components, fast (fAHP), a medium (mAHP), and a slow (sAHP), rely on Ca^{2+} [243]. The amplitude and duration of AHP is significantly enhanced in aged animals [44, 56, 66, 93, 94, 177, 222, 226, 244–246]. The inability to depolarize the cell is compounded, during patterned stimulation, due to the larger AHP. In fact, results suggest that it is the large AHP which underlies much of the LTP impairment [21, 22, 63, 92] and may even mask the propensity for enhanced LTP-induction during aging [223]. Normally, there is a relationship between the frequency of afferent stimulation required for LTP induction and the level of depolarization [247]. However, as noted above, a large and long-lasting AHP is observed following an action potential in older animals [44, 56, 66, 93, 94, 177, 222, 244–246]. The large AHP disrupts the integration of depolarizing postsynaptic potentials and the duration of this disruption is a function of the extent and duration of the AHP [21, 60, 92]. The disruption would increase the level of stimulation needed for LTP (Fig. 39.3). Result shows that pharmacological manipulations that reduce the AHP shift the frequency response functions such that LTP can be observed for much lower stimulation frequencies that would normally not elicit LTP in young or aged animals. The reduction in the AHP amplitude permits increased activation of NMDA receptor, to shift the threshold for induction of synaptic plasticity [39, 229]. It should be noted that L-channel blockade does not completely ameliorate age-related differences. The AHP amplitude is reduced but not to the levels observed in young animals [248]. In aged rats, blockade of VDCCs [39] or inhibition of Ca^{2+} stores [223] reduces the AHP and facilitates induction of LTP. The process can be reversed such that an increase in the AHP following the addition of an L-channel agonist prevents LTP-induction by 5 Hz stimulation [223]. Thus, an interesting aspect of this work is the fact that while induction of LTP depends on a large rise in intracellular Ca^{2+}, LTP-induction is facilitated by

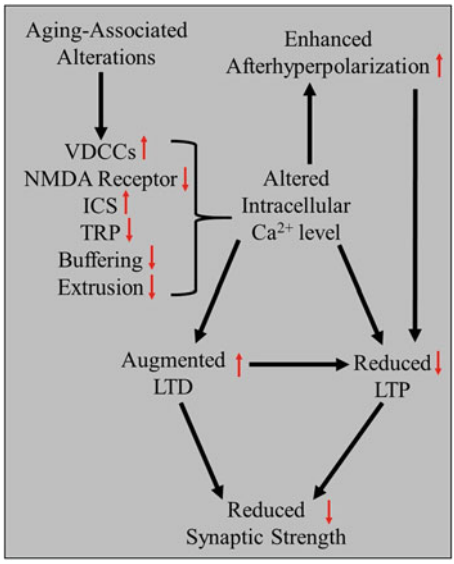

Fig. 39.3 Diagrammatic illustration of the relationship between altered Ca^{2+} regulation and synaptic plasticity during aging. An age-related alterations in Ca^{2+} regulation (increased release from voltage-dependent Ca^{2+} channels-VDCCs, intracellular stores-ICS, and transient receptor potential channels-TRP channels, and decreased NMDA receptor function) augments intracellular Ca^{2+} concentration during neural activity, which facilitates LTD-induction in response to low synaptic activity and increases the degree and duration of the afterhyperpolarization. In turn, a reduction in the level of depolarization due to a decline in cooperativity of decreased strength of synaptic contacts and an enhanced afterhyperpolarization acts to impair NMDA receptor activation and subsequent LTP-induction. The shift in the balance of LTP/LTD, preferring LTD, acts to decline synaptic strength with advanced age

blocking several Ca^{2+} sources that contribute to the AHP. The augmentation in the AHP amplitude diminishes the activation of NMDA channels, further contributing to impaired synaptic plasticity [60, 63]. The enhanced AHP with age is linked to increased involvement of VDCCs and internal Ca^{2+} stores [44, 46, 66, 93, 94, 177, 222, 223, 237, 248–254]. Thus, changes in Ca^{2+} from VDCCs or ICS can act through the AHP to impair NMDA receptor function.

A complimentary method for investigating the relationship between the AHP and LTP threshold is to reduce the AHP through manipulation of the potassium channels. For example, blockade of SK channels by apamin increases cell excitability and facilitates LTP-induction [39]. Moreover, deletion of the Kvβ1.1 subunit results in enhanced cell repolarization during repetitive firing by preventing A-type potassium channel inactivation. In turn, the normal spike broadening and increased Ca^{2+} influx through VDCCs is impaired by rapid repolarization. In aged, Kvβ1.1 knockout mice, the AHP is reduced, LTP is facilitated, and spatial memory is enhanced [255]. The results emphasize that the source of Ca^{2+} provides an overriding control of synaptic modifiability, shifting the threshold frequency of LTP-induction.

The shift in Ca^{2+} sources, increased AHP, and altered Ca^{2+} signaling, involving a shift in the activity of phosphatases and kinases also give rise to increased susceptibility to induction of LTD during aging. As described earlier, the induction of LTD depends on a modest rise in Ca^{2+}, which activates a signaling cascade to dephosphorylate glutamate receptors. Studies indicate that induction of LTD depends on suppression of NMDA receptors through a process in which Ca^{2+} influx through L-channels activates the Ca^{2+}-dependent phosphatase, CaN, resulting in reduced NMDA receptor function [247]. In aged animals, blockade of NMDA receptors can reduce, but does not necessarily prevent LTD [39]. In fact, LTD induction is facilitated by treatments that enhance potassium channel currents, hyperpolarizing the cell and limiting NMDA receptor activity [256]. Treatments that reduce the amplitude of the AHP including blockade of L-channels [39], depletion of Ca^{2+} stores [38], or treatment with estrogen [93, 238] impairs LTD induction in aged animals. The increase in CICR activates Ca^{2+}-dependent potassium channels in the membrane, inducing larger AHP. Attenuating CICR, by blocking RyR or depletion of Ca^{2+} from ICS, has a greater influence in reducing the amplitude of the AHP in aged animals [177, 222, 223], indicating an aging-specific mechanism. Thus, like LTP, the source of Ca^{2+} is important in determining synapse modifiability and LTD depends on Ca^{2+} from VDCCs and intracellular stores rather than NMDA receptors.

These results suggest a shift in Ca^{2+} homeostasis such that aging cells exhibit reduced Ca^{2+} influx from NMDA receptors and an increase contribution from VDCCs and ICS to intracellular Ca^{2+} during neural activity [21, 22, 63, 92]. In addition, it is likely that aged neurons exhibit changes in intracellular buffering and processes for extrusion of Ca^{2+} [257]. Collectively, this shift results in changes in Ca^{2+}-related physiology including an increase in the AHP amplitude and impaired LTP induction, at least under physiological Ca^{2+}/Mg^{2+} conditions. The change in Ca^{2} regulation, which shifts the cell away from Ca^{2+} influx through NMDA receptors, may be neuroprotective against Ca^{2+} mediated damage and thus act as compensation for increased vulnerability to neurotoxicity [258]. Physiological studies consistently indicate that NMDA receptor mediated excitatory postsynaptic potentials in the Schaffer collateral pathway of the hippocampus are significantly reduced in aged animals [110, 111, 117–120, 128, 176]. In turn, a decrease in NMDA receptor function is likely to influence induction of synaptic plasticity [259, 260] (i.e. metaplasticity [261]).

Alternatively, the shift in Ca^{2+} homeostasis could result from age-related increase in oxidative stress [262–264]. Reactive oxygen species could induce a rise in intracellular Ca^{2+} through release of Ca^{2+} from Ca^{2+} binding proteins (i.e. decreased buffering), and oxidation of Ca^{2+} regulatory proteins (calmodulin, SERCA, PMCA) would disrupt intracellular stores, and increase entry through Ca^{2+} channels [263, 265]. In the hippocampus, oxidative stress has effects which mimic aging; increasing Ca^{2+} influx through L-channels [266, 267], increasing the function of Ca^{2+}-dependent K^{+} channels [251, 268], and decreasing NMDA receptor function [269]. Furthermore, oxygen radicals can influence the activity of

Ca^{2+} dependent enzymes. The unstable super oxide ($O^{\cdot}$) or high levels of H_2O_2 (beyond the physiological range) inhibit CaN in tissue homogenates [270, 271]. However, in intact tissue, reactive oxygen species increase CaN activity, either through changes in the CaN inhibitory protein [272] or altered Ca^{2+} regulation involving increased Ca^{2+} from intracellular stores and VDCCs, leading to impaired induction of LTP [270]. Recent results provide evidence that enhanced oxidative stress also contributes to a reduction in Ca^{2+} influx [273].

Several recent studies have provided ample evidence that FK506-binding protein 12.6/1b (FKBP1b), a regulator of neuronal intracellular Ca^{2+}, negatively regulates Ca^{2+} release from RyRs, and attenuates influx of Ca^{2+} from L-type VDCCs. In addition, selective down regulation of FKBP1b in the hippocampus of young animals induced RyR-mediated dysregulation of Ca^{2+} homeostasis similar to that observed in aged animals [56, 274, 275]. Finally, viral-mediated upregulation of FKBP1b in the hippocampus reverses aging-associated dysregulation of Ca^{2+} signaling, reduces age-associated augmented AHP amplitude, restores genomic regulation, and ameliorates cognitive performance [55, 56]. Latest results demonstrated that age-associated enhanced oxidation of RyR contributes to decreased LTP induction and cognitive impairment [221].

39.7 Conclusion

The Ca^{2+} ion is a central signaling molecule in a wide range of cellular processes including synaptic plasticity, and the proper functioning of Ca^{2+} signaling machinery is essential for normal neuronal function. Alterations in neuronal Ca^{2+} homeostasis and Ca^{2+}-dependent physiological processes are the most consistent neurobiological manifestations of normal brain aging. Ca^{2+} dysregulation is not ubiquitous and mechanisms of altered regulation are restricted to specific cell populations. For example, an age-related increase in L-type Ca^{2+} channels is relatively specific to hippocampal pyramidal cells. Furthermore, an age-related decrease in NMDA receptor function, specifically in the hippocampus, suggests a possible compensatory mechanism to limit intracellular Ca^{2+} levels. However, such a mechanism may protect the cell at the expense of cell function. Cell specific susceptibility to Ca^{2+} dysregulation depends on environmental and genomic factors in addition to the availability of mechanisms for handling Ca^{2+}. The level of neural activity may render some regions more susceptible to oxidative stress, resulting in multiple changes to increase intracellular Ca^{2+} concentration including increased release of Ca^{2+} from ICS, impaired Ca^{2+} pumps, and weakened Ca^{2+} buffering. In turn, gene mutations may interact with age and cell specific alterations in Ca^{2+} regulation to produce the pattern of neuronal death, which characterizes neurodegenerative diseases. Due to the importance of Ca^{2+} as a crucial signaling molecule, selective regulation of Ca^{2+} in a particular set of neurons may be a daunting task for treating age-related diseases. Clearly, future studies are needed to delineate

the contribution of several mechanisms in optimizing neuronal Ca^{2+} regulating machinery and the influence of abnormal Ca^{2+} signaling in age-associated altered synaptic plasticity processes and cognitive function.

Acknowledgements Supported by National Institute of Aging grants R37AG036800, RO1AG049711, RO1AG037984, and RO1AG052258 and the Evelyn F. McKnight Brain Research Foundation.

References

1. Carafoli E (2002) Calcium signaling: a tale for all seasons. Proc Natl Acad Sci U S A 99(3):1115–1122
2. Capiod T (2016) Extracellular calcium has multiple targets to control cell proliferation. Adv Exp Med Biol 898:133–156
3. Clapham DE (2007) Calcium signaling. Cell 131(6):1047–1058
4. Toth AB, Shum AK, Prakriya M (2016) Regulation of neurogenesis by calcium signaling. Cell Calcium 59(2–3):124–134
5. Berridge MJ (2012) Calcium signalling remodelling and disease. Biochem Soc Trans 40(2):297–309
6. Berridge MJ, Lipp P, Bootman MD (2000) The versatility and universality of calcium signalling. Nat Rev Mol Cell Biol 1(1):11–21
7. Orrenius S, Zhivotovsky B, Nicotera P (2003) Regulation of cell death: the calcium-apoptosis link. Nat Rev Mol Cell Biol 4(7):552–565
8. Rizzuto R (2001) Intracellular Ca^{2+} pools in neuronal signalling. Curr Opin Neurobiol 11(3):306–311
9. Berridge MJ (1998) Neuronal calcium signaling. Neuron 21(1):13–26
10. Geiger JR, Melcher T, Koh DS, Sakmann B, Seeburg PH, Jonas P et al (1995) Relative abundance of subunit mRNAs determines gating and Ca^{2+} permeability of AMPA receptors in principal neurons and interneurons in rat CNS. Neuron 15(1):193–204
11. Ghosh A, Ginty DD, Bading H, Greenberg ME (1994) Calcium regulation of gene expression in neuronal cells. J Neurobiol 25(3):294–303
12. Parekh AB, Putney JW Jr (2005) Store-operated calcium channels. Physiol Rev 85(2):757–810
13. Prakriya M, Lewis RS (2015) Store-operated calcium channels. Physiol Rev 95(4):1383–1436
14. Clapham DE (2003) TRP channels as cellular sensors. Nature 426(6966):517–524
15. Moran MM, Xu H, Clapham DE (2004) TRP ion channels in the nervous system. Curr Opin Neurobiol 14(3):362–369
16. Ramsey IS, Delling M, Clapham DE (2006) An introduction to TRP channels. Annu Rev Physiol 68:619–647
17. Bai JZ, Lipski J (2014) Involvement of TRPV4 channels in Abeta(40)-induced hippocampal cell death and astrocytic Ca^{2+} signalling. Neurotoxicology 41:64–72
18. Hartmann J, Henning HA, Konnerth A (2011) mGluR1/TRPC3-mediated synaptic transmission and calcium signaling in mammalian central neurons. Cold Spring Harb Perspect Biol 3(4):pii: a006726
19. Zhang H, Sun S, Wu L, Pchitskaya E, Zakharova O, Fon Tacer K et al (2016) Store-operated Calcium Channel complex in postsynaptic spines: a new therapeutic target for Alzheimer's disease treatment. J Neurosci 36(47):11837–11850
20. Cavazzini M, Bliss T, Emptage N (2005) Ca^{2+} and synaptic plasticity. Cell Calcium 38(3–4):355–367

21. Foster TC (1999) Involvement of hippocampal synaptic plasticity in age-related memory decline. Brain Res Rev 30(3):236–249
22. Foster TC (2007) Calcium homeostasis and modulation of synaptic plasticity in the aged brain. Aging Cell 6(3):319–325
23. Bear MF, Abraham WC (1996) Long-term depression in hippocampus. Annu Rev Neurosci 19:437–462
24. Malenka RC, Bear MF (2004) LTP and LTD: an embarrassment of riches. Neuron 44(1):5–21
25. Collingridge G (1987) Synaptic plasticity. The role of NMDA receptors in learning and memory. Nature 330(6149):604–605
26. Collingridge GL, Bliss TV (1995) Memories of NMDA receptors and LTP. Trends Neurosci 18(2):54–56
27. Collingridge GL, Peineau S, Howland JG, Wang YT (2010) Long-term depression in the CNS. Nat Rev Neurosci 11(7):459–473
28. Bliss TV, Collingridge GL (1993) A synaptic model of memory: long-term potentiation in the hippocampus. Nature 361(6407):31–39
29. Kumar A (2011) Long-term potentiation at CA3-CA1 hippocampal synapses with special emphasis on aging, disease, and stress. Front Aging Neurosci 3:7
30. Muller W, Connor JA (1991) Dendritic spines as individual neuronal compartments for synaptic Ca^{2+} responses. Nature 354(6348):73–76
31. Nicoll RA, Malenka RC (1999) Expression mechanisms underlying NMDA receptor-dependent long-term potentiation. Ann N Y Acad Sci 868:515–525
32. Conti R, Lisman J (2002) A large sustained Ca^{2+} elevation occurs in unstimulated spines during the LTP pairing protocol but does not change synaptic strength. Hippocampus 12(5):667–679
33. Matsuzaki M, Honkura N, Ellis-Davies GC, Kasai H (2004) Structural basis of long-term potentiation in single dendritic spines. Nature 429(6993):761–766
34. Lisman J, Yasuda R, Raghavachari S (2012) Mechanisms of CaMKII action in long-term potentiation. Nat Rev Neurosci 13(3):169–182
35. Chang JY, Parra-Bueno P, Laviv T, Szatmari EM, Lee SR, Yasuda R (2017) CaMKII autophosphorylation is necessary for optimal integration of Ca^{2+} signals during LTP induction, but not maintenance. Neuron 94(4):800–808 e4
36. Dudek SM, Bear MF (1992) Homosynaptic long-term depression in area CA1 of hippocampus and effects of N-methyl-D-aspartate receptor blockade. Proc Natl Acad Sci U S A 89(10):4363–4367
37. Dunwiddie T, Lynch G (1978) Long-term potentiation and depression of synaptic responses in the rat hippocampus: localization and frequency dependency. J Physiol 276:353–367
38. Kumar A, Foster TC (2005) Intracellular calcium stores contribute to increased susceptibility to LTD induction during aging. Brain Res 1031(1):125–128
39. Norris CM, Halpain S, Foster TC (1998) Reversal of age-related alterations in synaptic plasticity by blockade of L-type Ca^{2+} channels. J Neurosci 18(9):3171–3179
40. Artola A, Singer W (1993) Long-term depression of excitatory synaptic transmission and its relationship to long-term potentiation. Trends Neurosci 16(11):480–487
41. Lee HK, Kameyama K, Huganir RL, Bear MF (1998) NMDA induces long-term synaptic depression and dephosphorylation of the GluR1 subunit of AMPA receptors in hippocampus. Neuron 21(5):1151–1162
42. Bienenstock EL, Cooper LN, Munro PW (1982) Theory for the development of neuron selectivity: orientation specificity and binocular interaction in visual cortex. J Neurosci 2(1):32–48
43. Khachaturian ZS (1989) Calcium, membranes, aging, and Alzheimer's disease. Introduction and overview. Ann N Y Acad Sci 568:1–4
44. Landfield PW, Pitler TA (1984) Prolonged Ca^{2+}−dependent afterhyperpolarizations in hippocampal neurons of aged rats. Science 226(4678):1089–1092
45. Gibson GE, Peterson C (1987) Calcium and the aging nervous system. Neurobiol Aging 8(4):329–343

46. Disterhoft JF, Thompson LT, Moyer JR, Mogul DJ (1996) Calcium-dependent afterhyperpolarization and learning in young and aging hippocampus. Life Sci 59(5–6):413–420
47. Alzheimer's Association Calcium Hypothesis W (2017) Calcium hypothesis of Alzheimer's disease and brain aging: a framework for integrating new evidence into a comprehensive theory of pathogenesis. Alzheimers Dement 13(2):178–182 e17
48. Frazier HN, Maimaiti S, Anderson KL, Brewer LD, Gant JC, Porter NM et al (2017) Calcium's role as nuanced modulator of cellular physiology in the brain. Biochem Biophys Res Commun 483(4):981–987
49. Gibson GE, Thakkar A (2017) Interactions of mitochondria/metabolism and calcium regulation in Alzheimer's disease: a calcinist point of view. Neurochem Res 42(6):1636–1648
50. Pchitskaya E, Popugaeva E, Bezprozvanny I (2018) Calcium signaling and molecular mechanisms underlying neurodegenerative diseases. Cell Calcium 70:87–94
51. Sompol P, Norris CM (2018) Ca^{2+}, Astrocyte activation and calcineurin/NFAT signaling in age-related neurodegenerative diseases. Front Aging Neurosci 10:199
52. Vardjan N, Verkhratsky A, Zorec R (2017) Astrocytic pathological calcium homeostasis and impaired vesicle trafficking in neurodegeneration. Int J Mol Sci 18(2):358
53. Verkhratsky A, Rodriguez-Arellano JJ, Parpura V, Zorec R (2017) Astroglial calcium signalling in Alzheimer's disease. Biochem Biophys Res Commun 483(4):1005–1012
54. Zorec R, Parpura V, Verkhratsky A (2018) Astroglial vesicular network: evolutionary trends, physiology and pathophysiology. Acta Physiol (Oxford) 222(2)
55. Gant JC, Blalock EM, Chen KC, Kadish I, Thibault O, Porter NM et al (2018) FK506-binding protein 12.6/1b, a negative regulator of [Ca^{2+}], rescues memory and restores genomic regulation in the Hippocampus of aging rats. J Neurosci 38(4):1030–1041
56. Gant JC, Chen KC, Kadish I, Blalock EM, Thibault O, Porter NM et al (2015) Reversal of aging-related neuronal Ca^{2+} dysregulation and cognitive impairment by delivery of a transgene encoding FK506-binding protein 12.6/1b to the Hippocampus. J Neurosci 35(30):10878–10887
57. Toescu EC, Verkhratsky A (2007) The importance of being subtle: small changes in calcium homeostasis control cognitive decline in normal aging. Aging Cell 6(3):267–273
58. Murchison D, Griffith WH (2007) Calcium buffering systems and calcium signaling in aged rat basal forebrain neurons. Aging Cell 6(3):297–305
59. Thibault O, Gant JC, Landfield PW (2007) Expansion of the calcium hypothesis of brain aging and Alzheimer's disease: minding the store. Aging Cell 6(3):307–317
60. Foster TC, Norris CM (1997) Age-associated changes in Ca^{2+}−dependent processes: relation to hippocampal synaptic plasticity. Hippocampus 7(6):602–612
61. Rapp PR, Gallagher M (1996) Preserved neuron number in the hippocampus of aged rats with spatial learning deficits. Proc Natl Acad Sci U S A 93(18):9926–9930
62. West MJ (1993) Regionally specific loss of neurons in the aging human hippocampus. Neurobiol Aging 14(4):287–293
63. Foster TC (2012) Dissecting the age-related decline on spatial learning and memory tasks in rodent models: N-methyl-D-aspartate receptors and voltage-dependent Ca(2)(+) channels in senescent synaptic plasticity. Prog Neurobiol 96(3):283–303
64. Kumar A, Foster TC (2018) Alteration in NMDA receptor mediated glutamatergic neurotransmission in the Hippocampus during senescence. Neurochem Res 44(1):38–48
65. Thibault O, Landfield PW (1996) Increase in single L-type calcium channels in hippocampal neurons during aging. Science 272(5264):1017–1020
66. Tombaugh GC, Rowe WB, Rose GM (2005) The slow afterhyperpolarization in hippocampal CA1 neurons covaries with spatial learning ability in aged Fisher 344 rats. J Neurosci 25(10):2609–2616
67. Murphy GG, Rahnama NP, Silva AJ (2006) Investigation of age-related cognitive decline using mice as a model system: behavioral correlates. Am J Geriatr Psychiatry 14(12):1004–1011
68. Abu-Omar N, Das J, Szeto V, Feng ZP (2018) Neuronal ryanodine receptors in development and aging. Mol Neurobiol 55(2):1183–1192

69. Catterall WA (2000) Structure and regulation of voltage-gated Ca^{2+} channels. Annu Rev Cell Dev Biol 16:521–555
70. Dolphin AC (2006) A short history of voltage-gated calcium channels. Br J Pharmacol 147(Suppl 1):S56–S62
71. Jones SW (1998) Overview of voltage-dependent calcium channels. J Bioenerg Biomembr 30(4):299–312
72. Kang MG, Chen CC, Felix R, Letts VA, Frankel WN, Mori Y et al (2001) Biochemical and biophysical evidence for gamma 2 subunit association with neuronal voltage-activated Ca^{2+} channels. J Biol Chem 276(35):32917–32924
73. Bertolino M, Llinas RR (1992) The central role of voltage-activated and receptor-operated calcium channels in neuronal cells. Annu Rev Pharmacol Toxicol 32:399–421
74. Veselovskii NS, Fedulova SA (1983) 2 types of calcium channels in the somatic membrane of spinal ganglion neurons in the rat. Dokl Akad Nauk SSSR 268(3):747–750
75. Nowycky MC, Fox AP, Tsien RW (1985) Three types of neuronal calcium channel with different calcium agonist sensitivity. Nature 316(6027):440–443
76. Bean BP (1989) Classes of calcium channels in vertebrate cells. Annu Rev Physiol 51:367–384
77. Carbone E, Lux HD (1984) A low voltage-activated, fully inactivating Ca channel in vertebrate sensory neurones. Nature 310(5977):501–502
78. Fedulova SA, Kostyuk PG, Veselovsky NS (1985) Two types of calcium channels in the somatic membrane of new-born rat dorsal root ganglion neurones. J Physiol 359:431–446
79. Soong TW, Stea A, Hodson CD, Dubel SJ, Vincent SR, Snutch TP (1993) Structure and functional expression of a member of the low voltage-activated calcium channel family. Science 260(5111):1133–1136
80. Nilius B, Hess P, Lansman JB, Tsien RW (1985) A novel type of cardiac calcium channel in ventricular cells. Nature 316(6027):443–446
81. Campbell LW, Hao SY, Thibault O, Blalock EM, Landfield PW (1996) Aging changes in voltage-gated calcium currents in hippocampal CA1 neurons. J Neurosci 16(19):6286–6295
82. Brewer LD, Dowling AL, Curran-Rauhut MA, Landfield PW, Porter NM, Blalock EM (2009) Estradiol reverses a calcium-related biomarker of brain aging in female rats. J Neurosci 29(19):6058–6067
83. Herman JP, Chen KC, Booze R, Landfield PW (1998) Up-regulation of alpha1D Ca^{2+} channel subunit mRNA expression in the hippocampus of aged F344 rats. Neurobiol Aging 19(6):581–587
84. Veng LM, Mesches MH, Browning MD (2003) Age-related working memory impairment is correlated with increases in the L-type calcium channel protein alpha1D (Cav1.3) in area CA1 of the hippocampus and both are ameliorated by chronic nimodipine treatment. Brain Res Mol Brain Res 110(2):193–202
85. Chen KC, Blalock EM, Thibault O, Kaminker P, Landfield PW (2000) Expression of alpha 1D subunit mRNA is correlated with L-type Ca^{2+} channel activity in single neurons of hippocampal "zipper" slices. Proc Natl Acad Sci U S A 97(8):4357–4362
86. Nunez-Santana FL, Oh MM, Antion MD, Lee A, Hell JW, Disterhoft JF (2014) Surface L-type Ca^{2+} channel expression levels are increased in aged hippocampus. Aging Cell 13(1):111–120
87. Davare MA, Hell JW (2003) Increased phosphorylation of the neuronal L-type Ca^{2+} channel Ca(v)1.2 during aging. Proc Natl Acad Sci U S A 100(26):16018–16023
88. Norris CM, Halpain S, Foster TC (1998) Alterations in the balance of protein kinase/phosphatase activities parallel reduced synaptic strength during aging. J Neurophysiol 80(3):1567–1570
89. Norris CM, Blalock EM, Chen KC, Porter NM, Landfield PW (2002) Calcineurin enhances L-type Ca^{2+} channel activity in hippocampal neurons: increased effect with age in culture. Neuroscience 110(2):213–225

90. Lu CB, Hamilton JB, Powell AD, Toescu EC, Vreugdenhil M (2009) Effect of ageing on CA3 interneuron sAHP and gamma oscillations is activity-dependent. Neurobiol Aging 32(5):956–965. [epub ahead of print]
91. Foster TC (2005) Interaction of rapid signal transduction cascades and gene expression in mediating estrogen effects on memory over the life span. Front Neuroendocrinol 26(2):51–64
92. Foster TC, Kumar A (2002) Calcium dysregulation in the aging brain. Neuroscientist 8(4):297–301
93. Kumar A, Foster TC (2002) 17beta-estradiol benzoate decreases the AHP amplitude in CA1 pyramidal neurons. J Neurophysiol 88(2):621–626
94. Moyer JR Jr, Thompson LT, Black JP, Disterhoft JF (1992) Nimodipine increases excitability of rabbit CA1 pyramidal neurons in an age- and concentration-dependent manner. J Neurophysiol 68(6):2100–2109
95. Cull-Candy S, Brickley S, Farrant M (2001) NMDA receptor subunits: diversity, development and disease. Curr Opin Neurobiol 11(3):327–335
96. Kutsuwada T, Kashiwabuchi N, Mori H, Sakimura K, Kushiya E, Araki K et al (1992) Molecular diversity of the NMDA receptor channel. Nature 358(6381):36–41
97. Meguro H, Mori H, Araki K, Kushiya E, Kutsuwada T, Yamazaki M et al (1992) Functional characterization of a heteromeric NMDA receptor channel expressed from cloned cDNAs. Nature 357(6373):70–74
98. Monyer H, Sprengel R, Schoepfer R, Herb A, Higuchi M, Lomeli H et al (1992) Heteromeric NMDA receptors: molecular and functional distinction of subtypes. Science 256(5060):1217–1221
99. Moriyoshi K, Masu M, Ishii T, Shigemoto R, Mizuno N, Nakanishi S (1991) Molecular cloning and characterization of the rat NMDA receptor. Nature 354(6348):31–37
100. Kumar A (2015) NMDA receptor function during senescence: implication on cognitive performance. Front Neurosci 9:473
101. Laube B, Kuhse J, Betz H (1998) Evidence for a tetrameric structure of recombinant NMDA receptors. J Neurosci 18(8):2954–2961
102. Al-Hallaq RA, Jarabek BR, Fu Z, Vicini S, Wolfe BB, Yasuda RP (2002) Association of NR3A with the N-methyl-D-aspartate receptor NR1 and NR2 subunits. Mol Pharmacol 62(5):1119–1127
103. Schuler T, Mesic I, Madry C, Bartholomaus I, Laube B (2008) Formation of NR1/NR2 and NR1/NR3 heterodimers constitutes the initial step in N-methyl-D-aspartate receptor assembly. J Biol Chem 283(1):37–46
104. Sucher NJ, Akbarian S, Chi CL, Leclerc CL, Awobuluyi M, Deitcher DL et al (1995) Developmental and regional expression pattern of a novel NMDA receptor-like subunit (NMDAR-L) in the rodent brain. J Neurosci 15(10):6509–6520
105. Low CM, Wee KS (2010) New insights into the not-so-new NR3 subunits of N-methyl-D-aspartate receptor: localization, structure, and function. Mol Pharmacol 78(1):1–11
106. Chen PE, Geballe MT, Stansfeld PJ, Johnston AR, Yuan H, Jacob AL et al (2005) Structural features of the glutamate binding site in recombinant NR1/NR2A N-methyl-D-aspartate receptors determined by site-directed mutagenesis and molecular modeling. Mol Pharmacol 67(5):1470–1484
107. Garaschuk O, Schneggenburger R, Schirra C, Tempia F, Konnerth A (1996) Fractional Ca^{2+} currents through somatic and dendritic glutamate receptor channels of rat hippocampal CA1 pyramidal neurones. J Physiol 491(Pt 3):757–772
108. Gonzales RA, Brown LM, Jones TW, Trent RD, Westbrook SL, Leslie SW (1991) N-methyl-D-aspartate mediated responses decrease with age in Fischer 344 rat brain. Neurobiol Aging 12(3):219–225
109. Pittaluga A, Fedele E, Risiglione C, Raiteri M (1993) Age-related decrease of the NMDA receptor-mediated noradrenaline release in rat hippocampus and partial restoration by D-cycloserine. Eur J Pharmacol 231(1):129–134

110. Barnes CA, Rao G, Shen J (1997) Age-related decrease in the N-methyl-D-aspartateR-mediated excitatory postsynaptic potential in hippocampal region CA1. Neurobiol Aging 18(4):445–452
111. Eckles-Smith K, Clayton D, Bickford P, Browning MD (2000) Caloric restriction prevents age-related deficits in LTP and in NMDA receptor expression. Brain Res Mol Brain Res 78(1–2):154–162
112. Magnusson KR (1998) The aging of the NMDA receptor complex. Front Biosci 3:e70–e80
113. Gore AC, Oung T, Woller MJ (2002) Age-related changes in hypothalamic gonadotropin-releasing hormone and N-methyl-D-aspartate receptor gene expression, and their regulation by oestrogen, in the female rat. J Neuroendocrinol 14(4):300–309
114. Liu P, Smith PF, Darlington CL (2008) Glutamate receptor subunits expression in memory-associated brain structures: regional variations and effects of aging. Synapse 62(11):834–841
115. Zhao X, Rosenke R, Kronemann D, Brim B, Das SR, Dunah AW et al (2009) The effects of aging on N-methyl-d-aspartate receptor subunits in the synaptic membrane and relationships to long-term spatial memory. Neuroscience 162(4):933–945
116. Bodhinathan K, Kumar A, Foster TC (2007) Oxidative stress decreases NMDA receptor function in the hippocampus of aged animals. Soc Neurosci Abstr:N18/256.8
117. Brim BL, Haskell R, Awedikian R, Ellinwood NM, Jin L, Kumar A et al (2013) Memory in aged mice is rescued by enhanced expression of the GluN2B subunit of the NMDA receptor. Behav Brain Res 238:211–226
118. Kumar A, Foster TC (2013) Linking redox regulation of NMDAR synaptic function to cognitive decline during aging. J Neurosci 33(40):15710–15715
119. Lee WH, Kumar A, Rani A, Foster TC (2014) Role of antioxidant enzymes in redox regulation of N-methyl-D-aspartate receptor function and memory in middle-aged rats. Neurobiol Aging 35(6):1459–1468
120. Kumar A, Rani A, Scheinert RB, Ormerod BK, Foster TC (2018) Nonsteroidal anti-inflammatory drug, indomethacin improves spatial memory and NMDA receptor function in aged animals. Neurobiol Aging 70:184–193
121. Bonhaus DW, Perry WB, McNamara JO (1990) Decreased density, but not number, of N-methyl-D-aspartate, glycine and phencyclidine binding sites in hippocampus of senescent rats. Brain Res 532(1–2):82–86
122. Kito S, Miyoshi R, Nomoto T (1990) Influence of age on NMDA receptor complex in rat brain studied by in vitro autoradiography. J Histochem Cytochem 38(12):1725–1731
123. Magnusson KR (1995) Differential effects of aging on binding sites of the activated NMDA receptor complex in mice. Mech Ageing Dev 84(3):227–243
124. Magnusson KR, Kresge D, Supon J (2006) Differential effects of aging on NMDA receptors in the intermediate versus the dorsal hippocampus. Neurobiol Aging 27(2):324–333
125. Miyoshi R, Kito S, Doudou N, Nomoto T (1991) Influence of age on N-methyl-D-aspartate antagonist binding sites in the rat brain studied by in vitro autoradiography. Synapse 8(3):212–217
126. Tamaru M, Yoneda Y, Ogita K, Shimizu J, Nagata Y (1991) Age-related decreases of the N-methyl-D-aspartate receptor complex in the rat cerebral cortex and hippocampus. Brain Res 542(1):83–90
127. Wenk GL, Walker LC, Price DL, Cork LC (1991) Loss of NMDA, but not GABA-A, binding in the brains of aged rats and monkeys. Neurobiol Aging 12(2):93–98
128. Billard JM, Rouaud E (2007) Deficit of NMDA receptor activation in CA1 hippocampal area of aged rats is rescued by D-cycloserine. Eur J Neurosci 25(8):2260–2268
129. Das SR, Magnusson KR (2008) Relationship between mRNA expression of splice forms of the zeta1 subunit of the N-methyl-D-aspartate receptor and spatial memory in aged mice. Brain Res 1207:142–154
130. Gazzaley AH, Weiland NG, McEwen BS, Morrison JH (1996) Differential regulation of NMDAR1 mRNA and protein by estradiol in the rat hippocampus. J Neurosci 16(21):6830–6838

131. Magnusson KR, Cotman CW (1993) Age-related changes in excitatory amino acid receptors in two mouse strains. Neurobiol Aging 14(3):197–206
132. Wenk GL, Barnes CA (2000) Regional changes in the hippocampal density of AMPA and NMDA receptors across the lifespan of the rat. Brain Res 885(1):1–5
133. Araki T, Kato H, Nagaki S, Shuto K, Fujiwara T, Itoyama Y (1997) Effects of vinconate on age-related alterations in [3H]MK-801, [3H]glycine, sodium-dependent D-[3H]aspartate, [3H]FK-506 and [3H]PN200-110 binding in rats. Mech Ageing Dev 95(1–2):13–29
134. Shimada A, Mukhin A, Ingram DK, London ED (1997) N-methyl-D-aspartate receptor binding in brains of rats at different ages. Neurobiol Aging 18(3):329–333
135. Ingram DK, Garofalo P, Spangler EL, Mantione CR, Odano I, London ED (1992) Reduced density of NMDA receptors and increased sensitivity to dizocilpine-induced learning impairment in aged rats. Brain Res 580(1–2):273–280
136. Topic B, Willuhn I, Palomero-Gallagher N, Zilles K, Huston JP, Hasenohrl RU (2007) Impaired maze performance in aged rats is accompanied by increased density of NMDA, 5-HT1A, and alpha-adrenoceptor binding in hippocampus. Hippocampus 17(1):68–77
137. Serra M, Ghiani CA, Foddi MC, Motzo C, Biggio G (1994) NMDA receptor function is enhanced in the hippocampus of aged rats. Neurochem Res 19(4):483–487
138. Magnusson KR (2000) Declines in mRNA expression of different subunits may account for differential effects of aging on agonist and antagonist binding to the NMDA receptor. J Neurosci 20(5):1666–1674
139. Liu F, Day M, Muniz LC, Bitran D, Arias R, Revilla-Sanchez R et al (2008) Activation of estrogen receptor-beta regulates hippocampal synaptic plasticity and improves memory. Nat Neurosci 11(3):334–343
140. Mesches MH, Gemma C, Veng LM, Allgeier C, Young DA, Browning MD et al (2004) Sulindac improves memory and increases NMDA receptor subunits in aged Fischer 344 rats. Neurobiol Aging 25(3):315–324
141. Adams MM, Morrison JH, Gore AC (2001) N-methyl-D-aspartate receptor mRNA levels change during reproductive senescence in the hippocampus of female rats. Exp Neurol 170(1):171–179
142. Sonntag WE, Bennett SA, Khan AS, Thornton PL, Xu X, Ingram RL et al (2000) Age and insulin-like growth factor-1 modulate N-methyl-D-aspartate receptor subtype expression in rats. Brain Res Bull 51(4):331–338
143. Magnusson KR, Bai L, Zhao X (2005) The effects of aging on different C-terminal splice forms of the zeta1(NR1) subunit of the N-methyl-d-aspartate receptor in mice. Brain Res Mol Brain Res 135(1–2):141–149
144. Martinez Villayandre B, Paniagua MA, Fernandez-Lopez A, Chinchetru MA, Calvo P (2004) Effect of vitamin E treatment on N-methyl-D-aspartate receptor at different ages in the rat brain. Brain Res 1028(2):148–155
145. Magnusson KR (2001) Influence of diet restriction on NMDA receptor subunits and learning during aging. Neurobiol Aging 22(4):613–627
146. Dumas TC (2005) Developmental regulation of cognitive abilities: modified composition of a molecular switch turns on associative learning. Prog Neurobiol 76(3):189–211
147. Massey PV, Johnson BE, Moult PR, Auberson YP, Brown MW, Molnar E et al (2004) Differential roles of NR2A and NR2B-containing NMDA receptors in cortical long-term potentiation and long-term depression. J Neurosci 24(36):7821–7828
148. Blanpied TA, Scott DB, Ehlers MD (2002) Dynamics and regulation of clathrin coats at specialized endocytic zones of dendrites and spines. Neuron 36(3):435–449
149. Lau CG, Zukin RS (2007) NMDA receptor trafficking in synaptic plasticity and neuropsychiatric disorders. Nat Rev Neurosci 8(6):413–426
150. Hardingham GE, Fukunaga Y, Bading H (2002) Extrasynaptic NMDARs oppose synaptic NMDARs by triggering CREB shut-off and cell death pathways. Nat Neurosci 5(5):405–414
151. Vanhoutte P, Bading H (2003) Opposing roles of synaptic and extrasynaptic NMDA receptors in neuronal calcium signalling and BDNF gene regulation. Curr Opin Neurobiol 13(3):366–371

152. Heidinger V, Manzerra P, Wang XQ, Strasser U, Yu SP, Choi DW et al (2002) Metabotropic glutamate receptor 1-induced upregulation of NMDA receptor current: mediation through the Pyk2/Src-family kinase pathway in cortical neurons. J Neurosci 22(13):5452–5461
153. Wang LY, Orser BA, Brautigan DL, MacDonald JF (1994) Regulation of NMDA receptors in cultured hippocampal neurons by protein phosphatases 1 and 2A. Nature 369(6477):230–232
154. Ben-Ari Y, Aniksztejn L, Bregestovski P (1992) Protein kinase C modulation of NMDA currents: an important link for LTP induction. Trends Neurosci 15(9):333–339
155. Chen L, Huang LY (1992) Protein kinase C reduces Mg2+ block of NMDA-receptor channels as a mechanism of modulation. Nature 356(6369):521–523
156. Raman IM, Tong G, Jahr CE (1996) Beta-adrenergic regulation of synaptic NMDA receptors by cAMP-dependent protein kinase. Neuron 16(2):415–421
157. Lieberman DN, Mody I (1994) Regulation of NMDA channel function by endogenous Ca^{2+}-dependent phosphatase. Nature 369(6477):235–239
158. Chung HJ, Huang YH, Lau LF, Huganir RL (2004) Regulation of the NMDA receptor complex and trafficking by activity-dependent phosphorylation of the NR2B subunit PDZ ligand. J Neurosci 24(45):10248–10259
159. Gardoni F, Schrama LH, Kamal A, Gispen WH, Cattabeni F, Di Luca M (2001) Hippocampal synaptic plasticity involves competition between Ca^{2+}/calmodulin-dependent protein kinase II and postsynaptic density 95 for binding to the NR2A subunit of the NMDA receptor. J Neurosci 21(5):1501–1509
160. Hallett PJ, Spoelgen R, Hyman BT, Standaert DG, Dunah AW (2006) Dopamine D1 activation potentiates striatal NMDA receptors by tyrosine phosphorylation-dependent subunit trafficking. J Neurosci 26(17):4690–4700
161. Lin Y, Jover-Mengual T, Wong J, Bennett MV, Zukin RS (2006) PSD-95 and PKC converge in regulating NMDA receptor trafficking and gating. Proc Natl Acad Sci U S A 103(52):19902–19907
162. Carroll RC, Zukin RS (2002) NMDA-receptor trafficking and targeting: implications for synaptic transmission and plasticity. Trends Neurosci 25(11):571–577
163. Scott DB, Blanpied TA, Swanson GT, Zhang C, Ehlers MD (2001) An NMDA receptor ER retention signal regulated by phosphorylation and alternative splicing. J Neurosci 21(9):3063–3072
164. Snyder EM, Nong Y, Almeida CG, Paul S, Moran T, Choi EY et al (2005) Regulation of NMDA receptor trafficking by amyloid-beta. Nat Neurosci 8(8):1051–1058
165. Foster TC, Sharrow KM, Masse JR, Norris CM, Kumar A (2001) Calcineurin links Ca^{2+} dysregulation with brain aging. J Neurosci 21(11):4066–4073
166. Coultrap SJ, Bickford PC, Browning MD (2008) Blueberry-enriched diet ameliorates age-related declines in NMDA receptor-dependent LTP. Age 30(4):263–272
167. Aizenman E, Lipton SA, Loring RH (1989) Selective modulation of NMDA responses by reduction and oxidation. Neuron 2(3):1257–1263
168. Aizenman E (1995) Modulation of N-methyl-D-aspartate receptors by hydroxyl radicals in rat cortical neurons in vitro. Neurosci Lett 189(1):57–59
169. Sucher NJ, Lipton SA (1991) Redox modulatory site of the NMDA receptor-channel complex: regulation by oxidized glutathione. J Neurosci Res 30(3):582–591
170. Aizenman E, Hartnett KA, Reynolds IJ (1990) Oxygen free radicals regulate NMDA receptor function via a redox modulatory site. Neuron 5(6):841–846
171. Choi Y, Chen HV, Lipton SA (2001) Three pairs of cysteine residues mediate both redox and zn2+ modulation of the nmda receptor. J Neurosci 21(2):392–400
172. Sullivan JM, Traynelis SF, Chen HS, Escobar W, Heinemann SF, Lipton SA (1994) Identification of two cysteine residues that are required for redox modulation of the NMDA subtype of glutamate receptor. Neuron 13(4):929–936
173. Foster TC (2006) Biological markers of age-related memory deficits: treatment of senescent physiology. CNS Drugs 20(2):153–166

174. Parihar MS, Kunz EA, Brewer GJ (2008) Age-related decreases in NAD(P)H and glutathione cause redox declines before ATP loss during glutamate treatment of hippocampal neurons. J Neurosci Res 86(10):2339–2352
175. Poon HF, Calabrese V, Calvani M, Butterfield DA (2006) Proteomics analyses of specific protein oxidation and protein expression in aged rat brain and its modulation by L-acetylcarnitine: insights into the mechanisms of action of this proposed therapeutic agent for CNS disorders associated with oxidative stress. Antioxid Redox Signal 8(3–4):381–394
176. Bodhinathan K, Kumar A, Foster TC (2010) Intracellular redox state alters NMDA receptor response during aging through Ca^{2+}/calmodulin-dependent protein kinase II. J Neurosci 30(5):1914–1924
177. Bodhinathan K, Kumar A, Foster TC (2010) Redox sensitive calcium stores underlie enhanced after hyperpolarization of aged neurons: role for ryanodine receptor mediated calcium signaling. J Neurophysiol 104(5):2586–2593
178. Haxaire C, Turpin FR, Potier B, Kervern M, Sinet PM, Barbanel G et al (2012) Reversal of age-related oxidative stress prevents hippocampal synaptic plasticity deficits by protecting d-serine-dependent NMDA receptor activation. Aging Cell 11(2):336–344
179. Robillard JM, Gordon GR, Choi HB, Christie BR, MacVicar BA (2011) Glutathione restores the mechanism of synaptic plasticity in aged mice to that of the adult. PLoS One 6(5):e20676
180. Kumar A, Yegla B, Foster TC (2018) Redox signaling in neurotransmission and cognition during aging. Antioxid Redox Signal 28(18):1724–1745
181. Schell MJ, Molliver ME, Snyder SH (1995) D-serine, an endogenous synaptic modulator: localization to astrocytes and glutamate-stimulated release. Proc Natl Acad Sci U S A 92(9):3948–3952
182. Williams SM, Diaz CM, Macnab LT, Sullivan RK, Pow DV (2006) Immunocytochemical analysis of D-serine distribution in the mammalian brain reveals novel anatomical compartmentalizations in glia and neurons. Glia 53(4):401–411
183. Wu S, Barger SW (2004) Induction of serine racemase by inflammatory stimuli is dependent on AP-1. Ann N Y Acad Sci 1035:133–146
184. Wu SZ, Bodles AM, Porter MM, Griffin WS, Basile AS, Barger SW (2004) Induction of serine racemase expression and D-serine release from microglia by amyloid beta-peptide. J Neuroinflammation 1(1):2
185. Hayashi Y, Ishibashi H, Hashimoto K, Nakanishi H (2006) Potentiation of the NMDA receptor-mediated responses through the activation of the glycine site by microglia secreting soluble factors. Glia 53(6):660–668
186. Moriguchi S, Mizoguchi Y, Tomimatsu Y, Hayashi Y, Kadowaki T, Kagamiishi Y et al (2003) Potentiation of NMDA receptor-mediated synaptic responses by microglia. Brain Res Mol Brain Res 119(2):160–169
187. Rosi S, Ramirez-Amaya V, Hauss-Wegrzyniak B, Wenk GL (2004) Chronic brain inflammation leads to a decline in hippocampal NMDA-R1 receptors. J Neuroinflammation 1(1):12
188. Rosi S, Vazdarjanova A, Ramirez-Amaya V, Worley PF, Barnes CA, Wenk GL (2006) Memantine protects against LPS-induced neuroinflammation, restores behaviorally-induced gene expression and spatial learning in the rat. Neuroscience 142(4):1303–1315
189. Cao X, Cui Z, Feng R, Tang YP, Qin Z, Mei B et al (2007) Maintenance of superior learning and memory function in NR2B transgenic mice during ageing. Eur J Neurosci 25(6):1815–1822
190. Ly CV, Verstreken P (2006) Mitochondria at the synapse. Neuroscientist 12(4):291–299
191. Mattson MP, LaFerla FM, Chan SL, Leissring MA, Shepel PN, Geiger JD (2000) Calcium signaling in the ER: its role in neuronal plasticity and neurodegenerative disorders. Trends Neurosci 23(5):222–229
192. Verkhratsky A, Toescu EC (1998) Calcium and neuronal ageing. Trends Neurosci 21(1):2–7
193. Verkhratsky AJ, Petersen OH (1998) Neuronal calcium stores. Cell Calcium 24(5–6):333–343
194. Petersen OH, Gerasimenko OV, Gerasimenko JV, Mogami H, Tepikin AV (1998) The calcium store in the nuclear envelope. Cell Calcium 23(2–3):87–90

195. Petersen OH, Michalak M, Verkhratsky A (2005) Calcium signalling: past, present and future. Cell Calcium 38(3–4):161–169
196. Toescu EC, Verkhratsky A (2004) Ca^{2+} and mitochondria as substrates for deficits in synaptic plasticity in normal brain ageing. J Cell Mol Med 8(2):181–190
197. Duchen MR (2000) Mitochondria and calcium: from cell signalling to cell death. J Physiol 529(Pt 1):57–68
198. Nicholls DG, Budd SL (2000) Mitochondria and neuronal survival. Physiol Rev 80(1):315–360
199. Solovyova N, Veselovsky N, Toescu EC, Verkhratsky A (2002) Ca^{2+} dynamics in the lumen of the endoplasmic reticulum in sensory neurons: direct visualization of Ca^{2+}-induced Ca^{2+} release triggered by physiological Ca^{2+} entry. EMBO J 21(4):622–630
200. McGuinness L, Bardo SJ, Emptage NJ (2007) The lysosome or lysosome-related organelle may serve as a Ca^{2+} store in the boutons of hippocampal pyramidal cells. Neuropharmacology 52(1):126–135
201. Toescu EC, Myronova N, Verkhratsky A (2000) Age-related structural and functional changes of brain mitochondria. Cell Calcium 28(5–6):329–338
202. Sanmartin CD, Paula-Lima AC, Garcia A, Barattini P, Hartel S, Nunez MT et al (2014) Ryanodine receptor-mediated Ca^{2+} release underlies iron-induced mitochondrial fission and stimulates mitochondrial Ca^{2+} uptake in primary hippocampal neurons. Front Mol Neurosci 7:13
203. Roth GS (1995) Changes in tissue responsiveness to hormones and neurotransmitters during aging. Exp Gerontol 30(3–4):361–368
204. Mizutani T, Nakashima S, Nozawa Y (1998) Changes in the expression of protein kinase C (PKC), phospholipases C (PLC) and D (PLD) isoforms in spleen, brain and kidney of the aged rat: RT-PCR and Western blot analysis. Mech Ageing Dev 105(1–2):151–172
205. Nicolle MM, Colombo PJ, Gallagher M, McKinney M (1999) Metabotropic glutamate receptor-mediated hippocampal phosphoinositide turnover is blunted in spatial learning-impaired aged rats. J Neurosci 19(21):9604–9610
206. Burnett DM, Daniell LC, Zahniser NR (1990) Decreased efficacy of inositol 1,4,5-trisphosphate to elicit calcium mobilization from cerebrocortical microsomes of aged rats. Mol Pharmacol 37(4):566–571
207. Stutzmann GE, Smith I, Caccamo A, Oddo S, Laferla FM, Parker I (2006) Enhanced ryanodine receptor recruitment contributes to Ca^{2+} disruptions in young, adult, and aged Alzheimer's disease mice. J Neurosci 26(19):5180–5189
208. Igwe OJ, Ning L (1993) Inositol 1,4,5-trisphosphate arm of the phosphatidylinositide signal transduction pathway in the rat cerebellum during aging. Neurosci Lett 164(1–2):167–170
209. Martini A, Battaini F, Govoni S, Volpe P (1994) Inositol 1,4,5-trisphosphate receptor and ryanodine receptor in the aging brain of Wistar rats. Neurobiol Aging 15(2):203–206
210. Simonyi A, Xia J, Igbavboa U, Wood WG, Sun GY (1998) Age differences in the expression of metabotropic glutamate receptor 1 and inositol 1,4,5-trisphosphate receptor in mouse cerebellum. Neurosci Lett 244(1):29–32
211. Long LH, Liu J, Liu RL, Wang F, Hu ZL, Xie N et al (2009) Differential effects of methionine and cysteine oxidation on [Ca^{2+}] i in cultured hippocampal neurons. Cell Mol Neurobiol 29(1):7–15
212. Peuchen S, Duchen MR, Clark JB (1996) Energy metabolism of adult astrocytes in vitro. Neuroscience 71(3):855–870
213. Bull R, Finkelstein JP, Humeres A, Behrens MI, Hidalgo C (2007) Effects of ATP, Mg2+, and redox agents on the Ca^{2+} dependence of RyR channels from rat brain cortex. Am J Physiol Cell Physiol 293(1):C162–C171
214. Gokulrangan G, Zaidi A, Michaelis ML, Schoneich C (2007) Proteomic analysis of protein nitration in rat cerebellum: effect of biological aging. J Neurochem 100(6):1494–1504
215. Hidalgo C, Bull R, Behrens MI, Donoso P (2004) Redox regulation of RyR-mediated Ca^{2+} release in muscle and neurons. Biol Res 37(4):539–552

216. Alford S, Frenguelli BG, Schofield JG, Collingridge GL (1993) Characterization of Ca^{2+} signals induced in hippocampal CA1 neurones by the synaptic activation of NMDA receptors. J Physiol 469:693–716
217. Matias C, Dionisio JC, Quinta-Ferreira ME (2002) Thapsigargin blocks STP and LTP related calcium enhancements in hippocampal CA1 area. Neuroreport 13(18):2577–2580
218. Yamazaki Y, Fujii S, Goto JI, Fujiwara H, Mikoshiba K (2015) Activation of inositol 1,4,5-trisphosphate receptors during preconditioning low-frequency stimulation suppresses subsequent induction of long-term potentiation in hippocampal CA1 neurons. Neuroscience 311:195–206
219. Sugita M, Yamazaki Y, Goto JI, Fujiwara H, Aihara T, Mikoshiba K et al (2016) Role of postsynaptic inositol 1, 4, 5-trisphosphate receptors in depotentiation in guinea pig hippocampal CA1 neurons. Brain Res 1642:154–162
220. Arias-Cavieres A, Adasme T, Sanchez G, Munoz P, Hidalgo C (2018) Raynodine receptor-mediated calcium release has a key role in hippocampal LTD induction. Front Cell Neurosci 12:403
221. Arias-Cavieres A, Adasme T, Sanchez G, Munoz P, Hidalgo C (2017) Aging impairs hippocampal- dependent recognition memory and LTP and prevents the associated RyR up-regulation. Front Aging Neurosci 9:111
222. Gant JC, Sama MM, Landfield PW, Thibault O (2006) Early and simultaneous emergence of multiple hippocampal biomarkers of aging is mediated by $Ca^{2+}-$induced Ca^{2+} release. J Neurosci 26(13):3482–3490
223. Kumar A, Foster TC (2004) Enhanced long-term potentiation during aging is masked by processes involving intracellular calcium stores. J Neurophysiol 91(6):2437–2444
224. Paula-Lima AC, Adasme T, Hidalgo C (2014) Contribution of Ca^{2+} release channels to hippocampal synaptic plasticity and spatial memory: potential redox modulation. Antioxid Redox Signal 21(6):892–914
225. Disterhoft JF, Oh MM (2006) Learning, aging and intrinsic neuronal plasticity. Trends Neurosci 29(10):587–599
226. Disterhoft JF, Oh MM (2007) Alterations in intrinsic neuronal excitability during normal aging. Aging Cell 6(3):327–336
227. Rex CS, Kramar EA, Colgin LL, Lin B, Gall CM, Lynch G (2005) Long-term potentiation is impaired in middle-aged rats: regional specificity and reversal by adenosine receptor antagonists. J Neurosci 25(25):5956–5966
228. Norris CM, Korol DL, Foster TC (1996) Increased susceptibility to induction of long-term depression and long- term potentiation reversal during aging. J Neurosci 16(17):5382–5392
229. Shankar S, Teyler TJ, Robbins N (1998) Aging differentially alters forms of long-term potentiation in rat hippocampal area CA1. J Neurophysiol 79(1):334–341
230. Diana G, Domenici MR, Loizzo A (1994) Scotti de Carolis A, Sagratella S. Age and strain differences in rat place learning and hippocampal dentate gyrus frequency-potentiation. Neurosci Lett 171(1–2):113–116
231. Kumar A, Thinschmidt JS, Foster TC, King MA (2007) Aging effects on the limits and stability of Long-term synaptic potentiation and depression in rat hippocampal area CA1. J Neurophysiol 98(2):594–601
232. Barnes CA, Rao G, McNaughton BL (1996) Functional integrity of NMDA-dependent LTP induction mechanisms across the lifespan of F-344 rats. Learn Mem 3(2–3):124–137
233. Watabe AM, O'Dell TJ (2003) Age-related changes in theta frequency stimulation-induced long-term potentiation. Neurobiol Aging 24(2):267–272
234. Zamani MR, Desmond NL, Levy WB (2000) Estradiol modulates long-term synaptic depression in female rat hippocampus. J Neurophysiol 84(4):1800–1808
235. Kemp N, McQueen J, Faulkes S, Bashir ZI (2000) Different forms of LTD in the CA1 region of the hippocampus: role of age and stimulus protocol. Eur J Neurosci 12(1):360–366
236. Dudek SM, Bear MF (1993) Bidirectional long-term modification of synaptic effectiveness in the adult and immature hippocampus. J Neurosci 13(7):2910–2918

237. Hsu KS, Huang CC, Liang YC, Wu HM, Chen YL, Lo SW et al (2002) Alterations in the balance of protein kinase and phosphatase activities and age-related impairments of synaptic transmission and long-term potentiation. Hippocampus 12(6):787–802
238. Vouimba RM, Foy MR, Foy JG, Thompson RF (2000) 17beta-estradiol suppresses expression of long-term depression in aged rats. Brain Res Bull 53(6):783–787
239. Moore CI, Browning MD, Rose GM (1993) Hippocampal plasticity induced by primed burst, but not long-term potentiation, stimulation is impaired in area CA1 of aged Fischer 344 rats. Hippocampus 3(1):57–66
240. Deupree DL, Bradley J, Turner DA (1993) Age-related alterations in potentiation in the CA1 region in F344 rats. Neurobiol Aging 14(3):249–258
241. Rosenzweig ES, Rao G, McNaughton BL, Barnes CA (1997) Role of temporal summation in age-related long-term potentiation- induction deficits. Hippocampus 7(5):549–558
242. Tong G, Jahr CE (1994) Regulation of glycine-insensitive desensitization of the NMDA receptor in outside-out patches. J Neurophysiol 72(2):754–761
243. Sah P, Faber ES (2002) Channels underlying neuronal calcium-activated potassium currents. Prog Neurobiol 66(5):345–353
244. Kumar A, Foster T (2007) Environmental enrichment decreases the afterhyperpolarization in senescent rats. Brain Res 1130(1):103–107
245. Disterhoft JF, Oh MM (2006) Pharmacological and molecular enhancement of learning in aging and Alzheimer's disease. J Physiol Paris 99(2–3):180–192
246. Kumar A, Rani A, Tchigranova O, Lee WH, Foster TC (2012) Influence of late-life exposure to environmental enrichment or exercise on hippocampal function and CA1 senescent physiology. Neurobiol Aging 33(4):828 e1–e17
247. Froemke RC, Poo MM, Dan Y (2005) Spike-timing-dependent synaptic plasticity depends on dendritic location. Nature 434(7030):221–225
248. Power JM, Wu WW, Sametsky E, Oh MM, Disterhoft JF (2002) Age-related enhancement of the slow outward calcium-activated potassium current in hippocampal CA1 pyramidal neurons in vitro. J Neurosci 22(16):7234–7243
249. Kerr DS, Campbell LW, Hao SY, Landfield PW (1989) Corticosteroid modulation of hippocampal potentials: increased effect with aging. Science 245(4925):1505–1509
250. Pitler TA, Landfield PW (1990) Aging-related prolongation of calcium spike duration in rat hippocampal slice neurons. Brain Res 508(1):1–6
251. Gong LW, Gao TM, Huang H, Zhou KX, Tong Z (2002) ATP modulation of large conductance Ca^{2+}-activated K(+) channels via a functionally associated protein kinase A in CA1 pyramidal neurons from rat hippocampus. Brain Res 951(1):130–134
252. Disterhoft JF, Moyer JR Jr, Thompson LT, Kowalska M (1993) Functional aspects of calcium-channel modulation. Clin Neuropharmacol 16(Suppl 1):S12–S24
253. Power JM, Oh MM, Disterhoft JF (2001) Metrifonate decreases sI(AHP) in CA1 pyramidal neurons in vitro. J Neurophysiol 85(1):319–322
254. Moyer JR Jr, Power JM, Thompson LT, Disterhoft JF (2000) Increased excitability of aged rabbit CA1 neurons after trace eyeblink conditioning. J Neurosci 20(14):5476–5482
255. Murphy GG, Fedorov NB, Giese KP, Ohno M, Friedman E, Chen R et al (2004) Increased neuronal excitability, synaptic plasticity, and learning in aged Kvbeta1.1 knockout mice. Curr Biol 14(21):1907–1915
256. Azad SC, Eder M, Simon W, Hapfelmeier G, Dodt HU, Zieglgansberger W et al (2004) The potassium channel modulator flupirtine shifts the frequency-response function of hippocampal synapses to favour LTD in mice. Neurosci Lett 370(2–3):186–190
257. Kumar A, Bodhinathan K, Foster TC (2009) Susceptibility to calcium dysregulation during brain aging. Front Aging Neurosci 1:2
258. Phillips RG, Meier TJ, Giuli LC, McLaughlin JR, Ho DY, Sapolsky RM (1999) Calbindin D28K gene transfer via herpes simplex virus amplicon vector decreases hippocampal damage in vivo following neurotoxic insults. J Neurochem 73(3):1200–1205
259. Dore K, Stein IS, Brock JA, Castillo PE, Zito K, Sjostrom PJ (2017) Unconventional NMDA receptor signaling. J Neurosci 37(45):10800–10807

260. Zorumski CF, Izumi Y (2012) NMDA receptors and metaplasticity: mechanisms and possible roles in neuropsychiatric disorders. Neurosci Biobehav Rev 36(3):989–1000
261. Abraham WC, Williams JM (2008) LTP maintenance and its protein synthesis-dependence. Neurobiol Learn Mem 89(3):260–268
262. Annunziato L, Amoroso S, Pannaccione A, Cataldi M, Pignataro G, D'Alessio A et al (2003) Apoptosis induced in neuronal cells by oxidative stress: role played by caspases and intracellular calcium ions. Toxicol Lett 139(2–3):125–133
263. Squier TC (2001) Oxidative stress and protein aggregation during biological aging. Exp Gerontol 36(9):1539–1550
264. Serrano F, Klann E (2004) Reactive oxygen species and synaptic plasticity in the aging hippocampus. Ageing Res Rev 3(4):431–443
265. Suzuki K, Nakamura M, Hatanaka Y, Kayanoki Y, Tatsumi H, Taniguchi N (1997) Induction of apoptotic cell death in human endothelial cells treated with snake venom: implication of intracellular reactive oxygen species and protective effects of glutathione and superoxide dismutases. J Biochem (Tokyo) 122(6):1260–1264
266. Lu C, Chan SL, Fu W, Mattson MP (2002) The lipid peroxidation product 4-hydroxynonenal facilitates opening of voltage-dependent Ca^{2+} channels in neurons by increasing protein tyrosine phosphorylation. J Biol Chem 277(27):24368–24375
267. Akaishi T, Nakazawa K, Sato K, Saito H, Ohno Y, Ito Y (2004) Modulation of voltage-gated Ca^{2+} current by 4-hydroxynonenal in dentate granule cells. Biol Pharm Bull 27(2):174–179
268. Gong L, Gao TM, Huang H, Tong Z (2000) Redox modulation of large conductance calcium-activated potassium channels in CA1 pyramidal neurons from adult rat hippocampus. Neurosci Lett 286(3):191–194
269. Lu C, Chan SL, Haughey N, Lee WT, Mattson MP (2001) Selective and biphasic effect of the membrane lipid peroxidation product 4-hydroxy-2,3-nonenal on N-methyl-D-aspartate channels. J Neurochem 78(3):577–589
270. Kamsler A, Segal M (2004) Hydrogen peroxide as a diffusible signal molecule in synaptic plasticity. Mol Neurobiol 29(2):167–178
271. Ullrich V, Namgaladze D, Frein D (2003) Superoxide as inhibitor of calcineurin and mediator of redox regulation. Toxicol Lett 139(2–3):107–110
272. Lin CH, Yeh SH, Leu TH, Chang WC, Wang ST, Gean PW (2003) Identification of calcineurin as a key signal in the extinction of fear memory. J Neurosci 23(5):1574–1579
273. Gorlach A, Bertram K, Hudecova S, Krizanova O (2015) Calcium and ROS: a mutual interplay. Redox Biol 6:260–271
274. Gant JC, Blalock EM, Chen KC, Kadish I, Porter NM, Norris CM et al (2014) FK506-binding protein 1b/12.6: a key to aging-related hippocampal Ca^{2+} dysregulation? Eur J Pharmacol 739:74–82
275. Gant JC, Chen KC, Norris CM, Kadish I, Thibault O, Blalock EM et al (2011) Disrupting function of FK506-binding protein 1b/12.6 induces the Ca(2)+−dysregulation aging phenotype in hippocampal neurons. J Neurosci 31(5):1693–1703

Chapter 40
Calcium Signaling in Endothelial Colony Forming Cells in Health and Disease

Francesco Moccia

Abstract Endothelial colony forming cells (ECFCs) represent the only known truly endothelial precursors. ECFCs are released in peripheral circulation to restore the vascular networks dismantled by an ischemic insult or to sustain the early phases of the angiogenic switch in solid tumors. A growing number of studies demonstrated that intracellular Ca^{2+} signaling plays a crucial role in driving ECFC proliferation, migration, homing and neovessel formation. For instance, vascular endothelial growth factor (VEGF) triggers intracellular Ca^{2+} oscillations and stimulates angiogenesis in healthy ECFCs, whereas stromal derived factor-1α promotes ECFC migration through a biphasic Ca^{2+} signal. The Ca^{2+} toolkit endowed to circulating ECFCs is extremely plastic and shows striking differences depending on the physiological background of the donor. For instance, inositol-1,4,5-trisphosphate-induced Ca^{2+} release from the endoplasmic reticulum is downregulated in tumor-derived ECFCs, while agonists-induced store-operated Ca^{2+} entry is up-regulated in renal cellular carcinoma and is unaltered in breast cancer and reduced in infantile hemangioma. This remodeling of the Ca^{2+} toolkit prevents VEGF-induced pro-angiogenic Ca^{2+} oscillations in tumor-derived ECFCs. An emerging theme of research is the dysregulation of the Ca^{2+} toolkit in primary myelofibrosis-derived ECFCs, as this myeloproliferative disorder may depend on a driver mutation in the calreticulin gene. In this chapter, I provide a comprehensive, but succinct, description on the architecture and role of the intracellular Ca^{2+} signaling toolkit in ECFCs derived from umbilical cord blood and from peripheral blood of healthy donors, cancer patients and subjects affected by primary myelofibrosis.

Keywords Endothelial colony forming cells · Ca^{2+} signaling · Inositol-1 · 4 · 5-trisphosphate receptors · Two-pore channel 1 · STIM1 · Orai1 · TRPC1 · TRPC3 · VEGF · SDF-1α

F. Moccia (✉)
Laboratory of General Physiology, Department of Biology and Biotechnology "L. Spallanzani", University of Pavia, Pavia, Italy
e-mail: francesco.moccia@unipv.it

M. S. Islam (ed.), *Calcium Signaling*, Advances in Experimental Medicine and Biology 1131, https://doi.org/10.1007/978-3-030-12457-1_40

40.1 Introduction

Endothelial progenitor cells (EPCs) are released in the bloodstream to replace senescent or injured endothelial cells and to restore the vascular networks disrupted by an ischemic insult [1, 2]. Moreover, EPCs sustain tumor angiogenesis and metastasis by providing the building blocks for nascent vasculature and by stimulating local angiogenesis in a paracrine manner [3]. Circulating EPCs can be subdivided into two main cellular populations based on their hematopoietic or endothelial lineage [1]. Myeloid angiogenic cells (MACs), also known as circulating angiogenic cells (CACs) or "early" EPCs, represent a population of hematopoietic EPCs that are released from bone marrow and promote vascular repair in a paracrine manner, even though they are not able to physically engraft within neovessels and show limited proliferative potential. Endothelial colony forming cells (ECFCs), also known as blood outgrowth endothelial cells (BOECs) or "late" EPCs, constitute the only known truly endothelial precursors with an enormous potential for vascular reconstruction [1, 4]. ECFCs express the surface antigens CD31, CD105, CD144, CD146, von Willebrand factor (vWF), VEGFR-2 (KDR) and display the ability to ingest the ability to ingest acetylated low density lipoprotein (AcLDL). Furthermore, ECFCs lack the hematopoietic or monocytes/macrophage surface antigens CD14, CD45, or CD115 [5]. ECFCs mainly reside within vascular stem cell niches, display a robust clonogenic potential, assemble into capillary-like structures in vitro and give raise to durable and functional blood vessels in multiple murine models of cardiovascular disorders [1, 4]. Moreover, ECFCs drive the angiogenic switch during the early phases of vascular growth in many types of solid cancers, including melanoma and breast cancer [4, 6]. Therefore, ECFCs are regarded as the most suitable cellular candidates for regenerative stem cell therapy of cardiovascular disorders [7] and the most promising target for anti-angiogenic therapy [3, 8].

Intracellular Ca^{2+} signaling has long been known to stimulate angiogenesis under both physiological and pathological conditions [9]. Growth factors and cytokines, such as vascular endothelial growth factor (VEGF), basic fibroblast growth factor (bFGF), epidermal growth factor (EGF), angiopoietins, and stromal cell-derived factor-1α (SDF-1α), stimulate endothelial proliferation, migration, and tube formation through an increase in intracellular Ca^{2+} concentration ($[Ca^{2+}]_i$) [10–17]. Recent studies demonstrated that Ca^{2+} signaling plays a key role in ECFC proliferation, tube formation and neovessel formation [18, 19]. This review discusses how insulin-like growth factor 2 (IGF2), SDF-1α and VEGF impinge on distinct Ca^{2+} waveforms to regulate the angiogenic behavior of ECFCs derived from human peripheral blood and umbilical cord blood (PB-ECFCs and UCB-ECFCs, respectively). Furthermore, this review discusses how the remodeling of the Ca^{2+} toolkit in PB-ECFCs may contribute to the development of resistance to anti-angiogenic therapies in renal cellular carcinoma (RCC), breast cancer (BC), and infantile hemangioma (IH) patients. Finally, this review discusses how the Ca^{2+} signaling machinery undergoes an extensive rewiring also in ECFCs deriving from

subjects affected by primary myelofibrosis (PMF-ECFCs), a myeloproliferative disorder that may include a driver mutation in the calreticulin gene [20].

40.2 The Intracellular Ca^{2+} Toolkit in Peripheral Blood-Derived Endothelial Colony Forming Cells

The concerted interaction of multiple Ca^{2+}-transporting systems contributes to maintain the resting $[Ca^{2+}]_i$ in ECFCs and to clear cytosolic Ca^{2+} upon extracellular stimulation [18, 19]. A thorough transcriptomic analysis revealed that ECFCs express some of the most widespread endothelial transporter and pump isoforms [21]. These include Sarco-Endoplasmic Reticulum Ca^{2+}-ATPase 2B (SERCA2B), which sequesters cytosolic Ca^{2+} into the endoplasmic reticulum (ER) lumen, the most abundant intracellular Ca^{2+} reservoir; Plasma Membrane Ca^{2+}-ATPase 1B (PMCA1B) and PMCA4B, which extrude Ca^{2+} towards the extracellular space. Surprisingly, ECFCs lack the endothelial isoforms of the Na^+/Ca^{2+} exchanger (NCX), e.g. NCX1.3 and NCX1.7, which sustain PMCA-mediated Ca^{2+} extrusion across the plasma membrane in vascular endothelial cells [22]. In agreement with this observation, reverting the Na^+ gradient through Na^+ substitution, which induces NCX to switch from the forward (3 Na^+ in: 1 Ca^{2+} out) to the reverse (3 Na^+ out: 1 Ca^{2+} in) Ca^{2+} entry mode [23], did not cause any detectable increase in $[Ca^{2+}]_i$ in ECFCs [18].

ECFCs impinge on two main Ca^{2+} sources to generate intracellular Ca^{2+} signals in response to extracellular stimulation [18, 19], namely the ER and the extracellular milieu (Fig. 40.1). Growth factors and cytokines bind, respectively, to their specific Tyrosine Kinase Receptors (TRKs), such as VEGFR2 (for VEGF), and G-Protein Coupled Receptors (GPCRs), such as IGF2 receptor (IGFR2) and CXCR4 (for SDF-1α), thereby causing an increase in $[Ca^{2+}]_i$ through the activation of multiple isoforms of phospholipase C (PLC) [19, 24–26]. Accordingly, GPCRs and TKRs recruit, respectively, PLCβ and PLCγ, which cleave phosphatidylinositol 4,5-bisphosphate (PIP_2), a minor phospholipid component of the plasma membrane, into the intracellular second messengers, inositol-1,4,5-trisphosphate ($InsP_3$) and diacylglycerol (DAG) [19]. ECFCs are endowed with PLCβ2, which may be recruited by IGF2 and SDF-1α through the $G_{\beta\gamma}$ dimer [24], while it is still unclear which PLCγ isoforms (PLCγ1–4) they express. In addition, ECFCs express all the three $InsP_3$ receptor isoforms ($InsP_3$Rs), namely $InsP_3$R1, $InsP_3$R2 and $InsP_3$R3 (Table 40.1) [26]. $InsP_3$, therefore, binds to ER-embedded $InsP_3$Rs and causes transient or rhythmical Ca^{2+} release into the cytosol, leading to a massive reduction in ER Ca^{2+} concentration [24, 26, 27]. Conversely, ECFCs lack ryanodine receptors (RyRs) (Table 40.1) and do not produce Ca^{2+} signals in response to caffeine [27, 28]. In addition, endogenous Ca^{2+} may be accumulated within the acidic vesicles of the endolysosomal (EL) compartment [29]. ECFCs express high protein levels of the two-pore channel 1 (TPC1) (Table 40.1), which is gated by the newly discovered

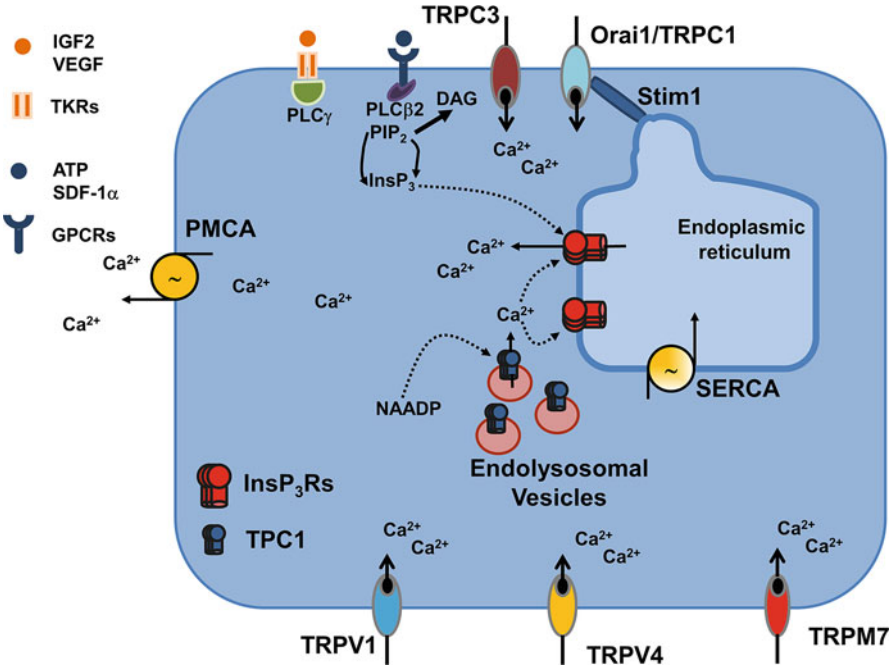

Fig. 40.1 The intracellular Ca^{2+} toolkit in human endothelial colony forming cells. Extracellular autacoids bind to specific G-protein Coupled Receptors (GPCRs) or Tyrosin Kinase Receptors (TKRs), thereby activating PLCβ2 and PLCγ, respectively, which cleave PIP_2 into $InsP_3$ and DAG. $InsP_3$ triggers ER-dependent Ca^{2+} release through $InsP_3Rs$, while DAG gates TRPC3 in UCB-ECFCs. The newly discovered second messenger NAADP stimulates TPC1 to cause Ca^{2+} release from the acidic vesicles of the endolysosomal (EL) system. NAADP-induced Ca^{2+} release could, in turn, recruit $InsP_3Rs$ through the Ca^{2+}-induced Ca^{2+} release process. The $InsP_3$-dependent drop in ER Ca^{2+} levels induces SOCE, which is mediated by the interaction between STIM1, Orai1 and TRPC1. Moreover, extracellular Ca^{2+} entry may occur through TRPV1, TRPV4 and TRPM7. TKRs and GPCRs are representative of IGFR2 and VEGFRs and of P_{2Y} receptors and CXCR4, respectively

second messenger, nicotinic acid adenine dinucleotide phosphate (NAADP), and mediates massive EL Ca^{2+} release into the cytoplasm [28, 30]. Mitochondria may also modulate intracellular Ca^{2+} signals by buffering $InsP_3$-dependent Ca^{2+} release and extracellular Ca^{2+} influx in ECFCs [21, 31]. For instance, $InsP_3$-driven mitochondrial Ca^{2+} signals sustain ECFC bioenergetics [32], as reported in vascular endothelium [33].

Extracellular Ca^{2+} entry in ECFCs is mediated by store-operated Ca^{2+} entry (SOCE) and members of the Transient Receptor Potential (TRP) superfamily of non-selective cation channels (Table 40.1) [19, 34]. SOCE is physiologically activated by the $InsP_3$-induced depletion of the ER Ca^{2+} store and is accomplished

Table 40.1 Composition of the Ca^{2+} toolkit in different types of endothelial colony forming cells

Parameter	PB-ECFCs	RCC-ECFCs	BC-ECFCs	IH-ECFCs	PMF-ECFCs	UCB-ECFCs
$[Ca^{2+}]_{ER}$	/	No [21]	No [76]	No [43]	No [99]	ND
SOCE	No [27]	No [35]	=	=	No [99]	No [27]
VEGF sensitivity	No [26]	No [35]	No [76]	No [43]	No [101]	No [48]
$InsP_3R1–3$	No [26], mRNA	No [35], mRNA	No [76]	No [43]	No [99]	No [48], mRNA
RyR1–3	No [27], mRNA	ND	ND	ND	ND	ND
TPC1	No [28], mRNA	ND	ND	ND	ND	ND
STIM1	No [27], mRNA & protein	No [35], mRNA & protein	No [76], mRNA & protein	No [43], mRNA & protein	No [99], mRNA & protein	No [27], mRNA & protein
STIM2	No [27], mRNA & protein	No [35], mRNA & protein	No [76], mRNA & protein	No [43], mRNA & protein	No [99], mRNA & protein	No [27], mRNA & protein
Orai1	No [27], mRNA & protein	No [35], mRNA & protein	No [76], mRNA & protein	No [43], mRNA & protein	No [99], mRNA & protein	No [27], mRNA & protein
Orai2	No [27], mRNA	No [35], mRNA	No [76], mRNA	No [43], mRNA	No [99], mRNA	No [27], mRNA
Orai3	No [27], mRNA & protein	No [35], mRNA	No [76], mRNA	No [43], mRNA	No [99], mRNA	No [27], mRNA
TRPC1	No [27], mRNA & protein	No [35], mRNA & protein	No [76], mRNA & protein	No [43], mRNA & protein	No [99], mRNA & protein	No [27], mRNA & protein
TRPC3	No [27, 48], mRNA & protein	No [35], mRNA	No [76], mRNA	No [43], mRNA	No, [99], mRNA	No [48], mRNA & protein
TRPC4	No [27], mRNA & protein	No [35], mRNA & protein	No [76], mRNA & protein	No [43], mRNA & protein	No [99], mRNA & protein	No [27], mRNA & protein
TRPC5–7	No [27], mRNA	No [35], mRNA	No [76], mRNA	No [43], mRNA	No [99], mRNA	No [27], mRNA
TRPV1	No [27], Protein	ND	ND	ND	ND	ND
TRPV4	No [52], mRNA & protein	ND	ND	ND	ND	ND
TRPM7	No [54], mRNA & protein	ND	ND	ND	ND	ND

Abbreviations: *$InsP_3R$* inositol-1,4,5-trisphosphate receptors, *ND* not defined, *RyR* ryanodine receptors, *SOCE* store-operated Ca^{2+} entry, *TPC* two-pore channels, *TRPC* Canonical Transient Receptor Potential, *TRPM* Melastatin Transient Receptor Potential, *TRPV* Vanilloid Transient Receptor Potential

by the interaction between Stromal Interaction Molecule 1 (STIM1), a sensor of ER Ca^{2+} levels, and Orai1 and Transient Receptor Potential (TRP) Canonical 1 (TRPC1), which form the Ca^{2+}-permeable channel(s) on the plasma membrane [19, 27, 35, 36]. $InsP_3$-evoked ER-dependent Ca^{2+} release induced STIM1 aggregation into ER-plasma membrane clusters, known as *puncta*, in which STIM1 interacts with and activates Orai1 and TRPC1 [19, 36]. It is, however, still unknown whether Orai1 and TRPC1 assemble into a unique supermolecular complex, as observed in human megakaryocytes [37] and platelets [38], or mediate two distinct STIM1-dependent channels, as described in human submandibular gland cells [39], mouse salivary acinar cells [40] and mouse pancreatic acinar cells [41]. TRPC1 has been shown to contribute to SOCE also in mouse bone marrow-derived ECFCs [42]. SOCE in ECFCs is blocked by 10 μM La^{3+} or Gd^{3+}, YM-58483/BTP-2, which lacks side effects in ECFCs [34], Pyr6 and carboxyamidotriazole (CAI) [27, 35, 43].

The TRP superfamily consists of 28 (27 human) members which fall into six subfamilies based on amino acid sequence similarity and function [44]: TRPC for canonical (TRPC1–7), TRPV for vanilloid (TRPV1–6), TRPM for melastatin (TRPM1–8), TRPA for ankyrin (TRPA1), TRPML for mucolipin (TRPML1–3), and TRPP for polycystin (TRPP; TRPP2, TRPP3 and TRPP5) [44]. Little information is available regarding TRP channel expression in human ECFCs. Apart from TRPC1, PB-ECFCs express TRPC4, while they lack TRPC3, TRPC5 and TRPC6, which play a crucial role in angiogenesis and blood pressure regulation in vascular endothelial cells [45–47]. Nevertheless, TRPC3 is abundantly expressed in UCB-ECFCs (Table 40.1) [48]. On the other hand, PB-ECFCs possess multiple TRP channel isoforms, i.e. TRPV1, TRPV4 and TRPM7 (Table 40.1) [19]. TRPV1 is a polymodal non-selective cation channel that is gated by noxious heat (>43 °C), protons (pH < 5.9), endovanilloids, and many natural products, including dietary compounds, such as capsaicin, eugenol, and gingerol [49]. A recent study showed that TRPV1 mediates cell proliferation and tube formation in ECFCs by promoting anandamide uptake in a Ca^{2+}-independent manner [50]. This effect was further enhanced by capsaicin [50]. Similar to TRPV1, TRPV4 is a polymodal Ca^{2+}-permeable channel that is activated by a disparate array of stimuli, including heat (>25 °C), hypotonicity, acidic pH, arachidonic acid (AA) and phospholipase A2-mediated AA metabolites [51]. AA stimulates TRPV4 to stimulate ECFC proliferation by recruiting the endothelial nitric oxide (NO) synthase (eNOS) and triggering robust NO release [28, 52]. Finally, TRPM7 is a constitutively active non-selective cation channel which is highly permeable to extracellular divalent cations, i.e. Ca^{2+} and Mg^{2+}, and is physiologically regulated by multiple mechanisms, including: a reduction in intracellular Mg^{2+} and Mg-ATP, depletion of PIP_2 in the plasma membrane upon PLC activation, laminar shear stress and membrane stretch [53]. Recent work showed that TRPM7 has no impact on ECFC growth, although it stimulates proliferation in human microvascular endothelial cells [54].

40.3 IGF2 and SDF-1α Stimulate ECFC Homing Through an Increase in $[Ca^{2+}]_i$

Ischemic tissues release a multitude of cytokines, including IGF2 and SDF-1α, which recruit circulating ECFCs or stimulate ECFC mobilization from the vascular niches and promote their physical incorporation within nascent neovessels [24, 55]. IGF2 stimulated IGFR2 to cause an increase in $[Ca^{2+}]_i$ through the recruitment of PLCβ2 [24]. Intracellular Ca^{2+} mobilization was, in turn, required to drive UCB-ECFC chemotaxis and adhesion to a fibronectin matrix in vitro. Furthermore, IGF2-evoked Ca^{2+} signals induced UCB-ECFC recruitment to injured vessels and incorporation into newly formed vessels in vivo, thereby promoting vascular repair in a murine model of hindlimb ischemia [24]. Subsequent work demonstrated that also SDF-1α stimulates PB-ECFC migration in vitro and neovessel formation in vivo through intracellular Ca^{2+} signaling [25]. SDF-1α-evoked increase in $[Ca^{2+}]_i$ was mediated by CXCR4 and achieved the largest magnitude at 10 ng/mL, whereas it desensitized at higher concentrations (i.e. 50 ng/mL). The Ca^{2+} response to SDF-1α consisted in an initial Ca^{2+} peak, which was mediated by $InsP_3$-dependent ER Ca^{2+} release, followed by a prolonged plateau phase, which was due to SOCE activation [25]. SDF-1α induced Ca^{2+} signaling, in turn, engaged the phosphoinositide 3-kinase (PI3K)/Akt and extracellular signal–regulated kinase (ERK) signaling pathways [25], which are both necessary for ECFC migration and neovessel formation [25, 56]. Therefore, intracellular Ca^{2+} signaling plays a crucial role in promoting ECFC homing to hypoxic tissues by mediating the chemotactic effect of multiple cytokines.

40.4 VEGF-Induced Intracellular Ca^{2+} Oscillations Stimulate ECFC Proliferation and Tube Formation

VEGF is massively released from hypoxic cells to stimulate sprouting angiogenesis and promote proliferation in EPCs (i.e. MACs and ECFCs) recruited to injured vessels [2, 57]. VEGF promotes the angiogenic activity of ECFCs by binding to VEGFR-2 [57, 58], which activates multiple downstream signaling pathways [59], including an increase in $[Ca^{2+}]_i$ [10, 14, 60]. A recent investigation demonstrated that VEGF-induced intracellular Ca^{2+} oscillations drive cell proliferation and tube formation in PB-ECFCs (Table 40.1) [26, 36]. VEGF-induced Ca^{2+} spikes were asynchronous between individual PB-ECFCs from the same coverslip and displayed a dose-response activity. The magnitude of the first Ca^{2+} spike increases while latency of the oscillatory response decreases when VEGF concentration was increased from 1 ng/ml to 50 ng/ml, with maximal frequency of Ca^{2+} oscillations attained at 10 ng/mL [26]. Pharmacological manipulation revealed that VEGF-induced intracellular Ca^{2+} oscillations were triggered by rhythmical $InsP_3$-dependent Ca^{2+} release from the ER and maintained over time by SOCE

in a SERCA-dependent manner [26]. The transcription factor, Nuclear factor kappa enhancer binding protein (NF-κB), represents the Ca^{2+}-dependent decoder which translates intracellular Ca^{2+} oscillations into a mitogenic output in vascular endothelial cells [61, 62]. The NF-κB family of transcription factors comprises five members: p50, p52, p65 (also known as REL-A), c-REL and REL-B, which assemble with each other into homo- or heterodimeric complexes [63]. Under resting conditions, NF-κB dimers are retained within the cytosol through the physical interaction with the inhibitory IkB proteins, which masks their nuclear localization sequence (NLS). Intracellular Ca^{2+} oscillations recruit the Ca^{2+}/Calmodulin (CaM)-dependent protein kinase IV (CaMKIV), which phosphorylates and activates two IκB kinases, i.e. IKKα and IKKβ. In turn, these kinases phosphorylate IκB at S32 and S36, respectively [19, 61, 62]. In particular, IKKβ-induced phosphorylation leads to IκB ubiquitination and subsequent proteosomal degradation, thereby exposing the previously masked NLS of NF-κB, which is free to translocate into the nucleus and initiate the transcription of target genes [63, 64]. VEGF-induced intracellular Ca^{2+} oscillations promoted IκB phosphorylation, whereby thimoquinone, a rather selective NF-κB inhibitor, prevented VEGF-dependent PB-ECFC proliferation and tube formation [26].

Earlier work demonstrated that UCB-ECFCs are more sensitive to VEGF compared to their circulating counterparts [65], although there is no significant difference in VEGFR-2 expression between the two cell types [27, 48]. This finding suggests that the pro-angiogenic signaling pathway recruited downstream of VEGFR-2 is more robustly activated in UCB-ECFCs [2, 66]. In agreement with this hypothesis, the oscillatory Ca^{2+} activity induced by VEGF is significantly enhanced in UCB-ECFCs compared to PB-ECFCs (Table 40.1) [2, 48]. The oscillatory response to VEGF was triggered by TRPC3, which is gated by DAG and is selectively expressed in UCB-, but not PB-ECFCs (Fig. 40.1) [48]. TRPC3-mediated extracellular Ca^{2+} entry, in turn, triggered the dynamic interplay between rhythmical $InsP_3$-dependent ER Ca^{2+} release and SOCE, which maintains the oscillations over time [48]. This observation showed that the Ca^{2+} toolkit endowed to ECFCs is extremely plastic and varies depending on the source (Table 40.1), i.e. PB vs. UCB. Furthermore, it led to the hypothesis that introducing TRPC3 in autologous aging or dysfunctional ECFCs could rejuvenate or partially rescue their reparative phenotype [66].

40.5 The Intracellular Ca^{2+} Toolkit Is Remodeled in Tumor-Derived ECFCs

The Ca^{2+} toolkit is dramatically altered not only in cancer cells [67, 68], but also in tumor stromal cells [69–74], thereby contributing to establish many cancer hallmarks, such as aberrant angiogenesis, invasion and metastasis. Tumor-derived ECFCs were isolated from peripheral blood of cancer patients, as described in the pioneering study by Yoder and coworkers [65]. The frequency of ECFCs is

significantly increased in peripheral blood of RCC and BC patients [75], which is consistent with their role in tumor vascularization [4, 6]. Furthermore, RCC- and BC-derived ECFCs (termed, respectively, RCC-ECFCs and BC-ECFCs) show significant ultrastructural differences when compared to healthy ECFCs. For instance, the mitochondria were more numerous and displayed an elongated and branched shape, which reflects fusion or incomplete separation, in tumor-derived ECFCs [21, 76]. Moreover, cisternae of rough ER (rER) were more widely spaced and occupied a wider area in RCC- and BC-ECFCs compared to healthy ECFCs. Similarly, smooth ER (sER) vesicles occupied a large part of the cytoplasm in tumor-derived, but not healthy, ECFCs [21, 76]. Ca^{2+} imaging recordings revealed that these major morphological differences were accompanied by a dramatic remodeling of the Ca^{2+} toolkit. An earlier report showed that $InsP_3$-dependent ER Ca^{2+} release was significantly reduced in RCC-ECFCs [35], due to the reduction in the ER Ca^{2+} concentration ($[Ca^{2+}]_{ER}$) (Table 40.1) [21] and the downregulation of $InsP_3R$ transcripts (Table 40.1) [35]. Conversely, SOCE amplitude was enhanced due to the up-regulation of STIM1, Orai1 and TRPC1 expression (Table 40.1) [35]. The reduction in $[Ca^{2+}]_{ER}$ could be due to the slowing down of SERCA pump activity [21], which is associated with the up-regulation of TMTC1, a tetratricopeptide repeats (TPR)-containing protein that physically interacts with and inhibits SERCA [77]. On the other hand, there was no difference in the expression levels of SERCA2B, PMCA1B, PMCA4B and of the two major ER Ca^{2+} buffering proteins, calreticulin and calnexin, between normal and RCC-derived ECFCs [21]. Remodeling of the Ca^{2+} toolkit has the potential to modulate ECFC resistance to a number of anticancer therapies [18, 69]. For instance, the reduction in $[Ca^{2+}]_{ER}$ and $InsP_3R$ expression resulted in lower sensitivity to pro-apoptotic stimulation in RCC-ECFCs [21], as routinely observed in cancer cells [68, 78], due to the impairment of $InsP_3$-driven ER-to-mitochondria Ca^{2+} transfer [21]. Conversely, there was no difference in the expression levels of the anti-apoptotic protein, Bcl-2, and of the pro-apoptotic protein, Bak [21]. Furthermore, RCC-ECFCs became insensitive to VEGF (Table 40.1), which failed to trigger $InsP_3$-dependent intracellular Ca^{2+} oscillations [18, 35]. This finding could explain why anti-VEGF therapy does not improve the overall survival of RCC patients and why a remarkable fraction of these subjects manifest resistance at the start of treatment [3, 18, 79]. Nevertheless, the pharmacological blockade of SOCE with 10 μM La^{3+} or Gd^{3+}, YM-58483/BTP-2 or CAI, inhibited RCC-ECFC proliferation and tube formation [35]. This finding suggested that SOCE could provide a reliable target for anti-angiogenic therapies in RCC [18, 34, 79].

A subsequent investigation showed that the intracellular Ca^{2+} toolkit is also remodeled in BC-ECFCs [76]. These cells displayed a significant reduction in the $InsP_3$-regulated ER Ca^{2+} pool (Table 40.1), although $InsP_3Rs$ were normally expressed. Although $[Ca^{2+}]_{ER}$ has not been directly measured in BC-ECFCs [76], TMTC1 was overexpressed in these cells and may be responsible for the down-regulation of $InsP_3$-sensitive Ca^{2+} store [75]. Conversely, the amplitude of SOCE was not enhanced as only STIM1, but not Orai1 and TRPC1, was up-regulated (Table 40.1) [76]. Similar to RCC-ECFCs, the reduction in the $InsP_3$-releasable ER

Ca^{2+} pool prevented VEGF from triggering robust intracellular Ca^{2+} oscillations in BC-ECFCs (Table 40.1), although there was no difference in VEGFR-2 expression compared to healthy cells. As a consequence, VEGF failed to promote proliferation and tube formation in BC-ECFCs [76]. As for RCC, this feature could explain why anti-VEGF drugs do not significantly improve the overall survival of BCC patients [80]. It should, however, be pointed out that the pharmacological blockade of SOCE did suppress BC-ECFC proliferation and tube formation.

Finally, the Ca^{2+} toolkit is also subtly remodeled in ECFCs derived from children suffering from infantile hemangioma (IH-ECFCs) [43]. IH is a benign vascular tumor that arises a few weeks after birth and can undergo spontaneous regression over the next 7–10 years [81]. Unfortunately, 24–38% of IH patients can develop complications that induce severe comorbidities and require medical interventions in 24–38% of the patients [82]. The aberrant vascular growth that results in IH is exacerbated by a population of resident endothelial precursors [81, 83], that are likely to be ECFCs. A recent study revealed that the $InsP_3$-releasable ER Ca^{2+} pool is dramatically reduced in IH-ECFCs, although $InsP_3Rs$ are normally expressed (Table 40.1). Interestingly, the amplitude of SOCE was dampened, although there was no change in the expression levels of STIM1, Orai1 and TRPC1 (Table 40.1) [43]. These findings led to the hypothesis that SOCE was constitutively activated in IH-ECFCs, so that STIM1, Orai1 and TRPC1 could not be fully recruited by extracellular stimulation [43]. The Mn^{2+} quenching technique is a widely employed strategy to evaluate resting Ca^{2+} permeability in vascular endothelial cells [84, 85]. This approach revealed that IH-ECFCs, but not healthy ECFCs, exhibit a constitutive SOCE which refills the ER and maintains the Ca^{2+} response to $InsP_3$ in a SERCA-dependent manner [43]. Similar to agonists-induced SOCE [35, 76], this constitutive Ca^{2+} entry was blocked by YM-58483/BTP-2 and 10 μM La^{3+} [43]. Therefore, it has been suggested that the chronic reduction in $[Ca^{2+}]_{ER}$ leads to the basal activation of store-operated channels to prevent excessive ER Ca^{2+} depletion. Constitutive SOCE, in turn, drives IH-ECFC proliferation by recruiting eNOS and enhancing basal NO release [43]. Of note, VEGF was not able to stimulate intracellular Ca^{2+} oscillations in IH-ECFCs (Table 40.1) [28].

Overall, these findings confirm that the Ca^{2+} toolkit in ECFCs is differently remodeled depending on the tumor type (Table 40.1). Nevertheless, tumor-derived ECFCs share three common features: (1) they display a significant reduction in the $InsP_3$-releasable ER Ca^{2+} pool, which could be due to a reduction in $[Ca^{2+}]_{ER}$ (and to $InsP_3Rs$ down-regulation in RCC-ECFCs); (2) they are insensitive to VEGF, which does not trigger intracellular Ca^{2+} oscillations and do not promote in vitro angiogenesis; and (3) they require SOCE to proliferate and assemble into capillary-like tubular structures. The molecular determinants that remodel the Ca^{2+} toolkit in tumor-derived ECFCs are not clear. It has been shown that BC-derived TRPC5-containing exosomes determine the up-regulation of TRPC5 expression in human dermal microvascular endothelial cells [86]. Moreover, the angiogenic behavior of several EPC subsets, including ECFCs, may be reprogrammed by circulating microRNAs (miRNAs) resident in exosomes and microvesicles [58, 87–89].

40.6 The Intracellular Ca^{2+} Toolkit Is Remodeled in Primary Myelofibrosis-Derived ECFCs

Primary myelofibrosis (PMF) is a Philadelphia chromosome-negative (Ph-neg) chronic myeloproliferative neoplasm which is characterized by bone marrow fibrosis, myeloid metaplasia, and splenomegaly. Splenomegaly, in turn, is sustained by enhanced mobilization of bone marrow-derived hematopoietic stem cells and circulating ECFCs, which support neovessel formation in the spleen [90, 91]. PMF is caused by somatic mutation in the JAK2 gene, resulting in a valine to phenylalanine substitution at position 617 (JAK2-V617F) in ≈60% of patients, in the calreticulin gene in 25% of patients, or in the gene encoding for the receptor for thrombopoietin (myeloproliferative leukemia virus oncogene, MPL) in 5% of patients [92]. Conversely, ≈10% of patients do not harbor any recognized mutation in their hematopoietic cells [20]. Calreticulin is a major ER Ca^{2+}-binding protein that exerts a multilevel control of intracellular Ca^{2+} dynamics. For instance, calreticulin determines the amount of ER-releasable Ca^{2+} [93], controls SOCE [94], and finely modulates SERCA2B activity [95]. The CALR mutation in PMF consists of either a 52-bp deletion (type 1) or a 5 bp TGTC insertion at the COOH-terminal, which contains the Ca^{2+}-binding site and the ER-retention domain [96]. Since the high capacity Ca^{2+}-binding domain of calreticulin is also able to impede SOCE activation [94], a mutation in this domain causes a decrease in the ER Ca^{2+} storage ability and an increase in SOCE amplitude in megakaryocytes from PMF patients, which are more evident for type 1 CALR mutation [97]. Long before the discovery of the driver role of calreticulin in PMF, a dramatic remodeling of the Ca^{2+} toolkit was described in ECFCs isolated from subjects carrying the JAK2 mutation (PMF-ECFCs). Although PMF-ECFCs do not belong to the neoplastic clone [98], they displayed a remarkable increase in the ER-releasable Ca^{2+} pool (Table 40.1) [99]. Nevertheless, $InsP_3$-dependent Ca^{2+} mobilization was attenuated (Table 40.1), although all the $InsP_3R$ isoforms were up-regulated [99]. SOCE was up-regulated and displayed additional molecular, pharmacological and functional differences when compared to healthy ECFCs (Table 40.1). Expression of STIM1, Orai1, Orai3, TRPC1 and TRPC4 proteins were also sup-regulated in PMF-ECFCs (Table 40.1). Intriguingly, two distinct store-operated channels were activated upon ER Ca^{2+} depletion in PMF-ECFCs. One channel was activated by $InsP_3$-dependent Ca^{2+} mobilization and was inhibited by YM-58483/BTP-2 and 10 μM La^{3+} and Gd^{3+}. The other channel was stimulated by pharmacological depletion of the ER Ca^{2+} pool with cyclopiazonic acid (CPA), a selective inhibitor of SERCA activity, but was insensitive to Gd^{3+}. The pharmacological profile of the $InsP_3$-sensitive SOCE was compatible with that described in RCC-ECFCs [35], BC-ECFCs [76] and IH-ECFCs [43] and strongly suggests that this pathway is mediated by STIM1, Orai1 and TRPC1. Molecular identity of the CPA-induced, Gd^{3+}-resistant SOCE is far less clear. Nevertheless, it has been shown that Orai1 may interact with TRPC1 and TRPC4 to form a STIM1-regulated channel that is insensitive to Gd^{3+} in a heterologous expression system, such as HEK-293 cells

[100]. Of note, YM-58483/BTP-2 only weakly affected PMF-ECFC proliferation, while Gd^{3+} was ineffective [99]. A subsequent report demonstrated that VEGF is able to trigger intracellular Ca^{2+} oscillations in PMF-ECFCs (Table 40.1), but this oscillatory activity is down-regulated compared to normal ECFCs and does not promote proliferation and tube formation [101]. Furthermore, the dynamic interplay between $InsP_3$-dependent ER Ca^{2+} release and SOCE, which shapes the periodic Ca^{2+} transients, was initiated by TRPC1-mediated Ca^{2+} entry. TRPC1 was, in turn, gated by DAG in a store-independent manner [52]. Notably, 1-oleoyl-2-acetyl-sn-glycerol, a membrane permeable DAG analogue, did not cause any detectable increase in $[Ca^{2+}]_i$ in PB-ECFCs [45]. The data described above can be attributed to the changes observed in the intracellular Ca^{2+} toolkits of differently sourced ECFCs (as shown in Table 40.1).

40.7 Conclusion

ECFCs represent a sharp double-edged sword. They are released in the blood to restore local blood perfusion by regenerating the vascular network injured by an ischemic event. Hence, these cells are regarded as one of the most suitable candidates for regenerative treatment of multiple cardiovascular disorders. On the other hand, ECFCs sustain the early phases of the angiogenic switch in a growing number of solid tumors and provide a promising target for developing alternative anti-angiogenic therapies. Intracellular Ca^{2+} signaling plays a key role in promoting proliferation, tube formation, homing and neovessel formation in both healthy and tumor-derived ECFCs. Therefore, it has been suggested that the Ca^{2+} toolkit could be genetically manipulated to rejuvenate or restore the reparative phenotype of autologous ECFCs [2, 66], or to interfere with tumor vascularization and prevent cancer growth and metastasis [18, 79]. For instance, autologous senescent ECFCs could be engineered to overexpress TRPC3, thereby increasing their sensitivity to VEGF, as reported in umbilical cord blood-derived ECFCs [2, 66, 102]. The molecular components of SOCE can be pharmacologically targeted to either prevent or minimize neovascularization in RCC, BC and IH [18, 79]. A fascinating feature of the Ca^{2+} toolkit expressed by ECFCs resides in its sensitivity to the pathophysiological conditions of the donors. Peripheral blood-derived ECFCs differ from UCB-ECFCs and from tumor-derived ECFCs. For instance, they lack $InsP_3R1$, but are endowed with TRPC3 which boosts their sensitivity to VEGF [48]. Furthermore, RCC-, BC-, IH- and PMF-derived ECFCs display distinct Ca^{2+} signaling machineries, although they all show a reduction in $[Ca^{2+}]_{ER}$, which prevents them from responding to VEGF. Understanding how solid cancers and myeloproliferative disorders, such as PMF, differently alter the Ca^{2+} toolkit in ECFCs will be a challenging field of research. Furthermore, it is predictable that the Ca^{2+} toolkit is also remodeled in ECFCs deriving from individuals affected by cardiovascular disorders, as recently shown in mouse MACs [103].

References

1. Medina RJ, Barber CL, Sabatier F, Dignat-George F, Melero-Martin JM, Khosrotehrani K et al (2017) Endothelial progenitors: a consensus statement on nomenclature. Stem Cells Transl Med 6(5):1316–1320
2. Moccia F, Ruffinatti FA, Zuccolo E (2015) Intracellular Ca(2)(+) signals to reconstruct a broken heart: still a theoretical approach? Curr Drug Targets 16(8):793–815
3. Moccia F, Zuccolo E, Poletto V, Cinelli M, Bonetti E, Guerra G et al (2015) Endothelial progenitor cells support tumour growth and metastatisation: implications for the resistance to anti-angiogenic therapy. Tumour Biol 36(9):6603–6614
4. Banno K, Yoder MC (2018) Tissue regeneration using endothelial colony-forming cells: promising cells for vascular repair. Pediatr Res 83(1–2):283–290
5. Yoder MC (2012) Human endothelial progenitor cells. Cold Spring Harb Perspect Med 2(7):a006692
6. Naito H, Wakabayashi T, Kidoya H, Muramatsu F, Takara K, Eino D et al (2016) Endothelial side population cells contribute to tumor angiogenesis and antiangiogenic drug resistance. Cancer Res 76(11):3200–3210
7. Tasev D, Koolwijk P, van Hinsbergh VW (2016) Therapeutic potential of human-derived endothelial colony-forming cells in animal models. Tissue Eng Part B Rev 22(5):371–382
8. Laurenzana A, Margheri F, Chilla A, Biagioni A, Margheri G, Calorini L et al (2016) Endothelial progenitor cells as shuttle of anticancer agents. Hum Gene Ther 27:784–791
9. Moccia F, Tanzi F, Munaron L (2014) Endothelial remodelling and intracellular calcium machinery. Curr Mol Med 14(4):457–480
10. Noren DP, Chou WH, Lee SH, Qutub AA, Warmflash A, Wagner DS et al (2016) Endothelial cells decode VEGF-mediated Ca^{2+} signaling patterns to produce distinct functional responses. Sci Signal 9(416):ra20
11. Pafumi I, Favia A, Gambara G, Papacci F, Ziparo E, Palombi F et al (2015) Regulation of angiogenic functions by angiopoietins through calcium-dependent signaling pathways. Biomed Res Int 2015:965271
12. Moccia F, Berra-Romani R, Tritto S, Signorelli S, Taglietti V, Tanzi F (2003) Epidermal growth factor induces intracellular Ca^{2+} oscillations in microvascular endothelial cells. J Cell Physiol 194:139–150
13. Munaron L, Fiorio Pla A (2000) Calcium influx induced by activation of tyrosine kinase receptors in cultured bovine aortic endothelial cells. J Cell Physiol 185(3):454–463
14. Yokota Y, Nakajima H, Wakayama Y, Muto A, Kawakami K, Fukuhara S et al (2015) Endothelial Ca^{2+} oscillations reflect VEGFR signaling-regulated angiogenic capacity in vivo. Elife 4:e08817
15. Sameermahmood Z, Balasubramanyam M, Saravanan T, Rema M (2008) Curcumin modulates SDF-1alpha/CXCR4-induced migration of human retinal endothelial cells (HRECs). Invest Ophthalmol Vis Sci 49(8):3305–3311
16. Fiorio Pla A, Gkika D (2013) Emerging role of TRP channels in cell migration: from tumor vascularization to metastasis. Front Physiol 4:311
17. Antoniotti S, Lovisolo D, Fiorio Pla A, Munaron L (2002) Expression and functional role of bTRPC1 channels in native endothelial cells. FEBS Lett 510(3):189–195
18. Moccia F, Poletto V (2015) May the remodeling of the Ca(2)(+) toolkit in endothelial progenitor cells derived from cancer patients suggest alternative targets for anti-angiogenic treatment? Biochim Biophys Acta 1853(9):1958–1973
19. Moccia F, Guerra G (2016) Ca^{2+} Signalling in endothelial progenitor cells: friend or foe? J Cell Physiol 231(2):314–327
20. Rumi E, Pietra D, Pascutto C, Guglielmelli P, Martínez-Trillos A, Casetti I et al (2014) Clinical effect of driver mutations of JAK2, CALR, or MPL in primary myelofibrosis. Blood 124(7):1062–1069

21. Poletto V, Dragoni S, Lim D, Biggiogera M, Aronica A, Cinelli M et al (2016) Endoplasmic reticulum Ca^{2+} handling and apoptotic resistance in tumor-derived endothelial colony forming cells. J Cell Biochem 117(10):2260–2271
22. Moccia F, Berra-Romani R, Tanzi F (2012) Update on vascular endothelial Ca^{2+} signalling: a tale of ion channels, pumps and transporters. World J Biol Chem 3(7):127–158
23. Berra-Romani R, Raqeeb A, Guzman-Silva A, Torres-Jacome J, Tanzi F, Moccia F (2010) Na^{+}-Ca^{2+} exchanger contributes to Ca^{2+} extrusion in ATP-stimulated endothelium of intact rat aorta. Biochem Biophys Res Commun 395(1):126–130
24. Maeng YS, Choi HJ, Kwon JY, Park YW, Choi KS, Min JK et al (2009) Endothelial progenitor cell homing: prominent role of the IGF2-IGF2R-PLCbeta2 axis. Blood 113(1):233–243
25. Zuccolo E, Di Buduo C, Lodola F, Orecchioni S, Scarpellino G, Kheder DA et al (2018) Stromal cell-derived factor-1alpha promotes endothelial colony-forming cell migration through the Ca^{2+}-dependent activation of the extracellular signal-regulated kinase 1/2 and phosphoinositide 3-kinase/AKT pathways. Stem Cells Dev 27(1):23–34
26. Dragoni S, Laforenza U, Bonetti E, Lodola F, Bottino C, Berra-Romani R et al (2011) Vascular endothelial growth factor stimulates endothelial colony forming cells proliferation and tubulogenesis by inducing oscillations in intracellular Ca^{2+} concentration. Stem Cells 29(11):1898–1907
27. Sanchez-Hernandez Y, Laforenza U, Bonetti E, Fontana J, Dragoni S, Russo M et al (2010) Store-operated Ca^{2+} entry is expressed in human endothelial progenitor cells. Stem Cells Dev 19(12):1967–1981
28. Zuccolo E, Dragoni S, Poletto V, Catarsi P, Guido D, Rappa A et al (2016) Arachidonic acid-evoked Ca^{2+} signals promote nitric oxide release and proliferation in human endothelial colony forming cells. Vasc Pharmacol 87:159–171
29. Morgan AJ, Platt FM, Lloyd-Evans E, Galione A (2011) Molecular mechanisms of endolysosomal Ca^{2+} signalling in health and disease. Biochem J 439(3):349–374
30. Di Nezza F, Zuccolo E, Poletto V, Rosti V, De Luca A, Moccia F et al (2017) Liposomes as a putative tool to investigate NAADP signaling in vasculogenesis. J Cell Biochem 118: 3722–3729
31. Wang YW, Zhang JH, Yu Y, Yu J, Huang L (2016) Inhibition of store-operated calcium entry protects endothelial progenitor cells from H2O2-induced apoptosis. Biomol Ther (Seoul) 24(4):371–379
32. Choi JW, Son SM, Mook-Jung I, Moon YJ, Lee JY, Wang KC et al (2017) Mitochondrial abnormalities related to the dysfunction of circulating endothelial colony-forming cells in moyamoya disease. J Neurosurg 129:1–9
33. Kluge MA, Fetterman JL, Vita JA (2013) Mitochondria and endothelial function. Circ Res 112(8):1171–1188
34. Moccia F, Dragoni S, Lodola F, Bonetti E, Bottino C, Guerra G et al (2012) Store-dependent Ca^{2+} entry in endothelial progenitor cells as a perspective tool to enhance cell-based therapy and adverse tumour vascularization. Curr Med Chem 19(34):5802–5818
35. Lodola F, Laforenza U, Bonetti E, Lim D, Dragoni S, Bottino C et al (2012) Store-operated Ca^{2+} entry is remodelled and controls in vitro angiogenesis in endothelial progenitor cells isolated from tumoral patients. PLoS One 7(9):e42541
36. Li J, Cubbon RM, Wilson LA, Amer MS, McKeown L, Hou B et al (2011) Orai1 and CRAC channel dependence of VEGF-activated Ca^{2+} entry and endothelial tube formation. Circ Res 108(10):1190–1198
37. Di Buduo CA, Balduini A, Moccia F (2016) Pathophysiological significance of store-operated calcium entry in megakaryocyte function: opening new paths for understanding the role of calcium in thrombopoiesis. Int J Mol Sci 17(12):2055
38. Jardin I, Lopez JJ, Salido GM, Rosado JA (2008) Orai1 mediates the interaction between STIM1 and hTRPC1 and regulates the mode of activation of hTRPC1-forming Ca^{2+} channels. J Biol Chem 283(37):25296–25304

39. Cheng KT, Liu X, Ong HL, Swaim W, Ambudkar IS (2011) Local Ca(2)+ entry via Orai1 regulates plasma membrane recruitment of TRPC1 and controls cytosolic Ca(2)+ signals required for specific cell functions. PLoS Biol 9(3):e1001025
40. Pani B, Liu X, Bollimuntha S, Cheng KT, Niesman IR, Zheng C et al (2013) Impairment of TRPC1-STIM1 channel assembly and AQP5 translocation compromise agonist-stimulated fluid secretion in mice lacking caveolin1. J Cell Sci 126(Pt 2):667–675
41. Hong JH, Li Q, Kim MS, Shin DM, Feske S, Birnbaumer L et al (2011) Polarized but differential localization and recruitment of STIM1, Orai1 and TRPC channels in secretory cells. Traffic 12(2):232–245
42. Du LL, Shen Z, Li Z, Ye X, Wu M, Hong L et al (2018) TRPC1 deficiency impairs the endothelial progenitor cell function via inhibition of calmodulin/eNOS pathway. J Cardiovasc Transl Res 11:339–345
43. Zuccolo E, Bottino C, Diofano F, Poletto V, Codazzi AC, Mannarino S et al (2016) Constitutive store-operated Ca^{2+} entry leads to enhanced nitric oxide production and proliferation in infantile hemangioma-derived endothelial Colony-forming cells. Stem Cells Dev 25(4):301–319
44. Gees M, Colsoul B, Nilius B (2010) The role of transient receptor potential cation channels in Ca^{2+} signaling. Cold Spring Harb Perspect Biol 2(10):a003962
45. Guerra G, Lucariello A, Perna A, Botta L, De Luca A, Moccia F (2018) The role of endothelial Ca^{2+} signaling in neurovascular coupling: a view from the lumen. Int J Mol Sci 19(4). https://doi.org/10.3390/ijms19040938
46. Hamdollah Zadeh MA, Glass CA, Magnussen A, Hancox JC, Bates DO (2008) VEGF-mediated elevated intracellular calcium and angiogenesis in human microvascular endothelial cells in vitro are inhibited by dominant negative TRPC6. Microcirculation 15(7):605–614
47. Antigny F, Girardin N, Frieden M (2012) Transient receptor potential canonical channels are required for in vitro endothelial tube formation. J Biol Chem 287(8):5917–5927
48. Dragoni S, Laforenza U, Bonetti E, Lodola F, Bottino C, Guerra G et al (2013) Canonical transient receptor potential 3 channel triggers vascular endothelial growth factor-induced intracellular Ca^{2+} oscillations in endothelial progenitor cells isolated from umbilical cord blood. Stem Cells Dev 22(19):2561–2580
49. Vriens J, Appendino G, Nilius B (2009) Pharmacology of vanilloid transient receptor potential cation channels. Mol Pharmacol 75(6):1262–1279
50. Hofmann NA, Barth S, Waldeck-Weiermair M, Klec C, Strunk D, Malli R et al (2014) TRPV1 mediates cellular uptake of anandamide and thus promotes endothelial cell proliferation and network-formation. Biol Open 3(12):1164–1172
51. White JP, Cibelli M, Urban L, Nilius B, McGeown JG, Nagy I (2016) TRPV4: molecular conductor of a diverse orchestra. Physiol Rev 96(3):911–973
52. Dragoni S, Guerra G, Fiorio Pla A, Bertoni G, Rappa A, Poletto V et al (2015) A functional transient receptor potential vanilloid 4 (TRPV4) channel is expressed in human endothelial progenitor cells. J Cell Physiol 230(1):95–104
53. Fleig A, Chubanov V (2014) Trpm7. Handb Exp Pharmacol 222:521–546
54. Baldoli E, Maier JA (2012) Silencing TRPM7 mimics the effects of magnesium deficiency in human microvascular endothelial cells. Angiogenesis 15(1):47–57
55. Tu TC, Nagano M, Yamashita T, Hamada H, Ohneda K, Kimura K et al (2016) A chemokine receptor, CXCR4, which is regulated by hypoxia-inducible factor 2alpha, is crucial for functional endothelial progenitor cells migration to ischemic tissue and wound repair. Stem Cells Dev 25(3):266–276
56. Oh BJ, Kim DK, Kim BJ, Yoon KS, Park SG, Park KS et al (2010) Differences in donor CXCR4 expression levels are correlated with functional capacity and therapeutic outcome of angiogenic treatment with endothelial colony forming cells. Biochem Biophys Res Commun 398(4):627–633
57. Joo HJ, Song S, Seo HR, Shin JH, Choi SC, Park JH et al (2015) Human endothelial colony forming cells from adult peripheral blood have enhanced sprouting angiogenic potential through up-regulating VEGFR2 signaling. Int J Cardiol 197:33–43

58. Su SH, Wu CH, Chiu YL, Chang SJ, Lo HH, Liao KH et al (2017) Dysregulation of vascular endothelial growth factor receptor-2 by multiple miRNAs in endothelial colony-forming cells of coronary artery disease. J Vasc Res 54(1):22–32
59. Koch S, Claesson-Welsh L (2012) Signal transduction by vascular endothelial growth factor receptors. Cold Spring Harb Perspect Med 2(7):a006502
60. Potenza DM, Guerra G, Avanzato D, Poletto V, Pareek S, Guido D et al (2014) Hydrogen sulphide triggers VEGF-induced intracellular Ca^{2+} signals in human endothelial cells but not in their immature progenitors. Cell Calcium 56:225–234
61. Zhu L, Song S, Pi Y, Yu Y, She W, Ye H et al (2011) Cumulated Ca2(+) spike duration underlies Ca2(+) oscillation frequency-regulated NFkappaB transcriptional activity. J Cell Sci 124(Pt 15):2591–2601
62. Zhu LP, Luo YG, Chen TX, Chen FR, Wang T, Hu Q (2008) Ca^{2+} oscillation frequency regulates agonist-stimulated gene expression in vascular endothelial cells. J Cell Sci 121(15):2511–2518
63. Chen ZJ (2005) Ubiquitin signalling in the NF-kappaB pathway. Nat Cell Biol 7(8):758–765
64. Oeckinghaus A, Ghosh S (2009) The NF-kappaB family of transcription factors and its regulation. Cold Spring Harb Perspect Biol 1(4):a000034
65. Ingram DA, Mead LE, Tanaka H, Meade V, Fenoglio A, Mortell K et al (2004) Identification of a novel hierarchy of endothelial progenitor cells using human peripheral and umbilical cord blood. Blood 104(9):2752–2760
66. Moccia F, Lucariello A, Guerra G (2018) TRPC3-mediated Ca^{2+} signals as a promising strategy to boost therapeutic angiogenesis in failing hearts: the role of autologous endothelial colony forming cells. J Cell Physiol 233(5):3901–3917
67. Monteith GR, Prevarskaya N, Roberts-Thomson SJ (2017) The calcium-cancer signalling nexus. Nat Rev Cancer 17(6):367–380
68. Prevarskaya N, Ouadid-Ahidouch H, Skryma R, Shuba Y (2014) Remodelling of Ca^{2+} transport in cancer: how it contributes to cancer hallmarks? Philos Trans R Soc Lond Ser B Biol Sci 369(1638):20130097
69. Moccia F (2018) Endothelial Ca^{2+} signaling and the resistance to anticancer treatments: partners in crime. Int J Mol Sci 19(1):E217
70. Pupo E, Pla AF, Avanzato D, Moccia F, Cruz JE, Tanzi F et al (2011) Hydrogen sulfide promotes calcium signals and migration in tumor-derived endothelial cells. Free Radic Biol Med 51(9):1765–1773
71. Fiorio Pla A, Ong HL, Cheng KT, Brossa A, Bussolati B, Lockwich T et al (2012) TRPV4 mediates tumor-derived endothelial cell migration via arachidonic acid-activated actin remodeling. Oncogene 31(2):200–212
72. Avanzato D, Genova T, Fiorio Pla A, Bernardini M, Bianco S, Bussolati B et al (2016) Activation of P2X7 and P2Y11 purinergic receptors inhibits migration and normalizes tumor-derived endothelial cells via cAMP signaling. Sci Rep 6:32602
73. Fiorio Pla A, Grange C, Antoniotti S, Tomatis C, Merlino A, Bussolati B et al (2008) Arachidonic acid-induced Ca^{2+} entry is involved in early steps of tumor angiogenesis. Mol Cancer Res 6(4):535–545
74. Genova T, Grolez GP, Camillo C, Bernardini M, Bokhobza A, Richard E et al (2017) TRPM8 inhibits endothelial cell migration via a non-channel function by trapping the small GTPase Rap1. J Cell Biol 216(7):2107–2130
75. Moccia F, Fotia V, Tancredi R, Della Porta MG, Rosti V, Bonetti E et al (2017) Breast and renal cancer-derived endothelial colony forming cells share a common gene signature. Eur J Cancer 77:155–164
76. Lodola F, Laforenza U, Cattaneo F, Ruffinatti FA, Poletto V, Massa M et al (2017) VEGF-induced intracellular Ca^{2+} oscillations are down-regulated and do not stimulate angiogenesis in breast cancer-derived endothelial colony forming cells. Oncotarget 8:95223–95246
77. Sunryd JC, Cheon B, Graham JB, Giorda KM, Fissore RA, Hebert DN (2014) TMTC1 and TMTC2 are novel endoplasmic reticulum tetratricopeptide repeat-containing adapter proteins involved in calcium homeostasis. J Biol Chem 289(23):16085–16099

78. Vanoverberghe K, Vanden Abeele F, Mariot P, Lepage G, Roudbaraki M, Bonnal JL et al (2004) Ca^{2+} homeostasis and apoptotic resistance of neuroendocrine-differentiated prostate cancer cells. Cell Death Differ 11(3):321–330
79. Moccia F, Dragoni S, Poletto V, Rosti V, Tanzi F, Ganini C et al (2014) Orai1 and transient receptor potential channels as novel molecular targets to impair tumor neovascularisation in renal cell carcinoma and other malignancies. Anti Cancer Agents Med Chem 14(2):296–312
80. Carmeliet P, Jain RK (2011) Molecular mechanisms and clinical applications of angiogenesis. Nature 473(7347):298–307
81. Greenberger S, Bischoff J (2013) Pathogenesis of infantile haemangioma. Br J Dermatol 169(1):12–19
82. Grzesik P, Wu JK (2017) Current perspectives on the optimal management of infantile hemangioma. Pediatr Health Med Ther 8:107–116
83. Bischoff J (2009) Progenitor cells in infantile hemangioma. J Craniofac Surg 20(Suppl 1):695–697
84. Zuccolo E, Lim D, Kheder DA, Perna A, Catarsi P, Botta L et al (2017) Acetylcholine induces intracellular Ca^{2+} oscillations and nitric oxide release in mouse brain endothelial cells. Cell Calcium 66:33–47
85. Moccia F, Berra-Romani R, Baruffi S, Spaggiari S, Adams DJ, Taglietti V et al (2002) Basal nonselective cation permeability in rat cardiac microvascular endothelial cells. Microvasc Res 64(2):187–197
86. Ma X, Chen Z, Hua D, He D, Wang L, Zhang P et al (2014) Essential role for TrpC5-containing extracellular vesicles in breast cancer with chemotherapeutic resistance. Proc Natl Acad Sci U S A 111(17):6389–6394
87. Plummer PN, Freeman R, Taft RJ, Vider J, Sax M, Umer BA et al (2013) MicroRNAs regulate tumor angiogenesis modulated by endothelial progenitor cells. Cancer Res 73(1):341–352
88. Katoh M (2013) Therapeutics targeting angiogenesis: genetics and epigenetics, extracellular miRNAs and signaling networks (review). Int J Mol Med 32(4):763–767
89. Chang TY, Tsai WC, Huang TS, Su SH, Chang CY, Ma HY et al (2017) Dysregulation of endothelial colony-forming cell function by a negative feedback loop of circulating miR-146a and -146b in cardiovascular disease patients. PLoS One 12(7):e0181562
90. Rosti V, Bonetti E, Bergamaschi G, Campanelli R, Guglielmelli P, Maestri M et al (2010) High frequency of endothelial colony forming cells marks a non-active myeloproliferative neoplasm with high risk of splanchnic vein thrombosis. PLoS One 5(12):e15277
91. Barosi G, Rosti V, Massa M, Viarengo GL, Pecci A, Necchi V et al (2004) Spleen neoangiogenesis in patients with myelofibrosis with myeloid metaplasia. Br J Haematol 124(5):618–625
92. Szuber N, Tefferi A (2018) Driver mutations in primary myelofibrosis and their implications. Curr Opin Hematol 25(2):129–135
93. Mesaeli N, Nakamura K, Zvaritch E, Dickie P, Dziak E, Krause KH et al (1999) Calreticulin is essential for cardiac development. J Cell Biol 144(5):857–868
94. Fasolato C, Pizzo P, Pozzan T (1998) Delayed activation of the store-operated calcium current induced by calreticulin overexpression in RBL-1 cells. Mol Biol Cell 9(6):1513–1522
95. John LM, Lechleiter JD, Camacho P (1998) Differential modulation of SERCA2 isoforms by calreticulin. J Cell Biol 142(4):963–973
96. Klampfl T, Gisslinger H, Harutyunyan AS, Nivarthi H, Rumi E, Milosevic JD et al (2013) Somatic mutations of calreticulin in myeloproliferative neoplasms. N Engl J Med 369(25):2379–2390
97. Pietra D, Rumi E, Ferretti VV, Di Buduo CA, Milanesi C, Cavalloni C et al (2016) Differential clinical effects of different mutation subtypes in CALR-mutant myeloproliferative neoplasms. Leukemia 30(2):431–438
98. Piaggio G, Rosti V, Corselli M, Bertolotti F, Bergamaschi G, Pozzi S et al (2009) Endothelial colony-forming cells from patients with chronic myeloproliferative disorders lack the disease-specific molecular clonality marker. Blood 114(14):3127–3130

99. Dragoni S, Laforenza U, Bonetti E, Reforgiato M, Poletto V, Lodola F et al (2014) Enhanced expression of Stim, orai, and TRPC transcripts and proteins in endothelial progenitor cells isolated from patients with primary myelofibrosis. PLoS One 9(3):e91099
100. Liao Y, Plummer NW, George MD, Abramowitz J, Zhu MX, Birnbaumer L (2009) A role for Orai in TRPC-mediated Ca^{2+} entry suggests that a TRPC:Orai complex may mediate store and receptor operated Ca^{2+} entry. Proc Natl Acad Sci U S A 106(9):3202–3206
101. Dragoni S, Reforgiato M, Zuccolo E, Poletto V, Lodola F, Ruffinatti FA et al (2015) Dysregulation of VEGF-induced proangiogenic Ca^{2+} oscillations in primary myelofibrosis-derived endothelial colony-forming cells. Exp Hematol 43(12):1019–30 e3
102. Moccia F, Dragoni S, Cinelli M, Montagnani S, Amato B, Rosti V et al (2013) How to utilize Ca^{2+} signals to rejuvenate the repairative phenotype of senescent endothelial progenitor cells in elderly patients affected by cardiovascular diseases: a useful therapeutic support of surgical approach? BMC Surg 13(Suppl 2):S46
103. Wang LY, Zhang JH, Yu J, Yang J, Deng MY, Kang HL et al (2015) Reduction of store-operated Ca^{2+} entry correlates with endothelial progenitor cell dysfunction in atherosclerotic mice. Stem Cells Dev 24(13):1582–1590

Chapter 41
Sensing Extracellular Calcium – An Insight into the Structure and Function of the Calcium-Sensing Receptor (CaSR)

Sergei Chavez-Abiega, Iris Mos, Patricia P. Centeno, Taha Elajnaf, Wolfgang Schlattl, Donald T. Ward, Joachim Goedhart, and Enikö Kallay

Author contributed equally with all other contributors. Sergei Chavez-Abiega, Iris Mos and Patricia P. Centeno

S. Chavez-Abiega
Systems Bioinformatics, Amsterdam Institute for Molecules, Medicines, and Systems, VU University, Amsterdam, The Netherlands

Section of Molecular Cytology, van Leeuwenhoek Centre for Advanced Microscopy, Swammerdam Institute for Life Sciences, University of Amsterdam, Amsterdam, The Netherlands
e-mail: s.chavezabiega@vu.nl

I. Mos
Department of Drug Design and Pharmacology, Faculty of Health and Medical Sciences, University of Copenhagen, Copenhagen, Denmark
e-mail: iris.mos@sund.ku.dk

P. P. Centeno · D. T. Ward
Faculty of Biology Medicine and Health, The University of Manchester, Manchester, UK
e-mail: patricia.pacioscenteno@postgrad.manchester.ac.uk; d.ward@manchester.ac.uk

T. Elajnaf · E. Kallay (✉)
Department of Pathophysiology and Allergy Research, Center of Pathophysiology, Infectiology & Immunology, Medical University of Vienna, Vienna, Austria
e-mail: taha.elajnaf@meduniwien.ac.at; enikoe.kallay@meduniwien.ac.at

W. Schlattl
Computer Science Department, University of Torino; S.A.F.AN. BIOINFORMATICS, Torino, Italy
e-mail: wolfgang.schlattl@unito.it

J. Goedhart
Section of Molecular Cytology, van Leeuwenhoek Centre for Advanced Microscopy, Swammerdam Institute for Life Sciences, University of Amsterdam, Amsterdam, The Netherlands
e-mail: j.goedhart@uva.nl

M. S. Islam (ed.), *Calcium Signaling*, Advances in Experimental Medicine and Biology 1131, https://doi.org/10.1007/978-3-030-12457-1_41

Abstract The calcium-sensing receptor (CaSR) is a G protein-coupled receptor that plays a key role in calcium homeostasis, by sensing free calcium levels in blood and regulating parathyroid hormone secretion in response. The CaSR is highly expressed in parathyroid gland and kidney where its role is well characterised, but also in other tissues where its function remains to be determined. The CaSR can be activated by a variety of endogenous ligands, as well as by synthetic modulators such as Cinacalcet, used in the clinic to treat secondary hyperparathyroidism in patients with chronic kidney disease. The CaSR couples to multiple G proteins, in a tissue-specific manner, activating several signalling pathways and thus regulating diverse intracellular events. The multifaceted nature of this receptor makes it a valuable therapeutic target for calciotropic and non-calciotropic diseases. It is therefore essential to understand the complexity behind the pharmacology, trafficking, and signalling characteristics of this receptor. This review provides an overview of the latest knowledge about the CaSR and discusses future hot topics in this field.

Keywords Extracellular calcium · Parathyroid hormone · G protein-coupled receptor · G proteins · Biased signalling · Calcimimetics · Calcilytics · Allosteric modulators · Orthosteric ligands · Cellular trafficking

Abbreviations

1,25D3	1α,25-dihydroxyvitamin D3
AC	Adenylate cyclase
ADH	Autosomal dominant hypocalcaemia
AP2	Adaptor protein-2
cAMP	Cyclic adenosine monophosphate
Ca^{2+}	Calcium
CaSR	Calcium-sensing receptor
CR	Cysteine rich domain
$[Ca^{2+}]_o$	Extracellular calcium concentration
$Ca^{2+}{}_i$	Intracellular calcium
$[Ca^{2+}]_i$	Intracellular calcium concentration
CKD	Chronic kidney disease
DAG	Diacylglycerol
ECD	Extracellular domain
ER	Endoplasmic reticulum
ERK	Extracellular signal-regulated kinase
FHH	Familial hypocalciuric hypercalcaemia
GABA	Gamma-aminobutyric acid
GAPs	GTPase-activating proteins
GEFs	Guanine nucleotide exchange factors
GDIs	Guanine nucleotide dissociation inhibitors
GPCR	G protein-coupled receptor

GRKs	G protein-coupled receptor kinases
GSK3	Glycogen synthase kinase-3
HEK	Human embryonic kidney
HEK-CaSR	HEK293 cells stably expressing the CaSR
ICD	Intracellular domain
IGF-1	Insulin-like growth factor 1
IP3	Inositol 1,4,5-trisphosphate
JNK	C-Jun amino-terminal kinases
mGlu	Metabotropic glutamate receptor
NAM	Negative allosteric modulator
LB	Lobe-shaped domain
MAPKs	Mitogen-activated protein kinases
NAM	Negative allosteric modulator
NSHPT	Neonatal severe hyperparathyroidism
NKCC2	Na-K-Cl cotransporter 2
PA	Phosphatidic acid
PAM	Positive allosteric modulator
PDEs	Phosphodiesterases
Pi	Inorganic phosphate
PI3Ks	Phosphoinositide 3-kinases
PIP2	Phosphatidylinositol 4,5-bisphosphate
PKA	Protein Kinase A
PKB	Protein Kinase B
PKC	Protein Kinase C
PLA2	Phospholipase A2
PLC	Phospholipase C
PLD	Phospholipase D
PreProPTH	Prepro-parathyroid hormone
PT	Parathyroid
PTH	Parathyroid hormone
PTHrP	Parathyroid hormone-related protein
PTx	Pertussis-toxin
RGS	Regulator of G protein signalling
RAMPs	Receptor activity-modifying proteins
TMD	Transmembrane domain
TAS1R	Taste 1 receptors
VFD	Venus flytrap domain

41.1 Introduction

Calcium (Ca^{2+}) is a macro element representing 1.5–2% of an adult's total body weight and is mostly found in bones and teeth. Only 1% of the body's Ca^{2+} is located in cells and tissues, where it regulates numerous critical cellular responses.

The extracellular calcium concentration $[Ca^{2+}]_o$ is much higher (20,000-fold) than in the cytosol and changes in this balance trigger various signalling pathways. This gradient allows Ca^{2+} to act as a second messenger in intracellular signalling [1]. Many tissues are equipped with a cell-surface sensor for Ca^{2+} that extends the signalling properties of Ca^{2+} to being an extracellular first messenger also. This receptor is known as the extracellular calcium-sensing receptor (CaSR) and is a G protein-coupled receptor (GPCR).

CaSR is a member of the class C GPCRs which also includes the metabotropic glutamate (mGlu) receptors, the gamma-aminobutyric acid (GABA) receptors, the taste 1 receptors (TAS1R) and 8 orphan receptors [2]. The class C orphan receptor GPRC6 shares the highest sequence similarity with the CaSR (Fig. 41.1).

The CaSR plays an essential role in calcium homeostasis and its existence was confirmed by cloning in 1993 [3]. CaSR senses changes in $[Ca^{2+}]_o$ and also interacts with other multivalent cations (Mg^{2+}, Gd^{3+}), organic cations (neomycin), polyamines (spermine, polyarginine and polylysine) and possibly even beta amyloid [4]. It is highly expressed in the parathyroid glands, pancreas, duodenum and kidney and less in the digestive system, stomach and respiratory system [5]. This review will give an overview of the (patho)physiological roles, structure, ligands, trafficking, signalling pathways and tissue specific functions of the CaSR.

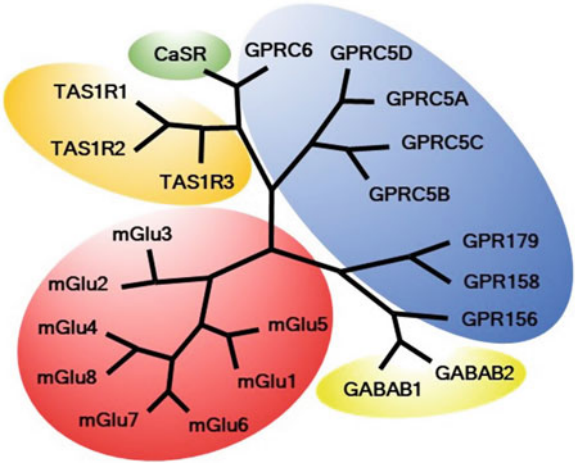

Fig. 41.1 Phylogenetic tree of the class C GPCRs generated with the neighbour-joining method of the full receptor sequences; The different colors represent the receptor families based on the endogenous ligand affiliation: CaSR family: calcium-sensing receptor (green), GPR family: class C orphan receptors with unknown endogenous ligands (blue), GABA family: gamma-aminobutyric acid receptors (yellow), mGlu family: metabotropic glutamate receptors (red), TAS1R family: taste 1 receptors (orange)

41.1.1 Physiological Role of the CaSR in Calcium Regulation

The blood $[Ca^{2+}]_o$ is influenced by parathyroid hormone (PTH), 1α,25-dihydroxyvitamin D_3 ($1,25D_3$) and calcitonin [4, 6]. PTH is expressed by and secreted from chief cells of the parathyroid gland and acts upon the kidneys, bones, and intestines. In the kidney, CaSR stimulates Ca^{2+} and Mg^{2+} reabsorption in the distal tubules whereas in the proximal tubules it promotes the excretion of hydrogen phosphate and dihydrogen phosphate. PTH induces the 25-hydroxyvitamin D_3 1α-hydroxylase to produce 1,25D3 which is essential for intestinal Ca^{2+} absorption [7]. Hypercalcaemia is prevented by CaSR, which inhibits PTH secretion and suppresses the transcription of PreProPTH and cell proliferation (Fig. 41.2) [8]. PTH stimulates bone remodelling. Calcitonin protects against hypercalcaemia and inhibits osteoclast activity and consequently the release of Ca^{2+} from bones. The transcription of calcitonin in thyroidal C-cells is inhibited by increasing 1,25D3 concentrations [6]. However, the impact of calcitonin in maintaining systemic

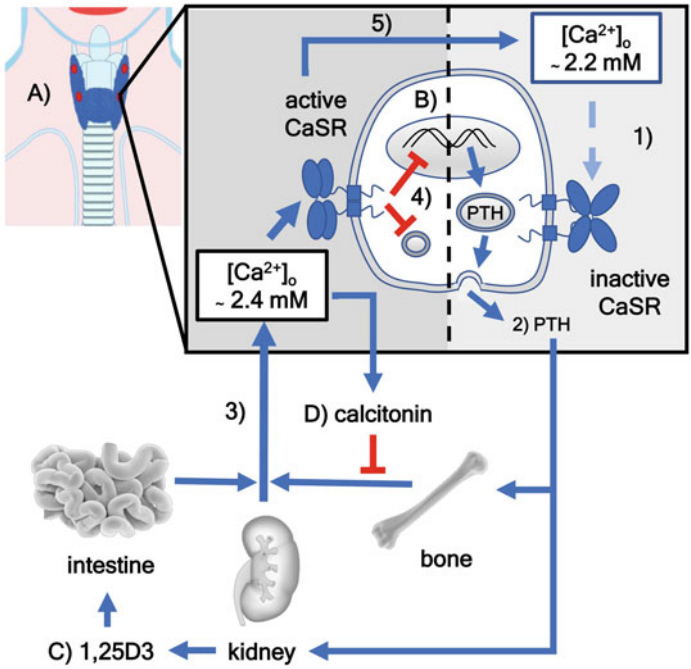

Fig. 41.2 Overview of the calcium homeostasis. (**a**) Location of the parathyroid glands (red dots); (**b**) Chief cell of the parathyroid gland, 1) CaSR is inactive at low $[Ca^{2+}]_o$ and PTH is secreted; 2) PTH stimulates Ca^{2+} release from bone, the reabsorption from the kidney and the $1,25D_3$ synthesis which induces Ca^{2+} uptake from the intestine (**c**); 3) The resulting increase in blood Ca^{2+} activates CaSR and at high concentrations calcitonin secretion; (**d**) Calcitonin inhibits the osteoclast activity and transiently the Ca^{2+} release from bone; 4) The active CaSR inhibits the PTH expression and secretion and consequently lowers the blood Ca^{2+} level; 5) Until the process starts again at 1)

blood Ca^{2+} is still contradictory because its absence or excess does not result in any significant metabolic abnormalities.

The physiological range of serum $[Ca^{2+}]_o$ is tightly regulated between 2.2 and 2.4 mM by the CaSR, facilitated by the high cooperativity of Ca^{2+} on the receptor. About half of the $[Ca^{2+}]_o$ is free, and the rest of it is bound mainly to albumin. PTH secretion is induced when the free $[Ca^{2+}]_o$ drops below 1.2 mM (to ~2.2 mM total Ca^{2+}) and it is effectively suppressed by CaSR activation when free $[Ca^{2+}]_o$ rises above 1.2 mM (towards 2.5 mM) [9]. High free $[Ca^{2+}]_o$ activates renal CaSR leading to inhibition of Ca^{2+} reabsorption resulting in elevated renal Ca^{2+} excretion [10, 11].

41.1.2 Pathophysiological Role of the CaSR

After the successful cloning of the bovine parathyroid CaSR [3], a number of diseases were identified which are caused by CaSR mutations.

Heterozygous loss-of-function mutations in CaSR are associated with familial hypocalciuric hypercalcaemia (FHH1) and homozygous CaSR mutations to neonatal severe hyperparathyroidism (NSHPT) [12]. FHH1 is characterised by disabled Ca^{2+} reabsorption causing hypocalciuria, moderate hypercalcaemia, hypermagnesaemia and a disabled inhibition of PTH secretion which leads to an elevated steady-state $[Ca^{2+}]_o$ level [4, 13]. Usually this disease remains asymptomatic over one's lifetime, but a few patients show signs of pancreatitis or chondrocalcinosis. FHH2 and FHH3 are the result of mutations in the G protein GNA11 and APS1 gene, respectively [13], these proteins acting downstream of CaSR signalling.

NSHPT is characterised by severe hypercalcaemia and very high PTH levels. The defective feedback regulation of the CaSR leads to bone demineralisation and to pathological fractures [4]. It is currently treated with bisphosphonates, dialysis, calcimimetics or by total parathyroidectomy [13, 14].

In contrast, autosomal dominant hypocalcaemia type 1 (ADH1) and type 2 (ADH2) are caused by gain-of-function mutations of the CaSR and the GNA11 gene, respectively. ADH1 results in a reduced steady-state of blood $[Ca^{2+}]_o$ and causes low PTH levels, hypercalciuria, hypomagnesaemia, and hyperphosphataemia. Symptoms of type 1 are paraesthesia, tetany, epilepsy, severe hypocalcaemia and basal ganglia calcification which are the same for ADH2 but without hypercalciuria and hypomagnesaemia [12]. Another gain-of-function disease is connected to a renal salt-wasting form called Bartter Syndrome type-5. It is the result of unrestrained CaSR activity which leads to dysfunctional Na-K-Cl cotransporter (NKCC2)-dependent NaCl reabsorption [4].

Autoimmune diseases of the CaSR have also been described in rare cases due to the presence of anti-CaSR antibodies. These antibodies can have CaSR-stimulating or CaSR-blocking effects causing a form of acquired autoimmune hypoparathyroidism or autoimmune hypocalciuric hypercalcaemia, respectively [13].

Mutations of the CaSR are also observed in a variety of non-calciotropic diseases, for example the R990G variant is associated with an elevated risk for hypercalciuria and nephrolithiasis [15]. Other diseases are connected to changed expression levels of the receptor. In colorectal and parathyroid cancer CaSR expression is decreased or lost, attenuating its tumour preventive effect. In breast and prostate tumours, CaSR is overexpressed which correlates with an increasing risk for metastases to the bone [16]. There is also evidence that changes in CaSR activity or expression are associated with alterations in cardiac function, insulin secretion, postprandial blood glucose regulation, lipolysis and inhibition of myocardial cell proliferation. In the digestive tract, CaSR shows anti-inflammatory, anti-secretory, pro-absorbent, and obstructive properties while in the respiratory tract CaSR activation is associated with inflammation and nonspecific hyperresponsiveness in asthma [13, 17].

41.2 Structure of the CaSR

The CaSR functions as a disulphide-tethered homodimer composed of three main domains: an extracellular domain (ECD), a heptahelical transmembrane domain (TMD) and an intracellular C-terminal domain (ICD) [18] (Fig. 41.3).

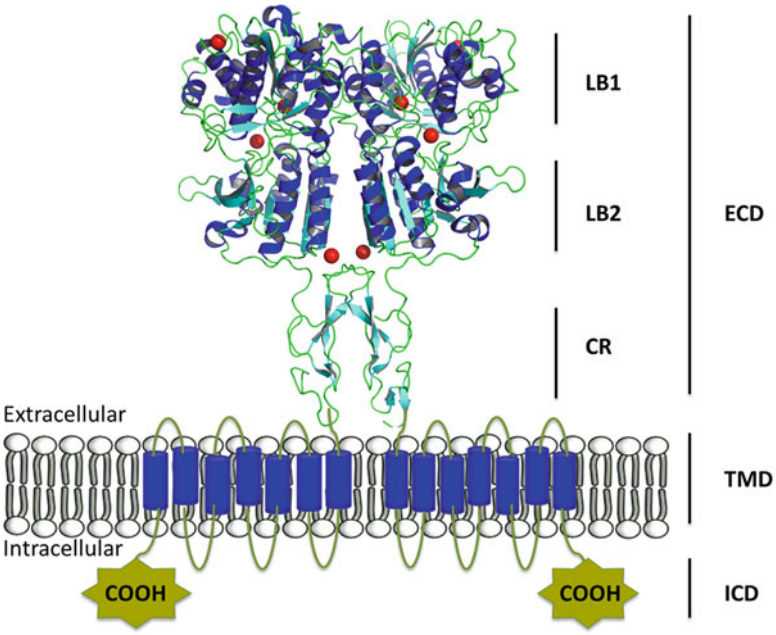

Fig. 41.3 Structure of the CaSR including the crystal structure of the ECD from the human CaSR, formed by LB1, LB2 and CR (PDB: 5k5s), and a schematic representation of the TMD formed by the seven transmembrane helixes followed by the ICD. Calcium ions are represented as red spheres in the ECD

The human CaSR ECD contains 612 amino acids and consists of two lobe-shaped domains (LB1 and LB2) that form the N-terminal Venus Fly Trap (VFT) domain, and the cysteine-rich (CR) domain [19]. The VFT is the ligand-binding region, reminiscent of gram-negative bacterial periplasmic binding proteins [20]. Both LB domains are formed by typical β-sheets and α-helices, where the central parallel β-sheets are sandwiched by α-helices [21]. The CR region, located between the ECD and the TMD contains nine-conserved cysteines. It transmits and amplifies signals from the VFT domain to the intracellular loops of the TMD [22]. The CR region is present in all class C GPCRs except in GABA B receptors and is required for receptor activation [21–23].

CaSR is expressed on the cell surface as a homodimer formed by direct interactions involving the ECD and the TMD. The ECDs of both monomers interact in a side-by-side fashion by a covalent disulphide bridge involving residues Cys-129 and Cys-131, whereas the TMDs establish hydrophobic interactions between them [24, 25]. However, there is also evidence suggesting heterodimerisation with other class C GPCRs. These heterodimers are considered new types of receptors that lead to changes in CaSR expression, signalling and sensitivity. For instance, CaSR may form dimers with mGlu1a or mGlu5, in hippocampal and cerebellar neurons, and with GABA B receptors [26, 27].

The CaSR ECD also includes 20–40 kDa of either high mannose or complex carbohydrates. These glycosylations are believed to be important for cell-surface localisation of the CaSR, intracellular trafficking, protein folding and secretion [25].

Recently, two different groups have simultaneously resolved the crystal structures of the human CaSR ECD in resting and active conformations [28, 29]. Zhang and partners crystallised the ECD in the active conformation and identified two Ca^{2+} binding sites plus an additional orthosteric binding site for L-Trp. The Ca^{2+} binding sites can also be occupied by other divalent metals such as Mg^{2+} whereas, the additional orthosteric binding site was occupied by a L-Trp derivate, L-1,2,3,4,-tetrahydronorharman-3-carboxylic acid and it was located in the hinge region between the two subdomains. The L-Trp binding site was described as crucial for receptor activation and stabilisation of the active conformation [29]. Meanwhile, Geng and colleagues crystallised the receptor in its active and inactive conformations. The active structure was obtained in the presence of 10 mM Ca^{2+} and 10 mM L-Trp, when the receptor is in its closed conformation (active state, closed-closed) (Fig. 41.4 left). They also identified the same orthosteric binding site described by Zhang and partners, located in the ligand-binding cleft of each protomer and also occupied by L-Trp. In this model, the authors defined four different Ca^{2+}-binding sites in the active structure, including one Ca^{2+}-binding site in each protomer that is common in the active and inactive structures suggesting an integral part of the receptor. On the other hand, the inactive CaSR ECD structure was obtained in the presence and absence of 2 mM Ca^{2+}, when the receptor is in open conformation (inactive state, open-open) and the interdomain cleft is empty (Fig. 41.4 right). In this model, they also defined three anion-binding sites. The authors proposed a CaSR activation model where L-Trp facilitates the CaSR-ECD closure by contacting LB1 and LB2 domains of the VFT module to bring the CR domains

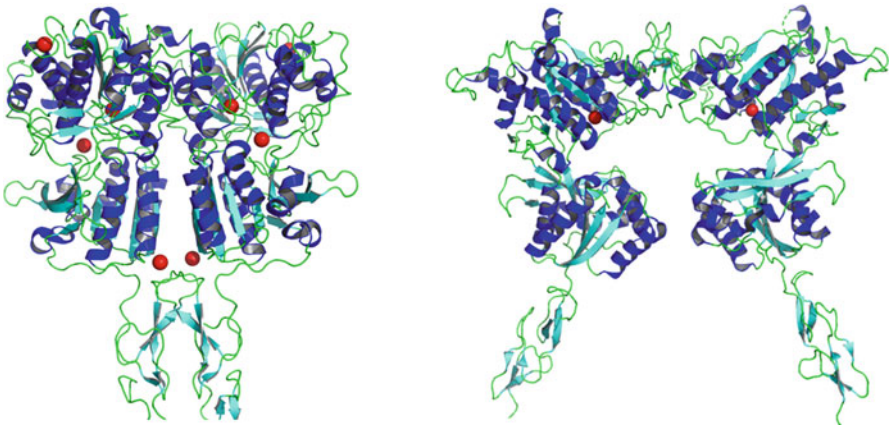

Fig. 41.4 Crystal structure of the human CaSR ECD in its active (left) and inactive (right) conformations. In the active conformation the VFT is closed and LB1 and LB2 interact to bring the CR domains closer together. In the inactive conformation the VFT is open and the interactions between LB1 and LB2 are minimal, therefore the CR domains do not interact. Calcium ions are shown as red spheres. PDB accession numbers: 5k5s and 5k5t [28]

closer together. These interactions form a large homodimer interface that is unique for the active state, reduce the distance between the C-terminal tails and might cause a rearrangement of the TMD [28] (Fig. 41.4).

Results from both groups suggest that the CaSR follows a universal activation mechanism similar for all class C GPCRs, despite the low sequence similarity (20–30%) [30]. This mechanism can be summarised in three steps. First, agonist binding causes the closure of the VFT. Second, membrane-proximal domains associate forming a homodimer interface between LB2 and CR domains. Third, agonist binding is accompanied by an approach between the C-terminal ends of ECDs of both protomers suggesting rearrangement of the TMD [31].

The ICD allows accurate receptor-specific control of diverse downstream signalling pathways. It represents the most diverse region of the class C GPCRs and determines selectivity of CaSR by coupling to different G proteins through the intracellular loops [32]. The ICD is exposed to the cytoplasm and begins with Lys-863 [33]. The amino acid sequence of the ICD is well conserved among species, although amino acids in the C-terminal tail are quite diverse [32]. Until now, two residues (Phe-706 and Leu-703) in intracellular loop two and eight residues (including Leu-797 and Phe-801) in intracellular loop three have been shown to be important for activating phospholipase C (PLC), the major pathway of the CaSR intracellular signalling [34]. Furthermore, there are several well-defined phosphorylation sites, especially Thr-888, in the ICD that are important for protein kinase C (PKC)-dependent inhibition of CaSR [22, 35, 36]. Also, this inhibitory effect may be counteracted by a protein phosphatase (most likely PP2A) that dephosphorylates Thr-888, restoring CaSR responsiveness [37].

41.3 CaSR Modulation

GPCRs can recognise diverse extracellular stimuli and are one of the most successful pharmaceutical target classes for different disorders. The ligands for GPCRs are typically polypeptides, amino acids and/or other small biological molecules that bind in well-defined pockets [38]. The CaSR, as a multifaceted receptor, is able to bind a broad range of molecules in addition to Ca^{2+}, its primary ligand. CaSR modulators can be divided into two groups: type I or orthosteric modulators, which bind to the active site, and type II or allosteric modulators, which bind elsewhere in the receptor.

41.3.1 Orthosteric Modulators of the CaSR

Orthosteric modulators are type I CaSR agonists and include all ligands that are thought to compete with Ca^{2+} for the same binding sites on the receptor. In addition, they are sufficient to activate the CaSR on their own, in the absence of Ca^{2+}.

Although Ca^{2+} is crucial for CaSR function, many other organic cations can activate CaSR in vitro for instance the divalent cations Mg^{2+} and Sr^{2+} and trivalent cations such as Gd^{3+}, as well as heavy metals such as Pb^{2+} and Co^{2+} which are more potent than Ca^{2+} [39]. In fact, the order of agonist potency for inositol metabolism in bovine parathyroid cells depends on two factors; the charge of the ion and the ionic radii. Thus, among ions with the same charge, those with greater radius have a greater potency and among ions of a similar size those with greater charge have a greater potency [40]. The order of potency for the main orthosteric modulators is as follows: $Gd^{3+} > La^{3+} > Ca^{2+} = Ba^{2+} > Sr^{2+} > Mg^{2+}$ [39]. Many organic polycations, such as the poly-amino acids poly-L-lysine or poly-arginine and aminoglycoside antibiotics such as neomycin, are also orthosteric modulators of the CaSR [41–43]. Polyamines produced in the gut and in the synaptic cleft in vivo, are also CaSR agonists. Spermine is the most potent polyamine followed by spermidine and putrescine. In this case, potency is linked to the number of amine groups in the ligand [44].

41.3.2 Allosteric Modulators of the CaSR

In addition to orthosteric agonists, the CaSR can also be activated by allosteric modulators, sometimes referred to as type II CaSR agonists, and these do not compete for the same binding sites as Ca^{2+}, instead they allosterically modify the endogenous affinity of the receptor for $Ca^{2+}{}_{o}$ [45]. The allosteric modulators affect the conformational equilibrium of the receptor and they can be divided into

two groups: activators or positive allosteric modulators (PAM) if they shift the equilibrium towards the active state, and inhibitors or negative allosteric modulators (NAM), if they stabilise the inactive state. Both types of modulators include compounds that can be found in the body under physiological conditions like L-aromatic amino acids, glutathione, ionic strength and alkalinisation [46], but also synthetic compounds like calcimimetic drugs [47].

L-aromatic amino acids were the first endogenous PAMs identified and these include L-Phe, L-Tyr, L-His and L-Trp, with the short aliphatic amino acids L-Thr and L-Ala also effective [48]. L-amino acids increase CaSR sensitivity in the presence of other agonists, such as Ca^{2+} or Gd^{3+}. This demonstrates that CaSR is able to sense a broad range of nutrients having special relevance in the gastrointestinal tract where the CaSR has been identified as an L-amino acid sensor for macronutrient-dependent hormone secretion [49, 50]. In addition, increased aromatic L-amino acid concentration suppresses PTH secretion stereoselectively by activating endogenous CaSR [51]. Therefore, L-amino acids may play an important role as physiological regulators of PTH secretion and calcium metabolism via CaSR modulation.

Interestingly, pH and ionic strength play a double role in modulating CaSR sensitivity. In the case of pH, CaSR sensitivity can be enhanced when pH is elevated (>7.5), but also reduced when pH is low (<7.3) [52]. Decreasing blood pH by only 0.2–0.4 units significantly increases PTH secretion, suggesting a functionally less active CaSR [53]. In contrast, moderate alkalinisation equivalent to that seen in metabolic alkalosis significantly inhibits PTH secretion independently of a change in $[Ca^{2+}]_o$, suggestive of a more sensitive CaSR [54]. This has been confirmed in vitro, whereby small pathophysiologic pH changes (0.2 units) significantly inhibit CaSR-induced intracellular calcium $Ca^{2+}{}_i$ mobilisation (and also extracellular signal-regulated kinase (ERK1/2) phosphorylation and actin polymerisation [55]) in CaSR-HEK cells and in bovine parathyroid cells [34]. Similarly, increasing the ionic strength of the surrounding buffer can also reduce CaSR sensitivity, whereas reducing the buffer's ionic strength enhances CaSR sensitivity [46]. This suggests that protons and Na^+ can both act as NAMs of the CaSR.

41.3.3 Synthetic Modulators of the CaSR

Over the last 20 years, scientists have been looking for drugs to alleviate pathological abnormalities in plasma PTH and Ca^{2+} levels. As the secretion of PTH is mainly regulated by CaSR, compounds that affect this receptor are good candidates to treat PTH disorders. Thus, new synthetic allosteric modulators with higher potency and specificity have been developed.

Nemeth and colleagues at NPS Pharmaceuticals Inc. successfully identified two small organic molecules that caused a leftward shift in the concentration-response

curve of the CaSR for $[Ca^{2+}]_o$. They named them calcimimetics. These compounds are able to potentiate the effects of $[Ca^{2+}]_o$ probably by stabilising the active conformation of the receptor by binding to the TMD [56–58]. Calcimimetics are considered type II CaSR agonists and most of them are phenylalkylamines and derivatives of Ca^{2+} channel blockers [57, 59]. Some Ca^{2+} channel blockers can also activate the CaSR, worsening the effects in pulmonary arterial hypertension [60].

Cinacalcet, a calcimimetic molecule more easily absorbed than the initially identified analogue NPS R-568, was the first PAM acting on a GPCR to receive FDA approval and enter the clinic. It represents a targeted therapy for the treatment of disorders linked to hyperparathyroidism, including chronic kidney disease (CKD), life-threatening NSHPT, and parathyroid carcinoma [61–63]. In patients with end-stage CKD, treatment with Cinacalcet lowers PTH levels after 2–4 h [64]. However, calcimimetics can evoke significant side effects including adverse gastrointestinal effects, due to the fact that the CaSR is expressed in many other tissues, where it activates different signalling pathways [64, 65]. Apart from nausea, the main side effect of Cinacalcet is hypocalcaemia [66]. Recently, a new peptide calcimimetic called Etelcalcetide (Parsabiv) has just received FDA approval for the treatment of secondary hyperparathyroidism in adult haemodialysis patients with CKD [66, 67]. Other calcimimetics in use either as research tools or as potential clinical agents include Calindol (AC265347) and Velcalcetide (AMG416) [68].

In contrast, synthetic CaSR NAMs called calcilytics have opposite effects to calcimimetics. Calcilytics include the substituted phenyl-O-alkylamine NPS 2143 and NPS 89636 [56]. Their binding site is located within the CaSR TMD and is partly overlapping with the calcimimetic binding site. Two other structural types of compounds, amino alcohols (e.g. Ronacaleret) and quinazolinones (e.g. ATF936), were identified by high-throughput screening and shown to reduce CaSR affinity for $[Ca^{2+}]_o$ [56, 69]. As calcilytics can increase endogenous PTH secretion by inhibiting CaSR they were initially developed to treat osteoporosis by delivering endogenous, anabolic pulses of PTH but they had insufficient efficacy [65]. Currently, calcilytics are being studied in different drug repurposing projects, including asthma and other lung-related diseases [70].

41.4 CaSR Trafficking

Receptor trafficking plays a critical role in GPCR activity through tight regulation of GPCR expression levels at the cellular surface. This regulation can be divided into two opposing routes: (1) trafficking of newly synthesised GPCRs to the cellular surface (i.e. exocytic trafficking) and (2) removal of GPCRs from the cell surface to intracellular compartments (i.e. endocytic trafficking) [71]. This section will focus on the processes and interacting partners involved in CaSR trafficking.

41.4.1 From Protein Synthesis to the Cellular Surface

To initiate downstream signalling, a GPCR is required to be present at the cellular surface where the agonist binding site is accessible to ligand stimulation and its intracellular part can interact with G proteins or other binding partners [71–73]. The outward motion of newly synthesised GPCRs to the cellular surface is driven by exocytic receptor trafficking. In this section, the term exocytic trafficking will be used in the broadest sense to refer to protein synthesis, protein maturation and the transport of newly synthesised GPCRs from the endoplasmic reticulum (ER) and Golgi system to the cellular surface [74].

To date, the processes and binding partners involved in exocytic CaSR trafficking are poorly understood. In humans, the gene that encodes for CaSR is located on chromosome 3q13.3-21 [75]. The CaSR protein is transcribed from six out of the eight mapped exons in this gene and transcription can be initiated from two different promoter sites (i.e. promoter P1 or P2) [76, 77]. In an investigation into the regulation of CaSR transcription, Canaff and Hendy have identified functional vitamin D and NF-κB response elements within both promoters of the CaSR gene [78, 79]. In agreement with these findings, vitamin D and several proinflammatory cytokines have been reported to upregulate rodent and human CaSR expression [79–82].

Correct protein folding and protein maturation through post-translational modifications are essential for cell-surface targeting of GPCRs. Protein folding into the GPCR's functional three-dimensional conformation is assisted by chaperones. To date, a large number of chaperones or GPCR-interacting proteins with chaperone function have been identified, but none of these proteins have been associated with CaSR folding [72, 83]. CaSR maturation involves extensive N-linked glycosylation in the ECD. A total of 11 potential N-linked glycosylation sites have been identified in the CaSR protein. Glycosylation of at least three sites have been found crucial for cell-surface expression. Moreover, western blot analyses of cell lysates containing CaSR demonstrate immunoreactive bands at approximately 140–160 kDa corresponding to immature monomeric CaSR and fully mature monomeric CaSR respectively [25, 84–86].

As mentioned earlier, the CaSR predominantly exists on the cell surface as a homodimer, but with evidence suggesting potential heterodimerisation with other class C GPCR members including mGlu and GABA B receptors [26, 87]. The CaSR homodimerisation process takes place in the ER and is directed by the formation of disulphide linkages and non-covalent interactions at the dimer interface, as confirmed by the recently resolved crystal structures of the CaSR ECD [28, 29].

Protein synthesis and maturation are strictly regulated by the cell to ensure that only correctly folded and fully matured GPCRs are targeted for trafficking towards the cellular surface. This quality control system is proposed to be regulated by GPCR-interacting proteins such as the previously mentioned chaperones as well as by recognition of conserved retention or export motifs [71, 83]. Bouschet et al. have investigated the involvement of receptor activity-modifying proteins (RAMPs)

in exocytic CaSR trafficking. According to Bouschet et al., CaSR interaction with RAMP subtype 1 or 3 facilitates delivery to the cellular surface [88]. This view is supported by Desai and co-workers who demonstrated direct interactions between CaSR and both RAMP subtypes at the cellular surface using FRET-based stoichiometry [89]. The CaSR-interacting protein dorfin mediates ER-associated degradation of the receptor, while filamin A, another interacting protein, protects CaSR from degradation [90–93]. Furthermore, an extended phosphorylation-regulated arginine-rich region was identified in the carboxyl terminus of CaSR which has been shown to be involved in intracellular retention through interaction with 14-3-3 proteins [94–97].

In general, the number of receptors expressed at the cellular surface influences the magnitude of downstream signalling responses. Multiple studies have demonstrated that differences in cell surface expression levels influence CaSR-mediated signalling. Cell surface expression levels of CaSR can be influenced by multiple factors [84, 98, 99]. First, CaSR expression is affected by numerous naturally occurring mutations and polymorphisms. Interestingly, cell surface expression levels of most CaSR mutants could be effectively rectified towards wild-type expression levels upon treatment with calcimimetics or calcilytics [90, 94, 100–102]. Second, phosphorylation at residue Ser-899, a protein kinase A (PKA) phosphorylation site located next to the extended arginine-rich region, has been reported to increase CaSR surface localisation by disruption of 14-3-3 protein binding [94, 95]. Third, a novel trafficking mechanism, referred to as agonist-driven insertional signalling, has been proposed to regulate cell surface expression in response to CaSR activation. According to this mechanism, agonist binding promotes an increase in the forward trafficking of newly synthesised CaSR to the cellular surface from a consistently present intracellular CaSR pool [95].

41.4.2 From the Cellular Surface to Protein Degradation

Endocytic receptor trafficking, also commonly referred to as receptor endocytosis or receptor internalisation, regulates the duration and magnitude of GPCR-activated G protein signalling responses by effective removal of GPCRs from the cellular surface. Besides its crucial role in the termination of GPCR activity, multiple studies have linked receptor endocytosis to the initiation of non-canonical G protein-independent signalling pathways [71, 103]. Endocytic trafficking of CaSR was described to play a role in parathyroid hormone-related protein (PTHrP) secretion and ERK1/2 activation [104, 105].

The molecular mechanism underlying endocytic CaSR trafficking is still poorly investigated. The reported experimental data is rather controversial, and there is no general agreement about the endocytic trafficking route of CaSR. One of the main findings related to CaSR endocytosis is the ability to initiate endocytic trafficking independently of ligand activation [95, 104, 106]. Pi and colleagues stated that phosphorylation preferentially by GRK4 promotes ß-arrestin binding

[107]. However, Lorenz et al. argue that phosphorylation by PKC rather than GRKs mediates ß-arrestin recruitment [108]. This disagreement could potentially be linked to receptor origin as Pi et al. measured desensitisation of rat CaSR while the studies of Lorenz et al. were conducted with human CaSR.

The internalised CaSR can be either recycled or degraded [95, 104, 106, 109]. Similarly as for the exocytic trafficking pathway, the endocytic trafficking pathway is strongly regulated by GPCR-interacting proteins and conserved motifs [103, 110, 111]. In 2012, a presumed internalisation motif linked to lysosomal degradation has been discovered at the CaSR carboxyl terminus [106]. Interestingly, this motif shows an overlap with the filamin A binding site indicating that filamin A might be involved in both exocytic and endocytic trafficking of the CaSR [91]. This hypothesis is supported by the finding that filamin A contributes to the localisation of CaSR to caveolae, a specialised cell membrane region known to be involved in clathrin-independent endocytosis [92, 112, 113]. Furthermore, the CaSR-interacting protein AMSH-1 (associated molecule with the SH3 domain of STAM) has been reported to promote ubiquitin-mediated degradation of internalised CaSR [104, 114].

The ability to rectify the expression of disease-related mutants by calcimimetics and calcilytics highlights the therapeutic potential of modulating endocytic CaSR trafficking in the treatment of CaSR-related diseases. However, further research is needed to fully understand the molecular mechanism underlying CaSR trafficking and its potential as therapeutic target.

41.5 Overview of Signalling Pathways Activated by the CaSR

This section will focus on the signalling pathways mediated by the CaSR, with special attention to the diversity of responses elicited upon activation of the receptor in different tissues. Figure 41.5 shows a simplified overview of what is known to date about CaSR signalling.

41.5.1 G Proteins Activated by the CaSR

G proteins, also called guanine nucleotide-binding proteins, can bind the guanine nucleotides GDP and GTP. GTP-bound, active G proteins have GTPase activity, hydrolysing GTP into GDP and inorganic phosphate (Pi), returning the G protein to its inactive GDP-bound form. The equilibrium of GDP- and GTP-bound forms of the G proteins is a result of the activities of three groups of molecules. Guanine nucleotide exchange factors (GEFs) activate the G proteins by exchanging GDP for GTP. GTPase-activating proteins (GAPs) accelerate the GTPase activity of the G protein and thus terminate its activity. Guanine nucleotide dissociation inhibitors (GDIs) bind GDP-bound G proteins and inhibit activation by the GEFs. G proteins

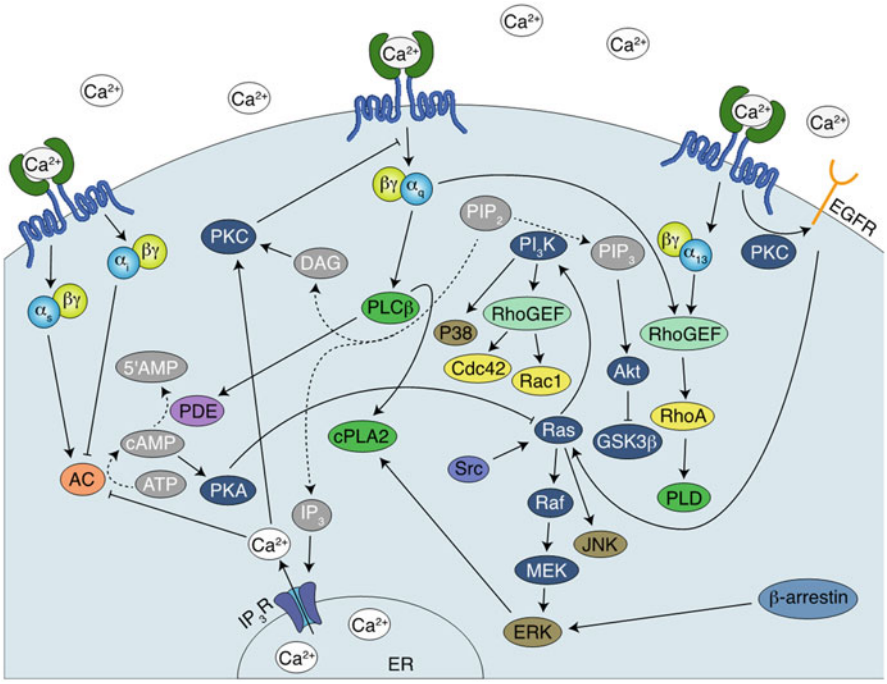

Fig. 41.5 General representation of the signalling pathways activated by CaSR. Arrows, bar-headed lines, and dashed arrows represent activation, inhibition, and a chemical reaction respectively. In green and blue, a CaSR homodimer; in light blue and yellow, the α and βγ subunits of the G proteins; in dark blue, kinases; in light green, phospholipases; in light brown, MAP kinases; in light yellow, Rho GTPases; in grey, second messengers and derivatives

can be either heterotrimeric or monomeric. In this section we will refer to them as "G proteins" and "small GTPases" respectively.

G proteins are heterotrimers composed of α, β, and γ subunits. To date, a total of 21 α, 6 β, and 12 different γ subunits have been identified in humans. G proteins are activated by GPCRs, such as the CaSR, which act as GEFs. The exchange of GDP for GTP, bound to the α subunit, results in the dissociation of the α subunit from the βγ dimer. Subsequently, both the GTP-bound α subunit and the βγ heterodimer activate signalling pathways until the GTP is hydrolysed into GDP and the heterotrimer is reassembled. GAPs accelerate the hydrolysis and are also known as regulators of G protein signalling (RGS). These events are illustrated in Fig. 41.6.

Among the well-accepted effects of the βγ dimer are the regulation of K^+ and voltage-dependent Ca^{2+} channels, adenylyl cyclases (ACs), phospholipases C (PLCs), and phosphoinositide 3-kinases (PI_3Ks) [115]. In addition, βγ heterodimers have been suggested to affect transcription, trafficking and signalling at different subcellular locations [116].

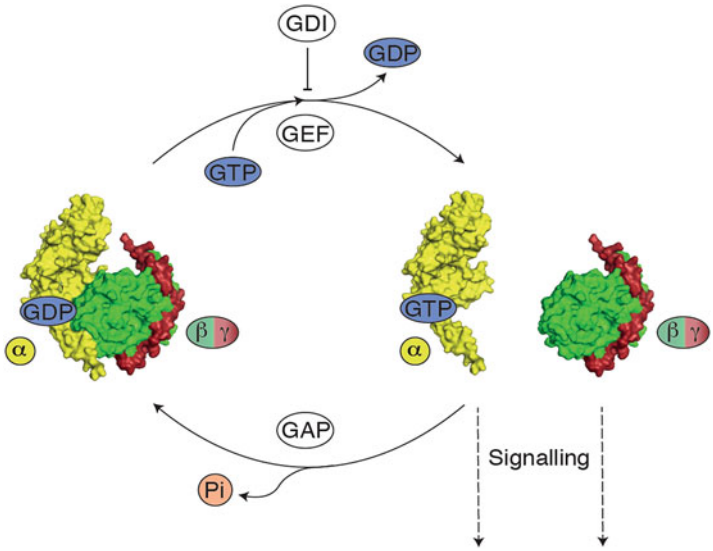

Fig. 41.6 Simplified representation of the cycles of activation and deactivation of G proteins

As for many GPCRs, the CaSR couples to more than one family of heterotrimeric G proteins, especially to $G_{q/11}$ and $G_{i/o}$. However several studies also suggest that the CaSR may couple to members of the $G_{12/13}$ family, and also to G_s in cancer-derived cell lines [18].

41.5.1.1 $G_{q/11}$

G_q and G_{11} share 90% sequence homology, are ubiquitously expressed, and have similar functions. For historic reasons, most studies focus on G_q and to a lesser extent on G_{11} [117]. The α subunits of $G_{q/11}$ activate PLCβ, which cleaves membrane-located phosphatidylinositol 4,5-bisphosphate (PIP_2) into the second messengers 1,2-diacylglycerol (DAG) and inositol 1,4,5-trisphosphate (IP_3). IP_3 diffuses into the cytosol and binds the IP_3 receptors that reside in the ER, causing the release of $Ca^{2+}{}_i$. IP_3 is then metabolised to IP_2 and IP_1. Increased $[Ca^{2+}]_i$ together with DAG, localised in the plasma membrane, results in the recruitment and activation of multiple isoforms of PKC. PKC phosphorylates numerous other proteins [118], including CaSR at Thr-888 to regulate $Ca^{2+}{}_i$ oscillations [119]. CaSR-induced IP_3 generation and $Ca^{2+}{}_i$ mobilisation was first shown in *Xenopus laevis* oocytes expressing the bovine parathyroid CaSR in the original cloning paper [3] but is more commonly investigated in HEK293 cells stably expressing the CaSR (HEK-CaSR) [18] [120] thus confirming the central role of the $G_{q/11}$-PLCβ pathway in CaSR signalling.

In addition to the classic $G_{q/11}$-PLCβ pathway, recent studies have shown that $G_{q/11}$ can also activate other signalling pathways via RhoGEFs such as RhoA [121–123], although the relevance of this pathway for the CaSR has not yet been determined.

41.5.1.2 $G_{i/o}$

The members of the $G_{i/o}$ family are characterised by their sensitivity to pertussis toxin (PTx), which inhibits their interaction with the GPCR, the only exception being G_z [124]. G_{i1}, G_{i2}, G_{i3} and G_o subtypes share a high sequence homology and probably have overlapping functions, although G_o is localised predominantly in the central nervous system [125]. Due to the relatively high abundance of this family of G proteins compared to the others, and since the majority of signalling events activated by βγ are sensitive to PTx [126], the signalling by βγ dimers is often attributed to activation of $G_{i/o}$ [127].

Activation of G_i inhibits several types of ACs. ACs increase cytosolic levels of cAMP and therefore G_i activation lowers cAMP levels. Studies in HEK-CaSR cells show that increased $[Ca^{2+}]_o$ decreases forskolin-induced increase in cAMP, suggesting the activation of G_i [120]. In bovine parathyroid and HEK-CaSR cells, CaSR stimulates ERK1/2 phosphorylation via $G_{q/11}$ and G_i pathways [128]. A later study suggested that G_{i2} is the $G_{i/o}$ subtype responsible for ERK1/2 activation [105].

41.5.1.3 $G_{12/13}$

The activation of $G_{12/13}$ proteins recruit to the membrane and activate RhoGEFs that specifically activate RhoA, such as p115-RhoGEF, which also acts as a GAP through its RGS domain terminating the activity of $G_{12/13}$ [129]. Using Madin-Darby canine kidney cells stably overexpressing CaSR, Miller and collaborators found that $[Ca^{2+}]_o$ activated phospholipase D via RhoA, and that this was mediated by $G_{12/13}$ and independent of $G_{q/11}$ and G_i [130]. Another study, suggested a pathway specifically activated by L-Phe via $G_{12/13}$ in mouse embryonic fibroblasts that resulted in $Ca^{2+}{}_i$ oscillations [131].

41.5.1.4 G_s

A few studies have reported G_s coupling to the CaSR. Wysolmerski and collaborators first showed that CaSR couples to G_i in healthy mammary epithelial cells, but then switches to G_s in both MCF-7 human breast cancer cells, and in Comma-D immortalised murine mammary cells. Surprisingly, no IP_1 accumulation was observed, whereas the levels of active mitogen-activated protein kinases (MAPKs)

were increased upon stimulation with high $[Ca^{2+}]_o$. They also found that cAMP regulated the secretion of PTHrP via PKA [132], which was corroborated in a recent study [133]. In mouse pituitary gland tumour derived AtT-20 cells, the same group showed that CaSR activation stimulated PTHrP via the same mechanism, G_s-cAMP-PKA, independently of PLC or PKC [134]. In a previous study using the same cell line, increases in IP_1 concentrations were sensitive to PTx, showing simultaneous coupling both to G_i and G_s [135]. G protein switching has been observed also for the β2-adrenergic receptor, where PKA phosphorylates the receptor, increasing its affinity for G_i versus G_s. As a result, it switches signalling from cAMP/PKA to MAPK activation [136].

41.5.2 Rho GTPases

Rho GTPases belong to the Ras family of GTPases, which are the most known small monomeric GTPases. Among the Rho GTPases, the best characterised are RhoA, Rac1 and Cdc42. Rho GTPases play a central role in cell migration, cell polarity, and cell cycle progression, by regulating cell adhesion and actin cytoskeleton dynamics [137]. The activation of RhoA has been traditionally associated exclusively with $G_{12/13}$ signalling, however there is increasing evidence of activation by $G_{q/11}$ via RhoGEFs and independent of PLCβ [138]. It has been suggested that the CaSR activates PI_4-kinase via Rho [139]. CaSR activation produced actin stress fibre assembly in HEK-CaSR, in a Rho kinase-dependent mechanism. This phenomenon was PTx-insensitive and the PLCβ inhibitor U73122 showed no effect [140]. Since U73122 can activate ion channels at the concentrations used to inhibit PLCβ [141] the recently available potent and specific $G_{q/11}$ inhibitors FR900359 and YM-254890 may prove better reagents for the investigation of $G_{q/11}$ signalling [142].

A study in human keratinocytes showed that CaSR-dependent activation of RhoA plays a role in cell-cell adhesion [143], whereas experiments in human podocytes showed that CaSR activated RhoA via $Ca^{2+}{}_i$ mobilisation, in a mechanism dependent of the ion channel TRPC6 [144].

The activation of Rac and Cdc42 by G proteins is less clearly defined. In highly motile cells βγ-mediated activation of PI_3K and the GEF PRex resulted in Rac1 activity. Whether these signalling modules play a role in CaSR signal transduction remains to be demonstrated [145]. In primary human monocyte-derived macrophages CaSR activated Rac and/or Cdc42, but no RhoA, to regulate membrane ruffling via a mechanism dependent on PI_3K [146]. A study in a human T cell line found that CaSR can promote cell migration by activating Cdc42, also via a PI_3K-dependent mechanism [147]. A study in HEK-CaSR cells showed that membrane ruffling is $G_{q/11}$-dependent and $G_{12/13}$-independent, suggesting activation of Rho GTPases by $G_{q/11}$ [148].

41.5.3 β-Arrestins

In addition to their key role in terminating G protein signalling pathways activated by GPCRs, β-arrestins can also activate signalling events [149]. Specifically in HEK-CaSR cells, β-arrestin 1 is involved in CaSR-induced plasma membrane ruffling [150] while β-arrestins 1 and 2 are involved in CaSR-induced ERK1/2 activation [151].

41.5.4 CaSR-Induced Protein Kinase Activation

The CaSR activates a number of protein kinase families including glycogen synthase kinase-3 (GSK3), Akt, and the MAPKs, and these will be detailed in turn.

41.5.4.1 Akt and GSK-3β

Akt, or protein kinase B, is a protein kinase that regulates multiple functions such as growth, proliferation and transcription. The first step for Akt activation is binding to PIP_3 in the membrane. PIP_3-bound Akt is sequentially phosphorylated first at Thr-308 and then at Ser-473 for full activation [152]. GSK3 is involved in the phosphorylation of over a hundred substrates, and it interacts with multiple types of receptors. It exists in two isoforms, α and β, and it can be phosphorylated by PKA, PKC, and Akt, among others. Phosphorylation of GSK3-β at Ser-9 results in inhibition of the binding to certain substrates that require binding to a domain in the protein prior to phosphorylation [153].

Studies in fetal rat calvarial cells, murine osteoblast 2T3 cells, and human osteoblasts, show that CaSR activation results in phosphorylation of Akt at Thr-308 and Ser-473, and of GSK3-β at Ser-9 [154, 155]. Further, in proximal tubular opossum kidney cells, the CaSR ligands neomycin and gentamicin elicit phosphorylation of Akt and GSK3-β in a PI_3K-dependent fashion [42].

41.5.4.2 MAPKs

Several studies have recently explored the role played by CaSR in the phosphorylation of protein kinases, both in healthy tissue and in disease models. The MAPKs include ERK, c-Jun amino-terminal kinases (JNK), and P38. These proteins are activated by phosphorylation and thus we will refer to the active phosphorylated forms as p-ERK1/2, p-JNK and p-P38.

Activation of ERK1/2 can be Ras- or PKC-dependent. Ras-dependent activation involves PI_3K, Src family kinases, and receptor tyrosine kinases such as the epidermal growth factor receptor. A study in HEK-CaSR cells showed that ERK1/2

activation by CaSR was Ras-dependent, relied largely on PI_3K activity, and was independent of tyrosine kinase activity [156]. In contrast, another study in HEK-CaSR cells and in bovine parathyroid cells, showed that the cytoplasmic tyrosine kinase inhibitor, herbimycin, inhibited ERK1/2 phosphorylation [128]. A similar result was observed for ERK1 in Rat-1 fibroblasts [157]. In proximal tubular opossum-kidney cells, activation of CaSR by neomycin induced P38 activation via a PI_3K-mediated mechanism [41].

Across different tissues, increased CaSR expression and activation correlates positively with an increase in p-ERK1/2 levels [41, 154, 158–162], except for a study on hearts of a rat epilepsy model where p-ERK1/2 levels decreased [163]. A similar positive correlation was observed for p-JNK [161–164], whereas one study showed no effect [160]. As for p-P38, a similar number of studies show a positive correlation [41, 161, 163, 164] or no effect [158, 160, 162].

Overall, a prolonged exposure to CaSR agonists increases mRNA or protein expression levels of CaSR, and this phenomenon often correlates positively with an increase in active ERK1/2, JNK, and P38. Differences in phosphorylation are observed reflecting the different signalling profiles of CaSR in different tissues.

41.6 Ligand-Biased Signalling Through the CaSR

Ligand-biased signalling is a relatively new concept based on the idea that a receptor can exist in multiple active conformations, each stabilised by a specific ligand, with characteristic binding kinetics, and therefore with a particular signalling profile [165]. For GPCRs, this would translate into different coupling behaviours towards G proteins and β-arrestins [166]. For allosteric modulators, the concept extends to how these molecules affect positively or negatively each of the pathways activated by the orthosteric ligands. Exploiting this phenomenon offers great potential for the discovery and development of new drugs with increased efficacy and safety, which is of course of interest for the pharmaceutical industry [167].

Several studies have used the CaSR as a model to study ligand-biased signalling, given that it can activate multiple signalling pathways and it can be modulated by a wide range of different ligands [168]. This phenomenon has been studied using pharmacological assays, applied in a high-throughput manner, and using multiple agonists. The receptor readouts usually follow changes in $Ca^{2+}{}_i$ mobilisation, IP_1 accumulation, cAMP levels, phosphorylation of ERK1/2, and plasma membrane ruffling. The first two provide information on the $G_{q/11}$-PLCβ pathway; cAMP on G_i and G_s activity; p-ERK1/2 on G_q, G_i, and β-arrestins; and PM ruffling on Rho GTPases and β-arrestins.

These studies often rely on obtaining concentration-response curves for different ligands, and comparing calculated values such as EC_{50}, dissociation constant, maximum response, or cooperativity αβ for allosteric modulators. Additionally, receptor expression levels are often also determined, and in fact regulation of cell surface expression has been proposed as a mechanism of bias by allosteric

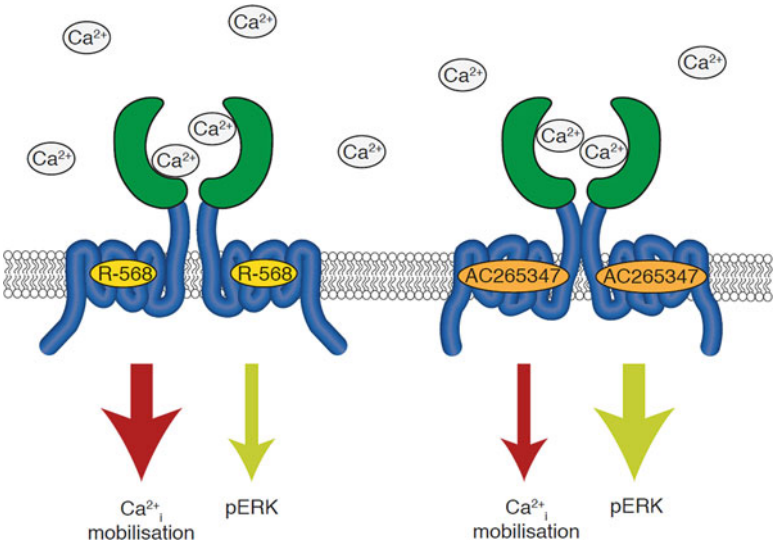

Fig. 41.7 Representation of bias by the positive allosteric modulators R-568 and AC265347 in $Ca^{2+}{}_i$ mobilisation and phosphorylation of ERK1/2 upon activation of the CaSR by $Ca^{2+}{}_o$

modulators [100, 169]. Multiple studies in HEK-CaSR cells have addressed ligand-bias by orthosteric ligands, as well as positive and negative allosteric modulators [151, 170–173], including one that explored the effect of naturally occurring CaSR mutations on ligand-bias [102].

These systematic in vitro studies provide valuable information to understand the differences in the effects of the ligands in vivo. For example, Leach and collaborators found that the calcimimetic AC265347 tunes the effect of $[Ca^{2+}]_o$ to favour phosphorylation of ERK1/2 and accumulation of IP_1, as compared to $Ca^{2+}{}_i$ mobilisation. Interestingly, AC265347 did not increase trafficking of loss-of-expression CaSR mutants, an effect observed by other calcimimetics, suggesting that it may act via a new mechanism [170]. Figure 41.7 shows an example of the signalling bias caused by two of the allosteric modulators used in this study.

41.7 Tissue-Specific Signalling of the CaSR

The pleiotropy of the CaSR arises as a result of its ability to couple to various G proteins and thus to mediate distinct signalling pathways. Consequently, the CaSR may fine-tune several physiological processes in a tissue-specific manner. The ability of GPCRs to mediate tissue-specific signalling is dictated by the cellular environment, as evidenced by recombinant systems where the same GPCR can have different pharmacological profiles in different cellular backgrounds. This

phenomenon is termed tissue-specific signalling or system bias. It arises when ligands favour the interaction of a receptor ensemble to auxiliary proteins, or when receptors form heterodimers with distinct pharmacological signatures [174]. The capacity of CaSR ligands to promote coupling to multiple G proteins and to differing extents was previously discussed in the context of biased signalling. Here, tissue-specific signalling is discussed in light of the evidence showing interaction of the CaSR with other proteins and the formation of heterodimers in different cellular environments.

The CaSR interacts with various proteins that influence its signalling signature. Several CaSR interacting proteins have been identified and these include inwardly-rectifying potassium channels [175] and the previously described filamin A [92, 93, 176] as well as the RAMPs [88]. In addition, the CaSR may form heterodimers with other class C GPCRs including mGlu1a, mGlu5 and GABA B receptors, as shown in endogenous and recombinant systems [87]. Such heterodimerisation could thus provide the CaSR another mechanism for tissue-specific signalling.

41.8 Future Topics and Concluding Remarks

The recently published crystallographic data of the CaSR ECD structure has shed some light on CaSR ligand recognition, receptor activation, allosteric modulation, as well as on the structural basis of dimerisation. The medicinal importance of CaSR modulation is clear and therefore obtaining the ECD structure will facilitate structure-based drug discovery and might open up further therapeutic approaches. These data also raise the question of whether L-aromatic amino acids and relevant anions should be added to the experimental buffers when studying CaSR function to preserve the receptor's native conformation. The full structure of the CaSR has yet to be determined and thus obtaining the crystal structures of the CaSR's TMD and ICD is a high priority in the field as this will help understanding effector interactions. In addition, the current structural data provides only a snapshot of the receptor in a fixed conformation, whereas in physiology the receptor is a dynamic molecule wobbling between multiple conformations. Thus, we need a new and more dynamic approach able to reveal a protein's structure in its transition states, ideally allowing us to see conformational changes upon agonist/antagonist binding at the receptor.

The CaSR field would also benefit from new reagents such as a CaSR-selective radioligand, as calcium itself is a too low-affinity ligand to be of use in binding studies. Such a radioligand would allow researchers to investigate whether CaSR biased signalling might be driven by ligand binding kinetics. Moreover, the radioligand could be used to study CaSR expression in native tissues and cells as CaSR expression analysis is currently hampered by nonspecific staining of commercially available CaSR antibodies. Next, the newly emerging FRET-based biosensors can be used to observe G protein activation of the CaSR directly, providing dynamic information on the first step in the signalling cascade [177]. Indeed by taking

advantage of the plethora of fluorescent biosensors available, given particular spectroscopic properties, it is possible to measure activation of multiple proteins simultaneously and in real-time [178]. This would be of particular value when studying biased signalling, as current protocols are susceptible to time- and assay-specific artefacts.

Finally, a recent publication suggested that internalised CaSR could have a role in sustained signalling [148]. This phenomenon has been proposed before for some class A GPCRs [179], and implies a new signalling mechanism by CaSR. The relevance of the observations for internalised CaSR signalling needs to be addressed in follow-up studies.

We can conclude therefore that CaSR activation results in a wide range of downstream signals and functions at different timescales and across a variety of tissues. To make sense of this complexity will require better understanding of a range of factors including differential ligand affinity and bias, receptor heterodimerisation, as well as downstream effector selection. The benefit of such information could be the rational development of novel drugs with improved efficacy and safety.

Acknowledgements The authors thank Hans Bräuner-Osborne for critical review of the manuscript. The authors of this chapter have received funding from the European Union's Horizon 2020 research and innovation programme under grant agreement No 675228 (CaSR Biomedicine).

References

1. Crichton RR (2008) Biological inorganic chemistry. Biological inorganic chemistry
2. Alexander SPH, Christopoulos A, Davenport AP, Kelly E, Marrion NV, Peters JA et al (2017) The concise guide to pharmacology 2017/18: G protein-coupled receptors. Br J Pharmacol 174:S17–S129
3. Brown EM, Gamba G, RIccardi D, Lombardi M, Butters R, Kifor O et al (1993) Cloning and characterization of an extracellular Ca^{2+}-sensing receptor from bovine parathyroid. Nature 366:461–464
4. Conigrave AD (2016) The calcium-sensing receptor and the parathyroid: past, present, future. Front Physiol 7:563
5. Uhlen M, Fagerberg L, Hallstrom BM, Lindskog C, Oksvold P, Mardinoglu A et al (2015) Tissue-based map of the human proteome. Science 347(6220):1260419–1260419
6. Felsenfeld AJ, Levine BS (2015) Calcitonin, the forgotten hormone: does it deserve to be forgotten? Clin Kidney J 8(2):180–187
7. Mutschler E, Geisslinger G, Kroemer HK, Menzel S, Ruth P Mutschler Arzneimittelwirkungen – Pharmakologie, Klinische Pharmakologie, Toxikologie. Lehrbuch der Pharmakologie, der klinischen Pharmakologie und Toxikologie; mit einführenden Kapiteln in die Anatomie, Physiologie und Pathophysiologie; mit 257 Tabellen und 1417 Strukturformeln. 2013. XXIII, 1197 Seiten
8. Brown EM, MacLeod RJ (2001) Extracellular calcium sensing and extracellular calcium signaling. Physiol Rev 81(1):239–297
9. Conigrave AD, Quinn SJ, Brown EM (2000) Cooperative multi-modal sensing and therapeutic implications of the extracellular Ca^{2+} sensing receptor. Trends Pharmacol Sci 21:401–407

10. Kantham L, Quinn SJ, Egbuna OI, Baxi K, Butters R, Pang JL et al (2009) The calcium-sensing receptor (CaSR) defends against hypercalcemia independently of its regulation of parathyroid hormone secretion. Am J Physiol Endocrinol Metab 297(4):E915–E923
11. Loupy A, Ramakrishnan SK, Wootla B, Chambrey R, De La Faille R, Bourgeois S et al (2012) PTH-independent regulation of blood calcium concentration by the calcium-sensing receptor. J Clin Invest 122(9):3355–3367
12. Ward BK, Magno AL, Davis EA, Hanyaloglu AC, Stuckey BGA, Burrows M et al (2004) Functional deletion of the calcium-sensing receptor in a case of neonatal severe hyperparathyroidism. J Clin Endocrinol Metab 89:3721–3730
13. Vahe C, Benomar K, Espiard S, Coppin L, Jannin A, Odou MF et al (2017) Diseases associated with calcium-sensing receptor. Orphanet J Rare Dis 12:19
14. Pallan S, Rahman MO, Khan AA (2012) Diagnosis and management of primary hyperparathyroidism. BMJ 344(7849):181–192
15. Assimos DG (2015) The G allele of CaSR R990G polymorphism increases susceptibility to urolithiasis and hypercalciuria: evidences from a comprehensive meta-analysis. J Urol 194:1014
16. Tennakoon S, Aggarwal A, Kallay E (2016) The calcium-sensing receptor and the hallmarks of cancer. Biochim Biophys Acta 1863(6 Pt B):1398–1407
17. Yarova PL, Stewart AL, Sathish V, Britt RD, Thompson MA, Lowe APP et al (2015) Calcium-sensing receptor antagonists abrogate airway hyperresponsiveness and inflammation in allergic asthma. Sci Transl Med 7(284):284ra58
18. Conigrave AD, Ward DT (2013) Calcium-sensing receptor (CaSR): pharmacological properties and signaling pathways. Best Pract Res Clin Endocrinol Metab 27(3):315–331
19. Muto T, Tsuchiya D, Morikawa K, Jingami H (2007) Structures of the extracellular regions of the group II/III metabotropic glutamate receptors. Proc Natl Acad Sci 104(10):3759–3764
20. Silve C, Petrel C, Leroy C, Bruel H, Mallet E, Rognan D et al (2005) Delineating a Ca^{2+} binding pocket within the venus flytrap module of the human calcium-sensing receptor. J Biol Chem 280(45):37917–37923
21. Hendy GN, Canaff L, Cole DEC (2013) The CASR gene: alternative splicing and transcriptional control, and calcium-sensing receptor (CaSR) protein: structure and ligand binding sites. Best Pract Res Clin Endocrinol Metab 27:285–301
22. Bai M (2004) Structure-function relationship of the extracellular calcium-sensing receptor. Cell Calcium 35:197–207
23. Hauache OM, Hu J, Ray K, Spiegel AM (2000 Aug) Functional interactions between the extracellular domain and the seven-transmembrane domain in Ca^{2+} receptor activation. Endocrine 13(1):63–70
24. Ward DT, Brown EM, Harris HW (1998) Disulfide bonds in the extracellular calcium-polyvalent cation-sensing receptor correlate with dimer formation and its response to divalent cations in vitro. J Biol Chem 273(23):14476–14483
25. Ray K, Clapp P, Goldsmith PK, Spiegel AM (1998) Identification of the sites of N-linked glycosylation on the human calcium receptor and assessment of their role in cell surface expression and signal transduction. J Biol Chem 273(51):34558–34567
26. Gama L, Wilt SG, Breitwieser GE (2001) Heterodimerization of calcium sensing receptors with metabotropic glutamate receptors in neurons. J Biol Chem 276(42):39053–39059
27. Chang W, Tu C, Cheng Z, Rodriguez L, Chen T-H, Gassmann M et al (2007) Complex formation with the Type B gamma-aminobutyric acid receptor affects the expression and signal transduction of the extracellular calcium-sensing receptor. Studies with HEK-293 cells and neurons. J Biol Chem 282(34):25030–25040
28. Geng Y, Mosyak L, Kurinov I, Zuo H, Sturchler E, Cheng TC et al (2016) Structural mechanism of ligand activation in human calcium-sensing receptor. elife 5(July):1–25
29. Zhang C, Zhang T, Zou J, Miller CL, Gorkhali R, Yang J et al (2016) Structural basis for regulation of human calcium-sensing receptor by magnesium ions and an unexpected tryptophan derivative co-agonist. Sci Adv 2(5):e1600241

30. Kunishima N, Shimada Y, Tsuji Y, Sato T, Yamamoto M, Kumasaka T et al (2000) Structural basis of glutamate recognition by a dimeric metabotropic glutamate receptor. Nature 407(6807):971–977
31. Matsushita S, Nakata H, Kubo Y, Tateyama M (2010) Ligand-induced rearrangements of the GABAB receptor revealed by fluorescence resonance energy transfer. J Biol Chem 285(14):10291–10299
32. Tfelt-Hansen J, Brown EM (2005) The calcium-sensing receptor in normal physiology and pathophysiology: a review. Crit Rev Clin Lab Sci 42:35–70
33. Garrett JE, Capuano IV, Hammerland LG, Hung BC, Brown EM, Hebert SC et al (1995) Molecular cloning and functional expression of human parathyroid calcium receptor cDNAs. J Biol Chem 270(21):12919–12925
34. Chang W, Chen TH, Pratt S, Shoback D (2000) Amino acids in the second and third intracellular loops of the parathyroid Ca^{2+}-sensing receptor mediate efficient coupling to phospholipase C. J Biol Chem 275(26):19955–19963
35. Brown EM, Lian JB (2008) New insights in bone biology: unmasking skeletal effects of the extracellular calcium-sensing receptor. Sci Signal 1:pe40
36. Bai M, Trivedi S, Brown EM (1998) Dimerization of the extracellular calcium-sensing receptor (CaR) on the cell surface of CaR-transfected HEK293 cells. J Biol Chem 273(36):23605–23610
37. McCormick WD, Atkinson-Dell R, Campion KL, Mun HC, Conigrave AD, Ward DT (2010) Increased receptor stimulation elicits differential calcium-sensing receptorT888 dephosphorylation. J Biol Chem 285(19):14170–14177
38. Granier S, Kobilka B (2012) A new era of GPCR structural and chemical biology. Nat Chem Biol 8:670–673
39. Handlogten ME, Shiraishi N, Awata H, Huang CF, Miller RT (2000) Extracellular Ca^{2+}-sensing receptor is a promiscuous divalent cation sensor that responds to lead. Am J Physiol Physiol 279(6):F1083–F1091
40. Quinn SJ, Ye CP, Diaz R, Kifor O, Bai M, Vassilev P et al (1997) The Ca^{2+}-sensing receptor: a target for polyamines. Am J Phys 273:C1315–C1323
41. Ward DT, McLarnon SJ, Riccardi D (2002) Aminoglycosides increase intracellular calcium levels and ERK activity in proximal tubular OK cells expressing the extracellular calcium-sensing receptor. J Am Soc Nephrol 13(6):1481–1489
42. Ward DT, Maldonado-Pérez D, Hollins L, Riccardi D (2005) Aminoglycosides induce acute cell signaling and chronic cell death in renal cells that express the calcium-sensing receptor. J Am Soc Nephrol 16(5):1236–1244
43. Brauner-Osborne H, Wellendorph P, Jensen A (2007) Structure, pharmacology and therapeutic prospects of family C G-protein coupled receptors. Curr Drug Targets 8(1):169–184
44. Chang W, Shoback D (2004) Extracellular Ca^{2+}-sensing receptors – an overview. Cell Calcium 35(3):183–196
45. Nemeth EF (2004) Calcimimetic and calcilytic drugs: just for parathyroid cells? Cell Calcium 35(3):283–289
46. Bandyopadhyay S, Tfelt-Hansen J, Chattopadhyay N (2010) Diverse roles of extracellular calcium-sensing receptor in the central nervous system. J Neurosci Res 88:2073–2082
47. Ward DT, Riccardi D (2012) New concepts in calcium-sensing receptor pharmacology and signalling. Br J Pharmacol 165:35–48
48. Conigrave AD, Quinn SJ, Brown EM (2000 Apr) L-amino acid sensing by the extracellular Ca^{2+}-sensing receptor. Proc Natl Acad Sci U S A 97(9):4814–4819
49. Liou AP, Sei Y, Zhao X, Feng J, Lu X, Thomas C et al (2011) The extracellular calcium-sensing receptor is required for cholecystokinin secretion in response to L-phenylalanine in acutely isolated intestinal I cells. Am J Physiol Gastrointest Liver Physiol 300(4):G538–G546
50. Feng J, Petersen CD, Coy DH, Jiang J-K, Thomas CJ, Pollak MR et al (2010 Oct) Calcium-sensing receptor is a physiologic multimodal chemosensor regulating gastric G-cell growth and gastrin secretion. Proc Natl Acad Sci U S A 107(41):17791–17796

51. Conigrave AD, Mun H-C, Delbridge L, Quinn SJ, Wilkinson M, Brown EM (2004 Sep) L-amino acids regulate parathyroid hormone secretion. J Biol Chem 279(37):38151–38159
52. Quinn SJ, Bai M, Brown EM (2004) pH sensing by the calcium-sensing receptor. J Biol Chem 279(36):37241–37249
53. López I, Aguilera-Tejero E, Estepa JC, Rodriguez M, Felsenfeld AJ (2004) Role of acidosis-induced increases in calcium on PTH secretion in acute metabolic and respiratory acidosis in the dog. Am J Physiol Endocrinol Metab 286(5):E780–E785
54. Lopez I, Rodriguez M, Felsenfeld AJ, Estepa JC, Aguilera-Tejero E (2003) Direct suppressive effect of acute metabolic and respiratory alkalosis on parathyroid hormone secretion in the dog. J Bone Miner Res 18(8):1478–1485
55. Campion KL, McCormick WD, Warwicker J, Khayat MEB, Atkinson-Dell R, Steward MC et al (2015) Pathophysiologic changes in extracellular pH modulate parathyroid calcium-sensing receptor activity and secretion via a histidine-independent mechanism. J Am Soc Nephrol 26(9):2163–2171
56. Nemeth EF (2002) The search for calcium receptor antagonists (calcilytics). J Mol Endocrinol 29(1):15–21
57. Nemeth EF, Steffey ME, Hammerland LG, Hung BC, Van Wagenen BC, DelMar EG et al (1998) Calcimimetics with potent and selective activity on the parathyroid calcium receptor. Proc Natl Acad Sci U S A 95(March):4040–4045
58. Miedlich S, Gama L, Breitwieser GE (2002) Calcium sensing receptor activation by a calcimimetic suggests a link between cooperativity and intracellular calcium oscillations. J Biol Chem 277(51):49691–49699
59. Saidak Z, Brazier M, Kamel S, Mentaverri R (2009) Agonists and allosteric modulators of the calcium-sensing receptor and their therapeutic applications. Mol Pharmacol 76(6):1131–1144
60. Yamamura A (2016) Molecular mechanism of Dihydropyridine Ca^{2+} channel blockers in pulmonary hypertension. Yakugaku Zasshi 136(10):1373–1377
61. Block GA, Zaun D, Smits G, Persky M, Brillhart S, Nieman K et al (2010) Cinacalcet hydrochloride treatment significantly improves all-cause and cardiovascular survival in a large cohort of hemodialysis patients. Kidney Int 78(6):578–589
62. Gannon AW, Monk HM, Levine MA (2014) Cinacalcet monotherapy in neonatal severe hyperparathyroidism: a case study and review. J Clin Endocrinol Metab 99(1):7–11
63. Silverberg SJ, Rubin MR, Faiman C, Peacock M, Shoback DM, Smallridge RC et al (2007) Cinacalcet hydrochloride reduces the serum calcium concentration in inoperable parathyroid carcinoma. J Clin Endocrinol Metab 92(10):3803–3808
64. Nemeth EF, Goodman WG (2016) Calcimimetic and calcilytic drugs: feats, flops, and futures. Calcif Tissue Int 98:341–358
65. Steddon SJ, Cunningham J (2005) Calcimimetics and calcilytics – fooling the calcium receptor. Lancet 365(9478):2237–2239
66. Block GA, Bushinsky DA, Cheng S, Cunningham J, Dehmel B, Drueke TB et al (2017) Effect of etelcalcetide vs cinacalcet on serum parathyroid hormone in patients receiving hemodialysis with secondary hyperparathyroidism. JAMA 317(2):156–164
67. Eidman KE, Wetmore JB (2018) Managing hyperparathyroidism in hemodialysis: role of etelcalcetide. Int J Nephrol Renovasc Dis 11:69–80
68. Ma J-N, Owens M, Gustafsson M, Jensen J, Tabatabaei A, Schmelzer K et al (2011) Characterization of highly efficacious allosteric agonists of the human calcium-sensing receptor. J Pharmacol Exp Ther 337(1):275–284
69. Nemeth EF, Delmar EG, Heaton WL, Miller MA, Lambert LD, Conklin RL et al (2001) Calcilytic compounds: potent and selective Ca^{2+} receptor antagonists that stimulate secretion of parathyroid hormone. J Pharmacol Exp Ther 299(1):323–331
70. Lembrechts R, Brouns I, Schnorbusch K, Pintelon I, Kemp PJ, Timmermans J-P et al (2013) Functional expression of the multimodal extracellular calcium-sensing receptor in pulmonary neuroendocrine cells. J Cell Sci 126(Pt 19):4490–4501

71. Drake MT, Shenoy SK, Lefkowitz RJ (2006) Trafficking of G protein-coupled receptors. Circ Res 99(6):570–582
72. Ritter SL, Hall RA (2009) Fine-tuning of GPCR activity by receptor-interacting proteins. Nat Rev Mol Cell Biol 10(12):819–830
73. Pierce KL, Premont RT, Lefkowitz RJ (2002) Seven-transmembrane receptors. Nat Rev Mol Cell Biol 3(9):639–650
74. Tokarev AA, Alfonso A, Segev N (2009) Overview of intracellular compartments and trafficking pathways. In: Trafficking inside cells: pathways, mechanisms and regulation. Springer, New York, pp 3–14
75. Janicic N, S E, Pausova Z, Seldin MF, Rivi M, Szpirer J et al (1995) Mapping of the calcium-sensing receptor gene (CASR) to human chromosome 3q13. 3-21 by fluorescence in situ hybridization, vol 801. Springer, New York, pp 798–801
76. Chikatsu N, Fukumoto S, Takeuchi Y, Suzawa M, Obara T, Matsumoto T et al (2000) Cloning and characterization of two promoters for the human calcium-sensing receptor (CaSR) and changes of CaSR expression in parathyroid adenomas. J Biol Chem 275(11):7553–7557
77. Yun FHJ, Wong BYL, Chase M, Shuen AY, Canaff L, Thongthai K et al (2007) Genetic variation at the calcium-sensing receptor (CASR) locus: implications for clinical molecular diagnostics. Clin Biochem 40(8):551–561
78. Canaff L, Hendy GN (2002) Human calcium-sensing receptor gene. Vitamin D response elements in promoters P1 and P2 confer transcriptional responsiveness to 1,25-dihydroxyvitamin D. J Biol Chem 277(33):30337–30350
79. Canaff L, Hendy GN (2005) Calcium-sensing receptor gene transcription is up-regulated by the proinflammatory cytokine, interleukin-1β: role of the NF-κB pathway and κB elements. J Biol Chem 280(14):14177–14188
80. Brown AJ, Zhong M, Finch J, Ritter C, McCracken R, Morrissey J et al (1996) Rat calcium-sensing receptor is regulated by vitamin D but not by calcium. Am J Phys 270(3 Pt 2):F454–F460
81. Yao JJ (2005) Regulation of renal calcium receptor gene expression by 1,25-dihydroxyvitamin D3 in genetic hypercalciuric stone-forming rats. J Am Soc Nephrol 16(5):1300–1308
82. Fetahu IS, Hummel DM, Manhardt T, Aggarwal A, Baumgartner-Parzer S, Kállay E (2014) Regulation of the calcium-sensing receptor expression by 1,25-dihydroxyvitamin D3, interleukin-6, and tumor necrosis factor alpha in colon cancer cells. J Steroid Biochem Mol Biol 144:228–231
83. Dong C, Filipeanu CM, Duvernay MT, Wu G (2007) Regulation of G protein-coupled receptor export trafficking. Biochim Biophys Acta Biomembr 1768(4):853–870
84. Ray K, Fan GF, Goldsmith PK, Spiegel AM (1997) The carboxyl terminus of the human calcium receptor. Requirements for cell-surface expression and signal transduction. J Biol Chem 272(50):31355–31361
85. Fan G, Goldsmith PK, Collins R, Dunn CK, Krapcho KJ, Rogers KV et al (1997) N-linked glycosylation of the human Ca^{2+} receptor is essential for its expression at the cell surface. Endocrinology 138(5):1916–1922
86. Aida K, Koishi S, Tawata M, Onaya T (1995) Molecular cloning of a putative Ca^{2+}-sensing receptor cDNA from human kidney. Biochem Biophys Res Commun 214(2):524–529
87. Chang W, Tu C, Cheng Z, Rodriguez L, Chen TH, Gassmann M et al (2007) Complex formation with the type B γ-aminobutyric acid receptor affects the expression and signal transduction of the extracellular calcium-sensing receptor: studies with HEK-293 cells and neurons. J Biol Chem 282(34):25030–25040
88. Bouschet T, Stéphane M, Henley JM (2005) Receptor-activity-modifying proteins are required for forward trafficking of the calcium-sensing receptor to the plasma membrane. J Cell Sci 118(20):4709–4720
89. Desai AJ, Roberts DJ, Richards GO, Skerry TM (2014) Role of receptor activity modifying protein 1 in function of the calcium sensing receptor in the human TT thyroid carcinoma cell line. PLoS One 9(1):e85237

90. Huang Y, Breitwieser GE (2007) Rescue of calcium-sensing receptor mutants by allosteric modulators reveals a conformational checkpoint in receptor biogenesis. J Biol Chem 282(13):9517–9525
91. Zhang M, Breitwieser GE (2005) High affinity interaction with filamin A protects against calcium-sensing receptor degradation. J Biol Chem 280(12):11140–11146
92. Hjälm G, MacLeod RJ, Kifor O, Chattopadhyay N, Brown EM (2001) Filamin-A binds to the carboxyl-terminal tail of the calcium-sensing receptor, an interaction that participates in CaR-mediated activation of mitogen-activated protein kinase. J Biol Chem 276(37):34880–34887
93. Awata H, Huang C, Handlogten ME, Miller RT (2001) Interaction of the calcium-sensing receptor and filamin, a potential scaffolding protein. J Biol Chem 276(37):34871–34879
94. Stepanchick A, McKenna J, McGovern O, Huang Y, Breitwieser GE (2010) Calcium sensing receptor mutations implicated in pancreatitis and idiopathic epilepsy syndrome disrupt an arginine-rich retention motif. Cell Physiol Biochem 26(3):363–374
95. Grant MP, Stepanchick A, Cavanaugh A, Breitwieser GE (2011) Agonist-driven maturation and plasma membrane insertion of calcium-sensing receptors dynamically control signal amplitude. Sci Signal 4(200):1–9
96. Grant MP, Cavanaugh A, Breitwieser GE (2015) 14-3-3 proteins buffer intracellular calcium sensing receptors to constrain signaling. PLoS One 10(8):1–20
97. Arulpragasam A, Magno AL, Ingley E, Brown SJ, Conigrave AD, Ratajczak T et al (2012) The adaptor protein 14-3-3 binds to the calcium-sensing receptor and attenuates receptor-mediated Rho kinase signalling. Biochem J 441(3):995–1007
98. Brennan SC, Mun H-C, Leach K, Kuchel PW, Christopoulos A, Conigrave AD (2015) Receptor expression modulates calcium-sensing receptor mediated intracellular Ca^{2+} mobilization. Endocrinology 156(4):1330–1342
99. Chang W, Pratt S, Chen TH, Bourguignon L, Shoback D (2001) Amino acids in the cytoplasmic C terminus of the parathyroid Ca^{2+}−sensing receptor mediate efficient cell-surface expression and phospholipase C activation. J Biol Chem 276(47):44129–44136
100. Leach K, Wen A, Cook AE, Sexton PM, Conigrave AD, Christopoulos A (2013) Impact of clinically relevant mutations on the pharmacoregulation and signaling bias of the calcium-sensing receptor by positive and negative allosteric modulators. Endocrinology 154(3):1105–1116
101. White E, McKenna J, Cavanaugh A, Breitwieser GE (2009) Pharmacochaperone-mediated rescue of calcium-sensing receptor loss-of-function mutants. Mol Endocrinol 23(7):1115–1123
102. Leach K, Wen A, Davey AE, Sexton PM, Conigrave AD, Christopoulos A (2012) Identification of molecular phenotypes and biased signaling induced by naturally occurring mutations of the human calcium-sensing receptor. Endocrinology 153(9):4304–4316
103. Moore CAC, Milano SK, Benovic JL (2007) Regulation of receptor trafficking by GRKs and arrestins. Annu Rev Physiol 69(1):451–482
104. Reyes-Ibarra AP, García-Regalado A, Ramírez-Rangel I, Esparza-Silva AL, Valadez-Sánchez M, Vázquez-Prado J et al (2007) Calcium-sensing receptor endocytosis links extracellular calcium signaling to parathyroid hormone-related peptide secretion via a Rab11a-dependent and AMSH-sensitive mechanism. Mol Endocrinol 21(6):1394–1407
105. Holstein DM, Berg KA, Leeb-Lundberg LMF, Olson MS, Saunders C (2004) Calcium-sensing receptor-mediated ERK1/2 activation requires Gα i2 coupling and dynamin-independent receptor internalization. J Biol Chem 279(11):10060–10069
106. Zhuang X, Northup JK, Ray K (2012) Large putative PEST-like sequence motif at the carboxyl tail of human calcium receptor directs lysosomal degradation and regulates cell surface receptor level. J Biol Chem 287(6):4165–4176
107. Pi M, Oakley RH, Gesty-Palmer D, Cruickshank RD, Spurney RF, Luttrell LM et al (2005) β-arrestin- and G protein receptor kinase-mediated calcium-sensing receptor desensitization. Mol Endocrinol 19(4):1078–1087

108. Lorenz S, Frenzel R, Paschke R, Breitwieser GE, Miedlich SU (2007) Functional desensitization of the extracellular calcium-sensing receptor is regulated via distinct mechanisms: role of G protein-coupled receptor kinases, protein kinase C and β-arrestins. Endocrinology 148(5):2398–2404
109. Huang Y, Niwa JI, Sobue G, Breitwieser GE (2006) Calcium-sensing receptor ubiquitination and degradation mediated by the E3 ubiquitin ligase dorfin. J Biol Chem 281(17):11610–11617
110. Marchese A, Paing MM, Temple BRS, Trejo J (2008) G protein–coupled receptor sorting to endosomes and lysosomes. Annu Rev Pharmacol Toxicol 48(1):601–629
111. Magalhaes AC, Dunn H, Ferguson SSG (2012) Regulation of GPCR activity, trafficking and localization by GPCR-interacting proteins. Br J Pharmacol 165(6):1717–1736
112. Kifor O, Diaz R, Butters R, Kifor I, Brown EM (1998) The calcium-sensing receptor is localized in caveolin-rich plasma membrane domains of bovine parathyroid cells. J Biol Chem 273(34):21708–21713
113. Chini B, Parenti M (2004) G-protein coupled receptors in lipid rafts and caveolae: how, when and why do they go there? J Mol Endocrinol 32(2):325–338
114. Herrera-Vigenor F, Hernández-García R, Valadez-Sánchez M, Vázquez-Prado J, Reyes-Cruz G (2006) AMSH regulates calcium-sensing receptor signaling through direct interactions. Biochem Biophys Res Commun 347(4):924–930
115. Khan SM, Sleno R, Gora S, Zylbergold P, Laverdure J-P, Labbe J-C et al (2013) The expanding roles of Gβγ subunits in G protein-coupled receptor signaling and drug action. Pharmacol Rev 65(2):545–577
116. Khan SM, Sung JY, Hébert TE (2016) Gβγ subunits—different spaces, different faces. Pharmacol Res 111:434–441
117. Hubbard KB, Hepler JR (2006) Cell signalling diversity of the Gqα family of heterotrimeric G proteins. Cell Signal 18(2):135–150
118. Newton AC (2018) Protein kinase C: perfectly balanced. Crit Rev Biochem Mol Biol 53(2):208–230
119. Davies SL, Ozawa A, McCormick WD, Dvorak MM, Ward DT (2007) Protein kinase C-mediated phosphorylation of the calcium-sensing receptor is stimulated by receptor activation and attenuated by calyculin-sensitive phosphatase activity. J Biol Chem 282(20):15048–15056
120. Chang W, Pratt S, Chen TH, Nemeth E, Huang Z, Shoback D (1998) Coupling of calcium receptors to inositol phosphate and cyclic AMP generation in mammalian cells and Xenopus laevis oocytes and immunodetection of receptor protein by region-specific antipeptide antisera. J Bone Miner Res 13(4):570–580
121. Rojas RJ, Yohe ME, Gershburg S, Kawano T, Kozasa T, Sondek J (2007) Gαq directly activates p63RhoGEF and trio via a conserved extension of the Dbl homology-associated pleckstrin homology domain. J Biol Chem 282(40):29201–29210
122. Lutz S, Shankaranarayanan A, Coco C, Ridilla M, Nance MR, Vettel C et al (2007) Structure of Gaq-p63RhoGEF-RhoA complex reveals a pathway for the activation of RhoA by GPCRs. Science 318:1923–1927
123. Van Unen J, Reinhard NR, Yin T, Wu YI, Postma M, Gadella TWJ et al (2015) Plasma membrane restricted RhoGEF activity is sufficient for RhoA-mediated actin polymerization. Sci Rep 5(October):1–16
124. Gagnon AW, Manning DR, Catani L, Gewirtz A, Poncz M, Brass LF (1991) Identification of Gz as a pertussis toxin-insensitive G protein in human platelets and megakaryocytes. Blood 78:1247–1254
125. Jiang M, Bajpayee NS (2009) Molecular mechanisms of go signaling. Neurosignals 17(1):23–41
126. Smrcka AV (2008) G protein βɣ subunits: central mediators of G protein-coupled receptor signaling. Cell Mol Life Sci 65:2191–2214
127. Wettschureck N, Offermanns S (2005) Mammalian G proteins and their cell type specific functions. Physiol Rev 85:1159–1204

128. Kifor O, MacLeod RJ, Diaz R, Bai M, Yamaguchi T, Yao T et al (2001) Regulation of MAP kinase by calcium-sensing receptor in bovine parathyroid and CaR-transfected HEK293 cells. Am J Physiol Renal Physiol 280(2):F291–F302
129. Kozasa T, Hajicek N, Chow CR, Suzuki N (2011) Signalling mechanisms of RhoGTPase regulation by the heterotrimeric G proteins G12 and G13. J Biochem 150(4):357–369
130. Huang CF, Hujer KM, Wu ZZ, Miller RT (2004) The Ca^{2+}-sensing receptor couples to G alpha(12/13) to activate phospholipase D in Madin-Darby canine kidney cells. Am J Physiol Physiol 286(1):C22–C30
131. Rey O, Young SH, Yuan J, Slice L, Rozengurt E (2005) Amino acid-stimulated Ca^{2+} oscillations produced by the Ca^{2+}-sensing receptor are mediated by a phospholipase C/inositol 1,4,5-trisphosphate-independent pathway that requires G12, Rho, filamin-A, and the actin cytoskeleton. J Biol Chem 280(24):22875–22882
132. Mamillapalli R, VanHouten J, Zawalich W, Wysolmerski J (2008) Switching of G-protein usage by the calcium-sensing receptor reverses its effect on parathyroid hormone-related protein secretion in normal versus malignant breast cells. J Biol Chem 283(36):24435–24447
133. Kim W, Takyar FM, Swan K, Jeong J, Vanhouten J, Sullivan C et al (2016) Calcium-sensing receptor promotes breast cancer by stimulating intracrine actions of parathyroid hormone-related protein. Cancer Res 76(18):5348–5360
134. Mamillapalli R, Wysolmerski J (2010) The calcium-sensing receptor couples to Galpha(s) and regulates PTHrP and ACTH secretion in pituitary cells. J Endocrinol 204(3):287–297
135. Emanuel RL, Adler GK, Kifor O, Quinn SJ, Fuller F, Krapcho K et al (1996) CaSR expression and regulation by extracellular calcium in the AtT-20 pituitary cell line. Mol Endocrinol 10(5):555–565
136. Daaka Y, Luttrell LM, Lefkowitz RJ (1997) Switching of the coupling of the beta2-adrenergic receptor to different G proteins by protein kinase A. Nature 390(November):88–91
137. Hodge RG, Ridley AJ (2016) Regulating Rho GTPases and their regulators. Nat Rev Mol Cell Biol 17(8):496–510
138. Vogt S, Grosse R, Schultz G, Offermanns S (2003) Receptor-dependent RhoA activation in G12/G13-deficient cells. Genetic evidence for an involvement of Gq/G11. J Biol Chem 278(31):28743–28749
139. Huang C, Handlogten ME, Tyler Miller R (2002) Parallel activation of phosphatidylinositol 4-kinase and phospholipase C by the extracellular calcium-sensing receptor. J Biol Chem 277(23):20293–20300
140. Davies SL, Gibbons CE, Vizard T, Ward DT, Sarah L, Gibbons CE et al (2006) CaSR induces Rho kinase-mediated actin stress fiber assembly and altered cell morphology, but not in response to aromatic amino acids. Am J Physiol Cell Physiol 290:1543–1551
141. Leitner MG, Michel N, Behrendt M, Dierich M, Dembla S, Wilke BU et al (2016) Direct modulation of TRPM4 and TRPM3 channels by the phospholipase C inhibitor U73122. Br J Pharmacol 173:2555–2569
142. Kukkonen JP (2016) G-protein inhibition profile of the reported Gq/11 inhibitor UBO-QIC. Biochem Biophys Res Commun 469(1):101–107
143. Tu CL, Chang W, Bikle DD (2011) The calcium-sensing receptor-dependent regulation of cell-cell adhesion and keratinocyte differentiation requires rho and filamin a. J Invest Dermatol 131(5):1119–1128
144. Zhang L, Ji T, Wang Q, Meng K, Zhang R, Yang H et al (2017) Calcium-sensing receptor stimulation in cultured glomerular podocytes induces TRPC6-dependent calcium entry and RhoA activation. Cell Physiol Biochem 43:1777–1789
145. Vazquez-Prado J, Bracho-Valdes I, Cervantes-Villagrana RD, Reyes-Cruz G (2016) G pathways in cell polarity and migration linked to oncogenic GPCR signaling: potential relevance in tumor microenvironment. Mol Pharmacol 90(5):573–586
146. Canton J, Schlam D, Breuer C, Gütschow M, Glogauer M, Grinstein S (2016) Calcium-sensing receptors signal constitutive macropinocytosis and facilitate the uptake of NOD2 ligands in macrophages. Nat Commun 7(11284):1–12

147. Chang F, Kim JM, Choi Y, Park K (2018) MTA promotes chemotaxis and chemokinesis of immune cells through distinct calcium-sensing receptor signaling pathways. Biomaterials 150:14–24
148. Gorvin CM, Rogers A, Hastoy B, Tarasov AI, Frost M, Sposini S et al (2018) AP2σ mutations impair calcium-sensing receptor trafficking and signaling, and show an endosomal pathway to spatially direct G-protein selectivity. Cell Rep 22(4):1054–1066
149. Lefkowitz R (2007) Introduction to special section on β-Arrestins. Annu Rev Physiol 69(1)
150. Bouschet T, Martin S, Kanamarlapudi V, Mundell S, Henley JM (2007) The calcium-sensing receptor changes cell shape via a beta-arrestin-1 ARNO ARF6 ELMO protein network. J Cell Sci 120(Pt):2489–2497
151. Thomsen ARB, Hvidtfeldt M, Bräuner-Osborne H (2012) Biased agonism of the calcium-sensing receptor. Cell Calcium 51(2):107–116
152. Hemmings BA, Restuccia DF, Wrana JL, Alto NM, Orth K, Kopan R et al (2012) PI3K-PKB/Akt pathway. Cold Spring Harb Perspect Biol 4:a011189
153. Beurel E, Grieco SF, Jope RS (2015) Glycogen synthase kinase-3 (GSK3): regulation, actions, and diseases. Pharmacol Ther 148:114–131
154. Dvorak MM, Siddiqua A, Ward DT, Carter DH, Dallas SL, Nemeth EF et al (2004) Physiological changes in extracellular calcium concentration directly control osteoblast function in the absence of calciotropic hormones. Proc Natl Acad Sci U S A 101(14):5140–5145
155. Rybchyn MS, Slater M, Conigrave AD, Mason RS (2011) An Akt-dependent increase in canonical Wnt signaling and a decrease in sclerostin protein levels are involved in strontium ranelate-induced osteogenic effects in human osteoblasts. J Biol Chem 286(27):23771–23779
156. Hobson SA, Wright J, Lee F, McNeil SE, Bilderback T, Rodland KD (2003) Activation of the MAP kinase cascade by exogenous calcium-sensing receptor. Mol Cell Endocrinol 200:189–198
157. McNeil SE, Hobson SA, Nipper V, Rodland KD (1998) Functional calcium-sensing receptors in rat fibroblasts are required for activation of SRC kinase and mitogen-activated protein kinase in response to extracellular calcium. J Biol Chem 273(2):1114–1120
158. Wang P, Wang L, Wang S, Li S, Li Y, Zhang L (2015) Effects of calcium-sensing receptors on apoptosis in rat hippocampus during hypoxia/reoxygenation through the ERK1/2 pathway. Int J Clin Exp Pathol 8(9):10808–10815
159. Mizumachi H, Yoshida S, Tomokiyo A, Hasegawa D, Hamano S, Yuda A et al (2017) Calcium-sensing receptor-ERK signaling promotes odontoblastic differentiation of human dental pulp cells. Bone 101:191–201
160. Li T, Sun M, Yin X, Wu C, Wu Q, Feng S et al (2013) Expression of the calcium sensing receptor in human peripheral blood T lymphocyte and its contribution to cytokine secretion through MAPKs or NF-κB pathways. Mol Immunol 53(4):414–420
161. Kong W-Y, Tong L-Q, Zhang H-J, Cao Y-G, Wang G-C, Zhu J-Z et al (2016) The calcium-sensing receptor participates in testicular damage in streptozotocin-induced diabetic rats. Asian J Androl 18:803–808
162. Qi H, Cao Y, Huang W, Liu Y, Wang Y, Li L et al (2013) Crucial role of calcium-sensing receptor activation in cardiac injury of diabetic rats. PLoS One 8(5):e65147
163. Li L, Chen F, Cao YG, Qi HP, Huang W, Wang Y et al (2015) Role of calcium-sensing receptor in cardiac injury of hereditary epileptic rats. Pharmacology 95:10–21
164. Zhen Y, Ding C, Sun J, Wang Y, Li S, Dong L (2016) Activation of the calcium-sensing receptor promotes apoptosis by modulating the JNK/p38 MAPK pathway in focal cerebral ischemia-reperfusion in mice. Am J Transl Res 8(2):911–921
165. Herenbrink CK, Sykes DA, Donthamsetti P, Canals M, Coudrat T, Shonberg J et al (2016) The role of kinetic context in apparent biased agonism at GPCRs. Nat Commun 7:1–14
166. Kenakin T (2011) Functional selectivity and biased receptor signaling. J Pharmacol Exp Ther 336(2):296–302
167. Kenakin T, Christopoulos A (2013) Signalling bias in new drug discovery: detection, quantification and therapeutic impact. Nat Rev Drug Discov 12(3):205–216

168. Leach K, Conigrave AD, Sexton PM, Christopoulos A (2015) Towards tissue-specific pharmacology: insights from the calcium-sensing receptor as a paradigm for GPCR (patho)physiological bias. Trends Pharmacol Sci 36(4):215–225
169. Cavanaugh A, Huang Y, Breitwieser GE (2012) Behind the curtain: cellular mechanisms for allosteric modulation of calcium-sensing receptors. Br J Pharmacol 165(6):1670–1677
170. Cook AE, Mistry SN, Gregory KJ, Furness SGB, Sexton PM, Scammells PJ et al (2015) Biased allosteric modulation at the CaS receptor engendered by structurally diverse calcimimetics. Br J Pharmacol 172(1):185–200
171. Davey AE, Leach K, Valant C, Conigrave AD, Sexton PM, Christopoulos A (2012) Positive and negative allosteric modulators promote biased signaling at the calcium-sensing receptor. Endocrinology 153(3):1232–1241
172. Leach K, Gregory KJ, Kufareva I, Khajehali E, Cook AE, Abagyan R et al (2016) Towards a structural understanding of allosteric drugs at the human calcium-sensing receptor. Cell Res 26(5):574–592
173. Thomsen ARB, Worm J, Jacobsen SE, Stahlhut M, Latta M, Brauner-Osborne H (2012) Strontium is a biased agonist of the calcium-sensing receptor in rat medullary thyroid carcinoma 6-23 cells. J Pharmacol Exp Ther 343(3):638–649
174. Kenakin T (2002) Drug efficacy at G protein–coupled receptors. Annu Rev Pharmacol Toxicol 42(1):349–379
175. Huang C, Sindic A, Hill CE, Hujer KM, Chan KW, Sassen M et al (2007) Interaction of the Ca^{2+}-sensing receptor with the inwardly rectifying potassium channels Kir4.1 and Kir4.2 results in inhibition of channel function. Am J Physiol Renal Physiol 44106:1073–1081
176. Pi M, Spurney RF, Tu Q, Hinson T, Quarles LD (2018) Calcium-sensing receptor activation of Rho involves filamin and Rho-guanine nucleotide exchange factor. Endocrinology 143(January):3830–3838
177. Adjobo-Hermans MJW, Goedhart J, van Weeren L, Nijmeijer S, Manders EMM, Offermanns S et al (2011) Real-time visualization of heterotrimeric G protein Gq activation in living cells. BMC Biol 9(1):32
178. Depry C, Mehta S, Zhang J (2013) Multiplexed visualization of dynamic signaling networks using genetically encoded fluorescent protein-based biosensors. Pflugers Arch Eur J Physiol 465(3):373–381
179. Jean-Alphonse F, Bowersox S, Chen S, Beard G, Puthenveedu MA, Hanyaloglu AC (2014) Spatially restricted G protein-coupled receptor activity via divergent endocytic compartments. J Biol Chem 289(7):3960–3977

Chapter 42
Extracellular Ca^{2+} in Bone Marrow

Ryota Hashimoto

Abstract Our blood serum Ca^{2+} levels are maintained within a narrow range (Ca^{2+} homeostasis) through a complex feedback system. However, local bone marrow Ca^{2+} levels can reach high concentrations, at least transiently, due to bone resorption, which is one of the notable features of the bone marrow stroma. Bone homeostasis is maintained by both the balance between osteoblastic bone formation and osteoclastic bone resorption and the balance of mesenchymal stem cell differentiation into osteoblasts and adipocytes. It has been reported that under culture conditions of infrequent adipocyte differentiation (no treatment with insulin or dexamethasone), high extracellular Ca^{2+} enhances osteoblast but not adipocyte accumulation in bone marrow stromal cells. In contrast, under culture conditions of predominant adipocyte differentiation (treatment with insulin and dexamethasone), high extracellular Ca^{2+} enhances adipocyte but not osteoblast accumulation in bone marrow stromal cells. Thus, the increased extracellular Ca^{2+} caused by bone resorption might enhance osteoblast development to reform missing bone under conditions of infrequent adipocyte differentiation (such as the normal physiological state) and might accelerate adipocyte accumulation instead of osteoblastic bone formation under conditions of predominant adipocyte differentiation (such as aging, obesity, use of glucocorticoids, and postmenopause). Moreover, increased adipocyte accumulation in bone marrow suppresses lymphohematopoiesis and contributes to a dysfunction of osteogenesis.

Keywords Extracellular Ca^{2+} · Hypercalcemia · Hypocalcemia · Bone marrow · Mesenchymal stem cells · Osteoblasts · Adipocytes

R. Hashimoto (✉)
Department of Physiology, Juntendo University Faculty of Medicine, Bunkyo-ku, Tokyo, Japan
e-mail: hryota@juntendo.ac.jp

M. S. Islam (ed.), *Calcium Signaling*, Advances in Experimental Medicine and Biology 1131, https://doi.org/10.1007/978-3-030-12457-1_42

42.1 Introduction

The concentration of calcium ions (Ca^{2+}) is well-controlled both intracellularly and extracellularly to maintain homeostasis in various vertebrates. Although the extracellular concentration of Ca^{2+} is on the order of 1 mM, the intracellular Ca^{2+} concentration ($[Ca^{2+}]_i$) is maintained on the order of 100 nM. Cells can increase their $[Ca^{2+}]_i$ to approximately 1 μM after stimulation. Increased intracellular Ca^{2+} works as a second messenger to control various cell functions (including fertilization, proliferation, differentiation, muscle contraction, and secretion) [1, 2]. The reader can reference other chapters in this book for more information regarding intracellular Ca^{2+}. Changes in extracellular Ca^{2+} concentration also seem to be important in cell functions. The molecular identification of the extracellular calcium-sensing receptor (CaSR), which is a monitor for extracellular Ca^{2+}, has opened up the possibility that Ca^{2+} might also function as a first messenger [3–5]. In this chapter, I focus on extracellular Ca^{2+}, particularly in bone marrow.

42.2 Significance of Maintaining Extracellular Ca^{2+} Levels within a Narrow Range

There is approximately 1.2 kg of total body Ca in adult humans, and approximately 99% of total body Ca exists in bones and teeth, where it is important for supporting the three-dimensional structure of the body. Approximately 1% of total body Ca is present in cells, and 0.1% is present in the extracellular fluid [6–8]. These numbers appear contradictory because the volume of intracellular fluid is approximately twice as great as that of the extracellular fluid,and the intracellular concentration of Ca^{2+} is approximately 10,000 times lower than the extracellular Ca^{2+} concentration. Although the cytoplasmic Ca^{2+} concentration is low, a substantial amount of Ca is intracellularly stored in the endoplasmic reticulum (ER; the ER in striated muscle is structurally and functionally different from that in other cells and is named the sarcoplasmic reticulum (SR)) and mitochondria [9], which results in more Ca content in cells than in the extracellular fluid. Despite the low amount of extracellular Ca^{2+}, the concentration of extracellular Ca^{2+} in blood serum must be strictly regulated within a narrow range. The normal range of blood serum Ca concentrations is 2.2–2.6 mmol/L (8.5–10.5 mg/dL). Blood serum Ca levels greater than 2.6 mmol/L are defined as hypercalcemia, whereas levels less than 2.2 mmol/L are defined as hypocalcemia [10, 11]. Approximately 40% of plasma Ca is protein-bound, and 10% of Ca is in a complex with anions, such as phosphate and citrate; thus, approximately half of plasma Ca is in its free form (ionized form; Ca^{2+}), which is physiologically important [1, 2].

The symptoms of hypercalcemia include drowsiness, constipation, nausea, cardiac arrhythmias, etc., while the typical symptom of hypocalcemia is a tetany, which is a continuous tonic muscle spasm. As Ca^{2+} blocks sodium channels

and inhibits the depolarization of neurons, hypercalcemia raises the threshold for depolarization, while hypocalcemia lowers the threshold for depolarization [12–14]. Thus, high levels of Ca^{2+} decrease the conductance of the neuronal membrane to Na^{+}, which leads to decreased excitability, resulting in hypotonus of muscles. This relation can explain the drowsiness, constipation and nausea in hypercalcemia and tetany in hypocalcemia. This mechanism can also explain bradycardia and atrioventricular block in hypercalcemia. On the other hand, QT shortening in hypercalcemia is explained by a rapid influx of Ca^{2+} through L-type Ca^{2+} channels in cardiomyocytes. The rapid influx of Ca^{2+} quickly reaches the threshold to close the L-type Ca^{2+} channels, thus reducing the duration of phase 2 of the myocardial action potential, which results in QT shortening in hypercalcemia [15, 16]. It has also been suggested that reducing the duration of both phases 2 and 3, during which time Ca^{2+}-activated K^{+} channels increase outward K^{+} currents and accelerate the process of repolarization, contributes to shortening the QT interval in hypercalcemia [17].

42.3 Mechanisms to Maintain Extracellular Ca^{2+} Levels Within a Narrow Range

To prevent these unfavorable symptoms, our blood serum Ca^{2+} levels are maintained within a narrow range (Ca^{2+} homeostasis) through a complex feedback system that involves hormones. First, the CaSR is a G protein-coupled receptor and a monitor of extracellular [Ca^{2+}] [3–5]. In response to increased serum Ca^{2+} levels, the C cells (parafollicular cells) of the thyroid gland [18, 19] increase the secretion of calcitonin (CT). In response to decreased serum Ca^{2+} levels, the chief cells of the parathyroid gland increase parathyroid hormone (PTH) secretion [20].

The main target organs of these hormones are bone, the small intestine, and the kidney (Fig. 42.1). Bone is a vast reservoir of Ca, and the resorption of bone mineral releases Ca^{2+} into the blood [21]. The small intestine is the site where dietary Ca^{2+} is absorbed [22], and the kidney regulates Ca^{2+} excretion [23]. The input of Ca^{2+} into the blood can originate from bone mineral resorption and intestinal Ca^{2+} absorption. Moreover, the output of Ca^{2+} from the blood can occur through bone formation and renal Ca^{2+} excretion. The Ca^{2+} balance is the net sum of these Ca^{2+} inputs and outputs in the body.

PTH increases Ca^{2+} levels in the blood through bone and the kidneys (Figs. 42.2 and 42.4):

1. PTH promotes the absorption of Ca^{2+} from the bone in 2 ways. The rapid phase is an increase in serum Ca^{2+} within minutes. Bone surfaces are covered with a cellular layer containing both osteocytes and osteoblasts that is referred to as the osteocytic membrane. Between the osteocytic membrane and the solid bone, there is bone material, which is not fully crystallized and is referred to as the bone fluid. When PTH binds to receptors on osteoblasts and osteocytes,

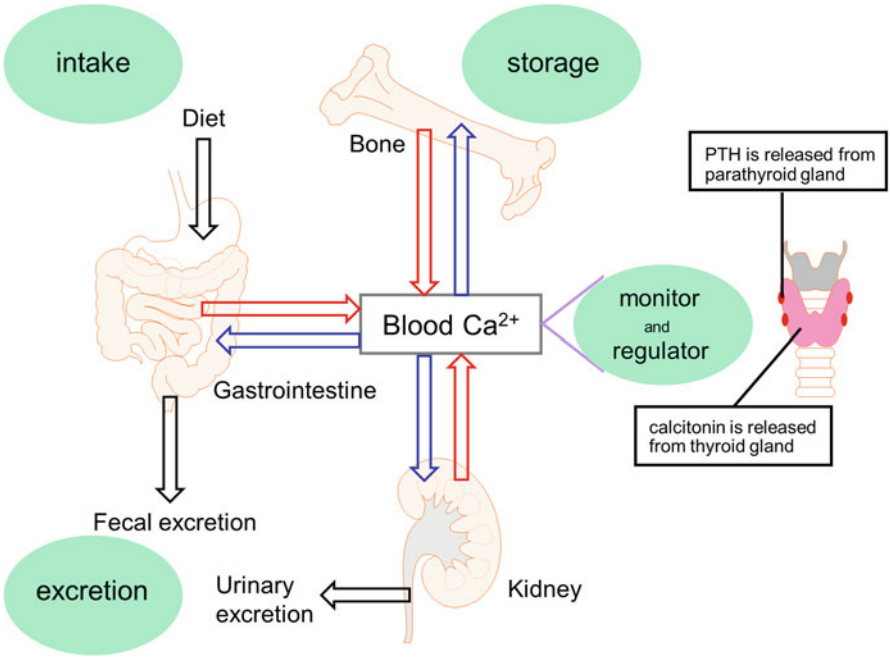

Fig. 42.1 Ca inputs and outputs in the body
Arrows show Ca flows; arrows indicating the increasing and decreasing of blood Ca^{2+} are red and blue, respectively. Bone is a vast reservoir of Ca, and resorption of bone mineral releases Ca^{2+} into the blood. The small intestine is the site where dietary Ca^{2+} is absorbed, and the kidney regulates Ca^{2+} excretion. Input of Ca^{2+} into the blood can originate from bone mineral resorption, intestinal Ca^{2+} absorption, and reabsorption from the kidney. Output of Ca^{2+} from the blood can occur through bone formation, secretion in the colon, and filtration in the kidney. The Ca^{2+} balance is the net sum of these Ca^{2+} inputs and outputs in the body. In response to increased blood Ca^{2+} levels, the C cells of the thyroid gland increase the secretion of calcitonin. In response to decreased blood Ca^{2+} levels, the chief cells of the parathyroid gland increase parathyroid hormone (PTH) secretion

the osteocytic membrane pumps Ca^{2+} from the bone fluid into the extracellular fluid. The slow phase of bone resorption occurs over several days. When osteoblasts and osteocytes are stimulated by PTH, they upregulate the expression of RANK ligand (RANKL) on the plasma membrane. RANKL binds to the receptor activator of the nuclear factor-kappa B (RANK) of osteoclast precursors, which activates signaling pathways that promote osteoclast differentiation and activation. Osteoclasts are bone-resorbing cells and produce a release of Ca^{2+} [24–27].

2. PTH increases the reabsorption of Ca^{2+} in the kidney (i.e., PTH suppresses renal Ca^{2+} excretion) [23].

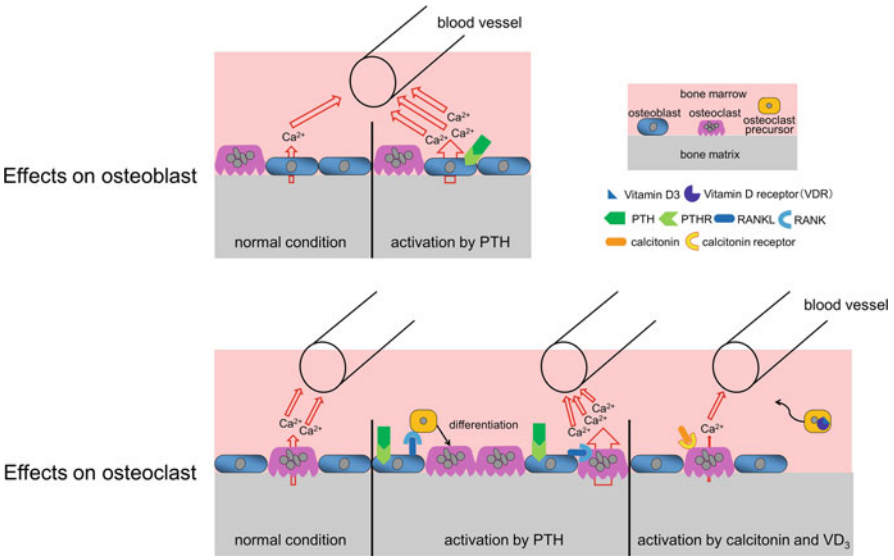

Fig. 42.2 Bone is a vast reservoir of Ca
Bone is a vast reservoir of Ca, and absorption of bone mineral releases Ca^{2+} into the blood. PTH promotes the absorption of Ca^{2+} from the bone in 2 ways. The rapid phase is an increase in serum Ca^{2+} within minutes, which appears to occur through the activation of osteoblasts. The slow phase of bone resorption occurs over several days. When osteoblasts are stimulated by PTH, they upregulate the expression of RANK ligand (RANKL). RANKL binds to receptor activator of nuclear factor-kappa B (RANK) of osteoclast precursors, which activates signaling pathways that promote osteoclast differentiation and activation. Osteoclasts are bone-resorbing cells and produce a release of Ca^{2+}. Calcitonin inhibits the activity of osteoclasts. Active vitamin D enhances the mobilization of osteoclast precursors from the bone to the blood. Thus, calcitonin and vitamin D suppress the absorption of Ca^{2+} from the bone

PTH also converts 25-hydroxyvitamin D to its most active metabolite, 1,25-dihydroxyvitamin D-3 [1,25-$(OH)_2D_3$], in the kidney. Active vitamin D, in turn, acts to suppress PTH production in the parathyroid gland, which is a mild inhibitory system of PTH release [28, 29]. The inhibition of PTH release primarily occurs by a direct effect of the Ca^{2+} concentration at the parathyroid gland as previously described.

Active vitamin D works as a hormone and increases Ca^{2+} levels in the blood through the small intestine and kidney (Figs. 42.2, 42.3 and 42.4):

1. Active vitamin D increases intestinal Ca^{2+} absorption from ingested food [30, 31].
2. Active vitamin D increases the reabsorption of Ca^{2+} in the kidney (i.e., active vitamin D suppresses renal Ca^{2+} excretion) [23].

Active vitamin D has been widely used in the treatment of rickets, osteomalacia, and osteoporosis to prevent bone loss. Active vitamin D enhances the mobilization of osteoclast precursors from the bone to the blood through the suppression of

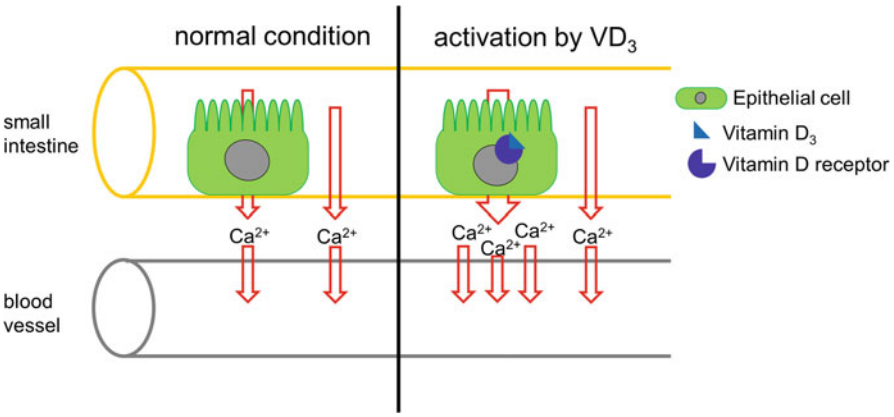

Fig. 42.3 The small intestine is the site where dietary Ca is absorbed
Intestinal Ca^{2+} absorption results in the input of Ca^{2+} into the blood through the transcellular and paracellular pathways. Active vitamin D causes changes in the function of epithelial cells, which enhance Ca^{2+} transport across the intestine

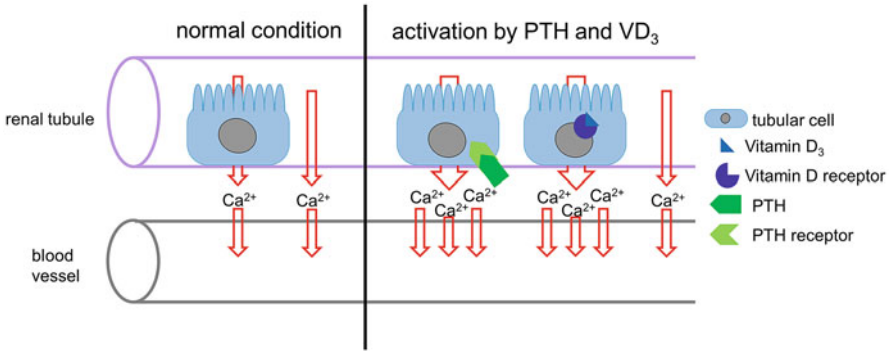

Fig. 42.4 The kidney regulates Ca excretion
The ionized and complexed form of blood Ca (excluding the protein bound form) is freely filtered through the renal glomerulus. Approximately 99% of filtered Ca is reabsorbed in the normal condition into the blood along the renal tubules through the transcellular and paracellular pathways. PTH and active vitamin D change the function of tubular cells, which increase the reabsorption of Ca^{2+} in the kidney (i.e., PTH and active vitamin D suppress renal Ca excretion)

sphingosine-1-phosphate receptor-2 (S1PR2) expression, thereby contributing to limiting osteoclastic bone resorption [32]. This report resolves the discrepancy of in vitro studies that have shown active vitamin D increases the expression of RANKL in osteoblasts and osteocytes, thereby acting as osteoclastogenic, bone-resorbing factors, which is inconsistent with the action of vitamin D on bone in vivo [33].

Calcitonin reduces Ca^{2+} levels in the blood through bone (Fig. 42.2):

1. Calcitonin inhibits the activity of osteoclasts. The osteoclast inhibition reduces the amount of Ca^{2+} released into the blood from bone [34].

The importance of human calcitonin for Ca^{2+} homeostasis in humans has not been established. However, calcitonin of fish (particularly salmon) actively affects human Ca^{2+} homeostasis [34]. In fact, salmon calcitonin has been used therapeutically for the treatment of hypercalcemia and osteoporosis. However, the use of salmon calcitonin is limited because of its involvement in prostate cancer and bone metastasis [35]. Thus, in various ways, these hormones and organs participate in supplying Ca^{2+} to the blood and removing it from the blood when necessary (Figs. 42.1, 42.2, 42.3 and 42.4).

42.4 Extracellular Ca^{2+} in Bone Marrow

42.4.1 In the Developing Skeletal Tissue

Our body length rapidly increases during fetal life and early childhood; however, linear growth progressively slows and eventually ceases during adolescence. Thus, skeletal development begins in the early stages of embryogenesis and continues postnatally until the peak bone mass is achieved in early adulthood. Longitudinal bone growth occurs at the growth plate of the long bone by endochondral ossification, a two-step process in which cartilage is first formed and then remodeled into bone. In the growth plate, chondrocytes proliferate, mature, hypertrophy, reach terminal differentiation and then deposit Ca^{2+}/phosphate-containing mineral in the surrounding matrix. Within this mineralized matrix, chondrocytes release growth factors to induce vascular invasion and guide the differentiation of incoming osteoclast progenitors and osteoblasts, which have respective bone resorbing and bone forming activities that replace cartilage with bone [24, 36, 37]. It has also been reported that hypertrophic chondrocytes can survive and become osteoblasts and osteocytes during endochondral bone formation [38]. Growth plates exist throughout adolescence to support longitudinal bone growth by repeating the previously described cell differentiation programs until the time of growth plate closure in early adulthood.

Accelerated or delayed chondrocyte differentiation leads to disorganized growth plates and retarded bone growth. Various factors, such as PTH-related protein (PTHrP) and insulin-like growth factor 1 (IGF1), and their receptors control the pace of chondrocyte differentiation [39, 40]. Here, I introduce Ca^{2+} and the CaSR as key modulators of chondrocyte differentiation. As previously described, blood serum Ca^{2+} levels are maintained within a narrow range. However, local bone marrow Ca^{2+} levels can reach high concentrations due to bone resorption [41], which is one of the notable features of the bone marrow stroma, indicating that bone marrow stroma can have elevated extracellular Ca^{2+} in vivo, at least transiently. It has been reported that high Ca^{2+} reduces the expression of early differentiation markers of chondrocytes, increases the expression of late differentiation markers, and increases mineral accumulation [42, 43]. In the growth plates, the CaSR is

detected in chondrocytes, and its expression increases as cells hypertrophy [44]. In addition, mice with chondrocyte-specific ablation of the CaSR gene exhibit a shorter, undermineralized skeleton due to delayed differentiation of hypertrophic chondrocytes [45]. These reports suggest that Ca^{2+} promotes chondrocyte differentiation.

42.4.2 In Adulthood – Under a Normal Physiological State

The mature skeleton in adulthood (following growth plate closure) is subsequently maintained by continuous bone remodeling; approximately 10% of the total adult bone mass turns over each year, resulting in a complete regeneration of the adult skeleton every 10 years [46, 47]. Bone remodeling is the replacement of old bone tissue by new bone tissue. It involves the processes of bone resorption by osteoclasts and bone deposition by osteoblasts. Bone homeostasis is maintained by the balance between osteoclastic bone resorption and osteoblastic bone formation [48].

Bone resorption by osteoclasts, which are derived from hematopoietic stem cells, gives rise to the release of Ca^{2+}. Increased Ca^{2+} enhances the proliferation [49, 50], differentiation [51, 52], and chemotaxis [49, 53] of osteoblasts to reform missing bone under a normal physiological state. In bone, the CaSR is detected in osteoblasts and osteocytes [44]. In mice that lack CaSR in immature osteoblasts, bone defects, which result from decreased osteoblast numbers, abnormal mineralizing activities, and increased osteoclast numbers and activities, are observed [45, 54]. These results indicate that the CaSR is directly essential for the proliferation, survival, and maturation of immature osteoblasts and that both the numbers and activities of osteoclasts are regulated through the CaSR of osteoblasts.

The increased Ca^{2+} also directly affects osteoclasts to prevent their further expansion and aberrant bone resorption. High Ca^{2+} inhibits the differentiation [55, 56] and bone-resorbing functions in osteoclasts [57–59] and increases the apoptosis of osteoclasts [56]. CaSR expression has been detected in osteoclasts, and the CaSR is involved in these functions [55, 56, 59]. These balanced bone-resorbing and bone-forming activities through Ca^{2+} sustain a steady bone turnover rate to continuously remodel the skeleton without bone loss [24, 36, 37].

42.4.3 In Adulthood – Under Aging, Obesity, Use of Glucocorticoids, and Postmenopause

Bone marrow stromal cells include mesenchymal stem cells, which are capable of differentiating into osteoblasts, chondrocytes, and adipocytes [60]. Bone homeostasis is maintained by both the balance between osteoblastic bone formation and osteoclastic bone resorption [48] and the balance of mesenchymal stem cell

differentiation into osteoblasts and adipocytes. As described in (42.4.2), high Ca^{2+} enhances the chemotaxis, proliferation, and differentiation of osteoblasts. However, despite the increased Ca^{2+} that results from bone resorption, bone mass declines and adipocyte levels in the marrow increase during aging [61], obesity [61], the use of glucocorticoids [62, 63], and postmenopause [64, 65]. Adipocyte accumulation in bone marrow suppresses lymphohematopoiesis [66, 67] and contributes to a dysfunction of osteogenesis [68–71]. Aging impairs the osteogenic lineage, and high-fat diet feeding activates the expansion of the adipogenic lineage in bone marrow [61]. Glucocorticoids are used in the treatment of a wide range of diseases, and glucocorticoid-induced osteoporosis is the most common secondary cause of osteoporosis. Glucocorticoids commit the differentiation of stem cells to adipocytes in preference to osteoblasts, which results in decreased numbers of osteoblasts. In addition, glucocorticoids enhance the differentiation and activities of osteoclasts [62, 63]. Postmenopausal osteoporosis is associated with estrogen deficiency because the loss of estrogens leads to a reduction in bone formation, an increase in bone resorption, and higher levels of marrow adipogenesis [72–75]. Estrogen promotes osteoblast differentiation and inhibits adipocyte differentiation in bone marrow stromal cells [76]. Osteoporotic fractures are common in patients with chronic kidney disease [77]. However, there are no significant differences in the gene expression of stemness markers or the morphology of adipocytes and osteoblasts differentiated from mesenchymal stem cells between chronic kidney disease and control groups [78].

We have reported that under culture conditions of infrequent adipocyte differentiation (no treatment with insulin or dexamethasone), high extracellular Ca^{2+} enhances osteoblast but not adipocyte accumulation in bone marrow stromal cells [79]. It is important to note that under culture conditions of predominant adipocyte differentiation (treatment with insulin and dexamethasone), high extracellular Ca^{2+} enhances adipocyte but not osteoblast accumulation in bone marrow stromal cells (Fig. 42.5, [79]). In addition, we have reported that another CaSR agonist, Sr^{2+}, enhances adipocyte accumulation under culture conditions of predominant adipocyte differentiation [80]. We have also reported that high extracellular Ca^{2+} enhances the proliferation of bone marrow stromal cells by increasing $[Ca^{2+}]_i$ and enhances their differentiation into adipocytes by decreasing intracellular cAMP (Fig. 42.5, [80, 81]). I propose that the increased extracellular Ca^{2+} caused by bone resorption might enhance osteoblast development to form bone under conditions of infrequent adipocyte differentiation (such as the normal physiological state) and might accelerate adipocyte accumulation instead of osteoblastic bone formation under conditions of predominant adipocyte differentiation (such as aging, obesity, the use of glucocorticoids, and postmenopause). Moreover, increased adipocyte accumulation in bone marrow suppresses lymphohematopoiesis and contributes to a dysfunction of osteogenesis.

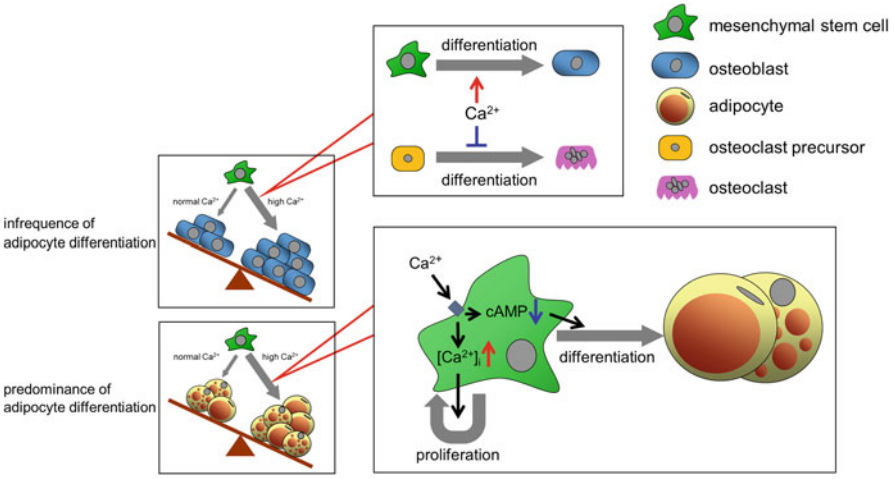

Fig. 42.5 Effects of extracellular Ca^{2+} on bone marrow cells
Bone marrow contains mesenchymal stem cells, which are capable of differentiating into osteoblasts, chondrocytes, and adipocytes. Under conditions of infrequent adipocyte differentiation, high Ca^{2+} enhances the proliferation and osteochondrogenesis of mesenchymal stem cells and suppresses the differentiation of osteoclast precursors. Under conditions of predominant adipocyte differentiation, high Ca^{2+} enhances the proliferation and adipogenesis of mesenchymal stem cells, which might accelerate adipocyte accumulation instead of osteoblastic bone formation. High Ca^{2+} enhances the proliferation of bone marrow stromal cells by increasing $[Ca^{2+}]_i$ and enhances their differentiation into adipocytes by decreasing intracellular cAMP

References

1. Berridge MJ, Bootman MD, Lipp P (1998) Calcium – a life and death signal. Nature 395:645–648
2. Mikoshiba K (2015) Role of IP3 receptor signaling in cell functions and diseases. Adv Biol Reg 57:217–227
3. Brown EM, Gamba G, Riccardi D, Lombardi M, Butters R, Kifor O, Sun A, Hediger MA, Lytton J, Hebert SC (1993) Cloning and characterization of an extracellular Ca^{2+}-sensing receptor from bovine parathyroid. Nature 366:575–580
4. Bouschet T, Henley JM (2005) Calcium as an extracellular signalling molecule: perspectives on the calcium sensing receptor in the brain. C R Biol 328:691–700
5. Hofer AM, Brown EM (2003) Extracellular calcium sensing and signalling. Nat Rev Mol Cell Biol 4:530–538
6. Weaver CM, Gordon CM, Janz KF, Kalkwarf HJ, Lappe JM, Lewis R, O'Karma M, Wallace TC, Zemel BS (2016) The National Osteoporosis Foundation's position statement on peak bone mass development and lifestyle factors: a systematic review and implementation recommendations. Osteoporos Int 27:1281–1386
7. Bushinsky, D. A. (2010) Contribution of intestine, bone, kidney, and dialysis to extracellular fluid calcium content, Clin J Am Soc Nephrol*: CJASN.* 5 Suppl 1, S12-S22
8. Peacock M (2010) Calcium metabolism in health and disease. Clin J Am Soc Nephrol 5(Suppl 1):S23–S30
9. Pizzo P, Pozzan T (2007) Mitochondria-endoplasmic reticulum choreography: structure and signaling dynamics. Trends Cell Biol 17:511–517

10. Stokes VJ, Nielsen MF, Hannan FM, Thakker RV (2017) Hypercalcemic disorders in children. J Bone Miner Res 32:2157–2170
11. Mirrakhimov AE (2015) Hypercalcemia of malignancy: an update on pathogenesis and management. N Am J Med Sci 7:483–493
12. Frankenhaeuser B, Hodgkin AL (1957) The action of calcium on the electrical properties of squid axons. J Physiol 137:218–244
13. Yamamoto D, Yeh JZ, Narahashi T (1984) Voltage-dependent calcium block of normal and tetramethrin-modified single sodium channels. Biophys J 45:337–344
14. Armstrong CM, Cota G (1999) Calcium block of Na^{+} channels and its effect on closing rate. Proc Natl Acad Sci U S A 96:4154–4157
15. Ahmed R, Hashiba K (1988) Reliability of QT intervals as indicators of clinical hypercalcemia. Clin Cardiol 11:395–400
16. Grandi E, Pasqualini FS, Pes C, Corsi C, Zaza A, Severi S (2009) Theoretical investigation of action potential duration dependence on extracellular Ca^{2+} in human cardiomyocytes. J Mol Cell Cardiol 46:332–342
17. Kazama I (2017) High-calcium exposure to frog heart: a simple model representing hypercalcemia-induced ECG abnormalities. J Vet Med Sci 79:71–75
18. Freichel M, Zink-Lorenz A, Holloschi A, Hafner M, Flockerzi V, Raue F (1996) Expression of a calcium-sensing receptor in a human medullary thyroid carcinoma cell line and its contribution to calcitonin secretion. Endocrinology 137:3842–3848
19. McGehee DS, Aldersberg M, Liu KP, Hsuing S, Heath MJ, Tamir H (1997) Mechanism of extracellular Ca^{2+} receptor-stimulated hormone release from sheep thyroid parafollicular cells. J Physiol 502. (Pt 1:31–44
20. Nemeth EF, Steffey ME, Hammerland LG, Hung BC, Van Wagenen BC, DelMar EG, Balandrin MF (1998) Calcimimetics with potent and selective activity on the parathyroid calcium receptor. Proc Natl Acad Sci U S A 95:4040–4045
21. Blair HC, Robinson LJ, Huang CL, Sun L, Friedman PA, Schlesinger PH, Zaidi M (2011) Calcium and bone disease. BioFactors (Oxford, England) 37:159–167
22. Bronner F (2003) Mechanisms of intestinal calcium absorption. J Cell Biochem 88:387–393
23. Jeon US (2008) Kidney and calcium homeostasis. Electrolyte Blood Press 6:68–76
24. Santa Maria C, Cheng Z, Li A, Wang J, Shoback D, Tu CL, Chang W (2016) Interplay between CaSR and PTH1R signaling in skeletal development and osteoanabolism. Semin Cell Dev Biol 49:11–23
25. Levine BS, Rodriguez M, Felsenfeld AJ (2014) Serum calcium and bone: effect of PTH, phosphate, vitamin D and uremia. Nefrologia Publ oficial de la Sociedad Espanola Nefrologia 34:658–669
26. Nakashima T, Hayashi M, Fukunaga T, Kurata K, Oh-Hora M, Feng JQ, Bonewald LF, Kodama T, Wutz A, Wagner EF, Penninger JM, Takayanagi H (2011) Evidence for osteocyte regulation of bone homeostasis through RANKL expression. Nat Med 17:1231–1234
27. Xiong J, Onal M, Jilka RL, Weinstein RS, Manolagas SC, O'Brien CA (2011) Matrix-embedded cells control osteoclast formation. Nat Med 17:1235–1241
28. Henry HL (2011) Regulation of vitamin D metabolism. Best Pract Res Clin Endocrinol Metab 25:531–541
29. Brenza HL, DeLuca HF (2000) Regulation of 25-hydroxyvitamin D3 1alpha-hydroxylase gene expression by parathyroid hormone and 1,25-dihydroxyvitamin D3. Arch Biochem Biophys 381:143–152
30. Veldurthy V, Wei R, Oz L, Dhawan P, Jeon YH, Christakos S (2016) Vitamin D, calcium homeostasis and aging. Bone research 4:16041
31. Bouillon R, Suda T (2014) Vitamin D: calcium and bone homeostasis during evolution. BoneKEy reports 3:480
32. Kikuta J, Kawamura S, Okiji F, Shirazaki M, Sakai S, Saito H, Ishii M (2013) Sphingosine-1-phosphate-mediated osteoclast precursor monocyte migration is a critical point of control in antibone-resorptive action of active vitamin D. Proc Natl Acad Sci U S A 110:7009–7013

33. Suda T, Takahashi F, Takahashi N (2012) Bone effects of vitamin D – discrepancies between in vivo and in vitro studies. Arch Biochem Biophys 523:22–29
34. Naot D, Cornish J (2008) The role of peptides and receptors of the calcitonin family in the regulation of bone metabolism. Bone 43:813–818
35. Warrington JI, Richards GO, Wang N (2017) The role of the calcitonin peptide family in prostate cancer and bone metastasis. Curr Mol Biol Rep 3:197–203
36. Goltzman D, Hendy GN (2015) The calcium-sensing receptor in bone–mechanistic and therapeutic insights. Nat Rev Endocrinol 11:298–307
37. Riccardi D, Brennan SC, Chang W (2013) The extracellular calcium-sensing receptor, CaSR, in fetal development. Best Pract Res Clin Endocrinol Metab 27:443–453
38. Yang L, Tsang KY, Tang HC, Chan D, Cheah KS (2014) Hypertrophic chondrocytes can become osteoblasts and osteocytes in endochondral bone formation. Proc Natl Acad Sci U S A 111:12097–12102
39. Kronenberg HM (2003) Developmental regulation of the growth plate. Nature 423:332–336
40. Wang Y, Cheng Z, Elalieh HZ, Nakamura E, Nguyen MT, Mackem S, Clemens TL, Bikle DD, Chang W (2011) IGF-1R signaling in chondrocytes modulates growth plate development by interacting with the PTHrP/Ihh pathway. J Bone Miner Res 26:1437–1446
41. Silver IA, Murrills RJ, Etherington DJ (1988) Microelectrode studies on the acid microenvironment beneath adherent macrophages and osteoclasts. Exp Cell Res 175:266–276
42. Bonen DK, Schmid TM (1991) Elevated extracellular calcium concentrations induce type X collagen synthesis in chondrocyte cultures. J Cell Biol 115:1171–1178
43. Rodriguez L, Tu C, Cheng Z, Chen TH, Bikle D, Shoback D, Chang W (2005) Expression and functional assessment of an alternatively spliced extracellular Ca^{2+}−sensing receptor in growth plate chondrocytes. Endocrinology 146:5294–5303
44. Chang W, Tu C, Chen TH, Komuves L, Oda Y, Pratt SA, Miller S, Shoback D (1999) Expression and signal transduction of calcium-sensing receptors in cartilage and bone. Endocrinology 140:5883–5893
45. Chang W, Tu C, Chen TH, Bikle D, Shoback D (2008) The extracellular calcium-sensing receptor (CaSR) is a critical modulator of skeletal development. Sci Signal 1:ra1
46. Manolagas SC (2000) Birth and death of bone cells: basic regulatory mechanisms and implications for the pathogenesis and treatment of osteoporosis. Endocr Rev 21:115–137
47. van Schaick E, Zheng J, Perez Ruixo JJ, Gieschke R, Jacqmin P (2015) A semi-mechanistic model of bone mineral density and bone turnover based on a circular model of bone remodeling. J Pharmacokinet Pharmacodyn 42:315–332
48. Sharan K, Siddiqui JA, Swarnkar G, Chattopadhyay N (2008) Role of calcium-sensing receptor in bone biology. Indian J Med Res 127:274–286
49. Yamaguchi, T., Chattopadhyay, N., Kifor, O., Butters, R. R., Jr., Sugimoto, T. & Brown, E. M. (1998) Mouse osteoblastic cell line (MC3T3-E1) expresses extracellular calcium (Ca^{2+}o)-sensing receptor and its agonists stimulate chemotaxis and proliferation of MC3T3-E1 cells, J Bone Miner Res 13, 1530-1538
50. Quarles, L. D., Hartle, J. E., 2nd, Siddhanti, S. R., Guo, R. & Hinson, T. K. (1997) A distinct cation-sensing mechanism in MC3T3-E1 osteoblasts functionally related to the calcium receptor, J Bone Miner Res 12, 393-402
51. Dvorak MM, Siddiqua A, Ward DT, Carter DH, Dallas SL, Nemeth EF, Riccardi D (2004) Physiological changes in extracellular calcium concentration directly control osteoblast function in the absence of calciotropic hormones. Proc Natl Acad Sci U S A 101:5140–5145
52. Yamauchi M, Yamaguchi T, Kaji H, Sugimoto T, Chihara K (2005) Involvement of calcium-sensing receptor in osteoblastic differentiation of mouse MC3T3-E1 cells. Am J Physiol Endocrinol Metab 288:E608–E616
53. Godwin SL, Soltoff SP (1997) Extracellular calcium and platelet-derived growth factor promote receptor-mediated chemotaxis in osteoblasts through different signaling pathways. J Biol Chem 272:11307–11312

54. Dvorak-Ewell MM, Chen TH, Liang N, Garvey C, Liu B, Tu C, Chang W, Bikle DD, Shoback DM (2011) Osteoblast extracellular Ca^{2+} −sensing receptor regulates bone development, mineralization, and turnover. J Bone Miner Res 26:2935–2947
55. Kanatani M, Sugimoto T, Kanzawa M, Yano S, Chihara K (1999) High extracellular calcium inhibits osteoclast-like cell formation by directly acting on the calcium-sensing receptor existing in osteoclast precursor cells. Biochem Biophys Res Commun 261:144–148
56. Mentaverri R, Yano S, Chattopadhyay N, Petit L, Kifor O, Kamel S, Terwilliger EF, Brazier M, Brown EM (2006) The calcium sensing receptor is directly involved in both osteoclast differentiation and apoptosis. FASEB J 20:2562–2564
57. Datta HK, MacIntyre I, Zaidi M (1989) The effect of extracellular calcium elevation on morphology and function of isolated rat osteoclasts. Biosci Rep 9:747–751
58. Zaidi M, Kerby J, Huang CL, Alam T, Rathod H, Chambers TJ, Moonga BS (1991) Divalent cations mimic the inhibitory effect of extracellular ionised calcium on bone resorption by isolated rat osteoclasts: further evidence for a "calcium receptor". J Cell Physiol 149:422–427
59. Kameda T, Mano H, Yamada Y, Takai H, Amizuka N, Kobori M, Izumi N, Kawashima H, Ozawa H, Ikeda K, Kameda A, Hakeda Y, Kumegawa M (1998) Calcium-sensing receptor in mature osteoclasts, which are bone resorbing cells. Biochem Biophys Res Commun 245:419–422
60. Friedenstein AJ, Gorskaja JF, Kulagina NN (1976) Fibroblast precursors in normal and irradiated mouse hematopoietic organs. Exp Hematol 4:267–274
61. Ambrosi TH, Scialdone A, Graja A, Gohlke S, Jank AM, Bocian C, Woelk L, Fan H, Logan DW, Schurmann A, Saraiva LR, Schulz TJ (2017) Adipocyte accumulation in the bone marrow during obesity and aging impairs stem cell-based hematopoietic and bone regeneration. Cell Stem Cell 20:771–784.e6
62. Compston J (2018) Glucocorticoid-induced osteoporosis: an update. Endocrine 61:7–16
63. Hachemi Y, Rapp AE, Picke AK, Weidinger G, Ignatius A, Tuckermann J (2018) Molecular mechanisms of glucocorticoids on skeleton and bone regeneration after fracture. J Mol Endocrinol 61:R75–r90
64. Beekman KM, Veldhuis-Vlug AG, den Heijer M, Maas M, Oleksik AM, Tanck MW, Ott SM, van't Hof RJ, Lips P, Bisschop PH, Bravenboer N (2017) The effect of raloxifene on bone marrow adipose tissue and bone turnover in postmenopausal women with osteoporosis. Bone
65. Syed FA, Oursler MJ, Hefferanm TE, Peterson JM, Riggs BL, Khosla S (2008) Effects of estrogen therapy on bone marrow adipocytes in postmenopausal osteoporotic women. Osteoporos Int 19:1323–1330
66. Naveiras O, Nardi V, Wenzel PL, Hauschka PV, Fahey F, Daley GQ (2009) Bone-marrow adipocytes as negative regulators of the haematopoietic microenvironment. Nature 460:259–263
67. Payne MW, Uhthoff HK, Trudel G (2007) Anemia of immobility: caused by adipocyte accumulation in bone marrow. Med Hypotheses 69:778–786
68. Elbaz A, Wu X, Rivas D, Gimble JM, Duque G (2010) Inhibition of fatty acid biosynthesis prevents adipocyte lipotoxicity on human osteoblasts in vitro. J Cell Mol Med 14:982–991
69. Maurin AC, Chavassieux PM, Frappart L, Delmas PD, Serre CM, Meunier PJ (2000) Influence of mature adipocytes on osteoblast proliferation in human primary cocultures. Bone 26:485–489
70. Maurin AC, Chavassieux PM, Vericel E, Meunier PJ (2002) Role of polyunsaturated fatty acids in the inhibitory effect of human adipocytes on osteoblastic proliferation. Bone 31:260–266
71. Lecka-Czernik B, Moerman EJ, Grant DF, Lehmann JM, Manolagas SC, Jilka RL (2002) Divergent effects of selective peroxisome proliferator-activated receptor-gamma 2 ligands on adipocyte versus osteoblast differentiation. Endocrinology 143:2376–2384
72. Eastell R, O'Neill TW, Hofbauer LC, Langdahl B, Reid IR, Gold DT, Cummings SR (2016) Postmenopausal osteoporosis. Nat Rev Dis Primers 2:16069
73. Levin VA, Jiang X, Kagan R (2018) Estrogen therapy for osteoporosis in the modern era. Osteoporos Int 29:1049–1055

74. Nuttall ME, Gimble JM (2000) Is there a therapeutic opportunity to either prevent or treat osteopenic disorders by inhibiting marrow adipogenesis? Bone 27:177–184
75. Zallone A (2006) Direct and indirect estrogen actions on osteoblasts and osteoclasts. Ann N Y Acad Sci 1068:173–179
76. Okazaki R, Inoue D, Shibata M, Saika M, Kido S, Ooka H, Tomiyama H, Sakamoto Y, Matsumoto T (2002) Estrogen promotes early osteoblast differentiation and inhibits adipocyte differentiation in mouse bone marrow stromal cell lines that express estrogen receptor (ER) alpha or beta. Endocrinology 143:2349–2356
77. Lips P, Goldsmith D, de Jongh R (2017) Vitamin D and osteoporosis in chronic kidney disease. J Nephrol 30:671–675
78. Yamada A, Yokoo T, Yokote S, Yamanaka S, Izuhara L, Katsuoka Y, Shimada Y, Shukuya A, Okano HJ, Ohashi T, Ida H (2014) Comparison of multipotency and molecular profile of MSCs between CKD and healthy rats. Hum Cell 27:59–67
79. Hashimoto R, Katoh Y, Nakamura K, Itoh S, Iesaki T, Daida H, Nakazato Y, Okada T (2012) Enhanced accumulation of adipocytes in bone marrow stromal cells in the presence of increased extracellular and intracellular [Ca(2)(+)]. Biochem Biophys Res Commun 423:672–678
80. Hashimoto R, Katoh Y, Miyamoto Y, Itoh S, Daida H, Nakazato Y, Okada T (2015) Increased extracellular and intracellular Ca(2)(+) lead to adipocyte accumulation in bone marrow stromal cells by different mechanisms. Biochem Biophys Res Commun 457:647–652
81. Hashimoto R, Katoh Y, Miyamoto Y, Nakamura K, Itoh S, Daida H, Nakazato Y, Okada T (2017) High extracellular Ca^{2+} enhances the adipocyte accumulation of bone marrow stromal cells through a decrease in cAMP. Cell Calcium 67:74–80

Chapter 43
Calcium in Cell-Extracellular Matrix Interactions

Sandeep Gopal, Hinke A. B. Multhaupt, and John R. Couchman

Abstract In multicellular organisms, the cells are surrounded by persistent, dynamic extracellular matrix (ECM), the largest calcium reservoir in animals. ECM regulates several aspects of cell behavior including cell migration and adhesion, survival, gene expression and differentiation, thus playing a significant role in health and disease. Calcium is reported to be important in the assembly of ECM, where it binds to many ECM proteins. While serving as a calcium reservoir, ECM macromolecules can directly interact with cell surface receptors resulting in calcium transport across the membrane. This chapter mainly focusses on the role of cell-ECM interactions in cellular calcium regulation and how calcium itself mediates these interactions.

Keywords Extracellular matrix · Cell adhesion · Calcium · Proteoglycans · Integrins · Syndecans · TRP channels · Focal adhesions · Actin cytoskeleton · Mechanosensing

43.1 Introduction

Extracellular matrix (ECM) is a complex network of proteins and polysaccharides that provides mechanical stability for tissues while maintaining its dynamic nature. Major structural proteins in the ECM include collagens, elastin and their associated

S. Gopal (✉)
Development and Stem Cells Program, Monash Biomedicine Discovery Institute, Department of Anatomy and Developmental Biology, Monash University, Clayton, VIC, Australia
e-mail: sandeep.gopal@monash.edu

H. A. B. Multhaupt · J. R. Couchman
Biotech Research & Innovation Center, University of Copenhagen, Copenhagen, Denmark
e-mail: hinke.multhaupt@bric.ku.dk; john.couchman@bric.ku.dk

M. S. Islam (ed.), *Calcium Signaling*, Advances in Experimental Medicine and Biology 1131, https://doi.org/10.1007/978-3-030-12457-1_43

glycoproteins, laminins, fibronectin, proteoglycans and matricellular proteins (e.g. tenascins, osteopontin, thrombospondins). The proportion of structural proteins in the ECM varies between tissue types, thus providing a varying degree of stiffness and elasticity to ECM as required [1]. ECM composition is known to change both spatially and temporally as well as in response to inflammation and disease. ECM, initially purported to be an inert support structure, in fact regulates many functions in animals including cell adhesion, durotaxis, gene expression and cell differentiation.

ECM is the largest source of free calcium ions in a multicellular organism, with a 10,000 fold higher concentration than cytosol [2]. The free calcium ion concentration in ECM is approximately 1.2 mM. From the ECM, calcium enters cells via voltage gated or ligand gated calcium channels present in the plasma membrane. As with many interactions, ECM-calcium cross-talk is a two-way conversation that plays a significant role in cell signaling pathways. While ECM regulates the calcium entry into the cell by various means, the calcium maintains a strong influence over several cell-ECM interactions. The entry of calcium from ECM into the cells is a tightly regulated process that involves several calcium channels and regulators, and sometimes cell structures such as focal adhesions and cytoskeleton [3–5].

Calcium can affect most of the aspects of a cell's life from fertilization to apoptosis [6, 7]. At cellular level, calcium ions are a key second messenger in many signaling pathways. It can bind to hundreds of molecules, in some cases to trigger various cellular signaling pathways and in others to regulate intracellular calcium level itself. Binding affinities of calcium to cellular proteins range from nM to mM range with many protein conformational properties dependent on the interaction. This chapter focusses on the role of calcium in regulating cell-ECM interactions and the role of ECM in controlling cellular calcium.

43.2 Role of Calcium in ECM and Cells

In a multicellular mammalian system, cells are always under persistent, dynamic mechanical tension [8–10]. Cells exert tension not only on extracellular matrix but also on neighboring cells. The mechanical tension exerted on the matrix is mediated through junctions such as focal adhesions that are connected to the actin cytoskeleton. Intra- and extracellular calcium levels are powerful regulators of cytoskeletal dynamics and cell-matrix adhesion [11]. Such effects of calcium on cytoskeletal assembly and contractility are due to the results of calcium interaction with several cytoskeletal proteins [12–14] . Roles for calcium in cytoskeletal maintenance are well known, though a comprehensive picture of the mechanisms remains unclear. This is mainly due to the presence of a multitude of protein networks in the cytoskeleton and junctions, which are subject to both rapid and long-term dynamics.

43.2.1 Matrix proteins

Mechanotransduction is an important component of cell survival, where mechanical forces influence signaling cascades and cell behavior. As ECM directly interacts with cells, there will be a significant tension applied to the cell membrane. While mechanotransduction pathways involve cell surface receptors, ion channels, actin cytoskeleton and tyrosine protein kinases, the role of ECM proteins appears to be essential. Previous reports have shown that the several of the ECM components regulate cytosolic calcium levels. At the same time, they have the ability to bind to calcium in the ECM. Depleting or enriching ECM components can significantly alter the mechanical properties of the matrix, which in turn affects the mechanically sensitive channels. For instance, TRP channels, also known as stretch activated channels, are regulated by extracellular tension derived from cell-ECM interactions. This section lists some ECM proteins and how they are connected with calcium homeostasis in the tissues.

43.2.1.1 Fibronectin

Fibronectin is a well characterized and abundant ECM proteins of vertebrates [15]. It can interact with transmembrane proteoglycans and integrins, two major cell surface receptor families that can initiate an array of downstream signaling. Early reports using *Entamoeba histolytica* trophozoites, an active feeding stage of a sporozoan parasite, showed that direct contact with fibronectin induces the cytosolic calcium spikes [16]. Similar results were observed in multiple cell types where fibronectin influenced the cytosolic calcium level [17]. The effect of fibronectin on calcium was later shown to be the result of engagement of its integrin-binding Arg-Gly-Asp motif with subsequent activation of stretch-activated calcium channels (Fig. 43.1) [18]. On the other hand, the significant increase in the fibronectin deposition in the ECM during wound healing is achieved through the TRPC3-induced transcription of fibronectin [19]. Recently identified role of syndecan-4 proteoglycan in cytosolic calcium regulation also appeared to be initiated by fibronectin. It has been demonstrated that the fibroblasts plated on the integrin-binding region of fibronectin (FN110-KDa, Fig. 43.1a) have an elevated calcium level, which can be reduced to the levels observed on whole fibronectin by the addition of solution containing the heparin-binding region, Hep II (fibronectin type III repeats 12–15, Fig. 43.1) [20]. This addition of Hep II domain also rectified the defects in focal adhesions and cytoskeleton observed in the fibroblasts plated on FN110-KDa [21]. Other syndecans also regulate cytosolic calcium, though their connection with fibronectin is unclear. This role of proteoglycans in calcium regulation will be discussed below.

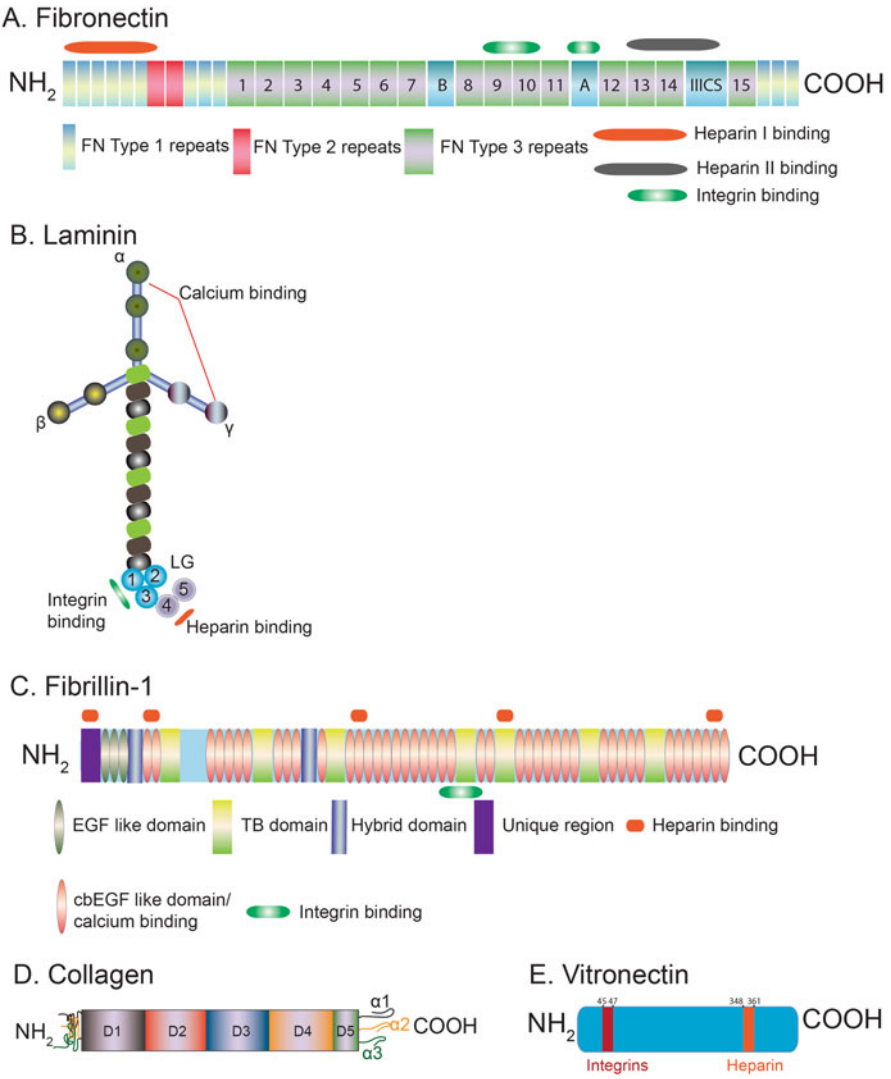

Fig. 43.1 Schematics of major calcium responsive/ regulating ECM molecules. (**a**) Fibronectin structure showing the integrin and heparin (heparan sulfate analogue) interacting domains. (**b**) Laminins are formed of one α, one β and one γ chains. The integrin and heparin interacting regions are shown in the figure. Calcium binding domains of laminins are located on the α and γ arms. (**c**) Fibrillin-1 structure showing the integrin and heparin interacting domains and high calcium affinity cbEGF like domains. (**d**) Collagen I monomer is comprised of three alpha chains forming a supercoiled triple helix. Final structure of collagen monomer assumes a rod-like structure of 300 nm length. Like other ECM molecules, collagen interacts with integrins and heparan sulfate chains. *E* Vitronectin interacts with integrins and heparan sulfate chains

43.2.1.2 Laminins

Laminins are the second most abundant structural component of basement membranes, with an ability to interact with integrins, dystroglycan receptors and negatively charged moieties such as heparan sulfate chains and sulfatides. A total 15 laminin polypeptides are expressed in vertebrates and several of them appear to have calcium binding sites or calcium-induced self-assembly mechanisms [22–24]. Laminins are composed of three distinct subunits (α, β, and γ) (Fig. 43.1b) that self-assemble in a calcium-dependent manner [24]. The self-assembly of laminin is further enhanced during their aggregation onto lipid bilayers where both aggregation and self-assembly depends on calcium binding [25]. There is a limited knowledge regarding the role of laminins in regulating cytosolic calcium. Addition of soluble laminin-211 (α2β1γ1), but not laminin-111 (α1β1γ1) to osteoclast precursor cells resulted in the release of calcium from intracellular calcium stores [26]. The more recent reports suggest that the laminin β2 chain interacts directly with voltage-gated calcium channels in neuromuscular junctions [27–29] where they control calcium sensitivity during neurotransmission [30]. This interaction between laminin β2 and voltage gated calcium channels may involve cytoskeletal proteins such as spectrins, plectin 1, dystrophin, myosin-1and α3 integrin cell surface receptor, though the details remain unknown [29, 31]. It is unclear how widespread the interaction between laminin β2 and voltage gated calcium channel property may be. However, a mutation in laminin α1 subunit in patients with cerebellar ataxia resulted in defective cellular calcium homeostasis [32]. Taken together, it is clear that laminins require calcium for structural integrity, but in turn may influence cytosolic calcium levels.

43.2.1.3 Fibrillin

Fibrillins are large ECM proteins that polymerize to form microfibrils, which can contribute to the architecture of extracellular matrix, including elastic fiber assemblies. Mutations in fibrillins are known to be associated with Marfan syndrome [33], a genetic disease leading to structural defects in connective tissue. At least four isoforms (fibrillin 1–4) of fibrillins are identified so far, with fibrillin-1 being the most studied. The role of calcium in microfibril organization was identified when incubation with EGTA or EDTA resulted in the disintegration of microfibril structure [34, 35]. Fibrillins possess multiple tandem repeats of epidermal growth factor-like motifs that can bind calcium with high affinity, an essential requirement in microfibril formation [36, 37]. Reports suggest that fibrillins contain calcium-binding epidermal growth factor (cbEGF) like domains that are interspersed with TGF-β binding protein like domains [38]. The interdomain interactions between cbEGF and TGF-β binding protein like domain appear to be strongly dependent on calcium [39]. It was shown that the calcium binding to cbEGF like domain plays a major role in maintaining fibrillin-1 structure by restricting the mobility of the interdomain regions [40]. In addition, calcium also appears to be essential for the homotypic and heterotypic interactions between fibrillin isoforms [41, 42].

Finally, calcium plays important role in fibrillin interactions with several matrix proteins including versican, aggrecan, fibulins and HSPGs [43–46]. The presence of calcium ions in the ECM embued fibrillin with resistance to proteolytic enzymes such as trypsin, matrix metalloproteinases and plasmin [47, 48]. While fibrillins can initiate cell signaling through cell surface receptors such as integrins and syndecan HSPGs [43, 49, 50], currently there is no direct evidence to suggest they can regulate cytosolic calcium, but seems likely given other data on these receptor systems.

43.2.1.4 Collagen

Collagens are the most abundant proteins of the ECM. There are at least 28 types of chronologically named (I–XXVIII, Fig. 43.1d) collagens identified in vertebrates. While collagens are important in calcification of cartilage during aging, this section of the chapter focuses only on the role of collagen in calcium mobility in cells. It has been debated for a long time whether the collagen can induce a calcium rise in cells. Most of the information about the role of collagen in calcium regulation comes from platelets. Some reports suggest that collagen raises cytosolic calcium levels in human platelets, possibly by activating calcium channels via phospholipase C and inositol 1,4,5 trisphosphate [51–53]. This observation was later supported when the platelets showed a steep increase in calcium levels when they were in contact with type 1 Collagen [54]. As the most abundant protein in ECM, the collagen contributes to the stiffness and tensile strength of the matrix. As mentioned previously, the ECM-mediated tension can alter calcium levels in cells. Studies using human mesenchymal stem cells plated on the collagen showed that calcium oscillations in the cells vary depending on the rigidity of the collagen matrix [55]. The average calcium spikes in the cells were increased with the increase in rigidity of the collagen matrix, indicating the calcium oscillations are sensitive to mechanical cues. While the study addressed the role of collagen rigidity, it may well be true for several other proteins since nearly all structural ECM proteins can contribute to matrix stiffness.

43.2.2 Focal Adhesions

Aside from hemidesmosomes, the major points of contacts with cells and ECM are focal adhesions (Fig. 43.2), a group of mechanosensitive, macromolecular assemblies that anchor cells to ECM. While multiple studies collectively identified a total of 2000 proteins in the focal adhesions depending on the cell types and the analysis methods, the core adhesome formed of approximately 60 proteins [56]. Focal adhesions are formed at a specific range when the plasma membrane is at a distance of 15 nm from the ECM. Focal adhesions are present at the termini of

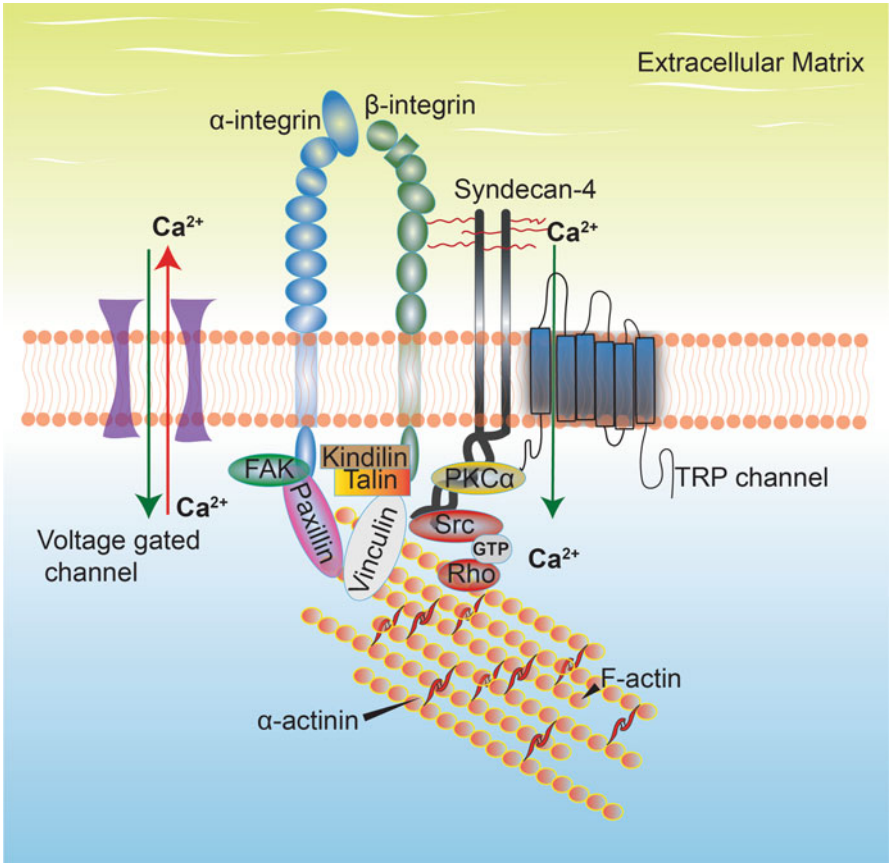

Fig. 43.2 Cell surface receptors in the focal adhesion formation, cytoskeletal organization and calcium regulation. The cell surface receptors integrins and syndecan-4 bind with ECM proteins to activate a large group of downstream signaling molecules to control focal adhesion and cytoskeletal dynamics. Integrins bind directly or indirectly to FAK, talin, kindlin and paxillin through its cytoplasmic domain to trigger focal adhesion formation, whereas syndecan-4 interacts with PKCα and trigger further downstream signaling. The focal adhesions are attached to the actin cytoskeleton formed by F-actin bundles connected by α-actinin, where the vinculin acts as a mechano-transducer between the cytoskeleton and focal adhesions. The synergistic action of integrins and syndecan-4 is essential for the formation of focal adhesions and organized cytoskeleton. Mechano-sensitive (TRP channels) and/or voltage gated channels are regulated by both integrins and syndecans, where they form complexes and appear to co-localize with other focal adhesion molecules

actin bundles (stress fibers), where, in a protein-dense plaque, they are connected to receptors, notably integrins (Fig. 43.2). Key protein components of the plaque include talin, vinculin, paxillin, kindlins and kinases (Fig. 43.2) [56–58]. Focal adhesion dynamics are maintained by localized cooperative signaling between integrins and syndecan-4 proteoglycans [59, 60]. While integrins and syndecans may be mechanoreceptors and have limited effects on transcription, they control

the localization of several focal adhesion proteins and signal survival in anchorage-dependent cells. It has been shown that the absence of integrin or syndecan can cause a significant reduction in the number and size of focal adhesions formed by cells.

It is well known that the focal adhesions respond to calcium changes in the cells. An early report showed that calcium affects the morphology of spreading human platelets. While the report did not specifically use the terminology 'focal adhesions', it mentioned the calcium dependent formation of small discrete, optically denser regions suggesting the presence of focal specializations at the ventral cell surface [61]. Later reports showed cells attach to fibronectin in calcium dependent manner. Even though the cell surface receptors involved was unknown at the time, one mechanism of attachment to fibronectin was shown to be mediated by glycosaminoglycan sugar chains, specifically heparan sulfate chains [62].

The role of calcium in adherent cells was further emphasized when enhanced calcium influx was shown to induce phosphorylation of focal adhesion-associated tyrosine kinase, FAK in adherent cells [63, 64]. Later reports suggested that FAK phosphorylation was coordinated by protein kinase C and integrins [65] and calcium spikes have been reported in focal adhesion complexes. Reports later indicated that protein kinase C inhibition resulted in marked reduction in tyrosine phosphorylation of paxillin [66, 67]. Recently, it was found that the PKC inhibition indeed resulted in an elevation of cytosolic calcium [20]. Similar mechanisms were identified with FAK and paxillin phosphorylation in response to external mechanical force, a known inducer of calcium changes in the cytosol [18, 68, 69]. A clearer observation regarding the role of calcium in focal adhesion turnover came from studies where fluorescent-tagged FAK was followed during focal adhesion formation. It appeared that the post photo-bleaching recovery of FAK at the focal adhesions was slowed by calcium elevation [11].

Until recently, no calcium channels were identified in any focal adhesion specific proteomic analysis (see review by [70]. However, it could be due to the low expression of channels in the focal adhesions making them difficult to detect. One of the latest mass spectrometry analyses of focal adhesions revealed that the presence of SLC9A1, SLC16A3, KCNH2, PKD-1 and TRPM7 in the focal adhesions. Recent studies by immunofluorescence showed that focal adhesions contain stretch-activated channels TRPC7 (Fig. 43.3) and TRPM4 whose expression changes appears to affect focal adhesion size [20, 71]. Currently, there is no evidence indicating that these channels form heterodimers in the focal adhesions. The observation that these channels are present in focal adhesions is very recent and their function in the focal adhesions remains unclear. TRPM4 itself is not a calcium channel, though it can be activated by calcium. Given the presence of TRPC7, it is possible the TRPM4 is activated by the calcium entry through TRPC7. The transient silencing of TRPM4 appears to lead to larger focal adhesions, leading to the speculation that TRPM4 is involved in focal adhesion turnover [71].

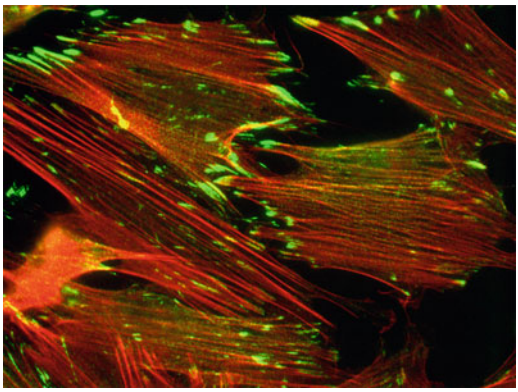

Fig. 43.3 The cells showing staining for TRPC7 channel (green) and filamentous actin (red). The TRPC7 channels appears to localize at the end of actin filaments, where the actin cytoskeleton attaches to the focal adhesions

43.2.3 The Actin Cytoskeleton

Cytoskeleton provides rigidity to the cells and facilitates cell shape maintenance. In addition, the actin cytoskeleton plays important roles in cell migration and tension sensing [72–74]. Actin forms filamentous bundles that are bridged by a second protein called α-actinin [75, 76]. In non-muscle cells, these structures are mostly visible in activated (myo)fibroblasts. Over 20 years ago the ability of the cells to contract in response to external mechanical forces was shown to be dependent on calcium influx from the ECM [77]. One of the initial observations showed that the addition of calcium to *Dictyostelium*, an eukaryotic, phagotrophic bacterivore led to restricted depolymerization of actin filaments where ends of the actin filaments were resistant to depolymerization [78]. Later, α-actinin, a 34 kDa actin-bundling protein and gelation factor (ABP-120) were identified as the components that bind to calcium in order to promote this process [79–81]. Studies using mutant α-actinin, 34 kDa actin-bundling protein, and knock-out models showed that the actin bundling was reduced in the cells and leading to a fragile, loose cytoskeleton [82]. Research from Edwards and Booth suggested a number of cytoskeletal proteins of molecular mass 72, 69, 38, 36 and 32 kDa were regulated by calcium concentration. Depletion of calcium using EGTA suggested the release of these proteins from their complexes led to a more open meshwork of disorganized cytoskeleton. This research also provided the first evidence for a possible effect of local calcium concentration on cytoskeletal proteins [83]. Previously, it was shown that increase in calcium concentration induced degeneration of monkey and human peripheral nerves due to cytoskeletal collapse [84]. Peripheral nerves already have comparatively high calcium concentrations and further increase in this calcium initiated the cytoskeletal collapse. However, lowering the calcium concentration did not produce significant changes during the examined time period [84]. These findings were further consolidated when the role of calcium in actin cytoskeletal organization was identified in osteoblasts [85]. Parathyroid hormone is necessary for maintaining optimum blood calcium concentration level by controlling calcium

release from bone. The treatment of osteoblasts with parathyroid hormone resulted in changes in osteoblast cytoskeletal organization due to an elevation in cytosolic calcium. This increase in the intracellular calcium concentration resulted in an impaired cytoskeleton leading to the retraction of the cells and a reduction of triton X-100 insoluble cytoskeletal components, suggesting a decrease in polymerized actin and tubulin in the cytoskeleton [85]. Furthermore, later research showed that the force-induced actin reorganization depended on cytosolic calcium levels and tyrosine phosphorylation of several cytoskeletal proteins including paxillin [86]. Another output of calcium-cytoskeleton cross-talk is the rapid actin assembly and disassembly caused by calcium oscillations in response to local flux through the membrane [87]. These observations essentially led to the idea that the integrity of cytoskeleton depends on maintaining optimum intracellular calcium concentrations.

Eukaryotic cells respond to a calcium-mediated effect on cytoskeleton mainly through calmodulin (**CAL**cium-**MODUL**ated prote**IN,** CaM), a calcium binding messenger protein [88]. Calmodulin is a small protein (17 kDa) with four helix-loop-helix structural domains called EF hands. Similar to another cytoskeleton protein α-actinin, calmodulin can sequester calcium ions in the EF hands which are essential for their structure [89, 90]. Calmodulin also possesses a hinged region giving structural flexibility to the backbone that helps to wrap around the target molecule. The calcium interaction property of calmodulin is interesting since it can target several cellular proteins that are not able to interact directly with calcium, thus acting as a signal transducer. The role of calcium/calmodulin in cell signaling is best exemplified by the major effector protein, calcium/calmodulin-dependent protein kinase II (CaMKII), a family of serine/threonine-specific protein kinases. CaMKII is often identified as a 'structural kinase' that can interact with cytoskeleton, a process that can be influenced by laminin interactions at the cell surface [91]. For instance, the variable region of oligomeric CaMKIIβ has an F-actin binding domain that directs CaMKIIβ to stress fibers. This promotes the localization of CaMKIIβ to the cytoskeleton [92, 93]. Calcium/calmodulin interactions triggers CaMKII phosphorylation by direct binding. As the calcium/calmodulin and F-actin binding site in CaMKII are located in proximity, it is possible that calcium/calmodulin binding may block CaMKII-F-actin interaction leading to cytoskeletal changes [93]. This observation was supported by using CaMKII mutant that was unable to interact with calcium/calmodulin, where the CaMKII interaction with filamentous actin was enhanced. Taken together, current knowledge suggests that the increase in calcium in cells may lead to calcium/calmodulin binding to CaMKII that governs the removal of CaMKII from actin cytoskeleton. Since binding of CaMKII to F-actin is required for stability of F-actin bundles [94], the increase in calcium may eventually results in a disassembled cytoskeleton. These observations were confirmed by biochemical assays suggesting CaMKII indeed regulates actin assembly, structure and remodeling [95]. In addition, in vitro studies suggested that actin could be phosphorylated exclusively by CaMKIIβ but not by other isoforms. This could be enhanced by the depletion of calcium/calmodulin complexes [96]. A more recent observation aligns with the findings where elevation of calcium through TRPC7 channel resulted in disorganized cytoskeleton [20]. The GTPase activating protein,

IQGAP was identified as another modulator between calmodulin and cytoskeleton. Knocking down of IQGAP1 led to the reduction of calmodulin in the actin rich cortex of mast cells. Cells exhibited changes in local calcium concentration followed by reorganization of cytoskeleton [97].

Importantly, cytosolic calcium regulates not only the cytoskeletal organization but also contractility. In this respect, myosin is the key protein. Myosins are family of at least 20 motor proteins involved in actin-based eukaryotic cell motility [98–100]. The head of the myosin protein contains the actin- and nucleotide-binding sites and the catalytic domain consisting of an α-helical strand, which is stabilized by the binding of calmodulin or calmodulin-like light chain subunits [101]. The C-terminal region, which is distinct for each myosin class, mediates the association of myosins with each other and anchoring them for movement relative to actin filaments [102]. Intracellular calcium levels heavily influence the activity of specific myosins. Most of the members of myosin family are inactive in the absence of calcium. For example, myosin V and VII have been shown by electron microscopy and analytical ultracentrifugation to fold into a more compact, inactive structure in the absence of calcium [103]. On the other hand increased cytosolic calcium leads to reductions in the progressive movement of motor proteins, which is speculated to result from the dissociation of calmodulin light chain from heavy chain affecting the stability of myosin [104]. Moreover, calcium levels have a major influence on interactions mediated by myosin head and tail [105]. Another calcium binding molecule that controls cytoskeletal contractility is troponin, which consists of a calcium binding subunit (troponin C), inhibitory subunit (troponin L) and tropomyosin-binding subunit (troponin T). Troponin mainly appears on the actin bundles of striated muscles, where they activate muscle contraction. Like several other cytoskeletal proteins, troponin C contains multiple EF hand domains. The two EF hands at the C-terminus troponin C harbor two high affinity calcium binding sites, whereas the single EF hands on the N-terminus have a low affinity calcium binding site [106, 107]. Depending on calcium levels, troponin regulates the interaction between myosin and actin filaments in striated muscles, thus affecting the contractility of the cytoskeleton [108–111].

The ability of calcium to alter cytoskeletal organization and contractility may have a broad impact on the life of an organism, emanating from the control of cell morphology. For example, the organization of dendritic spines depends on the local calcium concentration in neurons [112, 113]. Dendritic spines are highly motile structures whose morphology is cytoskeleton-dependent. Rapid reorganization of spines is crucial for the synapses residing on it, which eventually affects the neural transmission [114]. Observations from starfish oocytes suggest that calcium signals are increased with the increase in the expression of cofilin, an actin-depolymerizing factor that modulates cytoskeletal dynamics, cell motility and cytokinesis. Increased cofilin expression promotes hormone-induced oocyte maturation and fertilization [115]. More important aspects of cytosolic calcium levels came from the studies of cardiac physiology. The impaired diastolic function of the heart is believed be the result of dysfunctional calcium regulation, which can be improved through modulation of myofilament calcium sensitivity [116]. At this point it is worthy

to note that none of the studies indicated a change in protein level expression of any of the cytoskeletal proteins in response to change in cytosolic calcium. This means the changes in cytoskeletal structures are simply due to altered localization and function of various cytoskeletal proteins. For example, studies on roles of the cytoskeleton in exocytosis suggested that increased cytosolic calcium concentration directly affecting F-actin organization might cause the relocation of actin from the bundles, rather than affecting protein synthesis [117].

43.2.4 Cell Surface Receptors

43.2.4.1 Proteoglycans

Proteoglycans are composed of a core protein with glycosaminoglycan sugar chains covalently attached to the core protein. Proteoglycans are an important component of the ECM, but others at the cell surface function as receptors. Proteoglycans interact with ECM molecules, mainly through their glycosaminoglycan chains. Over 30 proteoglycans are encoded in mammals where many maintain tissue specific expression [118]. Proteoglycans of the syndecan family control multiple cellular functions, including cell adhesion, cytoskeletal organization, cell migration and protein transport [118–120]. Syndecans are the only proteoglycans identified to regulate cytosolic calcium (Fig. 43.4). They are transmembrane receptors that can interact with the extracellular ligands such as fibronectin, laminin and collagen [22]. Recently, syndecans were identified as regulators of mechanosensitive transient receptor potential (TRP) channels. Syndecans-1 and -4 were shown to regulate transient receptor potential (TRP) channels. Syndecan-1, a prominent syndecan of epithelial cells appeared to control TRPC4 channels [20]. Similarly, ubiquitously expressed syndecan-4 controls TRPC7 channels in mesenchymal cells [20]. While these two syndecans can associate with TRPC channels, it is highly likely that other syndecans regulate other members from TRP family, not least since similar properties could be shown in the single syndecan of *Caenorhabditis elegans* [20]. Syndecan-4 mediated regulation of TRP channel seems to be maintained through PKC activation and direct complex formation between syndecan, the channels and the cytoskeletal protein α-actinin [20]. This agrees with a previous observation made in goldfish retinal bipolar cells where calcium was altered with the activation of PKC by PMA. Both researches, performed over a decade apart in two different systems, found that the PKC induced calcium modification results in F-actin filament reorganization.

Syndecan-4, perhaps through ligand-induced clustering, can activate PKCα through direct interaction. It has been reported that TRP channels are negatively regulated by a PKC mediated phosphorylation of a regulatory serine residue situated near the C- terminus of the channel [121]. It is speculated that the active PKCα near the cytoplasmic domain of syndecan-4 can phosphorylate this regulatory serine residue of the channel, thus leading to the closure of the channel (Fig. 43.4).

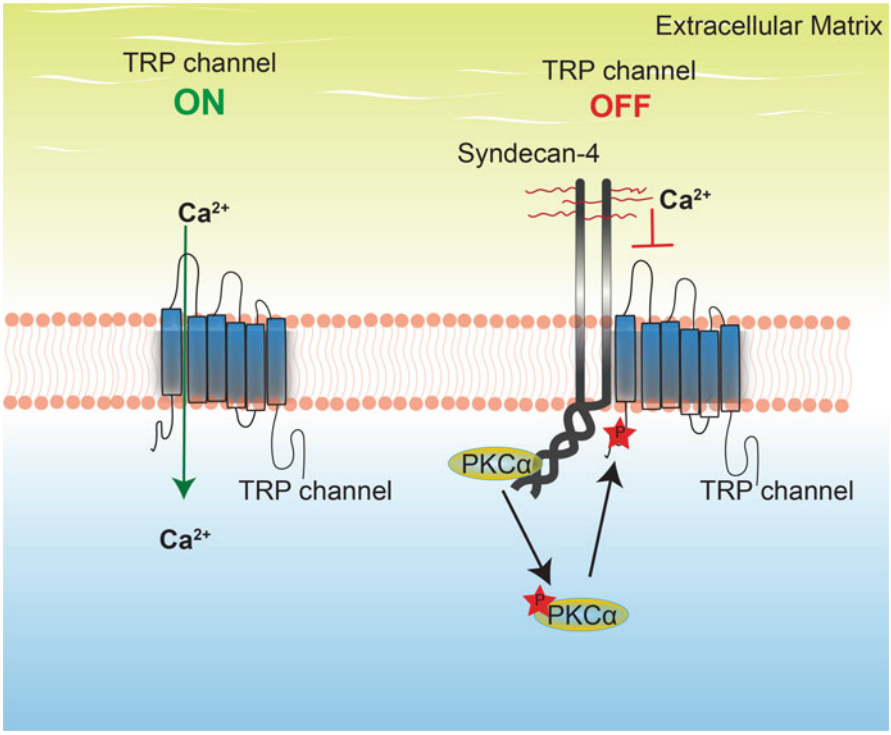

Fig. 43.4 Syndecan mediated regulation of TRP channels: In the presence of syndecan-4, the active PKCα phosphorylates TRP channels. This leads to the closing of the channel

The complex formed between TRP channels and syndecan-4 should enable the channel to be in the close proximity of the PKCα. Interestingly, the complex formation between syndecan-4 and the TRP channels appears to be independent of heparan sulfate chains on the ectodomain of syndecan-4, whereas the channel regulation results from heparan sulfate chain interactions with extracellular matrix [20]. Syndecan-4 interacts with the fibronectin, specifically the 31kD HepII domain of fibronectin through heparan sulfate chains. This classic interaction is known to trigger PKCα activation in the presence of the membrane phospholipid, PtdIns4,5P_2 [122–125]. Therefore, it can be speculated that the active PKCα phosphorylates the TRP channel and other cytoskeletal regulatory proteins [121, 126, 127]. Overall, these findings support the idea that the syndecan mediated calcium control is initiated by the heparan sulfate chain engagement with ECM, that transduces PKCα activation and channel regulation. Currently, fibronectin is the paradigmatic ECM component that was shown to have the ability to initiate syndecan-4 mediated control of TRP channels. This property could, however, be common to many ECM molecules and awaits investigation. Previous observations support the idea that heparan sulfate chains are essential for this process. One report showed that adding

heparin, a highly sulfated analogue of heparan sulfate, to epithelial cells inhibited calcium oscillations [128]. This could be due to the competition between heparin and endogenous heparan sulfate for interactions with ligands such as fibronectin. Recent reports reiterate this, where syndecan-4 without heparan sulfate chains failed to maintain the cytosolic calcium levels in embryonic fibroblasts [20].

The syndecan-4 mediated control of TRP channels is essential for the maintenance of cytoskeleton and formation of focal adhesions. Experiments in embryonic fibroblasts revealed that elevated calcium levels seen in syndecan-4 null fibroblasts result in disorganized cytoskeleton and smaller focal adhesions [20]. Currently, several syndecan-dependent phenotypes may be explained as secondary effects of their role in cytosolic calcium regulation. However, there is no significant information available regarding the organismal effect of syndecan-TRP channel cross talk in mammals. However, one report suggests that syndecan-4 and TRPC6 may regulate glomerular permeability [129]. Recent reviews also highlighted that syndecan controlled calcium may be of importance in cardiac diseases, cancers, neuronal patterning and development [130–134].

43.2.4.2 Integrins

The role of integrins in calcium regulation has been known for over three decades. Like syndecans, integrins are transmembrane receptors that can interact with a large number of cell ECM molecules such as fibronectin, vitronectin, collagens and laminins, and participate in signal transduction (Figs. 43.1 and 43.2). Integrins are composed of transmembrane α- and a β- subunits, where they can assume active or inactive conformations. There are 24 integrin heterodimers in vertebrates formed by different combinations of 18 α- and 8 β- subunits [135, 136]. Structural analysis revealed that calcium ions compete with manganese ions for integrin binding [137–139], in regulating the switch between active and inactive integrin conformations. This was further confirmed when removal of calcium appeared to increase ligand binding affinity of the integrin [140]. The divalent ion interaction with integrin also known to stabilize the integrin interaction with its ligands [139], though this is attributed to manganese rather than calcium ions.

A number of integrins can facilitate calcium entry into cells, thus affecting cellular processes including cell-ECM adhesion and cytoskeletal regulation. On the other hand, integrin -mediated cell adhesion was also shown to be controlled by cytosolic calcium levels. A subset of integrins interact with ECM proteins through an Arg-Gly-Asp motif on the ECM protein (e.g. fibronectin and vitronectin interactions with αV or α5β1 integrins) [141–144]. It has been shown that supplying cells with Arg-Gly-Asp peptides elicited a transient change in intracellular calcium levels [145–147], likely due to the integrin engagement with the peptide ligand.

Integrin-induced calcium changes are mainly associated with voltage-gated calcium channels. For instance, integrins differentially control L-type calcium channels in vascular smooth cells, where αVβ3 integrin may negatively regulate the channel while α5β1 integrin may enhance calcium entry [148]. Subsequent

research showed that the α5β1 integrin mediated control of L-type channels may be maintained via a tyrosine phosphorylation cascade, signaling between focal adhesion kinase, vinculin, paxillin and c-Src [12, 149]. This signaling appeared to be initiated by the interaction of integrins with extracellular proteins such as fibronectin and vitronectin, probably through the Arg-Gly-Asp motif. Currently the reason behind differential regulation of channels in response to Arg-Gly-Asp interaction is unclear. One possibility is that other calcium channels or internal calcium stores might be compensating the effects of integrin-ECM induced calcium changes. Alternatively, each integrin may associate with distinct channels, an area in need of further research. A more recent report showed that α4β1 integrin can similarly influence L-type calcium channels as a result of their interaction with the Leu-Asp-Val sequence of an alternately spliced fibronectin variant [150]. Finally, the interaction of α7 integrin with laminin in skeletal muscle resulted in not only the activation of L-type channels, but also calcium release from intracellular calcium stores [151]. As mentioned before, integrins and laminins may form complexes with voltage gated channel Ca(v)α in other systems such as synapses. However, the direct role of integrin in calcium release from intracellular calcium stores remains unclear. Finally, integrins are also involved in controlling mechanosensitive channels either directly or indirectly. Applying mechanical forces directly to integrins evoked an increase in cytosolic calcium levels, which seems to require a reciprocal force from the cytoskeleton [152, 153]. However, the application of the force may lead to more global effects on the plasma membrane. Therefore, the increase in calcium might be a combined result of the force applied on the plasma membrane and cytoskeleton instead of, or in addition to, an integrin-specific one.

While the role of integrin in calcium regulation is well established, the directionality of the regulation appeared to depend on cell and mode of integrin involvement. For instance, αVβ3 integrin appears to negatively regulate calcium entry in vascular smooth cells [148] whereas it increases calcium levels in rat osteoclasts [154]. These experiments were, however, different in terms of integrin presentation to cells. The experiments with vascular smooth cells were based on the integrin present on the cell surface whereas the αVβ3 integrin was supplied in solution to rat osteoclasts. This may have resulted in a competition for ligand binding between cell surface and exogenous integrins. Overall, the consensus is that integrin-controlled calcium regulation is initiated by the clustering of integrins on the cell surface following their interaction with ECM proteins [155].

43.3 Conclusions

The ability of ECM proteins to regulate cytosolic calcium levels in addition to signaling through kinase networks is an indicator of the complexity of cell-ECM interactions. Over last two decades the role of ECM in controlling cell behavior has been increasingly elucidated and some of the pathways are controlled through calcium. On the other hand, the ability of calcium to control cell-ECM interactions,

mainly though focal adhesions is also well known. This two-way interaction indicates feedback mechanisms, though the precise control mechanisms remain elusive. Since cell surface receptors are the gatekeepers of these interactions, it is highly likely the decisive factor is the localization of these receptors on the cell surface and the formation of localized and functional signaling complexes. The recent addition of syndecans as calcium regulators along with integrins reveals a complex, yet a delicately controlled mechanism, subject to the balance of cell surface receptor expression and function.

43.4 Future Research

As expected, the role of calcium in cell-ECM cross talk is a complex research area. While ECM and tissue fluids remain the largest calcium storage sites, intracellular calcium stores play a significant role in calcium regulation that impacts cell adhesion and morphology. The most challenging aspect of calcium studies is the identification of relevant calcium sources that are involved in specific cell signaling. Secondly, there is a need to identify exactly how the localized calcium is controlled. Microdomains within the cell with regard to ions, mRNAs and junctions are apparent. For example, calcium dynamics in focal adhesions may have a decisive effect on the focal adhesion turnover, yet there is no significant information available on its regulation. In addition, further information needs to be elucidated on the mechanosensitive calcium channels where cell-ECM interactions play a major role. It is not yet fully clear which TRP channels are regulated by which syndecans and how much redundancy may be in the system. It is also possible that other TRP subfamilies could be similarly regulated, but this is currently unknown. Applying computational models may be in the realm of possibilities to elucidate mechanotransduction between cell and ECM. By incorporating calcium regulation in the computational models may help to understand the complexity of calcium in cell-ECM interactions.

Acknowledgments Authors thank Ms. Ioli Mitsou for images for Fig. 43.3. SG is supported by Senior Postdoctoral Fellowship from Monash University.

References

1. Janson IA, Putnam AJ (2015) Extracellular matrix elasticity and topography: material-based cues that affect cell function via conserved mechanisms. J Biomed Mater Res A 103(3):1246–1258
2. Carafoli E, Krebs J (2016) Why calcium? How calcium became the best communicator. J Biol Chem 291(40):20849–20857
3. Avila-Medina J, Mayoral-Gonzalez I, Dominguez-Rodriguez A, Gallardo-Castillo I, Ribas J, Ordonez A et al (2018) The complex role of store operated calcium entry pathways and

related proteins in the function of cardiac, skeletal and vascular smooth muscle cells. Front Physiol 9:257
4. Zhang AH, Sharma G, Undheim EAB, Jia X, Mobli M (2018) A complicated complex: ion channels, voltage sensing, cell membranes and peptide inhibitors. Neurosci Lett
5. Kobayashi T, Sokabe M (2010) Sensing substrate rigidity by mechanosensitive ion channels with stress fibers and focal adhesions. Curr Opin Cell Biol 22(5):669–676
6. Whitaker M (2006) Calcium at fertilization and in early development. Physiol Rev 86(1):25–88
7. Mattson MP, Chan SL (2003) Calcium orchestrates apoptosis. Nat Cell Biol 5(12):1041–1043
8. Orr AW, Helmke BP, Blackman BR, Schwartz MA (2006) Mechanisms of mechanotransduction. Dev Cell 10(1):11–20
9. Vogel V, Sheetz M (2006) Local force and geometry sensing regulate cell functions. Nat Rev Mol Cell Biol 7(4):265–275
10. Ringer P, Colo G, Fassler R, Grashoff C (2017) Sensing the mechano-chemical properties of the extracellular matrix. Matrix Biol 64:6–16
11. Giannone G, Ronde P, Gaire M, Beaudouin J, Haiech J, Ellenberg J et al (2004) Calcium rises locally trigger focal adhesion disassembly and enhance residency of focal adhesion kinase at focal adhesions. J Biol Chem 279(27):28715–28723
12. Wu X, Davis GE, Meininger GA, Wilson E, Davis MJ (2001) Regulation of the L-type calcium channel by alpha 5beta 1 integrin requires signaling between focal adhesion proteins. J Biol Chem 276(32):30285–30292
13. Ciobanasu C, Faivre B, Le Clainche C (2014) Actomyosin-dependent formation of the mechanosensitive talin-vinculin complex reinforces actin anchoring. Nat Commun 5:3095
14. Drmota Prebil S, Slapsak U, Pavsic M, Ilc G, Puz V, de Almeida RE et al (2016) Structure and calcium-binding studies of calmodulin-like domain of human non-muscle alpha-actinin-1. Sci Rep 6:27383
15. Naba A, Clauser KR, Hoersch S, Liu H, Carr SA, Hynes RO (2012) The matrisome: in silico definition and in vivo characterization by proteomics of normal and tumor extracellular matrices. Mol Cell Proteomics 11(4):M111.014647
16. Carbajal ME, Manning-Cela R, Pina A, Franco E, Meza I (1996) Fibronectin-induced intracellular calcium rise in Entamoeba histolytica trophozoites: effect on adhesion and the actin cytoskeleton. Exp Parasitol 82(1):11–20
17. Nebe B, Rychly J, Knopp A, Bohn W (1995) Mechanical induction of beta 1-integrin-mediated calcium signaling in a hepatocyte cell line. Exp Cell Res 218(2):479–484
18. Lee HS, Millward-Sadler SJ, Wright MO, Nuki G, Salter DM (2000) Integrin and mechanosensitive ion channel-dependent tyrosine phosphorylation of focal adhesion proteins and beta-catenin in human articular chondrocytes after mechanical stimulation. J Bone Miner Res 15(8):1501–1509
19. Ishise H, Larson B, Hirata Y, Fujiwara T, Nishimoto S, Kubo T et al (2015) Hypertrophic scar contracture is mediated by the TRPC3 mechanical force transducer via NFkB activation. Sci Rep 5:11620
20. Gopal S, Sogaard P, Multhaupt HA, Pataki C, Okina E, Xian X et al (2015) Transmembrane proteoglycans control stretch-activated channels to set cytosolic calcium levels. J Cell Biol 210(7):1199–1211
21. Gopal S, Bober A, Whiteford JR, Multhaupt HA, Yoneda A, Couchman JR (2010) Heparan sulfate chain valency controls syndecan-4 function in cell adhesion. J Biol Chem 285(19):14247–14258
22. Xian X, Gopal S, Couchman JR (2010) Syndecans as receptors and organizers of the extracellular matrix. Cell Tissue Res 339(1):31–46
23. Yurchenco PD, Cheng YS (1993) Self-assembly and calcium-binding sites in laminin. A three-arm interaction model. J Biol Chem 268(23):17286–17299
24. Cheng YS, Champliaud MF, Burgeson RE, Marinkovich MP, Yurchenco PD (1997) Self-assembly of laminin isoforms. J Biol Chem 272(50):31525–31532

25. Kalb E, Engel J (1991) Binding and calcium-induced aggregation of laminin onto lipid bilayers. J Biol Chem 266(28):19047–19052
26. Colucci S, Giannelli G, Grano M, Faccio R, Quaranta V, Zallone AZ (1996) Human osteoclast-like cells selectively recognize laminin isoforms, an event that induces migration and activates Ca^{2+} mediated signals. J Cell Sci 109(Pt 6):1527–1535
27. Nishimune H (2012) Molecular mechanism of active zone organization at vertebrate neuromuscular junctions. Mol Neurobiol 45(1):1–16
28. Nishimune H, Sanes JR, Carlson SS (2004) A synaptic laminin-calcium channel interaction organizes active zones in motor nerve terminals. Nature 432(7017):580–587
29. Sunderland WJ, Son YJ, Miner JH, Sanes JR, Carlson SS (2000) The presynaptic calcium channel is part of a transmembrane complex linking a synaptic laminin (alpha4beta2gamma1) with non-erythroid spectrin. J Neurosci 20(3):1009–1019
30. Chand KK, Lee KM, Schenning MP, Lavidis NA, Noakes PG (2015) Loss of beta2-laminin alters calcium sensitivity and voltage-gated calcium channel maturation of neurotransmission at the neuromuscular junction. J Physiol 593(1):245–265
31. Carlson SS, Valdez G, Sanes JR (2010) Presynaptic calcium channels and alpha3-integrins are complexed with synaptic cleft laminins, cytoskeletal elements and active zone components. J Neurochem 115(3):654–666
32. Cali T, Lopreiato R, Shimony J, Vineyard M, Frizzarin M, Zanni G et al (2015) A novel mutation in isoform 3 of the plasma membrane Ca^{2+} pump impairs cellular Ca^{2+} homeostasis in a patient with cerebellar ataxia and laminin subunit 1alpha mutations. J Biol Chem 290(26):16132–16141
33. Dietz HC, Pyeritz RE (1995) Mutations in the human gene for fibrillin-1 (FBN1) in the Marfan syndrome and related disorders. Hum Mol Genet 4 Spec No:1799–1809
34. Handford PA (2000) Fibrillin-1, a calcium binding protein of extracellular matrix. Biochim Biophys Acta 1498(2–3):84–90
35. Kielty CM, Shuttleworth CA (1993) The role of calcium in the organization of fibrillin microfibrils. FEBS Lett 336(2):323–326
36. Sakai LY, Keene DR, Engvall E (1986) Fibrillin, a new 350-kD glycoprotein, is a component of extracellular microfibrils. J Cell Biol 103(6 Pt 1):2499–2509
37. Reinhardt DP, Mechling DE, Boswell BA, Keene DR, Sakai LY, Bachinger HP (1997) Calcium determines the shape of fibrillin. J Biol Chem 272(11):7368–7373
38. Corson GM, Chalberg SC, Dietz HC, Charbonneau NL, Sakai LY (1993) Fibrillin binds calcium and is coded by cDNAs that reveal a multidomain structure and alternatively spliced exons at the 5′ end. Genomics 17(2):476–484
39. Jensen SA, Corbett AR, Knott V, Redfield C, Handford PA (2005) Ca^{2+}−dependent interface formation in fibrillin-1. J Biol Chem 280(14):14076–14084
40. Smallridge RS, Whiteman P, Werner JM, Campbell ID, Handford PA, Downing AK (2003) Solution structure and dynamics of a calcium binding epidermal growth factor-like domain pair from the neonatal region of human fibrillin-1. J Biol Chem 278(14):12199–12206
41. Lin G, Tiedemann K, Vollbrandt T, Peters H, Batge B, Brinckmann J et al (2002) Homo- and heterotypic fibrillin-1 and -2 interactions constitute the basis for the assembly of microfibrils. J Biol Chem 277(52):50795–50804
42. Marson A, Rock MJ, Cain SA, Freeman LJ, Morgan A, Mellody K et al (2005) Homotypic fibrillin-1 interactions in microfibril assembly. J Biol Chem 280(6):5013–5021
43. Cain SA, Baldock C, Gallagher J, Morgan A, Bax DV, Weiss AS et al (2005) Fibrillin-1 interactions with heparin. Implications for microfibril and elastic fiber assembly. J Biol Chem 280(34):30526–30537
44. Tiedemann K, Batge B, Muller PK, Reinhardt DP (2001) Interactions of fibrillin-1 with heparin/heparan sulfate, implications for microfibrillar assembly. J Biol Chem 276(38):36035–36042
45. Isogai Z, Aspberg A, Keene DR, Ono RN, Reinhardt DP, Sakai LY (2002) Versican interacts with fibrillin-1 and links extracellular microfibrils to other connective tissue networks. J Biol Chem 277(6):4565–4572

46. El-Hallous E, Sasaki T, Hubmacher D, Getie M, Tiedemann K, Brinckmann J et al (2007) Fibrillin-1 interactions with fibulins depend on the first hybrid domain and provide an adaptor function to tropoelastin. J Biol Chem 282(12):8935–8946
47. Reinhardt DP, Ono RN, Sakai LY (1997) Calcium stabilizes fibrillin-1 against proteolytic degradation. J Biol Chem 272(2):1231–1236
48. Ashworth JL, Murphy G, Rock MJ, Sherratt MJ, Shapiro SD, Shuttleworth CA et al (1999) Fibrillin degradation by matrix metalloproteinases: implications for connective tissue remodelling. Biochem J 340(Pt 1):171–181
49. Mariko B, Ghandour Z, Raveaud S, Quentin M, Usson Y, Verdetti J et al (2010) Microfibrils and fibrillin-1 induce integrin-mediated signaling, proliferation and migration in human endothelial cells. Am J Physiol Cell Physiol 299(5):C977–C987
50. Massam-Wu T, Chiu M, Choudhury R, Chaudhry SS, Baldwin AK, McGovern A et al (2010) Assembly of fibrillin microfibrils governs extracellular deposition of latent TGF beta. J Cell Sci 123(Pt 17):3006–3018
51. Poole AW, Watson SP (1995) Regulation of cytosolic calcium by collagen in single human platelets. Br J Pharmacol 115(1):101–106
52. Shiraishi M, Ikeda M, Ogawa H, Tu CH, Ito K (1998) Impaired cytosolic calcium mobilization and aggregation in response to collagen in platelets from Japanese black cattle with Chediak-Higashi syndrome. Am J Vet Res 59(6):744–749
53. Roberts DE, McNicol A, Bose R (2004) Mechanism of collagen activation in human platelets. J Biol Chem 279(19):19421–19430
54. Nesbitt WS, Giuliano S, Kulkarni S, Dopheide SM, Harper IS, Jackson SP (2003) Intercellular calcium communication regulates platelet aggregation and thrombus growth. J Cell Biol 160(7):1151–1161
55. Shih YR, Tseng KF, Lai HY, Lin CH, Lee OK (2011) Matrix stiffness regulation of integrin-mediated mechanotransduction during osteogenic differentiation of human mesenchymal stem cells. J Bone Miner Res 26(4):730–738
56. Horton ER, Byron A, Askari JA, DHJ N, Millon-Fremillon A, Robertson J et al (2015) Definition of a consensus integrin adhesome and its dynamics during adhesion complex assembly and disassembly. Nat Cell Biol 17(12):1577–1587
57. Byron A, Humphries JD, Craig SE, Knight D, Humphries MJ (2012) Proteomic analysis of alpha4beta1 integrin adhesion complexes reveals alpha-subunit-dependent protein recruitment. Proteomics 12(13):2107–2114
58. Carisey A, Tsang R, Greiner AM, Nijenhuis N, Heath N, Nazgiewicz A et al (2013) Vinculin regulates the recruitment and release of core focal adhesion proteins in a force-dependent manner. Curr Biol 23(4):271–281
59. Morgan MR, Humphries MJ, Bass MD (2007) Synergistic control of cell adhesion by integrins and syndecans. Nat Rev Mol Cell Biol 8(12):957–969
60. Roper JA, Williamson RC, Bass MD (2012) Syndecan and integrin interactomes: large complexes in small spaces. Curr Opin Struct Biol 22(5):583–590
61. Zobel CR, Woods A (1983) Effect of calcium on the morphology of human platelets spread on glass substrates. Eur J Cell Biol 30(1):83–92
62. Laterra J, Norton EK, Izzard CS, Culp LA (1983) Contact formation by fibroblasts adhering to heparan sulfate-binding substrata (fibronectin or platelet factor 4). Exp Cell Res 146(1):15–27
63. Hamawy MM, Mergenhagen SE, Siraganian RP (1993) Tyrosine phosphorylation of pp125FAK by the aggregation of high affinity immunoglobulin E receptors requires cell adherence. J Biol Chem 268(10):6851–6854
64. Schaller MD, Borgman CA, Cobb BS, Vines RR, Reynolds AB, Parsons JT (1992) pp125FAK a structurally distinctive protein-tyrosine kinase associated with focal adhesions. Proc Natl Acad Sci USA 89(11):5192–5196
65. Shattil SJ, Haimovich B, Cunningham M, Lipfert L, Parsons JT, Ginsberg MH et al (1994) Tyrosine phosphorylation of pp125FAK in platelets requires coordinated signaling through integrin and agonist receptors. J Biol Chem 269(20):14738–14745

66. Zachary I, Sinnett-Smith J, Turner CE, Rozengurt E (1993) Bombesin, vasopressin, and endothelin rapidly stimulate tyrosine phosphorylation of the focal adhesion-associated protein paxillin in Swiss 3T3 cells. J Biol Chem 268(29):22060–22065
67. Turner CE (2000) Paxillin and focal adhesion signalling. Nat Cell Biol 2(12):E231–E236
68. Gopal S, Multhaupt HA, Pocock R, Couchman JR (2016) Cell-extracellular matrix and cell-cell adhesion are linked by syndecan-4. Matrix Biol
69. Sachs F (2010) Stretch-activated ion channels: what are they? Physiology (Bethesda) 25(1):50–56
70. Mitsou I, Multhaupt HAB, Couchman JR (2017) Proteoglycans, ion channels and cell-matrix adhesion. Biochem J 474(12):1965–1979
71. Caceres M, Ortiz L, Recabarren T, Romero A, Colombo A, Leiva-Salcedo E et al (2015) TRPM4 Is a novel component of the adhesome required for focal adhesion disassembly, migration and contractility. PloS One 10(6):e0130540
72. Tang DD, Gerlach BD (2017) The roles and regulation of the actin cytoskeleton, intermediate filaments and microtubules in smooth muscle cell migration. Respir Res 18(1):54
73. Oishi T, Kimura K, Hanada M, Samejima M (1982) Assistance extended to patients with poor prognosis and their families – a lesson in role playing. Kango Gijutsu 28(16):2183–2188
74. Hayakawa K, Tatsumi H, Sokabe M (2011) Actin filaments function as a tension sensor by tension-dependent binding of cofilin to the filament. J Cell Biol 195(5):721–727
75. Hampton CM, Taylor DW, Taylor KA (2007) Novel structures for alpha-actinin:F-actin interactions and their implications for actin-membrane attachment and tension sensing in the cytoskeleton. J Mol Biol 368(1):92–104
76. Meyer RK, Aebi U (1990) Bundling of actin filaments by alpha-actinin depends on its molecular length. J Cell Biol 110(6):2013–2024
77. Sharp WW, Simpson DG, Borg TK, Samarel AM, Terracio L (1997) Mechanical forces regulate focal adhesion and costamere assembly in cardiac myocytes. Am J Phys 273(2 Pt 2):H546–H556
78. Brown SS, Yamamoto K, Spudich JA (1982) A 40,000-dalton protein from Dictyostelium discoideum affects assembly properties of actin in a Ca^{2+}−dependent manner. J Cell Biol 93(1):205–210
79. Fechheimer M, Taylor DL (1984) Isolation and characterization of a 30,000-dalton calcium-sensitive actin cross-linking protein from Dictyostelium discoideum. J Biol Chem 259(7):4514–4520
80. Rivero F, Furukawa R, Fechheimer M, Noegel AA (1999) Three actin cross-linking proteins, the 34 kDa actin-bundling protein, alpha-actinin and gelation factor (ABP-120), have both unique and redundant roles in the growth and development of Dictyostelium. J Cell Sci 112(Pt 16):2737–2751
81. Witke W, Hofmann A, Koppel B, Schleicher M, Noegel AA (1993) The Ca^{2+}-binding domains in non-muscle type alpha-actinin: biochemical and genetic analysis. J Cell Biol 121(3):599–606
82. Furukawa R, Maselli A, Thomson SA, Lim RW, Stokes JV, Fechheimer M (2003) Calcium regulation of actin crosslinking is important for function of the actin cytoskeleton in Dictyostelium. J Cell Sci 116(Pt 1):187–196
83. Edwards HC, Booth AG (1987) Calcium-sensitive, lipid-binding cytoskeletal proteins of the human placental microvillar region. J Cell Biol 105(1):303–311
84. Badalamente MA, Hurst LC, Stracher A (1986) Calcium-induced degeneration of the cytoskeleton in monkey and human peripheral nerves. J Hand Surg (Br) 11(3):337–340
85. Lomri A, Marie PJ (1990) Distinct effects of calcium- and cyclic AMP-enhancing factors on cytoskeletal synthesis and assembly in mouse osteoblastic cells. Biochim Biophys Acta 1052(1):179–186
86. Glogauer M, Arora P, Yao G, Sokholov I, Ferrier J, McCulloch CA (1997) Calcium ions and tyrosine phosphorylation interact coordinately with actin to regulate cytoprotective responses to stretching. J Cell Sci 110(Pt 1):11–21

87. Veksler A, Gov NS (2009) Calcium-actin waves and oscillations of cellular membranes. Biophys J 97(6):1558–1568
88. Stevens FC (1983) Calmodulin: an introduction. Can J Biochem Cell Biol 61(8):906–910
89. Chin D, Means AR (2000) Calmodulin: a prototypical calcium sensor. Trends Cell Biol 10(8):322–328
90. Chou JJ, Li S, Klee CB, Bax A (2001) Solution structure of Ca^{2+}-calmodulin reveals flexible hand-like properties of its domains. Nat Struct Biol 8(11):990–997
91. Easley CA, Faison MO, Kirsch TL, Lee JA, Seward ME, Tombes RM (2006) Laminin activates CaMK-II to stabilize nascent embryonic axons. Brain Res 1092(1):59–68
92. Shen K, Teruel MN, Subramanian K, Meyer T (1998) CaMKIIbeta functions as an F-actin targeting module that localizes CaMKIIalpha/beta heterooligomers to dendritic spines. Neuron 21(3):593–606
93. Lin YC, Redmond L (2008) CaMKIIbeta binding to stable F-actin in vivo regulates F-actin filament stability. Proc Natl Acad Sci USA 105(41):15791–15796
94. Okamoto K, Narayanan R, Lee SH, Murata K, Hayashi Y (2007) The role of CaMKII as an F-actin-bundling protein crucial for maintenance of dendritic spine structure. Proc Natl Acad Sci USA 104(15):6418–6423
95. Sanabria H, Swulius MT, Kolodziej SJ, Liu J, Waxham MN (2009) {beta}CaMKII regulates actin assembly and structure. J Biol Chem 284(15):9770–9780
96. O'Leary H, Lasda E, Bayer KU (2006) CaMKIIbeta association with the actin cytoskeleton is regulated by alternative splicing. Mol Biol Cell 17(11):4656–4665
97. Psatha MI, Razi M, Koffer A, Moss SE, Sacks DB, Bolsover SR (2007) Targeting of calcium:calmodulin signals to the cytoskeleton by IQGAP1. Cell Calcium 41(6):593–605
98. Sellers JR (2000) Myosins: a diverse superfamily. Biochim Biophys Acta 1496(1):3–22
99. Hartman MA, Spudich JA (2012) The myosin superfamily at a glance. J Cell Sci 125(Pt 7):1627–1632
100. Syamaladevi DP, Spudich JA, Sowdhamini R (2012) Structural and functional insights on the Myosin superfamily. Bioinf Biol Insights 6:11–21
101. Preller M, Manstein DJ (2013) Myosin structure, allostery, and mechano-chemistry. Structure 21(11):1911–1922
102. Foth BJ, Goedecke MC, Soldati D (2006) New insights into myosin evolution and classification. Proc Natl Acad Sci USA 103(10):3681–3686
103. Wang F, Thirumurugan K, Stafford WF, Hammer JA 3rd, Knight PJ, Sellers JR (2004) Regulated conformation of myosin V. J Biol Chem 279(4):2333–2336
104. Lu H, Krementsova EB, Trybus KM (2006) Regulation of myosin V processivity by calcium at the single molecule level. J Biol Chem 281(42):31987–31994
105. Jung HS, Komatsu S, Ikebe M, Craig R (2008) Head-head and head-tail interaction: a general mechanism for switching off myosin II activity in cells. Mol Biol Cell 19(8):3234–3242
106. Li MX, Saude EJ, Wang X, Pearlstone JR, Smillie LB, Sykes BD (2002) Kinetic studies of calcium and cardiac troponin I peptide binding to human cardiac troponin C using NMR spectroscopy. Eur Biophys J 31(4):245–256
107. Herzberg O, Moult J, James MN (1986) Calcium binding to skeletal muscle troponin C and the regulation of muscle contraction. Ciba Found Symp 122:120–144
108. Murakami K, Yumoto F, Ohki SY, Yasunaga T, Tanokura M, Wakabayashi T (2005) Structural basis for Ca^{2+}−regulated muscle relaxation at interaction sites of troponin with actin and tropomyosin. J Mol Biol 352(1):178–201
109. Lehman W, Hatch V, Korman V, Rosol M, Thomas L, Maytum R et al (2000) Tropomyosin and actin isoforms modulate the localization of tropomyosin strands on actin filaments. J Mol Biol 302(3):593–606
110. McKillop DF, Geeves MA (1993) Regulation of the interaction between actin and myosin subfragment 1: evidence for three states of the thin filament. Biophys J 65(2):693–701
111. Sequeira V, Nijenkamp LL, Regan JA, van der Velden J (2014) The physiological role of cardiac cytoskeleton and its alterations in heart failure. Biochim Biophys Acta 1838(2):700–722

112. Engert F, Bonhoeffer T (1999) Dendritic spine changes associated with hippocampal long-term synaptic plasticity. Nature 399(6731):66–70
113. Toni N, Buchs PA, Nikonenko I, Bron CR, Muller D (1999) LTP promotes formation of multiple spine synapses between a single axon terminal and a dendrite. Nature 402(6760):421–425
114. Oertner TG, Matus A (2005) Calcium regulation of actin dynamics in dendritic spines. Cell Calcium 37(5):477–482
115. Nusco GA, Chun JT, Ercolano E, Lim D, Gragnaniello G, Kyozuka K et al (2006) Modulation of calcium signalling by the actin-binding protein cofilin. Biochem Biophys Res Commun 348(1):109–114
116. Lovelock JD, Monasky MM, Jeong EM, Lardin HA, Liu H, Patel BG et al (2012) Ranolazine improves cardiac diastolic dysfunction through modulation of myofilament calcium sensitivity. Circ Res 110(6):841–850
117. Yoneda M, Nishizaki T, Tasaka K, Kurachi H, Miyake A, Murata Y (2000) Changes in actin network during calcium-induced exocytosis in permeabilized GH3 cells: calcium directly regulates F-actin disassembly. J Endocrinol 166(3):677–687
118. Couchman JR, Pataki CA (2012) An introduction to proteoglycans and their localization. J Histochem Cytochem 60(12):885–897
119. Afratis NA, Nikitovic D, Multhaupt HA, Theocharis AD, Couchman JR, Karamanos NK (2017) Syndecans - key regulators of cell signaling and biological functions. FEBS J 284(1):27–41
120. Couchman JR (2010) Transmembrane signaling proteoglycans. Annu Rev Cell Dev Biol 26:89–114
121. Trebak M, Hempel N, Wedel BJ, Smyth JT, Bird GS, Putney JW Jr (2005) Negative regulation of TRPC3 channels by protein kinase C-mediated phosphorylation of serine 712. Mol Pharmacol 67(2):558–563
122. Oh ES, Woods A, Couchman JR (1997) Syndecan-4 proteoglycan regulates the distribution and activity of protein kinase C. J Biol Chem 272(13):8133–8136
123. Keum E, Kim Y, Kim J, Kwon S, Lim Y, Han I et al (2004) Syndecan-4 regulates localization, activity and stability of protein kinase C-alpha. Biochem J 378(Pt 3):1007–1014
124. Horowitz A, Murakami M, Gao Y, Simons M (1999) Phosphatidylinositol-4,5-bisphosphate mediates the interaction of syndecan-4 with protein kinase C. Biochemistry 38(48):15871–15877
125. Oh ES, Woods A, Lim ST, Theibert AW, Couchman JR (1998) Syndecan-4 proteoglycan cytoplasmic domain and phosphatidylinositol 4,5-bisphosphate coordinately regulate protein kinase C activity. J Biol Chem 273(17):10624–10629
126. Tu LC, Chou CK, Chen HC, Yeh SF (2001) Protein kinase C-mediated tyrosine phosphorylation of paxillin and focal adhesion kinase requires cytoskeletal integrity and is uncoupled to mitogen-activated protein kinase activation in human hepatoma cells. J Biomed Sci 8(2):184–190
127. Fogh BS, Multhaupt HA, Couchman JR (2014) Protein kinase C, focal adhesions and the regulation of cell migration. J Histochem Cytochem 62(3):172–184
128. Trinkaus-Randall V, Kewalramani R, Payne J, Cornell-Bell A (2000) Calcium signaling induced by adhesion mediates protein tyrosine phosphorylation and is independent of pHi. J Cell Physiol 184(3):385–399
129. Liu Y, Echtermeyer F, Thilo F, Theilmeier G, Schmidt A, Schulein R et al (2012) The proteoglycan syndecan 4 regulates transient receptor potential canonical 6 channels via RhoA/Rho-associated protein kinase signaling. Arterioscler Thromb Vasc Biol 32(2):378–385
130. Lunde IG, Herum KM, Carlson CC, Christensen G (2016) Syndecans in heart fibrosis. Cell Tissue Res 365(3):539–552
131. Couchman JR, Multhaupt H, Sanderson RD (2016) Recent insights into cell surface heparan sulphate proteoglycans and cancer. F1000Res 5

132. Saied-Santiago K, Bulow HE (2018) Diverse roles for glycosaminoglycans in neural patterning. Dev Dyn 247(1):54–74
133. Christensen G, Herum KM, Lunde IG (2018) Sweet, yet underappreciated: Proteoglycans and extracellular matrix remodeling in heart disease. Matrix Biol
134. Gopal S, Couchman J, Pocock R (2016) Redefining the role of syndecans in C. elegans biology. Worm 5(1):e1142042
135. Humphries JD, Byron A, Humphries MJ (2006) Integrin ligands at a glance. J Cell Sci 119(Pt 19):3901–3903
136. Hynes RO (2002) Integrins: bidirectional, allosteric signaling machines. Cell 110(6):673–687
137. Xiong JP, Stehle T, Goodman SL, Arnaout MA (2003) Integrins, cations and ligands: making the connection. J Thromb Haemost 1(7):1642–1654
138. Luo BH, Carman CV, Springer TA (2007) Structural basis of integrin regulation and signaling. Annu Rev Immunol 25:619–647
139. Craig D, Gao M, Schulten K, Vogel V (2004) Structural insights into how the MIDAS ion stabilizes integrin binding to an RGD peptide under force. Structure 12(11):2049–2058
140. Zhang K, Chen J (2012) The regulation of integrin function by divalent cations. Cell Adhes Migr 6(1):20–29
141. Stefansson S, Su EJ, Ishigami S, Cale JM, Gao Y, Gorlatova N et al (2007) The contributions of integrin affinity and integrin-cytoskeletal engagement in endothelial and smooth muscle cell adhesion to vitronectin. J Biol Chem 282(21):15679–15689
142. Cherny RC, Honan MA, Thiagarajan P (1993) Site-directed mutagenesis of the arginine-glycine-aspartic acid in vitronectin abolishes cell adhesion. J Biol Chem 268(13):9725–9729
143. Charo IF, Nannizzi L, Smith JW, Cheresh DA (1990) The vitronectin receptor alpha v beta 3 binds fibronectin and acts in concert with alpha 5 beta 1 in promoting cellular attachment and spreading on fibronectin. J Cell Biol 111(6 Pt 1):2795–2800
144. Chen J, Maeda T, Sekiguchi K, Sheppard D (1996) Distinct structural requirements for interaction of the integrins alpha 5 beta 1, alpha v beta 5, and alpha v beta 6 with the central cell binding domain in fibronectin. Cell Adhes Commun 4(4–5):237–250
145. Sjaastad MD, Angres B, Lewis RS, Nelson WJ (1994) Feedback regulation of cell-substratum adhesion by integrin-mediated intracellular Ca^{2+} signaling. Proc Natl Acad Sci USA 91(17):8214–8218
146. Sarin V, Gaffin RD, Meininger GA, Muthuchamy M (2005) Arginine-glycine-aspartic acid (RGD)-containing peptides inhibit the force production of mouse papillary muscle bundles via alpha 5 beta 1 integrin. J Physiol 564(Pt 2):603–617
147. Lin CY, Hilgenberg LG, Smith MA, Lynch G, Gall CM (2008) Integrin regulation of cytoplasmic calcium in excitatory neurons depends upon glutamate receptors and release from intracellular stores. Mol Cell Neurosci 37(4):770–780
148. Wu X, Mogford JE, Platts SH, Davis GE, Meininger GA, Davis MJ (1998) Modulation of calcium current in arteriolar smooth muscle by alphav beta3 and alpha5 beta1 integrin ligands. J Cell Biol 143(1):241–252
149. Gui P, Wu X, Ling S, Stotz SC, Winkfein RJ, Wilson E et al (2006) Integrin receptor activation triggers converging regulation of Cav1.2 calcium channels by c-Src and protein kinase A pathways. J Biol Chem 281(20):14015–14025
150. Waitkus-Edwards KR, Martinez-Lemus LA, Wu X, Trzeciakowski JP, Davis MJ, Davis GE et al (2002) alpha(4)beta(1) Integrin activation of L-type calcium channels in vascular smooth muscle causes arteriole vasoconstriction. Circ Res 90(4):473–480
151. Kwon MS, Park CS, Choi K, Ahnn J, Kim JI, Eom SH et al (2000) Calreticulin couples calcium release and calcium influx in integrin-mediated calcium signaling. Mol Biol Cell 11(4):1433–1443
152. Jiao R, Cui D, Wang SC, Li D, Wang YF (2017) Interactions of the mechanosensitive channels with extracellular matrix, integrins, and cytoskeletal network in osmosensation. Front Mol Neurosci 10:96

153. Matthews BD, Thodeti CK, Tytell JD, Mammoto A, Overby DR, Ingber DE (2010) Ultra-rapid activation of TRPV4 ion channels by mechanical forces applied to cell surface beta1 integrins. Integr Biol (Camb) 2(9):435–442
154. Zimolo Z, Wesolowski G, Tanaka H, Hyman JL, Hoyer JR, Rodan GA (1994) Soluble alpha v beta 3-integrin ligands raise $[Ca^{2+}]i$ in rat osteoclasts and mouse-derived osteoclast-like cells. Am J Phys 266(2 Pt 1):C376–C381
155. Bhattacharya S, Ying X, Fu C, Patel R, Kuebler W, Greenberg S et al (2000) alpha(v)beta(3) integrin induces tyrosine phosphorylation-dependent Ca^{2+} influx in pulmonary endothelial cells. Circ Res 86(4):456–462

Index

M. S. Islam (ed.), *Calcium Signaling*, Advances in Experimental Medicine and Biology 1131, https://doi.org/10.1007/978-3-030-12457-1